EANM'20

Annual Congress of the

European Association of Nuclear Medicine
October 22 – 30, 2020
Virtual

Abstracts

European Journal of Nuclear Medicine and
Molecular Imaging (2020) 47 (Suppl 1): S1–S753
10.1007/s00259-020-04988-4

This supplement was not sponsored by outside commercial interests. It was funded entirely by the association's own resources.

Dear colleagues, dear friends,

On behalf of the European Association of Nuclear Medicine, it is my great honour to invite you to the 33rd Annual EANM Congress, which will take place virtually from 22 to 30 October 2020.

Nuclear Medicine keeps on growing in many clinical areas, from diagnostic imaging to therapy: our procedures are increasingly being incorporated into clinical practice, in a variety of settings and diseases. This success is mostly related to a peculiar characteristic of our specialty, namely the functional approach to medicine. PET imaging works so well because of the unique functional information provided to clinicians, and this feature is the key to the ongoing rapid diffusion of Nuclear Medicine.

In recent years, the status of the EANM Congress as the world-leading meeting in Nuclear Medicine has been firmly established. The number of attendees in 2019 exceeded that in any previous year, with more than 6950 participants, but we are working to make the 2020 event even bigger, more memorable, and virtual.

EANM cares for its members, participants and patients, with safety being our primary concern as COVID-19 continues to pose a major health threat worldwide. Therefore, it was decided that it is in the best interest of the entire NM community to go virtual only.

The Virtual EANM Congress will still have all the features that made the event successful in the past. The usual excellent tracks and sessions, from CME to joint sessions, have already been confirmed. A number of newer features are also being planned and we will have a new format for the plenary sessions, new top-rated oral presentation sessions and a new 'Top Trials' session.

A further characteristic of our Congress is its multidisciplinarity, and this will be emphasised in 2020, with a number of sessions bringing together physicians from many specialties as well as specialists in radiochemistry and pharmacy, physicists and other professionals. In addition, a dedicated track for technologists will be provided.

If all of this still isn't enough to motivate you to attend the EANM'20 Congress virtually, we are working on providing some extra entertainment to make your virtual experience even more fun. This will include a daily nuclear quiz, daily programme highlights' announcements, games and social opportunities.

Stefano Fanti

EANM Congress Chair 2020–2022

THURSDAY | October 22, 2020

Time (CEST)	Channel 1	Channel 2	Channel 3	Channel 4	Channel 5	Channel 6	Channel 7	Channel 8	Channel 9	Channel 10	Channel 11	Time (CEST)
13:00 - 13:25	**Welcome and Practical Info - A Virtual Introduction**											13:00 - 13:25
13:25 - 13:30												13:25 - 13:30
13:30 - 15:00	101 CME **CME 1** Translational Molecular Imaging and Therapy + Oncology & Theranostics Committee **Radar on Gynaecological Cancers**	102 **Joint Symposium 1** Drug Development Committee / EFMC **Imaging Neuroinflammation**	103 **Joint Symposium 2** TMIT + Drug Development + Radiopharmacy + Oncology & Theranostics Committee / WMIS **Nano- and Micro-Particles in Nuclear Medicine (Incl. Radioembolisation)**	104 **Technologists' Opening** (13:30-13:40) **CTE 1** (13:40-15:00) Technologist Committee **Tech Guide Launch**	105 **M2M Track TROP Session** Radiopharmacy + Translational Molecular Imaging and Therapy Committee **Translational Oncology Imaging**	106 **Cutting Edge Science Track TROP Session** Physics Committee **Quantification**	107 **Pitfalls & Artefacts 1** Neuroimaging Committee **Unexpected Findings in Brain Imaging**	108 **Clinical Oncology Track Featured Session** Oncology & Theranostics Committee **Prostate Beyond Staging and Restaging**	109 **TROP Session** Thyroid Committee **Therapeutic Options in Thyroid Cancer - Radioiodine and Beyond**	110 **Featured Session** Cardiovascular Committee **Advances in PET-MPI / CT**	111 **e-Poster Presentation Session 1** Oncology & Theranostics Committee **PET Diagnostics - Part 1**	13:30 - 15:00
15:00 - 15:10												15:00 - 15:10
15:10 - 16:25	201 **Plenary 1 incl. Marie Curie Lecture** **Total Body PET**											15:10 - 16:25
16:25 - 16:35												16:25 - 16:35
16:35 - 18:05	301 CME **CME 2** Neuroimaging + Physics Committee **Software Tools and Approaches to Measure Nuclear Brain Images**	302 **Joint Symposium 3** Oncology & Theranostics Committee / EAU **Primary Staging of Prostate Cancer Reloaded**	303 **Joint Symposium 4** Radiation Protection Committee / EURADOS **Hot Topics in Radiation Protection**	304 **CTE 2** Technologist + Paediatrics Committee **Update in Paediatric Imaging**	305 **M2M Track TROP Session** Radiopharmacy + Translational Molecular Imaging and Therapy Committee **Cardiology Translational**	306 **Cutting Edge Science Track TROP Session** Dosimetry Committee **Preclinical Dosimetry and Radiobiology**	307 **Pitfalls & Artefacts 2** Thyroid Committee **Pre- and Post Therapeutic Imaging in Thyroid Cancer**	308 **Clinical Oncology Track TROP Session** Oncology & Theranostics Committee **Interventional Nuclear Medicine - Local Interventions**			311 **e-Poster Presentation Session 2** Oncology & Theranostics Committee **PET Diagnostics - Part 2**	16:35 - 18:05
18:05 - 18:10												18:05 - 18:10
18:10 - 19:00	**Virtual Congress Opening**											18:10 - 19:00
19:00 - 20:00	**Welcome Social Hour**											19:00 - 20:00

FRIDAY | October 23, 2020

Time (CEST)	Channel 1	Channel 2	Channel 3	Channel 4	Channel 5	Channel 6	Channel 7	Channel 8	Channel 9	Channel 10	Channel 11	Time (CEST)
08:30 - 08:45	**Nuclear Quiz**											08:30 - 08:45
08:45 - 08:55	**Daily Highlights**											08:45 - 08:55
08:55 - 09:00												08:55 - 09:00
09:00 - 10:30	401 CME **CME 3** Radiopharmacy + Oncology & Theranostics + Translational Molecular Imaging and Therapy Committee **Finding the Right PET Companion for ImmunoOncology**	402 **Joint Symposium 5** Oncology & Theranostics Committee / EHA **Use of PET in Multiple Myeloma**	403 **Joint Symposium 6** Cardiovascular Committee / ASNC **Detecting Cardiac Toxicity of Cancer Therapies with Nuclear Imaging**	404a **Mini Course 1** (09:00 - 09:50) Technologist Committee **New Developments in Cardiac Imaging Instrumentation** 404b **Mini Course 2** (10:00 - 10:50) Technologist Committee **Advanced Practice in Hybrid Nuclear Medicine**	405 **M2M Track TROP Session** Radiopharmacy + Translational Molecular Imaging and Therapy Committee **Pharmacokinetics and Chelators - Best of Both Worlds**	406 **Cutting Edge Science Track Featured Session** Radiation Protection Committee **Patient Radiation Protection**	407 **Teaching Session 1** TMIT + Physics Committee / EARL **Quantification and Standardisation in Clinical and Preclinical Molecular Imaging**	408 **Clinical Oncology Track Featured Session** Oncology & Theranostics Committee **PRRT for NETs**	409 **TROP Session** Neuroimaging Committee **Molecular Imaging of Movement Disorders**	410 **Featured Session** Bone & Joint Committee **Molecular Bone Imaging - Nuclear Medicine's Swiss Army Knife!**	411 **e-Poster Presentation Session 3** Dosimetry Committee **Clinical Dosimetry Methods**	09:00 - 10:30
10:30 - 10:40												10:30 - 10:40
10:40 - 12:10	501 CME **CME 4** Bone & Joint Committee **Multimodality Imaging-Based Problem Solving for Multiple Bone Lesions**	502 **Joint Symposium 7** Neuroimaging Committee / EAN / ECTRIMS **Multiple Sclerosis - Update in Neuroimaging**	503 **Joint Symposium 8** Radiopharmacy + Drug Development Committee / SRS **The Revival of Radiometals**	404c **Mini Course 3** (11:00 - 11:50) Technologist Committee **Alpha Emitters in Therapy**	505 **M2M Track TROP Session** Drug Development + Translational Molecular Imaging and Therapy Committee **It Takes Place in the Brain - New Neuro Tracers**	506 **Cutting Edge Science Track TROP Session** Physics Committee **New Technologies and Imaging Techniques**	507 **Teaching Session 2** **The Uncomfortable Truth - Are Nuclear Medicine Physicians Viewed as Second Class Doctors Compared to Radiologists?**	508 **Clinical Oncology Track TROP Session** Oncology & Theranostics Committee **PET for Haematological Tumours**	509 **Featured Session** Thyroid Committee **Parathyroid Imaging - Who Scores the Best Goals in this Champions League?**	510 **Clinical Oncology Track TROP Session** Oncology & Theranostics Committee **NET Diagnostics**	511 **e-Poster Presentation Session 4** Cardiovascular Committee **The Best of Cardiovascular Imaging in Short**	10:40 - 12:10
12:10 - 12:15												12:10 - 12:15
12:15 - 13:45	**Lunch Break**											12:15 - 13:45
13:45 - 13:50												13:45 - 13:50
13:50 - 15:20	601 CME **CME 5** Oncology & Theranostics Committee **Imaging Hepatobiliary and Pancreatic Tumours - Pearls, Patterns and Pitfalls**	602 **Joint Symposium 9** Inflammation & Infection Committee / ESMI / ESCMID **Imaging Pulmonary Fungal Infections**	603 **Joint Symposium 10** Cardiovascular Committee / JSNM **Nuclear Cardiology Beyond Perfusion Imaging**	604 **Technologists Oral Presentations 1 - Featured Session** **MATTER - MultidisciplinAry TechnologisT rEseaRch**	605 **M2M Track Featured Session** Radiopharmacy + Translational Molecular Imaging and Therapy Committee **Immune and Microenvironment Imaging**	606 **Cutting Edge Science Track TROP Session** Physics Committee **Image Processing - Neurology**	607 **Pitfalls & Artefacts 3** Dosimetry Committee **Dosimetry as Part of Patient Care**	608 **Clinical Oncology Track Featured Session** Oncology & Theranostics Committee **BCR Detection with Ga-PSMA and Beyond**	609 **TROP Session** Paediatrics Committee **Nuclear Playground - Nuclear Medicine in Children and Adolescents**	610 **Featured Session** Neuroimaging Committee **Molecular Brain Tumour Imaging**	611 **e-Poster Presentation Session 5** Thyroid Committee **The Thyroid and its Neighbours (The Parathyroids)**	13:50 - 15:20
15:20 - 15:30												15:20 - 15:30
15:30 - 16:45	701 **Plenary 2** **Cardiac Nuclear Medicine - Present and Future**											15:30 - 16:45
16:45 - 16:55												16:45 - 16:55
16:55 - 18:25	801 CME **CME 6** Drug Development + Radiopharmacy + Neuroimaging Committee **Bloody Hell!!! Impact on Quantitation of Blood Radiotracer Measurements**	802 **Joint Symposium 11** Oncology & Theranostics Committee / ESTRO **How Much PET does Radiation Oncology Require?**	803 **Joint Symposium 12** Cardiovascular Committee / EACVI **Selecting the Right Imaging for the Right Patient in CAD**	804 Technologists **Technologis e-Poster Presentation Session 1**	805 **M2M Track Featured Session** Radiopharmacy + TMIT + Oncology & Theranostics Committee **Translational Interventional Nuclear Medicine**	806 **Cutting Edge Science Track TROP Session** Radiation Protection Committee **Radiation Protection of Staff, and Advances in Technology**	807 **Pitfalls & Artefacts 4** Oncology & Theranostics + Inflammation & Infection Committee **Interpretation of Response Monitoring During Immune Therapy**	808 **Clinical Oncology Track TROP Session** Oncology & Theranostics Committee **Breast PET**			811 Technologists **Technologist e-Poster Presentation Session 2**	16:55 - 18:25

Plenary Sessions | CME Sessions | Joint/Special Symposia | Technologist Track | M2M Track | Cutting Edge Science Track | Pitfalls & Artefacts / Teaching Sessions | Clinical Oncology Track | Mid-Congress-Symposia | Further TROP/Featured Sessions | e-Poster Presentation Sessions | Special Sessions

SATURDAY | October 24, 2020

Time (CEST)	Channel 1	Channel 2	Channel 3	Channel 4	Channel 5	Channel 6	Channel 7	Channel 8	Channel 9	Channel 10	Channel 11	Time (CEST)
08:30 - 08:45	Nuclear Quiz											08:30 - 08:45
08:45 - 08:55	Daily Highlights											08:45 - 08:55
08:55 - 09:00												08:55 - 09:00
09:00 - 10:30	901 CME 7 Inflammation & Infection + Paediatrics Committee Nuclear Medicine in Paediatric Infections	902 Joint Symposium 13 Oncology & Theranostics Committee / EHA Metabolic Tumour Volume (MTV) in Lymphoma	903 Joint Symposium 14 Drug Development Committee / SRS Transporter's Imaging	904 CTE 3 Technologist + Dosimetry Committee Calibration for Instrumentation for Dosimetry	905 M2M Track TROP Session Translational Molecular Imaging and Therapy + Oncology & Theranostics Committee Image Guided Treatment and Biopsy	906 Cutting Edge Science Track TROP Session Dosimetry Committee Dosimetry Methods and Models - Part 1	907 Teaching Session 3 A Practical Guide to MR when Reading PET/MR	908 Clinical Oncology Track Featured Session Oncology & Theranostics Committee PET Diagnostics in Head Neck Cancers and Melanoma		910 TROP Session Thyroid Committee Nuclear Endocrinology in Diagnosis and Therapy	911 e-Poster Presentation Session 6 Physics Committee Physics - Hardware and Optimisation	09:00 - 10:30
10:30 - 10:40												10:30 - 10:40
10:40 - 12:10	1001 CME 8 Paediatrics Committee Emergency Conditions in Paediatric Nuclear Medicine	1002 Joint Symposium 15 Thyroid Committee / ETA-CG Systemic Therapeutic Options in Advanced Thyroid Cancer	1003 Joint Symposium 16 Bone & Joint Committee / EACMFS Role of Hybrid Imaging in Jaw and Skull Conditions	1004 CTE 4 Technologist Committee NET Imaging and Therapy	1005 M2M Track TROP Session Radiopharmacy + Translational Molecular Imaging and Therapy + Drug Development Committee New Kids on the Block - New Tracers	1006 Cutting Edge Science Track TROP Session Physics Committee AI - Radiomics and Modelling	1007 Teaching Session 4 The Intellectual and Emotional Journey to Radiology and Nuclear Equality	1008 Clinical Oncology Track Featured Session Oncology & Theranostics Committee Best of Nuclear Medicine Therapy	1009 Clinical Oncology Track Featured Session Oncology & Theranostics Committee Onco Diagnostics Miscellaneous	1010 Featured Session Cardiovascular Committee Nuclear Imaging in Cardiac Arrhythmias	1011 e-Poster Presentation Session 7 Inflammation & Infection Committee Nuclear Medicine for Infection & Inflammation - The Story Continues	10:40 - 12:10

SUNDAY | October 25, 2020

Time (CET)	Channel 1	Channel 2	Channel 3	Channel 4	Channel 5	Channel 6	Channel 7	Channel 8	Channel 9	Channel 10	Channel 11	Time (CET)
	Free											

MONDAY | October 26, 2020

Time (CET)	Channel 1	Channel 2	Channel 3	Channel 4	Channel 5	Channel 6	Channel 7	Channel 8	Channel 9	Channel 10	Channel 11	Time (CET)
09:30 - 12:15	CME Mid-Congress-Symposium 1 Cardiovascular + Inflammation & Infection Committee / EACVI Detecting Cardiac Amyloidosis - Increasing Role of Nuclear Medicine	CME Mid-Congress-Symposium 2 Physics + Dosimetry Committee Artificial Intelligence in Image Acquisition, Reconstruction and Processing										09:30 - 12:15
12:15 - 12:20												12:15 - 12:20
12:20 - 13:50	EANM Young Daily Forum 1 Simply the Best – Presentation Skills for Medical Professionals											12:20 - 13:50
13:50 - 14:00												13:50 - 14:00
14:00 - 16:45	CME Mid-Congress-Symposium 3 Oncology & Theranostics + Radiopharmacy + Drug Development Committee / ESMO Clinical Development of Radioligand Therapy	CME Mid-Congress-Symposium 4 Translational Molecular Imaging and Therapy + Oncology & Theranostics Committee Image Guided Surgery										14:00 - 16:45

TUESDAY | October 27, 2020

Time (CET)	Channel 1	Channel 2	Channel 3	Channel 4	Channel 5	Channel 6	Channel 7	Channel 8	Channel 9	Channel 10	Channel 11	Time (CET)
09:30 - 12:15	CME Mid-Congress-Symposium 5 Oncology & Theranostics Committee How to Read PET/CT - Different Shades of Sugar (FDG)	CME Mid-Congress-Symposium 6 Dosimetry + TMIT + Onco. & Theran. + Rad. Prot. + Infl. & Inf. Committee Improved Insights into Radiobiology - Key for Radionuclide Therapy										09:30 - 12:15
12:15 - 12:20												12:15 - 12:20
12:20 - 13:50	EANM Young Daily Forum 2 I will survive - Managing Work Stress and Building Your Resilience											12:20 - 13:50
13:50 - 14:00												13:50 - 14:00
14:00 - 16:45	CME Mid-Congress-Symposium 7 Dosimetry + Oncology & Theranostics + Physics Committee Lutetium Therapy	CME Mid-Congress-Symposium 8 For Youngsters - Essential Oncology for Young Nuclear Medicine Physicians										14:00 - 16:45

Plenary Sessions | CME Sessions | Joint/Special Symposia | Technologist Track | M2M Track | Cutting Edge Science Track | Pitfalls & Artefacts / Teaching Sessions | Clinical Oncology Track | Mid-Congress-Symposia | Further TROP/Featured Sessions | e-Poster Presentation Sessions | Special Sessions

WEDNESDAY | October 28, 2020

Time (CET)	Channel 1	Channel 2	Channel 3	Channel 4	Channel 5	Channel 6	Channel 7	Channel 8	Channel 9	Channel 10	Channel 11	Time (CET)
09:00 - 09:30			Mid-Congress-Symposium 13 (09:00 - 16:00) Technologist + Dosimetry + Physics Committee Introduction to Dosimetry									09:00 - 09:30
09:30 - 12:15	Mid-Congress-Symposium 9 Thyroid + Radiation Protection Committee / ETA / ESES Update on Treatment of Hyperthyroidism	Mid-Congress-Symposium 10 Inflammation & Infection Committee Diagnostic Flowcharts on Musculoskeletal Infections										09:30 - 12:15
12:15 - 12:20												12:15 - 12:20
12:20 - 13:50	EANM Young Daily Forum 3 Nothing else matters - Get your paper published in a top journal											12:20 - 13:50
13:50 - 14:00												13:50 - 14:00
14:00 - 16:45	Mid-Congress-Symposium 11 Neuroimaging + Radiopharmacy Committee Current State and Future of Tau PET Imaging	Mid-Congress-Symposium 12 For Youngsters - Emergency During Nuclear Medicine Procedures - What to Know and What to Do?										14:00 - 16:45

THURSDAY | October 29, 2020

Time (CET)	Channel 1	Channel 2	Channel 3	Channel 4	Channel 5	Channel 6	Channel 7	Channel 8	Channel 9	Channel 10	Channel 11	Time (CET)
13:00 - 13:15	Nuclear Quiz											13:00 - 13:15
13:15 - 13:25	Daily Highlights											13:15 - 13:25
13:25 - 13:30												13:25 - 13:30
13:30 - 15:00	1101 CME 9 Oncology & Theranostics + Physics Committee New PET Technologies - Digital Revolution or Big Bust?	1102 Joint Symposium 17 Drug Development Committee / EORTC Benchside to Bedside and Back - What do we Learn from the Clinic?	1103 Joint Symposium 18 Oncology & Theranostics + Inflammation & Infection Committee / AIO Imaging Tumour Microenvironment	1104 Technologists Oral Presentations 2 - Featured Session TOP - Technologist Overview and Practice Impact		1106 Cutting Edge Science Track TROP Session Dosimetry Committee Dosimetry Methods and Models - Part 2	1107 Pitfalls & Artefacts 5 Inflammation & Infection Committee FDG-PET Performed or Suspicious for Infections and Inflammation, Including COVID-19	1108 Clinical Oncology Track TROP Session Oncology & Theranostics Committee Detecting BCR with [68Ga]Ga-PSMA	1109 Featured Session Cardiovascular Committee Advances in SPECT-MPI	1110 Cutting Edge Science Track Featured Session Physics Committee Radiomics		13:30 - 15:00
15:00 - 15:10												15:00 - 15:10
15:10 - 16:25	1201 Plenary 3 What's Cooking? Next Generation Radiopharmaceuticals											15:10 - 16:25
16:25 - 16:35												16:25 - 16:35
16:35 - 18:05	1301 CME 10 Thyroid Committee Radiomics in Thyroid Imaging	1302 Joint Symposium 19 Oncology & Theranostics Committee / ENETS Impacting the Outcome of High Grade NET Patients	1303 Joint Symposium 20 Neuroimaging Committee / ECNP Simultaneous PET/MR Imaging of Neuroreceptor Systems	1304 Technologists Oral Presentations 3 - Featured Session BOTH ART - The Beauty Of The HeART and mind	1305 M2M Track Featured Session Drug Development + Radiopharmacy Committee The Revival of Pre-Targeting	1306 Cutting Edge Science Track Featured Session Physics Committee Intra-Operative Nuclear Medicine	1307 Pitfalls & Artefacts 6 Paediatrics Committee Pitfalls and Artefacts in Paediatric Nuclear Medicine	1308 Clinical Oncology Track TROP Session Oncology & Theranostics Committee PET Diagnostics of Lung Cancer and Mesothelioma	1309 Hot Topic Session Best Clinical Trials		1311 e-Poster Presentation Session 8 Oncology & Theranostics Committee All About the Prostate - Staging, Restaging and Beyond	16:35 - 18:05

Plenary Sessions | CME Sessions | Joint/Special Symposia | Technologist Track | M2M Track | Cutting Edge Science Track | Pitfalls & Artefacts / Teaching Sessions | Clinical Oncology Track | Mid-Congress-Symposia | Further TROP/Featured Sessions | e-Poster Presentation Sessions | Special Sessions

FRIDAY | October 30, 2020

Time (CET)	Channel 1	Channel 2	Channel 3	Channel 4	Channel 5	Channel 6	Channel 7	Channel 8	Channel 9	Channel 10	Channel 11	Time (CET)
08:30 - 08:45	Nuclear Quiz											08:30 - 08:45
08:45 - 08:55	Daily Highlights											08:45 - 08:55
08:55 - 09:00												
09:00 - 10:30	1401 CME 11 Oncology & Theranostics + Translational Molecular Imaging and Therapy Committee **SLN - Past and Future**	1402 **Joint Symposium 21** Drug Development + Physics Committee / IEEE **Total Body PET Imaging**	1403 **Joint Symposium 22** Paediatrics Committee / ESPGHAN **Nuclear Medicine Techniques in the Evaluation of GI Motility in Children**	1404 **CTE 5** Technologist Committee **Departmental Organisation**	1405 **M2M Track TROP Session** Drug Development + Radiopharmacy Committee **New and Established Tracers - Prostate only!**	1406 **Cutting Edge Science Track TROP Session** Dosimetry Committee **Dosimetry for PRRT and PSMA**	1407 **Teaching Session 5** Oncology & Theranostics Committee **PET/CT Guided Biopsy**	1408 **Clinical Oncology Track Featured Session** Oncology & Theranostics Committee **PET Diagnostics of Gynaecological and GI Tumours**	1409 **Featured Session** Cardiovascular Committee **Nuclear Imaging in Inflammatory and Infiltrative Cardiovascular Diseases**	1410 **TROP Session** **General Nuclear Medicine**	1411 **e-Poster Presentation Session 9** Physics Committee **Physics - Software and Image Processing**	09:00 - 10:30
10:30 - 10:40												10:30 - 10:40
10:40 - 12:10	1501 CME 12 Dosimetry Committee **Alpha Particle Therapy Without Imaging - Options for Dosimetry, the Alpha and Omega**	1502 **Joint Symposium 23** Oncology & Theranostics Committee / ESDO **New Diagnostic and Therapeutic Frontiers in Digestive Oncology**	1503 **Joint Symposium 24** Physics + Paediatrics Committee / EFOMP **Technical Advances in Paediatric Dose Reduction**	1504 **CTE 6** Technologist Committee **Advanced Competencies**	1505 **M2M Track Featured Session** Translational Molecular Imaging and Therapy + Radiopharmacy Committee **Targeted Radionuclide Therapy - Trick or Treat?**	1506 **Cutting Edge Science Track TROP Session** Physics Committee **Image Reconstruction and Corrections**	1507 **Teaching Session 6** Cardiovascular Committee **Difficult Cases in Cardiac Imaging**	1508 **Clinical Oncology Track Featured Session** Oncology & Theranostics Committee **Prostate Cancer Therapy - PSMA, ^{225}Ra and More...**	1509 **TROP Session** Thyroid Committee **Is It or Is It Not Malignant? - Diagnostic/Predictive Options in Thyroid Nodules**	1510 **TROP Session** Inflammation & Infection Committee **Our Army at War - Nuclear Medicine and COVID-19**	1511 **e-Poster Presentation Session 10** Neuroimaging Committee **Molecular Brain Imaging**	10:40 - 12:10
12:10 - 12:15												12:10 - 12:15
12:15 - 13:45	**Lunch Break**											12:15 - 13:45
13:45 - 13:50												13:45 - 13:50
13:50 - 15:20	1601 CME 13 Translational Molecular Imaging and Therapy + Physics + Oncology & Theranostics + Technologist Committee **Radiomics in a Preclinical and a Clinical Setting**	1602 **Joint Symposium 25** Neuroimaging Committee / EANO **Immunotherapy in Brain Tumours**	1603 **Joint Symposium 26** Physics + Oncology & Theranostics Committee / AAPM **Quantitative SPECT - An Essential Tool?**			1606 **Cutting Edge Science Track TROP Session** Physics Committee **Harmonisation & Standardisation**	1607 **Pitfalls & Artefacts 7** Bone & Joint Committee **Bone SPECT/CT Revisited - Learning an Old Fox New Tricks**	1608 **Clinical Oncology Track TROP Session** Oncology & Theranostics Committee **All About Staging the Prostate**	1609 **TROP Session** Inflammation & Infection Committee **PET for Infection and Inflammation - A New Story**		1611 **e-Poster Presentation Session 11** Oncology & Theranostics Committee **Nuclear Medicine Therapy Beyond Thyroid**	13:50 - 15:20
15:20 - 15:30												15:20 - 15:30
15:30 - 17:00	1701 CME 14 Oncology & Theranostics Committee **Molecular Drug Imaging of Solid Tumours Including Microenvironment**	1702 **Joint Symposium 27** TMIT + Oncology & Theranostics + Cardiovascular + Inflammation & Infection Committee / ESMI **Radar on Immune Cell Imaging**	1703 **Joint Symposium 28** Cardiovascular + Translational Molecular Imaging and Therapy + Drug Development Committee / AHA **New Approaches for Cardiovascular Imaging**	1704 **CTE 7** Technologist Committee **Quality Control of Imaging Instrumentation**	1705 **M2M Track TROP Session** Drug Development + Radiopharmacy Committee **Hot Stuff - Radionuclide Production**	1706 **Cutting Edge Science Track TROP Session** Physics Committee **AI - Image Processing and Data Corrections**	1707 **Teaching Session 7** Thyroid Committee **Molecular Imaging in Thyroid Nodules**	1708 **Clinical Oncology Track TROP Session** Oncology & Theranostics Committee **[^{177}Lu]Lu-PSMA Radioligand Therapy**	1709 **TROP Session** Neuroimaging Committee **Novel Molecular Brain Imaging Approaches**		1711 **e-Poster Presentation Session 12** Oncology & Theranostics Committee **Onco Diagnostics - Mixed Bag**	15:30 - 17:00
17:00 - 17:05												17:00 - 17:05

Plenary Sessions | CME Sessions | Joint/Special Symposia | Technologist Track | M2M Track | Cutting Edge Science Track | Pitfalls & Artefacts / Teaching Sessions | Clinical Oncology Track | Mid-Congress-Symposia | Further TROP/Featured Sessions | e-Poster Presentation Sessions | Special Sessions

101

CME 1: Radar on Gynaecological Cancers

Thursday, October 22, 2020, 13:30 - 15:00 Channel 1

OP-001
PET/CT Guided Response Assessment in Gynaecological Tumours
C. Nanni; Nuclear Medicine Unit, Policlinico Sant'Orsola Malpighi, Bologna, ITALY.

OP-002
PET/CT in Radiotherapy Treatment Planning
J. Adam; Department of Radiology and Nuclear Medicine, Amsterdam University Medical Center, Amsterdam, NETHERLANDS.

OP-003
Interventional Nuclear Medicine Techniques for Gynaecological Tumours
S. Vidal Sicart; Nuclear Medicine Hospital Clinic de Barcelona, Barcelona, SPAIN.

OP-004
New Radiopharmaceuticals for Improved Diagnosis in Gynaecological Tumours - What is the Future?
S. Kossatz; Technical University of Munich, Department of Nuclear Medicine, Munich, GERMANY.

102

Joint Symposium 1 (EANM/EFMC): Imaging Neuroinflammation

Thursday, October 22, 2020, 13:30 - 15:00 Channel 2

OP-005
Introduction Talk
D. van Weehaeghe; Division of Nuclear Medicine and Molecular Imaging, University Hospitals of Leuven and KU Leuven, Leuven, BELGIUM.

OP-006
Target Identification and Tracer Design and Development
A. Windhorst; Amsterdam UMC/VUMC, Department of Radiology and Nuclear Medicine, Amsterdam, NETHERLANDS.

OP-007
Clinical Directions for Neuroinflammation Imaging
A. Jacobs; European Institute for Molecular Imaging, University Hospital Muenster, Muenster, GERMANY .

OP-008
Clinical Trials of P2X7 Targeted Radiotracers
K. van Laere; Division of Nuclear Medicine and Molecular Imaging, University Hospitals of Leuven and KU Leuven, Leuven, BELGIUM.

103

Joint Symposium 2 (EANM/WMIS): Nano- and Micro-Particles in Nuclear Medicine (Incl. Radioembolisation)

Thursday, October 22, 2020, 13:30 - 15:00 Channel 3

OP-009
Introduction to Nanoparticles in Medicine
T. Lammers; RWTH Aachen, Experimental Molecular Imaging, Aachen, GERMANY.

OP-010
Nanocolloids in Theranostics
T. Buckle; Leiden University Hospital, Radiology, Leiden, NETHERLANDS.

OP-011
Radioembolization with Microparticles
M. Wildgruber; University Hospital Muenster, Radiology, Muenster, GERMANY.

104

CTE 1: Tech Guide Launch

Thursday, October 22, 2020, 13:30 - 15:00 Channel 4

OP-012
Technologists' Opening
A. Santos; Hospital CUF Descobertas, Medicina Nuclear Department, Lisbon, PORTUGAL.

OP-013
QC of Hybrid Systems
S. Rep; University Medical Centre, Department of Nuclera Medicine, Ljubljana, SLOVENIA.

OP-014
The Contribution of Hybrid Imaging to Radionuclide Therapy
C. Abreu; The Royal Marsden Hospital, Sutton, UNITED KINGDOM.

OP-015
Quantitative Methods in SPECT/CT
A. L. Strömvall; Umeå University Hospital, Dept. of Radiation Physics, Umeå, SWEDEN.

105

M2M Track - TROP Session: Translational Oncology Imaging

Thursday, October 22, 2020, 13:30 - 15:00 Channel 5

OP-016

Phase I study of 99mTc-ADAPT6, a scaffold protein-based probe for visualization of HER2 expression in breast cancer

O. Bragina[1,2], E. von Witting[3], J. Garousi[4], R. Zelchan[1,2], M. Sandström[4], A. Orlova[1,4], A. Medvedeva[2], A. Doroshenko[2], A. Vorobyeva[1,4], S. Lindbo[3], J. Borin[3], N. Tarabanovskaya[2], J. Sörensen[4], S. Hober[3], V. Chernov[1,2], V. Tolmachev[1,4];
[1]Research Centrum for Oncotheranostics, Tomsk Polytechnic University, Tomsk, RUSSIAN FEDERATION, [2]Tomsk National Research Medical Center Russian Academy of Sciences, Tomsk, RUSSIAN FEDERATION, [3]KTH Royal Institute of Technology, Stockholm, SWEDEN, [4]Uppsala University, Uppsala, SWEDEN.

Aim/Introduction: Radionuclide molecular imaging of human epidermal growth factor (HER2) expression may be helpful to stratify breast and gastroesophageal cancer patients for HER2-targeting therapies. ADAPTs (albumin-binding domain derived affinity proteins) are a new type of small (5-2-7 kDa) proteins useful as probes for molecular imaging. ^{99m}Tc-ADAPT6 binds with high affinity to HER2. It demonstrated a high-contrast imaging of HER2-expressing human xenografts in mice in preclinical studies. The primary objective of this Phase I study was to evaluate biodistribution, dosimetry, and safety of the HER2-specific ^{99m}Tc-ADAPT6. The secondary objective was to compare the tumour imaging data with the data concerning HER2 expression obtained by immunohistochemistry (IHC) or fluorescent in situ hybridisation (FISH) analysis of biopsy samples. ***Materials and Methods:*** Twenty-nine breast cancer patients were included. Twenty-two patients with HER2-positive (n=11) or HER2-negative (n=11) histopathology were randomized to injection of either 500 µg (n=11) or 1000 µg (n=11) of ^{99m}Tc-ADAPT6, The injected activity was 385±125 MBq. Planar scintigraphy and SPECT imaging was performed after 2, 4, 6 and 24 h. An additional cohort of seven patients was injected with 165±29 MBq (injected protein mass 250 µg) and imaging was performed after 2 h only. ***Results:*** Injections of ^{99m}Tc-ADAPT6 at any injected mass were not associated with adverse effects. ^{99m}Tc-ADAPT6 had a rapid clearance from blood. The normal organs with the highest accumulation were kidney, liver and lung. Effective dose was 0.009±0.002 and 0.010±0.003 mSv/MBq for injected protein mass of 500 and 1000 µg, respectively. Injection of 500 µg resulted in an excellent discrimination between HER2-positive and HER2-negative tumors already 2 h after injection. The tumor-to-contralateral breast ratio was 37±19 for HER2-positive and 5±2 for HER2-negative tumors at this time point ($p< 0.01$). The tumor-to-contralateral breast ratios for HER2-positive tumors were significantly ($p <0.05$) higher for injected mass of 500 µg than for both 250 and 1000 µg. In one patient, the imaging using ^{99m}Tc-ADAPT6 revealed three bone metastases, which were not found at the time of diagnosis by CT or ^{99m}Tc-pyrophosphate bone scan. MRI imaging confirmed this finding. ***Conclusion:*** Injections of ^{99m}Tc-ADAPT6 are safe, well tolerated and associated with low absorbed and effective doses. Protein dose of 500 µg provided the best discrimination between HER2-positive and HER2-negative tumors. ^{99m}Tc-ADAPT6 is a promising imaging probe for stratification of patients for HER2-targeting therapy. ***References:*** Garousi J, et al. ADAPT, a Novel Scaffold Protein-Based Probe for Radionuclide Imaging of Molecular Targets. Cancer Res. 2015;75:4364-4371

OP-017

Radiolabelling and Preliminary in vivo Study of a Small Molecule-based Ligand for CCK2 Receptors Targeting

M. Asti[1], M. Verona[2], S. Rubagotti[1], F. Mastrotto[2], G. Marzaro[2], V. Di Marco[2], S. Corradetti[3], N. Realdon[2], A. Andrighetto[3];
[1]AUSL-IRCCS, Reggio Emilia, ITALY, [2]University of Padua, Padua, ITALY, [3]National Institute of Nuclear Physics, Legnaro (PD), ITALY.

Aim/Introduction: Receptors-specific targeting ligands were recently exploited to selectively deliver both imaging and therapeutic agents to cancer tissues in vivo. The cholecystokinin 2 receptor (CCK2R) is overexpressed in various human cancers (e.g. lung, medullary thyroid, pancreatic, colon, and gastrointestinal stromal tumors) but displays limited expression in normal tissues. For this reason, it is a suitable diagnostic and therapeutic target. In this study, a non-peptide-based ligand (namely IP2) functionalized with a DOTA chelator was synthesized and labelled with indium-111. ***Materials and Methods:*** The targeting agent Z-360, a benzodiazepine-derived CCK2R antagonist, was synthetized optimizing a previously published procedure. The synthesis pathway consists in a six steps reaction where the benzodiazepine structure was first formed and then functionalized with a di-ethylglycol spacer connecting the pharmacophore to a DOTA chelator (IP2). The ligand was radiolabeled in a pH 4 buffered environment with indium-111 and the reactions were optimized for precursor amount. Stability in human blood and lipophilicity by shake-flask method were evaluated as well. In vitro uptake and affinity of [^{111}In]In-IP2 were assessed at different time (2, 4, 8, 24 h) on a high CCK2R expressing tumor cell line (A549) and biodistribution, pharmacokinetic and specificity in vivo were evaluated on nude mice bearing A549 xenograft tumors. ***Results:*** The Z-360 core was obtained with an overall moderate yield (23%). IP2 was synthetized in good amounts and then purified with preparative HPLC. The radiolabeling process yields >95% with a molar activity of ca. 10 MBq/nmol and a radiochemical purity (assessed by RP-HPLC) >98%. Stability studies showed an amount of intact radiotracer higher than 93% after 2 hours of incubation. Computed

logP was 0.45. Cellular uptake showed a maximum after 4 hours of incubation. Tumors could be clearly visualized in vivo already after 2 hours although high amount of radiotracer was also found in the gastro-intestinal tract and other organs. Tumour retention persisted up to 24 hours and clearing was slow mainly by hepatobiliary excretion. Blocking experiments showed receptors mediated specific uptake. ***Conclusion:*** In this study a CCK2R antagonist ligands not based on a peptide sequence was synthetized and labelled with indium-111. In vitro and in vivo studies showed good potential but, due to the lipophilic nature of the targeting agent, a more hydrophilic spacer should be selected in order to improve biodistribution. Structural studies are on-going for enhancing receptor affinity as well. This study is a part of the so called "Isolpharm project". ***References:*** None

OP-018

Evaluation of Molecular Design of HER2-targeting Affibody-drug Conjugates for Drug Delivery to Ovarian Cancer

T. Xu[1], *H. Ding*[2], *A. Vorobyeva*[1,3], *M. Oroujeni*[1], *T. Gräslund*[2], *A. Orlova*[4,3,5], *V. Tolmachev*[1,3];
[1]*Department of Immunology, Genetics and Pathology, Uppsala University, Uppsala, SWEDEN,* [2]*Department of Protein Science, KTH Royal Institute of Technology, Stockholm, SWEDEN,* [3]*Research Centrum for Oncotheranostics, Research School of Chemistry and Applied Biomedical Sciences, Tomsk Polytechnic University, Tomsk, RUSSIAN FEDERATION,* [4]*Department of Medicinal Chemistry, Uppsala University, Uppsala, SWEDEN,* [5]*Science for Life Laboratory, Uppsala University, Uppsala, SWEDEN.*

Aim/Introduction: Human epidermal growth factor receptor 2 (HER2) is overexpressed in ca. 30% of ovarian cancer patients, which offers an opportunity for HER2-targeting therapy. Antibody-drug conjugates (ADCs) permit specific delivery of cytotoxic drugs to antigen-expressing cancer cells. An alternative to ADCs are Affibody molecules. They are small engineered scaffold proteins that bind with high affinity and specificity to selected antigens. We previously demonstrated that the anti-HER2 Affibody-drug conjugates (AffiDCs) containing an albumin binding domain (ABD) for half-life extension and a cytotoxic drug DM1 prolonged survival of mice bearing HER2-expressing SKOV-3 xenografts. However, moderate hepatic uptake was observed that could pose a risk of hepatotoxicity. This study aimed to evaluate the influence of molecular design of AffiDCs on the biodistribution and drug delivery to tumors. ***Materials and Methods:*** Three monomer and dimer formats of anti-HER2 AffiDCs having a tri-glutamate or a tri-glycine linker $Z_{HER2:2891}$-$Z_{HER2:2891}$-ABD-EEE-DM1, $Z_{HER2:2891}$-ABD-EEE-DM1 and $Z_{HER2:2891}$-ABD-GGG-DM1 were labeled with $^{99m}Tc(CO)_3^+$ via N-terminal $(HE)_3$-tag. Binding affinity to living SKOV-3 cells was measured using LigandTracer instrument. In vitro specificity of the labeled AffiDCs to HER2-overexpressing SKOV-3 and BT474 cells was evaluated. The internalization rate during continuous incubation in SKOV-3 and BT474 was studied. Biodistribution was measured in Balb/c nu/nu mice bearing SKOV-3 xenografts at 4 h and 24 h after injection. ***Results:*** The radiochemical purity of conjugates after NAP-5 purification was ≥95%. All tested compounds were stable in the presence of large excess of histidine. Radiolabeled AffiDCs demonstrated specific HER2-mediated binding to SKOV-3 and BT474 cells. Affinity measurements showed dissociation equilibrium constants to SKOV-3 cells in the single digit nanomolar range. The cellular processing assay showed rapid binding of all conjugates to HER2-expressing cells and a similar internalization pattern with internalized activity increasing over time and reaching 40% of total cell-associated activity by 24 h. Biodistribution in SKOV-3 tumor-bearing mice demonstrated slow blood clearance for all tested compounds. Among the three compounds, $Z_{HER2:2891}$-ABD-EEE-DM1 had the lowest uptake in liver, spleen and large intestine while the tumor uptake was the same as the other compounds. Compared to tri-glycine linker, the tri-glutamate spacer provided 36% and 10% reduction in hepatic uptake by 4 h and 24 h, respectively. ***Conclusion:*** This study showed the importance of molecular design of AffiDCs for decreasing undesirable uptake in normal organs. Among all tested constructs, $Z_{HER2:2891}$-ABD-EEE-DM1 demonstrated equally high tumor uptake with the best tumor-to-liver ratio and is a promising candidate for HER2-targeted therapy of ovarian cancer. ***References:*** None

OP-019

Optimization of the biodistribution of 1C1m-Fc anti TEM-1 antibody fusion protein in soft tissue sarcoma model in mice

J. Delage[1], *A. Faivre-Chauvet*[2], *J. K. Fierle*[3], *N. Schaefer*[4], *G. Coukos*[5], *S. M. Dunn*[3], *D. Viertl*[4], *J. O. Prior*[4];
[1]*Radiopharmacy Unit, Pharmacy Department, Lausanne University Hospital, Lausanne, SWITZERLAND,* [2]*CRCINA, INSERM 1232-CNRS ERL 6001, University of Angers, University of Nantes, Nantes, FRANCE,* [3]*LAbCore, Ludwig Institute for Cancer Research, Lausanne University Hospital and University of Lausanne, Lausanne, SWITZERLAND,* [4]*Department of Nuclear Medicine and Molecular Imaging, Lausanne University Hospital and University of Lausanne, Lausanne, SWITZERLAND,* [5]*Ludwig Institute for Cancer Research and Department of Oncology, Lausanne University Hospital and University of Lausanne, Lausanne, SWITZERLAND.*

Aim/Introduction: 1C1m-Fc is an anti TEM-1 scFv-Fc fusion antibody developed in Lausanne. Our previous study showed the interest of this new compound radiolabeled with ^{177}Lu for molecular imaging in soft tissue sarcoma. Even if the TEM-1 positive uptake was specific, we also observed an important liver uptake that was not saturation-dependent. Our hypothesis for this phenomenon was the influence of the number of DOTA on the biodistribution. The aim of this

study was to verify this hypothesis and find the best ratio of DOTA per antibody to develop an optimal radiolabeled 1C1m-Fc for theranostic applications. ***Materials and Methods:*** 1C1m was conjugated with six different concentrations of DOTA. The number of DOTA per antibody fusion protein was evaluated by mass spectrometry and was respectively 1.5; 2.5; 3; 6; 8.5 and 11. Tumors expressing huTEM-1 were established by subcutaneous injection of $3x10^6$ SK-N-AS cells in mouse flank of 8-10-week-old female Balb/c nude mice. Tumors were allowed to grow to 5-10mm (largest diameter) before initiating studies. After radiolabeling, ^{177}Lu-1C1m-Fc conjugated with 1.5 to 11 DOTA was injected into the lateral tail vein of the mice. In each group, three animals were euthanized by CO_2 inhalation and exsanguinated at 24h after injection of the radiolabeled product. Blood was collected, organs and tumors were removed, weighed, and the activity was measured by gamma counter. ***Results:*** A significant decrease of the tumor uptake was observed with the antibodies conjugated with more than 3 DOTA (18%IA/g up to 3 DOTA to 7.5%IA/g for 11 DOTA). In parallel, the blood uptake at 24 h varied between 10.2 % for 1.5 DOTA per antibody to 2.5% for 11 DOTA per antibody. We observed an inverse correlation of the tumor/liver ratio with the increasing number of DOTA per antibody, from 2 with 1.5 DOTA per antibody to 0.17 with 11 DOTA per antibody (rho=-0.99, $p<0.0001$). ***Conclusion:*** The number of DOTA molecules attached per antibody moiety plays a significant role in determining successful tumor targeting with radiolabeled antibodies. 1.5 DOTA per antibody seems to be the best ratio to maintaining a balance between radiochemical yield, immunoreactivity and pharmacokinetic behavior. Our next step would be to measure immunoreactivity to gain more insight about the possible mechanism. ***References:*** None

OP-020

68Ga-NT-20.3 for imaging of neurotensin receptor: first human study

F. Wang[1], *W. Wu*[1], *I. Virgolini*[2], *M. Hodlic*[3];
[1]*Nanjing Medical University, Nanjing, CHINA,* [2]*Medical University Innsbruck, Innsbruck, AUSTRIA,* [3]*Palacký University Olomouc, Olomouc, CZECH REPUBLIC.*

Aim/Introduction: Over the last decades, multiple peptide receptors were recognized as potential diagnostic and therapeutic targets in nuclear medicine. The peptide neurotensin (NT) acts via seven-transmembrane, G-protein-coupled receptor called NT receptor (NTR). Three NTR subtypes have been cloned: NTR-1 (high-affinity NTR), NTR-2 (low-affinity NTR) and NTR-3 (Sortilin 1, a single transmembrane domain sorting receptor). NTR-1 is the most expressed NTR.High NTR-1 expression has been observed in various tumours, from pancreatic ductal adenocarcinoma (PDAC), mesothelioma and breast cancer to prostate cancer. With intention to quantitate NTR expression in various tumours, ^{68}Ga-NT-20.3 radiopharmaceutical has been developed. After demonstration of binding affinity to cell lines, ^{68}Ga labelled NT surrogate was successfully applied in animal model.The purpose of this study was to evaluate the safety and tolerability of ^{68}Ga-NT-20.3 radiopharmaceutical in the first human study. ***Materials and Methods:*** This study was performed in accordance with Declaration of Helsinki and the Enforcement Decree of Pharmaceutical Affairs Good Clinical Practice after Ethical committee approval.DOTA-NT-20.3 was dissolved in sodium acetate buffer (0.25 M) and sent into the pre-heated reactor. ^{68}Ga eluting from the ^{68}Ge/^{68}Ga generator with 0.05 M HCl was added to the reaction vial. ^{68}Ga-DOTA-NT-20.3 was synthesized automatically with ITM module. Quality control was performed with HPLC, only radiolabeled ligand with 99% radiochemical purity was used in the clinical . Finally, the labeled product was eluted from the C18 cartridge with ethanol and collected in the product vial.52 year old male with PDAC metastasised to liver was involved in this study. After 6 hours of fasting, 378 MBq (2.5 MBq/kg) of 68Ga-NT-20.3 was administered intravenously.All subjective and physician´s observations as well as vital parameters (systolic and diastolic blood pressure, heart rate, respiratory rate and body temperature) were checked before, immediately after and 3h after ^{68}Ga-NT-20.3 injection. ***Results:*** After intravenous injection of ^{68}Ga-NT-20.3, there was no side events neither from the perspective of patient neither from the perspective of nuclear medicine physician. No dizziness, shortness of breath, palpitations, nausea, vomiting or any gastrointestinal symptoms were registered.Vital parameters before injection, immediately after and 3h after injection were as follows: blood pressure (mmHg): 145/95, 146/101, 146/99; heart rate (beat/min): 89, 93, 92; respiratory rate (number of breaths/min): 20, 22, 22; body temperature (°C): 36.2, 36.2, 36.4. ***Conclusion:*** The first in human injection of ^{68}Ga-NT-20.3, PET radiopharmaceutical for imaging of neurotensin receptors, was performed without adverse events and seems to be tolerable in clinical work. ***References:*** None

OP-021

Molecular imaging of monocarboxylate transporters with PET - development and biological evaluation of novel 2-fluoropyridinyl analogs of FACH

M. Sadeghzadeh[1], *W. Deuther-Conrad*[1], *B. Wenzel*[1], *D. Gündel*[1], *M. Toussaint*[1], *R. P. Moldovan*[1], *S. Fischer*[1], *F. A. Ludwig*[1], *R. Teodoro*[1], *S. Jonnalagadda*[2], *S. K. Jonnalagadda*[2], *V. R. Mereddy*[2], *L. R. Drewes*[3], *P. Brust*[1];
[1]*Department of Neuroradiopharmaceuticals, Institute of Radiopharmaceutical Cancer Research, Helmholtz-Zentrum Dresden-Rossendorf, Leipzig, GERMANY,* [2]*Department of Chemistry and Biochemistry, Department of Pharmacy Practice & Pharmaceutical Sciences, University of Minnesota, Duluth, MN, UNITED STATES OF AMERICA,* [3]*Department of Biomedical Sciences, University of Minnesota Medical School Duluth, Duluth, MN, UNITED STATES OF AMERICA.*

Aim/Introduction: Monocarboxylate transporters 1-4 (MCT1-4) are involved in several metabolism-related diseases, especially cancer, providing the chance to be considered as relevant targets for diagnosis and therapy. Recently, we reported on [^{18}F]FACH as a novel MCT-targeting imaging agent (1), whose limited blood-brain barrier permeability, however, excludes application in brain diseases. Accordingly, we aimed to develop a more lipophilic FACH-derived radiotracer possessing higher brain uptake. ***Materials and Methods:*** Two 2-fluoropyridinyl-substituted analogs of FACH (***1*** and ***2***) were obtained by Buchwald-Hartwig cross coupling reaction. The potency of ***1*** and ***2*** to inhibit MCT1 was measured by [^{14}C]lactate uptake assay using rat brain endothelial-4 cells. Radiolabeling of [^{18}F]***1*** was proceeded using 1 mg nitro precursor and [^{18}F]fluoride in the presence of Kryptofix and K_2CO_3 in dimethyl sulfoxide at 130 °C within 15 min. The $logD_{7.4}$ value of [^{18}F]***1*** was experimentally determined in the n-octanol-PBS system. For biological evaluation of [^{18}F]***1,*** in vitro autoradiography on cryosections of mouse kidney and small animal PET-MRI studies in female CD-1 mice were performed. Target specificity was proven by using the sodium salt of the MCT inhibitor α-cyano-4-hydroxycinnamic acid (α-CCA-Na). ***Results:*** The analogs ***1*** and ***2*** inhibited MCT1 with IC_{50} values of 118 and 274 nM, respectively. [^{18}F]***1*** was obtained by radiofluorination of the nitro precursor via nucleophilic aromatic substitution reaction with radiochemical yields of 73 ± 12% (n = 4, non-isolated, radio-HPLC), a high radiochemical purity of > 98% and molar activities in the range of 180-200 GBq/µmol (n = 3, end of synthesis) using starting activities of 2-3 GBq. The $logD_{7.4}$ value of 0.82 achieved for [^{18}F]***1*** indicated 2-fold higher lipophilicity in comparison to [^{18}F]FACH (2). In vivo and in vitro studies revealed high uptake of the new radiotracer in kidney and other peripheral MCT-expressing organs together with significant reduction by using α-CCA-Na (10 µM). The brain uptake of [^{18}F]***1*** was similar to [^{18}F]FACH without significant washout and an almost unchanged SUV of 0.15 between 15 and 60 min p.i. ***Conclusion:*** Despite a higher lipophilicity of [^{18}F]***1*** compared to [^{18}F]FACH, the brain uptake of [^{18}F]***1*** was in a similar low range, revealing the need for further structural modification. However, a high and specific uptake of the new radiotracer in the kidneys suggests suitability of [^{18}F]***1*** for investigations on the expression of MCT in vivo. ***References:*** (1) Sadeghzadeh M, et al. J Label Compd Radiopharm. 2019; 62: 411-424. (2) Sadeghzadeh M, et al. Sci Rep. 2019; 9: 18890-18897.

OP-022

2-[^{18}F]FDG metabolism: The role of alternative metabolic pathways

E. Klebermass[1,2], *M. Mahmudi*[1], *A. Miller*[3], *V. Pichler*[1], *C. Vraka*[1], *T. Balber*[4], *A. Haschemi*[3], *W. Wadsak*[1,5], *M. Hacker*[1], *H. Viernstein*[2], *M. Mitterhauser*[1,4];

[1]*Department of Biomedical Imaging and Image-guided Therapy, Division of Nuclear Medicine, Medical University of Vienna, Vienna, AUSTRIA,* [2]*Department of Pharmaceutical Technology and Biopharmaceutics, University of Vienna, Vienna, AUSTRIA,* [3]*Department of Laboratory Medicine, Medical University of Vienna, Vienna, AUSTRIA,* [4]*Ludwig Boltzmann Institute Applied Diagnostics, Vienna, AUSTRIA,* [5]*CBmed GmbH - Center for Biomarker Research in Medicine, Graz, AUSTRIA.*

Aim/Introduction: Studies show that the PET-tracer 2-[^{18}F]FDG can be further metabolized via alternative metabolic pathways, such as the oxidative pentose phosphate pathway (oxPPP) after its phosphorylation (1), questioning the exact trapping mechanism and current PET-signal quantification. Recent discoveries further propose that 2-[^{18}F]FDG accumulation in brain is largely independent of glucose consumption, but reflects the activation of a metabolic pathway in the endoplasmic reticulum, triggered by the oxPPP isoenzyme hexose-6-phosphate-dehydrogenase (H6PD) (2). The aim of this study is to examine 2-[^{18}F]FDG metabolism in the light of these findings in order to better understand its influence on the tracer's accumulation and kinetics. ***Materials and Methods:*** Accumulation experiments and metabolism studies were performed using 3 different human cancer cell lines (HT29, Huh7, HT1080). Cells were pre-treated with oxPPP inhibitors (e.g. DHEA) and different media, incubated with 2-[^{18}F]FDG, lysed and analyzed with a gamma counter or radio-HPLC. Previously characterized metabolites were produced as references following published procedures (3). OxPPP enzyme activities were determined spectrophotometrically in equally treated cell lysates by measuring NADPH. In addition, in vitro kinetics were analyzed with LigandTracer technology. ***Results:*** Up to 95% 2-[^{18}F]FDG-6-phosphate conversion and 11 metabolites were detected, which was most pronounced in HT29 and enhanced by fasting or DHEA treatment. The combination led to a substantial formation of the oxPPP metabolite (up to 60%), deceleration of 2-[^{18}F]FDG uptake and substantial decrease in total accumulation (down to 35%). HPLC measurements revealed that the oxPPP enzyme glucose-6-phosphate-dehydrogenase (G6PD) can also process 2-[^{18}F]FDG-6-P. In enzyme activity measurements, G6PD/H6PD activity was shown to be lowered or unaffected by DHEA under starving when tested with glucose-6-phosphate, but enhanced using FDG-6-phosphate. ***Conclusion:*** Metabolism of 2-[^{18}F]FDG can be substantial in vitro and enhanced by fasting or oxPPP manipulation. Our enzyme activity data support the hypothesis that 2-[^{18}F]FDG may not be sweepingly seen as glucose surrogate. Contradicting Marini et al. (4), we found that 2-[^{18}F]FDG is not only processed by H6PD, but also by G6PD, adding another layer of complexity to its intracellular fate. Enhanced metabolism via oxPPP enzymes correlates with a significant reduction of 2-[^{18}F]FDG accumulation under glucose deprivation, however, further evaluations are needed to prove causality. ***References:*** (1) Bender D., et al. J Nucl Med. 2001 Nov, (2) Cossu V., et al. Eur J Nucl Med Mol

Imaging. 2019 May, (3) Rokka J., et al. J Chromatogr B Analyt Technol Biomed Life Sci. 2017 Mar, (4) Marini C., et al. Sci Rep. 2016 Apr

OP-023

High-Contrast Radionuclide Imaging of EpCAM Expression in Ovarian Cancer Using DARPin Labeled With a Non-Residualizing Label

A. Vorobyeva[1,2], E. Konovalova[3], T. Xu[1], A. Schulga[3], M. Altai[1], J. Garousi[1], S. S. Rinne[1], A. Orlova[1,2], S. M. Deyev[3,2,4], V. Tolmachev[1,2];
[1]Uppsala University, Uppsala, SWEDEN, [2]National Research Tomsk Polytechnic University, Tomsk, RUSSIAN FEDERATION, [3]Shemyakin & Ovchinnikov Institute of Bioorganic Chemistry, Moscow, RUSSIAN FEDERATION, [4]Sechenov University, Moscow, RUSSIAN FEDERATION.

Aim/Introduction: Disseminated ovarian cancer is often diagnosed at late stages and requires effective and safe systemic treatment. Epithelial cell adhesion molecule (EpCAM) has intense overexpression in up to 75% of ovarian cancers and is a promising therapeutic target. To identify patients with high EpCAM expression for targeted treatment, radionuclide molecular imaging could be performed. Designed ankyrin repeat protein (DARPin) Ec1 has high affinity to EpCAM (68 pM), small size (18 kDa) and was shown to be slowly internalized by pancreatic cancer cells. This provided preconditions for using a non-residualizing label in this study. The primary aim was to test a hypothesis that internalization of Ec1/EpCAM complex by ovarian cancer cells is slow to permit imaging hours after injection. The secondary aim was to evaluate what dose of Ec1 would permit DARPin-mediated delivery of cytotoxic payload to ovarian cancer xenografts. ***Materials and Methods:*** Ec1 was indirectly radioiodinated using N-succinimidyl-3-methylstannyl-benzoate to provide non-residualizing [^{125}I]I-PIB label. EpCAM-expressing OVCAR-3 and SKOV-3 ovarian cancer cells were used for characterisation of [^{125}I]I-PIB-Ec1 in vitro and in vivo. Biodistribution was measured in BALB/C nu/nu mice bearing OVCAR-3, SKOV-3 and Ramos (negative control) xenografts 6 h after injection. MicroSPECT/CT imaging was used to confirm the biodistribution data. To investigate the effect of protein dose on tumor uptake, mice bearing SKOV-3 xenografts were injected with [^{125}I]I-PIB-Ec1 at 0.8, 4, 40 and 640 μg total protein doses. ***Results:*** Ec1 was labeled with a radiochemical yield of 20±5%. Size exclusion purification provided radiochemical purity over 95%. Binding of [^{125}I]I-PIB-Ec1 to ovarian cancer cells was specific and had picomolar affinity. Slow internalization of [^{125}I]I-PIB-Ec1 by ovarian cancer cells confirmed utility of non-residualizing label for in vivo imaging. Six hours after injection [^{125}I]I-PIB-Ec1 provided tumor-to-blood ratios of 30 ± 11 and 48 ± 12 for OVCAR-3 and SKOV-3 xenografts, respectively, and high contrast to other organs. Tumor targeting was highly specific. MicroSPECT/CT imaging confirmed high-contrast visualization of OVCAR-3 and SKOV-3 xenografts. High doses of Ec1 can be administered to mice bearing SKOV-3 xenografts without saturating the tumor uptake. ***Conclusion:*** DARPin [^{125}I]I-PIB-Ec1 provided high-contrast imaging of EpCAM a few hours after injection in two models of ovarian cancer. This can be applied for clinical imaging of EpCAM using SPECT with ^{123}I label, as well as PET with ^{124}I and, potentially, with non-residualizing [^{18}F]-fluorobenzaldehyde label. Dose-finding experiment provided a rationale for dose selection in further studies using therapeutic conjugates of Ec1 for targeted therapy. ***References:*** None

OP-024

Affibody-based Theranostics for HER3-expressing cancers: tumor growth inhibition, and PET-imaging of HER3 for therapy monitoring in a preclinical model

A. Orlova[1], S. S. Rinne[1], M. Altai[1], C. Dahlsson Leitao[2], S. Ståhl[2], J. Löfblom[2], V. Tolmachev[1];
[1]Uppsala University, Uppsala, SWEDEN, [2]Royal Institute of Technology, Stockholm, SWEDEN.

Aim/Introduction: } The human epidermal growth factor receptor type 3 (HER3) is involved in tumor progression and therapy resistance, and a potential therapeutic target in cancer. HER3-targeting affibody molecules (Z) are a promising theranostic approach for diagnostic imaging of HER3 expression and tumor growth inhibition. The aim of this study was to investigate the therapeutic efficacy of HER3-targeting affibody-conjugates fused to an albumin binding domain (ABD) (Z-ABD, Z-Z-ABD, Z-ABD-Z, ABD-Z-Z-, ABD-Z) and the potential of affibody-based imaging of HER3 expression for therapy monitoring in a preclinical model. ***Materials and Methods:*** The new conjugates were labeled with indium-111 via C-terminal maleimide DOTA and their biodistribution was studied in tumor bearing mice. Inhibition of cell proliferation and receptor phosphorylation was studied in vitro using HER3-expressing BxPC-3 cells. For the in vivo therapy BxPC-3 xenografted mice (n=10/group) with were treated (ip, three times/week) with Z-ABD, Z-Z-ABD, Z-ABD-Z, control groups were treated with seribantumab or PBS. Affibody [^{68}Ga]Ga-HE$_3$-Z-NODAGA was used to study receptor occupancy by microPET/CT imaging. ***Results:*** Residence time in blood was found the longest for Z-ABD and Z-ABD-Z and tumor accumulation the highest for Z-ABD, Z-Z-ABD, Z-ABD-Z. These conjugates inhibited cell proliferation and HER3 phosphorylation in vitro. In vivo, treatment was well tolerated without adverse effects. All treatment groups showed significantly inhibited tumor growth and significantly prolonged survival compared to PBS control. Treatment effect of Z-ABD and Z-ABD-Z (median survival 80.5 d), was significantly stronger than Z-Z-ABD (72 d), and comparable with seribantumab (83 d). microPET/CT imaging with [^{68}Ga]Ga-HE$_3$-Z-NODAGA showed uptake of the radiotracer in the tumor in PBS group, but not in the treated groups, due blocking of HER3 by the therapeutic agents.

Accumulation of [^{68}Ga]Ga-HE$_3$-Z-NODAGA was observed in livers (mErbB3 expressing) in groups treated with PBS and non-cross-reactive seribantumab; in group treated with Z-ABD liver uptake was lower and no uptake was observed in groups treated with Z-Z-ABD, Z-ABD-Z. HER3 expression in tumors was confirmed in all groups at end-point by IHC. ***Conclusion:*** Combination of different HER3-affibody-constructs could be used for theranostic approaches in HER3-expressing cancer. The molecular design of the ABD-fused HER3 targeting agents affected their therapeutic efficacy. We have demonstrated that radiolabeling of therapeutic proteins helped to select the most promising candidates for further evaluation. The use of PET imaging with companion agent allowed therapy monitoring demonstrating receptor occupancy during HER3-targeted therapy. ***References:*** None

OP-025

In vitro receptor autoradiography utilising a novel ^{111}In-labeled GIP receptor antagonist reveal high signals in neuroendocrine tumours: A comparative study to ^{111}In-DOTATATE and ^{111}In-JR11

A. Schumann[1], C. Haase[1], U. Reineke[1], C. Smerling[1], J. C. Reubi[2], I. Eichhorn[3], B. Wiedenmann[3], C. Roderburg[3]; [1]3B Pharmaceuticals GmbH, Berlin, GERMANY, [2]Institute of Pathology, University of Berne, Berne, SWITZERLAND, [3]Charité-Universitätsmedizin, Berlin, GERMANY.

Aim/Introduction: The gastric inhibitory polypeptide receptor (GIPR) represents a promising structure for targeted radionuclide therapy. Autoradiography studies employing the agonistic peptide GIP(1-30) revealed substantial GIPR expression in numerous cancer types such as NETs and MTC and virtual absence in normal tissues [1]. We hypothesised that a GIPR antagonist might increase the detection of binding sites, as shown for the SSTR2 antagonist JR11 in comparison to the agonist DOTATATE [2]. 3B Pharmaceuticals has developed a high affinity GIPR antagonist (3BP-Tracer) for targeted radiotherapy of GIPR-positive tumours. In this study, we show a clear ranking of GEP-NETs visualising compounds based on autoradiographic signal intensity: ^{111}In-3BP-Tracer ~ ^{111}In-JR11 > ^{111}In-DOTATATE > ^{111}In-GIP(1-30). ***Materials and Methods:*** The novel 3BP-Tracer consists of a GIPR targeting moiety that is conjugated to DOTA enabling complexation of both diagnostic and therapeutic radionuclides. A human GIPR- transfected cell line was used for affinity assessment of the 3BP-Tracer by flow cytometry and radioligand binding assay. Antagonism was verified via Ca^{2+} signalling assay. In vitro receptor autoradiography was performed on GEP-NETs, their metastases, and corresponding normal tissues using the following tracers: ^{111}In-3BP-Tracer, ^{111}In-GIP(1-30), ^{111}In-DOTATATE, and ^{111}In-JR11. ***Results:*** Antagonism of the 3BP-Tracer was confirmed by the absence of Ca^{2+} release after binding of 3BP-Tracer with single digit nanomolar affinity to the hGIPR transfected cell line and by inhibition of GIP(1-30) binding mediated Ca^{2+} signalling. In vitro receptor autoradiography in GEP-NETs revealed up to 6-fold higher signals of the ^{111}In-labelled GIPR antagonist, relative to the clinically relevant SSTR2 agonist DOTATATE. Binding signals of both GIPR and SSTR2 antagonists were equally strong in most GEP-NETs and all metastases. However, in contrast to ^{111}In-JR11, ^{111}In-3BP-Tracer showed no off-target binding to normal tissues. Signal strength of the GIPR agonist ^{111}In-GIP(1-30) was close to background in all investigated tumour samples. In SSTR2-positive tumours and liver metastases, ^{111}In-JR11 showed 3- to 6-fold increased uptake compared to ^{111}In-DOTATATE. However, ^{111}In-JR11 was found to bind non-specifically to normal tissues such as ileum and liver. ***Conclusion:*** The antagonist ^{111}In-3BP-Tracer was found to bind in a receptor-specific manner to GEP-NETs and corresponding metastases without unexpected off-target binding in normal tissues. Since ^{111}In-3BP-Tracer revealed substantially higher GIPR signals relative to previous autoradiography studies with GIP(1-30), our results strongly emphasise the clinical potential of the novel GIPR antagonist for targeted radiotherapy in NETs. ***References:*** [1] Waser, B., J Clin Endocrinol Metab, 2011. [2] Reubi, J.C., JNM, 2017. 58(2): p. 300-306.

OP-026

Multimodal In Ovo Imaging: The chicken embyro as an alternative model in preclinical research

***T. Balber[1,2]**, J. Christl[1], J. Friske[3], S. M. Bugayong[2], V. Fröhlich[3], A. S. Zacher[2], L. Nics[2], W. Wadsak[2,4], M. Hacker[2], T. Helbich[3], M. Mitterhauser[1,2];*

[1]Ludwig Boltzmann Institute Applied Diagnostics, Vienna, AUSTRIA, [2]Division of Nuclear Medicine, Department of Biomedical Imaging and Image-guided Therapy, Medical University of Vienna, Vienna, AUSTRIA, [3]Division of General Radiology, Department of Biomedical Imaging and Image-guided Therapy, Medical University of Vienna, Vienna, AUSTRIA, [4]Center for biomarker research in medicine, CBmed GmbH, Graz, AUSTRIA.

Aim/Introduction: The preclinical evaluation of novel PET diagnostics is time-consuming and costly, but many tracer candidates ultimately fail in vivo. We lack an adequate, but affordable model for preselecting high-potential candidates while reducing animal experimentation. This need has already been recognised by others and comparable in vivo distribution of several PET and SPECT tracers have been demonstrated in mice and chicken embryos post mortem.(1) In addition, the Chorion Allantois Membrane (CAM), as a highly vascularized membrane on the periphery of the embryo, in combination with the natural embryonic immunodeficiency makes xenotransplantation possible. Previously, in vivo PET/CT has been successfully performed in a human glioblastoma CAM model including dynamic imaging protocols.(2) Thus, we aim to further explore the potential and possible limitations of this model in preclinical tracer development. ***Materials and Methods:*** To this, specific-pathogen free, fertilized chicken

eggs were incubated for 18 days to allow for embryonic development and formation of the CAM. Xenografts were generated by opening the eggshell and inoculating the CAM with human prostate cancer cells. PET-tracers (e.g. [^{18}F]FDG, [^{18}F]FEC, [^{18}F]PSMA-1007) were applied intravenously to a CAM-vessel. Immobilization of the embryo during imaging was achieved by applying volatile anesthetics or inducing hypothermia. Multimodal imaging was performed on a preclinical PET/CT scanner or using a PET Insert and a 9.4 Tesla micro-MRT. ***Results:*** Growth and vascularization of implanted tumor cells could be achieved within 5 to 7 days after inoculation depending on the cell line. Multimodal imaging (PET/MRI, contrast-enhanced PET/CT) enabled a clear delineation of tracer-accumulating tumor grafts. Due to the high soft tissue contrast, combined PET/ MRI significantly improved the accurate assessment of the organ-specific tracer distribution including brain uptake in the living chicken embryo. ***Conclusion:*** The in ovo model provides an affordable preclinical system of medium physiological complexity that has proven useful in tracer development, reducing the use of small animals in the future. The established workflow and imaging protocols demonstrate the resolution required for PET imaging of oncological models, and in ovo µPET/MRI opens a new perspective in neurological imaging. ***References:*** (1) Haller S et al, Nucl Med Biol 42 (2015) 226-233, (2) Warnock G et al, J Nucl Med 2013; 54 (10)

OP-027

Reducing abdominal background in 4FMFES-PET using intestinal peristalsis inhibitors: a translational study

M. Paquette*, E. Espinosa-Bentancourt, É. Lavallée, S. Phoenix, B. Guérin, É. E. Turcotte;*
Université de Sherbrooke, Sherbrooke, QC, CANADA.

Aim/Introduction: Like every steroidal compounds, the Estrogen Receptor (ER) targeting PET tracer 4-fluoro-11β-methoxy-16α-[18F]fluoroestradiol (4FMFES) is mainly eliminated via the hepatobiliary pathway. While 4FMFES allows unprecedentedly background-free assessment of thoracic ER+ lesions, gynaeco-oncological applications are more likely to be impaired by the overwhelming presence of radioactive intestinal content in the lower abdomen. In this project we sought to investigate the use of different pharmacological interventions, first in mice, then in uterine cancer patients, to slow down progression of the intestinal bolus sufficiently to reduce abdominal background at the time of imaging. ***Materials and Methods:*** Small cohorts (n = 4 each) of Balb-c mice received either 100 µl saline (control) or 80 µg loperamide per os 15 minutes prior injection of 4FMFES, or repeated intravenous administration of 10 µg hyoscine butylbromide at 0, 20- and 40-minute post tracer injection. Mice were imaged on a small animal PET scanner for 90 minutes. Images were reconstructed using 1-minute time frames, and progression of the intestinal content was tracked. In parallel, uterine cancer patients (n = 20) were recruited to evaluate 4FMFES-PET/CT for this new application. All patients were fasted for 5 hours before imaging, then were given either a 4 mg loperamide tablet 15 minutes prior 4FMFES injection or were injected with 20 mg hyoscine butylbromide at 0, 20 and 40 minutes after administration of the tracer. All patients also received furosemide after tracer injection to clear the bladder. Head-to-thigh acquisition occurred at 60 minutes post-injection. Abdominal background surrounding the uterine area was reported as SUVMean and intestinal progression was qualitatively evaluated. ***Results:*** While no differences could be observed for the distance traveled by the intestinal content between the control group and the hyoscine butylbromide treatment in mice (90.6 ± 13.4 mm and 85.4 ± 19.1 mm, respectively), loperamide pre-treatment had a significant effect (57.6 ± 21.9 mm; $p < 0.01$). In contrast, no improvement in abdominal background was observed in patients receiving loperamide prior to 4FMFES, whereas repeated injection of hyoscine butylbromide allowed substantial reduction of abdominal uptake and improvement in image quality in most patients receiving this drug. ***Conclusion:*** It is possible to reduce abdominal background of 4FMFES-PET using drugs inhibiting intestinal peristalsis in combination with diuretic agents to clear the bladder. Other steroidal PET tracers might benefit from this protocol. Other pharmacological agents, such as low-dose opioids will be investigated in the near future. ***References:*** None

106

Cutting Edge Science Track - TROP Session: Quantification

Thursday, October 22, 2020, 13:30 - 15:00 Channel 6

OP-028

An international quantitative SPECT/CT imaging exercise for Lu-177

J. Tran-Gia[1]*, A. P. Robinson*[2]*, N. Calvert*[3]*, A. M. Denis-Bacelar*[2]*, A. J. Fenwick*[2,4]*, K. M. Ferreira*[2]*, D. Finocchiaro*[5,6]*, F. Fioroni*[5]*, E. Grassi*[5]*, W. Heetun*[2]*, S. J. Jewitt*[7]*, T. Kalathas*[8]*, M. Kotzasarlidou*[8]*, M. Ljungberg*[9]*, D. R. McGowan*[7,10]*, J. Scuffham*[11]*, K. Sjögreen Gleisner*[9]*, J. Tipping*[3]*, J. Wevrett*[11]*, M. Lassmann*[1]*;*
[1]Department of Nuclear Medicine, University of Würzburg, Würzburg, GERMANY, [2]National Physical Laboratory, Teddington, UNITED KINGDOM, [3]The Christie NHS FT, Manchester, UNITED KINGDOM, [4]Cardiff University, Cardiff, UNITED KINGDOM, [5]Azienda Unità Sanitaria Locale di Reggio Emilia - IRCCS, Medical Physics Unit, Reggio Emilia, ITALY, [6]Department of Physics and Astronomy, University of Bologna, Bologna, ITALY, [7]Oxford University Hospitals NHS FT, Oxford, UNITED KINGDOM, [8]"THEAGENIO" Anticancer Hospital, Thessaloniki, GREECE, [9]Department of Medical Radiation Physics, Lund, SWEDEN, [10]University of Oxford, Oxford, UNITED KINGDOM, [11]Royal Surrey NHS FT, Guildford, UNITED KINGDOM.

Aim/Introduction: Patient-specific dosimetry is required to ensure the safety of molecular radiotherapy treatments and to predict response. Dosimetry involves several steps, the first of which is the determination of the activity of the radiopharmaceutical taken up by an organ/lesion over time. As uncertainties propagate along each of the subsequent steps (integration of the time-activity curve, absorbed dose calculation), establishing a reliable activity quantification is essential. The MRTDosimetry project was a European initiative to bring together expertise in metrology and nuclear medicine research, with one main goal of standardising quantitative Lu-177 SPECT/CT imaging based on a calibration protocol developed and tested in a multicentre intercomparison. ***Materials and Methods:*** The intercomparison included eight SPECT/CT systems (3×Siemens, 4×GE, 1×Mediso). Each site performed three measurements using the same acquisition (medium energy collimator, 2×60 projections of 60s, 208keV main energy windows) and reconstruction (OSEM with 25 iterations, 2 subsets, no postfiltering, attenuation correction [CT-based], triple-energy-window scatter correction [6%-20%-6% scatter-main-scatter], and resolution recovery [if available]): 1. Determination of image calibration factor (ICF): Counts (enlarged VOI around 216-mm Jaszczak cylinder filled with ~400MBq) divided by activity and scan duration (unit: cps/MBq). 2. Determination of recovery coefficients (RCs) for partial-volume correction (PVC) in IEC NEMA body phantom with 6 hot spheres (activity concentration ~2.0MBq/mL): Activity in CT-based VOI (counts/ICF/scan_duration) divided by each sphere's activity. Recovery curve: Comparison of weighted 3-parameter (b1/(1+(b2/volume)^b3)) and 2-parameter fit (b1:=1) of RCs against sphere volumes. 3. Validation of quantitative imaging setup in 3D-printed kidney and spleen phantoms filled with different activity concentrations (kidney cortex & spleen: ~1.5 MBq/mL, kidney medulla: ~0.5 MBq/mL) assembled in Jaszczak cylinder (custom-made baseplate for repeatable positioning): Activity in CT-based VOI (counts/ICF/scan_duration) divided by volume-dependent recovery value. An uncertainty analysis was performed for all measurements. ***Results:*** Similar combinations of imaging system and reconstruction led to similar ICF values (Siemens 3/8": [21.5±1.6] cps/MBq, GE 3/8": [45.4±2.5] cps/MBq). In the anthropomorphic phantom validation, the mean ratios between SPECT-based and radionuclide calibrator-based activity were very close to the ideal value of 1 for the 3-parameter fit: 1.02±0.10 (kidney), 1.07±0.11 (spleen). Larger deviations were seen for the 2-parameter-fit: 0.89±0.06 (kidney), 0.94±0.06 (spleen). ***Conclusion:*** This comparison exercise shows that reliable quantitative SPECT/CT is feasible when following the very specific recommendations of the dedicated calibration protocol developed within MRTDosimetry. In addition, for an anthropomorphic phantom, the count loss due to spill-out was successfully compensated by using a standardized PVC based on sphere-based RCs. ***References:*** http://mrtdosimetry-empir.eu/wp-content/uploads/2019/08/15HLT06_Publishable_Report_M36_Final.pdf

OP-029

An in silico study on the influence of radiosensitivity and tumor growth on the total tumor volume in ^{177}Lu-PSMA therapy

P. Kletting[1], *A. Gafita*[2], *H. Wang*[2], *A. Beer*[1], *W. Weber*[2], *M. Eiber*[2], *G. Glatting*[1];
[1]*Universität Ulm, Ulm, GERMANY,* [2]*Technische Universität München, München, GERMANY.*

Aim/Introduction: Physiologically-based pharmacokinetic/-dynamic modeling (PBPK/PD) allows to estimate important physiological and pathophysiological parameters using time activity data and tumor volume changes over time. The aim of this work was to 1) estimate tumor growth rates and radiosensitivities in patients with metastatic castration-resistant prostate cancer (mCRPC) and 2) to determine which combinations of tumor growth rate and radiosensitivity lead to a reduction of total tumor volume following ^{177}Lu-PSMA radioligand therapy (RLT) by model simulations. ***Materials and Methods:*** A PBPK/PD-model was developed describing the pharmacokinetics, tumor growth according to the power-law model and treatment effect in terms of the linear-quadratic model. The tumor is considered to be a sphere whose radius grows linearly, and the average size of the tumor lesions depends on the total tumor volume (TTV) of the patient. The radiosensitivity parameter α and the growth rate λg (tumor volume radius change per day) of the model were fitted to data derived from PSMA-targeted PET/CT prior to and following the first cycle of 177Lu-PSMA-targeted therapy. The employed data were PSMA-positive TTV and total tumor activity concentration (TTA) determined semi-automatically in 30 patients using the qPSMA software. To obtain additional information on the global pharmacokinetics in the patient, the kidneys volume and activity were determined in the PET/CT prior and post treatment and in one peri-therapeutic SPECT/CT. Based on the estimated parameter values, simulations were performed for various combinations of radiosensitivity (α=0.001-0.1 Gy-1) and tumor growth rate (λg=0.0004-0.04 cm/day). For each combination, the TTV was simulated after 6 cycles of ^{177}Lu-PSMA RLT using a 6-week regimen of 7.4 GBq and 80 nmol amount of substance. ***Results:*** The growth rates (λg=0.016±0.010 cm/day) and radiosensitivities (α=0.04±0.03 Gy^{-1}) of the PBPK/PD model were determined by fitting to the patients data. These parameter values compare favorably with literature values from radiotherapy and brachytherapy. The TTV simulations after 6 cycles show that for average tumor growth and radiosensitivity within this patient population, a ^{177}Lu-PSMA RLT 6-week regimen of 6 cycles leads to a TTV reduction in 8 out of 30 patients. ***Conclusion:*** This PBPK/PD modeling approach allowed to separately investigate the influence of radiosensitivity and

tumor growth on the total tumor volume after therapy. The identification of subpopulations with specific ranges of radiosensitivities or tumor growth values in a large patient population might improve patient selection for therapy. ***References:*** None

OP-030

Impact of gamma camera uniformity calibration methods in SPECT Imaging

***K. Ferreira**, W. Heetun, A. P. Robinson;*
National Physical Laboratory, Teddington, UNITED KINGDOM.

Aim/Introduction: The performance of conventional gamma cameras currently used in nuclear medicine is inherently non-uniform due to the underlying technology. The impact of non-uniformities in SPECT imaging has been widely recognised but more work is necessary to quantify the differences in corrections generated from different measurement techniques. In this work the impact of applying different uniformity calibration maps in SPECT imaging will be investigated. ***Materials and Methods:*** In this work, the uniformity of a Mediso AnyScan SPECT-CT camera was calibrated for Tc-99m imaging using a range of intrinsic and extrinsic methods. For intrinsic calibrations the following source geometries were used: ^{99m}Tc point Source, ^{57}Co point source and a ^{99m}Tc flood source. For extrinsic uniformity calibration a ^{99m}Tc and a ^{57}Co flood sources were used. To assess the impact of the choice of correction on SPECT/CT imaging data was acquired for: a cylindrical Jaczszak phantom, a NEMA phantom and a 3D-printed organ phantom filled with a known amount of ^{99m}Tc using the different uniformity calibration maps. The images were assessed visually to check for differences; and the Mean Squared Error (MSE) and respective uncertainties were calculated to estimate the possible differences between images. The percentage difference between total counts in the images was calculated to estimate the impact on quantitative imaging of using different uniformity calibration maps. ***Results:*** The use of intrinsic calibration maps was found to reduce the system sensitivity (total counts) compared to the corresponding extrinsic calibration. Changes in the sensitivity of the system were reported in terms of percentage when using different uniformity calibration maps, for the cylindrical phantom variations between -5.8 % and 5.2 % were estimated; for the NEMA phantom the differences ranged between -6.5 % and 6.3 % and for the 3D-printed organ differences between -3.4 % and 3.3 % were reported. ***Conclusion:*** This work showed that the method used for uniformity calibration has an impact in image quantification for SPECT. In molecular radiotherapy, these differences can be propagated to the absorbed dose calculations resulting in an underestimation or overestimation of the absorbed dose depending on the calibration map used. ***References:*** None

OP-031

Verification of xSPECT Quant for Quantitative ^{123}I-mIBG SPECT/CT Imaging

***K. Baete**, M. Sevenois, E. Pauwels, C. M. Deroose;*
Nuclear Medicine, University Hospitals Leuven; Nuclear Medicine and Molecular Imaging, Department of Imaging and Pathology, Leuven, BELGIUM.

Aim/Introduction: We have verified the accuracy of xSPECT Quant, a quantitative SPECT/CT imaging technique (Siemens Healthineers, Erlangen, Germany), for neuroendocrine tumor imaging using ^{123}I-meta-iodobenzylguanidine (^{123}I-mIBG). Image quantification in SPECT/CT is useful when comparing ^{123}I-mIBG with alternative PET/CT theranostics agents, such as ^{68}Ga-labeled somatostatin analogues or the recently introduced ^{18}F-meta-fluorobenzylguanidine. For that, SPECT/CT requires advanced QC and reliable activity determination. We assessed long-term stability of radionuclide calibrator and SPECT/CT cross-calibration accuracy using gamma spectrometry analysis. ***Materials and Methods:*** We verified the calibration factor settings of a radionuclide calibrator (IBC-LITE, VIK-202, Comecer) using the reported ^{123}I activity of an AdreView™ vial (GE Healthcare). We studied the influence of the used recipients (vial, syringe) with and without a copper filter insert. We transferred the ^{123}I activity uniformly in 1000 ml water in a plastic bottle. We weighed the recipients before and after activity transfer (analytical balance, Mettler), and corrected for residual syringe activity. From the ^{123}I solution, we pipetted and weighed three 1 ml samples for gamma spectrometry. Subsequently, we prepared a Symbia Intevo Bold (Siemens Healthineers, Erlangen, Germany) SPECT-CT camera for quantitative image analysis by performing standard maintenance and quality control procedures. We calibrated the SPECT camera for absolute ^{123}I quantification using the xSPECT Quant Calibration Source Kit, containing a NIST traceable ^{75}Se reference source. Using MELP collimators and factory based xSPECT acquisition and reconstruction settings, we performed a SPECT/CT acquisition of the bottle with the ^{123}I solution. We reconstructed the projection data using the xSPECT reconstruction method, and we analyzed the SPECT images, corrected for scatter, attenuation, decay, and expressed in Bq/ml, using MIM Encore (MIM Software, Cleveland, OH). We measured the samples using a 3-inch gamma counter (Wizard 1480, Perkin Elmer) with adjusted energy window settings to avoid the low-energy influence of possible ^{125}I contamination. We also verified the linearity of the gamma counter count-rate using the decaying samples. ***Results:*** At reference time, the prepared phantom activity concentration was 200.8 kBq/ml. In a central volume-of-interest in the bottle, the measured activity concentration of the xSPECT image measured 201.5 kBq/ml. Hence, the SUV deviation is 0.3 %. The gamma counter efficiency measured 0.778 ± 0.001 cps/Bq. The deviation from linearity between 400 Bq and 50 kBq ^{123}I was below 0.4%. ***Conclusion:*** We

established quantitative SPECT/CT imaging for ^{123}I, using a ^{75}Se reference source based calibration, and introduced quality assurance measures to perform follow-up analysis of the involved equipment. ***References:*** None

OP-032

Experimental validation of absolute SPECT/CT quantification for response monitoring in patients with coronary artery disease

A. van de Burgt[1], *P. Dibbets-Schneider*[1], *C. H. Slump*[2], *A. J. H. A. Scholte*[1], *D. E. Atsma*[1], *L. F. de Geus-Oei*[1,2], *F. H. P. van Velden*[1]; [1]*Leiden University Medical Center, Leiden, NETHERLANDS,* [2]*University of Twente, Enschede, NETHERLANDS.*

Aim/Introduction: Myocardial perfusion scintigraphy (MPS) is based on visual interpretation of relative myocardial perfusion and might underestimate the severity of ischemia due to global hypoperfusion. Quantification of SPECT imaging enables absolute measurement of perfusion defects. The aim of this experimental study is to assess quantitative accuracy and precision of a novel iterative reconstruction technique (Evolution; GE Healthcare, Milwaukee, USA) for the potential application of response monitoring using ^{99m}Tc-tetrofosmin SPECT/CT in patients with coronary artery disease (CAD). ***Materials and Methods:*** Acquisitions of an anthropomorphic torso phantom, with cardiac insert containing defects (with varying sizes) filled with ^{99m}Tc-pertechnetate, were performed on a SPECT/CT camera (Discovery 670 Pro, GE Healthcare). Subsequently, volumes-of-interest of the defects were manually drawn on CT to assess the recovery coefficient (RC). Bull's eye plots were composed to evaluate the uptake per segment. Finally, ^{99m}Tc-tetrofosmin SPECT/CT scans of 10 CAD patients were collected retrospectively before and after bone marrow cell (BMC) injection and used as a patient feasibility study to illustrate and test Evolution for clinical application. ***Results:*** The phantom study showed that the activity concentration converged after seven iterations (ten subsets). The average repeatability deviation of all configurations was 2.91% and 3.15% (%SD mean) for filtered (Butterworth) and unfiltered data, respectively. The accuracy after post-filtering was lower compared to the unfiltered data with a mean(SD) RC of 0.63(0.05) and 0.70(0.07), respectively ($p<0.05$). More artificial defects were found on Bull's eye plots created with the unfiltered data compared to filtered data. Eight out of ten patients showed significant changes in uptake before and after BMC injection ($p<0.05$). The median time between the SPECT/CT scans before and after BMC injection was 9 months. ***Conclusion:*** In a phantom study, it was demonstrated that absolute quantification of ^{99m}Tc-tetrofosmin SPECT/CT is feasible, when seven iterations (ten subsets), Butterworth post-filtering (cut off frequency 0.52 in cycles/cm, power 5) and manual delineation on CT images are applied. To show sufficient evidence for the use of Evolution in clinical practice for treatment response monitoring, validation should take place in a future clinical study. ***References:*** None

OP-033

Effect of Respiratory Motion on Dosimetric Measurements for ^{99m}Tc-MAA SPECT/CT

Z. Lu*, G. Mok;*
Biomedical Imaging Laboratory (BIG), Department of Electrical and Computer Engineering, Faculty of Science and Technology, University of Macau, Taipa, MACAO.

Aim/Introduction: Respiratory motion compromises ^{99m}Tc-MAA SPECT image quality and quantitation accuracy especially near the diaphragmatic region [1]. This study aims to systematically investigate the effect of breathing motion on lung shunt fraction (LSF), tumor-to-normal liver ratio (TNR), injected activity (IA) and absorbed dose estimation in ^{99m}Tc-MAA SPECT/CT for ^{90}Y microsphere radioembolization treatment planning. ***Materials and Methods:*** The 4D extended cardiac torso (XCAT) phantom was used to simulate a phantom population of 72 phantoms, modelling 6 different anatomies, 2 TNRs (8.2 and 13), 2 tumor sizes (3.0 and 4.5 cm diameter), 4 tumor locations and 3 axial/anterior-posterior motion amplitudes of 1/0.6, 2/1.2 and 3/1.8 (cm), mimicking ^{99m}Tc-MAA distribution with LSF of 5%, 10% and 15%. Phantoms with no motion were also generated for reference. An analytical projector for low energy high resolution parallel-hole collimator was used to simulate 128 projections over 360° for SPECT, modeling attenuation, scatter and geometric collimator-detector-response (GCDR). The OS-EM algorithm was employed for image reconstruction with 4 iterations and 16 subsets with attenuation correction using averaged attenuation map, effective source scatter estimation and GCDR modelling. The volumes-of-interest (VOIs) for liver, lungs and tumor were mapped out from the reconstructed images based on the original phantom organ maps. The LSF, TNR, IA, absorbed dose of normal liver, tumor and lungs were calculated based on the measured counts from different VOIs and the partition model [2]. ***Results:*** Generally, along with the increase of breathing motion amplitude, the absolute errors of LSF, TNR, IA and absorbed dose increase. The LSF and lung dose are overestimated while TNR and tumor dose are underestimated due to the respiratory motion. Larger LSF errors associate with tumors located closer to the lung-liver interface while larger TNR errors associate with smaller tumor size and higher TNR due to respiration. For axial respiratory motion of 2 cm and LSF of 10%, the mean errors of LSF, TNR, IA, absorbed dose of normal liver, tumor and lungs are 69.8±8.2%, -27.0±7.1%, -12.7±10.4%, -2.3±2.5%, -28.6±8.3% and 69.8±8.2%, respectively. ***Conclusion:*** Respiration motion has a strong impact for ^{99m}Tc-MAA SPECT/CT based dosimetry and may change the patient management due to overestimation of LSF and underestimated IA may lead to under treatment. Further studies to minimize the impact of respiration on ^{99m}Tc-MAA SPECT/CT are warranted. ***References:*** [1] Bastiaannet R, et al. Medical Physics. 2017;44(10):5270-9. [2] Ho S, et al. Eur J Nucl Med. 1996;23(8):947-5.

OP-034

Quantitation of small lesions by routine PET imaging protocols in Finland

J. Liukkonen[1], O. Sipilä[2], T. Tolvanen[3,4], H. Halme[2], M. Hakulinen[5,6], T. Kangasmaa[7], A. Kangasmäki[8], A. Manninen[9], T. Ollikainen[10], A. Sohlberg[11], K. Tahvanainen[12], V. Tunninen[13], J. Vuorela[14];
[1]Radiation and Nuclear Safety Authority (STUK), Helsinki, FINLAND, [2]HUS Medical Imaging Center, Clinical Physiology and Nuclear Medicine, University of Helsinki and Helsinki University Hospital, Helsinki, FINLAND, [3]Turku PET Centre, Turku University Hospital, Turku, FINLAND, [4]Department of Medical Physics, Turku University Hospital, Turku, FINLAND, [5]Dept. of Clinical Physiology and Nuclear Medicine, Diagnostic Imaging Center, Kuopio University Hospital, Kuopio, FINLAND, [6]Dept. of Applied Physics, University of Eastern Finland, Kuopio, FINLAND, [7]Department of Clinical physiology and nuclear medicine, Vaasa Central Hospital, Vaasa, FINLAND, [8]Departments of Imaging and Radiotherapy, Docrates Cancer Center, Helsinki, FINLAND, [9]OYS Department of Nuclear Medicine and Radiology, Oulu University Hospital, Oulu, FINLAND, [10]Clinical physiology and Neurophysiology North Karelia Central Hospital, Joensuu, FINLAND, [11]Laboratory of Clinical Physiology and Nuclear Medicine, Päijät-Häme Central Hospital, Lahti, FINLAND, [12]HUS Diagnostic Center, South Karelia Central Hospital, Department of Clinical Physiology and Nuclear Medicine, Lappeenranta, FINLAND, [13]Department of Clinical Physiology and Nuclear Medicine, Satakunta Central Hospital, Pori, FINLAND, [14]Clinical physiology and nuclear medicine, Central Finland Health Care District, Jyväskylä, FINLAND.

Aim/Introduction: The aim of the study was to compare relative quantitation accuracy of the routine whole-body imaging protocols in Finnish PET centers. ***Materials and Methods:*** To avoid re-filling the phantom in every center, a NEMA-2018-IQ phantom with Ge-68 was utilized, including six hot spheres with diameters of 10, 13, 17, 22, 28 and 37 mm with a concentration ratio of 4:1 to background. During five months period, the phantom was imaged in 11 PET centers with altogether 14 PET-CT scanners, including analog and digital systems from two major vendors. In every center, the local clinical imaging protocol for the whole body F-18-FDG studies was used. The imaging time was adjusted according to the average activity concentration of the phantom in the imaging day, varying from 3.2 to 2.1 MBq/kg, and the patient activity concentration as well as the patient resting and imaging times used in the particular center. In every scanning session, PET imaging was repeated 20 times, except for one scanner with 10 repetitions. In addition, for one scanner, the scanning sessions were repeated five times during 5.5 months. The peak, mean and max activity concentrations were measured from the 20 images and divided by the known activity concentration of the hot spheres. The results from the 20 repetitions were then averaged. The average values for different scanners were compared. Also, the standard deviations from the five scanning sessions of the same scanner were compared to the standard deviations for the 14 different scanners. ***Results:*** Measurements from one scanner produced unexplainable high concentration values and were excluded from the further comparisons for now. The minimum-maximum results for the peak activity concentration ratios for hot spheres with radius of 10, 13, 17, 22, 28 and 37 mm were 0.35-0.48, 0.47-0.68, 0.58-0.89, 0.74-0.99, 0.85-1.02 and 0.93-1.04, respectively. The corresponding mean value ratios were 0.27-0.49, 0.39-0.68, 0.49-0.79, 0.59-0.85, 0.68-0.86 and 0.74-0.89, and max value ratios 0.43-0.77, 0.60-1.03, 0.76-1.22, 0.86-1.32, 0.99-1.36 and 1.08-1.43. The same scanner standard deviations for different spheres resulted in 0.02-0.06, 0.01-0.01 and 0.01-0.02 for the peak, mean and max value ratios. As expected, the different scanner standard deviations were clearly bigger, 0.03-0.09, 0.04-0.09 and 0.11-0.14. ***Conclusion:*** According to these results, 30 % difference in quantitation of activity concentrations of relatively small lesions can occur depending on the imaging site. The peak activity concentration value seemed to give more accurate concentration results than the mean and max values. ***References:*** None

OP-035

Application of a novel image-based partial volume correction method on a multi-reconstructed phantom

***N. Cole**, S. Lindler, K. Krawiec, P. Wilson, D. Nelson, J. Sunderland, A. S. Nelson;*
MIM Software, Cleveland, OH, UNITED STATES OF AMERICA.

Aim/Introduction: Quantification of images can be heavily impacted by the resolution of the imaging system used. This is notably demonstrated with the partial volume effect (PVE) which causes an apparent decrease in activity in small regions of interest (ROI) due to a reduced system resolution. With resolution quality varying across cameras, reconstructions, institutions, and exam types, it is imperative to develop a partial volume correction (PVC) method that can correct PVE across a range of image resolutions. The aim of this study was to evaluate the performance of a novel image-based PVC method that uses system resolution to correct a phantom image reconstructed with multiple resolutions and varying degrees of PVE with known full-width-half-max (FWHM) values (Radial/Axial values ranging from 4.4/6 to 10.7/8.8 and 5/5 to 10/10). ***Materials and Methods:*** The SNMMI CTN oncology PET phantom containing twelve spheres of varying diameters (7 - 37mm) was acquired using a GE Discovery MI PET/CT system. Thirty reconstructions were created with various iterations, subsets, and smoothing filters. The image-based PVC method utilized known resolution values for each reconstruction parameter set to model the "spill-in" and "spill-out" of counts from each source and the background repeating over an optimized 4 iterations to correct the PVE. Spheres were segmented with the known sphere size (GS) and a clinically-used hybrid intensity and gradient-based

segmentation method (Hybrid). Mean activity (Bq/ml) was calculated for each ROI before and after PVC, then compared to measured activity. ***Results:*** Measured activity in each sphere was 25897 Bq/ml. Mean activity across all sphere sizes without PVC was 14818.9 ± 4966 Bq/ml and 15355.1 ± 4296 Bq/ml, yielding errors of 42.8% and 41.3% for the GS and Hybrid ROIs respectively. With PVC, mean activity was 20450.8 ± 3623 Bq/ml and 22584.7 ± 5235 Bq/ml reducing the error to 21.1% (GS) and 20.8% (Hybrid). This reflects an error reduction from 20% to 8.5% for 37mm spheres and 72.9% to 48.3% for 7mm spheres using the GS ROIs. Using Hybrid ROIs, the error was reduced from 22.8% to 12.1% for 37mm spheres and 71.7% to 47.1% for 7mm spheres. ***Conclusion:*** The image-based PVC method consistently improved activity quantification across a range of resolutions by iteratively modeling the PVE; accounting for a known resolution. This method significantly reduced errors for small volumes which can lead to improved accuracy in image analysis and treatment planning. ***References:*** Wan, H. et al. EJNMMI (2018) 45 (Suppl 1): S1-S844

OP-036

Tracer effect on partial volume correction of Brain PET/MR imaging

E. Balci[1], Ü. Akdemir[2], L. Ö. Atay[2];
[1]Gazi University Medical Faculty Department of Nuclear Medicine, Ankara, TURKEY, [2]Gazi University Medical Faculty Department of Nuclear Medicine, Ankara, TURKEY.

Aim/Introduction: Partial volume effect correction (PVEc) is very important in PET brain imaging in terms of getting regionally accurate tracer uptake values. In this study, regional tracer uptake values from metabolic and amyloid brain PET/MR imaging data that were obtained with/without PVEc (no-PVEc) were compared in the same group of patients with clinically suspected Alzheimer's disease (AD). ***Materials and Methods:*** Fourteen patients with clinically suspected AD were included in the neurodegenerative group (NG) and 44 subjects as control group (CG) in the study. The tracers used were (F^{18})fluorodeoxyglucose and (F^{18})flutemetamol, respectively, for the metabolic and amyloid PET/MR scans in the NG. Only metabolic PET/MR imaging was performed in the CG. Segmentation of T1-weighted brain MRI images and its co-registration with PET was done with the FreeSufer software. PVEc was applied using the Müller-Gärtner method in the PetSurfer code. The total uptake values from PVEc/no-PVEc PET images were recorded using 93 anatomical regions covering the cortical-gray-matter (GM) regions, subcortical-GM structures, and white-matter (WM) regions. The percent change of values from no-PVEc to PVEc PET images were calculated by the formula: (PVEc-(no-PVEc))/(no-PVEc). ***Results:*** Regional uptake values were increased by an average of 32% when PVEc was applied to the metabolic PET images in the NG patients. The highest increase was observed in the pericalcarine-transverse temporal in cortex-GM regions and the putamen-caudate-nucleus-accumbens areas while WM uptake values decreased. The results observed in the CG were similar. For the amyloid PET images the change in regional uptake values were heterogenous: While the cortical GM regions showed an average increase of uptake by 10% when PVEc was applied in 11 subjects with visually positive amyloid PET scans; the cortical uptake of amyloid tracer was decreased with PVEc in three patients with visually negative amyloid PET scans. For amyloid PET imaging, the uptake in WM regions increased and the subcortical GM structures showed a similar trend with the cortex. ***Conclusion:*** The effects of PVEc on regional uptake values were higher in metabolic PET imaging than amyloid PET imaging. In the metabolic PET imaging, the total counts in cortical GM regions were increased with PVEc. However, the changes observed in the amyloid PET data were dependent on the amyloid positivity of the patients. While increasing the quantitative accuracy of data analysis, the opposite effects of PVEc observed in amyloid PET according to the amyloid positivity can useful terms of classification of amyloid PET images. ***References:*** None

OP-037

Effect of temporal sampling on myocardial blood flow measurements using Rubidium-82 PET

S. Koenders[1,2], J. D. van Dijk[1], P. L. Jager[1], M. Mouden[3], C. H. Slump[2], A. G. Tegelaar[1], J. A. van Dalen[4];
[1]Isala Hospital, Department of Nuclear Medicine, Zwolle, NETHERLANDS, [2]Technical Medical Center, University of Twente, Enschede, NETHERLANDS, [3]Isala Hospital, Department of Cardiology, Zwolle, NETHERLANDS, [4]Isala Hospital, Department of Medical Physics, Zwolle, NETHERLANDS.

Aim/Introduction: Myocardial blood flow (MBF) quantification is increasingly used when performing myocardial perfusion imaging (MPI) using Rubidium-82 (Rb-82) PET. This has resulted in a wide variety of temporal sampling protocols applied in dynamic imaging. Both the length and number of time-frames in the temporal sampling protocol may influence the time-activity curves and may therefore alter MBF and myocardial flow reserve (MFR) measurements. To be able to use and interpret MBF and MFR values interchangeably between different sites, it is important to know the effect of temporal sampling on MBF and MFR measurements. Our aim was to assess the effect of different clinically used temporal sampling protocols on MBF and MFR measurements. ***Materials and Methods:*** First, we performed a literature search to find all clinically applied Rb-82 temporal sampling protocols. Next, we retrospectively included 20 consecutive patients referred for rest and regadenoson-induced stress MPI using Rb-82 PET (Discovery 690, GE Healthcare). The Rb-82 PET data were acquired and then reconstructed with the different temporal sampling protocols. Using the one-tissue compartment model of Lortie et al., rest and stress MBF and

MFR were calculated for all protocols and compared to the reference protocol with 26 time-frames (24x5s, 2x120s). ***Results:*** After screening 103 articles with potential protocols, we included 14 different temporal sampling protocols using: 14 frames (9x10s, 3x30s, 1x60s, 1x120s), 16 frames (12x10s, 2x30s, 1x60s, 1x120s), 18 frames (1x10s, 8x5s, 3x10s, 2x20s, 4x60s), 20 frames (12x8s, 5x12s, 1x30s, 1x60s, 1x120s), 22 frames (18x10s, 4x60s), 23 frames (15x6s, 5x12s, 1x30s, 1x60s, 1x120s), 26 frames (A:12x5s, 6x10s, 4x20s, 4x40s and B:18x5s, 6x15s, 1x120s, 1x60s), 27 frames (A:20x6s, 4x30s, 3x60s and B:14x5s, 6x10s, 3x20s, 3x30s, 1x90s), 30 frames (16x5s, 6x10s, 3x20s, 4x30s, 1x80s), 31 frames (20x6s, 5x12s, 4x30s, 2x60s), 32 frames (24x5s, 8x30s) and 48 frames (36x5s, 8x15s, 4x30s). Rest and stress MBF measurements differed in six (43%) temporal sampling protocols as compared to the reference protocol ($p<0.01$): the protocols using 22 frames, 27A, 30, 31, 32 and 48 frames. In addition, differences were found for rest MBF using 18 frames ($p=0.007$) and for stress MBF using the 26A frames ($p=0.006$). None of the tested protocols showed a significant difference in MFR. ***Conclusion:*** Different temporal sampling protocols result in different stress and rest MBF values. Therefore, temporal sampling protocols cannot be used interchangeably when considering MBF but can be used interchangeably when solely comparing MFR values. ***References:*** None

OP-038

Estimating Input Function with Incomplete Blood Samples for Quantification of Nonhuman Primate Dynamic F-18-FDG PET/CT Using a Patlak Plot-based Optimization Method

R. Wang[1,2], *S. Zhang*[1], *X. Chen*[1], *J. Zhang*[1], *L. Chen*[1], *Y. Zhou*[3];
[1]*Peking University First Hospital, Beijing, CHINA,* [2]*Peking University International Hospital, Beijing, CHINA,* [3]*Washington University School of Medicine, St Louis, MO, UNITED STATES OF AMERICA.*

Aim/Introduction: FDG uptake rate constant K_i is a main physiology parameter measured by dynamic PET study. A model-independent graphical analysis using Patlak plot with plasma input function is a standard approach used to estimate K_i. The plasma input function is the FDG time activity curve in plasma obtained by arterial blood sampling. The purpose of the study is to evaluate a Patlak plot-based optimization approach for noninvasive quantification of dynamic FDG PET. ***Materials and Methods:*** Eight 60-min monkey dynamic FDG PET studies with arterial blood samples were collected. The measured plasma input function (mPIF) was determined by arterial blood samples. Time activity curves of seven cerebral regions of interest were generated from each study. With a given number of blood samples, the estimated PIF (ePIF) was determined by either interpolation or extrapolation method using scale calibrated population mean of normalized PIF. The optimal time points for those blood samples to estimate PIF (ePIF) was determined by maximizing the correlations between the K_i estimated ePIF and ones estimated mPIF. A leave-two-out cross-validation method was used for evaluation. ***Results:*** The linear correlations between the K_i estimates from ePIF with optimal sampling schemes and those from measured PIF were: Ki (ePIF 1 sample) = 1.09 Ki (mPIF) - 0.00, R^2 =0.95±0.08; Ki (ePIF 2 samples) = 1.09 K_i (mPIF) - 0.00, R^2 =0.95±0.07; K_i (ePIF 3 samples) = 1.04 Ki (mPIF) - 0.00, R^2 =0.96±0.05; and K_i (ePIF 4 samples) = 1.02 K_i (mPIF)-0.00, R^2 =0.97±0.04. As sample size became greater or equal 4, the K_i estimates from ePIF with optimal protocol were almost identical to those from mPIF. ***Conclusion:*** The Patlak plot-based optimization approach is a robust method to estimate plasma input function for noninvasive quantification of non-human primate dynamic FDG PET. ***References:*** None

OP-039

Investigation of Optimal Beta Value with Frame Duration for PET Bayesian Penalized-Likelihood Reconstructions

S. Jewitt[1], *M. D. Walker*[1], *D. R. McGowan*[1,2];
[1]*Oxford University Hospitals NHS FT, Oxford, UNITED KINGDOM,* [2]*University of Oxford, Oxford, UNITED KINGDOM.*

Aim/Introduction: This research aims to assess how the optimal penalization factor (beta) in a Bayesian penalized-likelihood (BPL) PET reconstruction algorithm (Q.Clear) varies with frame duration. The results of the investigation will be used to determine the impact of gating on the optimal beta value. ***Materials and Methods:*** A solid Ge-68 phantom containing 7 hot spheres in a low activity concentration background was scanned in list-mode on a time-of-flight PET/CT scanner (GE Discovery 710) and reconstructed using ordered-subset expectation maximisation (OSEM) and BPL. The ratio of the activity concentration in the spheres to the background was approximately 4:1. The acquisition was retrospectively rebinned with frame durations from 10 seconds to 10 minutes. For each of these frame durations, 10 independent repeats were reconstructed. Contrast recovery (CR) and background variability (BV) were calculated for each dataset as per the NEMA 2001 protocol, but using volumes-of-interest rather than regions-of-interest. The contrast to noise ratio (CNR=CR/BV) for each hot sphere was calculated and compared as a function of beta value and frame duration. The average CNR was calculated from the 10 repeats. The beta value that resulted in the highest average CNR was taken to be the optimal beta value for a given frame duration. A paired t-test was used to determine if there was a significant difference ($p<0.05$) in the optimal beta value for acquisitions with different frame durations. ***Results:*** A preliminary analysis of the BPL reconstructions with beta values of 500, 1000, 1500, 2000 and 3000; and frame durations of 30 seconds and 3 minutes, was performed. For the 3 minute and 30 second acquisitions the optimal beta was found to be around 1000 and 2000 respectively. For the 30 second acquisitions there was a significant difference in

CNR for all sphere sizes when comparing CNRs for beta of 2000 vs. 1000 ($p<0.001$). This indicates that the optimal beta for a 30-second and a 3-minute acquisition is different. Work is ongoing to determine the optimal beta value for a range of frame durations from 10 seconds to 10 minutes. ***Conclusion:*** Preliminary results indicate that the optimal beta value varies with frame duration. Shorter frame durations produce noisier data and therefore require a higher beta value to maximize the CNR, providing better image quality and improved detection of small lesions. The results can be applied to gated PET acquisitions to optimise the image quality. ***References:*** None

107

Pitfalls & Artefacts 1: Unexpected Findings in Brain Imaging

Thursday, October 22, 2020, 13:30 - 15:00 Channel 7

OP-040

Unexpected Findings on Coregistered MRI or CT in Hybrid PET and SPECT Imaging

E. van de Giessen*; Department of Nuclear Medicine, Academic Medical Center, University of Amsterdam, Amsterdam, NETHERLANDS.*

OP-041

Unexpected Findings of PET Imaging in Brain Tumours

J. Arbizu*; University of Navarra, Clinica Universidad de Navarra, Department of Nuclear Medicine, Pamplona, SPAIN.*

OP-042

Unexpected Findings of PET and SPECT Imaging in Neurodegenerative Diseases

D. Cecchin*; University of Padua, Department of Medicine, Padova, ITALY.*

108

Clinical Oncology Track - Featured Session: Prostate Beyond Staging and Restaging

Thursday, October 22, 2020, 13:30 - 15:00 Channel 8

OP-043

Prostate PET Applications Beyond Staging and Restaging

W. Fendler*; Universitätsklinikum Essen, Nuclear Medicine, Essen, GERMANY.*

OP-044

Impact of PSMA PET/CT on SRT planning: Preliminary results from a randomized phaseIII trial

J. Calais*, W. R. Armstrong, A. U. Kishan, K. M. Booker, J. Czernin, N. G. Nickols;*
UCLA, Los Angeles, CA, UNITED STATES OF AMERICA.

Aim/Introduction: The purpose of this trial is to evaluate the success rate of salvage radiotherapy (SRT) for recurrent prostate cancer after prostatectomy with versus without planning based on PSMA PET. ***Materials and Methods:*** This is a Randomized, controlled, prospective, open label, phase 3 clinical trial with institutional funding. 193 patients are randomized to proceed with standard SRT allowing for any conventional imaging aside from PSMA PET/CT (control arm 1) or undergo a 68Ga-PSMA-11 PET/CT scan prior to SRT planning (investigational arm 2). The primary endpoint is the success rate of SRT measured as biochemical progression-free survival (PFS) at 5 years. We hypothesized that the incorporation of PSMA PET to SRT planning will improve 5-year PFS survival by 20%: 60% in Arm 1 and 80% in Arm 2. We report here the preliminary results of the impact of PSMA PET on SRT planning by comparing the pre-randomization RT plans prospectively obtained on surveys to the actually delivered RT plans. ***Results:*** 153 patients were enrolled from 09.06.2018 to 01.24.2020. 7/75 patients (9%) in the control arm dropped-out the study to undergo a PSMA PET at another institution. After a median follow-up of 10.6 months delivered RT plans were obtained in 44/68(65%) and 50/78(64%) of patients of the control and the PSMA arms, respectively. In these, median PSA at enrollment was 0.42 ng/ml (IQR 0.20-1.75) in the control arm and 0.22 ng/ml (IQR 0.13-0.59) in the PSMA arm. PSMA PET was positive in 24/50(48%): 5/50(10%) showed prostate cancer outside of the pelvis, 12/50(24%) in pelvic nodes and 8/50(16%) in the prostate bed only. There was a change between the intended pre-randomization RT plan and the actually delivered RT plan in 28/50(56%) and 14/44(32%) of the patients in the PSMA arm and the control arm, respectively ($p=0.019$). SRT was aborted in favor of systemic therapy and/or metastasis directed RT for extra-pelvic M1 disease in 4/50(8%) of the PSMA arm vs. 1/44(2%) in the control arm ($p=0.21$). Dose prescription and/or target volume delineation was changed in 14/50(28%) in the PSMA arm vs. 3/44(7%) in the control arm ($p=0.008$). ***Conclusion:*** In this prospective randomized phase 3 study, PSMA PET had an impact on the RT plan in more than half of the patients. Notably, 8% of PSMA PET patients did not undergo SRT because the scan revealed extra-pelvic metastases. Long-term follow-up will show if the impact of PSMA PET on SRT planning improves PFS. ***References:*** None

OP-045

Urokinase Plasminogen Activator Receptor (uPAR) PET/MRI of Prostate Cancer for Non-invasive Evaluation of Aggressiveness: a Prospective Phase II Clinical Trial Comparing with Gleason Score

M. Fosbøl, *S. Kurbegovic, H. H. Johannesen, M. A. Røder, A. E. Hansen, J. Mortensen, A. Loft, P. M. Petersen, J. Madsen, K. Brasso, A. Kjaer;*
Rigshospitalet, Copenhagen, DENMARK.

Aim/Introduction: Overexpression of urokinase-type plasminogen activator receptor (uPAR) is an important biomarker for aggressiveness in prostate cancer. uPAR expression can now be imaged and non-invasively quantified by using the novel positron emission tomography (PET) ligand ^{68}Ga-NOTA-AE105. The aim of this study was to evaluate the correlation between uptake of uPAR ligand and Gleason score in patients undergoing prostate biopsy. ***Materials and Methods:*** Patients with clinical suspicion of prostate cancer (PCa) or previously diagnosed with PCa were prospectively enrolled in this phase II trial. A combined uPAR PET, multiparametric magnetic resonance imaging (mpMRI) was performed and standardized uptake value (SUV) from primary tumor, as delineated by mpMRI, was measured by two independent readers. Correlation between SUV_{max} and Gleason score obtained by biopsy was assessed. ***Results:*** A total of 27 patients had histologically verified PCa visible on mpMRI and constituted the study population. There was a positive correlation between SUV_{max} and Gleason score (Spearman's rho= 0.55; p=0.003). Receiver operating characteristics (ROC) analysis showed an area under the curve (AUC) of 0.88 (95%CI: 0.67-1.00) in discriminating Gleason score ≥3+4 from ≤3+3. A cut-off for tumor SUVmax could be established with a sensitivity of 96% (79-99%) and specificity of 75% (30-95%) in detecting Gleason Scores ≥3+4. For discriminating Gleason score ≥ 4+3 vs. ≤ 3+4, a cut-off could be established for detecting Gleason score ≥ 4+3 with a sensitivity of 93% (69-99%) and specificity of 62% (36-82%). ***Conclusion:*** SUV measurements from uPAR PET in primary tumors as delineated by mpMRI showed a significant correlation with Gleason score, and tumor SUV_{max} was able to discriminate between low-risk and intermediate risk Gleason score profiles with high diagnostic accuracy. Consequently, uPAR PET/MRI could be a promising method for non-invasive evaluation of PCa, which may in the future potentially reduce the need for repeated biopsies, e.g. in active surveillance. ***References:*** None

OP-046

Prospective study on PSMA flare phenomenon after androgen deprivation therapy evaluated with ^{18}F-PSMA-1007 PET/CT in treatment naïve metastatic prostate cancer: any link to glucose metabolism?

S. Malaspina[1], *O. Ettala*[2], *T. Tolvanen*[3], *S. Forsback*[1], *P. J. Boström*[2], *J. Kemppainen*[1];
[1]*Turku PET Centre, University of Turku and Turku University Hospital, Turku, FINLAND,* [2]*Department of Urology, University of Turku and Turku University Hospital, Turku, FINLAND,* [3]*Department of Medical Physics and Turku PET Centre, University of Turku and Turku University Hospital, Turku, FINLAND.*

Aim/Introduction: Our previous clinical trial demonstrated that short-term androgen deprivation therapy (ADT) increases heterogeneously PSMA-uptake in hormone-sensitive prostate cancer (Pca). This PSMA-flare phenomenon needs validation, since possible factors associated with it remain unknown. We hypothesize that lesions having PSMA-flare might have a different potential to respond to ADT or progress. This prospective trial aims to validate our previous results and to observe whether FDG-PET might provide additional molecular imaging information, given that aggressive Pca tends to display FDG-uptake. ***Materials and Methods:*** This prospective, registered (NCT03876912), single-centre trial enrolls patients with newly diagnosed metastatic Pca, that undergo ^{18}F-PSMA-1007 PET/CT before and 3-4 weeks after the initiation of Degarelix. At baseline,^{18}F-FDG PET/CT is also performed. SUVmax on primary tumor and metastatic lesions is calculated. The increase, decrease or no-change of PSMA-uptake after ADT is represented as ΔSUVmax%. ***Results:*** To date, 8 patients (mean age: 71 years, median PSA: 59 ng/ml, range 8-130) completed all PET/CT scans. All patients reached castration levels (s-testo <1.7nmol/L) before the second PSMA PET/CT scan, performed with a 21-days median interval (range 17-31) after initiation of ADT. One patient had bone-only, one nodal-only and six bone and nodal metastases. In total 159 bone metastases, 53 lymph nodes (LN) and 12 prostate lesions were analysed. Out of the total, 116/224 (52%) lesions were FDG-positive. After ADT, 90/159 (57%) bone, 10/53 (19%) LN and 2/12 (17%) prostate lesions showed an increase of PSMA-uptake, with a median ΔSUVmax% of 47% (range 11-136), 33% (range 14-172) and 28% (range 14-43), respectively. The remaining lesions showed either a decrease or no-change (ΔSUVmax ±10%) of PSMA-uptake. According to lesions presenting PSMA-flare, 50/90 (56%) bone, 4/10 (40%) LN and 1/2 (50%) prostate lesions were FDG-positive (median FDG-SUVmax: 4,8). Out of the lesions presenting decrease of PSMA-uptake, 30/54 (56%) bone, 16/41 (39%) LN and 5/9 (56%) prostate lesions showed FDG-uptake (median FDG-SUVmax: 9,8). ***Conclusion:*** These preliminary results confirmed a heterogeneous increase of PSMA-uptake after ADT, most evidently seen in bone metastases. It appears that this phenomenon is not associated with glucose metabolism.

Nevertheless, the lowest FDG-uptake was observed in lesions that presented with PSMA-flare, suggesting that these lesions might potentially be less aggressive and have a better response to ADT. ***References:*** Ettala et al. Prospective study on the effect of short-term androgen deprivation therapy on PSMA uptake evaluated with 68Ga-PSMA-11 PET/MRI in men with treatment-naïve prostate cancer. Eur J Nucl Med Mol Imaging. 2020; 47(3): 665-673.

OP-047

Predictors of Intertumoral Heterogeneity of ^{18}F-FDG and ^{68}Ga-PSMA Uptake in Patients with Prostate Cancer

T. Telli, M. Tuncel, M. Caglar;
Hacettepe University Faculty of Medicine, Ankara, TURKEY.

Aim/Introduction: ^{68}Ga-PSMA PET/CT plays a pivotal role in patients with prostate cancer. It changes treatment plans and guides new therapy options. Although the sensitivity of PSMA PET is higher than other PET tracers, FDG PET/CT may detect PSMA-negative disease, in patients with metastatic castration-resistant prostate cancer(mCRPC) and change treatment decisions. The study aims, to evaluate baseline clinical, biochemical, ^{68}Ga-PSMA PET-related parameters that can predict patients in whom FDG PET showed additional lesions when compared to ^{68}Ga-PSMA PET/CT (FDG>^{68}Ga-PSMA). ***Materials and Methods:*** Sixty-three patients with mCRPCa who underwent both FDG and ^{68}Ga-PSMA PET/CT within two months were evaluated. The number and SUVmax of metastatic foci, total lesion-PSMA(TL-PSMA), total tumor volume-PSMA(TV-PSMA) were calculated. Patients' clinical parameters, sites of metastases, performance status, and bone pain score (VAS) were recorded. Baseline laboratory tests including PSA kinetics, complete blood counts, serum liver and kidney function tests, neuron-specific enolase (NSE), carcinoembryonic-antigen (CEA), lactate dehydrogenase (LDH), alkaline phosphatase (ALP), C-reactive-protein (CRP), and erythrocyte sedimentation rate (ESR) results were correlated with PET results. Based on FDG and ^{68}Ga-PSMA PET/CT images, patients were grouped into two categories: patients who had FDG PET/CT avid but ^{68}Ga-PSMA negative lesion (FDG>^{68}Ga-PSMA) and patients who had same or more number of lesions on PSMA PET compared to FDG PET (^{68}Ga-PSMA≥FDG). Variables associated with FDG>^{68}Ga-PSMA disease were investigated using logistic regression analysis. ***Results:*** 25/63 (39,7%) patients had FDG>^{68}Ga-PSMA disease. Discordant lesions were present in the bones (20/25), lymph nodes (12/25), liver (11/25), lung (2/25), pancreas (1/25). Five patients showed discordance in the local disease of the prostate, bladder wall, or seminal vesicles. Univariate analysis revealed that stage at the diagnosis (stage4b), higher ECOG, lower Karnofsky PS, higher pain score, not using 2nd generation anti-androgen therapy, higher baseline LDH, ESR, AST, GGT values, lower baseline hemoglobin (Hb) and visceral metastases were potential predictive factors for FDG>^{68}Ga-PSMA disease. On multivariate analysis, elevated AST (p: 0,012, RR: 1,145, CI: 1,056-1,26) and presence of visceral metastases (p: 0,02, RR: 33,479, CI:1,833-611,5) were significant for predicting FDG>^{68}Ga-PSMA disease. ***Conclusion:*** In patients with mCRPC, increased incidence of PSMA negative disease may have both diagnostic and therapeutic consequences. Our findings showed that patients with poor health performance and advanced disease on PSMA PET, especially with visceral metastases, may benefit from additional imaging like FDG PET. ***References:*** None

OP-048

The prognostic power of 18F-FDG PET/CT extends to the estimation of systemic treatment response duration in metastatic castration-resistant prostate cancer (mCRPC) patients

M. Bauckneht[1], *F. Bertagna*[2], *M. Donegani*[1], *R. Durmo*[3], *A. Miceli*[1], *V. De Biasi*[3], *R. Laudicella*[4], *S. Baldari*[4], *A. Versari*[3], *R. Giubbini*[2], *G. Sambuceti*[1], *S. Morbelli*[1], *D. Albano*[2];
[1]*IRCCS Ospedale Policlinico San Martino, Genova, ITALY,* [2]*Spedali Civili of Brescia and University of Brescia, Brescia, ITALY,* [3]*Nuclear Medicine, AUSL-IRCCS of Reggio Emilia, Reggio Emilia, ITALY,* [4]*Department of Biomedical and Dental Sciences and of Morpho-functional Imaging, University of Messina, Messina, ITALY.*

Aim/Introduction: In the last years, the therapeutic strategy for metastatic castration-resistant prostate cancer (mCRPC) radically changed due to improved knowledge of PC biology and progression mechanisms. However, clinicians presently face critical therapeutic challenges mainly related to the choice of the best treatment sequencing for each specific patient. In this scenario, there is an urgent need for the identification of reliable biomarkers to early and non-invasively determine treatment efficacy (possibly improving patients' selection). 18F-Fluorodeoxyglucose (FDG)-avidity is low in naïve prostate cancer, but it is enhanced in advanced mCRPC, providing prognostic insights. We thus aimed to verify whether the prognostic power of FDG PET/CT extends to the estimation of systemic treatment response duration in mCRPC. ***Materials and Methods:*** We conducted a retrospective review of mCRPC patients who were submitted to FDG PET/CT for prognostic purposes in four Italian centers from 2005 to 2020. Patient's age, Gleason Score (GS), prostate-specific antigen (PSA), Lactate dehydrogenase (LDH), and Alkaline Phosphatase (AP) at the time of imaging were collected. From PET/CT images SUVmax of the hottest lesion, total metabolic tumor volume (MTV) and total lesion glycolysis (TLG) were computed. The correlation between PET- and biochemical-derived parameters with Overall Survival (OS) was calculated by Kaplan-Meier, univariate and multivariate analyses. The prediction of duration of treatment response was also assessed in the subgroup submitted to FDG imaging before systemic therapy administration. ***Results:*** We enrolled 116 mCRPC patients clinically followed-up for a median

interval lasting seven months. PSA, MTV, and TLG significantly predicted long term OS in this cohort (p<0.01). Moreover, PSA and TLG evaluation of baseline metabolically active disease were able to predict OS with an additive independent value, as documented by multivariate Cox regression analysis, even after adjusting for patient's age, GS, LDH, and AP. When FDG imaging was performed at baseline before systemic treatment administration (40 patients), only MTV and TLG were able to significantly and independently predict therapy response duration (p<0.01 in either chemotherapy or Androgen Receptor-Targeted Agents treatment subgroups). ***Conclusion:*** FDG PET/CT imaging provides robust prognostic insights in hormone-refractory prostate cancer. This prognostic power may predict treatment response duration when FDG imaging is performed before systemic treatment administration. Prospective studies are needed to verify whether PET-derived parameters may also improve the selection of systemic treatment. ***References:*** None

OP-049

^{68}Ga- PSMA PET/CT on Local Disease Detection: The Added Value of Early Dynamic Imaging After Radical Prostatectomy

M. Monteiro[1], R. Silva[1,2], T. Saraiva[1], G. Costa[1,3], J. Pedroso de Lima[1,2,3];
[1]Centro Hospitalar e Universitário de Coimbra, Coimbra, PORTUGAL, [2]Instituto de Ciências Nucleares Aplicadas à Saúde (ICNAS), Coimbra, PORTUGAL, [3]Faculdade de Medicina da Universidade de Coimbra, Coimbra, PORTUGAL.

Aim/Introduction: ^{68}Ga-labelled prostate-specific membrane antigen positron emission tomography/computed tomography (^{68}Ga-PSMA PET/CT) is a non-invasive diagnostic technique to image prostate cancer with increased PSMA expression. Bladder activity may hinder local disease detection, particularly in patients submitted to prostatectomy. To overcome this limitation, some authors recommend early dynamic imaging of the pelvis. In this retrospective work, we aim to assess the added value of early dynamic imaging on local disease detection, when compared to whole body PET/CT only. ***Materials and Methods:*** A total of 229 ^{68}Ga-PSMA PET/CT scans, performed between April 2019 and March 2020, were reviewed. All prostate cancer patients submitted to radical prostatectomy who performed early dynamic imaging of the pelvis (4 min dynamic acquisition starting immediately after injection) and whole body PET/CT were selected and two databases were created after anonymization. Database A: including only whole body PET/CT scans; Database B: including dynamic images of the pelvis and whole body PET/CT scans. All scans were reviewed and patients were categorized in each database as: 1-negative for local disease; 2-positive for local disease; 3-doubtful for local disease. All relevant demographic and clinical data was recorded (when available), such as PSA values and tumor characteristics. Statistical analysis was performed using SPSS version 25.0. ***Results:*** Seventy-nine patients were included (age: 71.3±6.4 years, 53-85). Median PSA was 0.66 (interquartile amplitude = 1.66; 0.00-5060.60). In database A 62 patients (78.5%) were categorized as negative, 9 (11.4%) as positive and 8 (10.1%) as doubtful for local disease. While in database B 58 patients (73.4%) were categorized as negative, 19 (24.1%) as positive and 2 (2.5%) as doubtful for local disease. Thus, with dynamic imaging 9 patients previously categorized as negative were re-categorized either as positive (7) or doubtful (2) for local disease, and all 8 patients previously categorized as doubtful were re-categorized either as negative (5) or as positive (3) for local disease. No change was recorded for patients categorized as positive for local disease in Database A. A statistically significant difference in patient categorization between databases was found (McNemar, p<0.01). ***Conclusion:*** Early dynamic imaging altered local disease detection in ^{68}Ga-PSMA PET/CT, in a statistically significant manner, by increasing positive findings and decreasing doubtful results. Remarkably, dynamic imaging had no effect on positive whole body ^{68}Ga-PSMA PET/CT results. ***References:*** None

OP-050

Bone marrow expansion in patients with prostate cancer bone metastases: prognostic role and correlation with tumour load, based on ^{18}F-FDG PET/CT segmentation analysis

F. Fiz[1], M. Bauckneht[2], S. Morbelli[2], A. Miceli[3], I. Donegani[3], C. Campi[4], M. Piana[5], G. Sambuceti[2];
[1]Humanitas Clinical and Research Center - IRCCS, Milan, ITALY, [2]IRCCS Ospedale Policlinico San Martino, Genoa, ITALY, [3]University of Genoa, Genoa, ITALY, [4]Dipartimento di Matematica "Tullio Levi-Civita", Università di Padova, Padua, ITALY, [5]Department of Mathematics, University of Genoa, Genoa, ITALY.

Aim/Introduction: Bone marrow (BM) failure is a major cause of morbidity and mortality in patients affected by metastatic, castration-resistant prostate cancer (mCRPC). Bone metastases from mCRPC seed into the axial skeleton preferentially, thus reducing the space available for normal BM. We hypothesized that this phenomenon could cause an increase of active BM in the peripheral skeleton and that BM relocation has a prognostic role for patients' survival. ***Materials and Methods:*** Thirty-seven mCRPC, with evidence of bone metastases in the axial skeleton, underwent a whole-body PET/CT with ^{18}F-FDG before treatment with $^{223}RaCl_2$. Each PET/CT was analysed by a semi-automated segmentation software, which identifies the skeletal tissue on the CT images and automatically separates the cortical bone volume, the trabecular bone volume (IBV) and the bone metastases (MBV). From IBV, it extracts the FDG PET information, to calculate the volume of active BM and its SUV, based on a published statistical criterion. Axial (spine

and sternum) and appendicular (humeral, femoral, and tibial bone shafts) values were computed separately. The results were compared with age- and sex-matched controls from a published normalcy database. The mCRPC patients were followed up, and overall survival (OS) was calculated. ***Results:*** Appendicular active BM volume and SUV were both greater in mCRPC patients than in controls (35,8±15,9 ml Vs. 9,9±13,9 ml, p<0,01 and 1,3±0,1 Vs. 1,1±0,2, p<0,05, respectively). Axial active BM volume and SUV were not significantly different between cases and controls. Appendicular active BM volume directly correlated with haemoglobin levels at the time of PET/CT (R= 0,68, p<0,01). MBV directly correlated with appendicular BM volume (R=0,49, p<0,05) and SUV (R=0,65, p<0,01); it inversely correlates with OS (R= -0,71, p<0,001). ***Conclusion:*** The presence of metastases in the axial skeleton causes a measurable increase in BM metabolic activity in the appendicular bones. This phenomenon is linked with BM haematopoietic capability, as well as overall survival. ***References:*** Sambuceti G et a. Estimating the whole bone-marrow asset in humans by a computational approach to integrated PET/CT imaging. Eur J Nucl Med Mol Imaging. 2012 Aug;39(8):1326-38.

OP-051

Clinical significance of 68Ga-DOTATOC prostatic uptake on PET/CT: A ten-year review

F. Gossili[1], C. E. Almasi[1], H. D. Zacho[1,2], L. J. Petersen[1,2];
[1]Department of Nuclear Medicine, Aalborg University Hospital, Aalborg, DENMARK, [2]Department of Clinical Medicine, Aalborg University, Aalborg, DENMARK.

Aim/Introduction: Gallium68 DOTATyr3octreotide (68Ga-DOTATOC) is a radiolabeled somatostatin receptor (SSTR) analogue that is widely used in positron emission tomography/computed tomography (PET/CT), especially in the imaging of neuroendocrine tumors (NETs). Benign and malignant prostate tumors have been observed to express SSTR. Diffuse symmetric DOTATOC uptake in prostate is a normal PET-finding. The aim of this study was to evaluate the frequency and clinical significance of incidental atypical prostatic uptake in men undergoing 68Ga-DOTATOC PET/CT. ***Materials and Methods:*** A retrospective review of male patients who underwent 68Ga-DOTATOC PET/CT studies at our department from November, 2010 to April, 2020 was performed. PET/CT reports were searched for text words or phrases indicating incidental atypical prostatic uptake. The DOTATOC uptake in the prostate gland was categorized as focal, diffuse or mixed. The intensity of the uptake was visually graded by comparing the prostatic uptake to the background uptake in the liver and the spleen uptake (Krenning visual score). Follow up was based on available clinical, biochemical, imaging, and pathology follow up. ***Results:*** 188 male patients underwent 68Ga-DOTATOC PET/CT. Incidental atypical uptake of 68Ga-DOTATOC on PET/CT in the prostatic bed was observed in eight patients (4%) (mean age 68 years, range 58-77 years). Four patients (50%) had diffuse uptake, four (50%) patients had mixed uptake. One patient (13%) had low uptake (Kenning grade 1), four patients (50%) had moderate uptake (grade 2) and three patients (37%) showed grade 3 uptake. Follow up was conducted in all patients (median follow up of 29 months (range 56-7 months)). All patients had measurements of prostate-specific antigen and were referred for urological evaluation. Five patients (62%) underwent a transrectal, ultrasound-guided biopsy. No cases of prostate malignancy (including prostatic cancer) were diagnosed. ***Conclusion:*** During a 10-year period, we found that 4% of men exhibited prostate incidentalomas on 68Ga-DOTATOC PET/CT. No malignancy was found in the prostate in this population despite thorough examination and long-follow up. Our preliminary data indicate low or absent malignancy among incidental 68Ga-DOTATOC findings in the prostate. ***References:*** None

OP-052

Radiolabeled PSMA And Choline PET/MRI In Prostate Cancer: A Systematic Review And Meta-Analysis

L. Evangelista[1], F. Zattoni[2], G. Cassarino[1], P. Artioli[1], D. Cecchin[1], P. Zucchetta[1];
[1]University of Padua, Padua, ITALY, [2]Hospital of Udine, Udine, ITALY.

Aim/Introduction: In prostate cancer (PCa) patients, large experiences have been conducted by using PET/computed tomography (CT). However, the implementation of magnetic resonance imaging (MRI) in the hybrid systems with PET has conjugated the "real" potential of metabolic/receptorial imaging to functional parameters. The aim of the current systematic review and meta-analysis is to summarize the diagnostic information provided by PET/MRI in PCa patients. ***Materials and Methods:*** A bibliographic search was performed by including the following databases: Pubmed, Scopus and Web of Science. The terms used were "Choline" or "prostate specific antigen membrane-PSMA" AND "prostate cancer" or "prostate" AND "PET/MRI" or "positron emission tomography/magnetic resonance imaging". All recognized records were combined and the full texts were retrieved. Full texts were further evaluated, by also checking the references in order to improve the eligibility. Reports were excluded if they did not 1-consider hybrid PET/MRI scanners or 2-a sample size <10 patients, or 3-sufficient raw data was provided for completion of a 2×2 contingency table; 4-the performances' outcomes. ***Results:*** 50 articles were eligible for the systematic revision and 23 for meta-analysis. Overall, the number of included patients was 2313 of which 2104 (91%) underwent hybrid PET/MRI. Initial staging of disease was the most common indication (n=23 studies). Radiolabeled PSMA was used in the majority of case. In primary tumor, the pooled sensitivity was 94.9% (95% confidence interval-CI: 87.5-98.6%), at patient-based analysis. In restaging, the pooled detection rate was 80.9%

(95%CI: 73.0-86.9%), being higher for radiolabeled PSMA than radiolabeled Choline (81.8% vs. 77.3%, respectively). ***Conclusion:*** PET/MRI has a high sensitivity for the detection of primary PCa and a high detection rate for recurrent disease, particularly with radiolabeled PSMA. It would be of great importance for the detection of primary tumor and early recurrence of disease. ***References:*** 1. Kranzbuhler et al. J Nucl Med 2020; 61:194-201

OP-053

Evaluation of ^{68}Ga-PSMA PET/CT Images Acquired with a Reduced Scan Time Duration in Prostate Cancer Patients using a Digital PET/CT Scanner

M. Weber[1], *R. Hofferber*[1], *K. Herrmann*[1], *W. P. Fendler*[1], *M. Conti*[2], *A. Wetter*[3], *D. Kersting*[1], *C. Rischpler*[1], *W. Jentzen*[1], *P. Costa*[1];
[1]*Department of Nuclear Medicine, University of Duisburg-Essen and German Cancer Consortium (DKTK)-University Hospital Essen, Essen, GERMANY,* [2]*Siemens Medical Solutions USA, INC, Essen, GERMANY,* [3]*Institute for Diagnostic and Interventional Radiology and Neuroradiology University Hospital Essen, Essen, GERMANY.*

Aim/Introduction: PET/CT with ^{68}Ga-PSMA allows for a superior detection of prostate cancer tissue, especially in context of a low tumor burden. Digital PET/CT bears the potential of reducing scan time duration or administered tracer activity due to, for instance, its higher sensitivity and improved time coincidence resolution. It might thereby expand ^{68}Ga-PSMA PET/CT availibility currently limited by ^{68}Ge/^{68}Ga-generator yield. Our aim was to clinically evaluate the influence of a reduced scan time duration in combination with different image reconstruction algorithms on the diagnostic performance. ***Materials and Methods:*** Twenty prostate cancer patients (11 for biochemical recurrence, 5 for initial staging, and 4 for metastatic disease) sequentially underwent ^{68}Ga-PSMA PET/CT examination on a digital Siemens Biograph Vision. In 11 of these PET data were collected in continuous-bed-motion mode with a scan time duration of approximately 15 min (reference acquisition protocol) and 5 min (reduced acquisition protocol). For both protocols, 4 iterative reconstruction algorithms were applied using a time-of-flight (TOF) approach alone or combined with point-spread-function (PSF) correction, each with 2 or 4 iterations. To evaluate the diagnostic performance, the following metrics were chosen: (a) per-region detectability, (b) the tumor maximum and peak standardized uptake values (SUVmax and SUVpeak) and (c) image noise using the liver's activity distribution. ***Results:*** Overall, 98% of regions (91% of affected regions) were correctly classified in the reduced acquisition protocol independent of the image reconstruction algorithm. Two pelvic nodal lesions (each ≤4 mm in size) were not identified at 5 min vs 15 min scan duration leading to downstaging in 1 of 20 cases. Mean absolute percentage deviation of SUVmax and SUVpeak was approximately 9% and 6% respectively for each reconstruction algorithm. The mean image noise increased approximately from 13% to 21% (4 iterations) and from 10% to 15% (2 iterations) for both PSF+TOF and TOF images. ***Conclusion:*** Using a digital PET/CT, three-fold reduction of scan time resulted in near equalper-tumor region detection (98 % of regions) and image quantification (mean deviation ≤ 10 %); however, small lesions can be missed in about 5% of patients. Our results suggest that a reduction of scan time duration or administered ^{68}Ga-PSMA activities can be considered in patients with more advanced or extra-pelvic disease. ***References:*** None

109

TROP Session: Therapeutic Options in Thyroid Cancer - Radioiodine and Beyond

Thursday, October 22, 2020, 13:30 - 15:00 Channel 9

OP-054

The effectiveness of 177Lu-DOTATATE in patients with metastatic medullary thyroid cancer

S. Bilgic*, M. S. Sağer, M. F. Beytur, A. Nazari, R. L. Uslu Beşli, S. Asa, L. Kabasakal, H. B. Sayman, K. Sönmezoğlu;*
Istanbul University - Cerrahpasa, Istanbul, TURKEY.

Aim/Introduction: The current therapeutic options in metastatic medullary cancer (mMTC) are limited. Although tyrosine kinase inhibitors are recommended as a first-line therapy, these treatments have considerable side effects, which often limit the therapy effect. Peptide receptor radionuclide therapy (PRRT) is another possible treatment modality in patients with mMTC. The purpose of this study is to investigate the effectiveness of ^{177}Lu-DOTATATE in patients with mMTC. ***Materials and Methods:*** 19 mMTC patients (6 female and 13 male) treated by ^{177}Lu-DOTATATE in our institution between the years of 2012 and 2018 were retrospectively analyzed. Pretreatment 68Ga- DOTATATE-PET-CT imaging was performed. Pretreatment serum calcitonin (Ctn) values were assessed. The primary endpoints are: 1) increase in Ctn value more than 50% 2) post-therapy progression confirmed via ^{68}Ga-DOTATATE PET/CT scan. ***Results:*** 19 patients (aged: 32 - 87 years) with mMTC were enrolled. Only 1 patient (5.3%) had familial MTC (MEN2A). All patients underwent total thyroidectomy and bilateral central and lateral neck dissection. The median Ctn values before treatment were 1723 pg/ml (60 - 4840). 15 patients had no previous treatments, 4 patients were previously treated with other systemic agents (1 vandetanib, 1 sorafenib, 2 somatostatin analogs). Local recurrence was present in 8 patients. The most frequent sites of metastases were cervical lymph nodes (15), bone (12), mediastinum (5), liver (4), and lungs (3). Four patients were in stage IVB, and 15 patients were in stage IVC. The median of administrated activity was

177 mCi (11-214) in a median of 3 cycles with a range of 1 to 8 cycles with 2 months and longer intervals. The median Ctn values after treatment were 1291 pg/ml (20 - 9855). No patient had a complete response at the Ctn level. 8 patients had a partial response, 7 patients a disease stabilization, and 4 patients a disease progression. The biochemical disease control rate was 79%. Post-therapy ^{68}Ga-DOTATATE-PET-CT results and post-therapy Ctn levels were discordant. Based on ^{68}Ga- DOTATATE-PET-CT, no patient had a complete response, 2 patients had a partial response, while 15 patients had a disease stabilization, and 2 patients had a disease progression. The disease control rate was 89%. There was no grade 3/4 toxicity. ***Conclusion:*** In patients with mMTC, ^{177}Lu-DOTATATE therapy appears to be effective in disease control. ***References:*** Makis W, McCann K, McEwan AJ. Medullary thyroid carcinoma (MTC) treated with 177Lu-DOTATATE PRRT: a report of two cases. Clinical nuclear medicine. 2015;40:408-12. doi:10.1097/rlu.0000000000000706

OP-055

The Effectiveness of 177Lu-DOTA TATE in Radioiodine-Refractory Differentiated Thyroid Cancer

A. Nazari*, M. S. Sağer, S. Bilgiç, F. Beytur, R. L. Uslu Beşli, S. Asa, L. Kabasakal, H. B. Sayman, K. Sönmezoğlu;*
Department of Medicine, Istanbul University Cerrahpasa, Istanbul, TURKEY.

Aim/Introduction: Differentiated thyroid carcinomas (DTC) are cancers that develop from thyroid follicle epithelial cells and makeup 90% of all thyroid carcinomas. Radioiodine-Refractory (RAIR) DTC has a poor prognosis and fewer treatment options. In this study, we aimed to investigate the effectiveness of 177Lu-DOTATATE treatment in patients with RAIR DTC. ***Materials and Methods:*** 28 patients who underwent 177Lu-DOTATATE treatment in our institution between 2011-2020 were examined retrospectively. The study includes patients with total thyroidectomy (TT), followed by RIT but considered RAIR, biochemically progressive, and a positive somatostatin receptor in 68Ga-DOTATATE PET/CT. ***Results:*** 28 patients, 17 women (60.7%), and 11 men (39.3%) with a mean age of 62.8 (42-81) were included in the study. Papillary thyroid carcinoma (PTK) in 21 patients (53.8%), follicular thyroid carcinoma (FTK) in 5 patients (12.8%), Hürthle cell carcinoma (HCC) in 1 patient (2.6%), poorly differentiated thyroid carcinoma (PDTC) in 1 patient (2.6%). Patients were classified according to TNM classification before treatment; 27 patients (96.4%) evaluated as stage 4C, one patient as stage 4A. Median 2 cycles (1-12) of 177Lu-DOTATATE treatment was applied with an average dose of 454 mCi (149-1376) at intervals of 2 months and longer. Patients had a history of TT before treatment and received a median of 500 mCi (100-1100) RIT therapy. 11 patients (39.3%) received lymph node dissection (LND), 5 patients (17.9%) tyrosine kinase inhibitor (TKI), 3 patients (10.7%) Radiotherapy (RT). Prior treatment median thyroglobulin (Tg) value was measured as 238.5 ng/mL (2.12-1804). 12 patients (42.9%) had metastatic lesions in the thyroid region, 9 patients (32.1%) in the cervical lymphatic stations, 18 patients (64.3%) in the lungs, 10 patients (35.7%) in the skeletal system, and 2 patients (7.1%) in the muscles. ***Conclusion:*** No hepatotoxicity/nephrotoxicity was observed in patients during and after treatment. The median Tg values measured after treatment were as 300 ng/mL (7-5000). None of the patients had complete Tg response, a partial response in 4 patients (16%), and progressive Tg response in 21 patients (84%). No complete morphological response was observed in any patient; Partial response was detected in 1 patient (4.8%), stable disease in 3 patients (14.3%), and progressive disease in 17 patients (81%). 177Lu-DOTATATE treatment is an alternative treatment method in patients with RAIR DTC. ***References:*** 1. Czepczynski R, Matysiak-Grzes M, Gryczynska M, Baczyk M, Wyszomirska A, Stajgis M, et al. Peptide receptor radionuclide therapy of differentiated thyroid cancer: efficacy and toxicity. Arch Immunol Ther Exp (Warsz). 2015;63

OP-056

PRRT with the CCK-2 receptor Agonist ^{177}Lu-PP-F11N - First results of a Phase 1 "LUMED" Study

C. Rottenburger*[1], G. Nicolas[1], L. McDougall[1], M. Fürstner[2], M. Hentschel[2], F. Kaul[1], E. R. Christ[3], M. Cachovan[4], H. A. Vija[5], R. Schibli[6], S. Geistlich[6], M. Béhé[6], D. Wild[1];*
[1]University Hospital Basel, Division of Nuclear Medicine, Basel, SWITZERLAND, [2]Department of Nuclear Medicine, Inselspital, Bern University Hospital, University of Bern, Bern, SWITZERLAND, [3]Division of Endocrinology, Diabetology and Metabolism, University Hospital Basel, Basel, SWITZERLAND, [4]Siemens Healthcare GmbH, Forchheim, GERMANY, [5]Molecular Imaging, Siemens Medical Solutions USA, Inc., Hoffman Estates, IL, UNITED STATES OF AMERICA, [6]Center for Radiopharmaceutical Sciences, Paul Scherrer Institute, Villigen, SWITZERLAND.

Aim/Introduction: Despite the introduction of new molecular targeted therapies, there is still an unmet need for an effective systemic therapy for advanced medullary thyroid carcinoma (MTC). Recently, we demonstrated that the administration of the novel CCK-2 receptor agonist [^{177}Lu-DOTA-$(DGlu)_6$-Ala-Tyr-Gly-Trp-Nleu-Asp-PheNH$_2$] (^{177}Lu-PP-F11N) is safe and enables for visualization of metastasized disease in patients with MTC. This subsequent phase 1 study aims to determine the maximum tolerated dose of ^{177}Lu-PP-F11N (ClinicalTrials.gov: NCT02088645). Here we present the preliminary results of the first activity escalation step. ***Materials and Methods:*** Two patients received three injections of 6 GBq ^{177}Lu-PP-F11N in an interval of 8 weeks and one patient received the first injection. Planar scintigraphy and SPECT/CT scans were performed at several time points for up to 72 h post injection in order to calculate tumour and organ radiation doses using 3D voxel- and MIRD based dosimetry (Dosimetry Research Tool v5.2, Siemens Medical Solutions, USA). Blood

samples were taken for bone marrow dose calculations as well as measurement of blood count and blood chemistry. ***Results:*** Adverse reactions (mainly hot flashes, nausea and hyperhidrosis) after injection of 3 x 6 GBq ^{177}Lu-PP-F11N were comparable to the phase 0 study and not higher than grade 2 according to CTCAE version 4.03. Follow up visits at 9 and 6 months after the last injection did not reveal any dose limiting toxicity in patient #1 and #2. Dosimetry results are available for patient #1. The median (range) radiation dose for lymph node metastases (n=4) was 0.96 Gy/GBq (0.88-1.46), resulting in a median cumulative dose of 18.3 Gy (16.8-27.9). Median radiation doses in Gy/GBq (range) for stomach, kidneys and bone marrow were 0.29 (0.25-0.32); 0.04 (0.04-0.05) and 0.04 (0.03-0.04). In patient #1, maximum reduction of calcitonin was 12% 4 months after the first injection and calcitonin remained below initial levels for further 3 months before increasing again above baseline. In patient #2, calcitonin was not reliable because of intermittent PPI therapy, but maximum CEA reduction was 36% 5 months after first application. At present, CEA still remains below baseline, despite stopping vandetanib therapy after enrolment. ***Conclusion:*** The administration of the novel CCK-2 receptor ligand ^{177}Lu-PP-F11N at a potentially therapeutic dose was observed to be safe in all patients. The first results of tumour and organ dosimetry suggests that the cumulative administrated activity dose (18 GBq) can be further increased without exceeding the threshold radiation dose for potential organs of risk. ***References:*** None

OP-057

Use Of Iodine-131 (RAI) For The Initial Diagnosis And Treatment Of Differentiated Thyroid Cancer (DTC) In Spain And Portugal (ERUDIT Study)

J. Vallejo Casas[1], *V. Pubul*[2], *R. Santos*[3], *M. Llanos*[4], *E. Navarro*[5], *J. Aller*[6], *M. Sambo*[7], *S. Guadalix*[8], *G. Crespo*[9], *C. Zafón*[10], *C. González*[11], *A. Segura*[12], *M. Navarro*[13], *J. Santamaría*[14], *P. Gajate*[15], *J. Valdivia*[16], *M. Gómez*[17], *C. López*[18], *B. Castelo*[19], *M. Puig*[20], *J. Galofré*[21], *M. Villanueva*[22], *I. Argüelles*[23], *F. Araujo*[24], *L. Orcajo*[24];
[1]*Hospital Universitario Reina Sofía, IMIBIC, Córdoba, SPAIN,* [2]*Complejo Hospitalari Universitario de Santiago, Santiago de Compostela, A Coruña, SPAIN,* [3]*Intitudo Português de Oncologia de Lisboa Francisco Gentil, Lisbon, PORTUGAL,* [4]*Hospital Universitario de Canarias, Santa Cruz de Tenerife, SPAIN,* [5]*Hospital Virgen del Rocio, Sevilla, SPAIN,* [6]*Hospital Puerta de Hierro, Madrid, SPAIN,* [7]*Hospital Gregorio Marañón, Madrid, SPAIN,* [8]*Hospital 12 de Octubre, Madrid, SPAIN,* [9]*Complejo Asistencial de Burgos, Burgos, SPAIN,* [10]*Hospital Vall d'Hebrón, Barcelona, SPAIN,* [11]*Hospital de la Santa Creu i Sant Pau, Barcelona, SPAIN,* [12]*Hospital La Fé, Valencia, SPAIN,* [13]*Hospital Universitario de Salamanca, Salamanca, SPAIN,* [14]*Hospital Universitario de Cruces, Vizcaya, SPAIN,* [15]*Hospital Ramón y Cajal, Madrid, SPAIN,* [16]*Hospital Virgen de las Nieves, Granada, SPAIN,* [17]*Hospital Universitario Doctor Peset, Valencia, SPAIN,* [18]*Hospital Universitario Marqués de Valdecilla, Santander, SPAIN,* [19]*Hospital La Paz, Madrid, SPAIN,* [20]*Hospital Universitari Germans Trias i Pujol, Barcelona, SPAIN,* [21]*Clínica Universidad de Navarra, Navarra, SPAIN,* [22]*Complejo Hospitalario Universitario de Vigo, Vigo, SPAIN,* [23]*Hospital Son Espases, Palma de Mallorca, SPAIN,* [24]*EISAI, Madrid, SPAIN.*

Aim/Introduction: Advanced differentiated thyroid carcinoma (aDTC) - herein defined as locally unresectable or metastatic disease - is one of the most common late-stage endocrine neoplasias. However, available data about its natural history is limited.ERUDIT is a multicenter, observational, retrospective study of patients diagnosed with aDTC in Spain and Portugal. The study describes its natural history from the initial diagnosis until the advanced stages of disease, focusing on specific characteristics of this subpopulation of DTC, as well as its treatment, response patterns and medical specialties involved in its management.The aim of this communication is to describe the patterns of use and efficacy of RAI as first intervention (RAI ± surgery) and at its relapse in patients with aDTC diagnosed in Spain and Portugal. ***Materials and Methods:*** Clinical records from patients ≥18 y-o diagnosed with aDTC (including poorly differentiated DTC) with first evidence of advanced disease documented between January 2007 and August 2017 were retrospectively reviewed until death or lost to follow-up. ***Results:*** 213 patients were identified in 23 centres. The median age at initial diagnosis was 63 years and 59% were women. 52% had metastatic disease at debut (de novo). Following surgery, patients received mostly one (34%) or two (28%) ablative RAI doses, with a median (Q1-Q3) of 150 (100-170) mCi per dose and total cumulative activity of 750 (600-800) mCi after 5 doses. Persistent structural disease was the most frequent response, seen on average in 50% of the patients after two doses. The median (95% CI) progression-free and overall survival (OS) after the first RAI were 1.5 (0.7-1.9) and 10.1 (8.2-17.5) years, respectively. After a first intervention, 46% of the patients relapsed to advanced disease and, of these, 33% received RAI with a medium dose (Q1-Q3) of 150 (140-180) mCi. In this context, the accumulated activity was 620 (560-700) mCi after 3 doses with the result of persistent structural disease in 49% of the cases. Although 99% of the patients were RAI-avid at diagnosis, 68% of them became RAI-refractory after 27.6 (9.7-50.6) months. The median (95% CI) of OS in RAI-refractory patients was 4.7 (3.4-8.0) years. ***Conclusion:*** Regardless of the initial type of diagnosis (de novo vs localized), in this DTC series, half of the cases maintained persistent disease after 620 mCi and two thirds became RAI-refractory after 27.6 months ***References:*** None

OP-058

Radioiodine therapy (RAIT) guided by 124I-PET/CT imaging in metastatic differentiated thyroid cancer (DTC): long-term follow-up of patients recruited in a prospective trial

E. Lodi Rizzini[1], C. Pettinato[2], L. Zanoni[1], V. Allegri[1], E. Tabacchi[1], A. Repaci[3], A. G. Morganti[4], S. Fanti[1], F. Monari[4];
[1]Nuclear Medicine Unit, S.Orsola-Malpighi Hospital, Bologna, ITALY, [2]Medical Physics Unit, S.Orsola-Malpighi Hospital, Bologna, ITALY, [3]Endocrinology Unit, S.Orsola-Malpighi Hospital, Bologna, ITALY, [4]Radiation Oncology Center, S.Orsola-Malpighi Hospital, Bologna, ITALY.

Aim/Introduction: Although RAIT was used for over 80 years in the metastatic-DTC management, number, frequency and optimal administrated 131I activity remain matter of debate. 124I-PET/CT can be a useful tool to identify lesions still iodine-avid with higher detection rate than post-treatment I-131 scan(RxWBS) and to perform personalized dosimetry to the lesions, particularly in the case of potentially curative RAIT. The aim of this study is to confirm with long-term follow-up(FU) data the utility of 124I-PET/CT in RAIT planning of metastatic-DTC. ***Materials and Methods:*** We collected long-term FU data of 30 patients(pts) affected by metastatic DTC and recruited in a prospective trial from July 2011 to July 2013, who underwent to a personalized RAIT after performing 124I-PET/CT imaging.Clinical/laboratory data were collected every 6/12months from February 2012 to March 2020. In the case of strong suspect of relapse, contrast-enhanced-TC and/or 18FDG-PET/CT were also performed. Response to therapy was assessed according to ATA2015 guidelines. ***Results:*** Mean FU was 73.5months(range:17-108months). All pts received prior RAIT, with an average administered 131I activity of 9195.5MBq(range:1110-25900MBq). 15/30(50%) pts had negative 124I-PET/CT and RxWBS scans;11/15 pts received 3700MBq while 4/15 pts refused treatment. At last FU, 4/15 pts had indeterminate response(IR), one pt had biochemical persistence(BP), 7/15 pts had structural persistence(SP), one pt died for disease not-related causes and 2/15 were lost at FU. 15/30(50%) pts had positive 124I-PET/CT and RxWBS scans but in 2/15 pts dosimetry was not performed because of the influence of intestinal activity. All those pts received an 131I activity of at least 7400MBq. Overall, dosimetry was performed to 34 lesions.In 5/13(38%) pts lesions received less than the target dose of 80Gy(average dose:14.25Gy;range:1.47-60.50Gy); at last FU 2/5 pts had SP and 3/5 pts died for progression disease. In 2/15(15%) pts the majority of lesions received less than 80Gy and at last FU one pt had SP and one had IR. In 6/13(46%) pts lesions received more than 80Gy(average dose:393Gy;range:163.73-1283.12Gy);at last FU 2/5 pts had SP, 2/5 pts had an excellent response, one pt died for disease not-related causes and one pt was lost at FU. ***Conclusion:*** 124I-PET/CT imaging guided us to choice the optimal 131I administered activity; long-term FU data confirmed that pts who received more than 80 Gy to the lesions have a better response disease than those who received lower activities. ***References:*** Pretherapeutic dosimetry in patients affected by metastatic thyroid cancer using 124I PET/CT sequential scans for 131I treatment planning.Pettinato et al.ClinNuclMed2014;39(8):e367-e374.

OP-059

Variations in Radioiodine Therapy in Europe- Decision Making after total Thyroidectomy

F. Forrer[1], G. Fischer[1], M. Putora[1], L. Giovnella[2], M. Hoffmann[3], I. Iakovou[4], M. Luster[5], J. Mihailovic[6], P. Petranović[7], A. Vrachimis[8], S. Zerdoud[9], O. Maas[1];
[1]Kantonsspital St. Gallen, St. Gallen, SWITZERLAND, [2]Ospedale Regionale di Lugano, Lugano, SWITZERLAND, [3]University Viennna, Vienna, AUSTRIA, [4]Aristotle University AHEPA Academic Hospital, Thessaloniki, GREECE, [5]Universitätsklinikum Marburg, Marburg, GERMANY, [6]Oncology Institute of Vojvodina, Novi Sad, SERBIA, [7]University Hospital Center, Zagreb, CROATIA, [8]German Oncology Center, Limassol, CYPRUS, [9]Institut Universitaire du Cancer Toulouse, Toulouse, FRANCE.

Aim/Introduction: The role of radioiodine therapy (RIT) (used as ablation therapy or adjuvant therapy) following total thyroidectomy for differentiated thyroid cancer (DTC) changed over the last decade. Major revisions of the American Thyroid Association Guidelines in 2015 resulted in significant differences in treatment recommendations in comparison to the European Association of Nuclear Medicine (EANM) 2008 guidelines. Recently, we presented the effects on daily practice for RIT among Swiss Nuclear Medicine centers[1]. We now performed a project at the European level and hypothesized that there is also considerable variability regarding the use of RIT among recognized European experts. ***Materials and Methods:*** We performed a decision-tree based analysis of management strategies from all members of the EANM thyroid committee to map current practice among experts. Within this analysis, we collected data on whether or not RIT is administered, on which criteria these decisions are based, and collected details on treatment activities and patient preparation. ***Results:*** Our survey shows discrepancies for low risk DTC after thyroidectomy, where "follow-up only" is recommended by some experts while RIT with significant doses is used by other experts in the same situation. E.g. for pT1b tumors without evidence of metastases the level of agreement for the use of RIT, depending on histologic features, is as low as 50%. If RIT is administered in this setting, activities of I-131 range from 1.1 GBq to 3.0 GBq. In other constellations (e.g. pT1a) experts diverge from current clinical guidelines as up to 75% administer RIT in certain cases. For intermediate and high-risk patients, RIT is generally recommended. However, dosing and treatment preparation (rTSH vs. THW) vary distinctly. In comparison to the Swiss study, the general level of agreement

is higher among European experts. ***Conclusion:*** Currently, existing variety in the use of RIT after total thyroidectomy by European experts reflects differences in clinical guidelines as well as the lack of high level evidence. The recently proposed approach on the use of RIT, based on integrated post-surgery assessment (Martinique paper)[2] and results of ongoing prospective randomized studies are likely to reduce uncertainty in approaching RIT treatment in DTC patients. In certain constellations, consensus identified among European experts might be helpful in formulating future guidelines. ***References:*** 1. Maas et al. Variations in radioiodine ablation: decision-making after total thyroidectomy. Eur J Nucl Med Mol Imaging.2020;47:554-560. 2. Tuttle et al. Controversies, Consensus, and Collaboration in the Use of I-131 Therapy in differentiated Thyroid Cancer. Thyroid.2019;29:461-470.

OP-060

Prognostic Factors and Disease-Specific Survival of Recurrent Differentiated Thyroid Carcinoma Patients

J. Mihailovic*, V. Cimbaljevic, J. Roganovic, N. Prvulovic Bunovic; Institute of Oncology, Sremska Kamenica, SERBIA.*

Aim/Introduction: Differentiated thyroid carcinoma (DTC) patients with recurrent disease (RD) have worse prognosis than patients without recurrence. However, they usually get cured if RD is detected and treated on time. The aim of this study was to analyze prognostic factors and disease-specific survival (DSS) in recurrent DTC patients. ***Materials and Methods:*** Among 680 DTC patients treated in our institution between 2007 and 2019, 67 patients had recurrent disease (RD): 39 females, 28 males; 23 patients <45 years, 44 patients ≥45 years; median follow-up of 3,3 years; 5 follicular, 56 papillary carcinomas and 6 unfavourable types; T stage 1, 2, 3 and 4 included 16, 5, 37 and 9 patients, respectively. Initial nodal-(N1) and distant metastases (M1) and combined metastases (N1M1) were detected in: 34, 2 and 6 patients, retrospectively. DSS was analyzed by Kaplan-Meier method/Log-rank test. ***Results:*** RD appeared in 67/680 (9.9%) patients. The probability of recurrence was 8.4% at 5 y, 14.2% at 10 y, 32.1% at 15 y, and 49.7% at 19 years after the initial treatment. Strong predictors of RD were: gender, T stage, N stage, M stage, and initial treatment (p=0.0001). No significant difference was associated with the following prognostic factors: age, histologic type of the tumor, and presence of second primary neoplasm (p=0.208, p=0.531, and p=0.993, respectively). The 5-, 10-, 15-, 20- and 26-year DSS was: 0.966±0.24, 0.804±0.064, 0.76±0.074, 0.608±0.148, and 0.228±0.183, respectively. Patients with RD were treated with surgery, followed by radioiodine therapy (several courses if necessary). Additionally, in patients with advanced disease and iodine non-avid DTC, external radiation, chemo-therapy and Lu-177 DOTATATE treatment were performed (in 12, 1, and 2 patients, respectively). At last check up, there were 14 (20.9%) deaths: [12 (17.9%) of disease-related deaths, while 2 (3%) patients have died from other causes], and 53 (79%) patients were alive [complete remission was achieved in 18 (26.9%) patients, partial remission in 11 (16.4%) patients, stable disease in 7 (10.4%) patients while 17 (25.4%) patients had progressive disease]. ***Conclusion:*** Since recurrent disease may appear at any time, life-long monitoring of DTC patients is necessary. Recurrent disease should be treated until remission (surgery followed by RAI, and radiation therapy if necessary). ***References:*** Leboulleux S, Rubino C, Baudin E, et al. Prognostic factors for persistent or recurrent disease of papillary thyroid carcinoma with neck lymph node metastases and/or tumor extension beyond the thyroid capsule at initial diagnosis. J Clin Endocrinol Metab 2005;90:5723-5729.

OP-061

CRISPR/Cas9-mediated knockout of ESRRG gene (Estrogen-related Receptor gamma) restore the radioiodine avidity in poorly differentiated thyroid cancer

Y. Jeon*[1], H. Ji[2], S. Kim[1], J. Lee[1], S. Lee[3]; [1]Laboratory Animal Center, Daegu-Gyeongbuk Medical Innovation Foundation, Daegu, KOREA, REPUBLIC OF, [2]Department of Nuclear Medicine, School of Medicine, Kyungpook National University Hospital, Daegu, KOREA, REPUBLIC OF, [3]Kyungpook National University, Daegu, KOREA, REPUBLIC OF.*

Aim/Introduction: The resistance of radioiodine therapy in poorly differentiated thyroid cancer (PDC) is associated with insufficient function of the sodium iodide symporter (NIS). Recently, we have reported the important role of estrogen-related receptor gamma (ESRRG; also known as ERRγ) as a member of the orphan nuclear receptors on the regulation of NIS function in poorly differentiated thyroid cancer. Herein, we evaluated the effects of silencing of ERRγ on NIS function in poorly differentiated thyroid cancer cells using CRISPR/Cas9 gene editing system. ***Materials and Methods:*** Stable cell lines were generated by transducing CAL62 cells of human poorly differentiated thyroid cancer cells with the lentiviral CRISPR/Cas9 ERRγ or mock gRNA vectors, which was referred to as CAL62/ERRγ KO and CAL62/Mock cells, respectively. Iodine uptake was conducted to evaluate the NIS function in the presence or absence of $KClO_4$, a specific inhibitor of NIS using two cell lines. The mRNA and protein level of crucial gene expression related to iodine metabolism (NIS, TPO, TG, and TSHR) was determined in CAL62/Mock cells and CAL62/ERRγ KO by Q-PCR and western blotting assay. Finally, the cytotoxic effect of I-131 was determined by clonogenic assay. ***Results:*** Radioiodine avidity was increased in CAL62/ERRγ KO cells but not in CAL62/Mock cells. The increased radioiodine uptake of CAL62/ERRγ KO cells was completely inhibited by $KClO_4$. Q-PCR and western blotting assay revealed the up-regulation of NIS, TPO, TG, and TSHR genes in CAL62/ERRγ KO cells but not in CAL62/Mock cells. In vitro clonogenic assay demonstrated drastic reduction in the colony formation of

CAL62/ERRγ KO cells. ***Conclusion:*** These findings suggest that CRISPR/Cas9-mediated ERRγ gene editing may serve as novel therapeutic approach for enhancing the responsiveness of radioiodine therapy by modulating NIS function in poorly differentiated thyroid cancer. ***References:*** None

OP-062

Dosimetric study for refractory metastatic differentiated thyroid with RAS or BRAFV600 mutation treated with MEK +/- BRAF inhibitors followed by radioactive iodine treatment

N. Anizan[1], *G. Lion*[2], *Y. Godbert*[3], *C. Bournaud*[4], *D. Taieb*[5], *S. Bardet*[6], *D. Benisvy*[7], *S. Zerdoud*[8], *I. Borget*[9], *S. Leboulleux*[9];
[1]*Gustave Roussy, Villejuif, FRANCE,* [2]*CHRU de Lille - Hôpital Claude Huriez, Lille, FRANCE,* [3]*CLCC Institut Bergonié, Bordeaux, FRANCE,* [4]*CHU Lyon - Groupement Hospitalier Est, Lyon, FRANCE,* [5]*CHU de Marseille - Hôpital de la Timone, Marseille, FRANCE,* [6]*CLCC François Baclesse, Caen, FRANCE,* [7]*CLCC Antoine Lacassagne, Nice, FRANCE,* [8]*IUCT Oncopole - CLCC Institut Claudius Regaud, Toulouse, FRANCE,* [9]*Gustave Roussy, Villejuif, FRANCE.*

Aim/Introduction: The MERAIODE study is a prospective multicentric study evaluating the efficacy of selective MEK (trametinib) and BRAFV600E (dabrafenib) inhibitors associated with radioactive iodine (RAI) for the treatment of refractory metastatic differentiated thyroid cancer (DTC) with RAS or BRAFV600E mutation. A dosimetric evaluation was planned as an additional index to understand response to treatment. Results of the first available data on dosimetry of the BRAF cohort are presented. ***Materials and Methods:*** Following 5 weeks of trametinib plus dabrafenib, patients were given 5500 MBq of RAI after recombinant human TSH stimulation. Whole-body scans were performed 1, 2, 3 and 4 days after RAI administration and a SPECT/CT acquisition was done on day 4. To quantify I-131 uptake, SPECT/CT images were calibrated using a phantom acquisition with a I-131 source. The present work shows the dosimetric evaluation of patients treated in one center where whole-body retention was measured using NaI counter positioned in the room. Whole-body absorbed dose was estimated using S factor function of patient mass. Time activity curves in lesions and lungs were extracted from images using PLANET® Dose then corrected for deadtime. Absorbed doses were calculated using IDAC_DOSE 2.1. ***Results:*** Dosimetric evaluation was performed for 5 patients with BRAFV600E mutation. None of them disclosed RAI uptake on a diagnostic whole-body scan performed prior to treatment initiation and all did after MEK and BRAF inhibitors. Absorbed doses were calculated for 18 metastases with a median diameter of 10 mm (range: 4-24). Median whole-body absorbed dose was 322 mGy (range: 172-571 mGy). Median absorbed dose to the lungs was 10.8 Gy (range: 0.62-19.1 Gy) with 3 patients with an absorbed dose greater than 10 Gy. Mono-exponential fit was used for lesions and the median effective half-life of RAI was 53 hours (range: 21-81 h) with a median calculated absorbed dose of 211 Gy (range: 17-2764 Gy). ***Conclusion:*** Dosimetric evaluation is under investigation for all patients included in the study. First patients treated in one center show encouraging results regarding RAI uptake with some patients showing high absorbed dose in the lesions. RECIST evaluation is ongoing and correlation between tumor response and absorbed dose calculation remains to be evaluated. In the light of the high lungs absorbed dose, toxicity to the lungs should be evaluated. Funded by InCA, ClinicalTrials.gov number, NCT NCT03244956 ***References:*** None

OP-063

Value of interim F-18 FDG PET/CT imaging in patients with metastatic radioiodine-refractory thyroid carcinoma undergoing tyrosine-kinase inhibition therapy

G. Rendl[1], *B. Sipos*[1], *L. Hehenwarter*[1], *G. Schweighofer-Zwink*[1], *H. Gallowitsch*[2], *C. Pirich*[1];
[1]*Department of Nuclear Medicine and Endocrinology, University Hospital Salzburg, Paracelsus Medical University Salzburg, Salzburg, AUSTRIA,* [2]*Department of Nuclear Medicine and Endocrinology, PET/CT Centre, Klinikum Klagenfurt am Wörthersee, Klagenfurt, AUSTRIA.*

Aim/Introduction: This retrospective study aimed to analyse the predictive value of interim F-18 fluorodesoxyglucose (FDG) PET/CT in patients with radioiodine (RAI)-refractory thyroid carcinoma (TC) and treated with the tyrosine-kinase inhibitor therapy lenvatinib. ***Materials and Methods:*** Metabolic data from F-18 FDG PET/CT imaging were obtained from 21 patients with metastatic RAI-refactory TC (11 males, 10 females) with a median age of 67 years (range 39 - 80 years). The interval between PET/CT and start of lenvatinib therapy was 16 ± 30 days and the first interim PET/CT was performed 4 ± 1 months later. Compartmental analysis (locoregional uptake, lymph node, visceral and bone metastasis) was performed using an index lesion in the respective lesion. PERCIST was used to categorize the metabolic response in patients. ***Results:*** Mean survival was 29 months (4 - 56 months) in all patients. Five out of 21 patients died (24 %) and 4 patients discontinued lenvatinib (19 %). Overall, mean locoregional SUV was 12.23 ± 11.42 versus (vs) 11.36 ± 13.94, in lymph nodes 12.64 ± 11.90 vs 14.18 ± 15.72, in visceral metastases 10.98 ± 13.76 vs 5.87 ± 7.35 and 8.23 ± 4.51 vs 9.38 ± 7.58 in bone metastases in PET/CT at beginning and interim, respectively. Patients with complete metabolic response (CMR, n=2, 10 %) showed a mean survival of 45 months (36 - 53 months), patients with partial metabolic response (PMR, n=11, 52 %) of 28 months (4 - 53 months) and patients with progressive metabolic disease (PMD, n=8, 38 %) 26 months (7 - 56 months), respectively. ***Conclusion:*** In our patient cohort, complete metabolic response as defined by interim PET was rare but associated with a trend towards longer disease control with lenvatinib. However, the absence

of metabolic response at first interim PET indicated no worse prognosis when compared to patients with PMR, possibly due to timely treatment changes. ***References:*** None

OP-064

Prediction of treatment response to Lenvatinib with 18F-FDG-PET/CT in patients with advanced thyroid cancer

F. Ahmaddy, L. Beyer, V. Wenter, P. Bartenstein, A. Todica; LMU, München, GERMANY.

Aim/Introduction: In patients with advanced thyroid cancer, Lenvatinib is a promising treatment option for prolonged progression free survival (PFS). We aimed to assess the role of 18F-FDG-PET/CT in monitoring treatment response and predict prognosis using quantitative PET-parameters. ***Materials and Methods:*** Patients with advanced thyroid carcinoma who underwent baseline FDG-PET/CT shortly before and 3, 6, 9, 12 months after initiation of the treatment were included. PET-parameters (SUVpeak, TV=tumor volume, TLG=total lesion glycolysis) as well as clinical parameters (age, sex, tumour stage) were assessed. Treatment response was evaluated according to PET Response Criteria in Solid Tumors (PERCIST) as well as Response Evaluation Criteria in Solid Tumors 1.1 (RECIST) and correlated with clinical outcome (disease-specific survival (DSS) and PFS) and PET-parameters using Kaplan-Meier-Survival analysis. ***Results:*** 21 patients met the inclusion criteria. Within a median follow up time of 2.5±1.0 years, 11 patients died (DSS 2.5±0.2 years). DSS could be predicted using treatment response by RECIST (p=0.001) and PERCIST (p=0.026) in PET/CT after 12 months; PFS only by RECIST (p=0.027) after 9 months. Evaluating single PET-parameters, DSS and PFS could be predicted even earlier at 6 months after treatment start (DSS: pSUVpeak=0.007, pTV=0.001, pTLG=0.004; PFS: pSUVpeak=0.009, pTV=0.012, pTLG=0.012). ***Conclusion:*** Response evaluation with 18F-FDG-PET/CT prior and after initiation of Lenvatinib treatment can predict the DSS and PFS in patients with advanced thyroid cancer. PET-parameters can be used for early (6 months) prediction of DSS and PFS. ***References:*** None

OP-065

^{18}F-FDG PET/CT whole body volumetric evaluation in iodine-refractory differentiated thyroid cancer as predictors of Lenvatinib response

E. Califaretti[1], *P. Thuillier*[1,2], *V. Liberini*[1], *A. Ragni*[3], *A. Nervo*[3], *M. Gallo*[3], *A. Piovesan*[3], *E. Arvat*[3], *S. Grimaldi*[1], *D. Deandreis*[1]; [1]*Division of Nuclear Medicine, Department of Medical Sciences, University of Turin, Turin, ITALY,* [2]*Department of Endocrinology, University Hospital of Brest, Brest, FRANCE,* [3]*Oncological Endocrinology Unit, Department of Medical Sciences, University of Turin, Turin, ITALY.*

Aim/Introduction: Tyrosine kinase inhibitors (TKI) improve progression free survival in patients with metastatic iodine-refractory differentiated thyroid cancer (RDTC) but considering TKI frequent side effects and high costs, a careful selection of patients is necessary. Currently, there is no consensus on the selection of patients and the role of ^{18}F-FDG PET/CT. The main objective of this retrospective study was to evaluate pre-therapy ^{18}F-FDG-PET/CT quantitative volumetric and metabolic parameters in order to identify prognostic indices of clinical benefit. ***Materials and Methods:*** Ten patients with metastatic RDTC treated with Lenvatinib and with a pre-treatment ^{18}F-FDG PET/CT were retrospectively analyzed. Lesions contouring was performed by one operator with an isocountouring method with a SUVmax fixed threshold of 41% using LifeX v5.1. For each lesion, semi-quantitative parameters were evaluated: standard uptake value (SUVmax), metabolic tumor volume (MTV) and total lesion glycolysis (TLG). Moreover, whole-body and total-bone MTV (MTVwb and MTVbone) and TLG (TLGwb and TLGbone) were assessed. Bone-to-total MTV and bone-to-total TLG ratios (%MTVb/wb and %TLGb/wb respectively) were calculated. Therapy response was assessed according to RECIST 1.1 criteria on CT scan. Patients were divided in two groups according to the best RECIST 1.1 response: complete/partial response (group A) and stable disease/progression (group B). PET parameters were compared between the 2 groups with Mann-Whitney test. Results are expressed as median [range]. ***Results:*** Ten patients (F:M=5:5; median age=68y) with metastatic RDTC (3 follicular, 4 papillary and 3 poorly differentiated) were included; 8/10 patients had bone metastases. Contouring was performed on 121 lesions: 46 bone (38%), 36 lung (30%), 20 lymph nodes (16%), 7 thyroid bed (6%) and 12 other sites (10%). Group A included 3 patients with partial response, group B included 5 patients with stable disease and 2 with progressive disease. In group B, 65.4% [20-83] of analyzed lesions were bone metastases compared to 0% [0-6] in group A. Group B showed higher median values of %MTVb/wb (49% [18-89] vs 0% [0-7]) and %TLGb/wb (53% [17-92] vs 0% [0-9]) compared to group A (p=0.016). A similar trend was observed for MTVbone and TLGbone, but the difference did not reach statistical significance. All other PET parameters (SUVmax, MTVwb and TLGwb) were not significantly different between the two groups. ***Conclusion:*** In RDTC patients treated by Lenvatinib, ^{18}F-FDG PET/CT performed before starting treatment might be an important tool to predict response to treatment. Bone tumor burden might be one of the main predictive factors in these patients. ***References:*** None

110

Featured Session: Advances in PET-MPI / CT

Thursday, October 22, 2020, 13:30 - 15:00 Channel 10

OP-066

Quantification of MBF with PET - How Can Technology Improve Accuracy?

M. Lubberink; Uppsala University Hospital, PET Center, Uppsala, SWEDEN.

OP-067

Patient motion influence on the quantitative accuracyof cardiac ^{15}O-water PET

J. Nordström[1], H. J. Harms[2], T. Kero[1], J. Sörensen[1], M. Lubberink[1]; [1]PET Center Uppsala Akademiska sjukhuset, Uppsala, SWEDEN, [2]Medtrace Pharma A/S, Lyngby, DENMARK.

Aim/Introduction: Cardiac PET is increasingly being used in the clinical assessment of coronary artery disease (CAD). ^{15}O-water PET is considered gold standard for non-invasive quantification of myocardial blood flow (MBF), which has been shown to improve detection of CAD over qualitative assessments. Cardiac PET is, though, prone to motion artefacts arising from the cardiac and respiratory cycle, or from patient motion. Therefore, the purpose of the present study was to investigate to what extent motion influences quantitative MBF from ^{15}O-water PET/CT. ***Materials and Methods:*** Clinical stress scans from 10 patients referred for assessment of ischemia with ^{15}O-water PET/CT were included. Motion in the original scan was ruled out by visual assessment. A total of 17 different types of motion were simulated, divided into 3 different types of patient body motion and cardiac creep. The 3 body motions simulated 1) a stress agent reaction, 2) a caudal linear slide and 3) a cough at first pass and after 1 min. Maximum displacement for all motions relative to the original scan position ranged between 5-20 mm. All simulated motions and the original scan were quantitatively analyzed in aQuant (MedTrace Pharma A/S, Lyngby, Denmark). MBF and transmural MBF (MBFt) were study for all three coronary territories. ***Results:*** MBF and MBFt was generally shown to be decreased in the region of myocardium in which direction the motion occurred (e.g. in inferior wall for motion in inferior direction). PTF trended in the opposite direction. However, even if a clear pattern for each simulated motion type could be seen, the effect of motion is not completely predictable even when the exact same motions were simulated for each patient. A high inter-patient variance was seen in the deviation of the simulated motions from the original scan for all parameters, probably explained by different patient anatomy. On the global level MBF was significantly affected in 8 motions with average deviation 6.3% ± 5.6% and non-significantly affected in 9 motions with average deviation 2.8% ± 4.0%. MBFt was significantly affected in 4 motions with average deviation 8.0% ± 5.5% and non-significantly affected in 13 motions with average deviation 1.8% ± 5.0%. ***Conclusion:*** Patient motion can impair the quantitative accuracy of ^{15}O-water cardiac PET and may induce false positive or false negative results in the most severe cases. Understanding how motion affects the quantification and knowledge on how to detect motion artifacts is important in the clinical evaluation. ***References:*** None

OP-068

Clinical use of a Rb-82 simplified myocardial flow reserve model using myocardial activity ratio: Comparison to full-kinetics myocardial flow reserve quantitation

C. Kamani, M. Jreige, M. Pappon, P. Genoud, G. Allenbach, J. Prior; University Hospital Lausanne, Lausanne, SWITZERLAND.

Aim/Introduction: Myocardial flow reserve (MFR) measurement is a well-validated independent predictor of major adverse cardiovascular events and can be used to guide myocardial revascularization. Due to non-linear radiotracer extraction, its estimation requires kinetic modeling with specialized software packages.We aimed to investigate the correlation between a simplified model using only the stress/rest myocardial activity ratio (MAR) and the MFR corrected for partial volume effect (MFR_rc) in patients undergoing rest/stress perfusion study using Rubidium-82 chloride (Rb-82) PET/CT. ***Materials and Methods:*** In total, 439 patients referred to our institution underwent rest and pharmaceutical (adenosine or regadenoson) stress dynamic PET imaging. Stress/rest myocardial activity ratio (MAR) was obtained using the left ventricular (LV) mean count activity from the 2-6-minutes post-injection images. Simplified estimates of MFR (MFR_est) was obtained from MAR, and compared with the gold standard reference MFR_rc, obtained from a one-tissue compartment model. The correlation between MFR_est and MFR_rc has been further assessed. Using the Receiver Operator characteristic (ROC) analysis, the accuracy of the MFR_est was assessed for diagnosing impaired MFR<2. ***Results:*** There was significant correlation between MFR_est and MFR_rc (R= 0.57, p<0.001). The overall diagnostic performance of MFR_est to identify an impaired MFR_rc<2 was good, with AUC=0.76. There were fair sensitivity (75%) and specificity (78%), with a good negative predictive value (87%). However, the corresponding positive predictive value was poor (60%). ***Conclusion:*** Using a simplified method based on the MAR following a stress/rest Rb-82 perfusion PET, an impaired MFR_rc<2 can be estimated with a good sensibility and specificity, as well as a good negative predictive value without the need for kinetic flow modeling. ***References:*** None

OP-069

^{13}N-ammonia Regadenoson Stress PET/CT MPI: The Impact Of Persistent Caffeine Blood Levels On Myocardial Blood Flow Metrics Utilizing A Low-Dose Rest/High-Dose Stress Protocol

U. Mahmood, W. Yap, J. Donald, A. Diliberto, B. Press, M. Feldkamp, T. Rosamond;
The University of Kansas Health System, Kansas City, KS, UNITED STATES OF AMERICA.

Aim/Introduction: The quantification of myocardial blood flow (MBF) and myocardial flow reserve (MFR) utilizing ^{13}N-ammonia regadenoson low dose rest/high dose stress MPI provides additional diagnostic value for detection of CAD. Patients are typically instructed to avoid caffeinated beverages for at least 12 hours prior to the study. The impact of persistently measurable caffeine in the blood on MBF and MFR quantification with ^{13}N-ammonia, despite this period of supervised abstinence, remains uncertain. ***Materials and Methods:*** 76 consecutive inpatient subjects who were admitted with chest pain (64% female, age 66 ± 11 years, BMI 30.2 ± 8) underwent a low-dose rest/ high-dose regadenoson stress MPI protocol with a fully digital PET/CT hybrid scanner having had their blood caffeine level checked immediately prior to the study. Per standardized MPI protocol, all had been placed on a caffeine free diet for at least 12 hours prior to the exam in a supervised inpatient setting. MBF and MFR were calculated using proprietary software and adjusted to the resting heart rate x systolic blood pressure product and motion correction methodology. Intention to treat methodology was utilized for analysis. The study readers were blinded to caffeine levels and were interpreted by consensus between two qualified physicians from both Cardiology and Radiology. ***Results:*** Eight (6 female) of 76 inpatients (10.5%) had significant blood levels of caffeine in samples drawn just before the PET/CT exam (mean caffeine blood level=2.6± 2.1 µg/mL, range: 1-7 µg/mL). In the caffeinated group, the average age was 70 ± 9 years (range: 55-84 years), mean global MFR= 3.0 ± 0.7, mean resting global MBF = 0.86 ± 0.1 ml/min/gram and stress global MBF was 2.95± 0.86 ml/min/gram. Four of the eight patient studies with residual blood caffeine were read as ischemic by standard MPI qualitative and quantitative imaging criteria. ***Conclusion:*** A significant percentage of inpatients that are supervised regarding caffeine abstinence for at least 12 hours prior to a MPI exam still have detectable blood caffeine levels. At these levels, however, global MBF metrics are not meaningfully impeded when using ^{13} N-ammonia low-dose rest/high-dose regadenoson stress protocols. More vigorous dietary control is needed to prevent unrecognized persistent caffeine blood levels due to surreptitious or accidental intake by inpatients. It is likely that this phenomenon is more prevalent in the unsupervised outpatient population. ***References:*** None

OP-070

Effect of PET CT misalignment on the quantitative accuracy of cardiac ^{15}O-water PET

J. Nordström[1], H. J. Harms[2], T. Kero[1], M. Ebrahimi[1], J. Sörensen[1], M. Lubberink[1];
[1]PET Center Uppsala Academic Hospital, Uppsala, SWEDEN, [2]Medtrace, Lynby, DENMARK.

Aim/Introduction: Cardiac PET is increasingly being used in the clinical evaluation of coronary artery disease and ^{15}O-water PET is considered gold standard for non-invasive quantification of myocardial blood flow (MBF). For all PET tracers except ^{15}O-water, MBF is determined based on the uptake rate of the tracer. For accurate estimation of tracer uptake, accurate attenuation correction and consequently correct alignment between PET and the attenuation CT is critical. Misalignment is a common problem and may induce artifacts in uptake rates. With ^{15}O-water, MBF is determined based on washout rather than uptake rate. Since attenuation correction mainly affects the amplitude of tissue time-activity curves, but not its shape, we hypothesize that misalignment has minimal effect on washout-based MBF estimates of ^{15}O-water. This study aims to investigate the impact of misalignment on the quantitative accuracy of cardiac ^{15}O-water PET. ***Materials and Methods:*** Clinical adenosine-induced stress scans from 10 randomly selected patients referred for evaluation of ischemia were included in the study. Misalignment between PET and CT was ruled out by visual assessments. Eleven different misalignments were induced in six different directions with 10 and 20 mm amplitudes: caudal (-Z), cranial (+Z), lateral (±X), anterior (+Y), and anterior combined with cranial (+Y+Z). All scans were analyzed in aQuant software (MedTrace Pharma A/S, Lyngby, Denmark) for calculation of MBF, uptake-based MBF (MBFt) and perfusable tissue fraction (PTF), and the results were compared with the original, non-misaligned data. ***Results:*** On the global level, washout-based MBF was not significantly different for misalignments +X, +Y, +Y+Z, and -Z with average deviation of 0.9% ± 1.7% and significantly different for -X and +Z with average deviation of 2.0% ± 1.7%. Uptake-based MBFt, however, was significantly affected by all misalignment directions with average deviation of 7.4% ± 3.0% and not significantly affected in 20 mm +X and 10 mm +Z with average deviation 6.5% ± 4.2%. Larger effects were seen in LAD- and LCX-regions compared with the RCA-region. ***Conclusion:*** Misalignment between PET and CT has only margin effects in the quantitative accuracy of ^{15}O-water PET using washout-based MBF estimates. Uptake rate (MBFt) on the other hand was more affected by misalignment. Overall, however, additional co-registration between PET and CT images is not necessary. ***References:*** None

OP-071

Identification of predictors for myocardial blood flow using Rubidium-82 PET

R. Metselaar[1,2], J. A. van Dalen[3], B. N. Vendel[1], J. R. Timmer[4], M. Mouden[4], J. D. van Dijk[1];
[1]Isala Hospital, department of Nuclear Medicine, Zwolle, NETHERLANDS, [2]University of Twente, Enschede, NETHERLANDS, [3]Isala Hospital, department of Medical Physics, Zwolle, NETHERLANDS, [4]Isala Hospital, department of Cardiology, Zwolle, NETHERLANDS.

Aim/Introduction: Myocardial blood flow (MBF) measurements using Rubidium-82 PET provides incremental diagnostic and prognostic information in the evaluation of coronary artery disease (CAD). In particular, high myocardial flow reserve (MFR) values have a high negative predictive value for obstructive CAD. Understanding which features are characteristic for normal MBF and MFR values can aid in the risk stratification of patients with suspected obstructive CAD. The aim of this study was to identify these features for developing a clinical decision tool. ***Materials and Methods:*** We retrospectively included 997 patients with suspected CAD (50,7% Male, age 65,99 ± 10.43 years), who were referred for rest and regadenoson-induced stress Rubidium-82 PET/CT (Discovery 690, GE Healthcare). Cardiac risk factors; cigarette smoking, hypertension, hypercholesterolemia, diabetes, positive family history of CAD; prior medical history; age; gender; body mass index (BMI); creatinine serum values; coronary artery calcification (CAC) score and medication usage were registered at time of the PET/CT examination. All variables except CAC score, age, resting heart rate and BMI were transformed to categorical variables. Multiple linear regression with forward stepwise selection (F-to-enter < 0.050) was calculated to correlate variables with rest and stress MBF and MFR. The importance of significant predictors was determined by ranking using the incremental increase in adjusted R^2. ***Results:*** Significant predictors for high rest MBF were, in order of importance, high heart rate, female sex, calcium-channel blocker usage, low BMI, calcium-channel blocker usage, hypertension, no acenocoumerol usage and older age. The adjusted R^2 was 0.34. Furthermore, the significant predictors for high stress MBF were, in order of importance, female sex, high heart rate, low CAC score, low BMI, younger age, clopidogrel usage, no beta blocker usage, COPD. (Adjusted R^2: 0.23). The predictors for high MFR were younger age, low heart rate, low CAC score, no calcium-channel blocker usage, no underlying diabetes mellitus, positive family history of CAD normal creatinine serum levels and male. (Adjusted R^2: 0.19). ***Conclusion:*** We identified several features that correlate with MBF and MFR measurements using Rubidium-82 PET. These features can be used in a clinical decision tool for risk stratification of patients with CAD. Further studies are needed to determine the prognostic value of the identified features in combination with MBF and MFR. ***References:*** None

OP-072

Myocardial flow reserve could predict major adverse cardio and cerebrovascular event in the dialysis dependent end stage renal disease patients even without myocardial perfusion abnormality

S. Ohshima;
Nagoya Kyoritsu Hospital, Nagoya, JAPAN.

Aim/Introduction: Advanced atherosclerosis in dialysis dependent end stage renal disease (dd-ESRD) patient is critical issue to be solved. In prior studies, we reported a clinical usefulness of myocardial flow reserve (MFR) evaluated with ^{13}N-ammonia positron emission tomography ($^{13}NH_3$-PET) in prediction of poor prognosis in dd-ESRD population. However, no data were shown about the significance of MFR in the patients without myocardial perfusion abnormality. In this study, we investigated the relations between MFR and clinical events in the dd-ESRD patients without myocardial perfusion abnormality. ***Materials and Methods:*** We investigated 182 patients without myocardial perfusion abnormality (SSS≤3), of consecutive 438 dd-ESRD patients for suspected ischemic heart disease. The patients undergone any revascularization within 60 days after $^{13}NH_3$-PET were excluded. Patients were divided into two groups according to MFR=2.0: MFR<2.0 as the lower MFR(LM) group (n=56), and others as the higher MFR(HM) group(n=126). We followed up 1,509 days(median=900) and analyzed for major adverse cardio cerebrovascular event (MACCE), all-cause death and cardiovascular (CV) death. ***Results:*** There were significant differences in age, myocardial blood flow and MFR. There were no differences in SSS, SRS and SDS. Kaplan-Meyer analysis showed that LM group had significantly poorer prognosis than HM group (log rank p= 0.03) in MACCE. On the other hand, there were no difference in all-cause mortality (log rank p= 0.22) and CV death (log rank p= 0.30). Cox regression model showed relative risk ratio 2.29 (95% confidential interval 1.05 -4.99, p=0.04). Furthermore, multivariate cox regression model showed the continuous value of MFR was an independent risk factor for MACCE (risk ratio 0.56, 95% CI 0.31-0.98, p=0.04), considering risk factors that showed univariate assessment p value under 0.10. ***Conclusion:*** In the patients without myocardial perfusion abnormality, MFR would have predictability for MACCE in dd-ESRD population. ***References:*** None

OP-073

Coronary microvascular dysfunction as early marker of cardiac involvement in patients with Anderson-Fabry Disease

T. Mannarino[1], R. Assante[1], C. Nappi[1], V. Gaudieri[1], A. Ponsiglione[1], E. Zampella[1], A. D'Antonio[1], A. Giordano[1], P. Buongiorno[1], A. Pisani[2], M. Imbriaco[1], W. Acampa[1], A. Cuocolo[1];
[1]Department of Advanced Biomedical Sciences, University Federico II, Naples, ITALY, [2]Department of Public Health, University Federico II, Naples, ITALY.

Aim/Introduction: Cardiac involvement in Anderson-Fabry disease (AFD) is characterized by left ventricular hypertrophy, cardiomyopathy and heart failure. ^{18}F-fluorodeoxyglucose (FDG) metabolic activity by positron emission tomography (PET)/computed tomography (CT) and late gadolinium enhancement (LGE) by magnetic resonance imaging (MRI) are able to identify different patterns of cardiac involvement in AFD. ^{82}Rb PET/CT allows non-invasive measurement of stress myocardial perfusion and myocardial perfusion reserve (MPR). We investigated the relationship among metabolic activity, coronary microvascular function and LGE to define the progression of the pathophysiological patterns in AFD. ***Materials and Methods:*** We studied 31 asymptomatic AFD patients (14 men, mean age 49±11 years) without overt coronary artery disease. Eight patients were receiving enzyme replacement therapy (ERT) at the time of the study. All patients underwent cardiac imaging by ^{18}F-FDG and rest/stress ^{82}Rb PET/CT. Sixteen (52%) patients also underwent cardiac MRI. A focal increase of FDG uptake was considered as positive finding for presence of active inflammation. Myocardial perfusion was considered normal in presence of a summed stress score <3. Absolute myocardial blood flow (MBF) was computed from dynamic rest and stress imaging. MPR was defined as ratio of hyperemic to baseline MBF and considered reduced when <2. Focal LGE on MRI indicated intramyocardial fibrosis. ***Results:*** Myocardial perfusion imaging was normal in all 31 patients, while 11 (35%) patients had a reduced MPR. A significant relationship between reduced MPR and focal FDG uptake was found (chi-square=9.85, p<0.01). Among 14 patients with focal FDG uptake 10 (71%) had reduced MPR and 4 (29%) preserved MPR. In 17 patients with homogenous FDG uptake, only 1 patient (6%) had reduced MPR. Reduced MPR was not significantly related to ERT (chi square=0.08, p=0.7). Among the 16 patients undergoing MRI, 5 (31%) had left ventricular hypertrophy associated with focal FDG uptake and focal LGE in corresponding regions. Among these 5 patients, 3 had preserved MPR and 2 reduced MPR. Among 11 (69%) patients without LGE, 2 showed both focal FDG uptake and reduced MPR while 9 patients had homogeneous uptake of FDG, and 8 (82%) of them had preserved MPR. ***Conclusion:*** In patients with AFD, reduction of MPR may represent not only an evidence of coronary microvascular dysfunction, but also a very early sign of cardiac involvement anticipating active inflammation and more severe fibrosis. Evidence of different pathophysiological patterns in AFD would help in customization of therapeutic strategy to prevent progression of cardiac involvement. ***References:*** None

OP-074

Prognostic value of peri-coronary adipose tissue and coronary vascular function by cardiac^{82}Rb PET/CT imaging in patients with suspected coronary artery disease and normal perfusion imaging

V. Gaudieri[1], *E. Zampella*[1], *C. Nappi*[1], *R. Assante*[1], *T. Mannarino*[1], *A. D'Antonio*[1], *A. Giordano*[1], *P. Buongiorno*[1], *M. Petretta*[2], *P. Arumugam*[3], *W. Acampa*[1], *A. Cuocolo*[1];
[1]*Department of Advanced Biomedical Sciences, University Federico II, Naples, ITALY,* [2]*Department of Translational Medical Sciences, University Federico II, Naples, ITALY,* [3]*Department of Nuclear Medicine, Central Manchester University Hospitals, Manchester, UNITED KINGDOM.*

Aim/Introduction: Peri-coronary fat thickness (PCFT), by releasing inflammatory mediators, demonstrated a local pro-atherosclerotic effect. We evaluated the prognostic value of PCFT, coronary artery calcium (CAC), and myocardial perfusion reserve (MPR), in patients with suspected coronary artery disease (CAD) and normal myocardial perfusion imaging (MPI). ***Materials and Methods:*** A total of 640 patients without overt CAD and with normal ^{82}Rb PET/CT MPI were studied. PCFT was calculated on CT images as the maximum fat thickness (mm) between heart surface and visceral epicardium surrounding the main coronary arteries. CAC score was categorized as <400 or ≥400. MPR was considered reduced when <2. Endpoints were cardiac death, nonfatal myocardial infarction and coronary revascularization. ***Results:*** During a follow-up of 42±13 months, 29 events occurred (cumulative event rate 5%). Patients with events were older (66±13 vs. 60±13 years, p<0.01), had higher PCFT (13±2 vs 11±2 mm, p<0.001), higher prevalence of CAC score ≥400 (48% vs. 21%, p<0.01), and lower MPR (2.1±0.7 vs. 2.7±0.7, p<0.001) compared to those without. A higher prevalence of MPR <2 was observed in patients with events (48% vs. 18%, p<0.001) compared to those without. Patients with reduced MPR had higher PCFT compared to those with normal MPR (12±2 vs. 11±1 mm, p<0.01). A PCFT value of 11.2 mm was the best trade-off between sensitivity and specificity to detect reduced MPR. Event rate was higher in patients above this threshold compared to those below (8% vs. 1.5%, p<0.001). At Cox univariate analysis, age (p<0.05), PCFT >11.2 mm (p<0.001), CAC score ≥400 (p<0.01), and MPR <2 (p<0.001) were predictors of events. At multivariate analysis, only PCFT >11.2 mm and MPR <2 were independent predictors of events (both p<0.01). At incremental analysis, adding PCFT >11.2 to a model including clinical data and MPR <2 increased the global chi-square from 26 to 35 (p<0.01). Classification tree analysis produced 3 terminal groups. For patients with MPR <2, no further split was needed (event rate 12% vs. 3%, p<0.001). On the contrary, patients with MPR ≥2 were further stratified by PCFT (event rate 7% in patients with and 0.3% in those without (p<0.001) PCFT >11.2. ***Conclusion:*** In patients with suspected CAD and normal stress MPI, coronary

vascular dysfunction and high PCFT are associated with increased cardiac risk. PCFT could help in identifying patients at higher risk of events. Combined evaluation of anatomical and functional vascular abnormalities by ^{82}Rb PET/CT might allow a better risk stratification. ***References:*** None

OP-075

Does a Clinical Risk Score Improve the Negative Diagnostic Utility of a Zero Calcium Score?

C. Nappi[1], R. Megna[2], V. Gaudieri[1,2], T. Mannarino[1], R. Assante[1], E. Zampella[1], R. Green[1], V. Cantoni[1], A. D'Antonio[1], P. Arumugam[3], W. Acampa[1], M. Petretta[4], A. Cuocolo[1];
[1]Department of Advanced Biomedical Sciences, University Federico II, Naples, ITALY, [2]Institute of Biostructure and Bioimaging, National Council of Research, Naples, ITALY, [3]Department of Nuclear Medicine, Central Manchester Foundation Trust, Manchester, UNITED KINGDOM, [4]Department of Translational Medical Sciences, University Federico II, Naples, ITALY.

Aim/Introduction: Coronary artery calcium (CAC) score is a useful diagnostic and prognostic marker of coronary artery disease (CAD). The probability of obstructive CAD based on clinical variables and CAC score was first determined by Genders et et al.[1]. More recently, Alshahrani et et al.[2] proposed and validated a scoring system including clinical variables in patients with zero CAC score (ZCS) to drive the obstructive CAD ruling out. We evaluated if these risk scores may be also useful to predict a normal stress myocardial perfusion imaging (MPI) study in patients with ZCS. ***Materials and Methods:*** Our cohort included a total of 1,422 consecutive patients with ZCS who underwent rest-stress ^{82}Rb PET/CT for evaluation of suspected CAD. Predictive models were constructed as reported by Genders et al.[1] and Alshahrani et al.[2] and the probability of abnormal (>3) summed stress score (SSS) and of reduced (<2) myocardial perfusion reserve (MPR) based on these risk scores was assessed. ***Results:*** In the overall population, the prevalence of abnormal SSS was 0.10 and the prevalence of reduced MPR was 0.17 (both P<0.001). The observed frequencies of abnormal SSS and reduced MPR versus the probabilities predicted by the Genders and Alshahrani models were above the diagonal identity line, highlighting an underestimation of the observed occurrence by these models. The areas under the receiving operating characteristic curve of the Genders and Alshahrani models were fail, indicating lack of discriminative ability for predicting abnormal SSS (0.547 and 0.527) and reduced MPR (0.509 and 0.538). The Hosmer-Lemeshow test indicated that both models underestimated the observed occurrence of abnormal SSS and reduced MPR. ***Conclusion:*** Available models were unable to identify among patients with ZCS those with a low probability of a normal stress MPI study. Even using a low probability threshold, many positive MPI tests would have been missed. Thus, an optimal approach to rule out from MPI patients without detectable coronary calcium still needs to be improved. ***References:*** 1. Genders TS, Steyerberg EW, Hunink MG, Nieman K, Galema TW, Mollet NR, et al. Prediction model to estimate presence of coronary artery disease: retrospective pooled analysis of existing cohorts. BMJ. 2012;344:e3485. 2. Alshahrani AM, Mahmood H, Wells GA, Hossain A, Rybicki FJ, Achenbach S, et al. Point of care clinical risk score to improve the negative diagnostic utility of an Agatston score of zero: averting the need for coronary computed tomography angiography. Circ Cardiovasc Imaging. 2019;12:e008737.

OP-076

Ultra-low-dose coronary artery calcium scoring yields equivalent results compared to standard protocol: a study on 919 consecutive patients

F. Caobelli[1], I. Allio[1], C. E. Popescu[2], M. Zellweger[1];
[1]Universitätsspital Basel, Basel, SWITZERLAND, [2]Kantonsspital Baden, Baden, SWITZERLAND.

Aim/Introduction: Recent studies featuring small patients' populations suggest that the assessment of coronary artery calcium (CAC) scoring with computed tomography (CT) with 80 kilovolt-peak (kVp) tube voltage yields comparable results to the standard 120-kVp protocol. However, these preliminary findings still need to be validated in larger patients' populations. ***Materials and Methods:*** We included consecutive patients undergoing myocardial perfusion scintigraphy as part of clinical care. All underwent standard CT scanning with 120-kVp tube voltage and an additional scan with 80 kVp, which was also used for attenuation correction purpose. All patients had suspected but no prior coronary artery disease. Mean body mass index (BMI) was 28.3±6.1kg/m^2. CAC score was calculated on both CT images using the Agatston score, thus generating two datasets (low-dose and standard protocol), which were compared with linear regression and Bland-Altman analysis. Furthermore, risk-class (0-25, 25-50, 50-75, 75-90 and >90 percentiles according to data of the literature [1]) were recorded. ***Results:*** 919 patients were included (443 females, age 67.3±11.5). Estimated mean radiation doses were 0.6 mSv for standard CT and 0.2 mSv for the ultra low-dose CT, respectively. Median CAC score from 120 kVp scans was 104 (inter-quartile range 5-551). 179 (19.5%) patients had CAC score=0. Median CAC score from 80 kVp scans was 39 (inter-quartile range 0-330). 273 (29.7%) patients had CAC score=0. Scores calculated with 80 kVp scans showed a very good correlation with those calculated with standard 120 kVp scans ($r = 0.947$, $r^2 = 0.867$, $p<0.001$), with Bland-Altman limits of agreement of -495.9 to 739.4 and a bias of -121.7 The correlation across percentiles classes was also good ($r = 0.857$, $r^2 = 0.74$, $p<0.001$). ***Conclusion:*** In a large consecutive patient population, CAC scores calculated with ultra low-dose CT scan and those assessed with standard protocol correlated well regarding numeric CAC scores and CAC score classes. Thus, a substantial further radiation dose reduction (about 0.6 mSv) can be pursued by omitting

a standard scan for CAC assessment, while preserving diagnostic and prognostic accuracy. ***References:*** [1] Hoff JA et al. Am J Cardiol. 2001;87:1335-9

111

e-Poster Presentation Session 1: PET Diagnostics - Part 1

Thursday, October 22, 2020, 13:30 - 15:00 Channel 11

EPS-001

Role of FDG-PET/CT in patients with Non-Hodgkin Lymphoma treated with Chimeric Antigen Receptor T Cells

C. Bailly, B. Tessoulin, T. Eugene, T. Gastinne, F. Kraeber-Bodere, S. Le Gouill, C. Bodet-Milin;
CHU Nantes, Nantes, FRANCE.

Aim/Introduction: CD19-targeting chimeric-antigen-receptor (CAR)-T-cells has changed the landscape of immunotherapy in relapsed or refractory B-cell non-Hodgkin's lymphoma (NHL). Given the role that FDG-PET/CT already plays in the management of lymphoma, this study explored the potential prognostic or predictive values of this imaging modality in CAR-T-cells therapy. ***Materials and Methods:*** We retrospectively reviewed patients with NHL who received CD19-targeting CAR-T-cells therapy at our hospital between November 2018 and December 2019 and who underwent FDG-PET/CT imaging at the time of enrolment, showing relapsed or refractory disease (FDG-PET/$CT_{baseline}$), before CAR-T-cells injection (FDG-PET/$CT_{pre\text{-}infusion}$) and at 1 month after treatment (FDG-PET/$CT_{post\text{-}infusion}$). Most patients had repeated FDG-PET/CT scans during follow-up at 2, 3 or 4 months after CAR-T-cells injection. SUVmax, whole-body functional volume (MTV) and whole-body total lesion glycolysis (TLG) were extracted. Lugano criteria (LC) were used to evaluate therapeutic response. ***Results:*** Thirteen patients were enrolled. All patients had FDG-PET/$CT_{baseline}$ with active disease. Most patients received salvage chemotherapy before leukapheresis (92.7%;12 patients) and 8 patients (61.5 %) bridging chemotherapy before CAR-T-cells infusion. After a median follow-up of 9.9 months [range 3.2-15.9], overall response rate to CAR-T-cells therapy was 46.1%. Only the six patients (41.6 %) who presented objective response (complete or partial response) according to LC on FDG-PET/$CT_{pre\text{-}infusion}$ remained disease-free after CAR-T-cells infusion. On FDG-PET/$CT_{pre\text{-}infusion}$, SUVmax (medianSUVmax: 15.06 [range 4.08-23.19] vs 25.15 [range 9.33-32.58]; p = 0.23), MTV (medianMTV: 42.72 cm^3 [range 6.29-407.68] vs 111.95 cm^3 [range 10.09-877.53]; p=0.35) and TLG (medianTLG: 111.66 [range 32.62-1147.78] vs 1968.25 [range 45.39-8696.18]; p=0.11) seemed to be higher in non-responding patients but with no significant difference. At 1 month after treatment, changes in SUVmax or volumetric measures were not correlated to improved survival. All patients achieving a complete response according to LC on follow-up FDG-PET/CT scans (41.6%; 6 patients) between 1 and 4 months post-CAR-T-cells infusion remain disease-free >10 months post-therapy. Supplementary early FDG-PET/CT 15-days post-infusion showed one pseudoprogression with no predictive or prognostic value. Development of Cytokine Release Syndrome was not correlated to FDG-PET/CT findings. ***Conclusion:*** These preliminary results show the importance of the "dynamic" of response on FDG-PET/$CT_{pre\text{-}infusion}$, as all patients presenting a semblance of response using LC, consolidate this latter. Quantitative metrics determined on FDG-PET/$CT_{pre\text{-}infusion}$ seemed to be higher in non-responding patients with no significant difference at this time of analysis. LC allowed good prediction of response during follow-up. The study is ongoing and supplementary data including more patients will be presented at the congress. ***References:*** None

EPS-002

Chimeric Antigen Receptors T Cell Therapy in the Treatment of Non-Hogdkin Lymphoma. Assessment of Response and Side Effects using ^{18}F-FDG-PET / CT

J. Ardila Mantilla, I. Gómez Fernández, A. Rotger Regí, M. Kwon, J. Orcajo Rincón, M. Baquero Oliveros, C. Durán Barquero, D. Zamudio Rodríguez, A. Marí Hualde, Y. Henao Celada, J. Atance García de la Santa, J. C. Alonso Farto;
Hospital General Univeristario Gregorio Marañón, Madrid, SPAIN.

Aim/Introduction: CD19-targeting chimeric antigen receptor (CAR)-T cell therapy has shown great efficacy in patients with relapsed/refractory non-Hodgkin lymphoma (NHL) but has been associated with serious adverse effects, such as cytokine release syndrome (CRS), making necessary to search metabolic parameters that apart from predicting the response to treatment can also identify those patients with a higher risk of presenting CRS, who can benefit from cytoreductive therapy before CAR-T injection. Our aim is to assess the usefulness of ^{18}F-FDG-PET / CT in response evaluation to CAR-T therapy and to determine the value of metabolic tumor volume (MTV) and total lesion glycolysis (TLG) as a prognostic factor in development of CRS. ***Materials and Methods:*** Retrospective, descriptive, observational study; we included 13 patients with CAR-T therapy. Multiple variables were extracted (age, sex, Ann Arbor, histological type, previous treatment lines and dose). We performed baseline 18F-FDG-PET / CT (prior to therapy), at 30, 100, and 180 days. In baseline PET / CT, the tumor burden was evaluated, classifying it as high (MTV> 1781.19 cm3 and TLG> 16254) and intermediate-low (MTV <1781.19 cm3 and TLG <16254) and correlated it with clinical and analytical data after treatment (severe SLC grade 3-4 and mild-moderate SLC grade 1-2). The response to CAR-T therapy was evaluated using the Deauville scale classifying them as stable disease, pseudoprogression, progression and

hyperprogression. ***Results:*** We included 13 patients treated with CAR-T therapy, 7 women and 6 men, the mean age was 50.7 years; 10 NHL BDCG and 3 follicular lymphoma. 1 patient was assessed on PET / CT + 30 + 100 + 180 days, 2 PET / CT +30 +100 and 9 PET / CT on day +30. 10 patients showed baseline PET / CT (76%) with low tumor load, presenting no serious later complications and 3 high tumor load (24%) of which 1 died from SLC and in 2, the CAR-T infusion was delayed, administering cytoreductive treatment prior to the CAR-T infusion. ***Conclusion:*** Baseline ^{18}F-FDG-PET / CT prior to CAR-T therapy can predict the appearance of serious adverse effects and we can identify those patients with high tumor load that can benefit from cytoreductive treatments prior to the therapy administration. ***References:*** None

EPS-003

Possibility of 18F-FDG activity reduction for Hodgkin lymphoma patients performed on high sensitivity PET/CT camera

M. Dziuk[1,2], *E. Witkowska-Patena*[2], *A. Gizewska*[1], *A. Mazurek*[2], *M. Koza*[1], *A. Pieczonka*[3], *M. Chojnowska*[2], *Z. Podgajny*[3];
[1]*Affidea, PET-CT, Warsaw, POLAND,* [2]*Military Institute of Medicine, Warsaw, POLAND,* [3]*Affidea, PET-CT, Wroclaw, POLAND.*

Aim/Introduction: We aimed to investigate the dose reduction of fluorodeoxyglucose (18F-FDG) in positron emission tomography/computed tomography (PET/CT) of Hodgkin lymphoma patients performed on a camera with bismuth germanate (BGO) crystals. ***Materials and Methods:*** Ninety-one 18F-FDG PET/CT scans (each in seven Bayesian Penalised Likelihood [BPL] reconstructions with varying acquisition time per bed position - 2 min, 1.5 min, 1 min, 50 sec, 40 sec, 30 sec and 20 sec) were independently assessed by three physicians to evaluate image quality. Mean administered dose was 3.0±0.1 MBq/kg and mean uptake time was 54.0±8.7 min. Each time series quality was subjectively marked in 1-10 scale and then ranked 1-7 basing on the mean mark. Series with mean mark ≥7 were regarded as good quality appropriate for assessment, mean mark 5-6 was mediocre quality and mean <5 was poor quality (inappropriate for assessment). Interobserver rank correlation and intraclass correlation within each time series for the three observers were calculated. Phantom studies were also performed to find a correlation between reduced acquisition time and dose reduction. ***Results:*** Time series were marked and ranked unanimously - the longer the time of acquisition the higher the mark and rank. The interobserver agreement in ranking was excellent (100%) with kappa coefficient of 1.00 (95% CI [0.83-1.0]). The general intraclass correlation coefficient (agreement between the marks observers gave each time series) was very high (0.952, 95% CI [0,946-0,958]) and was the higher the shorter the time per bed. According to all three observers only the series with 2 min and 1.5 min acquisition time were appropriate for assessment (mean mark ≥7). In phantom studies the time of acquisition was strongly linked with the tracer activity. A reduction of acquisition time of 25% (from 2 min to 1.5 min) corresponded to a 25% dose reduction (with 1,64% error). Further reduction (to 1 min and less) resulted in an error of ≥16%. ***Conclusion:*** In a BGO crystal camera, 18F-FDG dose can be reduced by up to 25% without substantial compromising PET/CT image quality in patients with Hodgkin lymphoma. ***References:*** None

EPS-004

Influence of digital PET/CT and Q.Clear algorithm on determination of response to chemotherapy in patients with diffuse large B-cell lymphoma

C. Arede[1], *J. M. Riedinger*[1], *J. M. Vrigneaud*[1,2], *C. Tabouret-Viaud*[1], *J. L. Alberini*[1,2], *C. Drouet*[1], *Y. E Silva*[1], *R. Popoff*[1,2], *C. Rossi*[3], *O. Casasnovas*[3], *A. Berriolo-Riedinger*[1], *A. Cochet*[1,2];
[1]*Department of Nuclear Medicine, Centre Georges-François Leclerc, Dijon, FRANCE,* [2]*ImVIA, EA 7535, University of Burgundy, Dijon, FRANCE,* [3]*Department of Haematology, University Hospital, Dijon, FRANCE.*

Aim/Introduction: Baseline and interim 18F-FDG PET/CT are performed to monitor the early response to chemotherapy in diffuse large B-cell lymphoma (DLBCL) patients, using residual tumor metabolism compared to liver metabolism with the Deauville 5-point scale (DS), but also metabolic response using ΔSUV. However, the impact of digital PET/CT coupled with iterative Bayesian penalized-likelihood algorithm (Q.Clear), which improves signal-to-background ratio, has yet to be determined. ***Materials and Methods:*** Forty-four patients (23 men, 21 women, mean age=64±15y) with newly diagnosed DLBCL were prospectively included between February 2018 and February 2020. Each patient had interim 18F-FDG PET/CT after two cycles of chemotherapy (PET2). Among them, 29 had previously baseline 18F-FDG PET/CT (PET0). All acquisitions were performed on the same digital PET/CT (Discovery MI 4, GEHC, injected dose 3MBq/kg). PET images were all reconstructed using two algorithms: one optimized for harmonized quantification (EARL; OSEM with 2 iterations and 34 subsets) and one optimized for lesion detection (Q.Clear, beta=800). PET images (EARL and Q.Clear) were visually and semi-quantitatively analysed. SUVmax of the tumor and the liver were determined to calculate a Tumor to Liver ratio (T/L). Moreover, ΔSUV was calculated for patients who had PET0 and PET2. T/L ratios and ΔSUV determined with EARL and Q.Clear algorithms were compared using Bland-Altman plots. Finally, tumor response was determined based on both reconstruction algorithms using DS, and ΔSUV (cut-off -66%). ***Results:*** T/L ratio was significantly higher with Q.Clear reconstruction than with EARL, both at PET0 (8.5±4.9 vs 6.7±4.0, bias=+1.8, p<0.0001) and PET2 (1.7±1.5 vs 1.4±1.1, bias=+0.4, p<0.0001). However, there was no significant difference concerning ΔSUV (-69.2% vs -68.9%, bias=-0.3%, p=NS). Concerning response evaluated

with DS based on Q.Clear reconstructions, 29 patients were responders (DS 1-3) and 15 were non-responders (DS 4-5), including 3 with progression. Only one non-responder (DS 4) was found to be responder (DS 3) on EARL reconstructions. Concerning response evaluated with ΔSUV, 24 patients were responders on Q.Clear reconstructions (ΔSUV<-66%) and 5 were non-responders. Only 2 responders were classified as non-responders on EARL reconstructions; these patients had a low baseline tumor metabolism on EARL reconstructions (SUVmax < 10) which is a well-known limitation of ΔSUV. ***Conclusion:*** In patients with diffuse large B-cell lymphoma, the use of digital PET/CT and Q.Clear algorithm improve tumor-to-background ratio, with a limited impact on the interpretation of tumor response to chemotherapy, based on Deauville score and ΔSUV. ***References:*** None

EPS-005

Is visual residual lymphoma on FDG PET concordant with it's quantitative assessment?

A. Al-Busaidi[1,2], Z. Al-Bimani[1,2], A. Miglietta[1], W. Zeng[1];
[1]Division of Nuclear Medicine, Department of Medicine, University of Ottawa, Ottawa, ON, CANADA, [2]Ministry of Health, Muscat, OMAN.

Aim/Introduction: ^{18}F-FDG PET/CT is the current standard of care for aggressive lymphoma. Based on the NCCN guidelines (2018) and Consensus of the International Conference on Malignant Lymphomas Imaging Working Group (2014) the FDG PET assessment is visual. However, in clinical practice, SUV_{max} is often used to derive the Deauville score as it is considered less subjective. The aim of this study is to compare the visual and quantitative assessment for residual or resolved lymphoma. ***Materials and Methods:*** Consecutive patients with Hodgkin's lymphoma or diffuse large B-call lymphoma following chemotherapy referred for FDG PET/CT from January, 2016 to October, 2019 with a Deauville score of 3 and 4 based on SUV_{max} (3=above mediastinal blood pool and below liver, 4=above liver) were included. All lesions with a Deauville score other than 3 and 4 or small size (<1.0 cm) were excluded. Visual assessment was performed by experienced radiologist (Reader 1) and technologist (Reader 2) independently for Deauville score. Both were blinded to clinical and other imaging results including SUV_{max} of the lesions. SUV_{max} of tumor lesions, liver and mediastinal blood pool was measured by an experienced nuclear medicine physician. Both the visual and quantitative Deauville score as well as the score between two readers were compared with Cohen's Kappa. ***Results:*** 120 lesions from 100 patients (age: 58.0± 19.2, F:M=36:64) were analyzed. The mean tumor and liver SUV_{max} was 3.65 ±1.0 and 3.1±0.5 respectively, with 56 lesions (47%) at the Deauville score 4 category. The percentage agreement between quantitative and visual assessment was 73% for both readers. The agreement by taking into account the chance agreement was 43% for Reader 1 and 52% for Reader 2 with Cohen's Kappa calculation. Of note there were 32 lesions (27%) scored 3 by Reader 1 but scored 4 by SUV_{max}. There agreement between readers was fair with a Cohen's Kappa at 0.38 (38% of agreement). ***Conclusion:*** A lesion with a Deauville score of 4 following chemotherapy is usually considered residual lymphoma while a score of 3 is resolved or borderline lymphoma. There appears to be suboptimal agreement between the visual and quantitative methods. The difference in approaches should receive more attention as this could lead to changes in patient's management and continues to be a challenge to all reporting and referring physicians. ***References:*** None

EPS-006

Comparison of ^{68}Ga-PSMA and ^{18}F-FDG PET/CT Uptake in Different Lymphoma Subtypes: Preliminary Results

C. Ramos[1], S. Souza[1], N. Tobar[1], V. Castro[1], F. Frasson[1], B. Amorim[1], E. Etchebehere[1], M. Lima[1], J. Mengatti[2], E. Araujo[2], E. Perini[2], C. Souza[1], I. Lorand-Metze[1], A. Santos[1], M. Delamain[1];
[1]University of Campinas, Campinas, BRAZIL, [2]Nuclear and Energy Research Institute (IPEN), Sao Paulo, BRAZIL.

Aim/Introduction: Few reports have documented the uptake of radiolabeled Prostate-Specific Membrane Antigen (PSMA) in lymphomas [1,2]. It is not known how PSMA uptake varies among various histological subtypes and how it correlates with 18F-FDG uptake in lymphomas. This study aimed to compare 68Ga-PSMA and 18F-FDG in different lymphoma subtypes. ***Materials and Methods:*** Nine randomly selected patients with biopsy-proven lymphoma -median age 43 (32-70) years, 5 female - were submitted to whole-body ^{18}F-FDG and ^{68}Ga- PSMA PET/CT (time interval: 1-6 days between procedures). Lymphoma subtypes included: nodular-sclerosis Hodgkin's lymphoma (HL; 2 patients); diffuse large B-cell lymphoma (DLBCL; 1); marginal-zone lymphoma (2); MALT lymphoma (ML; 1); follicular lymphoma (FL; 1); lymphoplasmacytic lymphoma (1); and B-cell non-Hodgkin's lymphoma, unspecified (BCNHL-U; 1). Eight patients were under initial staging, and 1 (HL) with disease relapse after treatment. Two experienced nuclear physicians analyzed the images by consensus. The intensity of tracer uptake was visually classified as marked, moderate or mild. The affected sites (lymph node chains, spleen, diffuse bone marrow involvement and non-lymphatic focal lesions) were counted in both sets of images and their respective maximum SUV (SUVmax) were measured. ***Results:*** PSMA PET/CT was positive in all patients except for one with ML. FDG PET/CT was positive in all patients. At visual analyses, FDG uptake was higher than PSMA uptake in all patients, except for one patient with BCNHL-U (both tracers with similar low-intensity uptake). The intensity of FDG and PSMA uptake was respectively classified as marked in 3/9 and 0/8 patients, moderate in 4/9 and 1/8 and mild in 2/9 and 7/8. One patient (FL) presented a "mismatch" uptake pattern with different

parts of an extensive lesion presenting predominant uptake of PSMA or FDG. Brain infiltration in one patient (DLBCL) was more easily identified on PSMA than on FDG images. FDG detected a total of 58/58 and PSMA 43/58 affected sites in all patients with a median SUVmax of respectively 5.4 (2.0-31.1) and 2.8 (1.3-5.4), p<0.0001. The median SUVs of the 43 lesions with uptake of both tracers was respectively 5.5 (2.0-28.9) and 2.8 (1.3-P5.4) for FDG and PSMA, p<0.0001. ***Conclusion:*** Distinct lymphoma subtypes present PSMA uptake, with less intensity than FDG uptake. Although PSMA uptake is usually mild, several lymphoma subtypes might cause false-positive results in PSMA PET/CT performed to assess prostate cancer. ***References:*** [1] Kanthan GL, et al. Clin Nucl Med.2016;41(6):500-501. [2] Vamadevan S, et al. Clin Nucl Med.2016;41(12):980-981.

EPS-007

Artificial intelligence can warn for focal skeleton/bone marrow uptake in Hodgkin lymphoma patients staged with FDG-PET/CT

M. Sadik[1], J. Lopes-Urdaneta[1], J. Ullén[2], O. Enqvist[3], A. Krupic[1], R. Kumar[4], P. Andersson[5], E. Trägårdh[6], L. Edenbrandt[7]; [1]Nuclear Medicine, Gothenburg, SWEDEN, [2]Eigenvision AB, Malmö, SWEDEN, [3]Image Analysis and Computer Vision, Gothenburg, SWEDEN, [4]Nuclear Medicine, Chandigarh, INDIA, [5]Hematology and Medicine, Borås and Gothenburg, SWEDEN, [6]Nuclear Medicine, Malmö, SWEDEN, [7]Nuclear Medicine, Malmö and Gothenburg, SWEDEN.

Aim/Introduction: To develop an artificial intelligence (AI) method for the detection of focal skeleton/bone marrow uptake and quantification of diffuse bone marrow uptake (BMU) in patients with Hodgkin lymphoma undergoing staging with FDG-PET/CT. The results of the AI-method were compared to image interpretations of a group of physicians from different hospitals. ***Materials and Methods:*** Forty-eight non-treated patients who had undergone a staging FDG-PET/CT between 2017-2018, with biopsy proven Hodgkin lymphoma, were retrospectively included. The skeleton and bone marrow were segmented using a convolutional neural network [1] . To detect focal uptake, bone uptake significantly higher than the mean bone marrow uptake was marked as abnormal and an index, based on the total squared abnormal uptake, was computed. Patients with an index above a predefined threshold was interpreted as having focal uptake. Diffuse BMU was classified as high if the patient had a SUVmedian spine bone marrow uptake larger than the liver (>1,0). Ten physicians, with 2-12 years of PET/CT-experience, working in three different hospitals classified the cases regarding focal skeleton/bone marrow uptake and diffuse BMU. ***Results:*** AI agreed with the majority of the readers in 39 of the 48 cases (81%) regarding focal skeleton/bone marrow involvement. While for diffuse BMU AI agreed in 33 (69%) cases with the majority of the physicians, in 1 case half of the physicians agreed with AI and in 14 cases most physicians disagreed with AI. Inter-observer agreement between the physicians, both regarding focal and diffuse BMU was moderate, Kappa 0,53 (range 0,25-0,80) and Kappa 0,41 (range 0,03-0,68), respectively. ***Conclusion:*** An AI-method can be developed to highlight suspicious focal skeleton/bone marrow uptake in Hodgkin lymphoma patients staged with FDG-PET/CT. This AI-method can also objectively present high versus low BMU by calculating median SUV-values in the whole spine marrow and the liver. We have demonstrated that inter-observer agreement regarding both focal and diffuse BMU are moderate among nuclear medicine physicians. ***References:*** 1. Lindgren Belal S, Sadik M, Kaboteh R, Enqvist O, Ulén J, Poulsen MH, Simonsen J, Høilund-Carlsen PF, Edenbrandt L, Trägårdh E. Deep learning for segmentation of 49 selected bones in CT scans: First step in automated PET/CT-based 3D quantification of skeletal metastases. Eur J Radiol. 2019;113:89-95.

EPS-008

Bone Marrow 18F-FDG Uptake Patterns to Evaluate Infiltration in Mantle Cell Lymphoma

A. Sabaté-Llobera[1], M. Cortés-Romera[1], A. Palomar-Muñoz[1], E. Llinares-Tello[1], C. Soldevila-Lozano[1], L. Rodríguez-Bel[1], M. Martínez de Bourio-Allona[1], F. Climent-Esteller[2], E. M. González-Barca[3]; [1]IDI - Hospital Universitari de Bellvitge - IDIBELL, L'Hospitalet de Llobregat, SPAIN, [2]Hospital Universitari de Bellvitge - IDIBELL, L'Hospitalet de Llobregat, SPAIN, [3]ICO - Hospital Duran i Reynals - IDIBELL, L'Hospitalet de Llobregat, SPAIN.

Aim/Introduction: To determine the utility of establishing patterns of 18F-FDG uptake in the bone marrow to evaluate bone marrow infiltration (BMI) in mantle cell lymphoma (MCL). ***Materials and Methods:*** Retrospective review of PET/CT of 42 patients with MCL (3 women, average age 62.5 years), treatment-naïve and with bone marrow biopsy (BMB) as part of the diagnostic work-up study. PET/CT images were visually evaluated, defining five patterns of 18F-FDG uptake in the bone marrow: A-focal (uni or multifocal), B-diffuse homogeneous similar to liver activity, C-diffuse homogeneous above liver activity, D-heterogeneous, E-no uptake/below liver activity. All the patterns except the last one were considered as BMI. Results of image evaluation were compared with BMB. ***Results:*** PET/CT considered BMI in 30 cases (71.4%), most of them with pattern B (40.5%), while BMB revealed involvement in 35 patients (83.3%). There were 17 discordant results (40.5%), 11 of which were interpreted as no-BMI by PET/CT but BMB proved as infiltrated by lymphoma. At least 75% of the cases with uptake pattern C and 88.9% of those with pattern D showed disease at the BMB. No cases with pattern A were identified. ***Conclusion:*** Establishing patterns of FDG uptake in the bone marrow helps standardizing the visual evaluation of PET/CT to determine BMI in MCL, obtaining concordant results with the

BMB in most of the cases with diffuse homogeneous uptake of activity similar or above the liver, or with heterogeneous uptake. However, many cases with no uptake/below liver activity are misinterpreted as no-BMI, so BMB is still mandatory, especially in these patients. ***References:*** None

EPS-009

Assessment of the Predictive Capacity of Pretreatment 18F-FDG PET/CT in Gastric Mucosa-associated Lymphoid Tissue (MALT) Lymphoma

C. Jiang[1], C. Ding[2], Z. Zhou[1];
[1]Department of Nuclear Medicine, Nanjing Drum Tower Hospital,the Affiliated Hospital of Nanjing Unive, Nanjing, CHINA, [2]Department of Nuclear Medicine,the First Affiliated Hospital of Nanjing Medical University,Jiangsu Province Hospital, Nanjing, CHINA.

Aim/Introduction: The predictive capacity of positron emission tomography/computed tomography (PET/CT) using [18F]-fluorodeoxyglucose (18F-FDG) for gastric mucosa-associated lymphoid tissue (MALT) lymphoma (GML) remains still not determined. Therefore, we evaluated the predictive capacity of pretreatment 18F-FDG PET/CT in GML patients. ***Materials and Methods:*** Thirty-six patients with newly diagnosed GML were enrolled in this retrospective study. Each patient underwent 18F-FDG PET/CT scans before treatment. 18F-FDG PET/CT results were analyzed visually, and the lesion with the highest maximum standardized uptake value (SUVmax) was recorded. The predictive capacity of PET positivity, SUVmax and other clinical parameters were assessed. ***Results:*** Over a median follow-up of 38.2 months, PET positivity,SUVmax as well as large B cell transformation were the significant predictors of PFS.Multivariate analysis showed that SUVmax was the only independent predictor of PFS (P=0.027). SUVmax can independently predict the treatment response (P=0.016).Patients who presented with SUV ≥6.5 had a higher rate of large cell transformation. ***Conclusion:*** A high 18F-FDG uptakes prior to treatment can predict unfavorable outcomes and are associated with large cell transformation in GML patients. ***References:*** None

EPS-011

Impact of Gender on Metabolic Response in Patients with Head and Neck Cancers using End of Treatment ^{18}FDG PET/CT

M. Zaman[1], N. Fatima[1], U. Zaman[2], A. Zaman[3], S. Zaman[4], R. Tahseen[5];
[1]AKUH, Karachi, PAKISTAN, [2]Dept of Medicine Suny Downstate, Hospital, New York, NY, UNITED STATES OF AMERICA, [3]Department of Medicine, Dr Ruth Hospital, Karachi, PAKISTAN, [4]Dow Medical College, Dow University of Health Sciences (DUHS), Karachi, PAKISTAN, [5]Department of Radiation Oncology, Aga Khan University Hospital (AKUH), Karachi, PAKISTAN.

Aim/Introduction: The purpose of this study was to determine the impact of gender on response in patients with head and neck cancers (HNC) based on end of treatment (EoT) 18-fluorodeoxyglucose (^{18}FDG) positron-emission tomography/computed tomography (PET/CT). ***Materials and Methods:*** This retrospective study was conducted at PET/CT section of a JCI-accredited healthcare facility from January 2017 to February 2020. Patients with baseline (pre-treatment) and EoT ^{18}FDG PET/CT (12 week post-treatment) scans were selected. Based on EoT scans findings patients were categorized as responders and non-responders. Study population was divided on the basis of gender and various demographic factors were compared among them. Furthermore, Kaplan Meier analysis was used to see the impact of age, BMI, nodal status, size and SUVmax of primary tumor in non-responders. ***Results:*** Total 323 patients with HNC (oral cavity cancers: 201/323; larynx cancers: 97/323; sinonasal cancers: 12/323; submandibular cancers: 13/323) were categorized on the basis of gender into male (236/323; 73%) and female (87/323; 27%; P<0.05) cohorts. Female group was significantly obese (Body Mass Index ≥30 kg/m^2) and elder. Rest of demographic factors (age, fasting blood level, ^{18}FDG dose, uptake time, mean liver uptake, baseline highest SUVmax and primary tumor size) show no significant difference. Males had significantly higher incidence of throat cancers while no significant gender predisposition seen in oral, sinonasal and submandibular cancers. Left sided cancers were significantly higher in both genders than right side and mid line disease. No significant gender based difference was seen for cervical or extra-cervical nodal disease and intracranial extension. Male had significantly higher advanced disease with local bony destruction and stage IV disease as well. EoT PET/CT revealed metabolic response in 59% female and 51% of male participants (non-significant p-value). Kaplan Meier curves showed negative correlation between age, nodal status, primary tumor size and SUVmax for metabolic response without gender biasness. However, obesity was found a predictor in non-responder females (Log rank value: 6.336; F:M odd ratio: 1.61; p <0.05). ***Conclusion:*** We conclude that prevalence of HNC is higher in males with a higher tendency of local bony destruction and stage IV disease on baseline ^{18}FDG PET/CT. Male had significantly higher laryngeal cancers with left laterality in both genders. EoT ^{18}FDG PET/CT revealed no significant gender biasness on metabolic response. In non-responders, no significant impact of age, nodal status, primary tumor size and SUVmax in either gender noted. However, obesity was found a significant predictor in female non-responders. ***References:*** None

EPS-012

Image quality and interpretation of [18F]-FES-PET: is there any effect of food intake?

J. Boers[1], K. Giatagana[1], G. A. P. Hospers[1], C. P. Schröder[1], E. F. J. de Vries[2], A. W. J. M. Glaudemans[2];
[1]Department of Medical Oncology, University Medical Center Groningen, Groningen, NETHERLANDS, [2]Department of Nuclear Medicine and Molecular Imaging, University Medical Center Groningen, Groningen, NETHERLANDS.

Aim/Introduction: Whole-body estrogen receptor (ER) expression can be visualized with 16α-[18F]-fluoro-17β-estradiol ([18F]-FES) positron emission tomography (PET). This imaging technique may improve diagnostic understanding and help in therapy decision-making. However, high physiological [18F]-FES uptake in the liver, gall bladder and gastrointestinal tract may limit scan interpretation in these regions. We hypothesized that eating a (fatty) meal before [18F]-FES-PET imaging would lead to lower [18F]-FES uptake in the upper abdomen due to faster gall excretion, thereby improving scan interpretation of the upper abdomen. Therefore, in this exploratory study we investigated the effect of food intake prior to PET acquisition on abdominal background activity in [18F]-FES-PET scans. ***Materials and Methods:*** Breast cancer patients referred to the UMCG for [18F]-FES-PET due to a clinical dilemma between February 2012 and August 2019 were included. Three groups were designed: 1) patients who consumed a chocolate bar (fatty meal) between tracer injection and [18F]-FES-PET acquisition (n=20), 2) patients without diet restrictions before tracer injection (control group, n=20), and 3) patients that fasted for 4-6 h before tracer injection (n=20). We compared the physiological [18F]-FES uptake, expressed as mean standardized uptake value (SUV_{mean}), in the gall bladder and gastrointestinal tract between groups. ***Results:*** After chocolate, the median [18F]-FES uptake (SUV_{mean}) in the gall bladder was 71 [interquartile range 38-91], compared to 85 [62-128] for the control group, and 102 [68-140] for the fasting group (P=0.015). This [18F]-FES uptake pattern was similar in the lumen of the stomach, with the lowest values for the chocolate group: 0.55 [0.19-0.80], compared to 0.65 [0.48-0.92], and 0.90 [0.67-1.11] for the control and fasting group, respectively (P=0.011). [18F]-FES uptake in other abdominal regions was not different between groups. Post hoc analysis showed significant differences in gall bladder and stomach lumen [18F]-FES uptake between the fasting and chocolate group, but not between the chocolate and control group. ***Conclusion:*** In this exploratory study we showed that, compared to fasting, eating chocolate decreases physiological [18F]-FES uptake in the upper abdomen. Eating a fatty meal (chocolate) does not significantly decrease [18F]-FES uptake further compared to a normal diet. Therefore, eating before the scan may increase passage of the tracer. We suggest, particularly for patients suspected of metastases in the upper abdomen, that fasting is not recommended and eating (chocolate) prior to [18F]-FES-PET could help to lower the physiological uptake in gall bladder and stomach. ***References:*** None

EPS-013

18F-FLT PET/CT in locally advanced breast cancer: texture analysis and image quantification

A. Capozza[1], *B. Padovano[1], G. Serafini[1], A. Lorenzoni[1], G. Infante[2], R. Agresti[2], R. Miceli[2], E. Seregni[1], A. Alessi[1];*
[1]Nuclear Medicine Unit, IRCCS Istituto Nazionale dei Tumori di Milano, Milan, ITALY, [2]IRCCS Istituto Nazionale dei Tumori di Milano, Milan, ITALY.

Aim/Introduction: Radiomics studies intratumoral heterogeneity, relying on the assumption that quantitative data are expression of molecular mechanisms determining cancer behavior. Breast cancer (BC) is a highly heterogeneous disease, with severely different outcomes based on biological subtypes and molecular profile. Our pilot study[1] showed that the uptake of 18F-FLT, a tracer of proliferation, in BC, identifies patients that will achieve a complete response on final histology, after neoadjuvant chemotherapy (NCT). Aim of this study is to deepen the potentiality of 18F-FLT PET/CT advanced image analysis in BC. ***Materials and Methods:*** Enrolled patients underwent NCT and performed 18F-FLT PET/CT at baseline (PET0) and after first (PET1) and last (PET2) NCT cycles. Semi-quantitative analysis of 18F-FLT uptake of breast and nodal lesions was performed using semi-automatic segmentation method with fixed threshold (SUVmax 40%). Standard parameters and advanced imaging features were derived using statistic based method (LifeX software). Overtime variation of radiomic parameters (delta-features) were analyzed among PET0, PET1 and PET2. Hierarchical clustering analysis was performed to evaluate correlations between baseline- and delta-radiomic features, pathological response (RCB), histo-pathological data. Pathological analysis was performed on pre-treatment biopsy or surgical histological specimen. Pathological response was assessed using Anderson Residual Cancer Burden (RCB). ***Results:*** Fifteen female patients, with locally advanced T2-3-4 N0-1 BC, were evaluated. Median age at diagnosis was 42 years (range 29-63y); median follow-up 7 years. At time of our analysis, 27% patients had died for disease progression, 11/15 patients were progression-free. Histopathological analysis showed median Ki67 index= 50 (range 12-90). A significant correlation was found between a cluster of features, from texture analysis on PET0 images, and Ki67 expression, evaluated according to the standard cut-off Ki67 ≥20. Patients' population was then classified according to pathological response in two groups: responders (RCB 0+I) vs non-responders (RCB II+III). Cluster analysis, with heatmap designed on delta-features, showed a correlation between a group of specific radiomic

parameters (entropy and correlation derived from grey-level co-occurrence matrix, and histogram-based entropy) and pathological response. ***Conclusion:*** Whilst confirming previously reported data, on the potentiality of FLT in BC[1], texture-analysis may have a complementary role and offer adjunctive informations to in-vivo characterize BC lesions. Of the over 90 features analyzed, only a cluster of parameters (related to texture and homogeneity) has been found to correlate with pathological response and histopathological characteristics, thus allowing early prediction of NCT response and outcome. ***References:*** 1.Crippa F, et al. Eur J Nucl Med Mol Imaging. 2015 May;42:818-30.

EPS-015

Multiple bone scintigraphy metastatic lesions in correlation with breast carcinoma human epidermal growth factor receptor 2 neu and hormone receptor expression

S. Stojanoski[1,2], A. Jankulovska[1], E. Lazareva[1], T. Makazlieva[1], M. Iljovska[1], N. Manevska[1], M. Jovanovski Srceva[1], S. Smichkoska[1], D. Miladinova[1];
[1]Medical Faculty, Skopje, NORTH MACEDONIA, [2]Medical Faculty, Lazarski University, Warsaw, POLAND.

Aim/Introduction: Bone scintigraphy is a useful tool for the accurate diagnosis of skeletal metastatic lesions among oncological patients. Several factors have been proposed for the prediction of osseous and/or visceral metastatic disease onset in breast cancer patients. The aim of our study was to determine the correlation between multiple bone metastatic lesions initially diagnosed with bone scintigraphy and tumor receptor characteristics of breast cancer patients. ***Materials and Methods:*** We performed a monocentric (University Clinic ``Mother Theresa``), retrospective, observational study at the Institute of Pathophysiology and Nuclear Medicine and the Institute for Radiotherapy and Oncology in Skopje. Between January 2013 and December 2018, 66 female breast cancer patients (mean age 52,51 ± 10,64 years) who underwent initial ^{99m}Tc-MDP bone scintigraphy procedure and were diagnosed with multiple skeletal metastatic lesions were included in the study. Primary tumor characteristics regarding the human epidermal growth factor receptor 2 neu - HER2neu and hormone receptor - HR (estrogen receptor - ER and/or progesterone receptor - PR) expression of each patient were evaluated for association with multifocal osseous metastasis. ***Results:*** Bone metastatic lesions were initially detected 5,59 ± 2,72 years after the breast cancer diagnosis confirmation. The axial skeleton was affected in 29% of patients and in 71% the affection was both axial and appendicular. In our study cohort, the spine (predominantly the thoracic segment), the ribs and the pelvis were the most common sites of metastatic involvement (p = 0.013). ER+ were 86% (57/66) of the patients, PR+ were 74% (49/66) and HER2neu+ were 35% (23/66). HR+/HER2neu- were 65% (43/66) of the patients, HR+/HER2neu+ were 29% (19/66) and HR-/HE2neu+ were 6% (4/66). Multiple bone scintigraphy metastatic lesions significantly correlated with HR+ status of breast cancer patients (p = 0.021). ***Conclusion:*** Breast cancer patients with hormone receptor-positive status present significant predilection for skeletal metastatic patterns. ***References:*** None

EPS-016

^{18}F-FDG PET/CT Volume-based Metabolic Parameters in Advanced Non-Small-Cell Lung Cancer Patients Treated with anti PD-1 Immunotherapy: A Potential Biomarker for Predicting Prognosis

M. Rashki[1], E. Triviño-Ibañez[1], V. Amezcua Hernández[2], J. Valdivia Bautista[2], T. Rudolphi Solero[1], J. Fernández Fernández[1], J. Llamas-Elvira[1], A. Rodríguez-Fernández[1];
[1]Servicio de Medicina Nuclear, Hospital Virgen de las Nieves, Granada, SPAIN, [2]Servicio de Oncología Médica, Hospital Virgen de las Nieves, Granada, SPAIN.

Aim/Introduction: Pembrolizumab and Nivolumab are anti-programmed death-1 (PD-1) antibodies, that are used as treatment for previously treated non-small-cell lung carcinoma (NSCLC). We evaluated the potential predictive value of metabolic parameters of 18F-FDG PET/CT before treatment with anti-PD 1 immunotherapy, in patients with NSCLC and the association with therapeutic response and survival. ***Materials and Methods:*** We retrospectively analyzed the data from stage IV, NSCLC patients who underwent a PET scan before treatment with anti-PD 1 immunotherapy. Images were qualitatively and semiquantitative analyzed by measuring the volumetric parameters: total metabolic tumor volume (TMTV), total lesion glycolysis (TLGt), and SUVmax, SUVmean, SUVpeak, SUVmin, MTV and TLG of the lesion with the highest SUVmax value. Treatment response was evaluated at 3 months (RECISTv1.1). The correlation between metabolic parameters and early treatment response, progression-free survival (PFS), and overall survival (OS) were analyzed. ***Results:*** 54 patients were enrolled (mean age: 66.26±8.73, 68.5% male), followed until last observation or death (mean 23.9 months). The most frequent histological type was adenocarcinoma 64.8% followed by squamous cell carcinoma 24.1%. 66,7% were treated with Pembrolizumab and 33,3% with Nivolumab. 39/54 patients (72.2%) relapsed or progressed and 30/54 (55.6%) died. Response assessment, 3 months after immunotherapy showed two groups: responders (including patients with complete/partial response or stable disease) and non-responders. The expression of PD-L1 was higher in the responders' group (74.7 vs 54.7, p=0.038). TMTV and TLG were higher in the nonrespondents group. We found a low-moderate correlation between SUVmax, SUVpeak, SUVmean, and SUVmin and PDL1 expression (kappa coefficient 0.32-0.35; p<0.05). The median OS and PFS were 17.15 and 4.8 months, respectively. The mean TMTV was significantly higher in the patients who died (165.81 ± 159.07 vs. 87.92 ±

95.08, p=0.039). The baseline PET/CT metabolic parameters (TMTV, TLGt, and also MTV and TLG of the main lesion) were associated with a shorter OS and FPS (p< 0.05). ROC curves analysis showed an optimal cut-off point of 80cm3 for TMTV and 478cm3 for TLG. These values were associated with shorter OS (HR: 2.47 y 2.75; p=0.021 y p=0.012 respectively). ***Conclusion:*** In this study, a higher tumor burden assessed by PET MTV and TLG showed a significant association with overall and progression-free survival in patients with NSCLC treated with anti-PD1 immunotherapy. ***References:*** None

EPS-017

Low-activity digital PET emulation from decimated statistics applied to lung nodules detection

M. Jreige[1], *S. Gnesin*[1], *P. Schleyer*[2], *M. Conti*[3], *J. O. Prior*[1]; [1]*Lausanne University Hospital, Lausanne, SWITZERLAND,* [2]*Siemens Healthineers UK, Frimley, Camberley, UNITED KINGDOM,* [3]*Siemens Healthineers, Knoxville, TN, UNITED STATES OF AMERICA.*

Aim/Introduction: Functional imaging by F-18-fluorodeoxyglucose (FDG) SiPM PET/CT can potentially be used as a stand-alone modality in lung cancer screening, allowing nodule characterization for malignancy and staging. Recent studies have shown that statistical decimation of standard dose scans can generate new emulated scans from identical radiotracer spatial distributions, even when simulating extremely low-count conditions [1]. We present the first results of low-dose simulated PET/CT derived from decimated reconstruction (up to 10% of the original activity) applied to malignant lung nodule detection. ***Materials and Methods:*** Six patients investigated for lung nodules were enrolled in this study and underwent a standard-activity (2 MBq/kg) PET/CT (Siemens Biograph Vision 600) with standard free-breathing trunk acquisition (FB, continuous bed motion 1.4mm/s equivalent to 90-s per bed position). Low-activity emulations were reconstructed to simulate scans with 75%, 50%, 25% and 10% of the standard injected activity (2MBq/kg). SUVmax and SUVmean were measured for malignant nodules, in addition to lung background SUVmean allowing to calculate a Signal-to-Background-Ratio (SBR) across scans. ***Results:*** Six malignant lung nodules, measuring 15.3±7.6 mm, showed increased FDG uptake with SUVmax, SUVmean (g/mL) of 8±3.6 and 4.7±2.2, respectively. Low-activity simulation scans of 75%, 50%, 25% and 10% the injected activity led to a mean variation (%) of 1.3, 1.1, 10.8 and 42.4 of SUVmax and 1.8, 4, 9.6 and -16.6 of SUVmean in lung nodules, respectively. SBR was 17±6, 17±7, 17±6, 18±7 and 22±9, respectively for the standard dose, 75%, 50%, 25% and 10% emulations. ***Conclusion:*** This study shows that low-activity (10%) PET/CT is feasible for lung nodule evaluation, allowing for a potential application in lung cancer screening. Lower emulated dose PET/CT showed a slightly higher FDG uptake in nodule with good SBR, allowing the identification of the malignant lesions. ***References:*** [1] Schaefferkoetter J, Nai YH1, Reilhac A, et al. Low dose positron emission tomography emulation from decimated high statistics: A clinical validation study. Med Phys. 2019 Jun;46(6):2638-2645. doi: 10.1002/mp.13517.

201

Plenary 1 (incl. Marie Curie Lecture): Total Body PET

Thursday, October 22, 2020, 15:10 - 16:25 Channel 1

OP-077

A Game Changer for the Future of PET

D. Visvikis; INSERM UMR1101, LaTIM, CHRU Morvan, Bat 1, et 1, Brest, FRANCE.

OP-078

Marie Curie Lecture:Physics and Development of Total Body PET

S. Cherry; University of California, Biomedical Engineering, Davis, UNITED STATES OF AMERICA.

OP-079

Is Dynamic PET Imaging Ready for Prime Time?

I. Buvat; Unité Imagerie Moléculaire In Vivo, CEA/DRF/Service, Hospitalier Frédéric Joliot, Orsay, FRANCE.

OP-080

Drug Development and Evaluation with Total Body PET

J. Czernin; University of California Los Angeles, Molecular and Medical Pharmacology, Los Angeles, UNITED STATES OF AMERICA .

OP-081

Scientific Opportunities and their Use

B. Pichler; University Hospital Tübingen, Department of Preclinical Imaging and Radiopharmacy, Tübingen, GERMANY.

OP-082

Challenge for Technologists

A. Santos; Hospital CUF Descobertas, Medicina Nuclear Department, Lisbon, PORTUGAL.

OP-083

A Must Have or Another Expensive Luxury Tool?

K. Herrmann; Universitätsklinikum Essen, Nuclear Medicine, Essen, GERMANY.

OP-083a

Discussion

301

CME 2: Software Tools and Approaches to Measure Nuclear Brain Images

Thursday, October 22, 2020, 16:35 - 18:05 Channel 1

OP-084
Software Tools and Approaches to Measure FDG PET Brain Images
V. Berti; Careggi, University of Florence, Departement of Clinical and Experimental Biomedical Sciences, Florence, ITALY.

OP-085
Software Tools and Approaches to Measure Amyloid PET Brain Images
J. Gispert; Barcelonabeta Brain Research Center, Department of Neuroimaging, Barcelona, SPAIN.

OP-086
Software Tools and Approaches to Measure Dopaminergic Brain Imaging
J. Darcourt; Centre Antoine Lacassagne/ Université Cote d'Azur, Nice, FRANCE.

302

Joint Symposium 3 (EANM/EAU): Primary Staging of Prostate Cancer Reloaded

Thursday, October 22, 2020, 16:35 - 18:05 Channel 2

OP-087
Clinical Challenges in Primary Staging of Prostate Cancer
J. Walz; Institut Paoli-Calmettes Cancer Centre, Department of Urology, Marseille, FRANCE.

OP-088
mpMRI: Only PC Detection or also for Staging?
A. Wetter; University Essen, Department of Radiology, Essen, GERMANY .

OP-089
Can PSMA PET Contribute for Primary Loco-Regional Staging?
M. Eiber; Technical University Munich, Department of Nuclear Medicine, Munich, GERMANY.

OP-090
Influence of PSMA PET for Treatment Decision in Primary Prostate Cancer
I. Burger; University of Zurich, Deparment of Nuclear Medicine, Zurich, SWITZERLAND.

303

Joint Symposium 4 (EANM/EURADOS): Hot Topics in Radiation Protection

Thursday, October 22, 2020, 16:35 - 18:05 Channel 3

OP-091
LNT Model - Understanding, Applications and Limitations
N. Varmenot; Institut de Cancérologie de l'Ouest, Nantes, FRANCE.

OP-092
Breastfeeding - The Confusing Status of Rules and Guidelines - The Need for Harmonization
S. Leide-Svegborn; Lund University, Department of Radiation Physics, Malmö, SWEDEN.

OP-093
External Dose Rates from Nuclear Medicine Patients to Specific Patient-Carers Geometries - A Computational Approach
L. Struelens; Belgian Nuclear Research Centre, Institute for Environment, Health and Safety, Mol, BELGIUM.

OP-094
Selecting Biokinetic Models for TAC Calculations and Issues with MIRD Compartmental Model of 18F-FDG
W. Li; Helmholtz Zentrum München, Deutsches Forschungszentrum für Gesundheit und Umwelt (GmbH), Institute of Radiation Medicine, Neuherberg, GERMANY.

304

CTE 2: Update in Paediatric Imaging

Thursday, October 22, 2020, 16:35 - 18:05 Channel 4

OP-095
Technical Perspective and Challenges in Paediatric Imaging
A. Santos; Hospital CUF Descobertas, Medicina Nuclear Department, Lisbon, PORTUGAL.

OP-096
Nuclear Medicine in Paediatric Tumours - Past, Present and the Future
P. Ozgen Kiratli; Hacettepe University Medical Center, Ankara, TURKEY.

OP-097
PET/MR in Paediatric Imaging
C. Nappi; University Federico II, Department of Advanced Biomedical Sciences, Naples, ITALY.

305

M2M Track - TROP Session: Cardiovascular Imaging Translational

Thursday, October 22, 2020, 16:35 - 17:40 Channel 5

OP-098

Synthesis and Characterization of ^{18}F-Lableled 4-Thia-oleic Acid Derivatives for Fatty Acid Beta-Oxidation Imaging

Y. Murakami, Y. Fujita, H. Fushiki;
Astellas Pharma Inc., Tsukuba, JAPAN.

Aim/Introduction: To develop novel PET tracers for fatty acid oxidation, we have tried to modify 18-[^{18}F]fluoro-4-thia-oleate ([^{18}F]FTO) which was reported by DeGrado et al (1). [^{18}F]AS3504073-00 (7-[^{18}F]fluoro-4-thia-oleate) was successfully discovered as an excellent PET tracer for beta-oxidation imaging as previously reported (2) (3) (4). [^{18}F]AS3504073-00 has an ideal characteristics, high accumulation in heart and no bone accumulation by defluorination, even though only the ^{18}F labeling position is different from that on [^{18}F]FTO. In the present study, more several analogs of [^{18}F]FTO were synthesized and evaluated in monkey PET studies to clarify the relationship between the ^{18}F-position on 4-thia-oleate and the imaging characteristics as a PET tracer. ***Materials and Methods:*** Several secondary ^{18}F-fluorinated analogs, 17-fluoro-4-thia-oleate (17-FTO), 15-fluoro-4-thia-oleate (15-FTO), 12-fluoro-4-thia-oleate (12-FTO), 7-fluoro-4-thia-oleate, (7-FTO, AS3504073-00) and 6-fluoro-4-thia-oleate (6-FTO) were prepared from each tosylate or bromide-precursor in a similar manner. Nucleophilic ^{18}F fluorination on each precursor using [^{18}F]TBAF/TBAHCO$_3$, and then hydrolysis of methylester was performed. The obtained all ^{18}F-labeled compounds were administered to cynomolgus monkeys and PET measurements were performed. ***Results:*** All five compounds were successfully synthesized with enough quality and stability for animal experiment, although the radiochemical yield of 6-[^{18}F]FTO was lower than those of other compounds. In monkey PET studies, 12-[^{18}F]FTO, 7-[^{18}F]FTO ([^{18}F]AS3504073-00) and 6-[^{18}F]FTO showed higher accumulation in heart than [^{18}F]FTO. However, only [^{18}F]AS3504073-00 showed no significant accumulation of radioactivity in the bone. The SUV values of 12-[^{18}F]FTO, 7-[^{18}F]FTO ([^{18}F]AS3504073-00) and 6-[^{18}F]FTO in the heart and bone were 9.77 (heart), 3.17 (bone), 9.26, n.d. and 7.25, 1.96 at 60 min after administration, respectively. ***Conclusion:*** In the present study, we clarified the relationship between the ^{18}F position on 4-thia-oleate and the characteristics as a PET tracer. The only 7-position of ^{18}F on 4-thia oleate was metabolically stable. With regard to the accumulation in heart, compounds in which the closer position of ^{18}F to the olefin showed higher uptake. Taken together, we concluded [^{18}F]AS3504073-00 was the best tracer among [^{18}F]fluoro-4-thia oleates. ***References:*** (1) DeGrado TR et al., J Nucl Med. 2010;51:1310-1317., (2) Murakami Y et al, SNMMI 2020 Annual meeting in New Orleans., (3) Fushiki H et al, SNMMI 2020 Annual meeting in New Orleans., (4)Ohshima Y et al, SNMMI 2020 Annual meeting in New Orleans.

OP-099

Production of [^{18}F]AS3504073-00 for Investigational PET Imaging of Fatty Acid Beta-Oxidation in Human Subjects

Y. Murakami, H. Fushiki;
Astellas Pharma Inc., Tsukuba, JAPAN.

Aim/Introduction: Fatty acid beta-oxidation is a complex process involving several enzymes and transport proteins, and several SPECT and PET tracers have been developed. 3-{[(3RS,5Z)-3-[^{18}F]Fluorotetradec-5-en-1-yl]sulfanyl} propanoic acid ([^{18}F]AS3504073-00) was discovered as a novel PET tracer for fatty acid beta-oxidation, and showed high accumulation in heart and metabolically stable character. Preclinical toxicity studies of AS3504073-00 was already conducted, and the safety of [^{18}F]AS3504073-00 for human administration was verified. In the present study, our goal is to establish the synthetic method of [^{18}F]AS3504073-00 which meets the requirement of cGMP regulation. ***Materials and Methods:*** [^{18}F]AS3504073-00 was prepared by two subsequent reactions, (i) a nucleophilic fluorination of the corresponding tosylate precursor with [^{18}F]fluoride in the presence of tetrabutylammonium hydrogen carbonate in acetonitrile at 120 °C, for 10 min; (ii) hydrolysis of methyl ester with KOH at 110 °C, for 4 min. Product purification was done by semi-prep HPLC (Waters XBridge C18 column, 0.1 M HCl/CH3CN=30/70), followed by solid phase extraction eluted with ethanol and saline dilution including ascorbic acid. The resulting solution is passed through a sterilizing 0.2 µm membrane filter into a sterile vial. ***Results:*** Progress with process validation demonstrated that 78.3 ± 3.7 mCi (EOS;11.4 ± 0.6% RCY (DC)) of formulated [^{18}F]AS3504073-00 could be made. Full QC was performed on these preparations to show that they met or exceeded the acceptance specifications required for the release of the drug product. The radiochemical purity was more than 97%, and the specific activity was over 5.1 Ci/micromol. Stability of the radiopharmaceutical was evaluated after storage in the final dosage form. The radiochemical purity of the product remained higher level, >95% up to at least 8 h after EOS at room temperature. ***Conclusion:*** An automated radiosynthesis of [^{18}F]AS3504073-00 has been developed, and the procedure intended for clinical use meets the requirements of cGMP regulatory bodies. ***References:*** None

OP-100

Longitudinal evaluation of myocardial fatty acid metabolism post-myocardial ischemia/reperfusion injury in the border and remote myocardium using^{18}F-fluoro-6-

thia-heptadecanoic acid PET imaging in swine model

F. Zhang[1,2], Y. Wang[1,2];
[1]The Third Affiliated Hospital of Soochow University, Changzhou, CHINA, [2]Changzhou Key Laboratory of Molecular Imaging, Changzhou, Jiangsu Province, CHINA.

Aim/Introduction: Myocardial ischemia/reperfusion injury (MI/RI) is a pivotal therapeutic target to optimize revascularization therapy for acute coronary syndrome. Previous studies have found that reduced myocardial fatty acid (FA) uptake in ischemic myocardium, to date there have been no reports focusing on the myocardialsubstrate metabolismin the border and remote areas and its longitudinal changes. Thus, we used PET imaging to noninvasively evaluate the longitudinal uptake of 14(R,S)-^{18}F-fluoro-6-thia-heptadecanoic acid (^{18}F-FTHA) as analogs of FA to quantify myocardial metabolic substrate change in a swine model of MI/RI. ***Materials and Methods:*** Five male Bama miniature swine(weight 30-35 kg) were modeled by catheter-based 30 mins occlusion of left anterior descending coronary artery followed by reperfusion. 18F-FTHA PET, ^{99m}technetium-sestamibi (^{99m}Tc-MIBI) SPECT myocardial perfusion imaging (MPI), and echocardiography were performed simultaneously at baseline and 2h, 1, 5, 21, and 30 days post-MI/RI. The Left ventricular myocardium was divided into the infarct, border, and remote areas. FA metabolism in different regions were assessed as ^{18}F-FTHA uptake ratio (calculated as the ratio of Myocardium$_{SUVmean}$to Mediastinal Blood Pool$_{SUVmean}$) on PET imaging. The longitudinal changes of FA metabolism and differences between ischemic, border and remote areas were analyzed by repeated measurement ANOVAand generalized estimating equations. ***Results:*** 18F-FTHA uptake ratio in the three regions significantly decreased at 2h post MI/RI, reached the lowest point at 1 day, partial recovered at 5 days (All $P < 0.05$), and no significant differences were observed during the following 30-day follow-up period (All $P > 0.05$). FA metabolism in the ischemic area was significantly less than the border and remote areas at every time points post MI/RI. The ischemic area was the lowest, the border area was the second, and then was the remote area (All $P < 0.05$). Interestingly, reduced ^{18}F-FTHA uptake ratio in the border and remote areas revealed very similar trends when compared with ischemic area in the progression of FA metabolism disorder following MI/RI. ***Conclusion:*** ^{18}F-FTHA PET metabolism imaging, as an noninvasive molecular imaging, is an useful tool to monitor myocardial metabolism in vivo. FA metabolism in the LV myocardium decreased and changed dynamically after MI/RI.In addition to the ischemic region, myocardium FA metabolism were also impaired to varying degrees even in the border and remote regions after the onset of MI/RI, although the three showed an similar trend. This finding may suggest the mechanism underlying MI/RI and has important implications from the viewpoint of myocardial substrate metabolism. ***References:*** None

OP-101

Predicting post-ischemic angiogenesis with an APJ-specific PET radiotracer

B. Louis[1], *A. Moyon[2], A. Bouhlel[1], L. Balasse[1], S. Fernandez[1], S. Simoncini[3], G. Hache[2], F. Dignat-George[4], P. Garrigue[2], B. Guillet[2];*
[1]C2VN INSERM 1263 INRA 1260 CERIMED Aix-Marseille Université, Marseille, FRANCE, [2]C2VN INSERM 1263 INRA 1260 CERIMED, APHM, Aix-Marseille Université, Marseille, FRANCE, [3]C2VN INSERM 1263 INRA 1260 Aix-Marseille Université, Marseille, FRANCE, [4]C2VN INSERM 1263 INRA 1260, APHM, Aix-Marseille Université, Marseille, FRANCE.

Aim/Introduction: APJ receptor, expressed in various tissues has recently been identified as a key player in angiogenesis and as an innovative pharmacological target to promote angiogenesis. Thereby, we aimed to evaluate an innovative PET imaging agent specific of APJ, [^{68}Ga]Ga-AP747, in two preclinical models of angiogenesis. ***Materials and Methods:*** AP747 was designed, synthetized, radiolabeling with gallium-68 and specificity was setup. Radiochemical stability in NaCl 0.9% and in human serum was validated up to 2h after synthesis by TLC.Swiss mice were subcutaneously implanted behind their neck with 400µL of Matrigel supplemented with 10% fetal bovine serum, described as a simple hypoxic model (n=7).Unilateral hindlimb ischemia (HLI) mouse model was initiated by femoral artery resection (n=8). LASER-Doppler perfusion imaging was performed up to day 21 after surgery and expressed as ischemic to non-ischemic limb blood flow ratio (i/c).On days 1, 3, 7, 10, 13 and 21 post-surgery, mice were IV injected with 5-10 MBq (50µL,0.17µg) of [^{68}Ga]Ga-AP747. PET images were acquired 60 min after IV injection on a Mediso Nanoscan PET/CT and compared to PET images obtained after IV injection of 5-10 MBq (50µL,0.17µg) of [^{68}Ga]Ga-NODAGA-RGD$_2$. ***Results:*** [^{68}Ga]Ga-AP747 was produced with a radiochemical purity of 96.7%±2.0 and radiochemical stability in serum evaluated at 2h (95.0±1.5%).In a simple hypoxic model, [^{68}Ga]Ga-AP747 accumulated in Matrigel and this accumulation was significantly higher than that of [^{68}Ga]Ga-NODAGA-RGD$_2$ from day 10 (*P=0.036), to day 21 (**P=0.002).In the ischemic model, we observed an intense, earlier and higher [^{68}Ga]Ga-AP747 PET signal in the ischemic hindlimb (peaking on day 7, i/c=5.49± 5.98) than with [^{68}Ga]Ga-NODAGA-RGD$_2$ (peaking on Day 10, i/c=2,51±1,29;*P=0.066). Day 7 [^{68}Ga]Ga-AP747 PET signal in ischemic hindlimb was negatively correlated to LASER-Doppler signal at day of surgery (R^2=0.6291; P=0.02),seeming to highlight that [^{68}Ga]Ga-AP747 PET signal within ischemic limb increased with tissue ischemia intensity. [^{68}Ga]Ga-AP747 PET signal in ischemic limb is more important when reperfusion is longer: signal at Day 7 (peak) is correlated to late reperfusion index (Day 21/ Day 1)(R^2= 0.6245;P=0.02). ***Conclusion:*** We initially developed AP747 as a companion tool for APJ-modulating therapeutic strategies. We additionally postulate that PET imaging of APJ using AP747 could be a potential tool to

evaluate tissue angiogenesis. [^{68}Ga]Ga-AP747 PET imaging in two angiogenesis models: simple hypoxic model (Matrigel) and hypoxo-ischemic model (hindlimb ischemia), not only outbroke [^{68}Ga]Ga-RGD-based PET imaging, the actual reference in angiogenesis molecular imaging, but also was positively correlated with late reperfusion. ***References:*** None

OP-102

Dynamic evaluation of diastolic dyssynchrony by SPECT gated myocardial perfusion imaging early after acute myocardial infarction and the relationship with progression of left ventricular remodeling in swine model

F. Zhang[1,2], J. Wang[3], X. Shao[3], Y. Wang[1,2];
[1]The Third Affiliated Hospital of Soochow University, Changzhou, CHINA, [2]Changzhou Key Laboratory of Molecular Imaging, Changzhou, Jiangsu Province, CHINA, [3]The Third Affiliated Hospital of Soochow University, Changzhou, China Changzhou Key Laboratory of Molecular Imaging, Changzhou, Jiangsu Province, CHINA.

Aim/Introduction: Left ventricular diastolic asynchrony (LVDD), a dyssynchronous relaxation pattern, was known to develop after myocardial damage. We aimed to evaluate the dynamic changes of LVDD in the early stage of acute myocardial infarction (AMI) by phase analysis of ^{99m}technetium-sestamibi (^{99m}Tc-MIBI) SPECT gated myocardial perfusion imaging (GMPI) and its relationship with theprogression of left ventricular remodeling (LVR). ***Materials and Methods:*** The left anterior descending coronary artery of 16 Bama miniature swine were occluded by balloon to build AMI models. Animals were imaged before AMI and at 1 day, 1 week and 4 weeks after AMI by SPECT GMPI, and quantitative analysis was performed to obtain the extent of myocardial perfusion defect (Extent), and LVDD parameters: phase histogram bandwidth (PBW) and phase standard deviation (PSD). Echocardiography was simultaneously applied to evaluate left ventricular end-diastolic volume (LVEDV), left ventricular end-systolic volume (LVESV) and left ventricular ejection fraction (LVEF). Both myocardial injury markers and 12-lead ECG were measured.The degree of LVR progression was defined as LVESV (%) = ($LVESV_{AMI4\ weeks}$-$LVESV_{AMI1\ day}$) / $LVESV_{AMI1\ day}$.Generalized estimating equations and pearson linear correlation analysis were mainly used for data analysis. ***Results:*** Thirteen swine were successfully completed the study. LVDD changes dynamically at different time points after AMI. LVDD occurred as early as 1 day after AMI, peaked at 1 week, and there wasa partial recovery trendin 4 weeks. PBW, PSD on 1 day after AMI were associated withLVRP, respectively (r = 0.662, 0.617, both P <0.05). After adjusted for QRS duration and Extent,PBW, PSD on 1 day after AMI were independently associated with progression of LVR (PBW, OR=1.004, 95%CI: 1.001-1.007, P=0.017; PSD, OR=1.008, 95%CI: 1.000-1.017, P=0.049). In addition, the repeatability and reproducibility of LVDD by phase analysis of SPECT GMPI were all excellent (ICCs: PBW: 0.948, 0.921; PSD: 0.977, 0.914, all P < 0.001). ***Conclusion:*** LVDD occurred on the first day of AMI, reaches its peak in 1 week and partly recovered in 4 weeks after AMI. LVDD evaluated by phase analysisof SPECT GMPIearly after AMI could independentlypredict progression of LVRafter adjusted for QRS duration and Extent. The earlyassessment of LVDD after AMI may provide helpful information for predicting the progression of LVR in the future. ***References:*** None

OP-103

[^{18}F]AS3504073-00, Reflects Mitochondrial Fatty-Acid Oxidation in Physiological Alterations and Cardiac Disfunctions

H. Fushiki*, Y. Murakami;*
Astellas Pharma Inc., Tsukuba, Ibaraki, JAPAN.

Aim/Introduction: Myocardial energy metabolism is mainly dependent on Fatty Acid Oxidation (FAO) in ATP production, however, FAO alteration in cardiac dysfunction is still unclear. We reported [^{18}F]AS3504073-00 as a novel PET probe for FAO with good property on higher uptake in heart and no defluorination in vivo. Here we report further evaluation of the accumulation in mitochondria and the character of [^{18}F]AS3504073-00 in physiological alterations and cardiac disfunctions. ***Materials and Methods:*** [^{18}F]AS3504073-00 was synthesized in house. DBA2 mice were used for biostribution study of [^{18}F]AS3504073-00 with or without etomoxir, an inhibitor for CPT-1, to understand specificity of accumulation of [^{18}F]AS3504073-00 inside mitochondria. To understand the alteration of FAO in several physiological properties, uptake studies of [^{18}F]AS3504073-00 were performed under starvation or exercising burden in DBA2 mice. Longitudinal PET imaging with [^{18}F]AS3504073-00 was demonstrated to monitor the FAO status in both animals. Heart infraction model in monkey was established by occluding left anterior descending coronary artery (LAD). Head-to head comparison of PET imaging with [^{18}F]AS3504073-00 in acute (1-week) and subchronic (1-month) phase was conducted in ischemic heart disease monkey models. ***Results:*** [^{18}F]AS3504073-00 was successfully synthesized with enough quality and purity. In the biodistribution study with etomoxir in mice, [^{18}F] AS3504073-00 was mainly accumulated into brown adipose tissue, heart and diaphragm and these accumulations were inhibited with etomoxir. Food-restricting starvation and running burden, which induce upregulation of FAO, increased [^{18}F]AS3504073-00 accumulation in several organs, including heart, diaphragm and skeletal muscle. In monkey LAD occlusion model, [^{18}F]AS3504073-00 was visualized ischemic region at acute and subchronic phase. The higher uptake of [^{18}F]AS3504073-00 was observed in non-ischemic heart region at subchronic phase rather than that at acute phase. These observations might reflect the metabolic dysfunction and the remodeling in ischemic heart disease.

Conclusion: [^{18}F]AS3504073-00 is shown to be a potential tool of mitochondrial FAO specific PET probe. The character of [^{18}F] AS3504073-00 warrants the usefulness with good specificity and imaging efficacious window in clarifying the several heart disease mechanism and region from FAO point of view. ***References:*** (1) DeGrado TR et al., J Nucl Med. 2010;51:1310-1317., (2) Murakami Y et al, SNMMI 2020 Annual meeting in New Orleans., (3) Fushiki H et al, SNMMI 2020 Annual meeting in New Orleans., (4)Ohshima Y et al, SNMMI 2020 Annual meeting in New Orleans.

OP-104

Multitracer PET imaging for characterization of the IDH mutation in glioma: a translational in vitro and in vivo study

A. Clement[1], *T. Zaragori*[1], *M. Doyen*[1], *R. Filosa*[1], *O. Ovdiichuk*[1], *G. Hossu*[2], *C. Collet*[1], *F. Maskali*[1], *J. Pierson*[3], *E. Roeder*[1], *G. Karcher*[4], *A. Verger*[4];
[1]*Nancyclotep, Vandoeuvre-Les-Nancy, FRANCE,* [2]*IADI UMR 1254, Vandoeuvre-Les-Nancy, FRANCE,* [3]*CRAN UMR 7039, Vandoeuvre-Les-Nancy, FRANCE,* [4]*Nuclear Medicine, Vandoeuvre-Les-Nancy, FRANCE.*

Aim/Introduction: PET imaging is currently proposed as an adjunct to MRI for brain tumor characterization. This translational research project proposes to explore multi-tracer PET imaging for the non-invasive characterization of the mutation IDH1 in glioma, a factor of good prognosis. ***Materials and Methods:*** U87 high-grade glioma isogenic cell lines with (CRISP/Cas9 method) or without IDH1 mutation (IDH1+/-) were studied in vitro and in vivo after stereotactic grafts into brain rats through a 4 consecutive days protocol with static and dynamic PET imaging of glycolytic metabolism ([18F]FDG), amino acid metabolism ([18F]FDopa, [11C]MET and [18F]FET), angiogenesis ([68Ga]NODAGA-$(RGD)_2$) and inflammation ([18F]DPA-714), in association with anatomical MRI. In vitro, the radiotracer uptake was expressed as a percentage per million cells. In vivo, maximal and mean tumor-to-background ratios (TBR_{max} and TBR_{mean}) for static analysis, time-to-peak and slope curve parameters for dynamic analysis were calculated for each radiotracer. ***Results:*** In vitro, IDH1+ cells showed significant lower levels of [68Ga]NODAGA-$(RGD)_2$ and [18F]DPA-714 uptake at all times of concentration measurements ($p \leq 0.04$ for all), in comparison to the IDH1- cells. These results were confirmed by in vivo analyses where lower uptake with [68Ga]NODAGA-$(RGD)_2$ (7.19 vs. 9.70 for TBR_{max}, p=0.01) but significantly higher decreasing curves for [68Ga]NODAGA-$(RGD)_2$ and [18F]DPA-714 (respectively, -0.15 vs. 0.02 and -0.18 vs. 0.23, p=0.04) were observed in IDH1+ tumors. In univariate analysis, no other significant result was obtained in vitro and in vivo for the other tracers. In multivariate analysis, the combination of TBR_{max} and slope of [68Ga]NODAGA-$(RGD)_2$ and slope of [18F]DPA-714 provided the best diagnostic performances to discriminate between the two isogenic cell lines (AUC of 0.87, $p<0.01$). ***Conclusion:*** [68Ga]NODAGA-$(RGD)_2$ and [18F] DPA-714, reflecting lower angiogenesis and inflammation in IDH1+ tumors, are two independent tracers of choice for characterizing the IDH1 mutation in high-grade gliomas and should be translationally studied for clinical applications in patients. ***References:*** None

OP-105

Towards simultaneous extracorporeal recordings of PET and MRI arterial input functions in mice

P. Backhaus[1,2,3], *F. Büther*[1,2], *L. Wachsmuth*[3], *S. Hermann*[2], *K. Schäfers*[2], *C. Faber*[3], *M. Schäfers*[1,2];
[1]*University Hospital Münster, Department of Nuclear Medicine, Münster, GERMANY,* [2]*University of Münster, European Institute for Molecular Imaging (EIMI), Münster, GERMANY,* [3]*University of Münster, Translational Research Imaging Center (TRIC), Münster, GERMANY.*

Aim/Introduction: Compartmental modeling in small animal PET and MRI can serve to better judge the performance of radiotracer candidates and the translational potential of contrast agent-driven perfusion studies. Precise recording of the arterial input function (AIF) is a key prerequisite for modeling, but its acquisition is very challenging in small animals. So far, no method for simultaneous recordings of PET radiotracers and MR contrast agent AIFs has been reported in mice. We recently introduced a novel experimental setup allowing to record perfusion MRI AIFs in mice using an extracorporeal circulation. The shunted blood perfuses two reservoirs that reside in the field of view of a 9.4 T Bruker MRI for dynamic recording of the arterial contrast agent concentration (Backhaus et al. 2020). This study aims to explore simultaneous recordings of the radiotracer AIF using MR compatible measuring units. ***Materials and Methods:*** We performed recordings of the extracorporeal radiotracer AIF with two MR-compatible measurement systems: (1) a Polyether ether ketone (PEEK) measuring chamber equipped with a plastic scintillator (beta microprobe, Biospace Lab) and (2) the Twilight blood sampler (SwissTrace, Zurich). The validity of the extracorporeal measurements and different approaches of dispersion correction were tested by comparison to the undispersed recorded AIF using a pair of beta microprobes inside the aortic arch and the mediastinum. ***Results:*** We could perform simultaneous measurements of PET and DCE-MRI AIF in mice using the beta microprobe measuring chamber after intravenous co-injection of Gadobutrol (Gadovist®) and ^{18}F-PSMA-1007 (14 - 38 MBq). The blood concentration peaks of the 2 agents showed very good quantitative agreement. In the validation experiments, the height of the dispersion corrected AIF peaks inside the measuring chamber were significantly smaller than simultaneously measured in vivo signals using the infraaortal and mediastinal microprobes in some animals.

Numerical simulations show that this may be explained by small accumulations of radioactivity within the chamber over the duration of the measurement. The two extracorporeal measurement systems showed comparable sensitivities. ***Conclusion:*** We demonstrate that recordings of the PET radiotracer AIFs can be simultaneously combined with the novel perfusion MRI extracorporeal circulation model using the two tested systems. This allows to firstly explore the potential synergistic effects for dual AIF recordings and integrated modeling in PET/MRI imaging in mice. ***References:*** Backhaus P, Büther F, Wachsmuth L, et al. Toward precise arterial input functions derived from DCE-MRI through a novel extracorporeal circulation approach in mice. Magn Reson Med. 2020;:1-12. doi:10.1002/mrm.28214

OP-106

Succinate promotes neovascularization in a peripheric ischemia rodent model: a microPET/CT study

A. Moyon*, L. Balasse, S. Fernandez, G. Hache, F. Dignat-George, P. Garrigue, D. Taïeb, B. Guillet;*
APHM, Marseille, FRANCE.

Aim/Introduction: Beyond its role in carbohydrate metabolism as a tricarboxylic acid cycle intermediate, succinate has a hormone-like function acting in various tissues and in tumors (1). GPR91 is a G protein-coupled receptor activated by specific binding with extracellular succinate. In recent years, it has been described that activation of the GPR91-ERK1/2-C/EBP-β signaling pathway played an important role in regulating angiogenesis through VEGF transcription (2) and was associated with neovascularization notably in diabetic retinopathies (3) and rheumatoid arthritis (4). Therefore, we hypothesized that succinate could be a simple and original key promoter of therapeutic angiogenesis and vascular regeneration in peripheric ischemia. ***Materials and Methods:*** Swiss mice (n=18) were subjected to right hindlimb ischemia induced by ligation and partial resection of the right femoral artery. Ischemic mice were daily injected with succinate solution (1mM in PBS pH7.4, 10µL, n=10) or with PBS (10µL, n=8) in the gastrocnemius muscle up to day 23 post-ischemia. Hindlimb perfusion was measured in vivo by LASER Doppler on days 1, 3, 8, 15, and 24 after ischemia, and results were expressed as mean±s_d ipsi- to contralateral ratios (i/c). To assess in vivo angiogenesis, mice were injected in the caudal vein with 5.8±1.5 MBq/50µL [^{68}Ga]Ga-RGD_2 allowed to rest for 60 min then underwent a 20min-long microPET/CT scan on days 4, 7, 10 and 14 after ischemia. Quantifications from [^{68}Ga]Ga-RGD_2 microPET/CT in ischemic hindlimb were expressed as percentage of the injected dose per gram of tissue (%ID/g). Statistical analysis was performed with Prism v8.4.2 (Graphpad software). ***Results:*** Over the 24-day follow-up by LASER-Doppler, succinate treatment enabled an earlier and more intense reperfusion of the ischemic hindlimb compared to PBS treatment (*P=0.0189) and especially on day 8 (i/c succinate: 72.3±18.5%; i/c PBS: 49.3±20.8%; *P=0.0110) and on day 15 (i/c succinate: 75.8±8.9%; i/c PBS: 50.6±23.4%; **P=0.0040). Interestingly, [^{68}Ga]Ga-RGD_2 microPET quantifications on day 4 (succinate: 0.32±0.17%ID/g; PBS: 0.10±0.07%ID/g; *P=0.0295) translating an earlier angiogenic activation maintained up to day 10 post-ischemia enabled by succinate treatment, corroborating with the clinical benefits on hindlimb perfusion. ***Conclusion:*** The present study shows that intramuscular injections of succinate promote earlier angiogenesis resulting in earlier and more intense revascularization in a hindlimb ischemia mouse model. This microPET/CT study provides an impetus to better characterize the determinants of post-ischemic vascular regeneration through GPR91 and downstream signaling pathways. ***References:*** (1) https://doi.org/10.2967/jnumed.117.192674(2) https://doi.org/10.18632/oncotarget.14485(3) https://doi.org/10.1038/srep45807(4) https://doi.org/10.1016/j.freeradbiomed.2018.07.009

306

Cutting Edge Science Track - TROP Session: Preclinical Dosimetry and Radiobiology

Thursday, October 22, 2020, 16:35 – 17:45 Channel 6

OP-107

Modeling DNA damage induced by targeted radionuclide therapy

G. Tamborino[1,2]*, M. De Saint-Hubert*[1]*, L. Struelens*[1]*, J. Nonnekens*[2,3]*, M. W. Konijnenberg*[2]*, M. De Jong*[2]*, Y. Perrot*[4]*, C. Villagrasa*[4]*;*
[1]Research in Dosimetric Applications, Belgian Nuclear Research Centre (SCK•CEN), Mol, BELGIUM, [2]Department of Radiology & Nuclear Medicine, Erasmus MC, University Medical Center Rotterdam, Rotterdam, NETHERLANDS, [3]Department of Molecular Genetics, Erasmus MC, University Medical Center Rotterdam, Rotterdam, NETHERLANDS, [4]Institut de Radioprotection et de Sûreté Nucléaire (IRSN), Fontenay aux Roses, FRANCE.

Aim/Introduction: The aim of this study is to build a simulation framework to evaluate the number of DNA double strand breaks (DSBs) occurring during in vitro targeted radionuclide therapy (TRNT), adapting a simulation chain that has been benchmarked against external beam radiotherapy. This work represents the first step towards modeling DSBs during TRNT with the ultimate goal of exploring underlying biological mechanisms and influence of physical/chemical parameters to enable a better response prediction in patients. This tool characterized early DSB induction by [^{177}Lu]Lu-DOTA-[Tyr^3] octreotate (^{177}Lu-DOTATATE), a commonly used TRNT for neuroendocrine tumors. ***Materials and Methods:*** A multiscale approach is implemented to simulate the number of DSBs produced by the cumulated decays of ^{177}Lu-DOTATATE, preliminary assumed as purely beta emitter, without

including any repair. The approach involves 2 sequential simulations performed with Geant4/Geant4-DNA and accounts for a realistic geometry of the cell population and detailed sampling of the activity distribution within it. In order to reproduce the exposure conditions of cells incubated 4h with ^{177}Lu-DOTATATE(2.5MBq/ml), a phase space is scored by recording particles that enter the nucleus of a cell belonging to a population modelled by realistic polygonal mesh structures. The radioactive source is sampled according to previous uptake experiments on the distribution of activities within medium and cells, assuming instant and permanent internalization. Following, the particles recorded in the phase space file are released within an ellipsoidal nucleus geometry, including a multi-scale description of the DNA. DnaFabric software is used to model the entire human genome with a continuous chromatin fiber per chromosome. This geometry is used to simulate the physical, physicochemical and chemical stages in Geant4-DNA in order to score the number of DSB/decay. ***Results:*** Our results reveal induction of 6-10 DSBs/cell, depending on the confluence level of the cell population, compared to on average 11±2 DSBs/cell which were experimentally measured. This slight difference may arise from neglected or simplified contributions dealing with physics (i.e. ^{177}Lu spectrum, radionuclide localization, morphological variation within a cell population, chromatin compaction, nuclear size), chemistry (i.e. extended chemical stage simulation time) or biology (i.e. other pathways for DSB formation) that are currently under investigation. ***Conclusion:*** Monte Carlo Track Structure codes, such as Geant4-DNA, are considered as suitable tools for the study of biological responses to ionizing radiation. Overall a better understanding of the mechanisms and biophysical parameters characterizing biological damage will allow to improve our ability to predict responses on a clinical scale. ***References:*** None

OP-108

Understanding the LET dependence of the RBE observed in cell assays irradiation

S. Walrand, M. Hesse, R. Lhommel, F. Jamar;
Université Catholique de Louvain, Brussels, BELGIUM.

Aim/Introduction: to derive an analytical expression for the RBE in term of the particle track structure properties which can be computed in water using Geant4-DNA. ***Materials and Methods:*** the DSB probability resulting from n SSB produced in n_{bp} base-pairs by a particle track is $n(n-1)/4n_{bp}$ (1).The probability distribution and geometric considerations governing the SSB induction by a free radical, the production of a free radical by a particle track and the number of track corresponding to a given nucleus dose were identified. These processes were successively mathematically applied to eq. 1 an resulted in a simple mathematical expression for the DSB probability. ***Results:*** The radiosensitivity was found to be $\alpha(LET) = N_{bp}\, F\, f(LET)^2\, Y(LET)$, where N_{bp} is the total genome length in base-pair units, F is a form factor depending on the nucleus and on the DNA compaction geometry, f is the particle track structure radius FWHM and Y is the free radicals yields. Both parameters f and Y were computed for various particles and LET values using Geant4-DNA. Using a single fitted F value for all, the RBE was rightly predicted for hamster V79 cells irradiated with proton, deuteron, He3 and alpha particle for LET ranging from 10 up to 150 keV/µm. ***Conclusion:*** The RBE is simply the product of 4 distinct quantities: the genome length, a form factor F depending on the spatial DNA compaction, the particle track FWHM and the free radicals yield in water. ***References:*** None

OP-109

Strand DNA break non-linear dynamics equations perfectly predict the asymptotic high dose behaviour of log cells survival fraction post irradiation

S. Walrand, M. Hesse, R. Lhommel, F. Jamar;
Université Catholique de Louvain, Brussels, BELGIUM.

Aim/Introduction: the multiple-target model (MTM) requires an additional empiric term to explain the non-null slope of the log-survival curve at low dose, while the linear-quadratic model (LQM) requires an additional one to reproduce the linear asymptotical behaviour of the log-survival fraction at high dose. Our aim is to solve the full DNA SSB dynamics equations system including all non linear effects to overcome these models drawbacks. ***Materials and Methods:*** The equation governing the number N of viable cells is: $dN = -(Y\, N_{bp}\, N\, dD)\, (n/(2\, N_{bp}\, N)) - \alpha N\, dD$ (1) , the first term is the SSB production (Y is the free radicals yield) and the second one is the probability that the SSB occurs in the mirror base of an already existing SSB in order to produce a DSB. The last term is the probability of a direct DSB production. The total number n of SSB inside these viable cells is governed by: $dn = (Y\, N_{bp}\, N\, dD)\, P + n/N\, dN$ (2), the second term takes into account that when a cell is condemned its SSB leaves the pool N of viable cells. $P = (1-n/(N_{bp}\, N))$ (3) takes into account that a new SSB is produced only if the free radical hits an intact base-pair. ***Results:*** Taking into account that $Y << \alpha$, the analytical integration of eq. 1-3 shows that the LQM β term is simply multiplied by: $eff(D) = (\alpha D + e^{-\alpha D} - 1)/(\alpha^2 D^2/2)$. At low dose this efficacy term tends to unity giving back the conventional LQM β term, at high dose it tends to $2/(\alpha D)$ explaining the linear asymptotical behaviour. Assuming n proportional to N D in eq. 1 gives back the conventional LQM at any dose. Confrontation with cell assay survival curves proves eff(D) quantitatively predicting the linear asymptotic position. ***Conclusion:*** Linear asymptotic behaviour of the log-survival curve simply results from the non-linear feature of the SSB dynamics equations. ***References:*** McParland BJ. Nuclear medicine radiation dosimetry: advanced theoretical principles. Springer Science & Business Media; 2010 Jul 3.

OP-110

Radiobiology of Auger Electron-emitter Technetium-99m: In Vitro Toxicity in Triple Negative Breast Cancer Cells Expressing Human Sodium Iodide Symporter

I. Costa[1], *N. Siksek*[1], *K. Osytek*[1], *A. Volpe*[1], *F. Man*[1], *E. Verger*[1], *G. Schettino*[2,3], *G. O. Fruhwirth*[1], *S. Y. A. Terry*[1];
[1]*King's College London, London, UNITED KINGDOM,* [2]*National Physical Laboratory, Teddington, UNITED KINGDOM,* [3]*University of Surrey, Guilford, UNITED KINGDOM.*

Aim/Introduction: Gamma-emitting technetium-99m is widely used in nuclear medicine diagnostic scans. It also emits on average 4 Auger electrons and 1.1 internal conversion electrons per decay(1). Despite increasing use of Auger electrons for molecular radionuclide therapy (MRT)(1), technetium-99m derived Auger electrons remain unexplored. This study explores the potential of technetium-99m for MRT and its imaging safety in triple negative breast cancer cells. ***Materials and Methods:*** MDA-MB-231 cells expressing human sodium iodide symporter (hNIS) were incubated with [^{99m}Tc]TcO_4 at activities up to 4 MBq/mL and for up to 24 hours. Efflux and intracellular location of [^{99m}Tc]TcO_4 using fractionation methods were determined and absorbed dose to the nucleus calculated. Toxicity in both parental and hNIS-expressing cells of [^{99m}Tc]TcO_4 was determined using clonogenic assays and compared to untreated cells, [^{99}Tc]TcO_4 and Caesium-137. Direct and indirect formation of DNA damage was determined using the γ-H2AX assay and radical scavenger Dimethyl sulfoxide (DMSO). A preliminary in vivo study was carried out by establishing orthotopic breast cancer models using hNIS-expressing cells and the biodistribution of [^{99m}Tc]TcO_4 determined at 30 minutes and 24 hours post-intravenous administration of [^{99m}Tc]TcO_4 by SPECT/CT imaging. ***Results:*** Intracellular uptake of [^{99m}Tc]TcO_4 peaked at 30 minutes, reaching a maximum intracellular activity of 1.9 ± 0.2 Bq/cell, with 50% efflux observed after 35.6 ± 0.2 minutes post-incubation, contributing to a maximum nuclear absorbed dose of 1.85 Gy at 24 hours. Following 30 minutes and 24 hours incubation with 4 MBq/mL, the average foci/nucleus increased by 13.4 ± 3.1 and 18.7 ± 3.1 compared to untreated cells, respectively. No decrease in average foci/nucleus was observed with DMSO and 24 hours post-incubation values were still greater than control. No DNA damage was observed in parental cells nor with [^{99}Tc]TcO_4. Survival fraction was reduced only in hNIS-expressing cells at 24 hours (A_{50}=0.76 Bq added/cell). In vivo, [^{99m}Tc]TcO_4 was taken up by endogenously hNIS-expressing organs and tumours at 30 minutes and at 24 hours post-administration [^{99m}Tc]TcO_4 was retained only in the hNIS-expressing tumours (28 ± 2.3%ID/g). ***Conclusion:*** In vitro toxicity, direct and partially repaired DNA damage following intracellular uptake of [^{99m}Tc]TcO_4^- and its in vivo retention in hNIS-expressing tumours at 24 hours show that technetium-99m derived Auger electrons must not be neglected in dosimetry calculations. Further research is needed to determine the potential and limitations of technetium-99m for MRT/theragnostics and the appropriate doses for use in imaging without safety concerns. ***References:*** (1)Ku, A. et al. EJNMMI radiopharm (2019)

OP-111

Ratiometric relationship between γH2AX imaging and Lutetium-177 is predictive of survival following radionuclide therapy in vivo

E. O'Neill*, G. M. Dias, B. Cornelissen;*
University of Oxford, Oxford, UNITED KINGDOM.

Aim/Introduction: There is growing interest in progressing radionuclide therapies such as [^{177}Lu]Lu-DOTATATE from a palliative treatment with effective symptom control into a treatment with curative intent. Yet to justify any increase in radionuclide dose to patients and risk additional normal toxicity, a suitable metric is needed to determine the required ^{177}Lu dose for each tumour within a patient. We have previously shown that [^{111}In]In-anti-γH2AX-TAT is capable of visualising the DNA double strand break damage response to the radionuclide therapy [^{177}Lu]Lu-DOTATATE. Here, we demonstrate that by using the gamma emissions from [^{111}In]In-anti-γH2AX-TAT alongside those of the ^{177}Lu, a suitable SPECT image-based metric can be calculated that is predictive of in vivo therapeutic effect. ***Materials and Methods:*** Athymic mice bearing CA20948 somatostatin receptor positive tumour xenografts were treated with varying levels of [^{177}Lu]Lu-DOTATATE (5 to 30 MBq), staggered into two cohorts and injected with [^{111}In]In-anti-γH2AX-TAT at either day 0 or day 4 of treatment and imaged by SPECT to image γH2AX formation kinetics and ^{177}Lu retention over days 1,3,5,7,9 and 11 of treatment. Tumour growth was monitored by calliper up to 90 days and survival determined by tumour doubling times and ethical biological endpoints. The daily kinetics of γH2AX foci formation were investigated using CA20948 cells in vitro in response to varying levels of [^{177}Lu]Lu-DOTATATE by immunofluorescence up to day 11. ***Results:*** Voxel-based SPECT analysis of dual isotope images revealed the linear relationship between ^{111}In and ^{177}Lu within each xenograft tumour to undergo a pivotal change between days 5 and 7 post-injection of [^{177}Lu]Lu-DOTATATE. The ratio between day 5 and 7 of the linear gradient of ^{111}In: ^{177}Lu correlated significantly with survival ($r = 0.98$, $P<0.0001$), representing both loss of ^{177}Lu from cell death, and sustained γH2AX expression in tumour regions with retained lower ^{177}Lu levels. This pivot was investigated in vitro by immunofluorescence and revealed widespread apoptosis at day 6 with γH2AX foci counts negatively correlating with [^{177}Lu]Lu-DOTATATE clonogenic survival ($r = -0.995$, $P = 0.0005$). ***Conclusion:*** We describe the use of γH2AX imaging with ^{111}In: ^{177}Lu dual isotope imaging following ^{177}Lu radionuclide therapy as an attractive strategy to predict tumour growth inhibition. This

temporal ratiometric contrast approach can therefore be used to measure therapeutic success and as any potential inter-individual differences in [^{111}In]In-anti-γH2AX-TAT uptake is in effect normalised within each individual by temporal comparison it presents a promising dual isotope imaging strategy to support personalised radionuclide therapy. ***References:*** None

OP-112

Differences of ex vivo and in vivo DSB induction and repair after internal irradiation in PMBCs during radioiodine therapy

S. Schumann[1], H. Scherthan[2], P. E. Hartrampf[1], A. K. Buck[1], M. Port[2], M. Lassmann[1], U. Eberlein[1];
[1]Department of Nuclear Medicine, University of Würzburg, Würzburg, GERMANY, [2]Bundeswehr Institute of Radiobiology affiliated to the University of Ulm, Munich, GERMANY.

Aim/Introduction: A sub-study of the MEDIRAD project investigates the effects of low doses in patients with differentiated thyroid cancer (DTC) during radioiodine therapy. One aim is to analyse the time- and dose-dependent induction and repair of DNA double-strand breaks (DSBs) in peripheral blood mononuclear cells (PBMCs) in vivo and ex vivo after internal irradiation with [^{131}I]NaI. ***Materials and Methods:*** Radiation-induced DSBs were quantified in blood samples of 7 DTC patients taken before, and 1h, 2h, 3h, 4h and 24h after [^{131}I]NaI administration. One part of the blood sample taken before therapy start was exposed internally by adding [^{131}I]NaI to reach, after 1h incubation, an absorbed dose to the blood of 50mGy. The remaining non-irradiated blood served as baseline sample. To investigate the ex vivo repair, PBMCs isolated from all samples were either directly ethanol-fixed, or fixed after short time culture in RPMI for 4h and 24h. For the samples taken during the therapy, PBMCs were directly isolated and ethanol-fixed. All samples were immuno-stained with γ-H2AX and 53BP1 antibodies and co-localized foci were counted manually. ***Results:*** After ex vivo irradiation, a mean of 0.57±0.14 radiation-induced foci per cell (RIF) was observed after direct fixation. The mean number of RIF decreased to 0.27±0.09 after 4h and 0.06±0.04 after 24h. In vivo, the mean number of RIF was 0.40±0.20, 0.58±0.21, 0.67±0.18, 0.73±0.18, and 0.42±0.17 at 1h, 2h, 3h, 4h and 24h after therapy start, respectively. The mean absorbed dose to the blood at the five time points was (15±2)mGy, (29±5)mGy, (47±8)mGy, (65±12)mGy and (193±37)mGy. Comparing the directly fixed ex vivo values to the in vivo results, the number of RIF is comparable to the value 3h after therapy start at a similar absorbed dose to the blood. ***Conclusion:*** Due to the continuous irradiation in vivo, the number of DSBs increased up to 4h after therapy start and DSBs were not completely repaired 24h after administration. Ex vivo, DSB numbers were decreased 4h after washing out the activity and DSB repair was almost completed after 24h. This study shows that the continuous irradiation with decreasing, however non-negligible, dose rates in patients leads to altered repair kinetics in vivo, as there is most likely still DSB induction competing with repair. This finding contrasts with the ex vivo exposure, where irradiation is stopped by removing the activity. Future steps involve patient-specific calculations of the dose-dependent repair kinetics and the inclusion of more patients. ***References:*** None

OP-113

A whole-body physiologically-based pharmacokinetic model of [^{212}Pb]Pb-DOTAMTATE in neuroendocrine-tumour bearing mice

N. Zaid*, P. Kletting, A. Beer, G. Glatting;*
Ulm University, Ulm, GERMANY.

Aim/Introduction: The use of alpha-emitter labelled somatostatin analogues for peptide receptor radionuclide therapy (PRRT) is a promising therapeutic option for neuroendocrine tumours (NETs). The short-range cytotoxic alpha particles reduce the nephrotoxicity and overcome the radioresistance of NETs to beta emitters in PRRT. Mathematical modelling helps performing cost- and animal-free investigations to study the pharmacokinetics of alpha-emitter labelled somatostatin analogues and speeds up the translation from bench to bedside. Therefore, we developed a physiologically-based pharmacokinetic (PBPK) model to describe the pharmacokinetics of [^{212}Pb]Pb-DOTAMTATE targeting somatostatin receptor type2 in AR42J-bearing mice to improve treatment planning in alpha-emitter based PRRT for NETs. ***Materials and Methods:*** A whole-body compartmental model was developed and selected among other developed models based on the Akaike Information Criterion (AIC) using the modelling software SAAM II (v2.3, The Epsilon Group, TEG, USA). The model describes all major physiological mechanisms (peptide distribution, extravasation, receptor binding, specific and non-specific uptake in the kidneys, internalization and excretion) and physicochemical decays (physical decay and chelator stability) with parameter values from the literature. Data of [^{212}Pb]Pb-DOTAMTATE biodistribution in mice bearing AR42J rat xenografts were used for evaluating the developed model[1]. The fit was performed by intravenous injection of 0.0015 nmol of [^{212}Pb]Pb-DOTAMTATE with a molar activity of 0.13 GBq/nmol in a 30 g mouse. The time-activity curves for the tumour, pancreas, kidneys, spleen and lung were fitted to estimate the receptor densities as well as the plasma flow-rate to the tumour. The calculated receptor density responsible for non-specific uptake in the kidneys was 17 nmol/l. ***Results:*** The developed model could successfully describe the published experimental data. The fitted curves were good by visual inspection and R^2>77%. The tumour-specific receptor density and plasma flow-rate were (27±33) nmol/l and (0.05±0.03) ml/min/g, respectively. The specific receptor

densities in pancreas, spleen, kidneys and lung were (5.8±2.0) nmol/l, (0.8±0.3) nmol/l, (3.7±1.6) nmol/l and (1.8±0.7) nmol/l, respectively. ***Conclusion:*** The model best supported by the data successfully simulated the [^{212}Pb]Pb-DOTAMTATE biodistribution study. The developed ^{212}Pb-PBPK model allows for simulating the biokinetics of radiolabelled and unlabelled pharmaceuticals and free radionuclides in the whole mouse body. The ability of the model to estimate important physiological parameters, such as receptor densities and specific and non-specific uptakes, and subsequently predict optimal dosing regimens will reduce the required time for translation from bench to bedside. Consequently, the model allows for generating hypotheses for experiments leading to improve alpha-emitter-based PRRT for NET. ***References:*** 1. Stallons et al.,MolCancerTher.2019;18(5):1012-1021.

OP-114

Modelling Show Alpha-emitter Astatine-211 is an Apposite Candidate for Intra-thecal Radioimmunotherapy of Neuroblastoma Metastasized to the Central Nervous System

S. Palm[1], *T. Bäck*[1], *E. Leidermark*[1], *S. Lindegren*[1], *E. Aneheim*[1], *H. Jensen*[2], *R. Hultborn*[1], *P. Albertsson*[1], *L. Jacobsson*[1];
[1]*University of Gothenburg, Gothenburg, SWEDEN,*
[2]*Rigshospitalet, Copenhagen, DENMARK.*

Aim/Introduction: At least two antibodies, 3F8 and 8H9, have been used in clinical trials with the beta-emitting radionuclide ^{131}I for intra-thecal radioimmunotherapy of neuroblastoma metastasized to the central nervous system (1,2). Published models indicates that a better ratio of absorbed dose to tumor over that to critical healthy tissues can likely be achieved by instead using alpha-emitting radionuclides (3). In the current work, we model the possible effect of using alpha-emitter astatine-211 (half-life 7.2h) as radiolabel for 3F8 and 8H9. ***Materials and Methods:*** 3F8 antigen binding properties were taken from (4). The transport mechanisms were simulated using the software package STELLA (ISEE Systems, Inc.). The resulting time-dependent biodistribution was then used as input for dosimetry. Microdosimetry was performed by an in-house-constructed Monte Carlo program. ***Results:*** The model allow estimates of efficacy and toxicity for varying a range of input parameters. Based on this optimization of the therapy can be done. An example is provided for specific activity where 1 of 100 mAbs are radiolabeled with At-211 and cancer cells have 500.000 antigens specific for 3F8. For a maximum of 0.4 Gy to the bone marrow, 83 MBq ^{211}At-3F8 can be infused intra-thecally to a 20 kg patient. Absorbed dose to single cancer cells within the cerebrospinal fluid (CSF) is estimated to 19 Gy. Unspecific absorbed dose to CSF surfaces is 5 Gy. Cancer cells directly accessed by blood will receive 5.2 Gy. ***Conclusion:*** Modelling show that safe amounts of ^{211}At-labelled 3F8 antibodies, delivered intra-thecally, could eradicate neuroblastoma cells accessed by the cerebrospinal fluid, and possibly also cells accessed by blood. ***References:*** 1. J Clin Oncol 25:5465-5470 2. J Nucl Med 2019; 60:1794-1801 3. Eur J Nucl Med Mol Imaging (2011) 38:334-342 4. Oncoimmunology. 2012 Jul 1;1(4):477-486.

OP-115

Biodistribution and dosimetry studies for the optimization of pre-targeted radionuclide therapy using ^{211}At-labeled modified biotin

N. Ukon[1], *K. Washiyama*[1], *A. Sugiyama*[2], *S. Zhao*[1], *T. Tatsumi*[2], *M. Aoki*[1], *K. Yamatsugu*[2], *K. Nishijima*[1], *S. Shimoyama*[1], *C. Tan*[1], *T. Joho*[1], *N. Oriuchi*[1], *M. Kanai*[2], *K. Takahashi*[1], *T. Kodama*[2];
[1]*Fukushima Medical University, Fukushima, JAPAN,*
[2]*The University of Tokyo, Tokyo, JAPAN.*

Aim/Introduction: The pre-targeting strategy increases the absorbed dose to a tumor while reducing the side effects affecting normal tissues, resulting in a high therapeutic effect. Although the pre-targeting system has been selected and characterized, at least four variables remain to be adjusted: the dosage of the pre-targeting agent, pre-targeting interval (time between injections of the pre-targeting agent and radiolabeled effector), dosage of the effector, and detection time (time to sacrifice post-injection of the radiolabeled effector). The aim of this study was to optimize the pre-targeting interval time between injections of the pre-targeting agent and radiolabeled effector in our developed system. ***Materials and Methods:*** We used both mutated streptavidin with low immunogenicity, which can fuse to four single-chain variable fragments (scFv), called "Cupid", and a modified bis-iminobiotin corresponding to Cupid with a specific affinity, called "Psyche". Psyche-B, which is a Psyche, was labeled with ^{211}At. Anti-CEACAM5 scFv-conjugated streptavidin (CEA-Cupid, 100 pmol) was administered to carcinoembryonic antigen (CEA)-positive human gastric cancer cells xenograft BALB/c nu/nu mice. After 24, 48, and 72 h, the mice were injected with 250 kBq of ^{211}At-labeled Psyche-B (^{211}At-Psyche-B) and sacrificed at 1 min, 1 h, 6 h, and 24 h after the ^{211}At-Psyche-B injection. Samples were collected and measured for radioactivity using a gamma counter. The absorbed radiation dose for each interval condition was calculated using OLINDA/EXM ver. 2.0. ***Results:*** At the 24-h interval, ^{211}At-Psyche-B in blood decreased with time, and approximately 94% of the injected dose was excreted within 24 h. The tumor accumulation was 16.3 ± 4.1 %ID/g at 24 h after the ^{211}At-Psyche-B injection; this decreased to 11.28 ± 3.33 %ID/g and 1.47 ± 0.23 %ID/g at 24 h after ^{211}At-Psyche-B injection when the interval condition changed to 48 h and 74 h, respectively. The absorbed dose to the kidneys was greater as the pre-targeting interval condition was longer in the mouse model. The absorbed dose of the tumor was calculated using the sphere model, and the tumor-to-kidney ratio was calculated. The absorbed dose to the tumor was higher when the pre-targeting

interval condition was shorter. The tumor-to-kidney ratios showed the same trend. ***Conclusion:*** Tumor accumulation of ^{211}At-Psyche-B increased over time when the pre-targeting interval was 24 h. The results of our study suggested that a pre-targeting interval of 24 h may be optimal for our pre-targeted radionuclide therapy using Cupid and Psyche-B. ***References:*** Sugiyama et al., Prc. Jpn. Acad. Ser. B 95:602, 2019

OP-116

Multi-regional dosimetry of mouse kidneys for beta-emitters

C. Saldarriaga Vargas[1,2], P. Covens[2], M. D'Huyvetter[2], V. Caveliers[2], B. W. Miller[3,4], L. Struelens[1];
[1]Belgian Nuclear Research Centre (SCK CEN), Mol, BELGIUM, [2]Vrije Universiteit Brussel, Jette, BELGIUM, [3]University of Colorado School of Medicine, Aurora, CO, UNITED STATES OF AMERICA, [4]University of Arizona, Tucson, AZ, UNITED STATES OF AMERICA.

Aim/Introduction: Conventional preclinical internal dose estimates typically assume a uniform distribution of radioactivity and dose deposition throughout organ tissues. This assumption can deviate from reality for β$^-$/α-emitting radioligands with a heterogeneous tissue activity distribution. In this study S-values for internal dosimetry of β$^-$ emitters were calculated for a multi-region model of a mouse kidney. The significance of regional S-values was demonstrated for the mouse kidney biodistribution of a ^{131}I-labeled single-domain anti-HER2 antibody fragment with predominant uptake in the outer medulla outer stripe. ***Materials and Methods:*** A stylized computational model of a mouse kidney was developed, consisting on ellipsoids delimiting 5 tissue compartments: cortex, outer medulla outer/inner stripes (IS/OS), inner medulla and papilla. Electron energy absorbed fractions (Ø) for the different kidney regions were calculated for ^{131}I and ^{90}Y, from photon-electron transport simulations using MCNP6.2 code. A sensitivity study on the influence of model specifications (kidney volume, cortex occupancy) was performed. For the ^{131}I mouse study, time-dependent regional kidney-tissue activities were determined from the relative regional activity concentrations of kidney sections measured with digital β$^-$-particle autoradiography (using an iQID system), relative to the whole-kidney activity measured with conventional gamma counting. ***Results:*** For ^{131}I, a large fraction of the emitted β$^-$ energy is absorbed within the sub-kidney source region itself (Ø ≥0.60). Because of this and the smaller masses of sub-kidney tissues, the self-irradiation regional S-values are considerably higher (30% to >200% depending on kidney region) than whole-kidney S-values. Compared to ^{131}I, ^{90}Y regional self-absorbed fractions are lower (Ø <0.35). Yet, the difference between self-irradiation regional and whole-kidney S-values is still very large (≥100%) for most renal tissues. β$^-$ cross-irradiation is significant (Ø often >0.10) between most regions for ^{90}Y and between adjacent regions for ^{131}I (e.g. cortex/OS, OS/IS). The sensitivity of self-absorbed fractions to the kidney model specifications was typically small for ^{131}I (<5% deviation between models) and moderate for ^{90}Y (<20%). For the ^{131}I mouse study, regional dose rates and time-integrated doses based on a heterogeneous activity distribution differ largely (-60% to >100% depending on region) from the uniform whole-kidney dose based on a homogeneous activity distribution. ***Conclusion:*** The calculated regional S-values, in combination with sub-kidney activity information, allow a more realistic estimation of the doses absorbed by different renal tissues from β$^-$-emitting radioligands with a heterogeneous kidney uptake. This provides new dose information relevant for preclinical investigations studying the risk of radiation-induced nephrotoxicity of these therapies. ***References:*** None

307

Pitfalls & Artefacts 2: Pre- and Post Therapeutic Imaging in Thyroid Cancer

Thursday, October 22, 2020, 16:35 - 18:05 Channel 7

OP-117

Molecular Imaging before Radioiodine Therapy

L. Giovanella; Imaging Institute of Southern Switzerland, Clinic for Nuclear Medicine, Bellinzona, SWITZERLAND.

OP-118

Cross-Sectional Imaging Possibilities

M. Radzina; Pauls Stradins Clinical University Hospital, Institute of Diagnostic Radiology, Riga, LATVIA .

OP-119

Molecular Imaging after Radioiodine Therapy

M. Luster; University Hospital Marburg, Department of Nuclear Medicine, Marburg, GERMANY

308

Clinical Oncology Track - TROP Session: Interventional Nuclear Medicine - Local Interventions

Thursday, October 22, 2020, 16:35 - 18:05 Channel 8

OP-120

Transarterial radioembolization versus drug-eluting beads chemoembolization for treatment of inoperable early and intermediate hepatocellular carcinoma: interim results of the randomized controlled TRACE trial

B. Lambert[1], E. Dhondt[2], L. Hermie[2], X. Verhelst[2], L. Defreyne[2];
[1]Ghent University, Gent, BELGIUM, [2]Ghent University Hospital, Gent, BELGIUM.

Aim/Introduction: To compare the efficacy of Y90 radioembolization (TARE) with drug-eluting beads chemoembolization (DEB-TACE) for early and intermediate hepatocellular carcinoma (HCC), not amenable to curative treatment modalities. ***Materials and Methods:*** Patients with HCC in an early or intermediate Barcelona Clinic Liver Cancer (BCLC) stage A-B, extended to patients with ECOG 1 performance status and/or segmental portal vein thrombosis (PVT), and not eligible for surgery or thermo-ablation were included in a randomized controlled trial comparing TARE with DEB-TACE. Exclusion criteria were: prior tumor treatment in the same segment, > 50% tumor involvement, main and lobar PVT, a Child-Pugh score > 7 and ECOG ≥ 2. DEB-TACE was performed as selective as possible with 100-300 µm and 300-500 µm DEB loaded with a total of 150 mg doxorubicin. DEB-TACE could be repeated up to 3 times per lesion. TARE, using Y90 glass microspheres, was administered lobar or more selective if possible. Bilobar disease was treated with a 30-45 days interval. The administered activity was calculated to deliver an 80-150 Gy dose in the targeted area. The primary endpoint was time to progression (TTP) at 2 years and was assessed by blinded, non-chronological central review according modified Response Evaluation Criteria In Solid Tumors (mRECIST). Secondary endpoints were time to local tumor progression (TLP) in the treated liver volume at 2 years, safety (adverse events and 30-day mortality) and overall survival. Adverse events were recorded according to the Common Terminology Criteria for Adverse Events (CTCAE). ***Results:*** 73 patients were included. Five patients were post-hoc excluded. 32 patients received TARE and 36 patients DEB-TACE. Median TTP in the TARE group was 514 days versus 285 days in the DEB-TACE group (p<0.001). Median TLP for TARE was 514 days versus 300 days for DEB-TACE (p=0.001). Median survival in the TARE group was 906 days versus 455 days in the DEB-TACE group (p= 0.005).Adverse events CTCAE grade ≥3 (p=0.3) and 30-day mortality (p=0.2) were similar in both treatment groups. ***Conclusion:*** In the selected BCLC stage A and B HCC patients, TARE was superior to DEB-TACE for tumor control and survival. Safety was similar for both groups. ***References:*** None

OP-121

Clinical and Dosimetric Parameters Associated with Contralateral Liver Hypertrophy after Lobar SIRT

F. Grisanti*, P. Rodrigo, J. F. Bastidas, J. J. Rosales, A. Bronte, E. Prieto, C. Beorlegui, M. Iñarrairaegui, B. Sangro, M. Rodríguez-Fraile;*
Clinica Universidad de Navarra, Pamplona, SPAIN.

Aim/Introduction: To identify clinical and dosimetric parameters associated with contralateral hepatic hypertrophy after lobar selective internal radiation therapy (SIRT) with 90Y-resin microspheres. ***Materials and Methods:*** Patients underwent 90Y-PET/CT after lobar or extended lobar (right + segment IV) SIRT and were retrospectively studied with a 90Y-PET-based voxel dosimetry software (PLANET Dose; DOSIsoft SA). Mean absorbed doses to tumoral and non-tumoral volumes (defined by excluding the tumor volume from the target liver; NTL) were obtained. Metrics were extracted from dose-volume histograms: D50, D70, D90, D95 and D98, as well as V30, V40, V50, V70, V100 and V120. Clinical variables were collected. Changes in volume of the treated and untreated lobes were calculated in imaging studies at <2 months (T1), 2-5 months (T2), and 6-12 months (T3) post-SIRT. The maximum percentage of hypertrophy of the untreated lobe (MHT) was obtained. Multivariable linear regression analyses were performed to identify predictors of MHT. Regression assumptions were verified (normality, homoscedasticity, and non-multicollinearity of residuals, as well as linearity of predictors). The best cut-off value to predict MHT ≥ 20% was defined using ROC analysis. ***Results:*** Fifty patients were studied; most had primary liver tumours (74%), 50% had chronic liver disease, and 42% had been treated with chemotherapy prior to SIRT. Hypertrophy of the untreated lobe was found in T1 (21.6% ± 28.9), T2 (38.6% ± 56.5) and T3 (34.2% ± 35.8). The ratio of spared volume to total liver volume increased from 39.2% at baseline to 46% at T1, 51.1% at T2 and 64.7% at T3. Mean MHT occurred at an average of 4.4 months (41.94% ± 51.26). NTL-V30 (NTL volume receiving at least 30 Gy; p=0.001) and baseline untreated volume (p=0.014) were found to be independent predictors of MHT (R2=0.263, adjusted R2=0.231). Mean MHT increased 0.85% for each percent increase in NTL-V30 and decreased 3.6% for each 100 ml increase in baseline untreated volume. Regression assumptions were respected. Factors selected from the univariate analysis (p<0.2) not significant in the multivariate analysis were: absence of cirrhosis, no previous transarterial chemoembolization, number of chemotherapy cycles, total administered activity and NTL-D98 (dose to 98% of the NTL volume). When 50% of NTL received at least 30 Gy, MHT ≥ 20% was observed (sensitivity: 74.2%, specificity: 61.11%, AUC: 0.654). ***Conclusion:*** NTL-V30 and baseline volume of the untreated lobe are independent predictors of hypertrophy of the untreated liver lobe after lobar or extended lobar SIRT with 90Y-resin microspheres. ***References:*** None

OP-122

Predictive value of ^{99m}Tc-MAA SPECT-CT based dosimetry in liver radioembolization with resin microspheres

P. D'Abadie*, N. Amini, P. Goffette, S. Walrand, M. Hesse, I. Borbath, M. Van den Eynde, R. Lhommel, F. Jamar;*
Cliniques universitaires Saint Luc, Brussels, BELGIUM.

Aim/Introduction: ^{99m}Tc- macroaggregated albumin SPECT/CT (^{99}Tc-MAA) is performed before ^{90}Y liver radioembolization (RE) for evaluating lung shunt, ruling out extrahepatic deposition and sometimes for calculating the delivered activity for treatment using the partition model[1]. This dosimetric model assumes a perfect correlation between ^{99m}Tc-MAA and ^{90}Y microspheres in the tumor and the normal

liver compartments. The aim of this study is to compare tumor doses (TD) and normal liver dose (NLD) observed on ^{99m}Tc-MAA SPECT-CT to the real doses observed with ^{90}Y PET-CT. ***Materials and Methods:*** Patients treated with resin ^{90}Y microspheres (SIR-spheres) between 2011 and 2020 were retrospectively analyzed. Only procedures with catheter tips in similar locations on both angiograms (^{99}Tc-MAA and ^{90}Y resin microspheres) were selected, as determined by a senior interventional radiologist. $TD_{MAA}$was compared to $TD_{90Y}$for each lesion and NLD_{MAA}compared to $NLD_{90Y}$for each procedure, as determined using MIM software. The accuracy of the prediction of $TD_{MAA}$and $NLD_{MAA}$was estimated using the standard error of the estimate (SEE). ***Results:*** 66 procedures with 171 lesions were identified. ^{99m}Tc- MAA SPECT-CT predicts very poorly the real tumor dose with a SEE of 89.5 Gy. $NLD_{MAA}$was very close to $NLD_{90Y}$with a SEE of 2.7 Gy in the 66 procedures. ***Conclusion:*** ^{99}Tc-MAA SPECT/CT predicts TD with large errors, which may result in significant inaccuracies using the dosimetric partition model. However, NLD is very well predicted using ^{99}Tc-MAA SPECT/CT. Delivered activities could be calculated using a new personalized dosimetric model based only on the ^{99}Tc-MAA dose in the non target liver volume. ***References:*** 1- Bastiaannet, R., Kappadath, S.C., Kunnen, B. et al. The physics of radioembolization.EJNMMI Phys 5, 22 (2018).

OP-123

Antireflux catheter improves tumor targeting in liver radioembolization

P. D'Abadie*, N. Amini, P. Goffette, I. Borbath, M. Van Den Eynde, R. Lhommel, A. Van Maanen, F. Jamar;*
Cliniques universitaires Saint Luc- Institut Roi Albert II, Brussels, BELGIUM.

Aim/Introduction: Liver radioembolization aims at reaching an efficient absorbed dose to tumors for tumor control. A better tumor targetting could improve clinical results of this treatment. The purpose of this study is to determine if antireflux catheter (Surefire System) is responsible for better tumor targeting in liver radioembolization. ***Materials and Methods:*** Patients treated by resin microspheres for primary and secondary liver malignancies were retrospectively analysed. Each patient realized a ^{99m}Tc-macroaggregated albumin (^{99m}Tc-MAA) SPECT/CT after the preliminary arteriography and a ^{90}Yttrium (^{90}Y) PET/CT after the therapeutic arteriography. MAA SPECT and 90Y PET were matched with the baseline imaging to determine a tumor to normal liver ratio (T/NL MAA or 90Y) and tumor dose (TD MAA or 90Y). End-hole catheter was used for all preliminary arteriography (MAA injection). For 90Y microspheres injection, two groups were defined depending of the type of catheter used : a Surefire group (antireflux catheter) and a control group (end-hole catheter). ***Results:*** 38 patients (115 lesions) and 23 patients (75 lesions) were analysed in the Surfire and the control groups respectively. In the Surfire group, T/NL_{90Y} and TD_{90Y} were significantly higher than T/NL_{MAA} and TD_{MAA} (medians : 2,2 and 91 Gy versus 1.7 and 74 Gy, $p < 0.001$). Subgroups analyses demontrated highly significant differences for neuroendocrine metastases and hepatocellular carcinoma and less spectacular differences for colorectal metastases. In the control group, no differences were found comparing T/NL_{90Y} and TD_{90Y} to T/NL_{MAA} and TD_{MAA}. ***Conclusion:*** Antireflux catheter significantly improves tumor microsphere deposition in liver radioembolization. ***References:*** None

OP-124

Radioembolization of hepatocarcinoma with ^{90}Y glass microspheres: impact of the basal bilirubin level on treatment planning

C. Chiesa*[1], M. Mira[1], M. Maccauro[1], S. Bhoori[2], G. Bormolini[2], C. Spreafico[3], A. Cavallo[4], S. Mazzaglia[1], G. Tagliabue[5], A. Marchiano[3], E. Seregni[1], V. Mazzaferro[2];*
[1]Nuclear Medicine, Foundation IRCCS Istituto Nazionale Tumori, Milan, ITALY, [2]HPB Surgery, Hepatology and Liver Transplantation, Foundation IRCCS Istituto Nazionale Tumori, Milan, ITALY, [3]Interventional Radiology, Foundation IRCCS Istituto Nazionale Tumori, Milan, ITALY, [4]Medical Physics, Foundation IRCCS Istituto Nazionale Tumori, Milan, ITALY, [5]Tumour Registry, Foundation IRCCS Istituto Nazionale Tumori, Milan, ITALY.

Aim/Introduction: According to all published papers reporting comparison between pre- and peri-treatment evaluations, absorbed dose predictions obtained with ^{99m}Tc albumin macro-aggregates SPECT/CT on non-tumoral liver (NT) are much more accurate than on tumours (T). Therefore, personalized treatment planning should focus mainly on the NT liver absorbed dose. Aim of this study was to determine the safety threshold to limit the risk of treatment related liver decompensation, in order to deliver the maximum tolerable absorbed dose. ***Materials and Methods:*** We analysed data of intermediate/advanced hepato-cellular carcinoma (HCC) patients with well compensated cirrhosis (Child-Pugh score A) treated with ^{90}Y glass microspheres. Injection was lobar in 133/139 patients (96%) and performed 4 days after the calibration date. Only treatment related liver decompensation requiring a medical action (LDC) was considered as toxicity event. We report LDC rates, ROC analysis between LDC and NO LDC absorbed dose distributions, NT complication probability (NTCP) curves, as well as univariate and multivariate analysis of risk factors associated with toxicity. We considered the whole cohort and stratifications on previous transarterial chemo embolization (TACE), presence/absence of portal vein tumoral thrombosis (PVTT), tumour pattern (nodular versus infiltrative), basal bilirubin level (high/low with cut-off 1.1 mg/dL). ***Results:*** A six month timeline was necessary to capture treatment-related toxicity events. Toxicity rate was 11% for the whole cohort. Significant difference in LDC rates

was obtained only according to the basal bilirubin level (20% versus 6%, p=0.01) with a relative risk of 3.7 for patients with values > 1.1 mg/dL. At the multivariate analysis, absorbed dose averaged over the whole non tumoral parenchyma (including the non injected lobe) was associated with liver decompensation (odds ratio=4.24). High bilirubin level was the second even more significant risk factor (odds ratio= 6.35). NTCP analysis determined a 15% liver decompensation risk at 50 Gy / 90 Gy for bilirubin > / < 1.1 mg/dL. Limits of the study were absence of scatter correction in SPECT/CT, absence of ^{90}Y PET verification and segmentation on pure SPECT images. ***Conclusion:*** given the low accuracy of ^{99m}Tc-MAA on lesion absorbed dose prediciton reported by all authors, an optimized TARE on HCC with ^{90}Y glass microspheres with lobar injection should aim to an absorbed dose averaged over the whole non tumoral liver of 50 Gy / 90 Gy for basal bilirubin higher / lower than 1.1 mg/dL respectively. This Investigator Initiated Study was supported by Biocompatibles UK Ltd, a Boston Scientific company. ***References:*** None

OP-125

The response and survival rates of Y-90 radioembolization in patients with unresectable liver tumors; a single-centre experience

O. Ekmekcioglu[1], *O. Tabakci*[2], *D. Has Simsek*[1], *A. Hasanefendioglu Bayrak*[2], *S. Bilgic*[3], *G. Berk*[1], *C. Simsek*[1], *N. Kaplan*[4], *M. Battal*[5]; [1]*Nuclear Medicine Dept, Sisli Etfal Education and Research Hospital, Istanbul, TURKEY,* [2]*Interventional Radiology Dept, Sisli Etfal Education and Research Hospital, Istanbul, TURKEY,* [3]*Nuclear Medicine Dept, Cerrahpasa Medical Faculty, Istanbul, TURKEY,* [4]*Medical Oncology Dept, Sisli Etfal Education and Research Hospital, Istanbul, TURKEY,* [5]*General and Hepatobiliary Surgery Dept, Sisli Etfal Education and Research Hospital, Istanbul, TURKEY.*

Aim/Introduction: Locoregional therapies are successfully used in unresectable primary or metastatic liver tumors. Y-90 treatment has been shown to have advantages for patients with less side effects. Aim of this study is to share the experience from the patients we treated with Y-90 radioembolization in our department. ***Materials and Methods:*** The patients, referred to our department and planned to receive Y-90 treatment by the hepatobiliary council, were analyzed retrospectively. All patients were scanned either with PET, MRI or CT before and after treatment due to patient condition or type of the tumor. Patient selection for Y-90 treatment was evaluated due to recommendations from guidelines[1]. All patients were performed hepatic angiography to investigate tumor vascular anatomy before treatment. Tc99m Macroaggregated albumin scintigraphy was performed for calculation of tumor uptake and lung shunt fraction during the first angiography session. Patients received Y-90 treatment during the second session in the week following after first angiography. All has been followed up for side effects. mRECIST criteria was used evaluating response 3 months after therapy. ***Results:*** Sixty-four (38 male, 26 female) of 93 patients were eligible for treatment. Hepatocellulary cancer was the most common type of tumor (40,6%). Colorectal tumor metastases (29,6%), cholangiocarcinoma (4,6%), neuroendocrine tumor metastases (15,6%) and the other types of tumors were in our patient group. Mean age was 62,5±9,7(36-82). Mean dose for the treatment was 127 Gy (80-340). Abdominal pain discomfort (35%) and nausea (15%) were the most common clinical toxicities. Patients' survival data demonstrated that; %32,8 of the patients were alive during time of our data analysis. The maximum follow up duration was 44 months and median survival after treatment was 10 months. The response rates were 46,5% for partial and 6,2% for complete. Furthermore; 12,5% has stable disease and 14% of patients were progressive after treatment. From the partial response group; 10,9% of the patients' tumor were nearly totally decreased in size and activity. Additionally, 7,8% of the patients had substantially response in treatment region. Since some of the patients were followed-up in other centers 20% of the data were not found in our archives. ***Conclusion:*** For unresectable liver tumors, radioembolization with Y-90 is a safe and well-tolerated procedure. Our experience demonstrated that a significant percentage of patients had clinical benefit. Even it is more effective in hepatocellulary carcinomas; hypervascular tumors like colon cancer and neuroendocrine tumor metastases are also shown to get advantage. ***References:*** 1.https://www.eanm.org/publications/guidelines/EANM_liver_treatment_guidelines_2012.pdf

OP-126

Trans-arterial Rhenium (Re) -188 lipiodol therapy in advanced hepatocellular carcinoma: HDD vs N-DEDC

S. Datta Gupta[1], *S. A. Shamim*[1], *Shalimar*[1], *S. Gamanagatti*[1], *P. Gupta*[1], *M. B. Mallia*[2], *V. Chirayil*[2], *A. K. Dash*[2], *C. S. Bal*[1]; [1]*All India Institute of Medical Sciences, New Delhi, INDIA,* [2]*Bhabha Atomic Research Centre, Mumbai, INDIA.*

Aim/Introduction: Advanced hepatocellular carcinoma (HCC) with portal vein thrombosis (PVT) contributes to 35-50% of all HCC. Conventional first line therapy in them remains tyrosine kinase inhibitors (TKIs), which prolongs overall survival from a mere 2-4 months to 6-8 months although with poor compliance. Rhenium (Re)-188 lipiodol based trans-arterial radionuclide therapy (TART) is a promising alternative in HCC with PVT. Various complexes have been developed to prepare Re-188 lipiodol, with 4-hexadecyl-1,2,9,9-tetramethyl-4,7-diaza-1,10-decanethiol (HDD) being used more widely. We attempt to explore novel agent bis-(diethyldithiocarbamato) nitrido (N-DEDC), attributed with higher labeling yield and lower cost, and compare its response and survival outcomes with Re-188 HDD lipiodol in HCC with PVT. ***Materials and Methods:*** Patients of radiological proven HCC with PVT were recruited for therapy. Those with ECOG

performance status more than 2, contrast allergy, Child-Pugh C or elevated PT/INR were excluded. Re-188 was eluted from W-188/Re-188 generator and in-house labeling with lipiodol was done using HDD and N-DEDC kits. Under fluoroscopy, trans-arterial injection of Re-188 lipiodol complex into tumor feeding vessels was performed. Response was assessed on MRI using mRECIST at 3 months and survival was assessed every 3 months till completion of study. ***Results:*** Fifteen therapies were performed in fourteen patients (13 male, 2 female). Eight therapies were done using Re-188 HDD lipiodol and seven with Re-188 N-DEDC lipiodol. The patients' characteristics and dose injected (HDD vs N-DEDC: 68.6±11.2mCi vs 72.7±7.1mCi, p = 0.955) in both groups were comparable. Overall objective response rate was 30.7 % with no difference in the two groups (p = 0.424). Disease control rate in HDD and N-DEDC groups were similar (85.7% vs 83.3%, p = 0.727). Mean completed follow-up duration in HDD group was 14 months and in N-DEDC group was 9.5 months. Overall survival (OS) and progression free survival (PFS) in both groups were 14.2 (95% CI: 7.8-20.5) months and 10.2 (95% CI: 7.2 -13.3) months, respectively. Mean OS in HDD and N-DEDC groups was 14.3 and 11.3 months (p =0.999) and mean PFS was 10.7 and 11.0 months (p = 0.781), both being comparable. ***Conclusion:*** Re-188 lipiodol TART in advanced HCC shows favorable response and survival outcome, compared to available data on TKIs in literature. In this pilot study, novel N-DEDC labeled Re-188 lipiodol therapy appears comparable in response and survival, to Re-188 HDD lipiodol TART, with the said advantage of higher labeling efficiency and affordability. ***References:*** None

OP-127

Boosting 90Y SIRT with SBRT: a planning study with 90Y PET and TCP/NTCP models

J. Mikell*, K. Cuneo, Y. K. Dewaraja;*
University of Michigan, Ann Arbor, MI, UNITED STATES OF AMERICA.

Aim/Introduction: Selective internal radiation therapy (SIRT) with microspheres is an established therapeutic intervention and has made strides focusing on earlier stage disease. In this work, we focus on multifocal disease within the liver and perform retrospective planning to combine lobar injection of Y90 glass microspheres followed by stereotactic body radiation therapy (SBRT). The idea being microspheres will successfully treat most of the lesions and then SBRT can be used to target underdosed lesions. The aim of this work is to compare differences in mean nontumoral liver dose (MLD) and liver normal tissue complication probability (NTCP) between the boost SBRT plan with a hypothetical SBRT plan to all the detectable lesions ***Materials and Methods:*** Prior study established a tumor control probability (TCP) curve for liver lesions treated with glass microspheres[1]. Retrospectively, 5 HCC patients were selected after SIRT. Lesion absorbed doses from 90Y- PET/CT were evaluated with our TCP model to predict response. An SBRT plan was created to target lesions with TCP < 50%, corresponding to mean Y90 dose of 290 Gy with recovery coefficients included. The entire lesion was not targeted, only regions receiving < 70 Gy, a threshold based on D90 TCP analysis to determine a minimum dose. SBRT plans were created to deliver 36 Gy in 3 fractions, assumed breath hold and used 5 mm isotropic margins. ***Results:*** Based on lobar Y90, 3/5, 1/1, 8/9, 4/4, and 1/2 lesions were predicted to have TCP < 50%. Planning tumor volumes in the boost decreased on average by 52% +- 14% (112 cc +- 81 cc) compared to treating with SBRT alone. The MLD from SBRT decreased in the combined treatment by 25% on average with decreases from 15% to 43%. The NTCP for RILD was on average 10% less for the boost SBRT; this was dominated by a single patient whose NTCP went from 59% to 5% when comparing SBRT alone to the SBRT boost after SIRT. ***Conclusion:*** For multifocal HCC, lobar 90Y SIRT followed by an SBRT boost may enhance the therapeutic ratio by increasing TCP due to the two pass treatment and decreasing NTCP compared to SBRT alone due to less liver parenchyma irradiated by external beam when targeting several lesions. Additional research is needed to combine 90Y and SBRT absorbed doses to develop reliable combined TCP and NTCP predictions. ***References:*** 1. J Nucl Med 2020 61:104-111

OP-128

Evaluation of PRRT after Selective Catheterization of the Hepatic Artery as Established Technique ('Aretaieion' Protocol) using ^{111}In-DTPA-Phe^{1} Octreotide in Inoperable Liver Metastases Due to Neuroendocrine Tumors

G. Limouris[1]*, I. Kyriazanos*[2]*, A. Zafeirakis*[3]*;*
[1]*Nuclear Medicine, Medical School, National and Kapodistrian University of Athens, Athens, GREECE,* [2]*I Surgery Clinic, Army Naval and Veterans Hospital of Athens, Athens, GREECE,*
[3]*Army Share Fund Hospital of Athens, Athens, GREECE.*

Aim/Introduction: To evaluate the efficacy of Auger and Internal Conversion Electron Emission of ^{111}In-DTPA-Phe^{1}-Octreotide and their tumoricidal effectiveness due to their high LET, in inoperable liver metastases, positive for sst2 receptor over-expression (verified by Octreoscan and confirmed by biopsy) due to neuroendocrine tumours (NETs). ***Materials and Methods:*** In 86 patients ^{111}In-DTPA-Phe^{1}-Octreotide was implemented after selective catheterization of the hepatic artery, in an average activity of 6.3±1.3 GBq per patient/per session, consecutively, with a time interval between sessions of 6-8 weeks. Infusion repetition did not exceed the 12 sessions. Patients, being under repeated Sandostatin - LAR treatment (30 mg per 20 days) did not discontinued the dosage but they were intramuscularly injected 15 -20 days prior to the radioactive session. To reduce myelotoxicity, 75 mg of DTPA in trip-trop diluted in about 200 ml normal saline water was infused 30 min before the initialization of the radiopeptide therapy, lasting for about 4 hrs. For the

assessment of response, RECIST 1.1 standards were used. CT/MRI scans before, during and after the end of the whole procedure, as well as U/S images at monthly basis were performed. Absorbed doses delivered to metastases, kidneys and red marrow were calculated according to OLINDA/EXM 1.1 program. Toxicity (World Health Organization criteria) was measured using blood and urine tests of renal, hepatic and bone marrow function. ***Results:*** Three patients resulted in complete response (3.5%); partial response was assessed in 46 (53.5 %), disease stabilization in 21 (24.4 %) and progressive disease in 16 (18.6%). The median PFS and OS were estimated to be 32 and 47.5 months, respectively. The organ average radiation dose was estimated as follows: (a) Liver Tumor 15.2 mGy/MBq, (b) Liver 0.14 mGy/MBq, (c) Kidneys 0.41 mGy/MBq, (d) Spleen 1.4 mGy/MBq and (f) Bone marrow 0.0032 mGy/MBq. The average absorbed dose per session to a tumour for a spherical mass of 10 gr was estimated to be 10.8 mGy/MBq, depending on the histotype of the tumour. WHO toxicity grade 2 to 3 erythro-, leuko- and thrombocytopenia occurred in 9 (10.5%) cases observed about after the 3rd session. ***Conclusion:*** In unresectable metastatic liver lesions, positive for somatostatin receptors, repeated, trans-hepatic high doses of ^{111}In-DTPA-Phe^{1}-Octreotide resulted in an optimal therapeutic outcome with a disease control (CR+PR+SD) in an about 82 % of the treated patients. Thus, ^{111}In-DTPA-Phe^{1}-Octreotide, intra-arterially applied, can be considered as a potent candidate in the therapeutic pharetra against NETs. ***References:*** None

OP-129

Sequential PRRT and SIRT. Evaluation of safety and best sequence treatment in liver dominant GEPNETs

F. Scalorbi*, A. Lorenzoni, S. Mazzaglia, E. Garanzini, C. Chiesa, G. Aliberti, V. Fuoco, G. Argiroffi, S. Pusceddu, N. Prinzi, C. Spreafico, G. Centonze, J. Coppa, A. Marchiano', M. Milione, V. Mazzaferro, E. Seregni, M. Maccauro;*
Istituto Nazionale Tumori Milano, Milan, ITALY.

Aim/Introduction: To investigate safety, tolerability and best sequence treatment in patients subjected to Peptide Radio-Receptor Therapy (PRRT) and Selective Internal Radiation Therapy (SIRT) for metastatic liver-dominant Gastroenteropancreatic neuroendocrine tumors (GEP-NETs) ***Materials and Methods:*** Ninety-eight GEP-NET patients treated with PRRT and SIRT in our Institute, from March 2012 to January 2016, were retrospectively reviewed. Treatment toxicity was assessed according to the Common Terminology Criteria for Adverse Events (CTCAE). Dosimetric analysis of dose administered by SIRT was estimated by 99mTc-MAA-angioscintigraphy. Disease Control Rate (DCR), PFS and OS were calculated. Treatment response was evaluated by RECIST1.1 criteria. Kaplan -Meier analysis was performed to calculate PFS and OS curves ***Results:*** Eight patients who underwent both SIRT and PRRT were identified. All the patients had histological diagnosis of G1-G2 GEP-NETs with unresectable liver-dominant metastasis. Among these patients, six were males, two were females (mean age 52 years-old, range 37-61). Five patients (Group 1) underwent SIRT before PRRT, three (Group 2) received PRRT followed by SIRT. In both groups the median interval between the last administration of first treatment (PRRT or SIRT) and the first administration of the second one was 18 months. Both therapeutic combinations showed limited toxicity, without delayed G3-G4 adverse events in accordance with CTCAE. The best SIRT response was observed at 3-months follow-up both in Group2 (DCR 66.7%) and in Group1 (DCR 60%). An excellent PRRT response (DCR 100%) was observed in Group2 at 3-months follow-up and was maintained at least for 12 months. Similarly, the DCR in Group1 was 100% at 3-month follow-up but decreased until 40% twelve months after PRRT. Dosimetric data obtained for SIRT planning were available for 7 of 13 procedures showing high cumulative dose to target lesions with low dose to healthy liver. Median PFS was briefer in Group1 than in Group 2 (26 vs 45 months) but Kaplan- Meier analysis fails to achieve statistical significance (Mantel- Cox 95% CI 17-60, P value: 0.655). OS curves show a strong evidence against the null hypothesis that the overall survival is the same in the two groups (Mantel- Cox 95% CI 14-59, P value: 0.024), with a median OS of 29 months in Group1 compared to 55 months in Group2. ***Conclusion:*** Therapeutic combination of PRRT and SIRT represented a reliable approach in terms of safety and tolerability in liver-dominant GEP-NETs. The preliminary results are favourable to opt for PRRT before SIRT, in the sequential treatment decision ***References:*** None

OP-130

High dose brachytherapy with not-sealed ^{188}Re (Rhenium) resin in patients with non melanoma skin cancers (NMSC): single center preliminary results

P. Castellucci[1]*, F. Savoia*[2]*, A. Farina*[3]*, G. Lima*[3]*, A. Patrizi*[2]*, F. Zagni*[4]*, C. Baraldi*[2]*, S. Vichi*[4]*, C. Pettinato*[4]*, L. Strigari*[4]*, A. Morganti*[5]*, S. Fanti*[3]*;*
[1]Nuclear Medicine Department, Sant'Orsola-Malpighi Hospital, University of Bologna, Bologna, ITALY, [2]Dermatology Unit, Sant'Orsola-Malpighi Hospital, Bologna, ITALY, [3]Nuclear Medicine Department, Sant'Orsola-Malpighi Hospital, Bologna, ITALY, [4]Medical Physics Department, Sant'Orsola-Malpighi Hospital, Bologna, ITALY, [5]Radiation Oncology Department, Sant'Orsola-Malpighi Hospital, Bologna, ITALY.

Aim/Introduction: High dose brachytherapy using a non-sealed ^{188}Rhenium resin (^{188}Rhenium SCT Oncobeta, Munich, Germany) is a recently EU approved treatment option for Non-Melanoma Skin Cancer (NMSC). The aim of this prospective pilot study was to assess the efficacy and the safety of a tailored brachytherapy using a single application of non-sealed ^{188}Rhenium resin source in the treatment of NMSC. ***Materials and Methods:*** From October 2017 to January

2020, overall 48 consecutive patients (15F,33M, age56-97, mean81) showing 57 histologically proven NMSC (40BCC; 14SCC; 2Spino-CC; 1BCC&SCC) at presentation (37/57), or who relapsed after multiple previous therapies (20/57), were enrolled. Lesions were located on the face, ears, nose or scalp (45), extremities (8), trunk (4). Mean surface areas 6.4 cm^2 (range 1-36cm^2); mean thickness invasion 1.1mm (range 0.2-2.5mm). Mean treatment time was 79 minutes (range 21-285 minutes). Mean radiation dose delivered to the whole volume of the lesion was 62 Gy (range 18-126 Gy depending on the location, the shape, the size and the thickness of each single lesion). Patients were followed-up after 14-30-60-90-180 days when a dermoscopy and a biopsy (if needed) were performed. Mean follow up was 18 months (range 3-30months) ***Results:*** Six months after ^{188}Rhenium treatment, 45 lesions have been studied with dermoscopy and/or biopsy: 44/45 lesions (97.7%) completely responded to ^{188}Rhenium SCT. One patient presenting a 9.5 cm^2 BCC in the nose showed a small (1 cm^2) persistence of disease that was subsequently treated by small surgical excision. Twelve months after treatment, 30/30 lesions were free from relapse. No patient report pain during or soon after the procedure or showed any significant late side effect during follow up. In 31/57 lesions early side effects, resolving within 32 days, were consistent with skin erythema, faint or moderate edema (Grade 1-2-3 of the ROTG scale). In the remaining 26/57 lesions, little ulcerations and faint hemorrages were observed (Grade 4). Only in 7/26 lesions these findings were more severe lasted up to 5-10 weeks, but resolved with optimal results except faint dischromia, slight atrophy of the skin or hair loss. ***Conclusion:*** High dose brachytherapy using a non-sealed ^{188}Re resin (^{188}Rhenium SCT) is a non-invasive, safe, easy to perform, effective and well tolerated approach to treat NMSC and it seems to be a useful alternative option when surgery is difficult to perform or not recommended. In our population 97% of the treated lesions responded completely after a single application. ***References:*** None

OP-131

Rhenium-188 Epidermal treatment for Non-melanoma Skin Cancers

K. Mokoala*, M. Vorster, L. Nonjola, N. P. Mokgoro, T. M. G. Boshomane, I. O. Lawal, M. M. Sathekge;*
University of Pretoria & Steve Biko Academic Hospital, Pretoria, SOUTH AFRICA.

Aim/Introduction: The incidence of non-melanoma skin cancers (NMSC), namely basal cell carcinoma (BCC) and squamous cell carcinoma (SCC) has been on the rise over the last three decades. With the growing demand on non-invasive treatment of NMSC with Rhenium-188 as an epidermal application is a growing modality in the management of skin cancers. We report on the clinical and cosmetic outcomes in patients treated for NMSC with Rhenium-188. ***Materials and Methods:*** We treated 20 patients (33 lesions) of NMSC who presented with recurrence following surgery or radiation therapy, those who were not candidates for surgery or radiotherapy and those who refused surgery or radiotherapy. Rheniumn-188 was delivered as a jelly-like matrix applied superficially on every target lesion. The duration per session ranged from 30 minutes to 4 hours depending on the activity administered and size of the lesion with the goal being to deliver 50Gy to the lesion per session. Participants were followed-up for 4-26 months to assess the side effects, cosmetic results, and local failures. ***Results:*** Out of the 33 histologically confirmed lesions, 30 were BCC and 3 were SCC lesions. There were 8 females and 12 males with a mean age of 70.17 (range: 34 - 84). The vast majority (90%) of the lesions were located in the head and neck region. The administered activity ranged from 64.2MBq to 479MBq. With the exception of one patient who was lost to follow-up, no recurrence or side effects were observed. The cosmetic results were excellent in 93.8% of treated lesions (n = 30), good in 3.1% (n = 1), fair in 3.1% (n = 1) after single application, applied in one single session. The one patient with fair results is scheduled for a second application because of the thickness of the tumour. ***Conclusion:*** Rhenium-188 as an epidermal application is a safe modality with excellent clinical and cosmetic results for the treatment of NMSC. ***References:*** None

311

e-Poster Presentation Session 2: PET Diagnostics - Part 2

Thursday, October 22, 2020, 16:35 - 18:05 Channel 11

EPS-018

18F-FDG PET/CT interpretation Criteria for the Assessment of Therapeutic Response in Patients with Advanced Stage of Lung Cancer: inter-reader reliability, accuracy and survival outcomes

M. Gazzilli[1]*, D. Albano*[2]*, E. Cerudelli*[1]*, F. Dondi*[3]*, A. Mazzoletti*[3]*, P. Bellini*[3]*, F. Bertagna*[2]*, R. Giubbini*[2]*;*
[1]Azienda Socio Sanitaria Territoriale degli Spedali Civili di Brescia, Brescia, ITALY, [2]Università di Brescia e Azienda Socio Sanitaria Territoriale degli Spedali Civili di Brescia, Brescia, ITALY, [3]Università di Brescia, Brescia, ITALY.

Aim/Introduction: 18Fluorine-fluorodeoxyglucose positron emission tomography/computed tomography (^{18}F-FDG-PET/CT) is useful in the evaluation of lung cancer (LC), both for staging and therapy assessment. For the evaluation of treatment response, shared criteria are not available. Recently Hopkins criteria, a 5-point score for qualitative interpretation of PET/CT, was introduced with promising results. We proposed a 3-point score, similar to Deauville score and compared its diagnostic accuracy with Hopkins

criteria for the evaluation of treatment response in LC. Our aim was to validate our qualitative interpretation system to assess therapy response and survival outcome in patients with advanced stage of lung cancer. ***Materials and Methods:*** We retrospectively included 93 patients with advanced stage (III-IV) LC who underwent ^{18}F-FDG-PET/CT assessment after completion of first-line treatment. PET/CT scans were interpreted by two nuclear medicine physicians with experience in this field and were evaluated according to a 3-point scale like Deauville score criteria (score 1=uptake lower than blood-pool activity; score 2=uptake higher than blood-pool but lower than liver activity; score 3= uptake higher than liver). Patients were followed up for a median of 18.5 months (range 2-139 months). Inter-reader variability was assessed using percent agreement and kappa statistics. Kaplan-Meier plots with a Mantel-Cox log-rank test were performed, considering death as the endpoint. ***Results:*** The sensitivity, specificity, positive predictive value, negative predictive value and accuracy of like Deauville score criteria were 91.9% [95% confidence interval (CI) 82.1-97.3%), 67.7% (95% CI 48.6-83.3%), 85% (95% CI 77.2-90.5%), 80.7% (95% CI 63.6-90.9%) and 83.8% (95% CI 74.8-90.6%), respectively. With the Hopkins criteria score we obtained sensitivity, specificity, positive predictive value, negative predictive value and accuracy of 85.4% [95% confidence interval (CI) 74.2-93.1%), 70.9% (95% CI 51.9-85.7%), 85.4% (95% CI 77-91.1%), 70.9% (95% CI 56.2-82.3%) and 80.6% (95% CI 71.1-88.1%), respectively. There was a high agreement between the two readers both using Hopkins criteria (k=0,912) and like Deauville score criteria (k=0,956).Applying 3-point scale criteria, patients with positive PET/CT after therapy had significantly shorter lower survival (p=0,0021). ***Conclusion:*** The use of 3-point scale criteria for post-therapy assessment in patients with advanced stage of LC represents an easy and reproducible method with substantial to almost perfect inter-observer agreement and high positive predictive value and accuracy; moreover, it is easily understood by referring physicians. ***References:*** None

EPS-019

SUV-derived Parameters Assessed on F-18-FDG PET/CT Predict EGFR Mutation in Lung Adenocarcinoma Patients: the Construction of CART Predictive Model

R. Wang[1,2], *X. Liao*[1], *S. Chen*[3], *M. Liu*[1], *X. Chen*[1], *L. Yin*[1], *D. Chen*[3];
[1]*Peking University First Hospital, Beijing, CHINA,*
[2]*Peking University International Hospital, Beijing, CHINA,* [3]*Peking University, Beijing, CHINA.*

Aim/Introduction: To investigate the potential relationship between Epidermal growth factor receptor gene (EGFR) mutation status and standardized uptake value (SUV)-derived parameters from ^{18}F-fluorodeoxyglucose (F-18-FDG) positron emission tomography/computed tomography (PET/CT) examinations combining with other clinical characteristics through classification and regression trees (CART) in patients with lung adenocarcinoma (ADC), in order to obtain the noninvasive predictive model for EGFR mutation. ***Materials and Methods:*** Data of 192 ADC patients pre-treatment, who underwent F-18-FDG PET/CT scans, EGFR gene mutations test for newly diagnosed ADC patients from December 2011 to April 2018, were retrospectively collected. Then a series of clinical parameters including EGFR mutation status, SUV-derived features of primary tumor [maximum standardized uptake value (SUV_{max}), average of standardized uptake value (SUV_{mean}), metabolic tumor volume (MTV), and total lesion glycolysis (TLG)], serum tumor markers and so on were gathered, which were analyzed through CART to build the model for EGFR mutation prediction. Predictive effectiveness of the model was validated by 1000-time Bootstrap. ***Results:*** Ratios of EGFR mutation were 33.3% (64/192). Age, smoking status, SUV_{mean}, pMTV(primary MTV), pTLG(primary TLG), CEA, SCC, NSE, TPA, and proGRP could be independently and significantly associated with EGFR mutation of ADC patients. The area under the curve (AUC) which for the predictive value of these factors were 0.785(95%CI: 0.743-0.827); Sensitivity and specificity were 85.5% and 71.4% respectively. ***Conclusion:*** SUV_{mean}, pMTV and pTLG were a set of independent predictors and could be integrated with other clinical factors (age, smoking status, CEA, SCC, NSE, TPA and proGRP) to enhance the discriminability on the EGFR mutation status in ADC patients. ***References:*** None

EPS-020

18F-FDG PET Parameters and Radiomics Features Analysis in Advanced NSCLC treated with Immunotherapy as Predictors of Therapy Response and Survival

G. Polverari[1], *F. Ceci*[2], *V. Bertaglia*[3], *M. Reale*[3], *O. Rampado*[4], *E. Gallio*[4], *R. Passera*[2], *V. Liberini*[2], *P. Scapoli*[5], *V. Arena*[1], *M. Racca*[5], *A. Veltri*[6], *S. Novello*[3], *D. Deandreis*[2];
[1]*Affidea Irmet PET/CT Center, Turin, ITALY,* [2]*Nuclear Medicine Unit, Department of Medical Sciences, University of Turin, Turin, ITALY,* [3]*Department of Oncology, University of Turin, San Luigi Gonzaga Hospital, Orbassano, ITALY,* [4]*Medical Physics Unit, S.C. Fisica Sanitaria, A.O.U. Città della Salute e della Scienza, Turin, ITALY,* [5]*Nuclear Medicine, Istituto per la Ricerca e la Cura del Cancro (IRCC), Candiolo, ITALY,* [6]*Radiology Unit, Department of Oncology, University of Turin, San Luigi Gonzaga Hospital, Orbassano, ITALY.*

Aim/Introduction: Objectives: 1.1) to evaluate the association between baseline 18F-FDG PET/CT semi-quantitative parameters with progression free survival (PFS), overall survival (OS) and response to immunotherapy, in advanced NSCLC patients eligible for immunotherapy; 1.2) to evaluate the application of radiomics analysis to identify features predictive of response to immunotherapy; 1.3) to evaluate if tumor burden assessed by 18F-FDG PET/CT (N and M factors) is associated with PFS and OS. ***Materials and Methods:*** We retrospectively analysed clinical records of advanced

NCSLC patients (stage IIIb/c or stage IV) candidate to immunotherapy who performed 18F-FDG PET/CT before treatment to stage the disease. 57 patients were included in the analysis (F:M 17:40; median age=69 yo). 38/57 of patients had adenocarcinoma (AC), 10/57 squamous cell carcinoma (SCC) and 9/57 not otherwise specified (NOS). 47.4% patients were stage IVA, 42.1% IVB and 8.8% IIIB. Immunotherapy was performed as front-line therapy in 42/57 patients and as second line therapy after chemotherapy platinum-based in 15/57. Median follow up after starting immunotherapy was 10 months (range:1.5-68.6). Therapy response was assessed by RECIST 1.1 criteria (CT evaluation every 4 cycles of therapy) in 48/57 patients or when not feasible by clinical and laboratory data (fast disease progression in 9 patients). Radiomics analysis was performed applying ROIs of the primary tumor delineated manually by two operators and semi-automatically applying a threshold at 40% of SUVmax. ***Results:*** 1.1) MTV (p=0.028) and TLG (p=0.035) were significantly associated with progressive vs. non-progressive disease status. Patients with higher values of MTV and TLG had higher probability of disease progression, compared to patients presenting with lower values. SUVmax did not showed correlation with PD status, PFS and OS. MTV (p=0.027) and TLG (p=0.022) resulted also to be significantly different among PR, SD and PD groups while SUVmax confirmed to be not associated with response to therapy (p=0.427). 1.2) We observed association of several radiomics features with PD status. Namely, patients with high tumor volume, TLG and heterogeneity expressed by "skewness" and "kurtosis" had higher probability to fail immunotherapy. 1.3) M status at 18F-FDG PET/CT was significantly associated with PFS (p=0.002) and OS (p=0.049). No significant associations were observed for N status. ***Conclusion:*** 18F-FDG PET/CT performed before the start of immunotherapy might be an important prognostic tool able to predict the disease progression and response to immunotherapy in patients with advanced NSCLC since MTV, TLG and radiomics features (volume and heterogeneity) are associated with disease progression. ***References:*** None

EPS-021

Predictive value of ^{18}F-FDG PET/CT based metabolic parameters in patients with non-small cell lung cancer treated with stereotactic body radiation therapy

L. García Belaústegui, M. Alcántara, R. Couto Caro, M. García García-Esquinas, J. Corona, J. Carreras Delgado;
Clinico San Carlos Hospital, Madrid, SPAIN.

Aim/Introduction: The aim was to determine temporal evolution and prognostic value of maximum standardized uptake value (SUV_{max}) and metabolic tumor volume (MTV) on the serial ^{18}F-FDG PET / CT scans performed on patients with non-small cell lung cancer (NSCLC) treated with stereotactic body radiation therapy (SBRT) with curative intention. ***Materials and Methods:*** This retrospective study evaluated 30 patients with T1-T3N0M0 NSCLC who had undergone SBRT between 2015 and 2017. Lesion size, SUV_{max}, $MTV_{2.5}$ and $MTV_{40\%}$ were measured from a total of 120 ^{18}F-FDG PET / CT scans performed at baseline and 24-48 hours, 3 and 6 months after hypofractionated radiation. Variation over time of these parameters and their correlation with clinical evolution of the disease (progression vs. stability / remission) were studied. ***Results:*** The mean age was 75 years and 93.5% of the patients were men. The group of patients with disease progression presented equal or higher mean values of tumor parameters (size of 25.6 mm, SUV_{max} 12.5, $MTV_{2.5}$ 12.0 cm^3 and $MTV_{40\%}$ 5.8cm^3) compared to those patients with stable disease / remission (size of 20.3 mm, SUV_{max} 12.5, $MTV_{2.5}$ 6.1 cm^3 and $VMT_{40\%}$ 3.12 cm^3). With respect to the baseline scan, we found a post-treatment mean decrease in tumor size of 6.5% at 24-48 hours, 28.6% at three months and 44% at six months; in SUV_{max} of 37.2%, 73.7% and 78.9%; in $MTV_{2.5}$ of 10.1%, 84.5% and 88.1% and in $MTV_{40\%}$ of 8.7%, 9.6% and 68.3%, respectively. ***Conclusion:*** While pretreatment SUV_{max} were similar for both groups, MTV was higher in those patients with a worse clinical outcome, therefore this parameter at baseline may provide additional prognostic information. In addition, after 6 months of treatment, MTV decreased an average of 88% while tumor size only 40%, for this post-treatment MTV could also be useful as a predictor of response. However, randomized studies are needed to confirm the results. ***References:*** None

EPS-022

Sensitivity and characterization of Lung Nodules (LNs) by using Fast-Recovery Fast Spin-Echo (FRFSE-XL) on PET/MR hybrid system

G. Salvatierra Apala[1,2,3], E. Marino[1,4], G. Peña[1];
[1]Fundación Escuela de Medicina Nuclear (FUESMEN), Mendoza, ARGENTINA, [2]Agencia Boliviana de Energía Nuclear (ABEN), La Paz, BOLIVIA, PLURINATIONAL STATE OF, [3]Investigación Aplicada (INVAP), Bariloche, ARGENTINA, [4]Comisión Nacional de Energía Atómica (CNEA), Bariloche, ARGENTINA.

Aim/Introduction: To compare sensitivity of detection of small lung nodules (LN) using STIR and FRFSE-XL magnetic resonance (MR) sequences and to characterize LN's malignancy by using two-point SUVmax measurement in a PET/MR hybrid system. ***Materials and Methods:*** LNs were identified by two radiologist-physicians in 16 oncological patients by using CT and PET/MR images. Intercomparison of sensitivity of MR-sequences using FRFSE-XL in respiratory gated ($S_{FRFSE-XL-GAT}$) and breath-hold ($S_{FRFSE-XL-BH}$), and STIR gated ($S_{STIR-GAT}$) were performed by LN's diameter interval (d1: d<4mm, d2: 4<=d<8mm, d3: d>=8mm), using CT as reference (S_{CT}=100%). Image performance was analyzed using signal-to-noise (SNR) and contrast-to-noise (CNR) ratios, and evaluating qualitatively noise and artifacts in

PET/MR images using 5-scored rating. LN's malignancy were classified by measuring SUVmax in two different times t1 and t2, at 60 and 105 minutes FDG post-injection. LNs were considered as: malignant ($SUVmax_{t2}$>=1.3*$SUVmax_{t1}$), probably malignant ($SUVmax_{t2}$>=$SUVmax_{t1}$ and $SUVmax_{t2}$<1.3*$SUVmax_{t1}$), probably benign ($SUVmax_{t2}$<=$SUVmax_{t1}$ and $SUVmax_{t2}$>=0.9*$SUVmax_{t1}$), and benign ($SUVmax_{t2}$<0.9*$SUVmax_{t1}$). ***Results:*** A total of 179 LNs were detected in CT images. At 95% of confidence level, $S_{FRFSE\text{-}XL\text{-}BH}$=34% [confidence interval (CI): 24-46%], $S_{FRFSE\text{-}XL\text{-}GAT}$=18%(CI:9-32%) and $S_{STIR\text{-}GAT}$=17%(CI:8-30%) for d1. $S_{FRFSE\text{-}XL\text{-}BH}$=71%(CI:60-80%), $S_{FRFSE\text{-}XL\text{-}GAT}$=68%(CI:53-80%) and $S_{STIR\text{-}GAT}$=60%(CI:46-72%) for d2. $S_{FRFSE\text{-}XL\text{-}BH}$=90%(CI:67-98%), $S_{FRFSE\text{-}XL\text{-}GAT}$=90%(CI: 66-98%) and $S_{STIR\text{-}GAT}$=69%(CI:39-90%) for d3. Qualitative analysis showed higher scores for FRFSE-XL-BH (4.5/5, p=0.37) followed by FRFSE-XL-GAT (3.6/5, p=0.18) and STIR (3.2/5, p=0.37). Relative SNR and CNR was 2.7 and 7 times higher in FRFSE-XL-GAT than in FRFSE-XL-BH and STIR respectively. Based on SUVmax, 24LNs were found to be malignant in 7 patients, 39LNs probably malignant in 13 patients, 6LNs as probably benign and 38LNs as benign in 8 patients. ***Conclusion:*** FRFSE-XL (gated and breath-hold) showed great potential for the detection of small LNs, with better performance in terms of sensitivity, qualitative and quantitative analysis as compared to STIR. SUVmax measurements at two different times suggest clear differences between malignant and benign LNs. Further analysis is required to more accurately estimate specificity and sensitivity. ***References:*** None

EPS-023

Relationships of semiquantitative parameters assessed on F-18-FDG PET/CT for predicting EGFR mutation subtypes in Lung Adenocarcinoma

R. Wang[1,2], X. Liao[1], M. Liu[1], X. Chen[1], Y. Cui[1], L. Di[1], L. Yin[1], Z. Tong[1], H. Sun[1], C. Wu[1];
[1]Peking University First Hospital, Beijing, CHINA, [2]Peking University International Hospital, Beijing, CHINA.

Aim/Introduction: To explore the relationship of F-18-FDG standardized uptake value (SUV)-derived parameters and mutation subtypes (delections in exon 19 and a mutation in exon 21) in lung adenocarcinomas parameters with mutant epidermal growth factor receptors (EGFR) gene. ***Materials and Methods:*** Data of 64 lung adenocarcinoma patients who underwent F-18-FDG PET/CT scans and EGFR gene mutation test were collected. The relationships of subtype mutation of EGFR gene with four parameters (maximum standardized uptake value, SUVmax), average of standardized uptake value(SUVmean), metabolic tumor volume(MTV) and total lesion glycolysis(TLG) of primary lesion based on F-18-FDG PET/CT and clinical characteristics were evaluated with univariate and multivariate Logistic regression, respectively. ***Results:*** The mutant ratio of exon 19 and exon 21 was 23:41. When the parameters were continuous variables, univariate logistic regression showed exon 21 mutations were found more frequently in the EGFR positive patients with shorter maximum diameter of primary lesion (OR=0.942, 95%CI[0.890.0998]) and low level of MTV of primary lesion (pMTV), (OR=0.957,95%CI [0.923,0.991]). As dichotomous variables, in univariate regression shorter maximum diameter of primary lesion (<26.5mm:OR=3.759,95%CI[1.284,11.005]), high level SUVmax(≥4.35: OR=4.267, 95%CI[1.088,16.726]), low level pMTV(<11.2cm^2: OR=7.000, 95%CI[1.798, 27.253]) would be significantly related to mutant exon 21 mutation. ***Conclusion:*** The primary-lesion SUV-derived parameters from F-18-FDG PET/CT of lung adenocarcinoma patients with EGFR-gene mutation associate with mutant subtypes (exon 19 and 21 mutation)to some extent, nut this correlation might be limited. ***References:*** None

EPS-024

Soluble PD-L1 in NSCLC Patients Treated with Checkpoint Inhibitors

A. Castello*, S. Rossi, L. Toschi, E. Lopci;*
Humanitas Clinical and Research Hospital, Rozzano (MI), ITALY.

Aim/Introduction: Soluble PD-L1 (sPD-L1) is a potential biomarker recently identified into bloodstream. Its predictive role is still under debate with contrast results, particularly in the immune checkpoint inhibitors (ICI) context. Therefore, we investigated the role of sPD-L1 in NSCLC patients treated with ICI and its association with clinical outcomes and metabolic parameters by 18F-FDG PET/CT. ***Materials and Methods:*** Between July 2017 and May 2019, we enrolled 20 patients candidate to ICI therapy who had serum frozen samples and 18F-FDG PET/CT available, both at baseline and at the first restaging after approximately 7-8 weeks. This analysis is embedded into a larger prospective study (NCT03563482). ***Results:*** Nivolumab was administered to 12 out of 20 patients , whereas the others received pembrolizumab. Median sPD-L1 level at baseline was 27.22 pg/ml (range 11.23-61.27). We found a significant association between patients with elevated sPD-L1, above the median value, and high metabolic tumor burden, expressed by metabolic tumor volume (MTV, 115.3 vs 35.5, p=0.034) and total lesion glycolysis (TLG, 687 vs 210.1, p=0.049). At the first restaging after 7-8 weeks, median sPD-L1 levels significantly increased as compared to baseline median value (43.9pg/ml, p=0.017). No significant differences in response rates were detected, according to both morphological and metabolic response criteria. Likewise, no difference in survival outcomes were observed between low sPD-L1 and high sPD-L1 patients. ***Conclusion:*** Based on our findings, we speculated that increase of sPD-L1 concentrations during ICI treatment may reflect the expansion of tumor volume and the tumor lysis. Moreover, it is supposed that sPD-L1 has its own biological action, either by reducing membrane PD-1 sites available for nivolumab

or by inducing lymphocytes exhaustion after binding their membrane PD-1. Further larger studies are needed to confirm our preliminary results on the role of sPD-L1 during ICI therapy. ***References:*** The Italian Association for Research on Cancer (AIRC - Associazione Italiana per la Ricerca sul Cancro) is acknowledged for the support on research with the grant nr. 18923.

EPS-025

Metabolic Characteristics of Non-Small Cell Lung Cancer Lesions as Potential Predictor of Immunotherapy Response

A. Tabain*, S. A. Rogan, S. Divošević;*
Polyclinic Medikol, Zagreb, CROATIA.

Aim/Introduction: Various innovative therapy options, including immunotherapy, are available for treatment of advanced non-small cell lung cancer (NSCLC). The expression of programmed cell death-ligand 1 (PD-L1) on the surface of NSCLC cells, considered as predictor of immunotherapy response, is one of the factors that affect the therapy approach. Recently, the presence of tumour necrosis was also recognised as potential inflammation trigger associated with higher PD-L1 expression. We aimed to evaluate metabolic characteristics of primary NSCLC lesions, obtained with 18F-FDG PET/CT, according to the PDL-1 positivity. ***Materials and Methods:*** We retrospectively analysed 40 NSCLC pts in different stages of the disease, confirmed with biopsy or surgical resection, referred to 18F-FDG PET/CT for detection of malignancy or staging of already verified disease. Maximum standardised uptake value (SUV max), diameter and metabolic pattern of necrosis were evaluated. PDL-1 expression was assessed by immunohistochemistry assay. Samples were divided in three groups regarding positivity of tumour cell membrane staining: highly positive with >=50%, mild positive between 1%-49% and negative <1%. ***Results:*** In total of 40 pts (17 females and 23 males, age range 41-88 years, 28 with smoking history, 25 in advanced stage of the disease) there were 25 pts with non-squamous and 15 with squamous NSCLC. Based on PD-L1 positivity: 11/40 (27.5%) pts were highly positive, with SUVmax values 6.4-35.7, 14.8, 13.9 (range, mean, median); 14/40 (35%) pts were mild positive, with SUVmax values 2.1-13.8, 7.6, 8.3 (range, mean, median) and 15/40 (37.5%) were PD-L1 negative with SUVmax values 1.7-15.9, 7.7, 6.9 (range, mean, median). Necrotic pattern of the lesion was observed in 24 pts, represented between PD-L1 positive, mild positive and negative pts with 72%, 50% and 60%, respectively. Mean diameter of necrotic lesions was 55 mm, related to 44 mm in case of lesions without typical photopenic necrotic sign. Squamous NSCLC pts dominated in the PD-L1 highly positive group (63.3% pts). ***Conclusion:*** Higher SUV max values observed in group of PD-L1 high positive samples could preliminarily indicate pts with favourable respond to immunotherapy. PD-L1 mild positive and PD-L1 negative lesions had overall lower metabolic activity and we were not able to distinguish them regarding metabolic characteristics. In our group of pts, necrosis was present in PD-L1 positive as well as in negative pts, possible due to overall greater dimensions of the lesions, in association with later detection and advanced stages of the disease ***References:*** None

EPS-026

The value of hybrid 18F-FDG PET / MR in lung cancer and comparing with PET / CT

Y. Xu;
Hangzhou Universal Imaging Diagnostic Center, Hangzhou, CHINA.

Aim/Introduction: To explore the value of hybrid 18F-FDG PET / MR in radiotherapy target delineation of lung cancer and compare with PET/CT. ***Materials and Methods:*** 30 lung cancer patients planning to undergo radiotherapy, underwent whole body PET/CT and chest PET/MR on the same day. CT and PET images were acquired in free breathing mode, and then a breath-hold CT was performed. PET/MR gated acquisition under free breathing, MR and PET images acquired at the end of expiratory period. In PET/MR imaging, 8 cases of MR image artifacts were heavier, and the images met the standard after repeated scanning; The other 3 cases still had poor image quality after repeated scanning. The remaining 27 cases were analyzed by an experienced nuclear medicine physician and a radiotherapy physician. Compare the matching of PET and MR/CT between the two devices. The SUVmax and SUVmaen of the lesion were measured. MTV(metabolic tumor volume) and TLG(total lesion glycolysis) were obtained with 30% of SUVmax as the threshold, GTV(gross tumor volume) was delineated on CT and MR images, and the PTV(Planning Target Volume) was obtained from the fusion image. Non-parametric test is used to compare the differences between the two devices' data. ***Results:*** Among the 27 cases, 18 cases had inaccurate matching between PET_{CT} and CT, with an average displacement of 1.3 (0.2, 1.5) cm and a maximum displacement of 2.5 cm, while PET_{MR} and MR were accurately matched. The radiation concentration of the lesions were more obvious in the PET/MR imges. $SUV_{max\text{-}PET/MR}$[26.43(23.42,33.38)] and $SUV_{mean\text{-}PET/MR}$[14.11(11.71,19.21)] were higher than $SUV_{max\text{-}PET/CT}$[19.16(12.22,20.87)] and $SUV_{mean\text{-}PET/CT}$[9.72(6.27,11.27)], ($Z=-2.934,-2.837$, $P<0.05$); $MTV_{PET/MR}$[52.30(31.11,109.00)] was lower than $MTV_{PET/CT}$[58.16(33.51,124.00)], ($Z=-2.845$,$P<0.05$); $TLG_{PET/MR}$[751.08(307.38,1835.29)] were higher than $TLG_{PET/CT}$[684.78(250.06,1503.14)],($Z=-2.936$,$P<0.05$). There were 18 cases of obstructive pulmonary atelectasis or obstructive pneumonia, in which PET_{MR} and MR could clearly distinguish the tumor from them in 16 and 15 cases, respectively;while PET_{CT} and CT could distinguish 10 and 8 cases, respectively($\chi^2=4.98,5.90$,$P<0.05$).GTV_{MR}[60.55(29.25,108.00)] was lower than GTV_{CT}[68.58(30.08,122.00)],($Z=-2.490$,$P<0.05$). There was no statistical difference between GTV_{MR} and $MTV_{PET/MR}$ ($Z=-1.956$,$P>0.05$), while GTV_{CT} was lower than $MTV_{PET/CT}$ ($Z=-$

2.401,P<0.05). $PTV_{PET/MR}$[55.65(29.52,107.00)] was lower than $PTV_{PET/CT}$[62.23(30.08,122.00)], (Z=-2.936,P<0.05). ***Conclusion:*** Compared with PET/CT, PET/MR has more accurate image matching in lung tumor imaging, it can more accurately locate the tumor body, and may become a more accurate imaging method for delineating target areas of radiotherapy. However, MR lung scanning technology is more demanding, the image is prone to artifacts, and often needs repeated scanning. ***References:*** None

EPS-027

Application Value of PET/MR Radiomics Featuresand Metabolic Parameters in Evaluating the Staging ofNasopharyngeal Carcinoma

J. Liang;
Hangzhou Universal Medical Imaging Diagnostic Center, Hangzhou, CHINA.

Aim/Introduction: The study aims to investigate the value of 18F-FDG PET/MR radiomics features and metabolic parameters in evaluating the T staging, N staging and clinical staging of nasopharyngeal carcinoma (NPC). ***Materials and Methods:*** The clinical data and PET/MR imaging data of 100 NPC patients with undifferentiated carcinoma from a medical center were collected. The patients were randomly divided into training group (n = 70) and test group (n = 30). The pathological and clinical diagnosis results were used as the gold standard for diagnosis. We measured the metabolic parameters (SUVmax, MTV, TLG) of the NPC primary focus, and used AK software to extract the most relevant radiomics features to NPC staging. To compare the differences of the parameters and features of different stages, and evaluate the diagnostic efficacy of statistically significant parameters and features through the receiver operating characteristic (ROC) curve in NPC staging,The cutoff value was calculated from the ROC curve. ***Results:*** We extracted 6 and 3 radiomics features most relevant to the staging of NPC from T2WI and PET images, respectively. The AUCs of the training and test group were 0.849 and 0.833 in the T2WI model. The AUCs of the training and test group were 0.840 and 0.815 in the PET model. The MTV, TLG, T2WI radiomics feature (MinIntensity) and PET radiomics feature (GLCMEntropy_angle0_offset4) had statistically significant differences between and within groups of T stages (P < 0.05). With the increase of T stage, the mean value of MinIntensity decreased gradually, while the others increased gradually. The MTV, TLG, MinIntensity, GLCMEntropy_angle0_offset4 had higher diagnostic efficiency in differentiating T-stage of NPC (AUC: 0.785-0.956). The TLG and PET radiomics feature (GLCMEntropy_angle0_offset4) had statistically significant differences between and within groups in clinical stages (P <0.01). With the increase of clinical staging, the mean value of the two gradually increased, and they had higher diagnostic efficacy in differentiating clinical stage of NPC (AUC: 0.775-0.953). The comparison between groups showed that the T2WI radiomics feature (GLCMEntropy_AllDirection_offset1_SD) was smaller in the patients with lymph node metastasis (P <0.05). ***Conclusion:*** PET/MR radiomics features and metabolic parameters were of great value in evaluating T-stage and clinical stage of NPC, but they had limited value in N-stage. In the future, radiomics features are expected to be a more useful and economical tool for predicting local invasion and distant metastasis of NPC. ***References:*** None

EPS-028

Predictive value of 18F-FDG PET/CT in treatment response of Head and Neck squamous cell carcinoma using Deauville criteria

C. Ferrari*, G. Santo, A. Nappi, A. Branca, C. Altini, A. Gaudiano, A. Di Palo, A. Pisani, V. Lavelli, G. Rubini;*
Nuclear Medicine Department, University of Bari "Aldo Moro", Bari, ITALY.

Aim/Introduction: Head and neck squamous cell carcinoma (HNSCC) is the six leading cancer by the incidence worldwide. The 5-years overall survival is 40-50% and recurrence rate reaches about 60%. For locally advanced disease, chemo-radiotherapy is usually the standard of care. 18F-FDG PET/CT has proven to be a useful tool in post-treatment evaluation avoiding unnecessary neck dissections. Deauville criteria (DC), a 5-point scale used to assess metabolic response already validate in Hodking lymphoma, are currently proposed also for HNSCC.The aim of this study is to evaluate the predictive value of post-treatment 18F-FDG PET/CT in HNSCC by using DC. ***Materials and Methods:*** We retrospectively evaluated 36 patients (mean age 57; range 26-80), with histological proven of HNSCC, who underwent baseline (PET1) and end-of-treatment (PET2) 18F-FDG-PET/CT after first-line therapy. PET2 scans were visually interpreted according to DC assigned on both primitive tumor site (T) and lymph node (N) and scored as follows: 1. complete metabolic response; 2. probably complete metabolic response; 3. probably post-radiation inflammation; 4. probably persistent tumor; 5. persistent tumor. Patients were subsequently dichotomized into responders (score 1-2-3) and non-responders (score 4-5) groups. Disease free survival (DFS) was estimated by the Kaplan-Meier method and groups were compared using long-rank test. ***Results:*** Among 36 patients, primitive tumor site was pharynx (n=12), tongue (n=6), oral cavity (n=6), larynx (n=5), salivary glands (n=3), tonsil (n=2), paranasal sinus (n=1), occult (n=1). The time between the end of treatment and PET2 was 4 months on average (range 1-7 mo). Twelve/36(33%) patients experienced disease persistence/recurrence.DC evaluation were able to significantly predict metabolic response and remission of both T and N status. In particular, a statistically significant difference was found in DFS and DC(T), both with dichotomization (p=0,015) and without dichotomization (p=0,019); similarly, a statistically

significant difference was found in DFS and DC(N), both considering responder/non-responder (p<0.0001) and for each score separately (p<0.0001). ***Conclusion:*** Our preliminary results suggest that 18F-FDG PET/CT could be useful in predicting treatment response, in particular considering N status. Further larger studies are needed to validate the Deauville criteria in the HNSCC in order to avoid unnecessary lymph node dissections. ***References:*** None

EPS-029

Correlation between Apparent Diffusion Coefficients, Standardised uptake values and histological differentiation : preliminary results in anal cancer

A. Parsai[1], *I. Zerizer*[2], *H. Jan*[3], *E. Nowosinska*[3], *S. Subhan*[4], *A. Haroon*[3], *Y. Bouchareb*[5], *M. E. Miquel*[1];
[1]*Queen Mary University London, London, UNITED KINGDOM,* [2]*Royal Marsden Hospital, London, UNITED KINGDOM,* [3]*BartsHealth NHS Trust, London, UNITED KINGDOM,* [4]*The Queen Elizabeth Hospital, London, UNITED KINGDOM,* [5]*Sultan Qaboos University, Oman, QATAR.*

Aim/Introduction: To assess ADC and SUVmax values as predictors of histological differentiation in patients with anal squamous cell carcinoma (ASCC) at baseline and determine if there is a statistically significant difference for each tumour grade (well, moderately, poorly differentiated ASCC). ***Materials and Methods:*** A retrospective review of 41 patients (14 males, 27 females; mean age 65 ±13 years) with ASCC after baseline FDG PET/CT and MRI (mean scan time interval 21 ± 11 days). SUVmax and ADC were measured using HERMES® and PACS respectively. The values were compared to histopathology and correlated with tumour grade (well, moderately or poorly differentiated) to assess for statistical difference using paired t-test. ***Results:*** The mean size and volume of the tumour was 3 cm and 16.5 cm3. The mean ADC value for well, moderately and poorly differentiated ASCC was 935, 952 and 809, respectively. The mean SUVmax for well, moderately and poorly differentiated ASCC was 8, 11.3 and 12.4, respectively. There was statistical difference between mean SUVmax values of poorly differentiated and well-differentiated ASCC (p= 0.008) as well as moderately differentiated and well-differentiated ASCC (p = 0.03). There was no significant statistical difference between mean ADC values and degree of tumour differentiation. ***Conclusion:*** There is a statistically significant correlation between SUVmax values and degree of differentiation in ASCC. There is however no statistical correlation with ADC values. This highlights the superiority of FDG PET/CT in predicting tumour grade and can be used as an adjunct to plan treatment. ***References:*** None

EPS-030

2-[^{18}F]FDG PET/CT in Colorectal Cancer Liver Metastases

P. Soeiro*, P. Lapa, R. Silva, G. Costa, J. Pedroso de Lima;*
Centro Hospitalar e Universitário de Coimbra, Coimbra, PORTUGAL.

Aim/Introduction: Resection of liver metastasis (LMCRC), in carefully selected colorectal cancer patients, can improve overall survival. However, selection criteria for surgery is a hotly debated subject. Some reports indicate that 2-[^{18}F] FDG PET/CT can improve patient selection. In this study we aim to identify quantitative functional variables in 2-[^{18}F] FDG PET/CT able to predict recurrence or mortality LMCRC. ***Materials and Methods:*** All LMCRC patients who underwent 2-[^{18}F]FDG PET/CT followed by liver metastasis resection, since 1-1-2005 to 31-12-2019, were retrospectively selected. Patients under chemotherapy in the month of the 2-[^{18}F] FDG PET/CT scan were exclued. PET/CT data was reviewed. All hepatic metastases uptake related variables, such as SUVmax, SUVmean, metabolic tumour volume (MTV) and total lesion glycolysis (TLG) were recorded. Three ratios were calculated: hepatic metastase SUVmax/normal liver SUVmax (MaxM_MaxL), hepatic metastases SUVmax/ normal liver SUVmean (MaxM_MeL), hepatic metastase SUVmean/normal liver SUVmean (MeM_MeL). Demographic, clinical, time to relapse, time to hepatic relapse, time to death and histological variables were recorded. ***Results:*** 73 patients fulfilled the inclusion criteria, 63% (n=46) men and 37% (n=27) women (62±11.7; 33-84 years). Most patients had sigmoid cancer (39,4%), followed by rectal cancer (18%). Almost half of the patient had pT3 (48%). The most frequent clinical stage was III (25%). The average number of hepatic metastases per patient was 2±1.7(1-12). 66% patients were also submitted to chemotherapy. Relapse rate was 79%. Median time to relapse was 512 ±456 days (41-1851). Hepatic relapse rate was 62%. Median time to hepatic relapse was 512 ±456 days (41-1851). Mortality rate was 68%. Median time to death was 1306 ±1093 days (78-5252). Median metastase SUVmax and SUVmean was 10.4±5.6 ng/ml (3.6-46.5) and 5.7±2.9ng/ml (2,5-23,6), respectively. Median normal liver SUVmax and SUVmean was 4.1 ±0.9 ng/ml (2.4-7.2) and 2.0 ±0.5 ng/ml (1.3-5.1), respectively. Median MTV was 50±87 ml (1.4-447.6) and median TLG was 288 ±523ml (5.6-2992.5). No statistical significant correlation or difference was observed between variables. ***Conclusion:*** In our sample, contrary to the literature, 2-[^{18}F]FDG PET/CT functional parameters were not able to predict recurrence or mortality, and therefore do not seem to be optimal for hepatic surgery selection in colon-rectal cancer. ***References:*** Shim JR, Lee SD, Han SS, Lee SJ, Lee DE, Kim SK, Kim SH, Park SJ, Oh JH, Prognostic significance of ^{18}F-FDG PET/CT in patients with colorectal cancer liver metastases after hepatectomy. Eur J Surg Oncol. 2018 May;44(5):670-676. DOI:10.1016/j.ejso.2018.01.243

EPS-031

Correlation of CEA levels with metabolic tumor volume, assessed by FDG PET and RECIST compliant size measurement in patients with recurrent and/or metastatic colorectal cancer

P. Bochev[1], *Y. Bocheva*[2], *G. Mateva*[1];
[1]*Acibadem Cityclinic UMBAL Mladost Oncology hospital, Sofia, BULGARIA,* [2]*Medical University "Prof.d-r Paraskev Stoyanov", Varna, BULGARIA.*

Aim/Introduction: Carcinoembryonic antigen (CEA) is a routine tumor marker in the management of patients with colorectal cancer (CRC) in staging, prognostication and surveillance. Its use in treatment response monitoring is less clear in terms of correlation with the actual tumor volume. Fluorodeoxyglucose Positron emission tomography (FDG PET CT) is frequently used in treatment response assessment to represent metabolic tumor volume (MTV). Data on direct correlation between tumor size assessed by contrast enhanced CT (CECT) and CEA levels is present, but those for MTV and CEA is scarce and unconvincing. Aim: To correlate the CEA levels with metabolic tumor volume and RECIST compliant size measurement in patients with recurrent/persistent/metastatic CRC. ***Materials and Methods:*** Inclusion criteria: CRC with recurrence/persistence/metastatic disease, which have measurable MTV on FDG PET/CT, RECIST compliant target lesions on CECT and has been monitored with CEA serum levels. CEA levels have been tested within 4 weeks of PET/CT and/or CECT. Only patients with ≥3 measure points were included. Exclusion criteria: CRC with measurable MTV, but normal CEA levels; Patients with high CEA levels, but low FDG uptake; Patients with only non-measurable disease on CECT; Chemo- or radiotherapy, applied between PET/CECT and CEA measurement. We retrospectively reviewed the database of Nuclear medicine department, Acibadem City clinic Oncology hospital, Sofia from Nov.2018 to Mar.2020. Eight patients met the inclusion criteria. All scans of those patients, that were coupled with CEA measurement were considered evaluable points and were further analyzed. A total of 90 evaluable points were identified (37 PET, 52 CECT, 1 PET with CECT). MTV and CEA level as well as CECT sum of largest diameters (target lesion only) and CEA were tested for correlation at individual level. CLIA method is used for CEA determination. ***Results:*** The correlation of CEA levels and MTV was strikingly high , r=0,97 (0,86 to 0,99). The correlation of CECT parameters ranged from low to high (0,27 to 0,99) with one case of negative correlation (r=-0,27) with CECT failing to correlate in cases of complex liver lesions with massive necrosis, after local treatment of liver metastases and in bone metastases. PET CT performed slightly worse in small volume lung metastases. ***Conclusion:*** MTV has an almost perfect positive correlation with CEA levels. RECIST measurements have highly variable correlation, ranging from low negative to high positive. In cases of major discrepancies between CEA dynamics and CECT assessed response, arbitrary FDG PET CT should be recommended. ***References:*** None

EPS-032

The Relationship Between Ca-125 Level and ^{18}F FDG PET/CT Findings in The Assessment of Progressive Disease in Epithelial Ovarian Carcinoma

S. Tatlidil*, B. Karasah, H. Sariyildiz, Z. Burak, Z. Ozcan;*
Ege University, Izmir, TURKEY.

Aim/Introduction: Elevated Ca-125 level in ovarian tumors might indicate disease progression and it is in use as an indication of ^{18}F FDG PET/CT for restaging. In the current study, we aimed to investigate the relationship between imaging findings and serum Ca-125 level in patients with ovarian surface epithelial tumors who underwent ^{18}F FDG PET/CT to evaluate the suspicion of recurrent disease. ***Materials and Methods:*** The database of 125 patients (pts) who underwent PET/CT for re-staging between 13.12.2011-29.05.2019 was reviewed. There were 88 pts fitting to the study inclusion criteria. The initial ^{18}F FDG PET/CT scan which is performed for restaging was involved. Those pts without a Ca-125 test and PET/CT within a 2 week interval, or who had a histological diagnosis other than surface epithelium-originated tumors, who had a second primary malignancy, progression under treatment, or those with chronic granulomatous disease were excluded. Increasing lesion size and new lesions were considered as progression criteria and verified with clinical follow-up, imaging/clinical findings, or histopathological examination. ***Results:*** There were 34 (39%) cases with high grade and 33 (38%) low grade serous tumors. Other tumor subtypes were mucinous: 8 (9%), clear cell: 5 (6%), and 8 others (9%). Serum Ca-125 levels ranged from 2 to 2456U/ml. In 72 (82%) out of 88 cases, Ca-125 levels were elevated. While progressive disease was confirmed in 62 (86%) out of these 72 pts, disease progression was suspicious in 5 cases (7%). Five 5 cases were clinically stable despite the increased Ca-125 level and PET/CT showed no evidence of disease progression in these pts. On the other hand, PET/CT showed progression of intra-abdominal lesions in 11 out of 16 patients (69%) whose serum Ca-125 levels were actually non-elevated. Tumor histology was high grade serous carcinoma in 10 (91%) of them. When Ca-125 levels during the last 6 months period were assessed it was stable in 10 (91%) pts. A gradual increasing trend of Ca-125 was noted in a single patient (9%) even though it was not exceeding the normal limit. ***Conclusion:*** Despite the limited number of cases, our findings indicate the detection of cases of with progressive findings on ^{18}F FDG PET/CT scan without corresponding high Ca-125 levels. Therefore, a whole-body ^{18}F FDG PET/CT scan might improve clinical evaluation particularly in cases with high grade serous carcinoma in which normal Ca-125 levels might be found at the time of recurrence. ***References:*** None

EPS-033

^{18}F-FDG PET/CT and Ca-125 in the evaluation of ovarian cancer relapse or persistence: is there any correlation?

F. Dondi[1], D. Albano[1], A. Calabrò[2], M. Gregorelli[2], A. Mazzoletti[2], P. Bellini[2], M. Gazzilli[3], E. Cerudelli[3], F. Bertagna[1], R. Giubbini[1]; [1]Università degli Studi di Brescia, Brescia, ITALY, [2]Università degli studi di Brescia, Brescia, ITALY, [3]Spedali Civili di Brescia, Brescia, ITALY.

Aim/Introduction: Ovarian cancer relapse can be diagnosed by serum tumor markers measurements and ^{18}F-fluorodoxyglucose positron emission tomography/computed tomography (^{18}F-FDG PET/CT) findings. The aim of our study was to analyze the potential relationship between cancer antigen 125 (Ca-125) and PET/CT results in patients affected by ovarian cancer. ***Materials and Methods:*** 92 ^{18}F-FDG PET/CT scans in 61 patients with diagnosis of ovarian cancer were analyzed and compared to Ca-125 values. PET/CT results were compared to other imaging modalities, histology or follow-up data in order to define its diagnostic accuracy. PET/CT studies were analyzed qualitatively and semiquantitatively by measuring the maximum and mean standardized uptake value body weight max (SUVbwmax, SUVbwmean), maximum SUV lean body mass (SUVlbm), maximum SUV body surface area (SUVbsa), metabolic tumor volume (MTV) and total lesion glycolysis (TLG) of hypermetabolic lesions. All measurements were compared with Ca-125 values. ***Results:*** 20 PET/CT studies were true negative, 63 true positive, 5 false positive and 4 false negative with sensitivity of 94%, specificity of 80%, negative predictive value of 83%, positive predictive value of 93% and accuracy of 90%. Ca-125 levels were significantly correlated with PET/CT results and all PET/CT semiquantitative parameters. Ca-125 cutoff values of 17 UI/mL is the best compromise between sensitivity and specificity in discriminating between positive and negative PET/CT result. ***Conclusion:*** ^{18}F-FDG PET/CT has good accuracy in evaluating patients with relapse or persistance of ovarian cancer. Ca-125 levels were significantly correlated with metabolic PET/CT parameters. ***References:*** None

EPS-034

Patterns and Time to Recurrence of Gynaecologic Malignancies on ^{18}F-FDG PET/CT

S. Gitau, K. Makhdomi, E. Nganga, K. Warfa; Aga Khan University, Nairobi, KENYA.

Aim/Introduction: Patients with gynaecologic malignancies have varied patterns of disease recurrence as well as time to recurrence. There is paucity of literature on these patterns as assessed by ^{18}F-Fluorodeoxyglucose positron emission tomography/computed tomography (^{18}F-FDG PET/CT). This study aimed to characterize patterns and time to recurrence of gynaecologic malignacies as assessed on 18F-FDG PET/CT. ***Materials and Methods:*** Clinical data of patients treated for gynaecologic malignancies (cervical, endometrial and ovarian cancers) and referred for a follow up FDG PET/CT to exclude recurrence was collected between January and December 2019. Patients with evidence of metabolically active recurrence were included in this study. Patients referred for staging FDG PET CT were excluded. The time to recurrence, in months, for the different gynaecologic malignancies was recorded. ***Results:*** A total of 84 (45 cervical cancer, 24 ovarian cancer and 16 endometrial cancer) patients met the inclusion criteria. 46/84 (55%) patients had metabolically active disease recurrence at completion of the initial treatment. This included 21/45(47%) cervical cancer, 14/24 (58%) ovarian cancer and 10/16 (63%) endometrial cancer) patients had Patterns of cervical cancer recurrence were as follows: 5 (24%) patients had central/local/vault recurrence, 3 (14%) had pelvic sidewall nodal recurrence and 13 (62%) had distant/multiple-site recurrence. Patterns of ovarian cancer recurrence were as follows: 12 (86%) patients had multiple-site recurrence and 2 (14%) had single-site nodal recurrence only. Patterns of endometrial cancer recurrence were as follows: 1 (10%) patient had central/local recurrence, 1 (10%) had pelvic nodal recurrence and 8 (80%) had distant/multiple-site recurrence. A total of 13/46 (28%) patients had recurrence above the diaphragm. The median time to relapse (TTR) in months was 32.5 for cervical cancer, 23 for ovarian cancer and 33.8 for endometrial cancer, an average of 30 months for the gynecologic malignancies. ***Conclusion:*** Gynaecologic malignancies predominantly recur at distant/multiple sites. The average time to recurrence for these malignancies is 2-3 years. ***References:*** Gerdin E, Cnattingius S, Johnson P, et al. Prognostic factors and relapse patterns in early-stage cervical carcinoma after brachytherapy and radical hysterectomy. Gynecol Oncol 1994; 53:314. Morice P, Deyrolle C, Rey A, et al. Value of routine follow-up procedures for patients with stage I/II cervical cancer treated with combined surgery-radiation therapy. Ann Oncol 2004; 15:218. Sorbe, B., Juresta, C., Ahlin, C." Natural history of recurrences in endometrial carcinoma". Oncology Letters 8.4 (2014): 1800-1806.

401

CME 3: Finding the Right PET Companion for ImmunoOncology

Friday, October 23, 2020, 09:00- 10:30 Channel 1

OP-133

Why Do we Need PET Companion Tracers in Immunooncology?

N. Aide; Centre Hospitalier Universitaire de Caen (CHU Caen), Nuclear Medicine and Medical Biophysics, Caen, FRANCE.

OP-134

Going Beyond FDG - Development of Tailored PET Companion Tracers

S. Heskamp; Radboud University Medical Centre (Radboudumc), Department of Radiology and Nuclear Medicine, Nijmegen, NETHERLANDS.

OP-135

The Next Step - From Companion Diagnostics Towards Immunotheranostics

N. Schaefer; Centre Hospitalier Universitaire Vaudois (CHUV), Department of Nuclear Medicine, Lausanne, SWITZERLAND.

402

Joint Symposium 5 (EANM/EHA): Use of PET in Multiple Myeloma

Friday, October 23, 2020, 09:00- 10:30 Channel 2

OP-136

Multiple Myeloma – MRD

E. Zamagni; Hematology Department, Seragnoli Institut, University of Bologna, Bologna, ITALY.

OP-137

Evaluation of Minimal Residual Disease with FDG PET/CT

C. Nanni; Nuclear Medicine department, AOU S.Orsola-Malpighi, Bologna, ITALY.

OP-138

Where are we now with Non-FDG

N. Withofs; 1- Division of Nuclear Medicine and Oncological Imaging, Department of Medical Physics, CHU of Liege; 2- GIGA-CRC in vivo imaging, University of Liège, Liege, BELGIUM.

OP-139

Theranostics in MM

C. Lapa; University Hospital Augsburg, Department of Nuclear Medicine, Augsburg, GERMANY.

403

Joint Symposium 6 (EANM/ASNC): Detecting Cardiac Toxicity of Cancer Therapies with Nuclear Imaging

Friday, October 23, 2020, 09:00 - 10:30 Channel 3

OP-140

Cardiac Complications of Cancer Therapy -A Clinical Perspective

J. Bergler-Klein; Department of Cardiology, Vienna, AUSTRIA.

OP-141

Assessing LV Dysfunction

R. Russell; Cardiovascular Institute of Lifespan, Warren Alpert Medical School of Brown University, Providence , R.I., UNITED STATES OF AMERICA.

OP-142

Detecting Myocardial Injury

C. Rischpler; University Hospital Essen, Essen, GERMANY.

OP-143

Perspectives for CV Imaging in Cardio-Oncology

S. Dorbala; Department of Nuclear Cardiology, Brigham and Women's Hospital, Boston, UNITED STATES OF AMERICA.

OP-144

404a

Mini Course 1: New Developments in Cardiac Imaging Instrumentation

Friday, October 23, 2020, 09:00 - 09:50 Channel 4

OP-145

Difference in Myocardial Perfusion Imaging Between Conventional SPECT Imaging and Imaging with Dedicated Cardiac Cameras

S. Rep; University Medical Centre, Department of Nuclera Medicine, Ljubljana, SLOVENIA.

OP-146

Diagnostic Performance of Dedicated Cardiac Cameras

J. Jamsek; University Medical Centre, Department of Nuclera Medicine, Ljubljana, SLOVENIA

405

M2M Track - TROP Session: Pharmacokinetics and Chelators - Best of Both Worlds

Friday, October 23, 2020, 09:00 - 10:30 Channel 5

OP-147

SPECT imaging of SST2-expressing tumors with ^{99m}Tc-labelled somatostatin receptor antagonists is feasible depending on the chelator and the spacer

R. Gaonkar[1], F. Wiesmann[1], E. Gourni[2], R. Mikołajczak[3], L. McDougall[1], L. Del Pozzo[1], H. R. Maecke[2], R. Mansi[1], M. Fani[1]; [1]Division of Radiopharmaceutical Chemistry, University Hospital Basel, Basel, SWITZERLAND, [2]Department of Nuclear Medicine, University Hospital Freiburg, Freiburg, GERMANY, [3]National Centre for Nuclear Research, Radioisotope Centre POLATOM, Otwock, POLAND.

Aim/Introduction: Somatostatin receptor subtype 2 (SST2) is an established biomarker today for imaging of neuroendocrine

tumors using ^{68}Ga-labelled somatostatin receptor agonists ([^{68}Ga]Ga-DOTA-TATE or [^{68}Ga]Ga-DOTA-TOC) and more recently antagonists ([^{68}Ga]Ga-NODAGA-JR11). Nevertheless, most of the nuclear medical examinations are conducted with ^{99m}Tc, and [^{99m}Tc]Tc-HYNIC-TOC is being used for SST2 imaging. Surprisingly, when [^{99m}Tc]Tc-HYNIC was conjugated to the antagonist SS01 (4-Cl-Phe-cyclo(D-Cys-Tyr-D-Trp-Lys-Thr-Cys)D-Tyr-NH_2) SST2 imaging was not feasible[1]. This was not the case for [^{99m}Tc]Tc-N4-SS01 (N4: 6-carboxy-1,4,8,11-tetraazaundecane). HYNIC, a common bifunctional chelator for ^{99m}Tc, seemed to be "incompatible" with SST2 antagonists. The aims of this work are to investigate whether: a) the "incompatibility" of HYNIC is a general phenomenon with SST2 antagonists and b) the introduction of spacers facilitates SST2 imaging with the HYNIC conjugates. ***Materials and Methods:*** The two somatostatin antagonists SS01 and JR11 having a distinct SST2 affinity were conjugated to N4, HYNIC and Ahx-HYNIC (Ahx: aminohexanoic acid). All six conjugates were labelled with ^{99m}Tc (EDDA was used as co-ligand for HYNIC) and evaluated head-to-head in vitro and in vivo using HEK-hSST2 cells. Their imaging properties were assessed by SPECT/CT in HEK-hSST2 xenografts. [^{99m}Tc]Tc-HYNIC-TOC was used as a reference radiotracer. ***Results:*** Both [^{99m}Tc]Tc-N4 conjugates showed very high cellular uptake (78.5±0.3% and 71.2±1.45% for [^{99m}Tc]Tc-N4-SS01 and [^{99m}Tc]Tc-N4-JR11 at 4h, respectively). On the contrary, the two [^{99m}Tc]Tc-HYNIC conjugates showed very low cellular uptake ([^{99m}Tc]Tc-HYNIC-SS01 <1% and [^{99m}Tc]Tc-HYNIC-JR11 only 13.9±1.0%, at 4h). The introduction of Ahx restored to a great extent the SST2-mediated cellular uptake, being 36.6±0.2% for [^{99m}Tc]Tc-HYNIC-Ahx-SS01 and 56.9±0.8% for [^{99m}Tc]Tc-HYNIC-Ahx-JR11; close to the level of [^{99m}Tc]Tc-HYNIC-TOC (49.4±1.2%). As a result, SST2 imaging by SPECT/CT was successful with both [^{99m}Tc]Tc-HYNIC-Ahx conjugates. With the exception of [^{99m}Tc]Tc-HYNIC-Ahx-JR11 at 1h p.i. showing some abdominal uptake (attributed to stomach and pancreas), all four ^{99m}Tc-labelled conjugates were accumulated in the tumors and the kidneys and revealed excellent tumor-to-background contrast. Visually, both [^{99m}Tc]Tc-HYNIC-Ahx conjugates show similar tumor uptake as the [^{99m}Tc]Tc-N4 counterparts, which in turn had distinguishingly higher kidney uptake. All four ^{99m}Tc-labelled conjugates illustrated similar or superior image contrast to [^{99m}Tc]Tc-HYNIC-TOC. Quantitative biodistribution studies are on-going. ***Conclusion:*** HYNIC is a suitable chelator for the development of ^{99m}Tc-labelled SST2-antagonists when a spacer of appropriate length, like Ahx, is used. [^{99m}Tc]Tc-HYNIC-Ahx-SS01 and [^{99m}Tc]Tc-HYNIC-Ahx-JR11 compare fairly well with [^{99m}Tc]Tc-HYNIC-TOC as imaging agents. N4 is also a suitable chelator, which leads though to a higher accumulation in the kidneys. ***References:*** 1. Abiraj K et al., EJNMMI Research 2018;8:75

OP-148

Preclinical characterization of two ^{99m}Tc-labelled SSTR2 antagonists: Selection of a candidate for clinical translation

C. Decristoforo[1], R. Mansi[2], V. Weingärtner[1], P. Kolenc-Peitl[3], P. Garnuszek[4], M. Kroselj[3], R. Mikolajczak[4], C. Rangger[1], A. Hubalewska-Dydejczyk[5], M. Fani[2];
[1]Department of Nuclear Medicine, Medical University Innsbruck, Innsbruck, AUSTRIA, [2]Division of Radiopharmaceutical Chemistry, University Hospital Basel, Basel, SWITZERLAND, [3]Department of Nuclear Medicine, University Medical Centre Ljubljana, Ljubljana, SLOVENIA, [4]Radioisotope Centre POLATOM, National Centre for Nuclear Research, Otwock, POLAND, [5]5Department of Endocrinology, Jagiellonian University Medical College, Cracow, POLAND.

Aim/Introduction: Somatostatin receptors, predominantly of subtype 2 (SSTR2), overexpressed in neuroendocrine neoplasms (NEN) are an established target for radiopharmaceuticals. Recently, radiolabelled SSTR2 antagonists have demonstrated superior properties over agonists (e.g. DOTA-TATE, DOTA-TOC), with promising developments for PET imaging and therapy.[1] Considering the availability and diagnostic performance of SPECT/CT scans, usage of a suitable ^{99m}Tc-labelled SSTR2 antagonist would offer a wider applicability of this approach. The development of such candidates is so far very limited, clinical data are lacking. Within the ERA-PerMed project "TECANT" [2] two SSTR2 antagonists with the Tetraamine (N4) chelator for ^{99m}Tc-labelling (TECANT 1 based on the antagonist LM3 and TECANT 2 based on BASS) were compared preclinically regarding their pharmacological properties in vitro and in vivo for the selection of the best candidate for clinical translation. ***Materials and Methods:*** Receptor affinity (IC_{50}) displacement assays, internalization and dissociation studies were performed in HEK293 cells transfected with human SSTR2 (HEK-SSTR2). LogD values were determined using octanol/water partition, protein binding and stability were assessed in human serum. Biodistribution and SPECT/CT studies were carried out in nude mice bearing HEK-SSTR2-xenografts. Biodistribution studies provided the basis for dosimetry estimations from mouse to man. ***Results:*** [^{99m}Tc]Tc-TECANT 1 showed higher hydrophilicity (logD=-2.53) and lower protein binding (20%) than [^{99m}Tc]Tc-TECANT 2 (-1.63 and 23%, respectively), stability was comparable. Competition assays revealed a high affinity of both [^{99m}Tc]Tc-TECANT 1 and [^{99m}Tc]Tc-TECANT 2 to SSTR2 with IC_{50} values of 4.1± 0.8 and 5.0 ± 1.1 nM, respectively. [^{99m}Tc]Tc-TECANT 1 showed higher SSTR2-mediated cellular uptake in vitro (>50%, @2h/37°C) and lower dissociation rate (<30%, @2h/37°C), as compared to [^{99m}Tc]Tc-TECANT 2 (<40% and >50%, respectively). [^{99m}Tc]Tc-TECANT 1 had lower blood values, kidney and muscles uptake than [^{99m}Tc]T c-TECANT 2. Tumour uptake was comparable between the two

probes (26.0±1.3 and 28.4±4.8 %IA/g for [^{99m}Tc]Tc-TECANT 1 and [^{99m}Tc]Tc-TECANT 2, respectively), which was proven to be specific (<1% %IA/g in SSTR2-negative tumours). MicroSPECT/CT images confirmed the biodistribution results and indicated superiority of [^{99m}Tc]Tc-TECANT 1 as an imaging agent for SSTR2-expressing tumours. ***Conclusion:*** The preclinical studies provided the basis for selection of [^{99m}Tc]Tc-TECANT 1 for further pharmaceutical development in a kit formulation. Toxicity studies will be needed to complete the preclinical characterisation and to translate the first ^{99m}Tc-labelled SSTR2 antagonist into a clinical feasibility study in NEN patients. ***References:*** [1] Fani M, et al. J Nucl Med 2017 58 (Suppl 2), 61S-66S [2] https://www.era-learn.eu/network-information/networks/era-permed/1st-joint-transnational-call-for-proposals-2018/

OP-149

PET-MRI imaging of neurotensin receptor-positive tumors with ^{68}Ga-labeled antagonists : "the chelate makes again the difference"

V. Goncalves[1], E. Renard[1], M. Moreau[1], P. S. Bellaye[2], M. Guillemin[2], F. Denat[1];
[1]Université Bourgogne Franche-Comté, Dijon, FRANCE,
[2]Georges-François Leclerc Cancer Center, Dijon, FRANCE.

Aim/Introduction: Neurotensin receptor 1 (NTS_1) is involved in the development and progression of numerous cancers. A small-molecule NTS_1 antagonist, named [^{177}Lu]Lu-IPN01087 (previously [^{177}Lu]Lu-3BP-227) is currently evaluated in phase I/II clinical trials for the targeted radiotherapy of NTS_1-positive cancers. The identification of a PET companion diagnostic agent would greatly facilitate the selection of patients eligible for NTS_1-targeted therapy. In this study, we evaluated the influence of the nature of the chelator on the biodistribution of NTS_1 antagonists. ***Materials and Methods:*** Seven compounds were synthesized, based on the structure of the NTS_1 antagonist SR142948A, using different chelators for gallium-68 (NOTA, (R)-NODAGA, DOTA, DOTAGA and THP). The compound 3BP-227 and the NTS_1 peptide agonist NT20.3 were used as references. All these compounds were metalated with ^{nat}Ga and their affinity for NTS_1 was determined on a competition assay on CHO cells overexpressing NTS_1. Their stability was assessed in mouse serum. The compounds were radiolabeled with ^{68}Ga, partition coefficients were measured and their biodistribution was studied in nude mice bearing a subcutaneous xenograft of HT-29 cells. PET-MRI images were recorded between 1.5 h and 2 h post-injection (3-8 MBq). Two hours post-injection, mice were sacrificed, organs were collected, weighed and γ-counted. ***Results:*** Seven novel antagonists were obtained through a convergent synthesis in 21 steps. K_i values were in the nanomolar range, demonstrating a high affinity for NTS_1. The NOTA/NODAGA/THP-based compounds were radiolabeled with ^{68}Ga in 5 min at 37°C, whereas 10 min at 95°C was required for the DOTA/DOTAGA-based compounds to achieve molar activities of ca. 15-20 MBq/nmol. Good radiochemical yields and purities (>95%) were obtained. PET-MRI images and ex vivo biodistribution studies showed significant differences between compounds. The THP derivative showed significant uptake in the lungs, spleen, and liver. The NOTA- and NODAGA-compounds showed a strong signal in gallbladder and intestines suggesting a partial hepatobiliary excretion pathway. All the other compounds were eliminated through kidneys. We identified a promising ^{68}Ga-PET tracer that showed rapid accumulation in the tumor (4.9%ID/g, 2 h p.i.) and fast clearance from healthy tissues. Blocking experiments confirmed the specificity of the uptake. ***Conclusion:*** Here, we evaluated, side-by-side, the influence of the nature and number of chelators on a series of NTS_1 small-molecule antagonists and identified a promising tracer, [^{68}Ga]Ga-bisNODAGA-16. We believe that this tracer could serve as a useful ^{68}Ga-PET diagnosis agent for multiple cancers and assist in the selection of patients eligible for NTS_1 radiotherapy. ***References:*** None

OP-150

Longitudinal PET Imaging Allows for Non-Invasive Assessment of TSPO Expression in a Glioblastoma Mouse Model

A. Holzgreve[1], D. Pötter[1], M. Brendel[1], M. Orth[2], L. Weidner[3], J. Maas[2], B. von Ungern-Sternberg[1], L. Gold[1], M. A. Kirchner[1], M. J. Riemenschneider[3], P. Bartenstein[1], K. Lauber[2], N. L. Albert[1];
[1]Department of Nuclear Medicine, University Hospital, LMU Munich, Munich, GERMANY, [2]Department of Radiation Oncology, University Hospital, LMU Munich, Munich, GERMANY, [3]Department of Neuropathology, Regensburg University Hospital, Regensburg, GERMANY.

Aim/Introduction: The 18kDa translocator protein (TSPO) is upregulated during activation of microglia and macrophages and has shown to be overexpressed in glioblastoma (GBM). However, few data exist on TSPO-targeted imaging of malignant brain tumors. Hence, we investigated the feasibility of longitudinal TSPO PET imaging in a GBM mouse model validated through autoradiography and immunohistochemistry. ***Materials and Methods:*** A total of 24 mice were orthotopically injected with either GL261 cells (GBM, n = 21 mice) or saline for control (sham, n = 3 mice). Longitudinal PET imaging with the TSPO ligand ^{18}F-GE-180 was performed in a subgroup of 12 mice at four time points (4, 7, 11 and 14 days post inoculation). Another subgroup (n = 12 mice) was scanned at one time point only (7, 11 or 14 days post inoculation). PET analysis consisted in quantification of tracer uptake at the site of inoculation and within a background region in the unaffected contralateral hemisphere. Mean and maximal SUVs as well as tumor-to-background ratios were calculated ($SUV_{mean/max;}TBR_{mean/max}$). Post-mortem analysis of TSPO expression was performed

by autoradiography and immunohistochemistry for qualitative comparison of regional distribution of TSPO with the tracer signal. T-test was used for group comparison between GBM and sham mice and analysis of variance for comparison between GBM mice at different time points. Level of significance was $p < 0.05$. ***Results:*** PET imaging, autoradiography and immunohistochemistry revealed elevated TSPO expression in all inoculated mice. Tumor extent was visually congruent between autoradiography, immunohistochemistry and histology. TSPO PET signal was significantly higher in GBM vs. sham mice (e.g. TBR_{max} 3.0 ± 0.4 vs. 2.2 ± 0.3, TBR_{mean} 1.9 ± 0.2 vs. 1.29 ± 0.03; $p < 0.001$) 14 days post inoculation. In GBM mice, longitudinal PET imaging showed an increase of tumoral tracer uptake between day 4 and day 14 post inoculation (+57% for SUV_{mean} ($p < 0.001$), +23% for TBR_{max} (p=0.013) and +22% for TBR_{mean} ($p < 0.001$)). Interestingly, PET imaging indicated a slightly increased TSPO signal in the contralateral hemisphere in GBM mice (SUV_{mean} 0.22 ± 0.02) compared to sham mice (SUV_{mean} 0.20 ± 0.02, p=0.02) 14 days after inoculation. ***Conclusion:*** TSPO-targeted PET imaging is feasible in a GBM mouse model. Qualitative and quantitative PET evaluation allows for non-invasive assessment of tumoral TSPO expression over time. A reference region in the contralateral hemisphere should be used with caution, as background signal was increased in all GBM mice. ***References:*** None

OP-151

Low temperature radiolabelling of human serum albumin constructs with terbium-161 and ex vivo biodistribution to assess in vivo stability

I. Cassells[1,2], *M. Ooms*[2], *J. Cornelis*[1], *A. R. Burgoyne*[2], *S. Ahenkorah*[1,2], *M. Van de Voorde*[2], *T. Cardinaels*[2,3], *C. M. Deroose*[4], *G. Bormans*[1], *F. Cleeren*[1];

[1]*Radiopharmaceutical Research, Department of Pharmaceutical and Pharmacological Science, University of Leuven, Leuven, BELGIUM,* [2]*Nuclear Materials Science Institute, Belgian Nuclear Research Centre (SCK CEN), Mol, BELGIUM,* [3]*Department of Chemistry, University of Leuven, Leuven, BELGIUM,* [4]*Nuclear Medicine, University Hospitals Leuven: Nuclear Medicine and Molecular Imaging, Department of Imaging and Pathology, Leuven, BELGIUM.*

Aim/Introduction: Targeted radionuclide therapy using Terbium-161 (^{161}Tb) is a promising approach for β^- and Auger electron therapy. Heat-sensitive biomolecules (e.g. nanobodies) are increasingly being used as carriers in radiometal-based pharmaceuticals, however current radiolabelling techniques require heating (>85 °C) incompatible with heat-sensitive carrier molecules. In this study, we evaluated bifunctional chelators that allow ^{161}Tb-labelling under mild conditions using human serum albumin (HSA) and assessed the in vivo stability of the constructs. ***Materials and Methods:*** ^{161}Tb was produced and purified at SCKCEN.[1] p-SCN-Bn-CHX-A"-DTPA (***L1***), p-SCN-Bn-DOTA (***L2***) and p-NCS-Bz-DOTA-GA (***L3***) were conjugated to HSA (0.1 M $NaHCO_3$, pH 8.5, 2h, 25°C) and purified (PD-10 column) resulting in HSA-***L1-3*** with a chelator-to-HSA ratio of 1-3, as determined with ESI-TOF-HRMS. The constructs were labelled with 54 MBq $^{161}TbCl_3$ (10 µM HSA-***L1-3***, 0.1 M NaOAc, pH 4.7, 1h, 40°C) and purified (PD-10 column, PBS, 5 mg/mL ascorbic acid). The in vitro stability was determined in human serum at 37°C (iTLC and SEC-HPLC). NMRI mice were injected with free $^{161}TbCl_3$ or ^{161}Tb-HSA-***L1-3*** (0.9-1.5 MBq, 0.2 mL, 10 nmoles) via a tail vein under anaesthesia, and sacrificed after 10 min, 1 h, 4 h, 24 h or 7 days (n=3/time point). Organs were harvested and the radioactivity quantified using a gamma counter. ***Results:*** All HSA constructs (HSA-***L1-3***) were labelled successfully with $^{161}TbCl_3$ at 40 °C (radiochemical yield >99 %). A limited amount of ^{161}Tb (7%) bound to unmodified HSA (negative control). ^{161}Tb-HSA-***L1-3*** demonstrated high stability in human serum, even after 24 hours at 37°C (>96 %). Free $^{161}TbCl_3$ in NMRI mice showed significant uptake in bone (SUV = 2.57 ± 0.46) at 1 h post injection, which was increased further after 7 days (SUV = 3.53 ± 1.01). The HSA-***L1*** construct showed increased bone uptake after 7 days (SUV = 1.1 ± 0.3), suggesting ***L1*** is not a suitable ligand for terbium. In contrast, the DOTA constructs (***L2*** and ***L3***) showed only minor uptake in bone (SUV = 0.13, p = 0.002), suggesting a more stable chelation of terbium. ***Conclusion:*** We radiolabelled heat-sensitive biomolecules with ^{161}Tb in quantitative yields for the first time. The DOTA variants (^{161}Tb-HSA-***L2-3***) demonstrated high in vitro and in vivo stability and are promising chelators for terbium labelling. More interesting vector molecules will be radiolabelled using this method with different terbium isotopes for theranostic applications. ***References:*** 1. M. Ooms, et al., Eur. J. Nucl. Med. Mol. Imaging, 46, 2019, p. S40 1 p., OP-088

OP-152

Sensitive imaging of αvβ6-Integrin using Ga-68 labelled nonapeptide trimers

J. Notni*, N. G. Quigley, F. Richter, K. Steiger, W. Weichert; Technical University of Munich, Munich, GERMANY.*

Aim/Introduction: αvβ6-Integrin binds to latency-associated peptide (LAP) via a RGD sequence contained therein, and is a major activator of transforming growth factor beta (TGF-β). Many carcinomas (esp. pancreatic and squamous cell) express αvβ6-integrin, but it is also upregulated in other conditions associated with TGF-β dysregulation, such as fibrosis. We structurally optimized a previously described αvβ6-integrin selective nonapeptide [1] and designed trimeric Ga-68-labeled TRAP-conjugates thereof, aiming to reduce unspecific in-vivo uptake in non-target organs while maintaining target affinity and target-specific accumulation and retention. ***Materials and Methods:*** Peptides were synthesized by Fmoc technique. Integrin affinities were

determined by ELISA as described.[1] Ga-68 labelled trimeric TRAP (triazacyclononane-triphosphinate) conjugates thereof were synthesized via Click Chemistry (CuAAC) as described,[2] and characterized in H2009 (αvβ6+) xenografted SCID mice by dynamic (90 min) and static (75 min p.i.) PET as well as ex-vivo biodistribution. Expression of αvβ6-integrin in tumor and non-target tissues was determined by β6-immunohistochemistry. ***Results:*** The effect of altering different amino acids in the sequence of cyclo(FRGDLAFp(NMe)K) was investigated, regarding binding affinity, polarity, and biodistribution of the respective TRAP-based, Ga-68 labeled trimeric conjugates. All investigated compounds exhibited comparable αvβ6-integrin affinities in the sub-nanomolar range. Depending on the substitution patterns, varying reductions of non-specific uptake was observed (e.g., ranges in blood, liver, and pancreas from 2.4-0.25, 7.7-0.6, and 1.0-0.27 %ID/g, respectively). Since tumor uptakes were comparable (range 7.5-8.7 %ID/g), corresponding tumor/background ratios could be increased from 2.2, 1.2, and 10.1 %ID/g to 7.5, 10.5, and 28.5 %ID/g, respectively, resulting in high-contrast PET images. ***Conclusion:*** αvβ6-Integrin PET using Ga-68-labeled nonapeptide trimers holds great promise for improved clinical PET-diagnostics of carcinomas and fibrosis. ***References:*** [1] Färber SF, et al., ACS Omega 2018;3:2428. [2] Baranyai Z, et al., Dalton Trans. 2015;44:11137-11146.

OP-153

Optimized Radiosynthesis of [3-^{11}C]Alanine and [3-^{11}C] Pyruvate for Imaging Central Carbon Metabolism In Vivo

J. Kelly, *T. M. Jeitner, N. Waterhouse, N. Karakatsanis, S. Nehmeh, J. W. Babich;*
Weill Cornell Medicine, New York, NY, UNITED STATES OF AMERICA.

Aim/Introduction: Many cancer cells undergo metabolic reprogramming leading to high glucose consumption; known as the Warburg effect. Such metabolic reprogramming is typically imaged using FDG. Although FDG captures changes in glucose uptake, it provides no information about glucose utilization. This is particularly true in prostate cancer (PCa), in which FDG uptake is highly variable. To better understand metabolic reprogramming in cancer, and its relationship with pathogenesis and progression, probes that directly interrogate central carbon metabolism (CCM) are required. Pyruvate lies at the nexus of CCM, and the alanine-pyruvate-lactate axis is frequently altered in cancer. Our aims were to develop syntheses of [3-^{11}C]alanine and [3-^{11}C] pyruvate that would enable automation, and to demonstrate the feasibility of these probes for imaging elements of CCM metabolism in vivo by positron emission tomography (PET). ***Materials and Methods:*** [3-^{11}C]Alanine was synthesized from N-(diphenylmethylene)glycine tert-butyl ester and converted to [3-^{11}C]pyruvate using D-amino acid oxidase. All solvent exchanges and purifications were performed by solid phase extraction (SPE). Uptake of [3-^{11}C]alanine and [3-^{11}C]pyruvate was determined in two PCa cell lines, and tissue distribution was visualized by microPET/CT in male athymic BALB/c nu/nu mice and healthy male Sprague-Dawley rats. ***Results:*** Racemic [3-^{11}C]Alanine and [3-^{11}C]pyruvate are isolated after 33±4 min and 53±7 min, respectively. Decay-corrected radiochemical yields were 68±13% and 22±7%. Radiochemical purity exceeded 98% for both tracers. [3-^{11}C] Alanine is taken up continuously by PC3 cells over 40 min, with a rate that exceeds that of FDG. In contrast, [3-^{11}C] Pyruvate is taken up very rapidly by both LNCaP and PC3 cells (t_{max} < 5 min). Activity clears more rapidly from PC3 cells. In vivo, [3-^{11}C]Alanine accumulates in the liver and thymus as well as in PCa xenografts. The distribution of [3-^{11}C]pyruvate in mouse and rat is characterized by high uptake in the heart, liver, brain, and eyes. ***Conclusion:*** Chemoenzymatic syntheses of [3-^{11}C]alanine and [3-^{11}C]pyruvate based on SPE have been developed. These syntheses are suitable for automation, allowing for large end-of-synthesis activities sufficient for clinical use. [3-^{11}C]Alanine clearly delineates tumors in vivo, [3-^{11}C]pyruvate highlights distinct metabolic fluxes in LNCaP and PC3 cells. Taken together, these early observations support a role for these tracers for imaging elements of CCM in tumors in vivo. ***References:*** None

OP-154

Synthesis and in vitro comparison of squaric acid coupled lysine-urea-glutamate and glutamate-urea-glutamate based PSMA-inhibitors

T. Grus, *H. Lahnif, M. Omralinov, F. Roesch;*
Department of Chemistry, Johannes Gutenberg-University Mainz, Mainz, GERMANY.

Aim/Introduction: Prostate cancer (PC) is one of the most common cancer types worldwide. A promising target for PC is the prostate-specific membrane antigen (PSMA), which is highly overexpressed in PC and correlates with the severity of PC. The urea-based-target vector KuE (L-lysine-urea-L-glutamate) is the most used binding motif in PSMA inhibitors. Similar in vitro and in vivo study results were achieved with EuE (L-glutamate-urea-L-glutamate) based PSMA-radiotracer (1,2). In preliminary studies, we have identified squaric acid (SA) as promising linker moiety between KuE target vector and radiolabeling unit. In this study, we compared the PSMA-affinity of different SA.KuE and SA.EuE based tracer. ***Materials and Methods:*** DATA^{5m}.SA.KuE, DOTAGA.NH_2.SA.KuE, DATA^{5m}.SA.EuE and DOTAGA.NH_2.SA.EuE were synthesized and the binding affinity was determined in a competitive cell assay using PSMA-expressing LNCaP-cells. LNCaP-cells were incubated with 0.75 nM ^{68}Ga-PSMA-10 in the presence of different concentrations of the non-labeled PSMA-ligands. After incubation at RT and removal of free radioactivity, cell-bound activity was measured. PSMA-11 was used as reference. For comparison, DATA^{5m}.PSMA617 and DOTAGA.NH_2.PSMA-617 were also evaluated. ***Results:*** The SA.KuE and

SA.EuE building blocks were synthesized in two and three steps, respectively. Subsequently, the chelators were linked at pH 9. The binding affinity was determined for DATA^{5m}.SA.KuE (51.1 ± 5.5 nM), DOTAGA.NH_2.SA.KuE (20.2 ± 3.5 nM), DATA^{5m}.SA.EuE (386.2 ± 81.0 nM), DOTAGA.NH_2.SA.EuE (407.1 ± 19.2 nM), DATA^{5m}.PSMA-617 (92.1 ± 11.7 nM) and DOTAGA.NH_2.PSMA-617 (20.6 ± 3.4 nM). ***Conclusion:*** The results of the competitive binding assay showed that there is no difference in the affinity of SA.KuE based and PSMA-617 based DOTAGA-tracer. On the other side, DATA^{5m}.SA.KuE shows a better PSMA-binding affinity than DATA^{5m}.PSMA-617. Significant higher affinities of SA.KuE based and PSMA-617 based tracer were achieved in contrast to SA.EuE based tracer. Comparing the affinity of the Sa.EuE target vector without chelator unit (12.9 ± 7.4 nM) with the affinities of the tracers, a significant decrease in affinity is noticeable. The chelators seems to have a negative influence on the PSMA binding. ***References:*** 1. Hillier, S. M. et al. ^{99m}Tc-Labeled Small-Molecule Inhibitors of Prostate-Specific Membrane Antigen for Molecular Imaging of Prostate Cancer, J Nucl Med, 2013, 54:1369-1376. 2. 2. Robu, S. et al. Synthesis and preclinical evaluation of novel ^{18}F-labeled Glu-urea-Glu-based PSMA inhibitors for prostate cancer imaging: a comparison with ^{18}F-DCFPyl and ^{18}F-PSMA-1007, EJNMMI Research, 2018, 8, 30.

OP-155

Evaluation and Specific Targets of a Novel Tc-99m-MAG_3-RRL Probe for Tumor Imaging in Hepatoma Xenografts Model: A Pilot Study

R. Wang[1,2], *Y. Du*[1], *Z. Chen*[1], *P. Yan*[1], *X. Duan*[1], *Q. Jiang*[1], *J. Zhang*[1];
[1]*Peking University First Hospital, Beijing, CHINA,* [2]*Peking University International Hospital, Beijing, CHINA.*

Aim/Introduction: Arg-Arg-Leu (RRL) selected from peptide display library is a functional tumor -homing tripeptide, but its binding target is unclear. So in this study, we intend to identify its binding targets and improve the imaging application. ***Materials and Methods:*** Fluorescence imaging and flow cytometry were used to screen appropriate cell sample. Immunoprecipitation-mass spectrometry (IP-MS) method was utilized to screen the RRL-targeted proteins. Fluorescence colonization and cell-uptake experiment were used to verify the binding proteins. Peptides were modified with bifunctional chelating agent MAG_3 and further were radiolabeled by a one-step method. Imaging value was evacuated by γ-camera imaging and biodistribution studies. ***Results:*** HepG2 was the suitable cell with highest mean fluorescence intensity (P<0.05). IP-MS analyze showed that the dominant RRL-targeted proteins were mainly from heat shock protein (HSPs) family, especially heat shock cognate 71kDa protein (HSC70). Fluorescent colocalization showed a strong colocalization signal with the Pearson correlation coefficient of 0.80±0.07 and the overlap coefficient of 0.85±0.06. The HSP70 family inhibitor VER-155008 can significantly reduce cell ^{99m}Tc-MAG_3-RRL uptake by a factor of 3 (P<0.05). Correlation analysis showed that there was a strong correlation trend between inhibitor and RRL with 0.98 correlation coefficient. The labeling efficiency and radiochemical purity of Tc-99m-MAG_3-RRL were 96.72±1.01% and 97.10±0.27% respectively. Imaging results showed that Tc-99m- MAG_3-RRL could be significantly concentrated in tumor lesion with the tumor-to- muscle (T/M) ratio reaching up to 6.54 ± 0.30 at 2h, when compared to Tc-99m-MAG_3-GGG group (P<0.05) and blocking group (P<0.05). The peak %ID/g values were 8.95±0.28 at 30min and the highest (T/M) ratio of the %ID/g values was 5.61±0.38, which were significantly higher than control group at each time point (P<0.05). ***Conclusion:*** These results suggest that Tc-99m-MAG_3-RRL can hold great promise for imaging malignant tumor and detection the tumor expression of HSPs would be a meaningful application. ***References:*** None

OP-156

Auger Electron Emitter Radionuclide Therapy: In vitro Study of Thallium-201 Kinetics and Toxicity in Breast and Prostate Cancer Cells

K. Osytek*, I. Costa, E. Verger, F. Al-Salemee, J. Cheng, S. Terry, V. Abbate, P. Blower;*
King's College London, London, UNITED KINGDOM.

Aim/Introduction: Auger electron emitters have potential in targeted treatment of small tumours due to their high-LET (linear energy transfer) but short range emissions. Thallium-201 (^{201}Tl), known for its previous use in myocardial perfusion scintigraphy, decays by electron capture releasing around 37 Auger electrons, with a total energy of 15.3keV, per decay (1). However, its radiotoxic and cancer therapeutic effects remain unexplored. In this study we assess ^{201}Tl kinetics, radiotoxicity and its potential for targeted radionuclide therapy. ***Materials and Methods:*** [^{201}Tl]TlCl was used for in vitro studies on two cell lines: breast cancer cells MDA-MB-231 and prostate cancer cells DU-145, treated with activities ranging from 50-2000kBq per 250 µl medium. For the purposes of radiobiological evaluation, we chose to use membrane potassium channels, such as the K^+/Na^+-ATPase pump, as the mechanism of accumulation in cells, despite this not offering tumour selectivity. Uptake and efflux assays were performed to establish accumulation and wash-out of ^{201}Tl. We used clonogenic assays to assess survival after 90 minute incubation with ^{201}Tl and non-radioactive thallium and mercury as controls. The γH2AX method was used to visualise and quantify nuclear DNA damage. Higher concentrations of KCl were used to block ^{201}Tl uptake in order to assess the impact of non-internalised ^{201}Tl. ***Results:*** Cellular uptake of ^{201}Tl ranged between 4-13% measured in 250000 cells. Intracellular to extracellular concentration ratio at equilibrium was estimated between 40-55. Accumulated ^{201}Tl 'washed out' from cells exponentially after the radioactive medium

was exchanged for fresh medium. Clonogenic assays showed significant reduction in the number of colonies formed for the highest ^{201}Tl activities used compared to non-treated cells, with an estimated average activity of 0.2-0.3Bq/cell for 90% reduction in clonogenicity. Non-radioactive thallium and mercury at comparable concentrations revealed no toxicity. ^{201}Tl ions present only in the external solution did not reduce clonogenic survival of cancer cells. ^{201}Tl caused on average significantly more DNA damage per nucleus compared to non-treated and ^{nat}Tl/^{201}Hg treated cells. ***Conclusion:*** Internalised ^{201}Tl showed considerable radiotoxicity, reducing cell proliferation and survival while increasing nuclear DNA damage. Furthermore, we confirmed that ^{201}Tl ions need to be internalised to exhibit the radiotoxic effect on cells. These findings justify more advanced in vitro studies and the design of ^{201}Tl therapeutic radiopharmaceuticals, including the development of suitable chelators, for an Auger electron emitter radionuclide therapy. ***References:*** 1. Buchegger F, Perillo-Adamer F, Dupertuis YM, Bischof Delaloye A. Eur. J. Nucl. Med. Mol. Imaging. 33(11):1352. (2006)

OP-157

Exploring the limits of intranuclear PET/SPECT imaging with IgG-TAT: how low can you go?

M. Veal*, G. M. Dias, V. Kersemans, D. Sneddon, S. Faulkner, B. Cornelissen;*
University of Oxford, Oxford, UNITED KINGDOM.

Aim/Introduction: Radioimmunoconjugate (RIC)-based PET/SPECT imaging has great potential for a variety of clinical applications. The conjugation of cell penetrating peptides (CPPs), such as TAT (GRKKRRQRRRPPQGYG), facilitate the imaging of intranuclear epitopes, greatly expanding the scope for RIC-based imaging possibilities. Here, we develop a nuclear EGFP targeting method to evaluate the detection limits of IgG-TAT-based imaging of intranuclear epitopes. We use this methodology to predict the lower target abundance limit in vitro and in vivo, critical to choosing future candidate imaging targets. ***Materials and Methods:*** We stably transfected H1299 cells with Histone 2B tagged Enhanced Green Fluorescent Protein (H2B-EGFP) and generated four cell lines expressing increasing levels of H2B-EGFP, quantified by ELISA. We evaluated the anti-GFP monoclonal antibody GFP-G1 for specificity and affinity using Western blot, immunofluorescence microscopy and flow cytometry. GFP-G1 was conjugated to the CPP TAT, and the chelating agent DTPA using SPAAC-based click chemistry prior to radiolabelling with $^{111}InCl_3$. In vitro radio-internalisation assays were carried out across all four transfected cell lines and WT H1299 cells to evaluate the uptake of ^{111}In-DTPA-GFP-G1-TAT with different expression levels of H2B-EGFP. Xenograft tumours with three of the H2B-EGFP cell lines plus WT H1299 cells were established on the flank of balb/c nu/nu mice. Animals were administered 5 µg (5 MBq) ^{111}In-DTPA-GFP-G1-TAT followed by SPECT imaging at 24 and 72 hours post injection prior to being sacrificed for ex vivo biodistribution studies. ***Results:*** We generated four H2B-EGFP transfected cell lines, with expression levels ranging from 180,000 ± 5,000 to 1,100,000 ± 91,000 copies/cell. Immunofluorescence microscopy showed that antibody GFP-G1 colocalised with H2B-EGFP and flow cytometry demonstrated that binding of GFP-G1 bound H2B-EGFP with a dissociation constant of 5.1 nM (1.5 to 10.4 nM). We conjugated GFP-G1 with CPP TAT and chelating agent DTPA prior to radiolabelling with $^{111}InCl_3$. In vitro radio-internalisation assays showed that uptake of ^{111}In-DTPA-GFP-G1-TAT correlated linearly with increasing H2B-EGFP expression ($r = 0.76$, $P < 0.001$) with a predicted lower detection threshold of 180,000 copies/cell. In vivo xenograft models also demonstrated ^{111}In-DTPA-GFP-G1-TAT uptake correlated linearly with H2B-EGFP expression ($r = 0.63$, $P = 0.004$) with a raised detection threshold of 240,000 copies/cell. ***Conclusion:*** The ability to test the detection limit of IgG-TAT-based intranuclear imaging probes is essential when evaluating potential candidate imaging targets. This study demonstrates the current capabilities of RIC based intranuclear imaging whilst simultaneously creating a methodology for further optimisation of novel imaging probe designs. ***References:*** None

OP-158

Increased Accumulation of ^{64}Cu-Labbeled Liposomes after Photothermal Therapy in Syngeneic Murine Model of Colorectal Cancer

J. Jørgensen[1]*, K. Norregaard*[1]*, M. Simón*[1]*, A. E. Hansen*[2]*, J. R. Henriksen*[2]*, T. L. Andresen*[2]*, A. Kjær*[1]*;*
[1]Dept. of Clinical Physiology, Nuclear Medicine & PET and Cluster for Molecular Imaging, Dept. of Biomedical Sciences, Rigshospitalet and University of Copenhagen, Copenhagen, DENMARK, [2]Department of Health Technology,Technical University of Denmark, Lyngby, DENMARK.

Aim/Introduction: Hyperthermia increases tumor blood flow and vascular permeability, and can thereby enhance liposomal drug delivery to tumors. Photothermal therapy (PTT) is a minimally invasive technique that utilizes light-absorbing nanoparticles and near infrared light to induce local hyperthermia. Using a murine model of colorectal cancer (CT26), we aimed to assess if PTT can be used to increase liposomal accumulation in tumor tissue. ***Materials and Methods:*** Labelling of liposomes with ^{64}Cu was performed as previously described [1]. Balb/c mice bearing subcutaneous CT26 tumors were grouped (n = 5), and PTT was performed by intravenously injecting gold nanoshells (190 µl and $4.9x10^{10}$ nanoshells/ml) and 24 h later irradiating the tumors with a laser ($P = 1.5$ W/cm^2 for 5 min). The change in temperature on the tumor surface was monitored with a thermal imaging camera. Subsequently, the groups were administered ^{64}Cu-loaded stealth liposomes immediately (0

h group), 6 h (6 h group), and 24 h (24 h group) after PTT. Additionally, a group of mice was administered ^{64}Cu-loaded stealth liposomes without any PTT (control group). All animals were PET/CT scanned 10 min and 24 h after liposome administration and the radioactivity concentration in tumors was quantified. ***Results:*** All groups receiving photothermal therapy had very similar heating profiles reaching an average maximum temperature after 5 min of irradiation of 48.9 ± 1.2 °C (0 h group), 50.0 ± 0.9 °C (6 h group), and 49.9 ± 1.2 °C (24 h group). When the ^{64}Cu-loaded liposomes were administered immediately after PTT, the mean tumor uptake of was significantly enhanced both 10 min (2.2 ± 0.4 %ID/g) and 24 h (11.6 ± 1.5 %ID/g) post injection, compared to control animals (1.2 ± 0.1 %ID/g and 4.3 ± 0.5 %ID/g, respectively). In contrast, no difference in tumor uptake was observed when the liposomes were administered at a later timepoint after PTT. ***Conclusion:*** A significant increase in tumor accumulation could be obtained when ^{64}Cu-labelled liposomes were administered immediately after PTT, suggesting that PTT could potentially be applied to induce local hyperthermia and improve accumulation of liposomal encapsulated drugs. ***References:*** [1] Henriksen et al. ACS Appl. Mater. Interfaces, 2015

406

Cutting Edge Science Track - Featured Session - Patient Radiation Protection

Friday, October 23, 2020, 09:00 - 10:30 Channel 6

OP-159

Introduction

S. Holm*; Rigshospitalet, Clinical Physiology, Nuclear Medicine & PET, Copenhagen, DENMARK.*

OP-160

European Diagnostic Reference Levels for Computed Tomography applications in nuclear medicine: results from the MEDIRAD project

G. Verfaillie*[1], Y. D'Asseler[2], K. Bacher[1];*
[1]Ghent University, Ghent, BELGIUM, [2]Ghent University Hospital, Ghent, BELGIUM.

Aim/Introduction: Depending on the clinical objective, CT image quality requirements and corresponding patient radiation doses in nuclear medicine may differ considerably. Unlike in diagnostic radiology, published national Diagnostic Reference Levels (DRLs) in Europe for CT acquisitions used in hybrid imaging are limited. This study aims to propose the first European DRLs for specific applications of CT in hybrid SPECT/CT and PET/CT. ***Materials and Methods:*** As part of the EU Horizon 2020 MEDIRAD project, a CT dosimetry survey was conducted from October 2018 until February 2020. Participating nuclear medicine departments were asked to provide patient-specific information (gender, age, length and weight) and CT dose indicators ($CTDI_{vol}$, DLP) from the most frequently performed diagnostic SPECT/CT and PET/CT examinations. Per scan type, data from 30 adult patients (weight of 70 ± 10 kg) were collected. In addition, information on the used instrumentation and the clinical purpose of the CT scan was collected. For each examination the minimum, 25th percentile, median, 75th percentile and maximum were then retrieved from the distribution of the median $CTDI_{vol}$ and DLP values calculated for each dataset. European DRLs were defined as the 75th percentile value and were derived for examinations that included data of at least 10 facilities. ***Results:*** Data were received from 50 nuclear medicine departments in 20 European countries, of which 22 centres were part of a university hospital. As expected, CT doses were lower for attenuation correction than for localisation or diagnostic hybrid CT scans. Large variations (min/max) in median $CTDI_{vol}$ and DLP values up to a factor of 16 were observed. Suggested European DRLs for $CTDI_{vol}$ (and DLP) of ^{18}F-FDG half body PET/CT examinations are 2.5 mGy (230 mGy.cm) and 6.3 mGy (580 mGy.cm) for attenuation correction only and localisation CT scans, respectively. A value of 6.4 mGy (160 mGy.cm) is proposed for attenuation correction only ^{18}F-FDG brain PET/CT studies. For ^{99m}Tc-bone (trunk) and parathyroid SPECT/CT examinations, a DRL of 4.4 mGy (160 mGy.cm) for attenuation correction and localisation CT scans is suggested. Finally, the proposed European DRL for attenuation correction CT scans of ^{99m}Tc-cardiac SPECT/CT studies is 3.1 mGy (60 mGy.cm). ***Conclusion:*** European DRLs for typical CT applications in nuclear medicine were derived. The large variations in observed CT doses highlights the need for optimisation. ***References:*** None

OP-161

Automatic Exposure Control techniques in low dose CT - what benefit in PET/CT studies?

R. Ferreira*, V. Sousa, M. R. Victor, S. Carmona, G. Cardoso, A. I. Santos;*
Hospital Garcia de Orta, Almada, PORTUGAL.

Aim/Introduction: Automatic exposure control (AEC) systems allow a reduction of patients' radiation dose during a CT acquisition, while maintaining image quality on diagnostic CT. But what can we expect from these techniques applied to low-dose CT for attenuation correction and anatomical reference, as performed on PET/CT? Our aim was to evaluate radiation dose and image quality associated with a low-dose CT (performed as part of a PET/CT study) using a combined tube current modulation technique (CARE Dose 4D) versus constant tube current values (CTCV). ***Materials and Methods:*** A retrospective sample of 978 PET/CT studies was collected and 7 studies were excluded because the maximum reference value of the tube current would be

exceeded if the AEC system was used. CARE Dose 4D was applied in 971 studies, performed to 601 (61,9%) males and 370 (38,1%) females; median age=67[P25:56.0;P75:74.0] years old and median weight=70[P25:60.8;P75:80.0]kg. The low-dose CT protocol acquisition parameters used were 110 kV and for mAs reference: 80 or 100 for obese patients. A whole-body CT protocol (comprising the head and torso) was applied in 712(73.3%) studies, with complementary body regions protocols in 259(26.7%). Dose Length Product (DLP) values were automatically generated by the scanner (DLP-AEC) and compared with those theoretically expected using CTCV (DLP-CTCV). Statistical analysis was performed with IBM SPSS Statistics. ***Results:*** The median DLP-AEC, equal to 353[P25:220.7;P75:442.3]mGy.cm, was statically significantly lower than the DLP-CTVC, equal to 563[P25:280.6;P75:634.3]mGy.cm [Related-Samples Wilcoxon Test;p<0.001], corresponding to a median dose reduction of 30[P25:16.8;P75:41.1]%. Adequate image quality was found in all 978 studies. The difference between DLP-AEC and DLP-CTCV was also statistically significant for different weight groups [Related-Samples Wilcoxon Test;p<0.001], with a median reduction of DLP using CARE Dose 4D equal to: 226[P25:111.7;P75:273.8]mGy.cm for patients weighing below 70 kg; 152[P25:60.8;P75:195.2]mGy.cm for patients weighing between 70 and 80 kg; and 47[P25:-1.9;P75:111.1] mGy.cm for patients weighing more than 80 kg. Regarding both acquisition protocols, there was also a statistically highly significant difference between DLP-AEC and DLP-CTCV [Related-Samples Wilcoxon Test;p<0.001], with a median reduction of DLP using CARE Dose 4D equal to 195[P25:130.4;P75:258.0]mGy.cm for whole-body acquisition; and 30[P25:7.8;P75:50.7]mGy.cm for complementary body-regions protocols. ***Conclusion:*** We found that combined tube current modulation techniques are effective in lowering the radiation dose in low-dose CT, as described in literature for diagnostic CT, performing better in slimmer patients and whole-body acquisitions. ***References:*** None

OP-162

Simple daily algorithm to reduce biological detriment by PET/CT on the basis of the patient age

P. Sannino[1], *M. Sicignano*[1], *L. Evangelista*[2], *E. Di Giorgio*[1], *S. Fiordoro*[1], *S. Imbimbo*[1], *V. Rizzo*[3], *C. Del Vasto*[1], *C. Lanotte*[1], *D. Palma*[1], *G. Pecchia*[1], *C. Mainolfi*[4], *M. Spadafora*[1];
[1]*Nuclear Medicine Unit Ospedale del Mare, Naples, ITALY,* [2]*Nuclear Medicine Unit, Department of Medicine (DIMED), University of Padua, Padua, ITALY,* [3]*Nuclear Medicine Unit Moscati Hospital, Avellino, ITALY,* [4]*Department of Advanced Biomedical Sciences, University of Naples Federico II, Naples, ITALY.*

Aim/Introduction: In adults, the current international guidelines recommend in administering 18F-fluorodexyglucose (FDG) activity on the basis of patient's weight and technical performance of PET scanner. However, age at exposure time and sex are key factors in increasing radiation risk detriment by a factor of 2 or more. Particularly, the rise in life expectancy also increases the cumulative risk of repeated exposures. ICRP Annals of 2020 suggests a sex- and age-nominal risk, avoiding average values, for a new radiation detriment calculation. Aim of the study was to develop a simple daily algorithm based on age to reduce the biological PET detriment in the execution of PET/CT. ***Materials and Methods:*** Twenty study sessions of whole-body PET/CT, including a total of 221 patients (56% male gender, mean age 64±15 years) were retrospectively analysed to estimate, for each age and sex category, scan-time and FDG dose, radiation exposure in effective dose (ED), and additional cancer risk (ACR) of PET. In the study population, these parameters were assessed in reference condition (REF) and after applying an algorithm (ALGO) that, on the base of time-dose equation, inversely modified the FDG dose and PET scan-time. To keep constant the overall scheduled times and FDG quantity, the ALGO changed in each study session, by ±20% time/dose relationship, in the opposite way between younger and older patients ***Results:*** In REF, mean scan-time of PET was 1155.5±160.3 sec, with a mean dose of 281.3±57.3 MBq. In the same group, the ED and ACR were 4.499±0.91 mSv and 0.0199±0.02%, respectively, whereas in ALGO they dropped to 4.488±1.1 mSv and to 0.0188±0.02% (both p<0.001). In REF, ACR was 0.0168±0.01% for males and 0.024±0.02%, for females, whereas in ALGO it dropped to 0.0162±0.01% (p<0.05) for males and to 0.0222±0.02% for females (p<0.001). ACR change was significant in each of the following age category: 17-45 years (p<0.001); 46-65 years (p<0.01); 65-89 years (p<0.001). ***Conclusion:*** The proposed protocol, acting by tailor changing the dose in relation to age, significantly affects ED and ACR of FDG-PET/CT. This protocol can be applied in a simple way in each daily study session, without any negative drawbacks in global time and tracer dose, in line with the most recent ICRP indications. ***References:*** None

OP-163

Low dose computed tomography protocol optimization and its influence in radiation dose to the patient

V. de Sousa*, G. Cardoso, B. Bento, S. Carmona, A. I. Santos;*
Hospital Garcia de Orta, E.P.E., Almada, PORTUGAL.

Aim/Introduction: The increasing use of PET/CT systems and the recent installation of one in the department lead to a need of protocol optimization in order to achieve the best compromise between dose and image quality, also considering that the CT acquisition is only used for attenuation correction and anatomic referral, not for radiological diagnosis, and is routinely acquired using an automatic exposure control system, which modulates the tube current. Therefore, the aim of this study was to optimize the CT protocol for whole-body [18F]FDG in order to reduce the dose-length product (DLP) to the patient. ***Materials***

and Methods: The department started using the protocol proposed by the manufacturer, with low dose CT scans acquired using 110 kV and 125 mAs of reference (group 1 - 16 male and 19 female). After a period of customization, reference mAs was first reduced to 100 (group 2 - 10 male and 6 female), and subsequently to 80 (group 3 - 153 male and 175 female). After each reduction, quality image was evaluated by clinicians. All scout scans were acquired with 110 kV and 25 mA and pitch was maintained constant through the study (p=0.8). DLP values were obtained from reports generated by the scanner. ***Results:*** The median value for DLP_{total} was initially 551.56 [P25:502.58; P75:647.64] mGy.cm. After the first step of optimization it decreased to 468.42 [P25:388.86; P75:551.13] mGy.cm. Finally, in group 3, a median DLP_{total} of 395.95 [P25:326.88;P75:469.18] mGy.cm was achieved. DLP_{total} is a sum of the DLP resulting from the scout acquisition and the DLP from the CT scan. In all groups, clinicians considered image quality acceptable for study reading. By applying Kruskal-Wallis test, no statistically significant differences where observed between patients' characteristics among the 3 groups, regarding both weight (p = 0.399) and height (p = 0.676). It was observed a strong positive correlation between mA_{max} and DLP_{total} (p=0.750) and a very strong positive correlation between mA_{med} and the DLP_{total} (p=0.962). ***Conclusion:*** Each step of the reduction in tube current led to a decrease in 15% of the DLP_{total}, allowing a total decrease of 28% from the first protocol to the actual protocol in use. Thus, there was clearly an optimization of the acquisition protocol, with dose reduction, keeping image quality acceptable for the diagnostic purposes of the studies. ***References:*** None

OP-164

Radiation Dose Optimization of a Dual Tracer PET/CT Protocol for Multiple Myeloma: a Whole Body Ultra-Low Dose CT

E. Prieto*, J. M. Martí-Climent, J. D. Aquerreta, V. Morán, L. Irazola, J. F. Bastidas, I. Soriano, J. J. Rosales, P. Rodríguez-Otero, M. J. García-Velloso;*
Clínica Universidad de Navarra, Pamplona, SPAIN.

Aim/Introduction: To design an optimized dual-tracer PET/CT protocol for multiple myeloma and to retrospectively review the radiation dose received by patients who underwent this procedure. ***Materials and Methods:*** In a research project carried out in our PET department, a dual-tracer PET/CT scan covering head to feet and a whole-body low dose CT (WBLDCT) were prescribed for patients with multiple myeloma. For the scope of optimization, PET/CT and WBLDCT were merged in a one-stop-shop. Thus, FDG PET/CT included a diagnostic CT (WBLDCT: 120 kV-80 mAs) while MET PET/CT included a CT dedicated only for attenuation correction, referred as whole body ultra-low dose CT (WBULDCT: 100 kV-40 mAs). Both PET/CT scans covered the whole patient from head to feet, in supine position with the arms beside the body. Thirty-one patients with proven multiple myeloma who underwent this protocol were retrospectively reviewed. Demographic data and dose parameters (dose-length product, DLP) were recorded. Effective doses were calculated with CT-Expo for the CT component and with dose coefficients for the PET contribution (0.019 mSv/MBq for FDG and 0.0084 mSv/MBq for MET). ***Results:*** We analyzed 31 patients, 23 males and 8 females, aged 59 ± 10 years, with BMI 27.0 ± 3.8 kg/m^2. DLP expressed as median (inter-quartile range, IQR) was 790 (IQR: 282) mGy·cm for WBLDCT and 262 (IQR: 123) mGy·cm for WBULDCT (p<0.0001). Patients received a median effective dose of 6.4 (IQR: 2.0) mSv from the WBLDCT and 2.1 (IQR: 0.8) mSv from the WBULDCT (p<0.0001). Patients were administered 327 ± 75 MBq of FDG and 469 ± 50 MBq of MET. The resultant effective doses (mean ± standard deviation) were 6.2 ± 1.4 mSv and 3.9 ± 0.4 mSv, respectively. Total effective dose for each PET/CT was 12.7 ± 3.0 mSv for FDG and 6.1 ± 0.8 mSv for MET. ***Conclusion:*** In this protocol for multiple myeloma evaluation, radiation dose optimization achieved due to both, the merge of nuclear medicine and radiological examinations, and to the inclusion of a WBULDCT (with a 66.7% dose reduction respect to the WBLDCT), entailed a great benefit for the patients. An effort in reviewing each PET/CT indication could lead to the customization and optimization of protocols and to the subsequent dose reduction. ***References:*** None

OP-165

Optimising CT scan range and dose levels for diagnosis of bone metastases for ^{18}F-NaF PET-CT

P. Holdgaard[1]*, N. A. Bebbington*[2]*;*
[1]*Lillebælt Hospital, Vejle, DENMARK,* [2]*Siemens Healthcare A/S, Aarhus, DENMARK.*

Aim/Introduction: Breast cancer patients are staged with radionuclide bone scintigraphy. Cross-sectional hybrid methods provide greater sensitivity and specificity than planar gamma-camera imaging, yet a disadvantage of ^{18}F-NaF is the additional radiation burden from the wholebody CT. Very-low-dose CT allows attenuation correction (AC) of PET data and low-dose CT allows localisation/characterisation of tracer uptake. AC of PET data is generally considered essential for diagnostic PET image quality and quantification. However, NaF demonstrates an exceptionally high abnormal-to-normal bone uptake ratio, thus providing good image quality even in the absence of AC. The aim was to investigate whether CT scan range could be optimised on an individual patient basis from the appearance of PET images, in breast cancer patients prior to neoadjuvant chemotherapy. ***Materials and Methods:*** An expert observer classified bone abnormalities in 25 NaF patients as malignant, equivocal or benign, for both non-AC and AC PET data in the absence of CT, to evaluate the need for AC of PET images. To evaluate

the need for localisation/characterisation CT, the required localisation/characterisation CT scan length was noted for each patient from the appearance of the non-AC PET. It was then determined from the reference standard AC PET with wholebody characterisation CT, whether any lesions were missed that required localisation/characterisation CT for diagnosis. ***Results:*** Non-AC versus AC PET only: Metastases were suspected (including equivocal lesions) in 52% of patients with non-AC images, compared with 64% with AC images. A total of 50 suspicious and 50 benign lesions were identified with non-AC images, compared with 87 suspicious and 61 benign with AC. Requirement for localisation/characterisation CT: 36% of patients were identified as requiring CT for localisation, 36% for characterisation and CT (beyond AC purposes) was not required in 28%. Mean required localisation/charaterisation CT scan range was 33±28cm (range 0-105cm), compared with the conventional mean 140cm wholebody characterisation CT. ***Conclusion:*** These findings demonstrate that CTAC of PET data is essential for the full PET scan range for evaluating bone metastases in ^{18}F-NaF examinations, despite the exceptionally high abnormal-to-normal tracer uptake ratio. However, performing very-low-dose wholebody CT for AC plus individualised localisation/characterisation CT confined to the clinical area of interest on the PET images, may allow radiation dose reduction without compromising diagnosis of bone metastases, in breast cancer patients prior to neoadjuvant chemotherapy. Future work should quantify dose savings via the proposed method and evaluate its feasibility in the clinical environment. ***References:*** None

OP-166

^{131}Iodine Concentration in mother's milk after treatment of a papillary thyroid cancer with 3700 MBq of Na^{131}I under rhTSH

G. Le Rouzic*, H. Besse, M. Bailly;*
Centre Hospitalier Régional d'Orléans, Orléans, FRANCE.

Aim/Introduction: Breastfeeding and Na131I thyroid cancer treatment under thyroid hormone withdrawal as thyrotropin-stimulation are considered incompatible[1-3]. No study described the breast milk 131Iodine concentration under recombinant human thyrotropin (rhTSH) as thyrotropin-stimulation. Our nuclear medicine department had to treat a lactating woman with 3700 MBq of Na131I whose thyrotropin-stimulation was rhTSH. ***Materials and Methods:*** We collected mother's milk all along the hospitalization of our patient and measured 131Iodine concentration to evaluate rhTSH influence. In order to guaranty the child radioprotection (effective dose < 1 mSv or thyroid equivalent dose < 10 mSv), we calculated concentration and time from which breastfeeding could be continued [4-7]. Assuming that 131Iodine concentration in the milk was the same than in breasts, we also evaluated the dose delivered to mother's breasts [1,8,9]. ***Results:*** Breastfeeding after the administration of 3700 MBq of Na131I could be discontinued at least 10 days after capsule ingestion according to the most optimistic hypothesis. Breasts dose for a lactating woman was evaluated at 1.08 Gy, inducing a 0.51% risk of breast cancer at some time following the treatment [4]. ***Conclusion:*** Even with the use of rhTSH stimulation in Na^{131}I thyroid cancer treatment, time to wait for resuming breastfeeding seems to be redhibitory and breast dose must still be taken into account into the benefit-risk balance. ***References:*** 1. Robinson PS et al. Iodine-131 in Breast Milk Following Therapy for Thyroid Carcinoma. J Nucl Med. 1994. 2. Grünwald F et al. Unilateral Iodine-131 Uptake in the Lactating Breast. J Nucl Med. 1995 3. Leide-Svegborn S et al. Excretion of radionuclides in human breast milk after nuclear medicine examinations. Biokinetic and dosimetric data and recommendations on breastfeeding interruption. Eur J Nucl Med Mol Imaging. 2016. 4. ICRP. The 2007 Recommendations of the ICRP. ICRP Publication 103. 2007; 5. ICRP. Doses to Infants from Ingestion of Radionuclides in Mothers' Milk. ICRP Publication 95. 2004; 6. ICRP. Age-dependent Doses to Members of the Public from Intake of Radionuclides - Part 2 Ingestion Dose Coefficients. ICRP Publication 67. Ann. 1993; 7. Leggett R. An age-specific biokinetic model for iodine. J Radiol Prot. 2017. ICRP. Basic Anatomical and Physiological Data for Use in Radiological Protection Reference Values. ICRP Publication 89. 2002; 9. Ellett WH, Humes RW. MIRD Pamphlet No. 8: Absorbed Fractions for Small Volumes Containing Photon Emitting Radioactivity (1971). J. Nucl. Med. 12, Supplement No. 5, 25-32.

OP-167

Preventive measures and management of radiopharmaceutical extravasation with[^{177}Lu]Lu-DOTA-TATE

N. Eftychiou*[1], R. Fernandez[1], S. Allen[1], V. Lewington[1,2];*
[1]Guy's and St Thomas Foundation Trust, London, UNITED KINGDOM, [2]King's College London, London, UNITED KINGDOM.

Aim/Introduction: Literature data regarding radiopharmaceutical extravasation is sparse - particularly for therapeutic administrations. We describe the management of an extravasation incident which occurred during [^{177}Lu]Lu-DOTA-TATE administration. A 38 year old NET patient attended for his second treatment cycle. Following amino-acid infusion, 7360MBq [^{177}Lu]Lu-DOTA-TATE was administered slowly using a syringe driver via the antecubital fossa vein. Prior administration the cannula was checked. Administration proceeded uneventfully without patient complaint. Shortly after completion the patient reported discomfort around the elbow. Upon examination there was soft tissue swelling of the distal forearm. ***Materials and Methods:*** Extravasation was confirmed by rapid imaging on gamma-camera. Measures were applied immediately: a heat pad, elevation of the arm and massage of the area. Subsequent 4-hour and 24-

hour whole-body imaging was performed and confirmed systematic radiopharmaceutical uptake with no significant residual uptake at the injection site Quantification was also performed using a sensitivity phantom and ROI analysis of planar images. Oral steroids and hydrocortisone cream were prescribed to prevent inflammation and skin irritation. ***Results:*** 1-hour post-extravasation analysis demonstrated approximately 5.3GBq [^{177}Lu]Lu-DOTA-TATE at the injection site, which reduced to 2.8GBq at 4-hours, following preventive measures. Redistribution of extravasated activity modelled using a dual compartment model and bi-exponential clearance. Extrapolation to 0-hours estimates 6.6GBq was initially extravasated. This corresponds to a maximum tissue dose of 17Gy at injection site and 11Gy to forearm/elbow following intervention and subsequent redistribution. Short-term side effects were minimal skin irritation. No long-term (follow-up>1year) effects were noted. ***Conclusion:*** Rapid response and straightforward conservative procedures are proposed to minimise the effects of radiopharmaceutical extravasation and recover the intended therapeutic aim. ***References:*** None

OP-168

Comparative Dosimetry for ^{68}Ga-PSMA with Updated Reference Data and Impact for Patient Specific Dose Calculations

P. Gape*, D. Rushforth, C. Abreu, I. Murray, J. Gear, G. Flux;*
The Royal Marsden Hosptial NHS Foundation Trust, London, UNITED KINGDOM.

Aim/Introduction: Most dosimetry reports for ^{68}Ga-PSMA were calculated using RADAR phantoms and dose factors, and ICRP 60 organ weighting factors. The aim of this study was to investigate the impact of calculating organ absorbed doses and effective doses using the more anatomically realistic ICRP 110 phantoms and updated ICRP 103 weighting factors. Differences between patient anatomy and anatomical phantoms contribute to the uncertainty in patient specific absorbed dose calculations. The relative importance of this contribution is indicated by the difference in calculated absorbed doses to RADAR and ICRP phantoms. This is compared to the uncertainty in calculating the time integrated activity coefficient (TIAC) to investigate the dominant contribution to absorbed dose uncertainty. ***Materials and Methods:*** Dosimetry was performed for three patients participating in the Simplification of Low Level Internal Dosimetry (SOLLID) trial from an early three-phase dynamic scan, the clinical scan (t = 1 hour), and two additional scans (t = 2, 4 hours). Organs were delineated on CT and time-activity curves produced. A multi-phase exponential was fit to the data to calculate TIAC.TIACs for normal organs for a further 27 patients were collated from the literature. OLINDA and IDAC were used to perform absorbed dose calculations based on the RADAR and ICRP 110 phantoms for the combined dataset (n = 30). Effective doses were calculated using both ICRP 60 and 103 weighting factors. The uncertainty in the TIAC for the patients in the SOLLID trial were calculated in accordance with EANM guidelines. ***Results:*** ICRP 110 based dosimetry with ICRP 103 weighting factors resulted in a lower effective dose for 28/30 patients (0.0156 mSv/MBq) compared with RADAR and ICRP 60 weighting factors (0.0213 mSv/MBq). The average disagreement between the two methods for each patient was 45.9% (standard deviation = 32.0%). The kidneys received the highest absorbed dose, and this was found to be lower based on the updated reference data (0.175 mGy/MBq vs. 0.257 mGy/MBq). The average uncertainty in the organ TIAC for the imaged patients was 5.44% (0.017% - 20.42%). ***Conclusion:*** Absorbed and effective dose estimates for ^{68}Ga-PSMA PET studies are likely to be significantly overestimated if not based on the most recent phantoms and weighting factors. For patient specific dosimetry, the contributions to the uncertainty in the absorbed dose from the TIAC and the dose factor are likely to be of similar magnitude. Both should be considered to improve the accuracy of absorbed dose calculations. ***References:*** None

OP-169

Solid-Phase Extraction of ^{225}Ac for Internal Dosimetry and Incorporation Measurements

R. Cusnir*[1,2], P. Froidevaux[1], L. Pfefferlé[1], M. Straub[1,2];*
[1]Institute of Radiation Physics, Lausanne University Hospital and University of Lausanne, Lausanne, SWITZERLAND, [2]European Organization for Nuclear Research (CERN), Geneva, SWITZERLAND.

Aim/Introduction: Emergence of ^{225}Ac (actinium-225, $t_{1/2}$ 10 days) as a promising alpha-emitting radionuclide for therapeutic applications demands adequate surveillance measures for occupational exposure of the personnel handling ^{225}Ac. Committed effective dose E_{50} of 1 mSv is attained by inhaling 154 Bq or by ingesting 42 kBq of ^{225}Ac. According to ICRP biokinetic model, a major fraction of ^{225}Ac is found in alimentary tract (≥ 50 %), while urinary excretion is in the order of 10^{-3} [1]. Urine is a convenient biological sample, however chemical separation of ^{225}Ac is indispensable to determine its concentration for a subsequent dose reconstruction in case of an accidental intake. We propose a method for radiochemical separation of ^{225}Ac in urine using a polymer resin imprinted with Y^{3+} ion [2]. ^{243}Am (americium-243, $t_{1/2}$ 7360 years) enables metrological traceability and quantification of ^{225}Ac with alpha spectrometry. ***Materials and Methods:*** To test the method, 500 mL urine sample was spiked with 50 mBq of ^{229}Th (providing ^{225}Ac in equilibrium) and 25 mBq of ^{243}Am tracers. Following acid digestion, actinides were pre-concentrated by co-precipitation with calcium phosphates. Solid phase extraction of [^{225}Ac]Ac^{3+} and [^{243}Am]Am^{3+} in diluted HCl at pH 3 was achieved on a 5 mL column containing 2 g of Y^{3+}-imprinted polymer resin. ^{225}Ac and ^{243}Am were released

from column with 1 M HCl, and electrodeposited on stainless steel discs for alpha spectrometry counting. ***Results:*** Alpha spectrometry counting of ^{225}Ac and ^{243}Am resulted in distinct peaks, enabling quantification of ^{225}Ac with reference to ^{243}Am internal tracer. Recovery yields of ^{225}Ac and ^{243}Am extracted from urine were equivalent, showing that ^{243}Am is a suitable metrological tracer for quantitative determination of ^{225}Ac. Overall recovery yield of ^{225}Ac and ^{243}Am from urine was 60 %. ***Conclusion:*** Solid-phase extraction on a Y^{3+}-imprinted polymer is suitable for chemical separation and quantitative determination of ^{225}Ac, while ^{243}Am as internal tracer confers metrological traceability. This method is amenable for determination of ^{225}Ac in other biological samples, such as biopsied tissues. Combined with a different detection technique, e.g. liquid scintillation counting or mass spectrometry, it can prove useful for analysis of other isotopes of actinium, such as ^{227}Ac. ***References:*** [1] ICRP, 2017. Occupational intakes of radionuclides: Part 3. ICRP Publication 137. Ann. ICRP 46(3/4) and OIR Data Viewer. [2] Chauvin et al., Chem. Eur. J. 2006, 12, 6852-6864

407

Teaching Session 1 (EANM/EARL): Quantification and Standardisation in Clinical and Preclinical Molecular Imaging

Friday, October 23, 2020, 09:00 - 10:30 Channel 7

OP-170

Molecular Imaging With Small Animal Architectures - Challenges and Chances

J. Mannheim; University of Tübingen, Department of Preclinical Imaging and Radiopharmacy, Tübingen, GERMANY.

OP-171

EARL and the Road to PET/CT Imaging Harmonisation

I. Hristova; Programme Director EARL, Vratsa, BULGARIA.

OP-172

Standardization and Harmonisation for Radiomics Analysis

M. Hatt; LaTIM, INSERM, UMR 1101, Univ Brest, Brest, FRANCE

408

Clinical Oncology Track - Featured Session: PRRT for NETs

Friday, October 23, 2020, 09:00 - 10:30 Channel 8

OP-173

The Future of PRRT

L. Bodei; Memorial Sloan-Kettering Cancer Center, Department of Radiology, New York, UNITED STATES OF AMERICA.

OP-174

First-in-human dose escalation of AlphaMedix for targeted alpha-emitter therapy of neuroendocrine tumors

I. Tworowska[1], E. S. Delpassand[1], R. Esfandiari[2], J. Torgue[3], J. D. Hurt[3], R. Nunez[2];
[1]RadioMedix Inc., Houston, TX, UNITED STATES OF AMERICA, [2]Excel Diagnostics and Nuclear Oncology Center, Houston, TX, UNITED STATES OF AMERICA, [3]Orano Med LLC, Plano, TX, UNITED STATES OF AMERICA.

Aim/Introduction: Peptide Receptor Radioligand Therapy (PRRT) is an effective treatment for patients with metastatic somatostatin-receptor (SSTR)-positive neuroendocrine tumors (NETs), however, interest in developing alpha-emitter-based therapies remains high. We present the initial results of the first-in-human (FIH) study of AlphaMedix™ (^{212}Pb-DOTAMTATE), a novel somatostatin-analog for Targeted Alpha-emitter-Therapy (TAT), in patients with SSTR-expressing-NETs (FDA IND 135150). The objective of this study is the determination of safety and pharmacokinetics, dosimetry and preliminary effectiveness of ascending doses of AlphaMedix™. ***Materials and Methods:*** 16 adult subjects, 7 men and 9 women, median-age 68 (range 27-75), with biopsy-proven unresectable or metastatic SSTR (+)-NETs from different primary sites (small bowel, pancreas, and lung) with at least one measurable lesion were enrolled in safety and dose escalation studies. Subjects with a history of prior PRRT were excluded. Patients enrolled in the first two cohorts received a Single, weight-based, Ascending-Doses (SAD) of AlphaMedix™. Once a partial response was observed, the third cord received the Multiple- Ascending-Doses (MAD-cohort) consisting of 3-cycles of AlphaMedix™ administrated every 8-weeks. All patients received amino acid for renal protection. Response to treatment was measured per RECIST 1.1 and the effect on the quality of life measured with the EORTC-QLQ-C30 -QOL. Patients enrolled in SAD1 and SAD2 received 30.7 and 40.0 µCi/kg, respectively. MAD3 cohort received 3-cycles of treatment (52.0 µCi/kg per cycle). MAD4 cohort completed 4-cycles of therapy (67.6 µCi/ kg per cycle) with a cumulative dose ranging from 19.2-22 mCi. This cohort was expanded and 3 new subjects received 3-cycles of treatment. ***Results:*** All 3 subjects in MAD 4-dosed with 4-cycles of treatment showed partial response with 73%, 71%, and 33% decrease in the size of the index-lesions, respectively. NETSPOT revealed almost a complete response in 2 subjects and a partial response in the third. There was no clinically significant investigational drug-related hematological and renal toxicity. The most common adverse events noted were alopecia 7/16 (43%), diarrhea 3/16 (19%), nausea 6/16 (38%), fatigue 7/16 (43%), hyperglycemia 8/16 (50%), lymphopenia 6/16 (38%), and decrease of WBC count 4/16 (21%). QOL parameters suggest significant improvement in pain, energy, and shortness of breath in the majority of subjects. ***Conclusion:*** This FIH-study

of AlphaMedix™ illustrates that PRRT with ^{212}Pb is feasible, well-tolerated, and provides an Objective Radiological response (ORR) in 100% of cases with substantial reduction in tumor burden in patients with unresectable, metastatic SSTR-expressing-NETs. The treatment was well tolerated with only mild adverse events. ***References:*** None

OP-175

Efficacy of ^{225}Ac-DOTATATE Targeted Alpha Therapy in Metastatic Gastroenteropancreatic Neuroendocrine Tumors Stable or Refractory to ^{177}Lu-DOTATATE PRRT

S. Ballal, M. Yadav, C. Bal;
All India Institute of Medical Sciences, New Delhi, INDIA.

Aim/Introduction: The objective of this study was to investigate and present the results on the efficacy, safety, and quality of life of ^{225}Ac-DOTATATE targeted alpha therapy (TAT) in patients with advanced, progressive, ^{177}Lu-DOTATATE refractory, and somatostatin receptor (SSTR) expressing metastatic GEP-NETs. ***Materials and Methods:*** In this prospective study, we recruited patients with metastatic GEP-NETs who demonstrated stable or progressive disease on ^{177}Lu-DOTATATE therapy. Patients underwent a screening ^{68}Ga-DOTANOC PET/CT scan to assure high SSTR expression and progressive disease to prior therapies. Systemic TAT was performed in all the patients with ^{225}Ac-DOTATATE (100 KBq/Kg body weight) at an interval of 8 weeks up to 7 cycles. The median follow-up duration was 13 months (range: 6 - 20 months).The primary end-point was to assess the objective response (measured by RECIST 1.1 and functional M. D. Anderson criteria). The secondary end-points included biochemical response assessment as per the Italian Trials in Medical Oncology (ITMO), adverse-event profile as per CTCAE v5.0, and clinical response assessment by the quality of life (assessed with EORTC QLQ-GI.NET21 patient-based questionnaire. ***Results:*** 65 patients (34 females, 31 males, mean age 57±7 years, 35 - 72 years) with either stable disease after completing ^{177}Lu-DOTATATE therapy (44%) or progressive disease on ^{177}Lu-DOTATATE therapy (56%) were included in the study. The morphological response was assessed in 53 patients and revealed complete remission in 1, partial remission in 41, stable disease in 9 and disease progression in 2 patients. Death was recorded in 1 patient. There was a significant decrease in the plasma chromogranin level post-^{225}Ac-DOTATATE therapy (P<0.0001). None of the patients experienced grade 3 or 4 hematotoxicity, renal insufficiencies or hepatotoxicity. The most common adverse effects (AEs) were nausea, vomiting, gastritis, and appetite loss, but were limited to grade 1 or 2. Majority of the patients experienced these AEs at the time of amino acid infusion which was administered during ^{225}Ac-DOTATATE therapy and was resolved after few hours of amino acid infusion. All the other AEs such as fatigue or asthenia, diarrhoea, appetite loss, abdominal pain, abdominal distension, weight loss, peripheral edema, headache, dizziness, and flushing were also identified which were limited to grade 1 or 2, except for 1 patient with grade 3 abdominal distension and fatigue. ***Conclusion:*** Our results indicate ^{225}Ac-DOTATATE TAT safe with low and transient side-effects. It add to a new dimension in the treatment of end-stage GEP-NET who have exhausted all the standard treatment options. ***References:*** None

OP-176

Tolerability and Efficacy of Peptide Receptor Radionuclide Therapy in Elderly Neuroendocrine Tumour Patients: Results of a Case-Control Single Centre Study

D. Theiler[1], *M. Cattaneo*[2], *L. O. Dierickx*[3], *P. Igaz*[4], *S. Grozinsky-Glasberg*[5], *C. Bournaud*[6], *T. O'Dorisio*[7], *D. Wild*[1,8], *E. Christ*[9,8], *G. P. Nicolas*[1,8];
[1]*Division of Nuclear Medicine, University Hospital of Basel, Basel, SWITZERLAND,* [2]*Department of Clinical Research, University of Basel, Basel, SWITZERLAND,* [3]*Department of Nuclear Medicine, ENETS CoE, Institut Universitaire du Cancer Toulouse - Oncopole, Toulouse, FRANCE,* [4]*Second Department of Internal Medicine, Semmelweis University, Budapest, HUNGARY,* [5]*Neuroendocrine Tumor Unit, ENETS Center of Excellence, Department of Endocrinology, Hadassah-Hebrew University Medical Center, Jerusalem, ISRAEL,* [6]*Department of Nuclear Medicine, Hospices Civils de Lyon, Lyon, FRANCE,* [7]*University of Iowa, Iowa City, IA, UNITED STATES OF AMERICA,* [8]*Endocrine and Neuroendocrine Tumour Centre, ENETS CoE, University Hospital of Basel, Basel, SWITZERLAND,* [9]*Department of Endocrinology, University Hospital of Basel, Basel, SWITZERLAND.*

Aim/Introduction: Peptide-Receptor Radionuclide Therapy (PRRT) is an effective and well-tolerated treatment for inoperable/metastatic, somatostatin receptor expressing neuroendocrine tumours (NET). Although, caution is recommended for patients ≥70y due to potential toxicity, tolerability and efficacy of PRRT in elderly patients have not been systematically investigated, e.g. Netter-1 study: 63±9 (years, mean±SD). The aim was to investigate safety and efficacy of PRRT in elderly patients (EP). ***Materials and Methods:*** All consecutive patients with inoperable/metastatic/progressive, G1/G2 NET, aged ≥79y, treated with PRRT at the University Hospital Basel between 2006 and 2018, were enrolled in this case-control study. Each patient was manually matched with ≥1 younger patient (YP) aged between 60 and 70y (same gender, primary tumour location, grading, functional activity and estimated tumour load). The primary endpoint was safety and tolerability. Cell-blood count and eGFR were measured at baseline, 2-weekly after each PRRT cycle and 1, 2 and 3y after completion of PRRT. Subacute and long term toxicity were scored according to the common terminology criteria for adverse events (CTCAE) v5.0. All toxicity scores ≥3, or whose delta to baseline was ≥2 (≥1 for eGFR), were considered significant. Differences in odds ratio for the occurrence of toxicity between cohorts was tested for non-inferiority. Overall survival (OS), with

or without correction for differences in the residual life expectancy, and clinical response to PRRT were assessed as secondary outcome measures. Kaplan-Meier curves and mortality hazard ratio were compared using a non-inferiority test and a Cox-regression stratified model. ***Results:*** Forty-eight elderly patients (EP) and 68 younger patients (YP) were enrolled, aged 81.7±1.5 vs 67.6±1.7 (years, mean±SD), respectively. EP and YP were balanced with regards to median time-since-diagnosis, tumour location, grading, treatment scheme (Lutetium-177-DOTATOC (14.8 [9.3-25.1] vs 14.8 [7.4-22.1] and Yttrium-90-DOTATOC (0 [0-6.5] vs 5.6 [0-7.4] (GBq, median[IQR] for EP vs YP, respectively) and baseline biochemical parameters, except eGFR: 61±16 vs 78±19 (ml/min/1.73m^2) for EP vs YP. Grade≥3 or Δ≥2 subacute haematotoxicity occurred in 10 EP (21%) vs 19 in the YP (28%, p=NS). Long-term grade≥3 renal toxicity was 20% vs 5%, for EP vs YP (Odds-ratio 5.25 [1.02, 27.14], p=NS). The median OS was 3.4. vs 6.0 (years, EP vs YP) (Hazard-ratio (HR): 1.50 [0.75, 2.98], p= 0.094; HR after adjusting for life-expectancy residual: 0.41 [0.17, 0.96], p = 0.014 (relative non-inferiority margin: 1.2). ***Conclusion:*** In selected EP, PRRT is a valid therapeutic option with similar toxicity and non-inferior survival compared to the YP. ***References:*** None

OP-177

Survey of Challenges in Access to Diagnostics and Treatment for Neuroendocrine Tumor (NET) Patients (SCAN) - Usage & Affordability of Nuclear Medicine Tools, a comparative perspective

S. Dureja[1], *M. McDonnell*[2], *D. Van Genechten*[3], *C. Bouvier*[4], *S. Leyden*[5], *T. Kolarova*[6], *D. O'Toole*[7], *H. Singh*[8], *J. Chen*[9], *J. Howe*[10], *S. Singh*[11], *R. Hicks*[12], *C. Rodien-Louw*[13];

[1]*SMH Cancer Centre, New Delhi, INDIA,* [2]*NET Patient Network, Dublin, IRELAND,* [3]*vzw NET & MEN Kanker Belgium, Kortrijk, BELGIUM,* [4]*Neuroendocrine Cancer UK, Leamington Spa, UNITED KINGDOM,* [5]*NeuroEndocrine Cancer Australia, Victoria, AUSTRALIA,* [6]*International Neuroendocrine Cancer Alliance, Boston, MA, UNITED STATES OF AMERICA,* [7]*National Centre for Neuroendocrine Tumours, St. Vincent's University and Department of Clinical Medicine, St. James Hospital and Trinity College, Dublin, IRELAND,* [8]*Prince Court Medical Centre, Kuala Lumpur, MALAYSIA,* [9]*The First Affiliated Hospital, Sun Yat-sen University, Guangdong, CHINA,* [10]*University of Iowa Carver College of Medicine, Iowa City, IA, UNITED STATES OF AMERICA,* [11]*Sunnybrook Odette Cancer Centre, University of Toronto, Toronto, ON, CANADA,* [12]*Peter MacCallum Cancer Centre, Melbourne, AUSTRALIA,* [13]*APTED Association de Patients porteurs de Tumeurs Endocrines Diverses, Lyon, FRANCE.*

Aim/Introduction: SCAN assessed awareness, availability, quality and affordability of NET diagnostics and treatments. This analysis explored nuclear medicine (NM) tools' usage and affordability. ***Materials and Methods:*** During Sept-Nov-19, NET patients/carers and healthcare professionals (HCP) involved in NET management completed an online survey (14 languages). ***Results:*** There were 2795 respondents from 68 countries across 6 continents (2359 patients/carers [Europe 1102; North America (NA) 727; Asia 280]; 436 HCPs [37 NM specialists; NMS). NM tools commonly led to NET diagnosis, particularly in Europe (All: Europe 58% [641/1102] vs. NA 43% [309/727] vs. Asia 42% [118/280], p<0.0001 [Chi-squared]; FDG-PET: 13% [143/1102] vs. 9% [65/727] vs. 16% [46/280]; ^{68}Ga-DOTA-PET/CT: 19% [213/1102] vs. 11% [78/727] vs. 17% [48/280]; octreotide scan: 20% [221/1102] vs. 20% [145/727] vs. 8% [22/280]). NM treatment use appeared more infrequent (All: Europe 12% [136/1102] vs. NA 12% [85/727] vs. 7% Asia [19/280], p=0.0311; mIBG: 0.3% [3/1102] vs. 0% [0/727] vs. 0% [0/280]; PRRT: 12% [128/1102] vs. 11% [82/727] vs. 7% [19/280]; SIRT: 0.5% [5/1102] vs. 0.4% [3/727] vs. 0% [0/280]). Ongoing monitoring with NM tools was prevalent globally (Total: Europe 43% [475/1102] vs. NA 42% [305/727] vs. Asia 38% [107/280]; ^{68}Ga-DOTA-PET/CT: 27% [299/1102] vs. 32% [230/727] vs. 23% [65/280]; FDG-PET: 16% [176/1102] vs. 10% [75/727] vs. 15% [42/280]). NMS reported greater availability of NM diagnostics (86% [159/185] vs. 60% [1317/2180], p<0.0001) and treatment (PRRT: 92% [34/37] vs. 64% [277/436], p=0.0005) than other HCPs. NMS believed NM diagnostics (34% [62/185] vs. 26% [560/2180], p=0.0203) and treatments (PRRT: 46% [17/37] vs. 28% [123/436], p=0.0203), were more affordable than other HCPs. For patients receiving PRRT, household income used for NET treatment was lower in Europe and NA than Asia (0-20%: 55% [70/128] vs. 52% [43/82] vs. 16% [3/19], respectively; ≥21%: 13% [16/128] vs. 10% [3/82] vs. 68% [13/19]; no costs: 22% [28/128] vs. 21% [17/82] vs. 0% [0/19]; unknown: 11% [12/128] vs. 17% [12/82] vs. 16% [3/19]). Out-of-pocket costs over 12 months were lowest in Europe for ^{68}Ga-DOTA-PET/CT (median $112 vs. NA $500 vs. Asia $1120) and PRRT ($288 vs. $406 vs. $5600). Pricing was cheaper in Europe for ^{68}Ga-DOTA-PET/CT ($105 vs. NA $500 vs. Asia $840) and PRRT ($225 vs. $202 vs. $2800). ***Conclusion:*** NM tool usage is highest in Europe and NA, potentially due to affordability issues in developing countries. NMS state greater availability and affordability than other HCPs. Improving NM tools' accessibility and use can enhance NETs care worldwide. ***References:*** None

OP-178

PRRT of 200 patients from the SEPTRALU registry: real-world data

M. Mitjavila Casanovas[1], *A. Carmona Bayonas*[2], *P. Belló*[3], *V. Pubul*[4], *L. García-Cañamaque*[5], *J. Arbizu*[6], *A. Rotger*[7], *B. Llana*[8], *T. Navarro*[9], *M. Castellón*[10], *C. Field*[5], *M. Estorch*[11], *C. Riesco*[12], *A. Teule*[13], *M. Muro*[14], *P. García-Alonso*[15], *A. Repetto*[16], *M. Miguel*[17], *E. Caballero*[18], *M. Navarro*[19], *J. Aller*[1], *M. del Olmo*[3], *C. Blanco*[20], *P. Jimenez-Fonseca*[8];

[1]*Hospital Universitario Puerta de Hierro Majadahonda, Madrid, SPAIN,* [2]*Hospital Universitario Morales Meseguer, UMU, IMIB, Murcia, SPAIN,* [3]*Hospital Universitario La Fe, Valencia, SPAIN,* [4]*Hospital Universitario de Santiago Compostela, Santiago de*

Compostela, SPAIN, [5]Hospital Universitario HM Sanchinarro, Madrid, SPAIN, [6]Clínica Universidad de Navarra, Pamplona, SPAIN, [7]Hospital Universitario Gregorio Marañón, Madrid, SPAIN, [8]Hospital Universitario Central de Asturias, Oviedo, SPAIN, [9]Hospital Universitario Ramón y Cajal, Madrid, SPAIN, [10]Hospital Universitario Virgen de la Arrixaca, Murcia, SPAIN, [11]Hospital de la Santa Creu i Sant Pau, Barcelona, SPAIN, [12]Hospital Universitario Doce de Octubre, Madrid, SPAIN, [13]ICO-Bellvitge, Barcelona, SPAIN, [14]Hospital Universitario Virgen de las Nieves, Granada, SPAIN, [15]Hospital Universitario Getafe, Madrid, SPAIN, [16]Hospital Universitario Son Espases, Palma de Mallorca, SPAIN, [17]Hospital Universitario Burgos, Burgos, SPAIN, [18]Hospital Universitario Dr Peset, Valencia, SPAIN, [19]Hospital Universitario Salamanca, Salamanca, SPAIN, [20]Hospital Universitario Príncipe de Asturias, Madrid, SPAIN.

Aim/Introduction: The aim was to describe the characteristics of patients with advanced somatostatin receptor-positive neuroendocrine tumours (TNE) treated with 177Lu-DOTATATE (PRRT) and to evaluate the efficacy and safety of the treatment. ***Materials and Methods:*** The data comes from the national and multicentre study SEPTRALU in which a multidisciplinary team of 18 centers participate. Survival was evaluated using the Kaplan-Meier method and Cox proportional risk regression. Toxicity was recorded according to CTCAEv3.0 criteria. ***Results:*** 200 patients were recruited. 51% were women. The median age was 57 years (range, 18-89) and the ECOG performance status was 1-2 in 92%. 57% were functional and Ki-67 was <20% in 93%. The most frequent primary site was gastrointestinal (44%), and pancreatic (37%). Metastases were mainly located in: liver (86%), lymph nodes (42%) and bone (26%). Prior to PRRT, patients had received a median of 3 lines (range, 1-7). Four cycles of PRRT were administered to 66% of patients (96% with 7.4 GBq). Partial response rate was 27%, complete response 3%, stable disease 57% and progression 13%. The median progression-free survival (PFS)and overall survival (OS) were 26.6 months (95% CI, 21.5-NA), and 38.2 months (27.6-NA), respectively. Grade 3-4 toxicities were recorded in 9%. In multivariate analysis, the factors associated with OS were ECOG (HR 1.16, p=0.001), Ki-67% index (HR 1.02, p=0.026) and the presence of extrahepatic/extranodal metastases (HR 2.63, p=0.018).The greater the number of pre-radionuclide treatment lines, and the increment of previous lines was associated with worse PFS (HR 1.33; (95% CI, 1.04-1.68), p=0.018), and increased mortality: OS (HR 1.25; (95% CI, 0.96-1.62), p=0.092). Patients who received >2 previous lines vs. those who received ≤2 had worse PFS, with median of 15.8 months (95% CI, 10.5-NC) vs 45.3 months (95% CI, 24.0-NC) (Log-rank, p=0.02), and worse OS, 26 months (95% CI, 19.5-NC), vs not reached (Log-rank, p=0.05). After adjusting for confounding factors, no evidence was found that these differences were attributed to specific previous therapies. ***Conclusion:*** Conclusions: Therapy with 177Lu-DOTATATE (PRRT) is safe in clinical practice, with survival data comparable to those shown in clinical trials, and better outcomes in those patients who are treated earlier. Prognostic factors have been identified, with potential impact on decision-making. ***References:*** None

OP-179

[177]Lu-PRRT in advanced gastrointestinal neuroendocrine tumors: ten-year follow up of the IRST-Phase II prospective study

M. Sansovini[1], *G. Paganelli*[1], *S. Nicolini*[1], *I. Grassi*[1], *V. Di Iorio*[1], *E. Amadori*[1], *E. Scarpi*[1], *A. Bongiovanni*[1], *C. Cittanti*[2], *L. Urso*[2], *S. Severi*[1]; *[1]IRST, Meldola (FC), ITALY, [2]Nuclear Medicine Unit, University of Ferrara, Ferrara, ITALY.*

Aim/Introduction: In March 2014, we reported the activity and safety of [177]Lu-Dota-octreotate Lu-PRRT at 2 different dosages (18.5GBq and 27.5 GBq in 5 cycles) in patients with progressive metastatic gastrointestinal neuroendocrine tumors (GI-NETs). Disease control rate and toxicity were addressed. Herein we report the late toxicity, progression-free (PFS) and overall survival (OS) in the same cohort after a ten-year follow-up. ***Materials and Methods:*** We conducted an open-label, disease-oriented prospective phase II trial. From March 2008 to June 2011 43 patients received 3.7 GBq or 5.5 GBq of Lu-PRRT every 6 to 8 weeks, each cycle repeated 5 times. All patients showed [68]Gallium-DOTA-peptide PET/Octreoscan® positivity (score 3-4 Rotterdam scale) in known lesions. Tumor burden was estimated radiologically. Time-to-event data (PFS and OS) were described using Kaplan-Meier curves and compared with the log-rank test ***Results:*** Forty-three patients (28 males and 15 females) were evaluable and were monitored for a median period of 118 months (range 12.6-139.6). Median PFS in patients receiving 18.5 GBq was 59.8 months (95% confidence interval [95% CI] 14.3-79.6), identical to that of patients treated with 27.5 GBq (59.8 months, 95% CI 23.4-82.0). Median OS was 71.0 months (95% CI 46.1-107.3) in the group who received 18.5 GBq and 97.6. months (95% CI 64.3-not reached) in the group treated with 27.5 GBq (P=0.22). Patients with progression limited to lymph nodes showed significantly longer median PFS and OS than those with hepatic lesions (P=0.02 for PFS and P=0.04 for OS). Age over 65 years at the time of PRRT was also significant for OS. Of note, no late hematological or renal toxicity was observed in either group. ***Conclusion:*** The long-term follow-up of the IRST-Phase II study shows that Lu-PRRT is a safe and effective therapy for patients with advanced GI-NET, the most important prognostic factor being tumor burden, hepatic lesions and age. We believe that Lu-PRRT should be offered to patients with early-stage disease. ***References:*** Paganelli G, et al. 177Lu-Dota-octreotate radionuclide therapy of advanced gastrointestinal neuroendocrine tumors: results from a phase II study. Eur J Nucl Med Mol Imaging. 2014;41(10):1845-51. Severi S, et al. Role of 18FDG PET/CT in patients treated with 177Lu-DOTATATE for advanced differentiated neuroendocrine tumours. Eur J Nucl Med Mol

Imaging. 2013;40(6):881-8. https://doi.org/10.1007/s00259-013-2369-z. Strosberg J, et al. NETTER-1 Trial Investigators. Phase 3 Trial of 177Lu-Dotatate for midgut neuroendocrine tumors. N Engl J Med. 2017;12;376(2):125-35. https://doi.org/10.1056/NEJMoa1607427

OP-180

Initial experience with ^{177}lutetium peptide receptor radionuclide therapy for pediatric patients with somatostatin-receptor-positive tumors

M. Pizzoferro[1], B. Cassano[2], C. Altini[1], A. Serra[3], M. Cefalo[3], A. Cacchione[3], M. Villani[1], A. Castellano[3], V. Cannatà[2], M. Garganese[1]; [1]IRCCS Bambino Gesù Children's Hospital, Nuclear Medicine Unit/ Imaging Department, Rome, ITALY, [2]IRCCS Bambino Gesù Children's Hospital, Medical Physics Unit, Rome, ITALY, [3]IRCCS Bambino Gesù Children's Hospital, Oncoemathology Unit, Rome, ITALY.

Aim/Introduction: Treatment of relapsed/refractory malignant pediatric tumor remains a clinical challenge by poor outcome despite intensive multimodal therapy. 177Lu-Peptide-Receptor Radionuclide Therapy (177Lu-PRRT) shows a promising role in somatostatin-receptor-positive tumors (SSTR-PT) with a potential clinical utility in pediatric patients. We report on our initial experience assessing somatostatin analogues therapy in heavily pretreated pediatric patients affected by progressive SSTR-PT. ***Materials and Methods:*** four pediatric patients with progressive tumor (2 boys and 2 girls, age range: 7-19 years) were submitted to 177Lu-PRRT for palliative purpose after molecular imaging showing an overexpression of somatostatin receptor in tumor sites and ethical committee approval. Two patients were affected by Relapsed/Refractory Metastatic High-Risk Neuroblastoma (HRNBL), one patient had bilateral metastatic pheochromocytoma and one had an advanced medulloblastoma. 4 cycles of PRRT (Lutathera®) were administered in 3 patients while one patient received the first cycle. Recommended administration procedure was applied and haematological exams were performed. An individualized dosimetry for red-marrow and kidneys was assessed collecting blood samples, and acquiring planar images. ***Results:*** HRNBL and pheochromocytoma patients received 4 cycles of palliative PRRT (4.4 GBq in the 1st cycle in the younger HRNBL patient; 7.4 GBq per administration in the other cycles). Medulloblastoma patient received a single cycles of 7.4 GBq. The absorbed doses to red-marrow and kidneys ranged from 0.6 to 1.1 Gy and from 40 to 54 Gy, respectively. No significant acute toxicity attributed to PRRT was registered. No regression of disease was obtained in HRNBL patients but early symptoms improvement (pain and/or dyspnea relief) was registered in both of them. In the patient with pheochromocytoma a stable disease was documented over one year even if there wasn't a significant tracer uptake in disease sites at post-therapy imaging. Medulloblastoma patient is on going and showed an intense uptake in cerebellar lesion after the first initial cycle, without side-effects. ***Conclusion:*** our preliminary experience documented the feasibility of 177Lu-PRRT in pediatric clinical practice suggesting a potential role as new targeted therapy for palliative intent in children affected by SSTR-PT. 177Lu-PRRT showed a high tolerability and a significant clinical impact on patient quality life. 177Lu-PRRT requires a multidisciplinary approach and dosimetric implementation is mandatory to ensure 177Lu-PRRT administration safety avoiding exceeding the dose limits for organ-at-risk. Clinical trials, in larger patient cohorts, is warranted for evaluation of response to PPRT and for defining new combined therapeutic strategies including somatostatin analogues treatment in children affected by advanced progressive SSTR-PT. ***References:*** None

OP-181

PRRT/PRCRT in ^{18}F-FDG-avid G3 NET-Patients

H. Svirydenka[1], L. Scarpa[1], B. Nilica[1], M. Rodrigues[1], S. Buxbaum[1], G. Di Santo[1], C. Uprimny[1], S. Bayerschmidt[1], B. Neururer[1], E. Gamper[2], I. Virgolini[1]; [1]Universitätsklinik für Nuklearmedizin, Innsbruck, AUSTRIA, [2]2Division of Psychiatry II,Department of Psychiatry, Psychotherapy and Psychosomatics, Innsbruck, AUSTRIA.

Aim/Introduction: The efficacy and safety of PRRT in G1 and G2 NET-patients has been established in recent years. The peptide receptor radionuclide/chemoradionuclide therapy (PRRT/PRCRT) might be more efficient in patients with G3-NETs. In this study we determined the efficacy of a combined therapy strategy in ^{18}F-FDG-avid NET-patients. ***Materials and Methods:*** Twenty patients (mean age 53± 15.3 years, range 29-79) with metastatic SSTR-avid NET on ^{68}Ga-DOTATOC PET/CT and at least one hypermetabolic lesion on ^{18}FDG-PET/CT, before or in follow-up after PRRT were analyzed. The observation time was at least 1 year after completion of 4 cycles of PRRT. Dual-tracer imaging was performed at 6 months interval for the assessment of response. We divided the response finding in four categories according to PERCIST 1.1. Criteria: Complete Response (CR), Partial Response (PR), Stable Disease (SD) and Progressive Disease (PD). CR and PR were considered as overall response and clinical benefit was defined as CR+PR+SD. As long term predictors, we calculated the Progression-Free-Survival (PFS) and Overall-Survival (OS) since initialization of PRRT by Kaplan-Meier. Three months after PRRT adverse events, according to the Common Terminology Criteria for Adverse Events (CTCAE) V.5.0., and treatment's tolerability by Health-Related-Quality-of-Life (HRQoL) were monitored. ***Results:*** 75% of our cohort presents foregut localization of NETs and 25% midgut (26.3% G2 Grade, 73.7% G3 Grade). PRRT/PRCRT was performed after 36.4±47 months from diagnosis. 30% of patients received a single period (4 cycles) of PRRT, 70% had re-challenge PRRT/PRCRT. The mean accumulated activity was 38.1±13.0 GBq. All patients received a long-acting somatostatin analog

and 20% a concomitant radiosensitizing chemotherapy (temozolomide). 70% of patients had performed the comparable dual tracer study during the observation (35% were almost FDG positive before target-therapy and 35% become FDG avidity during follow-up). According to the last available follow-up (with FDG-PET, if possible, or with other imaging or laboratory diagnostic) at the end of the observation's time, 20% had CR, 10% PR, 30% SD, 40% PD. The overall response was observed in 30% and the clinical benefit in 60% of patients. The mean calculated OS and PFS were 102.5 months (range 78.9-126; CI 95%) and 47.2 months (range 32.4-61.9; CI 95%), respectively. No significant difference for OS was observed between patients with PRRT and PRCRT (p=0.954). None of our patients showed serious adverse events after PRRT/PRCRT during follow-up. Overall stable HRQoL was observed. ***Conclusion:*** PRRT/PRCRT promises to be a safe and efficient treatment strategy for ^{18}F-FDG-avid metastatic NET-patients. ***References:*** None

OP-182

Peptide Receptor Radionuclide Therapy In Broncopulmonary Neuroendocrine Tumours - Results Of A Single Centre Experience

G. Ferreira*, S. Castro, C. Costa, L. Violante, J. Teixeira, H. Duarte, I. L. Sampaio;*
Instituto Português de Oncologia do Porto Francisco Gentil, Porto, PORTUGAL.

Aim/Introduction: Therapeutic options in unresectable and metastatic broncopulmonary neuroendocrine tumours (bpNET) remain limited. These tumours may overexpress somatostatin receptors (SSTr), allowing for Peptide Receptor Radionuclide Therapy (PRRT). The aim of this study was to explore the efficacy and safety of therapy with ^{177}Lu-DOTATATE in bpNET. ***Materials and Methods:*** We analyzed 20 patients with advanced or metastatic bpNET treated with PRRT between 2011 and 2018 in our institution, after progression on previous locoregional and/or systemic therapy. Adequate tumoral SSTr expression was confirmed according to a baseline ^{68}Ga-DOTANOC PET/CT scan, prior to the administration of 3 cycles of ^{177}Lu-DOTATATE (median cumulative activity 19.6 GBq). Patients were followed until last observation or death. We evaluated the objective response rate (ORR) according to morphologic criteria (modified RECIST), progression free survival (PFS) based on radiologic or ^{68}Ga-DOTANOC PET/CT findings, overall survival (OS), clinical benefit and treatment tolerability. We also investigated factors associated with PFS and OS according to LogRank tests and Cox regression analysis. ***Results:*** Patients were followed for 7.5 to 106.9 months (median 32.2). Median PFS was 19.2 months (95% CI 14.7-23.7) and median OS was not reached (estimated at 50.1 months). ORR was 50% (6 patients had partial and 4 had minor responses). None of the responders died during follow-up, while non-responders had a median OS of 24.6 months (95% CI 6.1-43.1, p<0,001). Semi-quantitative uptake intensity (SUVmax) and visual inter-lesional uptake heterogeneity on baseline 68Ga-DOTANOC PET/CT were independent predictors of PFS (HR 0.93 and 9.46, p=0.019 and p=0.013, respectively). Clinical benefit was attained in 6 of 11 previously symptomatic patients, whereas 7 of 9 patients remained asymptomatic during the entire follow-up period. No serious (grade 3/4) haematological, renal or hepatic toxicity was observed. ***Conclusion:*** PRRT demonstrated to be a compelling option in the management of bpNET, as it provided a good response rate, symptomatic control and favorable toxicity, whilst also being promising in prolonging patients' survival. Quantitative and qualitative parameters based on baseline ^{68}Ga-DOTANOC PET/CT may be useful in selecting patients for PRRT and prognostic stratification. ***References:*** None

OP-183

Comparison and Evaluation of n.c.a. ^{111}In-DTPA-Phe^{1}-Octreotide vs. n.c.a. 177Lu-[DOTA0, Tyr3] TATE / n.c.a. 177Lu-[DOTA0, Tyr3] TOC in (GEP-NENs) Treated Patients

G. Limouris*[1], V. Krylov[2], M. B. Dolgushin[3], M. Paphiti[4], R. V. McCready[5], A. Zafeirakis[6];*
[1]Nuclear Medicine, Medical School, National and Kapodistrian University of Athens, Athens, GREECE, [2]Nuclear Medicine Department, "A Tsyb Research Center", Obninsk, RUSSIAN FEDERATION, [3]N.N. Blokhin Russian Oncological Research Center, Moscow, RUSSIAN FEDERATION, [4]Nuclear Medicine Dept, National Health System, Athens, GREECE, [5]Institute Cancer Research, Sutton Surrey and Royal Sussex County Hospital, Brighton, UNITED KINGDOM, [6]Army Share Fund Hospital of Athens, Athens, GREECE.

Aim/Introduction: To evaluate and compare the dosimetry profile and efficacy of n.c.a. ^{111}In-DTPA-Phe^{1}-Octreotide vs. n.c.a. Lu-177 DOTA-TATE and n.c.a. Lu-177 DOTA-TOC in GEP-NEN patients, initially i.a. treated with ^{111}In-DTPA-Phe^{1}-Octreotide and after a median progression-free-survival (PFS) of more than 39 mo, further retreated with i.a. infusions with n.c.a. Lu-177 DOTA-TATE in combination with n.c.a. Lu-177 DOTA-TOC, the latter i.v. implemented, to confrontate the relapse observed. ***Materials and Methods:*** The average activity of n.c.a. ^{111}In-DTPA-Phe^{1}-Octreotide [Group A: 12 cases (63 liver trans-arterial catheterizations)] was 6.3±1.3 GBq per patient/per session whereas the activity of n.c.a. Lu-177 DOTA-TATE, [Group B: 4 cases (24 liver trans-arterial catheterizations)] in tandem infused with n.c.a. Lu-177 DOTA-TOC to the same 4 cases (12 i.v. infusions, antecubital)] was 7.3±2.3 GBq. For both groups repetitions were performed in intervals of 5-8 weeks to avoid a possible stunning effect. Blood samples were collected 30 min, 2, 4, 8 and 24 hrs p.i. as well as 24 hrs urine samples for dosimetry. The % max uptake in organs and tumours was estimated by creating ROIs. Tumour Dosimetric calculations were performed using the OLINDA/EXM 1.1 code. ***Results:*** Non-carrier-added 177Lu-

[DOTA0,Tyr3]TATE blood and urinary radioactivity, expressed as a percentage of the injected dose was significantly lower compared as to non-carrier-added 177Lu-[DOTA0,Tyr3]TOC, clearly depicted from the created time/activity curves; the tumour uptake (Bkg-corrected) was significantly higher as compared to non-carrier-added 177Lu-[DOTA0,Tyr3] TOC. Absorbed dose kidneys' difference has been measured to be almost the same. The organ average dose in mGy / MBq of n. c. a. ^{111}In-DTPA-Phe^{1}-Octreotide was found as follows: (a) Liver tumour of 10 gr spherical mass was estimated to be 10.80 (b) Liver 0.14, (c) Kidneys 0.41 and (d) Bone marrow 0.0032. The organ average dose in mGy / MBq of n. c. a. 177Lu-[DOTA0,Tyr3] TATE / TOC was found as follows: (a) Liver tumour of 10 gr spherical mass was estimated to be 33.0/ 13.0, (b) Liver 0.19 / 0.55, (c) Kidneys 0.46/ 0.66 and (d) Bone marrow 0.030 /0.036. ***Conclusion:*** Comparing the i.a. infused n.c.a. 177Lu-[DOTA0,Tyr3]-TATE vs. the i.v. implemented -TOC of β-low-LET emitters (a) a statistically significant 2.53-fold higher dose in tumour was found, in favor of 177Lu-[DOTA0,Tyr3]-TATE advocating the efficacy profile of i.v. infused-TOC and the feasible continuation of the re-treatment procedure. Analyzing the Auger and Internal Conversion Electron Emission -high-LET of ^{111}In-DTPA-Phe^{1}-Octreotide an advantageous 8.9-fold lower dose in bone marrow was observed. ***References:*** None

409

TROP Session: Molecular Imaging of Movement Disorders

Friday, October 23, 2020, 09:00 - 10:30 Channel 9

OP-184

Metabolic and Dopaminergic Correlates of intellectual enrichment in De novo PD patients

S. Raffa[1], *M. Donegani*[1], *M. Bauckneht*[2], *M. Balma*[2], *D. Arnaldi*[3], *N. Girtler*[3], *M. Pardini*[3], *A. Miceli*[1], *F. Biagini*[1], *F. Massa*[3], *L. Filippi*[3], *G. Sambuceti*[1], *M. Pagani*[4], *F. Nobili*[3], *S. Morbelli*[1];
[1]*Nuclear Medicine Unit, Department of Health Sciences, University of Genoa, Genoa, ITALY,* [2]*IRCCS Policlinico San Martino, Genoa, ITALY,* [3]*Clinical Neurology, Department of Neuroscience (DINOGMI, Dept. of Excellence of the Italian Ministry for University and Research- MIUR), University of Genoa., Genoa, ITALY,* [4]*Institute of Cognitive Sciences and Technologies, Consiglio Nazionale delle Ricerche (CNR), Rome, ITALY.*

Aim/Introduction: To disclose brain metabolic and dopaminergic correlates of intellectual enrichment and cognitive reserve in de novo PD patients. ***Materials and Methods:*** 62 de novo PD patients (36 m; Age 70.1±8.5; MDS-UPDRSIII 20±9.9; Education 12.1±4.7; MMSE 28±1.9) underwent both brain 18F-FDG-PET and Dopamine Transporter SPECT. CR-index questionnaire including a total score (Total-CR) and 3 subscores concerning education (educational-CR), occupational complexity (occupational-CR) and leisure activities (leisure-CR) was administered. Specific binding ratios (SBRs) in the basal ganglia were computed with 'BasGan V2'. Age and sex-adjusted Z-scores of SBR in caudate (C) and putamen (P) nuclei and P/C ratio were obtained by comparing patients with 122 CTR recruited in the 'ENC-DAT' study. Z-scores were used as the dependent variables in repeated measures of general linear model. Correlation between whole brain metabolism and CR-scores was evaluated by means of SPM8 (age, gender and UPDRS as nuisance). Moreover patients were divided according to the median value of CR scores. Clinical variables, brain metabolism and SBR-values were compared between patients with high and low CR-related scores (two-sample t-test). To evaluate the interplay between brain metabolism and dopaminergic function in these group of patients, voxel-based correlation between SBR values and FDG PET data was also assessed. ***Results:*** MDS-UPDRS score and brain metabolism were not significantly different in patients with high and low CR-scores. SBRs were significantly higher in patients with higher CR (especially higher leisure-CR) despite expressing the same level of motor impairment. A direct correlation was highlighted between CR-scores on one side and SBRs (namely P/C ratio and SBR of putamen of both hemispheres, $p<0.03$) while an inverse correlation was highlighted between total and occupational-CR and brain metabolism in cerebellum ($p<0.001$). SBR-values of both putamen were directly correlated with metabolism in right occipital and parietal cortex and again inversely correlated with cerebellum ($p<0.001$). ***Conclusion:*** Given the less marked dopaminergic deficit highlighted in patients with higher CR, it is likely that more active patients with high leisure-CR are earlier aware of their symptoms and are thus in an earlier stage of disease. This difference is captured by the sensitivity of DAT-SPECT and not yet by MDS-UPDRS. The inverse correlation of both CR-scores and SBR-values with the cerebellum support this hypothesis. Cerebellum is relatively hypermetabolic with respect to the cortex in PD. Accordingly this relative hypermetabolism may reflect a compensative mechanism less needed in PD de novo with high reserve given their lower dopaminergic deficit. ***References:*** None

OP-185

Striatal Dopamine Transporter SPECT Quantification: Head-To-Head Comparison Between Two Tridimensional Automatic Tools

S. Raffa[1], *E. Cella*[1], *M. Donegani*[1], *D. Arnaldi*[2,3], *F. Massa*[3], *S. Capitanio*[2], *M. Bauckneht*[2], *A. Miceli*[1], *S. Morbelli*[1,2], *F. Nobili*[2,3];
[1]*Dept of Health Science (DISSAL), University of Genoa, Genoa, ITALY,* [2]*IRCCS Ospedale Policlinico San Martino, Genoa, ITALY,* [3]*Dept of Neuroscience (DINOGMI), University of Genoa, Genoa, ITALY.*

Aim/Introduction: Several methods have been proposed for semiquantification of DAT SPECT with results varying depending upon region of interest (ROI) identification method. We aimed to perform a head-to-head comparison between two automatic tools for semi-quantification of striatal dopamine transporter (DAT) specific-to-non displaceable (SBR) ratio brain SPECT values and to comparatively correlated data with a clinical measure as an 'external' reference in a naturalistic cohort of patients. ***Materials and Methods:*** We analyzed DAT SPECT scans from one-hundred and fifty-one consecutive outpatients submitted to brain DAT SPECT for a suspected parkinsonism. The scans were corrected for attenuation using the Chang's method, were reconstructed with an OSEM algorithm (10 subset, 10 iterations). Images were post-processed using a commercial (Datquant®, G.E. Healthcare) and BasGanV2 (free software by the AIMN-Neurology study group) software. Then, the individual results were compared with the control population embedded in each software and were compared with reading by experts considered as the gold standard. Finally, caudate and putamen SBRs were correlated with the MDS-UPDRS-III score in a subset of thirty-five patients with altered DAT SPET according to experts and degenerative parkinsonism at follow up. ***Results:*** Good correlations were achieved between the two tools (right caudate r= 0.76; left caudate r= 0.73; right putamen r= 0.84; left putamen r= 0.82; right P/C ratio 0.76; left P/C ratio 0.65; all p<0.0001). Concordance with the gold standard was 82.5% for BasGan V2 and 84% for Datquant (p= n.s.). Correlations of BasGan V2 with UPDRS-III score was r=-0.44 with caudate SBRs of both sides (p<0.01), r=0.32 with left putamen SBR (p<0.05) and not significant with right putamen SBRs. Correlations of Datquant® with UPDRS-III score was r=-0.39 (p<0.01) with right caudate SBRs and r=-0.35 with left caudate SBRs (p<0.05), but not significant with putamen SBRs of both sides. ***Conclusion:*** Both Datquant® and BasGanV2 give highly correlated SBR values and performed equally well compared with the gold standard (although correspondence with expert reading was slightly higher with Datquant®). Correlation with severity of motor impairment was higher with BasGan V2 and was higher at the caudate level with both methods, and this finding expresses the better ability of caudate SBR to track disease severity for the nigro-caudate pathway than putamen SBR. Both tools have their own strength and pitfalls that must be known in detail by users in order to obtain the best help in visual reading and reporting of DAT SPECT. ***References:*** None

OP-186

Machine Learning Assisted DAT PET in the Discrimination of Parkinsonism Disorders

Q. Xu;
North Huashan Hospital, Shanghai, CHINA.

Aim/Introduction: To explore the discriminative performance of DAT PET in Parkinsonism disorders, including Parkinson's disease (PD), multiple system atrophy (MSA-P) and progressive supranuclear palsy (PSP), with the assistance of computer based automatic segmentation, feature extraction and machine learning. ***Materials and Methods:*** 107 confirmed idiopathic patients (50 PD, 37 MSA-P, and 20 PSP) were recruited in our study. Subjects have been screened by two senior specialists of movement disorders, and were divided into early/advanced stage (ES/AS) group based on disease duration (24 months) at PET imaging. 11C-CFT PET and T1-weighted MRI imaging were performed on each subject within one week. Firstly, Striatum and midbrain were segmented from MRI image and registered rigidly to corresponding PET image, and resulting transformation matrix was used to transfer label information to the PET image. Then, 14 sub-regions were isolated from the PET image using a k-means clustering algorithm, including bilateral anterior, middle and posterior caudate and putamen, and bilateral pallidum. Maximum, minimum, median, quantiles, and mean value of tracer uptake in above sub-regions were extracted as features and presented as striatal-to-occipital ratio (SOR). Afterwards, Support-Vector-Machine (SVM) was used to train the disease classifier to make diagnosis for each subject. Furthermore, we applied different training strategies with leave-one-out cross-validation method to assess the diagnostic ability of this method for ES patients. Lastly, the importance of striatum and midbrain during the diagnosis process was investigated using random forest algorithm. ***Results:*** Sensitivity, specificity, PPV and NPV was 86%, 84%, 83% and 87% for diagnosis of PD patients, 78%, 89%, 78% and 89% for MSA-P patients, and 70%, 95%, 78% and 93% for PSP patients. Classification accuracy of PD, MSA-P and PSP from others achieved 85%, 78%, 89% respectively. Diagnostic accuracy achieved 77.78% when using both ES and AS groups as training set, which was better than other strategies. The caudate and putamen showed significantly higher weight of diagnostic importance than pallidum, especially the anterior caudate (18.52%), middle putamen (16.87%) and middle caudate (16.27%). The accuracy of diagnosis was not obviously different with and without midbrain. ***Conclusion:*** DAT PET has been confirmed to have potential to be applied in the diagnosis of parkinsonism diseases with the assistance of computer based automatic segmentation, feature extraction and machine learning method, even in the early stage of diseases. Caudate and putamen were found to play important role in the diagnostic process, while pallidum and midbrain do almost no help. ***References:*** None

OP-187

Cerebral glucose metabolism abnormalities and dopaminergic dysfunction in patients with Parkinson's disease with bilateral onset

P. Wu[1], L. Li[1], J. Song[1], X. Li[1], J. Lu[1], J. Ge[1], J. Wu[2], J. Wang[2], C. Zuo[1];
[1]PET Center, Huashan Hospital, Fudan University, Shanghai, CHINA, [2]Department of Neurology, Huashan Hospital, Fudan University, Shanghai, CHINA.

Aim/Introduction: Parkinson's disease (PD) is usually characterized by unilateral onset and by loss of dopamine transporter (DAT) and a unique PD-related pattern (PDRP). However, we indeed found that some patients presented bilateral onset and were diagnosed as PD by follow-up in clinical practice. Thus, we conducted this study to explore the abnormal cerebral glucose metabolism and dopamine distribution in PD patients with bilateral onset and compare with those with unilateral onset. ***Materials and Methods:*** Twenty PD patients with bilateral onset (PD-Bi) and 45 with unilateral onset (PD-Uni), matched for age, sex, duration and UPDRS-III scores, were recruited. 20 age-matched normal controls (NC) were also recruited. All subjects underwent ^{18}F-FDG and ^{11}C-CFT PET at the same time. Scans from PD-Uni patients with predominantly right-sided symptoms were flipped and those from PD-Bi patients and NC were flipped randomly. PDRP expression was computed in each subject based on the PDRP we previously identified. Regional FDG metabolism was compared among groups using SPM. ^{11}C-CFT uptake of bilateral caudate, anterior and posterior putamen was calculated respectively by the striatal-to-occipital ratio (SOR) using ScAnVp toolbox and the asymmetric index was calculated as the absolute value of (bilateral SOR difference/bilateral SOR average). ***Results:*** The asymmetry indices of UPDRS-III scores were significantly lower in PD-Bi group than those in PD-Uni group (P<0.001). The PDRP scores significantly increased in both PD groups relative to NC (P<0.001), but there was no difference between the two PD groups. Compared with PD-Uni, PD-Bi patients presented hypometabolism in left middle frontal gyrus and inferior parietal lobule and relative hypermetabolism in the right temporal, left parietal lobe and bilateral limbic lobe (P<0.001). DAT level significantly decreased in both PD groups compared with NC (P<0.001), and was lower in the posterior putamen in PD-Bi group than that in PD-Uni group (P=0.035). The asymmetric indices of both anterior and posterior putamen in PD-Bi group were significantly lower than those in PD-Uni group (P<0.05). ***Conclusion:*** The difference of both cerebral glucose metabolism abnormalities and dopamine dysfunction between PD-Bi and PD-Uni patients suggests PD-Bi might be another clinical phenotype of the disease. ***References:*** None

OP-188

Cerebral glucose metabolism, cognitive performance and emotional state in tremor dominant and akinetic-rigid subtypes of Parkinson's disease

J. Khomenko[1], I. Miliukhina[2], G. Kataeva[1], E. Gracheva[2], E. Gromova[1];
[1]N.P. Bechtereva Institute of Human Brain of the Russian Academy of Sciences, Saint-Petersburg, RUSSIAN FEDERATION, [2]Institute of Experimental Medicine, Saint-Petersburg, RUSSIAN FEDERATION.

Aim/Introduction: Parkinson's disease (PD) has a significant phenotypic heterogeneity. Clinical differences between akinetic-rigid (AR) and tremor dominant (TD) PD subtypes PD, in addition to the specific motor disorders, include cognitive and emotional disfunction. Study of the pathogenesis of PD heterogeneity is important for the prognosis and therapy. ***Materials and Methods:*** 71 PD patient were examined (47 - AR, 24 - TD). PET study with 18F-fluorodeoxyglucose (FDG) was performed on GE-Discovery710 scanner. PET images were normalized with SPM8, regional cerebral glucose metabolism rate (rCMRglu) in Brodmann areas (BA) were calculated using WFU-Pickatlas. rCMRglu in sensorimotor cortex was used as a referent. Mini-mental State Examination (MMSE), Frontal Assesment Battery (FAB), Monreal Cognitive Assesment (MoCA), and Hospital Anxiety and Depression Scale (HADS) were used for neuropsycological evaluation. ***Results:*** CMRglu in the AR group was lower in frontal cortex (BA 6,8,9,46) in right hemisphere and left BA46 (p<0,05) compared to the TD group. Cognitive tests scores correlated with different cortical areas in the studied groups. In TD group, MMSE and MoCA scores correlated positively with rCMRglu in BA7 and 9 bilaterally, BAs 6,8,10,11,47,24 in right hemisphere, and left BAs 22,32,46. In AR group, MMSE and MoCA scores correlated with rCMRglu in BAs 7,23,26,29,30,31 in both hemispheres (r=0.4-0.6; p<0.05). In the TD group, the HADS-depression scores correlated negatively with rCMRglu in left frontal (BA 8,46), anterior cingulate (BA32) and parietal cortex (BA40), and right BA39 (r=-0.5-0.7; p<0.05). The HADS-anxiety scores in AR group correlated with rCMRglu in BA7 (bilateral), r=-0.4-0.5; p<0.05. At the same time, there were no significant differences in anxiety and depression scores in 2 groups. MOCA negatively correlated with depression score in both groups (r=-0.4, p<0.05). In TD group, both depression and anxiety scores correlated negatively with FAB score (r=-0.4, p<0.05). ***Conclusion:*** In different PD subtypes cognitive performance and emotional state was associated with rCMRglu in different cortical areas: frontal, temporal, parietal, and anterior cingulate in TD, and parietal and posterior cingulate in AR group. Presumably, it is a result of differences in the cognitive and emotional disorders pathogenesis in different PD types. ***References:*** None

OP-189

^{18}F-PI-2620 Tau-PET in Corticobasal Syndrome

M. Brendel[1], C. Palleis[1], C. Prix[1], A. Finze[1], K. Bötzel[1], A. Danek[1], M. Höllerhage[2], L. Beyer[1], J. Sauerbeck[1], B. Rauchmann[1], A. Stephens[3], A. Drzezga[4], T. van Eimeren[4], H. Barthel[5], M. Patt[5], O. Sabri[5], V. Villemagne[6], P. Bartenstein[1], R. Perneczky[1], C. Haass[7], J. Levin[1], G. Höglinger[8];
[1]University Hospital of Munich, Munich, GERMANY, [2]Technical University of Munich, Munich, GERMANY, [3]Life Molecular Imaging, Berlin, GERMANY, [4]University Hospital of Cologne, Cologne, GERMANY, [5]University of Leipzig, Leipzig, GERMANY, [6]University of Melbourne, Melbourne, AUSTRALIA, [7]DZNE Munich, Munich, GERMANY, [8]Hannover Medical School, Hannover, GERMANY.

Aim/Introduction: The pathology of Corticobasal syndrome (CBS) is characterized by 4-repeat (4R)-tau aggregation in Corticobasal Degeneration (CBD) and Progressive Supranuclear Palsy (PSP) in ~50%, or by (3/4R)-tau aggregation in Alzheimer's disease (AD) in ~25% of patients. The tau-PET ligand ^{18}F-PI2620 showed high affinity to 3/4R-tau in AD and also revealed affinity to 4R-tau pathology in vitro. The aim of this study was to investigate ^{18}F-PI2620 in patients with CBS that are part of the interdisciplinary AD study "Activity of Cerebral Networks, Amyloid and Microglia in Aging and Alzheimer's Disease (ActiGliA)". ***Materials and Methods:*** ActiGliA comprises a comprehensive clinical assessment, multimodal prospective imaging in vivo and fluid biomarker analyses. Thirty-six patients (70±8y) with probable or possible CBS according to MDS-PSP or Armstrong-criteria underwent ^{18}F-PI2620 PET together with ten age-matched healthy controls. Distribution volume ratios (DVR, 0-60 min) of subcortical and prefrontal cortical brain-regions were generated using cerebellar reference tissue. DVR-data were quantitatively and visually compared between CBS and healthy controls. Regional ^{18}F-PI2620 binding was compared with clinical severity (PSP Rating Scale), and disease duration. Amyloid-PET served for assessment of β-amyloid status. ***Results:*** 26% (9/36) of CBS patients (PSP Rating Scale: 25±13) were amyloid-positive. Overall, a visually discernible ^{18}F-PI2620 was observed in 27 subjects (75%) and in 89% of amyloid-positive CBS patients. Significantly elevated ^{18}F-PI2620 DVR was observed in the whole group of CBS patients versus healthy controls in the putamen, the globus pallidus, the subthalamic nucleus, the dentate nucleus and the prefrontal cortex (all $p<0.01$). The prefrontal cortical signal was higher in amyloid-positive when compared to amyloid-negative CBS patients. Visually assessed cortical binding in CBS was heterogeneous (positive in 50%; 18/36). Asymmetry of ^{18}F-PI2620 binding matched the contralateral clinical dominance in 94% of CBS cases. ^{18}F-PI2620 binding was associated with disease severity in the globus pallidus ($R=0.412$, $p=0.032$) and with disease duration in the prefrontal cortex ($R=0.426$, $p=0.021$), after controlling for age, sex and β-amyloid-status. ***Conclusion:*** ^{18}F-PI2620 tau-PET is a potential biomarker for evaluation of CBS, facilitating detection of heterogeneous neuropathology and variable cortical and subcortical deposition sites. Longitudinal and autopsy correlation studies need to evaluate the suitability of ^{18}F-PI2620 tau-PET as biomarker of disease progression and target engagement. ***References:*** None

OP-190

Brain metabolic correlates of gait initiation in Progressive Supranuclear Palsy

G. Marotta[1], C. Palmisano[2], M. Todisco[3], J. Volkmann[2], C. Pacchetti[3], C. Frigo[4], R. Leo[1], C. Sdraiati[1], D. Capolongo[1], E. Orunesu[1], G. Pezzoli[5], I. U. Isaias[2];
[1]Fondazione IRCCS Ca' Granda Ospedale Maggiore Policlinico, Milan, ITALY, [2]Department of Neurology, University Hospital and Julius Maximilian University of Würzburg, Würzburg, GERMANY, [3]Parkinson's Disease and Movement Disorders Unit, IRCCS Mondino Foundation, Pavia, ITALY, [4]MBMC Lab, Department of Electronics, Information and Bioengineering, Politecnico di Milano, Milan, ITALY, [5]Centro Parkinson ASST G. Pini-CTO, Milan, ITALY.

Aim/Introduction: Progressive supranuclear palsy (PSP) is a neurodegenerative disease characterized by early impairment of balance and frequent falls. Gait initiation (GI) is a centrally-mediated motion achieved in a principled, controlled manner, including predictive mechanisms (anticipatory postural adjustments, APA) that destabilize the antigravity postural set of body segments for the execution of functionally- optimized stepping. The neural correlates of postural imbalance and falls in PSP are largely unknown. We compared the biomechanical resultants of APA at gait initiation (imbalance, unloading, and stepping phases) with clinical findings and brain metabolic abnormalities measured using [18F]FDG-PET. ***Materials and Methods:*** We recruited 26 patients with probable PSP and 14 age-matched healthy controls (HC). Biomechanical data were correlated with clinical findings in all subjects, and with brain metabolic abnormalities measured using FDG-PET in 11 patients, compared with a group of 12 age- and gender-matched HC. PET data were analyzed using the Statistical Parametric Mapping (SPM 12). We considered the clusters with $k\geq200$ voxels and threshold of $p<0.05$ FWE- corrected as significant. SPM findings were confirmed by a post hoc volume of interest (VOI) analysis. For each VOI, we extracted the [18F]FDG uptake values that were divided by the whole cortex uptake to reduce between-patient variability. The resulting [18F]FDG uptake ratios were then used to explore correlations with GI parameters. ***Results:*** Patients with PSP showed impaired modulation of the center of pressure displacement for a proper setting of the center of mass momentum and subsequent efficient stepping. Biomechanical measurements correlated with "Limb

motor" and "Gait and midline" subscores of the PSP Rating Scale. We identified five hypometabolic brain regions in the PSP group: the right dorsolateral prefrontal cortex, the left supplementary motor area, the middle cingulate cortex, the left caudate nucleus and the medial thalamus. Hypometabolism of the caudate nucleus and the middle cingulate cortex correlated positively with a key kinematic feature of APA pre- programming of the GI task, and medial thalamic hypometabolism correlated with the resultants of APA efficacy for a proper forward stepping. ***Conclusion:*** Our results show that postural instability at gait initiation in patients with PSP correlates with deficient APA production and is associated with dysfunction of the basal ganglia, cingulum, and thalamus. In conclusion, specific brain regions selectively regulate different phases of GI: while the caudate nucleus and cingulate cortex could directly influence APA programming, the thalamus predominantly influenced the biomechanical resultants of the APA during the stepping phase. ***References:*** None

OP-191

Progressive supranuclear palsy and its variants: pattern similarities and differences in 18F-FDG-PET

G. Martí-Andrés[1], J. J. Rosales[1], E. Prieto[1], L. van Bommel[2], F. Grisanti[1], S. K. Meles[2], R. V. Kogan[2], V. Gurvits[2], R. Valentí[1], M. Riverol[1], M. R. Luquin[1], K. Leenders[2], J. Arbizu[1];
[1]Clínica Universidad de Navarra, Pamplona, SPAIN, [2]University Medical Center Groningen, Groningen, NETHERLANDS.

Aim/Introduction: An accurate early diagnosis of Progressive Supranuclear Palsy (PSP) is still a clinical challenge. In a previous study, we performed a multicentre study including patients with different variants of PSP and defined a PSP-related pattern based on covariance analysis techniques. The pattern showed an optimal diagnostic accuracy to differentiate PSP patients from Parkinson's Disease (PD) and healthy subjects (HC). Currently, we aim to identify similarities and differences in the metabolic pattern among the PSP variants. ***Materials and Methods:*** A retrospective study was conducted on a multicentre cohort of 73 early-stage PSP patients who were referred for an FDG-PET scan (longitudinal clinical diagnosis based on the Movement Disorders Society-PSP criteria 2017): Richardson's Syndrome (PSP-RS), n=47; parkinsonian variant (PSP-P), n=18; and progressive gait freezing, n=8. Additionally, we included 55 HC and 58 PD patients as reference groups. We used a univariate analysis (Statistical Parametric Mapping) to assess the regional similarities and differences in metabolism (ANCOVA test adjusted by age, sex and PET procedures, $p<0.05$ corrected by family-wise error or $p<0.001$ uncorrected). Additionally, we applied the AAL3 atlas and obtained the mean glucose metabolism per ROI and clinical group, which were correlated using Pearson's rho correlation coefficient. ***Results:*** The demographical and clinical data of each group studied are shown in table 1. Compared to HC and PD, all the PSP variants exhibited hypometabolism in the thalamus and caudate, and hypermetabolism in the sensorimotor cortex and cerebellum. PSP-P and PSP-RS showed a larger spread of the subcortical metabolic abnormalities than PSP-PGF, displaying a hypometabolism in the midbrain. PSP-RS also showed more severe and widespread cortical abnormalities, displaying hypometabolism in the frontoinsular cortex and, compared to PD, hypermetabolism in the occipital cortex. Moreover, the mean glucose metabolism in each ROI was highly correlated between PSP variants, but there was a low correlation between any of the PSP variants and PD patients (table 2). Interestingly, PSP-RS and PSP-P patients showed a parallel clinical progression, but PSP-P patients showed a significantly delayed onset regarding the PSP core features (O1-2 and P1-2, table 3a-b). PSP-PGF showed a parallel progression to PSP-RS regarding the postural instability domain, and parallel to PSP-P regarding the oculomotor dysfunction. ***Conclusion:*** While both cortical and subcortical abnormalities are present in PSP-RS, subcortical abnormalities are predominant in PSP-P and PSP-PGF variants. Nevertheless, the presence of an early core common subcortical metabolic pattern and progressive phenotypical convergence among PSP variants differ from PD. ***References:*** None

OP-192

[18F]PI-2620 Tau PET to Improve Imaging-Based Diagnosis of PSP

K. Messerschmidt[1], *H. Barthel[1], M. Brendel[2], T. Van Eimeren[3], K. Marek[4], V. Villemagne[5], J. Rumpf[1], D. Saur[1], M. Schroeter[1], M. Rullmann[1], K. Hoffmann[1], C. Scherlach[1], B. Rauchmann[2], A. Schildan[1], M. Patt[1], L. Beyer[2], M. Song[2], C. Palleis[2], M. Gehmeyr[2], U. Fietzek[2], G. Respondek[6], J. Sauerbeck[2], A. Nitschmann[2], C. Zach[2], J. Hammes[7], M. Barbe[4], Ö. Onur[4], F. Jessen[7], B. Neumaier[3], O. Barret[4], J. Madonia[4], D. Russell[4], A. Stephens[8], S. Roeber[2], J. Herms[2], K. Bötzel[2], P. Bartenstein[2], J. Levin[2], A. Drzezga[7], J. Seibyl[4], G. Hoeglinger[9], J. Classen[1], O. Sabri[1];*
[1]University Hospital Leipzig, Leipzig, GERMANY, [2]LMU Hospital Munich, Munich, GERMANY, [3]Research Center Juelich, Juelich, GERMANY, [4]InviCRO, Boston, MA, UNITED STATES OF AMERICA, [5]Austin Health, Heidelberg, AUSTRALIA, [6]DZNE, Bonn, GERMANY, [7]University Hospital Cologne, Cologne, GERMANY, [8]Life Molecular Imaging, Berlin, GERMANY, [9]Hannover Medical School, Hannover, GERMANY.

Aim/Introduction: The in vivo diagnosis of progressive supranuclear palsy (PSP) is currently established on clinical grounds and supported by MR imaging findings. As recently reported, the second-generation tau PET tracer [18F]PI-2620 is able to provide valuable diagnostic information in PSP patients. The aim of this follow-up evaluation was to investigate how the diagnostic potential

of [18F]PI-2620 relates to that of the current imaging gold standard in PSP, i.e. midbrain (MB) atrophy MRI. ***Materials and Methods:*** The [18F]PI2620 PET and structural MRI data of 36 patients with clinical diagnosis of PSP (age=71±8yrs, 16 female, n=22 with PSP-Richardson's syndrome (RS) and n=14 with PSP-non RS, disease duration=3.3±2.6yrs, PSP Rating Scale scores=31±13, Schwab and England Activities of Daily Living Scale scores=60±19) and those of 10 age- and gender-matched healthy controls (HCs) were analysed. PET imaging was carried out dynamically 0-60min p.i. of ~300MBq, and distribution volume ratios for the typical tau-in-PSP target regions (globus pallidus, putamen, subthalamic nucleus, substantia nigra and dentate nucleus) were determined in PMOD by MRTM2 and by taking the lower cerebellum as reference region. In the MR images, the MB diameter, MB area, MB/pons area ratio, and MR Parkinsonian Index which also considers the relative (in relation to the middle cerebellar peduncles) atrophy of the superior cerebellar peduncles were measured on a Hermes workstation. ***Results:*** For the MRI parameters, the MB/pons area ratios and the MR Parkinsonian Index discriminated best between the PSP patients and the HCs (Cohen's d effect sizes=1.96 and 1.54). For the PET parameters, this was the case for the globus pallidus internus and the globus pallidus externus DVRs (1.92 and 1.90). Taking the respective HC data to define normality (mv±2sd) resulted in sensitivities/specificities in the separation between PSPs and HCs of 69%/100% for MR Parkinsonian Index, and of 64%/100% for globus pallidus internus DVRs. Of interest, the combination of MR Parkinsonian Index and globus pallidus internus DVRs (≥1 abnormal parameter defined abnormality) resulted in 78% sensitivity and 100% specificity in discriminating PSPs from HCs. All of the above PET and MRI measures apart from the MR Parkinsonian Index correlated with age (p=0.017 to <0.007), while correlations with the PSP Rating Scale scores were only found for the MRI measures (p=0.001 to <0.001). ***Conclusion:*** [18F]PI-2620 tau PET has the potential to improve the MR imaging-based PSP diagnosis by providing super-additive information independent of the severity of the clinical phenotype. ***References:*** None

OP-193

Graph theoretical analysis of the structural connectivity in progressive supranuclear palsyin relation to tau burden: A [18F]PI-2620 PET/MRI study

G. Aghakhanyan[1,2], M. Rullmann[2], J. Rumpf[3], M. L. Schroeter[4], M. Patt[2], J. Classen[3], O. Sabri[2], H. Barthel[2];
[1]Regional Center of Nuclear Medicine, University Hospital of Pisa and Department of Translational Research on New Technologies in Medicine and Surgery, University of Pisa, Pisa, ITALY, [2]Department of Nuclear Medicine, University of Leipzig, Leipzig, GERMANY, [3]Department of Neurology, University of Leipzig, Leipzig, GERMANY, [4]Max Planck Institute for Human Cognitive and Brain Sciences, Leipzig, GERMANY.

Aim/Introduction: Progressive supranuclear palsy (PSP) is a primary 4R tauopathy. Evidence supports the concept of disrupted/reorganized structural connectivity in PSP as a consequence of accumulating tau pathology. We aimed to assess the structural connectivity network properties in PSP and their relation to tau burden. ***Materials and Methods:*** Ten PSP patients (age 72±7 years, 6 female) underwent 60 minutes of dynamic PET imaging following 300 MBq bolus injection of [18F]PI-2620 on an integrated 3T PET/MRI system. The binding potential (BP) was estimated using non-invasive pharmacokinetic modeling (MRTM2 in PMOD) for 88 cortical/subcortical brain regions. DTI was acquired simultaneously and compared to measurements of ten healthy controls (age 65±8 years, 4 female). A graph theory approach was applied to investigate PSP-related structural connectivity network characteristics derived from probabilistic tractography. A possible association between tau load and various graph/vertex attributes was studied. Between-group differences in a given vertex measure was assessed with a vertex-wise general linear model and false discovery rate (FDR)-corrected p<0.05 was considered as significant. Student's t-test and Spearman's rank correlation coefficient were used, respectively, for between-group differences of the global network attributes and their association with BP. ***Results:*** At the global network level, the number of triangles, density, and the spatial distance were lower, while assortativity degree and vulnerability were higher in PSP patients compared to controls (p<0.05). At the vertex level, transitivity, edge asymmetry, average nearest neighbor strength, "hubness" scores, vulnerability, and eccentricity showed variable group differences (pFDR<0.05). Positive relationships were found between BP in the right cerebellar crus and clustering coefficient (r=0.74, p<0.05); BP in the left rolandic operculum and the global efficiency (r=0.65, p<0.05). Inverse relationships were observed between BP in the right precentral, bilateral frontal regions, caudate and subthalamic nuclei and the network vulnerability (r>0.60, p<0.05). The "hubness" scores demonstrated a negative association with BP in the left cerebellar crus (r=-0.76, p<0.05), and a trend towards significance in the medulla, right cerebellar crus and bilateral cerebellum (r=0.60, p<0.08). ***Conclusion:*** Graph theory analysis of the brain connectomics depicted various divergences of the structural network properties in PSP patients compared to controls. It seems that PSP-related tau pathology is associated with lower network integration. Cerebellum, cerebellar crus and medulla might impede the smoothness of the information passage in association with increased tau load. These results support the network degradation/reorganization concept in response to tau pathology, and motivate future investigations in a larger PSP patient cohort. ***References:*** None

OP-194

Aberrant functional connectivity in progressive supranuclear palsy is associated with tau load in the dentate nucleus: A [18F]PI-2620 PET/MRI study

G. Aghakhanyan[1,2], M. Rullmann[2], J. Rumpf[3], M. L. Schroeter[4], M. Patt[2], J. Classen[3], O. Sabri[2], H. Barthel[2];
[1]Regional Center of Nuclear Medicine, University Hospital of Pisa and Department of Translational Research on New Technologies in Medicine and Surgery, University of Pisa, Pisa, ITALY, [2]Department of Nuclear Medicine, University of Leipzig, Leipzig, GERMANY, [3]Department of Neurology, University of Leipzig, Leipzig, GERMANY, [4]Max Planck Institute for Human Cognitive and Brain Sciences, Leipzig, GERMANY.

Aim/Introduction: Progressive supranuclear palsy (PSP) is a primary 4R tauopathy. The evidence supports an ongoing reorganization of cortical/subcortical functional connectivity in PSP that might be influenced by tau pathology. Thus, we assayed the functional network connectivity (FNC) with cluster-based inference and the impact of subcortical tau load on cortical/subcortical connectivity in PSP patients. ***Materials and Methods:*** Ten PSP patients with predominant PSP Richardson/parkinsonian/cortico-basal phenotype (age 72±7 years, 6 female) underwent 60 minutes dynamic PET imaging following 300 MBq bolus injection of [18F]PI-2620 on an integrated 3T PET/MRI system. The binding potential (BP) was estimated using non-invasive pharmacokinetic modeling (MRTM2 in PMOD) within thirteen selected PSP-target regions of interest (ROI), consisted of the putamen, globus palidus, subthalamic nucleus, substantia nigra, periaqueductal gray matter, red nucleus and cerebellar dentate nucleus (DN). Resting-state fMRI was acquired in 520 echo planar imaging (EPI) volumes in PSP patients and ten healthy controls (age 65±8 years, 4 female) for ROI-to-ROI functional connectivity (RRC) analysis. We used the default atlas-based definition of 132 cortical and subcortical ROIs (a combination of the Harvard-Oxford atlas and the AAL atlas) implemented in the CONN toolbox (v18.a). FNC with cluster-level inferences based on multivariate statistics was applied to create RRC matrices that represent the level of effective connectivity between each pair of ROIs after discounting effects that may be mediated or accounted for by other ROIs. Under the General Linear Model (GLM) framework the between-subject effect and regression model were designed and a two-sided cluster-level false discovery rate (FDR) for multiple testing correction of pFDR < 0.05 was applied. ***Results:*** In total, 17292 functional connections among 132 ROIs were analyzed. Between-subject effect depicted three clusters, showing increased connectivity between frontal-orbital cortex and cerebellar vermis and decreased connectivity between putamen and mid-temporal gyrus in PSP patients compared to controls (pFDR < 0.05). Regression analysis showed a negative relationship between BP in the bilateral DN and cerebellar-putaminal/cerebellar-pallidal connectivity (pFDR < 0.05). ***Conclusion:*** We demonstrated clusters of aberrant cortical-cerebellar and cortical-striatal FNC in PSP patients. Tau-pathology in the cerebellar DN seems to influence the frontal-cerebellar functional connectivity profile. ***References:*** None

OP-195

HDAC6 distribution in amyotrophic laterals sclerosis

D. Van Weehaeghe[1], M. Koole[1], J. De Vocht[1], T. M. Gilbert[2], F. A. Schroeder[2], J. E. Kranz[2], J. M. Hooker[3], P. Van Damme[1], K. Van Laere[1];
[1]UZ/KU Leuven, Leuven, BELGIUM, [2]Eikonizo, Cambridge, MA, UNITED STATES OF AMERICA, [3]Athinoula A. Martinos Center for Biomedical Imaging, Charlestown, MA, UNITED STATES OF AMERICA.

Aim/Introduction: Histone deacetylase 6 (HDAC6) is a class IIb deacetylase implicated in the deacetylation of the non-histone target tubulin, important for efficient axonal transport (1). In mice and human induced pluripotent stem cell models of amyotrophic lateral sclerosis (ALS) a beneficial effect of HDAC6 inhibition has been demonstrated. Nevertheless, in postmortem tissue no significant difference in HDAC6 mRNA expression level between ALS and controls has been observed.Therefore, in this pilot study we aimed to investigate in-vivo HDAC6 expression changes in ALS patients compared to controls, using ^{18}F-EKZ-001, a new, promising HDAC6 PET ligand. We hypothesized that HDAC6 expression is increased in patients with ALS as the expression of HDAC6 is co-regulated by TDP-43, a pathological hallmark of ALS. ***Materials and Methods:*** Ten symptomatic ALS patients (61.9±11.6 years, 5F) were recruited in a tertiary neuromuscular clinic. Ten age- and sex-matched controls (57.0±3.4 years, 5F) were selected from an existing image database (2). All subjects were imaged with ^{18}F-EKZ-001 using the GE Signa PET-MR scanner. For ALS patients a coffee break protocol, with scanning intervals from 0 to 60 minutes and from 90 to 120 minutes post injection, was used to facilitate patient recruitment and increase comfort (average injected dose 124.8±8.8 MBq). Distribution volume estimates were calculated using a Logan plot with a fixed blood volume of 5% and t* of 40 minutes post injection. VOI- and voxel-based group comparisons were performed (General Linear Model) (p_{height}<0.001 and $p_{cluster\ FWE\text{-}corr}$<0.05). Sex was used as covariate as the first-in-human study showed a significant sex difference in HDAC6 distribution volume (2). ***Results:*** The voxel-based analysis revealed a global decrease of distribution volume in ALS compared to controls in all cortical and subcortical regions, cerebellum and the brainstem. These findings were confirmed by the VOI-based analysis which showed a significantly decreased ^{18}F-EKZ-001 uptake in frontal, parietal, temporal, occipital, hippocampus,

pre- and postcentral cortex in ALS compared to controls (p<0.01). At a lower threshold (p<0.05), ^{18}F-EKZ-001 binding was also decreased in striata, thalami and brainstem. No significant interaction effects were observed between group and sex. ***Conclusion:*** Our results demonstrate HDAC6 is globally decreased in symptomatic ALS patients, in line with the findings of Chen et al. where HDAC6 expression in an ALS mice model was low at disease onset and decreased even more in later stages (3). ***References:*** 1. Guo et al. Nature Communications 2017. 2. Koole et al. 2020.Submitted. 3. Chen et al.Neurosci. Bull 2015.

410

Featured Session: Molecular Bone Imaging - Nuclear Medicine's Swiss Army Knife!

Friday, October 23, 2020, 09:00 - 10:30 Channel 10

OP-196

Molecular Bone Imaging - Nuclear Medicine's Swiss Army Knife!

D. Morland; Institut Godinot, Médecine Nucléaire, Reims, FRANCE

OP-197

^{18}F-NaF Activity Related with Fibrous Dysplasia of Bone Lesions is Positively Associated with Established Bone Turnover Markers (BTMs)

G. Papadakis[1,2,3], G. C. Manikis[2], A. H. Karantanas[1], K. Marias[2], M. T. Collins[3], A. M. Boyce[3];
[1]Department of Medical Imaging, Medical School, University of Crete, Heraklion, GREECE, [2]Computational Biomedicine Laboratory (CBML), Foundation for Research and Technology Hellas (FORTH), Heraklion, GREECE, [3]National Institute of Dental & Craniofacial Research (NIDCR), Bethesda, MD, UNITED STATES OF AMERICA.

Aim/Introduction: Fibrous dysplasia (FD) of bone is a benign skeletal disorder characterized by replacement of normal bone and normal bone marrow with abnormal fibro-osseous tissue leading to significant morbidity. In a cohort of 15 FD patients we reported positive association between FD-related ^{18}F-NaF activity in the entire skeleton, with established markers of bone activity, including serum levels of alkaline phosphatase (Alk Phos) and osteocalcin (OC), and urine levels of N-terminal telopeptide (NTX) [1]. Aim of the current study was to confirm these findings in a much larger cohort of 44 FD patients. ***Materials and Methods:*** Forty four FD patients (26 females, 18 males) underwent whole-body ^{18}F-NaF-PET/CT scans at the NIH Clinical Center. Mean age±std at the time of the scan was: 30.1±14.9 years. PET scans were obtained (mean ± SD) 61.8±5.1minutes after intravenous administration of an average±std of 2.69±0.73mCi of ^{18}F-NaF. Low dose, non-contrast, CT scans were acquired for co-registration and attenuation correction purposes. FD-related ^{18}F-NaF activity was assessed by using MIM vista (version 6.5.9). Firstly, a VOI encompassing the entire skeleton was drawn, and afterwards a SUVmax threshold-based approach -customized per patient- was employed in order to include all FD-related bone uptake. Separate VOIs encircling all areas above the SUVmax threshold, were automatically generated, while areas with physiologic or non-FD related ^{18}F-NaF activity (e.g. activity in the urinary tract, inflammatory uptake) were manually removed. Subsequently, the following skeletal disease indices were automatically ontained: Total Volume (TV) of all ^{18}F-NaF positive skeletal FD lesions and FD-related ^{18}F-NaF activity (TA) in the entire skeleton determined as the product of TV multiplied by SUVmean of all FD lesions (TA = TV×SUVmean). ***Results:*** Pearson's correlation test revealed that TV and TA obtained from ^{18}F-NaF-avid FD-lesions in the entire skeleton were positively associated with serum levels of alkaline phosphatase, osteocalcin and urine levels of NTX:(TV: r=0.744, p<0.001 Alk Phos; r=0.429, p=0.013 OC ; r=0.746, p<0.001 NTX)(TA: r=0.460, p=0.009 Alk Phos; r=0.382, p=0.022 OC ; r=0.475, p=0.007 NTX)(P-values were adjusted for false discovery rate) ***Conclusion:*** We confirm in a larger cohort of FD patients that FD-associated ^{18}F-NaF activity strongly correlates with established bone turnover markers, further enhancing the finding that ^{18}F-NaF-PET/CT accurately reflects underlying bone processes encountered in FD, and implying the employment of the modality for the in vivo assessment of FD activity. ***References:*** 1. Papadakis GZ, et al. "18F-NaF PET/CT IMAGING IN FIBROUS DYSPLASIA OF BONE." J Bone Miner Res. 2019 Sep;34(9):1619-1631.

OP-198

Lesional uptake decreases on [^{18}F]NaF PET-CT in patients with Fibrous Dysplasia/McCune Albright syndrome treated with Denosumab

W. van der Bruggen[1,2], M. E. Meier[3,4], F. Smit[1,5], P. D. S. Dijkstra[3,4], L. E. M. Winter[3], L. F. de Geus-Oei[1,6], N. M. Appelman-Dijkstra[3], D. Vriens[1];
[1]Section of Nuclear Medicine, dept. of Radiology, Leiden University Medical Center (LUMC), Leiden, NETHERLANDS, [2]Dept. of Nuclear Medicine, Slingeland Hospital, Doetinchem, NETHERLANDS, [3]Center for Bone Quality, dept. of Internal Medicine, division of Endocrinology, Leiden University Medical Center (LUMC), Leiden, NETHERLANDS, [4]Dept. of Orthopaedic surgery, Leiden University Medical Center (LUMC), Leiden, NETHERLANDS, [5]Dept. of Nuclear Medicine, Alrijne Hospital, Leiderdorp, NETHERLANDS, [6]Biomedical Photonic Imaging Group, University of Twente, Enschede, NETHERLANDS.

Aim/Introduction: [^{99m}Tc]-TcHDP uptake does not change after bisphosphonate-treated Fibrous Dysplasia (FD). Despite the recently described relation between FD

disease burden measured with [^{18}F]NaF PET-CT and serum biomarkers of bone turnover, the effect of treatment on lesional [^{18}F]NaF-uptake in patients with FD is unknown. ***Materials and Methods:*** We retrospectively studied fifteen FD patients who underwent [^{18}F]NaF PET-CT at least twice (37 scans) and received antiresorptive treatment. Baseline and follow-up [^{18}F]NaF-uptake parameters of healthy bone and FD-lesions and serum biomarkers of bone turnover around treatment with denosumab (n=8) or on bisphosphonates (n=7) were assessed. ***Results:*** Individualized patient healthy bone cut-offs on [^{18}F]NaF PET-CT were again found to be preferential over a fixed cut-off for adequate normalization. This individual cut-off did not change in the whole group (p=0.233), nor after denosumab (p=0.237) or bisphosphonates (p=0.575) treatment. However, volumetric parameters of FD-burden on [^{18}F]NaF PET-CT showed significant decrease after start of denosumab. Median fluoride total volume (FTV), previously shown to be the preferred [^{18}F]NaF PET-CT parameter to quantify FD burden [3], decreased from 199 cm^3 on baseline scan to 97 cm^3 during follow-up (p=0.030). However, FTV did not change in patients receiving bisphosphonates (p=0.249). FTV correlated positively with serum biomarkers Alkaline Phosphatase (ALP) ($\rho_{Spearman}$=0.406; p=0.006; n=37) and with P1NP ($\rho_{Spearman}$=0.730; p<0.001; n=36). Relative changes in FTV and either serum biomarker of bone turnover correlated positively (ΔFTV versus ΔALP and ΔP1NP, $\rho_{Spearman}$=0.518 and 0.489; p=0.024 and 0.032, respectively). When trichotomizing changes in imaging-parameters and serum biomarkers in 'increasing' (>+10%), 'unchanged' or 'decreasing' (<-10%), moderate agreement of categorized FTV change with categorized ALP change were observed (Cohen's κ = 0.432; p=0.007; n=35) and fair agreement with categorized P1NP change (Cohen's κ 0.391; p=0.017; n=34). In several patients, either ALP or P1NP (n=5) or both (n=3) were within laboratory reference ranges at both time points, still FTV adequately quantified disease and response to antiresorptive treatment, as measured by pain scores, and possibility to reduce pain medication. ***Conclusion:*** FD-disease burden measured by FTV on [^{18}F]NaF PET-CT correlates with changes in serum biomarkers of bone turnover after antiresorptive treatment. No changes were seen in healthy bone [^{18}F]NaF-metabolism during follow-up. Therefore [^{18}F]NaF PET-CT could be used as an objective parameter of local treatment response in FD in addition to serum biomarkers of bone turnover, pinpointing location and extension of FD-burden. [^{18}F]NaF PET-CT might be of paramount importance in patients with normal(ized) serum biomarkers but clinical complaints. ***References:*** None

OP-199

Ultrafast 10x whole-body Na^{18}F digital photon counting PET/CT for assessing osteoblastic metastases: A Phase 1a intra-individual comparison trial

C. Wright*, K. Binzel, Y. Hsieh, E. Folefac, D. A. Diaz Pardo, D. G. Stover, M. V. Knopp;*
The Ohio State University, Columbus, OH, UNITED STATES OF AMERICA.

Aim/Introduction: Sodium fluoride (Na^{18}F) PET/CT is used clinically for the detection and characterization of osteoblastic lesions in both oncologic and non-oncologic patients. In patients with symptomatic bony disease, standard whole-body Na^{18}F PET image acquisition times (60 - 120 s/bed) remain longer than desired and new approaches to meaningfully reduce whole-body PET image acquisition time are needed. New clinical PET/CT systems equipped with digital photon counting PET (dPET) detector technology enable new approaches to reduce PET image acquisition times even at reduced PET radiotracer doses. The aim is to assess a 10x faster, whole-body, Na^{18}F PET imaging approach using dPET/CT technology for the detection and assessment of osteoblastic lesions. ***Materials and Methods:*** This Phase Ia intra-individual comparison trial of whole-body Na^{18}F dPET/CT (Vereos, Philips) was performed using target Na^{18}F doses of 185 MBq in 55 oncologic patients. Investigational dPET acquisitions were performed at a 10x faster rate of 9 s/bed (~80 min post injection) and then at the standard 90 s/bed (~85 min post injection). All dPET image data sets were reconstructed using standard definition voxel volumes (4x4x4 mm^3) and Time-of-Flight. Using an Intellispace Portal workstation, all matched and individual data sets were reviewed by a blinded reader panel to assess lesion detectability as well as overall image quality and background quality. ***Results:*** All 55 patients had evaluable dPET datasets (n = 110) for qualitative and quantitative assessment of osteoblastic lesions and ^{18}F biodistribution. With ultrafast 9 s/bed dPET acquisitions, ^{18}F-avidity within normal bone and osteoblastic lesions was visually comparable to the standard 90 s/bed acquisitions and no discordant osteoblastic lesions were identified. Average SUVmean values were comparable for 9 s/bed and 90 s/bed acquisitions in terms of ^{18}F activity in normal vertebral bone (6 ± 1 and 6 ± 1, respectively) and background skeletal muscle (0.6 ± 0.1 and 0.7 ± 0.1, respectively). The average SUVmax of 85 osteoblastic metastases were also comparable for 9 s/bed and 90 s/bed acquisitions (31 ± 31 and 36 ± 32, respectively and not significantly different). ***Conclusion:*** Given the unmet clinical need for shorter PET image acquisition times in oncology patients with symptomatic body disease, this Phase 1a trial demonstrates that 10x faster whole-body Na^{18}F PET imaging (~3 min total PET imaging time) is achievable with digital photon counting PET detector technology without loss of overall image quality, lesion detectability or quantitative accuracy. ***References:*** None

OP-200

Hybrid bone SPECT/CT with diagnostic-quality CT for recurrent pain following spinal fusion surgery: accuracy and impact on clinical management

B. Lambert[1], *B. Van Den Bossche*[2], *J. Bleyen*[2], *J. Mertens*[2], *T. Matton*[2], *T. Vandekerckhove*[2], *T. Van den Wyngaert*[3];
[1]*Maria Middelares Hospital and Ghent University, Gent, BELGIUM,* [2]*Maria Middelares Hospital, Gent, BELGIUM,* [3]*UZA, Antwerp, BELGIUM.*

Aim/Introduction: We designed a retrospective study to 1. investigate the sensitivity and specificity of bone SPECT/CT for identifying a pain generator in the post-operative spine 2. document the impact of bone SPECT/CT on the clinical management. ***Materials and Methods:*** We selected patients referred to our department for bone scintigraphy because of recurrent pain following cervical or lumbar spondylodesis. We limited our search to patients referred by a single experienced neurosurgeon within a 6-24 months post-surgery. The SPECT/CT images with non contrast enhanced diagnostic quality CT were acquired on Symbia T6 and Intevo T6 SPECT/CT-cameras (Siemens). SPECT/CT-scans were re-read by 2 experienced nuclear medicine specialists, blinded to the clinical data. A radiologist read the diagnostic CT-scan and a joint diagnosis was proposed. A standardized scoring method was used, aiming to assess the surgical spine levels as well as potential pain generators outside the operated spine levels (adjacent disc-or facetarthrosis, referred pain from the pelvis, hips or shoulders). All patient files were reassessed and all the applied therapeutic strategies were listed. The neurosurgeon retrospectively established a final clinical diagnosis, taking into account all available follow up data. ***Results:*** We included 71 patients: 23 males vs 48 females, median age of 50 years (min 26-max 83 y). A total of 77 SPECT/CT-scans (18 cervical vs 59 lumbar spine) were included since 6 patients were scanned twice. The mean interval since surgery was 15 months. In 4 patients no explanation for the pain was found, when retrospectively reviewing the clinical file. In the other patients the final clinical diagnoses were pseudo-arthrosis or delayed union (32%), screw loosening (15%), screw irritation (16%), adjacent segment disease (26%), extraspinal referred pain (8%). Hybrid bone SPECT/CT did not yield any positive finding in 9 scans, of which 4 also remained clinically without diagnosis. At the fusion levels SPECT/CT showed a sensitivity of 98% and a specificity of 73%. For pain generators identified outside the fusion level, sensitivity and specificity of SPECT/CT were 97% and 94%. The positive SPECT/CT findings impacted the clinical management in 55 out of 77 cases. SPECT/CT-scan guided the treatment strategy completely and partly in 42% and 38%, respectively. ***Conclusion:*** A systematic reanalysis of bone SPECT/CT studies with diagnostic-quality CT acquisitions in homogeneous group of patients after spinal fusion surgery showed a good sensitivity and specificity for identifying the main pain generator. SPECT/CT affected clinical management in 80% of patients. ***References:*** None

OP-201

Tc-99m-diphosphonate bone scan quantification: Fibrous dysplasia versus metastasis of prostate cancer

M. Jreige, *F. Becce*, *B. Rozier Aubry*, *N. Schaefer*, *J. O. Prior*, *M. Nicod-Lalonde;*
Lausanne University Hospital, Lausanne, SWITZERLAND.

Aim/Introduction: Bone scintigraphy with Tc-99m-labeled diphosphonate can identify fibrous dysplasia (FD), which typically exhibits markedly increased tracer uptake. Metastatic bone lesions of prostate cancer also show similar scintigraphic aspect on delayed planar images. The aim of this study was to investigate the emerging role of Tc-99m DPD uptake quantification to compare the value of SUV in FD and metastases. ***Materials and Methods:*** We retrospectively assessed 8 patients (49±15y) with a confirmed diagnosis of FD and 9 patients (79±13y) with known bone metastases from prostate cancer. SPECT/CT images were acquired with the Siemens Symbia Intevo providing SUV quantification on post-processed images. SUVmax, SUVmean and SUVmin were measured in all suspicious bone lesions, as well as in normal bone in both groups. ***Results:*** A total number of 77 FD and 73 metastatic bone lesions were analyzed, showing a median SUVmax, SUVmeanand SUVmin (g/mL) with a 95% CI of 10.1 (3-44.8), 6.2 (1.9-25.3) and 4.3 (1.2-17.9), and 28.5 (9.8-114), 17.2 (6.3-85.3) and 11.4 (3.9-45.6), respectively. SUVmax, SUVmean and SUVmin were significantly lower in FD compared to metastases ($p<0.001$). Normal bone uptake showed significantly lower uptake value of SUVmax, SUVmean and SUVmin in the FD group as compared the metastatic groups ($p\leq0.005$). ***Conclusion:*** This study shows a significant difference in diphosphonate uptake on bone scan between FD and prostate metastases based on quantitative data analysis, with lower SUVmax, SUVmean and SUVmin in FD. Therefore, further analysis of bone scan quantitative data can be helpful in characterizing bone lesions. ***References:*** None

OP-202

SPECT/CT with ^{99m}Tc-Tektrotyd in imaging tumors secreting fibroblast growth factor 23 (tumor-induced osteomalacia)

K. Slashchuk, *M. Degtyarev*, *P. Rumyantsev*, *S. Serzhenko*, *O. Baranova*, *A. Trukhin;*
Endocrinology Research Center, Moscow, RUSSIAN FEDERATION.

Aim/Introduction: Tumor-induced osteomalacia (TIO) is a rare paraneoplastic syndrome usually caused by tumors that overexpress fibroblast growth factor 23 (FGF23) with phosphaturic effect. The clinical signs of TIO are non-

specific and include fatigue, bone pain, muscle weakness, pathological bone fractures and compression fractures of the vertebrae, which makes timely diagnosis of the disease difficult and treatment is often delayed. Well-timed diagnosis is essential and if combined with complete tumor resection leads to complete relief of symptoms. Due to the risk of recurrence or metastases, patients with TIO require long-term management and follow-up. The article presents an analysis of 10 patients with TIO of various localizations who underwent somatostatin receptor scintigraphy (SRS) and SPECT/CT. Radiopharmaceutical was used as a tracer for SRS: it was prepared on the basis of a lyophilisate developed by Polatom (Poland) — Tektrotyd, EDDA/HYNIC-TOC labeled with ^{99m}Tc. ***Materials and Methods:*** Prospective study included 10 cases of patients aged 20-62 years (mean age 39,9±9,4), mean duration of osteomalacia was 7,4 years. Female to male ratio was 1:1. In all cases of biochemically confirmed TIO, the average levels were, blood P: 0,49±0,09 mmol/l (N:0,74-1,52); urine P in 24hours: 43,3±18,1 mmol/l (N: 12,9-43,9); alkaline phosphatase 366,7± 220,9 U/l (N: 40-150). Scintigraphy was performed with SPECT/CT (GE model 670 Discovery NM/CT) in 2-4 hours after intravenous administration of 500-700 MBq of ^{99m}Tc-Tektrotyd. ***Results:*** Tumor localization was determined in 9 (90%) of 10 patients. In 3 cases the tumor found in soft tissue of: popliteal region, 2 - femur, 1 - tibia, 1 - inguinal region, 1 - plantar side of the foot, 1 - in the left ethmoid labyrinth of the skull bones. In 3 cases imaging was performed after previous surgical treatment (tumor recurrence). All 9 patients underwent surgery with the diagnosis being confirmed by histological examination. In 1 case tumor was not visualized and patient is following up. ***Conclusion:*** SPECT/CT with ^{99m}Tc-Tektrotyd demonstrated good capacity in molecular imaging of osteolytic tumors secreting fibroblast growth factor 23 that cause the phosphopenic form of tumor-induced osteomalacia with severe bone disorders. It can be used as an alternative to PET/CT with ^{68}Ga-labeled octreotide peptides if it's not available. Further investigations of diagnostics accuracy in compare with PET/CT have to be evaluated. ***References:*** None

OP-203

Bone scintigraphy in oncological patients: The added value of SPECT-CT

D. Vega*, M. J. Tabuenca Mateo, V. Godigna Guilloteau, A. Galiana Moron, S. Ruiz Solis, M. Martin Ferrer, E. Martinez Albero, P. Pilkington Woll, P. Sarandeses Fernandez, A. Gomez Grande, J. M. Estenoz Alfaro;*
Hospital 12 de Octubre, Madrid, SPAIN.

Aim/Introduction: The objective of this study is to determine the impact of carrying out an additional study SPECT-CT in cancer patients who have undergone a total body scan with bone scintigraphy showing indeterminate findings. ***Materials and Methods:*** For our study, we have retrospectively selected in our hospital all SPECT-CT (Single-photon emission computed tomography-computerized tomography) studies performed in cancer patients with undetermined bone scans during the year 2019. A total of 73 SPECT-CT studies were performed in patients with various oncological pathologies (15.07% prostate, 31.51% breast, 9.59%, lung, 2.74%, kidney, 19.18%, gastrointestinal, 2.74%, melanoma, 15.07% head and neck, and 4.1% other tumors). The mean age was 66 years (35-91 years), 43.83% were men and 56.17% women. Bone scintigraphy, SPECT-CT, CT and MRI (performed when necessary) were analyzed in each patient. The findings were divided into two categories: malignant lesions and benign / indeterminate lesions in each of the imaging tests. The lesions were considered malignant on the SPECT-CT when areas appeared with increased uptake distributed asymmetrically, longitudinal rib lesions and, in regards to the spine, lesions with increased uptake in the pedicles, the posterior segment or the entire vertebral body. Afterwards, a comparison was made between these findings and the final diagnosis established by the oncologist, based on the results (laboratory and imaging studies) and the treatment received focusing on the newly diagnosed lesions. ***Results:*** The analysis of the lesions detected with bone scintigraphy obtained a sensitivity of 96%, and a specificity of 35%. SPECT-CT obtained a sensitivity of 96% and a specificity of 95%. CT achieved a sensitivity of 92% and a specificity of 92%, and MRI had a sensitivity and specificity of 100% in the 10 indeterminate cases, in which it was necessary to clarify the nature of the lesions. ***Conclusion:*** The increased sensitivity and specificity of SPECT-CT compared to conventional bone scintigraphy in cancer patients allows to determine more precisely the nature of the lesions and reduces the number of additional diagnostic test, thus allowing for earlier and more specific treatment. ***References:*** None

OP-204

^{18}F- FDG PET/CT in Synovial Sarcoma: Staging, Response and Surveillance

S. Datta Gupta*, G. Arora, S. Shamim, T. P. Singh, P. Kaushik, R. Kumar;*
All India Institute of Medical Sciences, New Delhi, INDIA.

Aim/Introduction: Synovial sarcoma (SS), a rare soft tissue sarcoma (STS), contributes to 6-10% of all STS. Due its insidious nature of onset, diagnosis and induction of treatment is often delayed. Long term local as well as metastatic recurrence is often seen, with up to 50% of local recurrence occurring in 2 years and 50-70% of metastases in 5 years after completion of treatment. We aimed to assess the role of ^{18}F-FDG PET-CT in staging at baseline, treatment monitoring and long-term follow-up of SS. ***Materials and Methods:*** All patients of SS, who were referred for ^{18}F-FDG

PET/CT to our department from July 2017 to February 2020, were retrospectively analyzed in this study. Indications for PET/CT included baseline staging, post excision residual disease, response assessment and surveillance. PET/CT was acquired 45-60 minutes after i.v. injection of 8-10mCi ^{18}F-FDG. Two expert nuclear physicians independently analyzed the images of PET/CT. Response was assessed as per PERCIST criteria. Cases were followed up clinically thereafter. ***Results:*** Fifty studies in 33 patients (17 male; 16 female) were analyzed. Mean age of the patients was 27.7±10.5 years. Ten of the 50 scans (20%) were referred for baseline staging, 9 (18%) for post excisional status, 24 (48%) for response assessment and remaining 7 (14%) were for surveillance. Among the baseline evaluations most common site of primary was found to be lower limbs (50%), and additional involvement of lung (50%), lymph nodes (40%) and skeletal (10%) sites were also observed. Of the nine post-resection scans, four showed residual disease, 2 had lung nodules, 5 had lymph nodal involvement and two scans were normal. Of the 24 response scans, eight (33%) showed complete metabolic response, 7 (29%) had partial metabolic response, 8 (33%) had stable disease and 1 (5%) had progression on FDG scan. Amongst the seven patients on surveillance post completion of treatment, four were positive on PET/CT. Two of these four cases revealed local recurrence (1 in lower limb, 1 in neck), one showed local recurrence (in lower limb) along with lung metastases and another scan revealed only pulmonary metastases. ***Conclusion:*** ^{18}F-FDG PET-CT may have a significant role in steering the management of synovial sarcoma by baseline staging, response assessment as well as detecting recurrent and residual disease. Since its long-term recurrence is relatively common, ^{18}F-FDG PET-CT can be considered as an important tool in the surveillance of synovial sarcoma for timely detection and management of recurrence. ***References:*** None

OP-205

Role of ^{18}FDG PET/CT in Staging and Determining the Grade of Soft Tissue Sarcoma. Relationship between Metabolic Parameters and Histopathological Features in Primary Lesion

A. Blanes*, M. N. Cabrera Martín, L. García Beláustegui, C. G. Wakfie Corieh, R. Valhondo Rama, M. García García-Esquinas, A. Crespo Rodríguez, L. Ortega Medina, J. L. Carreras Delgado; Hospital Clínico San Carlos, Madrid, SPAIN.*

Aim/Introduction: The aim of this study was to analyze different metabolic biomarkers of pretreatment ^{18}F-FDG PET/CT in soft tissue sarcoma (STS) located in trunk and limbs and to correlate them with tumor grade and necrosis. ***Materials and Methods:*** Consecutive patients (five years) with ^{18}F-FDG PET/CT for initial staging of STS with histopathological study (surgical specimen) of the primary tumor (gold standard). SUVmax, SUVpeak, MTV, TLG and texture parameters (first and second order, LIFEx software) were calculated. Statistical analysis with non-parametric tests and ROC curves. ***Results:*** 50 patients (32 males), 59.9 years (18-90). 34 local disease, 4 N1 and 8 N1M1. SUVmax/SUVpeak/TG2.5 ($p < 0.05$) differences between degrees were observed. SUVmax was the best predictor of tumor grade. In grade 1 (N = 7) SUVmax average 3.2, grade 2 (N = 11) of 11.2 and grade 3 (N = 32) of 19.8; $p < 0.05$. Optimal SUVmax to predict high grade was 10.9 (AUC-ROC: 0.865), sensitivity 78%, specificity 88.9%. Malignant fibrous histiocytoma (SUVmax 30.1), angiosarcoma (25.1), malignant peripheral nerve sheath tumor (24.1), leiomyosarcoma (16.7), and liposarcoma (10.9) showed higher uptake intensity. SUVmax/SUVpeak were significantly higher in those patients with lymph node extension and distance disease ($p < 0.05$). Subtypes with the highest dissemination were: malignant fibrous histiocytoma (4/8), malignant peripheral nerve sheath tumor (4/7), leiomyosarcoma (2/8) and desmoplastic round cells (2/2). First order texture parameters (entropy, energy and obliqueness) and most of second order parameters showed significant differences between necrotic tumors (scores 1-2) and non-necrotic tumors (score 0) and between histological grades. However, these data have not been contrasted with progression-free survival and overall survival, because most of patients have been recently diagnosed. ***Conclusion:*** ^{18}F-FDG PET/CT can be an useful tool in the staging of STS, especially in grades 2-3 and in subtypes with a greater probability of distant spread. Texture parameters could provide additional prognostic information. ***References:*** None

OP-206

SCOREp of clinical and FDG-PET/CT features at staging as risk index of poor response and relapse in Ewing Sarcoma

A. Martini*[1], M. Allocca[1], R. Di Dato[1], M. Di Paolantonio[1], I. Paglianiti[2], E. Spinelli[2], D. Volterrani[2], R. Sciagrà[1], C. Olianti[1];*
[1]University of Florence, Florence, ITALY,
[2]University of Pisa, Pisa, ITALY.

Aim/Introduction: The risk of poor histo-pathological response (HP-R) after induction-chemotherapy (i-CHT) and primary tumor (PT) surgery and relapse in Ewing Sarcoma (ES), is not evaluable at staging. Prognosis depends overall from the necrosis percentage found after i-CHT and PT surgical resection. We tested the prognostic power of clinical and ^{18}FDG-PET/CT features for predicting risk of poor response and relapse in a 5-years follow up. ***Materials and Methods:*** 39 Patients with ES, 24 males (61%) and 15 females (39%) were enrolled in ISG-EW1(26) and ISG-EW2(13) protocols. We evaluated age at staging, PT SUVmax, TLG41% (Tumor Lesion Glycolysis 41%) and diameters ratio at the staging vertex-feet ^{18}FDG-PET/CT. Than SCOREp was calculated as the value attributed to

each parameter proportionally (p) to the Exp(B) of Cox regression, by multiplying it by 10 and approximating to the unit: 10 for age<12.5y, 12 for SUVmax>4.8; 3 for TLG41%>136.13, and 10 for diameters ratio<1.46. Otherwise the SCOREp was considered null. Total SCOREp was the sum of the single values. For statistical analysis we used U-test of Mann-Whitney, ROC-analysis, univariate/multivariate Cox regression and Kaplan-Maier curve-analysis. ***Results:*** Patient age was 13.9+/-6.2y (range: 2-29); 28 localized (72%) and 11 metastatic (28%) ES. ROC-analysis related to HP-R showed a significant AUC for SUVmax (0.76, p = 0.02; cut-off 5.5, 79% spec., 60% sens.) and TLG41% (0.72, p = 0.04; cut-off 127.69, 71% spec., 67% sens.). ROC-analysis for relapse showed AUC for SUVmax (0.81, p = 0.03; cut-off 4.8, 71% sens., 86% spec.), TLG41% (0.80, p = 0.03; cut-off 136.13, 79% sens., 86% spec.), age (0.80, p = 0.03; cut-off 12.5y , 64% sens., 86% spec.) and diameters ratio (0.83, p = 0.02; cut off 1.46, 86 % sens., 71 % spec.). Mean+/-SD SCOREp was 9.7+/-1.57 for Good Responders (48%) and 23.29+/-0.43 for Poor Responders (52%) (p <0.001). Mean+/-SD SCOREp was 13.24+/-2.42 for not-relapsed ES and 23.72+/-0.6 for relapsed-ES (p <0.008). ROC-analysis for SCOREp revealed statistical significance AUC for HP-R (0.81, p = 0.001) and the risk of relapse (0.75, p = 0.007) with a cut-off SCOREp value of 24 (80% sens., 79.2% spec., 79% accuracy for HP-R and 77,8% sens., 67% spec. and 69% accuracy for risk of relapse). ***Conclusion:*** SCOREp seems able to summarize the capability of baseline variables to predict the evolution of HP-R in good or poor responders, and the risk of relapse. It could be therefore useful to stratify ES prognosis at staging PET/CT. ***References:*** None

411

e-Poster Presentation Session 3: Clinical Dosimetry Methods

Friday, October 23, 2020, 09:00 - 10:30 Channel 11

EPS-035

Salivary gland dosimetry in therapy of metastatic castrate-resistant prostate cancer with ^{177}Lu-PSMA-617

C. Happel, L. Völler, W. T. Kranert, J. Baumgarten, D. Gröner, F. Grünwald, A. Sabet;
University Medical Center Frankfurt, Department of Nuclear Medicine, Frankfurt, GERMANY.

Aim/Introduction: Therapy with ^{177}Lu-PSMA-617 is established for the treatment of metastatic castrate-resistant prostate cancer. Prostate-specific membrane antigen (PSMA) is a surface protein expressed on prostate cancer cells and is the target structure for the therapeutic radioligand ^{177}Lu-PSMA-617. It is also expressed physiologically on kidney and salivary gland (SG) tissue. Therefore, these tissues should be monitored for accumulated dose. The German Society of Nuclear Medicine recommends a non-dose limiting toxicity limit of 40Gy for SGs. Aim of this study was to calculate the dose to the salivary glands and to evaluate it in comparison to the above recommendation. ***Materials and Methods:*** Sixty ^{177}Lu-PSMA-617 therapy cycles of 21 patients were evaluated retrospectively. Median age of the patients was 74.7 years (59.6-88.8) at administration and median administered activity was 7.1 GBq (1.1-11.2). The masses of the SGs were determined by PET/CT-isocontouring (40%) with an assumed volumic mass of 1g/cm^3. Dosimetry of 120 parotid and 104 submandibular glands was performed. To ensure reliable measurement quality of the two smaller major SGs the calculation of both the submandibular and sublingual glands was summed-up. The monitoring process implemented whole-body scintigraphy imaging 24, 48 and 72h after administration from which doses were calculated with a mono-exponential fit in MS-EXCEL-2010 describing the activity over time. ***Results:*** Mean masses of the parotid and submandibular glands were 21.4±11.8 and 7.46±2.96 g, respectively. Mean activity of parotid and submandibular glands was 7.05±5.92 and 3.67±3.52 MBq correlating to 0.10 and 0.05% of the administered activity. Mean dose of the parotid and submandibular glands was 1.59±1.75 and 2.43±2.79 Gy. Mean dose per administered activity of the parotid glands was 0.25±0.27 Gy/GBq and of the submandibular glands 0.36±0.50 Gy/GBq. The mean effective half-life was 29.1±9.81 and 32.7±22.2 h for the parotid and submandibular glands. ***Conclusion:*** The accumulated dose could be reliably monitored applying the presented method. Assuming an administered activity of 6 GBq per cycle and postulating the calculated mean dose, 20 treatment cycles are necessary to exceed the dose limit of 40 Gy. However, assuming the maximum calculated dose (2.8 Gy/GBq) the dose to the SGs may converge to that limit in rare individual cases within 3 treatment cycles. In special cases when SGs may be affected in the past, their function should be monitored dosimetrically and included in the therapeutic considerations. ***References:*** None

EPS-036

Dosimetric evaluation of the lacrimal glands in patients undergoing therapy with ^{177}Lu-PSMA

C. Happel, L. Völler, W. T. Kranert, D. Gröner, B. Bockisch, C. Nguyen Ngoc, F. Grünwald, A. Sabet;
University Medical Center Frankfurt, Department of Nuclear Medicine, Frankfurt, GERMANY.

Aim/Introduction: Targeted treatment with ^{177}Lu-labelled prostate-specific membrane antigen ligands (^{177}Lu-PSMA-617) represents a promising therapeutic option for patients with metastatic castration-resistant prostate cancer. It is amply documented and investigated that ^{177}Lu-PSMA physiologically accumulates in the kidneys and the salivary glands. Although the lacrimal glands (LG) are

affected as well, it is unusual to monitor them dosimetrically in daily routine. This study aims to calculate and discuss the organ dose to the LG of patients undergoing ^{177}Lu-PSMA therapy. ***Materials and Methods:*** For dosimetric evaluation 50 ^{177}Lu-PSMA therapies with a total of 100 LGs were included. The mean administered activity was 6,809 MBq±29%. The mean age of the patients was 75 years±9%. Dosimetric analysis was performed by a region-based analysis using the ventral views of scintigraphic scatter corrected whole-body images one, two and three days post administration with an Anyscan scintillation camera (Mediso) (scan speed: 20 cm/min; matrix 256x1024 pixel, symmetric window at 208 keV; width 20%; 3-window scatter correction). Absolute quantification was achieved by previous performed sensitivity calibration for ^{177}Lu for the scintillation camera. ***Results:*** The mass of each LG was calculated by a region-based analysis using the metabolic volume (40% isocontour) from accompanying ^{68}Ga-PSMA-PET/CT. The density of LGs was assumed as 1 g/cm^3. The mean mass of the 100 LGs was 1.9 g±49%. The calculated mean accumulated activity in the LGs was 1.6 MBq±74% corresponding to 0.023%±65% of the administered activity. The organ dose was calculated by integration of the exponentially fitted time activity curve. ^{177}Lu-PSMA dosimetry indicated a mean organ dose of 4.57 Gy±111% per administration, corresponding to a mean activity-related dose of 700 mGy/GBq±105%. Mean effective half-life in the LG was 27.8 h±33%. ***Conclusion:*** Assuming a dose of 700 mGy/GBq and an administered activity of 7.4 GBq, a total of eight ^{177}Lu-PSMA therapy cycles is possible without exceeding the threshold of 40 Gy to the LGs that is known to cause organ damage. However, assuming the worst-case scenario of the maximum determined dose (3.490 mGy/GBq), two ^{177}Lu-PSMA therapy cycles may lead to an exceedance of the threshold. A ROI-evaluation of the ventral views of scintigraphic whole-body images 1, 2 and 3d post administration appears to be adequate for dosimetry of the LG. The LG are not dose-limiting organs at risk. However, an individual calculation of the organ dose may help to explain affections of dry eyes and initiate therapy especially when patients are treated with several cycles. ***References:*** None

EPS-037

Performance comparison of different dosimetry methods with respect to complexity and accuracy

J. Brosch[1], C. Uribe[2], A. Gosewisch[1], L. Kaiser[1], P. Bartenstein[1], A. Todica[1], H. Ilhan[1], A. Rahmim[3], A. Celler[3], S. Ziegler[1], G. Böning[1]; [1]University Hospital, LMU Munich, Munich, GERMANY, [2]PET Functional Imaging, BC Cancer, Vancouver, BC, CANADA, [3]Department of Radiology, University of British Columbia, Vancouver, BC, CANADA.

Aim/Introduction: Personalized dosimetry is of great importance for the improvement of therapy outcome. Different facts hinder the implementation of dosimetry in clinical workflows. The existing dosimetric approaches require varying numbers of processing steps, computation effort, manpower and time. The aim of this study is to directly compare the required resources and the accuracy of the absorbed dose estimates of three different dosimetry approaches using organ-specific S-values derived from simulations with reference phantoms, more advanced voxel-S-values (VSVs) simulated for a specific tissue type, and patient-specific full Monte Carlo (MC) simulation. ***Materials and Methods:*** Seven Lutetium-177-PSMA-I&T patients (8.12±0.78GBq) with QSPECT/CT 24h, 48h, 72h p.i. were evaluated. Rigid registration was applied based on CTs. Whole-body and kidneys were delineated on the 24h CT. Tumor lesions were segmented via k-means algorithm on 24h SPECT (PMOD v4.005). VOI-based effective half-life was determined from mono-exponential fitting. Subsequently a time-integrated activity map (TIAM) was generated for each patient. Doses to kidneys and bone lesions estimated with OLINDA and with soft-tissue Lu-177-VSVs from GATE v8.2 MC simulations convolved with TIAM (with MATLAB R2019b) were compared with values from GATE MC simulations using patient CT and TIAM. Processing times and required staff were compared. ***Results:*** OLINDA S-values were adjusted for patient organ/tumor mass. The mean percentage difference compared to MC for kidneys was -2% (OLINDA), +1% (VSVs); for 102 tumors +9% (OLINDA), +19% (VSVs). MC simulation of VSVs and full patient MC required a physicist. All methods required the same segmentation efforts. OLINDA requires fitting and no image creation and is fast (incl. pre-processing <30min). VSVs need to be simulated only once. VSV dosimetry performance was as fast as OLINDA. Full MC simulation per patient was run on 20 parallel CPUs and took 5h (simulation+preprocessing). ***Conclusion:*** For kidney dosimetry, all approaches revealed comparable dose results. OLINDA and VSV showed a strong overestimation and are therefore less appropriate for bone lesion dosimetry. OLINDA and VSVs assume soft tissue density instead of the actual bone density. However, OLINDA and VSVs were comparable with respect to organ dosimetry and time effort. MC, in contrast, requires powerful computers, is slow compared to both other methods, and requires specially trained personnel. Yet, MC can account for tissue heterogeneities and provides most accurate dose estimates for all volumes of interest (organs+tumors). Further investigations regarding bone lesion dosimetry methods, e.g. with density adjustments, are required. ***References:*** None

EPS-038

Determination of tumour control probability curves for treatments with ^{225}Ac-PSMA of metastatic castration resistant prostate cancer by means of microdosimetry calculations

P. Minguez Gabiña, A. Esteban Figueruelo, M. Nevares Herrero, R. Valverde Jorge, R. Nuñez Muñoz, Y. Carreres Ortega, I. Fernandez Tercero, E. Rodeño Ortiz de Zarate;
Osakidetza, Barakaldo, SPAIN.

Aim/Introduction: The aim of this study was to determine tumour control probability curves (TCP) for treatments with ^{225}Ac-PSMA of metastatic castration resistant prostate cancer (mCRPC) by means of microdosimetry calculations of the alpha-particle emissions. ***Materials and Methods:*** We performed Monte Carlo simulations with a previously tested program to determine by means of microdosimetry calculations the average number of hits to the cell nucleus required to reach a given TCP and the single-event mean specific energy for the α particles emitted by ^{225}Ac. The absorbed dose to reach a given TCP was calculated as the product of these two variables. The main alpha particle emissions in the ^{225}Ac to ^{209}Bi decay were considered. Realistic values of cell radiosensitivity, lesion size and cell size were considered, as well as non-uniform PSMA expression. For cell radiosensitivity, values of the specific energy deposited within an individual cell that reduces the average cell survival to 1/e, z_0, of 0.3 Gy and 0.7 Gy were considered; for lesion sizes values of 1 cm^3, 10 cm^3 and 100 cm^3; and for cell sizes nucleus radii values of 5µm, 7.5 µm and 10 µm (ratio of cell radius to nucleus radius of 1.5:1). The following distributions of the ^{225}Ac atoms were considered: ^{225}Ac atoms homogeneously distributed without any constraint (Case I); a distribution of ^{225}Ac atoms excluding the nuclei (Case II) and ^{225}Ac atoms distributed only in the cytoplasm (Case III). ***Results:*** Absorbed doses to reach a TCP of 0.9 ranged from 7.0 Gy (z_0=0.3 Gy, lesion size 1 cm^3 and nucleus radius 10 µm) to 23.3 Gy (z_0=0.7 Gy, lesion size 100 cm^3 and nucleus radius 5 µm). Assuming a relative biological effectiveness (RBE) of 5 for α particles, the absorbed doses to reach a TCP=0.9 ranged between 35.0 Gy and 116.5 Gy. The smaller the cell size, the larger the lesion size and the lower the cell radiosensitivity, the higher the absorbed dose to reach a given TCP, the highest variations occurring with cell radiosensitivity. The different ^{225}Ac distributions resulted in changes of absorbed dose to reach a TCP of 0.9 < 5%. ***Conclusion:*** We determined TCP curves for treatments with ^{225}Ac-PSMA of mCRPC by means of microdosimetry calculations. The obtained results can be a first step in the process of individualisation of the activities to administer in these treatments ***References:*** None

EPS-039

Towards in-silico dosimetry studies for (novel) radiopharmaceuticals based on physiology based pharmacokinetic models

R. Bouwman, G. de With;
NRG, Arnhem, NETHERLANDS.

Aim/Introduction: Physiology based pharmacokinetic (PBPK) models have the potential to be used as part of the individual dosimetry assessment of therapeutic radiopharmaceuticals. For somatostatin (SST2) targeting ligands for the treatment of neuroendocrine tumours a PBPK model has been developed. Currently SST2 targeting ligands are labelled with βemitting radionuclides while research focusses on a translation to alfaemitting radionuclides. In this study we show the potential value of PBPK model to conduct insilico dosimetry studies for the development of novel radiopharmaceuticals and to define future steps to develop and optimize them. ***Materials and Methods:*** A previously developed PBPK model has been implemented and results were reproduced to generate a virtual patient dataset. Subsequently simulations were conducted using the half maximum inhibitory concentration of three different radiopharmaceuticals: ^{177}LuDOTATATE, ^{90}Y-DOTATATE and ^{213}Bi-DOTATATE. From the time activity curves, ratios of accumulated activity in the organ at risk (kidney) and the target (tumour) compartment are determined for a fixed administrated activity. Subsequently for ^{90}YDOTATATE the equilibrium dissociation constant (k_D), an important parameter related to the binding, was varied to quantify its importance. ***Results:*** The simulations show that based on pre-therapeutic scans and individual physiologic characteristics individual time activity curves for the three different radiopharmaceuticals can be obtained. The ratios of the accumulated activity had the lowest value for ^{177}Lu-DOTATATE for 3 out 4 data points and for ^{213}Bi-DOTATATE for 1 out 4 (lowest dose to the organ at risk, compared to the tumour dose), indicating that there is room to optimize the optimal radionuclide with a specific ligand. Varying k_D (0.05 - 10 nmol l^{-1}) for a single subject and radiopharmaceutical, the tumour dose may decrease 50 to 90% compared to the highest value but also affected the dose ratio for organs at risk and the tumour. Suggesting that k_D is indeed important. ***Conclusion:*** PBPK-models seems to have potential to be used for in-silico dosimetry studies of novel radiopharmaceuticals for known targeting ligands. However further research is needed to validate and optimize the approach before implementing the model for in-silico dosimetry studies. This includes selection of appropriate boundary conditions and more experimental data to obtain more knowledge regarding the uncertainty in model parameters. For radiopharmaceuticals based on endocytosis, knowledge of binding is one of the most important parameters. ***References:*** Kletting, P. et al. Differences in predicted and actually absorbed doses in peptide receptor radionuclide therapy. Med. Phys. 39, 5708-5717 (2012).

EPS-040

Gamma Camera Calibration to Perform SPECT/CT-based Dosimetry in ^{177}Lu-DOTATATE Treatments

T. Monserrat Fuertes[1], N. Montenegro Iglesias[1], D. Álvarez

Llorente[1], M. Peinado Montes[1], D. San José Olmedo[1], P. Mínguez Gabiña[2];
[1]Hospital Universitario Central de Asturias, Oviedo, SPAIN, [2]Hospital Universitario Cruces/Gurutzeta, Bilbao, SPAIN.

Aim/Introduction: The objective of this work is to establish the acquisition and processing parameters that optimize the quantification of the SPECT images of ^{177}Lu, as well as obtaining the appropriate calibration and correction factors to calculate dose in patients. ***Materials and Methods:*** All acquisitions were performed on a Discovery NM/CT 670 gamma camera from General Electric (GE). Data were reconstructed in a GE Xeleris workstation using the ordered-subset expectation maximization (OSEM) method. To compare the quantification accuracy of the different options under study, four different phantoms were used: three spheres of 5.6, 11.2 and 28.8 cm^3 and one cylindrical phantom of 300 cm^3, all of them inside warm backgrounds of different activity concentrations. The activity measured in each of them was compared with the actual activity. Calibration geometry. Two geometries were compared: point source and cylindrical volume of 5677 cm^3. Acquisitions parameters. Two SPECT options were compared: 120 projections of 30 seconds/projection and 60 projections of 60 seconds/projection. Dead time. Several acquisitions were made of a 28 cm^3 spherical insert with different activity concentrations in a water background. The relationship between activity and SPECT counts for a wide range of activities of ^{177}Lu was analyzed. Scatter correction. To analyze scattered radiation correction, the results obtained with the dual (DEW) and triple (TEW) energy window scatter correction methods were compared, as well as those obtained with no scatter correction at all. Detector-collimator effect. The effect of introducing the information of the point spread function (PSF) in the reconstruction was studied. Partial volume effect (PVE). The NEMA image quality phantom with 6 spheres of different volumes and concentrations inside a water background was used to calculate the recovery coefficients. The effect of changing the number of iterations and subsets on the OSEM reconstruction was analyzed. ***Results:*** The conditions and parameters that resulted in greater accuracy in the quantification were: cylindrical calibration phantom, acquisition with 120 projections, 30 seconds/projection, scattered radiation correction with DEW, correction with PSF applied and OSEM reconstruction with (8 iterations, 10 subsets). Correction for dead time is not necessary, since dead time effects begin to be relevant at activity concentrations much higher than those observed in clinical practice. ***Conclusion:*** The parameters obtained have been established in the clinical routine of patient dosimetry in treatments with ^{177}Lu-DOTATATE. ***References:*** None

EPS-041

Patient Specific Peri- and Post-Treatment Analysis of ^{177}Lu-DOTATATE Injected NET Patients

*O. Yaylali[1], **S. Beykan**[2], D. Yüksel[3], G. Ergiyen Buldu[4], B. Nacar[4], A. Gültekin[3], T. Şengöz[3], M. Lassmann[2], I. Karaaslan[4];*
[1]Pamukkale University Medical Faculty Departement of Nuclear Medicine, Denizli, TURKEY, [2]Department of Nuclear Medicine, University of Würzburg, Würzburg, GERMANY, [3]Pamukkale University Medical Faculty Department of Nuclear Medicine, Denizli, TURKEY, [4]Graduate School of Health Sciences, Yeditepe University, İstanbul, TURKEY.

Aim/Introduction: Main goal is to perform the patient specific kidney and tumor analysis for the NET patients in each peri- and post-treatment of ^{177}Lu-DOTATATE. In addition, the influence of used imaging method was investigated by comparing the single time-point SPECT/CT dosimetry (STS) results with combination of 2D/3D imaging dosimetry (MP1S). ***Materials and Methods:*** 24h SPECT/CT and 6 WB planar images (up to 150h) were acquired for 11 NET patients after an administration of 6.5-7.4 GBq ^{177}Lu-DOTATATE. Amino acid kidney protection was performed to all patients. Kidneys and tumor' time-integrated activity coefficients (TIACs) were calculated for each treatment cycle by using NUKFIT. Kidney absorbed doses(ADs) per treatment cycle were calculated by using OLINDA/EXM and compared with the STS. ***Results:*** MP1S based KidneyADs were in the range of 5.7-13 Gy. Nevertheless 24h STS based KidneyADs resulted in either underestimations up to 33% or overestimations up to 25% in compare to MP1S. Instead of empiric treatment, with the aim of administration of maximum-possible-activity with avoiding 23Gy kidneyAD, up to 22 GBq of ^{177}Lu-DOTATATE can be safely administered to the patients. And as a result, by a factor of 2-4 higher tumorADs can be received. Direct relationship between the kidney and tumor TIACs per treatments is observed. Varied DOTATATE uptide of the liver for the patients 3/11 (20-40%) decreased, 6/11 stayed constant and 2/11 increased. ***Conclusion:*** The inconsistent DOTATATE uptake pattern in the kidneys for each treatment cycle is highly associated with the tumor regression or receptor- binding probabilities. Dosimetry results, biokinetics analysis, varied DOTATATE uptake-pattern and TIACs for kidneys and tumors per treatment cycle showed the necessity of patient-specific treatment protocol especially after the first ^{177}Lu-DOTATATE treatment. In addition, if the treatments were performed based on maximum-possible-activity administration, the tumors will receive higher doses with avoiding kidney toxicity, which may result in better treatment responses. ake-pattern, kidneyTIACs and tumorsTIACs were observed in 7/11 patients. Similar KidneyTIACs resulted in similar TumorTIACs and no change in tumor volumes (4/11 patients) per treatment cycle whereas decreased KidneyTIACs resulted in either stable tumor stage (2/11 patients) or progress (2/11 patients). Increased KidneyTIAC resulted in tumor regression (3/11patients).Additionally it's

observed that the tumors' volumes located outs ***References:*** None

EPS-042

Establishing a clinical dosimetry protocol for 177Lu-DOTATATE peptide receptor radionuclide therapy

S. Bissell[1], *E. Ross*[1], *H. McMeekin*[2], *E. Seal*[1], *K. Ogunwale*[1]; [1]*University Hospitals Birmingham, Birmingham, UNITED KINGDOM,* [2]*Hermes Medical Solutions, London, UNITED KINGDOM.*

Aim/Introduction: In the UK NET patients can undergo 4 cycles of ^{177}Lu-Dotatate therapy. Dosimetry is required to evaluate the effectiveness of this therapy and to establish dose-response relationships. The long term aim of this project is to establish a practical dosimetry method providing quantitative assessment of uptake which can be related to clinical response. The current focus is selection of a dosimetry software package. ***Materials and Methods:*** During cycle 1 of ^{177}Lu-Dotatate therapy patients undergo imaging at four time points: SPECT-CT acquired 4 hours post-administration and SPECT only acquisitions acquired on day 1, 5 and 7. SPECT-CT systems have been calibrated to provide quantitative image reconstructions that can be fed into dosimetry software. Patient variables were used for reconstructing images for a sample of 10 patients. Two software packages were used for quantitative comparison. The first package performs Organ Dosimetry (OD) using OLINDA based on the MIRD formalism; the second employs Voxel Based Dosimetry (VBD). VOIs of the spleen and kidneys were delineated by 4 operators using CT images obtained on day 0. The OD software was used to register the VOIs to each time point image, creating time activity curves and organ doses. For VBD the 4 SPECT images were co-registered and therapy variables used to create dosemaps. The previously delineated VOIs were registered to the dosemaps to calculate mean organ doses. ***Results:*** Average organ doses were calculated with the standard deviation resulting from operator variability expressed as a percentage. Using OD the mean organ dose for the kidneys was 3.76Gy ± 4.45% and for the spleen 4.01Gy ± 3.52% . Using VBD mean organ doses were 3.81Gy ± 7.10% for the left kidney, 4.69Gy ± 4.48% for the right kidney. Combined kidney dose was 4.25Gy ± 8.76% and spleen dose was 3.74Gy ± 10.32%. Direct comparison of both software packages reveals a 12% increase in dose using VBD ($p<0.005$) and a 7% decrease in dose for the spleen ($p<0.1$). ***Conclusion:*** Our results suggest that there is a significant difference in kidney dose between OD and VBD ($p<0.005$), with statistically insignificant variation for the spleen ($p<0.1$). This is likely due to the inclusion of cross-talk in VBD. Operator variability was lower than anticipated. Work has begun to assess the dose delivered to tumours and how this relates to clinical response. ***References:*** None

EPS-043

Comparison of the 24h-uptake value obtained from planar images with a gamma camera and from measurements with a thyroid uptake probe in patients with benign thyroid disease

P. Minguez Gabiña*, A. Esteban Figueruelo, M. Nevares Herrero, R. Valverde Jorge, R. Nuñez Muñoz, Y. Carreres Ortega, J. Genolla Subirats, E. Rodeño Ortiz de Zarate; Osakidetza, Barakaldo, SPAIN.*

Aim/Introduction: We aimed to compare the 24h-uptake value in patients with hyperthyroidism when it is determined from measurements with a thyroid uptake probe and from planar images with a gamma camera. ***Materials and Methods:*** Forty patients with different types of hyperthyroidism were included (15 Graves, 10 autonomous adenoma and 15 multinodular goitre). A capsule of ^{131}I(1.5MBq-3.0MBq) was administered to patients in order to perform treatment planning. Approximately 24h after the administration, uptake was first measured by trained staff with a thyroid uptake probe. The probe was centred at the patients' neck and counts were obtained during 60s. The acquisition window was centred at 364keV. A background measurement was performed with the probe in contact with the patients' thigh. A capsule of the same activity given to patients was measured at the time of the administration in order to obtain the relative thyroid uptake. A static planar image of the neck region was acquired in a gamma camera with a HEGP collimator during 600s. An energy window centred at 364keV with a 20% width was used, and a matrix size of 256×256. A 3x3 smoothing filter was applied. A ROI was delineated for the thyroid region with a 20% threshold of the pixel with maximum counts. Counts of this ROI were background corrected from the counts of a ROI taken below the thyroid. The camera was calibrated with a capsule of the same activity given to the patients, and the relative thyroid uptake was obtained. No attenuation correction was performed in either of the methods. The uptake values obtained for each of the two methods were tested for normality using the Shapiro-Wilks test. The differences between both groups were tested to see if they were significant. A Pearson correlation test was performed to study the correlation of that difference with the uptake value and with the type of hyperthyroidism. ***Results:*** Both groups followed normal distributions and after performing an independent samples t-test, it was found that uptake values obtained with the probe were significantly lower than those obtained with the gamma camera($p<0.05$). No correlation was found, either with the uptake value or with the type of hyperthyroidism. ***Conclusion:*** The unexpected significant differences between both methods call for research to find the reason for which one of the two methods is overestimating or underestimating the relative uptake value, as it may be relevant in regular treatment

planning of some centres. ***References:*** None

EPS-044

Improved patient dosimetry for radioactive iodide by adjusting the ICRP iodide compartment model to individual thyroid uptake

M. Andersson*, S. Mattsson;*
Medical Radiation Physics, Malmö, SWEDEN.

Aim/Introduction: Iodine is an essential component of the thyroid hormones thyroxine (T4) and triiodothyronine (T3), which regulate metabolic processes and are critical to growth and development. The thyroid uptake of iodide depends both of the hormone levels of T4, T3 and on the dietary intake of iodide. In the ICRP biokinetic compartment model for iodine the daily intake set to 160 µg. However, patient treated with iodide can both deviate from the hormone levels of T3, and T4 and the daily iodide intake. These patients often undergo thyroid activity measurements and therefore the actual uptake is known. The aim of this project is to automatically adjust the ICRP iodide compartment model to the measured individual patient thyroid uptake. This will provide not only a better and more representative absorbed dose to the thyroid, but also a realistic absorbed dose to all other tissues and organs. ***Materials and Methods:*** The biokinetic model of iodide includes 30 different compartments and 48 transfer coefficients to model the bio-distribution of iodide in the human body. Of these are two compartments used to describe the iodide uptake and retention in the thyroid, one for inorganic iodide and one for organic iodide, with four transfer coefficients. It is these four transfer compartments which are optimized to fit the biokinetic model to the patient specific uptake. However, as the model is a recirculation iodine model the optimization is performed using the whole model. Absorbed dose calculations are performed for all 30 different compartments. ***Results:*** The mathematical code was tested on measured activity data for I-131 for a Graves' hyperthyroidism patient. The transfer coefficient from blood to thyroid was changed from 7.2 day^{-1} to 16.2 day^{-1}. The increased thyroid uptake from blood will decrease the excretion to faeces and urine and 1.6 more thyroid I-131 decays will occur within the body. This increased thyroid uptake will also result in a 2.5 times higher thyroid absorbed dose (from 0.364 mGy/MBq to 0.939 mGy/MBq). For all other radiosensitive organs, the absorbed dose will in average increase with a factor of 2,due to adjusting the biokinetic model to the measured patient data. ***Conclusion:*** The uptake of iodide in thyroid can deviate between patients and healthy persons. The goal of this project is to adjust for this differences to perform more representative absorbed dose calculations for both the thyroid and all other radiosensitive organs. ***References:*** Rich Leggett.An age-specific biokinetic model for iodine.J.Radiol. Prot.37(4),864-882,2017

EPS-045

The tribulations of multi-centre clinical trials dosimetry

N. Clayton*[1], J. Ocampo-Ramos[1], G. Flux[2,3], J. Taprogge[2,3], M. Bardiès[1];*
[1]CRCT, UMR 1037, INSERM, Université Toulouse III Paul Sabatier, Toulouse, FRANCE, [2]Royal Marsden NHSFT, London, UNITED KINGDOM, [3]The Institute of Cancer Research, London, UNITED KINGDOM.

Aim/Introduction: Background: Multi-centre trials are often required within molecular radiotherapy (MRT) to acquire sufficient data to power the trial. For many trials involving a novel pharmaceutical, detailed administration protocols and common patient questionnaires ensure compatibility across centres. However, trials involving radiopharmaceuticals can be particularly complex, especially where dosimetry is required, due to the number of stages required in the production of quality data.Recent experience has highlighted challenges that may arise within multi-centre MRT trials that involve dosimetry. The aim of this review was to address aspects of the trial structure and consider recommendations for future trial design in order to prevent future complications. ***Materials and Methods:*** ***Results:*** Recommendations for trial design: Compromises may be necessary where teams of varying expertise participate in the trial particularly with budgetary or times constraints. ***Conclusion:*** The challenges arising within a multi-centre clinical trial that involves patient-specific dosimetry necessitate a high level of comprehension at all participating sites and clear communication throughout. Issues faced by a trial coordinator and a lack of comprehension by all parties can affect the quality of their individual contributions. These considerations should be taken into account at the initial design phase. ***References:*** None

EPS-046

International recommendations for personalised selective internal radiation therapy with yttrium-90 resin microspheres

H. Levillain*[1], O. Bagni[2], C. M. Deroose[3], A. Dieudonne[4], S. Gnesin[5], O. S. Grosser[6], S. Kappadath[7], A. Kennedy[8], N. Kokabi[9], D. Liu[10], D. Madoff[11], A. Mahvash[7], A. Martinez de la Cuesta[12], D. Ng[13], P. M. Paprottka[14], C. Pettinato[15], M. Rodriguez Fraile[12], R. Salem[16], B. Sangro[12], L. Strigari[15], D. Y. Sze[17], L. de Wit Van der Veen[18], P. Flamen[1];*
[1]Jules Bordet Institute, Brussels, BELGIUM, [2]Santa Maria Goretti Hospital, Latina, ITALY, [3]University Hospitals Leuven and Nuclear Medicine and Molecular Imaging KU Leuven, Leuven, BELGIUM, [4]Hôpital Beaujon, AP-HP.Nord, DMU DREAM and Inserm U1149, Clichy, FRANCE, [5]Institute of Radiation Physics, Lausanne University Hospital and University of Lausanne,

Lausanne, SWITZERLAND, [6]University Hospital Magdeburg, Magdeburg, GERMANY, [7]University of Texas MD Anderson Cancer Center, Houston, TX, UNITED STATES OF AMERICA, [8]Sarah Cannon Research Institute, Nashville, TN, UNITED STATES OF AMERICA, [9]Emory University School of Medicine, Atlanta, GA, UNITED STATES OF AMERICA, [10]Vancouver General Hospital, University of British Columbia, Vancouver, BC, CANADA, [11]Yale School of Medicine, New Haven, CT, UNITED STATES OF AMERICA, [12]Clinica Universidad de Navarra-IDISNA and CIBEREHD, Pamplona, SPAIN, [13]Singapore General Hospital, Singapore, SINGAPORE, [14]Technical University of Munich, Munich, GERMANY, [15]S. Orsola Malpighi University Hospital, Bologna, ITALY, [16]Northwestern University, Chicago, IL, UNITED STATES OF AMERICA, [17]Stanford University School of Medicine, Palo Alto, CA, UNITED STATES OF AMERICA, [18]The Netherlands Cancer Institute, Amsterdam, NETHERLANDS.

Aim/Introduction: A multidisciplinary expert panel convened to formulate state-of-the-art recommendations for optimisation of selective internal radiation therapy (SIRT) with yttrium-90 (^{90}Y) resin microspheres, by standardisation of multimodality treatment approaches, personalisation of activity prescription methods, and performance of post-treatment dosimetry. ***Materials and Methods:*** A steering committee of 23 international experts representing all participating specialties formulated recommendations for SIRT with ^{90}Y resin microspheres activity prescription and post-treatment dosimetry based on literature searches and the responses to a 61-question survey that was completed by 43 leading experts (including the steering committee members). The survey asked for opinions on best practice in areas of pre-SIRT work-up and interventional strategy, dosimetry method for activity prescription, dose thresholds for normal-liver and tumours, and post-treatment dosimetry. The survey was validated by the steering committee and completed anonymously. In a face-to-face meeting, the results of the survey were presented and discussed. Recommendations were derived and level of agreement defined (strong agreement ≥80%, moderate agreement 50%-79%, no agreement ≤49%). A follow-up meeting allowed the committee to consolidate these recommendations and levels of agreement. ***Results:*** Survey participants had a median of 14 years of experience with ^{90}Y resin microspheres. Fifty-two recommendations were made, which included: a multidisciplinary team should define treatment strategy and therapeutic intent (strong agreement); 3D imaging with CT in an angiography suite such as cone-beam CT and ^{99m}Tc-MAA-SPECT/CT are recommended for extra-/intra-hepatic deposition assessment, treatment field definition and calculation of the ^{90}Y resin microspheres activity needed (moderate/strong agreement). A personalised approach, using dosimetry (partition model [MIRD-based] and/or 3D voxel-based dosimetry), is recommended for activity prescription, when either whole liver or selective, non-ablative or ablative SIRT is planned (strong agreement). A mean absorbed dose to non-tumoural healthy liver of 40 Gy or less is considered safe (strong agreement). To target tumour ablation a minimum mean-absorbed dose to tumour of 100-120 Gy is recommended in hepatocellular carcinoma, liver-metastatic colorectal cancer and cholangiocarcinoma (moderate/strong agreement). Post-SIRT imaging evaluation should be visual and quantitative, and therefore, post-SIRT ^{90}Y-PET/CT or SPECT/CT is highly recommended, and ^{90}Y-PET/CT is preferred for accuracy of quantitative imaging (strong agreement). Post-SIRT dosimetry is also recommended (strong agreement). ***Conclusion:*** Optimised SIRT with ^{90}Y resin microspheres requires personalised activity prescription and dosimetry (voxel-based or MIRD-based partition method) and multidisciplinary management for safety and efficacy. Practitioners are encouraged to work towards adoption of these recommendations. ***References:*** None

EPS-047

Combined Quality and Dose Volume Histograms demonstrates the predictive value of ^{99m}Tc-MAA SPECT/CT simulation for personalizing radioembolization treatment in liver metastatic colorectal cancer

H. Levillain[1,2], *M. Burghelea*[1], *I. Duran Derijckere*[2], *T. Guiot*[1], *A. Gulyban*[1], *B. Vanderlinden*[1], *M. Vouche*[3], *P. Flamen*[2], *N. Reynaert*[1]; [1]*Medical Physics Department, Jules Bordet Institute, Brussels, BELGIUM,* [2]*Nuclear Medicine Department, Jules Bordet Institute, Brussels, BELGIUM,* [3]*Radiology Department, Jules Bordet Institute, Brussels, BELGIUM.*

Aim/Introduction: The aim of this work was to analyse differences between simulation ^{99m}Tc-MAA-SPECT/CT and treatment ^{90}Y-microsphere-PET/CT dosimetry using different metrics. Dose distribution was compared voxel-to-voxel using quality-volume-histograms (QVH), which was further used for identifying potential clinical parameters that induce discrepancies between simulation and treatment dosimetry. ***Materials and Methods:*** Thirty liver-only metastatic colorectal cancer patients were included in this monocentric retrospective investigation. Individual lesions were delineated on baseline FDG-PET/CT using a fixed SUV threshold (130 delineated lesions). Clinical workstation was used for initial co-registration and 3D voxel-based dosimetry computation for simulation and treatment dosimetry ($D^{Simulated}$ and $D^{Treatment}$ respectively). Lesions delineated on FDG-PET/CT were projected on the anatomically registered $D^{Treatment}$ and whole tumoral-liver (TL) and non-tumoral-liver (NTL) were delineated. Dose-volume-histograms were computed from $D^{Simulated}$ and $D^{Treatment}$ for each individual lesion, TL and NTL. The DVH-based indices D90, D70, D50, Dmean and D20 were analysed for all predefined volumes. The QVH were computed using an in-house Python code. QVHs represent decumulative histograms of the voxel-

based quality ratio, defined as: $\log_{10}(D^{Treatment}/D^{Simulated})$. When the simulated dose distribution perfectly matches the treatment dose distribution, the ratio is equal to 0 for every voxel within the given volume. QVHs were computed for TL, NTL and all lesions.Quality-factors representing the spread of the QVH curve around 0 (ideal QF=0) were determined for lesions, TL and NTL. QVHs were classified into good, acceptable and poor correspondence based on QF-values. ***Results:*** DVH indices showed no statistically significant differences between simulation and treatment across all volumes. Furthermore, in agreement with previous studies, the DVH analysis showed no difference in terms of D_{mean}. For lesions and TL, dose- and quality-volumes-histograms were mostly concordant: 69% of lesions had a QF within the good/acceptable categories (40% good) and 65% of TL had a QF within the good/acceptable categories (23% good). For NTL mixed results were obtained with 48% QF within the poor concordance category.The delay between simulation and treatment (>9days vs. ≤9days) was a significant predictor of discrepancies between simulation and treatment dosimetry, the median QF was 0.53 vs. 0.39 (p=0.04) for individual lesions, 0.62 vs. 0.42 (p=0.02) for TL and 1.20 vs. 0.60 (p=0.002) for NTL. ***Conclusion:*** The combination of DVH and QVH confirmed the predictive value of ^{99m}Tc-MAA SPECT/CT simulation for personalizing radioembolization activity prescription and could be used as a quality assurance process in mono/multi-centre trials as well as in clinical routine. ***References:*** None

EPS-048

Radioembolization of hepatocarcinoma with ^{90}Y glass microspheres: voxel dosimetry or mean dose approach to predict clinical outcomes?

C. Romanò[1], *S. Mazzaglia*[1], *M. C. De Nile*[2], *S. Bhoori*[3], *A. Gabutti*[4], *G. Maffi*[4], *C. Spreafico*[4], *A. Marchianò*[4], *V. Mazzaferro*[3], *M. Maccauro*[1], *E. Seregni*[1], *C. Chiesa*[1];
[1]*Nuclear Medicine Division, Foundation IRCCS Istituto Nazionale Tumori, Milan, ITALY,* [2]*Postgraduate Specialization School in Medical Physics, University of Milan, Milan, ITALY,* [3]*HPB Surgery, Hepatology and Liver Transplantation, Foundation IRCCS Istituto Nazionale Tumori, Milan, ITALY,* [4]*Radiology 2, Foundation IRCCS Istituto Nazionale Tumori, Milan, ITALY.*

Aim/Introduction: To retrospectively investigate if voxel dosimetry could improve correlation with clinical outcomes with respect to mean absorbed dose in hepatocellular carcinoma patients which underwent trans-arterial radioembolization (TARE). Our previous published study showed that no voxel dosimetry variable (Ψ) could significantly improve clinical outcome prediction with respect to the mean absorbed dose. However that study suffered from several methodological limitations: a limited number of cases (43), a non-consolidated method for radiological response evaluation, absence of hybrid SPECT/CT, scatter correction, and post-therapy ^{90}Y-PET verification. In this study, a larger patient cohort was considered, and all the previous limitations were overcome. ***Materials and Methods:*** We retrospectively evaluated ^{99m}Tc-MAA SPECT/CT ^{90}Y-PET/CT data of 101 patients treated with ^{90}Y glass microsphere 8 days after the calibration day. The following voxel-based Ψ were computed both for liver healthy parenchyma and tumours: mean absorbed dose (D), Equivalent Uniform Dose (EUD), average of the Biologically Effective Dose (BEDave), Equivalent Uniform Biologically Effective Dose (EUBED), the minimal dose of the 98%, 70%, 50% and 2% of the VOI (D_{98}, D_{70}, D_{50} and D_{2}), and homogeneity index (HI). We studied the correlation between each Ψ and liver decompensation (LD) or lesion local mRECIST response. Tumour control probability (TCP) curves were assessed. The area under the receiver-operating characteristic (ROC) curve (AUC) of the two classes with/without LD and of responding/non-responding lesions was calculated. ***Results:*** 4 over 101 patients presented LD. This scarce number of LD cases hinder the Ψ-toxicity analysis. A local disease control rate of 97% for measurable lesions was reported. An unexpectedly poor Ψ-response correlation was obtained in both pre- and post-treatment data. No Ψ reached an AUC value significantly higher than the mean absorbed dose. (AUC=0.56±0.06). The poor class separation in terms of any Ψ between responding and non-responding lesions prevented to derive a reliable treatment efficacy threshold. ^{90}Y-PET data presented slightly higher AUC values than ^{99m}Tc-MAA SPECT data. Despite high D up to 800 Gy, TCP curves did not reach 100%, rather showing an unexpected plateau at 75%. Lesion radiosensitivity α from TCP fit was confirmed (0.003/Gy). ***Conclusion:*** This study confirms that no voxel dosimetry based parameter, neither using pre- nor post-therapy imaging, significantly improved clinical outcome prediction with respect to the mean absorbed dose. These findings, the poor dose-response correlation obtained and the TCP curve plateau can be explained by the clustering effect of 8-days decayed microspheres and maybe other biological factors. ***References:*** None

EPS-049

Absorbed dose assessment in ^{90}Y radioembolization patients with GATE: a comparison between total-body PET and conventional PET imaging

G. Costa*, B. Spencer, M. Rusnak, D. T. Caudle, C. Foster, C. T. Vu, E. Roncali;*
University of California, Davis, CA, UNITED STATES OF AMERICA.

Aim/Introduction: Radioembolization based on the delivery of ^{90}Y microspheres to liver tumors through selective hepatic artery branches is an established radionuclide therapy, although current methods of verifying dose delivery suffer from poor accuracy. Despite the difficulties of measuring and quantifying the very low branching ratio

of ^{90}Y positron emission (32 ppm) [1], ^{90}Y PET can be used for therapy evaluation to estimate the absorbed dose [2] in the liver/tumor using Monte Carlo simulations. ***Materials and Methods:*** The patient received three injections of ^{90}Y microspheres (Theraspheres, BTG) with a total activity of 3.363 GBq and was scanned on both the total-body PET scanner uEXPLORER (United Imaging Healthcare) and the mCT Biograph (Siemens) five hours after injection. The dose distribution was estimated using Monte Carlo simulations (GATE 8.2), in which PET images were used as the activity distribution (source) and the CTs provided the tissue properties and anatomy. Volumes of interest (VOI) were created as image masks where the mCT mask was co-registered on uEXPLORER and vice-versa. These VOIs were overlaid with both the source images to force primary events to be generated only inside the VOI, and with the output dose-map to estimate the absorbed dose. ***Results:*** The number of counts obtained in the VOIs was significantly higher (up to 35.1%) on uEXPLORER as a result of its higher sensitivity. Absorbed doses estimations were 223.2 Gy and 230.7 Gy (3.2 % difference) for uEXPLORER and mCT simulations, respectively, with uEXPLORER mask, while the values with mCT's mask were 247.5 Gy and 260.6 Gy (5.0 %). ***Conclusion:*** GATE simulations showed promising results to estimate the absorbed dose from PET images. It must be noted that the absorbed dose is dependent on the VOI, for example, uEXPLORER simulations showed values of 223.2 Gy and 245.5 Gy with uEXPLORER and mCT masks, respectively. Furthermore, it is equally important to properly identify the volumes where primary events will occur while keeping noise and artefacts to a minimum. Further studies will be conducted to assess the impact of noise and artefacts on absorbed dose estimation. ***References:*** 1 - Strydhorst, Jared et al. "A gate evaluation of the sources of error in quantitative ^{90}Y PET". Medical Physics 43 (2016); 2 - Sarrut, David et al. "A review of the use and potential of the GATE Monte Carlo simulation code for radiation therapy and dosimetry applications." Medical Physics 41 (2014)

EPS-050

Comparison of Pre-Treatment Imaging for Radioembolization Using Tc-99m, Ho-166 and Y-90

J. Wielaard[1,2], *B. Kunnen*[1], *G. C. Krijger*[1], *R. van Rooij*[1], *H. W. A. M. de Jong*[1];
[1]*University Medical Center Utrecht, Utrecht, NETHERLANDS,*
[2]*St. Antonius hospital, Nieuwegein, NETHERLANDS.*

Aim/Introduction: Tc-99m-macroaggregated albumin particles are commonly used as a surrogate to therapeutic Y-90 microspheres to identify lung shunting and extrahepatic depositions in radioembolization. A potential better estimation can be derived by using a safe low dosage of the therapeutic microsphere, as is clinically studied for Ho-166 radioembolization, but also suggested for Y-90 microspheres[1,2]. This phantom study is performed to compare quantitative accuracy of the lung shunt fraction (LSF) estimation and detection of extrahepatic deposition, based on planar scintigraphy and SPECT/CT (Siemens Intevo) for Tc-99m, Ho-166 and Y-90. ***Materials and Methods:*** An anthropomorphic phantom (model ECT/TOR/P, IEL, Chilcompton, UK) with liver, lung (filled with styrofoam beads) and extrahepatic deposition compartments (2 and 8 mL) was filled several times to acquire an LSF of 0, 5, 15 and 20% in combination with activity concentrations in the extrahepatic depositions of 10 times the liver concentration. The total activity of the liver and lung compartments was kept at either 150 MBq, 250 MBq and 100 MBq, in 0.5 M HCl, for Tc-99m, Ho-166 and Y-90 respectively. Planar scintigraphy and SPECT/CT images were acquired and reconstructed with our current clinical protocols. In addition, for Y-90 and Ho-166 SPECT/CT, Monte Carlo (MC)-based reconstruction was performed. The LSF as well as the contrast-to-noise ratio (CNR) of the extrahepatic depositions were retrieved by automatic registration of CT-defined masks. ***Results:*** In all cases SPECT/CT imaging was more accurate than planar imaging for LSF estimations and resulted in higher CNRs for the extrahepatic depositions. However, Y90 and Ho-166 SPECT/CT still overestimated the LSF. MC-based reconstructions led to more accurate LSF estimations and increased CNRs. ***Conclusion:*** This study shows that all three radioisotopes led to comparable LSF estimations. The advantage of using Ho-166 and Y-90 for the pre-treatment procedure is the use of a low dosage identical therapeutic microspheres. For both radioisotopes MC-based reconstructions improved image quality and lowered LSF overestimation. ***References:*** [1] Braat, A. et al. Eur Radiol. 2019; 28(3): 920-928. [2] Kunnen, B. et al. Med Phys. 2020 Mar; 47(3): 1105-1114.

EPS-051

Comparison of Different Time-Activity Curve-Fitting Methods for Voxel-based In-111 Zevalin SPECT Targeted Radionuclide Therapy Dosimetry

Y. Lyu, *G. Chen, G. Mok;*
Biomedical Imaging Laboratory (BIG), Department of Electrical and Computer Engineering, Faculty of Science and Technology, University of Macau, Taipa, MACAO.

Aim/Introduction: Curve fitting is commonly applied on sequential activity data to calculate the time-integrated activity (TA) for targeted radionuclide therapy dosimetry. This study aims to compare different exponential curve fitting methods (mono-, bi- and tri-) on voxel-based dosimetry based on In-111 Zevalin SPECT scans with 3 or 5 imaging time points. ***Materials and Methods:*** We used an analytical projector of a medium energy general purpose collimator to generate 128 realistic noisy SPECT projections, modeling attenuation, scatter, and geometric collimator-detector-

response (GCDR), based on a population of 9 4D XCAT phantoms varying in anatomies and In-111 Zevalin activity distributions. The noisy projections were reconstructed using the OS-EM algorithm (8 iterations and 16 subsets) with attenuation, effective source scatter estimation and GCDR compensation. The time-activity curves for each voxel were fitted individually with mono-, bi- and tri-exponential functions (vox_adj) using the nonlinear least squares method based on sequential quantitative SPECT images, i.e., 3 time points of 1, 24 and 144 hrs, or 5 time points of 1, 12, 24, 72 and 144 hrs post injection, assuming physical decay after the last time point. The area under curves were then obtained to get the TA for kidneys, spleen and liver. Fitting parameters were also determined for the individual organ and fixed for voxels of the same organ (vox_fixed). Sum of squares for error (SSE) was calculated for all fitting methods while TA differences were compared using ANOVA test with Bonferonni correction by SPSS. ***Results:*** SSE_{vox_adj} is much smaller than SSE_{vox_fixed}, i.e., the average %difference is up to ~-300% for 3 time points and -145% for 5 time points. The median SSE of bi-exponential function is smallest generally. The TA obtained from mono-exponential fitting is generally larger than other fitting methods. Using bi-exponential method as reference, the % of TA absolute difference is <4% for all organs of interest when using mono- or tri-exponential method. There is no statistically significant difference between TA obtained from 3- and 5-time-point regardless of the fitting methods, and there is also no statistically significant difference among TA obtained from different fitting methods regardless of number of imaging time points. ***Conclusion:*** There is no substantial difference in terms of TA for different curve-fitting methods and imaging time points for In-111 Zevalin SPECT-based dosimetry yet bi-exponential voxel-based fitting provides the lowest SSE. Considering clinical resource and computational time, bi-exponential fitting using 3-time point data is recommended for this application. ***References:*** None

404b

Mini Course 2: Advanced Practice in Hybrid Nuclear Medicine

Friday, October 23, 2020, 10:00 - 10:50 Channel 4

OP-207

Clinical Applications of PET/CT

L. Lezaic; University Medical Center, Ljubljana, SLOVENIA.

OP-208

Hybrid Imaging in Nuclear Cardiology

W. Noordzij; University Medical Centre Groningen, Groningen, NETHERLANDS.

501

CME 4: Multimodality Imaging-Based Problem Solving for Multiple Bone Lesions

Friday, October 23, 2020, 10:40 - 12:10 Channel 1

OP-209

Multiple Osteolytic/Osteoclastic Lesions in the Axial Skeleton - Multimodality Imaging-Based Problem Solving

A. Bazzocchi; Diagnostic and Interventional Radiology, IRCCS Istituto Ortopedico Rizzoli, Bologna, ITALY .

OP-210

Multiple Osteolytic/Osteoclastic Lesions in the Peripheral Skeleton - Multimodality Imaging-Based Problem Solving

S. Carrilho Vaz; Nuclear Medicine-Radiopharmacology, Champalimaud Centre for the Unknown, Lisbon, PORTUGAL.

OP-211

Multiple Osteosclerotic/Osteoblastic Lesions in the Axial Skeleton - Multimodality Imaging-Based Problem Solving

F. Paycha; Department of Nuclear Medicine, Lariboisière Hospital, Assistance Publique-Hôpitaux de Paris, Paris, FRANCE.

OP-212

Multiple Osteosclerotic/Osteoblastic Lesions in the Peripheral Skeleton - Multimodality Imaging-Based Problem Solving

B. Jonca; Department of Nuclear Medicine, Bichat Hospital, Assistance Publique-Hôpitaux de Paris, Paris, FRANCE.

502

Joint Symposium 7 (EANM/EAN/ECTRIMS): Multiple Sclerosis - Update in Neuroimaging

Friday, October 23, 2020, 10:40 - 12:10 Channel 2

OP-213

MRI - What is Conventional and What is New?

M. Assunta Rocca; San Raffaele Hospital/ Università Vita-Salute San Raffaele, Division of Neuroscience, Milan, ITALY.

OP-214

Imaging Neuroinflammation with PET - Added Value of Studying the White Matter Involvement

L. Airas; University of Turku, Turku, FINLAND.

OP-215

Amyloid PET - A Potential Biomarker of De- and Re-Myelinization in MS

B. Stankoff; Saint-Antoine Hospital / Pierre and Marie Curie University, Department, Paris, FRANCE.

503

Joint Symposium 8 (EANM/SRS): The Revival of Radiometals

Friday, October 23, 2020, 10:40 - 12:10 Channel 3

OP-216

Production of New Radiometals

U. Köster; Institut Laue-Langevin (ILL),Grenoble,FRANCEInstitut Laue-Langevin (ILL), Grenoble, FRANCE.

OP-217

Chelators for New Radiometals

F. Rösch; Johannes Gutenberg-University Mainz, Institute of Nuclear Chemistry, Mainz, GERMANY.

OP-218

Strenghts and Limitations of New Radiometals

C. Cutler; Brookhaven National Laboratory, NY, New York, UNITED STATES OF AMERICA.

505

M2M Track - TROP Session: It Takes Place in the Brain - New Neuro Tracers

Friday, October 23, 2020, 10:40 - 12:10 Channel 5

OP-219

Changes in D_2R and SERT Availability in the Rat Brain After Depressive-like Behavior Recovery in the Repeated Social Defeat Model

R. Moraga-Amaro[1], D. A. Vazquez-Matias[1], L. Reali Nazario[1], J. Stehberg[2], R. A. J. O. Dierckx[1], J. Doorduin[1], E. F. J. de Vries[1]; [1]Department of Nuclear Medicine and Molecular Imaging, University of Groningen, University Medical Center Groningen, Groningen, NETHERLANDS, [2]Laboratorio de Neurobiología, Instituto de Ciencias Biomédicas, Facultad de Medicina y Facultad de Ciencias de la vida, Universidad Andres Bello, Santiago, CHILE.

Aim/Introduction: Dopaminergic and serotonergic neurotransmission are believed to play an important role development and progression of major depressive disorder (MDD). Studying neurotransmission changes in a longitudinal manner in animal models of depression, promise to be useful for further understanding of disease mechanisms, potentially leading to improved therapy. In this regard, Positron emission tomography (PET) scanning is a valuable resource for studying longitudinal changes in the brain in a non-invasive way. To determine the dopaminergic and serotonergic neurotransmission changes in animals submitted to the repeated social defeat (RSD) model of depression, by measuring changes in dopamine receptor 2 (D2R) and serotonin transporter (SERT) availability in the brain after depressive-like behavior recovery, using PET. *Materials and Methods:* Experimental male Wistar rats (RSD group) were exposed to social defeat by larger male Long-Evans rats during 5 consecutive days. Changes in depressive-like behavior were assessed with the sucrose preference test (SPT) before RSD (baseline), 1 day and 14 days after RSD. Bodyweight changes were used as an additional parameter to validate the RSD model. Changes in brain availability of D2R and SERT was measured by PET in the same animal after RSD using [^{11}C]-Raclopride (day1 and 14) and [^{11}C]-DASB (day2 and 15) 60-min dynamic scans respectively. The non-displaceable binding potential (BP_{ND}) was calculated regionally with a SRTM (cerebellum as reference) for both tracers. General estimated equations (GEE) models were used to analyze all parameters in a longitudinal way, using as control group animals not exposed to RSD. *Results:* RSD induced a reduction in body weight gain on day1 after RSD ($p<0.0001$), which was recovered at day14. Additionally, animals submitted to RSD showed a decrease in sucrose preference on day1 ($p<0.0001$) which did not last until day14, indicating that animals recovered from depressive-like behavior. PET imaging showed an increase in [^{11}C] Raclopride BP_{ND} in the caudate putamen ($p<0.05$), and in [^{11}C]DASB BP_{ND} in the whole brain ($p<0.01$), insular cortex ($p<0.01$), thalamus ($p<0.05$), brainstem ($p<0.05$), midbrain ($p<0.05$), but only after recovery of symptoms (day14 and day15 respectively). *Conclusion:* Our results showed changes in dopaminergic and serotonergic neurotransmission when animals recovered from the depressive-like behavior (day14), but not after its development (day1). These results support the idea that time-points in disease progression are important for the treatment of the disease. Further studies are needed to determine if these changes are due to changes in SERT or D2R availability, or changes of neurotransmitter concentrations in the brain. *References:* None

OP-220

In vivo comparison of the sensitivity of PET radioligands to detect moderate changes in P-gp function at the blood-brain barrier

L. Breuil, F. Caillé, S. Marie, S. Goutal, S. Auvity, M. Goislard, C. Coulon, T. Lekieffre, W. Saba, N. Tournier; Laboratoire d'Imagerie Biomédicale Multimodale (BIOMAPS), Université Paris-Saclay, CEA, CNRS UMR9011, Inserm UMR1281, Service Hospitalier Frédéric Joliot, Orsay, FRANCE.

Aim/Introduction: The P-glycoprotein (P-gp) is a major efflux transporter expressed at the blood-brain barrier (BBB) which plays a key role in brain protection and homeostasis. In patients, complete repression or inhibition of P-gp function is not likely to occur. However, partial inhibition/deficit is suspected in pathophysiological situations and

drug-drug interactions. PET imaging using radiolabeled substrates of the P-gp is the most advanced technique to study this transporter at the human BBB. However, the sensitivity of current radiolabeled P-gp substrates to detect moderate changes in P-gp function remains to be compared. We conducted an in vivo study to compare the sensitivity of the clinically validated P-gp substrates ^{11}C-metoclopramide, ^{11}C-verapamil and ^{11}C-N-desmethyl-loperamide (^{11}C-NdLop) to partial inhibition of P-gp function by tariquidar (TQD). ***Materials and Methods:*** First, the effect of increasing doses of TQD (injected i.v. 15 minutes before PET imaging) on the brain kinetics of ^{11}C-metoclopramide were studied using microPET imaging in rats. Brain exposure was estimated by the area under the time-activity curve of brain kinetics from 10 to 30 min ($AUC_{10\text{-}30min}$). The doses that inhibited 50% and 100% of the P-gp mediated transport of ^{11}C-metoclopramide ($ID_{50\%/Meto}$ and $ID_{100\%/Meto}$, respectively) were graphically estimated with brain $AUC_{10\text{-}30min}$ as a function of injected dose of TQD (0, 1, 1.4, 2, 3, 4 and 8 mg/kg). Then, PET experiments were performed using ^{11}C-metoclopramide, ^{11}C-verapamil and ^{11}C-NdLop at baseline (0% inhibition) and after injection of TQD at either $ID_{50\%/Meto}$ or $ID_{100\%/Meto}$ (n=2-7 per condition). Mean $AUC_{10\text{-}30min}$ obtained in each condition for each radiotracer were compared using an ANOVA and Tukey's post-hoc analysis. ***Results:*** $ID_{50\%/Meto}$ was estimated at 1±0,15 mg/kg TQD dose. The 1 mg/kg dose of TQD increased the brain exposure to ^{11}C-metoclopramide and ^{11}C-verapamil by 2.0 and 2.5-fold respectively but did not increase the brain uptake of ^{11}C-NdLop. The $ID_{100\%/Meto}$ of TQD was estimated at 8 mg/kg. This dose significantly increased the brain exposure to ^{11}C-metoclopramide (+3.0 and 1.5-fold), ^{11}C-verapamil (+8.8 and 2.4-fold) and ^{11}C-NdLop (+6.8 and 4.4-fold) compared with baseline and $ID_{50\%/Meto}$, respectively. ***Conclusion:*** P-gp substrates probes show significantly different sensitivity to inhibition. Especially, ^{11}C-NdLop may lack sensitivity to detect partial (50%) decrease in P-gp function at the BBB, which may be detected using either ^{11}C-metoclopramide or ^{11}C-verapamil, that both show similar sensitivity to TQD inhibition. Sensitivity should be considered when selecting radiolabeled substrate for PET imaging to explore situations where moderate decline in P-gp function at the BBB is expected. ***References:*** None

OP-221

Evaluation of a Novel P-glycoprotein Inducer Using [^{18}F] MC225 and PET

L. Garcia Varela[1], *D. Vállez García*[1], *M. Perez Rodriguez*[2], *R. Moraga-Amaro*[1], *N. A. Colabufo*[3], *P. Aguiar*[4], *T. Sobrino*[2], *R. A. J. O. Dierckx*[1], *A. van Waarde*[1], *P. H. Elsinga*[1], *G. Luurtsema*[1];
[1]*University of Groningen, University Medical Center of Groningen, Department of Nuclear Medicine and Molecular Imaging, Groningen, NETHERLANDS,* [2]*IDIS Health Research Institute, Clinical Neurosciences Research Laboratory, Santiago de Compostela, SPAIN,* [3]*University of Bari Aldo Moro, Department of Pharmacy, Bari, ITALY,* [4]*Clinical University Hospital, IDIS Health Research Institute, Department of Nuclear Medicine and Molecular Imaging, Santiago de Compostela, SPAIN.*

Aim/Introduction: P-glycoprotein (P-gp) is an efflux pump located at the blood-brain barrier (BBB). Its main function is the protection of the central nervous system via the efflux of neurotoxic compounds from the brain (1). A decline in P-gp function has been related to the pathogenesis of neurodegenerative diseases, like Alzheimer's and Parkinson's disease (2). Drugs called P-gp inducers have the potential to restore the P-gp function and are considered as possible candidates for the treatment of neurodegenerative diseases. MC111, (4'-((4-cyclohexylpiperazin-1-yl)methyl)-[1,1'-biphenyl-4-ol)), was selected as a promising P-gp inducer due to its ability to increase P-gp expression and function in colo-320 cells (3). Our study aims to evaluate the P-gp inducing effect of MC111 in vivo using the P-gp tracer [^{18}F]MC225 (4) and Positron Emission Tomography (PET). ***Materials and Methods:*** Eighteen healthy male Wistar rats were treated with either vehicle solution, 4.5mg/kg of MC111 (low-dose group) or 6mg/kg of MC111 (high-dose group) (n=6 per group). Animals underwent a 60-minutes dynamic-PET scan with arterial-blood sampling, 24 hours after the treatment with the inducer. Data were analysed using a 1-Tissue-Compartment-Model fit, fixing the volume of blood to 5% and using metabolite-corrected plasma as input function. K_1 and V_T were used to measure the P-gp function (4). ***Results:*** The administration of MC111 decreased K_1 and V_T of [^{18}F]MC225 in the whole-brain and all the selected brain regions. In the high-dose group, whole-brain K_1 decreased by 34% (K_1-high-dose=0.2±0.02 vs K_1-control=0.3±0.02; p≤0.001) and in the low-dose group by 7% (K_1-low-dose=0.28±0.02 vs K_1-control=0.3±0.02; p=0.411) compared to controls. Whole-brain V_T decreased by 25% in the high-dose group (V_T-high-dose=5.8±0.37 vs V_T-control=7.8±0.37; p≤0.001) and by 6% in the low-dose group (V_T-low-dose=7.35±0.37 vs V_T-control=7.8±0.37; p=0.371) compared to controls. k_2 values did not vary after treatment. Moreover, the treatment did not affect the metabolism of [^{18}F]MC225. ***Conclusion:*** The decrease in K_1 and V_T values after treatment with the inducer indicates an increase in the P-gp functionality at the BBB of treated rats. Therefore, the results verify that MC111 has an induction effect in vivo. These data also confirm the ability of [^{18}F] MC225 to measure increases in the P-gp function at the BBB in rats. ***References:*** 1. Mahringer A, Fricker G. Expert Opin Drug Metab Toxicol. 2016;12:499-508. 2. Löscher W, Potschka H. Prog Neurobiol. 2005;76:22-76. 3. Colabufo NA, Contino M, et al. RSC Adv. 2018;8:5451-8. 4. Savolainen H, Windhorst AD, et al. J Cereb Blood Flow Metab. 2017;37:1286-98.

OP-222

Binding of the experimental dual-action antiparkinsonian drug AG-0029 to dopamine D2 and histamine H3 receptors: a PET study in healthy rats

A. Van Waarde[1], N. Ghazanfari[1], J. W. A. Sijbesma[1], D. Vállez García[1], M. Kominia[2], M. Koelewijn[2], K. Attia[1], T. J. Visser[2], A. Heeres[2], A. T. M. Willemsen[1], R. A. J. O. Dierckx[1], P. H. Elsinga[1]; [1]University Medical Center Groningen, Groningen, NETHERLANDS, [2]Syncom, Groningen, NETHERLANDS.

Aim/Introduction: Drugs interacting with multiple targets are under study for the treatment of disorders of the central nervous system. AG-0029[1] combines very potent agonist affinity (0.08 nM) to the dopamine D_2 receptor with moderate antagonist affinity (111 nM) to the histamine H_3 receptor. These receptor interactions of AG-0029 were proven by measurement of extracellular dopamine levels in rat striatum and histamine levels in rat prefrontal cortex by microdialysis. AG-0029 showed anti-Parkinson action (contralateral rotation), and a cognition-enhancing effect in the novel object recognition test of 6-OHDA-lesioned rats. This drug may improve both the motor and cognitive symptoms of Parkinson disease. The present study aims to quantify the target engagement of AG-0029. ***Materials and Methods:*** Healthy male Wistar rats were scanned in a small animal PET camera (μPET Focus 220), using the dopamine D2/D3 receptor ligand [^{11}C]raclopride or the histamine H3 receptor ligand [^{11}C]GSK189254, before and after treatment with an intravenous, acute, single dose of AG-0029 (0.1 or 1 mg/kg for [^{11}C]raclopride, 1 mg/kg for [^{11}C]GSK189254). Dynamic [^{11}C]raclopride scans (60 min duration) were made without arterial blood sampling, and were analysed using the simplified reference tissue model with cerebellum as reference tissue. Dynamic [^{11}C]GSK189254 scans (90 min duration) were made with arterial blood sampling. ***Results:*** Binding potential values of [^{11}C]raclopride in the striatum were dose-dependently reduced after administration of AG-0029 (10 min before tracer injection), from 1.45±0.10 (n=9) to 1.04±0.17 (after a 0.1 mg/kg dose, n=4) and to 0.33±0.18 (after a 1 mg/kg dose, n=5), corresponding to D_2/D_3 receptor occupancy values of 27±12 and 78±4%. These data (0, 0.1, 1 mg/kg dose) are well-fitted by a one-site model for receptor binding (r^2>0.99), half-maximal receptor occupancy being reached at a dose of 0.27 mg/kg and maximal occupancy being 99.3%. Data acquisition and analysis for the [^{11}C]GSK189254 scans is still in progress. Frontal/occipital cortex ratios of radioactivity were reduced from 3.04±0.74 (n=4) at baseline to 2.58±0.13 (n=3) after administration of 1 mg/kg AG-0029, which may correspond to a H_3 receptor occupancy of 23%. However, due to high variability of [^{11}C]GSK189254 binding at baseline, the decline of binding potential at this dose was not statistically significant. ***Conclusion:*** Dopamine D_2/D_3 receptor occupancy by the agonist AG-0029 could be reliably measured with [^{11}C]raclopride and small animal PET. Histamine H_3 receptor occupancy by AG-0029 may be detectable in PET scans with [^{11}C]GSK189254, but may require a higher dose than 1 mg/kg. ***References:*** [1] 7-(4-(3-(4-(morpholinomethyl)phenoxy)propyl)piperazin-1-yl)benzo[d]oxazol-2(3H)-one.

OP-223

Impact of A_{2A}R agonist and antagonist on binding of the dopamine D_2receptor ligand [^{11}C]raclopride in the rodent striatum

K. Prasad, E. F. J. de Vries, J. W. A. Sijbesma, K. A. Attia, C. Kwizera, L. Garcia-Varela, D. A. Vazquez-Matias, R. Moraga-Amaro, D. Vallez-Garcia, A. T. Willemsen, R. A. J. O. Dierckx, A. van Waarde; University Medical Center Groningen (UMCG), Groningen, NETHERLANDS.

Aim/Introduction: Adenosine A_{2A} and dopamine D_2 receptors in the basal ganglia form heterotetrameric structures that are involved in the regulation of motor activity and neuropsychiatric functions. Although allosteric interactions between the receptors were established in-vitro and in-vivo in immunoprecipitation studies, further studies are required to demonstrate their functions. The present study examines the A_{2A} receptor-mediated modulation of D_2 receptor binding in vivo using PET with the D_2 antagonist tracer [^{11}C]raclopride. ***Materials and Methods:*** Healthy male Wistar rats (n=8) were scanned (60-min dynamic) with [^{11}C]raclopride at baseline and following the administration of A_{2A} agonist CGS21680 (1mg/kg), using a μPET Focus-220 camera. Binding potential (BP) values were calculated, using a simplified reference tissue model (SRTM) and cerebellum as the reference tissue. Other rats underwent dynamic [^{11}C]raclopride scans with arterial-blood sampling after pretreatment with vehicle(n=4), a single dose of CGS21680 (1mg/kg, n=5) or A_{2A} antagonist KW6002 (1mg/kg, n=4). BP values were calculated using a reversible two tissue compartment model (2TCM) and a metabolite-corrected plasma input function. Time-activity curves were extracted by projecting voxels of interest onto a dynamic scan. ***Results:*** Striatal and cerebellar areas-under-the-curve (AUC) were significantly higher after CGS21680 administration ($p<0.05$, Cohen's d=2.4) compared to baseline. SRTM analysis did not find significant changes in BP (p=0.102, Cohen's d=0.6), but relative tracer delivery (R_1) with respect to the reference was significantly increased after treatment (p=0.049, Cohen's d=0.84) compared to the baseline. Since tracer kinetics in the reference region were altered by the treatment, we performed arterial-blood sampling to obtain BP in a second group of animals. Tracer concentration in whole-blood or plasma was not significantly changed by the pretreatments (Cohen's d=0.07-0.27). The striatal AUC was significantly higher in CGS21680 compared to control and KW6002 rats (p=0.02, Cohen's d=2.4). BP decreased significantly from 2.43±0.52 in vehicle to 1.15±0.2 after administration

of CGS21680 and non-significantly to 1.69±0.41 after administration of KW6002. The efflux constant (k_2) was significantly reduced in CGS21680-treated animals (p=0.01, Cohen's d=2.79) compared to control and KW6002 groups. ***Conclusion:*** A_{2A} receptor stimulation causes changes in the binding characteristics of dopamine D_2 receptors. Since [^{11}C]raclopride uptake in the reference region is affected by agonist treatment, BP values obtained from SRTM are not reliable, but changes in BP can be reliably measured using a 2TCM with arterial input. Altered D_2 receptor affinity as a consequence of allosteric interactions in A_{2A}-D_2 receptor heterotetramers can be detected with PET. ***References:*** None

OP-224

Development and Identification of [^{18}F]SNFT-1 (THK-5562), a Promising Candidate for Selective Tau PET Tracer in Alzheimer's disease

P. Lerdsirisuk[1,2], R. Harada[3,4], Y. Shimizu[2,5], Y. Du[3], Y. Ishikawa[2], R. Iwata[2], K. Yanai[3], Y. Kudo[4], N. Okamura[2,6], S. Furumoto[2];
[1]Radiopharmaceutical chemistry, Graduate School of Pharmaceutical Science, Tohoku University, Sendai, JAPAN, [2]Cyclotron and Radioisotope Center (CYRIC), Tohoku University, Sendai, JAPAN, [3]Department of Pharmacology, Graduate School of Medicine, Tohoku University, Sendai, JAPAN, [4]Department of Gerontology and Geriatrics, Division of Brain Science, Institute of Development Aging and Cancer (IDAC), Tohoku University, Sendai, JAPAN, [5]Department of Pharmacy, Faculty of Pharmaceutical Science, Tohoku University, Sendai, JAPAN, [6]Division of Pharmacology, Faculty of Medicine, Tohoku Medical and Pharmaceutical University, Sendai, JAPAN.

Aim/Introduction: Base on the clinical studied, [^{18}F]THK-5351, originally developed as a PET imaging tracer for detection the accumulated tau proteins in Alzheimer's disease (AD), have been revealed to show an off-target binding to monoamine oxidase B (MAO-B) with high affinity. This limitation led us aim to optimise the structure for higher selective binding to aggregated tau proteins and for the optimal pharmacokinetic profile. In this study, we designed and synthesised new heteroaromatic compounds for tau imaging and then investigated in vitro and in vivo profiles of them. ***Materials and Methods:*** The newly designed derivatives were synthesised and evaluated the binding affinity for tau and MAO-B by in vitro competitive binding assay using [^{3}H]MK-6240 and [^{3}H]THK-5351. The new tracers were prepared from the corresponding precursors and an activated fluorine-18 (^{18}F)/K222 by microscale one-pot radiosynthesis method developed in-house. Then the binding properties of the ^{18}F-derivatives were characterised by in vitro autoradiography of frozen human AD brain sections and by competitive binding assay using AD brain homogenate rich in neurofibrillary tangles (NFTs) and recombinant MAO-A and MAO-B. Pharmacokinetics and metabolism were assessed in normal mice after intravenous injection of the ^{18}F-derivatives as well. ***Results:*** Through the analysis of the structure-activity (binding) relationship among the new derivatives, we found a novel core structure suitable for detection of tau-rich proteins in human AD. The derivatives with the core structure showed higher binding affinity for NFTs as sub-nanomolar range and less binding affinity for MAO-B in comparison to the 2-arylquinoline derivatives such as THK-5351. The microscale one-pot radiosynthsis of the derivatives were successfully synthesised in moderate to good radiochemical yields and the preclinical biological properties were also acceptable. Among the derivatives, [^{18}F]SNFT-1 (THK-5562) was found as the potent candidate for a tau selective PET tracer (IC_{50}: 0.8 nM for tau; >1000 nM for beta-amyloid, MAO-A and MAO-B). In vitro autoradiogram of the AD brain sections with [^{18}F]SNFT-1 displayed no off-target binding to MAO-A and MAO-B and an intense laminar binding to neocortex. The distribution of radioactivity was well consistent with the immunohistochemical distribution of tau. Additionally, [^{18}F]SNFT-1 showed high initial brain uptake and rapid clearance suitable for brain PET imaging. Preferably, the radiolabelled metabolites of [^{18}F]SNFT-1 did not penetrate the blood-brain barrier in mice. ***Conclusion:*** These results suggested that the novel ^{18}F-labelled tracer [^{18}F]SNFT-1 is a promising candidate for visualising the accumulated tau proteins in the AD brain with less of off-target binding. ***References:*** None

OP-225

[^{18}F]FEPPA PET/CT Imaging to Assess STAT Inhibitor Effect in LPS-induced Neuroinflammation Mouse Models

C. San[1,2], P. Millot[1,3], M. Brault[2], F. Hontonnou[2], L. Sarda-Mantel[2,4], N. Vignal[1,2,4], F. Mouton-Liger[1,3], B. Hosten[1,2];
[1]INSERM UMR-S 1144, Université de Paris, Paris, FRANCE, [2]Unité Claude Kellershohn, Institut de Recherche Saint-Louis, Hôpital Saint-Louis, APHP, Paris, FRANCE, [3]Centre de Neurologie Cognitive/CMRR Paris Nord Ile de France, Hôpital Lariboisière, APHP, Paris, FRANCE, [4]Service de Médecine Nucléaire, Hôpital Lariboisière, APHP, Paris, FRANCE.

Aim/Introduction: Signal transducer and activator of transcription 3 (STAT3) is a transcription factor involved in the regulation of several cellular activities. STAT3 abnormal activation promotes tumour growth and proliferation and plays a key role in mediating inflammatory signals. Thus, STAT3 inhibitors have become of major interest for treatment of cancers but also chronic inflammatory diseases such as neurodegenerative diseases. Our previous work has shown that our lipopolysaccharides (LPS)-induced neuroinflammation models present a translocator protein (TSPO) overexpression and STAT3 excessive activation. Besides, these models have also been studied by PET imaging with a TSPO ligand, [^{18}F]FEPPA. The aim of the study was to investigate the anti-inflammatory response

of a STAT3 inhibitor (Stattic) with [18F]FEPPA PET imaging in these models. ***Materials and Methods:*** Eight-week-old C57Bl/6 male mice (n=5/group) were used for this study. Two groups of neuroinflammation model induced by i.p injection of LPS (acute: 5mg/kg for 1 day and chronic: 1mg/kg for 3 days) and a saline control group were explored. Each mouse also received an i.p injection of either 20mg/kg Stattic or a vehicle composed of 2% DMSO and 30% PEG300. 24 hours after the treatment, mice received 10MBq of [18F]FEPPA and underwent a 1-hour dynamic PET followed by a CT scan. Image analysis and pharmacokinetic modelling using 2TCM-1K model were performed with Pmod v3.9: cerebral time activity curves (TAC) were obtained after ROI automatic drawing based on an atlas. To confirm LPS effect on STAT3 phosphorylation and STAT3 effect on microglial activation, immunoblot of phospho-STAT3/STAT3 and Iba1 immunofluorescence coupled with morphometric analysis of microglia were respectively performed on mouse hippocampus (n=7-9/group). ***Results:*** [18F]FEPPA cerebral uptake and phospho-STAT3/STAT3 ratio are significatively higher in chronic LPS group compared to control. However, no significant change in [18F]FEPPA cerebral uptake in the Stattic groups is observed compared to the vehicle groups. Interestingly, an increase of K1 (but not significant) is observed in the Stattic groups which might be explained by an increase of [18F]FEPPA plasmatic unbound fraction in these groups. STAT3 inhibition reduces significantly phospho-STAT3/STAT3 ratio and microglial activation as a decrease of microglial body size and an increase of branching processes size are observed in Stattic groups. ***Conclusion:*** Although biochemical analysis revealed a decrease of microglial activation by Stattic, this study suggests that TSPO PET imaging is not sensitive enough to investigate Stattic anti-inflammatory effect. Besides, further studies should be pursued to evaluate Stattic effect on [18F]FEPPA plasmatic unbound fraction. ***References:*** None

OP-226

Brain distribution and retention of ^{89}Zr and ^{111}In labeled bispecific antibody in an amyloid beta mouse model

T. Gustavsson[1], T. Tran[2], S. Syvänen[1], D. Sehlin[1];
[1]Department of Public Health and Caring Sciences, Uppsala University, Uppsala, SWEDEN, [2]Department of Radiopharmacy, Karolinska University Hospital, Stockholm, SWEDEN.

Aim/Introduction: Brain uptake of antibodies is restricted by the blood-brain barrier (BBB) at the vasculature of the brain. We have created a bispecific antibody, RmAb158-scFv8D3, which binds to the mouse transferrin receptor (8D3 moeity) and is transpored over the BBB via trancytosis. We have previously used it as a PET ligand to target amyloid-beta (Aβ) in the brain [1]. The aim of this study was to evaluate brain uptake and retention, blood pharmacokinetics, and biodistribution of RmAb158-scFv8D3 labeled with ^{89}Zr and ^{111}In in a mouse model of Aβ pathology (tg-ArcSwe). ***Materials and Methods:*** RmAb158-scFv8D3 conjugated with DFO* or CHX-A"-DTPA was labeled with ^{89}Zr or ^{111}In, respectively. Binding of RmAb158-scFv8D3 following labeling was evaluated with ELISA. Radiolabeled products were incubated in plasma and stability was assessed with instant thin-layer chromatography. Labeled RmAb158-scFv8D3 was i.v. injected in 18 months old tg-ArcSwe and wild type mice (WT) and blood pharmacokinetics were evaluated from 4 h to 72 h after injection. Mice receiving [^{111}In]-RmAb158-scFv8D3 were SPECT scanned after 3 days. Ex vivo brain uptake of [^{89}Zr]RmAb158-scFv8D3 and [^{111}In]RmAb158-scFv8D3 was quantified at 2 h and 72 h after injection in tg-ArcSwe and WT mice. Biodistribution and ex vivo brain autoradiography were performed after 72 h. ***Results:*** Specific activity for ^{89}Zr and ^{111}In labeled RmAb158-scFv8D3 was 74 MBq/ng and 280 MBq/ng, respectively. Post-labeling ELISA demonstrated that labeled RmAb158-scFv8D3 retained binding to transferrin receptor and Aβ protofibrils, and was stable in plasma for 24 h. Half-life in blood for [^{89}Zr]RmAb158-scFv8D3 and [^{111}In]RmAb158-scFv8D3 were 19 h and 9 h, respectively. SPECT scanning demonstrated no difference between tg-ArcSwe and WT mice 3 days after injection of [^{111}In]RmAb158-scFv8D3, which displayed ex vivo brain concentrations (%ID/g(brain)) of 1.31±0.13 at 2 h post injection and 0.7 after 72 h. Brain uptake of [^{89}Zr]RmAb158-scFv8D3 was 1.12±0.67 at 2 h after injection, and 0.42±0.04 and 0.24±0.07 in tg-ArcSwe and WT mice, respectively, after 72 h. Ex vivo brain autoradiography showed a high and specific [^{89}Zr]RmAb158-scFv8D3 signal in brain regions with abundant Aβ pathology. Both ^{89}Zr and ^{111}In were highly retained in liver, spleen, and bone. ***Conclusion:*** This study demonstrates that bispecific brain penetrating antibodies labeled with radiometals are retained in the brain 2 h after injection. Still, the in vivo stability of radiometal labeled antibodies during transcytosis and prolonged retention in brain parenchyma needs further investigation. ***References:*** [1] Theranostics. 2017 Jan 1;7(2):308-318

OP-227

TSPO expression in vivo is moderated by sex in response to amyloidosis but not to tau pathology in mouse models of neurodegenerative diseases

G. Biechele[1], N. Franzmeier[1], M. Ewers[1], T. Blume[2], F. Eckenweber[1], C. Sacher[1], J. Luque[2], L. Beyer[1], F. Ruch-Rubinstein[1], S. Lindner[1], F. Gildehaus[1], B. von Ungern-Sternberg[1], P. Bartenstein[1], A. Rominger[3], G. Höglinger[4], J. Herms[1], M. Brendel[1];
[1]University Hospital of Munich, Munich, GERMANY, [2]DZNE Munich, Munich, GERMANY, [3]Inselspital Bern, Bern, SWITZERLAND, [4]Hannover Medical School, Hannover, GERMANY.

Aim/Introduction: In vivo assessment of neuroinflammation by 18 kDa translocator protein positron-emission-

tomography (TSPO-PET) ligands receives growing interest in preclinical and clinical research of neurodegenerative disorders. Higher TSPO expression in females has been reported for cognitively normal humans, but such effects have not yet been evaluated in rodent models of neurodegeneration and their controls. Thus, we aimed to investigate the impact of sex on TSPO expression in amyloid and tau mouse models and wild-type controls. ***Materials and Methods:*** Longitudinal ^{18}F-GE-180 TSPO-PET (^{18}F-GE180) data of C57Bl/6 (wild-type), App^{NL-G-F} (β-amyloid model), and P301S (tau model) mice were evaluated between two and twelve months of age. App^{NL-G-F} received additional longitudinal β-amyloid-PET imaging (Aβ-PET; ^{18}F-florbetaben). Immunohistochemistry served for validation of PET data by microglial (Iba1, CD68) and tau (AT8) markers. PET and immunohistochemistry were quantified in cortical regions and compared by linear mixed models (PET) and analysis of variance (immunohistochemistry) between sexes. ***Results:*** TSPO-PET values in wild-type mice indicated an increase with time (female: +23%, male +4%) and a significant time x sex interaction was found (T=-4.171, p<0.001). The Aβ model App^{NL-G-F} revealed a distinct cortical increase of TSPO-PET values from 2.5 to 10 months in female mice (+31%), whereas male App^{NL-G-F} mice only showed minor increases (+6%). The linear mixed model indicated a significant sex x time interaction (T=-2.953, p=0.0048), validated by Iba1 and CD68 immunohistochemistry. Aβ-PET quantification in the same App^{NL-G-F} mice indicated no significant time x sex interaction (T=0.425, p=0.673). The P301S tau model showed strong cortical increases of TSPO-PET from 2 to 8.5 months of age (female: +32%, male: +36%) but no significant sex x time interaction (T=-0.671, p=0.504) and no sex differences in Iba1, CD68 or AT8 were observed. ***Conclusion:*** Female mice indicate a sex dependent elevation of TSPO expression in response to amyloidosis but not to tau pathology. Sex requires attention when TSPO-PET is used as biomarker of glial activation in mouse models of neurodegeneration and requires detailed studies in human disease. ***References:*** None

OP-228

Identification and in vitrocharacterization of C05-01, a PPB3 derivative with improved affinity for α-synuclein

P. Miranda Azpiazu[1], *M. Svedberg*[1], *M. Higuchi*[2], *M. Ono*[2], *Z. Jia*[3], *D. Sunnemark*[4,5], *C. Elmore*[6], *M. Schou*[1,7], *A. Varrone*[1];
[1]Centre for Psychiatry Research, Department of Clinical Neuroscience, Karolinska Institutet, & Stockholm Health Care Services, Region Stockholm, Stockholm, SWEDEN, [2]Department of Functional Brain Imaging Research, National Institute of Radiological Sciences, National Institutes for Quantum and Radiological Science and Technology, Chiba, JAPAN, [3]Karolinska Institutet, Solna, SWEDEN, [4]Applied Immunology, Department of Clinical Neuroscience, Karolinska Institutet, Stockholm, SWEDEN, [5]Offspring Biosciences, Offspring Biosciences, Sweden AB, SWEDEN, [6]Early Chemical Development, Pharmaceutical Sciences, R&D, AstraZeneca, Gothenburg, SWEDEN, [7]PET Science Centre, Precision Medicine, Oncology R&D, AstraZeneca, Stockholm, SWEDEN.

Aim/Introduction: Accumulation of α-synuclein is a neuropathological hallmark of Parkinson´s disease, multiple system atrophy, and dementia with Lewy bodies. There is an unmet need for the development of an imaging biomarker for α-syn. Initial studies suggested that the tau tracer [^{11}C]PBB3 displays some degree of binding to α-syn [1,2]. Based on these findings, a library of compounds structurally related to PBB3 was developed. The aim of the present study was to identify the compound(s) displaying the strongest fluorescence signal to Lewy aggregates and to characterize the binding properties of the best candidate (C05-01) using in vitro binding techniques. ***Materials and Methods:*** A series of 44 compounds derived from the PBB3 scaffold were examined with fluorescence imaging using a qualitative assessment of the strength of the signal to α-synuclein, amyloid-β and tau aggregates. Five compounds were selected and the fluorescence signal was assessed semiquantitatively using tissue microarrays (TMAs) derived from brain samples with different proteinopathies. In vitro binding studies using α-synuclein fibrils and human brain homogenates were performed to measure the affinity for α-synuclein. Autoradiography studies using fresh frozen tissue and TMAs were performed to assess the binding in brain tissue. ***Results:*** C05-01 was the compound selected from the initial screening and semiquantitative assay. In vitro binding assays using human brain homogenates and recombinant fibrils indicated that C05-01 had higher affinity for α-synuclein (K_D/K_i ≈ 25 nM for fibrils, Ki ≈ 3.5 nM for brain homogenates) as compared with PBB3 (K_D ≈ 60 nM). In autoradiography studies using fresh frozen human tissue and TMAs, [^{3}H]C05-01 displayed specific binding in cases with α-synuclein pathology. C05-01 showed specific binding also in AD tissue with amyloid-β and tau pathology, as well as relatively high non-specific and off-target binding. None of the possible off binding target studied, such as MAO-A, MAO-B, amyloid-β, Tau, Sigma 1 receptors seemed to be responsible for this off-target binding. ***Conclusion:*** C05-01 is the first PBB3 analogue developed as potential compound targeting α-synuclein. Despite improved affinity for α-synuclein, additional efforts are needed to optimize the pharmacological and physicochemical properties of this series of compounds as ligands for α-synuclein. This study also showed that the construction of TMAs from different proteinopathies provides a tool for evaluation of fluorescent or radiolabeled compounds binding to misfolded proteins. ***References:*** 1. 1. Koga, S., et al. Mov Disord 2017;32:884-892. 2. Perez-Soriano, et al., Mov Disord 2017; 32:1016-1024.

OP-229

Amyloid beta (Aβ) imaging in transgenic mice - comparison of [11C]PiB and an antibody-based ligand

S. Meier[1], J. Rokka[2], J. Eriksson[2], S. Roshabin[1], U. Neumann[3], D. Sehlin[1], S. Syvänen[1];
[1]Department of Public Health and Caring Sciences, Uppsala, SWEDEN, [2]Department of Medicinal Chemistry, Uppsala, SWEDEN, [3]Neuroscience Research, Novartis Institutes for BioMedical Research, Uppsala, SWITZERLAND.

Aim/Introduction: Amyloid-beta (Aβ) positron emission tomography (PET) has become an important inclusion criterion for enrolment of patients with Alzheimer's disease (AD) in clinical trials. However, all available radioligands for Aβ, such as [11C]PIB, reflect levels of insoluble Aβ plaques. Thus, they may not be able to quantify effects of candidate drugs aimed at reducing other forms of Aβ, e.g. by decreasing the intra-brain production of Aβ and early formed soluble Aβ aggregates. In a previous study, we showed that PET with a radiolabeled antibody could quantify a reduction in soluble Aβ aggregates after treatment with a BACE-1 inhibitor in an early stage of Aβ pathology in a mouse model(1). The aim of the present study was to compare the antibody-based PET approach to [11C]PIB in transgenic mice with advanced Aβ pathology, including mice that underwent treatment with a BACE-1 inhibitor. ***Materials and Methods:*** Transgenic animals (tg-ArcSwe), model of Aβ pathology) at the age of 16 months when the study started, were treated during 2 months with BACE-1 inhibitor NB-360(2) (n=14) and compared to an untreated control group (n=14). After treatment, the animals received a [11C]PiB PET scan followed by a scan with the Aβ protofibril selective radioligand [124I] RmAb158-scFv8D3(5). A baseline group (n=14), aged 16 months, also underwent [11C]PiB and [124I]RmAb158-scFv8D3 PET scanning. Brain tissue was isolated after PET and analyzed ex vivo. ***Results:*** Hippocampal SUV for [124I] RmAb158-scFv8D3 in treated animals was 0.059 ± 0.021 and significantly lower compared to controls 0.078 ± 0.022 (P=0.023) (Figure 1A). Hippocampal [124I]RmAb158-scFv8D3 SUV of treated animals and baseline group (0.052 ±0.023) was not statistically different. In contrast, hippocampal SUV quantified with [11C]PiB was not significantly different between the treated animals 0.26 ± 0.18 and the controls 0.28 ± 0.16. In the baseline group the hippocampal SUV was 0.13 ± 0.07. ***Conclusion:*** Protofibril selective radioligand [124I]RmAb158-scFv8D3 was able to monitor treatment effects with PET imaging in tg-ArcSwe mice with advanced Aβ pathology. [11C]PiB PET was not able to detect these changes in side by side comparison, indicating a need for improved PET imaging to study effects of AD treatments in clinical trials. ***References:*** 1. Meier, S.R. et al. Antibody-based in vivo PET imaging detects amyloid-β reduction in Alzheimer transgenic mice after BACE-1 inhibition. J. Nucl. Med. (2018) 2. Neumann, U. et al. A novel BACE inhibitor NB-360 shows a superior pharmacological profile and robust reduction of amyloid-β and neuroinflammation in APP transgenic mice. Mol. Neurodegener(2016)

506

Cutting Edge Science Track - TROP Session: New Technologies and Imaging Techniques

Friday, October 23, 2020, 10:40 - 12:10 Channel 6

OP-230

Simulation and first measurements of a prototype ultra-long FOV PET/CT scanner

***M. Conti**, M. Aykac, H. Bal, B. Bendriem, D. Bharkhada, J. Cabello, L. Eriksson, V. Panin, H. Rothfuss, S. Siegel;*
Siemens Medical Solutions, Knoxville, TN, UNITED STATES OF AMERICA.

Aim/Introduction: There is great interest in long axial field-of-view (FOV) PET/CT scanners: their capability to simultaneously image multiple organs and their high sensitivity enables novel research and clinical applications. Design criteria of such devices must include state-of-the-art technology that not only exploit the very high sensitivity, but also offers excellent time of flight (TOF) performance and spatial resolution. Furthermore, the design should consider trade-off between performance and cost. Using Monte Carlo (MC) simulation, this work focuses on axial coverage, acceptance angle for lines-of-response (LORs), time coincidence window, and their effects on spatial resolution and sensitivity. Based on the technology introduced with Biograph Vision, a 106-cm long axial FOV prototype was designed and assembled, and initial characterization and phantom experiments are presented. ***Materials and Methods:*** The work included Monte Carlo GATE and numerical simulation of the scanner, with incorporation of synthetic images derived from patient data sets acquired on Vision scanners. Sensitivity was studied as a function of the axial coverage of a PET scanner, of the LOR acceptance angle, and of the time coincidence window. Preliminary time and spatial resolution, and sensitivity measurements, as well as a standard image quality phantom, were performed on a 106-cm long prototype. ***Results:*** The MC simulation confirmed the excellent sensitivity a 106-cm long PET/CT scanner, together with other design choices: a time coincidence window below 5 ns allowed to collect more than 90% of the true coincidences in typical patient scans, thus reducing excessive random coincidences; opening the acceptance angle from 20° to 52° (full acceptance angle for the 106-cm long prototype) increases the sensitivity by about a factor 2; the simulated spatial resolution is very similar to that of the Biograph Vision. The experimental data confirmed excellent spatial

and time resolution, comparable to previously published values for the Biograph Vision scanners. The increase in sensitivity enables dose and/or scan time reduction, while maintaining the phantom image quality of the Biograph Vision: a visual and quantitative comparison with Vision data is presented. ***Conclusion:*** Simulation and preliminary data from a 106-cm long prototype PET/CT scanner are presented. Excellent time and spatial resolution, as well as sensitivity, are demonstrated by preliminary measurements. Phantom images demonstrate the feasibility of lower dose or shorter scan time. ***References:*** None

OP-231

Fully digital-PET is unaffected by any deterioration in TOF resolution and TOF image quality in the wide range of routine PET count rates

J. Salvadori[1], F. Odille[1], G. Karcher[2], P. Marie[3], L. Imbert[1]; [1]IADI UMR1254, Vandoeuvre-lès-Nancy, FRANCE, [2]Nancyclotep molecular imaging platform, Vandoeuvre-lès-Nancy, FRANCE, [3]UMR1116, Vandoeuvre-lès-Nancy, FRANCE.

Aim/Introduction: Digital PET involving silicon photomultipliers (SiPM) provides an enhanced time-of-flight (TOF) resolution, as compared with photomultiplier (PMT)-based PET, but also, a better prevention of the count-related rises in dead time and pile-up effects mainly due to smaller trigger domains (i.e. the detection surfaces associated to each trigger circuit). This study aimed to determine whether this latter property could help prevent against deteriorations in TOF resolution and TOF image quality in the wide range of the PET count rates documented in clinical routine. ***Materials and Methods:*** Variations, according to count rates, in timing resolution and in TOF-related enhancement of the quality of phantom images, were compared between the first fully digitalPET (Vereos) and a PMT-based PET (Ingenuity). Single count rates values were additionally extracted from the list mode data of routine analog- and digital-PET exams at each 500-ms interval, in order to determine the ranges of routine PET count rates. ***Results:*** Routine PET count rates were lower for the Vereos than for the Ingenuity for which the upper limits were estimated at approximately 21.7 and 33.2 Mcps after the injection of respectively 3 and 5 MBq.kg-1 of current 18F-labeled tracers. At 5.8 Mcps, corresponding to the lower limit of the routine count rates documented with the Ingenuity, timing resolutions provided by the scatter phantom were 326 and 621 ps for Vereos and Ingenuity, respectively. At higher count rates, timing resolution was remarkably stable for Vereos but exhibited a progressive deterioration for Ingenuity, respectively reaching 732 and 847 at the upper limits of 21.7 and 33.2 Mcps. The averaged TOF-related gain in signal/noise ratio was stable at approx. 2 for Vereos but decreased from 1.37 at 5.8 Mcps to 1.15 and 1.01 at respectively 21.7 and 33.2 Mcps for Ingenuity. ***Conclusion:*** Contrary to the Ingenuity PMT-based PET, the Vereos fully digital PET is unaffected by any deterioration in TOF resolution and consequently, in the quality of TOF images, in the wide range of routine PET count rates. This advantage is even more striking with higher count-rates for which the preferential use of digital-PET should be further recommended (i.e. dynamic PET recording, higher injected activities). ***References:*** None

OP-232

Clinical impact of fully automated multiparametric PET imaging using direct Patlak reconstruction: Evaluation of 100 dynamic whole-body 18F-FDG PET/CT scans

A. H. Dias, M. F. Pedersen, H. Danielsen, O. L. Munk, L. C. Gormsen; Aarhus Universitetshospital, Aarhus, DENMARK.

Aim/Introduction: Imaging guidelines for 18F-FDG PET/CT endorse static images at a single time-point, usually 60 minutes after tracer administration. The method is well-proven, but hampered by the inherent omission of tracer kinetics from injection to acquisition. Recent methodology allows for whole-body dynamic PET/CT scaning using conventional PET-cameras. The dynamic whole-body data can be used for direct reconstruction of parametric images of the metabolic rate of glucose using Patlak linearization1, thus utilizing the entire information contained in the blood input function and tissue time-activity curves. Our goal was to evaluate whether parametric images have superior lesion target-to-background and if this translates clinically. ***Materials and Methods:*** Retrospective analysis of 100 patients spanning a range of mostly malignant diseases, scanned using a multiparametric PET acquisition protocol on a Siemens Biograph Vision 600 PET/CT scanner. A 70-min dynamic whole-body PET scan was performed immediately after injection of 18F-FDG. The scan included a 6-min dynamic scan of the chest region followed by multiple whole-body passes from 6-70 min. Parametric Patlak images were reconstructed using data from 40-70 min and an image-derived aorta input function. In addition, a standard-of-care static PET image was reconstructed using data from 60-70min. Patlak images of metabolic rate (K) and distribution volume (V) were compared to standard 60-min static SUV images. Standard SUV values of target regions were compared with parameters obtained from dynamic scanning using Patlak reconstructions. ***Results:*** Whole-body parametric Patlak images were of good visual quality and comparable to standard static SUV images. Observed lesion target to background contrast was superior in the parametric K images ($p<0.001$), allowing for easier detection of lesions, particularly in organs with high blood pool signal. There was no observable difference between disease groups in background normalized K/SUV ratios. In four patients with focal FDG uptake in the upper arm, Patlak imaging correctly omitted the signal from the K-image avoiding false positives

and subsequent biopsies. However, although lesions were easier to detect by Patlak K-images, no additional lesions were detected. ***Conclusion:*** Whole-body parametric Patlak-PET/CT imaging provides supplementary information, which may improve the evaluation of PET images. Pointedly, parametric imaging reduced the number of false positive lesions and had superior target-to-background ratios enabling easier image interpretation. Future prospective studies will clarify if parametric PET/CT may also detect more lesions in diseases characterized by relatively low target-to-background ratios on conventional static PET/CT. ***References:*** 1.Patlak,C,et al. Graphical evaluation of blood-to-brain transfer constants from multiple-time uptake data. J.Cereb.BloodFlowMetab.1983.

OP-233

Use of population input functions for FDG whole-body Patlak imaging

J. van Sluis[1], M. Yaqub[2], A. H. Brouwers[1], W. Noordzij[1], R. Boellaard[2];
[1]University Medical Center Groningen, Groningen, NETHERLANDS, [2]Amsterdam University Medical Center, Amsterdam, NETHERLANDS.

Aim/Introduction: SUV derived from PET scans are widely used in clinical practice for diagnosing and evaluating treatment response in oncology. However, SUV can be influenced by changes in plasma kinetics due to treatment possibly causing inaccurate assessments. Recently, whole-body Patlak images can be obtained from a combined acquisition of first 10 min of dynamic imaging over the heart to obtain the arterial input function (IF) followed by multiple whole-body sweeps up to 60 min pi. Population averaged input function (PIF) could exclude the first dynamic scan and minimize whole-body sweeps to an interval of 30-60 min pi. Here, the effects of (incorrect) PIFs on the accuracy of the proposed Patlak method were assessed. In addition, the extent of mitigating these biases through rescaling of the PIF to image derived values at 30-60 min pi was evaluated. ***Materials and Methods:*** Using a representative IF and rate constants from literature, various tumor time activity curves (TACs) were simulated. Variations included multiplication of the IF with a positive and negative gradual bias over 60 min of 5, 10, 15, 20, and 25% and use of rate constants (K1, k3, and both K1 and k2) multiplied by 2, 1.5, and 0.75. The blood volume fraction was fixed at 8.9%. Subsequent Patlak analysis using the original IF (representing the PIF) was used to obtain the influx constant (Ki) for the differently simulated TACs. In addition, the PIF was scaled towards the correct value using the 30-60 min pi time-interval, simulating scaling of the PIF to image derived values. Next, Ki were obtained using these rescaled PIFs. Influence of variabilities in IF and rate constants, and rescaling the PIF on bias in Ki was evaluated. ***Results:*** Percentage bias in Ki seen using simulated incorrect IFs varied from -15 to 15% depending on the simulated amplitude and direction of the IF modifications. Subsequent scaling of the PIF reduced these Ki biases between -2 and 4% and between -0.9 and 1%, respectively. Bias in Ki due to use of non-rescaled incorrect PIFs tended to be larger for TACs with higher simulated Ki. In most cases, rescaling the PIF mitigated these Ki biases to below 5%. ***Conclusion:*** Simulations suggest that scaling of an (incorrect) PIF to IF values seen in whole-body dynamic imaging from 30-60 min pi will provide accurate Ki estimates (<5% bias). Consequently, whole-body Patlak imaging from 30-60 min pi offers possibilities for clinical application. ***References:*** None

OP-234

Two short ^{18}F-FDG PET/CT dynamic acquisitions to evaluate with accuracy the influx constant with Patlak method in patients with lung cancer

V. Scolozzi[1], A. Capotosti[2], L. Indovina[2], S. Taralli[1], M. Lorusso[1], C. Caldarella[1], M. L. Calcagni[1,3];
[1]Fondazione Policlinico Universitario A. Gemelli IRCCS, UOC Medicina Nucleare, Dipartimento di Diagnostica per Immagini, Radioterapia Oncologica ed Ematologia, Rome, ITALY, [2]Fondazione Policlinico Universitario A. Gemelli IRCCS, UOS Dosimetria Clinica e Radioprotezione, Dipartimento di Diagnostica per Immagini, Radioterapia Oncologica ed Ematologia, Rome, ITALY, [3]Università Cattolica del Sacro Cuore, Istituto di Medicina Nucleare, Rome, ITALY.

Aim/Introduction: Patlak graphical analysis is a quantitative method that allows an accurate estimation of ^{18}F-FDG influx constant (K_i), known to be more reliable than more common semiquantitative parameters. It is less used in clinical practice since it requires a long-lasting (60min) dynamic acquisition. Aim: to propose a new approach for estimating K_i with Patlak method using two short dynamic acquisitions ($K_{i,SDA}$) instead of the standard one (K_i). ***Materials and Methods:*** Twenty-four non-small-cell lung cancer patients, prospectively enrolled, underwent 60min dynamic PET acquisition over the thorax after ^{18}F-FDG injection (134-507MBq). A venous blood sampling was performed at 45min to obtain ^{18}F-FDG plasmatic activity. To estimate K_i, the entire dynamic acquisition was used: image derived input function (IDIF) was obtained drawing VOI on descending aorta (0-60min) using the plasmatic activity as quality control; tissue response drawing VOI on tumour (10-60min). To estimate $K_{i,SDA}$, only the early (0-10min) and the late phase (40-60min) of dynamic acquisition were used. $IDIF_{SDA}$ was obtained utilizing data of early phase (0-10min) of dynamic acquisition and reconstructing the last part with mean values of mono-exponential fitting of all patients (since it can be expressed by a mono-exponential function), and using the plasmatic activity at 45min as constrain. Spearman's rank, Intraclass Correlation Coefficient, Passing-

Bablok regression and Bland-Altman method were used for correlation and concordance between K_i and $K_{i,SDA}$. ***Results:*** In all patients (n=24) the correlation coefficient (R^2) between Integral IDIF and Integral $IDIF_{SDA}$ was equal to 0.9977. The mean values of K_i and $K_{i,SDA}$ were 0.0388±0.0268 and 0.0374±0.0261, respectively. Spearmen's correlation coefficient (ρ) between K_i and $K_{i,SDA}$ was equal to 0.991 (p<0.001). The comparison between the two methods showed a slope of 0.97 (95%CI:0.91-1.00) and intercept of 0.00005 (95%CI:-0.00132-0.00118) and mean of differences of 0.001497 (95%CI:0.0007-0.0021). ***Conclusion:*** Our approach is reliable and easily achievable. The excellent correlation between Integral IDIF and Integral $IDIF_{SDA}$ demonstrates that only a short early dynamic acquisition and a venous sample are enough to accurately reconstruct IDIF. The great correlation between K_i and $K_{i,SDA}$ supports the possibility to apply Patlak method using two short dynamic acquisitions, instead of the standard longer one. The use of two short acquisitions in order to perform Patlak method implies two important practical advantages in clinical routine: 1) more comfort for patients and less risk of movement artefacts; 2) the possibility to obtain the influx constant, especially useful in the response assessment, in a larger number of patients. ***References:*** None

OP-235

Comparing the accuracy of global and blockwise deadtime correction for the BrainPET scanner

A. Issa[1], *J. Scheins*[1], *L. Tellmann*[1], *C. Régio Brambilla*[1,2], *H. Xu*[1], *N. Shah*[1,2,3], *C. Lerche*[1];
[1]*Institute of Neuroscience and Medicine 4, INM-4, Forschungszentrum Jülich, Jülich, GERMANY,* [2]*Institute of Neuroscience and Medicine 11, INM-11, JARA, Forschungszentrum Jülich, Jülich, GERMANY,* [3]*JARA - BRAIN - Translational Medicine, Aachen, GERMANY.*

Aim/Introduction: All components in the PET detector system contribute to dead time (DT) losses. DT affects the quantitation of PET, especially for high activity in the field of view. Thus, DT distorts the measured time-activity curves (TAC). The uncorrected count rate in each detector block varies significantly which leads to different DT for each block. Therefore, processing the DT losses on the block-wise DT correction frame potentially provides more accurate results. The main goal of this work is to improve the DT correction by implementing an independent DT correction for each block of the Siemens 3T MR/BrainPET scanner. ***Materials and Methods:*** On our Siemens 3T MR/BrainPET scanner, the standardly applied DT correction has been implemented as a global, count rate-dependent, average correction factor. For this, the constant fraction discriminator (CFD) counts for each block are summed to estimate the global single counts, and the overall DT induced single count losses. For typical PET measurements, global single count rates (sum of all 192 blocks) and the corresponding corrections are compared to individual single count rates and the corresponding corrections. ***Phantom measurements.*** Decay experiments using a cylindrical phantom filled with high activity (685 MBq and 257 MBq) of [18F, 20 hours' duration] centered inside of FOV. ***Patient measurements***. ([18F] FET, 50 minutes' duration) measurement for brain tumors, the injected activity of 234 MBq. Moreover, ([11C] ABP688, 65 minutes' duration) measurement, the injected activity of 437 MBq. ***Results:*** DT losses are very different for each detector block according to the various count rates, which is caused by the block position concerning the activity distribution. For the phantom measurements, the blockwise single counts follow the non-paralyzable model (NPM). For the NPM, the average of blockwise dead time was about 200 ns (Scheins, 2018). For the patients' measurements, the single counts of the 192 blocks depend strongly on the angular and axial block positions, due to the cylindrical geometry of the BrainPET insert. Therefore, global dead time correction is potentially insufficient for high activity and diverse blockwise count rates. Therefore, the independent DT correction for each detector block is necessary to achieve higher accuracy in quantitative imaging. ***Conclusion:*** The block counts follow the non-paralyzable model in the Siemens Brain PET insert. There are important differences between average single counts and blockwise single counts for the different blocks depending on their geometrical positions. ***References:*** Scheins, J. J., et al. "PET Quantification." Hybrid MR-PET Imaging. 2018. 162-182.

OP-236

Characteristics and properties of a novel cost-effective preclinical PET scanner for high performance molecular imaging of small animal models

F. Castro[1,2], *P. M. M. Correia*[2,1], *P. M. C. C. Encarnação*[2], *A. L. M. Silva*[2,1], *F. M. Rodrigues*[1], *A. G. Sá*[1], *A. C. Azevedo*[1], *F. M. Ribeiro*[2], *I. Mohammadi*[2], *R. Oliveira*[2], *A. I. Veloso*[3], *A. C. Santos*[4], *N. A. Gomes*[5], *M. F. L. Loureiro*[5], *P. Mar*[5], *M. Inocêncio*[5], *J. F. C. A. Veloso*[2,1];
[1]*RI-TE Radiation Imaging Technologies, Lda, Ílhavo, PORTUGAL,* [2]*Institute for Nanostructures, Nanomodelling and Nanofabrication (i3N), University of Aveiro, Aveiro, PORTUGAL,* [3]*DigiMedia, University of Aveiro, Aveiro, PORTUGAL,* [4]*Institute for Clinical and Biomedical Research (iCBR), Center for Innovative Biomedicine and Biotechnology (CIBB), Coimbra, PORTUGAL,* [5]*Exatronic, Lda, Aveiro, PORTUGAL.*

Aim/Introduction: EasyPET technology is a novel concept for high-resolution PET imaging based on the smart rotation of detector modules. Its uniquely cost-effective scanning method achieves excellent imaging performance with only 10-20% of the components used in other PET systems, being able to finely scan millions of LORs in minutes and cover full body mouse axial imaging with a much smaller number of detectors. EasyPET achieves a great level of

detail and spatial resolution, very uniform in all the FOV due to the intrinsic capacity to mitigate parallax errors, since its detectors are always collinear, unlike ring-based scanners. Detector arrays can have different geometries and each scan can be performed with different parameters in order to achieve different sensitivity, level of desired detail/speed or image specific regions of interest within the FOV, which is also a unique capability of this technology. This study aims to present and characterize the performance of iPET, a new preclinical scanner based on easyPET technology, following NEMA NU 4-2008 standards. ***Materials and Methods:*** The iPET system uses 2 arrays of 50x6 LYSO crystals of 1.5x1.5x20 mm^3 pixel size coupled to corresponding arrays of silicon photomultipliers with 1 mm^2 active area, covering an axial FOV of 8 cm length and maximum radial FOV of 6 cm diameter. A dedicated 3D reconstruction method was developed based on OSEM and MLEM algorithms, considering the original geometry of the scanner and high number of possible LORs. ***Results:*** Based on NEMA NU 4-2008 standards, scans of NEMA IQ and NEC phantoms filled with ^{18}F-FDG and a point-like ^{22}Na source were simulated and carried out in available systems, in order to determine spatial resolution, sensitivity, uniformity and other results achieved by easyPET based scanners. Imaging studies of murine models of disease carried out at iCBR will also be presented. Image improvements based on the selection of regions of interest and a dedicated reconstruction algorithm will be shown. ***Conclusion:*** EasyPET is the most efficient technology for cost reduction of preclinical PET scanners, without compromising their capacity for high-resolution molecular imaging of small animal models of disease including fast dynamic studies with short-lived radionuclides such as ^{18}F or ^{68}Ga. ***References:*** Patent WO/2016/147130. Acknowledgement: this work was supported by project CENTRO-01-0247-FEDER-039880, co-financed by the EU through ERDF (CENTRO2020 program).

OP-237

Channel-based Energy Resolution of TOFPET2C-read PET Detectors

V. Nadig[1], *D. Schug*[1,2], *H. Radermacher*[1], *B. Weissler*[1,2], *V. Schulz*[1,2,3]*;*
[1]Physics of Molecular Imaging Systems, RWTH Aachen University, Aachen, GERMANY, [2]Hyperion Hybrid Imaging Systems GmbH, Aachen, GERMANY, [3]Institute of Physics III B, RWTH Aachen University, Aachen, GERMANY.

Aim/Introduction: In time-of-flight positron emission tomography (ToF-PET), clinical systems aim to resolve the timing information of a coincidence event with a resolution of around 200 ps, resulting in a high gain in the signal-to-noise ratio of PET images [1]. Additionally, an energy resolution of about 10 - 12 % is required to reliably filter out scatter. Whether this resolution can be achieved, strongly depends on the employed detector blocks, i.e., the scintillators, photo-sensors, and readout electronics used. Amongst others, important advances have been accomplished in electronics during the past decades [2]. A ToF-PET system constitutes ten-thousands of detector channels requiring several hundred application-specific circuits (ASICs) for readout. Thus, it is essential to consider the performance spread of individual readout channels and its impact on the system resolution. ***Materials and Methods:*** We used two detector blocks, each consisting of a 8 x 8 12-mm-high lutetium-yttrium-oxyorthosilicate (LYSO) scintillator matrix one-to-one coupled to a S14161-3050-HS-08 photo-sensor (pitch 3.2 mm) using a two-component dielectric gel. Signals from the 64 channels of each detector block were read out consecutively by twelve samples of the latest version of the TOFPET2 ASIC (version 2c), in which research and industry developed an increasing interest in recent years. This way, the impact of the ASIC on the performance of individual channels is tested. Employing Sodium-22 point sources with a total activity of approximately 2 MBq, the linearity of the energy spectra and the energy resolution of each of the in total 768 ASIC channels was determined. ***Results:*** For each ASIC sample, channel linearity ratios and energy resolutions showed Gaussian distributions. Effects of single channels, i.e., border effects, non-linearities and short circuits, can be identified and excluded from further evaluation or noted for an adjustment of their configuration, e.g., applied thresholds. Computing the performance globally, all ASIC samples achieved energy resolutions of approx. 10.3 %. ***Conclusion:*** We found a low spread in channel energy resolution, which supports the usage of a large number of TOFPET2 ASICs as readout electronics in a clinical ToF-PET system, without the need for excessive calibration/matching effort or the risk of ASIC-dependent performance variation. Still, the possibility to identify individual channels behaving differently allows for the adjustment of their configuration parameters. The low energy resolution can be used to filter out scatter. ***References:*** [1] Surti et al. (2015): Advances in time-of-flight PET, doi:10.1016/j.ejmp.2015.12.007. [2] Berg et al. (2018): Innovations in Instrumentation for positron emission tomography, doi:10.1053/j.semnuclmed.2018.02.006.

OP-238

Optimizing energy window width for digital SPECT-CT in myocardial perfusion imaging

R. Hirvilammi[1], *M. Seppänen*[1,2], *M. Hakulinen*[3], *J. Knuuti*[2], *T. Noponen*[1,4]*;*
[1]Department of Clinical Physiology and Nuclear Medicine, Turku University Hospital, Turku, FINLAND, [2]Turku PET Centre, Turku University Hospital, Turku, FINLAND, [3]Department of Clinical Physiology and Nuclear Medicine, Kuopio University Hospital, Kuopio, FINLAND, [4]Department of Medical Physics, Turku University Hospital, Turku, FINLAND.

Aim/Introduction: Good energy resolution of digital SPECT-CT systems allow imaging with a narrow energy window. Narrow energy window can reduce the number of scattered photons improving image quality. In this study the benefits of narrowing the energy window was studied with cardiac phantoms. ***Materials and Methods:*** Two custom designed 3D printed cardiac phantoms (Kuopio Cardiac Phantom) modeling the left ventricles were used. Other phantom included 5 and other 9 mm long cube shaped defects located in the middle of cylindrical wall. Both phantoms were filled with 99mTc-pertechnetate with activity concentration of 67.5 kBq/ml. Phantoms were fixed inside a plastic background box containing 24.5 l of 99mTc-pertechnetate with the concentration of 10.6 kBq/ml. Data were acquired using Discovery NM/CT 670 CZT system (GE Healthcare, Tirat Hacarmel, Israel) with wide-energy high resolution collimators using following parameters: 60 projections over 180° with 40-s time-per-projection, L-mode, 64X64 matrix and energy window of 140 keV ± 7.5%. Attenuation correction was done using low-dose CT. The data acquisition was carried out in list-mode which allowed the changing of energy window afterwards. New sinograms were created with energy windows from ±6 to ±2%. Sinograms were reconstructed using iterative OSEM based algorithm with and without collimator correction. From reconstructed images count profiles containing the cube shaped defects were extracted using MATLAB (version R2020A, Natick, Massachusetts, USA). Double Gaussian function was fitted to count profiles to calculate the contrasts of defects. Also, noise was calculated as standard deviation from the apical data points of the phantoms. ***Results:*** When the energy window was narrowed from ±7.5 to ±4% the contrast of defects increased from 28% to 32%. When the energy window was further narrowed to ±3% the contrast decreased by 2 percentage points compared to the contrast in images with ±7,5% energy window. Collimator correction decreased noise especially in images with energy window of ±7.5 - ±4% and increased the contrast by 2.1 percentage point when ±7.5% energy window images were compared with and without the correction. In images with ±4% or narrower energy windows the contrast decreased with collimator correction when compared to the images without the correction. ***Conclusion:*** Narrowing energy window can improve the contrast of defects in myocardial perfusion imaging. Energy window of ±4% seems to produce the best contrast. By using collimator correction it is possible to decrease noise in myocardial images to further improve their quality. ***References:*** None

OP-239

Bone metabolism may be monitored through the absolute quantification provided by a whole-body 360° CZT SPECT/CT camera during the healing period of vertebral fractures

A. Bahloul*, L. Imbert, A. Blum, G. Karcher, A. Verger, P. Marie; Nancy University Hospital, Vandoeuvre-les-Nancy, FRANCE.*

Aim/Introduction: Bone scintigraphy (BS) is routinely performed for assessing vertebral fractures (VF) and subsequent follow-up, although this investigation is mainly based on subjective visual analysis. Nowadays, absolute quantification with SUV values may be obtained on bone SPECT recordings provided by new SPECT/CT systems. This study aimed to determine whether the absolute quantification of bone scintigraphy provided by the Veriton® CZT-SPECT/CT system (Spectrum Dynamics Medical) is reliable, as assessed through phantom experiments, and whether it provides consistent results for monitoring VF healing. ***Materials and Methods:*** SPECT/CT images were recorded with the Veriton® system and reconstructed with corrections of attenuation, scatter and partial volume. In a first step, absolute quantification was assessed on an IEC phantom filled-in with a ^{99m}Tc-solution, with spheres of various diameters. In a second step, this quantification was applied on 29 paired ^{99m}Tc hydroxymethylene diphosphonate-scintigraphy recordings, each pair obtained in the same patient (age: 71±13 years, 38% male) who had first been imaged at 2.0±2.0 months from the date of an acute VF (ie. baseline) and subsequently at 5.4±2.2 months for a control whilst under medical treatment. ***Results:*** On the IEC phantom, the % errors in SUV measurement were: 2.3%, 0.2%, 3.8%, 1.2%, 5.7% for spheres with respective diameters of 37, 28, 22, 17 and 13 mm. In patients, the SUVmax from VF exhibited a marked decrease between baseline (12.9±6.8) and control scans (7.5±2.7, $p<0.001$), whereas the corresponding values for the non-fractured vertebrae were much lower (for the T1 vertebra: 4.2±1.8 at baseline and 3.3±1.5 at control). The relationship between all VF SUVmax values recorded at baseline or control and the time elapsed since fracture, corresponded to a decreasing logarithmic function ($p<0.001$, $R^2=0.21$). The duration of the healing period, to the point of normalized VF SUVmax values, was estimated to be 9-months on average, but with marked inter-individual variations. ***Conclusion:*** The time taken for a return to normal bone metabolism is lengthy and highly variable in acute VF treated medically, however this may be monitored with the absolute quantification of bone scintigraphy provided by the whole-body Veriton® CZT-SPECT/CT system. ***References:*** 1. Van den Wyngaert T, Strobel K, Kampen WU et al. The EANM practice guidelines for bone scintigraphy. Eur J Nucl Med Mol Imaging 2016;43:1723-38. 2. Beck M, Sanders JC, Ritt P, Reinfelder J, Kuwert T. Longitudinal analysis of bone metabolism using SPECT/CT and ^{99m}Tc-diphosphono- propanedicarboxylic acid: comparison of visual and quantitative analysis. EJNMMI Research 2016;6:60.

OP-240

Compared visual analyses of whole-body planar bone scintigraphies obtained from conventional Anger camera and from retro-projections after CT-based corrections of a high-speed SPECT recording using a 360° CZT-camera

A. Bahloul, A. Verger, M. Perrin, M. Claudin, G. Karcher, P. Marie, L. Imbert;
Nancy University Hospital, Vandoeuvre Les Nancy, FRANCE.

Aim/Introduction: Reconstructed planar projections (the so-called "MVP" or multi-view planar) may be obtained from a single high-speed whole-body 3D SPECT recording (6 to 7 bed positions of 3 minutes each) using the Veriton® 360° CZT-SPECT camera (Spectrum Dynamics Medical) after CT-based corrections of attenuation and of partial volume effect. This study aimed to assess the concordance of results from visual analysis of such MVP bone scans in comparison with analysis of conventional planar images from an Anger camera (Symbia, Siemens Healthineers). *Materials and Methods:* Whole-body anterior and posterior bone scans were obtained in the same 25 patients (67±14 years, 11 women, 22 with known or suspected bone metastasis) consecutively with an Anger camera and with the CZT-camera. Presence or absence of definite uptake abnormalities was scored by two blinded experienced nuclear physicians on all scans, presented in a random order, and by using a 24-segment division of the skeleton. *Results:* The global concordance of image analyses between the two systems was excellent for both observers (with respective global accuracies of 92 and 96% and kappa scores of 0.78±0.03 and 0.87±0.03). Discordant results affected only 77 of the total 1200 segments analyzed by the two observers. Interestingly, 34 of these discordant results corresponded to abnormalities documented only on MVP scans, with 23 being documented on the few segments corresponding to the axial skeleton. *Conclusion:* Visual analysis of MVP whole-body bone scintigraphy obtained with this CZT-camera is highly concordant with the visual analysis of corresponding planar images from an Anger-camera. However, these MVP images are associated with higher detection rate of abnormalities on the axial skeleton, a location where the detection sensitivity of conventional planar images is known to be rather low. *References:* None

OP-241

Going quicker for dopamine transporter DaTSCAN imaging using SPECTStep & Shoot Continuous

M. Bailly[1], G. Le Rouzic[1], G. Metrard[1], M. Ribeiro[2];
[1]CHR Orléans, Orleans, FRANCE, [2]CHRU Tours, Tours, FRANCE.

Aim/Introduction: Dopamine transporter imaging with ^{123}I-DaTSCAN is an established diagnostic tool in parkinsonism and dementia. Conventional DaTSCAN SPECT acquisitions are quite long-lasting in those difficult patients. In this study, we evaluated a 25% reduction of the acquisition time using a Low Energy High Resolution and Sensitivity (LEHRS) collimator and step-and-shoot continuous scanning mode, and its effect on visual or quantitative analysis. *Materials and Methods:* An anthropomorphic striatal phantom filled with ^{123}I solution at different striatum-to-background radioactivity ratios was acquired with low energy high sensitivity (LEHR) collimator and LEHRS collimator with and without step-and-shoot continuous mode. 25%-time reduction was also assessed on the LEHRS step-and-shoot continuous SPECT phantom data. SPECT data from 30 normal individuals (12 men, 18 women; age range 39 - 91 years, mean 71 years) and 30 Parkinson disease (16 men, 14 women; age range 43 - 84 years, mean 69 years) were retrospectively included. All clinical data were acquired using LEHRS collimator and step-and-shoot continuous scanning mode. Data were retrospectively reconstructed with full time and 25%-time reduction and were visually analyzed by multiples raters. In addition, Striatal Binding Ratios (SBRs) were calculated. *Results:* Visual analysis remained stable and SBRs differences were insignificant whether using full time or with 25%-time reduction ($p<0.001$) both on phantom and clinical study. There was an excellent inter-rater agreement and no effect of time-reduction on diagnosis, nor on user-rated image quality. *Conclusion:* Using LEHRS step-and-shoot continuous SPECT mode, 25%-time reduction can be applied to DaTSCAN acquisition protocols, without impairing visual or quantitative analysis. Dose reduction could also be applied without shortening time of acquisition. *References:* None

507

Teaching Session 2: Nodal Anatomy Required for Lymphoma, Lung and Head/Neck Cancer

Friday, October 23, 2020, 10:40 - 11:40 Channel 7

OP-242

TBA

T. Lynch; Belfast, UNITED KINGDOM.

OP-243

TBA

TBA

508

Clinical Oncology Track - TROP Session: PET for Haematological Tumours

Friday, October 23, 2020, 10:40 - 12:10 Channel 8

OP-247

^{18}F-FDG PET/CT baseline radiomics features are predictive of outcome in diffuse large B-cell lymphoma patients

J. Eertink[1], T. van de Brug[2], S. E. Wiegers[1], G. J. C. Zwezerijnen[3], E. Pfaehler[4], P. J. Lugtenburg[5], B. van der Holt[6], H. C. W. de Vet[2], O. S. Hoekstra[3], R. Boellaard[3], J. M. Zijlstra[1];
[1]Amsterdam UMC, Vrije Universiteit Amsterdam, department of Hematology, Cancer Center Amsterdam, Amsterdam, NETHERLANDS, [2]Amsterdam UMC, Vrije Universiteit Amsterdam, department of Epidemiology and Biostatistics, Amsterdam Public Health research institute, Amsterdam, NETHERLANDS, [3]Amsterdam UMC, Vrije Universiteit Amsterdam, department of Radiology and Nuclear Medicine, Cancer Center Amsterdam, Amsterdam, NETHERLANDS, [4]Department of Nuclear Medicine and Molecular Imaging, University of Groningen, University Medical Center Groningen, Groningen, NETHERLANDS, [5]Erasmus MC Cancer Institute, department of Hematology, Rotterdam, NETHERLANDS, [6]Erasmus MC Cancer Institute, HOVON Data Center, department of Hematology, Amsterdam, NETHERLANDS.

Aim/Introduction: Up to one third of diffuse large B-cell lymphoma (DLBCL) patients experience relapse or fail to achieve complete remission during first-line treatment. Identification of poor prognosis patients might be further improved by radiomics. Radiomics analysis of imaging data provides quantitative features of tumor characteristics such as intensity, shape, volume, texture and intra- and inter-lesion heterogeneity. The aim of this study is to develop a prediction model for 2-year time to progression (TTP) using baseline quantitative radiomics features. ***Materials and Methods:*** 296 newly diagnosed DLBCL patients with baseline ^{18}F-FDG PET/CT scans from the HOVON84 trial (EudraCT: 2006-005174-42) were included. Lesions were delineated using a fully automated preselection of ^{18}F-FDG avid structures defined by a SUV ≥ 4.0 and volume >3mL. Missed lesions were added and non-tumour regions were removed (accurate tool, https://petralymphoma.org). Next, 490 radiomics features were extracted from the total metabolic tumor volume (MTV) using RaCat (Pfaehler et al, 2019). To reduce feature space dimensions, we made a preselection of clinically most relevant radiomics features (SUV_{max}, SUV_{mean}, SUV_{peak}, TLG, MTV, dissemination features and sphericity) and used logistic regression with backward feature selection to predict 2-year TTP, defined as time from baseline PET/CT to progression. Patients who died without progression were censored at date of death. Furthermore, we tested the predictive value of known clinical predictors (age, WHO performance status (WHO), Ann Arbor stage, extranodal involvement, lactate dehydrogenase (LDH) level and bulky disease) and of a model that combined radiomics and clinical parameters. Model performance was assessed using repeated cross-validation (5 folds, 2000 repeats) yielding the mean receiver-operator-characteristics curve integral (AUC). ***Results:*** The highest performance for the radiomics model was observed for MTV combined with SUV_{peak} and the maximal distance between the largest lesion and any other lesion ($Dmax_{bulk}$), which yielded in a cross-validated AUC (CV-AUC) of 0.75±0.07, which was significantly higher than the MTV model (CV-AUC: 0.66±0.08, p = 0.01). LDH, WHO and extranodal involvement showed the highest performance for the clinical prediction model with a CV-AUC of 0.71±0.08. When combining radiomics features with clinical predictors, the highest performance was observed for MTV combined with SUV_{peak}, $Dmax_{bulk}$, WHO and age, with a CV-AUC of 0.77±0.07. ***Conclusion:*** Prediction models using quantitative radiomics features extracted from baseline ^{18}F-FDG PET/CT scans are able to identify patients at risk of relapse at baseline and have added value compared to currently used clinical and PET predictors. ***References:*** None

OP-248

Correlation of baseline TMTV/TLG with early metabolic response in Hodgkin Lymphoma and integration with the iPET gene-based predictive model

R. Durmo*, B. Donati, S. Luminari, M. Casali, A. Ruffini, M. Zanelli, A. Ciarrocchi, F. Merli, A. Versari;*
AUSL-IRCCS of Reggio Emilia, Reggio Emilia, ITALY.

Aim/Introduction: Interim-PET (iPET) is prognostic for classical Hodgkin Lymphoma (cHL). However, iPET response is defined two months after treatment start and cannot be anticipated at the time of diagnosis. Total metabolic volume (TMTV) and total lesion glycolysis (TLG) are promising prognostic metabolic parameters in cHL. We recently developed and validated a 5-gene signature (iPET predictive model) from pre-treatment biopsies that anticipates at diagnosis the iPET response in cHL patients. The aim of this study was to investigate the predictive significance of baseline TMTV and TLG and their value in addition to the iPET gene-based predictive model in cHL patients. ***Materials and Methods:*** We selected a retrospective cohort of 150 stage I-IV cHL patients who underwent baseline 18F-FDG PET/CT between 2007-2019 with available iPET after 2 ABVD courses. TMTV and TLG were computed from baseline PET. iPET was reported according to the five-point Deauville scale (DS1-5). iPET were considered positive for DS4-5 (iPET+). TMTV and TLG were dichotomized according to the median value within our cohort. iPET predictive model from our previous study was included (Score positivity ≥-0.93). Univariate and multivariate analyses were performed by generalized linear

model to test the relationship between these variables and iPET response. ROC curve was built to determine variables' performance in predicting iPET+. ***Results:*** Median TMTV was 106 cm3(range 6-1196) and median TLG was 601(range 52-6453). iPET predictive model was available for 116 patients. Median age was 38years (15-79); 64(55%), 18(16%), and 34 patients (29%) had stage I-II, III and IV respectively. Twenty-three patients (19,8%) had iPET+. In univariate analysis, TMTV (OR 2.60, CI 1.00-6.72, p=0.05), TLG (OR 4,29, CI 1.55-11.88, p=0.005) and iPET model (OR 10.34, CI 3.60-29.67, p<0.001) were associated with iPET+. In multivariate analysis, TLG (OR 8.71, CI 1.24-61.40, p 0.03) and iPET model (OR 10.41, CI 3.44-31.50, p<0.001) were confirmed independent predictor of iPET+. No significant correlation of histotype, age, stage and risk group with iPET was observed. Integrating iPET model with TMTV and TLG we were able to increase AUC of the model obtained by ROC analysis from 0.76 (CI 0.66-0.86) to 0.83 (CI 0.75-0.92); main difference was observed for specificity that changed from 78% to 81%. ***Conclusion:*** TLG is an independent predictor factor of iPET+ and improves risk stratification of patients with cHL. Integration of TMTV and TLG to iPET gene-based predictive model improved specificity of the model. ***References:*** Luminari et al. ClinCancerRes.2020;26(2):373-383. doi:10.1158/1078-0432.CCR-19-2356

OP-249

Aberrant patterns of PET-CT response for diffuse large B-cell lymphoma patients with MYC rearrangement

J. Eertink[1], *F. Celik*[2], *J. Huijbregts*[3], *A. I. J. Arens*[4], *S. E. Wiegers*[1], *C. N. Burggraaff*[1], *O. S. Hoekstra*[5], *S. Stroobants*[6], *R. Boellaard*[5], *H. C. W. de Vet*[7], *M. E. D. Chamuleau*[1], *J. M. Zijlstra*[1];
[1]*Amsterdam UMC, Vrije Universiteit Amsterdam, department of Hematology, Cancer Center Amsterdam, Amsterdam, NETHERLANDS,* [2]*Department of Radiology and Nuclear Medicine, Deventer Ziekenhuis, Deventer, NETHERLANDS,* [3]*Department of Radiology and Nuclear Medicine, Gelre Ziekenhuis, Apeldoorn, NETHERLANDS,* [4]*Department of Radiology and Nuclear Medicine, Radboud University Medical Center, Nijmegen, NETHERLANDS,* [5]*Amsterdam UMC, Vrije Universiteit Amsterdam, department of Radiology and Nuclear Medicine, Cancer Center Amsterdam, Amsterdam, NETHERLANDS,* [6]*Department of Nuclear Medicine, Antwerp University Hospital (UZA), Antwerp, BELGIUM,* [7]*Amsterdam UMC, Vrije Universiteit Amsterdam, department of Epidemiology and Biostatistics, Amsterdam Public Health research institute, Amsterdam, NETHERLANDS.*

Aim/Introduction: Diffuse large B-cell lymphoma (DLBCL) is a heterogeneous subtype of malignant lymphoma. DLBCL generally tends to relapse in previously involved sites. MYC oncogene rearrangement occurs in approximately 10-15% of DLBCL patients and has been associated with a poor prognosis. The aim of this study was to analyse the patterns of response for MYC-rearrangement positive DLBCL (MYC+ LBCL) patients. ***Materials and Methods:*** 82 Patients from the prospective phase II HOVON130 study (Eudra-CT: 2014-002654-39, Chamuleau et al, Haematologica 2019) were included for this analysis. ^{18}F-fluorodeoxyglucose positron emission tomography computed tomography (^{18}F-FDG PET/CT) scans were performed at baseline, after 3 cycles of treatment (I-PET) and at end of treatment (EoT) and were centrally reviewed. I-PET and EoT scans were evaluated according to the Deauville 5-point scale (DS). DS 1-3 was regarded as PET-negative and DS 4-5 as PET-positive. To assess volumetric changes, Metabolic tumour volume (MTV) was calculated using a fully automated preselection of ^{18}F-FDG avid structures defined by an SUV ≥ 4.0 at baseline using the ACCURATE tool. For I-PET and EoT, we used the method with the most complete tumour segmentation without flooding, which could be either SUV4.0, SUV2.5, 41%max, 50%peak, MV2 or MV3. Progression was defined as an increase in MTV and/or the presence of new lesions. ***Results:*** 79 I-PET scans and EoT scans were centrally reviewed. At I-PET, 24 patients were PET-positive (30.3%), whereas 55 patients were PET-negative (69,7%). 1 patient showed progression compared to baseline. At EoT, 26 patients were PET-positive (32.9%), of which 23 showed progression compared to I-PET. 12 I-PET positive patients remained PET-positive at EoT. From these 12 patients, 7 patients also presented with new extranodal and nodal lesions. 14 out of 55 I-PET negative patients were PET-positive at EoT. In total, 21 out of 26 PET-positive patients at EoT presented with new nodal and/or extranodal lesions compared to I-PET. From these 21 patients, 9 patients showed new lesions at EoT in regions that were not initially involved at baseline. 23 out of 26 PET-positive patients at EoT showed increased MTV compared to I-PET. ***Conclusion:*** MYC+ LBCL patients demonstrate aberrant PET response patterns with progressive disease during treatment after I-PET negative assessment with nodal and extranodal lesions at sites that were not initially involved. ***References:*** None

OP-250

Baseline ^{18}F-FDG PET/CT Metabolic Parameters Combined with Interim PET/CT Improve Risk Stratification in Patients with Hodgkin Lymphoma

M. Rashki[1], *E. Triviño-Ibáñez*[1], *L. Lamarca Eraso*[2], *E. Gámez Jiménez*[2], *F. Hernández Mohedo*[2], *C. Ramos Font*[1];
[1]*Servicio de Medicina Nuclear. Hospital Virgen de las Nieves, Granada, SPAIN,* [2]*Servicio de Hematología y Hemoterapia. Hospital Virgen de las Nieves, Granada, SPAIN.*

Aim/Introduction: To study the predictive value of baseline volumetric parameters in combination with interim PET/CT (iPET) to improve risk stratification in Hodgkin lymphoma patients. ***Materials and Methods:*** Between 2013 and 2018, 92 patients with newly diagnosed HL were retrospectively

evaluated. Baseline PET/CT images were qualitatively and semiquantitative analyzed by measuring the volumetric parameters: total metabolic tumor volume (TMTV), total lesion glycolysis (TLG), and SUV_{max}, SUV_{mean}, SUV_{peak}, SUV_{min} of the lesion with the highest SUV_{max} value. All iPET scans were defined as PET/CT performed after 2-4 cycles of chemotherapy. Response on iPET and end-of-treatment PET was assessed using the Deauville 5-point scale, with a score of 4-5 reflecting positivity. The therapeutic response was established based on the Lugano´s criteria. We analyzed the relation between qualitative and semiquantitative PET/CT features and OS and PFS. ***Results:*** 92 patients (mean age: 36.74±16.51, 55% male). 49% were stage II, followed by stage III (23%) and IV (16%). 90% received treatment according to the ABVD scheme. Nineteen patients (21%) relapsed or progressed and 7 (8%) died. Median OS was 42.2 months and PFS of 36.5 months. Factors associated with survival were: younger age at diagnosis (35.2±15.7 vs 58±25.5; p<0.001), advanced stage (p=0.025), positive iPET (OR 9.71, p<0.001) and positive end-of-treatment PET (OR: 28.83, p<0.001). Factor associated with recurrence were: SUV_{peak} of baseline PET/CT study (p=0.038), SUV_{mean} (p=0.044), IPI (P=0.006), iPET positive (p <0.001). TMTV and TLGt were associated with shorter PFS (p<0.05). ROC curves analysis showed an optimal cut-off point of 150cm^3 for TMTV and 790cm^3 for TLGt. Predictive factors of survival in univariate analysis (Cox´s regression) were: TMTV>150cm^3 (HR4.65, p=0.003), TLGt>790cm^3 (HR: 4.90, p=0.002) and positive iPET (HR: 8.25, p<0.001). In multivariate analysis, only positive iPET was a prognostic factor. A combination of the baseline TMTV and iPET variables stratifies patients into 4 risk categories from worst to best prognosis: baseline MTVt>150+iPET(+), baseline MTVt<150+iPET(+), baseline MTVt>150+iPET(-), baseline MTVt<150+iPET(-). A statistically significant difference was observed between the four groups (p<0.001) in the Cox proportional hazard regression analysis. ***Conclusion:*** Tumor burden determined by volumetric parameters in basal PET/TC and positive iPET were associated with relapse of HL and PFS. The combination of both parameters can help identify the worst prognosis group of patients. ***References:*** None

OP-251

Comparison between 18F-FDG PET/CT and endoscopy in the staging of gastrointestinal involvement in Mantle Cell Lymphoma: A multi-centre study

C. Ferrari[1], *C. Minoia*[2], *V. Lavelli*[1], *T. Skrypets*[2], *L. Nassi*[3], *G. Margiotta Casaluci*[3], *B. Puccini*[4], *L. Manelli*[4], *S. Kovalchuk*[4], *M. Frugis*[1], *K. Filonenko*[5], *I. Kryachok*[5], *A. Sciacovelli*[2], *M. Vegliante*[2], *A. Daniele*[2], *G. Sacchetti*[6], *A. Guarini*[2], *G. Rubini*[1];
[1]*Nuclear Medicine Department, University of Bari "Aldo Moro", Bari, ITALY,* [2]*Haematology Unit, IRCCS Istituto Tumori "Giovanni Paolo II", Bari, ITALY,* [3]*Haematology Department, Azienda Ospedaliero-Universitaria Maggiore della Carità, Novara, ITALY,* [4]*Haematology, University of Firenze, Firenze, ITALY,* [5]*Oncohematology department, National Cancer Institute, Kiev, UKRAINE,* [6]*Nuclear Medicine, AOU Maggiore della Carità, Novara, ITALY.*

Aim/Introduction: Mantle-cell lymphoma (MCL) represents 2-10% of all B-NHL. In 15-30% of cases, MCL may affect the gastrointestinal tract (GI), but the real frequency could be underestimated. It is unknown if the 18F-FDG-PET/CT is able to detect the GI involvement and eventually guide or omit the endoscopic exams.The objective of the study was to evaluate Sensitivity, Specificity, PPV, NPV and Accuracy of 18F-FDG-PET/CT in GI involvement detection in patients with MCL, in comparison to endoscopy with biopsy. ***Materials and Methods:*** We retrospectively evaluated 79 patients (median age: 66.8 years, range 27-83) with newly diagnosed MCL from 7 centres. All patients performed a pre-/post-treatment 18F-FDG-PET/CT scan and esophagogastroduodenoscopy (EGD)/colonoscopy at staging, according to the best clinical local practice. EGD/colonoscopy were repeated only if it was positive at staging. ***Results:*** Patients were staged III-IV in 89.9%, with B-symptoms observed in only 8%. Mostly, MIPI score was intermediate (35.5%) or high (39.2%).EGD with gastric biopsy was performed in 52 pts (65.8%); colonoscopy with colorectal biopsy in 31 (39.2%).At staging, gastric biopsy was positive in 13 pts (29.5%), while colorectal biopsy was positive in 11 pts (28.2%).At re-staging, only 1 patient presented a persistent colorectal positivity confirmed with biopsy.We found a GI positivity in 30 18F-FDG-PET/CT: upper GI involvement in 18 patients vs colorectal in 12 patients.In upper GI tract, false-negative 18F-FDG-PET/CT were observed in 8 patients; while 5 pts were false-positive. Sensitivity, specificity, PPV, NPV and accuracy were 61.90% (38.44-81.89%), 83.87% (66.27-94.55%), 72.22% (52.14% to 86.12%), 76.47% (64.84% to 85.14%) and 75.00% (61.05% to 85.97%) respectively.Comparing 18F-FDG-PET/CT and colorectal biopsy, false-negative results were in 5 and a false-positive only in 1 patient. Sensitivity, specificity, PPV, NPV and accuracy were 68.75% (41.34-88.98%), 93.33% (68.05-99.83%), 91.67% (61.67% to 98.69), 73.68% (57.21% to 85.43%), 80.65% (62.53% to 92.55%) respectively. ***Conclusion:*** Our data demonstrated a better performance of 18F-FDG PET/CT in detecting colorectal involvement compared to the upper GI one. Endoscopy with biopsy still need to be considered the gold standard in MCL patients. However, these promising results suggest that molecular imaging could replace colonoscopy if they will be confirmed on larger and prospective cohort. ***References:*** None

OP-252

Total Metabolic Tumor Volume Measured on Baseline 18F-FDG PET/CT Gaves Added Predictive Value to the Four Prognostic Scores in Patients with Peripheral T-cell lymphoma (PTCL)

C. Jiang[1], *C. Ding*[2], *Z. Zhou*[1], *J. Xu*[3];
[1]*Department of Nuclear Medicine, Nanjing Drum Tower Hospital,the Affiliated Hospital of Nanjing Unive, Nanjing, CHINA,* [2]*Department of Nuclear Medicine,the First Affiliated Hospital of Nanjing Medical University,Jiangsu Province Hospital, Nanjing, CHINA,* [3]*Department of Hematology, Nanjing Drum Tower Hospital,the Affiliated Hospital of Nanjing University Medical School, Nanjing, CHINA.*

Aim/Introduction: The aim was to explore the prognostic value of total metabolic tumor volume (TMTV) on baseline 18F-FDG PET/CT in patients diagnosed with peripheral T-cell lymphoma (PTCL). ***Materials and Methods:*** Fifty-seven PTCL patients who underwent baseline 18F-FDG PET/CT between December 2012 and January 2019 and did not receive any treatment were enrolled in this retrospective study. The FDG-avid lesions in each patient were segmented using semiautomated software to calculate the maximum standardized uptake value (SUVmax), total metabolic tumor volume (TMTV), and total lesion glycolysis (TLG) values using the boundaries of voxels presenting with SUV ≥2.5. Progression-free survival (PFS) and overall survival (OS) were used as end points to evaluate patient prognosis. The log-rank test and Cox regression analyses were used to evaluate PFS and OS. ***Results:*** ROC curve analysis demonstrated that the ideal TMTV cut-off value was 418.9 cm3. During the follow-up period of 5-70 months (23.1±16.9 months), high TMTV was significantly associated with worse PFS and OS. Multivariate analysis revealed that TMTV and the modified prognostic index for T-cell lymphoma (m-PIT) were independent predictors of PFS and OS.The combination of TMTV and International prognostic index(IPI),Prognostic index for T-cell lymphoma(PIT) International peripheral T-cell lymphoma Project score (IPTCLP) as well as m-PIT can be allowed for a significantly better risk sub-stratification in PFS and OS of PTCL patients. ***Conclusion:*** Both TMTV and m-PIT are independent predictors of the PTCL patient survival outcome. Moreover, the combination of TMTV and IPI,PIT,IPTCLP as well as m-PIT improved patient risk stratification and might contribute to the ability to personalize therapeutic regimens. ***References:*** None

OP-253

PET/CT-based Prognostic Biomarkers in Diffuse Large B-cell Lymphoma

S. Czibor[1], *F. Redondo*[2], *R. Carr*[3], *J. Cerci*[4], *D. Paez*[5], *S. Fanti*[6], *T. Györke*[1];
[1]*Semmelweis University, Budapest, HUNGARY,* [2]*Fundación Arturo Lopez Perez, Santiago, CHILE,* [3]*Guy's & St. Thomas' Hospital, King's College London, London, UNITED KINGDOM,* [4]*Quanta Diagnóstico e Terapia, Curitiba, Sao Paolo, BRAZIL,* [5]*International Atomic Energy Agency, Vienna, AUSTRIA,* [6]*Policlinico S. Orsola Malpighi, University of Bologna, Bologna, ITALY.*

Aim/Introduction: In diffuse large B-cell lymphoma (DLBCL) several F-18-fluoro-deoxy-glucose (FDG) positron emission tomography/computed tomography (PET/CT) based biomarkers have emerged in the last decade to define prognosis. Our aim was to investigate some of these in patients recruited into a previously reported international multicentre study. ***Materials and Methods:*** We report analysis of 107 patients with de novo DLBCL (mean age: 53.7y; range: 16-83y), most were recruited in Hungary (57) and Chile (36), others from Thailand (8), Philippines (4), and Italy (2). 58% patients presented with advanced stage disease. Lymphoma lesions on baseline PET/CT images were delineated with >SUV4 method. Metabolic Tumour Volume (MTV) and Total Lesion Glycolysis (TLG) values were calculated, as well as introducing body weight-adjusted (bwa) MTV and TLG values, normalised for patient body weight. Interim PET/CT (I-PET) scans were analyzed visually according to the Deauville criteria, (DS 1-5), and semiquantitatively with the calculation of ΔSUVmax, modified qPET [mqPET, calculated as SUVpeak(lesion)/SUVmean(liver)] and rPET [SUVmax(lesion)/SUVmax(liver)] values. The outcome assessed was 24-month progression-free survival (PFS). Receiver operating characteristics analyses were performed to define optimal cut-off points for baseline (MTV, TLG, bwaMTV, bwaTLG) and I-PET (ΔSUVmax, mqPET, rPET) values. ***Results:*** Two-year PFS in the whole cohort was 75%. Dividing the patients into two groups according to calculated optimal PET/CT cut-offs or pre-defined values (1-3 vs. 4-5 in case of DS) resulted in significantly different PFS between low- and high-risk groups for baseline MTV, bwaMTV, TLG, bwaTLG, as well as I-PET parameters DS, ΔSUVmax, mqPET, and rPET. Univariate Cox-regression analyses showed significant survival difference between low- and high-risk groups except for low/high bwaTLG, with calculated hazard ratios (HRs) lowest for bwaMTV (HR=2.3) and highest for rPET (HR=9.09) among the remaining PET parameters. Combined analysis was performed based on four groups defined by low/high MTV and DS 1-3 vs. 4-5. Kaplan-Meier curves showed good survival rate for DS 1-3 patients and poor PFS for DS 4-5 patients, irrespective of MTV. A similar analysis with ΔSUVmax and MTV resulted in relatively good PFS for all ΔSUVmax negative patients and also ΔSUVmax positive patients with low MTV. ΔSUVmax positive patients with high MTV formed a group with distinctly poor PFS. ***Conclusion:*** PET/CT baseline volumetric parameters and response assessment can be analyzed to generate several different prognostic biomarkers in DLBCL. The analyses reported here demonstrate that early treatment response has a greater

impact on survival than baseline volumetric assessment. ***References:*** None

OP-254

Imaging CXCR4 receptors expression for staging multiple myeloma by using 68Ga-Pentixafor PET-CT: Comparison with 18F-FDG PET-CT

B. Singh[1,2], *A. S. Shekhawat*[2], *A. Watts*[2], *H. Singh*[2], *R. K. Basher*[2], *P. Malhotra*[2];
[1]*Society of Nuclear Medicine, India, Chandigarh, INDIA,* [2]*PGIMER, Chandigarh, INDIA.*

Aim/Introduction: 68Ga-Pentixafor PET imaging targets CXCR4 expression which is over-expressed in multiple myeloma (1,2)**.** In this study, we evaluated the diagnostic utility of 68Ga-Pentixafor PET/CT for imaging CXCR-4 expression in multiple myeloma and compared results with 18F-FDG PET/CT. ***Materials and Methods:*** Thirty-four (21M; 13F; median age= 57.5 years) treatment naive multiple myeloma patients were recruited. All the patients underwent 18F-FDG-PET/CT and 68Ga-Pentixafor PET/CT imaging within one week. Freshly prepared 68Ga-Pentixafor (148-185 MBq) was injected intravenously and whole-body PET/CT (low dose CT) was acquired at 1-h post-injection. The pattern of uptake (diffuse, focal or mixed) and the mean SUV_{max} value of all lesions (when lesions were ≤ 5) or of the 5 most tracer avid lesions (when lesions was > 5) were evaluated. Tumor to background ratio (TBR_{max}) was calculated for both the tracers. Durie Salmon plus staging (DSPS) was used for disease staging on PET and the results were compared with International staging system (ISS). ***Results:*** 68Ga-Pentixafor PET-CT showed higher disease extent than seen on 18F-FDG PET in 23/34 patients (68.0%), lesser disease extent in 2/34 (6%) and similar disease extent in 9/34 (26%) patients. Significantly (p<0.001) higher TBR_{max} values (5.7; IQR 9.1) were obseved on 68Ga-Pentixafor PET as compared (2.9; IQR =4.0) to 18F-FDG PET values. Both the techniques detected extramedullary lesions in 6 patients. On the other hand, 68Ga-Pentixafor detected medullary lesions in 5, whereas, 18F-FDG PET in 3 patients. Further, only 68Ga-Pentixafor TBR_{max} correlated significantly (rho =0.421; 0.013) with bone marrow plasma cell percentage. When compared to ISS, 68Ga-Pentixafor PET upstaged more number (9/29) of patients as compared to (4/29) on 18F-FDG PET imaging. On the other hand, 18F-FDG-PET down-staged 9/29, whereas. 68Ga-Pentixafor PET down-staged only 3/29 patients. ***Conclusion:*** 68Ga-Pentixafor PET imaging detected more number of involved sites than 18F-FDG PET. The dual tracers imaging may provide additional information on spatial and temporal heterogeneity of MM and may have significance for response evaluation to CXCR4 targeting pharmacologic or endoradiotherapeutic therapies in $CXCR4^+$ and FDG^- disease variant of multiple myeloma. ***References:*** Herrmann K, Schottelius M, Lapa C, et al. First-in-Human Experience of CXCR4 Directed Endoradiotherapy with 177Lu- and 90Y-Labeled Pentixather in Advanced-Stage Multiple Myeloma with Extensive Intra- and Extramedullary Disease. J Nucl Med. 2016 ; 57 :248-5 Philipp-Abbrederis K, Herrmann K, Knop S et al. In vivo molecular imaging of chemokine receptor CXCR4 expression in patients with advanced multiple myeloma. EMBO molecular medicine [Internet]. BlackWell Publishing Ltd; 2015;7:477-87

OP-255

^{18}F-FDG PET/CT role in detecting Richter's transformation of Chronic Lymphocytic Leukemia and predicting overall survival

D. Albano[1], *E. Cerudelli*[2], *M. Gazzilli*[2], *F. Dondi*[1], *A. Mazzoletti*[1], *P. Bellini*[1], *L. Camoni*[2], *F. Bertagna*[1], *R. Giubbini*[1];
[1]*University of Brescia and Spedali Civili of Brescia, Brescia, ITALY,* [2]*Spedali Civili of Brescia, Brescia, ITALY.*

Aim/Introduction: Chronic lymphocytic leukemia (CLL) is an indolent, low-grade B cell lymphoproliferative disorder, which may transformed into aggressive lymphoma, called Richter's syndrome (RS). Our aim was to study the accuracy of ^{18}F-FDG-PET/CT and its semiquantitative parameters for the detection of RS and the impact on overall survival (OS). ***Materials and Methods:*** Between January 2009 and December 2019, 80 patients with histologically proven CLL were retrospectively enrolled; all patients underwent ^{18}F-FDG-PET/CT for the suspicious of RS in presence of enlarged lymph nodes. The PET images were analyzed visually and semi-quantitatively by measuring the maximum standardized uptake value body weight (SUVbw), the maximum standardized uptake value lean body mass (SUVlbm), the maximum standardized uptake value body surface area (SUVbsa), lesion to liver SUVmax ratio (L-L SUV R), lesion to blood-pool SUVmax ratio (L-BP SUV R), metabolic tumor volume (MTV) and total lesion glycolysis (TLG) of the hypermetabolic lesion then submitted to biopsy. For the entire population, receiver operating characteristic curve analysis was used to identify the optimal cutoff point of semiquantitative parameters in the light of risk of RS. OS curves were plotted according to the Kaplan-Meier method. ***Results:*** Seventy-eight patients had positive 18F-FDG-PET/CT, while the remaining 2 were not ^{18}F-FDG-avid. RS was diagnosed in 18 cases (22.5%): final diagnosis was DLBCL in 13 patients and HL in 5. All PET/CT metabolic parameters were significantly higher in RS groups compared to no RS group, except of metabolic volumes (MTV and TLG). Using ROC curves analysis, the best threshold identified were 9 for SUVbw, 5.3 for SUVlbm, 1.7 for SUVbsa, 2 for L-L SUV R and 4.8 for L-BP SUV R. After a median follow-up of 32 months, 24 patients died; OS was significantly shorter in patients with RS than patients without RS (27.8 vs 16.5 months, p 0.001). SUVbw ≥9, SUVlbm≥5.3, SUVbsa≥1.7,

L-L SUV R≥2, L-BP SUV R≥4.8 PS≥2, Binet stage and B symptoms were independently associated with shorter OS. ***Conclusion:*** In conclusion, in our study we demonstrated that semiquantitative PET/CT parameters SUV-related may be useful in discriminating patients with high risk to RS and also for predicting outcome survival. Instead, MTV and TLG showed no significant impact on predicting RS and OS. ***References:*** None

OP-256

Patients with Erdheim-Chester Disease who Harbor the BRAF V600E Mutation, Exhibit Significantly Higher Metabolic Activity in the Adrenal glands Assessed by ^{18}F-FDG PET/CT, when Compared to Mutation-Negative Counterparts

G. Papadakis[1,2], *F. Hannah-Shmouni*[3], *G. C. Manikis*[2], *A. H. Karantanas*[1], *K. Marias*[2], *K. J. O' Brien*[4], *W. A. Gahl*[4], *J. I. Estrada-Veras*[5];

[1]*Department of Medical Imaging, Medical School, University of Crete, Heraklion, GREECE,* [2]*Computational Biomedicine Laboratory (CBML), Foundation for Research and Technology Hellas (FORTH), Heraklion, GREECE,* [3]*Section on Endocrinology and Genetics, Eunice Kennedy Shriver National Institute of Child Health and Human Development, Bethesda, MD, UNITED STATES OF AMERICA,* [4]*Office of the Clinical Director, National Human Genome Research Institute, National Institutes of Health, Bethesda, Bethesda, MD, UNITED STATES OF AMERICA,* [5]*Medical Genetics Branch, National Human Genome Research Institute, National Institutes of Health, Bethesda, MD, UNITED STATES OF AMERICA.*

Aim/Introduction: Erdheim-Chester disease (ECD) is a rare non-Langerhans cell histiocytosis characterized by uncontrolled inflammation resulting in fibro-inflammatory damage in multiple organs, including the hypothalamic-pituitary-adrenal axis (1). The aim of the current study was to investigate potential associations between disease-causing BRAF V600E variants and adrenal metabolic activity assessed by ^{18}F-FDG PET/CT imaging (2). ***Materials and Methods:*** 20 ECD patients (mean age ± SD at first ECD manifestations: 56.3 ±10.25 y.o.) were evaluated with whole-body ^{18}F-FDG-PET/CT scans. 13 patients harbored the BRAF V600E mutation, while 7 were BRAFnegative. PET-acquisition commenced 60 minutes after intravenous administration of approximately 10mCi of ^{18}F-FDG, while a non-contrast, low dose CT scan was performed for attenuation correction and co-registration purposes. Metabolism in the adrenal glands was assessed by quantifying ^{18}F-FDG uptake, using the MIM Vista workstation (version 6.5.9). A VOI encompassing both adrenal glands was drawn, and an automated SUVmax threshold-based approach was applied in order to include all ^{18}F-FDG-avid regions of the adrenal glands, while excluding low-level background activity (SUVmax threshold was set at 1.5). The software enables automatic generation of separate VOIs encircling all areas above the SUVmax threshold set by the user. Afterwards, the following parameters were automatically obtained: SUVmax, SUVmean (average SUV), total ^{18}F-FDG-avid adrenal volume (Metabolic Tumor Volume; MTV) and total glycolytic activity (TGA) of the adrenal glands, determined as the product of SUVmean multiplied by MTV (TGA=SUVmean x MTV). Finally, statistical analysis was performed using R software (version 3.3.3). ***Results:*** Mann-Whitney-Wilcoxon test revealed statistical differences ($p<0.05$) between BRAF-positive and BRAF-negative ECD patients, with mutation carriers exhibiting significantly higher ^{18}F-FDG activity by the adrenal glands in terms of all the obtained PET-parameters: SUVmax $p=0.018$, SUVmean $p=0.026$, MTV $p<0.01$, and TGA $p<0.001$. (P-values were adjusted using false discovery rate (FDR) correction to account for multiple hypothesis testing.) ***Conclusion:*** ECD patients who harbor the disease-causing BRAF V600E variant present with hypermetabolic adrenal glands when compared to mutation negative ECD patients, implying increased susceptibility of BRAF-positive ECD-patients to adrenal involvement and potentially adrenal insufficiency. ***References:*** 1. Estrada-Veras JI, et al "The clinical spectrum of Erdheim-Chester disease: an observational cohort study." Blood Adv. 2017 Feb 14;1(6):357-366. 2. Papadakis GZ, et al "Adrenal cryptococcosis in an immunosuppressed patient showing intensely increased metabolic activity on ^{18}F-FDG PET/CT". Endocrine 2016 Dec;54(3):834-836.

OP-257

Role of [^{18}F]FDG PET/CT in patients with Monoclonar Gammopathy of Unknown Significance (MGUS)

T. Rudolphi-Solero*, R. Sánchez Sánchez, E. Triviño-Ibáñez, M. Rashki, J. Fernández Fernández, Á. C. Rebollo Aguirre;*
SAS, Granada, SPAIN.

Aim/Introduction: The monoclonal gammopathy of undetermined significance (MGUS) is a clinically asymptomatic premalignant clonal plasma cell or lymphoplasmacytic proliferative disorder. It is the most common type of plasma cell dyscrasia. The risk of progression to multiple myeloma and associated malignancies is variable depending on risk stratification.The aim of this study is to evaluate the role of [18F]FDG PET/CT in the correct classification and monitoring of MGUS patients. ***Materials and Methods:*** Retrospective analysis of patients who underwent [18F]FDG PET/CT, after MGUS diagnosis from 2012 to 2018. They were classified in three subgroups according to the risk of progression to myeloma (low, intermediate, high). A positive [18F]FDG PET/CT study for myeloma is considered if it presents areas of focal hypermetabolism outside of areas of physiological distribution or diffuse increase in bone marrow of activity, superior to the background seen in patients without infiltration of the marrow.All statistical analysis was carried

out using SSPS version 23.The descriptive analysis of categorical variables were described as frequencies and the numeric variables as mean and standard deviation. We studied the possible association between all the collected variables and a positive [18F]FDG PET/CT result through bivariate analysis.After the non-normality confirmation of the population regarding the monoclonal component rate by Kolgomorov-Smirnov test, the Mann-Whitney U test was performed. Significant differences were observed respecting the PET/CT result. Receiver Operating Characteristics (ROC) curve analysis was done to assess a cutoff representing the best accuracy in terms of best compromise between sensitivity and specificity in evaluating active myeloma. ***Results:*** A total of 255 patients with MGUS (mean age 72,1±12,5 years old, 50,2% women) were included. 25 had a positive [18F]FDG PET/CT, 15 in diagnosis and 10 in follow-up (average time to progression: 21,3±10,4 months). We found a significant statistical association between the monoclonal component rate and a positive [18F]FDG PET/CT. The cut-off point with a better sensitivity and specificity relation (S=70% and E=70%) through ROC curve analysis was 1 g/dL (AUC 0,795). ***Conclusion:*** [18F]FDG PET/CT allows the correct classification of patients with MGUS, highlighting those patients with a small monoclonal component or even non-secretors who have active bone disease and therefore are already myeloma. The monoclonal component rate seems to be the variable most related to the probability of presenting a positive [18F]FDG PET/CT study for myeloma. ***References:*** None

OP-258

Prognostic value of FDG-PET/CT derived visual and semi-quantitative parameters in Multiple Myeloma (MM) patients

A. Farina[1], *E. Zamagni*[2], *S. Strolin*[3], *L. Strigari*[3], *L. Dozza*[2], *M. Cavo*[2], *S. Fanti*[1], *C. Nanni*[1];
[1]*Nuclear Medicine Department, Sant'Orsola-Malpighi Hospital, University of Bologna, Bologna, ITALY,* [2]*Hematology Department, Sant'Orsola-Malpighi Hospital, University of Bologna, Bologna, ITALY,* [3]*Medical Physics Department, Sant'Orsola-Malpighi Hospital, University of Bologna, Bologna, ITALY.*

Aim/Introduction: At staging and before maintenance PET/CT provides prognostic parameters such as the number of hot focal lesions and the diffuse involvement of the bone marrow(BM).However, they are a surrogate for the volume of active disease, that can be more accurately measured with dedicated semi-automatic softwares.Aim of this study is to explore the prognostic value of metabolic tumor volume(MTV)and total lesion glycolysis(TLG)in the context of other PET parameters MM patients. ***Materials and Methods:*** We conducted a retrospective study on a group of patients affected by MM referred from the Hematology-Unit of AOU S.Orsola-Malpighi for a basal and a post therapy scan. MTV,TLG,DS of the hottest focal lesion, SUVmax of the hottest focal lesion,DS of the BM uptake were measured before and at completion of therapy.Overall Survival(OS) and Progression free survival(PFS)were analyzed from the begin of therapy. Possible prognostic values were extracted from Volumes-of-Interests(VOIs)contoured on co-registered basal and interim scans using MIM Vista Software with semiautomatic approach. The Kaplan-Meier-method was used to estimate PFS and OS.Survival curves were compared using the log-rank test. ROC-curves were used to select cut-offs.Cox-multivariate proportional hazard models were used to identify indipendent prognostic factors affecting to PFS and OS.Furthermore, the predicticted probalities of PFS and OS were presented with help of nomograms reporting all the statistically significant covariates included in the fitted models. ***Results:*** 42 patients (20F, 22M,mean age5 yo, mean follow up51months) were retrospectively enrolled from2011to2014.Several prognostic parameters were found. Survival curves allowed to stratify patients into2risks groups with appropriate cut-offs, even though most of them demonstrated a p-value only close to significance level probably because of the relatively low number of patients. In particular at staging: presence of FDG avid extramedullary disease($p<0.001$) and MTV>130($p=0.07$) were predictive for a worse OS.At completion of therapy,DS≥4of the diffuse BM uptake(0.06) was predictive both for worse PFS and OS while MTV>2and TLG>5.2were both predictive for worse OS($p=0.04$ both). On a multivariate analysis, MTV after therapy, TLG after therapy and SUV max of the hottest focal lesion seems to be indipendent factors affecting OS (Overall model P-value=0.07). ***Conclusion:*** The novel tools seem to provide promising parameters for the risk stratification of MM pts, both at staging and after therapy.These parameters can be included into nomograms for risk assessment, an easy and useful method to employ in the clinical practice. However, these parameters need to be tested on a wider population of patients to better confirm a statistical significance. ***References:*** None

509

Featured Session: Parathyroid Imaging - Who Scores the Best Goals in this Champions League?

Friday, October 23, 2020, 10:40 - 12:10 Channel 9

OP-259

Starters and Backups in Parathyroid Imaging

P. Petranovic*; University Hospital Center Sestre milosrdnice, Oncology and nuclear medicine, Zagreb, CROATIA.*

OP-260

Parathyroid scintigraphy pre-surgery: comparison between methods in primary hyperparathyroidism

L. Torres, A. Oliveira, J. Pereira;
Centro Hospitalar Universitário São João, Porto, PORTUGAL.

Aim/Introduction: Most of primary hyperparathyroidism (pHPT) cases are due to a single hyperfunctioning adenoma (about 85%) (1), occasionally more, surgical excision being the only cure. In the age of minimally invasive parathyroidectomy, preoperative parathyroid scintigraphy can be useful in reducing the duration and extent of surgical exploration. Different protocols and techniques include dual-phase, double tracer and SPECT-CT. We aimed to study each of these methods' diagnostic value in detecting abnormal parathyroid glands, as well as the possible influence of concomitant thyroid disease. ***Materials and Methods:*** We retrospectively reviewed patients with biochemical pHPT who underwent parathyroid scintigraphy in our department from June/2018 to December/2019. Out of 164 patients who met these criteria, 47 had undergone surgery with histological analysis (gold standard), and were included in the study. All patients were submitted to a 3-method protocol consisting of planar imaging using ^{99m}Tc-Sestamibi at 15 mins and 2 h post-injection, SPECT-CT acquisition, 2 h post-injection, followed by ^{99m}Tc-pertechnetate injection and final planar imaging. The acquired ^{99m}Tc-pertechnetate thyroid planar image was then subtracted from the early ^{99m}Tc-Sestamibi planar image. Results of the different techniques were analyzed and compared. ***Results:*** 30 patients (64%) had previously documented thyroid disease. Review of the hispatological reports revealed 39 single parathyroid adenomas (83%), three multiple adenomas (6%), one parathyroid carcinoma (2%) and four cases (9%) with no lesions. Overall sensitivity, specificity, PPV, NPV and accuracy values of the three methods were: 91,4%, 16,7%, 0,76, 0,40 and 72,4% for SPECT-CT; 77,8%, 27,3%, 0,78, 0,27 and 66,0% for dual-phase; 70,3%, 30,0%, 0,79, 0,21, and 61,7% for the subtraction method. In patients with thyroid disease, the sensitivity and diagnostic accuracy values were lower when compared to patients with no thyroid disease in SPECT-CT (90,0% vs 92,3% and 73,3% vs 75,0%, respectively), and more significantly in dual-phase (69,6% vs 92,3% and 63,3% vs 70,6%) and subtraction (62,5% vs 84,6% and 60,0% vs 73,3%). ***Conclusion:*** Our results suggest that, despite its lower specificity, parathyroid imaging with SPECT-CT is a more sensitive and accurate method in detecting abnormal parathyroid glands than the dual-phase or subtraction. In accordance with previous literature, concomitant thyroid disease seems to lower the diagnostic performance of this exam. ***References:*** 1. Hindié E, Ugur O, Fuster D, O'Doherty M, Grassetto G, Ureña P, Kettle A, Gulec SA, Pons F, Rubello D, Parathyroid Task Group of the EANM (2009) 2009 EANM parathyroid guidelines. Eur J Nucl Med Mol Imaging 36:1201-1216.

OP-261

The contribution of protocol selection to diagnostic accuracy in MIBI parathyroid scintigraphy: reevaluation with SPECT/CT and histopathologic findings

***B. Özdemir**, Ü. Korkmaz, S. Soyluoğlu, E. Gökdemir, G. Durmuş Altun;*
Department of Nuclear Medicine, Trakya University, Edirne, TURKEY.

Aim/Introduction: The evolving procedures provide additional information about localization of parathyroid lesions after SPECT/CT added in routine protocols. Dual phase parathyroid scintigraphy has been used to determine parathyroid lesions and to assist minimally invasive procedures. Thyroid lesions is the main cause of misdiagnosis and additionally the most important lesions that reduces sensitivity and diagnostic accuracy. In our study, we aimed searching the optimal imaging time to revised protocols, also determining the SPECT/CT's contribution to dual phase parathyroid scintigraphy. ***Materials and Methods:*** We studied 188 patients (mean age 57±12,8 years; 40 male, 144 female) who underwent preoperative parathyroid scintigraphy and ultrasonography between January 2017 and September 2019. İmaging included dynamic blood flow, blood pool ,15-60th images as early Tc 99m MIBI images and 2nd-4th hour Tc99m MIBI images as delayed ones. Also was added 60th minute Tc 99m MIBI SPECT/CT images and Tc99m pertechnetate thyroid images. Lesions characterized with visual analog scale (0-3) according to the MIBI accumulation pattern. Each data was evaluated with clinical information, histopathologic and laboratory findings. ***Results:*** In 95 of 188 patients, scintigraphic findings showed parathyroid lesions at any side. At the 60th minute, 71 (sensitivity 75%) patients became positive, while 87 (sensitivity 92%) focus was detected on the SPECT / CT that taken right after 60th minute. Eight of 95 lesions were detected as ectopic foci. In 87 patients ; lesions were localized on perithyroidal area. One patient was diagnosed with parathyroid carcinoma and 3 patients were diagnosed with parathyroid hyperplasia based on histopathological findings. Benign/malignant thyroid disease was detected in 9 patients, and this patient group was accepted as the ones that caused false positivity. Thyroid pathology was detected in 6 patients, but dual phase parathyroid scintigraphy did not show a positivity. Diagnostic accuracy of the SPECT/CT was calculated as 82.5% based on histopathological data. ***Conclusion:*** In detecting parathyroid lesions, SPECT / CT sensitivity was 92% and diagnostic accuracy was 83%. The false positivity rates of the lesions were high in early images and these false positivity rates decreased with delayed images or SPECT/CT. Also we found out 4th hour images didn't make significant contribution to second hours.

SPECT/CT is the most accurate method to localisation of biochemically proven parathyroid lesions. ***References:*** None

OP-262

F-18 Choline PET-CT is valuable in the assessment of normocalcemic primary hyperparathyroidism

C. Pirich[1], D. Schaffler-Schaden[2], G. Schweighofer-Zwink[1], G. Rendl[1], L. Hehenwarter[1], M. Beheshti[3];
[1]Dpt. of Nuclear Medicine and Endocrinology, University Hospital Salzburg, Salzburg, AUSTRIA, [2]Institute of General Practice, Family Medicine and Preventive Medicine Paracelsus Medical University, Salzburg, AUSTRIA, [3]Clinic for Nuclear Medicine, RWTH, University Aachen, Aachen, GERMANY.

Aim/Introduction: Normocalcemic primary hyperparathyroidismhas (pHPT) is increasingly seen as clinically relevant condition. In this prospective study, we evaluated the value of ^{18}F-choline (FCH) PET-CT for detection of parathyroid adenoma in patients with normocalcemic pHPT. ***Materials and Methods:*** FCH PET-CT was performed on a Philips Ingenuity TF (Philips Healthcare, PC Best, The Netherlands) in 90 patients (mean age 56,7±7,0 years) with biochemical evidence of pHPT (median 142 pg/ml, range: 68-246), and normal serum calcium level (median: 2.53 mmol/l, range: 2,09-2,63). A median activity of 197 MBq F-18 choline was injected intravenously and imaging performed 1 hour later. Images were reconstructed using a three-dimensional ordered-subsets iterative TOF (BLOB-OS-TF) algorithm after correction for scatter and attenuation. At least one abnormal FCH focus corresponding to a parathyroid gland or ectopic parathyroid tissue was considered as positive finding by visual analysis. Histopathological analysis was performed from any surgically removed parathyroid tissue. Based on WHO classification of bone mineral density measurement by DXA 35, 43, and 12 patients had osteoporosis, osteopenia or normal bone mineral density, respectively. Three patients with secondary HPT were excluded from statistical analysis. ***Results:*** Among 87 patients 36 (41%) had positive imaging findings by visual analysis. .Surgery for primary HPT was clinically indicated and performed in 19 patients, the remaining were followed-up biochemically. In patient-based analysis, FCH PET-CT was able to detect parathyroid adenoma in 89% of patients eligible for surgery (17/19). Two patients had biglandular disease, and one patient ectopic disease. In lesion-based analysis, FCH PET-CT showed a sensitivity of 86% (18/21). Semi-quantitative analysis of FCH-positive lesions exhibited that the mean SUVmax of parathyroid adenoma was trendwise higher in patients with surgical than in those with conservative follow-up (7.4±4.2, vs. 4.67±3.46). ***Conclusion:*** In this prospective study, FCH PET-CT showed promising results for the detection of parathyroid adenoma even in patients with normocalcemic pHPT. In those patients high at risk for osteoporotic fractures parathyroid imaging using FCH PET/CT might guide successful surgical removal of parathyroid adenoma. ***References:*** None

OP-263

Early-phase SPECT/CT, as part of a hybrid dual-phase/double-tracer protocol, improves detection of rapid washout hyperfunctioning parathyroid glands

L. Lemos[1], P. Soeiro[1], R. Ferreira[1,2], G. Costa[1,3], J. Pedroso de Lima[1,2,3];
[1]Centro Hospitalar e Universitário de Coimbra, Coimbra, PORTUGAL, [2]Instituto de Ciências Nucleares Aplicadas à Saúde (ICNAS), Faculdade de Medicina, Universidade de Coimbra, Coimbra, PORTUGAL, [3]Faculdade de Medicina, Universidade de Coimbra, Coimbra, PORTUGAL.

Aim/Introduction: Rapid washout of the radiopharmaceutical is a cause of false negative studies in [^{99m}Tc]Tc-sestamibi parathyroid scintigraphy (PS), particularly in dual-phase protocols (with an early phase at 15-20 minutes and a late phase at 2-3 hours). While SPECT/CT imaging can improve diagnostic accuracy, the ideal timing of acquisition is not yet clear. This study aims to evaluate whether early-phase SPECT/CT improves detection of rapid washout hyperfunctioning parathyroid glands (HPG) as part of a hybrid dual-phase/double-tracer protocol. ***Materials and Methods:*** We reviewed the clinical charts of 122 patients (94 female, 28 male; mean age: 61.95±14.76) with hyperthyroidism who underwent PS, between March 2019 and March 2020. In that cohort of patients we used a new hybrid dual-phase/double-tracer protocol imaging acquisition protocol, with cervical SPECT/CT being performed in every patient, immediately after planar early-phase images. Digital subtraction was performed whenever possible, using the [^{99m}Tc]TcO_4^- and the early-phase [^{99m}Tc]Tc-sestamibi planar images. All scintigraphic studies were reviewed and classified in two groups: negative (no abnormal findings were observed in both phases) and positive (if findings suggesting HPG were detected in, at least, one of the two phases). In positive scans, the abnormal parathyroid gland was considered to display rapid washout of the radiopharmaceutical if it was not visible on late-phase images. Relevant demographic and clinical data were also collected, regarding biochemical parameters (PTH, calcium, phosphates, vitamin D, creatinine), other imaging studies, surgery and pathology reports. ***Results:*** Of the 122 studies analysed, 106 patients (86,9%) were referred for primary hyperparathyroidism, whereas 16 (13,1%) had secondary or tertiary hyperparathyroidism. 50 (41.0%) had positive studies, 8 (16.0%) of which showing rapid washout HPG (6 in primary hyperparathyroidism, 2 in secondary/tertiary hyperparathyroidism). Multiple HPG were reported in three patients, all of which with secondary/tertiary hyperparathyroidism. Patients with positive studies had significantly higher PTH ($p<0.01$) and calcium ($p<0.01$) levels than those with negative studies. We found no statistically significant differences in biochemical markers between

patients with rapid washout and delayed washout HPGs. Four patients with primary hyperthyroidism underwent surgery and the HPG was correctly located by scintigraphy in every case. ***Conclusion:*** In this series, the inclusion of early-phase SPECT/CT, as part of a hybrid dual-phase/double-tracer protocol, significantly improves the detection rates of rapid washout parathyroid glands. No predictive factors were found for rapid washout hyperfunctioning parathyroid glands in patients with primary or secondary/tertiary hyperparathyroidism. ***References:*** None

OP-264

Detection of hyperfunctioning parathyroid tissue with F18-fluorocholine PET/CT in patients with hyperparathyroidism

T. Nazerani Hooshmand[1], B. Pernthaler[1], A. Ntoumanoglou-Schuiki[2], P. Ofner-Kopeinig[3], R. M. Aigner[1];
[1]Medical University of Graz, Department of Radiology, Division of Nuclear Medicine, Graz, AUSTRIA, [2]Medical University of Graz, Department of Obstetrics and Gynecology, Graz, AUSTRIA, [3]Medical University of Graz, Institue for Medical Informatics, Statics and Documentation, Graz, AUSTRIA.

Aim/Introduction: Exact localization of a hyperfunctioning parathyroid tissue in hyperparathyroidism (HPT) is highly advantageous for an exact preoperative plan to acquire the best possible results. Recent studies show the high accuracy of F18-fluorocholin (FCH) PET/CT in finding parathyroid adenomas; however, there is no consensus for the optimal acquisition time after intravenous application of the tracer. The aim of our study is to determine a proper FCH PET/CT protocol and to find if there is any correlation between PET/CT results and laboratory parameters in patients with HPT. ***Materials and Methods:*** Forty six patients with biochemical proven HPT were enrolled in this retrospective study. FCH PET/CT scan was performed and the acquisitions were conducted dynamically in the cervical region over 15 minutes, followed by static images of the neck and mediastinum at 15, 30, 45- and 60-minutes after tracer injection. The SUVmax (standardized maximum uptake value) of the suspected parathyroid lesion was measured in the dynamic and in all static images. The laboratory results of our patients including parathyroid hormone level, calcium and phosphate serum level and vitamin D levels were included in our database. ***Results:*** In 57% of patients (26/46) the suspected parathyroid lesion showed the highest tracer uptake at 45 minutes post injection with a SUVmax of 8, 23 ±3,07. In 22% of patients (10/46) the highest SUVmax was at 15 minutes post injection. There was no significant correlation between parathyroid hormone level, calcium and phosphate serum level and vitamin D and the SUVmax of the parathyroid lesions. ***Conclusion:*** Our study shows that the best acquisition time point for parathyroid gland is at the 45 minutes after tracer injection; however, it is yet to be investigated if the dynamic phase is needed. Our study shows that the biochemical parameters such as parathyroid hormone level, calcium and phosphate serum level and vitamin D do not correlate with the intensity of the tracer uptake in hyperfunctioning parathyroid lesion. ***References:*** 1. Broos WAM, Wondergem M, van der Zant FM, Knol RJJ. Dual-Time-Point (18)F-Fluorocholine PET/CT in Parathyroid Imaging. J Nucl Med. 2019;60(11):1605-102. Fischli S, Suter-Widmer I, Nguyen BT, Muller W, Metzger J, Strobel K, et al. The Significance of 18F-Fluorocholine-PET/CT as Localizing Imaging Technique in Patients with Primary Hyperparathyroidism and Negative Conventional Imaging. Front Endocrinol (Lausanne). 2017;8:380

OP-265

A Prospective GCP-Controlled Study of 60 Patients Regarding the Location of Hyperfunctioning Parathyroid Glands in PHPT Using 11C-Choline PET/CT vs. Dual Isotope SPECT/CT

***J. Christensen[1]**, A. Ismail[1], M. Krakauer[2], F. N. Bennedbæk[3], B. Zerahn[1], B. Kristensen[1], S. B. Søndergaard[1], L. T. Jensen[1];*
[1]Dept. of Nuclear Medicine, Herlev & Gentofte University Hospital, Herlev, DENMARK, [2]Dept. of Nuclear Medicine, Herlev & Gentofte University Hospital, Gentofte, DENMARK, [3]Dept. of Endocrinology, Herlev & Gentofte University Hospital, Herlev, DENMARK.

Aim/Introduction: In primary hyperparathyroidism (PHPT), one or more parathyroid gland(s) produce(s) excess parathyroid hormone (PTH), causing increased p-Ca^{2+}. The only cure is surgical removal of the hyperfunctioning parathyroid gland(s) (HPGs). Preoperative location imaging is essential to insure minimally invasive surgery. The standard method is dual-isotope subtraction scintigraphy (SPECT/CT) using ^{99m}Tc-sestamibi/^{123}I-iodide. While accurate (sensitivity 93% (86%-97%), specificity 99% (97%-100%)) this method is time consuming. We compare the "standard method" to ^{11}C-Choline PET/CT, a faster method (10 minutes vs. up to 4 hours) with lower effective dose (6.6 mSv vs. 12.9 mSv) in a GCP-controlled prospective trial of 60 patients. ***Materials and Methods:*** Calculations of effect measures involve multiple observations per patient. Observations within patients are often positively correlated (i.e. the likelihood of a second HPG is higher than the first HPG). This may lead to biased estimates of sensitivity and specificity when correlation is ignored. More importantly, analyses ignoring correlation often yield misleadingly small estimated standard errors for sensitivity and specificity because observations are counted as independent. Thus, analyses of data that include multiple observations per patient require adjustment to account for possible correlation. We calculated effect measures at the patient level rather than using multiple observations per patient. Patients diagnosed with PHPT and referred to preoperative imaging are included in the present

study and undergo additional preoperative ^{11}C-Choline PET/CT.Number of HPGs, location relative to the thyroid gland (left/right and upper/middle/lower third/ectopic) are noted for each imaging modality and during surgery. Surgical results, confirmed by pathology and biochemistry serves as the gold standard. ***Results:*** The presented data is an interim analysis of the first 60 patients in an ongoing project. Patients are predominately female (75 %) with a mean age of 62 years (range 24-83). Sensitivities of dual isotope subtraction scintigraphy and 11C-Choline PET/CT are 98% (90%-100%) and 100% (93%-100%) respectively. Calculations for specificities have been done, but are omitted. As all included patients have PHPT, they must have at least one HPG per definition, and no patient should be a "truenegative". ***Conclusion:*** Patient-level analysis yields high sensitivities for both scintigraphy and PET/CT.Sensitivities were higher than previously found analysis at the gland level, because in the latter, every gland must be identified separately to count as true positive. These interim results are optimistic, but more statistical power is needed to warrant a change in recommended method. Project inclusion continues with next interim analysis at 100 patients. ***References:*** None

OP-266

Comparison between digital and analog 18F-Fluorocholine PET/CT detection rate of parathyroid adenomas

M. Sizova*, D. López-Mora, M. Estorch, F. Fuentes- Ocampo, S. Abouzian, A. Flotats, V. Camacho, J. Pérez García, I. Carrió;*
Hospital de la Santa Creu i Sant Pau, Barcelona, SPAIN.

Aim/Introduction: To compare the detection rate of hyperfunctioning parathyroid tissue (HPT) between digital and analog PET/CT with 18F-fluorocholine in patients with primary hyperparathyroidism (PHPT) and negative or inconclusive 99mTc-MIBI scan. ***Materials and Methods:*** Forty-eight patients (35 females; 58 ± 14,8 years) with PHPT and negative or inconclusive 99mTc-MIBI scintigraphy/SPECT/CT were prospectively included from January 2018 to June 2019. All patients consecutively underwent a dual imaging protocol (digital and analog PET/CT, in random order) on the same day, after a single injection of 18F-fluorocholine. Three nuclear medicine physicians assessed the detection rate by identifying focal radiotracer uptake suspicious of HPT. ***Results:*** HPT was detected in 42/48 (88%) patients by the digital system, whereas it was detected in 32/48 (67%) patients by the analog system ($p<0.01$). Parathyroidectomy was performed in 33/48 patients. HPT was confirmed in 30/33 (91%) patients by the digital system, whereas in 22/33 (67%) patients by the analog system ($p<0.01$). All HPT suspected lesions that were resected and detected only by the digital system were <10mm (7.5 mm ± 1.3 mm), while those detected by both systems were >10mm (13 mm ± 3.8 mm). The elevated baseline preoperative parathyroid hormone plasma levels decreased 10 minutes after parathyroidectomy (13.6 ± 10.1 pmol/L vs. 2.9 ± 2.5 pmol/L). Fifteen patients are still waiting for parathyroidectomy. In 11/15 patients, focal radiotracer uptake suspicious HTP was detected, 10 detected by both systems and 2 detected only by the digital PET/CT ($p<0.01$). In 4 patients neither the digital nor the analog PET/CT detected focal radiotracer uptake suspicious of HTP. ***Conclusion:*** In patients with PHPT and negative or inconclusive 99mTc-MIBI scan, digital PET/CT offers a superior detection rate of HPT than the analog PET/CT, particularly in subcentimeter parathyroid adenomas. ***References:*** None

OP-267

^{11}C-Methionine PET/CT in Patients with Primary Hyperparathyroidism and Inconclusive Pre-Operative Work-Up: Diagnostic Accuracy and Role of Semi-quantitative Analysis

D. Maccora*[1], C. Caldarella[2], M. L. Calcagni[1,2];*
[1]Istituto di Medicina Nucleare, Università Cattolica del Sacro Cuore, Rome, ITALY, [2]Dipartimento di Diagnostica per Immagini, Radioterapia Oncologica ed Ematologia, UOC di Medicina Nucleare, Fondazione Policlinico Universitario A. Gemelli IRCCS, Rome, ITALY.

Aim/Introduction: PET/CT using Carbon-11-Methionine (C-MET) is a promising method in detecting abnormal parathyroid glands in patients with hyperparathyroidism (HPT) and inconclusive standard diagnostic work-up. The first aim of the study was to evaluate which is the diagnostic role of C-MET in patients with primary HPT and inconclusive pre-operative imaging. Secondly, we aimed to investigate whatever C-MET semi-quantitative parameters may reflect biochemical and histological characteristics of involved glands. ***Materials and Methods:*** Patients with primary HPT, undergoing C-MET after an inconclusive pre-operative imaging and having a parathyroid surgery, were retrospectively included. Histological diagnosis, post-operative normalization of serum calcium and parathyroid hormone (PTH) were the reference standard. C-MET diagnostic performances were evaluated by visual assessment and semi-quantitative analysis. Parameters, as SUV_{max}, SUV_{peak}, SUV_{mean}, functional lesion volume (FLV) and total lesion activity (TLA), were measured for each detected lesion; SUV_{mean}, FLV and TLA were calculated on 40%-90% thresholds of SUV_{max} to define $SUV_{mean40\text{-}90}$, $FLV_{40\text{-}90}$ and $TLA_{40\text{-}90}$. Results were correlated with patients' clinical-laboratory and histological data (calcium and PTH values; main size/weight of excised glands). Mann-Whitney test was used and P value <0.05 was considered significant. ***Results:*** Thirty-eight patients were included. Median calcium and PTH values were 11.1 mg/dl [interquartile range (IQR) 10.6 - 11.5] and 154.6 pg/ml (IQR 101.8 - 227.0), respectively. C-MET

sensitivity, specificity and accuracy in detecting the correct side in the neck of the abnormal gland were 79%, 75% and 79%, while in detecting its correct position were 75%, 50% and 71%, respectively. A per-patient analysis showed sensitivity, specificity, accuracy of 85%, 75% and 84% in detecting the side, 84%, 50% and 79% in detecting the exact position, respectively. Clinical-laboratory and histological data were not significantly different according to C-MET performance. Calcium results were not significantly related to any C-MET semi-quantitative parameters (P=ns), while SUV_{peak}, FLV_{50-70} and TLA_{40-70} were significantly higher in cases with higher PTH results (P<0.05, respectively). The size of the excised gland showed a significant positive correlation with SUV_{max}, SUV_{peak}, FLV_{40-80} and TLA_{40-90}, its weight with SUV_{peak}, $SUV_{mean40-50}$, FLV_{40-80} and TLA_{40-90} (P<0.05, respectively). ***Conclusion:*** C-MET showed a good performance in detecting hyperfunctioning parathyroid glands in selected patients with inconclusive diagnostic work-up. Although clinical data did not guide in predicting C-MET performance, some semi-quantitative PET-derived parameters (i.e. SUV_{peak}, FLV_{50-70} and TLA_{40-70}) closely correlated with pre-operative PTH as well as with size and weight of the excised gland, thus reflecting some biochemical and histological characteristics of involved glands. ***References:*** None

OP-268

The value of PET/CT in patients with primary hyperparathyroidism and negative or inconclusive neck ultrasound and MIBI scintigraphy

D. Huic[1,2], A. Golubić[1], E. Pasini Nemir[1];
[1]Department of Nuclear Medicine and Radiation Protection, University Hospital Centre Zagreb, Zagreb, CROATIA,
[2]School of Medicine Zagreb, Zagreb, CROATIA.

Aim/Introduction: Primary hyperparathyroidism (PHPT) is a common endocrine disorder and parathyroid surgery still represents the only curative approach. Preoperative localization of hyperfunctioning parathyroid glands is very challenging, but it is crucial for focused and minimally invasive parathyroid surgery. The aim of our study was to assess the value of ^{18}F-fluorocholine positron emission tomography (PET/CT) in very selected group of patients with negative or inconclusive neck ultrasound and MIBI scintigraphy and history of hyperparathyroidism of several years. ***Materials and Methods:*** We performed PET/CT with 100-150 MBq of ^{18}F-fluorocholine in 42 patients (female 36, male 6, mean age 57years) in 18 months' period. Low-dose PET/CT acquisition was done 15-30 minutes' post injection. The regions of neck and thorax were scanned, 3 min per bed position. ***Results:*** In 40 patients (95%) 42 foci of increased tracer uptake suggestive for hyperactive parathyroid gland have been found, single in 38 patients, and two in two patients. One patient was negative and the other one judged as false positive after surgery. Most often localisation of the hyperactive parathyroid gland in the neck region was in the level of the lower pole of thyroid lobe (11 on the right side,10 on the left. Less common we found lesions in the level of the upper pole of thyroid lobe (7 right, 5 left). Usually parathyroid glands in the neck were localised very deeply prevertebral. In 8 patients (19%) we found ectopic parathyroid gland in mediastinum. The average maximum diameter of the lesions was 8 mm (range 4-30 mm), and median SUV value was 6 (range 2-10,6). 17 patients underwent surgery, and 18 parathyroid glands were removed. Pathology confirmed parathyroid hyperplasia in 13 glands and adenoma in 5 cases. The mean PTH and Ca serum values postoperatively dropped significantly (PTH from 19,1 to 6 pmol/L; Ca from 2,8 to 2,4 mmol/L), and normalized in all patients. ***Conclusion:*** In conclusion, PET/CT with ^{18}F-fluorocholine is very sensitive and simple method for localisation of hyperactive parathyroid glands in very demanding patients with the long history of primary hyperparathyroidism. The data about specificity will be more detailed when surgery will be completed in majority of our patients. ***References:*** None

510

Clinical Oncology Track - TROP Session: NET Diagnostics

Friday, October 23, 2020, 10:40 - 12:10 Channel 10

OP-269

Optimal Dose of ^{68}Ga-Satoreotide Trizoxetan as a PET Imaging Agent in Patients with Gastroenteropancreatic Neuroendocrine Tumours: Qualitative Analysis of PET Images

I. Virgolini[1], S. Bahri[2], H. Grønbæk[3], A. Kjær[4], J. Czernin[2], E. von Guggenberg[1], C. Powell[5], S. McEwan[6], C. G. Miller[5];
[1]Medical University Innsbruck, Department of Nuclear Medicine, Innsbruck, AUSTRIA, [2]University of California, Los Angeles, CA, UNITED STATES OF AMERICA, [3]Aarhus University Hospital, Aarhus, DENMARK, [4]Rigshospitalet and University of Copenhagen, Copenhagen, DENMARK, [5]Ipsen, Cambridge, MA, UNITED STATES OF AMERICA, [6]Ipsen, Toronto, ON, CANADA.

Aim/Introduction: ^{68}Ga-satoreotide trizoxetan (also known as ^{68}Ga-IPN01070, ^{68}Ga-NODAGA-JR11, or ^{68}Ga-OPS202), a novel somatostatin receptor 2 (sstr2) antagonist, showed improved diagnostic performance as a PET imaging agent versus the agonist ^{68}Ga-DOTA-TOC in a single-centre study.[1] This analysis from the phase II study aimed to confirm the optimal dose range for peptide mass and radioactivity of ^{68}Ga-satoreotide trizoxetan based on quantitative maximum standardized uptake value (SUV_{max}) and other quality parameters. ***Materials and Methods:*** This international, open-label, factorial-design, phase II study investigated two

peptide mass dose ranges and three radioactivity ranges of ^{68}Ga-satoreotide trizoxetan (NCT03220217). 24 participants with well-differentiated metastatic sstr2-expressing gastroenteropancreatic neuroendocrine tumours were randomized to one of three study arms (n=8 per arm), each patient received two different peptide mass/activity range combinations at two consecutive visits 2-3 weeks apart with PET/CT images obtained at 60±10 minutes post intravenous injection. Participants were allocated to 5-20 µg of peptide mass at visit-1 and 30-45 µg at visit-2, with one of three gallium-68 radioactivity ranges (40-80 [low], 100-140 [mid] or 160-200 [high] MBq) per visit. Comparative image quality was reported by independent blinded readers and the 5 most avid lesions in the liver and lymph nodes were selected for quantification (SUV_{max}). The reference tissue was either non-diseased liver parenchyma or aorta. The study design allowed for review of paired images of different activity doses. ***Results:*** The median SUV_{max} ratio (SUV_{max} lesion/ SUV_{mean} reference tissue) in the liver at low/mid/high activity was 9.9, 6.0 and 7.2 in the 5-20 µg subgroups, and 9.3, 8.4 and 7.0 in the 30-45 µg subgroups, respectively. The mean [median] signal-to-noise-ratios (SNR) in liver for low/mid/high activity were 3.9 [2.8], 4.9 [4.3] and 6.1 [4.5], respectively. There was no noticeable effect of peptide mass on SUV_{max}. Radioactivity evaluated as MBq/kg of participant bodyweight was weight independent. The comparative quality of the images was more often suboptimal in the low radioactivity range. No serious adverse events (AEs) and a total of 14 related Grade 1 or 2 AEs from 7 participants were reported. ***Conclusion:*** No safety concerns arose in this phase II study of ^{68}Ga-satoreotide trizoxetan, which confirmed the optimal dose of 150±50 MBq delivered with a peptide mass range up to 50 µg, and will form the basis of a future development of a phase III program. ***References:*** 1. Nicolas et al. J Nucl Med. 2018 Jun;59(6):915-921.

OP-270

[^{18}F]AlF-NOTA-octreotide PET imaging: Pharmacokinetics, biodistribution, and head-to-head comparison with [^{68}Ga]Ga-DOTATATE in neuroendocrine tumour patients

E. Pauwels[1], *F. Cleeren*[2], *T. Tshibangu*[2], *M. Koole*[1], *K. Serdons*[1], *J. Dekervel*[3], *E. Van Cutsem*[3], *C. Verslype*[3], *K. Van Laere*[1], *G. Bormans*[2], *C. M. Deroose*[1];

[1]Nuclear Medicine, University Hospitals Leuven; Nuclear Medicine and Molecular Imaging, Department of Imaging and Pathology, KU Leuven, Leuven, BELGIUM, [2]Radiopharmaceutical Research, Department of Pharmacy and Pharmacology, KU Leuven, Leuven, BELGIUM, [3]Digestive Oncology, University Hospitals Leuven, Leuven, BELGIUM.

Aim/Introduction: While gallium-68-labelled somatostatin analogue (SSA) PET is the current gold standard for somatostatin receptor imaging, its widespread use is hampered by practical, regulatory and economic challenges associated with ^{68}Ga/^{68}Ga-generators. These challenges could be largely overcome by a fluorine-18-labelled alternative. This prospective trial aimed to evaluate pharmacokinetics, biodistribution and lesion targeting of [^{18}F]AlF-NOTA-octreotide ([^{18}F]AlF-OC) and perform a first head-to-head comparison with [^{68}Ga]Ga-DOTATATE in neuroendocrine tumour (NET) patients. ***Materials and Methods:*** Six NET patients (5M/1F; age 48-74y) with a previous clinical [^{68}Ga]Ga-DOTATATE PET were included. After injection of 4 MBq/kg [^{18}F]AlF-OC, a 45-minute dynamic PET of a thoraco-abdominal region, containing several tumour lesions, was acquired, followed by 3 whole-body PET scans at 1h, 2h and 3h post-injection (PI). Pharmacokinetic analysis was performed using PMOD v3.9. Per patient, 4 to 6 target lesions were delineated on the dynamic scan (32 in total). For each lesion, the net influx rate K_i was determined using the Patlak plot, with an image-derived input function retrieved from the radioactivity concentration in the descending thoracic aorta. The relation between K_i and SUV_{mean} of the target lesions on the static scans was evaluated. Furthermore, normal organ uptake (SUV_{mean}), tumour uptake (SUV_{max} and tumour-to-background ratio (TBR)) and detection ratio (fraction of detected lesions; DR) with [^{18}F]AlF-OC and [^{68}Ga]Ga-DOTATATE were compared. ***Results:*** The median K_i was 0.066 (0.012-0.126). Between K_i and SUV_{mean} a moderate to good linear correlation was observed, somewhat decreasing over time (R^2=0.73 at 1h PI; R^2=0.68 at 2h PI; R^2=0.60 at 3h PI). Biodistribution of [^{18}F]AlF-OC was similar to [^{68}Ga]Ga-DOTATATE, except for the salivary glands, where [^{68}Ga]Ga-DOTATATE uptake was about 5-fold higher (p=0.002). In total, 242 lesions were detected with a high DR that was comparable for both tracers (86.0% for [^{68}Ga]Ga-DOTATATE at 30-45min PI vs. 83.1%, 90.1% and 91.7% for [^{18}F]AlF-OC at 1h, 2h and 3h PI; p>0.05). However, the DR for [^{18}F]AlF-OC was significantly lower at 1h PI, compared to 2h and 3h PI (p=0.005 and p<0.001). Mean tumour SUV_{max} was significantly lower for [^{18}F]AlF-OC at 1h and 2h PI (p=0.016 and p=0.033), but not at 3h PI (p=0.065). Moreover, SUV_{max} significantly increased with time from 10.7±5.7 to 12.3±6.5 and 13.1±6.9 at 1h, 2h and 3h PI, respectively (p=0.3 for all). No significant differences were observed in TBR between [^{68}Ga]Ga-DOTATATE and [^{18}F]AlF-OC. ***Conclusion:*** [^{18}F]AlF-OC shows favourable kinetics and equivalent lesion targeting in NET patients compared to gallium-68-labelled SSA PET, warranting further head-to-head validation. ***References:*** None

OP-271

Improving target volume delineation for 3D image-based dosimetry in Peptide Receptor Radionuclide Therapy

S. Berenato[1,2], *E. Grassi*[3], *F. Fioroni*[3], *D. Finocchiaro*[3,4], *M. Iori*[3], *G. Lewis*[2], *E. Spezi*[2,1];

[1]Department of Medical Physics, Velindre Cancer Centre, Cardiff, UNITED KINGDOM, [2]School of Engineering, Cardiff

University, Cardiff, UNITED KINGDOM, [3]Medical Physics Unit, Azienda Unità Sanitaria Locale - IRCCS, Reggio Emilia, ITALY, [4]Department of Physics, University of Bologna, Bologna, ITALY.

Aim/Introduction: To create an accurate map of the distribution of radiation dose deposition during radionuclide therapy it is important to measure the 3D activity after administration of the radioactive material [1]. In Peptide Receptor Radionuclide Therapy (PRRT) the total activity can be derived from sequential SPECT/CT scans. In this process, lesions are typically outlined on the scan showing the maximum uptake. This however does not reflect the nonuniform nature of activity distributions arising over time in the patient's anatomy. This can lead to a non-optimal definition of target volume and dose assessment. We describe a novel approach to the segmentation of the target volume based on 3D image-based dosimetry that takes into account the total activity accumulated over time. ***Materials and Methods:*** 100 patients treated with PRRT were imaged 5 times with a SPECT/CT scanner, after therapeutic administration of 177Lu-labeled peptides. Sequential scans were co-registered to the reference scan and used to calculate a personalised 3D dose map using the Raydose Monte Carlo code [2]. For each patient, lesions were segmented on the dose map using a variable threshold method. Dose and volume statistics were compared with those extracted from lesions manually contoured by expert clinicians on the SPECT with maximum uptake. Quantitative differences between the two methods were evaluated with the Jaccard conformity index (JCI) and Centre of Mass (CoM) distance. ***Results:*** 85.7% of the cases had a JCI lower than 0.5 and no cases had an index higher than 0.8. On average, a 0.29 conformity value was found. 71% of the cases had CoM shift between 0.3 and 1.5 cm. Some cases had a CoM shift up to 3.6 cm. 3D dose analysis showed an overestimation of absorbed doses in the 97% of the cases and an underestimation of the target volumes in 79% of the cases. According to Bland-Altmann analysis, differences in doses and volumes were found to be statistically significant (p-value<0.01). ***Conclusion:*** The novel approach described in this study provides visually accurate target volume delineations for PRRT which are based on the actual biodistribution of the administered radioactive compound. This method has the potential to minimise inter-observer variability and could be implemented as a standardised process to improve efficiency and accuracy of image-based treatment planning for radionuclide therapy. ***References:*** 1. Dewaraja YK et al. 2012. J Nucl Med. (53) 1310 2. Marcatili S et al. 2013. Phys Med Biol. (51) 2491

OP-272

Serum succinate as a marker of tumor metabolic burden in patients with 18F-FDG-PET positive sporadic or SDHB-mutated metastatic malignant pheochromocytomas/paragangliomas

H. Tissot[1], *C. Lamy*[2], *M. Faron*[3,4], *A. Paci*[5,2], *E. Baudin*[6], *S. Leboulleux*[1], *J. Hadoux*[6], *S. Broutin*[5,2]; *[1]Nuclear Medecine Department, Gustave Roussy, Villejuif, FRANCE, [2]INSERM, U1030, Villejuif, FRANCE, [3]Department of Surgical Oncology, Gustave Roussy, Villejuif, FRANCE, [4]Department of Biostatistics and Epidemiology, INSERM U1018 CESP, Oncostat, Gustave Roussy, Villejuif, FRANCE, [5]Department of Pharmacology, Gustave Roussy, University Paris-Saclay, Villejuif, FRANCE, [6]Endocrine Oncology, Gustave Roussy, Villejuif, FRANCE.*

Aim/Introduction: 18F-FDG-PET/CT is a well-validated method for extension assessment (or for the follow-up) of metastatic malignant pheochromocytomas/paragangliomas (MPP). SDHB-mutated MPP are characterized by high 18F-FDG avidity and metastatic risk. On the other hand, SDHB mutations lead to succinate accumulation, making the serum succinate assay a potential tumor biomarker. Our objective is to determine whether the serum succinate levels reflect the metabolic tumor burden in 18F-FDG-PET/CT positive metastatic MPP patients according to their genetic status. ***Materials and Methods:*** This is a retrospective monocentric study on 32 patients with clinical, 18F-FDG-PET/CT and biological data available. 18F-FDG-PET/CT data were extracted using PET-VCAR software (GE Healthcare): TMTV (Total Metabolic Tumor Volume), TLG (Total Lesion Glycolysis) and SUVmax. MTV was measured setting a threshold of 40% of SUVmax. Serum succinate levels were quantified using a fully validated LC-MS/MS method (Xevo TQS, Waters). Spearman's rank correlation coefficient was used to test the correlation between PET markers and serum succinate levels. ***Results:*** Forty six 18F-FDG-PET/CT and succinate assays from 32 metastatic MPP patients (15 sporadic and 17 SDHB) were analyzed. Primary tumor site was abdominal, neck or adrenal for 13, 7 and 12 patients respectively. Twenty of the 46 18F-FDG-PET/CT and serum succinate assays were performed during locoregional or systemic treatment. In the sporadic group, median serum succinate level of 17 assays was 6,6 µM (range 3,1-33,6) for a median TMTV, TLG and SUVmax of 69,6 cm^3 (range 0-3173.7), 662 (range 0-24196) and 9,5 (range 0-35,6) respectively. In the SDHB group, median serum succinate level of 29 assays was 17,9 µM (range 5,5-274,9) for a median TMTV, TLG and SUVmax of 175,9 cm^3 (range 3,0-2409,4), 1126 (range 6-24724) and 22,0 (range 2,4-40,4) respectively. Strong and equivalent relationships were documented between the serum succinate level and TMTV (r=0,75) and TLG (r=0,76) in the overall study population. Moderate and equivalent relationship was observed between the serum succinate level and SUVmax (r=0,6). In the SDHB group,

patients with the highest tumor burden (3rd and 4th TLG quartiles ; range 1135-5129 and 5136-24725 respectively) showed significant increased succinate levels compared to the sporadic group (p< 0.001 and p<0.0001 respectively). ***Conclusion:*** Serum succinate levels correlate well with TMTV and TLG and may be used as a marker of tumor metabolic burden in patients with 18F-FDG-PET/CT positive sporadic or SDHB-mutated metastatic MPP. This confirms its status as a potential biomarker of MPP. ***References:*** None

OP-273

68Ga-DOTATOC PET/CT in patients with paraganglioma/pheochromocytoma. Interest of combination with other PET/CT methods according to a monocentric experience

C. Morvant*, D. Drui, C. Ferron, M. Le Bras, E. Langlois-Mourrain, F. Toulgoat, E. Mirallie, K. Renaudin-Autin, P. Baumgartner, F. Kraeber-Bodere, C. Ansquer;*
University Hospital of Nantes, Nantes, FRANCE.

Aim/Introduction: 68Ga-DOTATOC-PET/CT is recommended in patients with paraganglioma/pheochromocytoma (PGL/PHEO). Our retrospective study analyzed the sensitivity of 68Ga-DOTATOC-PET/CT in PGL/PHEO patients explored in the University Hospital of Nantes between 2016 and 2019. ***Materials and Methods:*** Thirty three patients (16 men and 17 women), median age 50 years, with PGL/PHEO underwent a 68Ga-DOTATOC-PET/CT in addition to morphological imaging (thoraco-abdomino-pelvic CT, head and neck MR-angiography or MR on another area) for initial staging or follow up. 18F-DOPA-PET/CT and 18F-FDG-PET/CT were also performed in 14 and 24 patients, respectively. Seventeen (52%) patients had localized PGL/PHEO and 16 (48%) metastatic or multifocal disease. Genetic mutations were identified in 13 (40%) patients (1 SDHA, 8 SDHB, 1 SDHC, 3 SDHD), not identified in 15 (45%) patients and indeterminate in 5 patients (15%). Uptake higher than physiological background was considered as pathological and was confirmed by the gold standard (histological proof or positivity of at least another imaging modality). ***Results:*** The 170 lesions identified by PET/CT in the 33 patients were all confirmed by the gold standard, corresponding to 46 primary tumors or local recurrences and 124 metastases. In the whole population, the per-patient sensitivities were 97% (32/33) with 68Ga-DOTATOC, 96% (23/24) with 18F-FDG and 93% (13/14) with 18F-DOPA. The per-lesion sensitivities were 91% (155/170) with 68Ga-DOTATOC, 90% (145/161) with 18F-FDG and 79% (44/56) with 18F-DOPA. A sub-analysis was performed in the 11 (33%) patients explored with the 3 tracers, 3 of them with localized disease and 8 with metastatic or multifocal disease. In this sub-group, the per-patient sensitivities were 91% (10/11) with each tracer and the per-lesion sensitivities were 77% (41/53) for 68Ga-DOTATOC and 18F-DOPA and 83% for 18F-FDG (44/53). Twelve 68Ga-DOTATOC false negative lesions were found in 6 patients, corresponding to 6 sub-diaphragmatic lesions (5 primaries and 1 lymph node), and 6 visceral metastases (lung = 5, liver = 1). These 6 patients presented with several mutation status : 1 SDHA, 1 SDHB, 1 SDHD, 2 not mutated, 1 indeterminate. Interestingly, among these 12 lesions, 5 were detected by 18F-DOPA-PET, 9 by 18F-FDG-PET and all of them by the combination of 18F-FDG and 18F-DOPA. ***Conclusion:*** Our study confirms the accuracy of 68Ga-DOTATOC-PET/CT for the exploration of PGL/PHEO. Nevertheless, and as already reported with 18F-FDG and 18F-DOPA, 68Ga-DOTATOC alone does not detect all the lesions. Best performances are obtained by combining nuclear imaging modalities, in particular in metastatic and multifocal disease. ***References:*** None

OP-274

Fully hybrid 68Ga-DOTATOC PET/MRI in NET patients evaluation: assessment of synergic value of 68Ga-DOTATOC PET and MRI

P. Mapelli*[1,2], G. Ironi[3], F. Fallanca[2], S. Partelli[1,4], V. Bettinardi[2], F. Muffatti[4], V. Andreasi[1,4], P. Scifo[2], R. Rigamonti[2], A. Savi[2], L. Gianolli[2], M. Falconi[1,4], F. De Cobelli[1,3], M. Picchio[1,2];*
[1]Vita-Salute San Raffaele University, Milan, ITALY, [2]Nuclear Medicine Department, IRCCS San Raffaele Scientific Institute, Milan, ITALY, [3]Radiology Department, IRCCS San Raffaele Scientific Institute, Milan, ITALY, [4]Pancreatic Surgery Unit, Pancreas Translational & Clinical Research Centre, IRCCS San Raffaele Scientific Institute, Milan, ITALY.

Aim/Introduction: The simultaneous acquisition of 68Ga-DOTATOC PET and functional MRI by using fully hybrid PET/MRI scanners represent and innovation in the field of molecular imaging with relevant implication in the field of Neuroendocrine Tumours (NETs). The aim of the present study is to evaluate the synergic value of fully hybrid 68Ga-DOTATOC PET/MRI in the management of NETs. ***Materials and Methods:*** Forty-three patients with diagnosis or imaging suspicion of NET underwent 68Ga-DOTATOC PET/MRI for staging (30 pts) or restaging (13 pts) purpose from September 2018 to November 2019. Whole-body PET/MRI scan started approximately 60 minutes after 68GA-DOTATOC injection, followed by a dedicated MRI protocol on the upper and/or lower abdomen. Using an axial LAVA-FLEX acquisition during contrast, two arterial phases and a portal venous phase before and after the injection of a gadolinium-based contrast agent have been performed. These sequences were followed by axial SSFSE and axial echo planar DWI. Axial and coronal breath-hold hepatobiliary phase (HBP) were finally performed. PET images were also acquired simultaneously to the diagnostic MRI. An experienced Nuclear Medicine Physician analyzed the 68Ga-DOTATOC PET scans, while the diagnostic MRI examshave been reviewed by an expert Radiologist. For each 68Ga-DOTATOC PET/MRI scan, an additional analysis combining

PET and MRI findings (concordant and/or discordant) was performed. ***Results:*** In 7/43 pts (16.2%; 5 in the staging group and 2 in the restaging group) discordances between PET and MRI were observed. Diagnostic MRI (at abdominal level) could not detect extra-abdominal lesions detected by whole body 68Ga-DOTATOC PET (lung findings in 1/7 pts). In 3 staging patients, PET detected the presence of 68Ga-DOTATOC uptake within the pancreas, in correspondence of small lesions (<8mm) not clearly identifiable on MRI images. Finally, MRI detected liver metastases not seen on 68Ga-DOTATOC PET (2/7 pts; 1 in the staging group and 1 in the restaging group). In a MEN1 patient, both PET and MRI detected a major pancreatic lesion, with only PET identifying several additional uptakes within the pancreatic gland as site of additional NETs (histological examination confirmed multiple pancreatic NETs). ***Conclusion:*** In both staging and restaging phases of NETs patients, 68Ga-DOTATOC PET and MRI provide synergic information. The major strength of PET is the ability to provide a whole-body assessment of receptor expression, also in small lesions hardly detected by MRI. On the other hand, MRI confirmed its undisputed role in liver disease detection and monitoring. ***References:*** None

OP-275

F-18 DOPA PET imaging in hyperinsulinemic hypoglicemia

K. Toplutas*, L. Uslu-Besli, S. Asa, S. Sager, E. Karayel, H. Pehlivanoğlu, K. Sönmezoğlu;*
Istanbul University-Cerrahpasa, Cerrahpasa Medical Faculty, Department of Nuclear Medicine, Istanbul, TURKEY.

Aim/Introduction: Hyperinsulinemic hypoglycemia (HH) is a disorder developing due to focal or general insulin hypersecretion by pancreatic islet cells and is generally seen as insulinoma in adults and congenital hyperinsulinism in newborns. Focal and diffuse hyperplasia of the endocrine pancreas is involved in the etiopathogenesis and their differential diagnosis is important in planning surgical treatment. In this study, we evaluated patients who underwent F-18 DOPA (FDOPA)-PET with the indication of HH. ***Materials and Methods:*** Twelve HH patients, who were resistant or unresponsive to medical treatment and had negative or inconclusive radiological imaging results were referred to our department for FDOPA-PET. Ten patients (age range: 2 months-15 years) were children and two were young adults (age: 29 and 34 years). Dynamic PET imaging of the abdomen and whole-body imaging at 45-60 minutes post-injection were performed after FDOPA injection using either PET/CT or PET/MRI according to the patients' medical condition. Carbidopa premedication could not be used. ***Results:*** Among five children who had heterozygous ABCC8/KJCN11 mutation suggesting focal disease, focal FDOPA uptake was detected in two and diffuse uptake was present in the remaining three. Islet cell hyperplasia was histopathologically confirmed in one child with focal uptake who had focal pancreatectomy and no medication was needed during follow-up. The other child with focal uptake has not been operated yet and is still under investigation. Among five other children without genetic mutation, two had focal uptake and three had diffuse uptake. Of these, two with focal uptake had further imaging for preoperative evaluation and pancreatic lesion was confirmed in abdominal MRI in one of them. Patients with diffuse uptake were not operated. Both young adult patients had focal FDOPA uptake. One of these adults, who was previously diagnosed with insulinoma and had a history of pancreatectomy, underwent a second operation after FDOPA-PET and recurrence of insulinoma in the splenic hilum, which was in accordance with FDOPA PET, was histopathologically confirmed. Also, in the other adult patient, histopathology confirmed islet cell hyperplasia. While the patient with insulinoma continued medication, the other patient was followed without medication. ***Conclusion:*** FDOPA-PET imaging is the most promising method for the identification of preoperative lesions in HH patients who are resistant/unresponsive to medical treatment. In our cohort, FDOPA-PET was useful in identification of focal lesions and planning focal pancreatectomy, thus helped us to refrain from long-term side effects of subtotal pancreatectomy. ***References:*** None

OP-276

Early response assessment and prediction of overall survival after peptide receptor radionuclide therapy

D. Huizing*, E. A. Aalbersberg, M. W. J. Versleijen, M. E. T. Tesselaar, I. Walraven, M. J. Lahaye, B. J. de Wit - van der Veen, M. P. M. Stokkel;*
Netherlands Cancer Institute, Amsterdam, NETHERLANDS.

Aim/Introduction: Response after peptide receptor radionuclide therapy (PRRT) can be evaluated using anatomical imaging (CT/MRI), somatostatin receptor imaging ([^{68}Ga]Ga-DOTA-TATE PET/CT), and serum Chromogranin-A (CgA). The aim of this study is to assess the role of these response evaluation methods and their predictive value for overall survival (OS). ***Materials and Methods:*** Imaging and serum CgA levels were acquired prior to start of PRRT, 3 and 9 months after completion. Tumor size was measured on anatomical imaging and response was categorized according to RECIST and Choi criteria. [^{68}Ga]Ga-DOTA-TATE uptake was quantified in both the target lesions depicted on anatomical imaging and separately identified PET target lesions, which were either followed over time or newly identified on each scan. OS was calculated from PRRT start until death from any cause. The association of response determination methods and OS was assessed with univariate Cox regression analyses. ***Results:*** A total of 44 patients were included with a median follow-up of 31 months (IQR 26-36 months) and a median OS of 39 months

(IQR 32mo-not reached). Anatomical imaging analysis after 3 months was not associated with OS. Progressive disease after 9 months (according to RECIST) was significantly associated with worse OS compared to stable disease [HR 9.04 (95% CI 2.10-38.85)], however not compared to patients with response [HR 3.951, 95% CI 0.459-34.006]. According to the Choi criteria, progressive disease was also significantly associated with worse OS compared to stable disease [HR 6.10 (95% CI 1.38-27.05)] and compared to patients with response [HR 22.66 (95% CI 2.33-219.99)]. In some patients, new lesions were detected earlier with [^{68}Ga]Ga-DOTA-TATE PET/CT than with anatomical imaging. After 3 months, new lesions on [^{68}Ga]Ga-DOTA-TATE PET/CT which were not visible on anatomical imaging, were detected in 4/42 (10%) patients and in another 3/27 (11%) patients after 9 months. However, no associations between change in uptake on ^{68}Ga-DOTA-TATE PET/CT using any of the four quantification methods or serum CgA measurements and OS was observed. ***Conclusion:*** Progression on anatomical imaging after 9 months is associated with worse OS. In some patients, new lesions were detected earlier with [^{68}Ga]Ga-DOTA-TATE PET/CT than with anatomical imaging, however the numbers are too small for associations with OS. Overall, changes in [^{68}Ga]Ga-DOTA-TATE uptake, and serum CgA after PRRT were not predictive for OS in this series. ***References:*** None

OP-277

The role of ^{18}F-FDG PET/CT in the prediction of overall survival of patients with GEP-NECs

M. Aly[1,2], *H. L. Stokmo*[3,4], *S. M. Seraj*[1], *R. Ghorpade*[1], *A. J. Borja*[1,5], *X. Miao*[1], *G. O. Hjortland*[6], *E. Malinen*[7], *T. J. Werner*[1], *A. Alavi*[1], *M. E. Revheim*[1,3,4];
[1]*Department of Radiology, University of Pennsylvania, Philadelphia, PA, UNITED STATES OF AMERICA,* [2]*Department of Radiology, Asyut University Hospital, Asyut, EGYPT,* [3]*Division of Radiology and Nuclear Medicine, Oslo University Hospital, Oslo, NORWAY,* [4]*Institute of Clinical Medicine, Faculty of Medicine, University of Oslo, Oslo, NORWAY,* [5]*Perelman School of Medicine at the University of Pennsylvania, Philadelphia, PA, UNITED STATES OF AMERICA,* [6]*Department of Oncology, Oslo University Hospital, Oslo, NORWAY,* [7]*Department of Radiotherapy, Oslo University Hospital, Oslo, NORWAY.*

Aim/Introduction: The clinical usefulness of ^{18}F-FDG PET/CT is emerging in the evaluation and management of high-grade neuroendocrine neoplasms (NENs). A few studies have demonstrated the presence of increased glucose metabolism in NENs correlates with the aggressiveness of tumors and bad prognosis. Herein, we performed a study to evaluate the prognostic value of the volumetric and metabolic information derived from ^{18}F-FDG PET/CT. ***Materials and Methods:*** Patient selection: This study includes 71 (40 males, 31 females) patients with median age 66 (range 31 - 80y) diagnosed with advanced neuroendocrine carcinoma who underwent a 18F-FDG PET/CT examination and a biopsy within 90 days (median -22, range -85 - 89d) of the PET-study.Image acquisition: ^{18}F-FDG PET/CTs were performed on EARL-accredited (EANM Research Ltd) PET/CT systems (mCT 16, Siemens Medical Systems, Erlangen, Germany (n=63), Siemens Biograph 64/16 (n=6) and GE Discovery 690 (n=2)). The patients fasted for at least 6 hours and blood samples were obtained to document blood glucose levels (median 5.6, range 3.7 - 13.6 mmol/l) prior to intravenous administration of median 236 MBq ^{18}F-FDG (range 154.7 - 400 MBq). Images were obtained approximately 60 min. post-injection (median 63, range 44 - 134 min).Image analysis: All the scans were analyzed using an adaptive thresholding system (ROVER software; ABX GmbH, Radeberg, Germany). Spherical or cylindrical masks were placed over the active malignant lesions, and the adaptive thresholding algorithm of ROVER delineated the boundaries of active lesions giving the metabolic tumor volume (MTV). Standardized uptake values (SUV) lik SUV_{mean} and SUV_{max}, in addition to partial volume corrected (pvc) SUV_{mean} and SUV_{max} were calculated by the software. Total lesion glycolosis (TLG) were calculated by the software by multiplying with SUV_{mean}. Global scores were calculated by summing all the patient lesions. The cut-off value for MTV dividing the patients into two groups was based on the median MTV (150.91 cm^3). Overall survival (OS) for patients over- and under the cut-off value were compared using the Kaplan-Meier method, and the log rank test. ***Results:*** Median survival in the group with low global MTV was 694 days, compared to 226 days for the group with high global MTV. Global MTV under the cut-off value were significantly correlated to improved OS (X^2=9.21, p=0.0024). Estimated 1-year OS was (X2=11.53, p=0.00068), and estimated 3-year OS was (X2=4.18, p=0.04). ***Conclusion:*** NECs with higher global MTV have poorer survival and hence indicate more aggressive disease. ***References:*** None

OP-278

Investigation of parameters impacting 68Ga-DOTATOC PET image quality and quantification: a clinical and phantom study

M. Bernardini*, C. Smadja, N. Ghazzar;*
European Hospital Georges Pompidou, Paris, FRANCE.

Aim/Introduction: 68Ga-DOTATOC PET/CT has emerged as a highly accurate imaging method for patients with neuroendocrine tumors (NETs). In our institution, we recently provided PET exams with 68Ga-DOTATOC and we investigated the way to optimize the acquisition parameters and the differences of quantification between 18F-FDG, 18F-DOPA and 68Ga-DOTATOC patient images. ***Materials and Methods:*** To investigate the influence of several parameters, as the delay after injection, injected activity, BMI and

acquisition time per bed position on 68Ga-DOTATOC PET exams, 24 patients were analyzed. Moreover, several 68Ga NEMA phantoms were acquired to explore the influence of positon energy and its pathway in water and air on the quantification, together with spatial resolution and volumes thresholding. ***Results:*** We did not found any correlation between SUV values and the delay after injection (varying from 48 min to 1h40), nor the injected activity (varying from 102 MBq to 198 MBq), neither the BMI (varying from 17 to 45). In the same way, the liver and sternum signal to noise ratio (S/N) did not show any correlation with the parameters cited above. When increasing time acquisition from 2min to 2min30sec per bed step, on 11 patients and 21 lesions analyzed, the signal globally decreases: SUVmax median value decreases of -3.6% for lesions (ranging from -15% to 42%), -4.7% for liver (varying from -10% to 6%) and -11.4% for sternum (ranging from -27% to -1%). NEMA phantoms analysis showed that the mean radioactive concentration (Bq/ml) outside spheres ranges from 10.3% (26.5ml sphere) to 20.3% (0.5ml sphere). Concerning the total activity (Bq) outside the spheres, it ranges from 24.6% (26.5ml sphere) to 139.2% (0.5ml sphere). ***Conclusion:*** The very high specificity of 68Ga-DOTATOC explains the absence of correlation between the signal quantification and the parameters that typically influence the F-18 FDG signal (injected activity, BMI, delay after injection), at the clinical values applied. SUV values decrease globally when the time per bed position increases, underlying the predominant effect of short half-life of Ga-68 (68 min) on quantification. Analysis of 68Ga-NEMA phantoms, showed lower recovery coefficient than F-18: mean radioactivity concentration in the edge of spheres ranging from 10.3% to 20.3% involves important amount of radioactivity detected out of the spheres, ranging from 24.6% to 139.2%. These results show that clinical volume thresholding and quantification methods applied for 18F-FDG or 18F-DOPA should be revised for 68Ga-DOTATOC exams. ***References:*** None

OP-279

Comparison between metastatic neuroendocrine tumours and carcinomas somatostatin receptor expression on ^{99m}Tc-EDDA/HYNIC-TOC SPECT/CT with immunohistochemical, histopathological and laboratory parameters

G. Sipka*, Z. Besenyi, I. Farkas, T. Czékus, Z. Mikó, A. Bakos, S. Urbán, L. Pávics;*
University of Szeged, Department of Nuclear Medicine, Szeged, HUNGARY.

Aim/Introduction: Neuroendocrine tumours can occur anywhere in the body, however these are treated as a common group because the cells of these neoplasms share multiple common features. The somatostatin receptor scintigraphy helps to visualize one of these feature, which is especially essential in the advanced stages of these neoplasms. The aim of our study was to compare the somatostatin receptor expression of the pathological lesions from different origins on ^{99m}Tc-EDDA/HYNIC-TOC SPECT/CT images with other specific or aspecific histological, immunohistochemical and laboratory results to find any relevant correlations between these parameters. ***Materials and Methods:*** In our retrospective analysis, 38 histologically proven, advanced neuroendocrine tumour or carcinoma patients' (14 women, 24 men, mean age: 59 years) 53 ^{99m}Tc-EDDA/HYNIC-TOC SPECT/CT examinations were analysed. The detected pathological lesions somatostatin receptor expressions were standardly quantified and also a patient- and lesion-based semiquantitative assessment was performed. The obtained results were compared with each other and with the laboratory findings (Chromogranin-A, Neuronspecific enolase and other specific tumour markers), with histopathological results (Grade, Ki-67, TNM) and with immunohistochemistry reports (Chromogranin-A, Synaptophysin, CD56, Somatostatin receptor, SyntaxinA1, CK7, CK20, TTF-1, S100 and other markers). ***Results:*** In total 315 pathological lesions were detected on 53 ^{99m}Tc-EDDA/HYNIC-TOC SPECT/CT scans, which majority (235/315) located in the liver, lymph nodes and bones. The somatostatin receptor density quantification confirmed the different uptake between the neuroendocrine carcinomas and neuroendocrine tumours (Kruskal-Wallis, P<0,0001). The gastrointestinal tumours had higher somatostatin receptor expression, than other neuroendocrine malignancies (Mann-Whitney, P<0,0001). Most of the tumours were chromogranin-A, synaptophysin, and CD56 positive, but in addition to the widely known immunohistochemical parameters the CK7 (Mann-Whitney, P=0,0138) and TTF-1 negative (Mann-Whitney, P<0,0001), and moreover SyntaxinA1 (Mann-Whitney, P<0,0001), CK20 (Mann-Whitney, P=0,0128), S100 (Mann-Whitney, P=0,0067) and as expected the somatostatin receptor (Mann-Whitney, P=0,0001) positive lesions showed higher uptake. The somatostatin receptor density was not correlated between laboratory parameters and lesions. ***Conclusion:*** These data show that the ^{99m}Tc-EDDA/HYNIC-TOC SPECT/CT has the potential to differentiate between neuroendocrin tumours and carcinomas. Our study also confirms that the CK7, TTF-1 negativity and CK20, syntaxin A1, S100 positivity could be a good prognostic factor to predict the high somatostatin receptor expression. This correlation between certain immunohistochemical factors and somatostatin receptor expression may lead to a better understanding of the biochemical behaviour of the neuroendocrine tumours. ***References:*** None

OP-280

Normal pancreatic appearances of [^{68}Ga]Ga-DOTA-TATE

G. La Torre, S. Hughes;
University Hospital Birmingham, Birmingham, UNITED KINGDOM.

Aim/Introduction: [^{68}Ga]Ga-DOTA-TATE is a radiotracer for PET/CT imaging of neuroendocrine tumours (NETs). A thorough knowledge of the normal patterns of tracer uptake is needed to interpret these images accurately. Our study focuses on describing the normal patterns of pancreatic ^{68}Ga-DOTA-TATE uptake which is particularly important in pancreatic NETs (PNETs). ***Materials and Methods:*** We conducted a retrospective study of 163 consecutive routine [^{68}Ga]Ga-DOTA-TATE PET/CT scans carried out the Queen Elizabeth Hospital Birmingham between 2017-2018. The patients with known PNETS were excluded. The normal appearance of the pancreas on the CT component of the PETCT in the presence of pathologically confirmed NET elsewhere were interpreted as no evidence for second DOTA-TATE positive pancreatic pathology. We described the patterns of uptake in the anatomical regions of uncinate process, head, neck, body and tail of the pancreas defined by the regions correlating with the co-registered CT component. The pattern seen was recorded as being focal or diffuse. The maximum semi-quantitative uptake value (SUVmax) was recorded for qualitatively abnormal regions. ***Results:*** 27 patients had evidence of PNET or other pathology, these were removed from our analysis with a further 14 because images were not retrievable. 122 scans were analysed. 5.7% showed no detectable qualitative uptake. 18.0% showed whole pancreatic uptake in with diffuse patterns (highest SUVmax: 16.5). 41.8% of scans showed evidence of uncinate uptake (Focal:57%, Diffuse:43%, SUVmax Focal:65.6, Diffuse:24.1). 14.5% showed uptake in the head of the pancreas (Focal:10.5%, Diffuse:89.5%, SUVmax Focal:38.7, Diffuse:27.1); 4.5% showed uptake in the neck (Focal:37.5%, Diffuse:62.5%, SUVmax Focal:23.4, Diffuse:9); 21.2% in the body (Focal:10.5%, Diffuse:89.5%, SUVmax Focal:39.3, Diffuse:9.7) and 17.8% in the pancreatic tail (Focal:12.5%, Diffuse:87.5%, SUVmax Focal:92.7, Diffuse:17.7). Only 1 scan had evidence of 4 areas of uptake, 14 had 3 areas of uptake, 41 had 2 areas of uptake and 37 had only 1 area of uptake. Compared to previous studies, our results show a more complex pattern of normal uptake with both diffuse and focal regions of uptake. ***Conclusion:*** To the best of our knowledge, this is the most detailed description of probable normal patterns of pancreatic uptake of [^{68}Ga]Ga-DOTA-TATE. We show that normal uptake is not limited to the uncinate process and head of the pancreas, albeit the most common, and other important complex patterns are seen. We show that [^{68}Ga]Ga-DOTA-TATE PET/CT imaging may be a misleading tool for the local assessment of small PNETs without anatomical imaging. ***References:*** None

511

e-Poster Presentation Session 4: The Best of Cardiovascular Imaging in Short

Friday, October 23, 2020, 10:40 - 12:10 Channel 11

EPS-052

Identifying and quantification of cardiovascular calcification by 18F-NaF PET/CT in alkaptonuria patients

E. Alawadhi[1], *S. Vinjamuri*[2], *J. A. Gallagher*[1], *R. Lakshminarayan*[3], *J. Dillon*[1];
[1]*Institute of Ageing & Chronic Disease, William Henry Duncan Building, the University of Liverpool, Liverpool, UNITED KINGDOM,* [2]*Department of Nuclear Medicine Royal Liverpool University Hospital, Liverpool, UNITED KINGDOM,* [3]*Liverpool Clinical Laboratories, Royal Liverpool & Broadgreen University Hospitals Trust, Liverpool, UNITED KINGDOM.*

Aim/Introduction: Alkaptonuria is characterised by increased homogentisic acid (HGA) in the blood and tissues. The main pathophysiological event in alkaptonuria is the binding of an HGA-derived pigment to connective tissue, termed ochronosis. The ochronotic pigment can be deposited in the cardiovascular system causing severe cardiovascular involvement such as heart valve stenosis[1]. Microcalcification and active calcification have been detected and identified using 18F-NaF PET/CT imaging[2]. The study aimed to evaluate regional cardiac calcification by semi-quantifying the sodium fluoride uptake from PET images and attenuation coefficient from CT images as evidence of calcification in the main cardiac arterial regions within AKU patients. ***Materials and Methods:*** 18F-NaF PET/CT images from 40 AKU patients (24 males, 16 females) were analysed quantitively in this study using HOROS software. Maximum standardised uptake value (SUV_{max}), maximum target-to-background ratio (TBR_{max}), and mean Hounsfield units (HU_{mean}) were generated from PET/CT images for the main cardiac arterial regions, including coronary and aortic arterial regions. SUV_{max}, $TBR_{max,}$ and HU_{mean} from each region were correlated with gender and age using the Pearson correlation coefficient. ***Results:*** The average (±SD) SUV_{max} value of all measured coronary arteries was 1.39 ±0.49, and for the aorta was 2.06 ±0.84. The average TBR_{max} for the coronary arteries (1.80 ±0.80) was significantly lower than the aorta TBR_{max} (2.7 ±1.24, $p < 0.005$). The average HU_{mean} of all measured coronary arteries was 138.18 ±139.41, and was 133.71 ±143.48 for the aorta, with no significant differences ($p > 0.05$). Regional coronary arteries and aortic arteries 18F-NaF uptake values were not clearly correlated with age ($p > 0.05$), while HU_{mean} values were positively correlated with age ($p < 0.05$). Males had higher average coronary arteries SUV_{max} and TBR_{max} values compared to females ($p = 0.036$, $p = 0.012$). Almost similar aortic findings have been

noted between male and female subjects in all measured regions, with no significant confounding differences ($p > 0.05$). ***Conclusion:*** Quantitative assessment of cardiovascular molecular calcification by 18F-NaF can be considered as a novel and practical tool for investigating the early vascular calcification in AKU patients. The findings from this initial study demonstrate the potential feasibility of using 18F-F-NaF as a biomarker for in vivo quantification of molecular cardiovascular calcification as an early feature of cardiovascular ochronosis. ***References:*** 1.Hannoush, Hwaida, et al. Molecular genetics and metabolism 105.2 (2012): 198-202.2.Dweck, Marc R., et al. Journal of the American College of Cardiology 59.17 (2012): 1539-1548.

EPS-053

Combined Thoracic Contrast-Enhanced CT with PET/CT in Assessment of Primary Cardiac Tumors in Adult Patients

E. Liu*, T. Sun, S. Wang, Z. Chen, H. Dong, C. Liu, D. Shao, Z. Lian, Q. Xie, S. Wang; Guangdong Provincial People's Hospital, Guangdong Academy of Medical Sciences, Guangzhou, CHINA.*

Aim/Introduction: AIM^{18}F-FDG PET/CT is a key molecular imaging modality to noninvasively assess and differentiate benign and malignant cardiac tumors. However, few benign cardiac tumors can be characterized by increased ^{18}F-FDG uptake, which makes differential diagnosis difficult. This study sought to retrospectively evaluate whether combined thoracic contrast-enhanced CT (CECT) with 18F-FDG PET/CT helps in assessing primary cardiac tumors in adult patients, compared with CECT or PET/CT alone. ***Materials and Methods:*** A retrospective study was conducted using 109 consecutive patients with cardiac masses suspected by transthoracic echocardiography (TTE) and/or thoracic CT. All patients underwent ^{18}F-FDG PET/CT, followed by thoracic CECT on the same day. Visual qualitative interpretation and quantitative analysis were performed and diagnostic performance was evaluated using the receiver operating characteristic (ROC) analysis, with the area under the ROC curve (AUC) for multi-parameters. ***Results:*** A total of 46 patients with 46 tumors (29 benign, 17 malignant) were enrolled; 55.2% of benign tumors showed visually increased ^{18}F-FDG uptake. There were significant differences in the level of ^{18}F-FDG uptake and the degree of absolute enhancement between benign and malignant tumors ($P < 0.001$). The combination of two modalities (PET/CT and thoracic CECT) improved the specificity from 79% to 93%, the positive predictive value from 73% to 89%, and the accuracy of diagnosis from 85% to 93%. There were significant differences between PET/CT alone or thoracic CECT alone and combined modalities ($P = 0.034$ and $P = 0.026$, respectively). The combination with the optimal SUVmax cutoff value generated 94% sensitivity, 100% specificity, 97% negative predictive values, 100% positive predictive values, and 98% accuracy rates. ***Conclusion:*** Combining thoracic CECT with ^{18}F-FDG PET/C significantly improved specificity and accuracy compared to CECT or PET/CT alone in detecting tumors. This combination of diagnostic imaging is effective in differentiating malignant from benign masses. ***References:*** None

EPS-054

V/Q scintigraphy and SPECT for the diagnosis of Chronic Thromboembolic Pulmonary Hypertension: Experience from a reference centre

D. Vega*, P. Pilkington Woll, V. Godigna Guilloteau, A. Galiana Moron, S. Ruiz Solis, E. Martinez Albero, M. J. Tabuenca Mateo, M. D. Martin Ferrer, M. P. Sarandeses Fernandez, A. Gomez Grande, J. M. Estenoz Alfaro;*
Hospital 12 de Octubre, Madrid, SPAIN.

Aim/Introduction: Our goal is to determine the diagnostic accuracy of the V/Q scintigraphy and SPECT in patients with suspected CTPH (Chronic Thromboembolic Pulmonary Hypertension) in our hospital. ***Materials and Methods:*** Patients with suspected CTPH referred from the CTPH multidisciplinary committee who later underwent ventilation/perfusion (V/Q) SPECT were analyzed retrospectively between the years 2018 and 2020. We registered the final diagnosis of each patient based on clinical management or surgical treatment/angioplasty performed, obtaining two groups: patients with CTPH and without CTPH. The results of V/Q SPECT were analyzed, considering as positive result the presence of perfusion defects of triangular morphology (with peripheral base) and not concordant with the ventilation study. Subsequently, we calculated the sensitivity (S), specificity (E), negative predictive value (NPV) and positive predictive value (PPV) of the V/Q scintigraphy and SPECT for the diagnosis of CTPH with the STATA statistical program. A sub-analysis was performed on 24 patients who had also undergone CTPA (CT Pulmonary Angiography) to compare the diagnostic accuracy of both tests. ***Results:*** A total of 45 studies were carried out, with a mean age of 65.6 years (from 31 to 95 years), 35.5% men and 64.5% women. Of these patients, 35.5% had CTPH as a definitive diagnosis. The statistical analysis determined that the diagnosis of CTPH with the V/Q SPECT obtained S:93%, E:96%, PPV:93% and NPV:96%. The results of the sub-analysis (CTPA VS SPECT) were:- CTPA: S: 83%, E: 91%, PPV: 90% and NPV: 84%.- SPECT: S: 100%, E: 91%, VPP: 92% and VPN: 100%. ***Conclusion:*** The performance of V/Q SPECT for the diagnosis of CTPH has a high diagnostic accuracy (similar to that described in the literature), therefore able to confirm it as the first-choice diagnostic test, increasing its importance when diagnosing accurately a pathology with significant morbidity and mortality. ***References:*** None

EPS-055

Nuclear medicine techniques for the assessment of cardiac sarcoidosis and cardiac amyloidosis.Preliminary results of a European survey

P. Erba[1], R. Slart[2], A. Saraste[3], O. Gheysens[4], J. Bucerius[5], M. Dweck[6], F. Hyafil[7], A. Glaudemans[2], H. Verberne[8], M. Lubberink[9], O. Gämperli[10], G. Habib[11], A. Gimelli[12];
[1]Regional Center of Nuclear Medicine, Department of Translational Research and New Technology in Medicine, University of Pisa and AOUP, Pisa, ITALY, [2]Department of Nuclear Medicine and Molecular Imaging, Medical Imaging Center, University Medical Center Groningen, University of Groningen, Groningen, NETHERLANDS, [3]PET Centre, Turku University Hospital and University of Turku, Turku, FINLAND, [4]Department of Nuclear Medicine, Cliniques Universitaires Saint-Luc, Université Catholique de Louvain (UCL), Brussels, BELGIUM, [5]Department of Radiology and Nuclear Medicine, Maastricht University Medical Center (MUMC+), Maastricht, NETHERLANDS, [6]BHF Centre for Cardiovascular Science, University of Edinburgh, Edinburgh, UNITED KINGDOM, [7]Department of Nuclear Medicine, Bichat University Hospital, Paris, FRANCE, [8]Department of Radiology and Nuclear Medicine, Amsterdam University Medical Centers, Location AMC, University of Amsterdam, Amsterdam, NETHERLANDS, [9]Nuclear Medicine and PET, Department of Surgical Sciences, Uppsala University, Uppsala, SWEDEN, [10]Heart Clinic Zurich Hirslanden, Zurich, SWITZERLAND, [11]Aix-Marseille Université, IRD, APHM, MEPHI, IHU Méditerranée Infection, Marseille, France; Département de cardiologie, Hôpital de la Timone, AP-HM, boulevard Jean-Moulin, Marseille, FRANCE, [12]Fondazione Toscana Gabriele Monasterio, Pisa, ITALY.

Aim/Introduction: Despite nuclear imaging techniques have the potential to provide unique information in cardiac sarcoidosis/amyloidosis, an overview of the current clinical use in Europe is lacking. Therefore, we design a survey to evaluate the current clinical practice in imaging cardiac sarcoidosis/amyloidosis with nuclear techniques. In this abstract we present the results of the first round of the survey which was held between February 15 -April 15, 2020. ***Materials and Methods:*** none ***Results:*** Information was collected using an electronic questionnaire, consisting of 16 questions. Responses were obtained from 50 professionals, the majority of which were in the middle career stage working in center where < 10 patients with sarcoidosis and between 10-40 patients with amyloidosis are studied each year. Only a very few sites assessed > 40 patients per year. The large majority of the responders used nuclear imaging in patients with cardiac sarcoidosis/amyloidosis (40/50 (80%) and 46/50 (92%), respectively). The most common reasons for nuclear imaging in sarcoidosis were: staging of extracardiac disease, 2nd line imaging to establish the diagnosis in uncertain cases, and treatment response. [^{18}F]FDG PET/CT, either whole body or cardiac, followed by MPI PET or SPECT were the most frequently used technique.In case of cardiac amyloidosis, imaging was more often requested as either 1st line imaging test to establish a diagnosis or 2nd line imaging to establish the diagnosis in uncertain cases. Scintigraphy with bone-seeking radiopharmaceuticals was the most used imaging modality with ^{99m}Tc-DPD being used in almost 50% of the cases followed by ^{99m}Tc-HPD and ^{99m}Tc-PYP. Cardiac ^{123}I-MIBG was the second most used technique.The primary reasons not to study these patients were i) lack of referrals/interest from the referring clinicians and of proper equipment or radiopharmaceuticals; ii) lack of reimbursement and iii) use of echocardiography or MRI.Management of patients with cardiac sarcoidosis by a multimodality imaging team was present in less than 50% of the participating centers while it's slightly more common in case of amyloidosis. Almost all responders indicated willing to be involved in a European network registry/study, therefore underlying the interest for the topic. ***Conclusion:*** These preliminary results encourage the creation of coordinated European effort rto promote clinical practice and research in cardiac sarcoidosis/amyloidosis. A second round of the questionnaire (June 2020), aiming at increasing the number of responders, will most likely strengthen the results. ***References:*** None

EPS-056

High Sympathetic Activity in Raynaud's Disease

L. Lindberg[1], B. Kristensen[1], T. W. Hansen[2], P. Hasbak[3], J. F. Thomsen[4], E. Eldrup[5], L. T. Jensen[1];
[1]Department of Nuclear Medicine, Copenhagen University Hospital, Herlev Hospital, Herlev, DENMARK, [2]Steno Diabetes Center Copenhagen, Gentofte, DENMARK, [3]Department of Clinical Physiology, Nuclear Medicine & PET, Rigshospitalet, University of Copenhagen, Copenhagen, DENMARK, [4]Department of Occupational and Environmental Medicine, Copenhagen University Hospital, Bispebjerg and Frederiksberg Hospital, Copenhagen, DENMARK, [5]Department of Endocrinology, Copenhagen University Hospital, Herlev Hospital, Herlev, DENMARK.

Aim/Introduction: Raynaud's disease (RD) is characterized by episodic whitening of the fingers without an underlying cause. The disease is usually considered benign and of peripheral location. However, studies have indicated an increased sympathetic activity[1] as well as increased cardiovascular morbidity and mortality in patients with RD[2,3]. Therefore, the aim of the study was to examine the sympathetic nervous system in patients with RD to elucidate a possible central nervous component of the disease. ***Materials and Methods:*** [^{123}I]MIBG heart scintigraphy was performed on 22 patients with RD. The diagnosis was verified by international consensus criteria. Early and late images were acquired. Regions of interest (ROIs) were drawn over the myocardium and the upper mediastinum, and the heart-to-mediastinum ratio (HMR_{late}) was calculated

upon analysis of the late images. Results were compared with results from 14 healthy subjects examined in a previous study. ***Results:*** The mean (SD) HMR_{late} in the patients with RD was 2.4 (0.4), and in the healthy subjects, it was 2.9 (0.4). The difference was statistically significant (p = 0.0004). Multiple linear regression analysis showed that a lower HMR_{late} was associated with higher age (p = 0.03) and the presence of RD (0.0002). Regression analysis including the patient group showed no association between HMR_{late} and severity of RD. ***Conclusion:*** The study supports the hypothesis that RD affects the central sympathetic nervous system, which seems to be overactive in these patients compared to healthy subjects. Although recommendations cannot be made based solely on results from the present study, more attention to the prevention of cardiovascular disease in RD might be advised. ***References:*** 1. Olsen, N., Petring, O. U. & Rossing, N. Exaggerated postural vasoconstrictor reflex in Raynaud's phenomenon. Br Med J (Clin Res Ed) 294, 1186-1188 (1987)2. Nietert, P. J. et al. Raynaud phenomenon and mortality: 20+ years of follow-up of the Charleston Heart Study cohort. Clin Epidemiol 7, 161-168 (2015)3. Suter, L. G., Murabito, J. M., Felson, D. T. & Fraenkel, L. Smoking, alcohol consumption, and Raynaud's phenomenon in middle age. Am J Med 120, 264-271 (2007)

EPS-057

The improvement of hibernating myocardium analyzed by gated ^{99m}Tc-sestamibi SPECT/CT and gated ^{18}F-FDG PET/CT in patients with ischemic cardiomyopathy were associated with the reversal of left ventricular remodeling after revascularization

Y. Lu[1], *J. Cao*[2], *J. Tian*[1], *Y. Tian*[1], *W. Dong*[1], *M. Hacker*[3], *R. Dong*[2], *X. Li*[1], *X. Zhang*[1];
[1]*Department of Nuclear Medicine, Beijing Anzhen Hospital, Capital Medical University, Beijing, CHINA,* [2]*Department of Cardiac Surgery, Beijing Anzhen Hospital, Capital Medical University, Beijing, CHINA,* [3]*Division of Nuclear Medicine, Department of Biomedical Imaging and Image-guided Therapy. Medical University of Vienna, Vienna, AUSTRIA.*

Aim/Introduction: In this study, we aimed to evaluate the changes of hibernating myocardium after revascularization, and its association with the changes of cardiac function as well as left ventricular(LV) remodeling in patients with ischemic cardiomyopathy and severe heart failure (HF) after revascularization at different time points. ***Materials and Methods:*** Ischemic cardiomyopathy patients who were referred to revascularization underwent gated ^{99m}Tc-MIBI SPECT/CT myocardial perfusion imaging (GSPECT) and gated ^{18}F-FDG PET/CT metabolism imaging (GPET) pre-operation. 29 (age 56.7±9.6 y, 26 male) patients with LV ejection fraction (LVEF, %) by GSPECT less than 35% were recruited, who performed followed-up GSPECT and GPET at different time points after revascularization. Total perfusion defect (TPD, %), hibernating myocardium (HM, %), and infarcted myocardium (SCAR, %) were analyzed by 17-segment and 5 score system. GSPCT and GPET images were analyzed by QGS software, summed motion score (SMS), summed thickening score (STS), end-diastolic volume (EDV, mL), end-systolic volume (ESV, mL) and LVEF were obtained. Patients were divided into three groups according to the followed-up scan time (Group1 n = 6, at 3months, Group 2 n=7, at 6months, Group3 n=16, at 12months). The changes of TPD, HM, SCAR, SMS, STS, EDV, ESV, LVEF were evaluated, in addition, the correlation between the changes (Δ) of HM and function as well as remodeling parameters was analyzed by Pearson and Spearman rank correlation analysis. P value<0.05 was considered as statistical significance. ***Results:*** In comparison with pre-revascularization, both TPD (27.9±16.5% vs 19.1±15.7%, p<0.05) and HM (14.8±10.9% vs.7.8±6.5%, p<0.05) after revascularization were significantly improved in Group 3, LVEF were improved in Group 2 (20.3±12.4% vs 25.5±14.0% , p<0.05) and Group 3 (32.8±13.2% vs. 38.6±14.2%, p<0.05). In addition, STS was decreased in Group 2 (29.8±8.7 vs 25.5±10.0, p<0.05) and Group 3 (20.9±10.5 vs 17.3±10.6 , p<0.05). Besides, there was a significant correlation between ΔHM and ΔTPD (r=0.71, p=0.001), ΔHM and ΔSMS by GPET (r=0.386, p=0.039), and ΔHM and ΔEDV by GPET (r=0.374, p=0.046). While no correlation between ΔSCAR and these parameters. ***Conclusion:*** In patients with ischemic cardiomyopathy and HF, global function could be improved after revascularization. The improvement of hibernating myocardium was correlated with the improvement of myocardial perfusion, regional LV function and the reversal of LV remodeling after revascularization. Acknowledgements: This project was sponsored by National Natural Science Foundation of China(81871377), Capital Characteristic Clinical Application Research (Z181100001718071). ***References:*** None

EPS-058

Combining Genetic Evidence with Myocardial Perfusion Imaging: Correlations Between RAAS-related Gene Polymorphisms and SPECT Quantitative Parameters

G. Angelidis[1], *M. Samara*[1], *M. Papathanassiou*[1], *M. Satra*[1], *V. Valotassiou*[1], *I. Tsougos*[1], *D. Psimadas*[1], *C. Tzavara*[1], *S. Alexiou*[1], *J. Koutsikos*[2], *N. Demakopoulos*[3], *G. Giamouzis*[1], *F. Triposkiadis*[1], *J. Skoularigis*[1], *P. Kollia*[4], *P. Georgoulias*[1];
[1]*University of Thessaly, Larissa, GREECE,* [2]*401 General Military Hospital, Athens, GREECE,* [3]*Army Share Fund Hospital (417 NIMTS), Athens, GREECE,* [4]*National & Kapodistrian University, Athens, GREECE.*

Aim/Introduction: Coronary artery disease (CAD) represents one of the main causes of morbidity and mortality worldwide. The non-Mendelian heritable basis of common CAD presentations in middle to late adulthood, as well as the

significance of a positive family history, has been supported by clinical observations. Recently, based on genome-wide association studies (GWAS), several single nucleotide polymorphisms (SNPs) have reached genome-wide significance for CAD. In particular, the renin-angiotensin-aldosterone system (RAAS) has been reported to play an important role in the development of atherosclerosis. In the present study, we aim to investigate the correlations of RAAS-related SNPs with myocardial perfusion, as evaluated through myocardial perfusion single photon emission computed tomography (SPECT). ***Materials and Methods:*** The study sample consisted of 619 males and 191 females, referred to our departments for a clinically indicated stress-rest myocardial SPECT. Summed stress score (SSS), summed rest score (SRS), summed difference score (SDS), transient ischemic dilation (TID), and lung/heart ratio (LHR) were recorded. The following gene polymorphisms were studied: angiotensin-converting enzyme (ACE) insertion/deletion (I/D), angiotensinogen (AGT) M235T and T174M, angiotensin II type 1 receptor (AT1R) A1166C, angiotensin II type 2 receptor (AT2R) C3123A, and renin (REN) C5312T. ***Results:*** The heterozygotes or homozygotes on ACE D allele were 7.54 times more likely to have abnormal SSS and the AGT (T174M) heterozygotes were 5.19 times more likely to have abnormal SSS, while the AT1R heterozygotes had greater odds for having SSS≥3. The homozygotes of ACE D and the patients carried AT1R homozygosity of C allele had significantly higher values on TID. Further, the AGT (T174M) heterozygotes had higher values on TID. Finally, the homozygotes of ACE D and the heterozygotes of AT1R had significantly higher values on LHR. ***Conclusion:*** Among the polymorphisms studied, ACE D allele had the strongest association with abnormal myocardial perfusion. Genetic analysis combined with functional imaging may provide an efficient way to dissect the genetic basis of CAD. This approach could improve our ability to identify subjects at higher risk of developing CAD, and the use of additional prognostic parameters may improve patient risk stratification. ***References:*** None

EPS-059

Gated myocardial SPECT results in patients with chronic heart failure before and after cardiac contractility modulator implantation

A. Ansheles*, V. Amanatova, T. Uskach, S. Tereschenko, V. Sergienko;*
National Medical Research Center of Cardiology, Ministry of Healthcare, Moscow, RUSSIAN FEDERATION.

Aim/Introduction: Cardiac contractility modulation (CCM) is a relatively new method of non-drug treatment in patients with chronic heart failure (HF) without indications for cardiac resynchronization therapy. Myocardial perfusion SPECT has proved reproducibility in serial assessment of cellular left ventricular (LV) perfusion with comparison of LV contractility in patients with HF. The purpose of the study was to assess gated myocardial SPECT data in patients with chronic heart failure before and after CCM device implantation. ***Materials and Methods:*** 28 patients with chronic heart failure due to LV dilation (12 - ischemic, 16 - non-ischemic, including 8 idiopathic and 8 - other non-ischemic, i.e. hypertensive or combined) underwent rest myocardial perfusion CT-AC SPECT with ^{99m}Tc-MIBI before Optimizer Smart implantable pulse generator installment and 6 months after. LV perfusion impairments were evaluated using summed rest score (SRS) parameter, gated SPECT analysis included end diastolic volume (EDV, ml) and LV ejection fraction (EF). ***Results:*** Before CCM mean EDV in the whole group was 253 ± 121 ml, EF - 23.4 ± 9.5%, with no difference between ischemic and non-ischemic subgroups, while LV perfusion impairments were more severe in ischemic subgroup (mean SRS: 30.0 [22.0-34.0] vs 13.5 [7.5-24]). After 6 months of CCM device implantation mean EDV lowered (227 ± 102 ml) and LV EF increased (28.7 ± 11.2%), both insignificantly (p=0.39 and 0.14, respectively). LV contractility increased predominantly in non-ischemic patients (mean Δ EF +10,5 ± 3,9 units %), while patients with large perfusion defects detected by SPECT were mostly non-responders (mean Δ EF -4,9 ± 6,4 units %). Larger SRS values (higher than cut-off value of 14) predicted absent or worse LV EF response. Baseline SRS values correlated well with LV EF decrease (r=-0.67, p=0.002). ***Conclusion:*** We suggest that gated perfusion SPECT data allowed to identify areas of a viable (perfused but hypokinetic) myocardium in patients with LV dilation and low EF. Preserved perfusion with no severe focal impairments was a good prognostic factor for CCM responce. Also, performing myocardial perfusion SPECT in the framework of preoperative preparation allowed to determine the most accurate electrode positioning at the viable interventricular septum zones. ***References:*** None

EPS-060

Stress gated blood pool SPECT: the prognosis of left ventricle repeated remodeling in 12 month after surgical correction of ischemic cardiomyopathy

V. Shipulin*, K. Zavadovsky, S. Andreev, A. Pryakhin, V. M. Shipulin;*
Cardiology Research Institute, Tomsk National Research Medical Centre, Russian Academy of Sciences, Tomsk, RUSSIAN FEDERATION.

Aim/Introduction: To assess the value of gated blood pool SPECT (GBPS) with dobutamine in the prognosis of left ventricular (LV) repeated remodeling after surgical treatment of patients with ischemic cardiomyopathy (ICM). ***Materials and Methods:*** A total of 30 patients with ICM [1] were enrolled. Prior to surgery patients underwent GBPS at rest and at stress (5/10/15 μg/kg /min increasing doses of dopamine). The duration of each dosage was 5 minutes.

The values of LV volumes, global contractile function and dissynchrony were calculated. In the follow-up period (476 ± 36 days), patients were divided into two groups. Group 1 (n=20) - patients with repeated LV myocardial remodeling (an increase of LV end-systolic volume (LVESV) or decrease of LVESV≤10% according to 2D echocardiography in comparison to early postoperative period study). Group 2 (n=10) - reverse LV remodeling (reduction >10% in LVESV). ***Results:*** Stress study showed differences between groups in terms of stress-induced changes of LVEF (Δ LVEF): 2(2;8) vs. 11(5;2), p=0.02; LV dissynchrony - ΔPSD: 3(0;7) vs. -2(-9;3), p=0.004; ΔEntropy: 2(-1;6) vs. 0(-4;2), p=0.01, respectively. Multivariate logistic regression analysis showed that ΔLVEF (OR = 0,88; 95% CI 0,8; 0,97; p = 0.008), ΔPSD (OR=1,13; 95% CI 1,03; 1,25; p=0.005) and the number of coronary arteries with stenosis> 75% (CAS) (OR = 4.25; CI 1.57; 11.48; p = 0.001) were independent predictors of myocardial remodeling in the long term follow-up. The ROC analysis revealed that ΔPSD showed a sensitivity of 87% and a specificity of 64% (cut-off value >-1; AUC, 0.727), ΔLVEF had a sensitivity of 65% and a specificity of 82% (cut-off value ≤4; AUC 0.674) and CAS had a sensitivity of 84% and a specificity of 46% (cut-off value >2; AUC 0.691) in myocardial remodeling prediction. Based on multivariate logistic regression the prognostic model was estimated (including indices above and presence of diabetes mellitus). According to the ROC analysis, the AUC of this model (0.907) was significantly higher in comparison to AUC values of indices alone. ***Conclusion:*** In patients after surgical ICM correction, the values of ΔLVEF and ΔSDLV obtained with the preoperative stress GBPS are associated with the repeated left ventricular remodeling in the long-term follow-up period. ***References:*** 1. Shipulin V. M., Pryakhin A. S., Andreev S. L. et all. Surgical Treatment of Ischemic Cardiomyopathy: Current State of the Problem. Kardiologiia. 2019;59(9):71-82. DOI: 10.18087//cardio.2019.9.n329

EPS-061

Patient Safety in MPI: Role of the Radiopharmacist in a Multidisciplinary Team

A. Jimenez-Heffernan*, C. Salgado-Garcia, T. Aroui-Luquin, E. Sanchez de Mora, A. Amr-Rey, A. Ramirez-Navarro;*
Hospital Juan Ramon Jimenez, Huelva, SPAIN.

Aim/Introduction: To assess the radiopharmacist's role in a multidisciplinary team together with nuclear physcians and nurses, after a short period of specific training focused on the clinical contraindications of regadenoson and adenosine, in order to ensure the safe use of pharmacologic vasodilator stress agents in patients undergoing SPECT-MPI. ***Materials and Methods:*** We prospectively studied the safe use of regadenoson in 557 consecutive patients undergoing MPI (57.4% female, mean age: 67.2±11.2 years, range: 32-90 years). Gender, age, medical history, medications, drug allergies and contraindications for stress testing were registered together with the recommendations to the nuclear physician in charge. ***Results:*** The situations and contraindications found together with the corresponding recommendation to the nuclear physician were as follows: prior stroke or TIA 3.9%-consider carotid stenosis assessment; salicylates/sulfonamides allergy 3.8%- use 99mTc-sestamibi as the radiopharmaceutical; epilepsy/seizures 2.2%- reconsider test indication; risk factors for QTc interval prolongation 2.0%-extravigilance of ECG during test for QTc prolongation; systemic corticosteroid therapy for severe COPD 1.4%-do not perform test; acute exacerbation of COPD 1.1%-defer test until acute episode is over; severe asthma 0.7%-do not perform test; methylxanthine ingestion 0.4%-reassessment of patient's condition on the appointment day; other 6.5%-evaluation of other contraindications. No contraindications were detected in 78% of patients. ***Conclusion:*** Working in a systematic way, the radiopharmacist was able to detect a high number of issues related to the safe use of regadenoson in MPI studies, with one out of four patients presenting some drug interaction or clinical contraindication. The recommendations given by the radiopharmacist were well accepted by the nuclear physicians who changed their approach, thus contributing to increase the safety of patients referred for MPI. ***References:*** None

EPS-062

Added value of Myocardial Flow Reserve measurement during SPECT perfusion: correlation with invasive coronary angiography

M. Bailly[1]*, F. Thibault*[1]*, M. Courtehoux*[2]*, G. Metrard*[1]*, D. Angoulvant*[2]*, M. Ribeiro*[2]*;*
[1]*CHR Orléans, Orleans, FRANCE,* [2]*CHRU Tours, Tours, FRANCE.*

Aim/Introduction: Myocardial blood flow (MBF) and flow reserve (MFR) measurement have been shown to improve diagnostic performances of coronary artery disease (CAD). Dedicated CZT cardiac cameras provide accurate evaluation of MBF and MFR. In this pilot study we correlated the results of SPECT myocardial perfusion imaging (MPI) and MFR measurement with invasive coronary angiography (ICA) findings. ***Materials and Methods:*** Patients referred for dynamic MPI for CAD screening between November 2018 and March 2020 and for whom coronary angiography was performed within 3 months were included. Symptoms and risk factors were collected. SPECT data were acquired on a CZT-based pinhole cardiac camera using a stress (251 ± 12 MBq) / rest (513 ± 25 MBq) one-day Tc-99m-tetrofosmin protocol. Kinetic analysis was done with Corridor 4DM™software using a 1-tissue-compartment model and converted to MBF using a previously determined extraction fraction correction. ICA was performed upon decision of the referring cardiologist and considered normal if no

stenosis > 30% or with impaired FFR was found. The results of ICA were compared to global MFR. ***Results:*** 35 patients (21 male, 14 female) were analyzed. MPI was visually normal in 25 patients, among them 16 had pathological ICA. Mean global MFR was 1.94 ± 0.77. Global MFR was impaired (<2) in 25 patients; among them only 7 patients had abnormal visual MPI. This threshold could be considered as the optimal one and allowed a safe exclusion for asking an ICA: sensitivity 95.5%, specificity 69.2% and negative predictive value 99.3%, area under Receiver-Operator-Characteristic curve: 0.83. MFR is related to epicardial coronary arteries and to microvascular arteries; this can explain the limited specificity, with 4 patients having normal ICA but impaired MFR potentially due to microvascular dysfunction (diabetes with target organ damage such as proteinuria-). Only one patient had normal global MFR of 2.68, but abnormal ICA with severe stenosis on right coronary artery (inferior MFR was 1.68). ***Conclusion:*** Global MFR measured during MPI for CAD screening on CZT camera significantly enhances SPECT diagnostic performances and could be a safe exclusion or a strong motivation for asking an ICA. ***References:*** None

EPS-063

SPECT Myocardial Blood Flow and Calcium Scoring measurement in patients referred for Coronary Artery Disease screening

M. Bailly[1], F. Thibault[1], M. Courtehoux[2], G. Metrard[1], D. Angoulvant[2], M. Ribeiro[2];
[1]CHR Orléans, Orleans, FRANCE, [2]CHRU Tours, Tours, FRANCE.

Aim/Introduction: Dedicated CZT cardiac cameras provide accurate measurements of absolute myocardial blood flow (MBF) and flow reserve (MFR). PET MBF studies using either Rb-82 or N-13-ammonia have shown that MFR was predictive of major adverse cardiovascular (CV) events. Coronary calcium score (CCS) is also predictive of CV events, especially in diabetic patients. In this study, we evaluated the results of SPECT global MFR measurement and CCS evaluation in patients referred for Coronary Artery Disease (CAD) screening. ***Materials and Methods:*** Patients referred for Myocardial Perfusion Imaging (MPI) for CAD screening between November 2018 and March 2020 were included in a prospective trial (CFR-OR). Clinical and CV risk factors were collected to classify patients in 3 groups: moderate, high and very high risk. HeartScore (SCORE) according to the European Society of Cardiology was calculated. SPECT data were acquired on a CZT-based pinhole cardiac cameras in listmode using a stress (251 ± 11 MBq) / rest (512 ± 23 MBq) one-day Tc-99m-tetrofosmin protocol. Kinetic analysis was done with Corridor4DM™software using a 1-tissue-compartment model and converted to MBF using a previously determined extraction fraction correction. Low dose thoracic CT was acquired on the same day using another SPECT/CT camera in the same position and used for CCS evaluation. ***Results:*** 136 patients (60 male, 76 female) were included and classified in 3 clinical CV risk groups: 50 moderate, 36 high and 50 very high risk. Mean SCORE was 4 ±3.1 %. Mean global MFR was 2.50 ± 0.74; 34 patients had impaired CFR (using a threshold of 2). MFR wasn't significantly different between the three groups of CV risk (p=0.09), but MFR was significantly reduced in high and very-high risk patients (p=0.05). CCS was not different according to risk categories (p=0.32). There was a significant inverse correlation between MFR and SCORE (p=0.009) and gender (p=0.026). Significant correlation was also found between CCS and SCORE (p=0.001) and gender (p=0.05). MFR was not correlated to CCS (p=0.61). Regarding CV risk factors, CCS was significantly higher in smokers (p=0.05), but no other significant correlation was found between MFR or CCS and dyslipidemia, hypertension, diabetes or family history of coronary artery disease (p at least 0.41). ***Conclusion:*** CCS and MFR measured during MPI for CAD screening are significantly correlated with SCORE and gender. MFR was significantly reduced in high and very-high risk patients. CCS and MFR however weren't correlated together. ***References:*** None

EPS-064

The Dark Side Of Atrial Uptake On 99mTc-3,3-Diphosphono-1,2-Propanodicarboxylic Acid (99mTC-DPD) Bone Scintigraphy In Patients With Cardiac Amyloidosis

R. Mei[1], I. Diemberger[2], R. Bonfiglioli[1], A. Paccagnella[1], F. Mattana[1], C. Gagliardi[2], G. Caponetti[2], S. Longhi[2], P. Massa[2], G. Saturi[2], M. Sguazzotti[2], N. Galiè[2], S. Fanti[1];
[1]Nuclear Medicine Policlinico S.Orsola-Malpighi, Bologna, ITALY, [2]Cardio-Thoracic and Vascular Building, Department of Experimental, Diagnostic and Specialty Medicine, Bologna, ITALY.

Aim/Introduction: Bone scintigraphy with 99mTc-DPD is an excellent non-invasive diagnostic tool for cardiac amyloidosis, especially for the recognition of differential diagnosis between ATTR (amyloidosis with trans-tiretin deposition) and AL (amyloidosis with light-chains deposition). To date there is a lack of knowledge in recognizing atrial uptake (AU) and its possible clinical implications. We aimed to evaluate patterns of AU in patients with suspected or confirmed CA who undergone staging with 99mTc-DPD bone scintigraphy. ***Materials and Methods:*** Patients who had undergone bone scintigraphy with suspected or confirmed CA were retrospectively analyzed in the period 2016-2020. Inclusion criteria were: Perugini's score >=1, availability of clinical data, including comorbidities, laboratory exams, eventual supraventricular atrial disorders and echocardiographic anteroposterior atrial diameter. All planar and SPECT/CT images (when available) were revised by two experienced nuclear physicians; diffuse atrial and left ventricular uptake data were collected. Interobserver agreement (IA) analysis was performed (Cohen's k). Correlation between AU and supraventricular

rhythm disorders were evaluated with Pearson's chi square. ***Results:*** Sixty patients were finally selected (53M; 7F); mean age of 77 (+-9.9). 48.3% of them had sinus rhythm, while 31 pts had different arrhythmias (permanent and paroxysistic atrial fibrillation 30% and 16.7%; atrial flutter 1.7%). Mean left anteroposterior atrial diameter was 46mm (+-6.3mm). Out of 60, twenty-seven pts (45%) were still ongoing diagnosis pathway for amyloidosis (i.e. differential diagnosis between ATTRvs.AL), while 32 pts (55%) had ATTR and 1 with AL. An overall left ventricular cardiac uptake was observed in 60/60 by each two observers, with IA between mild versus moderate/severe uptake of 0.90 ($p<0.0001$). AU was observed in planar images in 36/60 and 42/60 respectively by each two physicians, with an IA of 0.49 ($p<0.0001$). SPECT/CT was performed in 17/60 pts; AU was observed in 14/17 and 15/17 pts respectively, IA=0.77 ($p=0.001$). No significant correlation was observed between AU and current presence or history of supraventricular arrhythmias, nor with left atrial enlargement. ***Conclusion:*** Standard planar images of bone scintigraphy are a validated approach for detection and differentiation of CA. Our analysis evidenced limitations of this technique in identifying atrial involvement that can be at least mitigated by adoption of SPECT/TC scan. The association of AU with atrial enlargement and/or arrhythmias was not evidenced by our analysis but larger prospective studies systematically adopting SPET/TC are needed. Gaining insight into these possible relationships may help to better understand the real meaning of cardiac uptake, which still remains eclipsed. ***References:*** None

EPS-065

Electromechanical Decoupling Associated With Cardiac Transthyretin Amyloidosis. A Small Case Series Characterization of Left Ventricle Dyssynchrony Applying Gated-SPECT Phase Analysis

F. Ferrando-Castagnetto[1], *C. G. Wakfie Corieh*[2], *J. C. Rodríguez Gómez*[2], *K. Bayardo*[3], *P. Romero Fernández*[2], *M. Pedrera Canal*[2], *I. Vilacosta*[4], *A. Sánchez*[2], *F. Mut*[5], *R. Ferrando*[3], *M. Pérez Castejón*[2], *J. Carreras Delgado*[2];
[1]*Departamento de Cardiología - CCVU, Hospital de Clínicas, FM, UdelaR, Montevideo, URUGUAY,* [2]*Servicio de Medicina Nuclear, Hospital Clínico San Carlos, Madrid, SPAIN,* [3]*Departamento de Medicina Nuclear e Imagen Molecular, Hospital de Clínicas, FM, UdelaR, Montevideo, URUGUAY,* [4]*Instituto Cardiovascular, Hospital Clínico San Carlos, Madrid, SPAIN,* [5]*Sevicio de Medicina Nuclear, Asociación Española Primera de Socorros Mutuos, Montevideo, URUGUAY.*

Aim/Introduction: Myocardial amyloid deposition can alter the regional cardiac mechanics of the left ventricle (LV). Recent findings of Doppler tissue velocity imaging suggest that patients with early light-chain cardiac amyloidosis have increased segmental dyssynchrony compared to controls. (1) However, LV mechanical dyssynchrony (LVMD) has not been assessed in transthyretin cardiac amyloidosis (ATTR). ***Materials and Methods:*** Consecutive patients with high clinical and imaging suspicion of ATTR and no coronary artery disease referred to bone-seeking scintigraphy during the last 6 months were included. Patients were studied using ^{99m}Tc-DPD and ^{99m}Tc-PYP with planar imaging and gated-SPECT/CT obtained 1-3 hours after injection. Peak amplitude (PA), phase standard deviation (PSD) and phase bandwidth (PBW) were calculated from phase histogram applying SyncTool (Emory Cardiac Toolbox®) and compared with normal values obtained with perfusion tracers as previously reported (2) and with a group of patients with normal gated-SPECT ^{99m}Tc-MIBI images (n = 24). The site of the onset of mechanical LV contraction (OMC) was detected in a digital video of contractile dynamics. ***Results:*** Six patients were included, 4 with ^{99m}Tc-DPD and 2 with ^{99m}Tc-PYP, all men, aged 70-89 years, LVEF = 41 + 18%. Two patients exhibited left bundle branch block in baseline ECG. The mean H/CL score was 2.83, all cases were graded as Perugini category 3. Patients with ATTR presented a marked LVMD (PA = 137.5 + 64.6, PSD = 57.1 + 21.9, PBW = 184.5 + 64.4 degrees (p-value < 0.05 for comparisons of PSD and PBW with both control groups). A multisite OMC was found in 33% of cases. ***Conclusion:*** Results of gated-SPECT phase analysis obtained using bone-seeking radiotracers suggest an underlying mechanical substrate of marked LVMD that could be correlated with a severe amyloid burden. This could be an unrecognized mechanism contributing to heart failure in ATTR subjects. However, phase histogram measures obtained with bone-seeking tracers should be validated by comparison with perfusion imaging tracers through large series, ideally on a per-patient, dual-isotope basis. ***References:*** 1) Migrino RQ, Harmann L, Woods T, et al. Intraventricular dyssynchrony in light chain amyloidosis: a new mechanism of systolic dysfunction assessed by 3-dimensional echocardiography. Cardiovasc Ultrasound 2008;7:40. 2) Chen J, Garcia EV, Folks RD, et al. Onset of left ventricular mechanical contraction as determined by phase analysis of ECG-gated myocardial perfusion SPECT imaging: development of a diagnostic tool for assessment of cardiac mechanical dyssynchrony. J Nucl Cardiol 2005;12:687-695.

EPS-066

The Importance Of Monoclonal Proteins Determination For The Correct Diagnosis Of Transthyretin Cardiac Amyloidosis By [^{99m}Tc]Tc-diphosphonates

A. Roteta*, D. Nogueira Souto, A. Andrés Gracia, L. Tardin Cardoso, P. Razola Alba, M. Delgado Castro, T. Escalera Temprado, E. Prats Rivera, M. Abós Olivares;*
Clinic Hospital "Lozano Blesa", Zaragoza, SPAIN.

Aim/Introduction: To analyze the influence of the determination of free monoclonal proteins in blood and urine in the final diagnosis of Transthyretin Cardiac

Amyloidosis (TTRA). ***Materials and Methods:*** We have analyzed 200 [99mTc]Tc-diphosphonates scans: 192 performed on 190 patients under suspicion of TTRA and 7 patients with grade II-III radiotracer myocardial deposit as a casual finding (November/2013 - January/2020). Likewise, clinical and laboratory characteristics (heart failure, LVEF, proBNP levels, immunofixation in serum and/or urine for the detection of monoclonal chains and chronic renal failure) have been evaluated. A positive case has been considered for TTRAwt or senile (Score Perugini II-III scan, negative immunofixation in serum and/or urine, negative genetic study), positive case for hereditary TTRA (Score Perugini II-III scan, negative immunofixation and positive genetic study), positive case for secondary amyloidosis (positive immunofixation and presence of hematologic malignancy) and undetermined amyloidosis (immunofixation not performed or positive and absence of haematologic malignancies at follow-up). ***Results:*** 59 positive scans have been detected, 47 men (79'7%) and 12 women (20'3%). The mean age of the group of positives was 82'66 years, while that of the negatives was 72'15. The mean proBNP levels in the positives are 7561, compared to 5869 in the negative group. Immunofixation (serum and/or urine for detection of kappa or lambda monoclonal chains at 30 (50.8%) has been performed on these patients. Finally, 37.2% (22/59) resulted in ATTRwt, 3.4% (2/59) hereditary ATTR (genetic study: variant E54Q and mutation c.424> A (p.Va.122Ile) in exon 4 of TTR) and 1.7% (1/59) secondary amyloidosis. The remaining 34/59 (57.7%) cases were undetermined amyloidosis (6 positive immunofixation and 27 without monoclonal proteins determination). ***Conclusion:*** Determination of monoclonal bands in blood and urine is mandatory to correctly characterize cases of cardiac amyloidosis and, in presence of monoclonal bands, to assess the existence of underlying haematological malignancies. ***References:*** None

EPS-067

Left Ventricle Mechanical Response to Induced Ischemia In Patients With Narrow QRS and Normal Systolic Function Derived To Gated-SPECT

F. Ferrando-Castagnetto[1], M. Pedrera Canal[2], M. Ollarves Carrero[2], L. García Belaustegui[2], C. Real[3], I. Vilacosta[3], R. Ricca-Mallada[1], F. Mut[4], R. Ferrando[5], R. Lluberas[1], M. Pérez Castejón[2], J. Carreras Delgado[2];
[1]Departamento de Cardiología - CCVU, Hospital de Clínicas, FM, UdelaR, Montevideo, URUGUAY, [2]Servicio de Medicina Nuclear, Hospital Clínico San Carlos, Madrid, SPAIN, [3]Instituto Cardiovascular, Hospital Clínico San Carlos, Madrid, SPAIN, [4]Servicio de Medicina Nuclear, Asociación Española Primera de Socorros Mutuos, Montevideo, URUGUAY, [5]Departamento de Medicina Nuclear e Imagen Molecular, Hospital de Clínicas, FM, UdelaR, Montevideo, URUGUAY.

Aim/Introduction: Gated-SPECT phase analysis is a novel, noninvasive and reliable method to quantify left ventricular mechanical dyssynchrony. However, the contributions of this technique as ancillary criteria to the diagnosis of induced myocardial ischemia have been scarcely evaluated. In this research, we characterized the contractile response of the left ventricle associated with post-stress myocardial ischemia in subjects without baseline electrical dyssynchrony. ***Materials and Methods:*** Phase histograms were obtained under basal and post-stress conditions in a sample of consecutive patients referred to gated-SPECT with normal systolic function and narrow QRS complex in 12-lead ECG. Gated-SPECT myocardial perfusion imaging with 99mTc-MIBI was performed following a two-days stress-rest protocol. Post-stress images were acquired 0.5 - 2.0 hours after exercise or vasodilator challenge. Patients in non-sinus rhythm, renal failure or mitro-aortic valve disease were excluded. The resting/post-stress changes (pre/post measurements) in phase standard deviation (PSD) and phase bandwidth (PBW) indices were compared between patients with and without myocardial ischemia on images. Continuous variables were expressed in means + SEM. The magnitude of these changes was evaluated using paired "t" test. ***Results:*** A total of 118 consecutive patients were included, 61% male, 68 + 12 years old; 46% of them completed a treadmill exercise protocol (Bruce). An increasing trend in the post-stress mechanical dyssynchrony indices was observed in patients with perfusion defects interpreted as ischemia, although not reaching statistical significance (PSDpre = 24.38 + 1.85, PSDpost = 26.36 + 2.12 degrees, p = 0.22; PBWpre = 73.04 + 6.17, PBWpost = 82.38 + 7.68 degrees, p = 0.08). The biggest change was observed in patients with reversible defects interpreted as ischemia and fixed defects compatible with infarct sequelae, either remote or perilesional (PBWpre = 79.11 + 9.37, PBWpost = 91.50 + 11.79 degrees, p = 0.06). ***Conclusion:*** Induced myocardial ischemia tended to be associated with increased dyssynchrony measured by gated-SPECT phase analysis obtained in post-stress images, especially in the subgroup of patients with myocardial scar. This response should be tested by acquiring immediate post-stress images and correlated with the amount (quantum) of ischemic burden, the extension of stenotic coronary lesions, and the presence of microvascular dysfunction. ***References:*** None

EPS-068

The Diagnostic Role Of ^{99m}Tc-DPD Scintigraphy In TTR Cardiac Amyloidosis And Its Corelation With Clinical And Radiological Findings, Our Experience

J. Cañadas Salazar[1], B. LucasVelázquez[2], L. G. Díaz González[2], F. Gómez-Caminero López[2], P. García-Talavera-San-Miguel[2], A. C. Peñaherrera Cepeda[2], J. G. Villanueva Curto[2], S. López Puche[2], E. Martin Gomez[2], M. P. Tamayo Alonso[2];
[1]Sacyl, Salamanca, SPAIN, [2]CAUSA, Salamanca, SPAIN.

Aim/Introduction: To evaluate the relation of 99mTc-DPD scintigraphy in patients with suspected TTR cardiac amyloidosis with clinical and radiological findings in echocardiogram and magnetic resonance imaging (MRI). *Materials and Methods:* 118 patients were reviewed from 2016 to 2020 (85 male / 33 female, with a mean age of 79±9 years) with the suspicion of cardiac amyloidosis (AcTTR variant). A total body planar image and SPECT / CT hybrid imaging (acquisition of 90 views / 6s, reconstruction with an iterative method) using 740MBq of 99mTc-DPD , were performed. The interpretation of the images was carried out by visual assessment according to the Perugini scale, establishing those with grade 2 or 3 uptake as positive for AcTTR. Clinical and radiological parameters obtained by echocardiography or MRI were reviewed: ventricular function, hypertrophy, atrial dilation and enhancement. gadolinium late. *Results:* The scintigraphy was positive for AcTTR in 60/118 patients and all of them obtained the diagnosis of AcTTR based on this result and complementary non-invasive tests. In this subgroup of patients, heart failure was observed in 86%, atrial fibrillation in 70%, conduction disorders in 51%, and a pseudoinfarction pattern in 16%. Preserved left ventricular function was detected in 62%, ventricular hypertrophy in 100% and atrial dilation in 83%. Gadolinium MRI was performed in 42/60 patients, of which 38 (91%) showed a late enhancement pattern suggestive of amyloidosis. A genetic study was performed in 28 patients, 6 of them carrying an AcTTR-associated mutation. 58/118 patients with a negative scan for AcTTR were diagnosed with other cardiac diseases, the most frequent being valvular heart disease. *Conclusion:* In our experience 99mTc-DPD scintigraphy is a very useful technique in the non-invasive differential diagnosis of ATTR with a sensitivity and PPV of 100%, demonstrating its relationship and agreement with clinical alterations and structural parameters of cardiac imaging. *References:* None

404c

Mini Course 3: Alpha Emitters in Therapy

Friday, October 23, 2020, 11:00 - 11:50 Channel 4

OP-281

Radionuclide Therapy with Radium-223 of Metastatic Castration-Resistant Prostate Cancer

V. Frantellizzi; Department of Molecular Medicine, Sapienza University of Rome, Rome, ITALY.

OP-282

An Overview of Targeted Alpha Therapy with Actinium-225 and Bismuth-213

M. Ooms; SCK-CEN Academy, Brussels, BELGIUM.

601

CME 5: Imaging Hepatobiliary and Pancreatic Tumours - Pearls, Patterns and Pitfalls

Friday, October 23, 2020, 13:50 - 15:20 Channel 1

OP-283

What Do we Need from Imaging in Hepatobiliary and Pancreatic Tumours - A Clinician's View

C. Carvalho; Champalimaud Clinical Centre, Digestive Unit, Lisbon, PORTUGAL.

OP-284

Abdominal 3T MRI and Spectral CT Imaging of Pancreatic and Biliary Cancer - Review of Imaging Techniques, Protocols and Findings

R. Braren; Technische Universität München, Klinikum rechts der Isar, Institute of Diagnostic and Interventional Radiology, Munich, GERMANY.

OP-285

Hepatic and Biliary System - Pearls, Patterns and Pitfalls of PET/CT Imaging

S. Carrilho Vaz; Champalimaud Clinical Centre, Nuclear Medicine - Radiopharmacology, Lisbon, PORTUGAL.

OP-286

Pancreas and Gallbladder- Pearls, Patterns and Pitfalls of PET/CT Imaging

G. Gnanasegaran; Royal Free London NHS Foundation Trust, Department of Nuclear Medicine, London, UNITED KINGDOM.

602

Joint Symposium 9 (EANM/ESMI/ESCMID): Imaging Pulmonary Fungal Infections

Friday, October 23, 2020, 13:50 - 15:20 Channel 2

OP-287

Current Dilemmas in Fungal Treatment

M. Sanguinetti; Universita Cattolica del S.Cuore (UNICATT), Dept. of Laboratory Sciences and Infectious Diseases,Rome,ITALY.

OP-288

Preclinical Tools to Study Fungal Infections

G. Vande Velde; Katholieke Universiteit (KU) Leuven, Dept. Imaging and Pathology, Leuven, BELGIUM.

OP-289

In vivo Imaging of Host Responses

L. Carlin; Beatson Institute for Cancer Research, Glasgow, UNITED KINGDOM.

OP-290

Imaging Pulmonary Infections in the Clinic

M. Gunzer; University Duisburg-Essen, Center for Medical Biotechnology, Essen, GERMANY.

603

Joint Symposium 10 (EANM/JSNM): Nuclear Cardiology Beyond Perfusion Imaging

Friday, October 23, 2020, 13:50 - 15:20 Channel 3

OP-291

Imaging Innervation with MIBG

K. Nakajima; Department of Functional Imaging and Artificial Intelligence, Kanazawa University, Kanazawa, JAPAN.

OP-292

Diagnostic Application of BMIPP Imaging in Clinical Practice

T. Chikamori; Department of Cardiology, Tokyo Medical University, Tokyo, JAPAN.

OP-293

Imaging Cardiac Amyloidosis with Bone Tracers

K. Wechalekar; Department of Nuclear Medicine, Royal Brompton Hospital, Imperial College, London, UNITED KINGDOM.

OP-294

Imaging Endocarditis with Radiolabeled WBC

P. Erba; Department of Translational Research and New Technology in Medicine, University of Pisa, Pisa, ITALY.

604

Technologists Oral Presentations 1 - Featured Session: MATTER - MultidisciplinAry TechnologisT rEseaRch

Friday, October 23, 2020, 13:50 - 15:20 Channel 4

OP-295

Introduction

P. Fragoso-Costa; Clinic for Nuclear Medicine, University Hospital Essen, Essen, GERMANY.

OP-296

The effect of Artificial Intelligence (AI) on lung perfusion SPECT-CT segmentation analysis

A. Willems van Beveren, G. T. Nauta, A. van Erp-Zeilstra, A. Heus, J. Pruim;
UMCG NGMB, Groningen, NETHERLANDS.

Aim/Introduction: The use of AI in nuclear medicine is increasing. We tested an AI application in a group of severe COPD patients in order to assess the accuracy of segmentation and the consequences for the calculation of segmental lung perfusion. ***Materials and Methods:*** The data of 7 patients with COPD GOLD IV, that underwent a lung perfusion scan and SPECT CT with 99mTcMAA because of intended lung volume reduction surgery, were fed to a newly developed Siemens AI application. The application was trained on approx. 8500 normal people, patients with lung cancer and patients with COPD. A 4-point Likert scale was used by 3 observers independently to assess the quality of the outlining by the system (0= bad match, 1= moderate match, 2= reasonable match, 3= good match): total overview of AI segmentation, pleural confection and the interlobular fissures. In case of discrepancies a radiology resident with subspecialisation in cardiothoracic imaging examined the results in addition. Also, the ratios of the left and right lung and as well the ratios of the respective inferior and the superior lobes from the AI application were compared to the static SPECT results. ***Results:*** In all but 1 delineation the segmentation by the system was considered to be reasonable to good. However, in 1 patient with a congenital absence of the right horizontal fissure the AI "created" a fissure from interlobular septae. The ratio between the right and left lung of the analysis suite application versus the static SPECT results were almost identical. However, the ratios between the left superior and inferior lobes, and between the right superior and inferior lung fields differed greatly from static SPECT: left 1% to 20% (mean 10%); right 3% to 34% (mean 17%.) ***Conclusion:*** The AI application can reliably detect interlobular fissures in COPD GOLD IV patients although trained on normal thoracic CT scans. Introduction will most likely improve the accuracy of estimated perfusion of pulmonary lobes in lung perfusion scans. ***References:*** Lung Analysis suite 002_MI_RCCCA_S_LAS_V01, prototype User Guide, Siemens Healthineers, USA.

OP-297

The choice of colour scale for reconstruction of ^{68}Ga-PSMA-11 PET/CT images impacts upon diagnostic performance

R. Schepers[1], C. Sachpekidis[1,2], J. Hünermund[1], K. P. Bohn[1], V. Fech[1], A. Rominger[1], A. Afshar-Oromieh[1], I. Alberts[1], C. Mingels[1];
[1]Department of Nuclear Medicine, Inselspital, Bern University Hospital, University of Bern, Bern, SWITZERLAND,
[2]Clinical Cooperation Unit Nuclear Medicine, German Cancer Research Center, Heidelberg, GERMANY.

Aim/Introduction: The aim of this study is to assess the lesion based inter-observer agreement between non-linear and linear colour scales of ^{68}Ga-PSMA-11 PET/CT in patients with recurrent prostate cancer. ***Materials and Methods:*** ^{68}Ga-PSMA-11 PET/CT scans for biochemical recurrence of prostate cancer (PCa) for 50 consecutive patients were

evaluated retrospectively. Scans were prepared in both a non-linear 'PET-rainbow' and a linear colour scale 'hot-metal new'. All images were reconstructed using Siemens Syngovia. Two readers (one consultant and one junior resident), read all scans in a randomised order. Both were blinded to patient data, clinical details and each other's analyses. ^{68}Ga-PSMA-11-avid lesions were classified into benign and pathological in both colour scales. Confirmatory clinical follow-up was available for 68% of the patients. Only fusion PET/CT-datasets and stand-alone CT-images were analysed. The number of lesions (benign or pathological) was ascertained. Bland-Altman statistics (bias±95% limits of agreement) was used to assess agreement in number of lesions between the two readers and the colour scales for benign lesions as well as for pathological lesions. ***Results:*** Both readers described greater numbers of pathological lesions in 'PET-rainbow' compered to 'hot-metal new' (junior reader 142 vs. 117, consultant 119 vs 112). Likewise, Bland-Altman analysis confirmed bias towards 'PET-rainbow' in the detection of pathological lesions (-0.50±1.32). For the detection of benign lesions, no difference was seen (0.02±2.48). We also found a difference between the consultant and junior reader, with a greater bias towards the junior reader for pathological lesions in 'PET-rainbow' (0.46±1.25) than for 'hot-metal new' (0.10±0.75). ***Conclusion:*** Greater numbers of pathological lesions were found in 'PET-rainbow' than in 'hot-metal new'. Likewise, Bland-Altman analysis confirmed a bias towards 'PET-rainbow' for pathological lesions, but not for benign. Emphasising that increased pathological lesion detection was not at cost of increased unspecific findings in 'PET-rainbow'. We found that the bias towards 'PET-rainbow' was greater for the junior reader, suggesting that 'PET-rainbow' was most beneficial for the less experienced physician. It can be shown from basic science that, non-linear colour scales aid lesion discrimination. We therefore suggest that ^{68}Ga-PSMA-11 PET/CT images shall be reconstructed in a non-linear colour scale as 'PET-rainbow' rather than in a linear colour scale like 'hot-metal new', owing to its improved performance. ***References:*** None

OP-298

Hand-foot contamination monitoring in hospital radiopharmacy laboratory: one-year data

K. Levänen[1], C. Lehtinen[1], M. Kullberg[1], N. Hänninen[2], J. Heikkinen[2];
[1]Department of Radiology and Nuclear Medicine, Social and healtcare joint authority of South Savo, Mikkeli, FINLAND, [2]Department of Medical Physics, Social and healtcare joint authority of South Savo, Mikkeli, FINLAND.

Aim/Introduction: After the preparation of radiopharmaceuticals, contamination control is important in reducing unneeded doses to personnel or patients. A hand-foot monitor is useful in detecting possible contaminations in gloves or shoes. In our facility, the hand-foot monitor was connected to cloud service, to allow real-time monitoring of the contamination measurements, in addition to easy record keeping and data collection. In this study, the collected data was analyzed to provide information about how common glove and shoe contaminations are and how they could be further prevented. ***Materials and Methods:*** Measurements were recorded for the duration of one year from February 2019 to February 2020. During that time, radiopharmacy laboratory was mainly used by four radiographers. After each of their visit to the lab, they measured the dose rate of their gloves and shoes with hand-foot monitor from eight target areas: right/left hand palm/back, right/left foot front/back. All the targets were measured simultaneously in one measurement instance. Radiographers identified their measurements by personal labels. Data was recorded by a cloud system connected to the monitor. ***Results:*** The threshold of contamination of clothes of personnel or the environment outside radio laboratory is defined as a dose rate of 4 Bq/cm^2 or more (Radiation and Nuclear Safety Authority STUK Finland). In total the four radiographers completed 237 measurement instances, of which in 16% cases (38 instances) the contamination threshold was exceeded in at least for one target area. Some activity in at least one target was detected in 73% of measurement cases (173 instances). Most common contamination target was right hand palm (87% or 33 of cases above threshold, 39% or 68 of cases of any activity). Foot contamination never exceeded the contamination threshold, though some activity was detected in 73% of measurement cases. When threshold was exceeded the average dose rate was 45 Bq/cm^2. Overall the average dose rate was 22 Bq/cm^2 (range from 0.01 to 248 Bq/cm^2). Usually when one target was contaminated, some of the others were too. Average number of contaminated targets was 2.9 when threshold was exceeded, and 2.8 when any activity was detected. ***Conclusion:*** The contamination of the gloves and shoes in radiopharmacy laboratory of the hospital is common. Right hand was most commonly contaminated target, as the four radiographers were all right-handed. Based on the collected data, more precautions can be applied, e.g. changing the gloves more often in the laboratory. ***References:*** None

OP-299

Difficulties in achieving compliance with the dose limit requirements for the skin exposure of workers handling radiopharmaceuticals

J. Sabol[1], J. Hudzietzová[2], M. Fülöp[3];
[1]Department of Crisis Management, PACR, Prague, CZECH REPUBLIC, [2]Faculty of Biomedical Engineering, CTU, Prague, CZECH REPUBLIC, [3]Slovak Medical University, Bratislava, SLOVAKIA.

Aim/Introduction: The purpose of this paper is to summarize

the present regulatory requirements concerning compliance with the dose limit associated with the skin exposure of workers at Nuclear Medicine Departments. The difficulties in monitoring of the equivalent dose to skin in accordance with the definition of this quantity are highlighted. In addition, some results of monitoring are presented where appropriate correction factors converting ring dosimeters reading to the relevant personal dose equivalent approximate the equivalent dose at the location with the maximum exposure. ***Materials and Methods:*** More than 100 measurements were carried out at two nuclear medicine departments applying radiopharmaceuticals labelled with ^{18}F, ^{131}I, ^{11}C and ^{68}Ga. In each monitoring, 12 TLDs fixed on workers' hands were used. The readings of these dosimeters were compared with the personal equivalent dose $H_{skin}(0.07)$ corresponding to the location showing the maximum exposure, i.e. $H_{skin,max}(0.07)$, the value of which was correlated with the relevant dose limit 500 mSv/y. The correction factor, corresponding to the ratio of $H_{skin\ max}(0.07)/H_{skin}(0.07)$, was assessed taking also into account specific handling techniques workers used. ***Results:*** The results of the correction factors was found to be in the range of 2-6 depending on the individual radionuclide handled and also on the worker´s specific routine adopted in manipulating radiopharmaceuticals. In the case of ^{131}I, ^{11}C and ^{18}F, the mean value of this factor amounted to 2, 2.8 and 3.5, respectively. The highest value was observed for ^{68}Ga being close to 6. ***Conclusion:*** Our previous studies as well as the results presented by other authors indicate that nearly one in five workers in nuclear medicine might exceed the legal dose limit for skin. This is why it is important to pay attention to adopting a reliable approach to monitor the equivalent skin dose consistent with the definition of the relevant quantity. Since in most cases, the dosimeter is not located at the position with the maximum exposure, the use of the appropriate correction factor is the only way to ensure that the readings of routine dosimeters can be interpreted in terms of the equivalent skin dose. The results presented demonstrate that the difference between the reading of the dosimeter and actual equivalent dose may differ more than five times. This is a serious inconsistency in reliability of controlling of skin exposure based on routine monitoring where the position of the dosimeter has not up to now been normalized. ***References:*** None

OP-300

Reduction of [^{18}F]-FDG activity applied is feasible in clinical routine for 3D TOF PET/CT scanner: A retrospective patient study

J. Pilz, *L. Hehenwarter, G. Rendl, G. Schweighofer-Zwink, C. Pirich; Department of Nuclear Medicine and Endocrinology, University Hospital Salzburg, Paracelsus Medical University, Salzburg, AUSTRIA.*

Aim/Introduction: Phantom studies demonstrated that PET imaging data using a reduced acquisition time of 57s per bed position still fulfil international EARL criteria. Therefore, we investigated PET/CT studies of oncological patients with standard and reduced PET acquisition times. This study aimed to evaluate the equivalence of acquisition times of 75 and 57 seconds per bed position translating into an activity reduction from 4MBq to 3MBq per kg bodyweight (bw) ***Materials and Methods:*** 96 patients (60 men, 36 women, age 27-87, mean +- SD 65 +- 11.6 years) with melanoma, lung or head and neck cancer were divided into three different bw classes (<75kg, 75-100kg, >100kg) and underwent a standard whole-body or skull base-to-thigh [^{18}F]-FDG PET/CT examination using the Philips Ingenuity TF PET/CT scanner. The [^{18}F]-FDG activity applied was equal to 4MBq per kg bw (MBq range 246-479, mean +- SD 345.3 +- 71.1). Retrospectively, PET list-mode data were recalculated gaining a second PET study per patient with a reduced acquisition time of 57s instead of 75s per bed position. PET/CT data were reconstructed using a 3D OSEM TOF algorithm. Blinded patient data were analysed by two nuclear medicine physicians. The number of PET-positive lesions per body region (head and neck, thorax, abdomen, bone, extremity) and image quality (grade 1-5) were evaluated. Standardised uptake values (SUVs) were calculated with the help of 3D volume of interests in order to be able to compare the PET-positive lesions in the standard as well as the recalculated PET/CT study with reduced acquisition time. Statistical analyses were performed by equivalence testing using the R software version 3.6.3 and Bland-Altman Plots were created with graph pad prism version 6. PET-positive lesions were confirmed histologically or by clinical follow-up. ***Results:*** Lesion detection rate per patient´s body region matched in > 98% comparing 57s and 75s datasets. Overall subjective image quality was assessed as even or superior in 80 and 69%, respectively. Equivalence was established in 214 PET-positive lesions (164 malignant: mean SUV_{max} +- SD of 7.9 +- 4.0, 50 benign: mean SUV_{max} +- SD of 6.0 +- 3.3) matched per patient between the 75s and 57s PET studies for SUV_{max} (mean of differences: 0.008411, equivalence bounds +-0.0974, 90% CI -0.047-0.063, p=0.00405). ***Conclusion:*** This retrospective patient study demonstrates that an activity reduction of [^{18}F]-FDG from 4MBq to 3MBq per kg bw beyond the current EANM guidelines is feasible in clinical routine employing a 3D TOF PET/CT. ***References:*** None

OP-301

Dose reduction in FDG-PET by reconstruction optimization using resolution modelling

*A. Tegelaar - Kuiper[1], **S. Koenders**[1,2], D. Koopman[1], P. G. Sanches[3], B. N. Vendel[1], H. Arkies[1], J. A. van Dalen[4];*
[1]Department of Nuclear Medicine, Isala Hospital, Zwolle, NETHERLANDS, [2]Technical Medical Centre, University of Twente, Enschede, NETHERLANDS, [3]Health Systems, Philips

Benelux, Eindhoven, NETHERLANDS, [4]Department of Medical Physics, Isala Hospital, Zwolle, NETHERLANDS.

Aim/Introduction: Image quality of FDG-PET greatly depends on administered tracer dose and applied reconstruction settings. Especially by lowering the number of updates (iterations x subsets) and applying resolution modelling (RM) in iterative reconstructions, noise can be reduced while maintaining lesion's uptake value. Our aim was to determine the FDG-dose reduction that can be obtained using RM-reconstruction, compared to a high-resolution reconstruction without RM. ***Materials and Methods:*** Using the NEMA image quality phantom with fillable spheres (diameters 10-37mm), FDG-PET imaging (Vereos, Philips Healthcare) was performed using a sphere-to-background ratio of 10. We applied multiple reconstructions using updates ranging from 12 to 39 and RM (point-spread-function: 1 iteration; 4 regularizations). No post-smoothing filter was applied in order to maximize contrast recovery coefficients (CRCs) of the spheres. Reconstructed images were compared to a reference high-resolution reconstruction using 39 updates without RM nor filtering, as previously determined to maximize CRCs. The RM-reconstruction with similar CRCs and background noise as compared to our reference was applied to FDG-PET data of 10 consecutive oncology patients. Extra reconstructions simulating dose reductions up to 40% using clipped list-mode data were made. We measured maximum SUVs of reported lesions and the noise in the liver to verify our phantom results and to determine the maximum dose reduction without significantly altering SUVs or noise. Furthermore, three expert readers scored the image quality on a four-point scale (bad, moderate, good, excellent). ***Results:*** Reducing the number of updates resulted in both lower CRCs and noise. The reconstruction with 15 updates and RM had similar CRCs compared to our reference without RM. Applying this RM-reconstruction to patient data provided similar SUVs and an average noise reduction of 32%, as compared to the reference reconstruction. RM-reconstructions using 15 updates and simulating 40% dose reduction still showed similar SUVs and also similar noise levels, as compared to the reference. Expert readers scored the image quality of all RM-reconstructions using 15 updates to be at least 'good' and to be equal or even better compared to our reference. ***Conclusion:*** An FDG-dose reduction of 40% can be obtained when using iterative reconstruction with 15 updates and RM, compared to a high-resolution reconstruction without RM. For each PET/CT-facility it is recommended to investigate optimal reconstruction settings when using RM. Specifically, it gives the opportunity to minimize noise by reducing the number of updates without altering SUVs. ***References:*** None

OP-302

Optimal Balance between Patient Comfort, Received Dose and Image Quality for Block Sequential Regularized Expectation Maximization Reconstruction and Digital PET/CT

D. Klagyvik[1], *F. Nagy*[2], *A. Ács-Nagy*[1], *P. Szabó*[1], *I. Garai*[2], *A. Forgács*[2], *Á. K. Krizsán*[2];
[1]*ScanoMed Nuclear Medicine Centers, Budapest, HUNGARY,*
[2]*ScanoMed Nuclear Medicine Centers, Debrecen, HUNGARY.*

Aim/Introduction: The present study focuses on a quantitative and qualitative comparative evaluation of clinical whole-body ^{18}F-FDG images acquired on a SiPM-based digital PET/CT scanner using Block Sequential Regularized Expectation Maximization reconstruction (BSREM). The aim of this study was to find the optimal reconstruction parameter β value for the reduced injected activity examination protocol, without the degradation of image quality. ***Materials and Methods:*** Whole-body ^{18}F-FDG patient scans including wide range of BMIs (19.7 - 36.8) were acquired with 1.5 min/bed positions. Two reconstruction algorithms were compared in case of ^{18}F-FDG studies with oncological indications. Patients were divided into two separate groups: „Low dose" and „Normal dose" radiopharmaceutical injection protocol. The two groups were divided into further subgroups according to their body habitus: BMI=20, 25, 30, 35. The „Normal dose" group included 8 patients receiving 3.0, 3.5, 4.0 MBq/kg, while in the „Low dose"group 8 patients receiving 2.0, 2.5, 3.0 MBq/kg for BMIs ≤ 20, between 20 and 30, >30 respectively. The Whole Body PET images were created with various β values of 500, 1000, 1500, 2000. In addition to the four BSREM reconstruction, one TOF OSEM reconstruction was performed per patient with a total of 80 reconstructions. Evaluation of the reconstructed images in terms of ranking the overall image quality was performed by an experienced nuclear medicine physician and quantitatively analysed with fix 40 mm VOIs on the liver in each cases. ***Results:*** It can be clearly stated that „Low-dose" injected activity protocol using higher β values resulted in better image quality, i.e higher contrast and reduced noise. Medical reading revealed that β value 1000 resulted excellent image quality for all BMI categories except Low-dose injected patient with BMI=30, (preferred β value was 500) and showed similar qualitative result for both injected activity protocols. Liver VOI analysis revealed that SUV mean ranged between (1.87-2.88), and $(St.Dev./Mean)^2$ values were significantly lower compared to conventional (TOF OSEM with PSF correction) reconstructions for both injected activity protocols. ***Conclusion:*** Q.Clear image reconstruction could provide good image quality performance when using β value 1000 at short total acquisition times for better patient comfort, even in case of low injected activity protocols. According to the most important result of this study, it is feasible to reduce the amount of injected activity and increase the β

value for the proper quality of Whole Body ^{18}F-FDG PET/CT images. ***References:*** None

OP-303

Image quality performance of Block Sequential Regularized Expectation Maximization and digital PET/CT with the Kyoto IB-10 brain phantom

A. Ács-Nagy[1], *D. K. Klagyvik*[1], *F. Nagy*[2], *P. Szabó*[1], *I. Garai*[2], *Á. K. Krizsán*[2];
[1]*ScanoMed Kft., Budapest, HUNGARY,*
[2]*ScanoMed Kft., Debrecen, HUNGARY.*

Aim/Introduction: This study focused on the evaluation of the image quality performance of a SiPM-based digital PET/CT scanner using Block Sequential Regularized Expectation Maximization reconstruction (BSREM, also called as Q.Clear) for 18F-FDG Brain images. ***Materials and Methods:*** All phantom measurements were performed on a GE Discovery MI PET/CT system. We used the Kyoto IB-10 phantom that includes a linearity and an anthropomorphic compartment. 5 chambers of linearity compartment was filled with 18F-FDG with the following activity concentrations: 2.13, 5.22, 12.68, 26.84, 53.06 kBq/ml, while one chamber was filled with water only. The anthropomorphic phantom compartment was filled with 18F-FDG solution in a 3.67 ratio for grey/white matter. Single bed position PET scans with 5 minutes acquisition time durations were performed for both Kyoto IB-10 phantom compartments. BSREM reconstruction β values were varied between 100 and 4000 using increments of 100 for both phantom compartments, while in case of the anthropomorphic compartment additional reconstruction series were performed with β values from 20 to 200 with increments of 20. ***Results:*** Following the image reconstructions, Standard Deviation/Mean values were calculated for Volume of Interests (VOIs) applied on all chambers of the linearity compartment images. This evaluation revealed that image noise reaches a minimum at 400 β value for lower activity concentrations and 200 β value for higher activity concentrations, while significant image degradation and spill over occurs above 2000 β value. In addition, the activity concentration in the water-only compartment (caused by the spill-over effect) reaches minimum in Standard Deviation/Mean around β value of 1000. For optimal reconstruction in case of brain studies these limitations should be also taken into consideration. The anthropomorphic compartment was evaluated with calculating the mean activity concentration ratios using VOIs on the gray matter, thalamus, putamen, caudate nucleus region compared to the VOI applied on the white matter region. These ratios are monotonously increasing towards the lower β values, and reaches the real activity concentration ratio for grey/white matter at β value of 80. ***Conclusion:*** The Kyoto IB-10 phantom set gave us opportunity to comprehensively evaluate imaging performance and quantitative accuracy of digital PET/CT technology with BSREM reconstruction for brain ^{18}F-FDG studies. Definition of optimal BSREM β value for ^{18}F-FDG PET/CT images still remain a complex topic. The optimal noise values appear between 200 and 400 β values, while the reconstructed activity concentration ratios are close to the real ratio at β value of 80. ***References:*** None

OP-304

A Comparative Study Between Conventional & Digital PET-CT For Detection of Lymph Node Metastases in Patients with High-Risk Prostate Cancer Using 18F-Flourocholine

M. Björsdorff[1], *J. Oddstig*[2], *A. Bjartell*[3], *C. Puterman*[4], *H. Kjölhede*[5], *E. Trägårdh*[6];
[1]*Department of Translational Medicine, Malmö, SWEDEN,* [2]*Radiation Physics, Skåne University Hospital and Lund University, Lund, SWEDEN,* [3]*Department of Urology, Skåne University Hospital and Und University, Malmö, SWEDEN,* [4]*Department of Urology, Skåne University Hospital and Lund University, Malmö, SWEDEN,* [5]*Department of Urology, Sahlgrenska University Hospital, University of Gothenburg, Gothenburg, SWEDEN,* [6]*Clinical Physiology and Nuclear Medicine, Skåne University Hospital and Wallenberg Center for Molecular Medicine, Lund University, Malmö, SWEDEN.*

Aim/Introduction: In 2017, new digital PET-CT technology were installed at Skåne University Hospital, Sweden. The diagnostic performance for detection of lymph node metastases for digital PET-CT compared with conventional technology remains largely unknown. The aim was to compare the diagnostic performance of conventional and digital PET-CT for detecting pelvic lymph node metastases in patients with high-risk prostate cancer (PCa) referred to for 18F-flourocholine (FCH) PET-CT, using histopathology as reference method. ***Materials and Methods:*** 176 high-risk PCa patients were included, examined on either the conventional Philips Gemini TF PET-CT, (n= 91) or on the digital GE Discovery MI PET-CT (DMI) (n= 85). Patients were referred for initial staging of high-risk prostate cancer. All were injected with 4 MBq/kg FCH and the PET data was collected one hour after injection. The medical reports regarding lymph node metastases were compared to the medical report from histopathology after extended pelvic lymph node dissection for calculation of sensitivity, specificity, positive predictive value (PPV) and negative predictive value (NPV). ***Results:*** The examinations performed on Philips Gemini showed 72 patients (72.9%) having no lymph node metastases and 19 patients (20.8%) having suspected lymph node metastases. 31 patients (34%) had lymph node metastases on histopathology. The sensitivity, specificity, PPV and NPV for Philips Gemini were 29.0%, 83.3%, 47.4% and 69.4%, respectively. The examinations performed on DMI showed 44 patients (51.8%) having no

lymph node metastases and 41 patients (48.2%) having suspected lymph node metastases. 21 (25%) had lymph node metastases on histopathology. The sensitivity, specificity, PPV and NPV for DMI resulted in 61.9%, 56.3%, 31.7% and 81.8% respectively. The area under the ROC curve was 0.56 for Philips Gemini and 0.59 for DMI. ***Conclusion:*** The present study showed similar overall accuracy (ROC analysis) but large differences in sensitivity, specificity, PPV and NPV between conventional and digital PET-CT. Potential reasons for the differences needs further investigations. ***References:*** None

OP-305

A PET Technologist's Role in Imaging Research

D. Ribeiro*, R. Janisch;*
Invicro, A Konica Minolta Company, London, UNITED KINGDOM.

Aim/Introduction: Positron Emission Tomography (PET) is best known for its contribution in cancer diagnostics and follow up, however, this imaging modality can also be used in research. Common applications in research span from investigation of neurodegenerative and psychiatric diseases to drug development. The aim of this project is to provide an overview of PET technologist's role in the field of imaging research. ***Materials and Methods:*** Research sites with an in situ cyclotron and manufacturing capabilities are able to produce a broader range of isotopes and radiopharmaceuticals than the ones used clinically and, after undergoing preclinical trials, they can be used in human research studies. These studies must be conducted in accordance with the International Council for Harmonisation (ICH) Good Clinical Practice (GCP) and the guiding principles of the 2013 Declaration of Helsinki [1]. Unlike clinical scans, most research scans are acquired in a dynamic format for 90 minutes or longer, which poses unique challenges in movement correction, and are often processed with analytic rather than iterative reconstructive algorithms, as accurate quantification is paramount [2]. ***Results:*** Biodistribution and imaging studies that use tracers for which the pharmacokinetics cannot be described by 2-tissue compartment models, require arterial blood sampling and analysis. Usually, the first 15min after tracer administration provide information regarding initial peak radioactivity and blood clearance. Discrete blood samples thereafter are used for investigation of whole-blood-to-plasma radioactivity concentration and metabolites. Ethical concerns must always be weighed particularly in situations of lack of understanding, inappropriate consent or lack of an impartial interpreter. PET Technologists may also be involved in providing practical and technical perspectives on imaging protocols and reviewing associated documentation, writing PET-related study documentation and Standard Operating Procedures, accurately maintaining records to a very high standard of GCP compliance, performing internal audits and actively assisting in external audits. ***Conclusion:*** As the field of medical imaging technologies continues to develop, it's important to demonstrate that the roles and responsibilities of PET Technologists have evolved alongside. PET Technologists form a vital part of a team and with appropriate training and competency assessments, these multidisciplinary teams make valuable contributions to research. ***References:*** [1] Vijayananthan A, Nawawi O. The importance of Good Clinical Practice guidelines and its role in clinical trials. Biomed Imaging Interv J. 2008;4(1):e5. [2] Verhaeghe J and Reader AJ, "Lower variance FBP image reconstruction via new filter families," IEEE Nuclear Science Symposium & Medical Imaging Conference, Knoxville, TN, 2010, pp. 2277-2281.

605

M2M Track - Featured Session: Immune and Microenvironment Imaging

Friday, October 23, 2020, 13:50 - 15:20 Channel 5

OP-306

Immunotherapy and the TME - Expanding the Scope

M. Schottelius*; CHUV, Lausanne, SWITZERLAND*

OP-307

FAPI PET/CT: Tracer- biodistribution in patients with head and neck-, lung-, pancreatic- and colorectal- cancer

F. Staudinger*[1], J. Schlittenhardt[1], T. Lindner[1], H. Rathke[1], M. Röhrich[1], S. Körber[2,3,4], J. Debus[2,3,4], C. Kratochwil[5,6], U. Haberkorn[1,6,7], F. Giesel[1,6,8];*
[1]Department of Nuclear Medicine, Heidelberg University Hospital, Heidelberg, GERMANY, [2]Department of Radiation Oncology, Heidelberg University Hospital, Heidelberg, GERMANY, [3]National Center for Tumor diseases (NCT), Heidelberg, GERMANY, [4]Heidelberg Institute of Radiation Oncology (HIRO), Heidelberg, GERMANY, [5]Department of Nuclear Medicine, University Hospital Heidelberg, Heidelberg, GERMANY, [6]Clinical Cooperation Unit Nuclear Medicine, German Cancer Research Center (DKFZ), Heidelberg, GERMANY, [7]Translational Lung Research Center Heidelberg (TLRC), German Center for Lung Research (DZL), Heidelberg, GERMANY, [8]Clinical Cooperation Unit Radiation Oncology, German Cancer Research Center (DKFZ), Heidelberg, GERMANY.

Aim/Introduction: Fibroblast activation protein inhibitor (FAPI)-positron-emission tomography (PET) / computed tomography (CT) is a promising staging tool for detecting a variety of solid cancers. Here we describe the in vivo biodistribution of the FAPI-tracer head and neck-, lung-, pancreatic- and colorectal- cancer patients. ***Materials and Methods:*** A mean of 245 MBq (range 111-336 MBq) ^{64}Ga-FAPI-02/ -04/ -46 and ^{18}F-FAPI-74 was administered and PET/

CT imaging was acquired at 1h post injection (p.i.). FAPI-PET/CT was performed in a cohort of 81 patients (median age 63 years) including 20 patients with head- and neck-cancer, 18 patients with lung-cancer, 21 patients with pancreatic-cancer and 22 patients with colorectal-cancer. Normal organ distribution and tumor uptake were semi-quantitatively evaluated based on the standardized uptake values (SUV)$_{max}$ and SUV$_{mean}$ at the 1h time-point. ***Results:*** The overall SUV$_{max}$ average at 1h in primary tumors was 12,93; in lymph node metastases it was 9,82; in distant metastases 8,32. Thus, due to rapid kidney clearance of non-tumor-bound tracer and moderate nonspecific uptake in normal organs, promising tumor-to-background-ratios could be achieved: tumor/bloodpool: 7; tumor/muscle: 9; tumor/fat: 24; tumor/spinal: 18. A direct quantitative comparison of the different tumor entities presented no significant differences in the SUV$_{max}$ of primary cancers (p=0,38), lymph node metastases (p=0,117) and distant metastases (p=0,212). ***Conclusion:*** The present study demonstrates that FAPI-PET/CT can achieve equal or even superior results in patients with head and neck-, lung-, pancreatic- and colorectal-cancer compared to gold standard imaging modality for staging/-restaging cancer strateficatoin. Due to a low background activity in normal tissue, there was a high tumor-to-background ratio in most lesions. The high contrast tumor delineation of FAPI indicates potential usefulness for multiple clinical applications. ***References:*** None

OP-308

FAPI-74 PET/CT Using Either ^{18}F-AlF or Cold-kit ^{68}Ga-labeling: Biodistribution, Radiation Dosimetry and Tumor Delineation in Lung Cancer Patients

F. Giesel[1], *S. Adeberg*[1], *M. Syed*[1], *T. Lindner*[1], *L. Jiménez-Franco*[2], *F. Staudinger*[1], *E. Tonndorf-Martini*[1], *S. Regnery*[1], *S. Rieken*[3], *R. El Shafie*[1], *M. Roehrich*[1], *P. Flechsig*[1], *A. Kluge*[4], *A. Altmann*[1], *J. Debus*[1], *U. Haberkorn*[1], *C. Kratochwil*[1];
[1]*University Hospital Heidelberg, Heidelberg, GERMANY,* [2]*ABX CRO advanced pharmaceutical services, Dresden, GERMANY,* [3]*University Hospital Goettingen, Goettingen, GERMANY,* [4]*ABX advanced pharmaceutical services, Dresden, GERMANY.*

Aim/Introduction: ^{68}Ga-FAPI-2/4/46 have already been proposed as promising PET-tracers. However, the short half-life of ^{68}Ga ($T_{1/2}$ 68 min) creates problems with manufacture and delivery. ^{18}F ($T_{1/2}$ 110 min) labeling would result in a more practical large scale production and a cold-kit formulation would improve the spontaneous availability. The NOTA-chelator ligand FAPI-74 can be labeled with both ^{18}F-AlF (Aluminum-Fluoride) and ^{68}Ga. Here we describe the in-vivo evaluation of ^{18}F-FAPI-74 and a proof-of-mechanism of ^{68}Ga-FAPI-74 labeled at ambient temperature. ***Materials and Methods:*** In ten patients with lung cancer PET-scans were acquired at 10 min, 1h and 3h after administration of 259±26 MBq ^{18}F-FAPI-74. Physiological biodistribution and tumor uptake were semi-quantitatively evaluated based on SUV at each time-point. Absorbed doses were evaluated using OLINDA/EXM 1.1 and QDOSE dosimetry software with the dose calculator IDAC-Dose 2.1. Identical methods were used to evaluate one exam after injection of 263 MBq ^{68}Ga-FAPI-74. ***Results:*** The highest contrast was achieved 1 h p.i. in primary tumors, lymph node and distant metastases with SUVmax >10, respectively. The effective dose per 100 MBq administered activity of ^{18}F-FAPI-74 was 1.4±0.2 mSv and for ^{68}Ga-FAPI-74 it was 1.6 mSv. Thus, the radiation burden of a diagnostic ^{18}F-FAPI-74 PET-scan is even lower than that of PET-scans with ^{18}F-FDG and other ^{18}F-tracers; ^{68}Ga-FAPI-74 is comparable to other ^{68}Ga-ligands. FAPI-PET/CT supported target volume definition for guiding radiotherapy. ***Conclusion:*** High contrast and low radiation burden of FAPI-74 PET/CT favors multiple clinical applications. Centralized large-scale production of ^{18}F-FAPI-74 or decentralized cold-kit labeling of ^{68}Ga-FAPI-74 allows flexible routine use. ***References:*** None

OP-309

Reversing cold tumor microenvironment with targeted alpha-therapy

J. Perrin*, M. Capitao, S. Gouard, C. Maurel, C. Louvet, M. Lancien, F. Bruchertseifer, A. Morgenstern, M. Cherel, J. Gaschet, Y. Guilloux; INSERM, Nantes, FRANCE.*

Aim/Introduction: Actual cancer therapies are facing numerous challenges towards tumor cell destruction : tumor microenvironment involves immunoregulatory cells and cytokines, which prevent anti-tumoral immune response. Therapeutic combination could be the key to turn these « cold » tumor microenvironment into « hot » ones : more vascularised and infiltrated with immune cells. To this end, this project focus on combining targeted alpha-therapy (TAT) and adoptive T-cells transfer (ACT). ***Materials and Methods:*** This therapeutic combination was conducted in a Multiple Myeloma (MM) murine model using a 5T33-OVA MM cell line expressing the CD138 antigen and H_2K^b/$OVA_{257-264}$ complexes grafted subcutaneously to C57BL6/KalwRij mice. TAT was delivered through intraveinous injection of a 213-bismuth radiolabelled anti-CD138 antibody. To further reinforce its efficiency, TAT was combined with an ACT of tumor specific OT-1 T-cells. This therapeutic combination resulted in a significant tumor growth delay and improved survival, compared to ACT or TAT alone (Ménager and al. 2015). Based on these results, the aim of this project was then to understand the impact of TAT on the "cold" tumor microenvironment and on ACT efficacy. Tumor infiltrated cells were analysed by flow cytometry to identify in situ immune populations, and cytokines production were assessed by RT-qPCR on tumor fragment. ***Results:*** Although OT-1 T cells infiltrated the tumor after ACT, only combination with TAT resulted in regulatory CD4 T cell drop and

production of IL-2 and IFNγ within the tumor. Futhermore, OT-1 T cells motility was increased on TAT treated tumor slices as observed by ex vivo time lapse. ***Conclusion:*** Combining TAT and ACT appears to turn this "cold" tumor model into a "hot" one with regulatory T cells depleted, proportion and motility of tumor-specific CD8 T cells increased and IL-2 and IFNγ produced in the tumor. Next, we aim to investigate impact of this combination on metabolism and hypoxia in tumor microenvironment. ***References:*** ADDIN Mendeley Bibliography CSL_BIBLIOGRAPHY Ménager, J. et al. (2015) 'Combining α-radioimmunotherapy and adoptive T cell therapy to potentiate tumor destruction', PLoS ONE, 10(6), pp. 1-14. doi: 10.1371/journal.pone.0130249. <![endif]-->

OP-310

PET Imaging of PD-L1 Expression in NSCLC: Pharmacokinetic Comparison of an Antibody and its Fab Fragment

A. Bouleau[1], H. Nozach[2], M. Richard[1], S. Dubois[2], G. Torquet[1], B. Kuhnast[1], B. Maillère[2], V. Lebon[1], C. Truillet[1];
[1]Université Paris-Saclay, CEA, CNRS, Inserm, BioMaps, Service Hospitalier Frédéric Joliot, Orsay, FRANCE, [2]Département Médicaments et technologies pour la santé, SIMoS, Université Paris-Saclay, CEA-Saclay, Gif-sur-Yvette, FRANCE.

Aim/Introduction: The interaction of programmed death ligand 1 (PD-L1) with its receptor PD-1 on T-cells promotes tumour cell immuno-escape. In solid cancers, including non-small cell lung cancer (NSCLC), the PD-L1$^+$ status, assessed via immunohistochemistry (IHC) on tumour biopsies, was associated with the efficacy of PD-1/PD-L1 immunotherapy. However, IHC ignores spatial and temporal dynamics of PD-L1 expression within and across lesions of a patient. Immuno-PET with radiolabelled antibody-based PD-L1 ligands provides non-invasive whole-body visualization of PD-L1 expression, and may thus help to improve patient stratification and response monitoring for PD-1/PD-L1 immunotherapy. To select the most appropriate PET imaging tool to assess in vivo PD-L1 expression, for obtaining high-contrast images at early time points, we compared the pharmacokinetics (PK) of an anti-PD-L1 IgG and its Fab fragment radiolabelled with ^{89}Zr in NSCLC xenograft models. ***Materials and Methods:*** A cross-species anti-PD-L1 antibody C4 and its Fab fragment (50 kDa), with nanomolar affinities for human and mouse PD-L1, were developed. PK and biodistribution of the ^{89}Zr-labelled IgG C4 and Fab C4 were evaluated with PET/CT imaging in nude mice bearing subcutaneous human NSCLC xenografts with different PD-L1 expression levels. ***Results:*** Specific tumour uptake of ^{89}Zr-IgG C4 and ^{89}Zr-Fab C4 was observed in PD-L1$^+$ H1975 xenografts, with the highest tumour-to-muscle ratio (TMR) at 50 h post-injection (pi) for ^{89}Zr-IgG C4 (TMR = 8.3 ± 0.6) and at 4 h pi for ^{89}Zr-Fab C4 (TMR = 4.7 ± 0.5). ^{89}Zr-Fab C4 uptake was significantly lower in PD-L1$^-$ A549 xenografts (TMR = 2.9 ± 0.2 at 4h) as compared to PD-L1$^+$ H1975 xenografts (P = 0.004). Uptakes correlated to PD-L1 expression levels in tumour tissues determined by flux cytometry. ***Conclusion:*** The Fab C4 achieved maximum TMR quickly (4 h pi), although it was lower (≈2x) than the IgG C4 maximum TMR (48 h pi). The faster Fab tumour diffusion allows tracer injection and imaging on the same day. It would reduce patient radiation exposure with the use of shorter-lived isotopes like ^{18}F. ^{89}Zr-Fab C4 was mainly cleared via the urinary tract, resulting in high kidney signal, whereas ^{89}Zr-IgG C4 was excreted through the hepatobiliary route. PK and biodistribution of the fragment scFv C4 (30 kDa) will be assessed in the same NSCLC H1975 xenograft model. Murine 3D imaging-based dosimetry analysis will also be performed for the ^{89}Zr-IgG C4 and its fragments. ***References:*** Truillet C, et al. Imaging PD-L1 expression with ImmunoPET. Bioconjug Chem. 2018; 29: 96-103.

OP-311

^{90}Y-NM600 Combined with Bempegaldesleukin (NKTR-214) Improves Response to Immune Checkpoint Inhibition in a Syngeneic Murine Model of Head and Neck Cancer

J. Grudzinski[1], A. Bates[1], R. Hernandez[1], G. Sosa[1], E. Nystuen[1], S. Emma[1], E. G. Sumiec[1], A. Pieper[1], R. Patel[2], E. Aluicio-Sarduy[1], J. Engle[1], I. Marsh[1], B. Bednarz[1], J. Weichert[1], Z. Morris[1];
[1]University of Wisconsin, Madison, WI, UNITED STATES OF AMERICA, [2]University of Pittsburgh, Pittsburgh, PA, UNITED STATES OF AMERICA.

Aim/Introduction: Combining low-dose targeted radionuclide therapy with a CD122 agonist like NKTR-214, which exhibits greater serum half-life, more preferential CD8+ T cell and NK cell activation, and improved tolerability compared to native IL-2, is one possible approach to improving low response rates of immunotherapies in unresectable recurrent or metastatic head and neck squamous cell carcinoma (HNSCC). The aim of this study was to test whether NKTR-214 and ^{90}Y-NM600 increases the response to anti-CTLA-4 immune checkpoint blockade in an immunologically "cold" and spontaneously metastatic MOC2 syngeneic mouse model of HNSCC. ***Materials and Methods:*** C57BL/6 female mice (n = 4) bearing MOC2 tumors were administered 9.25 MBq of ^{86}Y-NM600, and longitudinal static microPET/CT scans were acquired at 3, 24, 48, and 72 h post-injection. Region-of-interest analysis of the images afforded dosimetry estimation of ^{90}Y-NM600 using Monte Carlo simulation. In therapy studies, mice bearing subcutaneous MOC2 tumors (n = 8; 100 mm^3) received combinations of NKTR-214, ^{90}Y-NM600, and anti-CTLA-4. 3.7 MBq of ^{90}Y-NM600, estimated to deliver a tumor dose of 8 Gy (2.17 Gy/MBq), was administered i.v. on Day 1 followed by anti-CTLA-4 (200 µg) i.p. injections on days 4, 7, and 10. NKTR-214 (16 µg) was given i.v. on days 6, 15, and 24 post administration of ^{90}Y-NM600. Tumors from a subgroup of treated mice were collected at Day 14 for

flow cytometry analysis. Survival and tumor growth were tracked until Day 60. ***Results:*** Imaging confirmed selective uptake and retention of NM600 in MOC2 tumors and gradual clearance from normal tissues. Absorbed doses per ^{90}Y-NM600 injected activity of 3.15, 1.52, and 0.65 Gy/MBq were estimated for the tumor, spleen, and muscle, respectively**.** In the MOC2 tumor model, 62.5% of mice treated with the combination of ^{90}Y-NM600, NKTR-214, and anti-CTLA4 experienced complete tumor response, and these mice showed no observable primary or metastatic disease 60 days after treatment initiation. No mice receiving single or dual therapy combinations exhibited complete tumor response ($p < 0.01$). Treatment with NKTR-214 and ^{90}Y-NM600 resulted in increased tumor infiltration by CD8+ T cells. Interestingly, ^{90}Y-NM600 triggered increased expression of the IL2-beta receptor, CD122, on tumor infiltrating CD8+ T cells, indicating a sensitization of T-cells for NKTR-214. ***Conclusion:*** NKTR-214 combined with ^{90}Y-NM600, and anti-CTLA-4 resulted in complete and durable tumor response in a murine model of HNSCC. Low-dose TRT may enhance the effect of NKTR-214 by increasing the expression of the IL2-beta receptor on tumor infiltrating T-cells. ***References:*** None

OP-312

^{18}F-FDG-PET for the Evaluation of Response to Therapy of Triple-NegativeBreast Cancer Bearing Nude Mice to Pembrolizumab(anti-programmed death 1 (PD-1) monoclonal antibody)

L. Shi[1], *S. An*[2], *J. Fu*[1], *F. Wang*[1];
[1]*Nanjing First Hospital, Nanjing Medical University, Nanjing, CHINA,* [2]*Department of Nuclear Medicine, Ren Ji Hospital, School of Medicine, Shanghai, CHINA.*

Aim/Introduction: This study evaluated the usefulness of micro-positron emission tomography (micro-PET) with ^{18}F-fluorodeoxyglucose (^{18}F-FDG) in assessing response to anti-programmed death 1 (PD-1) monoclonal antibody pembrolizumab in triple-negative breast cancer (TNBC) cell MDA-MB-231 xenograft and to investigate whether the molecular mechanism involves hypoxia-inducible factor 1-α (HIF1α) . ***Materials and Methods:*** Methods: Five-week-old female BALB/c nude mice received subcutaneous injections of 5×10^6 MDA-MB-231 cells in 100μL of saline at the right dorsal flank. Fourteen days after tumour implantation, the mice were randomly assigned to a treatment group receiving anti-programmed death 1 (PD-1) monoclonal antibody pembrolizumab (200μg/per mouse) or a control group receiving saline three times per week intraperitoneally for 21 days. The status of the nude mice,tumor growth rate and size changes in both groups were observed. ^{18}F-FDG microPET scan was performed before and after treatment to calculate the maximum tumor uptake rate per gram(%ID/gmax)for efficacy evaluation. At the end of the experiment, animals were sacrificed, and tumour tissues were collected for weighing and immunohistochemistry for Ki-67, cysteine proteinase 3 (Caspase-3), HIF1α, glucose trans porter-1 (GLUT1), and lactate dehydrogenase A (LDHA). The lactic acid production of xenografts was investigated with enzymic method. The mRNA expression and the protein expression levels of glycolytic metabolic enzymes in xenografts were detected by real-time PCR and western blotting. ***Results:*** Results: Compared with PBS-control group, tumors derived from pembrolizumab treatment group had decreased glucose uptake as shown by ^{18}F-FDG microPET imaging ($P<0.01$). Furthermore, compared with the tumors in the PBS-control group, tumors in mice treated with pembrolizumab were smaller and lighter ($P<0.05$). IHC analysis of tumours revealed that pembrolizumab reduced Ki-67, HIF1α, GLUT1, and LDHA protein levels and increased Caspase-3 expression. Lactic acid analysis of the tumor masses further confirmed that pembrolizumab decreased lactate production. Real-time PCR and western blotting showed that under pembrolizumab treatment, the protein and mRNA expression levels of HIF1α and its downstream glycolytic metabolic enzymes such as GLUT1, HK2 and LDHA were significantly inhibited. ***Conclusion:*** Conclusion: The anti-programmed death 1 (PD-1) monoclonal antibody pembrolizumab has a significant inhibitory effect on the growth of TNBC MDA-MB-231 transplanted tumors. ^{18}F-FDG PET plays an important role in the early evaluation of pembrolizumab for TNBC. The molecular mechanism may be related to the pembrolizumab-induced HIF1α/Glut1 pathway. ***References:*** None

OP-313

Immune-checkpoint blockade enhances^{225}Ac-PSMA617 efficacy in a mouse model of prostate cancer

K. Lueckerath*, K. Current, C. E. Mona, L. Nyiranshut, F. Hikmat, C. G. Radu, J. Czernin;*
University of California Los Angeles, Los Angeles, CA, UNITED STATES OF AMERICA.

Aim/Introduction: Radionuclide therapy (RNT) may increase tumour immunogenicity. We aimed at exploiting this effect by combining PSMA-targeted RNT with immunotherapy in a mouse model of prostate cancer (PC). ***Materials and Methods:*** C57BL/6 mice bearing syngeneic RM1-PGLS tumours were treated with ^{225}Ac-PSMA617 (30 kBq, i.v.), an anti-PD-1 antibody (10 mg/kg, i.p., q3d for 4 doses) or both. Therapeutic efficacy was assessed by tumour volume measurements (computed tomography), time to progression (TTP) and survival. ***Results:*** PSMA-RNT or anti-PD-1 alone tended to prolong TTP (isotype control 25d; anti-PD-1 33.5d, p=0.0153; RNT 30d, p=0.1038) and survival (control 28d; anti-PD-1 37d, p=0.0098; RLT 32d, p=0.1018). Combining PSMA-RNT and anti-PD-1 significantly improved disease control compared to either monotherapy. TTP was

extended to 47.5d ($p<0.0199$ vs. monotherapies), and survival to 51.5d ($p<0.0251$ vs. monotherapies). In mice with smaller tumours, complete responses were observed with RNT/anti-PD-1. Complete-responders were immune to tumour re-challenge. ***Conclusion:*** PSMA-RNT and PD-1 blockade synergistically improve therapeutic outcomes in our PC model and might facilitate generation of an immunological memory. Thus, RNT might aid the conversion of PC into immunological "hot" tumours. Together, our data support the evaluation of RNT/immunotherapy combination regimens for PC patients. ***References:*** None

OP-314

PD-L1 targeted Ga-68-PET imaging in human lung adenocarcinoma xenografts

J. Notni*, K. Steiger, N. G. Quigley, F. Richter, W. Weichert;*
Technical University of Munich, Munich, GERMANY.

Aim/Introduction: Immune checkpoint therapy with PD-L1 targeted antibodies is characterized by low response rates and high costs. Therefore, eligible cancer patients must be carefully selected, while selections are based on tumoral PD-L1 status. At present, such decisions rely on histological analysis of biopsies, which however are characterized by low reliability due to small volume of specimen and a high degree of heterogeneity of PD-L1 expression. Consequently, non-invasive mapping of PD-L1 expression could significantly improve patient management. ***Materials and Methods:*** The peptidic PD-L1 ligand WL12 [1] was decorated with the Ga-68-chelator TRAP employing Click Chemistry (CuAAC) as described [2]. The resulting Ga-68 labelled compounds were evaluated in H2009 (human lung adenocarcinoma) xenografted SCID mice employing dynamic (90 min) and static (60 and 120 min p.i.) PET as well as biodistribution (60 min p.i.). PD-L1 expression in tumors and organs was determined by immunohistochemistry. ***Results:*** In analogy to the clinical picture observed in lung cancer patients, subcutaneous H2009 tumors were characterized by a low and heterogeneous PD-L1 expression density (overall approx 20% of positive tumor cells, with large regional differences). Nevertheless, Ga-68-TRAP-WL12 showed a high and persistent tumor accumulation (approx. 7 %ID/g). Comparably low uptakes in liver (6.1 %ID/g), lung (5.0 %ID/g), and blood pool (2.2±0.6 %ID/g) resulted in favorable tumor/organ ratios (T/liver: 1.2; T/lung: 2.4; T/blood: 3.4, 60 min p.i.). Dynamic PET data indicated no significant washout from tumor but a strongly decreasing activity in blood and organs, resulting in an increase of image contrast over time. ***Conclusion:*** Conjugation of a hydrophilic Ga-68-TRAP chelate to the lipophilic WL-12 peptide yielded a renally excreted PET tracer with higher overall hydrophilicity and less non-specific uptake, as compared to other radiolabelled WL-12 derivatives [1,3]. Ga-68-TRAP-WL12 is characterized by a high PD-L1 detection sensitivity. Thus, it appears suitable for PET-based patient selection of possible responders to PD-L1 immune checkpoint therapy, potentially enhancing the overall performance of PD-L1 directed personalized cancer therapy regimen. ***References:*** [1] R. A. De Silva et al., Mol Pharmaceutics 2018;15:3946. [2] Baranyai Z, et al., Dalton Trans. 2015;44:11137-11146. [3] Lesniak WG, et al., Mol. Imaging 2019;18:1536012119852189.

OP-315

Imaging tumour CD8+ T-cell infiltrates following radioimmunotherapy in an immunocompetent mouse model

B. Cornelissen*[1], G. Dias[1], E. O'Neill[1], C. Bristow[1], F. Salazar[2], R. Tavare[2], N. Sibson[1], A. Wu[2];*
[1]University of Oxford, Oxford, UNITED KINGDOM, [2]City of Hope, Duarte, CA, UNITED STATES OF AMERICA.

Aim/Introduction: Combination of irradiation (IR) and immunotherapy (IT) has been shown to be an effective regime for cancer therapy in certain settings. This approach however requires optimized IR and IT regimes. To measure the effects of anti-CTLA-4 on CD8+ T-cell infiltrates in multiple lesions in the same individual during radiotherapy, we used SPECT imaging with a radiolabelled anti-CD8-cys-diabody (α-CD8-CDb). ***Materials and Methods:*** Female immunocompetent Balb/c mice were inoculated with murine CT-26 cancer cells on the left and right lower flank. Fourteen days after, only the right-hand side tumours were irradiated (4 Gy). On day 15, half of the mice were administered a therapeutic dose of anti-CTLA4 antibody (250 µg). αCD8-CDb was labelled with ^{111}In through maleimide-DTPA. [^{111}In]In-mDTPA-αCD8-CDb (1.9 MBq, 10 µg) was administered intravenously on day 21, and SPECT/CT images acquired on day 22 (MILabs VECTor^{4}CT). Tumours and organs were excised, weighed and measured on a gamma counter. Flash frozen tumours were sectioned and processed for autoradiography, and stained with a rat anti-CD8 antibody. ***Results:*** Tumour growth was not significantly different within the studies time frame comparing the irradiated (right, RT) and the non-irradiated (left, LT) tumours. SPECT/CT images showed uptake of the [^{111}In]In-anti-CD8-CDb in spleen, kidneys, tumours and lymph nodes. The axillary and brachial nodes were clearly visible with the [^{111}In]In-anti-CD8-CDb, while any signal from inguinal nodes was overshadowed by tumour location. IR +αCTLA4-treated mice showed a greater uptake of ^{111}In in the non-IR tumour compared to the IR tumour, contrary to mice that did not receive anti-CTLA4. Heterogeneity within tumours was evident from autoradiographs and immunohistochemistry staining, showing the presence of CD8 in the tumours. ***Conclusion:*** In vivo CD8 expression was assessed post irradiation and αCTLA4 treatment using a radiolabelled anti-CD8-cys-diabody. The differences between the uptake of [^{111}In]In-anti CD8-CDb in LT and RT between the IR only and

combo group suggest further investigation to the effects of αCTLA4 in T-cell infiltrate recruitment. Further analysis is underway to relate the amount of staining to the amount of [^{111}In]In-anti CD8-CDb. ***References:*** Tavaré R, Escuin-Ordinas H, Mok S, et al. An Effective Immuno-PET Imaging Method to Monitor CD8-Dependent Responses to Immunotherapy. Cancer Res. 2016;76(1):73-82.

OP-316

Development of [^{18}F]AlF-NODA-CTHRSSVVC for imaging M2 macrophages with PET

B. Fernandes[1], I. F. Antunes[2], C. M. M. Jeckel[3], E. F. J. de Vries[2], P. H. Elsinga[2];
[1]UMCG, Groningen, NETHERLANDS, [2]University of Groningen, University Medical Center Groningen (UMCG), Groningen, NETHERLANDS, [3]Graduate Program in Biomedical Gerontology, School of Medicine, Pontifical Catholic University of Rio Grande do Sul (PUCRS), Porto Alegre, BRAZIL.

Aim/Introduction: Macrophages are specialized cells that play an important role in the immune system and the tumor microenvironment. Macrophages can be activated into the pro-inflammatory M1 phenotype or the anti-inflammatory M2 phenotype[1]. Since these phenotypes have opposing effects, it is important to be able to discriminate them, e.g. by PET imaging. The haptoglobin-hemoglobin scavenger receptor (CD163) is selectively expressed by the M2 macrophage phenotype. CTHRSSVVC is a peptide that binds to the CD163 receptor. In this study, the peptide was radiolabeled with fluorine-18 and evaluated as a novel agent PET imaging of M2-type macrophages. ***Materials and Methods:*** NODA-CTHRSSVVC was labeled with [^{18}F]AlF^{2+}. The labeling conditions were optimized using different concentrations of NODA-CTHRSSVVC (15, 30, 60, and 90 µg/mL) and reaction times. The logD and in vitro stability were determined. In Balb-c mice, dynamic PET scans were acquired and ex vivo biodistribution was performed at 30, 60, and 90 minutes post-injection. ***Results:*** Radiolabeling of NODA-CTHRSSVVC with [^{18}F]AlF^{2+} gave the highest conversion after 20 minutes of reaction using 90 µg of precursor in 1mL of sodium acetate pH 4.5 (29.3±6.5%). If 30 µg or less precursor was used, the conversion dropped to <11%. Under the optimal conditions, [^{18}F]AlF-NODA-CTHRSSVVC was obtained in a radiochemical yield of 9.2 ± 4.9% after HPLC purification and formulation. The product had a purity of 96.4 ± 2.5% and a molar activity of 281 ± 388 GBq/µmol. In the formulation solution, [^{18}F]AlF-NODA-CTHRSSVVC was stable at least for 2 hours. The PET imaging and ex vivo biodistribution studies in balb/c mice showed the highest tracer uptake in kidneys, bladder, duodenum, liver, and spleen. The tracer showed fast clearance mainly via kidneys due to its high hydrophilicity (Log D = -4.6). Moreover, low bone uptake was observed, suggesting little defluorination or release of [^{18}F]AlF^{+2}. ***Conclusion:*** [^{18}F]AlF-NODA-CTHRSSVVC was successfully labeled and is stable in vitro. The radiotracer shows fast renal clearance and accumulation in organs with high amounts of resident M2 macrophages (liver, spleen). Further validation in an in vivo immune disease model is warranted. ***References:*** 1. Silva et al. Int J Mol Sci. 2016;17(9).

606

Cutting Edge Science Track - TROP Session: Image Processing - Neurology

Friday, October 23, 2020, 13:50 - 15:20 Channel 6

OP-317

Multimodal assessment of test-retest reliability using functional PET, ASL and BOLD imaging in a complex visuo-spatial motor task

L. Rischka[1], G. M. Godbersen[1], V. Pichler[2], P. Michenthaler[1], S. Klug[1], M. Klöbl[1], V. Ritter[1], W. Wadsak[2], M. Hacker[2], S. Kasper[1], R. Lanzenberger[1], A. Hahn[1];
[1]Department of Psychiatry and Psychotherapy, Medical University of Vienna, Vienna, AUSTRIA, [2]Department of Biomedical Imaging and Image-guided Therapy, Division of Nuclear Medicine, Medical University of Vienna, Vienna, AUSTRIA.

Aim/Introduction: Cerebral glucose metabolism is commonly assessed to examine disease status and cognitive processes. The recent introduction of functional PET (fPET) enabled the quantification of glucose metabolism at rest and task within a single measurement[1], showing high signal-to-noise ratio and task sensitivity[2]. However, for clinical applicability, new methods also require testing for a stable longitudinal performance. We therefore investigated the test-retest reliability of fPET, using a complex visuo-spatial motor task. In a multimodal approach, ASL and BOLD contrast imaging were acquired within the same session as fPET, enabling a direct comparison. ***Materials and Methods:*** Twenty healthy subjects underwent two measurements on a hybrid PET/MR scanner, approximately 4 weeks apart. The radiotracer [^{18}F]FDG was administered in a bolus+constant infusion protocol. After 8 minutes of rest, a visuo-spatial motor task was carried out in two difficulty levels (2 easy, 2 hard, 6 minutes) each followed by 5 minutes of rest. ASL was acquired at rest and simultaneously with fPET during one easy and one hard period. Immediately after fPET, BOLD imaging was carried out in a block design with the same difficulty levels (12x30 sec, 10 sec rest). Cerebral glucose metabolism (influx constant K_i) was assessed with a general linear model and the Gjedde-Patlak plot. Cerebral blood flow (CBF) and BOLD changes were estimated with standard procedures[2,3]. Functional regions of interest were defined as the intersection of group t-maps in the hard condition (p<0.05 FWE corrected voxel level), across

all three modalities. Finally, intraclass correlation ($ICC_{3,1}$), median coefficient of variation (CoV) and DICE coefficient were estimated for each difficulty. ***Results:*** The intersection revealed task changes in the frontal eye field, intraparietal sulcus and occipital cortex. Highest reliability was achieved with K_i at rest (CoV: 4.6-5.8%, ICC: 0.87-0.89). Although reliability decreased during task performance (CoV: 15.7-40.6%), this was similar to CBF (CoV: 9.5-38.7%) and higher than BOLD (CoV: 16.0-66.2%). BOLD imaging exhibited the highest DICE coefficient (0.8) compared to CBF (0.7) and K_i (0.6). ***Conclusion:*** Task-specific changes can be detected with all three modalities. However, fPET achieved similar or even superior test-retest reliability compared to well-established modalities. Since fPET is still novel, further optimisation procedures will also enhance its reliability. We therefore suggest fPET as valuable tool for application in clinical routine, enabling the assessment of metabolic dynamics in a reasonable time frame of 30 minutes for enhanced diagnosis. ***References:*** [1]Hahn (2016) J.Nucl.Med 57:1933-1940 [2]Rischka (2018) Neuroimage 181:323-330 [3]Wang (2005) Radiology 235:218-228

OP-318

Improvement of FDG PETCT and MRI concordance in Temporal Lobe Epilepsy Pre-surgical Assessment using Statistical Parametric Mapping Z-scores

M. Kershaw[1], *H. Amada*[2], *L. Yiping*[3], *V. Sawlani*[4], *S. Hughes*[4]; *[1]University of Birmingham, Birmingham, UNITED KINGDOM, [2]Sandwell and West Birmingham NHS Trust, Birmingham, UNITED KINGDOM, [3]Fudan University, Fudan, CHINA, [4]University Hospitals Birmingham, Birmingham, UNITED KINGDOM.*

Aim/Introduction: This study evaluates the diagnostic performance of statistical parametric mapping (SPM) analysis of PET-CT in temporal lobe epilepsy (TLE). Our aim is to increase consistency in image reporting and increase confidence in the surgical evaluation of TLE patients. ***Materials and Methods:*** Thirty-eight patients with TLE who underwent MRI and PET-CT imaging at the Queen Elizabeth Hospital in Birmingham were included in this study. Images were interpreted by visual assessment by radiologists. Quantitative analysis for PET-CT was performed using SPM. Statistical analyses performed include the Kruskal-Wallis and Game Howell tests, analysis of Receiver Operating Characteristic (ROC) curve and Cohen's κ statistics. ***Results:*** The standardised uptake value (SUV) ratio for left temporal epilepsy, non-epilepsy and right temporal epilepsy were -1.06±1.01, 0.08±0.79, 0.39±0.73 respectively, exhibiting significant difference between the three groups ($p<0.01$). In the left/non-left group, the area under curve (AUC) was 0.881 while the cut-off value to separate left temporal epilepsy from non-epilepsy and right temporal epilepsy was -0.305 with 89.7% sensitivity and 88.9% specificity. In the right/non-right group, the AUC was 0.792 while the cut-off value to separate left temporal epilepsy from non-epilepsy and right temporal epilepsy was 0.190 with 83.3% sensitivity and 81.3% specificity. When patients were divided into three groups based on SUV ratio (left temporal epilepsy, non-epilepsy and right temporal epilepsy), there was good inter-method agreement between MRI and SUV ratio ($\kappa = 0.63$, 95% CI, 0.42-0.85). ***Conclusion:*** These results indicate that PET-CT-based SUV ratios may have promising diagnostic value in future clinical practice. ***References:*** None

OP-319

Clinical impact of digital vs conventional healthy control databases for semi-quantitative analysis of brain 18F-FDG PET scans

M. Doyen[1], *E. Mairal*[2], *T. Rivasseau Jonveaux*[3], *C. Malaplate-Armand*[4], *V. Roch*[5], *G. Karcher*[5], *E. Guedj*[6], *A. Verger*[1]; *[1]Department of Nuclear Medicine & Nancyclotep Molecular Imaging platform, CHRU Nancy; IADI, INSERM U1254, University of Lorraine, Nancy, FRANCE, [2]Department of Nuclear Medicine, CHRU Nancy, Nancy, FRANCE, [3]Department of Geriatrics, Université de Lorraine, CHRU Nancy; 2LPN, University of Lorraine, Nancy, FRANCE, [4]Department of Biochemistry, Molecular Biology and Nutrition, CHRU Nancy; AFPA laboratory, ENSAIA, University of Lorraine, Nancy, FRANCE, [5]Department of Nuclear Medicine & Nancyclotep Molecular Imaging platform, CHRU Nancy, Nancy, FRANCE, [6]Department of Nuclear Medicine, Timone University Hospital; CERIMED, Aix-Marseille Université; CNRS, Ecole Centrale de Marseille, UMR 7249, Institut Fresnel, Marseille, FRANCE.*

Aim/Introduction: Digital PET cameras offer clear improvements in brain 18F-FDG PET image quality as compared to conventional PET cameras. However, the clinical impact of such image quality enhancements on the semi-quantitative analysis (SQA) of brain 18F-FDG PET scans remains unknown. The aim of this study was to evaluate performances of digital PET SQA of brain 18F-FDG PET scans over conventional PET cameras. ***Materials and Methods:*** Twenty-seven patients with moderate to severe Alzheimer's disease (AD) with cerebro-spinal fluid confirmation and 22 age and gender-matched healthy patients (H) without any neurological antecedent were included. They had a brain 18F-FDG PET on a digital PET camera (Vereos, Philips®) with SQA in comparison to two normal age and gender-matched healthy control databases acquired respectively with a digital PET (n=20, Vereos, Philips®) and a conventional PET (n=19, Biograph 6, Siemens®) cameras. Results are presented at the group-level, and with visual analyses at the individual level for the positive diagnosis of AD by a consensual analysis of 3 experimented readers, using SPM T-maps representations. SQA involved an inclusive AD mask and the sensitivo-motor cortex as reference for the intensity normalization. ***Results:*** At the group level, digital database SQA showed more marked hypometabolism in AD (+22 cm3 at $p<0.001$ for the voxel, corrected for the expected

cluster volume) and less extensive hypometabolism in H (-2 cm3) when compared to conventional database SQA. At the individual level, accuracy of digital database SQA was higher than those of conventional database SQA (78 vs. 65%, p<0.01, at p<0.005 for the voxel, corrected for the expected cluster volume), with lower specificity (64 vs. 91%) but much higher sensitivity (89 vs. 44%). ***Conclusion:*** There is an urgent need to develop digital PET databases for brain 18F-FDG PET SQA as it is associated with improved accuracy of AD diagnosis, in particular higher detection sensitivity, as compared to conventional database SQA. ***References:*** None

OP-320

Understanding gender pattern differences in 11C-Methionine PET Glioma patients with radiomics analysis

L. Papp*, S. Rasul, M. Weber, M. Grahovac, T. Beyer, M. Hacker, T. Traub-Weidinger;*
Medical University of Vienna, Vienna, AUSTRIA.

Aim/Introduction: PET-tracer uptake in glioma patients may vary with gender and histological subgroups. Here, we study gender differences in Glioma histological subgroups by the means of imaging patterns and radiomics analysis. ***Materials and Methods:*** 56 11C-MET-PET positive cases were included. Each case underwent semi-automated tumour delineation (Hybrid 3D, Hermes Nuclear Diagnostics, Sweden) as well as a normal background definition in the contra-lateral region. PET voxel values were normalized to the mean of the respective background to provide TBR values. Extraction of 50 radiomic features from each TBR-normalized VOI was performed. Matched-size male-female cohorts with similar characteristics (histology, WHO stage, age, IDH mutation status) were categorized to Astrocytoma (n=14, Oligodendroglioma (n=16), Oligoastrocytoma (n=14) and Glioblastoma multiforme (n=12) subgroups according to the WHO 2007 classification system. Radiomics feature weighting was performed based on establishing gender prediction models by ensemble learning in all the four pairwise subgroups. The three most prominent radiomic features in each of the four subgroups were analyzed to identify gender differences in each subgroup. ***Results:*** All subgroups demonstrated TBR heterogeneity differences, with Glioblastoma multiforme having the most prominent textural feature pattern differences within gender. The Oligoastrocytoma subgroup was an exception, where the most prominent feature to differentiate genders was sphericity-based, followed by textural features. ***Conclusion:*** Our pairwise radiomic analysis indicates that significant heterogeneity pattern differences are present between gender in glioma patients. Our results may support why Oligoastrocytoma presented a challenge in the interpretation according to the WHO 2007 system. Even though the WHO 2016 system eliminates the term Oligoastrocytoma, our results imply that future classification systems shall also consider a gender specificity. ***References:*** None

OP-321

Age correction has only minor impact on the diagnostic accuracy of the specific binding ratio in dopamine transporter SPECT in the diagnosis of parkinsonian syndromes

I. Apostolova[1]*, H. Schmitz-Steinkrüger*[1]*, C. Lange*[2]*, L. Frings*[3]*, S. Klutmann*[1]*, S. Hellwig*[3]*, P. T. Meyer*[3]*, R. Buchert*[1]*;*
[1]*University Hospital Hamburg Eppendorf, Hamburg, GERMANY,* [2]*Charité - Universitätsmedizin Berlin, Corporate Member of Freie Universität Berlin, Humboldt-Universität zu Berlin, and Berlin Institute of Health, Berlin, GERMANY,* [3]*Medical Center - University of Freiburg, Faculty of Medicine, Freiburg, GERMANY.*

Aim/Introduction: Several studies in healthy volunteers covering a wide age range consistently demonstrated an age-related decline of the [^{123}I]FP-CIT specific binding ratio (SBR) in the striatum and striatal subregions with healthy aging of about 5% per decade. However, age explains less than 10% of the SBR variability in healthy volunteers aged 50y and older. Therefore, the necessity of age correction of the SBR to support interpretation of [^{123}I]FP-CIT SPECT in clinical routine is still a matter of debate. The present study tested the impact of age correction on the diagnostic SBR performance in three different settings. ***Materials and Methods:*** Research setting: The putaminal SBR of 210 healthy controls (HC) and 446 Parkinson's disease (PD) patients of the Parkinson's Progression Marker Initiative (PPMI) was downloaded from the PPMI homepage. Clinical setting A: 186 patients with neurodegenerative PS and 186 patients with non-neurodegenerative PS were recruited retrospectively from one clinical site. The putaminal SBR was obtained by hottest voxels analysis of SPECT images reconstructed by filtered backprojection. Clinical setting B: 84 patients with neurodegenerative PS and 38 patients with non-neurodegenerative PS were recruited retrospectively from another clinical site. The putaminal SBR was obtained by applying anatomical standard ROIs (AAL atlas) to iteratively (OSEM) reconstructed SPECT images. The minimum of left and right putamen SBR was used in all settings. Age correction was based on linear regression of the minimum putamen SBR with age as independent variable in the HC subjects / patients with non-neurodegenerative PS, separately in each setting. The area (AUC) under the ROC curve for identification of PD / neurodegenerative PS was used as performance measure. ***Results:*** The AUC without/with age correction was 0.982 (95%-CI: 0.971-0.992) / 0.980 (0.971-0.990) in the research setting, 0.949 (0.927-0.972) / 0.945 (0.921-0.969) in clinical setting A, and 0.965 (0.937-0.993) / 0.974 (0.950-0.998) in clinical setting B. Only the small loss of AUC by age correction in clinical setting A was

statistically significant (DeLong p = 0.029, research setting: p = 0.600, clinical setting B: p = 0.220). ***Conclusion:*** These findings do not support age correction of the specific [123I]FP-CIT binding ratio in the etiological diagnosis of parkinsonian syndromes. ***References:*** None

OP-322

Quantification of 18F-Florbetaben amyloid PET images in patients with Alzheimer's disease

N. H. Patel[1], *L. Perry*[1], *J. Lilja*[2,3], *M. Golemme*[1], *H. McMeekin*[4], *L. Alves*[1], *K. S. Nijran*[1], *P. Malhotra*[1,5], *R. J. Perry*[1,5], *Z. Win*[1];
[1]*Imperial College Healthcare NHS Trust, London, UNITED KINGDOM,* [2]*Uppsala University, Uppsala, SWEDEN,* [3]*Hermes Medical Solutions, Stockholm, SWEDEN,* [4]*Hermes Medical Solutions, London, UNITED KINGDOM,* [5]*Imperial College London, London, UNITED KINGDOM.*

Aim/Introduction: 18F-Florbetaben PET/CT estimates beta-amyloid plaque density in patients with cognitive impairment under evaluation for Alzheimer's disease. Quantitative analysis can be performed using BRASSv4.0 software, with an automated PET only registration method, utilising an adaptive template based on principal component analysis to register PET data to a regional template. This approach could be beneficial as spatial normalisation of amyloid images is challenging due to different cortical uptake patterns in positive and negative scans. The aim of this work was to assess the ability of BRASSv4.0 software to quantify and aid identification of positive and negative 18F-Florbetaben scans. ***Materials and Methods:*** Patients (n=194) who underwent 18F-Florbetaben PET scan for a minimum 20 minutes were included in this study. Brain beta-amyloid was quantified using BRASSv4.0 software and compared with the final clinical report. The binary result and brain amyloid plaque load (BAPL) sub-group classification were identified in the double reported and independently reviewed clinical report (reference standard). The two experienced clinicians reached a consensus in cases of disagreement. Regional values from BRASSv4.0 were normalised using the Pons region as reference to give regional amyloid uptake ratios (SUV_R). The mean SUV_R value across all regions was calculated ($meanSUV_R$). A coefficient within the linear registration model which correlated with amyloid load was identified for all scans (Aβ-index). ROC curves were used to evaluate the most useful regions for accurate diagnosis, and threshold values were determined which minimised errors in diagnosis (false positive and false negative scans). ***Results:*** Of 194 18F-Florbetaben scans, 100 were classified as negative (BAPL1) and 94 as positive (8 BAPL2, 86 BAPL3). The optimum threshold for Aβ-index and $meanSUV_R$ was found to be 0.041 (AUC 0.989) and 0.74 (AUC 0.982) respectively for all data. Region-wise the left and right anterior cingulate, left and right frontal cortex, left and right lateral temporal cortex had best separation between the positive and negative cohorts. Optimal SUV_R thresholds were found to be 0.79 (AUC 0.972, 0.962), 0.77 (AUC 0.985, 0.978) and 0.73 (AUC 0.985, 0.972) respectively. ***Conclusion:*** BRASSv4.0 performed well for 18F-Florbetaben scans giving very good agreement with the final clinical report and could be utilised to aid identification of positive and negative scans. A threshold value for $meanSUV_R$=0.74 (sensitivity 97%, specificity 96%) and Aβ-index=0.041 (sensitivity 94% specificity 97%) is suitable for classification of typical 18F-Florbetaben studies. As shown, high sensitivity and specificity were obtained when adopting these recommended thresholds. ***References:*** None

OP-323

Correlation assessment between brain ^{18}F-Florbetaben PET/CT SUVR late acquisitions and parametric images obtained from dynamic acquisitions compartmental analysis

S. Ferreira[1,2,3], *F. Oliveira*[1], *M. Silva*[1], *R. Oliveira*[1], *Â. Silva*[1], *C. Oliveira*[1], *J. Castanheira*[1], *S. Vaz*[1], *N. Matela*[3], *P. Maniawski*[4], *D. C. Costa*[1];
[1]*Champalimaud Centre for the Unknown, Champalimaud Foundation, Lisbon, PORTUGAL,* [2]*Philips Portuguesa S.A., Lisbon, PORTUGAL,* [3]*Institute of Biophysics and Biomedical Engineering, Faculty of Sciences of the University of Lisbon, Lisbon, PORTUGAL,* [4]*Philips Medical Systems, Cleveland, OH, UNITED STATES OF AMERICA.*

Aim/Introduction: ^{18}F-Florbetaben PET/CT is widely used to access amyloid burden in the central nervous system. Data analysis is usually based on static late acquisition (90 min. pi.). However, refinement with kinetic parameters extracted from dynamic acquisitions and compartmental analysis may be useful. This work aims to evaluate the correlation between late image SUVR and BP, DVR and K (parametric images) obtained from the kinetic compartmental analysis. ***Materials and Methods:*** Data from twenty-five patients with cognitive impairment (14 females and 11 males, mean age 68±11 years, 11 amyloid positive and 14 amyloid negative) were retrospectively studied. Dynamic PET/CT scans were 45 minutes long and started immediately post-injection of 291±24 MBq of ^{18}F-Flobetaben. Late acquisitions started 90 minutes post-injection for 20 minutes. All studies were acquired in the Philips Vereos Digital PET/CT. Four kinetic methods were used: simplified reference region method (SRTM2), modified reference region method (MRTM2), Logan plot and Patlak plot. The parametric images BP-SRTM2, BP-MRTM2, DVR-Logan and K-Patlak were extracted from the dynamic acquisitions using the respective kinetic models. All images (including late acquisitions) were registered to Montreal Neurological Institute (MNI) space using deformable geometric transformations. Cerebellar gray matter was the reference region used both for kinetic models and SUVR computation. Voxelwise within subject and regional correlations were accessed between SUVR

images and the four parametric images. ***Results:*** Mean brain voxelwise within subject correlation between SUVR images and BP-SRTM2, BP-MRTM2, DVR-Logan and K-Patlak parametric images were 0.91±0.04, 0.94±0.02, 0.85±0.09 and 0.78±0.09, respectively. Regarding the voxelwise regional correlation between SUVR images and the kinetic parametric images, similar correlation patterns were obtained in all cases. However, the following variations were found: higher correlations between the SUVR image and BP-SRTM2 and BP-MRTM2 images; very high correlation (r>0.90) in most of the brain cortex; fair correlation (0.4<r<0.7) around the ventricles and fissures. ***Conclusion:*** Good voxelwise within correlation was obtained between SUVR images and all parametric images. The inferior correlation obtained with the K-Patlak does not mean worse performance than the BP, since there is no ground true of the real amyloid burden. They may measure different things. Regional voxelwise correlation, in general, was very high for most of the brain. The inferior correlation around the ventricles and fissures may be explained by imperfection of the image registration and the variability among the subjects in terms of brain atrophy in these regions. ***References:*** None

OP-324

Dual-time-window dynamic [^{18}F]MK-6240 PET protocols for improved quantification in longitudinal studies and stroke patients

G. D. Kolinger[1], *D. Vállez García*[1], *R. Boellaard*[1,2], *T. G. Lohith*[3], *E. D. Hostetler*[3], *C. Sur*[3], *A. Struyk*[3], *M. Koole*[4];
[1]*Medical Imaging Center, University Medical Center Groningen, University of Groningen, Groningen, NETHERLANDS,* [2]*Department of Radiology and Nuclear Medicine, Amsterdam University Medical Centers, location VU Medical Center, Amsterdam, NETHERLANDS,* [3]*Merck & Co., Inc., Kenilworth, NJ, UNITED STATES OF AMERICA,* [4]*Department of Nuclear Medicine and Molecular Imaging, KU Leuven, Leuven, BELGIUM.*

Aim/Introduction: Kinetic modeling of [^{18}F]MK-6240 brain uptake requires long dynamic PET scans up to 2 h due to slow kinetics in regions with high tau load. Therefore, dual-time-window (DTW) protocols were evaluated to reduce the total acquisition time and make [^{18}F]MK-6240 PET procedures more tolerable for patients. ***Materials and Methods:*** A plasma input two-tissue compartment model (2TCM) was fitted to 90min dynamic [^{18}F]MK-6240 PET scans using individual metabolite corrected plasma input functions from three healthy control (HC) and five mild cognitive impairment/Alzheimer's Disease (MCI/AD) subjects showing various levels of specific tracer binding. The 2TCM fit parameters were then used to simulate various 120 min time activity curves (TAC). Additional TACs for target regions based on PET-Braak stages were generated by varying the relative influx rate ($R1=K1/K1_{ref}$ changes; range: -50% to 50%) while keeping K1/k2 constant to mimic changes of blood flow and blood brain barrier functionality. Using cerebellar cortex as reference tissue, distribution volume ratios (DVR) were estimated with the reference Logan model (RefLogan). Standardized uptake value ratios (SUVR) were calculated for the 90-120min interval. To simulate different DTW protocols, four break intervals were introduced in the TACs: 20-90min, 30-90min, 40-90min and 50-90min. Breaks in the simulated DTW-TACs were filled using linear interpolation. DVRs from DTW-TACs were compared with 120min TACs. ***Results:*** For the HC subjects, DVR bias was less than 2.5% for all break intervals. For the MCI/AD subjects, DTW with 20-90min break had an average DVR bias up to 7% while shorter breaks resulted in less than 2.5% DVR underestimation. In terms of K1 changes, average SUVR bias ranged from -5.3% to 11% (regional standard deviation (SD) up to 14%), while 30-90min DTW DVR bias ranged from -5.9% to 1.3% (SD<4% for all regions). ***Conclusion:*** The DTW protocol with 30-90min interval using RefLogan and cerebellar cortex as reference tissue is suitable for clinical routine allowing to estimate tracer influx rate in addition to binding parameter DVR. Compared to 90-120min SUVR, a 30-90min DTW quantification is less susceptible to reduced K1 values which can be expected in stroke patients and potentially in longitudinal MCI/AD studies. (This project is partially funded by European Union's Horizon 2020 research and innovation programme under the Marie Skłodowska-Curie grant agreement No 764458.) ***References:*** None

OP-325

Optimizing of the white matter reference region for synaptic density imaging with [^{11}C]UCB-J PET

N. Mertens[1], *L. Michiels*[2,3], *B. Lacroix*[4], *J. Mercier*[4], *R. P. Maguire*[4], *R. Lemmens*[2,3], *K. Van Laere*[1], *M. Koole*[1];
[1]*Nuclear Medicine and Molecular Imaging, University Hospital and KU Leuven, Leuven, BELGIUM,* [2]*UZ Leuven/KU Leuven, Neurology, Neurosciences, Experimental Neurology, Leuven, BELGIUM,* [3]*VIB, Center for Brain & Disease Research, Laboratory of Neurobiology, Leuven, BELGIUM,* [4]*UCB Pharma, Braine-l'Alleud, BELGIUM.*

Aim/Introduction: [^{11}C]UCB-J PET, targeting synaptic vesicle glycoprotein 2A (SV2A), has been widely used as in vivo proxy for synaptic density. For non-invasive quantification, subcortical white matter (centrum semiovale - SO), restricted to white matter (WM) with only very limited partial volume effects (PVE), has been proposed as reference region (=method 1)[1]. However, in brain disorders with WM pathology this region reduces the potential to exclude pathological WM without affecting statistics. Therefore, we considered more expanded subcortical WM (=method 2) and cerebellar WM (=method 3) as candidate reference tissues while using a partial volume correction (PVC). ***Materials and Methods:*** 10 healthy volunteers (8M/2F;27.6±10.0yrs)

underwent a 90-min dynamic [11C]UCB-J PET/MR scan (GE Signa) with full arterial sampling under baseline and dosing conditions using a compound with selective affinity for SV2A. Six subjects received a second post dose scan. Cerebellar WM and SO were obtained by 3-tissue class segmentation of T1-weighted MR. WM standarized uptake values (SUV;60-90min post injection) in both regions was estimated by a four-tissue compartment model including white and gray matter within and outside of the predefined regions and applying Gaussian smoothing to mimic limited PET resolution. SUV of method 2 and 3 was compared to method 1. Baseline and post dose SUV was evaluated for displacement for both new methods. SUVR-based occupancy was compared with occupancy using full kinetic modeling. ***Results:*** PVC with a 6mm Gaussian filter resulted in no significance difference between baseline and post dose SUV in method 2, while a significant difference was detected in method 3 ($p<0.05$). For the latter, increased smoothing of 7.5mm resulted in similar baseline and post dose SUV. For these filter settings, SUV was similar when using method 2 ($p>0.05$;bias: 2.2%±7.8%) while higher bias was observed in method 3 ($p<0.001$;bias: -29.3%±22.5%). Bland-Altman revealed SUVR-based occupancies in line with method 1 [1] for method 2 ($p>0.05$;bias: 3.5%±9.2%) and method 3 ($p>0.05$;bias: -2.3%±10.3%) but a higher variation in method 3. ***Conclusion:*** PVC allows the use of a more extensive and robust subcortical WM reference region (method 2) for non-invasive [11C]UCB-J quantification, while the use of cerebellar WM (method 3) seems to be more challenging as it may produce bias. ***References:*** M. Koole et al., "Quantifying SV2A density and drug occupancy in the human brain using [11C]UCB-J PET imaging and subcortical white matter as reference tissue," Eur. J. Nucl. Med. Mol. Imaging, pp. 1-11, Aug. 2018.

OP-326

Reliability of occipital reference region in [123I]-FP-CIT SPECT

T. Noponen[1,2], *E. Jaakkola*[3], *E. Mäkinen*[3], *M. Eklund*[3], *S. Nuuttila*[3], *K. Lindholm*[3], *J. Joutsa*[3], *M. Seppänen*[1,4], *V. Kaasinen*[3];
[1]*Department of Clinical Physiology and Nuclear Medicine, Turku University Hospital, Turku, FINLAND,* [2]*Department of Medical Physics, Turku University Hospital, Turku, FINLAND,* [3]*Department of Clinical Neurosciences, Turku University Hospital and University of Turku, Turku, FINLAND,* [4]*Turku PET Centre, Turku, FINLAND.*

Aim/Introduction: Dopamine transporter (DAT) imaging using [123I]-FP-CIT SPECT is a routine clinical method to examine patients with suspected Parkinson's disease (PD). Currently there is, however, no straightforward method to estimate the reliability of reference region values for specific binding ratio (SBR) calculations. In this study the stability of counts-per-voxel values of occipital cortex in DAT imaging were investigated. ***Materials and Methods:*** [123I]-FP-CIT SPECT imaging was carried out for 89 patients with clinically uncertain parkinsonian syndrome. The injected activity was 185 MBq and the imaging was started 3 h after injection with GE Infinia II Hawkeye or Siemens Symbia T6 SPECT/CT scanner using LEHR collimators. To prevent thyroid uptake, potassium perchlorate was given 30-60 min before the injection. Data were acquired using 120 projections with 30-s time per projection and matrix size of 128x128. The data were reconstructed with 3D OSEM based iterative algorithm including Chang's attenuation, collimator and Monte-Carlo-based scatter correction and Gaussian post-filtering.Regional specific-binding ratios (rSBR) were calculated with Brass software (Hermes Medical Solutions, Sweden). The patient data were automatically registered with the template volume using a traditional nine parameter transformation. Before registration the data were resampled to the template size and after the registration slices with zero intensity were removed. Then six constant size striatal volume-of-interests (VOIs) (the right and left anterior putamen, the right and left posterior putamen, the right and left caudate nucleus) and the reference occipital VOI were transferred from the template volume to the patient image.Average counts-per-voxel values of occipital reference VOIs and the correlation of those values with the striatal rSBRs were analyzed. ***Results:*** The occipital reference VOIs included in average 8200 ± 189 (mean ± sd) voxels. The occipital mean (± sd) counts-per-voxel value was 116.4 ± 1.3, sd being 1.1% of the mean. The correlation coefficients between occipital cortex counts-per-voxel values and rSBRs ranged from 0.00 to 0.14 meaning non-significant correlations ($p = 0.19 - 0.96$). ***Conclusion:*** Average occipital counts-per-voxel values in [123I]-FP-CIT imaging have a low variation between patients. Non-specific [123I]-FP-CIT binding in occipital cortex is therefore very constant and occipital cortex can be used as a reliable reference region in [123I]-FP-CIT imaging. These findings also suggest that average counts-per-voxel values are useful as a quality control measure, e.g., to estimate the success of radiopharmaceutical injection in [123I]-FP-CIT imaging in clinical routine. ***References:*** None

OP-327

Multicenter intensity harmonization of dopamine SPECT studies without previous in-site scanner calibration

J. Silva-Rodríguez[1], *A. Moscoso*[2], *A. Niñerola-Baizán*[3], *J. Cortés*[4], *B. Aradas-Cabado*[4], *Á. Ruibal*[4], *P. Aguiar*[1];
[1]*Health Research Institute of Santiago de Compostela, Santiago de Compostela, SPAIN,* [2]*Wallenberg Centre For Molecular and Translational Medicine, Gothenburg, SWEDEN,* [3]*Nuclear Medicine Department, Hospital Clinic, Barcelona, SPAIN,* [4]*Nuclear Medicine Department, University Hospital of Santiago de Compostela, Santiago de Compostela, SPAIN.*

Aim/Introduction: Specific binding ratios (SBR) used for the

semiquantification in DAT-SPECT are largely dependent on the scanner, the used collimator, and the acquisition and reconstruction parameters [1]. Conventionally, SBRs are harmonized by calculating calibration factors for different camera-collimator combinations using physical phantoms [2]. Nevertheless, the harmonization of SBRs through image postprocessing is of great interest for several applications [3]. In this work, we study the feasibility of different implementations histogram matching (HM) as a post-processing only harmonization method. ***Materials and Methods:*** Striatum SBRs were quantified for 183 healthy controls (HC) and 470 Parkinson's Disease (PD) patients DAT-SPECT images acquired at 6 different gammacameras. HC SBRs variations across scanners were evaluated for unprocessed images and for four different implementations of HM: Conventional HM (HM), exact HM (EHM), bi-histogram HM (BiHM) and LogPow HM (LpHM). Potential changes in spatial information due to the image processing were assessed by evaluating the preservation of asymmetry and caudate-to-putamen ratios (CPRs) for the different methods on PD patients. Binary classification (HC vs. PD) for each of the proposed methods and for the unprocessed images was evaluated by calculating receiver operating curves (ROC). ***Results:*** While the median voxel-wise standard deviation for the original images was 13.6%, the evaluated methods reduced it to 4.5% (EHM), 5.5% (HM), 6.6% (LpHM) and 8.2% (BiHM). When focusing on SBR values, EHM and LpHM were able to eliminate all the significant difference between scanners (on 1 vs. 1 comparisons). EHM was the only method altering asymmetry values ($p < 0.001$) while all the methods presented significant changes on the CPRs (LpHM provided the best preservation). In terms of classification, EHM, HM and LpHM provided great improvements (AUC= 0.91-0.94) in comparison with unharmonized images (0.77). ***Conclusion:*** HM is a suitable methodology for the harmonization of HC and PD DAT-SPECT images, both visually and in terms of SBR. Of the tested implementations, LpHM was the most promising method both in terms of classification and spatial feature preservation. ***References:*** [1] Tossici-Bolt L, Dickson JC, Sera T, et al. [123I]FP-CIT ENC-DAT normal database: the impact of the reconstruction and quantification methods. EJNMMI Phys. 2017;4:8.[2] Tossici-Bolt L, Dickson JC, Sera T, et al. Calibration of gamma camera systems for a multicentre European 123I-FP-CIT SPECT normal database. Eur J Nucl Med Mol Imaging. 2011;38:1529-1540.[3] Llera A, Huertas I, Mir P, Beckmann CF. Quantitative Intensity Harmonization of Dopamine Transporter SPECT Images Using Gamma Mixture Models. Mol Imaging Biol. 2019;21:339-347.

OP-328

Partial volume correction improves the diagnostic capacity of quantitative amyloid PET imaging for both clinical and biomarker-assisted criteria for Alzheimer's disease

M. Shekari[1,2,3], G. Salvadó[1,3], A. Sala[4,5,6], E. Rodriguez-Vieitez[4], J. L. Molinuevo[1,2,3], J. D. Gispert[1,2,3], for the ADNI study;
[1]BarcelonaBeta Brain Research Center, Barcelona, SPAIN, [2]Universitat Pompeu Fabra, Barcelona, SPAIN, [3]Hospital del Mar Medical Research Institute (IMIM), Barcelona, SPAIN, [4]Department of Neurobiology, Care Sciences and Society, Karolinska Institutet, Stockholm, SWEDEN, [5]Vita-Salute San Raffaele University, Milan, ITALY, [6]In Vivo Human Molecular and Structural Neuroimaging Unit, Division of Neuroscience, IRCCS San Raffaele Scientific Institute, Milan, ITALY.

Aim/Introduction: Quantification has been proposed as an aid to improve the accuracy and confidence of visual interpretation of amyloid PET scans of patients with suspected Alzheimer's disease(AD). However, the limited spatial resolution of PET scanners may hamper the diagnostic capacity of amyloid PET. This study assesses the impact of partial volume correction(PVC) on the diagnostic capacity of quantitative amyloid PET against clinical and biomarker-assisted diagnostic criteria for AD. ***Materials and Methods:*** A total of 864 participants from ADNI cohort(185 healthy controls(HC), 90 subjects with significant memory concern, 443 subjects with mild cognitive impairment, 146 patients with AD dementia) were included in this study. AV45-PET, T1-MRIs, CSF Abeta1-42, p-tau, and clinical diagnosis were available for all participants. PVC was done using a region-based method(Rousset et al, JNM,1998). Global cortical amyloid was quantified for both non-PVC and PVC PET images normalized to the whole cerebellum as reference region. Optimal diagnostic cut-offs were calculated on the PVC and non-PVC corrected images using a Gaussian Mixture Model(GMM) by selecting the mean of the 'normal' Gaussian plus 2 standard deviations. Receiver Operating Curve(ROC) analysis was conducted for global SUVR to discriminate HC.vs.AD dementia(clinical diagnosis of AD), as well as participants with Low.vs.High pTau/Abeta1-42 ratios(cutoff=0.11,biomarker-assisted AD definition). The area under the curve(AUC) was measured, as well as the sensitivity at 90%specificity(Sens@90%Spec). ***Results:*** After applying PVC, global SUVR of the subjects with high amyloid level increased 12.73%±5.59% which is due to recovering the cortex signal spilled out to the white matter, while global SUVR of subjects with low amyloid burden decreased 26.11%±11.97% due to reducing activity contamination spilled in the cortex from the white matter regions. The optimal SUVR cutoff for clinical diagnostic classification decreased from 1.02±0.12 to 0.88±0.06 after PVC. In the ROC analysis, AUC for differentiating between HC and AD dementia significantly improved from

0.83(95%Confidence Interval: 0.78-0.87) to 0.87(0.83-0.91) (p<0.0001) and the sensitivity at 90% specificity increased from 54.8% to 68.5%. Accordingly, the optimal SUVR cutoff for biomarker-assisted diagnostic classification decreased from 1.03±0.08 to 0.89±0.1 after PVC. For predicting high pTau/Abeta1-42 ratio, PVC significantly improved the AUC from 0.81(0.79-0.84) to 0.84(0.81-0.86)(p=0.003) and the Sens@90%Spec was improved from 65.6% to 68.7%. ***Conclusion:*** Our results show that PVC can improve the diagnostic capacity of amyloid PET quantification using both clinical and biomarker-assisted criteria. These results suggest that quantification using PVC can serve as an aid to the visual interpretation of amyloid PET scans for diagnostic purposes. ***References:*** None

607

Pitfalls & Artefacts 3: Dosimetry as Part of Patient Care

Friday, October 23, 2020, 13:50 - 15:20 Channel 7

OP-329

Patient Specific Therapy in PRRT - The Bright Future

M. Cremonesi; Istituto Europeo di Oncologia (IEO), Radiation Research Unit, Milan, ITALY.

OP-330

Patient Specific Therapy with 177Lu PSMA

J. Violet; Peter MacCallum Cancer Centre, Radiation Therapy Division, Melbourne, AUSTRALIA

608

Clinical Oncology Track - Featured Session: BCR Detection with Ga-PSMA and Beyond

Friday, October 23, 2020, 13:50 - 15:20 Channel 8

OP-331

PET Tracer Landscape in Prostate Cancer

I. Burger; University of Zurich, Deparment of Nuclear Medicine, Zurich, SWITZERLAND.

OP-332

Matched-pair comparison of ^{68}Ga-PSMA-11 and ^{18}F-rhPSMA-7 PET/CT in patients with primary and biochemical recurrent prostate cancer

I. Rauscher[1], M. Krönke[1], A. Wurzer[2], H. Wester[2], W. Weber[1], M. Eiber[1];
[1]Department of Nuclear Medicine, Technical University of Munich, Klinikum rechts der Isar, Munich, GERMANY, [2]Department of Pharmaceutical Radiochemistry, Technical University of Munich, Klinikum rechts der Isar, Munich, GERMANY.

Aim/Introduction: ^{18}F-labeled prostate-specific membrane antigen (PSMA)-ligand positron emission tomography/computed tomography (PET/CT) is increasingly used for prostate cancer imaging due to several major principal advantages (image contrast/noise, logistics, positron range) compared to ^{68}Ga-PSMA-11. We aimed to evaluate frequency of non-tumor related uptake and tumor positivity comparing ^{68}Ga-PSMA-11 and recently introduced ^{18}F-rhPSMA-7 (providing low urinary excretion) in patients with both primary and recurrent prostate cancer (PC). ***Materials and Methods:*** This retrospective matched-pair comparison included 160 ^{18}F-rhPSMA-7 PET/CT and 160 ^{68}Ga-PSMA-11 PET/CT studies both for primary staging (n=33) and biochemical recurrence (n=127) matched by various clinical variables. All PET/CTs were reviewed by two nuclear medicine physicians in consensus. First, all PET positive lesions, defined as focal uptake above surrounding background and not physiological distribution, were identified. Then, lesions suspicious for PC were differentiated from lesions attributed to benign origin based on known pitfalls and information from CT. For each region, SUVmax of the lesion with the highest PSMA-ligand uptake was noted. Tumor positivity rates were determined and SUVmax were compared separately for ^{68}Ga-PSMA-11 and ^{18}F-rhPSMA-7. ***Results:*** In total, ^{18}F-rhPSMA-7 PET and ^{68}Ga-PSMA-11 revealed 532 and 293 PSMA-ligand positive lesions, respectively. The absolute number of lesions attributed to benign origin was 3.3 times higher for ^{18}F-rhPSMA-7 PET compared to ^{68}Ga-PSMA-11 PET (351 vs. 105 lesions, respectively), whilst the distribution of their etiology was relatively similar (46%, 27%, 20% in ^{18}F-rhPSMA-7 vs. 30%, 40%, 20% in ^{68}Ga-PSMA-11 for ganglia, unspecific LN and bone lesions, respectively). All primary tumors were positive in ^{18}F-rhPSMA-7 and ^{68}Ga-PSMA-11 (n=33 each) while a slightly higher number of metastatic lesions was observed with ^{68}Ga-PSMA-11 in primary staging (16 for ^{18}F-rhPSMA-7 and 21 for ^{68}Ga-PSMA-11). In biochemical recurrence a similar number of malignant lesions (132 for ^{18}F-rhPSMA-7 and 134 for ^{68}Ga-PSMA-11) were detected. SUVmax of all malignant lesions was significantly higher (p<0.01) in ^{18}F-rhPSMA-7 PET (SUVmax 26.7±28.8 for ^{18}F-rhPSMA-7 PET and 17.9±18.7 for ^{68}Ga-PSMA-11 PET, respectively) while SUVmax of the urinary bladder was significantly lower in ^{18}F-rhPSMA-7 PET (SUVmax 3.8±1.9 for ^{18}F-rhPSMA-7 PET and 11.2±14.0 for ^{68}Ga-PSMA-11 PET, respectively). ***Conclusion:*** While tumor positivity rate is consistently high for ^{18}F-rhPSMA-7, a considerably higher number of lesions with increased PSMA-ligand uptake attributed to benign lesions is present compared to ^{68}Ga-PSMA-11. However, after adequate reader training, physicians should be well equipped to distinguish likely malignant lesions from those that are most probably benign, while fully exploiting the logistical advantages of ^{18}F-labeled PSMA-ligands. ***References:*** None

OP-333

Prospective Single Institution Study of F18-DCFPyL PET/CT in Biochemically Recurrent Prostate Cancer: An Analysis of Lesions Detection and Localization

A. Iagaru, H. Song, H. Duan, C. Harrison, K. Guja, N. Hatami, B. Franc, J. Nguyen, F. Moradi, C. Mari, G. Davidzon;
Stanford University, Stanford, CA, UNITED STATES OF AMERICA.

Aim/Introduction: F18-DCFPyL, a promising PET agent targeting prostate specific membrane antigen (PSMA), is prospectively evaluated in a single academic center for detecting recurrent lesions in prostate cancer patients with biochemical recurrence (BCR). ***Materials and Methods:*** We prospectively enrolled 170 men (49-91 years old, mean ± SD: 69.6±8.0) with biochemical recurrence (PSA median 2.27 ng/mL, range 0.12 to 698.4) after primary definitive treatment with prostatectomy (67%), radiotherapy (33%) or both (22%). All patients were scanned using a SiPM-based PET/CT (GE Discovery MI). The F18-DCFPyL positive lesions compatible with prostate cancer were evaluated by two independent readers. Impact of F18-DCFPyL PET/CT on patient management was recorded from clinical chart review. ***Results:*** F18-DCFPyL PET/CT had an overall positivity rate of 84% (142 scans), which increased with higher prostate specific antigen (PSA) levels (ng/mL): 67% (PSA<0.5), 71% (0.5≤PSA<1), 93% (1≤PSA<2), 93% (2≤PSA<5) and 98% (PSA≥5), respectively. In the cohort who underwent prostatectomy, F18-DCFPyL PET/CT had higher positivity rate in patients with shorter PSA doubling time (PSAdt) (95% in PSAdt 0-3 months vs. 56% in PSAdt > 12 months, P<0.01). No difference of F18-DCFPyL positivity rate was observed in post-radiation patients with different PSAdt, nor were there differences between patients with low grade (Gleason 6) or higher-grade prostate cancer (Gleason 7-10). 21 patients (12%) had lesions in the prostate bed only and 50 patients (29%) had oligometastatic disease (1-3 lesions), making them candidates for locally targeted therapy. We identified a total of 1573 F18-DCFPyL positive lesions, including 57 lesions in the prostate bed, 316 pelvic and 506 extra-pelvic lymph nodes, approximately 594 osseous lesions, including 5 patients with diffuse osseous metastases, and 100 lesions in other organs (most commonly in the lungs). 105 out of 170 patients (62%) had change in treatment after F18-DCFPyL PET and, most noticeably, 57 of these patients (34% total) had lesions only localized on F18-DCFPyL PET/CT despite negative conventional imaging. ***Conclusion:*** F18-DCFPyL PET/CT holds great potential to be a "one-stop shop" diagnostic tool in the work-up of BCR prostate cancer, with high (62%) impact on the management of these patients. ***References:*** None

OP-334

The role of ^{64}Cu-PSMA PET/CT in the early diagnosis of prostate cancer recurrence: preliminary results on a prospective cohort of 127 patients

S. Annunziata, R. Sciuto, S. Rea, A. Annovazzi, R. Pasqualoni, S. Bergomi, L. Romano, C. Mazzone, S. Di Traglia, G. Sanguineti;
IRCCS Regina Elena National Cancer Institute, Rome, ITALY.

Aim/Introduction: Prostate-specific membrane antigen (PSMA) positron emission tomography/computed tomography (PET/CT) emerged as an accurate imaging method for prostate cancer (PC). Until now, the most investigated PSMA tracers are labelled with ^{68}Ga. Recent studies on small series have demonstrated the potential of ^{64}Cu-labeled PSMA in patients with recurrent PC. ^{64}Cu-PSMA may also offer the possibility of pre-therapeutic dosimetry in the theragnostic approach. The aim of this study is to investigate the diagnostic role of ^{64}Cu-PSMA PET/CT in a large prospective cohort of PC patients with early recurrence of disease. ***Materials and Methods:*** The study was approved by the local Ethical Committee as a prospective trial on a cohort of 162 patients with PC biochemical recurrence (BCR). The primary endpoint was to verify the diagnostic accuracy of ^{64}Cu-PSMA PET/CT compared to ^{18}F-Choline PET/CT in the early identification of PC recurrence with low values of prostate specific antigen (PSA). All patients underwent to ^{64}Cu-PSMA-617 and ^{18}F-choline PET/CT in a maximum time of two months. ^{64}Cu-PSMA and ^{18}F-Choline results were compared and verified by histology, other imaging, or on follow-up. Thereafter, patients underwent to secondary treatment (target radiotherapy or surgery as appropriate). The clinical impact of ^{64}Cu-PSMA was discussed in a multidisciplinary setting. ***Results:*** A preliminary analysis was performed on 127 patients. At the time of ^{64}Cu-PSMA PET/CT, PSA values ranged from 0,17 ng/ml to 3,2 ng/ml with a median value of 0,76 ng/ml. Patient-based PET/CT sensitivity was of 57% for 18F-choline and of 89% for ^{64}Cu-PSMA, respectively. ^{64}Cu-PSMA PET/CT identified 209 lesions while 18F-choline PET/CT identified 122 lesions, showing ^{64}Cu-PSMA higher sensitivity (41% more identified lesions than ^{18}F-choline). Small local recurrence (up to a minimum of 3 mm) were identified by ^{64}Cu-PSMA in 60% of cases, while only 20% identified by 18F-Choline. Node metastasis sensitivity was of 15% and 35% for ^{18}F-Choline and ^{64}Cu-PSMA, respectively. Moreover 15% of bone lesions showed by ^{64}Cu-PSMA PET/CT were missed by ^{18}F-choline. ^{64}Cu-PSMA specificity was higher than ^{18}F-Choline, differentiating aspecific nodal and bone uptake in more than 5% of cases. ^{64}Cu-PSMA PET/CT changed clinical management in more than 90% of cases, guiding treatment choice and target therapy. ***Conclusion:*** ^{64}Cu-PSMA PET/CT is an accurate imaging tool in a large prospective cohort of patients with early recurrence of PC, showing higher sensitivity than ^{18}F-Choline PET/CT and

significantly impacting on further clinical management. A future role of ^{64}Cu-PSMA as theragnostic agent is worth exploring. ***References:*** None

OP-335

In-vivo D'Amico score for predicting low-vs-high risk and biochemical recurrence in prostate patients from PET/MRI with machine learning

L. Papp, C. P. Spielvogel, D. Krajnc, M. Grahovac, T. Beyer, M. Hartenbach, M. Hacker;
Medical University of Vienna, Vienna, AUSTRIA.

Aim/Introduction: Combined PET/MR imaging is a useful approach to localize and characterize prostate cancer lesions. Nonetheless, the pre-operative diagnosis of prostate cancer is still performed by the D'Amico score, which builds on clinical stage, PSA and biopsy-based Gleason scoring. Our goal was to establish an in-vivo D'Amico score for post-operative and biochemical risk predictions utilizing PET/MRI risk scores provided by machine learning (ML) as the replacement of biopsy-derived risk scores. ***Materials and Methods:*** This study included 74 multi-parametric prostate PET/MRI cases with ^{18}F-FMC, ^{18}F-FMC+^{68}Ga-PSMA$^{HBED-CC}$ (dual-tracer) PET, and T2, ADC, iAUC, KEP, Ktrans and Ve MRI images. Based on annotated, full-mount histopathological slices, 120 lesions representing different Gleason patterns were delineated and annotated as of the histopathological data (Hermes Nuclear Diagnostics, Sweden). Extraction of 56 radiomics features from PET/MR image sets was performed for all 120 lesions. Ensemble learning was utilized to build lesion-specific low (<=G3) vs. high (>=G4) as well as benign (<G3) vs malign (>=G3) risk probability predictors (LH and BM respectively). The summed LH and BM prediction probabilities across the two largest lesions were categorized as +3 (BM+LH>T & LH>BM), +2 (BM+LH>T & LH<BM) and +1 (BM+LH<T) risk score, as the replacement of the biopsy Gleason +3, +2 and +1 risk scores in the D'Amico scheme. 1000-fold Monte Carlo (MC) cross-validation was performed to estimate the performance of the in-vivo D'Amico score. For all the MC folds, T=0.3 and T=0.9 were selected based on the first MC fold training data analysis to predict in-vivo D'Amico post-operative low-high risk (IPR) and in-vivo biochemical recurrence (IBCR) no-yes scores respectively. ***Results:*** IPR prediction performance values were SENS 83%, SPEC 88% and ACC 84% compared to reference D'Amico SENS 74%, SPEC 94% and ACC 80%. The IBCR performance values were SENS 100%, SPEC 81% and ACC 86% compared to reference D'Amico SENS 78%, SPEC 65% and ACC 69%. ***Conclusion:*** We have presented a novel in-vivo D'Amico score utilizing PET/MRI-derived ML risk values to predict post-operative risk as well as biochemical recurrence in prostate patients. Our results indicate that such predictions can be improved alternatives of the gold-standard D'Amico score system. ***References:*** None

OP-336

The impact of 18F-Choline (FCH) PET/MRI on PSA response in patients with oligometastatic prostate cancer (PCa)

L. Evangelista[1], G. Cassarino[1], C. Lacognata[2], S. Da Pozzo[2], D. Cecchin[1], P. Zucchetta[1];
[1]University of Padua, Padua, ITALY,
[2]Hospital of Padua, Padua, ITALY.

Aim/Introduction: Oligometastatic disease (OMD) in PCa represents a clinical condition that significantly influences the optimal choice of treatment. PET/MRI with radiolabeled PSMA and Choline (FCH) has showed a high detection rate in patients with an early (i.e. PSA levels ≤ 1 ng/mL) recurrence of PCa. The aim of the study was to assess the impact of FCH PET/MRI on PSA response in patients with oligometastatic PCa. ***Materials and Methods:*** We retrospectively analyzed a cohort of 108 patients who underwent FCH PET/MRI for biochemical recurrence of PCa. The inclusion criteria were: 1) PSA ≤ 1 ng/mL at PET time; 2) OMD defined as < 5 lesions at PET/MRI scan; and 3) available follow-up data of at least 6 months after PET. T2-weighted turbo spin-echo, T1-vibe after contrast enhancement, T2-haste, T1-vibe fat saturated and diffusion weighted image (DWI) sequences were used for the MRI component. PET images were acquired using a dedicated (>20 min) acquisition of the pelvis, followed by a whole-body scan. Attenuation correction was performed using a mu-map obtained from a MR sequence with a 2-point Dixon fat and water separation for a segmentation into 4 tissue classes (air, lungs, fat, and soft tissue). All images were revised jointly by two nuclear medicine physicians and a radiologist. ***Results:*** Out of 108 patients, 67 (62%) were eligible. Fifty-five patients presented with OMD at PET/MRI. Nine patients were lost at follow-up. In 46 patients sixty lesions were detected: 39 in the prostatic fossa (20 at MRI and 19 at PET/MRI), 20 in local and distant lymph nodes (2 at MRI, 12 at PET and 6 at PET/MRI) and 1 lesion in bone visible only at MRI. Twenty-six (57%) patients were treated with radiotherapy (RT), 9 (20%) with hormonal therapy (HT), 3 (6%) with a combined therapy (RT+HT) and 8 (17%) underwent a PSA surveillance. At follow-up, PSA levels decreased in 35 (76%) patients mostly in those undergoing RT or RT+HT. In the subset of patients with a reduction of PSA levels, PET/MRI detected more lesions than MRI alone (87% vs 71%). ***Conclusion:*** FCH PET/MRI showed an higher detection rate than MRI alone in oligometastatic PCa patients, with a PSA ≤ 1 ng/mL. Therefore, It could be used as a tool to optimize treatments in OMD. ***References:*** 1. Kranzbuhler et al. J Nucl Med 2020; 61:194-201 2. Evangelista et al. Nuclear Med Comm 2018; 39:260-7.

OP-337

Clinical utility of PET/CT with ^{18}F-FSU880 in patients with biochemical recurrence after curative treatment of prostate cancer

Y. Nakamoto, Y. Shimizu, T. Ishimori, T. Otani, T. Saga; Kyoto University, Kyoto, JAPAN.

Aim/Introduction: We have developed a new ^{18}F-labeled compound, called ^{18}F-FSU880 [1], for targeting prostate-specific membrane antigen with higher affinity, and our feasibility assessment has been already reported [2]. The purpose of this study was to investigate the clinical utility of PET/CT with ^{18}F-FSU880 for detecting suspected recurrent lesions in biochemical recurrence after curative treatment of prostate cancer. ***Materials and Methods:*** A total of 14 male patients (58-79 yr, mean 69 yr) were assessed who had undergone curative treatment for prostate cancer by surgery (n=8) or radiation therapy (n=6), who had been suspected of having recurrence due to increase of serum PSA level (0.266 - 11.74 ng/mL), and for whom conventional imaging was inconclusive. All patients were scanned using a combined PET/CT scanner twice one hour and three hours after administration of ^{18}F-FSU880. PET/CT images were interpreted visually. Quantitative values in suspected lesions and physiological uptake were evaluated. ***Results:*** FSU880-PET/CT demonstrated positive findings in 8 of 14 patients (57%); however, one patient was finally diagnosed to have hemangioma in the rib, i.e. false positive. Other suspected findings, suggesting bone metastasis (n=2), lymph node metastasis (n=5), lung metastasis (n=1), and local recurrence (n=1) in seven patients were considered recurrence/metastasis, based on clinical follow-up. The detection rates for suspected lesions were comparable between 1-hr and 3-hr post-injection, while maximum standardized uptake value (SUVmax) tended to be higher in 3-hr images (5.3-26.5) than in 1-hr post-injection (2.7-15.2). Positive results were obtained in all patients when their PSA levels exceeded 2 ng/mL. Physiological uptake was seen in lacrimal glands (mean SUVmax at 1h, mean SUVmax at 3h = 9.4, 11.8), parotid glands (12.1, 15.4), submandibular glands (12.2, 16.0), sublingual glands (6.3, 7.3), liver (5.3, 6.8)*, spleen (4.1, 3.3), renal cortex (21.2, 22.9), and duodenum (7.4, 10.9), and they increased over time except in the spleen. *: SUVmean ***Conclusion:*** Our preliminary data suggest that ^{18}F-FSU880 would be a new promising tracer for detecting metastasis/recurrence in patients with biochemical recurrence of prostate cancer. ***References:*** [1] Harada N, Kimura H, Onoe S, et al. Synthesis and biologic evaluation of novel 18F-labeled probes targeting prostate-specific membrane antigen for PET of prostate cancer. J Nucl Med. 2016; 57: 1978-1984. [2] Saga T, Nakamoto Y, Ishimori T, et al. Initial evaluation of PET/CT with (18) F-FSU-880 targeting prostate-specific membrane antigen in prostate cancer patients. Cancer Sci. 2019; 110: 742-750.

OP-338

Impact of Targeted Molecular Imaging with ^{18}F-PSMA-1007 and ^{68}Ga-PSMA-11 PET/CT in Multimodal Evaluation of Local Recurrence of Prostate Cancer

L. Dronka[1,2], M. Radzina[1,2], M. Tirane[1,2], L. Zemniece[1], M. Kalnina[1,3], L. Roznere[2,3], I. Briede[4], V. Lietuvietis[5], A. Freimanis[5], E. Vjaters[6]; [1]Institute of Radiology, Pauls Stradins Clinical University Hospital, Riga, LATVIA, [2]Riga Stradins University Radiology Research Laboratory, Riga, LATVIA, [3]Riga Stradins University Nuclear Medicine Clinic, Riga, LATVIA, [4]Center of Patology, Pauls Stradins Clinical University Hospital, Riga, LATVIA, [5]Center of Urology, Riga East University Hospital, Riga, LATVIA, [6]Center of Urology, Pauls Stradins Clinical University Hospital, Riga, LATVIA.

Aim/Introduction: Recurrent prostate cancer (PCa) can be assessed by magnetic resonance imaging (MRI) and positron emission tomography (PET/CT). The aim was to compare the diagnostic tools - MRI, ^{68}Ga-PSMA-11 and ^{18}F-PSMA-1007 PET/CT for evaluation of local recurrence. ***Materials and Methods:*** In this prospective study were included 54 patients (32 patients underwent ^{68}Ga-PSMA-11 PET/CT and 22 patients - ^{18}F-PSMA-1007 PET/CT) with biochemical recurrent PCa (with PSA ≥0.2 ng/ml) who were previously treated with radical prostatectomy and/or radiation therapy of prostate bed. The probability of a ^{68}Ga-PSMA-11 or ^{18}F-PSMA-1007 PET/CT scan suggestive of pathology was compared with the MRI Imaging results. The results of MRI and PET/CT were compared using reference standard that was based on clinical data of patient and/or results of histology material and/or follow-up information. ***Results:*** Total 54 patients were divided in two groups - ^{68}Ga-PSMA-11 and ^{18}F-PSMA-1007 group. Mean patient age in groups - 63±7 vs. 66±7 years, age range 49-81 vs. 52-77. Mean PSA value at the time of the studies were 2.27 ng/ml vs. 1.97 ng/ml, median PSA 1.07 ng/ml vs. 0.86 ng/ml. Median Gleason score 7 vs. 7, range 5-10 vs. 5-9. PSA median doubling time 4.63 months vs. 5.73 months. PET/CT ^{68}Ga-PSMA-11 local recurrence findings were in 38% (n=12/32) patients, in MRI - 37 % (n=11/30). The mean SUVmax value of recurrent local lesions was 5.3. Against the standard of reference, sensitivity, specificity, accuracy, PPV and NPV for local recurrence of PET/CT were 63.6 %; 73.7%; 77.8; 58.3% and 77.8%, respectively. MRI reached 90.9%; 94.7%; 92.3%, 90.9% and 94.7% respectively. In PET/CT ^{18}F-PSMA-1007 group local recurrence findings were detected by PET/CT in 41 % (n=9/22), in MRI - 30% (n=6/20). The mean SUVmax value of recurrent local lesions was 7.1. Sensitivity, specificity, accuracy, PPV and NPV for ^{18}F-PSMA-1007 PET/CT and MRI were 100%, 92.9%, 95.5%, 88.9%, 100% and 62.5%, 91.7%, 80%, 83.3%, 78.6%, respectively. ***Conclusion:*** Our comparative study results revealed ^{18}F-PSMA-1007 PET/CT as superior diagnostic tool to MRI and ^{68}Ga-PSMA-11 PET/CT for evaluation of local recurrence. Low urinary background clearance of ^{18}F-PSMA-1007 provide higher diagnostic value

of PET/CT in evaluation of the prostate bed and pelvis in recurrent PCa patients. ***References:*** None

OP-339

Parameters Predicting [^{18}F]PSMA-1007 scan Positivity and Type and Number of Detected Lesions in patients with Biochemical Recurrence of Prostate Cancer

N. Ahmadi Bidakhvidi[1], *A. Laenen*[2], *S. Jentjens*[1], *C. M. Deroose*[1], *K. Van Laere*[1], *C. Berghen*[3], *K. Haustermans*[3], *S. Joniau*[4], *W. Everaerts*[4], *K. Goffin*[1];
[1]*Nuclear Medicine, University Hospitals Leuven, Leuven, BELGIUM,* [2]*Interuniversity Institute for Biostatistics and Statistical Bioinformatics, Leuven, BELGIUM,* [3]*Radiation Oncology, University Hospitals Leuven, Leuven, BELGIUM,* [4]*Urology, University Hospitals Leuven, Leuven, BELGIUM.*

Aim/Introduction: Biochemical recurrence of prostate cancer (PCa) after primary treatment with curative intent occurs in 30-50% of patients within 10 years. Detection of the site of recurrence using PSMA-PET/CT is important to guide further treatment. The aim of this study was to evaluate the positivity rate of [^{18}F]PSMA-1007-PET/CT in patients with biochemically recurrent PCa and identify parameters that predict [^{18}F]PSMA-1007-PET/CT positivity and the type and number of identified lesions. ***Materials and Methods:*** This monocentric retrospective study included 137 PCa patients with biochemical recurrence who underwent one or more [^{18}F]PSMA-1007-PET/CT scans between August 2018 and June 2019. [^{18}F]PSMA-1007-PET/CT was considered positive if at least one PET-positive lesion was identified (focal non-physiological tracer uptake above local background with high suspicion of malignancy). PET-positive lesions were classified as local recurrence, lymph node, bone or soft tissue metastases. A maximum of 10 PET-positive lesions per lesion type were analysed. We evaluated the influence of serum PSA, PSA doubling time and velocity, Gleason score, neo-adjuvant treatment, primary treatment, PSA after radical prostatectomy (RP), adjuvant radiation therapy (RT), salvage therapy (surgery or RT), ongoing/prior androgen deprivation therapy (ADT), injected activity and tracer uptake-time on scan positivity and type and number of detected lesions using logistic regression analysis (binary outcomes) and Poisson models (count-type outcomes). ***Results:*** We included 175 [^{18}F]PSMA-1007-PET/CTs after RP (78%), RT (9%), ADT (7%), brachytherapy (5%) and high intensity focused ultrasound (1%) as primary treatment. Median PSA and PSA velocity at moment of PET/CT were 1.6 ng/ml and 0.10 ng/ml/month, respectively. Positivity rate was 80%. PSA velocity and PSA at moment of PET/CT were significant predictors of scan positivity and were also significantly correlated with the number of detected lymph nodes, bone and soft tissue metastases. Salvage therapy was a significant negative predictor of local recurrence. Higher Gleason score was a positive predictor of the number of bone and soft tissue metastases. Increased PSA level after RP was significantly correlated with the number of bone metastases. Ongoing/prior ADT was significantly correlated with detection of bone metastases and the number of lymph node/soft tissue metastases. The other parameters were not correlated with scan positivity or number/type of detected lesions. ***Conclusion:*** [^{18}F]PSMA-1007-PET/CT showed a high positivity rate in patients with biochemically recurrent PCa. PSA velocity and PSA value at moment of scan were significant predictors of scan positivity. Together with parameters of the patient's PCa history, they also predicted the number of detected metastases. ***References:*** None

OP-340

Management impact and detection rate of 18F- Prostate-Specific Membrane Antigen (18F-PSMA) PET/CT imaging for biochemically recurrent prostate cancer

E. Panagiotidis*, A. Paschali, A. Klampatsas, A. Pipintakou, A. Makridou, V. Chatzipavlidou;*
Theageneio Cancer Center, Thessaloniki, GREECE.

Aim/Introduction: To determine the impact on clinical management of patients with biochemical recurrence (BCR) of prostate cancer using 18F- Prostate-Specific Membrane Antigen (18F-PSMA) with positron emission tomography-computed tomography (PET-CT). ***Materials and Methods:*** Sixty-eight (68) patients (pts) had management plans documented at a multidisciplinary meeting before 18F-PSMA PET-CT. Three group of patients underwent PET-CT scans 90-min post-injection of 18F-PSMA (mean 171 ± 31.2 MBq), 47 pts had radical prostatectomy, (Group 1), 1 pts had implementation of radioactive I125 (Group 2) and 20 pts had radiotherapy in the prostatic bed (Group 3) (median age 71years, range : 50-82). Post-scan management plans, TNM score, Gleason score, prostate-specific antigen (PSA), PSA velocity and PSA doubling time (PSAdt) were recorded. ***Results:*** In total, 262 pathological lesions depicted by PET/CT. 32/68 (47%) pts had management changed. Patients with PSA < 4 μg/L had more frequent management changes (18/32, 56.25%) compared with PSA > 4 μg/L (14/32, 43.75%). Forty out of 68 (59%) scans were positive. Positivity rate increased with PSA level (PSA < 0.5 μg/L, 0%; PSA 0.5-1.0 μg/L, 25%; PSA 1.0-5.0 μg/L, 59%; PSA 5.0-10.0 μg/L, 93%), PSAdt of < 6 months (59% vs 46%) and Gleason score > 8 (81% vs 53%). ***Conclusion:*** 18F-PSMA PET-CT influences clinical management in significant numbers of patient with biochemical recurrent prostate cancer. Therapeutic alteration is associated with PSA and Gleason score, despite lower scan positivity rates at low PSA levels < 0.5 μg/L. ***References:*** None

OP-341

18F-Choline PET/CT in the evaluation of high-risk prostate cancer outcome: an explorative study on radiomics feature classification for prediction of disease progression

P. Alongi[1], A. Stefano[2], A. Comelli[3], R. Laudicella[4], G. Arnone[5], S. Barone[5], M. Midiri[5], G. Russo[2];
[1]Istituto San Raffaele G.Giglio, Cefalù PA, ITALY, [2]Institute of Molecular Bioimaging and Physiology, National Research Council (CNR), Cefalù PA, ITALY, [3]Department of Electrical and Computer Engineering, Georgia Institute of Technology, Atlanta, GA, UNITED STATES OF AMERICA, [4]Department of Biomedical and Dental Sciences and of Morpho-functional Imaging, Nuclear Medicine Unit, University of Messina, Messina, ITALY, [5]University of Palermo, Palermo, ITALY.

Aim/Introduction: The aim of the study was to investigate the potential application of texture analysis of Cho-PET/CT images in prostate cancer and to propose a model incorporating a new machine-learning radiomics model to select PET imaging features able to predict disease progression in prostate cancer (PCa) in patients with the same class of risk at re-staging. ***Materials and Methods:*** We retrospectively analyzed 94 high-risk PC patients who underwent restaging Cho-PET/CT after first-line therapy. Follow-up data about clinical, laboratory and radiological exams were recorded for a time of 24 months after PET. PET studies and related structures containing volumetric segmentation using an active contour method were imported in LifeX toolbox to extract 51 imaging features from each lesion by defining subgroups as follow: primary or local relapse; lymph-nodal disease; bone metastasis; whole sample). In addition, PSA and Gleason score features were considered (51+2=53 features). Due to the redundancy, heterogeneity and uncertainty of the information represented by radiomics features, a novel statistical system based on correlation matrix and point-biserial correlation coefficient has been implemented for feature reduction and selection, while Discriminant Analysis (DA) was used as a method for feature classification in a whole sample (all lesions in 94 patients) and in sub-group analysis for T, N and M. ***Results:*** The most Cho-PET avid lesions (for T, N and M = 134 lesions) were examined for texture analysis in the whole group (N=94): 53 features were extracted for each lesion for a total of 7102. After statistical reduction and selection in the whole group, 2 features (HISTO_Entropy_log10; HISTO_Energy_Uniformity)) resulted able to discriminate the occurrence of disease progression at follow-up, obtaining the best performance in DA classification and improving the FU status assessment (Sensitivity 47.11%, Specificity 76.54%, Precision 46.78%, and Accuracy 67.66%). In the sub-group analysis, the same method demonstrates the best performance in DA classification for T (N=38) in 3 features (SUVmin; SHAPE_Sphericity; GLCM_Correlation) with Sensitivity 91.59%, Specificity 84.06%, Precision 79.14, and Accuracy 86.99%, for N (N=44) in 2 features (HIST=_Energy Uniformity; GLZLM_SZLGE) with Sensitivity 68.09%, Specificity 91.42%, Precision 83.00%, and Accuracy 82.59%, and for M (N=52) 2 Features (HISTO_Entropy_log10 - HISTO_Entropy_log2) with Sensitivity 64.39 %, Specificity 74.60 %, Precision 40.55 %, and Accuracy 72.52 %. ***Conclusion:*** The presented artificial intelligence model demonstrated to be feasible and potentially useful to select Cho-PET features for T , N and M with valuable association with High-Risk PCa patients' outcomes. ***References:*** None

609

TROP Session: Nuclear Playground - Nuclear Medicine in Children and Adolescents

Friday, October 23, 2020, 13:50 - 15:20 Channel 9

OP-342

PET metabolic tumor volume as a prognostic factor in childhood rhabdomyosarcoma: a cohort study

H. Fayolle[1], N. Jehanno[2], V. Cances-Lauwers[3], M. Castex[4], D. Orbach[5], P. Payoux[6], A. Hitzel[1];
[1]Nuclear Medicine Department, CHU Purpan, Toulouse, FRANCE, [2]Nuclear Medicine Department, Institut Curie, Paris, FRANCE, [3]Epidemiology and Public Health department, Toulouse, FRANCE, [4]Pediatric Hemato-oncology Department, Toulouse, FRANCE, [5]IREDO Oncology Center, PSL University, Institut Curie, Paris, FRANCE, [6]ToNIC, INSERM, Toulouse, FRANCE.

Aim/Introduction: Childhood rhabdomyosarcoma (RMS) is a rare and serious disease in which evaluation at diagnosis is essential for therapeutic management. We studied the prognostic value of the metabolic tumor volume measured from a pre-treatment18F-FDG PET scan in this disease. ***Materials and Methods:*** This multicenter study examined the prognosis accuracy of the metabolic tumor volume at diagnosis of patients with RMS from the last ten years, for overall survival and progression-free survival. Then we looked at of other prognostic parameters such as SUVmax, SUVpeak or bone lysis. ***Results:*** A total of 101 patients were included in 6 French university hospitals. In univariate analysis a metabolic volume greater than 200 cm^3 was predictive of overall survival ((HR = 3.47 [1.79; 6.74], p <0.001) and progression-free survival (HR = 3.03 [1.51; 6.07], p=0.002). SUVmax, SUVpeak and bone lysis were prognostic of overall survival (p=0.005, p=0.004 and p=0.007) and progression-free survival (p=0.029, p=0.019 and p=0.015). In the multivariate analysis a metabolic volume greater than 200 cm^3 was predictive of overall survival (HR= 2.642 [1.272;5.486], p=0.009) and progression-free survival (HR=2.707 [1.322;5.547], p=0.006) after adjustment for confounding factors including SUVmax, SUVpeak and

bone lysis. ***Conclusion:*** 18F-FDG PET imaging is currently used for RMS disease staging. In our study, a metabolic tumor volume greater than 200 cm^3, SUVmax, SUVpeak and bone lysis in the pre-treatment assessment were poor prognostic factors for overall survival and progression-free survival. Children presenting tumors with a metabolic volume of more than 200 cm3 had approximately 2.6 and 2.7 times the risk of death and progression, respectively, after adjusting for confounding factors. It should be worth validating the prognostic advantage of measuring the metabolic volume on a larger patient population. ***References:*** 1. Casey DL, Wexler LH, Fox JJ, Dharmarajan KV, Schoder H, Price AN, et al. Predicting outcome in patients with rhabdomyosarcoma: role of [(18)f]fluorodeoxyglucose positron emission tomography. Int J Radiat Oncol Biol Phys. 1 déc 2014;90(5):113642. 2. Ferrari A, Miceli R, Meazza C, Casanova M, Favini F, Morosi C, et al. Comparison of the prognostic value of assessing tumor diameter versus tumor volume at diagnosis or in response to initial chemotherapy in rhabdomyosarcoma. J Clin Oncol Off J Am Soc Clin Oncol. 10 mars 2010;28(8):13228. 3. Baum SH, Frühwald M, Rahbar K, Wessling J, Schober O, Weckesser M. Contribution of PET/CT to prediction of outcome in children and young adults with rhabdomyosarcoma. J Nucl Med Off Publ Soc Nucl Med. oct 2011;52(10):153540.

OP-343

Risk Stratification Using 18 FDG PET/CT In High Risk Neuroblastomas :Is It Comparable With 131I-Metaiodobenzylguanidine (MIBG)

C. Bongulwar*, S. Shah, N. Purandare, A. Agrawal, V. Rangarajan;*
Tata Memorial Hospital, Mumbai, INDIA.

Aim/Introduction:Radioiodinatedmetaiodobenzylguanidine (mIBG) is an established imaging modality in neuroblastoma. Semiquantiative scoring -SIOPEN [International Society of Pediatric Oncology Europe Neuroblastoma Group] and Modified Curie using radiolabelled MIBG are used for prognostication in high risk neuroblastomas. The present study aims to use 18F -fluorodeoxyglucose (FDG) for semiquantitative scoring and compares it with mIBG scores thereby validating it for risk stratification. ***Materials and Methods:*** Data of 90 patients were retrospectively analyzed diagnosed to have stage IV high risk neuroblastoma. MIBG scans were assessed according to the SIOPEN and the modified Curie scoring method .Similarly 18 F FDG PET/CT scans were also scored using these semi quantitative systems. The paired scans were compared at initial staging and end of induction therapy. A Curie score of </=2 and > 2 and a SIOPEN score </=4 and >4 (best cutoff) described in previous studies was used to classify these scans into low and high risk and subsequently correlated with the clinical course of the disease. ***Results:*** At initial staging there was a statistically significant difference between the Curie-FDG scores of (10.94 ± 10.0)as compared to mIBG score of (7.99 ± 9.00)with an increase of 2.94 with p=0.001.Also for SIOPEN -FDG scores of (20.00 ± 26.00) against mIBG (11.72 ± 20.00) with a difference of 8.27 and p=0.12.At end of induction therapy there was no statistically significant difference (p >0.01)between the Curie FDG and MIBG scores. Using the standard cut off values for Curie and SIOPEN scores 18 patients show discordance out of which 6 patients (33%) showed disease progression or death. ***Conclusion:*** Modified CURIE score and SIOPEN score using 18F FDG shows an incremental value over MIBG score and can be correlated with the clinical outcome of the disease .The Modified Curie and SIOPEN score can be validated using 18 F FDG PET/CT establishing their role in risk stratification ***References:*** Borris decoralis et al Boris Decarolis, Christina Schneider, Barbara Hero, Thorsten Simon, Ruth Volland, Frederick Roels,Markus Dietlein, Frank Berthold, and Matthias Schmidt Iodine-123 Metaiodobenzylguanidine Scintigraphy Scoring allows Prediction of Outcome in Patients With Stage 4 Neuroblastoma:Results of the Cologne Interscore Comparison Study2013 -JCO Matthay KK, Edeline V, Lombroso J, et al: Correlation of early metastatic response by123Imetaiodobenzylguanidinescintigraphy with overall response and event-free survivalin stage IV neuroblastoma. J Clin Oncol 21:2486-2491, 2003

OP-344

Comparison of ^{18}F-FDG PET/CT with Anatomic Imaging Methods in Pediatric Neuroblastoma

M. Engin*, A. Arcay, Z. G. Kiprak, C. N. Dundar Caglayan, G. G. Bural, A. Boz;*
Akdeniz university faculty of medicine nuclear medicine department, Antalya, TURKEY.

Aim/Introduction: Neuroblastoma is the most common extracranial malignant solid tumor in the pediatric age group and ranks high among the causes of cancer-related death in children with a rate of approximately 15% (1). Performing appropriate imaging modalities during staging and follow-up would lead to selection of appropriate treatment protocols and improve patient survival. In this study, it was aimed to compare the effectiveness of ^{18}F-FDG PET/CT imaging with anatomical imaging methods (CT, MRI) in patients with neuroblastoma. ***Materials and Methods:*** We enrolled 15 pediatric patients (7 girls, 8 boys; age range 1-10 years) with histopathologically proven neuroblastoma, who had both FDG PET/CT and anatomical imaging (CT or MRI) between November 2015 and March 2020 for staging and restaging. Twenty FDG PET/CT studies were compared with the findings of anatomical imaging methods (CT, MRI). Equivocal findings were correlated with clinical and follow-up imaging. ***Results:*** Of the 20 FDG PET/CT images included in the study, 11 were for

staging, 6 for treatment response evaluation, and 3 for restaging. All primary tumors were detected by both FDG PET/CT and anatomical imaging methods. In 8/20 (40%) examination bone and bone marrow metastases and in 5/20 (25%) examination, cervical, supraclavicular, mediastinal, anterior diaphragmatic and pelvic metastatic lymph nodes were detected by only FDG PET/CT. Findings suggesting pulmonary infection on anatomical imaging in one patient were evaluated in favor of metastasis on FDG PET/CT, and lesions were compatible with metastasis in accordance with clinical and follow-up findings. In one patient, the findings interpreted in favor of metastatic lung nodules with FDG PET/CT resulted in diagnosis of infection in accordance with anatomical imaging methods, clinical and laboratory findings. In four patients; liver metastasis, millimetric metastatic abdominal and pelvic lymph nodes, millimetric lytic bone metastases, spinal canal invasion and adrenal recurrence detected on CT or MRI, could not be detected with FDG PET/CT. ***Conclusion:*** In the pediatric patients diagnosed with neuroblastoma, ^{18}F-FDG PET/CT is superior to the anatomical imaging methods in the detection of bone, bone marrow and distant lymph node metastases. In a few cases, with small lesion size and extra-adrenal organ metastases, anatomical imaging methods may be required as a complementary examination. For the detection of the primary tumor site, there was no difference between ^{18}F-FDG PET/CT and anatomical imaging methods. ***References:*** 1-Park J.R., Eggert A.,and Caron H.: Neuroblastoma: biology, prognosis, and treatment.Pediatric Clin North Am 2008; 55: pp.97-120

OP-346

SIOPEN SCORING vs 3 Simplified Scoring Systems in Pediatric Patients with HR-NB-1 and L2-NB

C. Olianti[1], A. Martini[1], R. Di Dato[1], M. Allocca[1], A. Tondo[2], H. Gauthier[3];
[1]University Hospital of Florence, Florence, ITALY, [2]University Hospital Meyer of Florence, Florence, ITALY, [3]Oscar Lamberet Center, Lille, FRANCE.

Aim/Introduction: SIOPEN scoring system SIOPEN-SS (12 anatomical body segments with a 0-6 scale and 72 as maximal score) is used to semiquantify metastatic tumor load (TL) in HR-NB to stratify patients with good versus poor response to therapy (1): a cut-off score &#8804 3 was the most useful predictor across trials to define good responders and a tumor load at staging 0-23 correlates with a better EFS vs 24-47 and 48-72. We tested the ability of 3 simplified methods to define TL and response to therapy. ***Materials and Methods:*** To compare the SIOPEN-SS and the three proposed Simplified Scoring System (SSS), 14 pediatric patients HR-NB-1 and 14 intermediate or low risk-NB referred to Nuclear Medicine for I-123 MIBG scintigraphy (January 2009 - February 2019) were investigated by 123I-MIBG scans for staging, response to therapy, after surgery, after radiotherapy, off-therapy for a total of 92 planar whole-body plus SPECT scans. The studies included 9 F and 19 M (mean age 4.14 &#177 2.85 years at the first scintigraphy). SSS1 analyzes three great sector: neural, body and arms, with the same SIOPEN 0-6 scale, SSS2 analyzes three great sector: neural, body and arms, with a simplified 0-4 scale, SSS3 analysis 12 body segments as SIOPEN scoring, with a simplified 0-2 scale. Total number of discrete lesions is also reported. ***Results:*** Obviously statistical analysis showed a huge correlation between SIOPEN and three SSS scorings : Rho Spearman : 1.000, 0.988 and 0.982 between SIOPEN and respectively SSS1, SSS2 and SSS3 ($p<0.000$). Graphical representation of SSS 1, 2 and 3 versus SIOPEN-SS taken as gold standard, shows an exponential trend of values with a plateau towards 24 in SSS3, towards 12 in SSS2 and a linear correlation in SSS1 (R^2linear =0,993). Regression Analysis with estimate of curves shows a logarithm trend for SSS2 and a hyperbolic trend for 1/SSS2 vs SIOPEN. ***Conclusion:*** SSS1 and SSS3 don't bring a real advantage respect SIOPEN-SS cause the first has the same grading in lesions-extension characterization, and the second has the same numbers of segments. Otherwise the SSS2 seems bring a real benefit in terms of simplification both for number of segments and grading of lesion-extension without a significant lost of accuracy for each patient. SSS2 should be tested on a selected larger cohort of HR-NB, to verify prognostic impact respect SIOPEN scoring system. ***References:*** 1) Eur J Nucl Med Mol Imaging. 2018 February; 45:292-305, DOI 10.1007/s00259-017-3829-7

OP-347

Do SUV values reflect completely accurate results especially in pediatric cases?

O. Ozmen[1]*, S. Beykan[2], E. Tatcı[1];*
[1]University of Health Sciences Atatürk Chest Diseases and Thoracic Surgery Training and Research Hospital, Ankara, TURKEY, [2]Klinik fuer Nuklearmedizin Universitaetsklinikum Wuerzburg, Wuerzburg, GERMANY.

Aim/Introduction: In FDG PET/CT studies, SUV is a useful parameter in distinguishing malignant lesions from benign lesions and evaluating the treatment response in cancer patients. SUVs are mainly depend on patients' weight and injected activity, however, in practice there are several sources of bias and variance of calculation. The variety might be critical especially pediatric patients due to significant change in weight and brain volume. The aim is to analyze the patient-specific FDG uptake in brain and liver of pediatric and adult patients. And investigate the correlation of the SUVweight and SUVlbm of liver between pediatric and adult patients ***Materials and Methods:*** Images of 53 pediatric (23F,30M age:3-17y , weight:12-97kg , injected activity: 90-519 MBq) and 25 adult patients (7F,18M

age:22-86y, weight:60-104 kg, injected activity:310 - 565 MBq) who underwent FDG PET/CT imaging for oncological purposes were evaluated retrospectively. Pediatric patients were investigated in three groups as 3-7 years, 8-12 years, 13-17 years. The percentage injected activities (A%) in brain, bladder, liver and whole-body are calculated for all patients. In addition, Liver SUVweight and SUVlbm were calculated for all patients. ***Results***: A% of brain per injected activity was higher in pediatric patients approximately as a factor of 8 (for 3-7 years), 5 (for 8-12 years), and 2 (for 13-17 years) in compare to adults. This is highly related to brain volume. The difference between liver SUVweight and SUVlbm were 20% for adult and patient group-iii whereas the difference was ±2% for others. There is little to no gender dependent correlation on liver SUV values in the pediatric patient groups 3-7year and 8-12year whereas ±12% difference was observed for other patients. Adult liver SUVs were lower than pediatric patients 57% for 3-7 years, 43% for 8-12 years and 26% for 13-17 years. ***Conclusion:*** In compare to adults, for pediatric patients, majority of the injected activity accumulated in the brain since brain-to-Whole-body volume ratio in pediatric patients are higher than adults. This directly resulted in lower SUV for other tissues and tumors which may be confusing for the physician. In pediatric patients adults based reference SUVs should be carefully take into account for diagnostic evaluation. ***References:*** None

OP-348

^{18}F-FDG-PET/MR Semiquantitative Response Assessment Methods in Paediatric Hodgkin Lymphoma Patients

S. Gusella[1], *A. Spimpolo*[2], *S. Berti*[3], *F. Menegatti*[3], *C. Campi*[4,5], *M. Pillon*[6], *C. Giraudo*[7], *D. Cecchin*[3], *P. Zucchetta*[3];
[1]*Nuclear Medicine Unit, Ospedale di Bolzano, Bolzano, ITALY,* [2]*Nuclear Medicine Unit, Department of Medicine, PhD Student International PhD Program in Arterial Hypertension and Vascular Biology, University of Padova, Padua, ITALY,* [3]*Nuclear Medicine Unit, Department of Medicine, University of Padova, Padua, ITALY,* [4]*Department of Mathematics "Tullio Levi-Civita", University of Padova, Padua, ITALY,* [5]*Padova Neuroscience Center, University of Padova, Padua, ITALY,* [6]*Clinic of Paediatric Haematology-Oncology, Department of Women's and Children's Health, University of Padova, Padua, ITALY,* [7]*Institute of Radiology, Department of Medicine, University of Padova, Padua, ITALY.*

Aim/Introduction: Deauville score (DS) has proved to be a reliable qualitative method for ^{18}F-FDG-PET-based response assessment in paediatric Hodgkin Lymphoma (HL). PET/MR is a recommended imaging modality for paediatric patients, thanks to its lower radiation exposure in comparison with PET/CT. A number of semiquantitative measures might be derived, whose consistency is still to be validated. The aim of our study was to evaluate the correlation between commonly used semiquantitative parameters, such as ΔSUVmax, ΔSUVpeak and qPET with DS and response categories (CMR, PMR, NMR, PMD) in paediatric HL patients undergoing ^{18}F-FDG-PET/MRI scans both at baseline (sPET) and at interim (iPET). ***Materials and Methods:*** We retrospectively evaluated 30 consecutive paediatric HL patients who underwent n. 60 ^{18}F-FDG-PET/MR investigations (sPET and iPET) at Our Institution. All PET images were analysed using a research-dedicated software. Spherical VOIs were manually drawn on the 6 hottest lesions of sPET and on areas of residual uptake of iPET images. After isocontouring with a fixed 41%-of-SUVmax threshold, lesion ΔSUVmax and ΔSUVpeak were calculated. In order to derive the qPET parameter, liver uptake was used according to Hasenclever et al.[1] Each parameter was calculated using bw-, bsa-, and lbm-SUV values. Treatment response categories (CMR, PMR, NMR and PMD) were determined according to the Lugano criteria and correlation with the above-mentioned parameters was calculated. Kruskal-Wallis nonparametric test was used to compare median values of each semiquantitative parameter both in the different DS and response categories subgroups. ***Results:*** Two out of thirty HL patients (M:F=12:18, age range: 8-18) were excluded since no iPET residual uptake areas were present or brown fat activation impaired VOIs positioning. The SUV normalization method did not influence the qPET capacity of differentiating between DS3, DS4 and DS5, and between PMR and CMR categories ($p < 0.01$). Similar results were obtained for ΔSUVmax and ΔSUVpeak even if more intra-group variability was observed ($p \leq 0.01$). ***Conclusion:*** In paediatric HL patients undergoing ^{18}F-FDG-PET/MR at interim, qPET proved to reliably differentiate among DS and response categories. The use of different SUV normalization methods did not significantly affect the qPET performance. ***References:*** 1. Hasenclever D, Kurch L, Mauz-Körholz C, et al. qPET - a quantitative extension of the Deauville scale to assess response in interim FDG-PET scans in lymphoma. Eur J Nucl Med Mol Imaging 2014;41(7):1301-8.

OP-349

Assessment of prognostic value of baseline ^{18}FDG PET/CT metabolic parameters (SUV max, MTV and TLG) and treatment response on ^{18}FDG PET/CT scan in patients of Langerhan Cell histiocytosis

M. Pereira, *S. Shah, A. Puranik, A. Bedmutha, A. Agrawal, N. Purandare, V. Rangarajan;*
Tata Memorial Hospital, HBNI, Mumbai, INDIA.

Aim/Introduction: To assess prognostic value of baseline FDG PET/CT metabolic parameters (SUV max, MTV and TLG) and treatment response on FDG PET/CT scan in patients of Langerhan Cell histiocytosis (LCH) ***Materials and Methods:*** Between August 2010 and March 2019, 36 paediatric patients with LCH were treated with chemotherapy in our institution and their baseline and post chemotherapy

PET/CT scans were reviewed. The SUV max, MTV and TLG parameters of LCH lesions were recorded.These PET parameters were correlated with disease free survival. Also post chemotherapy PET-CT scans were reviewed for treatment response into categories based on visual scoring (good response: uptake<= liver; no response : uptake > liver)The treatment response on FDG PET/CT was correlated DFS.Follow-up time was analyzed from the last day of chemotherapy to the date of the last follow-up, recurrence, or death. DFS rate was calculated using Kaplan-Meier analysis stratified according to cut-off value (median value) and compared using the log-rank test. ***Results:*** At a median follow-up time of 27 months (range, 1 to 100 months), the disease-freesurvival (DFS) rate was 83.4% respectively.Baseline PET parameters, SUV max, MTV and TLG of LCH lesions showed no statistically significant correlation with DFS (p=0.8, p=0.9, p=0.5 respectively) Of the 36 patients of LCH, 8 patients (22%) developed recurrence, from which 5 patients had complete response and 3 showed stable or progressive disease post treatment. Hence correlation of treatment response on PET-CT with clinical outcome of patients did not achieve a statistical significance (p =0.1). ***Conclusion:*** None of the baseline PET-CT parameters were an independent prognosticator of disease free survivalTreatment response on FDG PET/CT did not correlate with clinical outcome in patients with LCH ***References:*** None

OP-350

Correlation between ^{18}F-DOPA PET/CT findings and genetic mutation analysis in patients with persistent hyperinsulinemic hypoglycemia

S. Sagar*, N. Damle, R. Sharma, K. Reddy, T. Subudhi, V. Jain, C. Bal, M. Tripathi, M. Jana;*
AIIMS, Delhi, INDIA.

Aim/Introduction: Persistent hyperinsulinemic hypoglycaemia is a rare but life threatening disease of infancy and childhood. ^{18}F-DOPA PET/CT has been shown to be a useful modality in the localization of focal pancreatic lesions in these patients. We aimed to assess the role of ^{18}F-DOPA PET/CT in such patients at our institution. ***Materials and Methods:*** ^{18}F-DOPA PET/CT scans and clinical details of 22 children with clinical diagnosis of hyperinsulinemic hypoglycemia were reviewed. Scans were acquired at 5 min post-injection of 2-3 mCi of ^{18}F-DOPA on dedicated PET/CT scanners (Biograph mCT, Siemens Inc and Discovery PET/CT, GE). Abdominal spot images over 1-2 bed positions were acquired. Additionally, genetic mutation status was correlated to the scan findings in some children. ***Results:*** In this ethically approved study, out of 22 children (9 female and 13 male), 14 were infants. The age of the children ranged from 1 month to 8 years. Sixteen children had undergone gene analysis, 13 were positive for ABCC8, 1 for GLUD-1, 1 for GCK mutations and 1 had not showed any mutation. ^{18}F-DOPA PET/CT scan showed 5 focal pancreatic lesions in 5 children (1 in each), two focal lesions in 1 child and diffuse pancreatic uptake in 16 children. Of the 13 ABCC8 mutation positive children, ^{18}F-DOPA PET scan showed focal pancreatic lesion in 5 (38.4%) and diffuse uptake in 8. Of the 7 children who inherited ABCC8 paternal monoallelic recessive mutation, 5 (71.4%) were having focal pancreatic lesions on ^{18}F-DOPA PET scan. One child with GLUD-1 mutation showed multifocal pancreatic uptake, 1 with GCK mutation showed diffuse pancreatic uptake and one child with no mutation on gene analysis showed mild diffuse uptake on PET scan. However, in 6 children with unknown mutation status, ^{18}F-DOPA scan showed diffuse uptake. Two patients underwent surgery and are thriving on regular food without any complications post-surgery 19 and 8 months back respectively. Both the patients have paternally inherited ABCC8 gene mutation. All the remaining 20 patients are being managed medically with 17 patients maintained on octreotide and rest 3 maintained on diazoxide medication. ***Conclusion:*** ^{18}F-DOPA PET/CT is a useful modality for localising focal pancreatic lesions in children with persistent hyperinsulinemic hypoglycemia. The detection rate is significantly higher in patients with ABCC8 paternal monoallelic recessive gene mutation. ^{18}F-DOPA PET scan driven by genetic analysis appears to be useful in planning the management of children with hyperinsulinemic hypoglycemia . ***References:*** None

OP-351

Risk of structural persistent disease in pediatric patients with low or intermediate risk differentiated thyroid cancer

M. Manganelli[1]*, M. Klain*[1]*, E. Zampella*[1]*, F. Volpe*[1]*, L. Piscopo*[1]*, M. De Risi*[1]*, M. De Risi*[1]*, V. Gaudieri*[1]*, C. Nappi*[1]*, A. D' Antonio*[1]*, S. Limone*[1]*, L. Pace*[2]*, A. Cuocolo*[1]*;*
[1]Department of Advanced Biomedical Sciences, University Federico II of Naples, Naples, ITALY, [2]Department of Medicine, Surgery and Dentistry, University of Salerno, Salerno, ITALY.

Aim/Introduction: In pediatric patients with differentiated thyroid cancer (DTC), the risk of recurrence is high and the indication for post-operative ^{131}I administration is still debated. Aim of this study was to assess the risk of structural recurrence in pediatric DTC patients at low-intermediate risk. ***Materials and Methods:*** We retrospectively evaluated 69 pediatric patients with DTC, treated with surgery and ^{131}I. The patients were classified as low, intermediate or high risk of recurrence according to the American Thyroid Association (ATA) guidelines. We excluded 8 patients with positive serum anti-thyroglobulin antibody and 7 patients with post-operative ATA high risk, leaving 54 subjects. Follow-up was performed. The need of additional therapy or the observation of structural disease persistence, defined

as defined by histology or imaging procedures, were considered as end-point. Annualized event rate (AER), was calculated. Hazard ratios were obtained by Cox regression analyses. Disease free survival analysis was performed by Kaplan-Meier method. ***Results:*** Follow-up was available in 45 subjects. During a mean time of 64±53 months, 15 structural events occurred (33% cumulative event rate). The patients with events had higher pre-therapy thyroglobulin values (82±21 vs. 13±18, P &lt 0.001), as well as a higher prevalence of age ≤14years (53% vs. 23%, P &lt 0.05) and intermediate ATA risk (80% vs. 30%, P &lt 0.01), as compared to those without events. A TSH stimulated thyroglobulin value &gt 10 ng/ml before post-operative RAI therapy resulted the best trade-off in predicting the occurrence of events. The occurrence rate of structural events was higher in patients with thyroglobulin &gt 10 (AER 15% vs. 0.5%) and those at intermediate risk (AER 11% vs. 1.5%) (both P&lt 0.01). At multivariate analysis, a thyroglobulin level &gt 10 ng/ml resulted the only independent significant prognostic factor of structural recurrence (P &lt 0.001). At Kaplan Meier analysis, the worst prognosis was observed in patients with a serum thyroglobulin level &gt 10 ng/mL in both ATA risk and age categories (both P for trend &lt 0.001) ***Conclusion:*** In this retrospective series of pediatric patients with ATA low or intermediate risk DTC treated with surgery and RAI, post-operative elevated thyroglobulin values (&gt 10 ng/mL) have a high independent prognostic impact independently from age and ATA risk. The detection of a high serum thyroglobulin value could improve the post-surgical risk stratification and indicate RAI treatment. ***References:*** None

OP-352

Renogram Image Features and the Reproducibility of Differential Renal Function Measurements

A. Brink[1], *M. Levin*[1], *E. Libhaber*[2], *M. D. Mann*[1];
[1]*Red Cross War Memorial Children's Hospital, Department of Paediatrics, University of Cape Town, Cape Town, SOUTH AFRICA,* [2]*School of Clinical Medicine and Health Sciences Research Office, Faculty of Health Sciences, University of the Witwatersrand, Johannesburg, SOUTH AFRICA.*

Aim/Introduction: The reproducibility of differential renal function (DRF) measurements on ^{99m}Tcmercaptoacetyltriglycine (^{99m}TcMAG3) is good in most children. There is however a group with poor reproducibility which could affect clinical decision making. Factors, such as age and glomerular filtration rate (GFR), have been implicated as causes for poor reproducibility. The aim of this study is to investigate image features associated with the reproducibility of DRF measurements. ***Materials and Methods:*** The image features and reproducibility of the DRF estimates of cohort 1 (n=127) was used to identify the factors associated with reproducibility. The associations between these image features and reproducibility were then tested in a second cohort (n=227). The DRF measurements were calculated using the area under the curve method (AUC) and the Rutland Patlak method (RP). The images were visually inspected to categorise the categorical variables and processed to obtain the values of the continuous variables. The variables investigated included age and measured/ estimated GFR. The association between each variable and the reproducibility of DRF measurement was tested with univariate linear regression. The results of the univariate linear regression were used to plan the multiple linear regression combinations. All possible combinations were tested with multiple linear regression. ***Results:*** The R^2-values for goodness-to-fit for the multiple regression models ranged from 0.35 to 0.49 for AUC and 0.33 to 0.45 for RP in cohort 1 and they ranged from 0.17 to 0.22 for AUC, and 0.17 to 0.22 for RP in cohort 2. One variable, left kidney to background ratio, was significant in all the multiple linear regression combinations ($p < 0.05$). Age, right kidney to background ratio, right renal margins well defined, right renal margins poorly visualised and time visualisation right calyces were significant in most of the combinations analysed. The reproducibility of DRF measurement was decreased when the kidney to background ratio was < 2. ***Conclusion:*** The variables which predicted reproducibility for the measurement of DRF on ^{99m}TcMAG3 renograms using AUC and RP methods were left kidney to background ratio, right kidney to background ratio, right renal margins well defined, age and time visualisation right calyces. Consideration should be given to incorporating the kidney to background ratio into the renal processing screen display as a valuable quality control step. The DRF values should be interpreted with caution if the kidney to background ratio is < 2.0. ***References:*** None

OP-353

DMSA renal investigations performed with a 360° whole-body CZT SPECT camera as compared with the conventional method based on planar images from an Anger camera

A. Bahloul*, L. Imbert, G. Karcher, P. Marie, A. Verger;*
Nancy University Hospital, Vandoeuvre Les Nancy, FRANCE.

Aim/Introduction: The whole-body Veriton™ CZT-camera (Spectrum Dynamics Medical) is equipped with 12 swiveling high-resolution detectors regularly spaced over 360 degrees and covering an axial field-of view of 32 cm. These detectors may be placed in close proximity with the abdomen for adults or children and SPECT recordings may additionally be focalized on the kidney area. This study aimed to assess the results of DMSA renal scintigraphy recorded with the 360° CZT-SPECT system, as compared with results provided by conventional planar images from an Anger camera (Ecam, Siemens Healthineers). ***Materials and Methods:*** A total of 21 patients, with an age range from 6 months to

85 years (mean: 21±23 years) and who were referred for DMSA scintigraphy, were selected. The protocol involved conventional planar images on an Anger camera, equipped with a conventional high-resolution parallel hole collimator, immediately followed by an abdominal SPECT recording obtained with the CZT camera and with the addition (n=13) or not (n=8) of a focalized recording on the kidney area. Routine acquisition and reconstruction parameters were used for both cameras. The count sensitivity and the relative renal functions from right and left kidneys were compared between the two cameras, as well as the rate of visual detection of renal sequelae made by two experimented nuclear physicians. ***Results:*** Marked enhancements in count sensitivity were observed with the CZT-SPECT recording, as compared with the conventional planar recording, with mean relative increases of 70% and 180% for the recordings planned respectively without or with the use of a kidney focus. A close correlation was documented between the relative kidney functions determined with the CZT-SPECT and those obtained with the conventional camera ($y=0.92x+3.9$; $R^2=0.98$) with a mean relative difference of only 2.2±1.9% between the two modalities. The visual identification of renal sequelae was concordant in 19 of the 21 patients (90%) and on the basis of additional clinical and imaging data, the 2 discordant cases were ultimately considered as corresponding to an accurate diagnosis for the CZT-camera and not for the Anger-camera (one false-positive result and one false-negative result for the latter). ***Conclusion:*** Results from the DMSA scintigraphy recorded with this CZT-SPECT camera are highly concordant with those from the conventional planar method, but with the advantages of: (i) high diagnostic quality provided by the 3-dimensional CZT-SPECT images and (ii) high count sensitivity using CZT-SPECT, a property that might allow reduction in scan recording times and/or injected activities. ***References:*** None

610

Featured Session: Molecular Brain Tumour Imaging

Friday, October 23, 2020, 13:50 - 15:20 Channel 10

OP-354

Amino Acid PET of Brain Tumours - An Update

N. Galldiks; University Hospital Cologne, Department of Neurology, Cologne, GERMANY

OP-355

Spatial relationship between brain tumor regions assessed by 11C-Methionine and perfusion weighted imaging (PWI) in neuro-oncological lesions assessed by fully hybrid PET/MRI

P. Mapelli[1,2], *P. Scifo*[2], *M. Barbera*[3], *F. Fallanca*[2], *A. Castellano*[1,3], *V. Bettinardi*[2], *R. Menichini*[2], *A. Savi*[2], *L. Gianolli*[2], *N. Anzalone*[1,3], *M. Picchio*[1,2];

[1]*Vita-Salute San Raffaele University, Milan, ITALY,* [2]*Nuclear Medicine Department, IRCCS San Raffaele Scientific Institute, Milan, ITALY,* [3]*Neuroradiology Unit and CERMAC, IRCCS San Raffaele Scientific Institute, Milan, ITALY.*

Aim/Introduction: The aim of this analysis is to investigate the spatial relationship between PW-MRI maps and MET-PET in brain tumors by using a fully integrated PET/MRI system. ***Materials and Methods:*** Ten patients (13 lesions) with primary or secondary cerebral neoplastic diseases, characterized by Gd enhancement, underwent simultaneous 11C-MET PET/MRI. MR protocol included T1w, T2w, FLAIR, DWI, DCE and DSC PWI sequences with double Gd bolus injections and a 3D T1w post-contrast scan. Simultaneous MET-PET acquisition lasted 20 minutes on brain level. ZTE-based attenuation correction was used to account for the head bone. After the assessment of the optimal co-registration of PW-MRI and MET-PET over 3D post-contrast T1w images, a neuro-radiologist and a nuclear medicine physician manually defined the segmentation of the lesions using PMOD software. MRI lesions (Gd-VOIs) and PET lesions (PET-VOIs) have been defined on T1w enhancement and on the PET images, respectively. PET-VOIs were used to measure SUVmax, MTV and SUVmean for each lesion seen on MET-PET. Ktrans, Vp and rCBV maps have been calculated using OLEA software and the Gd-VOIs have been used to mask Ktrans, Vp and rCBV maps. DICE coefficient for each lesion of each patient was calculated to measure the overlap between the corresponding VOIs on PET and Gd-enhanced MRI. The Center of Masses (CoM) of each masked map (Ktrans, Vp, CBV and MET-PET) have been localized and the distances between MET-PET CoM and PWI CoMs have been calculated. ***Results:*** Eleven/13 lesions showed both Gd-enhancement and MET-PET uptake (mean SUVmax: 4,5; range: 2,5-10,8; mean SUVmean: 2,7; range: 1,5-6,5; MTV: 21,7, range: 0,5-94,6). Mean DICE index between PET and Gd-VOIs of the lesions was moderate (0.58 ± 015). PET-VOIs were significantly larger than Gd-VOIs (median PET-VOI: 47 cc; range 9.9-2499; median Gd-VOI: 33cc; range 4,4-1097). The distances between PWI-CoMs and PET CoM were: mean Ktrans-PET distance = 2,79 mm ± 2,60; mean Vp-PET distance = 2,82 mm ± 2,32, mean rCBV-PET distance = 3,81 mm ± 3,52, without statistical difference between distances of PWI-CoMs from PET. ***Conclusion:*** Areas defined by MET-PET and Gd-MRI seem to be able to characterize different tumour aspects (metabolic active lesions within not-enhancement and vice-versa) with moderate overlapping. Although heterogeneous histology of the lesions included in this study may have hampered the analysis, no statistical difference between distances of PWI-CoMs from PET-CoM have been observed. Our findings suggest that MET-PET

and PW-MRI provide complementary information on brain tumor biology. ***References:*** None

OP-356

Photopenic defects in gliomas with amino-acid PET and relative prognostic value: a multicentric ^{11}C-Methionine and ^{18}F-FDOPA PET experience

A. Verger[1], *T. Zaragori*[1], *A. Castello*[2], *E. Guedj*[3], *A. Girard*[4], *N. Galldiks*[5], *N. Albert*[6], *E. Lopci*[2];
[1]*Department of Nuclear Medicine and Nancyclotep Imaging Platform, CHRU Nancy, Nancy, FRANCE,* [2]*Nuclear Medicine Department, Humanitas Clinical and Research Hospital, Milan, ITALY,* [3]*Department of Nuclear Medicine, Assistance Publique Hôpitaux de Marseille, Timone University Hospital, Marseille, FRANCE,* [4]*Department of Nuclear Medicine, Eugène Marquis Center, Rennes 1 University, Rennes, FRANCE,* [5]*Dept. of Neurology, Faculty of Medicine and University Hospital Cologne, University of Cologne, Cologne, GERMANY,* [6]*Department of Nuclear Medicine, University Hospital, LMU Munich, Munich, GERMANY.*

Aim/Introduction: As an adjunct to MRI, amino-acid PET is currently recommended in newly-diagnosed gliomas. Among negative amino-acid PET scans at initial diagnosis, photopenic defects in gliomas have been reported with ^{18}F-FET PET, associated to a more aggressive clinical course as compared to isometabolic gliomas. In line with this emerging concept, we aimed to explore photopenic defects in newly diagnosed glioma patients and their prognostic value using the other two widely used amino-acid radiotracers, ^{11}C-MET and ^{18}F-FDOPA. ***Materials and Methods:*** Patients with newly diagnosed glioma and ^{11}C-MET or ^{18}F-FDOPA negative PET were retrospectively selected in this European multicentric study. Photopenic defects were identified visually and semi-quantitatively using mean tumor-to-brain ratios (TBR_{mean}), extracted from FLAIR MR image volumes. Progression free survival (PFS) calculation was based on the RANO criteria. ***Results:*** 32 ^{11}C-MET and 26 ^{18}F-FDOPA PET scans with amino-acid PET-negative gliomas were selected. Out of these 58 patients examined gliomas 16 ^{11}C-MET and 10 ^{18}F-FDOPA PET scans with photopenic defects were identified, exhibiting lower TBR_{mean} as compared to isometabolic gliomas (P<0.001). Gliomas with photopenic defects had not significantly different PFS than isometabolic gliomas in the whole-population (P=0.40), but shorter PFS in the subgroup of WHO grade II IDH-mutant astrocytomas (median PFS, 35 vs. 68 months; P=0.047). ***Conclusion:*** Photopenic defects observed with ^{11}C-MET and ^{18}F-FDOPA are able to delineate subgroups of patients with poorer outcome for patients with WHO grade II IDH-mutant astrocytomas. ***References:*** Albert NL, Weller M, Suchorska B, et al. Response Assessment in Neuro-Oncology working group and European Association for Neuro-Oncology recommendations for the clinical use of PET imaging in gliomas. Neuro-Oncol. 2016;18:1199-1208. Galldiks N, Unterrainer M, Judov N, et al. Photopenic defects on O-(2-[18F]-fluoroethyl)-L-tyrosine PET: clinical relevance in glioma patients. Neuro-Oncol. 2019;21:1331-1338.

OP-357

11C-Methionine Positron Emission Tomography/ Computed Tomography (PET/CT): a prognostic factor for disease progression and survival in patients with suspected recurrence of glioma

M. Mattoli[1], *V. Scolozzi*[2], *F. Cocciolillo*[2], *I. Marini*[2], *G. Trevisi*[3], *M. Caulo*[4], *A. Saponiero*[5], *M. Balducci*[6], *M. Calcagni*[7];
[1]*Department of Neurosciences, Imaging and Clinical Sciences, "G. d'Annunzio" Chieti-Pescara Universit, Chieti, ITALY,* [2]*Fondazione Policlinico Universitario A. Gemelli IRCCS, UOC di Medicina Nucleare, Dipartimento di Diagnostica per Immagini, Radioterapia Oncologica ed Ematologia, Rome, ITALY,* [3]*Neurosurgical Unit, Presidio Ospedaliero Santo Spirito, Pescara, ITALY,* [4]*Department of Radiology, University "G. d'Annunzio" of Chieti, Chieti, ITALY,* [5]*UOSD di Oncologia, Dipartimento di Oncologia, Presidio Cassia - S. Andrea - ASL RM1, Rome, ITALY,* [6]*Fondazione Policlinico Universitario A. Gemelli IRCCS, UOC Radioterapia Oncologica Dipartimento di Diagnostica per immagini, Radioterapia Oncologica ed Ematologia, Rome, ITALY,* [7]*Istituto di Medicina Nucleare, Università Cattolica del Sacro Cuore, Rome, ITALY.*

Aim/Introduction: Gliomas, the most common primary brain tumours, have poor prognosis. The prognostic evaluation is a crucial step in the therapeutic strategies planning. Aim: to investigate the prognostic value of 11C-methionine PET/CT (MET-PET) in patients with suspected glioma recurrence. ***Materials and Methods:*** We retrospectively analysed MET-PET of 67 patients (40males; age:48±15years) with a histological diagnosis of glioma (37/67 high-grade) performed for suspected recurrence at MRI. A 15min brain static acquisition was performed 20min after ^{11}C-methionine injection (185-200MBq). MET-PET images were qualitatively and semi-quantitively analysed. After PET-MR images co-registration, regions of interest were manually drown over the lesion (T) and contralateral normal cortex (N). SUVmax, SUVmean, SUVratio (SUVmaxT/SUVmeanN) were calculated. Mann-Whitney test was used to compare parameters between groups. ROC analysis was performed to determine the optimal parameters' threshold. Progression-free and overall survival (PFS, OS) were calculated from the MET-PET date using Kaplan-Meier method and compared using log-rank test. ***Results:*** MET-PET was positive in 46/67 (68.7%) patients. The overall median follow-up was 19 months. The one-year PFS and OS rates were 42% and 75% respectively. During follow-up, recurrence occurred in 3/21 and 43/46 patients with negative and positive MET-PET, respectively; death occurred in 1/21 and 22/46 patients with negative and positive MET-PET, respectively. Negative MET-PET patients had significant better PFS (p<0.0001) and OS

(p=0.0013) than positive MET-PET patients. Recurrence patients (46/67) showed higher SUVmax (median: 3.36vs1.1; p<0.0001), SUVmean (1.76vs1.1; p=0.0009) and SUVratio (3.38vs2.13; p<0.0001) than non-recurrence patients (21/67). The optimal thresholds indicating recurrence patients were: SUVmax>3.01 (S=67%; Sp=81%; p=0.0002), SUVmean>1.58 (S=65%; Sp=81%; p=0.0002), SUVratio>2.39 (S=80%; Sp=71%; p<0.0001). Patients with SUVmax>3.01, SUVmean>1.58 and SUVratio>2.39 had significant worse PFS (p<0.0001, p=0.0001, p<0.0001, respectively). No significant differences in PFS between high-grade and low-grade glioma patients were found. Deceased patients (23/67) showed higher SUVratio (median: 3.76vs2.43; p=0.0045) than alive patients (44/67). No significant difference in SUVmax and SUVmean between deceased and alive patients was found. The optimal threshold indicating alive patients was SUVratio<3.67 (S=52%; Sp=84%;p=0.0014). Patients with SUVratio<3.67 and low-grade glioma had better OS (p=0.0005, p=<0.0001, respectively). ***Conclusion:*** In patients with suspected glioma recurrence, qualitative and semiqualitative evaluation of MET-PET were able to predict both disease progression and survival, unlike the histological grade tumour. This clinically relevant finding highlight the better ability of functional imaging to reflect the tumour cells' behaviour, compared to grade tumour. Future PET studies with more sophisticated analysis, including dynamic quantitative parameters or machine learning-driven approaches, could identify new prognostic factors. ***References:*** None

OP-358

Clinical value of ^{18}F-FET-PET/CT in pediatric patients with central nervous system tumors

O. Kertels[1], J. Krauß[2], C. M. Monoranu[3], S. Samnick[4], A. Dierks[4], A. K. Buck[4], B. Bison[5], C. Lapa[6];
[1]Institute of Diagnostic and Interventional Radiology, University Hospital Würzburg, Würzburg, GERMANY, [2]Department of Neurosurgery, University Hospital Würzburg, Würzburg, GERMANY, [3]Department of Neuropathology, Institute for Pathology, University of Würzburg, Würzburg, GERMANY, [4]Department of Nuclear Medicine, University Hospital Würzburg, Würzburg, GERMANY, [5]Department of Neuroradiology, University Hospital Würzburg, Würzburg, GERMANY, [6]Department of Nuclear Medicine, University Hospital Augsburg, Augsburg, GERMANY.

Aim/Introduction: Positron emission tomography/computed tomography (PET/CT) with O-(2-[^{18}F]fluoroethyl)-L-tyrosine ([^{18}F]FET) is a well-established tool for the non-invasive assessment of brain tumors. However, data on its diagnostic utility and impact on clinical management in children and adolescents is limited. ***Materials and Methods:*** 21 children and young adults (13 males; mean age, 9.3 ± 5.2 years; range, 1-19 at initial diagnosis) with both [^{18}F]FET-PET/CT as well as cranial magnetic resonance imaging (cMRI) were retrospectively analyzed. Five patients presented with newly diagnosed brain tumors, in the remaining sixteen, tumor recurrence after resection and/or radio-chemotherapy was suspected. Beyond its diagnostic accuracy, impact of PET imaging on clinical decision making was assessed. Histopathology (n=12) and/or clinical and imaging follow-up (n=9) served as reference. ***Results:*** [^{18}F]FET-PET/CT was rated correctly in 16 out of 21 patients with a very good inter-reader consensus with κ = 0.83. [^{18}F]FET-PET/CT had an impact on further treatment decisions in 17 out of 21 patients with avoidance of invasive surgery or biopsy in seven patients, exact biopsy guidance in five patients, change of further treatment in another three patients and confirmation of the diagnosis in two patients. ***Conclusion:*** [^{18}F]FET-PET/CT can provide important additional information for treatment decisions in pediatric and adolescent patients with CNS tumors. ***References:*** None

OP-359

Primary diagnosis of low-grade glioma: ^{18}F-FET or ^{18}F-FCH PET? A pilot study

M. Hodolic[1], A. Golubic[2], A. Misir Krpan[3], M. Zuvic[2], M. Baucic[3], G. Mrak[4], J. Nemir[4], D. Huic[2];
[1]Nuclear Medicine Department, Faculty of Medicine and Dentistry, Palacký University Olomouc, Olomouc, CZECH REPUBLIC, [2]Department of Nuclear Medicine and Radiation Protection, University Hospital Centre Zagreb, Zagreb, CROATIA, [3]Department of Oncology, University Hospital Centre Zagreb, Zagreb, CROATIA, [4]Department of Neurosurgery, University Hospital Centre Zagreb, Zagreb, CROATIA.

Aim/Introduction: Gliomas, as one of the more commonly diagnosed primary brain tumours, are associated with variable survival, in part linked with their histological type. The diagnosis of low grade gliomas (LGG) is challenging, as results of radiological imaging modalities can often be inconclusive or equivocal. Functional imaging modalities have been introduced to provide additional metabolic information. O- (2-[18F]-fluoroethyl) -L-tyrosine (^{18}F-FET) is PET radiopharmaceutical approved for the characterisation of glioma-suggestive brain lesions. ^{18}F-FET displays a high tumour-to-background ratio and minimal accumulation in inflammatory lesions. Because of low uptake in healthy brain parenchyma, fluoromethyl-(^{18}F)-dimethyl-2-hydroxyethyl-ammonium chloride (^{18}F-FCH) has also been used for diagnosis of LGG is some european nuclear medicine units. The objective of this pilot study was to investigate the diagnostic accuracy of ^{18}F-FET and ^{18}F-FCH PET in patients with primary LGG. ***Materials and Methods:*** Eleven patients aged 21-80 years with MRI-suspected LGG were involved in this study. Patients underwent both ^{18}F-FET and ^{18}F-FCH PET/CT within one week. Brain PET/CT was performed according to standard protocol: 20 minutes after intravenous injection of 185 MBq of ^{18}F-FET and 185 MBq of ^{18}F-FCH PET. Surgery

and histological diagnoses were performed in the next two weeks. ***Results:*** Eleven out of 11 patients with suspected LGG underwent MRI, ^{18}F-FET and ^{18}F-FCH PET/CT. All patients had LGG according to MRI. In all PET positive patients, tumour location on MRI was consistent with region of PET/CT positivity. Nine out of 11 patients with suspected LGG had final histological diagnosis after the surgery. Two out of 11 patients included in this study did not undergo surgery or biopsy for histological confirmation. Both had negative ^{18}F-FET and negative ^{18}F-FCH PET scan, so they declined surgery and multidisciplinary tumour board recommended follow-up. Seven lesions positive on ^{18}F-FET PET and negative on ^{18}F-FCH PET scan were diffuse astrocytoma (grade II), ganglioma (grade I) and anaplastic astrocytoma (grade III) by pathohistology. Two lesions positive on ^{18}F-FET PET and positive on ^{18}F-FCH PET scan were glioblastoma multiforme (grade IV) by pathohistology. ***Conclusion:*** Preliminary results on a small patient sample suggest appropriate radiopharmaceutical should be chosen before performing PET/CT scan in patients with newly diagnosed LGG. ^{18}F-FET is more accurate radiopharmaceutical than ^{18}F-FCH in detection of LGG, while increased lipid synthesis seems to correlate with higher grade and more aggressive gliomas. ***References:*** None

OP-360

Is there a need for premedication with Carbidopa for static and dynamic ^{18}F-FDOPA PET imaging of brain tumors?

M. Bros*, T. Zaragori, F. Rech, M. Blonski, L. Taillandier, A. Verger; Centre Hospitalier Régional Universitaire de Nancy, Nancy, FRANCE.*

Aim/Introduction: ^{18}F-FDOPA is a PET amino-acid tracer recommended in brain tumor imaging for glioma assessment. There is currently no evidence-based recommendation for the use in this clinical setting of a premedication with Carbidopa, an inhibitor of peripheral DOPA metabolism, which increases ^{18}F-FDOPA availability during acquisitions. This study aimed to determine the impact of this premedication on conventional quantitative parameters used in the ^{18}F-FDOPA PET imaging of brain tumors. ***Materials and Methods:*** Ninety-four patients having undergone a ^{18}F-FDOPA PET for newly-diagnosed glioma, among which 72 also had dynamic acquisitions, and whom respectively 56 and 40 patients were premedicated with 100 mg of Carbidopa, were retrospectively included. Mean Standardized Uptake Values (SUVmean) were calculated on static images, as well the Time-To-Peak (TTP) and curve slope dynamic parameters, on the reference striatum and on the tumors regions. These previous quantitative parameters were also evaluated through ratios to the background. ***Results:*** In patients with Carbidopa premedication, significant higher values for SUVmean, longer TTP and more increasing slope curves were observed in the striatum as compared to quantitative parameters obtained in patients without any premedication (respective values of 3.04 vs. 2.50; 29.9 vs. 28.9 min; and 1.9 vs. 0.7 SUV/h, $p \leq 0.01$). All these differences were no more documented after using ratios to the background (1.82 vs. 1.80; 30 vs. 29.1 min; and 1.1 vs. 1.3.h^{-1}, $p > 0.29$). In tumors regions, significant higher SUVmean values (2.75 vs. 2.25, $p < 0.01$) and a tendency to a longer TTP (14.6 vs. 10.9, $p = 0.06$) were also observed in patients with Carbidopa premedication, but no significant difference remained after using ratios to the background (1.67 vs. 1.66; 8.1 vs. 11.1 min, $p > 0.13$), no differences being observed between the two groups of patients regarding the tumor molecular status ($p > 0.31$). ***Conclusion:*** The effects of Carbidopa, mainly observed for static parameters, are no more documented after using ratios to the background parameters used in clinical routine. This potentially limits the added-value of this costly and not always easily available premedication in ^{18}F-FDOPA PET imaging of brain tumors. ***References:*** Law I, Albert NL, Arbizu J, et al. Joint EANM/EANO/RANO practice guidelines/SNMMI procedure standards for imaging of gliomas using PET with radiolablled amino acids and 18F-FDG: version 1.0. Eur J Nucl Med Mol Imaging. 2019;46:540-57

OP-361

Multicentre evaluation of the clinical impact of 18F-FDOPA brain PET in the management of high grade gliomas

J. Darcourt*[1], J. Gal[1], R. Schiappa[1], V. Bourg[2], L. Taillandier[3], F. Le Jeune[4], L. Collombier[5], A. Kas[6], A. Verger[3];*
[1]Centre Antoine Lacassagne - UCA, Nice, FRANCE, [2]CHU - UCA, Nice, FRANCE, [3]CHRU, Nancy, FRANCE, [4]Centre Eugène Marquis, Rennes, FRANCE, [5]CHU, Nîmes, FRANCE, [6]CHU Hôpital Pitié-Salpêtrière, Paris, FRANCE.

Aim/Introduction: 18F-FDOPA PET is one of the nuclear medicine recommended methods for response assessment after initial treatment of high-grade gliomas (HGG) improving the differential diagnosis between tumour progression/recurrence and treatment-related changes. We present the preliminary results of a prospective multicentre trial to evaluate its practical clinical impact in this situation. ***Materials and Methods:*** 94 patients (mean age 54.7) followed after initial HGG treatment were included in 6 different centres. When MRI was not fully conclusive, a 18F-FDOPA PET-CT static acquisition was performed (10-20 min post injection of 2-3 MBq/kg of 18F-DOPA) within 28 days. PET and MRI images were coregistered. Images were visually analysed comparing tumour uptake to striatal activity (Lizarraga scale). They were considered positive when tumour uptake was equal or superior to striatal uptake. PET results were included in the clinical management of patients as follows. Multidisciplinary Neuro Oncology Board (MNOB)

meetings considered first clinical and MRI data (including perfusion and spectrometry) without knowledge of PET data and proposed a first diagnosis and a preferred treatment option (MNOB1). Then, 18F-DOPA PET images were shown and diagnosis and management were reconsidered for final decision (MNOB2). The role of PET data was evaluated by assessing the number of changes in patients' management decisions and, when unchanged, by the level of confidence in the final decision assessed on a 3 levels scale. ***Results:*** 78 patients were discussed once during MNOB meetings and 16 several times (2 to 3) leading a total of 115 studied cases. Between MNOB1 and MNOB2, diagnosis was changed in 18 cases (15.6%); leading to upstaging in 14 (12.6%) and downstaging in 4 (3.6%); management was changed in 27 cases (23.5 %). When management was unchanged, the confidence in final decision increased in 73 cases (82.9%), was unchanged in 14 cases (15.9%) and decreased in 1 cases (1.1%). ***Conclusion:*** This study confirms the usefulness of 18F-DOPA brain PET to differentiate progression/recurrence from treatment-induced changes during the follow-up of HGG. TEP-DOPA results modified patient's management in 23.5 % of the cases and improved the decision's confidence in most of the other cases. ***References:*** None

OP-362

Evaluation of PSMA expression in high grade gliomas using ^{68}Ga-PSMA PET/CT

A. Kumar[1], *S. T. ArunRaj*[1], *M. P. Yadav*[1], *S. Ballal*[1], *R. Kumar*[1], *D. Khan*[1], *A. Hemrom*[1], *K. P. Haresh*[2], *S. Gupta*[2], *N. A. Damle*[1], *A. Garg*[3], *M. Singh*[4], *M. Tripathi*[1], *C. Bal*[1];
[1]*Department of Nuclear Medicine and PET/CT, All India Institute of Medical Sciences, New Delhi, INDIA,* [2]*Department of Radiation Oncology, All India Institute of Medical Sciences, New Delhi, INDIA,* [3]*Department of Department of Neuroimaging & Interventional Neuroradiology, All India Institute of Medical Sciences, New Delhi, INDIA,* [4]*Department of Neurosurgery, All India Institute of Medical Sciences, New Delhi, INDIA.*

Aim/Introduction: Evaluation of Prostate Specific Membrane Antigen (PSMA) expression in high grade gliomas using Glu-NH-CO-NH-Lys-(Ahx)[Ga-68(HBED-CC)])(Ga-68 PSMA 11) positron emission tomography (PET) for its potential theranostic application- with the background that recurrent high grade gliomas (HGG) and brainstem (BSG) gliomas have limited therapy options. ***Materials and Methods:*** Twenty-seven patients (M:F=16:11, Age:20-60, Median-37years) with recurrent HGG (Grade III and IV of WHO classification) on follow up MRI after treatment completion and five BSG patients (M:F=1.5:1, Age:5-18 , median=11) with residual disease after treatment were prospectively evaluated using Ga-68 PSMA PET/CT. Images were acquired on Biograph-mCT scanner (Siemens Inc.) 45-60minutes after intravenous administration of 3-5mCi of Ga-68 PSMA-11. Scans were evaluated qualitatively by two experienced Nuclear medicine physicians and analysed semiquantitatively using SUVmax of the target lesion, contralateral hemisphere [Target to contralateral ratio (TCR) for HGG], parotid and centrum semiovale (CS) [Target to CS ratio for BSG]. For HGG correlation of tumor MIB-index with SUVmax tumor and TCR, difference in SUVmax values in patients with positive and negative mutations for IDH and p53 were evaluated. ***Results:*** Twenty-seven patients with recurrent HGG included 10 grade III and 17 grade IV gliomas with median MIB index of 18% (8-20%, IQR). All had recurrent lesions reported on MRI and showed increased radiotracer uptake on PSMA PET/CT (100% detection rate) with median SUVmax of 6.2 (IQR- 3.9-8.5), median SUVmean of 3.36 (IQR- 2.7-3.7) and median TCR of 35.1 (IQR, 22.1-51.9). Median recurrent lesion to parotid SUVmax ratios were 0.34 (IQR, 0.27-0.54). Two glioblastoma multiforme patients had maximum lesion to parotid ratio (>1). No significant correlation with tumor MIB index and the uptake values was noted. Significantly high SUVmax and TCR values were observed in IDH wild type gliomas (p value of 0.02). Significant difference in distribution of SUVmax was also observed between positive and negative p53 gene mutations. Among 5 patients of brain stem glioma one was midbrain glioma and 4 were diffuse intrinsic pontine glioma with median SUVmax of 4.4 (IQR- 3.5-7.9), median SUVmean of 3.0 (IQR- 2.5-4.4) and median T/CSR of 33.9 (IQR-29.8-176.0). ***Conclusion:*** High TCR of recurrent HGG and high TCSR of BSG on Ga-68 PSMA PET/CT suggest potential for theranostics with Lu-177 PSMA-617 however tumor to parotid ratios will be the limiting factor limiting patient eligibility for therapy. Significantly high SUVmax and TCR values observed in IDH wild type gliomas suggest PSMA expression to be a potential biomarker for poor prognosis. ***References:*** None

OP-363

Imaging of androgen receptor by [^{18}F]-FDHT PET/CT in patients with GBM

O. Shamni[1], *N. Zalcman*[1], *A. Mordechai*[1], *S. Moscovici*[1], *C. Alexandre*[1], *Y. Shoshan*[1], *T. Shahar*[2], *H. Charbit*[1], *M. Guterman*[1], *I. Paldor*[1], *E. Mishani*[1], *A. Lossos*[1], *M. Orevi*[1], *I. Lavon*[1];
[1]*Hadassah medical center, Jerusalem, ISRAEL,* [2]*Shaare Zedek medical center, Jerusalem, ISRAEL.*

Aim/Introduction: Glioblastoma multiforme (GBM) is the most malignant form of brain tumor and is associated with a median overall survival of 14.6 months. The androgen receptor (AR) is a member of the steroid hormone receptor superfamily which function through their ability to regulate the transcription of specific genes, some of which can promote cancer cell survival and growth. The 16β-18F-fluoro-5α-dihydrotestosterone ([^{18}F]-FDHT) PET tracer has been used clinically in metastatic prostate cancer patients and permits the detection and relative quantification of the AR. Recently we showed that AR is overexpressed in

vast majority of GBM specimens. Ninety-three percent of the GBM samples showed AR RNA overexpression and 56% demonstrated AR-protein induction. Inhibition of AR signaling with FDA approved AR antagonists induced dose-dependent death in several glioblastoma cell lines and significantly reduced the growth of human glioblastoma in a xenograft mouse model. The aim of this study was to evaluate whether [^{18}F]-FDHT PET can be employed to detect and quantify AR expression in GMB patients, and enable selection of candidates who might benefit from AR antagonist therapy. ***Materials and Methods:*** Twelve patients suspected of having GBM underwent dynamic (first 30 min) and whole-body static (later 60-80 min) [^{18}F]-FDHT PET/CT (296-370 MBq) scans, 2-4 days prior to the surgery or biopsy. Tumor tissues were collected for pathology and AR-protein expression levels were measured by western blot analysis. AR expression levels were compared to [^{18}F]-FDHT uptake (SUV_{mean} and SUV_{max}) and a correlation between AR-protein expression and [^{18}F]-FDHT tumor uptake was calculated. ***Results:*** At 60 min after injection, 7 of the 12 patients showed significantly higher tumor accumulation of [^{18}F]-FDHT, compared to reference tissue ($(SUV/Control)_{mean}$: 1.3-2.6 fold, $(SUV/control)_{max}$: 1.3-3.4 fold). The AR protein expression from the specimen was measured. In 6 of the 7 patients who had higher tumor accumulation of [^{18}F]-FDHT, the AR protein expression was also increased, in comparison to the AR protein expression of normal brain tissue (1.4-2.3 fold higher). Pearson correlation coefficient for the $(SUV/Control)_{mean}$ at 60 min after the injection versus AR protein expression was calculated and showed a high positive correlation r=0.88 (p &lt 0.002). ***Conclusion:*** The findings indicate that [^{18}F]-FDHT PET/CT can be used as a screening tool for selecting GBM patients who are candidates for therapy with AR antagonists. In addition, [^{18}F]-FDHT PET/CT could possibly be employed to monitor treatment response and/or progression during the course of AR antagonist therapy. ***References:*** None

OP-364

Hypoxia characterization in high-grade glioma: complementary role and spatial relationship of 18F-FAZA PET/CT, perfusion and diffusion brain MRI

P. Mapelli[1,2], P. Scifo[2], A. Castellano[1,3], F. Fallanca[2], G. Conte[3], V. Bettinardi[2], A. Savi[2], E. Incerti[2], A. Coliva[2], A. Compierchio[2], N. Anzalone[1,3], L. Gianolli[2], M. Picchio[1,2];
[1]Vita-Salute San Raffaele University, Milan, ITALY, [2]Nuclear Medicine Department, IRCCS San Raffaele Scientific Institute, Milan, ITALY, [3]Neuroradiology Unit and CERMAC, IRCCS San Raffaele Scientific Institute, Milan, ITALY.

Aim/Introduction: Definition of complementary value of 18F-FAZA PET/CT, perfusion and diffusion weighted MRI in assessing functional status of high-grade glioma (HGG), by assessing the mutual spatial relationship of co-registered PET and MR acquisitions. ***Materials and Methods:*** Prospective study including 20 pts with HGG. Eighteen/20 pts underwent pre-treatment 18F-FAZA PET/CT. SUV was derived for each 18-FAZA PET scan. All pts also underwent MRI (FLAIR, T2w, 3D-T1w pre- and post-contrast, diffusion and perfusion images); however, only 11/20 have been considered for analysis with 18F-FAZA in this preliminary work. FAZA-PET, MR Perfusion and Diffusion images were firstly co-registered to 3D-T1 MR. Ktrans, Vp and CBV maps were calculated from Dynamic contrast enhanced (DCE) and Dynamic Susceptibility contrast (DSC) MR images. Mean Diffusivity (MD) was calculated from Diffusion Tensor MR (DTI). 18F-FAZA SUV maps were divided by the muscle value uptake to calculate defined maps. A threshold of tumour-to-muscle (T/M)>1.2 was used to define FAZA-based VOIs (VOIsFAZA). By using these VOIsFAZA, Spearman correlations between FAZA SUV and perfusion parameters have been calculated for each subject. A second VOI has been defined in pw-maps and MD based on the Gd-enhanced regions on 3D T1 post contrast images (VOIsGd). Then, the spatial coordinates of center-of-mass (CoM) of VOI_{Gd}s in each parametric map (Ktrans, Vp, CBV,MD, FAZA) were found and relative distances were calculated for each patient. ***Results:*** With a T/M threshold of 1.2 for FAZA SUV and the 3D T1 Gd-enhancement, mean values ± SD of the volumes were: 12.4 ± 12.3cc for VOIsFAZA and 26.6±22.1cc for VOIsGd, respectively. Tumour volumes were different between the two modalities (p<0.004). Using FAZA and VOIsGd, mean values of Dice and Jaccard coefficients were 0.588±0.166 and 0.434±0.165; volume overlap was 0.612±0.254. CoMs of pw-maps and MD in the VOIsGd, were in different positions depending on the map. The relative distances from FAZA CoMs of some MR CoMs were correlated: Ktrans and Vp (p=0.000), Vp and CBV (p=0.002), Vp and MD (p=0.007) and CBV and MD (p=0.002). No differences in the distances were found between the different CoMs, neither normalizing with the volume extension. ***Conclusion:*** FAZA PET and Gd-MR enhancement provide different information on tumour hypoxia as indicated by the low similarity indexes; the similar relative distances of MR CoMs from FAZA CoM suggest that all MR parameters are more correlated among them compared to FAZA. This suggests that FAZA PET and MRI provide complementary information in HGG patients. ***References:*** None

611

e-Poster Presentation Session 5: The Thyroid and its Neighbours (The Parathyroids)

Friday, October 23, 2020, 13:50 - 15:20 Channel 11

EPS-069

Clinical Significance of Extra-thyroid ^{99m}Tc-Pertechnetate

Uptake before Initial Radioiodine Therapy for Differentiated Thyroid Carcinoma

B. Long[1,2,3], L. Yao[1,2,3], H. Yi[1,2,3], S. Chen[1,2,3], S. Jin[1,2,3], X. Ye[1,2,3], C. Lou[4];
[1]Institute of Cancer and Basic Medicine (ICBM), Chinese Academy of Science, Hangzhou, CHINA, [2]Department of Nuclear Medicine, Cancer Hospital of the University of Chinese Academy of Sciences, Hangzhou, CHINA, [3]Department of Nuclear Medicine, Zhejiang Cancer Hospital, Hangzhou, CHINA, [4]Department of Nuclear Medicine, Sir Run Run Shaw Hospital, Zhejiang University School of Medicine, Hangzhou, CHINA.

Aim/Introduction: ^{99m}Tc-pertechnetate scanning is commonly used to evaluate thyroid remnants before the initial radioiodine (RAI) therapy for differentiated thyroid carcinoma (DTC). However, extra-thyroid ^{99m}Tc-pertechnetate uptake is rarely reported. This study aimed to investigate the clinical significance of extra-thyroid ^{99m}Tc-pertechnetate uptake before the initial RAI therapy for DTC. ***Materials and Methods:*** We retrospectively analyzed 4930 RAI-treated DTC patients. Thirty-eight cases of extra-thyroid ^{99m}Tc-pertechnetate uptake were selected. The clinical features, location, location count, and extra-thyroid ^{99m}Tc-pertechnetate uptake distribution were analyzed, combined with the uptake rate, stimulated thyroglobulin (sTg) level, post-therapy whole-body scan, and curative effect. ***Results:*** Sixty-five extra-thyroid ^{99m}Tc-pertechnetate foci were detected in 38 patients. The patient proportions with abnormal uptake in the lymph nodes, lungs, and bones ere 68.4%, 10.5%, and 10.5%, respectively. The corresponding uptake rates were 0.2%, 0.2%, and 0.8%. The uptake rate was significantly lower in the lymph nodes than in the bones ($Z = -2.722$, $p = 0.019$). The uptake rate and sTg were positively correlated ($r = 0.36$, $p = 0.027$). ^{131}I uptake was found in 36 cases at the technetium uptake site, and the number of iodine uptake foci was significantly higher than that of ^{99m}Tc-pertechnetate uptake foci. The sTg value and pathological staging significantly differed between the excellent and nonexcellent response groups ($Z = 2.947$,$p = 0.003$, and $Z = 2.348$, $p = 0.019$, respectively). ***Conclusion:*** In most cases, extra-thyroid ^{99m}Tc-pertechnetate uptake before RAI therapy for DTC indicated metastasis with specific clinical features, which may have prognostic value for the judgment of the iodine uptake function and RAI therapy plan. ***References:*** None

EPS-071

Association between clinical and tumor features with postoperative thyroglobulin in pediatric papillary thyroid cancer

T. Tian, B. Liu;
West China Hospital, Sichuan University, Chengdu, CHINA.

Aim/Introduction: Postoperative pre-ablation stimulated thyroglobulin (s-Tg) has the capability of predicting the clinical outcomes in children and adolescents with thyroid cancer. However, the exact reason for the prevalence of elevated pre-ablation s-Tg in certain thyroid cancer patients without distant metastasis is unknown. The aim of our study was to systematically investigate the associations of pre-ablation s-Tg with clinical and tumor characteristics in children and adolescents with papillary thyroid cancer. ***Materials and Methods:*** A retrospective analysis of 93 children and adolescents without initial distant metastases who underwent remnant ablation was performed. Pre-ablation s-Tg after thyroid hormone withdrawal and clinical and histopathologic characteristics, according to American Thyroid Association pediatric initial risk classification system, was assessed. ***Results:*** The median age was 18 years, and the majority were female (79.6%). The pre-ablation s-Tg ranged from 0.02–902.00 ng/mL, with a median of 9.2 ng/mL. Forty-five (48.4%) patients presented elevated pre-ablation s-Tg (> 10 ng/mL). In multi-variate analyses of clinical and tumor characteristics, high-risk stratification and high neck uptake (>2%) were the independent predictive factors for the presence of elevated pre-ablation s-Tg. ***Conclusion:*** Children and adolescents with high-risk stratification and high neck uptake are likely to present a high level of pre-ablation s-Tg after surgery. Our study confirms that pre-ablation s-Tg is a useful biomarker for monitoring post-operative residual disease in pediatric thyroid cancer. ***References:*** 1. Klein Hesselink MS, Nies M, Bocca G, et al. Pediatric Differentiated Thyroid Carcinoma in The Netherlands: A Nationwide Follow-Up Study. J Clin Endocrinol Metab. 2016;101(5):2031-9.2. Schmidt Jensen J, Gronhoj C, Mirian C, et al. Incidence and Survival of Thyroid Cancer in Children, Adolescents, and Young Adults in Denmark: A Nationwide Study from 1980 to 2014. Thyroid. 2018;28(9):1128-1133. 3. Qian ZJ, Jin MC, Meister KD, et al. Pediatric Thyroid Cancer Incidence and Mortality Trends in the United States, 1973-2013. JAMA Otolaryngol Head Neck Surg. 2019; 145(7):617-6234. Bernier MO, Withrow DR, Berrington de Gonzalez A, et al. Trends in pediatric thyroid cancer incidence in the United States, 1998-2013. Cancer. 2019;125(14):2497-2505. 5. Wang J, Yu F, Shang Y, et al. Thyroid cancer: incidence and mortality trends in China, 2005-2015. Endocrine. 2020;68(1):163-173

EPS-072

Radiation dose to family members during hospitalization of pediatric thyroid cancer patients treated with radioactive iodine

H. Tissot[1], T. Henry[1], A. Cosse[2], L. Lamartina[3], M. Terroir[1], J. Hadoux[3], D. Hartl[4], E. Baudin[3], M. Schlumberger[5], N. Guilabert[2], S. Leboulleux[1];
[1]Nuclear Medecine Department, Gustave Roussy, Villejuif, FRANCE, [2]Service de Radioprotection, Gustave Roussy, Villejuif, FRANCE, [3]Endocrine Oncology, Gustave Roussy, Villejuif, FRANCE, [4]Department of Head and Neck Oncology, Thyroid Surgery Unit, Gustave Roussy, Villejuif, FRANCE, [5]Departments

of Nuclear Medicine and Endocrine Oncology, Gustave Roussy and University Paris-Saclay, Villejuif, FRANCE.

Aim/Introduction: Radioactive iodine (RAI) is often used for the treatment of pediatric thyroid cancer (TC). Given the young age of the patients, support from family members (FM) is often needed during hospitalization. RAI is a source of radiation exposure to FM that should be minimized. A dose constraint of 5 mSv per episode is deemed reasonable according to the International Atomic Energy Agency. The aim of this retrospective monocentric study was to evaluate the radiation dose received by FM accompanying pediatric patients treated with RAI in our center. ***Materials and Methods:*** Prior to hospitalization for RAI administration, FM were given an operational dosimeter to be carried when present in the hospital room. The following radiation protection recommendations were given: entering the room was allowed from RAI administration until discharge (72 hours post treatment). We encouraged multiple FM to visit a given patient, but only one relative at a time was allowed in the room; staying in the room was allowed for one person. Radiation exposure of 28 FM from 17 pediatric patients (median age 12 years, 13 females, 7 with distant metastases) treated with RAI (median 131-I activity: 2265 MBq; range: 967-3745) between 2014 and 2019 was recorded. ***Results:*** The median time during which a pediatric TC was accompanied by a FM was 20h17 (range: 3h10-64h20). During the first 24h following RAI administration, the median time spent by each FM in the room was 4h05 min (range: 51min-20h29). During the first night, 12 FM stayed in the room, 9 during the 2nd night and 10 the 3rd night. Four FM stayed 3 nights in the room. Each RAI treatment was associated with a median cumulative radiation dose for the entire family of 74.5 µSv (range: 8-545). The median cumulative radiation dose to each of the 28 FM during their entire stay at the hospital was 66 µSv (range: 2-374), and the median duration of time spent in the room was 16h35 (range: 0h51-59h50). The median cumulative radiation dose to each FM was 93 µSv during the 1st night (range: 25-229), 30 µSv during the 2nd night (range: 6-98) and 9 µSv during the 3rd night (range: 3-110). ***Conclusion:*** Levels of radiation received by family members who stay and sleep in the hospital room of pediatric TC patients treated with RAI were low. This should permit relatives to stay with their child even during the nights whenever needed. ***References:*** None

EPS-073

Post-therapeutic dosimetry and thyroglobulin concentrations are predictors of thyroid remnant tissue after radioiodine therapy

M. Herchuelz[1], *I. Duran Derijckere*[1], *B. Vanderlinden*[1], *G. Costante*[2], *R. Moreno-Reyes*[3], *P. Bourgeois*[1], *P. Flamen*[1];
[1]*Nuclear medicine department, Institut Jules Bordet, Université Libre de Bruxelles (ULB), Brussels, BELGIUM,* [2]*Endocrinology clinic, medicine department, Institut Jules Bordet Université Libre de Bruxelles (ULB), Brussels, BELGIUM,* [3]*Nuclear medicine departement, Hopital Erasme, Université Libre de Bruxelles (ULB), Brussels, BELGIUM.*

Aim/Introduction: Differentiated Thyroid Cancer (DTC) is one of the most frequent malignancies, especially among women and young adults. Radioiodine therapy (RAIT) is performed to achieve full ablation of thyroid remnants after thyroidectomy. However, persistence or recurrence of DTC after RAIT is observed in around 12.5% of patients, often requiring subsequent therapy. The aim of our study was to evaluate the predictive value of post-therapeutic dosimetry and thyroglobulin measurements to identify patients at risk for persistent or recurrent DTC post RAIT. ***Materials and Methods:*** This monocentric retrospective study enrolled patients with DTC treated with RAIT between January 2010 and October 2019. All patients were iodine-naive, non-metastatic and RAIT was realized after thyroid hormone withdrawal. Patients with positive anti-thyroglobulin antibodies were excluded. All patients performed two post-therapeutic planar scintigraphies centered on the neck area for intended dosimetry using identical acquisition parameters 24-48 hours and 120-168 hours after RAIT. Thyroglobulin (Tg) concentrations were measured the day 0 of RAIT (Tg_0) and after therapy at the same time-points as post-therapeutic scintigraphy (Tg_1). Tg_1/Tg_0 ratios were calculated, for each patient the highest ratio reached at different post-therapeutic Tg was considered for analysis. Absorbed energy to the remnants (AER) was measured in mJoules (mJ) using anterior planar scintigraphy and normalized for Tg_0. Persistence or recurrence of DTC was defined at one-year follow-up after RAIT either as nonstimulated Tg level ≥0.2 µg/L or stimulated Tg level ≥1.0 µg/L, positive thyroid bed uptake observed at WBS or suspicious finding on neck ultrasonography with pathological confirmation. ***Results:*** Out of 103 patients, 24/103 (26.2%) presented persistent or recurrent DTC at 1-year follow-up. Median Tg_0 was significantly higher (28.0 µg/L vs 3.2 µg/L, p<0.0001) and Tg_1/Tg_0 ratio were significantly lower (2.7 vs 11.9, p<0.0001) in the recurrence group as compared to the complete ablation group, ROC analysis of Tg_0 and Tg_1/Tg_0 ratio showed an AUC of 0.86 (CI95%=0.78-0.94) and 0.75 (CI95%=0.63-0.86) respectively. Median normalized AER was significantly lower in the recurrence group compared to the complete ablation group (6.7 mJ/µgTg/L vs 71.4 mJ/µgTg/L, p<0.0001). ROC analysis of normalized AER showed an AUC of 0.86 (CI95%=0.76-0.97). A cut-off value of <20 mJ/µgTg/L AER predicted persistent or recurrent DTC with a sensitivity and a specificity of 85.2% and 86.8% respectively (PPV=70%, NPV=94%). ***Conclusion:*** Post-therapeutic dosimetry and circulating Tg evaluation before and after RAIT allows more precise risk stratification of DTC after ablative radioiodine

therapy. ***References:*** None

EPS-074

Is endogenous TSH-stimulation associated with more violent cell destruction during radioiodine therapy than exogenous TSH?

I. Lopo[1], *P. Lapa*[1,2], *G. Costa*[1,2], *J. Pedroso de Lima*[1,2,3];
[1]*Serviço de Medicina Nuclear do Centro Hospitalar e Universitário de Coimbra, Coimbra, PORTUGAL,* [2]*Faculdade de Medicina da Universidade de Coimbra, Coimbra, PORTUGAL,* [3]*Instituto de Ciências Nucleares Aplicadas à Saúde (ICNAS), Coimbra, PORTUGAL.*

Aim/Introduction: Thyroglobulin (Tg) is release into the blood along with thyroid hormones. This physiologic leak is amplified by situations that promote cell destruction, like radioiodine therapy (RAI-T). It is therefore reasonable to think that the increase in serum Tg, during the days following iodine administration, may reflect the magnitude of the target cell death. In RAI-T for differentiated thyroid carcinoma (DTC), patient's preparation can be done either by thyroid hormone withdraw or by exogenous administration of rhTSH. With this study, we aim to compare the magnitude of the variation of TSH-stimulated Tg (stTg) between the two preparation methods. ***Materials and Methods:*** A total of 107 patients with DTC, admitted in our Department for the first RAI-T (January/2016-December/2019), were selected. During hospitalization for RAI-T, we collected two blood samples to measure stTg level: stTg0h (just before the radioiodine administration) and stTg48h (48 hours after radioiodine). The RAI-T variation of serum stTg was defined as the ratio between stTg48h and stTg0h (stTg-ratio). All patients were considered to have an adequate TSH stimulation and were negative for serum Tg-autoantibodies. According to the method of TSH stimulation, patients were divided in two groups: endogenous (n=47; 43.93%) vs exogenous with rhTSH (n=60; 56.07%). During follow-up, and according to the established criteria based on international guidelines, each patient was then classified as responder or no-responder to the initial treatment. Relevant demographic and clinical data available were collected (age, gender, histology, TNM-classification, radioiodine administered activity). Using SPSS for statistical analysis, a comparison between the stTg-ratio in both groups (Mann-Whitney U test) and the association between the TSH stimulation method and the therapeutic response (Chi-square test) were evaluated. ***Results:*** Statistically significant higher values of stTg-ratio were found in the group of patients prepared with endogenous-TSH (p<0.001). No difference was found between the two groups regarding to gender, tumour histology and TNM-classification. Patients in exogenous group were older (p=0.002) and were exposed to a higher radioiodine activity (p=0.002) compared to endogenous one. Responders rate were slightly better in patients prepared with thyroid hormone withdraw (p=0.046). ***Conclusion:*** Our results suggest that endogenous stimulation of TSH is associated with a more intense release of tissue-stored-Tg into the blood, indicating faster or more extensively cell destruction than the exogenous TSH-stimulation, impacting in some way the responder's rate. ***References:*** None

EPS-075

Long-term outcome of RAI remnant ablation in low-risk differentiated thyroid cancer patients

A. Tupalli*, B. Mangu, A. Hemrom, N. Mohan, C. Bal;*
All India Institute of Medical Sciences, New Delhi, INDIA.

Aim/Introduction: Post definitive surgery for thyroid carcinoma, all patients are stratified into low, intermediate, or high-risk categories, which helps in surveillance and therapeutic management decisions. If the significant remnant is present post-surgery, radioactive iodine (RAI) ablation was indicated earlier. This retrospective cohort study was designed to assess the long-term outcomes, namely, the recurrence rate and overall survival (OS) in low-risk DTC patients. ***Materials and Methods:*** The cohort of DTC patients at our center is being meticulously followed in Thyroid Clinic, Department of Nuclear Medicine, AIIMS, New Delhi since 1967. In our previous 3 randomized control trials since 1990, we had recruited 1080 (149 +509 +422) low-risk DTC patients for remnant ablation. The data of 390/1080 patients who were administered ≤30 mCi of 131I were analyzed for long term outcomes, i.e., recurrence, OS, and prognostic factors. ***Results:*** Out of 390 patients, 300 were females, and 90 were males. The median follows up period was 122.6 months. The recurrences were developed in 4/390 (1%) patients. The median time to recurrence was 77.5 months, ranging from 54 to 108 months. Two patients had loco-regional failures, 1 had pulmonary recurrence alone, and 4th one had both pulmonary and skeletal recurrences. The patient who had a recurrence in lungs and bones received 150 mCi RAI therapy, on scan proved to have TENIS, thus was put on TKI (Sorafenib). Initial serum Tg was >300 ng/ml, and subsequently, become biochemical and radiological disease-free at the end follow-up. The patient who had a recurrence in the lungs alone did not respond to RAI therapy, and TKI continued on progression but still surviving with the disease at last contact. Out of 2 Patients who had cervical lymph nodal recurrence, surgery could not be performed due to co-morbid conditions; one progressed even after RAI therapy, and TKI and other person lost to follow up immediately after recurrence. None of the low-risk patients died even after recurrence. No associated factors could be found for recurrence. Until now, no secondary hematological malignancy or any other solid organ malignancy has been observed. ***Conclusion:*** The results are very reassuring. In ATA low-risk

DTC patients, with a median follow up of 10 years, loco-regional and distant failure combined is 1%, who had received remnant ablation less than or equal to 30 mCi of 131I. ***References:*** None

EPS-076

Prognostic factors for patients with lowrisk differentiated thyroid cancer after surgery and the first I131 therapy

M. Xiao li[1,2], H. Xingmin[1,2], L. Baoping[1,2];
[1]The First Affiliated Hospital of Zhengzhou University, Zhengzhou, CHINA, [2]Henan Medical Key Laboratory of Molecular Imaging, Zhengzhou, CHINA.

Aim/Introduction: Radioactive iodine (RAI) therapy for thyroid remnant ablation is used to treat differentiated thyroid carcinoma (DTC). This study aimed to evaluate the prognostic factors for patients with low-risk DTC after surgery and adjuvant RAI therapy. ***Materials and Methods:*** From March 2015 to October 2017, patients with low-risk DTC who underwent I-131 therapy after total thyroidectomy were retrospectively analyzed. Multivariate logistic regression analyses were performed using eight variables, including age, gender, pathological type, size of primary tumor, lymph node metastasis, interval between surgery and I-131 therapy, thyroid-stimulating hormone (TSH) and stimulated postoperative thyroglobulin (sPOTg) levels before I-131 therapy. The predictive value of the independent associated factors on prognosis was assessed by receiver operating characteristic (ROC) curve ***Results:*** A total of 158 patients were included in the study, 94 (59.5%) of them were disease free after the first postoperative I-131 therapy. There were no statistical differences in any of the variables between the disease free group and persistent disease group except that of TSH and sPOTg levels before I-131 therapy (P <0.05). Multivariate analysis showed that sPOTg level was an independent prognostic factor (OR=1.100, 95%CI:1.056-1.146, P<0.001). The area under ROC curve was 0.806(95%CI: 0.739-0.873). The corresponding sensitivity and specificity of sPOTg level was 92.2% and 58.5%, respectively ***Conclusion:*** sPOTg is a prognostic factor for patients with low-risk DTC who received surgery and adjuvant I-131 therapy, and it maybe be a clinically useful marker ***References:*** None

EPS-077

Radioiodine-131 therapy during preimplantation period of pregnancy: Evaluation of uterus exposition of a patient with differentiated thyroid carcinoma

C. Happel[1], D. Gröner[1], M. Borowski[2], M. Fiebich[3], B. Schulze[4], A. Sabet[1], W. T. Kranert[1], F. Grünwald[1];
[1]University Medical Center Frankfurt, Department of Nuclear Medicine, Frankfurt, GERMANY, [2]Städtisches Klinikum Braunschweig GmbH; Institut für Röntgendiagnostik und Nuklearmedizin, Braunschweig, GERMANY, [3]Technische Hochschule Mittelhessen Gießen; Institut für Medizinische Physik und Strahlenschutz, Gießen, GERMANY, [4]Genetische Beratung und Diagnostik; Kaiserstraße 6; Frankfurt am Main, Frankfurt, GERMANY.

Aim/Introduction: To protect the unborn life, pregnancy is an absolute contraindication for radioiodine-131 therapy (RIT). Therefore, ruling out pregnancy by beta hCG pregnancy testing (PT) can be considered mandatory prior to RIT. However, a sufficient amount of hCG can at the earliest be proven in a blood sample seven days after fertilization, resulting in a given time gap of proof. ***Materials and Methods:*** A 39-year-old patient with differentiated papillary thyroid cancer (DTC) was treated with RIT. The patient declared not to be pregnant and the PT performed upon administration was negative. Subsequently, 3.721MBq of radioiodine-131 were administrated orally. One month after discharge pregnancy was detected. Conception was dated about 5 days prior to the administration of radioiodine-131 by the gynecologist. Therefore, a reasonable recommendation concerning the further course of the pregnancy was requested. ***Results:*** Radiation dose to the uterus was estimated according to the 2019 revised DGMP report No. 7 [1]. It subdivides the human development into preimplantation period (0-10d p.c.), organ building period (10d-8w p.c.) and fetal period (3-9m p.c.). A radiation exposure (>100 mSv) during the preimplantation period leads to either cessation of pregnancy or regular implantation (all-or-nothing effect). No other detriments are to be expected during this period. In the presented case the exposure likely occurred during this period. However, an exposition during the organ building might lead to severe malformations. As, within the given uncertainty, conception might be more than 10d before dose application and from the fact that the exposure lasted for a longer period, dose to the uterus was calculated. The dose to the uterus was calculated to be 283mSv, using a conversion factor of 76µGy/MBq as stated in [1]. This dose is clearly above the threshold for anatomic malformations, growth disturbance and mental retardation, which is expected to be 100mGy. After genetic counseling and detailed discussion with the patient the pregnancy was continued until a healthy child was delivered. ***Conclusion:*** The DGMP report is an indispensable guideline for nuclear medicine physicians, medical physicists and gynecologist to assess the uterus dose of pregnant women, who were exposed to radiation [1]. Additionally, detailed genetic counselling is indispensable. The dose consideration and the resulting potential consequences for the health of the child show the importance of a reliable PT prior to RIT. ***References:*** Pränatale Strahlenexposition aus medizinischer Indikation. Dosisermittlung, Folgerungen für die Ärztin/den Arzt und Schwangere. DGMP-Bericht Nr.7; Überarbeitete und ergänzte Neuauflage 2019; ISBN 978-3-00-064613-3.

EPS-078

Variation of serum thyroglobulin during the first radioiodine therapy: a prognostic marker in patients with thyroid carcinoma?

I. Lopo[1], P. Lapa[1,2], G. Costa[1,2], J. Pedroso de Lima[1,2,3];
[1]Serviço de Medicina Nuclear do Centro Hospitalar e Universitário de Coimbra, Coimbra, PORTUGAL, [2]Faculdade de Medicina da Universidade de Coimbra, Coimbra, PORTUGAL, [3]Instituto de Ciências Nucleares Aplicadas à Saúde (ICNAS), Coimbra, PORTUGAL.

Aim/Introduction: In patients with differentiated thyroid carcinoma (DTC), serum thyroglobulin (Tg) is extensively used for postoperative initial risk stratification and for disease monitoring, during life-long follow-up. Low Tg levels are expected to be associated with better outcome. However, a few days after radioiodine therapy (RAI-T), a dramatic transient serum Tg level elevations could be observed, reflecting benign/malignant thyroid tissue destruction. Our aim is to evaluate the value of the variation of TSH-stimulated Tg (stTg) during the first RAI-T, as prognostic marker. ***Materials and Methods:*** We review the clinical chart of all patients with DTC submitted to the first RAI-T in our Department, between January-2016 and December-2019. During hospitalization for RAI-T, a dual time stTg measurements were performed: stTg0h (just before the radioiodine administration) and stTg48h (48 hours after radioiodine administration). The variation of serum stTg was defined as the ratio between stTg48h and stTg0h (stTg-ratio). All patients were negative for serum Tg autoantibodies. Based on therapeutic responses at follow-up, and according to ATA guidelines, patients were divided in two groups: excellent or indeterminate/incomplete responses. To evaluate the association between stTg-ratio and therapeutic responses, a Mann-Whitney U test and ROC curve were performed. All relevant clinical data available were collected, either those known at the RAI-T (histology, TNM-classification, TSH-stimulation method, post-therapy whole-body scan) or those registered later, during the follow-up (Tg level and neck ultrasound, performed 6-30 and 4-36 months after RAI-T, respectively). ***Results:*** One hundred and eight patients were enrolled (mean age 52.4±15.5 years; 75.0% women; 89.8% papillary carcinoma; TMN: T1=27.8%, T2=24.1%, T3=47.2%, T0=0.9%). Statistical analysis showed that stTg-ratio was significantly higher in the group of 66 patients (61%), with excellent RAI-T response, than in the group of indeterminate/incomplete RAI-T response (p<0.001). However, when grouping for the TSH-stimulation method, just thyroid hormone withdrawal (n=48 patients; 44%) showed association between stTg-ratio and therapeutic response (p=0.001). For this group, a ROC curve analysis predicted an optimal stTg-ratio cutoff value of 2.41, with a sensitivity of 88.6% and specificity of 76.9% for an excellent response (AUC=0.813, 95%CI 0.669-0.957; p=0.001). ***Conclusion:*** Our study suggest that when endogenous TSH stimulation is used, stTg-ratio is a potential predictor of response to the initial RAI-T, pointing to an excellent result if higher than 2.41. ***References:*** None

EPS-079

Efficacy of a 740 MBq Single Fixed Radioactive Iodine Dose for Subclinical Hyperthyroidism Treatment and Implications of Pretreatment Thyroid Antibodies Levels

F. Cañete*, P. Garrastachu, X. Boulvard, L. Romero, M. Mangas, A. Cabrera, R. Delgado-Bolton, R. Ramírez;*
Centre for Biomedical Research of La Rioja (CIBIR), Logroño, SPAIN.

Aim/Introduction: There is an emerging role for I-131 in the treatment of so-called subclinical hyperthyroidism[1]. Our study first aimed to evaluate the efficacy of a fixed dose of 740MBq of I-131 in subclinical hyperthyroidism treatment and to assess the secondary effects frequency. A second aim is to see if there is any correlation between previous elevated thyroid antibodies and final thyroid function status. ***Materials and Methods:*** We retrospectively studied patients with normal thyroid hormone levels and suppressed thyroid-stimulating hormone concentrations persistent for at least six months, with no previous antithyroid drugs treatment, recent Tc-99m pertechnetate thyroid scan (to discard low thyroid uptake) and neck ultrasound, treated with a fixed dose of 740Mbq of I-131. Clinical and thyroid function test were periodically reviewed thereafter for a minimum period of eight months. Also, 36 patients had antithyroid peroxidase and antithyroid stimulating antibodies tests previous to radioiodine treatment. The elevation of any or both of them was considered as positive, and normal or negative values were considered negative. Chi-square test was used for the comparison between categorical variables. A p<0.05 was considered statistically significant. ***Results:*** 62 patients (21%males, 79% females; age: 70±11,8, 45-94 years) treated from October 2009 to November 2015 met inclusion criteria. Of this group, 85% were toxic multinodular goiter and 15% single hyperfunctioning adenoma. 100% of our patients achieved response, out of which 32% finally became hypothyroid and 68% euthyroid. After a clinical following mean period of 4 years and 7 months (range 8 months to 8 years and 8 months), only one patient (1.6%) presented secondary effect, which was transient gastritis. The majority of patients with negative antibodies (74%) were euthyroid and most of those with positive antibodies (89%) became hipothyroid after radioiodine treatment (p=0,001). ***Conclusion:*** Using a fixed dose of radioactive iodine dose of 740MBq for treating toxic multinodular goiter and single hyperfunctioning adenoma subclinical hyperthyroidism, successful treatment can be achieved in 100% of the patients, with very low (1.6%) side effects rate. Furthermore, there is a good correlation between elevated thyroid antibodies previous radioiodine treatment

and getting hypothyroid status after it. Normal or negative antibodies pretreatment leads to euthyroidism. ***References:*** [1] Stokkel MP, Handkiewicz Junak D, et al. EANM procedure guidelines for therapy of benign thyroid disease. Eur J Nucl Med Mol Imaging. 2010 Nov;37(11):2218-28.

EPS-080

Assessment of preoperative imaging techniques in patients with primary hyperparathyroidism treated in an unique endocrine surgical unit

I. Saura Lopez*, M. J. Ribelles Segura, I. Blanco Saiz, L. Paruta Araez, M. I. Morales Lozano, J. García Torres, N. A. Rudic Chipe, F. Gomez Sainz, M. Díaz Tobarra, Á. O. Rabines Juarez, E. Anda Apiñaniz, H. Gomez Herrero, A. Echegoyen Silanes, A. Camarero Salazar, P. Salvador Egea, E. Goñi Gironés;*
Navarra Hospital Complex, Pamplona/Iruña, SPAIN.

Aim/Introduction: Because the only treatment of primary hyperparathyroidism (pHPT) is the surgery management, evidence-based recommendations enhance the appropriate and effective practice in reference hospitals. We want to evaluate the records of our unit in order to check that the results of our team are within the current standards. The aim of this study was to determine the diagnostic performance of [^{99m}Tc]Tc-MIBI SPECT/CT and ultrasonography (US) for preoperative localization of parathyroid adenoma. ***Materials and Methods:*** Retrospective study of 152 patients with a median (interquartile range, IQR) of age 63 (52-71) and 80.3% women, from August 2016 to December 2019 in Complejo Hospitalario de Navarra. All patients underwent [^{99m}Tc]Tc-MIBI dual-phase scintigraphy with early SPECT/CT and US prior to surgery. In doubtful cases, L-[methyl-^{11}C]-methionine PET/CT and/or CT were added. Sensitivity and positive predictive value (PPV) were calculated. Histopathology was used as reference value. ***Results:*** Preoperative laboratory data were median (IQR) of calcium 11 mg/dL (IQR 10.7-11.5) ,PTH 181 pg/mL (IQR 144-249) and 25-hydroxyvitamin D 18 ng/mL (IQR:13-26). More than one surgical criterion was found in 26 cases (17.1%) and the most frequent surgical procedure was minimally invasive parathyroidectomy (121 cases; 79.6%). Parathyroid lesion was successfully removed in 142 (93.4%) patients, corresponding 139 (91.4 %) to adenomas (5 double), 2 hyperplasias and 1 carcinoma. Sensitivity and PPV were 83% and 94% for [^{99m}Tc]Tc-MIBI; 74% and 95% for US, respectively. Parathyroid [^{99m}Tc]Tc-MIBI scintigraphy had reported the accurate surgical location in 116 (76.7%) patients (102 eutopic and 14 ectopic), whereas US located in 100 (68.5%) patients (94 eutopic and 6 ectopic). The difference was statistically significant (p = 0.03). Both, [^{99m}Tc]Tc-MIBI and US were concordant in the precise localization of the lesion in 94 (61.8%) patients, corresponding to adenoma 88 (93.6%). The remaining 58 (38%) patients in whose there were discordant results or both failed results were explored with PET/CT (36 cases) and/or CT (14) being diagnostic 10 and 11 patients, respectively, thereby achieving the correct excision of the pathological gland in 54/58 (93.1%) patients. ***Conclusion:*** [^{99m}Tc]Tc-MIBI scintigraphy shows significantly higher sensitivity and accuracy than US in anatomical presurgical localization in primary hyperparathyroidism. The combined use of both techniques provides the necessary information for the surgical decision in most patients. However, radioguided surgery should be considered in the subgroup of patients in which, despite the addition of other available diagnostic tests, removal of the adenoma is not achieved. ***References:*** None

EPS-081

^{11}C-methionine PET/CT for the evaluation of patients with recurrent or persistent secondary hyperparathyroidism after surgery and negative or inconclusive ^{99m}Tc-MIBI scintigraphy

A. Damian*[1,2], A. Quagliata[1], S. San Roman[3], E. Silvera[2], M. Rodriguez Taroco[1], N. Niell[1,2], R. Castro[1], R. Silvariño[3], O. Alonso[1,2];*
[1]Uruguayan Centre of Molecular Imaging (CUDIM), Montevideo, URUGUAY, [2]Centro de Medicina Nuclear e Imagenología Molecular, Hospital de Clínicas, UdelaR, Montevideo, URUGUAY, [3]Centro de Nefrología, Hospital de Clínicas, UdelaR, Montevideo, URUGUAY.

Aim/Introduction: Persistent or recurrent secondary hyperparathyroidism (sHPT) after parathyroidectomy is a complex clinical scenario and constitutes a diagnostic and therapeutic challenge. Few studies have assessed the additional value of ^{11}C-methionine PET/CT in the evaluation of patients with primary hyperparathyroidism and negative MIBI scans that previously underwent surgery. However, no study has explored the diagnostic performance of this modality in patients with sHPT. Thus, the objective was to evaluate the detection capability of ^{11}C-methionine PET/CT in these patients. ***Materials and Methods:*** We included 16 patients (5 women, median age 57.5 years, range 39-72 years) with chronic renal failure, persistent or recurrent sHPT after surgery and a negative or inconclusive dual-phase ^{99m}Tc-MIBI scintigraphy. PET/CT was acquired 10 minutes after the administration of a dose of approximately 400 MBq of ^{11}C-methionine. SUVmax, SUV parathyroid/cervical soft tissue and SUV parathyroid/thyroid index were calculated for each positive lesion. ***Results:*** ^{11}C-methionine PET/CT was positive for the detection of hyperfunctioning parathyroid tissue in 14 patients (87.5 %). Three patients (18.8%) had multiple gland foci. Serum PTH ranged from 288 to 3000 pg/mL (median 1450 pg/mL). In eleven patients (68.8%) the hyperfunctioning tissue was located in the neck and in three patients (18.8%) it was located in the mediastinum. Lesion size measured on axial CT ranged from 6 to 25 mm (median 9 mm). Median SUVmax of the

positive lesions was 3.7 (range from 2 to 7.1), while median SUV parathyroid/cervical soft tissue index was 2.6 (range from 1.7 to 4), and median SUV parathyroid/thyroid index was 1.4 (range 1 to 2.85). Four of the patients underwent a second or third parathyroidectomy after PET. ***Conclusion:*** ^{11}C-methionine PET/CT may provide valuable information for the localization of hyperfunctioning parathyroid tissue in patients with persistent or recurrent sHPT after surgery. ***References:*** None

EPS-082

F18-choline PET/CT in primary hyperparathyroidism when conventional tests are negative or inconclusive

J. Atance García de la Santa, D. Zamudio Rodríguez, R. Pérez Pascual, J. J. Ardila Mantilla, Y. K. Henao Celada, M. Baquero Oliveros, M. I. Gómez Fernández, A. Rotger Regí, C. M. Durán Barquero, A. Marí Hualde, J. E. Orcajo Rincón, J. C. Alonso Farto, S. Vargas Martín;
Hospital Universitario Gregorio Marañón, Madrid, SPAIN.

Aim/Introduction: To assess the sensitivity of F18-choline PET/CT for parathyroid adenoma detection in patients with primary hyperparathyroidism (PHPT) and negative or inconclusive Tc99m-MIBI scintigraphy (planar and SPECT/CT) result. ***Materials and Methods:*** Prospective study of a series of patients with PHPT and previous negative or inconclusive results in conventional tests. All patients underwent F18-choline PET/CT; the result was scored as positive, inconclusive or negative. The number of uptake foci and their sites were recorded. The result of the F18-choline PET/CT guided the surgical procedure (selective parathyroidectomy or bilateral cervical exploration). The results were compared with the pathological findings. ***Results:*** 46 patients were included: 30 (65.2%) with a negative and 16 (34.8%) with an inconclusive previous Tc99m-MIBI scintigraphy result. 9 of them had a persistent/recurrent PHPT despite previous parathyroid surgery (8 after a negative and 1 after an inconclusive Tc99m-MIBI scintigraphy result). 38 (82.6%) F18-choline PET/CT were scored positive, 2 (4.4%) inconclusive and 6 (13%) negative, showing 45 cases of uniglandular disease, including 2 ectopic localizations and 1 case of multiglandular (2 foci) disease. 16 patients have already undergone surgery. In 14 patients (87.5%) a positive F18-choline PET/CT result guided surgery: 9 selective parathyroidectomies (64%) and 5 bilateral cervical explorations. The PHPT of these 14 patients was solved after surgery (their levels of PTH and calcium decreased) and pathological findings was adenoma in everyone of them (14 true positives). 1 patient with a positive F18-choline PET/CT result underwent a bilateral cervical exploration in another hospital regardless of this result. In this patient the PHPT persisted after surgery and no adenoma was found in the pathological examination. 1 patient with a negative F18-choline PET/CT result underwent bilateral cervical exploration, with resolution of the PHPT, and was considered 1 false negative. With current data, sensitivity and positive predictive value were both 93%. ***Conclusion:*** Preoperative F18-choline PET/CT appears to have a high sensitivity and positive predictive value for parathyroid adenoma detection in patients with PHPT and negative or inconclusive conventional tests. Bilateral cervical exploration could be avoided in up to 60% of patients. ***References:*** None

EPS-083

Pre-surgical imaging tests in the diagnosis of primary hyperthyroidism in adverse scenarios: low weight adenomas and concomitant thyroid disease

***L. Paruta Araez**, I. Blanco Saiz, M. Ribelles Segura, M. Morales Lozano, J. García Torres, M. Díaz Tobarra, I. Saura López, N. Rudic Chipe, A. Rabines Juárez, F. Gomez Sainz, B. Alvarez Galán, P. Caballero García, A. Goikoetxea Urdiain, A. Camarero Salazar, E. Goñi Gironés, P. Salvador Egea;*
Complejo Hospitalario de Navarra, Pamplona, SPAIN.

Aim/Introduction: BACKGROUND: Parathyroid scintigraphy and ultrasonography are the routine preoperative localization procedures. However, when thyroid disease coexists and the lesion has low weight, their diagnostic accuracy is possibly diminished. AIM: To analyze the factors that influence in the success of localization with [^{99m}Tc]Tc-MIBI SPECT/CT and ultrasound in the primary hyperthyroidism. ***Materials and Methods:*** Retrospective descriptive review of 152 patients from Aug 2016 to Dec 2019 with primary hyperparathyroidism and surgical criteria. [^{99m}Tc]Tc-MIBI dual phase scintigraphy (early SPECT/CT) and cervical ultrasonography were the pre-surgical methods of localization in all patients; [$^{99m}TcO_4^-$] thyroid scintigraphy (planar and SPECT-CT acquisition) was added in doubtful cases. Different results and statistics parameters were compared. Data were recorded for the following study variables: gender, age, gland weight (mg), calcemia (mg/dL), preoperative PTH (pg/mL) and 25-hydroxyvitamin D (ng/mL), associated thyroid nodular disease, previous cervical surgery and results of imaging techniques performed. ***Results:*** The study included 122 (74.8%) females. The median age was 63 y/o (IQR: 52-71). BMI over 30 was registered in 34 (22.4%). Median pre-surgical calcium was 11 mg/dL (IQR:10.7-11.5), median PTH 183 pg/mL (IQR:144-251), and median 25-hydroxyvitamin D 18 ng/mL (IQR:13-26). Neither [^{99m}Tc]Tc-MIBI SPECT/CT nor ultrasound found statistically significant difference in the location of the lesion with respect to sex, age, BMI, calcium, PTH and 25-hydroxyvitamin D levels. In [^{99m}Tc]Tc-MIBI SPECT/CT negative patients the media weight of the lesion was 602.9 mg (95%CI 389.3-816.5), whereas

in those positive was 1147.4 mg (95%CI 962.6-1332.1), p=0.002. This regard was not significant on ultrasound. MIBI localization was not significantly affected by concomitant thyroid nodular pathology, meanwhile ultrasound was diminished, although in the limit of statistically significance (p=0.05). Considering 84 (55.2%) patients with underlying nodular thyroid pathology, ultrasound was positive in 56 (66.7%), doubtful or negative in 28 (33.3%); while [^{99m}Tc] Tc-MIBI SPECT/CT was positive in 72 (85.7%) and doubtful or negative in 12 (14.3%).The addition of the thyroid scan was conclusive for the diagnosis of adenoma in 12 of these patients and to exclude it in 5, who in the absence of this test would have been misclassified. ***Conclusion:*** The only factor significantly related with the diagnostic accuracy to [^{99m}Tc] Tc-MIBI SPECT/CT is the weight of the gland. Underlying nodular thyroid pathology causes a decreased of the ultrasound detection rate, not so in the [^{99m}Tc]Tc-MIBI SPECT/CT thanks to the added value of thyroid scan. ***References:*** None

EPS-084

Brown Tumors Secondary To Tertiary Hyperparathyroidisim Masqeurading As A Lytic Or Sclerotic Skeletal Metastases On Preoperative/ Postoperative 18F-FDG PET/CT: A Case Report

C. Engur, *T. Ones, N. Filizoglu, S. Kesim, S. Ozguven, K. Oksuzoglu, H. T. Turoglu, S. Inanir, T. Y. Erdil;*
Marmara University Pendik Training and Research Hospital, Department of Nuclear Medicine, Istanbul, TURKEY.

Aim/Introduction: Tertiary hyperparathyroidism(THPT) develops from secondary hyperparathyroidism in cases when the secretion becomes autonomous. Brown Tumors are rare skeletal lesions of hyperparathyroidism that may mimic cancer metastasis. In this case report, we discuss the FDG PET/CT findings of a patient with tertiary hyperparathyroidism with multiple Brown Tumors which mimics osteolytic/osteoblastic metastases. ***Materials and Methods:*** We report a case of a patient who was diagnosed with tetiary hyperparathyoidism that evaluated with two FDG PET scans with an interval of 23 months in the preoperative and postoperative period. ***Results:*** Thorax CT imaging of this patient was revealed multiple lytic lesions evaluated in favor of bone metastasis and FDG PET/CT (first scan) was performed to detect the primary focus. In the first PET scan intense hypermetabolic lytic/destructive multiple lesions were observed in the skeleton. When these lesions were evaluated together with the patient history, the diagnosis was in favor of multiple Brown Tumors secondary to tertiary hyperparathyroidism. After this first PET scan parathyroidectomy was performed. Twenty-three months after the surgical procedure the patient evaluated with new PET scan for another reason. The second PET scan revealed multiple sklerotic bone lesions in the skeleton (which were descr,bed as intensely hypermetabolic lytic/destructive lesions previously). ***Conclusion:*** Although they are benign lesions giant cell reperative granuloma, aneurysmal bone cyst, giant cell tumor of bone and osteoclast-like giant cell containing lesions of bone show increased FDG uptake in favor of malignancy. These benign lesions contain giant cells and/or histiocytes derived from monocyte-macrophage group and provide their energy mostly by glucose metabolism. Brown tumors contain mononuclear cells and fibroblasts that derived from the same cell group. They provide their energy as the same way. Radiologic characteristics of 18F-FDG PET/CT between Brown Tumors and skeletal metastases are similar and it should be kept in mind that Brown Tumors can imitate both osteolytic and osteosclerotic metastas depending on the surgical history especially in patients with diagnosed tertiary hyperparathyroidism. ***References:*** None

EPS-085

Evaluation of Primary Hyperparathyroidism in Hormone Receptor- Positive Breast Cancer Patients Using [^{99m}Tc] Tc-MIBI SPECT/CT and Ultrasound

M. Punda, *P. Petranovic Ovcaricek, V. Gladic Nenadic, I. Sisko Markos, M. Franceschi, T. Jukic;*
UHC Sestre Milosrdnice, Zagreb, CROATIA.

Aim/Introduction: Breast cancer (BC) patients receiving advanced specific anti-neoplastic treatments are at increased risk for cancer treatment-induced bone loss. The guidelines recommend bone mineral density (BMD) testing by dual-energy X-ray absorptiometry (DXA) and exclusion of secondary causes for low BMD such as primary hyperparathyroidism (PHPT). The number of studies that describe PHPT in BC patients are scarce and show conflicting results. Several reports documented an increased frequency of PHPT in BC patients, particularly associated with the use of aromatase inhibitors (AIs) in hormone receptor-positive breast cancer (HRBC). Hence, we aimed to determine the prevalence of PHPT among our HRBC patients to provide better clinical insight into this condition. ***Materials and Methods:*** We examined 169 HRBC patients referred to our Osteoporosis Clinic Unit between January 2014 and November 2019. BMD by DXA, serum PTH, serum calcium and thyroid function was assessed in all patients. The patients with biochemical evidence of PHPT and no evidence of bone metastasis underwent dual-phase [99mTc]Tc-MIBI SPECT/CT parathyroid scintigraphy, a high-resolution ultrasound (US) and ultrasound-guided fine-needle biopsy with measurement of PTH levels in the needle washout (FNB-PTH). ***Results:*** Six (3.6%) patients had biochemically proven PHPT (mean ± SD: serum PTH 154.6±78.82 pg/mL, serum calcium 2.70 ±0.14 mmol/L) and low BMD (mean T-scores of -2.23 at the lumbar spine and -1.35 at the femoral neck). The patients aged 58.6±9.24

years (mean, ± SD) were evaluated for PHPT 26.5 months (median, range 11-180 months) after BC diagnosis. The subjects previously underwent postoperative radiotherapy (6/6 patients), chemotherapy (2/6 patients) and five out of 6 patients were taking AIs for a median time of 15 months (range 4-24 months). One patient has completed tamoxifen treatment for recurrent BC. The longest US-diameter of parathyroid lesions was 10.5±3.39 mm. PHPT was confirmed in 6/6 patients based on concordant [99mTc]Tc-MIBI SPECT/CT, US and FNB-PTH findings: 4 patients underwent surgery for a single parathyroid adenoma, in one patient surgery was canceled due to advanced age and severe comorbidities, and one patient with asymptomatic disease was advised to closer follow-up. Three patients had co-existing Hashimoto thyroiditis and 2 patients had nodular goiter. ***Conclusion:*** We found PHPT in 3.6% of our HRBC patients which is consistent with the increased prevalence of PHPT observed in several reports (2.88-7%) compared to the adult female population without BC (<1.5%). Among cancer-treated HRBC patients with low BMD and hypercalcemia a careful diagnostic evaluation is required to rule out PHPT. ***References:*** None

701

Plenary 2: Cardiac Nuclear Medicine - Present and Future

Friday, October 23, 2020, 15:30 - 16:45 Channel 1

OP-373
Renew or Fade Away
H. Verberne; Academic Medical Center, Department of Nuclear Medicine, Amsterdam, NETHERLANDS.

OP-374
Do we meet the Clinical Demand?
W. Acampa; Univ. Federico II di Napoli, Scienze Biomorphologiche e Funzionali, Naples, ITALY.

OP-375
MBF - Lost in Clinical Translation?
R. Buechel; Department of Nuclear Medicine, Cardiac Imaging, University Hospital Zurich, Zurich, SWITZERLAND.

OP-376
Imaging Cardiac Amyloidosis
S. Dorbala; Brigham and Women's Hospital, Boston, UNITED STATES OF AMERICA.

OP-377
Endocarditis
P. Erba; Nuclear Medicine, Department of Translational Research and New Technology in Medicine, University of Pisa and Azienda Ospedialiero Universitaria Pisana, Pisa, ITALY.

OP-377a
Discussion

801

CME 6: Bloody Hell!!! Impact on Quantitation of Blood Radiotracer Measurements

Friday, October 23, 2020, 16:55 - 18:25 Channel 1

OP-378
True Blood - The Story of How to Quantify Plasma Radio-Metabolites
C. Vraka; Department of Biomedical Imaging and Image-guided Therapy, Medical University of Vienna, Vienna, AUSTRIA.

OP-379
Compartmental Modelling for Kinetic Quantification with Arterial Input Function and Alternatives
N. Costes; CNRS Research Engineer, CERMEP- Imagerie du vivant, PET-MR department,Lyon,FRANCE.

OP-380
Bloody Hell, Why Do we Need Metabolite Corrections for Uptake Quantification
R. Boellaard; Amsterdam University Medical Centres, location VUMC, Radiology and Nuclear Medicine, Amsterdam, NETHERLANDS.

802

Joint Symposium 11 (EANM/ESTRO): How Much PET does Radiation Oncology Require?

Friday, October 23, 2020, 16:55 - 18:25 Channel 2

OP-381
FDG-PET for Radiation Target Volume Delineation
E. Troost; Faculty of Medicine and University Hospital Carl Gustav Carus, Department of Radiotherapy and Radiation Oncology, Dresden, GERMANY.

OP-382
PET Beyond FDG
S. Carrilho Vaz; Champalimaud Clinical Centre, Nuclear Medicine - Radiopharmacology, Lisbon, PORTUGAL.

OP-383
PET & Radiomics - Does it Matter?
B. Fischer; PET Centre, School of Biomedical Engineering and Imaging Sciences KCL, St Thomas' Hospital, London, UNITED KINGDOM.

803

Joint Symposium 12 (EANM/EACVI): Selecting the Right Imaging for the Right Patient in CAD

Friday, October 23, 2020, 16:55 - 18:25 Channel 3

OP-385

Which Patients Should be Evaluated with CCTA?

I. Danad; Amsterdam University Medical Centers, Department of Cardiology, Amsterdam, NETHERLANDS.

OP-386

Which Patients Should be Evaluated with Cardiac MRI?

F. Bandera; San Donato Milanese, Cardiology, Milano, ITALY.

OP-387

Which Patients Should be Evaluated with Cardiac SPECT?

R. Assante; University Federico II, Department of Advanced Biomedical Sciences, Naples, ITALY.

OP-388

Which Patients Should be Evaluated with Cardiac PET?

P. Arumugam; Central Manchester Foundation Trust, Department of Nuclear Medicine, Manchester, UNITED KINGDOM.

804

Technologists e-Poster Presentation Session 1

Friday, October 23, 2020, 16:55 - 18:25 Channel 4

TEPS-01

The Increase In The Activity Of Technetium-99m, Isolated From The Routine Activity Generator

A. Rogov, E. Stasyuk;
National Research Tomsk Polytechnic University, Tomsk, RUSSIAN FEDERATION.

Aim/Introduction: Currently, more than 80% of all radionuclide studies are performed using radiopharmaceuticals based on technetium-99m. To obtain the isotope it installations called technetium generators are used. Organization of 99Mo production by the reaction of radiative capture (n,γ) using enriched molybdenum-98 at research reactors widespread in Russia and in the world. This technology has virtually no waste, but the resulting product has a low specific activity 6-10 Cu/g. The use of such low active materials for the production of generators requires the use of columns of increased size, which increases eluation profile of generators and as a consequence, to a decrease in the volume activity of eluted preparation of technetium-99m. Aim:To investigate the factors influencing the eluation characteristics of generators of technetium-99m, manufactured by neutron irradiation of enriched molybdenum oxide 98. ***Materials and Methods:*** Elution of technetium-99m from generators in the form of sodium pertechnetate solution was carried out by pumping of 0.9% solution of NaCl (eluent) in portions of~2 ml into 10 ml vials through columns followed by measuring the activity of 99mTc on the radiometer RIS-01A. Based on these results, the dependence of changes of the yield of 99mTc on the volume of passed eluent, as well as dependence of changes of eluation yield from the adsorbed mass of molybdenum-98 for different volumes of the eluent are developed. Changes in the activity of adsorbed 99Mo along the length of chromatographic column was determined by single-channel pulse-height analyzer Strahlungsmessgerat 20 046 (Germany) by scanning the columns above the detector with collimator. ***Results:*** We show that with an increase of molybdenum mass eluation profile of generator becomes narrower. For example, for the complete elution of 99mTc from generator with adsorbed weight of 0.070 g it is necessary to pass 16-17 ml of eluent through its column and 8-9 ml will be enough at a weight of 0.177 g. Accordingly, even at the same total activity of 99mTc eluted from generators the volumetric activity of the preparation will be about 2 times higher in the latter case than in the first. ***Conclusion:*** The width of eluation profile of generators depends on the adsorbed mass of molybdenum. At the same time, with its increase the profile of generators becomes narrower, reaching a minimum at a certain limiting mass. ***References:*** National Research Tomsk Polytechnic University

TEPS-02

Research To Create A Miniature Generator Of Technetium-99m

A. Rogov;
National Research Tomsk Polytechnic University, Tomsk, RUSSIAN FEDERATION.

Aim/Introduction: Radiopharmaceuticals based on short-lived technetium-99m (^{99m}Tc) radionuclides are used for diagnostic studies in many areas of medicine. Most of the global market is for chromatographic generators based on fission products of uranium-235. Their manufacture requires a high activity of ^{99}Mo (200 Ci / g), produced by environmentally hazardous technologies. The proposed possibility of obtaining ^{99}Mo by radiation capture (n, γ) when molybdenum-98 is exposed to the neutron field of a nuclear reactor. The described technology has virtually no waste, and the resulting product has a low specific activity of ^{99}Mo at 7-9 Ci / g. In this regard, it becomes necessary to use a large amount of ^{99}Mo, about 150-190 mg. This necessitates the use of a large amount of sorbent, aluminum oxide. ***Materials and Methods:*** Mo aluminum oxide capacity has a saturation limit of 22-25 mg per gram of sorbent. The

required activity of the obtained technetium-99m product is possible only when 190 mg of Mo is adsorbed onto the surface of the sorbent. In this case, it is necessary to use from 7.6 to 8.6 g of sorbent. Such conditions require an increase in the size of the column and the device delivered to the clinic (technetium-99m generator). ***Results:*** Studies of the possibility of creating a sorption generator of technetium-99m in a reduced form were carried out in a number of experiments to increase the sorption capacity of aluminum oxide. Depending on the initial (production) and subsequent processing of the sorbent, it becomes possible to prepare a sorbent capacity of Mo, approximately equal to 34 mg / g This is achieved through the use of a set of measures for the preparation of the sorbent and methods of densifying the structure of the active centers of the sorbent. These conditions increase the capacity of the sorbent from a solution containing ^{99}Mo. ***Conclusion:*** By reducing the required volume of the sorbent by 26.4%, there is a decrease in the weight of the sorbent and the device itself. The mass of the used sorbent is reduced to 5.6 g from the starting position of 8.6 g. This allows to reduce the columns and frames of the generator. As a result of research, the design of the compact technetium-99m generator and a number of methods used for their manufacture were designed. ***References:*** None

TEPS-03

Development methods for 99mTc-labeled nanocolloidal preparations

V. Sadkin[1], *E. Nesterov*[1], *V. Skuridin*[1], *E. Stasyuk*[1], *A. Rogov*[1], *N. Varlamova*[1], *R. Zelchan*[2];
[1]*National Research Tomsk Polytechnic University, Tomsk, RUSSIAN FEDERATION,* [2]*Cancer Research Institute, Tomsk National Research Medical Center, Tomsk, RUSSIAN FEDERATION.*

Aim/Introduction: The work considers the problem of obtaining nanocolloid radiopharmaceuticals (RPs) and studying their functional suitability for diagnosing sentinel lymph nodes (SLN) in cancer patients. ***Materials and Methods:*** All the reagents were purchased from Sigma-Aldrich ACS grade and used without further purification. Technetium-99m was obtained from chromatographic ^{99}Mo/^{99m}Tc generator «^{99m}Tc-GT-TOM» produced by Tomsk Polytechnic university (TPU) - Tomsk, Russia.Methods use:Method for preparation of ^{99m}Tc labeled nanocells. Determination of the size of ^{99m}Tc labeled colloidal particles. Thin-layer chromatography (TLC) procedure. Determination of the functional suitability of preparations for scintigraphic detection of SLN. ***Results:*** As a result of the studies, the composition of the reagents and the conditions for the synthesis of three nanocolloid RPs were determined. An experimental dependence of the change in the content of 99mTc (VII) impurities on the concentration of tin (II) was established and its minimum amount (0.175 mg/ml) was determined to reach a RHP greater than 94%. In this case, the yield of the target colloid with particle sizes of 50 ± 100 nm is 42 - 76%. Preliminary tests of the developed preparations on experimental animals showed that accumulation of RP in lymph nodes is practically not observed, although the sizes of colloidal particles are in the required range. Increase in the speed of "transportation" of colloids through the lymphatic system was achieved by the introduction of gelatin in the composition (2.5-4 mg/ml). In addition, there was an increase in the yield of the colloid with particle sizes of 50-100 nm to 76-97% with radiochemical purity of the preparations of 94-95%. ***Conclusion:*** Repeated studies in experimental animals have shown that all synthesized nanocolloid preparations provide a good level of accumulation in the SLN. Thus, the level of accumulation of RP "^{99m}Tc-DTPAmod" and RP "^{99m}Tc-Fe@C(ADT)" in the SLN is 1.5% and 1.71% respectively. At the same time, the accumulation level of the preparation based on aluminum oxide is 8.6% of the total input activity, which is several times greater than all known analogues. ***References:*** None

TEPS-04

Sedimentation of Radioactive-labelled Colloid During Transport

M. Rode Pedersen*, B. Hoyer Mathiasen;*
Hospital Lillebaelt, Vejle, DENMARK.

Aim/Introduction: At our department we use a Tc-99m-labelled pharmaceutical containing human serum albumin nano-colloid, requiring suspension prior to extraction. After daily preparation, we deliver a multi-dose vial to a collaborating hospital. Due to recent requirements from the Danish Health Authorities, the pharmaceutical now has to be transported in prepared syringes, instead of the glass vial. The aim of our study was to investigate whether the radioactive nano-colloid would sediment in the syringes during different settings, to determine if the required practice would be feasible in regards to product quality. ***Materials and Methods:*** The study was conducted over the course of four days under different settings; Day 1: Syringes placed horizontal without air, Day 2: Syringes placed vertically without air, Day 3: Syringes placed horizontally with air, Day 4: Syringes placed vertically with air. Each day, two syringes containing 0.8 mL of the pharmaceutical was prepared into 1 mL syringes, with a concentration of 100 MBq/mL at time of preparation. The syringes containing air, was suspended prior to acquisition. Distribution of radioactivity within the syringes was imaged and analyzed after four and six hours. Each acquisition was done on a Siemens Symbia Intevo SPECT/CT scanner, as a five minute static acquisition. Images were analyzed using a ROI-tool from Hermes Medical Solutions, by dividing the image into 12-14 ROIs and plotting them into a graphic display. ***Results:*** By analyzing the number of counts in each ROI, we were able to graphically show the distribution of radioactive

nano-colloid the syringes at 4 and 6 post-preparation. In each setting, it showed a rapid increase in activity, after which the graph stabilized, before a rapid decrease, thus indicating a homogenous distribution throughout the syringe. The graphs showed that the distribution of radioactive nano-colloid was homogenous in all instances, regardless of orientation or suspension. Furthermore, the measurement of activity in the syringes before and after imaging indicated the nano-colloid does not adhere to the inside of the syringes, as only 10 % of activity remains after discharge, which corresponds to the syringe tip. ***Conclusion:*** Our study could not provide evidence that orientation or suspension of syringes has any effect on the distribution of radioactive nano-colloid. We were not able to prove, that the nano-colloid would sediment, even after 4 or 6 hours. Thus, we assess that the transport of prepared syringes containing radioactive human serum albumin nano-colloid, is feasible and without risk of sedimentation. ***References:*** None

TEPS-05

Review of the radiosynthesis preparation of 68Ga-labelled PSMA in a fully automated system - a routine procedure

M. Paula*, C. Capelo, A. Fonseca, L. Ribeiro, H. Duarte;*
Ipo Porto, Porto, PORTUGAL.

Aim/Introduction: The PET imaging of the prostate-specific membrane antigen (PSMA) using ([68Ga]Ga-PSMA-HBED-CC) has gained highest clinical impact. The application of ^{68}Ga-labeled peptides has considerable interest for cancer imaging due to the physical characteristics of ^{68}Ga and the availability of reliable GMP-compliant ^{68}Ge/^{68}Ga generators. Although 68Ga-labeled PSMA individual doses can be purchased it is economically and strategically important to have the possibility of synthesizing the radiopharmaceutical on-site. In 20016 we present the data of our initial experience with the firsts radiosynthesis of ^{68}Ga-labeled HBEC-CC-PSMA ; after 4 years we propose to review what has become a routine procedure in our Nuclear Medicine Department. ***Materials and Methods:*** In the radiolabeling we used a cassette based automated synthesis module; the^{68}Ge/^{68}Ga generator, eluition solvent HCl 0.1M. Preconcentration: SCX cartridge, elution with NaCl/HCl mixture (3 ml) Labelling buffer: sodium acetate/ hydrochloric acid buffer pH 4.5+/-0.1 (400 µl) Precursor amount: 10-20 µg; Reaction time/Incubation: 5 min at 95°C at pH ~4 Purification with C-18 light, product elution from C18 cartridge with ethanol/water solution (50%) into product vial and dilution with saline. All patients had a histopatological confirmation of prostate cancer and/ or increased values of PSA. PSMA images were acquired with a mCT FlowMotion continuous bed motion PET/CT equipment. ***Results:*** Between October 2015 and February of 2020, we performed 390 synthesis of ([68Ga] Ga-PSMA-HBED-CC) and PET/CT imaging in about 1164 patients. We had better results achieving higher specific activity labelling using precursor amount> 10 µg, the synthesis time was 14+/-3min. The success rate of the synthesis was very high, just 10 of them had failure. ***Conclusion:*** The radiosynthesis of [68Ga] Ga-PSMA-HBED-CC as described it prove to be a method fast and reliably over the past 4 years and it has become a routine procedure in our department. Is suitable for being used in Nuclear Medicine Departments for clinical use with hight reproducibility and robustness. One of the biggest challenge is manage the validity of the Ge / Ga generators, which is 9-12 months and the activity obtained by synthesis gradually decreases. Since our first syntheses in 2016, little or nothing has changed in the process, which has been more significant is the operator's ability to solve problems faster and more effectively with the synthesis module or the generator or even problems with the computer programs. ***References:*** None

TEPS-06

Contribution of Information Technology systems in the planning of radiopharmaceuticals purchase: an ongoing experience

M. Maccagnani*, A. Farina, R. Bonfiglioli, C. Malizia, S. Fanti;*
Azienda Ospedaliero-Universitaria S.Orsola-Malpighi, Bologna, ITALY.

Aim/Introduction: The application of the best practice in radiopharmacy has required to Nuclear Medicine Centers, to implement quality assurance systems to allow complete traceability of their activities. In many cases, Information Technology System(NMIS) was employed to manage the required documentation. The aim of this work was to investigate the possible use of NMIS database in the planning of radiopharmaceuticals purchase in order to move from short term (3-months) planning to long term (1-year) planning. ***Materials and Methods:*** The NMIS for they use need and collect a variety of data that is possible to infer and analyze to describe the macroscopic profile of both main and side activities in radiopharmacy. The information about each warehouse movement of the radiopharmaceutical in use was extracted in monthly step for the period2016-2018and used to plan the purchase activity for the year2019. Especially, we extract the data about purchase, use and expire of every radiopharmaceuticals in use. As a first step, the average of the products used annually was calculated and a value equal to10%was set to resize the minimum amounts always available in the radiopharmacy warehouse. Secondly, the average of the products purchased annually was calculated and the value obtained, increased by5%, was set as standard annual order. Then the value divided over the12months according to the scheduled activity to plane the arrive in the radiopharmacy. These values have been

approximated to multiples of the minimum purchasable quantity. The quantities calculated so far, theoretically, allow to always have sufficient products in the radiopharmacy warehouse to cope with both radiopharmaceutical labelling and/or supply problems without interfering with the scheduled activity. ***Results:*** 2019 was a year of transition between the supply management method and therefore not decisive to evaluate the effectiveness of the change. However, data analysis shows some interesting effects: 1)both the supply and warehouse volumes of the radiopharmaceuticals were sufficient to guarantee the diagnostic activities; 2)a widespread drop in the number of expired radiopharmaceuticals without being used; 3)a drop in spending on radiopharmaceuticals from €1,369,617.75 to €1,150,781.17, with saving around16%. ***Conclusion:*** The use of NMIS was appropriate in the management of purchases of the radiopharmaceuticals. In light of these positive data, the same calculation method for supplies was applied for2020, with a prediction of savings between 5%-7% compared to2019. Due to the ongoing health emergency, expenditure data for the first quarter of2020 was not available yet, therefore early verification was not possible. ***References:*** None

TEPS-07

Normal values of ^{201}Tl myocardial uptake at stress using a CZT SPECT and IQ-SPECT

A. Matsumoto[1], S. Yoshimura[1], S. Tomiguchi[2], S. Shiraishi[3], Y. Nakamura[4], H. Sakamoto[2];
[1]Graduate School of Health Sciences, Kumamoto University, Kumamoto, JAPAN, [2]Faculty of Life Sciences, Kumamoto University, Kumamoto, JAPAN, [3]Kumamoto University, Hospital, Kumamoto, JAPAN, [4]Division of medical technology, Kumamoto University, Hospital, Kumamoto, JAPAN.

Aim/Introduction: A cadmium zinc telluride (CZT) single-photon emission-computed tomography (SPECT) device (CZT SPECT: NM530c:GE) and IQ-SPECT(Siemens) have higher count sensitivity than a conventional NaI SPECT device. Both SPECT devices are therefore feasible to investigate the myocardial perfusion quantitatively. Stress ^{201}Tl myocardial uptake (myocardial uptake index: MUI) presumed to be useful index for the diagnosis of coronary arterial disease (CAD). The aim of this study was to assess the normal values of MUI obtained by CZT SPECT and IQ-SPECT. ***Materials and Methods:*** 7 patients using a CZT camera (Discovery NM 530c, GE) and 11 patients using IQ-SPECT without coronary arterial stenosis (normal subjects) performed stress ^{201}Tl SPECT-myocardial perfusion imaging (MPI) were enrolled. MUI was calculated by dividing estimated radioactivity of whole left ventricular myocardium by injected dose. Estimated activity was obtained by multiplying SPECT counts by Cross Calibration Factor (CCF). No attenuation correction or scatter correction was performed on the reconstructed images. ***Results:*** CCF was 5.05 for CZT SPECT and 0.50 for IQ-SPECT, respectively. The mean of MUI value using the CZT SPECT was 6.0%, and that using the IQ-SPECT was 10.7%. Scaling factor may be one of the factors of difference in normal values of MUI between CZT SPECT and IQ-SPECT. ***Conclusion:*** It should be careful that the normal value of MUI on IQ-SPECT is higher than that on CZT-SPECT in the quantitative evaluation of myocardial blood flow. ***References:*** None

TEPS-08

Usefulness of CT attenuation correction for ^{201}Tl/^{123}I-BMIPP dual-isotope myocardial SPECT on CZT camera

***S. Yoshimura[1]**, S. Tomiguchi[2], F. Sakamoto[3], T. Matsubara[4], S. Shiraishi[4];*
[1]Graduate School of Health Sciences , Kumamoto University, Kumamoto, JAPAN, [2]Faculty of Life Sciences, Kumamoto University, Kumamoto, JAPAN, [3]Facility of Life Sciences, Kumamoto University, Kumamoto, JAPAN, [4]Kumamoto University, Hospital, Kumamoto, JAPAN.

Aim/Introduction: Dual-isotope myocardial single-photon emission-tomography (SPECT) using ^{201}Tl and ^{123}I-BMIPP is better to undergo with a CZT camera than with a conventional NaI camera because of high energy resolution on CZT camera. Precise assessment on ischemic myocardium can be performed by combining the information of fatty acid metabolism from ^{123}I-BMIPP SPECT with that of myocardial perfusion from stress ^{201}Tl myocardial SPECT. The myocardial uptake ratio of ^{123}I-BMIPP / ^{201}Tl (BM/Tl ratio) is considered to be a useful index for evaluation the myocardial ischemia. The effectiveness of CT attenuation correction (CT-AC) for quantitative assessment has not been fully studied on the CZT camera. The aim of this study was to evaluate the usefulness of CT attenuation correction for diagnosing a coronary arterial disease (CAD) using stress ^{201}Tl/ rest ^{123}I-BMIPP dual-isotope myocardial SPECT on CZT camera. ***Materials and Methods:*** 26 patients underwent dual-isotope myocardial SPECT combining stress ^{201}Tl with rest ^{123}I-BMIPP studies on CZT camera (NM530c:GE) were enrolled. They were 10 patients with CAD and 16 without CAD, respectively. In 10 patients with CAD, 2 patients have a coronary arterial stenosis of more than 75% luminal diameter (severe CAD patients). BM/Tl ratio was obtained by dividing ^{123}I-BMIPP myocardial uptake at rest by ^{201}Tl myocardial uptake at stress. Each uptake calculated from myocardial counts corrected cross calibration factors divided by injected dose. The diagnostic performance for CAD was evaluated by ROC analysis. ***Results:*** BM/Tl ratio is significantly higher in patients with CAD than those without CAD. However, BM/Tl ratio in severe CAD patients showed higher value than that in patients without CAD. The AUC of ROC curve was 0.83 without CT-AC and 0.90 with CT-AC, respectively. The AUC increase in 0.98 with CT-AC excluding

severe CAD patients. ***Conclusion:*** CT-AC is useful to diagnose the CAD using the BM/Tl ratio on stress ^{201}Tl / rest ^{123}I-BMIPP dual-isotope myocardial SPECT. BM/Tl ratio is considered to be the useful index for diagnosing CAD patients with mild coronary arterial stenosis. ***References:*** None

TEPS-09

Studies on Decision of the Cut-off Standardized Uptake Values for Normal Bones and Bone Metastases in the Vertebrae in ^{18}F-fluoride PET/CT and ^{18}F-FDG PET/CT

R. Ono[1], *N. Fujita*[1,2], *Y. Ito*[1], *T. Tada*[1], *R. Murayama*[1], *H. Ikeda*[3], *Y. Ochi*[3], *M. Nishio*[3], *Y. Tsutsumi*[2], *T. Odagawa*[1], *M. Tamura*[1], *S. Abe*[2], *K. Kato*[3];

[1]*Department of Radiological and Medical Laboratory Sciences, Nagoya University Graduate School of Medicine, Nagoya, JAPAN,* [2]*Department of Radiological Technology, Nagoya University Hospital, Nagoya, JAPAN,* [3]*Department of Integrated Health Science, Nagoya University Graduate School of Medicine, Nagoya, JAPAN.*

Aim/Introduction: For the detection of bone metastases, ^{18}F-fluoride PET/CT and ^{18}F-FDG PET/CT are used as imaging modalities and standardized uptake value (SUV) is often used besides visual image interpretation. According to previous studies, different vertebral regions have different normal SUVs. If the cut-off SUVs for normal bones and bone metastases in the cervical to lumbar vertebrae are established, they can be used for the assessment of bone metastases in the vertebrae. The aim of this study is to determine the cut-off SUVs for normal bones and bone metastases in the cervical to lumbar vertebrae in ^{18}F-fluoride PET/CT and ^{18}F-FDG PET/CT. ***Materials and Methods:*** Our study subjects were 24 patients who underwent ^{18}F-fluoride PET/CT and ^{18}F-FDG PET/CT within 2 months at our Hospital. We measured SUVmax and SUVpeak from the vertebral bodies of the cervical, thoracic, and lumbar vertebrae, and calculated the mean ± standard deviation of SUVmax and SUVpeak in the cervical, thoracic, lumbar, and cervical-lumbar vertebrae. We analyzed differences between SUVs of normal bones and bone metastases by Mann-Whitney U test. We calculated the cut-off values and area under the curve (AUC) with its associated 95% confidence interval (95%CI) of SUVmax and SUVpeak using the receiver operating characteristic curve (ROC) analysis. ***Results:*** SUVs of bone metastases were significantly higher than those of normal bones in the cervical, thoracic, lumbar, and cervical-lumbar vertebrae in ^{18}F-fluoride PET/CT and ^{18}F-FDG PET/CT. In ^{18}F-fluoride PET/CT, the cut-off SUVmax (AUCs) of the cervical, thoracic, lumbar, cervical-lumbar vertebrae were 9.3 (0.96), 10.0 (0.89), 13.4 (0.96), and 10.0 (0.92), respectively, and the cut-off SUVpeak (AUCs) of those were 8.4 (0.95), 8.5 (0.87), 10.9 (0.95), and 8.4 (0.91), respectively. In ^{18}F-FDG PET/CT, the cut-off SUVmax (AUCs) of those were 2.4 (0.77), 3.0 (0.66), 3.1 (0.77), and 3.0 (0.71), respectively, and the cut-off SUVpeak (AUCs) of those were 2.0 (0.77), 2.2 (0.64), 2.4 (0.69), and 2.1 (0.69), respectively. ***Conclusion:*** In order to differentiate bone metastases from normal bones in the cervical to lumbar vertebrae with the cut-off values, both SUVmax and SUVpeak are useful in ^{18}F-fluoride PET/CT, and SUVmax is useful in ^{18}F-FDG PET/CT. ***References:*** None

TEPS-10

Improved TEW method estimating primary photons in the energy tail in ^{201}Tl SPECT-MPI on CZT camera

K. Yoshimura[1], *S. Tomiguchi*[2], *S. Shiraishi*[3], *F. Sakamoto*[2], *R. Kamezaki*[3];

[1]*Graduate School of Health Sciences, Kumamoto, JAPAN,* [2]*Faculty of Life Sciences, Kumamoto, JAPAN,* [3]*Kumamoto University Hospital, Kumamoto, JAPAN.*

Aim/Introduction: A tailing effect has been observed in energy spectrum of ^{201}Tl using a CZT camera (NM-530c;GE) for single-photon emission-tomography myocardial perfusion imaging(SPECT-MPI). Scatter photons in the tail of energy spectrum is overestimated by scatter correction using TEW method because primary photon also includes in the tail. On the other hands, scatter correction has been performed if the primary photons or scatter photons in the tail is estimated. The aim of this study was to investigate the usefulness of scatter correction method of a combination of the TEW method and the model of primary photons in the tails by simulation. ***Materials and Methods:*** All simulations with a CZT detector fitted with a single pinhole collimator were executed using SIMIND developed by Ljungberg M. et al. First, we simulated a scatter-free point source energy spectrum at distances of 19 cm~24 cm from the detector and energy windows were set on 50-64keV (scatter window including tail effect), 64-77 keV(narrow main window for ^{201}Tl), and 64-86.1keV (wide main window for ^{201}Tl), respectively. Next, the scatter -free count ratio of the scatter window to the main window at each distance (primary photon fraction in the scatter window) was calculated and averaged. The modelling of primary photon fraction in the scatter windows at various distance was then fitted by the Gaussian function. SPECT-MPI images were reconstructed by ML-EM algorithm using this modeling. Finally, digital myocardial phantom filled with ^{201}Tl was reconstructed without scatter correction, with conventional TEW and improved TEW method, respectively. Average count ratio of myocardium to ventricular cavity (myocardial S/N) and coefficient of variation (CV) of counts in the myocardium (count uniformity) were evaluated. ***Results:*** In both narrow and wide main energy windows, myocardial S/N of new TEW method improved approximately 1.2 times greater than that of the conventional TEW method and 1.5 times greater than that without scatter correction. CV decrease in about 30% in both windows as compared with conventional TEW method. CV in the narrow main energy window was

6% lower and that in wide energy window was 6% higher than that without scatter correction. ***Conclusion:*** Improved TEW method is superior to conventional TEW method with higher myocardial S/N. The narrow main energy window shows better count uniformity in the myocardium than the wide main energy window. ***References:*** None

TEPS-11

Nuclear Medicine Dynamic Cardiac Phantom Implemented by 3D Printing Technique

H. Park[1], *J. Lee*[2];
[1]*Shingu University, Seongnam, KOREA, REPUBLIC OF,*
[2]*Songho University, Hoengseong, KOREA, REPUBLIC OF.*

Aim/Introduction: The static phantom of international standard is widely used in the field of nuclear medicine. Although the heart is a moving organ, only a fixed situation can be reproduced and evaluated, so a study on the dynamic situation is necessary. More research is necessary to address these challenges. ***Materials and Methods:*** This study used 3D printing techniques to design dynamic cardiac phantom. It also intended to reproduce the images through dynamic cardiac flow to confirm the usefulness of the proposed technique. The frame of dynamic cardiac phantom was produced based on the international standard phantom and a nuclear medicine dynamic cardiac phantom was produced based on the myocardium implemented by 3D printing technique. In this way, we compared the quantitative and qualitative properties of the static and the dynamic cardiac phantom, as well as the clinical and the dynamic cardiac phantom images. ***Results:*** In the quantitative analysis of the static and the dynamic cardiac phantoms, the SRS(Summed Rest Score) indicated 5.80 ± 0.45 points in static cardiac phantom, 3.40 ± 0.89 points in 10 stroke rate, 2.40 ± 0.55 points in 20 stroke rate, and 1.40 ± 0.55 points in 30 stroke rate in dynamic cardiac phantom. The SRS was the highest in the static cardiac phantom, followed by SRS in the order of 10, 20 and 30 stroke rate in the dynamic cardiac phantom($P<0.05$). The TPD(Total Perfusion Deficit) was the highest in the static cardiac phantom, followed by TPD in the order of 20, 10 and 30 stroke rate in the dynamic cardiac phantom. The Adjusted Man-Whitney test was conducted to determine which groups showed significant differences between the static and dynamic cardiac phantom 30 stroke rates, with a very significant difference of <.0001, but no significant difference between the static and dynamic cardiac phantom 10 and 20 stroke rates, respectively, was found to be 0.899. ***Conclusion:*** The potential for clinical application of the proposed method was confirmed in the dynamic cardiac phantom implemented with 3D printing technique. It is believed that the objective information secures the reliability of the inspection equipment and it contributes to improve the value of diagnosis of nuclear medicine. ***References:*** None

TEPS-12

Phantom analysis in hybrid imaging

S. Rep, *S. Kotar;*
University Medical Centre Ljubljana, Ljubljana, SLOVENIA.

Aim/Introduction: The distribution of radiopharmaceuticals in the body after administration can be demonstrated with two tomography methods. The first is a single-photon emission computed tomography and the second positron emission tomography, which (in combination with computer tomography) enables the viewing of physiological and morphological information from the body. The purpose of research is qualitatively and quantitatively evaluating the contrast-to-noise ratio (CNR) and the signal-to-noise ratio (SNR) in PET/CT and SPECT/CT images obtained with a NEMA body phantom. ***Materials and Methods:*** The NEMA body phantom was filled with 99mTc and 18F FDG in ratios of 1 : 2, 1 : 4, and 1 : 8. Phantom imaging was done with SPECT/CT and PET/CT. The obtained scintigrams were evaluated qualitatively and quantitatively by using the OASIS processing software. The SNR was quantitatively evaluated for the background of phantoms and CNRs for assessing the spheres according to the background. SPSS 21 software was used for analysis. ***Results:*** Quantitative analysis of spheres in the NEMA body phantom shows spheres with diameters of 17, 22, 28 and 37 mm in ratios of 1 : 2, 1 : 4, and 1 : 8 on SPECT/CT. In a ratio 1 : 8, SPECT/CT also shows spheres with diameters of 13 mm. All spheres in the NEMA body phantom are visible on the PET/CT at ratios of 1 : 4 and 1 : 8, and at a ratio of 1 : 2 only spheres with diameters of 17, 22, 28, and 37 mm are visible. The quantitative value of the SNR for the background was higher in PET/CT according to SPECT/CT. A comparison of CNR for PET/CT and SPECT/CT showed a significant difference between the two methods ($p = 0.002$). For both methods, the SNR value is higher in relation to the height of the ratio and shows a good correlation between ($r = 0.85$ and $p < 0.001$). ***Conclusion:*** The results of the analysis between SPECT/CT and PET/CT methods showed a better SNR and CNR ratio in the PET/CT image method compared to SPECT/CT. ***References:*** Lee TC, Alessio AM, Miyaoka RM, Kinahan PE (2016). Morphology supporting function: attenuation correction for SPECT/CT, PET/CT, and PET/MR imaging. J Nucl Med Mol Imaging 60(1): 25-39. Beijst C, de Keizer B, Lam MGEH, Janssens GO, Tytgat GAM, de Jong HWAM (2017). A phantom study: Should 124 I-mIBG PET/CT replace 123 I-mIBG SPECT/CT?. Med Phys 44(5): 1624-1631. doi: 10.1002/mp.12202.

TEPS-13

Evaluation of the Usefulness of SPECT Brain Phantom Based on 3D printing

H. Park[1], *Y. Lee*[2], *H. Lee*[1], *J. Lee*[3];
[1]*Shingu University, Seongnam, KOREA, REPUBLIC*

OF, [2]Kismits, Seoul, KOREA, REPUBLIC OF, [3]Songho University, Hoengseong, KOREA, REPUBLIC OF.

Aim/Introduction: Although an experiment was shown that 3D printing material such as ABS(acrylonitrile butadiene styrene) and PLA(polylactic acid) showed a possibility to replace the PMMA(Polymethylmethacrylate) which is normally used for phantom, a lot of experiment haven't been performed to compare the usefulness of these 3D printing materials and PMMA in nuclear medicine. In this experiment, SPECT(Single-photon emission computed tomography) brain phantom which was made with 3D printing material and 3D printing technology was used for it to evaluate the applicability of it. ***Materials and Methods:*** The information from the original phantom using CT(computed tomography) were obtained. The acquired file was printed by the SLA(Stereo lithography apparatus) method of ABS materials. SPECT-CT was used to obtain images. We filled the both Phantom with a solution mixed with 1 mCi ^{99m}Tc in 1 liter of water and acquired images in accordance with the standard protocol. Using Image J, the SNR(signal to noise ratio) for each slice of the image was obtained. As a reference images, AC(Attenuation correction) images were used. For the analysis of acquired images, ROI(region of interest) was set in the white matter and gray matter sections of each image, and the average Intensity Value within the ROI were compared. ***Results:*** The 3D printed phantom had 5.43 average SNR and the original phantom had 5.32 average SNR. It showed that the 3D printed phantom had 0.1 higher SNR. However, white matter and gray matter of the original phantom had 9.59 and 32.64 intensity value while the 3D printed phantom had 13.32 intensity value for white matter and 42.98 for gray matter. The ratio of intensity value of them was 1:3.4 for white matter and gray matter of the original phantom and 1:3.2 3D printed phantom. ***Conclusion:*** Therefore, if calibration value is applied, it is believed that contributing effective examination of quality control and cost reduction. Since there were technical limitations and we used only one radioactive isotope, solving the technical problem and variety radioactive isotope would be required for further study. ***References:*** None

TEPS-14

Implementation of an automatically quantification package (Hone Graph) for phantom-based image quality assessment of bone SPECT: computerized self-classification of detectability using a novel index

H. Ichikawa[1,2], *T. Shibutani*[2], *M. Onoguchi*[2], *K. Kawakami*[3], *K. Nagatake*[4], *T. Ito*[5], *T. Kato*[1];
[1]Department of Radiology, Toyohashi Municipal Hospital, Toyohashi, JAPAN, [2]Department of Quantum Medical Technology, Graduate School of Medical Sciences, Kanazawa University, Kanazawa, JAPAN, [3]Products Marketing Dept., FUJIFILM Toyama Chemical Co., Ltd., Tokyo, JAPAN, [4]Quality Assurance Dept., FUJIFILM Toyama Chemical Co., Ltd., Tokyo, JAPAN, [5]Department of Radiology, Saiseikai Yokohamashi Tobu Hospital, Yokohama, JAPAN.

Aim/Introduction: We have already developed a custom-design thoracic bone scintigraphy-specific phantom (hereafter referred to as "SIM^{2}bone phantom") to assess image quality in bone SPECT imaging. The purpose of this study was to develop and demonstrate the validity of an automatically assessment system for imaging technology in bone SPECT. ***Materials and Methods:*** We were able to make more realistic phantom configurations of the thorax, spines, mediastinum, lung and bone metastases. SIM^2 bone phantom was constructed with an elliptical shape with a major axis of 310 mm, a minor axis of 210 mm, and a height of 320 mm. The vertebral body and reference section were constructed in a cylinder shape with a diameter of 36 mm, and height of 207 and 35 mm, respectively. Spherical lesion with diameters of 13, 17, 22 and 28 mm inserted in the vertebral body. The developed software was fully automatically calculated quantitative indexes (e.g. contrast-to-noise ratio, % coefficient of variance, % detectability equivalence volume, sharpness index, etc.). The repeatability and reproducibility of each index was assessed and compared between automatically and manually methods. A detectability score (DS) was defined four observation types to score the hot spherical lesions with the following value and was classified with the quantitative indexes by using decision tree analysis. The DS of lesions is 1) poor, 2) average, 3) adequate, 4) excellent. The validity of DS was assessed by comparison with visual analysis. ***Results:*** The repeatability and reproducibility of the software were excellent, and the automatically classified DSs exhibited an almost perfect agreement with those of classified by three expert board-certified nuclear medicine technologists. Decision tree analysis produced seven terminal groups, and four quantitative indexes were used for classifying the DS. Percentage agreement between Hone Graph and experienced, moderately experienced and inexperienced were almost perfect agreement, substantial and moderate, respectively. ***Conclusion:*** The software could automatically classify the detectability of hot lesion in the SIM2 bone phantom using the quantitative indexes, which were calculated by itself. It is suggested that this software is excellent in convenience or repeatability in order to fully automatically perform from analysis after data input to output result. ***References:*** None

TEPS-15

^{125}I Radiation protection

J. Bartl*, R. Bartlova;*
Masaryk Memorial Cancer Institute, Brno, CZECH REPUBLIC.

Aim/Introduction: Radionuclide source ^{125}I is

intended for medical use for its introduction into close proximity to the tumor centre for its precise localization and subsequent operative extirpation. ***Materials and Methods:*** Type-approved small closed radionuclide sources (Iodine grain IsoAid ^{125}I) in localization needles. Package of iodine grains is taken from the supplier by radiation worker of the Pharmacy Department and in a shielded container is placed in a reserved place. Prior to the planned administration of iodine grains, the radiological assistant of the Radio Diagnostics (RD) Department will take a predetermined number of sources (maximum 3 pcs per day) that inserts into the portable shielded container and deposits it in the storage area behind the mammographic intervention room. The individual iodine grain is applied by the radiologist directly on the mammographic intervention scan to the patient's breast tissue. After implantation of the grain, the patient goes to the operating room of Surgical Department. Iodine grains are removed from the patient's breasts during radio-guided surgery. The extirpated node with iodine grain is transported from the operating room by elevator for pathological samples to the pathology site. After the removal of the grain by the pathologist and after purification in the formaldehyde solution, all iodine grains from the same working day are handed over to the supervising person on the Nuclear Medicine (NM) Department, who puts them in the transport shielded container, which is transferred to the storage areas of the NM Department. Here is stored in the form of solid waste for the period of release limits compliance, and then released into the environment within municipal waste. ***Results:*** The staff for handling of ionizing sources are trained in occupational safety and radiation protection by supervising persons of RD and NM Departments. The patient's written informed consent to the application of radionuclide grain and its familiarity with other procedures and behavior during application is prepared by the supervising person and the head of RD Department. Pathologists are not guided as radiation workers. Prior to the start of this work, must be demonstrably trained by the supervising person of NM Department in radiation protection and occupational safety with this type of radionuclide. ***Conclusion:*** The employees of RD and NM Departments for handling of ionizing sources are radiation workers equipped with full-body OSL personal dosimeters, finger thermo luminescent dosimeters (TLD) and electronic direct reading personal dosimeters. Pathologists are equipped with finger TLDs. ***References:*** None

TEPS-16

Simultaneous myocardial Tc-99m/I-123 imaging using a cadmium-zinc-telluride camera: Validation of triglyceride deposit cardiomyopathy diagnosis

T. Niimi[1], *M. Sugimoto*[1], *K. Unno*[1], *S. Yoshida*[2];
[1]*Nagoya Daini Red Cross Hospital, Nagoya, JAPAN,*
[2]*Nagoya University, Nagoya, JAPAN.*

Aim/Introduction: Simultaneous myocardial Tc-99m/I-123 (Tc/I) imaging using a cadmium-zinc-telluride (CZT) camera allows for the concomitant evaluation of the processes targeted by the two radioisotopes with reduced radiation exposure. Recently, attention has been paid to myocardial scintigraphy with I-123-β-methyl iodophenyl-pentadecanoic acid (^{123}I-BMIPP) as a diagnostic imaging method for triglyceride deposit cardiomyopathy (TGCV). Among the features of ^{123}I-BMIPP scintigraphy, the washout rate is a major diagnostic criterion (less than 10%) in addition to myocardial perfusion and metabolism. To validate a CZT camera's (D-SPECT) response to TGCV diagnosis, simultaneous myocardial Tc/I imaging results were quantitatively evaluated. ***Materials and Methods:*** The impacts of cross-talk and reconstructed image contrast were quantified by measuring the contrast-to-noise ratio (CNR) and transmural defect contrast in the left ventricle wall (C_{TD}) induced by the difference in energy for combinations of Tc/I using a cardiac phantom. The collected data were reformatted by reconstruction without scatter correction and reorientation. We also verified the appropriate dose ratio, including the cross-talk rate of the energy spectra of both nuclides. The washout rate of I-123 was calculated using a cardio-hepatic phantom filled with clinically simulated proportions of I-123 for each organ. After acquiring the early images, the delay images were acquired 4 times with any time interval for the calculation of the washout rate (with decay correction). ***Results:*** The C_{TD} values of Tc/I were 91% for Tc-99m and 95% for I-123 in the anterior wall without scatter correction. Regarding the inferior wall, the C_{TD} was approximately 20% lower than that of the anterior wall. No notable difference was confirmed in the CNRs of the anterior and inferior walls. Higher Tc/I dose ratios for Tc-99m resulted in lower cross-talk rates for I-123, and Tc-99m exhibited a cross-talk rate of about 5% at 3 times the dose of I-123. The mean error of the washout rate for the combination of the data of the five measurements was 3%. ***Conclusion:*** The D-SPECT system features a difference in detectability between the anterior and inferior walls; however, it is capable of performing high-quality simultaneous dual-isotope imaging using Tc/I to facilitate TGCV diagnosis. The criteria for TGCV diagnosis using the D-SPECT system should be judged based on a washout rate error of 3%. ***References:*** None

TEPS-17

Effect of Reconstruction Parameters on Lu-177 SPECT Imaging

Y. Parlak, *D. Goksoy, C. Sezgin, G. Mutevelizade;*
Celal Bayar University, Faculty of Medicine, Department of Nuclear Medicine, Manisa, TURKEY.

Aim/Introduction: Lutetium-177 is a radionuclide used for the treatment of the neuroendocrine tumors, bone pain from metastatic disease, and prostate cancer. For lesion dosimetry based 177Lu, resolution and reconstruction parameters are critical and should be considered. In this study, 177Lu was evaluated of activity quantification and reconstruction parameters for different combinations on planar and SPECT imaging. ***Materials and Methods:*** A uniform "body phantom" was used with 6 lesions (6900 ml; distance; 10 mm to 35 mm) and filled with 444 MBq 177Lu-water. First, the calibration factor of the gamma camera was calculated using a point source with known radioactivity. The phantom was scanned by positioning in the center of the gamma camera (GE, Infinia) gantry. Planar images were acquired for 10 min 256 x 256 matrix at a single bed position and multiple time points. The SPECT acquisition parameters were performed for 120 projections, 30 s per projection, a non-circular step-and-shoot acquisition orbit and 128 × 128 matrix. Projection data were acquired using two gamma rays of 113±15 keV with a 6% abundance factor and 208±15 keV with an 11% abundance factor using a parallel-hole medium-energy general-purpose (MEGP) collimator. The concentration of activity in the signal-to-background ratio was performed by manually drawing regions of interest (ROIs). All images were reconstructed with OSEM 3D, Flash 3D and filtered back-projection algorithms for different combinations. ***Results:*** The gamma camera calibration was calculated as 7.1 cps/MBq from planar scans. All reconstructions were processed in terms of the signal to background ratio in each sphere. According to the analyzes, the highest SNRs were calculated as 2.97, 3.4, 3.61 for OSEM, FBP and Flash 3D reconstructions, respectively. The SNR obtained with the Flash 3D algorithm were found statistically different ($p<0.05$). ***Conclusion:*** The accuracy of activity determination was evaluated for 177Lu imaging studies. Our results indicate that the methods used in this study allow for accurate determination of 177Lu activity, and also suggest that standardizing reconstruction settings decreases inter-system variability for quantification of 177Lu. This has an important role in dosimetry studies ***References:*** None

TEPS-18

A comparison of the results of myocardial perfusion analysis software for ischemia diagnosis between each coronary artery branch area

T. Iimori[1], *H. Miyauchi*[2], *T. Sada*[1], *T. Umezawa*[1], *K. Sawada*[1], *Y. Masuda*[1], *Y. Kuwabara*[2], *T. Uno*[3], *Y. Kobayashi*[2];
[1]*Department of Radiology, Chiba University Hospital, Chiba, JAPAN,* [2]*Department of Cardiovascular Medicine, Chiba University Graduate School of Medicine, Chiba, JAPAN,* [3]*Department of Diagnostic Radiology and Radiation Oncology, Chiba University Graduate School of Medicine, Chiba, JAPAN.*

Aim/Introduction: The results of stress myocardial perfusion single-photon emission computed tomography (SPECT), can be quantitatively evaluated by calculating the grade of ischemia or infarction using a myocardial perfusion analysis software. CardioREPO provided by FUJIFILM Toyama Chemical Co., Ltd. is a myocardial perfusion analysis software, and various verification studies have been performed regarding its ischemia diagnostic ability. However, there are few reports of its verification of ischemia diagnostic capability based on the coronary artery branch region[1,2]. The concordance rates of CardioREPO results, quantitative perfusion SPECT (QPS) scores, and coronary angiographic findings were evaluated for each coronary artery branch (right coronary artery: RCA, left anterior descending: LAD, and left circumflex: LCX). ***Materials and Methods:*** Sixty-two patients who underwent both technetium-99m-methoxy-isobutyl-isonitrile myocardial perfusion SPECT and coronary angiography were evaluated. Using stress myocardial perfusion SPECT, the total value of the regions corresponding to the RCA, LAD, and LCX was calculated based on CardioREPO and QPS from the myocardial data divided into 17 segments. 1) The correlation coefficient was calculated for each coronary artery branch based on CardioREPO and QPS from the calculated scores. 2) When coronary angiography showed vascular stenosis of 75% or greater, the region was defined as "with ischemia." Based on these results of coronary angiography, the ischemia diagnostic ability of CardioREPO and QPS was evaluated using the receiver operator characteristic (ROC) curves. ***Results:*** 1) Correlation between CardioREPO results and total defect score of QPS The rank correlation coefficients for each coronary artery governing region were determined in all regions of the RCA, LAD, and LCX.2) Results of ROC analysis of coronary angiography, CardioREPO, and QPS Although there was no difference between CardioREPO and QPS in terms of the summed stress score, the results of the analysis for each coronary artery branch showed that CardioREPO had a higher area-under-the-curve value than that of the QPS in all coronary artery branch regions. ***Conclusion:*** In this study, the evaluation of coronary branch ischemia using CardioREPO was shown to be useful. ***References:*** 1). Nakajima K, et al. Diagnostic Performance of Artificial Neural Network for Detecting Ischemia in Myocardial Perfusion Imaging. Circ J 2015; 79: 1549-1556.2). Gräni C, Benz DC, Schmied C, et al. Hybrid CCTA/SPECT myocardial perfusion imaging findings in patients with anomalous origin of coronary arteries from the opposite sinus and suspected concomitant coronary artery disease. J Nucl Cardiol. 2017 Feb;24(1):226-234.

TEPS-19

Immediate adverse effects recorded in patients with neuroendocrine tumors undergoing treatment with ^{177}Lu-oxodoteotridre, using Lysine and Arginine at a

slower rate of infusion. Nursing management

S. Lopez Gandul, E. Albuixech, J. Arcos, S. Garcia, F. Hernando, M. Iniesta, E. Lopez, L. Lozano, Y. Samadi, C. Sanchez, I. Garlito, D. Villasboas, A. Garcia, J. Castell;
Hospital Universitari Vall d'Hebrón, Barcelona, SPAIN.

Aim/Introduction: To record the immediate adverse effects (IAEs) in cancer patients undergoing treatment with ^{177}Lu-oxodoteotride, using amino acid formula Lysine and Arginine, by Metabolic Therapy Unit staff. ***Materials and Methods:*** Thirty-four patients (9 women and 25 men, 22±83 age) with gastroenteropancreatic neuroendocrine tumors and paragangliomas, underwent treatment with ^{177}Lu-oxodoteotride in our Metabolic Therapy Unit (July 2016 to April 2020). Protocol: intravenous premedication with Ondasentron (8mg) and Pantropazol (40mg); was followed by a continuous perfusion of amino acid Lysine and Arginine formula (1500cc /6hours). 30 minutes into the aminoacid perfusion, ^{177}Lu-oxodoteotride (200mCi/7400MBq) was administered using intravenous infusion pumps (lasting up to 1 hour in some cases, to avoid some adverse reactions). The hospital protocol establishes the administration of four doses of ^{177}Lu-oxodoteotride every 2 months, depending on the patients evolution and response to treatment. IAEs were recorded during the administration of amino acid formula. ***Results:*** Thyrty-four patients underwent eighty-nine ^{177}Lu-oxodoteotride treatments and 16,8% had IAEs (nausea 5, vomiting 3, abdominal pain 1, diarrhea 2, headache 1, flushing 1, dizziness 1 and muskuloeskeletal pain 1). ***Conclusion:*** According to our experience, the use of our protocol of administration of Lysine and Arginine administrated at a slower infusion rate significatively reduces the appearence of IAEs in patients with ^{177}Lu-oxodoteotride treatment. ***References:*** None

TEPS-20

Incidental suspicious COVID-19 findings in asymptomatic patient during ^{18}F-FDG PET/CT follow-up

***M. Paula**, A. Fonseca, C. Marques, L. Ribeiro, S. Sequeira, H. Duarte; Ipo Porto, Porto, PORTUGAL.*

Aim/Introduction: Although nuclear medicine procedures are unlikely to have a role in the primary diagnosis of COVID-19, there may be incidental detection found in PET/CT patients with history of neoplasic disease. These findings have implications in the hospital daily routines. Furthermore in addition, it is our task as Nuclear Medicine Technologists to know and follow the institution's guidelines for safely dealing with patients suspected of having COVID-19 infection, protecting staff and other patients. ***Materials and Methods:*** A 41-year-old woman with a 1-year history of breast cancer underwent a follow-up 18F-FDG PET/CT during COVID-19 outbreak. After the PET/CT acquisition abnormalities in parenchyma lung have been reported. It was suspected that the changes presented on CT could be related to infection by COVID-19. At the end of the examination, the patient was treated as potentially infected with COVID-19 and was referred to a COVID-19 diagnosis area that was created at the institution to assist patients who, during examinations or consultations, present suspicious criteria of infection ***Results:*** The PET/CT was report as "No evidence of hypermetabolic lesions. Hyperactivity in poorly defined peripheral pulmonary densifications scattered in the right lung of probable nature inflammatory (infectious? iatrogenic?)…". The patient was forwarded, according to the rules instituted in our hospital, to the department responsible for testing patients with suspected COVIDE-19. The patient remained in the hospital until the test result was obtained, which in this case was a negative test for COVID-19. ***Conclusion:*** The CT patterns of respiratory infection in PET / CT has been described as subcapsular densifications attributed to recent RT. Nonspecific symptoms or asymptomatic patients that present suspicious images should be quickly tested and monitored for SARS-CoV-2 nucleic acid. The COVID-19 infection changed the way we work. The health system and professionals must be alert and should aim to provide safe patient care, workplace safety and well-defined rules for dealing with suspected cases that may occur according to the National and International recommendations. ***References:*** None

TEPS-21

The impact of SARS-Cov-2 emergency in the activity of the Nuclear Medicine Department, a single-center experience

***M. Maccagnani**, A. Farina, R. Bonfiglioli, S. Fanti;*
Azienda Ospedaliero-Universitaria S.Orsola-Malpighi, Bologna, ITALY.

Aim/Introduction: The SARS-Cov-2 emergency was declared in Italy on January 31th. It progressed in steps until March 11th, when all the Italian territory was involved in extremely severe restrictive measurements. The emergency had a substantial impact on all the activities of the hospital. The aim of this work was to investigate the real effect of this restriction on the management of the patients and on the volume of examinations performed in our Nuclear Medicine Center (NMC). ***Materials and Methods:*** Nuclear medicine diagnostic methods are classified as second-level, and thus the NMC was not directly involved in the confirmation of SARS-CoV-2 infections. However, access to the NMC by positive cases cannot be excluded. Moreover, both oncological and non-oncological pathologies may present with the same symptoms of COVID-19, and the etiopathogenesis of the infection does not ease the rapid identification of possible infects patients. For this reason, the NMC first step was the creation of a "checkpoint",

surveilled by a nuclear physician and a nurse, where all the outpatients were taken the temperature and examined about COVID-19-like symptoms. Secondly, the NMC medical team assessed all the scheduled examinations until the end of April and postponed the non-urgent exams. The same approach was put in place for all the exams carried out in collaboration with other specialists due to the change in their volume of activities. In collaboration with the Clinical Hygiene Department, new and more precise procedures were prepared regarding the reception and admittance of patients in the diagnostic areas, their discharge, the cleaning and disinfection of furniture and equipment in between examinations. In the same way, some patients contacted the ward expressing the will to postpone, or cancel, the exams already scheduled. ***Results:*** As a result, there was a significant drop in the activities carried out in the NMC compared to the same period (March-April) of the previous year: - 27% of PET activity (from 2038 to 10495 exam) and -40% of conventional nuclear medicine activity (from 1050 to 629 exams). ***Conclusion:*** In conclusion, the decrease in activity was a key factor to safeguard the health of patients and operators. In fact, no new case of COVID-19 infection related to the presence or to the diagnostic activity of the unit was reported in patients or even in the staff. ***References:*** None

TEPS-22

Covid19 emergency: how the Nuclear Medicine dept of Verona reacted

L. Pavanello, F. Sciume, D. Grigolato, M. Cucca, L. Locantore, E. Biggi, M. Naseri, M. Zuffante;
AOUI di Verona, Verona, ITALY.

Aim/Introduction: We describe our experience to contain and reduce the ongoing transmission of the virus while ensuring scintigraphy or PET/CT in patients who need it for diagnostic purpose and monitoring response to therapy. Our operating unit has implemented all the legal provisions given by the Ministry of Health involving the Nuclear Medicine staff to contain the infection. ***Materials and Methods:*** Our actions have been: hang signboards with the instructions for hand washing, use of mask and social distancing at the hall of our department. Give new surgical masks to all our patients. Ensure that all patients do the hand washing with the available gel as soon as they enter in the hall. Reduce the number of people entering the dept. Modify the Appointment Agenda, in order to avoid gathering in the waiting room. The diagnostic activity was reviewed on the basis of urgency and priority. The day before the exam our nurses call patients and do a triage, asking information on their health. The day of the exam their temperature is checked, in diagnostic, the patients remove their gloves and wash again their hands, the staff ensures that patient mask is well kept during the examination. When the scan is completed, the patient waits for the doctor's approval in the same diagnostic room, this to prevent the patient to stay in different waiting rooms. If patients have a temperature on the day of the scanning they are invited to go home and contact their GP. In case the scans are needful and still the test, the patients are considered suspected for coronavisus and they are asked to come at the end of the day. ***Results:*** Our operativity has changed by raising the level of attention to the highest risk, this to limit or contain the coronavirus contagion between operators and patients as low as possible. We work with even more attention to the behavior and management of the patient, who is always seen as potentially infected. ***Conclusion:*** To date, after 2 months of emergency, being in a location where the infection is at a high level and having had few patients in our dept where viral pneumonia was discovered at PET/CT and subsequently tested positive with the swab, nobody of the staff had the coronavirus disease. Our personnel was tested once or twice for the virus. This validate the management policy in our service as a good one. ***References:*** None

805

M2M Track - Featured Session: Translational Interventional Nuclear Medicine

Friday, October 23, 2020, 16:55 - 18:00 Channel 5

OP-411

From Lab to Clinic - Moving Forward in Urologic Surgery

O. Brouwer; The Netherlands Cancer Institute, Antoni van Leeuwenhoek Hospital, Urology, Amsterdam, NETHERLANDS.

OP-412

A Novel Clickable MSAP Agent for Dual Fluorescence/ Nuclear Labeling of a GRPR-Targeted Peptide

K. Chen, J. Nieuwenhuizen, M. Handula, Y. Seimbille;
Erasmus MC, Rotterdam, NETHERLANDS.

Aim/Introduction: Dual-modality optical/radio-imaging has received great attention in preoperative surgical planning and intraoperative optical guidance for tumor therapy.[1] Gastrin-releasing peptide receptor (GRPR) is an established target for many cancers, such as prostate and breast cancers.[2] We herein describe the development of a novel dual-modality agent for site-specific labeling of a GRPR-targeted peptide through a 2-cyanobenzothiazole (CBT)/1,2-aminothiol click reaction. Notably, the CBT-based multifunctional single-attachment-point (MSAP) agent enables a general and single-step synthesis of the dual-modality probe. In this study, the radiolabeling protocol was optimized by using CBT-scavenger to improve the reaction rate and molar activity of the imaging probe. ***Materials and Methods:*** DOTA-Cy5.5-CBT (1) and the GRPR-targeted

peptide (Cys-d-Phe-Gln-Trp-Ala-Val-Gly-His-NHCH[CH_2-$CH(CH_3)_2$]$_2$, 2) were prepared by solid phase synthesis. The DOTA chelator was labeled with ^{68}Ga (or ^{111}In) in a NaOAc buffer (pH 5.5) at 100 °C for 15 min. The CBT/1,2-aminothiol click reaction was performed by mixing [^{68}Ga]-1 (or [^{111}In]-1) with the peptide 2 in a molar ratio of 1:20 at 37 °C in PBS buffer (pH 7.4) and in the presence of TCEP. After 20 min, the mixture was incubated with CBT-magnetic beads for another 5 min. The radiolabeling and scavenger reaction was monitored by RP-C18 HPLC. ***Results:*** CBT-bearing chelator 1 and peptide 2 were obtained in a yield of 45% and 23% after purification by RP-C18 HPLC, respectively. Labeling of 1 with ^{68}Ga and ^{111}In was successfully achieved in slightly acidic aqueous conditions to give [^{68}Ga]-1 and [^{111}In]-1 with high RCYs (> 99%). Two-step radiolabeling of 2 with [^{68}Ga]-1 or [^{111}In]-1, provided the corresponding radiolabeled GRPR-targeted peptides with high RCYs (> 99%) and molar activities (~10 MBq/nmol). Completely removal of non-reacted 2 from the solution was successful with using CBT-scavenger. ***Conclusion:*** The novel dual-modality GRPR-targeted probe was successfully synthesized and labeled with ^{111}In and ^{68}Ga for respective SPECT/fluorescence and PET/fluorescence imaging studies. The MSAP radiolabeling approach based on the orthogonal CBT/1,2-aminothiol click reaction is very practical for regioselective labeling of N-terminal cysteine-containing sensitive biomolecules. Further in vitro stability, biodistribution and imaging studies of the GRPR ligand are currently underway in our laboratory. ***References:*** (1) Kuil, J.; Velders, A. H.; van Leeuwen, F. W. Bioconjug Chem 2010, 21, 1709. (2) Kaloudi, A.; Lymperis, E.; Giarika, A.; Dalm, S.; Orlandi, F.; Barbato, D.; Tedesco, M.; Maina, T.; de Jong, M.; Nock, B. A. Molecules 2017, 22.

OP-413

Fluorescence-based video tracking of the DROP-IN gamma probe during robotic surgery - technological evaluation in porcine models

M. van Oosterom[1,2], K. M. Houwing[1], P. R. Roos[1], T. Buckle[1,2], D. M. van Willigen[1], E. Mazzone[3,4], K. Bauwens[4], P. Dell'Oglio[1,4], F. W. B. van Leeuwen[1,2,4];
[1]IMI-Lab, Dept. of Radiology, Leiden University Medical Center, Leiden, NETHERLANDS, [2]Department of Urology, Netherlands Cancer Institute - Antoni van Leeuwenhoek Hospital, Amsterdam, NETHERLANDS, [3]Division of Oncology/Unit of Urology, URI, IRCCS Ospedale San Raffaele; Vita-Salute San Raffaele University, Milan, ITALY, [4]ORSI Academy, Melle, BELGIUM.

Aim/Introduction: Minimally invasive interventions in the form of robot-assisted laparoscopic surgery, are claiming an increasing share of the surgeries performed. Through the clinical introduction of the DROP-IN gamma probe, surgical robotic systems have become compatible with radioguided surgery (e.g. sentinel node or PSMA-targeted dissection) [1,2,3]. 'GPS-like' surgical navigation of laparoscopic detection modalities based on preoperative roadmaps has been suggested to further advance the realization of precision surgery [4]. The tool-tracking needed for navigation, however, is complex in a laparoscopic setting. In an effort to integrate the DROP-IN modality in a robotic navigated workflow, a fluorescence-based video-tracking method was developed and validate in a surgical setting. ***Materials and Methods:*** A clinical grade multispectral-fluorescence laparoscope, capable of detecting fluorescein (Λ_{ex}=488 nm, Λ_{em}=515 nm) and indocyanine green (ICG; Λ_{ex}=800 nm, Λ_{em}=820 nm), was used [5]. Dedicated video-processing algorithms were developed to detect and segment fluorescent markers on the DROP-IN gamma probe. Based on this information the relative position and orientation (pose) of the DROP-IN could be calculated, in real time, with respect to the fluorescence laparoscope. Tracking algorithms were integrated with a surgical navigation system able to optically track the pose of the laparoscope and the patient. In a robotic torso phantom this allowed DROP-IN probe navigation towards radioactive lesions (^{99m}Tc) identified on SPECT/CT. The functionality of the DROP-IN probe navigation was further validated during robotic surgery in porcine models (n=4). ***Results:*** Using multispectral fluorescence imaging, the DROP-IN markers could be differentiated from ICG-positive lesions based on emission wavelength. Maintaining a direct line-of-sight with respect to the fluorescent markers enabled intraoperative tracking of the DROP-IN probe with respect to lesions even under surgical conditions. Augmented reality overlays, indicating the real-time distance between the DROP-IN and the lesion targets, were visualized in the surgical robotic console. Integration with the SPECT navigation workflow, allowed accurate positioning of the DROP-IN probe relative to radioactive lesions as defined in preoperative SPECT/CT scans. Real-time audible and numerical feedback provided by the DROP-IN gamma probe verified that the localization was correct. ***Conclusion:*** We have shown that the implementation of the DROP-IN probe technology can in the future be expanded with (multispectral) fluorescence imaging-based surgical navigation towards lesions identified in preoperative images. With that a next step has been taken towards creating impact on clinical care using radioguided surgery in the robotic setting. ***References:*** [1] M.N.van_Oosterom_et_al.,AJNMMI,2016; [2]P.Meershoek_et_al.,EJNMMI,2019; [3]F.W.B.van_Leeuwen_et_al.,Clin_Nucl_Med,2019; [4]M.N.van_Oosterom_et_al.,J_Urol,2018; [5]P.Meershoek_et_al.,J_Nucl_Med,2018.

OP-414

Tumor-targeting potential and photodynamic therapy efficacy of dual-labeled PSMA-N064: An ex vivo incubation study on human prostate cancer samples

Y. Derks[1], M. Rijpkema[1], M. Schilham[1], H. Amatdjais-Groenen[2], A. Kip[1], S. van Lith[1], M. Sedelaar[1], D. Somford[3], M. Simons[1], P.

Laverman[1], M. Gotthardt[1], D. Löwik[2], S. Lütje[4], S. Heskamp[1]; [1]Radboud university medical center, Nijmegen, NETHERLANDS, [2]Radboud University, Nijmegen, NETHERLANDS, [3]Canisius Wilhelmina Hospital, Nijmegen, NETHERLANDS, [4]University hospital Bonn, Nijmegen, NETHERLANDS.

Aim/Introduction: Incomplete resection of prostate cancer (PCa) leads to disease recurrence and consequently poor oncological outcome. To achieve complete resection, prostate specific membrane antigen (PSMA) targeting multimodal ligands may be used for intraoperative tumor detection, delineation, and targeted photodynamic therapy (tPDT). Previously, we demonstrated that PSMA-N064, a PSMA ligand conjugated with IRDye700DX and labeled with ^{111}In via DOTAGA, shows promising tumor-targeting properties and tPDT efficacy in preclinical tumor models. Here, we aimed to evaluate its potential for intraoperative multimodal imaging and tPDT using human PCa samples in an ex vivo incubation study. ***Materials and Methods:*** Eleven patients scheduled for radical prostatectomy were included. Biopsy samples were obtained from the surgically removed prostate, both from the tumor and from contralateral (healthy) prostate tissue. To study the tumor-binding potential of PSMA-N064 ex vivo, tissue samples (n=10) were incubated with ^{111}In-labeled PSMA-N064 (0.025 nmol, 26.3 MBq/nmol, 4 hrs). To study the efficacy of tPDT (n=1, patient inclusion is ongoing), tissue samples were incubated with PSMA-N064 (0.05 nmol, 4 hrs), washed and exposed to near infrared (NIR) light (100 J/cm^2). Cellular distribution of the ligands within the tissue sample was evaluated macroscopically using fluorescence flatbed scanning and autoradiography. Subsequently, tissue samples were sectioned and analyzed immunohistochemically (H&E, PSMA, Caspase-3 and γH2AX). Discrimination between tumor and normal tissue regions within the tumor sample was performed by a pathologist based on H&E staining. Localization of the marked tumor regions was compared with autoradiography, fluorescence imaging, and PSMA immunohistochemistry. ***Results:*** Macroscopic fluorescence imaging and autoradiography of ^{111}In-PSMA-N064 showed preferential accumulation in tumor tissue. A significant difference in fluorescence intensity was observed when comparing tumor regions of ^{111}In-PSMA-N064-incubated tissue samples (mean fluorescence intensity 58,143 ± 17,267) to either adjacent normal tissue regions within the same tissue sample (23,712 ± 10,364, $p < 0.01$) or the contralateral control sample from healthy tissue (20,220 ± 10,871, $p < 0.001$). Moreover, co-localization of the radiosignal, fluorescence signal and PSMA expression in the marked tumor regions was observed. tPDT treatment with NIR light increased Caspase-3 and γH2AX staining in tumor samples compared with healthy prostate tissue. ***Conclusion:*** The current results strongly suggest a PSMA-specific accumulation of ^{111}In-PSMA-N064 in human PCa samples, that can be visualized by both radionuclide and fluorescence imaging. Although patient inclusion has to be completed, preliminary results point towards increased cell death, as proven by Caspase-3 and γH2AX staining, upon PSMA-N064 mediated tPDT on human PCa samples. ***References:*** None

OP-415

C-Met receptor-specific fluorescence-guided surgery in penile cancer patients

***H. M. de Vries[1]**, M. N. van Oosterom[2], D. M. van Willigen[2], H. G. van der Poel[1], F. W. B. van Leeuwen[2], O. R. Brouwer[1], T. Buckle[2]; [1]Netherlands Cancer Institute - Antoni van Leeuwenhoek hospital, Amsterdam, NETHERLANDS, [2]Leiden University Medical Center, Leiden, NETHERLANDS.*

Aim/Introduction: Surgery is still mainstay of treatment in penile squamous cell carcinoma (pSCC). During surgery, the goal is to find the optimal balance between an oncologically safe surgical margin, while minimizing unnecessary mutilation. Unfortunately, positive margins currently occur in 7-36% of patients. As c-Met receptor over-expression is reported for 87% pSCC, the feasibility of targeting this receptor to support image-guided surgery applications was clinically investigated. ***Materials and Methods:*** A total of fifteen patients (≥ 18 years of age with ≥T1 pSCC undergoing primary tumour surgery) were included in a prospective pilot study. For initial ex vivo assessment of tracer performance (N=10) surgically excised penile tumour samples were incubated in a solution containing the Cy5 labelled C-Met targeting tracer EMI137 [1]. In vivo assessment of EMI137 was performed in five patients (0.13mg/kg; imaging at 3h p.i.). White light and fluorescence imaging were conducted using a prototype STORZ fluorescence laparoscope complemented with in-house developed image-processing software. The location and intensity of signal enhancement in the fluorescence images were correlated to standard pathological assessment including c-Met immunohistochemistry (% positive cells and combined c-Met score (mean multiple regions per tumour)) and H&E staining. ***Results:*** C-Met mediated fluorescence imaging combined with image-processing allowed tumour identification in all tumour specimens (diameter 5-55mm and infiltration depth 2-24mm). Tumour-to-background ratios did not significantly differ between ex vivo (range: 2.0 ± 0.6 - 3.4 ±0.3) and in vivo (range: 2.0 ± 0.4 - 4.2 ± 0.9) sample analyses. In line with previous in vivo studies in colon cancer [1], no tracer-related adverse effects occurred. Microscopic immunohistochemistry showed a possible correlation of macroscopic tumour-to-background ratios with the percentage of c-Met expressing cells in the surgical specimens, suggesting that this application could potentially be used for tumour margin visualization. Inter-patient differences were observed in

the percentage of c-Met positive cells (30-100%) and the combined c-Met score (0.3-2.3). ***Conclusion:*** C-Met receptor-specific fluorescence imaging of primary pSCC tumours using EMI137 appears to be feasible. This pilot study is the first to report in vivo application of a targeted fluorescent tracer in pSCC and paves the way for further development of this surgical guidance approach in order to visualize surgical margins and (potentially) assess tumour spread using c-MET specific (PET) tracers. ***References:*** 1. Burggraaf et al. Detection of colorectal polyps in humans using an intravenously administered fluorescent peptide targeted against c-Met. Nat Med. 2015; 21: 955-61.

OP-416

Accuracy of 68Ga-PSMA-11 for pelvic nodal metastasis detection prior to radical prostatectomy and pelvic lymph node dissection:A multicenter prospective phase III imaging study

J. Calais[1], W. R. Armstrong[1], V. Murthy[2], C. L. Heath[2], S. Behr[2], F. Barbato[3], F. Ceci[4], A. Farolfi[5], S. Schwarzenboeck[6], M. Unterrainer[7], H. Zacho[8], M. R. Cooperberg[2], H. G. Nguyen[2], R. E. Reiter[1], S. Holden[1], K. Herrmann[1], W. P. Fendler[3], M. Eiber[9], J. Czernin[1], T. A. Hope[2];

[1]University of California, Los Angeles, CA, UNITED STATES OF AMERICA, [2]University of California, San Francisco, CA, UNITED STATES OF AMERICA, [3]University Hospital Essen, Essen, GERMANY, [4]University of Turin, Turin, ITALY, [5]S.Orsola University Hospital, Bologna, ITALY, [6]Rostock University Medical Centre, Rostock, GERMANY, [7]Ludwig-Maximilians-University Munich, Munich, GERMANY, [8]Aalborg University Hospital, Aalborg, DENMARK, [9]Technical University Munich, Munich, GERMANY.

Aim/Introduction: To determine the accuracy of 68Ga-PSMA-11 PET for the detection of pelvic nodal metastases (N1) compared to histopathology at time of radical prostatectomy (RP). ***Materials and Methods:*** This is a prospective multicenter single-arm open-label phase 3 imaging trial. Patients with intermediate to high risk prostate cancer (PCa) considered for RP with lymph node dissection (PLND) were enrolled at the University of California, Los Angeles (UCLA) and at the San Francisco (UCSF) (NCT03368547, NCT02611882, NCT02919111), and underwent one 68Ga-PSMA-11 PET. The primary endpoint was the sensitivity (Se) and specificity (Sp) of 68Ga-PSMA-11 PET for the N1 detection compared to PLND histopathology (reference-standard) on a per patient basis using nodal region-based correlation. Each scan was read by three blinded independent central readers (BICR). Consensus was based on majority rule. ***Results:*** From December 2015 to August 2019, 633 patients underwent one 68Ga-PSMA-11 PET for primary staging, and 277/633 (44%) subsequently underwent RP and PLND. The median initial PSA was 11.1 [0.04-147]. 75/277 patients (27%) had N1 disease per histopathology. Using a regional based analysis, Se, Sp, positive predictive value (PPV) and negative predictive value (NPV) for N1 detection was 0.40 [0.34, 0.46], 0.95 [0.92, 0.97], 0.75 [0.70, 0.80], 0.81 [0.76, 0.85], respectively. Se was higher for patients with higher PSA: 0.29 [0.24, 0.35] for PSA < 11 ng/ml versus 0.48 [0.42, 0.54] for PSA > 11. Se was higher when the nodes were larger: 0.30 [0.25, 0.36] for nodes < 10 mm versus 0.68 [0.63, 0.74] for nodes > 10. The average node size in true positive patients was 10 mm versus 4 mm in false negative patients. ***Conclusion:*** In intermediate to high risk PCa patients who underwent RP and PLND, 68Ga-PSMA-11 PET detected pelvic nodal metastases with a sensitivity of 0.40 and a specificity of 0.95. Higher PSAs and larger node size correlated with increased sensitivity. ***References:*** None

OP-417

Local recurrence after radical prostatectomy and additive radiation - can PSMA-radioguided surgery prolong therapy-free survival?

*S. Knipper[1], L. Ascalone[1], B. Ziegler[1], R. Simon[2], C. Berliner[3], M. Graefen[1], M. Eiber[4], M. Heck[2], T. Horn[2], **T. Maurer**[1];*

[1]Martini-Klinik Prostate Cancer Center, University Hospital Hamburg-Eppendorf, Hamburg, GERMANY, [2]Department of Urology, Technical University of Munich, Munich, GERMANY, [3]Department of Radiology and Nuclear Medicine, University Hospital Hamburg-Eppendorf, Hamburg, GERMANY, [4]Department of Nuclear Medicine, Technical University of Munich, Munich, GERMANY.

Aim/Introduction: Since the introduction of prostate specific membrane antigen (PSMA)-positron emission tomography (PET) imaging, isolated local recurrence may be precisely detected after radical prostatectomy (RP). We aimed at evaluating the biochemical response and therapy-free survival after salvage surgery in patients with local recurrence in the area of the former seminal vesicles. ***Materials and Methods:*** We assessed 32 patients treated with PSMA-radioguided surgery (PSMA-RGS) between 04/2014 and 02/2020 in two centers. All patients presented with biochemical recurrence after RP with a singular local recurrence at PSMA PET imaging. Previous radiation therapy was administered in 18 patients. PSA nadir without further treatment, as well as percentage of patients with complete biochemical response (cBR, PSA <0.2 ng/ml) after 6-16 weeks were assessed. BCR-free survival and therapy-free survival (TFS) were calculated using Kaplan-Meier. Moreover, Clavien-Dindo complications were evaluated. ***Results:*** Prior to PSMA-RGS, overall median PSA was 1.1 ng/ml (interquartile range [IQR]: 0.7-1.8 ng/ml). Post PSMA-RGS, overall median PSA Nadir was 0.1 (IQR: 0-0.4 ng/ml). In 26 patients (81.3 %), cBR was observed. During the median follow-up of 27.0 months (IQR: 17.1-44.7 months), 16 patients experienced BCR and 11 patients received further therapy. At 2 years of follow-up, BCR-free survival rate was

58.7% and TFS rate was 81.3%. Three Clavien-Dindo Grade III complication were observed (ureter injury, rectal injury, suprapubic catherization). ***Conclusion:*** Salvage surgery of local recurrence within the seminal vesicle bed with PSMA-RGS is feasible and may present an opportunity in highly selected patients with local recurrence to prolong BCR-free survival and therefore possibly increase therapy-free survival. Further studies are needed to confirm our findings. ***References:*** None

OP-418

Between pathological prostate cancer lymph node and sentinel lymph node status : which one is the most informative ?

A. Morel[1], *V. Fleury*[1], *M. Le Thiec*[1], *B. Maucherat*[1], *M. Colombié*[1], *D. Rusu*[1], *G. Aillet*[2], *F. Kraeber-Bodéré*[1,3], *T. Rousseau*[4], *L. Campion*[1,3], *C. Rousseau*[1,3];
[1]*ICO René Gauducheau, Saint-Herblain, FRANCE,* [2]*Histopathology Institute, Nantes, FRANCE,* [3]*Nantes University, CNRS, Inserm, CRCINA, Nantes, FRANCE,* [4]*Urologic Clinic Nantes-Atlantis, Saint-Herblain, FRANCE.*

Aim/Introduction: Due to the concept of sentinel lymph node (SLN) where the pathologic status of SLN reflects the other pathologic lymph nodes status,SLN should contain decisive information for clinical outcome. This study assessed the clinical outcome after laparoscopic prostatectomy associated with isotopic SLN detection and extensive pelvic resection (ePLND) in localized prostate cancer (PCa) patients. ***Materials and Methods:*** From February 2009 until October 2015, a total of 231 consecutive patients were analyzed.Biochemical Progression-Free Survival (PFS) was assessed with Kaplan-Meier curves. Various histopathological parameters were analyzed by univariate and multivariate analysis by Cox regression analysis. ***Results:*** The study median follow-up was 7.1 years (95% CI: [6.6-7.5]). Lymph node (LN) metastases occurred in 38 patients.We removed an average of 20.2±9.2 LNs via ePLND and 6.05±3.99 SLN. At the time of final follow-up, 36.4% (84/231) patients had recurrence and we noticed 11 specific mortalities. In univariate analysis, characteristics of primary tumour, as pT stage, ISUP Grade Group, percentage of positive biopsy cores, intersection margin, vesicles and prostate capsule involved, significantly affected the PFS from $p<10^{-4}$ to 10^{-6}. Concerning LN metastases, the most relevant data were the number of metastases both in LN and in SLN and particularly the presence of SLN and LN macro-metastases($p<10^{-12}$ to 10^{-15}). In the multivariate analysis evaluating PFS, the most significant prognostic factor was evidence of macro- or micro-metastases in SLN (adjusted hazard ratio of 3.88 [95%CI: 2.24-6.71], $p< 2.10^{-6}$) but very interestingly not in extra SLN (adjusted hazard ratio of 0.85 [95%CI: 0.37-1.97], p=0.71). ***Conclusion:*** SLN detection seems to contain decisive information for the clinical outcome of patients with localized PCa because metastatic or non-metastatic status of SLN had a strong impact on the PFS.The question arises as to propose immediate postoperative additional treatment to patients with metastatic SLN as temporarily received adjuvant androgen deprivation therapy[1] ***References:*** [1]Muck A et al. Urol Int. 2015;94(3):296-306

806

Cutting Edge Science Track - TROP Session: Radiation Protection of Staff, and Advances in Technology

Friday, October 23, 2020, 16:55 - 18:05 Channel 6

OP-419

Extremity dose in nuclear medicine: EURADOS initiative to update the ORAMED results

R. Kollaard[1], *A. Zorz*[2], *N. Cherbuin*[3], *J. Cooke*[4], *P. Covens*[5], *M. Crabbé*[6], *L. Cunha*[7], *J. Dabin*[6], *A. Dowling*[8], *M. Ginjaume*[9], *S. Haruz-Waschitz*[10], *A. Kyriakidou*[11], *A. McCann*[8], *L. McNamara*[12];
[1]*Nuclear Research and Consultancy Group (NRG), Arnhem, NETHERLANDS,* [2]*Istituto Oncologico Veneto IOV - IRCCS, Padua, ITALY,* [3]*HUG-CHUV, Lausanne, SWITZERLAND,* [4]*St. James Hospital, Dublin, IRELAND,* [5]*VUB, Bruxelles, BELGIUM,* [6]*SCK.CEN, Mol, BELGIUM,* [7]*IsoPor-Azores, Angra do Heroismo, PORTUGAL,* [8]*St. Vincent's University Hospital, Dublin, IRELAND,* [9]*UPC, Barcelona, SPAIN,* [10]*Shamir Medical Center, Shamir, ISRAEL,* [11]*EEAE, Athens, GREECE,* [12]*University Hospital Limerick, Limerick, IRELAND.*

Aim/Introduction: Extremity dose is a radioprotection concern for Nuclear Medicine (NM) departments. According to the ORAMED study, nearly one of five workers could receive an equivalent skin dose over the annual limit. Since the publication of the ORAMED project results in 2011, NM departments have undergone several novelties. New isotopes have been introduced, like ^{68}Ga or ^{177}Lu, and radiation protection devices, such as (semi-)automatic dose dispensers, are now widely used. A subgroup of the EURADOS working group 12 has been established in order to update the results of ORAMED project according to the actual state of the NM departments in Europe. ***Materials and Methods:*** A detailed literature review regarding the extremity exposures of NM workers has been performed. A questionnaire has been distributed to the European regulators, to investigate the extremity doses collected in national dose registries as well as some issues related to the use of dosimeters for extremities. A second questionnaire is in preparation to be submitted to single European NM departments. ***Results:*** Regarding the literature review, more than 150 papers published between 1985 and 2019 have been analyzed. Articles were stratified according to the type of isotopes and procedures. 44% of the articles

cover diagnostic PET acquisition (92%, 5% and 3% related respectively to ^{18}F, ^{68}Ga and ^{124}I), 38% of articles cover therapeutic procedures with beta isotopes, while only 18% cover ^{99m}Tc diagnostic scintigraphy. Several articles evaluate the use of automatic dispensers, especially for ^{18}F. Regarding therapeutic procedures, the majority of the articles consider consolidated therapies with ^{90}Y (60%), ^{131}I (15%), ^{153}Sm (6%), ^{188}Re (6%),^{186}Re (3%) and ^{169}Er (2%). Very few works consider innovative therapies such as ^{166}Ho (3%) or ^{177}Lu (5%). The questionnaire was sent to 25 countries in October 2019. The average doses in NM, as reported by 15 European regulators are between 4-14 mSv, with a very low number of doses over the limit of 50 mSv (< 5%). A questionnaire focused on the use of radiation protection devices in Europe is under evaluation in a pilot court of NM departments. ***Conclusion:*** The literature review shows that there is a lack of data for radioisotopes introduced in the last 10 years. The task group is preparing pilots to investigate extremity exposure for ^{68}Ga and ^{177}Lu. The questionnaire that will be distributed to single hospitals will help to validate data from regulators, as well as to investigate the radiation protection measures in use. ***References:*** None

OP-420

Optimization of the exposure to workers handling of radiopharmaceuticals

M. Fulop[1], *J. Hudzietzová*[2], *J. Sabol*[3], *P. Povinec*[4], *A. Vondrák*[5], *D. Baček*[4], *P. Ragan*[1], *L. Foltínová*[6], *I. Benkovský*[7];
[1]*ABRS, s.r.o., Samorin, SLOVAKIA,* [2]*Faculty of Biomedical Engineering, Czech Technical University in Prague, Prague, CZECH REPUBLIC,* [3]*Faculty of Security Management PACR in Prague, Prague, CZECH REPUBLIC,* [4]*PET center BIONT, a.s., Bratislava, SLOVAKIA,* [5]*IZOTOPCENTRUM, s.r.o., Nitra, SLOVAKIA,* [6]*University of Economics in Bratislava, Bratislava, SLOVAKIA,* [7]*Faculty of Pharmacy, Comenius University in Bratislava, Bratislava, SLOVAKIA.*

Aim/Introduction: Contacts of workers with radiopharmaceuticals during their preparation and application include a number of operations, which, depending on the geometry and duration of irradiation, cause different exposure of the skin on the hands. The results of personal monitoring show that approximately 10% of workers at nuclear medicine departments in Slovakia and in the Czech Republic regularly receive an increased skin exposure reaching the investigation level set by the respective regulatory authorities. The reasons for such elevated exposure are not always understood and identified. The paper proposes a new approach in identifying a probable cause of elevated exposure associated with the specific working procedures. ***Materials and Methods:*** The contact of workers with radioactive sources include preparation and application of radiopharmaceuticals. The ORAMED studies found a direct relationship between the total distribution of the personal dose equivalent $H_p(0.07)$ characterizing skin exposure when preparing or administering radiopharmaceuticals to patients and various individual working approach or techniques used. In case of overexposure the dose distribution of workers is visibly distorted. By comparing the analysis of this distribution using the multiple linear regression (taken into account spatial distributions from individual operations) with a similar analysis of a worker normally exposed under the same radiopharmaceutical manipulation procedures, it is possible to identify possible reasons causing excessive exposure. The dose distribution matrix have been determined by the measurement on a physical phantom in combination with Monte Carlo calculations using MCNP5 code and a voxel hand phantom. Ten TLDs positioned on gloves were used to map the overall dose distribution during the administration. ***Results:*** The method of identifying the operations or procedures causing excessive exposure was used for the investigation of two overexposed workers. The matrix of the mean hand dose distribution was determined by measuring on the physical hand phantom in combination with Monte Carlo code calculations (MCNP5) using a hand voxel phantom. As to the first investigated worker, the most serious procedures behind the excessive skin exposure was attributed to the non-reported administration of FDG to patients by unshielded syringe while in the second case, the overexposure was caused by the undetected surface contamination of the hands. ***Conclusion:*** The proposed new method of the optimization of handling of radiopharmaceuticals allows for effective disclosures of the cases of reducing hand exposure in individual steps of handling radiopharmaceuticals related to their preparation or application to patients. ***Acknowledgments:*** The paper was partially supported by project SGS18/100/OHK4/1T/17. ***References:*** None

OP-421

Femur surgery and clinical management of a patient hospitalized after 131 Iodine cancer radiometabolic therapy: dosimetry evaluations for healthcare personnel

F. Zito[1], *M. Schiavini*[1], *E. Cristini*[1], *S. Mazzola*[1], *M. Tolentini*[1], *F. La Fauci*[2], *A. Gebbia*[2], *L. Solimeno*[1];
[1]*Fondazione IRCCS Cà Granda Ospedale Maggiore Policlinico, Milan, ITALY,* [2]*University of Milan Specialization in Medical Physics, Milan, ITALY.*

Aim/Introduction: To report our experience in managing femur surgery and ten day hospitalization for a 84 old patient admitted the 4th day after administration of 5.55 GBq of 131-I for thyroid carcinoma metastases. ***Materials and Methods:*** The patient had a femur fracture at home and was admitted in emergency. He had surgery 8 days after 131-I administration. The 131-I radioactivity was mainly distributed in lung and thorax metastases. Radioactive

patient was isolated in a room in the peripheral zone of emergency unit. For involved operators (nurses, physicians, surgeons) a radiation protection program was planned. All healthcare personnel involved was alerted about entity of exposure for irradiations and risk for contaminations. To all staff was recommended to wear protective disposable clothes, to increase distance, whenever possible speed up procedures, to collect and differentiate as radioactive all produced wastes (disposable clothes, objects touched by the patient or cloths used for cleaning surfaces and room floor) and to control laundry radioactivity. Personal dosimeters were worn by 2 of eight nurses, considered the most exposed persons. For femur surgery only 3 orthopaedists, 1 anaesthetist and 2 nurses were asked to participate; all operators wore dosimeters during surgery. At the end of surgery, contaminations of staff, object surfaces, floor, surgery instruments and waste were checked. Contaminations of hospitalization room were also controlled after patient discharge. ***Results:*** At admission 131-I retained activity in patient body was about 600 MBq. For the 10 days hospitalization, exposure doses for nurses was maximum 0.16 mSv and none reported individual contaminations. For surgery treatment, exposure rate at 1 m from the patient thorax was 20 µSv/h (about 220 µSv/h at contact) and blood activity concentration 22.6 KBq/ml. Surgery lasted 2 hours, an operator had 0.6 mSv/cm^2 contamination on forearm skin. Irradiation doses for surgery staff were between 0.035 - 0.240 mSv (maximum value reported by the surgeon attending closer to the patient trunk). Contaminated surgery instruments were completely cleaned after washings in chloride solutions. No surface contaminations were detected in surgery room and floor. After patient discharge, contaminations were detected on porous-plastic surfaces of bed handles (30 Bq/cm^2) and on floor near the bed (15 Bq/cm^2). Produced wastes, 1 m^3 (17 boxes of 60 L), contained almost 70 MBq of 131-I. ***Conclusion:*** Specific recommendations to prevent exposures and contaminations as well as to collect radioactive wastes correctly are mandatory. Safety precaution observation and collaboration among professionals are crucial. ***References:*** None

OP-422

Preliminary Investigations on Radiation Exposure in [^{68}Ga]Ga-PSMA-11 based Cerenkov Luminescence Imaging Procedures

P. Fragoso Costa[1], W. Sonnenschein[1], I. Binse[1], W. P. Fendler[1], K. Herrmann[1], M. R. Grootendorst[2], U. Krafft[3], J. P. Radtke[3], B. Hadaschik[3], C. Darr[3];
[1]University Hospital Essen, Universty of Duisburg-Essen, Department of Nuclear Medicine, Essen, GERMANY, [2]Lightpoint Medical Ltd., Clinical Research, Chesham, UNITED KINGDOM, [3]University Hospital Essen, Universty of Duisburg-Essen, Department of Urology, Essen, GERMANY.

Aim/Introduction: The current study was designed to provide a quantitative description on the occupational exposure to surgery and histopathology personnel from image-guided robotic surgery using a [^{68}Ga]Ga-PSMA-11 one day PET/CT / Cherenkov Luminescence Imaging (CLI) protocol. ***Materials and Methods:*** In this ongoing study (DRKS00020942), the dose rate in the patient's environment was assessed in four patients in supine position following [^{68}Ga]Ga-PSMA-11 PET/CT imaging. Four positions were measured (head, feet, left/right abdomen) at one meter distance. Exposure to the medical personnel was assessed in ten procedures using electronic personal dosimeters (EPD). Measurements included the first assistant, scrub nurse and the surgeon (representing CLI operator), encompassing the duration of surgery. A simple point source model was used to compare the calculated dose rate with the EPD readouts. Finally, to measure pathologist's skin exposure, eight prostate specimens were placed in a semiconductor radiation detector after CLI to quantify the tracer activity decay-corrected to the time of excision. As a threshold, we use the nuclide-specific exemption limit in Germany (Ga-68 < 100 kBq). ***Results:*** All presented results refer to median (range). The patients included in this study were injected with a median of 122 MBq (79-203 MBq) [^{68}Ga]Ga-PSMA-11. Measurements of the ambient dose rate were performed at median 101 min (88-151 min) post tracer administration. The median dose rate measurements were 0.38, 1.13, 0.99 and 0.27 µSv/hour corresponding to head, abdomen right, abdomen left and feet, respectively. After correcting for physical decay and normalizing for activity, a specific dose rate (SDR) of 0.011, 0.026, 0.021 and 0.006 µSv MBq^{-1} m^{-2} were obtained for the same positions. Surgery started at median 192 min (141-330 min) after [^{68}Ga]Ga-PSMA-11 administration and lasted for 240 min (209-264 min). The median personal dose equivalent was 6.5 (1-10), 2 (1-5), and 0.5 (0-1) µSv for first assistant, scrub nurse and surgeon, respectively. The time-integrated point source SDR model provided 7.9 (1-13), 2 (1-3), 0.7 (0-1) µSv. Semiconductor measurements revealed a median tracer activity of 3.0 (0.9-38.6) kBq on the excised prostate specimen, decay-corrected to the time of excision. ***Conclusion:*** Our results suggest that the current CLI protocol is very low in occupational exposure, and that there is no need for monitoring in the operating room or histopathology department (up to 153 procedures/year for the first assistant). A SDR point source model should be used to predict occupational exposure if other radionuclides are to be used on CLI. ***References:*** None

OP-423

National survey and research on actual circumstances of radiation exposure and reduction of staff members working in nuclear medicine and other radiological procedures in Japan

M. Hosono[1], Y. Mikami[2], H. Watanabe[3], M. Takenaka[1], Y. Koba[4],

R. Kanda[4], K. Akahane[4], T. Yamada[5], K. Torisu[2], H. Sakamoto[6], K. Yamamoto[7];
[1]Kindai University Faculty of Medicine, Osaka-Sayama, JAPAN, [2]Yokohama Rosai Hospital, Yokohama, JAPAN, [3]Gunma Paz University, Takasaki, JAPAN, [4]QST National Institute of Radiological Sciences, Chiba, JAPAN, [5]Kindai University Atomic Energy Research Institute, Higashi-Osaka, JAPAN, [6]Juntendo University Faculty of Health Science, Tokyo, JAPAN, [7]Tokai University Hospital, Isehara, JAPAN.

Aim/Introduction: This study was conducted as a research project that was supported by Ministry of Health, Labour and Welfare, Japan. We surveyed the occupational radiation exposure of staff members in nuclear medicine and other radiological procedures. We also investigated how radiation exposure of staff was managed in hospitals by correlating it with exposure doses of staff. And the goal was to propose countermeasures of reducing occupational exposure by improving management and implementing PDCA (plan-do-check-act) cycle on the basis of data. ***Materials and Methods:*** We investigated the radiation exposures of radiological staff members including radiological practitioners, technologists, and nurses who were serving in nuclear medicine, X-ray fluoroscopy procedures, and brachytherapy in hospitals across Japan. The exposure doses included the effective dose and equivalent doses to the lens and the skin. Also we investigated the management status in 49 hospitals by sending a questionnaire including individual dose measurements, protection countermeasures, work environment, occupational health education, and how PDCA cycle worked in hospitals. We also focused on exposure of the lens by measuring 3-mm-depth dose equivalent using a dedicated dosimeter DOSIRIS™ and by comparing the values with those measured as 10-mm- or 70-μm-depth dose equivalent. ***Results:*** Nuclear medicine physicians received lower exposure than cardiologists and other physicians who used X-ray fluoroscopy, however, nuclear medicine technologists received higher effective dose (mean 0.13 mSv/month) among technologists in all radiological practices. Among all, cardiologists received a higher effective dose (mean 0.19 and maximum 0.7 mSv/month), and cardiologists and IVR radiologists received a higher equivalent dose to the lens (mean 1.03 and 0.55 mSv/month). Among nurses, those who worked at endoscopy facilities received higher equivalent doses to the skin and the lens (mean 0.13 and 0.13 mSv/month). To the questionnaire on the management of occupational exposure, 31 hospitals of 49 replied, resulting in a response rate of 63%. The implementation rate of training for workers on radiation protection was 60%. There was a shortage in the deployment of protective equipment in the X-ray facilities, which might increase the equivalent dose of the lens. ***Conclusion:*** This study can provide fundamental materials and suggestions for advancing radiation protection of staff through clarifying exposure dose and management status in hospitals. ***References:*** ICRP, 2018. Occupational radiological protection in interventional procedures. ICRP Publication 139. Ann. ICRP 47(2).Taniguchi Y et al. Radiation exposure in nurses during care of 131I-MIBG therapy for pediatric patients with high-risk neuroblastoma. Ann Nucl Med. 2020 Apr 15.

OP-424

The current situation and problems in quantifying radiation exposure of workers and patients in nuclear medicine

J. Sabol;
Department of Crisis Management PACR, Prague, CZECH REPUBLIC.

Aim/Introduction: The purpose of this paper is to summarize the present situation regarding quantities used for the quantification of radiation exposure of persons and, based on the analysis performed, some relevant suggestions aimed at the simplification of the current system are proposed. ***Materials and Methods:*** The overview and assessment of the present system of radiation protection quantities, with special emphasis on their use in nuclear medicine, took into account the latest recommendations by the ICRP, ICRU, EANM and other professional expert bodies. A new modified and simplified approach in the quantification of the radiation exposure of persons has been proposed in order to reduce confusion associated with the excessive number of quantities and units used at present and defined in a rather complicated manner. ***Results:*** Analysis of the present situation has shown that it would be most appropriate to clearly distinguish between the quantification of stochastic and deterministic health effects, where quite often in both cases the unit Sv is generally used without mentioning the relevant quantity. Moreover, the same unit is also applied for the assessment of deterministic effects where the most appropriate unit should be Gy-Eq. It is proposed to rely only on the following five quantities for the assessment of personal exposures: the organ dose in Gy, equivalent organ dose in Sv, RBE-weighted organ dose in Gy-Eq, effective whole-body dose in Sv, and RBE-weighted whole-body dose in Gy-Eq, these quantities reflecting the detriment of individual organs and the whole body in terms of stochastic and deterministic effects, respectively. The monitoring of these quantities should rely on measurements of particle fluence and fluence rate at the point of interest weighted by the conversion factors that relate to the measured quantities to appropriate radiation protection quantities. ***Conclusion:*** The proposed system of quantities would significantly simplify the present system, which is based on too many quantities, some of which are defined in a somewhat complicated way so that even those responsible for radiation protection at nuclear medicine workplaces are

confused and are not in a position to correctly interpret the results of their radiation monitoring. Even in some scientific literature, everything related to the exposure is a dose and unit Sv, which are often used for deterministic assessment. Sometimes, many commercially available monitors are "calibrated" in the range of the "dose" up to 10 Sv. For such high exposure, this unit obviously cannot be used under any circumstances. ***References:*** None

OP-425

The current use of multi-modality imaging in nuclear medicine in Europe: results from the MEDIRAD project

G. Verfaillie[1], *Y. D'Asseler*[2], *K. Bacher*[1];
[1]*Ghent University, Ghent, BELGIUM,* [2]*Ghent University Hospital, Ghent, BELGIUM.*

Aim/Introduction: The use of CT in multimodality SPECT/CT and PET/CT systems is increasing. This study presents the status of the use of these multi-modality imaging systems in nuclear medicine in Europe. ***Materials and Methods:*** As a part of the Horizon 2020 MEDIRAD project, a European-wide online survey was set up to gather information on the current implementation and use of hybrid imaging in nuclear medicine. Special attention was paid to the clinical use of CT, CT technology and dosimetry in PET/CT and SPECT/CT. ***Results:*** 109 responses from 38 countries, of which 58.3% came from university hospitals, were received until October 2019. Overall, 85% of the reported PET systems are equipped with CT, whereas for SPECT systems, CT is integrated in only 40% of the cases. More than half of the responders indicated that they will invest into a new PET/CT or SPECT/CT in the near future. In PET/CT, CT is performed routinely (about 90%) in clinical practice, while for SPECT/CT this seems less systematic and standardized. For both SPECT/CT and PET/CT, the majority of the CTs are linked to attenuation correction and anatomical localisation. Full diagnostic CT scans are used more often in PET/CT than in SPECT/CT. Modern dose reduction techniques (such as iterative reconstruction and tube current modulation) are widely available in hybrid imaging systems. Automatic tube current modulation is used in about 80% and 45% of the PET/CT and SPECT/CT systems, respectively. Iterative reconstruction is available in about 51% and 62% of the SPECT/CT and PET/CT systems, respectively, and is routinely used. In the large majority (70%) of nuclear medicine departments, CT doses are centrally stored in a database or dose management system. The survey revealed that there are no specific paediatric CT protocols available in about 30% and 65% of the PET/CT and SPECT/CT systems, respectively. About 70% of nuclear medicine physicians and nuclear medicine technologists indicate a need for additional education in CT technology and CT dosimetry. ***Conclusion:*** The survey indicated the wide spread use of CT in nuclear medicine departments. Especially in PET/CT, modern CT dose reduction techniques are widely available. While the use of CT in SPECT examinations seems less systematic and standardized, CT acquisitions in PET examinations are performed in about 90% of the cases. ***References:*** None

OP-426

Comparative Study of PET injectors in the routine practice of Nuclear Medicine

M. Costa[1], *M. Silva*[1], *R. Parafita*[2], *A. Canudo*[1], *B. Freitas*[1], *H. Delgado*[1], *J. M. Correia*[1], *M. Andrade*[1], *M. Machado*[1], *R. Oliveira*[1], *S. Teixeira*[1], *F. Oliveira*[1], *P. Ferreira*[1], *D. Costa*[1];
[1]*Champalimaud Foundation, Lisbon, PORTUGAL,* [2]*Mercurius Health, Lisbon, PORTUGAL.*

Aim/Introduction: Staff radiation protection is more and more a concern in the practice of clinical Nuclear Medicine. There are, nowadays, several PET automatic injectors for use in the daily routine practice to help and reduce staff radiation daily exposures. Our work's purpose was to try and find the most suitable equipment to fulfil our nuclear medicine service needs. The following properties were chosen to be tested: radiation safety, costs and user-friendliness of the equipment. ***Materials and Methods:*** The selected injectors were MedRad's Intego, Comecer's IRIS and Tema Sinergie's Karl100. In order to monitor the equivalent dose rate (using Thermo-Scientific RadEye B20-ER) being received by the injector's operator, a set of regions of interest were established on the surface and all sides of the equipment, during the injection procedure. The measurements were done on the surface (worst case scenario) making sure that at a reasonable operating usage (40-50 cm) all staff will be significantly less exposed to the radiation. Considering the "worst case scenario" we decided to calculate the equivalent dose assuming that all measures were obtained for a single operator, for an entire working year. It was taken into consideration the mean exposure time throughout the procedure, at the different regions of interest and for a single injection. The received equivalent dose rate was always assumed on contact with the equipment. In average, six measurement sets were obtained with an average initial vial activity of 2.8±0.9 GBq of ^{18}F-FDG, performing a total of more than 30 measurement sets for each injector. ***Results:*** The determined equivalent dose per year for single user, showed the following values: Intego 0.9±0.4 mSv/year, IRIS 1.7±0.6 mSv/year and Karl100 4.2±1.3 mSv/year. However, Karl100 in our practice conditions, obliges to handle the injection procedure by hand, increasing the dose rate to 38±14 mSv/year. Regarding equipment's interface and costs, Karl100 offered a more user-friendly interface and IRIS (plus accessories) by the end of one full year, was the less expensive and in addition it is registered for the use of other radiopharmaceuticals, in particular Gallium-68 and Luthetium-177. ***Conclusion:*** Taking into account the chosen

properties to be tested, the most adequate injector for our routine practice is IRIS, which excels by being registered for the usage of Gallium-68 and Luthetium-177. Intego does not have this feature and Karl100 delivers higher equivalent dose rates and therefore fails in reducing significantly, as we wish, radiation exposure to staff. ***References:*** None

OP-427

Amyloid hybrid membranes for the treatment of radioactive wastewater from nuclear medicine and nuclear industry

G. Prenosil[1], *S. Bolisetty*[2], *N. M. Coray*[2], *A. Palika*[2], *R. Mezzenga*[2]; [1]*1Department of Nuclear Medicine, Inselspital, Bern University Hospital, University of Bern, Bern, SWITZERLAND,* [2]*Department of Health Science and Technology, ETH Zürich, Zürich, SWITZERLAND.*

Aim/Introduction: Before being discharged to the municipal sewage system, medium lived radioactive waste from nuclear medicine must be stored until sufficiently decayed. To this end, costly storage facilities for monitoring and holding large volumes of liquid nuclear waste are employed. The nuclear power industry produces even larger amounts of long-lived nuclear waste, which needs to be conditioned before final storage. Previously, we reported hybrid membranes composed of amyloid fibrils produced from cheap and readily available proteins and activated carbon, which efficiently removed heavy metal ions and radioactive compounds from water. Here, we show that these membranes are highly efficient in the removal of diverse, clinically relevant radioactive compounds from hospital wastewater by single-step filtration. Our aim was to initiate the development of a cost-efficient method for volume reduction of liquid radioactive waste. ***Materials and Methods:*** Aqueous solutions containing Technetium (Tc-99m), Iodine (I-123) and Gallium (Ga-68) at clinically relevant concentrations were passed in a single step through amyloid membranes. Additionally, real clinical wastewater from a Swiss hospital containing Iodine (I-131) and Lutetium (Lu-177) was purified by tangential filtration using our membranes. Radioactivity was measured with a gamma counter in the feed and the filtrate, and accumulation of radioactive compounds in the membranes was visualized by PET/CT and SPECT imaging. Filtration of clinical wastewater with amyloid membranes was compared against filtration with cellulose and activated carbon. Saturation experiments with increasing nuclide concentrations and with multiple filtration rounds per membrane were performed. ***Results:*** The single filtration removed Tc-99m, I-123, and Ga-68 from the water with efficiencies above 99.8%. Similar efficiencies were found for the removal of I-131 Lu-177 from wastewater, whereas cellulose and pure carbon removed nothing. Nuclear imaging confirmed the buildup of radioactive isotopes in the membranes and revealed the flow in the filtration systems. The removal efficiency still did not decrease with multiple cycles of wastewater filtration. ***Conclusion:*** The radioactivity of the water after filtration was below the level of detection and thus could be considered as non-radioactive. By converting large volumes of radioactive wastewater into low volumes of solid radioactive waste, the present technology emerges as a possible game changer in the treatment and conditioning of nuclear wastewater. Additionally, our approach shows that the tracer principle and nuclear imaging can help in engineering better filtration systems. ***References:*** [1] S. Bolisetty, R. Mezzenga, Nat Nanotechnol 2016, 11, 365-371

OP-428

Calibration, radioprotection and dosimetry in Lu-177 treatment of Neuro Endocrine tumours

P. Saletti[1], *S. Raspanti*[2], *A. D'Agata*[1], *F. Rossi*[1], *M. Papi*[1], *G. Belli*[1]; [1]*Azienda Ospedaliero-Universitaria Careggi, Florence, ITALY,* [2]*University of Florence, Florence, ITALY.*

Aim/Introduction: A ^{177}Lu based radiopharmaceutical was recently employed for the first time at Careggi hospital for radiometabolic neuroendocrine tumors treatment. First of all, dose calibrator adjustment was necessary because ^{177}Lu was not included in control unit. Dose rate measurements and estimate were then carried out in vial and in phantom to evaluate dosimetric impact on operators. ***Materials and Methods:*** A calibrated vial of ^{177}Lu was used to adjust two Biodex Atomlab100 dose calibrators. This was achieved by inserting the vial in the housing and tuning the calibration factor to match the exact activity reported in calibration certificate. The same vial was then inserted in a home-made phantom (consisting of two 5 liters water bags arranged in sandwich around the vial) and dose rate measurements were made at various distances with a Victoreen 450P ionization chamber. Approximately 40 days later, the same vial was used for irradiating for 88 hours a set of 10 TLD LiF100 which were then read in a Harshaw 6600 reader. Finally, a therapeutic dose of 7400MBq of ^{177}Lu was injected by infusion pump in approximately 40 minutes to the first patient. Radiopharmaceutical manipulation, administration and patient assistance timing were measured together with dose rate and distances between operators and radioactive sources (vial, patient) for an accurate radioprotection evaluation. ***Results:*** A calibration factor of 116 was found for both Atomlab 100 dose calibrators, in perfect agreement with manufacturer suggested value of 115 for ^{177}Lu. Dose rate measurements with ionization chamber were normalized per activity and plotted as a function of distance for vial and phantom to obtain exposition at any distance. A dose rate of 6.57μSv/(h*GBq) at 1 meter was found for vial source while 3.16μSv/(h*GBq) is the dose rate from phantom at the same distance. From manipulation, administration and assistance

measured timing an effective dose of respectively 0.13µSv, 6.2µSv and 14.4µSv resulted for involved operators. A very good agreement was found with 10 exposed TLD reading proving that routine dosimetry with LiF100 is reliable even for β emitters such as ^{177}Lu. ***Conclusion:*** Dose calibrator adjustment, dose rate measurements and timing to carry out specific tasks (radiopharmaceutical manipulation and administration, patient assistance) have made it possible a first assessment of radiological impact on operators envolved in treatment with ^{177}Lu for neuroendocrine tumours. This is the starting point for subsequent and more detailed evaluations that will also be compared with operators TLD dosimetry evidences. ***References:*** None

807

Pitfalls & Artefacts 4: Interpretation of Response Monitoring During Immune Therapy

Friday, October 23, 2020, 16:55 - 18:25 Channel 7

OP-429

Current Systems for Response Classification

J. O'Connor; Division of Cancer Sciences, The University of Manchester, Manchester, UNITED KINGDOM.

OP-430

The Role of 18F-FDG-PET Monitoring During Immune Therapy

E. Lopci; Humanitas Clinical and Research Hospital – IRCCS, Rozzano (MI), ITALY.

OP-431

Pitfalls in Interpretation of Response to Immune Therapy

W. Noordzij; Department of Nuclear Medicine and Molecular Imaging, University of Groningen, UMCG, Groningen, NETHERLANDS.

808

Clinical Oncology Track - TROP Session: Breast PET

Friday, October 23, 2020, 16:55 - 18:15 Channel 8

OP-433

The Predictive Value of Visual Evaluation and Quantitative Metabolic Parameters for Axillary Lymph Node Metastasis on FDG PET/MRI in Breast Cancer

U. Aydos[1], L. Atay[1], O. Kurukahvecioglu[2], U. Akdemir[1], P. Uyar Gocun[3], S. Gulbahar Ates[1], K. Seker[1], C. Cifter[2]; [1]Gazi University Faculty of Medicine, Department of Nuclear Medicine, Ankara, TURKEY, [2]Gazi University Faculty of Medicine, Department of General Surgery, Ankara, TURKEY, [3]Gazi University Faculty of Medicine, Department of Medical Pathology, Ankara, TURKEY.

Aim/Introduction: The aim of this study was to evaluate the role of visual assessment and quantitative metabolic parameters for predicting axillary lymph node (AxLN) metastasis on F-18 FDG PET/MRI in newly diagnosed patients with invasive ductal carcinoma (IDC) of breast. ***Materials and Methods:*** Histopathological and imaging data of 265 female patients who underwent PET/MRI for primary staging between 2016-2019 in our department were analyzed retrospectively. In visual assessment, AxLNs were scored as 0 (negative) and 1 (positive) according to the presence of FDG uptake above background. In quantitative evaluation of PET positive group, maximum standardized uptake values (SUVmax) of AxLNs (SUV-LN) and AxLN/Primary tumor SUVmax ratios (Ax/T) were obtained from PET/MR images. The presence of AxLN metastasis was accepted as positive according to the i) histopathological verification or ii) AxLN FDG uptake intensities on baseline and follow-up imaging in patients who received neoadjuvant treatment. Statistical analyses were performed on SPSS version 23.0. ***Results:*** The characteristics of patients were shown in Table 1. The sensitivity, specificity, positive predictive value, negative predictive value and accuracy of visual evaluation were 89.8 %, 78.2 %, 89.4 %, 79.0 % and 86.0 %, respectively. 8 of 18 patients with false negative PET had micrometastasis. In ROC curve analysis, SUV-LN and Ax/T had the AUCs of 0.88 and 0.89, respectively. The optimal cut-offs were 2.95 for SUV-LN and 0.31 for Ax/T. Using the set cut-off values, the sensitivities of SUV-LN and Ax/T were 77.5% and 90.6% ($p<0.001$), their specificities were 94.7% and 84.2% ($p=0.625$), and their diagnostic accuracies were 79.2 % and 89.9%, respectively. In patients with micrometastasis (n=9), only 1 patient had PET positive AxLN, with an SUV-LN of 1.2 but an Ax/T of 0.43. In patients with SUV-LN ≤ 2.95 and Ax/T > 0.31 the rate of AxLN metastasis was 89 % (24/27). In patients with SUV-LN > 2.95 and Ax/T ≤ 0.31 this rate was 75% (3/4). ***Conclusion:*** Visual evaluation of AxLN on FDG PET/MRI had high diagnostic performance, and nearly half of patients with false negative PET had micrometastasis. With respect to the quantitative parameters, Ax/T values demonstrated better diagnostic performance for predicting AxLN metastasis than SUV-LN in patients with IDC. Ax/T had added diagnostic value especially in patients with lower SUV-LN. For the evaluation of AxLN status, visual assessment and quantitative parameters seem to be complementary to each other. ***References:*** None

OP-434

Identification of aggressive breast cancer lesions with [18F]-FDG-PET/CT in combination with machine learning and data pre-processing

D. Krajnc, L. Papp, T. S. Nakuz, H. F. Magometschnigg, M.

Grahovac, C. P. Spielvogel, Z. Bago-Horvath, A. Haug, G. Karanikas, T. Beyer, M. Hacker, T. H. Helbich, K. Pinker;
Medical University of Vienna, Vienna, AUSTRIA.

Aim/Introduction: Breast cancer is the common cancer in women and the 2nd most common cause of female cancer deaths. [18F]-FDG-PET/CT has been established as a sensitive diagnostic test for detecting distant metastases and lymph node infiltration in high-risk breast cancer patients as well as for assessing treatment response. The aim of this study was to investigate the performance of breast cancer detection and the identification of aggressive breast cancer from [18F]-FDG-PET/CT incorporating data pre-processing algorithms in machine learning predictive models. ***Materials and Methods:*** A cohort of 170 patients with suspicious imaging finding (BI-RADS 4/5) was examined with [18F]-FDG-PET/CT imaging as part of a prospective study. Histopathology was used as the standard of reference. Breast tumours were classified as benign or malignant. Lesions were classified as (a) less aggressive to targeted treatment (luminal A/B, Her2-positive) and (b) more aggressive (ER, PR, Her2-negative, triple negative (TN) breast cancer) based on immunohistochemical (IHC) receptor status (estrogen (ER), progesterone (PR), Her2) and proliferation rate (ki-67). 173 lesions from 170 patients were delineated in the Hermes Hybrid 3D software. Radiomic features were extracted from all 173 delineated 18F-FDG-PET/CT lesions. Ensemble learning approaches were applied to predict tumour malignancy as well as IHC triple negative subgroup in a 100-fold Monte Carlo cross-validation scheme. This step was performed twice for both reference labels: (a) with training the predictive models on the original training datasets, and (b) with processing the training datasets by data pre-processing approaches for class imbalance and feature redundancy correction, noisy data samples cleansing as well as outlier detection. Predictive performance was estimated over the ML fold validation cases with confusion matrix calculations (sensitivity (SENS), specificity (SPEC) and overall accuracy (ACC)). ***Results:*** The validation performance of [18F]-FDG-PET/CT ML models built over the original training data was 83% (SENS), 68% (SPEC) and 76% (ACC) for breast cancer detection, and 58% (SENS), 90% (SPEC) and 74% (ACC) for identification of aggressive breast cancer. The validation performance of [18F]-FDG-PET/CT ML models built over the pre-processed training data was improved to 82% (SENS), 78% (SPEC) and 80% (ACC) for breast cancer detection and 67% (SENS), 92% (SPEC) and 80% (ACC) for identification of aggressive breast cancer. ***Conclusion:*** We demonstrated that ML models based on radiomic tumour features extracted from [18F]-FDG-PET/CT in conjunction with the utilization of data preparation approaches provide breast cancer detection and identification of aggressive breast cancers with high accuracy. ***References:*** None

OP-435

Incidental Focal Breast Uptake On ^{18}F-FDG PET-TC. Our Center Experience

C. Wakfie Corieh[1], *C. Rodríguez Rey*[1], *A. Ortega Candil*[1], *R. Valhondo-Rama*[1], *A. Blanes García*[1], *L. García Beláustegui*[1], *M. Ruiz Tolón*[1], *B. Lannegrand*[1], *A. Pascual Martín*[1], *F. Ferrando-Castagnetto*[2], *J. Carreras Delgado*[1];
[1]*Hospital Clínico San Carlos, Madrid, SPAIN,* [2]*Hospital de Clínicas Dr. Manuel Quintela, Facultad de Medicina, Universidad de la República, Montevideo, URUGUAY.*

Aim/Introduction: Breast incidental ^{18}F-FDG uptake (BIU) in patients undergoing PET-CT for reasons nonrelated to breast pathology represent a diagnostic challenge. In this study we aim to determine the frequency and clinical significance of focal breast incidental ^{18}F-FDG uptake detected with this technique. ***Materials and Methods:*** From January 2017 to January 2020, a total of 10,615 whole-body (WB) ^{18}F-FDG PET-CT studies were performed in our center. We retrospectively identified 26 patients showing incidental focal hypermetabolic activity in breast, we measured SUVmax and the maximum diameter of the lesion. We also analyzed the clinical management, images (ultrasound/mammography) and pathology reports (with or without histopathological confirmation). ***Results:*** We found BIU in 0.3% (27 scans of 26 patients) of the studies. The mean age was 62.2 years. 88.5% (23/26) of the patients were women. Among the reasons for the request, 84.6% (22/26) were oncological and 15.4% (4/26) non-oncological. On 23 patients (88.5%) ultrasound/mammography was performed consequently PET-CT findings, showing BIRADS-5 in 30.4% (7/23), BIRADS-4C in 13% (3/23), BIRADS-4A in 8.7% (2/23), BIRADS-3 in 13% (3/23) and BIRADS-2 in 34.8% (8/23). The remaining 11.5% (3/26) of the patients had no ultrasound/mammography reports, one patient died shortly after PET-CT was performed, another patient progressed into palliative care and the last one carries out gynecological controls in a private center (we have no access to this information). Of the 23 patients studied with ultrasound/mammography and histological correlation (BIRADS-4 and 5), the findings were benign in 60.9% (14/23) of which 8.7% (2/23) have risk of malignancy, and malignant in 39.1% (9/23). The mean SUVmax of the 14 benign lesions and 9 malignant lesions were 2.6±1.4 and 5.8±3.7, respectively (p=0.0019). At a cut-off value of 4.0, the rate of malignancy and specificity of the mean SUVmax for differentiating benign and malignant breast lesions were 67% and 93%, respectively. The CT data from PET-CT revealed that the mean diameters of benign and malignant lesions were 1.3±0.5 cm and 2.0±0.5 cm, respectively (p=0.019). ***Conclusion:*** Although BIU detected by WB ^{18}F-FDG PET-CT is very rare (0.3% of our studies), it was indicative of malignancy and benign with risk of malignancy lesions in 39.18% (11/23) and 8.7% (2/23) of our patients, respectively. Both mean SUVmax and diameter

of the lesion were greater for malignant than benign lesions. According to our experience, we consider essential exhaustive study (ultrasound/mammography and even histopathological study) in case of BIU findings in ^{18}F-FDG PET-CT studies. ***References:*** None

OP-436

Dual Tracers of 18F-FES and 18F-FDG for Prediction of Progression-Free Survival After Fulvestrant Therapy in Patients with HR+/HER2- Metastatic Breast Cancer

Z. Yang;
Fudan University Shanghai Cancer Center, Shanghai, CHINA.

Aim/Introduction: The purpose of this study was to use dual tracers 18 F-fluoroestradiol (18 F-FES) and 18 F-fluorodeoxyglucose (18 F -FDG) as imaging biomarkers in predicting progression-free survival (PFS) in ER-positive MBC patients receiving fulvestrant therapy. ***Materials and Methods:*** We retrospectively analyzed thirty-five HR+HER2- metastatic breast cancer patients who underwent 18 F-FES and 18 F-FDG PET/CT scans prior to fulvestrant therapy in our centre. The SUVmax across all metastatic lesions on the baseline PET/CT were assessed. The heterogeneity of ER expression was assigned by presence of 18 F-FES negative lesions, for patients with 100% 18 F-FES positive lesions were categorized into two groups by the median ratio of FES/FDG SUVmax, low FES/FDG and high FES/FDG. PFS were estimated by the Kaplan-Meier method and compared by the log-rank test . Univariate and multivariate analyses were performed using the Cox proportional hazard model. ***Results:*** In total, 12 of 35 patients' presence of 18 F-FES negative lesion(s), suggesting that heterogeneity of ER expression in metastatic lesions. These patients had a low median PFS of 5.5 months (95%CI 2.3-8.7). Of patients with 100% 18 F- FES positive lesions, 11 had a low FES/FDG and 12 had a high FES/FDG. These groups had a median PFS of 29.4 months (95%CI 2.3-56.5) and 14.7 months (95%CI 10.9-18.5), respectively. The patients were stratified in three categories based on incorporating both 18 F-FES and 18 F-FDG imaging results that were significantly correlated with PFS by univariate analysis ($P < 0.001$) and multivariate analysis ($P = 0.006$). ***Conclusion:*** Our data suggest that dual 18F-FDG and 18F-FES PET imaging could be a potential predictor of efficacy to fulvestrant therapy among HR+HER2- MBC patients. These findings indicate that endocrine therapy should be individualized for patients with ER-positive MBC, particularly that presence of 18F- FES negative lesions. ***References:*** None

OP-437

Standarisation Of Normalized Workflow For 18F-FDG PET/MRI Studies In Staging Of Patients With Breast Cancer

J. Garcia*, A. Compte, E. Valls, S. Mourelo, M. Buxeda, T. Blanch, P. Bassa, M. Soler, E. Riera;*
CETIR ASCIRES Grupo biomédico, Barcelona, SPAIN.

Aim/Introduction: We aimed to apply a Standard Operating Procedure (SOP) on ^{18}F-FDG PET/MRI studies for local-regional and distant staging in patients with ductal breast carcinoma. ***Materials and Methods:*** A theoretical SOP on ^{18}F-FDG PET/MRI in breast study was developed and optimized, and which included the following acquisition parameters: Whole-body synchronic PET+MRI acquisition, 1 h after 18F-FDG injection (dose 2.5 MBq/Kg) .Body PET acquisition (5 beds; 4 min/bed).Body MRI acquisition (Axial LAVA Flex, Axial MRAC, Axial DWE, Axial T2 SSFSE sequences). Selective breast synchronic PET+MRI acquisition, with patient lying in prone position, 2 h after tracer injection. .Breast PET acquisition (1 bed;10 min). .Breast MRI acquisition: 3D Axial T2, 3D T2 Fat, 3DT1, Axial DWE, Gradient Coronal, 3D Axial VIBRANT dynamic sequences (Gadolinium dose 0.2 ml/Kg). In order to assess its clinical role, the above SOP was applied over the first 15 patients who were referred to our clinic for primary staging of a ductal breast carcinoma (cT2-4N0 or cT1-4N+). Selective and whole-body PET, MRI and PET/MRI studies were all jointly reviewed by a specialist in Nuclear Medicine and a Radiologist, both with extensive expertise in breast oncology studies.A consensus was reached over the T-staging, as well as for nodal disease and distant metastases detection. Results were compared with histopathological study and/or other diagnostic procedures available. ***Results:*** PET/MRI procedures performed in our first 15 patients did not show artifacts due to synchronous acquisition, or incidences due to technical reasons, or claustrophobia events. Not performing the whole-body CT on a standard ^{18}F-FDG PET/CT study meant a radiation dose reduction of 50% for every patient. Mean time of our studies was 60 min, divided into 35 min for the breast PET/MRI acquisition, and 25 min for the whole-body PET/MRI acquisition. Preliminary assessment of the simultaneous/synchronous PET/MRI studies in our first 15 patients was as follows: T-staging: Agreement (n:8), better boundary detection (n:5), hypermetabolic uptake not depicted on MRI (n:2). N-staging: Axilla (n:9): infracentimetric in 5 (PET and Diffusion agreement). Internal mammary chain (n:3). M-staging: Bone metastases (n:2): Lung metastases (n:2): Liver metastases (n:1). ***Conclusion:*** Our SOP on ^{18}F-FDG PET/MRI studies provided us with us global information on the local-regional and distant staging of patients with breast cancer, with an optimized procedure time due to synchronous acquisition, as well as a significant reduction in radiation dose in comparison to performing a breast MRI and a whole-body ^{18}F-FDG PET/CT procedures consecutively . ***References:*** doi:10.1007/s00259-017-3823-0doi:10.3892/ijo.2017.4012

OP-438

Radionuclide bone scans can be removed from the pathway for staging breast cancer patients prior to neoadjuvant chemotherapy after introduction of FDG PET-CT

P. Holdgaard[1], *S. T. Nygaard*[2], *E. H. Jakobsen*[2], *S. Hess*[3,4];
[1]*Department of Nuclear Medicine, Lillebælt Hospital, Vejle, DENMARK,* [2]*Department of Oncology, Lillebælt Hospital, Vejle, DENMARK,* [3]*Department of Radiology and Nuclear Medicine, Hospital Southwest Jutland, Esbjerg, DENMARK,* [4]*Department of Regional Health Research, Faculty of Health Sciences, University of Southern Denmark, Odense, DENMARK.*

Aim/Introduction: Breast cancer patients were originally staged with CT and Tc99m bone imaging. Recently FDG PET-CT was added prior to neoadjuvant treatment. Some departments have replaced Tc99m scanning with NaF PET-CT. The aim was to evaluate the added clinical benefit of NaF PET-CT in addition to FDG PET-CT. ***Materials and Methods:*** Retrospective evaluations were made for 200 consecutive breast cancer patients prior to neoadjuvant chemotherapy from Lillebælt Hospital (2017-2019) with <14 days between FDG and NaF, and agreement in presence or absence of bone metastases assessed. True bone disease status was determined using all image and biopsy data available up to April 2020. FDG and NaF images for all examinations with bone findings were reviewed and any disagreement in diagnoses recorded. ***Results:*** 187/200 patients demonstrated agreement in reported presence or absence of bone metastases between FDG and NaF examinations (reported metastases were present in 16 patients (all true positive) and absent in 171). 13 patients demonstrated disagreement, with presence of metastases reported on FDG with absence on NaF in 4 patients (1 false-negative NaF, 3 false-positive FDG) and 9 patients with absence of metastases reported on FDG with presence on NaF (8 false-positive NaF, 1 false-negative FDG). All patients with confirmed metastases showed bone lesions with both tracers. 6 patients showed more lesions on FDG, 6 showed more on NaF, and 6 demonstrated the same lesions. The patient reported false negative with NaF had bone lesions misinterpreted as benign but was correctly identified as metastases by FDG. The false negative FDG patient also had misinterpreted FDG uptake in bone correctly identified as metastases by NaF. The 3 false-positive FDG scan results were owing to a solitary lesion being interpreted as malignant which NaF confirmed to be benign, demonstrating importance of dual FDG/NaF scanning in the case of solitary lesions. In the remaining 196 patients (98%), NaF scanning did not add clinical value to the FDG scan. ***Conclusion:*** FDG and NaF scans provide comparable outcomes in evaluating presence or absence of bone metastases in staging breast cancer prior to neoadjuvant therapy. This obviates the need for the bone scan in the vast majority of patients. However, the small proportion of patients demonstrating FDG uptake in solitary lesions may still benefit from a NaF scan in addition to confirm diagnosis. FDG is preferred to NaF scanning due to additional detection of soft tissue metastases and a lower number of false-positives. ***References:*** None

OP-439

Pretreatment 18F-FDG-PET/CT Parameters Predict Treatment Outcome of First-Line Therapy in Patients with Metastatic Breast Cancer

Z. Yang;
Fudan University Shanghai Cancer Center, Shanghai, CHINA.

Aim/Introduction: 18F- fluorodeoxyglucose positron emission tomography/computed tomography (18F-FDG-PET/CT) imaging could provide prognostic information, especially the 18F-FDG uptake has proven to be a predicting marker for treatment outcome in various tumors. However, the prognosis of other PET parameters in metastatic diseases is still unclear. The aim of this study was to evaluate pretreatment18F-FDG-PET/CT based parameters for the prediction of the progression free survival (PFS) of first-line treatment in metastatic breast cancer (MBC). ***Materials and Methods:*** MBC patients with whole-body 18F-FDG PET/CT scans before first-line treatment were included. In PET/CT scans, conventional parameters (maximum and mean standardized uptake value, metabolic tumor volume [MTV], total lesion glycolysis [TLG]) and heterogeneity parameters: intra-tumor heterogeneity index [HI] were analyzed. PFS was mainly assessed for efficacy. The survival analyses were performed using the Kaplan-Meier method and compared by the log-rank test. ***Results:*** A total of 177 patients with MBC were enrolled in this study, of which 68 were De novo stage IV. Among 177 MBC patients, 87 patients with hormone receptor (HR) positive and human epidermal growth factor receptor 2 (HER2) negative, 30 patients with HER2 positive and 60 patients with triple-negative. In the overall population, patients with high SUVmax, high SUVmean, high MTV, high TLG and high tumor HI at baseline were associated with lower PFS ((P=0.028, P=0.005, P=0.017, P=0.026, P=0.035, respectively). In Patients with De novo stage IV, patients with high HI had significantly shorter PFS (P=0.001). In HR+/HER2- and HER2+ subgroups, only baseline HI showed the predictive value of PFS (P=0.023, P=0.049, respectively). In the triple-negative subgroup, high SUVmax, MTV and TLG showed predictive value of worse PFS (P=0.030, P = 0.011 and P=0.023, respectively). ***Conclusion:*** Pretreatment 18F-FDG-PET/CT Parameters showed the prediction value of PFS of first-line therapy in MBC patients. However, in patients with De novo stage IV and different molecular subtypes, the predictive PET-CT parameters may be different. ***References:*** None

OP-440

Role of ^{18}F-FDG PET/CT metabolic/volumetric parameters to predict response to neoadjuvant chemotherapy/ chemo-immunotherapy and risk stratification in patients with Triple-Negative (TNBC) and HER2+breast cancer (HER2+)

G. Paone[1], *S. Di Lascio*[2], *L. Knappe*[1], *T. Ruberto*[1], *G. Treglia*[1], *L. Ceriani*[1], *L. Giovanella*[1];
[1]*IIMSI, Bellinzona, SWITZERLAND,* [2]*IOSI, Bellinzona, SWITZERLAND.*

Aim/Introduction: The aim of this study was to assess response to NAC and prognostic value considering dynamic evolution of metabolic/volumetric parameters measured on 18F-FDG PET/CT in TNBC and HER2+. ***Materials and Methods:*** We retrospectively analyzed 50 patients with TNBC and HER2+, who performed a staging PET/CT before and after neo-adjuvant chemotherapy (for TNBC) and chemo-immunotherapy (for HER2+). Treatment-related changes in SUVmax, MTV and TLG were evaluated (ΔSUVmax, ΔMTV and ΔTLG) in the primary tumor and nodal lesions. To identify the optimal cut-off value of these parameters a receiver-operating curve analysis was performed. Kaplan-Meier method was used to evaluate prognostic value. The associations between early metabolic/volumetric changes, pathological complete response (pCR), and event-free survival (EFS) were examined. ***Results:*** Of the 50 patients, 16 (32%) achieved pCR, 13 (26%) relapsed and 8 of them died (median FU, 48 mo). 1 relapse and no deaths were observed in patients with pCR. A multivariate analysis underlined that ΔSUVmax was significantly associated with pCR (p 0.028) with an optimal percent of decrease (cutoff value ΔSUVmax 81%, p 0.010). Kaplan-Meier analysis underlined that pCR showed a significant difference for predicting EFS (p 0.036) and OS (p 0.045). A subgroup analysis in no-pCR patients showed a close correlation positive between high reduction gradients of metabolic/ volumetric parameters and less postoperative morbidity. Nevertheless, a multivariate analysis underlined that only pretreatment SUVmax absolute value was significantly associated with disease recurrence (with a cutoff value of SUV 7.28 p 0.0069). No significant correlation was found with MTV and TLG absolute value, age, Ki-67, NLR ratio and adjuvant regimen. ***Conclusion:*** Our data suggest that the dynamic variation of metabolic/volumetric parameters could be a useful predictive marker for pCR and EFS in TNBC and HER2+. The Pretreatment SUVmax absolute value is the only parameter in no-pCR subgroup to predict higher risk of relapse. Prospective studies are needed to validate these tools to evaluate the response to neoadjuvant treatment and the risk stratification in these patients. ***References:*** None

OP-441

Diagnostic performance and impact on management of 18F-FDG PET/CT for suspected recurrence in Invasive Lobular Breast Carcinoma

J. Alberini[1], *D. Bonnin*[1], *S. Ladoire*[1], *A. Bertaut*[1], *N. Briot*[1], *C. Drouet*[1], *Y. E Silva*[1], *G. Nodari*[1], *C. Tabouret-Viaud*[1], *A. Berriolo-Riedinger*[1], *I. Dygai-Cochet*[1], *H. Boulahdour*[2], *A. Cochet*[1];
[1]*Centre Leclerc - University Hospital, Dijon, FRANCE,*
[2]*University Hospital, Besancon, FRANCE.*

Aim/Introduction: Invasive Lobular Carcinoma (ILC), which accounts for 10-15% of all breast cancers, is usually characterized by a low FDG uptake of primary tumor and metastases, when compared with invasive ductal carcinoma (IDC), during initial staging. The aim of this retrospective monocentric study was to examine the diagnostic performance of 18F-FDG PET/CT to detect sites of recurrence when first recurrence was suspected in women previously treated for ILC, and the impact on management. The final diagnosis of recurrence made by the oncologist was used for reference. Results were correlated with the pathological and biological prognostic factors of the primary tumor. ***Materials and Methods:*** 64 patients (mean age: 60.3±12.4 years [32-86]), for whom a PET/CT scan (Gemini TF, Philips and Discovery MI, GEHC) was performed between January 2011 and May 2019, were included. The association with IDC was an exclusion criterion. Recurrence was suspected based on clinical symptoms (48%), conventional imaging findings (42%) and/or an increase in tumor markers (30%). The mean time between initial diagnosis and suspicion of recurrence was 5.2 years. ***Results:*** ILC primary tumors were mainly grade II (75%), expressing estrogen receptors (95%) or Her2 negative (95%). 40 patients out of 64 (62.5%) underwent a biopsy, of which 32 were in favor of a local or metastatic ILC recurrence. In the 8 remaining patients, pathological findings corresponded to the IDC subtype, primary pulmonary or gastric tumors, lymphoma or benign material. Among the 64 patients, 48 were judged to be recurrent by the oncologist: 16 local recurrences and/or 41 metastatic with mainly bone (n=24), lymph node (n=14) and liver (n=10) metastases. Bone metastases were mainly sclerotic or mixed (14/24) on CT. PET sensitivity, specificity, PPV and NPV were 87%, 87%, 95% and 70%, respectively. SUVmax at recurrence sites was generally high (mean: 6.4±2.7; 1.9-17.3). The 6 false negative PET results corresponded to local (n=2), bone (n=1), meningeal (n=1), peritoneal (n=1) or bladder (n=1) recurrences, sites for which 18F-FDG PET may lack sensitivity. The detection of a recurrence resulted in a change in treatment in 44 patients (92%). No correlation with the pathological prognostic factors of the primary tumors was demonstrated. ***Conclusion:*** While highlighting its limits in relation to certain recurrence sites specific to ILC, the present study demonstrates that 18F-FDG PET/CT remains an effective and reliable tool for the detection of

ILC recurrence. ***References:*** None

OP-442

18F-FES PET/CT influences the diagnosis and management of stage IV patients with dual primary malignancies: ER-positive breast cancer combined with another primary tumour

Z. Yang;
Fudan University Shanghai Cancer Center, Shanghai, CHINA.

Aim/Introduction: We aimed to investigate the clinical value of 18F-fluoroestradiol (18F-FES) positron emission tomography (PET)/computed tomography (CT) in stage IV patients previously diagnosed with oestrogen receptor (ER)-positive breast cancer and another primary malignancy. ***Materials and Methods:*** We retrospectively analysed 20 female patients who had been diagnosed with ER- positive breast cancer and another primary tumour and underwent 18F-FES PET/CT scans in our centre. To investigate the definite clinical impact of 18 F-FES on managing such patients, we designed questionnaires. Physicians completed the questionnaires, including diagnosis and treatment decisions, before and after the imaging reports of 18F-FES. ***Results:*** In total, eleven physicians were given questionnaires referring to the treatment strategy of the 20 patients. The application of 18F-FES had reference significance for management decisions in 80% (n = 16) of the patients. Out of the 16 patients with consideration of profit from 18F-FES PET/CT reports, 8 patients were considered to have definite changes in the treatment strategies. And the scan was considered to be instructive to develop management plans in 8 patients. Most physicians (86.7%, 52/60) considered that 18F-FES PET/CT scans played definitely instructive roles in the decision-making of the treatment strategy in these patients (0.032, 95% CI 0.024- 0.042). The intended diagnosis was changed by 71.7% of physicians (0.033, 95% CI 0.023-0.056) and the treatment strategy was changed by 68.3% of physicians (0.032, 95% CI 0.023-0.045), respectively. ***Conclusion:*** 18F-FES PET/CT scans in stage IV patients diagnosed with ER-positive breast cancer combined with another primary tumour have significantly clinical value for diagnosis and treatment management. ***References:*** None

OP-443

68-Ga PSMA and 18-F FDG PET/CT Imaging in Triple-Negative Breast Cancer

E. Arslan[1], *N. Ergül*[1], *F. D. Can Trabulus*[2], *Ö. Mermut*[3], *S. Akbaş*[4], *M. Cin*[5], *T. F. Çermik*[1];
[1]*University of Health and Sciences, Istanbul Training and Research Hospital, Clinic of Nuclear Medicine, Istanbul, TURKEY,* [2]*University of Health and Sciences, Istanbul Training and Research Hospital, Clinic of Surgery, Istanbul, TURKEY,* [3]*University of Health and Sciences, Istanbul Training and Research Hospital, Department of Radiation Oncology, Istanbul, TURKEY,* [4]*University of Health and Sciences, Istanbul Training and Research Hospital, Department of Medical Oncology, Istanbul, TURKEY,* [5]*University of Health and Sciences, Istanbul Training and Research Hospital, Department of Pathology, Istanbul, TURKEY.*

Aim/Introduction: Limited studies about using 68-Ga prostate specific membrane antigen (PSMA) PET/CT imaging have been published on breast-cancers, especially in triple negative subtype (TN) and Her2 positive NST subtypes.High endothelial PSMA expression has been demonstrated in 60% of breast cancer patients. In this study, we aimed to determine the possible contributions of 68-Ga PSMA PET/CT to 18-F FDG PET/CT imaging for TN breast cancer staging and restaging ***Materials and Methods:*** Fifteen women patients with 18 primary lesions (Age range: 26-67 years; mean: 50,3 years) underwent prospective assessment with 18-F FDG and 68-Ga PSMA PET/CT imaging. PSMA expression and FDG uptake were semiquantitatively (SUVmax) compared in primary tumor, metastatic axillary lymph nodes, as well as distant metastases such as bone and liver. ***Results:*** Primary lesions were detected in all 15 patients with 68-Ga PSMA PET/CT (median SUVmax: 4.5, range: 1.6-10.7), and also high FDG uptake was observed in primary tumors and metastatic lesions of the entire patient group. Fourteen patients with FDG avid lesions showed substantial PSMA expression but one patient with multiple bone and distant metastatic lesions has very low PSMA expression. ***Conclusion:*** 68-Ga PSMA PET/CT showed similar results to 18-F FDG PET/CT staging in patients with TN breast cancer. For this reason, it also may play a guiding role in targeted radionuclide therapies in this breast cancer subtype with a high risk of recurrence. ***References:*** None

811

Technologists e-Poster Presentation Session Technologists 2

Friday, October 23, 2020, 16:55 - 18:05 Channel 11

TEPS-23

Is there a role for ^{99m}Tc-PSMA in times of ^{18}F-PSMA?

T. Oliveira*, B. Beier, J. Sailer, P. Peloscheck, M. Hoffmann;*
Radiology Center, Vienna, AUSTRIA.

Aim/Introduction: Prostate cancer is the second most common cause of death in developed countries and is the most common type of cancer in men. PSMA provides a promising target for prostate cancer specific imaging. ^{99m}Tc-labelled PSMA for planar and SPECT/CT imaging appears a promising alternative to PET tracers for diagnostic work-up of prostate cancer patients. We present a retrospective single-center experience with ^{99m}Tc-PSMA and ^{18}F-PSMA. ***Materials and Methods:*** From December 2018 to March 2020,

22 patients were examined for staging of prostate cancer. In 16/22 patients ^{99m}Tc-PSMA whole-body scintigraphy followed by SPECT/CT was performed. In 8/22 patients ^{18}F-PSMA PET/CT was performed. In 2 patients, both scans were used during follow up.The inclusion criteria for the performance of any of these studies was a bioptic diagnosis of prostate cancer, an elevated PSA or clinical suspicion of recurrence with detectable PSA level during or following therapy. A whole-body scan and SPECT/CT of the thorax and abdomen were performed earliest 6 hours after administration of 720 MBq (mean activity) ^{99m}Tc-PSMA. ^{18}F-PSMA-PET/CT was performed 2 hours after injection of 453 MBq (mean activity) with IV contrast enhancement. ***Results:*** Local prostatic uptake of ^{99m}Tc-PSMA was found in 5/16 patients. Another 5 patients showed lymph node metastases, predominantly local and iliacal but also in paraortal regions. In 1 of these patients also distant spread was detected, namely bone metastases. A total of 8 patients were examined prior to surgery. In 3 patients with ^{99m}Tc-PSMA positive lymph nodes, a gamma probe was used for surgical resection, which was carried out on the same day or the morning of the following day. In 8 patients who have undergone the study with ^{18}F-PSMA, local uptake was found in 1/8 patient. In 6/8 patients, the study showed lymph node metastases and distant osseous spread was detected in 4 patients. ***Conclusion:*** For staging and follow up in prostate cancer ^{68}Ga PSMA or ^{18} F PSMA will stay to be the tracers of first choice. Yet, PSMA scintigraphy including SPECT/CT is an acceptable alternative when no PET/CT machine or tracer for prostate cancer are available. Especially, when applied preoperatively it allows the specific localization of involved lymph nodes metastases during surgery with the use of a gamma probe. ***References:*** None

TEPS-24

Cardiac Inhibition Protocol For The Diagnosis Of Infective Endocarditis Wth 18F-FDG PET/CT

M. Cabanillas Perez*, S. Ruiz Solis, P. Pilkington Wol, J. Sánchez Redondo, J. Estenoz Alfaro;*
Hospital Universitario 12 Octubre, Madrid, SPAIN.

Aim/Introduction: Inhibition of the physiological cardiac activity on 18F-FDG PET/CT is essential for the diagnosis of infective valve endocarditis. The objective of this work is to determine the effectiveness of the cardiac inhibition protocol used in our department. ***Materials and Methods:*** We retrospectively analyzed all the PET/CT studies done to patients with suspected infective endocarditis from April 2019 to January 2020. Previous to the scan, these patients are contacted to explain the cardiac inhibition protocol used in our department and which they have to follow. This protocol consists in a low-carbohydrate and high-fat diet for at least 24 hours, and an 8 hour period of fasting previous to the scan. Good hydration is also recommended. The PET/CT used was a Siemens Biograph 6. Following glycemic control, a standard dose of 5 MBq/kg of 18F-FDG was injected intravenously. After 50 - 60min a standard acquisition protocol was followed, which consists in performing images from the base of the skull to the mid-thighs, with a 3min per bed position acquisition in a cranial to caudal direction and using a low dose CT (mAs modulated with CARE Dose4D, 130 kV, 4mm slices). Following the scan acquisition, images were evaluated for total, partial or no cardiac inhibition by a nuclear medicine physician. ***Results:*** Twenty studies performed with the cardiac inhibition protocol were evaluated. After analysis, we found that 11 patients (55%) had total cardiac inhibition, 8 patients (40%) had partial cardiac inhibition (never the less only in 1 case this partial inhibition affected image interpretation) and only 1 patient (5%) had no cardiac inhibition (we suspect that this result is because the patient did not follow the protocol). Therefore, taking into account our results, we can say that a satisfactory cardiac inhibition was achieved in 90% of patients (18 patients). ***Conclusion:*** The cardiac inhibition protocol used in our department allowed for a correct cardiac evaluation in 90% patients with suspected infective endocarditis following 18F-FDG PET/CT scan. ***References:*** None

TEPS-25

The Use Of Fatty Acids Labeled With Technetium-99m For Visualization Of The Cardiac Muscle

A. Rogov*, E. Stasyuk, E. Nesterov;*
National Research Tomsk Polytechnic University,
Tomsk, RUSSIAN FEDERATION.

Aim/Introduction: The results of studies on the development of methods for the synthesis of new X-ray diagnostic tools based on a modified fatty acid are presented. Labelled technetium-99m fatty acid is necessary for a detailed scintigraphic evaluation of myocardial metabolism. In the process of synthesis of the radiopharmaceutical, the interaction of the substance with technetium-99m in an alcohol medium was studied using ethanol as a solvent. Aim: Developing methods for the synthesis of a new radiopharmaceutical based on modified fatty acid labelled with technetium-99m. ***Materials and Methods:*** This agent is intended for studying the metabolism of cardiac muscle and this will allow differentiating viable heart and scar tissue. An important task of cardiology is the diagnosis of viable myocardium, since its presence in an ischemic area is a direct indication for invasive correction of coronary insufficiency. As a substance for radiolabelling fatty acid was synthesized derivative (PDA-DTPA). PDA-DTPA molecule includes two structural fragments ensuring successful functioning of the radiopharmaceutical. The first is that provided bioavailability acid fragment of the radiopharmaceutical to myocardium. The second fragment which serves for chelate binding of ^{99m}Tc. Ethanol was used as solvent for PDA-DTPA but it acts as a reducing agent for $SnCl_2 \cdot 2H_2O$. To perform labelling

1mg PDA-DTPA dissolved by heating in 1.0 ml 96% ethanol. Then 1.0ml ^{99m}Tc, 50 mcl Sn(II) solution and 50mcl ascorbic acid as a stabilizing additive were successively placed in a test tube. Determine radiochemical purity was carried out by thin layer chromatography. Determine radiochemical purity was carried out by thin layer chromatography. As mobile phases have been identified Chloroform and Acetone. Acetone was selected for comparing mobility ^{99m}Tc(VII). ***Results:*** Determine radiochemical purity was carried out by thin layer chromatography. As mobile phases have been identified Chloroform and Acetone. Acetone was selected for comparing mobility ^{99m}Tc(VII). Radiometer «RIS-A1» was used to measure the total activity of the vial. After incubating the mixture for 15min and it is heated on a steam bath for 30min at temperature to 98°C. Then was carried out repeated sampling for chromatography in the same media. ***Conclusion:*** The experiments carried out show that receiving PDA-DTPA-^{99m}Tc, having a pH of~6, the desired product yield is insufficient. The next stage of our research will be the study of PDA-DTPA behavior in aqueous media and effect on solubility of the pH medium. ***References:*** None

TEPS-26

Comparison of quantitative assessment for cardiac sarcoidosis inflammation site using ^{18}F-FDG PET / CT images

R. Murayama[1], *R. Morimoto*[2], *N. Fujita*[1,3], *Y. Ito*[1], *R. Ono*[1], *T. Tada*[1], *H. Ikeda*[4], *Y. Ochi*[4], *M. Nishio*[4], *Y. Tsutsumi*[3], *M. Tamura*[1], *T. Odagawa*[1], *S. Abe*[3], *K. Kato*[4];
[1]*Department of Radiological and Medical Laboratory Sciences, Nagoya University Graduate School of Medicine, Nagoya, JAPAN,* [2]*Department of Cardiology, Nagoya University Graduate School of Medicine, Nagoya, JAPAN,* [3]*Department of Radiological Technology, Nagoya University Hospital, Nagoya, JAPAN,* [4]*Department of Integrated Health Sciences, Nagoya University Graduate School of Medicine, Nagoya, JAPAN.*

Aim/Introduction: Cardiac involvement in sarcoidosis is associated with a worse prognosis and accounts for 25% of deaths from sarcoidosis, so early diagnosis and treatment of cardiac sarcoidosis (CS) are very important. ^{18}F-FDG PET/CT detects CS inflammation site as focal areas of FDG uptake with high sensitivity, so that cardiac imaging is a useful method for diagnosis of CS. For CS ^{18}F-FDG PET/CT, indices such as standardized uptake value (SUV), cardiac metabolic volume (CMV), and cardiac metabolic activity (CMA) are used to evaluate CS inflammation site. These indices are calculated by volume of interest (VOI) setting at CS inflammation site using a threshold value. However, the thresholds for calculating these indices have not been clarified. The aim of this study was to verify whether VOI set using the threshold from the liver SUV normalized by lean body mass (SUL) or the left ventricular blood pool (LVBP) SUL was consistent with CS inflammation site confirmed by clinical diagnosis. ***Materials and Methods:*** Study subjects were 50 patients (62 examinations in total) who underwent CS ^{18}F-FDG PET/CT studies and diagnosed with CS at Nagoya University Hospital. Analyzing software programs PMOD (PMOD Technologies) was used for measurement of the liver SUL and the LVBP SUL, and calculation of the threshold value. VOI was set at the heart using the threshold from the liver SUL or the LVBP SUL and was compared with CS inflammation sites confirmed by clinical diagnosis. CMA inside VOI set at the heart was measured. To select the best threshold for CMA, receiver-operator curves (ROC) analysis was used, and the sensitivity, specificity and area under the curve (AUC) were calculated. ***Results:*** CS inflammation sites set using threshold from the LVBP SUL were better consistent with CS inflammation sites confirmed by clinical diagnosis than those set using threshold from the liver SUL. CS inflammation sites set using the threshold from the liver SUL were mostly not consistent with CS inflammation sites confirmed by clinical diagnosis in the cases on the way of treatment. Since the visual assessment of CS evaluated the difference of uptake between CS inflammation sites and LVBP, VOI using threshold from the LVBP SUL could be set exactly. ***Conclusion:*** CS inflammation sites set using threshold from the LVBP SUL were comparatively well consistent with CS inflammation sites confirmed by clinical diagnosis. ***References:*** None

TEPS-27

Patient Non-Compliance Rates in Following Dietary Instructions for Cardiac Inflammation/Infection Imaging with FDG PET/CT

N. Martins*, F. Alves, K. Wechalekar;*
Royal Brompton & Harefield NHS Foundation Trust, London, UNITED KINGDOM.

Aim/Introduction: 18F- Fluorodeoxyglucose (FDG) has a high physiological uptake in the heart. Hence, it is difficult to evaluate pathologies such as cardiac involvement of sarcoidosis and heart infections. Our protocol of no-carbohydrate diet on day prior followed by fasting (18 hours) before scan deprives the heart from using glucose as a substrate for metabolism allowing us to secure diagnosis of cardiac inflammation/infection. Despite providing patients with elaborate instructions on how to follow this diet, some patients fail to adhere to these dietary restrictions leading to cancellations and ultimately delaying their diagnosis and subsequent management. We have been working to improve on protocol compliance. This follow up study was performed after introducing new dietary menus and multi-lingual text. Our aim was to identify potential reasons for cancellations. ***Materials and Methods:*** All planned cases from October 2019 to February 2020 were checked for cancellations. The percentage of failing dietary restrictions in comparison to total FDG doses was calculated. The

reasons for failing the dietary restrictions were gathered from the patients. ***Results:*** In the 5 months, 26 FDG doses out of 599 were cancelled due to patients failing the dietary restrictions (4.34%). The reasons for this can be divided into patient related and voluntary (misunderstanding/not reading the instructions and ingesting carbohydrates), patient related and involuntary (hypoglycaemia due to change in diet) and non-patient related (interpreters providing incorrect information to the patients). The first category accounts for most of the cancellations. Hence to tackle this problem, changes such as the inclusion of new menu choices and translation of menus were made. In a similar study concerning the five months prior, the percentage of cancellations due to failing the diet was of 3.57%. One of the main reasons of cancellation in that study was the disregard for the diet and after changes to the patient's letter, this is rarely the reason for cancellation. ***Conclusion:*** Cancellations due to failing the diet restrictions are mostly due to human error which can never be brought to 'zero'. However, studies such as these help technologists understand the reasons behind compliance, so measures can be implemented to keep them to minimum. By doing so, delays in clinical pathways can be avoided and save the cost of cancelled FDG exams. The study aims to share our experience to raise awareness for the potential problems that arise and what measures can be implemented to tackle them. ***References:*** None

TEPS-28

Sweet child of mine: the use of music in dynamic renal scintigraphy in pediatric patients

M. Maccagnani*, A. Farina, R. Bonfiglioli, M. Levorato, S. Fanti;*
Nuclear Medicine Department, Sant'Orsola-Malpighi Hospital, University of Bologna, Bologna, ITALY.

Aim/Introduction: Dynamic renal scintigraphy in pediatric patients is one of the most demanding examinations depending on the way children relate to their surroundings. The aim of this work is to describe our center experience and a new strategy to increase the quality of the examination and reduce the stress in little patients and their parents. ***Materials and Methods:*** The dynamic renal scintigraphy is one of the stressful examinations for paediatrics patients due to the injection of the radiopharmaceutical and the need to remain as still as possible for a long time. The help of the parents is not always sufficient to guarantee a successful exam. Over the years we have applied different strategies to calm down young patients: the use of sucrose drops for infants from 1 to 6 months and the use of a tablet with cartoons for children from 2 to 6 years obtaining excellent results. We still miss a strategy for children from 6 months to 2 years. In summer2019 during the injection of the radiotracer for dynamic renal scintigraphy to a 7-month-old infant, doctors began to sing the popular Korean song "Baby Shark" for fun. The baby calmed down quickly making the injection easier. It was decided to keep listening to the song, via-Youtube, for the duration of the exam. As a result, the child remained serene throughout the procedure and the examination required a reduced intervention of realignment of the images, increasing their general quality. In light of this incidental experience, in the following weeks, the same attempt has been repeated on every possible occasion always leading to remarkable results. ***Results:*** Since September2019 the use of music while performing dynamic renal scintigraphy in pediatric patients has been adopted as a standard procedure. From July2019 to April2020, dynamic renal scintigraphy was acquired for 35 children in the age group from 6 months to 2 years, every time background music was used throughout the exam. This strategy seems to decrease stress in children and consequently the same effect on parents, thus eliminating emotional feedback. ***Conclusion:*** In all cases examinated, the benefits of music have been significant: the increased complement of the child during the injection and acquisition phase of the examination resulted in a reduced need for post-image processing. A playlist containing several children's songs has been uploaded on a tablet but "Baby Shark" seems to remain the favourite song of younger children and doctors. ***References:*** None

TEPS-29

Psychosocial characteristics of patients with coronary artery disease during imaging examinations in the Nuclear Medicine Department

M. Stolidou[1]*, F. Rondoyanni*[1]*, I. Datseris*[1]*, G. Alexias*[2]*;*
[1]*Evaggelismos Hospital, Athens, GREECE,*
[2]*Panteion University, Athens, GREECE.*

Aim/Introduction: To explore the effect of anxiety and depression, as well as social support, on patients with coronary artery disease. ***Materials and Methods:*** 155 patients with known coronary artery disease were subjected to myocardial perfusion imaging at the Nuclear Medicine Department of "Evaggelismos" Hospital. Data were collected by the completion of questionnaires, which apart from the socio-demographic and clinical variables, included the Hospital Anxiety and Depression Scale (HADS) and the short form of the Social Support Questionnaire (SSQ-6). The statistical analysis was conducted by using the statistical software SPSS 19.0. ***Results:*** From the participants 85.2% were 51-80 years old, 80.6% were men, 71.6% married and 55.5% retired. As to their educational level, 42.6% were high school/college graduates and 31.0% were graduates of elementary school. Regarding the clinical characteristics of the sample-studied, 71.6% had myocardial infarction and 71.0% angioplasty. 34.2% of patients had cardiovascular disease of 2-5 years' duration, 23.2% were diagnosed within the last year, while 94.8% of patients had been hospitalized

for the same reason. Also, 74.2% of the participants had hypertension, 51.0% had family history of cardiovascular disease, 43.9% obesity, 34.8% diabetes, and 36.8% were smokers. 44.5% of patients experienced a myocardial perfusion imaging for the first time. Regarding social support, higher levels were found for the most educated and those who had children. In addition, angina pectoris patients had significantly less social support than non-angina patients. In addition, in terms of satisfaction with their social support, multivariate linear regression showed that women were significantly more satisfied with their social support than men. Higher levels of depression based on the HADS questionnaire were found according to multifactorial analysis in women and patients with arrhythmias. In addition, it was found that the more social support the patients had, the less depressive symptoms they experienced. In terms of anxiety levels as measured by the HADS questionnaire, it was found to be higher in women, in patients suffering from angina pectoris, while the more social support the patients had, the fewer the symptoms of anxiety were. ***Conclusion:*** For the holistic treatment of coronary artery disease the systematic approach of anxiety and depression, as well as social support, should be an integral part of the patients' treatment. ***References:*** None

TEPS-30

Flow motion modality reduce the patient radiation exposure of whole-body PET-CT

G. Pecchia[1], *E. Palladino*[2], *S. Amabile*[1], *G. Borselleca*[1], *C. Del Vasto*[1], *C. Lanotte*[1], *U. Marra*[1], *V. Milone*[1], *D. Palma*[1], *S. Piccolo*[1], *A. D'Acunzo*[1], *M. Spadafora*[1];
[1]*Nuclear Medicine Unit, Ospedale del Mare, Naples, ITALY,* [2]*Ospedale Civile Lipari, Messina, ITALY.*

Aim/Introduction: The first priority of actual ICRP Strategic Plan, as well as the basic principle of radioprotection, is to reduce radiation exposure maintaining diagnostic information. Continuous motion in flow modality (FM) of the patient table has recently been introduced in modern PET/CT tomograph. This individualized acquisition, without the limitations of multi-bed position-based planning (MB),increased patient comfort with image quality at least comparable to that step-and-shoot acquisition. FM, avoiding additional CT range scanning, can be conceptually advantageous from a dosimetric point of view. However, to our knowledge no studies explored the effect of two modalities in reducing CTpatient dose. Aim of this study was to compare the patient radiation exposure of FM and MB acquisition modality, related to whole-body (wb) PET/CT scan. ***Materials and Methods:*** We have collected our first 80 patients referred for whole-body FDG-PET/CT for different malignancies. PET/CT images were acquired using an integrated 3-D mode PET/CT systems, from the base or top of the skull to mid-thigh (wb-PET/CT), starting 60 min after tracer administration. In each patient, after the topogram, two acquisition mode, FM and MB, were set in order to preliminarily obtain an estimate of both dose-length product (DLP) and scan length (in mm) for FM and MB modality. At the end of the PET/CT study, the effective values of both DLP and ED were recorded. DLP was calculated as CTDI vol*length of scan in mGy*cm. The transformation of DLP in Effective Dose (ED in mSv) was made accordingly ICRP 103. The relative risk of cancer was evaluated by the software X-ray risk, based on the BEIR VII report. Differences between continuous data were assessed using paired Student's t test. ***Results:*** In study population estimate mean values of both DLP and scan length was significantly higher by MB than FM modality of whole-body PET/CT (762.8+381.8 vs 744.3+376.0 mGy*cm, p<0.0001; 963.5+78.0 vs 928.2+75.2 mm, p<0.0001, respectively). Similarly, estimate ED was significantly higher by MB than FM modality (13.7+6.9 vs 13.4+6.8 mSv, p<0.0001). The effective values of both DLP and ED were slightly lower than the same parameters estimate before the study (662.0+342.8 mGy*cm and 12.0+6.2 mSv, respectively). The lower DLP in FM than in MB modality produces e lower relative risk of cancer due to whole-body PET/CT procedure (0.059+0.05 vs 0.058+0.05, p<0.0001). ***Conclusion:*** Compared to standard MB modality, the flexibility of FM significantly reduces the radiation exposure and relative cancer-risk of wb-PET/CT, according to ICRP provisions. ***References:*** None

TEPS-31

Occupational Radiation Exposure in the Department of Nuclear Medicine - the Effect of Distance and Shielding Material on the Dose Rate

T. Saila[1], *S. Hakkarainen*[1], *K. Hirsimäki*[1], *T. Taatila*[2], *H. Vilpas*[2];
[1]*Tampere University of Applied Sciences, Tampere, FINLAND,* [2]*Tampere University Hospital, Tampere, FINLAND.*

Aim/Introduction: To increase knowledge related to the importance of radiation safety procedures which permit safe working in the Department of Nuclear Medicine. An answer was sought to the question of how distance and shielding material affect dose rate when dealing with Tc99m-labeled radiopharmaceuticals. ***Materials and Methods:*** The entire data comprises two parts: the first data were collected during Myocardial perfusion SPECT and Bone scan and the second data were related to syringe measurements. In the case of imaging situations, the dose rate was measured at different distances (2 m, 1 m, 50 cm, 25 cm) from the patient who had received the radiopharmaceutical. Myocardial perfusion SPECT and bone scan were chosen because both examinations are common, and the activity used in these examinations is relatively high. The effect of distance (1 cm, 20 cm) and syringe shield (2 mm tungsten) on the dose rate was investigated with syringe measurements. The radioactive component to be measured was

technetium-99m eluate. The measurements were made with several activities (805.1 MBq, 600.4 MBq, 502.6 MBq, 402.6 MBq, 311.8 MBq). Instructions and data collection forms were prepared in advance for the measurements. Their purpose was to ensure that no errors occur during the measurements. The dose rates were measured with a radiation meter calibrated by the Radiation and Nuclear Safety Authority. ***Results:*** The study is currently in process, so the results are still underway. The results related to the patient examinations determine how extensive the change (%) in dose rate is when the distance increases. The dose rates will be described using tables and graphs, separately from skeletal and myocardial perfusion examinations. The results of the syringe measurements determine how much (%) the syringe shield affects the dose rate. In addition, average dose rates in the immediate vicinity of the syringe (0-1 cm) and at 20 cm from the syringe will be compared. ***Conclusion:*** The dose rates will be presented in a concrete way. The radiographers and nuclear medicine technologists working in the department of NM ought to understand the importance of distance and shielding material in their daily routine. Dose rates are illustrated by describing how long it takes for the worker's effective dose limit of 20 mSv or the finger dose limit of 500 mSv to be reached, at different distances, or without and with a syringe shield. Dose rates will be also compared to air travelling and natural background radiation. ***References:*** None

TEPS-32

Hand exposure in nuclear medicine technologists working in the radiopharmaceutical laboratory in diagnostic nuclear medicine

C. Sobral*, J. O. Prior, E. Perez;*
Centre hospitalier universitaire vaudois (CHUV), Lausanne, SWITZERLAND.

Aim/Introduction: We aimed to assess dose-extremity, its distribution and to define a personal correction factor from measurements on the hands of technologists working in a radiopharmaceutical laboratory. ***Materials and Methods:*** From October-November 2019, five technologists were equipped with 22 thermoluminescent dosimeters (TLDs) (11 positions by hand) to measure their personal dose equivalent Hp (0.07). We used TLD-100 LiF 3.2x3.2x0.9mm, GIM1, calibrated on 23/05/2019, and measured with a reader Harshaw 5500 with a Co-60 beam. Measurements were repeated twice over 1 week for 2 out of the 5 participants. A TLD was used to measure the background activity in the laboratory. ***Results:*** For all 5 technologists, the index tip of the non-dominant hand demonstrated the maximum received dose, followed by the ipsilateral thumb. A comparison of dose measurements between the maximum dose position and the base of the index finger of the non-dominant hand where it is routinely measured showed values for the correction factors ranging from 2 to 2.7 (2.3±0.3). On average, the non-dominant hand received 1.7±6.2mGy (or 59%) more dose than the dominant hand (laboratory background activity was 0.159mGy). ***Conclusion:*** According to our results, we recommended wearing of the extremity dosimeter at the base of the index finger of the non-dominant hand facing its palm. In addition, an average correction factor of 3 can be applied to estimate the absorbed dose on the position with the most exposure, the tip of the index finger of the non-dominant hand; this compares to the factor of 5 taken by default in the Swiss Radioprotection Ordinance. ***References:*** Carnicer, A., Sans-Merce, M., Baechler, S., Barth, I., Donadille, L., Ferrari, P., ... Vanhavere, F. (2011). Hand exposure in diagnostic nuclear medicine with 18F- and 99mTc-labelled radiopharmaceuticals - Results of the ORAMED project. Radiation Measurements, 46(11), 12771282. https://doi.org/10.1016/j.radmeas.2011.07.019

TEPS-33

Using common tungsten vs. special plastic syringe shield with yttrium-90: more radiation exposure to staff or not?

E. Tyyskä*, N. Takalo, M. Ladev, M. Eskola, J. Hyypiä, M. Tenhunen, V. Reijonen;*
Helsinki University Hospital Cancer Center, Helsinki, FINLAND.

Aim/Introduction: Yttrium-90 is a high-energy beta emitter used in radionuclide therapy such as radioembolization. Handling an unshielded syringe containing yttrium-90 can quickly lead to significant skin exposure. Syringe shielding is thus very important. Beta radiation produces Bremsstrahlung X-rays as it travels through medium, and using right shielding materials is essential. Lead/tungsten shields are commonly used when handling radiopharmaceuticals; however, for yttrium-90, plastic or aluminium-based low-Z special syringe shields are recommended as they produce a softer Bremsstrahlung spectrum. On the other hand, there are results suggesting that tungsten is the shield material of choice for yttrium-90. ***Materials and Methods:*** We drew 0.54 GBq of yttrium-90 resin microspheres into a 5 ml plastic syringe (polypropylene, wall thickness 1 mm) and placed it into three different syringe shields at a time: a plastic (PMMA) 12 mm thick syringe shield used in radioembolization, a "high energy" tungsten syringe shield (5 mm tungsten, 9 mm lead glass window) and a "low/medium energy" tungsten syringe shield (2 mm tungsten, 6 mm lead glass window). All beta radiation is absorbed in the three syringe shields and the exposure is due to Bremsstrahlung only. We measured dose rates with a multi-purpose survey meter (gamma/X-ray detection range: 48 keV-3 MeV, energy response according to ambient dose equivalent H*(10)) at the distances of 1.0 m and 10 cm from the shielded syringe, and in close contact to the shield. ***Results:*** For the plastic syringe shield, the measured dose rates were 1 µSv/h at 1.0 m, 75 µSv/h at 10 cm and 500 µSv/h in close contact

to the shield. For the "HE" tungsten syringe shield the dose rates were 0.4 µSv/h, 17 µSv/h and 165 µSv/h, respectively. For the "ME/LE" tungsten syringe shield the dose rates were 0.6 µSv/h, 30 µSv/h and 265 µSv/h, respectively. Earlier, our technologist used by error the "HE" tungsten syringe shield instead of the plastic special syringe shield while handling yttrium-90 microspheres. The personal dosimeter (TLD based, worn three weeks before read-out) readings were H*(10)=0.13 mSv and Hp(0.07)=1.85 mSv (finger). These values do not differ from the average doses recorded in normal working conditions at our radionuclide therapy unit. ***Conclusion:*** Common tungsten syringe shields appear to provide adequate shielding with yttrium-90. It is important to use shielding meticulously when handling yttrium-90 radiopharmaceuticals, and finding a consensus on the optimal shielding solutions is encouraged. ***References:*** None

TEPS-34

Image quality improvement method for nuclear medicine images based on deep learning

R. Yamada[1], M. Momiuchi[1], T. Hara[1], T. Katafuchi[2], X. Zhou[1], H. Fujita[1];
[1]Gifu University, Gifu, JAPAN, [2]Gifu University of Medical Science, Seki, JAPAN.

Aim/Introduction: Nuclear medicine images can acquire functional information of organs that cannot be imaged by other radiological modalities, but it is difficult to extract detailed structures of organs. In this study, we examined an image quality improvement method of nuclear medicine images with low spatial resolution by using a super-resolution technique with deep learning and an original dataset. ***Materials and Methods:*** In this study, low resolution (LR) images were created from high resolution (HR) data using a food printer containing RI materials in the ink. 108 pairs of the LR and HR images were employed as image database for the deep learning. The image database contains a medical image set using CT and MRI, and a natural image set as the HR images. These HR images were printed on paper by a food printer using specialized ink mixed with a radiopharmaceutical, and the printed images on the paper were captured by using a gamma camera. The captured images were defined as the LR images. Four-fold cross-validation was performed using a network created based on SRResNet. The input image size was 64 × 64 [pixels] and the output image size was 256 × 256 [pixels]. We compared the proposed method with the Bi-cubic method by numerical evaluation using PSNR and SSMI and subjective evaluation. ***Results:*** In the numerical evaluation, PSNR and SSIM were 33.71 and 0.861 in the proposed method and 32.53 and 0.808 in Bi-cubic method, respectively. ***Conclusion:*** We have suggested a supuer-resolution method using deep learning and a creation method for the image database using a food printer. These approaches can contribute to improve the visibility of nuclear medicine images with low spatial resolution. ***References:*** None

TEPS-35

Striatum extraction using deep learning in ioflupane brain scintigraphy - Learning using Monte Carlo simulation images -

H. Tsushima[1], R. Murakawa[1], S. Kurata[2,1], R. Ishitsuka[3], H. Nosaka[4], A. Onoma[5], S. Koike[6,1];
[1]Ibaraki Prefectural University of Health Sciences, Ami-machi, Ibaraki, JAPAN, [2]Ibaraki Prefectural Central Hospital, Kasama, Ibaraki, JAPAN, [3]Chiba University Hospital, Chiba, JAPAN, [4]Clinical Imaging Center for Healthcare, Nippon Medical School, Bunkyo-ku, Tokyo, JAPAN, [5]Yokohama City University Hospital, Yokohama, Japan, JAPAN, [6]University of Tsukuba Hospital, Tsukuba, Ibaraki, JAPAN.

Aim/Introduction: Ioflupane brain scintigraphy is evaluated by the accumulated amount and shape of the radiopharmaceutical accumulation in the striatum. The Specific Binding Ratio proposed by Bolt et al. (SBR_{Bolt}) is widely used for quantitative evaluation of the accumulated amount; however, this method underestimates because the region of interest (ROI) is set larger than the striatum and includes the ventricle. In order to improve the accuracy of these evaluations, attempts have been made to extract only the striatum. In this study, we examined whether deep learning with Monte Carlo simulation images can be applied to the extraction of the striatum. ***Materials and Methods:*** First, single-photon emission computerized tomography (SPECT) images, with an accumulation ratio of 1: 2 to 1: 8 between the brain parenchyma and the striatum, were created by Monte Carlo simulation (SIMIND ver.6.1.0 Lund university) based on the striatum phantom as training data. Furthermore, SPECT images, with no accumulation in the brain parenchyma but only in the striatum, were similarly created as reference images. The network then trained on these SPECT images. Using the U-net and Convolutional Neural Network (CNN) for the network, the results of the extraction of the striatum were compared by Dice coefficient to evaluate the extraction accuracy. Furthermore, the same comparison was performed for the extraction results using 2D data and 3D data as learning data. ***Results:*** The Dice coefficients of U-net and CNN were 0.9 and 0.5 in normal striatum models, respectively. The Dice coefficients of 2D data and 3D data were 0.93 and 0.99 in normal striatum models, respectively. When 3D data was used as learning data, it was possible to extract from the top to the bottom of the striatum. However, some images with low accumulation were not extracted by the 3D algorithm. ***Conclusion:*** On the basis of the findings of this study, U-net is more suitable than CNN and 3D data is more suitable for learning data than 2D data in striatal scintigraphy. It was suggested that the underestimation of SBR_{Bolt} would

be improved by the accurate extraction because the ROI of the striatum does not include the ventricle. It was also suggested that it can be applied to quantitative evaluation methods for accumulated shape. In the future, it will be necessary to improve the extraction accuracy by learning more low accumulation images on a 3D U-net algorithm. ***References:*** None

TEPS-36

Development of the pulmonary artery region of interest setting program using deep neural networks for the ^{123}I-MIBG myocardial quantification

S. Itoyama[1], *Y. Uchiyama*[2], *K. Yamashita*[1], *A. Takaki*[3], *S. Ito*[2]; [1]*Graduate school of health sciences, Kumamoto University, Kumamoto, JAPAN,* [2]*Faculty of Life Sciences, Kumamoto University, Kumamoto, JAPAN,* [3]*Faculty of Fukuoka Medical Technology, Teikyo University, Fukuoka, JAPAN.*

Aim/Introduction: In this study, we developed a fully automatic myocardial uptake quantification analytical program for the Iodine-123 metaiod-obenzylguanidine (^{123}I-MIBG) myocardial uptake quantification method. The input function of this method was determined using the administered dose, which was obtained by analysing the count-time activity curve of the pulmonary artery (PA) in dynamic chest images. The automatic region of interest (ROI) setting program for the PA was developed by mathematically and statistically analysing a chest RI angiogram (mathematical method). The coincidence ratio between the location of the PA-ROI obtained using the mathematical method and that obtained using manual methods was approximately 90%. However, to practically use this program, further improvements of 10% are required. If the PA region can be determined by using deep neural networks for segmentation, the accuracy of the PA-ROI setting program can be improved in terms of simple analytical operations, repeatability, and reproducibility. The purpose of this study is to develop a new PA-ROI setting program by using deep neural networks. ***Materials and Methods:*** A U-Net architecture based on convolutional neural networks was used to determine the PA candidate region. Images of 364 patients who underwent the chest RI angiography were used as training images. An ROI with a radius of 4 pixels (8.76 mm) was set on the candidate PA region, and the highest mean pixel value on the ROI was identified. To confirm the usefulness of this program, 44 patients were examined using the PA-ROI setting program, and the results ware compared with those obtained through the manual method. ***Results:*** The dice coefficient between the training PA regions and the segmented PA regions was 76.5%. The coincidence ratio between the location of the PA-ROI obtained using this program and that obtained using manual methods was 98%. A strong correlation was observed between the PA-ROI setting method and the manual setting methods. ***Conclusion:*** We developed a fully automated PA-ROI setting program using deep neural networks for ^{123}I-MIBG myocardial quantification. This program improves the reproducibility, repeatability, and accuracy of the ROI setting. ***References:*** None

TEPS-37

Computer-aided detection of cancer on PET/CT images based on anomaly detection using GAN-based deep learning

T. Maeda[1], *M. Haga*[1], *T. Hara*[1], *T. Katafuchi*[2], *X. Zhou*[1], *M. Matsusako*[3], *S. Ito*[4], *M. Kato*[4], *A. Yamada*[5], *H. Fujita*[1]; [1]*Gifu University, Gifu, JAPAN,* [2]*Gifu University of Medical Science, Seki, JAPAN,* [3]*St. Luke's International Hospital, Tokyo, JAPAN,* [4]*Daiyukai General Hospital, Ichinomiya, JAPAN,* [5]*Shinshu University, Matsumoto, JAPAN.*

Aim/Introduction: Reducing false positives (FPs) is also an important issue in computer-aided diagnostic system as an interpretation help for radiologists. We propose an automated detection method for cancer-screening on PET/CT images based on anomaly detection using Generative adversarial networks (GANs). ***Materials and Methods:*** In this study, both of PET and CT images are used to detect cancer regions. OCGAN[1] is a deep learning model proposed for anomaly detection in two-dimensional images. We apply the GAN's model to PET images. The model trained axial, coronal and sagittal slices of many normal PET images. After that, the model would then produce a normal image even if the input image contains cancer regions as abnormal region. Subsequently, cancer regions were identified by a dynamic threshold processing on the differential image between the input and output of the model. Since the same process was performed for each cross-section. Areas where the results of the three cross-sections did not match were removed as FPs. The FPs were eliminated by using a gradient of voxel values within an organ on the CT images. ***Results:*** The detection performance was evaluated using 71 PET/CT images included 38 normal cases for a training dataset and 33 anomaly cases for a test dataset. The sensitivity was 87.6% with 84.4 FPs per case. The area of FPs was 904.7 voxels per case, which showed that FPs of small size were seen interspersed. ***Conclusion:*** We have developed a detection method based on anomaly detection using GANs for screening of cancer in PET/CT images. GANs trained only normal cases were contributed to correctly detection of cancer. ***References:*** [1] P. Perera et al. , " OCGAN: One Class Novelty Detection Using GANs With Constrained Latent Representations", The IEEE Conference on Computer Vision and Pattern Recognition (CVPR), pp. 2898-2906, 2019

TEPS-38

Use of artifical neural network for the diagnosis of myocardial ischemia :Comparison of imaging diagnosis between two devices in the clinical conditions

M. Kano[1], D. Ogura[1], T. Ino[2], T. Toyama[3], K. Koyama[1]; [1]Gunma Prefectural Cardiovascular Center, Maebashi-shi, Gumma-ken, JAPAN, [2]Gunma Prefectural Phychiatric Medical Center, Isesaki-shi, Gumma-ken, JAPAN, [3]Toyama cardiovasculary Clinic, Maebashi-shi, Gumma-ken, JAPAN.

Aim/Introduction: The advances in the myocardial perfusion analysis software have enabled the diagnosis of myocardial ischemia using artificial neural network (ANN). ANN supports radiological technologists and less-experienced physicians in interpreting images. Two different devices using for nuclear medicine examination are used in our hospital, both requiring the same diagnostic results. Here, we compared ANN values and summed stress scores (SSS) for a cardiac phantom and patients between the two devices. Although there are a few diagnostic studies using ANN, no studies have compared two different devices. ***Materials and Methods:*** The used devices were PRISM-IRIX: LEGAP and Infinia 8 Hawkeye 4: LEHR. The phantom study was performed using a heart/liver phantom without defects or with 2-cm defects in the anterior and inferior walls of the left myocardium. Imaging was performed under various conditions with two different devices. Thirty patients with proven or suspected ischemic heart disease underwent stress myocardial perfusion imaging with the two devices. ANN values and SSS were calculated from the images using myocardial perfusion analysis software. The results were compared between the two devices, and also compared with those by expert image interpreters. ***Results:*** In the phantom study, the ANN values of both devices showed normal in phantom without defect and abnormal in phantom with defects. In the clinical conditions, ANN values and SSS did not differ significantly between the two devices (P=0.131 and P=0.118, respectively). Using ANN normal and abnormal values obtained by expert interpreters as standard, the sensitivity and specificity were 78% and 95% for PRISM, and 78% and 95% for Infinia, respectively. When SSS were categorized into normal, mild, moderate, and severe abnormalities, the concordance rate between the SSS categories and expert interpretations was 70% (21/30) for both devices.The discrimination of normal from abnormal ANN values was possible even with different devices in both phantom and clinical studies. However, it is important to use not only ANN values but also other parameters such as SSS with an understanding of the device characteristics and imaging findings. Different results from those based on expert interpretations were influenced by extracardiac accumulation, inferior wall artifact, and cardiac enlargement. ***Conclusion:*** By using ANN in myocardial perfusion analysis software even with different devices may allow imaging diagnosis. Japan has a shortage of diagnostic radiologists, given that certain skills are required for diagnosis, a diagnostic support system using ANN is anticipated. ***References:*** None

901

CME 7: Nuclear Medicine in Paediatric Infections

Saturday, October 24, 2020, 09:00 - 10:30 Channel 1

OP-445

Clinical Perspective From a Paediatrician About Paediatric Infections

G. Milani; Pediatric Unit, University of Milan, Milan, ITALY.

OP-446

Conventional NM in Paediatric Infections

D. de Palma; Nuclear Medicine Unit, "Circolo" Hospital, Varese, ITALY.

OP-447

PET and Fever of Unknown Origin in the Child

M. Parisi; Seattle Childrens Hospital, Seattle, UNITED STATES OF AMERICA.

902

Joint Symposium 13 (EANM/EHA): Metabolic Tumour Volume (MTV) in Lymphoma

Saturday, October 24, 2020, 09:00 - 10:30 Channel 2

OP-448

How to Use MTV in Therapy Guiding Lymphoma?

J. Mettler; University Hospital of Cologne, Department for Nuclear Medicine, Cologne, GERMANY.

OP-449

How to Calculate MTV?

R. Boellaard; Dept. of Radiology and Nuclear Medicine, Amsterdam University Medical Centres, location VUMC, Amsterdam, NETHERLANDS.

OP-450

How does MTV fit in with Liquid Biopsy, Circulating Tumour Cells, etc.

C. Schmitz; West German Cancer Center (WTZ), Faculty of Medicine and University Hospital Essen, Department of Hematology, Essen, GERMANY.

903

Joint Symposium 14 (EANM/SRS): Transporter's Imaging

Saturday, October 24, 2020, 09:00 - 10:30 Channel 3

OP-451

PET Imaging of P-Glycoprotein Activity at the Blood-Brain Barrier

O. Langer; Medical University of Vienna, Department of Clinical Pharmacology, Vienna, AUSTRIA.

OP-452

Design and Modification of Labeled Antibodies for Active Transport Across the Blood-Brain Barrier

D. Sehlin; Uppsala University, Department of Public Health and Caring Sciences, Uppsala, SWEDEN.

OP-453

PET Imaging of P-gp Function at the Blood-Brain Barrier in CNS Diseases

P. Mossel; University of Groningen, University Medical Center Groningen, Department of Nuclear Medicine and Molecular Imaging, Groningen, NETHERLANDS.

904

CTE 3: Calibration for Instrumentation for Dosimetry

Saturday, October 24, 2020, 09:00 - 10:30 Channel 4

OP-454

Calibration of Instrumentation for Dosimetry - Principles and Applications

L. Beels; AZ Groeninge Kortrijk, Nuclear Medicine, Kortrijk, BELGIUM.

OP-455

Calibration of the Non-Imaging Instrumentation for Dosimetry

K. Baete; University Hospitals Leuven, Nuclear Medicine, Leuven, BELGIUM.

OP-456

Calibration of the Imaging Instrumentation for Dosimetry

J. Gear; The Royal Marsden NHS Foundation Trust, Joint Department of Physics, London, UNITED KINGDOM.

905

M2M Track - TROP Session: Image Guided Treatment and Biopsy

Saturday, October 24, 2020, 09:00 - 10:20 Channel 5

OP-457

Clinical impact of Molecular Breast Imaging as adjunct diagnostic modality in evaluation of indeterminate breast abnormalities and unresolved diagnostic concerns

C. Corion[1], A. Loevezijn[2], R. Smithuis[3], L. Wijers[4], A. Zeillemaker[5], R. Valdes Omos[1], L. de Geus-Oei[1], J. van der Hage[1], L. Pereira Arias-Bouda[1];
[1]LUMC, Leiden, NETHERLANDS, [2]AVL, Amsterdam, NETHERLANDS, [3]Alrijne Zieknhuis Leiderdorp, Leiderdorp, NETHERLANDS, [4]Alrijne Ziekenhuis Leiderdorp, Leiderdorp, NETHERLANDS, [5]Alrijne ziekenhuis leiderdorp, Leiderdorp, NETHERLANDS.

Aim/Introduction: To evaluate the value of Molecular Breast Imaging (MBI) in patients with indeterminate breast abnormalities and unresolved diagnostic concerns, especially in terms of its ability to rule out malignancy. ***Materials and Methods:*** Data of patients who underwent MBI because of equivocal findings or diagnostic concerns on conventional diagnostic (CD) work up in the period from March 2012 until February 2015 were analysed retrospectively. All patients underwent digital mammography, ultrasound and MBI. MBI was performed using a Dilon 6800 gamma camera 5 min after administration of 600 MBq ^{99m}Tc-sestamibi intravenously. Pathological findings or follow-up imaging for at least 6 months were used as the reference standard. Sensitivity and specificity rates for CD alone and MBI adjunct to CD were statistically compared using McNemar's test ***Results:*** Out of 226 women, 25 (11%) patients were diagnosed with breast malignancies. Histopathological data were available for 106 (47%) patients and mean follow-up time was 5.4 years (IQR 3.9-7.1). In 68 out of 226 (30%) patients, MBI showed discordant findings with CD. MBI correctly adjusted treatment strategy in 46/226 (20%) patients and detected 21 out of 25 malignancies, including 15 (7%) patients categorised BI-RADS ≤ 3 on CD imaging. MBI correctly downstaged 31 of 33 patients categorised BI-RADS 4 or 5 on CD. In this highly selected study population with complex cases sensitivity of CD combined with MBI was, as expected, higher compared to CD alone (84% vs. 32%) but specificity did not differ significantly (86% vs. 81%). PPV and NPV for CD plus MBI were 43% and 98%, respectively, compared to 17% and 91% for CD alone. In the subgroup of 42 patients with nipple discharge, sensitivity of MBI was 88%; all malignancies were occult on CD. In the subgroup of 113 patients with BI-RADS 3 lesions on CD, MBI detected 7/8 malignancies and correctly categorized 99/113 (88%)

patients in the 'benign' or 'malignant' category. ***Conclusion:*** MBI as problem solving modality in patients with equivocal breast abnormalities or unresolved diagnostic concerns changed clinical treatment strategy in 20% of patients and could safely rule out malignancy with a high NPV of 98%. ***References:*** None

OP-458

Selective sentinel node biopsy in ductal carcinoma in situ of the breast. Is it justified?

P. Fernández-Rodríguez*, Á. De Bonilla Damia, J. De León Carrillo, R. Álvarez Pérez, J. Jiménez-Hoyuela García;*
Virgen del Rocio University Hospital, Seville, SPAIN.

Aim/Introduction: Ductal carcinoma in situ (DCIS) of the breast is a pre-invasive malignancy without periductal stromal invasion, theoretically unable to metastasize. The incidence has experienced an important increase with the introduction of mammography screening. Currently, sentinel lymph node biopsy (SLNB) procedure for DCIS is controversial and is not standard of care. Aim of the study was to identify the existence of lymphatic involvement through SLNB and preoperative features predictive of nodal involvement in DCIS patients. ***Materials and Methods:*** We have retrospectively reviewed 212 patients with a preoperative diagnosis of DCIS in vacuum-assisted breast biopsy (VABB) undergoing surgery with sentinel node biopsy from January 2015 to December 2018 with an average follow-up of 32 months [range, 7-53 months]. From this group, 129 patients with preoperative histopathology of pure DCIS and criteria for SLNB with not microinvasive disease and ultrasound or MRI evidence of lymph node involvement (pTis cN0) were included in the analysis The variables distribution were compared between patients with positive vs. negative sentinel node as well as invasion criteria in the final histopathology. The Van Nuys index was calculated for each patient. ***Results:*** The final histopathology result of breast exeresis determined the presence of infiltrating carcinoma (upstaging disease) in 35/129 patients (27.1%). The SLNB was positive for DCIS in 20/129 (15.5%) of the patients; 11 presented macrometastasis (55%) and 9 micrometastasis (45%). In this subgroup, 13/20 patients presented infiltration in the final breast exeresis. Nevertheless, pure DCIS was confirmed in 7/20 patients (35%). Several predictive factors of nodal involvement were observed such as a BI-RADS≥4, size>20mm, multicentricity/multifocality, nuclear grade 2-3, presence of necrosis and a cribriform and solid pattern. Upstaging disease was directly related to lymph node involvement, however, it was not a predictive preoperative factor. ***Conclusion:*** The role of SLNB in DCIS is controversial. However, the non-implementation of this technique could increase the risk of underestimation and therefore undertreatment of these patients. The presence of axillary lymph nodes involvement could change the subsequent adjuvant treatment. A particular subgroup of DCIS patients with the factors described would have an increased risk of developing SLNB+, requiring axillary evaluation to define the most appropriate clinical treatment. ***References:*** None

OP-459

Utility Whole Body PET/CT Scan In Malignant Melanoma. Can The Location Of The Primary Tumor Guide Image Planning?

V. Godigna Guilloteau*, J. P. Pilkington Woll, E. Martínez Albero, A. Galiana Morón, D. Vega Pérez, S. Ruiz Solis, A. Gomez Grande, M. Tabuenca Mateo, M. Sarandeses Fernandez, M. Marin Ferrer, J. Estenoz Alfaro;*
Hospital Universitario 12 de Octubre, Madrid, SPAIN.

Aim/Introduction: To determine the value of systematically performing whole-body (head-to-toe) PET/CT images (WB-PET) in the evaluation of patients with malignant melanoma and propose a criteria of when standard imaging can be performed. ***Materials and Methods:*** Retrospective study of all WB-PET scans performed in patients with malignant melanoma in our hospital, either for staging, restaging, recurrence or post-treatment follow-up, between January 2011 and January 2020. We looked for any FDG avid foci in the lower extremities. The findings were considered as true positives if histopathological findings were confirmed, if the lesion was treated as melanoma because of other complementary findings (physical exploration, ultrasound, etc) or if during follow-up it was determined as malignant in nature. We also analyzed if the true positive findings had any change in patients management. ***Results:*** We analyzed 367 WB-PET studies belonging to 169 patients, 93 male (55%) and 76 female (45%), with a mean age of 56.4 years (range 19- 90 years). Of the 367 studies performed 170 (46,3%) where for staging (all at least stage IIIB), and 197 (53,7%) for suspected recurrence or post treatment follow-up. From all the WB-PET scans we observed that 19 (5 %) had positive findings in the lower extremities, 11 (3%) of which were true-positive findings (all with histopathological confirmation), 8 (2%) scans were false positive (5 inflammatory foci demonstrated by clinical follow-up and 3 benign lesions (dermatophibroma, nevus and encondroma). From the 11 true-positive findings, 8 (2%) had the primary lesion in an infra-umbilical location; 1 (0.2%) was an extracutaneous melanoma (paranasal) but the finding could be included on a standard study, and the other 2(0,4%), had disseminated disease so the findings did not change clinical management. Also, none of these findings generated a change in management. ***Conclusion:*** In our cohort, we found that WB-PET in patients with melanoma had no additional value to standard (head-to-mid-thigh) PET/CT images. We propose to perform WB-PET only in patients with the primary melanoma lesion located

below the umbilical line. PET/CT acquisition of the lower extremities results in increased scan time and unnecessary radiation dose without generated therapeutic impact. ***References:*** Clinical and therapeutic impact of 18F-FDG PET/CT whole-body acquisition including lower limbs in patients with malignant melanoma Solene Querellou. Nuclear Medicine Communications 2010 - Clinical relevance of 18F-FDG PET/CT lower-limb imaging in patients with malignant cutaneous melanoma Nicolas Plouznikoff, Nuclear Medicine Communications 2017.

OP-460

The value of lymph node ultrasound and [18F]FDG PET/CT in stage IIB/C melanoma patients prior to sentinel lymph node biopsy

B. van der Hiel, *E. Stahlie, A. Bruining, B. van de Wiel, Y. Schrage, M. Wouters, W. van Houdt, A. van Akkooi;*
the Netherlands Cancer Institute - Antoni van Leeuwenhoek Hospital, Amsterdam, NETHERLANDS.

Aim/Introduction: Stage IIB/IIC (pT3b-T4N0) patients are known to have high-risk primary tumors, even higher risk than some stage IIIA/B melanomas (AJCC Staging System 8th edition), however they follow the same routine to sentinel lymph node biopsy (SLNB) as more low risk tumors. A priori the risk of finding positive SLN or other metastases is much higher for these thick and/or ulcerated primary melanomas compared to the thinner ones. Guidelines are not conclusive regarding the use of preoperative imaging in these cases. Recently, a trend to more frequently use cross-sectional imaging has been noticed. However, others have previously shown that preoperative ultrasound (US) was the most sensitive. The aim of this pilot study was to assess the value of US and whole body [18F]FDG PET/CT prior to lymphoscintigraphy (LSG) and SLNB for stage IIB/C (pT3b-T4N0) melanoma patients. ***Materials and Methods:*** Starting 2019-04, all patients with a pT3b melanoma or higher (8th AJCC) were included. All patients underwent US and [18F]FDG PET/CT before their planned LSG and routine SLNB. Suspected metastases were confirmed with fine needle aspiration (FNA). ***Results:*** A total of 23 patients were screened. Six patients (26%) had metastases detected by imaging: five by ultrasound and four by PET/CT. Three of these metastases were detected by US as well as PET/CT. All metastases were nodal. For all patients, treatment was altered to lymph node dissection, all but one also received adjuvant therapy. Of the 17 patients in whom no metastases were identified by imaging, 8 (47%) still had a positive sentinel node. ***Conclusion:*** This study suggests that nodal staging with US is sufficient in the work-up of stage IIB and IIC melanoma. Staging with whole body [18F]FDG PET/CT is not of added value prior to LSG and SLNB and should therefore not be used. Despite normal imaging result, SLNB cannot be foregone for pT3b-pT4N0 melanoma, as many patients still have an involved SN. Cross-sectional imaging should be reserved for patients after positive FNA or SN to confirm the absence of distant visceral metastases. ***References:*** None

OP-461

Sentinel node lymphoscintigrapy reproducibility in melanoma

P. Soeiro, *R. Silva, F. Morgado, A. Albuquerque, G. Costa, J. Pedroso de Lima;*
Centro Hospitalar e Universitário de Coimbra, Coimbra, PORTUGAL.

Aim/Introduction: Sentinel lymph node biopsy (SNB) is based on the identification of the node(s) that directly drain the lymph vessel(s) originating in the tumour. Several techniques are available to identify these nodes, lymphoscintigraphy being one of the most commonly used. Despite its popularity, reproducibility remains mostly untested. The aim of this study was to assess the reproducibility of lymphoscintigraphy in melanoma patients. ***Materials and Methods:*** Melanoma patients proposed for SNB in a tertiary hospital center from January 2005 to December 2019, and who underwent two separate lymphocintigraphy exams in a very short time period, were retrospectively included. These paired lymphoscintigraphies were compared regarding the number and location of sentinel nodes (SN) and drainage pathways and classified accordingly into 2 different groups: group: 1 - perfect overlap (same number of SN and in the same clusters); 2 - partial or no overlap (different number of SN and/or in different clusters). ***Results:*** 17 patients were included (mean age 66 ± 10.8 years). The average time between paired exams was 15 ± 8 days. Perfect overlap was found in 82% (14) of the patients (same number of SN and in the same clusters). Two patients did not show the same number of SN, in the same clusters, and one patient that did not show a perfect overlap, with one additional SN in a different cluster. In the latter case, this SN had very few radioactive counts per minute and was not surgically removed in the operating theatre the following day due to the absence of measurable radioactivity. ***Conclusion:*** Sentinel node lymphoscintigraphy is an extremely reproducible technique. ***References:*** None

OP-462

Diagnostic performance and predictive value of fully hybrid 18F-FDG PET/MRI in preoperative endometrial cancer patients

P. Mapelli[1,2], *F. Fallanca*[2], *G. Ironi*[3], *A. Bergamini*[1,4], *P. Rancoita*[5], *L. Bocciolone*[4], *P. Scifo*[2], *V. Bettinardi*[2], *G. Orlandi*[2], *F. Turba*[4], *A. Savi*[2], *G. Candotti*[1,4], *F. Vasta*[1,4], *R. Cioffi*[1,4], *G. Taccagni*[6], *G. Mangili*[4], *L. Gianolli*[2], *F. De Cobelli*[1,3], *M. Picchio*[1,2];
[1]*Vita-Salute San Raffaele University, Milan, ITALY,* [2]*Nuclear Medicine Department, IRCCS San Raffaele Scientific Institute,*

Milan, ITALY, [3]Radiology Department, IRCCS San Raffaele Scientific Institute, Milan, ITALY, [4]Unit of Obstetrics and Gynaecology, IRCCS San Raffaele Scientific Institute, Milan, ITALY, [5]University Centre of Statistics in the Biomedical Sciences, Vita-Salute San Raffaele University, Milan, ITALY, [6]Unit of Pathology, IRCCS San Raffaele Scientific Institute, Milan, ITALY.

Aim/Introduction: The aim of the present study is to explore the diagnostic performance and predictive value of fully hybrid 18F-FDG PET/MRI in the preoperative staging of endometrial cancer. ***Materials and Methods:*** 16 pts with biopsy-proven endometrial cancer were prospectively enrolled. All pts underwent preoperative fully hybrid 18F-FDG-PET/MRI for initial staging, between December 2018 and May 2019. All patients underwent surgery, with availability of histological examination as reference standard to assess the diagnostic performances. PET/MRI findings were compared to FIGO staging score. In addition to qualitatively evaluation, semi-quantitative PET (SUVmax, SUVmean, MTV, TLG) and MRI (Volume index, ADCmean, ADCmin, Ktrans and Kep) parameters were evaluated on the primary tumour and their role in predicting myometrial invasion (MI) or lymphovascular invasion (LVSI) was assessed. ***Results:*** Patients' median age was 65 yrs (range: 52-86). 18F-FDG PET/MRI identified the primary tumour in all pts. Thirteen/16 patients had endometrioid tumor, 1/6 had mixed-serous carcinoma, 1/6 had a malignant mixed-mullerian tumour and 1/16 serous histotype. 18F-FDG PET/MRI detected lymphnodal involvement in 5/16 pts, confirmed by histology in 4/5 while in 1/4 chronic reactive lymphadenitis was diagnosed. Accuracy, sensitivity, specificity and PPV in the assessment of lymph node metastases were 93%, 100%, 91%, 80% and 100%, respectively. 18F-FDG PET/MRI was in agreement with FIGO score in 10/16 pts (62.5%). Discordant results were: histologically proven micrometastatic peritoneal (2/6) or lymphnodal (1/6) involvement not detected by PET/MRI; lymphnodal chronic inflammation (1/6) reported as metastatic on PET/MRI; myometrial invasion higher than 50% (1/6) at HE, compared to MRI finding of myometrial invasion <50%; presence of lung metastases assessed only by PET/MRI. MTV predicted LVI with a cut-off value of 18.9 and correspondent sensitivity and specificity of 80% and 90%, respectively (p=0.0495). MRI volume index was able to predict LVI (p=0.0207). Neither PET nor MRI parameters were able to predict myometrial invasion. ***Conclusion:*** 18F-FDG PET/MRI has good diagnostic performance in preoperative staging of endometrial cancer; despite the possibility of false positive and negative results, it provides a whole body staging with detection of distant metastases beyond the surgical FIGO staging. PET and MRI parameters has synergic role in preoperatively predicting myometrial and lymphovascular invasion. ***References:*** None

OP-463

Validation Study Of Sentinel Lymph Node Biopsy In The Staging And Treatment Of Endometrial Cancer

D. Patrut, *J. Alors Ruiz, I. Sanchez Urbaneja, O. Rahmouni, J. Oliva Pastor, S. Sanz Viedma;*
University Hospital Virgen de la Victoria, Málaga, SPAIN.

Aim/Introduction: Sentinel Lymph Node Biopsy (SLNB) emerged as an alternative to complete lymphadenectomy in patients with endometrial cancer. The aim of this study is to evaluate the utility of SLNB in the staging and treatment of women diagnosed with endometrial cancer. ***Materials and Methods:*** 64 patients with endometrial cancer were prospectively included between January 2014 and December 2019. A lymphoscintigraphy was performed the day prior to the intervention by injecting the patients with 4mCi of ^{99m}Tc-nanocolloid. Static planar images at 30 minutes and 3 hours post-injection, and a SPECT/CT were acquired. After the induction of general anesthesia, methylene blue dye was injected in the cervix, prior to the surgical procedure. The SLN was identified with the laparoscopic or conventional gamma-detection probe. Completion pelvic/para-aortic lymphadenectomy was performed, regardless of the SLNB result. The SLN was analyzed by hematoxylin-eosin staining and immunohistochemistry. ***Results:*** SLN detection rate was 81.25%, with 41.67% bilateral detection. SLN was negative in 45 cases (25 being low-risk, 13 intermediate-risk and 7 high-risk) with posterior negative lymphadenectomy. There were no false negatives (NPV: 100%, Sensitivity: 100%). The incidence of metastases was 10.7% (7 patients): 5 macrometastases and 2 micrometastases. Intraoperative analysis of SLN showed a false negative rate of 57.1%. Ultrastaging in SLN detected 28% more metastases. 3 out of 60 performed lymphadenectomies showed positive lymph nodes. In the pre-operative staging, 40 cases were classified as low-risk, 14 as intermediate-risk and 4 as high-risk, while post-operative staging modified the stage in 39.7% of the cases. ***Conclusion:*** SLNB can be considered an adequate technique for standardizing the surgical management of the lymphatic system (mainly in low and intermediate risk cases), allowing the selection of patients who would truly benefit from a lymphadenectomy, and those in whom this procedure could be avoided. ***References:*** None

OP-464

18F-FDG PET/CT Radiomics Of Cervical Cancer In Predicting Lymph Node Metastasis

L. Monaco[1], *G. Mathoux[1], C. Crivellaro[2], F. Elisei[2], A. Buda[3], R. Fruscio[4,3], C. Landoni[4,2], L. Guerra[4,2], C. Messa[5], E. De Bernardi[4];*
[1]University of Milan–Bicocca, Milan, Lombardia, ITALY, [2]Nuclear Medicine Department, ASST Monza San Gerardo Hospital, Monza, ITALY, [3]Gynaecologic Oncology Surgical Unit, Obstetrics and Gynaecology Department, ASST Monza San Gerardo Hospital, Monza, ITALY, [4]School of Medicine and Surgery,

University of Milan-Bicocca, Milan, Lombardia, ITALY, [5]Tecnomed Foundation,University of Milan–Bicocca, Milan, Lombardia, ITALY.

Aim/Introduction: Cervical cancer is the second most frequent diagnosed gynecological tumor and the third leading cause of cancer death among females in less developed countries. The aim of the study was to evaluate the role of 18F-FDG PET/CT in preoperative assessment of N-staging in early stage cervical cancer patients. In addition, radiomics features extracted from primary lesion FDG uptake were correlated to the presence of lymph node metastases. ***Materials and Methods:*** From March 2006 to April 2019, 74 cervical cancer patients in early stages were retrospectively considered. All women underwent 18F-FDG PET/CT before surgical staging with pelvic lymphadenectomy. Histology was used as standard reference. PET cervical lesions were contoured with PETVCAR (GE Healthcare) by using iterative threshold. SUVmax, SUVmean, MTV, TLG and radiomics features were computed inside tumor contours using standard Image Biomarker Standardization Initiative (IBSI) methods. Radiomics features associated with lymph-node metastases were identified by Mann-Whitney test. Receiver operating characteristic (ROC) curves and area under the curve (AUC) values were computed and optimal cut-off (Youden index) was assessed. ***Results:*** In our study 14/74 patients had nodal metastases at histology (18.9%): 5/14 correctly identified by PET/CT with 9 false negative cases. Sensitivity, specificity, accuracy, positive predictive value and negative predictive value of PET/CT for pelvic nodal metastases were 36%,93%,82%,55%,86%,respectively. A significant correlation was observed between MTV (p value= 0,013; AUC= 0,72 ; cut-off= 17ml) and the presence of nodal metastasis. Among radiomics features, a significant correlation was found between the presence of nodal metastases and Inverse Difference- Grey Level Co-occurrence Matrix (p value=0,03, AUC=0,76, cut-off =0,17), that is an homogeneity index. No significant correlation was found for SUV parameters. ***Conclusion:*** PET/CT demonstrated low sensitivity, high specificity and high NPV in detecting pelvic nodal metastases in preoperative staging of cervical cancer. These preliminary data suggest a promising application of radiomics PET for predicting the presence of nodal metastases in cervical cancer; further studies on larger populations are needed. ***References:*** None

OP-465

Sentinel lymph node detection in oral cancer: a head to head comparison between [^{99m}Tc]Tc-Tilmanocept and [^{99m}Tc]Tc-Nanocoll

R. Mahieu, *I. J. den Toom, R. van Rooij, R. J. J. van Es, M. G. Hobbelink, G. C. Krijger, B. M. Tijink, B. de Keizer, R. de Bree; University Medical Center Utrecht, Utrecht, NETHERLANDS.*

Aim/Introduction: Sentinel lymph node (SLN) biopsy has proven to reliably stage the clinically negative neck in early-stage oral cavity squamous cell carcinoma (OSCC). [^{99m}Tc]Tc-Tilmanocept has been specifically designed for SLN detection. Due to its proposed rapid clearance from the injection site, rapid uptake and high retention within SLNs, and low uptake in higher echelon nodes, [^{99m}Tc]Tc-Tilmanocept may be of benefit in OSCC with complex drainage patterns and close spatial relation to SLNs. ***Materials and Methods:*** A monocenter prospective within-patient evaluation study was designed to compare [^{99m}Tc]Tc-Tilmanocept (74MBq) with [^{99m}Tc]Tc-Nanocoll (120MBq; 74MBq) for SLN detection. A total of 20 patients with early-stage OSCC were included, who underwent lymphoscintigraphy for both [^{99m}Tc]Tc-Tilmanocept and [^{99m}Tc]Tc-Nanocoll. Both lymphoscintigraphic images of each patient were evaluated for SLN detection and radiotracer distribution at 2-4 hours postinjection (i.e. injection site retention, uptake in SLNs). ***Results:*** A median of 3.0 and 2.5 SLNs were identified with [^{99m}Tc]Tc-Tilmanocept and [^{99m}Tc]Tc-Nanocoll, respectively (p=0.271). A median of 2.0 and 2.5 higher echelon nodes were identified with [^{99m}Tc]Tc-Tilmanocept and [^{99m}Tc]Tc-Nanocoll, respectively (p=0.103). Radioactive uptake in SLNs was significantly higher for [^{99m}Tc]Tc-Nanocoll (3.16%) compared to [^{99m}Tc]Tc-Tilmanocept (1.95%) (p=0.010). Radioactive uptake in higher echelon nodes was not significantly different between [^{99m}Tc]Tc-Nanocoll (0.86%) and [^{99m}Tc]Tc-Tilmanocept (0.57%) (p=0.052). The injection site's remaining radioactivity was significantly lower for [^{99m}Tc]Tc-Tilmanocept (29.9%; SD±7.6), compared to [^{99m}Tc]Tc-Nanocoll (60.9%; SD±16.1) (p<0.001). No significant difference was seen in SLN to injection site ratio in radioactivity between [^{99m}Tc]Tc-Nanocoll (0.054) and [^{99m}Tc]Tc-Tilmanocept (0.067) (p=0.232). ***Conclusion:*** The significantly higher injection site clearance and slightly, although not statistically significant, improved SLN to injection site ratio of [^{99m}Tc]Tc-Tilmanocept may benefit SLN detection, particularly in situations with close spatial relation between injection site and SLNs. However, the relatively low radioactive uptake in SLNs of [^{99m}Tc]Tc-Tilmanocept may limit intraoperative detection of SLNs, but can probably be overcome by higher injection dose ***References:*** None

OP-466

Use of ^{99m}Tc-Tilmanocept for selective sentinel lymph node biopsy in oral cavity tumours. Our experience at Hospital Clínic in Barcelona, Spain

R. Valhondo-Rama[1,2], *C. Martí Pagés*[1], *A. Perissinotti*[1], *A. Tapias Mesa*[1], *N. Sánchez Izquierdo*[1], *A. Ferrer Fuertes*[1], *R. Sieira Gil*[1], *M. Cámara Vallejo*[1], *E. García Díez*[1], *S. Vidal-Sicart*[1]; *[1]Hospital Clínic, Barcelona, SPAIN, [2]Hospital Clínico San Carlos, Madrid, SPAIN.*

Aim/Introduction: To assess our initial experience with ^{99m}Tc-Tilmanocept for selective sentinel lymph node biopsy (SLNB)

in oral cavity tumours. ***Materials and Methods:*** Retrospective analysis of 16 patients with oral cavity cancer who underwent a SLNB procedure by means of perilesional injection of ^{99m}Tc-Tilmanocept. The variables collected were the following: age, sex, type of tumour, laterality, initial stage, number of sentinel nodes (SN) visualized by lymphoscintigraphy, if there was secondary drainage, number of SN biopsied, anatomical territories, anatomopathological result and if there were relapses. ***Results:*** The mean age was 68.9 years (range 57-90). 50% males and 50% females. One of the 16 cases (6.25%) presented melanoma on the palate. The rest (93.75%) were diagnosed of squamous cell carcinoma: 8 on the tongue (53.33%), 3 on the gingiva (maxillary-mandibular) (20%), 2 on the floor of the mouth (13.33%), 1 on the palate (6.67%) and 1 in the jugal mucosa (6.67%). Six cases had the primary tumour involvement in their left side (37.5%), 6 right (37.5%) and 4 bilateral or midline (25%). Ten had initial T1N0 stage (62.5%). Lymphoscintigraphy showed 52 SN in total (11 at cervical level I, 20 at level II, 13 at level III, 4 at level IV and 4 at level V), obtaining a mean of 3.25 SN per patient. Secondary drainage was evident in 10 cases (62.5%). Intraoperatively, 51 SN (10 at level I, 20 at II, 13 at III, 4 at IV and 4 at V) were biopsied, resulting in 3.19 SN/patient. Two out of 16 patients (12.5%) had metastatic SN. Regional lymphadenectomy was performed in one of them (6+/8), who subsequently suffered a relapse. The other patient with positive SN is awaiting lymphadenectomy. Another patient (12.5%) - whose SN had been negative - developed a second primary tumour of the oral cavity with lymph node involvement 10 months later. ***Conclusion:*** ^{99m}Tc-Tilmanocept is a valid radiotracer for SLNB in tumours of the oral cavity, with good results in locating SN at cervical lymphatic level I. Secondary drainage is also observed with ^{99m}Tc-Tilmanocept. ***References:*** None

OP-467

Improved radiooncological management by FAPI-PET/CT as primary staging for patients with esophageal cancer

S. Koerber[1,2,3], J. Ristau[1,2,3], F. Staudinger[4], J. Schlittenhardt[4], M. F. Haefner[1,2,3], C. Kratochwil[4,5], T. Lindner[4], J. Debus[1,2,6], U. Haberkorn[4,5,6], F. L. Giesel[4,5,6];
[1]Department of Radiation Oncology, Heidelberg University Hospital, Heidelberg, GERMANY, [2]Heidelberg Institute of Radiation Oncology (HIRO), Heidelberg, GERMANY, [3]National Center for Tumor diseases (NCT), Heidelberg, GERMANY, [4]Department of Nuclear Medicine, Heidelberg University Hospital, Heidelberg, GERMANY, [5]Clinical Cooperation Unit Nuclear Medicine, German Cancer Research Center (DKFZ), Heidelberg, GERMANY, [6]German Cancer Consortium (DKTK), partner site Heidelberg, Heidelberg, GERMANY.

Aim/Introduction: FAP-ligands in oncology has recently shown as very promising PET tracers with also equal or even superiority to FDG. Therefore, the current study aimed to evaluate the potential of FAPI-PET/CT for the primary assessment of patients with esophageal cancer and its usefulness in radiotherapy planning as a first clinical analysis. ***Materials and Methods:*** FAPI-PET/CT imaging was performed for a cohort of seven patients (median age: 63.5 years) with treatment-naïve esophageal carcinoma undergoing irradiation. Six patients obtained definitive radio(chemo)therapy, one patient had an indication for neoadjuvant chemoradiation. All patients were referred to the experimental diagnostics by their caring oncologist/therapist. Tumor uptake was quantified by standardized uptake value (SUV)max and SUVmean (60% isocontour). Consequences for radiooncological management were documented after image evaluation and comparison with conventional imaging and/or clipping. ***Results:*** For almost all patients, uptake of FAPI tracer was high in primary tumor tissue with a median SUVmax of 17.23. Excellent tumor-to-background ratios resulted in improved target volume delineation. FAPI imaging led to dose escalation (simultaneous integrated boost) for nodal metastases in two patients. For three patients (42.9%) with multiple small nodes, boost irradiation was omitted due to absence of significant FAPI tracer uptake. In all patients who underwent pretherapeutic endoscopic clipping of the tumor margins, conformity of tracer uptake and clipping distance was considerably well-matching. ***Conclusion:*** FAPI-PET/CT was able to demonstrate very promising results in esophageal cancer for tumor delineation and tumor-to-background contrast in radiooncological management. With these very promising results, FAPI should be more explored in other cancer entities for improved radiooncological treatment purposes. ***References:*** None

906

Cutting Edge Science Track - TROP Session: Dosimetry Methods and Models - Part 1

Saturday, October 24, 2020, 09:00 - 10:30 Channel 6

OP-468

Is a single late SPECT/CT-based kidney ^{177}Lu-dosimetry superior to dosimetry with sequential whole-body scans in combination with an early SPECT/CT?

S. Beykan[1], J. Tran-Gia[1], S. B. Jensen[2,3], M. Lassmann[1];
[1]Department of Nuclear Medicine, University of Würzburg, Würzburg, GERMANY, [2]Department of Nuclear Medicine, Aalborg University Hospital, Aalborg, DENMARK, [3]Department of Chemistry and Bioscience, Aalborg University, Aalborg, DENMARK.

Aim/Introduction: The aim is to find a more practical and equally accurate alternative for the time-consuming multiple SPECT/CT based dosimetry. For that reason, dosimetry was performed based on data from an in-vivo

pig study (1) as well as data from a 3D-printed kidney phantom using three different dosimetry approaches (multiple SPECT/CT [MS, gold standard], multiple planar + 1 SPECT/CT [MP1S], single time-point SPECT/CT (2)[STS]). ***Materials and Methods:*** Planar and SPECT/CT scans were performed for five ^{177}Lu-OPS201 injected pigs at 4h-298h (injected activity: 102-113 MBq) and a phantom (injected activity: 4 MBq, time-points simulated by adjusting acquisition duration based on pig 1 data). The kidney time-integrated activity coefficients (TIACs) and absorbed doses (kidneyADs) of the pigs and phantom were calculated applying three methods MS,MS1P, STS at 54h, 101h, 148h, 293h. In addition, to show the effect of late scans on AD calculation, MS- and MS1P-based TIACs difference of pig 1 and phantom were calculated by eliminating the late two time-points. ***Results:*** In comparison to MS, the mean difference in kidneyADs of pigs was −31±19% for MP1S (pig 2 excluded: +40%) and it was in the range of −23±12% to −13±9% for STS. The STS-based kidneyADs of pigs at all time-points resulted in lower kidneyADs in comparison to MS. STS at 101h showed the best agreement with MS-based kidneyADs (mean deviation: −12.5±9%). Higher differences were observed between MP1S- and MS-based kidneyADs associated with organ activity overlay on planar scans. Based on phantom and pig 1 experiments, MP1S-based kidney TIAC was lower than MS results respectively 42% for pig 1 and 3% for the phantom. Eliminating late time-points resulted in up to 56% higher TIACs for pig 1 (MS) and the phantom (MS and MP1S), whereas the MP1S-based TIACs for pig 1 decreased by 10%. ***Conclusion:*** MS gives the most accurate results, but it is time-consuming and, therefore, difficult to integrate in clinical routine. For MS, scans acquired after 120h are essential for accurate absorbed dose calculations since lack of late follow-up scan time points results in over- or underestimations of the ADs. MP1S, considered as a potential alternative, showed, however, high differences associated with organ overlay. STS-based dosimetry, with a single SPECT/CT acquired after ~4 days, is less time-consuming and results in ADs, which are systematically lower with a small deviation (12.5±9%) compared to MS. ***References:*** 1.Beykan S, et al. EJNMMI Res. 2016;6:50 2.Hänscheid H, et al. J Nucl Med. 2018;59:75-81.

OP-469

In pursuit of fully automated dosimetry: evaluation of an automatic VOI propagation algorithm using contour intensity-based SPECT alignments

D. Mirando[1], *Y. K. Dewaraja*[2], *N. M. Cole*[1], *A. S. Nelson*[1]; *[1]MIM Software, Cleveland, OH, UNITED STATES OF AMERICA, [2]University of Michigan, Ann Arbor, MI, UNITED STATES OF AMERICA.*

Aim/Introduction: Personalised dosimetry has emerged as a promising tool for treatment planning and prediction of patient outcomes in molecular radiotherapies. Time requirements of image segmentation contribute to high burdens associated with dosimetry, especially dosimetry with multiple SPECT/CTs for which 3D segmentation is required on all timepoints. Here, a fully automated method of propagating kidney and tumour volumes of interest (VOIs) to subsequent timepoints is compared to manual transfer and adjustment. ***Materials and Methods:*** After the first cycle of 177Lu-DOTATATE in 10 patients, SPECT/CT images were acquired. Kidney VOIs were manually segmented on the first post-injection CT image, while a radiologist defined tumour VOIs on the diagnostic CT and rigidly transferred these to the first CT. In the manual method of propagation, VOIs were rigidly transferred to each subsequent SPECT/CT timepoint before visual fine-tuning by the radiologist. In the automatic approach, subsequent SPECT images were first rigidly registered to the first SPECT. The SPECT intensity information within a 1cm expansion zone around each VOI was then used to perform local rigid registrations between the images, which were spliced together to generate a composite image aligned to the first SPECT. VOIs were then directly propagated to each timepoint. For both VOI propagation methods, total activity in each VOI was recorded at each timepoint and organ-level biexponential fitting was applied and integrated [1]. ***Results:*** Fully automatic VOI propagation resulted in average activity measurements on subsequent SPECT scans that deviated from the manual method by 3.6% (95% CI: [-8.4%, 10.5%]) in kidneys and 2.3% (95% CI: [-8.0%, 12.5%]) in tumours, excluding 1 outlier with minimal uptake where the difference was 30.4%. The time-integrated activity deviated by 0.3% (95% CI: [-8.0%, 8.7%]) for kidneys and 1.9% (95% CI: [-17.8%, 21.7%]) for tumours (12.8% for the outlier). ***Conclusion:*** Automatic VOI propagation using contour intensity-based SPECT alignments showed good agreement with the activity from manual propagation/adjustment. It is worth emphasizing that the manual reference method is not a gold standard. Indeed, visual inspection reveals cases where the automatic propagation worked excellently despite moderate deviations from the manual method, suggesting that it can sometimes outperform the manual method. Notably, the generation of composite aligned SPECTs in this automatic method permits voxel-based activity integration and dose calculation. Combined with recent advances in neural network-based segmentation [2], such a technique can allow for completely automated dosimetry. ***References:*** [1] Sarrut et al, MedPhys, 2017. [2]Lamba et al, JNM, 2019.

OP-470

^{177}Lu dosimetry may be obtained on a whole-body scale through serial high-speed CZT-SPECT recordings

L. Imbert*, E. Chevalier, C. Boursier, V. Roch, G. Karcher, P. Marie; CHU Nancy Hopital Brabois Adultes, Vandœuvre-lès-Nancy, FRANCE.*

Aim/Introduction: Although ^{177}Lu radionuclide therapy is increasingly used in clinical routine, its dosimetry remains difficult to assess, requiring long recording times on standard gamma-camera systems. However, this issue could be overcome with new CZT-SPECT imaging systems. The whole-body Veriton® 360° CZT-camera (Spectrum Dynamics Medical) is equipped with 12 swiveling detectors, which can be positioned in very close proximity to each part of the body during acquisitions, thereby providing a high count-sensitivity that is particularly advantageous for the current low-count rate conditions of ^{177}Lu imaging. The aim of this study was to evaluate the feasibility of monitoring Lutathera® dosimetry on a whole-body scale through serial high-speed recordings provided by this CZT camera. ***Materials and Methods:*** SPECT and low-dose CT whole-body recordings lasting 20 minutes or less were obtained with the Veriton® camera at 4, 24 and 48 hours, and at 7 days after a full-dose Lutathera® injection in 3 patients with neuroendocrine tumors. SPECT images were recorded on the 113 keV (±10%) energy peak and reconstructed with CT-based attenuation correction, scatter correction and resolution recovery, a method already validated for absolute quantification on an IEC body phantom. The total-body dose, as well as individual doses received by kidneys, liver, spleen, bone marrow and tumors, were calculated using MIM SurePlan™ MRT software. ***Results:*** The whole-body SPECT images exhibited a high signal-to-noise ratio, even at 7 days after injection. For the three patients, mean absorbed doses expressed per MBq of injected Lutathera® were variable and ranged from 0.07 to 0.09 mGy/MBq for bone marrow, 0.21 to 0.30 mGy/MBq for kidneys, 0.16 to 0.78 mGy/MBq for liver, and 0.17 to 0.48 mGy/MBq for spleen. These values are in the range of those documented within the literature for ^{177}Lu dosimetry measured on thoracic and abdominal recordings provided by conventional gamma-camera systems. Mean tumor doses ranged from 1.15 to 2.55 mGy/MBq and finally, the mean total-body dose ranged from 0.028 to 0.037 mGy/MBq, a variability due to differences in body size and in the elimination rate of Lutathera®. ***Conclusion:*** from the Veriton® camera**.** This original tool could help enhance the medical monitoring of ^{177}Lu-based therapy in clinical routine. ***References:*** 1. Cremonesi M, Ferrari M, Bodei L, Tosi G, Paganelli G. Dosimetry in peptideradionuclide receptor therapy: a review. J Nucl Med. 2006;47(9):1467-75. 2. Santoro L, Mora-Ramirez E, Trauchessec D et al. Implementation of patient dosimetry in the clinical practice after targeted radiotherapy using [177Lu-DOTA0,Tyr3]-octreotate. EJNMMI Research 2018;8:103.

OP-471

Voxel-wise Prediction of Post-therapy Dosimetry for 177Lu-PSMA I&T Therapyusing Deep Learning

S. Xue[1], *A. Gafita*[2], *Y. Zhao*[2], *A. Afshar-Oromieh*[1], *M. Eiber*[2], *A. Rominger*[1], *K. Shi*[1,2];
[1]*University of Bern, Bern, SWITZERLAND,* [2]*Technical University of Munich, Munich, GERMANY.*

Aim/Introduction: PSMA-directed radioligand therapy (RLT) has become one of the effective treatment options for metastatic castration-resistant prostate cancer (mCRPC). However, individual treatment planning is still not feasible as it is for the external beam radiotherapy. Our group has presented an organ-based research in the prediction of post-therapy dosimetry in EANM 2019. However, an organ-based approach is unable to reveal the heterogeneity of dose distribution and therefore is not sufficient for the realization of treatment planning. In this study, we propose an approach for voxel-wise prediction of post-therapy dosimetry from pre-therapy positron emission tomography (PET) using deep learning. ***Materials and Methods:*** 30 patients with mCRPC treated with 177Lu-PSMA I&T RLT were retrospectively included in this study. Totally 48 treatment cycles with68Ga-PSMA-11 PET/CT directly before the treatment and at least 3 post-therapeutic SPECT/CT dosimetry imaging were considered for this proof-of-concept study. Post-therapy voxel-wise dosimetry was calculated using Hermes Voxel Dosimetry. 3D RLT Dose generative adversarial networks (GANs) were developed with a 3D U-net generator and a convolutional neural network (CNN) based discriminator. A dual-input-model was designed to incorporate both information from PET and CT, for the purpose of anatomical coregistration. Both voxel-wise content loss alongside image-wise loss were taken into account for better synthesis performance. 5-fold cross validation was applied to verify the trained network. ***Results:*** The proposed 3D RLT Dose GANs achieved the voxel-wise mean absolute percentage error (MAPE) of 17.56%±5.42%. The dual-input-model was able to synthesize dose maps with comparable accuracy while preserving anatomical consistency, which achieved a MAPE of 18.94%±5.65%. ***Conclusion:*** Our preliminary results demonstrate the potential of artificial intelligence to estimate voxel-wise post-therapy dosimetry both qualitatively and quantitatively. This may provide a practical solution to improve the dosimetry-guided treatment planning for RLT. ***References:*** 1. Sumanasuriya, S. and J. De Bono, Treatment of Advanced Prostate Cancer-A Review of Current Therapies and Future Promise.Cold Spring Harb Perspect Med, 2018. 8(6).2. Stokke, C., et al., Dosimetry-based treatment planning for molecular radiotherapy: a summary of the 2017 report from the Internal Dosimetry Task Force.EJNMMI Phys, 2017. 4(1): p. 27.3. Erdi, A.K., et al., Treatment planning for radio-immunotherapy.Phys Med Biol, 1996. 41(10): p. 2009-26.4.

Goodfellow, I., et al. Generative adversarial nets. in Advances in neural information processing systems. 2014.5. Yi, X., E. Walia, and P. Babyn, Generative adversarial network in medical imaging: A review.Medical image analysis, 2019: p. 101552.

OP-472

Combined planar and SPECT image method for bone marrow dosimetry during ^{177}Lu-DOTATATE treatmens using deep learning generated synthesized projections

L. Hagmarker[1], J. Svensson[2], T. Ryden[1], M. van Essen[3], A. Sundlöv[4], K. Sjögreen Gleisner[5], P. Gjertsson[3], P. Bernhardt[1];
[1]Department of Radiation Physics, Sahlgrenska Academy, University of Gothenburg, Gothenburg, SWEDEN, [2]Department of Oncology, Sahlgrenska Academy, University of Gothenburg, Gothenburg, SWEDEN, [3]Department of Clinical Physiology, Sahlgrenska academy, University of Gothenburg, Gothenburg, SWEDEN, [4]Department of Oncology and Pathology, Clinical Sciences, Lund University, Lund, SWEDEN, [5]Department of Radiation Physics, University of Lund, Lund, SWEDEN.

Aim/Introduction: Post-therapy imaging during treatment with ^{177}Lu-DOTATATE is time-consuming and at many centres the camera availability is limited. A recent study by Ryden et al showed that it is possible to reduce the number of sampled projections by adding deep learning generated synthesized projections (SIPs), thereby decreasing the acquisition time, without impairing image quality. This study aims to investigate how this approach affects the bone marrow absorbed doses (ADs) determined using a hybrid planar and SPECT-image method, and if it allows for a less demanding strategy for volume-of-interest (VOI) delineation. Evaluation was performed by comparing the ADs when using the full and reduced projection sets, and by analyses of predictive ability of haematological response. *Materials and Methods:* This study included 44 patients with advanced neuroendocrine tumours treated with ^{177}Lu-DOTATATE at Sahlgrenska University Hospital (ILUMINET-study, EUDRACT nr 2011-etc). ADs were calculated using a hybrid planar and SPECT-image method. Cross-doses from high-uptake organs and the remainder of the body were determined by time-activity curves created using planar images. The self-dose was determined using the time-activity concentration curve for the remainder of the body adjusted by the activity concentration determined in VOIs placed in the lumbar vertebral bodies in SPECT-images collected at 24 h.p.i. Three VOIs were studied; spheres with radius of 5.5 mm (r5.5) and 10 mm (r10) and the complete lumbar vertebral body (LV). Three reconstructions were performed; using all 120 projections (120), using 30 of the 120 projections (30) and using 30 projections together with 90 synthetic intermediate projections created by a deep Convolutional U-net shaped neural network (30-120SIP). The SPECT-images were reconstructed using the Monte-Carlo based reconstruction code SARec in the image-platform phONSAi, developed in-house. *Results:* The hybrid method 120 using r5.5, r10 and LV yielded ADs after treatment cycle one of 0.44 (0.22-1.73), 0.45 (0.20-1.64), and 0.45 (0.19-1.51) Gy/7.4 GBq, respectively. There were no significant differences between ADs determined using the 120 and 30-120SIP or using r5.5 and r10. Small differences were found when using only 30 projections and the VOI LV. Significant dose-response relationships were observed between decreased platelet counts and ADs using all reconstruction methods and all VOIs with r-values between -0.53 and -0.57. *Conclusion:* Reducing the number of sampled projections to decrease the acquisition time without significantly affecting the ADs and the dose-response relationships is possible. Smaller spheres might be used instead of a more time-consuming VOI containing the complete vertebral body. *References:* None

OP-473

Bone Marrow Dosimetry for Peptide Receptor Radionuclide Therapy using Patient-specific Pharmacokinetic Models

L. Carnegie-Peake, J. Taprogge, J. Gear, G. Flux;
Royal Marsden Hospital NHS FT, London, UNITED KINGDOM.

Aim/Introduction: A bone marrow (BM) absorbed dose limit of 2 Gy is typically prescribed in peptide receptor radionuclide therapy (PRRT) due to the radiation-induced haematological toxicity [1,2]. BM dosimetry is therefore necessary to ensure this limit is not exceeded. According to EANM guidance, the activity retention in blood can be used as a surrogate for the activity retention in bone marrow. However, if blood samples are not routinely acquired, whole-body (WB) and organ activity retention data can be used to develop patient-specific pharmacokinetic (PK) models to determine the activity retention in blood from which the BM dosimetry may be obtained. *Materials and Methods:* Bone marrow dosimetry for 9 patients treated with Y-90 DOTATATE was derived from the absorbed dose delivered to blood, calculated from patient-specific PK models constructed from activity retention data for liver, spleen, kidneys, whole-body and tumours [3]. Published OLINDA S-values were applied to the TIAs to calculate bone marrow absorbed doses. *Results:* Serum TIA values ranged from 1004MBq.h to 7411MBq.h (4030 ± 2217MBq.h) were determined. The serum TIAs ranged from 0.7% to 8.4% of the WB TIA (4.5±2.7%). WB and serum TIAs predicted by the PK model were used to perform bone marrow dosimetry. Bone marrow absorbed doses ranged from 0.5Gy to 2.1Gy (1.2±0.7Gy). The PK-derived serum activity retention curves and the bone marrow absorbed doses showed good agreement with previously published values. *Conclusion:* It has been shown that it is feasible to extract serum activity retention curves in PRRT using patient-specific PK models

in the absence of blood samples. Direct validation of PK-derived serum activity retention curves is required through prospective blood sample collection on future patients. ***References:*** [1] Bergsma, H., et al., Subacute haematotoxicity after PRRT with (177) LuDOTA-octreotate: prognostic factors, incidence and course. Eur J Nucl Med Mol Imaging, 2016. 43(3): p. 453-63. [2] Forrer, F., et al., Bone marrow dosimetry in peptide receptor radionuclide therapy with [177Lu-DOTA(0),Tyr(3)]octreotate. Eur J Nucl Med Mol Imaging, 2009. 36(7): p. 1138-46. [3] Kletting, P., et al., Differences in predicted and actually absorbed doses in peptide receptor radionuclide therapy. Med Phys, 2012. 39(9): p. 5708-17.

OP-474

Improved prediction of haematological toxicity during [177Lu]Lu-DOTA-TATE therapy by optimising serial SPECT-CT red marrow dosimetry

J. Tipping[1], E. Page[1], N. Calvert[1], D. Hamilton[1], D. Cullen[2], E. Price[2], S. Pells[2], G. Needham[2], P. Manoharan[1];
[1]The Christie NHS Foundation Trust, Manchester, UNITED KINGDOM, [2]The University of Manchester, Manchester, UNITED KINGDOM.

Aim/Introduction: This research compared red marrow absorbed dose estimations following Peptide Receptor Radionuclide Therapy (3D Image Based (IB) versus Blood Based (BB) methods), and dose correlations with haematological toxicity. ***Materials and Methods:*** Data were acquired during cycle 1 of [177Lu]Lu-DOTA-TATE therapy for a cohort of PRRT patients. Red marrow dosimetry was performed using BB methods and IB methods using serial SPECT/CT methods, with dose uncertainties estimated. The effect on total dose (due to self & cross-irradiation) was assessed for two different cross-irradiation models (simplistic versus realistic). The strength and significance of the correlation between dose and post therapy platelet toxicity were assessed for each dosimetry method. The effect of exposure to prior treatments on dose toxicity correlations was also assessed. ***Results:*** Early results indicate that IB methods delivered significantly higher red marrow absorbed doses than BB methods (mean increase of a factor of 3 when cross-irradiation was included). Choice of cross-irradiation model had a significant impact on total dose magnitude for both BB and IB techniques. Dose response analysis of these initial results indicate that the simplistic cross-irradiation model gave the strongest and most significant dose - toxicity correlations for both IB and BB methods. The most realistic activity distribution model produced significant correlations only with IB methods for therapy naïve patients. ***Conclusion:*** Red marrow absorbed doses measured from serial SPECT were significantly higher than those from serial blood measurements. IB absorbed doses produced stronger and more significant correlations for therapy naïve patients than BB absorbed doses. ***References:*** None

OP-475

Calculation of absorbed dose distribution for Selective Internal Radiation Therapy (SIRT) using Monte Carlo Method

M. Maciak[1], P. Piasecki[2], E. Iller[3];
[1]National Centre for Nuclear Research, Otwock, POLAND, [2]Department of Interventional Radiology, Military Institute of Medicine, Warsaw, POLAND, [3]National Centre for Nuclear Research, Radioisotope Centre POLATOM, Otwock, POLAND.

Aim/Introduction: Radioembolization or Selective Internal Radiation Therapy, SIRT is one of the method applied to treat liver cancer, mainly hepatocellular carcinoma and colorectal metastases. Therapy involves the administration of microspheres containing beta radiation emitter directly to the liver circulatory system. Currently used dosimetry models assumes uniform distribution of the microspheres within the tumor volume but there are some evidences that heterogeneous distribution, especially in large metastases, results in ineffective treatment and finally shortening of the survival time. The aim of this study was to prepare a computational dosimetry model using Monte Carlo Method-based tool, to estimate the distribution of the absorbed dose at the cellular, microscopic level. ***Materials and Methods:*** To build a computational dosimetry model the FLUKA simulation package was used [1,2]. The distribution of microspheres implemented in the model, based on microscopic images obtained for different relative concentration of resin microspheres used for different experiment described elsewhere. Microspheres were defined as pure yttrium spheres with diameter of 32,5 μm (median diameter of resin spheres) and sphere specific activity of 55 Bq per sphere. As the estimator for the absorbed dose calculation, the USRBIN estimator, defined as cuboid of dimensions of 1800 μm x 1300 μm times sphere diameter was used. ***Results:*** Monte Carlo model for calculation of the absorbed dose and the distribution of the absorbed dose at the microscopic level was prepared. For the microscopic data available for the preparation of the model absorbed dose distributions and total absorbed dose for the samples were calculated and biological studies of the samples were correlated with the doses calculated using the model. ***Conclusion:*** FLUKA is a valuable tool for preparation dosimetry model for absorbed dose calculation at the microscopic level and it seems to be possible to extend the application of the model to the macroscopic level using DICOM files of the patients who underwent the SIRT therapy to validate the relation of the heterogeneous distribution and the shortening of the survival time. ***References:*** [1] The FLUKA Code: Developments and Challenges for High Energy and Medical Applications, T.T. Böhlen, F. Cerutti, M.P.W. Chin, A. Fassò, A. Ferrari, P.G. Ortega,

A. Mairani, P.R. Sala, G. Smirnov and V. Vlachoudis, Nuclear Data Sheets 120, 211-214 (2014); [2] FLUKA: a multi-particle transport code, A. Ferrari, P.R. Sala, A. Fasso`, and J. Ranft, CERN-2005-10 (2005), INFN/TC_05/11, SLAC-R-773

OP-476

Impact of tumour contouring method on prediction of survival with ^{99m}Tc-MAA-based dosimetry in HCC patients treated with selective internal radiation therapy

G. Nodari[1], R. Popoff[1,2], J. Riedinger[1], O. Lopez[3], J. Pellegrinelli[3], I. Dygai-Cochet[1], C. Tabouret-Viaud[1], B. Presles[2], O. Chevallier[2,3], S. Gehin[3], M. Gallet[1], M. Latournerie[4], S. Manfredi[4], R. Loffroy[2,3], J. Vrigneaud[1,2], A. Cochet[1,2];
[1]Centre Georges-François Leclerc, Dijon, FRANCE, [2]ImVIA, EA 7535, University of Burgundy, Dijon, FRANCE, [3]Department of Vascular & Interventional Radiology, University hospital, Dijon, FRANCE, [4]Gastroenterology Department, University hospital, Dijon, FRANCE.

Aim/Introduction: Selective internal radiation therapy (SIRT) with ^{90}Y microspheres is an effective option for treatment of advanced hepatocellular carcinoma (HCC). ^{99m}TcMAA-SPECT-CT pre-treatment dosimetry is systematically performed to estimate the lung shunt fraction and the absorbed doses to tumor and healthy liver. However, the optimal method for determination of target (tumors) contours has not yet been validated. Our aim was here to correlate different ^{99m}TcMAA-SPECT-CT based dosimetry data and contouring methods with overall survival (OS) in HCC patients treated with SIRT. ***Materials and Methods:*** 56 patients who underwent SIRT between 2012 and 2019 (33 resin microspheres and 23 glass microspheres) were retrospectively included. Tumours were delineated using 3 methods: MRI-based contours manually drawn by a radiologist and then registered on SPECT-CT via deformable registration (C_{MRI}); MAA-SPECT 10% threshold contouring (C_{SPECT}); overlapping of both volumes ($C_{MRI/SPECT}$). Three-dimensional voxel-based dosimetries were computed with a research workflow in MiM SurePlan 7.0.1 software. Doses were calculated with the Local Deposition Method. The mean absorbed dose (Dmean) and the Tumor-to-Normal liver uptake Ratio (TNR) were evaluated for all 3 contouring methods. Tumor Response was based on follow-up MRI using mRECIST criteria. Optimal cut-off for each parameter were determined with Receiver Operating Characteristic (ROC) method based on tumor response at 6 months. Univariate and multivariate Cox proportional hazard regression analyses were performed to identify associations with outcome. ***Results:*** Median follow-up was 34 months during which 24 patients died. The median (IQR) Dmean were 107 Gy (60-169), 134 Gy (76-181) and 164 Gy (106-222) for C_{MRI}, C_{SPECT}, and $C_{MRI/SPECT}$, respectively. Areas under ROC curves were predictive for all 3 Dmean contouring methods, and for TNR with C_{MRI} method only. By multivariate analysis, only Dmean associated with TNR, both based on C_{MRI} method, were independent prognostic factors for OS ($p < 0.05$ for both). Patients with Dmean C_{MRI} > 107 Gy had an OS = 48.6 vs 15.3 months for others, and patients with TNR C_{MRI} > 7.7 an OS = 48.6 vs 15.7 months ($p < 0.0037$). ***Conclusion:*** In advanced HCC treated with SIRT, dosimetry based on pre-treatment ^{99m}Tc-MAA SPECT/CT is predictive of tumor response whatever the contouring method. However, only Dmean and TNR determined with radiologic contours (C_{MRI}) are independent predictive factors of survival. The use of radiologic contours registered on ^{99m}Tc-MAA SPECT/CT images should be prospectively considered for helping therapeutic strategy. ***References:*** None

OP-477

Radioembolization of hepatocarcinoma: dose-response assessment with mRECIST and with a new densitometric method

C. Romanò[1], S. Mazzaglia[1], M. C. De Nile[2], S. Bhoori[3], A. Gabutti[4], G. Maffi[4], V. Mazzaferro[3], M. Maccauro[1], C. Spreafico[4], E. Seregni[1], C. Chiesa[1];
[1]Nuclear Medicine, Foundation IRCCS Istituto Nazionale Tumori, Milan, ITALY, [2]Postgraduate Specialization School in Medical Physics , University of Milan, Milan, ITALY, [3]HPB Surgery, Hepatology and Liver Transplantation, Foundation IRCCS Istituto Nazionale Tumori, Milan, ITALY, [4]Radiology 2, Foundation IRCCS Istituto Nazionale Tumori, Milan, ITALY.

Aim/Introduction: Radiological response evaluation after radioembolization of hepatocarcinoma is often difficult and uncertain with the current consolidated dimensional criteria. We studied a new densitometric response assessment method in comparison with mRECIST in a dose-response study of hepatocarcinoma patients treated with ^{90}Y glass microspheres. ***Materials and Methods:*** 106 lesions of patients treated 8 days after calibration day were retrospectively analysed. In all the cases, both pre- (^{99m}Tc-MAA SPECT) and post-therapy (^{90}Y-PET) voxel-based dosimetry parameters were computed. In particular, the following variables (Ψ) were considered: mean dose (D), Equivalent Uniform Dose (EUD), average of the Biologically Effective Dose (BEDave), Equivalent Uniform Biologically Effective Dose (EUBED), the minimal dose of the 98%, 70%, 50% and 2% of the VOI (D_{98}, D_{70}, $D_{50,}$ and D_2), and homogeneity index (HI). The consolidated mRECIST and the proposed densitometric criterion were adopted to assess lesion responses. According to the densitometric criterion, the Hounsfield Units (HU) variation within a circular ROI lesion is considered. The response threshold was optimized at 20% of HU decrease in the arterial CT phase. The Ψ-response correlation was assessed. The area under the receiver-operating characteristic (ROC) curve (AUC) of responding/not responding lesions was evaluated. The analysis was repeated stratifying on lesion mass with the median lesion mass as cut-off value (56 g).

Results: The mRECIST method did not show statistically significant Ψ-response correlation, neither with ^{99m}Tc-MAA SPECT nor ^{90}Y-PET dosimetric data. On the contrary, the densitometric method returned statistically significant Ψ-response correlation for all the dosimetric variables with post-therapy ^{90}Y-PET data, and with D, BED_{ave}, D_{50}, and D_2 using pre-therapy ^{99m}Tc-MAA SPECT images. Higher AUC values were reported with the densitometric (0.71±0.05) with respect to the mRECIST (0.57±0.06) criterion. In all the cases, post-therapy data returned higher AUC values with respect to pre-therapy evaluations, for the low predictive accuracy of MAA simulation. After the stratification on mass, mRECIST gave higher AUC values with respect to the densitometric method when large lesions were considered (mass ≥ 56 g, 4.7 cm diameter if spherical), while the opposite situation was obtained when small lesions (mass < 56 g) were considered. ***Conclusion:*** The densitometric method gave better correlation between dose and response, and, in general, improved the dose separation between responding and non-responding lesions. Moreover it allowed measuring a higher number of lesions. After lesion mass stratification, it gave better AUC values for small lesions, whereas the mRECIST method showed better AUC for large lesions. ***References:*** None

OP-478

Radioembolization of hepatocarcinoma with ^{90}Y glass microspheres: clinical implications of low precision of ^{99m}Tc-MAA SPECT/CT dosimetry on lungs and lesions

C. Chiesa[1], S. Mazzaglia[1], M. Maccauro[1], M. C. De Nile[2], C. Romano[1], M. Mira[1], A. Marchiano[3], E. Seregni[1], V. Mazzaferro[4], C. Spreafico[3];
[1]Nuclear Medicine, Foundation IRCCS Istituto Nazionale Tumori, Milan, ITALY, [2]Post graduate specialization school in Medical Physics, Milan, ITALY, [3]Interventional Radiology, Foundation IRCCS Istituto Nazionale Tumori, Milan, ITALY, [4]HPB Surgery, Hepatology and Liver Transplantation, Foundation IRCCS Istituto Nazionale Tumori, Milan, ITALY.

Aim/Introduction: In order to define the most accurate individualised treatment planning strategy in radioembolization of hepato-carcinoma with ^{90}Y glass microspheres, we evaluated the frequency and the amount of differences between predicted and actual absorbed doses (AD). ***Materials and Methods:*** We evaluated two sequential groups of 43+189=232 hepato-carcinoma patients, with 56 and 309 lesions, respectively, with ^{99m}Tc-MAA SPECT/CT and ^{90}Y-PET. They were injected after a decay time of 3.75 and 7.75 days from the calibration time (therefore named "Few-spheres" and "Many-spheres"), with 1 and 2.8 million of microspheres per GBq, respectively. PET images were automatically coregistered to SPECT in order to copy identical VOIs. Incidence of presence of Lung Shunt Fraction (LSF) was compared between planar MAA and ^{90}Y-PET scans. For patients showing MAA-LSF, lung was included in PET scan. In liver, the difference between paired AD values AD(^{90}Y)-AD(^{99m}Tc) and their ratio ADR=AD(^{99m}Tc)/AD(^{90}Y) of lesions and whole non-tumoural tissue were analyzed both as dichotomic and as continuous dependent variables. Independent covariates considered in the univariate analyses were: DA=Different catheter tip positions during Angiography (>2 mm), different interventional radiologist, the time interval between the two sessions; lesion location in anterior/posterior segment; VOI mass (39 g median value adopted as cut-off). ***Results:*** MAA-LSF was present in 82/232 (35%) patients, while PET-LSF in 16/232 (7%) (p<0.0001). PET-LSF was clinically relevant (>10%) in only 6/232 cases (2.5%). For lesions, Bland-Altman bias (mean difference) and [95% C.I.] were, for "Few-spheres" and "Many-spheres", respectively: -29[-324,+265]Gy and -61[-416,+294]Gy for lesions; 0.7[-18,+20]Gy and +5[-13,+22]Gy for non tumoural tissue. "Few-spheres" showed a significantly better bias, while only a non-significant reduction trend for the 95% C.I.. Exclusion of cases with biasing factors (DA, MAA-LSF, coregistration problem) did not improved these values significantly. The Lin Concordance parameter was affected by low precision (0.70-0.80) for lesions in both groups. Lesion dose difference was associated only with DA (p=0.0009) and with lesion mass, with larger ADR (overestimation in simulation) for small masses. ADR was also weakly but significantly correlated with lesion mass (Spearman r=-0.17, p=0.04), converging with an asymmetric bi-logarithmic funnel-shaped plot to 1 for large masses. ***Conclusion:*** For lung prediction, ^{99m}Tc-MAA is inadequate. In liver, ^{99m}Tc-MAA predictions on lesions are largely inaccurate on the individual case. The relatively limited mean lesion differences allow to improve average cohort properties (OS, PFS), as reported in literature. However, further improvement may be obtainable trough planning on much more accurate whole non-tumoural liver AD. ***References:*** None

OP-479

Comparison of different voxel-S-value methods for quantitative Y-90 TOF PET dosimetry

G. Chen[1], Y. Dewaraja[2], G. Mok[1];
[1]University of Macau, Taipa, MACAO, [2]University of Michigan, Ann Arbor, MI, UNITED STATES OF AMERICA.

Aim/Introduction: Converting time-integrated activity to absorbed dose using voxel-S-values (VSV) is an efficient method for voxel-based dosimetry yet its limitation in heterogeneous media is recognized. This study aims to assess the differences among different VSV methods as compared to Monte Carlo (MC) methods for lung, liver, lung-liver interface and tumor absorbed dose based on Y-90 microsphere TOF PET/CT images. ***Materials and Methods:*** This study included four sets of Y-90 microsphere TOF PET/CT patient data available from the University of

Michigan Deep Blue Data Repository. The PET matrix size was 200*200*122 with a voxel size of 4.07*4.07*3 mm. VSV (Gy/MBq-s) were generated by GATE v.8.0 with a matrix size of 21*21*21 and same voxel size as PET images. Liver, lungs and tumors were manually segmented from CT images and mapped to the corresponding PET images. Tumors could only be delineated on two patients while liver and lungs could be segmented from all patients. Time-integrated activity maps were generated from PET images assuming only physical decay after the acquisition. Investigated VSV methods were liver kernel with density correction (LKD), constant liver kernel (LK), central voxel scaling kernel (CK), lung+liver kernels (LLK) and local deposition (LD). MC results were used as the gold standard. Mean absorbed doses were calculated for tumors, liver, lungs, lung-liver interface, i.e., liver_i and lung_i which are 1.5 cm slabs of liver and lungs extended from the interface, respectively. ***Results:*** LKD, LK, CK, LLK and LD methods were within 3% of MC for mean liver and tumor absorbed dose. Compared to MC, their average differences were 26%±4.6%, -47.6%±36.2%, -8.6%±34.4%, -8.5%±2.0% and 19.9%±3.6%, for mean lung absorbed dose, 53.2%±10.8%, -61.7%±2.7%, 24.9%±5.7%, -12.8%±3.2% and 46.4%±5.8%, for lung_i, and 4.4%±3.3%, -4.4±3.4%, 6.1%±1.7%, 19.2%±8.0% and -6.7%±4.8% for liver_i. ***Conclusion:*** Absorbed doses from five VSVs are similar to MC for liver and tumors which are located far from the lung-liver interface. LKD and LD overestimate lung absorbed dose whereas others underestimate it. For the interface, LKD and LK perform reasonably well on liver_i, while LLK performs better on lung_i as compared to others. VSV poses more errors in lung absorbed dose as compared to the liver, especially manifests in the interface. LLK is suggested to obtain the lung absorbed dose, and LKD or LK is suggested to obtain the liver or tumor absorbed dose. ***References:*** [1] Mikell et al. EJNMMI physics, 2015; 2(1): 16. [2] Götz et al. Phys. Med. Biol 2019; 64(24):245011.

907

Teaching Session 3: A Practical Guide to MR when Reading PET/MR

Saturday, October 24, 2020, 09:00 - 10:30 Channel 7

OP-480

Non-Prostate Oncologic Body PET/MR. MR Needs and Expectation. The Nuclear Medicine's Perspective

C. Field Galán; *HM Hospitales/Hospital Universitario Madrid Sanchinarro, Nuclear Medicine, Madrid, SPAIN.*

OP-481

Non-Prostate Oncologic Body PET/MR. MR Needs and Expectation. The MR Expert's Perspective

O. Catalano; Harvard University, Massachusetts General Hospital, Radiology, WHT 270, Boston MA, UNITED STATES OF AMERICA.

OP-482

Prostate PET/MR. MR Needs and Expectation. The Nuclear Medicine's Perspective

H. Bernstine; Assuta Medical Center/ Sackler School of Medicine, Tel Aviv University, Tel Aviv, ISRAEL.

OP-483

Prostate PET/MR. MR Needs and Expectation. The MR Expert's Perspective

L. Domachevsky; Sheba Medical Center, Radiology and Nuclear Medicine, Radiology, Tel Aviv, ISRAEL.

908

Clinical Oncology Track - Featured Session: PET Diagnostics in Head Neck Cancers and Melanoma

Saturday, October 24, 2020, 09:00 - 10:30 Channel 8

OP-485

An introduction to PET Radiomics and Texture Analysis

J. Kleesiek; UK Essen, Essen, GERMANY.

OP-486

Correlation Study between PET/MR Radiomics Features, Metabolic Parameters and Staging of Nasopharyngeal Carcinoma

J. Liang;
Hangzhou Universal Medical Imaging Diagnostic Center, Hangzhou, CHINA.

Aim/Introduction: The study aims to investigate the correlations between PET/MR radiomics features and three metabolic parameters: the maximum standardized uptake value(SUVmax), tumor metabolic volume(MTV), total lesion glycolysis (TLG) , as well as their correlation with TNM staging of Nasopharyngeal Carcinoma(NPC). ***Materials and Methods:*** The PET/MR imaging data of 100 NPC patients with undifferentiated carcinoma from a medical center were collected. The patients were randomly divided into training group (n = 70) and test group (n = 30). We measured the metabolic parameters (SUVmax, MTV, TLG) of the NPC primary focus with GE post-processing workstation, and used AK software to extract the most relevant radiomics features to NPC staging. Finally, we used the selected radiomics features to establish a logistic regression model. To analyze the correlation between radiomics features, metabolic parameters and the TNM staging, and analyze the correlation between radiomics features and metabolic parameters. ***Results:*** We extracted 396 radiomics features from the T2WI and the PET image respectively. After the

feature selection, 6 and 3 features were retained. The AUCs of the training and test group of the T2WI model were 0.85 and 0.83, the AUCs of the training and test group of the PET model were 0.84 and 0.82. Spearman correlation analysis showed that metabolic parameters (MTV, TLG), PET radiomics features (GLCMEnergy_AllDirection_offset1_SD, GLCMEntropy_angle0_offset4) were correlated with T stage, and the correlation coefficients were 0.608, 0.770, -0.752, 0.688, respectively; MTV, TLG, PET radiomics features (GLCMEnergy_AllDirection_offset1_SD, GLCMEntropy_angle0_offset4) were correlated with clinical stage, and the correlation coefficients were 0.430, 0.511, -0.470, 0.471, respectively; All metabolic parameters and radiomics features were not correlated with N stage. Pearson correlation analysis showed that T2WI radiomics feature (MinIntensity) was negatively correlated with MTV and TLG, and the correlation coefficients were -0.502, -0.566; PET radiomics feature (GLCMEntropy_angle0_offset4) was positively correlated with MTV and TLG, and the correlation coefficients were 0.692, 0.738, respectively; all features were not correlated with SUVmax. ***Conclusion:*** PET radiomics features (GLCMEnergy_AllDirection_offset1_SD, GLCMEntropy_angle0_offset4) and metabolic parameters (MTV, TLG) have a strong correlation with T staging and clinical staging of NPC, and all metabolic parameters and radiomics features have no correlation with N staging. T2WI radiomics features (MinIntensity), PET radiomics features (GLCMEntropy_angle0_offset4) are correlated with metabolic parameters (MTV, TLG), while the remaining features are not correlated with metabolic parameters. ***References:*** None

OP-487

Application Value of PET/MR Radiomics Analysis in Evaluating the Clinical Staging of Nasopharyngeal Carcinoma

J. Liang;
Hangzhou Universal Medical Imaging Diagnostic Center, Hangzhou, CHINA.

Aim/Introduction: To investigate the value of ^{18}F-FDG PET/MR radiomics model in evaluating the clinical staging of nasopharyngeal carcinoma (NPC). ***Materials and Methods:*** From June 2017 to October 2019, the clinical data and PET/MR imaging data of 100 NPC patients with undifferentiated carcinoma from a medical center were collected. The patients were randomly divided into training group (n = 70) and verification group (n = 30). All patients were divided into early stage (I - II stage) and advanced stage (III - IV stage). We measured the metabolic parameters (SUVmax, MTV, TLG) of the NPC primary focus with GE post-processing workstation, and used AK software to extract the most relevant radiomics features to NPC staging, then constructed the corresponding radiomics signature. Multivariable logistic regression analysis was performed with radiomics signature and clinical variables for developing the prediction model. The receiver operating characteristic(ROC) analysis was used to evaluate the prediction model. ***Results:*** The established radiomics signature has better prediction efficiency for identifying the clinical stage of NPC. The AUCs were 0.749 (95% CI: 0.696 - 0.858) and 0.733 (95% CI: 0.631 - 0.835) in the training group and the verification group, respectively. On multivariable logistic regression, the radiomics signature and total lesion glycolysis (TLG) were considered to be independent and significant risk factors for the stage (I-II stage vs. III-IVb stage) of NPC. The prediction model showed good discrimination in both training group (AUC=0.851, 95%CI:0.799 to 0.893; sensitivity=0.801, specificity=0.734, positive predictive value=0.811, negative predictive value=0.890) and verification group (AUC=0.876, 95% CI: 0.781 to 0.903, sensitivity=0.893, specificity=0.718, positive predictive value=0.701, negative predictive value=0.912). ***Conclusion:*** The radiomics predictive model which integrated with the radiomics signature and metabolic parameters (TLG) can be used as a promising and applicable adjunct approach for predicting the clinical stage (I-II stage vs. III-IVb stage) of patients with NPC. ***References:*** None

OP-488

Impact of Primary Tumor Size, SUV_{max} of Primary Tumor and the Most Avid Neck Node on Baseline ^{18}FDG PET/CT Upon Disease Recurrence in Head and Neck Ooropharyngeal SCC using Standardized Imaging Protocol

M. Zaman[1], *N. Fatima*[1], *A. Zaman*[2], *U. Zaman*[3], *S. Zaman*[4], *R. Tahseen*[1];
[1]*AKUH, Karachi, PAKISTAN,* [2]*Dow University of Health Sciences (DUHS), Karachi, PAKISTAN,* [3]*Dept of Medicine Suny Downstate, Hospital, New York, NY, UNITED STATES OF AMERICA,* [4]*Dow Medical College, Dow University of Health Sciences (DUHS), Karachi, PAKISTAN.*

Aim/Introduction: Purpose of this prospective study was to find the impact of primary tumor size (Ts), standardized uptake values (SUVmax) of primary tumor and the most avid neck node on disease recurrence in patients with head and neck oropharyngeal squamous cell carcinoma (HNOP-SCC). ***Materials and Methods:*** We included patients with HNOP-SCC (without distant metastasis - M0 disease) who had pre and post-treatment ^{18}FDG PET/CT using strict standardized imaging protocol from 2017-2019. Based on follow-up ^{18}FDG PET/CT findings patients were categorized as disease free (no or minimal ^{18}FDG uptake ≤ background over surgical bed and no distant metastasis) and disease recurrence (^{18}FDG uptake > background over surgical bed with or without nodal and/or distant metastasis). Ts and SUVmax of primary tumor and the most avid neck

node were compared and impact of these were studied upon disease recurrence. ***Results:*** Total 112 patients were included. No significant difference was seen in mean age (overall: 60 ±14 yr.), gender distribution (overall M:F: 69:31%), body mass index (overall: 25.20 ±5.82) and history of diabetes (overall: 19%) between disease free and disease recurrence groups. Similarly, no significant difference was observed for fasting blood sugar (overall: 110 ±28 mg%), ^{18}FDG dose (overall: 169 ±37 MBq) and uptake period (overall: 70 ±12 min) between two groups ensuring strict adherence to standardized imaging protocol. Significant difference (p <0.05) was observed between disease free and disease recurrence for Ts (25 ±10 mm vs. 33 ±14 mm), SUVmax of primary tumor (6.2 ±6.8 vs 9.3 ±7.2) and the most avid neck node (2.1 ±3.3 vs. 4.7 ±5.9) and median follow-up (13 ±12 vs 08 ±13 months) respectively. Using receiver operating characteristic (ROC) analysis, Ts > 29 mm, baseline tumor SUVmax >4.6 and nodal SUVmax >6.2 were found independent predictors for disease recurrence. Nodal SUVmax >6.2 was found an independent predictor of shortest DFS than Ts and tumor SUVmax. ***Conclusion:*** We conclude that in HNOP-SCC, primary tumor size (>29 mm), SUVmax of primary tumor (>4.6) and the most avid neck node (>6.2) in baseline ^{18}FDG PET/CT using standardized imaging protocol are the independent predictors of disease recurrence. Furthermore, SUVmax >6.2 of the most avid node predicts the shortest DFS than primary tumor size and SUVmax of primary tumor. ***References:*** None

OP-489

Comparison of 18F-FDG PET / MR and enhanced MR in skull-base bone invasion of nasopharyngeal carcinoma

Y. Xu, S. Wang;
Hangzhou Universal Imaging Diagnostic Center, Hangzhou, CHINA.

Aim/Introduction: To explore the value of 18F-FDG PET/MR in evaluating skull-base bone invasion of nasopharyngeal carcinoma ***Materials and Methods:*** 124 patients with NPC who underwent PET/MR and enhanced MR scan. Difference between GTV_{PET}(gross tumor volume), a tumor target region delineated with 30% of SUVmax as a threshold, and GTV_{MR}, a tumor target region delineated with fat suppression enhanced T2 sequence was compared. ***Results:*** 68 patients showed skull-base bone erosion, of the 68 patients, 24 showed osteolytic bone destruction and 44 showed bone marrow infiltration. The osteolytic bone destruction area is characterized by soft tissue mass signals. The bone marrow infiltration type is characterized by low signal intensity replaced high signal intensity in the bone marrow on the T1-weighted images or when hyperintensity was observed on the fat-suppressed T2WI, and a high signal was seen on DWI. All enhanced scans of the bone invasion area showed abnormal enhancement. The SUVmax [3.31(1.64,4.95)]of the skull base lesion area was significantly lower than that [9.77(6.47,11.54)]of the main body of the nasopharyngeal lesion (Z=-7.143,P<0.01). The SUVmax [3.22(2.44,3.60)] of bone lesions in bone marrow infiltrating cases was significantly lower than that[6.18(4.72,7.45)] of osteolytic bone destruction (Z=-6.776,P<0.01). Among the 44 cases of bone marrow infiltration, FDG metabolism in the visible lesion area was higher than that in the contralateral or surrounding normal bone in 23 cases, and no intense high metabolic region was observed in 21 cases. The area under the ROC curve (AUC) for the evaluation of skull base invasion by SUVmax was 0.866, the SUVmax corresponding to the most approximate index was 1.5, and the sensitivity and specificity were 79.4% and 46.0%, respectively. In osteolytic bone destruction cases, 4.17% (1/24) of the cases of skull-base bone lesions were located outside the GTV_{PET} area, and 61.36% (27/44) of bone marrow infiltration cases were located outside the GTV_{PET} area,there were statistical differences(χ^2=20.97,P<0.01). GTV_{PET} [35.46(25.27,43.56)] is smaller than GTV_{MR} [41.27(30.45,29.58)] (Z=-5.316,P<0.01). ***Conclusion:*** Although PET / MR is of great value for staging of nasopharyngeal carcinoma, FDG uptake in the area of skull base invasion is lower than that of nasopharyngeal lesions, and false negatives often occur in bone marrow infiltrating types. Evaluation of skull base bone invasion and radiotherapy target region with PET metabolic range may not be accurate, and enhanced MR is still a necessary detection method for pre-treatment evaluation and efficacy evaluation. ***References:*** None

OP-490

18F-FDG PET/Low Dose CT as unique multimodality imaging method to assess bone involvement in Multiple Myeloma patients

C. Ferrari[1], A. Nappi[1], C. Minoia[2], M. Zappia[3], G. Santo[1], P. Mammucci[1], N. Merenda[1], A. Guarini[2], L. Brunese[3], N. Maggialetti[3], G. Rubini[1];
[1]Nuclear Medicine Department, University of Bari "Aldo Moro", Bari, ITALY, [2]Haematology Unit, IRCCS Istituto Tumori "Giovanni Paolo II", Bari, ITALY, [3]Radiology Department, University of Campobasso, Campobasso, ITALY.

Aim/Introduction: Imaging plays a crucial role to assess bone involvement in Multiple Myeloma (MM) patients. The International Myeloma Working Group recommends the use of Whole-body Low Dose CT (WBLDCT) instead of conventional skeletal survey in the baseline workup.In the last years, 18F-FDG PET/CT, including both functional and morphological evaluation, has changed the clinical approach to MM patients in staging, restaging and therapy response assessment, particularly in accurately distinguishing active from inactive bone lesions.We aimed to compare the performance of 18F-FDG PET-coregistrated low dose CT (PET/LDCT) with WBLDCT in MM patients.

Materials and Methods: Since July 2018 to September 2019, 33 consecutive MM patients (mean age 67y, range: 53-82y) were prospectively enrolled and underwent WBLDCT during their staging/restaging work-up and PET/LDCT within 30 days. CT acquisition parameters of both WBLDCT and PET/LDCT had been defined to reduce dose exposition (120kV, 50 mAs/rotation, Pitch 0.984, FOV/Matrix 500mm/512, thickness 3.75). WBLDCT and PET/LDCT were evaluated by two independent readers and assessed as positive in the presence of at least one lytic bone lesion, evaluating as both patient-based analysis and region-based analysis, including skull, cervical, dorsal, lumbo-sacral spine, thorax (ribs, sternum, scapula), pelvis, upper and lower limbs.Concordance between the two methods were analyzed by Cohen's k test. ***Results:*** According to patient-based analysis, WBLDCT and PET/LDCT resulted negative concordant in 3/33 (9%) patients and positive concordant in 29/33 (88%) (k=0.841, p<0.001). In region-based analysis, concordances in different anatomic regions were: skull (k=0.937, p<0.001), cervical (k=1.000, p<0.001), dorsal (k=0.809, p<0.001), lumbo-sacral spine (k=0.878, p<0.001), thorax (k=0.756, p<0.001), pelvis (k=0.814, p<0.001), upper limbs (k=0.655, p<0.05) and lower limbs (k=1.000, p<0.001). No statistically significance differences were found between the two exams both in patient-based analysis and region-based analysis. ***Conclusion:*** According our experience, PET/LDCT showed comparable performances to WBLDCT. Our preliminary data need to be confirmed in larger cohorts and, if confirmed, lead us to suggest the use of PET/LDCT to assess bone involvement in MM patients as unique morphological and functional imaging method in staging and restaging disease. The combined radiologist-nuclear physician report could allow to avoid further investigations, with impact on patient compliance, radiation exposure and health care spending. ***References:*** None

OP-491

FDG-PET/CT in early assessment of immune-related adverse events during first treatment response assessment in melanoma patients treated with immune checkpoint inhibitors

K. Kudura[1,2], L. Nussbaumer[2], S. Bengs[1,2], A. Haider[1,2], D. A. Ferraro[1,2], L. Basler[3,2], R. Förster[3,2], M. Hüllner[1,2], L. Husmann[1,2], C. Deubelbeiss[4,2], F. Dimitriou[4,2], R. Dummer[4], J. Mangana[4,2]; [1]Department of Nuclear Medicine University Hospital Zurich, Zürich, SWITZERLAND, [2]University of Zurich, Zurich, SWITZERLAND, [3]Department of Radiation Oncology University Hospital Zurich, Zürich, SWITZERLAND, [4]Department of Dermatology University Hospital Zurich, Zürich, SWITZERLAND.

Aim/Introduction: The recently introduced immune checkpoint inhibitors already represent an important treatment option in advanced tumor stages including malignant melanoma. Immune checkpoint inhibitors favour the onset of autoimmune manifestations, often termed immune-related adverse events (IRAEs). Considering their high frequency but also still controversial discussed presumed interaction with treatment outcome an early detection of IRAEs is essential.Aim of this retrospective study is to investigate whether early findings suspicious of common immune-related adverse events after immune checkpoint blockade initiation assessed by FDG-PET/CT performed for early treatment response assessment three months after treatment initiation can be validated by laboratory, radiological findings and/or occurrence of clinical symptoms under immune checkpoint blockade in metastatic melanoma patients. ***Materials and Methods:*** FDG-PET/CT scans at baseline, 3 months and 12 months after first drug infusion between 2015 and 2017 were retrospectively separately analyzed. Patients were enrolled when FDG-PET/CT scan at 3 months showed new signs of IRAEs compared to previous FDG-PET/CT at baseline. In total 25 patients with histologic proven malignant metastatic melanoma all treated with immune checkpoint blockade. The new findings suspicious of IRAEs on FDG-PET/CT at three months after the first drug infusion were then retrospectively validated by laboratory or radiological findings or onset of new symptoms. FDG-PET/CT scans at 12 months after first treatment were analyzed according to the PET/CT based immune-related response criteria and our cohort dichotomized into two groups: clinical benefit (CR, PR and SD) vs. no clinical benefit (PD). ***Results:*** Approximately half of our population (n=12) showed new findings suspicious of thyroiditis on FDG-PET/CT three months after first drug infusion, followed by 32 % (n=8) presenting signs of colitis, 12% (n=3) sarcoid-like lymphadenopathy, 4% (n=1) hypophysitis and 4% (n=1) hepatitis. In 80% (n=20) of our patients hybrid imaging based new findings suspicious of IRAEs could be verified by the onset of new symptoms, clinical or radiological findings (p=0.003 < 0.05). 68% (n=17) of our metastatic melanoma patients benefit from immune checkpoint blockade one year after first drug infusion. ***Conclusion:*** FDG-PET/CT enables an early reliable detection of immune-related adverse events three months after treatment initiation concordant with clinical, laboratory and radiological findings in metastatic melanoma patients under immune checkpoint blockade. In daily clinical practice, as part of an interdisciplinary tumorboard, FDG-PET/CT performed for first treatment response assessment can also help to detect and treat immune-related adverse events at an early stage and so potentially prevent from possible interaction with treatment outcome. ***References:*** None

OP-492

Can [18F]FDG PET/CT predict histopathologic response or recurrence after complete surgical resection in prior unresectable stage III melanoma patients treated with

neoadjuvant targeted therapy?

B. van der Hiel*, S. Blankenstein, E. Aalbersberg, M. Stokkel, B. van de Wiel, W. Klop, A. van Akkooi, J. Haanen;*
the Netherlands Cancer Institute - Antoni van Leeuwenhoek Hospital, Amsterdam, NETHERLANDS.

Aim/Introduction: In unresectable stage III BRAF-mutated melanoma patients, neoadjuvant treatment with BRAF/MEK inhibitors enables surgical resection after sufficient downsizing of the tumour. However, recurrences after radical surgery still occur in these patients. The degree of pathologic (PA) response might act as a predictive biomarker for recurrent disease or survival. [18F]FDG uptake on PET/CT shows a rapid decrease in patients treated with BRAF/MEK inhibitors, even shortly after the initiation of treatment. With this study we aim to investigate whether response monitoring with PET/CT prior to- and during treatment with dabrafenib and trametinib can predict histopathological response or recurrence after complete surgical resection. ***Materials and Methods:*** Patients with BRAF-mutated, unresectable locally advanced stage III melanoma were included and treated with BRAF- and MEK-inhibitor dabrafenib and trametinib for eight weeks. [18F]FDG PET/CT was performed at baseline and two and eight weeks after the initiation of therapy. Pathological response was assessed on the dissection specimen after surgical resection. Body weight based SUVmax, SUVpeak, and Total Lesion Glycolysis (TLG) were measured. Tumour SUVmean and SULpeak were measured for response monitoring according to EORTC-criteria and PERCIST. Patients underwent PET/CT at follow up every 3 months for 2 years, then every 6 months for 2 years, and once in year 5. ***Results:*** Twenty patients were included in the study. In eighteen patients sufficient downsizing occurred to perform a resection and assess pathological response. Eight patients (44%) had a pathologic Complete Response (pCR) and ten patients (56%) had a non-pathologic Complete Response (non-pCR). EORTC or PERCIST response measurements did not correspond with pathologic outcome. Median and interquartile range of SUVmax, SUVpeak and TLG at baseline, 2 weeks or 8 weeks did not differ between the pCR and pPR/NR group, nor did absolute or percentage change between baseline and two weeks, baseline and eight weeks or two weeks and eight weeks. Recurrence was evaluated in sixteen patients with R0 resection and no evidence of disease elsewhere in the body. Eight (50%) patients developed recurrence. Six recurrences were detected with imaging only, four of which with PET/CT within 6 months after surgery. PET parameters prior to surgery could not predict recurrence. ***Conclusion:*** Baseline PET or (early) PET response in previous unresectable stage III melanoma patients could not predict pathologic response or recurrence after treatment with BRAF/MEK inhibitors. However, [18F]FDG PET/CT seems valuable in detecting recurrence after surgery in these patients. ***References:*** None

OP-493

The use of [18F]FDG PET/CT to detect early recurrence after resection of high-risk stage III melanoma

B. van der Hiel*, E. Stahlie, M. Stokkel, Y. Schrage, W. van Houdt, M. Wouters, A. van Akkooi;*
the Netherlands Cancer Institute - Antoni van Leeuwenhoek Hospital, Amsterdam, NETHERLANDS.

Aim/Introduction: To date, international consensus concerning the use of [18F]FDG PET/CT as a surveillance tool in the follow-up of high-risk melanoma patients after complete resection of disease is lacking. Moreover, with the rise of adjuvant therapy it seems appropriate to investigate the role of this imaging modality to exclude newly developed metastases after resection and prior to starting treatment. The aim of this study was to investigate the use of PET/CT in detecting (early) recurrences after complete resection of stage IIIB-D melanoma, either prior to starting adjuvant systemic therapy or within a surveillance program without adjuvant therapy in asymptomatic patients. ***Materials and Methods:*** Prospectively two cohorts were set up with stage III melanoma patients with complete resection of disease. In the first cohort (stage IIIB/C AJCC 7th) surveillance [18F]FDG PET/CT was performed 6-monthly for two years if patients stayed asymptomatic with normal serum S100B, with a final scan at three years. In the second cohort (stage IIIB/C/D AJCC 8th) patients underwent one screening [18F]FDG PET/CT after resection and prior to starting adjuvant treatment. ***Results:*** Thirty-five patients were included in cohort one (105 scans) with a median follow-up of 33 months. Twelve patients (34.3%) developed a recurrence which were all discovered by PET/CT, of which seven (20.0%) were detected at the first scan after six months. Seven recurrences occurred in stage IIIC patients, five in stage IIIB patients. Sensitivity and specificity were 92.3% and 100% respectively. Forty-two patients were included in cohort two. Recurrence was suspected on nine scans (21.4%), four (9.5%) of which were true positive. Five (11.9%) scans were false positive. The number of scans needed to find one asymptomatic recurrence were 8.8 and 10.5 in cohort one and two respectively. ***Conclusion:*** This study demonstrates that [18F]FDG PET/CT is useful for detecting recurrence in high-risk resected stage III melanoma patients, especially within the first six months after surgery. Therefore, PET/CT should be considered when monitoring these patients after complete resection either prior to starting adjuvant therapy and during follow-up protocols. ***References:*** None

OP-494

PET/CT Evaluation and Patterns of Response to Different Type of Therapies in Patients with Disseminated Melanoma

S. Divosevic[1], *M. Sunjic*[2];
[1]*Medikol Polyclinic, Zagreb, CROATIA,* [2]*Clinical Hospital Centre Sisters of Mercy, Zagreb, CROATIA.*

Aim/Introduction: To evaluate the benefit of F 18 FDG PET/CT in follow-up of efficacy of different types of therapy modalities in patients with disseminated melanoma. ***Materials and Methods:*** We examined 171 patients, 91 men, 62 women, 70 on molecular targeted therapy (40 vemurafenib-kobimetinib, 30 dabrafenib-trametinib, group A), 101 patients on immunotherapy (91 pembrolizumab, 10 nivolumab, group B), and 16 on combined therapy (group C). The mean age of patients was 60 years, in the time of primary tumor excision 62 years, in the time of metastases appearance 62 years, approximately 3 years from the primary diagnosis to disseminated disease. We found totally 363 metastases, mainly in the lymph nodes, lung, subcutaneous tissue, skeleton, liver, brain, skin, muscles, spleen, adrenal glands and bowel, consecutively. We performed totally 132 FDG PET/CT scans (52 in group A, 80 in group B, 87 in group C), although 106 patients were followed every time with PET/CT, thus the numbers were 36 patients in group A, 54 in group B, and 16 in group C. ***Results:*** In the group A, 89% of patients were in regression of the disease, 11% in progression, in group B we had 63% of patients in regression and 37% in progression, and in group C 31% of patients were in regression and 69% in progression of the disease. We found 5 pseudoprogressions in 3 immunotherapy patients, in the period of 4-19 months since the beginning of the therapy, which is in concordance to known results from previous studies, but we have only two patients with hypreprogression, which is significantly less than usually known. We found iatrogenic pneumonitis in 3 patients. ***Conclusion:*** Since the new modalities of therapy for melanoma patients are expensive, and beacuse melanoma can spread throughout the whole body, including skin, subcutaneous tissue and muscles, our results support the importance of PET/CT in evaluation of all the modalities of specific therapy, evaluating the need for continuation or cessation of therapy, changing of treatment modalities, and diagnosis of different side-effects, thus influencing strongly on the quality of patient's life, being at the same moment cost-effective. ***References:*** None

OP-495

Clinical significance of FDG-PET/CT for Mucosal Melanomas

K. Kitaguchi*, Y. Nakamoto, T. Nomashi, S. Koyasu, K. Miyake, T. Ishimori, T. Saga;*
Kyoto University Hospital, Kyoto, JAPAN.

Aim/Introduction: Mucosal melanoma (MM) is a rare and aggressive tumor, which arises in extracutaneous sites from melanocytes present in mucosal membranes of the respiratory, gastrointestinal and urogenital tracts. Clinical role of positron emission tomography/computed tomography (PET/CT) in skin melanoma has been established [1)]. However, its utility for MM has not been fully investigated [2)]. The aim of this study was to evaluate the clinical significance of FDG-PET/CT for MM. ***Materials and Methods:*** A total of 28 patients (median 65 yr, M: F= 15:13) with histologically-proven MM, who underwent PET/CT between May 2009 and September 2019 at our institution, were included in this study. PET/CT was performed for staging in 21 patients and for restaging in 7 patients. Based on the final diagnosis obtained by histopathology or clinical follow-up, the diagnostic performance of PET/CT was evaluated. The prognostic value of multiple PET parameters (SUVmax, SUVmean, metabolic tumor volume (MTV) and total lesion glycolysis (TLG) for the primary tumor) with respect to progression free survival was assessed with the Cox proportional hazards regression model as a sub-analysis. ***Results:*** The 21 primary sites were as follows: nasal sinus (n=6), digestive tract (n=6), uterus (n=5), oral cavity (n=2), and tracheal bronchus (n=2). The sensitivity and positive predictive value (PPV) of FDG-PET/CT were all 100% for detection of primary sites. For metastases, sensitivity and PPV were 93% and 98%, respectively. There were some lesions identified only by FDG-PET/CT in palate(n=1), paranasal sinus(n=1), esophagus(n=1), small intestine(n=1), and bone(n=11), while brain (n=2) and liver (n=7) metastases were missed. In 18 patients who underwent surgical resection or chemotherapy for a primary tumor in our institution, 16 patients had a recurrence during follow-up (median time, 11.9 months). Higher MTV ($p = 0.039$) and TLG ($p = 0.031$) correlated with poorer progression free survival. However, SUVmax, SUVmean, number of lesions were not identified as a significant predictor. ***Conclusion:*** FDG-PET/CT is a valuable imaging modality for staging and re-staging in mucosal melanoma. Some PET quantitative parameters were suggested to be important prognostic factors for progression free survival. ***References:*** 1. Perng P, et al. AJR Am J Roentgenol. 2015 Aug;205(2):259-70.2. Goerres GW, et al. Laryngoscope. 2002 Feb;112(2):381-5.

910

TROP Session: Nuclear Endocrinology in Diagnosis and Therapy

Saturday, October 24, 2020, 09:00 - 10:30 Channel 10

OP-507

Increased cerebral glucose consumption during hypoglycemia in obese patients measured using dynamic bolus-injection ^{18}F-FDG PET/MR during hyperinsulinemic euglycemic and hypoglycemic clamp

M. Lubberink, S. Kvernby, N. Abrahamsson, K. Almby, M. Fahlström, M. Gingnell, S. Haller, J. Wikström, M. Sundbom, A. Karlsson, J. Eriksson;
Uppsala University, Uppsala, SWEDEN.

Aim/Introduction: Obese patients develop less symptoms and hormonal response during hypoglycemia after gastric bypass surgery (GBP) than before[1]. However, it is not known whether cerebral glucose consumption and/or blood flow (CBF), and their response to hypoglycemia, change in obese patients after gastric bypass surgery. The aim of the present work was to develop methodology and assess glucose metabolism and cerebral blood flow (CBF) response to hypoglycemia in obese patients using simultaneous PET/MR. ***Materials and Methods:*** Eight non-diabetic obese subjects (BMI 35-45) underwent 120-min dynamic scans after bolus injection of 5 MBq/kg ^{18}F-FDG on a Signa PET/MR. Plasma glucose levels were stabilized using a hyperinsulinemic-euglycemic clamp, resulting in normal glycemia with a plasma glucose concentration of 5 mmol/L during the first 50 min of the scan. Between circa 50 and 80 min p.i., plasma glucose concentration was decreased to 2.7 mmol/L. Blood samples were taken to measure plasma glucose and radioactivity. Net uptake rate of ^{18}F-FDG (K_i) and metabolic rate of glucose (MRglu) during euglycemia and hypoglycemia were calculated using a dual-phase basis function implementation of the irreversible two-tissue compartment (2T3k) model allowing for a change in rate constants during the glucose reduction phase, both for whole brain grey matter and at the voxel level. Changes between euglycemic and hypoglycemic CBF were assessed using simultaneous pseudo-continuous arterial spin labelling (pcASL). Accuracy and precision of the dual-phase model were assessed using numerical simulations. ***Results:*** Mean Ki increased significantly from 0.025±0.003 mL/cm^3/min during normal glycemia to 0.059±0012 mL/cm^3/min during hypoglycemia (p=0.08, Wilcoxon), corresponding to a significant increase of MRglu from 0.13±0.01 to 0.16±0.03 µmol/cm^3/min (p=0.015). No significant changes in CBF were found. Agreement between K_i values for normal glycemia based on the dual-phase model and 2T3k was high. Simulations showed a high correlation and agreement between simulated and fitted K_i values both at normal glycemia and hypoglycemia. Voxel-based results agreed well with whole brain gray matter results, showing a uniform significant increase in K_i in cortex but not in cerebellum. A significant decrease in K_i was found in hypothalamus. ***Conclusion:*** Simulations indicate that the dual-phase basis function method is able to robustly measure changes in glucose metabolism. Hypoglycemia appears to result in an overcompensation of cortical glucose uptake rate, but a reduction in hypothalamus, in obese patients. This results in slightly but significantly increased average whole brain glucose metabolism compared to normal glycemia.

References: 1 Abrahamsson et al, Diabetes 2016

OP-508

The Assessment of Intrahepatic Islet Transplantation with Dynamic Exendin PET Imaging

T. J. P. Jansen[1], *M. Buitinga*[1,2], *M. Boss*[1], *M. van der Graaf*[1], *E. J. P. de Koning*[3], *M. A. Engelse*[3], *M. F. Nijhoff*[3], *I. Velikyan*[4], *O. Korsgren*[4], *O. Eriksson*[4], *M. Brom*[1], *M. Gotthardt*[1];
[1]*Radboudumc, Nijmegen, NETHERLANDS,* [2]*KU Leuven, Leuven, BELGIUM,* [3]*LUMC, Leiden, NETHERLANDS,*
[4]*Uppsala University, Uppsala, SWEDEN.*

Aim/Introduction: Intrahepatic transplantation of islets is performed in patients with complicated type 1 diabetes (T1D) and unstable glycemic control. This procedure leads to improved glycemic control and quality of life. Graft function can however deteriorate over time due to various factors. A tool for the assessment of transplantation success and to measure islet survival in addition to functionality would be of great clinical value. We used dynamic PET imaging with the beta cell-specific tracer ^{68}Ga-exendin to study the presence of intrahepatic islet grafts in T1D patients. ***Materials and Methods:*** Dynamic PET scans were acquired after intravenous injection with [^{68}Ga]Ga-NODAGA-exendin-4 of 8 T1D patients with functional intrahepatic islet grafts (Tx-group: 4 men, 4 women), and 3 control patients with T1D awaiting islet transplantation (2 men, 1 woman). Islet functionality was biochemically assessed prior to imaging with a mixed-meal tolerance test (MMTT), and presented as C-peptide AUC and peak. Hepatic regions were identified with a minimum uptake (mean+2SD) based on controls. Kinetic modeling was applied to measure tracer accumulation in these regions to determine the distribution volume. Subsequently, the relation between PET signal and islet function was determined. Proton Magnetic Resonance Spectroscopy (1H-MRS) of a voxel positioned in the center of the liver was performed at 3T to check for hepatic steatosis. Relative lipid content was determined by time-domain fitting of the methylene lipid signal at 1.3 ppm and water signal at 4.7 ppm. ***Results:*** The control and Tx-group did not differ in age (58.7±5.5 vs. 57.6±9.1 years, p=1.00), BMI (24.5±4.5 vs. 24.2±3.8 kg/m^2, p=0.92) and HbA1c (62.3±6.1

vs. 46.3±10.0 mmol/mol, p=0.052), though C-peptide AUC (22.6 vs. 145.2 nmol.min/L, p=0.01)) and peak C-peptide (0.24 vs. 1.69 nmol/L, p=0.01)) significantly differed. The distribution volume (Vt) of the PET tracer was significantly higher in the Tx-group, indicating an increased retention of ^{68}Ga-exendin in the liver (0.43±0.02 vs. 0.57±0.08, p=0.01). There was no significant correlation found in the Tx-group between Vt and C-peptide production, nor between Vt and islet equivalents. No hepatic steatosis was observed in the subjects using 1H-MRS. ***Conclusion:*** These preliminary data of this explorative study indicate that dynamic PET imaging using ^{68}Ga-labeled exendin is a highly promising tool to monitor survival of pancreatic islet grafts in T1D patients. Imaging can contribute to further elucidate the correlation between beta cell mass measurements and C-peptide production using larger datasets. ***References:*** None

OP-509

Pancreatic uptake of radiolabeled exendin as a measure of beta cell mass in T2DM before and after bariatric surgery

L. Deden[1], M. Boss[2], F. Berends[3], H. de Boer[3], E. Hazebroek[1,4], M. Gotthardt[2];
[1]Vitalys, Rijnstate, Arnhem, NETHERLANDS, [2]RadboudUMC, Nijmegen, NETHERLANDS, [3]Rijnstate, Arnhem, NETHERLANDS, [4]Wageningen University & Research, Wageningen, NETHERLANDS.

Aim/Introduction: An approach for in vivo beta cell imaging is targeting the glucagon-like peptide-1 (GLP-1) receptor by radiolabeled exendin-4. Currently, the role of beta cells in onset, course and remission type 2 diabetes mellitus (T2DM) is not clear. Beta cell mass (BCM) and function (BCF) might be related to T2DM remission after gastric bypass surgery (RYGB). The aim of this study is examining BCF and pancreatic uptake of ^{68}Ga-exendin-4 before and after RYGB in patients with T2DM. ***Materials and Methods:*** Thirteen patients were included between December 2017 and June 2019. Arginine stimulation test, oral glucose tolerance test (OGTT) and ^{68}Ga-exendin-4-PET/CT were performed pre- and one year post-RYGB. Total pancreatic uptake of ^{68}Ga-exendin-4 per injected activity (kBq/MBq) was measured quantitatively on PET/CT as marker for BCM. ***Results:*** Preliminary analysis in nine patients with complete follow-up was performed. Six were female, mean age of 54 years and mean duration of T2DM was 12 years. Six patients were on insulin therapy (104±53IU/day), three on metformin (1-2g/day) preoperatively. Postoperatively, average BMI decreased from 39±4.7 to 27±3.7 kg/m^2 and HbA1c from 63±10 to 47±17 mmol/mol. Preoperatively, pancreatic uptake of ^{68}Ga-exendin-4 was lower in the insulin than in the metformin group; 1.55 [0.53-2.66] vs 2.95 [2.47-3.20] kBq/MBq (p=0.017). Also, c-peptide response during OGTT was smaller in the insulin than the metformin group (1.1 vs 2.9 nmol/l, p=0.015). Postoperatively, in the insulin group, one patient had complete remission (no antidiabetics, normal HbA1c), two patients had little improvement (insulin or sulfonylurea, unchanged HbA1c), three patients had improvements in between. Pancreatic uptake increased to 2.29 [1.86-3.06] kBq/MBq (p=0.025) in this group, which seems to be related to the degree of improvement; relative increase of 56-340% in three patients with most improvement, and 8-30% in patients with least improvement. In the metformin group all patients had complete remission. Pancreatic uptake decreased or remained stable; the relative change varied from -47% to +13%. ***Conclusion:*** As could be expected, patients with insulin dependent T2DM have lower beta cell mass and function compared to patients with non-insulin dependent T2DM. In the metformin group, average pancreatic uptake of ^{68}Ga-exendin-4 decreased after RYGB, probably reflecting reduction of beta cell hyperplasia. Contrary, insulin-dependent patients with remission or large improvement of T2DM, had increased pancreatic uptake. This may indicate towards recovered beta cell mass and has not been observed in patients so far. Mechanisms of recovering BCM and increasing pancreatic ^{68}Ga-exendin-4 uptake need further investigation. ***References:*** None

OP-510

Peptide Receptor Radionuclide Therapy in Patients with Neurofibromatosis Type 2 - Initial Experience

O. Kertels[1], M. Breun[2], H. Hänscheid[3], M. Kircher[4], P. Hartrampf[3], A. Schirbel[3], C. M. Monoranu[5], R. I. Ernestus[2], A. K. Buck[3], M. Löhr[2], C. Matthies[6], C. Lapa[4];
[1]Institute of Diagnostic Radiology, University Hospital Würzburg, Würzburg, GERMANY, [2]Department of Neurosurgery, University Hospital Würzburg, Würzburg, GERMANY, [3]Department of Nuclear Medicine, University Hospital Würzburg, Würzburg, GERMANY, [4]Department of Nuclear Medicine, University Hospital Augsburg, Augsburg, GERMANY, [5]Department of Neuropathology, Institute of Pathology, University of Würzburg, Würzburg, GERMANY, [6]Department of Neurosurgery, University Hospital Würzburg, Würzburg, GERMANY.

Aim/Introduction: Neurofibromatosis type 2 (NF2) is a genetic disorder that is associated with multiple tumors of the nervous system and approximately one-half of patients present with meningiomas. For patients with multifocal disease, somatostatin receptor (SSTR)-targeted peptide receptor radionuclide therapy (PRRT) might be a suitable systemic treatment option. ***Materials and Methods:*** Between March 2015 and August 2017, eleven NF2 patients (7 females and 4 males; mean age, 39 ± 12 years) with multifocal, progressive meningiomas underwent a median of 4 cycles of PRRT (range, 2 - 6 cycles). Acute and chronic adverse events were recorded according to NIH Common Toxicity Criteria (CTC) version 5.0. Follow-up magnetic resonance imaging (every 3 to 6 months), using the Response Assessment in

Neuro-Oncology response criteria for meningiomas, were used to assess treatment responses. ***Results:*** PRRT was well tolerated in all patients without any relevant acute adverse effects. Transient hematologic toxicity (CTC grade 3) was observed in 2 subjects. SSTR-directed radiopeptide therapy resulted in radiological disease stabilization in 6 out of 11 patients. Median progression-free survival of the entire cohort was 12 months (range, 1 - 55 months), overall survival was 37 months (range, 5 - 61 months), respectively. ***Conclusion:*** PRRT is feasible and well-tolerated in NF2 patients. It might be a suitable treatment option in subjects with multifocal disease. ***References:*** None

OP-511

Radiosynovectomy is effective in patients with knee replacement and chronic synovitis

K. Liepe*, M. Baehr;*
Klinikum Frankfurt, Frankfurt (Oder), GERMANY.

Aim/Introduction: After knee replacement, therapy resistant, chronic synovitis is a common problem which causes effusion and pain. Even after arthroscopic surgery of synovitis the rate of relapse is high. It has been hypothesized that radiosynovectomy (RSO) is a useful therapeutic modality in patients with knee replacement and chronic synovitis. ***Materials and Methods:*** In a single center study, a cohort of 55 patients with 57 knee replacements and chronic synovitis underwent RSO. In summary, 101 joints were treated using 182 ± 9 MBq of ^{90}Y-citrate. The number of performed RSOs ranged from 1 to 4 (53%, 21%, 23%, and 4%). Every patient received a ^{99m}Tc-MDP scintigraphy before first RSO and three months after every RSO. Long-term follow-up ranged from 5.7 to 86.7 months with a mean of 23.2 months. For qualitative analysis, an established 4 steps scoring was used (0 = no response or worsening, 1 = slight response, 2 = good response, 3 = excellent response). For quantification, the uptake was determined within the ^{99m}Tc-MDP scintigraphy soft tissue phase before and after therapy. ***Results:*** At the end of long-term follow-up 27% of patients have an excellent, 24% a good, 30% a slight and 20% no response. The duration of response was 7.5 ± 8.3 months with a maximum of 27 months. In patients with repeated treatment, the effect after the first therapy was lesser than in patients who received a single treatment in total. However, three months after the last RSO, patients with repeated treatment showed a similar effectiveness than single treated patients. At the end of long-term follow-up, patients with repeated RSOs had a higher effectiveness at similar duration response. In the ^{99m}Tc-MDP scan 65% of patients showed a reduction of uptake. When comparing subjective and objective response 78% of patients showed a concordance in both, symptoms and scintigraphy. Pilot histological analysis revealed that the synovitis is triggered by small plastic particles. ***Conclusion:*** RSO is an effective therapy in patients with knee replacement and chronic synovitis. It shows good subjective and objective response rates and long response duration. ^{99m}Tc-MDP scintigraphy is suitable for evaluation of response, since the results correlate with the symptoms. Repeated treatment leads to a stronger long-time response. The chronic synovitis is caused by plastic particles, which result from the abrasion of the polymeric inlay of endoprothesis. Consequently, the effect of RSO is restricted by the amount of foreign material within the knee joint. ***References:*** None

OP-512

Off the beaten path in oncology: active BAT by virtue of ^{18}F-FDG PET/CT

W. Jalloul[1]*, I. C. Grierosu*[1]*, T. Ionescu*[1]*, C. Stolniceanu*[1]*, R. Iacob*[2]*, R. Tibu*[1]*, A. Tarca*[1]*, M. Gutu*[1]*, D. Chetan*[2]*, C. Ştefănescu*[1]*, A. Naum*[2]*;*
[1]Biophysics and Medical Physics-Nuclear Medicine Laboratory, University of Medicine and Pharmacy „Grigore T. Popa", Iasi, ROMANIA, [2]Nuclear Medicine Laboratory, Regional Institute of Oncology, Iasi, ROMANIA.

Aim/Introduction: Brown Adipose Tissue (BAT) is a complex tissue which participates in the regulation of the whole body metabolism by producing a variety of adipokines. ^{18}F-FDG PET/CT, as a common imaging modality used in cancer assessment, can identify the hypermetabolic activity in activated BAT, also. The aim of this study is to emphasize the contribution of ^{18}F-FDG PET/CT to BAT detection, quantification and better understanding of this tissue biodistribution in oncological patients. ***Materials and Methods:*** After investigating ^{18}F-FDG PET/CT scans performed on the total number of patients, who were referred to our Nuclear Medicine Laboratory-between January 2018 and June 2019 for various oncological diagnoses, we selected the images with active BAT. We studied the BAT imaging pattern and measured SUV_{max} in multiple hyperfunctional tissue's localizations (cervical, supraclavicular, paravertebral, axillary, mediastinal and abdominal). ***Results:*** 42 positive scans were described in 38 patients with median age of 34.5 years. Female patients represented the highest rate of active BAT (57.89%). We noticed that 50% of patients were initially diagnosed with Hodgkin's Lymphoma (HL), 13.15% with Non-Hodgkin's Lymphoma (NHL), 10.53% with Cervical Cancer (CC), and with other cancer types under 5% each. ^{18}F-FDG high uptake in BAT was symmetric (sym) and homogeneous (hom), respectively, in 71.42% and 42.85% of images. The highest percentages were identified in NHL patients: 80% sym and 60% hom versus 66.7% sym and 38.1% hom in HL patients, versus 60% sym and 20% hom in CC patients. SUV_{max} in functional BAT ranged between 1.8 and 21.76 g/ml, with the highest median value of 5.98 g/ml in HL patients, followed by 5.68 g/ml in NHL patients and 4.73 g/ml in CC patients. Its maximum individual value was reached in supraclavicular localization in a HL patient (21.76

g/ml); however, the maximum uptake was identified in paravertebral region in a CC patient (8.67 g/ml). ***Conclusion:*** Biodistribution and SUV_{max} variation in different active BAT localizations raise a compelling hypothesis, of potential correlation between the oncological diagnosis and BAT activation, which needs further investigation. ***References:*** None

OP-513

The effectiveness predictive model of radioiodine therapy for Graves' disease in children and adolescents

A. Trukhin[1], *P. Rumyantsev*[1], *V. Saenko*[2], *D. Dzeytova*[1], *M. Sheremeta*[1], *V. Degtyarev*[1], *V. Yasuchenya*[1], *K. Slaschuck*[1], *S. Serzhenko*[1], *Y. Sirota*[1], *S. Zakharova*[1];
[1]*Endocrinology Research Cener, Moscow, RUSSIAN FEDERATION,* [2]*Nagasaki University, Nagasaki, JAPAN.*

Aim/Introduction: Graves' disease (GD) is a common cause of hyperthyroidism in patients of any age. In order to keep up with desirable effect and safety, radioiodine treatment (RIT) for hyperthyroidism accompanied by dosimetric estimations of therapeutic activity in children and adolescents requires preliminary risk assessment using predictive models. ***Materials and Methods:*** Study includes 55 children and adolescents (48 girls and 7 boys): age - 8÷17 (14.4±2.8) years; thyroid volume - 7.1÷94.5 (35.4±20.1) ml; Graves' orbitopathy in 32% patients; antithyroid drug (ATD) treatment - 3÷144 (38.9±26.3) months; thyrotoxicosis recurrence after ATD reduction - 40% patients; thyroid uptake 1.8÷41.2 (16.2±11.4) %; prescribed ^{131}I activities - 534÷1396 (896±203) MBq; maximum thyroid ^{131}I-uptake - 10÷60 (43.2±10.3) %; specific ^{131}I activity - 4.1÷27.0 (14.3±5.5) MBq/ml; maximum thyroid absorbed dose rate - 0.44÷2.9 (1.6±0.6) Gy/h. Follow-up period ranged from 6÷36 months (18.8±2.8); TSH, fT3, fT4 before RIT. Follow-up: monthly - TSH, fT3 and fT4; half-annually - TRAb, thyroid volume. Effect evaluation: positive outcome - 6 months hypothyroidism. Predictors of RIT success evaluation - multivariate logistic regression modeling, cross-validation; quasi-complete separation of predictors: the Firth's penalized likelihood method. Effect achievement assessment - Cox proportional hazard model. ***Results:*** Effect: hypothyroidism - 45 (81.8%) patients; euthyroidism - 2 (3.6%) patients; hyperthyroidism - 8 (14.6%). Thyroid volume reduction - 12.2÷94.3 (70.0±15.7) %. Predictors of effect: age (OR=1.31, 95%CI 1.06-1.60), thyroid volume (OR=0.90, 95%CI 0.83-0.96); fT4 prior RIT (OR=1.23 95%CI 1.03-1.48). ROC analysis: continuous variables {age, thyroid volume, fT4} - AUC=0.94 (95%CI 0.88-1.00), accuracy=0.86, SE=0.93, SP=0.50, PPV=0.89, NPV=0.63; AUC cross-validated = 0,91 (95%CI 0.846-0.99); categorical variables {age ≥11 years, thyroid volume≥43 ml, fT4≥13.5 pmol/l} - AUC=0.92 (95%CI 0.81-1.00), Accuracy=0.93, SE=0.93; SP=0.90, PPV=0.98, NPV=0.75; AUC cross-validated =0.87 (95%CI 0.73-1.00). The Cox modeling: volume affected the achievement of hypothyroidism: continuous variable - HR=0.98 (95%CI 0.96-0.99), categorical ≥43 ml - HR=0.32 (95%CI 0.15-0.71). Chance of achieving hypothyroidism: decreases effect by 2% per each additional 1 ml of thyroid volume each month; 3-fold lower in patients with thyroid volume≥43 ml. ***Conclusion:*** Developed models are useful instruments for RIT planning and prospective evaluation of outcome in children and adolescents with GD. Key efficacy predictors prior RIT - age, thyroid volume and fT4. Thyroid volume less than 43 ml, age older than 11 years and fT4 level higher than 13.5 pmol/l were associated with favorable result. Knowledge of pivotal factors of RIT efficacy provides broader opportunities for the exploration of more sophisticated predictive models. ***References:*** None

OP-514

^{18}F-FDG -PET/MRI in patients with Graves'orbitopathy

M. Weber[1], *J. Koenen*[2], *C. Deuschl*[3], *N. Bechrakis*[2], *K. Herrmann*[1], *A. Eckstein*[2], *I. Binse*[1], *M. Oeverhaus*[2];
[1]*Department of Nuclear medicine, University Hospital Essen, Essen, GERMANY,* [2]*Department of Ophthalmology, University Hospital Essen, Essen, GERMANY,* [3]*Institute for Diagnostic and Interventional Radiology and Neuroradiology University Hospital Essen, Essen, GERMANY.*

Aim/Introduction: Currently therapeutic management of patients with Graves' orbitopathy (GO) relies on clinical assessments and MRI scans. However, monitoring of inflammation remains difficult since external inflammatory signs like injection and chemosis do not necessarily represent the orbital disease activity and MRI scans cannot be used for follow-up examinations. Therefore, we aimed to evaluate the diagnostic value of ^{18}F-FDG-PET/MRI to assess the inflammation of GO patients. ***Materials and Methods:*** Patients with new onset of GO who were examined in our EUGOGO tertiary referral center were enrolled in this trial. All patients underwent ophthalmological and orthoptic examinations to evaluate the activity and severity of GO, as well as an ^{18}F-FDG-PET/MRI (Siemens Biograph mMR) with dual-time-point-imaging (immediately post injection and 60 minutes p.i.). A subset of PET parameters including maximum standardized uptake value (SUVmax), metabolic target volume (MTV), and total lesion glycolysis (TLG) were obtained separately per-eye and per-extraocular eye muscle (EOM). EOM thickness was measured on the co-registered MRI. Subsequently, differences in PET parameters among severity grades were analyzed and correlation with clinical findings assessed using Pearson's correlation coefficient (R^2). ***Results:*** Fourteen GO patients were enrolled and analyzed. Three showed mild, seven moderate-to-severe and four sight-threatening GO. Patients with severe GO showed statistically significant higher TLG than patients with mild GO (11.5 vs. 4; p=0.02) and higher MTV than patients with mild (11.8 vs. 4.7; p=0.03) and moderate (11.8

vs. 6.3; p=0.04) GO on the per-eye analysis of early static images. PET parameters did not show statistically significant differences among groups on the late acquisition images. Correlation between NOSPECS on one hand and MTV and TLG on the other was comparable among early and late static images (R^2= 0.49-0.61). Parameters obtained from individual EOMs were not correlated with its motility (p=0.17-1.0). ***Conclusion:*** TLG and MTV appear to be good discriminators for severe vs. mild/ moderate GO and show a significant correlation with NOSPECS. Whereas early PET acquisition compares favorably for GO severity assessment, the correlation of NOSPECS with PET parameters was equal for both time points. As expected, PET parameters of individual eye muscles were not correlated with associated eye motility, since fibrosis and not inflammation is mainly responsible for motility disorders. In conclusion, ^{18}F-FDG-PET/MRI is a promising modality for the assessment of GO severity with the potential to address limitations of current diagnostic standard procedures. Therefore, its diagnostic value should be subject of further studies on larger collectives. ***References:*** None

OP-515

Level of Thyrotropin Receptor Antibodies after Treatment with Radioactive Iodine

S. Gaberscek[1,2], D. Šfiligoj Planjšek[1], E. Pirnat[1], K. Zaletel[1], P. Jaki Mekjavić[3,2];
[1]Department of Nuclear Medicine, University Medical Centre Ljubljana, Ljubljana, SLOVENIA, [2]Faculty of Medicine, University of Ljubljana, Ljubljana, SLOVENIA, [3]Department of Ophthalmology, University Medical Centre Ljubljana, Ljubljana, SLOVENIA.

Aim/Introduction: For decades, radioiodine (I-131) therapy is effectively used for the treatment of Graves' disease (GD). It is known, that after I-131, serum level of thyrotropin (TSH) receptor antibodies (anti TSH-R) usually increases. Our aim was to evaluate the dynamic of this increase, since antiTSH-R may influence the course of Graves' orbitopathy. ***Materials and Methods:*** We reviewed medical records of all patients who were for the first time diagnosed with GD between the years 2005 and 2009. After initial treatment with antithyroid drugs, all patients were eventually treated with I-131. With respect to thyroid volume they received 555, 740, 925 or 1110 MBq of I-131. Serum level of antiTSH-R was measured with a second-generation human TRAK RIA kit (Brahms, Hennigsdorf, Germany). Values above 1.5 U/L were considered positive. Only patients with the known antiTSH-R value were included in the study. Results are expressed as median values and range. ***Results:*** Out of 724 patients, 335 patients, 253 females and 82 males, aged 45 (16-87) years had the known value of antiTSH-R before the first dose of I-131, 6 (2-12) weeks, 3 (2-10) months, 6 (3-15) months, 9 (3-43) months, and 12 (1-71) months after the first dose of I-131. Treatment with I-131 was performed 9 (0-31) months after the first presentation of GD. Out of 335 patients, 295 (88.1%) patients were cured with the first dose of I-131, while 40 (11.9%) patients needed the second dose of I-131 to achieve hypothyroidism or euthyroidism. When compared with the level before I-131 therapy (6.2 (0-41) U/L), level of antiTSH-R was significantly higher (p<0.001 for all) six weeks after I-131 therapy (10, (0-40) U/L), three months after I-131 therapy (31, (0-40) U/L), six months after I-131 therapy (30, (0-40) U/L), nine months after I-131 therapy (21, (0-40) U/L), as well as twelve months after I-131 therapy (12, (0-40) U/L). When compared with the highest level three and six months after I-131 therapy, level of antiTSH-R was significantly lower nine and twelve months after I-131 (p<0.001 for all). When compared with the level nine months after I-131, level of antiTSH-R was significantly lower twelve months after I-131 (p<0.001). ***Conclusion:*** Level of antiTSH-R increases up to six months after I-131 therapy and, afterwards, gradually decreases. This finding helps to plan a successful follow-up strategy for patients with GD, treated with I-131 therapy. ***References:*** None

OP-516

Therapeutic ^{131}I dose for the treatment of hyperthyroidism due to unifocal autonomy in compliance with the optimization principle of Council Directive 2013/59/EURATOM

C. Canzi, V. Longari, L. Florimonte, F. Buffoni, M. Castellani;
Fondazione IRCCS Ca' Granda Ospedale Maggiore Policlinico, Milan, ITALY.

Aim/Introduction: European guidelines for hyperthyroidism radiometabolic treatment suggest a target dose of 300-400Gy for unifocal autonomy. Aim of this study was to demonstrate that a lower dose and a personalised pretreatment dosimetric study can be effective in obtaining a stable euthyroid status avoiding both hyperthyroidism persistence and onset of hypothyroidism and in complying with the Council Directive 2013/59/Euratom optimization principle. ***Materials and Methods:*** We considered 123 patients with a minimum follow-up of 12 months (85F, mean age 61±13y, 78 with subclinical hyperthyroidism and 45 with overt hyperthyroidism) with a single nodule of mean weight of 14.6±10.4g (range: 3.8-57.3g). They were studied with a pretreatment patient-specific dosimetric study (based on administration of 48-111MBq of ^{123}I, on multiple uptake measurements with a gammacamera and on the MIRD formula corrected for the reduced uptake in therapy with respect to dosimetry) in order to calculate the therapeutic ^{131}I activity necessary to release to the nodule a dose of 140Gy. Afterwards, the dose released after the administration of the calculated ^{131}I therapeutic activity was evaluated by means of 6 uptake measurements at 2, 4, 24, 48, 96 and 168 hours and the use of the MIRD formula. Uptake measurements were performed with a gammacamera

equipped with a high energy collimator. After the first 12 months each patient clinical outcome was monitored with biochemical analysis (TSH, FT3 and FT4) once a year. Two subgroups of 72 and 41 patients had a follow-up of 5 and 10 years, respectively. ***Results:*** All patients were given a single therapeutic ^{131}I administration with a mean activity of 292±146MBq [range: 87-625MBq]. The mean dose released to the nodule was 143±37 Gy. Twelve months after therapy hyperthyroidism was healed in 97% of the patients and 8% were hypothyroid (serum TSH level over 4.2 uU/ml). In the subgroup followed for 5 years, 100% of the patients solved hyperthyroidism and 22% became hypothyroid and in the subgroup followed for 10 years they were 29%. ***Conclusion:*** This study demonstrated that a released target dose of about 140 Gy is effective in solving hyperthyroidism due to unifocal autonomy and in maintaining a long lasting euthyroid state in the most of the patients. This dose is quite lower than the value indicated by the European guidelines for hyperthyroidism treatment. The wide range of administered activity indicates the importance of a personalized pretreatment dosimetric study in order to obtain the clinical goal with the lowest activity. ***References:*** None

OP-517

Hyperactive thyroid nodules treated by radiofrequency ablation

F. Joosten*, H. de Boer, P. Veendrick, W. Bom, E. Bom, M. van Borren; Rijnstate Hospital, Arnhem, NETHERLANDS.*

Aim/Introduction: Toxic thyroid nodules are usually treated with radioactive iodine. This is associated with a high risk of permanent hypothyroidism. Radiofrequency ablation (RFA) may be a good alternative. ***Materials and Methods:*** Patients with a symptomatic toxic thyroid nodule, documented by suppressed TSH levels and a hot nodule on I-123 scan were treated by transisthmic, ultrasound-guided RFA, in an outpatient setting under local anesthesia. Follow-up was at least one year. ***Results:*** Over 40 patients were included, ranging in age from 37 - 75 years. All subjects had suppressed TSH levels. RFA was not associated with clinically significant adverse effects. Euthyroidism was achieved in the first 21 patients 11/21 patients (52%). A partial response with normalization of FT4 and FT3, and an incomplete improvement of TSH levels was observed in 6/21 patients (29%). Durin g the meeting the data of 20 more patients with a follow up of 1 year at least will be presented. Recurrence of hyperthyroidism has not been observed so far. ***Conclusion:*** These data suggest that radiofrequency ablation is a safe and promising treatment for symptomatic toxic thyroid nodules, with a low risk of permanent hypothyroidism. The recurrence risk of hyperthyroidism cannot be established due to the short follow up, however did not occur in this group of patients ***References:*** None

OP-518

HIFU For Thyroid Nodules An Effective Therapy For The Volume Reduction Of Thyroid Nodules

C. Körber*, N. Körber-Hafner; Nuclearmedicine, Fulda, GERMANY.*

Aim/Introduction: Themoablative therapies have been established as additional therapy options for thyroid nodules with local symptoms in comparison to thyroid surgery or radioiodine therapy in the last years. Therefore we used and analysed the HIFU therapy as a mean for the volume reduction of thyroid nodules. ***Materials and Methods:*** Since January 2019 we used the HIFU device of Theraclion SA (92240 Malakoff, France) for the therapy of thyroid nodules and fibroadenomas of the female breast. Only patients with local symptoms and often visible cervical protrusion underwent a therapeutic procedure. The volume of the thyroid nodules were analysed by two independent investigators 4, 12 and 36 weeks after therapy using ultrasound (My lab 9, Esaote, 15 MHZ) and the results were compared to the nodule volume before echotherapy. All possible side effects were registered as well as a possible palsy of the N laryngeus recurrens. We further analysed the statistical relation between the dose administered and the pretherapeutic volume. The statistical analysis was performed using Statistica 10, the significance level was defined with $p<0,05$. ***Results:*** 75 patients were treated in the time period. 36 weeks after the therapy 52 patients could be analysed (male 6, female 46). The pretherapeutic volume of the total volume was 26 ± 10 (ml), the pretherapeutic volume of the thyroid nodules volume was 4,9 ± 2,6 (ml) , after 4 weeks 2,6 ± 0,76 (ml) and after 36 weeks 0,6 ± 0,1 ml. (t-Test pretherapeutic volume//thyroid nodule volume after 36 weeks $p> 0,0003$). The mean volume reduction was 58 ± 12 %. Furthermore a good correlation between the administered dose and the pretherapeutic volume could be shown. A significant drop of the adminienstered dose could only be found for thyroid volume greater than 16 ml. ***Conclusion:*** HIFU therapy is a great non surgical therapy for thyroid nodules without any side effects discovered. After 36 weeks a good reduction of the thyroid nodule could be seen, even with thyroid volumes up to 16 ml. At all patients an improvement of the local symptoms could be observed without recognizable side effects. ***References:*** None

911

e-Poster Presentation Session 6: Physics - Hardware and Optimisation

Saturday, October 24, 2020, 09:00 - 10:30 Channel 11

EPS-086

Assessment of high-speed recording lung perfusion images provided by a high sensitivity 360° whole-body CZT camera in the pre-operative workup of lung cancer

***S. Melki**, A. Verger, G. Karcher, P. Marie, L. Imbert;*
CHRU Nancy, Vandoeuvre-lès-Nancy, FRANCE.

Aim/Introduction: The whole-body Veriton® 360° CZT-camera (Spectrum Dynamics Medical) is equipped with high-resolution detectors which can be positioned in close proximity to the chest, allowing high-speed recordings and further reconstructions of SPECT images using CT-based attenuation correction, not only for 3D images, but also for retro-projected images in a 2D planar mode (i.e. the multi-view planar (MVP) images). This study aimed to assess the relative percentages of right- and left lung-perfusions obtained with these MVP images, as well as with the 3D CZT-SPECT images, in comparison with those provided by conventional planar images from an Anger camera (Symbia, Siemens Healthineers), in lung cancer patients undergoing pre-operative workup. ***Materials and Methods:*** A SPECT/CT acquisition of less than 5 minutes was obtained with the 360° whole-body CZT camera after 370 MBq injection of 99mTc-labelled macroaggregate of albumin, and was immediately followed by a conventional Anger camera planar scintigraphy acquisition in 41 consecutive patients (66±12 years, 16 women) for whom this investigation was planned as part of pre-operative workup of a lung cancer. Right- and left-lung counts, obtained using dedicated software, were expressed in percentages of total pulmonary counts and comparisons made between values provided by the Anger camera planar views, and both the MVP and the SPECT images from the CZT-camera. ***Results:*** The percentages of lung perfusion obtained with the MVP images from the CZT-camera were strongly linked to those obtained with conventional planar images ($y = 0.99x + 0.38$, $R^2 = 0.98$), as well as to those obtained from the 3D CZT-SPECT images ($y = 1.02x - 1.46$, $R^2 = 0.99$). Values obtained with the 3D CZT-SPECT images and the conventional planar images were also strongly inter-correlated between each other ($y = 0.97x + 2.07$, $R^2 = 0.98$). Finally, each of the 3 image methods identified the same 21 patients, and no additional patients, as having an asymmetrical lung function (i.e. with a relative right lung function setting outside the 45 to 55% normal range). Additionally, high-speed 3D CZT-SPECT enabled per lobe assessment. ***Conclusion:*** Both MVP and native 3D SPECT images from this CZT-camera may be used instead of conventional planar scintigraphy for quantitative assessment of relative lung perfusion and function in the pre-operative workup of lung cancer. However, only the 3D images provide additional values at the lobar scale. ***References:*** None

EPS-087

An Assessment of the Accuracy of Quantitative SPECT/CT Imaging Using Tc99m and Lu177

***J. Johnson**, K. Adamson, T. Alkahtani;*
Guy's and St Thomas' Hospitals NHS Foundation Trust, London, UNITED KINGDOM.

Aim/Introduction: Quantitative SPECT imaging is a valuable tool in the diagnosis and staging of disease, and for assessing therapeutic response. An increasing number of such commercial applications are being developed and it's important that the accuracy, precision and source of errors for quantitative data is known. Calibration of the imaging system and optimisation of imaging and reconstruction parameters ensures the uncertainties are established. This study validated quantitative data for Tc99m and Lu177 acquired on two Siemens Symbia Intevo Bold SPECT/CT systems, using Siemens xSPECT Broad Quantification. ***Materials and Methods:*** The imaging systems were calibrated for each isotope using a point source and a homogeneous cylindrical source of known Tc99m and Lu177 activity. An IEC NEMA Image Quality phantom comprising 6 spherical inserts of 10mm-37mm diameter was filled with an activity concentration ratio of 10:1 between the spheres and background for Tc99m and Lu177 on separate occasions. Following imaging using a clinical protocol and reconstruction using xSPECT Broad Quantification workflows, SUV-based quantitative analysis was performed and resolution recovery coefficient (RRC) curves generated. RRC is defined as the ratio of the measured to expected SUV. Two SUV parameters were calculated for each sphere; SUV_{max} and $SUV_{50,meas.}$ $SUV_{50,meas}$ is defined as the average SUV in the VOI defined by the 50% isocontour of the sphere. ***Results:*** The SUV_{max} and $SUV_{50,meas}$ for Tc99m and Lu177 clearly exhibited the impact of the partial volume effect for smaller volumes. The RRC results show that for the smallest volume (10mm) using $SUV_{50,meas}$ the uptake of Tc99m was underestimated by up to 83%, and 89% for Lu177. For SUV_{max} RRC for the 10mm sphere was 0.182 and 0.174 for Tc99m images on each of the systems, and 0.134 and 0.110 for Lu177. For the largest sphere (37mm), the RRC using SUV_{max} for Tc99m was 1.298 and 1.208, and for Lu-177 0.687 and 0.629. For Tc99m, for spheres between 10mm and 37mm, the RRC using SUV_{max} ranged from a significant underestimation to an overestimation. The great variation in results for volumes comparative to those in clinical images could greatly

impact conclusions drawn. For Lu177, the RRC shows the significant underestimation of Lu177 uptake for all spheres. This understanding is key for accurately reporting clinical images and assessing therapeutic response. ***Conclusion:*** Validation of software providing quantitative data from SPECT/CT imaging is essential before its application in clinical setting to ensure understanding of accuracy and impact on patient management. ***References:*** None

EPS-088

Can Half-Time Bone SPECT Replace the Standard Bone SPECT?

M. El-Sayed*, J. O'Brien, T. Jones, A. D'Sa, A. Notghi;*
Sandwell & West Birmingham Hospitals NHS Trust, Birmingham, UNITED KINGDOM.

Aim/Introduction: At our centre, SPECT-CT is performed as an add-on to planar bone scan (BS) in oncology patients who have focal increased uptake of unclear cause. The additional SPECT-CT increases the total scan time which affects the patient throughput. This study evaluates if add-on SPECT-CT with reduced scan time can replace standard time SPECT-CT for oncology patients. ***Materials and Methods:*** 20 BS for oncology patients who had add-on SPECT-CT were selected. Images were acquired using a dual-head gamma camera. Acquisition parameters were as follows: imaging performed 2 hours after 550-650 MBq [99mTc]-HDP injection, 128 x 128 matrix, 120 steps, 10 seconds/step. Poisson resampling was used to mimic reduced scan time of 5 seconds/step & 3 seconds/step. The scans were processed using GE Xeleris resolution recovery software producing 3 data sets; SPECT-CT10, SPECT-CT5 & SPECT-CT3. This resulted in 60 scans. These were anonymised, randomised, then reported by 2 radionuclide radiology consultants. The number of lesions on SPECT-CT and final diagnoses were recorded. Using a visual analogue scale (1-10), the scans were scored for quality and reporter confidence. Wilcoxon signed-rank test was used for comparisons. ***Results:*** Comparing SPECT-CT10 (gold standard) to SPECT-CT5, the latter showed statistically significant inferior quality (p=0.027). However, all lesions were detected and their were no errors in the final diagnosis. There was no difference in reporter confidence (p=0.982). Comparing SPECT-CT10 to SPECT-CT3, 12/20 SPECT-CT3 had interpretation errors (missed lesions=58%. False positive lesions=42%). SPECT-CT3 was significantly inferior in quality and reporter confidence (p=0.000 & 0.019 respectively). ***Conclusion:*** We conclude that SPECT-CT5 can replace SPECT-CT10 as add-on to inconclusive planar BS in oncology patients at our centre. This will reduce SPECT acquisition time by 50% without compromising the clinical diagnosis or reporter confidence. However, SPECT-CT3 is not acceptable with our current scanning protocol. ***References:*** None

EPS-089

Design and implementation of a network-based educational platform for simulation of a benchtop PET system

I. Mohammadi[1,2]*, P. M. M. Correia*[1]*, I. F. C. Castro*[1]*, P. M. C. C. Encarnação*[1]*, A. L. M. Silva*[1]*, J. F. C. A. Veloso*[1]*;*
[1]*i3N-Physics Department, University of Aveiro, 3810-193, Aveiro, PORTUGAL,* [2]*Department of Basic Sciences, Faculty of Medicine, Sari Branch, Islamic Azad University, Sari, IRAN, ISLAMIC REPUBLIC OF.*

Aim/Introduction: Nuclear medical imaging has the power of bringing together different areas of scientific knowledge: mathematics, physics, biochemistry, engineering and medical sciences. Using an efficient way to deliver medical imaging knowledge and establishing an effective learning environment for students, technologists and medical specialists has long been a goal for educators. Limited efforts have been made for step-by-step interactive education of the nuclear medical imaging data generation process, the fundamental education component of tomographic imaging. Based on this idea, a network-based user-interactive learning system including a graphical user interface simulation script creator to run on GATE platform was implemented, featuring text, animation, data acquisition, mathematical concepts of image creation, simulation and image reconstruction courses, so as to optimally fulfill PET imaging education tasks. ***Materials and Methods:*** A benchtop PET scanner considered for training and entry-level research. Using SQL as database and ASP.NET as server-end language, ADO.NET database access technology was adopted to design and implement the educational platform's structural functions, question/answer module and exam creation with hierarchical subject categorization. In addition, a dedicated graphical interface webform page provides flexibility and simplicity in defining an input file for simulating a benchtop PET system on the already popular GATE Monte Carlo simulation platform, benefiting from the existing capabilities and large selection of underlying Geant4 libraries for physical processes. ***Results:*** The system's interactive learning environments provided multiple means of representation and expression for the learner through text and graphics, animated simulations and other media combinations. Interactive education aids in increasing students' comprehension, motivation level and learning perception. The implemented system is widely accessible using any web browser and multiple users can work individually and simultaneously. Furthermore, to simplify the selection of parameters like phantom materials, source type, position and activity, a single configuration page lets the user control simulation parameters by setting their respective values, replacing aliases in correspondent macro files. Default properties will be used when undefined by the user. GATE macros are

subdivided into major parts, describing the phantom(s), source selection, digitizer, selection of physics models and visualization options. Scripts that used to be entered in GATE have been generated and compiled by the program as a single compressed file accessible by authenticated users. ***Conclusion:*** This system allows generalizing the practical learning of PET imaging, a valuable resource for students, technologists and researchers of nuclear medicine, medical imaging, biomedical engineering and other fields that imply the knowledge of PET imaging. ***References:*** None

EPS-090

Emission time optimisation for [^{68}Ga]Ga-PSMA-11 with a SiPM PET/CT based on phantom measurements

P. Fragoso Costa[1], W. Jentzen[1], F. Süßelbeck[1], W. P. Fendler[1,2], C. Rischpler[1], K. Herrmann[1], M. Conti[3], D. Kersting[1], M. Weber[1]; [1]Department of Nuclear Medicine, University Hospital Essen, University of Duisburg-Essen, Essen, GERMANY, [2]German Cancer Consortium (DKTK)-University Hospital Essen, Essen, GERMANY, [3]Siemens Medical Solutions, Knoxville, TN, UNITED STATES OF AMERICA.

Aim/Introduction: In clinical routine protocols with [^{68}Ga]Ga-PSMA-11, the emission time per bed position is currently 2-4 min. The potential for reducing the total acquisition time is particularly valuable for prostate cancer patients undergoing [^{68}Ga]Ga-PSMA-11 PET/CT examinations enhancing patient comfort and throughput. The aim of this study was to identify the optimal reconstruction parameters allowing a minimal acquisition time in [^{68}Ga]Ga-PSMA-11 examinations on a Biograph Vision using silicon photomultipliers (SiPM) PET/CT, preserving acceptable lesion detectability and spatial resolution. ***Materials and Methods:*** Two phantoms were used: a soft-tissue tumour phantom consisting of six spheres (ranging from 6.5 mm to 28.0 mm in diameter) mounted in an abdominal cavity, and a line phantom to estimate the reconstructed PET spatial resolution. The soft-tissue tumour spheres were filled with activity concentrations (ACs) that were derived from clinical data. Phantom data were acquired in list-mode, single bed position. Images with emission data ranging from 30 to 300 s, in 30-s increments, and a reference image with 10-min emission data were reconstructed. Iterative image reconstruction (OSEM) with and without point-spread-function (PSF) and/or time-of-flight (TOF) options were applied using different iterations, Gaussian filters, and voxel sizes. The resulting image quality was assessed using the following metrics: lesion detectability of each sphere was assessed using the contrast-to-noise ratio (CNR); a CNR equal or larger than 8 was considered acceptable. For image quantification, the percentage maximum AC (AC-max) deviations between the images at different emission times and the reference image were calculated; a percentage deviation range of ±20% was considered acceptable. ***Results:*** Sphere and background ACs of 20 kBq/mL and 1 kBq/mL were selected, respectively. The line sources were filled with an AC of 10 MBq/mL (approximately 30 MBq in the field-of-view). The optimized emission time duration was 60 s using OSEM-TOF or OSEM-TOF+PSF (4 iterations, 4-mm Gaussian filter, and almost isotropic voxel size of 3-mm side length), resulting in a PET spatial resolution of 6.3 mm. The metrics at 60 s were $CNR_{OSEM+TOF}$=15 and $CNR_{OSEM+TOF+PSF}$=24; AC-max deviations were below 20%. ***Conclusion:*** Based on the phantom data, acquisition time on a SiPM PET/CT can be reduced by a factor of 2-3, while maintaining lesion detectability similar to our standard clinical protocol. Spatial resolution was maintained at the same order than the smallest lymphatic lesions in prostate cancer. Impact of reduced acquisition time on patient comfort, image quality/pelvic urine background, and throughput will be assessed in future clinical studies. ***References:*** None

EPS-091

Optimization of 18F-FDG oncological examination on a TOF-PET/CT scanner: results of a multicenter preliminary study

A. Zorz[1], E. Richetta[2], M. Poli[2], M. A. Rossato[1], R. E. Pellerito[2], G. M. Sacchetti[3], M. Burei[1], R. Matheoud[3]; [1]Istituto Oncologico Veneto IOV - IRCCS, Padua, ITALY, [2]AO Ordine Mauriziano di Torino, Turin, ITALY, [3]AOU Maggiore della Carità, Novara, ITALY.

Aim/Introduction: In PET/CT 18F-FDG oncology practice, image quality is influenced by different factors, such as the administered activity, patient dimension, acquisition and reconstruction parameters. The aim of this study was to investigate the possible dependence of image quality and lesion detectability on emission scan duration and patient Body Mass Index (BMI), in order to optimize oncological acquisition protocol. ***Materials and Methods:*** 30 oncological patients were selected for the study (15 with BMI<25 kg/m^2 (L) and 15 with BMI>25 kg/m^2 (H)) and acquired on three Philips Ingenuity TF PET/CT scanners installed in different Italian hospitals. Patients were injected with 3 MBq/kg of 18F-FDG. PET images were acquired in list-mode with an emission scan duration (ESD) of 120 seconds per bed position and retrospectively reconstructed at 120, 90, 75, 60 (default scan time), 45 and 30 seconds. Images were reconstructed by using the default clinical protocol. Image quality was described by using the Coefficient of Variation (CV), defined as the ratio between the standard deviation and the average activity concentration on a 1500 mm^2 ROI placed in the central part of the liver. For the lesions outlined in whole body examinations, Contrast-to noise ratio (CNR) was evaluated as ((CL-CB)/CB)/(σB/CB)), where CL, CB and σB are the average concentration in the lesion, the average concentration in the background and the standard deviation in the background, respectively. Overall,

31 lesions were analysed. The impact of ESD and BMI as independent variables was assessed separately on CV and CNR by means of the ANOVA test ($p<0.05$). ***Results:*** Both ESD and BMI resulted to be predictors of CV and CNR. In particular, CV decreases by increasing ESD ($p<0.05$), though a significant increase in CV can be observed only between ESD=60s vs ESD=120s and ESD=60s vs ESD=30s. As expected, CV increases by increasing the patient's BMI, with an average increase of 22% from L to H BMI group. As for CNR, ANOVA showed a significant increase with increasing ESD and by decreasing patient's BMI (+23%). ***Conclusion:*** Our preliminary data suggest that an improvement in image quality in terms of noise and contrast-to-noise ratio is still achievable on a TOF-PET/CT scanner by increasing ESD. Overweight patients will further benefit from such protocol optimization. ***References:*** None

EPS-092

The impact of patient's body shape on PET image quality in digital and analogic PET/CT

K. Weyts*, E. Quak, I. Licaj, C. Lasnon, R. Ciappuccini, J. Savigny, G. Foucras, S. Bardet, C. Jaudet;*
Centre François Baclesse, Caen, FRANCE.

Aim/Introduction: New digital PET shows higher temporal resolution and more stable count rate than analogic PET. This could limit PET image quality degradation with increasing patient's body mass (index) (BMI) observed in analogic PET/CT. We wanted to describe patient's body shape's influence on PET image quality in digital (dPET/CT) and analogic PET/CT (aPET/CT). The robustness was tested by using 2 different protocols for dPET/CT. ***Materials and Methods:*** We retrospectively studied the relation between patient's weight, BMI, fatty mass and FDG PET image quality, evaluated by liver coefficient of variance (CV_{liv}) and visually by 2 specialists. 177 unique patients and exams were performed on dPET/CT (weight 35-127 kg; BMI 15-44 kg/m^2): with Protocol 1 (N=52) : 3MBq/kg FDG (±8%) - 2min/bed position- 3D OSEM with point spread function (PSF) reconstruction; 2 iterations 10 subsets (2i10s) and 2mm voxel size diameter, or Protocol 2 (N=125): 4MBq/kg FDG (±8%) -1min/bed position-3D OSEM PSF reconstruction ; 4i4s, 2mm voxel size diameter), implemented in a period of increased patient number scanning. 77 different patients and exams were analyzed on aPET/CT (weight 38-130 kg; BMI 14 -52 kg/m^2) with following imaging protocol: 4MBq/kg FDG (±8%) - 2min40s/bed position if BMI < 25 kg/m^2 and 3min40s/bed position if BMI ≥ 25 kg/m^2 - 3D OSEM PSF reconstruction ; 3i21s, 4mm voxel size diameter. We used STATA version 15 for statistical analyses, with two sided $p<0.05$ considered to be statistically significant. ***Results:*** In multivariable analyses we found a positive association between weight, BMI, fatty mass and CV_{liv} on each camera and in each protocol ($p\leq0.004$ for dPET/CT; $p\leq0.04$ for aPET/CT). Best linear fit ($r^2=0,61$) and highest correlation Pearson coefficient (R=0,78) was obtained between CV_{liv} and weight as well as fatty mass on dPET/CT with 3MBq protocol 1; $p\leq0,046$. No significant inferiority was observed between dPET/CT protocol 2 (Pearson R= 0,61 for weight) and aPET/CT (Pearson R= 0,42 for weight) with substantially longer scanning time (p=0,07). For dPET/CT a significant increase by 23% of mean CV_{liv} was found in weight category ≥90 kg (CV_{liv}=0,149 +/-0,018) versus <70kg (CV_{liv}=0,121+/- 0,009) for the 3MBq protocol 1 (p=0,0001), and 25% with the 4MBq protocol 2 (CV_{liv}= 0,142+/-0,014 versus 0,113 +/-0,013; $p<0,0001$). A concordant, inverse association was found between body shape and visual scores on each camera ($p\leq0.001$). ***Conclusion:*** FDG PET image quality decreases especially with increasing patient's weight on digital and analogic PET/CT, imposing an adaptive imaging protocol also on digital PET/CT. ***References:*** None

EPS-093

Emission time reduction for 2-[^{18}F]FDG examinations in lymphoma patients with a PET/CT with SiPM - a feasibility phantom study

P. Fragoso Costa[1]*, A. Bramer*[1]*, M. Weber*[1]*, D. Kersting*[1]*, M. Conti*[2]*, W. P. Fendler*[1,3]*, C. Rischpler*[1]*, K. Herrmann*[1]*, W. Jentzen*[1]*;*
[1]Department of Nuclear Medicine, University Hospital Essen, University of Duisburg-Essen, Essen, GERMANY, [2]Siemens Medical Solutions, Knoxville, TN, UNITED STATES OF AMERICA, [3]German Cancer Consortium (DKTK)-University Hospital Essen, Essen, GERMANY.

Aim/Introduction: A new generation of PET/CT scanners, equipped with silicon photomultipliers (SiPM), provide increased sensitivity and faster coincidence timing resolution. These improvements may translate in reduced acquisition time or administered activity without compromising lesion detectability and quantitative accuracy. In the case of paediatric patients undergoing 2-[^{18}F]FDG PET/CT for malignant lymphomas, a decrease of either acquisition time or administered activity is particularly beneficial for the patient. The aim of this study is to optimise the standard emission time (140-s emission time per bed, 70-kg patient and 210-MBq tracer activity) from 2-[^{18}F]FDG PET/CT procedures in lymphoma patients on a Biograph Vision using SiPM PET/CT using an abdominal tumour phantom. ***Materials and Methods:*** The phantom consists of 6 spheres with inner diameters of 6.5 to 28.0 mm inserted on a torso-like background cavity. Injected sphere and background activity concentrations (ACs) were derived from clinical data. Phantom data were acquired in list mode with a scan time duration of 10 min. Different image reconstructions with varying iterations and Gaussian filters were performed using emission data between 30 and 300 s in 30-s increments. A reference image was reconstructed with 10 min emission time per bed position. Detectability was assessed using the

contrast-to-noise ratio (CNR); a CNR equal or larger than 8 was considered to be sufficiently visible. Quantification was assessed using the maximum AC (AC-max). The percentage AC-max deviations were calculated between the images at different emission times and the reference image; a percentage deviation range of ±20% was considered acceptable. ***Results:*** A representative signal-to-background ratio of 5:1 and a sphere AC of approximately 13 kBq/mL was selected based on the clinical data. The smallest lesion identified on the clinical dataset was comparable to the 9.7-mm diameter sphere. The following metrics refer to the 9.7-mm diameter sphere as larger spheres possess CNR values above 8, irrespective of image reconstruction methods and parameters. The optimised emission time per bed position was 60 s using OSEM+TOF or OSEM+TOF+PSF (4 iterations, 4-mm Gauss and 2-mm nearly cuboid voxel size). At 60 s emission time, $CNR_{OSEM+TOF}$ and $CNR_{OSEM+TOF+PSF}$ values were 8 and 12, respectively. Absolute AC-max percentage deviations were below 20%. ***Conclusion:*** In this phantom study, acquisition time on a PET/CT with SiPM allows a reduction of approximately a factor 2-3 while maintaining lesion detectability. Impact on a reduced acquisition time will be assessed in future clinical studies. ***References:*** None

EPS-094

Gender related difference in PET SUV in overweight and obese people

I. Sarikaya[1], *A. Sarikaya*[2], *A. N. Albatineh*[1];
[1]*Kuwait University Faculty of Medicine, Kuwait, KUWAIT,*
[2]*Trakya University Faculty of Medicine, Edirne, TURKEY.*

Aim/Introduction: It is well known that standardized uptake value (SUV) is overestimated in patients with high body mass index (BMI). In this study we aimed to determine the gender related difference in SUV in overweight and obese patients. ***Materials and Methods:*** F-18 fluorodeoxyglucose (FDG) whole body positron emission tomography/computed tomography (PET/CT) images of the patients with BMI higher than normal (overweight: 25-29.9 and obese: 30 and above) were analyzed retrospectively. SUV_{max} and SUV_{mean} of the liver and blood pool were measured. BMI and lean body mass (LBM) were measured via online calculators. SUVs were corrected by LBM to obtain SUV_{LBM} (SUL). ***Results:*** Thirty four (34) females (mean age 58 ± 9 years) and 33 males (mean age 63 ± 7 years) were included. Among females, 31 were obese and 3 overweight. Among males, 20 were overweight and 13 obese. There was a significant difference between median SUV-SUL differences among males and females in all patients (overweight and obese) and also in obese patients (P value < 0.001). Including all patients, SUVs were approximately 43.4% higher than SULs in females and 35.5% higher than SULs in males. Including only obese patients (31 female and 13 male), SUVs were approximately 45.3% higher than SUL in females and 39.5% higher than SULs in males. Mean weight of the patients was 86.8 kg (44.9% fat) in obese females and 103 kg in obese males (39.9% fat). ***Conclusion:*** SUVs are overestimated in both genders who are overweight and obese but overestimation of SUVs is higher in females as compared to males. This is mainly due to higher percentage of body fat in females. ***References:*** 1. Lucignani G, Paganelli G, Bombardieri E. The use of standardized uptake values for assessing FDG uptake with PET in oncology: a clinical perspective. Nucl Med Commun. 2004;25:651-6.2. Zasadny KR, Wahl RL. Standardized uptake values of normal tissues at PET with 2-[fluorine 18]fluoro-2-deoxy-D-glucose: variations with body weight and a method for correction. Radiology 1993; 189:847-850.3. Sugawara Y, Zasadny KR, Neuhoff AW, et al. Reevaluation of the standardized uptake value for FDG: variations with body weight and methods for correction. Radiology. 1999;213:521-5.4. Sarikaya I, Albatineh A, Sarikaya A. Re-visiting SUV-weight and SUV-lean body mass in FDG PET studies. J Nucl Med Technol. Accepted for publication 2019.

EPS-095

Study on the difference between peripheral lung cancer and inflammatory pseudotumor based on the method of image histology

C. Ma;
Shandong Cancer Hospital and Institute, Shandong First Medical University and Shandong Academy of Me, Jinan, CHINA.

Aim/Introduction: This study is to distinguish peripheral lung cancer and pulmonary inflammatory pseudotumor using CT-radiomics features extracted from PET/CT images. ***Materials and Methods:*** In this study, the standard 18 F-flurodeoxyglucose positron emission tomography/computed tomography (18 F-FDG PET/CT) images of 21 patients with pulmonary inflammatory pseudotumor (PIPT) and 21 patients with peripheral lung cancer were restrospectively collected. The dataset was used to extract CT-radiomics features from regions of interest (ROI),using,then,statistical methods to screen CT-radiomics features,which could distinguish peripheral lung cancer and PIPT. And the ability of radiomics features distinguished peripheral lung cancer and PIPT was estimated by receiver operating characteristic (ROC) curves. ***Results:*** A total of 435 radiomics features were extracted, of which 20 could difference between peripheral lung cancer and PIPT. these features were seen in 16 of 330 Gray-Level Co-occurrence Matrix features, 1 of 49 Intensity Histogram features, 1 of 5 Neighbor Intensity Difference features, 2 of 18 Shape features. area under the curve (AUC) of these features were 0.7310.075, 0.717, 0.737, 0.7480.038, respectively. ***Conclusion:*** Radiomics features extracted from non-contrast CT based on PET/CT images can help distinguish peripheral lung cancer and PIPT. ***References:*** [1] Vanderhoek M, Perlman SB , Jeraj

R.Impact of different standardized uptake value measures on PET-based quantification of treatment response.[J]. Journal of nuclear medicine : official publication, Society of Nuclear Medicine,2013,54(8):1188-94. DOI: 10.2967/jnumed.112.113332[2] Westerterp M , Pruim J , Oyen W , et al. Quantification of FDG PET studies usingstandardised uptake values in multi-centre trials: effects of image reconstruction, resolution and ROI definition parameters [J]. European Journal of Nuclear Medicine and Molecular Imaging, 2007, 34(3):392-404. DOI: 10.1007/s00259-006-0224-1[3] Zhang J,Qiu QT,Duan JH,et al. Variability of radiomic features extracted from multi-b-value diffusion-weighted images in hepatocellular carcinoma[J]Translational cancer research,2019,48(1), 152-163,DOI: 10.1002/jmri.26037

EPS-096

Development of an anthropomorphic rodent phantom

W. McDougald[1], N. Weir[2], R. Collins[3], A. Tavares[1];
[1]BHF-Centre for Cardiovascular Science, College of Medicine & Veterinary Medicine, Edinburgh, UNITED KINGDOM, [2]Department of Medical Physics, NHS Lothian, Edinburgh, UNITED KINGDOM, [3]University of Edinburgh College of Arts, Edinburgh School of Architecture and Landscape Architecture, Edinburgh, UNITED KINGDOM.

Aim/Introduction: Develop a 3D printed tissue equivalent material (TEM) anthropomorphic rodent phantom with the intent to replace using animals when optimizing imaging protocols and assist in accurate scanner quality control validation. Research using positron emission tomography/computed tomography (PET/CT) continues its rapid increase as a key imaging technique across multiple biomedical preclinical research fields. Preclinical PET/CT is a powerful, pivotal imaging tool supporting investigations and evaluations of underlining biological mechanisms. Preclinical PET/CT is fully quantitative, providing biological functional information, whilst CT provides anatomical information. Additionally, the expansion of utilizing CT, as a dedicated system and with PET, SPECT or optical increases the need for new imaging protocols in several biomedical research fields. When designing or optimizing a preclinical experimental imaging protocol, usually, a priori knowledge of obtainable optimization is not known. To gain this information, small laboratory animals are generally used for testing. ***Materials and Methods:*** A CT acquisition of a scheduled 1 rodent was exported into OsiriX and PMOD for volume and surface rendering. The rodent's brain, heart, liver, kidney and lungs were imaged and exported in the same manner. All files were exported into Rhinoceros 3D CAD software. The prepared CAD files were used for 3D printing the anthropomorphic TEM rodent phantom. Phantoms were made with combinations of Tango Black Plus M, Vero Clear and Vero White Plus M 830. Furthermore, the phantom was designed with a void for lungs and a calcium hydroxyapatite (CaHA) skeletal insert. HU values were extracted by dawning volumes of interested using PMOD. Calculated 3D material linear attenuation coefficient were compared to tissue. ***Results:*** Selected commercially available 3D printing materials produced measured HUs within accepted ranges for soft tissue. Calculated 3D material linear attenuation coefficient compared well to measured attenuation coefficients. Tango Black Plus M measured the lowest values at -38HU. Perspex and Vero Clear measured -12HU and -17HU, respectively. Vero White Plus measured the greatest at 22HU. No tissue measured HUs for lung or cortical bone at the preclinical tube voltage. ***Conclusion:*** X-ray properties and HUs of materials corresponded to those of human tissues at diagnostic and preclinical energies for soft tissue. No 3D material measured a close similarity to lung or cortical bone. Collected data and the developed 3D printed TEM phantom support the usage of an anthropomorphic rodent phantom for preclinical protocol optimizations and quality control; replacing the use of animals. ***References:*** None

EPS-097

Optimization of Quantitative ^{18}F-DCFPyL PET using a Realistic Anthropomorphic Phantom with Shell-less Radioactive Epoxy Lesions

R. Fedrigo[1,2], D. Kadrmas[3], P. Edem[4], L. Fougner[4], I. S. Klyuzhin[1,2], M. P. Petric[4], F. Bénard[1,2,4], A. Rahmim[1,2,4], C. Uribe[2,4];
[1]BC Cancer Research Centre, Vancouver, BC, CANADA, [2]University of British Columbia, Vancouver, BC, CANADA, [3]University of Utah, Salt Lake City, UT, UNITED STATES OF AMERICA, [4]BC Cancer, Vancouver, BC, CANADA.

Aim/Introduction: Block sequential regularized expectation maximization (BSREM), as compared to OSEM reconstruction, has received significant interest for its ability to reach convergence with minimal noise amplifications. PET images with ^{18}F-DCFPyL (a PSMA-based tracer) have shown superior results in detecting prostate cancer. However, few phantom studies have evaluated the quantitative accuracy of BSREM for high contrast, small diameter (sub-10mm) lesions observed in ^{18}F-DCFPyL scans. This study aimed to design a realistic phantom experiment to optimize the reconstruction parameter (β) of the BSREM algorithm for quantification of prostate cancer metastasis imaged with ^{18}F-DCFPyL. In addition, the quality of the reconstructed images was also evaluated. ***Materials and Methods:*** Twenty-seven spherical lesions (diameters 3mm-16mm) were cast using Epoxy resin infused with 3 activity concentrations of ^{22}Na-NaCl. The diameters and concentrations were chosen based on an analysis of 10 prostate cancer patients imaged with ^{18}F-DCFPyL. A highly realistic anthropomorphic phantom [1] which features a liver, lungs, bladder, and ureters, was filled with ^{18}F-FDG

to achieve target concentrations determined from the patient segmentations. Ten scans were performed at 30min intervals using a GE Discovery D690 PET/CT scanner. Bed and scan durations were scaled to maintain similar count statistics. Images were reconstructed with OSEM (24,32 subsets, 1-4 iterations) and BSREM (32 subsets, 25 iterations, γ=2, β=100,150,200,250,300,400,500,650,800). Regions-of-interest were drawn with MIM (MIM Software Inc.) using a 40% of SUV_{max} fixed threshold and MIM's PET Edge+ method. ^{22}Na lesion ground truth activity concentrations were determined from a scan with fully decayed background. Metabolic tumour volume (MTV), contrast, signal-to-noise ratio, and recovery coefficients (max, mean, and peak) were calculated for each sphere size. ***Results:*** SUV_{mean} recovery coefficients were 130.4+/-13.5% and 98.3+/-6.9% (16mm), and 99.7+/-4.7% and 69.4+/-0.8% (10mm), for β=150 and β=300 respectively. Contrast-to-noise ratios for β=150 and β=300 were 55.3+/-14.4 and 65.3+/-5.6 (16mm), and were 15.4+/-1.8 and 4.6+/-1.4 (6mm). Signal-to-noise ratios were comparable with maximum values 81.2+/-1.0 (β =150) and 105.2+/-0.07 (β =300). PET Edge+ MTV bias was 0.2+/-0.01% at 6mm, but deviated 56.2+/-1.7% at 12mm. The 40% threshold deviated by over 176% for spheres smaller than 10mm, but reduced to 14.9% at 12mm. ***Conclusion:*** Our results suggest that β=150 and β=300 are optimal parameters for quantification of ^{18}F-DCFPyL PET scans for lesions of sizes of 3-10mm and 12-16mm, respectively. PET Edge+ segmentation is recommended for segmenting lesions of 3-10mm, while the 40% threshold showed better results on larger 12-16mm lesions. ***References:*** [1] Kadrmas,et al. J. Nucl. Med.,50,8,1315-1323, 2009.

EPS-098

Dose-scan-time optimization for ^{18}F-PSMA-PET using a digital PET scanner

P. Bergwerff[1,2], D. Koopman[2], B. N. Vendel[2], C. H. Slump[3], J. A. van Dalen[4];
[1]Technical Medicine, University of Twente, Enschede, NETHERLANDS, [2]Department of Nuclear Medicine, Isala hospital, Zwolle, NETHERLANDS, [3]TechMed Centre, University of Twente, Enschede, NETHERLANDS, [4]Department of Medical Physics, Isala hospital, Zwolle, NETHERLANDS.

Aim/Introduction: There is an increasing use of prostate specific membrane antigen (PSMA) in PET imaging of patients with prostate cancer. Current literature suggests to use a tracer dose of typically 2 MBq/kg without specifying the scan-time. We aimed to determine the dose-scan-time product (DSTP) that is needed for adequate ^{18}F-PSMA-PET imaging using a digital PET/CT scanner. ***Materials and Methods:*** ^{18}F-PSMA-1007 PET/CT scans (Vereos, Philips Healthcare) of 10 consecutive patients (mean weight 81 kg, range 54-100 kg) with initial or recurrent prostate cancer were used. Data were acquired using 2 MBq/kg and 4 minutes per bed position (DSTP=8). Previously, we determined optimal image reconstruction settings using ordered subset expectation maximization and DSTP=8 for ^{18}F-PSMA-PET, and we applied those optimized parameters in this study: 3 iterations, 7 subsets and point spread function modelling. Images based on DSTPs of 4, 5, 6 and 7 were simulated by reconstruction of clipped list-mode data. Three nuclear medicine physicians assessed the image quality based on a 4-point scale. Moreover, a semi-quantitative assesment was performed by measuring the SUV of reported lesions and background noise in the aorta. ***Results:*** Visual assessment of 50 ^{18}F-PSMA-PET datasets (10 patients × 5 reconstructions) showed comparable and adequate image quality for all DSTPs (p=0.72, p=0.72, p=1.0, p=1.0 for DSTPs of 4, 5, 6 and 7, respectively). There was a tendency towards lower scores for patients with the highest body weight. Reducing DSTP resulted in a noise increase up to 20% for DSTP=4, but SUVs of reported lesions (n=32) remained stable. The standard deviation of differences in SUV between default and reduced DSTPs increased up to 14%. ***Conclusion:*** Using optimized reconstruction settings for ^{18}F-PSMA-PET, the dose-scan-time product can be reduced to at least 4 MBq/kg/min for the Vereos PET/CT scanner. For example, when applying a tracer-dose of 2 MBq/kg, an acquisition time of 2 minutes is suggested. Future studies could investigate the relation between patient's bodyweight and ^{18}F-PSMA tracer dose for a constant image quality across all patients. ***References:*** None

EPS-099

Results of different formulations on hepatic Standardized Uptake Value in pediatric FDG PET

B. de Keizer[1,2], A. F. van der Hoeven[1], L. Miltenburg[1], R. van Rooij[1];
[1]UMC Utrecht, Utrecht, NETHERLANDS, [2]Prinses Maxima Center for Pediatric Oncology, Utrecht, NETHERLANDS.

Aim/Introduction: [^{18}F]FDG PET is increasingly used in diagnosis and follow-up of pediatric cancer patients(1). For quantification of FDG uptake in tissue, the standardized uptake value (SUV) is used. SUV can be calculated using different formulations. The body weight (BW) corrected formulation and lean body mass (LBM) corrected formulations (according to James or Janmahasatian) are mostly used. For measurements in adults the LBM janmahasatian formulation is advised(2). It is not known which formulation is best for use in pediatric patients. To investigate results of different formulations for hepatic SUV in paediatric patients, a retrospective analysis was performed. ***Materials and Methods:*** Consecutive [^{18}F]FDG PET performed in pediatric aged <16 years between December 2018 and April 2020 were retrospectively reviewed. Liver SUV was measured with a 3-cm-diameter spheric region of interest in the right liver lobe. SUV was calculated using BW (SUVbw) and sex specific LBM formulations according to James and

Janmahasatian (SULjames and SULjanmaha). ***Results:*** A total of 236 patients were reviewed (92 female and 144 male). Mean age was 9.9 (range 0.8 - 15.8) and 9.8 (range 0.4 - 15.7) for female and male patients respectively. Mean weight was 36.5 (range 7 - 96) and 38.9 (range 7 - 99) for female and male patients respectively. Mean SUVbw was 1.41 (1.46 female; 1.37 male), mean SULjames was 1.21 (1.26 female; 1.18 male), mean SULjanmaha was 1.22 (female 1.30; male 1.19). All measurements had a positive correlation with weight ranging from r = 0.71, for SULjanma for male patients till r = 0.82 for SUVbw for female patients. ***Conclusion:*** The used formulations lead to different mean hepatic SUV, with highest values for SUVbw and lower values for SULjames and SULjanma. All formulations have positive correlation with weight, leading to increasing liver SUV with increasing weight. ***References:*** 1. Uslu L, Donig J, Link M, Rosenberg J, Quon A, Daldrup-Link HE. Value of18F-FDG PET and PET/CT for evaluation of pediatric malignancies. J Nucl Med. 2015.2. Tahari AK, Chien D, Azadi JR, Wahl RL. Optimum lean body formulation for correction of standardized uptake value in PET imaging. J Nucl Med. 2014.

EPS-100

SPECT/CT with 99mTc MIBI Diagnostic Value In HyperparathyroidismComparsion To Other Alternative Ultrasound & Four-dimensional parathyroid CT

M. Algarni*; KFMMC, Dhahran, SAUDI ARABIA.*

Aim/Introduction: Accurate preoperative anatomic localization of hyperfunctioning parathyroid adenoma (HTP) critical importance in surgical planning for minimally invasive parathyroidectomy. SPECT/CT with 99mTc-sestamibi (99mTc-MIBI) important for detection of any metabolic active hyperfunctioning gland(s) localized in the neck or mediastinum. Ultrasonography(US) and Four-dimensional parathyroid CT (4D CT) increasingly offers potential advantages as an alternative primary investigation and is a common second-line investigation. ***Materials and Methods:*** Retrospective study included 28 patients aged 26 - 87 years (mean age 49±7). Female to male ratio was 4:1. The follow-up period ranged from 3 to12 months, the mean being 6months. In all cases of biochemically confirmed hyperparathyroidism, the average levels were: Ca total - 2.65±0.05mmol/l (NV 2.12-2,52), PTH=72±32pg/ml (NV 1.5-9.2). Allunderwent parathyroidectomy, and an adenoma was confirmed. Scintigraphy was performed with SPECT/CT (GE model 670pro NM/CT). 4D CT done with Toshiba aquilion 64.Ultrasonography (US) was done with ACUSON SC2000 by means of 10MHz linear probe. ***Results:*** The exact localization hyperfunctioning parathyroid gland was identified 23 (82.2%) out of 28 patients by means of SPECT/CT. The remaining 5 patients need an alternativeinvestigation and second-line investigation which we started with US parathyroid adenomia was identified 2 (40%) out of 5 patients. All remaining 5 patients further invastigatedwith 4D-parathyroid CT scan hyperfunctioning parathyroid gland was identified 4 (80%) out of 5 patients. One patients (3.5%) out of 28 patients was dignosed intraoperatively. ***Conclusion:*** SPECT/CT with 99mTc-sestamibi appears promising with an important key role in diagnosis hyperfunctioning parathyroid gland but further imaging with 4D-parathyroid CT scanmay needed particularly when we attempting to diagnose the precise site of disease localization in presurgical planning. ***References:*** 1-Casara D et al. 99mTc-MIBI radio-guided minimally invasive parathyroid surgery planned basis of a preoperative 99mc-pertechnetate/99mTc-MIBI and ultrasound. Eur J Nucl Med 2000;27:1300-4. 2- Casara et al. 99mTc-MIBI radio-guided minimally invasive parathyroidectomy: Nucl Med Commun 2019;40:96-105.3- Beheshti M et al. PET/CT in the assessment of primary hyperparathyroidism compared with 99mTc-MIBI SPECT/CT: a prospective dual-centre study in 100 patients. Eur J Nucl Med Mol Imaging 2018;45:1762-71. 4- Huber GF et al. Benefit of PET imaging in parathyroid surgery. Eur Radiol 2018;28:2700-7.5- Kluijfhout WP et al. PET/MR imaging in patients with primary hyperparathyroidism. Radiology 2017;284:460-7. 6- Haciyanli M et al. Accuracy of preoperative localization studies J Am Coll Surg 2003;197:739-46. 7- Doppman JL et al. parathyroid hormone assay. Radiology 1983;148:31-5. 8- Gooding GA et al. Parathyroid aspiration biopsy under ultrasound guidance in the postoperative hyperparathyroid patient. Radiology 1985;155:193-6.

EPS-101

Recent Developments in Beta Radio Guided Surgery

F. Collamati*[1], S. Morganti[1], E. Bertani[2], M. Colandrea[2], M. Ferrari[2], L. Funicelli[2], S. Papi[2], E. Pisa[2], A. Collarino[3], A. Giordano[3], D. Maccora[3], C. Mancini-Terracciano[1], M. Cremonesi[4], C. M. Grana[5], A. Florit[6], N. Bizzarri[7], G. Scambia[7], F. Fanfani[7], R. Faccini[8]; [1]INFN Rome, Rome, ITALY, [2]Istituto Europeo di Oncologia, Milan, ITALY, [3]Istituto di Medicina Nucleare, Fondazione Policlinico A. Gemelli IRCCS - Università Cattolica del Sacro Cuore, Rome, ITALY, [4]Unità Ricerca sulle Radiazioni, Istituto Europeo di Oncologia, Milan, ITALY, [5]Divisione di Medicina Nucleare, Istituto Europeo di Oncologia, Milan, ITALY, [6]Istituto di Medicina Nucleare, Università Cattolica del Sacro Cuore, Rome, ITALY, [7]Fondazione Policlinico Universitario A. Gemelli, IRCCS, UOC Ginecologia Oncologica, Dipartimento per la salute della Donna e del Bambino e della Salute Pubblica, Rome, ITALY, [8]Università Sapienza, Rome, ITALY.*

Aim/Introduction: Radio Guided Surgery (RGS) is a technique helping the surgeon to achieve complete resection of tumours, using a radio tracer injected to the patient before surgery, and detecting emitted radiation by means of a dedicated probe.This technique today uses gamma emitting isotopes together with gamma detectors. A novel approach to RGS using pure beta- decaying isotopes

was recently proposed [1], aiming at overcoming major limitations of the current one, that are given by the high penetration of gamma particles.First validation case has been Y90 as radio isotope (pure B- decay, Emax=2.23MeV) and an organic scintillator as detector element of the probe. Despite having shown a good sensitivity and high efficacy in Y90-DOTATOC applications, in particular in Meningioma and gastrointestinal NET ex-vivo samples, the limited number of pure beta- emitting radio pharmaceuticals limits the applicability of this promising technique ***Materials and Methods:*** : In this context, i.e. to increase the number of application cases of the beta-RGS technique, we have been investigating new detector technologies/solutions (including solid state detectors), aimed at increasing the sensitivity to low energy particles, that would allow the technique to be performed also with lower-endpoint radio pharmaceuticals. Moreover, we also investigated the possibility to use positron emitting radio pharmaceuticals, exploiting the high sensitivity to beta particles of our detector, together with its substantial transparency to photons. In parallel with an experimental campaign of ex-vivo tests on Ga-PSMA prostate tumor samples, we developed laboratory measurements and Monte Carlo simulations regarding a possible application with F18 and Cu isotopes (64-67), in particular in gynaecologic applications. Also a possible application to pancreatic tumours is under study, using 90Y-DOTATOC. ***Results:*** The novel approach to beta RGS demonstrated to be highly effective if performed with pure beta- emitting radiopharmaceuticals in meningioma and gastrointestinal NET ex vivo samples. Moreover, pancreatic NETs are expected to be a possible application case. Furthermore, improved detectors allow also the use of positron emitting radio pharmaceuticals, as demonstrated by Ga-PSMA prostate cancer ex-vivo tests, and the use of 18F is also likely to be a possibility. ***Conclusion:*** The novel approach to beta RGS we proposed in the past years, initially tailored at pure beta- emitting isotopes, thanks to retrospective studies, ex-vivo tests and detector optimisation is now expanding towards a higher number of application cases. ***References:*** [1] E. S. Camillocci et al., Scientific Reports, 4 (2014), "A novel radioguided surgery technique exploiting beta- decays" 4401.

EPS-102

An IAEA tool to assess staffing needs in Nuclear Medicine

M. Marengo[1], *M. Dondi*[2], *J. Bomanji*[3], *S. A. Baigorria*[4], *S. Bouyoucef*[5], *E. W. Elias*[6], *T. E. Pascual*[7], *D. Paez*[2];
[1]*University of Bologna, Bologna, ITALY,* [2]*Nuclear Medicine and Diagnostic Imaging Section - IAEA, Vienna, AUSTRIA,* [3]*Institute of Nuclear Medicine - University College of London, London, UNITED KINGDOM,* [4]*Fundacion Escuela Medicina Nuclear, Mendoza, ARGENTINA,* [5]*Department of Nuclear Medicine CHU Bab el Oued, Algiers, ALGERIA,* [6]*Department of Nuclear Medicine - Singapore General Hospital, Singapore, SINGAPORE,* [7]*Philippine Nuclear Research Institute - St Lukes Medical Center, Gloabal City, PHILIPPINES.*

Aim/Introduction: Staff costs are one of the most expensive components of nuclear medicine services (NMS). Introduction of new imaging modalities or therapies, new roles and responsibilities, let alone a fresh new start of a new NMS, may require assessment or re-assessment of staffing needs to ensure the most efficient use of resources. To the best of our knowledge, there are no models, applicable to NMS of different complexity, to assess staffing needs. ***Materials and Methods:*** A model was created, based not only on clinical workload but also on "infrastructure" parameters, such as number and type of equipment; level of Radiopharmacy activity and presence of in-house cyclotron. Indeed, additionally to the clinical work, which include attendance to multidisciplinary meetings and discussion with referring physicians, staff need to spend time for setting the equipment; run QA/QC and user-operated maintenance and patient- and equipment-related administrative tasks. In case of teaching hospitals, a slightly higher weight has been given. In our model, considering annual leaves, sick leaves, absences for training, working time is set at 1640 hours/year, down from an average of 2000 hours, and is consistent with a replacement factor of 1.22, frequently used by Human Resources. The most relevant factor, however, is the amount of time required to carry out clinical procedures, i.e. their "weight". As suggested by the Center for Medicare and Medicaid Services, a standard basic "work unit" has been set at 15 min. Then weights of each procedure consider the number of "15-minutes work units", needed to covering all aspects, from patient admission and interview, discussion with referring physicians and attendance to meetings, through administration of radiopharmaceuticals and other medication, reporting, patients assistance, data processing, storing, archiving, etc. The needs for Radiopharmacy staff are based on previous IAEA publication, while contribution of medical physicists is not included, since another IAEA tool already exists. ***Results:*** This model was tested on data existing in an IAEA data base for NMS of different levels and by an international panel, considering their own Departments and other simulated or real configurations. The agreement between existing staff and calculated needs was found to be within 15 %. ***Conclusion:*** This model calculates staffing needs in term of FTE nuclear medicine physicians, radiopharmacists, NM technologists, and nurses and could be used for planning new departments, before introduction of new technologies or for periodical reviews of resources utilization. ***References:*** None

1001

CME 8: Emergency Conditions in Paediatric Nuclear Medicine

Saturday, October 24, 2020, 10:40 - 12:10 Channel 1

OP-519

Nuclear Medicine in Urgent Paediatric Conditions - A Clinical Perspective

A. Yaari; Schneider Children's Medical Center, Emergency Medicine Department (ER), Petah Tikva, ISRAEL.

OP-520

Nuclear Medicine Techniques in Urgent Paediatric Conditions - Part 1

Z. Bar-Sever; Schneider Children's Medical Center in Israel, Nuclear Medicine Department, Petah Tikva, ISRAEL.

OP-521

Nuclear Medicine Techniques in Urgent Paediatric Conditions - Part 2

I. Roca Bielsa; HU Vall Hebron, Paediatric Nuclear Medicine Unit, Barcelona, SPAIN.

1002

Joint Symposium 15 (EANM/ETA-CG): Systemic Therapeutic Options in Advanced Thyroid Cancer

Saturday, October 24, 2020, 10:40 - 12:10 Channel 2

OP-522

Personalized Therapy in View of Molecular Signatures

C. Spitzweg; Medizinische Klinik und Poliklinik IV, Ludwig-Maximilians-University Munich, Munich, GERMANY.

OP-523

Update on Tyrosine Kinase Inhibitors

D. Handkiewicz-Junak; Department of Nuclear Medicine and Endocrine Oncology, Maria Sklodowska-Curie Memorial Cancer Center and Institute of Oncology, Gliwice, POLAND.

OP-524

News from Redifferentiation

J. Nagarajah; Radboud University Medical Centre, (Radboudumc), Department of Radiology and Nuclear Medicine, Nijmegen, NETHERLANDS.

1003

Joint Symposium 16 (EANM/EACMFS): Role of Hybrid Imaging in Jaw and Skull Conditions

Saturday, October 24, 2020, 10:40 - 12:10 Channel 3

OP-525

Jaw Osteomyelitis / Osteonecrosis - Clinical Presentation, Diagnosis, Therapy

B. Brokstad Herlofson; Department of Oral Surgery and Oral Medicine, Oslo, NORWAY.

OP-526

Jaw Osteomyelitis / Osteonecrosis – Imaging

K. Strobel; Radiology and Nuclear Medicine, Cantonal Hospital Lucerne, Lucerne, SWITZERLAND.

OP-527

Incidental Findings in Jaw and Skull on Bone Scan and SPECT/CT

E. Panagiotidis; Theageneio Cancer Center, Thessaloniki, GREECE.

1004

CTE 4: NET Imaging and Therapy

Saturday, October 24, 2020, 10:40 - 12:10 Channel 4

OP-529

NET Imaging in Conventional NM - Is There Still a Role for Conventional NM in NET Imaging?

N. Girotto; Klinički bolnički centar Rijeka, Clinical department of nuclear medicine (Head of Department of Diagnostic imaging), Rijeka, CROATIA.

OP-530

PET/CT in NET Tumours - Applications and Novelties

W. Cholewinski; Poznan University of Medical Sciences, Electroradiology Department, Poznan, POLAND.

OP-531

NET Therapy – Oncologist's Point of View

P. Martenka; Greater Poland Cancer Centre, Radiotherapy Department, Poznan, POLAND.

1005

M2M Track - TROP Session: New Kids on the Block - New Tracers

Saturday, October 24, 2020, 10:40 - 12:10 Channel 5

OP-532

[18F]Crizotinib PET imaging to address the impact of the P-glycoprotein transport function at the blood-brain barrier on the brain delivery of the drug

F. Caillé[1], M. Sardana[2], M. Goislard[1], L. Breuil[1], M. Schou[3], G. Wrigley[4], N. Tournier[1], C. Elmore[2], B. Kuhnast[1]; [1]CEA, Orsay, FRANCE, [2]Astra Zeneca, Gothenburg, SWEDEN, [3]Astra Zeneca, Stockholm, SWEDEN, [4]Astra Zeneca, Cambridge, UNITED KINGDOM.

Aim/Introduction: Crizotinib is a tyrosine kinase inhibitor approved for non-small cells lung carcinoma. The brain accumulation of crizotinib is mainly restricted by the P-glycoprotein (P-gp, ABCB1), a major efflux transporter at the blood-brain barrier, which limits its efficacy against CNS metastases. We hypothesized that the brain delivery of crizotinib can be improved using a clinically feasible pharmacological protocol of P-gp inhibition. We report the preparation of an original precursor for isotopic radiolabelling of [18F](R,S)-crizotinib and the first brain PET images in rats with and without ABCB1 inhibition. ***Materials and Methods:*** A racemic spirocyclic hypervalent iodine(III) complex was synthesized for radiosynthesis with [18F] fluoride. Radiofluorination was realized using a TRACERlab FX_{FN} module and conditions were optimized monitoring the conversion rate by radio-TLC. The crude radiotracer was purified by semi-preparative HPLC. Radiochemical yield (RCY) and molar activity (A_m) were assessed by radio-HPLC. Dynamic PET acquisitions were performed in anesthetized rats during 60 min after [18F](R,S)-crizotinib injection (37 ± 5 MBq) with or without ABCB1 inhibition using tariquidar (8 mg/kg, 15 min i.v. prior to radiotracer injection). ***Results:*** The racemic precursor was synthesized from 2,4-dichloro-1-iodobenzene in 5 steps and 2% yield. Up to 52% radiochemical conversion was obtained using fluorine-18 and tetraethylammonium bicarbonate as a base in DMF at 160 °C for 10 minutes. Deprotection with 3 M $HCl_{(aq)}$ at the same temperature for 10 minutes was quantitative. Ready-to-inject [18F](R,S)-crizotinib was obtained in 5 % RCY and 60 ± 10 GBq/µmol (n = 7) A_m. PET baseline experiments showed no penetration in the rat brain whereas [18F](R,S)-crizotinib enters the brain under ABCB1 inhibition using tariquidar. ***Conclusion:*** An original precursor for crizotinib radiofluorination was synthesized and [18F](R,S)-crizotinib was successfully radiolabelled. The first PET images of [18F](R,S)-crizotinib in the rat brain demonstrated the relevance of P-gp inhibition to improve its brain delivery. Investigation with the enantiomerically pure [18F](R)-crizotinib are ongoing. ***References:*** None

OP-533

Validation of [11C]glyburide as PET probe for imaging OATP function in humans

S. Marie[1,2], L. Breuil[1], Z. Chalampalakis[1], L. Becquemont[2], M. Goislard[1], F. Caillé[1], C. Comtat[1], M. Bottlaender[1], N. Tournier[1]; [1]Laboratoire d'Imagerie Biomédicale Multimodale (BIOMAPS), Université Paris-Saclay, CEA, CNRS UMR9011, Inserm UMR1281, Service Hospitalier Frédéric Joliot, Orsay, FRANCE, [2]Hôpital Bicêtre, Assistance Publique des Hôpitaux de Paris, Le Kremlin Bicêtre, FRANCE.

Aim/Introduction: Organic Anion Transporting Polypeptides (OATP, SLCO) transporters control the influx of many endo/exogeneous compounds across biological membranes. OATPs are mainly expressed in hepatocytes (OATP1B1/1B3/2B1) where they mediate the hepatic uptake of many drugs and control hepatobiliary elimination. OATPs have also been detected at other blood-tissue interfaces (OATP1A2/2B1) suggesting a role for drug distribution to tissues. Imaging probes with improved pharmacokinetic properties are needed for determination of OATP function at the blood-tissue interface. Glyburide (GLB) is transported by OATP1B1/1A2/2B1 and [11C]GLB successfully revealed OATP function using PET imaging in non-human primates[1]. ***Materials and Methods:*** Three healthy male volunteers (< 30 years) underwent two consecutive [11C]GLB dynamic PET/MR scans (126±55 MBq i.v.; 30 min), before and after an injection of the prototypical OATP-inhibitor rifampicin (9 mg/kg i.v.). Time-activity curves (TAC) were obtained in the liver and the arterial blood-pool (left ventricle + aorta). During PET acquisitions, venous blood samples were withdrawn to test [11C]GLB metabolism and binding to plasma proteins. Liver distribution was estimated by the ratio of areas under the curves $AUC_R = AUC_{liver}/AUC_{blood}$. The initial uptake clearance of [11C]GLB from blood to liver (CL_{uptake}) was estimated using an integration plot analysis. Paired t-test were used to compare outcome parameters obtained in each subject. ***Results:*** PET images revealed the predominant uptake of [11C]GLB in the liver. Rifampicin drastically decreased the PET signal in the liver while obviously increasing radioactivity in the vasculature. With or without rifampicin-pretreatment, [11C]GLB was slowly metabolized with >90 % parent compound at 30 min and binding to plasma proteins was >99 %. There was a significant 2.62±0.24-fold decrease in AUC_R consistent with the 3.90±0.99-fold decrease in CL_{uptake} obtained after rifampicin inhibition. ***Conclusion:*** [11C]GLB benefits from suitable in vivo stability and its liver uptake is inhibited by rifampicin, thus demonstrating an importance of OATP-mediated transport. The decrease in CL_{uptake} induced by rifampicin is higher than that of previous PET radioligands used for imaging OATP in humans. This may be explained by the limited passive diffusion of [11C]GLB, probably related to highly lipophilic physico-chemical properties and high binding to plasma proteins. Thus, transport of [11C]GLB across membranes is predominantly governed by OATP-mediated transport which makes it a sensitive and quantitative probe to investigate the importance of extra-

hepatic OATP-function in humans. ***References:*** 1. Tournier and al. Effects of Selected OATP and/or ABC Transporter Inhibitors on the Brain and Whole-Body Distribution of Glyburide. AAPS J. 15, 1082-1090 (2013).

OP-534

^{18}F-VUIIS1008 as a potential novel PET probe for PET imaging of rheumatoid arthritis in a rat model

X. Su[1], L. Wang[1], W. Dong[1], Z. Guo[2];
[1]Department of Nuclear Medicine, Zhongshan Hospital Xiamen University, Xiamen, CHINA, [2]Center for Molecular Imaging and Translational Medicine, Xiamen University, Xiamen, CHINA.

Aim/Introduction: Early diagnosis and therapy are crucial to control optimally disease progression and achieve good prognosis in Rheumatoid arthritis (RA). Currently, it is difficult to efficiently diagnose and monitor early-stage RA. The aim of the present study is to developd ^{18}F-labeled TSPO ligand VUIIS1008 (^{18}F-VUIIS1008) as a novel PET probe for imaging of rheumatoid arthritis. ***Materials and Methods:*** The tosylate substrate was labeled with fluorine-18 at its 2-fluoroethylmoiety using a tosyloxy-for-fluorine nucleophilic aliphatic substitution labeled to obtain ^{18}F-VUIIS1008. The labeling efficiency, radiochemical purity, lipophilicity and stability were determined in vitro. In vitro cellular uptake and competitive binding assays were performed on RAW264.7 macrophage cells. Micro-PET studies were conducted on mice with rheumatoid arthritis induced by Complete Freund's Adjuvant. ***Results:*** The labeling yields and radiochemical purity of ^{18}F-VUIIS1008 were (41±5) % and more than 98 %, respectively. Lipophilicity was 1.58±0.03 and specific radioactivity was 4107 Ci/mmol. ^{18}F-VUIIS1008 displayed good stability, which the radiochemical purity was more than > 98%, in saline at 4 h. It also exhibited high specific TSPO binding in RAW264.7 macrophage cells in vitro. The uptake ratio was (14.0 ± 0.3) % at 1 h after incubation, and decreased significantly after adding cold ligand (Figure 1). The competitive binding study showed that^{18}F-VUIIS1008 has high affinity for TSPO with IC50 0.05nM (Figure 2). Micro-PET imaging demonstrated uptake of ^{18}F-VUIIS1008 on the left arthritic ankles was gradually increased from 0.5 h to 1 h, which was (1.33±0.01) % ID/g at 1 h. The uptake was 2-2.5 times compared with contralateral normal ankles. The uptake of ^{18}F-VUIIS1008 Micro PET imaging showed different levels at various days in inflammation models, with a peak of inflammation at day 7 and 29 (Figure 3), suggesting that it was associated with the mechanism that the inflammation model was performed by CFA. ^{18}F-VUIIS1008 Uptake in the arthritic ankles could be largely blocked by PK11195 or cold ligand (VUIIS1008) (Figure 4). ***Conclusion:*** ^{18}F-VUIIS1008 can be readily radiolabelled, clearly visualized arthritis and exhibited low background, suggesting its potential as a novel promising molecular probe targeting TSPO for arthritic PET imaging. ***References:*** None

OP-535

Preliminary evaluation of a novel PET tracer for fatty acid oxidation, ^{18}F-AS3504073-00

Y. Ohshima[1,2], Y. Yagi[1,2], X. Chen[1,2], S. Mühlig[1,2], H. Fushiki[3], Y. Murakami[3], T. Higuchi[1,2,4];
[1]Department of Nuclear Medicine, University Hospital, University of Würzburg, Würzburg, GERMANY, [2]Comprehensive Heart Failure Center, University Hospital, University of Würzburg, Würzburg, GERMANY, [3]Bioimaging Research Laboratories, Astellas Pharma Inc., Tsukuba, JAPAN, [4]Okayama University, Graduate School of Medicine, Dentistry and Pharmaceutical Sciences, Okayama, JAPAN.

Aim/Introduction: Fatty acid oxidation (FAO) is a major process to satisfy the high-energy requirement of the myocardium and is a promising therapeutic target for heart failure. Radiolabeled thia-substituted fatty acid, such as 18-^{18}F-fluoro-4-thia-oleate (FTO), has been introduced as a marker of myocardial FAO. A newly developed FTO analogue ^{18}F-AS3504073-00 has been reported aiming to improve tracer characteristics for cardiac imaging. In this study, the subcellular kinetics of uptake and trapping of ^{18}F-AS3504073-00 was characterized and compared to ^{125}I-15-(p-iodophenyl)-3(R,S)-methylpentadecanoic acid (^{125}I-BMIPP) and 1-^{14}C-palmitate in freshly isolated mouse cardiomyocytes. Furthermore, biodistribution studies were performed with ^{18}F-AS3504073-00 in mice. ***Materials and Methods:*** All animal experiments were conducted in compliance with the current laws of the Federal Republic of Germany. Cardiomyocytes were freshly isolated from healthy mice according to the previous reports with some modifications (1). Cardiomyocytes were treated with ^{18}F-AS3504073-00, ^{125}I-BMIPP or 1-^{14}C-palmitate in 0.5% BSA/DMEM at 37°C or 4°C. CD36-dependent uptake and metabolic trapping were examined by treating cardiomyocytes with each tracer in the presence of specific inhibitors. For biodistribution studies, mice were euthanized at 60 min after intravenous injection of ^{18}F-AS3504073-00 and the radioactivity in the tissues of interest was measured. ***Results:*** ^{18}F-AS3504073-00, ^{125}I-BMIPP, and 1-^{14}C-palmitate were time-dependently taken up into cardiomyocytes, while CD36 inhibitor, sulfo-succinimidyl oleate, could significantly inhibit the uptake of these tracers ($P<0.01$). The cell-associated radioactivity of three tracers was significantly reduced in the presence of etomoxir, a specific inhibitor for carnitine palmitoyltransferase-1 (CPT-1) ($P<0.05$). These results indicate that ^{18}F-AS3504073-00, as well as ^{125}I-BMIPP and 1-^{14}C-palmitate, was taken up into cardiomyocytes via CD36, then transported into mitochondria via CPT-1. Extracellular release after exposure of the tracers in the presence or absence of etomoxir showed that ^{18}F-AS3504073-00 was rapidly washed out from

cytosol, but remained in mitochondria. While ^{125}I-BMIPP and 1-^{14}C-palmitate remained in both cytosol and mitochondria. Biodistribution studies showed that ^{18}F-AS3504073-00 was rapidly cleared from the blood and accumulated significantly in the heart and liver. The SUV in the heart, heart-to-blood ratio, and heart-to-muscle ratio were 4.9±0.5, 22.0±3.2, 27.8±1.2, respectively. ***Conclusion:*** ^{18}F-AS3504073-00 was taken up into cardiomyocytes via fatty-acid transporter CD36 and specifically trapped in mitochondria due to FAO. Furthermore, biodistribution study with ^{18}F-AS3504073-00 showed high heart-to-background ratios. Therefore, the new class of PET tracer ^{18}F-AS3504073-00 is worthy of further pursuit as a marker of altered cardiac metabolic phenotype in heart failure. ***References:*** (1) O'Connell TD, et al. Methods Mol Biol 2007;357:271-96.

OP-536

Characterization of a new panel of ^{89}Zr-labeled RON targeting monoclonal antibodies as a targeting agent for molecular imaging

D. Spiegelberg[1,2], *P. Jha*[1], *X. Y. Koh*[3], *D. Lane*[3,4], *M. Nestor*[1];
[1]*Dep of Immunology, Genetics and Pathology, Uppsala University, Uppsala, SWEDEN,* [2]*Dep of Surgical Sciences, Uppsala University, Uppsala, SWEDEN,* [3]*P53 Laboratory, Agency for Science, Technology and Research (A*STAR), Singapore, SINGAPORE,* [4]*Dep of Microbiology, Tumor and Cell Biology, Science for Life Laboratory, Karolinska Institutet, Stockholm, SWEDEN.*

Aim/Introduction: The tyrosine kinase of the Recepteur D'origine Nantais (RON) receptor, also called macrophage-stimulating protein receptor (MST1R), is associated with the progression and metastasis of cancer. Only expressed in small amounts on epithelial cells, it is often overexpressed and alternatively spliced in cancer, including constitutively active isoforms. In addition, aberrant glycosylated RTKs like RON tend to increase the kinase activity of the receptor and lead to poor outcomes. RON is therefore an attractive target for diagnostic imaging and cancer therapeutics. Particularly, RON targeting monoclonal antibodies that also inhibit aberrantly glycosylated RON, which might have greater therapeutic efficacy in the treatment of cancer, is of great value. The objective of the present study was to evaluate for the first time the in vitro and in vivo binding properties of a new panel of RON targeting monoclonal antibodies to assess their utility as a targeting agent for molecular imaging using PET/CT. ***Materials and Methods:*** In the current study we examined a new panel of monoclonal antibodies binding not only of the glycosylated RON but also of the non-glycosylated and aberrant glycosylated RON receptor. The antibodies were labeled with ^{89}Zr using the siderophore-derived chelator desferrioxamine (DFO) and the stability was evaluated by chromatography. In vitro binding properties were assessed by LigandTracer measurements and cell specificity studies. For the in vivo investigations, tracer distribution was studied in a double tumor model with RON knockout and RON-overexpressing colon cancer xenografts using PET/CT imaging, followed by biodistribution and autoradiography. ***Results:*** The in vitro characterizations of the tracers demonstrated long shelf life and antigen specific binding. Repeated PET/CT imaging after 24, 48 and 72 hours demonstrated excellent imaging properties for all tested tracers, with the best contrast images occurring 48 hours post injection. The highest uptake was detected in the RON expressing tumor with no uptake in healthy tissue. The biodistribution data and ex vivo autoradiography results confirmed the specific binding of the novel tracer to the RON-positive tumors, significantly higher than for the negative control tumors. ***Conclusion:*** PET imaging with ^{89}Zr-DFO-anti RON Ab's is a promising approach for cancer diagnostics and could be further utilized for patient stratification and treatment response monitoring of RON targeting therapeutics. ***References:*** None

OP-537

D-Peptide-based probes for CXCR4-targeted molecular imaging and radionuclide therapy

F. Cleeren[1], *C. Cawthorne*[2], *T. Van Loy*[3], *J. Kleynhans*[4], *K. Leys*[1], *M. M. Sathekge*[4], *D. Schols*[3], *C. M. Deroose*[5], *G. Bormans*[1];
[1]*Radiopharmaceutical Research, Department of Pharmacy and Pharmacology, KU Leuven, Leuven, BELGIUM,* [2]*Nuclear Medicine and Molecular Imaging, Department of Imaging and Pathology, KU Leuven, Leuven, BELGIUM,* [3]*Rega Institute for Medical Research, KU Leuven, Leuven, BELGIUM,* [4]*Department of Nuclear Medicine, University of Pretoria & Steve Biko Academic Hospital, Pretoria, SOUTH AFRICA,* [5]*Nuclear Medicine, University Hospitals Leuven; Nuclear Medicine and Molecular Imaging, Department of Imaging and Pathology, KU Leuven, Leuven, BELGIUM.*

Aim/Introduction: Attempts to make a suitable fluorine-18 derivative of [^{68}Ga]Pentixafor[1] were unsuccessful due to the pronounced sensitivity of the Pentixafor scaffold towards even minor structural modifications, leading to strongly decreased CXCR4 binding affinity. Results with the therapeutic companion radiopharmaceutical [^{177}Lu] Pentixather are promising, but there is still room for improvement regarding pharmacokinetics and dosimetry profile.[2] Moreover, an anti-CXCR4 radiopharmaceutical labelled with an α-emitter might present a breakthrough in therapy of various CXCR4-expressing tumours. Therefore, the aim of this study is to develop innovative CXCR4 radiopharmaceuticals, both for diagnostic and therapeutic purposes, starting from D-Peptide-based probes (vMIP-II-derived CXCR4 antagonists composed entirely of D-amino acids)[3] that have not been explored yet for nuclear medicine applications. ***Materials and Methods:*** The high affinity (~4.6 nM) bivalent construct DV1-K-(DV3)[3] was site-specifically derivatised with 2tBu-NOTA and 3tBu-DOTA to obtain NOTA-DV1-K(DV3) and DOTA-DV1-K-(DV3), after deprotection

respectively. After purification and characterization, the CXCR4 binding affinity of the derivatized peptides was determined before and after complexation of stable gallium and lutetium. NOTA-DV1-K(DV3) was labelled using the Al^{18}F-method (NaOAc 0.1M, pH 4.1, 15 min 95°C) on an automated synthesis platform (Trasis AllinOne). DOTA-DV1-K-DV3 was labelled manually with galium-68 (NH_4OAc 0.1M, pH 3.5), lutetium-177 (0.1M NaOAc, pH 4.1, 15 min 95°C) and actinium-225 (Tris 0.1M, pH 9, 5 min µwave 95°C). The in vitro stability of the radiopharmaceuticals was determined in human serum at 37°C (iTLC and HPLC). Finally, the pharmacokinetic properties and specificity of the Al^{18}F-labeled anti-CXCR4 radiopharmaceutical was evaluated in healthy mice using µPET/CT with or without co-injection of 5 mg/kg AMD3100, followed by ex vivo biodistribution at 75 min. ***Results:*** The probes were succesfully radiolabelled with [^{18}F]AlF, [^{68}Ga]Ga, [^{177}Lu]Lu or [^{225}Ac]Ac and demonstrated high in vitro stability (>95% after 2h). [^{18}F]AlF-NOTA-DV1-K-(DV3) showed excellent pharmacokinetic properties with fast renal clearance and high and specific targeting of CXCR4 expressing tissues such as liver (SUV 7.38±0.49 vs. 0.96±0.13) and spleen (SUV 3.15±0.80 vs. 0.88±0.25). Moreover, in vitro binding studies of the probes confirmed high-affinity binding (5-15 nM) towards human CXCR4. Tumour targeting studies in CXCR4-positive xenografts and further affinity studies (AlF, La complex) are ongoing. ***Conclusion:*** The new probes demonstrated excellent pharmacokinetic properties and are expected to have a strong impact on CXCR4-targeted diagnostic imaging and targeted radionuclide therapy. ***References:*** 1. Wester, HJ. et al. Theranostics. 2015; 5: 618-630. 2. Maurer, S. et al., J Nucl Med. 2019; 60:1399-1405 3. Mao, Y. et al. Cell Transplantation. 2018; 27: 1249-1255.

OP-538

Development of a specific PET radiotracer of APJ: in vitro and in vivo evaluation in a colon adenocarcinoma model

B. Louis[1], *A. Moyon*[2], *A. Bouhlel*[1], *L. Balasse*[1], *S. Fernandez*[1], *S. Simoncini*[3], *G. Hache*[2], *F. Dignat-George*[4], *P. Garrigue*[2], *B. Guillet*[2]; [1]*C2VN INSERM 1263 INRA 1260 CERIMED Aix-Marseille Université, Marseille, FRANCE,* [2]*C2VN INSERM 1263 INRA 1260 CERIMED, APHM, Aix-Marseille Université, Marseille, FRANCE,* [3]*C2VN INSERM 1263 INRA 1260 Aix-Marseille Université, Marseille, FRANCE,* [4]*C2VN INSERM 1263 INRA 1260, APHM, Aix-Marseille Université, Marseille, FRANCE.*

Aim/Introduction: APJ receptor has been recently identified as overexpressed in various cancer cell lineages. To date, several APJ-targeted antitumor strategies are explored. We developed [^{68}Ga]Ga-AP747 as an APJ-targeted PET radiotracer, evaluated its biodistribution in healthy animals, and its specificity towards APJ in vitro and in vivo in a human colon carcinoma mouse model. ***Materials and Methods:*** AP747 was synthetized and radiolabeled with gallium-68. Radiochemical stability in 0.9% NaCl and in human serum was validated up to 2h after synthesis by radioTLC (iTLC-SG, sodium citrate 0.1M pH5).To evaluate [^{68}Ga]Ga-AP747 biodistribution, 4.3±0.44MBq/50µL (0.17µg) of [^{68}Ga]Ga-AP747 were IV injected to healthy mice (n=3), and µPET/CT acquisition was performed.In vitro characterization of [^{68}Ga]Ga-AP747 specificity towards APJ was performed on APJ-overexpressing human colon carcinoma T84 cells, as verified by western-blot. Blocking was performed using a 50-fold excess of APJ natural ligand. Quantification of radioactivity was realized on background-corrected autoradiographs (n=6).Mice (n=6) were subcutaneously xenografted with human colon adenocarcinoma T84 cells. 5.1±1.1MBq/50µL (0.17µg) of [^{68}Ga]Ga-AP747 were IV injected to the mice (n=3), and a µPET/CT acquisition was performed. In vivo blocking was realized by injecting a large excess of 50µg apelin 30min before injecting 5.3±0.9MBq/50µL (0.17µg) of [^{68}Ga]Ga-AP747 (n=3) and a µPET/CT acquisition was performed 1h after injection. µPET/CT acquisitions were performed on a Nanoscan PET/CT camera. PET signal quantification was corrected by physical decay and expressed as percentage of injected dose per gram of tissue (%ID/g) for the biodistribution study, and as tumor-to-background ratios (t/b) for the in vivo blocking study, the gastrocnemius muscle taken as reference for background. ***Results:*** [^{68}Ga]Ga-AP747 was produced with a radiochemical purity of 96.7±2.0% and a radiochemical stability confirmed in serum up to 2h after synthesis (95.0±1.5%). In healthy animals, [^{68}Ga]Ga-AP747 was rapidly cleared from the circulation through early renal elimination with a resulting low background signal as soon as 30min after injection and notably a low hepatic uptake. In vitro blocking resulted in a significant 65% signal abolishment compared to non-blocked condition (***P= 0.0003).In T84-tumor bearing mice, [^{68}Ga]Ga-AP747 showed a high tumor uptake (t/b : 7.93±2.17) nearly totally abolished In blocking conditions (t/b: 1.03±0.32, n=3,*P=0.0235)) ***Conclusion:*** [^{68}Ga]Ga-AP747 presents a highly favorable biodistribution profile for PET imaging. Specificity of AP747 PET imaging signal towards APJ was demonstrated in vitro and in vivo. Evaluating in vivo tissue APJ overexpression may represent an efficient companion tool of experimental APJ-inhibiting therapies, to determine therapeutic eligibility or to monitor therapeutic follow-up. ***References:*** None

OP-539

Preclinical evaluation of ^{68}Ga-Desferal for bacterial infection imaging

M. Petrik[1], *E. Umlaufova*[1], *V. Raclavsky*[2], *A. Palyzova*[3], *V. Havlicek*[3], *J. Pfister*[4], *Z. Novy*[1], *M. Popper*[1], *M. Hajduch*[1], *C. Decristoforo*[4]; [1]*Institute of Molecular and Translational Medicine, Faculty of Medicine and Dentistry, Palacky University, Olomouc, CZECH REPUBLIC,* [2]*Department of Microbiology, Faculty of Medicine and Dentistry, Palacky University, Olomouc, CZECH REPUBLIC,*

[3]Institute of Microbiology of the Czech Academy of Sciences, Prague, CZECH REPUBLIC, [4]Clinical Department of Nuclear Medicine, Medical University Innsbruck, Innsbruck, AUSTRIA.

Aim/Introduction: Bacterial infections are a serious global healthcare problem. Early and accurate identification and localization of infection is the critical first step in effective patient care. Molecular imaging has the potential for specific and sensitive detection of infections. The siderophore-based iron acquisition system represents one of few fundamental differences between bacterial and mammalian cells. Bacteria possess dedicated transporters for uptake of siderophores. Siderophores are low-molecular mass, iron specific chelators secreted by microorganisms. We have recently demonstrated that siderophores can be radiolabelled, replacing iron by gallium-68 without loss of bioactivity and allowing molecular imaging of fungal infections by positron emission tomography (PET). Here we report on the preclinical evaluation of clinically used siderophore, deferoxamine, marketed under the brand name Desferal (DFO), radiolabelled with Ga-68 for imaging of bacterial infections. ***Materials and Methods:*** DFO was labelled with Ga-68 in sodium acetate. In vitro characterization of ^{68}Ga-DFO including the determination of partition coefficient, protein binding and stability in various media was performed. In vitro uptake of ^{68}Ga-DFO was tested in different microbial cultures. In vivo biodistribution was studied in healthy mice. PET/CT imaging of ^{68}Ga-DFO was performed in suitable animal infection models. ***Results:*** DFO was labelled with Ga-68 with high radiochemical purity. In vitro assays showed hydrophilic properties of ^{68}Ga-DFO with low protein binding and high stability in human serum and PBS. The high in vitro uptake of ^{68}Ga-DFO in selected strains of Pseudomonas aeruginosa (P.a.), Staphylococcus aureus (S.a.) and Streptococcus agalactiae (S.ag.) could be blocked with an excess of cold iron-DFO. Ex vivo biodistribution data and PET/CT imaging acquired from experiments with healthy mice displayed rapid excretion of ^{68}Ga-DFO via the renal system and showed minimal retention in blood and other organs. PET/CT images of animal infection models displayed high and specific accumulation of ^{68}Ga-DFO in both P.a. and S.a. infection with excellent image contrast. No uptake was found in sterile inflammation, heat inactivated P.a. or S.a. and Escherichia coli lacking DFO transporters. ***Conclusion:*** We have shown that DFO can be labelled with Ga-68 with high radiochemical purity. ^{68}Ga-DFO displayed suitable in vitro characteristics and excellent pharmacokinetics in healthy mice. The high and specific uptake of ^{68}Ga-DFO by P.a. and S.a. was confirmed both in vitro and in vivo, proving the potential of DFO for specific imaging of bacterial infections. Whereas DFO is accepted in clinic for many years, we believe that ^{68}Ga-DFO has a great potential to clinical translation. ***References:*** None

OP-540

Fluorine-18 isotopic radiolabelling of the MEK inhibitor drug Binimetinib as a new PET imaging tool

S. Specklin*, R. Pelletier, C. Truillet, B. Kuhnast;*
CEA, Orsay, FRANCE.

Aim/Introduction: Mitogen-activated protein kinases (MAPK) signaling pathway plays an important role in cell proliferation. Mutation of BRAF gene induces an upregulation of this pathway that is involved in the development of several cancers. Binimetinib is a selective inhibitor of the MEK kinase involved in this signaling cascade and has been approved by the FDA for the treatment of BRAF positive melanoma.[1] Radiolabelling of this compound could thus lead to interesting PET imaging applications, from preclinical studies of the signaling pathway, to a potential selective clinical tracer to monitor BRAF mutation. However, the structure of Binimetinib exhibits two aromatic fluorine atoms located on unactivated positions, therefore making its isotopic labelling a strong radiochemistry challenge. ***Materials and Methods:*** The most promising radiofluorination position was selected and the labelling development was performed from a model derived from the Binimetinib whose hydroxamic ester was replaced by a methyl ester. A large number of aromatic radiofluorination methods was screened in an informative comparative benchmark. For each method, the corresponding labelling precursor was synthesized in a few steps from a commercial Binimetininb precursor. Evaluation of the radiofluorination was performed on the advanced intermediate and applied to the whole compound in case of success. ***Results:*** Seven labelling precursors of the model intermediate were synthesized in one to six synthesis steps. Most of the radiofluorination methods were ineffective, highlighting a significant electronic enrichment of the arene. A low radiochemical conversion (RCC) of 5% was surprisingly observed via a Balz-Schiemann reaction and the best results were observed from copper mediated radiofluorination from stannyl or boronate precursors. After a careful optimization of the conditions, the model intermediate was radiolabelled with RCC up to 70% from the boronate precursor. However, the translation of these conditions to the whole Binimetinib precursor was unsuccessful. This prompted us to develop an optimized labelling strategy starting from the radiofluorination of the model intermediate first, followed by the hydrolysis of the methyl ester, its activation and coupling to the corresponding alkylhydroxylamine prior to a final deprotection. ***Conclusion:*** Using copper mediated radiolabelling of a boronate precursor, [^{18}F]Binimetinib was obtained in a fully automated radiosynthesis involving a 5 steps / one pot sequence with 6% RCY. These first results will enable the first preclinical evaluation of [^{18}F] Binimetinib. ***References:*** [1] Specenier, P. An Overview of Binimetinib for the Treatment of Melanoma. Expert Opinion

on Pharmacotherapy 2020 https://doi.org/10.1080/14656566.2020.1729122.

OP-541

Development of a new fluorine-18-labelled PET tracer targeting norepinephrine transporter and evaluation on rodent and large animal models

X. Chen[1,2,3], S. Mühlig[2,3], Y. Ohshima[2,3,4], Y. Yagi[5], H. Kimura[5], K. Koshino[6], N. Nose[7], C. Lapa[1], A. Buck[2], T. Higuchi[2,3,7];
[1]Department of Nuclear Medicine, University Hospital of Augsburg, Augsburg, GERMANY, [2]Department of Nuclear Medicine, University Hospital of Würzburg, Würzburg, GERMANY, [3]Comprehensive Heart Failure Center, University Hospital of Würzburg, Würzburg, GERMANY, [4]Department of Radiation-Applied Biology Research, Quantum Beam Science Research Directorate, National Institutes for Quantum and Radiological Science and Technology, Gunma, JAPAN, [5]Department of Analytical and Bioinorganic Chemistry, Kyoto Pharmaceutical University, Kyoto, JAPAN, [6]Department of Systems and Informatics, Hokkaido Information University, Ebetsu, Hokkaido, JAPAN, [7]Graduate School of Medicine, Dentistry and Pharmaceutical Sciences, Okayama University, Okayama, JAPAN.

Aim/Introduction: Norepinephrine transporter (NET) is one of the major targets for diagnosis of heart failure and neuroendocrine tumours. Exemplified by clinically used SPECT tracer MIBG, a few NET-targeting radiotracers structurally derived from norepinephrine have been reported. We intend to develop a new fluorine-18-labelled PET tracer, 1-(3-fluoro-4-(3-^{18}F-(fluoropropoxy)phenethyl) guanidine, with convenient radiolabelling procedure and high yield while keeping the high NET affinity. ***Materials and Methods:*** Starting from 4-methoxy-3-fluorobenzaldehyde, followed with Wittig reaction and Mitsunobu reaction for the synthesis. The NET affinity of the non-radioactive (cold) reference was evaluated in neuroblastoma SK-N-SH cell lines against ^{131}I-MIBG. Different fluorine salts, catalysts and reaction temperature were examined for optimal radiolabelling condition. After successful radiofluorination, the radiotracer was evaluated in both rodents (n=4) and large animals (n=4) for biodistribution and cardiac uptake studies. ***Results:*** The precursor and the corresponding cold reference were synthesized. The cold reference shows essentially identical affinity at NET as norepinephrine (1.38 vs 2.57 µM against ^{131}I-IBG). The radiofluorination of the tracer could be achieved using [^{18}F]KF/K_{222}in DMF with high yield (28 %) and specific activity (54 GBq/mol). The dynamic imaging of the ^{18}F-labelled tracer in rats has demonstrated stable and long-term cardiac uptake. Specific uptake was confirmed by blocking studies (administration of phenoxybenzamine before the injection of the radiotracer, heart-to-liver ratio: blocking 1.30 ± 0.54 vs control 6.14 ± 0.35 p<0.001) in both ex vivo autoradiography and in vivo imaging. A further evaluation of the radiotracer in cynomolgus monkeys has demonstrated desipramine-sensitive high cardiac uptake and long-term retention (standardized uptake value 60 min postinjection of the tracer: heart 1.47 ± 0.18 vs liver 0.91 ± 0.47, p<0.05). ***Conclusion:*** We have successfully developed a new ^{18}F-labelled PET tracer targeting NET, which showed almost identical affinity as MIBG in cell uptake studies and favourable biodistribution in both rodents and large animals showing distinct heart delineation and long-term desipramine-sensitive cardiac uptake. It provides not only potentially new PET clinical option, but also alternatives to investigate insights into the structure-affinity relationships for NET. ***References:*** None

OP-542

Preclinical Evaluation of [^{18}F]OF-NB1, a Promising Radioligand for Imaging GluN2B Subunits of the NMDA Receptor in Rodents and Human Brain Tissues

H. Ahmed[1], A. Haider[1], V. Hosseini[2], R. Wallimann[1], I. Iten[1], M. Robledo[1], T. A. N. Nguyen[1], A. Herde[1], C. Keller[1], S. Gruber[1], V. Vogel[2], R. Schibli[1,3], L. Mu[1,3], B. Wünsch[4], S. M. Ametamey[1];
[1]Institute of Pharmaceutical Sciences, Department of Chemistry and Applied Biosciences, ETH Zürich, Zürich, SWITZERLAND, [2]Laboratory of Applied Mechanobiology, Institute of Translational Medicine, Department of Health Sciences and Technology, ETH Zürich, Zürich, SWITZERLAND, [3]Department of Nuclear Medicine, University Hospital Zürich, Zürich, SWITZERLAND, [4]Institute of Pharmaceutical and Medicinal Chemistry, University of Münster, Münster, GERMANY.

Aim/Introduction: GluN2B subunit-containing NMDA receptors are involved in various neurodegenerative pathologies and hence a critical therapeutic drug target. We have previously reported on a GluN2B PET radioligand codenamed [^{18}F]PF-NB1. Despite the remarkable in vitro specificity and selectivity, [^{18}F]PF-NB1 exhibited only moderately higher in vivo binding to GluN2B-rich brain regions, as compared to the GluN2B-deficient cerebellum. With the aim to improve the in vivo selectivity, we evaluated OF-NB1 and MF-NB1, both constitutional isomers of [^{18}F]PF-NB1[1]. ***Materials and Methods:*** Multi-step synthesis of OF-NB1 and MF-NB1 was followed by in vitro binding affinity determination of both ligands towards GluN2B subunits and sigma-1 receptors (off-target binding). A two-step method involving radiofluorination and cleavage of the protecting groups was used for the radiosynthesis of [^{18}F] OF-NB1. In vitro autoradiography using rat and postmortem human ALS brain tissue slices, confocal microscopy, PET imaging, ex vivo biodistribution and metabolite studies were performed. Receptor occupancy experiments were carried out using CP-101,606 (0.5-15 mg/kg), a GluN2B antagonist with documented clinical efficacy. ***Results:*** OF-NB1 and MF-NB1 were synthesized in 24% and 14% overall yields, respectively. OF-NB1 exhibited a binding affinity value of 10.4±4.7 nM towards GluN2B subunits and a 39-

fold selectivity over sigma-1 receptors. MF-NB1 displayed a lower GluN2B subunit affinity of 590±36 nM. [^{18}F]OF-NB1 was synthesized in isolated radiochemical yields of 5.5±0.1% (n=6) and molar activities of 192±33 GBq/μmol. In rat autoradiographic experiments, [^{18}F]OF-NB1 displayed higher accumulation in GluN2B-rich regions (cortex, striatum, thalamus and hippocampus) than the GluN2B-poor cerebellar region, which was blockable with GluN2B ligands, EVT-101 and CERC-301, but not with sigma-1 receptor ligands, fluspidine and SA4503. These findings were corroborated by PET imaging in Wistar rats using CP-101,606. Only intact [^{18}F]OF-NB1 was found in the rat brain 60 min postinjection. Biodistribution studies indicated higher GluN2B-rich regions/cerebellum ratios when compared to our previously reported [^{18}F]PF-NB1. A dose-dependent blocking effect was observed with CP-101,606 and resulted in a D_{50} of 8.1 μmol/kg. Lower GluN2B subunit expression was observed in ALS brain tissue sections compared to healthy controls, as indicated by autoradiography and confocal microscopy. ***Conclusion:*** [^{18}F]OF-NB1 is by far the most promising fluorinated radioligand for the in vivo PET imaging of GluN2B-containing NMDA receptors and drug receptor occupancy studies, and has potential for PET imaging studies in ALS patients and GluN2B subunit-related brain disorders. ***References:*** [1] Ahmed H, et al. Journal of medicinal chemistry. 2019;62(21):9450-9470. This project was supported by the Swiss National Science Foundation Grant Nr. 310030E-160403/1 and 310030E_182872/1.

OP-543

Biodistribution and Pharmacokinetics of Long-acting Radiolabeled Cyclic RGD Peptide in MDA-MB-231 Breast Cancer Model

Y. Huang, M. Chen, S. Lee, S. Lo, S. Chen, L. Chen, M. Li, C. Chang; Institute of Nuclear Energy Research, Taoyuan, TAIWAN.

Aim/Introduction: Integrin $\alpha_v\beta_3$ plays a very important role in tumor angiogenesis which is significantly up-regulated on activated endothelial cells during angiogenesis. The majority of integrin-targeted imaging tracers are based on the tripeptide Arg-Gly-Asp (RGD) acid sequence because of its high affinity and specificity for integrin $\alpha_v\beta_3$. Some studies had proved that the conjugation of an albumin-binding motif, truncated Evans blue (EB), to radiolabeled cyclic RGD peptides significantly enhance imaging performance and therapeutic efficacy in a glioblastoma model. Aims of this study were to evaluate the improvement of pharmacokinetics, nanoSPECT imaging performance and biodistribution of the novel ^{111}In-DOTA-EB-cRGDfK in MDA-MB-231 breast cancer model. We demonstrated that ^{111}In-DOTA-EB-cRGDfK may offer diagnostic images for triple-negative breast cancer in the future. ***Materials and Methods:*** After intravenous injection of ^{111}In-DOTA-EB-cRGDfK and ^{111}In-DOTA-cRGDfK, blood samples from MDA-MB-231 tumor-xenografted mouse model were collected through cardiac puncture at various time points. The pharmacokinetic parameters were estimated with the WinNonlin. Comparative study of nanoSPECT/CT imaging was processed by manually drawing regions of interest (ROIs) on tumor/kidney/liver/muscle and calculating the value of ROIs in PMOD. For ^{111}In-DOTA-EB-cRGDfK biodistribution analysis, organs of interest were removed, washed and weighed, and the radioactivity was measured with gamma counter. ***Results:*** The radiochemical purity of ^{111}In-radiopharmaceuticals was more than 90% analyzed by using radio-TLC and radio-HPLC. The clearance rate (Cl) of ^{111}In-DOTA-cRGDfK was 12.9 g/h, which is 94.9-fold higher than that of ^{111}In-DOTA-EB-cRGDfK (0.136 g/h). The area under the time curve($AUC_{0\rightarrow\infty}$) of ^{111}In-DOTA-EB-cRGDfK and ^{111}In-DOTA-cRGDfK was 375 and 1.02 %ID/g*h. The results of nanoSPECT/CT imaging presented cRGDfK peptide with a truncated albumin-binding motif EB enhanced tumor accumulation. ^{111}In-DOTA-EB-cRGDfK showed the highest tumor uptake at 24 h postinjection (10.93 ± 3.22 %ID/g), whereas ^{111}In-DOTA-cRGDfK was almost washout at the same time point (0.32 ± 0.18 %ID/g). The tumor accumulation of ^{111}In-DOTA-EB-cRGDfK was maintained at least 96 h (9.22 ± 2.65 %ID/g). The biodistribution result showed the highest tumor uptake was found to be 7.19 ± 0.45% at 24 h after ^{111}In-DOTA-EB-cRGDfK administration. ***Conclusion:*** These results of pharmacokinetics and nanoSPECT/CT imaging showed albumin-binding motif could improve circulation time of cRGDfK peptide, and the slow release of ^{111}In-DOTA-EB-cRGDfK from albumin might allow continual uptake in MDA-MB-231 breast tumor. It has been proved that ^{111}In-DOTA-EB-cRGDfK provided high contrast for the diagnostic image of triple-negative breast cancer. We are going to evaluate the capability as a radiotherapy tool of DOTA-EB-cRGDfK for $\alpha_v\beta_3$-positive tumors in the future. ***References:*** None

1006

Cutting Edge Science Track - TROP Session: AI - Radiomics and Modelling

Saturday, October 24, 2020, 10:40 - 12:10 Channel 6

OP-544

Application of artificial neural network to preoperative ^{18}F-FDG PET/CT for predicting pathological nodal involvement in NSCLC patients

S. Taralli[1], V. Scolozzi[1], L. Boldrini[2], J. Lenkowicz[2], A. Pelliccioni[3], M. Lorusso[1], O. Attieh[4], G. Cardillo[5], M. L. Calcagni[6]; [1]Fondazione Policlinico Universitario A. Gemelli IRCCS; UOC Medicina Nucleare, Rome, ITALY, [2]Fondazione Policlinico Universitario A. Gemelli IRCCS; UOC Radioterapia Oncologica, Rome, ITALY, [3]INAIL, Department of Occupational and

Environmental Medicine, Rome, ITALY, [4]Nuclear Medicine Department, Jordanian Royal Medical Services, Amman, JORDAN, [5]Unit of Thoracic Surgery, San Camillo Forlanini Hospital, Rome, ITALY, [6]Fondazione Policlinico Universitario A. Gemelli IRCCS; UOC Medicina Nucleare-Università Cattolica S. Cuore, Rome, ITALY.

Aim/Introduction: In non-small-cell lung cancer (NSCLC) staging, the evaluation of lymph nodal status is of paramount importance for selecting the optimal therapeutic approach. Study aim is to evaluate the performance of artificial neural network (NN) applied to preoperatively ^{18}F-FDG PET/CT for predicting pathological nodal involvement in NSCLC patients. ***Materials and Methods:*** We retrospectively analyzed clinical, anatomic, metabolic and histopathological data from 540 consecutive clinically resectable NSCLC patients (333M; mean age: 67.4±9 years), who underwent pre-operative ^{18}F-FDG PET/CT and subsequent pulmonary resection with hilo-mediastinal lymphadenectomy. From a set of features, Boruta algorithm selects 13 relevant features as input parameters (>60% PET-derived): patients'age, tumor size (mm), PET tumor result (positive: uptake ≥mediastinal blood-pool; SUVmax, SUVmean, TLG, MTV), PET nodal result (positive: at least one node with uptake ≥mediastinal blood-pool), PET nodal staging (N0/N1/N2), tumor histotype and grading. The dataset was randomly splitted into 2/3 training and 1/3 testing, with no features differences ($p>0.05$) between the two groups. Both logistic regression (LR) and a 3-layers NN (with 12, 6 and 2 neurons, respectively) models were applied, with NN trained for 500 epochs with 150 batch size and 0.1 validation split. With surgically-proven nodal status as gold standard (pN0 vs pN+ patients), diagnostic performance of NN for nodal staging was calculated by ROC analysis and compared with LR in terms of area under the curve (AUC), accuracy (ACC), sensitivity (SE), specificity (SP), positive and negative predictive values (PPV, NPV); comparison with visual PET nodal staging was also performed. ***Results:*** Histopathological nodal involvement (pN+) was detected in 108/540 (20%) patients. Training NN performance (AUC=0.849): ACC=80%, SE=72%, SP=81%; PPV=50%, NPV=92%. Test NN performance (AUC=0.769): ACC=77%, SE=58%, SP=81%; PPV=44%, NPV=89%. Training LR performance (AUC=0.795): ACC=75%, SE=68%, SP=77%; PPV=43%, NPV=90%. Test LR performance (AUC=0.763): ACC=77%, SE=55%, SP=82%; PPV=43%, NPV=88%. Visual PET analysis performance: ACC=0.82, SE=32%, SP=94%; PPV=57%, NPV=85%. ***Conclusion:*** Application of artificial NN to preoperative ^{18}F-FDG PET/CT provides overall good performance for predicting pathological nodal status in NSCLC patients candidates for surgical resection, especially for ruling out nodal metastases due to high specificity. In clinical practice, our results suggest that application of NN allows to reduce the chance of false negative results at visual ^{18}F-FDG PET/CT analysis. This finding assumes greater relevance in a population of clinically resectable NSCLCs, with "a priori" low probability of lymph nodal involvement. Further studies are ongoing on NN application for categorizing pathological nodal involvement in N1 vs N2 status. ***References:*** None

OP-545

Weakly-supervised deep learning for the exploration of the prognostic value of ^{18}F-FDG PET/CT in extranodal natural killer/T-cell lymphoma, nasal type

B. Li[1], *R. Guo*[1], *X. Hu*[2], *H. Song*[2], *P. Xu*[3], *H. Xu*[4], *A. Rominger*[5], *C. Sun*[1], *X. Lin*[1], *B. Menze*[2], *K. Shi*[2,5];

[1]Department of Nuclear Medicine, Ruijin Hospital, Shanghai Jiao Tong University School of Medicine, Shanghai, CHINA, [2]Department of Computer Science, Technical University of Munich, Munich, GERMANY, [3]State Key Laboratory of Medical Genomics, Shanghai Institute of Hematology, Rui Jin Hospital, School of Medicine, Shanghai Jiao Tong University, Shanghai, CHINA, [4]Department of Radiation, Rui Jin Hospital, School of Medicine, Shanghai Jiao Tong University, Shanghai, CHINA, [5]Lab for Artificial Intelligence Translational Theranostics, Department of Nuclear Medicine, University of Bern, Bern, SWITZERLAND.

Aim/Introduction: Survival follow-up is often incomplete or missed in clinical trials, which restricts the availability of extensive data in the development of artificial intelligence (AI) in prognosis prediction. We aimed to develop a weakly-supervised deep learning technology to utilize incomplete survival data in the prognosis of extranodal natural killer/T-cell lymphoma, nasal type (ENKTL) based on pre-treatment ^{18}F-FDG PET/CT. ***Materials and Methods:*** One hundred and twenty-three ENKTL patients underwent ^{18}F-FDG PET/CT before the treatment for the purpose of staging were retrospectively collected. Among them, 72 were followed-up for at least 2 years and 20% (14 randomly selected) were reserved for the test. In order to use the 51 patients without follow-up data, positive-negative-unlabeled classification (PNU) was developed to create pseudo labels for the training of survival prediction. Deep learning features were extracted from the PET/CT images in a training set (n=109) and a prediction similarity index (PSI) was derived from these features. The sensitivity, specificity and accuracy of PSI based progression-free survival (PFS) prediction were calculated. It was compared with the no pseudo-labels data. Survival curves were obtained using Kaplan-Meier analysis, followed by multivariate analysis to assess the independent effects of PSI and clinical features of the disease on PFS. ***Results:*** Deep learning features were extracted and PSI>1 was set as positive. In the training set with PNU, PSI got an AUC score of 0.995 in prediction of PFS. The prognosis are significantly different between the two groups divided by PSI (P=0.000). Prognostic performances were validated with the corresponding AUC score of 0.875 in prediction of PFS in the test set. A prediction sensitivity, specificity and accuracy were 83.33%, 87.50% and 85.71%, respectively.

The prognosis are significantly different between the two groups divided by PSI (P=0.019). In the control group without PNU, PSI got an AUC score of 0.771 in the test set. A prediction sensitivity, specificity and accuracy were 66.67%, 87.50% and 78.57%, respectively. PNU group (0.708) achieved Youden's index higher than that of non-PNU group (0.542) in the test set. Multivariate analysis showed that PSI with PNU or without PNU remained independent significant factors for PFS. ***Conclusion:*** Data-enhanced deep learning can utilize the data of incomplete to improve survival prediction. The method revealed the potential of the AI-extracted ^{18}F-FDG PET/CT features as a surrogate for the prognosis prediction of ENKTL. Future prospective studies with external validation are needed to validate our findings. ***References:*** None

OP-546

Performance of 18F-FDG PET/CT based on machine-learning defined diagnostic criteria is not inferior to a consensus review by experts to detect pelvic lymph node involvement in bladder cancer

A. Girard[1], L. Dercle[2], H. Vila Reyes[3], E. Le Stanc[4], O. Delcroix[5], M. Rouanne[6];
[1]Department of Nuclear Medicine, Centre Eugène Marquis, Rennes, FRANCE, [2]Department of Radiology, Columbia University Medical Center, New York, NY, UNITED STATES OF AMERICA, [3]Department of Urology, Columbia University Medical Center, New York, NY, UNITED STATES OF AMERICA, [4]Department of Nuclear Medicine, Hôpital Foch, Suresnes, FRANCE, [5]Department of Nuclear Medicine, CHU de Brest, Brest, FRANCE, [6]Department of Urology, Hôpital Foch, Suresnes, FRANCE.

Aim/Introduction: The diagnosis of pelvic lymph node (LN) involvement of muscle invasive bladder cancer (MIBC) is critical to guide patients' management. Heterogeneous metabolic and morphological criteria have been suggested in the litterature. In this study, we aimed to develop and validate an PET/CT-based decision-making algorithm for use by the non-expert clinician that helps diagnose LN extent in patients with MIBC. ***Materials and Methods:*** Out of 238 screened patients retrospectively screened, 173 were included. All 18F-FDG PET/CT were performed within 90 days before radical cystectomy and extended pelvic LN dissection, and were reviewed independently by two nuclear medicine physicians. Morphological and metabolic features were collected for visible LN in each pelvic area, as well as physician the subjective conclusion regarding LN involvement. The reference standard was pathological examination of LN dissection samples. Patients were randomly assigned to the training set (n=115) or the validation set (n=58). Using machine learning (random forest tree algorithm) with 20 features, a multivariable prediction model (the signature) was developed and validated for diagnosing LN involvement. Signature performance was evaluated using area under a receiver operating characteristic curves (AUCs). ***Results:*** Thirty (26%) patients presented pelvic LN involvement in the training set, and twelve (21%) in the validation set. In a per-patient analysis in the training set, the top 5 features for the diagnosis of LN involvement were LN SUVmax, product of diameters of the largest LN, the sum of the products of diameters of LN, the bladder tumor largest diameter and the SUVmax of urine. In the training set, the signature reached an AUC of 79.2 (95%CI 70.5-87.9) and the consensus of expert an AUC of 71.5 (95%CI 62.0-81.0), p = 0.24. In the validation set, AUCs were 66.7 (95%CI 49.7-83.6) and 62.3 (95%CI 47.8-76.8) p = 0.70, respectively. ***Conclusion:*** A PET/CT-based signature was developed with machine learning and validated for diagnosis of LN involvement on a per patient analysis, in patients with MIBC. The diagnostic performance of 18F-FDG PET/CT provided by this tool was not significantly inferior to a consensus of experts, and could be used for enhanced decision-making. ***References:*** None

OP-547

A convolutional neural network for fully automated blood SUV determination in oncological FDG-PET

P. Nikulin[1], *F. Hofheinz[1], J. Maus[1], Y. Li[2], R. Bütof[3], C. Lange[4], C. Furth[4], S. Zschaeck[4], M. Kreißl[5], J. Kotzerke[3], J. van den Hoff[1];*
[1]Helmholtz-Zentrum Dresden-Rossendorf, Institute of Radiopharmaceutical Cancer Research, Dresden, GERMANY, [2]Xiamen Cancer Hospital, The First Affiliated Hospital of Xiamen University, Xiamen, CHINA, [3]University Hospital Carl Gustav Carus, Technische Universität Dresden, Dresden, GERMANY, [4]Charité – Universitätsmedizin Berlin, corporate member of Freie Universität Berlin, Humboldt-Universität zu Berlin, and Berlin Institute of Health, Berlin, GERMANY, [5]Klinik für Radiologie und Nuklearmedizin, Universitätsklinikum Magdeburg A.ö.R., Magdeburg, GERMANY.

Aim/Introduction: The standardized uptake value (SUV) is widely used for quantitative evaluation in oncological FDG-PET but has well-known shortcomings as a measure of the tumor's glucose consumption. The standard uptake ratio (SUR) of tumor SUV and arterial blood SUV (BSUV) possesses an increased prognostic value [1,2] but requires image-based BSUV determination, typically in the aortic lumen. However, accurate manual ROI delineation requires care and imposes an additional workload which makes the SUR approach less attractive for clinical routine. The goal of the present work was the development of a fully automated method for BSUV determination in whole-body PET/CT. ***Materials and Methods:*** Automatic delineation of the aortic lumen was performed with a convolutional neural network (CNN), using the U-Net architecture. 946 FDG PET/CT scans from several sites were used for network training (N=366) and testing (N=580). For all scans, the aortic lumen was manually delineated, avoiding areas affected by motion-

induced attenuation artifacts or potential spill-over from adjacent FDG-avid regions. Performance of the network was assessed using the fractional deviations of automatically and manually derived BSUVs in the test data. ***Results:*** The trained U-Net yields BSUVs in close agreement with those obtained from manual delineation. Notably, using both CT and PET data as input for network training allows the trained network to derive unbiased BSUVs by detecting and excluding aorta segments affected by attenuation artifacts or spill-over. Comparison of manually (M) and automatically (A) derived BSUVs shows excellent concordance: the mean paired M-A difference was (mean +/- SD)=(-0.5 +/- 3.1)% with a 95% confidence interval of [-7.0, 6.6]% and a total range of [-10.2, 13.3]%. For four test cases the derived ROI volume was below the predefined threshold (< 1ml). ***Conclusion:*** CNNs offer a viable approach for automatic BSUV determination. Our trained network exhibits a performance comparable to an experienced human observer and might already be considered suitable for supervised clinical use. ***References:*** [1] van den Hoff J, Oehme L, Schramm G, Maus J, Lougovski A, Petr J, et al., EJNMMI Res. 2013;3(1):77 [2] Hofheinz F, Li Y, Steffen IG, Lin Q, Lili C, Hua W, et al., EJNMMI 2019;46(7):1485

OP-548

Deep Learning-Enabled Comprehensive Detection and Quantification of 18FDCFPyL (PyL-PSMA) PET/CT

J. Brynolfsson[1], K. Johnsson[1], H. Sahlstedt[1], J. Richter[1], K. Sjöstrand[1], N. G. Nickols[2], M. B. Rettig[2], L. Edenbrandt[1,3], A. Anand[1]; [1]Exini Diagnostics AB, Lund, SWEDEN, [2]VA Greater Los Angeles, Los Angeles, CA, UNITED STATES OF AMERICA, [3]University of Gothenburg, Gothenburg, SWEDEN.

Aim/Introduction: Comprehensive and automated quantification of PyL-PSMA PET/CT findings has the potential to be of great value in routine clinical practice as well as in clinical trials. We have developed the automated Prostate Cancer Molecular Imaging Standardized Evaluation (aPROMISE): a tool for automated, structured, and quantitative reporting of PET/CT findings. aPROMISE is based upon, but extends the PROMISE framework (Eiber et al, 2017). aPROMISE automates the process of lesion identification and quantification of e.g. Standard Uptake Values (SUVs). It may improve consistency of both inter- and intra-physician PSMA PET/CT assessments of disease. ***Materials and Methods:*** aPROMISE creates a deep-learning based semantic segmentation of the CT image. The segmentation is transferred to the PET image where reference SUVs for liver and blood pool are calculated. Suspicious hotspots, i.e., regions with high uptake in the PET image that may be consistent with disease, are identified and their volumes outlined. For each identified hotspot a range of quantitative measurements are generated, e.g., SUV max and lesion volume, as well as the miPSMA index (Johnsson et al, 2020). Finally, a structured report is generated, summarizing the study data of the patient, together with a detailed list of detected lesions and their respective quantitative measurements. For development of the hotspot detection and delineation algorithm, a data set comprised of 266 PyL-PSMA PET/CT scans with manually annotated lesions was used. Evaluation of reference value computation was performed on 86 independent PyL-PSMA PET/CT images and compared with values estimated by 3 manual readers. ***Results:*** For bone, lymph and prostate lesions respectively, 91%, 92% and 93% were automatically detected. The Pearson correlation coefficient between reader-generated reference values were in the range 0.73-0.78 for blood pool and 0.78-0.97 for liver. The correlation between the software and reader generated reference values were in the range 0.82-0.88 for blood pool and 0.81-0.95 for liver. The standard deviation of manually generated reference values were 0.24 and 1.29 for blood pool and liver, respectively, whereas the corresponding standard deviations for aPROMISE were 0.21 and 1.15. ***Conclusion:*** An efficient automatic detection coupled with delineation of lesions in aPROMISE can enable standardized comprehensive quantification. Computation of reference SUVs with aPROMISE demonstrated better consistency than the manual readers. Future work would focus on evaluating the consistent and quantitative reporting of aPROMISE in management of patients with prostate cancer. ***References:*** None

OP-549

Whole-body lesion detection and prostate cancer staging in ^{68}Ga-PSMA-11 PET/CT using deep learning

N. Capobianco[1], A. Gafita[2], G. Platsch[1], L. Sibille[3], B. Spottiswoode[3], M. Eiber[2], W. A. Weber[2], N. Navab[4], S. G. Nekolla[2]; [1]Siemens Healthcare GmbH, Erlangen, GERMANY, [2]Department of Nuclear Medicine, Klinikum rechts der Isar, Technical University of Munich, Munich, GERMANY, [3]Siemens Medical Solutions USA Inc., Knoxville, TN, UNITED STATES OF AMERICA, [4]Computer Aided Medical Procedures (CAMP), Technical University of Munich, Munich, GERMANY.

Aim/Introduction: PSMA-ligand PET/CT has shown high accuracy for prostate cancer staging. Nevertheless, accurate interpretation of ^{68}Ga-PSMA-11 PET/CT images can be challenging with possible tracer uptake in sub-milliliter lesions and known pitfalls (1). We developed and evaluated a deep learning method to detect lesions in whole-body ^{68}Ga-PSMA-11 PET/CT and classify them following a standardized staging framework. ***Materials and Methods:*** ^{68}Ga-PSMA-11 PET/CT images of 93 patients with proven prostate cancer were annotated by two expert physicians (AG, GP). Each region with increased tracer uptake was segmented, labeled as physiological or suspicious and assigned an anatomical localization from a set of physiological uptake

sites and sites relevant for staging according to the PROMISE framework (2). PET/CT images and expert annotations were used for training a convolutional neural network (CNN) to detect and classify sites of suspicious tracer uptake. A hold-out set of 30 patients was used exclusively to evaluate performance. The CNN detection accuracy was evaluated by the fraction of suspicious sites successfully detected per subject (sensitivity) and the number of false positive sites identified per subject; compared to expert visual assessment. The CNN anatomical localization performance was evaluated by the ability to predict miN0 or miN1 stage, as presence or absence of suspicious pelvic lymph nodes, and miM0 or miM1 stage, as presence or absence of lesions in extrapelvic lymph nodes, bone or other organs. ***Results:*** In total, 2919 regions with elevated tracer uptake were annotated (average 31.4 per subject), including 2589 physiological uptake regions and 570 suspicious regions, of which 81 were pelvic lymph nodes, 157 were distant lymph nodes and 295 were bone lesions. The median segmented volume of suspicious lesions was 1.2 mL [interquartile range (IQR) 0.6-2.9mL]. The CNN showed good ability to detect suspicious sites, with 0.84 average sensitivity per subject (IQR 0.74-1) and a median of 2.5 false positives per subject (IQR 1.2-7.8). Based on the anatomical localization of lesions determined using the CNN, miN0 stage was correctly predicted in 18/22 subjects, miN1 in 8/8 subjects, miM0 in 2/5 subjects, miM1 in 25/25 subjects. ***Conclusion:*** The investigated deep learning method showed promising results for detection and anatomical localization of suspicious uptake sites in whole-body PSMA-targeted PET/CT, including sites with small volume. The anatomical localization is shown to have utility in providing staging support for prostate cancer. ***References:*** (1) Hofman MS, et al. Radiographics. 2018;38:200-217. (2) Eiber M, et al. J Nucl Med. 2018;59:469-478.

OP-550

Improved 3D Tumour Definition and Quantification of Radiotracer Uptake Using Deep Learning

L. Dal Toso[1], *Z. Chalampalakis*[2], *I. Buvat*[2], *C. Comtat*[2], *J. A. Schnabel*[1], *P. K. Marsden*[1];
[1]*King's College London, London, UNITED KINGDOM,* [2]*CEA, Paris, FRANCE.*

Aim/Introduction: Positron Emission tomography (PET) is used in oncology to detect and stage tumours. Quantification of tumour radiotracer uptake is often performed using the standardized uptake value. However, its accuracy is limited by the poor spatial resolution and noise properties of PET images. There is need for new methods that allow for accurate and reproducible quantification of radiotracer uptake. We developed a deep learning approach using a 3D convolutional neural network (CNN), trained on simulated data, to improve uptake quantification and tumour shape definition. ***Materials and Methods:*** Tumours with different shapes and dimensions, spanning 0.01 to 200 ml, were simulated. We generated 1000 tumours with uniform activity, 700 tumours split into halves, with different activities, and 700 hollow tumours. Each tumour was pasted in a random position within a lung of an anthropomorphic phantom. 'Ground truth' images with 2.08x2.08x2.03 mm^3 voxels were generated by assigning appropriate activities to each organ, then input to an analytical simulator with the corresponding attenuation maps to create realistic PET data. PET images were reconstructed using CASToR, with the OSEM algorithm including PSF modelling. Small regions (50x50x50 voxels) cropped from the ground truth images and reconstructed PET images were used to train a CNN with six convolutional layers, each followed by batch normalisation except for the final layer. ***Results:*** The CNN was first trained and tested on 980 tumours with uniform activity and 580 hollow tumours. The network yielded denoised images, with sharper tumour edges. Improved estimates of the maximum activity were extracted from the predicted tumours and increased values of mean structural similarity (MSSIM) were measured between ground truth and predicted tumours. When testing this network on tumours divided into halves, similar improvements of tumour shape and maximum activity were observed, but some predicted tumours contained areas with non-uniform activities, in regions where the ground truth activity distribution was uniform. When training and testing this network on 2200 simulated tumours, better defined tumours were predicted but non-uniform activities could be observed. The average percentage difference between the maximum tumour intensity, extracted from the reconstructed PET and from the ground truth images was 75%±43%. The average percentage difference between maximum activities calculated using the predicted and ground truth images was 25%±33%. ***Conclusion:*** This approach improved the estimation of maximum activity in the simulated tumours and yielded better defined tumours. Future plans include applying the CNN on phantom PET images and on real patients. ***References:*** None

OP-551

Influence of delineation modality on overall accuracy of machine learning predictive model on colorectal carcinoma

M. Grahovac*, L. Papp, C. P. Spielvogel, D. Krajnc, A. Leisser, A. Strassl, J. Bozic-Pavletic, T. Beyer, M. Hacker, A. Haug;
Medical University Vienna, Vienna, AUSTRIA.*

Aim/Introduction: Positron Emission Tomography (PET) / Computer Tomography (CT) support diagnosis and follow-up of patients with colorectal cancer (CRC). To date, the association of the PET and CT-driven in vivo radiomics features with the overall survival (OS) is not well explored.

The aim of this study was to investigate the differences in the performance of predictive models depending of PET- and CT-driven delineation with the help of machine learning. ***Materials and Methods:*** 73 ^{18}F-FDG PET/CT patients were included in this study. 319 lesions were delineated twice: once based on PET and once based on contrast enhanced CT. Optimized radiomics feature extraction in both cases was performed from the PET/CT images [1]. Additionally, demographic information (gender, weight, height and age group), clinical features (TNM staging, location of primary tumor, treatment response, K-ras mutation status, grading, number and location of metastases) and laboratory findings, which may be associated with worse outcome (elevated creatinine, LDH- and CRP values, leukocytopenia, thrombocytopenia and anemia), were merged with the extracted imaging features. 12-month OS predictor models were established utilizing embedded feature selection [2] for both the PET and CT-driven delineation approaches. Monte Carlo cross-validation with 90% training and 10% validation sets in 100-fold cross-validation scheme was performed to estimate the sensitivity (SENS), specificity (SPEC), accuracy (ACC), positive-predictive-value (PPV) and negative-predictive-value (NPV) of both predictive models. Class imbalance was handled with random undersampling. ***Results:*** The predictive model based on PET-driven delineation outperformed the CT-driven predictive model (ACC: 74% vs 66%, SENS: 69% vs 68%, SPEC: 78% vs. 64%, PPV: 76% vs 65%, NPV: 72% vs 67% respectively). ***Conclusion:*** The PET-driven delineation approach outperformed the CT-driven approach. This indicates that PET heterogeneity combined with including the surrounding tissue of the lesions in CT - due to larger PET delineation masks as of the partial-volume effect - seems to provide additional supporting information for survival prediction in colorectal cancer patients. ***References:*** 1.Papp L, et al: Optimized feature extraction for radiomics analysis of 18F-FDG-PET imaging. JNM 2018, 10.2967/jnumed.118.217612. 2.Papp L. et al: Glioma Survival Prediction with Combined Analysis of In Vivo 11C-MET PET Features, Ex Vivo Features, and Patient Features by Supervised Machine Learning. JNM, 2018(59):892-899

OP-552

Deep learning radiomics for prediction of Alzheimer disease by usingamyloid PET images

G. Giovacchini[1], *E. Giovannini*[1], *M. Riondato*[1], *O. Ferrando*[2], *F. Foppiano*[2], *M. De Biasi*[3], *C. Passera*[3], *A. Tartaglione*[3], *P. Lazzeri*[1], *A. Ciarmiello*[1];

[1]*Nuclear Medicine Unit, S. Andrea Hospital, La Spezia, ITALY,*
[2]*Medical Physics Unit, S. Andrea Hospital, La Spezia, ITALY,*
[3]*Neurology Unit, S. Andrea Hospital, La Spezia, ITALY.*

Aim/Introduction: Preliminary data suggest that radiomics may be used as a non invasive tool for diagnosis prediction among normal control (NC), mild cognitive impairment and Alzheimer's disease (AD). This study was aimed to predict different disease stages and disease progression using deep learning approach and radiomic textural data derived by amyloid PET images. ***Materials and Methods:*** 328 subjects from ADNI database and EudraCT 2015-001184-39 trial (159 male, 169 female), mean age 72 ± 7.4 years underwent PET/CT with 18F-Florbetaben. Study subjects cohort consisted of normal controls (n=149), MCIs (n=144) and AD (n=35). A total of 42 radiomics features and SUV were extracted from PET/CT studies on the whole brain and at lobar level. Whole cortical burden (Aß burden) was defined by frontal, parietal, temporal, occipital and cingulate VOIs.SUV was corrected for cerebellar activity (SUVr). The neighborhood component analysis (NCA) was applied to reduce the high features dimensionality and selecting the most powerful for diagnosis prediction. NCA weighs each feature according to classification accuracy using Leave-One-Out (LOO) approach. The features selected were grouped in all possible combination and tested for the accuracy to discriminate among subject's group. Support vector machine (SVM) was used to estimate the performance of each feature combination by using misclassification error (MCE) as classifier. General linear model (GLM) was used for testing the relantionship of SUV and radiomic model on Minimental State Examination (MMSE) and Clinical Dementia Rate scale Sum Of Boxes (CDR-SB). Significant differences between AUCs computed using different prediction models were tested using the Hanley and McNeil method.Effect size was assessed with Cohen's f statistic and evaluated as f;: 0.10 = small, 0.25 = medium, and 0.40 = large. Analysis was implemented under Matlab 2019b using Deep Learning Toolbox. ***Results:*** Eight of 42 textural features were selected by NCA alghorithm. Feature combination with the best diagnostic performance included the following 4 textural variables: (Global_Skewness, GLCM_AutoCorrelation, GLRLM_LRHGE, GLSZM_LZHGE) which emerged as being more useful to distinguish between groups as compared to the SUVmax (AUC: 0.74 vs. 0.63, P<0.01). Radiomic model compared to SUVmax significantly improved the relatioship with MMSE (R2=0.28 vs. 0.20; cohen's f=0.28 vs. 0.25) and CDR-SB (R2=0.26 vs. 0.20; cohen's f=0.35 vs. 0.26. ***Conclusion:*** Deep-Learning radiomics is a promising approach for prediction of diagnosis and disease progression in AD. Although there results require validation in a larger population, this technique may support clinical decision strategy with complementary information. ***References:*** None

OP-553

In-vivo survival prediction of glioma patients from [11C]MET-PET using advanced data pre-processing and machine learning

D. Krajnc*, L. Papp, C. P. Spielvogel, M. Grahovac, T. Beyer, M. Hacker, T. Traub-Weidinger;*

Medical University of Vienna, Vienna, AUSTRIA.

Aim/Introduction: [^{11}C]Methionine (MET) PET is an established nuclear medicine procedure for glioma imaging. 3-years survival built on in vivo features extracted from MET-PET glioma patients was demonstrated with moderate performance [1]. We hypothesize that such performance was biased by lack of proper data pre-processing of training datasets utilized for machine learning. Here, we compare predictive performance of 3-years survival of glioma patients with and without a novel data pre-processing approach. ***Materials and Methods:*** 105 MET-PET positive glioma cases were included. Primary tumour volume of interest (VOI) and a contra-lateral reference background region were defined using a semi-automated delineation procedure. Following tumour-to-background ratio normalization 49 radiomics feature were extracted per case. A 100-fold Monte Carlo cross-validation scheme was executed resulting in 90% training and 10% validation set in each MC fold. The training dataset of the MC folds were inputs of ensemble learning to establish 3-years survival predictive models in two schemes, without data preparation and after applying data pre-processing algorithms. We performed class imbalance correction, sample and feature redundancy cleansing, as well as outlier detection. Predictive performance was estimated for both executions over the validation cases of each MC fold by confusion matrix calculations (SENS, SPEC, ACC, PPV and NPV). ***Results:*** The validation performance of ML models with the original training data was 76% (SENS), 64% (SPEC) and 71% (ACC). In contrast, the performance with ML models built on the pre-processed training data was 71% (SENS), 82% (SPEC) and 80% (ACC), where we recorded sensitivity decrease due to original model overfitting when building on imbalanced dataset, while specificity and overall accuracy increased significantly. ***Conclusion:*** The accuracy of 3-y survival prediction in glioma patients, built on in vivo features, undergoing MET-PET can be improved significantly following advanced data preparation methods. ***References:*** 1. Papp L, et al: Glioma Survival Prediction with Combined Analysis of In Vivo ^{11}C-MET PET Features, Ex Vivo Features, and Patient Features by Supervised Machine Learning. JNM, 2018, DOI: 10.2967/jnumed.117.202267

OP-554

Data-driven identification of diagnostically useful extrastriatal signal in dopamine transporter SPECT using explainable AI

M. Nazari[1,2], *I. Apostolova*[3], *A. Kluge*[2], *S. Kimiaei*[2], *R. Buchert*[3];
[1]*TU-Dresden, Dresden, GERMANY,* [2]*ABX-CRO, Dresden, GERMANY,* [3]*University Medical Center Hamburg- Eppendorf, Hamburg, GERMANY.*

Aim/Introduction: In clinical routine, the interpretation of dopamine transporter (DAT) SPECT for the diagnosis of clinically uncertain parkinsonian syndromes usually is entirely based on striatal tracer uptake. However, there is some evidence that tracer uptake in other brain regions including insula, cingulate cortex, ventromedial prefrontal cortex, thalamus, hypothalamus and brain stem might also provide clinically useful information. The aim of the present study was to use explainable artificial intelligence (AI) for purely data-driven identification of extrastriatal brain regions that can contribute to the classification of DAT-SPECT beyond the striatal signal. ***Materials and Methods:*** Projection data from 1306 DAT-SPECT studies performed in clinical routine during 12/2008 and 01/2020 at a single center using 3 different SPECT camera models from two different manufactures equipped with low-energy-high-resolution collimators were retrieved from the PACS. Images were reconstructed by filtered backprojection using MATLAB. Reconstructed SPECT images were stereotactically normalized into the anatomical space of the Montreal Neurological Institute using SPM12 and a custom-made DAT-SPECT template. From each SPECT, a 2-dimensional slab view image of 12mm thickness was obtained by adding transaxial slices through the striatum. A convolutional neuronal network was trained with 1006 randomly selected slab views using visual binary interpretation as 'normal' or 'reduced' by an experienced reader as standard of truth. The convolutional neuronal network consisted of 14 convolutional layers followed by 3 fully connected neural network layers and had a total of 1,459,266 trainable parameters. The independent test set comprising the remaining 300 slab views was used to assess classification performance of the network. Layer-wise relevance propagation was used to quantify the relevance for the classification on a voxel-by-voxel base for each of the 300 slab views in the test set. A mean relevance map was obtained by averaging the relevance maps over all test slab views. ***Results:*** Overall accuracy, sensitivity, and specificity of the convolutional neuronal network were 97.0, 94.4, and 99.4%, respectively. Prominent contribution in the relevance map beyond the striatum (mainly putamen) was located in lateral frontal and lateral occipital cortex. Neither insula nor thalamus contributed relevantly. ***Conclusion:*** These findings suggest that tracer uptake in lateral frontal and lateral occipital cortex but not in insula and thalamus provides useful independent information for the interpretation of DAT-SPECT beyond striatal tracer uptake. ***References:*** None

OP-555

Evaluation of quantum-encoding for machine learning features in neural network-based predictive models

C. Spielvogel*, M. Grahovac, D. Krajnc, M. Hacker, T. Beyer, A. R. Haug, L. Papp;*
Medical University of Vienna, Vienna, AUSTRIA.

Aim/Introduction: Quantum neural network machine

learning approaches have been recently proposed [1] . The goal of the study was to compare the performance of predictive models established by quantum neural network and classic neural network approaches including three different radiomic cohorts. ***Materials and Methods:*** Three study cohorts were selected: 73 PET/CT cases of colorectal cancer patients, 120 CT cases of pancreatic cancer patients and 84 PSMA-11 PET cases of prostate cancer patients. The binary prediction targets were tumor presence for the colon cancer and the pancreatic cancer cohorts. For the prostate cohort the prediction target was low versus high risk. The class ratio was balanced for the prostate and pancreatic cohort while for the colon cancer cohort, 77 % of the samples corresponded to the non-tumor class. The radiomics features were scaled to values between 0.0 and 1.0 before executing both quantum and classic neural network approaches. The evaluation was performed using a nested, stratified Monte-Carlo cross-validation with 10 folds with a validation ratio of 25 % and a test ratio of 10 % in each predictive model. Evaluated performance metrics on the independent test set included sensitivity, specificity and accuracy for all predictive models. ***Results:*** The classic neural network models outperformed the corresponding quantum approaches in all cohorts. The accuracies were 0.69, 0.54 and 0.51 for the quantum approach for the colon cancer, pancreatic cancer and prostate cancer respectively while they were 0.74, 0.90 and 0.84 for the classic neural network respectively. The performance in the classic neural network was 17 % and 30 % higher for sensitivity and specificity respectively. ***Conclusion:*** Current solutions to perform quantum encoding of radiomics features appear to be inferior for neural network-based predictive models. Future approaches shall further optimize the way of encoding radiomics features to the quantum problem domain. ***References:*** [1] Broughton, Michael, et al. "TensorFlow Quantum: A Software Framework for Quantum Machine Learning." arXiv preprint arXiv:2003.02989 (2020).

1007

Teaching Session 4: Using Nodal Knowledge to Improve PET/CT Reporting for Lymphoma, Lung and Head/Neck Cancer

Saturday, October 24, 2020, 10:40 - 11:40 Channel 7

OP-556

TBA

T. Lynch; Belfast, UNITED KINGDOM.

OP-557

TBA

TBA.

1008

Clinical Oncology Track - Featured Session: Best of Nuclear Medicine Therapy

Saturday, October 24, 2020, 10:40 - 12:10 Channel 8

OP-561

Future of NM Therapy Beyond PSMA and PRRT

V. Lewington; Kings College London, Guys Hospital, Nuclear Medicine, London, UNITED KINGDOM.

OP-562

Patients with Progressive Paraganglioma Consecutively Treated with 177Lu-Dotatate or 90Y-Dotatoc PRRT. Toxicity, Efficacy and Prognostic Biomarker Results after Long-Term Follow-Up

S. Severi[1], S. Zovato[2], S. Nicolini[1], I. Grassi[1], M. Sansovini[1], E. Tardelli[3], E. Scarpi[1], E. Mezzenga[1], V. Di Iorio[1], G. Paganelli[1]; [1]IRST IRCCS, Meldola, ITALY, [2]Familial Cancer Clinic, Istituto OncologicoVeneto (IOV) IRCCS, Padua, ITALY, [3]Nuclear Medicine Unit, Department of Diagnostic Imaging, San Luca Hospital, Lucca, ITALY.

Aim/Introduction: At present there are no active therapies available for patients with progressive paraganglioma (mPPGLs) in either post-surgery or inoperable settings. However, these rare tumors overexpress somatostatin receptors and can thus be treated with peptide receptor radionuclide therapy (PRRT). We present our 10-year experience treating 46 consecutive mPPGL patients with 90Y-Dotatoc or 177Lu-Dotatate. ***Materials and Methods:*** All patients (20 men and 26 women, median age 52 years) showed positive scintigraphic imaging at 111In-octreoscan or 68Ga-Dotatoc PET/CT. 90Y-Dotatoc was administered in 12 patients, with cumulative dosages ranging from 7.4 GBq to 11 GBq, while 34 patients received 18.5 GBq or 27.5GBq of 177Lu-Dotatate. We used SWOG/RECIST criteria to evaluate treatment efficacy and CTCAE criteria to assess toxicity. The prognostic role of primary tumor site, hormone secretion, SDHx mutation, disease extension and metastatic involvement was also evaluated. ***Results:*** Both 90Y-Dotatoc and 177Lu-Dotatate PRRT were well tolerated by patients, without renal or bone marrow toxicity. The median follow-up was 60 months (range 11-146). The overall disease control rate (DCR) was 80.4% (95% CI 68.9-91.9) and was similar for both treatments. However, 177Lu-Dotatate patients showed a better median overall survival (mOS) than those receiving 90Y-Dotatoc and a better DCR when higher dosages were administered (P=0.03). Syndromic patients had a poorer mOS, and SDHx mutations did not interfere with treatment efficacy. ***Conclusion:*** PRRT is safe and effective for the treatment of patients with progressive mPPGL, especially at higher dosages. The better outcome

of 177Lu-Dotatate-treated patients indicates the former radiopharmaceutical as the best candidate for further clinical application. ***References:*** None

OP-563

Personalized Thera(g)nostic Approach in Patients with Pheochromocytoma and Paraganglioma: ^{131}I-mIBG and / or Peptide Receptor Radionuclide Therapy

H. Svirydenka*, B. Nilica, C. Mair, L. Rossetti, A. Kroiss, G. Di Santo, S. Buxbaum, C. Decristoforo, C. Uprimny, M. Gabriel, I. Virgolini;*
Universitätsklinik für Nuklearmedizin, Innsbruck, AUSTRIA.

Aim/Introduction: The experience with ^{131}Iodine metaiodobenzylguanidine (^{131}I-mIBG) and somatostatin-receptor (SSTR)-based-peptide-radionuclide therapy (PRRT) in patients with phaeochromocytomas (PCC) and paragangliomas (PGL) is limited. We report our experience for the treatment of malignant PCC and PGL (PPGL). ***Materials and Methods:*** Malignant PPGL patients treated at the Medical University Innsbruck, Department of Nuclear Medicine between 2006-2019 with ^{131}I-mIBG / ^{90}Y-DOTATOC / ^{177}Lu-DOTATATE, were retrospectively reviewed. Response to treatment was evaluated according to RECIST 1.0/ PERCIST 1.1 Criteria: Complete Response (CR), Partial Response (PR), Stable Disease (SD) and Progressive Disease (PD). The observation time was at least 1 year after completion of PRRT. As long term predictors we calculated the Progression-Free-Survival (PFS) and Overall-Survival (OS) since initialization of PRRT by Kaplan-Meier. ***Results:*** Twenty-seven patients (age range 18-74 years) with PPGL (8 PCC, 19 PGL) were analyzed. Pre-therapeutic scanning was positive in 7/8 PCC-patients with ^{123}I-mIBG and in 7/8 PCC-patients with ^{68}Ga-DOTATOC. 5/8 PCC-patients received ^{131}I-mIBG therapy (accumulated activity (ACC) range 3.6-47.48 GBq, absorbed tumour dose (ATD) range 0.8-673.2 Gy), from those 2 patients received additional tandem therapy with ^{90}Y-DOTATOC (ACC 11.2 and 15.5 GBq, ATD range 10.5-225.7 Gy). 2/8 PCC-patients were treated with ^{177}Lu-DOTATATE (ACC 25.8 and 30.4 GBq, ATD range 92-191.7 Gy) and 1/8 patients refused the therapy after performing dosimetry with ^{131}I-mIBG. 6/8 patients demonstrated PD, 1/8 PR, 1/8 CR by RECIST 1.0/ PERCIST 1.1 Criteria. The median PFS and OS of PCC-patients was 10 (range 8-108) and 30 months (range 12-156), respectively. Pre-therapeutic scanning was positive in 19/19 PGL-patients with ^{68}Ga-DOTATOC. However, 5/19 PGL-patients performed ^{123}I-mIBG, only in 1/5 patients, a positive uptake was observed. Additionally, 7/19 patients performed ^{18}F-DOPA and ^{18}F-FDG PET/CT, with evidence of positivity in 7/7 and 5/7 patients, respectively. 13/19 PGL-patients received ^{90}Y-DOTATOC (ACC range 8.07-16.44 GBq, ATD range 4.6-152.8 Gy), 4/19 PGL-patients ^{177}Lu-DOTATATE (ACC range 8.49-55.42 GBq, ATD range 14.1-235.3 Gy). 2/19 patients were lost to follow-up. In 16/17 patients SD and in 1/17 PD were recorded by RECIST 1.0/ PERCIST 1.1 Criteria. The median PFS and OS of PGL-patients was 96 (range 10-180) and 99.5 months (range 24-180), respectively. ***Conclusion:*** Both ^{131}I-mIBG and ^{90}Y / ^{177}Lu-SSTR-targeting peptides may be beneficial for long-term disease control in some patients with locally advanced or metastatic PPGL when applied in several treatment cycles that could reach meaningful absorbed tumour doses. Pretherapeutic imaging allows a personalized, tailored treatment by selecting the radiopharmaceutical resulting in the highest tumour dose. ***References:*** None

OP-564

Transarterial radioembolization of unresectable intrahepatic cholangiocarcinoma with ^{90}Y glass microspheres: results of a single institution study

A. Lorenzoni*, S. Mazzaglia, C. Spreafico, F. Scalorbi, G. Argiroffi, S. Bhoori, C. Chiesa, V. Fuoco, T. Cascella, E. Seregni, V. Mazzaferro, M. Maccauro;*
Fondazione IRCCS Istituto Nazionale Tumori, Milan, ITALY.

Aim/Introduction: To investigate safety and efficacy of yttrium-90 transarterial radioembolization (^{90}Y-TARE) in patients with unresectable intrahepatic cholangiocarcinoma (ICC). ***Materials and Methods:*** We retrospectively evaluated data of 23 consecutive patients (10 males, 13 females; mean 66, range 45-83 years) with locally advance ICC treated with ^{90}Y glass microspheres as first-line therapy or after chemotherapy failure. Macroaggregated albumin (MAA)-based SPECT/CT dosimetry was used to plan treatment through tumor dose (TD) and non-tumoural whole liver dose (NTWLD). Tumor response was assessed using mRECIST criteria 3-6 months after each TARE. Side effects were assessed using NCI-CTCAE version 5 criteria. Overall Survival (OS) and Progression-Free Survival (PFS) were evaluated from the first TARE (Kaplan-Meier methodology). ***Results:*** ^{90}Y-TARE was administered 30 times (7 repeated administrations), for a total of 35 lesions treated. Eight out of 30 treatments were performed as first line therapy. The mean ^{90}Y-loaded glass microsphere injected activity was 2.5 GBq (95% CI: 2.1-2.9). Mean NTWLD was 42.4 Gy (95% CI: 34.5-50.3). One grade 3 treatment-related irreversible liver toxicity was observed. No clinically relevant extra-hepatic toxicity was recorded. We obtained 1 complete response (CR 1/30=3%), 1 partial response (PR 1/30=3%), 26 stable disease (SD 26/30=87%) and 2 progression of disease (PD 2/30=7%). Objective response rate (CR+PR) was 7%; disease control rate (CR+PR+SD) was 93%. Two patients underwent post-TARE tumor resection and 1 patients orthotopic liver transplantation. Median OS was 21 months (95% CI: 12-34), median PFS was 9 months (95% CI: 6-17). Single-lesion dosimetric data were available in 25 out of 35 lesions (single-lesion response: 1 CR, 2 PR, 22 SD). Mean TD of all lesions was 309 (95% CI: 235-384) Gy, mean TD to responding lesions (CR+PR) was 384 (95% CI:

-129-898) Gy and mean TD to stable lesions was 280 (95% CI: 206-354) Gy. ***Conclusion:*** Our results show that ^{90}Y-TARE was safe and effective in controlling the disease. Dosimetric data of NTWLD suggest the possibility to increase ^{90}Y- glass microsphere administered activity to safely improve efficacy ***References:*** None

OP-565

Effectiveness of high-dose ^{131}I-MIBG as consolidation therapy for the patients with high-risk neuroblastoma

A. Inaki*, R. Kuroda, H. Wakabayashi, N. Akatani, T. Yamase, Y. Kunita, S. Watanabe, T. Hiromasa, H. Mori, S. Saito, Y. Ikawa, D. Kayano, S. Kinuya;*
Kanazawa University Hospital, Kanazawa, JAPAN.

Aim/Introduction: High-risk neuroblastoma is a childhood solid tumor with poor prognosis despite modern multimodality therapy. We have performed ^{131}I-metaiodobenzylguanidine (^{131}I-MIBG) internal radiotherapy with myeloablative dose combined with high-dose chemotherapy and blood stem cell transplantation as consolidation therapy for these patients. The aim of this study is to investigate whether our treatment protocol improved the remission induction rate and the long-term survival rate compared with conventional treatments. ***Materials and Methods:*** A total of 16 patients with primary or first-relapsed high-risk neuroblastoma were enrolled. Patients received high-dose (666 MBq/kg as a target dose) ^{131}I-MIBG and then received high-dose chemotherapy and stem cell transplantation after conventional induction chemotherapy. ***Results:*** The mean age was 3.6 ± 2.8 (range 0 - 10 years old) and the mean ^{131}I-MIBG dose was 648.1 ± 49.3 MBq/kg (range 526.9 - 730.3 MBq/kg). Thirteen and 3 patients received MEC (melphalan, VP-16 and carboplatin) and BuMel (busulfan and melphalan) as high-dose chemotherapy, respectively. Fourteen and 2 patients received peripheral blood stem cell transplantation and cord blood transplantation, respectively. Fourteen patients (87.5%) succeeded to reach complete remission. The mean follow-up period was 1460.8 ± 999.5 days. Two patients relapsed and 1 patient died of the primary disease. Nine patients were followed up over 3 years and 3-year overall survival rate was 100%. ***Conclusion:*** ^{131}I-MIBG therapy increased the success rate of consolidation therapy and may improve the long term prognosis in patients with high-risk neuroblastoma. ***References:*** None

OP-566

PRRT Efficacy of ^{111}In-DTPA-Octreotide Auger and Internal Conversion Electron Emission after Intra-arterial Implementation in Liver Metastasized Colorectal NETs

G. Limouris[1]*, V. Krylov*[2]*, M. B. Dolgushin*[3]*, I. Kyriazanos*[4]*, A. Zafeirakis*[5]*;*
[1]*Nuclear Medicine, Medical School, National and Kapodistrian University of Athens, Athens, GREECE,* [2]*Nuclear Medicine Dpt. "A. Tsyb Research Center", Obninsk, RUSSIAN FEDERATION,* [3]*N.N. Blokhin Russian Oncological Research Center, Moscow, RUSSIAN FEDERATION,* [4]*I Surgery Clinic, Army Naval and Veterans Hospital of Athens, Athens, GREECE,* [5]*Army Share Fund Hospital of Athens, Athens, GREECE.*

Aim/Introduction: Colorectal originated NETs are less commonly metastatic; however, when present, patients' survival is rather mediocre. Evidence guiding optimal treatment of such patients is practically lacking. By the present it was aimed to evaluate the efficacy of ^{111}In-DTPA-Octreotide Auger and Internal Conversion Electron Emission by assessing PRRT outcomes in patients with somatostatin receptor (SSTR) positive liver metastasized colorectal NETs. ***Materials and Methods:*** Eleven patients (m=3, f=8, age range 49-79 years) were included in the study. All eleven had ^{111}In-DTPA-Octreotide avid disease (visual score IV). Patients treated with PRRT were retrospectively reviewed. Morphologic (RECIST 1.1), SSTR imaging responses and toxicity were assessed, three-monthly post-PRRT. Kaplan-Meier estimate was used to determine progression-free survival (PFS) and overall survival (OS) from the beginning of the therapy. ^{111}In-DTPA-Phe^{1}-Octreotide was implemented after selective catheterization of the hepatic artery, in an average activity of 6.3±1.3 GBq per patient/per session, consecutively, with a time interval between sessions of 6-8 weeks. Infusion repetition did not exceed the 12 fold. ***Results:*** None of the eleven treated patients resulted in complete response and partial response was assessed in eight cases (72.72%), disease stabilization in one (9.10 %) and progressive disease in two (18.18%). The median PFS and OS were estimated to be 36 and 48 months, respectively. The organ average radiation dose was estimated as follows: (a) Liver Tumor 15.2 mGy/MBq, (b) Liver 0.14 mGy/MBq, (c) Kidneys 0.41 mGy/MBq, (d) Spleen 1.4 mGy/MBq and (f) Bone marrow 0.0032 mGy/MBq. The average absorbed dose per session to a tumour for a spherical mass of 10 gr was estimated to be 15 mGy/MBq, depending on the histotype of the tumour. Distinctive side effects were not noticed except a WHO toxicity grade 1 to 2 erythro-, leuko- and thrombocytopenia occurred in 9 (81.81%) cases observed about after the 9th session. ***Conclusion:*** The study indicates the high efficacy of ^{111}In-DTPA-Octreotide Auger and Internal Conversion electron emission due to their high LET, the morphologic responses with minimal toxicity and the very encouraging survival in patients with metastatic colorectal NETs despite the mediocre prognostic features of this cohort. Further larger prospective PRRT trials are warranted in this NET-subgroup. ***References:*** None

OP-567

Feasibility, Biodistribution and Preliminary Dosimetry in Peptide-Targeted Radionuclide Therapy (PTRT) of Diverse Adenocarcinomas using ^{177}Lu-FAP-2286: First-in-Human Results

H. Kulkarni[1], C. Smerling[2], C. Schuchardt[1], A. Singh[1], F. Robiller[1], M. Chantadisai[1,3], A. Eismant[1], D. Mueller[1], D. Zboralski[2], F. Osterkamp[2], A. Hoehne[2], U. Reineke[2], R. P. Baum[1];
[1]Zentralklinik Bad Berka, Bad Berka, GERMANY, [2]3B Pharmaceuticals GmbH, Berlin, GERMANY, [3]King Chulalongkorn Memorial Hospital, Bangkok, THAILAND.

Aim/Introduction: Fibroblast activation protein (FAP) is of great interest as target for diagnosis and therapy of numerous malignant tumors. In preclinical models, FAP-2286 has shown high uptake and long retention in tumors. Here we present first-in-human results. ***Materials and Methods:*** PTRT was performed in 11 patients with advanced adenocarcinomas using 2.5 - 9.9 GBq ^{177}Lu-FAP-2286 after prior confirmation of significant tumor uptake (SUV tumor-to-background ratio > 3) on ^{68}Ga-FAP (n =10)/FAPI PET/CT. A second cycle was administered to 9 patients, one patient underwent 3 cycles. Laboratory parameters including tumor markers were monitored. Biodistribution was analyzed by post-therapy planar and SPECT/CT images. Preliminary dosimetry estimations were performed in 7 patients. Clinical parameters including laboratory findings were monitored. ***Results:*** Metastases from adenocarcinomas of the pancreas (n=5), breast (n=4), rectum (n=1) and ovary (n=1).were present in the following localization: lymph node (n=6), lung (n=3), pleura (n=1), peritoneum (n=3), liver (n=7) and bone (n=5). Significant uptake and long tumor retention on delayed ^{177}Lu-FAP-2286 imaging (72h to 10 days post-injection) was observed in all patients. The mean absorbed whole body dose ranged from 0.05 - 0.1 Gy/GBq, red marrow received 0.04 - 0.09 Gy/GBq, and kidneys 0.6 - 0.9 Gy/GBq (comparable to ^{177}Lu-DOTATOC). Intensification of pre-existing abdominal pain with nausea and vomiting was noted in a pancreatic carcinoma patient with coeliac lymph node metastases, whereas short-lasting, severe headache was seen in a patient with skull metastases. There was mild, self-limiting headache in 3 patients, otherwise no relevant short-term side effects occurred. Pain decreased in 3 patients, one patient reported long-term clinical improvement. CTCAE v5.0 grade (G) 1 anemia emerging after treatment was noted in three patients. Anemia and leukocytopenia worsened from pre-existing G2 to G3 in one patient with bone-marrow involvement, who also experienced G3 renal insufficiency on follow-up (considered not related to PTRT). There was one new G3 thrombocytopenia. Follow-up using molecular imaging with ^{68}Ga-FAP-2286 PET/CT, RECIST 1.1 (CT/MRI) and tumor markers revealed stable disease in 3, and progressive disease in 8 patients. One patient with pre-existing, very advanced disease died of progression 4 weeks after the second cycle. ***Conclusion:*** FAP-targeted theranostics appears to be feasible and relatively safe. ^{68}Ga-FAP-2286 PET/CT can be used for patient selection and follow-up. Due to long tumor retention, PTRT using ^{177}Lu-FAP-2286 seems to be a promising treatment option in a broad spectrum of cancers. Further follow-up of patients as well as prospective clinical studies are warranted. ***References:*** None

OP-568

IPAX-1: Phase 1/2 study of 4-L-[^{131}I]-iodo-phenylalanine (^{131}I-IPA) administered concomitantly to second line external radiation therapy (XRT) in patients with recurrent glioblastoma multiforme (GBM)

T. Traub-Weidinger[1], R. Wilson[2], J. Pichler[3];
[1]Medical University of Vienna, Vienna, AUSTRIA, [2]Telix Pharmaceuticals, Melbourne, AUSTRALIA, [3]Kepler Universitätsklinikum, Linz, AUSTRIA.

Aim/Introduction: Many tumour types, including GBM, overexpress the L-type amino transporter 1 (LAT-1). ^{131}I-IPA is a small-molecule amino acid derivative internalised by LAT-1. Preclinical studies showed additive cytotoxic effects of ^{131}I-IPA + XRT[1]. Tumour accumulation of ^{131}I-IPA was shown in a proof-of-principle study[2] and confirmed with single dosing of 2-7 GBq ^{131}I-IPA in combination with XRT in patients with recurrent GBM[3]. The ^{131}I-IPA + XRT in Recurrent GBM (IPAX-1) study evaluates safety, dosing schedule and preliminary efficacy of ^{131}I-IPA combined with second-line XRT in patients with recurrent GBM. ***Materials and Methods:*** IPAX-1 is a multicentre, open-label, Phase 1/2, dose-finding study 131I-IPA + XRT in patients with histologically confirmed GBM experiencing first recurrence. Three dosing regimens are being evaluated at 2.0 GBq with subsequent dose escalation: Single dose ^{131}I-IPA administered 1-3 days prior to 1st XRT (N=3). Fractionated (parallel) ^{131}I-IPA in three fractions (3 x 0.67 GBq) administered throughout XRT, commencing 1-3 days prior to 1st XRT and subsequently every 5-9 XRT fractions (N=3). Fractionated (sequential) ^{131}I-IPA in three fractions (3 x 0.67 GBq) with fraction 1 administered 1-3 days prior to 1st XRT and fractions 2 and 3 administered after completion of XRT (N=3). 36 Gy of XRT will be delivered in 18 fractions of 2 Gy. The best regimen at 2.0 GBq will proceed to dose escalation in 2.0 GBq increments, up to 8.0 GBq or until the maximum tolerated dose (MTD) is reached (N=3 per cohort). The primary study objective is to assess safety and tolerability of ^{131}I-IPA + XRT. Secondary objectives include establishing MTD and optimal dosing schedule, dosimetry, biodistribution and preliminary efficacy. IPAX-1 will enroll up to 44 patients in Europe and Australia. Clinical trial number: NCT03849105. ***Results:*** As of May 2020, four patients have been randomised to the single dose and fractionated parallel groups. Up to 9.6 months post-treatment, one patient has stable disease

(SD, 9.6 months) and three patients have progressed (PD, 7.1, 4.8 and 2.5 months) using the Revised Assessment in Neuro-Oncology (RANO) criteria. No serious adverse events have been reported. ***Conclusion:*** ^{131}I-IPA (2 GBq) + XRT is safe and well tolerated. Preliminary results in the first 4 patients evaluated show best tumour response of SD up to 9.6 months post-treatment. ***References:*** 1. Israel et al. Nucl Med Biol 20112. Baum et al. Nucl Med Mol Imaging 20113. Verburg et al. Nuklearmedizin 2013

OP-569

Comparison of 99mTc-MAA SPECT/CT predictive dosimetry and 90Y PET/CT posttreatment dosimetry in Radioembolization of Hepatic Tumours

O. Ferrando[1], *F. Foppiano*[2], *A. Ciarmiello*[3];
[1]*ASL5 Spezzino, La Spezia, ITALY,* [2]*Medical Physics Department - ASL5 Spezzino, La Spezia, ITALY,* [3]*Nuclear Medicine Department - ASL5 Spezzino, La Spezia, ITALY.*

Aim/Introduction: The aim of this study was to evaluate the agreement between the predictive dosimetry based on 99mTc-MAA SPECT/CT and the post-treatment dosimetry based on 90Y PET/CT acquisitions. ***Materials and Methods:*** The study was applied to 20 patients with hepato-cellular carcinoma who underwent radioembolization with 90Y-resin spheres. We compared pre-treatment dosimetry based on 99mTc-MAA SPECT/CT and post-treatment dosimetry based on 90Y PET/CT. 3D dose maps and dose- volume histograms (DVH_spect, DVH_pet) were calculated using the methodology proposed in [1]. Mean absorbed dose in tumour volumes (D_{spect} and D_{pet}) were calculated using the MIRD method [2]. SPECT and PET volumes of interest (tumour volume) were delineated with a thresholding method using the AMIDE software [3], lobar and whole liver volumes were determined from CT images. Patient administered activity was calculated using the Body Surface Area method as recommended by the sphere manufacturer. Concordance between D_{spect} and D_{pet}, DVH_spect and DVH_pet were evaluated with the Wilcoxon Signed Ranked test. ***Results:*** Patient administered activity ranged from 0.4 GBq to 2.2 GBq. Tumour volumes ranged from 75mL to 1012 mL. The mean absorbed doses for tumour volume were 161±66 Gy (D_{spect}) and 173 ±79 Gy (D_{pet}). The comparison between D_{spect} and D_{pet} and the comparison between DVH_spect and DVH_pet evaluated with the Wilcoxon Signed Ranked test were statistically significant with α=0.01. ***Conclusion:*** Even if our results are limited to the restricted population analysed in this study, we have found a quantitative agreement between predictive and post dosimetry of 90Y-radioembolisation. From our point of view predictive dosimetry with 99mTc-MAA SPECT/CT can provide valuable estimation of tumour and non-tumour tissues absorbed doses and these information can help in the decision of a more personalised activity administration. ***References:*** [1] A.C. Traino et all. Dosimetry for nonuniform activity distributions: A method for the calculation of 3D absorbed-dose distribution without the use of voxel S-values, point kernels, or Monte Carlo simulations. Med. Phys. 40 (4), April 2013 [2] M.G. Stabin et all. Recommendations of the American Association of Physicists in Medicine on dosimetry, imaging, and quality assurance procedures for 90Y microsphere brachytherapy in the treatment of hepatic malignancies. Med. Phys. 38 (8), August 2011 [3] AMIDE 1.0.4 open source software

OP-570

Effectiveness and safety of multiple 90Y-radioembolization in patients with primary and secondary liver tumors

A. Di Palo*, C. Ferrari, C. D'Alò, P. Mammucci, M. Frugis, R. Ruta, V. Lavelli, G. Rubini;*
Nuclear Medicine Department, University of Bari "Aldo Moro", Bari, ITALY.

Aim/Introduction: The purpose of this study was to assess the effectiveness and safety of multiple 90Y radioembolization with microspheres (TARE) in patients with primary and secondary liver tumors to complete the first treatment. ***Materials and Methods:*** Between 2016 and 2020, 20 patients (9 women, 11 men; mean age, 70 y) with nonresectable advanced liver tumors (6 colorectal liver metastases;12 hepatocellular carcinoma; 2 cholangiocellular carcinoma) were treated by TARE twice. 12/20 patients received a whole-liver treatment with sequential TARE sessions of the left and right liver lobes (group A) while an uni-lobar treatment was performed in 8/20 patients (group B) within a mean of 6 months. Safety was the primary endpoint. Toxicity was documented according to Common Terminology Criteria for Adverse Events 4.0 (CTCAE) criteria based on laboratory parameters and clinical examinations 3 days, 6 weeks, and every 3 months after every TARE session. Response to treatment was assessed by CT scan according to RECIST criteria. Both CT scan and PET/CT imaging were used for patients' follow up to evaluate time to progression disease (TTP). TTP was estimated by the Kaplan-Meier method and results were compared using long-rank test. ***Results:*** In group A, after the first treatment 8/12 were PR, 2/12 SD and 2/12 PD, while in group B all patients (8/20) presented PR. After the second treatment, in group A 1/12 patients was CR, 2/12 were PR, 2/12 were SD and 7/12 were PD; in group B, 2/8 patients were CR, 1/8 were PR, 2/8 were SD and 3/8 were PD. No radioembolization-induced liver disease was observed. The most common adverse effects were ascites, reversible increasing of bilirubin and liver enzymes levels and transient abdominal pain. According to CTCAE criteria 3/20 patients showed reversible grade III to IV toxicities based on laboratory values, which returned to pretreatment levels after 6 weeks. Dorsal radiodermatitis occurred in 2/20

patients due to the interventional procedure. No case of RE-induced liver disease was registered. Median of TTP after the first treatment was 12,5 months.In particular a statistically significant difference was found in TTP and the patients' response to TARE (p=0,002), while no statistically significant difference was found in TTP and the number of lobes undergoing the treatment. ***Conclusion:*** In advanced liver tumors, multiple treatments with 90Y radioembolization can be performed with an acceptable toxicity profile. Furthermore, multiple treatments do not affect the disease control both in unilobar and whole-liver TARE. ***References:*** None

OP-571

Role of ^{90}Y- microspheres PET based tumor to normal (T/N) dosimetry to assess response in HCC selective internal radiation therapy

R. B. Martinez, S. Gavane, ***K. Knesaurek****;*
Icahn School of Medicine at Mount Sinai, New York, NY, UNITED STATES OF AMERICA.

Aim/Introduction: The aim of our work is to assess role of tumor-to-normal tissue (T/N) dosimetry ratios for predicting response in patients undergoing liver treatment with ^{90}Y microspheres. ***Materials and Methods:*** After treatment with ^{90}Y microspheres, 33 patients (5 females and 28 males, mean age 64.0± 8.1y), underwent PET/CT imaging. The low mA, non-diagnostic CT images from PET/CT were used for attenuation correction and localization of the ^{90}Y microspheres. Images were acquired for 15 min with the reconstruction matrix size of 200x200x75 mm and voxel size 4.07x4.07x3.00 mm. Local deposition method with known activity of ^{90}Y was used for dosimetry calculations. For each patient, volume-of-interest (VOI) for whole liver and tumor(s) was manually created and program automatically created normal tissue VOI. Response was assessed on MRI by mRECIST criteria done at a month post treatment and subsequently every 3 months after ^{90}Y treatment. ***Results:*** For 33 patients, the mean liver, tumor and normal tissue doses (mean ± SD) were, 55.37±25.83 Gy, 913.15±796.54 Gy and 54.64 ±25.55 Gy respectively. Among these patients, 29 (88%) have shown complete response (CR) and 4 (12%) have shown progression of disease (PD). For CR patients, the mean T/N dose ratio obtained was 20.14 (range 2.16 - 67.48) and for PD patients, the mean T/N dose ratio was significantly lower 6.57 (range 0.65-13.02). ***Conclusion:*** Our data indicates that patients with PD usually have T/N dose ratio lower than those with CR. However, further investigation is warranted because the number of PD cases was limited, and partial volume effect was not considered. ***References:*** None

1009

Clinical Oncology Track - Featured Session: Onco Diagnostics Miscellaneous

Saturday, October 24, 2020, 10:40 - 12:10 Channel 9

OP-572

PET Beyond FDG

D. Taïeb*; Centre hospitalo-universitaire Timone, Médecine Nucléaire, Marseille, FRANCE.*

OP-573

Comparison of ^{68}Ga-FAPI and ^{18}F-FDG PET/CT for the diagnosis of primary and metastatic lesions in patients with various types of cancer

H. Chen*, L. Zhao, Y. Pang, Q. Lin, L. Sun, H. Wu;*
The First Affiliated Hospital of Xiamen University, Xiamen, CHINA.

Aim/Introduction: 68Ga-FAPI serves as a promising alternative to ^{18}F-FDG for the assessment of malignant tumours and adds important diagnostic value in the context of challenging ^{18}F-FDG PET cancer subtypes. In this study, we evaluated the potential usefulness of ^{68}Ga-FAPI positron emission tomography/computed tomography (PET/CT) for the diagnosis of primary and metastatic lesions in various types of cancer, compared with ^{18}F-FDG PET/CT. ***Materials and Methods:*** A total of 75 patients with various types of cancer underwent contemporaneous ^{68}Ga-FAPI and ^{18}F-FDG PET/CT either for an initial assessment or for recurrence detection. Tumour uptake was quantified by the maximum standard uptake value (SUV_{max}). The sensitivity, specificity, positive predictive value (PPV), negative predictive value (NPV), and accuracy of ^{18}F-FDG and ^{68}Ga-FAPI PET/CT were calculated and compared to evaluate the diagnostic efficacy. ***Results:*** The study cohort consisted of 75 patients (47 male and 28 female; median age, 61.5 years; age range, 32-85 years). Fifty-four patients with 12 different tumour entities underwent paired ^{68}Ga-FAPI and ^{18}F-FDG PET/CT for initial assessment, while the other 21 patients underwent paired scans for recurrence detection. ^{68}Ga-FAPI PET/CT was able to clearly identify 12 types of malignant tumours with favourable tumour-to-background contrast, which resulted in a higher detection rate of primary tumours than did ^{18}F-FDG PET/CT (98.2% vs. 82.1%, P=0.021). Meanwhile, ^{68}Ga-FAPI PET/CT showed a better sensitivity than ^{18}F-FDG PET/CT in the detection of lymph nodes (86.4% vs. 45.5%, P=0.004) and bone and visceral metastases (83.8% vs. 59.5%, P=0.004). By contrast, ^{68}Ga-FAPI PET/CT was found to yield more false-positive findings compared to ^{18}F-FDG PET/CT, which resulted in its lower specificity for lymph nodes (76.5% vs. 58.8%, P=0.250) and bone and visceral metastases (58.3% vs. 41.7%, P=0.500). ***Conclusion:*** This study revealed that the primary tumour and most sites of

tumour involvement in patients with various cancers are well-visualised using ^{68}Ga-FAPI PET/CT. Tumour sites in the liver, abdomen, and brain were particularly evident because of the strong tumour uptake and low background uptake of ^{68}Ga-FAPI in these areas. ^{68}Ga-FAPI PET/CT was revealed to have better sensitivity and accuracy for the detection of both primary and metastatic lesions than did ^{18}F-FDG PET/CT. By contrast, ^{68}Ga-FAPI PET was found to yield more false-positive findings compared with ^{18}F-FDG PET, which resulted in its lower specificity for metastatic lesions (although this difference was not statistically significant). ***References:*** None

OP-574

^{18}F-FDG PET/CT in muscle-invasive urothelial bladder cancer: the role of functional imaging in neoadjuvant immunotherapy, an ancillary analysis of PURE-01 protocol

A. Capozza[1], L. Marandino[2], B. Padovano[1], G. Serafini[1], A. Briganti[3], D. Raggi[2], E. Farè[2], F. Pederzoli[3], A. Gallina[4], M. Bandini[3], U. Capitanio[3], M. Bianchi[4], G. Gandaglia[4], N. Fossati[3], P. Giannatempo[2], A. Salonia[4], F. Montorsi[3], A. Necchi[2], E. Seregni[1], A. Alessi[1];

[1]Nuclear Medicine Unit, IRCCS Istituto Nazionale dei Tumori di Milano, Milan, ITALY, [2]IRCCS Istituto Nazionale dei Tumori di Milano, Milan, ITALY, [3]Vita-Salute San Raffaele University, Milan, ITALY, [4]IRCCS San Raffaele Hospital, Milan, ITALY.

Aim/Introduction: Nodal disease, in bladder cancer staging, has a significant impact on patients' prognosis; yet accurate lymph nodes (LN) staging is an ongoing challenge for oncologic imaging. In clinical practice, computed-tomography (CT) and magnetic-resonance are the standard staging methods, however conventional imaging is burdened by high false-negative rates. Currently, there are no consensus recommendations on the routine use of ^{18}F-FDG PET/CT in abdomino-pelvic nodal staging of bladder cancer. In this secondary analysis of PURE-01 clinical trial (NCT02736266), we exploited the role of ^{18}F-FDG PET/CT in patients with muscle-invasive bladder cancer (MIBC) treated with neoadjuvant immunotherapy and radical cystectomy. ***Materials and Methods:*** Enrolled MIBC patients were treated with 3 courses of 200 mg pembrolizumab, followed by radical cystectomy. They were assessed with thorax-abdomen CT scan and with ^{18}F-FDG PET/CT scan during screening and before surgery. All patients underwent extended pelvic LN dissection with packeted node submission. ^{18}F-FDG PET/CT results were compared with histopathological findings. ^{18}F-FDG PET/CT scans were reviewed to assess the onset of immune-related adverse events (irAEs) during pembrolizumab treatment, as well. ***Results:*** From 02/2017 to 08/2019, 106 evaluable patients were enrolled and treated; 212 PET/CT scans were internally performed and reviewed. Seven patients (6%) had nodal uptake at baseline PET/CT; whereas eight patients (7%) had LN uptake at PET/CT post-neoadjuvant immunotherapy. After lymphadenectomy, the rate of pathologic LN was 15% (n=16). The performance of post-pembrolizumab PET/CT, in predicting pathologic LN, is as follows: Sensitivity 37% (15.2-64.6, 95% CI); Specificity 98% (91.9-99.7, 95% CI); Negative Predictive Value 89% (85.3-92.6, 95% CI); Positive Predictive Value 75% (39.9-92.6, 95% CI), Accuracy 88%. Overall, 4/6 patients (67%) with baseline FDG uptake revealed as true positive versus 12/97 (12%) false negative cases. As it concerns irAEs, a total of 40 patients (38%) developed inflammatory FDG-uptakes post-pembrolizumab in several target regions. Thyroid gland was the most frequently involved organ (n=21; 52%), followed by stomach (n=14; 35%), mediastinum (n=13; 32%) and lung (n=10; 25%). Only 15/40 (37%) patients had clinical manifestations of irAEs, i.e. signs, symptoms or laboratory alterations. ***Conclusion:*** ^{18}F-FDG PET/CT could find a role in bladder cancer LN staging, as it enforces conventional imaging in diagnosing nodal disease, especially in patients tested for eligibility in clinical trials, and to improve clinical management, as well. Immunotherapy determines profound inflammatory adverse events that could affect the safety profile of these treatments. ^{18}F-FDG PET/CT should be proposed to precociously recognize and diagnose irAEs. ***References:*** None

OP-575

^{18}F-PSMA-1007 PET/CT for response assessment in patients with metastatic renal cell carcinoma undergoing tyrosine kinase or checkpoint inhibitor therapy

L. Mittlmeier[1], M. Unterrainer[2], S. Rodler[3], A. Todica[1], N. L. Albert[1], C. Burgard[1], C. C. Cyran[2], W. G. Kunz[2], J. Ricke[2], P. Bartenstein[1], C. G. Stief[3], M. Staehler[3], H. Ilhan[1];

[1]LMU Munich, Department of Nuclear Medicine, Munich, GERMANY, [2]LMU Munich, Department of Radiology, Munich, GERMANY, [3]LMU Munich, Department of Urology, Munich, GERMANY.

Aim/Introduction: The implementation of tyrosine-kinase and checkpoint inhibitors improved overall survival for metastatic renal cell carcinoma (mRCC). However, serum biochemistry is unable to predict therapeutic efficacy whereas early prediction of treatment response is highly desirable for the individualization of patient management and improvement of therapeutic outcome. Initial data showed promising results for PSMA-targeted PET imaging in mRCC due to a high PSMA-expression of the neovasculature of RCC. Therefore, we aimed at evaluating ^{18}F-PSMA-1007 PET imaging for response assessment in mRCC patients undergoing tyrosine-kinase or checkpoint inhibitor therapy compared to CT-based response assessment as the current imaging reference standard. ***Materials and Methods:*** ^{18}F-PSMA-1007 PET/CT was performed in 11 mRCC patients

prior to initiation of systemic treatment and 8 weeks after therapy initiation. Treatment response was evaluated separately on ^{18}F-PSMA PET and CT. Changes in uptake on PSMA-PET (SUV_{mean}) were assessed on a per-patient basis using a modified PERCIST scoring system. Complete response (CR_{PET}) was defined as absence of any uptake in all target lesions on posttreatment PSMA-PET. Partial response (PR_{PET}) was defined as decrease in summed SUV_{mean} of >30%. The appearance of a new PET-positive lesion or an increase in summed SUV_{mean} of >30% was defined as progressive disease (PD_{PET}). A change in summed SUV_{mean} of ±30% was classified as stable disease (SD_{PET}). RECIST 1.1 criteria were used for response assessment on CT. Subsequently, results of radiographic response assessment on PSMA-PET and CT were compared. ***Results:*** At baseline PSMA-PET_1, every mRCC patient showed at least one PSMA-avid lesion. On follow-up PET_2, 3 patients showed CR_{PET}, 3 PR_{PET}, 4 SD_{PET} and 1 PD_{PET}. According to RECIST 1.1, 1 patient showed PR_{CT}, 9 SD_{CT} and 1 PD_{CT}. Overall, concordant classifications were found in only 2 cases (2 SD_{CT+PET}). Patients with CR_{PET} on PET were classified as 3 SD_{CT} on CT using RECIST 1.1. By contrast, the patient classified as PR_{CT} on CT showed PSMA-uptake without major changes during therapy (SD_{PET}). However, among 9 patients with SD_{CT} on CT, 3 were classified as CR_{PET}, 3 as PR_{PET}, 1 as PD_{PET} and only 2 as SD_{PET} on PSMA-PET. ***Conclusion:*** On baseline PSMA-PET, heterogenous courses were observed during systemic treatment in mRCC patients with highly diverging results compared to RECIST 1.1. PSMA-PET for response assessment in mRCC patients undergoing tyrosine-kinase or checkpoint inhibitor therapy might provide additional information beyond the morphologic information on CT that might highly influence patient management. ***References:*** None

OP-576

Phosphoenolpyruvate Carboxykinase1Reduces ^{18}F-FDG Uptake in Clear Cell Renal CellCarcinoma

L. Shi[1], S. An[2], Y. Liu[3], J. Liu[2], F. Wang[1];
[1]Nanjing First Hospital, Nanjing Medical University, Nanjing, CHINA, [2]Department of Nuclear Medicine, Ren Ji Hospital, School of Medicine, Shanghai Jiao Tong University, Shanghai, CHINA, [3]Department of Nuclear Medicine, Shanghai Tenth People's Hospital, Tongji University School of Medicine, Shanghai, CHINA.

Aim/Introduction: Phosphoenolpyruvate carboxykinase (PCK1) plays an important role in gluconeogenesis. Suppressing gluconeogenesis is a component of glucose metabolism change in clear cell renal cell carcinoma (ccRCC). Fluorine 18 (^{18}F) fluorodeoxyglucose (FDG) positron emission tomography and computed tomography (PET/CT) is based on the abnormally high rate of glucose metabolism found in cancer cells and is widely used in diagnose and management of many malignant tumors. However, to date, the relationship between ^{18}F-FDG uptake and PCK1 expression has not been investigated. ***Materials and Methods:*** Retrospective analysis was conducted on 68 patients with ccRCC who underwent ^{18}F-FDG PET/CT. The relationship between maximum standardized uptake (SUV_{max}) and the expression of PCK1, glucose transporter 1 (GLUT1) was analyzed with immunohistochemical analysis. PCK1 knockdown and overexpression in ccRCC cells were used to examine the role of PCK1 in tumor metabolism, tumorigenesis, and its effect on the expression of hypoxia inducible factor-1α (HIF-1α), GLUT1, and lactate dehydrogenase A (LDHA). ***Results:*** An inverse relationship between SUV_{max} and PCK1 expression ($P < 0.001$) was noted. The higher-grade ccRCC tumors exhibited a significantly greater SUV_{max} than lower-grade ccRCC tumors ($P < 0.001$). The PCK1 expression was also significantly lower in the patients with higher-grade ccRCC ($P = 0.001$) as revealed by ANOVA. PCK1 expression influenced glucose uptake, utilization and tumorigenesis in vitro and in vivo. PCK1 silencing-regulated expression of HIF-1α mediates such metabolic reprogramming. ***Conclusion:*** PCK1 expression is inversely associated with SUV_{max} in patients with ccRCC, and PCK1 inhibits ^{18}F-FDG uptake and utilization via the HIF-1α pathway. SUV_{max} is higher in patients with higher-grade ccRCC than in those with lower-grade ccRCC; this result may be due to the lower PCK1 expression in the former. ***References:*** None

OP-577

Auxiliary Diagnostic Utility of Partial 18F-FDG PETMR on Whole-Body 18F-FDG PETCT

Y. Xu;
Hangzhou Universal Imaging Diagnostic Center, Hangzhou, CHINA.

Aim/Introduction: To explore the value of selectively adding partial PET/MR after Whole-Body PET/CT. ***Materials and Methods:*** 296 cases of whole body PET/CT were analyzed retrospectively, those cases were all selectively added partial PET/MR due to the difficulty of diagnose on whole body PET/CT. 238 patients among those 296 patients were suffered from malignant tumor. Partial PET/MR covers multiple organs, which include 32 intracranial cases, 21 nasopharynx cases, 18 thoracic cases, 59 breast cases, 147 abdominal cases and 65 pelvic cases. The utility of adding partial PET/MR was valued ccording to the subsequent pathologic findings of those cases. ***Results:*** Partial PET/MR has a significant diagnostic value on most of the cases with a positive rate of 81.76%(242/296) among those cases, 14.86%(44/296)of the cases has no obvious value on further diagnose, yet another 3.38%(10/296) of the cases were misdiagnosed because of selectively adding partial PET/MR. 130 out of 216 cases which covers intracranial, breast, hepato, pancreas, renal and prostatic lesions have already acquired or changed the initial diagnose after partial PET/

MR was added, which covered 325 lesions including 191 malignant lesions. 81 cases have negative FDG uptake on PET-CT yet with a positive FDG uptake on PET-MR, mostly distributed in thoracic and abdominal areas. Among 80 cases of nasopharyngeal carcinoma, central primary bronchogenic carcinoma, rectal carcinoma and cervical carcinoma, 67 of those cases changed or pointed to a clear diagnose after adding partial PET-MR. ***Conclusion:*** Partial PET/MR has a significant value on those with diagnostic difficulties cases by only depending on whole body PET/CT. The appropriate timing, organ and sequences were highly depending on the experience of the radiologists. ***References:*** [1] Catalano O A, Rosen B R, Sahani D V, et al. Clinical impact of PET/MR imaging in patients with cancer undergoing same-day PET/CT: initial experience in 134 patients--a hypothesis-generating exploratory study[J]. Radiology,2013,269(3):857-869.[2] Dunet V , Maeder P , Nicodlalonde M , et al. Combination of MRI and dynamic FET PET for initial glioma grading.[J]. Nuklearmedizin, 2014, 53(4):155-161.[3] Kubiessa K, Purz S, Gawlitza M, et al. Initial clinical results of simultaneous 18F-FDG PET/MRI in comparison to 18F-FDG PET/CT in patients with head and neck cancer. Eur J Nucl Med Mol Imaging, 2014,41(4):639-648. [4] Partovi S, Kohan A, Vercher-Conejero JL, et al. Qualitative and quantitative performance of 18F-FDG-PET/MRI versus 18F-FDG-PET/CT in patients with head and neck cancer. AJNR, 2014,35(10):1970-1975.

OP-578

Imaging-based score and diagnostic flow-chart for malignant adrenal lesions

A. Farolfi[1], *E. Maietti*[2], *F. Piperno*[1], *P. Coppolino*[3], *A. Lambertini*[4], *R. Mei*[1], *L. Calderoni*[1], *C. Balacchi*[5], *R. Golfieri*[5], *U. Pagotto*[6], *S. Fanti*[1], *S. Selva*[2], *D. Santini*[7], *A. De Leo*[7], *C. Mosconi*[5], *G. Di Dalmazi*[6], *V. Vicennati*[6], *C. Nanni*[1];
[1]*Nuclear Medicine Unit, S. Orsola Hospital, University of Bologna, Bologna, ITALY,* [2]*Department of Medical and Surgical Sciences, University of Bologna, Bologna, ITALY,* [3]*Radiodiagnostic and Radiotherapy Unit, Department of Medical and Surgical Sciences and Advanced Technologies, "GF Ingrassia", Catania, ITALY,* [4]*Department of Nuclear Medicine, Würzburg University Hospital, Würzburg, GERMANY,* [5]*Radiology Unit, S. Orsola Hospital, University of Bologna, Bologna, ITALY,* [6]*Endocrinology Unit, S. Orsola Hospital, University of Bologna, Bologna, ITALY,* [7]*Pathology Unit, S. Orsola Hospital, University of Bologna, Bologna, ITALY.*

Aim/Introduction: Hormonal assessment (HA) and contrast-enhanced CT (ceCT) show insufficient sensitivity and specificity when staging adrenal lesions (AL), while FDG-PET does not hold an established role during the diagnostic work-up. We aimed at: 1) developing an imaging-based (ceCT and FDG-PET) score to predict the probability of malignancy and 2) identifying a diagnostic flow-chart able to possibly discriminate between malignant and benign lesions by the means of a composite reference standard. ***Materials and Methods:*** From 2007 to 2018 we retrospectively enrolled patients referred to our hospital for evaluation of unilateral adrenal mass with: a) a ceCT made up of unenhanced, arterial, venous and delayed phase (15 minutes); b)FDG-PET within one month of the ceCT; c) HA if available; d) histopathology after adrenalectomy or if unavailable, a clinical follow-up of at least 2 years as reference standard. Firstly, multivariable logistic regression analysis was employed to determine predictors of malignant AL and ROC curves were calculated. Second, regression-based coefficients were used to develop a score predicting malignant AL. Finally, cut-offs were calculated and a diagnostic flow-chart able to distinguish malignant versus benign AL was defined. ***Results:*** 51 patients were enrolled (41F, 10M; mean age 61 years). Twenty-four (47%) had malignant AL (14 pheochromocytomas, 5 carcinomas, 5 others). The remaining 27 presented with lesions benign AL (22 adenoma, 2 haemangioma and 3 others). Norepinephrine, maximum lesion diameter, HU at the delayed phase (HU15min), relative and absolute washout, AL-SUV_{max}, AL-SUV_{mean}, ratio AL-SUV_{max}/liver SUV_{max} (R-SUV_{max}) were associated with the presence of a malignant lesion (all $p<0.05$). Regarding FDG-PET parameters, R-SUV_{max} had the highest AUC (0.796) and a 1.5 cut-off showed a 75% sensitivity and a 75% specificity. A model including only R-SUV_{max} and HU15min had an AUC of 0.893 and the following score was developed: "score=40*(R-SUV_{max} -1) +1*HU15min". Excluding FDG-PET parameters, we calculated cut-offs of ceCT and HA parameters to discriminate malignant versus benign AL, finding 83% of malignant and 78% of benign lesions. Applying the R-SUV_{max} cut-off of 1.5 to those remaining patients with uncertain diagnosis, we found an overall 96%sensitivity and 89% specificity for malignant AL. ***Conclusion:*** This study shows that combined morphological and metabolic parameters may predict the presence of malignant AL. An imaging-based score may be successfully applied to selected patients. Even more important is the availability of a reliable diagnostic flow-chart to stratify patients on the basis of malignancy risks, thus guiding undefined adrenal lesions to FDG-PET imaging. ***References:*** None

OP-579

Contribution of open mouth technique in F-18 FDG PET/CT imaging of patients with malignant lip neoplasm

G. Mutevelizade*, C. Sezgin, E. Sayit, G. Gumuser;*
Celal Bayar University, Faculty of Medicine, Department of Nuclear Medicine, Manisa, TURKEY.

Aim/Introduction: F-18 FDG PET/CT has an important role for evaluating head and neck cancers. On the other hand, localization and size evaluation of this region can be rough due to the multitude of the anatomic structures and

physiologic uptakes. The aim of this study is to evaluate the contrubition of open-mouth imaging technique at F-18 FDG PET/CT while staging malignant lip neoplasms. ***Materials and Methods:*** Thirty-four patients (9 women, 25 men; mean age 70.9 ± 9.6 years) with histopathologically proven malignant lip neoplasm underwent F -18 FDG PET/CT (Philips, True Flight Select, USA) imaging for initial staging. Each patient imaged twice as whole-body F -18 FDG PET/CT with routine closed-mouth (CM) position; and open-mouth (OM) head and neck image, standardized with a special device. Open-mouth and CM images were evaluated by two nuclear medicine specialists blinded to each other. Lesion SUV max, localization, size and involvement of lymph nodes were evaluated. The data were compared to histopathological, clinical and radiological results ***Results:*** SUV max were calculated as 7.61±6.4 and 7.57±6.9 for CM and OM, respectively. There was no statistical significant difference between OM and CM SUV max. This revealed that openness or closure of the mouth did not affect SUVmax. Lesion localization was compared with clinical and radiological (MRI&CT) results and the localization was concordant at 50% of CM and 92% of OM images. Lesion size in F-18 FDG PET/CT was compared with histopathological findings and the size measurement was coherent at 47% and 79% for CM and OM images, respectively. Lesion size was also compared with MRI and it was consistent at 38% of CM and 74% of OM images. Regional lymph node metastasis were detected in 12 (35%) patient. It was observed that open-mouth acquisition did not contribute additionally in detecting the presence of regional lymph node metastasis. Statistical analysis was performed using SPSS 21.0 ($p<0.05$ was considered as statistically significant). ***Conclusion:*** We conclude that additional open-mouth head and neck imaging is useful and necessary for the accurate determination of the localization and size of the tumour, thus enhancing the value of PET/CT in staging, re-staging and response to the treatment of malignant lip neoplasms. ***References:*** None

OP-580

Role of F-18 FDG PET/CT in Hemophagocytic Lymphohistocytosis (HLH)

T. T, S. Datta Gupta, S. Shamim, R. Kumar, C. Bal;
All India Institute Of Medical Sciences, New Delhi, INDIA.

Aim/Introduction: Hemophagocytic lymphohistiocytosis (HLH) is an infrequent disorder seen primarily in paediatric age group, marked by persistent fever, splenomegaly with cytopenia, hypertriglyceridemia, and hypofibrinogenemia. Primary HLH may be managed by hematopoietic stem cell transplantation. However secondary HLH, usually associated with underlying infection, autoimmune diseases and malignancies, is managed as per its provoking cause. This study was performed to assess the role of F-18 FDG PET/CT in detection of underlying cause in secondary HLH. ***Materials and Methods:*** We retrospectively analysed patients referred for FDG PET/CT with clinical suspicion of HLH. Clinical diagnosis was made using the HLH- 2004 criteria. Five out of 8 criteria were needed to be fulfilled for inclusion. Criteria included were fever, splenomegaly, cytopenia (Hb <9.0 g/dl, platelets <100,000/µl, and neutrophils <1,000/µl), hypertriglyceridemia and/or hypofibrinogenemia (high triglycerides >3.0 mmol/l or low fibrinogen <150 mg/dl), low NK cell activity, hyperferritinemia (>500 ng/ml), high sIL-2R (>2,400 U/ml) and histological finding of hemophagocytosis. All referred patients underwent F18- FDG PET/CT study, which was reported independently by two experienced nuclear medicine physicians. Histopathological correlation was sought for PET positive lesions. ***Results:*** Seven patients (6 male, 1female) with mean age of 18.45 years were included. All seven patients showed positive findings on PET/CT. FDG PET/CT revealed metabolically active lymphadenopathy, focal or diffuse splenic and marrow uptake in six (85%) of the seven included patients. One patient had FDG avid skin lesions and hepatomegaly with no splenic involvement. Five out of the seven patients underwent histopathological correlation. Out of these 5, biopsy of two revealed Hodgkin Lymphoma and one lupus disorder; 1 patient showed necrotising lymphadenitis on biopsy suggestive of autoimmune disorder, however serum antibody profile was negative; 1 case with focal marrow uptake was negative on bone marrow biopsy, (site of biopsy did not correlate to uptake); For the remaining two patients with PET positive lymphadenopathy histopathological correlation is awaited. Three out of five (60%) PET positive cases were true positives and two were false positive on biopsy. ***Conclusion:*** In conclusion, F-18 FDG PET/CT can be a useful tool in detecting the associated cause in cases of secondary HLH and thereby in guiding the management. Although a rare disease, studies with larger sample size may be appropriate to assess the accuracy of FDG PET/CT in HLH. ***References:*** None

OP-581

Non-conformist intracranial Ga-DOTATATE uptake

C. Millo, A. Jha, K. Pacak;
NIH, Bethesda, MD, UNITED STATES OF AMERICA.

Aim/Introduction: Incidental intracranial SSTR-2 positive lesions have been reported in patients with neuroendocrine tumors, including Pheo/PGL, and commonly represent benign tumors such as meningiomas, pituitary tumors, both more commonly encountered in MEN1 patients, and hemangioblastomas seen in VHL patients. However, nefarious causes/lesions can also be detected, albeit rarely. The focus of our study was to highlight the rare cases of positive Ga-DOTATATAE intracranial lesions, other than the benign ones comprised of the tumors mentioned above, that were found in our patient population. ***Materials and Methods:*** 1200 patients with neuroendocrine tumors, including familial genetic syndromes such as MEN1 and VHL, and Phe/PGL, underwent Ga-Dotatate PET/CT scanning between 11/2014 and 12/2019. Patients in which the abnormal intracranial uptake was due to known or MRI confirmed meningiomas, pituitary tumors, and hemangioblastmas, were excluded from the analysis. ***Results:*** 6 patients (0.5%) demonstrated abnormal intracranial uptake that was not explained by corresponding meningiomas, pituitary tumors, or hemangioblastomas, as verified by their clinical history and CT/MRI. One patient with history of familial midgut carcinoid presented with LLL mass c/w atypical carcinoid; the Ga-DOTATATE scan revealed a biopsy proven cerebellar lesion c/w NET. A second patient had history of cardiac PGL and developed brain lesions with evidence of SSTR-2 expression proven by biopsy to represent PGL. A third patient presented with biopsy proven brain PGL. A fourth patient had history of abdominal PGL and CBT and developed extensive intracranial uptake with involvement of the sinuses. A fifth patient had with history of abdominal PGL and CBT and presented with suspicious intracranial lesion that remained unelucidated. A sixth patient had known spinal cord PGL and demonstrated separate brain lesions with positive biopsy for PGL. ***Conclusion:*** These anecdotal cases depict a spectrum of Dotatate avid intracranial brain lesions beyond the more common benign tumors that are known to demonstrate SSTR-2. Though very rare, primary or metastatic NET and paragangliomas can involve the brain parenchyma and intracranial structures. Although not difficult to detect in the normally absent background intracranial Ga-DOTATATE uptake (with the exception of pituitary), the localization and extension of these abnormalities can be challenging and unexpected. Therefore, we recommend that Ga-DOTATATE studies include by default the entire head in their FOV followed by careful evaluation of intracranial activity. ***References:*** None

OP-582

Role of ^{18}F-FDG PET/CT in detecting recurrent transitional cell carcinoma

S. Shamim*, P. Kaushik, J. Hussain, G. Arora, S. Datta Gupta, R. Kumar, C. Bal;*
AIIMS, New Delhi, INDIA.

Aim/Introduction: There is paucity of literature on utility of ^{18}F-FDG PET/CT in transitional cell carcinoma (TCC), possibly because the tracer is excreted in urine which makes scan interpretation difficult. Conventional imaging using cystoscopy, CT or MRI may be equivocal in detecting recurrence in presence of post-surgical changes, especially in upper urinary tract lesions. Hybrid PET/CT imaging and use of dual time point imaging with diuresis can overcome these problems. The present study was aimed at determining the role of ^{18}F-FDG PET/CT in detecting recurrent TCC. ***Materials and Methods:*** Treated follow up cases of TCC (post-surgery and chemotherapy) who underwent FDG PET/CT for suspected recurrence, were retrospectively included in the study. Recurrence was suspected based on clinical features and/or conventional imaging. Whole body PET/CT scan was acquired on dedicated PET/CT scanner (Biograph mCT, Siemens, Germany and 710 Discovery, GE, USA) 45-60 minutes after injection of 10 mCi of FDG intravenously, following which 1mg/kg (maximum 40 mg) of furosemide was injected i.v. and a spot image with kidneys and bladder in field of view was acquired 110-120 minutes post-injection of FDG. All images were visually analyzed by two nuclear medicine physicians independently, who were blinded to each other's scan findings. ***Results:*** Twenty-nine patients of TCC underwent FDG PET/CT in our department since 2014, of which 12 patients (10 male and 2 female) with query of recurrence were included in this retrospective study. Mean age of the patients was 57.4±11.9 years. The primary site of TCC was kidney in 9, urinary bladder in 2 and ureter in 1 patient. FDG PET/CT was positive for recurrent disease in 10/12 (83%) patients and negative in 2 (17%) patients. Of the patients with recurrent disease, 2 patients had only local recurrence, 6 patients had recurrent metastatic disease while both local and metastatic recurrence was seen in 2 patients. The site of recurrent disease was lymph nodes in 4 patients, visceral disease in 4 patients and both in 2 patients. ***Conclusion:*** FDG PET/CT may be used for detection of local as well as metastatic recurrence in TCC particularly in patients with upper urinary tract TCC where cystoscopy is not feasible. Dual time point imaging with diuresis can help in avoiding pitfalls and artifacts due to urinary excretion of FDG. ***References:*** None

1010

Featured Session: Nuclear Imaging in Cardiac Arrhythmias

Saturday, October 24, 2020, 10:40 - 12:10 Channel 10

OP-583

Nuclear Imaging in Cardiac Arrhythmias - What do we have? What do we still need?

F. Rouzet; Hopital Bichat Claude Bernard, Service de Médecine Nucléaire, Paris, FRANCE.

OP-584

The value of cardiac sympathetic nervous system activity in predicting the effectiveness of radiofrequency ablation of atrial fibrillation

Y. Varlamova, K. Zavadovsky, I. Kisteneva, S. Sazonova, R. Batalov; Cardiology Research Institute, Tomsk NRMC, Tomsk, RUSSIAN FEDERATION.

Aim/Introduction: Atrial fibrillation (AF) is one of the widest spread forms of arrhythmia worldwide. To date, radiofrequency catheter ablation (RFCA) of AF is a valuable treatment option. So far there are no clear predictors of the effectiveness of AF ablation. Nowadays, the association of cardiac sympathetic nervous system and the development and maintenance of AF has been showed. However, the association between sympathetic innervation disturbances and AF RFCA effectiveness remains inconclusive. The aim of the study was to evaluate the prognostic significance of cardiac sympathetic activity, assessed by ^{123}I-MIBG scintigraphy, in AF RFCA efficacy. ***Materials and Methods:*** The study included 46 patients. All patients were divided into 2 groups: I group - AF patients (n=36), II group - sinus rhythm patients (n=10). All patients underwent ^{123}I-MIBG and ^{99m}Tc-MIBI scintigraphy (planar and SPECT) to evaluate the cardiac sympathetic activity and myocardial perfusion, respectively. Echocardiography was performed in all patients to assess the cardiac contractile function. The effectiveness of interventional treatment was assessed in one year by 24 hour Holter monitoring. ***Results:*** During a median follow-up of 12±6 month, arrhythmia recurrence was observed in 15 patients. The univariate regression analysis showed that the left atrial diameter, ^{123}I-MIBG washout rate (WR), late ^{123}I-MIBG defect score and ^{123}I-MIBG/^{99m}Tc-MIBI mismatch score were predictors of AF recurrence. According to multivariate analysis only WR (odds ratio: 1.691, 95% confidence interval: 1.096-2.647, p = 0.012) and ^{123}I-MIBG/^{99m}Tc-MIBI mismatch score (odds ratio: 1.995, 95% confidence interval: 1.192-2.992, p = 0.023) were an independent predictors of AF RFCA effectiveness. The receiver operator characteristics curve (ROC) analysis indicated the potential diagnostic value of WR to predict recurrence of AF after RFCA with an area under the curve of 0.996 (P < 0.05; sensitivity = 98%, specificity = 50%), and an optimum cut-off value of 21.5 %. ROC analysis gave an optimum cut-off value of 12 % for the ^{123}I-MIBG/^{99m}Tc-MIBI mismatch score with an area under the curve of 0.940 to predict of AF RFCA effectiveness (p<0.05, sensitivity = 75%, specificity = 45%). ***Conclusion:*** To sum up, the prognosis of AF recurrence has a link with pre-ablation abnormalities of cardiac sympathetic innervation. *References:* None

OP-585

Relationship between heart rate response and cardiac innervation in patients with suspected or known coronary artery disease

C. Nappi[1], R. Assante[1], E. Zampella[1], V. Gaudieri[1], G. De Simini[1], A. Giordano[1], A. D'Antonio[1], W. Acampa[1], M. Petretta[2], A. Cuocolo[1]; [1]Department of Advanced Biomedical Sciences, University Federico II, Naples, ITALY, [2]Department of Translational Medical Sciences, University Federico II, Naples, ITALY.

Aim/Introduction: Chronotropic response to pharmacological stress test is blunted in patients with autonomic neuropathy. The relationship between heart rate (HR) changes during pharmacological stress test and cardiac autonomic dysfunction has not been fully investigated. We assessed the potential interplay between HR response (HRR) and myocardial innervation in patients with suspected or known coronary artery disease (CAD). ***Materials and Methods:*** We considered 71 consecutive patients with suspected or known CAD referred to pharmacological stress myocardial perfusion imaging (MPI) for the assessment of myocardial ischemia and to ^{123}I-metaiodobenzylguanidine (MIBG) imaging for the evaluation of cardiac innervation within one month from each other as part of their diagnostic work-up planned by the attending physician. HRR was calculated as the maximum percent change from baseline according to the formula: (peak HR - rest HR)/rest HR × 100. ^{123}I-MIBG heart-to-mediastinum (H/M) ratio was calculated and a late H/M ratio <1.6 was considered abnormal. ***Results:*** The majority of patients (56 out of 71, 79%) had known CAD while the remaining patients were evaluated due to primary dilated cardiomyopathy. No differences in demographic data and clinical characteristics were observed between patients with normal and abnormal H/M ratio. Similarly, hemodynamic data and MPI findings were comparable between the two groups, while left ventricular ejection fraction was significantly lower in patients with abnormal compared to those with normal H/M ratio (34±10% vs. 40±10%, P<0.05). A significant response to stress test was observed in both categories; however, HRR was lower in patients with abnormal as compared to those with normal late H/M ratio (18±9 vs. 26±14, P<0.05). HRR progressively decreased with decreasing late H/M ratio tertiles (P for trend =0.02). In particular, HRR mean value was 17±10

in the low, 20±12 in the middle, and 27±16 in the high tertile. A significant correlation between HRR and H/M ratio (r=0.28, P=0.03) was also detectable. Finally, the addition of HRR to a model including age, diabetes, known CAD, left ventricular ejection fraction, and stress-induced ischemia added incremental value in predicting an abnormal late H/M ratio, increasing the global chi-square from 8.09 to 13.8 (P=0.02). ***Conclusion:*** In patients with suspected or known CAD undergoing pharmacological stress MPI and 123I-MIBG cardiac imaging there was a significant relationship between HRR and late H/M ratio. HRR was an independent predictor of abnormal late H/M ratio, suggesting a strong interplay between cardiac response to stress test and cardiac innervation. ***References:*** None

OP-586

A novel method for regional innervation/perfusion mismatch assessed by cardiac ^{123}I-mIBG and rest ^{99m}Tc-tetrofosmin SPECT to predict arrhythmic events in ischemic heart failure

D. Verschure[1,2], E. Poel[1], A. F. Jacobson[3], H. J. Verberne[1]; [1]Amsterdam UMC, Amsterdam, NETHERLANDS, [2]Zaans Medical Center, Zaandam, NETHERLANDS, [3]Diagram Consulting, Kihei, HI, UNITED STATES OF AMERICA.

Aim/Introduction: Cardiac ^{123}I-mIBG SPECT imaging provides information on regional myocardial innervation. However, there is no consensus on how to use a, sometimes cumbersomely assessed, 17-segment based score to assess prognosis. The present study examined whether a simpler regional scoring approach for evaluation of ^{123}I-mIBG SPECT combined with rest ^{99m}Tc-tetrofosmin SPECT myocardial perfusion imaging (MPI) could be used for the prediction of arrhythmic events (AEs) in patients with ischemic heart failure (HF). ***Materials and Methods:*** 502 ischemic HF subjects (NYHA II/III, LVEF ≤35%) of the ADMIRE-HF study cohort with complete cardiac ^{123}I-mIBG and rest ^{99m}Tc-tetrofosmin SPECT studies were enrolled. Both SPECT image sets were read together by 2 experienced nuclear imagers and scored by consensus. In addition to standard 17 segments scoring, the readers classified walls (i.e. anterior, lateral, inferior, septum and apex) as normal, matched defect of innervation and perfusion, mismatched (i.e., innervation defect lager than perfusion defect) or reverse mismatched (i.e., innervation defect smaller than perfusion defect). Cox proportional hazards ratios (HR) were used to determine if the visual segmental wall classification innervation/perfusion mismatch score, ^{123}I-mIBG summed defect scores (SDS), ^{99m}Tc-tetrofosmin SDS and innervation/perfusion mismatch SDS, LVEF, NYHA class, B-type natriuretic peptide (BNP) were associated with occurrence of AEs (i.e. sudden cardiac death, sustained VT, resuscitated cardiac arrest, appropriate ICD therapy). ***Results:*** At 2-year median follow-up, 52 subjects (10.4%) had AEs. Subjects with 1 or 2 mismatched walls were twice as likely to have AEs compared with subjects with either 0 or 3-5 mismatched walls (16.3% vs 8.3%, p = 0.010). Cox regression analyses showed that the combination of BNP and the presence of visual mismatch in 1-2 walls were independent predictors of AEs (HR 2.084 [1.109-3.914], p = 0.001) However, compared to the visual mismatch, the contribution of BNP is relatively small (i.e., HR 1.001 [1.000-1.001]). None of the other innervation, perfusion and mismatch scores using standard 17 segments were associated with AEs. ***Conclusion:*** In ischemic HF the highest risk of AEs occurs in subjects with intermediate levels of visual wall-level innervation/perfusion mismatches. Therefore, a simple visual wall-level based assessment of combined cardiac ^{123}I-mIBG and rest ^{99m}Tc-tetrofosmin SPECT can be used to differentiate those HF patients at higher AE risk from those with relatively low AE risk. ***References:*** None

OP-587

Low-dose dual-isotope by CZT camera: single imaging to assess cardiac function, myocardial perfusion and adrenergic innervation in heart failure

A. Giordano*, G. De Simini, R. Assante, C. Nappi, A. D'Antonio, E. Zampella, V. Gaudieri, T. Mannarino, R. Green, V. Cantoni, P. Buongiorno, W. Acampa, A. Cuocolo;*
Department of advanced biomedical sciences, University Federico II of Naples, Naples, ITALY.

Aim/Introduction: We assessed the feasibility of a low-dose dual isotope ^{123}I/^{99m}Tc-acquisition protocol by a cadmium-zinc-telluride (CZT) dedicated camera for the simultaneous evaluation of left ventricular (LV) function, myocardial perfusion and adrenergic innervation in patients with heart failure (HF). ***Materials and Methods:*** A total of 36 patients (34 men, mean age 64±9 years) with HF underwent simultaneous dual-isotope ^{123}I-metaiodobenzylguanidine (MIBG)/^{99m}Tc-sestamibi (74 MBq/185 MBq) cardiac gated CZT imaging with a single acquisition. Early and late heart to mediastinum ratio (H/M), washout rate (WR) and total defect score (TDS) were assessed from ^{123}I-MIBG images; while summed rest score (SRS) was computed from ^{99m}Tc-sestamibi images. Difference between innervation and perfusion were identified as innervation/perfusion mismatch (%). LV systolic function was considered reduced when ejection fraction (EF) was <45%. ***Results:*** LVEF was normal in 13 (36%) patients and reduced in 23 (64%). Clinical characteristics were comparable in patients with normal and reduced LVEF. TDS (r=0.51, P=0.001) and SRS (r=0.56, P<0.001) resulted correlated with LVEF. A significant relation between early (r =0.45, P=0.005) and late (r=0.50, P<0.005) H/M ratio and LVEF and was also found. Patients with reduced LVEF compared to those with normal LVEF had higher SRS (15±12 vs. 6±8, P<0.05), TDS (29±15 vs. 19±8, P<0.05) and WR (34±22% vs. 16±34%, P<0.05) and

lower values of early (1.60±0.3 vs 1.84±0.3, P<0.05) and late (1.50±0.3 vs 1.9±0.3, P<0.01) H/M ratio. Conversely, myocardial mismatch was comparable in patients with normal and reduced LVEF (19±18% vs. 18±12%, P=0.81). Late H/M ratio resulted the only independent predictor of reduced LVEF (P=0.05). Although TDS correlated with SRS (r=0.77, P<0.001), ^{123}I-MIBG defect size was larger than perfusion defects (25±14 vs. 12±11, P<0.001). WR was the only independent predictor of myocardial mismatch (P<0.05). ***Conclusion:*** In patients with HF, a low-dose dual isotope ^{123}I/^{99m}Tc with a single acquisition protocol using a CZT camera is clinically feasible and allows simultaneous evaluation of LV function, myocardial perfusion and adrenergic innervation. WR measurements provided by CZT camera could integrate the clinical value of innervation/perfusion assessment in heart failure patients. ***References:*** None

OP-588

The ability of ^{123}I-mIBG/199Tl SPECT to predict appropriate ICD therapy in patients with ischemic heart failure

S. Sazonova*, T. A. Atabekov, R. E. Batalov, J. N. Ilushenkova, Y. B. Lishmanov, S. V. Popov;*
Cardiology Research Institute, Tomsk NRMC, Tomsk, RUSSIAN FEDERATION.

Aim/Introduction: Last years was shown the ability of ^{123}I-mIBG/perfusion cardiac scintigraphy to predict arrhythmic events in patient (pts) with heart failure (HF). However, the application of these methods as a predictor of appropriate ICD therapy in pts with HF after myocardial infarction (MI) remains questionable. ***Aim.*** To evaluate the ability of ^{123}I-mIBG and myocardial perfusion scintigraphy with ^{199}Tl to predict ICD-therapy in candidates for primary and secondary SCD prevention. ***Materials and Methods:*** The study included 80 pts (63,7±9.7 years) with a MI (>3 month) and indications for ICD implantation for primary (1st group, n=49) and secondary prevention (2 group, n=31). All pts underwent cardiac scintigraphy with ^{123}I-mIBG and ^{199}Tl at 5 days before ICD implantation. ICD interrogation was performed at 6, 12, and 18 months. ^{123}I-MIBG (i.v.a. 300 MBq) planar and SPECT images were acquired at 15 minutes (early) and 4 hours (delayed). On planar images the heart/mediastinum ratios (H/Me, H/Md) , washout rate (WR) were calculated. ^{199}Tl (i.v.a. 185 MBq) SPECT was performed according to the rest/4 h redistribution protocol. ^{123}I-MIBG and ^{199}Tl images were analyzed by a 17-segment model with a 5-point scoring. ^{123}I-MIBG scores (SMSe%, SMSd %), ^{199}Tl summed scores (SRS%, SDS%) , trigger zone (TZ%) as SDS%-SMSd% were calculated. Both groups were subdivided according to the presence or absence of appropriate ICD therapy and compared by U-test. ***Results:*** During follow-up appropriate ICD-therapy (ATP or shocks) was registered in 6 pts (12,2%) of the 1 group and in 11 pts (35%) of the 2 group. In the 1 group H/Me=1,88±0,56, H/Md=1,71±0,42, SMSe=23,4±10,07%, SMSd=33,95±16,11%, WR=28.87±21,14; SRS=17,46±14,88, SDS=18,6±16,23%, TZ=15,0±10,19%. In the 2 group H/Me=1,97±0,53, H/Md=1,9±0,59, SMSe=22,61±18,1%, SMSd=24,6±18,28% (p=0,028), WR=16,03±8,26; SRS=17,87±15,13% (p=0,69), SDS=15,94±15,84%, TZ=8,31±7,39%. In the 1 group there were no statistical differences at scintigraphic parameters between subgroups of pts with and without appropriate ICD therapy. In the 2 group pts with appropriate ICD therapy had significantly lager SMSe (40,1±16,97% vs 13,0±9,59%, p=0,00015), SMSd (42,18±16,46% vs 15,0±10,44%, p=0,00012), WR (20,09±8,32 vs 13,85±7,51, p=0,049), TZ (12,44±5,13% vs 6,79±8,17%, p=0,025), SRS (31,4±17,44% vs 10,75±7,69%, p=0,0052), SDS (30,22±20,3% vs 9,4±7,76%, p=0,03). ***Conclusion:*** Both ^{123}I-mIBG and ^{199}Tl SPECT demonstrated disability to predict appropriate ICD therapy in candidates for primary SCD prevention. The good relationship between size of denervated and/or hypoperfused myocardium and appropriate ICD therapy was shown in candidates for secondary SCD prevention. Probably the scar structure is more significant, than scar size in appearance of life-threatening arrhythmia ***References:*** None

OP-589

Myocardial 123I-Metaiodobenzylguanidine Scintigraphy in Patient with Heart Failure: a Gender Study

M. Conte[1]*, A. Di Rocco*[2]*, C. De Angelis*[1]*, V. Frantellizzi*[1]*, A. Farcomeni*[3]*, G. De Vincentis*[1]*;*
[1]Department of Radiological Sciences, Oncology and Anatomical Patology, "Sapienza" University of Rome, Rome, ITALY, [2]Department of Public Health and Infectious Diseases, "Sapienza" University of Rome, Rome, ITALY, [3]"Tor Vergata" University of Rome, Rome, ITALY.

Aim/Introduction: The aim of the study was to evaluate the prognostic significance differences of myocardial 123I-metaiodobenzylguanidine (123I-MIBG) scan between males and females in patients with heart failure (HF). ***Materials and Methods:*** Patients with HF prior to implantable cardioverter-defibrillator (ICD) implantation were consecutively enrolled. They underwent 123I-mIBG scintigraphy using a dual-head gamma camera and a LEHR collimator. Planar anterior thoracic and Single Photon Emission Computed Tomography (SPECT) images were acquired at 15 and 240 minutes after tracer injection. Region of interest were manually drawn over the heart and the upper mediastinum and Early and late heart-to-mediastinum ratios (eHM, lHM) as well as myocardial washout rate (WR)were calculated. Early and late summed SPECT scores (ESS, LSS) were calculated. A statistical analysis was conducted taking into account age, body mass index

(BMI), males rate, comorbidities (diabetes, dyslipidemia, chronic renal failure, chronic obstructive pulmonary disease), smoke habits, administered treatment (ACE-inhibitors, α and β-blockers, potassium-sparing diuretics, calcium antagonists, sartans, amiodarone and digitalis), ESS, LSS, eHM, lHM, WR and ejection fraction. ***Results:*** 306 consecutive patients (247 males) were enrolled, 115 had arrhythmic events (AE). The median follow-up was of 85 months. In general population at univariate analysis ESS (HR= 1.023 CI95% 1.008-1.039;p=0.003) and LSS (HR=1.02 CI95% 1.005-1.035; p=0.009) resulted as risk factor in the prediction of AE. Moreover, eHM (HR= 0.326 CI95% 0.143-0.742; p=0.008) and lHM (HR=0.215 CI95% 0.094-1.002; p=0.001) resulted as protective factor in the prediction of AE, with AUC of 0.625 and 0.645 respectively. Gender analysis: in female no MIBG parameters gained statistical significance in the prediction of AE (p>0.05). Male group data results were similar to the total population, and also slightly better (eHM - AUC=0.677; lHM - AUC= 0.693). ***Conclusion:*** Our results indicated that MIBG represents a tool to predict AE in male patients: ESS and LSS are risk factors while eHM and lHM are protective factors. However, MIBG showed lower specificity and sensibility in long term analysis and in female predictive estimation. ***References:*** None

OP-590

Altered Electromechanical Coupling With Multisite Onset of Left Ventricle Mechanical Contraction Associated With Advanced Coronary Heart Disease

F. Ferrando-Castagnetto[1], *M. Pedrera Canal*[2], *I. Vilacosta*[3], *C. Real*[3], *M. Ollarves Carrero*[2], *L. García Belaustegui*[2], *M. Olivan*[2], *R. Ricca-Mallada*[1], *M. Pérez Castejón*[2], *J. Carreras Delgado*[2];
[1]*Departamento de Cardiología - CCVU, Hospital de Clínicas, FM, UdelaR, Montevideo, URUGUAY,* [2]*Servicio de Medicina Nuclear, Hospital Clínico San Carlos, Madrid, SPAIN,* [3]*Instituto Cardiovascular, Hospital Clínico San Carlos, Madrid, SPAIN.*

Aim/Introduction: Left ventricle (LV) mechanical dynamics have been poorly characterized in patients with ischemic heart disease not legible for resynchronization therapy (CRT). Some experimental evidence suggests that, in certain patients with chronic coronary artery disease (CAD), there may be considerable LV mechanical dyssynchrony in the absence of severe systolic dysfunction or electrical dyssynchrony. We evaluated LV contractile dynamics in patients with advanced CAD. ***Materials and Methods:*** Phase histograms at rest were obtained in a sample of patients with known coronary artery disease (severe coronary malformation, old infarct, primary or delayed angioplasty and/or coronary bypass surgery) derived to 99mTc-MIBI gated-SPECT between July 2019 and March 2020. The site of onset of mechanical LV contraction (SOMC) was defined through SyncTool of Emory Cardiac Toolbox®, detecting those patients with "multisite" OMC, defined as the onset in at least 3 of 17 segments. Peak amplitude (PA), phase standard deviation (PSD), and phase bandwidth (PBW) were compared with controls (n = 24). ***Results:*** We detected thirteen patients with multisite OMC and chronic coronary disease, 63 + 13 years old, 38% diabetic, LVEF = 39.8 + 13.6%, VTS = 112.4 + 64.9 ml, averaged summed rest score = 12.5 and summed difference score = 2.8. Indexes derived from phase analysis at rest showed values compatible with severe LV mechanical dyssynchrony (PA = 120.2 + 15.0, PSD = 50.3 + 18.1, PBW = 160.0 + 65.2 degrees, p <0.05 for all comparisons with controls). A multisite latest mechanical contraction was also detected in 4 of them (30.8%). ***Conclusion:*** Advanced CAD is associated with altered electromechanical coupling, characterized by multisite OMC, even in the absence of prolonged QRS duration. Prognostic and therapeutic implications of this mechanical substrate deserve to be evaluated in larger series that include CRT candidates with different underlying heart diseases. ***References:*** None

OP-591

Left Ventricular Diastolic Asynchrony Combined with Left Ventricular Ejection Fraction Decline Based on Gated Myocardial Perfusion Imaging Can Early Predict Cardiotoxicity Caused by Anthracyclines

J. Wang*, Y. Lin, W. Gu, C. Qiu, R. Niu, Y. Wang;*
The Third Affiliated Hospital of Soochow University, Changzhou, CHINA.

Aim/Introduction: To explore the value of quantitative parameters of gated myocardial perfusion imaging (GMPI) in early prediction of anthracycline treat - related cardiotoxicity (ATRC). ***Materials and Methods:*** Fifty-eight patients with newly diagnosed diffuse large B-cell lymphoma (DLBCL) were enrolled. All patients were administered 6 cycles of R-CHOP chemotherapy. Rest GMPI was performed before and after anthracycline chemotherapy. Myocardial perfusion abnormal extent (Extent), Left ventricular ejection fraction (LVEF), end diastolic and systolic volumes (EDV and ESV), peak filling rate (PFR) , left ventricular systolic and diastolic synchronization parameters such as phase standard deviation (SD), phase histogram bandwidth (BW) were calculated at automatically using the ECToolbox program. ATRC was defined as symptomatic heart failure; cardiac death, arrhythmia, or infarction; a decrease in LVEF of >15% from baseline; or a decrease in LVEF of >10% to <50%. Univariate logistic regressions were performed first. Factors with p values <0.20 in the univariate model were included in multivariate models. Receiver-operating characteristic (ROC) curves were used to assess the performance of linear predictors of risk for ATRC. ***Results:*** ATRC occurred in 14 of 58 patients. There were no statistically significant differences between ATRC group and Non-ATRC group in terms of gender, age, BMI, hypertension, diabetes, hyperlipidemia

(all P >0.05). Compared with before chemotherapy, the value of QTc interval of electrocardiogram, LVEF, PFR, $SD_{systolic}$, $BW_{systolic}$, $SD_{diastolic}$, $BW_{diastolic}$ were significantly changed after chemotherapy (all P < 0.05). The ΔQTC,ΔLVEF,ΔPFR,$\Delta SD_{systolic}$, $\Delta SD_{diastolic}$ were separately calculated as the difference of the indicators before and after chemotherapy. The multivariate logistic regressions revealed both ΔLVEF (OR: 0.846; 95% CI: 0.739 to 0.969; P = 0.016) and $\Delta SD_{diastolic}$ (OR: 1.186; 95% CI: 1.040 to 1.353; P = 0.011) as significant predictors of ATRC. ROC analysis revealed the AUC of ΔLVEF and $\Delta SD_{diastolic}$ in predicting ATRC were 0.774, 0.827 separately(all P < 0.001), while the AUC of $\Delta SD_{diastolic}$ combined with ΔLVEF in predicting ATRC was 0.869(P < 0.001), which higher than single ΔLVEF and single $\Delta SD_{diastolic}$, its diagnostic sensitivity and specificity were 92.9% and 65.9%. ***Conclusion:*** Left ventricular diastolic asynchrony and LVEF decline post-anthracycline were both independent predictors of ATRC, the combination of ΔLVEF and $\Delta SD_{diastolic}$ have a good efficacy for early prediction of ATRC in DLBCL patients. ***References:*** None

OP-592

The diagnostic accuracy of cardiac I-123-mIBG scintigraphy as a biomarker for mild cognitive impairment with Lewy bodies

G. Roberts[1,2], R. Durcan[1], P. C. Donaghy[1], S. Barker[1], S. Lawley[1], C. A. Hamilton[1], J. Ciafone[1], G. Petrides[2], K. Howe[2], N. Barnett[1], M. Firbank[1], J. P. Taylor[1], J. O'Brien[3], A. J. Thomas[1];
[1]Newcastle University, Newcastle upon Tyne, UNITED KINGDOM, [2]Newcastle upon Tyne Hospitals, Newcastle upon Tyne, UNITED KINGDOM, [3]University of Cambridge, Cambridge, UNITED KINGDOM.

Aim/Introduction: Cardiac mIBG scintigraphy (cardiac mIBG) is recommended as a biomarker in the 2020 research criteria for mild cognitive impairment with Lewy bodies (MCI-LB) [1]. Prospective studies assessing the accuracy of mIBG for the detection of MCI-LB are required. Objective: To examine the diagnostic accuracy of cardiac mIBG for differentiating probable MCI-LB from MCI due to Alzheimer's disease (MCI-AD). ***Materials and Methods:*** We conducted a prospective cohort study into the accuracy of cardiac mIBG in the diagnosis of MCI-LB. Ninety-five people over 60 years of age with MCI were recruited. MCI-LB was diagnosed in individuals with two or more core features (fluctuating cognition, visual hallucinations, REM sleep behaviour disorder, parkinsonism) or one core feature with abnormal dopaminergic imaging. MCI due to probable Alzheimer's disease (MCI-AD) was diagnosed in individuals with no core features of Lewy body disease and who met the Alzheimer's Association criteria [2]. Individuals with just one core feature or abnormal dopaminergic imaging only were excluded due to lack of certainty as to whether their MCI could be attributed to Lewy body disease. All recruits were administered 111 MBq (±10%) mIBG and scanned 4 hours later. Anterior planar images were processed to obtain the heart-to-mediastinum ratio (HMR). Thirty-two age-matched controls without cognitive impairment were used to set a cardiac mIBG diagnostic threshold two standard deviations below mean age-matched control heart-to-mediastinum ratio. ***Results:*** Thirty-seven patients were diagnosed with MCI-LB, of which 22 had an abnormal MIBG scan, resulting in a sensitivity of 59% (95% CI: 42-75%). Forty-three patients were diagnosed with MCI-AD, of which 38 had a normal scan, resulting in a specificity of 88% (95% CI: 75-96%). The overall accuracy was 75% (95% CI: 64-84%). The positive likelihood ratio was 5.1 and negative likelihood ratio 0.46. ***Conclusion:*** At the MCI stage, over half of patients with probable Lewy body disease already have positive cardiac MIBG scans. Combined with high specificity, this means cardiac MIBG is a useful biomarker even at the MCI stage (likelihood ratio 5.1). ***References:*** 1. McKeith, I., et al., Research criteria for the diagnosis of prodromal dementia with Lewy bodies. Neurology, 2020. 2. Jack, C.R., Jr., et al., NIA-AA Research Framework: Toward a biological definition of Alzheimer's disease. Alzheimers Dement, 2018. 14(4): p. 535-562.

OP-593

Predictive value of the cardiac sympathetic innervation and contractile function in cardiac resynchronization therapy

***A. Mishkina**, K. Zavadovsky, V. Saushkin, D. Lebedev, Y. Lishmanov;*
Cardiology Research Institute, Tomsk National Research Medical Centre, Russian Academy of Sciences, Tomsk, RUSSIAN FEDERATION.

Aim/Introduction: To evaluate the predictive value of the cardiac sympathetic activity and contractility, assessed by radionuclide methods, in the prediction of cardiac resynchronization therapy (CRT) response. ***Materials and Methods:*** This study included 38 heart failure (HF) patients with ischemic (n=16) and non-ischemic (n=22) etiology. Before CRT all patients underwent ^{123}I-metaiodobenzylguanidine (^{123}I-MIBG) imaging for cardiac sympathetic activity evaluating. The following indexes were estimated: early and delayed heart to mediastinum ratio (eH/M and dH/M), summed MIBG Score (eSMS and dSMS). All patients underwent gated myocardial perfusion scintigraphy with assessments of LV dyssynchrony indexes: standard deviation (SD) and histogram bandwidth (HBW). Additionally, all patients underwent gated-blood-pool-SPECT with both ventricles ejection fraction (EF) and stroke volume (SV) assessment. ***Results:*** One year after CRT patients were divided into two groups: responders (n=26) and non-responders (n=12). The response was defined as LV_ESV decreased greater than or equal to 15% or

LV_EF increase greater than or equal to 5%. The following differences in the preoperative scintigraphic parameters between responders and non-responders were found: eH/M (2.16 and 1.74; p < 0.05), dH/M (1.94 and 1.53; p < 0.05), dSMS (13 and 16.5; p < 0.05), SD (101.9 and 141.8ms; p < 0.05). According to logistic regression analysis eH/M (OR=1.25 per 0.1 unit increase; 95% CI 1.054-1.49; p < 0.05), dH/M (OR=1.43 per 0.1 unit increase; 95% CI 1.09-1.87; p < 0.05), dSMS (OR=0.91; 95% CI 0.84-0.99; p < 0.05), SD (OR=0.97; 95% CI 0.95-0.98; p < 0.05) were related to CRT response. In patients with ischemic HF SD (OR=1.55; 95% CI 1.09-2.2; p < 0.05) and HBW (OR=1.13; 95% CI 1.02-1.24; p < 0.05), and right ventricle (RV) EF (OR=1.11; 95% CI 1.001-1.23; p < 0.05), RV_SV (OR=1.07; 95% CI 1.003-1.138; p < 0.05) were predictors of CRT response. In non-ischemic HF patients dH/M (OR=1.47 per 0.1 unit increase; 95% CI 1.08-2; p < 0.05), SD (OR=0.83; 95% CI 0.73-0.95; p < 0.05), HBW (OR=0.96; 95% CI 0.93-0.99; p < 0.05) showed the predictive value in terms of CRT response. ***Conclusion:*** ^{123}I-MIBG scintigraphy and gated myocardial perfusion scintigraphy can be used as additional methods for predicting the effectiveness of CRT. In ischemic HF patients preoperative values of LV dyssynchrony and RV contractility were independent predictors of response to CRT. In non-ischemic HF patients cardiac sympathetic activity, as well as LV dyssynchrony can be used as prognostic criteria for a positive response to CRT. ***References:*** None

1011

e-Poster Presentation Session 7: Nuclear Medicine for Infection & Inflammation - The Story Continues

Saturday, October 24, 2020, 10:40 - 12:10 Channel 11

EPS-103

The role of nuclear medicine imaging with ^{18}F-FDG PET/CT, combined ^{111}In-WBC/^{99m}Tc-Nanocoll and ^{99m}Tc-HDP SPECT/CT in evaluation of patients with chronic problem after TKA or THA in a prospective study

R. Aleksyniene[1], *V. Iyer*[2], *H. C. Bertelsen*[1], *M. Frost*[1], *V. Khalid*[3], *H. C. Schønheyder*[4], *L. H. Larsen*[4], *P. T. Nielsen*[3], *A. Kappel*[3], *T. R. Thomsen*[5], *J. Lorenzen*[6], *I. Ørsted*[7], *O. Simonsen*[3], *P. L. Jordal*[6], *S. Rasmussen*[3], *PRIS Study Group;*

[1]Department of Nuclear Medicine, Aalborg University Hospital, Aalborg, DENMARK, [2]Department of Nuclear Medicine, Uppsala University Hospital, Uppsala, SWEDEN, [3]Department of Orthopaedic Surgery, Aalborg University Hospital, Aalborg, DENMARK, [4]Department of Clinical Microbiology, Aalborg University Hospital, Aalborg, DENMARK, [5]Center for Microbial Communities, Aalborg University, Aalborg East, Life Science Division, The Danish Technology Institute, Aarhus, DENMARK, [6]Life Science Division, The Danish Technology Institute, Aarhus, DENMARK, [7]Department of Infectious Disease, Aalborg University Hospital, Aalborg, DENMARK.

Aim/Introduction: The aim was to assess the diagnostic value of nuclear imaging with ^{18}F-FDG PET/CT, combined ^{111}In-WBC/^{99m}Tc-Nanocoll and ^{99m}Tc-HDP SPECT/CT for patients with chronic problem related to knee or hip prosthesis (TKA or THA) scheduled by the structured multidisciplinary algorithm within the prospective study. ***Materials and Methods:*** The study was a part of a prospective study conducted in Denmark from December 2011 to January 2014 within the framework of an innovation consortium (Danish acronym PRIS). Fifty five patients (26 women and 29 men, mean age 64 years) with persisting pain and/or a mechanical problem but without clinical or radiological signs for aseptic loosening or prosthetic joint infection (PJI) (29 knee and 26 hip) underwent imaging with ^{99m}Tc - HDP SPECT/CT, combined ^{111}In-labeled WBC/^{99m}Tc-Nanocoll bone marrow SPECT/CT, and ^{18}F-FDG PET/CT. The combined imaging report in conjunction with the clinical data were evaluated at multidisciplinary conferences and guided patient management. The final diagnosis of PJI infection and/or loosening was based on the intraoperative findings and microbiological culture results and the clinical follow-up 2-3 years after inclusion. ***Results:*** 23 patients (42%) underwent percutaneous biopsies/ joint aspirates or revision surgery after imaging and the final diagnosis was obtained by microbiological culturing. 20 patients (38%) were scheduled for clinical follow-up due to negative all three scans in 6 patients. 14 patients with no suggestive periprosthetic infection or loosening on both ^{18}F-FDG PET/CT and ^{111}In-labeled WBC/^{99m}Tc-Nanocoll bone marrow SPECT/CT. Remaining patients with findings suggestive for PJI or aseptic loosening were scheduled for clinical follow-up due to other reasons (severe comorbidity, mild symptoms). Clinical follow-up (median follow-up 438 days) was performed on all 55 patients. 11 patients excluded from final statistical analysis (4 patients due missing leucocyte/ bone marrow imaging and 7 patients due to equivocal clinical follow-up results). The diagnostic performance of ^{111}In-labeled WBC/^{99m}Tc-Nanocoll bone marrow SPECT/CT for PJI showed sensitivity of 100% (CI 0.74-1.00), specificity 97% (CI 0.82-1.00), PPV 92% (CI 0.64-1.00), NPN 100% (0.88 - 1.00) and accuracy 98% (CI 0.88-1.00), for PET/CT -the sensitivity 100% (CI 0.74-1.00), specificity 76% (CI 0.56-0.90), PPV 63% (CI 0.38-0.84), NPN 100% (0.85 - 1.00) and accuracy 83% (CI 0.68-0.93). ***Conclusion:*** In a standardized prospectively scheduled patient group the results showed highly specific performance of combined ^{111}InWBC/^{99m}Tc-Nanocoll SPECT/CT in confirming chronic PJI after TKA or THA. ^{18}F-FDG PET/CT has an appropriate accuracy but the utility of use in the diagnostic algorithm of suspected PJI needs further evidence. ***References:*** None

EPS-104

The Use of a Novel Semiquantitave Parameter in the Three-phase Bone Scan to Predict the Results of ^{99m}Tc-HMPAO-labeled Leukocyte Scintigraphy in Patients with Suspected Septic Loosening of Unilateral Knee Prosthesis

N. Quartuccio[1], L. Sturiale[1], M. Siracusa[2], A. Arnone[1], R. Laudicella[2], M. T. Arnone[1], P. Alongi[3], G. L. Mauro[4], L. Camarda[5], M. D'Arienzo[5], R. Sciortino[6], S. Baldari[2], G. Arnone[1];
[1]Nuclear Medicine Unit, A.R.N.A.S. Ospedali Civico, Di Cristina e Benfratelli, Palermo, ITALY, [2]Department of Biomedical and Dental Sciences and of Morpho-functional Imaging, Nuclear Medicine Unit, University of Messina, Messina, ITALY, [3]Nuclear Medicine Unit, Fondazione Istituto G.Giglio, Cefalù, ITALY, [4]Rehabilitation Unit, Paolo Giaccone Hospital, Palermo, ITALY, [5]Department of Orthopaedic Surgery (DICHIRONS), University of Palermo, Palermo, ITALY, [6]Department of Orthopaedic Surgery, Ospedale Civico ARNAS, Palermo, ITALY.

Aim/Introduction: The evaluation of the three-phase bone scan in patients with possible loosening of knee prosthesis is based on the assessment of asymmetry of counts in the different phases of the exam between the prothesized and the healthy knee. Scintigraphy with autologous leucocytes is the imaging technique of choice to discriminate between aseptic and septic loosening. Nevertheless, it is a more complicated, costly and longer exam. Our aim was to assess different semiquantitive parameters in three-phase bone scan, including a novel parameter named perfusion-to-blood pool ratio (P/BP ratio) for the prediction of the results of autologous leukocyte scintigraphy. ***Materials and Methods:*** 30 patients with unilateral knee arthroplasty were evaluated by three-phase bone scan (after at least 1 year from arthroplasty) and ^{99m}Tc-HMPAO-labeled leucocytes scintigraphy (within an interval of 2 months from the three-phase bone scan). In three-phase bone scan, a region of interest (ROI) was drawn in the perfusion and blood-pool phase images, including the prosthetic region and using an isocontour with threshold of 40% of the maximum pixel activity within the ROI. A mirror ROIs were placed on the healthy knee. Perfusion (Pr) and Blood Pool (BPr) ratios were calculated by dividing the total counts in the ROI including the prosthetic region for the total counts in the ROI including the healthy knee; P/BP ratio was obtained using the formula {[(Pr/BPr) x 100] - 100}. ROC curves were created in order to determine the optimal cutoff value for each semiquantitative parameter to predict the positivity of the autologous leukocyte scintigraphy. ***Results:*** Autologous leukocyte scintigraphy revealed 13 cases suggestive for septic loosening and 17 negative cases. Positive cases presented values of Pr, BPr and P/BP ratio above the optimal cutoff values, which resulted 1.91 for Pr (sensitivity = 100%, specificity = 58.8%), 1.5 for BPr (sensitivity = 92.3% , specificity = 41.18%) and 25% for P/BP ratio (sensitivity = 100%, specificity = 76.47%). Corresponding areas under the curve for the Pr, BPr and P/BP ratio were 0.72, 0.67 and 0.82. ***Conclusion:*** P/BP ratio appears the semiquantitative parameter with the highest predictive capability and may reinforce the clinical suspicion of septic loosening in patients with unilateral knee prosthesis. These results warrant studies in larger patient populations; we will evaluate whether the use of P/BP ratio may anticipate differential diagnosis between aseptic and septic loosening and have an impact on clinical decision making. ***References:*** None

EPS-105

White blood cells scintigraphy as an alternative to the arthrocentesis in suspected periprosthetic knee infection

E. Noriega-Álvarez*, A. M. García Vicente, V. M. Poblete García, M. E. Bellón Guardia, F. J. Pena Pardo, M. P. Talavera Rubio, B. González García, E. Casillas Sagrado, Á. M. Soriano Castrejón; University Hospital of Ciudad Real, Ciudad Real, SPAIN.*

Aim/Introduction: To analyse the diagnostic accuracy of 99mTc-HMPAO-labeled white blood cells scintigraphy (WBCS) to consider it as a reliable alternative to avoid arthrocentesis in patients with suspected periprosthetic knee infections (PKI). ***Materials and Methods:*** This retrospective study included 24 patients (13 women, mean age 68 years) with suspected PKI undergoing a WBCS and an arthrocentesis between 2017 and 2019. In WBCS a time decay-corrected acquisition was performed, obtaining serial planar images at 30 minutes, 3 hours and 8 hours after injection, although in some patients the third planar image (at 8 hours) could not be obtained. WBCS were visually classified as: "negative for infection" if no uptake was seen in planar images or when the uptake was decreasing over time, or "positive for infection" when at least one focus of abnormal uptake increased its intensity or extension from 3 to 8 hours. Subsequently, WBCS results were compared with final diagnosis. The final diagnosis was based on the results of the arthrocentesis. Then, sensitivity, specificity, accuracy, and positive and negative predictive values of WBCS were determined, as well as Kappa index and ROC curve. ***Results:*** The final diagnosis showed PKI in 13 patients and it was ruled out in 11. On the other hand, WBCS was positive for infection in 10 patients and negative in 14 (3 false negative, though these patients did not undergo the late image at 8 hours, very useful to differentiate infection from inflammation as recommended by the EANM guidelines[1])(table 1). The values of sensitivity, specificity, positive predictive value, negative predictive value and diagnostic accuracy were 76.9%; 100%; 100%; 78.6% and 87.5%, respectively. Comparing final diagnosis with WBCS a substantial Kappa agreement of 0.75 ($p < 0.01$), and an area under the ROC curve of 0.885 ($p < 0.01$) were obtained. ***Conclusion:*** The high specificity, positive predictive value, and diagnostic accuracy of WBCS denote its value as a non-invasive technique to confirm PKI, representing

a reliable alternative to arthrocentesis. Nevertheless, prospective studies with a larger number of patients are required. ***References:*** 1-Signore A, Sconfienza LM, Borens O, Glaudemans AWJM, Cassar-Pullicino V, Trampuz A, et al. Consensus document for the diagnosis of prosthetic joint infections: a joint paper by the EANM, EBJIS, and ESR (with ESCMID endorsement). Eur J NuclMed Mol Imaging. 2019;46:971-88.

EPS-106

One-year follow-up with ^{18}F-FDG PET/CT of large vessel vasculitis treated with tocilizumab

I. Martinez-Rodriguez[1], D. Prieto-Peña[2], R. Quirce[1], J. Jiménez-Bonilla[1], M. de Arcocha-Torres[1], A. Sánchez-Salmón[1], N. Martínez-Amador[1], G. Molina-Mendoza[1], O. Cuenca-Vera[1], J. Andrés-Pacheco[1], Á. Gutiérrez-González[1], S. Ruiz Llama[1], F. J. Gómez-de la Fuente[1], M. Calderón-Goerke[2], R. Blanco[2], M. A. González-Gay[2], I. Banzo[1];

[1]Nuclear Medicine Service. Marqués de Valdecilla University Hospital. Molecular Imaging Group (IDIVAL). University of Cantabria, Santander, SPAIN, [2]Rheumatology Service. Marqués de Valdecilla University Hospital. IDIVAL, Santander, SPAIN.

Aim/Introduction: Large vessel vasculitis (LVV) treatment is based on corticosteroids, although sometimes other immunosuppressive drugs, like methotrexate, are necessary due to frequent relapses after decreasing prednisone dose. In recent years, new biological therapies, such as tocilizumab (TCZ), have been incorporated into the therapeutic arsenal with good initial results. Our aim was to evaluate the usefulness of ^{18}F-FDG PET/CT (PET/CT) in the one-year follow-up of patients with LVV treated with TCZ. ***Materials and Methods:*** An observational study was carried out including 23 patients (19 women, 66 ± 11 years) with a diagnosis of LVV and an initial positive PET/CT scan. In all the patients a follow-up PET/CT scan was performed at ≤1 year after the onset of TCZ. PET/CT scans were obtained 180' after intravenous injection of 7 MBq/Kg of ^{18}F-FDG. PET/CT images were assessed both visually and semiquantitatively. For the visual analysis ^{18}F-FDG uptake (graded from 0-3 in comparison to liver uptake) was evaluated in 5 vascular territories: supraaortic trunks (SAT), thoracic aorta (TA), abdominal aorta (AA), iliac arteries (IA) and femorotibial arteries (FTA). A total vascular score (from 0-15) was also calculated. For the semiquantitative analysis a target to background ratio (TBR: SUVmax thoracic aorta wall/ SUVmax vascular background) was calculated. ***Results:*** In the visual analysis, the overall total vascular score decreased from 4.87 ± 2.85 to 3.36 ± 1.56 (p = 0.0065). Per patient, the score decreased in 69.6% of them, did not change in 17.4% and increased in 13%. When we considered the different vascular territories, the percentage of patients with ^{18}F-FDG uptake grade 2-3 decreased on PET/CT follow-up from 26.1% to 4.4% in SAT, from 91.3% to 65.2% in TA, from 17.4% to 0% in AA, from 8.7% to 0% in IA and from 17.4% to 8.7% in FTA. Overall, in the semiquantitative analysis the TBR decreased significantly from 1.73 ± 0.58 to 1.48 ± 0.26 (p = 0.0025). Per patient, the TBR decreased in 18/23 patients (78.3%) and increased in 5/23 (21.7%). Furthermore, a decrease in the TBR below 1.34 (cut-off level establish in a control population) was observed in 7/23 patients (30.4%). ***Conclusion:*** Visual and semiquantitative analysis of PET/CT images showed a significant decrease of ^{18}F-FDG vascular uptake at one-year follow-up of patients with LVV under TCZ therapy. A decrease of TBR below the cut-off level established in controls was observed in one third of the patients. ***References:*** None

EPS-107

Correlation of clinical and biochemical parameters with ^{18}F-FDG PET/CT in patients with large vessel vasculitis under biological therapy with tocilizumab

I. Martínez-Rodríguez[1], D. Prieto-Peña[2], R. Quirce[1], J. Jiménez-Bonilla[1], M. de Arcocha-Torres[1], A. Sánchez-Salmón[1], N. Martínez-Amador[1], G. Molina-Mendoza[1], O. Cuenca-Vera[1], J. Andrés-Pacheco[1], Á. Gutiérrez-González[1], S. Ruiz Llama[1], F. J. Gómez-de la Fuente[1], M. Calderón-Goerke[2], R. Blanco[2], M. A. González-Gay[2], I. Banzo[1];

[1]Nuclear Medicine Service. Marqués de Valdecilla University Hospital. Molecular Imaging Group (IDIVAL). University of Cantabria, Santander, SPAIN, [2]Rheumatology Service. Marqués de Valdecilla University Hospital. IDIVAL, Santander, SPAIN.

Aim/Introduction: The recent incorporation of biological therapies such as tocilizumab (TCZ) to the therapeutic strategy of large vessel vasculitis (LVV) has been a notable advance. The classic inflammatory parameters, erythrocyte sedimentation rate (ESR) and C-reactive protein (CRP), are ineffective in the follow-up of the patients since they normalize rapidly. Our aim was to study if there is a correlation between different clinical and biochemical parameters and ^{18}F-FDG PET/CT (PET/CT) findings in the follow-up of patients with LVV treated with TCZ. ***Materials and Methods:*** We included 23 patients (19 women) with a diagnosis of LVV and positive initial PET/CT scan treated with TCZ due to steroid-refractory LVV, relapse or atypical polymialgic syndrome. Clinical outcome (complete response / partial response / no response), ESR, CRP, and initial and follow-up PET/CT results at ≤1 year from the start of TCZ (mean: 10.34 ± 3.13 months) were evaluated. PET/CT scans were obtained 180' after intravenous injection of 7 MBq/Kg of ^{18}F-FDG.PET/CT images were analyzed visually (total vascular score of 5 territories) and semiquantitatively (TBR: SUVmax thoracic aorta wall/ SUVmax vascular background). ***Results:*** Of the 23 patients included, 19 (82.6%) had a clinical complete response and 4 (17.4%) had a partial response. The TBR decreased significantly in patients with complete response (1.75 ± 0.63 vs. 1.49 ± 0.28; p = 0.0126) and there was no

difference in patients with partial response (1.63 ± 0.18 vs. 1.46 ± 0.16; p = ns). The total vascular score established by PET/CT showed similar behavior to the TBR, decreasing in patients with complete response (4.95 ± 3.06 vs. 3.00 ± 1.73; p = 0.0038) and showing no significant differences in those patients with partial response (4.50 ± 1.73 vs. 4.25 ± 0.96; p = ns). ESR and CRP decreased in patients with complete response (ESR: 31.42 ± 26.03 vs. 2.42 ± 1.12 mm/1h; CRP: 1.54 ± 1.64 vs. 0.13 ± 0.07 mg/dL; p <0.001). These parameters also decreased in patients with partial response (ESR: 27.0 ± 41.61 vs. 2.75 ± 0.96mm/1h; CRP: 1.23 ±1.27 vs. 0.1 ± 0.0mg/dL), although the differences were not significant. No correlation was observed between inflammatory parameters and the TBR. ***Conclusion:*** ^{18}F-FDGPET/CT demonstrated its utility for assessing inflammatory vascular activity in relation to clinical outcome in patients with LVV treated with TCZ. No correlation was observed between PET/CT findings and biochemical inflammatory parameters. These promising results should be confirmed in a larger population. ***References:*** None

EPS-108

Chasing Infection: Is There An Specific ^{18}F-FDG Pattern To Accurately Differentiate Septic From Aseptic Inflammation In Aortic Root/Ascending Aorta Graft Replacement?

B. Rodriguez-Alfonso*, D. Martinez-Lopez, L. Canales-Rodriguez, A. Forteza-Gil, A. Ramos-Martinez, R. Jimeno-Pernett, A. Sanfiel Delgado, M. Mitjavila-Casanovas;*
Hospital Universitario Puerta De Hierro, Majadahonda, SPAIN.

Aim/Introduction: Infective endocarditis in patient with graft replacement of the aortic root and ascending aorta is infrequent (0,2%/patient/year) but life-threatening. Accurate and prompt diagnosis is challenging. Imaging test contribute to the assessment of infection. The use of ^{18}F-FDG-PET/CT has been previously reported in these patients. Nevertheless, the lack of uniform interpretation criteria and misleading diagnosis due to inflammatory changes limit its use, especially the first year after surgery. The aim of this study was to detect a "normal" pattern of ^{18}F-FDG distribution along the graft during the first year after surgery in non-infected subjects. ***Materials and Methods:*** Prospectively designed study including patients with aortic root or ascending aorta replacement undergoing serial PET/CT at 3, 6 and 12 months after surgery. CRP and blood cultures were obtained the day of each PET/CT study. Patients with clinical or analytical suspicion of infection were excluded. Myocardial suppression protocol was applied. Selective thoracic images were acquired 60 minutes after the injection of 180MBq of ^{18}F-FDG. Studies were visually and semiquantitatively assessed regarding the pattern of radiotracer distribution along the graft (homogeneous/heterogenous) and the intensity of uptaking areas (SUVmax, SUVratio). Fluid collections or other significative findings were also determined. ***Results:*** Eighteen patients were included. Significative ^{18}F-FDG uptake along the graft was detected in all the studies with a mean SUVmax 4.79 (SD 1.2), 4.28 (SD 0,85) and 4.29 (SD 0.94) at 3, 6 and 12 months respectively. Heterogenous distribution along the graft was noticed in 55% of the studies at 3 months, 44% at 6 months and 72% at 12 months. Six patients (33%) showed retrosternal fluid collections that persisted throughout the year, with progressive growth in one case. An unsuspected stage I sarcoidosis was depicted in one patient. ***Conclusion:*** Cautious interpretation should be made in patients with aortic root or ascending aorta replacement undergoing PET/CT for suspicion of infective endocarditis because significant inflammatory uptake persists the first year after surgery. Uptake level in postsurgical inflammation overlap to those reported in literature in septic inflammation[1]. Heterogeneous pattern in non-infected patients is highly depicted and thus it should not be considered as a specific criteria for infection. ***References:*** 1.Daniel García-Arribas, Isidre Vilacosta, Aida Ortega-Candil, Cristina Rodríguez-Rey, Carmen Olmos, María Jesús Pérez-Castejón, et al. Usefulness of positron emission tomography/ computed tomography in patients with valve-tube graft infection. Heart. 2018; 104 (17): 1447-54.

EPS-109

^{18}F-FDG-PET/CT in the Diagnosis of Infective Endocarditis in Patient with Electronic Cardiac Device and Fever of Unknown Origin and/or Bacteriemia

S. Guzmán Ortiz*, B. Rodríguez Alfonso, A. Ramos-Martinez, M. Cobo Marcos, S. Pérez Quirós, M. Mitjavila Casanovas;*
University Hospital Puerta de Hierro Majadahonda, Madrid, SPAIN.

Aim/Introduction: To asses diagnosis performance of ^{18}F-FDG-PET/CT for the detection of infective endocarditis (IE) in patients with electronic cardiac device (ECD) presenting fever of unknown origin and/or positive blood cultures. ***Materials and Methods:*** We retrospectively analysed all PET/CT studies conducted in our hospital from 01/2018 to 01/2020 in patients with ECD and fever of unknown origin (FUO) and/or bacteraemia to rule out IE. Patients with sing or symptoms of pocket-generator infection were excluded. Results of both imaging tests (Ecocardiography and PET/CT) were compared with final diagnosis to asses sensitivity, specificity and positive and negative predictive values (PPV, NPV). Duke criteria obtain by the conventional approach (Duke-1) and after the addition of PET/CT (Duke-2) were compared to final-Duke criteria to assed the better correlation. For the final diagnosis, culture of explanted devices or consensual decision of the multidisciplinary endocarditis team and a follow-up period not inferior to 4,86 weeks were considered as gold-standar (GS). ***Results:*** Twenty-two patients were included. Fever was the only

symptom in 4, positive blood culture in 3 and 15 presented both. All patients had echocardiography previous to PET/CT (82% transoesophageal echocardiography). According to GS, IE was stablished in 5 patients (25%) and discarded in 17 (75%). Just 1 patient underwent device explantation and culture, demonstrating S. aureus IE. Both, sensitivity and specificity were higher for PET/CT compared to echocardiography (0.66 vs 0.33 and 0.87 vs 0.75 respectively). When considering results of both imaging studies, sensitivity reach 1 but specificity decreased to 0.62. Duke-1 was concordant to final-Duke classification in 5 patients (23%), 2 definite-IE and 3 rejected-IE, whereas Duke-2 was concordant in 8 patients (36%), the 5 patients with definite-IE and 3 rejected-IE. In the possible-IE group according to Duke-1 (14 patients), the addition of PET/CT correctly re-classified 3 definite-IE but it also misclassified 3 rejected-IE as definite-IE. ***Conclusion:*** Patients with ECD and FUO and/or bacteraemia are a particular subgroup in which PET/CT shows moderate sensitivity and high specificity in the detection of IE, improving the low-moderate yield of echocardiography. Duke criteria performed poorly even after adding PET/CT results showing a low concordance with final-Duke. ***References:*** None

EPS-110

Visual Vascular Score with 2-[^{18}F]FDG: validation on a control sample

R. Ferreira*, M. R. Victor, S. Carmona, A. I. Santos;*
Hospital Garcia de Orta, Almada, PORTUGAL.

Aim/Introduction: To assess interobserver agreement and validate a visual vascular score (Eur J Nucl Med Mol Imaging.2018;45:1250-1269) of 2-[^{18}F]FDG physiological arterial uptake, in a possible control group for suspected large vessel vasculitis. ***Materials and Methods:*** Retrospective analysis of 2-[^{18}F]FDG PET/CT oncological scans from an occasional sample of patients 50 or more years' old, without suspicion of inflammatory disease, characterizing age, gender, known risk factors for atherosclerosis, blood glucose level and activity administered. To obtain a total vascular score, all PET/CT scans were attributed a visual vascular score to 7 arterial compartments (carotid, subclavian, axillary, thoracic aorta, abdominal aorta, iliac and femoral) by 3 observers with different years of practice: 1 over 10 (obs1), 1 about 3 (obs2) and 1 less than 1 (obs3). Statistical analysis was performed using IBM SPSS Statistics. ***Results:*** A total of 51 scans from 51 patients were evaluated, the most common diagnosis being lung cancer (n=21;41%). Fever of unknown origin, infection and hepatic lesions were exclusion criteria. The mean age was 69[sd=9.4;min=50;max=90] years' old and 32/51(63%) patients were male. Thirty-two (63%) had arterial hypertension, 18(35%) dyslipidaemia, 13(25%) diabetes, 21(41%) history of smoking, 5(10%) ischemic heart disease and 6(12%) peripheral arterial disease. Blood glucose levels prior to the acquisition had a median value of 102[P25:92;P75:116] mg/dL and the 2-[^{18}F]FDG administered activity had a mean value of 247[sd=67;min=102;max=398] MBq. The vascular score for each compartment was assumed as the concordant classification between 2 out of 3 observers, 3 out of 3, or the score attributed by the most experienced observer in one case of total disagreement. Total score was 0 in 30(59%) patients, 1 in 9(18%), 2 in 3(6%), 3 in 5(10%), 4 in 3(6%) and 5 in 1(2%). Kappa index showed moderate agreement for the: subclavian territory- obs1/obs2 (k=0.563;p=0.001), obs1/obs3 (k=0.505;p=0.004), obs2/obs3 (k=0.491,p=0.009); axillary territory- obs1/obs3 (k=0.506;p=0.002); thoracic aorta- obs1/obs2 (k=0.489;p<0.001); abdominal aorta-obs1/obs2 (k=0.510,p<0.001); and femoral territory-obs1/obs2 (k=0.527,p<0.001). ***Conclusion:*** All patients were classified as having a total vascular visual score ≤5, translating a relatively homogeneous sample. The majority of the arterial territories were scored as 0/1 and none was scored as 3, and so this sample might be considered as a control group when evaluating the presence of vasculitis. However, the interobserver agreement was weak and should also be evaluated in a pathological sample. This classification might also need a learning curve and/or could benefit from a semiquantitative analysis. ***References:*** None

EPS-111

FDG-PET imaging of gastrointestinal Graft-versus-Host disease

W. Roll[1]*, G. Evers*[2]*, R. Strotmann*[1]*, J. Albring*[2]*, B. Noto*[1]*, M. Weckesser*[1]*, M. Stelljes*[2]*, M. Schäfers*[1]*;*
[1]Department of Nuclear Medicine, University Hospital Münster, Münster, GERMANY, [2]Department of Medicine A, Hematology, Oncology and Pulmonary Medicine, University Hospital Münster, Münster, GERMANY.

Aim/Introduction: Following Allogeneic stem cell transplantation (alloSCT), a potentially curative treatment for many refractory and high-risk hematologic malignancies, intestinal Graft-versus-Host disease (GvHD) is a frequent complication, associated with a significant morbidity and mortality. As previously shown, FDG-PET can be used for diagnostic purposes and might have a prognostic value for patients suffering from intestinal GvHD. The aim of this retrospective analysis was to further elaborate the value of FDG-PET in a larger patient cohort with intestinal GvHD. ***Materials and Methods:*** Between 06/2011 and 02/2019, 101 patients with suspected acute intestinal GvHD underwent FDG-PET examination. Complete clinical and FDG-PET data sets were reviewed for presence of intestinal inflammation. 74 of the 101 patients with clinically and/or histologically proven intestinal GvHD and signs of inflammation in FDG-PET were analyzed in detail. Quantitative PET parameters, as well as clinical data, were compared between patients

with fast and slow / no response to immunosuppressive treatment. ***Results:*** 18F-FDG-PET detected intestinal GvHD with a sensitivity and specificity of 93.0% (95% CI: 84.9 - 97.1) and 73.3% (95% CI: 44.8 - 91.1), respectively. Patients with subsequent rapid relief of GvHD symptoms had significantly higher standard uptake values for SUVmax (mean 13.5, 95% CI: 10.7 - 16.4) and SUV peak levels (mean 9.2, 95% CI: 7.3 - 11.1) compared to patients with slow or no response to immunosuppressive therapy (mean SUVmax: 7.7; 95% CI: 7.0 - 8.4; mean SUVpeak: 5.4, 95% CI: 4.9 - 5.8; p .005). ***Conclusion:*** This retrospective analysis indicates that 18F-FDG-PET detects acute intestinal GvHD with good sensitivity and specificity. Of further interest, our results suggest potential significance of FDG-PET in predicting treatment response following immunosuppressive therapy. Before implementation into clinics prospective studies are needed to corroborate our results. ***References:*** None

EPS-112

Simple radiosynthesis of ^{68}Ga-desferrioxamine B (^{68}GaDFO) for infection imaging

A. Darwesh*, R. Wellman, V. Abbate, M. S. Cooper, R. Hider, M. Morais, S. Y. A. Terry, M. T. M. Ma, P. J. Blower;*
King's College London, London, UNITED KINGDOM.

Aim/Introduction: Endovascular stent graft infections are difficult to diagnose.[1]A PET radiotracer that is taken up selectively by microorganisms could provide more specific detection than currently used [^{18}F]FDG. The Fe^{3+} complex of DFO, a siderophore, is taken up by bacteria, making its isostructural ^{68}Ga complex applicable for imaging infection.[2] DFO is a clinically approved drug[3], hence its ^{68}Ga complex has a low regulatory barrier to clinical translation. Here, we report a GMP method for ^{68}GaDFO preparation, its bacterial binding in vitro, and its in vivo pharmacokinetics in healthy mice. ***Materials and Methods:*** ^{68}GaDFO was radiolabelled by mixing aqueous DFO (20µl), aqueous solution of sodium acetate (3.6 M) (20/30 µl), and ^{68}Ga chloride (200µl). The mixture was diluted with water to 1 ml then incubated for 10 min at room temperature. The radiochemical purity was assessed by TLC and HPLC. ^{nat}GaDFO was added to ^{68}GaDFO and analysed by LC-MS. Stability in human serum was measured by RP-HPLC after 60-min incubation at 37° C. ^{68}GaDFO uptake in E. coli was studied in vitro and compared to ^{68}Ga ferrichrome-C, enterobactin, and siderophore-free ^{68}Ga. Mice were injected intravenously with ^{68}GaDFO and PET/CT scanned for 60 min. Mice were sacrificed at 60 min, and organs were counted in a gamma-counter ***Results:*** ^{68}GaDFO was labelled with high radiochemical purity (≥ 95%) as measured by TLC and HPLC. ^{68}GaDFO demonstrated no binding to serum proteins at any time point by RP-HPLC. All ^{68}Ga labelled siderophores showed higher E. coli uptake than siderophore free ^{68}Ga, with ^{68}Ga ferrichrome-C showing the highest uptake. ^{68}GaDFO exhibited rapid renal excretion and low blood retention. Ex vivo biodistribution at 60 min showed most of the activity resided in urine ***Conclusion:*** ^{68}GaDFO radiolabelling with GMP graded reagents gave a product with high radiochemical purity identified as a 1:1 complex of Ga^{3+} with DFO. The complex showed specific uptake in E. coli. ^{68}GaDFO did not release ^{68}Ga to serum proteins, indicating high stability of the compound in serum. ^{68}GaDFO is rapidly cleared with no significant retention in any organ except kidneys. In vivo biodistribution of ^{68}GaDFO on infected animal models is now planned ***References:*** 1. J. C. Marc Elieson,T. Mixon, Case Reports, 2012, 39, 884-889. 2. W. Rabsch and G. Winkelmann, Biol. Met., 1991, 4, 244-250. 3. M. Naser, S. Mehrnoosh, E. Hassan, N. Hajar, S. Mehdi, S. Mohsen, G. Mehdi, P. Hoda and A. Mehdi, Int. J. Hematol. stem cell Res., 2016, 10, 239-247.

EPS-113

FDG-PET/CT is clinically valuable in the majority of patients referred from Emergency Department with unclarified systemic inflammation

S. Hess*[1,2], R. Horvat[3];*
[1]Dept. of Radiology and Nuclear Medicine, Hospital South West Jutland, University Hospital of Souther, Esbjerg, DENMARK, [2]Department of Regional Health Research, University of Southern Denmark, Odense, DENMARK, [3]Dept. of Radiology and Nuclear Medicine, Hospital South West Jutland, University Hospital of Southern Denmark, Esbjerg, DENMARK.

Aim/Introduction: FDG-PET/CT is increasingly used to assess infection and inflammation, not only in well-defined clinical entities, but also in heterogeneous populations from Emergency Departments (ED) with unclarified systemic inflammation. It remains controversial when to introduce FDG-PET/CT, but some advocate introduction early in the course of admission. We retrospectively assessed the clinical value of all FDG-PET/CT performed in ED-patients with suspected or unclarified inflammation of unknown origin. ***Materials and Methods:*** All patients referred to FDG-PET/CT from the ED during 2019 for unclarified inflammation, unresolved infection or bacteremia, or fever of unknown origin were included. Medical records were comprehensively reviewed for baseline characteristics, results of FDG-PET/CT and clinical conclusions at discharge, which constituted the reference standard. ***Results:*** Forty-four consecutive patients were included (52% males, mean age 70 years [22-92]) and divided into three groups according to results of PET/CT. Group 1 (n=22/44, 50%): Directly helpful results, i.e. true positive diagnoses [pneumonia (n=5), abscess (n=4), spondylodiscitis (n=3), catheter-related infection (n=2), novel cancers (n=2), progressive known cancer (n=1), giant-cell arteritis (n=1), or endocarditis (n=1)], or patients with established infections but poor treatment response where PET/CT ruled-out suspected additional occult infectious foci. Group 2 (n=10/44, 23%): Potentially

helpful, i.e. focal findings ruled out with negative PET/CT scans, no complications, and a discharge diagnosis of non-specific, self-limiting infection. Group 3 (n=12/44, 26%): Not helpful, non-specific findings and discharge diagnoses other than simple, self-limiting infections. Of note, in half of these cases, the final diagnoses are not usually detectable by PET, i.e. urinary tract infection (n=3), native-valve endocarditis (n=2), and erysipelas outside the scan area (n=1). Baseline characteristics were similar in the three groups 1-3, e.g. mean body temperature (i.e. 37.8 C, 37.6 C, and 37.5 C, respectively) and C-reactive protein (i.e. 154 mg/L, 152 mg/L, and 167 mg/L, respectively). Bacteremia was present in 17 patients; most in group 1 (n=10) compared to group 2 (n=2), and group 3 (n=5), with comparable fractions in groups 1 and 3 (i.e. 46% and 47%, respectively), but lower in group 2 (20%). ***Conclusion:*** FDG-PET/CT is clinically helpful in establishing a diagnosis in the majority of patients with unclarified or unresolved inflammation in a heterogenic ED-population, i.e. 50-73% (group 1 or group 1+2) depending on how "helpful" is defined. Patients' basic baseline characteristics are not useful for discriminating patients with useful or not useful FDG-PET/CT. Further studies on optimal patient selection in prospective settings are highly desirable. ***References:*** None

EPS-114

Contribution of ^{18}F-FDG-PET/CT in the diagnosis of patients with fever of unknown origin

S. Georga[1], P. Exadaktylou[1], I. Petrou[1], D. Katsampoukas[1], E. Moralidis[1], K. Arvaniti[2], G. Giataganas[3], G. Arsos[1];
[1]3rd Department of Nuclear Medicine, Aristotle University Medical School, Papageorgiou Hospital, Thessaloniki, GREECE, [2]ICU and Antimicrobial Stewardship Unit, Papageorgiou Hospital, Thessaloniki, GREECE, [3]Department of Radiology, Papageorgiou Hospital, Thessaloniki, GREECE.

Aim/Introduction: Conventional laboratory and imaging investigation despite being time-consuming and costly, are often inconclusive in revealing the underlying cause of fever of unknown origin (FUO). 18F-fluorodeoxyglucose (18F-FDG) accumulates in malignant lesions as well as at sites of active infection or inflammation, the three major causes of FUO, thus making 18F-FDG-PET/CT a useful tool for approximation of the underlying cause of FUO, especially when potential diagnostic clues are missing. The aim of the study was to assess the diagnostic contribution of 18F-FDG-PET/CT in a small, representative series of FUO patients of a tertiary hospital. ***Materials and Methods:*** We retrospectively reviewed whole-body 18F-FDG-PET/CT scans performed in 50 consecutive, non-immunocompromised, adult patients referred to our department for further FUO investigation. 18F-FDG-PET/CT scans were considered positive for active disease if any focus of increased 18F-FDG uptake other than physiological uptake was observed. Scans showing normal 18F-FDG distribution throughout the body and no hypermetabolic foci, were considered negative for active disease. Positive and negative 18F-FDG-PET/CT scans were compared to the final diagnosis based on histopathological and microbiological findings, generally acceptable clinical criteria or a minimum of 6 months of clinical follow-up. 18F-FDG-PET/CT scan was considered contributory to the diagnosis when detected the underlying cause of FUO or correctly suggested the most appropriate site for a biopsy leading to an accurate diagnosis. ***Results:*** Final diagnosis was established in 39/50 (78%) of the patients. The underlying cause of FUO was malignancy in 8 (16%), infection in 20 (40%), noninfectious inflammatory diseases in 11 (22%), while fever remained unexplained in 11/50 (22%) of the patients. 18-F-FDG-PET/CT scan was positive for active disease in 42/50 (84%) of patients and was negative for active disease in 8/50 (16%) of patients. There were 36 TP, 6 FP, 6TN and 2 FN results. Accordingly, the sensitivity, specificity, accuracy, positive predictive value and negative predictive value of 18F-FDG-PET/CT for active disease detection in patients with FUO were 94.7%, 50.0%, 84.0%, 85.7%, and 75.0%, respectively. 18F-FDG-PET/CT scan was considered clinically helpful and contributory to the diagnosis in 35/50 (70%) of patients. ***Conclusion:*** 18F-FDG-PET/CT is a valuable diagnostic modality in the evaluation of patients with FUO, substantially contributing in our study to the diagnosis in 70% of patients, by either identifying the underlying cause of FUO or correctly targeting suspect lesions for further evaluation. Earlier application of 18F-FDG-PET/CT in FUO investigation, could be cost-effective by means of shortening the diagnostic workup period. ***References:*** None

EPS-115

The role of ^{18}FDG-PET/CT in the diagnostic work-up of fever of unknown origin (FUO) and inflammation of unknown origin (IUO)

M. Allocca, T. Tagliente, D. Malandrino, A. Berni, M. Di Paolantonio, A. Martini, C. Olianti, P. Saletti, L. Poggesi, R. Sciagrà; University of Florence, Florence, ITALY.

Aim/Introduction: Fever of unknown origin (FUO) and inflammation of unknown origin (IUO) are diagnostically challenging conditions. ^{18}FDG PET/CT is a sensitive diagnostic technique that may improve diagnosis. The aim of this study was to assess the problem-solving value of ^{18}FDG-PET/CT in FUO/IUO, taking into account the following diagnostic sub-categories: infections, non-infectious inflammatory disease (NIID), neoplasm, miscellaneous causes, no diagnosis. ***Materials and Methods:*** 50 patients aged 18-86, admitted to Internal Medicine Unit for FUO/IUO from January 2016 to December 2019, and who underwent ^{18}FDG-PET/CT vertex-pelvis scan, were retrospectively evaluated. On ^{18}FDG-PET/CT images lesion SUVmax and SUVpeak, SUVmax and a Deauville-

like score for the evaluation of spleen and bone-marrow uptake were assessed. Besides, clinically and laboratory parameters usefull to final diagnosis were examined. ***Results:*** No significant differences in main vital parameters and laboratory values were found in FUO vs. IUO, except for body temperature, according to definition (mean±sd in FUO= 38.4°C±0.4 vs. IUO= 37.4°C±0.3; p<0.001). Diagnosis was established in 45 patients: 18 neoplasms (36%), 13NIIDs (26%), 12 infections (24%), 2 miscellanies (4%). In 5 patients, who had spontaneous regression of symptoms, no abnormalities were found.[18]FDG-PET/CT played a decisive role in 25/45 cases (55%), identifying possible, not previously detected causes. PCR was found as the best predictors of [18]FDG-PET/CT diagnostic usefulness (p=0.005) and in particular for PCR>40mg/L (Wilks' Λ=0.078; p=0.006; accuracy=75%). In our sample, lesion SUVmax and SUVpeak resulted significantly higher (p<0.001) in neoplasms vs other diagnostic sub-categories (mean±sd: 12.64±7.68 vs 4.50±2.20 for lesion SUVmax; 9.97±6.36 vs 3.63±1.70 for lesion SUVpeak). The qualitative assessment of bone marrow metabolism (Deauville-like score) showed an uptake ≥ liver in 50% of NIID cases, while in 23% only of the infection group. However, no significant difference (p=0.09) in marrow SUVmax values was found between NIID and infection groups (mean±sd: 3.54±1.00 vs 2.94±0.63, respectively). ***Conclusion:*** The study demonstrated a determinant diagnostic role of [18]FDG-PET/CT in more than a half of FUO/IUO patients, with a possible relationship with higher PCR values. The observation of a trend for bone marrow uptake to be higher in NIID vs infections is intriguing and should be further expanded. ***References:*** Schönau V, et al. The value of 18F-FDG-PET/CT in identifying the cause of fever of unknown origin (FUO) and inflammation of unknown origin (IUO): data from a prospective study; Ann Rheum Dis 2018;77:70-77. doi:10.1136/annrheumdis-2017-211687

EPS-116

Does FDG-PET contribute to patients diagnosed with Primary and Secondary Hypophysitis?

S. Asa[1], Ö. Korkmaz[2], M. Beytur[1], R. Uslu Beşli[1], P. Kadıoğlu[2], M. Sağer[1], K. Sönmezoğlu[1];
[1]Istanbul University-Cerrahpaşa Faculty of Medicine, Department of Nuclear Medicine, Istanbul, TURKEY, [2]Istanbul University-Cerrahpaşa Faculty of Medicine, Department of Internal Medicine, Endocrinology Department, Istanbul, TURKEY.

Aim/Introduction: Hypophysitis is a rare inflammatory disease of the pituitary gland that mostly mimics the pituitary masses. It is divided into two groups as primary and secondary. It is crucial to make the correct differential diagnosis in these patients. In this study, we aimed to examine the contribution of FDG PET imaging in determining the underlying inflammatory etiology in patients diagnosed with hypophysitis. ***Materials and Methods:*** In our retrospective study, 11 patients were sent to FDG PET imaging was performed with PET / CT and PET / MR systems. In patients with focal activity involvement, the presence of pituitary stalk involvement with the parenchyma, or the proximity of the lesion to the optical resection was evaluated. Also, SUV maximum and SUV mean values were calculated from the lesion areas determined visually. The Mann-Whitney U test was used for comparisons. ***Results:*** The patient group was 7 male and 4 women. Pathological focal activity involvement was detected in 3 of 8 patients diagnosed with primary hypophysitis, while PET was negative in 5 patients. PET was positive in all 3 patients diagnosed with secondary hypophysitis Non-pituitary findings related to other involvement of secondary disease in PET were also detected in 2 of the patients. In PET, only one patient with involvement in the pituitary was operated due to visual impairment and pressure findings, and diagnosed as germinoma and was accepted as SH. The diagnosis of the other two SH patients was IgG4 related disease and Erdeim Chester disease. There was a significant difference between the SUV parameters and the SUV values of the control group in a total of 6 patients with focal activity involvement in PET. found (p = 0). Besides, SUV values (median SUVmax: 4.94; median SUVmean: 3.11) showed a significant difference from the control group in patients diagnosed as hypophysitis clinically-radiologically whether or not focal lesions were selected (p = 0.001). ***Conclusion:*** Despite the limitation of the resolution, it may be possible to determine the inflammatory reaction in the pituitary by PET imaging. The differential diagnosis becomes easier when the FDG-positive lesions of the underlying disease other than pituitary are detected in secondary hypophysitis cases. The evaluation of the biological information provided by FDG using PET / MR in conjunction with the morphological detail provided by MR may have an essential contribution to the management of patients with pituitary disease ***References:*** None

EPS-117

COVID-19 related findings assessed by dual reporting in our series of [18]F-FDG PET/CT studies performed over the coronavirus pandemic

J. Garcia, S. Ortiz, A. Compte, P. Bassa, S. Mourelo, M. Soler, M. Buxeda, T. Blanch, E. Valls, E. Riera;
CETIR ASCIRES Grupo biomédico, Barcelona, SPAIN.

Aim/Introduction: To assess incidence in radiological and metabolic findings due to COVID-19 in our oncology patients referred for an [18]F-FDG PET/CT study, and reported by a Nuclear Medicine physician and a Radiologist over the coronavirus pandemic. ***Materials and Methods:*** From January 15th through April 15th 2020, a total of 877 [18]F-FDG PET/CT procedures were performed in oncology patients. All patients were symptom-free at the time of the PET/CT

procedure, especially with no fever or respiratory distress. Each patient fasted for > 6 hours before imaging. After ensuring that blood glucose was < 160 mg/dL, 0.125 mCi/kg ^{18}F-FDG were administered i.v. 1 hour before image acquisition. Imaging was performed with PET/CT scanner (Gemini.Philip) equipped with LSO crystals and 16-slice CT. A CT scan in maximum inspiration (120kV, 25 mAs, axial slice thickness 2.5 mm) was first acquired followed by a second CT with same parameters but patient breathing normally, for attenuation correction of PET images. A whole-body PET imaging was then taken from the base of the skull to the upper-thigh (3 min/bed). Images were visually inspected by experienced Nuclear Medicine and Radiologist specialists jointly. Inspiratory CT was assessed according to the CORADS classification by the Dutch Radiological Society. SUVmax values were also calculated in lung involvement. ***Results:*** Out of 877 studies performed, 784 (89.4%) did not show lung involvement (CORADS 1). Ninety-three studies (10.6%) showed lung disease on CT as follows: 5.9% CORADS 2 (52 cases), 1.6% CORADS.3 (14 cases), 2.5% CORADS.4 (22 cases), 0.6% CORADS.5 (5 cases). Therefore CT detected in 27 cases (3.1%) a high/very high likelihood of COVID-19 lung disease. There were only 2 cases with mediastinal lymphadenopathy, rated CORADS 2. In 23 patients (44.2%) with low probability of COVID-19 (CORADS.2), abnormal lung ^{18}F-FDG uptake was detected. However, none of the cases with intermediate/high/very high probability of COVID-19 (CORADS.3-4-5) showed abnormal ^{18}F-FDG uptake. ***Conclusion:*** Dual specialist interpretation of ^{18}F-FDG PET/CT studies allowed detection of lung involvement consistent with COVID-19 according to CORADS classification. Uptake of ^{18}F-FDG limited only to low probability cases of lung involvement (CORADS.1), due to inflammatory/infectious disease. Lack of abnormal ^{18}F-FDG uptake seen in all intermediate/high/very high probability (CORADS.3-4-5) cases may be due to an early phase of the disease, since no symptoms were reported. Further studies are warranted to assess the predictive value of ^{18}F-FDG uptake in the remaining clinical stages of the lung disease. ***References:*** EJNMIM. doi:10.1007/s00259-020-04767-1. EJNMIM. doi:10.1007/s00259-020-04762-6. EJNMIM. doi:10.1007/s00259-020-04734-w.

EPS-118

^{18}F-fluorodeoxyglucose (FDG) PET/CT findings in patients with CT lung abnormalities suggestive of COVID-19 infection

C. Aveline, Q. Pouliot, M. Gauthé, L. Turpin, K. Kerrou, M. Calzada, V. Gaura-Schmidt, B. Sgard, J. Zhang, J. Talbot, F. Montravers; Hôpital Tenon, Paris, FRANCE.

Aim/Introduction: In relation with the Covid-19 outbreak in the Paris area, we determined the incidence of lung lesions on CT suspicious for Covid-19 pneumonia in patients referred to FDG PET/CT and the FDG uptake by those. We also aimed to evaluate the proportion of those patients finally diagnosed with SARS-CoV-2 infection. ***Materials and Methods:*** We retrospectively reviewed the FDG PET/CTs of patients referred to our nuclear medicine department during the COVID-19 pandemic outbreak in Paris, France. We searched for typical lung findings on CT suggestive of COVID-19 pneumonia (bilateral subpleural ground glass opacities and/or consolidations in multiple segments). If this pattern was observed, we determined the FDG uptake by the pulmonary lesions and collected the medical data of the patient, in order to determine the aetiology: SARS-CoV-2 related pneumonia or other causes. ***Results:*** 617 patients were referred for FDG PET/CT between March 1st and April 30th 2020,mainly for initial assessment or follow-up of malignancies; 31 showed pulmonary lesions on CT (without contrast medium injection) which were compatible with COVID-19 pneumonia (5%). All lesions showed an increased FDG uptake (mean SUVmax 3.44, median 2.8, range 1.1-10.9). In 7 of them (23% of patients with CT lung abnormalities and overall about 1 % of patients) referred for cancer imaging, this FDG PET/CT pattern was confirmed to be due to Covid-19 pneumonia (diagnosis based on highly evocative clinical symptoms and/or positive RT-PCR for SARS-CoV-2). Three of these 7 patients were asymptomatic at the time of FDG PET/CT but became symptomatic about 10 days later; the Covid-19 infection was already known for the 4 other patients. In 4/7 patients, bilateral mediastinal nodes took-up FDG (mean SUVmax 3.87). The 24 other patients (77%) had a different final aetiological diagnosis: other viral or bacterial infections, consequences of a recent bronchoalveolar lavage, and known pulmonary lesions of autoimmune diseases. There was no difference in FDG uptake by lung lesions between Covid-19 patients and others (mean, median [range] SUVmax 3.13, 1.7 [1.1-6.4] vs. 3.53, 2.85 [1.2-10.9] respectively, p =0.71). ***Conclusion:*** In our area with relatively high prevalence of Covid-19, about 1 in 4 patients showing evocative pulmonary CT patterns on FDG PET/CT was considered to be infected by this virus. The FDG uptake by parenchymal lesions was usually moderately increased, and may also be observed in bilateral mediastinal nodes. Moreover, FDG PET/CT identified some patients in the early phase of the Covid-19 infection, before symptoms onset. ***References:*** None

EPS-119

Incidental Findings Suggestive of COVID-19 Pneumonia in Asymptomatic Patients Derived to ^{18}F-FDGPET/CT. Preliminary Results Obtained in a Reference Single Center During the Pandemia in Spain

A. Blanes[1], C. G. Wakfie Corieh[1], R. Valhondo Rama[1], L. García Beláustegui[1], M. N. Cabrera Martín[1], C. Rodríguez Rey[1], R. Couto Caro[1], A. Ortega Candil[1], M. García García-Esquinas[1], F. Ferrando-Castagnetto[2], J. L. Carreras Delgado[1];

[1]*Hospital Clinico San Carlos, Madrid, SPAIN,* [2]*Hospital de Clínicas Dr. Manuel Quintela, Facultad de Medicina, Universidad de la República, Montevideo, URUGUAY.*

Aim/Introduction: The objective of the study is to evaluate the prevalence of incidental findings suggestive of COVID-19 pneumonia in a sample of patients referred for a ^{18}F-FDG PET/CT study, asymptomatic for inflammatory lung disease, in a period corresponding to a high rate of contagion from COVID-19 in Hospital Clínico San Carlos (Madrid, Spain). We aim to contrast these findings with their real-time reverse polymerase chain reaction (rRT-PCR) result and to described radiological and metabolic findings of pneumonia. ***Materials and Methods:*** Consecutive patients with whole-body (WB) ^{18}F-FDG PET/CT from February 20th to April 30th 2020. Intravenous contrast-enhanced CT was always used except contraindications. The CO-RADS criteria (1-6) was applied to classify the probability of COVID-19 pneumonia on chest CT and the maximum standardized uptake value (SUVmax) was evaluated to measure metabolic behavior of the lungs. We compared these radiological and metabolic findings with rRT-PCR result (gold standard). All patients were carefully interrogated about coronavirus-like symptoms prior to PET/CT acquisition and all of them were asymptomatic. All the studies were acquired on a Biograph 6 True Point PET/CT (Siemens, Germany) following European Association of Nuclear Medicine Guidelines. ***Results:*** We identified 46 asymptomatic patients with incidental findings suggestive of COVID-19 pneumonia for a total of 507 WB ^{18}F-FDG PET/CT studies, what it means a percentage of 9.1%. The mean age was 66.4 years. 54.3% (25/46) of the patients were men. Among the reasons for the request, 76.1% (35/46) were oncological and 23.9% (11/46) non-oncological. On 14 patients (30.4%) rRT-PCR for COVID-19 were performed consequently PET/CT findings, being positive for 64.3% (9/14). The remaining 69.6% (32/46) of the patients had no rRT-PCR for COVID-19 reports. The mean SUVmax of the lung glass opacities and/or consolidations were measured, obtaining 6.2±3.7, 5.5±2.5 and 4.3±2.5 for positive, negative and non-performed rPCR, respectively. ***Conclusion:*** ^{18}F-FDG PET/CT may detect incidental finding COVID-19 pneumonia in asymptomatic patients in regions with high SARS-CoV-2 prevalence. Although suspicion of COVID-19 pneumonia shows FDG uptake in most cases of our sample, the additional diagnostic value of pulmonary metabolic activity should be defined in larger series of patients. Nuclear Medicine workers need to be aware of the possibility of contact with patients infected even if they are asymptomatic and should be prepared accordingly. ***References:*** None

MCS1

Mid-Congress-Symposium 1 (EANM/EACVI): Detecting Cardiac Amyloidosis - Increasing Role of Nuclear Medicine

Monday, October 26, 2020, 09:30 - 12:15 Channel 1

MCS-01

Introduction Cardiac Amyloidosis and New Treatment Options

H. Nienhuis; University Medical Center Groningen, Groningen, NETHERLANDS.

MCS-02

Echocardiography and Cardiac MRI in Cardiac Amyloidosis

O. Lairez; University Hospital Toulouse, Toulouse, FRANCE.

MCS-03

Cardiac Bone Scans -Protocols, Interpretation, Quantification

R. Slart; University Medical Center Groningen, University of Groningen, Groningen, NETHERLANDS.

MCS-05

Cardiac MIBG - Protocols, Interpretation, Quantification

E. Piekarski; Bichat Claude Bernard Hospital, Paris, FRANCE .

MCS-06

New PET Radiopharmaceuticals in Cardiac Amyloidosis, Perspectives

J. Sörensen; Department of Nuclear Medicine & PET, Uppsala University Hospital, Uppsala, SWEDEN .

MCS-07

Results EU Questionnaire on Cardiac Amyloidosis and Cardiac Sarcoidosis & Clinical cases

A. Gimelli; Fondazione Toscana-CNR Gabriele Monasterio, Pisa, ITALY.

MCS2

Mid-Congress-Symposium 2: Artificial Intelligence in Image Acquisition, Reconstruction and Processing

Monday, October 26, 2020, 09:30 - 12:15 Channel 2

MCS-08

AI in Image Reconstruction

A. Reader; King's College London, Biomedical Engineering and Imaging Sciences, London, UNITED KINGDOM.

MCS-09
AI for Image Corrections
J. Lee; Seoul National University College of Medicine, Seoul, REPUBLIC OF KOREA.

MCS-10
AI and Imaging Biomarkers
D. Visvikis; INSERM, LaTIM, Brest, FRANCE.

MCS-12
AI for Monte Carlo Simulations
D. Sarrut; CNRS, CREATIS, Lyon, FRANCE.

MCS-13
AI for Dosimetry Applications
J. Bert; University Hospital Brest, LaTIM, Brest, FRANCE.

MCS-14
Potential Clinical Applications of AI in NM
M. Sollini; Department of Biomedical Sciences, Humanitas University, Milan, ITALY.

YDF1

EANM Young Daily Forum 1: Simply the Best - Presentation Skills for Medical Professionals

Monday, October 26, 2020, 12:20 - 13:50 Channel 1

OP-132
Simply the Best - Presentation Skills for Medical Professionals
R. Sheppard; London, UNITED KINGDOM

MCS3

Mid-Congress-Symposium 3 (EANM/ESMO): Clinical Development of Radioligand Therapy

Monday, October 26, 2020, 14:00 - 16:45 Channel 1

MCS-15
Overview of Clinical Development (From Phase 0 to 3)
A. Stathis; Oncology Institute of Southern Switzerland, Ospedale Regionale die Bellinzona e Valli, Bellinzona, SWITZERLAND.

MCS-16
Early Development of New Therapeutic Approaches - A Break with the Past
A. Awada; Institut Jules Bordet, Department of Medicine, Brussels, BELGIUM.

MCS-17
Regulatory Aspects and (Potential) Hurdles for Clinical Development and Approval of Radioligand Therapies
G. Waxenecker; Vienna, AUSTRIA.

MCS-19
Current Status of Radioligand Therapy
D. Oprea-Lager; Universitair Medische Centra, Department of Radiology and Nuclear Medicine, Amsterdam, NETHERLANDS.

MCS-20
Identification of New Targets and New Ligands
U. Haberkorn; University of Heidelberg, Department of Nuclear Medicine, Heidelberg, GERMANY.

MCS4

Mid-Congress-Symposium 4: Image Guided Surgery

Monday, October 26, 2020, 14:00 - 16:45 Channel 2

MCS-21
Sentinel Lymph Node – An Overview of the Different Tracers/Technologies for SLN. Strengths and Limitations
S. Vidal-Sicart; Consultant in Nuclear Medicine. Staff member of Diagnostic Imaging Institute Hospital Clinic Barcelona, Barcelona, SPAIN.

MCS-22
Image Guidance Using Common PET Tracers such as 18F-FDG
J. Grimm; Radiologist and Nuclear Medicine physician, Memorial Sloan-Kettering Cancer Center, New York, UNITED STATES OF AMERICA.

MCS-23
From PET to SPECT - Optimizing Surgical Guidance in Pelvic Cancers
T. Maurer; Urologist, Martini-Klinik Prostate Cancer Center, University of Hamburg-Eppendorf, Hamburg, GERMANY.

MCS-25
The Next Step in Image-Guided Surgery, Tracer Refinements and Complementary Use of Different Tracers
T. Buckle; Dept of Radiology, Leiden University Medical Centre, Leiden, NETHERLANDS.

MCS-26
Using Navigation and Hybrid Tracer or Radiotracer + ICG in Head and Neck Cancers
C. Schilling; Consultant Head & Neck Surgeon, University College London Hospitals NHS Foundation Trust, London, UNITED KINGDOM.

MCS5

Mid-Congress-Symposium 5: How to Read PET/CT - Different Shades of Sugar (FDG)

Tuesday, October 27, 2020, 09:30 - 12:15 Channel 1

MCS-27
How to Read PET/CT - Chemotherapy Setting
N. Aide; Centre Hosptalier Universitaire de Caen, Caen, FRANCE.

MCS-28
How to Read PET/CT - Radiotherapy Setting
A. Loft Jakobsen; Dept of Clinical physiology, Nuclear Medicine & PET, Copenhagen, DENMARK.

MCS-29
How to Read PET/CT - Post-Surgical Setting
A. Agrawal; Dept of Nuclear Medicine & Molecular Imaging, Tata Memorial Centre, Mumbai, INDIA.

MCS-31
How to Read PET/CT - Immumotherapy Setting
E. Lopci; Instituto Clinico Humanitas IRCCS (Humanitas), Milan, ITALY.

MCS-32
How to Deal with Incidental Findings
K. Strobel; Head of Nuclear Medicine, Kantonsspital Luzern, Lucerne, SWITZERLAND.

MCS-33
How to Read PET/CT - Tumours with Low FDG Uptake
T. van den Wyngaert; Dept of Nuclear Medicine and Molecular Imaging University of Antwerp, Antwerp, BELGIUM.

MCS6

Mid-Congress-Symposium 6: Improved Insights into Radiobiology - Key for Radionuclide Therapy

Tuesday, October 27, 2020, 09:30 - 12:15 Channel 2

MCS-34
Five For the Price of One - Alternatives to the Linear-No-Threshold Theory
M. Verslegers; Belgian Nuclear Research Centre, SCK CEN, Radiobiology Unit, Mol, BELGIUM.

MCS-35
Differences Between EBRT and MRT Radiobiology
J. Pouget; French Institute of Health and Medical Research (Inserm) Montpellier Cancer Research Institute (IRCM), Montpellier, FRANCE.

MCS-36
Why Dosimetry Alone is Not the Answer
A. Sundlöv; Skåne University Hospital, Unit for Endocrine Tumors and Radionuclide Therapy, Dept of Hematology, Oncology and Radiation Physics, Lund, SWEDEN.

MCS-38
How to Combine Dosimetry and Radiobiology
U. Eberlein; University of Würzburg, Department of Nuclear Medicine, Würzburg, GERMANY .

MCS-39
Biological Aspects of Radionuclide Therapy
J. Nonnekens; Erasmus MC, Molecular Genetics and Radiology & Nuclear Medicine, Rotterdam, NETHERLANDS.

YDF2

EANM Young Daily Forum 2: I will Survive - Managing Work Stress and Building Your Resilience

Tuesday, October 27, 2020, 12:20 - 13:50 Channel 1

OP-444
I will Survive - Managing Work Stress and Building Your Resilience
R. Sheppard; London, UNITED KINGDOM

MCS7

Mid-Congress-Symposium 7: Lutetium Therapy

Tuesday, October 27, 2020, 14:00 - 16:45 Channel 1

MCS-40
Treatments using 177Lu - The Roles of Image Analysis and Dosimetry
C. Kratochwil; Universität Heidelberg, Department of Nuclear Medicine, Heidelberg, GERMANY.

MCS-41
Dosimetry & Radiobiology for [177Lu]Lu-PSMA-Treatments, Whole-Body Tumour Dose
J. Violet; Peter MacCallum Cancer Centre, Radiation Therapy Division, Melbourne, AUSTRALIA.

MCS-42
Dosimetry & Radiobiology for Tumours in Preclinical [177Lu]Lu-DOTA-TATE Exposures
M. Konijnenberg; Erasmus MC, Department of Nuclear Medicine, Rotterdam, NETHERLANDS.

MCS-44
Salivary Gland Uptake in [177Lu]Lu-PSMA Therapy - Current Status and Novel Approaches
A. Eder; University of Freiburg, University Medical Center Freiburg, Freiburg, GERMANY.

MCS-45
Image-Based Dosimetry for Bone Marrow in [177Lu]Lu-PSMA Therapy
A. Gosewisch; University Hospital, Ludwig-Maximilians-University of Munich, Department of Nuclear Medicine, Munich, GERMANY.

MCS-46
Texture Analysis for Quantification of Non-Uniformity
F. Botta; Istituto Europeo di Oncologia IRCCS, Medical Physics Unit, Milan, ITALY.

MCS8
Mid-Congress-Symposium 8: For Youngsters - Essential Oncology for Young Nuclear Medicine Physicians

Tuesday, October 27, 2020, 14:00 - 16:45 Channel 2

MCS-47
Essential Oncology - The Young Nuke`s Need
S. Telo; Policlinico S.Orsola-Malpighi, Nuclear Medicine, Bologna, ITALY.

MCS-48
Lung Cancer
A. Berghoff; Berghoff, Medical University of Vienna, Clinic for Internal Medicine I, Division of Oncology, Vienna, AUSTRIA.

MCS-49
Lymphoma
B. Kiesewetter-Wiederkehr; Medical University of Vienna, Clinic for Internal Medicine I, Division of Oncology, Vienna, AUSTRIA.

MCS-51
Breast Cancer
K. Strasser-Weippl; MBA, Wilheminenspital Vienna, Center for oncology and hematology, Vienna, AUSTRIA.

MCS-52
Prostate Cancer
G. Kramer; Medical University of Vienna, Clinic for Urology, Vienna, AUSTRIA.

MCS-53
Discussion
M. Hacker; Medical University of Vienna, Clinic for Urology, Vienna, AUSTRIA.

MCS9
Mid-Congress-Symposium 9 (EANM/ETA/ESES): Update on Treatment of Hyperthyroidism

Wednesday, October 28, 2020, 09:30 - 12:15 Channel 1

MCS-54
Diagnosis of Diseases Leading to Hyperthyroidism
L. Giovanella; Imaging Institute of Southern Switzerland, Clinic for Nuclear Medicine, Bellinzona, SWITZERLAND.

MCS-55
Medical Treatment of Hyperthyroidism
K. Boelaert; Queen Elizabeth Hospital, Endocrinology, Birmingham, UNITED KINGDOM.

MCS-56
Surgical Treatment of Hyperthyroidism
P. Riss; University Hospital of Wien, Endocrine Surgery, Vienna, AUSTRIA.

MCS-58
Radioiodine Treatment of Hyperthyroidism
D. Deandreis; University Hospital Molinette, Nuclear Medicine, Torino, ITALY.

MCS-59
Radioiodine for Benign Disease - Radiation Protection
L. Cunha; IsoPor-Azores, Ermesinde, PORTUGAL.

MCS-60
Risk of Cancer Following Radioiodine Treatment for Hyperthyroidism
I. Iakovou; Aristotle University, Nuclear Medicine, Thessaloniki, GREECE.

MCS10
Mid-Congress-Symposium 10: Diagnostic Flowcharts on Musculoskeletal Infections

Wednesday, October 28, 2020, 09:30 - 12:15 Channel 2

MCS-61
Correct protocols for WBC imaging
E. Noriega Alvarez; Hospital General Universitario de Ciudad Real, Department of Nuclear Medicine, Ciudad Real, SPAIN.

MCS-62
Correct protocols for FDG-PET/CT imaging
O. Gheysens; University Hospitals Leuven, Department of Nuclear Medicine, Leuven, BELGIUM.

MCS-63
When do we need imaging in PJI?
R. Trebse; Medical University Ljubljana, Valdoltra Orthopaedic Hospital, Ljubljana, SLOVENIA.

MCS-64
Diagnostic flowcharts in PJI
A. Signore; Sapienza University, Department of Medical-Surgical Sciences and Translational Medicine, Rome, ITALY.

MCS-66
When do we need imaging in spine infections?
B. Bouyer; Unité de Chirurgie du rachis, Service d'orthopédie-traumatologie, University Hospital of Bordeaux, Bordeaux, FRANCE.

MCS-67
Diagnostic flowcharts in spine infections
E. Lazzeri; Pisa University Hospital, Regional Center of Nuclear Medicine, Pisa, ITALY.

MCS-68
When do need imaging in FRI?
G. Govaert; University Medical Center Utrecht, Department of Trauma Surgery, Utrecht, NETHERLANDS.

MCS-69
Diagnostic flowcharts in FRI
A. Glaudemans; University Medical Center Groningen, Medical Imaging Center, Groningen, NETHERLANDS.

YDF3

EANM Young Daily Forum 3: Nothing else matters - Get your paper published in a top journal

Wednesday, October 28, 2020, 12:20 - 13:50 Channel 1

OP-730
Round Table Discussion
A. Chiti; Humanitas University, Nuclear Medicine, Milan, ITALY.

OP-731
Round Table Discussion
I. Carrio; Hospital de la Santa Creu i Sant Pau, Department of Nuclear Medicine, Barcelona, SPAIN.

OP-732
Round Table Discussion
J. Czernin; University of California Los Angeles, Molecular and Medical Pharmacology, Los Angeles, UNITED STATES OF AMERICA.

MCS11

Mid-Congress-Symposium 11: Current State and Future of Tau PET Imaging

Wednesday, October 28, 2020, 14:00 - 16:45 Channel 1

MCS-70
The Clinical Need for Tau PET Tracers
V. Garibotto; Nuclear Medicine and Molecular Imaging Division, Geneva University Hospitals, Geneva, SWITZERLAND.

MCS-71
Lessons Learnt from the First-Generation Tau PET Tracers
R. Ossenkoppele; Alzheimer Center, Amsterdam University Medical Center, Amsterdam, NETHERLANDS.

MCS-72
Design Goals for the Ideal Tau PET Tracer
A. Nordberg; Karolinska University Hospital, Department NVS, Clinical Geriatrics, Center for Alzheimer Research, Stockholm, SWEDEN.

MCS-74
Second-Generation Tau PET Tracers
J. Seibyl; Institute for Neurodegenerative Disorders, New Haven, UNITED STATES OF AMERICA.

MCS-75
Tau and Other Imaging in Alzheimer's Disease
G. Bischof; University Hospital Cologne, Department of Nuclear Medicine, Cologne, GERMANY.

MCS-76
Tau Imaging in Non-AD Neurodegeneration
M. Brendel; University Hospital of Munich, LMU Munich, Department of Nuclear Medicine, Munich, GERMANY

MCS12

Mid-Congress-Symposium 12: For Youngsters - Emergency During Nuclear Medicine Procedures - What to Know and What to Do?

Wednesday, October 28, 2020, 14:00 - 16:45 Channel 2

MCS-77
Emergencies During Nuclear Medicine Applications - The Young Nuke`s Need
F. Mattana; Bologna, ITALY.

MCS-78
Myocardial Scintigraphy
S. Graf; Medical University of Vienna, Clinic for Internal

Medicine II, Division of Cardiology, Vienna, AUSTRIA.

MCS-79

Lung Scintigraphy

H. Domanovits; Medical University of Vienna, Clinic for Emergency Medicine, Vienna, AUSTRIA.

MCS-81

Claustrophobia, CT Contrast Agents and Incidental Findings

TBA.

MCS-82

Therapy Associated Emergencies

E. Kretschmer-Chott; Medical University of Vienna, Department of Biomedical Imaging and Image-guided Therapy, Division of Nuclear Medicine, Vienna, AUSTRIA .

MCS-83

Discussion

T. Traub-Weidinger; Medical University of Vienna, Department of Biomedical Imaging and Image-guided Therapy, Division of Nuclear Medicine, Vienna, AUSTRIA.

MCS13

Mid-Congress-Symposium 13 - Technologists: Introduction to Dosimetry

Wednesday, October 28, 2020, 09:00 - 16:00 Channel 3

MCS-84

Welcome by the EANM Technologist Committee Chair

A. Santos; Hospital CUF Descobertas, Medicina Nuclear Dep., Lisbon, PORTUGAL.

MCS-85

MIRD Scheme

J. Gear; The Royal Marsden NHS Foundation Trust, Joint Department of Physics, London, UNITED KINGDOM.

MCS-87

Principles of Dosimetry

G. Marin; Institut Jules Bordet, Nuclear Medicine,Brussels,BELGIUM.

MCS-89

Dosimetry in Radionuclide Therapy Planning - Neuroendocrine Tumours (Interactive Cases)

J. Gear; The Royal Marsden NHS Foundation Trust, Joint Department of Physics, London, UNITED KINGDOM.

MCS-91

Dosimetry in Radionuclide Therapy Planning - Primary and Metastatic Liver Tumours (Interactive Cases)

G. Marin; Institut Jules Bordet, Nuclear Medicine, Brussels, BELGIUM.

MCS-93

Quantitative Imaging

I. Armstrong; Manchester University NHS Foundation Trust, Department of Nuclear Medicine, Manchester, UNITED KINGDOM.

MCS-95

Artificial Intelligence in Nuclear Medicine

D. Visvikis; INSERM UMR 1101 LaTIM UBO, Brest, FRANCE.

1101

CME 9: New PET Technologies - Digital Revolution or Big Bust?

Thursday, October 29, 2020, 13:30 - 15:00 Channel 1

OP-594

Background on the Recent Developments in PET Technology

I. Armstrong; Manchester University NHS Foundation Trust, Nuclear Medicine Department, Manchester, UNITED KINGDOM.

OP-595

Challenges for Heterogeneity Evaluation in the Era of New PET Technologies

I. Buvat; Paris Diderot University, UMR 8165, Paris, FRANCE.

OP-596

New PET Technology - Pushing the Limits

N. Aide; University Hospital, Nuclear Medicine Department, Caen, FRANCE.

OP-597

New PET Technology - Clinical Implications

C. Kobe; University Hospital, Nuclear Medicine Department, Cologne, GERMANY.

1102

Joint Symposium 17 (EANM/EORTC): Benchside to Bedside and Back - What do we Learn from the Clinic?

Thursday, October 29, 2020, 13:30 - 15:00 Channel 2

OP-599

Immuno-PET to Assess Response to PD-L1 Blockade

F. Bensch; Department of Pulmonary Diseases, University

Medical Center Groningen, Groningen, NETHERLANDS.

OP-600

Imaging Tumour Metabolism in Response to Immunotherapy

E. Lopci; Department of Nuclear Medicine, Humanitas Clinical and Research Center-IRCCS, Milan, ITALY.

OP-601

Application of Radiolabelled Amino Acids to Brain Tumour Imaging

M. Glas; Department of Neurology, University Hospital Essen, University Duisburg-Essen, Essen, GERMANY.

OP-602

Development of New Radiolabelled Amino Acids for Neuro-Oncology Applications

F. de Vos; Ghent University, Department of Radiopharmacy, Ghent, BELGIUM.

1103

Joint Symposium 18 (EANM/AIO): Imaging Tumour Microenvironment

Thursday, October 29, 2020, 13:30 - 15:00 Channel 3

OP-604

The Clinical Relevance of Tumour Microenvironment in Solid Tumours

M. Trajkovic-Arsic; German Cancer Consortium (DKTK) and German Cancer Research Center (DKFZ), Heidelberg, GERMANY.

OP-605

Imaging Cellular Components of the Tumour Microenvironment

S. Heskamp; Radboud University Medical Center, Radiology and Nuclear Medicine, Nijmegen, NETHERLANDS.

OP-606

Imaging Metabolic Components of the Tumour Microenvironment

T. Witney; King's College London, School of Biomedical Engineering and Imaging Sciences, London, UNITED KINGDOM.

1104

Technologists Oral Presentations 2 - Featured Session: TOP - Technologist Overview and Practice impact

Thursday, October 29, 2020, 13:30 - 15:00 Channel 4

OP-608

Introduction

M. Attard; UMC Radboud, Radiology and Nuclear Medicine Department, Nijmegen, NETHERLANDS.

OP-610

Investigation into theImpact Manufacturers have uponSyringe Residuesin Different Volumes of Radiopharmaceuticals

T. Stephens;
University Hospitals Birmingham, Birmingham, UNITED KINGDOM.

Aim/Introduction: Diagnostic Reference Levels (DRL) when using Tc DMSA were noted to be reduced at imaging and later found to be due to syringe residue. These residues had measured at a 60-70% of the original dose in some instances and the issue appeared to be random when using 3ml and 5ml syringes with this particular radioisotope. An investigation was carried out to determine which syringes caused high residue and correlate a factor for the increase. As there was an initial question whether the time the dose spent in the syringe pre-injection or the time post kit manufacture was a contributing factor, this was also examined. ***Materials and Methods:*** The method involved testing every 3ml and 5ml syringe available within the department. Two separate doses were drawn up in each syringe and measured. One dose was left to incubate at room temperature for one hour before being emptied and the other emptied 5-10 minutes post dispensing. After being re-measured each syringe was washed out with saline to see the effect on its residue. This whole method was repeated twice, the second was to assess the shelf life and its effect on the residue. ***Results:*** It was found that two syringe manufactures left a residue of 4-5% of the original dose. Four syringe types had 30-50% residue and two syringes had 70-80% residue remaining. The washout with the saline was deemed ineffective as each washout would remove <0.5% of the residue. It was concluded that certain manufacturers had packaging that looked very similar which explained how the residue amounts seemed to randomly occur. ***Conclusion:*** The outcome of this study has highlighted that patient doses have been affected by high residual activity in certain syringes leading to the increased risk of undiagnostic studies being carried out. Further work involving investigation of syringe residue with other

radiopharmaceuticals, syringe manufacturer and syringe volume is already under way to ensure DRL's are met thus providing a consistent and standardised service. Important for other centres to make sure that they are measuring their residues post injection and working out exact dose administered ***References:*** None

OP-611

Two Deep Inspirations - Friend or Foe?

J. Terzic, M. Rode Pedersen, S. Monrad Laugesen, B. Hoyer Mathiasen;
Department of Nuclear Medicine, Hospital Lillebaelt, Vejle, DENMARK.

Aim/Introduction: Patients at our department are instructed to take two deep inspirations prior to FDG-PET/CT scan. The purpose of this procedure is to ensure well ventilated and expanded lungs, thus eliminating or reducing the occurrence of atelectasis. However, as this procedure is not, to our knowledge, applied at other departments, we wanted to investigate its actual effects. The aim of this study was to evaluate, if there was any significant differences in the prevalence of atelectasis between a control group and a trial group. ***Materials and Methods:*** A total of 179 patients, who underwent FDG-PET/CT, at our department during March 2020, were included in the study. By using two identical scanners, patients were randomized daily to either the control or the trial group. The control group were instructed to take two deep inspirations prior to scan, and the trial group were not. Scans were performed at low dose (ref. mAs 40, kV 120) and dose modulated using CARE Dose 4D. Nuclear physicians evaluated the image quality to determine whether atelectasis was present for each patient. Furthermore, atelectasis diagnosis was separated into a set of four pre-defined categories; Subsegmental atelectasis, Segmental atelectasis (dependent on other pathologies), Gravity dependent atelectasis or Uncertain. To ensure the quality of the study, physicians were blinded in regards to which group patients belonged to. ***Results:*** After randomization of patients, there were 75 in the control group and 104 in the trial group. 60% of patients in the control group was not presented with any type of atelectasis, compared to 50% of patients in the trial group (p=0.185). The prevalence of subsegmental atelectasis was identical in the control and trial group, (17.3%), while segmental atelectasis was present in 9.3% of the control group and 11.5% of the trial group (p=0.637). The prevalence of gravity dependent atelectasis in the control and trial group was 10.7% and 17.3%, respectively (p=0.213). Although differences between the control and trial groups were observed, none of these were statistically significant. Furthermore, instructing patients to take two deep inspirations would in several cases induce severe cough, potentially causing motion artefacts. ***Conclusion:*** Our study did not find any significant differences in the prevalence of atelectasis between patients who were instructed to take two deep inspirations prior to a FDG-PET/CT scan and patients who did not receive instructions. This does not emphasize the use of deep inspirations prior to low dose FDG-PET/CT. ***References:*** None

OP-612

Evaluation of data-driven gating for ^{68}Ga-DOTATOC PET-CT in patients with neuroendocrine tumors

J. Sigfridsson[1], H. Romelin[1], E. Lindström[2,3], S. Kvernby[2,3], I. Velikyan[1,3], A. Sundin[1,3], M. Lubberink[1,3];
[1]PET Centre, Uppsala University Hospital, Uppsala, SWEDEN, [2]Medical Physics, Uppsala University Hospital, Uppsala, SWEDEN, [3]Radiology & Nuclear Medicine, Department of Surgical Sciences, Uppsala University, Uppsala, SWEDEN.

Aim/Introduction: In PET imaging, respiratory motion can severely impair image quality, especially in tissues near the diaphragm, and consequently may lead to poorer lesion detection, delineation and quantitation. Respiratory gating has been available for many years. Previously available gating techniques involve separate devices and are hard to implement in routine clinical practice, respiratory gating has therefore often not been utilized to its full extent. Data-driven gating (DDG), based on detection of respiratory signal using principal component analysis of dynamic sinogram data, would allow for routine implementation of respiratory gating. To date, DDG has only been validated for FDG-PET. The aim of the present work was to assess the effectivity of respiratory signal detection in DDG and its effect on standardized uptake values (SUV) for ^{68}Ga-DOTATOC. ***Materials and Methods:*** Fifteen patients underwent a whole-body PET-CT scan 1 h after injection of 1.5 MBq/kg body weight of ^{68}Ga-DOTATOC on a General Electric Discovery MI 4-ring PET-Scanner, with 2 min acquisition per bed position. MotionFree (GE-Healthcare), a principal component analysis based respiratory DDG software, was applied prospectively and the scan time per bed position was doubled for beds where a respiratory motion signal was detected in the raw data. Quiescent period gated images, containing 50 % of the doubled scan time data, were reconstructed with Q. Static software (GE Healthcare). All images were reconstructed using TOF-OSEM (3 iterations, 16 subsets) with resolution recovery. SUV_{max} measurements on ^{68}Ga-DOTATOC positive lesions (n=22) without and with DDG were compared. Also, the effectiveness of the detection of respiratory signal was evaluated retrospectively. ***Results:*** Using the same threshold value for respiratory motion detection as recommended by the manufacturer for FDG (r = 15), motion was detected on mean 2.2 bed positions per scan. DDG resulted in a mean 16% increase in SUV_{max} (p = 0.0001). ***Conclusion:*** Using the same threshold as for FDG, respiration signals were detected in considerably more bed positions than

previously reported for FDG (mean 2.2 versus 1.2), likely due to the higher image contrast for ^{68}Ga-DOTATOC than for FDG. DDG yielded significantly higher SUV_{max} values as compared to non-gated images. ***References:*** None

OP-613

Predictive value of multiparametric PET/MR in patients with head and neck squamous cell carcinoma treated with chemoradiotherapy

A. Kedves[1,2,3], *M. Emri*[2], *K. Fabian*[1], *D. Sipos*[1,2,3], *O. Freihat*[3], *J. Tollar*[1], *Z. Cselik*[4], *G. Bajzik*[2], *I. Repa*[2], *A. Kovacs*[1], *Z. Toth*[3,5];
[1]*Department of Medical Imaging, Faculty of Health Sciences, University of Pecs, Kaposvar, HUNGARY,* [2]*Dr. Jozsef Baka Diagnostic, Radiation Oncology, Research and Teaching Center, Kaposvar, HUNGARY,* [3]*Doctoral School of Health Sciences, University of Pecs, Pecs, HUNGARY,* [4]*Oncoradiology, Csolnoky Ferenc County Hospital, Veszprem, HUNGARY,* [5]*MEDICOPUS Healthcare Provider and Public Nonprofit Ltd., Somogy County Moritz Kaposi Teaching Hospital, Kaposvar, HUNGARY.*

Aim/Introduction: The aim of the study was to evaluate the predictive value of the pretreatment, simultaneously acquired PET/MR based metabolic, and diffusion parameters of head and neck squamous cell carcinoma treated with chemoradiotherapy (CRT). ***Materials and Methods:*** Retrospective evaluation was performed using pretreatment and post CRT PET/MR image datasets of 68 histologically proven head and neck cancer patients. PET SUV_{max}, $SUL_{peak,}$ MTV and TLG parameters and MR ADC_{mean} values were calculated using pretreatment imaging data. Therapeutic response was evaluated using posttreatment scans, two patient subgroups were created according to the presence or absence of viable tumor. For statistical analysis, Spearman's correlation and Wilcoxon's test were used. ***Results:*** After completing the CRT, a viable residual tumor was detected in 36/68 (53%) cases, while 32/68 (47%) patients showed complete remission. Significant correlation was not found between the pretreatment ADC_{mean} parameter and the therapeutic success ($p = 0.88$). The PET parameters, SUV_{max} and SUL_{peak}, MTV, and TLG were statistically significantly different between the two patient subgroups ($p = 0.032$, $p = 0.01$, $p < 0.0001$, $p = 0.0004$). ***Conclusion:*** Our preliminary result suggests that MR ADC_{mean} data originating from pretreatment PET/MR is not useful for therapeutic response prediction, while the evaluated PET parameters (SUV_{max}, SUL_{peak}, MTV, and TLG) seems to be more promising for that purpose, thus their inclusion to risk stratification may also be of additional value. ***References:***

OP-614

Comprehensive Review of Zr-89 Immuno-PET in Emerging Clinical Use: What the Technologist Needs to Know

A. Scott[1], *M. Morris*[2];
[1]*Advanced Molecular Imaging and Therapy, LLC, Glen Burnie, MD, UNITED STATES OF AMERICA,* [2]*Advanced Molecular Imaging and Therapy, Glen Burnie, MD, UNITED STATES OF AMERICA.*

Aim/Introduction: The modern paradigm of medical oncology therapy is personalized treatment planning based on molecular and genomic characteristics. Molecular histopathology is a current standard of care for guiding therapy regimens. Emergence of Zr-89 immuno-PET agents introduces the opportunity for an evolution to in vivo, whole-tumor, whole-body molecular diagnostics. The half-life of Zr-89 (78.41 hours) allows for various types of immuno-PET tracers, with different characteristics. Technologists need to understand the washout characteristics of types of immuno-PET tracers and their safety considerations, as well as radiation safety considerations related to Zr-89 emission properties (approximately 23% positron and 77% gamma at 909 keV). ***Materials and Methods:*** Comprehensive literature review using pubmed with the search term "Zr AND 89 AND immuno AND PET" was performed. Review articles were excluded. Remaining resulting articles were included and evaluated for molecular tracer utilized, administration technique, imaging technique, and patient safety considerations from the nuclear medicine technologist's perspective. ***Results:*** There were 107 articles identified meeting the search criteria. There were 11 review articles identified and excluded leaving 96 articles for evaluation. Articles were categorized by those describing studies in human subjects, by specific Zr-89 immuno-PET tracer, and by physical, technical, and safety aspects for human use. Specific aspects of each Zr-89 Immuno-PET agent in current human use were assessed and detailed from the technologist's perspective. ***Conclusion:*** Zr-89 immuno-PET is an important emerging area of molecular imaging in oncology, yet the technologist community still has limited exposure to this diverse category of radiotracer in humans in everyday clinical practice. This comprehensive review is intended to provide a single source of information for technologists to better understand Zr-89 immuno-PET agents and their practical considerations related to image quality and safety at the point of care. ***References:*** 107 Literature articles meetings search criteria can be provided as a supplemental upon request.

OP-615

Clinical Usefulness of ^{99m}Tc-DMSA SPECT/CT in Evaluating Focal Defects in Transplanted Kidneys

B. Ferreira*, A. Parthipun;*
Royal Free London, NHS Foundation Trust, London, UNITED KINGDOM.

Aim/Introduction: There are several imaging modalities at our disposal in order to aid the diagnosis of complications in transplanted kidneys (e.g. ultrasonography, magnetic

resonance imaging, Computed Tomography or Scintigraphic Renogram studies with ^{99m}Tc-MAG3). ^{99m}Tc-DMSA studies are often used to identify focal parenchymal defects, the presence of which alters the clinical management. Although ^{99m}Tc-DMSA SPECT studies improve accuracy of identifying defects compared to planar scintigraphy, it still remains non-specific and cannot differentiate between multiple causes of defects. The aim of this study is to evaluate whether adding anatomical correlation through the execution of simultaneously acquired SPECT and CT studies can improve on the lack of specificity of performing a simple SPECT study. ***Materials and Methods:*** 26 transplanted kidney ^{99m}Tc-DMSA SPECT/CT cases, from January 2019 until January 2020 were reviewed by a Nuclear Medicine Consultant. Images were reconstructed using a Hermes' Hybrid ViewerTM. SPECT images were analysed and areas with defect/reduced radiopharmaceutical uptake were identified; these findings were respectively compared with the co-registered non-contrast CT images. ***Results:*** Of 26 kidneys reviewed, 2 were normal on both modalities, and 2 had diffuse parenchymal disease on SPECT with no focal defects nor CT abnormality. From the remaining 21 kidneys, there were 41 focal defects on ^{99m}Tc-DMSA SPECT: 25 of the SPECT defects had corresponding CT defects, 1 (2.4%) corresponded to foetal lobulation, 1 (2.4%) to a renal mass, 4 (10%) to cysts and 19 (46%) were linked to parenchymal scars. There were 16 (39%) defects on SPECT which were unmatched on CT, suggesting focal nephritis. ***Conclusion:*** The combination of non-contrast CT images adds value to ^{99m}Tc-DMSA SPECT studies. This technique allows the identification of space occupying lesions or masses that can cause focal uptake defects observed in SPECT studies, and differentiate them from 'normal' findings such as cysts' or anatomical variants (e.g. foetal lobulation). Furthermore, it also differentiates scarring (indicated by the presence of cortical thinning on CT) from focal nephritis (unmatched SPECT defects), with its respective impact on therapeutic management. ***References:*** 1) H. Cairns et al., 99mTc-DMSA imaging with tomography in renal transplant recipients with abnormal lower urinary tracts; Nephrology Dialysis Transplantation, Vol.9, 1157-1161; 2) J. Craig et al., How accurate is Dimerscaptosuccinic Acid Scintigraphy for the Diagnosis of Acute Pyelonephritis? A Meta-Analysis of Experimental Studies; The Journal of Nuclear Medicine, Vol.41, 986-993; 3) B. Natasa et al., Revelance of Tc-99m DMSA scintigraphy in renal transplant parenchymal imaging. Clinical Nuclear Medicine, Vol.19, 782-784.

OP-616

Serum Creatinine Measurement as a Predictor for Single Sample GFR using [^{99m}Tc]Tc-DTPA

A. Matos*, C. Findlay, G. Hilland, S. Small;*
Department of Nuclear Medicine, Gartnavel General Hospital, NHS Greater Glasgow and Clyde, Glasgow, UNITED KINGDOM.

Aim/Introduction: The purpose of this study was to compare slope intercept (SI) glomerular filtration rate (GFR) and the single sample (SS) GFR measurements to aid confidence in transitioning to a SS-GFR method. We also wished to assess at the validity of using estimated GFR (eGFR) as a single sample time predictor. ***Materials and Methods:*** Using 4-sample SI-GFR measurements, the equivalent SS-GFR was calculated using the single sample time point identified in the BNMS guidelines[(1)]. The patient's most recent eGFR measurement was used to identify which of the 4 blood samples would be the SS equivalent. eGFR was calculated using the Chronic Kidney Disease Epidemiology Collaboration Creatinine 2009 equation. ***Results:*** One hundred and forty-two [^{99m}Tc]Tc-DTPA SI-GFR patients were retrospectively reviewed with an average eGFR of 92.2 ± 25.4 mL/min/1.73m^2. The average SI-GFR and SS-GFRs were 85.4 ± 24.3 and 85.4 ± 23.2 mL/min/1.73m^2 respectively. Time between eGFR and measure GFR (mGFR) was 19.1 ± 39.8 days. Using t-Test: Paired Two Sample for Means, recommended SS times across all eGFRs values demonstrated no statistically significance between SI-GFR and SS-GFR (p=0.81, N=142) with an absolute average difference between the SI-GFR and SS-GFR of 1.95 ± 1.7 mL/min/1.73m^2. Using the non-parametric Wilcoxon Signed Rank test to analyse sub-groups, investigation revealed that there were no statistically significant differences between the SI-GFR and SS-GFR for eGFRs >100 mL/min/1.73m^2 (p= 0.05, N=58) and eGFRs 70-100 mL/min/1.73m^2 (p= 0.09, N=58). However, there were statistically significant differences for eGFRs between 25-70 mL/min/1.73m^2 (p< 0.00, N=24). ***Conclusion:*** Preliminary findings using eGFR to determine SS times for [^{99m}Tc]Tc-DTPA mGFRs showed that SS-GFRs taken at 2 hours (eGFRs >100 mL/min/1.73m^2) and 3 hours (eGFRs 70-100 mL/min/1.73m^2) correlate with SI-GFRs. However, results from this group of patients demonstrated that SS-GFRs taken at 4 and 6 hours (eGFRs 25-70 mL/min/1.73m^2) were different from the SI-GFR measurement. This could indicate that low eGFRs are a bad predictor for SS-GFR times, but further work is needed to develop on the results of this group. It will also be valuable to investigate if there is improved accordance between the two methods if a recent eGFR measurement is available to assist the SS-GFR time identification. Finally, the clinical significance of any discrepancies between SS and SI GFRs will also be of relevance during this transition period. ***References:*** (1) Burniston, M. (2018). Clinical Guideline for the measurement of glomerular filtration rate (GFR) using plasma sampling. British Nuclear Medicine Society.

OP-617

Improved Comfort and Image Quality When Using Purpose-Built Support For Hand and Wrist SPECT/CT In Supine Position

A. Leite*, M. Humphrys, B. Walker, M. Jessop;*
Brighton and Sussex University Hospitals NHS

Trust, Brighton, UNITED KINGDOM.

Aim/Introduction: Current methods of upper extremity positioning and immobilisation, such as the 'superman position', can be very difficult for patients to tolerate (especially if they have poor mobility) with increased risk of movement while performing a SPECT/CT scan. This project aimed to minimize patient movement and improve patient comfort when performing SPECT/CT of wrist and hands. In addition, the improved positioning was aimed at producing higher quality images. ***Materials and Methods:*** A new support was created allowing the patient to lie in the supine position with arms raised above the head. A purpose-built extension was built to work in combination with an existing support, which then allowed immobilization of hands and wrist. Attached to this new support made from perspex, were hand and wrist orthotic devices (splints) made out of plastic with hook and loop fasteners. In addition, disposable bandages were used to immobilise the elbows. The hands were centred in the CT field of view (FOV). During image processing, when creating fused SPECT/CT images, the support and table were cropped. A maximum intensity projection (MIP) was created using settings C=1500 W=2000. ***Results:*** Initially, a number of trial acquisitions were performed to ensure that the hands would be correctly centred in the FOV, to avoid image distortion of the CT. To facilitate this, a standard bed height was set in the imaging protocol. The support was used with two patients. Both patients gave good feedback about the support. The patients commented that staying still in the 'superman position' would be extremely painful in their specific circumstances, as one had a shoulder injury while the other had a hernia and reflux. The use of the bandages on the elbows gave more support to the patient which ensured the elbows remained still throughout the scan, without the arms relaxing downwards. Improved positioning allowed for better image interpretation. Cropping the table and support produced improved image aesthetics. The MIP reconstructed at the settings used, produced an image with a transparent appearance which allowed good visualisation of functional abnormality and localization, especially when rotating the image. ***Conclusion:*** This immobilization device has allowed patients to lie in the supine position for hand and wrist SPECT/CT. This has successfully minimized patient movement and improved patient comfort, while improving image quality. ***References:*** None

OP-618

Somatostatin Receptor-Based Imaging with 99mTc-EDDA/HYNIC-TOC: Departmental Protocol Update to Include Whole Body SPECT-CT

R. Martins*, L. Aloj, I. Harper;*
Addenbrooke's Hospital, CUH, Cambridge, UNITED KINGDOM.

Aim/Introduction: Neuroendocrine tumours (NETs) can vary in histology and biological behaviour, which results in various responses to therapy. Determining these factors through different diagnostic tools helps develop specific therapy adjustments for each patient. As part of the diagnosis and follow-up, somatostatin receptors' (STTR) imaging plays an essential role in both differentiating NETs and staging the disease progression. Alongside computed tomography (CT), magnetic resonance imaging (MRI) and positron emission tomography (PET), Nuclear Medicine (NM) STTR scintigraphies with ^{111}In-Diethylene Triamine Pentaacetic Acid -Octreotide (^{111}In-DTPA-Octreotide) or with ^{99m}Tc-HYNIC-[D-Phe1, Tyr^3-Octreotide] Trifluoroacetate (^{99m}Tc-EDDA/HYNIC-TOC) are performed in the first instance to locate and assess NETs, as well as to predict eventual therapy response. (Maxwell and Howe, 2015) (Tsoli et al, 2019) The purpose of this study is to analyse imaging data collected from ^{99m}Tc-EDDA/HYNIC-TOC scans in order to update current scanning protocols within the Department of Nuclear Medicine (DNM). ***Materials and Methods:*** The DNM has recently moved from using ^{111}In-DTPA-Octreotide to ^{99m}Tc-EDDA/HYNIC-TOC. Both tracers' cost-effectiveness was briefly compared in terms of radiotracer availability, image quality and patient compliance. Images of 19 ^{99m}Tc-EDDA/HYNIC-TOC scans in patients with NETs were also reviewed by main reporting consultant in order to update existing scanning protocols. ***Results:*** Despite being more expensive, patient compliance and management have improved with the use of ^{99m}Tc-EDDA/HYNIC-TOC, for the scan is performed only during the course of one day. ^{99m}Tc-EDDA/HYNIC-TOC scans provide better image quality and overall tracer distribution due to its pharmacokinetic properties when compared to ^{111}In-DTPA-Octreotide. From the imaging data analysis, consultants found no evidence to suggest whole body (WB) images provided information not visible on the SPECT-CT performed 3 to 4 hours post-injection, where the contrast between lesions and background is better. ***Conclusion:*** Scanning protocols with ^{99m}Tc-HYNIC-TOC can be updated to only perform neck to pelvis SPECT-CT at 3 to 4 hours post-injection, without the need of a late WB scan. This protocol change maximizes clinical information obtained and overall image quality, which can prove very useful in diagnosing and staging NETs whenever higher resolution imaging through PET-CT is not immediately available to patients. ***References:*** Maxwell, J.E and Howe, J.R., 2015. Imaging in Neuroendocrine Tumors: an Update for the Clinician. International Journal of Endocrine Oncology, 2(2), pp.159-168. Tsoli, M., Chatzellis, E., Koumarianou, A., Kolomodi, D. and Kaltsas, G., 2019. Current Best Practice in the Management of Neuroendocrine Tumors. Therapeutic Advances in Endocrinology and Metabolism, 10, pp.1-18.

1106

Cutting Edge Science Track - TROP Session: Dosimetry Methods and Models - Part 2

Thursday, October 29, 2020, 13:30 - 15:00 Channel 6

OP-619

3D Anthropomorphic Phantom Facilitates Accurate Dosimetry for Head and Neck Radiopharmaceutical Therapy Trials

D. Adam, J. Grudzinski, B. Cox, I. R. Marsh, T. Bradshaw, P. Hill, P. Harari, B. P. Bednarz;
University of Wisconsin-Madison, Madison, WI, UNITED STATES OF AMERICA.

Aim/Introduction: Accurate and personalized dosimetry is important for combined external beam radiotherapy and radiopharmaceutical therapy (RPT) treatment regimens in which a cumulative target tumor dose is delivered. The accuracy of RPT dosimetry is limited by uncertainties related to quantitative nuclear medicine scans (i.e. PET, SPECT). Measurements to quantify recovery coefficients (RC), a form of partial volume corrections (PVC), are often taken with nuclear medicine phantoms with idealized geometries and activity distributions which address the size but not the shape of a structure. A 3D printed anthropomorphic phantom with replaceable, patient-specific, 3D printed inserts facilitates a way to standardize activity quantification for more accurate, personalized RPT dosimetry. This work details the construction of a 3D printed head and neck phantom and the dosimetric impact of RCs derived from the phantom are studied using a Monte Carlo (MC) RPT dose calculation platform [1]. ***Materials and Methods:*** The phantom is based upon open-access CT data provided by the Radiation Therapy Oncology Group (RTOG) 0522 study [2]. The main chamber, a fused thyroid gland void, and removeable parotid and tumor voids were 3D printed using stereolithography (SL) out of a photopolymer resin. The skull, spine, and lacrimal gland voids were 3D printed using SL out of a photopolymer resin mimicking bone material. RCs were calculated for the phantom that was filled with an Iodine-131 solution and imaged using SPECT/CT (120 projections, 60s/projection). The phantom was imaged after injecting the ~20ml tumor insert with 6.99 µCi/ml and the main phantom with 0.71 µCi/ml (9.88:1 insert/background ratio). Jaszczak phantom hot sphere measurements were also conducted to compare to the anthropomorphic phantom. ***Results:*** A RC of 0.47 was calculated for the tumor region. The impact of RC was compared against a ground truth MC scenario in which uniform activity concentrations were assigned to the tumor and main chamber. In comparison to the ground truth, the mean dose to the tumor was underestimated by 57% and 9% before and after applying the RC, respectively. ***Conclusion:*** This work highlights the importance of accurate RC calculations for PVC of SPECT-based Iodine-131 RPT dosimetry and offers a method to integrate patient-specific SPECT PVC into dosimetry workflows. Future work will include 3D printing multiple phantom inserts based on patient-specific contours and characterizing the PVCs and resultant dosimetry. ***References:*** [1] Besemer, A, et al. Cancer biotherapy & radiopharmaceuticals 33.4 (2018): 155-165. [2] Ang KK, et al. RTOG 0522. J Clin Oncol. 2014; 32:2940-2950.

OP-620

Making a copy of conventional anthropomorphic phantom section by 3D printing

S. Stuchebrov[1], A. Bulavskaya[1], Y. Cherepennikov[1], A. Grigorieva[1], I. Miloichikova[1,2], E. Gargioni[3];
[1]Tomsk Polytechnic University, Tomsk, RUSSIAN FEDERATION, [2]Cancer research institute of Tomsk national research medical center of the Russian academy of sciences, Tomsk, RUSSIAN FEDERATION, [3]University Medical Center Hamburg-Eppendorf, Hamburg, GERMANY.

Aim/Introduction: Currently, along with rising radiation exposure in single radiotherapy sessions and growing complexity of dose planning, rigorous verification using phantoms, which simulate patients' anatomy taking into account properties of different tissues and organs, is also required. For this purpose, conventional anthropomorphic phantoms simulating certain organs and bone tissues, made of different tissue equivalent materials are used. Authors propose making of anthropomorphic phantoms by the means of 3D-printing. The aim of this study is to design and produce a copy of conventional anthropomorphic phantom section using proposed approach, and compare its tomography data with default data. ***Materials and Methods:*** Authors obtained computed tomography (CT) images of the Alderson Radiation Therapy male phantom using Siemens Somatom Definition AS CT-scanner at the University Medical Center Hamburg-Eppendorf. These data were used to develop a 3D model of the eighth phantom section (neck area), simulating larynx, bone marrow, muscle and bone. The model is designed using Slicer and Meshmixer software. CT-indices of different volumes were used to choose suitable materials and printing parameters. The phantom section is made using 3D printer Prusa i3 Multi Material 2.0. The phantom thicknesses equals to 1 inch. After that, CT-imaging of the printed section was performed, and CT-images of the printed and default phantom sections were compared in order to check the geometry and the matching of CT-indices. ***Results:*** The result of this study proves the possibility to produce an anthropomorphic phantom by 3D-printing. Comparison of CT-images shows that 3D-printing allows making an object on the base of its DICOM data with 1 mm accuracy throughout the whole

volume that is comparable to CT-tomography data accuracy. The difference of CT-indices for each printed volume is less than 5%. The value of CT-indices for default and printed sections equals to: 980 (default) and 940 (printed) for larynx; 30 (default) and 15 (printed) for bone marrow; 15 (default) and 17 (printed) for muscle; 400 (default) and 380 (printed) for bone. The results match within the variation of CT-indices in conventional clinical CT-images of corresponding tissues of real patients. ***Conclusion:*** In this study, we demonstrate the possibility to make an anthropomorphic phantom by 3D printing with reproducing shapes and CT-indices of a conventional phantom. Considered approach allows making of inserts for a conventional phantom with unique geometry corresponding to clinical verification tasks for radiotherapy plan. This work is supported by the Russian Science Foundation, project No. 19-79-10014. ***References:*** None

OP-621

The dosimetric impact of deformable image registration on multi-timepoint internal dosimetry studies

I. Marsh*, J. J. Grudzinski, R. Hernandez, M. M. Turek, D. M. Vail, Z. S. Morris, J. P. Weichert, B. P. Bednarz;*
University of Wisconsin-Madison, Madison, WI, UNITED STATES OF AMERICA.

Aim/Introduction: Accurate voxel-based personalized dosimetry for targeted radionuclide therapy relies on the temporal coregistration of serial PET/CT or SPECT/CT images. In regions where uptake varies both spatially and temporally, coregistration can have a significant impact. This work investigates the impact of incorporating locoregional affine and deformable image registration (DIR) in the calculation of 3D internal dose distributions. ***Materials and Methods:*** Five companion canine patients presenting with widespread metastatic disease were administered ^{86}Y-NM600 and scanned via PET/CT at 2, 24, and 48 h post-injection. Tumor and normal tissue volumes were contoured at each timepoint and absorbed dose rate (ADR) distributions from ^{90}Y-NM600 were estimated using a Geant4-based Monte Carlo internal dosimetry platform. Absorbed dose distributions were generated using either whole-body or locoregional CT-CT affine coregistration (WAC or LAC, respectively) prior to applying demons-based DIR. The 48 h PET/CT, corresponding to peak differential tumor uptake, served as the reference to which all other timepoints were registered. CT-CT image transformations were applied to the corresponding ADR distribution and voxel-level absorbed dose was integrated within each region of interest. ***Results:*** The Sørensen-Dice index measured overlap of locoregionally registered tumor (n = 11) and liver (n = 5) volumes was 17 ± 29% and 5 ± 6% higher than that achieved using the whole-body approach, respectively. The incorporation of DIR further improved temporal coregistration by an average of 6% for tumor volumes and 18% for liver volumes when compared to LAC. Differences in reported D90 for tumor DVHs ranged from -19.7 to 3.0% for WAC vs LAC+DIR and -2.2 to 1.7% for LAC vs LAC+DIR. In the liver these differences ranged from -9.5 to 4.1% and -9.2 to 3.3%, respectively. ***Conclusion:*** This work shows that the approach used for temporal coregistration will have a meaningful impact on multi-timepoint personalized dosimetry calculations. Incorporating DIR can improve coregistration of tumor and normal tissue volumes across an imaging series and potentially lead to more accurate internal dose distributions. ***References:*** None

OP-622

OpenDose3D: A free, collaborative 3D Slicer module for patient-specific dosimetry

A. Vergara Gil[1]*, E. Amato*[2,3]*, L. Auditore*[2]*, M. Brenet*[4]*, M. Chauvin*[1]*, N. Clayton*[1]*, L. Ferrer*[5,6]*, B. Gibaud*[4]*, S. Gnesin*[7]*, A. Italiano*[3,8]*, G. Kayal*[1,9]*, T. Lima*[7,10,11]*, J. Ocampo*[1]*, D. Pistone*[3,8]*, G. Quan*[1]*, E. Mora Ramirez*[12]*, J. Ruegger*[10]*, M. Bardies*[1]*;*
[1]CRCT, UMR 1037, INSERM, Université Toulouse III Paul Sabatier, Toulouse, FRANCE, [2]Department of Biomedical and Dental Sciences and of Morphologic and Functional Imaging, University of Messina, Messina, ITALY, [3]Istituto Nazionale di Fisica Nucleare, Sezione di Catania, Messina, ITALY, [4]Univ Rennes, Inserm, LTSI UMR 1099, Rennes, FRANCE, [5]Université de Nantes, CNRS, Inserm, CRCINA, F-44000, Nantes, FRANCE, [6]ICO René Gauducheau, F-44800, Saint-Herblain, FRANCE, [7]Institute of Radiation Physics, Lausanne University Hospital, Lausanne, SWITZERLAND, [8]Department of Mathematics, Computer Science, Physics and Earth Science, University of Messina, Messina, ITALY, [9]SCK CEN, Belgian Nuclear Research Centre, Boeretang 200, Mol 2400, BELGIUM, [10]Radiation Protection Group, Kantonsspital Aarau, Lausanne, SWITZERLAND, [11]Institute of Radiology and Nuclear Medicine, Luzerner Kantonsspital, Lausanne, SWITZERLAND, [12]Universidad de Costa Rica, Escuela de Física, CICANUM, San Jose, COSTA RICA.

Aim/Introduction: The availability of software solutions is instrumental in the development of clinical dosimetry. Both academic and commercial solutions are available, each with advantages and drawbacks. In this work, we present a free, open source software, based on 3D-Slicer designed to perform patient-specific dosimetry. ***Materials and Methods:*** 3D Slicer is an open source software platform for medical imaging, image processing, and three-dimensional visualisation. Its modules already include tools suitable for dosimetry, such as: Dicom import, 3D image display, registration and segmentation. We developed additional features needed for patient-specific dosimetry: •Handling (import and co-register) multiple time-points Dicom images from PET/CT or SPECT/CT reconstructed images • Specific module for calibrations/corrections (sensitivity, contrast recovery and dead-time) • Fitting and integration

time-related events (activity and absorbed dose rates) • Calculating absorbed doses via local energy deposition or convolution, in both homogeneous and heterogeneous media (including density correction). • Generating Monte Carlo input files for absorbed dose calculation. OpenDose3D is able to report cumulated activity and residence times, absorbed dose rates, mean absorbed doses with uncertainties. The validation of this tool covered: sanity checks of its interface and dosimetry calculations following different scenarios. ***Results:*** Absorbed dose kernels for convolution in homogeneous or heterogeneous media were implemented for several radionuclides, and, depending on the user's requirements, more can be added.Thanks to the scripting capabilities of 3D Slicer, all calculation steps of the dosimetry process can be automated (except the VOI/organ segmentation). Conversely, the modular nature of the tool allows the saving and retrieval of intermediary steps within the process. The OpenDose3D module is fully functional and currently being tested on several clinical datasets including sequential PET (90Y-labelled glass microspheres for transarterial radioembolization - TARE) and SPECT/CT (^{131}I for thyroid cancer remnant ablation and ^{177}Lu-DOTATATE for peptide receptor radionuclide therapy). Preliminary results for TARE cases, using local energy deposition, indicate good agreement with direct Monte Carlo simulations performed with GAMOS. ***Conclusion:*** We developed a 3D Slicer scripted module to perform patient-specific dosimetry for molecular radiotherapy. The module has been developed collaboratively in order to establish mechanisms through which it can continue to evolve with the clinical need. Users can engage directly in the development, and provide new functionality with addition and support. Being part of the OpenDose collaboration[1], the whole project is publicly available/accessible. ***References:*** [1]Chauvin et al. 2020 jnumed.119.240366

OP-623

An International Multi-Center Investigation on the Accuracy of Radionuclide Calibrators for Theranostics in Nuclear Medicine

C. Saldarriaga Vargas[1,2], M. Bauwens[3], I. N. A. Pooters[3], S. Pommé[4], S. M. B. Peters[5], M. Segbers[6], W. Jentzen[7], A. Vogg[8], F. H. P. van Velden[9], S. L. Meyer Viol[10], M. Gotthard[5], F. M. Mottaghy[3,8], J. E. Wildberger[3], P. Covens[2], R. Wierts[3];

[1]Belgian Nuclear Research Centre (SCK CEN), Mol, BELGIUM, [2]Vrije Universiteit Brussel, Jette, BELGIUM, [3]Maastricht University Medical Center, Maastricht, NETHERLANDS, [4]European Commission Joint Research Centre (JRC), Geel, BELGIUM, [5]Radboudumc, Nijmegen, NETHERLANDS, [6]Erasmus MC, Rotterdam, NETHERLANDS, [7]University of Duisburg-Essen, Essen, GERMANY, [8]University Hospital RWTH Aachen University, Aachen, GERMANY, [9]Leiden University Medical Center, Leiden, NETHERLANDS, [10]University Medical Center Utrecht, Utrecht, NETHERLANDS.

Aim/Introduction: Personalized molecular radiotherapy based on theranostics requires accurate quantification of the amount of radiopharmaceutical activity administered to patients both in diagnostic and therapeutic applications. This international multi-center study aims to investigate the clinical measurement accuracy of radionuclide calibrators for 7 radionuclides used in theranostics: ^{99m}Tc, ^{111}In, ^{123}I, ^{124}I, ^{131}I, ^{177}Lu and ^{90}Y. ***Materials and Methods:*** In total, 32 radionuclide calibrators from 8 hospitals located in the Netherlands, Belgium and Germany were tested. For each radionuclide, a set of four samples comprising two clinical containers (10-mL glass vial and 3-mL syringe) with two filling volumes were measured. The reference value of each sample was determined using two secondary standard ionization chambers of certified radioactivity calibration centers (Belgian Nuclear Research Centre SCK CEN and Joint Research Centre Geel). The deviation in measured activity with respect to the reference value was determined for each radionuclide and each measurement geometry. In addition, the combined systematic deviation of activity measurements in a theranostic setting was evaluated for 5 clinically-relevant theranostic pairs: ^{131}I/^{123}I, ^{131}I/^{124}I, ^{177}Lu/^{111}In, ^{90}Y/^{99m}Tc and ^{90}Y/^{111}In. ***Results:*** For ^{99m}Tc, ^{131}I, and ^{177}Lu, a small minority of measurements were not within ±5% range from the reference activity (percentage of measurements not within range: ^{99m}Tc: 6%, ^{131}I: 14%, ^{177}Lu: 24%) and almost none were outside ±10% range. However, for ^{111}In, ^{123}I, ^{124}I and ^{90}Y more than half of all measurements were not accurate within ±5% range (^{111}In: 51%, ^{123}I: 83%, ^{124}I: 63%, ^{90}Y: 61%) and not all were within ±10% margin (^{111}In: 22%, ^{123}I: 35%, ^{124}I: 15%, ^{90}Y: 25%). A large variability in measurement accuracy is observed between radionuclide calibrator systems, type of sample container (vial vs syringe), and source-geometry calibration/correction settings used. Consequently, we observed large combined deviations (percentage deviation >10%) for the investigated theranostic pairs, in particular for ^{90}Y/^{111}In, ^{131}I/^{123}I and ^{90}Y/^{99m}Tc. ***Conclusion:*** Our study shows that substantial over- or under-estimation of therapeutic tissue doses are likely to occur in a theranostic setting when radionuclide calibrators are used with factory-set calibration factors. These findings underline the importance of thorough validation of radionuclide calibrator systems for each clinically-relevant radionuclide and sample geometry. ***References:*** None

OP-624

A correlation study between clinical outcome and absorbed dose to organs at risk and lesions for patients with High-Risk Neuroblastoma administered with high-activity therapy of 131I-mIBG

B. Cassano[1], M. Pizzoferro[2], S. Valeri[3], S. Donatiello[1], C. Polito[1,4], D. Ciucci[1,3], F. Martire[1,3], A. Castellano[5], C. Altini[2], M. C. Garganese[2], V. Cannatà[1];

[1]IRCCS Bambino Gesù Children's Hospital, Medical Physics

Unit, Rome, ITALY, [2]IRCCS Bambino Gesù Children's Hospital, Nuclear Medicine Unit/Imaging Department, Rome, ITALY, [3]Tor Vergata Postgraduate School of Medical Physics, Rome, ITALY, [4]Sapienza University of Rome, Postgraduate School of Medical Physics, Rome, ITALY, [5]IRCCS Bambino Gesù Children's Hospital, Oncoemathology Unit, Rome, ITALY.

Aim/Introduction: The administration of high-activity of ^{131}I-metaiodobenzylguanidine (^{131}I-mIBG) is a gold standard for treating patients affected by relapsed/refractory metastatic high-risk neuroblastoma (HR-NBL). One of the most promising strategies is the tandem high-activity therapy, which consists of two administrations of ^{131}I-mIBG separated by 15 days. The aim of this study was to report the absorbed dose to WB, red marrow (RM) and tumours in order to correlate them with clinical outcome of the patients. ***Materials and Methods:*** 20 patients (10 boys and 10 girls, age range [3;20] years) affected by relapsed-refractory HR-NBL and treated with tandem high activity therapy were enrolled. The first administration was weight-based (444 MBq/kg) [6.6;17.5] GBq, while the second one was dosimetry-based, achieving 4 Gy to WB. Data collection for the assessment of absorbed dose to WB and RM (D_{WB} and D_{RM}) was performed taking measurement in a time window [0.5;144] hours after the administration, according to the MIRD and EANM guidelines. The WB dose-rate has been measured with an external probe placed at 2 meters distance while a well counter was used to measure the blood activity. Lesion dosimetry (D_{Lesion}) was performed on 13 patients following the conjugated view method acquiring five static images in a time window [2;144] h for a total of 13 lesions evaluated. The response was classified in Progression and Stable Disease (PD and SD), Partial and Complete Response (PR and CR) according to semiquantitative assessment based on SIOPEN-mIBG score system. ***Results:*** The cumulative D_{WB}, D_{RM} and D_{Lesion} ranged from [2.5; 4.8], [0.7; 2.4] and [13;464] Gy. A linear correlation between the absorbed dose to WB and RM were obtained with a correlation coefficient equals to R^2=0.97. After 131I-mIBG therapy, combined with chemotherapy, patient 3, 4, 7 and 6 showed CR, PR, SD and PD respectively. A correlation between the clinical outcome and the absorbed dose to lesion was obtained with a threshold at 80 Gy. ***Conclusion:*** The dosimetric approach was necessary to perform a patient-specific treatment both to administer the maximum tolerable activity to the patients and to evaluate the efficacy of the therapy. The absorbed dose to lesion ranged in a very wide interval and could be a predictor of the outcome of the treatment. Tandem high-activity therapy, in combination with chemotherapy treatment, was well tolerated and effective in patients with HR-NBL. Benefits were observed in the treatment of relapse/progression, improving survival rates without severe toxicities. ***References:*** None

OP-625

The MEDIRAD imaging network - Standardisation of quantitative radioiodine imaging

J. Taprogge[1,2], *F. Leek*[1,2], *M. Bardiès*[3], *A. Buck*[4], *N. Clayton*[3], *F. Courbon*[5], *U. Eberlein*[4], *C. Lapa*[4], *M. Lassmann*[4], *M. Luster*[6], *E. Mora-Ramirez*[3], *K. Newbold*[1], *S. Schlögl*[4], *S. Schumann*[4], *T. Schurrat*[6], *J. Tran-Gia*[4], *D. Vallot*[5], *F. Verburg*[6], *L. Vija*[5], *A. Vergara Gil*[3], *S. Zerdoud*[5], *G. D. Flux*[1,2];
[1]Royal Marsden Hospital NHSFT, London, UNITED KINGDOM, [2]Institute of Cancer Research, London, UNITED KINGDOM, [3]Centre de Recherches en Cancérologie de Toulouse INSERM, Toulouse, FRANCE, [4]Department of Nuclear Medicine, University of Würzburg, Würzburg, GERMANY, [5]IUCT Oncopole, Toulouse, FRANCE, [6]Department of Nuclear Medicine, Philipps-University Marburg, Marburg, GERMANY.

Aim/Introduction: Treatment of differentiated thyroid cancer with radioiodine has been performed for almost 80 years. Nevertheless, controversies remain over the related radiation risks and the optimal treatment regimen for individual patients. Large-scale prospective multi-centre studies are essential to resolve these controversies. Multi-national multi-centre clinical studies will allow sufficient patient recruitment to achieve the statistical significance required to address these issues. Optimisation and standardisation of data acquisition and processing are essential to ensure quantitative imaging so that patient-specific dosimetry may be compared between centres. We report here on the set-up of a European network of centres able to perform standardised quantitative imaging of radioiodine within the EU consortium MEDIRAD. ***Materials and Methods:*** Four SPECT/CT systems and one SPECT system at four European centres were characterised with respect to their system volume sensitivity, recovery coefficients and dead-time to enable quantitative imaging of patients administered with radioiodine for the treatment of thyroid cancer. A site set-up protocol was developed that complied with varying local and national interpretation of radiation protection guidance and laws. Furthermore, image acquisition protocols were developed that allowed for flexible imaging schedules based on local requirements and availability of equipment to allow a wide range of centres to be included in the studies. Reconstructions were performed locally using Flash3D and Volumetrix MI, respectively, with OSEM (4 iterations, 10 subsets), CT (SPECT/CT) and Chang (SPECT) attenuation correction and triple-energy window scatter correction with no post-reconstruction filtering. ***Results:*** System volume sensitivities of three 3/8" Siemens Intevo SPECT/CT systems were found to be in the range from 62 to 74 cps/MBq. A 5/8" GE Discovery 670 SPECT/CT was found to have a sensitivity of 92.2 cps/MBq. Lastly, a Siemens Symbia S SPECT system was found to have a sensitivity of 55.6 cps/MBq. Recovery coefficients measured on the Siemens Intevo systems agreed within the uncertainties

on all systems. ***Conclusion:*** This network has been set-up to support a series of clinical studies to determine accurately absorbed doses for thyroid cancer patients treated with radioiodine. Results from the site set-up indicate that global calibration parameters for similar set-ups (camera and reconstruction) may be used for an extension of the imaging network. Standardisation of the imaging and dosimetry protocol, however, was found to be challenging due to local differences in ethical approval, radiation protection and availability of equipment. ***References:*** None Acknowledgments: MEDIRAD project received funding from Euratom research and training programme 2014-2018 under grant agreement No 755523.

OP-626

Predictive accuracy of pre-therapy ^{123}I-NaI dosimetry for patients treated with ^{131}I-NaI as part of the UK multi-centre SELIMETRY trial

J. Taprogge[1,2], S. Yusuf[1], J. Gear[1,2], I. Murray[1,2], F. Leek[1], R. A. Gregory[3], J. Wevrett[4], J. Scuffham[5,4], J. Tipping[6], B. Murby[6], S. Jeans[6], M. Stuffins[4], S. Michopoulou[7], M. Guy[7], D. Morgan[8], A. Hallam[8], D. Hall[9], H. Polydor[9], C. Brown[10], G. Gillen[10], N. Dickinson[11], S. Brown[12], G. Ainsworth[12], J. Wadsley[13], G. D. Flux[1,2];
[1]Royal Marsden Hospital NHSFT, London, UNITED KINGDOM, [2]Institute of Cancer Research, London, UNITED KINGDOM, [3]Barts Health NHS Trust, London, UNITED KINGDOM, [4]Royal Surrey County Hospital NHS Foundation Trust, Guildford, UNITED KINGDOM, [5]National Physical Laboratory, Teddington, UNITED KINGDOM, [6]The Christie NHS Foundation Trust, Manchester, UNITED KINGDOM, [7]University Hospital Southampton NHS Foundation Trust, Southampton, UNITED KINGDOM, [8]Oxford University Hospitals NHS Foundation Trust, Oxford, UNITED KINGDOM, [9]University Hospitals Bristol NHS Foundation Trust, Bristol, UNITED KINGDOM, [10]NHS Greater Glasgow and Clyde, Glasgow, UNITED KINGDOM, [11]Nottingham University Hospitals NHS Trust, Nottingham, UNITED KINGDOM, [12]CTRU, University of Leeds, Leeds, UNITED KINGDOM, [13]Weston Park Hospital, Sheffield, UNITED KINGDOM.

Aim/Introduction: The aim of the UK-based multi-centre clinical trial SELIMETRY (EudraCT No 2015-002269-47) is to investigate the potential use of the MEK 1/2 inhibitor, Selumetinib (AZD6244, ARRY-142886), to re-sensitise patients with iodine refractory differentiated thyroid cancer to radioiodine therapy. Lesion biokinetic analysis is performed both for the pre-treatment ^{123}I-NaI and for the subsequent ^{131}I-NaI therapy. The aim of this study was to evaluate the potential for the ^{123}I-NaI study to predict the biokinetics following the therapeutic administration. ***Materials and Methods:*** Pre-treatment dosimetry involved up to five SPECT/CT scans at 5, 24, 30, 48 and 72 hours after a 370 MBq ^{123}I-NaI administration following four weeks of Selumetinib therapy. Four post-therapy SPECT/CT scans were performed at 24, 48, 72 and 144 hours following radioiodine therapy with 5.5 GBq of ^{131}I-NaI. rhTSH stimulation was used before ^{123}I-NaI scans and ^{131}I-NaI therapy. The SPECT scans were quantified using system calibration factors [1]. Activity retention in lesions was determined from large VOIs placed on the SPECT scans to include spill-out due to the partial-volume effect. Activity in the large VOIs was corrected for background activity. Lesions were outlined on the CT scans by a trained radiologist to obtain lesion volumes. Absorbed doses were calculated using the MIRD formalism. Uncertainties in the absorbed doses were estimated using recent EANM guidance. Pearson product-moment correlation coefficients were computed to assess relationships between results from pre-treatment and post-therapy dosimetry. ***Results:*** Preliminary results obtained for 10 lesions (lesion size range: 0.4 - 42 .3 ml), in 3 patients treated as part of the clinical trial suggest a strong, positive correlation between predicted activity retention at 24 hours from the pre-treatment dosimetry and measured activity retention post-therapy ($r=0.98$, $n=10$, $p<0.001$). Predicted and measured activity retention at 24 hours after administration agreed in the majority of cases (8/10) within the associated uncertainties. Furthermore, a strong, positive correlation between predicted and measured effective half-lives of activity retention in lesions assuming a single exponential decay was found ($r=0.96$, $n=10$, $p<0.001$). ***Conclusion:*** Preliminary results suggest that the lesion biokinetics of pre-treatment ^{123}I-NaI are applicable to subsequent ^{131}I-NaI therapy of advanced thyroid cancer. This will potentially allow for a more personalised approach in the treatment of patients with metastatic thyroid cancer based on patient-specific dosimetry. ***References:*** [1] Gregory RA et al. Phys Med Biol. 2019;64(24):24501. ***Acknowledgments:*** The SEL-I-METRY trial is supported by a Cancer Research UK Grant (trial number CRUK/14/041), AstraZeneca and Genzyme Corporation.

OP-627

Absorbed dose estimation of thyroid residues, salivary glands and distal metastases after ^{131}I therapy using SPECT/CT with scatter, dead time and partial volume correction

M. Abuqbeitah*, M. Demir, S. Sager, N. Yeyin, K. Sonmezoglu; Istanbul University, Istanbul, TURKEY.*

Aim/Introduction: It was aimed to calculate the absorbed dose of salivary glands, thyroid residues and distal metastases after ^{131}I therapy with resolving the quantification degrading factors. ***Materials and Methods:*** IEC body phantom was filled by 1983.2 MBq ^{131}I followed by 20 SPECT/CT scans . Recovery coefficients were calculated for 26.51,11.49, 5.57, 2.57,and 0.52 cm^3 spheres. Triple energy window (6%) was used for scatter correction and special equations were derived for dead time correction. 31 patients (73±16 kg, 46±17 years) were scanned (1 bed) involving salivary glands and lungs at

6, 24, and 168 hours following administration of 5069±1924 MBq ^{131}I. CT images were used to draw the salivary glands ROIs, while the thyroid residues (n=22) and the distal lesions (n=10) were delineated by 30% iso-contour owing to its superior accuracy over 40 and 50% iso-contour. The absorbed doses were calculated using IDAC-Dose 2.1 for salivary glands, and sphere model for thyroid residues and lesions. ***Results:*** The mean residence time of single parotid gland (n = 31) and single submandibular gland (n=25) was 8.6±11.2 and 3.1±2.2 minutes, respectively. While that was 3.52±4.54 h for thyroid residues and 0.31±0.34 h for the distal lesions. The range of the salivary glands uptake (%) at 6 h was 0.27-1.67 and 0.03-0.99 at 24 h, while thyroid residues uptake ranged from 0.06 to 10.9 at 2 h, and it was 0.04-18.3 at 24 h. The parotid glands dose was 0.46 ± 0.47 Gy/GBq, and the submandibular glands dose was 0.16 ± 0.10 Gy/GBq. The total salivary glands (n = 26) mean dose was 0.41 (0.21-1.11) Gy/GBq, whereas 78 (0.5-400) Gy/GBq was found as thyroid residues dose, and 2 (0.8-15) Gy/GBq for the distal lesions. 100% of the distal lesions and 30% of the thyroid residues received dose ≤ 70 Gy. ***Conclusion:*** The salivary glands doses were comparable with few studies conducted with ^{131}I tracer that verifies the accuracy of the present methodology . Also, salivary glands uptake might largely affect the thyroid uptake during the first hours when using the thyroid probe for uptake measurement, while this impact decreases at 24 h due to the activity clearance. The salivary glands failure may occur after total administration of 54.5 GBq ^{131}I with respect to 60 Gy tolerated dose and 1.1 Gy/GBq. The resultant low dose of the lesions emphasizes the importance of dosimetry based therapy to deliver effective and successive absorbed dose. ***References:*** None

OP-628

Optimization of a dual-energy quantitative computed tomography (DEQCT) method to quantify the mineral bone volume fraction (MBVF) for bone marrow dosimetry in molecular radiotherapy

M. Salas Ramírez, J. Tran-Gia, M. Lassmann;
Department of Nuclear Medicine, University of Würzburg, Würzburg, GERMANY.

Aim/Introduction: The quantification of the absorbed dose to active bone marrow is essential for determining the risk of marrow toxicity in patients undergoing molecular radiotherapy. The development of parameterized computational models of bone marrow for calculating patient-specific radionuclide S-values requires the implementation of imaging methods for quantifying the mineral bone volume fraction (MBVF). This study aims to optimize a phantom-independent dual-energy quantitative computed tomography (PI-DEQCT) method (without external calibration standards) for a SPECT/CT system to enable the calculation of MBVF for bone marrow dosimetry in molecular radiotherapy. ***Materials and Methods:*** First, a previously implemented PI-DEQCT method (validated in a Siemens Healthineers Symbia Intevo Bold (SPECT/)CT system [1]) was optimized (improvement: inclusion of soft tissue-equivalent materials in the beam hardening correction). Subsequently, the MBVF was measured in a phantom simulating the vertebral geometry (European Spine Phantom, ESP) using the non-optimized and optimized PI-DEQCT method. Then, the MBVF in the spongiosa region of the head and neck of two femoral bones from an adult boar was measured using the optimized PI-DEQCT method. The two bone samples were located in a plastic box without dispersion material and imaged with a dual-energy CT acquisition protocol. For comparison, four external standards (water and three water-pHEMA mixtures, each with a different MBVF (0.03, 0.07, and 0.10)) were attached to the box to enable a phantom-dependent MBVF quantification (PD-DEQCT) method [2]. Lastly, the effective atomic number (Z_{eff}) and the effective density (Rho_{eff}) of the analyzed volume were obtained using the PI-DEQCT method and compared with the values provided by a commercially available tool for DECT systems (syngo. CT DE Rho/Z, Siemens Healthineers). ***Results:*** As previously reported, the BMVF quantification errors in the ESP with the non-optimized method ranged between 5.4% and 31.7% [1], while for the new optimized method, it ranged between -12.1% and -3.3%. The errors between the MBVF quantification with PI-DEQCT and PD-DEQCT in the boar bones were -1.84% (bone 1) and 2.48% (bone 2). Lastly, the Rho_{eff}/Z_{eff} values showed a good agreement between PI-DEQCT and the Rho/Z tool (relative errors 5.23%/3.2% [bone 1] and 6.7%/2.46% [bone 2]). ***Conclusion:*** The good agreement between both DEQCT methods provides evidence for the feasibility of a phantom-independent MBVF quantification using the presented PI-DEQCT method with a commercial hybrid (SPECT/)CT system. Moreover, PI-DEQCT enables a good characterization of the spongiosa region based on the obtained Rho_{eff}/Z_{eff} values. ***References:*** [1] Salas-Ramirez et al., PhysMedBiol 2019;64(20). [2] Goodsitt et al., MedPhys 2014;41(9).

OP-629

Implementation of SPECT auto-contouring detector motion in GATE Monte Carlo simulation for ^{177}Lu and ^{131}I Molecular Radiotherapy (MRT) dosimetry

G. Kayal[1,2], M. Chauvin[1], E. Mora-Ramirez[3], L. Struelens[2], M. Bardiès[1];
[1]CRCT, INSERM, Toulouse, FRANCE, [2]SCK CEN, Belgian Nuclear Research Centre, Mol, BELGIUM, [3]Universidad de Costa Rica, Escuela de Física, CICANUM, San José, COSTA RICA.

Aim/Introduction: Monte Carlo (MC) modeling of SPECT imaging systems provides unique insight to evaluate quantitative imaging procedures in Molecular Radiotherapy

(MRT) dosimetry. The modeling of time dependent phenomena, including detector movement allows the simulation of more realistic acquisition conditions. To date, SPECT modeling in GATE cannot account for body contour acquisitions where detector heads move as close as possible to the patient resulting in a non-circular orbit (NCO), which improves image resolution and uniformity. In this work we developed and validated NCO - step and shoot acquisition mode for use in GATE SPECT modeling. ***Materials and Methods:*** We modelled ^{177}Lu SPECT experimental acquisitions performed on a Siemens Symbia T2 dual headed gamma camera with MELP collimator. SPECT projections were obtained for cylindrical (with 2 organ inserts) and elliptical (with 4 organ inserts) phantoms[1], using a matrix size of 128 x 128, 60 projections per head, acquisition time of 20 and 30 seconds per projection and total activity of 303.4 MBq and 1190.3 MBq for the 2-organ and 4-organ phantom respectively. A GATE (v8.2) model implementing NCO acquisitions was designed and validated based on the experimental settings.Additionally, ^{131}I and ^{177}Lu circular orbit (CO) and NCO SPECT projections were simulated using the 4-organ phantom model for the same Siemens Symbia T2 gamma camera, with MELP (for ^{177}Lu) and HE (for ^{131}I) collimator and the same acquisition parameters to highlight the relevance of NCO modeling. ***Results:*** Simulation time for 2-organ (3.6e+11 primaries) and 4-organ (2.1e+12 primaries) phantoms were 5h and 9.5h respectively using the regional HPC centre CALMIP. Simulated images were compared with experimental images and were found to be in good agreement with a high similarity of 94% using structural similarity index (SSIM) and a relative difference of less than 5% from profiles. Simulated images for ^{177}Lu and ^{131}I were compared between circular and body contouring motion (using both SSIM and profiles). The maximum difference in the counts between the two gamma camera motions CO and NCO (taking into account all the projections) was less than 1% for ^{177}Lu and up to 10.6% for ^{131}I. This difference arises from the higher septal penetration of ^{131}I compared to ^{177}Lu. ***Conclusion:*** We developed and validated NCO acquisition modes for GATE SPECT modeling. This implementation is recommended for all NCO acquisitions and essential in the case of radionuclides with high septal penetration such as ^{131}I. ***References:*** 1. Gear J et. al., Med. Phys. 41(8),082502-1, 2014.

OP-630

Generation of realistic SPECT/CT images for ^{177}Lu dosimetry in Molecular Radiotherapy (MRT) based on Monte Carlo simulation with GATE

G. Kayal[1,2], M. Chauvin[1], A. Vergara-Gil[1], N. Clayton[1], L. Struelens[2], M. Bardiès[1];
[1]CRCT, INSERM, Toulouse, FRANCE, [2]SCK CEN, Belgian Nuclear Research Centre, Mol, BELGIUM.

Aim/Introduction: Patient-specific dosimetry in MRT relies on quantitative imaging, pharmacokinetic assessment and absorbed dose calculation. The DosiTest[1] project was initiated to evaluate the uncertainties associated with each step of the clinical dosimetry pathway, via a virtual multicentric intercomparison based on Monte Carlo modeling. The first phase of the project considered only planar imaging[2]. This work presents the generation of 'virtual' clinical SPECT/CT datasets based on GATE Monte Carlo modelling, which can subsequently be integrated in commercial image workstations as if they were real patient datasets. ***Materials and Methods:*** Our study considered a therapy cycle of 6.85 GBq ^{177}Lu-labelled DOTATATE derived from an IAEA-CRP project (E23005) on "Dosimetry in Radiopharmaceutical therapy for personalised patient treatment". Patient images were obtained from a GE Infinia gamma camera with MEGP collimator. A patient model was generated by segmenting and labelling volumes of interest on the patient CT image and modeled SPECT projections (matrix size of 128 X 128 with 15 seconds per projection and energy window of 208 keV ± 20%) were generated based on experimental time points at 1h, 4h, 24h, 48h and 96h. Next, these simulated projections were integrated in the SPECT/CT DICOM envelopes from the patient, allowing the integration of the modelled projections into a commercial workstation. Simulated projections were validated against real SPECT projections for similarity using the SSIM (Structural Similarity Index Metric) index. Finally, images were reconstructed using a standard reconstruction algorithm (5 iterations, 16 subsets OSEM reconstruction and CT-based attenuation correction). ***Results:*** Simulated images produced with GATE were very close to experimental images with SSIM indices ranging from 85 % to 90 % among the different time points. Image reconstruction of the simulated projections were performed on a HERMES workstation. Simulation of SPECT projections with realistic activities in a therapeutic context took 11.5 hours to compute using 3560 CPU cores at the regional HPC centre CALMIP (instead of 5.4 years with a single CPU), thus making it feasible to perform multicentric virtual intercomparison with simulated SPECT images. ***Conclusion:*** These results demonstrate that GATE can be used for realistic simulation of ^{177}Lu SPECT/CT acquisitions. Now, the modelled datasets will be circulated to clinical departments, in order to allow them to benchmark their clinical dosimetry procedure on a common reference dataset, so as to further assess the uncertainties in the entire dosimetric chain. ***References:*** 1 Garcia et al. 2015 Med Phys 42(12):6885-94. 2 Costa et al. 2017 Physica Medica 42:292-7.

1107

Pitfalls & Artefacts 5: FDG-PET Performed or Suspicious for Infections and Inflammation, Including COVID-19 - Fever, Vascular Graft, Granulomatosis, Covid-19

Thursday, October 29, 2020, 13:30 - 15:00 Channel 7

OP-631

Fever or Inflammatory Syndrome of Unknown Origin

S. Balogova; Comenius University and St. Elisabeth Oncology Institute, Nuclear Medicine, Bratislava, SLOVAKIA.

OP-632

Vascular Grafts Infections

C. Lauri; Sant'Andrea Hospital of Rome, Nuclear Medicine Unit, Rome, ITALY.

OP-633

Granulomatous Diseases

V. Ambrosini; University of Bologna, S.Orsola-Malpighi Hospital, Nuclear Medicine DIMES, Bologna, ITALY .

OP-634

Covid-19 Infection

J. Talbot; Hopital Tenon & Sorbonne Université, Nuclear Medicine, Paris, FRANCE.

1108

Clinical Oncology Track - TROP Session: Detecting BCR with [68Ga]Ga-PSMA

Thursday, October 29, 2020, 13:30 - 15:00 Channel 8

OP-635

Multicentre External Validation of a Prediction Nomogram for 68Ga-PSMA-11 PET/CT in different Clinical Settings of PSA Failure, after Radical Treatment for Prostate Cancer

F. Ceci[1], L. Bianchi[2,3], P. Castellucci[4], C. Artigas[5], J. Leite[6], P. Corona[7], A. Farolfi[4], Q. A. Shagera[5], R. Moreira[6], C. González[7], D. Deandreis[1], S. Fanti[4,3];

[1]Nuclear Medicine, Department of Medical Sciences, University of Turin, Turin, ITALY, [2]Department of Urology, S.Orsola-Malpighi University Hospital, Bologna, ITALY, [3]Department of Specialistic, Diagnostic and Experimental Medicine, University of Bologna, Bologna, ITALY, [4]Nuclear Medicine, S.Orsola-Malpighi University Hospital, Bologna, ITALY, [5]Department of Nuclear Medicine, Institut Jules Bordet, Université Libre de Bruxelles, Bruxelles, BELGIUM, [6]PET/CT Center, DASA - Diagnósticos da Américc, Rio de Janeiro, BRAZIL, [7]Fundación Centro Diagnóstico Nuclear (FCDN), Buenos Aires, ARGENTINA.

Aim/Introduction: A clinical nomogram has been recently developed to predict 68Ga-PSMA-11-PET/CT positivity in different clinical setting of PSA failure, after radical therapy in prostate cancer (PCa) [1]. Since its implementation in clinical practice is still limited by lack of a formal external validation, we aimed to validate this tool in a large multicentre cohort. ***Materials and Methods:*** We retrospectively included 1515 PCa patients with confirmed PSA failure after radical therapy (surgery n=1428; radiotherapy n=87), from five high-volume PET-centres (University of Bologna n=682; DASA-Rio de Janeiro n=295; Bruxelles-Bordet n=255; University of Turin n=223; FCDN-Buenos Aires n=60). All patients had complete clinical/pathologic/laboratory information. The external cohort was stratified according to clinical setting categories as defined in the original population: a) Group-1: first-time biochemical recurrence (BCR), n=668; Group-2: BCR after salvage therapy, n=506; Group-3: biochemical persistence (BCP) after radical prostatectomy, n=202; Group-4: advanced stage PCa before second-line systemic therapies, n=139. 68Ga-PSMA-11-PET/CT detection rate in the overall population and in each sub-group was assessed. A multivariable logistic regression model was produced to assess the predictors of positive scan. Third, the performance characteristics of the model were assessed by quantifying the predictive accuracy, according to model calibration and Yuden's index was used to find the best nomogram's cut-off. Finally, decision curve analysis (DCA) was implemented to quantify the nomogram's clinical value. ***Results:*** In the external cohort, the overall detection rate was 54.6% vs. 51.2% in the original population. PET/CT detection rates in different clinical setting were: Group-1 43.4% vs. 40.3%; Group-2: 58.1% vs- 54.0%; Group-3 60.4% vs. 60.5%; Group-4 88.2% vs. 86%. In the multivariate analysis, ISUP grade (p=0.004), PSA (p<0.001), PSA doubling time (p<0.001) and clinical setting (p<0.001) were independent predictors of positive scan. The predictive accuracy of the nomogram was optimal and comparable to the original model (82.6% vs. 82.3%,). The calibration plot indicated ideal concordance between actual and predicted probability of positive 68Ga-PSMA-11-PET/CT. In DCA, the nomogram revealed clinical net benefit when the threshold probabilities of positive scan was >10%. ***Conclusion:*** The original nomogram exhibited excellent characteristics on multicentre external validation. Given its optimal accuracy, this prediction nomogram might be an easy tool to help clinicians in the decision-making process of recurrent PCa and to reduce the incidence of false-negative scan. ***References:*** Ceci F, et al. Prediction nomogram for 68Ga PSMA-11 PET/CT in different clinical settings of PSA failure after radical treatment for prostate cancer. Eur J Nucl Med Mol Imaging. 2020;47(1):136-146.

OP-636

A phase II, open-label single-arm study to assess safety, clinical utility of disease burden assessments with 68Ga-

PSMA-11 PET/CT in localizing recurrent prostate cancer

M. Piert[1], *M. Abghari-Gerst*[2], *M. Rodnick*[2], *J. Hearn*[2], *J. S. Montgomery*[2], *A. Alva*[2], *Z. Reichert*[2], *D. Spratt*[2], *P. J. H. Scott*[2]; [1]*University of Michigan, Ann Arbor, MI, UNITED STATES OF AMERICA,* [2]*University of Michigan, Ann Arbor, MI, UNITED STATES OF AMERICA.*

Aim/Introduction: While PET/CT with the prostate-specific membrane antigen (PSMA) ligand 68Ga-PSMA-11 is widely used at the time of biochemically recurrent (BCR) prostate cancer, prospective and quantitative data of the utility and disease burden from the United States are still scarce. ***Materials and Methods:*** In this registered trial, 671 patients with BCR after radical prostatectomy (RP) (n=275, 41%), definitive radiation therapy (RT) (n=167, 25%), or RP with post-operative RT (PORT) (n=229, 34%) underwent 68Ga-PSMA-11 PET/CT. Presence of prostate cancer was assessed qualitatively and quantitatively using a user-assisted semi-automatic segmentation routine on a per-patient and per-region base. Lesions were validated by histopathologic analysis and a composite reference standard including follow-up imaging and prostate-specific antigen (PSA) response criteria in absence of systemic treatment. Study endpoints were the detection rate, positive predictive value (PPV), PSMA-positive disease burden, and safety. ***Results:*** 68Ga-PSMA-11 PET/CT localized prostate cancer sites in 567 of 671 (84.5%) of patients. The overall detection rate increased with PSA levels (ng/mL): 59% for <0.5 (n=102), 77% for 0.5 to <1.0 (n=87), 87% for 1.0 to <2.0 (n=113), 90% for 2.0 to <5.0 (n=142), and 94% for >=5.0 (n=227, p<0.001). On a per-patient basis, PPV was 0.88 (95% CI, 0.81-0.92) by histopathologic validation (n=59) and 0.93 (95% CI, 0.91-0.95) by the composite reference standard (n=243). In patients with positive scans, the number of identified lesions, the whole-body PSMA tumor volume (PSMA-TV) and whole-body total lesion PSMA (TL-PSMA, normalized by body weight or lean body mass) correlated positively with the PSA level, while no correlation was found with the PSA doubling time or Gleason score at diagnosis. The detected PSMA-TV and TL-PSMA significantly (p<0.001) increased with escalation of interval treatment (from surveillance, over PORT, to ADT). Based on the scan results the intended therapeutic management (at 1-month) changed in 74% of cases (n=461), while actual management changes at 12-months were noted in 77% of cases (n=353). Heart rate and blood pressure reading were stable before and after 68Ga-PSMA-11 administration, and no serious adverse events associated with 68Ga-PSMA-11 administration were observed. ***Conclusion:*** 68Ga-PSMA-11 PET/CT is safe, has an excellent detection rate and PVP in BCR prostate cancer and has high impact on therapeutic decision making. ***References:*** None

OP-637

Patterns of failure on ^{68}Ga-PSMA-11 PET/CT after radical prostatectomy (RP), radiotherapy (RT), and RP with post-operative RT (RP-PORT)

M. Rodnick*, M. Abghari-Gerst, J. W. D. Hearn, J. S. Montgomery, A. Alva, Z. Reichert, D. E. Spratt, T. D. Johnson, P. J. H. Scott, M. Piert; The University of Michigan, Ann Arbor, MI, UNITED STATES OF AMERICA.*

Aim/Introduction: Conventional imaging has demonstrated different failure patterns based on initial treatment of prostate cancer. Such information is helpful to inform adaptation and optimization of treatment techniques. Given the improved sensitivity and specificity of PSMA-ligands, we performed a propensity matched analysis of the relapse patterns after definitive treatment (RP, RT, or RP-PORT). ***Materials and Methods:*** Within a registered prospective single-center trial investigating the diagnostic performance of ^{68}Ga-PSMA-11 PET/CT, 592 subjects received approx. 300 MBq ^{68}Ga-PSMA-11 PET/CT, 60 min. p.i. Patient and disease characteristics, treatment details and PSMA-scan results (total PSMA-positive tumor volume, identified disease location [local (prostate/prostate bed/seminal vesicles), pelvic nodal, soft tissue (including extra-pelvic nodal), and/or bone] were recorded. Propensity score matching on age, PSA at initial treatment, Gleason grade group, types of interval treatments, time-interval between definitive treatment to scan, and PSMA-positive tumor burden was performed, followed by logistic regression analysis on propensity score matched cases to determine the multiple comparison corrected odds ratio (OR). ***Results:*** Five hundred of 592 scans resulted positive for recurrent prostate cancer [(194 RP, 130 RT, and 176 RP-PORT; age: 69.5,70(68.9-70.1) years. The PSA (ng/mL) at time of scan was 4.5,1.5(3.3-5.8) for RP, 10.7,5.5(8.2-13.2) for RT, and 4.9,2.0(3.7-6.1) for RP-PORT (mean/median (95%CI)]. In matched cohorts, the odds of local recurrence after RT were significantly higher than following RP (OR 8.0 (98.75%CI 3.8-16.8; n=267) and RP-PORT (OR 18.8 (98.75%CI 7.7-45.8, n=288; p<0.001). Conversely, the odds for nodal recurrence in the pelvis were significantly higher after RP compared to RT (OR 2.3 (98.75%CI 1.2-4.4) and RP-PORT (OR 3.3 (98.75%CI 1.8-6.7; p<0.001). Compared to RT, the odds for distant metastatic disease in bone was higher after RP (OR 2.6 (98.75%CI 1.1-5.9) and RP-PORT (OR 2.3 (98.75%CI 1.0-5.3; p<0.001). Significant differences were absent for any comparison regarding soft tissue metastases. ***Conclusion:*** This study evaluated only patients who experienced treatment failure and therefore this analysis cannot quantify the overall probability of recurrence across treatment modalities, especially given lack of randomization. Nevertheless, among patients with positive scans, different patterns of failure were observed based on the initial treatment, with a higher rate of local recurrence after RT, and higher rates of nodal and osseous

metastases after RP. These findings may inform treatment techniques and warrant further investigation. ***References:*** None

OP-638

Recurrence patterns after radical prostatectomy, definitive radiation therapy and salvage radiation therapy with 68Ga-PSMA-11 PET/CT in non-metastatic castrate sensitive prostate cancer patients: a single center post-hoc retrospective analysis

W. Armstrong, P. Thin, R. Alano, K. Nguyen, K. Booker, J. Gartmann, V. Lok, S. Lira, I. Sonnie, N. G. Nickols, A. U. Kishan, J. Czernin, J. Calais;
University of California, Los Angeles, Los Angeles, CA, UNITED STATES OF AMERICA.

Aim/Introduction: 20 to 50% of prostate cancer (PCa) patients undergoing radical prostatectomy (RP) or definitive radiation therapy (dRT) will experience disease recurrence. However, anatomical recurrence patterns may differ depending on the therapeutic approaches. The aim of this post-hoc retrospective analysis was to investigate if the relapse pattern as assessed by 68Ga-PSMA-11 PET/CT was different depending on the type of local pelvic therapy (RP, dRT, salvage RT (SRT), pelvic lymph node dissection (PLND), pelvic lymph node RT (PLNRT)) in patients with non-metastatic castrate sensitive (nmCS) recurrent disease after primary definitive therapy. ***Materials and Methods:*** Patients who underwent a 68Ga-PSMA-11 PET/CT for nmCS PCa recurrent disease after primary definitive therapy were screened from a database of 4 prospective studies (NCT02940262, NCT03515577, NCT04050215, NCT03582774). Patients who underwent primary staging (n = 95), without definitive therapy (n = 68), with known metastatic disease (M1) (n = 68) or with castrate resistant (CR) disease (n = 291) were excluded. We examined the relationship between recurrence patterns as assessed by 68Ga-PSMA-11 PET/CT (PROMISE criteria) and prior local treatments: i) RP, ii) dRT, iii) RP + SRT. ***Results:*** 787 patients were included in the analysis. Positive scan rates were 60%, 94% and 75% in RP, dRT and RP + SRT populations, respectively. Median pre-scan PSA levels were 0.50 (0.02-72.5) ng/ml, 4.4 (0.1-202) ng/ml, and 1.07 (0.04-33) ng/ml for patients who underwent RP (n = 464), dRT (n = 109) and post-RP SRT (n = 214). Median time to first recurrence was 27.7 after RP and 54.6 months after dRT (p = < 0.0001). Patients who underwent RP had lower local recurrence (LR) pattern (T+) rates by PSMA PET than those with dRT (99/464; 21% vs 69/109; 63%; p=< 0.0001). Nodal metastasis (N1) positivity rate was similar between RP and dRT (179/464; 39% vs 43/109; 39%; p = 0.87). Extrapelvic metastasis (M1) positivity rate was lower for RP than dRT (93/464; 20% vs 51/109; 47%; p=< 0.0001). Median time from post-RP SRT to second recurrence was 22.3 months. In patients who had a second recurrence after RP and SRT the positivity rate of LR (T+), N1 disease and M1 disease by PSMA PET/CT was 12% (24/214), 46% (99/214) and 44% (95/214). ***Conclusion:*** In this cohort of patients with nmCS PCa recurrent disease after primary definitive therapy, the anatomic patterns of failure assessed by PSMA PET differ based on prior local and systemic treatments. ***References:*** None

OP-639

Performance of ^{68}Ga-PSMA-11 PET/CT in patients with recurrent prostate cancer. A multi-centre evaluation of 2533 patients

A. Afshar-Oromieh[1], M. Livorsi da Cunha[2], J. Wagner[2], U. Haberkorn[3], W. Weber[4], M. Eiber[4], T. Holland-Letz[5], I. Rauscher[4];
[1]Department of Nuclear Medicine, University Hospital of Bern, University of Bern, Bern, SWITZERLAND, [2]Department of Nuclear Medicine, Hospital Israelita Albert-Einstein, Sao Paulo, BRAZIL, [3]Department of Nuclear Medicine, Heidelberg University Hospital, Heidelberg, GERMANY, [4]Department of Nuclear Medicine, Technical University of Munich, Munich, GERMANY, [5]Department of Biostatistics, German Cancer Research Center, Heidelberg, GERMANY.

Aim/Introduction: To evaluate the performance of ^{68}Ga-PSMA-11 PET/CT in the diagnosis of recurrent prostate cancer (PCa) in a large patient's cohort. ***Materials and Methods:*** The initial database included 6758 patients scanned with ^{68}Ga-PSMA-11 PET/CT at 1h p.i. in the departments of nuclear medicine of Heidelberg (Germany), Technical University of Munich (Germany) and Albert-Einstein Hospital of São Paulo (Brazil). Of these patients, those with untreated Primary PCa, undergoing androgen-deprivation therapy, referred for PSMA-Endoradiotherapy and those previously treated with chemotherapy or exclusively external beam radiation therapy were excluded from the analysis, giving a total of 2533 included patients. Potential influences of different factors such as PSA-level, PSA-doubling-time (PSA_{DT}), PSA-velocity (PSA_{Vel}), Gleason Score (GSC, including the separate analysis of 7a and 7b), age and amount of injected tracer were evaluated in a multivariate analysis. ***Results:*** The rate of pathological PET/CT-scans was 43% for PSA less than 0.2 ng/ml, 58% for PSA between 0.2 and 0.5ng/ml, 72% for PSA between 0.5 and 1.0ng/ml and increased to a maximum of 93% for PSA bigger than 10ng/ml. A pathologic PET/CT was significantly (p=0.001) associated with PSA level and higher GSC. Amount of injected tracer, age, PSA-DT and PSA-Vel were not associated with a higher probability of a positive PET/CT. ***Conclusion:*** ^{68}Ga-PSMA-11 PET/CT conducted at 1h p.i. demonstrated its high performance in the largest patient cohort yet analysed. Tumour detection showed a clear association with higher PSA and higher GSC. No association was found between a pathological ^{68}Ga-PSMA-11 PET/CT and age, amount of injected tracer, PSA_{DT} or PSA_{Vel}. ***References:*** None

OP-640

Early BCR: in which patients is it worth performing a further PSMA scan?

A. Paccagnella[1], A. Farolfi[1], G. Ricci[2], P. Castellucci[1], F. Mattana[1], L. Muraglia[1], S. Fanti[1];
[1]Department of Nuclear Medicine, Policlinico S.Orsola, University of Bologna, Bologna, ITALY, [2]Department of Nuclear Medicine, M. Bufalini Hospital, Cesena, ITALY.

Aim/Introduction: to identify potential factors able to predict 68Ga-PSMA-11 PET/CT (PSMA-PET) positivity after a previous negative PSMA-PET performed in patients with early biochemical recurrence (BCR). ***Materials and Methods:*** from March 2016 to March 2020 we retrospectively reviewed patients with the following inclusion criteria: 1) diagnosis of prostate cancer treated with radical prostatectomy; 2) BCR defined by PSA measurement ≥ 0.2 ng/mL; 3) a negative PSMA-PET during early phases of BCR (PET1); 4) a subsequent PSMA-PET (PET2) within 20 months; 5) no treatment between PET1 and PET2, with exception of hormonal therapy (HT). Imaging dataset was evaluated by two independent experienced readers and in case of disagreement by the opinion of a third reader. We considered: PSA values at the time of the scans, PSAdt, PSAvel, ΔPSA and Δtime between PET1 and PET2. Mann-Whitney U test and Chi-Square test were used to compare the distribution of patients' characteristics across PET2 results. Regression analyses were employed to determine predictors of a positive PET2; ROC curves were calculated. ***Results:*** 431 patients had a negative PSMA-PET during early phases of BCR, 73/431 (17%) patients met all the inclusion criteria. 32/73 (44%) were T3a or grater, 14/73 (19%) were N1, 31/73 (42%) had a GS≥8. Mean-PSA1 was 0.88 ng/ml (median 0.5; range 0.2-9.5); mean-PSA2 was 2.5 ng/ml (median 1.13; range 0.23-43.8); mean-Δtime was 8.5 months (2-20); mean-ΔPSA was 1.65 ng/ml; mean-PSAdt was 14.1 months; mean-PSAvel was 2.2 ng/ml/years. 13/73 (18%) patients were on HT at the time of PET2. PET2 was positive in 29/73 (40%); 21/29 (72%) had loco-regional disease and 8/29 (28%) had distant metastasis. ΔPSA, PSAdt, PSAvel and HT were associated with a positive PET2 (all $p<0.05$). On univariate regression analysis PSAdt and being on HT were predictors of a positive PET2, but on multivariate only PSAdt was significant (OR 0.9, CI95% 0,886-0,998, p=0,044). PSAdt had an AUC of 0.69 and a 7.3 months cut-off showed a 69% sensitivity and a 70% specificity. PET2 was positive in 13/45 (29%) patients with PSAdt>7 months and in 16/28 (57%) patients with PSAdt≤7. ***Conclusion:*** this study shows that PSA kinetics and being on HT during PET2 are predictors of a positive PSMA-PET after a first negative in patients with early BCR. A cut off PSAdt of 7 months could be used to improve the selection of patients for a second scan, reducing the number of negative scans and increasing detection rate. ***References:*** None

OP-641

68Ga-PSMA PET/CT prospective study in prostate cancer occult recurrence patients: diagnostic performance, impact on therapeutic decision-making and long-term benefits

C. Rousseau[1], L. Ferrer[1], M. Le Thiec[2], V. Fleury[2], M. Frindel[2], D. Rusu[2], B. Maucherat[2], A. Rauscher[2], P. Baumgartner[2], A. Morel[2], N. Varmenot[1], L. Campion[1], F. Kraeber-Bodéré[1];
[1]ICO René Gauducheau, F-44000 Saint-Herblain; Nantes University, CNRS, Inserm, CRCINA, F-44000, Nantes, FRANCE, [2]ICO René Gauducheau, F-44000, St Herblain, FRANCE.

Aim/Introduction: The aim of this prospective study was to investigate the impact of 68Ga-PSMA-11 PET/CT on management of prostate cancer patients with occult biochemical recurrence (OBR). ***Materials and Methods:*** 130 hormone-naïve OBR (PSA from 0.05 to 1.5 ng/mL) patients were enrolled in the study (NCT03443609), whose design was described previously in preliminary results report[1]. PSMA detection rates were determined and correlated to various clinical variables using univariate and multivariable analyses (Cox regression analysis). ***Results:*** After pre-screening, 13 patients were excluded due to positive pelvic mpMRI (9 pts) or bone scan (4 pts). The median time from radical prostatectomy +/- radiotherapy to OBR was 5.2 y [0.2-17.1]. Ninety-two among the 130 patients (70.8%) had a positive PSMA PET/CT. One hundred eighty-four lesions were detected, 97/184 in lymph nodes (52.7%), 47/184 in bone (25.5%), 34/184 into prostate bed (18.5%) and 6/184 (3.3%) in peritoneal nodules. PSMA detection rates were 59.6 %, 73.9 % and 81.1% for patients with PSA value ranging from 0.05 to 0.29, 0.3 to 0.59 and 0.6 to 1.59 ng/ml respectively. Univariate analysis revealed PSA value before PSMA, PSA doubling time and PSA velocity as potential predictive factors for positive 68Ga-PSMA PET/CT ($p=0.008$ to 10^{-4}). In multivariate analysis, only PSA velocity was identified as significant independent predictor of positive 68Ga-PSMA PET (adjusted odd of 4.35 - 95%CI: [1.79-10.58], p=0.001). Thanks to PSMA PET/CT, therapeutic management changed in 71/130 patients (54.6%). Take the example of 33 patients, previously treated by surgery and bed prostate radiotherapy, who would have a surveillance due to low PSA increase: 23 of them (70%) were able to have stereotactic radiotherapy on PSMA positive areas. For 5/23 (21.7%) and 12/23 (52.2%) of them, a decrease of more than 90% or 50% of PSA level after treatment was observed respectively. Considered all the cohort, a major impact on PSA value was observed with a decrease of more than 90% or 50% of PSA level from few weeks after treatment in 34/130 (28.4%) and 62/130 (47.7%) respectively. This continues for 46/130 patients (35.5%) who were still in biochemical complete remission, after PSMA based treatment with a median follow-up of 23.4 months [14.5-30.5]. ***Conclusion:*** Results showed, in more than half of patients, a major impact of PSMA PET/CT on treatment

management allowing them to benefit very early from focal PSMA based therapy with a long-term biochemical complete response for 35.5% of them. ***References:*** Rousseau C et al., doi: 10.1002/pros.23869.

OP-642

Forced diuresis with furosemide increases diagnostic certainty in the assessment of local recurrence in prostate cancer patients with biochemical recurrence referred for [^{68}Ga]Ga-PSMA-11-PET/CT compared to patients without preparation

C. Uprimny*, S. Bayerschmidt, A. S. Kroiss, H. Svirydenka, G. di Santo, B. Nilica, S. Rauch, E. von Guggenberg, C. Decristoforo, I. J. Virgolini;*
Medical University of Innsbruck, Innsbruck, AUSTRIA.

Aim/Introduction: On [^{68}Ga]Ga-PSMA-11-PET/CT tracer accumulation in the bladder is reduced with furosemide. The purpose of the study was (a) to evaluate whether forced diuresis with furosemide has the potential to increase diagnostic certainty in the assessment of local recurrence (LR) in prostate cancer patients with biochemical recurrence in comparison with patients without preparation and (b) whether furosemide has an influence on biodistribution and uptake of [^{68}Ga]Ga-PSMA-11 in organs with physiologic tracer accumulation. ***Materials and Methods:*** two groups with 140 prostate cancer patients each, referred for [^{68}Ga]Ga-PSMA-11-PET/CT because of biochemical recurrence after primary were compared: group one (median PSA: 1.39 ng/ml) receiving no preparation prior to imaging, whereas patients in group two (median PSA: 0.87 ng/ml) were injected with 20 mg furosemide shortly after tracer injection. Evaluation of presence of LR was performed visually. In addition intensity of tracer accumulation in lesions suspicious of LR and in organs with physiologic tracer uptake was assessed using maximum standardized uptake value (SUV_{max}). ***Results:*** Lesions with pathologic tracer uptake judged as LR were found in 26 cases of group one (18.6%), compared with 39 cases in group two (27.9%), showing a median SUV_{max} of 9.3 (range: 3.9-37.0) and 8.0 (range: 3.2-52.7), respectively. In 21 cases of group one an equivocal finding was present (21%), compared with 17 cases in group two (12.1%). No LR was detected in 93 cases of group one (66.4%) and in 84 cases of group two (60%). Findings between both groups differed statistically significantly. Median SUV_{max} values of organs and tissues with physiologic uptake of [^{68}Ga]Ga-PSMA-11 in group one and two were: liver (10.3 vs 10.2), spleen (11.6 vs 12.1), parotid gland (19.7 vs 19.7), lacrimal gland (8.5 vs 10.2), small bowel (16.2 vs 17.0), bone (1.6 vs 1.7), vascular activity (2.2 vs 2.4), kidney (55.8 vs 55.7) and bladder (62.4 vs 9.7). Apart from bladder activity no statistically significant difference between the two groups was found. ***Conclusion:*** Forced diuresis with 20 mg furosemide increases detection rate of local recurrence in patients with biochemical recurrence referred for [^{68}Ga]Ga-PSMA-11-PET/CT in comparison with patients without preparation. Apart from a significant reduction in bladder activity injection of furosemide shortly after tracer administration did not influence intensity of tracer uptake in organs with physiologic tracer accumulation. ***References:*** None

OP-643

The influence of digital PET/CT on diagnostic certainty and interrater reliability in ^{68}Ga-PSMA-11 PET/CT for recurrent prostate cancer

I. Alberts*, J. Hünermund, C. Sachpekidis, C. Mingels, V. Fech, K. Bohn, A. Rominger, A. Afhsar-Oromieh;*
Institut für Nuklearmedizin, Bern, SWITZERLAND.

Aim/Introduction: To evaluate the influence of digital PET/CT on diagnostic certainty, sensitivity and inter-rater reliability. ***Materials and Methods:*** This retrospective study compared two cohorts of patients who underwent ^{68}Ga-PSMA-11 PET/CT on a digital PET/CT (dPET/CT) (n=82) or an analogue scanner (aPET/CT) (n=82) for recurrent prostate cancer (PC). Both cohorts were matched for clinical parameters. Four physicians (consultant nuclear medicine physician, two experienced residents and a junior resident) read each scan independently and were blinded to clinical details and each other's results. Lesions were rated according to PSMA-RADS criteria. The number of equivocal and pathological lesions as well as the frequency of discrepant findings and the interrater reliability for the two scanners were compared. ***Results:*** Overall dPET/CT detected greater numbers of all lesion types compared to aPET/CT (benign $p<0.001$, equivocal $p=0.005$, pathological $p=0.05155$). Likewise, a significantly higher patient-based sensitivity (number of scans rated by all four readers as pathological) was observed for dPET/CT (84% vs. 58%, $p<0.05$). The higher number of lesions detected resulted in a higher false discovery rate (proportion of non-pathological lesions as a total of all lesions detected) for dPET/CT compared to aPET/CT (60.7% vs 56.4%, $p=0.008$), but not at the cost of increased diagnostic uncertainty (equivocal lesions for dPET/CT 11.6% vs aPET/CT 12.6%. $p=0.4$). No significantly increased rate of discrepant scans (where one or more readers differed in opinion as to whether the scan is pathological) was observed for dPET/CT compared to aPET/CT (20% vs. 16% respectively, $p=0.18$). However, interrater reliability was slightly lower for dPET/CT (PET/CT Krippendorf's $\alpha=0.72$ substantial agreement,) compared to aPET/CT ($\alpha=0.82$ almost perfect agreement). Interrater reliability did not improve with reader experience and did not correlate with the number of, or discrepancies in, the finding of equivocal lesions. ***Conclusion:*** Our results demonstrate a higher rate of detection for pathological lesions and higher patient based sensitivity for dPET/CT compared with aPET/CT, in

keeping with the known improved sensitivity and tumour-to-background ratio in dPET/CT. This improved sensitivity was coupled with slightly improved diagnostic certainty, with a lower rate of equivocal results. The higher sensitivity, however, was at the cost of higher false detection rates and lower interrater agreement, although interrater agreement showed no relationship with diagnostic uncertainty. ***References:*** None

OP-644

The value of early dynamic imaging in ^{68}Ga-PSMA PET/CT in prostate cancer patients with biochemical recurrence

S. Castro*, G. Ferreira, L. Violante, J. Teixeira, I. Sampaio Lucena, H. Duarte;*
Portuguese Institute of Oncology - Porto, Porto, PORTUGAL.

Aim/Introduction: ^{68}Ga-PSMA urinary bladder accumulation may hinder locoregional prostate cancer (PC) lesion detection. The aim of this study is to determinate if an early ^{68}Ga-PSMA-PET/CT acquisition may improve PSMA-avid lesion detection in patients with biochemical recurrence. ***Materials and Methods:*** Retrospective study of 148 patients with PC biochemical relapse (after prostatectomy/radiotherapy), referred for ^{68}Ga-PSMA-PET/CT scan between 01/01/2018 and 30/06/2018 (mean age 71 ±7.8 years; median prostate specific antigen: 3.5 [IQR 7.0] ng/mL; median Gleason score 7). Early dynamic pelvic ^{68}Ga-PSMA-PET/CT scans were acquired immediately after tracer injection during 10 minutes, and whole-body ^{68}Ga-PSMA-PET/CT scans were acquired 42-79 (mean 60.9 ±8.9) minutes after tracer injection (median activity 108.2MBq). Images were reviewed by two Nuclear Medicine physicians and suspicious lesions for PC were noted. Quantitative uptake (SUVmax) of PC lesions and background tissue (gluteus muscle, left external iliac artery and bladder) was evaluated in both sets of images and compared using Intraclass Correlation Coefficient (ICC), Wilcoxon matched-pair signed-rank test and Bland-Altman analysis. ***Results:*** A total of 114 patients presented PC lesions (detection rate: 77%) and 149 lesions were analyzed: 43 within the prostate gland/prostatic fossa, 101 lymph node and 5 bone metastasis. There was a strong correlation between initial and late images' quantitative uptake in total (ICC 0.943 [p<0.001]), prostate (ICC 0.864 [p<0.001]), lymph node (ICC 0.949 [p<0.001]) and bone lesions (ICC 0.846 [p=0.056]). No significant difference was found in the quantitative uptake of total, lymph node and bone lesions across the two measured time points, while prostate lesions exhibited only slightly higher tracer uptake on late images (median SUVmax 9.10 [IQR 7.30] initial vs 10.13 [IQR 11.70] late, mean bias -2.34 ±5.42, p<0.001).On the other hand, bladder activity was much higher on late images (median SUVmax 1.83 [IQR 2.50] initial vs 47.40 [IQR 52.00] late, mean bias -54.82 ±46.18, p<0.001), hindering PC lesions detection in 4 cases, which were only visible in early images and later confirmed with a post-diuretic acquisition. Muscle and vascular activity was higher in early images (median SUVmax 1.70 [IQR 0.70] and 5.72 [IQR 2.00] initial vs 0.73 [IQR 0.30] and 1.53 [IQR 0.50] late, p<0.01). ***Conclusion:*** Early dynamic ^{68}Ga-PSMA-PET/CT imaging showed comparable lesion uptake to late whole-body imaging, while bladder activity was significantly higher at later time points. Performing an additional early acquisition provides a window of opportunity to identify lesions with low back1ground activity and may improve the detection rate of pelvic lesions in PC patients. ***References:*** None.

OP-645

Is there any clinical-pathological variable able to predict a true positive ^{68}Ga- PSMA PET/CT result?

J. Bastidas*, F. Grisanti, J. J. Rosales, A. Bronte, A. Erhard, B. Miñana, C. Guitierrez, J. Perez Gracia, J. A. Richter, M. Rodriguez;*
Clinica Universidad de Navarra, Pamplona, SPAIN.

Aim/Introduction: To define clinical-pathological variables that allow to predict the positivity of ^{68}Ga-prostate-specific membrane antigen (PSMA) PET/CT for detecting relapse of treated prostate cancer (PCa). ***Materials and Methods:*** Inclusion criteria was: Patients with biochemical recurrence (BQR) in whom PSMA findings should be confirmed by 1) histopathological study; 2) Prostate-specific agent (PSA) response after salvage therapy (radiotherapy or surgery); 3) other image methods. Clinical and pathological variables were also collected. Patients were stratified into three different clinical scenarios: persisting detectable PSA after radical prostatectomy (Group-1), first-time BQR after curative intent treatment (Group-2), and BQR after salvage therapy (Group-3). By definition, negative PSMA results were considered False Negative (FN). The association between variables was assessed using univariate and multivariate Cox regression analysis. For categorical variables, Chi-square was used, and for continuous variables, Mann-Whitney test was used. Values are expressed as mean (±standard deviation) or median (P25-P75). ***Results:*** Sixty-eight patients were retrospectively studied. The PSA at PSMA study was 2.5 (±6.6) ng/ml, the PSA-doubling time was 8.5 (±10.2) months and the PSA-velocity was 0.17 (±0.37) ng/ml/month. The Gleason score was ≤7 in 45/68 (66%). Eleven patients (18%) were under androgen-deprivation therapy. The True Positive (TP) rate was 70,5% (48/68) confirmed by a histopathological study in 4 patients, PSA response after salvage therapy in 28 and by other image methods in 16. The FN were 20/68 (29,4%). No clinical-pathological variables were found to be significantly correlated with a TP PSMA result. However, when patients were studied by clinical scenarios, to belong to Groups 1 (n=13) and 2 (n=14) multiplied by 5 (OR = 5, 95% CI: 1.64-15.29, p = 0.005) the probability of having an FN result. Moreover, Group 3 (n=41)

FN patients had lower values than TP patients for: PSA 1.08 (0.95-1.76) vs. 1.63 (0.89-2.9) p>0.5; PSA-doubling time 10.67 (3.36-16.17) vs. 4.09 (1.9-8.6) p>0.5 and PSA-velocity 0.03 (0.015-0.08) vs. 0.08 (0.04-0.18) p=0.1. ***Conclusion:*** In this study, no clinical-pathological variable was found to predict a true positive PSMA result. Nevertheless, differences were found between clinical scenarios. With patients who have persisting detectable PSA after radical prostatectomy or patients with first-time BQR after curative intent treatment, have a five times greater probability of an FN result. Interestingly, patients with an FN result in the group with BQR after rescue therapy had lower values of PSA, PSAdt at PSMA, being almost statistically significant for PSA velocity. ***References:*** None

OP-646

Pathological lesions are at risk to be missed in linear colour scales in ^{68}Ga-PSMA-11 PET/CT

C. Mingels[1], C. Sachpekidis[1,2], J. Hünermund[1], K. P. Bohn[1], V. Fech[1], A. Rominger[1], A. Afshar-Oromieh[1], I. Alberts[1];
[1]Department of Nuclear Medicine, Inselspital, Bern University Hospital, University of Bern, Bern, SWITZERLAND, [2]Clinical Cooperation Unit Nuclear Medicine, German Cancer Research Center, Heidelberg, GERMANY.

Aim/Introduction: Despite being a primarily visual speciality, the optimal colour scale for viewing fused images in PET/CT has been inadequately investigated. The aim of this study was to evaluate the influence of linear and non-linear colour scales in ^{68}Ga-PSMA-11 PET/CT for recurrent prostate cancer. ***Materials and Methods:*** A retrospective evaluation of 50 consecutive patients undergoing PET/CT for recurrent prostate cancer with ^{68}Ga-PSMA-11 was performed. Three separate readers (one consultant and two experienced residents) read all scans in randomised order and were blinded to clinical details and each other's analyses. Each scan was read first using the non-linear "PET-rainbow" look-up table, re-randomised and then read in the linear "hot-metal new" look-up table. Readers were blinded to the maximum intensity projection and stand-alone PET images. They were asked to rate all lesions using only the fusion PET/CT for each colour look-up table. Lesions were classified with a three-point scale (benign, pathological and equivocal). The average number of pathological lesions per patient (paired t-test) and inter-rater reliability (Fleiss'κ) were compared for each colour scale. Lesions were validated by composite follow-up of histology, radiology and laboratory parameters. ***Results:*** A greater number of lesions per patient (p=0.002) rated as pathological were reported by all three readers in the "PET-rainbow" scale (mean 2.98±2.47) compared to the "hot-metal new" scale (mean 2.63±2.45). On a per patient basis, a total of 40 scans (80%) were rated as pathological in "PET-rainbow" and 37 (74%) in "hot-metal new" respectively. Clinical follow up was available for 30 patients, confirming 27/30 true positive scans for "PET-rainbow", 25/30 true positive scans for "hot-metal new", and two false negative scans in "hot-metal new". Both colour scales correctly identified one true negative patient. Follow-up identified no false positive scans for either scale. However, inter-rater reliability was slightly higher for "hot-metal new" (Fleiss' κ: 0.64) compared to "PET-rainbow" (κ: 0.58). ***Conclusion:*** A linear colour scale like "hot-metal new" demonstrated lower patient-based sensitivity, and incorrectly identified two patients as having negative scans (false negatives at follow-up). Conversely, the non-linear colour scale "PET-rainbow" showed superior sensitivity and positive predictive value, albeit with a slightly lower inter-rater agreement. The differences between the two colour-scales find explanation in the physical properties of the tracers and colour scales. Our results suggest that use of PET-rainbow is better suited to imaging with ^{68}Ga-PSMA-11 PET/CT and should be implemented for clinical routine use as well as for clinical studies. ***References:*** None

1109

Featured Session: Advances in SPECT-MPI

Thursday, October 29, 2020, 13:30 - 15:00 Channel 9

OP-647

Quantification of MBF with SPECT - Ready for Clinical Use?

A. Manrique; Normandie Université - EA 4650, CHU de Caen, Caen, FRANCE.

OP-648

Fully-automatic data-driven motion correction improves the diagnostic performance of myocardial perfusion imaging with CZT cameras

C. Ko[1,2], K. Ko[1], R. Yen[1], C. Chen[2];
[1]National Taiwan University Hospital, Taipei, TAIWAN, [2]Biomedical Engineering, National Taiwan University, Taipei, TAIWAN.

Aim/Introduction: Myocardial perfusion imaging (MPI) sometimes suffered from motion artifacts. The motion artifacts can cause image blurring and may degrade the diagnostic accuracy. Data-driven motion correction can be performed on list-mode enabled CZT cameras, and this may reduce the artifacts. We have developed a fully-automatic motion correction algorithm (NoMo software) with the aid of deep-learning technique. This study aimed to evaluate the effects of this algorithm on the diagnostic performance of coronary artery disease (CAD). ***Materials and Methods:*** We unselectively recruited 9469 consecutive subjects referred for routine treadmill-exercise MPI between June 2011 and Dec 2017. Among them, 1115 subjects with subsequent coronary angiography within 180 days were analyzed.

The images were automatically segmented and rotated with the aid of a trained deep-learning model for further analysis. The emitted photon events were binned into five respiratory gates and were reconstructed into motion-corrected images. The original and corrected images were independently scored on the AHA 17-segment model with manual verification. Summed scores were used to predict obstructive CAD (≥70% stenosis). Receiver operating characteristics (ROC) analysis was used to evaluate the diagnostic performance. A p-value of less than 0.05 was considered significant. ***Results:*** The heart excursed more in post-stress images than in redistribution images (10.0±3.9mm vs. 7.6±3.1mm, p<0.01). ROC analysis showed significantly increased area under curve (AUC) for corrected images in prediction of CAD (0.796 vs 0.741, p<0.01). Vessel-based analysis also showed significantly increased AUC (LAD: 0.750 vs. 0.696, LCX: 0.754 vs. 0.716, RCA: 0.729 vs. 0.672, all p<0.01). One-third of the falsely positive studies can be avoided with motion correction. ***Conclusion:*** The diagnostic performance of MPI can be improved with fully automatic motion correction. This technique can reduce significant amount of falsely positive studies. ***References:*** None

OP-649

Evaluation Of Coronary Flow Reserve By A New Method Using Routine Myocardial SPECT And Comparison To Dynamic SPECT With The Same Patients For Both Methods

L. Philippe[1], *M. Bailly*[2], *Y. El Yaagoubi*[1], *C. Prunier-Aesch*[1];
[1]*Medecine Nucleaire Tourangelle, Chambray-les-Tours, FRANCE,*
[2]*Médecine Nucléaire - CHR Orléans, Orléans - La Source, FRANCE.*

Aim/Introduction: Coronary Reserve assessment in Nuclear Medicine is usually performed using the "Dynamic SPECT" method with a CZT gamma-camera. We evaluate a new method, previously described (EANM 2019), without first-pass, using the short axis slices of a routine 99mTc-Tetrofosmin SPECT, providing an estimation of the Coronary Flow Reserve (CFR) by means of a Coronary Reserve Index (CRI). Counts ratio (myocardial Stress/Rest) represents the CRI, after adjustments with 5 corrective factors.In order to validate the CRI method, we compare results obtained with both methods (Dynamic SPECT and routine SPECT). ***Materials and Methods:*** Patients referred for dynamic Myocardial Perfusion Image (MPI) between November 2018 and March 2020 with Invasive Coronary Angiography (ICA) performed within 3 months were included. SPECT data were acquired on a CZT-based pinhole cardiac camera using Stress / Rest one-day Tc-99m-tetrofosmin protocol. Kinetic analysis was done with Corridor 4DM™software using a 1-tissue-compartment model and converted to MBF using a previously determined extraction fraction correction. Furthermore, we applied the new CRI method, to the data SPECT of a series of 25 patients who previously underwent a Dynamic SPECT. Unlike Dynamic SPECT, CRI method can be applied subsequently to the SPECT acquisition, or can be linked to the standard SPECT processing. Comparison of the 2 methods ("Dynamic" and CRI) concern the diagnosis of CAD: according to ICA , 15 patients had significant CAD: 3 patients had 3-vessels disease, 8 patients 2-vessels disease, and 4 patients one-vessel disease. A coronary stenosis was considered as significant over 30% . ***Results:*** For "Dynamic" SPECT method, the cut-off value Normal vs CAD, was 2.0 . Among the 25 patients, this method induced 14 true positives, 7 true negatives , 1 false negative , and 3 false positives (probably related to microvascular alteration), giving 93% Sensitivity - 70% Specificity - 82% Positive Predictive Value - 88% Negative Predictive Value. 21/25 patients are well classified, and the ROC AUC = 0.78 . For the CRI method, we observe 15 true positives, 7 true negatives , 0 false negative , and 3 false positives (different of "Dynamic" SPECT), giving 100% Sensitivity - 70.0% Specificity - 83% Positive Predictive Value - 100% Negative Predictive Value. 22/25 patients are well classified, and the ROC AUC = 0.78. ***Conclusion:*** The diagnostic value of both methods are good and quite similar. Results show that maybe, these methods don't evaluate exactly the same physiological process (epicardial CFR ± micro-circulation). ***References:*** None

OP-650

The evaluation of myocardial blood flow and coronary flow reserve in myocardial infarction with non-obstructive coronary arteries patients

K. Zavadovsky, *A. Mochula, A. Maltseva, D. Vorobyeva, M. Gulya, V. Shipulin, V. Ryabov;*
Cardiology Research Institute, Tomsk National Research Medical Centre, Russian Academy of Sciences, Tomsk, RUSSIAN FEDERATION.

Aim/Introduction: To elucidate the severity of myocardial perfusion, myocardial blood flow (MBF) and myocardial flow reserve (MFR) impairment in patients with myocardial infarction with non-obstructive coronary arteries (MINOCA) in comparison to those with MI with obstructive coronary artery disease (MICAD) and non-obstructive stable coronary artery disease (CAD). ***Materials and Methods:*** The study group comprised 40 patients (29 men, age 62.9±10.7years) who underwent ECG and invasive coronary angiography (ICA). Based on ICA results three groups were created: 1. MINOCA (n=11); 2. MICAD (n=17); 3. Control group - stable CAD with non-obstructive coronary arteries (n=12). A total of 12/17 (71%) MICAD patients underwent PCI with stenting; in 2/12 cases two arteries were revascularized. The first and the second groups of patients underwent Creatine phosphokinase-MB (CPK-MB) and Troponin I (TnI) assessment at admission and after 24 hours. In 7-10 days all patients underwent myocardial perfusion CZT

gamma-camera with the assessment of standard indices of myocardial perfusion (SSS, SRS, SDS) and quantitative parameters: rest MBF (rMBF), stress MBF (sMBF) and MFR. ***Results:*** After 24 hours cardiospecific biomarkers levels in MINOCA group were significantly (p<0.05) lower compared to MICAD group patients: CPK-MB 21.5 (IQR 13.7;45.0) vs. 94.4 (53.1;217.0) U/L; TnI 0.5 (0.1;3.3) vs. 9.8 (2.0;23.0) ng/ml. Standard myocardial perfusion indices differed significantly (p<0.05) among all three groups (except SDS between the first and second groups): MINOCA: SSS 5.0 (3.0;6.0), SDS 2.0 (1.0;3.0); MICAD: SSS 9.0 (5.0;13.0), SDS 3.0 (2,0;5.0); control group: SSS 1.5 (0.5;2.0), SDS 0.0 (0.0;2.0). Hoverer, sMBF and MFR differed significantly in all three groups of patients: MINOCA: sMBF 1.2 (0.8;1.7) ml/min/g, MFR 2.0 (1.2;2.4); MICAD: sMBF 0.7 (0.6;1.0) ml/min/g, MFR 1.2 (1.1;1.5); control group: sMBF 2.2 (2.1;2.3) ml/min/g, MFR 2.6 (2.5;2.8). In 7/11 (64%) of MINOCA patients the value of sMBF was ≤1.5 ml/min/g. In the MICAD group 16/17 (94%) had sMBF ≤1.5 ml/min/g and all control group patients had sMBF >1.5 ml/min/g. In 4/11 (36%) of MINOCA patients MFR values were less than 2; in MICAD group MFR<2 was observed in 15/17 (88%) patients. ***Conclusion:*** MINOCA patients are heterogeneous in terms of myocardial perfusion, MBF and MFR impairment. Despite the absence of obstructive coronary artery lesion, myocardial perfusion and blood flow assessed semiquantitatively and quantitatively are impaired more severely in MINOCA group, compared to stable CAD patients. This study was supported by the Russian Federation President Grant MK-1347.2020.7. ***References:*** None

OP-651

Determinants of myocardial perfusion reserve assessed by dynamic stress 201Tl/rest99mTc-tetrofosmin single photon emission computed tomography in patients with diabetes mellitus and stable coronary artery disease

J. Choi, E. Shin, M. Oh, S. Chae, C. Lee, D. Moon;
Asan Medical Center, Seoul, KOREA, REPUBLIC OF.

Aim/Introduction: Quantification of myocardial perfusion reserve (MPR) provides predictive information on cardiovascular outcome. We aimed to identify determinants of myocardial flow reserve in patients with type 2 diabetes mellitus and stable coronary artery disease. ***Materials and Methods:*** We conducted a prospective study to enroll consecutive patients who were aged 19 years or older, and had type 2 diabetes mellitus and stable coronary artery disease. All patients underwent dynamic stress ^{201}Tl/rest ^{99m}Tc-tetrofosmin single photon emission computed tomography (SPECT) using a dedicated multiple pinhole camera with cadmium-zinc-telluride detectors. ***Results:*** Between July 2017 and September 2019, we included 277 patients for analysis. There were 236 men, and 41 women. The median age was 65 [interquartile range (IQR), 59-71]. The median global MPR was 2.4 [1.9-3.0]. Characteristics of patients that showed a significantly lower MPR were advanced age of more than 70 years (n=74, 2.2 [1.8-2.6] vs. 2.4 [2.0-3.0], P=0.034), smoking history (n=63, 2.2 [1.8-2.4] vs. 2.5 [2.0-3.1], P=0.0004), hyperlipidemia (n=85, 2.2 [1.9-2.6] vs. 2.5 [1.9-3.1], P=0.021), hypertension (n=204, 2.3 [1.9-2.8] vs. 2.6 [2.0-3.2], P=0.013), and abnormal summed stress score of myocardial perfusion scan (n=136, 2.2 [1.7-2.7] vs. 2.5 [2.1-3.1], P<0.0001). Body mass index of 30 or higher, prior history of myocardial infarction or coronary intervention, and left ventricular dysfunction were not associated with global MPR (P>0.1). Multivariate linear regression analysis showed that age of more than 70 years (P=0.0098), smoking history (P=0.0012), hypertension (P=0.013), and abnormal summed stress score of myocardial perfusion scan (P=0.0011) were independent determinants of MPR. ***Conclusion:*** Advanced age and cardiovascular risk factors are determinants of MPR assessed by dynamic stress ^{201}Tl/rest ^{99m}Tc-tetrofosmin SPECT in patients with type 2 diabetes and stable coronary artery disease. ***References:*** None

OP-652

Comparison of dynamic SPECT Myocardial Blood Flow and Flow Reserve with regadenoson and dipyridamole

M. Bailly[1]*, Q. Brana*[1]*, F. Thibault*[1]*, M. Courtehoux*[2]*, G. Metrard*[1]*, D. Angoulvant*[2]*, M. Ribeiro*[2]*;*
[1]*CHR Orléans, Orleans, FRANCE,* [2]*CHRU Tours, Tours, FRANCE.*

Aim/Introduction: Regadenoson is a recent selective A2A adenosine receptor agonist. It is currently unclear if the absolute stress flow increase differs between pharmacological stress agents. We compared dipyridamole and regadenoson Myocardial Blood Flow (MBF) and Myocardial Flow Reserve (MFR) values obtained with dynamic Cadmium Zinc Telluride (CZT) SPECT Myocardial Perfusion Imaging (MPI), to evaluate if they could induce the same level of hyperemia. ***Materials and Methods:*** Patients referred for dynamic MPI for Coronary Artery Disease (CAD) screening between November 2018 and March 2020 were retrospectively analyzed. SPECT data were acquired on a CZT camera, using 1-day stress/rest 99mTc-tetrofosmin dynamic protocol. All analysis was performed using Corridor 4DM. To rule out confounding factors, patients with prior cardiac disease, ischemia or infarction and diabetes were excluded in a sub-group analysis. The remaining patients were matched for clinical characteristics (age, gender, BMI, cardiovascular risk factors) and compared in terms of stress MBF and MFR. ***Results:*** 162 patients stressed with dipyridamole were compared with 66 patients stressed with regadenoson. Global MFR wasn't different between regadenoson and dipyridamole groups (2.46 ± 0.87 vs. 2.64 ± 1.02 respectively for dipyridamole and regadenoson, p=0.36) but stress MBF was higher in regadenoson group (1.71 ± 0.73 vs. 1.44 ± 0.55 ml/min/g respectively for regadenoson and dipyridamole, p<0.05). When potential pathological patients were

excluded, two groups of 41 patients comparable in terms of age, gender, BMI, resting left ventricular ejection fraction, cardiac risk factors and cardiovascular treatments at the time of evaluation (p=0.2 at least) were analyzed. Mean global MFR wasn't different between the two groups: 2.62 ± 0.77 and 2.46 ± 0.76 respectively for dipyridamole and regadenoson (p=0.88). Stress MBF wasn't significantly different between dipyridamole (1.57 ± 0.56 ml/min/g) and regadenoson patients (1.61 ± 0.62 ml/min/g) (p=0.88). ***Conclusion:*** Regadenoson showed higher stress MBF values in our global results, but dipyridamole and regadenoson induced equivalent hyperemia with similar global stress MBF and MFR when confounding factors were ruled out. These results should be confirmed on a large, prospective and randomized study. ***References:*** None

OP-653

Quantification of Myocardial Flow Reserve using Dynamic CZT camera in Symptomatic Patients with Multiple Vessels Disease

D. Agostini[1], *G. Liu*[2], *A. Manrique*[1], *H. Shi*[2];
[1]*Department of Nuclear Medicine, CHU Caen Normandy, Caen, FRANCE,* [2]*Department of Nuclear Medicine, Zhongshan Hospital Fudan University, Shanghai, CHINA.*

Aim/Introduction: Quantification of myocardial flow reserve (MFR) by CZT has previously demonstrated diagnostic value in patients with stable CAD in comparison with PET and FFR (Agostini D et al 2018). We appraised the feasibility of myocardial blood flow (MBF), MFR and LVEF estimation using dynamic CZT camera in symptomatic patients with multiple vessels disease (MVD). ***Materials and Methods:*** 52 patients (42M, 10F; 60± 12 yrs) with chest pain and-or dyspnea underwent dynamic CZT and angiography within a 3 month timeframe. A stenosis was considered obstructive if greater than 50%. All pts had MVD. All pts underwent one-day dynamic rest (296±29 MBq)/regadenoson stress (865 ± 95 MBq) myocardial perfusion imaging by ^{99m}Tc-sestamibi CZT SPECT to measure MBF and LVEF. For SPECT, reconstructed frames were automatically segmented to extract the vascular input function and the LV uptake curve. A net retention model was used to estimate global uptake values, and then MBF was derived using Leppo correction. MFR was defined as the ratio of stress MBF over rest MBF using a commercially available software (4DM, Invia, Ann Arbor, MI). ***Results:*** We divided pts into 2 groups: G1 with normal stress LVEF>50%, n=43; and G2 with LVEF<50%; n=9. Stress MBF in G1 was significantly higher (2.35± 0.86) than in G2 (1.38± 0.62 ml/min/g; P= 0.0006). Rest MBF was identical in G1 (0.96± 0.29) and in G2 (0.81± 0.22 ml/min/g; P= ns). MFR in G1 was significantly higher (2.59± 1.04) than in G2 (1.66± 0.42; P<0.0001). Stress MBF and MFR correlated well with stress LVEF (r=0.54; r=0.45; P=0.0008). No gender variation was observed for MBF and MFR. ***Conclusion:*** Stress MBF and MFR data using dynamic 99mTc-sestamibi CZT were decreased in pts with LV dysfunction and appeared to correlate well with stress LVEF in pts with MVD. ***References:*** Agostini D et al. Eur J Nucl Med Mol Imaging. 2018;45(7):1079-1090

OP-654

The detection of multivessel coronary artery disease: the value of SPECT CZT myocardial blood flow and coronary flow reserve assessment

K. Zavadovsky[1], *A. Mochula*[1], *A. Maltseva*[1], *A. Baev*[1], *S. Andreev*[1], *R. Liga*[2], *A. Gimelli*[3];
[1]*Cardiology Research Institute, Tomsk National Research Medical Centre, Russian Academy of Sciences, Tomsk, RUSSIAN FEDERATION,* [2]*Università di Pisa, Pisa, ITALY,* [3]*Fondazione Toscana/CNR Gabriele Monasterio, Pisa, ITALY.*

Aim/Introduction: The recent Cadmium-Zinc-Telluride (CZT) camera for myocardial perfusion scintigraphy allows evaluating absolute myocardial blood flow (MBF) and coronary flow reserve (CFR), possibly increasing the accuracy in detecting of multivessel coronary artery disease (CAD). The aim of this study is to evaluate the accuracy of stress MBF and CFR quantitation performed by myocardial perfusion scintigraphy for the detection of multivessel CAD. ***Materials and Methods:*** Fifty-two patients with suspected or known CAD were enrolled in the study. All patients underwent CZT MPS, with the evaluation of MBF and CFR, followed by invasive coronary angiography. According to MPS and coronary angiography results, patients were divided into three groups. 1) non-obstructive CAD and normal MPS scan (control group) (n=7), 2) one vessel disease (1VD) (n=16), with significant coronary stenosis (≥70%) in one major epicardial coronary artery, 3) multivessel disease (MVD) group (n=29), with two or more major epicardial coronary arteries with (≥70%) stenoses or with ≥50% LMA stenosis. ***Results:*** Absolute MBF and CFR were significantly reduced in patients with MVD as compared to those with 1VD [0.93 (IQR 0.76; 1.39) vs 1.94 (1.37; 2.21) ml/min/g, p=0.00012] and [1.4 (IQR 1.02; 1.85) vs 2.3 (1.8; 2.67), p=0.0004], respectively. The Syntax score correlated with global stress MBF (ρ=-0.64; p<0.0001) and CFR (ρ=-0.53; p=0.0003). ROC analysis showed higher sensitivity and specificity for stress MBF (85.2% and 81%), and CFR (88.9% and 80%) compared with semiquantitative MPS stress evaluation (69% and 69%). Multivariate regression analysis showed that only stress MBF [OR (95% CI) 0.59 (0.42-0.82); p<0.0003] was an independent predictor of MVD. ***Conclusion:*** The use of absolute myocardial blood flow analysis with the CZT camera may identify high risk patients, such as those with multivessel disease. This approach could be used in clinical practice, increasing the accuracy in the evaluation of patients with known or suspected coronary artery disease. ***References:*** None

OP-655

Assessment Of Coronary Flow Reserve By Routine Tetrofosmin SPECT, Without First Pass: Comparison With Invasive Coronary Angiography And With Visual Calcium Score

L. Philippe, Y. El Yaagoubi, C. Prunier-Aesch;
Medecine Nucleaire Tourangelle, Chambray-les-Tours, FRANCE.

Aim/Introduction: Coronary Flow Reserve (CFR) assessed by SPECT is not always in agreement with the evaluation of the % stenosis. At least two reasons can explain these discrepancies: Invasive Coronary Angiography (ICA) provides anatomic approach, while SPECT gives a functional evaluation. Secondly, pathologies other than CAD can affect the CFR: dyslipidemia, HBP, diabetes, myocardial hypertrophy, ···We evaluate CFR by routine 99mTc-tetrofosmin-SPECT to assess the CAD severity, ICA nevertheless being the "gold" standard for CAD diagnosis. ***Materials and Methods:*** CFR is evaluated by computation using a 5 steps correction of the myocardial Stress/Rest counts-ratio as described previously, with slight algorithm improvement mainly related to the mathematical fit of the extraction curve (exponential model instead of polynomial fit) and to the more accurate time data directly obtained from the gamma-camera acquisition data. The 5 steps processing produces a Coronary Reserve Index (CRI) which was calculated in a series of 101 patients addressed to our institution for routine myocardial stress and rest perfusion SPECT. Among these patients, 56 patients underwent also ICA, 50 patients had visual estimation of the Calcium Score (vCS) and 5 patients, both vCS and ICA. vCS was performed using a 3 grades scale: normal (0), low to intermediate (1), important to severe (2). This evaluation was performed by means of the low dose CT used for attenuation correction (not sufficient for a quantitative score). We used only non-attenuation corrected short-axis SPECT slices for CRI computation. ***Results:*** The 56 ICA indicated, for an optimal discrimination between normal and CAD patients, a 3.0 CRI cut-off. Using this value, we observe 92% Sensitivity, 75% Specificity, 98% Positive Predictive value, and 43% Negative Predictive Value. The area under the ROC curve is 0.73 . The comparison of the CRI and the 50 vCS shows a decrease of CRI when the vCS worsens:(mean CRI ± 1 SD) Grade0: 3.28 ± 1.29 Grade1: 3.00 ± 1.25 Grade2: 2.62 ±1.44 . The differences are not significant, mainly due to the small number of patients in each group. ***Conclusion:*** CFR assessment by means of a CRI computed at the end of the routine 99mTc-tetrofosmin-SPECT is of value for CAD diagnosis. This assessment can be performed automatically for each patient, without additional time, and without additional injected dose activity. The CRI information, associated to the vCS improves the efficiency and reliability of the SPECT report. ***References:*** None

OP-656

Stunned Myocardium is Associated with Low Myocardial Flow Reserve using Dynamic CZT camera in Symptomatic Patients with Multiple Vessels Disease

D. Agostini[1], G. Liu[2], A. Manrique[1], H. Shi[2];
[1]Department of Nuclear Medicine, CHU Caen Normandy, Caen, FRANCE, [2]Department of Nuclear Medicine, Zhongshan Hospital Fudan University, Shanghai, CHINA.

Aim/Introduction: Stunned myocardium is defined as a post-ischemic drop of LVEF >5% compared to rest conditions. We aimed to determine the myocardial blood flow (MBF) and flow reserve (MFR) using CZT camera in patients with multiple vessels disease (MVD) and stunned myocardium. ***Materials and Methods:*** 52 symptomatic patients (42M, 10F; 60± 12 yrs) with chest pain and-or dyspnea and angiographically proven MVD underwent dynamic CZT and angiography within a 3 month timeframe. A stenosis was considered obstructive if greater than 50%. All pts underwent one-day dynamic rest (296±29 MBq)/ regadenoson stress (865 ± 95 MBq) myocardial perfusion imaging by ^{99m}Tc-sestamibi CZT SPECT to measure MBF and LVEF at both stress and rest. For SPECT, reconstructed frames were automatically segmented to extract the vascular input function and the LV uptake curve. A net retention model was used to estimate global uptake values, and then MBF was derived using Leppo correction. MFR was defined as the ratio of stress MBF over rest MBF using a commercially available software (4DM, Invia, Ann Arbor, MI). ***Results:*** We divided pts into 2 groups: G1 with a post stress reduction of LVEF >5%, n=14; and G2 without reduction of LVEF; n=38. Stress MBF was identical in G1 (1.91± 0.98) and in G2 (2.28± 0.62 ml/min/g; P= ns). Rest MBF was identical in G1 (0.93± 0.29) and in G2 (0.95± 0.29 ml/min/g; P= ns). However, MFR in G1 was significantly lower (1.93± 0.55) than in G2 (2.61± 1.1; P=0.005). No gender variation was observed for MBF and MFR. ***Conclusion:*** Stunned myocardium is associated with a low MFR using dynamic 99mTc-sestamibi CZT in symptomatic pts with MVD. ***References:*** None

OP-657

Long-term prognostic value of gated SPECT after acute myocardial infarction and primary percutaneous coronary intervention

A. D'Antonio, E. Zampella, R. Assante, V. Gaudieri, C. Nappi, T. Mannarino, G. De Simini, A. Giordano, V. Cantoni, R. Green, P. Buongiorno, W. Acampa, A. Cuocolo;
Department of Advanced Biomedical Sciences, University "Federico II" of Naples, Naples, ITALY.

Aim/Introduction: We evaluated whether changes in myocardial perfusion after acute myocardial infarction (AMI) and primary percutaneous coronary intervention (PCI) predict cardiac events at long-term follow-up. ***Materials and***

Methods: We enrolled 112 patients referred to stress-rest gated SPECT myocardial perfusion imaging (MPI) at 1 month (baseline) and 6 months (control) after an AMI treated with primary PCI. Summed stress (SSS), summed rest (SRS), summed difference scores and left ventricular (LV) ejection fraction (EF) were obtained. MPI was considered worsened or improved according to ≥5% change from baseline to control. End-diastolic (EDV) and end-systolic (ESV) volumes were measured and expressed as indexes (I). Remodeling was defined as an increase in LVEDVI ≥20% from baseline to control. Patient follow-up was obtained and occurrence of cardiac death, MI and unstable angina requiring revascularization were considered as events. *Results:* During follow-up (86±38 months), 21 events occurred (19% cumulative event rate). Patients with events compared to those without at baseline had lower stress (43±11% vs. 48±10%, p< 0.05) and rest (42±10% vs. 48±10%, p<0.05) EF, and higher stress (38±16 ml/m^2 vs. 30±14 ml/m^2, p<0.05) and rest (38±17 ml/m^2 vs. 30±14 ml/m^2, p<0.05) ESVI. At control, patients with events had higher stress ESVI (44±26 ml/m^2 vs. 29±14 ml/m^2, p<0.01) and rest ESVI (41±20 ml/m^2 vs. 29±16 ml/m^2, p<0.01) and lower rest EF (44±11% vs. 50±11%, p<0.01), stress EF (44±11% vs. 51±11%, p<0.05), rest EDVI (69±24 ml/m^2, vs. 54±18 ml/m^2, p<0.01). Myocardial perfusion status worsened in 17 (15%) patients, improved in 43 (38%), and unchanged in 52 (46%). Annual event rate (AER) was higher (7%) in patients with worsening compared to both those with improvement (1%) and unchanged (2%) SSS (both p<0.001). Resting remodeling was found in 13 (12%) patients. AER was higher in patients with remodeling compared to those without (9% vs. 1%, p<0.001). At multivariate Cox analysis, SSS worsening (p<0.01) and rest remodeling (p<0.001), resulted independent predictors of events. At Kaplan-Meier analysis, event-free survival was lower in both patients with remodeling and SSS worsening (p for trend <0.001). *Conclusion:* After AMI and primary PCI, worsening of SSS and cardiac remodeling are related to higher risk of cardiac events at long-term follow-up. Serial MPI is useful to improve risk stratification at long-term follow-up in patients after AMI and primary PCI. *References:* None

1110

Cutting Edge Science Track - Featured Session: Radiomics

Thursday, October 29, 2020, 13:30 - 15:00 Channel 10

OP-658

Introduction

M. Hatt; LaTIM, INSERM, UMR 1101, Univ Brest, Brest, FRANCE.

OP-659

Complementary diagnostic value of PSMA PET and MR radiomics for prostate cancer staging

E. Solari[1], A. Gafita[1], D. Visvikis[2], W. Weber[1], M. Eiber[1], M. Hatt[2], S. G. Nekolla[1];
[1]Nuklearmedizinische Klinik, Klinikum rechts der Isar, München, GERMANY, [2]LaTIM, INSERM, Univ. Brest, Brest, FRANCE.

Aim/Introduction: Prostate-specific membrane antigen (PSMA)-targeted positron emission tomography (PET) and magnetic resonance imaging (MRI) are the main imaging techniques for prostate cancer (PC) diagnosis. We previously showed that PSMA PET radiomics can predict Gleason scores. We investigated here the potential additive value of MR images (T1w, T2w, ADC maps) for PC staging. *Materials and Methods:* Simultaneous PSMA PET/MR studies for primary staging of PC from a single scanner were retrospectively included. Gleason score (GS) was obtained in histopathology after radical prostatectomy. The entire prostate was manually segmented in PET and MR (T1w, T2w, ADC maps) images. Image biomarker standardization initiative (IBSI)-compliant handcrafted features (first order intensity, shape, texture) with fixed bin widths (8-128 discrete values) were extracted from both PET and MR prostate volumes. The train and validation scheme was stratified 5-fold cross-validation, balancing the training data with SMOTE. Between 1 and 20 features were extracted through recursive feature elimination (RFE). A radial-basis support vector machine (SVM) model with hyperparameter tuning was trained for the classification of GS by groups (≤7, 8, ≥9). The performance (balanced accuracy , specificity and sensitivity) of the best classifiers on the validation data is reported as mean and standard deviation over the 5 folds. *Results:* 130 patients were included in the analysis. 64% (83) of the patients exhibited a GS of 7, 21% (27) a GS of 8 and 15% (20) a GS of 9. The 5-fold averaged balanced accuracy of radiomics from T2w images (77.8 +/-7.6%) was superior to that of PET (73.7 +/-8.6%), ADC (71.3 +/-12.0%) and T1w (73.2 +/-12.3%). Combined PET+T2w radiomics accuracy (acc. 80.0 +/-6.2%), sensitivities (GS≤7: 86.3%, GS=8: 70.6%, GS≥9: 78.0%) and specificities (GS≤7: 74.0%, GS=8: 90.5%, GS≥9: 92%) were superior to other combinations, including T2w-only radiomics (acc.: 77.8%; sens.: 78.7%, 75.0%, 72.2%; spec.: 84.2%, 82.3%, 85.9%). The combination of PET and all three MR image types did not improve the results from PET+T2w.*Conclusion:* Despite the unbalanced dataset, an accurate prediction of GS was achieved. The combined information gathered from PET and MR radiomics features slightly improved performance compared to PET-only and MR-only. The combination of PET and T2w images produced the best results. *References:* *This project is funded by the European Union's Horizon 2020 research and innovation programme under the Marie Sklodowska-Curie grant agreement No 764458

OP-660

Complementarity of PET and MR radiomic features for the characterization of lung cancers

F. Orlhac[1], M. Lacroix[1,2], I. Buvat[1], J. Bernaudin[3], C. Nioche[1], M. Soussan[1,4], P. Brillet[2], F. Frouin[1];
[1]Institut Curie, Inserm, U1288 LITO, Orsay, FRANCE, [2]AP-HP, Hôpital Avicenne, Service de radiologie, Bobigny, FRANCE, [3]Université Paris 13, Inserm, UMR 1272 Hypoxie et Poumon, Bobigny, FRANCE, [4]AP-HP, Hôpital Avicenne, Service de médecine nucléaire, Bobigny, FRANCE.

Aim/Introduction: To study the complementarity of radiomic features extracted from PET and MR images of lung cancer patients for the development of radiomic signatures distinguishing between adenocarcinoma and other histological types. ***Materials and Methods:*** A prospective cohort of N=52 patients with an advanced lung cancer was studied. All patients underwent a pretreatment 18F-FDG PET scan and a T2-weighted MR at 3 Teslas. The tumor lesion was segmented with an adaptative threshold in the PET images. The MR images were preprocessed using a bias field correction and a normalization of voxel intensities with fat as a reference region [1], before lesion segmentation based on an intensity threshold manually set for each patient. Radiomic features were computed in 3D for PET images (48 features) and in 2.5D for MR images (44 features corresponding to the median value over all slices of each patient) with LIFEx [2]. A screening procedure based on leave-one-out cross-validation was used to identify radiomic models able to distinguish between adenocarcinoma and other lesion subtypes. The procedure involved: 1) selection of all features with a p-value of univariate Wilcoxon test lower than 0.005, 0.01, 0.05 or 0.10 for (N-1) learning patients, 2) based on these features, selection of only one feature among correlated features using a Pearson correlation cut-off varying from 0.95 to 0.50, 3) building of a radiomic signature using the linear discriminant analysis, 4) test of the model on the N^{th} patient. The performance was evaluated using the Youden Index (sensitivity+specificity-1). ***Results:*** 32 lesions were adenocarcinomas and 20 were another subtype. The screening procedure consistently demonstrated the best classification performance after strong univariate selection of features ($p<0.01$ in Wilcoxon test). Focusing on this selection setting, Youden Index was no greater than 0.33 for PET features, between 0.24 and 0.46 for MR features and between 0.30 and 0.54 when combining PET and MR features. In each case, the best performance was obtained with a small number of features: 1 feature for PET-only models, between 2 and 6 for MR-only models, and between 3 and 5 for PET-MR based models. ***Conclusion:*** Lung cancer subtypes can be better distinguished when combining a small number of PET and MR radiomic features than with many PET or many MR features separately, highlighting the potential contribution of MR on top of PET for charactering lung lesions. ***References:*** [1] Lacroix et al. Front Oncol 2020. [2] Nioche et al. Cancer Res 2018.

OP-661

Radiomics and FDG PET/CT in cervical cancer: a single centre experience

F. Mattana[1], A. Farina[1], S. Telo[1], N. Fraccascia[1], G. M. Lima[2], S. Strolin[3], E. Loi[3], E. De Crescenzo[4], A. M. Perrone[4], P. De Iaco[4], L. Strigari[3], C. Nanni[1], S. Fanti[1];
[1]Department of Nuclear Medicine, S.Orsola-Malpighi University Hospital, Bologna, ITALY, [2]Department of Nuclear Medicine, Modena University Hospital, Modena, ITALY, [3]Medical Physics Unit, S.Orsola-Malpighi University Hospital, Bologna, ITALY, [4]Department of Obstetrics and Gynecology, S.Orsola-Malpighi University Hospital, Bologna, ITALY.

Aim/Introduction: To investigate the prognostic value of baseline 18F-FDG-PET/CT analysing the correlation between its radiomic variables (RV) with progression-free survival (PFS) and overall survival (OS) rates in patients with locally advanced cervical cancer (LACC) treated with concomitant-chemoradiation-therapy (CCRT). ***Materials and Methods:*** In our single center retrospective study, we have selected LACC patients treated with CCRT, who underwent baseline 18F-FDG-PET/CT from August 2007 to October 2017, performed using hybrid PET/CT scanners, according to EANM guidelines. Metabolic tumor volumes (MTV, i.e. volume of interest consisting of all spatially connected voxels within a fixed threshold of 40% of the SUVmax) was calculated following the TNM criteria: primary tumour, local/distant pathologic lymph nodes and metastasis were segmented using PET-edge tool included in the MIM software. RV extraction was performed with PyRadiomics version 2.0.1. A total of 99 RV were extracted from each region of interest and for each modality (PET or CT) and PFS and OS were calculated. The correlation between RV, OS and PFS was analyzed by both the univariate and multivariate analyses (UVA and MVA, respectively) using the Kaplan-Meier method and long-rank tests. ***Results:*** According to our inclusion criteria, we enrolled 114 patients. Patients characteristic were: median age: 61 (range 28-94); lesion histotypes: 90 squamous cell carcinomas, 16 adenocarcinomas and 7 of other histotypes; FIGO class: F2=1, F3=3, F4=77, F5=9, F6=13, F7=11 patients. At the UVA, assuming a cutoff of $p<0.10$, 25 RV and SUVmax were significantly associated with OS rates. Higher-CT-Difference-Entropy (p=0.019), CT-Difference-Average (p=0.048), CT-Zone-Entropy (p=0.044), PET-Small-Dependence-High-Gray-Level-Emphasis (p=0.003), PET-Small-Dependence-Emphasis (p=0.0061), PET-Small-Area-Emphasis (p=0.006) and Lower-PET-Large-Dependence-Low-Gray-Level-Emphasis (p=0.006), CT-Contrast (p=0.0218), PET-Large-Dependence-High-

Gray-Level-Emphasis (p=0.0198) and SUVmax (p=0.028) resulted as significant prognostic factors (p=0.0091) and were significantly associated with higher OS rates. Of note, lower p-values were registered using parameters extracted from PET than CT images. A prognostic nomogram was developed using the most significative values to assign the OS probability at 60 months after baseline PET/CT (Concordance indexes=0.68). ***Conclusion:*** Despite our small cohort of patients, this preliminary study revealed that various RV, in particular CT-Contrast and PET-Large-Dependence-High-Gray-Level-Emphasis, are significantly associated with OS rates in patients with LACC treated with CRT. Further analyses are ongoing to validate this data in a larger population, which may help for stratifying the patient's pre-therapy risk. The prognostic nomogram, if validate with prospective study, could be introduced in LACC management and easily used in the clinical practice. ***References:*** None

OP-662

Relationship between histopathological parameters and ^{18}F-FDG PET radiomic features in breast cancer patients

F. Görtan*, N. Coskun, N. C. M. Gülaldi;*
Turkish Ministry of Heath, Ankara City Hospital, Department of Nuclear Medicine, Ankara, TURKEY.

Aim/Introduction: The aim of this study is to evaluate the relationship between histopathological parameters and textural radiomic features of ^{18}F-FDG PET images in patients with breast cancer. ***Materials and Methods:*** Forty-three patients with histopathologically proven breast cancer who were referred to our department for pretreatment ^{18}F-FDG PET-CT scan were retrospectively enrolled in this study. Histopathological parameters including tumor type, histologic grade, estrogen and progesterone receptor status, Ki67 index and HER2 (Human Epidermal Growth Factor) status were derived from pathology specimens. ^{18}F-FDG PET/CT images were acquired from vertex to midthigh 60 minutes after i.v. injection of 6 MBq/kg ^{18}F-FDG at 2 minutes per bed position. SUV based parameters, as well as histogram, shape and textural radiomic features were extracted from PET images using a medical image analysis software. ***Results:*** Analysis between hormone receptor status and imaging features revealed statistically higher SUVmax (p=0,016; p=0,005), SUVmean (p=0,020; p=0,005), Histogram Entropy (p=0,005; p=0,019), GLCM Entropy (p=0,001; p=0,014), GLRLM HGRE (p=0,023; p=0,040), GLRLM SRHGE (p=0,015; p=0,002) and GLZLM HGZE (p=0,017; p=0,002) values in estrogen receptor negative and progesterone receptor negative patients respectively. Patients with higher Ki67 index demonstrated statistically higher SUVmax (p=0,033), SUVmean (p=0,042), Histogram Entropy (p=0,008), GLCM Entropy (p=0,002), GLRLM SRE (p=0,015), GLRLM RP (p=0,026), but lower GLCM Homogeneity (p=0,014), GLRLM LRE (p=0,014), GLRLM LGRE (p=0,000), GLRLM SRLGE (p=0,000), GLRLM LRLGE (s=0,003), NGLDM Coarseness (p=0,006), GLZLM LZE (p=0,044), GLZLM LGZE (p=0,000), GLZLM SZLGE (p=0,001), GLZLM LZLGE (p=0,011) values. Triple negative patients had statistically higher SUVmax (p=0,004), SUVmean (p=0,004), Histogram Entropy (p=0,004), GLCM Entropy (p=0,001), GLRLM Dissimilarity (p =0,022), GLRLM HGRE (p =0,003), GLRLM SRHGE (p =0,001), GLZLM HGZE (p =0,002), GLZLM SZHGE (p =0,008), GLZLM ZP (p =0,042) but lower GLCM Homogeneity (p =0,037) values. ***Conclusion:*** Our study results indicate that radiomic features of ^{18}F-FDG PET images of pretreatment breast cancer patients, consistent with estrogen, progesterone and HER2 receptor negativity as well as high Ki67 index values, contain inherent intratumoral heterogeneity. These may correlate with poor therapy response or high frequency of relapses during the course of the disease. Although higher SUVmax values generally correlates well with aggressiveness of the disease, revealing heterogeneous nature of the tumor at the beginning of treatment process will make clinicians to choose more aggressive treatment procedures for these patients. ***References:*** None

OP-663

Preliminary comparative results between FES and FDG in ER+ metastatic breast cancer: a radiomic approach

L. Ferrer[1,2]*, B. Maucherat*[1]*, T. Carlier*[2,3]*, F. Kraeber-Bodéré*[1,2,3]*, C. Rousseau*[1,2]*;*
[1]ICO René Gauducheau, St Herblain cedex, FRANCE, [2]University of Nantes, CNRS, INSERM CRCINA, Nantes, FRANCE, [3]University hospital, Nantes, FRANCE.

Aim/Introduction: 16α-18Fluoro-17β-Oestradiol (FES) PET-imaging provides a non-invasive, in vivo measurement of the ligand binding function of estrogen-receptor (ER) in situ of metastatic breast cancer. We conducted a multicentric study (NCT03442504) to predict the value of FES PET at patient level, before a second hormonotherapy based on FDG response obtained at follow up. The aim of this work is to explore the correlation between FDG and FES PET examinations performed few days apart using radiomics features. ***Materials and Methods:*** Two FDG and FES PET examinations were performed for 20 patients from march 2017 to november 2019. The 5 most intense lesions visible in both PET images were delineated with DOSISOFT software (v.3.1.1.20L). We used all the software's algorithms to delineate each lesion for both examination. Thanks to a label majoritary voting approach [1], we created a unique mask from each lesion from which selected radiomics features were extracted [Table 1] using pyradiomics library (v.3.0). This selection was arbitrarily based on our previously work [2] related to radiomics reproducibility in multicentric trials. FES and FDG images were normalized in

SUV and resampled with a 0.4x0.4x0.2 cm^3 pixel size using BSpline algorithm. Gray value histograms were discretized with a fixed 0.5 SUV bin size. We only considered for this analysis volumes greater than 64 voxels (2 cm^3). Statistical analysis were conducted with scipy stats module (v.1.3.1). ***Results:*** Among 96 delineated lesions, only 43 paired lesions remained after applying the 64 voxels cut-off. Hence, 4 patients did not exhibit FES-FDG any paired lesions. Spearman correlation and regression slopes are presented in table1. Among all compared features, no correlation was observed except than a weak one for coarseness (rho=0.5, p=0.002) in neibourghood grey tone difference matrices. This suggests that higher values are observed in FES than in FDG respective volume, implying that textures tends to be more locally uniform in former than in latter volume. ***Conclusion:*** In ER+ metastatic breast cancer, intra-tumoral textural properties extracted from correlated FES and FDG volumes seem to be different. These preliminary findings should be confirmed and this work should be extended to assert whether both FES and FDG intra-tumoral properties assessed using handcrafted radiomics are related to patient outcomes. ***References:*** 1. T. Rohlfing et al, "Multi-classifier framework for atlas-based image segmentation," Pattern Recognition Letters, 2005 2. C. Bailly et al., "Revisiting the Robustness of PET-Based Textural Features in the Context of Multi-Centric Trials". PLOS ONE 11: e0159984, 2016

OP-664

Identifying a reliable radiomic signature from scarce data: illustration for 18F-FDOPA PET images in glioblastoma patients

F. Orlhac[1,2], A. Rollet[3], I. Buvat[1], J. Darcourt[3,4], V. Bourg[5], C. Nioche[1], C. Bouveyron[6], N. Ayache[2], O. Humbert[3,4];
[1]Institut Curie, Inserm, U1288 LITO, Orsay, FRANCE, [2]Université Côte d'Azur, Inria, Epione, Sophia-Antipolis, FRANCE, [3]Université Côté d'Azur, Centre Antoine Lacassagne, Service de Médecine Nucléaire, Nice, FRANCE, [4]Université Côté d'Azur, CEA, TIRO, Nice, FRANCE, [5]Université Côté d'Azur, CHU Pasteur 2, Service de Neurologie, Nice, FRANCE, [6]Université Côte d'Azur, Inria, MAASAI, Nice, FRANCE.

Aim/Introduction: The design and validation of a reliable radiomic signature is challenging when few patients are available because the disease is rare, the imaging protocol is specific and/or the classes are unbalanced. In this context, we propose an approach to identify a signature and estimate its reliability. ***Materials and Methods:*** 84 patients with a clinical and MRI suspicion of recurrent glioblastoma were retrospectively included. Each patient underwent a 18F-FDOPA PET-CT scan. For each patient, the suspicious lesion was segmented and 49 radiomic features were calculated using LIFEx [1]. Our goal was to distinguish between tumor recurrence and radiation-induced necrosis as confirmed on pathological data, or on a 3-month clinical/imaging follow-up. A screening procedure was developed to identify a signature using leave-one-out (LOO) cross-validation. The procedure involved: 1) selection of all features with a p-value of univariate Wilcoxon test lower than alpha varying from 0.005 to 0.10 for (N-1) learning patients, 2) based on these features, selection of only one feature among correlated features using a Pearson correlation cut-off R varying from 0.95 to 0.50, 3) building of a radiomic signature involving the resulting features using a linear discriminant analysis, 4) test of the model on the N^{th} patient, 5) characterization of the model performance using the Youden Index (Y=sensitivity+specificity-1). The final model selection was based on the consistency of Y values as a function of alpha and R, on the consistency of selected features between the different models, and favored models involving a low number of features. To test the reliability of the selected signature, we repeated the process by excluding one patient using a jackknife procedure (ie, 84 LOO of 83 patients each). We compared the results with those obtained with the same alpha and R when randomly assigning a label to each patient (sham task). ***Results:*** 61 patients had tumor recurrence and 23 had radiation necrosis. Visual interpretation yielded Y equal to 0.35 (Lizarraga scale, Se=100%, Sp=35%). Using LOO, 10/28 radiomic models had Y>0.35. The largest Y (Y=0.49, Se=62%, Sp=87%) were obtained with 4 features on average, reflecting the volume, sphericity and heterogeneity (GLCM_Correlation, GLCM_Contrast) of the lesion uptake. Using the jackknife procedure, Y was 0.47±0.06 (range: [0.32;0.56]), significantly higher (Wilcoxon $p < 0.05$) than for the sham task (Y=0.06±0.18, range: [-0.52;0.47]). ***Conclusion:*** The proposed systematic screening procedure enabled the identification of a parsimonious radiomic signature from scarce data. ***References:*** [1] Nioche et al. Cancer Res 2018.

OP-665

Textural features combined with static and dynamic parameters of ^{18}F-FDopa PET imaging for the non-invasive prediction of the IDH mutation status in glioma

T. Zaragori[1,2], J. Oster[1], M. B. Chawki[2], B. Chen[1,3], V. Roch[2], L. Taillandier[4,5], G. Karcher[2], L. Imbert[2,1], A. Verger[2,1];
[1]Université de Lorraine, IADI, INSERM, UMR 1254, Vandoeuvre-lès-Nancy, FRANCE, [2]CHRU-Nancy, Université de Lorraine, Department of Nuclear Medicine & Nancyclotep Imaging platform, Vandoeuvre-lès-Nancy, FRANCE, [3]CIC-IT 1433, INSERM, CHRU de Nancy and Université de Lorraine, Vandoeuvre-lès-Nancy, FRANCE, [4]CHRU-Nancy, Université de Lorraine, Department of Neuro-oncology, Vandoeuvre-lès-Nancy, FRANCE, [5]Université de Lorraine, Centre de Recherche en Automatique de Nancy CRAN, CNRS UMR 7039, Vandoeuvre-lès-Nancy, FRANCE.

Aim/Introduction: The IDH mutation is a key-factor of favorable prognosis in patients with glioma. ^{18}F-FDopa PET imaging, currently recommended in glioma assessment,

has shown good performances by combining static and dynamic parameters for the non-invasive prediction of this mutation. The aim of this study was to evaluate whether textural features extracted from the ^{18}F-FDopa PET images can further enhance the performances of this prediction over static and dynamic parameters. ***Materials and Methods:*** Seventy-five patients having undergone a ^{18}F-FDopa PET scan with dynamic acquisitions for glioma assessment at initial diagnosis were retrospectively included. Seven conventional static parameters (S) and one-hundred-twenty-seven textural features (T) were extracted from 10-to-30 min post-injection static images as well as two conventional dynamic parameters (D) from the 30-min duration dynamic acquisitions. Features were extracted from gliomas metabolic volume segmented with Nestle's method. Four models were trained to predict the patient's IDH mutation status with respectively S, S+D, S+T and S+D+T features. These models were based on a SVM classifier with a linear kernel, and an automated selection of the 10 best metafeatures. The latter were first built by combining highly correlated normalized features using a hierarchical clustering approach. These 10 best metafeatures were then selected according to the Wilcoxon score ranking obtained during 100 bootstrap iterations. A nested cross-validation with 1000 bootstrap iterations of outer loop results was performed for each model and performances were expressed through an AUC score using the neuropathological result as a reference. ***Results:*** The S+T model achieved better results than the S model (AUC of 0.652 (95% Confidence Interval): [0.614;0.691] vs 0.567[0.517;0.618]) but with lower performances as compared to the S+D model (AUC of 0.755[0.718;0.788]). Moreover, results were not improved when adding textural features to the S+D model (AUC of 0.734[0.697;0.767] for the S+D+T model), highlighting the fact that most of the information is provided by dynamic parameters. ***Conclusion:*** The integration of textural features improves the prediction of the IDH mutation status of ^{18}F-FDopa PET imaging in patients with glioma only if compared to a model based on conventional static parameters. The inclusion of dynamical parameters yields the best performances, strengthening the case for integrating them into clinical routine. ***References:*** 1. Ginet et al.,Integration of dynamic parameters in the analysis of 18F-FDopa PET imaging improves the prediction of molecular features of gliomas.EJNMMI,2019 2. Leger et al.,A comparative study of machine learning methods for time-to-event survival data for radiomics risk modelling. Scientific Reports,2017

OP-666

The influence of central necrosis on radiomic analysis

W. A. Noortman[1,2], *D. Vriens*[1], *C. D. Y. Mooij*[1,3], *E. H. Aarntzen*[4], *A. van Berkel*[4], *H. J. L. M. Timmers*[4], *J. Bussink*[4], *T. W. H. Meijer*[4], *L. F. de Geus-Oei*[1,2], *F. H. P. van Velden*[1];

[1]Leiden University Medical Center, Leiden, NETHERLANDS, [2]University of Twente, Enschede, NETHERLANDS, [3]Delft University of Technology, Delft, NETHERLANDS, [4]Radboud University Medical Center, Nijmegen, NETHERLANDS.

Aim/Introduction: Central necrosis (CN) often occurs as a result of hypoxia and glucose deprivation, caused when fast tumour growth and oxygen consumption are left unmatched by sufficient blood supply. CN manifests itself predominantly in aggressive cancers and is associated with poor prognosis. It can be detected by [^{18}F]FDG PET as an often central region with little to no tracer uptake. Currently, radiomics does not provide guidelines whether or not to include CN during volume of interest (VOI) delineation. Isocontour methods inherently exclude CN. In some studies, these CN-subvolumes are added manually, but this is not always reported. The aim of this study was to assess how CN influences PET radiomic analysis. ***Materials and Methods:*** Two cohorts of patients visually selected for showing CN on the [^{18}F]FDG PET/CT scan were included retrospectively: patients with pheochromocytomas and paragangliomas (PPGL, n=24) and patients with non-small cell lung carcinomas (NSCLC, n=12). VOIs were delineated using a 50% isocontour method based on the peak standardized uptake value or a fuzzy locally adaptive Bayesian method for the PPGL and NSCLC cohort, respectively ($VOI_{vital\text{-}tumour}$). In addition, VOIs were generated by manually adding the volumes of CN to the delineations ($VOI_{gross\text{-}tumour}$). The necrotic tumour fraction was determined by: $NTF = 1 - VOI_{vital\text{-}tumour}/VOI_{gross\text{-}tumour}$. From each of these 72 VOIs, 90 radiomic features were extracted. Per cohort, differences in radiomic features between delineation with and without CN were assessed using a paired T-test with Benjamini-Hochberg correction for multiple testing. ***Results:*** Median NTFs were 0.27 and 0.11 for the PPGL and NSCLC cohort, respectively (range 0.01-0.78 and 0.03-0.60, non-different for both cohorts, p=0.280). At least 46% of the features were significantly different between either $VOI_{vital\text{-}tumour}$ and $VOI_{gross\text{-}tumour}$ (46% and 50% (p=0.551) for the PPGL and NSCLC cohort, respectively), where first order features (n=18) were affected the most (61% and 56% (p=0.735) for the PPGL and NSCLC cohort, respectively), shape features (n=13) the least (23% for both cohorts (p=1.000) and texture features (n=59) 46% and 54% (p=0.357), respectively. ***Conclusion:*** In both tumour types, almost 50% of features were affected, demonstrating that the impact of whether or not to include CN in the VOI on the radiomic analysis is significant. Until preference of delineation method, including the choice to add or leave out CN, has been investigated, radiomic studies should report whether or not CN was included in the VOI. ***References:*** None

OP-667

A Phantom Study to Evaluate the Stability of PET Images Radiomic Features with Time of Acquisition

E. Alsyed[1], R. Smith[2], L. Bartley[2], C. Marshall[2], E. Spezi[1];
[1]Cardiff University, Cardiff, UNITED KINGDOM, [2]Wales Research & Diagnostic PET Imaging Centre, Cardiff, UNITED KINGDOM.

Aim/Introduction: The term radiomics refers to a method of extracting quantitative features from radiographic medical images, some of which cannot be seen by the human eye. In recent years, there has been an increasing interest in utilising radiomic features extracted from positron emission tomography (PET) images which may serve as biomarkers to monitor cancer prognosis and treatments. One major issue effecting confidence in adopting radiomic features as key prognostic indicators clinically is their stability under varying PET image acquisition parameters. The main goal of this phantom study is to assess the stability of PET image radiomic features with varying time duration before image acquisition. ***Materials and Methods:*** Artificially constructed tumour inserts using an array of radioactivity filled syringes were used to model four tumours with varying degrees of heterogeneity. The inserts were placed into a cylindrical uniform water filled phantom and imaged using a GE690 PET/CT for 80 minutes. Images were re-binned into 4x20 minutes PET scans. Region of interests (ROI) were segmented (cylindrical delineation) in the first configuration and copied to all other configurations.SPAARC [1] was utilised to extract 78 3D-radiomic features for each tumour volume at each time point. The Coefficient of Variation (COV) was calculated for each feature to analyse it's stability with imaging time. Stabilities were categorized into four groups including stable (COV≤5%), moderately stable (5%<COV≤10%), poorly stable (10%<COV≤20%) and unstable (COV>20%) were assessed [2]. ***Results:*** More than 32(41%) features showed stability (COV≤5%) for all four configurations. Eleven (14%) and seven (9%) features exhibited instability (COV>20%) for homogeneous shapes 1 and 3, respectively. Eleven (14%) and thirteen (16%) features showed instability (COV>20%) for inhomogeneous shapes 2 and 4, respectively. Twenty-three (29%),Six(7%),nine(11%) and three (4%) features showed poor stability (10%<COV≤20%) for configuration 1,2,3 and 4, respectively. ***Conclusion:*** PET image radiomics features may be affected by varying acquisition time. Further clinical studies are needed to evaluate the stability of PET images radiomic features over different acquisition time. Radiomic features with high (unstable) COV should be omitted in radiomic studies. ***References:*** [1] P.Whybra, C.Parkinson, K. Foley,J Staffurth and E. Spezi"Assessing radiomic feature robustness to interpolation in F-FDG PET imaging,"Sci. Rep.,no.December,pp.0-10,2019.Sci Rep 9,9649(2019).[2] F.Gallivanone, M.Interlenghi, D.D.Ambrosio, I.Castiglioni, and G. Trifir, "Parameters Influencing PET Imaging Features : A Phantom Study with Irregular and Heterogeneous Synthetic Lesions,"vol.2018,2018.[3] E. Alsyed, R. Smith, C. Marshall, E. Spezi, and S. Paisey, "Stability of PET Radiomic Features: A Preclinical Study,"in EJNMMI,2019,p.S759.

OP-668

A transfer learning approach to facilitate ComBat-based harmonization of multicentre radiomic features in new datasets

M. Hatt[1], F. Lucia[2,1], I. Masson[3], A. Mervoyer[3], C. Reinhold[4], P. Robin[5], J. Alfieri[6], C. Rousseau[7], O. Pradier[2,1], U. Schick[2,1], D. Visvikis[1], R. Da-ano[1];
[1]INSERM, LaTIM, UMR 1101, Brest, FRANCE, [2]CHU Brest, radiotherapy department, Brest, FRANCE, [3]Department of Radiation Oncology, Institut de cancérologie de l'Ouest René-Gauducheau, Saint-Herblain, FRANCE, [4]Department of Radiology, McGill University Health Centre, Montreal, QC, CANADA, [5]CHU Brest, Department of Nuclear Medicine, Brest, FRANCE, [6]Department of Radiation Oncology, McGill University Health Centre, Montreal, QC, CANADA, [7]Department of Nuclear Medicine, Institut de cancérologie de l'Ouest René-Gauducheau, Saint-Herblain, FRANCE.

Aim/Introduction: In order to demonstrate the clinical potential value of radiomics, multi-center studies are needed. They are challenging, as the variability in scanner manufacturers and models, acquisition protocols and reconstruction settings hamper the ability to pool radiomic features for modeling. ComBat is a harmonization method able to eliminate such "center-effect", however it suffers from limitations when dealing with new, unseen data (i.e., patients and/or centers not included in the initial harmonization). Our objective was to develop a novel method based on transfer learning (TL) in order to facilitate the use of ComBat in that context. ***Materials and Methods:*** The TL-based ComBat implements three steps: i) save the parametric empirical estimates obtained in the initial data harmonization on the available data, ii) use the initial estimates in step 1 to calculate the new adjusted batch effect estimators and iii) calculate the final adjusted data using the estimators obtained in step 2. It was evaluated on a dataset of radiomic features extracted from PET and MRI images of 197 patients with cervical cancer from 3 centers, with the task of predicting local failure (LF) using 3 different machine learning methods (support vector machine (SVM) and random forest (RF), both with embedded feature selection, as well as logistic regression (LR) combined with least absolute shrinkage and selection operator). Two experiments were carried out: 1) stratified random sampling was used to split the data from 3 centers into training (n=140 with 51 LF) and testing (n=57 with 16 LF) sets. In the TL case, all patients from the testing set were set aside and not used in the initial harmonization. 2) Brest and McGill (n=147 with 52 LF) were used as the training set, whereas Nantes (n=50 with 15 LF) was the testing set. In

the TL case, all patients from Nantes were set aside in the initial harmonization. ***Results:*** In both experiments, the TL approach led to models with accuracy very close to the reference (all data available for harmonization), across all three ML methods. In most cases the resulting performance was exactly the same, the accuracy values being within 1 to 3 points (e.g., RF accuracy of 0.90 with TL vs. 0.93 using all data). ***Conclusion:*** The proposed approach was successful in applying the previously determined harmonization transform to the radiomic features values of new patients, in both configurations of new patients from a known center or a new center. ***References:*** None

1201

Plenary 3: What's Cooking? Next Generation Radiopharmaceuticals

Thursday, October 29, 2020, 15:10 - 16:25 Channel 1

OP-669
What's New?
M. Fani; University Hospital Basel, Nuclear Medicine, Basel, SWITZERLAND.

OP-670
FAP-Inhibitors are the Future - For Everything?
U. Haberkorn; Heidelberg University Hopsital, Department of Nuclear Medicine, Heidelberg, GERMANY.

OP-671
Brain Tracers - Finally for Clinical Application?
V. Garibotto; Nuclear Medicine and Molecular Imaging Division, Geneva University Hospitals, Geneva, SWITZERLAND.

OP-672
Is Theranostics the Future in Nuclear Medicine?
M. Hofman; Peter MacCallum Cancer Centre, Molecular Imaging, Melbourne, AUSTRALIA.

OP-673
Do we need Specific Tracers in the Clinics?
E. Ocak; Istanbul University, Pharmacy Faculty, Department of Pharmaceutical Technology, Istanbul, TURKEY.

OP-674
Why does it take so long?
J. Sosabowski; Queen Mary University of London, Barts Cancer Institute, Centre for Molecular Oncology, London, UNITED KINGDOM.

OP-675
Discussion

1301

CME 10: Radiomics in Thyroid Imaging

Thursday, October 29, 2020, 16:35 - 18:05 Channel 1

OP-676
Imaging Biomarkers in Thyroid Nodules and Cancer (General Concept, Omics)
M. Sollini; Nuclear Medicine Department, Humanitas Clinical and Research Center - IRCCS; Department of Biomedical Sciences, Humanitas University, Milan, ITALY.

OP-677
PET Radiomics in the Characterization of Thyroid Nodules (FDG/PSMA/FDOPA/DOTA)
C. Lapa; Nuclear Medicine Department, University Hospital Augsburg, Ausburg, GERMANY .

OP-678
Perspectives of Artificial Intelligence and Radiomics in Thyroid Imaging (Studies with US and MR)
M. Kirienko; Department of Biomedical Sciences, Humanitas University, Milan, ITALY.

1302

Joint Symposium 19 (EANM/ENETS): Impacting the Outcome of High Grade NET Patients

Thursday, October 29, 2020, 16:35 - 18:05 Channel 2

OP-679
Nuclear Medicine Physicians´ View (PRRT; SIRT)
H. Ahmadzadehfar; Westfalen Clinic (Knappschaftskrankenhaus), Department of Nuclear Medicine, Dortmund, GERMANY.

OP-680
Oncologists´ View
N. Fazio; European Institute of oncology, IEO, Division of Gastrointestinal Medical Oncology and Neuroendocrine Tumors ,Milan, ITALY.

OP-681
Surgeons´ View
A. Frilling; Imperial Collage London / Hammersmith Campus, Department of Surgery and Cancer, London, UNITED KINGDOM.

1303

Joint Symposium 20 (EANM/ECNP): Simultaneous PET/MR Imaging of Neuroreceptor Systems

Thursday, October 29, 2020, 16:35 - 18:05 Channel 3

OP-682

Functional Characterization of Drugs Targeting the 5-HT 1B Receptors

H. Hansen; Massachusetts General Hospital, Athinoula A. Martinos Center for Biomedical Imaging, Charlestown, MA, UNITED STATES OF AMERICA.

OP-683

PET and MR Studies of the μ-Opioid and Dopamine Receptor Systems

L. Nummenmaa; University of Turku, Turky PET Center,Turku,FINLAND.

OP-684

Demonstrating Biased Agonism of Neuroreceptors with Simultaneous PET/MRI

L. Zimmer; Lyon University Hospital, Lyon Neuroscience Research Center, Lyon, FRANCE.

1304

Technologists Oral Presentations 3 - Featured Session: BOTH ART - The Beauty Of The HeART and mind

Thursday, October 29, 2020, 16:35 - 18:05 Channel 4

OP-685

Introduction to Brain Imaging

A. Pietrzak; Greater Poland Cancer Centre and Poznan University of Medical Sciences, Nuclear Medicine Dep./Electroradiology Dep., Poznan, POLAND.

OP-686

Traumatic Brain Injury Induced Amyloid Plaque Scintigraphy

A. Datta[1], G. Mann[1,2], A. Kaul[1], M. Thirumal[2], A. Mishra[1]; [1]Institute of Nuclear Medicine and Allied Sciences, Delhi, INDIA, [2]University of Delhi, Delhi, INDIA.

Aim/Introduction: Epidemiological evidence implicates formation of diffused amyloid plaques after incident of Traumatic Brain Injury as a risk factor for developing associated neurodegenerative disorders. Early detection of these plaques consequently remains vital for better regulation of these diseases. Considering this, we developed a cost-effective, homodimeric chalcone scaffold-based SPECT radiotracer which specifically binds detrimental $A\beta_{1-42}$ plaques. The bifunctional chelating agent, pentapa-en-NH_2 was explored for the development of SPECT agent. We hypothesise the developed bivalent homodimeric molecule to display enhanced binding affinity and blood brain barrier penetration. ***Materials and Methods:*** The bifunctional chelator was synthesised through a series of steps in high purity and further conjugated to the chalcone derivative using bivalent approach. The molecule was conjugated to ^{99m}Tc and further used for pre-clinical studies. A repetitive mild TBI mouse model was developed and uptake of tracer was studied. ***Results:*** The molecular docking studies reported multiple binding of tracer at the recognition sites of Aβ fibrils with a significantly high binding score (-12.64) as compared to known Aβ ligands. Bischalcone derivative, 6,6′-(((2-(bis(2-(4-((E)-3-(4 (dimethylamino)phenyl)acryloyl) phenoxy)ethyl)amino)ethyl)azanediyl)bis(methylene)) dipicolinic acid, $(Ch)_2$pa was synthesized in 95% yield with high purity. Radiolabelling was carried out with ^{99m}Tc under mild conditions with 95.4% efficiency and 103-124 MBq μmol^{-1} specific activity. In vitro binding assay with $A\beta_{1-42}$ aggregates displayed high binding affinity of $(Ch)_2$pa. The fluorescent data displayed absorption/emission at 410/540 nm and exhibited blue shift with 10-fold increase in emission intensity on binding with Aβ aggregates. Blood kinetics performed on normal rabbit displayed fast clearance ($t_{1/2}$(F) = 32 ± 0.04 min; $t_{1/2}$(S) = 3h 55min ± 0.03 min). A repetitive mild TBI mice model was established and ex vivo staining of TBI mice model brain sections with $(Ch)_2$pa showed specific binding of complex to amyloid plaques. In vivo scintigraphy displayed two-fold increase of radioligand concentration in TBI model as compared to sham mice owing to higher amyloid burden in TBI model. Ex vivo biodistribution analysis demonstrated high blood brain barrier penetration in TBI model mice with brain uptake of 5.24 ± 0.31% ID g^{-1} at 2 min p.i. and 3-fold higher than brain uptake in sham mice. ***Conclusion:*** These preliminary studies reveal the enhanced amyloid binding affinity by bivalent approach and offers a new perspective in ^{99m}Tc probes for β-amyloid imaging. The study also highlights the increased amyloid burden in traumatic brain injury cases and provides a novel approach for prognosis and ultimately better regulation of TBI induced dementia. ***References:*** None

OP-687

Does gadolinium deposition in the brain affect to F18-FDG brain uptake?

R. Sanchez Jurado[1], E. Blanco Perez[2]; [1]ERESA, Valencia, SPAIN, [2]Alzira's Hospital, Valencia, SPAIN.

Aim/Introduction: Gadolinium-based contrast agents have revolutionized MRI and diagnostic medicine. They have allowed us to detect diseases that would otherwise be

extremely difficult to diagnose. However, new publications affirm that minute traces of gadolinium are often retained in the brain tissue of patient years after undergoing an MRI.The purpose of this study was to determine whether repeated administrations of gadolinium in brain MRI studies would affect the uptake of 18F-FDG in brain PET-CT. ***Materials and Methods:*** More than three thousand patients from two different hospitals, those who underwent both contrast-enhanced MR (CE MR) of the brain and F18-FDG brain PET/CT from January 2009 to January 2019 were identified. The SUVmax was measured in the globus pallidus (GP), thalamus (T), dentate nucleus (DN), pons (P), substantia nigra (SN) and red nucleus (RN) on the PET/CT scanners in patients which had 3-12 successive CE MR brain studies. The SUVmax of the corresponding areas in the control group of patients that had not undergone previous CE MR was also measured. ***Results:*** Seventeen patients (mean age ± SD, 52 ± 12 y; 11 men and 6 women) finally were included in the subject group, which were divided in two groups: Group A 'elderly' (mean age ± SD, 59 ± 5,8 y; 9 men and 3 women) and Group B 'early' (mean age ± SD, 36 ± 4,8 y; 2 men and 3 women). Seventeen patients were included in the control group and they were divided in Group C 'elderly' (mean age ± SD, 56 ± 5,1 y; 7 men and 5 women) and Group D 'early' (mean age ± SD, 32 ± 5,1 y; 4 men and 1 women). The median DN, GP, T and P SUVmax were significantly lower in the subject group than in the control group. However, SN and RN were significantly higher in the subject group than in the control group. ***Conclusion:*** The median SUVmax in the DN, GP, T and P were 6%, 54%, 48% and 44% lower, respectively, in the Group A respect to Group C; and 16%, 19%, 4% and 12%, respectively, in the Group B respect to Group D. Highlight the results obtained in SN and RN that were 6% and 10% higher, respectively, in the Group A to Group C; and 16% and 24% higher, respectively, in the Group B to Group D. ***References:*** None

OP-688

Preliminary Results of Developing a Planar Camera for Building an Open-type Brain-PET scanner

H. Liang*, H. Wu, C. Cheng, C. Lin;*
INER (Institute of Nuclear Energy Research), Taoyuan, TAIWAN.

Aim/Introduction: A project of developing a planar PET scanner for brain function imaging was raised. In our current design, two planar cameras are arranged in a sliding scan scheme. Due to camera sliding, it is required the proposed camera to have whole imaging area successive. However, due to Anger logic not able dealing with inter-detector information, missing rows/columns of crystals in the cross-over regions in a crystal 2D map was observed. Therefore, it is necessary to build a position decoding algorithm capable of solving crossover problems, to make our camera have a whole successive imaging area. ***Materials and Methods:*** The proposed planar PET camera is composed of 9 imaging detectors, connecting with a plate of 2-mm-thick window. Each detector is composed of a scintillation layer (31×31, 1.5-mm-pixel-LYSO-crystal array), a photonic layer (144-pixels SiPM), and a readout circuit (1:12 weighting). Instead of Anger logic, the ratios of the 4 acquired weighted signals, i.e. x+/x- and y+/y-, from each detector are applied to decode the event positions. Due to the pre-designed weights in the readout, a position mapping curve vs. weighted signal ratios (i.e. x+/x- and y+/y-) is built. Such curve is applied for position decoding of event signals to realize event positions. When the signal ratios approaching two ends of the mapping curve (i.e. 12.004 and 0.0833), it indicates that the incident events occurred in crossover region crystals. Thus, position correction calculations by using neighbor detector signals are applied for such events. In such position decoding algorithm (weighted signal ratio driven), it is expected to recover the event counts of the crossover region crystals. ***Results:*** From a crystal 2D map obtained by Anger logic, it is observed that 2 rows/columns of crystals are missing in the cross-over regions, and thus makes a countable crystal array of 29×29 for each detector. With applying the proposed position decoding calculation to the same experimental data, it is observed that the lost 2 rows/columns of crystals are recovered, and thus makes the countable crystal array to be 30×30. It implies that our new position decoding calculations work for making the camera imaging area successive. ***Conclusion:*** In this study, a set of position decoding calculations is built, and its effectiveness is proved. However, the crystals in the peripheral edges are still missing. The following efforts will be put on searching a similar way of position decoding calculations to recover the edge rows/columns. ***References:*** None

OP-689

Introduction to Cardiac Imaging

L. Camoni*; Università & Spedali Civili di Brescia, Brescia, ITALY*

OP-690

Start of a new Cardiac PET service with Rb-82 in a UK based hospital: operational management of patients pathway

G. Testanera*, L. Menezes, L. Price, M. Burniston, R. Gregory, C. Copland;*
Barts Health NHS Trust, London, UNITED KINGDOM.

Aim/Introduction: Coronary Arterial Disease (CAD) is the disease responsible for most deaths in UK and consequently Myocardial Perfusion Scintigraphy (MPS) is one of the most common examinations performed in Nuclear Medicine (NM). In our hospital, the MPS output was an average of 1650 MPS scans a year divided across 4 sites. To improve our service, In 2018 we started a project to introduce cardiac PET-CT with Rb-82 which provides diagnostic information

on CAD competitive with Cardiac CT, with less radiation dose to the patient. The project included switching 50% of MPS scans from conventional NM to Cardiac PET-CT. This new procedure allows rest and stress images of the heart to be achieved in one short appointment of 30 minutes and radiotracer Rb-82 is produced internally from a Sr-82/Rb-82 generator enabling the service to be more operationally flexible. ***Materials and Methods:*** The PET-CT service is equipped with a GE-Discovery 710 PET system with a 128 slice CT enabling for a diagnostic CT for calcium scoring. To set up the service we required a cart for Rb-82 infusion, Sr-82/Rb-82 generator, adenosine infusion pump, 3 lead ECG and dedicated training for technologist, physics and nursing staff. Corridor 4DM, a suite for cardiac post processing was installed to support reporting on the Hermes Medical platform. ***Results:*** The service started in November 2019 with 10 patients a week and in 2 months the number of scans performed reached 24 a week, consisting of about 45% of overall MPS scans, very near to the original plan of 50% conversion. The triage was actioned prioritising clinical appropriateness over operational reasons. Oncology scan capacity was preserved with a mobile PET-CT support installed. Only 1 minor adverse event was observed and patients feedback showed improved satisfaction. Cardiac PET proved also to be much more suitable during the pandemic, since only one appointment was needed. ***Conclusion:*** Rb-82 Cardiac PET-CT proved to be a game changer in CAD patient pathway[1] , improving diagnostic accuracy, patient experience and reducing radiation dose by 80% .The service requires a massive amount of effort from the PET team and a very careful triaging of patients, to ensure appropriateness of scans and to preserve oncology patient slots when limited resources are available in the PET service. It also proved to be safer for patients in the unexpected pandemic event. ***References:*** [1] Jaarsma et al.J Am Coll Cardiol. 2012 May 8;59(19):1719-28.

OP-691

Assessment of the effect of fasting on stomach interference on Rubidium-82 PET-CT MPI

G. Testanera, B. Ribeiro, R. Gregory, M. Costa, S. Ferreira, S. Townrow, A. Simeonova, C. Copland, L. Price, M. Burniston, L. Menezes;
Barts Health NHS Trust, London, UNITED KINGDOM.

Aim/Introduction: Rubidium-82 chloride (^{82}Rb) PET/CT has revolutionised how myocardial perfusion imaging (MPI) is performed. This method allows MPI within a 30 minute appointment and is more accurate than the equivalent nuclear medicine techniques. However ^{82}Rb PET/CT images can suffer from interference from stomach and liver activity. This study aims to determine whether implementing a protocol that instructs the patient to fast for 6 hours prior to their appointment reduces the interference from sub-diaphragmatic activity. ***Materials and Methods:*** The level of stomach interference was assessed for rest and stress PET/CT MPI images sets, for one group of 59 patients that had fasted for 6 hours and a separate group of 59 patients that had not been instructed to fast. Images were viewed using Corridor 4DM with a 10 step colour map. This map allows the viewer to identify areas that are less than 40%; 40-60%; 60-70%; and>70% of the maximum image count. The interference was therefore scored based on the level of counts in the region between the myocardium and gastric wall, as absent (1) if <40%, mild (2) if 40-60%, moderate (3) if 60-70% and severe (4) if >70% of the maximum. These areas had to cover at least 4 slices with 20% angular coverage. All 236 images were scored by an experienced technologist, physicist and nuclear medicine cardiologist. The median of the 3 scores for each image were compared between the image sets for each protocol, the statistical significance of the results was assessed using a Mann-Whitney U-test. ***Results:*** Demographics for both patient groups were similar (average BMI 28.8±8.13 kg/m^2 and 28.97±5.66 kg/m^2 , age 63.54±12.28 years and 66.77±10.76 years for 6 hour fasted and unfasted groups respectively). For the rest studies, there was a statistically significant difference between the two patient groups, with interference scores higher in the non-fast patients (1.93±1.06 and 1.48±0.73 for no fast and 6 hour fast patients respectively, p=0.036). For the stress studies the average interference scores were also higher for the non-fast compared to the 6hr fast patients (1.79±0.95 and 1.52±10.78 respectively, p=0.13). ***Conclusion:*** The level of interference from sub-diaphragmatic activity was on average significantly lower in the rest images when the patients were asked to fast for 6-hours prior to their appointment; this provides support for the ASNC/SNMMI guidelines. ***References:*** Dilsizian et al. ASNC imaging guidelines/SNMMI procedure standard for positron emission tomography (PET) nuclear cardiology procedures. J Nucl Cardiol. 2016;23(5):1187-1226.

OP-693

The investigation of automated region growing method for the detection of heart to streamline calculation of ^{201}Tl-MUI at stress in patients

K. Nishimoto[1], S. Tomiguchi[2], F. Sakamoto[2], S. Shiraishi[3], Y. Kawamata[3];
[1]Graduate School of Health Science Kumamoto University, Kumamoto, JAPAN, [2]Faculty of Life Sciences Kumamoto Univercity, Kumamoto, JAPAN, [3]Kumamoto University Hospital, Kumamoto, JAPAN.

Aim/Introduction: Quantitative index such as ^{201}Tl Myocardial Uptake at stress(MUI) is useful for the diagnosis of coronary arterial disease(CAD) on stress ^{201}Tl single photon emission computed tomography-myocardial perfusion imaging(^{201}Tl-SPECT-MPI). However, it is necessary to

extract the left ventricular contour for calculation of the left ventricular myocardial counts. The aim of this study was to evaluate the feasibility of automated program for extracting the left ventricular myocardium(LVM) by comparing number of voxels in LVM estimated with the automated program and that obtained with manually extracting LVM on stress ^{201}Tl SPECT-MPI using a CZT camera(NM530c;GE). ***Materials and Methods:*** The automatic program for extracting LVM based on region growing method was developed. We obtained the number of voxels in LVM by using this program and manually set ROI on LVM, respectively. Three different radioactivity in myocardium of phantom images(74,37,18.5kBq/ml) and normal 95 patients (SSS=0) performed stress ^{201}Tl SPECT-MPI were enrolled. We evaluated the concordance of the number of voxels in LVM obtained by two methods with Jaccard similarity coefficient. ***Results:*** Jaccard similarity coefficient in all cases of phantom images and 94 patients of 95 clinical images showed equal 1. ***Conclusion:*** The developed automatic program for extracting LVM is feasible to use in patients with normal myocardial perfusion. ***References:*** None

OP-694

Evaluation of extent and severity of myocardial perfusion defects: quantitative [perfusion SCOREs] and qualitative [segments] analysis

A. Ghilardi[1], *G. Medolago*[2];
[1]*ASST-PG23, Bergamo, ITALY,* [2]*Humanitas Gavazzeni, Bergamo, ITALY.*

Aim/Introduction: Determination of amount of ischemia/scar or viable myocardium is essential for patient management. It is important to report amount of ischemic/scarred/viable myocardium, by qualitative analysis [#segments hypoperfused] or quantitatively [#SCOREs], anyway as a percentage of left ventricle, taking into account that ESC recommends that patients with stable angina or silent ischemia with proven large area of ischemia (10-12%) should receive revascularization . We Evaluated variability/differences of assessing extent of reversibile/fixed perfusion defects obtained by qualitative and quantitative analysis, to better determine extent and severity of hypoperfused myocardium for clinical decision making ***Materials and Methods:*** All patients with known/suspected coronary artery disease underwent stress exercise/rest single day protocol using Tc^{99m}_Sestamibi as radiophamaceutical. Gated_SPECT was performed using double-head Siemens_Symbia_S equipped with LEHR collimators; short-and-long (sagittal-horizontal)-axis oblique slices were obtained by reorienting transaxial image data using iterative filtering and displayed with different pixel thickness and colour grading windows to better visualize ischemic/scar/viable myocardium. Gated_SPECT images were interpreted based on a 17-segment model. Qualitative analysis categorized images either normal or ischemic/necrotic/viable [0-4 score]. Quantitative perfusion and functional parameters were derived fully automatically using commercially available software program [Cedars-Sinai QPS and QGS]. ***Results:*** Comparing qualitative slices imaging [hypoperfused #segments] and quantitative data [#SCOREs] diagnostic mismatch was frequently found. #SCOREs value is objective/operator_independent, easily repeatable and mostly a powerful prognostic tool. However it may not fit absolute segmental myocardial uptake of Tc^{99m}_Sestamibi, referring to commercial normal [albeit validated] database. Furthermore even if #SCOREs can be converted to percent of total myocardium (% myocardium) involved with ischemic/fixed defects [by dividing the summed scores by 68, the maximum potential score (4*17), and multiplying by 100], it doesn't often correlate to segmental hypoperfused defect size. Qualitative analysis allows to assess hypoperfused defect size in terms of extent: #segments, severity: "0-4 score [normal, moderate,severe, absent uptake]" and percentage of hypoperfused myocardium[by multiplying 6% [100%/17segments] by #segmental defects] differentiating small [6%], moderate[12%], large[18%] and viable/not viable defects ***Conclusion:*** Both qualitative and quantitative analysis are needed for accurate evaluation of myocardial perfusion defects size for patient management. In our experience qualitative analysis showed to be more convenient/suitable to assess accurately, promptly ischemic/scarred/viable myocardium for clinical decision making, using a more standardize model ***References:*** Germano G, Kavanagh P, Waechter P, Areeda J, Sharir T, Lewin H, Berman D. A new automatic approach to myocardial perfusion SPECT quantitation. J Nucl Med 1998 (abstract); 39(5):62P.

OP-695

Introduction to COVID-19 Pandemic

L. Camoni; Università & Spedali Civili di Brescia, Brescia, ITALY

OP-696

Ventilation scintigraphy: is it really safe now with COVID-19 pandemic?

S. Mendes, I. Ferreira, J. Isidoro, G. Costa, P. Soeiro, J. P. Lima;
Hospitais da Universidade de Coimbra, Coimbra, PORTUGAL.

Aim/Introduction: Ventilation-perfusion scintigraphy in the emergency setting is essential for some patients. However, with the COVID-19 pandemic and most infected patient beings asymptomatic, ventilation procedure became particularly challenging due to the generation of extremely small carbon aerosols (0.005-0.2 µm). Nuclear medicine technicians may therefore be at higher risk of COVID-19. The aim of these work was to assess the risk of infection and thereby implement additional procedure safety standards if necessary. ***Materials and Methods:*** Ventilation

simulation with Thecnegas generator and phantom able to perform inspiration and exhale was performed. Technicians individual equipment used for protection was head cover, face protection, mask N95, gown and foot protection. Millenium VH gamma camera without collimators was used to measure the activity in individual equipment, technician lung, walls, the floor and the Thecnegas generator. All the data was corrected for the background and for decay. ***Results:*** Gown had the higher particles contamination (17KBq). Relative to gown the head cover had 5% (0.9 KBq), face protection 3% (0.5 KBq), mask N95 9% (1.5 KBq),foot protection 6%(1.0 KBq). The personal uniform was evaluated and the pants had 5% (0.8 KBq) and the shirt had 1% (0.2 KBq). The total contamination of the components of the room had a medium of contamination of 0.9 KBq (min. 0.004 KBq; máx. 5.5 KBq). The lungs and the face radioactive contamination after the removal of all the protection equipment, even without a shower, were lower than the detection sensitive of the gamma camera. ***Conclusion:*** These preliminary results suggest that protective individual equipment reduce the probability of particle lung aspiration by the technicians, aspect very important when we perform this procedure in a patient infected with the corona virus. ***References:*** None

OP-697

Management of COVID-19 pandemic in Nuclear Medicine Departments: a contribute for the Portuguese community

P. Costa*, J. Lemos, D. Vieira, N. Arantes;*
Nuclear Medicine Department, School of Health, Politécnico do Porto, Porto, PORTUGAL.

Aim/Introduction: Considering the infection with the new Coronavirus (SARS-CoV-2), which may evolve into CoronaVirus Disease 2019 (COVID-19), and the pandemic that is active, standards, guidelines and recommendations have been issued by diverse entities at the governmental, professional and scientific levels. During this pandemic, it is mandatory that the operation of Nuclear Medicine (NM) Departments will be conditioned restricted and internal protocols and practices adjusted accordingly. NM Departments integrated in hospital institutions are included in their contingency plans, generally, and currently operate under the contingency regulations in place, who report to the best available evidence. It was conducted a literature review that aims to aggregate international recommendations and to document practices for the management of the COVID-19 pandemic in NM Departments. The pertinence relies in a possible lack of practical information reporting to the specific context of NM, as well as lack of time to do the careful research of the best available evidence. This work aims to describe the gathered information, and share the process of research, revision, and dissemination amongst the Portuguese community of NM Departments and the feedback obtained. ***Materials and Methods:*** An informal literature review was conducted in scientific databases, but also in other sources of information such as scientific and/or professional entities involved in the NM field, concerning scientific articles, clinical studies or other reports or guidelines that are relevant for the operation or management of NM Departments. Results were disseminated among Portuguese NM community and feedback was obtained via e-mail and social media. ***Results:*** A total of 13 references were found and reviewed by the authors, leading to the compilation of a document divided in these topics: i) General measures for infection prevention and control; ii) Management of staff and work routines; iii) Management of scheduled procedures and future appointments; iv) Measures for patients and accompanying persons; and v) Special care in the interpretation of NM examinations. Feedback obtained will be compiled and shared, but preliminary evaluation resulted in an overall positive acceptance of the document and the recognition of the efforts conducted given the lack of specific and direct indications for NM Departments. ***Conclusion:*** The current pandemic of COVID-19 has brought some necessities and challenges to the reality of NM that will remain relevant in the near future, at least, thus being very important to adapt and adjust the management and operation of NM Departments always based on scientific evidence available. ***References:*** None

1305

M2M Track - Featured Session: The Revival of Pre-Targeting

Thursday, October 29, 2020, 16:35 – 17:45 Channel 5

OP-698

Pretargeting From Past to Present

J. Barbet*; GIP Arronax, Université de Nantes, Centre de Recherche en Cancérologie de Nantes-Angers, U892, Nantes, FRANCE.*

OP-699

Search for the optimal bis-iminobiotin for the pretargeting strategy using a mutated low immunogenic streptavidin

K. Washiyama*[1], T. Tatsumi[2], S. Zhao[1], A. Sugiyama[2], M. Aoki[1], K. Yamatsugu[2], N. Ukon[1], K. Nishijima[1], S. Shimoyama[1], C. Tan[1], T. Joho[1], N. Oriuchi[1], M. Kanai[2], K. Takahashi[1], T. Kodama[2];*
[1]Fukushima Medical University, Fukushima, JAPAN,
[2]The University of Tokyo, Tokyo, JAPAN.

Aim/Introduction: By separating the role of an antibody and a radioligand, the pretargeting strategy has been expected to increase the therapeutic effect of radioimmunotherapy.

We have developed a pretargeting system using a mutated low immunogenic streptavidin denoted as Cupid, which can fuse to scFV mAb, and a bis-iminobiotin compound denoted Psyche that specifically binds to Cupid [1]. The purpose of this study was to explorer the relationships between the molecular structure of a series of Psyches, binding stabilities to Cupid, and pharmacokinetics of ^{211}At-labeled Psyches in mice in order to identify the optimal candidates for pretargeting radionuclide therapy. ***Materials and Methods:*** We synthesized several trimethylstannylated bis-iminobiotins called Psyche-B, -J, -N, and -P, and evaluated its affinity to Cupid using surface plasmon resonance (SPR). ^{211}At was manufactured in our facility and isolated through dry distillation. ^{211}At was labeled to Psyches and purified as no-carrier-added products using RP-HPLC. For the stability evaluation, ^{211}At-Psyches were incubated with PBS and serum for 24 hours. For the biodistribution studies, a series of ^{211}At-Psyches were administered to CEA-expressing xenograft mice with and without a 100 pmol of anti-CEA scFv-Cupid. The interval between ^{211}At-Psyches and anti-CEA scFv-Cupid administration was set 24 h. ***Results:*** SPR results showed that all Psyches have a high affinity to Cupid, especially Psyche-B has K_D=5.1E^{-11} M. The logD values of ^{211}At-Psyches differed depending on their structure, eg. ^{211}At-Psyche-P (0.37), ^{211}At-Psyche-J (-1.26). All ^{211}At-Psyches showed high stability in PBS. However, while ^{211}At-Psyche-N and -P are relatively stable in plasma, ^{211}At-Psyche-B dissociated in serum within 1 hour. The biodistribution of all ^{211}At-Psyches in mice without Cupid showed the same trends; the blood clearance was fast, showing <1% ID/g at 6 hours after administration. However, the biodistribution of all ^{211}At-Psyches when 100 pmol of Cupid was administered 24 hours before showed different patterns for each compound. ^{211}At-Psyche-P showed almost the same pharmacokinetics with and without Cupid. In contrast, ^{211}At-Psyche-J and B showed increased uptake in the tumor up to the experimental period (24h). Despite being unstable in plasma, ^{211}At-Psyche-B have reached 16.3 ± 4.1 %ID/g at 24 hours after administration. ***Conclusion:*** Although ^{211}At-Psyche-B showed serum instability ex vivo, the high affinity of Psyche-B to cupid compensates the tumor uptake and its accumulation increased over time in vivo. Based on the encouraging results, we will evaluate ^{211}At-Psyche-B as a promising candidate for further pretargeting optimization. ***References:*** [1] Sugiyama et al., Prc. Jpn. Acad. Ser. B 95:602, 2019

OP-700

Design and evaluation oflactosaminated cetuximabas a clearing agent for antibody-based PNA-mediated pretargeting

M. Altai[1,2], *A. Vorobyeva*[1], *A. Myrhammar*[3], *K. Westerlund*[3], *S. Yoneoka*[4], *T. Tsukahara*[4], *A. Eriksson-Karlström*[3], *A. Orlova*[5], *V. Tolmachev*[1];

[1]*Immunology, Genetics and Pathology, Uppsala, SWEDEN,* [2]*Division of Oncology and Pathology, Department of Clinical Sciences, Lund, SWEDEN,* [3]*Department of Protein Science, KTH, Stockholm, SWEDEN,* [4]*Laboratory for Advanced Nuclear Energy, Tokyo, JAPAN,* [5]*Department of Medicinal Chemistry, Uppsala, SWEDEN.*

Aim/Introduction: Pretargeting is a promising strategy allowing for the rational use of long circulating, monoclonal antibodies (mAbs) in therapy. We developed a pretargeting approach based on hybridization between peptide nucleic acids (PNAs). The anti-HER2 mAb trastuzumab (T) was coupled to the HP1 PNA-probe (T-ZHP1) and injected first. Forty-eight hours later, a complementary radiolabeled HP2 PNA-secondary probe was injected. Pretargeting resulted in 2-fold increase in tumor-to-blood radioactivity uptake ratio compared to direct targeting using trastuzumab. Here, we extend further on this strategy by developing a clearing agent (CA) aimed at chasing the primary T-ZHP1 in vivo to clear it faster from the circulation prior to the injection of the secondary radiolabeled-HP2 probe. ***Materials and Methods:*** We designed a CA based on the mAb cetuximab, site-specifically conjugated to a PNA HP2 probe recognizing T-ZHP1 using a photoactivatable Fc-binding Z domain. Thereafter, the CA was galactosylated to improve hepatic clearance through binding to asialoglycoprotein receptors. Binding interaction of ^{125}I-radiolabeled CA (cetuximab-galact$_{35}$-ZHP2) with primary-T-ZHP1 was evaluated using cell dishes coated with T-ZHP1. The influence of galactosylation and conjugation of PNA-modified Z-domain on cetuximab biodistribution was evaluated in normal mice injected with [^{125}I]I-radiolabeled CA and the controls cetuximab, cetuximab-ZHP2 or cetuximab-galactose. The blood clearance of primary T-ZHP1 radiolabeled with [^{131}I]I, with and without CA administration (6h post-T-ZHP1 injection) was also evaluated in normal mice. Blood samples from mice (1 h post-CA injection) were collected and analyzed using size-exclusion chromatography. ***Results:*** Cetuximab was efficiently photoconjugated with Z-HP2. Lactosamination resulted in an average of 35 lactose units per cetuximab molecule. Binding of [^{125}I]I-CA to T-ZHP1-coated dishes was 1.5-4-fold ($p<0.05$) higher than to controls, were an excess of the complementary-PNA, HP2, was added to T-ZHP1 before the addition of [^{125}I]I-CA or when no T-ZHP1 was added. Results from the biodistribution study demonstrated that the CA cleared from the blood to the liver more rapidly than the parental cetuximab in as early as 1 h p.i. Injection of the CA 6 h p.i. of the primary T-ZHP1 resulted in a modest but significant ($p<0.05$) increase in clearance of T-ZHP1 from the blood, compared to T-ZHP1 alone (8.5±1.8 vs. 6.0±0.4 %ID/g). Analysis of blood-borne radioactivity demonstrated that 90.8± 1.8% of the total serum-associated radioactivity post-[^{131}I]I-T-ZHP1 administration followed by injection of the CA, is still in high molecular weight form i.e. intact

T-ZHP1. ***Conclusion:*** The obtained results provide an initial proof-of-principle and efforts to further optimize the CA are ongoing. ***References:*** None

OP-701

Comparative evaluation of novel ^{177}Lu-labeled PNA conjugates for affibody mediated PNA-based pretargeting

M. Oroujeni[1], A. Vorobyeva[1,2], Y. Liu[1], T. Xu[1], H. Tano[3], L. Vasconcelos[3], K. Westerlund[3], A. Karlström[3], A. Orlova[4,2], V. Tolmachev[1,2];
[1]Department of Immunology, Genetics and Pathology, Uppsala University, Uppsala, SWEDEN, [2]Research Centrum for Oncotheranostics, Research School of Chemistry and Applied Biomedical Sciences, Tomsk Polytechnic University, Tomsk, RUSSIAN FEDERATION, [3]Department of Protein Science, School of Engineering Sciences in Chemistry, Biotechnology and Health, KTH Royal Institute of Technology, Stockholm, SWEDEN, [4]Department of Medicinal Chemistry, Uppsala University, Uppsala, SWEDEN.

Aim/Introduction: Affibody molecules are engineered scaffold proteins, which demonstrated excellent imaging of HER2 expression in breast cancer metastases using SPECT and PET. Radiometal-labelled affibody molecules show high renal uptake, which prevented the use of them in targeted therapy. Earlier, we have demonstrated that affibody-mediated peptide nucleic acid (PNA)-based pretargeting provides low kidney uptake and significantly extends survival of mice bearing HER2-expressing xenografts without renal toxicity. The aim of this study was to evaluate the targeting properties of three novel secondary DOTA-conjugated pretargeting agents, HP16, HP17 and HP18, and compare them directly with the properties of the first generation secondary probe, HP2. ***Materials and Methods:*** The primary probe was created by the coupling of a novel HP15 recognition tag to the HER2-binding ZHER2:342 affibody molecule. Radiolabelling of secondary probes with ^{177}Lu was performed at 95 °C for 60 min. In vitro stability of ^{177}Lu-labels was tested by a challenge with a 500-fold molar excess of EDTA. In vitro specificity of pretargeting was tested and cellular processing was evaluated using HER2-expressing SKOV3 and BT474 cell lines. Biodistribution was measured in Balb/c nu/nu mice bearing SKOV3 xenografts. The radiolabelled secondary probes were injected 16 after injection of the primary probe. The distribution of activity was measured at 4 and 144 h after injection of the radiolabelled secondary agent. In vivo specificity of pretargeting was tested by injection of ^{177}Lu-secondary agent without preinjection of primary agent. ***Results:*** Radiolabelling with ^{177}Lu resulted in high yield and over 95% radiochemical purity. All labels were stable under the EDTA challenge. In vitro pretargeting specificity test showed that binding of the ^{177}Lu-secondary agent to cells was mediated by PNA-PNA hybridization. Cellular processing revealed high cellular retention over time and slow internalization rate. With a preinjection of the primary probe, the tumour uptake of all secondary probes at 4 h was in the range of 19-24%ID/g. Without primary probe preinjection, the tumour uptake was 0.08-0.12%ID/g. Uptake in normal tissues (except kidneys) was negligible, several hundreds fold lower than in tumours. The renal uptake ranged from 6±1%ID/g for HP16 to 12±1%ID/g for HP18 at 4 h pi. The ratios of areas under the curve for tumour and kidneys was 3.8, 2.9, 1.9 and 2.0 for HP16, HP17, HP18 and HP2, respectively. This indicates that 177Lu-HP16 would provide the most favourable dosimetry. ***Conclusion:*** This study showed that HP16 is the best variant among all secondary agents. ***References:*** None

OP-702

Tetrazine-functionalized clearing agent to increase contrast in antibody imaging

E. Schlein[1], J. Rokka[1], T. Gustavsson[1], J. Eriksson[2,3], S. Syvänen[1], D. Sehlin[1];
[1]Department of Public Health and Caring Sciences, Uppsala University, Uppsala, SWEDEN, [2]PET Centre, Uppsala University Hospital, Uppsala, SWEDEN, [3]Department of Medical Chemistry, Uppsala University, Uppsala, SWEDEN.

Aim/Introduction: Antibodies, engineered to enter the brain, can reach concentrations up to 80-fold higher than unmodified antibodies, similar to those observed with small, lipophilic radioligands [1]. Due to the long biological half-life of a radiolabelled antibody, imaging of brain targets with antibody-based ligands must be performed several days after injection. To overcome this problem we used clearing agents (CA), which induce accelerated peripheral clearance immediately after administration [2, 3]. Here, we aimed to combine antibody-based imaging with a CA to allow imaging shortly after administration of an amyloid-β (Aβ) antibody. ***Materials and Methods:*** The Aβ antibody RmAb158 [4] and its bispecific, brain penetrating variant RmAb158-scFv8D3 [1] were modified with mannose for direct increased clearance or with trans-Cyclooctene (TCO) for induced clearance. The mannose modified [^{125}I]antibody was studied in wildtype mice using ex vivo biodistribution 24h after injection. Transgenic (tg-ArcSwe [5], Aβ pathology model) and wildtype mice were administered with [^{125}I] RmAb158-TCO and SPECT/CT scanned 3 days later. Immediately after, CA was administered and additional SPECT/CT scans were taken after 1 h and 1 day post CA injection. The tetrazine-functionalised CA reacts quickly with the TCO-modified antibody (invers electron-demand Diels-Adler reaction) to induce radioligand clearance from blood. Blood was sampled at defined time points after antibody injection for analysis. The perfused brain tissue was cryosectioned for subsequent ex vivo autoradiography analysis. ***Results:*** Both strategies cleared efficiently, with

a decrease of up to 90% of RmAb158. The bispecific RmAb158-scFv8D3 could not be cleared from the blood, likely due to its binding to blood cells. Hence we used RmAb158 for imaging, in combination with the tetrazine-functionalized CA, which was more efficient and has the advantage of inducible clearance. [^{125}I]RmAb158 SPECT/CT images obtained 3 days after antibody injection showed immediate liver accumulation upon CA administration, which substantially reduced antibody concentration in blood (Fig. 1). Contrast of the brain derived signal increased after 1 h CA administration and further improved after 24 h (Fig. 2). ***Conclusion:*** Results indicate that the method works as intended and that the use of clearing agents may be a promising strategy for antibody-based imaging in combination with more short-lived radionuclides. ***References:*** 1. Hultqvist G, et al. Theranostics 2017. 7:308-318 2. Rossin R, et al. Journal of Nuclear Medicine 2013. 54, 1989-1995 3. Lee S-P, et al. Theranostics 2017. 7, 413-424 4. Englund H, et al. Journal of Neurochemistry 2007. 103, 334-345 5. Lord A, et al. Neurobiol. Aging 2006. 27, 67-77

OP-703

Evaluation of therapeutic effect of the targeted alpha therapy using Cupid-^{211}At-labeled Psyche-B pretargeting system in a human gastric cancer cell xenograft

S. Zhao[1], *A. Sugiyama*[2], *N. Ukon*[1], *S. Shimoyama*[1], *T. Tatsumi*[2], *M. Aoki*[1], *F. Gao*[1], *K. Yamatsugu*[2], *K. Nishijima*[1], *T. Joho*[1], *N. Oriuchi*[1], *K. Takahashi*[1], *M. Kanai*[2], *T. Kodama*[2], *K. Washiyama*[1];
[1]*Fukushima Medical University, Fukushima, JAPAN,*
[2]*The University of Tokyo, Tokyo, JAPAN.*

Aim/Introduction: Targeted alpha therapy using astatine-211 (^{211}At) is one of the most promising anticancer therapies. Recently, we have developed a novel Cupid-Psyche pretargeting system [Cupid, a mutated low-immunogenicity streptavidin; Psyche, a modified bis-biotin with specific affinity to Cupid. Single-chain variable fragment (scFv) antibodies against various cancer cell surface antigens can be fused with Cupid, which specifically marks malignant cells (Ref. 1)]. In this study, we evaluated the therapeutic effect of the anti-carcinoembryonic antigen (CEA) scFV-Cupid and ^{211}At-labeled Psyche-B (^{211}At-Psyche-B) pretargeting system on high-level CEA-expressing xenograft mice. ***Materials and Methods:*** A CEA high-level expressing human gastric cancer cell xenograft (MKN-45) was established in nude mice. In the biodistribution study, the mice were intravenously injected with100 pmol of anti-CEA scFv-Cupid antibodies. After 24 h, they were injected with 250 kBq of ^{211}At-Psyche-B (n=3 in each group). Blood, organs, and tumor tissues were collected, weighed, and measured for radioactivity using a gamma counter. In the treatment study, the mice were assigned to a control group and three treatment groups (n=5, in each group), and received 100 pmol of anti-CEA scFv-Cupid antibodies. Twenty-four hours after the injection, the mice in the treatment groups were injected with a single dose of ^{211}At-Psyche-B (0.37, 1.11, and 1.85 MBq or vehicle solvent). The tumor volumes were measured three times per week for 26 days. To determine safety, we also measured the body weight three times per week. ***Results:*** The accumulation levels of ^{211}At-Psyche-B in the tumor significantly increased over time. There were no significant differences in tumor volume among the four groups at the initial treatment time. After 26 days, the tumor volume significantly increased in the control group (347.0 ± 101.6 to 1837.5 ± 430.7 mm^3, $P<0.01$). In contrast, the tumor volume dose-dependently suppressed over time in the groups treated with 0.37, 1.11 and 1.85 MBq of ^{211}At-Psyche-B. There were no significant differences in body weight among the four groups at the initial treatment time and 26 days after the treatment despite the transient body weight loss observed in the groups treated with ^{211}At-Psyche-B. ***Conclusion:*** A high accumulation level of ^{211}At-Psyche-B was observed in the CEA high-expression tumor, and the tumor volume was suppressed dose-dependently by the Cupid-^{211}At-Psyche-B treatment. Therefore, the CEA scFv-Cupid and ^{211}At-labeled Psyche-B pretargeting system might be an effective targeted treatment for cancers expressing CEA. ***References:*** 1. Sugiyama et al., Proc Jpn Acad Ser B. 2019;95:602

OP-704

Successful Pretargeting Approach for Peptide Receptor Radionuclide Therapy of GRPR-positive Prostate Cancer

M. Verhoeven*, M. Handula, K. Chen, M. de Jong, Y. Seimbille, S. U. Dalm;*
Erasmus MC, Rotterdam, NETHERLANDS.

Aim/Introduction: The gastrin-releasing peptide receptor (GRPR) is overexpressed on prostate cancer and is therefore a suitable target for imaging and therapy using high-affinity GRPR-targeting radioligands. Unfortunately, studies have revealed that it is not only the tumor that will show high radiotracer uptake; the tracer also accumulates in the GRPR-expressing pancreas. However, the radiotracer clears relatively fast from this healthy organ while tumor radioactivity retains much better. This study aims to overcome pancreatic irradiation and herewith associated side effects when GRPR-targeting radioligands are applied for cancer treatment by applying a pretargeting strategy based on the inverse electron demand Diels-Alder click reaction. ***Materials and Methods:*** A panel of 6 vectors with structures containing the binding domain of the GRPR antagonist NeoB coupled to trans-cyclooctene with various linkers and spacer lengths were synthesized. The IC_{50} values were determined with a competition binding assay on PC3 prostate cancer cells. Cells were incubated with 0.5 mL of 1 nM [^{111}In]In-NeoB (50MBq/nmol) +/- increasing concentrations (10^{-12}-10^{-6} M) of the unlabeled

vectors. Membrane-bound fractions and internalized fractions of 4 DOTA-containing vectors were identified via an internalization assay in which PC3 cells were exposed to 0.5 mL of 1 nM indium-111 radiolabeled vectors (50MBq/nmol) +/- 1 µM unlabeled NeoB. To verify the click reaction between vector and [^{111}In]In-Tz-PEG$_{11}$-DOTA (effector) both were added in a 1:1 ratio in PBS. After incubation, the mixture containing the collected click product was verified using HPLC and mass spectrometry. Additionally, a pilot in vivo study was performed in PC3 xenografted Balb/c nu/nu mice. Animals were first injected with 600 pmol vector and 4 h later with ~20 MBq/600 pmol effector. One hour after the second injection SPECT/CT imaging was performed. ***Results:*** The IC_{50} value of all vectors was in the 0.1-0.37 nM range. For the 4 DOTA-containing vectors, the membrane-bound fraction of 53.2-64.4% was higher than the internalized fraction (35.6-46.8%). In vitro, all vectors underwent a click reaction with the effector. The SPECT/CT images showed a clearly detectable signal in the tumor indicating an in vivo click reaction. ***Conclusion:*** Our findings provide evidence that a pretargeting approach is feasible for GRPR-mediated radionuclide therapy. All vectors have shown to be promising candidates as they possess high GRPR binding affinities and binding to the effector was successful. The results of the pilot in vivo study are encouraging. Further research is needed for optimization of conditions for future in vivo imaging and therapy studies. ***References:*** None

OP-705

The "click" chemistry approach as in vivo pre-targeting strategy for microspheres and bacteria

M. M. Welling[1], *N. Duszenko*[1,2], *D. M. van Willigen*[1], *T. Buckle*[1], *D. D. D. Rietbergen*[1,3], *M. Roestenberg*[2], *F. W. B. van Leeuwen*[1]; [1]*Interventional Molecular Imaging, Department of Radiology, Leiden University Medical Center, Leiden, NETHERLANDS,* [2]*Department of Parasitology and Department of Infectious Diseases, Leiden University Medical Center, Leiden, NETHERLANDS,* [3]*Section of Nuclear Medicine, Department of Radiology, Leiden University Medical Center, Leiden, NETHERLANDS.*

Aim/Introduction: Pre-targeting is a proven strategy for in vivo delivery of a diagnostic or therapeutic payloads. The pre-targeting concept can be realized through various conjugation strategies, one of which is copper-free "click" reactions, which have shown in vivo potential for imaging and radionuclide therapy. This conjugation strategy, however, has not yet been explored in combination with microspheres or unicellular organisms. Hence, we aimed to evaluate the in vivo efficacy of strain-promoted azide-alkyne cycloaddition (SPAAC) "click" reactions in the hepatic delivery of a payload. ***Materials and Methods:*** MAA microspheres (diameter 10-90 µm) were functionalized with a biorthogonal Cy5 fluorophore bearing an azide functionality (N_3) to generate MAA-Cy5-N_3. S. aureus (diameter ~ 1 µm) were functionalized with ^{99m}Tc-UBI$_{29-41}$-Cy5-N_3 to generate S. aureus-UBI$_{29-41}$-Cy5-N_3. In situ and in vitro "click" conjugation was studied over time using a radioactivity assay and fluorescence microscopy. To validate the pre-targeting strategy in vivo, both entities, radiolabeled with ^{99m}Tc, were locally delivered in the microvasculature of the liver. Secondary targeting was realized following reaction with intravenously administered indium-111-radiolabeled diethylenetriaminepentaacetic acid-dibenzocyclooctyne (^{111}In-DTPA-DBCO). Imaging of ^{111}In-DTPA-DBCO in mice without MAA deposits or mice infected with non-functionalized S. aureus served as controls. ***Results:*** In vitro data confirmed effective "click" reactions on both the MAA particles and the bacterial membrane. SPECT imaging and %ID/g biodistribution studies revealed significantly ($p < 0.05$) increased accumulation of ^{111}In-DTPA-DBCO at the sites where MAA-Cy5-N_3 (7.5±1.5%ID/g vs 3.5±0.5%ID/g in control mice) and S. aureus-UBI$_{29-41}$-Cy5-N_3 (9.3±1.3%ID/g vs. 6.0±0.5%ID/g in control mice) accumulated. Ex vivo fluorescence imaging confirmed the presence of either functionalized MAA or S. aureus in excised spleens and livers of mice. ***Conclusion:*** Copper-free "click" chemistry between a DBCO moiety and Cy5-N_3-functionalized microspheres or bacterial entities in the liver could be used to realize in vivo pre-targeting. Thereby demonstrating that this generic concept can serve both theragnostic radioembolization strategies and bacterial colonization applications. ***References:*** Welling et al. ACS Infect. Dis. 2019, 5;1160−1168Welling et al. J Contr. Rel. 2019, 293:126-134

1306

Cutting Edge Science Track - Featured Session: Intra-Operative Nuclear Medicine

Thursday, October 29, 2020, 16:35 – 17:50 Channel 6

OP-706

Introduction

B. Sattler*; University Hospital Leipzig, Department for Nuclear Medicine, Leipzig, GERMANY*

OP-707

First clinical experiences with an innovative Gamma-probe to guide parathyroid radio-guided surgery: Navigator and Lock-on-target functions of the Gonioprobe

V. Frantellizzi*, M. S. De Feo, S. Sollaku, R. Falconi, R. Pani, M. Bononi, J. Lazri, A. Matto, G. De Vincentis; Sapienza University of Rome, Rome, ITALY.*

Aim/Introduction: Minimally invasive radio-guided parathyroidectomy (MIRP) represents a validated surgical

approach in patients with primary hyperparathyroidism (PHPT) caused by single adenomas. To date, little attention has been paid to how the physical characteristics of gamma-probes may impact on intraoperative detection of abnormal tissue with increased uptake of 99mTc-sestamibi. The aim of this analysis was testing an innovative gamma-probe prototype, the Gonioprobe, in selected patients with parathyroid adenomas particularly difficult to identify due to anatomy modifications from previous neck surgery or concomitant thyroid goiter ***Materials and Methods:*** In the fall of 2019 three patients were submitted to MIRP with Gonioprobe in our center. The Gonioprobe performs the dual function of Navigator and Lock-on-target thanks to its 5 scintillating independent crystals. This innovative prototype was used to both detect abnormal parathyroid tissue during intervention, and to ensure no radioactivity in surgical bed after adenoma removal.All patients were administered a very low activity of 99mTc-sestamibi (111 MBq) 2 hours before intervention. Parathyroid hormone (PTH) assay and frozen biopsy were performed to confirm the successful excision of the adenoma. The intraoperative nerve monitoring system was used to protect the recurrent laryngeal nerve (RLN) from injuries ***Results:*** Thanks to its characteristics, our newly developed prototype allowed the immediate guidance of surgeon's hand towards the target with extreme precision and high spatial resolution, showing in-vivo target to background ratio higher than 1.5 in all cases, specifically 1.81 for case 1 and 1.57 and 1.89 for case 2 and 3 respectively. After the removal of the adenomas, high radioactivity levels in ex-vivo tissues and no residual radioactivity in surgical bed were detected, with the "Twenty percent rule" satisfied in all cases. A decrease of more than 50% of PTH levels was observed 10 minutes after the removal of the adenomas and frozen section analysis confirmed parathyroid tissue in all the excision materials. No RLN damage was registered. The mean operative time from the incision to the complete removal was 20 minutes. The postoperative course was uneventful for all patients who were discharged on the third postoperative day ***Conclusion:*** The intraoperative use of the Gonioprobe for MIRP allowed the accurate removal of parathyroid adenomas even in case of previous neck surgery or thyroid nodular diseaseand offered a significant advantage by reducing surgical time, radiation exposure to surgical staff, postoperative complications, as well as hospitalization and costs ***References:*** None

OP-708

Towards a drop-in beta probe for robotic radio guided surgery

F. Collamati[1], *C. Mancini-Terracciano*[1], *S. Morganti*[1], *E. Solfaroli-Camillocci*[1], *R. A. Valdes Olmos*[2], *F. W. B. van Leeuwen*[2], *M. N. van OOsterom*[2], *R. Faccini*[3];
[1]*INFN Rome, Rome, ITALY,* [2]*16Interventional Molecular Imaging Laboratory, Department of Radiology, Leiden University Medical Center, Leiden, NETHERLANDS,* [3]*Università degli studi di Roma Sapienza, Rome, ITALY.*

Aim/Introduction: Recently, a flexible design of DROP-IN gamma-probe was introduced for robot-assisted radioguided surgery, exploiting traditional low-energy SPECT-isotopes. This study explores the use of a novel DROP-IN beta-particle (DROP-IN) detection probe to support the implementation of the large number of PET-tracers available during robot-assisted tumor-receptor-targeted resections, together with beta-RGS intrinsic advantages ***Materials and Methods:*** Following engineering of the DROP-IN probe, robotic implementation was investigated using ex-vivo surgical specimens. Seven prostate cancer patients with PSMA-PET positive tumors received an intraoperative injection of ~70 MBq ^{68}Ga-PSMA-11, followed by prostatectomy and extended pelvic lymph node dissection. ***Results:*** The probe was able to identify the position of the tumor in the prostate specimens: S/B was > 5 when pathology confirmed that the tumor was located <1 mm below the specimen surface. PSMA-PET positive lymph nodes, as found in two patients, could be identified with the DROP-IN probe (S/B>3). ***Conclusion:*** This ex vivo study underlines the potential to use a DROP-IN probe for intraoperative tumor identification on the prostate surface and confirmation of PSMA-PET positive lymph nodes. In vivo tests are now on schedule to further validate this technique. ***References:*** None

OP-709

Development of the intraoperative movable PET imaging system for radio guided surgery

O. Kenichiro[1,2], *M. R. Liyanaarachchi*[3], *K. Shimazoe*[3], *H. Takahashi*[4], *S. Aiko*[1], *Y. Seto*[1], *M. Takahashi*[2], *T. Momose*[2];
[1]*Department of Surgical Science, The University of Tokyo, Tokyo, JAPAN,* [2]*Department of Nuclear Medicine, International University of Health and Welfare, Tokyo, JAPAN,* [3]*Department of Bio-engineering and Management, The University of Tokyo, Tokyo, JAPAN,* [4]*Department of Nuclear Engineering and Management, The University of Tokyo, Tokyo, JAPAN.*

Aim/Introduction: FDG-PET is one of the effective nuclear examinations to diagnose various cancers and identify lymph node (LN) metastasis preoperatively. However, it's too difficult to locate each metastatic LN during surgery. This difficulty usually leads to unnecessary node removal, in which impairment of neighboring nerves would be inevitable, resulting in a deterioration of a patient's quality of life. To overcome this problem, we developed an intraoperative PET imaging system. ***Materials and Methods:*** This system consists of an external detector array (49 pixels of 10mm x 10mm x 20mm, GAGG)(SiPM) connected to a patient's surgical bed and a movable detector probe (4

layers of 12 pixels of 2mm x 2mm x 3mm, GAGG)(SiPM) which is small enough to be inserted into peritoneal cavity along with a laparoscope tracked by an optical tracking system. In this proof-of-concept study, we imaged the ^{22}Na point source (290kBq) and FDG (0.6MBq/2mL) with/without the low concentration FDG background. PET scan was performed by swinging the movable detector at the speed of a few millimeters per second for 2 mins at the distance of about 2 cm above from the activity source. The image is reconstructed using a modified filtered back projection algorithm. ***Results:*** Our developed system reconstructed images of a ^{22}Na point source with 3 mm spatial resolution. And we could succeed in imaging FDG in a 2min-scan. It was confirmed that the accumulation could be imaged even in an environment with a low concentration of FDG in the background. Even if the probe was not fixed, the spatial resolution equivalent to that of the conventional fixed PET was obtained by integrating the position information. ***Conclusion:*** We could develop the intraoperative PET imaging system with a movable detector probe tracked by an optical tracking system. This system has potential to achieve the limited operations. ***References:*** None

OP-710

Preliminary study of the feasibility of Cerenkov luminescence imaging in metastasectomy

E. Ciarrocchi[1], S. Saponaro[1], F. Bartoli[2], A. G. Cataldi[2], S. Vitali[2], P. A. Erba[2], N. Belcari[1];
[1]University of Pisa, Department of Physics, Pisa, ITALY,
[2]University of Pisa and Azienda Ospedaliero Universitaria Pisana, Department of Translational Research and of New Surgical and Medical Technologies, Pisa, ITALY.

Aim/Introduction: Cerenkov luminescence imaging (CLI) is an imaging modality to detect distributions of radiopharmaceuticals that can allow intra-operative visualization of surgical margins and immediate surgery refinement. We are planning a pilot clinical study to evaluate its impact on pulmonary and hepatic metastasectomy, using ^{18}F-FDG and ^{68}Ga-DOTATOC. We are currently optimizing the clinical protocol regarding patient inclusion criteria, activity to inject, maximum allowed delay for imaging and radiation monitoring. ***Materials and Methods:*** To optimize the clinical protocol, we are performing a preliminary study, featuring, on one side, an analysis of patient PET/CT data (n=45) to determine typical uptake, lesion dimension, resection margins; on the other, an in-vitro study to determine the detection limits for ^{18}F and ^{68}Ga in animal tissue specimens as a function of the depth in tissue, using signal-to-noise ratio (SNR) as metrics. ^{18}F-FDG and ^{68}Ga-HCl were either diluted in distilled water inside Petri dishes or uniformly distributed in agar-based solid phantoms and placed under animal liver slabs. Acquisitions were performed with acceptable exposure times (no longer than five minutes) and spatial resolution (0.9375 mm/pixel). We have also acquired images with 550- and 800- nm short-pass filters to try estimating the source depth. We plan to repeat the same in-vitro measurements with animal lung specimens. ***Results:*** PET/CT data indicate tumor uptakes that vary from 4-11 kBq/cc at the time of CLI, assumed to be approximately 5 hours post-injection. So far, we have obtained the following in-vitro results: 1) the light yield of ^{68}Ga is 15 (22) times that of ^{18}F in agar (Petri); 2) when imaged in air, a certain amount of activity in a given volume produces in the agar phantoms a signal that is 2.3 (1.6) times that in a Petri for ^{68}Ga (^{18}F); 3) the average attenuation length of our animal liver specimens is ~1.5 mm; 4) the detection limits with SNR=2 for ^{68}Ga in a Petri dish are 0.93 kBq/cc in air, and 2.7 kBq/cc at a depth of 2.5 mm in liver. The detection limits for agar, for other depths and for ^{18}F agree well with the conversion factors given by 1)-3). ***Conclusion:*** The fact that clinical uptakes are larger than the detection limits we measured is promising, because it suggests that intra-operative Cerenkov luminescence imaging in the liver is likely to be feasible. ***References:*** None

OP-711

Cerenkov Luminescence Imaging in prostate cancer: unraveling of the basal halo

J. olde Heuvel[1], H. G. van der Poel[1], E. M. Bekers[1], M. P. M. Stokkel[1], C. H. Slump[2], B. J. de Wit-van der Veen[1];
[1]Netherlands Cancer Instititute, Amsterdam, NETHERLANDS,
[2]University of Twente, Enschede, NETHERLANDS.

Aim/Introduction: Positive surgical margins (PSM) are found in up to 38% of patients after radical prostatectomy. Cerenkov Luminescence Imaging (CLI) is a novel imaging technology that could be used for intra-operative margin assessment after injection of ^{68}Ga-PSMA [1]. In this ongoing clinical trial an area of increased signal intensity, referred to as halo, was visible on all images of the prostate base, despite the fact that the tumor was not located there in 6/13 patients. Since this basal halo might hamper visualization of PSMs, the study aim is to unravel its origin. ***Materials and Methods:*** The study was approved by local ethics committee and all patients signed informed consent. All CLI images were acquired at 150s, 8x8 binning, with and without 550nm shortpass filter and corrected for decay. Possible sources for the halo that were assessed are; 1) urine contamination and 2) chemiluminescence. First, two prostates of patients injected with ~100MBq ^{68}Ga-PSMA are imaged before and after rinsing it with sodium chloride. Subsequently, prostates of three patients who underwent surgery without ^{68}Ga-PSMA injection were imaged to assess signal intensities in non-radioactive specimens. The signal half-life, influence of a 550nm short-pass filter and 6µm thick scintillator sheet on the intensity of the halo signal were investigated. ***Results:*** Rinsing a radioactive prostate

did not reduce the signal both visually and quantitatively, suggesting the halo is not caused by urine contamination. The basal halo was also observed in non-radioactive specimens. The use of the 550nm short pass filter reduced this signal with 85%. The half-life of the basal halo was on average 50±12min. A scintillator sheet reduced the image intensity by 50% of its original signal, in both non-filtered and filtered setting. ***Conclusion:*** The basal halo is not caused by urine contamination, and importantly, is also visible in non-radioactive specimens. It is hypothesized that the halo is produced by chemiluminescence from radical oxygen species[2], generated by use of diathermia at the base to separate bladder from the prostate. The half-life of this diathermia halo and ^{68}Ga-Cerenkov signal is similar (50 vs. 68min), so it remains difficult to distinguish the two. ***References:*** 1. olde Heuvel J, de Wit-van der Veen BJ, van der Poel HG, et al. ^{68}Ga-PSMA Cerenkov luminescence imaging in primary prostate cancer: first-in-man series. Eur. J. Nucl. Med. Mol. Imaging. 2020; 2. Kobayashi K, Okabe H, Kawano S, Hidaka Y, Hara K. Biophoton emission induced by heat shock. PLoS One. 2014;9:e105700.

OP-712

A smart forceps for intraoperative fluorescence tissue characterisation during robotic surgery - technical development and validation in large animal models

M. van Oosterom[1,2], S. I. van Leeuwen[1], F. van Beurden[1,2], E. Mazzone[3,4], P. Dell'Oglio[1,4], T. Buckle[1,2], M. Boonekamp[5], K. Bauwens[4], H. Simon[6], P. J. van Leeuwen[2], H. G. van der Poel[2], F. W. B. van Leeuwen[1,2,4];
[1]IMI-Lab, Dept. of Radiology, Leiden University Medical Center, Leiden, NETHERLANDS, [2]Department of Urology, Netherlands Cancer Institute - Antoni van Leeuwenhoek Hospital, Amsterdam, NETHERLANDS, [3]Division of Oncology/Unit of Urology, URI, IRCCS Ospedale San Raffaele; Vita-Salute San Raffaele University, Milan, ITALY, [4]ORSI Academy, Melle, BELGIUM, [5]Medical Technology Center, Leiden University Medical Center, Leiden, NETHERLANDS, [6]Eurorad, Eckbolsheim, FRANCE.

Aim/Introduction: The introduction of a small and tethered DROP-IN gamma probe helped facilitate precision radioguided surgery in the robotic workflow by enhancing the manoeuvrability of the detection modality [1,2,3]. In addition to radioguidance, fluorescence guidance is increasingly being implemented during robotic surgery, in particular angiography and lymphatic mapping with indocyanine green (ICG). Next to issues in manoeuvrability of the fluorescence laparoscope, fluorescence imaging may limit the surgical logistics: during laparoscopic surgery its overall depiction of the patient anatomy (e.g. bleedings) has proven inferior to white light imaging. Hence implementation of fluorescence imaging requires a surgeon to pause the resection, interrupting the surgical workflow. In addition, this means fluorescent tracers are not detected during the actual resection under white light. To this end, we developed and investigated click-on fluorescence detectors that convert robotic surgical instruments into fluorescence imaging devices (so-called SmartForceps), detecting fluorescence tracers in the tissues grasped during every stage of the surgical procedure. ***Materials and Methods:*** A tailored fibre-based fluorescence detector for ICG was engineered so that it could be clicked-on to traditional instruments of the surgical robot. Translational performance evaluation was performed using: 1) phantoms; 2) during robotic surgery in pigs (n=5), evaluating angiography and lymph node localisation; and 3) on surgical specimens from clinical sentinel node procedures that made use of the hybrid tracer ICG-^{99m}Tc-nanocolloid (n= 2; prostate cancer). ***Results:*** The instruments, including detectors, could be introduced through standard 12 mm trocars. After insertion in the abdomen, the detectors did not interfere with the instruments grasping ability or manoeuvrability. Only in fluorescent samples, as confirmed with fluorescence imaging, fluorescent counts were detected using the SmartForceps. Porcine surgery demonstrated grasping of tissue allowed for the identification of blood vessels (bladder, bowel and kidney) and pelvic lymph nodes. During ex vivo evaluation with human prostate cancer related lymph nodes, the SmartForceps could distinguish sentinel nodes from non-sentinel nodes, as confirmed by fluorescence imaging and gamma probe detection. ***Conclusion:*** This study successfully introduces a click-on fluorescence-based sensing module for robotic surgical instruments, turning regular forceps into SmartForceps. This technology allows fluorescence sensing during white light resections. In addition, it opens the way for bio-sensing applications, where the surgical instruments can be used to characterise the molecular aspects of tissues. ***References:*** [1] M.N. van Oosterom et al., AJNMMI, 2016; [2] P. Meershoek et al., EJNMMI, 2019; [3] F.W.B. van Leeuwen et al., Clin Nucl Med, 2019

OP-713

Imaging Cancer Immunology: Magnetic Particle Imaging of Immunotherapy

J. Mansfield[1], G. Ren[1], M. Gerosa[2], J. Gaudet[1], N. Carvou[1], Y. Zhang[2], P. Goodwill[1], M. Wintermark[2];
[1]Magnetic Insight, Alameda, CA, UNITED STATES OF AMERICA, [2]Stanford University, Palo Alto, CA, UNITED STATES OF AMERICA.

Aim/Introduction: The rapid growth of immuno-oncology research has fueled a need to evaluate the location, quantity, and phenotype of immune cells. Tumour-associated macrophages (TAMs) play a pivotal role in cancer immunotherapy. However, current methods for qualitative and quantitative measurements of TAM accumulation are insufficient. Magnetic Particle Imaging (MPI) is a novel tomographic molecular imaging technique

used to non-invasively track cells labeled with magnetic nanoparticles. MPI provides sensitive (<50 attomole nanoparticle detection limit), depth-independent, 3D quantitative data and imagery (&gt3 logs linear dynamic range) about nanoparticle biodistribution in longitudinal studies. Phagocytotic cells, such as macrophages, become labeled with the nanoparticles in situ following intravenous injection. ***Materials and Methods:*** A murine breast tumour model was established by injecting 3 x 10^5 4T1 cells into the 5th mammary fat pad of 8-10-week-old female Balb/c mice. Immunotherapy treatment was with a CD47 mAb (200 ug x 5 days). Two groups were used: a CD47-treated group and an untreated control group. All mice were injected with an iron-oxide MPI tracer (Synomag PEG 50, Micromod GMBH, 5 mg/kg) and then 3D images were acquired on MPI and MRI (T2-weighted multi-slice, multi-echo sequences). Images were acquired at 1, 3, and 7 days after tracer injection. MPI and MRI images were co-registered and quantitated. Tumour, liver, spleen, and draining lymph nodes were harvested, imaged, fixed, and stained with Perls Prussian blue for analysis of iron content. ***Results:*** This preliminary study suggests that TAM accumulation increases following CD47 mAb treatment. All mice showed an accumulation of tracer in the tumor and liver following injection and signal was predominately detected in the expanding margins of the tumour. There was an increased tracer accumulation at the tumour site for the treated group compared to the control on days 1 and 3 following injection, but not on day 7 ($p = 0.002$, 0.243 and 0.075, respectively). ***Conclusion:*** MPI provides valuable quantitative and spatial distribution information for preclinical models. In combination with existing FDG-PET techniques for increased glucose consumption, in situ tagging of phagocytic cells with magnetic tracers and MPI could significantly improve the specificity of inflammation detection. This would enable researchers to monitor the efficacy of immunotherapies with the sensitivity, specificity and quantitation they require. ***References:*** None

OP-714

3D compton Imaging: A new modality for nuclear medicine at 511 KeV and above

A. Iltis[1], G. Zeufack[1], M. Lopez[1], H. Snoussi[2], L. Zimmer[3,4], N. Costes[3], C. Bouillot[3], Z. Hmissi[1], F. Lavenne[3], J. Redoute[3];
[1]Damavan Imaging, Rosieres pres Troyes, FRANCE, [2]Université de Technologie de Troyes (UTT), Troyes, FRANCE, [3]CERMEP-Imagerie du vivant, Bron, FRANCE, [4]INSERM, CNRS, Université de Lyon, Lyon, FRANCE.

Aim/Introduction: So far, the main imaging modalities for nuclear medicine are PET and SPECT scanners. Both modalities require a large number of views or many LOR to reconstruct a tomographic image of a patient. To populate all those views in a reasonable time, a large activity above 100 MBq must be injected to the patient. Besides for both modalities each detector element (Septa or pair of coincidence detector) has a limited field of view below 10°. Compton imaging offers wide FOV (90°x90°) and requires no collimation. 2D Compton imaging has been proposed as an alternative to SPECT, but Compton imaging doesn't work well at the low energies of SPECT tracers (140 KeV). ***Materials and Methods:*** We have developed a hand-held Compton camera based on temporal imaging and $CeBr_3$ monolithic scintillator plates for nuclear industry. This camera has the following characteristics:1) A 90x90° Field of view with small equipment allowing to study large animals (monkeys, horses…) 2) 3D imaging with 3-4 views only 3) Injection of a dose to the patient an order of magnitude lower than standard. Typically we would need less than 10 MBq for a human body. 4) Reasonable spatial resolution below 1cm^3 for human torso, probably below 0,1 cm^3 for brain. 5) Using well known isotopes as those used for PET imaging 6) But we could also use also radiotherapy isotopes having significant emissions above 400 KeV (^{131}I, ^{177}Lu, ^{211}At …) . 7) Digital photon counting allowing quantification with a good signal/noise ***Results:*** With this camera we have obtained first views of a mouse injected with Fluorine 18. We have obtained both 2D images from a single view and tomographic 3D image by using 3 views at right angle to the object, using only a 0,6MBq dose and 5 minutes exposures. The results presented here are very preliminary and the images obtained are in no way optimized, but they are very promising. ***Conclusion:*** 3D Compton imaging appears as a promising new imaging modality in complement to SPECT and PET as it allows: It seems possible with this technology to obtained tomographic 3D images with a voxel size below 1 cm3 in human patients with an injected dose an order of magnitude below standard practice in PET and with a portable equipment ***References:*** T Zafiarifety et al. (2019). "Temporal ImagingCeBr3 Compton camera: First imaging results and perspectives in medical imaging". In: SPIE, San Diego, California, United States.

1307

Pitfalls & Artefacts 6: Pitfalls and Artefacts in Paediatric Nuclear Medicine

Thursday, October 29, 2020, 16:35 - 18:05 Channel 7

OP-715

Paediatric Nuclear Medicine Specificities and Image Artefacts

C. Olianti; Florence University Hospital Careggi, Nuclear Medicine Department, Florence, ITALY.

OP-716

Imaging Artefacts in Paediatric Nuclear Medicine - Planar Imaging

A. Santos; Hospital Garcia de Orta, Nuclear Medicine Department, Almada, PORTUGAL.

OP-717

Imaging Artefacts in Paediatric Nuclear Medicine – SPET/CT, PET/CT and PET/MR

P. Zucchetta; Padua University Hospital, Nuclear Medicine Department, Padova, ITALY.

1308

Clinical Oncology Track - TROP Session: PET Diagnostics of Lung Cancer and Mesothelioma

Thursday, October 29, 2020, 16:35 - 18:05 Channel 8

OP-718

Concordance of PD-L1 status between image-guided percutaneous biopsies and matched surgical specimen in non-small cell lung cancer

L. Zhao, H. Chen, Y. Zhuang, Q. Lin;
the First Affiliated Hospital of Xiamen University, Xiamen, CHINA.

Aim/Introduction: Determining PD-L1 expression status could help select patients with non-small cell lung cancer (NSCLC) who will optimally benefit from anti-PD-1/PD-L1 immunotherapy.Currently, PD-L1 testing is mainly performed on biopsy samples because of diagnosis at the advanced stage. However, the inevitable intra-tumor heterogeneity would markedly affect the results of PD-L1 status investigations. As such, the concordance of PD-L1 status between biopsy samplesand matched resected specimens varied across previous studies [1, 2]. This study aimed to evaluate the concordance of PD-L1 expression between image-guided percutaneous biopsies and matched surgical specimens. *Materials and Methods:* We evaluated 157 patients diagnosed with operable NSCLC on both surgical tissue sections and matched lung biopsies retrospectively.The patients underwent either regular computed tomography (CT)-guided biopsy (n=82) or ^{18}F-FDG positron emission tomography (PET)/CT-guided biopsy (n=75). The diagnostic success rates of CT- and ^{18}F-FDG PET/CT-guided biopsy were scored. The concordance between surgical specimens and lung biopsies for PD-L1 TPS was evaluated using Cohen's kappa (κ) coefficient. *Results:* The diagnostic success rates of CT- and ^{18}F-FDG PET/CT-guided biopsy were 82.9% (68/82) and 93.3% (70/75), respectively. Immunohistochemical expression of PD-L1 was evaluated in both surgical resected specimens and matched biopsies in the eligible 138 patients. The concordance rate of PD-L1 expression between surgical tissue sections and matched biopsies was fairly high at 83.3% (115/138), and the κ value was 0.73 (95% CI: 0.63-0.83, $P < 0.001$). The concordance rate was higher for tissue sections from ^{18}F-FDG PET/CT-guided biopsy than for tissue sections from CT-guided biopsy (88.6% [62/70, κ value: 0.81] vs 77.9% [53/68, κ value: 0.66]). *Conclusion:* PD-L1 TPS was strongly concordant between surgical specimens and matched lung biopsies. Thus, routine evaluation of PD-L1 expression in diagnostic percutaneous biopsies could be reliable for identifying patients who will benefit from anti-PD-1/PD-L1 immunotherapy. Moreover, our result showed ^{18}F-FDG PET/CT-guided biopsy has higher diagnostic success rate and concordance compare with CT-guided biopsy. *References:* 1. Ilie, M., et al., Comparative study of the PD-L1 status between surgically resected specimens and matched biopsies of NSCLC patients reveal major discordances: a potential issue for anti-PD-L1 therapeutic strategies.Ann Oncol, 2016. 27(1): p. 147-53. 2. Thunnissen, E., et al., Programmed death-ligand 1 expression influenced by tissue sample size. Scoring based on tissue microarrays' and cross-validation with resections, in patients with, stage I-III, non-small cell lung carcinoma of the European Thoracic Oncology Platform Lungscape cohort.Mod Pathol, 2019.

OP-719

Differentiation of the histopathological types of solitary pulmonary nodules with ^{18}F-FDG PET/CT radiomic using machine-learning methods

Y. Zhou, R. Tian;
West China Hospital, Chengdu, CHINA.

Aim/Introduction: Our study assessed the ability of ^{18}F-fluorodeoxyglucose (FDG) positron emission tomography/computed tomography (PET/CT) radiomics features combined with a large panel of machine-learning methods to differentiate primary lung cancer from metastatic lung cancer and squamous cell carcinoma from adenocarcinoma, and secondly to identify optimal machine-learning methods. *Materials and Methods:* 775 patients pathologically diagnosed as primary or metastatic lung lesions were retrospectively studied. Radiomics features were extracted from semiautomatically segmented PET and CT images using the LIFEx package. Five feature selection methods and nine machine learning classifiers were used to establish the differentiate models. The patient cohort was randomly divided into a training and a validation group and the robustness of the procedure was tested by ten-fold cross validation. The areas under the receiver operating characteristic curve (AUC) , accuracy, sensitivity, and specificity were calculated to evaluate the discriminative ability of these models. *Results:* Forty-five differentiate models were established based on radiomics features from PET and CT images. Most of the classifiers represented feasible ability in differentiation, with AUC more than 0.8 when combined with suitable selection method. In the differentiation of primary lung cancer and metastatic lung cancer, for models based on PET

images, the combination of GBDT and AdaBoost classifier represented the highest AUC of 0.98 in the validation group, while the combination of Xgboost and GBDT classifier represented the highest AUC of 0.863 in the validation group for models based on CT images. In the differentiation of squamous cell carcinoma and adenocarcinoma, for models based on PET images, the combination of GBDT and GBDT classifier represented the highest AUC of 0.917 in the validation group, while the combination of GBDT and LDA classifier represented the highest AUC of 0.853 in the validation group for models based on CT images. Most of the DT-based models were overfitting, suggesting that this classifier was not suitable for application. ***Conclusion:*** Radiomics features extracted from ^{18}F-FDG PET and CT images are efficient to differentiate primary lung cancer from metastatic lung cancer and squamous cell carcinoma from adenocarcinoma using machine-learning methods. ***References:*** None

OP-720

Comparison of Metabolic and Morphological Response Criteria for Early Prediction of Response and Survival in NSCLC Patients Treated with Checkpoint Inhibitors

A. Castello*, S. Rossi, L. Toschi, E. Lopci;*
Humanitas Clinical and Research Hospital, Rozzano (MI), ITALY.

Aim/Introduction: Immunotherapy with immune checkpoint inhibitors (ICI) has positively changed the history of several malignant tumors. In parallel, new challenges have been arisen in the evaluation of treatment response due to their peculiar anticancer effect. In the current study we aim to compare different response criteria, both morphological and metabolic, for assessing response and outcome in patients with advanced non-small-cell lung cancer (NSCLC) treated with ICI. ***Materials and Methods:*** Overall, 52 patients with advanced NSCLC candidate to ICI were prospectively evaluated. Inclusion criteria comprised whole body contrast-enhanced CT and 18F-FDG PET/CT at baseline and at the first response evaluation after 3 or 4 cycles of ICI. Response assessment by CT was performed according to RECIST 1.1 and iRECIST criteria, whereas metabolic response on PET was computed by EORTC, PERCIST, imPERCIST, and PERCIMT criteria. The concordance among the different tumor response criteria and the performance of each criterion to predict PFS and OS were calculated. ***Results:*** Inclusion criteria were fulfilled in 35 out of 52 patients. We observed a low agreement between iRECIST and imPERCIST (κ=0.174) with discordant response in 14 patients (p=0.005), fair agreement between iRECIST and EORTC (κ=0.360), and PERCIST (κ=0.404), and moderate for PERCIMT (κ=0.484). Moreover, we found a moderate agreement between EORTC and imPERCIST (k=0.446) with discordant response in 21 patients (p<0.001), particularly regarding stable metabolic disease and progressive metabolic disease groups. All criteria were significantly associated with PFS, while only PERCIMT and imPERCIST were associated with OS. Of note, in patients classified as immune stable disease (iSD), imPERCIST well differentiated those with longer PFS (p<0.001) and OS (p=0.001). In the multivariate analysis, performance status (HR=0.278, p=0.015), iRECIST (HR=3.799, p=0.026), and imPERCIST (HR=4.064, p=0.014) were predictive factors for PFS, while only performance status (HR=0.327, p=0.035) and imPERCIST (HR= 3.247, p=0.007) were predictive for OS. ***Conclusion:*** At the first evaluation during treatment with ICI, imPERCIST criteria correctly evaluate treatment response and appear able to predict survival. Moreover, in patients with iSD on CT, imPERCIST was able to discriminate those with longer survival. This advantage might allow for earlier therapy modification based on the metabolic response. ***References:*** The Italian Association for Research on Cancer (AIRC - Associazione Italiana per la Ricerca sul Cancro) is acknowledged for the support on research with the grant nr. 18923.

OP-721

Analysis of the Association between SUV index in ^{18}F-FDG PET/CT Imaging and Malignant Risk of Ground-Glass nodules: A Retrospective Cohort Study

R. Niu*, X. Shao, X. Shao, J. Wang, M. Xu, Y. Wang;*
The Third Affiliated Hospital of Soochow University, Changzhou, CHINA.

Aim/Introduction: To explore the association between the SUV index (GGN SUVmax / liver SUVmean) in ^{18}F-FDG PET / CT imaging and the malignant risk of ground-glass nodules (GGNs). ***Materials and Methods:*** A retrospective analysis of 166 patients with GGN who underwent PET/CT from January 2012 to October 2019 was performed. There were 113 males and 53 females, aged (60.8 ± 9.1) years. 192 GGNs were confirmed by postoperative pathology, 22 in the benign group, and 170 in the adenocarcinoma group. The clinical and imaging data of all patients were collected and analyzed. The patients were grouped based on SUV index tertiles, and the differences of clinical and imaging parameters among groups were compared with analysis of ANOVA or Kruskal-Wallis test. Univariate logistic regression method was used to analyze the influencing factors of malignant GGN. Multivariate logistic regression and stratified analysis were used to correct for confounding factors. Generalized additive model was used to test the nonlinear relationship between the SUV index and the malignant risk of GGN. ***Results:*** The percentages of malignant GGN from Tertile 1 to Tertile 3 were 89.1%, 95.3%, and 81.2%, respectively. After adjusting for the potential confounding factors, we found that the malignancy risk of GGN significantly decreased as the SUV index increased (OR, 0.245; 95% CI, 0.119-0.504; P <0.001), and the increase of SUV index was significantly correlated with the reduction of malignant risk (OR, 0.099;

95% CI, 0.025-0.394; P = 0.001), especially between Tertile 3 and Tertile 1 (OR, 0.064; 95% CI, 0.012- 0.356; P = 0.002). Curve fitting showed that the SUV index was linearly and negatively correlated with the malignant risk of GGN, and the correlation was not affected by age, GGN number, type, shape, vacuolar signs, and CTR levels, indicating that SUV index had no significant interaction with these factors (P for interaction range: 0.187-1.000). ***Conclusion:*** The SUV index is an independent correlation factor for GGN malignant risk, and these two factors are linearly and negatively correlated. The understanding of this correlation will help to improve the accuracy of PET/CT in GGN diagnosis. ***References:*** None

OP-722

Prediction of mutational status in lung cancer using PET radiomics

M. Berraho[1], *O. Tankyevych*[1,2], *G. Tachon*[3], *M. Hatt*[2], *D. Visvikis*[2], *C. Cheze le Rest*[1,2];
[1]*Nuclear medicine, CHU de Poitiers, Poitiers, FRANCE,* [2]*LaTIM, INSERM, UMR1101, Brest, FRANCE,* [3]*Cancer biology, CHU Poitiers, Poitiers, FRANCE.*

Aim/Introduction: Nowadays, precise characterization of lung adenocarcinoma at the genetic level is a fundamental requirement for personalized therapy. The present work aims at evaluating radio-genomic associations of quantitative parameters derived from initial 18FDG PET/CT in lung adenocarcinoma. The study was retrospectively designed to assess feasibility of mutational status identification using pretreatment PET image derived parameters. ***Materials and Methods:*** 487 patients with pulmonary adenocarcinoma were included in this retrospective study. All patients underwent 18FDG PET/CT for initial staging and EGFR, KRAS, BRAF mutational status and PDL1 expression , ALK translocation and ROS1 fusion were assessed. All primary tumors were identified (volume larger than 4 cm3) on PET images and were automatically segmented using the FLAB algorithm, and radiomics parameters were derived. The association between PET parameters and biological characteristics were evaluated. ***Results:*** A total of 120 features were extracted from each PET image. Routinely used SUVmax had no efficient predictive value for any of the biological studied characteristics. In univariate and multivariate analysis, several PET parameters were associated with EGFR, PDL1, ROS1 and BRAF status, with individual AUC reaching 0.86. The best performing parameters were different depending on the studied gene. Textural parameters did better than any volume related ones. No parameter managed to predict efficiently KRAS and ALK translocation (AUC< 0.65). ***Conclusion:*** Our results confirm that PET radiomics could help detect lung adenocarcinoma harboring EGFR, BRAF mutation, ROS fusion, and PDL1 expression. PET radiomics could be a powerful approach to identify specific molecular subgroups of pulmonary carcinoma and should be considered to guide patient management. ***References:*** None

OP-723

PERCIST-derived metabolic volume response predicts overall and progression-free survival in patients with malignant pleural mesothelioma treated with Pembrolizumab

J. Ferdinandus*, F. Barbato, M. Chodyla, W. P. Fendler, L. Kessler, M. Metzenmacher, F. Krefting, T. Hager, K. Herrmann, D. C. Christoph; University Hospital Essen, Essen, GERMANY.*

Aim/Introduction: Despite promising response rates in phase 1b and 2 clinical trials, immune checkpoint inhibition (ICI) with pembrolizumab for the treatment of malignant pleural mesothelioma (MPM) did not result in survival benefit in the PROMISE-meso trial compared to 2nd-line chemotherapy. Due to lack of validated imaging response criteria, responder-subgroups with potential survival benefit have not yet been identified. Here, we assess the predictive value of PET metabolic response in patients undergoing four cycles of high-dose pembrolizumab (10 mg/kg, d_1, q2w) considering the KEYNOTE-028 trial procedure for chemotherapy-resistant malignant pleural or peritoneal mesothelioma. ***Materials and Methods:*** RECIST v1.1, mRECIST, PERCIST (using SULpeak, MTV and TLG) response assessment criteria were used separately to categorize responders in CT and PET imaging studies. Progression-free survival (PFS) and overall Survival (OS) of responders were compared to non-responders using Kaplan-Meier methods and log-rank comparisons. Fishers-exact testing was used to compare PD-L1e expression status of responders vs.non-responders. ***Results:*** Twenty-seven patients had [^{18}F]-FDG-PET/CT imaging at baseline and after four cycles of pembrolizumab. Response rates were 7%, 7%, 30%, 30% and 33% based on RECIST v1.1, mRECIST, PERCIST, MTV and TLG response criteria, respectively. Regarding PFS, only MTV and TLG response groups showed a significant different survival ($p < 0.01$, respectively). Regarding OS, only a reduction of MTV ≥30% predicted prolonged survival ($p < 0.01$). PD-L1 expression could not be associated with response rates or survival. ***Conclusion:*** PERCIST-derived metabolic volume response predicts survival in pretreated patients with malignant mesothelioma receiving high-dose pembrolizumab. These results warrant inclusion of PET response assessment in future clinical trials and routine practice. ***References:*** None

OP-724

Interobserver reliability in the quantitative assessment of [^{99m}Tc]-labeled anti-Programmed Death-Ligand 1 (PD-L1) SPECT/CT in non-small cell lung cancer

D. Hughes[1], *G. Chand*[1], *H. Ting*[2], *V. Warbey*[1], *V. Goh*[1], *G. Cook*[1];
[1]*Department of Cancer Imaging, School of Biomedical Sciences*

and Engineering, King's College London, London, UNITED KINGDOM, [2]Department of Research and Development, NanoMab Technology Limited, Shanghai, CHINA.

Aim/Introduction: Checkpoint inhibition using directed antibody therapy (e.g. antiprogrammed death-1 antibody) has become a standard of care in the management of non-small cell lung cancer (NSCLC). [^{99m}Tc]-labeled anti-PDL1 single-domain antibody single-photon emission computed tomography (SPECT) has been shown to demonstrate tumour to blood pool ratios that correlate with tumoural PD-L1 expression. In this study, we assessed whether this quantitative assessment demonstrated interobserver reliability. ***Materials and Methods:*** Using 1 and 2h post-injection [^{99m}Tc]sdAb-PD-L1 SPECT scans in 21 patients with NSCLC, three independent observers applied a manual technique for measurement of ROI_{max} of primary tumour, metastatic lesions and normal tissue references to determine PD-L1 expression. A two-way random effects model was applied to estimate the intraclass correlation coefficient (ICC) of single measurements and tumour (T) ROI_{max} to blood pool (BP) ROI_{max} ratio using SPSS. ***Results:*** Manual ROI_{max} scoring of primary tumour (0.95 confidence interval, 0.90.97), lung (0.99-1.0) and nodal (0.95-0.98) metastases all demonstrated an ICC of >0.9. Blood pool ROI_{max} score ICC was 0.9 (0.84-0.94) with a T:BP ICC of 0.83 (0.73-0.90). The ICC for normal lung tissue was 0.84 (0.75-0.90), however, applying an anatomically defined rule-based approach to scoring demonstrated a trend toward improved reliability (ICC 0.89; 0.82-0.93). ***Conclusion:*** Measurement of PD-L1 expression using [^{99m}Tc]-labeled anti-PD-L1 SPECT of primary tumour, lung and nodal metastases is achievable with excellent interobserver reliability. In addition, T:BP previously shown to correlate with tumoural PD-L1 expression demonstrated good interobserver reliability. ***References:*** None

OP-725

Role of texture parameters derived from baseline 18F-FDG PET/CT as prognostic markers in non-small cell lung cancer (NSCLC) patients undergoing platinum-based chemotherapy

A. Sharma*, A. K. Pandey, C. Bal, R. Kumar;*
All India Institute of Medical Sciences, New Delhi, INDIA.

Aim/Introduction: To prospectively evaluate the role of texture parameters evaluated from baseline 18F-FDG PET/CT in prediction of overall survival (OS) in biopsy proven NSCLC patients who were planned to undergo platinum-based chemotherapy. ***Materials and Methods:*** Forty five patients (36 male, 9 female) with biopsy proven NSCLC (22 adenocarcinoma, 17 Squamous cell carcinoma and 6 NSCLC NOS) and mean age 55.22±10.370 years were enrolled in the study. Each patient underwent a baseline whole body 18F-FDG PET/CT scan on Biograph mCT 64 slice after 60 minutes of injecting 5.18-7.77 MBq/kg of 18F-FDG intravenously. For texture analysis, the displayed PET/CT images with maximum tumor diameter were exported in JPEG format and analysis was performed using R version 3.4.3. Ten Intensity Histogram based first order and 21 GLCM based second order texture features (16 bins, zero degree direction, 1 pixel distance) were evaluated. SUV and MTV based parameters were also evaluated. Cut-off values for all significant parameters ($p < 0.05$) were calculated using ROC analysis. Univariate Survival analysis was performed in which survival patterns were compared by log rank method and presented using Kaplan-Meier curves. Multivariate analysis was performed and hazard ratios (HRs) were evaluated by Cox regression model. ***Results:*** Median follow up time of 45 patients was 9 months (range: 1 - 27 months) during which 27 patients died. In univariate survival analysis, 6 first order texture parameters i.e. entropy, skewness, uniformity, mean, median and RMS were found to be significantly associated with OS with cut-off values 3.37, -0.803, 0.130, 10.26, 12.50, 11.49 and HRs 4.908 (p=0.004), 4.006 (p=0.002), 2.649 (p=0.018), 3.573 (p=0.003), 3.153 (p=0.009), 2.685 (p=0.019), respectively. Among the second order parameters, mean, auto-correlation, energy, entropy, inverse variance, maximum probability, sum average, sum entropy, sum variance were significantly associated with OS with cut-off values 10.45, 131.70, 0.0725, 3.561, 0.3603, 0.211, 22.51, 4.164 and HRs 3.573 (p=0.003), 2.685 (p=0.019), 2.965 (p=0.015), 2.349 (p=0.038), 2.213 (p=0.048), 3.749 (p=0.003), 2.845 (p=0.018), 2.834 (p=0.014), respectively. Among the clinical parameters, only ECOG was significantly associated with OS (HR 2.839, p = 0.01). In multivariate cox regression analysis skewness was found to be the independent predictor of OS with HR 4.006 (p=0.002). None of the SUV and tumor volume based parameters were significantly associated with OS. ***Conclusion:*** Texture parameters evaluated from baseline 18F-FDG PET/CT performed better than routinely used metabolic parameters and can be used as reliable prognostic markers of OS in NSCLC. ***References:*** None

OP-726

Value of ^{18}F-FDG PET/CT-Based Radiomics Model to Distinguish the Growth Patterns of Early Invasive Lung Adenocarcinoma Manifesting as Ground-Glass Opacity Nodules

X. Shao*, R. Niu, X. Shao, Y. Wang;*
the Third Affiliated Hospital of Soochow University, Changzhou, CHINA.

Aim/Introduction: The growth pattern of invasive lung adenocarcinoma (IAC) manifesting as ground-glass opacity nodules (GGNs), is divided into lepidic, acinar, papillary, micropapillary, and solid predominant. The use of predominant growth patterns not only helps to classify IAC into subtypes but also serves as a prognostic

indicator independent of the clinical stage. Among the first three most common growth patterns, the prognosis of acinar or papillary types is worse than lepidic. The confirmation of the IAC growth pattern before surgery is essential for the risk stratification of GGN and personalized treatment. This study aimed to establish and validate the PET/CT-based radiomics model and use it to predict the intermediate-high risk growth patterns in early invasive adenocarcinoma (IAC). ***Materials and Methods:*** Eighty-two ground-glass nodules (GGNs) from 80 patients with stage IA who underwent a preoperative ^{18}F-FDG PET/CT scan and histopathological examination were included in this study. Texture analysis software was used to extract 52 PET and 49 CT radiomics features. The least absolute shrinkage and selection operator (LASSO) algorithm was used to select radiomics features and develop radiomics signatures. We used the receiver operating characteristics curve (ROC) to compare the predictive performance of conventional CT parameters, radiomics signatures, and the combination of these two. Also, a nomogram based on conventional CT indicators and radiomics signature score (rad-score) were developed. ***Results:*** GGNs were divided into lepidic group (n = 17) and acinar-papillary group (n = 65). Seven radiomics features were selected to calculate the rad-score (Rad-score = − 1.58597 × GLRLM_LRE + 0.00207 × GLZLM_LZE + 0.00058 × GLZLM_LZLGE − 0.00012 × GLZLM_LZHGE + 0.21479 × GLZLM_ZLNU + 3.05551 × GLZLM_ZP − 0.00138 × HUmax), and the area under the curve (AUC) of rad-score was 0.819, which was not significantly different as attenuation value of the ground-glass opacity component on CT (CT_{GGO}) (0.686). When rad-score was combined with CT_{GGO} (joint model, Logit (P) = 9.91059 + 0.00854 × CT_{GGO} + 1.82346 × rad-score), the AUC increased to 0.846 (95% CI [0.741-0.951]), which was significantly higher than CT_{GGO} (P = 0.007). Furthermore, the decision curve analysis of the three models also showed higher clinical value for the joint model. ***Conclusion:*** PET/CT-based radiomics model showed good performance in predicting intermediate-high risk growth patterns in early IAC, providing useful methods for risk stratification, clinical management, and personalized treatment. ***References:*** None

OP-727

18F fluorodeoxyglucose PET/CT Radiomic signature for prediction of lung cancer histology and outcome

E. Giovannini[1], *L. Florimonte*[2], *M. Cuzzocrea*[2], *M. Castellani*[2], *L. Dellavedova*[3], *E. Borsò*[1], *G. Giovacchini*[1], *C. Aschele*[4], *A. Ciarmiello*[1]; [1]*Nuclear Medicine U.O. - Sant'Andrea Hospital, La Spezia, ITALY,* [2]*Fondazione IRCCS Ca' Granda- Ospedale Maggiore Policlinico, Milan, ITALY,* [3]*ASST Ovest Milanese, Milan, ITALY,* [4]*Oncology OU- Sant'Andrea Hospital, La Spezia, ITALY.*

Aim/Introduction: Textural feature analysis, also known as part of radiomics, is an emerging field in quantitative medical imaging analysis, allowing to extract higher dimensional features from grey level distribution of image that are unrecognizable by visual inspection. Preliminary data suggest that radiomics may be used for histological features classification or prognostic evaluation. This study was aimed to evaluate deep learning radiomic approach as a non invasive tool for classification of tumor histology and outcome in lung cancer patients. ***Materials and Methods:*** 85 patients with lung cancer (58 male, 27 female), mean age 70 ± 10 years underwent PET/CT with FDG at initial staging. For data analysis, patients were grouped according to diagnosis in early stage (n=46) and metastatic stage (n=39). A total of 43 radiomics features and SUVmax were extracted from PET/CT for each primary tumor lesion. Receiver operating characteristic curve (AUC) was used to reduce the high dimensionality of radiomic features selecting for subsequent analysis only those exceeding the value of 0.6. The textural features survived to this cut-off were grouped in all possible combination and tested for the accuracy to discriminate among patient's group. The 632+ bootstrap method was used to assess the discrimination performance of each feature subset in terms of AUC. Comparison between textural features and SUVmax for group classification was explored. Statistical analysis was performed with Chi-Square test. Analysis was implemented under Matlab 2019b using Deep Learning Toolbox. ***Results:*** Twenty-four of 43 textural features showed an AUC value of>0.6. The combination with the best diagnostic performance included the following 7 textural features: (GLCM_Contrast, GLSZM_SZE, GLSZM_LZE, GLSZM_ZSN, GLSZM_ZP, GLSZM_LZHGE, NGTDM_Coarseness) which emerged as being more useful to distinguish between groups, compared to the SUVmax (AUC: 0.77 vs. 0.69, P<0.001). In comparison with SUVmax, radiomic model significantly improved the prediction of tumor histology (Chi2=25.2 vs. 2.4; P>0.00001 vs. P=0.12) and disease progression rate (chi2=5.9 vs. 4.8; P=0.01 vs. P=0.02). ***Conclusion:*** Radiomic modeling is a promising approach for prediction of lung cancer histology and outcome. Although this technique deserves validation on larger population it may support clinical decision strategy with complementary information. ***References:*** None

OP-728

A novel model for predicting the invasiveness of early lung adenocarcinoma by combining ^{18}F-FDG PET and HRCT

X. Shao, *X. Shao, R. Niu, M. Xu, Y. Wang; The Third Affiliated Hospital of Soochow University, Changzhou, CHINA.*

Aim/Introduction: To establish a novel model for predicting and validating the invasiveness of early lung adenocarcinoma by ^{18}F-FDG PET combined with HRCT. ***Materials and Methods:*** 149 patients with early stage lung

adenocarcinoma who underwent preoperative PET/CT and HRCT examination in our hospital from October 2011 to October 2019 were enrolled. 457 ground-glass nodules (GGN) were detected by PET/CT, 37.2% (170/457) of GGNs were surgically removed. In order to establish a new prediction model and verify its accuracy, we randomly divided the 170 GGNs resected into a modeling group (89) and a verification group (81), the two groups were divided into pre-invasive/minimally invasive adenocarcinoma (MIA) subgroup and invasive adenocarcinoma (IAC) subgroup according to pathological subtypes. The stepAIC (Akaike Information Criterion) method was used to build the PET/CT model, respectively. Receiver operating characteristic (ROC) curve analysis was used to compare the diagnostic efficacy of different models. ***Results:*** In the modeling group, the proportion of mixed GGNs, irregular shape, lobulation sign, bronchiectasis/distortion/truncation sign, D_{GGN}, D_{Solid}, CTR, CT_{GGO}, and SUV index in the IAC subgroup were significantly higher than those in the pre-invasive/MIA subgroup, the difference was statistically significant (all $P < 0.05$). Among the quantitative parameters of PET/CT (D_{GGN}, D_{Solid}, CTR, CT_{GGO}, SUV_{index}), the SUV_{index} had the best diagnostic efficacy (AUC = 0.854). Use the stepAIC method to build a multi-factor model: $\text{logit}(P) = 2.56455 + 0.00592 \times CT_{GGO} + 3.55028 \times SUV_{index}$. In the modeling group, the efficacy of the model in predicting early lung adenocarcinoma invasion was AUC = 0.854, and the sensitivity, specificity, and accuracy were 0.737, 0.923, and 0.764. In the validation group, the model predicted the early lung adenocarcinoma invasion: the efficacy was AUC = 0.802, and the sensitivity, specificity, and accuracy are 0.970, 0.643, and 0.914. The model has similar prediction performance in the modeling group and the validation group, and has good robustness. ***Conclusion:*** The novel model based on the combination of FDG PET and HRCT parameters has a good predictive value for early lung adenocarcinoma invasiveness and can effectively avoid misdiagnosis and missed diagnosis of IAC. ***References:*** None

OP-729

PD-L1 expressioncorrelation with metabolic parameters of ^{18}F-FDG PET/CTand clinicopathological characteristics in non-small cell lung cancer

L. Jiang;
Shanghai Pulmonary Hospital, Shanghai, CHINA.

Aim/Introduction: Immunotherapy targeting programmed cell death-ligand 1 (PD-L1) has shown promising results in non-small cell lung cancer (NSCLC) patients. Exploring PD-L1 expression could help to select NSCLC candidates for immunotherapy. ^{18}F-FDG PET/CT could provide phenotypic information of malignant tumors. Thus, this study investigated PD-L1 expression correlation with metabolic parameters of ^{18}F-FDG PET/CT and clinicopathological characteristics in NSCLC. ***Materials and Methods:*** ^{18}F-FDG PET/CT metabolic parameters including maximum standard uptake (SUVmax), metabolic tumor volume and total lesion glycolysis of primary lesion (MTV-P, TLG-P), and combination of primary lesion and metastases (MTV-C, TLG-C), were compared with PD-L1-positive expression in patients with NSCLC. Moreover, clinicopathological characteristics, including age, gender, smoking history, serum tumor markers, tumor location, size, TNM stage, and genetic mutation were also reviewed. ***Results:*** All 374 patients (215 men; 159 women; age: 63 ± 9 years) included 283 adenocarcinomas (ACs) and 91 squamous cell carcinomas (SCCs). PD-L1 expression was positive in 27.8% (104/374) cases. SUVmax, TLG-P, and TLG-C of PD-L1-positivity was significantly higher than PD-L1-negativity. Moreover, PD-L1 expression was obviously correlated with man, smoking, and central NSCLC. If ACs and SCCs were separately analyzed, PD-L1 positivity in ACs and SCCs was 21.6% (61/283) and 47.5% (43/91), respectively, and only SUVmax was obviously associated with PD-L1 expression. Furthermore, multivariate analysis revealed that only SUVmax was an independent predictor of PD-L1 positive expression in overall NSCLC, AC, and SCC, respectively. Using a SUVmax cut-off value of 9.8, PD-L1 status of NSCLC was predicted by ^{18}F-FDG PET/CT with sensitivity, specificity, and accuracy of 77.9%, 70.0%, and 72.2%, respectively. ***Conclusion:*** PD-L1 expression of NSCLC was related with SUVmax, TLG, man, smoking, and central location. However, only SUVmax was an independent predictor of PD-L1 positivity, which could help to select NSCLC candidates for immunotherapy. ***References:*** None

1309

Hot Topic Session - Best Clinical Trials

Thursday, October 29, 2020, 16:35 - 18:05 Channel 9

OP-496

Introduction

I.Burger; University of Zurich, Deparment of Nuclear Medicine, Zurich, SWITZERLAND.

OP-497

ProPSMA study - A prospective randomised multi-centre study of Prostate Specific Membrane Antigen (PSMA) PET/CT imaging for staging high-risk prostate cancer prior to curative-intent surgery or radiotherapy

M. Hofman; Peter MacCallum Cancer Centre, Molecular Imaging, Melbourne, AUSTRALIA.

OP-498

68Ga-RM2 Gastrin-Releasing Peptide Receptors PET Imaging for Biochemically Recurrent Prostate Cancer in the Era of PSMA: Results of a Prospective Study

A. Iagaru; Stanford University, Stanford, CA, UNITED STATES OF AMERICA.

OP-499

Characteristics of the relationship between MTV and survival in diffuse large B-cell lymphoma - A PETRA consortium study

N. Mikhaeel[1,2], *M. W. Heymans*[3], *H. C. W. de Vet*[3], *J. J. Eertink*[4], *R. Boellaard*[5], *U. Dührsen*[6], *A. Hüttmann*[6], *C. Schmitz*[6], *L. Ceriani*[7], *E. Zucca*[8], *O. S. Hoekstra*[5], *J. M. Zijlstra*[4], *S. Barrington*[9]; [1]*Guy's Cancer Centre, London, UNITED KINGDOM,* [2]*King's College London, School of Cancer and Pharmaceutical Sciences, London, UNITED KINGDOM,* [3]*Amsterdam UMC, Vrije Universiteit Amsterdam, department of Epidemiology and Biostatistics, Amsterdam Public Health research institute, De Boelelaan 1117, Amsterdam, NETHERLANDS,* [4]*Amsterdam UMC, Vrije Universiteit Amsterdam, department of Hematology, Cancer Center Amsterdam, De Boelelaan 1117, Amsterdam, NETHERLANDS,* [5]*Amsterdam UMC, Vrije Universiteit Amsterdam, department of Radiology and Nuclear Medicine, Cancer Center Amsterdam, De Boelelaan 1117, Amsterdam, NETHERLANDS,* [6]*Department of Hematology, West German Cancer Center, University Hospital Essen, University of Duisburg-Essen, Essen, GERMANY,* [7]*Department of Nuclear Medicine and PET/CT Centre, IIMSI - Imaging Institute of Southern Switzerland, Bellinzona, Switzerland; SAKK - Swiss Group for Clinical Cancer Research, Bern, SWITZERLAND,* [8]*Medical Oncology Clinics, IOSI - Oncology Institute of Southern Switzerland, Bellinzona; Università della Svizzera Italiana, Bellinzona, Switzerland; SAKK - Swiss Group for Clinical Cancer Research, Bern, SWITZERLAND,* [9]*King's College London and Guy's and St Thomas' PET Centre, School of Biomedical Engineering and Imaging Sciences, King's Health Partners, Kings College London, London, UNITED KINGDOM.*

Aim/Introduction: Increased metabolic tumour volume (MTV) in DLBCL is reported to be inversely related to progression-free (PFS) and/or overall survival (OS). However the characteristics of the relationship are not fully understood, as most studies have analysed continuous MTV data in a categorical fashion which is not recommended for optimizing predictive performance. Our aim was to study the relationship between MTV as a continuous variable with PFS and OS and determine the best statistical model to describe it. ***Materials and Methods:*** Patient level data from 1091 DLBCL patients enrolled in 4 studies collated by the PETRA consortium (https://petralymphoma.org) were used to examine the relationship between baseline MTV and 3-year PFS and OS using Cox regression models. MTV was calculated using a fixed SUV ≥ 4.0 threshold. To decide on the best shape and fit of MTV in these models, different transformations of the MTV variable (natural log transformation, MTV squared and linear spline (LSP) and restricted cubic spline (RCS) functions) were plotted and compared with a linear model where MTV was assumed to have a linear relationship with PFS and OS. A spline function describes the association for multiple intervals of MTV, without the assumption of linearity. These MTV transformations were added to the univariable Cox models and the models adjusted for international prognostic index (IPI). The fit of the models was tested and compared with likelihood-ratio tests, R squared and c-index values for discrimination. These analyses were repeated in the separate study cohorts and in the merged dataset. ***Results:*** The RCS models showed highest R-squared values and showed a significantly better ($p < 0.001$) fit for PFS and OS than the MTV squared and LSP model in the merged dataset, which was confirmed by the curved shape of the plot of the relationship between MTV and PFS and OS. The shape of the curve showed an increasing risk of progression, relapse or death with increasing values of MTV. The rise in risk was higher for lower MTV values. Results were consistent for IPI adjusted and unadjusted models in the separate research cohorts and in the merged dataset. Differences in discriminative ability of various transformations of MTV were less clear. ***Conclusion:*** We recommend that MTV is used as a restricted cubic spline function in future analyses to obtain the optimal predictive performance. ***References:*** None

OP-500

Hybrid ICG-^{99m}Tc-nanocolloid, on the road towards becoming the new standard for sentinel node biopsy in penile cancer? Results from 740 inguinal basins assessed at a single institution

H. M. de Vries[1], *P. Dell'Oglio*[2], *E. Mazzone*[3], *G. H. KleinJan*[3], *H. G. van der Poel*[1], *S. Horenblas*[1], *F. W. B. van Leeuwen*[3], *O. R. Brouwer*[1]; [1]*Netherlands Cancer Institute - Antoni van Leeuwenhoek hospital, Amsterdam, NETHERLANDS,* [2]*ASST Grande Ospedale Metropolitano Niguarda, Milan, ITALY,* [3]*Leiden University Medical Center, Leiden, NETHERLANDS.*

Aim/Introduction: Sentinel node (SN) biopsy in penile cancer (PeCa) is typically performed using ^{99m}Tc-nanocolloid and blue dye. Recent reports suggested that the hybrid radioactive and fluorescent tracer indocyanine green (ICG)-^{99m}Tc-nanocolloid may improve intraoperative optical SN identification. However, further investigation was required before this technique could be adopted at a larger scale. The aims of the current study were to confirm the reliability of ICG-^{99m}Tc-nanocolloid and to assess whether blue dye is still of added value, in the largest series of PeCa SN biopsies with ICG-^{99m}Tc-nanocolloid to date. ***Materials and Methods:*** 400 ≥T1G2N0 PeCa patients were scheduled for SN biopsy and treatment of the primary tumour at a single European centre. After peritumoural injection of ICG-^{99m}Tc-nanocolloid, SNs were preoperatively identified with lymphoscintigraphy and SPECT/CT. Intraoperatively, SNs were pursued via gamma tracing, visual identification (blue

dye) and near-infrared fluorescence imaging. In the overall cohort (n=400), intraoperative SN identification rates using radio- and fluorescence guidance were assessed. In those patients who received ICG-^{99m}Tc-nanocolloid and blue dye (n=266), fluorescence SN identification rates were compared with blue dye using a chi-square test. ***Results:*** 740 groins were assessed. No tracer-related adverse events were reported. All preoperatively defined SNs (n=1163) were intraoperatively localized. 98% of all excised SNs were detectable with gamma probe and 96% were visible with fluorescence imaging. The 95 SNs that were tumour-positive were all both radioactive and fluorescent. In the fluorescence vs. blue dye analysis (n=266), fluorescence imaging yielded a 39.2% higher SN detection-rate relative to blue dye (95.3 vs. 56.1%). 100% (n=58) of the SNs that were tumour-positive at pathology could be intraoperatively visualized by fluorescence imaging, whereas merely 69% (n=40) were stained blue. ***Conclusion:*** This study confirms that ICG-^{99m}Tc-nanocolloid is a reliable SN tracer for PeCa that significantly improves optical SN detection over blue dye. ***References:*** None

OP-501

Age and cognitive reserve affect the expression of cingulate island sign in patients with DLB: an European-DLB (E-DLB) consortium project

M. Donegani[1], *M. Bauckneht*[2], *A. Chincarini*[3], *M. Brendel*[4], *A. Rominger*[4], *L. Beyer*[4], *R. Bruffaerts*[5], *R. Vandenberghe*[5], *M. G. Kramberger*[6], *M. Trost*[6], *V. Garibotto*[7], *N. Nicastro*[8], *G. B. Frisoni*[9], *A. W. Lemstra*[10], *B. N. M. van Berckel*[11], *A. Pilotto*[12], *A. Padovani*[12], *M. A. Ochoa-Figueroa*[13], *A. Davidsson*[13], *V. Camacho*[14], *E. Peira*[3], *S. Raffa*[1], *A. Miceli*[1], *D. Aarsland*[15], *F. Nobili*[2], *S. Morbelli*[1];
[1]*Department of Health Sciences (DISSAL), University of Genoa, Genoa, ITALY,* [2]*IRCCS Ospedale Policlinico San Martino, Genoa, ITALY,* [3]*National Institute of Nuclear Physics (INFN), Genoa, ITALY,* [4]*University Hospital (LMU Munich), Munich, GERMANY,* [5]*Department of Neurosciences, Ku Leuven, Leuven, BELGIUM,* [6]*University Medical Centre, Ljubljana, SLOVENIA,* [7]*Geneva University Hospitals and NIMTLab, Geneva University, Geneva, SWITZERLAND,* [8]*Department of Clinical Neurosciences, Geneva University Hospitals, Geneva, SWITZERLAND,* [9]*LANVIE (Laboratoire de Neuroimagerie du Vieillissement), Geneva University Hospitals, Geneva, SWITZERLAND,* [10]*VU Medical Center Alzheimer Center, Amsterdam, NETHERLANDS,* [11]*Department of Radiology and Nuclear Medicine, Amsterdam University Medical Centres, Amsterdam, NETHERLANDS,* [12]*Department of Clinical and Experimental Sciences, University of Brescia, Brescia, ITALY,* [13]*Department of Clinical Physiology, Institution of Medicine and Health Sciences, Linköping, SWEDEN,* [14]*Hospital de la Santa Creu i Sant Pau, Universitat Autònoma de Barcelona, Barcelona, SPAIN,* [15]*Centre for Age-Related Medicine (SESAM), Stavanger University Hospital, Stavanger, NORWAY.*

Aim/Introduction: We previously identified brain regions whose metabolic impairment contributes to DLB clinical core features expression and we demonstrated an influence of severity of global cognitive impairment on the hypometabolic DLB pattern and in particular on the expression of the cingulate island sign (CIS) (1). In this study we aim to evaluate the impact of age and education (as a proxy of cognitive reserve, CR) on the DLB-related pattern in probable DLB patients belonging to E-DLB consortium database. Materials and Methods: Brain FDG-PET and clinical/demographic information were available in 168 patients recruited in 10 centers belonging to the E-DLB consortium (age 73.4±7.0; 93 males; MMSE-score 22.2±4.7; Education 10.4±4.0 years). Principal component analysis was applied to identify brain regions relevant to the local data variance. A regression analysis to the locally normalized intensities was performed to generate an age-sensitive map as well as a CR-sensitive map (both maps were also adjusted for the other confounding variables, i.e., MMSE score, Gender, Center, and either education or age, respectively). $p<0.05$ was regarded as significant. Results: Age negatively covaried with metabolism in fronto-mesial and fronto-insular cortex, anterior and posterior cingulate while it positively covaried with lateral temporal, occipital and posterior parietal metabolism in the left hemisphere. Education positively covaried with metabolism in insula, medial frontal gyrus, medial temporal lobe and basal ganglia in both hemispheres and negatively covaried with metabolism in left parietal cortex, and bilateral precuneus. Conclusion: CR-related mechanisms are at work in DLB. In particular education negatively affects metabolism in bilateral precuneus while not in PCC suggesting that the DLB-typical CIS (2) is more expressed in patients with high CR. By contrast the DLB-typical CIS may be blunted in older DLB patients. In fact, age negatively covaried with metabolism in bilateral posterior cingulate thus reducing the expression of the CIS. The present results suggest that non disease-specific variables such us CR and age may be a further source of heterogeneity in the relationship between clinical symptoms and related metabolic patterns in DLB patients. These findings point out the importance of tailoring the interpretation of biomarkers results considering individual patients' characteristics also in DLB patients. ***References***: (1) Morbelli S et al. Metabolic patterns across core features in dementia with lewy bodies. Ann Neurol. 2019, 85(5):715-725. (2) Lim SM et al. The 18F-FDG PET cingulate island sign and comparison to 123I-beta-CIT SPECT for diagnosis of dementia with Lewy bodies. J Nucl Med. 2009 50(10):1638-45

OP-502

Progression to overt Coronary artery disease in Patients with Diabetes Mellitus at High Coronary Risk: 5 year follow-up of the prospective multicenter BARDOT Trial

F. Caobelli*, P. Haaf, G. Haenny, M. Pfisterer, M. Zellweger;*

Universitätsspital Basel, Basel, SWITZERLAND.

Aim/Introduction: The Basel Asymptomatic high-Risk Diabetics' Outcome Trial (BARDOT) [1] demonstrated that asymptomatic diabetic patients with an abnormal myocardial perfusion scintigraphy (MPS) were at increased risk of major cardiac events (MACE) at 2-years follow-up. It remains unclear whether this finding holds true even for a longer follow-up. ***Materials and Methods:*** Four hundred patients with type-2 diabetes and neither history nor symptoms of CAD were evaluated. They underwent clinical evaluation and MPS with either physical or pharmacologic stress test. Patients were followed up for 5 years. MPS-based diagnosis of CAD was defined as summed stress score (SSS) ≥4 and/or summed difference score (SDS) ≥2. A fully unremarkable scan was defined as SSS and SDS=0. MACEs were defined as myocardial infarction, cardiac death or late coronary revascularization. Patients with detectable CAD were randomly assigned to medical or invasive treatment. ***Results:*** At baseline, an abnormal MPS was found in 87 of 400 patients (22%). MACE within 5 years occurred in 14 patients with abnormal MPS (16.1%) and in 22 with normal scan (1.7%, p=0.009); 15 deaths were recorded. An abnormal MPS was a predictor of MACEs occurrence: HR- (95% CI) 2.537 (1.238 - 5.199, p=0.011). At Kaplan-Meyer analysis, patients with normal MPS had lower rates of MACEs than patients with abnormal scans (p=0.016). Patients with SSS = 0 (n= 285) had also lower rate of all-cause death (2.5% vs. 7.1%, p=0.033). Patients undergoing revascularization experienced significant lower rate of MACE (n=2, 6.7%, p=0.007) and mortality (p=0.002) compared to those treated with optimal medical therapy ***Conclusion:*** High-risk asymptomatic patients with DM and normal MPS (78%) have a lower rate of first manifestations of coronary artery disease (CAD) even at 5-years follow-up. A SSS value =0 predicted a very low all-cause mortality rate, similar to that of a normal population. Conversely, patients with abnormal MPS at baseline (22%) have a 7-fold higher rate of progression to overt CAD. Our results confirm that if patients with diabetes are clinically at high risk of CAD as in BARDOT, they should be considered for ischemia testing. A normal scan predicts a good 5-year outcome, while evidence suggests that those with CAD should be treated with a combined invasive and medical approach. ***References:*** [1] JACC Cardiovasc Imaging. 2014;7:1001-10.

OP-503

Biodistribution and Dosimetry of ^{177}Lu-satoreotide-tetraxetan: an Interim Analysis of a Multi-Centre, Open-Label Phase I/II Study in Patients with Neuroendocrine Tumours

D. Wild[1], *S. Beykan*[2], *H. Grønbæk*[3], *J. Beauregard*[4], *C. Ansquer*[5], *A. Haug*[6], *N. Lenzo*[7], *S. Navalkissoor*[8], *G. Nicolas*[1], *L. Durand-Gasselin*[9], *C. Powell*[10], *B. Pais*[11], *R. Hicks*[12], *U. Eberlein*[2], *M. Lassmann*[2];

[1]*University Hospital Basel, Basel, SWITZERLAND,* [2]*University of Würzburg, Würzburg, GERMANY,* [3]*Aarhus University Hospital, Aarhus, DENMARK,* [4]*CHU de Quebec, Université Laval, Quebec, QC, CANADA,* [5]*CHU de Nantes, Nantes, FRANCE,* [6]*University Hospital Vienna, Vienna, AUSTRIA,* [7]*GenesisCare Theranostics, Ramsay Hollywood Private Hospital, Perth, AUSTRALIA,* [8]*Royal Free Hospital, London, UNITED KINGDOM,* [9]*Ipsen, Les Ulis, FRANCE,* [10]*Ipsen, Cambridge, MA, UNITED STATES OF AMERICA,* [11]*Ipsen, Hoofddorp, NETHERLANDS,* [12]*Peter McCallum Cancer Centre, Melbourne, AUSTRALIA.*

Aim/Introduction: ^{177}Lu-satoreotide-tetraxetan (^{177}Lu-IPN01072, ^{177}Lu-OPS201 or ^{177}Lu-DOTA-JR11), a novel somatostatin receptor 2 antagonist, has shown acceptable toxicity in patients with progressive neuroendocrine tumours (NETs) at approximately 4.5 GBq/cycle [1]. We report an interim analysis (IA) of ^{177}Lu-satoreotide-tetraxetan biodistribution and dosimetry from an on-going phase I/II study. ***Materials and Methods:*** Part A of the phase I study enrolled 15 patients with well-differentiated grade 1/2 NETs who each received 3 cycles of 4.5 GBq with 300 µg peptide mass ^{177}Lu-satoreotide-tetraxetan. Part B, which had enrolled 20 patients at the IA cut-off date, explored separately escalation of activity and peptide mass (up to 6 GBq/cycle, 300-1300 µg peptide/4.5GBq cycle). Cumulative renal, bone marrow (BM), splenic, hepatic and tumour dosimetry was assessed for each subject after each administration. ***Results:*** After the first 3 patients were enrolled in cohort 1 of part B, the planned administered activity of 6 GBq was reduced to 4.5 GBq due to cumulative BM absorbed dose exceeding the prespecified 1.5 Gy threshold in 2 patients, and thrombocytopenia in one patient. At the IA cut-off, dosimetry data was summarized for 25 patients having no major protocol violation affecting dosimetry variables. Among those, 16 (64%) had received all 3 treatment cycles (including 2 patients who received a fourth cycle) with a cumulative activity of 13.4±1.6 GBq. At cycle 1, ^{177}Lu-satoreotide-tetraxetan delivered radiation primarily to tumour lesions (specific absorbed dose [SAD] ranging from 0.43 to 27 Gy/GBq, median 2.9 Gy/GBq), followed by kidneys and spleen (median SAD 0.82 to 0.94 Gy/GBq and 0.86 Gy/GBq, respectively) and to a lesser extent to liver (median SAD 0.18 Gy/GBq) and BM (median SAD 0.090 Gy/GBq). Part A preliminary analysis showed comparable SAD (median percent change <15%, N=7-10) for kidneys, BM and liver between cycle 1 and cycle 3. Similarly, comparable BM SAD was observed when 300 µg or 700 µg were administered (cohort 3, N=4) but this finding shall be confirmed when more data is available. In the IA of safety population (N=35), haematological toxicity (grade≥3) consisted of lymphopenia (51.4% patients), thrombocytopenia (14.2%), neutropenia (8.6%), and anaemia (2.8%) but were not associated with bleedings or

infections. ***Conclusion:*** These preliminary results show that ^{177}Lu-satoreotide-tetraxetan efficiently targets tumours in patients with well-differentiated grade 1/2 NETs. Dosimetry supports the ^{177}Lu-satoreotide-tetraxetan acceptable safety profile at median cumulative activity of 13.0 GBq over 3 cycles in patients with NETs. ***References:*** 1. Wild et al. J Nucl Med. 2014; 55(8): 1248-1252

OP-504

Lymph node staging by FDG-PET/CT and MRI in cervical uterine cancer: the impact on FIGO stage migration and prognostic value

J. Holm[1], *A. Thomassen*[1], *O. Gerke*[1], *M. H. Vilstrup*[1], *D. Spasojevic*[2], *S. E. Sponholtz*[3], *K. M. Jochumsen*[3], *P. T. Jensen*[4], *M. G. Hildebrandt*[1]; [1]*Department of Nuclear Medicine, Odense University Hospital, Odense C, DENMARK,* [2]*Department of Radiology, Odense University Hospital, Odense C, DENMARK,* [3]*Department of Gynecology and Obstetrics, Odense University Hospital, Odense C, DENMARK,* [4]*Department of Obstetrics and Gynecology, Aarhus University Hospital, Aarhus, Denmark, Odense C, DENMARK.*

Aim/Introduction: The new and revised staging for carcinoma of the uterine cervix (CCU) proposed by the FIGO committee in 2018 includes imaging in the staging process. It suggests a stage migration of early-stage FIGO I and II patients with retroperitoneal lymph node metastasis to a new FIGO (2018) stage IIIC. We aimed to investigate the prognostic value of suspected lymph node metastases by FDG-PET/CT and MRI in women with early stages FIGO (2009) I and II. ***Materials and Methods:*** In this clinical register study, we included 535 women with biopsy verified uterine cervical cancer at Odense University Hospital, Denmark from 2007-2016. Women referred for diagnostic work-up underwent FDG-PET/CT and MRI before gynecological examination. Stratified analyses were performed for patients with CCU FIGO (2009) stage IA, IBI, IB2 and II. We compared disease-specific survival in each stage for patients with and without imaging signs of retroperitoneal lymph node involvement (N+, N0) and performed Kaplan-Meier analysis. Lymph node involvement was assessed by both imaging modalities combined: if either of the imaging modalities were lymph node positive, the result was regarded as positive (N+). If both modalities were lymph node negative, the result was regarded as negative (N0). ***Results:*** A total of 425 patients were clinically staged FIGO I and II: 36, 195, 30, and 164 women were staged FIGO IA, IB1, IB2, and II, respectively. Overall, 106 women (25%) had suspected lymph node metastases on imaging and stratified by FIGO stage the number was 0 (0%) in stage IA, 22 (11%) in IBI, 14 (47%) in IB2, and 70 (43%) women in II. The 5-year disease specific survival rates for women with FIGO stage IB1, IB2, and II comparing lymph node negative vs. lymph node positive patients were 99% (95% CI: 95-100) vs. 95% (72-99), 100% (NA) vs. 64% (34-83), and 82% (72-88) vs. 62% (49-72), respectively. ***Conclusion:*** One fourth of the patients in this study had suspected lymph node metastasis on imaging and would be upstaged to FIGO stage IIIC by the new FIGO classification. The 5-year disease-specific survival was significantly higher in the lymph node negative group compared with the lymph node positive group, based on imaging findings alone. The prognostic value of staging lymph node metastasis by imaging in FIGO stages I and II CCU in this study supports the migration of patients with signs of lymph node disease towards a more advanced stage. ***References:*** None

OP-505

Diagnostic Performance and Clinical Impact of Ga-68 PSMA PET/CT Imaging in Early Relapsed Prostate Cancer After Radical Therapy: Phase 3, Prospective, Multicenter Study (IAEA-PSMA Study)

E. Estrada-Lobato*; International Atomic Energy Agency, Nuclear Medicine and Diagnostic Imaging, Vienna, AUSTRIA.*

OP-506a

TheraP Study - A randomised phase II trial of 177Lu-PSMA-617 (Lu-PSMA) theranostic versus cabazitaxel in metastatic castration resistant prostate cancer (mCRPC) progressing after docetaxel

M. Hofman*; Peter MacCallum Cancer Centre, Molecular Imaging, Melbourne, AUSTRALIA.*

OP-506b

Summary

J. Bomanji*; University College Hospital NHS Trust, Institute of Nuclear Medicine, London, UNITED KINGDOM.*

1311

e-Poster Presentation Session 8: All About the Prostate - Staging, Restaging and Beyond

Thursday, October 29, 2020, 16:35 - 18:05 Channel 11

EPS-120

Diagnostic efficacy of F-18-rhPSMA-7.3 PET imaging for N-staging in Intermediate and High-Risk Prostate Cancer patients validated by histopathology

T. Langbein[1], *I. Rauscher*[1], *M. Kroenke*[1], *A. Wurzer*[2], *K. Schwamborn*[3], *H. Wörther*[1], *C. Franz*[1], *T. Maurer*[4], *T. Horn*[5], *H. Wester*[2], *W. Weber*[1], *M. Eiber*[1]; [1]*Technical University of Munich, School of Medicine, Klinikum rechts der Isar, Department of Nuclear Medicine, Munich, GERMANY,* [2]*Technical University of Munich, Chair of Radiopharmacy, Garching, GERMANY,* [3]*Technical University of Munich, School of Medicine, Klinikum rechts der Isar, Institute of Pathology, Munich, GERMANY,* [4]*University Hospital Hamburg-Eppendorf, Martini-Klinik, Hamburg, GERMANY,* [5]*Technical University of Munich, School of Medicine, Klinikum rechts der Isar, Department of Urology, Munich, GERMANY.*

Aim/Introduction: Radiohybrid PSMA (rhPSMA) ligands are a

new class of diagnostic/therapeutic PSMA-targeting agents which can be efficiently labeled with F-18 and radiometals and show only minimal renal excretion. Promising preliminary data have been reported for F-18-rhPSMA-7, which comprises four isomers. Based on preclinical findings, the single isomer, F-18-rhPSMA-7.3, was selected as the lead rhPSMA compound for clinical development. Here we report first efficacy data for primary N-staging in patients with intermediate and high-risk prostate cancer. Results were compared to morphological imaging and validated by histopathology. ***Materials and Methods:*** Fifty-six patients (median PSA 11.0 ng/mL, range: 2.4- 296.0) with intermediate or high-risk prostate cancer (defined by D'Amico), who had undergone F-18-rhPSMA-7.3 PET imaging (median injected activity 349 MBq; range: 240-449 MBq, median uptake time 72 min; range: 58-102 min) at our center before radical prostatectomy and extended pelvic lymph node dissection, were included. PET and morphologic images were retrospectively rated by one experienced reader for the presence of lymph node metastases using a standard surgical template. Each anatomical field was rated on a five-point-scale independently for PET and for morphological imaging. Results were compared to histopathology findings on patient-, right vs. left-, and template-based analyses. ***Results:*** Lymph node metastases were present in 18/56 patients (32.1 %), located in 33/319 templates (10.3%). On the patient-based analysis the sensitivity, specificity and accuracy of F-18-rhPSMA-7.3-PET were 81.3%, 87.5% and 85.7%, and those of morphological imaging 33.3%, 89.5% and 71.4%, respectively. For the right vs. left analysis the sensitivity, specificity and accuracy of F-18-rhPSMA-7.3-PET were 70.8%, 96.6% and 91.1%, and for morphological imaging 25.0%, 95.5% and 80.4%, respectively. The template-based analysis showed the sensitivity, specificity and accuracy of F-18-rhPSMA7.3-PET to be 63.6%, 97.9% and 94.4%, and those of morphological imaging to be 15.2%, 99.3% and 90.6%, respectively. On ROC analyses, F-18-rhPSMA-7.3-PET showed a significantly better performance than morphological imaging on patient-, right vs. left and template-based analyses, yielding AUC values of 0.842 vs. 0.697 ($p<0.05$), 0.843 vs. 0.631 ($p<0.001$) and 0.801 vs. 0.639 ($p<0.001$), respectively. ***Conclusion:*** Our preliminary data from this small cohort indicate that F-18-rhPSMA-7.3 PET might be superior to morphological imaging for primary N-staging of intermediate and high-risk prostate cancer. Data analysis from a larger cohort is planned to confirm this significant difference. ***References:*** None

EPS-121

Choosing Wisely recommendations compliance in bone scan scintigraphies of newly diagnosed prostate cancer patients

I. Saura Lopez*, Á. O. Rabines Juárez, N. A. Rudic Chipe, M. J. Ribelles Segura, M. I. Blanco Saiz, L. Paruta Araez, M. I. Morales Lozano, A. Camarero Salazar, E. Goñi Gironés; Navarra Hospital Complex, Pamplona, SPAIN.*

Aim/Introduction: To examine the appropriate use of Choosing Wisely recommendations (ChW) for bone scintigraphy (BS) in newly diagnosed prostate cancer patients in the Navarra Hospital Complex. Most reports demonstrated the over-use of imaging explorations in staging for patients with newly diagnosed prostate cancer. This practice produces consequences in all stakeholders : patients, health providers, health system and society. This consequences include emotional stress, exposition of harm without net benefits or increased financial burden on the healthcare systems. For this reason, it is necessary examine the appropriate use of existing recommendation in our services. ***Materials and Methods:*** This quantitative, observational and cross-sectional study included newly diagnosed prostate cancer patient undergoing bone scintigraphy within the Navarra Hospital Complex in 2019. A descriptive statistical analysis was performed to evaluate the characteristics of patient (age, PSA level, clinical manifestations suggestive of bone involvement, pre-existing bone lesion viewed in another imaging explorations); the frequency of results of bone scintigraphy (categorized as positive, negative or indefined for metatasis) and the frequency of compliance of ChW recommendations. An analysis using chi square test was used to determine whether there is a statistically significant difference between the frequencies of results of bone scintigraphy and compliance of ChW recommendations. ***Results:*** A total of 155 BS were included. The mean age was 70.46 +/- 8.30 y-o; 59.35% with PSA levels> = 10ng / ml. 5.81% had no previous biopsy. The Gleason score values were: 6 (12.90%), 7 (45.16%), 8 (17.42%), 9 (16.13%) and 10 (2.58%). Presence of symptoms of bone involvement and pre-existing bone lesions were viewed in 7.74% and 18.71% of patients, respectively. A 14.84% of overall patients were a positive BS , categorized as polyostotic (10.32%), monostotic (3.23%) and superscan (1.29%). The compliance of ChW recommendations was 72.26% of overall BS performed, with positive BS in 20.54% of those who met the criteria and none among those who did not met that ($p<0.001$). ***Conclusion:*** The compliance of ChW recommendations represents three quarters of newly diagnosed prostate cancer patient, this being a significant associated factor for the identification of bone metastases. ***References:*** None

EPS-122

Standardized Uptake Values are Adequate Measures of ^{18}F-DCFPyL Uptake in Patients with Low- to Intermediate Tumour Burden: a Comparison to Tumour-to-Blood Ratio, a Validated Simplified Pharmacokinetic Analysis

D. Oprea*, Y. J. L. Bodar, B. P. F. Koene, D. Meijer, B. H. E. Jansen, M. C. F. Cysouw, M. Yaqub, H. N. Hendrikse, A. N. Vis, R. Boellaard; Amsterdam UMC, Amsterdam, NETHERLANDS.*

Aim/Introduction: Prostate cancer (PCa) is the second most prevalent cancer in men. To diagnose PCa in its primary and metastatic form, radiolabelled prostate-specific membrane antigen (PSMA) positron emission tomography/ computed

tomography (PET/CT) has been successfully introduced. This imaging technique relies on radiotracers, e.g. ^{18}F-DCFPyL, to bind to the overexpressed PSMA, class II transmembrane glycoproteins, on malignant prostate cells. To reliably assess PET-scans, radiotracer-uptake quantification is required. True quantification remains an intricate process, hence simplified semi-quantitative methods are preferable for daily practice. From pharmacokinetic analysis, it was demonstrated that the uptake of ^{18}F-DCFPyL can be reliably approximated by the Tumour-to-Blood ratio (TBR) [1], derived by normalizing mean tumor uptake (either Bq/cm^3 or SUV) by the mean activity in the arterial blood pool (Bq/mL or SUV). However, TBR depends strongly on tracer uptake interval (i.e. time from injection to scan start), often difficult to adhere to in clinical practice. In this study we investigated whether the even more simple, and clinically preferred, standardized uptake value (SUV) could provide adequate quantification in selected patients. The aim was therefore to investigate whether SUV correlates to TBR for ^{18}F-DCFPyL PET/CT imaging, thereby providing a simplified measure that is less dependent on tracer uptake interval than TBR. ***Materials and Methods:*** A total of 116 PCa patients, in different stages of PCA (Primary staging, Biochemical Recurrence (BCR) or metastatic castration-resistant prostate cancer (mCRPC), that underwent ^{18}F-DCFPyL-PET/CT scans were analysed retrospectively. Reported suspicious lesions (suspect for intraprostatic tumours, lymph node, bone or visceral metastases) were delineated and assessed, using in-house developed software. SUVpeak was correlated to TBR and a sub-analysis was performed to assess the effect of total tumour volume (this included metastatic lesions), PSA and uptake time interval. ***Results:*** SUV highly correlated to TBR in PCa patients with a tumour volume <200cc (R^2 = 0.931). When the groups were plotted separately, this correlation remained high (R^2 = 0.950; 0.902; 0.956, in respectively Primary PCa, BCR and mCRPC). Tracer uptake interval did not affect the correlation between SUV and TBR and R^2, which measured in ascending order for tracer uptake interval was 0.907, 0.925 and 0.955 (respectively <110min, 110-130min and >130min). ***Conclusion:*** SUV is suitable as a simplified quantitative method in PCa patients with a tumour volume of <200cc, with high correlation to TBR. ***References:*** 1. Jansen, B.H.E., et al., Simplified Methods for Quantification of (18)F-DCFPyL Uptake in Patients with Prostate Cancer. J Nucl Med, 2019; 60(12):1730-35. PMID: 31000583.

EPS-123

Diagnostic accuracy of 68Ga-PSMA PET-CT at initial diagnosis in a population of prostate cancer patients submitted to radical prostatectomy as compared to pathology results

C. Varela Pinto, B. Martins, D. Calado, C. Loewenthal; Hospital da Luz Lisboa, Lisbon, PORTUGAL.

Aim/Introduction: To evaluate the diagnostic accuracy of 68Ga-PSMA PET-CT results at initial staging before radical prostatectomy in prostate carcinoma patients. Prostate-specific membrane antigen (PSMA) is a transmembrane protein expressed in prostatic tissues, including neoplastic tissue, with highest expression in undifferentiated, metastatic and hormone-resistant tumors. 68Ga-PSMA PET-CT detects lesions avid for PSMA and is currently one of the most sensitive and specific tests in disease detection, even at low PSA values. 68Ga-PSMA PET-CT is well established in high risk patients with biochemical recurrence. Due to high diagnostic yield, 68Ga-PSMA PET-CT can be also be useful at initial staging, in order to improve localization of cancer sites before therapy decision-making, namely radical prostatectomy. ***Materials and Methods:*** Retrospective evaluation of clinical electronic records of 150 patients (mean age 66.2 years, range 39-88) who underwent 68Ga-PSMA PET-CT for initial staging of prostate carcinoma between February 2017 and April 2020. Biochemical, clinical, imaging and pathological findings were reviewed. We compared 68Ga-PSMA PET-CT results prior to surgery with pathology reports of radical prostatectomy specimens, and evaluated diagnostic accuracy of PET-CT results in prostate disease, in locoregional extraprostatic extension and in locoregional lymph nodes metastases. ***Results:*** One hundred and fifty patients underwent 68Ga-PSMA PET-CT for initial staging of prostate carcinoma. Thirty-seven patients underwent radical prostatectomy after PET-CT. Lymphadenectomy was performed in all but 6 patients. In these 37 patients, the mean PSA initial value was 12.7 ± 15.5 ng/ml. Gleason score was 6 in 2 patients, 7(3+4) in 8, 7(4+3) in 12, 8(4+4) in 9 and 9(4+5) in 6. On PET-CT, 32 patients had disease confined to the prostate, 3 had locally advanced disease and 2 presented with locoregional lymph nodes. Compared to pathology results, 68Ga-PSMA PET-CT detected prostatic lesions in 37/37 patients and lymph nodes in 2/2 patients. PET-CT did not detect focal microscopic unilateral lesions in seminal vesicles in 7/37 patients (19%). PET-CT referred false positives lesions in seminal vesicles in 2/37 patients (5%). ***Conclusion:*** PET-CT with 68Ga-PSMA is a sensitive imaging procedure for localization of prostate cancer lesions. Its high sensitivity brings added value to conventional imaging, improving localization of prostate cancer sites at initial staging. Its accuracy in seminal vesicle invasion warrants further study. ***References:*** None

EPS-124

Diagnostic accuracy of ^{18}F-PSMA-1007-PET/CT imaging for lymph node staging in prostate carcinoma in primary and biochemical recurrence

K. Sprute[1], V. Kramer[2,3], S. Koerber[4,5,6], M. Meneses[7], R. Fernandez[3], C. Soza-Ried[3], M. Eiber[8], W. Weber[8], I. Rauscher[8], K. Rhabar[9], M. Schaefers[9], T. Watabe[10], M. Uemura[11], S. Naka[12], N. Nonomura[11], J. Hatazawa[13], C. Schwab[14], V. Schuetz[15], M. Hohenfellner[15], T.

Holland-Letz[16], J. Debus[4,5,6], C. Kratochwil[1,17], H. Amaral[18,2], P. Chokyke[19], U. Haberkorn[1,17], C. Sandoval[7], F. Giesel[1,17,20]; [1]Department Nuclear Medicine, Heidelberg University Hospital, Heidelberg, GERMANY, [2]Positronpharma SA, Santiago, CHILE, [3]Center of Nuclear Medicine PositronMed, Santiago, CHILE, [4]Department of Radiation Oncology, Heidelberg University Hospital, Heidelberg, GERMANY, [5]National center for tumor disease (NCT), Heidelberg, GERMANY, [6]Heidelberg Institute of Radiation Oncology (HIRO), Heidelberg, GERMANY, [7]Fundacion Arturo Lopez Perez, FALP, Santiago, CHILE, [8]Department Nuclear Medicine, Munich University Hospital, Munich, GERMANY, [9]Department Nuclear Medicine, Muenster University Hospital, Muenster, GERMANY, [10]Department Nuclear Medicine and Traer Kinetics, Osaka University Graduate School of Medicine, Osaka, JAPAN, [11]Department of Urology, Osaka University Graduate School of Medicine, Osaka, JAPAN, [12]Osaka University Hospital, Osaka, JAPAN, [13]Research Center for Nuclear Physics, Osaka University, Osaka, JAPAN, [14]Department of Pathology, Heidelberg University Hospital, Heidelberg, GERMANY, [15]Department of Urology, Heidelberg University Hospital, Heidelberg, GERMANY, [16]Department of Biostatistics, German Cancer Reasearch Center (DKFZ), Heidelberg, GERMANY, [17]Clinical Cooperation Nuclear Medicine, German Cancer Research Center (DKFZ), Heidelberg, GERMANY, [18]Center of Nuclear Medicine PostitronMed, Santiao, CHILE, [19]Molecular Imaging Program, Center for Cancer Research, National Cancer Institute of Health, Bethesda, MD, UNITED STATES OF AMERICA, [20]German Cancer Consortium (DKTK), Heidelberg, GERMANY.

Aim/Introduction: PSMA-ligand PET/CT is performed in patients with prostate cancer to stage the disease initially or to identify sites of recurrence after definitive therapy. ^{18}F-PSMA-1007 is a promising PSMA-PET tracer based on clinical results but detailed histologic confirmation has been lacking. ***Materials and Methods:*** 96 patients with prostate cancer received a ^{18}F-PSMA-PET/CT followed by either a radical prostatectomy with lymphadenectomy or a salvage lymphadenectomy. Patients undergoing radical prostatectomy without lymphadenectomy or biopsies were excluded. The histological findings of PSMA-PET-positive nodes were analysed retrospectively. A lesion and a patient-based analysis was performed comparing 1) all positive and 2) only lesions with a size larger than 3 mm in histopathology. ***Results:*** 90.6% of the patients received ^{18}F-PSMA-PET/CT for staging before the primary treatment, while 9.4 % of the cohort underwent imaging for biochemical recurrence. In 34.4% of the cohort positive lymph nodes were present in imaging. A total of 1746 lymph nodes were dissected in 96 patients. PSMA-PET had a lesion-based sensitivity of 81.7% a specificity of 99.6%, a positive predictive value (PPV) of 92.4%, a negative predictive value (NPV) of 98.9% for detecting positive lymph nodes larger than 3 mm. In the analysis of all malignant nodes regardless the size the overall sensitivity, specificity, PPV, NPV on lesion-based analysis was 71.2%, 99.5%, 91.3%, 97.9%. The patient-based analysis showed a sensitivity of 85.9% and a specificity of 99.5% for lymph nodes >3 mm. ***Conclusion:*** ^{18}F-PSMA-1007-PET/CT reliably detects malignant lymph nodes and has an exceptional specificity of >99% for nodal metastases. ***References:*** None

EPS-125

Pattern of prostate cancer recurrence in patients with biochemical failure following definitive therapy evaluated with [^{68}Ga]Ga-PSMA-11 PET/CT

I. Lawal[1,2], T. Lengana[1], K. Mokoala[1], T. Boshomane[1], J. Kleynhans[1,2], M. Vorster[1,2], N. Mokgoro[1], M. Sathekge[1,2]; [1]University of Pretoria, Pretoria, SOUTH AFRICA, [2]Nuclear Medicine Research Infrastructure (NuMeRI), Pretoria, SOUTH AFRICA.

Aim/Introduction: [^{68}Ga]Ga-PSMA PET/CT has emerged as a whole-body imaging technique with excellent accuracy in the detection of prostate cancer (PCa) recurrence. Pelvic MRI is commonly used for this indication. Whole-body imaging affords the opportunity to determine extra-pelvic sites of recurrence. We aimed to determine the distribution of PCa recurrence in men who experience biochemical failure (BF) after definitive radiotherapy or radical prostatectomy (RP) using [^{68}Ga]Ga-PSMA-11 PET/CT. ***Materials and Methods:*** We retrospectively reviewed the images of all patients who had [^{68}Ga]Ga-PSMA-11 PET/CT at first confirmation of BF after definitive radiotherapy or RP. We determined the diagnostic sensitivity of [^{68}Ga]Ga-PSMA-11 PET/CT for the localization of the site of recurrence. We also determined the distribution of the sites of PCa recurrence. We further evaluated the impact of the type of primary therapy and PSA level on the distribution of recurrence. ***Results:*** A total of 184 men were included, the median age of 66 years (range:47-87). The median PSA and Gleason scores (range) were 2.98 (0.05-10.24) ng/mL and 8 (6 - 9), respectively. Definitive therapy was by RP in 112 patients and by radiotherapy in 74 patients. A total of 314 sites of recurrence were seen with a median lesion per patient of one (range: 1 - 12) lesion. At least one site of recurrence was seen in 152 patients (sensitivity of 82.61%). Fifty-seven patients had more than one lesion due to PCa recurrence. Local recurrence in the prostate gland/prostate bed or seminal vesicles was the commonest site of recurrence across all PSA levels (n=109) followed by recurrence in pelvic nodes (n=61). Loco-regional recurrence (local and regional pelvic nodes) was prevalent at PSA<2ng/mL with extra-pelvic lesions seen in only two patients in this PSA group. Skeletal recurrence was more prevalent at high PSA levels as 17 of 18 patients with skeletal sites of recurrence had a PSA>2ng/mL. In 8 patients, extra-pelvic sites of recurrence were seen without associated loco-regional pelvic recurrent disease. Patients treated by definitive radiotherapy were more likely to have a local recurrence in the prostate gland/ seminal vesicles

compared with patients treated by RP (P<0.001). ***Conclusion:*** [^{68}Ga]Ga-PSMA-11 PET/CT has a high diagnostic sensitivity for the detection of PCa recurrence after definitive therapy. Loco-regional recurrence is commoner at lower PSA levels while skeletal recurrence is more prevalent at higher PSA levels. Whole-body imaging affords the opportunity to detect the extra-pelvic sites of recurrence. ***References:*** None

EPS-126

[^{68}Ga]Ga-PSMA-11 PET/CT in patients with recurrence of prostate cancer - usefulness of delayed phase in pelvic lesions detection

L. Krolicki*, K. Pełka, S. Kujda, J. Kunikowska;*
Medical University of Warsaw, Warsaw, POLAND.

Aim/Introduction: Prostate cancer is one of the most common cancers in men. The presence of prostate specific membrane antigen (PSMA) on the surface of prostate cancer cells and its metastases enables the use of this antigen in targeted diagnosis and therapy. ***The aim*** of this study was to evaluate the usefulness of delay phase image in the [^{68}Ga]Ga-PSMA-11 PET/CT. ***Materials and Methods:*** The study was performed in 64 patients aged 67.8±7.0 years with diagnosed prostate cancer, after radical treatment, referred for [^{68}Ga]Ga-PSMA-11 PET/CT due to biochemical relapse. In the study group 48 patients underwent prostatectomy, 14 radical radiotherapy, 2 HIFU. In the histopathological examination Gleason score 5, 6, 7, 8, 9 was described in 4, 6, 33, 10 and 11 patients, respectively. In the study group, the average PSA concentration at the time of PET scan was 4.1 ± 6.7 ng/ml (range: 0.3-39.0). All patients underwent PET/CT imaging with [^{68}Ga]Ga-PSMA-11 (Siemens, Biograph 64), 60 minutes after injection of 135-205 MBq, and additionally 120-180 minutes delay phase targeted on the pelvis. For semi-quantitative evaluation maximal standard uptake value (SUVmax) was used. ***Results:*** [^{68}Ga]Ga-PSMA-11 PET/CT showed lesions in 50/64 (78%) patients. In pelvis 45 patients had 74 foci of increased tracer accumulation in the both phases with $SUVmax_{60}$ 9.3 ±10.5 and $SUVmax_{120}$ 11.6 ± 12.8. 7 foci of increased uptake were seen only in the study after 60 min with $SUVmax_{60}$ 3.3 ± 1.2 , which was interpreted as physiological or inflammatory accumulation. 8 foci (in 7 patients) of increased tracer accumulation were visible only in delay image with $SUVmax_{120}$ 5.7 ± 2.0, on the CT part correspond - fine lymph nodes up to 4-5 mm and additional focus in the prostate gland. In the delayed phase additional lesions were seen in 11% of patients . The foci visible only in delayed phase: 3/8 with normal 60 minutes examination, 5/8 additional lesions. ***Conclusion:*** Delay phase of[^{68}Ga]Ga-PSMA-11 PET/CT doesn't significantly extend the duration of the examination, but it allows to visualize additional lesions in 11% of patients. The delayed phase should be considered in patients with biochemical relapse and negative examination after 60 min, and in patients with before radiotherapy to accurate treatment planning. ***References:*** None

EPS-127

Comparison of early imaging and imaging 60 minutes post injection after forced diuresis with furosemide in the assessment of local recurrence in prostate cancer patients with biochemical recurrence referred for [68Ga] Ga-PSMA-11-PET/CT

S. Bayerschmidt*, C. Uprimny, A. S. Kroiss, H. Svirydenka, G. di Santo, B. Nilica, S. Rauch, E. von Guggenberg, C. Decristoforo, I. Virgolini;*
Medizinische Universität Innsbruck, Innsbruck, AUSTRIA.

Aim/Introduction: [68Ga]Ga-PSMA-PET/CT is a promising method for the assessment of local recurrence in prostate cancer patients. The aim of this study was to evaluate the diagnostic performance of early [68Ga]Ga-PSMA-11 PET imaging in comparison to [68Ga]Ga-PSMA-11 PET imaging 60 minutes post injection (p.i.) in the detection of local recurrence in patients with biochemical recurrence of prostate carcinoma. ***Materials and Methods:*** 190 image sets of patients with biochemical recurrence in prostate cancer who underwent [68Ga]Ga-PSMA-11-PET/CT were assessed retrospectively [median prostate specific antigen (PSA) value 0.69 ng/ml (range 0.1 - 105.6)]. Patients received an early static scan of the pelvic area [mean 248 s p.i. (range 56 - 923 s)] and whole-body scan 60 minutes post injection after forced diuresis with furosemide 20mg i.v.. We based the assessment on visual analysis and calculation of maximum standardized uptake value (SUV_{max}) of pathologic lesions present in the pelvic area found on early PET imaging and on 60 min-PET scans. ***Results:*** Image assessment resulted in 30 (15.8%) positive and 17 (9.0%) equivocal findings in early scans, and 28 (14.7%) positive and 25 (13.2%) equivocal findings of local recurrence. 20 (66.7%) findings were positive and 9 (30.0%) findings were equivocal in both scans. ***Conclusion:*** While there was no significant difference between the detection rates of positive findings, early scans yielded a lower number of equivocal findings. These findings suggest that early [68Ga]Ga-PSMA-11-PET/CT scan is useful in the detection and characterization of local recurrence in prostate cancer. Combination of early scans and [68Ga]Ga-PSMA-11-PET/CT scans 60 min p.i. might lead to a better assessment of local recurrence in the clinical routine. ***References:*** None

EPS-128

Ga68 PSMA PET/CT in the restaging of patients with prostate cancer. Correlation to PSA levels

V. Prassopoulos*, T. Pipikos, D. Kechagias, M. Vogiatzis, V. Filippi, F. Vlachou, J. Andreou, K. Gogos, R. Efthymiadou;*
PET/CT Department, Hygeia Hospital, Athens, GREECE.

Aim/Introduction: In the follow up of prostate cancer patients, a usual diagnostic problem is biochemical recurrence with elevated PSA and no discovered underlying pathology in the conventional imaging. Ga68 PSMA is a specific agent for the investigation of prostate cancer. Aim of this study is to evaluate the effectiveness of Ga68 PSMA PET/CT in prostate cancer patients with biochemical recurrence ***Materials and Methods:*** The data of 138 patients that underwent a Ga68 PSMA PET/CT study in our department in the last year because of elevated PSA were evaluated. ***Results:*** Mean time after surgery was 5,3 years(0,3 to 22 years) with a mean patients' age of 69 years. 98 of these patients showed abnormal uptake (98/138-71%). 18 had uptake only in the prostatic bed indicative of local recurrence, with a mean SUVmax value of 36,62 (7-94), while 80 patients had extra-prostatic abnormal findings with mean SUVmax value of 17,45. In the latter patient group the most common site of abnormal uptake was lymph nodes (60/80- 75%) with mean SUVmax 12,33 (2,9-70). 34 patients (34/80-42%) had abnormal bone uptake with mean SUVmax of 26,4 (3,9-94), 2 patients had peritoneal implantations, 4 patients were presented with uptake indicative of liver metastasis, while three had lung foci. When categorizing the patients based on PSA levels, in the group of patients with PSA levels up to 0,5 ng/dl (42 patients) PET/CT pathology was discovered in 16/42(38%), while in the group with PSA values 0,51-0,99 ng/dl(20 patients) in 12/20(60%). Overall in the group of patients with PSA values up to 0,99 ng/dl abnormal lesions were found in 28/62(45%) of the patients. In the group with PSA values of 1ng/dl or higher the rate of positive studies was70/76(92%). ***Conclusion:*** Ga68 PSMA PET/CT study can be of great value in the restaging of patients with elevated PSA, especially in the group with PSA levels over 1 ng/dl. Although abnormal foci detection rate is lower in PSA levels<1 ng/dl, in the majority of the patients abnormal findings in the Ga68 PSMA PET/CT study are detected, with a great possible impact in the therapy planning especially in the early treatment. ***References:*** 1. Kopka, K.;etal. Glu-ureido-based inhibitors of prostate-specific membrane antigen: J. Nucl. Med. 2017, 58, 17s-26s. 2. Virgolini, I.; etal Current status of theranostics in prostate cancer. Eur. J. Nucl. Med. Mol. Imaging 2018, 45, 471-495.

EPS-129

Diagnostic value of Ga-68 PSMA PET/CT in biochemical progression in prostate cancer (PC) patients after radical prostatectomy in the low range values of prostate specific membrane antigen (PSA)

M. Dyankova[1,2], Z. Dancheva[1], T. Stoeva[1], S. Chausheva[1], T. Yordanova[1], B. Chaushev[1], A. Klisarova[1];
[1]St. Marina University Hospital, Varna, BULGARIA, [2]Medical University Varna Prof. Dr. Paraskev Stoyanov, Varna, BULGARIA.

Aim/Introduction: Currently Ga-68 PSMA PET/CT is making a significant shift in the diagnosis, staging and restaging of PC patients. There were many questions raised concerning indications and sensitivity of the method. Most of them concerning the PSA value in biochemical progression, specifically in the low values, PSA up to 2.00 ng/ml. The aim of this study was to analyze the influence of PSA value in BP on PSMA sensitivity, detection rate and the relationship with regional or metastatic lesions incidence in patients after radical prostatectomy. ***Materials and Methods:*** We performed a retrospective analysis in 144 consecutive patients with radical prostatectomy. The mean age of the patients was 67.3 years. The patients were divided into six groups according to the PSA value: 1) 0.00- 0.040 ng/ml; 2) 0.041- 0.160 ng/ml; 3) 0.161- 0.500 ng/ml; 4) 0.501-1.0 ng/ml; 5) 1.001- 2.00 ng/ml; 6) >2.001 ng/ml. The relationship between PSA levels in the groups and PSMA sensitivity, detection rate and regional or metastatic lesions incidence were examined. ***Results:*** A total of 63 patients (42.6%) showed at least one positive lesion. PSMA PET/CT detection rate into the different groups were: 1) 6 (12.3%); 2) 3 (15.0%); 3) 11 (50%); 4) 7 (53.8%); 5) 4 (57.1%); 6) 31 (93.9%). There was a significant relationship between the PSA level and the ability of PSMA to reveal metastatic lesions (p<0.001). Local recurrence was revealed in patients with higher PSA values, above 0.160 ng/ml. Distant metastases were seen most commonly in patients with low levels of PSA (up to 0.160 ng/ml) in 100.0% of patients, (p<0.001). Bone metastases were most commonly found in patients with low PSA levels, including five patients with PSA level below 0.04 (83.33% of patients in the first group). A PSA-based analysis of overall sensitivity and specificity revealed values of 58% and 87% respectively. A sensitivity of 15% was found at lower PSA levels (0.041- 0.160 ng/ml). In the other groups was higher 3) 50.0%; 4) 53.0%; 5) 57.0%; 6) 93.0. ***Conclusion:*** This study confirms that PSMA PET/CT is an excellent tool for the detection of recurrent prostate cancer and metastatic spread with high sensitivity even at low PSA levels, which may influence further clinical management. Detection of local recurrence was positively associated with PSA level. Low level PSA BP after radical prostatectomy is more commonly related with distant metastases, specifically bone metastases in patients with lower levels of PSA, even below 0.04. ***References:*** None

EPS-130

High detection sensitivity in [^{18}F]PSMA-1007 PET: initial experience focusing on biochemical recurrence in prostate cancer patients

T. Watabe[1], M. Uemura[1], F. Soeda[1], S. Naka[2], H. Sasaki[2], T. Kamiya[2], E. Shimosegawa[1], H. Kato[1], N. Nonomura[1], F. L. Giesel[3,1];
[1]Osaka University, Suita, JAPAN, [2]Osaka University Hospital, Suita, JAPAN, [3]University Hospital Heidelberg, Heidelberg, GERMANY.

Aim/Introduction: ^{18}F-labeled prostate-specific membrane

antigen (PSMA) ligand, [18F]PSMA-1007, is focusing attention for its higher synthetic yield and minimal excretion in the urine. High detection efficacy has been reported in biochemical recurrence (BCR) of prostate cancer after radical prostatectomy.[1] In this study, we evaluated diagnostic performance of [18F]PSMA-1007 PET in prostate cancer patients, focusing on the BCR. ***Materials and Methods:*** We enrolled consecutive 45 patients (age: 48-87) with prostate cancer (BCR: 24, recurrence: 7, Castration Resistant Prostate Cancer (CRPC) without metastasis: 6, metastatic CRPC (mCRPC): 7, and initial staging: 1). [18F]PSMA-1007 solution was synthesized using MPS200 (Sumitomo Heavy Industries). PSMA-PET scanning was performed 60 min after intravenous injection of [18F]PSMA-1007 (242 ± 24 MBq). PSMA-PET images were evaluated for its lesion detection as well as its relation to PSA values and location in BCR patients. Detection rates were compared with the previous reports using [68Ga]PSMA-11 PET.[2] ***Results:*** Abnormal uptakes, which suspected recurrent or metastatic legion, was detected in 97.8% (44/45) of the whole patients. SUVmax were 14.8 ± 12.6 in local recurrence, 16.7 ± 21.1 in pelvic lymph nodes (LN), 28.6 ± 23.3 in extra-pelvic LN, and 27.3 ± 21.9 in bone metastasis. In BCR patients (n=24), detection rates were 75% in low PSA group (0.1-0.5 ng/mL), 86% in medium PSA group (0.5-1.0 ng/mL), and 100% in high PSA group (above 1.0 ng/mL). Among the PET-positive BCR patients (n=23), local recurrence was detected in 48% (11/23), pelvic LN in 39% (9/23), and bone metastasis in 39% (9/23). These detection rates were higher than reported values in [68Ga]PSMA-11 PET. In 64% (7/11) of BCR patients who were suspected of local recurrence, focal uptakes were detected adjacent to the bladder on [18F]PSMA-1007 PET, suggesting its big advantage of low physiological urine excretion compared to [68Ga]PSMA-11 PET. ***Conclusion:*** Although further follow-up is essential to confirm the true positive, [18F]PSMA-1007 PET detected recurrent and metastatic lesion with high sensitivity. In BCR patients, its higher detection lead to proper treatment strategy, such as salvage radiation therapy with confidence, or surgical removal of recurrent lymph nodes. It was suggested that [18F]PSMA-1007 PET will contribute to improve the prognosis in prostate cancer patients. ***References:*** 1. Giesel FL, et al. J Nucl Med. 2019. 2. Afshar-Oromieh A, et al. Eur J Nucl Med Mol Imaging. 2017.

EPS-131

Assessment of early oxidative stress following the use of radiotheranostics agents 177Lu-PSMA for prostate cancer and 177Lu-DOTATATE for neuroendocrine tumors; radioprotective effect of vitamin C

M. Assadi[1], *E. Jafari*[1], *H. Ahmadzadehfar*[2], *D. Bagheri*[3], *A. Amini*[1];
[1]*Bushehr University of Medical Sciences (BUMS), Bushehr, IRAN, ISLAMIC REPUBLIC OF,* [2]*Klinikum Westfalen, Knappschaft Hospital, Dortmund, GERMANY,* [3]*Persian Gulf University, Bushehr, IRAN, ISLAMIC REPUBLIC OF.*

Aim/Introduction: In this study, we aimed first to evaluate the early oxidative stress changes following radionuclide therapy (RNT) with 177Lu-PSMA and 177Lu-DOTATATE and second to evaluate the protective effect of vitamin C on RNT-related oxidative stress. ***Materials and Methods:*** From December 2018 to October 2019, prostate cancer and neuroendocrine tumor (NET) patients referred to undergo radioligand therapy (RLT) with177Lu-PSMA and peptide receptor radionuclide therapy (PRRT) with177Lu-DOTATATE, respectively, were enrolled in this study. The patients were divided into two main groups; the control group underwent routine RNT without any intervention and the intervention group was asked to take effervescent tablets (500 mg) of vitamin C for two days prior to the RNT (three tablets per day). To measure oxidative stress, blood samples were taken immediately before treatment and 48 hours after treatment and the serums were separated and frozen. To evaluate oxidative stress, the serum levels of malondialdehyde (MDA) and glutathione (GSH) and the activity of glutathione reductase (GR) were measured before and two days after treatment. ***Results:*** 61 RNT cycles were evaluated in 34 patients with a mean age of 62.82±16.54 years (range of 27-99); this total included 20 (59%) prostate cancer patients (35 cycles (57.4%)) and 14 patients (41%) with NET (26 cycles (42.6%)) who received 177Lu-PSMA and 177Lu-DOTATATE, respectively. The NET patients included five females (36%) and nine males (64%). Of the 61 evaluated cycles, 27 cycles were given in the control group and 34 cycles were given in the intervention group. The serum level of MDA was significantly increased after treatment compared to before treatment (p=0.02) in the control group, while no significant change in the serum level of MDA was observed in the intervention group (p=0.52). The serum level of GSH was insignificantly decreased after treatment compared to before treatment in the control group and slightly increased after treatment in the intervention group (p>0.05). The serum level of GR was insignificantly increased in all groups of patients after treatment (p>0.05). ***Conclusion:*** According to the results, radionuclide therapy with177Lu-PSMA and 177Lu-DOTATATE induces oxidative stress which can be ameliorated with vitamin C. ***References:*** None

EPS-132

Prostate Primary Tumor Assessment by [68Ga]Ga-PSMA PET/CT

P. Soeiro*, R. Silva, R. Almeida, V. Sousa, G. Costa, J. Perdoso de Lima;*
Centro Hospitalar e Universitário de Coimbra, Coimbra, PORTUGAL.

Aim/Introduction: [68Ga]Ga-PSMA PET/CT is widely considered to be the most accurate imaging technique for

the distant staging of prostate adenocarcinoma (PCa). In this study we aim to assess its ability to identify and characterize the primitive tumour, which currently is considered to be lacking. ***Materials and Methods:*** All PCa patients who underwent [^{68}Ga]Ga-PSMA PET/CT followed by radical prostatectomy (RP) were retrospectively selected. PET/CT data was reviewed for any apparent area of focal uptake and seminal vesicle invasion(SVI). Semi-automatic VOIs centered on the highest uptake area were then generated according to 5 different SUV thresholds(2;2.5;3;3.5 and 4) to draw the tumour with as little operator intervention as possible. All [^{68}Ga]Ga-PSMA tumour uptake related variables, such SUVmax, SUVmean and Prostate Tumour Volume(PTV-PSMA) were recorded. A new variable, named Total Lesion PSMA expression(TL-PSMA), was calculated by multiplying the SUVmean by the PTV-PSMA. Demographic, clinical and histological variables were recorded. ***Results:*** Twenty-nine patients fulfilled the inclusion criteria (65±6.4; 52-76 years). Four patients had an ISUP score of 1 (14%), 12 patients a score 2 (41%), and 13 patients a score 3 (45%). Average staging PSA was 17.3±16.24ng/ml. The average elapsed time between PET/CT and surgery was 97±109days. On visual analysis, the primary tumour was detected in 26 patients (90%). Among the 3 undetected tumours, 2 were of intermediate risk, despite the fact that high risk tumors represented the vast majority (90%). According to a rough estimate, tumour localization agreement between PET/CT and the pathological report was 76%. Accuracy, sensitivity, specificity, PPV and NPV for SVI detection was 90, 57, 100, 100, 88%, respectively.Statistical significant correlations between tumour mass and PTV-PSMA were found, the highest for a SUV threshold of 3 (spearman-r^2:0.54, p:0.034). However, for the highest Gleason grade tumour mass(GTM) the strongest statistical significant correlation was found with TL-PSMA (spearman-r^2:0.567, p:0.014) also for a SUV threshold of 3. Globally, stronger correlations with clinical variables, such as staging PSMA (spearmanr^2:0.599, p:0.02), PSMA value at PET date (spearmanr^2:0.448, p:0.028), and stage group (spearman-r^2:0.432, p:0.035) were found for PTV-PSMA, than for TL-PSMA or SUVmax. ***Conclusion:*** [^{68}Ga]Ga-PSMA PET/CT was able to detect most PCa on visual analysis, especially high risk tumours, with only one being missed. Also, SVI was detected with extreme specificity and PPV, despite low sensitivity. Statistically significant correlations were found between PTV-PSMA and tumour mass and TL-PSMA and GTM. Correlations with clinical variables was globally stronger for PTV-PSMA, than for TL-PSMA or SUVmax. ***References:*** None

EPS-133

PSMA-positivity of the salivary glands in ^{68}Ga-PSMA-PET: Does fasting play a role?

K. Huang[1], *A. D. J. Baur*[2], *H. Hupperts*[1], *J. M. M. Rogasch*[1], *J. Albers*[1], *W. Brenner*[1], *C. Furth*[1], *J. Müller*[3], *H. Amthauer*[1];

[1]*Charité - Universitätsmedizin Berlin, Department of Nuclear Medicine, Berlin, GERMANY,* [2]*Charité - Universitätsmedizin Berlin, Department of Radiology, Berlin, GERMANY,* [3]*Vivantes Klinikum Spandau, Clinic for Neurology, Berlin, GERMANY.*

Aim/Introduction: Aim of the study was to evaluate the impact of fasting during the uptake-phase of a ^{68}Ga-PSMA-PET on PSMA-positivity of the parotid (PG), submandibular (SMG) and sublingual gland (SLG). ***Materials and Methods:*** From 145 consecutively examined patients with prostate cancer (median age: 72 [range 47-91] years; median activity 169 [132-203] MBq ^{68}Ga-PSMA; median uptake time: 99 [54-167] min), the PSMA-positivity of PG, SMG and SLG was retrospectively analyzed. The gastric filling was used as surrogate for fasting; additionally the patients were interviewed. SUVmax of PG, SMG and SLG were determined. A side-averaged ratio between SMG and PG (SMP-ratio) for each patient was calculated. 16 patients were excluded because of asymmetry of the salivary glands (>50% SUVmax of contralateral side). With Shapiro-Wilk-tests a normal distribution was excluded and Mann-Whitney-U-tests were performed. ***Results:*** Median SUVmax of PG was 21.8, of SMG 22.7 and of SLG 8.1. Median SMP-ratio was 1.11. SUVmax of PG for fasting patients (f) was lower than non-fasting patients (nf) (f: 20.6; nf: 22.9; p=0.004). SUVmax of SMG showed an converse behaviour (f: 24.4; nf: 19.8; p=0.001). SUVmax of SLG did not show significant differences (f: 8.5; nf: 7.5; p=0.117). Fasting had a high significant Impact on SMP-ratio (f: 1.27; nf: 0.89; p<0.001). ***Conclusion:*** The results show for the first time, that the physiological secretion at rest (f: SMG>PG>>SLG) and under stimulation (nf: SMG=PG>>SLG) relevantly affect the PSMA-positivity of salivary glands in ^{68}PSMA-PET. A preventive reduction of salivery gland activity / secretion could be a promising approach to minimize damage of salivery glands due to radioligand therapies with PSMA-ligands. ***References:*** None

EPS-134

The Role of Interleukin-23 in Prostate Adenocarcinoma; Comparison to Ga-68 PSMA PET/CT Findings

N. Ergul[1], *H. Serin*[2], *E. Beyhan*[1], *Ö. Erol*[1], *B. Yılmaz*[1], *C. Gündoğan*[1], *T. F. Çermik*[1];

[1]*Istanbul Training and Research Hospital, Department of Nuclear Medicine, Istanbul, TURKEY,* [2]*Istanbul Training and Research Hospital, Department of Biochemistry, Istanbul, TURKEY.*

Aim/Introduction: The first treatment option in advanced stage prostate cancer is androgen deprivation therapy. However, the majority of patients develop progression due to the resistance to castration. Recent studies have reported that immune cells in the tumor microenvironment and various cytokines may play a role in the development of this resistance. In this prospective study, the role of interleukin-23 (IL-23), a cytokine expressed in many types

of cancer, in prognosis of prostate cancer was investigated. ***Materials and Methods:*** Twenty-three patients diagnosed with prostate cancer, who were referred for Ga-68 PSMA PET / CT were included in the study. While 13 of the patients were newly diagnosed and had no treatment, 10 patients were found to have increased PSA and / or progression in Ga-68 PSMA PET / CT under hormonotherapy (HT). 5 ml of venous blood samples were derived from all patients on the day of Ga-68 PSMA PET / CT. Levels were measured by ELISA method using IL-23 receptor kit in serum separated from all samples. The relationship between the newly diagnosed patient group and the progressive patient group under HT, and the relationship between IL-23 levels, as well as Gleason scores, tPSA levels, bone and distant organ metastasis detection rates, prostate gland and pelvic lymph node SUVmax values and IL-23 levels were investigated. ***Results:*** In Gallium-68 PSMA PET / CT, 13 (56.5%) of all patients had bone metastasis, 10 (43.5%) had non-pelvic lymph nodes and organ metastases. While tPSA levels were stable in 2 of castration resistant patients, new developed metastases were detected in PET / CT. No significant difference was found between blood IL-23 levels of patients with newly diagnosed and no treatment was initiated and those who developed resistance to castration (P = 0.689). There was no significant difference in IL-23 levels between patients with and without bone and distant organ metastases. Also, there was no significant correlation between IL-23 levels and tPSA and primary tumor and pelvic lymph node SUVmax values. ***Conclusion:*** Since there was no significant relationship between serum IL-23 levels and development of castration resistance, metastatic disease and SUVmax values, it can be said that IL-23 has no place in the prognosis of prostate cancer. Ga-68 PSMA PET / CT has an important role in guiding the treatment by showing resistance to castration. ***References:*** 1. IL-23 secreted by myeloid cells drives castration-resistant prostate cancer. Calcinotto A et al. Nature. 2018 Jul;559:363-369

EPS-135

Detection of primary prostate cancer with ^{99m}Tc-PSMA-SPECT/CT

I. Farkas*, Z. Besenyi, G. Sipka, S. Urbán, A. Maráz, Z. Bajory, L. Pávics;*
University of Szeged, Szeged, HUNGARY.

Aim/Introduction: Although PSMA-PET tracers have been extensively studied in the last few years, it's role in primary prostate cancer diagnosis is unclear. ^{99m}Tc-PSMA -SPECT/CT could be a promising cost effective alternative for prostate cancer imaging. The aim of this study was to quantify the difference between the physiological and pathological intraprostatic tracer uptake on PSMA-SPECT scans. ***Materials and Methods:*** We retrospectively analysed the SPECT/CT images of 25 patients with primary prostate cancer (71±7 yo ISUP Grade 1-5, serum PSA level 85,51±226,41 ng/ml) and 5 healthy volunteers (70±5 yo, serum PSA level 4±3 ng/ml). All patients received androgen deprivation therapy during study. Whole-body PSMA-SPECT/CT imaging were performed with 660 ± 95 MBq of ^{99m}Tc-mas3-ynal-k(Sub-KuE). The images were evaluated visually and quantitatively. Normal and pathological tracer uptake was measured using maximum activity concentration within whole prostate gland. Tumour-to-background ratio (TBR) was calculated as maximum intraprostatic activity concentration physiological by mean mediastinal blood pool activity concentration. ***Results:*** ^{99m}Tc-PSMA -SPECT/CT sensitivity, specificity, positive predictive value, negative predictive value and accuracy for primary prostate adenocarcinoma were 80%, 100%, 100%, 50% and 83% respectively. In the case of 20 true positive lesions TBR was significantly higher (7,67±12,12) than the false negative cases (1,28±0,27); p<0,01 but no significant difference was found in relative tracer uptake between the false negative and true negative cases (normal prostate to background ratio: 1,67±0,36); p<0,05. ***Conclusion:*** These preliminary data show that quantitative assessment of ^{99m}Tc-PSMA -SPECT/CT has the potential to be used to differentiate between the physiological and pathological intraprostatic tracer uptake. Further clinical investigations are warranted in larger patient groups and prospective trials. ***References:*** None

1401

CME 11: SLN - Past and Future

Friday, October 30, 2020, 09:00 - 10:30 Channel 1

OP-735

Sentinel Node Biopsy in Prostate Cancer - Nomogram-Related Patient Selection and Clinical Reliability

N. Grivas*; Department of Urology, G.Hatzikosta General Hospital, Ioannina, GREECE.*

OP-736

Current Clinical Status of Sentinel Node Biopsy in Cervical and Endometrial Cancer

A. Collarino*; Fondazione Policlinico Universitario A. Gemelli IRCCS, Nuclear Medicine Unit, Rome, ITALY.*

OP-737

Contribution of SPECT/CT for Sentinel Node Mapping in Pelvic Malignancies

S. Sahbai*; Nuclear Medicine and Clinical Molecular Imaging, University Hospital Tuebingen, Tübingen, GERMANY.*

OP-738

Technological Advances in Robot-Assisted Radioguided Surgery in the Pelvis

M. van Oosterom; Interventional Molecular Imaging Lab, Department of Radiology, Leiden University Medical Center, Leiden, NETHERLANDS.

1402

Joint Symposium 21 (EANM/IEEE): Total Body PET Imaging

Friday, October 30, 2020, 09:00 - 10:30 Channel 2

OP-739
Opportunities and Challenges for Dynamic Imaging with Total Body PET
D. Visvikis; INSERM, LaTIM, Brest, FRANCE.

OP-740
New Opportunities and Clinical Investigations That a Total Body PET Can Offer
R. Boellaard; Amsterdam University Medical Centres, location VUMC, Radiology and Nuclear Medicine, Amsterdam, NETHERLANDS.

OP-741
Applications for Exploring Serotonergic Receptors and Drugs in the Periphery and Central Nervous System
H. Hansen; Massachusetts General Hospital, Athinoula A. Martinos Center for Biomedical Imaging, Charlestown, MA, UNITED STATES OF AMERICA.

1403

Joint Symposium 22 (EANM/ESPGHAN): Nuclear Medicine Techniques in the Evaluation of GI Motility in Children

Friday, October 30, 2020, 09:00 - 10:30 Channel 3

OP-742
Clinical Scenarios of GI Motility Disorders in Children
M. van Wijk; Amsterdam University Medical Centre, VUmc, Paediatric Gastroenterology Department, Amsterdam, NETHERLANDS.

OP-743
Non-Imaging Techniques in the Evaluation of GI Motility in Children
A. Rybak; Great Ormond Street Hospital for Children, Department of Gastroenterology, London, UNITED KINGDOM.

OP-744
Gastric Emptying Scintigraphy
Z. Bar-Sever; Schneider Children's Hospital, Department of Nuclear Medicine, Tel Aviv, ISRAEL.

OP-745
Nuclear Medicine Techniques in Intestinal Motility
L. Biassoni; Great Ormond Street Hospital for Children, Department of Radiology, London, UNITED KINGDOM.

1404

CTE 5: Departmental Organisation

Friday, October 30, 2020, 09:00 - 10:30 Channel 4

OP-747
Management Basics
W. Kemps; University Hospital Brussels, Brussels ,BELGIUM.

OP-748
Radiopharmacy
A. Socan; University Medical Centre Ljubljana, Ljubljana, SLOVENIA.

OP-749
Radiation Protection
K. Pathmaraj; Austin Health, Victoria, AUSTRALIA.

1405

M2M Track - TROP Session: New and Established Tracers - Prostate only!

Friday, October 30, 2020, 09:00 - 10:30 Channel 5

OP-750
Kinetic Modelling of ^{18}F-rhPSMA-7.3 Uptake in PET Imaging of Prostate Cancer
S. Malaspina[1], V. Oikonen[1], A. Kuisma[2], O. Ettala[3], K. Mattila[2], P. J. Boström[3], H. Minn[2], K. Kalliokoski[1], E. J. Postema[4], M. P. Miller[4], M. Scheinin[5];
[1]Turku PET Centre, University of Turku and Turku University Hospital, Turku, FINLAND, [2]Department of Oncology, University of Turku and Turku University Hospital, Turku, FINLAND, [3]Department of Urology, University of Turku and Turku University Hospital, Turku, FINLAND, [4]Blue Earth Diagnostics Ltd, Oxford, UNITED KINGDOM, [5]Clinical Research Services Turku - CRST Ltd, Turku, FINLAND.

Aim/Introduction: ^{18}F-labeling of prostate-specific membrane antigen (PSMA) PET imaging agents is increasingly used instead of ^{68}Ga because of their longer half-life and improved logistics. Radiohybrid PSMA (rhPSMA) ligands can be labelled with both diagnostic (^{18}F) and therapeutic (^{177}Lu) radionuclides. This phase 1 open-label study evaluated the uptake kinetics of a novel theranostic PET tracer, ^{18}F-rhPSMA-7.3, to optimize its use for PET/CT imaging of prostate cancer (PCa). ***Materials and***

Methods: Nine men, three with high-risk primary PCa, three with hormone-sensitive metastatic PCa and three with castration-resistant metastatic PCa, received a dynamic 45-min PET scan immediately after i.v. administration of 300 MBq ^{18}F-rhPSMA-7.3. Two whole-body PET/CT scans were then acquired 60 and 90 min post-injection. Venous blood samples were collected for pharmacokinetic analysis. Volumes of interest (VOIs) corresponding to PCa lesions and healthy reference tissues (bone marrow for bone lesions, blood pool for lymph node (LN) and prostate lesions) were recorded. SUV_{mean} and lesion-to-reference ratios were calculated from data collected at two time points: early (between 35 and 45 min) and late (between 60 and 118 min). Net influx rates (Ki) were calculated using Patlak plots. ***Results:*** Three patients had primary localized PCa, one had pelvic nodal metastases and five had distant metastatic disease, with lesions in LN only (n=2) or in bone and LN (n=3). All lesions analyzed (n=35) were clearly visualized by ^{18}F-rhPSMA-7.3 PET in the dynamic and whole-body scans, with optimal visual lesion detection starting 60 min post-injection. The ^{18}F signal from PCa lesions increased over time, while the signal from the reference tissues remained stable or decreased. The SUV_{mean} of all lesions increased by a mean±SD of 27±18 % from early to late time points (mean±SD SUV_{mean} 8.6±5.1 vs. 10.7±6.2 g/mL). Lesion-to-reference ratio±SD of prostate, LN and bone metastases increased from 2.4±0.9, 4.1±2.0 and 6.9±3.6 at the early time point to 3.2±1.9, 6.1±3.1 and 8.8±4.5 at the late time point, respectively. Patlak plots derived from the lesion VOIs were linear, with minor downward curvature when data from the static scans were included, signifying almost irreversible uptake kinetics during the PET scan. The Patlak-derived Ki estimates, SUVmean values, and lesion-to-reference ratios were in good agreement. ***Conclusion:*** ^{18}F-rhPSMA-7.3 showed high uptake in PCa lesions, with high lesion-to-background ratios. Optimal visual lesion detection started 60 min post-injection. Thus, ^{18}F-rhPSMA-7.3 emerges as a very promising radiotracer for diagnostic PET imaging of PCa, with possible further application in theranostics. ***References:*** None

OP-751

Pharmacokinetics of PSMA-617 - dynamics of radiopharmaceutical uptake in tumours

K. Bohn*, M. Fürstner, M. Hentschel, I. Alberts, A. Rominger, A. Afshar-Oromieh;*
Department of Nuclear Medicine, Inselspital/Bern University Hospital, University of Bern, Bern, SWITZERLAND.

Aim/Introduction: Following the introduction of PET-imaging with PSMA-ligands, a multitude of studies demonstrates that the majority of prostate cancer (PC) lesions present with an increasing tracer-uptake over time. For instance, scans at 3h p.i. show increased lesion contrast compared to those at 1h p.i. However, neither for diagnostic nor therapeutic PSMA-ligands has the time point of maximum uptake been adequately investigated. The aim of this study was to assess the time of maximum uptake for PSMA-617 in PC lesions. ***Materials and Methods:*** In the context of dosimetry of PSMA-based endoradiotherapy with ^{177}Lu-PSMA-617, five patients were scanned with SPECT/CT at four different time points (4h, 1d, 2d and 3d p.i.). Amongst these patients, fifteen representative PC lesions were selected by random and analysed with regard to their SUV values at all mentioned time points. Thereafter, time-activity curves were drawn. ***Results:*** For the majority of lesions a clear maximum and then constant fall in tracer uptake was observed: 10 lesions in three patients maximum at 1 day and 5 lesions in two patients maximum at 4h p.i. ***Conclusion:*** Our preliminary data (more analyses in progress) show that, for the majority of lesions, the maximum uptake of PSMA-617 in PC lesions can be expected between few hours and 1d p.i. This observation may find further relevance once PSMA-ligands labelled with isotopes of longer half-lives become available for PET-imaging (e.g. ^{44}Sc, $T_{1/2}$ 4h). In challenging patients, e.g. very early biochemical recurrence of PC, the maximum performance of PSMA-PET/CT could be achieved with scans conducted at 4h p.i., with the option of additional later imaging at 24h p.i. thereby showing PC lesions with the maximum uptake. ***References:*** None

OP-752

Heterodimeric Radiotracer Targeting PSMA and GRPR for Imaging of Prostate Cancer: Optimisation of the Affinity towards PSMA by Linker Modification

F. Lundmark*[1], A. Abouzayed[1], B. Mitran[1], S. S. Rinne[1], Z. Varasteh[2], M. Larhed[3], V. Tolmachev[4], U. Rosenström[1], A. Orlova[1];*
[1]Department of Medicinal Chemistry, Uppsala University, Uppsala, SWEDEN, [2]Nuclear Medicine, Klinikum rechts der Isar der TUM, Munich, GERMANY, [3]Science for Life Laboratory, Department of Medicinal Chemistry, Uppsala University, Uppsala, SWEDEN, [4]Department of Immunology, Genetics and Pathology, Uppsala University, Uppsala, SWEDEN.

Aim/Introduction: Prostate-specific membrane antigen (PSMA) and gastrin-releasing peptide receptor (GRPR) are promising targets for molecular imaging of prostate cancer (PCa) lesions. Due to the heterogenic overexpression of PSMA and GRPR in PCa, a bispecific heterodimeric radiotracer with the ability to bind both targets could be beneficial. Recently, our group reported the novel heterodimer BQ7800 consisting of a urea-based PSMA inhibitor, the peptide-based GRPR antagonist RM26, and NOTA chelator. BQ7800 demonstrated high affinity towards GRPR but only modest affinity towards PSMA together with short tumour retention. This study aimed to improve the affinity towards PSMA of this heterodimer by changing the composition of the two linkers connecting the PSMA- and

GRPR-targeting parts. ***Materials and Methods:*** Three novel heterodimeric analogues were synthesised using SPPS by incorporation of phenylalanine in the functional linker of the PSMA-binding part and/or shortening the PEG-linker coupled to RM26. The heterodimers were labelled with indium-111 and their affinity towards PSMA and GRPR was evaluated in vitro. Binding specificity to both targets was studied for the heterodimer [^{111}In]In-BQ7812 in mice bearing PC3-pip tumours (PSMA and GRPR positive). In vivo biodistribution of [^{111}In]In-BQ7812 was studied over time and compared with the biodistribution of [^{111}In]In-BQ7800. NanoScan SPECT/CT images were performed in tumour bearing mice 1 and 3 h pi. ***Results:*** In the competitive binding assay, BQ7812, featuring phenylalanine and shorter PEG-linker, demonstrated a nine-fold improved affinity towards PSMA (IC_{50} ~ 100 nM) without losing affinity towards GRPR (IC_{50} ~ 6 nM). In the biodistribution study of [^{111}In]In-BQ7812, the activity uptake was two-fold higher in the tumour and three-fold higher in kidneys compared to [^{111}In]In-BQ7800, which corroborates with the higher affinity to PSMA for BQ7812. However, no enhanced tumour retention was observed. The highest tumour-to-organ ratios were observed 3 h pi: tumour-to-blood and tumour-to-muscle ~70, tumour-to-bone ~30, and tumour-to-intestine ~15. The nanoScan SPECT/CT images confirmed ex vivo data. ***Conclusion:*** In this study, we demonstrated that the incorporation of hydrophobicity in the functional linker of a PSMA/GRPR targeting heterodimer was beneficial for the affinity towards PSMA. We also demonstrated that the length of the PEG-linker connected to the GRPR binding motif of the heterodimer affected the binding towards PSMA but not towards GRPR. ***References:*** None

OP-753

Correlation of PSMA-ligand uptake combining autoradiography, histopathology and immunohistochemistry in primary prostate cancer

H. Wang[1], *M. Reiser*[2], *T. Horn*[3], *K. Schwamborn*[2], *K. Steiger*[2], *H. Wester*[4], *M. Schottelius*[4], *W. Weber*[1], *M. Eiber*[1];
[1]*Department of Nuclear Medicine, Klinikum rechts der Isar, Munich, GERMANY,* [2]*Institute of Pathology, School of Medicine, Technical University Munich, Munich, GERMANY,* [3]*Department of Urology, Klinikum rechts der Isar, Technical University Munich, Munich, GERMANY,* [4]*Pharmaceutical Radiochemistry, Technical University Munich, Munich, GERMANY.*

Aim/Introduction: Targeting PSMA has been highly successful in imaging and treatment of prostate cancer. However, heterogeneity in immunohistochemistry indicates limitations in the effect of imaging and radionuclide therapy of multifocal disease. The goal of this study was to investigate the heterogeneity of PSMA ligand uptake in prostate cancer in close correlation with histopathology and to investigate its potential for prediction of tumor aggressiveness. ***Materials and Methods:*** To avoid the complexities and errors of co-registration of PSMA PET or SPECT images and histology we studied patients who underwent radioguided surgery (RGS) with ^{99m}Tc-PSMA-I&S for primary nodal positive prostate cancer and evaluated the distribution of ^{99m}Tc-PSMA-I&S within the resected specimens by autoradiography allowing a perfect spatial correlation to histopathology. ^{99m}Tc-PSMA-I&S was injected intravenously before surgery and autoradiography was performed with 5-7mm prostate specimen slices over 12-16 hours. The images were compared with H&E stained slides (Gleason Pattern [GP] and Gleason Score [GS]) and PSMA-immunohistochemistry. Radioactivity intensity was measured as CPM/mm^2 and after normalization as SUV, which was then matched with histology on a grid-base (3x3mm). The linear mixed model and the Kruskal-Wallis H test were used for statistics and "estimate" values indicating the power of the effect. ***Results:*** So far 9 patients (between 11/2018 and 05/2019) with a total of 1632 grids were included in the preliminary analysis. GP 4 (CPM/mm^2: estimate: 4470, p<0.001) and GP 5 (CPM/mm^2: estimate: 1675, p<0.001) correlated with higher uptake of ^{99m}Tc-PSMA-I&S compared with GP 3 and non-neoplastic tissue, and GP 4 showed stronger impact on PSMA uptake than GP 5. After standardization, we observed GP 4 strongly associated with higher uptake (SUV: estimate: 2.3, p<0.001), while GP 5 affected uptake in an intermediate level (SUV: estimate: 0.6, p<0.001) and GP3 weakly correlated to the higher uptake (SUV: estimate: 0.5, p<0.001). Regarding different GS groups, GS 6 was excluded because of the small sample size. Compared with normal tissue (12680±6810 CPM/mm^2, SUV: 7±3), GS 7a (24715±13054 CPM/mm^2, SUV: 15±5; p<0.001), 7b (23780±12969 CPM/mm^2, SUV: 16±7; p<0.001), 8 (28646±17351 CPM/mm^2, SUV: 15±8; p<0.001) and 9 (37667±14075 CPM/mm^2, SUV: 14±6; p<0.001) had significantly higher PSMA-ligand uptake. ***Conclusion:*** Prostate carcinoma with Gleason Pattern 4 showed significantly higher uptake compared with non-neoplastic prostate tissue. Therefore, our analyses indicate the potential of PSMA-ligands to identify high grade disease and imply its use as a noninvasive biomarker in prostate cancer. More samples are evaluated to confirm these results. ***References:*** None

OP-754

Gallium-66 PET: Production and characterization of ^{66}Ga-NOTA-PEG$_2$-RM26 for PET-imaging of GRPR expression in prostate cancer

S. Rinne[1], *A. Abouzayed*[1], *K. Gagnon*[2], *V. Tolmachev*[3], *A. Orlova*[1];
[1]*Department of Medicinal Chemistry, Uppsala University, Uppsala, SWEDEN,* [2]*GEMS PET Systems AB, Uppsala, SWEDEN,* [3]*Department of Immunology, Genetics and Pathology, Uppsala University, Uppsala, SWEDEN.*

Aim/Introduction: Gastrin releasing peptide receptor (GRPR) is an attractive molecular target in prostate cancer. RM26 is a GRPR-antagonist with promising characteristics for imaging and therapy of GRPR-expressing cancers. Earlier studies with RM26 have shown that next-day imaging could increase imaging sensitivity due to clearance of RM26 from healthy tissue. Gallium-66 is a positron-emitting radioisotope with an intermediate half-life (9.5 hours). We aimed to cyclotron-produce gallium-66 suitable for radiolabelling using a liquid target, and investigate the PET-imaging properties of ^{66}Ga for later-time-point-imaging of GRPR expression using the bombesin-like peptide NOTA-PEG_2-RM26 in a preclinical mouse model. ***Materials and Methods:*** ^{66}Ga was produced by proton irradiation(~25 μA; ~70 min) of 1 M enriched [^{66}Zn]Zn$(NO_3)_2$ in 0.3 M HNO_3 in a "^{68}Ga" PETtrace liquid target. To maximize specific activity, an additional intermediate strong anion exchange column (1x8) was included to published (1) method for [^{66}Ga]$GaCl_3$ isolation on FASTlab. NOTA-PEG_2-RM26 was labelled with gallium-66 and stability of the radiolabel was tested. Binding specificity, binding kinetics, and cellular processing were studied in GRPR-expressing PC-3 cells. In vivo, binding specificity and biodistribution of [^{66}Ga]Ga-NOTA-PEG_2-RM26 were studied using PC-3 xenografted Balb/c nu/nu mice 3 h and 22 h pi and compared with biodistribution of [^{68}Ga]Ga-NOTA-PEG_2-RM26. microPET/MR imaging of [^{66}Ga]Ga-NOTA-PEG_2-RM26 was performed 3 h and 22 h pi in tumour-bearing mice. ***Results:*** Total isolated [^{66}Ga]$GaCl_3$ activity was ~320-340 MBq, with an activity concentration of 160-280 MBq/mL used for labelling. NOTA-PEG_2-RM26 was stably labeled with [^{66}Ga]Ga with molar activity of 4-8 MBq/nmol. Binding was GRPR-specific with K_D of 188±50 pM. Fraction of internalized activity was less than 17% of cell-associated activity after 24 h. In vivo, clearance of [^{66}Ga]Ga-NOTA-PEG_2-RM26 was rapid and binding was GRPR-specific. Tumour uptake 3 h pi was 15±1 %ID/g and decreased 2-fold at 22 h pi. Tumour activity uptake exceeded uptake in all other organs. ^{66}Ga-NOTA-PEG_2-RM26 cleared from GRPR-positive pancreas with time, but other normal tissue clearance was limited, resulting in no improvement of tumour-to-organ ratios with time. Still, GRPR-expressing xenografts were clearly visualized with ^{66}Ga-NOTA-PEG_2-RM26 at both time points using microPET/MR. No difference in uptake in GRPR-positive organs and xenografts was observed between [^{66}Ga]- and [^{68}Ga]Ga-labeled NOTA-PEG_2-RM26, but uptake of [^{68}Ga]-NOTA-PEG_2-RM26 in normal tissue was significantly lower. ***Conclusion:*** In conclusion, we successfully produced gallium-66 suitable for radiolabelling and demonstrated that [^{66}Ga]Ga-PET-imaging can be used to visualize GRPR-expression using the GRPR-antagonist [^{66}Ga]Ga-NOTA-PEG_2-RM26. ***References:*** (1)Nair et al. Eur J Nucl Med Mol Imaging, 2017, 44, S2, OP439

OP-755

Evaluation of ^{64}Cu-labelled GRPR-antagonist RM26 for PET-imaging of prostate cancer in a preclinical model

S. Rinne[1], *B. Mitran*[1], *C. Baun*[2], *J. H. Dam*[2], *B. B. Olsen*[2], *V. Tolmachev*[3], *H. Thisgaard*[2], *A. Orlova*[1];
[1]*Department of Medicinal Chemistry, Uppsala University, Uppsala, SWEDEN,* [2]*Department of Nuclear Medicine, Odense University Hospital, Odense, DENMARK,* [3]*Department of Immunology, Genetics and Pathology, Uppsala University, Uppsala, SWEDEN.*

Aim/Introduction: Gastrin-releasing peptide receptor (GRPR) is a molecular target expressed in 65-100% of prostate cancers (PC) and a suitable target for diagnostic imaging of PC, especially in earlier stages. We have previously demonstrated that the bombesin-based GRPR-antagonist PEG_2-RM26 labeled with ^{55}Co ($T_{½}$=17.5 h, $β^+$-abundance: 76%) could visualize GRPR expression in preclinical models. PET-imaging at late time may allow clearance of radioactivity in normal tissues which could increase image contrast. ^{64}Cu ($T_{½}$=12.7 h, $β^+$-abundance: 17%) is an alternative nuclide for later time-point PET-imaging. Aim of this study was to investigate the potential of a [^{64}Cu]Cu-label for PET-imaging of GRPR expression using GRPR-targeting ligands NOTA-PEG_2-RM26 and NODAGA-PEG_2-RM26, and compare them head-to-head with their earlier reported radiocobalt-labelled counterparts in a preclinical PC-model. ***Materials and Methods:*** [^{55}Co]Co and [^{64}Cu]Cu were cyclotron-produced in house. NOTA/NODAGA-PEG_2-RM26 were labelled with [^{64}Cu]Cu and stability was tested. Novel [^{64}Cu]Cu-ligands were evaluated in GRPR-expressing PC-3 cells for binding specificity, cellular processing and retention. IC50 was estimated for ^{nat}Cu-labelled ligands by a competitive binding assay. Biodistribution of [^{64}Cu]Cu-NOTA/NODAGA-PEG_2-RM26 was studied in PC-3 xenografted mice (n=4/group, 45 pmol/mouse) and compared to radiocobalt-labelled NOTA/NODAGA-PEG_2-RM26 3 h and 24 h pi. Preclinical PET/CT (Siemens INVEON) was performed in tumour-bearing mice 3 h and 24 h after injection of 3.1-3.7 MBq (0.2 nmol [0.18-0.23]) [^{64}Cu]Cu-NOTA/NODAGA-PEG_2-RM26 and 2.0-2.9 MBq (0.3nmol [0.24-0.32]) of [^{55}Co]Co-NOTA/NODAGA-PEG_2-RM26. ***Results:*** NOTA/NODAGA-PEG2-RM26 were stably labelled with [^{64}Cu]Cu with almost quantitative yields. Binding was GRPR-specific and cellular processing pattern of [^{64}Cu]Cu-NOTA/NODAGA-PEG2-RM26 was similar to earlier observed patterns (rapid binding and low internalized fraction) without differences between the conjugates. IC50 value of [^{64}Cu]Cu-NOTA-PEG_2-RM26 (6.05 nM) was approximately 2-fold lower than for [^{64}Cu]Cu-NODAGA-PEG_2-RM26. In vivo, [^{64}Cu]Cu-NOTA/NODAGA-PEG_2-RM26 bound to GRPR-expressing tumours and displayed similar biodistribution profiles to [^{57}Co]Co-NOTA/NODAGA-PEG_2-RM26 with fast clearance from blood and normal organs. The choice of

chelator and radiolabel did not influence the tumor uptake significantly. Tumour uptake exceeded normal tissue uptake 3 h pi for all radioligands. Tumour-to-organ ratios did not increase with time, because of significant clearance of tumor activity, despite the good binding affinity to GRPR. Radiocobalt-labelled ligands demonstrated more efficient clearance from blood and higher tumour-to-organ ratios at both time points. All radioligands could visualize the GRPR-expressing xenografts in preclinical PET/CT and images confirmed the findings from the biodistribution study. ***Conclusion:*** ^{64}Cu-labelled PEG_2-RM26 was able to visualize GRPR-expression using PET at early and later-timepoints. However, radiocobalt-labelled PEG_2-RM26 provided favorable PET-imaging contrast compared to its radiocopper-labelled counterparts. ***References:*** None

OP-756

Influence of the Versatile Bifunctional Chelator AAZTA^{5}on the Radiometal Labelling Properties and the in vitro Performance of a GRPr Antagonist

M. Hofstetter[1], E. Moon[2], F. D'Angelo[1], L. Geissbühler[1], F. Rösch[2], A. Rominger[1], E. Gourni[1];
[1]Department of Nuclear Medicine, Inselspital, Bern University Hospital, Bern, SWITZERLAND, [2]Department of Chemistry – TRIGA site, Johannes Gutenberg - University Mainz, Mainz, GERMANY.

Aim/Introduction: GRPr-based radioligands, mainly antagonists, have shown great promise for diagnostic imaging of GRPr-positive cancers, such as prostate and breast. Prostate Specific Membrane Antigen (PSMA)-based theranostics have also proven great success in the recent years in prostate cancer managment. However, not all patients suffering from prostate cancer benefit from the advantages of PSMA targeting. Therefore, GRPr could play an essential complementary role for PSMA negative cancers, and for tumors characterized by a heterogeneity of receptors expressed on their cell surface. The present study aims at developing and evaluating a versatile GRPr-based probe for PET/SPECT imaging as well as intraoperative and therapeutic applications. Particular focus was given on the influence of the versatile chelator AAZTA^5 on the radiometal labelling properties and the in vitro performance of the generated radiotracers. ***Materials and Methods:*** The potent GRPr-based antagonist D-Phe-Gln-Trp-Ala-Val-Gly-His-Sta-Leu-NH_2 was functionalized with the chelator 6-[Bis(carboxymethyl)amino]-1,4-bis(carboyxmethyl)-6-methyl-1,4-diazepane (AAZTA^5) via the spacer 4-amino-1-carboxymethyl-piperidine (Pip) to obtain AAZTA^5-Pip-D-Phe-Gln-Trp-Ala-Val-Gly-His-Sta-Leu-NH_2 (LF1). LF1 was radiolabelled with ^{68}Ga (PET), ^{111}In (SPECT, intraoperative applications) and ^{177}Lu (therapy, SPECT). ^{68}Ga-, ^{111}In- and ^{177}Lu-LF1 were evaluated in vitro using the epithelial human prostate cancer cell line PC3. In vitro evaluation included stability studies, determination of lipophilicity, protein-binding studies, determination of K_d and B_{max} as well as internalization studies. ***Results:*** LF1 was labelled with ^{68}Ga, ^{111}In and ^{177}Lu within 10 min at RT with a labelling yield >98 %. The specific activities were ranging between 70-80 MBq/nmol for ^{68}Ga-LF1, 10-20 MBq/nmol for ^{111}In-LF1 and ^{177}Lu-LF1. The three tested radiotracers were found to be stable for a period of 4 h post labeling exhibiting a hydrophilic profile with an average of a $LogD_{octanol/PBS}$ of -3, and with the bound activity to the human serum proteins being 10%. They revealed high affinity for PC3 cells, with K_d values between 5 and 13 nM while the required concentration of the radiotracers to saturate the receptors (B_{max}) was between 0.6 and 0.7 nM which correspond to approximately 4 x 10^5 receptors per cell. Low specific internalization rate was found in cell culture with a maximum of 10.0 % at 6 h, while at the same time point the total specific cell surface bound uptake was about 30.0 %. ***Conclusion:*** LF1 can efficiently be labeled with ^{68}Ga, ^{111}In and ^{177}Lu leading to radiotracers with high affinity towards GRPr. The promising acquired in vitro data prompt us to further continue on the evaluation of this precursor in tumor models. ***References:*** None

OP-757

Characterisation of a cyclohexanediamine-triazole-PSMA conjugate on spheroids of prostate cancer cells

W. Sihver[1], M. Saager[1], M. Walther[1], R. Wodtke[1], F. Reissig[1,2], C. Mamat[1,2], K. Kopka[1,2], J. Pietzsch[1,2], H. Pietzsch[1];
[1]Helmholtz-Zentrum Dresden-Rossendorf, Dresden, GERMANY, [2]Technische Universität Dresden, Faculty of Chemistry and Food Chemistry, Dresden, GERMANY.

Aim/Introduction: A recently developed cyclohexanediamine-triazole-chelator enabling ^{18}F-labelling using the Al[^{18}F]F approach was conjugated via copper-catalysed azide-alkyne cycloaddition to the PSMA-binding motif glutamate-urea-lysine connected with 1-naphthyl-D-alanine [1] (ligand L). In the present study radiolabelled L will be characterized on PSMA-positive prostate cancer-spheroids. Three-dimensional cell models offer structure and functional properties closer to in vivo conditions than two-dimensional cell culture models. Spheroids show altered cell-cell and cell-extracellular matrix interactions and are useful for better understanding the nature of tumours concerning drug uptake, toxicity, hypoxia, tissue growth and therapeutic effects. The aim of this study was to investigate the radiopharmacological potential of ^{18}F- and ^{68}Ga-labelled L using LNCaP-spheroids regarding binding properties and internalisation behaviour. The results will be compared with data obtained from LNCaP-monolayer cell culture. ***Materials and Methods:*** Spheroids of LNCaP and PC3 (PSMA-negative) cells were created according to a protocol by the vendor. Freshly harvested cells were incubated with magnetic nanoparticles overnight. After loading, the cells were distributed in a 24-well-plate (10^{-4} cells/well), covered

with a lid equipped with 24 small magnet devices for 5 days and kept in an incubator so that the cells could form spheroids [2]. After incubation with radiolabelled ligand (RCY >95%) the spheroids were washed, exposed to a phosphor imaging plate and the data analysed. Internalisation experiments were carried out by the "acid wash" method. ***Results:*** The method of creating spheroids by magnetised prostate cancer cell lines and treating them with a magnet device was applied successfully and resulted in spheroids with a diameter size of about 500 µm. The evaluation of first saturation experiments with LNCaP spheroids provided preliminary affinity data with K_d values in the range of 30 to 40 nM. These results are comparable to that of monolayer cell homogenate. Internalisation experiments with LNCaP-spheroids are ongoing. ***Conclusion:*** The novel radiolabelled PSMA-ligand L can be radiopharmacologically characterised on prostate cancer cell homogenate but also spheroids. The establishing of three-dimensional cell aggregates by magnetised cells and, moreover, the investigation of new radiolabelled conjugates for potential PET/SPECT application or even therapeutic treatment of cancer entities using spheroids is a valuable and promising method. Next, it is planned to use the LNCaP-spheroids for evaluation of PSMA-radioligands in a proof-of-concept-study applying the technology of Micro-Physiological Systems (multiorgan-chips) [3]. ***References:*** [1] Sihver, Eur. J. Nucl. Med. Mol. Imaging 2019, 26 (Suppl 1), S132. [2] Turker, ACS Biomater. Sci. Eng. 2018, 4, 787. [3] Maschmeyer, Lab Chip 2015, 15, 2688.

OP-758

Development and preclinical evaluation of ^{177}Lu-AMTG, a novel pharmacophore-modified GRPR-targeted antagonist with improved metabolic stability

T. Günther*, R. Beck, V. Felber, S. Deiser, H. Wester;*
Technical University of Munich, Garching, GERMANY.

Aim/Introduction: In order to further improve the metabolic stability and thus pharmacokinetics of Gastrin-releasing peptide receptor (GRPR)-targeted antagonists, we substituted the tryptophan moiety within the metabolically unstable pharmacophore of the potent antagonist RM2 (DOTA-Pip^5-D-Phe^6-Gln^7-Trp^8-Ala^9-Val^{10}-Gly^{11}-His^{12}-Sta^{13}-Leu^{14}-NH_2) by the unnatural amino acid α-methyl tryptophan (α-Me-Trp^8). Results of the preclinical evaluation of [α-Me-Trp^8]RM2 (=AMTG) were compared with the current golden standards among GRPR-addressing compounds, RM2 and NeoBOMB1 (DOTA-pABzA-DIG-D-Phe-Gln-Trp-Ala-Val-Gly-His-NH-CH[CH_2-$CH(CH_3)_2$]$_2$). ***Materials and Methods:*** All compounds were synthesised via standard Fmoc-based solid-phase peptide synthesis (SPPS). ^{177}Lu-labelling was carried out at 95 °C within 10 min (1.0 M sodium acetate buffer, pH = 5.5, 0.1 M sodium ascorbate). GRPR affinity (IC_{50}) and internalisation (37 °C, 1 h) were evaluated on PC-3 cells. Hydrophilicity (expressed as n-octanol/PBS distribution coefficient; $logD_{7.4}$) and metabolic stability in vitro in murine as well as human plasma (37 °C, 72 ± 2 h) were investigated. Biodistribution studies at 24 h p.i. and µSPECT/CT imaging at 1, 4, 8, 24 and 28 h p.i. were carried out on PC-3 tumour-bearing CB17-SCID mice. ***Results:*** Synthesis of the three derivatives via SPPS yielded 6-11% HPLC-purified labelling precursor. ^{177}Lu-labelling proceeded quantitatively. All peptides showed comparable GRPR affinity (IC_{50} [nM] of Lu-RM2: 3.45 ± 0.18, Lu-NeoBOMB1: 4.22 ± 0.14, Lu-AMTG: 3.04 ± 0.08). Studies on the receptor mediated internalisation into PC-3 cells (37 °C, 1 h) displayed distinct differences for ^{177}Lu-RM2 (2.92 ± 0.20%), ^{177}Lu-NeoBOMB1 (13.91 ± 0.64%) and ^{177}Lu-AMTG (3.03 ± 0.18%). Hydrophilicity ($logD_{7.4}$) of the RM2-based compounds was higher than that of ^{177}Lu-NeoBOMB1 (^{177}Lu-RM2: −2.51 ± 0.02 and ^{177}Lu-AMTG: −2.28 ± 0.06 vs. ^{177}Lu-NeoBOMB1: −0.57 ± 0.03). Studies on the metabolic stability in vitro (37 °C, 72 ± 2 h) revealed comparable amounts of intact tracer in murine plasma (^{177}Lu-RM2: 71.2 ± 3.6%; ^{177}Lu-NeoBOMB1: 73.5 ± 3.4%; ^{177}Lu-AMTG: 75.0 ± 11.5%), but distinctly different intact tracer amounts in human plasma (^{177}Lu-RM2: 33.5 ± 2.7%; ^{177}Lu-NeoBOMB1: 60.8 ± 1.2%; ^{177}Lu-AMTG: 77.6 ± 10.1%). In vivo, ^{177}Lu-AMTG exhibited the highest tumour-to-blood and tumour-to-muscle ratios at 24 h p.i. As demonstrated by µSPECT/CT imaging, ^{177}Lu-RM2 showed a faster clearance from the tumour and the pancreas than ^{177}Lu-AMTG. Proof of concept studies in men have already been started. ***Conclusion:*** Based on its improved metabolic stability and very promising preclinical data, the novel GRPR-targeted antagonist AMTG might have the potential to compete with or even outperform the current golden standards among GRPR-targeted ligands (RM2, NeoBOMB1) for targeted radiotherapy in men. ***References:*** None

OP-759

A preclinical evaluation of ^{89}Zr-labeled PSMA ligands for pre-treatment dosimetry for ^{177}Lu-labeled PSMA therapy

B. Privé*, Y. H. W. Derks, G. M. Franssen, S. M. B. Peters, M. W. Konijnenberg, M. Gotthardt, M. J. R. Janssen, P. Laverman, J. Nagarajah, S. Heskamp;*
Radboudumc, Nijmegen, NETHERLANDS.

Aim/Introduction: [^{177}Lu]Lu-PSMA-I&T and [^{177}Lu]Lu-PSMA-617 are promising therapies for prostate cancer (PCa). To date, it is difficult to predict their efficacy up-front. While ^{177}Lu offers SPECT-based dosimetry, this is only possible after a therapeutic injection and because of the limited resolution, exclusively for larger tumours. Hence, PET based pre-treatment dosimetry may improve patient stratification. ^{89}Zr-labeled PSMA ligands could potentially be used for this, as ^{89}Zr has a longer $T_{1/2}$ compared to ^{68}Ga/^{18}F and may therefore be more suited to study uptake as well as retention of these ligands. Here, we describe

the radiolabelling of PSMA-I&T and PSMA-617 with ^{89}Zr. Furthermore, we compared their in vivo biodistribution and dosimetry with ^{177}Lu-labeled PSMA-I&T and PSMA-617 in tumour-bearing mice. ***Materials and Methods:*** [^{89}Zr]$ZrCl_4$ was produced from [^{89}Zr]$Zr(ox)_2$ using a strong anion exchanger.(1) PSMA ligands were labelled with [^{89}Zr]$ZrCl_4$ or [^{177}Lu]$LuCl_3$ in 0.5M MES buffer pH 5.5 and purified using C18 SPE cartridges. Labelling efficiency and radiochemical purity were analysed by TLC and HPLC. In total, 96 BALB/c nude mice bearing PSMA$^+$-LS174T and PSMA$^-$-LS174T xenografts received either 0.50 nmol (0.6 - 1 MBq) [^{89}Zr]Zr-PSMA-I&T, [^{89}Zr]Zr-PSMA-617, [^{177}Lu]Lu-PSMA-I&T or [^{177}Lu]Lu-PSMA-617 intravenously. Ex vivo biodistribution was performed at 2, 24, 72 and 168 h post injection. ***Results:*** [^{89}Zr]Zr-PSMA-I&T and [^{89}Zr]Zr-PSMA-617 were labeled with a radiochemical yield of 30-60%, resulting in molar activities of 2.4 MBq/nmol and 1.3 MBq/nmol, respectively. All four radiotracers demonstrated high tumour accumulation in PSMA$^+$ xenografts, with a mean uptake two hours p.i. of 8.8 ±1.6, 10.9 ±1.9, 11.6 ±1.4 and 10.2 ±1.0 %ID/g for [^{89}Zr]Zr-PSMA-I&T, [^{177}Lu]Lu-PSMA-I&T, [^{89}Zr]Zr-PSMA-617 and [^{177}Lu]Lu-PSMA-617, respectively. This resulted in a mean dose to the tumours of 143.1, 247.8, 381.5 and 309.0 mGy/MBq, respectively. Overall, ^{89}Zr-labeled PSMA ligands showed a comparable biodistribution to ^{177}Lu-labeled PSMA ligands (e.g. blood, salivary glands, liver). However, the mean doses in the skeleton and kidneys were 44.4, 5.0, 13.5 and 3.3 mGy/MBq, and 132.8, 357.9, 94.0 and 37.2 mGy/MBq for [^{89}Zr]Zr-PSMA-I&T, [^{177}Lu]Lu-PSMA-I&T, [^{89}Zr]Zr-PSMA-617 and [^{177}Lu]Lu-PSMA-617, respectively. ***Conclusion:*** PSMA-617 and PSMA-I&T were successfully labelled with ^{89}Zr and demonstrated high uptake in PSMA$^+$ xenografts. The overall biodistribution of [^{89}Zr]Zr-PSMA-I&T and [^{89}Zr]Zr-PSMA-617 resembled the distribution of [^{177}Lu]Lu-PSMA-I&T and [^{177}Lu]Lu-PSMA-617, respectively. However, the concentration of ^{89}Zr in bone was higher compared to ^{177}Lu. Furthermore, [^{89}Zr]Zr-PSMA-617 overestimated the kidney and tumour uptake, while [^{89}Zr]Zr-PSMA-I&T underestimated these. Future studies are needed to clarify these differences and to optimize radiolabelling and purification. ***References:*** 1. Pandya et al., J Nucl Med 2019; 60:696-701

OP-760

Does the Injected Mass influence the Biodistribution of F-18-rhPSMA-7.3 on Positron Emission Tomography in Prostate Cancer Patients?

T. Langbein[1], *A. Wurzer*[2], *A. Gafita*[1,3], *A. Robertson*[1], *H. Wang*[1], *A. Arçay*[1,4], *M. Herz*[1], *H. Wörther*[1], *C. Franz*[1], *W. Weber*[1], *H. Wester*[2], *M. Eiber*[1];

[1]Technical University of Munich, School of Medicine, Klinikum rechts der Isar, Department of Nuclear Medicine, Munich, GERMANY, [2]Technical University of Munich, Chair for Pharmaceutical Radiopharmacy, Garching, GERMANY, [3]Ahmanson Translational Theranostics Division, Department of Molecular and Medical Pharmacology, University of California Los Angeles, Los Angeles, CA, UNITED STATES OF AMERICA, [4]Department of Nuclear Medicine, Akdeniz University, Antalya, TURKEY.

Aim/Introduction: F-18-labeled PSMA ligands are increasingly used for prostate cancer imaging due to longer half-life and potential large batch productions in comparison with Ga-68-labeled counterparts allowing the use of a single batch for many patients over several hours. With defined activities for each patient the injected ligand mass substantially increases during the working day. Studies of F-18 labeled compounds in mice have shown a significant influence of the injected mass on the biodistribution of PSMA ligands. We investigated whether similar effects on organ uptake could be observed in patients using the novel PET radiotracer, F-18-rhPSMA-7.3. ***Materials and Methods:*** Patients with prostate cancer who underwent PET/CT with F-18-rhPSMA-7.3 at various timepoints after its production and therefore received different injected ligand masses were retrospectively grouped into two groups (low or high injected mass). Only patients with low tumour load were included to avoid variability due to "tumour sink" effects. The biodistribution of the PSMA ligand in the two groups was compared by drawing standardized isocontour-volumes of interest over normal organs and tumour lesions to detect SUVmean, and by obtaining full organ segmentation data using semiautomatic analysis with the software qPSMA. ***Results:*** Two groups, each with 42 patients, who either received a "low" or "high" mass of F-18-rhPSMA-7.3 (1.7±0.2µg vs. 18.4 ±3.6µg) were compiled from the database. Mean injected activities per body weight and uptake times did not vary significantly between the groups (3.95±0.13 vs. 3.84±0.37 MBq/kg; 72±10.0 vs. 77±12.5 min for low and high mass, respectively). SUVmean of the blood pool (2.1±0.5 vs. 2.2±0.4), liver (7.6±2.3 vs. 7.5±2.1), kidneys (35.4±9.9 vs. 34.9±9.4), bone (1.4±0.4 vs. 1.5±0.5) and muscle (0.8±0.1 vs. 0.8±0.2) showed no significant difference between the groups. There was also no significant difference in tumour uptake (10.0±8.5 vs. 14.4±14.8). A significantly decreased uptake by the parotid and submandibular glands was observed in patients with higher injected ligand mass compared with those with a lower injected mass (20.1±5.3 vs. 17.4±4.7; $p<0.05$ and 22.4±6.3 vs. 18.4±5.3; $p<0.01$, respectively). Similar results were found with spleen uptake (10.3±4.0 vs. 8.1±2.9; $p<0.05$). ***Conclusion:*** The injected mass of rhPSMA-7.3 had only minimal effects on its biodistribution and no impact on clinical imaging interpretation. The stability of biodistribution over a 10-fold range of injected masses supports central production and distribution of F-18 labeled PSMA ligands. The uptake by salivary glands and the spleen appears saturable with increased mass of cold ligand, which warrants further investigation. ***References:*** None

OP-761

Competition ('steal' phenomenon) between [68Ga]Ga-PSMA-11 uptake in prostate tumor and healthy tissue

E. C. A. van der Sar, S. van den Doel, B. de Keizer, M. G. E. H. Lam, A. J. A. T. Braat;
UMC Utrecht, Utrecht, NETHERLANDS.

Aim/Introduction: Prostate specific membrane antigen (PSMA)-targeted radionuclide therapy for prostate cancer (PCa) has shown to be effective but with some side effects (fatigue, nausea, diarrhea, and xerostomia), potentially caused by irradiation of organs with physiological PSMA uptake. Because PCa cells have an overexpression of PSMA, the total tumor volume (TTV) might affect PSMA distribution. Filss et al., 2018 suggested that competition might induce a 'steal' phenomenon, resulting in diminished uptake in healthy tissue. In the current study, we aimed to investigate the influence of TTV on [68Ga]Ga-PSMA-11 uptake in healthy tissue. If a 'steal' phenomenon exists, we might individualize PSMA-targeted radionuclide therapy based on TTV and potentially reduce/avoid unwanted side effects. ***Materials and Methods:*** Patients with PCa referred for a [68Ga]Ga-PSMA-11 PET/CT were identified retrospectively from a single center from March 2016 to January 2019. Patients with recent prostate specific antigen (PSA) values (±1 month) and ≥3 metastases on [68Ga]Ga-PSMA-11 PET/CT were included, as difference in ligand binding is only expected in case of sufficient competition between tumor and healthy tissue. Patients were excluded if imaging followed previous treatment with [177Lu]Lu-PSMA-617, 223Radium-dichloride, or external beam radiation of the head/neck region. Quantitative image analysis was performed using the Syngo.via-software (Siemens version 05.01) on EARL reconstructions. Values were collected in line with the PERCIST parameters; Total Lesion Volume (TLV, derived from TLG; defined as Total Lesion PMSA-binding in SUVlean body mass*cm^3 (SUV_{lbm}*cm^3)), and Metabolic Tissue Volume (MTV) of the lacrimal-,submandibular-,and parotid glands, kidneys and the TTV (SUV_{lbm}*cm^3, derived from total TLG) of the PCa. Relevant volumes of interest were (semi-)automatically segmented based on blood pool activity (i.e. in line with PERCIST). ***Results:*** 488 patients were screened, 92 patients met the inclusion criteria. Median TTV was 703.37 SUV_{lbm}*cm^3 (IQR 5.76-34043.37), median TLV of the lacrimal-,submandibular-,and parotid glands, kidneys was respectively 14.06 SUV_{lbm}*cm^3 (IQR 1.25-59.28), 194.75 SUV_{lbm}*cm^3 (IQR 22.99-576.83), 552.54 SUV_{lbm}*cm^3 (IQR 119.98-1544.73), and 8092.75 SUV_{lbm}*cm^3 (IQR 3209.20-15855.18). A significant (p-value<0.01) but weak correlation was found between the TTV and TLV of the parotid-,and submandibular glands and kidneys (correlation coefficient of respectively -0.447,-0.345, and -0.394). No correlation was found between TTV and TLV of the lacrimal glands. ***Conclusion:*** The weak correlation between the TTV and TLV of healthy tissue (salivary glands and kidneys) suggests that healthy tissue uptake of [68Ga]Ga-PSMA-11 is not solely influenced on TTV. Thus, modification of therapeutic [177Lu]Lu-PSMA activity should not be adjusted based on TTV alone. ***References:*** doi:10.3413/Nukmed-0937-17-10

1406

Cutting Edge Science Track - TROP Session: Dosimetry for PRRT and PSMA

Friday, October 30, 2020, 09:00 - 10:20 Channel 6

OP-762

Estimation of tumor burden from 68Ga- Dotatate-PET/CT and day-7 planar 177Lu images, for patients treated with 177Lu-Dotatate

K. Sjögreen Gleisner[1], J. Gustafsson[1], A. Stenvall[1], D. Roth[1], C. Hindorf[2], L. Jönsson[1], E. Larsson[2], T. Olsson[2], A. Sundlöv[3,1];
[1]Medical Radiation Physics, Clinical Sciences, Lund, SWEDEN, [2]Department of Radiation Physics, Skane University Hospital, Lund, SWEDEN, [3]Oncology and Pathology, Clinical Sciences Lund, Skane University Hospital, Lund, SWEDEN.

Aim/Introduction: The total tumor burden (TuB) has been identified as a factor that may affect the rate of peptide accumulation and thereby the absorbed dose to organs and tumors for NET patients treated with 177Lu-Dotatate. TuB refers to the total tumor volume and can be estimated from 3D images such as 68Ga-PET/CT. In the clinical trial Iluminet (EUDRACT 2011-000240-16), post-therapeutic 177Lu gamma-camera images were acquired for dosimetry. A hybrid planar-SPECT/CT protocol was used, where the last whole-body scan was made 7 days after administration, when mainly tumors retain activity. The aim was to develop a semi-automatic method for segmentation of the TuB, applicable in both 2D and 3D images, and to compare the TuB estimated from 68Ga-PET/CT to surrogate metrics from 177Lu day7-planar images. ***Materials and Methods:*** 68Ga-PET/CT and 177Lu planar whole-body images for 18 patients acquired within 20 weeks (14 pts within 10 weeks) were included. The planar images were processed for activity quantification, including pixel-wise attenuation correction using a CT-scout, and a deconvolution filter for scatter correction. The segmentation method was constructed as a difference of Gaussians (DOG) filter, implemented as a scale pyramid in which Gaussian filters (2D or 3D) with gradually increasing width were applied to the image. A sequence of high-pass filtered images were obtained by subtraction of the image from a lower level of filtering from the next level. A region-growing algorithm was applied to each of these high-pass filtered images, where seeds were automatically generated from the image coordinates whose value exceeded a predefined threshold in any of the high-pass

filtered images. The binary masks obtained from region-growing of each level were combined to form the final tumor-burden mask. The DOG filtering was implemented in a graphical user interface in which the number of levels and the gradient thresholds could be adjusted, and false positive regions removed. ***Results:*** Pearson's correlation coefficient was determined for the TuB determined from the 68Ga-PET/CT images versus different metrics determined for the day7-planar image (total activity in tumors, projected tumor area, total-body activity). The highest correlation coefficient (approximately 0.8) was obtained for the total activity in tumors, followed by the total-body activity. ***Conclusion:*** The DOG filtering enables fast assessment of the TuB in planar or tomographic images. The correlations obtained support the use of day7-planar 177Lu images for assessment of the TuB. ***References:*** None

OP-763

Comparison of The Effect of 1L Vs 2L Lysine/Arginine Solution (25g/L Each) on Kidney Absorbed Doses and Acute Side Effects in Patients Undergoing Lutathera Treatment

D. Gillett[1], *S. Ballout*[1], *E. Varzakis*[1], *I. Harper*[1], *D. Pitfield*[2], *A. Powell*[1], *R. T. Casey*[3,2], *S. Heard*[1], *L. Aloj*[4,1];
[1]*Department of Nuclear Medicine, Addenbrooke's Hospital CUHFT, Cambridge, UNITED KINGDOM,* [2]*Department of Endocrinology, Addenbrooke's Hospital CUHFT, Cambridge, UNITED KINGDOM,* [3]*Department of Genetics, University of Cambridge, Cambridge, UNITED KINGDOM,* [4]*Department of Radiology, University of Cambridge, Cambridge, UNITED KINGDOM.*

Aim/Introduction: Lu-177 DOTATATE (Lutathera®) is an approved treatment for patients with metastatic GEP-NET tumours. As with most small negatively-charged peptides there is significant kidney retention following infusion. Coadministration of high concentrations of Lysine and Arginine have been shown to reduce kidney retention and absorbed doses in patients undergoing treatment. Our institution traditionally used 2L of solution (25g Arginine/25g Lysine in 1L saline) injected at 333 mL/hour starting approximately 1h prior to Lutathera (7.4 GBq). Administering high doses of amino acids is known to cause acute side effects such as nausea and vomiting, which can persist for several days, as well as transient acute kidney toxicity, so we recently adopted a reduced regimen of 1L of the solution over 5h (200mL/hr) as recommended by the manufacturer.We aim to identify whether this change in regimen significantly impacts kidney absorbed doses and side effects. ***Materials and Methods:*** Patients undergoing Lutathera treatment were routinely imaged at three time points up to one week after radiopharmaceutical administration for each cycle. SPECT studies of the abdomen (one of which had a co-registered CT) were obtained at each time point. Absolute radioactivity concentrations were estimated using GE Xeleris Volumetrix AC OSEM reconstruction and a camera-specific sensitivity factor. Kidney volumes were determined from the CT component. Effective half-lives and absorbed dose estimates were obtained using 3D Slicer and RADAR dose factors. The incidence and severity of acute side effects and other laboratory findings of acute metabolic effects (where available) were also reviewed. ***Results:*** 23 treatment infusions were analysed for 6 patients whose treatment straddled the regime change in the period May 2019 to March 2020. The mean kidney effective half-lives and doses were calculated for each patient for both kidney blocking regimes. The mean patient-specific effective half-lives were found to be 4.31 and 4.58 days for regime A (2L of solution) and B (1L) respectively. Mean patient-specific kidney doses were found to be 2.13 and 2.58 Gy for regime A and B respectively. These results indicate increases of 6.3% and 21.1% for effective half-lives and absorbed doses respectively. ***Conclusion:*** Our initial experience with the manufacturer-recommended reduced regimen indicates a small increase to kidney half-lives, contributing to increased kidney absorbed doses. No significant acute side effects have been observed since modifying the amino acid infusion scheme. Data on whether these changes have any impact on long term kidney toxicity are not yet available. ***References:*** None

OP-764

Absorbed doses to kidneys based two SPECT measurements versus seven SPECT measurements patients with neuroendocrine tumours receiving ^{177}Lu-DOTATATE therapy

M. Sandstrom[1], *A. Sundin*[2], *M. Lubberink*[1];
[1]*Medical Physics, Uppsala, SWEDEN,* [2]*Nuclear medicine and PET, Uppsala, SWEDEN.*

Aim/Introduction: As in all therapies using ionizing radiation, a patient-specific optimization of the delivered radiation should be performed in therapy with ^{177}Lu-DOTATATE. At our centre, the number of treatments is based on the absorbed dose (AD) to the kidneys. For logistical reasons, estimation of absorbed doses should be performed with as few measurements as possible. The aim of the present work was to study how well kidney AD estimations using a method with two measurement points agree with a method that is based on seven imaging points. ***Materials and Methods:*** Six patients (three female and three male) with neuroendocrine tumors with high somatostatin receptor expression were included. They were injected with 500MBq 177Lu-DOTATATE and no kidney protection was used. SPECT/CT over the abdomen were acquired at 0.5, 1, 1.5, 2.5, 4, 24 and 96h after injection of ^{177}Lu-DOTATATE. AD were calculated using single exponential fits to data from 2 measurements (24-96) or trapezoidal integration up to 24h and then exponential fit after 24h. Bias of AD values relative

to those based on the seven-point measurement were calculated for both right and left kidney. To test statistical significance a Wilcoxon matched-pairs signed rank test with a P-value of 0.05 for significance was used. Median, Min and Max of the deviations were also calculated for the AD. For the early measurement points, estimations from the (24-96) for the time of measurement were compared with the measured values. ***Results:*** Bias versus AD(seven) was -0.4%(-1.1-3.8) (Median(Min-Max)) for the right kidney and -0.2%(-1.1-5.4) for the left kidney when the AD(24-96) method was used. The P-values were 0.69 for the right kidneys and 0.84 for the left kidneys and this show no significant difference between the two methods. With errors as small as these and using a fixed limit of the absorbed dose to the kidneys, this would mean that really few patients would be given unoptimized number of treatments. The difference of the estimated activity concentrations for every point was in general small (less than 5%) but could vary up to about 30% for single values. A larger study including more patients and preferably also a later timepoint (maybe 7 days) is highly warranted. ***Conclusion:*** With a difference of less than about 5% for all the measurements the results from this study indicate that the influence of early measurements (earlier than 24 h) is fairly small and can be ignored. ***References:*** None

OP-765

Preliminary results of a Phase II ^{177}Lu and ^{90}Y PRRT study: analysis of OAR dosimetry and dose-response relationship for NET liver metastases

E. Tonini[1], S. Panareo[2], M. Longo[3], L. Longo[4], L. Perrucci[5], E. Fortini[5], G. Di Domenico[4], L. Uccelli[2], C. Cittanti[2], A. Turra[1], M. Giganti[5], M. Bartolomei[2];
[1]Sant'Anna Hospital, Medical Physics Unit, Ferrara, ITALY, [2]Sant'Anna Hospital, Nuclear Medicine Unit, Ferrara, ITALY, [3]Sapienza University of Rome, Ph.D. Program in Morphogenesis & Tissue Engineering, Rome, ITALY, [4]Department of Physics and Earth Sciences, Ferrara University, Ferrara, ITALY, [5]Section of Diagnostic Imaging, Department of Morphology, Surgery and Experimental Medicine, University of Ferrara, Ferrara, ITALY.

Aim/Introduction: Peptide-receptor radionuclide-therapy (PRRT) has become a standard treatment modality for patients affected by neuroendocrine tumors. A phase II study FENET2016 (University Hospital Sant'Anna, Ferrara, Italy) is presented. Treatment protocol relies on either five PRRT cycles with ^{177}Lu-DOTATOC or a sequence of ^{177}Lu followed by ^{90}Y-DOTATOC spaced two months apart. We report about tumors and organ-at-risk (OAR) dosimetry and evaluation of the dose-response relationship for liver metastases. ***Materials and Methods:*** 80 patients underwent PRRT therapy with systemic administration of cumulative activities between 11 and 28 GBq. A validated method based on three-time-point (at 1, 24, 48 hours after administration) SPECT/CT was developed to calculate the absorbed doses (AD) to tumors and OARs. Tumors and kidneys AD were calculated according to MIRD scheme, while L2-L4 lumbar vertebrae imaging method was used to calculate AD to BM. Dosimetric results between first and fifth cycle were compared as well as those obtained with ^{177}Lu and ^{177}Lu\$^{90}$Y modalities. Tumor response was evaluated applying the Response Evaluation Criteria In Solid Tumors (RECIST 1.1) to hepatic lesions. The CTs were performed no earlier than 4 weeks before the treatment and no later than 12 weeks after it. By comparing the lesions in the CT with the areas of high uptake in SPECT\CT, only the superimposable lesions were selected, resulting in 29 lesions in 15 patients. The variations of lesion diameter recorded by CECT and the corresponding absorbed doses were correlated. ***Results:*** The cumulative doses ranged from 13 to 310 Gy for tumors, from 3.5 to 40 Gy for kidneys and from 0.03 to 1.2 Gy for BM. High variability in tumor AD per unit activity was observed with values ranging from 2.5 to 45 mGy/MBq and from 1 to 107 mGy/MBq for ^{177}Lu and ^{177}Lu\$^{90}$Y. The percentage reduction of lesion diameters treated with ^{177}Lu\$^{90}$Y resulted higher than those obtained with ^{177}Lu (mean=29.3%, SD=17.6 for ^{177}Lu\$^{90}$Y; mean=3.4%, SD=19.41 for ^{177}Lu\$^{90}$Y). The dose-response correlation (r=0.92) turned out to be highly significant with a level of sampling significance superior than 99% when considering lesions above 3 cm in diameter treated with ^{177}Lu\$^{90}$Y. No correlation was found below 80 Gy. ***Conclusion:*** The dosimetric protocol routinely established provides reproducible, standardized and patient-tailored dose estimates. The highly significant correlation between the lesion response and the absorbed dose we found for large metastases treated with ^{177}Lu\$^{90}$Y is highly promising for the clinical benefit derived from the implementation of dosimetry in PRRT. ***References:*** None

OP-766

Lesion-wise dosimetry for multiple bone metastases in mCRPC patients undergoing Lu-177-PSMA therapy: comparison of five dosimetric methods

J. Brosch[1], C. Uribe[2], A. Gosewisch[1], L. Kaiser[1], P. Bartenstein[1], A. Todica[1], H. Ilhan[1], A. Rahmim[3], A. Celler[3], S. Ziegler[1], G. Böning[1];
[1]Department of Nuclear Medicine, University Hospital, LMU Munich, Munich, GERMANY, [2]PET Functional Imaging, BC Cancer, Vancouver, BC, CANADA, [3]Department of Radiology, University of British Columbia, Vancouver, BC, CANADA.

Aim/Introduction: Although metastatic, castration-resistant prostate cancer (mCRPC) patients undergoing Lu-177-PSMA-therapy show a large number of bone metastases, tumor dosimetry is typically performed only for a limited number of lesions per patient. To differentiate between responding/non-responding bone lesions, dosimetric calculation for all bone lesions is required. We aimed to investigate the accuracy of 4 computationally-efficient

dosimetric methods against Monte-Carlo (MC) based dosimetry as gold-standard. ***Materials and Methods:*** 10 mCRPC patients, receiving their 1st cycle of Lu-177-PSMA-I&T-therapy (7.4-9GBq), were enrolled. Each patient underwent quantitative Lu-177-SPECT/CT at 24h, 48h and 72h p.i. with 3 bed positions (shoulders-knees). All lesions with volumes >1ml were segmented on the 24h SPECT (kmeans segmentation, PMOD v4.005) and the resulting volumes of interest (VOIs) were copied to the subsequent co-registered SPECTs. For each lesion, the effective half-life was obtained by mono-exponential fitting of activities in these VOIs. To preserve the 3D distribution information within the lesions, the time-integrated activity image was estimated based on the 24h SPECT. Dose estimates per lesion from MC (GATE v8.2) were compared with those from: A) OLINDA v.2.0 using unit-density sphere model, B) OLINDA weighted with CT-based average lesion density, C) ICRP soft tissue Lu-177 voxel-S-values (GATE), and D) voxel-S-values with CT-based voxel density weighting. ***Results:*** In total, 125 lesions (volumes 1.5-420.6ml) were analyzed. On average, method A overestimated doses for all lesions (mean: +10%, range: -12% to +47%), while method B underestimated them (mean: -14%, range: -28% to -2%). Similarly, method C overestimated the lesion doses (mean: +20%, range: -8% to 57%), whereas results from method D were closest to the MC dose estimates showing the smallest range of deviations (mean: -4%, range: -9% to -3%). ***Conclusion:*** Full MC dosimetry is complex and time-consuming, while commonly employed OLINDA is simple and fast. The advantage of MC and voxel-S-value methods is the generation of 3D dose distributions, contrary to OLINDA which assumes spherical tumors and provides only mean doses. Our results show that doses estimated by methods A and C (assuming unit density) reveal a large range of deviations from MC, which is reduced when CT-based density weighting (methods B and D) is applied. To conclude, dosimetric calculation using voxel-S-values with CT-based density weighting represents a simple, yet accurate dosimetric method compared to the gold-standard MC dose estimates. This practical approach would enable determination of dose estimates for all bone lesions in mCRPC patients and visualization of 3D dose maps. ***References:*** None

OP-767

Individualization of ^{177}Lu-PSMA Therapy based on important physiologic parameters using global sensitivity analysis and a physiologically-based pharmacokinetic model

G. Glatting[1,2], P. Kletting[1,2], N. J. Begum[1], M. Eiber[3], A. J. Beer[2], S. A. Pawiro[4], D. Hardiansyah[4];

[1]Medizinische Strahlenphysik, Nuklearmedizin, Universität Ulm, Ulm, GERMANY, [2]Klinik für Nuklearmedizin, Universität Ulm, Ulm, GERMANY, [3]Nuklearmedizin, Klinikum rechts der Isar, Technische Universität München, München, GERMANY, [4]Medical Physics and Biophysics, Physics Department, Faculty of Mathematics and Natural Sciences, Universitas Indonesia, Depok, INDONESIA.

Aim/Introduction: Individualized treatment planning is expected to improve outcome of radionuclide therapy. In this study, we identify the most important physiologic parameters for the determination of the individual kidneys and tumor absorbed doses (ADs) in ^{177}Lu-PSMA therapy. Therefore, a global sensitivity analysis (GSA) and a physiologically-based pharmacokinetic (PBPK) model are used. ***Materials and Methods:*** A whole-body PBPK model that has been developed for treatment planning in ^{177}Lu-PSMA therapy was used. As the fixed model parameters have a relatively small effect on the estimation of time-integrated activity coefficients (TIACs) and thus the ADs, the model parameters of interest for the GSA analysis in this study were the parameters that have been estimated from the biokinetic data such as the organ receptor densities Rdens, organ flows f and organ release rates. GSA with the extended Fourier Amplitude Sensitivity Test (eFAST) algorithm was chosen based on its high accuracy for non-linear models and the low number of model evaluations needed. An in-house GSA with eFAST program based on MATLAB software (version R2019b) was developed. The frequency-based sampling method with a log-normal distribution was used to avoid negative values of the sampled parameters. The main effects S_i and total effects S_{Ti} were calculated and analyzed using the GSA program and the PBPK model to identify the importance of each model parameter i for the individualization of the ADs in ^{177}Lu-PSMA therapy. To warrant the convergence of the calculated S_i and S_{Ti}, various numbers of model simulations were performed, i.e. 129, 257, 513, 1025, 2049, 4097 and 8193. ***Results:*** The inter-individual variability of tumor ADs (coefficients of variation CV around 60%) was higher than that in the kidneys (CV around 30%). Based on the GSA with the eFAST algorithm results, the individual calculated tumor ADs were mostly depending on the receptor density RdensTU (S_i and S_Ti values up to 0.72) for the tumor lesions. For the kidneys, receptor density in kidneys RdensK (S_i=0.25, S_{Ti}=0.30) and flows fK (S_i=0.36, S_{Ti}=0.43) were identified as the most important parameters determining the individual kidneys ADs. ***Conclusion:*** We have shown the first implementation of the GSA with the eFAST algorithm to identify the most important parameters that affect the individualization of the calculated ADs in ^{177}Lu-PSMA therapy. These results suggest an accurate measurement of these parameters, i.e. receptor density and blood flow, before ^{177}Lu-PSMA therapy to decrease the inter-individual variability of the ADs in kidneys and tumor. ***References:*** None

OP-768

[^{90}Y]Y-PSMA-617 -Post-therapeutic kidney, bone marrow and tumor dosimetry for individualized treatmentof metastatic castration-resistant prostate cancer

J. Kurth, B. J. Krause, O. W. Hakenberg, S. M. Schwarzenböck, M. Heuschkel;
Rostock University Medical Center, Rostock, GERMANY.

Aim/Introduction: PSMA ligands have been established as a treatment option for patients suffering from mCRPC. To date, Y-90 hasn't been extensively used for PSMA-targeted therapies, although it is hypothetically assumed that larger lesions could benefit from enhanced crossfire effects. As mCRPC-patients are heavily pretreated all reasonable efforts should be made to protect the organs at risk (OAR). Therefore, dosimetry accompanying therapy is indispensable. As intra-therapeutic quantitative Y-90-imaging is challenging, dosimetry of a previous study was only estimated based on previously performed [^{177}Lu]Y-PSMA-617 therapies [1], Therefore, aim of this study was to establish an imaging protocol and a workflow allowing post-therapeutic dosimetry for kidneys and bone marrow in [^{90}Y]Y-PSMA-617 therapy. ***Materials and Methods:*** 17 patients (mean age: 72y (range: 59-84ys)) presenting insufficient response to [^{177}Lu]Lu-PSMA-617 treatment were selected for [^{90}Y]Y-PSMA-617 therapy. For dosimetry, each patient underwent SPECT/CT imaging of the upper abdomen at approximately 2, 24, 48 and 72h p.i., (Siemens Symbia T6; HEGP-collimators; energy-window: 125keV±20%; matrix: 128x128; 64 projections, 35 sec each). Quantitative SPECT/CT reconstruction was performed (3D-OSEM; 5i15s) with corrections for attenuation, scatter and detector blurring using a fully Monte Carlo based collimator modeling (Hermes Hybrid Recon v.3.0) [2]. A special calibration factor adapted to the general kidney geometry was determined. The required phantom inserts were manufactured using a rapid prototyping technology [3] and inserted into a torso phantom. Absorbed doses (AD) of kidneys and tumor lesions were calculated based on a voxel level dosimetry scheme (Hermes Voxel Dosimetry, v.1.0.1). VOIs based on CT were applied to calculated dose map to extract AD for kidneys and tumor lesions. Red bone marrow dosimetry was performed based on blood sampling according to EANM guideline. ***Results:*** The therapy was well tolerated by all patients. Mean administered activity was 4.23±0.54 GBq. Mean AD in the kidneys was 2.1±1.0Gy/GBq and 0.19±0.18Gy/GBq for the red bone marrow. For tumor lesions (19 osseous and 15 soft tissue lesions) the mean AD was 16.4±7.8Gy/GBq. Compared to [^{177}Lu]Lu-PSMA-617, AD of the kidney and bone marrow are approximately 2.8 and 5 times higher, respectively. ***Conclusion:*** [^{90}Y]Y-PSMA-617 offers an alternative treatment option for patients without sufficient response to Lu-177-PSMA therapy. AD of tumor lesions are higher, but also OAR are more affected. However, quantification of the Y-90-SPECT/CT still needs further validation and critical discussion.***References:*** [1] Rathke H et al. JNM Nov 2, 2018 [2] Porter et al. EJNMMI Research (2018) 8:7 [3] Kurth J et al. JNM. 2013;54(suppl 2):2174

OP-769

Targeted Alpha PSMA-based Therapy of mCRPC patients: previsional dosimetry and radiobiological evaluation

A. Sarnelli[1], *M. Belli*[1], *E. Mezzenga*[1], *F. Cesarini*[1], *P. Caroli*[1], *V. Di Iorio*[1], *M. Cremonesi*[2], *L. Strigari*[3], *A. Romeo*[1], *S. Nicolini*[1], *F. Matteucci*[1], *S. Severi*[1], *G. Paganelli*[1];
[1]*Istituto Scientifico Romagnolo per lo Studio e la Cura dei Tumori (IRST) IRCCS, Meldola, ITALY,* [2]*European Institute of Oncology, IRCCS 20141 Milano, Milan, ITALY,* [3]*Policlinico S. Orsola-Malpighi, 40138 Bologna, Bologna, ITALY.*

Aim/Introduction: For tumors refractory to beta-radiation therapy, the use of alpha emitters in radiometabolic treatment is a promising option. Target-alpha therapy(TAT) combines high-LET ^{225}Ac alpha-emitter with PSMA(prostate-specific-membrane-antigen) carrier highly affine to tumor cells in metastatic prostate-cancer patients (mCRPC). Nevertheless,the therapeutic window is limited by high rate of xerostomia. A prospective trial is ongoing in our institute to test the efficacy of salivary gland protectors administered in combination with ^{177}Lu-PSMA therapy. In this study we explore a possible advantage of salivary gland protectors in TAT-PSMA by extrapolating provisional dosimetry for ^{225}Ac-PSMA from ^{177}Lu-PSMA absorbed doses(AD). ***Materials and Methods:*** Sequential planar images and blood samples were acquired for 13 ^{177}Lu-PSMA patients at 1,16-24,36-48, and 120h post-injection. The same biokinetics was assumed for both radionuclides and ^{177}Lu time-activity curves were corrected for ^{225}Ac physical decay. 100 MBq/kg injection activity was assumed for ^{225}Ac-PSMA, indicated as safe dosage with no salivary gland protectors [1]. Assuming all daughters in equilibrium, each contribution was summed for AD calculation. OLINDA/EXM adult male phantom was used for kidneys, red marrow (RM) and whole body (WB) AD estimation; spherical model was used for parotid and submandibular glands (PGs,SGs). Biologically effective dose (BED) was calculated for salivary glands and compared to the BED values of external-beam radiotherapy (EBRT) schedules. RBE values equal to 5 and 1 were used for alpha and beta/gamma radiation, respectively. Considered the data reported in [1] as reference for TAT without salivary gland protectors, we scaled our data accordingly to the ratio between the mean AD value of our data and this reference. The probability of xerostomia for ^{225}Ac-PSMA with and without salivary glands protector was estimated based on NTCP model derived from EBRT. ***Results:*** Median(range) AD/MBq were 0.67 $Bd_{RBE=5}$/MBq(0.15-1.81), 0.86 $Bd_{RBE=5}$/MBq(0.49-2.43), 1.05 $Bd_{RBE=5}$/MBq(0.42-1.98), 0.07 $Bd_{RBE=5}$/MBq(0.03-0.14), 0.04 $Bd_{RBE=5}$/MBq(0.02-0.11) for kidneys, PGs,

SGs, RM and WB, respectively. A reduction of 53% for salivary gland mean AD was observed as compared to previously published data (2.33 $Bd_{RBE=5}$/MBq[1]). Median (range) BED values were 2.1Gy(1.2-9.7) for PGs and 2.7Gy(0.9-8.1) for SGs vs. 33.5Gy of EBRT dose constraint on PGs. The predicted probability of acute G2+ xerostomia based on NTCP model were 49%(95%CI:18%-71%) vs 98%(82%-100%) with or without salivary gland protector administration. ***Conclusion:*** Our results suggest a possible efficacy of salivary gland protectors in TAT-PSMA. However, for toxicity evaluation, prospective clinical trials are required in order to confirm the promising extrapolation showed by our data. ***References:*** [1] Kratochwill(2017)JNM

OP-770

Pre-therapeutic dosimetry of ^{177}Lu-rhPSMA7.3 and ^{177}Lu-PSMA-I&T in patients with metastatic castration resistant prostate cancer

B. Feuerecker[1,2], *M. Chantadisai*[1,3], *A. Allmann*[1], *R. Tauber*[4], *J. Allmann*[1], *H. Wester*[5], *W. A. Weber*[1], *C. D'Alessandria*[1], *M. Eiber*[1]; *[1]Technical University of Munich, School of Medicine, Department of Nuclear Medicine, München, GERMANY, [2]German Cancer Consortium (DKTK), partnersite München, Heidelberg, GERMANY, [3]Division of Nuclear Medicine, Department of Radiology, Faculty of Medicine, Chulalongkorn University, King Chulalongkorn Memorial Hospital, The Thai Red Cross Society, Bangkok, THAILAND, [4]Technical University of Munich, School of Medicine, Department of Urology, München, GERMANY, [5]Technical University of Munich, Department of Pharmaceutical Radiochemistry, München, GERMANY.*

Aim/Introduction: Radiohybrid prostate-specific membrane antigen (rhPSMA)-ligands are a new class of theranostic radiopharmaceuticals currently under evaluation in patients with prostate cancer. Based on in vitro data the single isomer rhPSMA-7.3 is a promising candidate. We aimed to investigate ^{177}Lu-rhPSMA-7.3 in comparison with established agent, ^{177}Lu-PSMA-I&T, for potential endoradiotherapy in metastatic castration resistant prostate cancer (mCRPC) using pre-therapeutic comparative dosimetry. ***Materials and Methods:*** Three patients with mCRPC underwent both ^{177}Lu-rhPSMA-7.3 and ^{177}Lu-PSMA-I&T pre-therapeutic dosimetry after injection of 1 GBq of each ligand (mean for ^{177}Lu-PSMA-I&T: 1102.3±99.6 MBq and for ^{177}Lu-rhPSMA7.3: 1004±68.0 MBq). Whole-body scintigraphy was performed at 1h, 4h, 24h, 48h and 7d after administration. Regions of interest covering the whole body, organs of interest, and a total of 3 lymph node and 7 bone lesions were drawn. Organ and tumour masses were derived from pretherapeutic ^{18}F-rhPSMA-7.3 PET/CT. Absorbed doses for individual patients and pretherapeutic cycles were calculated using OLINDA/EXM. The "therapeutic index" defined as the activity in lesions divided by the activity in kidneys was used to compare the two agents in each patient. Subsequent radioligand therapy was performed with the superior ligand. ***Results:*** Mean effective doses of ^{177}Lu- rhPSMA-7.3 vs. ^{177}Lu-PSMA-I&T for the whole-body, liver and kidneys were 0.133±0.025 vs. 0.057±0.013 Sv/GBq, 0.134±0.013 vs. 0.053±0.006 Gy/GBq, and 1.680±0.235 Gy/GBq vs. 0.644±0.126 Gy/GBq, respectively. Tumour lesions absorbed a mean of 8.088±8.644 Gy/GBq (range 1.527-29.250 Gy/GBq) using ^{177}Lu- rhPSMA7.3 and a mean of 2.873±2.937 Gy/GBq (range 0.520-9.800 Gy/GBq]) using ^{177}Lu-PSMA-I&T. The "therapeutic indices" for ^{177}Lu-rhPSMA-7.3 vs. ^{177}Lu-PSMA-I&T were 1.27 vs. 1.60 for patient 1, 4.74 vs 3.71 for patient 2 and 7.83 vs 7.97 for patient 3, respectively. ***Conclusion:*** Pre-therapeutic organ- and tumour-absorbed activities for ^{177}Lu-rhPSMA-7.3 are higher than those for ^{177}Lu-PSMA-I&T with a similar increase for tumour lesions and kidneys as the most relevant organ at risk. These clinical dosimetric results hold promise that binding and kinetic characteristics of ^{177}Lu-rhPSMA-7.3 could lead to a similar therapeutic effect without increased side effects at substantial lower activity levels compared with ^{177}Lu-PSMA-I&T. Therefore, future ^{177}Lu-rhPSMA-7.3 radioligand therapy might be performed with lower costs and with potential advantages as a result of lower nuclide demand in case of upcoming shortages. ***References:*** None

OP-771

Quantitative SPECT imaging for Ac-225-based radionuclide therapy: a phantom feasibility study and first patient trial

A. Gosewisch, *M. Schleske, F. J. Gildehaus, A. Todica, J. Brosch, L. Kaiser, P. Bartenstein, H. Ilhan, G. Böning; Department of Nuclear Medicine, University Hospital, LMU Munich, Munich, GERMANY.*

Aim/Introduction: Ac-225-PSMA therapy is a promising option for patients suffering from metastasized prostate cancer. Although Ac-225 shows a noticeable gamma emission (e. g. 26 % for 440 keV), image-based dosimetry via quantitative SPECT is challenging due to the low therapeutic activities. Further, imaging of the 440 keV photopeak shows a complex detector point-spread-function (PSF), consisting of geometrical response, collimator scatter, and septal penetration. In this study, the feasibility of quantitative Ac-225 SPECT imaging with consideration of a distance-dependent 2D PSF model was investigated via a phantom experiment. Respective results from the simulation study were applied to a first patient case. ***Materials and Methods:*** A self-made cylindrical phantom (3.5 l) containing three inserts (20, 45, 200 ml), a total activity of 2.8 MBq, and a foreground-to-background ratio of approx. 10:1 was imaged on a Siemens Symbia Intevo T16 system equipped with a HEGP collimator (32 projections p. head, 128x128 pixel, 60 s p. projection, 440 keV +/- 10 %, lower adjascent scatter window (width 10 %)). Quantitative SPECT reconstruction

was carried out via an in-house MAP (15i4s), including CT-based attenuation and DEW scatter correction. Modelling of the collimator-detector-response was achieved via a distance-dependent 2D PSF model (2D-MAP), simulated for distances of up to 70 cm via SIMIND. For a prostate cancer patient, Ac-225 imaging of the abdomen was performed 24 h p. i. of 8.1 MBq Ac-225-PSMA-I&T (16 projections p. head, 128x128 pixel, 210 s p. projection). SPECT reconstruction was performed via the proposed 2D-MAP. The measured kidney uptake was combined with the patient-specific kidney effective half-life of a former Lu-177-PSMA-I&T cycle to derive a respective kidney absorbed dose estimate. ***Results:*** The phantom experiment resulted in recoveries of 72, 53, and 42 % and signal-to-noise ratios of 33, 24, and 18 for 200, 45, and 20 ml. Regarding the patient case, an absorbed dose of 1.6 $Sv_{RBE=5}$ and 1.4 $Sv_{RBE=5}$ was estimated for the left and right kidney, respectively (volume: 214 and 180 ml). A small lesion could be identified in the right hip, which was also noticeable in the pre-therapeutic F-18-PSMA-I&T PET/CT. ***Conclusion:*** Image-based kidney dosimetry for Ac-225 radionuclide therapy is feasible. Further effort has to be spent to improve Ac-225 imaging with regard to dosimetry for salivary glands or lesions, respectively to provide improved lesion detection. Further, a trade-off between image quality and patient examination time is required. ***References:*** None

OP-772

Patient-specific kidney absorbed doses in mCRPC patients treated with ^{177}Lu-PSMA-617: a post-hoc analysis of a prospective phase 2 study

C. Meyer[1], D. Mirando[2], T. Adams[2], D. Ranganathan[3], R. Esfandiari[4], E. Delpassand[4], J. Czernin[1], J. Calais[1], M. Dahlbom[1]; [1]Ahmanson Translational Theranostics Division, UCLA, Los Angeles, CA, UNITED STATES OF AMERICA, [2]MIM Software Inc, Cleveland, OH, UNITED STATES OF AMERICA, [3]Radiomedix, Houston, TX, UNITED STATES OF AMERICA, [4]Department of Clinical Nuclear Medicine, Excel Diagnostics Imaging Clinic, Houston, TX, UNITED STATES OF AMERICA.

Aim/Introduction: To move towards more personalized PSMA-targeted molecular radiotherapy, dosimetry can be used to devise safe therapeutic activities to deliver maximal tumor doses while delivering as low as achievable doses to non-target volumes. More investigation is needed on the performance of different imaging-based dosimetry methods. The aim of this study was to estimate the absorbed doses in the kidneys, salivary glands, and lesions in metastatic castrate-resistant prostate cancer (mCRPC) patients treated with ^{177}Lu-PSMA-617 using a hybrid approach: one single SPECT/CT and four planar imaging scans. ***Materials and Methods:*** This is a post-hoc retrospective dosimetry analysis in a cohort of patients treated with ^{177}Lu PSMA-617 who were included in a bi-centric single-arm prospective phase II trial (NCT03042312). Lutetium-177 gamma imaging was acquired after the administration of the first cycle of ^{177}Lu PSMA (5.9-8.1 GBq): whole body planar imaging at 4h, 24h, 48h, 72h, optional 9 days, and quantitative SPECT/CT at 24h. Image analysis was performed using commercial dosimetry software compatible with the hybrid SPECT and planar data. Kidneys were segmented on SPECT/CT images and the ROIs propagated to the serial planar images for background and activity overlap corrections. Time-activity curves were generated from the biokinetics in the planar images and scaled by the quantitative SPECT counts, followed by multiexponential decay function curve-fitting. Organ-level doses were calculated using a ^{177}Lu dose kernel derived from Monte Carlo simulations. ***Results:*** 11/51 mCRPC patients (age range 59 -76) were included in this preliminary report. Retrospective dosimetry calculations estimated radiation absorbed doses of 2.60 ± 1.31 Gy (mean ± SD) to each kidney, or 0.39 ± 0.20 Gy/GBq (range 0.12-0.79 Gy/GBq). This estimate is similar to other reports for ^{177}Lu-PSMA-617 using 3D multi-time point SPECT approaches up to 4 days following treatment (1). ***Conclusion:*** In mCRPC patients treated with ^{177}Lu-PSMA-617, dosimetry calculations based on a hybrid approach using one single quantitative SPECT/CT (+24h) and serial planar imaging (4h, 24h, 48h, 72h +/- 9 days) estimated kidney absorbed doses of approximately 0.39 Gy/GBq with significant inter-patient variability in absorbed doses. ***References:*** [1] Violet J, Jackson P, Ferdinandus J, et al. Dosimetry of (177)Lu-PSMA-617 in Metastatic Castration-Resistant Prostate Cancer: Correlations Between Pretherapeutic Imaging and Whole-Body Tumor Dosimetry with Treatment Outcomes. J Nucl Med. 2019;60:517-523.

1407

Teaching Session 5: PET/CT Guided Biopsy

Friday, October 30, 2020, 09:00 - 10:30 Channel 7

OP-773

Review Limitations of CT and US Guided Biopsy

F. Waneck; Division of Cardiovascular and Interventional Radiology, Department of Biomedical Imaging and Image-guided Therapy, Medical University of Vienna, Vienna, AUSTRIA.

OP-774

Review Indications of PET/CT Guided Biopsy

C. Nanni; Azienda Ospedaliero-Universitaria di Bologna Policlinico S.Orsola-Malpighi, Nuclear Medicine Dapartment, Bologna, ITALY.

OP-775

Review Techniques of PET/CT Guided Biopsy

J. Cerci; Quanta – Diagnostic and Therapy, PET/CT Department, Curitiba, BRAZIL.

1408

Clinical Oncology Track - Featured Session: PET Diagnostics of Gynaecological and GI Tumours

Friday, October 30, 2020, 09:00 - 10:30 Channel 8

OP-777

New Developments in PET of Gynaecological Tumours

L. de Geus-Oei; Nuclear Medicine Physician, Department of Radiology, Leiden University Medical Center (LUMC), Leiden, NETHERLANDS

OP-778

The potential role of dynamic PET with ^{13}N-ammonia for evaluating response to Sorafenib in advanced HCC patients. A preliminary report of a prospective study

V. Scolozzi[1], S. Taralli[1], A. Capotosti[2], G. Bencivenga[3], F. Ponziani[4], A. Nicoletti[4], M. Pompili[4], L. Indovina[2], M. L. Calcagni[1,5]; [1]Fondazione Policlinico Universitario A. Gemelli IRCCS; UOC Medicina Nucleare, Dipartimento di Diagnostica per Immagini, Radioterapia Oncologica ed Ematologia, Rome, ITALY, [2]Fondazione Policlinico Universitario A. Gemelli IRCCS; UOS Dosimetria Clinica e Radioprotezione, Dipartimento di Diagnostica per Immagini, Radioterapia Oncologica ed Ematologia, Rome, ITALY, [3]Fondazione Policlinico Universitario A. Gemelli IRCCS; PET-CT centre, Rome, ITALY, [4]Fondazione Policlinico Universitario A. Gemelli IRCCS; Division of Internal Medicine, Gastroenterology and Hepatology – Università Cattolica del Sacro Cuore, Rome, ITALY, [5]Università Cattolica del Sacro Cuore; Istituto di Medicina Nucleare, Rome, ITALY.

Aim/Introduction: Sorafenib, an anti-angiogenetic drug, is the standard of care in patients with advanced hepatocellular carcinoma (HCC). Due to its poor tolerability, narrow therapeutic effects and high costs, the early identification of patients who can benefit from Sorafenib is important. Aim: to investigate the potential role of PET with ^{13}N-ammonia (perfusion tracer) for evaluating response to Sorafenib (acting on angiogenesis) in patients with advanced HCC (highly vascularized cancer). ***Materials and Methods:*** Six male patients (mean age: 69.2±6.1years) with advanced HCC, prospectively enrolled, underwent contrast-enhanced CT and dynamic ^{13}N-ammonia PET (370MBq; 20min) before (baseline) and 8-10 weeks after (post-therapy) the beginning of Sorafenib treatment. Quantitative analysis: VOIs drawn on descending aorta (input function), on up to six HCC lesions and on two normal liver areas using baseline and post-therapy contrast-enhanced CT, and transferred on baseline and post-therapy PET, respectively. For each VOI, K_1 (ml/min/gr) and k_2 (min^{-1}) values were estimated using 1-tissue compartment model. For each patient, ΔK_1 and Δk_2 (percentage changes between baseline and post-therapy PET) in HCC lesions were compared with standard response, based on clinical evaluation and mRECIST criteria. ***Results:*** median K_1 and k_2 values were higher in HCC lesions (n=25) than in normal liver both at baseline (0.76 vs 0.38, p=0,0016 and 0.15 vs 0.05, p=0.0001, respectively) and at post-therapy PET (0.62 vs 0.29, p=0,0002 and 0.12 vs 0.03, p<0.0001, respectively). At standard response assessment, 4/6 patients were classified as "disease control" (3 with stable disease and 1 with partial response) and 2/6 patients as "no disease control" (progression). At post-therapy PET, a reduction in K_1 was observed in all patients; reduction was greater in patients with disease control compared to those with no disease control (mean ΔK_1= -31.7% vs -11.8%). A reduction in k_2 was observed in 5 patients (4 disease control, 1 progression), whereas one patient (progression) showed an increase of k_2. Overall, a greater change in k_2 was found in patients with disease control than other group (mean Δk_2= -30.0% vs -9.2%). ***Conclusion:*** Dynamic ^{13}N-ammonia PET seems a promising tool for evaluating response to anti-angiogenetic drugs used in highly vascularized cancer as HCC. Changes in quantitative parameters observed after treatment are in line with standard response assessment. The evaluation of the role of ^{13}N-ammonia perfusion changes for predicting tumour response is ongoing. This should assume an important clinical relevance in the selection of patients with "no control disease" candidates to Sorafenib discontinuation. ***References:*** None

OP-779

The Combination of Pretreatment Total Metabolic Tumor Volume on PET/CT and MYC/Bcl-2 Protein Dual Expression Further Improves Prognostic Stratification of Patients with Primary Gastrointestinal Diffuse Large B-cell Lymphoma

C. Jiang[1], C. Ding[2], Y. Teng[3], J. Xu[4], J. Chen[5], Z. Zhou[1]; [1]Department of Nuclear Medicine, Nanjing Drum Tower Hospital,the Affiliated Hospital of Nanjing Unive, Nanjing, CHINA, [2]Department of Nuclear Medicine,the First Affiliated Hospital of Nanjing Medical University,Jiangsu Province Hospital, Nanjing, CHINA, [3]Department of Nuclear Medicine, Nanjing Drum Tower Hospital,the Affiliated Hospital of Nanjing University Medical School, Nanjing, CHINA, [4]Department of Hematology, Nanjing Drum Tower Hospital,the Affiliated Hospital of Nanjing University Medical School, Nanjing, CHINA, [5]Department of Pathology, Nanjing Drum Tower Hospital,the Affiliated Hospital of Nanjing University Medical School, Nanjing, CHINA.

Aim/Introduction: The aim of the study was to explore whether a combination of pretreatment total metabolic tumor volume (TMTV) and MYC/BCL-2 protein dual expression (DE) would improve the prognostic stratification of primary gastrointestinal diffuse large B-cell lymphoma (PGI-DLBCL) patients. ***Materials and Methods:*** Eighty-three patients between March 2011 and July 2019, diagnosed with PGI DLBCL without any treatment, were enrolled in this

retrospective study. TMTV on pretreatment PET/CT scans were calculated using the boundaries of voxels presenting a SUVmax≥2.5. Expression patterns of MYC and BCL-2 were detected at protein levels via immunohistochemistry. The distributions of Progression-free survival (PFS) and overall survival (OS) rates were estimated using the Kaplan-Meier method and differences were compared using a log-rank test followed by multivariate analysis using the Cox proportional hazards model. ***Results:*** During the follow-up period of range between 3-96 months (32.1±19.7 months), high TMTV and DE were significantly associated with a worse PFS ($\chi2=26.054, P<0.001$; $\chi2=10.120, P=0.001$) and OS ($\chi2=1.462, P<0.001$; $\chi2=3.930, P=0.047$). Both TMTV and DE were each independent predictors of PFS ($P<0.001$, $P=0.021$), whereas TMTV was the only independent predictor of OS ($P<0.001$). A combination of TMTV and DE allowed for a significantly better division of PGI-DLBCL patients into three groups as follow:low-risk group, intermediate-risk group and high-risk group. ***Conclusion:*** High TMTV and DE identified a subset of PGI-DLBCL patients with dismal survival outcomes. Furthermore, a combination of TMTV and DE status may further improve the ability of clinicians to stratify PGI-DLBCL patients with differential prognosis. ***References:*** None

OP-780

Baseline Total Lesion Glycolysis on FDG PET/CT Improves the Prognostic Value of NCCN-IPI in Primary Gastric Diffuse Large B-cell Lymphoma Patients Treated with the R-CHOP Regimen

C. Jiang[1], *C. Ding*[2], *Y. Teng*[3], *J. Xu*[4], *Z. Wang*[5], *Z. Zhou*[1];
[1]*Department of Nuclear Medicine, Nanjing Drum Tower Hospital,the Affiliated Hospital of Nanjing Unive, Nanjing, CHINA,* [2]*Department of Nuclear Medicine,the First Affiliated Hospital of Nanjing Medical University,Jiangsu Province Hospital, Nanjing, CHINA,* [3]*Department of Nuclear Medicine, Nanjing Drum Tower Hospital,the Affiliated Hospital of Nanjing University Medical School, Nanjing, CHINA,* [4]*Department of Hematology, Nanjing Drum Tower Hospital,the Affiliated Hospital of Nanjing University Medical School, Nanjing, CHINA,* [5]*Department of Pathology,the First Affiliated Hospital of Nanjing Medical University, Jiangsu Province Hospital, Nanjing, CHINA.*

Aim/Introduction: The aim was to explore whether baseline total lesion glycolysis (TLG) can improve the prognostic value of the National Comprehensive Cancer Network-International Prognostic Index (NCCN-IPI) in patients diagnosed with primary gastric diffuse large B-cell lymphoma (PG-DLBCL) treated with the R-CHOP like regimen. ***Materials and Methods:*** Ninety-four PG-DLBCL patients who underwent baseline PET/CT between July 2010 and May 2019 were enrolled in this retrospective study. The FDG-avid lesions in each patient were segmented to calculate the maximum standardized uptake value (SUVmax), total metabolic tumor volume (TMTV), and TLG. Progression-free survival (PFS) and overall survival (OS) were used as end points to evaluate patient prognosis. ***Results:*** During the follow-up period of 5-108 months (35.3±23.5 months), high TLG and high NCCN-IPI were significantly associated with worse PFS and OS. TLG and NCCN-IPI were independent predictors of PFS and OS. The patients were stratified into three groups according to the combination of TLG and NCCN-IPI for PFS ($P < 0.001$) and OS ($P < 0.001$): high-risk group with TLG>1159.1 and an NCCN-IPI score of 4-8 (PFS and OS were 57.7% and 61.5%, respectively, n = 42), intermediate-risk group with TLG> 1159.1 or an NCCN-IPI score of 4-8 (PFS and OS were both 76.9%, n = 26), and low-risk group with TLG≤1159.1 and an NCCN-IPI score of 0-3 (PFS and OS were 97.6% and 100.0%, respectively, n = 26). For patients at stage I/II, the combination of TLG and NCCN-IPI can also be used to stratify the patients. ***Conclusion:*** Both TLG and NCCN-IPI are independent predictors of the PG-DLBCL patient survival outcome. Moreover, the combination of TLG and NCCN-IPI improved patient risk stratification and might contribute to the ability to personalize therapeutic regimens. ***References:*** None

OP-781

Dynamic PET Perfusion Imaging in Esophageal Cancer Patients Receiving Radiation Therapy

K. Binzel*, E. D. Miller, C. L. Wright, Y. Hsieh, A. Wollett, E. Ives, M. V. Knopp;*
The Ohio State University Wexner Medical Center, Columbus, OH, UNITED STATES OF AMERICA.

Aim/Introduction: To assess the utility of dynamic perfusion PET imaging for the evaluation of esophageal tumors over the course of radiation therapy. ***Materials and Methods:*** Ten patients with esophageal tumors were imaged over one bed position at the site of the primary tumor for 15 minutes immediately following injection of 185 MBq ^{18}F-FDG. Imaging was performed on a digital photon counting system (Philips Vereos). Patients spent the remaining uptake period in the injection suite followed by whole body imaging at 75 minutes post-injection as standard imaging. Listmode data from the dynamic acquisition were reconstructed with 1 minute per frame. Regions of interest were placed over the primary tumor, aorta, and a portion of healthy liver. Imaging was performed prior to radiation therapy, at a 3 month interim timepoint, and post-therapy, about 6 months after baseline imaging. ***Results:*** Excellent image quality and quantifiably robust data were produced for all acquisitions. Physiologic motion could readily be corrected for, however very little motion was observed. Differences in perfusion and dynamic uptake patterns in the individual tumors were identifiable. Most patients had tumors with small initial perfusion peaks followed by relatively stable uptake levels over the 15-minute dynamic acquisition. Three such

patients showed marked decreases in tumor uptake curves at both the interim and follow-up, averaging 35% decreases from baseline at both later timepoints. Four patients had similar baseline and interim curves, averaging 18% different at interim compared to baseline. However, these patients then had greater decreases in dynamic uptake at the follow-up timepoint, averaging a 47% decrease. Two patients had increased perfusion and dynamic uptake at the interim, 48% and 12% increases compared to baseline, respectively. At follow-up one of these patients had a continued increase compared to baseline while the other now presented with a 33% reduction as compared to baseline. One patient did have a strong initial perfusion peak and also had similar dynamic curves on all three acquisitions, only 0.6% and 8.5% changed from baseline values. Correlation with pathology results and clinical outcomes is ongoing. ***Conclusion:*** We have demonstrated that dynamic perfusion FDG PET/CT is robustly achievable. Quantification of tumor features is robust as well as changes in perfusion and uptake during therapy. This PET-based methodology can be applied to assess changes in rates of tumor perfusion and radiotracer uptake over the course of therapy, adding additional insight beyond delayed, static measures of SUV. ***References:*** None

OP-782

Utility of ^{18}F-FDG PET/CT in Management of Pancreatic and Periampullary Masses : Experience of a Tertiary Care Center in South India

C. Singareddy[1], R. Manthri[2], T. Kalawat[2], V. Venkatarami Reddy[2], H. Narendra[2], B. Vijaya Lakshmi Devi[2], A. Chowhan[2];
[1]SVIMS, Tirupati, INDIA, [2]Sri Venkateswara Institute Of Medical Sciences, Tirupati, INDIA.

Aim/Introduction: Characterizing a mass lesion in pancreas as benign or malignant on conventional imaging is difficult due to overlapping morphological features. 18F-FDG PET/CT is a molecular imaging technique that is reported to have higher sensitivity and specificity in the differentiation of benign and malignant pancreatic and periampullary masses. Aim of this study is to study the utility of 18F-FDG PET/CT in the diagnosis and treatment of pancreatic and periampullary masses. ***Materials and Methods:*** In this prospective study, we evaluated the utility of 18F-FDG PET/CT in patients with recently diagnosed pancreatic and periampullary masses. Based on FDG uptake pattern, diffuse or absent uptake was considered as benign and focal increased uptake as malignant. ***Results:*** Among the 32 patients included in the study, pathological examination confirmed 25 as positive for malignancy and remaining 7 as benign etiology. Based on FDG uptake pattern, sensitivity, specificity, PPV, NPV and accuracy of the study were 92%, 42.8%, 85.2%, 60%, and 81.3% respectively. 18F-FDG PET/CT had a statistically significant higher detection rate in evaluation of regional lymph nodes and distant organ metastases compared to radiological imaging. In 7/25 malignant cases, 18F-FDG PET/CT detected additional distant metastases which were not detected by conventional imaging and thus resulting in their change in management from curative resection to palliative therapy. ***Conclusion:*** 18F-FDG PET/CT uptake pattern can characterize pancreatic and periampullary masses as benign or malignant with good accuracy. But it has very limited role in the evaluation of pancreatic solid pseudopapillary neoplasm. Using 18F-FDG PET/CT for initial staging in pancreatic and periampullary cancer helps in accurate staging and optimal selection of treatment modality compared to conventional imaging techniques. ***References:*** 1. DeWitt J, Devereaux B, Chriswell M, McGreevy K, Howard T, Imperiale TF, et al. Comparison of endoscopic ultrasonography and multidetector computed tomography for detecting and staging pancreatic cancer. Ann Intern Med. 2004;141:753-63. 2. Santhosh S, Mittal BR, Bhasin D, Srinivasan R, Rana S, Das A, et al. Role of ^{18}F-fluorodeoxyglucose positron emission tomography/computed tomography in the characterization of pancreatic masses: Experience from tropics. J Gastroenterol Hepatol. 2013;28:255-61.

OP-783

Can FDG PET/CECT Accurately Restage Hilar Cholangiocarcinoma?

J. Paudel;
Chitwan Medical College, Bharatpur, NEPAL.

Aim/Introduction: To evaluate the diagnostic performance of contract enhanced F-18 FDG PET/CT in restaging hilar cholangiocarcinoma. ***Materials and Methods:*** A retrospective analysis of histopathological proven patients with hilar cholangiocarcinoma (age range 33-79 years; mean age 53.52 years; Male/ female 23/11) was performed in 34 patients. All patients had been treated previously with either surgery, radiotherapy or chemotherapy alone or in combination and referred for F-18 FDG PET/CT to rule out residual or recurrent disease. On FDG PET any abnormal tracer uptake with corresponding lesion on CECT was taken as positive. Histopathological examination and clinical or imaging follow up were taken as gold standard. ***Results:*** Out of the 34 patients, 21 patients were true positive for primary disease**.** FDG PET/CT detected abnormal FDG uptake in 27 patients. Uptake at the primary site was detected in 15 (44.1%) patients and only metastatic lesions in 11 (32.3%) patients. Out of 15 patients with primary lesions, 12 had adjacent liver involvement, 2 had adjacent pancreas involvement, 6 had regional lymph nodes, 7 had distant lymph nodes involvement, 6 had both regional and distant lymph nodes involvement, 10 had both regional and distant lesions and 6 had only primary lesion. On lesion based analyses in 21 patients with distant metastases, lymph nodes, abdominal wall/muscle metastases, peritoneal deposits, liver, lung,

adrenal, pancreas, omental and mesenteric deposits were noted in 17, 5, 15, 15, 4, 1, 2, 1, 4 patients respectively. Additionally we also detected metachronous primary in the thyroid in 1 patient and confirmed it on histopathology. We found FDG PET/CT sensitivity, specificity , PPV, NPV and accuracy 94%, 56%, 86%, 71% and 93% respectively for residual/recurrence detection (P <0.05). On ROC curve analysis, SUVmax >2.7 had sensitivity and specificity of 63.8% and 81.4% respectively for detection of residual/recurrent disease on F-18 FDG PET/CT (Area under the ROC curve is 0.729 at 95% confidence Interval (P value 0.0004). We also observed that there was no correlation between SUVmax and patient survival (Spearman's coefficient rank correlation). ***Conclusion:*** We concluded that 18F-FDG PET/CT had high diagnostic accuracy for suspected residual/recurrent disease in hilar cholagiocarcinoma patients and also useful in detection of additional metachronous second primary. ***References:*** None

OP-784

4FMFES and FDG-PET imaging in uterine cancer patients: preliminary assessment

M. Paquette[1], *E. Espinosa-Bentancourt*[1], *É. Lavallée*[1], *S. Phoenix*[1], *K. Lapointe-Milot*[2], *P. Bessette*[2], *B. Guérin*[1], *É. E. Turcotte*[1];
[1]*Université de Sherbrooke, Sherbrooke, QC, CANADA,*
[2]*CIUSSS de l'Estrie-CHUS, Sherbrooke, QC, CANADA.*

Aim/Introduction: In order to improve imaging of uterine cancers, other groups explored the use of the estrogen-like [18F]-16α-fluoroestradiol (FES) PET tracer in the clinical setting. FES tumor uptake was shown to correlate well with the biopsy-determined Estrogen receptor (ER) status in endometrial cancers. However, FES-PET has some shortcomings, including slow blood clearance and rapid metabolization, both factors increasing non-specific signal and hence reducing tumor detectability. In this phase II clinical trial, the metabolism-resistant, ER-targeting molecule, 4-fluoro-11β-methoxy-16α-[18F]fluoroestradiol (4FMFES), will be investigated in combination with FDG-PET for the diagnosis of uterine cancer patients. ***Materials and Methods:*** Uterine cancer patients (n = 20) were recruited in the imaging protocol in collaboration with our local gynaeco-oncology department before surgery. All patients harbored ER+ diseases. Among them, 7 patients had endometrial carcinoma, 11 had endometroid adenocarcinoma, 1 were diagnosed with endometrial intraepithelial neoplasia and 1 had a benign lesion. Patients were scheduled to undertake FDG- and 4FMFES-PET with less than 10 days apart, with injected doses of 3 MBq/kg for each tracer. Tumor uptake for each tracer was reported as SUVMax values, and background proximal to each lesion reported as SUVMean. Shortly before injection of 4FMFES, 15 patients received medication aiming to slow down progression of the radioactive intestinal bolus toward the lower abdomen resulting from the biliary excretion of the tracer. ***Results:*** 4FMFES primary tumor uptake ranged between 3.0 and 14.4 (9.7 ± 3.2), whereas FDG uptake spread between 0 and 22.0 (7.2 ± 5.4). One endometroid adenocarcinoma patient was FDG-negative (4FMFES SUVMax = 9.6). Tumor-to-background ratio were significantly higher ($p < 0.001$) for 4FMFES (17.8 ± 6.4) than for FDG (7.6 ± 5.0). Two of the endometrial carcinoma cases had sentinel node involvement according to pathology assessment that were FDG and 4FMFES-negative, but those nodal lesions were less than 5 mm in size. Tumor uptake for 4FMFES peaks at grade 2, whereas FDG uptake have a trend to increase according to grade. Apparent tumor volume is higher using 4FMFES than FDG in most cases, the latter being more representative of the true tumor size. ***Conclusion:*** 4FMFES-PET enables high-contrast detection of ER+ uterine tumors, regardless of grade and subtype. Size assessment is better defined using CT and FDG than 4FMFES. 4FMFES-PET is a good companion tracer for FDG-PET and improves diagnostic confidence. ***References:*** None

OP-785

Preliminary application of ^{68}Ga-PSMA PET/CT in detection of ovarian cancer

M. Xin*, L. Xu, Q. Xia, W. Lou, J. Liu;*
Renji hospital, School of medicine, Shanghai Jiao Tong university, Shanghai, CHINA.

Aim/Introduction: The extensive clinical adaptation of prostate-specific membrane antigen (PSMA)-targeted PET imaging has played crucial role in the evaluation of patients with prostate cancer. Meanwhile, PSMA overexpression in neovascular endothelium of some non-prostatic malignancies has motivated novel theranostic applications of anti-tumor strategies. The goal of the study was to explore the value of ^{68}Ga-PSMA PET/CT imaging in detection of female ovarian cancer, as PSMA-targeted therapy has showed a promise in treatment of advanced carcinomas. ***Materials and Methods:*** We prospectively investigated 9 female patients with suspected pelvic occupying diseases (carbohydrate antigen-125>35 U/mL) who underwent ^{68}Ga-PSMA PET/CT before surgery. The PET/CT scan was performed approximately 1 h after an intravenous injection of 2 MBq/Kg of ^{68}Ga-PSMA. Two nuclear medicine physicians independently recorded the sites of PSMA-PET/CT positivity. ***Results:*** The mean age of patients was 58.3±12.9 years (range: 36-79 years); mean carbohydrate antigen-125 was 1546.2±1825.0 U/mL (range: 63.5-5857.0 U/mL). 5/9 (55.5%) patients displayed bilateral foci, 1 patient presented unilateral lesion, and 3/9 (33.3%) patients had ambiguous pelvic mass. In CT imaging of pelvic primary lesions, 3/9 (33.3%) sites appeared as soft tissue density, and 6/9 (66.7%) presented a solid-cystic type. Determined by postoperative pathology, 6/9 (66.7%) were malignant lesions

including high grade serous carcinoma, endometrioid adenocarcinoma and neuroendocrine carcinoma, 1 case was borderline serous cystadenoma, and 2/9 (22.2%) were benign diseases. ^{68}Ga-PSMA PET/CT showed 100% positive in detecting ovarian malignant and borderline tumors, with an average uptake SUVmax of 7.5±1.6 (range: 6.1-10.1) in the primary lesions, and 7.1±1.4 (range: 5.6-8.7) in the peritoneal metastatic lesions. Less sensitivity of PSMA PET/CT detection was found in lymph node (2 cases) and distant organ metastasis (1 case). ***Conclusion:*** Our pilot study shows that ^{68}Ga-PSMA PET/CT could effectively detect primary ovarian cancer and peritoneal metastases, rendering it a potential molecular imaging modality in the monitoring and evaluation of advanced ovarian cancer therapies. ***Acknowledgements:*** This work was supported by grants from National Natural Science Foundation of China (No. 81701725), and Shanghai "Rising Stars of Medical Talent" Youth Development Program (SHDC2012105). ***References:*** 1. Sheikhbahaei S, Afshar-Oromieh A, Eiber M, et al. Pearls and pitfalls in clinical interpretation of prostate-specific membrane antigen (PSMA)-targeted PET imaging. Eur J Nucl Med Mol Imaging. 2017 Nov;44(12):2117-2136. 2. Wernicke AG, Kim S, Liu H, et al. Prostate-specific Membrane Antigen (PSMA) Expression in the Neovasculature of Gynecologic Malignancies: Implications for PSMA-targeted Therapy. Appl Immunohistochem Mol Morphol. 2017 Apr;25(4):271-276.

OP-786

Assessment of radiomic PET analysis in the evaluation of cervical cancer treatment

F. Scalorbi*, A. Alessi, G. Centonze, M. Signorelli, G. Calareso, M. Kirienko, A. Lorenzoni, G. Bogani, F. Martinelli, G. Argiroffi, F. Raspagliesi, E. Seregni;*
Istituto Nazionale Tumori Milano, Milan, ITALY.

Aim/Introduction: To investigate the possible value of radiomic ^{18}F-FDG-PET/CT analysis in the assessment of neoadjuvant chemotherapy response and post-surgery decision-making in locally advanced cervical cancer of uterus (LACC). ***Materials and Methods:*** We retrospectively enrolled patients with LACC diagnosis treated with cisplatin-based neoadjuvant chemotherapy (NACT) at our Institute, between 2014-2018. The patients were classified as Ib3-IIb in accordance with clinical FIGO classification. MRI was performed to evaluate the response to treatment and plan the radical surgery. A dedicated radiologist evaluated all the MRI and applied RECIST1.1 criteria defining good-responders (CR, PR>50%) vs poor-responders (PR<50%, SD, PD). All the patients performed a PET after NACT on the same tomograph. Primary tumor volume was delineated by a nuclear physician, applying an estimated SUVmax threshold and a semiautomatic algorithm (PET_Tumor_Segmentation_Effect) implemented on 3DSlicer. On the volume of interest, 136 fist-second order features were extracted per patient by Pyradiomics. After hysterectomy, patients were treated with adjuvant therapies or followed-up, according to Sedlis criteria. Wilcoxon's test was performed to compare every feature with NACT response (Outcome1) and post-surgery decision-making (Outcome2). Fisher's test was applied to evaluate possible interaction between FIGO, patient age and outcome1/outcome2 results. Principal component analysis (PCA) was carried out for reducing the dimension of radiomic features and investigate relationships between them. Group differences in the principal components were assessed using Hotelling's T-squared test. ***Results:*** We enrolled 27 women (mean age 46; range 24-77), 13/27 were classified as Ib3 FIGO, 14/27 as IIa-IIb. According to RECIST1.1, 21 (77.8%) patients were classified as good responders and 6 (22.3%) as poor responders . According to Seadlis criteria, 18 (66.7%) patients were followed-up and 9 (33.3%) were treated with adjuvant therapies . Considering radiomic PET analysis, 26 features resulted significant in distinguishing between responders and non-responders to NACT, 12 features in distinguishing follow-up from neoadjuvant therapy decision (Wilcoxon's test $p<0.05$). Considering PCA, the first (PC1) and the second (PC2) principal component explained 61.5% and 15.3% of the overall variability, respectively. PC1 had multiple significant positive correlations with 25 features and had negative correlation with 6 features. Evaluating Outcome1, the two principal components were statistically significant in predicting good- from poor-responders ($p= 0.04$). PC2 was significantly correlated to Dependence Non Uniformity Normalized. No statistical differences were found considering Outcome 2. Fisher's test was not significant. ***Conclusion:*** Radiomic analysis of ^{18}F-FDG-PET/CT performed after NACT can have a role in the assessment of therapy response and post-surgery decision-making. ***References:*** None

OP-787

18F-FDG PET/CT incidental gynecological uptake: a 8-year retrospective analysis

P. Bellini[1]*, D. Albano*[1]*, S. Lucchini*[2]*, F. Motta*[2]*, A. Peli*[2]*, M. Bertoli*[2]*, G. Bosio*[2]*, E. Cerudelli*[2]*, M. Gazzilli*[2]*, F. Dondi*[1]*, A. Mazzoletti*[1]*, A. Calabrò*[1]*, M. Gregorelli*[1]*, M. Bonacina*[3]*, F. Bertagna*[1]*, R. Giubbini*[1]*;*
[1]Nuclear Medicine, University of Brescia, Spedali Civili Brescia, Brescia, ITALY, [2]Nuclear Medicine, Spedali Civili Brescia, Brescia, ITALY, [3]Nuclear Medicine, Fondazione Poliambulanza, Brescia, ITALY.

Aim/Introduction: Incidentalomas are defined as asymptomatic and unexpected lesions, found during the course of examination and imaging for other reasons and related to a different organ. These lesions can be incidentally detected by several imaging techniques, like PET/CT. The description of an unexpected finding can trigger additional investigations including unnecessary

tests, other diagnostic examinations and sometimes treatments. For this reason, it is crucial to understand when proceeding with further investigations. The aim of this study was to establish the prevalence and the pathological nature of gynecological incidental uptake among patients studied with 18F-FDG-PET/CT between 2008 and 2015. ***Materials and Methods:*** We have retrospectively evaluated 11000 women who underwent 18F-FDG PET/CT from January 2008 to December 2015. The PET images were analyzed visually and semi-quantitatively by measuring the maximum standardized uptake value (SUVmax) of the gynecological incidentaloma; every focal tracer uptake deviating from physiological distribution and background was considered as suggestive of incidentaloma. Final diagnosis of gynecological incidentaloma was obtained by cytological/histological examination or other imaging examinations. ***Results:*** Unexpected FDG-uptake in female reproductive organs was found in 158 (1.4%) 18F-FDG PET scan performed in 158 different women (109 in reproductive age, 33 in menopause, 16 with unknown status). 103 focal uptake was in reported in uterus, 41 in ovaries and 14 in both sites. In 82 patients gynecological uptake was judged as physiological, in 54 as indeterminate and in 22 as malignant at PET/CT. After subsequent follow-up, 13 incidentalomas were classified as malignant (5 ovarian cancer, 3 endometrial cancer, 2 cervical cancer, 1 non-Hodgkin lymphoma, 2 with unknown origin), 19 as benign (11 fibromas, 2 myomas, 1 leiomyoma, 5 ovarian cysts) and 92 as physiological. In the remaining 34 patients, gynecological incidentaloma was not investigated subsequently. Average SUVmax in malignant lesions was significantly higher than non-malignant (19.64 vs 6.91; $p<0.001$). No patients with uptake judged as physiological found malignancy after follow-up exams. ***Conclusion:*** 18F-FDG PET/CT focal incidental gynecological uptake may be a relevant diagnostic reality which requires further investigations. 18F-FDG uptake in female reproductive organs can have many different meanings: PET images related with anamnesis could be effective and specific in characterization of physiological uptake[1]. SUVmax was significantly higher in malignant lesion. ***References:*** [1] Zhu ZH, Cheng WY, Cheng X et AL; Characteristics of physiological uptake of uterus and ovaries on 18F-fluorodeoxyglucose positron emission tomography; Acta Academiae Medicinae Sinica, 2007, 29(1): 124-129.

1409

Featured Session: Nuclear Imaging in Inflammatory and Infiltrative Cardiovascular Diseases

Friday, October 30, 2020, 09:00 - 10:30 Channel 9

OP-788

Nuclear Imaging in Inflammatory and Infiltrative Cardiovascular Diseases - How Far Can we Go?

E. Reyes*; PET imaging centre, St Thomas' Hospital, King's College London, Royal Brompton Hospital, Nuclear Medicine, London, UNITED KINGDOM.*

OP-789

Transthyretin gene mutation carriers: can bone scintigraphy identify disease markers early?

F. Mattana*[1], R. Bonfiglioli[1], L. Muraglia[1], A. Paccagnella[1], R. Mei[1], G. Caponetti[2], G. Saturi[2], P. Massa[2], M. Sguazzotti[2], A. Ponziani[2], C. Gagliardi[2], S. Longhi[2], N. Galiè[2], S. Fanti[1];*
[1]Department of Nuclear Medicine, S.Orsola-Malpighi University Hospital, Bologna, ITALY, [2]Department of Cardiology, S.Orsola-Malpighi University Hospital, Bologna, ITALY.

Aim/Introduction: Cardiac amyloidosis (CA) caused by amyloid-transthyretin (ATTR) deposition is a progressive and often fatal disease that may be easily underdiagnosed. Carriers are defined as patients with pathogenic transthyretin gene mutation (TTRm), asymptomatic and with no evidence of disease. Technetium-99m-DPD-scintigraphy (99mTc-DPD-S) is an important diagnostic and prognostic tool in amyloidosis patients, but in carriers its role is still unclear, considering that a cardiac uptake (CU) has been described in a few cases. There is no consensus on carriers management due to its wide range of clinic presentation, penetrance and clinical progression, but an early diagnosis is important above all considering that new specific therapies are now available. The present study was designed to evaluate the role of 99mTc-DPD-S in TTRm carriers management. ***Materials and Methods:*** We enrolled 50 consecutive patients with TTRm from 2004 to 2019. All patients underwent 99mTc-DPD-S using a dual-head camera (ECAM, Siemens Medical Systems; Discovery NM/CT 670, GE Healthcare), according to EANM guidelines. Visual image analysis was performed in consensus by two experienced nuclear medicine physicians blinded to all other patient data. Visual scoring of CU was scored on planar images using a scoring system (Perugini score). All patients were analysed at cardio lab using echocardiography, electrocardiography and, when diagnosis was unclear, with cardiac magnetic resonance. ***Results:*** In this group of TTRm carriers, 40 patients (23 female/27 male; group A) did not show myocardial tracer uptake (MTU), whereas 10 patients

(4 female/6 male; group B) showed MTU (Perugini score: mild in 3 case, moderate in 5, strong in 2 for operator one; mild in 4 case, moderate in 3, strong in 3 for operator two). In group B, cardio lab tests were normal at the time of the first positive scintigraphy; in all these patients a diagnosis of CA was settled within 3,5 years. When CU was not present, the patients showed no signs of cardiac amyloidosis after a median follow-up of 3,6 years. ***Conclusion:*** Our study, with the highest number of TTRm carriers, showed that 99mTc-DPD-S could play an important diagnostic role also in TTRm carriers with an high prognostic value and impact on the clinical management. In non Val30Met patients, the CU seems to be not correlated with a specific gene mutation, though some mutations seem to be correlated with a worst scintigraphic/clinical progression within 1 or 2 years. ***References:*** None

OP-790

Evaluation Of The Regional Distribution Of Tc99m-DPD In The Left Ventricle In Patients With Transthyretin Cardiac Amyloidosis

N. Martinez Amador[1], *I. Martínez-Rodríguez*[1], *A. Sánchez-Salmón*[1], *R. Quirce*[1], *J. Jiménez-Bonilla*[1], *M. de Arcocha-Torres*[1], *S. Ruiz-Llama*[1], *G. Molina-Mendoza*[1], *O. Cuenca-Vera*[1], *J. Andrés-Pacheco*[1], *A. Gutiérrez-González*[1], *M. J. Zarauza-Navarro*[2], *I. Banzo*[1];

[1]*Nuclear Medicine Service. Marqués de Valdecilla University Hospital. Molecular Imaging Group (IDIVAL). University of Cantabria, Santander, SPAIN,* [2]*Cardiology Service. Marqués de Valdecilla University Hospital, Santander, SPAIN.*

Aim/Introduction: To know the regional distribution of Tc99m 3,3-diphosphono-1,2-propanodicarboxylic acid (Tc99m-DPD) in the left ventricle of patients diagnosed with transthyretin cardiac amyloidosis (TTR-CA). ***Materials and Methods:*** This retrospective study included 60 patients (12 women, mean age 79.5±10.6 years) diagnosed with TTR-CA, in whom a bone scintigraphy (whole-body scan in anterior and posterior projections and chest SPECT) were carried out 2-3 hours after the i.v injection of 740 MBq Tc99m-DPD. Images of cardiac uptake were first assessed visually by two nuclear medicine specialists according to Perugini score system (grade 0: absent cardiac uptake and normal bone uptake, grade 1: mild cardiac uptake inferior to bone uptake, grade 2: moderate cardiac uptake associated with attenuated bone uptake, and grade 3: strong cardiac uptake with mild or absent bone uptake). Grades 2 and 3 were considered as positive for TTR-CA. Then, a semiquantitative analysis was performed using standardized 20-segment polar maps of the left ventricle to assess the amyloid burden in the left ventricle. ***Results:*** On visual analysis, 51/60 (85%) patients had grade 3 cardiac uptake and 9/60 (15%) patients had grade 2 cardiac uptake. According to polar maps, 50/51 (98%) patients included in the grade 3 group showed greater uptake in the septum wall: inferoseptal-mid (23/51), inferoseptal-apical (19/51), anteroseptal-mid (6/51) and anteroseptal-apical (2/51) segments. In 1/51 (2%) patient, the highest uptake was observed in the inferior-apical segment. On the other hand, 7/9 (77.8%) patients included in grade 2 group showed greater uptake as well in the septum wall: inferoseptal-mid (4/7) and inferoseptal-apical (3/7) segments. In 2/9 (22.2%) patients, the highest uptake was also found in the inferior-apical segment. Globally, the semiquantitative analysis revealed that the septal segments had the highest uptake, with a mean value 82.5±10.2 for grade 3 group and 74.5±3.5 for grade 2 group. These mean values had statistically significant differences with the remaining left ventricular segments ($p = 0.02$ for grade 3 and $p = 0.03$ for grade 2). ***Conclusion:*** Patients with TTR-CA and Perugini score grade 2 and 3 showed a higher percentage of Tc99m- DPD uptake in septum wall segments than in the remaining segments of the left ventricle, suggesting a relationship with the amount of amyloid fiber deposit, the ventricular wall involvement, and, finally, the cardiac dysfunction. ***References:*** None

OP-791

Quantifying Right Ventricle Uptake Of ^{99m}Tc-DPDIn Cardiac Transthyretin Amyloidosis Through SPECT/CT. Preliminary Results In A Single Center

J. Rodríguez Gomez[1], *F. Ferrando-Castagnetto*[2], *C. Wakfie Corieh*[1], *M. Pedrera Canal*[1], *M. Ollarves Carrero*[1], *M. Meneses Navas*[1], *J. Diz*[3], *E. Silvera*[4], *A. Zamarrón*[1], *Y. Santero*[1], *M. Pérez Castejón*[1], *J. Carreras Delgado*[1];

[1]*Servicio de Medicina Nuclear, Hospital Clínico San Carlos, Madrid, SPAIN,* [2]*Departamento de Cardiología-CCVU, Hospital de Clínicas, Facultad de Medicina, Universidad de la República., Montevideo, URUGUAY,* [3]*Instituto Cardiovascular, Hospital Clínico San Carlos, Madrid, SPAIN,* [4]*Departamento de Medicina Nuclear, Hospital de Clínicas, Facultad de Medicina, Universidad de la República, Montevideo, URUGUAY.*

Aim/Introduction: To characterized the right ventricle (RV) involvementin consecutive ATTR-CA patients referred to ^{99m}Tc-DPD scintigraphy with the aid of SPECT/CT quantified parameters. Myocardial uptake of phosphate bone-seeking radiotracerslike 99mTc-DPD are remarkably sensitive for detecting transthyretin cardiac amyloidosis (ATTR-CA). However, the diagnosis of cardiac amyloid deposit has mainly relied on the tracer affinity for left ventricular (LV) mass. ***Materials and Methods:*** Images were acquired in a sample of consecutive patients with ATTR-CA through a dual head hybrid SPECT/CT camera. Heart/Contralateral Lungratio activity (H/CL) and Perugini graded score were obtained in each case. Cardiac SPECT/CT images were processed to quantify RV involvement. A dedicated processing protocol was systematically applied to compare inter and intraventricular activities usin grounded ROIs of

12-16 pixels as maximal counts in RV/maximal counts in LV septum (RV/LVsept) in attenuation corrected (AC, applying iterative and filtered back projection methods) and non-corrected (NC) images. The site of maximal activity in RV was also documented. The relation between RV scores and H/CL ratio was estimated for NC and AC images through linear regression analysis. ***Results:*** Eleven consecutive patients with diagnosed ATTR-CA based on expert consensus criteria were included; 91% males, 70-92 years, 9/11with isolated ATTR-CA and 2/11 with combined TTR and light chain CA. The H/CL score was 2.9+0.5, grade 3 = 91% and LVEF was 49.0 + 14.8%. The percentage of LV mass showing a tracer activity of at least 40% was 24.3 + 17.5%. Although ECHO and cardiac nuclear resonance found RV hypertrophy and/or dysfunction in 40% of patients, myocardial uptake of ^{99m}Tc-DPD in RV was detected in all patients through SPECT/CT, mainly distributed onits anterior free wall. The RV/LVsept activity ratio tended to be associated inversely with H/CL ratio, especially when considering AC images. The best fit line was obtained after processing AC images by filtered back projection method (p-value =0.07). ***Conclusion:*** RV involvement is a constant finding in patients with ATTR-CA, as previously reported incardiac nuclear resonance case series. A trend toward more pronounced amyloid deposit in patients with greater activity in septal LV supports the hypothesis of a late RV involvement during slow natural course of ATTR-CA. The potential prognostic value of different patterns of biventricular myeloid deposit applying several image processing protocols deserves further evaluation. ***References:*** None

OP-792

Incidental Disphosphonate cardiac Uptake In Bone Scintigraphy As A Recommendation For Cardiological Monitoring

J. Bonilla*, M. Gomez Martinez, L. Rincon, O. Ajuria, P. Azpeitia, I. Lopez Villar, P. Jane, M. Rioja, M. Orduña Diez;*
Hospital Ramón y Cajal, Madrid, SPAIN.

Aim/Introduction: Imaging techniques have taken center stage in diagnostic algorithms for cardiac transthyretin amyloidosis (ATTR), eliminating the need for invasive tests. Scintigraphy with diphosphonates has become the diagnostic technique of choice. Our purpose is to analyze the frequency of incidental appearance of cardiac radiopharmaceutical uptake in patients undergoing bone scintigraphy for neoplastic or traumatic pathology and its relationship with concurrent cardiovascular pathology. ***Materials and Methods:*** 99mTc HDP bone scintigraphy performed from 2001 to 2018 with significant myocardial deposits (Perugini grade 2-3) were retrospectively analyzed. The mean time elapsed since the examination was 5.5 ± 3.3 years. The follow-up of patients was performed by reviewing the medical history. The incidental finding of significant cardiac uptake appeared in 74 patients (85% male; mean 83 ± 5 years). Most of them had attended the prostate cancer extension study (75.7%). ***Results:*** During follow-up, 76% of patients with significant deposits presented cardiovascular pathology: congestive heart failure with different degrees of myocardial hypertrophy on echocardiogram (53%), conduction disorders (12%), ischemic heart disease (4%) or mixed (7%). In the rest of the patients, the existence of cardiovascular pathology was not found. None were diagnosed with cardiac amyloidosis nor received specific treatment. Mortality was 52% (71% cardiovascular) during this period. ***Conclusion:*** Patients with significant myocardial radiopharmaceutical deposits in 99mTc HDP bone scintigraphy, even as an incidental finding, present a high frequency of concurrent cardiovascular disease. Given the possibility of ATTR once this deposit has been detected, we should recommend starting assessment and follow-up by Cardiology given the current possibility of using new treatments that may change the natural history of this pathology. ***References:*** None

OP-793

Optimising myocardial suppression and diagnostic confidence in cardiac ^{18}F-FDG PET/CT by adding a high-fat, low-carbohydrate dietary preparation

M. Naik*, K. L. Wallitt, S. R. Khan, L. Alves, C. Bowen, W. E. Svensson, N. D. R. Soneji;*
Imperial College Healthcare NHS Trust,
London, UNITED KINGDOM.

Aim/Introduction: Cardiac ^{18}F-FDG PET/CT (cPET/CT) is used in the assessment of active myocardial inflammation in cardiac sarcoidosis (CS). Several preparation techniques to suppress physiologic myocardial activity are described, including the implementation of a high-fat, low-carbohydrate (HFLC) diet before an extended fast. This study assesses whether the addition of a HFLC diet decreases physiologic myocardial activity, thereby increasing diagnostic confidence of the cPET/CT studies. ***Materials and Methods:*** A preliminary retrospective review of cPET/CT for CS was performed before and after the addition of a HFLC diet. Patients with diabetes, taking steroids or administered with heparin were excluded. Group 1 patients had an 18-hour fast pre-cPET/CT. Group 2 patients followed an additional 12-hour HFLC diet prior to the 18-hour fast. Ten consecutive cPET/CT studies in each group were independently reviewed by 3 nuclear medicine consultants. Myocardial suppression was graded as excellent, moderate or poor as per 2017 SNMMI-ASNC guidelines. Background myocardial uptake was visually compared with left ventricular blood pool activity (below, similar to, above or significantly above blood pool). Overall interpretation of the findings (positive, negative or indeterminate for active myocarditis) was recorded.

Confidence of interpretation was graded using a five-point scale (very low-very high). ***Results:*** There were 30 reads in each Group. In Group 1, background myocardial suppression was excellent in 9/30 (30%), moderate 5/30 (17%) and poor 16/30 (53%) with a significant improvement in Group 2 ($p<0.04$ for each reviewer independently); excellent 25/30 (83%) and moderate 5/30 (17%) with no cases interpreted as poor. Background myocardial uptake was below blood pool activity in only 5/30 (17%) in Group 1 compared to 23/30 (77%) in Group 2 ($p<0.02$ for each reviewer).There were more cases interpreted as 'indeterminate' in Group 1 (15/30; 50%) compared to Group 2 (2/30; 6%), statistically significant for 2/3 reviewers. Reviewers also scored improved diagnostic confidence in interpretation in Group 2 with confidence scored as high or very high in 25/30 (83%) compared to 11/30 (37%) in Group 1, again significant for 2/3 reviewers. ***Conclusion:*** These preliminary results suggest significantly improved myocardial suppression, fewer indeterminate studies and increased confidence in the interpretation of cPET/CT studies for CS following addition of a HFLC diet before an extended fast. A further 100 cPET/CT studies will be reviewed with presentation of full results and statistical analysis. ***References:*** Joint SNMMI-ASNC Expert Consensus Document on the Role of 18F-FDG PET/CT in Cardiac Sarcoid Detection and Therapy Monitoring. J Nucl Med. 2017.

OP-794

Dietary compliance and interpretability of ^{18}F-FDG PET-CT scans in diabetic population evaluated for cardiac sarcoidosis

K. Wechalekar*, S. Clark, S. Hatipoglu, S. R. Underwood, G. Keramida, A. Maenhout, R. Sharma, V. Kouranos;*
Royal Brompton and Harefield NHS Foundation Trust, London, UNITED KINGDOM.

Aim/Introduction: 18F-FDG PET-CT has important role in cardiac sarcoidosis (CS) with special dietary and fasting preparation to suppress normal myocardial uptake. If the preparation protocol is adhered to, only inflamed myocardium shows FDG uptake. Achieving appropriate preparation can be difficult in diabetes mellitus (DM) and there is less clarity on how it impacts on interpretation of images. We retrospectively analysed DM patients over last 7 years from electronic records. These were compared to age matched non-DM patients. We assessed the ability of reporters to confidently identify cardiac inflammation in these populations. ***Materials and Methods:*** Our preparation protocol for CS involves no carbohydrate diet- 1 day before the scan followed by 18 hours of fast. For DM patients the instructions include taking OHA or Insulin with food and avoid the doses during fasting period. Dietary preparation was extended for 48 hours in 2 Type II DM patients since the blood glucose levels were higher than 12mM/l. If preparation was not followed, scan was rescheduled. We identified 100 PET-CT scans in patients with a history of DM (Type I, II) referred for diagnosis or disease monitoring of CS between 2012-2019 at our institution. Average age 59 (38-80, median 58) years. 100 age matched non-DM scans, average age 57 (range 30-81, median 57) years on non-DM patients suspected for CS were analysed for comparison. ***Results:*** Out of 100, 97 scans with Type II DM, 3 scans were with Type I DM. 4 Patients were on diet control, 60 oral hypoglycaemic agents (OHA) and 33 on insulin. Out of 100 studies, 54 studies had no uptake in heart (negative for CS), 36 studies showed abnormal uptake in heart (positive) and 9 patients showed non-specific uptake (low-grade uptake in basal lateral wall) and 1 patient had protocol failure (intense homogeneous uptake in LV myocardium only) making 10% non-compliant. 7 patients had blood glucose level higher than 10mM/lit but scans were interpretable in 6 with 5 negative, 1 positive but 1 non-specific uptake due to suspected inadequate suppression. In the non-DM group, 50 negative, 32 positive, 14 with nonspecific uptake and 4 clear dietary non-compliance (18%) ***Conclusion:*** Compared to the DM population, non-DM patients had more failures with dietary compliance for CS assessment with FDG PET-CT scans. This is possible since diabetics are more aware of dietary composition, specially carbohydrates and are more likely to understand the preparation than nondiabetic patients. ***References:*** None

OP-795

Preliminary Results of ^{18}F-FSPG PET/CT in Patients Referred for Exclusion of Active Cardiac Sarcoidosis after Non-Contributory ^{18}F-FDG PET/CT

A. Iagaru*, H. Duan, L. Baratto, S. S. Gambhir, R. Witteles;*
Stanford University, Stanford, CA, UNITED STATES OF AMERICA.

Aim/Introduction: F18-FDG PET is recommended for the assessment of active cardiac sarcoidosis; however, up to 1/3 of patients fail to follow the required complex dietary restrictions, resulting in non-diagnostic scans. F18-labeled FSPG, an L-glutamate derivative, is a promising radiotracer for PET imaging of the aminoacid antiporter system xC- that is involved in detoxification processes and balancing oxidative stress, including in sarcoidosis. No dietary restrictions are required prior to F18-FSPG PET. Here we evaluated the utility of F18-FSPG PET for assessment of cardiac sarcoidosis, in comparison to negative, equivocal or non-diagnostic F18-FDG PET. ***Materials and Methods:*** Patients referred to Nuclear Medicine to rule out active cardiac sarcoidosis were prospectively enrolled after the F18-FDG PET/CT results were negative, equivocal or non-diagnostic. F18-FSPG whole-body imaging started 46-83 minutes (mean±SD: 56.3±8.8), while dedicated cardiac imaging started 55-99 minutes (mean±SD: 70.29.9) after injection of 7.1-8.9 mCi (mean±SD: 8.1±0.4). The mean

delay time between F18-FDG PET and F18-FSPG PET was 23.3 days. A state-of-the art SiPM-based PET/CT scanner (GE Discovery MI) was used for all scans. ***Results:*** Data from 6 women and 13 men, 32-79 year-old (mean±SD: 58.5±12.3) were collected. Eleven of the 19 participants had no F18-FDG uptake compatible with cardiac sarcoidosis; 2 of the 11 had F18-FDG uptake in lung nodules and mediastinal lymph nodes, while 4 of the 11 had F18-FDG uptake in mediastinal lymph nodes compatible with sarcoidosis. F18-FSPG uptake was seen in the lung nodules and mediastinal lymph nodes in the same 6 participants with F18-FDG uptake, while no F18-FSPG uptake was identified in the myocardium. Seven patients had non-diagnostic cardiac F18-FDG PET due to non-compliance with dietary instructions and 1 patient had equivocal findings; F18-FDG uptake in lung nodules and mediastinal lymph nodes was seen in 1 of these 8 patients. These lung nodules and mediastinal lymph nodes also had F18-FSPG uptake. No 18F-FSPG myocardial uptake was identified in the 8 patients with non-diagnostic or equivocal cardiac F18-FDG PET. ***Conclusion:*** F18-FSPG shows promising results in ruling out cardiac sarcoid involvement in a cohort with negative, equivocal or non-diagnostic F18-FDG PET. The F18-FSPG protocol does not require patient preparation. Further evaluation in larger cohorts is needed to confirm our data. In addition, future studies should evaluate F18-FSPG usage in patients with confirmed active cardiac sarcoidosis. ***References:*** None

OP-796

Effect of oral corticosteroids on cardiac 68Ga-DOTANOC uptake in inflammatory cardiomyopathy : a proof of concept study

P. Kaushik*, C. Patel, S. Seth, P. Gupta;*
All India Institute of Medical Sciences, New Delhi, INDIA.

Aim/Introduction: Somatostatin receptor imaging using 68Ga-DOTANOC PET/CT is an emerging technique to assess inflammatory activity in cardiac sarcoidosis and acute myocarditis. We hypothesized that if 68Ga-DOTANOC binds to receptors on inflammatory cells in the myocardium, oral corticosteroids should reduce its uptake by virtue of their immunosuppressant effect. This is a proof of concept study to test the same. ***Materials and Methods:*** Patients with cardiac sarcoidosis and acute myocarditis were included in the study. Diagnosis of cardiac sarcoidosis was based on revised Japanese Circulation Society criteria and acute myocarditis was diagnosed based on clinical features, endomyocardial biopsy, serum enzyme levels and imaging features. 68Ga-DOTANOC cardiac PET/CT scans done at diagnosis and after oral corticosteroids were analyzed visually and semi quantitatively. SUV_{max} of myocardial region with maximum uptake on visual analysis was calculated at baseline and after corticosteroid treatment. In addition, lesion to blood pool (L/BP) and lesion to remote myocardial (L/M) SUV_{max} ratios were calculated at both timepoints. The pre- and post-treatment values were compared using paired t test. ***Results:*** Eight patients (6 male and 2 female) were included in the study (6 with cardiac sarcoidosis and 2 with acute myocarditis). The median duration of steroid intake was 34 weeks. On visual analysis there was reduction in 68Ga-DOTANOC uptake in 7 out of 8 patients. The mean SUV_{max}, L/BP and L/M at baseline were 2.2, 2.6 and 2.3 respectively. Post treatment values of the parameters were 1.4, 1.4 and 1.3 respectively. There was significant reduction in values of all three parameters after treatment as calculated by paired t test (p value < 0.005). ***Conclusion:*** Oral corticosteroids cause a significant reduction in myocardial 68Ga-DOTANOC uptake in cardiac sarcoidosis and acute myocarditis as assessed by visual and semiquantitative analysis. This indirectly indicates that cardiac imaging with 68Ga-DOTANOC indeed measures myocardial inflammation and can potentially be used for monitoring effect of oral corticosteroid treatment. ***References:*** None

OP-797

Prognostic role of serial cardiac ^{18}F-FDG PET-MR imaging in Anderson-Fabry disease: preliminary results

C. Nappi[1]*, A. Ponsiglione*[1]*, A. Pisani*[2]*, E. Riccio*[2]*, E. Nicolai*[3]*, W. Acampa*[1]*, M. Imbriaco*[1]*, A. Cuocolo*[1]*;*
[1]Department of Advanced Biomedical Sciences, Federico II University, Naples, ITALY, [2]Department of Public Health, Nephrology Unit, Federico II University, Naples, ITALY, [3]IRCCS SDN, Naples, ITALY.

Aim/Introduction: Anderson-Fabry disease (AFD) is a rare genetic disorder. Early enzyme replacement therapy (ERT) before irreversible organ injury might lead to better outcome. Cardiac ^{18}F-FDG PET-MR imaging allows different disease patterns identification. The FASTEX score has been proposed for systemic disease progression estimation. We explored the prognostic role of cardiac ^{18}F-FDG PET-MR and its potential relationship with FASTEX score in AFD patients. ***Materials and Methods:*** We enrolled 16 consecutive AFD patients (8 males, mean age 44±14 years). The FASTEX score was calculated considering the weighted variation of neurological, renal and cardiac parameters across two different temporal points, at baseline and at follow-up (FU). Cardiac ^{18}F-FDG PET-MR imaging was performed at baseline and FU (58±13 months). Left ventricular (LV) volumes, hypertrophy and late-gadolinium enhancement (LGE) patterns were analysed. Focally increased cardiac ^{18}F-FDG uptake indicated active cardiac inflammation. ***Results:*** From the initial population of 16 patients, 3 patients did not perform FU ^{18}F-FDG PET-MR imaging due to ICD implantation. Therefore, 13 patients underwent both baseline and FU cardiac PET-MR. At baseline, 6/16 patients were already on ERT and among them 5 showed LGE at MR. Of the 9 (69%) patients without LGE at baseline MR that were not under

ERT, 6 demonstrated homogeneous ^{18}F-FDG uptake and 3 focally increased ^{18}F-FDG uptake localised in the infero-lateral region of the LV. At FU scan, while 7/9 patients were on ERT, negative PET-MR imaging findings were observed in all 9 patients, including those 3 demonstrating a focally increased ^{18}F-FDG uptake at baseline. Among the remaining 7 patients showing advanced disease at baseline, PET-MR imaging findings were confirmed at FU in the 4 patients who performed the scan. In the remaining 3 patients who did not undergo the FU scan, ICD implantation indicated disease worsening. With regard to FASTEX score, 2 patients not needing ERT yet, reported a FASTEX score of 0, indicating globally stable disease. Although all the remaining 14 patients showed systemic disease worsening, the FASTEX score was significantly lower in patients without LGE at baseline compared to the 7 patients with evidence of cardiac damage at baseline (41±14 vs. 80±26; P=0.004). ***Conclusion:*** ^{18}F-FDG PET/MR is effective in detecting cardiac involvement in AFD at early stage, to timely start ERT, thus improving patient outcome. FASTEX score, indicating systemic disease worsening, is lower in patients without evidence of cardiac fibrosis at baseline scan, highlighting greater benefits of early ERT before irreversible damage occurs. ***References:*** None

OP-798

Immune checkpoint inhibitor therapy affects inflammatory activity in large arteries - a retrospective analysis using 18[F]-FDG PET/CT imaging

R. Calabretta*, C. Hoeller, V. Pichler, M. Mitterhauser, G. Karanikas, A. Haug, X. Li, M. Hacker;*
Medical University of Vienna, Vienna, AUSTRIA.

Aim/Introduction: Besides typical cardiovascular risk factors, cardio-toxicity induced by antineoplastic drugs remains a critical issue. Cancer immunotherapy with immune checkpoint inhibitors (ICIs), such as monoclonal antibodies targeting PD-1 (Nivolumab, Pembrolizumab), PD-L1 (Atezolizumab), or CTLA-4 (Ipilimumab), stimulates previously inactivated cytotoxic T-cells to recognize and target cancer cells. Interference with the CTLA-4 and PD-1 axes can cause immune-related adverse events, which in some cases leads to serious and potentially fatal cardiovascular toxicity. PD-1/PD-L1 and CTLA-4 chemokine axes play important roles in limiting T-cell mediated autoimmune inflammation. The effect of T-cells produces large amounts of pro-atherogenic cytokines that may contribute to both the growth and destabilization of atherosclerotic plaques, suggesting cancer patients receiving ICIs therapy may be at an increased risk for atherosclerotic cardiovascular or cerebrovascular events. Previous studies suggested that PET/CT with 18[F] - Fluorodeoxyglucose (FDG) is a valid tool to assess and to reliably quantify atherosclerotic inflammatory activity by evaluating the glucose metabolism of corresponding immune cells and predicted severe cardio- and cerebrovascular events in oncological patients. ***Materials and Methods:*** 20 patients with melanoma treated with ICIs and available FDG PET/CT scans before and during/after treatment have been retrospectively analyzed. FDG maximum focal uptake in the arterial walls was evaluated visually and maximum standardized uptake values (SUVmax) were derived by placing 1 cm^3 volumes of interest (VOIs) along six artery segments (ascending aorta, aortic arch, descending and abdominal aorta, iliac arteries). For bloodpool correction of FDG, three cubic VOIs (1 cm^3) were placed within the lumen of the superior vena cava and the mean SUV was calculated as $SUV_{bloodpool}$. Target-to-background ratios (TBRs) were calculated by correcting SUV_{max} and SUV_{mean} values for $SUV_{bloodpool}$. As surrogate markers of systemic immune cell activation, FDG uptake was also measured in bone marrow and in spleen before and after ICIs therapy. ***Results:*** Cancer immunotherapy with ICIs resulted in a significant increase of inflammatory activity in 318 measured lesions of both the aorta and the iliac arteries (mean TBR_{max_pre}=2.18±0.84 vs. mean TBR_{max_post}=3.46±0.4; p<0.05). FDG uptake measured before and after ICIs therapy in bone marrow and in spleen did not show statistical differences ($SUV_{max\_bonemarrow\_pre}$=2.38±0.53 vs. $SUV_{max\_bonemarrow\_post}$=2.55±0.83, p=0.15; $SUV_{max\_spleen\_pre}$=3.76±1.14 vs. $SUV_{max\_spleen\_post}$=3.67±1.14, p=0.42). ***Conclusion:*** Significantly increasing FDG-uptake in the large arteries is pointing towards an induction of inflammatory activity after cancer immunotherapy with ICIs and might cause increased cardio-/cerebrovascular complications. ***References:*** None

1410

TROP Session: General Nuclear Medicine

Friday, October 30, 2020, 09:00 - 10:30 Channel 10

OP-799

SPECT-CT Optimimization of Lung Perfusion Quantification

S. Menendez Sanchez*, E. Carrillo Villamizar, A. Cardozo Saavedra, R. Bellviure Meiro, S. Aguade, J. Castell;*
Hospital Universitario Vall d'Hebron, Barcelona, SPAIN.

Aim/Introduction: The aim was to compare the presurgical lung perfusion quantification using planar geometric means of the upper and lower lung halves with that of SPECT-CT 3D anatomical lung lobes segmentation. ***Materials and Methods:*** 58 patients (mean age 64.5 years /17 women) from the thoracic surgery department were selected for pre-surgical quantification and subsequent surgery planning. Planar and SPECT-CT lung perfusion images were acquired with 99mTc-MAA on a GE Discovery

670 gamma camera. Geometric means of the upper and lower half of each lung (Lung Analysis, Xeleris GE) were used to quantify planar images (anterior and posterior acquisition) and (Q-Lung, Xeleris GE) was used to delineate each lung lobe on the CT and obtaining the lobar activity in perfusion images. Planar and SPECT-CT quantifications were compared by Student's T for paired data, considering p value &lt 0.05 as statistically significant. ***Results:*** Global planar quantification found an average uptake of the right lung (RL) of 52% ± 11.3, compared to the left lung (LL) of 48% ± 11.3. Global SPECT-CT quantifications results were: RL 52.3% ± 11.9 and LL 47.6% ± 11.9 (p ns). The planar halves subdivision results were: upper right 24.5% ± 7.4, lower right 27.5% ± 7.5, upper left 24.3% ± 5.9 and lower left 23.8 ± 7.7. Anatomical lobe based quantification was: right upper lobe (RUL) 17.4% ± 7.5, Right middle lobe (RML) 9.9% ± 5.1, right lower lobe (RLL) 25% ± 9%, left upper lobe (LUL) 47.6% ± 11.9 and left lower lobe (LLL) 24% ± 7, 8. Significant difference (p &lt 0.001) was obtained in RL delimitation: the upper half against RUL and the lower half against the sum of RML and RLL. No significant differences were found on LL. Planar method did not identify the functional contribution of each lobe. ***Conclusion:*** SPECT-CT anatomical lung lobes delineation allows more accurate quantification of the functional contribution of each lung lobe to predict the effect of surgical resection. ***References:*** None

OP-800

Pulmonary Ventilation / Perfusion Scintigraphy In Patients With Chronic Thromboembolic Disease With And Without Confirmed Pulmonary Hypertension. A Clinical-Radiological Prediction

J. Cañadas Salazar[1], F. Gómez-Caminero López[1], P. García-Talavera San Miguel[1], P. Álvarez-Vega[2], J. G. Villanueva Curto[1], A. C. Peñaherrera Cepeda[1], C. Riola Parada[1], M. P. Tamayo Alonso[1], S. Cadenas Menéndez[1];
[1]Sacyl, Salamanca, SPAIN, [2]SESPA, Gijón, SPAIN.

Aim/Introduction: To compare the findings of the ventilation / perfusion scintigraphy (V / Q) in patients diagnosed with chronic pulmonary thromboembolism (CTEP) with confirmed pulmonary hypertension (PH) and patients with CTEP without PH and its possible associations with the main pulmonary artery diameter (mPA) and functional classification (FC) of the patient according to NYHA score. ***Materials and Methods:*** We reviewed 387 lung perfusion and ventilation scans of patients with suspected chronic PE performed from July 2015 to October 2019. Visual analysis of each of the studies was performed by an experienced nuclear medicine physician, we observed 43 of the patients with suggestive scintigraphic criteria of CTEP, of which 15 were clinically and radiologically diagnosed with PH. The total number of visualized defects (nTD) was gathered in each of these, the mPA measurement was performed on a CT with contrast (Iohexol) in the axial plane, and later the functional clinical data of the patients was required to clinical medicine. ***Results:*** After conducting normality tests and showing an asymmetric distribution in the variable nTD and symmetric in mPA and FC, the results are described based on the interpretation of the total defects in the scintigraphy, in which no statistically significant association was found using Spearman's coefficient of correlation between nTD and mPA (p: 0.82) or CF (p: 0.85). ***Conclusion:*** Our study shows that greater scintigraphic involvement in patients with CTEP is associated with a trend of higher risk of developing HP and, apparently, a worse functional class. Although without statistical correlation, probably due to the sample size, the V / Q scan is a key test in the evaluation of chronic thromboembolic disease. ***References:*** None

OP-801

^{75}Se-SeHCAT test in bile acids malabsorption. Methodological contributions

A. Bronte*, J. Bastidas, J. Rosales, F. Grisanti, J. Zuaznabar, M. Herraiz, J. Richter;*
University Clinic of Navarra, Pamplona, SPAIN.

Aim/Introduction: To evaluate the kinetics of 75-Selenium-homocholic acid taurine (^{75}Se-SeHCAT) during the first 3 hours after oral administration and predict its association with the abdominal retention of ^{75}Se-SeHCAT measured after 7 days (AR_7). Moreover, to describe the results obtained in our center in the diagnosis of bile acids malabsorption (BAM). ***Materials and Methods:*** A total of 38 patients with chronic diarrhea were evaluated. Imaging protocol included abdominal static projections performed at 1, 2 and 3 hours and the 7th day after oral administration. 1 to 3 hours images determined 6 uptake patterns of ^{75}Se-SeHCAT enterohepatic recirculation: gallbladder at 3 hours, gallbladder-abdominal at 3 hours, gallbladder at 2 and 3 hours, lower abdominal at 3 hours, abdominal at 3 hours, upper left abdominal. The association of these patterns with the AR_7 (Fisher, STATA) were investigated. Patients were classified as non-MAB (AR_7>15%), mild-BAM (AR_7<15-10%), moderate-BAM (AR_7<10-5%), severe-BAM (AR_7<5%). The clinical characteristics of each patient such as digestive surgery (DS), intestinal biopsy, digestive pathologies and treatments (Trt) were collected. ***Results:*** In total 38 patients were included, 23 women and 15 men, age 18-81 years. Half patients (19/38) had an AR_7 diagnostic of BAM (7 mild-BAM, 5 moderate-BAM, 7 severe-BAM), and the other half had a non-BAM AR_7. In the BAM group, intestinal biopsy was performed in 7 patients in which 2 had an organic cause; 6 had a DS; 1 had pancreatic insufficiency and 1 received Trt with lenalidomide. 16/19 received standard Trt with cholestyramine (symptoms improved in 13 of them and clinical follow up is pending in 3 of them). In the non-BAM group 11 patients had another diagnosis confirmed.

Patients with MAB had a statistically significant association with "gallbladder-abdominal at 3 hours" uptake pattern (p-0.008), while patients with non-BAM had a statistically significant association with "gallbladder at 2 and 3 hours" uptake pattern (p-0.02). ***Conclusion:*** ^{75}Se-SeHCAT diagnosed MAB in 50% of patients, of which 47.37% had digestive pathologies. Gallbladder and abdominal uptake pattern at 3 hours was associated with the posterior diagnosis of MAB. Symptoms improved in 81.25% of the patients treated with cholestyramine. ***References:*** None

OP-802

Prevalence of Bile Acid Malabsorption Diagnosed by ^{75}SeHCAT Retention Test in the Last Decade at the Bellvitge University Hospital

M. Pudis, *P. C. Notta, A. Sabaté-Llobera, J. Suils, M. T. Bajen, A. Rodriguez-Gasen, J. Guardiola, M. Cortés; Bellvitge University Hospital, Barcelona, SPAIN.*

Aim/Introduction: Bile acid malabsorption (BAM) is a cause of several gut-related problems, the main one being chronic diarrhoea (CD). The purpose of this study was to evaluate the prevalence of BAM in patients with long lasting CD by performing a 75-selenium homotaurocholic acid retention test (^{75}SeHCAT). ***Materials and Methods:*** A retrospective assessment (from 2010 to 2018) of 2184 patients with long lasting (&gt 1 year) CD in whom a primary programme for diagnostic evaluation had not revealed a cause. The ^{75}Se-SeHCAT abdominal retention was measured in these patients, after 7 days of ^{75}SeHCAT capsule ingestion (370 kBq).A retention value (RV) of ≤10% was considered diagnostic of BAM. A severity classification into mild (≤10%), moderate (≤8%) and severe (≤4%), based on retention values on the seventh day, was applied. ***Results:*** MAB was the most common diagnosis in these patients. Out of 2184 patients studied, 946 (43.3%) had a RV of ≤10%. When classified by severity, 554 patients (58.5%) had mild, 323 (34.2%) moderate and 69 (7.3%) severe MAB. The second most prevalent diagnosis was irritable bowel syndrome (IBS), diagnosed in 359 patients (16.4%). ***Conclusion:*** This study reveals that the ^{75}SeHCAT retention test should be performed in all the patients with long lasting CD with an unknown cause because MAB is the most common diagnosis in this group of patients. IBS represents the second most common cause. ***References:*** None

OP-803

75SeHCAT scan in chronic diarrhea for bile acid malansorption: update of an Italian single center experience

N. Fraccascia[1], *E. Tabacchi*[1], *L. Zanoni*[1], *G. Barbara*[2], *V. Stanghellini*[2], *M. Bortolotti*[2], *L. Rotondo*[2], *M. Levorato*[1], *R. Bonfiglioli*[1], *S. Fanti*[1];
[1]*Nuclear Medicine-DIMES University of Bologna, S. Orsola-Malpighi Hospital, Bologna, ITALY,* [2]*Department of Digestive Diseases, University Hospital S. Orsola; DIMEC, University of Bologna, Bologna, ITALY.*

Aim/Introduction: Bile acid malabsorption (BAM) is a common and likely under-diagnosed and under-treated cause of chronic diarrhea. Diagnosis of BAM can be confirmed using 75 Selenium homotaurocholic acid test (75SeHCAT), a tool which is not consistently part of the diagnostic flow-chart, although regularly licensed in Italy, and remains unavailable in most centers and underutilized. The aim of our study was to update our experience with the use of 75SeHCAT test. ***Materials and Methods:*** A retrospective analysis on patients (pts) who routinely underwent 75SeHCAT in our Nuclear Medicine Unit was conducted. 75SeHCAT procedure was performed following the current standard prescribing information. According to 7-day retention, BAM status was reported as: normal>15% (borderline 15-20%), mild 10-15%, moderate 5-10%, severe<5%. Records detailing i.e. clinical history, results, treatment and clinical follow-up were collected. ***Results:*** Overall 64 pts underwent 75SeHCAT test in our Center (November 2017-January 2020): 32 F and 32 M; mean age 44 years (median 42, range 17-80); pts were referred by local gastroenterologists with clinical suspicion of BAM for chronic diarrhea without a recognizable cause by traditional diagnostic test (42/64, 65%) or IBS-D not responder to standard medications (17/64, 26%) (5/64: not available-na). Time of significant gastrointestinal symptoms varied: <12 months (5), 1-3 years (15), 3-5 years (7), >5 years (23), from birth (1), unknown (13). Concomitant anti-diarrheal medications, potentially influencing 75SeHCAT absorption, were assumed by most pts (61/64, 95%) but they were interrupted at least 1 week before, until the end of the test in all cases. Overall, the mean retention score was 22% (median 18%; range 1-88). BAM was confirmed in 30/64 (47%) pts (10 mild; 12 moderate; 8 severe; mean and median retention 8%, range 1-14); excluded in 25/64 (39%) pts (mean retention 40%, median 36% range 21-88), and resulted borderline in 9/64 (14%) cases (mean retention 18%, median 19%, range 16-20). Follow-up data was available in 51/64 (79%) pts. The diagnostic performance of 75SeHCAT led to a change in patient management in 35/50 (64%) cases, in particular 32/35 pts were addressed to bile acid sequestrant (BAS) therapy, with clinical benefit in 21/32 (65%). ***Conclusion:*** 75SeHCAT scan is a simple test able to reliably diagnose BAM and to select patients who might benefit treatment with BASs. Further analyses on larger population are warranted to establish a diagnostic algorithm of chronic diarrhea and to determine whether 75SeHCAT represents a cost-effective option in the differential diagnosis. ***References:*** None

OP-804

Usage of hepatobiliary scintigraphy imaging in stratification of patients with chronic viral hepatitis

D. Jocius[1], D. Vajauskas[2], A. E. Tamosiunas[1];
[1]Vilnius University Faculty of Medicine, Vilnius, LITHUANIA, [2]Lithuanian University of Health Science Kauno klinikos, Kaunas, LITHUANIA.

Aim/Introduction: Viral hepatitis B and C is the one of leading causes of chronic liver damage resulting liver fibrosis and cirrhosis.Routine work up for viral hepatitis patients includes laboratory testing, medical imaging and liver biopsy in selected cases.Liver biopsy used as the "gold standard", is widely questionable.Therefore quantitative medical imaging including magnetic resonance and ultrasound elastography are incorporated in clinical practice. Nuclear medicine imaging is not used as an option determining the degree of liver fibrosis and only scarce literature can be found on this topic. Nonetheless dynamic hepatobiliary scintigraphy with 99mTc labeled mebrofenin may have potential role assessing liver fibrosis.This is prospective study investigating the potential value of dynamic hepatobiliary scintigraphy with 99mTc labeled mebrofenin in staging chronic liver disease. ***Materials and Methods:*** We prospectively enrolled patients with chronic viral hepatitis B and C referred for liver biopsy prior to treatment. All patients underwent liver shear wave elastography followed by dynamic hepatobiliary scintigraphy with 99mTc-mebrofenin. Liver stiffness was measured in right liver lobe taking 10 measurements and results were expressed in kilopascals. Dynamic hepatobiliary scintigraphy was performed immediately after intravenous tracer injection for 30 minutes scanning time. Multiple quantitative scintigraphy parameters were assessed: whole liver lobe and focal area time to peak (ttp), 30 minutes to peak ratio (30/peak), whole lobe and focal area slope index in 350s (slope_350), remaining whole lobe and focal area uptake after 30 min. (BLUR). Liver biopsy took place shortly after imaging. ***Results:*** Total of 72 HCV (68) and HBV (4) patients were included in the study. All imaging parameters were compared to histological examination. Shear wave elastography correctly discriminated between each fibrosis stage (p value <0,0001) and also differentiated non-advanced and advanced fibrosis (p value <0,0001). Quantitative hepatobiliary scintigraphic parameters were found to be statistically significant differentiating significant and nonsignificant fibrosis (30/peak_dex - p 0,03; focal 30/peak_dex - p 0,016), also separating both advanced fibrosis (e.g. ttp_dex - p 0,007; focal ttp_dex - p 0,025; slope_dex - p 0,0001 etc) and cirrhosis (e.g. ttp_dex - p 0,024; 30/peak_dex - p 0,000006; slope_dex - p 0,00001 etc). ***Conclusion:*** Dynamic hepatobiliary scintigraphy with 99mTc labeled mebrofenin is good quantitative imaging tool evaluating patients with diffuse liver disease. Moreover, whole liver imaging may give additional information about fibrosis heterogeneity imaging whole liver. This feature could allow to compare different liver areas as a post processing feature. ***References:*** None

OP-805

The effect of protein binding on calculated glomerular filtration rates using [^{99m}Tc] Tc-DTPA: identifying, quantifying and resolving the issue

S. Townrow, M. Burniston, N. Sizer;
Barts Health NHS Trust, London, UNITED KINGDOM.

Aim/Introduction: An audit of glomerular filtration rate (GFR) studies for patients who required a blood sample 24 hours post-injection (n=58), either with suspected ascitic volume or poor renal functions, indicated that the inclusion of the 24 hour sample universally reduced the GFR (average 27%, minimum 13%, maximum 38%) independent of the extent of ascites or observed renal function. This suggested that the GFR tracer [^{99m}Tc]Tc-DTPA may be binding to proteins resulting in a complex that is unable to be filtered through the kidneys, delaying clearance of the tracer from the body and reducing the apparent GFR. ***Materials and Methods:*** Blood samples taken between 2 and 24 hours after the tracer was administered were processed and counted normally to establish a baseline before undergoing ultrafiltration at 2300g, with a molecular weight cut-off of 10kDa, to extract any protein-bound [^{99m}Tc]Tc-DTPA. The reduction in counts (after decay correction) has been used to estimate the fraction of each sample that was protein bound, and in conjunction with the intercept of the clearance curve (plasma count rate at the injection time) indicates how much of the tracer is protein bound. These results were compared with the radiopharmacy QC values to determine whether binding could be identified before the tracer was administered to patients. ***Results:*** The protein bound fraction of plasma samples at 2 hours ranged from negligible to 27% (n=36, average=11.5%) while at 24 hours it ranged from 7% to 93% (n=31, average=72%) indicating that this was strongly influencing the measured counts in the 24 hour samples. Replacing the original plasma count rate for the 24 hour sample with the value obtained after ultrafiltration increased the GFR in all 31 patients, by 2% to 52% (average=29%). ***Conclusion:*** The potential for protein binding for [^{99m}Tc]Tc-DTPA is hard to quantify before it is administered and can significantly reduce the GFR for patients requiring a 24 hour sample, but protein binding is also observed in blood samples taken at 2 hours and will affect the GFR for routine patients. Protein binding measurements will be required for all patients unless the manufacturing process can be validated as free from protein binding or a QC check can be developed prior to administration. The production process has been revised locally and provisional results are encouraging, but further validation is required. ***References:*** None

OP-806

Correlation of CT KUB based renal parenchymal abnormalities with 99m - Technitium Dimercaptosuccinic Acid SPECT Renal Scinitigraphy: A Specialized Centre Experience

M. Siddique[1], A. Iqbal[2], M. K. Nawaz[1];
[1]Pakistan Kidney and Liver Institute & Research Centre, Lahore, PAKISTAN, [2]LINCS Diagnostic & IR Services, Lahore, PAKISTAN.

Aim/Introduction: To assess the degree of correlation of renal parenchymal abnormalities on unenhanced multidetector CT KUB with 99m-Technetium Dimercaptosuccinic acid (99m-Tc DMSA) planar scintigraphy (PS) and the incremental diagnostic value of single photon emission tomography (SPECT). Secondly, our objective was to evaluate whether conventional radiological imaging results are equivalent or sufficient when compared to DMSA scintigraphy in the assessment of hydronephrosis/atrophy. ***Materials and Methods:*** Retrospectively 114 cases with renal abnormalities (obstructive hydronephrosis and/or atrophy, vesico-ureteric reflux or pyelonephritis) who underwent CT KUB and DMSA scans were evaluated. Detection rates and number for cortical defects in both kidneys were compared between PS and SPECT. Differential cortical uptake function was calculated by geometric mean method. Correlation between renal scintigraphy and CT KUB findings was done using Cohen's Kappa coefficient. ***Results:*** Of total 114 patients [male:female, 70:44; mean age 42±17.5, range: 2-70 years], 56(49%) had hydronephrosis, 27(24%) had unilateral atrophic kidney, 25(22%) patients had hydronephrosis with secondary parenchymal thinning and 6(5%) cases with pyelonephritis. On the basis of radiological imaging, 26% cases had congenital renal outflow obstruction and 74% had acquired obstructive nephropathy due to nephrolithiasis. Of cases with unilateral atrophic kidneys (maximum CT parenchymal thickness <5mm), DMSA revealed nonfunctioning kidneys (uptake<10%) in 93% cases and those with low to moderated degree hydronephrosis, bilateral scarring was seen on DMSA with variable CT KUB parenchymal thickness (mean: 16±1.2 mm). Negative findings on PI in 45 cases with low grade hydronephrosis (32%) were modified to positive findings by adding SPECT. The detection rate of SPECT was significantly higher than that of PI (92% vs. 56%, p<0.01) for small cortical defects as compared to the larger ones. DMSA imaging had significantly higher (p<0.001) diagnostic utility for interpreting renal abnormalities in pyelonephritis as compared to CT KUB with preserved parenchymal thickness (>15 mm). Overall mild agreement (K-value:0.19) was seen between CT KUB and Renal DMSA scintigraphy for interpreting scaring in cases with obstructive hydronephrosis. ***Conclusion:*** DMSA scintigraphy shows higher sensitivity for assessment of renal scarring in cases with high grade hydronephrosis and/or atrophy, and is particularly useful for evaluating functional status preoperatively. The study results emphasize that, compared with planar imaging, Tc-99m DMSA SPECT can detect small cortical defects with greater sensitivity. ***References:*** None

OP-807

Can Dynamic Renal Scintigraphy Predict Renal Outcome in Acute Kidney Injury?

M. Nicod Lalonde*, M. Altarelli, M. Jreige, G. Allenbach, N. Schaefer, J. O. Prior, A. Schneider;*
University hospital of Lausanne, Lausanne, SWITZERLAND.

Aim/Introduction: Acute kidney injury (AKI) is characterized by rapid loss of renal function (<48hrs). Dynamic Tc-99m-MAG3 or I-123-Hippuran renal scintigraphy (RS) is regularly requested by clinicians from our institution to evaluate renal function in patients with AKI. The aim of our study is to evaluate the ability of dynamic RS to predict renal recovery after AKI. ***Materials and Methods:*** We retrospectively included 115 patients (84M/31F) with a mean age of 63±15y, who underwent RS during AKI. During RS, the accumulation index (AI) defined as the percentage of injected activity extracted by the kidney during one minute was calculated and the slope of the accumulation curve (SAC) of the most functional kidney was measured. Renal function was assessed 3 months after RS, and patients were divided into two groups: patients with renal recovery and patients with no significant recovery, defined as recovery of less than 33% of the loss of function during AKI. ***Results:*** When RS was performed during AKI, the sum of the AI of both kidneys was significantly higher in patients with renal function recovery three months after AKI than in patients with no significant renal recovery (8.8 [5.9-10.9] versus 5.9 [4.8-7.0]; p<0.01). The SAC of the most functional kidney was also significantly higher in patients with renal function recovery (0.26 [0.16-0.47] than without 0.19 [0.10-0.27] (p=0.04). ***Conclusion:*** AI and SAC measured during RS seem to be useful indices to help predict renal function recovery after AKI. ***References:*** None

OP-808

Is there a relevance of Hystero-Salphingo-Scintigraphy in SPECT/CT era?

S. Barna*[1], J. Lőrincz[2], F. Dinko[3], I. Mihovk[4], T. Herman[5], P. Török[6], I. Garai[1,4];*
[1]Scanomed Ltd., Debrecen, HUNGARY, [2]University of Debrecen, Kenézy Gyula University Hospital, Department of Obstetrics and Gynecology, Debrecen, HUNGARY, [3]Faculty of Medicine, University of Debrecen, Debrecen, Hungary, Debrecen, HUNGARY, [4]Department of Medical Imaging, Faculty of Medicine, University of Debrecen, Debrecen, HUNGARY, [5]Assisted Reproduction Center, University of Debrecen, Debrecen, HUNGARY, [6]Department of Obstetrics and Gynecology, Faculty of Medicine, University of Debrecen, Debrecen, HUNGARY.

Aim/Introduction: The incidence of infertility is steadily increasing according to published WHO data. 8 to 12 % of couples with intentions of having a family are infertile. At the background of infertility might be anatomical, genetic, immunological, hormonal or psychic abnormality or alterations. 40 % of female infertilty can be traced back to ovarian problems, 30 % to the uterine tubes, and only 5-10 % are caused by genetic abnormalities. The permeability of the uterine tube can be examined by several methods, among these the hystero-contrast-sonography (HyCoSy), hysterosalpingography (HSG) and hysterosalpingoscintigraphy (HSSG) are routinly used. Nevertheless the invasive laporoscopic chromopertubation are used as the gold standart in assessment of uterine tube status. The aim of our study was to investigate the effectiveness of HSSG with SPECT/CT on assessment of the permeability of the Fallopian tubes. ***Materials and Methods:*** 70 infertile female patients (average age: 31 years) were studied between 01.03.2017 and 01.12.2019 in our Institution. The examinations were timing on the 7th-14th days of their menstrual cycle. The patient were lying in a supine position under the SPECT camera. With the assisstance of a gynecologist 37 MBq of 99mTc nanoalbumon were delivered through a cannula placed into the uterine cavity. Firstly we started 40x30 sec. dynamic images (simple dynamic). Then the flow of delivered radiopharmaceutical was forced with direct administration of 5 ml of physiological saline liquid and another dynamic acquisition was performed with 10x30 sec. images (forced dynamic). Finally additional SPECT/CT (128x128 matrix size, 10sec/frame, 120kV and 10 mAs) was done to localise activity in the pelvic area.(forced SPECT) ***Results:*** Different acquisition methods were evaluated in according their diagnostic performance. We found that forced SPECT showed the best diagnostic performance in contrast with simple and forced dynamic acquisition (sensitivity 100%, 87%, 87%, specificity 89%, 72% and 89%). All these methods have excellent negative predictive value (100% in forced SPECT and 97% in dynamic methods). CT did not povide significant additional information. ***Conclusion:*** The HSSG with good NPV is an excellent simple diagnostic method to evaluate permeability of Fallopian tubes. Using only forced SPECT we can improve the diagnostic accuracy without dynamic acquisition. It is time-consuming and more confortable for the patient. No need additional CT. ***References:*** Kissler S et. al. Uterine contractility and directed sperm transport assessed by hysterosalpingoscintigraphy (HSSG) and intrauterine pressure (IUP) measurement. Acta Obstet Gynecol Scand. 2004 Apr;83(4):369-74.

OP-809

Rest/Stress Intradermal Lymphoscintigraphy in Women with Lipedema

G. Tartaglione, F. P. Ieria;
Cristo Re Hospital, Rome, ITALY.

Aim/Introduction: Lipedema is a painful progressive disease due to an abnormal and disproportionate deposition of subcutaneous fat. It is characterized by a symmetrical and bilateral swelling of the lower limbs, but feet are not involved. Lipedema is believed to affect nearly 1 out of 9 of adult women worldwide. Despite this relatively common disease the lipedema is often confused with primary lymphedema or simple obesity. We proposed Rest/Stress Intradermal Lymphoscintigraphy to evaluate lymphatic drainage in women with a clinical diagnosis of lipedema. ***Materials and Methods:*** We studied 54 consecutive women, age 47.1 y +/-19.3 (range 17-86), with a clinical diagnosis of lower limbs lipedema. The mean Body Mass Index was 32.3 (range: 21.7- 58.5, normal value = 18.5 - 25). Two doses 50 MBq, 0.3-0.4 mL, of 99mTc-nanocolloid, were intradermally injected bilaterally in two sites: at the first intermetatarsal space and at the external malleolar area. Two planar static scans in anterior and posterior views were acquired at rest, immediately following the injection. Subsequently, all patients were asked to make an isotonic muscular exercise (stepping) for 2 minutes. Then, post exercise scans were performed to monitor the tracer pathway. After that, the patient performed a prolonged exercise limited by symptoms (walking), for 30-40 minutes. Delayed scans, including abdomen, were acquired 1 hour after tracer injection. ***Results:*** We imaged a total of 108 lower limbs. Rest scan showed a normal visualization of lymphatic vessel along the great saphenous vein and inguinal lymph nodes in 36 limbs (33.3%). Stress and Delayed scans showed collaterals and/or deep vessels in 53 limbs (49.1%) (Popliteal lymph node uptake appeared in 39 limbs); Tracer stagnation area in 16 limbs (14.8%); Dermal backflow in 3 limbs (2.8%). A tortuous course of lymph pathway was observed in about 75% of legs. The Tracer Appearance Time (TAT) in the inguinal lymph node was <10 mins in 100 Limbs (92.5%). The mean value of Trasport Index was 9 (range 3-16). ***Conclusion:*** A normal TAT with a tortuous course of lymphatic vessels and minor findings of lymphatic disorder are frequent in early clinical stage of Lipedema. Over time the lymph adapts its course to increasing deposit of fat in subcutaneous tissue. If the fat continues to build up, it might block the lymphatic vessels causing a secondary lymphedema (Lipo-Lymphedema). Major findings of lymphatic damage may appear in advanced clinical stages. ***References:*** Boursier V et al J Mal Vasc. 2004;29(5):257-61.

OP-810

Role of 18F-FDG PET/CT in the evaluation of pyrexia of unknown origin

D. Khan, S. Sagar, A. Raj ST, S. Kumar, M. Tripathi, M. Sharma, R. Kumar;
All India Institute of Medical Sciences, New Delhi, INDIA.

Aim/Introduction: To evaluate role of F-18 Fluorodeoxyglucose (FDG) positron emission tomography/computed tomography (PET/CT) in the evaluation of pyrexia of unknown origin (PUO). *Materials and Methods:* Four seventy eight patients who underwent 18-F-FDG PET/CT for the evaluation of PUO (by standard definition[1]) from 2016 to 2020 were evaluated retrospectively. Images were acquired on Biograph-mCT scanner (Siemens Inc.) 45-60 minutes after intravenous administration of 6-10mCi of 18-F-FDG. Scans were evaluated qualitatively by two experienced Nuclear medicine physicians. Each scan was read by two nuclear medicine physicians and based on the imaging findings, each scan was given three differential diagnosis by consensus. Histopathological reports of patients who underwent guided biopsy using FDG PET were analysed for final diagnosis and correlated with the first diagnosis by consensus. *Results:* Four seventy eight patients having mean age of 39.5±1.0 years (range 2-90 years), male : female= 1.4:1, with PUO underwent PET/CT. The diagnostic yield of 18-F-FDG PET/CT in PUO cases was found out to be 52%. Among one fifty three patients (153/478) underwent guided biopsy, conclusive histopathology report was available in 109 patients, remaining patients (44/153) had inconclusive reports. Most common reports were inflammatory/vasculitis, lymphoma, other malignancies and tuberculosis (35,20,22,17 respectively). Considering histopathological evidence as gold standard, guided biopsy had an accuracy of 54% and sensitivity of 84.6%. Out of the 14 patients (14/109) of whom we reported as negative, 4 patients were discharged with improved clinical outcome and negative biopsy report while 10 patients came out positive on biopsy. *Conclusion:* 18-F-FDG PET/CT is a valuable non-invasive tool in the evaluation of PUO and can guide biopsy site and direct treatment by identifying underlying pathophysiology of lesions and is most contributory to the diagnosis of lymphoma, malignancy and vasculitis. *References:* 1. Bharucha T, Rutherford A, Skeoch S, Alavi A, Brown M, Galloway J; FDG-PET/CT in fever of unknown origin working group. Diagnostic yield of FDG-PET/CT in fever of unknown origin: a systematic review, meta-analysis, and Delphi exercise. Clin Radiol. 2017 Sep;72(9):764-771.

1411

e-Poster Presentation Session 9: Physics - Software and Image Processing

Friday, October 30, 2020, 09:00 - 10:30 Channel 11

EPS-136

Digital PET/CT 4D: A Study Phantom On The Effect Of Respiratory Gating In Volumes And SUV Recoveries

A. Belly-Poinsignon[1], P. Finitzer[1], M. M. Alabdoaburas[1], C. Provost[2], L. Champion[3], L. Ammour[1], R. Belshi[1];
[1]Institut Curie-Saint Cloud, Medical Physics Department, Paris, FRANCE, [2]Institut Curie-Saint Cloud, Radiopharmacology Department, Paris, FRANCE, [3]Institut Curie-Saint Cloud, Medical Imaging Department, Paris, FRANCE.

Aim/Introduction: PET is established as one of the major biomedical imaging modality for diagnostic, staging and follow-up. In radiotherapy, PET images are used to determine irradiation volumes. However, artefacts due to respiration motion persist to be an important factor in degrading PET image quality and quantification. The aim of this study is to evaluate achievable accuracy of tumors volumes and Standard Uptakes Values (SUV) with 4D digital PET/CT acquisitions (Vereos, Philips Healthcare). *Materials and Methods:* Dynamic thorax phantom, (CIRS, Model 008A-15) with a hollow plastic sphere placed in the left lung region was used. To avoid partial volume effects, the 8ml sphere (diameter 24.8 mm) was chosen in this first study. ^{18}F-FDG activity concentration of 40 kBq/ml was prepared to fill the sphere to simulate a hot tumor in lung. Four different breathing motions (2 translations, hysteresis and pulmonary) were imposed on the sphere along the superior and inferior direction with an external motor. They are detected and recorded using a pressure sensor placed in a belt (Medspira Breath Hold ES). According to patients' protocols, the first two phantom acquisitions were non-gated 3D PET/CT, without, then with breathing motions. The third acquisition was a prospective gated 4D PET/CT. Delineation methodology was validated with a static NEMA phantom study in order to confirm the 40% threshold as the best value for volumes determination. Two commercial softwares, Mirada XD or IntelliSpace Portal, are used to calculate tumor spread, volumes, SUVmax. *Results:* Calculated volumes are largely degraded without respiratory correction and clearly improved with 4D PET/CT acquisitions. Deviations from nominal volume are respectively -5.7%/0.8% for hysteresis, -10.8%/0.8% for 1 cm translation, 111.6%/0.0% for 2 cm translation, -17.0%/3.2% for pulmonary motion. Results depend on sphere movement amplitude for SUVmax metric. In case of large range motion as 2 cm translation, SUVmax is 0.55 with 3D PET/CT and 0.95 with 4D PET/CT, whereas for

small pulmonary movement SUVmax is 1.20 versus 1.03 respectively. There is no significant improvement with 4D PET/CT for intermediate amplitude movements (hysteresis: 0.95/0.96 and 1 cm translation 1.04/0.97). ***Conclusion:*** Obtained results confirm the ability of the system to correct breathing movement by improving the recovering of volumes and SUVmax, particularly in case of large movement. Test for irregular pulmonary motions significant of patients showed the same trend. This study has to be completed for the smaller spheres in order to assess the contribution of digital technology. ***References:*** None

EPS-137

Negative oral contrast agents Utilization in PETCT studies

N. Bashank[1], *W. Diab*[1], *S. Hassanein*[2], *M. Abdel Tawab*[2], *M. S. Keshk*[1];
[1]*Assuit university,AUH, clinical oncology and nuclear medicine department, Assuit, EGYPT,* [2]*Assuit university,AUH, Diagnostic Radiology department, Assuit, EGYPT.*

Aim/Introduction: To compare the performance of different negative oral contrast agents in bowel distension in patient referred for PET/CT studies for various causes aiming for identification of ideal negative oral contrast agent(NOCA). ***Materials and Methods:*** 80 patients were included in this study divided into four groups of 20 patients each. Group I: No intervention (control).Group II: patients received 1500 ml water.Group III: patients received 1500 ml milk with 5% fat Group IV: patients received lactulose 40 gm dissolved in 1500 ml water. Patients received 1000 ml of the NOCA immediately after F18 FDG injection at a rate of 150 ml every 5-10 min for 45-60 min .another 500ml received 5-10 min before imaging Assessments of bowel distention at various levels with mural visability of bowel were studied and graded as follows: (0) No distension, (1) poor =1 cm distension, (2) reasonable =1-2 cm distension, (3) excellent = >2 cm distension. For the study analysis, % of patients with criteria 2 and 3 were considered as good visualization. The effect of oral contrast on F18FDG uptake on the gut was classified into (1) Minimal FDG gut uptake, (FDG activity less than the liver), (2)Moderate (FDG activity same as the liver), (3) Intense (FDG uptake more than the liver). Also gaseous distension was graded as(1) Mild amount of gas in the abdomen (2) Moderate gaseous distention (3) sever. Chi-square test was used as test of significance for qualitative data. ANOVA was the test of significance for quantitative data. Value <0.05 was considered as significant. ***Results:*** Bowel distention & mural visualization were significantly improved in group II,III,IV compared to group I ($p < 0.001$). No statistically significant differences were seen between group III and IV regarding the degree of bowel distention and mural visualization with significant difference between group III&II and group IV &II .Milk in group III was better tolerated and acceptable than water and lactulose in group II and IV with almost no abdominal side effects like abdominal discomfort, nausea,vomiting and diarrhea. Milk was the least agent to produce gasous distension and intense FDG uptake by the gut ***Conclusion:*** Distension and visualization of the bowel was significantly improved with NOCA utilization . Milk was comparable to lactulose regarding bowel distention and bowel wall visualization with a lower cost, better patient tolerability ,& fewer side effects. ***References:*** None

EPS-138

TOF Resolution Assessment based on Time Alignment Procedure

V. Panin*, D. Bharkhada, H. Rothfuss; Siemens Medical Solutions USA, Knoxville, TN, UNITED STATES OF AMERICA.*

Aim/Introduction: TOF resolution estimation is an important assessment of TOF PET scanner performance. Its NEMA standard methodology has evolved over years and current methodology is designed specifically for a line source in scattered media. A time alignment (TA), also referred to as timing calibration, procedure is performed on a regular basis and TOF resolution assessments results strongly depend on TA performance. With the introduction of SiPM scanners TA standards were tightened due to significant improvements in TOF resolution. The Siemens Biograph Vision scanner TA method is designed for arbitrary objects based on non-TOF data reconstruction. Practically, Vision TA is performed on a uniform cylindrical phantom, placed arbitrarily in the scanner. Nevertheless, the same TA can be executed on the line source, arbitrarily placed in the scanner. In addition, the mathematics behind the TA method, which differs from the NEMA method, can be used to estimate TOF resolution from a line phantom. The goal behind this study was to compare performances of NEMA and TA methods in estimation of TOF resolution from a line source after on either cylindrical or line phantom TA. ***Materials and Methods:*** A standard, 28 cm long Ge-68 uniform cylindrical phantom, TA procedure was performed on a Siemens Biograph Vision PET/CT scanner. The outcome of this procedure is the crystal time offsets (TO) array, which is downloaded by firmware for TOF bin index correction in the subsequent list mode data acquisitions. The Ge-68 line source was placed at the center of the scanner to evaluate time resolution according to the NEMA and TA method. Additional TA (self-TA) was performed for this phantom. Residual TOs were applied during list mode data re-writing by changing the TOF bin indexing. ***Results:*** The TOF resolution from the line source was 207ps with standard TA. After additional self-TA, time resolution was marginally improved by 4ps. NEMA and TA methods coincided in TOF resolution assessment within 0.3 ps. ***Conclusion:*** The TA procedure, performed on a wider cylindrical phantom and a line source, results in nearly the same line TOF resolution. Line source self-TA however is

optimized for a smaller amount of coincidence data. The TA is a necessary scanner procedure, designed for an arbitrary object. The proposed TA based TOF resolution assessment method, mostly performed in projection space, can be a suitable replacement of the current NEMA method, mostly performed in image space and designed for line sources only. ***References:*** None

EPS-139

Development of an automatic calculation method for the specific binding ratio in [I-123]ioflupne SPECT

H. Okazawa[1], M. M. Islam[1,2], M. G. M. Rahman[1], T. Tsujikawa[1]; [1]University of Fukui, Fukui, JAPAN, [2]Khulna University of Engineering & Technology, Khulna, BANGLADESH.

Aim/Introduction: A fully-automatic method for specific binding ratio (SBR) calculation in [^{123}I]ioflupane (FP-CIT) SPECT studies was proposed by creating volumes of interest of the striatum (VOI_{st}) and reference region (VOI_{ref}) without manual-handling steps to avoid operator-induced variability with rapid quantitative calculation. ***Materials and Methods:*** The present study involved 105 patients (72±10 years) suspected of parkinsonian syndrome (PS) who underwent FP-CIT SPECT. All patients were classified into PS and non-PS groups according to the results of clinical follow-up and SPECT images. The data from 200 patients in our previous study were used for evaluation and validation of the new program. The SPECT images were reconstructed with two methods; CT-attenuation correction with scatter (ACSC) and without scatter correction (CTAC). Consecutive slices containing striatal intensive counts were selected and a trapezoidal volume of interest (VOI_t) was created automatically. VOI_{st} was then created using our previous method [1]. SBR values were calculated from the mean values of VOI_{st}, and VOI_{ref} determined by the whole brain region outside of VOI_t. To exclude low count voxels in the VOI_{ref}, several thresholds were applied for choosing an appropriate cut-off level. The SBR values from the new method were compared with those from our previous semi-automatic method and the Tossic-Bolt (TB) method [2]. ***Results:*** The fully-automatic method with the VOI_{ref} threshold of 75% maximum reference count, determined from the previous data (200 patients), showed a good linear correlation between the SBRs from the semi- and fully-automatic methods in both patient data sets ($r > 0.98$). The areas under the curves (AUCs) of receiver operating characteristics (ROC) analysis showed no significant difference between the semi- and the fully-automatic methods for both our previous (AUC > 0.99) and new (AUC > 0.95) data. Diagnostic accuracy of the two methods with ACSC and CTAC reconstruction showed similar results (> 92%), and both were better than the TB method. The mean running time of the fully-automatic method was 9±1 sec for each patient. ***Conclusion:*** The proposed method successfully created the automatic VOIs and calculated SBR rapidly without any manual operation, avoiding the operator-induced variability and providing objective SBR results. ***References:*** 1) Rahman MGM, et al. Count-based method for specific binding ratio calculation in [I-123]FP-CIT SPECT analysis. Ann Nucl Med. 2019; 33: 14-21. 2) Tossic-Bolt, et al. Quantification of [^{123}I]FP-CIT SPECT brain images: an accurate technique for measurement of the specific binding ratio. Eur J Nucl Med Mol Imaging. 2006; 33: 1491-9.

EPS-140

A new automated method for analysis of cerebrovascular reserve capacity deficiency by rCBF SPECT with acetazolamide test: Preliminary results

***S. Urbán**[1], G. Sipka[1], A. Balogh[2], Z. Besenyi[1], J. Csirik[2], L. Pávics[1]; [1]Department of Nuclear Medicine, University of Szeged, Szeged, HUNGARY, [2]Institute of Informatics, University of Szeged, Szeged, HUNGARY.*

Aim/Introduction: The rCBF SPECT with acetazolamide test is a well-known, reliable method for the evaluation of cerebrovascular reserve capacity. The investigation could predict the increased risk for stroke in patient population with significant hemodynamic ischemia. Most nuclear medicine clinicians use visual assessment for the interpretation of rCBF SPECT. Quantitative assessment of the presence and degree of cerebrovascular reserve capacity could lead to more precise, patient-based treatment strategies. The aims of this study was to develop a new, automated method for quantification the difference between rCBF SPECTs before and after acetazolamide test and to validate with visual assessment. ***Materials and Methods:*** The automated method consists of five main steps: 1) SPECT brain images were translated into the MNI space (to ICBM Average Brain - ICBM152) using rigid and affine image registration methods; 2) Brain images were normalized by the average voxel value of the cerebellum (cerebellum atlas [1]); 3) the difference image obtained by subtracting the two aligned normalized SPECT images; 4) abnormal regions were detected using automated IQR analysis based on cortical and subcortical regions (Harvard-Oxford atlas); 5) for each detected subregion the size, median difference and anatomical region are extracted. The validation process contained two steps. Firstly, the founded subregions were evaluated based on the visual probability of decreased vascular reserve capacity using three main groups (proved, probable or not proved). Secondly, a region based comparison was performed between the visual assessment and the automated method. 15 patients' (7 men, 8 women, mean age: 66 years) rCBF SPECT images were evaluated. ***Results:*** All pathological cortical and subcortical regions were recognized by the automated method. In total 129 subregions with decreased vascular reserve were identified by the method. Forty two (32,56%)

visually proved or probable subregions were confirmed. The volume determined by our automated method in proved and probable subregions differed significantly from the not proved subregions (Kruskal-Wallis, P<0,0001). The proved subregions do not differed from probable subregions (Kruskal-Wallis, P>0,05). ***Conclusion:*** A new, automated method for analysis of brain perfusion reserve was developed. Based on the evaluation the method detected all of the affected regions. Despite the detected subregions large number based on our study in the future the clinically relevant subregions can be separated from the clinically irrelevant areas. ***References:*** [1] Diedrichsen, J. et al., A probabilistic MR atlas of the human cerebellum., Neuroimage, 2009 May 15;46(1):39-46

EPS-141

Quantification of 18F-Florbetapir amyloid brain PET scans using commercial software: a comparison with an experienced and independently reviewed clinical report

L. Perry[1], *N. H. Patel*[1], *J. Lilja*[2,3], *S. R. Khan*[1], *S. Curry*[4], *F. Loreto*[5], *M. Golemme*[1], *H. McMeekin*[6], *L. Alves*[1], *K. S. Nijran*[1], *P. Malhotra*[1,5], *R. J. Perry*[1,5], *Z. Win*[1];

[1]*Imperial College Healthcare NHS Trust, London, UNITED KINGDOM,* [2]*Uppsala University, Uppsala, SWEDEN,* [3]*Hermes Medical Solutions, Stockholm, SWEDEN,* [4]*King's College London, London, UNITED KINGDOM,* [5]*Imperial College London, London, UNITED KINGDOM,* [6]*Hermes Medical Solutions, London, UNITED KINGDOM.*

Aim/Introduction: BRASS software can be used to quantify 18F-Florbetapir amyloid PET/CT scans performed for suspected Alzheimer's disease. BRASSv4.0 applies an automated PET-only registration method utilising an adaptive template based on principal component analysis. Work by our group has shown accurate registration of amyloid PET images to a template is possible without need of an MR(T1) driven template registration (R^2=0.996). Previous versions of BRASS used a standard rather than adaptive PET template. The aim of this work was to assess the potential of the BRASSv4.0 software to aid interpretation of 18F-Florbetapir scans. ***Materials and Methods:*** The clinical report for 226 18F-Florbetapir scans was agreed by two experienced readers following independent review. The scans were classified as type A (typical features) or non-type A (atypical features including image noise and atrophy) for both positive and negative scans. Quantitative analysis was performed using BRASSv4.0 and the regional values were normalised using the Pons region to give regional amyloid uptake ratios (SUV_R). The mean SUV_R across the regions was recorded (meanSUV_R) together with a coefficient identified in the linear model that correlated with amyloid load (Aβ-index). The quantitative values were compared with the clinical report. ROC curves were used to evaluate regions and threshold values which minimised disagreement to the clinical report (false positive and false negative scans). These results were compared to those obtained using the software with standard template. ***Results:*** 183(81%) scans were classified as type A (87 positive,96 negative). 43(19%) scans were classified as non-type-A (23 positive,20 negative). In BRASSv4.0 the optimum threshold for Aβ-index and meanSUV_R was found to be -0.05(AUC 0.96) and 0.74 (AUC 0.96, 94% sensitivity and 93% specificity) respectively. The left and right (i)lateral temporal cortex (SUV_R=0.75,AUC=0.97; SUV_R=0.76,AUC=0.96), (ii)Precuneus (SUV_R=0.73,AUC=0.95; SUV_R=0.76,AUC=0.95) and (iii) frontal cortex (SUV_R=0.75,AUC 0.95; SUV_R=0.77,AUC=0.95) brain regions showed best separation between positive and negative cohorts. For atypical studies an increase in specificity (79% verses 37%) with preserved sensitivity (79%) was found when comparing results from BRASSv4.0 with the previous version. A small improvement in agreement with the report was seen for typical scans (97% compared to 89% agreement previously, 99% sensitivity, 91% specificity). ***Conclusion:*** The updated BRASSv4.0 software utilising an adaptive template registration shows improved agreement with clinical report for 18F-Florbetapir PET/CT scans compared to a standard template registration. This study has shown very good agreement of atypical scans which are often difficult to interpret and require high degree of experience. ***References:*** None

EPS-142

Evaluation of myocardial perfusion images in patients with left ventricular dilatation using software program provided Artificial Neural Network (ANN)

K. Koyama[1], *M. Kanou*[1], *T. Ogura*[1], *S. Naito*[1], *T. Higuchi*[2], *T. Toyama*[3];

[1]*Gunma prefectural cardiovascular center, Maebashi, JAPAN,* [2]*Gunma Faculity of medicine Graduate School, Maebashi, JAPAN,* [3]*Toyama cardiovasculary Clinic, Maebashi, JAPAN.*

Aim/Introduction: Left ventricular (LV) dilatation has several causes such as ischemic heart disease (IHD) or cardiomyopathy. Patients with LV dilatation and severely impaired LV function will be under heart failure condition. Heart failure is expected poor prognosis and is the leading cause of hospital admission in over 65s. Myocardial perfusion images (MPI) analyzed by ANN provides various indices. To investigate these indices, it will be possible to define the characteristic of myocardium and to approach proper treatment. We compared these indices of patients with LV dilatation caused by IHD and non-IHD. ***Materials and Methods:*** Thirty patients with LV dilatation were enrolled in this study. They were divided into two groups, IHD group (group A) and non-IHD group (group B). All of them underwent MPI. In visual assessment, two expert physicians in nuclear medicine detected myocardial abnormality. Indices from MPI analyzed by ANN were compared. ***Results:*** The age of

the patients range was from 47 to 74 years old. Average of LV ejection fraction (LVEF), end-diastolic volume(EDV) and summed rest score (SRS) of patients in group A were 47%, 214 mL and 24 and those in group B were 47%, 253mL and 25, respectively. In LV diastolic function analysis, peak filling rate and 1/3 mean filling rate of patients in group A were 1.87/ sec. and 0.93/sec. and those in group B were 2.32/sec. and 1.27/sec., respectively. In phase dyssynchrony analysis, Bandwidth, Phase standard deviation (SD) and Entropy in grope A were smaller than those in group B. In regional wall motion analysis, SD of time to end systolic of patients in group A was 9.68% and that in group B was 17.39% (p:0.07). ***Conclusion:*** MPI analyzed by ANN provides various indices. In LV diastolic function analysis, phase dyssynchrony analysis and regional wall motion analysis, indices showed the difference between IHD group and non-IHD group. They will offer valuable information and lead us to proper treatment. ***References:*** None

EPS-144

Deep learning image enhancement for short-duration whole-body FDG PET scans

A. Mehranian[1], *K. Su*[2], *M. D. Walker*[3], *M. Chetan*[3], *D. R. McGowan*[3,4], *F. Gleeson*[5], *A. Brown*[6], *R. Johnsen*[2], *S. D. Wollenweber*[2];
[1]*GE Healthcare, Oxford, UNITED KINGDOM,* [2]*GE Healthcare, Waukesha, WI, UNITED STATES OF AMERICA,* [3]*Oxford University Hospitals NHS FT, Oxford, UNITED KINGDOM,* [4]*University of Oxford, Oxford, UNITED KINGDOM,* [5]*National Consortium of Intelligent Medical Imaging(NCIMI), University of Oxford, Big Data Institute, Oxford, UNITED KINGDOM,* [6]*Oregon Health & Science University, Portland, OR, UNITED STATES OF AMERICA.*

Aim/Introduction: Reducing scan time in PET without compromising the diagnostic value of images is of importance for increasing patient throughput and follow-up exams. In this work, we aimed to leverage a deep learning image enhancement (DLE) model to reduce scan time in oncology whole-body FDG PET scans by up to half and reconstruction time by up to two-third. ***Materials and Methods:*** 137 ^{18}F-FDG PET scans were collected from two PET centers using different GE PET/CT scanners. List-mode data were retrospectively thinned into short-duration scans by factors of 3/4, 1/2 and, if feasible, 1/4. Full-duration datasets were reconstructed using the advanced Q-Clear (beta: 350-400) algorithm, whereas short-duration ones using the faster OSEM algorithm. The datasets were split into train (298), validation (30) and test (36) sets. A DLE model was trained to map short-duration images into their target full-duration ones. The best model was selected based on quantification analyses of lesions, liver and lungs in validation set. Test datasets included only 3-quarter and half-duration scans to avoid false findings caused by lack of signal or physiology mismatches. Beside quantitative evaluations, four experienced readers ranked the quality of images (85 series including Q-Clear) on a 4-point scale (1: very low, 2: acceptable, 3: good and 4: very good) ***Results:*** For 64 identified lesions, the ¾ - and ½ -duration OSEM images and their corresponding DLEs showed respectively SUV_{max} errors of -19±15, -18±16, -5±15, -6±17% with respect to their target full-duration Q-Clear images (all p-values <0.001). The SUV_{mean} errors for lungs and liver were below 4% for all four images. Standard deviation of SUVs in liver was on average 0.17, 0.25, 0.30, 0.16 and 0.18 for Q-Clear, ¾-OSEM, ½-OSEM, ¾-OSEM+DLE and ½-OSEM+DLE images, respectively. The scores rated by readers based on overall quality of the images were on average 3.3±0.4, 2.0±0.5, 1.5±0.4, 3.1±0.5, 3.0±0.5 for the above-mentioned methods, respectively. The readings showed that short-duration images depict an "acceptable" image quality, while DLE makes their quality as "good" as the target Q-Clear images ***Conclusion:*** The qualitative and quantitative results of this study show that the developed DLE model allows to reduce the scan time of whole-body FDG scans from 21±6 min to 10±3 min and the reconstruction time from 2.4 to 0.8 min/bed without substantially compromising the quantitative accuracy and diagnostic value of PET images. This work will be continued by including 2000 datasets provided by National Consortium of Intelligent Medical Imaging ***References:*** None

EPS-145

Deep-learning based urinary bladder segmentation using 18FDCFPyL (PyL-PSMA) PET/CT images

J. Brynolfsson[1], *K. Johnsson*[1], *H. Sahlstedt*[1], *J. Richter*[1], *K. Sjöstrand*[1], *L. Edenbrandt*[1,2], *A. Anand*[1];
[1]*Exini Diagnostics AB, Lund, SWEDEN,* [2]*University of Gothenburg, Gothenburg, SWEDEN.*

Aim/Introduction: Organ segmentation of medical images is an important step in clinical workflows, both when diagnosing and treating patients. Multiple different deep learning methods for automatic organ segmentation have been implemented to that end, usually based on CT or MRI images. When considering segmentation of the urinary bladder in prostate cancer patients, there may be multiple factors that make the delineation difficult. If the patient has a catheter, or has had a prostatectomy, this could change the anatomy and position of the urinary bladder, or the patient may have metallic implants creating image artifacts.When acquiring PET/CT images the PET tracer accumulates in the urinary bladder, making it clearly visible. One approach could be to segment the urinary bladder is segmented using the PET image instead of the CT. However, there may be lesions in the prostate gland or in nearby lymph nodes with high tracer uptake which might then erroneously be segmented as urinary bladder. In this study we evaluate a deep learning based method that takes

both PET and CT images as input to segment the urinary bladder. ***Materials and Methods:*** A data set consisting of 39 PYL-PSMA PET/CT images with manually crafted urinary bladder segmentations was used to train and evaluate the deep-learning segmentation. The network was trained on 31 images and evaluated on 8 images. Cross-validation was performed such that the evaluation set was rotated, and the network re-trained until evaluation had been performed on all 39 images. The Sørensen-Dice score was used to evaluate the performance of the segmentation. Two sets of U-net neural network structures were trained (Ronneberger et al, 2015), one which only received the CT image, and one which took both the CT and the PET image as input. ***Results:*** Evaluated on all images, the network using only low-dose CT as input achieved a mean Dice score of 0.73 with a standard deviation of 0.20. The network receiving the PET/CT image pair as input achieved a Dice score of 0.76 with a standard deviation of 0.14. ***Conclusion:*** By utilizing the PET image in addition to CT image as input to a deep-learning based semantic segmentation, bladder segmentation improves. We will continue to evaluate possible benefits of utilizing both PET and CT images for semantic segmentation, both on a larger data set as well as for additional organs. ***References:*** None

EPS-146

Impact of [^{18}F]FDG uptake time on non-small cell lung cancer PET radiomics and their repeatability

G. D. Kolinger[1], *D. Vállez García*[1], *A. S. Dirand*[2], *G. M. Kramer*[3], *V. Frings*[3], *O. S. Hoekstra*[3], *E. F. Smit*[4,5], *A. J. de Langen*[4,5], *R. A. J. O. Dierckx*[1], *I. Buvat*[2], *R. Boellaard*[1,3];
[1]*Medical Imaging Center, University Medical Center Groningen, University of Groningen, Groningen, NETHERLANDS,* [2]*Laboratoire d'Imagerie Translationnelle en Oncologie, INSERM, Institute Curie, Université Paris-Saclay, Orsay, FRANCE,* [3]*Department of Radiology and Nuclear Medicine, Amsterdam University Medical Centers, location VU Medical Center, Amsterdam, NETHERLANDS,* [4]*Department of Pulmunology, Amsterdam University Medical Centers, location VU Medical Center, Amsterdam, NETHERLANDS,* [5]*Department of Thoracic Oncology, Amsterdam University Medical Centers, location VU Medical Center, Amsterdam, NETHERLANDS.*

Aim/Introduction: In recent years, PET radiomics have gained increased interest. The impact of image reconstruction settings and lesion segmentation on radiomics features (RF) has been extensively studied, however, the influence of tracer uptake interval on RFs has not been explored yet. In this study, we explored the impact of tracer uptake time in combination with reconstruction settings and lesion delineation methods on PET RFs as well as the impact on RF repeatability. ***Materials and Methods:*** Ten NSCLC patients underwent two baseline [^{18}F]FDG-PET scans on two consecutive days (test-retest study) prior to systemic treatment. At each day, scans were obtained at both 60min and 90min post-injection and reconstructed following EARL1 and with point-spread-function resolution modelling (PSF-EARL2). Lesions were delineated using thresholds at SUV=4.0, 40% of SUV_{max}, and with a contrast-based isocontour (at $0.5*SUV_{peak}+SUV_{background}$). Then, RFs were calculated with LIFEx software and divided into classes: conventional, shape, histogram, grey-level co-occurrence matrix (GLCM), grey-level run-length matrix (GLRLM), grey-level zone-length matrix (GLZLM), and neighbourhood grey-level different matrix (NGLDM). Wilcoxon signed-rank tests were performed for statistical comparison and a significance level at 0.05 was considered. ***Results:*** Most shape features were not significantly impacted by tracer uptake time (median average difference and interquartile range of 2%[1%-3%]). On the other hand, conventional and grey-level-based features were significantly impacted by uptake interval, with median average differences of 12%[10%-13%] for conventional, 6%[3%-12%] for GLCM, 10%[1%-19%] for GLRLM, 14%[7%-23%] for GLZLM, and 14%[7%-17%] for NGLDM features. Features were not significantly different between test-retest (<10% changes) studies. Histogram (2%[1%-7%]), GLZLM (4%[2%-8%]), and NGLDM (4%[2%-7%]) had worse repeatability than other classes (median average differences of <2%). PSF-EARL2 images (3%[1%-6%]) had slightly worse repeatability than EARL1-images (2%[1%-4%]), and fixed SUV threshold delineation provided overall more repeatable RFs (1%[0.3%-4%]) than the use of other segmentation methods (3%[1%-5%]). Repeatability of RFs was improved with longer uptake time, with test-retest differences at 60min and 90min being, respectively, 2%[1%-5%] and 2%[1%-3%] for GLCM, 2%[0.5%-4%] and 1%[0.4%-3%] for GLRLM, 5%[3%-8%] and 3%[2%-7%] for GLZLM, and 6%[2%-9%] and 3%[2%-5%] for NGLDM. ***Conclusion:*** Radiomic features other than shape features were significantly impacted by tracer uptake time, emphasizing the need of timely procedures. A longer tracer uptake time improved the repeatability of radiomic features (90min vs 60min post-injection).(This project is funded by EC H2020 #764458.) ***References:*** None

EPS-147

Optimal ^{68}Ga-PSMA-11 and ^{18}F-PSMA-1007 PET window levelling for gross tumour volume delineation in primary prostate cancer

K. Goffin[1], *C. Draulans*[2], *R. De Roover*[2], *U. A. van der Heide*[3], *L. Kerkmeijer*[4], *R. J. Smeenk*[4], *F. Pos*[3], *W. V. Vogel*[3], *J. Nagarajah*[5], *M. Janssen*[5], *S. Isebaert*[2], *F. Maes*[6], *C. Mai*[7], *R. Oyen*[7], *S. Joniau*[8], *M. Kunze-Busch*[4], *K. Haustermans*[2];
[1]*Nuclear Medicine, University Hospitals Leuven, Leuven, BELGIUM,* [2]*Radiation Oncology, University Hospitals Leuven, Leuven, BELGIUM,* [3]*Radiation Oncology, The Netherlands Cancer Institute, Amsterdam, NETHERLANDS,* [4]*Radiation Oncology, Radboud University Medical Centre, Nijmegen, NETHERLANDS,* [5]*Radiology &*

Nuclear Medicine, Radboud University Medical Centre, Nijmegen, NETHERLANDS, [6]Electrical Engineering, ESAT/PSI, KU Leuven, Leuven, BELGIUM, [7]Radiology, University Hospitals Leuven, Leuven, BELGIUM, [8]Urology, University Hospitals Leuven, Leuven, BELGIUM.

Aim/Introduction: Using uniform window levels for PSMA PET-based gross tumour volume (GTV) contouring in primary prostate cancer focal boost strategies reduces interobserver variability. The aim of this study was to determine optimal threshold-based window levels for both ^{68}Ga-PSMA-11 and ^{18}F-PSMA-1007 PET-based GTV contouring. ***Materials and Methods:*** Nine ^{68}Ga-PSMA-11 and ten ^{18}F-PSMA-1007 PET scans including GTV-delineations of four expert teams (GTV_{manual}) and a majority-voted GTV (>50% of individual segmentations) ($GTV_{majority}$) were assessed with respect to a registered histopathological GTV (GTV_{histo}) as gold standard reference. The standard uptake values (SUVs) per voxel were converted to a percentage (SUV%) relative to the SUV_{max} measured in the corresponding prostate and seminal vesicles. The optimal threshold was defined as the threshold that maximizes accuracy for semi-automatic contouring. A leave-one-out cross validation receiver operating characteristic (ROC) curve analysis was performed to identify this statistically optimal SUV% thresholding (SOST) threshold for both tracers. The SOST-analysis was performed twice: once with the GTV_{histo} contour as training structure (GTV_{SOST-H}) and once with the $GTV_{majority}$ contour as training structure ($GTV_{SOST-MA}$) to correct for any limited misregistration. The accuracy of both SOST-based semi-automatic contours was calculated relative to the histological reference structure in the 'leave-one-out' patient of each fold and compared with those obtained by the manual contours. ***Results:*** A median voxel-wise accuracy for GTV_{manual} ranging between 85.7%-92.3% and between 72.1%-93.2% per team for ^{68}Ga-PSMA-11 and ^{18}F-PSMA-1007 PET-based contours, respectively, was found. ROC-curve analysis revealed a median GTV_{SOST-H} threshold of 24 SUV% (range, 22-27 SUV%) and 40 SUV% (range, 39-44 SUV%) ($p<0.001$) for ^{68}Ga-PSMA-11 and ^{18}F-PSMA-1007 PET, respectively. Median $GTV_{SOST-MA}$ thresholds of 41 SUV% (range, 40-43 SUV%) for ^{68}Ga-PSMA-11 PET and 45 SUV% (range, 43-46 SUV%) for ^{18}F-PSMA-1007 PET were calculated ($p<0.001$). A statistically significant pairwise difference in accuracy was found when comparing the accuracy of GTV_{SOST-H} contours with $GTV_{SOST-MA}$ contours for the 'leave-one-out'-patient of each fold (median, -5.7%; IQR, -16.6 - -0.2%; p=0.001). No significant pairwise difference was found when comparing the accuracy of $GTV_{SOST-MA}$ contours with the median accuracy of GTV_{manual} contours (median, -0.5%; IQR, -4.9 - 0.5%; p=0.184), whereas for the GTV_{SOST-H} contours a significant pairwise difference was observed (median, -6.5%; IQR, -27.8 - 0.3%; p=0.011). ***Conclusion:*** Semi-automatic $GTV_{majority}$-trained SOST-based contours achieve accuracy comparable to manual contours to delineate GTV_{histo}. The obtained optimal SUV% thresholds could serve as a base for optimal ^{68}Ga- and ^{18}F-PSMA PET window levelling to reduce interobserver and inter-tracer delineation variability. ***References:*** None

EPS-148

Methodological Quality of Guidelines for Positron Emission Tomography is Suboptimal

Q. Li[1,2], *W. Hou*[1], *L. Li*[2], *M. Su*[1], *Y. Ren*[2], *W. Wang*[2], *K. Zou*[2], *R. Tian*[1], *X. Sun*[2];

[1]Department of Nuclear Medicine, West China Hospital, Sichuan University, Chengdu, CHINA, [2]Chinese Evidence-based Medicine Center, West China Hospital, Sichuan University, Chengdu, CHINA.

Aim/Introduction: Facilitated by clinical application of novel tracers and imaging modalities, guidelines for positron emission tomography (PET) are released increasingly to assist patient care. The potential benefits of guidelines depend on the quality of themselves. However, the methodological quality of PET guidelines have never been examined. We hereby examined the methods used for evidence synthesis and recommendation formation in peer-reviewed guidelines for PET. ***Materials and Methods:*** We systematically searched PubMed from inception to 2 December 2019 for the latest version of PET guidelines published in English. Evaluation criteria were adapted from an internationally developed and validated guideline assessment instrument, the AGREE (Appraisal of Guidelines for Research and Evaluation) II instrument. We also examined the use of evidence in procedure guidelines released in recent five years. ***Results:*** We included 47 guidelines, published between 2004 and 2020, among which, 19 (40.4%) focused on the appropriate use of PET in diverse clinical indications, 27 (57.4%) were procedure guidelines providing step-by-step instructions, and one guideline (2.1%) equally discussed both. Guidelines for PET indications were mainly (17, 89.4%) based on literature review. 12 guidelines (63.1%) reported the level of evidence, 4 (21.0%) reported the strength of recommendations, 8 (42.1%) involved methodologist(s), and 3 (15.7%) described external review. The 2018 EANM/EAN series of guidelines for neurodegenerative conditions reported the most rigorous development methodology. Guidelines for procedures were mainly (24, 88.9%) consensuses without literature review. Only one guideline (3.7%) reported the level of evidence, one (3.7%) reported the strength of recommendations, 7 (25.9%) involved methodologist(s), and 3 (11.1%) described external review. Recent procedure guidelines poorly referenced evidence and varied in contents. Evidence-based recommendations were available in merely 7 guidelines (33.3%) on radiation safety, 8 (38.0%) on radiopharmaceutical dosage, 11 (52.3%) on patient preparation, and 12 (57.1%) on equipment quality control. No recommendation was provided for radiation safety in 10 guidelines (47.6%) and for personnel

qualification in 9 guidelines (42.9%). Two procedure guidelines presented evidence-based recommendations for all necessary contents: the 2019 joint EANM/EANO/RANO/SNMMI guideline for gliomas and the 2015 EANM guideline for tumour imaging. ***Conclusion:*** This is the first study on the methodological quality of guidelines for PET. Our results advised guideline users that the rigor of evidence synthesis and recommendation formation is suboptimal in PET guidelines, and suggested guideline developers that efforts are needed to improve the methodological quality. Critical appraisals are warranted to thoroughly examine the development and reporting of PET guidelines. ***References:*** None

EPS-149

Reporting Standards for Bland-Altman Agreement Analysis: a Systematic Review of Methodological Reviews

O. Gerke[1,2];
[1]*Dept. of Nuclear Medicine, Odense University Hospital, Odense C, DENMARK,* [2]*Dept. of Clinical Research, University of Southern Denmark, Odense C, DENMARK.*

Aim/Introduction: Bland-Altman Limits of Agreement (BA LoA) are a popular and widespread means of analyzing the agreement of two methods, instruments, or raters in quantitative outcomes. Agreement analysis could be reported as stand-alone research articles but are more often than not conducted as a minor quality assurance project in a subgroup of patients in a larger diagnostic accuracy study, clinical trial, or epidemiological survey, leading to brief descriptions and few details in the main report [1]. To this end, reporting items for Bland-Altman analysis have been proposed in different medical areas. The aim of this study was to identify such reporting standards proposals for BA agreement analysis, find the most comprehensive one, and exemplify it with interrater data of a Bland-Altman analysis from our institution. ***Materials and Methods:*** MEDLINE/PubMed was searched including publications until March 3, 2020. All papers that proposed a list of items for standardizing BA plots were included, irrespective of article type (systematic reviews, narrative reviews, original articles, commentaries, editorials, letters, and case studies). ***Results:*** The literature search resulted in 5,600 hits. Seven proposals were identified, three of which were derived from reviewing anesthesia journals. Four studies leaned on publications within 2-year time frames, and the number of included publications varied from 0 to 394 (median: 50). Across included studies, 16 reporting items were proposed. Broad consensus was seen for the a priori establishment of acceptability benchmarks, the estimation of repeatability of measurements, description of the data structure, visual assessment of the normality and homogeneity assumption, and plotting and numerically reporting of both bias and BA LoA including 95% confidence intervals. Abu-Arafeh et al. proposed the most comprehensive and prudent list, identifying 13 key items for reporting [2]. ***Conclusion:*** The unbowed popularity of BA plots, the limited extent as to which BA plots are reported and interpreted in the literature, and the associated need for standardization as evidently expressed by the included proposals obligate researchers to more diligence and warrant journal editors to consider the work of Abu-Arafeh et al. [2] as an essential supplement to GRRAS [1] with respect to statistical analysis of agreement with BA plots. ***References:*** (1) Kottner J, et al. Guidelines for Reporting Reliability and Agreement Studies (GRRAS) were proposed. J Clin Epidemiol.2011;64(1):96-106. https://doi.org/10.1016/j.jclinepi.2010.03.002. (2) Abu-Arafeh A, et al. Reporting of method comparison studies: a review of advice, an assessment of current practice, and specific suggestions for future reports. Br J Anaesth.2016;117(5):569-575. https://doi.org/10.1093/bja/aew320.

EPS-150

Bone metastasis classification in bone scintigraphy using densely-connected convolutional neural networks

N. Papandrianos[1], *E. I. Papageorgiou*[2], *A. Anagnostis*[3,4], *A. Feleki*[5], *K. Papageorgiou*[6], *D. J. Apostolopoulos*[7];
[1]*University of Thessaly, Lamia, GREECE,* [2]*Department of Energy Systems, Faculty of Technology, University of Thessaly, Geopolis Campus, Larissa, GREECE,* [3]*University of Thessaly, Computer Science and Telecommunications Department, Lamia, GREECE,* [4]*Institute for Bio-economy and Agri-technology, Center for Research and Technology Hellas, Volos, GREECE,* [5]*Faculty of Technology, University of Thessaly, Geopolis Campus, 41500, Larissa, GREECE,* [6]*University of Thessaly, Computer Science & Telecommunications Department, Lamia, GREECE,* [7]*University of Patras, Medical School, Department of Nuclear Medicine, PC 26504, Rio, Achaia, GREECE.*

Aim/Introduction: Bone metastasis is one of the most frequent cancer complications and mainly emerges in patients suffering from certain types of primary tumors. The development of automated image analysis tools for bone scans is a challenge to accurately classify patterns of bone lesions. This paper addresses the image recognition problem of bone metastasis diagnosis, using whole-body scans, by investigating the promising capabilities of densely connected convolutional neural networks (CNN). ***Materials and Methods:*** This study employs the dense convolutional network (DenseNET), as an efficient type of deep network with transfer learning capabilities, to recognize medical images by extracting their insightful features and using them for their precise classification. The retrospective study included 808 sequential male patients suffering from prostate cancer, who underwent whole-body bone scans. A nuclear medicine physician classified all the cases into 3 categories: normal, malignant, and degenerative, which was used as gold standard. The provided dataset

of images was shuffled and split into a 85% training and validation set and a 15% testing set. The network's weights were pre-trained using the ImageNet database with natural images, allowing the network to learn general image features. The network was then fine-tuned using the whole-body scans. The experiments were performed in a collaborative environment, with free GPU acceleration, called Google Colab. A meticulous CNN exploration process was accomplished, in which different sets of configurations, regarding various drop rates, epochs, number of dense nodes, pixel sizes and batch sizes, were explored. ***Results:*** After CNN exploration analysis, the best DenseNET-based model parameters include: batch-size=32, dropout=0.2, pixel=350x350x3, flatten, dense nodes=1024-1024, epochs=200. The network's accuracy (ACC), sensitivity (SEN), specificity (SPEC), and AUC were evaluated on an independent 15% testing dataset. The results revealed that the method is sufficiently precise when it comes to differentiate the metastatic bone from degenerative changes as well as from normal tissue (overall ACC = 91.26%±2.95%, loss 0.25±0.12, SEN 0.894, SPEC 0.946, and AUC 0.93). The accuracy of prostate cancer identification regarding normal, malignant or degenerative changes was up to 95.8±1.1%, 94.3±2.2% and 90.8±2.1%, respectively. To strengthen the outcomes of the study, authors further compared the proposed classifier with the popular VGG16 (ACC 89.47±4.53%, loss 0.33±0.16, SEN 0.882, SPEC 0.933, and AUC 0.906). ***Conclusion:*** The proposed approach is proven as an efficient and robust decision support tool that can help nuclear medicine physicians to make immediate and accurate diagnosis of bone metastasis in prostate cancer patients, using bone scans. ***References:*** colab.research.google.com

EPS-151

Segmentation Protocols in ^{99m}Tc-MAA SPECT/CT for ^{90}Y Radioembolization Treatment Planning

G. Mok*, Z. Lu;*
University of Macau, Taipa, MACAO.

Aim/Introduction: Segmentation of lungs, tumor and normal liver is a major source of errors for ^{99m}Tc-MAA SPECT/CT-based dosimetry for ^{90}Y radioembolization. The goal of this study is to assess different segmentation protocols for lung shunt fraction (LSF) and tumor-to-normal liver ratio (TNR) for ^{99m}Tc-MAA SPECT/CT. ***Materials and Methods:*** The XCAT phantom was used to simulate 10 patient anatomies with ^{99m}Tc-MAA distribution, with 5%-20% LSF, axial respiratory motion of 2 cm, different TNR and tumor size. An analytical projector for low energy high resolution parallel-hole collimator was used to simulate 128 realistic noisy projections. The OS-EM method was used for reconstruction with 4 iterations and 16 subsets with attenuation correction using averaged attenuation map, effective source scatter estimation and geometric collimator-detector-response modelling. For LSF, lungs were segmented based on different CT images, i.e., helical CT at end-inspiration (HCT-IN), helical CT at mid-respiration (HCT-MID), helical CT at end-expiration (HCT-EX) and cine averaged CT (CACT). For measuring the lung counts, 2.21 cm lung basal region was excluded to calculate the lung mean count density and then multiply with the original lung volume [1] from different CTs. Liver was segmented based on SPECT images with 2.5% lower threshold or contouring on respective CT images. For TNR, tumors and normal liver were segmented from intensity thresholding on SPECT, contouring on various contrast HCTs or by combining the information from both of them [2]. The mean errors of LSF and TNR for different phantoms were computed for different protocols. ***Results:*** For liver segmentation in various LSFs, the LSF errors are generally higher for CT-based segmentation as compared to those of SPECT-based segmentation, which can reach 15% when using HCT-EX to segment the lungs. The mean LSF error is lowest for the use of CACT to segment the lungs, i.e., <1%. The TNR errors can be over 30% when using contrast HCT-EX as the segmentation method. The mean TNR error is lowest for SPECT-based segmentation with 50% and 2.5% lower threshold for tumor and liver respectively. ***Conclusion:*** It is recommended to use SPECT thresholding based method to segment the liver and to use CACT to segment the lungs for LSF calculation. The TNR can be measured based on SPECT data with good quantitation accuracy without the use of contrast CT for ^{90}Y radioembolization treatment planning. ***References:*** [1] Yu N, et al. Int J Radiat Oncol Biol Phys. 2013;85(3):834-9. [2] Zeintl J, et al. J Nucl Med. 2010;51:921-928.

EPS-152

A new mathematical concept omitting fitting procedures to describe radio tracer processes in kidneys using linear response theory

B. Geist[1]*, M. Hacker*[1]*, H. Neufeld*[2]*;*
[1]*Medical University Vienna, Vienna, AUSTRIA,*
[2]*University of Vienna, Vienna, AUSTRIA.*

Aim/Introduction: Compartmental kinetic models (KM) are commonly used to mathematically describe a measured tracer time activity curve (TAC) of an organ, acquired from dynamically performed imaging scans. They ideally cover the main biochemical processes, which are quantified after applying fitting procedures to measured TACs. In case of the kidneys, the application of a KM is hampered due to the complexity of renal processes and intra-renal delays, leading to a high number of fit parameters or vague descriptions. We thus developed mathematical tools to describe renal TACs without the need for fitting procedures. ***Materials and Methods:*** The description follows the approach to track the tracer particles along their journey according to

the continuity equation. Employing the methods of linear response theory, a probability density function (PDF) is calculated, reflecting tracer processes at certain time points. The approach was applied on kidney TACs from an accomplished and a running study performed at the Division of Nuclear Medicine (Medical University of Vienna, ethical approval numbers 1068/2015 and 1734/2017): adult subjects were scanned twice, with a renal scintigraphy using [99mTc]-mercaptoacetyltriglycine (MAG3) and with a dynamic positron emission tomography (PET) scan using 2-deoxy-2-[18F]fluoro-D-glucose (FDG). While MAG3 is not filtered in the glomeruli and mainly excreted from the kidneys, FDG is filtered, partially re-absorbed and excreted. The obtained probabilities from the PDFs were compared to the clinical parameters renal blood flow (RBF), glomerular filtration rate (GFR), transit time (TT) and outflow efficiency (OE). ***Results:*** So far, the MAG3 and FDG TACs from 14 subjects were investigated. For MAG3, the PDF revealed a high initial venous outflow, correlating with the RBF by $r = 0.94$ ($P < 0.001$), no re-absorption from the renal system, and finally a high outflow at averaged 4.3 minutes, correlating with the OE by $r = 0.85$ ($P < 0.001$) and with the TT by $r = 0.90$ ($P < 0.001$), respectively. For FDG, the PDF revealed a continuous venous outflow matching with re-absorption of averaged 20 % within the first two minutes. The filtrated proportion correlated with the GFR by $r = 0.82$ ($P < 0.001$). FDG was excreted after averaged 3.8 minutes, correlating with the OE by $r = 0.62$ ($P < 0.001$). ***Conclusion:*** To describe the various renal processes and intra-renal delays, a new approach was developed omitting the usage of fits. A first evaluation showed promising results, which will be presented together with further analyzed data. ***References:*** None

1501

CME 12: Alpha Particle Therapy Without Imaging - Options for Dosimetry, the Alpha and Omega

Friday, October 30, 2020, 10:40 - 12:10 Channel 1

OP-811

Surrogate Imaging and Dosimetry with PET / SPECT

L. Bodei; Memorial Sloan-Kettering Cancer Center, Department of Radiology, New York, UNITED STATES OF AMERICA.

OP-812

Ac-225 Therapy, What Do We See and What Can We Measure?

C. Kratochwil; Heidelberg University Hospital, Department of Nuclear Medicine, Heidelberg, GERMANY.

OP-813

Ra-223 and Th-227 Just Dump it in the Body?

I. Murray; Royal Marsden NHS Foundation Trust, Joint Department of Physics, London, UNITED KINGDOM.

1502

Joint Symposium 23 (EANM/ESDO): New Diagnostic and Therapeutic Frontiers in Digestive Oncology

Friday, October 30, 2020, 10:40 - 12:10 Channel 2

OP-814

Therapeutic Combinations in Digestive Oncology

E. van Cutsem; Head of the Digestive Oncology Unit, University Hospital Gasthuisberg, Leuven, BELGIUM.

OP-815

Predictive Markers of Efficacy

C. Lepage; Hepato gastroenterology and digestive oncology, University Hospital Dijon, Dijon, FRANCE.

OP-816

Combined Imaging Approaches - From Bench to Bedside

L. De Geus-Oei; Nuclear Medicine Physician, Department of Radiology, Leiden University Medical Center (LUMC), Leiden, NETHERLANDS.

1503

Joint Symposium 24 (EANM/EFOMP): Technical Advances in Paediatric Dose Reduction

Friday, October 30, 2020, 10:40 - 12:10 Channel 3

OP-817

CT Dose Reduction Techniques

M. Kachelriess; German Cancer Research Center (DKFZ), Division of X-Ray Imaging and CT, Heidelberg, GERMANY.

OP-818

Dose Reduction in PET

A. Smith; University College London Hospitals, Institute of Nuclear Medicine, London, UNITED KINGDOM .

OP-819

Dose Reduction Approaches for Conventional Nuclear Medicine

M. Attard; UMC Radboud, Radiology and Nuclear Medicine Department, Nijmegen, NETHERLANDS.

1504

CTE 6: Advanced Competencies

Friday, October 30, 2020, 10:40 - 12:10 Channel 4

OP-821

NMT Advanced Competencies - A Decade in Review

G. Testanera; Bartshealth NHS Trust, Nuclear Medicine, London, UNITED KINGDOM.

OP-822

Radionuclide Therapy - Technologist's Role and Responsibilities

P. Silva; Jules Bordet Institut, Nuclear Medicine, Brussels, BELGIUM.

OP-823

Research in NM - Technologist's Role and Responsibilities

I. Costa; Kings College, London, UNITED KINGDOM

s1505

M2M Track - Featured Session: Targeted Radionuclide Therapy - Trick or Treat?

Friday, October 30, 2020, 10:40 - 11:55 Channel 5

OP-824

Therapy and Beyond

J. Nonnekens; Erasmus MC, Molecular Genetics and Radiology & Nuclear Medicine, Rotterdam, NETHERLANDS.

OP-825

Disturbing redox balance enhances the biological effect of PRRT but not EBRT in a panel of cancer cell lines

W. Delbart, G. E. Ghanem, P. Flamen, Z. Wimana; Institut Jules Bordet, Brussels, BELGIUM.

Aim/Introduction: Radiobiology of radionuclide therapy has often been extrapolated from external beam radiation therapy (EBRT), where DNA damage has been attributed a central role in ionizing radiation-induced cell death, via direct and indirect effects. In case of low LET radiation, such as with ^{177}Lu, biological effects are mostly relying on indirect effects, via reactive oxygen species (ROS) production. Hence oxidative damage to DNA and other macromolecules occur if ROS can exceed the cell antioxidant defenses. Our in vitro study aims at comparing the radiosensitizing potential of decreasing antioxidant defenses in combination with ^{177}Lu-DOTATATE versus EBRT. *Materials and Methods:* Human cancer cell lines expressing somatostatin receptors were selected for their different intrinsic radiosensitivities to radiation therapy: HBL and MM162 (melanoma-radioresistant), COLO-677 and EJM (multiple myeloma-radiosensitive), MIA-PACA-2 and HT-29 (pancreatic and colon carcinoma-intermediate radioresistance). Cells were irradiated at 2Gy of EBRT or exposed to 5MBq ^{177}Lu-DOTATATE during 4 hours. In the combination experiments, the glutathione (GSH) synthesis inhibitor, BSO (10^{-7} M), was already added 24h prior irradiation and was maintained during the entire experiment of 10 days. Cell survival was assessed using crystal violet. *Results:* Cell lines displayed various sensitivities to radiation therapy. Except in the radioresistant HT-29, cell survival was significantly decreased by ^{177}Lu-DOTATATE and EBRT in all cell lines. Supplementation with BSO could further significantly decrease cell survival of HBL (-40%), MM162 (-11%), EJM (-23%), and MIA-PACA-2 (-28%) compared to ^{177}Lu-DOTATATE alone (all p values < 0.05). When increasing BSO concentration to 10^{-6} M, its radiosensitizing effect was also observed in COLO-677 (-55%) and even in the radioresistant HT-29 (-20%). In contrast, BSO had no added value when added in combination with EBRT. *Conclusion:* Our results showed that disturbing the cell redox balance using a GSH synthesis inhibitor had a radiosensitizing effect in all cell lines when used in combination with ^{177}Lu-DOTATATE, while it had no additional benefit in combination with EBRT. This highlights differences in radiobiological mechanisms between these 2 radiation-based treatment modalities. Additionally, these encouraging results pave the way to new combination strategies not yet explored in the context of radionuclide therapy. *References:* None

OP-826

^{225}Ac-labeled anti-EphA2/EGFR bispecific radioimmunoconjugate prolongs survival of mice bearing triple negative breast cancer xenograft

B. Khan[1], R. Solomon[1], E. Alizadeh[1], N. Thiele[2], P. Causey[3], R. Perron[3], D. Gendron[3], J. Wilson[2], T. Behzad[1], F. Vizeacoumar[1], A. Freywald[1], H. Fonge[1];
[1]University Of Saskatchewan, Saskatoon, SK, CANADA, [2]Cornell University, Ithaca, NY, UNITED STATES OF AMERICA, [3]Canadian Nulear Laboratories, Chalk River, ON, CANADA.

Aim/Introduction: Triple negative breast cancer (TNBC) is deadly form of breast cancer (BC). Epidermal growth factor receptor I (EGFR) is overexpressed in over 85% of TNBC, anti-EGFR targeted therapies have been evaluated albeit with very limited success. In addition, about 70% of TNBC tumors overexpress the subtype A2 of the erythropoietin-producing hepatocellular (EphA2) tyrosine kinase. For the first time we have developed a bispecific antibody (bsAb) against EGFR and EphA2. Our hypothesis is simultaneous targeting of EGFR/EphA2 using alpha particle (^{225}Ac) labeled radioimmunoconjugates will prolong survival of mice bearing EGFR+/EphA2+ TNBC tumors. To accomplish this, we have developed ^{89}Zr-bsAb for microPET/CT imaging and ^{225}Ac-bsAb for alpha particle therapy in EGFR/EphA2 TNBC mouse models. *Materials and Methods:* Anti-EphA2/

EGFR bsAb was radiolabeled with ^{89}Zr for microPET imaging and biodistribution. Tumor uptake of ^{89}Zr-bsAb ,control ^{89}Zr-human IgG was studied in CD-1 nude mice inoculated with EphA2+/EGFR+ MDA-MB-231 TNBC cells. BsAb was radiolabeled with ^{225}Ac for alpha particle therapy. The (radio)immunoconjugates and controls were characterized by flow cytometry, HPLC and internalization rate (live-cell imaging). In vitro cytotoxicity was studied in EphA2+/EGFR+ MDA-MB-231. In vivo radioimmunotherapy using ^{225}Ac-bcAb was studied in EphA2+/EGFR+ MDA-MB-231 model following treatment with three doses of 350 nCi/dose administered 10 days apart. A panel of EphA2-/EGFR+, EphA2+/EGFR- and EphA2-/EGFR- cells are developed to further characterize the imaging properties of ^{89}Zr-bsAb and study in vitro cytotoxicity and in vivo efficacy of ^{225}Ac-bsAb. ***Results:*** Flow cytometry showed > 90% binding to the cells. The microPET imaging data showed persistently high tumor uptake of ^{89}Zr-bsAb in EphA2+/EGFR+ MDA-MB231 xenograft. The uptake of ^{89}Zr-bsAb was clearly visible as early as 24 h p.i. (6.1 ± 0.9 %IA/g) and peaked at around 48 h p.i. (6.6 ± 1.3 %IA/g). In vitro studies showed enhanced cytotoxicity (IC_{50}) of ^{225}Ac-bsAb (1.8 ± 0.6 nM; 0.5 nCi/mL) compared with control ^{225}Ac-IgG (5.8 ± 1.9 nM; 1.5 nCi/mL) and non-labeled antibodies: bsAb (113.5 ± 0.4 nM); human IgG (374.1 ± 1 nM), respectively. ^{225}Ac-bsAb prolonged the survival of mice bearing EphA2+/EGFR+ MDA-MB231 TNBC xenograft compared with control ^{225}Ac-human IgG or non-treated mice. 1/5 mice treated injected with ^{225}Ac-bsAb had complete remission. Median survival after > 90 days since start of treatment are: ^{225}Ac-bsAb (not yet reached); unlabeled bsAb (37 days), control ^{225}Ac-human IgG (24 days), non-treated (20 days). ***Conclusion:*** ^{225}Ac-labeled anti-EGFR/EphA2 bispecific radioimmunotherapeutic shows great promise in TNBC. Validation of this radioimmunoconjugate in other TNBC xenografts is ongoing. ***References:*** None

OP-828

Comparison of intravenous and intraperitoneal dosing of the Targeted Alpha Therapy Thorium-227-anetumab corixetan in a model of peritoneal carcinomatosis of mesothelioma

U. Hagemann[1], M. I. Suominen[2], I. Moen[3], M. Brand[1], C. Ellingsen[3], A. S. Cuthbertson[3], D. Mumberg[1];
[1]Bayer Ag, Berlin, GERMANY, [2]Pharmatest Services, Turku, FINLAND, [3]Bayer AS, Oslo, NORWAY.

Aim/Introduction: Peritoneal carcinomatosis is common in abdominal cancers of mesothelium and ovary appendix. The treatment may include cytoreductive surgery followed by hyperthermic intraperitoneal chemotherapy. Mesothelin-targeted thorium-227 conjugate (MSLN-TTC, ^{227}Th-anetumab corixetan) is a new targeted alpha therapy (TAT; 1, 2) currently being tested in phase 1 in patients suffering from mesothelioma and serous ovarian cancer (NCT03507452) and dose administration is pursued intravenously. An alternative treatment option could be administration of MSLN-TTC into the intraperitoneal cavity. We present the differences in biodistribution, efficacy and tolerability of the two administration routes, studied in a mouse model of peritoneal carcinomatosis of mesothelioma. ***Materials and Methods:*** Nude mice with established intraperitoneal (i.p.) luciferase-tagged mesothelioma NCI-H226 tumors were allocated to 7 groups (n=10 each) after stratification using bioluminescence imaging signals (BLI). Animals were treated either intravenously (i.v.) or intraperitoneally (i.p.) with MSLN-TTC (2 x 250 kBq/kg, 8 weeks apart, or 1 x 500 kBq/kg). Tumor burden was followed by weekly bioluminescence imaging (BLI). Mice were sacrificed when a critical BLI signal intensity was reached. Tolerability was followed by hematology measurements. In a biodistribution study, MSLN-TTC accumulation was compared to a murine cross-reactive MSLN-surrogate-TTC, both administered either i.v. or i.p. at a dose of 500 kBq/kg. Organs and tumors were harvested two weeks after administration to determine accumulated thorium-227. ***Results:*** In the biodistribution study, a statistically significant higher tumor accumulation was observed for MSLN-TTC after i.p. administration when compared to i.v. Accumulation in all organs, including isolated peritoneum, was not statistically significantly different. Similarly, there was no difference in organ and tumor accumulation between MSLN-TTC and the murine cross-reactive MSLN-surrogate-TTC. In the efficacy study, animals were euthanized upon reaching a critical BLI signal. Vehicle treated animals showed a medium survival time (MST) of 25 days and the MST for radiolabeled isotype control treated animals was 55 days after i.v. or i.p. administration. However, animals treated with MSLN-TTC showed MST of 80 to 98 days after i.v. or i.p. dose administration. However, based on tumor weight data upon sacrifice, i.p. administration of MSLN-TTC appeared to be more effective than i.v. administration. Intravenous administration of MSLN-TTC resulted in longer lasting leukopenia. ***Conclusion:*** Intraperitoneal administration of MSLN-TTC in an intraperitoneal model of mesothelioma resulted in increased efficacy and decreased myelosuppression. ***References:*** 1. Hagemann UB et al; Cancer Biother Radiopharm. 2020 Apr 7. doi: 10.1089/cbr.2020.3568. 2. Hagemann UB et al; Clin Cancer Res. 2019 Aug 1;25(15):4723-4734. doi: 10.1158/1078-0432.CCR-18-3476. Epub 2019 May 7

OP-829

Targeted alpha-therapy with ^{211}At-anti-mCD138 mAb in a syngeneic murine Multiple Myeloma model : can repeated doses or fractionation protocol overpass single dose efficiency?

S. Gouard[1], S. Marionneau-Lambot[1,2], J. Gaschet[1,3], N. Chouin[1,4], F. Haddad[5], C. Alliot[5], J. Gestin[1], F. Guérard[1], F. Kraeber-Bodéré[1,3,2], M.

Chérel[1,5,3];
[1]CRCINA, Nantes, FRANCE, [2]Nuclear Medicine Department, University Hospital, Nantes, FRANCE, [3]Nuclear Medicine Department, ICO-René Gauducheau Cancer Center, Saint Herblain, FRANCE, [4]Oniris, École Nationale Vétérinaire, Agroalimentaire et de l'alimentation de Nantes-Atlantique, Nantes, FRANCE, [5]Groupement d'Intérêt Public Arronax, Saint Herblain, FRANCE.

Aim/Introduction: Multiple myeloma (MM) is a B-cell malignancy of terminally differentiated plasma cells developing in the bone marrow. Despite a considerable improvement over the past 30 years, cure is almost never achieved. We have already demonstrated the usefulness of Targeted Alpha-Therapy (TAT) to eradicate residual cells in a MM preclinical syngeneic model by administrating a single high dose of monoclonal antibody anti-CD138 radiolabeled with astatine-211 as alpha particle-emitting radionuclide. The aim of this study was to evaluate the benefit of dose fractionation or repeated doses of an astatine-211-labelled anti-mouse CD138 antibody (^{211}At-9E7.4) in term of survival or side effects in the same syngeneic mouse MM model compared to one injection therapy. ***Materials and Methods:*** C57BL/KaLwRij mice were grafted with 10^6 5T33 MM cells by intravenous injection and received a first injection of ^{211}At-9E7.4 ten days after. A group of mice was used to evaluate the fractionated doses protocol in which a 660 kBq efficient activity was administered in one injection, in 2 fractions of 330 kBq or in 3 fractions of 220 kBq with 1 or 2 weeks interval. A second group was used to evaluate the repeated doses protocol: a 660 kBq activity was administered once or twice with 1 or 2 weeks interval. Hematologic parameters were monitored as well as survival. Data were compared to our previously data obtained with single-dose. ***Results:*** As a reminder, a single-dose of 740 kBq of ^{211}At-9E7.4 was able to cure 65% of mice until 150 days after engraftment while 1100 kBq provoked radiotoxic lethality 14 days after treatment injection. Without any treatment, mice died around 42 days after engraftment presenting paraplegia in most of the cases. In this study, a single-dose of 660 kBq cured 40% of mice at D100. The fractionation in 2 doses treated only 20% of mice regardless of the time interval between the 2 doses. By fractionating the dose of 660 kBq in 3 parts of 220 kBq, even less survival benefit was observed. Concerning the repeated dose protocol, an interval of one week between 2 injections of 660 kBq appeared lethal while an interval of 2 weeks appeared possible in term of early radiotoxicity but gave no benefit in term of survival. ***Conclusion:*** In the particular context of MM disseminated microlesions treatment, it appears that neither the split-dose protocol nor the repeat-dose protocol provided better results than the single-dose treatment. ***References:*** None

OP-830

Increased SST_2 Expression on Pulmonary Neuroendocrine Tumor Cells by Epigenetic Drug Treatment with Histone Deacetylase Inhibitors

I. Klomp*, S. U. Dalm, P. M. van Koetsveld, F. Dogan-Oruç, M. de Jong, L. J. Hofland;*
Erasmus MC, Rotterdam, NETHERLANDS.

Aim/Introduction: Our aim is to increase the expression of somatostatin type-2 receptors (SST_2) on the pulmonary neuroendocrine tumor (NET) cell line NCI-H727 by using epigenetic drugs. We tested the effect of six histone deacetylase inhibitors (HDACis), aiming to promote the euchromatin state supporting SST_2 gene transcription. This approach may possibly open up opportunities for NET patients with insufficient tumoral SST_2, thereby increasing the number of patients eligible for SST_2-targeted therapies such as peptide receptor radionuclide therapy (PRRT). We also compared our results with similar studies performed in the pancreatic NET cell line BON-1. ***Materials and Methods:*** EC_{50} values on cell growth were determined in NCI-H727 after 7-day HDACi treatment. Valproic acid (VPA), tacedinaline (TAC), entinostat (ENT), LMK-235, mocetinostat (MOC) and panobinostat (PAN) were evaluated. After a 7-day treatment, (1) samples were collected for RT-qPCR to determine SST_2 mRNA expression levels and (2) internalization studies were performed by incubating NCI-H727 with 1mL of 1nM [^{111}In]In-DOTA-TATE (50MBq/nmol), +/- 1µM unlabeled DOTA-TATE. To study the reversibility of the observed effects, samples were collected for RT-qPCR 1 and 3 days after HDACi-withdrawal. ***Results:*** For all HDACis, except MOC, the uptake of [^{111}In]In-DOTA-TATE was significantly increased, reaching a maximum upregulation of 4.2-fold for VPA. In line with this, SST_2 mRNA levels were upregulated as well, although statistical significance was not reached for LMK-235 and PAN. For MOC, both SST_2 mRNA levels and uptake of [^{111}In]In-DOTA-TATE were significantly downregulated. Already 1 day after HDACi-withdrawal, SST_2 mRNA levels were significantly lowered for 5 of the 6 HDACis. Only VPA-treated cells reached control levels at this time. Three days after drug withdrawal, SST_2 mRNA levels reached control levels for all treatments. In comparison, control levels were not reached yet in BON-1 7 days after HDACi-withdrawal for 4 of the 6 HDACis. Moreover, the percentage increased uptake of [^{111}In]In-DOTA-TATE was higher in BON-1. ***Conclusion:*** In conclusion, SST_2 expression is evidently upregulated by HDACi treatment in NCI-H727, characterized by intermediate basal SST_2 expression levels. Effects were more prominent in BON-1, probably due to lower basal expression levels of this cell line. Our results support the possibility for a combined treatment approach of HDACi and SST_2-targeted therapies. Furthermore, our in vitro results predict the importance of precise timing as SST_2 upregulation is reversible. Future studies focus

on confirming (1) upregulation of SST_2 protein levels and (2) the epigenetic mechanism-of-action, and (3) in vitro therapy studies by colony forming assays. ***References:*** None

OP-831

Preclinical Evaluation of [18F]F-DPA Uptake in Head and Neck Cancer Under Normal Conditions and After Radiotherapy

S. Tuominen[1,2,3], T. Keller[1], D. Eichin[4], N. Petruk[2,3], A. Verhassel[2,3], J. Rajander[5], F. López-Picón[1], E. Löyttyniemi[6], J. Sandholm[7], J. Tuomela[2,3], T. Grönroos[1,8];
[1]Turku PET Centre, University of Turku, Turku, FINLAND, [2]Institute of Biomedicine, University of Turku, Turku, FINLAND, [3]FICAN West Cancer Research Laboratory, University of Turku, Turku, FINLAND, [4]MediCity Research Laboratory, University of Turku, Turku, FINLAND, [5]Turku PET Centre, Åbo Akademi University, Turku, FINLAND, [6]Department of Biostatistics, University of Turku, Turku, FINLAND, [7]Turku Bioscience, University of Turku and Åbo Akademi University, Turku, FINLAND, [8]Department of Oncology and Radiotherapy, Turku University Hospital, Turku, FINLAND.

Aim/Introduction: Many cancer types exhibit increased translocator protein (TSPO) expression, which has been related to an aggressive phenotype and poor prognosis. Therefore, imaging of TSPO in cancer could be a useful tool for treatment planning and/or the development of new TSPO targeting drugs. In cancer, TSPO-PET imaging has been, with a few exceptions, focused to brain gliomas. Our aim of this study was to evaluate the usability of the TSPO-PET tracer [18F]F-FDPA in head and neck cancer (HNC). ***Materials and Methods:*** [18F]F-DPA uptake was measured in vivo in FaDu control and RT-treated (locally to tumour, 2 x 5 Gy) xenografts and compared to the uptake of [18F]FDG. Following imaging, ex vivo biodistribution, tumour autoradiography (ARG) and radioactive metabolite measurements were performed. The uptake of [18F]F-DPA was also measured in non-irradiated and irradiated parental and TSPO-silenced FaDu cells. TSPO and xCT (a cystine-glutamate transporter) protein expression levels were determined from the xenografts. In addition, TSPO and xCT mRNA expression was also determined from FaDu cells. Blocking studies were done with the TSPO ligand PK11195. ***Results:*** Significantly higher [18F]F-DPA uptake was measured in irradiated xenografts ($p < 0.001$) and cells ($p < 0.001$) compared to controls, whereas the [18F]FDG uptake remained either unchanged or decreased depending on the time after RT. Pre-treatment with PK11195 reduced [18F]F-DPA uptake by 70% and 85% in xenografts and cells, respectively. A moderate, yet not significant, increase in TSPO protein and mRNA levels was detected after RT. The effect of RT on xCT expression was significant, but changed during the time after RT. No effect of RT on [18F]F-DPA uptake was detected in TSPO-silenced cells, in which TSPO mRNA and protein levels were significantly ($p < 0.0001$ and $p < 0.01$, respectively) reduced. Ex vivo tissue measurements revealed significantly increased [18F]F-DPA uptake in adrenal glands ($p < 0.05$) and kidneys ($p < 0.05$) after local RT to tumours. The amount of radioactive metabolites was only approximately 5% in both control and RT treated tumours, whereas approximately 35% of [18F]F-DPA was metabolized in blood. ***Conclusion:*** Our results show that [18F]F-DPA can be used for TSPO imaging in HNC. Furthermore, [18F]F-DPA uptake did reveal RT-induced and TSPO-dependent changes in FaDu xenografts and cells, indicating that TSPO-PET imaging might be utilized in predicting and monitoring RT outcomes. Further studies are needed to determine whether the RT-induced [18F]F-DPA uptake reflects inflammation, reactive oxygen production, or changes in energy demand. ***References:*** None

OP-832

Ultrasound enhanced brain delivery of 89Zr-Cetuximab, an anti-EGFR based immunotherapy followed by immunoPET

A. Schweitzer-Chaput[1], A. Novell[1], N. Tournier[1], V. Tran[1], B. Jego[1], B. Larrat[2], C. Truillet[1];
[1]Université Paris-Saclay, cea, cnrs, inserm, BioMaps, Orsay, 91401, FRANCE, [2]Université Paris-Saclay, cea, cnrs, NeuroSpin/baobab, Gif sur Yvette, 91191, FRANCE.

Aim/Introduction: Glioblastoma (GBM) is the most common and aggressive malignant brain tumour in adults, with a survival rate of approximately 5% at five years. The main source of resistance is the blood brain barrier (BBB), regulating the access of molecules to the brain. Several methods of BBB opening have been developed, among which the use of focus ultrasound (FUS) with gas microbubbles, causing a transient and targeted opening. In this project, we studied the delivery and diffusion of an anti-EGFR monoclonal antibody, the cetuximab (CTX), after BBB opening by FUS of a large part of the brain of healthy mice and then of an orthotopic GBM mouse model monitored by positron emission tomography (PET). ***Materials and Methods:*** First, the affinity constant (K_d) of CTX for human and murine EGFR were determined. The CTX was then labelled with zirconium-89 (89Zr). In vivo experiments involved four groups of nude mice (n=8) with intact BBB: sham group (without FUS), Sham group with a pharmacologic dose of CTX, FUS group and FUS group with pharmacologic dose. BBB opening was achieved using a focused transducer on a large square region (6x6 mm). After FUS, all group received similar dose of 89Zr-DFO-CTX (0.24 ± 0.07 MBq/g) under the PET scanner. 60min dynamic PET acquisition were performed immediately after injection, then 30min static PET acquisition until 7 days after injection. ***Results:*** K_d of CTX for human EGFR was 950pM and 65nM for mouse EGFR, showing low affinity of CTX for murine EGFR. After FUS, 89Zr-DFO-CTX brain uptake was almost two

time higher in FUS groups compared to sham groups. The difference between FUS and sham remained significant even 168h after injection. The uptake of ^{89}Zr-DFO-CTX to the brain was not impacted by the addition of pharmacologic dose of CTX, showing that the ^{89}Zr-DFO-CTX diffusion was not due to specific binding. The elimination half-life from brain was 5.01 ±0.7h in sham and 21.4 ±1.7h in FUS group. ***Conclusion:*** In this study we have shown that with FUS we could increase significantly the uptake of ^{89}Zr-DFO-CTX across the BBB. Furthermore, after BBB opening, we observe a slight diffusion back to the blood compartment and a slow diffusion within brain parenchyma. Following these results, we are conducting a study of effectiveness of ^{89}Zr-DFO-CTX + FUS for treatment of orthotopic mice model of GBM. ***References:*** None

OP-833

Pharmacological inhibition of mTORC1 increases CCKBR-specific tumor uptake of radiolabeled minigastrin analogue [^{177}Lu]Lu-PP-F11N

M. Grzmil[1], Y. Qin[1], C. Schleuniger[1], S. Frank[2], S. Imobersteg[1], A. Blanc[1], R. Schibli[1,3], M. Behe[1];
[1]Paul Scherrer Institute, Villigen PSI, SWITZERLAND, [2]Institute of Pathology, University of Basel, SWITZERLAND, [3]Department of Chemistry and Applied Biosciences, ETH Zurich, SWITZERLAND.

Aim/Introduction: High expression of G-protein coupled receptors (GPCRs) that selectively bind their peptide ligands allowed the development of peptide receptor radionuclide therapy (PRRT) for human cancers. The molecular strategies, which increase uptake of radiolabeled peptides selectively in cancer tissue while sparing healthy organs from cytotoxic side effects, have huge potential to improve PRRT efficacy. In the present study, we searched for the novel opportunities to increase tumor-specific uptake of lutetium-177 labeled minigastrin analogue [^{177}Lu]Lu-PP-F11N that targets overexpressed cholecystokinin B receptor (CCKBR) in human cancers. ***Materials and Methods:*** Drug library screens followed by the proliferation and internalization assays were employed to identify compounds which can increase uptake of [^{177}Lu]Lu-PP-F11N in human epidermoid carcinoma A431 cells which overexpress CCKBR and in rat pancreatic acinar AR42J cells. Western blot (WB) analysis verified inhibition of signaling pathways and CCKBR level. Biodistribution and SPECT imaging of A431/CCKBR xenograft mouse model as well as histological analysis of dissected tumors were used for in vivo validation. ***Results:*** Our kinase inhibitor library screen identified the mammalian target of rapamycin in complex 1 (mTORC1) pathway, which inactivation increased cell uptake of [^{177}Lu]Lu-PP-F11N. Pharmacological mTORC1 inhibition by RAD001 or metformin increased internalization of [^{177}Lu]Lu-PP-F11N in A431/CCKBR and in AR42J cells. Analysis of the protein lysates from RAD001-treated cells revealed increased level of CCKBR and lack of mTORC1-regulated phosphorylation of ribosomal protein S6 at Ser235/236. In A431/CCKBR-tumor bearing nude mice, RAD001 pretreatment significantly enhanced tumor-specific uptake of [^{177}Lu]Lu-PP-F11N, whereas metformin treatment did not show a significant difference. Quantification of SPECT/CT images confirmed higher uptake of [^{177}Lu]Lu-PP-F11N in RAD001-treated tumors. The hematoxylin and eosin staining as well as immunohistochemistry of RAD001-treated tumors showed significant increase in the necrosis and a reduction in the number of proliferative and mitotically active cells. No significant difference in the tumor vascularization was observed after a five-day RAD001 or metformin treatment. Currently, our recent screens with FDA-approved drug library identified several other compounds, which can enhance uptake of radiolabeled minigastrin analogue [^{177}Lu]Lu-PP-F11N. ***Conclusion:*** Our data demonstrate that increasing CCKBR protein level by RAD001 pretreatment has the potential to improve tumor uptake of [^{177}Lu]Lu-PP-F11N and provide proof-of-concept for the development of molecular strategies aimed at enhancing level of the targeted receptor to increase efficacy of PRRT and nuclear imaging. The most recent results and their potential in the theranostics application will be presented and discussed. ***References:*** None

1506

Cutting Edge Science Track - TROP Session: Image Reconstruction and Corrections

Friday, October 30, 2020, 10:40 - 12:10 Channel 6

OP-834

The prevalence and severity of image degradation from motion in rest-stress rubidium-82 PET on a SiPM PET-CT system

I. Armstrong[1], M. Memmott[1], C. Hayden[2], P. Arumugam[1];
[1]Manchester University NHS Foundation Trust, Manchester, UNITED KINGDOM, [2]Siemens Medical Imaging Inc., Knoxville, TN, UNITED STATES OF AMERICA.

Aim/Introduction: We have previously demonstrated the benefit of a high temporal resolution data-driven motion correction (DDMC) algorithm for rubidium-82 relative perfusion PET images [1]. To date, there is limited data on the prevalence of motion degradation during perfusion PET studies. This work compares visual differences between non-corrected (NC) images and their corresponding DDMC images in a large number of cases to demonstrate the prevalence of motion degradation. ***Materials and Methods:*** Rest and stress relative perfusion images from 300 consecutive patients (181 male; stress agent: 266 adenosine, 34 regadenoson) were reconstructed with and

without DDMC. Patients were administered 740 MBq of Rb-82 for each acquisition with images acquired on a Siemens Biograph Vision and reconstructed with OSEM+PSF+TOF. The 600 image pairs (NC and DDMC) were blinded and shown to two observers who gave a visual difference score (VDS) of 0, 1 or 2 as such: 0 - no difference perceivable; 1 - subtle difference perceivable and 2 - a clear difference perceivable. The NC images from the pairs with a VDS of 2 were graded according to image quality as good, adequate or non-diagnostic. The number of non-diagnostic NC studies were further categorised where either rest or stress, or both images within the study were graded as non-diagnostic as a direct result of motion blurring. ***Results:*** The distribution of VDS 0, 1 and 2 were 200, 92 and 8 for rest images and 127, 145 and 28 for stress images respectively. Complete results are shown in the Table. For the 36 cases with a VDS of 2, the NC image quality was adequate in 29 images and non-diagnostic for 7 images (5 stress and 2 rest). None of these 36 images were graded as good quality. In one case, the non-diagnostic quality images were rest and stress from the same study while the 5 remaining non-diagnostic images were part of separate studies meaning that 6 of the 300 studies were non-diagnostic as a consequence of motion affecting one or both images within a study. ***Conclusion:*** The visual impact of motion was seen in 33% of rest and 58% of stress relative perfusion images from rubidium-82 studies. As a result of motion degradation, 2% of studies were considered to be non-diagnostic. This highlights the need for motion correction on modern high-resolution PET systems. ***References:*** [1] Armstrong IS, Hayden C, Arumugam P. Eur J Nucl Med Mol Imaging 2019; 46:S18-S19

OP-835

Comparison of respiratory motion estimation methods in cardiac PET/MR

A. Villagran Asiares[1], C. Munoz[2], T. Kuestner[2], T. Vitadello[3], C. Rischpler[4], T. Ibrahim[3], R. Botnar[2], C. Prieto[2], S. Nekolla[3];
[1]Klinikum rechts der Isar, München, GERMANY, [2]King's College London, London, UNITED KINGDOM, [3]Klinik und Poliklinik für Innere Medizin I, Klinikum rechts der Isar, School of Medicine, Technical University of Munich, Munich, GERMANY, [4]Department of Nuclear Medicine, University Hospital Essen, University of Duisburg-Essen, Essen, GERMANY.

Aim/Introduction: During the cardiac images acquisition, heart motion due to physiological processes degrades the image quality that might lead to misinterpretation of non-viable myocardial areas and misevaluation of cardiac morphology and function [1]. Particularly in cardiac PET studies, respiratory and cardiac cycles generate heart displacements greater than 1cm, and with that the blurring of myocardial structures and bias / underestimation in PET tracer uptake.Previous studies have tried to mitigate these effects using external devices (belt), PET data-driven (PDD) methods, or dedicated MR sequences (INAV) that track the position of the diaphragm. A novel PET/MR approach (INAV + CMRA) that uses INAV to directly localize the myocardium showed promising results[1]. In this ongoing study, we quantitatively compared different approaches for respiratory motion correction in cardiac PET images based on INAV, belt and PDDs techniques. ***Materials and Methods:*** PET/MR viability assessment exams were performed on 11 patients with chronic coronary diseases. INAV + CMRA sequences, acquired in the last 10 minutes of the protocol, were used to correct for respiratory motion the simultaneous FDG PET images. Respiratory cycles were tracked with an external belt. PDD tracking was obtained by computing the center of mass of the PET sinograms constructed every 250 ms and 1s (PDD1s and PDD250ms). On the other hand, PET reconstructions were carried out with motion corrected and uncorrected attenuation correction maps (MoCo and Static umap). To compare nongated-uncorrected PET images (reference) with gated PET images and motion corrected PET images, profile analysis was performed to compute the thickness and FDG uptake of the myocardial wall (Gaussian FWHM and height values) for all the PET images. ***Results:*** A preliminary analysis in the first patient showed that motion estimation based on INAV reduced FWHM up to 40% for gated PET images and up to 20% for motion corrected PET images, outperformed belt (dFWHM: -20% / -5%) and PDDs methods (dFWHM:-30% / -5% for 250ms, and -12% / +2% for 1s). ***Conclusion:*** In general, all the methods reduced the image blurring but the quantitative analysis showed that the INAV method outperformed belt and PDD corrections. As was expected, PDD motion estimation improved when increasing the time resolution. Similar results for motion corrected and uncorrected umaps. ***References:*** [1] Munoz, (2018). Motion-corrected whole-heart PET-MR for the simultaneous visualisation of coronary artery integrity and myocardial viability: an initial clinical validation. European journal of nuclear medicine and molecular imaging, 45(11), 1975-1986.

OP-836

Clinical impact of trigger attenuation correction combined with MR-gating in the correction of respiratory artifacts in thoracic-upper abdominal PET/MR

H. Li[1], X. Meng[1], X. Guan[1], H. Liu[2], Y. Zhang[1], B. Yu[1], H. Zhu[1], N. Li[1], Z. Yang[1];
[1]Peking University Cancer Hospital & Institute, Beijing, CHINA, [2]United Imaging Healthcare, Shanghai, CHINA.

Aim/Introduction: Respiratory motion often leads to blurry the PET images in thoracic-upper abdomen region. For the simultaneous PET/MR acquisition, the MR part can provide different sequences for motion correct, such as trigger, which reduce the lesion's uptake quantification error and align the PET and MRI images well. In this study, we

evaluated the clinical value of MR gated PET reconstruction combining with triggered attenuation correction (AC) in the thoracic-upper abdominal regions. ***Materials and Methods:*** In total, 20 oncologic patients with thoracic-upper abdominal hypermetabolic foci in FDG PET/CT were enrolled in this study, all patients were scanned in an integrated PET/MR system. 28 lesions (17 in liver, 3 in spleen, 3 in pancreas, 2 in peritoneum and 3 in lung) were selected as target lesions. The PET images were reconstructed into 4 groups with different combination of gating and AC (with MR triggered AC vs. breath-hold (BH) AC) techniques, including trigger AC + non MR-gated (group A), trigger AC + MR-gated (group B), BH AC + non MR-gated (group C) and BH AC + MR-gated (group D). A 4-piont visual scale was proposed (on the coronal T2WI, score the mismatch degree of liver anatomic image and PET image, from 0 to 3 points reflect well match to obvious mismatch) to evaluate the respiratory artifacts by 2 doctors independently. The quantitative analysis was assessed by SUV metrics and signal-noise ratio (SNR). ***Results:*** The patient-based analysis showed significant differences in visual respiratory artifact scores among 4 groups, with higher proportion of 0 point in group B (p=0.000). The lesion-based analysis demonstrated significant differences in SUV metrics and SNR. Group B showed significant higher SUVmax (7.49±3.37, 8.45±3.82, 6.90±3.24 and 7.69±3.50 in A, B, C and D groups, respectively, p=0.000), SUVmean (3.90±1.60, 4.34±1.84, 3.67±1.61 and 4.03±1.81, in A, B, C and D groups, respectively, p=0.000), SUVpeak (5.60±2.50, 6.10±2.80, 5.22±2.40 and 5.65±2.68, in A, B, C and D groups, respectively, p=0.000) and SNR values (136.06±90.58, 136.24±81.63, 99.52±53.16 and 107.57±69.05, in A, B, C and D groups, respectively, p=0.000). ***Conclusion:*** The MR gated reconstruction combining with triggered AC could improve the PET image quality and reduce the mismatch between MR and PET images for the thoracic-upper abdomen imaging in simultaneous PET/MR system. ***References:*** None

OP-837

Comparison of data-driven gating and external hardware-gating for ^{18}F-FDG PET/MRI in patients with esophageal tumors

S. Kvernby*, N. Korsavidou Hult, J. Sigfridsson, H. Ahlström, T. Bjerner, M. Lubberink;*
Akademiska hospital, Uppsala, SWEDEN.

Aim/Introduction: Respiratory motion during PET imaging reduces image quality, resulting in decreased lesion detection and quantitative accuracy by introducing an underestimation of the standardized uptake value (SUV) and an overestimation of the lesion volume. Data-driven gating (DDG) based on principal component analysis (PCA) can be used to identify respiratory signals, similarly as external hardware-gating does, and sort data into respiratory phases containing no respiratory motion. The use of DDG, without need for external devices, would greatly increase the feasibility of using respiratory gating in a routine clinical setting. The objective of this study is to evaluate data-driven gating in relation to external hardware-gating and regular static image acquisition on PET-MRI data. ***Materials and Methods:*** Ten patients with esophageal tumors underwent a 6 min PET scan on a Signa PET-MRI system (GE Healthcare) 1.5 hours after injection of 4 MBq/kg ^{18}F-FDG. External hardware gating was done using a respiratory bellow device (GE Healthcare) and DDG was performed using MotionFree (GE Healthcare). The DDG raw data files and the external hardware-gating raw files were created on a Matlab-based toolbox (Duetto v02.03, GE Healthcare) from the whole 6 min scan LIST-file. For comparison, a 3 min static raw file was also created for each patient. Images were reconstructed using TF-OSEM with resolution recovery with 2 iterations, 28 subsets and 3 mm post filter. SUV_{max} and lesion volume, based on a 41% SUV_{max} threshold, were measured in all visible lesions. ***Results:*** A total number of 20 lesions (up to 4 lesions per subject) were included in the study. Both DDG and external hardware-gating demonstrated significantly ($p<0.05$) higher SUV_{max} (9.2 % for DDG; 9.6 % for external hardware-gating) and smaller lesion volume (-4.2 % for DDG; -8.6 % for external gating) in comparison with non-gated static images. No significant differences and a high correlation between DDG and external hardware-gating SUV_{max} values or lesion volumes were found, R^2=0.967. ***Conclusion:*** Data-driven gating with MotionFree for PET-MRI improves image accuracy in comparison with non-gated static acquisition by increasing SUV_{max} and reducing lesion volume. A high agreement between SUV_{max} based on DDG and on external hardware-gating was found. ***References:*** None

OP-838

Effect of a motion correction algorithm on malignant lung nodule uptake: in comparison to ordinary and breath-hold PET/CT

M. Jreige[1]*, S. Gnesin*[1]*, P. Schleyer*[2]*, M. Conti*[3]*, J. O. Prior*[1]*;*
[1]*Lausanne University Hospital, Lausanne, SWITZERLAND,*
[2]*Siemens Healthineers UK, Frimley, Camberley, UNITED KINGDOM,*
[3]*Siemens Healthineers, Knoxville, TN, UNITED STATES OF AMERICA.*

Aim/Introduction: Functional imaging by F-18-fluorodeoxyglucose (FDG) SiPM PET/CT is considered an important tool for lung cancer detection and staging, with promising application for screening. We aimed to evaluate the use of a motion correction reconstruction algorithm (Siemens OncoFreeze) for malignant lung characterization in comparison to non-motion-corrected reconstructions and breath-hold PET/CT at full and up to 10% decimated dose. ***Materials and Methods:*** Six patients investigated for lung nodules were enrolled in this study and underwent a standard-activity (2 MBq/kg) PET/CT (Siemens Biograph

Vision 600) with standard free-breathing trunk acquisition (FB) with an ordinary non-motion-corrected reconstruction (ORD) and the motion-corrected reconstruction (EM), in addition to a dedicated lung Breath-Hold (BH) acquisition lasting between 20-40 s. Low-activity emulations were reconstructed to simulate scans with 10%, 25%, 50% and 75% of the standard injected activity (2MBq/kg) using ordinary and motion correction-algorithms. SUVmax, SUVmean, and Signal-to-Background-Ration (SBR) of malignant nodules were measured across scans. ***Results:*** Six malignant lung nodules, measuring 15.3±7.6 mm, showed increased FDG uptake with SUVmax, SUVmean (g/mL) and SBR of 7.6±3.7, 4.6±2.3 and 16.3±6.8 for ORD; 8.0±3.6, 4.7±2.2 and 17.1±6.4 for EM; and 10.2±5.1, 5.1±2.6 and 22.1±9.7 for BH respectively. EM and BH increased SUVmax by 23% and 34% in comparison to ORD, respectively. At low-activity simulation scans of 10%, 35%, 50% and 75% the injected activity, EM led to a minimal increase of SUVmax of 2.0%, 0.3%, 3.8% and 2.8% in comparison to ORD, with no effect on SBR, except a slight increase of 1.6% and 1.8% for 50% and 75% of the decimated activity, respectively. ***Conclusion:*** This study shows that the motion correction reconstruction algorithm can increase FDG uptake measured in malignant lung nodules with standard injected activity. The combination of breath-hold PET/CT and motion correction algorithm may optimize PET/CT performance in lung cancer evaluation. ***References:*** None

OP-839

Application of a generic dynamic reconstruction algorithm on PET whole-body pharmacokinetic studies

Z. Chalampalakis[1], S. Stute[2,3], M. Filipovic[1], S. Marie[1,4], M. Bottlaender[1], N. Tournier[1], C. Comtat[1];
[1]Service Hospitalier Frédéric Joliot, CEA, Inserm, CNRS, Univ. Paris Sud, Univ. Paris Saclay, Paris, FRANCE, [2]Nuclear Medicine Department, Nantes University Hospital, Nantes, FRANCE, [3]CRCINA, INSERM, Nantes University, Nantes, FRANCE, [4]Hôpital Bicêtre, Assistance Publique des Hôpitaux de Paris, Le Kremlin Bicêtre, Paris, FRANCE.

Aim/Introduction: Dynamic PET is an ideal tool to study in vivo pharmacokinetics. When applied to the whole-body with regular scanners, however, large temporal gaps in the acquisition result to low count statistics, making whole-body parametric imaging very challenging. The aim of this study is to improve whole-body parametric imaging, using a generic 4D reconstruction algorithm adapted for dynamic whole-body protocols that does not assume a specific kinetic model. Its application is demonstrated on a research protocol that studies the function of Organic Anion Transporting Polypeptides (OATP, SLCO) transporters in drug delivery to tissues. ***Materials and Methods:*** The acquisition protocol was implemented on a PET/MR scanner, with whole-body passes of five bed positions each. The data were reconstructed with a regular 3D-OSEM algorithm and a novel 4D reconstruction algorithm, adapted for imaging with overlapping beds and incorporating the dynamic spectral model [1]. From this model, whole-body images were estimated for each time frame in addition to the K_1 parametric map, assumed to reflect the activity of OATP transporters at the blood-tissue interface. ***Results:*** Visual comparison of the whole-body dynamic frame images shows clearly lower noise and higher contrast for the 4D reconstruction compared to 3D. The two reconstructions provide similar quantification over large organs/regions of interest in the body. In the liver the root mean square difference (RMSD) of the time activity curves of the two reconstructions is 50 Bq/cc, with an average reduction of variance across frames of 50% for the 4D reconstuction compared to 3D. ***Conclusion:*** The 4D reconstruction method using the spectral model has shown to greatly improve image quality in whole-body dynamic imaging while maintaining quantification. It also shows the feasibility of doing whole-body parametric imaging with currently available scanners, based on the proposed 4D reconstruction algorithm and minimum assumptions on the underlying kinetics. In the protocol demonstrated here, whole body parametric images provide a tool for direct detection of organs with OATP expression, such as the liver. Further work is required for improving quantification of regions in the field of view that are not completely modeled with the spectral model, like the bladder, using additional dynamic models. ***References:*** 1) Reader, A. J. & Verhaeghe, J. Phys. Med. Biol. 59, R371-R418 (2014).

OP-840

Voluntary body motion in WB dynamic PET imaging

J. Trinckauf[1], C. Weyermann[1], F. Kotasidis[2], M. Hug[1], V. Schober[1], V. Treyer[1], D. Ferraro[1], M. Huellner[1], K. Kudura[1], M. Messerli[1], I. Burger[1];
[1]University Hospital Zürich, Zurich, SWITZERLAND,
[2]GE Healthcare, Zurich, SWITZERLAND.

Aim/Introduction: Recent introduction of high sensitivity SIPM-based PET systems provides the ability to acquire WB dynamic protocols, leading to images of improved image quality and allowing the estimation of WB parametric maps. In such studies, patient body motion (BM), can manifest itself both across and within dynamic frames. Therefore understanding its prevalence in clinic and optimizing acquisition protocols, is of particular interest in order to maximize clinical potential. ***Materials and Methods:*** 37 WB dynamic ^{18}F-FDG patient datasets, were prospectively acquired on an 25cm FOV PETCT system (Discovery MI). Patients were injected on the scanner's bed (2±0.5MBq/kg) and dynamic acquisition over a large blood pool was initiated simultaneously (10±4 min), followed by multiple (11±3 frames) sequential WB passes (35sec/bed) for up to 60±10min post-injection. Data were reconstructed using

BSREM image reconstruction in a 256x256 image matrix. BM was then assessed qualitatively and quantitatively to investigate prevalence and was categorized. ***Results:*** In 73% (27/37) of the patients, some type of motion was visible in at least 1 dynamic frame with 13.5% having a stepped BM in less than 3 frames and 59.5% having stepped or slow drift motion in 4 frames or more. Slow drift was visible in 30% (11/37) of patients which involved mostly the head and neck region. 63% of patients which were involved in some kind of BM, exhibited a sustained step motion, while 37% were involved in a motion around a mean position. In patients that did move, 74% involved some motion in the head and neck region, either sustained or around a mean position. Extremity motion was seen also in 74% of the motion affected patients and these were mostly step movements. Lastly 6 subjects initiated a motion involving the torso either as a translation or rotation. ***Conclusion:*** Understanding motion types most frequently encountered in WB dynamic imaging, can guide mitigation strategies both during acquisition, reconstruction and analysis. Based on this interim analysis, BM mainly involved either the head or the extremities at the beginning or end of the acquisition but crucially less so involving the torso. Motion associated with any and injection associated procedures or other patient intervention, appears to have limited impact on the observed BM and subject to staff experience. These findings are indicative of this kind of protocols, while more clinically applicable dynamic protocols, starting after a normal uptake time, are expected to exhibit similar BM as in clinical static acquisitions ***References:*** None

OP-841

Impact of Point Spread Function (PSF) reconstruction on ^{68}Ga-DOTATOC PET/CT Quantitative Imaging Parameters - a patient and phantom pilot study

A. McCann[1,2], S. Liddy[2], D. Maguire[2], E. Loughman[2], A. Dowling[2], L. Harris[2], L. L. Vintro[3], S. Cournane[1,2], J. Lucey[2]; [1]Centre for Physics in Health & Medicine, School of Physics, University College Dublin, Dublin, IRELAND, [2]St Vincent's University Hospital, Dublin, IRELAND, [3]School of Physics, University College Dublin, Dublin, IRELAND.

Aim/Introduction: The aim of this pilot study was to assess the influence of PSF Reconstruction on ^{68}Ga-DOTATOC PET/CT quantitative parameters. ***Materials and Methods:*** Eight ^{68}Ga-DOTATOC PET/CT patient studies, with a total of 16 lesions were included in this study. The administered activity ranged from 94-127MBq, with patient weights ranging from 54-81kg. Following a one hour uptake period, wholebody images were acquired on a Siemens Biograph Horizon PET/CT scanner. All images were iteratively reconstructed with Time of Flight (TOF), and with and without PSF modulation (True X UltraHD-PET). For each lesion, the SUV_{max}, SUV_{mean}, SUV_{peak}, tumor volume and total lesion somatostatin avidity (TLSA) were measured. Uptake in the Liver and Spleen were analysed and their SNR calculated. Tumour-to-normal tissue uptake was analysed using both the Liver and Spleen as the background organ. Phantom studies were performed to determine the impact of PSF reconstruction on SUV accuracy and fixed threshold defined volume accuracy for varying target sizes using the NEMA IEC body phantom. All Images were analysed with Siemens Syngo.Via image software. ***Results:*** Comparing the PSF to non-PSF reconstruction, the Lesion SUV_{max}(SUV-bw), SUV_{mean}(SUV-bw) and volume(cm^3) were all found to be statistically significantly different ($p<0.05$). TLSA was not found to be statistically different ($p>0.05$). All quantitative values in the Liver, with the exception of SUV_{peak} were found to be statistically different ($p<0.05$). PSF modulation did not have a statistically significant impact on any metrics in the spleen with all metrics having a p-value >0.05. Tumour-to-normal tissue ratios were found to be statistically different for both the liver and the spleen ($p<0.05$). In the phantom study volume accuracy was improved with PSF modulation for all sphere sizes. However, even with PSF reconstruction the measured sphere volume was still >50% of the actual volume for spheres ≤ 2.8cm^3. PSF modulation resulted in improved SUV accuracy for all spheres compared to non-PSF reconstruction. However, even with PSF reconstruction the SUV_{mean} and SUV_{max} values were underestimated by >40% and >25% respectively, for volumes ≤ 2.8cm^3. ***Conclusion:*** Our results demonstrated that PSF-based reconstruction significantly impacted quantitative PET values, emphasising the need for a consistent, well informed approach when applying PSF techniques in clinical practice. Even when PSF reconstruction was employed partial volume effects were still apparent for volumes ≤ 2.8cm^3. Further results will be presented and their clinical significance discussed. ***References:*** None

OP-842

LM-MLEM for an Ultra-High VoR density PET

P. Encarnação[1], P. M. M. Correia[1], I. F. Castro[2], I. Mohammadi[1], F. M. Ribeiro[1], A. L. M. Silva[1], J. F. C. A. Veloso[1]; [1]I3N - Universidade de Aveiro, Aveiro, PORTUGAL, [2]RI-TE, Radiation Imaging Technology, Aveiro, PORTUGAL.

Aim/Introduction: EasyPET.3D is a cost-effective benchtop PET system using a patented method based on a 2-axes rotation of 2 detector modules achieving a very high spatial resolution and sampling with only a small number of cells. Since modules are always face-to-face, parallax errors are strongly reduced achieving high uniformity[1]. Due to its unique scanning method, a fine sampling granularity is achieved and more than 2600 million different positions can be detected, which requires new image reconstruction algorithm and computation strategies. List-mode (LM) based image reconstruction, implemented on graphical

processing units (GPU), has been achieving a significant importance in the last few years mainly due to its speed gain. Compared with other methods LM has several advantages, such as preserving the temporal sampling and ensuring the highest spatial sampling available for a given detector geometry[2].This work aims to develop a dedicated LM-MLEM/OSEM image reconstruction algorithm capable of ensuring a correct detector geometry description and speed reliability. ***Materials and Methods:*** A dedicated GPU-based LM-MLEM/OSEM algorithm was developed using a GPU GTX 1060 and a CPU core i7(8700) for EasyPET.3D data. In this algorithm, the correct modelling of the PET system is a critical factor for its imaging performance. Due to the uncommon large size of the EasyPET.3D system response matrix, the probability density function of each VoR (volume of response) is calculated on the fly. The system sensitivity and attenuation corrections were also included. In order to validate the algorithm, real and simulated (GATE) data from quality control phantoms (NEMA NU 4-2008) were used and filled with ^{18}F-FDG, as well as phantoms consisting of uniform cylinders filled with ^{18}F-FDG and ^{22}Na point-like sources. All data was reconstructed with different iterations and voxel sizes and was filtered with a 340-720 keV energy window. ***Results:*** A spatial resolution of about 1 mm, uniform in all the FOV, was oobtained accordimg to NEMA standards. The algorithms performance is currently being evaluated to define the best set of parameters for mice imaging. This includes image quality measurements such as SNR, PSNR, NCC and MSE. Image reconstructed results of the mentioned phantoms together and with in vivo Balb/c mice (20g) injected with 18F-NAF bone tracer and 18F-FDG will be presented. ***Conclusion:*** The reconstruction method was successfully applied to the complex geometry of easyPET.3D, resulting in high quality images of phantoms and Balb/c mice in preclinical studies. ***References:*** 1 - Patent WO2016/147130Al2 -Autret, A et al, hal-01006117

OP-843

Evaluation of Monte Carlo based reconstruction concerning visual assessment of liver metastases in ^{111}In-octreotide SPECT/CT imaging

E. Wikberg[1], M. van Essen[2], T. Rydén[1], J. Svensson[3], P. Gjertsson[2], P. Bernhardt[1];
[1]Institute of Clinical Sciences, Gothenburg, SWEDEN, [2]Department of Clinical Physiology, Sahlgrenska University Hospital, Gothenburg, SWEDEN, [3]Department of Oncology, Sahlgrenska University Hospital, Gothenburg, SWEDEN.

Aim/Introduction: Early cancer detection is crucial for patients' survival. Improvement of the image quality in ^{111}In-octreotide SPECT imaging can be accomplished using Monte Carlo (MC) based reconstruction. The aim of this observer study was to determine the detection rate of simulated liver metastases for MC based OSEM reconstruction compared to conventional attenuation corrected OSEM reconstruction. ***Materials and Methods:*** 37 SPECT/CT examinations with ^{111}In-octreotide (Octreoscan) where randomly chosen. The inclusion criteria were no liver metastases at the time of examination and three years forward. 26 SPECT images of spheres, radii 2.21 mm, representing metastases were simulated using MC. Raw data of the spheres were added to rawdata of the established healthy patients in 26 of the examinations (the remaining 11 patients were unchanged) and thereafter reconstructed using two different methods. The conventional reconstruction method was iterative reconstruction with attenuation correction, AC-OSEM. The other method was Sahlgrenska Academy Reconstruction Code where MC simulations were used in the forward projection of the OSEM algorithm (MC-OSEM). Two filters were used, a butterworth low-pass filter for AC-OSEM and a gaussian low-pass filter for MC-OSEM. MC-OSEM was also used unfiltered. Hence 37 SPECT/CT examinations (26 with a simulated liver metastasis and 11 healthy) were reconstructed and placed in three groups (AC-OSEM+filter, MC-OSEM+filter and MC-OSEM without filter). The 111 (37x3) images were visually evaluated by a nuclear medicine specialist, unaware of whether or not the patient had liver metastases or what type of reconstruction method or filter was used. Criteria evaluated were liver metastasis yes or no with confidence level 1-3. The image quality was evaluated on a scale of one to five and the presence of artifacts was evaluated as yes or no. If liver metastasis was judged being present the coordinates were requested so that the accuracy of the position could be evaluated. ***Results:*** The sensitivity and specificity were 30.8% and 81.8% for AC-OSEM+filter, 42.3% and 54.5% for MC-OSEM+filter and 50.0% and 63.6% for MC-OSEM. The observer's confidence level was highest in AC-OSEM+filter. Regarding the image quality it was rated higher in AC-OSEM+filter and MC-OSEM+filter than in MC-OSEM. ***Conclusion:*** One in two metastases were found using MC-OSEM versus one in three using conventional reconstruction. However, the specificity, confidence level as well as image quality were all lower for MC-OSEM. New reconstruction methods generate different-looking images and it is important that there is time to get used to these images before eventual method modification. ***References:*** None

OP-844

Towards a comprehensive validation of a Monte Carlo simulation for clinical SPECT acquisition protocol optimisation and image correction

S. Pells[1,2], D. M. Cullen[1], A. P. Robinson[2,1,3], B. Pietras[1], N. Calvert[3], D. Deidda[2], A. Fenwick[2,4], K. Ferreira[2], D. Hamilton[3], W. Heetun[2], P. Julyan[3], G. Needham[1], E. Page[1,3], E. Price[1], J. Tipping[3];
[1]The University of Manchester, Manchester, UNITED KINGDOM, [2]The National Physical Laboratory, Teddington, UNITED KINGDOM, [3]The Christie NHS Foundation Trust, Manchester,

UNITED KINGDOM, [4]Cardiff University, Cardiff, UNITED KINGDOM.

Aim/Introduction: Monte Carlo (MC) simulations are a valuable tool for the optimisation of acquisition protocols and image corrections in Single-Photon Emission Computed Tomography (SPECT). Simulations allow direct gamma tracking and show all interactions that occur during acquisition. They offer an unparalleled insight into processes that are not directly experimentally observable such as scatter and attenuation within the acquisition. As the need for quantitative SPECT becomes increasingly important for dosimetry calculations, accurate image corrections are essential, and their methodologies are increasingly based on results from MC. Whilst MC is often used to provide a 'ground-truth', this is only the case if the simulation is fully validated against experimental data. This is a vital part of confirming the performance of new scanners. This work aims to establish a validation protocol for MC SPECT simulations. ***Materials and Methods:*** A full MC simulation of the triple-head SPECT system installed at the National Physical Laboratory has been developed in the GATE (Geant4 Application for Tomographic Emission) [1] tool-kit. The simulation extensively models the components of each detector head and a range of collimators according to technical specifications provided. The simulation can run in both dual- and triple-head acquisition modes. Validation data has been collected in a range of geometries, including commercial and 3D-printed phantoms, for multiple therapeutic and diagnostic isotopes. ***Results:*** Experimental and simulated data have been compared for both the dual- and triple-head acquisitions, providing validation for all key experimental observables for a range of therapeutic and diagnostic isotopes. ***Conclusion:*** The validation procedure has demonstrated that the MC simulation accurately reproduces SPECT data. The validated simulation will be used to optimise clinical imaging protocols and image corrections, including for novel radioisotopes such as Tb-155 and Tb-161 where low availability of isotopes limits experimental studies. ***References:*** [1] Jan S. 2004, 49:4543-61 Phys. Med. Biol.

OP-845

Data-Driven Respiratory SPECT-Gating for Pre-Radio-Embolization Determination of Liver-Lung-Shunt Fraction

P. Ritt[1], *K. Seidl*[1], *M. Cachovan*[2], *A. H. Vija*[3], *T. Kuwert*[1]; *[1]Clinic for Nuclear Medicine, Erlangen, GERMANY, [2]Siemens Healthcare GmbH, Molecular Imaging, Forchheim, GERMANY, [3]Siemens Medical Solutions USA, Inc., Molecular Imaging, Hoffman Estates, MI, UNITED STATES OF AMERICA.*

Aim/Introduction: In hepatic radio-embolization, lungs are at risk of substantial radiation damage if resulting in a too high deposition of radioactive particles in lungs. For assessing this risk, each patient undergoes pre-therapeutic simulation with e.g. Tc-99m-macro-aggregated albumin in order to determine liver-lung-shunt fraction (LLSF). Depending on extent of LLSF, injected activity could be adapted or therapy even be precluded. ***Materials and Methods:*** As part of pre-radio-embolization work-up, n=12 patients (age 65 ± 11, BMI 24.8 ± 3.6) underwent SPECT/CT scans on a Siemens Symbia T2 system after intra-hepatic injection of Tc-99m-MAA (~150 MBq). SPECT was carried out in step-and-shoot fashion (60 views, 2 projections per view, 15 s dwell time per view) using LEHR collimators and a body-contouring scan. Patients were allowed to breathe freely during SPECT acquisition. Immediately following SPECT, a CT scan was carried out (130 kVp, 30 mAs effective). SPECT/CT consisted of a single bed-position (~40 cm axial field of view) and was set to include whole liver and as much of lungs as possible. Using research software, SPECT projection data was acquired in listmode format and retrospectively framed into four time bins representing different respiratory states. Gated SPECT data were reconstructed using ordered-subset conjugate-gradient algorithm (1 subset, 24 iterations). Only corrections for scattered radiation (dual energy window) were applied. Additionally, also ungated SPECT data was reconstructed, which represents projection data averaged over the whole acquisition time. Liver and lung compartments were manually segmented on CT. SPECT counts were extracted for gated and ungated data and LLSFs were computed. ***Results:*** Average segmented liver and lung volumes were 2111 ± 695 mL (ranging 980 - 3433 mL) and 1707 ± 657 mL (954 - 2769 mL). Average LLSF was 5.4 ± 2.9 % (1.5 - 11.2 %) for gated and 6.2 ± 2.3 % (2.1 - 9.6 %) for ungated data. The span, which here is the range from maximum to minimum LLSF of gated data for one individual patient, was 2.6 ± 3.0 % (0.2 - 9.1 %) in absolute units, which is equivalent to 46.1 ± 43.0 % (4.0 - 141.1 %) when expressed in percentages relative to mean LLSF. ***Conclusion:*** Data-driven respiratory gating of SPECT data is feasible. Respiratory movements lead to a bias, which could potentially lead to under- or overestimation of LLSF. Studies with an increased patient number will be carried out in order to determine relevancy in clinical practice. ***References:*** None

1507

Teaching Session 6: Difficult Cases in Cardiac Imaging

Friday, October 30, 2020, 10:40 - 12:10 Channel 7

OP-846

SPECT Myocardial Perfusion Imaging

R. Calabretta*; Division of Nuclear Medicine, Department of Biomedical Imaging and Image-guided Therapy,*

Medical University of Vienna, Vienna, AUSTRIA.

OP-847

PET Myocardial Perfusion Imaging

***J. Sörensen**; Radiology, Department of Surgical Sciences, University Hospital, Uppsala Unversity, Uppsala, SWEDEN.*

OP-848

PET in Inflammation/Infection

***B. Mahida**; Nuclear Medicine Department, Bichat Claude Bernard Hospital, Assistance Publique Hôpitaux de Paris (AP-HP), Paris Diderot University, Paris, FRANCE.*

OP-849

Cardiovascular Hybrid Imaging

***T. Maaniitty**; Department of clinical physiology, nuclear medicine and PET, Turku University Hospital, Turku, FINLAND.*

1508

Clinical Oncology Track - Featured Session: Prostate Cancer Therapy - PSMA, 223Ra and More...

Friday, October 30, 2020, 10:40 - 12:10 Channel 8

OP-851

Positioning PSMA-RLT in the Urooncologial Treatment Pathway

***B. Hadaschik**; Universitätsklinikum Essen, Urology, Essen, GERMANY.*

OP-852

Efficacy and Safety of ^{225}Ac-PSMA-617 Targeted Alpha Therapy in Metastatic Castration-Resistant Prostate Cancer Patients

***M. Yadav**, S. Ballal, C. Bal;*
All India Institute of Medical Sciences, New Delhi, INDIA.

Aim/Introduction: Metastatic castration-resistant prostate cancer (mCRPC) patients develop disease progression in spite of several current standard of care treatment offered. Managing these patients are currently challenging. Thus, there is need of new therapy options that induce anti-tumor activity and improve survival. The objective of this study was to assess the safety and therapeutic efficacy of ^{225}Ac-PSMA-617 targeted alpha therapy (TAT) in mCRPC patients in real world conditions. ***Materials and Methods:*** All consecutive mCRPC patients refractory to therapy options, including first and second-generation anti-androgen therapies, taxane-based chemotherapies, and ^{177}Lu-PSMA-617 therapy, were treated with ^{225}Ac-PSMA-617 TAT (100 KBq/Kg body weight) at an 8-weekly interval. The primary endpoint included the assessment of biochemical response by measuring the serum prostate-specific antigen (PSA) response rate as per the PCWG3 criteria. Secondary endpoints comprised the estimation of overall survival (OS), progression-free survival (PFS), molecular tumor response assessment (PERCIST 1 criteria), disease control rate, toxicity according to CTCAE v5.0, and clinical response evaluation. ***Results:*** Total 28 patients were recruited for this cohort study. The mean age was 69.7 years (range: 46-87 years). All patients, except one, had extensive skeletal metastases on baseline ^{68}Ga-PSMA-11 PET/CT scan; one patient had lymph node dominant disease and advance primary prostatic tumor. The mean activity administered was 26.5 ± 12 MBq (range: 9.25 - 62.9 MBq) [715.5 ± 327 µCi, range: 250 - 1700 µCi] with a median of 3 cycles. After the initial follow-up and the end of the assessment, >50% decline in PSA was observed in 25% and 39%, respectively. The median PFS and OS were 12 months (95% CI: 9 - 13 months) and 17 months (95% CI: 13 - 16 months), respectively. Molecular tumor response by PERCIST 1 criteria could be conducted in 22/28 (78.6%) patients, which revealed complete response in 2/22 (9%), partial response in 10/22 (45.4%) patients, 2/22 (9%) with stable disease, and 8/22 (36%) with progressive diseases. The disease control rate, according to the biochemical and molecular tumor response criteria, was 63.4%. Multivariate analysis revealed PSA progression and any PSA decline as prognostic indicators of OS and PFS, respectively. There was no Grade III/IV toxicity noted in this series. ***Conclusion:*** ^{225}Ac-PSMA-671 TAT showed promising disease control rate, even when all other therapeutic options were exhausted, with low treatment-related toxicities ***References:*** None

OP-853

Effects of one cycle of Actinium-225-PSMA-617 (AcPSMA) on the salivary glands compared to Lu-177-PSMA (LuPSMA)-prelimary results

***B. Feuerecker**[1,2], A. Gafita[1], R. Tauber[3], C. Seidl[1], F. Bruchertseifer[4], M. Retz[3], J. E. Gschwend[3], W. A. Weber[1], C. D'Alessandria[1], A. Morgenstern[4], M. Eiber[1];*
[1]Technical University of Munich, School of Medicine, Department of Nuclear Medicine, München, GERMANY, [2]German Cancer Consortium (DKTK), partnersite München, Heidelberg, GERMANY, [3]Technical University of Munich, School of Medicine, Department of Urology, München, GERMANY, [4]European Commission, Joint Research Centre, Directorate for Nuclear Safety and Security, Karlsruhe, GERMANY.

Aim/Introduction: ^{225}Ac-PSMA is a compassionate use treatment option in metastatic castration resistant prostate cancer (mCRPC) after failure of approved drugs and ^{177}Lu-PSMA. Xerostomia has been reported to be a relevant side effect of AcPSMA treatment impacting quality of life. The aim of this retrospective analysis was to assess the effects of one cycle of AcPSMA on the salivary glands using data from

pre- and post PSMA-PET/CT imaging and compare it to possible changes induced by previous LuPSMA treatment. ***Materials and Methods:*** In 18 patients with late stage mCRPC PSMA ligand uptake (16 PSMA-PET/CT, 2 PSMA/PET/MRI) and morphologic changes (CT/MRI) were retrospectively analyzed after one cycle of AcPSMA (9.0 MBq ± 1.6) and in 11 of these patients before and after a median of 2 cycles of LuPSMA (7346 MBq ± 529; 11 PSMA PET/CT). PSMA ligand uptake of the parotid and submandibular glands were quantified using qPSMA, the volume was measured slice based on CT/MRI. ***Results:*** Mean volume of the salivary glands was 50±13 ccm before and 39±11ccm after AcPSMA treatment (- 23% mean volume reduction). Mean PSMA-TV was 68±25 ccm before and 40±15 ccm after AcPSMA treatment (-40%). For LuPSMA mean CT volume of the salivary glands was 62±14 ccm before and 52±12 ccm after LuPSMA treatment (-13% mean volume reduction). Mean LuPSMA PSMA-TV of the salivary glands was ca. 89±16 ccm before and 78±21 after treatment (-11%). ***Conclusion:*** Volume and PSMA-uptake of salivary glands decrease both after LuPSMA and AcPSMA. However, the effect of one cycle AcPSMA is almost 4 times higher compared to 2 cycles LuPSMA which might be a potential correlate for its relevant xerostomia. Additional investigations including salivary gland scintigraphy and measurement of saliva gland production might help to further elucidate the differences between xerostomia after LuPSMA and AcPSMA. ***References:*** None

OP-854

Ac-225-PSMA I&T in patients with end stage mCRPC: First clinical results

M. Zacherl*, F. J. Gildehaus, A. Gosewisch, P. Bartenstein, A. Todica, H. Ilhan;*
University of Munich, Munich, GERMANY.

Aim/Introduction: After failure of approved therapy options, although several agents are available, end stage metastatic castration resistant prostate cancer (mCRPC) remains challenging. Radioligand therapy (RLT), using β- and α-emitter labeled PSMA-inhibitors, have been introduced with promising results. Here we present the first early clinical data for PSMA-directed α-therapy using Ac-225-PSMA I&T. ***Materials and Methods:*** 17 patients receiving Ac-225 PSMA I&T RLT between 08/18 and 12/19 have been included in this retrospective analysis. All but one patient had received second line antihormonal treatment using abiraterone and/or enzalutamide. 15 patients received prior chemotherapy. In 14 patients RLT using Lu-177-PSMA-ligands was performed prior to Ac-225 PSMA-ligandtherapy (median 2 cycles, rang 1-5). PSMA PET/CT was performed in all patients prior to Ac-225-PSMA I&T therapy to assess PSMA-expression in tumor lesions. Patients were treated at 7-8 weekly intervals until progression or intolerable side effects. Prostate-specific antigen (PSA) and blood cell count were measured every 2-3 weeks. We evaluated hematological and non-hematological side effects according to CTCAE 4.0 criteria and biochemical response. ***Results:*** A total of 33 cycles of Ac-225-PSMA I&T (median dose 7.8 MBq, range 6.7-8.2) were applied. 6 patients received 1 cycle, 7 patients 2 cycles, 3 patients 4 cycles and 1 patient 5 cycles. No acute toxicity was observed at the time of hospitalization. Baseline PSA was 228 ng/ml (range 13.4 - 1146). 5/17 patients had no follow-up and were excluded from the further study. 6/12 patients had a PSA-decline of more than 50%, 3/12 patients a decline of 40-50% and 2/12 patients a decline between 20-30%. Two patients had no PSA-decline at any time. Mild xerostomia (grade 1/2) was observed in 11 patients. Severe xerostomia (grade 3) was observed in 1 patient. No patient developed a new renal insufficiency. 6/12 patients had a grade 3-4 anemia. ***Conclusion:*** In this small cohort Ac-225-PSMA I&T RLT showed antitumor effect in end stage mCRPC even after failure of Lu-177 PSMA-ligand therapy in more than 40%. Grade 3/4 hematological side effects in 50% of patients and Grade 1-2 xerostomia in 11/12 patients indicate moderate tolerability in this heavily pretreated end stage patient group. These results are comparable to data for Ac225 PSMA-617 after failure of Lu-177 therapy. ***References:*** None

OP-855

Multicenter retrospective Study: Validation of the 3-variable prognostic score (3-PS) in a population with metastatic castration resistant prostatic cancer treated with Radium223-dichloride

C. De Angelis[1]*, F. Monari*[2]*, M. Mascia*[3]*, R. Costa*[4]*, G. Rubini*[5]*, A. Spanu*[6]*, A. Di Rocco*[7]*, E. Lodi Rizzini*[8]*, L. Cindolo*[9]*, M. Licari*[4]*, G. Santo*[5]*, S. Nuvoli*[6]*, V. Frantellizzi*[1]*, V. Dionisi*[2]*, C. Ferrari*[5]*, G. De Vincentis*[1]*;*
[1]Department of Radiological Sciences, Oncology and Anatomical Pathology, "Sapienza" University of Rome, Rome, ITALY, [2]Radiation Oncology Center, S Orsola-Malpighi Hospital, Bologna, ITALY, [3]Unit of Nuclear Medicine, "Spirito Santo" Hospital, Pescara, ITALY, [4]Unit of Nuclear Medicine, Biomedical Department of Internal and Specialist Medicine, University of Palermo, Palermo, ITALY, [5]Nuclear Medicine Department, University of Bari "Aldo Moro", Bari, ITALY, [6]Unit of Nuclear Medicine. Department of Medical, Surgical and Experimental Sciences. University of Sassari, Sassari, ITALY, [7]Department of Public Health and Infectious Diseases, "Sapienza" University of Rome, Rome, ITALY, [8]Nuclear Medicine Unit, S Orsola-Malpighi Hospital, Bologna, ITALY, [9]Department of Urology, "Villa Stuart" Private Hospital, Rome, ITALY.

Aim/Introduction: Since its introduction in clinical practice for metastatic Castration Resistant Prostatic Cancer (mCRPC) and bone metastasis, Radium-223 treatment has been proven to have not only a positive effect on pain but it can also increase overall survival (OS). However, several studies

are highlighting the fact that patient's baseline conditions are fundamental in order to maximize Radium-223 effects prolonging OS. Several studies tried to individuate a prognostic marker to better stratify patients eligible to Radium-223 treatment. Still, to date clinicians lack a valid and simple tool that allows a better selection of patients before starting therapy with this α-emitting radionuclide. A study conducted in 2017 proposed a 3-variable prognostic score (3-PS) using baseline Hemoglobin (Hb), baseline Prostatic Specific Antigen (PSA) and Eastern Cooperative Oncology Group Performance Status (ECOG PS) to stratify patients in five prognostic groups, each one with a different and specific predicted OS. The aim of this retrospective multicentric study was to validate the 3-PS score. ***Materials and Methods:*** 430 patients with mCRPC under treatment with Radium-223 were enrolled from six Italian centers. The 3-PS was firstly applied to the entire population (TOTAL group). Secondly, 92 patients from the 2017 3-PS study were subtracted from the TOTAL group (CLEAN group). The score was applied to this purified subgroup to furtherly validate the score. The prognostic significance of the scores was evaluated via time-dependent receiver operating characteristic (ROC) curves in the CLEAN GROUP. ***Results:*** The area under curve (AUC) estimated (0.74) falls within the confidential interval (CI) of the AUC calculated on the validation groups. In fact, the validity of the 3-PS score was confirmed on the TOTAL group as well as in the CLEAN group [95% CI 0.66 - 0.82]. ***Conclusion:*** This multicentric study confirms the validity, the simplicity and the applicability of the 3-PS score on patients with mCRPC. This tool can be used in clinical practice to select patients that will most probably benefit from Radium-223 treatment and to predict and assess OS. ***References:*** None

OP-856

Do the number of previous treatments and bone metastases impact Radium-223 therapy efficacy in mCRPC patients? A multicentre study

V. Lavelli[1], *V. Frantellizzi*[2], *E. Lodi Rizzini*[3], *M. Licari*[4], *L. Cindolo*[5], *M. Stazza*[6], *A. Nappi*[1], *M. Pontico*[2], *V. Dionisi*[7], *C. Ferrari*[1], *A. Spanu*[6], *M. Mascia*[8], *R. Costa*[4], *F. Monari*[7], *G. De Vincentis*[2], *G. Rubini*[1]; [1]*Nuclear Medicine Department, University of Bari "Aldo Moro", Bari, ITALY,* [2]*Department of Radiological Sciences, Oncology and Anatomical Pathology, Sapienza, "Sapienza" University of Rome, Rome, ITALY,* [3]*Nuclear Medicine Unit, S.Orsola-Malpighi Hospital, Bologna, ITALY,* [4]*Unit of Nuclear Medicine, Biomedical Department of Internal and Specialist Medicine, University of Palermo, Palermo, ITALY,* [5]*Department of Urology, "Villa Stuart" Private Hospital, Rome, ITALY,* [6]*Unit of Nuclear Medicine. Department of Medical, Surgical and Experimental Sciences. University of Sassari, Sassari, ITALY,* [7]*Radiation Oncology Center, S.Orsola-Malpighi Hospital, Bologna, ITALY,* [8]*Unit of Nuclear Medicine, "Spirito Santo" Hospital, Pescara, ITALY.*

Aim/Introduction: 223Radium-dichloride (Ra223)-therapy was approved for mCRPC patients with symptomatic bone metastases (BM) and no visceral involvement and scheduled with six intravenous injections every four weeks. Its clinical use was restricted since July 2018 to patients with at least two previous systemic treatments or without other therapeutic options and not recommended with a low burden of osteoblastic BM.We aimed to evaluate if the number of previous treatments and/or BM can impact Ra223-therapy completion and efficacy. ***Materials and Methods:*** We retrospectively evaluated 334 mCRPC patients (mean age 73y, range: 50-90), who received Ra223 between September 2013 and July 2019 in six Italian centres. We evaluated the association between two of current eligibility patient criteria (≥2 previous systemic treatments and ≥6 BM) and the completion of Ra223-therapy as well as its efficacy. Particularly, Ra223-therapy efficacy was measured as biochemical response (≤ ALP-post-therapy vs baseline), clinical response (< pain post-therapy vs baseline, assessed by Brief Pain Inventory-Short Form), instrumental response (partial response or stable disease at post-therapy Bone Scan vs baseline) and survival (alive vs dead patients). Both evaluations were calculated by using contingency tables and Chi-Square test. ***Results:*** 141/334 (42%) patients met current eligibility criteria, of which 80/141 (57%) completed Ra223 therapy; 193/334 (58%) patients did not meet these criteria, of which 121/193 (63%) completed Ra223 therapy. There was no statistically significant association between eligibility criteria and the completion of 223Ra-therapy ($\chi2=1.206$, $p=0.272$). As regarding treatment efficacy, the association with eligibility criteria resulted statistically significant only for instrumental response, in particular for the number of previous treatments ($\chi2=7.570$, $p=0.006$).In addition, a statistically significant association was found between the completion of Ra-223 therapy and biochemical ($\chi2=16.904$, $p<0.005$) and instrumental ($\chi2=5.002$, $p=0.025$) response as well as survival ($\chi2=19.546$, $p<0.005$). Conversely, even if no statistically significant association was found between the completion of Ra-223 therapy and clinical response ($\chi2=1.680$, $p<0.195$), pain reduced in a significant percentage of patients who completed treatment (65%). ***Conclusion:*** Our multicenter experience confirmed the efficacy of Ra223-therapy in patients who completed the six scheduled doses of treatment. The current use of Ra223 allows treating mainly advanced-disease patients. Our results suggest that neither ≥2 previous systemic treatments nor ≥6 BM impacts on both Ra223-therapy completion or efficacy. However, multi-treated patients showed worse response to Ra223-therapy, regardless of the number of doses received. ***References:*** None

OP-857

Overall survival in elderly mCRPC patients treated with Radium-223: a national multicenter study

V. Lavelli[1], L. Cosma[2], F. Monari[3], M. Mascia[4], R. Costa[5], G. Rubini[1], A. Spanu[6], A. Farcomeni[7], E. Lodi Rizzini[8], L. Cindolo[9], A. Murabito[5], S. Nuvoli[6], V. Frantellizzi[2], V. Dionisi[3], A. Nappi[1], G. De Vincentis[2]; [1]Nuclear Medicine Department, University of Bari "Aldo Moro", Bari, ITALY, [2]Department of Radiological Sciences, Oncology and Anatomical Pathology, "Sapienza" University of Rome, Rome, ITALY, [3]Radiation Oncology Center, S.Orsola-Malpighi Hospital, Bologna, ITALY, [4]Unit of Nuclear Medicine, "Spirito Santo" Hospital, Pescara, ITALY, [5]Unit of Nuclear Medicine, Biomedical Department of Internal and Specialist Medicine, University of Palermo, Palermo, ITALY, [6]Unit of Nuclear Medicine. Department of Medical, Surgical and Experimental Sciences, University of Sassari, Sassari, ITALY, [7]Department of Economics & Finance, University of Rome "Tor Vergata", Rome, ITALY, [8]Nuclear Medicine Unit, S.Orsola-Malpighi Hospital, Bologna, ITALY, [9]Department of Urology, "Villa Stuart" Private Hospital, Rome, ITALY.

Aim/Introduction: The purpose of this multicentre retrospective study is to analyze metastatic castration-resistant prostate cancer (mCRPC) patients treated with Radium-223 evaluating whether there are differences in overall survival (OS) between young and elderly and verifying efficacy and safety in the very elderly population (patients >75 years old). ***Materials and Methods:*** In our study 430 mCRPC patients treated with Radium-223 in six Italian Centres were examined.Clinical and diagnostic patients' characteristics were gathered at baseline and after each cycle of Radium-223: blood biochemical parameters, pain by Numeric Rating Scale (BPI) and ECOG-PS. Bone scintigraphy was performed before starting treatment, after the third cycle and at the end of therapy. All patients, according to their age (≤75 years old and >75 years old), were divided into two groups. Moreover we considered other clinical covariates: BMI, Gleason score, ECOG-PS, baseline hemoglobin, prostate specific antigen, total alkaline phosphatase, lactate dehydrogenase, platelets, absolute neutrophil counts. Our main endpoint was the evaluation of the overall survival (OS). Survival distributions were calculated using the Kaplan-Meyer product-limit estimator and compared using the log-rank test. The association of predictors with OS was evaluated by means of univariate Cox regression models. A multivariable Cox regression model was then selected using a stepwise forward procedure based on Akaike Information Criterion. ***Results:*** 51% of the patients were ≤75 years old and 49% were >75 years old. Considering those subjects with similar basal parameters, OS did not show significant differences between the two groups. Age had no significant impact on the OS (p=0.274) in multivariate models. The evaluation of clinical covariates in univariate models (p<0.05) showed that several of the examined clinical aspects had an impact on OS, but not age (p=0.072). Moreover, the toxic effects, in terms of hematological or symptomatic skeletal events, were few and similar in the two groups, continuing to guarantee the safety of Radium-223 even in very elderly patients. ***Conclusion:*** The management of elderly patients should not be based on age but on their health status. Radium-223 is well-tolerated and characterized by low rates of adverse effects and for these reasons it is suitable for treatment of younger and even more for older, frails and vulnerable patients. As demonstrated in our study, at the same baseline condition Radium-223 prolongs survival in both younger and older patients and is a good choice in the mCRPC setting compared to other agents, especially for men unsuitable for cytotoxic chemotherapy. ***References:*** None

OP-858

The effect of tumor burden in ^{68}GA-PSMA-PET/CT on tracer uptake into kidneys in ^{68}Ga-PSMA-PET/CT and the absorbed dose per administered GBq ^{177}Lu-PSMA-617 during a following therapy

J. Wichert*, C. Happel, W. T. Kranert, D. Gröner, J. Baumgarten, C. Nguyen Ngoc, N. Mader, S. Banek, F. Grünwald, A. Sabet; Goethe University Hospital Frankfurt, Frankfurt, GERMANY.*

Aim/Introduction: In patient therapy with Lu-177-PSMA-617, kidneys are regarded as dose limiting organs. We explored if the tumor load in pretherapeutic Ga-68-PSMA-PET/CT had an effect on the SUV-parameters of the kidneys and if it could be used as a predicting factor to dose to kidney/GBq Lu177-PSMA in a following therapy cycle. ***Materials and Methods:*** 265 kidneys in 152 patients with mCRPC who underwent a Ga-68-PSMA-11 PET/CT-baseline scan prior to the start of the Lu-177-PSMA-617 were analyzed. Tumor load was categorized as minor (n=31), intermediate (n=47) or high (n=74), based on miTNM classification (PROMISE). The relation of Ga-68-PSMA-uptake in the kidneys and tumorburden were checked. We evaluated the relation between SUV-parameters of each kidney and the absorbed dose / GBq Lu-177-617-PSMA after the first administration of Lu-177-PSMA-617 therapy to see if a correlation between the two parameters exists. We also compared tumorload and the dose to the kidneys/ GBq Lu-177-617-PSMA in the following cycle. The correlation was tested using nonparametric testing. ***Results:*** We compared the PET parameters with the kidney dose/ GBq Lu-177-PSMA in the following cycle. Looking at all patients, SUVmax (36+-15), SUVmean (24+-10), SULmax (26+-10) and SULmean (18+-7) ranged widely. All four parameters showed a strong negative correlation to the tumor burden in the PET-scan (P-values between: SUVmax/tb: 0,009; and SULmean/tb: 0,001). When comparing the groups, we found ~10% higher tracer uptake in patients with low tumor load and 30-35% lower tracer uptake in patients with higher tumor

load, both compared to intermediate load. All four PET parameters showed a strong positive correlation to the kidney dose/ GBq Lu177-PSMA in the first PET (P-values: SUVmax/Gy/GBq: <0,001; SUVmean/Gy/GBq: <0,001; SULmax/Gy/GBq: <0,001; SULmean/Gy/GBq: <0,001). Die kidney dose per GBq Lu-177-617-PSMA for all patients had an average of 0,277 Gy. When comparing the groups, we found in average a ~3,5% lower dose per GBq Lu-177-617-PSMA in patients with minor burden, and a ~9,5% lower dose per GBq Lu-177-617-PSMA in patients with high, both compared to intermediate burden . ***Conclusion:*** Tumor load correlates negatively with the SUV parameters in baseline PET/CT which in turn is associated with the absorbed dose/GBq Lu-177-PSMA. Further, a high tumor burden in the primary PSMA-PET-scan correlates with a lower dose to the kidneys per GBq Lu-177-617-PSMA in the following cycle. This finding encourages the consideration of higher activities of Lu177-PSMA in patients with high tumor load and low SUV-parameters in baseline PET-scan. ***References:*** None

OP-859

Prediction of therapy response in PSMA radioligand therapy with PSMA PET/CT

F. Völter*, A. Gosewisch, L. Kaiser, F. Gildehaus, A. Todica, P. Bartenstein, G. Böning, H. Ilhan;*
Ludwig-Maximilian-Universität, München, GERMANY.

Aim/Introduction: Prediction of therapy efficacy is of great importance in PSMA-based radioligand therapy (RLT). The purpose of this investigation was to assess the value of pretherapeutic Ga^{68}-PSMA-11 PET as a predictive marker for therapy efficacy and dosimetry in mCRPC patients receiving ^{177}Lu-PSMA-617. ***Materials and Methods:*** Pretherapeutic SUVmean and SUVmax in Ga^{68}-PSMA-11 PET were correlated with absorbed doses pre injected activity for 40 patients (age 72,9±9,7) and 211 tumor lesions. The administered activity of Lu^{177}-PSMA was 6.0 GBq in 35 and 3.7 GBq in 5 patients. Absorbed dose of the tumor lesions were analyzed with dose maps providing voxelwise dose distribution using quantitative 3D SPECT 24, 48 and 72 hours after injection of ^{177}Lu-PSMA. Correlation was analyzed with Pearson's correlation analysis. ***Results:*** SUVmean and SUVmax showed a broad range in bone (SUVmean 20.5±31.5; SUVmax 30,8±21.2) and lymph node metastases (SUVmean 20.9±16.0; SUVmax 37.2±53,4). Mean absorbed dose was 5.94±13.6 Gy/GBq in bone and 5.5±8.9 in lymph node metastases. There was a strong correlation of absorbed dose and pretherapeutic SUVmean (r=0.86) as well as pretherapeutic SUVmax (r= 0.7) in bone metastases. Lymph node metastases showed a strong correlation of SUVmean and absorbed dose (r=0.7) and a moderate correlation of SUVmax and absorbed dose (r=0,64). There was no correlation between PSA levels and SUVmean or SUVmax or absorbed dose. ***Conclusion:*** The strong correlation of pretherapeutic SUVmean and SUVmax with absorbed dose shows that pretherapeutic PSMA-PET can be used to predict therapy efficacy in ^{177}Lu- PSMA Radioligand therapy. ***References:*** None

OP-860

Clinical outcome of radioligand therapy with Lu-177 PSMA in metastatic prostate cancer: An initial experience from a tertiary care cancer hospital

M. Gupta[1,2]*, P. Choudhury*[1]*, G. Karthikeyan*[3]*, V. Talwar*[1]*, S. Rawal*[1]*;*
[1]Rajiv Gandhi Cancer Institute and Research Centre, Delhi, INDIA, [2]Amity Center of Radiation Biology, Amity University, Noida, INDIA, [3]Amity Institute of Virology and Immunology, Amity University, Noida, INDIA.

Aim/Introduction: Metastatic castration resistant prostate cancer (mCRPC) is an inevitable stage in management of prostate cancer. Eventually, all advanced prostate cancer patients developed resistant to known standard drugs and most of them land up with rising PSA, high volume of disease and diffuse bone pain. Hence, novel drugs with better efficacy are in-desired for patients' palliation. One such possible hope to these patients is to use 'Theranostic' approach using prostate specific membrane antigen (PSMA) as target. In this study, we analysed the clinical outcome of Lu177-PSMA in mCRPC patients in Indian population. ***Materials and Methods:*** Twenty five mPCs patients were treated with Lu177-PSMA on compassionate basis. Pre and 8-10 weeks post treatment PSA, Eastern cooperative oncology group (ECOG) performance status, Visual analogue scale (VAS) and Analgesic quantification scale (AQS) were recorded for clinical outcome. Based on three PSA response groups (partial response PR, stable disease SD, progressive disease PD), patients were categorized into responder (PR+SD) and non-responder (PD).Wilcoxon signed-rank, and Kruskal-Wallis test, Kaplan Meier with Log rant test were computed by MedCalc Statistical Software version 19.1.5. P value < 0.05 was considered statistically significant. ***Results:*** Twenty five mPCa patients with median gleason score 8.3 (range 7-10) with median 69 years of age (range 45-81) were treated with median 7.4 GBq (range 3.7-7.7 GBq) Lu177-PSMA. Overall PR, SD and PD were 24%, 60% and 16% respectively. Sixteen patients who received ≥ 7.4GBq Lu177-PSMA dose, PR and SD were seen in 31.2% and 68.8% respectively. We had 84% responders and 16% non-responders. Statistically significant difference (P <0.05) was seen in pre and post ECOG (Z value -2.5), VAS (Z value -3.9) and AQS (Z value -3.5) parameters on Wilcoxon signed-rank test while it was statistical in-significant for PSA (P value 0.170, Z value -1.6). We found that Lu177-PSMA dose was the only significant factor (P 0.024) on Kruskal-Wallis test for PSA response outcome. Overall median PFS was 24 weeks (95% CI: 9-52) in our study. Two years PFS of PR, SD and

PD response group was 50%, 37.3% and 0% respectively. Significant difference was seen in PFS of responder and non-responder groups (P value 0.0003 and Hazard ratio 0.16). ***Conclusion:*** We concluded that Lu177-PSMA was a fair palliative option in heavily per-treated mPCa patients for both pain and PSA response. It has a potential to become valid treatment option for these patients, however proper randomized studies are pending. ***References:*** None

OP-861

Selective Intraarterial Lu-177 PSMA Therapy for Castration Resistant Prostate Cancer: Preliminary Results of a Pilot Study

H. Sayman[1], F. Gulsen[1], S. Sager[1], E. Akgun[1], N. Yeyin[1], S. Bilgic[1], K. Toplutas[1], F. Beytur[1], R. Oklu[2], O. Aras[3];
[1]Istanbul University-Cerrahpasa, Istanbul, TURKEY, [2]Mayo Clinic Arizona, Phoenix, AZ, UNITED STATES OF AMERICA, [3]Memorial Sloan Kettering Cancer Center, New York, NY, UNITED STATES OF AMERICA.

Aim/Introduction: In patients with metastatic castration-resistant prostate cancer undergoing Lu-177 PSMA therapy, we aimed to determine the feasibility and safety of selective intraarterial administration compared with conventional intravenous administration. We further aimed to deliver the higher possible tumor dose in the primary site depending on the receptor density at first pass, without compromising uptake by any distant metastases. ***Materials and Methods:*** Four patients were treated in two visits whereby their total empiric therapeutic dose was divided equally between the two occasions. During the first visit, the first half of the selected dose was given through an intravenous line (IV treatment). One week after, the second half of the selected dose was administered selectively using bilateral internal iliac arteries consecutively (IA treatment); comparing the two treatments within the same patient. Accordingly, confrontation of maximum possible dose rate was established in the first pass of therapeutic agent in the primary cancer. Subsequently, the activity was circulated in consecutive cycles until it reached other possible metastatic sites. We acquired planar whole-body and SPECT/CT scans from prostate and/or metastatic bone lesion sites to calculate the absorbed doses, after both IV and IA applications. An additional acquisition was made just before the IA dose in order to obtain a baseline image that we may calculate leftover activity in tissues from the IV dose for background correction. Freehand ROIs were drawn over the composite image by adding all axial SPECT slices with increased tracer uptake, by anatomic correlation of CT in order to cover the lesions. Additionally, liver, kidneys, bone marrow, prostate and whole-body absorbed doses were also calculated. Lesion-to-liver, lesion-to-bone marrow and lesion-to-whole-body ratios were calculated. None of our patients experienced more than regularly expected side effects within first 8-16 weeks of follow-up and intra-arterial application was tolerated very well in all patients. Student's t-test was used and $p<0.05$ was accepted as statistically significant. ***Results:*** Having limited number of patients, the organs (except kidneys) and whole-body doses were not significantly different between two applications. Kidney doses, although not significant, were less in the IA Lu-177 PSMA application. The absorbed doses in bone metastases were significantly higher in IA Lu-177 PSMA than in IV Lu-177 PSMA application. ***Conclusion:*** This preliminary study shows that intraarterial administration of Lu-177 PSMA may serve as an alternative to the intravenous route and may be favourable in terms of absorbed doses in metastatic bone lesions. ***References:*** None

1509

TROP Session: Is It or Is It Not Malignant? - Diagnostic/Predictive Options in Thyroid Nodules

Friday, October 30, 2020, 10:40 - 12:10 Channel 9

OP-862

MIBI SPECT as first line diagnostic of hypofunctioning thyroid nodules - a long term study

M. Baehr, K. Liepe;
Klinikum Frankfurt (Oder), Dept. Nuclear Medicine, Frankfurt (Oder), GERMANY.

Aim/Introduction: Current guidelines recommend fine needle biopsy (FNB) in hypofunctioning thyroid nodules. We have postulated that ^{99m}Tc-MIBI SPECT with additional FNB of MIBI positive nodules is a safe, effective and least-invasive workflow. ***Materials and Methods:*** In a time-period of 69 months 705 patients with hypofunctioning thyroid nodules underwent administration of 418 MBq ± 33 MBq ^{99m}Tc-MIBI with SPECT 120 min p.i. Additional FNB was performed in high-risk nodules (EU-TIRADS 5), in symptomatic patients and in asymptomatic patients with MIBI SPECT positive nodules. Long-term follow-up ranged from 12 to 69 months with a mean of 30.7 months. ***Results:*** 55 patients showed positive MIBI SPECT and consequently received surgical resection. In 26% of these patients the suspected nodule was MIBI negative but another either small nodule, isthmus nodule or part of multinodous goiter was MIBI positive. 84 patients received surgical resection after negative MIBI SPECT because of strong symptoms or symptomatic high-volume multinodous goiter. Retrospectively histological diagnosis was concordant with positive MIBI SPECT and the additional FNB in 65% of cases, whereas in 32% MIBI was superior and in 3% FNB was superior. In long-term follow-up MIBI negative patients revealed malignancy in 0.6%,

three papillary carcinoma of 2-4mm and one medullary carcinoma with Ki-67 of 5%. Statistical analysis for MIBI SPECT showed an overall sensitivity of 73%, specificity of 95%, positive predictive value of 22% and negative-predictive value of 99%. MIBI SPECT was also positive in thyroid adenomas, which nevertheless required surgical resection, like hürthle cell adenoma, parathyroid adenoma or follicular adenoma. Assessing these patients as true-positive either, the corrected predictive statistics were 80%, 98%, 76% and 99%. ***Conclusion:*** First line diagnostic with MIBI SPECT is safe in the assessment of low to intermediate risk hypofunctioning thyroid nodules. With a negative predictive value of 99% after up to 69 months of follow-up, MIBI SPECT has proven as an excellent screening tool. Surgical resection of only MIBI positive and FNB positive hypofunctioning nodules could be reduce the frequency of thyroidectomies significantly. ***References:*** None

OP-863

Low-dose 18F-FDG thyroid PET/CT vs. Thyroid scintigraphy in indeterminate high-risk nodules: a pilot dosimetric assessment

E. Di Giorgio[1], *M. Sicignano*[1], *L. Evangelista*[2], *L. Mansi*[3], *P. Sannino*[1], *F. Masone*[1], *F. Squame*[1], *N. D'Acunzo*[1], *V. Nuzzo*[4], *S. Spiezia*[5], *M. Klain*[6], *M. Spadafora*[1];
[1]*Nuclear Medicine Unit, Ospedale del Mare, Naples, ITALY,* [2]*Nuclear Medicine Unit, Department of Medicine (DIMED), University of Padua, Padua, ITALY,* [3]*CIRPS, Rome. Interuniversity, reseach center for sustainability, Rome, ITALY,* [4]*Endocrinology Unit, Ospedale del Mare, Naples, ITALY,* [5]*Endocrino surgery Unit, Ospedale del Mare, Naples, ITALY,* [6]*Department of Advanced Biomedical Sciences, University of Naples Federico II, Naples, ITALY.*

Aim/Introduction: Thyroid nodules suspicious at ultrasounds necessitate fine-needle aspiration cytology as confirmative test, which suffers from high indeterminate reports, up to 25%.Indeed, these lesions are addressed to surgery, resulting as benign in ¾ of cases. In this population whole body FDG-PET/CT(wb-PET/CT) has a high negative predictive value for malignancy, ranging between 81% and 100%.However, this imaging modality is not recommended in the diagnostic workup, mainly because of high radiation exposure and costs.The aim of the study is to preliminary estimate tracer dose, dosimetric and scan-time impacts of low dose FDG-thyroid-PET/CT(t-PET/CT)either versus wb-PET/CT, in patients undergoing FDG PET/CT for an oncologic query, and 99m-TcO4–thyroid scintigraphy (t-S). ***Materials and Methods:*** Wb-PET/CT of 50 patients (64,7+12yy; 50%male) were retrospectively compared with t-PET/CT, defined as the cervical part (1 bed) of wb-PET/CT. The ratio between scan-length of t-PET/CT and wb-PET/CT was the basis to estimate temporal, tracer dose and radiation exposure relationship between the two modalities.Data obtained in a population matched by age and gender undergoing t-S were also evaluated.Tracers dose (FDGor99m-TcO4–, expressed in MBq), radiation exposure (ED, in mSv), scan-time and additional cancer risk (ACR) were assessed. ***Results:*** In wb-PET/CT, the radiation exposure is determined by CT (60.4%) and 18F-FDG (39.6%).The ratio between scan-length of t-PET/CT vs wb-PET/CT was 0,20. Mean scan-time and dose of wb-PET/CT were 17,9+1,9 min and 276,1+51 MBq, respectively.Based on the time-dose equation, t-PET/CT would need a mean dose of 55,2 MBq, which is 20% of wb-PET/CT, to obtain the same counting rate. Considering a cervical scan instead of a WB, ED decreases from 4,4 to 0,88 ($p< 0.0001$), from 6,7 to 1,34 ($p<0.0001$), and from 11,1 to 2,22 mSv ($p<0.0001$) for PET, CT and PET/CT, respectively. For t-S, using a 99m-Tc dose of 158,6+29 MBq, mean scan-time and ED were 5,4+1,7 min and 2,1+0,4 mSv, respectively. Considering prices in our Institution, tracer's cost was 9,4 euro for t-PET/CT and 5-10 euro for t-S. ACR was calculated 0,106% for wb-PET/CT vs 0,008% for t-PET/CT($p<0.0001$); 0,003% for t-PET vs 0,006% for t-S($p<0.0001$).Alternatively, using the same FDG dose of wb-PET/CT, the scan time of t-PET was 4,1 vs 5,4 min of t-S($p<0.0001$). ***Conclusion:*** These preliminary data support the hypothesis that low-dose t-PET/CT is a conceivable diagnostic strategy in patients with indeterminate high risk nodules. This imaging approach would be cost/effective in clinical setting, having a potential role in limiting the rate of futile thyroid surgery. ***References:*** None

OP-864

Ten-Year Follow-up and Clinical Outcome in Euthyroid Patients with Thyroid Nodules in an Iodine Sufficient Area

K. Bajuk Studen[1], *K. Zaletel*[1], *S. Gaberscek*[1,2];
[1]*Department of Nuclear Medicine, University Medical Centre Ljubljana, Ljubljana, SLOVENIA,* [2]*Faculty of Medicine, University of Ljubljana, Ljubljana, SLOVENIA.*

Aim/Introduction: The initial evaluation of patients with thyroid nodules should identify a small subgroup that harbor thyroid cancer, cause compressive symptoms or progress to functional disease and therefore need further clinical management. The rest can be managed with a surveillance program. Defining optimum surveillance intervals remains a challenge. The purpose of our study was to establish a natural history of thyroid nodules in a cohort of euthyroid patients 10 years after the diagnosis. ***Materials and Methods:*** Patients diagnosed with unsuspicious thyroid nodules in whom at the time of diagnosis no treatment was indicated and who did not have autoimmune thyroid disease were invited for re-evaluation 10 years after the diagnosis. Baseline patient parameters and ultrasound characteristics of the nodules were retrospectively collected. At follow-up, thyroid ultrasound was performed; in case of nodule growth, the patient was referred for a complete clinical evaluation. A significant change in

the size of thyroid nodule was defined as the increase or decrease that involved at least 2 nodule dimensions, each amounting to at least 2 mm and representing at least 20% of the baseline diameter. Data are presented as mean +/- standard deviation (SD). ***Results:*** Fourty-three (39 women/4 men, aged 54.2 +/- 13.6 years) patients were included in the study, having 65 nodules with maximum diameter 11.8 +/- 7.8 mm, mean thyrothropin (TSH) 1.73 +/- 1.00 mIU/L and thyroglobulin (Tg) 27.1 +/- 46.9 µg/l. After 10 years, 21 (32.3%) nodules significantly increased in size, 7 (10.8%) nodules significantly decreased in size, for 29 (44.6%) of nodules, no significant change in size of the nodules was noted. Furthermore, 8 (12.3%) disappeared and 16 new nodules were found. For the nodules that grew, change in nodule largest diameter was found to correlate significantly with baseline largest diameter ($p<0.05$), but not with baseline TSH, Tg or age. Regarding the clinical outcome, no new thyroid cancers were found. For 39 (90.7%) patients no further management was indicated. Two (4.7%) patients were referred to thyroidectomy because of the growth of the nodules. Two (4.7%) patients were treated for hyperthyroidism because of toxic multinodular goiter. ***Conclusion:*** We report a single centre experience of the natural history of unsuspicious thyroid nodules. Our results show that 67.7% of such nodules remain stable in size, decrease or even disappear and that the vast majority of the patients remain clinically stable with no treatment indication ten years after the diagnosis. ***References:*** None

OP-865

^{99m}Tc-3PRGD$_2$ SPECT/CT for predicting disease progression after initial therapy in high risk DTC patients

X. Jia*, Y. Wang, Y. Liu, X. Wang, X. Yao, A. Yang, R. Gao;*
The first affiliated hospital of Xi'an jiaotong university, Xi'an, CHINA.

Aim/Introduction: This study aimed to validate the effectiveness of integrin avb$_3$ imaging in predicting structural progression in high-risk differentiated thyroid cancer (DTC) patients. ***Materials and Methods:*** DTC patients evaluated as high risk of recurrence after initial surgery were enrolled and ^{99m}Tc-3PRGD$_2$ SPECT/CT was performed before radioiodine ablation (RAI). Clinical data obtained during follow-up were used to assess the response and outcome. Aggressive local surgery, another RAI, or targeted chemotherapy was performed if disease progression was detected. ***Results:*** A total of 25 patients were enrolled in this study because of the existence of gross extra-thyroidal extension (n=10), incomplete tumor resection (n=4), extensive vascular invasion (n=2), lung metastases (n=5), and elevated Tg suggestive of distant metastases (n=24). Nineteen out of the 25 cases demonstrated RGD-avid disease and the median T/B ratio of the lesions was 3.29 (range 1.8-15.5, n=19). The serum thyroglobulin (Tg) level of them was higher than that of the cases that showed non-RGD-avid disease, but without statistical difference (n=6; 77.30 vs. 27.75 ng/mL, p=0.105). Three cases demonstrated RGD-avid disease were excluded from further analysis because of loss to follow-up. During follow-up post initial treatment (median 16 months), no disease progression was detected and a decrease of Tg (ranged from 12.83% to 100%) was revealed in cases showed non-RGD-avid disease (n=6). While structural progression was detected in 11 out of the 16 (68.75%) cases demonstrated RGD-avid lesions. Among them, a second surgery was administered in four because of metastatic lymph nodes and another RAI was applied in three for progression of pulmonary disease. Kaplan-Meier curves showed a significant difference in terms of progression-free survival (PFS) between patients who demonstrated RGD-avid disease or not (p=0.033). ***Conclusion:*** ^{99m}Tc-3PRGD$_2$ imaging is a valuable initial predictor of treatment failure in high-risk DTC. A significant association emerged between 3PRGD$_2$ uptake and PFS. ***References:*** None

OP-866

Is BRAF^{V600E} mutation a risk factor for developing controlateral limph-node metastases in papillary thyroid cancer (PTC) patients?

A. Campenni'[1]*, R. Ruggeri*[2]*, M. Siracusa*[1]*, A. Alibrandi*[3]*, D. Cardile*[1]*, H. Lanzafame*[1]*, F. Panasiti*[1]*, F. La Torre*[1]*, G. Giacoppo*[1]*, A. Ieni*[4]*, G. Giuffrè*[4]*, G. Tuccari*[4]*, S. Baldari*[1]*;*
[1]Department of Biomedical and Dental Sciences and Morpho-Functional Imaging, Nuclear Medicine Unit, University of Messina, Messina, ITALY, [2]Department of Clinical and Experimental Medicine, Unit of Endocrinology, University of Messina, Messina, ITALY, [3]Department of Economical, Business and Environmental Sciences and Quantitative Methods, University of Messina, Messina, ITALY, [4]Department of Human Pathology in Adult and Developmental age "Gaetano Barresi", University of Messina, Messina, ITALY.

Aim/Introduction: Several molecular markers have been introduced to improve postoperative risk stratification of papillary thyroid cancer (PTC) patients. BRAF^{V600E}is the most common somatic point mutation in sporadic PTC and is frequently associated with aggressive behavior in intermediate-high risk PTC patients. The aim of our study was to evaluate if BRAF^{V600E} mutation was associated with more aggressive clinico-pathological features and could be considered as risk factor for developing contralateral lymph-node metastases in low-intermediate risk PTC patients with unilateral tumor. ***Materials and Methods:*** We reviewed the record of 354 out of 1185 patients (29.8%) affected by low or intermediate risk unilateral-PTC [pT1-T3,Nx(0/1),Mx; 269 women, 85 men; mean age (SD)=46.9 (13.6), median=47 yrs; female-to-male ratio: 3.16:1]. In all of these patients, BRAF^{V600E}mutation was evaluated and

131-radioiodine therapy (RaIT) was performed using ≥2220 MBq (2220-4588 MBq) with ablative or adjuvant intent. Neck-ultrasonography and laboratory test were obtained before RaIT. A post-therapy whole body scintigraphy (pT-WBS) was performed 5-7 days after RaIT. Neck-ultrasonography, computed tomography, magnetic resonance imaging were performed on request of attending nuclear medicine physician. ***Results:*** $BRAF^{V600E}$mutation was found in 170 out of 354 (48%) PTC patients (Group A) [F=126, M=44, mean age=47.2 yrs (14.4), median=47; female-to-male ratio: 2.9:1]. In the remaining patients (184/354, 52%), $BRAF^{V600E}$mutation was not found (Group B).The risk to have aggressive variant (eg. Tall-cell), intermediate risk PTC (2015 ATA) and disease staging II (AJCC 8_{th} edition) was significantly higher in Group A than B patients [Odds Ratio(OR)=3.509, 3.186, 20.646, respectively]. In addition, significant differences in the prevalence of intermediate risk PTC, Hashimoto thyroiditis, multifocality, aggressive variant as well as higher tumour size and disease staging were observed between Group A and B(p=<0.001, p=0.001, p=0.026, p=<0.001, p=<0.001, p=<0.001, respectively). Forty-two out of 170 Group A patients [F=27, M=15, mean age=48.8 yrs (14.3), median=50; female-to-male ratio: 1.9:1] had omolateral (n=24, 57.2%) or contralateral (n=18, 42.8%) loco-regional metastases at pT-WBS.Interestingly, the prevalence of both loco-regional and contralateral lymph-node metastases at pT-WBS was significantly higher in Group A than B patients [42/170 (24.7%) vs22/184 (11.9%), p=0.003 and 18/42 vs2/22, p=0.013, respectively]. ***Conclusion:*** $BRAF^{V600E}$ mutation is associated to more aggressive clinico-pathological features in our cohort of low and intermediate risk unilateral-PTC patients. Of note, $BRAF^{V600E}$mutation should be considered as a significant risk factor for having contralateral lymph-node metastases. pT-WBS is a useful diagnostic tool for improving postoperative risk stratification of PTC patients. ***References:*** None

OP-867

Comparison between PERCIST criteria, Metabolic Tumor Volume (MTV) and Total Lesion Glycolysis (TLG) in the evaluation of response to tyrosine kinase inhibitors in patients with radioactive iodine-refractory metastatic thyroid cancer

A. Miceli[1], *A. Borra*[1], *M. Bauckneht*[2], *S. Gay*[3], *S. Raffa*[1], *M. Albertelli*[3], *M. Donegani*[1], *S. Marra*[1], *G. Ferrarazzo*[2], *G. Sambuceti*[1], *D. Ferone*[3], *M. Glusti*[3], *S. Morbelli*[1];
[1]*DISSAL, Genoa, ITALY,* [2]*IRCCS Ospedale Policlinico San Martino, Genoa, ITALY,* [3]*DIMI, Genoa, ITALY.*

Aim/Introduction: Tyrosine kinase inhibitors (TKI) and, in particular, Lenvatinib, have been shown to delay disease progression and provide benefit in terms of overall survival (OS) in patients' with radioactive iodine-refractory (RAI-R) differentiated thyroid cancer (DTC). Effective methods for evaluating response to TKI are a critical unmet need owing to their expensive costs and unique adverse events. While computed tomography have been used to evaluate response to TKI in metastatic DTC by means of RECIST criteria, no PET-based criteria have been to-date validated in this clinical settings. We aimed to explore agreement between FDG-PET-based metabolic response to TKI measured with different criteria and their relationship with RECIST-based response at last follow up. ***Materials and Methods:*** We interrogated our database to identify metastatic DTC patients who performed FDG-PET just before and after therapy with TKI between January 2013 and December 2019. Both first response and following responses to TKI were considered. Baseline and post-treatment maximum standardized uptake value (SUVmax), SUVmean, metabolic tumor volume (MTV) and total lesion glycolysis (TLG) were measured at baseline and after therapy to compute PERCIST and MTV-, TLG-based responses. Concordance in terms of response between PERCIST, DELTA-MTV, DELTA-TLG was computed with kappa value. Evaluation of the predictive value of early metabolic response to the final CT-based RECIST 1.0 response was also assessed. ***Results:*** 45 scans in 15 metastatic DTC patients were included in the analysis (five patients had been initially treated with Sorafenib and then shifted to Lenvatinib). The median OS was 32 months. Considering both first and best response 40%, 27% and 33% of patients were classified as either stable metabolic disease (SMD) or partial metabolic response (PMR) by PERCIST, MTV and TLG respectively. Substantial agreement was observed between PERCIST and DELTA-MTV (K=0.66) while only a fair agreement was documented between DELTA-TLG and both PERCIST and MTV (k=0.4). Of note, all long term (> 41 months) SD according to RECIST 1.0 criteria at last follow up had been previously classified as in PMR according to TLG within one year after initiation of therapy with TKI (while no relationship was highlighted with PERCIST and MTV). ***Conclusion:*** A PERCIST-based single lesion approach reaches fair concordance with more complex metabolic response based on MTV and TLG. However, TLG computation potentially provides additive information. In fact, only depth of response as highlighted by TLG was able to early identify long term responders patients. ***References:*** None

OP-868

Thyroglobulin doubling time independently predicts 2-[^{18}F]-FDG-PET/CT results in Patients Affected by Differentiated Thyroid Carcinoma with Positive Thyroglobulin Level and Negative ^{131}I Whole Body Scan

D. Albano[1], *E. Cerudelli*[2], *M. Gazzilli*[2], *F. Dondi*[1], *A. Mazzoletti*[1], *P. Bellini*[1], *L. Camoni*[2], *F. Bertagna*[1], *R. Giubbini*[1];
[1]*University of Brescia and Spedali Civili of Brescia, Brescia, ITALY,* [2]*Spedali Civili of Brescia, Brescia, ITALY.*

Aim/Introduction: Serum thyroglobulin (Tg) is considered

the most sensitive marker of disease for monitoring patients affected by differentiate thyroid carcinoma (DTC) after surgery and ablation of thyroid remnants by iodine-131 (^{131}I). In patients with positive Tg and negative ^{131}I whole-body scan (^{131}I-WBS), 2-deoxy-2-[^{18}F]fluoro-D-glucose positron emission tomography/computed tomography (2-[^{18}F]-FDG PET/CT) can be considered useful to detect sites of disease. But the effective relationship of Tg-Doubling time (Tg-DT) and PET/CT results is lacking. ***Materials and Methods:*** From December 2006 to December 2019, 113 patients (median age 56 years, 61 female, 52 male) affected by DTC and treated with total thyroidectomy plus ^{131}I, with last ^{131}I-WBS negative and Tg≥1 ng/ml without detectable Tg-antibodies, underwent 2-[^{18}F]-FDG PET/CT and were retrospectively included in this study. Tg-DT was computed on the basis of at least three consecutive Tg measurements under TSH suppression performed prior to the PET/CT scan. Receiver operating characteristic (ROC) curve analysis was used to identify the optimal cutoff point of last stimulated Tg before PET/CT and Tg-DT in the light of which interpret the results of 2-[^{18}F]-FDG PET/CT. ***Results:*** Among 113 2-[^{18}F]-FDG PET/CT scans, 74 (65%) resulted positive showing the presence of hypermetabolic lesions consistent of DTC disease. Of these, 72 were confirmed as true-positive, in the remaining two cases, PET/CT were false-positive. In 39 (35%) patients, PET/CT was negative showing no increased FDG uptakes in whole body: 33 was true negative and 6 false negative. Sensitivity, specificity, positive predictive value, negative predictive value and accuracy of 2-[^{18}F]-FDG PET/CT were 92% (95% CI 84-97%), 94% (95% CI 81-99%), 97% (95% CI 90-99%), 87% (95% CI 72-92%), and 93% (95% CI 87-97%) with positive and negative likelihood ratios of 16.15 and 0.08, respectively. Serum Tg and Tg-DT were significantly higher in patients with negative PET/CT than positive (for Tg-DT median 4.52 year, mean 8.9 years, vs median 1.07 year, mean 1.3, p<0.001) ROC curve analysis revealed an optimal Tg cut-off of 19 ng/mL (sensitivity 78%, specificity 85%, AUC 0.844) and Tg-DT of 2.5 years (sensitivity 93%, specificity 87%, AUC 0.911). Tg-DT threshold of 2.5 years correctly predicted 66 of 72 (92%) true-positive and 31 of 33 (94%) true negative PET/CT. ***Conclusion:*** In conclusion, in DTC patients with negative ^{131}I-WBS and positive Tg, Tg-DT may predict 2-[^{18}F]-FDG PET/CT results with an accuracy higher than Tg as absolute value. Tg-DT less than 2.5 years can be considered a valid marker for predicting PET/CT results. ***References:*** None

OP-869

Comparison of Lesion Detectability and Image Quality among Digital and Analog PET Systems for Recurrence in Thyroid Cancer Patients Using I-124

D. Kersting[1], *M. Weber*[1], *M. Sraieb*[1], *P. Fragoso Costa*[1], *L. Umutlu*[2], *C. Rischpler*[1], *W. P. Fendler*[1], *M. Conti*[3], *K. Herrmann*[1], *W. Jentzen*[1]; [1]*Department of Nuclear Medicine, University Hospital Essen, Essen, GERMANY,* [2]*Department of Diagnostic and Interventional Radiology and Neuroradiology, University Hospital Essen, Essen, GERMANY,* [3]*Siemens Medical Solutions USA, Inc., Knoxville, TN, UNITED STATES OF AMERICA.*

Aim/Introduction: I-124 PET is limited by a low positron branching ratio and low image quality, especially for low-uptake lesions and at late dosimetry time points. In this study, we assess the improvement in lesion detectability in differentiated thyroid cancer (DTC) patients with low increasing thyroglobulin (TG) levels by a digital versus an analog PET/CT system with TOF capability and, in addition, compare the results to a neck scan on a non-TOF PET/MR system at standard and prolonged emission time (ET). Moreover, different image reconstruction algorithms are evaluated. The results are used to suggest scan protocol optimisations. ***Materials and Methods:*** Data sets of 10 DTC patients with low increasing TG levels after total thyroidectomy and radioiodine therapy were included. PET data were acquired within 24 h after administration of 38 MBq I-124 on a digital Siemens Biograph Vision and an analog Biograph mCT PET/CT system (both whole-body, 4-min ET per bed position, image reconstruction OSEM, OSEM+TOF and OSEM+TOF+PSF) and a non-TOF Biograph mMR PET/MR system (only neck region, 4-min and 20-min ET, only OSEM). All data were interpreted by 3 blinded nuclear medicine physicians. Apart from lesion detection, the image quality was rated on a five-point-scale from 1 to 5. ***Results:*** Across all systems, a total of 9 lesions was detected, all located in the neck region. The detectability was significantly higher (p<0.01) for the digital (OSEM 5/9, OSEM+TOF 8/9, OSEM+TOF+PSF 8/9) compared to the analog PET/CT (OSEM 2/9, OSEM+TOF 2/9, OSEM+TOF+PSF 3/9) and increased for the non-TOF PET/MR from 3/9 to 8/9 with increasing ET. TOF+PSF image reconstruction on the analog PET/CT induced two additional regions (hilar lymph node and bone) with artificially elevated uptake (as not discernible in any other imaging modality). The median visual image quality increased from the analog to the digital PET/CT from 1.5 to 3 (OSEM), from 2 to 4 (OSEM+TOF) and from 3 to 4 (OSEM+TOF+PSF), the PET/MR reached values of 1 (4-min ET) and 3 (20-min). ***Conclusion:*** Based on this study, several protocol optimisations may be considered to improve the detectability for low-uptake lesions. If available, digital PET/CT and TOF image reconstruction are preferable and revealed at 4-min ET a detectability comparable to non-TOF PET/MR at 20-min ET. Moreover, emphasis of the mostly affected neck region by a selectively prolonged scan duration can be useful. Images reconstructed with TOF+PSF can be critical due to artificial uptakes and should be carefully considered. ***References:*** None

OP-870

Do Histological Patterns of Primary Tumor Predict Metabolic Patterns detected by FDG PET/CT in

Differentiated Thyroid Cancer Patients

S. Soyluoglu, E. Tastekin, U. Korkmaz, S. Orum, G. Durmus Altun; Trakya University, Medical School, Edirne, TURKEY.

Aim/Introduction: Although differentiated thyroid cancers (DTC) generally has excellent prognosis, approximately 15% develop metastasis in follow-up. The clinical course of metastatic patients is quite variable. We aimed to investigate the relationship between primary tumor histopathological features and FDG PET/CT findings in patients with elevated thyroglobulin levels. ***Materials and Methods:*** DTC patients, who underwent PET/CT between January 2015 and December 2019 were scanned and all patients with accessible postoperative pathology and I-131 whole body scan (WBS) were included in the study. Primary tumor size, focality, positivite surgical margin (PSM), capsule invasion (CI), lymphovascular invasion (LVI), blood vessel invasion (BVI), perineural invasion (PNI), extrathyroidal invasion (ETI), intraglandular dissemination (IGD), mitoses, peritumoral lymphocytic infiltration (PTLI) were recorded. Patients were also grouped according to the ATA risk classification and follow-up thyroglobulin values, and the relationship between these groups, histopathological patterns, I-131 WBS and FDG PET/CT findings were evaluated statistically. ***Results:*** Total of 75 patients, 45 female and 30 male, included in the study. The average age at the time of diagnosis was 48.9 ± 7.8. The tumor size ranged from 0.2 to 8 cm, mean 2.3 mm (± 1.8). Multifocality, PSM, CI, LVI, ETI (56%, 60%, 39%, 39%, 55%) were frequently observed, while BVI, PNI, IGD were more rare (1%, 7% , 7%). PET/CT was positive in 54 patients (72%) and I-131 WBS was positive in 37 patients (49%). The average SUVmax in metastatic lesions was 6.2 ± 18.8. A significant correlation was found between PET positive metastatic disease and LVI ($p = 0.04$). The presence of LVI increased the risk of PET positivity by 3.9 times (95% Confidence Interval: 1.2-13.3; $p = 0.027$). SUVmax values were significantly associated with LVI ($p = 0.04$). There was also a significant relationship between mitosis, PTLI and PET positivity. A significant correlation was found between tumor size and SUVmax ($p = 0.04$), and between thyroglobulin groups and PSM, LVI, ETI ($p = 0.037$, $p = 0.004$, $p = 0.04$). There is a significant relationship between risk classification and PET positive bone metastasis ($p = 0.03$). ***Conclusion:*** LVI and mitosis detected in primary tumor and tumor size is correlated with the presence of FDG PET/BT positive metastases and higher SUVmax values in patients with DTC, which associated with more aggressive tumor behavior. Patients who identified as high risk according to initial risk stratification are more likely to develop PET positive bone lesions. ***References:*** None

OP-871

Comparison of simultaneous ^{18}F-FDG PET/MR and PET/CT in the follow-up of patients with differentiated thyroid cancer

L. Piscopo[1], *M. Klain*[1], *C. Nappi*[1], *M. Manganelli*[1], *E. Nicolai*[2], *V. Romeo*[1], *A. Giordano*[1], *V. Gaudieri*[1], *E. Zampella*[1], *F. Volpe*[1], *M. De Risi*[1], *L. Pace*[3], *A. Cuocolo*[1];
[1]*Department of Advanced Biomedical Sciences, University Federico II, Napoli, ITALY,* [2]*IRCCS-SDN, Napoli, ITALY,* [3]*Department of Medicine, Surgery and Dentistry, University of Salerno, Salerno, ITALY.*

Aim/Introduction: ^{18}F-FDG PET/CT is the most accurate imaging method in differentiated thyroid cancer (DTC) patients with either an aggressive histology, an absence of radioiodine uptake in neoplastic foci, or an elevated serum thyroglobulin (Tg) level that progresses with time in the absence of known imaging abnormalities. We evaluated the diagnostic performance of FDG PET/MR in comparison with that of PET/CT. ***Materials and Methods:*** Following the injection of a single ^{18}F-FDG activity, simultaneous PET/MR and PET/CT were sequentially performed in 40 consecutive patients with DTC previously treated with total thyroidectomy and radioiodine ablation. At PET/MR imaging, all areas with abnormal FDG uptake corresponding to a MR abnormality (tissue mass or lymph node) were considered as positive. In addition, any focal increased uptake of FDG that did not correspond to normal structures was also recorded as positive. A similar procedure was applied for PET/CT interpretation. Any morphological abnormality identified as lesion on MR or CT was recorded. All patients were followed-up for at least 6 months by serum Tg, Tg-Ab and thyroid-stimulating hormone determinations and neck ultrasonography. Other imaging procedures were performed as clinically indicated, whole-body scan was obtained in case of ^{131}I therapy, and histology was recorded in case of surgery. The date of recurrence or the most recent follow-up examination was recorded, as well as the clinical status at the end of the study. ***Results:*** All patients were treated in a range of 6-400 months before study. According to serum Tg levels, abnormal imaging findings were found in 10/22 patients (45%) with a serum Tg ≥2 ng/mL (range 20-1050 ng/mL) and in only 1/18 patients (5%) with a serum Tg <2 ng/mL. PET/MR was positive in 11 patients and PET/CT in 10 patients. PET/MR detected 33 tumor foci and PET/CT 30 tumor foci. During the follow-up of the 12 patients with negative initial PET studies and with detectable serum Tg, only one patient had a neck recurrence and the administration of an empiric high activity of ^{131}I in the other 11 patients did not reveal any unknown tumor focus. In the 17 patients with an initial serum Tg level <2 ng/mL, no recurrence occurred. ***Conclusion:*** This study confirms the high diagnostic accuracy of FDG PET studies in DTC patients with elevated serum Tg levels and shows that PET/MR does

not bring significant complementary information over PET/CT imaging. ***References:*** None

OP-872

Clinical Impact Of [^{68}Ga]Ga-DOTA-TATE Imaging In Patients With Medullary Thyroid Cancer

M. Tuncel*, S. Kılıckap, N. Suslu;*
Hacettepe University, Ankara, TURKEY.

Aim/Introduction: Medullary thyroid cancer(MTC) arises from the neuroendocrine C cells of the thyroid. There is no single diagnostic imaging method to reveal all MTC recurrences or metastases.[^{68}Ga]Ga-DOTA-TATE is an alternative PET-radiotracer that showed acceptable efficacy in the detection of MTC. In this study, we aimed to reveal the clinical impact of this radiotracer in the management of patients with MTC. ***Materials and Methods:*** [68Ga]Ga-DOTA-TATE-PET-CT records of 38 patients with confirmed MTC were included in the study. Demographic data, the clinical indication for the scan, previous therapies, and tumor marker levels were recorded. The site and SUVmax of the disease sites were noted. Consensus reached for the additional value of [68Ga]Ga-DOTA-TATE-PET-CT, and discordant sites with conventional imaging(CI) were recorded. Finally, changes in management after the scan were evaluated. ***Results:*** [^{68}Ga]Ga-DOTA-TATE-PET-CT outperformed CI in 14/38(37%) patients. It has detected metastatic lymph nodes in 8, bone metastases in 4, and both bone&lymph nodes in 2 of these 14 patients. In 16/38(42%) of patients,[^{68}Ga]Ga-DOTA-TATE PET-CT performed equally with CI. In 5/38(13%) patients CI outperformed PET-CT.[^{68}Ga]Ga-DOTA-TATE PET-CT positivity was also correlated with tumor markers(Ctn-median;PET-positive:743±5439 vs PET-negative:31±17(p:0.012) CEA median; PET-positive: 41±162 vs PET-negative:2,6±1,4(p:0,015).[^{68}Ga]Ga-DOTA-TATE PET-CT had changed clinical management in 13/38 (34%) patients. ***Conclusion:*** [^{68}Ga]Ga-DOTA-TATE is an essential part of the work-up of patients with MTC. It has outperformed CI in 14/38 (37%) patients and has changed the 34% of therapy decisions. Prospective studies with image-guided therapy decisions are needed further to reveal the impact of PET imaging in patients with MTC. ***References:*** None

OP-873

Long-term Outcome and Prognostic Features of Differentiated Thyroid Cancer Patients Treated at Croatian Referral Centre

T. Jukic[1,2]*, M. Franceschi*[3]*, I. Blažeković*[3]*, M. Punda*[3]*, J. Staničić*[3]*, R. Granić*[3]*, P. Petranović-Ovčariček*[3]*, V. Gladić-Nenadić*[3]*, I. Šiško-Markoš*[3]*, M. Bosak-Butković*[1]*, Z. Sonicki*[4,2]*, I. Mihaljević*[5]*, V. Bedeković*[6]*, A. Fröbe*[3]*, Z. Kusić*[7]*;*
[1]Sestre milosrdnice University Hospital Centre, Zagreb, CROATIA, [2]University of Zagreb, School of Medicine, Zagreb, CROATIA, [3]Sestre milosrdnice University Hospital Centre, Department of Nuclear Medicine and Oncology, Zagreb, CROATIA, [4]School of Public Health "Dr. Andrija Štampar", Zagreb, CROATIA, [5]Clinical Institute of Nuclear Medicine and Radiation Protection, University Hospital Osijek , Faculty of Medicine Osijek, Josip Juraj Strossmayer University of Osijek, Osijek, CROATIA, [6]Sestre milosrdnice University Hospital Centre, Department of Otorhinolaryngology, Head and Neck Surgery, University of Zagreb, School of Medicine, Zagreb, CROATIA, [7]Croatian Academy of Sciences and Arts, Zagreb, CROATIA.

Aim/Introduction: The aim of the study was to assess survival rates and prognostic features of papillary (PTC) and follicular (FTC) thyroid cancer patients (pts) treated and followed-up up to 50 years in one institution. ***Materials and Methods:*** The retrospective study enrolled 1167 PTC (F/M 4:1, median age 47, range 6-83 years) and 215 FTC pts (F/M 2.8:1, median age 48, range 13-81 years) operated between 1970-2012 and followed-up till April 2020. Mean follow-up in years of PTC pts was 12.0 (0.2-48) and FTC pts 11.0 (0.4-46). In >99% DTC pts total thyroidectomy was performed and 92% PTC and 96% FTC pts underwent 131-I therapy. Prognostic factors: age gender, tumor size, TNM stage, presence of local and distant metastases at presentation and disease recurrence were evaluated with univariate (Kaplan-Meier Survival Curves, Log-rank test) and multivariate analysis (Cox Regression) ($p<0.05$). ***Results:*** At initial presentation, cervical metastases were recorded in 252 (26%) PTC and 17 (7.9%) FTC pts ($p=0.033$), and distant metastases (M1) in 40 (3.4%) PTC and 29 (13.5%) FTC pts ($p<0.001$). Median tumour size in mm in PTCs vs FTCs was 12 (1-100) vs 32 (7-90) ($p<0.001$). During follow-up new M1 developed in 7 PTCs (overall 47, 4.0%) and 3 FTCs (overall 32, 14.9%) and loco-regional recurrence in 70 (6%) PTCs and 14 (6.5%) FTCs. Median tumor size in PTCs vs FTCs with M1 was 25 vs 64 mm. During follow-up 14 PTCs (F/M 0.6:1) and 20 FTCs (F/M 1.2:1) died from disease. In PTCs with fatal outcome, 8 died due to distant metastases and 6 due to advanced local disease. In FTCs with fatal outcome, 17 died due to distant metastases and 3 due to advanced local disease. Overall 10-year cancer specific survival rate for PTC and FTC was 98.8% and 92.7% (80% and 37% with M1) ($p<0.001$). All 7 risk factors affecting outcome in PTC and FTC pts showed statistically significant correlation in univariate analysis ($p<0.001$). Multivariate analysis demonstrated in PTCs older age ($p=0.005$), stage IV, larger tumor size and M1 ($p<0.001$) as prognostic factors affecting outcome, but for FTCs none reached statistical significance. ***Conclusion:*** DTCs are malignant tumors with low mortality rate as demonstrated in this study, especially PTCs. Recurrence rate in our study was low, probably due to total thyroidectomy and I-131 therapy in most of the pts. FTCs have less favourable outcome than PTCs due to more advanced tumour stages at initial presentation. ***References:*** None

1510

TROP Session: Our Army at War - Nuclear Medicine and COVID-19

Friday, October 30, 2020, 10:40 - 12:10 Channel 10

OP-874

Incidental lung findings suggestive of COVID-19 pneumonia in oncologic PET/CT studies

D. Monachello Araujo, M. Coronado Poggio, S. Rodado Marina, E. López Llobet, S. Rizkallal Monzón, D. Travaglio Morales, C. Lancha Hernández, L. García Zoghby, J. Cordero García, A. Guzmán Cruz, C. Escabias del Pozo, L. Domínguez Gadea; Hospital Universitario La Paz, Madrid, SPAIN.

Aim/Introduction: In Spain COVID-19 pandemia reached its outbreak in March 2020. For some weeks, patients without clinical diagnosis of COVID-19 infection underwent PET/CT studies for standard indications. The aim of this study is to report incidental PET/CT findings suggestive of COVID-19 associated pneumonia in this group of patients, who received medical attention in a third level hospital of Madrid during this "peak of infection" period. ***Materials and Methods:*** Whole body PET/CT studies from patients without clinical or microbiological diagnosis of COVID -19 infection, performed from March 3rd to April14th, were retrospectively reviewed by two nuclear medicine experts. Lung findings unrelated to their oncologic process or pulmonary chronic disease were noted. CT findings were classified in three categories following COVID-19 pneumonia classification for CT (Simpson S and cols, 2020): typical, indeterminate and atypical appearance; all of them were PET positive if they presented pathological radiotracer uptake.Final diagnosis was made based on PCR results and clinical follow up. Change in the patient management was also recorded. ***Results:*** 230 whole body PET/CT scans were reviewed. 33 of them (14.3%) had lung findings suggestive of COVID-19 associated pneumonia (30 18F-FDG, 3 18F-Fluorocholine). Twelve patients had typical pattern, 15 indeterminate pattern and 6 atypical pattern, all of them with pathologic radiotracer uptake. Patients characteristics: 20 male, 13 female, mean age 59 years old. PET/CT indication: 30 oncologic patients -head and neck (5), breast (4), lung (5), lymphoma (3), multiple myeloma (1), colorectal (3), sarcoma (1), unknown primary tumor (1), endometrium (1), melanoma (1), prostate (3), SPN (1), thyroid (1)- and 3 patients with fever of unknown origin.Based on PET/CT findings, PCR was performed in 22/33 (66.6%) patients 0-12 days after PET/CT, with 12 positive and 10 negative results. All patients with positive PCR received specific treatment and isolation measures, and two of them had surgery delayed. From the 10 patients with negative PCR results, three of them were symptomatic a few weeks before; 1 patient had Klebsiella pneumonie present in BAS; 6 patients don´t have more clinical data. 11 patients had no PCR done; 1 of them was found to be clinically suspicious, and was prescribed to start specific treatment, isolation, and surgery was delayed; the rest don´t have further clinical follow up. ***Conclusion:*** In the actual pandemic state, incidental PET/CT lung findings are useful to identify COVID-19 associated pneumonia, and can change patient´s medical and social management. ***References:*** None

OP-875

Incidental Interstitial Pneumonia Suggestive Of COVID-19 In Asymptomatic Patients Undergoing 18F-FDG PET/CT In A High Prevalence Area

***D. Albano**, E. Cerudelli, M. Gazzilli, F. Dondi, A. Mazzoletti, P. Bellini, L. Camoni, F. Bertagna, R. Giubbini;*
University of Brescia and Spedali Civili of Brescia, Brescia, ITALY.

Aim/Introduction: : An aggressive acute respiratory disease caused by SARS-CoV 2, called COVID-19, occurred initially during December 2019 in Wuhan, China, and then spread globally, becoming a pandemic. After China, Europe and especially Northern Italy were severely affected, with a dramatic increase of cases of pneumonia and respiratory distress syndrome is some cities, like Brescia and Bergamo. Chest radiographs and CT are the preferred examinations for screening, diagnosis and monitoring of COVID-19 pneumonia. CT findings are typically characterized by ground-glass opacities (GGOs) or bilateral pulmonary consolidations in multiple lobular and sub-segmental areas. Instead the potential role of 18F-FDG PET/CT in this field remains unclear. Our aim was to collect the cases of interstitial pneumonia COVID-19 suspected detected at 18F-FDG PET/CT in March 2020 , describe their metabolic and radiological features and compared these results with those of the same period of 2019. ***Materials and Methods:*** In march 2020, 145 ^{18}F-FDG PET/CT studies were performed for routine oncological indications in our Department of Nuclear Medicine in Brescia, Italy. Owing to the concurrent high prevalence and increasing dynamics of COVID-19 infections in the region, all patients were asymptomatic and carefully screened by a triage before general access to the hospital, and again before entering the nuclear medicine service unit. Accordingly, no suspicion of viral infection was present at the time of PET/CT in any patient. ***Results:*** Fifteen patients (10%) showed CT signs of interstitial pneumonia, suspicious for COVID-19. In most cases (73%), increased FDG uptake corresponding to areas of pneumonia were detected. RT-PCR test was performed in 12 cases and resulted positive for COVID-19 in 11. The frequency of incidental pneumonia was significantly higher when compared to PET/CT scans of the same period one year earlier (only 9 of 350 PET/CT studies performed during March 2019 had incidental pneumonia). In case of positive scans, average SUVmax

was 5.7 (range 2.6-13) and SUVmean 3.5 (1.7-8.8). FDG-avid mediastinal lymph nodes involvement was registered in 3/15 cases. ***Conclusion:*** COVID-19 suspected pneumonia may be detected as incidental finding in asymptomatic patients undergoing PET/CT for oncologic indications in regions with high COVID-19 prevalence, are characterized by GGO and/or consolidations FDG-avid in most cases, underlying a possible high metabolic rate of this disease. ***References:*** None

OP-876

Estimating the incidence of asymptomatic SARS-CoV-2 infection by frequency of CT findings in patients undergoing PET/CT

I. Alberts*, B. Vollnberg, C. Sachpekidis, C. Mingels, S. Weidner, A. Rominger;*
Institut für Nuklearmedizin, Bern, SWITZERLAND.

Aim/Introduction: To present a method to estimate the prevalence of asymptomatic SARS-CoV-2 infection in high-risk individuals undergoing PET/CT using frequency of CT findings. ***Materials and Methods:*** 562 consecutive patients underwent PET/CT scanning with different radiotracers in the period between the first confirmed SARS-CoV-2 case in Switzerland and 14.04.2020. All patients were asymptomatic for respiratory infection at the time of scanning and were at increased risk for SARS-CoV-2 infection. Cognisant of recent reports showing the high sensitivity of CT for SARS-CoV-2 (98%) [1], including in asymptomatic patients [2] when compared to conventional laboratory testing [3], we observed the frequency of incidental, SARS-CoV-2 related changes in PET/CT [4]. No SARS-CoV-2 related CT findings were observed, enabling an estimate of the prevalence in the asymptomatic population using the binomial proportion confidence interval (Wilson's test). ***Results:*** N=562 negative tests yields a point prevalence of asymptomatic patients with SARS-CoV-2 infection in the population as 0.325% (95% confidence interval (CI) 0-0.65). By comparison, at the time of analysis the Swiss Federal Office for Public Health (FOPH) reported 25826 laboratory confirmed cases (population prevalence 0.3%, 92.7% agreement). These results find broad agreement with estimates of SARS-CoV-2 infection in other similar populations for the limited number of peer-reviewed population prevalence studies published [5]. ***Conclusion:*** The frequency and number of CT findings in asymptomatic patients undergoing PET/CT scanning can be used to estimate the incidence for SARS-CoV-2 in the asymptomatic population who may otherwise not present for conventional testing. Hitherto, few prevalence studies in asymptomatic populations have been conducted as a result of limited testing capacity during the pandemic. The derived model has good agreement with other empirical parameters. ***References:*** [1] Shi H, et al. Radiological findings from 81 patients with COVID-19 pneumonia in Wuhan, China: a descriptive study. The Lancet Infectious Diseases. 2020;20(4):425-34. [2] Inui S, et al. Chest CT Findings in Cases from the Cruise Ship "Diamond Princess" with Coronavirus Disease 2019 (COVID-19). Radiology: Cardiothoracic Imaging. 2020;2(2):e200110. [3] Fang Y, et al. Sensitivity of Chest CT for COVID-19: Comparison to RT-PCR. Radiology. 2020:200432. [4] Polverari G, et al. (18)F-FDG uptake in Asymptomatic SARS-CoV-2 (COVID-19) patient, referred to PET/CT for Non-Small Cells Lung Cancer restaging. Journal of thoracic oncology : official publication of the International Association for the Study of Lung Cancer. 2020 [5] Gudbjartsson DF, et al. Spread of SARS-CoV-2 in the Icelandic Population. New England Journal of Medicine. 2020.

OP-877

Incidental lung findings suspicious for SARS-CoV-2 infection in patients undergoing PET/CT during COVID-19 pandemic

R. Mei[1,2]*, L. Zanoni*[1]*, A. Farolfi*[1]*, C. Nanni*[1]*, V. Ambrosini*[1]*, P. Castellucci*[1]*, G. Montini*[1]*, V. Allegri*[1]*, A. Musto*[3]*, A. Golemi*[3]*, S. Fanti*[1]*;*
[1]Nuclear Medicine Policlinico S.Orsola-Malpighi, Bologna, ITALY, [2]DIMES, University of Bologna, Bologna, ITALY, [3]Metropolitan Nuclear Medicine, AUSL di Bologna, Ospedale Maggiore, Bologna, ITALY.

Aim/Introduction: SARS-CoV-2 infection may remain asymptomatic/falsely negative at pharyngeal RT-PCR, thus leading to COVID-19 underdiagnosis. Incidental pneumonia suspicious for COVID-19 in routine PET/CT examinations is reported. ***Materials and Methods:*** During Italian-Phase1-COVID-19-restrictions (21Feb2020-April2020), among triage-selected PET/CT performed for standard-indication in our MNM-Institution (n=2025), we retrospectively, preliminary analysed patients with findings suspicious for COVID-19 pneumonia, respectively: SARS-CoV-2 -RT-PCR-negative (at least 1) at the time of PET/CT (n=53) who unexpectedly turned out positive at subsequent RT-PCR tests (n=4/53), and asymptomatic, with incidental suspected viral pneumonia at PET/CT, immediately addressed to further investigations (n=14).All PET/CT were retrospectively reviewed by at least 2 expert readers; any lung/mediastinal potentially infectious finding was reported at PET (visual and SUVmax interpretation) and low-dose-CT (LDCT) images. Short-term clinical/laboratory/diagnostic-CT follow-up data were collected for validation. COVID-19 likelihood was finally categorized as: "certain"(RT-PCR-positive), "probable"(RT-PCR-negative but likely infected, treated), "indeterminate"(RT-PCR negative but isolated), "excluded". ***Results:*** Overall 18 pts were included (M:F=16:2; mean 67[47-84] years; 6/18 inpatients). PET-clinical-indication were: FUO 4/18, oncological 14/18. Radiotracers: 18F-FDG 15/18, 11C-Choline 2/18 ; 68Ga-PSMA 1/18.Overall 17/18 (94%) presented tracer-avid suspicious

ground-glass(GG)/consolidations: 7/17 monolateral, 10/17 bilateral, mostly multilobar (8/17) but predominantly basal (16/17). Among the 15 18F-FDG-avid lung findings, SUVmax ranged 2-10 (median 3.7, mean 4.4±2.5). No suspicious avid/enlarged hilar/mediastinal nodes were found. Non-avid LDCT lung findings were detected in 12/18 (67%) (mainly GG/consolidation or combination, pleural-effusion, bibasal disventilation).All 18 pts were addressed to RT-PCR after PET/CT and finally classified for COVID-19 as: "certain" (5), "probable"(5), "indeterminate"(5), "excluded"(3). At least 7/18 patients were hospitalized in COVID-area.8/18 patients presented double RT-PCR negativity and no symptoms the day of PET/CT: 4/8 however subsequently turned out positive at 3rd RT-PCR (4th in 1 case) (mean 12 days from PET[9-15]), with concordant HRCT, later hospitalized and treated; to note 1 coinfection case (Pneumococcal remission/COVID-19 progression). Among the other 4/8 persistingly negative RT-PCR cases, 1 was "probable", 1 "indeterminate", 2 "excluded" (bacterial).Among the 10/18 asymptomatic cases, only 1/10 was "certain" (RT-PCR positive 13 days after PET) and responded to hydroxychloroquine.Among the remaining 9/10 asymptomatic and RT-PCR negative patients, 4/9 presented concordant HRCT and considered "probable"(2/4 hospitalized), 4/9 "indeterminate", 1 "excluded"(bacterial). ***Conclusion:*** During COVID-19 pandemic, incidental PET/CT detection of asymptomatic/previously RT-PCR-negative lung infection is not infrequent and should be reported "real-time" having relevant implications for further clinical/contact exposures management. LDCT findings are reliable whereas PET-tracer avidity is not able to discriminate aetiology. Isolation and rigorous monitoring is crucial when etiology remains indeterminate. ***References:*** None

OP-878

Cancer and COVID-19; Report of Cases in Nuclear Medicine Department during the Pandemia in Spain

J. Ardila Mantilla*, A. Rotger Regí, M. Baquero Oliveros, A. Marí Hualde, J. Orcajo Rincón, I. Gómez Fernández, C. Durán Barquero, D. Zamudio Rodríguez, Y. Henao Celada, J. Atance García de la Santa, J. C. Alonso Farto;*
Hospital General Univeristario Gregorio Marañón, Madrid, SPAIN.

Aim/Introduction: The association between COVID-19 and cancer, despite the limited experience available, has been described. However, there are few publications about metabolic imaging manifestations in these patients. Since the pandemic started, Spain is one of the countries that has been affected the most in terms of case numbers and deaths. During the declaration of the state of alarm, our service has only performed urgent PET/CT scans. The aim is to determine the association between cancer and COVID-19 among patients who underwent an 18FDG PET/CT study. ***Materials and Methods:*** From March 14 to April 24, 2020, we have performed 240 urgent 18FDG-PET/CT examinations most of them with oncologic indication. All of them underwent PET/CT using the usual protocol, carrying out, before the examination, a questionnaire for screening for COVID-19 infection. Those without any of the following clinical manifestations were considered asymptomatic: myalgia, cough, headache, fever, dyspnea or others and oligosymptomatic those who presented only one of the above symptoms. Imaging was considered positive for infection in the presence of hypermetabolic lung infiltrates unjustified by other causes. ***Results:*** In 16 patients (6.6% of the total PET performed), COVID-19 infection was diagnosed by polymerase chain reaction with reverse transcriptase (PCR). Oncological indication was: 37.5% lung cancer (6/16, 4 of them with solitary pulmonary nodule), 25% lymphomas (4/16). The rest were respectively esophageal, gastric, thyroid, urothelial carcinoma, soft tissue sarcoma and a tumor of unknown origin. In 12 patients PET was requested to diagnose malignancy or tumor staging, all except 2 were without treatment; 2 were to assess response to treatment (1 with chemotherapy and 1 with radiotherapy) and 2 for disease follow up without treatment. 3 of them were asymptomatic for COVID-19 and 5 were oligosymptomatic, in these patients the PCR was requested based on the findings of the PET/CT. The mean hospitalization time was 15 days and all except 4 required oxygentherapy. There was 1 exitus in a patient with stage IV lung carcinoma. ***Conclusion:*** The incidence of COVID-19 infection seems to be higher in cancer patients than in the general population that is 0,29% (Cancer Incidence in the General Chinese population, Bersanelli M. Controversies about COVID-19 and Anticancer Treatment with Immune Checkpoint Inhibitors. Immunotherapy. 2020) and 0,42% according to official data in Spain. Lung carcinoma and lymphomas are the tumors most frequently associated with this infection. Strikingly, up to 50% of the cases detected are asymptomatic or oligosymptomatic. ***References:*** None

OP-879

The rate of incidental pulmonary ground glass opacities (pGGOs) at 18F-Choline PET/CT in prostate cancer (PCa) patients

D. Donner[1]*, M. Burei*[2]*, S. Agostini*[1]*, L. Picori*[1]*, E. Bagatin*[1]*, M. Erini*[1]*, G. Carbone*[1]*, A. Palermo*[1]*, F. Chierichetti*[1]*, L. Evangelista*[3]*;*
[1]Nuclear Medicine, Santa Chiara Hospital APSS - Trento, ITALY, [2]Nuclear Medicine Unit, Veneto Institute of Oncology IOV-IRCSS, Padua, ITALY, [3]Nuclear Medicine Unit, Department of Medicine-DIMED, University of Padua, ITALY.

Aim/Introduction: the aim of the study was to evaluate the rate of pGGOs with or without 18F-Choline uptake in PCa patients during COVID-19 outbreak. ***Materials and Methods:*** 18F-Choline PET/CT images of 410 patients (pts), from two different Italian PET centers, were re-evaluated by nuclear medicine physicians. In case of discordance, a third nuclear

medicine physician was involved. Two different subsets of pts were included: those who underwent 18F-Choline PET/CT from 1st November 2019 to 24th April 2020 (called Group A) and from 1st November 2018 to 24th April 2019 (called Group B). Data about the number and percentage of pts with incidental pGGOs, with and without 18F-Choline uptake, were collected for each group. Information about therapy at the time of PET/CT and the number of pts submitted to the COVID-19 test were assessed by using the Hospital Information System (SIO). Moreover, the incidence of COVID-19 symptoms in health professionals was registered. ***Results:*** 164 pts were included in Group A, while 246 in Group B. The number of pts with incidental pGGOs at PET/CT was 14.6% for Group A and 3.2% for Group B. In Group B none of the pts had also an uptake of 18F-Choline in pGGOs. Conversely, 12 pts (7.3%) in Group B have both pGGOs and 18F-Choline uptake. 9/83 (10.8%) pts with incidental pGGOs were under hormonal therapy in Group A and 2/93 (2.1%) in Group B. All pts were asymptomatic for lung disease, at the time of PET/CT and none of them were submitted to the COVID-19 nasopharyngeal test. The percentage of pts with incidental pGGOs and significant uptake of 18F-Choline was 4.5 times more frequent in Group A compared to Group B. However, none of the health professionals showed symptoms relative to COVID-19 in the first four months of 2020. ***Conclusion:*** this descriptive and retrospective work shows a different rate of pts with an incidental abnormal lung pattern in pts undergoing 18F-Choline PET/CT during COVID-19 pandemic. The relative higher percentage of pts undergoing hormonal therapy with incidental pGGOs at PET/CT, but without symptoms, seems to suggest a sort of compliance face to a possible asymptomatic infection. However, the use of personal protective equipment (surgical masks) by all patients examined and by all health professionals, together with a telephone evaluation in order to exclude the presence of symptoms relative to COVID-19 and the frequent handwashing procedures, have probably allowed avoiding contagion among the professionals. ***References:*** None

OP-880

Signs of a diffuse and intense tracheobronchitis are commonly observed on ventilation scans obtained with ^{99m}Tc-labelled aerosols during the disease progression of coronavirus 2019

P. Marie*, A. Bahloul, S. Melki, G. Karcher, C. Selton, F. Goehringer, L. Imbert, A. Verger;*
CHRU Nancy, Vandoeuvre (Les Nancy), FRANCE.

Aim/Introduction: In addition to the lung parenchyma, the endothelial lining of the respiratory track is also vulnerable to SARS-CoV2 infection, due to high ACE2 receptor expression [1]. We report herein a particularly high rate of signs of intense tracheobronchitis observed on Technegas® ventilation scans from 12 consecutive patients (age 67±17 years, 9 men) for whom a pulmonary embolism was suspected during the progression of a coronavirus disease 2019 (COVID-19). ***Materials and Methods:*** Ventilation images were obtained with ^{99m}Tc-labelled Technegas® and blood perfusion images obtained with ^{99m}Tc-labelled albumin macro-aggregates. Imaging was recorded using a whole-body CZT SPECT-CT camera (Veriton-CT®). ***Results:*** All patients had CT abnormalities highly evocative of COVID-19; 8 had positive RT-PCR tests whereas 4 did not. No mismatch indicative of PE was documented on SPECT images, but matched ventilation/perfusion defects were documented in all patients at the sites of parenchymal lung sequelae identified on CT images. Moreover, a particularly intense and symmetrical increase in Technegas® uptake was observed within the overall tracheobronchial tract in 3 patients and in the bronchi only in 2 patients. There was no difference between the 5 patients with, and the 7 patients without, such tracheobronchial abnormalities when considering all clinical and biological data, including the time duration from onset of symptoms (18±14 days vs. 12±12 days) and the rate of previous history of pulmonary disease, which was very low in both groups (20% vs. 0%). ***Conclusion:*** Increased tracheobronchial uptake of Technegas® has previously been observed in patients with bronchitis or chronic obstructive pulmonary disease [2] however was particularly marked here, suggesting an intense tracheobronchitis. Although the mechanism is presumably not specific of the SARS-CoV2 virus, such signs may have diagnostic applications, especially in the absence of any previous history of pulmonary disease. ***References:*** 1 - Ren X, Glende J, Al-Falah M, de Vries V, Schwegmann-Wessels C, Qu X, et al. Analysis of ACE2 in polarized epithelial cells: surface expression and function as receptor for severe acute respiratory syndrome-associated coronavirus. J Gen Virol. 2006;87:1691-5. 2 - Bajc M, Schümichen C, Grüning T, Lindqvist A, Le Roux P-Y, Alatri A, et al. EANM guideline for ventilation/perfusion single-photon emission computed tomography (SPECT) for diagnosis of pulmonary embolism and beyond. Eur J Nucl Med Mol Imaging. 2019;46:2429-51.

OP-881

Impact of the COVID-19 pandemic in Nuclear Medicine departments: preliminary report of the first international survey

S. Annunziata*[1], M. Bauckneht[2], D. Albano[3], G. Argiroffi[4], D. Calabrò[5], E. Abenavoli[6], F. Linguanti[6], R. Laudicella[7], Young Group of the Italian Association of NuclearMedicine (AIMN);*
[1]IRCCS Regina Elena National Cancer Institute, Rome, ITALY, [2]IRCCS Ospedale Policlinico San Martino, Genova, ITALY, [3]University and Spedali Civili, Brescia, ITALY, [4]University of Milan, Milan, ITALY, [5]University of Bologna, S. Orsola-Malpighi, Bologna, ITALY, [6]University of Florence, Firenze, ITALY, [7]University of Messina, Messina, ITALY.

Aim/Introduction: COVID-19 pandemic is challenging the availability of hospital resources. Several departments are shifting their work to the management of COVID-19 patients. Healthcare professionals who work in Nuclear Medicine (NM) departments could have experienced changes and problems. The Young Group of the Italian Association of Nuclear Medicine (AIMN) developed the first international survey to evaluate different experiences in the international scenario. Aim of this study is to perform a preliminary report of the ongoing survey. ***Materials and Methods:*** A questionnaire of thirty questions was prepared for all healthcare professionals of NM departments (e.g., physicians, residents, technicians, nurses, researchers), addressing three main issues: 1) new scheduling praxes for diagnostic and therapeutic programs; 2) assistance of patients with diagnosed or suspected COVID-19; 3) prevention of COVID-19 spreading in the departments. Since the 1st of April 2020, an invitation to the survey was sent to the corresponding authors of NM scientific papers indexed in SCOPUS in 2019. Two reminders were mailed to non-responding recipients. Personal data were analysed per individual responder. Organization data were evaluated per single department. ***Results:*** Two-hundred and ninety-six individual responders from 220 departments were evaluated. The mean age of responders was of 42 years (range 22-69). Most of the responders were from Europe (199/296, 67%). At the time of the response, several departments (213/220, 97%) already changed their organization due to the pandemic. About new scheduling praxes, in most departments scheduled diagnostic and therapeutic procedures were allowed but quantitatively reduced (112/220, 51%). A significant reduction of diagnostic and therapeutic programs (more than 20%) affected 198/220 (90%) and 158/220 (72%) departments, respectively. Patients with COVID-19 or suspected symptoms were evaluated for possible NM procedures by both phone and on-site pre-triage in approximately all departments. Incidental COVID-19 signs in NM exams occurred in 106/220 departments (48%). Few departments were closed or shifted to directly assist patients with COVID-19 (36/220, 16%). About the prevention of COVID-19 spreading, most of departments ensured proper distancing and personal protective equipment for NM staff and patients (200/220, 91%), such as surgical masks and gloves. Finally, 189/296 professionals (64%) thought that pandemic would not permanently change the work of NM departments in the future. ***Conclusion:*** COVID-19 heavily impacted on NM departments and professionals according to the preliminary report of this first international survey. New praxes for NM scheduling, assistance and prevention of COVID-19 have been applied during the pandemic. ***References:*** None

OP-882

A pandemic's impact on a Nuclear Medicine Department: Contingency plan implementation and activity restrictions in a COVID-19 referral hospital

L. Torres[1], M. Monteiro[2], A. Oliveira[1], J. Pereira[1];
[1]Centro Hospitalar Universitário São João, Porto, PORTUGAL,
[2]Centro Hospitalar Universitário Coimbra, Coimbra, PORTUGAL.

Aim/Introduction: The COVID-19 pandemic has forced Nuclear Medicine departments to adjust their operating procedures, reducing activity to the context-relevant essential services, amongst other extraordinary measures. With this study, we aimed to analyze the changes in the day-to-day activity of a Nuclear Medicine Department in a COVID-19 referral hospital. ***Materials and Methods:*** In our department, a COVID-19 contingency plan was drafted and put into action on March 13th 2020, determining all non-urgent programmed procedures to be suspended, therefore restricting activity to hospitalized patients and oncologic or urgent exams/treatments. This plan also revised disinfection procedures, patient flow inside the department, repurposed a room for isolation in the event of a signaled or symptomatic patient, and assigned the staff to 2 mirror teams, for rotation purposes. We reviewed the exam requests and procedures performed in the department during the periods of March-April 2019 and March-April 2020, analyzing and comparing the data. ***Results:*** In the months of March and April 2020, 1000 requests for imaging/therapeutic procedures were received, a 42% reduction compared to the same period in 2019 (1727 requests). These requests included non-urgent patients, to be scheduled at a later date, when the contingency plan is no longer active. 322 procedures were performed in March 2020, and 101 in April 2020, versus 628 and 652 in March and April 2019, which signals a 49% and 85% decrease, respectively. These numbers translate the rescheduling of all non-urgent patients since March 13th, and do not include PET-CT's performed, which are outsourced and remained stable, with even a slight increase (186 in March-April 2020 vs 163 in March-April 2019). From March 13th to the 30th of April 2020, 89% of procedures were for oncologic diseases, and 11% for urgent cases (myocardial perfusion, pulmonary thromboembolism, kidney transplant and Meckel diverticulitis). Finally, in March-April 2020, we reported 3 members of the staff who developed symptoms, all of whom tested negative for COVID-19, and one symptomatic patient who tested positive 1 week after having performed an imaging exam in our department. ***Conclusion:*** Despite precipitating a sharp decrease in the workload, the COVID-19 contingency plan allowed for a safe and clean work environment, which in turn enabled our department to carefully attend to oncologic and other urgent patients, with only 1 case of a symptomatic patient, and no cases among healthcare professionals. The impact of this contingency plan on rescheduled patients will be

evaluated in months to come. ***References:*** None

OP-883

Usefulness of Triage in a Nuclear Medicine Unit during Covid-19 Pandemic

S. Telo*, A. Farolfi, L. Muraglia, D. Bezzi, F. Serani, E. Fortunati, S. Mattoni, L. Vetrone, P. Castellucci, C. Nanni, S. Fanti;*
Nuclear Medicine, Policlinico S.Orsola-Malpighi, Bologna, ITALY.

Aim/Introduction: Covid-19 pandemic heavily affected Northern Italy since late February, forcing many changes to routine activities of Nuclear Medicine units. These changes included postponing non necessary/urgent exams, systematic use of personal protective equipments (PPE), modifications of patients' pathways and standard operating procedures (SOP); furthermore, we introduced a Triage of all patients accessing the department. Aim of the study was to evaluate the usefulness of Triage in a Red Zone area. ***Materials and Methods:*** From March 9th to April 30th 2020, we daily run the Triage, aimed at identifying patients at risk of having Covid-19 infection. At the access of the building all patients were asked for possible exposure on days before; presence of symptoms on days before; temperature was also measured. We compared the data resulting from such activity to the number of cases as officially recorded by the hospital as being Covid-19 positive. ***Results:*** Overall, the Triage was done for 8 consecutive weeks, namely 38 consecutive working days; 2 employees/day were necessary to run it properly. 1952 patients (pts) were overall evaluated (avg: 51 pts/day), and 3 pts (0.15%) were identified as suspect for Covid-19 (all 3 due to high temperature > 38°C). All 3 cases were sent back home (as not requiring immediate hospitalization, being without further symptoms), and notified to public healthcare for further exams/therapies; 2/3 resulted not affected and then came back to have their scans regularly done, while the 3rd was lost at follow-up. Based on official hospital data, out of the 1949 patients scanned, 8 subsequently resulted Covid-19 positive and confirmed (0.4%), while other 4 resulted highly suspect, and treated for Covid-19 but not confirmed. All those 12 cases were not identified at Triage (0% sensitivity); nonetheless we received a number of congratulations for the reassuring role of Triage, either from patients and from hospitals operators. The study could have been biased because symptomatic out-patients have probably decided to not come to the unit, while symptomatic in-patients were asked to have a negative swab before being admitted. ***Conclusion:*** Our data indicate that Triage was ineffective at identifying Covid-19 patients in our experience; however, the Triage was perceived as useful either by patients and by caregivers. ***References:*** None

OP-884

Teaching PET/CT to medical students under the COVID-19 lockout: Implementing a new freeware client server PET/CT viewer in the university network

M. Biermann*[1,2], S. Kanoun[3], T. Davidsen[4], R. Gray[5];*
[1]Nuclear Medicine/PET centre, Haukeland University Hospital, Bergen, NORWAY, [2]Department of Clinical Medicine, University of Bergen, Bergen, NORWAY, [3]Nuclear Medicine/PET centre, Institut Claudius Regaud, Tolouse, FRANCE, [4]IT Department, University of Bergen, Bergen, NORWAY, [5]Department of Education, University of Bergen, Bergen, NORWAY.

Aim/Introduction: Since 2017, medical students in the third and the fifth years at the University of Bergen are taught PET/CT "hands-on" by mandatory exercises in the university's learning management system (LMS) paired to a diagnostic client-server viewing system in the hospital [1]. Following the COVID-19 pandemic, students were barred access to the hospital. To give students continued access to PET/CT studies in native format including interactive image fusion, a separate client server system based on the university network had to be established at short notice. ***Materials and Methods:*** All 77 fifth-year students participating in the course "Nuclear Medicine in Oncology" were requested to install the open source multiplatform Fiji viewer with Beth Israel PET/CT plugin (http://petctviewer.org/) on their personal computers. Anonymized DICOM images are hosted by the public domain orthanc server (https://orthanc-server.com) running under a virtual CentOS Linux host behind the university's firewall. Students connect via virtual private network (VPN) with individual logon. Transport Security Layer (TSL/https) encryption is provided by apache2 acting as a reverse proxy. Detailed end user documentation was provided by screencasts on https://www.uib.no/en/radioweb/nuclear and inside the LMS. ***Results:*** The new client-server solution was online with complete user documentation after just six days on 19 April 2020. Regulatory approval was obtained on 21 April 2020, in time for the electronic Team-Based Learning (TBL) session on 22 April 2020. Before the TBL, we performed in-depth usability testing with the first five student adopters, four of whom had been exposed to earlier practical teaching of PET/CT as part of their objective structured Clinical Examination (OSCE) at the end of their third year [1]. All five expressed their satisfaction with the new solution. Within ten days after the TBL, 25 % of the students (19/77) passed the course's introductory PET/CT tutorial, and none requested support. ***Conclusion:*** The freeware Fiji/orthanc PET/CT-viewer has made it possible for medical students to receive hands-on PET/CT training even when they have no access to the hospital infrastructure. We plan a detailed student survey at the conclusion of our course to determine if these changes, which were necessitated by the pandemic crisis, provide a benefit to our teaching that should be made

permanent. ***References:*** 1. Gulati, Ankush; Schwarzlmüller, Thomas; du Plessis, Elsa; Softeland, Eirik; Gray Jr, Robert; Biermann, Martin. 2019. Evaluation of a new e-learning framework for teaching nuclear medicine and radiology to undergraduate medical students. Acta radiologica open. 8: 1-6. doi: 10.1177/2058460119860231

OP-885

Radiopharmacy activity during SARS-CoV-2 pandemic: management and production

S. Migliari[1], *A. Sammartano*[1,2], *M. Scarlattei*[1,2], *G. Baldari*[1,2], *S. Bola*[1,2], *T. Graziani*[1,2], *L. Ruffini*[1,2];
[1]*AZ. Osp. Universitaria di Parma, Parma, ITALY,* [2]*Nuclear Medicine Department, University Hospital of Parma, Parma, ITALY.*

Aim/Introduction: A new coronavirus causing severe respiratory diseases, called SARS-CoV-2, was described for the first time in the Hubei province of China, on late December 2019. Since then the virus has spread in several countries being declared, on 30 January 2020, from the World Health Organisation (WHO) a Public Health Emergency of International Concern. On February 21, the first cluster of 16 Italian cases have been reported in the Italian Northern region of Lombardy and then other confirmed cases were reported in several Italian regions. In this unprecedented pandemic moment, Nuclear Medicine (NM) services as integral part of multi-speciality hospitals had to face the outbreak, especially assisting cancer patients. Aim of study was to assess the impact of pandemic challenge on a hospital-based radiopharmacy, especially considering the production phase and the related diagnostic sessions during current lockdown, the protection of the work team and the susceptible patients and the maintenance of medical quality and safety. ***Materials and Methods:*** We have collected data about radiopharmaceutical preparations and injected doses from February 2020 to April 2020 for both conventional NM and PET, comparing data with the same period of the previous year (2019), using Microsoft Software Excel version 2007. Moreover, we have created and adapted SOPs to minimize the risk to staff and patients, while continuing to provide the essential and critical services. ***Results:*** Radiopharmaceutical preparations showed an increase of 7.83% in February 2020 respect to 2019. In March and April 2020 the radiopharmcy reduced the activity with a decrease of 21.59% in March and 38.58% in April 2020 compared to the same months of 2019, due to the lockdown declaration. For the injected doses it was recorded an increase of 6.53% comparing February 2020 to 2019, and a reduction of 20.43% and 44.23% in March and April 2020, respectively. Regarding PET, it was recorded an increase of 2.36% of the injected doses comparing February 2020 to 2019, and a reduction of 2.1% and 12.64% for March and April 2020. Ga-68 based radiopharmaceuticals produced in house increased of 1.88%, 29.06% and 10.82% in February, March and April 2020 compared to 2019. No staff member have been diagnosed with infection as of April, 2020. ***Conclusion:*** The current COVID-19 pandemic poses many challenges for the practice of PET and NM. Nevertheless, we have successfully developed guidelines and strategies to guarantee essential services and to keep our facilities safe for patients and staff. ***References:*** None

1511

e-Poster Presentation Session 10: Molecular Brain Imaging

Friday, October 30, 2020, 10:40 - 12:10 Channel 11

EPS-153

Clinical value of FDG-PET and MRI coregistration in Focal Cortical dysplasia

D. Khan*, A. Raj ST, M. Tripathi, A. Garg, M. Tripathi, R. Bhargavi, P. Chandra, R. Doddamani, A. Kumar, C. Bal;*
All India Institute of Medical Sciences, New Delhi, INDIA.

Aim/Introduction: Utility of F-18 Fluorordeoxyglucose (FDG) Positron Emission Tomography (PET) and MRI coregistration in focal cortical dysplasia (FCD). ***Materials and Methods:*** This was a retrospective study in which we included 40 histopathologically proven cases of FCD (17 type I and 23 type II). Each difficult to treat refractory epilepsy (DTE) patient had been extensively worked up and discussed multiple times in the epilepsy surgery meeting and a working hypothesis was generated before the decision for surgery was taken. The pre-surgical evaluation in these patients had included MRI in epilepsy protocol and resting brain FDG-PET. In all those cases when MRI was non-lesional, PET/MRI fusion was done and evaluated with reference to the vEEG and MEG localisation. Following which the neuroradiologist had a relook at the MRI. ***Results:*** 17 DTE patients had FCD type 1. MRI had revealed the lesion in 5 cases while both MRI and PET revealed the lesion in 6 cases. 6 patients were non-lesional on MRI (normal in 2 and equivocal in 4). PET/MRI fusion was done in all 6 cases and lesion was confirmed on MRI with corresponding hypometabolism on PET. There were 23 cases of FCD type II. MRI was localising in 5, both MRI and PET were localising in 17 and one case was non-lesional on MRI. PET/MRI fusion subsequently helped in lesion localisation in this case. Thus in a total of 7/ 40 cases (17.5%) PET/MRI coregistration enabled lesion localisation and hypothesis generation with successful surgery in this group of patients with DTE. ***Conclusion:*** PET/MRI coregistration is a useful non-invasive investigation that should be included in all DTE especially when MRI is non-lesional. In patients with FCD, it can lead to lesion localisation in upto 17.5 % cases. ***References:*** None

EPS-154

The clinical value of 18F-FDG PET/CT in assessment of STN-DBS therapy in PD patients

Q. Zhao, H. Yang, J. Cao, R. Wang, F. Wang;
General Hospital of Ningxia Medical University, Yinchuan, CHINA.

Aim/Introduction: 18F-fluorodeoxyglucose (18F-FDG) PET/CT has been widely used in the assessment of neurodegenerative diseases. The immediate effects of deep brain stimulation (DBS) of subthalamic nucleus (STN) in PD patients on relative subcortices are still controversial. The aim of this study was to investigate the changing pattern of 18F-FDG metabolism in PD patients after STN-DBS therapy. ***Materials and Methods:*** Resting brain 18F-FDG PET/CT imaging on baseline and 6 months after STN-DBS surgery were performed on 6 PD patients (4 male, 2 female, mean age 62 ± 6.9 years). 18F-FDG PET/CT cerebral images and raw data were analyzed using SPM8. A volumes of interest (VOIs) based change in regional glucose metabolism was obtained. An AAL template was used to perform the ROI based semi-quantitative analysis. The correlation between glucose metabolism and clinical alleviation was also investigated. SPSS17.0 was applied as the statistical software. Paired samples t-test and Pearson correlation analysis were conducted. ***Results:*** Compared with baseline, the glucose metabolism in parietal lobe was significantly increased (P< 0.05) 6 months after STN-DBS, which was also correlated with the alleviation of body rigidity. In contrast, the 18F-FDG were shown as decreased areas in putamen, pons, cerebellum and motor cortex after STN-DBS. ***Conclusion:*** STN-DBS can inhibit the PD-related pattern in a short time after surgery. A large number of sample is needed to the further verification. ***References:*** None

EPS-155

Glucose metabolic pattern using ^{18}F-FDG PET/CT in Parkinson's disease patients

Q. Zhao, H. Yang, J. Cao, J. Li, F. Wang;
General Hospital of Ningxia Medical University, Yinchuan, CHINA.

Aim/Introduction: Parkinson's disease (PD) is associated with the progressive loss of dopaminergic neurons in the substantia nigra, characterized by motor symptoms including tremor, rigidity, bradykinesia, and postural imbalance. ^{18}F-fluorodeoxyglucose (18F-FDG) positron emission tomography/computed tomography (PET/CT) has been widely used in the assessment of neurodegenerative diseases. The aim of this study was to identify the brain glucose metabolic pattern in PD patients and the clinical utility of ^{18}F-FDG PET/CT for PD. ***Materials and Methods:*** A total of 62 patients (33 male, 29 female, mean age 58 ± 6.9 years) with idiopathic PD and 40 normal control (NC) (20 male, 20 female, mean age 62.3 ± 8.6 years) in the control group are enrolled for the ^{18}F-FDG PET/CT study. ^{18}F-FDG PET/CT cerebral images and raw data were analyzed using SPM8. A VOI based brain metabolism changing pattern image was obtained. An AAL template was used to perform the ROI based semi-quantitative analysis. SPSS17.0 was applied as the statistical software. Paired samples t-test and Pearson correlation analysis were conducted. ***Results:*** When compared with the NC group, the brain glucose metabolism of PD patients in thalamus, putamen, pons, cerebellum, and motor cortex were significantly increased (p< 0.05). In contrast, the glucose metabolism in posterior parietal, occipital, and frontal cortices showed a decrease of FDG uptake (p< 0.05). ***Conclusion:*** The PD-related pattern (PDRP) of ^{18}F-FDG PET/CT in Parkinson's disease was characterized and reproducible globally. Multi-centered, longitudinal and specific PD subtypes studies are needed to explore the clinical utilities of ^{18}F-FDG PET/CT. ***References:*** None

EPS-156

Metabolic network alterations in FDG-PET in prodromal Dementia with Lewy bodies

L. Beyer[1], *A. Stockbauer*[1], *S. Morbelli*[2], *A. Chincarini*[3], *R. Bruffaerts*[4], *K. Van Laere*[5], *M. Grmek*[6], *V. Garibotto*[7], *N. Nicastro*[8], *G. B. Frisoni*[9], *A. W. Lemstra*[10], *A. Pilotto*[11], *S. Garcia-Ptacek*[12], *I. Savitcheva*[13], *M. A. Ochoa-Figueroa*[14,15,16], *A. Davidsson*[17], *V. Camacho*[18], *J. Vöglein*[19], *M. Unterrainer*[1], *O. Pogarell*[20], *P. Bartenstein*[1], *M. Ewers*[21], *D. Aarsland*[22], *F. Nobili*[2], *A. Rominger*[23], *M. Brendel*[1];
[1]Department of Nuclear Medicine, University Hospital of Munich, LMU Munich, Munich, GERMANY, [2]IRCCS Ospedale Policlinico San Martino, Genoa, ITALY, [3]National Institute of Nuclear Physics (INFN), Genoa section, Genoa, ITALY, [4]Department of Neurosciences, Faculty of Medicine, KU Leuven, Leuven, BELGIUM, [5]Department of Nuclear Medicine, University Hopsitals Leuven, Leuven, BELGIUM, [6]Department of Nuclear Medicine, University Medical Centre, Ljubljana, SLOVENIA, [7]Division of Nuclear Medicine and Molecular Imaging, Geneva University Hospitals and NIMTLab, Geneva University, Geneva, SWITZERLAND, [8]Department of Clinical Neurosciences, Geneva University Hospitals, Geneva, SWITZERLAND, [9]LANVIE (Laboratoire de Neuroimagerie du Vieillissement), Department of Psychiatry, Geneva University Hospitals, Geneva, SWITZERLAND, [10]VU Medical Center Alzheimer Center, Amsterdam, NETHERLANDS, [11]Neurology Unit, University of Brescia, Brescia, ITALY, [12]Division of Clinical Geriatrics, Center for Alzheimer Research, Department of Neurobiology, Care Sciences and Society, Karolinska Institutet, Stockholm, SWEDEN, [13]Medical Radiation Physics and Nuclear Medicine, Karolinska University Hospital, Stockholm, SWEDEN, [14]University Hospital of Munich, LMU MunichDepartment of Clinical Physiology in Linköping, Department of Health, Medicine and Caring Sciences, Linköping University, Linköping, SWEDEN, [15]Department of Radiology, and Department of Medical and Health Sciences, Linköping University, Linköping, SWEDEN, [16]Center for Medical Image Science and Visualization (CMIV), Linköping University, Linköping, SWEDEN, [17]Department of Clinical Physiology in Linköping, Department of Health, Medicine and Caring Sciences, Linköping University, Linköping, SWEDEN, [18]Servicio de Medicina Nuclear, Hospital de la Santa

Creu i Sant Pau, Universitat Autònoma de Barcelona, Barcelona, SPAIN, [19]Department of Neurology, University Hospital of Munich, LMU Munich, Munich, GERMANY, [20]Department of Psychiatry and Psychotherapy, University Hospital, LMU Munich, Munich, GERMANY, [21]DZNE–German Center for Neurodegenerative Diseases, Munich, GERMANY, [22]Centre for Age-Related Medicine (SESAM), Stavanger University Hospital, Stavanger, NORWAY, [23]epartment of Nuclear Medicine, University of Bern, Inselspital, Bern, SWITZERLAND.

Aim/Introduction: Metabolic network analysis in FDG-PET has been proven to provide complementary information underlying the disease process in Parkinsonism. In other atypical parkinsonian syndromes, network expression was proposed as an additional supporting biomarker in early diagnosis (1). In Dementia with Lewy Bodies (DLB), decreasing dopamine availability correlates with decreasing metabolic connectivity in affected regions (2), but only a few cases at an early disease stage have been investigated yet (3). The goal of this study was to evaluate alterations of glucose metabolism and network connectivity in DLB subjects at early stages of dopaminergic loss. ***Materials and Methods:*** FDG-PETs of subjects with probable or possible prodromal DLB (4) without significant dopamine deficiency (Z-Score < 2 in DaT-SPECT compared to healthy controls) were analysed by volume-of-interest-based calculations after stereotactic normalisation and cerebellar scaling. Metabolic alterations and network connectivity were compared to healthy controls (n=28) for both subjects with (n=86) and without (n=22) significant dopamine deficiency. ***Results:*** Subjects without significant dopamine deficiency showed regions with significant relative hypo- (parietal- and occipital cortex) and hypermetabolism (basal ganglia, parts of the limbic system, motor cortices) compared to healthy controls. The metabolic alterations were less pronounced, but similar to those found in subjects with significant dopamine deficiency. Metabolic connectivity analyses revealed increasing connectivity between affected brain regions at early disease stages without significant dopamine deficiency when compared to healthy controls. ***Conclusion:*** Disease specific patterns of glucose metabolism and altered metabolic networks can be detected by FDG-PET in DLB subjects without significant dopaminergic loss. These findings underline the potential of FDG-PET to be used as a supporting biomarker at early stage DLB. ***References:*** 1. Ko JH, Lee CS, Eidelberg D. Metabolic network expression in parkinsonism: Clinical and dopaminergic correlations. Journal of cerebral blood flow and metabolism : official journal of the International Society of Cerebral Blood Flow and Metabolism. 2017;37(2):683-93. 2. Huber M, Beyer L, Prix C, Schonecker S, Palleis C, Rauchmann BS, et al. Metabolic Correlates of Dopaminergic Loss in Dementia with Lewy Bodies. Movement disorders : official journal of the Movement Disorder Society. 2020;35(4):595-605.3. Massa F, Arnaldi D, De Cesari F, Girtler N, Brugnolo A, Grazzini M, et al. Neuroimaging findings and clinical trajectories of Lewy body disease in patients with MCI. Neurobiology of aging. 2019;76:9-17.4. McKeith IG, Ferman TJ, Thomas AJ, Blanc F, Boeve BF, Fujishiro H, et al. Research criteria for the diagnosis of prodromal dementia with Lewy bodies. Neurology. 2020.

EPS-157

Value of 18F-FDG-PET in early and differential diagnosis of Frontotemporal dementia, a prospective study

I. López Villar[1], *P. Paredes Rodríguez*[1], *D. Lourido García*[2], *A. López-Frías López-Jurado*[2], *P. Jane Soler*[1], *J. Bonilla Plaza*[1], *P. Azpeitia Hernández*[1], *A. Martínez Lorca*[1], *A. B*[1], *A. B*[1], *J. Castro Beiras*[1], *M. Orduña Díez*[1];

[1]Ramón y Cajal University Hospital, Nuclear medicine, Madrid, SPAIN, [2]Ramón y Cajal University Hospital, Radiology, Madrid, SPAIN.

Aim/Introduction: Frontotemporal dementia FTD is a common type of dementia particularly in patients younger than 65, encompassing a group of neurodegenerative diseases classified into 3 clinical variants: non-fluent variant primary progressive aphasia (NFV-PPA), semantic-variant primary progressive aphasia (SV-PPA) and behavioral-variant (BV-FTD). The goal is to evaluate FDG-PET as a biomarker for early and differential diagnosis of FTD and to investigate for specific metabolic signs of the variants. ***Materials and Methods:*** A prospective study of 41 patients was carried out at University Hospital (July 2017-March 2019); All patients (20 men 21 women) with clinical diagnostic suspicion of FTD were consecutively evaluated with 18F-FDG-PET/CT. Age (59-87 mean 70). The data were compared with 41 controls screened by age and gender. In all cases, a careful history, detailed neurological examination, laboratory studies and neuroimaging were performed. In atypical cases (26p) the differential diagnosis of Alzheimer's disease, parkinsonisms and/or psychiatric disorders was evaluated with: cerebrospinal fluid biomarkers (14), at the dopaminergic level (9) (with pre- and postsynaptic Dopamine SPECT and transcranial sonography), amyloid PET (2) and/or genetic test C9orf72 (1). FDG-PET data was visually and semi-quantitatively analyzed using a standardized uptake value ratio (SUVr) with a reference region of the cerebellar cortex. ***Results:*** In 65% patients (26/41) FTD was diagnosed: (15 PPA, 9 BV-FTD, 1 SV-PPA and in 1 case PPA and Alzheimer's disease co-ocurred). The remaining 35% (15/41): (10 Alzheimer's disease, 2 corticobasal syndrome, 1 mild cognitive impairment, 1 drug-induced-parkinsonism and 1 progressive supranuclear palsy). Specificity of 87% (13 True Negatives / 2 False Positives) and Sensitivity of 100% (26 True Positives / 0 False Negatives). High negative predictive value. Compared to controls, FDG-PET showed hypometabolism in frontal and temporal regions in most of the patients with

FTD. It also proves useful for discriminating FTD and early Alzheimer's disease (where hypometabolism in precuneus is especially indicative). The specific metabolic signs of the FTD variants: in primary progressive aphasia (APP) leftward asymmetry in the hemispheric brain, with hypometabolism mainly in left fronto-temporal region; In the behavioral-variant (BV-FTD) we found hypometabolism in the frontal and anterior temporal lobes, with involvement of the anterior cingulate gyrus, as more prominent metabolic findings. ***Conclusion:*** FDG-PET is a sensitive metabolic marker for early and differential diagnosis of FTD, with high negative predictive value. Patients with FTD have distinctive metabolic characteristics. In addition we also found specific metabolic signs in PPA and BV-FTD variants, further research is needed. ***References:*** None

EPS-158

Utility of 18F-FDG PET/CT based Metabolic Parameters in Differentiating Malignant Brain SOLs

A. Bedmutha*, N. C. Purandare, A. D. Puranik, M. Pereira, A. Agrawal, S. Shah, V. Rangarajan; Tata Memorial Center, Mumbai, INDIA.*

Aim/Introduction: Brain space-occupying-lesions (SOLs) can be neoplastic (lymphoma, glioma, metastasis, etc.) or non-neoplastic (infection, demyelination, etc.). Although MRI is standard imaging modality for characterizing brain SOLs, features of different pathologies can sometimes overlap. Fluorine-18-fluorodeoxyglucose (18F-FDG) uptake correlates with tumoral glycolytic activity, a characteristic that can be exploited to differentiate between malignant brain lesions. In this study, we aimed to determine role of different 18F-FDG PET-based metabolic parameters in differentiating malignant brain pathologies ***Materials and Methods:*** 147 patients with brain SOL, referred for pre-treatment 18F-FDG PET/CT scan by a multidisciplinary team, were included in this retrospective study. Following semi-quantitative metabolic parameters of brain lesions were calculated: Maximum standardized uptake value normalized by body weight (SUVmax), maximum and mean standardized uptake values normalized by lean body mass (SULpeak and SULmean), tumor-to-background activity ratios, metabolic tumour volume (MTV) and total lesion glycolysis (TLG). Histopathological confirmation was used as the gold standard in all patients. Differences between metabolic parameters of three most common malignancies were compared using rank-based nonparametric statistical tests. Receiver operating characteristic (ROC) curve analysis was used to determine diagnostic abilities of various metabolic parameters, and to establish their optimal cut-offs to differentiate between pathologies ***Results:*** High grade glioma (HGG, n=43), lymphoma (n=33), and metastases (n=65) were most common brain SOL pathologies (95.9%). Lymphomas showed significantly higher metabolic uptake (Mean ± SD: SUVmax=29.3±12.7, SULpeak=19.2±9.1 and SULmean=14.4±6.9), as compared with HGG (Mean±SD: SUVmax=13.1±7.4, SULpeak=8.1±4.4 and SULmean=6±2.9) and metastases (Mean±SD: SUVmax=15.6±12.7, SULpeak=9.5±7.5 and SULmean=7.4±5.7), with $P<0.05$ on non-parametric tests. The tumour-to-background ratios for lymphomas were also significantly higher, while MTV and TLG were insignificant in this regard. SULpeak>12.7 showed 83% sensitivity and 88% specificity, while tumour-to-white matter ratio (T/Wm)>5.6 showed 83% sensitivity and 85% specificity to diagnose lymphomas (AUC=0.912 and 0.900 respectively, $P<0.05$). In a subset analysis, MTV>19.05 cm^3 (Sensitivity, specificity:71%,75%; AUC=0.747) and TLG>126.15 gm (Sensitivity, specificity:71%,71%; AUC=0.737) could fairly differentiate HGG from solitary metastasis, while only SULmean could differentiate between HGG and multiple metastases (AUC=0.700). Lung cancer was most common primary in patients with brain metastases (83%). Two cases of disseminated tuberculosis showed FDG-avid brain SOLs. ***Conclusion:*** CNS lymphomas demonstrate significantly higher metabolism than HGG and metastases, with SULpeak and T/Wm ratio being optimal differentiating parameters. SULmean, MTV and TLG have average ability in differentiating glioma from metastases, and could be useful in select scenarios. In patients with brain metastasis, 18F-FDG PET/CT contributes by detecting primary malignancy and extent of disease. ***References:*** None

EPS-159

Single-centre investigation on the prognostic role of semiquantitative FET PETparameters in patients with previously treated primary brain tumours

M. Celli[1]*, G. Ghigi*[2]*, P. Caroli*[1]*, D. Arpa*[3]*, I. Marini*[1]*, L. Fantini*[1]*, V. Rossetti*[1]*, P. Cenni*[4]*, E. Amadori*[5]*, A. Romeo*[3]*, M. Belli*[6]*, A. Sarnelli*[6]*, G. Paganelli*[1]*, F. Matteucci*[1]*;*
[1]Nuclear Medicine Unit, Istituto Scientifico Romagnolo per lo Studio e la Cura dei Tumori (IRST) IRCCS, Meldola, ITALY, [2]Radiation Therapy Unit, Istituto Scientifico Romagnolo per lo Studio e la Cura dei Tumori (IRST) IRCCS, Ravenna, ITALY, [3]Radiation Therapy Unit, Istituto Scientifico Romagnolo per lo Studio e la Cura dei Tumori (IRST) IRCCS, Meldola, ITALY, [4]Neuro-Radiology Unit, "Santa Maria delle Croci" General Hospital AUSL Romagna, Ravenna, ITALY, [5]Radiology Unit, Istituto Scientifico Romagnolo per lo Studio e la Cura dei Tumori (IRST) IRCCS, Meldola, ITALY, [6]Health Physics Unit, Istituto Scientifico Romagnolo per lo Studio e la Cura dei Tumori (IRST) IRCCS, Meldola, ITALY.

Aim/Introduction: treatment-induced changes (TIC) may mimic recurrent / progressive brain tumor (RP-BT) on Gadolinium-enhanced MRI (Gd-MRI) in up to 30% of primary brain tumour patients. FET PET has been increasingly utilised to assist Gd-MRI in differential diagnosis of such scenarios. We aim to investigate the potential prognostic value of FET-based semiquantitative parameters in brain tumour patients

previously treated with surgery and chemo-radiation. ***Materials and Methods:*** This is a retrospective analysis on the follow-up of 18 primary brain tumour patients (mean age: 49 years; range: 21-76; WHO grade II n = 5; grade III n = 5; IV n = 8) previously treated with surgery and chemoradiation therapy, referred for FET PET to help Gd-MRI differentiate TIC and RP-BT (n=15) and for systemic therapy response evaluation (n = 3). FET PETs were acquired as 40-minute dynamic brain scans and late static brain images (20-40 minutes) were generated from each FET PET. FET images were fused with Gd-enhanced T1-weighted MRI images for lesion co-registration. FET outcome (positive versus negative) was evaluated according to established criteria* and the following FET semiquantitative parameters were tested for association with 12-month overall survival (OS): 1)ROC analysis: lesion SUVmax-to-normal Brain SUVmean Ratio (LBRmax), Metabolic Lesion Volume (MLV 40% isocontour), Total Lesion Metabolism (TLM = MTV x lesion SUVmean): 2)Kruskal-Wallis: TAC patterns (1: increasing with no peak; 2: peak and plateau; 3: peak and wash-out). ***Results:*** the 12-month OS ROC analysis found AUC of 0,805 for MLV cut-off value of 37,2mm^3 [cohort range: 3,6-138,6mm^3] with sensitivity (SE), specificity (SP), positive predictive value (PPV) and negative predictive value (NPV) of, 92,1%, 81,8%, 71,4%, 81,8%, respectively (p = .005). AUC of 0,805 was found for TLM cut-off value of 119,0mm3 [cohort range: 1,2- 314,8mm3] with SE, SP, PPV and NPV of 71,4%, 90,9%, 83,3%, 83,3%, respectively (p = .0011). FET outcome (positive / negative) did not significantly distinguish patients 12-months OS (Fisher's exact Test; p = 0,59; Log-rank: 0,642; p = 0,423), nor did LBRmax (ROC analysis; p = .149) and TAC pattern (Kruskal-Wallis; p = .200). ***Conclusion:*** Our preliminary experience suggests that FET-derived MLV and TLM may serve as prognostic factors for 12-month OS in pretreated primary brain tumours. ***References:*** *Law I, Albert NA, Javier Arbizu J et Al. Joint EANM/EANO/RANO practice guidelines/SNMMI procedure standards for imaging of gliomas using PET with radiolabelled amino acids and [18F] FDG: version 1.0. European Journal of Nuclear Medicine and Molecular Imaging. 2019 Mar;46(3):540-557.

EPS-160

Dual Time-Point FET-PET/CT in Glioma Patients: a Single-Centre Preliminary Experience

A. Vento[1], *R. Laudicella*[1], *F. Minutoli*[1], *D. Romeo*[1], *S. Russo*[1], *D. Cardile*[1], *R. Filice*[1], *A. D. Comis*[1], *A. Mirabile*[1], *B. Pagano*[1], *S. Bisdas*[2,3], *S. Baldari*[1];

[1]*Nuclear Medicine Unit, Department of Biomedical and Dental Sciences and Morpho-Functional Imaging, Univeristy Of Messina, Messina, ITALY,* [2]*Department of Neuroradiology, University College London Hospitals NHS Trust, London, UNITED KINGDOM,* [3]*Department of Brain Repair and Rehabilitation, University College London, London, UNITED KINGDOM.*

Aim/Introduction: Fluoroethyltyrosine (FET), an L-tyrosine amino acid analogue whose transport is independent from blood-brain-barrier status, is a well-established PET 18F-labelled agent used in the evaluation of glioma patients. Dynamic acquisitions enable to obtain time-activity-curves (TACs), able to provide information for grading assessment: low-grade-gliomas (LGG) are usually characterized by a continuously increasing uptake, vice versa high-grade-gliomas (HGG) usually shows an early peak followed by a plateau or a decreasing TACs. However, dual time-point acquisition imaging is more feasible even due to an increase in patient comfort and quicker image interpretation. This preliminary study aims to evaluate the potential clinical advantages of FET-PET/CT in the management of glioma, also in comparison with MRI. ***Materials and Methods:*** We retrospectively analyzed data of 20 patients (15 male and 5 female, mean age 52 years old, range 22-75) affected by glioma (6 G2, 3 G3, and 11 G4 according to WHO classification) who underwent surveillance MRI and FET-PET/CT static acquisition 10 and 50 min after administration of a mean dose of 277,5 MBq of 18F-FET. We correlated PET findings with clinical, radiological (MRI) and follow-up data for a mean period of 3 months after the FET-PET/CT scan. ***Results:*** 12/20 patients resulted positive for recurrence at FET-PET/CT: among them, the dual time-point acquisition showed the usual trend in 9/12 patients (75%) with 2/2 LGG showing an increasing uptake, and 7/10 HGG showing an early peak followed by a decreasing uptake. Among positive FET-PET patients, 4 of the HGG (29%) patients experienced a change of management according to FET findings .FET-PET/CT resulted negative in 4/20 patients, and doubtfully in other 4/20.Among the four doubtful PET findings, 3 HGG were negative at MRI assessment and have resulted suspicious for recurrence at FET-PET/CT; however, follow-up evaluation confirmed the PET findings. In 12/20 patients, PET findings were in accordance with MRI findings and among them 9/12 were HGG. ***Conclusion:*** In our preliminary experience, the evaluation with 18F-FET PET/CT resulted as a useful tool in LGG and HGG gliomas evaluation, offering an imaging method able to identify tumour progression and malignant transformation, earlier than MRI. Hence, 18F-FET findings influence clinical and therapeutic strategy. ***References:*** None

EPS-161

Initial clinical experience on the complementary role of brain FET-PET imaging with respect to Gd-MRI in the differential diagnosis of treatment-induced changes and true disease progression in treated primary brain tumour patients and association with WHO grading and prognostic biomarkers

M. Celli[1], *G. Ghigi*[2], *P. Caroli*[1], *D. Arpa*[3], *I. Marini*[1], *L. Fantini*[1], *V. Rossetti*[1], *P. Cenni*[4], *E. Amadori*[5], *A. Romeo*[3], *E. Mezzenga*[6], *A. Sarnelli*[6], *G. Paganelli*[1], *F. Matteucci*[1];
[1]*Nuclear Medicine Unit, Istituto Scientifico Romagnolo per lo Studio e la Cura dei Tumori (IRST) IRCCS, Meldola, ITALY,* [2]*Radiation Therapy Unit, Istituto Scientifico Romagnolo per lo Studio e la Cura dei Tumori (IRST) IRCCS, Ravenna, ITALY,* [3]*Radiation Therapy Unit, Istituto Scientifico Romagnolo per lo Studio e la Cura dei Tumori (IRST) IRCCS, Meldola, ITALY,* [4]*Neuro-Radiology Unit, AUSL Romagna, Ravenna, ITALY,* [5]*Radiology Unit, Istituto Scientifico Romagnolo per lo Studio e la Cura dei Tumori (IRST) IRCCS, Meldola, ITALY,* [6]*Health Physics Unit, Istituto Scientifico Romagnolo per lo Studio e la Cura dei Tumori (IRST) IRCCS, Meldola, ITALY.*

Aim/Introduction: in treated primary brain tumours, treatment-induced changes (TIC) can mimic recurrent / progressive brain tumor (RP-BT) on Gadolinium-enhanced MRI (Gd-MRI) in up to 30% of cases. FET PET has been increasingly utilised to assist Gd-MRI in differential diagnosis of such scenarios. We aim to evaluate 1) diagnostic performance of established* FET semiquantitative parameters in distinguishing TIC and RP-BT; 2) association of FET outcome with WHO grade, IDH mutant status, MGMT methylation and Ki67%. ***Materials and Methods:*** 18 primary brain tumour patients (WHO grade II n = 5; grade III n = 5; IV n = 8) treated with surgery and chemoradiation underwent 25 FET PET scans to discriminate equivocal Gd-MRI findings for RP-BT and TIC.FET PETs were acquired as 40-minute dynamic brain scans and late static images (20-40 minutes) were generated. FET images were fused with Gd-MRI for lesion co-registration.FET PET was considered positive for RP-BT if lesion SUVmax-to-normal Brain SUVmean Ratio (LBRmax) was superior to cut-off values of 1,9 and 2,3 in the early (< 12 weeks) and late (> 12 weeks) period after chemo-radiation therapy, respectively. Gold standard was repeat Gd-MRI within 3 months from FET PET and clinical follow-up (n = 23) and pathology (n = 2). FET PET outcome (positive / negative) was tested for dependency on prognostic features (Fisher's Exact Test; alfa: 0,05): WHO grade (Grade II versus III-IV), IDH status (mutant versus wild-type), MGMT methylation (methylated versus unmethylated) and Ki67 (< 10% and 10%). ***Results:*** Positive LBRmax ranged between 2,3 and 5.0 resulting in 17 true positives and no false positives. Negative LBRmax ranged between 1,3 and 1,7 resulting in 5 true negatives and 3 false negatives.The diagnostic performance of FET PET resulted in 85% sensitivity, 100% specificity, 63% negative predictive value, 100% positive predictive value and 88% diagnostic accuracy.In the post-surgical and chemoradiation therapy scenario, no significant dependency of FET PET outcome was found for WHO grade (p = 1,000), IDH status (p = 0,308), MGMT methylation (p = 1,000) and Ki67 (p = 0,206). ***Conclusion:*** FET PET demonstrated good diagnostic performance in discriminating RP-BT and TIC. In this pre-treated cohort of patients prognostic features did not significantly associate with FET outcome. ***References:*** *Law I, Albert NA, Javier Arbizu J et Al. Joint EANM/EANO/RANO practice guidelines/ SNMMI procedure standards for imaging of gliomas using PET with radiolabelled amino acids and [18F]FDG: version 1.0. European Journal of Nuclear Medicine and Molecular Imaging. 2019 Mar;46(3):540-557.

EPS-162

Assessment of Glioma Aggressiveness Using Dynamic FDOPA PET/CT

A. Girard[1], *P. Le Reste*[2], *A. Metais*[3], *N. Chaboub*[4], *A. Devillers*[1], *H. Saint-Jalmes*[4], *F. Le Jeune*[1], *X. Palard-Novello*[1];
[1]*Department of Nuclear Medicine, Centre Eugène Marquis, Rennes, FRANCE,* [2]*Neurosurgery, University Hospital of Rennes, Rennes, FRANCE,* [3]*Department of Pathology, University Hospital of Rennes, Rennes, FRANCE,* [4]*Inserm, LTSI – UMR 1099 research unit - University Rennes 1, Rennes, FRANCE.*

Aim/Introduction: The aim of this study was to assess the diagnostic value of kinetic parameters extracted from dynamic FDOPA PET/CT for tumor grading in patients with newly diagnosed gliomas in a prospective study with biopsy validation. ***Materials and Methods:*** Fourteen patients with untreated gliomas were prospectively investigated with FDOPA PET/CT. Twenty minutes of dynamic PET imaging after FDOPA injection were reconstructed. Tumor volume-of-interest (VOI) were generated based on the MRI-guided brain biopsies. Static parameters (SUVmax and tumor-to-brain ratio (TBRmax)), kinetic parameters extracted using full kinetic analysis with the reversible single-tissue compartment model (K1 = rate constant from blood to tissue, k2 = rate constant from tissue to blood, VB = blood volume parameter and distribution volume (DV) = K1/k2) and distribution volume (Vt) extracted using Logan graphical analysis were provided. Diagnostic accuracies of FDOPA PET/CT parameters for differentiating low-grade gliomas (LGG) from high-grade gliomas (HGG) were evaluated by receiver-operating characteristic (ROC) analyses (area under the curve; AUC). ***Results:*** Thirty-three tumoral VOI were analysed. K1 and k2 were significantly higher for HGG than for LGG (respectively median K1 value 0.124 vs 0.073 ml/ccm/min, p = 0.025 and median k2 value 0.093 vs 0.063 min^{-1}, p = 0.024). No significant difference was observed for the other kinetic parameters and the static parameters. Using ROC analyses, the diagnostic

accuracy to discriminate LGG from HGG was the highest and similar for K1 and k2 parameters (AUC values = 0.76, p = 0.02). ***Conclusion:*** The present study confirms the significant added value of FDOPA PET/CT kinetic parameters for newly-diagnosed gliomas grading. ***References:*** None

EPS-163

Dopamine release after fear conditioning as measured using bolus-infusion ^{11}C-raclopride PET-MRI

M. Lubberink*, A. Frick, J. Björkstrand, F. Åhs, M. Fredriksson;*
Uppsala University, Uppsala, SWEDEN.

Aim/Introduction: Dopamine transmission is suggested to be crucial for aversive learning, as has been shown in animal studies. However, studies on the importance of dopamine release in human fear conditioning are lacking. The aim of the present study was to investigate dopamine release in striatum and amygdala during fear conditioning in healthy humans. In addition to equilibrium analysis and lp-ntPET[1], a nested version of SRTM[2] was evaluated for assessment of dopamine release. ***Materials and Methods:*** Eighteen volunteers underwent 90 min ^{11}C-raclopride scans using a bolus-infusion protocol on a Signa PET/MR scanner. Fifty minutes after injection start, participants underwent a 20 min differential fear conditioning paradigm, pairing one cue (CS+) with an aversive electrical shock while another cue (CS-) was never paired with a shock. Changes in raclopride binding were assessed by equilibrium analysis, using lp-ntPET, and using a nested version of SRTM (SRTMnt). In this last case, BP_{ND}, R_1 and k'_2 were estimated for the first 45 min, and then R_1 and k'_2 were fixed for a fit to the last 20 min of data after conditioning. Accuracy and precision of SRTMnt were evaluated using simulations where dopamine release was described by gamma variate functions. Skin conductance response (SCR) to CS+ minus CS- served as the autonomic fear conditioning index. ***Results:*** ^{11}C-raclopride BP_{ND} based on SRTMnt was significantly reduced following fear conditioning by 5.4, 5.1 and 13.4 % in putamen, caudate and amygdala, respectively ($p<0.03$). A significant correlation between changes in BP_{ND} across all three methods was found. Simulations showed that SRTMnt could accurately measure changes in BP_{ND} provided that dopamine release was persistent to the end of the scan, without requiring equilibrium, and that results were insensitive to changes in R_1. Changes in BP_{ND} based on SRTMnt and equilibrium analysis in amygdala correlated with SCR ($r=0.54$, $p=0.22$ for SRTMnt). ***Conclusion:*** SRTMnt provided a robust, easily implemented alternative for assessment of dopamine release induced changes in BP_{ND} provided that increased dopamine concentrations are persistent, which has previously been shown to be the case by microdialysis in amygdala in similar fear conditioning expertiments in rodents. A significant correlation between dopamine release induced changes in BP_{ND} in amygdala and fear conditioning was found. ***References:*** 1. Normandin MD, Schiffer WK, Morris ED, Neuroimage 2012. 2. Lammertsma AA, Hume SP, Neuroimage 1996

EPS-164

Clinical significance of 123I-MIBG and 123I-FP-CIT in patients with Parkinsonism

K. Maruyama*, K. Utsunomiya, H. Kishishita, Y. Kono, Y. Ueno, N. Tanigawa;*
Kansai Medical University, Osaka, JAPAN.

Aim/Introduction: To evaluate the usefulness of 123I-meta-iodobenzylguanidine (MIBG) myocardial scintigraphy and 123I-Ioflupane (FP-CIT) scintigraphy in patients with parkinsonism. We also compare the differences between Parkinson's disease (PD) and any other parkinsonism (nonPD). ***Materials and Methods:*** Seventy-six patients (mean age: 73, age range: 53-89 years) with parkinsonism were enrolled in this study. Myocardial MIBG uptake was evaluated as the heart to mediastinum count ratio (H/M) for early (e) and delayed (d) images, and the heart washout rate (WR). Striatum FP-CIT uptake was evaluated as (1) Striatum (S), Caudate (C), anterior Putamen (aP), posterior Putamen (pP), whole Putamen (P); (2) Caudate asymmetry index (Casy), Putamen asymmetry index (Pasy); (3) the Caudate to Putamen count ratio (C/P). ***Results:*** The patients have been eventually diagnosed PD (n = 52) and nonPD (n = 24) clinically. The nonPD comprise progressive supranuclear palsy (n = 10), corticobasal degeneration (n = 6), multiple system atrophy (n = 2), drug induced parkinsonism (n = 3), and unknown cause of parkinsonism (n = 3). For PD-nonPD differentiation using each scintigraphic approach alone, we obtained test accuracy (MIBG eH/M, 53.9%; dH/M, 69.7%; WR, 71.1%; FP-CIT S, 65.8%; C, 69.7%; aP, 65.8%; pP, 65.8%; P, 64.5%) and low accuracy using asymmetry (Casy 48.7%; Pasy, 43.4%). MIBG WR alone had a sensitivity of 82.7% for detecting PD, with low specificity of 45.8%. FP-CIT C alone had a sensitivity of 80.8% for detecting PD, with low specificity of 45.8%. For combined use, the highest test accuracy (71.1%) separated PD from nonPD resulted under the assumption that 2 of the 2 biological markers as follows: WR combined with C or dH/M combined with S, had a sensitivity of 71.2% and specificity of 70.8%. Mean MIBG uptake (H/M) in PD was significantly lower, which was greater in dH/M than in eH/M, and mean WR in PD was significantly higher than in nonPD (Mann-Whitney U test, eH/M P = 0.018; dH/M, P = 0.002; WR, P = 0.0001). ***Conclusion:*** Neuroimaging study with radiotracer (MIBG and/or FP-CIT) may help in the differential diagnosis of parkinsonism. It is important to diagnose with taking the clinical findings and the scintigraphic features into consideration. ***References:*** None

EPS-165

The homogeneity of beta amyloid PET: different white matter properties of [18F]Florbetaben and [11C]PiB

M. Rullmann[1], P. L. Flender[1], V. L. Villemagne[2], O. Sabri[1], H. Barthel[1];
[1]Department of Nuclear Medicine, University of Leipzig, Leipzig, GERMANY, [2]Department of Molecular Imaging and Therapy, Centre for PET, Austin Health, Heidelberg, AUSTRALIA.

Aim/Introduction: The visual reading of brain beta-amyloid (Aβ) PET images relies on the regional evaluation of the contrast between specific gray and unspecific white matter (WM) uptake. Thus, the degree and homogeneity of the WM uptake might influence the reading results. It is known for the approved [18F]-labeled Aβ tracer Florbetaben (FBB) that its WM uptake is relatively higher than that of [11C] PiB. We hypothesize, however, that the homogeneity of the tracer uptake within the WM is more important than its magnitude, and investigated this feature in the present study. ***Materials and Methods:*** We analyzed the data of (1) two matched (for the Aβ-neg. vs. -pos ratio, age and gender, n=67 each) patient cohorts who underwent [11C]PiB and [18F]Florbetaben PET, and those of (2) a head-to-head PiB vs. FBB comparison (10 young controls: 32.6±9yrs, 3 males; 25 elderly: 71.7±6yrs, 12 males) from the GAAIN database. For both tracers, we assessed the homogeneity, energy and contrast as WM uptake texture characteristics using the Radiomics toolbox in Matlab. ***Results:*** For (1), homogeneity, energy and contrast showed no tracer differences, but a smaller variance ($p<0.001$) for FBB independent of the Aβ status. Here, no age effect on the WM uptake texture parameters was seen. For (2), the FBB WM uptake data showed higher homogeneity ($p<0.001$), energy ($p<0.001$) and lower contrast ($p<0.001$) as compared to the PiB data. Here, the FBB data had a lower variance in homogeneity (young controls: $p=0.02$), energy (young controls: $p=0.006$) and contrast (elderly: $p=0.009$). While, in this cohort, for both tracers the WM uptake homogeneity correlated with age (FBB: $r=0.45$, $p=0.007$; PiB: $r=0.6$, $p<0.001$), only in the PiB data the WM uptake energy ($r=0.57$, $p<0.001$) and contrast ($r=-0.59$, $p<0.001$) was age-correlated. ***Conclusion:*** For PiB and FBB, the texture characteristics homogeneity, energy and contrast of the WM uptake differ, with favorable results for FBB. Further, an age effect on the WM uptake was evident for PiB, but not for FBB data. Further investigations on the expression of this feature over different patients and on its effect on the gray matter Aβ diagnosis are, thus, warranted. ***References:*** None

EPS-166

Myelin imaging with [^{11}C]MeDAS PET

C. W. J. van der Weijden*, J. F. Meilof, R. A. J. O. Dierckx, E. F. J. de Vries;*
UMCG, Groningen, NETHERLANDS.

Aim/Introduction: Magnetic resonance imaging (MRI) is important for the diagnosis of Multiple Sclerosis (MS), but lacks the specificity needed for evaluating demyelination and remyelination. Anti-inflammatory therapies are not able to treat MS adequately, therefore new therapies aim to stimulate remyelination. To determine the efficacy of remyelination therapies, it is necessary to have an accurate myelin imaging method. [^{11}C]MeDAS Positron Emission Tomography (PET) scanning was found to be a promising method for in vivo myelin quantification in animal models, but has not been used in humans yet. Our study aims to evaluate the feasibility of myelin imaging with [^{11}C]MeDAS PET in MS patients. ***Materials and Methods:*** A total of 10 MS patients will be included in the study. Following intravenous injection of [^{11}C]MeDAS, patients will receive a 60-min dynamic brain PET scan and subsequently a 10 min static spinal cord PET scan. Concomitant arterial blood sampling will be performed to obtain a metabolite-corrected plasma input function. Regional time-activity curves will be generated from the PET images using pMOD (version 4.004). These curves will be analysed using several pharmacokinetic models. Some preliminary results will be presented. ***Results:*** So far, 5 patients have been included. The data from these patients was analysed. Visual assessment of tracer binding in the first patients indicates that the tracer primarily binds to white matter. This was confirmed by quantitative analysis, showing a higher binding potential in white (4.02±1.37) than in grey matter (1.49±0.43). Furthermore, rapid metabolism of [^{11}C]MeDAS was observed, with 73% of the tracer being metabolized after 10 min. The kinetics of the tracer was best described by a reversible two tissue compartment model (AIC -15.9). Different amounts of tracer was observed per lesion. ***Conclusion:*** The first in human [^{11}C] MeDAS scans were successfully performed. No adverse events occurred and both the scan protocol as the scan itself were well tolerated. Preliminary results indicate that [^{11}C]MeDAS binds primarily to white matter and is rapidly metabolised, which leads to a fast clearance from the body. [^{11}C]MeDAS kinetics are well described by a reversible two tissue compartment model. The data suggests that [^{11}C] MeDAS might have the potential to determine the efficacy of remyelination therapies. More precise data will follow after more inclusions. ***References:*** None

EPS-167

Alterations in cerebral blood flow in patients with secondary progressive and stem cell-treated multiple sclerosis - a perfusion study with ^{15}O-water-PET

M. Lubberink*, L. Appel, A. Tolf, T. Danfors, E. Larsson, A. Landtblom, G. Antoni, J. Sörensen, J. Burman;*
Uppsala University, Uppsala, SWEDEN.

Aim/Introduction: Multiple sclerosis (MS) is an autoimmune and degenerative disorder where the immune system

malfunctions attack the central nervous system, leading to demyelination and neuronal/axonal loss. Impaired cerebral blood flow (CBF) has been associated with disease progression in neurodegenerative disorders. Chemotherapy combined with haematopoietic stem cell transplantation (HSCT) was introduced as an alternative treatment in 2004 at our hospital. Nowadays there is a growing evidence that HSCT is a successful treatment, but the question remains whether it is an ultimate cure for MS. This study aimed to investigate differences in CBF between three cohorts: patients with secondary progressive MS (SPMS), treated patients (HSCT) and healthy controls (HC). ***Materials and Methods:*** ^{15}O-water-PET scans with arterial blood sampling were acquired at rest for 10 SPMS, 9 HSCT (10 years after treatment), and 10 HC (age and gender matched). Arterial input functions were corrected for delay and dispersion. CBF and distribution volume (V_T) values were generated using a standard single-tissue compartment model including a fitted blood volume parameter. T1-weighted MR images were used for segmentation and automated definition of volumes of interest. Nonparametric tests were used to detect significant differences between cohorts ($p<0.05$). ***Results:*** Global CBF, including gray and white matter, was significantly lower in SPMS compared to HSCT (0.36±0.08 versus 0.50±0.11 mL/g/min, $p = 0.005$), whereas no significant differences were found between HSCT (0.46±0.09 mL/g/min) and HC ($p = 0.47$). Regional CBF revealed similar patterns for SPMS, and significant differences with HC and HSCT were especially found in subcortical regions. Further, V_T was significantly higher in HSCT and HC compared to SPMS, both globally and regionally, but not significantly different between HC and HSCT. ***Conclusion:*** These preliminary results revealed an impaired CBF and decreased V_T in SPMS. Similar levels of CBF and V_T for HSCT and HC indicates that HSCT treatment might restore overall brain functionality. In part, the current findings also confirm the outcome of clinical investigations/observations [1,2]. Specific CBF and V_T alterations in gray matter suggest a relationship with various disabilities in MS patients. ***References:*** 1 Burman J et al. J Neurol Neurosurg Psychiatry. 2014, 85(10):1116. 2 Tolf A et al. Acta Neurol Scand. 2019, 40(5):320-327.

EPS-168

Brain SPECT perfusion and PET metabolism as discordant biomarkers in major depressive disorder

E. Guedj[1], R. Richieri[1], L. Boyer[1], T. Korchia[2], G. Fond[2], C. Lançon[1], M. Tastevin[1];
[1]Aix Marseille Univ, Marseille, FRANCE, [2]APHM, Marseille, FRANCE.

Aim/Introduction: Brain SPECT perfusion and PET metabolism have been, most often interchangeably, proposed to study the underlying pathological process in major depressive disorder (MDD). It is hypothesized that the two biomarkers characterize the global synaptic activity through the neurovascular coupling. The objective of this study is to document similarities and inconsistencies between brain SPECT perfusion and PET metabolism according to global characteristics of the disease (number of previous episodes and illness duration) in patients with MDD. ***Materials and Methods:*** We conducted a retrospective pilot study in 16 patients suffering from unipolar depressive disorder who underwent a cerebral SPECT with 99mTc-HMPAO and 18F-FDG PET with an interval delay of less of 18 months (mean delay of 4.37 months ±4.89). Whole-brain voxel-based SPM(T) maps were generated in correlation with the number of depressive episodes and in correlation with the depression duration, separately for the two exams (p-voxel < 0.005 uncorrected, p-cluster < 0.05 uncorrected). ***Results:*** No significant correlations were found between brain PET metabolism and either the number of depressive episodes or the duration of the disease. On the contrary, significant correlations were found with SPECT perfusion: the increased number of depressive episodes was correlated with decreased perfusion of the right insula (k=515); the increased depression duration was correlated with bilateral decreased perfusion of the anterior cingulum (k=236). ***Conclusion:*** The study demonstrates that brain perfusion and glucose metabolism are not equivalent biomarkers in MDD, highlighting the value of brain perfusion SPECT despite less favorable instrumentation detection compared to metabolic PET. ***References:*** None

EPS-169

Effect of Statins on Brain Perfusion in Major Depression as an Addition to Standard Therapy. SPM Analysis of Inflammation, Platelet Activation, Endothelial Dysfunction and Neurocognitive Parameters

***T. Massardo[1]**, J. Quintana[2], J. Pereira[2], C. Sáez[2], L. Risco[1], S. Corral[1], N. Olivares[2], J. Spuler[1], G. Castro[1], D. Vicentini[2], B. Riedel[1], G. Valenzuela[2], C. Villa[3];*
[1]Hospital Clinico Universidad de Chile, Santiago, CHILE, [2]Pontificia Universidad Católica de Chile, Santiago, CHILE, [3]Instituto Psiquiátrico Dr. Horwitz, Santiago, CHILE.

Aim/Introduction: Major depressive disorder (MDD) is a prevalent condition, with a close bidirectional relation with cardiovascular disease and a significant proportion of relapse with serious quality of life and social impact. Statins may have some effect on MDD as observed in coronary heart disease and other vascular conditions. Aim: evaluate the effect of Rosuvastatin in MDD comparing changes in regional cerebral blood flow (rCBF), in neurocognitive performance and in serum biomarkers, affected by statins action. ***Materials and Methods:*** We studied 20 MDD patients free of specific therapy; 59% females; median age: 34 years; HAM-D 17 items greater than 15 and self-applied Beck´s Questionnaire greater than 12. All received specific serotonin receptor inhibitors; half rosuvastatin (10 mg/d)

and half placebo, randomized. We performed a rest brain perfusion SPECT with ^{99m}Tc-ECD at baseline and at 3 months of therapy. SPM12 analysis was employed to compare the differences in both groups between 3 months and baseline (perfusion deltas). Applied covariances (CoV) were the deltas from: Neurocognition Cambridge Battery CANTAB tasks; platelet activation, endothelial dysfunction, general inflammatory serum markers, Rho A / Rho kinase pathway and oxidative stress parameters, obtained the same days than the SPECT images. ***Results:*** HAM-D and Beck's scores decreased (p=0.0001); Beck´s presented a larger decrease with statins. Seven out of ten placebos were responders and 8/10 statins (p=ns). SPM12 analysis demonstrated significantly larger rCBF changes in the pregenual / subgenual anterior cingulate plus orbitofrontal cortex and a small area in the posterior cingulate gyrus in the statins group, not observed with placebo, when using HAM-D and Beck´s scores as CoV. Similar pattern of rCBF changes, when used as CoV, were observed with: A) emotion recognition, attentional, paired associates learning, spatial planning and working memory tasks; B) platelet activation markers: P-Selectin, RANTES, NAP-2 and Brain-derived Neurotrophic Factor; C) endothelial dysfunction markers: circulating endothelial cells, ICAM-1, VCAM and Monocyte Chemoattractant Protein; D) General inflammation markers: ESR, CRP and IL-6; E) Rho kinase pathway and F) oxidative stress: malondialdehyde; those changes were no present with placebo. ***Conclusion:*** Short-term use of low dose statins in MDD patients under standard therapy, results in important rCBF changes in key mood and cognitive control areas, associated to improvement in neurocognitive performance, platelet activation, oxidative stress and diverse inflammatory and endothelial function markers. These findings could open a new therapeutic approach to this relevant mood disorder. FONDECYT 1160885 ***References:*** None

1601

CME 13: Radiomics in a Precliniical and a Clinical Setting

Friday, October 30, 2020, 13:50 - 15:20 Channel 1

OP-886

Radiomics and Nuclear Medicine - The Basis for Understanding its Value and a Revision of Literature

M. Hatt; INSERM, LaTIM UMR 1101, Brest, FRANCE.

OP-887

Radiomics and Nuclear Medicine - Oncologist's Requests

N. Fazio; IRCCS IEO, European Institute of Oncology, Division of Gastrointestinal Medical Oncology and Neuroendocrine Tumours, Milan, ITALY.

OP-888

Radiomics and Nuclear Medicine - Nuclear Physician's Response

M. Kirienko; IRCCS Istituto Nazionale dei Tumori, Nuclear Medicine Division, Milan, ITALY.

OP-889

Radiomics and the Future - Where are we Going?

P. Lambin; Maastricht University, Precision Medicine, School for Oncology and Develop Biol, Fac. Health, Medicine and Life Sciences, Maastricht, NETHERLANDS.

1602

Joint Symposium 25 (EANM/EANO): Immunotherapy in Brain Tumours

Friday, October 30, 2020, 13:50 - 15:20 Channel 2

OP-890

Immunotherapy of Gliomas

M. Weller; Universitay Hospital Zurich, Department of Neurology, Zurich, SWITZERLAND.

OP-891

Immunotherapeutic Options in Brain Metastases

E. Le Rhun; University Hospital Lille, Department of Neurosurgery, Lille, FRANCE.

OP-892

PET Imaging of Response to Immunotherapy in Brain Tumours

N. Galldiks; University Hospital Cologne, Department of Neurology, Cologne, GERMANY.

1603

Joint Symposium 26 (EANM/AAPM): Quantitative SPECT - An Essential Tool?

Friday, October 30, 2020, 13:50 - 15:20 Channel 3

OP-894

How we get from SPECT to Quantitative SPECT

G. Roberts; The Newcastle upon Tyne Hospitals NHS Foundation Trust, Nuclear Medicine Department, Newcastle, UNITED KINGDOM.

OP-895

The Limitations and Pitfalls of Quantitative SPECT

C. Kappadath; University of Texas MD Anderson Cancer Center, Department of Imaging Physics, Houston, TX, UNITED STATES OF AMERICA.

OP-896

A Physicians View of Quantitative SPECT

S. Vöö; University College London Hospitals, Institute of Nuclear Medicine, London, UNITED KINGDOM.

1606

Cutting Edge Science Track - TROP Session: Harmonisation & Standardisation

Friday, October 30, 2020, 13:50 - 15:20 Channel 6

OP-898

Standardisation and Validation of ^{177}Lu Quantitative SUV-SPECT/CT

T. Alkahtani[1,2], J. Johnson[2], K. Adamson[2], V. Lewington[1,2], L. Livieratos[1,2];
[1]King's College London, London, UNITED KINGDOM, [2]Guy's & St Thomas' Hospitals NHS Foundation Trust, London, UNITED KINGDOM.

Aim/Introduction: Imaging as part of the patient workup for molecular radiotherapy (MRT) is often used in evaluation, verification and follow-up of treatment. Beyond its role as a visual assessment tool, image quantification may have a role in monitoring change as part of MRT. Recent advancements in SPECT imaging, such as improved image reconstruction and scatter and attenuation correction, allow for precise quantitative analysis and the calculation of standardised uptake value (SUV). This study aims to investigate optimal protocols for quantitative ^{177}Lu SPECT/CT by evaluating the accuracy of absolute SUV-SPECT/CT quantification. ***Materials and Methods:*** As part of setting the optimal 3D quantitative SUV-SPECT/CT protocol, since there are different quantitative tools proposed, phantom imaging was conducted to develop and validate image quantification method using ^{177}Lu including: · Cylindrical homogeneous phantom to assess scintillation camera calibration factor (CF) (cps/MBq) for planar and SPECT imaging. CF value was used by HERMES to estimate the SUV in the volume of interest (VOI). · The NEMA IEC Body Phantom consisting of a body/thorax-size compartment and six spherical inserts of various sizes (from 10mm to 37mm in diameter) was used to validate the accuracy of quantitative SUV by calculating the concentration recover coefficients (cRC) at various object sizes. ***Results:*** HERMES Hybrid3D 3.01 software (HERMES Medical Solutions, Sweden) was used to estimate CF and SUV values. An optimal CF of 11.1 cps/MBq results in most accurate activity estimates (1124MBq) with -1% difference from the actual activity (national primary standard calibrated well-counter) compared to a 16% difference reported with manually calculated CF (9.4 cps/MBq). With regard to OSEM iterations for optimised activity concentration values, good precision was observed over 80 sub-iterations as coefficient-of-variation became less than 3%. Relative error reached a plateau of minimum value above 80 sub-iterations. Activity concentration showed a minimum relative error of -4%. SUV-SPECT values presenting optimal SUVmean equal to 1 and measured activity concentration with less than 5% difference from the actual value for a Philips PRECEDENCE system and less than 2% for a Siemens INTEVO BOLD systems. ***Conclusion:*** SUV-SPECT/CT quantification can be optimised with implemented calibrations. CF and cRC are the primary aspects to be addressed with high accuracy and precision. Reliable estimation is achievable when attenuation, scatter, collimator-detector resolution, energy window, and OSEM iterative reconstructions are compensated. ***References:*** None

OP-899

An international quantitative SPECT/CT imaging exercise for assessment of Ba-133 as surrogate for I-131

J. Tran-Gia[1], A. P. Robinson[2], C. Bobin[3], N. Calvert[4], S. Collins[2,5], A. M. Denis-Bacelar[2], A. Fenwick[2,6], K. Ferreira[2], D. Finocchiaro[7,8], F. Fioroni[7], K. Gianopoulou[9], E. Grassi[7], W. Heetun[2], S. J. Jewitt[10], M. Kotzasarlidou[9], M. Ljungberg[11], V. Lourenço[3], D. R. McGowan[10,12], J. Scuffham[13], K. Sjögreen Gleisner[11], J. Solc[14], C. Thiam[3], J. Tipping[4], J. Wevrett[13], M. Lassmann[1];
[1]Department of Nuclear Medicine, University of Würzburg, Würzburg, GERMANY, [2]National Physical Laboratory, Teddington, UNITED KINGDOM, [3]CEA, LIST, Laboratoire national Henri Becquerel, (LNE-LNHB), Gif-sur-Yvette Cedex, FRANCE, [4]The Christie NHS FT, Manchester, UNITED KINGDOM, [5]Department of Physics, University of Surrey, Guildford, UNITED KINGDOM, [6]Cardiff University, Cardiff, UNITED KINGDOM, [7]Azienda Unità Sanitaria Locale di Reggio Emilia - IRCCS, Medical Physics Unit, Reggio Emilia, ITALY, [8]Department of Physics and Astronomy, University of Bologna, Bologna, ITALY, [9]"THEAGENIO" Anticancer Hospital, Thessaloniki, GREECE, [10]Oxford University Hospitals NHS FT, Oxford, UNITED KINGDOM, [11]Department of Medical Radiation Physics, Lund, SWEDEN, [12]University of Oxford, Oxford, UNITED KINGDOM, [13]Royal Surrey NHS FT, Guildford, UNITED KINGDOM, [14]Czech Metrology Institute, Brno, CZECH REPUBLIC.

Aim/Introduction: In nuclear medicine imaging, commissioning and quality control are typically performed based on hollow containers manually filled with radionuclide solutions. Most associated sources of uncertainty (e.g., filling volume, activity concentration) can be overcome by sealed, long-lived surrogate sources containing a radionuclide of comparable energies and emission probabilities, traceable to a primary standard. This study presents the results of a quantitative SPECT/CT imaging comparison exercise performed within the MRTDosimetry project to assess the applicability of Ba-133 sources as a surrogate for I-131 and to determine a cross-calibration factor. ***Materials and Methods:*** Cylinders of four

different dimensions (active volumes of diameters 7.5, 15, 30, and 60 mm and 38 mm height, resulting in volumes of 1.68, 6.72, 26.9 and 107.4 cm^3) and two different caps (one for complete closure, one with filling hole) were fabricated with a stereolithography 3D printing system (Formlabs Form 2, Tough resin). Optimal source placement in 216-mm Jaszczak cylinder was ensured by a laser-cut attachment baseplate designed based on simulations of spilled-out counts (Gaussian convolution with 20-mm FWHM). Solid Ba-133 surrogate sources were produced at two metrology institutions: CEA (activity concentration [206.2±5.8] kBq.mL^{-1}) and CMI ([99.8±1.6] kBq.mL^{-1}), with leakage and contamination tests according to ISO9978. The comparison exercise included eight SPECT/CT systems (3×Siemens, 5×GE). Each site had to perform three measurements with different sources attached in a water-filled Jaszczak cylinder: 1) Ba-133 CEA sources, 2) Ba-133 CMI sources, 3) identical containers filled with liquid I-131. Parameters: High-energy collimator, 2×60 projections of 30s, Ba-133: 356.0keV [5%-15%-10% scatter-main-scatter], I-131: 364.5keV [6%-20%-6%], low-dose CT, OSEM with standard corrections. A CT-based VOI analysis was carried out to compare differences in pseudo-ICF (image calibration factor including partial-volume related errors: counts in VOI per activity and scan duration). A regression analysis was performed to determine a cross-calibration factor. ***Results:*** Iodine-131 pseudo-ICFs were higher than Ba-133 pseudo-ICFs for all reconstructions and systems. Equivalent setups (camera and reconstruction) yielded comparable pseudo-ICFs (average relative error 5.6% between three equivalent GE setups). The regression analysis resulted in a cross-calibration factor of 0.70±0.02. This value is in agreement with the ratio 0.764±0.005 of the emission probabilities (62.05±0.19)% (Ba-133) and (81.2±0.5)% (I-131) [1]. ***Conclusion:*** Although this international comparison exercise was challenging due to varying transport regulations between countries, we could show that traceable solid Ba-133 sources can be used as surrogate for liquid I-131, thus potentially reducing inherent problems with on-site activity measurement and phantom preparation. ***References:*** [1] http://www.nucleide.org/DDEP_WG/DDEPdata.htm.

OP-900

Computer Aided Imaging Analysis software for SPECT/CT protocol comparisons

C. Jaudet*, E. Quak, K. Weyts, A. Corroyer Dulmont, C. Lasnon, R. Ciappuccini, J. Saviny, G. Foucras, A. Batalla, S. Bardet;*
Centre François Baclesse, Caen, FRANCE.

Aim/Introduction: Robust methodology to compare SPECT/CT protocol performance is lacking. Generally, a fillable phantom is used to create reproducible measurements and a simple recovery coefficient is used for comparison. We developed a new freely available software solution to extract more complex image features from SPECT/CT acquisitions, allowing for more accurate comparisons. This software solution was then used to reduce acquisition time and optimize image quality of ^{177}Lu SPECT/CT scans. ***Materials and Methods:*** We created a new module named Computer Aided Image Analysis in simpleITK in python [1]. It was implemented in 3dSlicer software in order to optimize this already usable graphical interface [2]. With this module, recovery coefficients, noise, spatial resolution and a shape index can be extracted from SPECT scans based on an ideal image created from CT[3]. Firstly, the module was validated and optimized on simulation data, by varying the spatial position and resolution of a SPECT degraded image in reference to an ideal one. Secondly, it was used on NEMA IEC phantom data (spheres to background ratio=10) to compare two ^{177}Lu SPECT/CT acquisition protocols for different activity concentration. The standard protocol of 32 projections of 30s in a step and shoot mode was compared to a new protocol of 60 projections of 15s in a continuous mode. ***Results:*** For simulation data the software was able to compare the recovery coefficient, noise, spatial resolution and form index with an accuracy of 100% for 3 different simulations. For the phantom data, the recovery coefficient, noise, spatial resolution and form index for the standard versus the new protocol were [42.2%, 54.9%], [8.7%, 10.2%], [22.5mm, 17.5mm], [70.4%, 83.8%] respectively for a sphere of 5.57ml (rod diameter=22mm) and a background activity of 150kBq/ml. Acquisition time was reduced from 35 to 30 min for a two bed position acquisition. Except for noise, the new continuous SPECT/CT protocol improved the recovery coefficient, spatial resolution and shape index in phantom data. ***Conclusion:*** Our program was successfully deployed in a clinical environment and allowed us to choose a faster and optimized 177 Lu SPECT/CT protocol. ***References:*** [1]Lowekamp BC et al., (2013) ,Front. Neuroinform. 7:45. doi: 10.3389/fninf.2013.00045 [2] Fedorov A. et al., Network.,(2012) Magn Reson Imaging. 2012 Nov;30(9):1323-41. PMID: 22770690. PMCID: PMC3466397. [3] Tran-Gia, J., & Lassmann, M. (2019)., Journal of Nuclear Medicine, 60(1), 50-59.

OP-901

Development and characterisation of a PET "painting" robotic phantom to generate pseudo-anthropomorphic brain and geometric test objects under digital computer control

A. Paramithas*, A. Britten;*
St. George's University Hospitals NHS Foundation Trust, London, UNITED KINGDOM.

Aim/Introduction: Moving radioactive source systems have been used for gamma camera and PET test objects in air (Forgacs et al., 2019). This work aims to extend the capability

to in-water objects to produce pseudo-anthropomorphic test objects to optimise brain PET. ***Materials and Methods:*** A computer controlled electro-mechanical system allows 3D positioning of a source (5 MBq ^{18}F), and control of the time spent at each location over a 12cm^3 volume in a water filled cylinder. The relative distribution of activity is achieved by varying the source dwell time, derived from MRI images or geometry files. Basic performance was characterised and a geometrical test object was defined representing the cerebellum and inferior temporal lobe with a clinically relevant SUVR of 1.8, as found in Alzheimer's patients imaged with novel tau tracer PI-2620. Another test object representing the 28 mm IEC sphere was digitally defined and imaged on GE Discovery 710 series scanners. ***Results:*** Simulated point sources had image locations measured within +/- 1.2 mm of those set. A linear relationship between dwell time and image counts was obtained (97% r^2 over 0.5 s to 2.5 s). The IEC sphere image matched the set 28 mm diameter. SUVR was in agreement with the set value. Painting of test objects took 40-60 minutes. Operators could change between test objects in under 15 minutes, with the only change being the digital control files. ***Conclusion:*** This first in-water robotic "painting" phantom shows the potential to produce pseudo anthropomorphic and geometric shape test objects, under highly flexible digital control. Further investigation of the inclusion of random counts is required and the painting speed needs to increase to allow larger organ or shape volumes to be produced. ***References:*** Forgacs A, Kallos-Balogh P, Nagy F, Krizsan AK, Garai I, Tron L, et al. (2019) Activity painting: PET images of freely defined activity distributions applying a novel phantom technique. PLoS ONE 14(1): e0207658

OP-902

Printing 3D Heterogeneous Activity Distributions for Quality Control of SPECT and PET

J. Gear, *G. Flux;*
The Royal Marsden NHSFT, Sutton, UNITED KINGDOM.

Aim/Introduction: Quality control tests of molecular imaging systems are hampered by the complexity required to prepare phantoms. It is proposed that radioisotopes can be directly incorporated into photo-polymer resins. Use of the radio-polymer in a 3D printer allows phantoms with complex and reliable activity distributions to be produced whilst simplifying source preparation. ***Materials and Methods:*** Initial tests have been performed to determine the practicality of integrating Tc-99m into a photo-polymer and example phantoms produced to test suitability for quality control. Samples of build and support resins were extracted from the print cartridges of an Objet30Pro Polyjet 3D printer. The response of the resin to external factors including ionising radiation, light and dilution with Tc-99m pertechnetate were explored. After success of the initial tests the radio-polymer was used in the production of different phantoms. Radionuclide dose calibrator and gamma camera acquisitions of the phantoms were used to test the accuracy of activity concentration, print consistency, uniformity and heterogeneous reproducibility. Tomographic phantoms were also produced including a uniform hot sphere, a complex configuration of spheres and interlacing torus's and a hot rod phantom. ***Results:*** The coefficient of variation between repeat prints of a 12 g disk phantom was 0.08%. Measured activity within the disks agreed to within 98 ± 2 % of the expected activity based on initial resin concentration. Gamma camera integral uniformity measured across a 3D printed flood field phantom was 5.2 % compared to 6.0 % measured with a commercial Co-57 flood source. Heterogeneous distributions of activity were successfully reproduced for both 2D and 3D imaging phantoms. Count concentration across regions of heterogeneity agreed with the planned activity assigned to those regions on the phantom design. ***Conclusion:*** 3D printing of radioactive phantoms has been successfully demonstrated and is a promising application for quality control of PET and SPECT systems. ***References:*** None

OP-903

Retrospective Quantitative Harmonization in PET Using Deconvolution and Optimal Filtering

D. Huff[1], *M. Namías*[2], *A. J. Weisman*[1], *T. J. Bradshaw*[3], *M. R. Albertini*[4], *R. Jeraj*[1,5];
[1]*Department of Medical Physics, University of Wisconsin-Madison, Madison, WI, UNITED STATES OF AMERICA,* [2]*Department of Medical Physics, Fundación Centro Diagnóstico Nuclear, Buenos Aires, ARGENTINA,* [3]*Department of Radiology, University of Wisconsin-Madison, Madison, WI, UNITED STATES OF AMERICA,* [4]*University of Wisconsin Carbone Cancer Center, Madison, WI, UNITED STATES OF AMERICA,* [5]*Faculty of Mathematics and Physics, University of Ljubljana, Ljubljana, SLOVENIA.*

Aim/Introduction: Quantitative analysis in longitudinal clinical assessments using PET imaging can be negatively impacted if multiple PET scanners are used. In this work, we describe a retrospective harmonization method that can be implemented to enable accurate, quantitative PET analysis across scanners which were not harmonized before the baseline PET assessment. ***Materials and Methods:*** Clinical reconstruction protocols for each scanner were identified from PET/CT image DICOM headers. NEMA phantom scans were acquired on each scanner using the identified reconstruction settings. Phantom images were deconvolved with the post-filters declared in the headers using Wiener deconvolution, giving unfiltered images as a result. Then, optimal isotropic 3D Gaussian filters were determined for each reconstruction setting combination by minimizing the dispersion in NEMA phantom contrast recovery coefficients

(CRC_{max}) via a downhill-simplex optimizer. Dispersion was defined as the root-mean-square sum over NEMA phantom spheres of the standard deviation of CRC_{max} values. After optimal filters were established, clinical PET images were also unfiltered using Wiener deconvolution, and then re-filtered with the optimal filters. The impact of the harmonization process was assessed by tracking SUV metric changes in 184 lesion response observations from 138 ^{18}F-FDG whole body scans of 20 patients with metastatic melanoma treated at the University of Wisconsin Carbone Cancer Center. ***Results:*** Seven unique sets of reconstruction settings from three GE PET/CT scanners (Discovery IQ, Discovery 710, Discovery VCT) were identified. Harmonization reduced the dispersion in CRC_{max} values by a factor of 3.4. After harmonization, 7/7 reconstruction setting combinations complied with EANM/EARL specifications, where only 1/7 had complied prior to harmonization. The optimal post filters for harmonization ranged between [7.6-8.1] mm FWHM. The harmonization process changed lesion response category as defined by ±30% change in lesion metric for at least one lesion in 11/20 patients. Lesion response assessment via SUV_{max} was changed by harmonization more frequently (18% of lesion observations) than assessment via SUV_{mean} (5%) or SUV_{total} (4%). ***Conclusion:*** The proposed method for quantitative harmonization can reduce differences due to imaging hardware and reconstruction settings for a retrospective PET dataset. Performing harmonization with this method had a significant impact on lesion response observations in more than half of a cohort of metastatic melanoma patients. ***References:*** None

OP-904

A realistic Phantom of the head for the Validation of attenuation corrections methods in PET-MRI

J. Harries[1,2], *T. H. Jochimsen*[2], *T. Scholz*[2], *T. Schlender*[2], *H. Barthel*[2], *O. Sabri*[2], *B. Sattler*[2];
[1]*Department of Medical Physics and Radiation Protection, Hannover Medical School, Hannover, GERMANY,* [2]*Department of Nuclear Medicine, Leipzig University Hospital, Leipzig, GERMANY.*

Aim/Introduction: The combination of positron emission tomography (PET) and magnetic resonance imaging (MRI) (PET-MRI) is a unique hybrid imaging modality mainly used in oncology and neurology. The MRI-based attenuation correction (MRAC) is crucial for correct quantification of PET data. A suitable phantom to validate quantitative results in PET-MRI is currently missing. In particular, the correction of attenuation due to bone is usually not verified by commonly available phantoms. The aim of this work was to develop such a phantom and to explore whether such a phantom can be used to validate MRACs. ***Materials and Methods:*** Various materials were investigated for their attenuation and MR properties. For the substitution of bone, water-saturated gypsum plaster was used. The attenuation of 511 keV annihilation photons was regulated by addition of iodine. Fatty tissue was imitated by silicone and brain tissue by agarose gel, respectively. The practicability with respect to the comparison of MRACs was checked as follows: A small flask inserted into the phantom and a large spherical phantom (serving as a reference with negligible error in MRAC) were filled with the very same stock solution. The activity concentration was measured and compared using clinical protocols on PET-MRI and different built-in and offline MRACs. The same measurements were carried out using PET-CT for comparison. ***Results:*** The phantom imitates the human head in sufficient detail. All tissue types including bone were detected as such so that the phantom-based comparison of the quantification accuracy of PET-MRI is possible. Quantitatively, the activity concentration in the brain, which was determined using different MRACs, showed a mean deviation of about 5% and a maximum deviation of 11% compared to the spherical phantom. For PET-CT, the deviation was 5%. ***Conclusion:*** The comparatively small error in quantification demonstrates that the phantom can be used to validate MRAC methods. Hence, a cross-system comparison towards standardization of the overall quantification performance of various PET-MRI systems, including their MRAC methods, seems to be possible for the first time for brain Imaging. ***References:*** None

OP-905

A PET/MRI phantom study using MRI based attenuation correction to account for attenuation of the phantom material

I. Rausch*, A. Valladares, T. Beyer, E. Unger;*
Medical University of Vienna, Vienna, AUSTRIA.

Aim/Introduction: PET/MRI phantom studies are challenged by the need of a phantom specific attenuation template to account for the attenuation of the phantom material. In this study we present a PET/MRI phantom built from MRI visible, 3D printable material for which attenuation correction (AC) can be performed using the standard MRI based AC. ***Materials and Methods:*** A water fillable phantom was 3D printed with a commercially available, MRI visible polymer. The phantom had a cylindrical shape and the fillable compartment consisted of a homogeneous region and a region with solid rods of different diameters. The phantom was filled with a solution of water and [18F]FDG. Sodium chloride (0.9%) and MR contrast agent was added to avoid MR artefacts. The phantom was placed in the FOV of a PET/MRI system and a 30 min PET acquisition including the standard Dixon based MR-AC method was performed. In addition, a CT scan of the Phantom was acquired on a PET/CT system. From the Dixon in-phase, opposed-phase and fat images, a phantom specific AC map (Phantom MR-AC) was produced by separating the phantom material from the water compartment using a thresholding-based

method and assigning fixed attenuation coefficients for water and the polymer to the individual compartments. The PET data was reconstructed using the original Dixon MR-AC, the Phantom MR-AC, an MR-AC just containing the water compartment (noWall-AC) to estimate the error of ignoring the phantom walls and a CT based AC as reference. We calculated average percent differences in measured activity between the CT corrected PET and the PET corrected with the other AC methods for the whole water compartment as well as for a 5 pixel wide region along the phantom material in a slice of the homogeneous- and the rod containing region. ***Results:*** Compared to the CT-AC PET, average differences in measured activity of 8.9%, 4.5% and -27.2% were found for Dixon MR-AC, Phantom MR-AC and noWall-AC based PET, respectively. Average differences near the phantom wall in the homogeneous region were 6.7%, 6.6% and -34.4%, respectively. Around the rods, activity differed from the CT-AC PET by 9.7%, 4.8% and -21.9%, respectively. ***Conclusion:*** The presented phantom material is visible using standard MR sequences, and thus, can be incorporated in the MR-AC. PET quantification was substantially improved when accounting for the phantom material. However, the presented MR-AC approaches did not show full equivalence to CT based AC. ***References:*** None

OP-906

Automated acceptance calibration and quality control for a compact benchtop SPECT system

P. Mollet*, S. Neyt, K. Braeckman, K. Deprez;*
Molecubes NV, Ghent, BELGIUM.

Aim/Introduction: Routine quality control measurements are often lacking in preclinical research, but are of paramount importance to standardize the use of high-performance imaging systems(1,2). In this study, we present automated QC for the ɣ-CUBE (MOLECUBES). To the best of our knowledge, these automated procedures do not exist in preclinical µSPECT. ***Materials and Methods:*** Daily QC (<1min) measures detector temperature and response, based on background activity. Monthly QC (<1min) evaluates the energy spectrum and uniformity of each detector using a 1ml syringe containing 35-50µCi 99m-Tc. Energy resolution and photopeak location are calculated using an automatic Gaussian fitting algorithm. The average standard deviation of detector flood maps is used as uniformity measure. An automated procedure using the syringe phantom has been included to allow acceptance calibration. This protocol will collect data at every position for all detectors. For each position on a 0.5 by 0.5mm pitch, an energy histogram is collected and the energy peak location is determined by fitting the spectrum using a Gaussian model. Using the new energy peak locations, the data is energy filtered and the detector flood maps are used to correct for detector gain variations. GPU acceleration is used to speed up the process. ***Results:*** Using the standard user interface, any user can start the procedures without specialized knowledge. All measurements and analyses are done automatically and results are reported in the GUI. The daily QC will evaluate whether a detector temperature between 20 and 26°C is measured, and whether counts are collected. The Monthly QC will report energy resolution (to be below 11%), maximum energy peak shift (<1.5 keV) and detector uniformity (<5%). The procedure was tested on an uncalibrated system leaving the production facility. After passing daily QC, monthly QC showed an energy peak at 124 keV, energy resolution of 10.8% and detector uniformity of 7.96%. After applying the automated calibration, the energy peak was centered at 140 keV and a resolution of 10.6% and a uniformity of 3.45% were obtained. ***Conclusion:*** We demonstrated the possibility to automatically evaluate detector stability, energy spectra and detector uniformity in combination with automated system calibration. This is a step forward in providing easy and straightforward QC procedures in preclinical imaging to improve standardization in the daily use of microSPECT and to ensure uniform performance over time. All procedures can easily be extended towards other isotopes. ***References:*** 1. Osborne et al. Mol Imaging Biol 2. Vanhove et al. EJNMMI Physics

OP-907

Performance Evaluation of a compact benchtop SPECT system for ^{99m}Tc, ^{111}In and ^{177}Lu

K. Deprez*, K. Braeckman, S. Neyt;*
MOLECUBES, Ghent, BELGIUM.

Aim/Introduction: The γ-CUBE is a compact high-sensitivity, high-resolution preclinical SPECT system for whole body mouse and rat imaging. The detectors of this system are based on SiPMs coupled to NaI(Tl) scintillators. The collimators use the lofthole geometry [1] and are produced by additive manufacturing [2]. In this study we evaluated the imaging capabilities for three isotopes using the methods published in [3]. ***Materials and Methods:*** The performance evaluation consists of spatial resolution, energy resolution and sensitivity measurements using 99m-Tc, 111-In and 177-Lu [3]. Spatial resolution measurements were done both with capillary tubes and with hot rod phantoms, scanned for one hour. Reconstructions were done using 500 or 300 iterations (mouse and rat respectively) and a voxel size of 250µm or 500µm (mouse and rat respectively). A low volume source (50uL, 3.7-37MBq) was used to perform the sensitivity and energy resolution measurements, scanned for 20 seconds. ***Results:*** The 99m-Tc measurements show a resolution of 456µm and 956µm and a sensitivity of 0.10% and 0.05%, for the mouse and rat collimator respectively. Using 111-In and the mouse collimator we obtained a spatial resolution of 503 µm and 801 µm for the 171keV and 245keV photon peak respectively and a similar sensitivity of

0.07%. With the rat collimator a resolution of 980µm and 1.57mm, and a sensitivity of 0.05% and 0.06% is obtained for the 171keV and 245keV photon peaks respectively. Results of the Lu177 measurements are reported for the 113keV and 208 keV photon peak respectively. A resolution (sensitivity) of 410µm (0.12%) and 564µm (0.08%) was measured for the mouse collimator and a resolution (sensitivity) of 898µm (0.07%) and 1.3mm (0.06%) was obtained for the rat collimator. The energy resolutions were: 9.7% (99m-Tc, 140keV), 9.3% (111-In, 171keV), 9.4% (111-In, 245keV), 10.5% (177-Lu, 113keV) and 9% (177-Lu, 208keV). ***Conclusion:*** This performance evaluation of the MOLECUBES γ-CUBE demonstrates that the system has ideal imaging capabilities for in vivo imaging of both rats and mice, and for a variety of radiopharmaceuticals. The high energy resolution also opens up possibilities for multi-isotope studies. ***References:*** 1. Deprez et al. Physics in Med & Biology 2. Deprez et al. Medical Physics 3. Deleye et al. Eur J Nucl Med Mol Imaging

OP-908

Performance of a Novel Small-Animal SPECT System with Two Stationary Detectors: A Comparison of Multi-Pinhole Collimators for Mouse Imaging

J. Hoffmann[1,2], J. Janssen[1,2], T. Kanno[2,3], T. Higuchi[1,2,4];
[1]Department of Nuclear Medicine, University Hospital of Würzburg, Würzburg, GERMANY, [2]Comprehensive Heart Failure Center, University Hospital of Würzburg, Würzburg, GERMANY, [3]Department of Quantum Medical Technology, Graduate School of Medical Sciences, Kanazawa University, Kanazawa, JAPAN, [4]Graduate School of Medicine, Dentistry and Pharmaceutical Sciences, Okayama University, Okayama, JAPAN.

Aim/Introduction: Small-animal SPECT systems with multi-pinhole collimation and three large stationary detectors have been shown their superiority when compared to systems with moving small detectors [1]. Recently an economically attractive version with two large stationary detectors has been introduced. We investigated the performance to analyze the capabilities of this novel SPECT system. ***Materials and Methods:*** A newly developed small-animal SPECT with two stationary detectors (size of detectors: 47.2 cm x 59.5 cm) and multi-pinhole collimation was used for acquiring data with point source, mini-Derenzo hot-rod and uniformity phantoms, filled with ^{99m}Tc (energy window centered at 140 keV), to analyze sensitivity, spatial resolution, uniformity and contrast-to-noise-ratio (CNR). Three dedicated mouse collimators with 75 pinholes each and diameters of 0.25 mm; 0.6 mm and 1.0 mm for extra ultra-high resolution (XUHR-M), general-purpose (GP-M) and ultra-high sensitivity (UHS-M) imaging were examined. Activity concentration was 309.7 ± 20.4 MBq/ml and scan time was 45 min. For CNR analysis, four different activity ranges representing low- and high-count setting were investigated. Raw data was reconstructed by using the novel SR-OSEM algorithm with 3 iterations and 128 subsets [2]. ***Results:*** The peak sensitivity achieved 237 cps/MBq (XUHR-M); 847 cps/MBq (GP-M); 2054 cps/MBq (UHS-M). Resolution in the visually analyzed sections of the reconstructed hot-rod phantom was 0.35 mm (XUHR-M); 0.50 mm (GP-M) and 0.70 mm (UHS-M). Uniformity for maximum resolution records 40.7% (XUHR-M); 29.1% (GP-M) and 24.5% (UHS-M), respectively. UHS-M reaches highest CNR values for low-count images, for rods smaller than 0.45 mm acceptable CNR was only achieved by XUHR-M. GP-M was superior for imaging rods sized from 1.5 - 0.6 mm for intermediate activity concentrations. To achieve the best possible image quality considering contrast and noise, each collimator showed its advantage close to its maximum spatial resolution. ***Conclusion:*** Although the investigated SPECT scanner uses only two stationary detectors instead of conventional three detectors, the system's performance records no significant deficits regarding the highest possible image quality. The effects of the lower sensitivity on the noise level might be improved by increasing either scanning time or injection dose, but further validation especially concerning animal models is necessary. ***References:*** 1. Deleye S, Van Holen R, Verhaeghe J, Vandenberghe S, Stroobants S, Staelens S. Performance evaluation of small-animal multipinhole muSPECT scanners for mouse imaging. Eur J Nucl Med Mol Imaging. 2013;40:744-58. doi:10.1007/s00259-012-2326-2.2. Vaissier PE, Beekman FJ, Goorden MC. Similarity-regulation of OS-EM for accelerated SPECT reconstruction. Phys Med Biol. 2016;61:4300-15. doi:10.1088/0031-9155/61/11/4300.

OP-909

Multi-pinhole SPECT Imaging of Rat Hearts and Bones: Image Quality under In Vivo Conditions

J. Janssen[1,2], J. Hoffmann[1,2], T. Kanno[2,3], T. Higuchi[1,2,4];
[1]Department of Nuclear Medicine, University Hospital of Würzburg, Würzburg, GERMANY, [2]Comprehensive Heart Failure Center, University Hospital of Würzburg, Würzburg, GERMANY, [3]Department of Quantum Medical Technology, Graduate School of Medical Sciences, Kanazawa University, Kanazawa, JAPAN, [4]Graduate School of Medicine, Dentistry and Pharmaceutical Sciences, Okayama University, Okayama, JAPAN.

Aim/Introduction: Preclinical multi-pinhole SPECT enables sub-half-millimeter spatial resolution, whereby the loss of sensitivity and its dependency on the scanned volume must be taken into account [1]. We investigated the capabilities of a new micro-SPECT, equipped with two large stationary detectors, to visualize rat hearts and bones using clinically available ^{99m}Tc tracers by maintaining high image quality. ***Materials and Methods:*** Sensitivity, count linearity, spatial resolution, uniformity, contrast-to-noise-ratio was measured by point source, hot-rod, and uniform phantoms for a small-animal SPECT with 2 stationary detectors using

an ultra-high-resolution rat and mouse multi-pinhole collimator. The phantoms filled with ^{99m}Tc were scanned for a high-count performance assessment and count levels equal to the animal scans. Reconstruction parameters were set to 4 iterations 128 subsets using the SR-OSEM algorithm with Gaussian smoothing [2]. Rats were injected with ~100 MBq ^{99m}Tc-MIBI or ~150 MBq ^{99m}Tc-HMDP and imaged with multiple frames in a 60-min scan after the tracer distribution (25 and 190 min, respectively). Phantom and in vivo scans, with different Gaussian filters to optimize image quality, were compared. Dependency of resolution on the injection dose and scan time was examined. ***Results:*** Sensitivity was 567 cps/MBq, count loss was less than 5% for up to 191 MBq (425 MBq/ml). Hot-rods as small as 1.2 mm were resolved, uniformity was 55.5 %. Resolution was 2.2 mm in the heart for 60 min acquisition time, 2.8 mm, for 30 min and 3.5 mm for 10 min, respectively. Left ventricle and bone structures of the rats were successfully visualized in the reconstructed SPECT images of the 60-min scans. The high image quality (visual observation) was maintained by Gaussian filtering with a minimum of 2.2, 2.8 and 3.5 mm FWHM for the 60, 30 and 10-min-measurement, validated by the corresponding phantom measurement. ***Conclusion:*** Optimizing the study design regarding injection dose, acquisition time, post-filtering and collimator choice is essential to maximize the potential of small-animal SPECT imaging. The algorithm SR-OSEM with fixed reconstruction parameters is simplifying the study planning, although there are still challenges concerning the low system sensitivity, limited injection dose and acquisition time in in-vivo settings especially concerning dynamic scans. ***References:*** 1. Ivashchenko O, van der Have F, Villena JL, Groen HC, Ramakers RM, Weinans HH, et al. Quarter-millimeter-resolution molecular mouse imaging with U-SPECT(+). Mol Imaging. 2014;13. doi:10.2310/7290.2014.00053. 2. Vaissier PE, Beekman FJ, Goorden MC. Similarity-regulation of OS-EM for accelerated SPECT reconstruction. Phys Med Biol. 2016;61:4300-15. doi:10.1088/0031-9155/61/11/4300.

1607

Pitfalls & Artefacts 7: Bone SPECT/CT Revisited – Learning an Old Fox New Tricks

Friday, October 30, 2020, 13:50 - 15:20 Channel 7

OP-910

The End of Planar - Optimizing SPECT/CT Acquisition, Interpretation, and Reporting

L. Antunovic; Department of Nuclear Medicine, Humanitas Research Hospital, Rozzano (MI), ITALY.

OP-911

Quantification by SPECT/CT

T. Kuwert; Department of Nuclear Medicine, University Hospital, Erlangen, GERMANY.

OP-912

Novel Hardware, Algorithms, and Protocols in Bone Hybrid Imaging

Z. Keidar; Department of Nuclear Medicine Rambam Health Care Campus, Haifa, ISRAEL.

1608

Clinical Oncology Track - TROP Session: All About Staging the Prostate

Friday, October 30, 2020, 13:50 - 15:20 Channel 8

OP-913

Is PSMA-PET/CT cost-effective for disease staging in men with high-risk prostate cancer? An analysis of the proPSMA randomised controlled trial

R. De Abreu Lourenco[1], R. de Feria Cardet[1], T. Segard[2], J. Yim[1], S. Williams[3], R. Francis[2], M. Frydenberg[4], N. Lawrentschuk[5], D. G. Murphy[5], M. S. Hofman[3];
[1]University of Technology Sydney, Sydney, AUSTRALIA, [2]Sir Charles Gairdner Hospital, Perth, AUSTRALIA, [3]Peter MacCallum Cancer Centre, Melbourne, AUSTRALIA, [4]Monash University, Melbourne, AUSTRALIA, [5]University of Melbourne, Melbourne, AUSTRALIA.

Aim/Introduction: The recently published proPSMA clinical trial demonstrated increased accuracy of PSMA-PET/CT compared with conventional imaging (CI; computed tomography plus bone imaging) in men with high risk prostate cancer. It is important to assess whether the additional benefits of increased accuracy are justified by potential differences in the use of resources of these two imaging approaches. Thus, we determined the cost-effectiveness of PSMA-PET/CT when compared with CI in men with high risk prostate cancer. ***Materials and Methods:*** This analysis was informed by data collected as part of the proPSMA study conducted in Australia. Patients in proPSMA had high-risk prostate cancer (PSA ≥ 20 ng/mL or International Society of UroPathology grade group 3-5, or clinical stage ≥ T3). A total of 300 patients were assigned to CI or ^{68}Ga-PSMA-11 PET/CT, with planned health economics data collected (including time required for scan delivery). These data informed a cost-effectiveness decision tree analysis to estimate the cost per accurate diagnosis for PSMA-PET/CT compared to CI. Cases detected flowed into a Markov model to assess longer-term costs and outcomes of lifetime treatment following initial disease staging. Treatment pathways for the Markov model reflected local Australian practice and costs, with probabilities for disease outcomes in terms of metastatic disease, quality of life and survival informed by the literature. Results from the Markov model were expressed as cost per quality adjusted life year (QALY) gained. ***Results:*** Analysis of data from proPSMA

resulted in a cost per scan of AUD$1,203 for PSMA-PET/CT and AUD$1,412 for CI. proPSMA showed that PSMA-PET/CT was more accurate, largely due to improved sensitivity of PSMA-PET/CT in nodal disease. Thus, PSMA-PET/CT was dominant, being more effective (accurate) and less costly. When analysed as part of the Markov model, improved diagnostic accuracy resulted in a higher proportion of men receiving the appropriate treatment for their disease, accumulating estimated improvements in survival and quality of life. This resulted in a cost per QALY of AUD$10,629. The results were most sensitive to variations in the accuracy of CI and the number of men that could be scanned for each ^{68}Ga-PSMA production. ***Conclusion:*** This analysis shows that PSMA-PET/CT is a cost-effective technology; based on the results of proPSMA it dominates CI for initial staging and translates into a cost-effective longer-term management strategy when combined with standard clinical pathways. ***References:*** None

OP-914

Prospective comparison of ^{18}F-PSMA-1007 PET/CT and whole-body MRI/DWI with CT for primary lymph node staging of unfavorable intermediate and high-risk prostate cancer

S. Malaspina[1], *M. Anttinen*[2], *I. Jambor*[3], *M. Sandell*[4], *I. Rinta-Kiikka*[5], *S. Kajander*[1], *J. Schildt*[6], *E. Saukko*[7], *T. Noponen*[8], *J. Saunavaara*[4], *P. Taimen*[9], *P. B. Dean*[7], *R. B. Sequeiros*[7], *H. J. Aronen*[7], *J. Kemppainen*[1], *M. Seppänen*[10], *P. J. Boström*[2], *O. Ettala*[2]; [1]*Turku PET Centre, University of Turku and Turku University Hospital, Turku, FINLAND,* [2]*Department of Urology, University of Turku and Turku University Hospital, Turku, FINLAND,* [3]*Department of Radiology, Icahn School of Medicine at Mount Sinai, New York, NY, UNITED STATES OF AMERICA,* [4]*Medical Imaging Centre of Southwest Finland, University of Turku and Turku University Hospital, Turku, FINLAND,* [5]*Department of Radiology, Tampere University Hospital, Tampere, FINLAND,* [6]*Department of Clinical Physiology and Nuclear Medicine, Helsinki University Central Hospital, Helsinki, FINLAND,* [7]*Department of Diagnostic Radiology, University of Turku and Turku University Hospital, Turku, FINLAND,* [8]*Department of Medical Physics and Nuclear Medicine, University of Turku and Turku University Hospital, Turku, FINLAND,* [9]*Institute of Biomedicine, University of Turku and Department of Pathology, Turku University Hospital, Turku, FINLAND,* [10]*Department of Clinical Physiology, Nuclear Medicine and Turku PET Centre, University of Turku and Turku University Hospital, Turku, FINLAND.*

Aim/Introduction: EAU guidelines recommend abdominopelvic computed tomography (CT) for primary nodal staging of intermediate to high-risk prostate cancer (PCa), although CT has low sensitivity for detection of pelvic lymph node metastases. We have studied two potentially more accurate imaging modalities, prostate-specific membrane antigen positron emission tomography/CT (PSMA PET/CT) and whole-body MRI (wbMRI) with diffusion-weighted imaging (DWI), comparing in a prospective study their diagnostic performance with clinical standard-of-care CT. ***Materials and Methods:*** This prospective, registered (NCT03537391), singlecenter trial enrolled 80 patients with newly diagnosed unfavorable intermediate or highrisk PCa according to the EAU risk group classification. After consent, patients underwent contrastenhanced abdominopelvic and chest CT as a clinical standard for nodal staging. Research scans included ^{18}FPSMA1007 PET/CT and 1.5 T wbMRI/DWI. Two separate modalitybased specialists reviewed independently each modality blinded for other modalities. Regional lymph nodes were reported as either benign, equivocal or malignant and recorded using the REDCap electronic data capture tool. Pessimistic analysis (equivocal considered malignant) was performed in cases with an equivocal modality status. Histology from pelvic lymph node dissection (n=17 patients), follow-up imaging (n=63 patients) and clinical data were used as reference standards and the ground truth was defined at a patient-level in multidisciplinary consensus meetings. ***Results:*** Seventy-nine patients (mean age: 70 years) completed all the imaging modalities, with an eight-day median interval between the first and last imaging study (IQR 7). Median PSA was 12 ng/ml (range: 3-2000). Twenty-five patients (32%) presented with unfavorable intermediate and 54 (68%) with highrisk PCa. Twenty patients (25%) had distant metastatic disease and pelvic nodal metastases were found in 31 (39%) patients. In patientlevel pessimistic analysis, the sensitivity of CT (reader 1 and reader 2), wbMRI/DWI (reader 3 and reader 4) and PSMA PET/CT (reader 5 and reader 6) were 0.44/0.36, 0.48/0.56 and 0.92/1 ($p<0.01$), respectively. The corresponding specificity and accuracy values were 0.89/0.93, 0.94/0.85, 0.91/0.89 ($p>0.05$) and 0.75/0.75, 0.79/0.75 and 0.91/0.92 ($p<0.05$), respectively. Inter-reader agreement values (κ = Kappa) were 0.86 for PSMA PET/CT, while the corresponding values for CT and wbMRI/DWI were 0.51 and 0.40, respectively. Furthermore, PSMA PET/CT detected regional lymph nodes metastases in 8/31 (26%) patients, in whom the other modalities were negative. ***Conclusion:*** In this prospective clinical trial 18F-PSMA-1007 PET/CT demonstrated superiority in sensitivity and accuracy to wbMRI with DWI and CT in primary nodal staging of unfavorable intermediate and highrisk PCa, while maintaining optimal specificity and showing the highest inter-reader agreement. ***References:*** None

OP-915

A Prospective Study to Compare the Role of ^{68}Ga-PSMA-11 PET-CT and ^{68}Ga-GUL-NOTA-PSMA PET-CT in the Evaluation of Prostate Cancer

S. Prakash*, C. S. Bal, A. Seth, M. Tripathi, S. Ballal, M. P. Yadav; All India Institute of Medical Sciences, New Delhi, INDIA.*

Aim/Introduction: • ^{68}Ga-PSMA-11 has proven to be highly sensitive and specific for detection of prostate cancer and its metastasis but its drawback is that it cannot bind to therapeutic radiometals, such as ^{177}Lu or ^{225}Ac. (1) A new PSMA ligand GUL-NOTA-PSMA can be feasibly linked to both ^{68}Ga and ^{177}Lu. This study compares the role of ^{68}Ga-PSMA-11 PET-CT and ^{68}Ga-GUL-NOTA-PSMA PET-CT in the evaluation of prostate cancer keeping in mind the potential for future theranostics with ^{177}Lu-GUL-NOTA-PSMA. ***Materials and Methods:*** 26 patients with histopathologically proven prostate cancer (age: 49-87 years, mean: 68 years) underwent ^{68}Ga-PSMA-11 PET-CT and ^{68}Ga-GUL-NOTA-PSMA PET-CT with a maximum gap of 2 weeks between the two scans. Radiotracer uptakes in the prostate cancer primary and its metastases to lymph nodes and bones were semi-quantitatively analysed by measuring the maximum standardised uptake values (SUV_{max}). SUV_{max} of physiological uptake in liver, mediastinum, parotid glands and kidney were measured. Comparison between the two tracers was done on a per lesion and per patient based analysis. Paired T test and Wilcoxon signed-rank test were used as statistical tests for significance. ***Results:*** Among a total of 26 patients, 25 patients had primary prostatic lesions, 23 had lymph nodal metastasis and 21 had skeletal metastasis. Both tracers detected lesions in all patients. In total, PSMA-11 PET-CT detected 738 lesions (394 skeletal, 319 lymph nodes, 25 in prostate bed) while GUL-NOTA-PSMA PET-CT detected 735 lesions (393 skeletal, 317 lymph nodes, 25 in prostate bed) (p=0.33) showing no significant difference in the lesion detection rate between the two tracers. There was no significant difference in the SUV_{max} of the lesions in the prostatic bed (p=0.9), lymph nodes (p=0.9) or bones (p=0.3) between the two tracers. Furthermore, the physiological radiotracer uptake (SUV_{max}) in liver (p=0.001), salivary glands (p=0.001) and kidneys (p=0.002) was significantly lower in GUL-NOTA-PSMA but mediastinal uptake (p=0.0003) was significantly lower in PSMA-11. ***Conclusion:*** There is no significant difference in the detection of prostate cancer lesions and its metastasis between ^{68}Ga-GUL-NOTA-PSMA and ^{68}Ga-PSMA-11 PET-CT. The physiological uptake in salivary glands, kidney and liver is lower with ^{68}Ga-GUL-NOTA-PSMA signifying potentially less toxicity when used as a theranostic agent which needs to be pursued with further studies. ***References:*** 1. Eder M, Neels O, Müller M, Bauder-Wüst U, Remde Y, Schäfer M, et al. Novel Preclinical and Radiopharmaceutical Aspects of [68Ga]-PSMA-HBED-CC: A New PET Tracer for Imaging of Prostate Cancer. Pharm Basel Switz. 2014 Jun 30;7(7):779-96.

OP-916

Novel [F18]siPSMA14 biodistribution at 60, 90 and 120 min p.i. showing most favourable kinetics at 90 min p.i. for staging and restaging of prostate cancer patients

J. Miksch[1], V. Prasad[1], D. Di Carlo[2], F. Zengerling[3], C. Bolenz[3], C. Solbach[1], M. Beer[4], T. Wiegel[5], H. J. Wester[2], A. J. Beer[1]; [1]Department of Nuclear Medicine, University Hospital Ulm, Ulm, GERMANY, [2]Pharmaceutical Radiochemistry, Technische Universität München, Garching, GERMANY, [3]Department of Urology and Pediatric Urology, University Hospital Ulm, Ulm, GERMANY, [4]Department of Radiology, University Hospital Ulm, Ulm, GERMANY, [5]Department of Radiation Oncology and Therapy, University Hospital Ulm, Ulm, GERMANY.

Aim/Introduction: Analysis of novel [F-18]siPSMA14 at different time points to assess biodistribution and the optimal time point for staging primary and metastatic prostate cancer. ***Materials and Methods:*** 47 prostate cancer patients (69 ± 7 y; GS 6-9, median (range) PSA 3.195 (0.09 - 1000) ng/ml) referred for PSMA PET/CT were scanned at three different time points T1 (n=7; 60min), T2 (n=40; 90 minutes), T3 (n=7; 120 min). PET/CT (with contrast enhanced CT, if not contraindicated) images were acquired after injection of [F18]siPSMA14 (344.08 ± 11.7 MBq, without furosemide), from head to mid-thigh (T1,T2) or from lower thorax to upper thigh (T3). SUVmean were measured for normal organs and malignant lesions (intraprostatic tumor/residual tumor (prostatic lesion(PL)), bone(BM), lymph(LM) and adrenal gland(AM) metastases). For analyzing changes between early and late uptake T1 and T3 were examined. Target / non target ratios (TnTR) were calculated by comparing SUVmean of tumor lesions with background activity. T-test was performed to compare the differences in the mean of SUVmean in normal organs. ***Results:*** In all patients examined no side effects occurred. In high PSMA expressing organs mean SUVmean ± SD (kidney cortex, duodenum) increased significantly at T1/T3 (kidney cortex 22.9 ± 5.2/26.7 ± 8.8; duodenum 7.8 ± 1.8/8.9 ± 2.7) whereas in liver, spleen and pancreas [F-18]siPSMA-14 uptake remained stable (liver 7.4 ± 3/7.2 ± 2.8; spleen 8.4 ± 5.6 /7.9 ± 5.4; pancreas 2.2 ± 0,9 /1.9 ± 0,9). The mean SUV mean of PL and metastatic lesions (ML) at T1/T3 were 6.9 ± 4.2/14.6 ± 6.2 and 12.6 ± 7.3/14.4 ± 8.1. Mean SUV mean TnTR at T1/T3 for PL (n=6); LM (N=2); BM (n=2) and AM (n=1) were 13.8/28.2; 21.4/24.2; 5.3/5,8; 41.2/46,8. The mean SUV mean of PL and ML at T2 were 9.6 ± 10.6 and 23.8 ± 9.6. Mean SUV mean TnTR at T2 for PL (n=11); LM (N=17); BM (n=11) and AM (n=1) were 16; 14.3; 18.6 and 30.2. SUV mean PL and bladder ratio at T1/T3 and T2 were 0.7/0.9 and 1.9. ***Conclusion:*** Novel [F-18]siPSMA-14 was well tolerated in all patients. All lesions were observed at all the time points and showed high [F-18]siPSMA-14 uptake. SUVmean in primary as well as in metastatic locations increased with time. Distribution in normal organs was similar to other known PSMA PET radiotracers. Without furosemide PL could be clearly delineated at 90min p.i., which seems to be the optimal time point. ***References:*** None

OP-917

Temporal accumulation patterns of ^{68}Ga-PSMA in primary prostate cancer: stable or steep?

J. olde Heuvel[1], M. Sinaasappel[1], M. P. M. Stokkel[1], C. H. Slump[2], B. J. de Wit-van der Veen[1];
[1]Netherlands Cancer Instititute, Amsterdam, NETHERLANDS, [2]University of Twente, Enschede, NETHERLANDS.

Aim/Introduction: Understanding the day-to-day variability of an imaging biomarker is key when using it to characterize lesions or quantify response to treatment. So, the objective of this study was to assess pharmacokinetics of ^{68}Ga-PSMA in patients suffering from primary prostate cancer in both tumour lesions and normal tissue. ***Materials and Methods:*** Five patients were enrolled in this prospective study. Before standard clinical PSMA-PET/CT, dynamic acquisitions were made for 30 minutes (Vereos, Philips). Acquisitions started directly after intravenous bolus injection of ~100MBq [^{68}Ga]Ga-PSMA-11. The same protocol was repeated ~four weeks later, without therapeutic interventions in between. List-mode data was binned in 1 minute frames, and reconstructed with 4mm voxel size (3it5sub, no PSF). Time-activity curves (TACs) were derived for the prostate tumour, gluteal muscle and common iliac artery. Intra-patient variability was expressed by median SUV_{mean} and coefficient of variation (CoV). ***Results:*** Median intra-patient CoV was within 3.3% for artery, 1.1% for tumour, and 0.3% for gluteal muscle. The median difference in SUV_{mean} of the common iliac artery and gluteal muscle was 0.08 and 0.04; these TACs plateaued after 8 and 5 minutes, respectively. Tumour TAC profiles showed marked differences between patients; in two patients uptake stabilized already after 5 minutes ('stable'-group), whereas in three patients the uptake kept increasing over time ('steep'-group). This resulted in a marked 3.0 times higher SUV_{mean} in the 'steep'-group (SUV_{mean} 2.8) compared to the 'stable'-group (SUV_{mean} 8.5) after 30 minutes, which was reproducible on the second PET/CT four weeks later ('steep'-SUV_{mean} 2.9; 'stable'-SUV_{mean} 8.6). No differences in systemic blood supply and perfusion were observed on PET. The only relevant distinction between these patients was tumour volume, which was on average 3cc vs. 36cc for stable and steep group, respectively. ***Conclusion:*** Dynamic ^{68}Ga-PSMA-PET/CT scans in a test-retest setting revealed that accumulation patterns are highly repeatable over time. Tumour accumulation is already visualized 5 minutes p.i., but marked difference between TAC-profiles are present. These temporal differences in tumour uptake might be beneficial for selecting patients for PSMA-targeted radionuclide therapy. ***References:*** None

OP-918

Is the increased ^{82}Rubidium uptake in prostate cancer explained by underlying Na^+/K^+-ATPase density?

M. Jochumsen[1,2], J. Sörensen[1,2], J. R. Nyengaard[3], S. R. P. Krag[4], B. G. Pedersen[5,2], M. Borre[6,2], J. Frøkiær[1,2], K. Bouchelouche[1,2], L. P. Tolbod[1,2];
[1]Aarhus University Hospital, Dept. of Nuclear Medicine and PET-Centre, Aarhus, DENMARK, [2]Aarhus University, Dept. of Clinical Medicine, Aarhus, DENMARK, [3]Department of Clinical Medicine, Core Centre for Molecular Morphology, Section for Stereology and Microscopy, Centre for Stochastic Geometry and Advanced Bioimaging, Aarhus University, Aarhus, DENMARK, [4]Aarhus University Hospital, Dept. of Pathology, Aarhus N, DENMARK, [5]Aarhus University Hospital, Dept. of Radiology, Aarhus N, DENMARK, [6]Aarhus University Hospital, Dept. of Urology, Aarhus, DENMARK.

Aim/Introduction: ^{82}Rubidium is clinically used as perfusion tracer for PET, as the cellular ^{82}Rubidium uptake is proportional to blood flow. However, as a potassium analogue, ^{82}Rubidium is also dependent on active transport by the Na^+/K^+-ATPase for cellular uptake. In recent studies, we found ^{82}Rubidium uptake and hence blood flow in prostate cancer (PCa) correlated with cancer aggressiveness [1]. The aim of this study was to examine the role of underlying Na^+/K^+-ATPase density in determining PCa ^{82}Rubidium uptake. ***Materials and Methods:*** One-hundred-and-two patients underwent pelvic ^{82}Rubidium PET prior to magnetic resonance imaging (MRI)-guided in-bore prostate biopsy. PCa was confirmed in 100 lesions in 86 patients, and 25 lesions in 16 patients were benign. Tumours were delineated on MRI and transferred to ^{82}Rubidium PET for SUV analysis. Immunohistochemical α1/α2-Na+/K+-ATPase staining was subsequently performed on biopsies. No expression of the α2-isoform was found. Quantification of the α1-Na+/K+-ATPase antibody staining intensity was performed using ImageJ. Additionally, cell profile density was calculated. ***Results:*** ^{82}Rubidium SUVmax and International Society of Urological Pathology (ISUP) Grade Group (GG) were moderately correlated (rho=0.68, p<0.0001), inflamed lesions excluded. ^{82}Rubidium SUVmax separated GGG2-5 from GGG1 and benign lesions with 96% sensitivity and 59% specificity with 2.92 as cut-off. Na^+/K^+-ATPase optical density per cell profile in benign prostate cells was 38% (1.38 with 95% CI [1.28; 1.49]) (p<0.0001) higher than in malignant cells. Na^+/K^+-ATPase density per cell was significantly lower in "high" grade tumours (ISUP GG≥2) (6.4E-5 [6.0E-5; 6.9E-5]) than in low grade tumours (ISUP GG-1) (7.7E-5 [6.5E-5; 8.9E-5]) (p=0.02). Mean cell density was 24% (1.24 with 95% CI [1.17; 1.33]) higher in PCa glands than in benign glands, corresponding to 96% higher (1.96 with 95% CI [1.83; 2.09]) (p<0.0001) in malignant areas than in benign areas. Driven by this higher cell density, malignant areas has 58% higher Na^+/K^+-ATPase optical density than the benign areas (p<0.0001). Still, no correlations between ^{82}Rubidium SUVmax and Na^+/K^+-ATPase density nor cell profile density were found. A near-significant positive correlation between cell density and GG was found (rho=0.21, p=0.06). ***Conclusion:*** Blood flow

in PCa measured with simple ^{82}Rubidium SUV correlates with ISUP GG independent of underlying Na^+/K^+-ATPase density. Consequently, the interpretation of ^{82}Rb uptake as a reflection of tumour blood flow is further consolidated. Na^+/K^+-ATPase density is reduced in PCa cells compared to benign cells, and slightly reduced in high-grade tumours compared to low-grade tumours. ***References:*** [1] MR Jochumsen et al., J Nucl Med 60(8), 1059 (2019).

OP-919

Prospective evaluation of medium and high risk prostate cancer patients at initial staging with (^{18}F)AlF-PSMA-HBED-CC: Intraindividual comparison with ^{68}Ga-PSMA-HBED-CC

O. Alonso Nunez[1,2], G. dos Santos[1,2], M. Rodriguez Taroco[1]; [1]Uruguayan Centre of Molecular Imaging (CUDIM), Montevideo, URUGUAY, [2]Nuclear Medicine Centre, Clinical Hospital, University of Uruguay, Montevideo, URUGUAY.

Aim/Introduction: ^{68}Ga-PSMA-HBED-CC (^{68}Ga-PSMA-611) PET/CT represents a clinically relevant and commonly used technique for the evaluation of prostate cancer (PCa) patients whereas [^{18}F]AlF-PSMA-HBED-CC (^{18}F-ALF-PSMA-11) is a novel tracer produced in our centre, with suitable radiochemical purity for clinical purposes. The aim of this study was to prospectively compare the diagnostic values of ^{18}F-AlF-PSMA-11 versus ^{68}Ga-PSMA-11 for the detection of metastatic disease in a sample of patients with intermediate and high-risk PCa at initial staging. ***Materials and Methods:*** We enrolled 66 patients (mean age: 63 years; range: 52-78 years) with medium and high-risk biopsy proven PCa prior therapy (Gleason ≥ 6; mean PSA: 26.45 ng/mL, median PSA: 14 ng/mL, range: 1.7-152 ng/mL). They prospectively underwent routine ^{68}Ga-PSMA-11 and ^{18}F-AlF-PSMA-11 PET/CT scanning within a time window of 1-2 weeks. Studies were performed with a 64-slice PET/CT scan with TOF correction. We measured the SUVmax in all coincident lesions. Open prostatectomy and pelvic lymph-node dissection were performed in non-metastatic patients. Histopathology, correlative imaging and/or clinical follow-up were considered as reference standard, with a follow-up of at least 4 months after PET/CT scanning (median 6.4, range 4-11 months). Sensitivity and specificity with their 95% C.I. were calculated. ***Results:*** Overall detection rate was 85% (56/66) for both ^{68}Ga-PSMA-11 and ^{18}F-AlF-PSMA-11 PET/CT. At least one suspicious lesion for prostate cancer metastasis was detected in 20 (30%) and 21 (32%) of 66 patients, for each tracer respectively. A total of 145 extra-prostatic lesions were detected in bone (n=56), lymph-nodes (n=88), and lung (n=1) by at least one radiopharmaceutical: 131 (90%) for ^{68}Ga-PSMA-11 and 123 (85%) for ^{18}F-AlF-PSMA-11. In concordant lesions a significant correlation was found between the SUVmax of both radiopharmaceuticals (r=0.90, P<0.001). ^{18}F-AlF-PSMA-11 SUVmax was higher in bone foci (n=39) compared to ^{68}Ga-PSMA-11 (7.2 vs 8.9, P=0.002), while no significant differences were found for lymph node and prostate lesions. On a per patient basis the sensitivity values were the same for both techniques: 0.90 (0.68-0.98). We calculated a specificity of 0.96 (0.85-0.99) and 0.94 (0.82-0.98) for ^{68}Ga-PSMA-11 and ^{18}F-AlF-PSMA-11, respectively. ***Conclusion:*** ^{68}Ga-PSMA-11 and Al^{18}F-PSMA-11 PET/CT seem to be clinically equivalent imaging techniques for the assessment of primary medium to high-risk PCa with great potential for the detection of metastatic spread that would impact patient management. ***References:*** None

OP-920

The clinical value of ^{68}Ga-PSMA-11 PET/CT in patients with newly diagnosed prostate cancer, ISUP grade 5 and no metastases based on standard imaging

H. Zacho[1,2], S. Nalliah[1], A. Petersen[1], L. J. Petersen[1,2]; [1]Aalborg University Hospital, Aalborg, DENMARK, [2]Aalborg University, Aalborg, DENMARK.

Aim/Introduction: To evaluate the clinical value of ^{68}Ga-PSMA-11 PET/CT in patients with newly diagnosed prostate cancer, ISUP grade 5 (Gleason score ≥9), and no metastases based on standard imaging ***Materials and Methods:*** We initiated a new clinical strategy for the clinical use of PSMA PET/CT for staging of patients with prostate cancer, which was based on the following eligibility criteria: 1) Newly diagnosed prostate cancer, 2) no prior treatment for prostate cancer, 3) ISUP grade 5 (Gleason score 9 or 10), 4) suitable for treatment with curative intend (radical prostatectomy or radiation therapy) based on co-morbidity and life expectancy, and 4) No definitive metastases on standard of care (SoC) imaging, which was contrast-enhanced CT (ceCT) and bone scintigraphy (BS). We present the results from the first 6 months of this new staging procedure. ***Results:*** During six months, 50 patients complied with the eligibility criteria and underwent a PSMA PET/CT (mean age 69.6 years, range 55-78). Median PSA was 14.0 ng/mL, and 28 patients (56%) had localized cancer, 22 patients (44%) had locally advanced prostate cancer according to the criteria from the European Association of Urology. Five patients had indeterminate findings on SoC imaging (three equivocal bone scans, two ceCTs suggesting lymph node metastases). Visual uptake of PSMA in the prostate was seen in all (50/50. 100%) patients. PSMA PET/CT showed pathological PSMA-uptake outside the prostate in 23 patients (46%); pelvic lymph node metastases in 13 patients (26%) and lymph node metastases outside the pelvis and/or bone metastases and/or visceral metastases in 10 patients (20%). Among the five patients with indeterminate findings on SoC imaging, PSMA PET/CT showed malignant findings in three patients (two patients with lymph node metastases and one with bone metastases). The result of the PSMA PET/CT changed the treatment strategy in 19 (38%) patients from curatively

intended treatment to palliative treatment, e.g. androgen deprivation therapy. ***Conclusion:*** PMSA PET/CT revealed metastatic disease in 46% of high-risk patients with no definitive metastases on SoC imaging and led to change of patient management in 38% of patients. ***References:*** None

OP-921

Investigation of 68-Ga PSMA PET and Multiparametric MRI imaging Radiomics based models in the prediction of ISUP score in prostate cancer patients

G. Feliciani[1], A. Savini[1], G. Bellomo[1], M. Celli[1], F. Ferroni[1], E. Menghi[1], M. Costantini[2], D. Barone[1], A. Sarnelli[1], G. Paganelli[1]; [1]Istituto Scientifico Romagnolo per lo Studio e la Cura dei Tumori (IRST) IRCCS, Meldola, ITALY, [2]Departement of Pathology Azienda Ospedaliera-Universitaria Policlinico di Modena, Modena, ITALY.

Aim/Introduction: The present study proposes a new model for predicting Epstein ISUP/WHO grade groupe based on the analysis of textural features on T2w, ADC and 68-Ga PSMA PET images. The first objective is to investigate the diagnostic performance of textural features to distinguish between well-differentiated and poorly differentiated forms and to improve accuracy of low-risk prostate cancer patients stratification. ***Materials and Methods:*** In this retrospective study, a dataset of T2w (MRI), ADC (MRI) and 68Ga-PSMA-PET images from 20 patients was analyzed. After the prostatectomy, the Pathology provided us with confirmation of histological diagnosis though Gleason score and ISUP/WHO grade group for each lesion. Therefore, we analysed 40 prostate lesions in T2w, ADC and 68GaPET images. Multiple patient lesions were treated as standalone after performing their direct comparison between histology and imaging location. The PIRADS associated to the patients by radiologists was assigned to the patient's corresponding lesions in MRI. All the MRI images were acquired in our department on a Philips Ingenia 3T MR scanner. All MRI study protocols included T2w sequences in the axial, coronal and sagittal plane and Apparent Diffusion Coefficient (ADC) maps, derived by DWI sequences, with ***b*** ranging from 0 to 1000. Patients injected with 68Ga-PSMA were then imaged on a PET/CT scanner. First-order, second-order and higher order imaging features were extracted with the open source software Lifex Ver 5.10 from each imaging modality contours. LASSO algorithm was used to select the best performing features in order to build an internally cross-validated statistical model. ***Results:*** Features extracted employing LASSO algorithm were used to build a model for each imaging modality. All the models were cross validated with 5-fold cross validation. The 68-Ga-PET-based model is based on a decision tree composed of 2 features (3rd Quartile of SUV histogram and Entropy) with a final accuracy of 80% to discriminate low-grade forms of prostate cancer with ISUP/WHO grade groupe 1 from others. The ADC-based model is a linear discriminant with an accuracy of 82% employing 3 features (mean, entropy and zone uniformity). Finally, the T2w-based model, another linear discriminant, produced an accuracy of 74% employing entropy and zone uniformity. ***Conclusion:*** The results of this study are in line with previous published data on the prediction power of ADC sequences. PET-PSMA in combination with MRI techniques can improve accurancy in diagnosis and patient treatment stratification. ***References:*** None

OP-922

^{68}Ga-PSMA PET/CT for Primary Staging of High-Risk Prostate Cancer: A High-Volume Center Study

S. Klingenberg[1,2,3], M. R. Jochumsen[1,2], B. P. Ulhøi[4], J. Fredsøe[2,3], K. D. Sørensen[2,3], M. Borre[2,5], K. Bouchelouche[1,2]; [1]Department of Nuclear Medicine & PET-Centre, Aarhus University Hospital, Aarhus N, DENMARK, [2]Department of Clinical Medicine, Aarhus University, Aarhus C, DENMARK, [3]Department of Molecular Medicine, Aarhus University Hospital, Aarhus N, DENMARK, [4]Department of Pathology, Aarhus University Hospital, Aarhus N, DENMARK, [5]Department of Urology, Aarhus University Hospital, Aarhus N, DENMARK.

Aim/Introduction: We present the largest cohort of high-risk prostate cancer (PCa) patients undergoing ^{68}Ga-PSMA PET/CT for primary staging to date. We aimed to investigate the metastatic spread of PCa and the relation to primary tumor ^{68}Ga-PSMA uptake and the D'Amico classification. Furthermore, we described the undetected lymph node metastases (LNMs) in the primary staging setting. ***Materials and Methods:*** We assembled a cohort of 691 consecutive newly diagnosed, D'Amico high-risk PCa patients primary staged by ^{68}Ga-PSMA PET/CT from April 2016 to March 2019 at our facility. PSMA maximum standardized uptake value (SUV_{max}) and advanced disease findings were compared to the traditional stratification parameters PSA level, International Society of Urologic Pathology (ISUP) grade, and clinical stage. In addition, ^{68}Ga-PSMA PET/CT findings were compared with lymph node histology in radical prostatectomy patients. Furthermore, six undetected lymph nodes above 5.0 mm in size was immunohistochemically stained with anti-PSMA. ***Results:*** Advanced disease (N1/M1) was observed in 35.3% of patients (244/691) and was associated with increasing PSA levels, ISUP grades, and clinical stages. Advanced disease frequencies in patients with ISUP grade 2 and 3 were 10.8% (11/102) and 37.1% (33/89), respectively, yet the risk of advanced disease for cT2a/cT2b/cT2c tumors were almost equal (24.2%, 27.9%, and 22.4%, respectively). We observed a weak positive correlation between SUV_{max} and biopsy ISUP grade ($\rho = 0.21$; $p < 0.001$) and a modest positive correlation between SUV_{max} and post-prostatectomy ISUP grade ($\rho = 0.38$; $p < 0.001$). The area under the receiver operating characteristic curve for SUV_{max} to predict ISUP grade ≤2 or >2 was 0.65

(95% CI 0.56 to 0.74). With an optimal cut-off of SUV_{max} of 11.4, the sensitivity and specificity were 51.2% and 77.4%, respectively. Sensitivity, specificity, positive and negative predictive value, and accuracy for LNMs detection on ^{68}Ga-PSMA PET/CT were 30.6%, 96.5%, 68.8%, 84.5%, and 83.1%, respectively. Undetected LNMs were either micrometastases located in the border of the lymph node cortex or had no PSMA expression. ***Conclusion:*** We identified advanced disease in 35.3% of high-risk PCa patients at diagnosis in this cohort with ISUP grade being the superior predictor of advanced disease at diagnosis. Likewise, we observed a major difference in frequency of advanced disease between ISUP grade 2 and 3, which supports the subdivision of Gleason Score 7. However, no significant differences in risk when comparing the different cT2 stages were demonstrated. The undetected LNMs on PSMA PET/CT were either PSMA-negative or micrometastases. ***References:*** None

OP-923

The impact of dual time point 68Ga-PSMA PET/CT imaging on PSMA uptake of primary tumor in prostate cancer

D. Has Simsek;
Istanbul University, Istanbul Faculty of Medicine, Istanbul, TURKEY.

Aim/Introduction: The goal of this study was to investigate the impact of early and late 68Ga-PSMA PET/CT on PSMA uptake of primary tumor in prostate cancer (PCa). ***Materials and Methods:*** A total of 313 patients who were performed 1h. and 2h. 68Ga-PSMA PET/CT scan for staging PCa were enrolled to this study. Median PSA was 13.59 ng/ml (X-X ng/ml) and median Gleason score (GS) was 8 (6-10). All clinical and histopathological data were documented. Early and late 68Ga-PSMA PET/CT scans were interpreted, and PSMA uptake in primary tumors were recorded separately by using SUVmax value based on the guidance of TRUS biopsy results. SUVmax values were correlated with GS. Statistical analysis was performed for patients who had increased PSMA in primary tumor on both 1h. and 2h. scans and more than 10% differences in primary tumor SUVmax value between 1h. and 2h. scans. SPSS version 24 was used for analyses. ***Results:*** According to histopathological results, 32 patients had GS:6, 114 patiens had GS:7, 75 patients had GS:8, 92 patients had GS:9-10 tumors. Increased PSMA uptake in primary tumor was detected in 295 (94.2%) patients, while 18 patients (%5.8%) had no PSMA uptake in primary tumor in 1h. or 2h. 68Ga-PSMA PET/CT imaging. PSMA uptake in primary tumor was increased in late imaging in 239 patients (76.4%), and in 158 of them (50.4%) the difference was more than 10%. In remaining 74 (23.6%) patients, PSMA uptake in primary tumor was decreased in late imaging and in 33 of them (10.5%) the difference was more than 10%. There was no statistical correlation between the differences of SUVmax values and GS (Pearson r= -0.125; p=0.084). GS and SUVmax values were correlated for both early (p=<0.001) and late (p=<0.001) imaging, according to Kruskal Wallis test. However, no statistical differences was found in SUVmax values between GS:3+4 and GS:4+3 patients for both 1h. (p=0.192) and 2h. imaging (p=0.117). ***Conclusion:*** Our results shows that early and late PSMA uptake in primary tumor is varied independently from GS, and mostly increased in late 68Ga-PSMA PET/CT imaging. PSMA uptake in primary tumor were well correlated with GS for dual time point imaging. ***References:*** None

OP-924

Diagnostic performance of the novel PSMA-specific PET radiotracer [F-18]siPSMA-14 in staging and restaging of prostate cancer

J. Miksch[1], *V. Prasad*[1], *D. DiCarlo*[2], *F. Zengerling*[3], *C. Bolenz*[3], *C. Solbach*[1], *M. Beer*[4], *T. Wiegel*[5], *H. J. Wester*[2], *A. J. Beer*[1];
[1]*Department of Nuclear Medicine, University Hospital Ulm, Ulm, GERMANY,* [2]*Pharmaceutical Radiochemistry, Technical University Munich, Garching, GERMANY,* [3]*Department of Urology and Pediatric Urology, University Hospital Ulm, Ulm, GERMANY,* [4]*Department of Radiology, University Hospital Ulm, Ulm, GERMANY,* [5]*Department of Radiation Oncology, University Hospital Ulm, Ulm, GERMANY.*

Aim/Introduction: F-18 labelled Prostate Specific Membrane Antigen (PSMA) radiotracers offer logistic and potential diagnostic advantages over Ga-68 PSMA. We evaluated the diagnostic performance of the novel F-18-labelled silicone fluorine acceptor based PET radiotracer [F18]siPSMA-14 in staging and restaging of patients with prostate cancer (PCa). ***Materials and Methods:*** 108 PCa patients (70 ± 7 y; GS 69) referred for PET/CT at our center were retrospectively analyzed. The indications for PET/CT were primary staging (n = 21); restaging due to biochemical recurrence (BCR) (n = 57) or progressive disease under systemic therapy (n = 30). Median PSA value of patients referred for primary staging was 8.7 (2.36 - 1000) ng/ml and for restaging 1.06 (0.02 1500) ng/ml. PET/CT images were acquired 90 minutes after i.v. injection of [F18]siPSMA14 (345.8 ± 9.1 MBq, without furosemide) with contrast enhanced CT scans from head to mid-thigh, if not contraindicated. ***Results:*** In primary staging, all biopsy proven primary prostate cancer lesions were visualized (21/21). In 33 % (7/21) of the patients metastatic findings occurred: lymph node metastases in 33 % (7/21) and bone metastases in 24 % (5/21). The overall detection rate in patients referred for restaging was 84 % (73/87). In the PSA subgroup analyses (0-0.5 ng/ml, 0.5-2 ng/ml, 2-10 ng/ml and > 10 ng/ml) detection rates were 61 % (17/28), 88 % (24/26), 93 % (13/14) and 100 % (19/19) respectively. In patients referred for restaging, the frequency of local recurrence, lymph node metastases and bone metastases was 45 % (39/87), 62 % (54/87), and 37

% (32/87) respectively. Low bladder activity provided an excellent contrast for visualization of lesions in the prostate bed. ***Conclusion:*** The novel [F18]siPSMA14 PET radiotracer showed high detection rates comparable to the reported data of other Ga-68 and F-18 labelled PSMA radiotracers with the advantage of a low urinary excretion and low bladder activity even without administration of furosemide. ***References:*** None

1609

TROP Session: PET for Infection and Inflammation - A New Story

Friday, October 30, 2020, 13:50 - 15:20 Channel 9

OP-925

Role of [^{18}F]FDG-PET/CT in the diagnosis of spondylodiscitis

R. Viglialoro*, R. Zanca, A. Marciano, F. Bartoli, P. Erba, E. Lazzeri; Regional Center of Nuclear Medicine, Department of Translational Research and New Technology in Med, Pisa, ITALY.*

Aim/Introduction: Spine can be infected by pathogens through haematogenous spread (primary spondylodiscitis (SD)) or directly by contiguous tissues (secondary SD). Diagnosis of SD is based on clinical, laboratory and imaging findings. We evaluated the role of [^{18}F]FDG-PET/CT, comparing with MRI, in primary and secondary SD diagnosis. ***Materials and Methods:*** Forty patients (pts), (14 women, 26 men; mean age 66±13 years) with suspected SD (26 primary and 14 secondary) presented back pain and increased flogosis indexes. All pts were retrospectively evaluated with [^{18}F]FDG-PET/CT and MRI, performed within 30 days. 10/40 pts were ongoing antimicrobial treatment. Qualitative analysis of [^{18}F]FDG- PET/CT was used, [^{18}F]FDG uptake patterns were scored in 5 Hungenbach grades, grade 0 and 1 (normal or slightly enhanced uptake of FDG in the inter/ paravertebral region) were negative for infection, score 2 (clearly enhanced uptake of [^{18}F]FDG with linear or disciform pattern in the intervertebral space) was consistent with discitis, scores 3 and 4 (enhanced uptake of [^{18}F]FDG with linear or disciform pattern in the intervertebral space with the involvement of adjacent vertebrae or paravertebral tissues) were consistent with SD. Final diagnosis was based on microbiological culture and/or clinical follow-up for at least 10 months. Statistical analysis was performed using McNemar's test and MedCalc. ***Results:*** 33 pts had spine infection (8/33 with positive microbiological culture, 25/33 with clinical follow-up diagnosis), 7 pts were not infected. In primary SD [^{18}F]FDG-PET/CT showed positive results in 22 pts (22 TP, 0 FP) and negative results in 4 pts (3 TN, 1 FN), MRI showed positive results in 25 pts (23 TP, 2 FP) and negative results in 1 pt (1 TN, 0 FN). [^{18}F]FDG-PET/CT and MRI showed the same diagnostic accuracy of 88%. In secondary SD [^{18}F]FDG-PET/CT showed positive results in 10 pts (10 TP, 0 FP) and negative results in 4 pts (4 TN, 0 FN), MRI showed positive results in 4 pts (4 TP, 0 FP) and negative results in 10 pts (4 TN, 6 FN). The diagnostic accuracy of [^{18}F]FDG-PET/CT was 100% and of MRI was 57%. McNemar's test was P=0.25. ***Conclusion:*** Despite the small number of patients population, our data confirm that MRI is the imaging of choice in patients with primary SD and [^{18}F]FDG-PET/CT should be performed in pts with contraindications to MRI. [^{18}F]FDG-PET/CT shows higher diagnostic accuracy in secondary SD compared with MRI, confirming its crucial role in the diagnostic algorithm of secondary SD in adults. ***References:*** None

OP-926

^{64}Cu-DOTA-Ubiquicidin 29-41 PET/CT in patients with suspected infectious process: Initial experience in a single center in Mexico

O. Garcia-Perez*[1,2], P. Munguia[1], H. Valdovinos[1], J. Vargas-Ahumada[1], F. Lemus[1], I. Soldevilla[1], N. Becerra[1], M. Acuña[3]; [1]Instituto Nacional de Cancerologia, Mexico City, MEXICO, [2]Imagenus - Diagnostics in Healthcare, Mexico City, MEXICO, [3]Clinica FOSCAL, Bucaramanga, COLOMBIA.*

Aim/Introduction: Molecular imaging has played a very important role in the management of infectious processes, the development of antimicrobial peptides such as ubiquicidine (UBI29-41) a fragment of a cationic synthetic peptide capable of binding to the anionic microbial cell membrane that has allow to improve decision making. In conventional nuclear medicine, radiolabelling is done with 99m Tc with quite encouraging results, however, in the field of PET/CT, 68Ga has been used but its short half-life limits the acquisition of late images, the use of radiometals with favorable physical and chemical characteristics such as Cooper 64 (64 Cu) (T 1/2 = 12.7 hrs; beta+: 17.6%) allows an efficient and accessible alternative for the study of infectious processes by molecular imaging. ***Materials and Methods:*** Fourteen patients were included in a period between November 2019 and March 2020 with suspected infectious process in the extremities. PET/CT was performed 4 hours after intravenous injection of 5 mCi of ^{64}Cu-DOTA-UBI 29-41. All patients were cultured after the PET study. 64Cu was produced in a IBA twin cyclotron, wich was produced in a silver disk wich was electroplated into solid target (Nirta Solid Target), the purity of the radiopharmaceutical was corroborated with HPLC analysis and mass spectrometry. ***Results:*** 9 women and 5 men were included, mean age was 45 years (+/-8,2). 9 patients were positive by 64Cu DOTA UBI 29-41 and 8 by culture, the most commonly bacteria found was staphilococus epidermidis (n=5), escherichia coli (n=2), pseudomonas aeruginosa (n=1). The mean SUV_{max} for the positive studies by culture and by PET was 1.6 (+/-

0.65), compared to 0.33 (+/-0.57) of the negative studies for infectious process. When estimating the lesion/background ratio in the patients with a positive study, the mean SUVmax was 4.58 (+/-5.2) compared to 0.95 (+/-1.0) for patients with a negative study. ROC curves were performed to estimate the cutoff values between positivity and negativity using SUVmax values and lesion/background ratio, finding a statistically significant association of 1.2 (p 0.02) and 1.5 (p 0.003) respectively. The false positive by PET was secondary to a recent surgical intervention with high inflammatory reaction. ***Conclusion:*** Imaging of UBI 29-41 radiolabeled with ^{64}Cu is a reliable alternative to assess active infectious processes, it allows us to define the infection sites with better spatial resolution, also the ability to acquire late images can improve the lesion/background ratio. ***References:*** None

OP-927

Could Hypermetabolism of the spleen or bone marrow improve the FDG-PET/CT diagnosis of Infective Endocarditis as indirect signs?

M. Gazzilli[1], D. Albano[2], E. Cerudelli[1], A. Mazzoletti[3], F. Dondi[3], P. Bellini[3], F. Bertagna[2], R. Giubbini[2];
[1]Azienda Socio Sanitaria Territoriale degli Spedali Civili di Brescia, Brescia, ITALY, [2]Università di Brescia e Azienda Socio Sanitaria Territoriale degli Spedali Civili di Brescia, Brescia, ITALY, [3]Università di Brescia, Brescia, ITALY.

Aim/Introduction: In the latest update of the European Society of Cardiology (ESC) [18F]FDG-PET/CT are been included in the diagnostic flow chart for the management of infective endocarditis (IE). FDG-PET may provide direct but also indirect signs of infections and/or inflammation, notably a diffuse increase in spleen and/or bone marrow (BM) uptake. In fact, the host defence against IE involves the activation of polymorphonuclear cells, macrophages and lymphocites leading to an increase in the glycolytic metabolism, which could be documented in BM and spleen. The aim of our study was to determine whether hypermetabolism of the spleen and/or BM (HSBM) could help in the FDG-PET-based diagnosis of IE. ***Materials and Methods:*** We included 108 patients who underwent 18F-FDG-PET/CT scan for suspicious of IE, all patients were prepared with a low carbohydrate, high fat and high protein diet. Nine patients were excluded because PET/CT's visual analysis demonstrated other inflammatory diseases. PET/CT images were analysed qualitatively, by experienced physicians, and semi-quantitatively by measuring maximum and mean Standardized Uptake Value (SUVmax and SUVmean) of the suspected valve lesion and liver by a ROI in the right lobe, SUVmean of the spleen was obtained from a ROI positioned in the center of the spleen and SUVmean of the BM was obtained from a ROI on the bodies of the five lumbar vertebrae. BM and spleen SUVmean values were normalized to those of the liver, and HSBM was defined as a BM or spleen-to-liver ratio>1. ***Results:*** Among the 99 patients enrolled in the study, 54 had a clinical final diagnosis of IE. HSBM was a predictor of IE (p<0,05), independently of the criterion of abnormal cardiac FDG uptake. A definite IE was documented in 83% (40/48) of patients showing both HSBM and abnormal cardiac uptake, 44% (4/9) of patients with only abnormal cardiac uptake, 28% (9/32) of patients with only HSBM and 10% (1/10) of patients with neither one. ***Conclusion:*** Our preliminary results demonstrated that HSBM is good indirect sign of IE and could strengthen the suspicion of IE, especially in the absence of any other infections, inflammatory or malignant disease. ***References:*** None

OP-928

A Qualitative Assessment System Proposed to Improve the Diagnosis of Infective Endocarditis with 18F-FDG PET/CT

M. Gazzilli[1], D. Albano[2], E. Cerudelli[1], A. Mazzoletti[2], F. Dondi[2], P. Bellini[2], F. Bertagna[2], R. Giubbini[2];
[1]Azienda Socio Sanitaria Territoriale degli Spedali Civili di Brescia, Brescia, ITALY, [2]Università di Brescia, Brescia, ITALY.

Aim/Introduction: Infective Endocarditis (IE) is a disease associated with high mortality rate and highly variable clinical history. ^{18}F-FDG-PET/CT was introduced in the latest update of the European Society of Cardiology (ESC) guidelines as a new tool for the diagnosis of IE, especially in patients with prosthetic valve and Implanted Cardiac Device (ICD). The use of a simple qualitative criteria with good interpreter reliability, easy reproducibility and good diagnostic performance will be of immense value in the diagnosis of this disease; for this reason we proposed a 3-point score, similar to Deauville score to estimate the accuracy of 18F-FDG PET/CT in detecting IE. The aim of our study was to evaluate the value of this 18F-FDG PET/CT-based interpretation system to assess the diagnosis of IE and to validate the reproducibility of this criterion. ***Materials and Methods:*** We retrospectively included 108 patients (M:F=57:51, mean age 62 years, range 18-88) who underwent ^{18}F-FDG-PET/CT for suspected IE. After clinical assessment and echocardiographic exams, the patients underwent to FDG PET/CT imaging after adequate preparation to reduce the physiological myocardial uptake of ^{18}F-FDG (a low carbohydrate, high protein, high fat (LCHPHF) diet starting 72 hours prior the scan). PET/CT scans were interpreted by two nuclear medicine physicians with experience in this field and were evaluated according to a 3-point scale like-Deauville score criteria (score 1=uptake in suspect lesion lower than blood-pool activity; score 2=uptake higher than blood-pool but lower than liver activity; score 3= uptake higher than liver). PET/CT was considered positive when like-Deauville score 3; negative like-Deauville score

1 and 2. Inter-reader variability was assessed using percent agreement and kappa statistics. ***Results:*** Of the 108 patients enrolled in the study, 54 had a clinical final diagnosis of IE. Comparing the score criteria results with the clinical final diagnosis the sensitivity, specificity, positive predictive value, negative predictive value and accuracy of like Deauville score criteria were 92.8% [95% confidence interval (CI) 82.7-98%), 80.7% (95% CI 67.4-90.3%), 83.8% (95% CI 74.7-90.1%), 91.3% (95% CI 80.1-96.4%) and 87% (95% CI 79.2-92.7%), respectively. There was a high agreement between the two readers applying our criteria (k=0,902). ***Conclusion:*** The proposed 3-point scale criteria is a simple, qualitative method with substantial inter-interpreter agreement and high positive predictive value and accuracy, and may have a significant impact in the diagnosis of IE with PET/CT. ***References:*** None

OP-929

Identification Of Brain 18F-FDG PET Metabolic Profile Of Encephalitis In Patients With Infective Endocarditis (IE): Relationships With Clinical/Biological Features And Prognosis

M. Philip*, E. Kaphan, L. Tessonnier, M. Mulatero, S. Cammilleri, F. Gouriet, J. Casalta, S. Hubert, A. Riberi, G. Habib, E. Guedj;*
Hôpital La Timone, Marseille, FRANCE.

Aim/Introduction: IE is associated with severe morbidity and mortality. ^{18F}FDG PET/CT is now included in ESC Guidelines for the IE positive diagnosis and peripheral complications detection. Among them, cerebral damages are frequent and break IE's prognosis. We observe strokes, hemorrhages, abscesses, usually diagnosed by MRI. In addition, some patients present with an impairment of cognitive or psychomotor functions, consistent with encephalitis, and inconsistent findings on brain morphological imaging. ^{18F}FDG PET is increasingly used for the diagnosis and the follow-up of encephalitis, with a specific metabolic profile characterized by global hypometabolism possibly associated with hypermetabolism of striata and of the medial temporal cortex. The primary objective of this study is to describe the metabolic brain PET profiles of patients with IE. We secondarily aim at determining the relationships between the PET profile of encephalitis and clinical/biological features and the prognosis. ***Materials and Methods:*** From November 2017 to July 2019, all patients admitted in the Cardiology Department of Timone Hospital in Marseille for IE suspicion were included and benefitted from a global evaluation and a whole-body PET including cerebral study. A first visual analysis was performed in order to determine the several brain metabolic profiles. Then we performed a quantitative whole-brain voxel-based analysis using SPM12, searching for correlation between cerebral metabolic rate of glucose and rate of C Reactive Protein using multiple comparison correction Family Wise Error method (p-voxel<0.05), and secondarily with clinical/biological features. ***Results:*** Were included 129 patients, among which 97 with definite IE according to an Expert Consensus were analyzed. Cerebral PET visual analysis permitted the identification of usual complications in 57 patients, already highlighted by morphological imaging, and mostly a new metabolic profile in 21 patients consistent with encephalitis. In quantification analysis, hypermetabolism of the left medial temporal was correlated with CRP increase. This quantitative metabolic profile of encephalitis was statistically (p<0.05) associated with clinical (age, neurological events history), biological (particularly inflammatory syndrome), microbiological (Staphylococcus aureus infections) features and prognosis events such as embolism. A positive trend is revealed as well concerning mortality (OR 2.23). ***Conclusion:*** This study describes, for the first time, cerebral ^{18}F-FDG PET/CT findings in a cohort of patients with suspected IE. We reveal in a proportion of these patients a metabolic brain PET entity similar to those reported in encephalitis, correlated to clinical/biological features and prognosis. Further studies will be needed to specify the possible impact on the clinical management of these patients. ***References:*** None

OP-930

The detectability of infective endocarditis is significantly enhanced when FDG-PET images are recorded in cine mode

C. Boursier*[1], X. Duval[2,3,4], L. Imbert[1,5], B. Mahida[6], B. Hoen[7], F. Goehringer[7], C. Selton-Suty[8], E. Chevalier[1], M. Claudin[1], V. Roch[1], Z. Lamiral[9], A. Bourdon[10], A. Cochet[11], F. Rouzet[6,12], P. Marie[1,13], the AEPEI-TEPvENDO study group;*
[1]CHRU-Nancy, Université de Lorraine, Department of Nuclear Medicine and Nancyclotep molecular imaging platform, Vandoeuvre-les-Nancy, FRANCE, [2]AP-HP, Hôpital de Bichat Claude Bernard, Department of Infectious Diseases, Paris, FRANCE, [3]Université Paris Diderot, INSERM, UMR 1137 (IAME), Paris, FRANCE, [4]INSERM, CIC 1425, AP-HP, Hôpital Bichat Claude Bernard, Paris, FRANCE, [5]Université de Lorraine, INSERM, UMR 1254, Nancy, FRANCE, [6]AP-HP, Hôpital Bichat Claude Bernard, Department of Nuclear Medicine, Paris, FRANCE, [7]CHRU-Nancy, Department of Infectious Diseases, Vandoeuvre-les-Nancy, FRANCE, [8]CHRU-Nancy, Department of Cardiology, Vandoeuvre-les-Nancy, FRANCE, [9]Université de Lorraine, CHRU-Nancy, INSERM, CIC 1433, Vandoeuvre-les-Nancy, FRANCE, [10]CHRU-Nancy,Department of Nuclear Medicine, Montpellier University Hospital, Montpellier, FRANCE, [11]Department of Nuclear Medicine, Georges-François Leclerc Cancer Center, Dijon, FRANCE, [12]Université Paris Diderot, INSERM, UMR 1148 (LVTS), Paris, FRANCE, [13]Université de Lorraine, INSERM, UMR 1116, Nancy, FRANCE.

Aim/Introduction: This explanatory study aimed at determining whether the detectability of infective endocarditis (IE) on ^{18}F-fluorodesoxyglucose Positron

Emission Tomography (FDG-PET) images is enhanced when recorded with an ECG-triggered cine mode (gated-PET).Conventional FDG-PET exams are poorly sensitive for detecting IE, which may be partly explained by the small size and high mobility of certain IE foci. ***Materials and Methods:*** Twenty-eight patients, 15 of whom had a cardiac prosthesis, and all having undergone a 10-min cardiac gated-PET recording after a whole-body FDG-PET in 4 centers involved in a multicenter IE study, were included. Static-PET images, as well as the gated-PET images reconstructed with an additional temporal Fourier filter, were analyzed by three blinded observers with the additional diagnostic criterion that the FDG-activity from IE foci should be nearly constant during cardiac contraction at gated-PET, contrary to myocardial areas of FDG-uptake. ***Results:*** IE was ultimately classified as definite in 19 cases, possible in 6 and rejected in 3. In these 3 groups, the pooled observers' rates of a positive PET for IE were respectively 44%, 11% and 0% with static-PET, compared to 70%, 39% and 0% with gated-PET (P<0.001). Gated-PET but not static-PET was positive for IE in 6 patients, whereas the converse was observed in none. At gated-PET, the FDG foci of definite IE exhibited a high mobility with systole-to-diastole displacements ranging from 6 to 18 mm (mean: 11±4 mm), and their mean activities, expressed relative to blood activities at end-diastole (2.48±0.96) and end-systole (2.60±1.02), were higher than corresponding values from static-PET images (2.05±0.89, both P<0.005). ***Conclusion:*** The detectability of IE is markedly enhanced for cardiac FDG-PET images displayed in an ECG-triggered cine mode and reconstructed with an adapted temporal filtering, in keeping with lower image blurring and with an easier differentiation from areas of myocardial FDG uptake. ***References:*** None

OP-931

Diagnostic Performance Of 18FDG-PET/CT In Discriminating Patients With/Without Cardiac Implantable Electronic Device Infection: A Case-Control Study

R. Mei[1], *V. Marinelli*[2], *R. Bonfiglioli*[1], *L. Calderoni*[1], *G. Massaro*[2], *S. Fanti*[1], *I. Diemberger*[2];
[1]*Nuclear Medicine Policlinico S.Orsola-Malpighi, Bologna, ITALY,* [2]*Cardio-Thoracic and Vascular Building, Department of Experimental, Diagnostic and Specialty Medicine, Bologna, ITALY.*

Aim/Introduction: Diagnosis of cardiac implantable electronic device infection (CIEDI) represents a real challenge for clinicians, radiologists and nuclear physicians. Modified Duke criteria gained higher accuracy with recently implementation of ^{18}F-FDG-PET/CT scan in the diagnostic management for suspected CIEDI. However, literature data about its real efficacy is still lacking. We aimed to explore the potential role of ^{18}F-FDG-PET/CT in general, asymptomatic CIED population, expanding this procedure to patients with CIED and without a suspected infection of the device. ***Materials and Methods:*** We have retrospectively analyzed 68 patients (Group 1, G1) with CIED who underwent ^{18}F-FDG-PET/CT scan (corrected for attenuation) for different reasons than suspected CIEDI (i.e. oncology or non-cardiovascular infection). A second control-group of 105 patients (Group 2, G2) with confirmed CIEDI who underwent ^{18}F-FDG-PET/CT prior to transvenous lead extraction (TLE) was considered. For both Group 1 and 2 general population characteristics, along with maximum standardized uptake value (SUVmax) and target to backround ratios (TBRs) related to pocket, leads and heart were collected. Clinical outcomes (mortality and all-cardiovascular complications) were also evaluated with an up to 3 years follow-up. ***Results:*** 9/68 patients (13.2%) in G1 had an ^{18}F-FDG-PET/CT report suspected for CIEDI. SUVmax on pocket and leads, as well as pocket/blood pool TBR, were statistically superior than G1 negative scans. Of positive G1 patients, no one developed CIEDI or any cardiovascular complications at follow-up. In pocket and/or lead SUVmax cut-off value of 3.5 (corresponding to 25th percentile with 82/105 patients, 79%) was assessed for G2 and then applied to G1. 14/68 patients (20%) of G1 had pocket and/or lead SUVmax higher than 3.5. According to these figures use of a cut-off value of 3.5 for SUV max in patients with suspect of CIEDI seems to provide an acceptable diagnostic performance with a sensitivity of 80% and a specificity of 79%. ***Conclusion:*** ^{18}F-FDG-PET/CT in patients with CIED demonstrated a potential key-role in detecting possible asymptomatic or silent infection of the device with round to 80% of sensibility and specificity. This procedure might be useful to rule out the possibility to assess early diagnosis of CIEDI in patients without any other diagnostic standard (imaging or laboratories) tool or even asymptomatic. ***References:*** None

OP-932

Semiquantitative Analysis Of 18F-FDG PET/CT Results In Patients With Cardiac Implantable Electronic Device Infection

D. Pursanova*, I. P. Aslanidis, O. V. Mukhortova, I. V. Shurupova, I. V. Ekaeva, T. A. Trifonova, D. A. Popov;*
A.N. Bakulev Scientific Center for Cardiovascular Surgery of the Ministry of Health of the Russian F, Moscow, RUSSIAN FEDERATION.

Aim/Introduction: to investigate the semi-quantitative assessment of 18F-fluorodeoxyglucose (18F-FDG) PET/CT in patients with infection of cardiac implantable electronic devices (CIED) and without it. ***Materials and Methods:*** The analysis included results of 18F-FDG PET/CT examinations performed in 50 patients (54+16 y.o.) with CIED (32+27 months after implantation) - with surgically confirmed infection (n = 20) and with malignancies used as control group (n = 30). PET/CT results were assessed visually

and semi-quantitatively with calculation of parameters of 18F-FDG uptake intensity - SUVmax and SUVratio - in whole device, pocket, extra- and intracardiac portions of leads. SUVratio was calculated as SUVmax in the CIED to SUVmean in the reference zone - aorta, liver and lung. ***Results:*** Visual analysis of PET/CT results revealed abnormal 18F-FDG uptake in all patients with CIED infection (n = 20) in different regions of interest: in pocket (n = 8), along extra- (n = 15) and intracardiac (n = 9) portions of leads. In control group (n = 30) 18F-FDG uptake was normal in all 90 regions of interest (n = 30 in each). In semiquantitative analysis all parameters - SUVmax and three types of SUVratios - in the CIED pocket and extracardiac portion of leads were higher in patients with confirmed infection, compared to patients without it ($p<0.05$). Along intracardiac portion of leads two types of SUVratios (using aorta and liver) were higher in patients with confirmed infection ($p<0.02$), but there was no statistical difference in the SUVmax and SUVratio using lung parenchyma ($p>0.05$).ROC-curve analysis for optimal thresholds of SUVmax and three types of SUVratios for the diagnosis of CIED infections (for whole device) by PET/CT was performed: SUVmax = 3.3 (AUC = 0.847), SUVratio (aorta) = 1.8 (AUC = 0.947), SUVratio (liver) = 1.2 (AUC = 0.881), SUVratio (lung) = 6.8 (AUC = 0,783). ***Conclusion:*** According to the obtained data visual analysis in combination with semi-quantitative assessment of 18F-FDG PET/CT images showed a good diagnostic performance in the detection of CIED infection. 18F-FDG uptake around non-infected CIED was low. SUVratio using aorta - in whole CIED, as well as in each of its various parts - pocket, extra- and intracardiac portions of leads - was found to give the greatest AUC. ***References:*** None

OP-933

PET-MRI in acute gastrointestinal graft versus host disease

W. Roll[1], G. Evers[2], P. Schindler[3], R. Strotmann[1], B. Noto[3], M. Masthoff[3], M. Stelljes[2], M. Schäfers[1,4];
[1]Department of Nuclear Medicine, University Hospital Münster, Münster, GERMANY, [2]Department of Medicine A, Hematology, Oncology and Pulmonary Medicine, University Hospital Münster, Münster, GERMANY, [3]Institute of Clinical Radiology, University Hospital Münster, Münster, GERMANY, [4]Europeam Institute for Molecular Imaging, Münster, GERMANY.

Aim/Introduction: Allogenic stem cell transplantation (alloSCT) is considered the only curative treatment option in numerous relapsed or refractory hematologic malignancies. Following alloSCT gastrointestinal Graft-versus-Host disease (GI-GvHD) is a common complication significantly increasing morbidity and mortality. There are only limited data on molecular (FDG-PET) or contrast enhanced (CE) morphological imaging assessment of GI-GvHD. The objective of this retrospective study was to further elucidate the diagnostic value of a combined FDG-PET/MR approach in patients with acute GI-GvHD. ***Materials and Methods:*** Between 2/2015 and 2/2019, 21 patients with suspected acute GI-GvHD underwent FDG PET-MRI. PET- (dataset 1), contrast enhanced MRI- (dataset 2) and PET-MR datasets (dataset 3) were independently reviewed by two nuclear medicine physicians (dataset 1 and 3) and two radiologists (dataset 2 and 3). In case of disagreement a consensus reading was performed. Readers assessed the certainty of the diagnosis on a 5-point likert scale (from "1=definitely no GvHD" to "5= definitely GvHD") and the number of affected segments of the lower GI-tract. Semi-quantitative (number of affected segments) and quantitative PET-parameter (SUVmax, SUVpeak and metabolic volume (MV)), as well as quantitative parameters from CE-MRI (wall thickness) were correlated with clinical parameters (stage and grade of acute GvHD). ***Results:*** Likert scale values were significantly different between the tree datasets, underlining the higher reliability of imaging based diagnosis with PET-MR (median: 5; range: 4-5) compared to PET (median: 4; range: 2-5; p=0.007) and compared to MRI (median: 4; range: 3-5; p=0.002). The correlation between affected segments in PET-MRI (r_s=0.677; p=0.001) and MV (r_s =0.692; p=0.001), to clinical stage were significant. SUVmax (r_s =0.345; p=0.14), SUVpeak (r_s =0.276; p=0.24) and wall thickening (r_s =0.174; p=0.17) did not show any significant correlation to clinical stage. ***Conclusion:*** Combined FDG PET-MRI contributes to a more sensitive detection and a more reliable diagnosis of acute GI-GvHD compared to single PET or MRI. Metabolic volume adds information indicating the clinical severity of acute GI-GvHD. Before implementation into clinical routine, FDG-PET-MRI should be further evaluated in prospective studies. ***References:*** None

OP-934

Association between residual FDG metabolic activity and CT features of active tuberculosis on end-of-treatment [^{18}F]F-FDG PET/CT in patients treated for pulmonary tuberculosis

I. Lawal[1,2], M. Mathebula[3], I. Moagi[3], T. Lengana[1], N. Moeketsi[3], M. Nchabeleng[3], G. Popoola[4], C. Hikuam[5], E. Douglass[6], J. Ellner[6], M. Hatherill[5], B. Fourie[1], M. Sathekge[1];
[1]University of Pretoria, Pretoria, SOUTH AFRICA, [2]Nuclear Medicine Research Infrastructure (NuMeRI), Pretoria, SOUTH AFRICA, [3]Sefako Makgatho University of Medical Science, Pretoria, SOUTH AFRICA, [4]University of Ilorin, Ilorin, NIGERIA, [5]University of Cape Town, Cape Town, SOUTH AFRICA, [6]Boston University, Boston, MA, UNITED STATES OF AMERICA.

Aim/Introduction: Residual metabolic activity (RMA) on [^{18}F]F-FDG PET/CT in the lungs of patients treated with a standard course of anti-tuberculous therapy (ATT) and declared cured based on the current standard of care including negative culture has been shown to be predictive

of disease relapse. Certain CT features including nodules, consolidation, and pleural effusion are also known to be suggestive of active pulmonary tuberculosis (PTB). We aimed to determine the association between RMA on PET and CT features of active tuberculosis in patients who completed a standard course of ATT for PTB. ***Materials and Methods:*** We prospectively recruited patients who completed a standard course of ATT and were declared cured based on clinical and microbiological assessments. All patients underwent [^{18}F]F-FDG PET/CT within two weeks of completing ATT. We determined the proportion of patients who had RMA in the lungs as well as CT features suggestive of active PTB including lung consolidation, pulmonary nodules, lung changes in tree-in-bud pattern, hilar/mediastinal lymphadenopathy, and pleural effusion. We determined the association between RMA and CT features of active PTB. ***Results:*** A total of 75 patients with a mean age of 30.09 ± 10.49 years were included. There were 47 males and 50 patients were HIV-infected. Forty-one patients had RMA. No significant difference in the prevalence of RMA in patients with HIV versus those without (p=0.01). Nodules, consolidation, tree-in-bud pattern, lymphadenopathy, and pleural effusion were seen in 53, 10, 29, 17, and 2 patients, respectively. CT features of active PTB that were significantly more prevalent among patients with RMA were nodules (Odds ratio, OR=10.41; p<0.001), consolidation (OR=9.28, p=0.018), tree-in-bud pattern (OR=30.86, p<0.001), and lymphadenopathy (OR=3.48, p=0.040). The Odds of having RMA in any patient with the combined CT features of active PTB was 24.97 (95%CI: 6.39 - 97.56), p<0.001. ***Conclusion:*** Residual FDG metabolic activity, a risk factor for relapse, is prevalent in the lungs of patients considered cured for PTB based on the current standard of care. There is a strong association between RMA and CT features suggestive of active PTB. ***References:*** None

OP-935

Visual 4-point scoring scale improves the yield of FDG PET/CT in the diagnosis of cyst infection in patients with autosomal dominant polycystic kidney disease

P. Lovinfosse, M. Neuville, ***A. Jadoul****, F. Jouret, R. Hustinx; CHU of Liege, Liege, BELGIUM.*

Aim/Introduction: FDG PET/CT proved useful in the diagnosis of cyst infection (CyI) in patients with autosomal dominant polycystic kidney disease (ADPKD). However, the definition of CyI by FDG PET/CT remains unclear. Here, we characterize the FDG uptake in case of CyI in ADPKD patients in order to infer a visual 4-point diagnostic scale. ***Materials and Methods:*** All ADPKD patients who were hospitalized between 2007 and 2019 and who underwent an FDG PET/CT within the 14 days preceding or following their admission, were identified. All files were systematically reviewed. CyI was defined on the basis of a constellation of 5 concomitant criteria: (i) fever ≥38°C; (ii) abdominal pain; (iii) peak plasma C-reactive protein (CRP) levels ≥70 mg/L; (iv) no other cause of inflammation; and (v) favorable outcomes after antibiotics for ≥21 days. First, all FDG PET/CT images were classically studied by 2 board-certified physicians in nuclear medicine unaware of the clinical and biological parameters, independently of the initial diagnosis. Next, the uptake of FDG around the suspected CyI was scored using a 4-point scale, in comparison to the physiological FDG blood-pool activity and liver uptake. ANOVA, Kruskal-Wallis test and Fisher exact test were used to compare clinical, (micro-) biological, and PET parameters between groups. Sensitivity, specificity, positive predictive value and negative predictive value of FDG PET/CT for the diagnosis of hepatic or renal cyst infection were calculated. The logistic regression was used to study the risk of cyst infection with respect to visual scale. Differences in P-values of less than 0.05 were considered statistically significant. ***Results:*** Sixty-one FDG PET/CT were performed for suspected CyI in 39 ADPKD patients. The mean age was 59, with a man/woman ratio of 33/28 and a history of kidney transplantation or nephrectomy in 72.1% and 27.9% of cases, respectively. Among these, 30 episodes met the gold-standard criteria for CyI. The first classical assessment of FDG PET/CT images reached a sensitivity of 74% and a specificity of 71%. Using the 4-point scale scoring system, the specificity of FDG PET/CT increased to 85%, with no significant change in sensitivity. ***Conclusion:*** In conclusion, the use of the visual 4-point visual scale of FDG uptake improves the specificity of FDG PET/CT in CyI diagnosis in ADPKD patients, thereby reaching positive and negative predictive values of 79% and 78%, respectively. External validation is required. ***References:*** None

OP-936

Automated Quantification of Bowel ^{18}F-FDG PET/CT Uptake for Early Detection of Immune-Related Colitis in Cancer Patients Receiving Immune Checkpoint Inhibitors

D. Huff*[1], H. Emamekhoo[2], S. B. Perlman[3], R. Jeraj[1,4]; [1]Department of Medical Physics, University of Wisconsin-Madison, Madison, WI, UNITED STATES OF AMERICA, [2]Department of Medicine, University of Wisconsin-Madison, Madison, WI, UNITED STATES OF AMERICA, [3]University of Wisconsin Carbone Cancer Center, Madison, WI, UNITED STATES OF AMERICA, [4]Faculty of Mathematics and Physics, University of Ljubljana, Ljubljana, SLOVENIA.*

Aim/Introduction: Immune-related colitis (irColitis) is a common and clinically impactful side effect of immune checkpoint inhibitors that benefits from early detection to expedite appropriate intervention and avoid unintended complications. Our purpose was to develop a biomarker for the prediction of irColitis onset from standard of care ^{18}F-FDG PET/CT. ***Materials and Methods:*** We retrospectively analyzed ^{18}F-FDG PET/CT scans of 40 patients receiving

ipilimumab and/or nivolumab for melanoma, lymphoma, or lung cancer. A convolutional neural network was trained to segment the bowel (small and large intestine) from low dose CT and was used to quantify bowel ^{18}F-FDG uptake. SUV metrics extracted from the bowel (SUV_{max}, SUV_{mean}, SUV_{total}, percentiles of the SUV histogram) were compared to clinical diagnoses of irColitis confirmed with colonoscopy and biopsy. Differences in metric between irColitis and non-irColitis groups were assessed with Wilcoxon sign-rank tests and Receiver Operating Characteristic (ROC) analysis. ***Results:*** Immune-related colitis was clinically diagnosed in 7/40 (18%) of reviewed patients. The median time to clinical diagnosis was 140 days after treatment start (range: 13-302). The most predictive biomarker of irColitis was the 95th percentile of the bowel SUV histogram ($SUV_{95\%}$). Patients who later received a clinical diagnosis of irColitis had a significantly higher increase in $SUV_{95\%}$ from baseline to first on-treatment PET than patients who did not experience irColitis (p=0.023). ROC analysis revealed that an increase in $SUV_{95\%}$ of greater than +40% indicated pre-colitis bowel change with a sensitivity of 75% and specificity of 88%. For these patients, elevated bowel ^{18}F-FDG uptake was seen a median of 115 days prior to clinical diagnosis (range: 30-206). However, in 2/7 irColitis patients, the clinical diagnosis occurred prior to the first on-treatment PET. ***Conclusion:*** Increased ^{18}F-FDG uptake in the bowel is a useful early indicator of immune-related colitis in patients receiving immune checkpoint inhibitors. Although standard of care ^{18}F-FDG PET/CT scans obtained for response evaluation provided sufficient information for early prediction of irColitis, an earlier timepoint scan after treatment initiation might further improve the predictive power. ***References:*** None

1611

e-Poster Presentation Session 11: Nuclear Medicine Therapy Beyond Thyroid

Friday, October 30, 2020, 13:50 - 15:00 Channel 11

EPS-170

Is It Safe Enough to Follow-up Patients Only with Post-therapy Whole-body Scan After PRRT?

T. Telli, M. Tuncel, P. Ozgen Kiratli;
Hacettepe University Faculty of Medicine, Ankara, TURKEY.

Aim/Introduction: There is an ongoing debate over the optimal post-peptide receptor radionuclide therapy(PRRT) imaging strategies. This study aimed to compare therapy response patterns of Ga-68-DOTATATE-PET/CT with post-PRRT whole-body scans(PT-WBS) and evaluate whether PT-WBS alone could play a decisive role in therapy response. ***Materials and Methods:*** Ga-68-DOTATATE-PET/CT and PT-WBS images of 60 patients (F/M:32/28, median age: 60(IQR: 51-69), median tumor grade: 2 (IQR: 1-2)) treated with at least two cycles of Lu-177-DOTATATE(37/60) or combination of Lu-177-DOTATATE and Y-90DOTATATE(23/60) were evaluated retrospectively. Ninety-four scan pairs of Ga-68-DOTATATE PET/CT and PT-WBS were compared for therapy response by three nuclear medicine physicians. SPECT/CT was also available in 23/94(25%) pairs. Pre-therapy PET/CTs were compared with PETs obtained six weeks after the second cycle of PRRT and PETs obtained 8-12 weeks after four cycles. Similarly, PT-WBSs after the first therapy were compared with PT-WBSs after the second and fourth therapy. For response assessment, EORTC criteria for Ga-68-DOTATATE-PET/CT and tumor/background ratios for Lu-177-DOTATATE-WBSs(PT-WBSs) were used. Critical differences between PET/CT and PT-WBS responses causing a change in the management were recorded. Tumor grade, total number of lesions, tumor volume, total lesion Ga-68-DOTATATE uptake, SUVmax of the most avid lesion, size of the largest avid lesion on pre-therapy Ga-68-DOTATATE-PET/CTs were analyzed as baseline predictor factors for the critical difference. ***Results:*** There was a moderate agreement between PET/CT and PT-WBS responses (kappa value:0,44, p<0,001). Critical differences were seen in 9/60 (15%) patients. Among these nine patients, eight patients were classified as PD with PET/CT, while SD/PR was reported on PT-WBS. Lastly, one patient who had PR with low tumor burden with mild uptake on PT-WBS accepted as CR with PET/CT. Overall PET/CT prevented further PRRT cycles in eight patients with PD and one with CR. Among the predictive factors analyzed for critical difference, only pre-therapy total lesion number was found to be statistically significant (p: 0,03, RR: 1,1, CI: 1-1,1). Patients with PD on PET/CT but SD/PR on PT-WBS, had discordant lesions with a median size of 11 mm(IQR:8-24 mm) and a median SUVmax of 6,1(IQR:2,7-10,7). Progressive lesions that were not detected with PT-WBS were mostly in the abdominopelvic region compared elsewhere (81% and 42,6% respectively,p:0,003). ***Conclusion:*** Agreement between PET/CT and PT-WBS responses was moderate, and critical inconsistencies were observed. PT-WBS can be insufficient, especially in patients with numerous lesions and may overlook progression of abdominopelvic lesions. ***References:*** None

EPS-171

Clinical outcome of 177Lu-PSMA-IT Therapy in Advanced metastatic prostate cancer patients in Asia

T. Bu, F. Yu, L. Zhang, F. Wang;
Nanjing First Hosptial China, Nanjing, CHINA.

Aim/Introduction: The aim of this study to evaluate the safety and efficacy of metastatic castration-resistant prostate cancer (mCRPC) patiets in Asia after several cycles of 177Lu PSMA-IT therapy, and to explore the factors that affect the

prognosis of treatment. ***Materials and Methods:*** From August 2018 to March 2020,42 patients(mean age:68.3 years old) with mCRPC were consecutively enrolled for one cycle of Lu-177-PSMA therapy, institutional review board approval and informed consent was obtained for this study. 68Ga-PSMA-11 PET/CT showed multiple PSMA-avid lesion sin all patients before the therapy. 177Lu-PSMA-I&T radioligand therapy with 2.0-7.7GBq were performed. Hematological status, liver and kidney function, and serum prostate specific antigen (PSA) levels were documented before and after treatment. Visual Analogue Scale/Score (VAS) was used to record changes in bone metastasis pain. The efficacy was evaluated by the changes of PSA, Eastern Cooperative Oncology Group (ECOG) , maximum standardized Uptake Value (SUVmax) and tumor size on 68Ga-PSMA-11 PET/CT, and clinical follow-up. Paired t test and rank-test was used to analyze the data. ***Results:*** Significant PSA reduction was associated with 177Lu-PSMA-I&T treatment(P=3.6×10-4),Of the 42 patients, 10 had elevated PSA levels and disease progression, while 32 patients had variable reduction of PSA, of which 11/32 decreased by <30%and 20/32 decreased by >50%. No evident hematotoxicity, hepatorenal toxicity was observed during the follow-up after treatment. The ECOG , VAS scores and SUVmax of metastatic lesions showed significant differences in pre and post treatment (P<0.05). This analysis determined that the average intensity of the mean of PSMA standardized uptake value (SUVmean) , tumor burden, lactate dehydrogenase(LDH), and alkaline phosphatase (ALP) were closely related to the prognosis. ***Conclusion:*** The present study in Asian population validated 177Lu-PSMA-I&T treatment achieve better response in the treatment of mCRPC, which is easy tolerable and safe. In addition, both biomarkers (ALP / LDH) and PSMA PET / CT parameters have important implications for the prognosis of men receiving LuPSMA. ***References:*** None

EPS-172

The Role of Ga-68 PSMA PET / CT in Predicting Lu-177 PSMA Effectiveness: Can We Project the Ga-68 DOTA PET / CT and Lu-177 DOTA Treatment Experience to PSMA?

U. Korkmaz*, F. S. Soyluoglu, G. Durmus-Altun;*
Trakya University, Edirne, TURKEY.

Aim/Introduction: Prostate cancer is the most common type of cancer in men, and the second most common cause of cancer death. Prostate Specific membrane antigen (PSMA) is expressed in prostate epithelial cells and highly expressed on prostate cancer. PSMA levels are directly related to androgen independence, metastasis and prostate cancer progression. Therefore, it is a good target for the diagnosis and treatment of prostate cancer. Lu 177-PSMA therapy is an effective type of "targeted therapy" used in the treatment of castration-resistant prostate cancers. Despite data showing significant clinical responses obtained with Lu 177-PSMA therapy, predictors of the treatment response in imaging were not clearly characterized yet. In this study, we evaluated the relationship between Ga68-PSMA imaging parameters and the therapeutic response obtained after Lu177-PSMA treatment, and analyzed the differences and similarities of Ga68-DOTA / Lu177-DOTA pair. ***Materials and Methods:*** Ga-68 DOTA and Ga 68-PSMA PET/CT images of patients who applied to the Nuclear Medicine Department and received Lu177-radiopeptide (DOTA and PSMA) treatment between January 2016 and January 2020 were included in the study. Pre-treatment, mid-treatment and post-treatment Ga68 (DOTA/PSMA) PET/CT images and also 177Lu whole body images taken after each treatment dose, which were all taken on the same system, were found from archive. Data of the patients were collected from the patient files. The patients were grouped as DOTA and PSMA according to their primary diagnosis and the peptide used in 68Ga-PET/CT. Metabolic PET parameters, 177Lu uptake, biochemical parameters and treatment response findings of both group were compared and evaluated separately. ***Results:*** Of the 46 patients included in the study, 14 were in the DOTA group and 32 were in the PSMA group. Most patients had widespread metastatic disease prior to the treatment. In the DOTA group, the liver was the most frequently metastatic site with the highest metabolic activity (36%), while bone was in the PSMA group (68%). TmSUVmax was similar for the DOTA and PSMA group after treatment (p= 0.11). ΔTmMTV, ΔTm / TotalMTV values were significantly different (p= 0.04 and p= 0.03). At the end of the treatment, the number of foci decreased in both groups. The highest treatment efficacy was achieved in soft tissue. The metabolic response of both groups to treatment was similar. ***Conclusion:*** 177Lu -radiopeptide therapy is an effective treatment method for both NET and prostate cancer. Tumor burden is significantly reduced and the most pronounced effect occurs in soft tissue. ***References:*** None

EPS-173

Peptide receptor radionuclide therapy (PRRT) for neuroendocrine tumors (NET): A single institution experience in the USA

H. Duan*, V. Ferri, P. L. Kunz, G. A. Fisher, F. Moradi, G. A. Davidzon, B. L. Franc, A. H. Iagaru, C. Aparici Mari;*
Stanford University, Stanford, CA, UNITED STATES OF AMERICA.

Aim/Introduction: Neuroendocrine tumors (NET) are a rare and heterogenous group of tumors with a rising incidence. NETs are often times indolent leading to a late diagnosis at an advanced, metastatic stage, making these patients ineligible for surgery, the only curative treatment. Peptide receptor radionuclide therapy (PRRT) with radiolabeled somatostatin analogues is an encouraging systemic treatment modality. It is not only known to reduce tumor burden but also leads to symptomatic relief and thus increases quality of life with

minimum side effects. Here we present our initial experience with PRRT since FDA approval in May 2018 in patients with NET and other somatostatin receptor (SSTR) positive tumors. ***Materials and Methods:*** Seventy-seven patients (38 males and 39 females; 37 - 81-year-old, mean ± SD: 63.1 ± 10.7 years), thereof 72 with progressing NETs (37 pancreas, 25 small intestine, 1 cecum, 1 appendix, 1 gastric, 1 atypical lung and 6 of unknown primary), 3 paragangliomas, and 2 pheochromocytomas underwent PRRT with ^{177}Lu-labeled Dotatate (Lutathera®) at our institution. ^{68}Ga-Dotatate PET/CT was performed at baseline, after 2 cycles, and following completion of treatment. RECIST and SSTR density based on change of SUV_{max} were used to evaluate response to therapy. Laboratory tests were obtained at baseline and 1 week before each cycle and every 2 months at follow up. Progression-free survival (PFS), objective response rate (ORR). Considering the short follow-up time, an interim overall survival (OS) analysis was performed. ***Results:*** 46/77 (59.7%) patients completed all 4 cycles of PRRT, 19/77 (24.7%) patients are still in treatment. 12/77 (15.6%) patients had to discontinue PRRT (5 after the 1st cycle, 4 after the 2nd cycle, and 3 after the 3rd cycle) due to worsening comorbidities. The 3-month PFS rate was 79% and the 6-month PFS rate was 84%. The ORR at 3-month follow-up was 56.1% and at 6-month 21.7%. Interim OS was 74% at 22 months. Patients had on average 3.4 ± 1.39 treatment lines prior to receiving PRRT. ***Conclusion:*** Our preliminary data show overall good results of PRRT with Lutathera® in patients with NETs. However, our results seem to be inferior to the NETTER -1 trial which is most likely due to the extensive pre-treatment before PRRT. ***References:*** None

EPS-174

Early change of ^{68}Ga-HA-DOTATATE uptake during PRRT prognosticates duration of response in patients with metastatic NET

F. Fiz[1], *H. Dittmann*[2], *G. Centurioni*[3], *C. la Fougère*[2];
[1]*Humanitas Clinical and Research Center - IRCCS, Milan, ITALY,* [2]*Nuclear Medicine Unit, Department of Radiology, University of Tübingen, Tübingen, GERMANY,* [3]*University of Tübingen, Tübingen, GERMANY.*

Aim/Introduction: Peptide-receptor radiotherapy (PRRT) is an effective treatment of metastatic neuroendocrine tumors (NET); however, time-to-progression (TTP) after PRRT varies significantly among patients. Moreover, early posttreatment PET/CT might not identify variation in lesion size or visual tracer uptake, thus identification of response is challenging. In this study, we assessed whether semiquantitative analysis of liver and bone metastases could prognosticate response duration in NET patients. ***Materials and Methods:*** Seventy-six NET patients underwent ^{68}Ga-HA-DOTATATE PET/CT before and after the first two cycles of PRRT with ^{177}Lu-HA-DOTATATE (7400 MBq per cycle, four cycles total). Mean, max, and peak target-to-background ratio (TBRmean, TBRmax, TBRpeak) was computed on the liver and bone metastases as the ratio between metastases and blood pool SUV (assessed in a 10-slices VOI, manually drawn on the inferior vena cava). Variation trend in TBR between the first and the second PET was defined as increasing (>10% TBR increase), decreasing (>10% TBR drop), or stable (all other cases). Patients were stratified according to the TTP median as long- or short-time responders (LR and SR). TBR, grading (G1, G", and G3), histology (midgut, pancreatic, bronchial, or other), and presence of bone metastases were used to stratify TTP in a Kaplan-Meier (KM) model. ***Results:*** Median TTP was 22 months (range 5-39). At KM analysis, patients with increasing, stable, or decreasing TBRmean (n= 35, 12, and 29, respectively) had a TTP of 31, 26, and 14 months, respectively ($p<0.001$ for increasing Vs. decreasing; $p<0.05$ for stable Vs. decreasing). When comparing the first and second PET, LR patients displayed a more positive variation in TBRpeak than SR (+30±49% Vs. -18±32%, $p<0.01$); the same difference was observed for TBRmean and TBRpeak as well ($p<0.05$ and $p<0.01$, respectively). KM identified a shorter TTP in G3 NET (n=9, 7 months, $p<0.001$ Vs. both G1 and G2) but found no difference between G1 and G2 tumors. Moreover, histology and the presence of bone metastases purported no differences in TTP. ***Conclusion:*** Decreasing SSR-Expression after 2 cycles of PRRT appears to be related to a shorter duration of response. This phenomenon might indicate the growth of less differentiated tumor components. ***References:*** None

EPS-175

Incidence of raised HbA1c and correlation with Somatostatin analogue therapy (SSA) in patients with Neuroendocrine Tumours (NET) receiving peptide receptor [^{177}Lu]Lu-DOTA-TATE radionuclide therapy (PRRT)

N. Eftychiou[1], *H. Ilyas*[1], *H. Ahmed*[1], *F. Hassan*[1], *A. Eccles*[1], *V. Lewington*[1,2];
[1]*Guy's and St Thomas Foundation Trust, London, UNITED KINGDOM,* [2]*King's College London, London, UNITED KINGDOM.*

Aim/Introduction: Administration of short course corticosteroids (dexamethasone) post peptide receptor radionuclide therapy (PRRT) is recommended for selected patients to mitigate radiation-related oedema. Hence, pre-assessment of HbA1c in patients with no previous diagnosis of impaired glucose tolerance (IGT) or diabetes mellitus (DM) is considered important. As Somatostatin Analogues (SSA) are widely used in patients with Neuroendocrine Tumours (NET) and have been associated with possible changes in glucose metabolism, we investigate the incidence of raised serum HbA1c in patients with NET receiving PRRT in combination with SSA. ***Materials and Methods:*** This is a retrospective study. We included all NET

patients who received [^{177}Lu]Lu-DOTA-TATE treatment at our centre between 01/01/2017 - 31/12/2019. Patient data were obtained from electronic patient records. Raised serum HbA1c was defined as ≥ 42 mmol/mol. ***Results:*** 138 patients were treated, of whom 19 were excluded as their baseline HbA1c was not recorded. Of 119 patients, 13% (16/119) had a prior diagnosis of DM or IGT while the majority, 87% (103/119) had no history of altered glucose metabolism. Of the 103 patient cohort, 46% (47/103) had raised HbA1c at baseline (54% (56/103) being within normal limits). 83% (85/103) were on SSA therapy. To determine the significance of SSA therapy upon mean HbA1c values in patients with no known history of DM or IGT, we performed t-test. The results show no significant difference between the 2 groups (43.3+/-6.3 Vs 44.1+/-11.0, p-value: 0.779). Of patients with a raised HbA1c (including both diagnosed and undiagnosed patients with DM or IGT) the commonest primary tumour origin was gastroenteropancreatic (GEP-NETs) 70%, (gastroenteric 51% and pancreatic 19%), followed by lung 13%, unknown primary 6%, pheochromocytoma 5%, paraganglioma 3%, mesenteric 1.5% and thymic 1.5%. ***Conclusion:*** The relatively high incidence (46%) of HbA1c ≥ 42 mmol/mol in NET patients undergoing PRRT with no known prior history of DM or IGT confirms the clinical relevance of documenting pre-treatment HbA1c status. No significant difference was observed between mean HbA1c levels among patients on SSA therapy vs those not on SSA. The most common primary site of origin among patients with raised HbA1C was GEP-NET. Statistical analysis will be performed to investigate whether an increased incidence of raised HbA1c is linked to certain primaries. ***References:*** None

EPS-176

Single-institution real-life experience of ^{177}Lu-DOTATATE treatment in progressive, well differentiated GEPNETs

F. Scalorbi*, A. Lorenzoni, E. Seregni, V. Fuoco, G. Argiroffi, N. Prinzi, S. Pusceddu, G. Aliberti, E. Garanzini, J. Coppa, F. De Braud, V. Mazzaferro, M. Maccauro; Istituto Nazionale Tumori Milano, Milan, ITALY.*

Aim/Introduction: To evaluate safety, toxicity and interim efficacy of ^{177}Lu-DOTATATE treatment (PPRT) in patients with progressive G1-G2 GEPNETs. ***Materials and Methods:*** We prospectively evaluated GEPNET patients treated with at least one PRRT cycle at our Institution from April 2019 to April 2020. PRRT treatment was given as 4 separate infusions, 7.4 GBq each, with 8-week interval. To evaluate the interim response, CT or MRI were performed after the second PRRT administration. Side effects were assessed applying NCI-CTCAE criteria meanwhile RECIST 1.1 criteria were applied to evaluate interim response to PRRT. ***Results:*** We evaluated 55 patients (21 males, 34 females; mean age 62.5, range 38-84) diagnosed as G1 (25, 44.6 %) or G2 (30, 53.6%) progressive metastatic GEPNETs. In the majority of cases the primary tumor was located in the ileum (60%) followed by pancreas (32.7%) and other sites (7.3%). PRRT was administered as fifth/sixth-line in 25 cases (45.4%) followed by third/fourth-line in 20 (36.4%) and second-line therapy in 10 (18.2%). Forty-four patients (80.3%) were treated with two, 35 (62.5%) with three and 22 (44.6%) completed the four administrations. PRRT was suspended in eight patients (14.5%), previously treated with two (4 cases), three (3 cases) and five (1 case) systemic therapeutic lines, due to toxicity (4 cases, 50%), radiological (2 cases, 25%) and clinical progression (2 case, 25%). The lasting two cases consisted of intestinal occlusion and progression of neoplastic ascites that needed medical intervention. The toxicity that caused PRRT interruption were: two G2 persistent thrombocytopenia, one G4 hyperbilirubinemia and one G4 renal failure. The lasting two cases were known to have G2 hyperbilirubinemia and G2 renal failure before the start of PRRT. In the remaining 51 patients, we observed hematological toxicities G1-G2 in 14 patients and G3 in one. Furthermore, G1 renal toxicity was shown in 1 patient and G3 in another one. Two patients experienced G1 hepatic toxicity. Data from 31 available interim CT or MRI scan showed stable disease in the majority of cases (90.3%), progression in two (6.5%) and partial response in one (3.2%). ***Conclusion:*** Considering our real-life experience, PRRT is a safe treatment option even in patient previously treated with numerous systemic therapeutic lines. PRRT is effective in early disease control, reaching stability in more than 90% of interim evaluations. However, effectiveness and safety could be improved if PRRT is early performed after disease progression. Further clinical studies are needed to confirm this hypothesis. ***References:*** None

EPS-177

Four-years experience in 177Lu-oxodotreotide therapy for patients with Neuroendocrine Tumors (NETs)

A. Cardozo Saavedra*, A. García-Burillo, D. Villasboas-Rosciolesi, M. Simó-Perdigó, J. Hernando-Cubero, J. Capdevila Castillón, E. M. Carrillo-Villamizar, S. Menendez Sanchez, J. Castell-Conesa; Hospital Universitari Vall D'Hebron, Barcelona, SPAIN.*

Aim/Introduction: Our aim is to evaluate our results with 177Lu-oxodotreotide therapy for patients with somatostatin-receptors-overexpressing NETs. ***Materials and Methods:*** We performed a descriptive and retrospective analysis in patients with a diagnosis of a disseminated NET in progression who underwent treatment with 177Lu-oxodotreotide from June 2016 to April 2020 at our center. The patients still ongoing treatment were excluded. We assessed the clinical and imaging response to treatment after the fourth dose, besides the presence of adverse effects. ***Results:*** A total of 21 patients (15 men and 6 women), with a mean age of 57.9 years (22-85) were

included. 17/21 patients had Gastroenteropancreatic-NETs (GEP-NET), 2/21 had Non-GEP-carcinoids and 2/21 had paragangliomas. 14/21 patients completed our standard treatment of 4 doses (ST4D) of 7.4GBq; of these, 12/14 had a GEP-NET. The post-therapeutic evaluation (PTE) showed: PR in 7/14, SD in 5/14 and PD in 1/14, it is pending in 1/14. Among the GEP-NETs the PTE showed: PR in 6/12, SD in 5/12 and in 1/12 it is pending (interim-SD). 7/21 patients received less than 4 doses, the causes were: complication directly related with treatment (DRT) in 1/7 (GEP-NET), complications not-DRT in 5/7 (4/7 GEP-NET) and voluntary resignation in 1/7 (Non-GEP-NET). The PTE showed: PR in 2/7, PD in 1/7, death in 2/7 and unknown in 2/7. Among the 5/7 patients with GEP-NETs, the PTE showed: PR in 2/5 (including the patient with relevant toxicity), death in 2/5 (Not-DRT) and unknown in 1/5. The mean progression-free survival (PFS) of the 19/21 patients with known outcome was of 15.6 months (2-41). The PFS for the GEP-NETs with ST4D was of 19.8 months (6-41) and for the Non-GEP-NETs it was of 9.5 months (9-10). Of the total, 11/21 patients reported symptomatic improvement, 9/21 showed no changes (2/21 asymptomatics) and 1/21 worsened. Of the 21 patients, 10/21 presented haematological toxicity, 3/10 required transfusion and 1/10 discontinued treatment for significant pancytopenia. None of them presented significantly renal toxicity. Of the 12 patients with GEP-NETs who received 4 doses, 4/12 died during follow-up (overall survival of 12, 19, 22 and 33 months); of these, 1/12 GEP-NET patient underwent a re-treatment and died after the fifth (accumulated) dose, for an intracranial hemorrhage of unclear etiology: traumatic versus unconfirmed metastasis. ***Conclusion:*** Benefits in PFS, symptomatic relief and an adequate tolerance was observed in patients with GEP-NETs treated with 4 doses of 177Lu-oxodotreotide. Benefits in Non-GEP-NETs are not clear. ***References:*** None

EPS-178

Treatment of Neuroendocrine Tumors with Lutetium-177 Oxodotretoide: First Results in our Institution

Á. Galiana*, A. Gardellini, M. Marín, E. Martínez, A. La Salvia, R. García-Carbonero, M. Tabuenca, S. Ruiz, V. Godigna, J. Pilkington, D. Vega, J. Estenoz;*
Hospital Universitario 12 de Octubre, Madrid, SPAIN.

Aim/Introduction: Theranostics is a powerful tool with enormous potential in the management of neoplasm. We analyze the first steps of our hospital in using Peptide Receptor Radionuclide Therapy with ^{177}Lu-oxodotreotide in neuroendocrine tumors (NET), its effectiveness and security in our practice. ***Materials and Methods:*** Nineteen patients (9 women, average age 60,4±12,6 years) were included, all of whom received at least one dose of ^{177}Lu-oxodotreotide (standard protocol of 4 doses of 7400MBq every 8 weeks) between March 2016 and November 2019. Thirteen patients completed the treatment (68,4%), 2 patients did not, due to toxicity/death, and 4 patients were pending completion. Fourteen patients had their primary tumor located in the digestive system (6 small intestine, 5 pancreas, 2 rectum,1 stomach), 13 of which were well differentiated (5 G1, 8 G2) and 1 was poorly differentiated; 5 were located in lungs (3 typical carcinoids, 2 atypical). We analyzed clinical characteristics during the treatment, biochemical and image response 2 months post-treatment with CT (progression criteria RECIST 1.1) and SPECT-CT Octreoscan (Krenning score and appearance of new lesions), and adverse effects (hematologic and nephrologic toxicity). Average follow-up time: 18,3±12,8 months. ***Results:*** All patients received previous treatments (11p: 3 or more lines of treatment, 6p: 2 previous treatments, and 2p: 1 treatment). Localization of metastasis were: 16p hepatic, 3p peritoneal, 6p osseous. Seven patients had functioning tumors (5p presented carcinoid syndrome and 2p insulinoma). Adverse reactions included gastrointestinal: nauseas 13p, vomits 6p, abdominal pain 4p; hematological: anemia 3p, thrombocytopenia 4p, leukopenia 5p, neutropenia 3p and lymphopenia 15p. No significant variations were observed in renal function before and post-treatment. Treatment response of the 13p receiving full dosage was evaluated with CT and SPECT-CT Octreoscan, showing stable disease in 9p(69,2%) with CT and in 3p(23,1%) with Octreoscan, partial response was shown in 2p(14,3%) with CT and in 9p(69,2%) with SPECT-CT, finally progression of the disease was observed in 2p(14,3%) and 1p(7,7%) respectively. During follow-up, disease progressed (average 20,8 months) in 5p(38,5%), and stable disease (16,6 months) 8p(61,5%). One patient died due to hemoptysis 7 months post-treatment. ***Conclusion:*** Treatment of NET with ^{177}Lu-oxodotreotide is a safe option with favourable outcomes in patients with previous treatments. The results obtained are similar to published bibliography[1]. ***References:*** [1]Strosberg, J., El-Haddad, G., Wolin, E., Hendifar, A., Yao, J., Chasen, B., ... & Yao, J. (2017). Phase 3 Trial of 177Lu-Dotatate for Midgut Neuroendocrine Tumors. The New England journal of medicine, 376(2), 125-35.

EPS-179

Evaluation of toxicity in peptide receptor radionuclide therapy (PRRT) for neuroendocrine tumors (NET)

H. Duan*, V. Ferri, P. L. Kunz, G. A. Fisher, F. Moradi, G. A. Davidzon, B. L. Franc, A. H. Iagaru, C. Aparici Mari;*
Stanford University, Stanford, CA, UNITED STATES OF AMERICA.

Aim/Introduction: Peptide receptor radionuclide therapy (PRRT) with radiolabeled somatostatin analogues is an encouraging systemic treatment modality for neuroendocrine tumors (NET). PRRT is generally safe and possesses little side effects. Renal toxicity and hematotoxicity have already been reported but little is known about liver

toxicity. ***Materials and Methods:*** Seventy-seven patients (38 males and 39 females; 37 - 81-year-old, mean ± SD: 63.1 ± 10.7 years) underwent PRRT with ^{177}Lu-labeled Dotatate (Lutathera®) at our institution. Thereof 72 had progressing NETs (37 pancreas, 25 small intestine, 1 cecum, 1 appendix, 1 gastric, 1 atypical lung and 6 of unknown primary), 3 had a paraganglioma, and 2 had a pheochromocytoma. Blood work was obtained 1 week before each cycle and every 2 months at follow up. Hematological parameters were determined with Common Terminology Criteria for Adverse Events (CTCAE) V5.0. The hematological guidelines for starting PRRT at our institution are based on the package insert. ***Results:*** 46/77 (59.7%) patients completed all 4 cycles of PRRT. 19/77 (24.7%) patients are still being treated. 12/77 (15.6%) patients did not finish all 4 cycles. Out of the patients who finished, we observed in regard to liver toxicity: One patient (2.2%) had an albumin value of 2.9 g/dl which is below the cut off for PRRT. We decided to treat for his overall benefit. Albumin increased shortly after the first cycle to 4.5 g/dl at last cycle and remained at that level. At 7-month follow up, this patient showed partial response to PRRT. 3/46 (6.5%) patients initially had albumin values within the limits for PRRT but decreased during treatment from 3.53 ± 0.61 (range 3 - 4.2) g/dl at first cycle to 2.6 ± 0.1 (range 2.5 - 2.7) g/dl at last cycle. At 6-month post-treatment follow up, 2 patients showed persistent hypoalbuminemia with 2.35 ± 0.07 (range 2.3 - 2.4) g/dl with one of them improving to normal limits at 1-year follow up (3.6 g/dl). Imaging follow-up showed that 1 patient had stable disease while the other 2 had an initial partial response and remained with a stable disease at 7 months post-treatment evaluation. All patients with a decreased albumin had previous liver-directed treatments (transarterial chemoembolization and radioembolization). ***Conclusion:*** Our preliminary data show that PRRT is overall a safe treatment. Hypoalbuminemia is the only liver related side effect observed. In our small cohort it appears to not affect response to treatment. ***References:*** None

EPS-180

Real-time MR imaging of holmium-166 microsphere distribution during SIRT in salvage patients: proof of principle

J. Roosen*, M. A. Arntz, M. Janssen, K. G. Overduin, M. W. Konijnenberg, J. J. Fütterer, F. W. Nijsen;*
Radboud University Medical Center, Nijmegen, NETHERLANDS.

Aim/Introduction: Selective internal radiation therapy (SIRT) is a local treatment for liver tumours during which radioactive microspheres are injected in the hepatic arterial system. To create better understanding of the distribution patterns in relation to the number of microspheres administered, we prospectively studied the microsphere distribution with radioactive holmium-166 poly(L-lactic) acid microspheres, using real-time MRI. ***Materials and Methods:*** Ethical committee approval was obtained for this feasibility study, in which 6 patients with unresectable liver tumours are treated. The SIRT procedure is split up: the catheter is placed under X-ray guidance as per usual, after which the patient is moved to an MRI scanner which is positioned directly adjacent to the hybrid OR. The total activity for each of the identified catheter positions is split in predefined fractions. MRI is performed during and after the administration of each fraction. All fractions for one catheter position are injected within one hour. Quantitative imaging is performed after each fraction and converted to dose maps using Q-Suite software to establish the T/L ratio and perform voxel-based dosimetry. ***Results:*** Recruitment is ongoing, with 3 out of 6 patients enrolled and treated successfully. The quantitative dose distributions provide promising insight into microsphere distribution in relation to the amount of microspheres administered. The intrahepatic distribution of microsphere fractions is not necessarily consistent between different fractions. ***Conclusion:*** This study is an important first step to better understand SIRT fundamentally and this may lead to improving the therapy by increasing the T/L ratio, ultimately resulting in better patient outcomes. ***References:*** None

EPS-181

Absorbed Dose in "Black Hole" as a predict of complete MRI response in HCC patients treated with Y-90 TARE

M. Meyer*, S. Boughdad, J. O. Prior, M. Da Mota, N. Schaefer, A. Hocquelet;*
CHUV, Lausanne, SWITZERLAND.

Aim/Introduction: Transarterial radioembolization (TARE) for hepatocellular carcinoma (HCC) induces various post-treatment radiologic changes, and it can take several months for evidencing tumor response. The lack of contrast enhancement or Black Hole (BH) on post-TARE Magnetic Resonance Imaging (MRI) is strongly associated with complete histological response. The aim of this study was to assess the absorbed dose associated with BH at 3-months post-TARE MRI. ***Materials and Methods:*** We retrospectively included all HCC patients treated by selective TARE (Y-90 glass microspheres) with a post-TARE Y-90 Positron Emission Tomography (PET) and a follow-up contrast enhanced MRI (06-2018 to 02-2020). BH was defined by the absence of contrast enhancement on MRI at arterial, venous and delayed (2-minute) phases. Using Simplicity software (BTG Biocompatibles Ltd, Farnham, UK), MRI was co-registered with Y-90 PET. Then, Y-90 PET perfused volume (PV) and MRI BH were semi-automatically segmented using thresholding by two experienced nuclear physician and radiologist. Enhanced-Perfused volume (E-PV) was defined by PV minus BH. We also defined margins volume (MV) corresponding to a 5-mm volume around the BH. Based

on a per-treatment analysis and considering the normal distribution of analyzed variables, absorbed dose of each volume were compared using T-test. ***Results:*** We included 13 treatments in 11 patients (2 patients have been treated with 2 consecutive TAREs in two different arterial territories with a few months interval): 5 lobar, 3 sectoral and 5 segmental. The mean injected activity was 2.3 ±0.85 GBq. No specific toxicities according to high-dose Y-90 TARE have been reported. The mean delay between Y-90 TARE and follow-up MRI was 2.9 ±0.8 months. BH was found in 11 treatments (84.6%). The mean volumes were 567.8 ±408.6 cm^3 for PV and 30.9 ±31.9 cm^3 for BH. The mean absorbed doses were 695.1 ±372.1 Gy for BH, 425.9 ±235.0 Gy for MV and 195.6 ±97.0 Gy for E-PV. Absorbed dose in BH was significantly higher than in MV (p=0.049) and in E-PV (p<0.0001). No BH was found below 306 Gy, which corresponded to D_{BH_min}. ***Conclusion:*** The response pattern after Y-90 TARE is dose dependent and complete lack of contrast enhancement in MRI ("Black-Hole") is associated with a high-absorbed dose. This observation adds to the ongoing debate on response assessment using MRI after Y-90 TARE. ***References:*** None

EPS-182

The effect of metabolic tumor volume and total lesion glycolysis on prognosis of pancreatic adenocarcinoma patients in staging with FDG PET/CT

O. Ekmekcioglu[1], M. Battal[2], O. Bostanci[2], P. Arican[1], B. Yilmaz Ozguven[3];
[1]Nuclear Medicine Dept, Sisli Etfal Education and Research Hospital, Istanbul, TURKEY, [2]General and Hepatobiliary Surgery Dept, Sisli Etfal Education and Research Hospital, Istanbul, TURKEY, [3]Pathology Dept, Sisli Etfal Education and Research Hospital, Istanbul, TURKEY.

Aim/Introduction: FDG PET/CT has shown to be useful staging in pancreas cancer especially illustrating the distant metastases. The prognosis of pancreatic adenocarcinoma is correlated with stage and the resectability of the tumor. SUVmax, Metabolic tumor volume (MTV) and total lesion glycolysis (TLG) of the primary tumor are the datas that has been shown to correlate with prognostic parameters in pancreas cancer. In this study, we aim to investigate FDG PET/CT findings with prognostic factors in our patient group with pancreatic adenocarcinoma. ***Materials and Methods:*** The patients with pancreas adenocarcinoma that were referred to our department between 2013 and 2020 for staging evaluated retrospectively. After at least 6 hours fasting FDG has been injected. Head to mid thigh images were revealed one hour after injection. The patient demographics, follow-up data including overall survival and reports from pathology of 39 patients, who were operated after PET/CT imaging, were gained. All the primary metabolic tumor volume, SUVmax, background SUVmax and total lesion glycolysis datas have been measured with GE Healthcare PET/CT workstation. ***Results:*** The images of 57 patients; 21 female and 36 male; mean age of 67,6(41-84) with pancreatic adenocarcinoma were evaluated. Twenty-seven patients has shown positive findings for distant metastases either in lung, liver or bone. The mean values of SUVmax, metabolic tumor volume (MTV 40%) and total lesion glycolysis (TLG) of primary tumor in pancreatic tissue were 7,3 (2,1-18,5), 24,3cm3 (1,4-77,9) and 98,5 g/ml 5,3-478,4) respectively. The average survival after diagnosis of the disease 17,7 (1-55) months. TLG values have demonstrated a significant relation with positive findings for distant metastases; SUVmax was significantly related with positivity for lymph node and distant metastases. The overall survival was significantly related with perineural invasion and distant metastases. ***Conclusion:*** FDG PET/CT is useful for staging and detecting distant metastases in pancreatic cancer. Furthermore, total lesion glycolysis and SUVmax could be helpful to understand the prognosis of pancreatic cancer before surgery or treatment decision. However, results of metabolic tumor volume analysis of our study was not compatible with the data published before which could be related to low number of our patients. Additionally, we did not exclude the metastatic patients from the survival analysis. From this point of view we are planning to investigate MTV and TLG as independent factors in a patient group without metastases. More patients without metastatic disease could give more accurate results for correlating MTV and TLG with survival. ***References:*** None

1701

CME 14: Molecular Drug Imaging of Solid Tumours Including Microenvironment

Friday, October 30, 2020, 15:30 - 17:00 Channel 1

OP-937

Tumor Immunotargeting Using Innovative Radionuclides

C. Bailly; Nuclear Medicine Department, University Hospital of Nantes and ICO-Gauducheau Cancer Center, Nantes, FRANCE.

OP-938

Protease Fibroblast Activation Protein (FAP)-Targeted Radiotracers for New Applications in Non-Invasive Tumour-Characterization, Staging or Radio-Ligand Therapy

U. Haberkorn; Department of Nuclear Medicine, Universität Heidelberg, and Clinical Cooperation Unit Nuclear Medicine, DKFZ, Heidelberg, GERMANY.

OP-939

Immuno-Positron Emission Tomography with Zirconium-89-Labeled Monoclonal Antibodies in Oncology - What Can We Learn From Initial Clinical Trials?

D. Vugts; VUmc Imaging Center AmsterdamRadiology & Nuclear Medicine, Amsterdam, NETHERLANDS.

1702

Joint Symposium 27 (EANM/ESMI): Radar on Immune Cell Imaging

Friday, October 30, 2020, 15:30 - 17:00 Channel 2

OP-940

Unravelling the Universe of the Immune System by Targeted Molecular Imaging

B. Pichler; University Hospital Tübingen, Department of Preclinical Imaging and Radiopharmacy, Tübingen, GERMANY.

OP-941

Clinical Experience in Immune Cell Imaging in Altherosclerosis

F. Hyafil; Centre Hospitalier Universitaire Bichat, Assistance Publique - Hôpitaux de Paris, Department of Nuclear Medicine, Paris, FRANCE.

OP-942

Clinical Experience in Immune Cell Imaging in Myocardial Infarction

F. Bengel; Hannover Medical School, Department of Nuclear Medicine, Hannover, GERMANY.

OP-943

Inflammation and Immunooncology - Same Targets, Different Story?

I. Grondman; Radboud University Medical Centre, Department of Internal Medicine and Radboud Center for Infectious Diseases, Nijmegen, NETHERLANDS.

1703

Joint Symposium 28 (EANM/AHA): New Approaches for Cardiovascular Imaging

Friday, October 30, 2020, 15:30 - 17:00 Channel 3

OP-944

Cardiologist's perspective : what do we need?

P. Soman; University of Pittsburgh Medical Center, Pittsburgh, UNITED STATES OF AMERICA.

OP-945

Physicist's perspective : what comes next ?

L. Imbert; Nuclear Medicine Department, CHRU Nancy Brabois, Nancy, FRANCE.

OP-946

Radiopharmacist's perspective : what comes next ?

B. Guillet; Radiopharmacy department, University Hospital Marseille, Marseille, FRANCE.

OP-947

Nuclear physician's perspective: what comes next ?

A. Saraste; Turku PET Centre and Heart Center, Turku University Hospital and University of Turku, Turku, FINLAND.

1704

CTE 7: Quality Control of Imaging Instrumentation

Friday, October 30, 2020, 15:30 - 17:00 Channel 4

OP-949

Routine QC Tests on SPECT and SPECT/CT

C. Pestean; Iuliu Hatieganu University of Medicine and Pharmacy, Nuclear Medicine Department, Cluj, ROMANIA.

OP-950

Routine QC Tests on PET and PET/CT

G. Testanera; Bartshealth NHS Trust, Nuclear Medicine, London, UNITED KINGDOM.

OP-951

Annual QC Tests on SPECT/CT and PET/CT and Annual Report

P. Tomse; University Medical Centre, Department of Nuclera Medicine, Ljubljana, SLOVENIA.

1705

M2M Track - TROP Session: Hot Stuff - Radionuclide Production

Friday, October 30, 2020, 15:30 - 17:00 Channel 5

OP-953

Automated Production of [^{61}Cu]CuCl$_2$ at UW-Madison

C. Kutyreff[1], J. Pettersson[2], K. Seeley[1], T. Barnhart[1], J. Engle[1,3], K. Gagnon[2];
[1]University of Wisconsin-Madison, School of Medicine and Public Health, Department of Medical Physics, Madison, WI, UNITED STATES OF AMERICA, [2]GEMS PET (GE Healthcare), Uppsala, SWEDEN, [3]University of Wisconsin-Madison, School of Medicine and Public Health, Department of Radiology, Madison, WI, UNITED STATES OF AMERICA.

Aim/Introduction: We sought to improve methods for isolating ^{61}Cu from irradiated ^{nat}Ni, ^{60}Ni, and ^{61}Ni targets to avoid high acid concentrations and large volume

formulations. We developed a cassette-based automated method for ^{61}Cu purification and Ni recovery using commercial extraction chromatography resins. ***Materials and Methods:*** Briefly, 99 ± 23 mg of ^{nat}Ni was electroplated (or recovered and re-plated) on silver discs following [1] and automatically transferred to/from the cyclotron (QIS). Targets were irradiated at 30 µA with 8.4 MeV deuterons for 30 minutes (n=5 [3 @ singly recycled; 2 @ doubly recycled]) or 200 minutes (n=1 [new target]) and dissolved in 1:1 7 M HCl:30% H_2O_2. The HCl concentration was adjusted to ≥6 M, and transferred to a FASTlab chemistry module whereby [^{61}Cu]$CuCl_2$ was isolated with a two-column process using TBP (as an Fe guard column) and TK201 resins. In short, the ^{61}Cu was trapped on the TK201, washed with 6 M and 4.5 M HCl to remove nickel and cobalt, and finally washed with 5 M NaCl prior to elution with 0.05 M HCl. ***Results:*** The isolated [^{61}Cu]$CuCl_2$ was collected 65 ± 3 minutes post EoB in ~2 mL of 0.057 ± 0.002 M HCl (n=5, assessed by titration). An overall radiochemical yield (including both the dissolution and separation chemistry) of 85 ±4% (n=6) is reported. The measured saturation yield of the isolated [^{61}Cu]$CuCl_2$ was 166 ± 31 MBq/µA (n=6), consistent across fresh and recycled targets. HPGe and MP-AES of the isolated [^{61}Cu]$CuCl_2$ (values decay corrected to EoB) measured Ni separation factors of ≥(6.0 ± 3.3)x10^5 (n=5, noting that the nickel content in the final products was below the minimum detectable limit), ^{58}Co content of (8.3 ± 0.6)x10^{-5} % (n=5) vs. ^{61}Cu activity, molar activities of 119 ± 32 MBq/nmol (n=5) for the 30 minute irradiations, and apparent molar activities of 31 ± 8 MBq/nmol (n=5) and 201 MBq/nmol using NOTA for the 30 and 200 minute irradiations, respectively. ***Conclusion:*** A cassette-based, automated method of producing high purity [^{61}Cu]$CuCl_2$ from recycled Ni targets has been developed that does not require dry-down for formulation. Molar and apparent molar activities are suitable for subsequent preparations of ^{61}Cu-based radiopharmaceuticals and are expected to increase with isotopically enriched Ni targets. ***References:*** [1] Piel H, et al. Radiochim Acta 1992; 57:1-6. doi:10.1524/ract.1992.57.1.1. Acknowledgment: Authors acknowledge support and collaborative efforts with Swiss Nuclides.

OP-954

Cyclotron-based ^{68}Ga production with dual liquid targets

K. Gagnon[1], M. E. Rodnick[2], C. Parr[1], M. Clark[2], S. A. Grosch[1], P. J. H. Scott[2];
[1]GEMS PET Systems, Uppsala, SWEDEN, [2]University of Michigan, Ann Arbor, MI, UNITED STATES OF AMERICA.

Aim/Introduction: At the University of Michigan, due to ongoing uncertainty in generator costs and delivery timelines, the clinical production of [^{68}Ga]Ga-PSMA-11 using cyclotron-produced ^{68}Ga from a liquid target was validated and implemented in early February 2019, with routine production of 1.3-1.7 GBq (35-45 mCi) final product demonstrated [1]. Aiming for further scale-up while maintaining liquid target infrastructure, we investigated, and present the preliminary results on the cyclotron-production of [^{68}Ga]$GaCl_3$ and [^{68}Ga]Ga-PSMA-11 using simultaneous production of ^{68}Ga in two liquid targets by dual beam irradiation. Following bombardment, the contents of both targets were combined and used for the production of [^{68}Ga]Ga-PSMA-11. ***Materials and Methods:*** ^{68}Ga was produced by proton irradiation of 1.0M [^{68}Zn]$Zn(NO_3)_2$ in dilute (i.e. 0.3M) HNO_3 on a PETtrace cyclotron per our previous report [1], albeit using dual targets. For these initial tests, targets were irradiated at 25-30 µA (port 3), and 30-35 µA (port 6) for ~60 minutes at a nominal proton energy of 14.3 MeV. Target solutions were delivered to the lab one at a time, with beam maintained on the second target while the first was being emptied. The target solutions were combined into an external vial which was connected to a FASTlab synthesis module. This vial was pre-loaded with 6 mL of metal free H_2O to ensure the HNO_3 concentration was ≤0.1M prior to column loading. The resulting solution was then either processed to isolate [^{68}Ga]$GaCl_3$ (n=2), or, for single cassette production of [^{68}Ga]Ga-PSMA-11 which includes also the [^{68}Ga]$GaCl_3$ purification (n=1) [1]. ***Results:*** The total time from EOB (counting from EOB of the 2nd target) to EOS was 42 and 43 min for the two [^{68}Ga]$GaCl_3$ runs, and following slight adjustments to delivery and column loading times, only 40 minutes from EOB to EOS for the single [^{68}Ga]Ga-PSMA-11 run. Yields were, 4.6±0.1 GBq (125±3 mCi) and 3.1 GBq (85 mCi) at EOS for [^{68}Ga]$GaCl_3$ (n=2) and [^{68}Ga]Ga-PSMA-11 (n=1), respectively. Both products met quality control criteria previously established in UM's [^{68}Ga]Ga-PSMA-11 IND application approved by the US FDA. ***Conclusion:*** Following modifications on dilution and column loading, successful combination of two simultaneously irradiated ^{68}Ga liquid targets to produce high quality [^{68}Ga]$GaCl_3$ and [^{68}Ga]Ga-PSMA-11 has been demonstrated, with >3.7 GBq (>100 mCi) of [^{68}Ga]$GaCl_3$ isolated. Further optimization efforts are underway with a goal of producing >3.7 GBq (>100 mCi) of [^{68}Ga]Ga-PSMA-11 from a single production run. ***References:*** [1] Rodnick et al., J. Label. Compd. Radiopharm. 62 (2019), S123-S588,P149.

OP-955

Selective, stable chelation of radioantimony for Sb-119 Targeted Radionuclide Therapy

A. Olson[1], Y. Feng[2], P. A. Ellison[1], E. Aluicio-Sarduy[1], T. E. Barnhart[1], R. J. Nickles[1], S. S. Jurisson[3], J. W. Engle[1];
[1]Department of Medical Physics, University of Wisconsin Madison, Madison, WI, UNITED STATES OF AMERICA, [2]Department of Radiology, Duke University, Durham, NC, UNITED STATES OF AMERICA, [3]Department of Chemistry, University of Missouri, Columbia, MO, UNITED STATES OF AMERICA.

Aim/Introduction: Antimony-119 ($t_{1/2}$=38.5h, EC = 100%)

emits a cascade of 23 - 24 low energy high LET electrons and no photons with energy above 30 keV [1], making it an ideal candidate for targeted radionuclide therapy (TRT). It is produced by the ^{119}Sn(p,n)^{119}Sb reaction but has not been chelated for practical medical applications [2]. We aim to develop antimony separation from tin through implementing direct radioantimony chelation in unseparated target solutions using a conjugatable chelator. ***Materials and Methods:*** Radioantimony was produced by 16 MeV proton irradiation of electroplated Sn [3]. The target (mass exceeding 350 mg/cm^2) was dissolved in 3 mL concentrated HCl (3h/90°C), and without purification, reacted in situ with a trithiol chelator developed at the University of Missouri [4]. HPLC was implemented to study reaction kinetics and resulting complex stability after C18 Sep-Pak purification (EtOH and H_2O pre-conditioning, load in diluted labelled target solution, 5mL H_2O wash). Sb-trithiol was eluted in 3mL of acetonitrile, dried, and resuspended in PBS. ***Results:*** The trithiol chelator rapidly (30 min) complexed no carrier added pmol of Sb in the presence of mmol of Sn (10^8-fold excess) at ligand concentrations down to 0.01 mM. The trithiol has strong selectivity of antimony over tin. Final decay corrected radiochemical yields of Sb-trithiol were 64.5% ±20% (N=3) via HPGe activity measurements. HPLC stability studies revealed undegraded Sb-ligand in 25 mM cysteine at 24 hours (99.7% ±0.5% stability, N=3) and in fetal bovine serum at 72 hours (92.8% ±5.5% stability, N=3). ***Conclusion:*** We report an elegant method for radioantimony chelation, circumventing usual radionuclide isolation from dissolved accelerator targets with a functionalizeable trithiol chelator. ***References:*** [1] K. F. Eckerman and A. Endo, MIRD: Radionuclide Data and Decay Schemes, 2nd ed. Society of Nuclear Medicine, 2008.[2] H. Thisgaard and M. Jensen, "Production of the Auger emitter 119Sb for targeted radionuclide therapy using a small PET-cyclotron," Appl. Radiat. Isot., vol. 67, pp. 34-38, 2009.[3] A. P. Olson, P. A. Ellison, V. Radchenko, T. E. Barnhart, and J. W. Engle, "Electrodeposition and recovery of Sn targets for Sb-119 production," in Workshop in Targetry and Target Chemistry 17, 2018.[4] Y. Feng and S. S. Jurisson, "Trithiol compounds—tricky but valuable: the design and synthesis of ligands for stabilizing radioarsenic for radiopharmaceutical development," Strateg. Tactics Org. Synth., vol. 14, pp. 207-224, 2019.

OP-956

Automated production of Ga-68 chloride and Ga-68-Dotatate on a low energy medical cyclotron

M. Malinconico[1], *C. Hollis*[2], *K. Kuan*[2], *C. Barkil*[2], *P. Takhar*[2], *A. Brunetti*[1], *W. Tieu*[2];
[1]*COMECER S.p.A., Castel Bolognese, ITALY,* [2]*Molecular Imaging and Therapy Research Unit, South Australian Health and Medical Research Institute, Adelaide, AUSTRALIA.*

Aim/Introduction: The demand for Gallium-68 (^{68}Ga) labelled PET radiopharmaceuticals and its source (^{68}Ge/^{68}Ga generators) have increased over the past few years. To keep up with the demand, new avenues for ^{68}Ga production are needed. The present work describes a rapid and automated production of [^{68}Ga]$GaCl_3$ and [^{68}Ga]Ga-DOTA-TATE on a low energy medical cyclotron. ***Materials and Methods:*** An automated process was developed for producing [^{68}Ga]$GaCl_3$ on a GE PETtrace 880 with Comecer PTS and Aleco system. ^{68}Zn was prepared by electrochemical deposition over 2.5 h on a dynamic electrochemical cell. The ^{68}Zn target was irradiated at 14.5 and 12.0 MeV incident energy with 10 - 35 µA proton beam for 8.5 - 20 min. The irradiated ^{68}Zn/^{68}Ga was purified on automated Taddeo unit using hydroxamate/tri octyl phosphine resin (29 min) or octanol resin (26 min). The automated radiolabelling of DOTA-TATE was performed on the Taddeo (15 min). ***Results:*** [^{68}Ga]$GaCl_3$ on a low energy cyclotron at 14.5 MeV gave production yield of 61.26 GBq.µA^{-1}.h^{-1} in 0.05 M HCl solution. The specific activity of [^{68}Ga]$GaCl_3$ was determined as 660 ± 164 GBq.µmol^{-1} following ICP-MS and effective specific activity of 14.6 GBq.µmol^{-1} following DOTA titration. Radionuclidic impurity 0.012 - 0.080% as determined by HPGe. Finally, the automated process was extended to include ^{68}Ga-dotatate labelling to give >3 GBq of ^{68}Ga-dotatate with RCY of >65%. The total process time from start of bombardment to [^{68}Ga]$GaCl_3$ (45 min) and [^{68}Ga]Ga-DOTA-TATE (<1 h). ***Conclusion:*** A rapid and automated solid targetry production was developed that yielded [^{68}Ga]$GaCl_3$ (>6 GBq) in <35 min and ^{68}Ga-Dotatate in <55 min after start of bombardment. [^{68}Ga]$GaCl_3$ obtained from solid targetry was found to be comparable to [^{68}Ga]$GaCl_3$ obtained from a ^{68}Ge/^{68}Ga generator. ***References:*** None

OP-957

Separation of Cyclotron-Produced ^{51}Mn from ^{54}Fe with DGA Resin

K. Barrett*, E. Aluicio-Sarduy, T. E. Barnhart, J. W. Engle;*
University of Wisconsin- Madison, Madison, WI, UNITED STATES OF AMERICA.

Aim/Introduction: ^{51}Mn has been isolated from target material with ion exchange and extraction chromatography and used for in vivo monitoring of pancreatic beta cell function [1]. We report a new method of isolating ^{51}Mn from isotopically enriched ^{54}Fe target material and trace stable contaminants with DGA (branched and unbranched) resins. ***Materials and Methods:*** Solutions containing representative masses of Fe(III) and Mn(II) were loaded onto 101±8mg resin columns equilibrated with HCl (0.1, 1.0, 3.0, 5.0M). Solutions were agitated then pushed through the resin. Metal concentrations were assayed by MP-AES to quantify masses adhered to the resin and eluted in solution. Affinity constants (kD values) were calculated from measured data.

The results of these batch studies were used to design dynamic separation experiments. A column containing 3.5g of resin was equilibrated with 30mL of 5M HCl. An ^{54}Fe target was irradiated and dissolved in 3mL of 6M HCl. To this solution, 1.8mL of H_2O_2 was added to promote oxidation of Fe(II) to Fe(III). This target solution was loaded onto the column, washed with 15mL of 5M HCl to elute the Mn(II), then washed with 15mL of 0.01M HCl to recover the Fe(III). Samples were collected in 5mL fractions and assayed to determine an elution profile. The final fraction of ^{51}Mn was complexed with DOTA, while the recovered Fe(III) was recycled and electroplated. ***Results:*** The produced kD values provided incentive to move to a dynamic column experiment. A target made of 51.5 ± 10.3mg of ^{54}Fe was irradiated at 16MeV, producing ^{51}Mn at a saturation bombardment yield of 44.0± 4.8 MBq/μAh. At end of chemistry, a separation factor of 1.03 x 10^6 ± 2.0 x 10^5 and a radiochemical yield of 99.3 ± 1.2% (N=3) were achieved. The measured apparent molar activity of the ^{51}Mn was 5.46 ± 0.8 GBq/μmol of DOTA. The enriched ^{54}Fe was recovered and electroplated with a recycling efficiency of 90.4 ± 12.6%. ***Conclusion:*** We report a rapid, high-yield, DGA-based purification of ^{51}Mn that efficiently recovers isotopically enriched ^{54}Fe material for target recycling. ***References:*** [1] S. A. Graves et al., "Preparation and in vivo characterization of $^{51}MnCl_2$as PET tracer of Ca2+ channel-mediated transport," Sci. Rep., vol. 7, no. 1, pp. 1-8, 2017.

OP-958

Re-Establishing of Production of ^{188}W/^{188}Re Generators Utilizing ^{188}W Activity Obtained from Irradiated $^{188}WO_3$ Ampoules and ^{188}W Solution

J. Jernstroem, M. Olmeda Palomar, J. Nikula, N. Vetter, I. Kuru, T. Nikula;
OncoBeta GmbH, Garching, GERMANY.

Aim/Introduction: Simultaneous long-term interruption in ^{188}W isotope production of the two main global manufacturers has created a shortage of ^{188}W/^{188}Re generators in the markets. In order to re-establish and stabilize the generator production it was necessary to develop a production chain which includes all the steps from raw material target irradiation and chemistry to loading and release of generator. Several generators were produced following the designed routes and methods. Comparison with generators loaded with commercially produced ^{188}W has given fundamental information on the quality of the developed processes. ***Materials and Methods:*** Enriched $^{186}WO_3$ powder packed in quartz glass ampoules was irradiated in high-flux nuclear research reactors in different irradiation cycles. After cooling, the ampoules were delivered to the production facility for chemical processing. Irradiated $^{188}WO_3$ powder was dissolved in hot oxidative alkaline conditions and chemically optimized for the loading of ^{188}W/^{188}Re generators. The processes were performed in a hot cell using a technical unit designed for the purpose. Additionally, ^{188}W/^{188}Re generators were produced using ^{188}W activity provided by a commercial source. ***Results:*** Several generators were produced during the period of six months, majority of them using the activity obtained from $^{188}WO_3$ ampoules. The measured ^{188}W activities of the ampoules varied between 92.3 - 39.4 GBq* depending on reactor and number of irradiation cycles in question. The activities of the generators in terms of elutable ^{188}Re varied between 57.9 - 17.4 GBq* when loaded with $^{188}WO_3$ based activity and 128.2 - 18.6 GBq when loaded with commercial ^{188}W solution. The reported activities of the generators partly varied depending on the intended use (customer order, etc.). In the quality control the monitored gamma-ray emitting radionuclidic impurities included ^{51}Cr, ^{95}Zr, ^{95}Nb, ^{99}Mo, ^{124}Sb, ^{187}W, ^{191}Os and ^{192}Ir (raw materials), and ^{60}Co, ^{124}Sb, ^{191}Os and ^{192}Ir (generator eluates). In the specifications of the ^{188}W/^{188}Re generators the amount of gamma-ray emitting radionuclidic impurities including breakthrough of ^{188}W in eluate is limited to < 1.0e-04 in relation to ^{188}Re at calibration time, and the radiochemical purity of eluate is limited to > 98 % as Re(VII). * Normalized to EOI ***Conclusion:*** The developed production chain utilizing irradiated $^{188}WO_3$ has made it possible to re-establish the full production of ^{188}W/^{188}Re generators at the time when the availability of commercially produced ^{188}W solution was scarce. In the future, this technology will be an important amendment to commercially produced ^{188}W in providing activity for generator production. ***References:*** None

OP-959

Development of an in-house ^{188}W/^{188}Re generator

M. Van de Voorde[1], *A. Burgoyne*[1], *B. Ponsard*[1], *E. Dennis*[1], *T. Cardinaels*[1,2], *M. Ooms*[1];
[1]*SCK CEN, Mol, BELGIUM,* [2]*KU Leuven, Leuven, BELGIUM.*

Aim/Introduction: ^{188}Re decays by emitting high-energy beta particles (E_{max}: 2.1 MeV, E_{av}: 784 keV), which can be used to kill targeted tumor cells. The short half-life ($t_{1/2}$ = 16.9 h) of ^{188}Re allows it to be used in targeted radionuclide therapy when linked to peptides or antibodies. ^{188}Re decays with a 155 keV (15%) gamma emission suitable for imaging and dosimetry. Combining these properties make ^{188}Re an ideal theranostic agent in clinical nuclear medicine. Furthermore, ^{188}Re is readily available from a ^{188}W/^{188}Re generator which enables the use of nca ^{188}Re in hospitals and remote locations [1]. ***Materials and Methods:*** In light of the recent shortage of ^{188}W/^{188}Re generators on the market we undertook efforts to prepare our own generator to provide a constant 188Re supply for our research into ^{188}Re-based radiopharmaceuticals. Enriched ^{186}W (99.7%) was irradiated at high fluxes in the BR2 reactor to produce MBq amounts of ^{188}W ($t_{1/2}$ = 69 d) via double neutron capture. Following a

significant cooling time to allow for ^{187}W decay ($t_{1/2}$ = 23.72 h), the ampoules were opened and the target dissolved and characterized. The tungsten solution was then loaded on an Al_2O_3 column from which ^{188}Re could be eluted. ^{188}W breakthrough was investigated in the initial ^{188}Re "milkings", finding a radionuclidic purity of >99.99% for ^{188}Re. The generator eluent was successfully concentrated (~800 µl) with the aid of cation exchange and anionic exchange cartridges. ***Results:*** Using this protocol, we developed small-scale $^{188}W/^{188}Re$ generator that allows production of MBq amounts of ^{188}Re for radiolabeling.To show that the ^{188}Re can be used for radiolabeling, we performed proof-of-concept radiolabeling experiments with MAG3 and an in-house developed chelator. Initial radiolabeling experiments showed that high radiolabeling yields could be achieved. ***Conclusion:*** We have developed and optimized an in-house $^{188}W/^{188}Re$ generator to provide MBq amounts of nca ^{188}Re on a daily basis. Upscaling of our $^{188}W/^{188}Re$ generator will lead to a reliable supply of ^{188}Re for our ongoing research towards ^{188}Re-radiopharmaceuticals. ***References:*** [1.] B. Ponsard et al., J. Radioanal. Nucl. Chem., 2003. 257, 169-174

OP-960

Exploring a new library of ligands for [^{68}Ga]Gallium radiopharmaceutical application

E. Cazzola[1], C. De Rosa[2], J. Amico[1], M. Malachini[1], C. Nardon[2], G. Gorgoni[1], F. Piccinelli[2];
[1]Radiopharmacy and Cyclotron Dept, IRCCS Sacro Cuore Hospital, Negrar, ITALY, [2]Biotechnology Dept, University of Verona, Verona, ITALY.

Aim/Introduction: In the last fifteen years radioactive [^{68}Ga] Gallium has gained more and more importance in Nuclear Medicine due to its favorable half-live, easy preparation and important theranostic pair in combination with [^{177}Lu] Lutetium. For this reason, many studies were focused to the design of new ligands capable to ensure more tunable radiopharmaceutical properties.Bpcd=N,N'-Bis(2-pyridylmethyl)-trans-1,2.diaminocyclohexane-N,N'-diacetic acid is an interesting diaminoacetic acidic ligand that can be potentially used to coordinate a group IIIA nuclide like [^{68}Ga]Gallium. The H_2bpcd is a 6-fold coordinating ligands (which employs two acetic acid functions, four nitrogen atoms). The rotational restriction about the C-C bond of the cyclohexane ring gives rise to a pre-organized configuration, which, from a coordination chemistry point of view, is thermodynamically convenient. The final complex will be positive charged. The aim of this study is the investigation of the coordination chemistry towards for the trivalent [^{68}Ga]Gallium ion, and the stability of the relative complexes. ***Materials and Methods:*** The [^{68}Ga] $GaCl_3$ solution from generator was used to test different reaction conditions using this class of new ligands. In particular, different concentrations, pH values and reaction temperatures have been investigated to find the optimal protocol. A kinetic study for all the samples was performed using the TLC and HPLC techniques over time. In detail, TLC analysis were performed with iTLC-SG mobile phase NH_4Ac (77 g/L; H_2O/MeOH). HPLC analysis were typically performed by means of Luna OMEGA 5 µm 100A Polar C18 column (250x4,6 mm) as stationary phase and a mixture of A=(H_2O +0.1TFA) and B=(ACN+0.1%TFA) as eluent. Flow: 1 mL/min, gradient 0-3 min from 0% B to 100% B (ranging 3-25 min). ***Results:*** To date, most of the explored ligands show a promising reactivity in the tested temperature interval with an almost total conversion of free [^{68}Ga]$GaCl_3$ to the complexed one in less than 15 minutes. A complete characterization of the complexes was carried out using ^{1}H-NMR spectroscopy and HPLC-mass spectrometry using the non-radioactive counterpart. ***Conclusion:*** Based on the high stability recorded under the reaction conditions, the collected results pave the way to further radiochemical characterization, as well as biological in vitro studies. ***References***: [1] Piccinelli, F.; De Rosa, C.; Melchior, A.; Faura, G.; Tolazzi, M.; Bettinelli, M. Eu(III) and Tb(III) Complexes of 6-Fold Coordinating Ligands Showing High Affinity for the Hydrogen Carbonate Ion: A Spectroscopic and Thermodynamic Study. Dalt. Trans. 2019, 48 (4), 1202-1216.

OP-961

Production of Ac-225 for Targeted Alpha Therapy using an Electron Linear Accelerator

T. Tadokoro[1], Y. Ueno[1], Y. Kani[1], M. Shimada[2], T. Sasaki[2], T. Watanabe[2], H. Kikunaga[3], S. Kashiwagi[3], S. Sekimoto[4], T. Ohtsuki[4];
[1]Hitachi, Ltd., Research & Development Group, Hitachi-shi, JAPAN, [2]Hitachi, Ltd., Healthcare Business Unit, Tokyo, JAPAN, [3]Research Center for Electron Photon Science, Tohoku University, Sendai, JAPAN, [4]Institute for Integrated Radiation and Nuclear Science, Kyoto University, Kumatori-cho, JAPAN.

Aim/Introduction: Ac-225 has nuclear properties well suited for use in targeted alpha therapy and clinical trials have demonstrated the applicability of radiopharmaceuticals containing Ac-225 to treat various cancers. Despite promising results from recent clinical trials, Ac-225-radiopharmaceutical development has been hindered by insufficient supply for the demand. An electron linear accelerator has many advantages, its size is relatively small and a high beam current is easily achieved. Hence, we have carried out a feasibility study of Ac-225 production by using an electron linear accelerator. ***Materials and Methods:*** We carried out a basic examination of Ac-225 production using the electron linear accelerator of the Tohoku University Research Center for Electron Photon Science. We used Ra-226•Cl_2 (Ra-226, 50 kBq) as a target nuclide, the electron beam energy was 35 MeV, the current was 140 µA and irradiation time was 5.25 h. Ac-225 is in radiation equilibrium with Fr-221 and Bi-213. Hence, we evaluated Ac-225 production

amount using gamma-ray counting rates of Fr-221 and Bi-213 measured with an HPGe detector. We also carried out an Ac-225 production calculation and compared calculated and experimental values of Ac-225 production amount. We derived the bremsstrahlung radiation distribution using the Monte Carlo radiation transport calculation code PHITS [1]. There are no experimental data for the Ra-226(γ,n)Ra-225 nuclear reaction, so we derived the production rate of Ra-225 using our derived bremsstrahlung radiation distribution and the theoretical reaction cross section data [2]. Ac-225 production amount was derived by calculation of radiation balance with Ra-225. Using these results, we also estimated the Ac-225 production amount in a real-scale system using the same calculation method. ***Results:*** We found that experimental Ac-225 production amounts were 1.42 times (using gamma-ray counting rate of Fr-221) and 1.37 times (using gamma-ray counting rate of Bi-213) larger than the calculated value. Based on these results, we evaluated the production amount of Ac-225 in the real-scale Ac-225 production system (Ra-226•Cl_2 , 3.85 g; acceleration energy, 35 MeV; current, 1 mA) and found that 56.5 GBq per 20-h irradiation could be produced. ***Conclusion:*** The amount of Ac-225 produced using an electron linear accelerator was estimated and the system was found to have a high Ac-225 production capability. ***References:*** [1] T. Sato et al. Features of Particle and Heavy Ion Transport code System (PHITS) version 3.02, J. Nucl. Sci. Technol. 55. 684-690 (2018). [2] TENDLE-2017 Nuclear data library Gamma sub-library for Ra(Z=88) and A=226, https://tendle.web.psi.ch/tendle_2017/gamma_html/Ra/GammaRa226xs.html (accessed on August 20, 2019)

OP-962

Fluorine-18 labelling of biomolecules via disulfide rebridging for PET imaging

M. Richard, B. Kuhnast;
Université Paris-Saclay, CEA, CNRS, Inserm, BioMaps, Service Hospitalier Frédéric Joliot, Orsay, FRANCE.

Aim/Introduction: Fluorine-18 labelled biomolecules are increasingly employed in clinical imaging for diagnosis purposes. Given their fragility and complexity, it necessitates the development of site-selective labelling techniques in mild conditions. Besides, it is essential to develop labelling procedures with minimal modification of the tertiary structure, as it is fundamental for biological activity. Disulfide rebridging is a promising possibility since it allows protein modification as well as conservation of the tertiary structure (1). In this context, we have developed an original method for the radiofluorination of disulfide containing biomolecules via disulfide rebridging. We applied it to the labelling of octreotide, a somatostatin analogue employed for the imaging of neuroendocrine tumours, and to the labelling of trastuzumab, a monoclonal antibody used to treat HER2-positive breast cancer. ***Materials and Methods:*** The labelling strategy relies on the preparation of a radiofluorinated prosthetic group presenting a disulfide rebridging moiety followed by rebridging of the reduced biomolecule. To this end, the synthesis of a labelling precursor presenting both a dithiophenolmaleimide group (rebridging moiety) and an activated pyridine group containing a trialkylammonium leaving group for nucleophilic substitution with Fluorine-18 was carried out. ***Results:*** The labelling precursor was reacted with K[^{18}F]F-K_{222} complex for 30 minutes at 40°C affording the radiofluorinated dithiophenolmaleimide in a 25 % radiochemical yield (d.c.) after reformulation on a C18 cartridge. This prosthetic group was then reacted with the biomolecules previously reduced with TCEP. In the case of octreotide, radioHPLC analysis showed complete rebridging after 10 minutes at room temperature. Affinity of the rebridged octreotide was evaluated (Ki = 2.04 nM). Regarding trastuzumab, initial experiments showed the formation of the expected radiolabelled antibody with a 13 % radiochemical yield (d.c.) after 60 minutes at room temperature. ***Conclusion:*** The preparation of a highly reactive radiofluorinated maleimide was carried out and enabled the selective rebridging of the native disulfide bond of octreotide in 10 minutes. To test the scope of this original radiolabeling strategy, the method was also applied on a more complex biomolecule (trastuzumab) and showed promising results. To go one step further, the preparation of DFO- or DOTA-containing maleimides will be implemented and radiolabelling of biomolecules with Zirconium-89 or Copper-64 viarebridging will thus be explored in the near future. ***References:*** (1) Kuan, S. L.; Wang, T.; Weil, T. Chemistry - A European Journal 2016, 22, 17112-17129

OP-963

[^{89}Zr]ZrTrastuzumab preparation based on commercial cassette base synthesis module

E. Cazzola[1], *J. Amico*[1], *P. Martini*[2,3], *M. Malachini*[1], *G. Sciacca*[2], *J. Esposito*[2], *G. Gorgoni*[1];
[1]*Radiopharmacy and Cyclotron Dept, IRCCS Sacro Cuore Hospital, Negrar, ITALY,* [2]*INFN- Legnaro National Laboratories (LNL), Legnaro, ITALY,* [3]*Unife - Ferrara University, Ferrara, ITALY.*

Aim/Introduction: [^{89}Zr]Zirconium is one of the emergent isotopes due to its favorable PET imaging characteristics (β+max 0.395 MeV; 22.7%) and half-life (T½78.4h) ideal for antibodies labeling. Monoclonal antibodies (MAbs) are the most approved biopharmaceutical in the word with multiple and selective targets. The immunoPET can facilitate the approval for new MAbs and can help on patient selection. Due to these needs, a robust production, purification and labelling procedure should be optimized on automatic modules in order to minimize the operator dosimetry and increase the reproducibility.Aim of this work is based on easy modifications of an automatic, cassette-

based, commercial module in order to dissolve the solid target and purify the [89Zr]Zirconium in oxalate form. After the formulation, in the same cassette, the [^{89}Zr]ZrOx will be used to label Trastuzumab and finally purify the [^{89}Zr]ZrTrastuzumab. The use of disposable cassettes reduce the possibility to accumulate metal impurities, avoids cleaning step, which are instead mandatory when working with synthesis modules based on fixed tubes technology. ***Materials and Methods:*** A cassette-based module was used to set up an automatic dissolution, purification and labelling procedure. The solid [^{89}Y]Yttrium target was bombarded on cyclotron at 12.5 MeV, without degrader, at different currents (20-60 μA) for a variable time 30-240 minutes. The coin was transferred to a dedicated coated hotcell and finally inserted on a cassette module in order to dissolve and purify the [^{89}Zr]/[^{89}Y] material. A 2 N HCl solution was used to dissolve the target material, the solution was transferred to a ZR resin and recovered in the oxalate form. The [^{89}Zr]ZrOx solution was used to label DFOTrastuzumab. The final purification based on PD10 was performed and the final solution, was evaluated on a standard quality control profile including immunoreactivity. ***Results:*** To date, all the process take place in less than 2h starting to target management up to radiopharmaceutical formulation. ***Conclusion:*** What we described on this work is one of the possible way to optimize the automatic [^{89}Zr]Zirconium production starting from [^{89}Y]Yttrium solid target including: dissolution, purification, MAb labelling, [^{89}Zr]ZirconiumMAb purification and formulation. This process is based on cassette module to minimize the impurities, avoid any manual operation on radioactive material management and facilitate the regulatory process for radiopharmaceutical application. ***References:*** Fully automated 89Zr labeling and purification of antibodies; Poot A, Adamzek K, Windhorst A, Vosjan M, Kropf S, Wester H, Van Dongen G, Vugts D; Journal of Nuclear Medicine (2019) 60(5) 691-695

1706

Cutting Edge Science Track - TROP Session: AI - Image Processing and Data Corrections

Friday, October 30, 2020, 15:30 - 17:00 Channel 6

OP-964

An automated method for locating a liver reference region in PET/CT scans

A. Goddard[1,2], G. Platsch[3], C. Gall[1], L. Sibille[1], B. Spottiswoode[1], V. Shah[1];

[1]Siemens Medical Solutions USA, Inc., Knoxville, TN, UNITED STATES OF AMERICA, [2]Illinois Institute of Technology, Chicago, IL, UNITED STATES OF AMERICA, [3]Siemens Healthcare GmbH, Erlangen, GERMANY.

Aim/Introduction: A reference region in the liver is commonly used to determine threshold values for segmentation (e.g.-PERCIST) or provide disease scoring (e.g.-Deauville criteria). This work proposes an automated method to find an optimal liver reference region on PET/CT images. ***Materials and Methods:*** The proposed method consists of automatically segmenting the liver[1] and placing a 3-cm diameter sphere (as-per-PERCIST) at a homogenous position within the liver. The spherical VOI was placed on all voxel positions within the liver (segmented-mask-eroded-1.5cm). For each position the coefficient of variance (CoV) was separately calculated for PET and CT, and combined to determine a joint score. The VOI with the lowest joint score was selected as the optimal liver reference region. For comparison, a 3-cm sphere was centered on a liver landmark automatically detected using ALPHA-technology[2]. Two-experienced nuclear medicine physicians [CvG-reader1,GP-reader2] reviewed the position of the ALPHA-derived landmark and if required moved the VOI to avoid vessels or liver metastases. 205,^{18}F-FDG PET/CT scans evaluated: lung cancer[43%], lymphoma[24%], melanoma[10%], colorectal[3%], other[20%] cancers. Six-scans were excluded due to failure of automated technology (4-ALPHA landmarking,2-Liver Segmentation). Data was acquired on a range of scanners Siemens-(TruePoint[4%], mCT[52%],Horizon[18%], Vision[13%]) and GE-Discovery[13%][3,4]. ***Results:*** The reference region CoV across all patients [mean±stdev] for [reader1 (11.9±5.0%), reader2 (11.6±5.2%), ALPHA-Landmark (12.5±5.8%), proposed-method (9.1±3.9%)]. The landmark obtained by ALPHA-technology was moved in 68-scans[reader1-only:48, reader2-only:6, both:14]. When both clinicians corrected the reference region the SUVmean±SUVstdev: average of two readers: 2.2±0.4, proposed-method: 2.2±0.4, and ALPHA-method: 2.4±1.2. The percent difference in the PERCIST-threshold-value(1.5*SUVmean±2*SUVstdev) compared to the average of the readers for all 14 scans was 15.5±61.8% for the ALPHA method and -1.2±4.2% for the proposed method. ***Conclusion:*** This study shows selecting liver reference regions based on minimum CoV in the PET CT volumes is more robust than performing landmarking only on CT scans. Early evidence is shown that the organ segmentation seems to be more robust in terms of failure in this small cohort. For subjects where both readers moved the reference region on old method, the mean SUV and PERCIST threshold values of the proposed algorithm were consistent with the clinician-placed regions. These early results are promising to provide a new tool for improving the use of PERCIST by using a hybrid approach to identify the optimal placement of the input VOI. ***References:*** [1]Yang.et.al.(2017)."Automatic-liver-segmentation using an adversarial image-to-image network."Proc.MICCAI,pp.207-515. [2]Tao.et.al.(2011)."Robust learning based parsing and annotation of medical radiographs."IEEETMI-V:30:pp.338-350. [3]Madhavi.et.al.(2019)."Data from Anti-

PD-1 Immunotherapy Lung [Data set].TCIA."DOI:10.7937/tcia.2019.zjjwb9ip [4]Clark.et.al.(2013)"The Cancer Imaging Archive(TCIA),"JDI:v26(6),pp:(1045-1057)DOI:10.1007/s10278-013-9622-7

OP-965

Effectively Detecting Left Bundle Branch Block Artefacts With a Convolutional Neural Network (CNN) Using a Very Small Training Dataset

M. Abdi[1], Q. Naili[1], M. Habbache[1], B. Said[1], A. Boumenir[1], T. Douibi[1], D. Djermane[2], S. Berrani[3];
[1]Centre d'imagerie scintigraphique, Blida, ALGERIA, [2]Cardio A2, Mustapha Bacha, Algiers, ALGERIA, [3]Ecole Nationale Polytechnique, Algiers, ALGERIA.

Aim/Introduction: Left bundle branch block (LBBB) is a frequent source of false positive reports in myocardial perfusion imaging[1]. In this work, we evaluated the ability of a CNN-based solution, using transfer learning, to produce an expert-like judgment in differentiating LBBB artefacts from left anterior descending artery (LAD) perfusion defects. The study was conducted considering a very small training dataset, because collecting a larger dataset needs a proof of utility. ***Materials and Methods:*** The study covered two groups, collected retrospectively. (i) The LBBB group included patients with LBBB on ECG, along with mild to severe fixed anteroseptal perfusion defect, that was judged as false positive by two experts (based on clinical assessment, GATED-SPECT[1], and having no cardiovascular events after 3 years of follow-up). (ii) The LAD group included patients without LBBB, with mild to severe anteroseptal perfusion defect, that was judged as a true positive by two experts (confirmed by angiography; >70% narrowing of LAD artery). The dataset was composed of 107 perfusion polar maps (42 images in each class for training, with 29% for validation). Several CNN were tested[2], and ResNet50V2 was chosen for achieving the best results. Only the classification part of the network was re-trained, following a transfer learning approach. After 60 iterations, the reached accuracy plateau was 0.98, and the loss was 0.19 (the validation accuracy and loss were 0.91 and 0.25, respectively, demonstrating low overfit). ***Results:*** A set of 23 test images was used (11 LBBB, and 12 LAD). The empiric ROC Area[3] was estimated at 0.98, with 95.7% accuracy. Two blinded experts were asked to classify the testing images. The results of empiric ROC area for them were 0.97 and 0.91, respectively. Another test set (18x2 images) was collected after the final results (without follow-up for the LBBB group). The ROC area was estimated again at 0.98. The results showed that our CNN-based approach can reproduce expert-like judgment for this problem. ***Conclusion:*** Artificial intelligence, using CNN and transfer learning -even on a very small training dataset- could reproduce an expert-like judgment in differentiating between LBBB artefacts and LAD perfusion defects. These results are motivating for a multicenter prospective study. ***References:*** 1. Left bundle-branch block artifact on single photon emission computed tomography with technetium Tc 99m (Tc-99m) agents: Mechanisms and a method to decrease false-positive interpretations John P. Higgins et al 2. https://keras.io/applications/ 3. Johns Hopkins University School of Medicine web-based calculator (John Eng, M.D.)

OP-966

Metabolic tumour volume segmentation for oesophageal cancer on hybrid PET/CT using convolutional network architecture

***E. Spezi[1]**, C. Parkinson[1], S. Berenato[2], W. Riviera[3], S. Sobhee[4], C. Stylianou[5], T. Crosby[2], K. Foley[2];*
[1]Cardiff University, Cardiff, UNITED KINGDOM, [2]Velindre Cancer Centre, Cardiff, UNITED KINGDOM, [3]Intel Corporation, London, UNITED KINGDOM, [4]Intel Corporation, Munich, GERMANY, [5]Intel Corporation Limited, London, UNITED KINGDOM.

Aim/Introduction: Oesophageal cancer (OC) has a particularly poor prognosis with an overall 5-year survival rate of only 15%. OC is rising in incidence and is a cancer with unmet clinical need. The segmentation of metabolic tumour volume (MTV) is time consuming and subject to intra and inter-observer variability. This study aims to increase the efficiency of MTV segmentation in OC by developing a hybrid PET/CT deep-learned model based on convolutional network architecture. ***Materials and Methods:*** A data set of 440 patients with biopsy-proven OC tumours was included in this study. All patients had PET/CT acquisition using a GE 690 scanner with time of flight. Details of patient selection and image acquisition parameters were published by our group [1,2,3].Only primary tumours were used in this study for the development of a deep-learning model. The primary MTV was delineated on PET imaging using a previously published segmentation method[4,5] and reviewed by a consultant radiologist. For the convolutional network architecture, we used a 2-dimensional (2D) based U-Net architecture[6]. The developed model was trained using a cluster consisting of 2 nodes. Each node contained 2 CPU's running at 2.10Ghz, resulting in total of 88 threads per node. Contours delineated with the proposed deep-learned model were assessed using a Turing test including a total 376 images with associated contours for evaluation by 5 independent radiologists (Ob1 - Ob5). ***Results:*** The mean Dice Similarity Coefficient (DSC) of the U-net architecture, when compared to manual outlines, was 0.73. In the Turing test, Ob1 to Ob5 had accuracies of 0.55, 0.73, 0.47, 0.64 and 0.46, respectively. Sensitivity for Ob1 to Ob5 was 0.66, 0.64, 0.38, 0.56, and 0.47 respectively. Specificity for Ob1 to Ob5 was 0.44, 0.83, 0.57, 0.71, 0.46. The area under the curve values ranged from 0.46 to 0.73. ***Conclusion:*** We successfully trained a convolutional network to segment the metabolic tumour volume on hybrid PET/CT oesophageal cancer.

The performance of the network was confirmed to be equivalent to expert delineation. ***References:*** 1. Foley, K.G. et al., 2018. Eur. Radiol. 28, 428-436. 2. Foley, K.G., et al. 2019. Radiother. Oncol. 133, 205-212. 3. Parkinson, C., et al 2018. EJNMMI Res. 8-29.4. Berthon, B., et al. 2017. Radiother. Oncol. 122, 242-247. 5. Berthon, B. et al 2016. Phys. Med. Biol. 61, 4855-4869.6. Ronneberger, O. et al 2015. Lect. Notes Comput. Sci. 9351, 234-241.

OP-967

A tool for AI-driven Organ Segmentation and quantification in SSTR- imaging - Development and external validation

P. Jackson[1], B. M. Fischer[2], S. F. Barrington[2], L. McIntosh[1], T. Kotwal[2], G. Krokos[2], J. Callahan[1], J. Korte[1], R. Alipour[1], M. Hofman[1], R. J. Hicks[1];
[1]Peter MacCallum Cancer Centre, Melbourne, AUSTRALIA, [2]King's College London & Guy's and St Thomas' PET Centre, London, UNITED KINGDOM.

Aim/Introduction: AI methods are showing potential for automatic delineation of organs using CT imaging. Our aim was to determine if convolutional neural networks could rapidly and reliably delineate organs on the CT component of PET/CT and SPECT/CT somatostatin receptor (SSTR) imaging, namely kidneys, spleen, bladder, & liver. These organ segmentations facilitate assessment of lesional Krenning score for radionuclide therapy, prediction of potential toxicities, discrimination between malignant and physiological uptake in somatostatin-avid tissues, or selection of novel adaptive thresholds to characterise highly avid regions in SSTR imaging. ***Materials and Methods:*** Organs were contoured on CT by first aligning to a reference coordinate system using a novel 2D image recognition neural network. Subsequently, organ-specific crop regions were selected and labelled by conventional 3D U-Net. Training data for kidney (n=93) and bladder (n=110) were manually contoured from clinical data. Contours for liver (n=161) and spleen (n=41) were taken from a publicly-available dataset[1]. The tool was assessed in an external dataset of 20 FDG PET/CT images. Accuracy was scored visually by an independent experienced nuclear medicine physician rating reliability of automated contouring as follows: 1 good agreement, no correction needed 2- minimal correction required, 3- major editing required 4- no contour identified. ***Results:*** Images were rated as showing good agreement or minimal correction needed in 16/20 cases for liver, 12/20 for bladder, 18/20 for left kidney, and 13/20 for right kidney. The mean and standard deviation of accuracy scores for liver, bladder, left kidney, and right kidney were 1.7±0.7, 2.1±1.0, 1.5±0.7, and 2.0±1.1, respectively. Results were worse for splenic contouring with the fewest available training cases. Spleen was not identified in 4/20 cases, accuracy score=2.2±1.2. The algorithm was incorporated into a DICOM processing pipeline. Contours were generated automatically as an RT-structure set on a typical desktop computer. Workflows that automated removal of labelled somatostatin-avid organs reduced the time required to remove physiological uptake and assess tumour burden in a modified PERCIST workflow for SSTR imaging. ***Conclusion:*** It is feasible to rapidly contour organs using an AI -driven tool for the purpose of assessment of functional imaging in neuroendocrine cancer with reasonable accuracy. Further work is warranted to refine the model with additional training cases to develop a mature tool for clinical application. ***References:*** [1]Simpson, Amber L., et al. "A large annotated medical image dataset for the development and evaluation of segmentation algorithms." arXiv preprint arXiv:1902.09063 (2019).

OP-968

Automatic Image Subtraction in Parathyroid Scintigraphy using Rotated Principal Components

I. Marikova[1], S. Balogova[2], J. Talbot[3], M. Samal[1];
[1]Institute of Nuclear Medicine, First Faculty of Medicine, Charles University and the General University Hospital in Prague, Prague, CZECH REPUBLIC, [2]Department of Nuclear Medicine, Comenius University, Faculty of Medicine & St. Elisabeth Cancer Institute, Bratislava, SLOVAKIA, [3]Department of Nuclear Medicine, Hôpital Tenon APHP and Sorbonne University, Paris, FRANCE.

Aim/Introduction: Image subtraction in parathyroid scintigraphy requires registration of the two images and estimation of subtraction weights reflecting different count rate produced by different radiopharmaceuticals. Pixel values in both images are usually converted to similar scales and subtraction weights derived stepwise by trials and errors under visual supervision. Our motivation was to simplify and accelerate manual procedure by using rotated principal components (RPC) where both scaling and weighting can be optimized automatically. The aim was to assess performance of RPC with perfectly registered pairs of 99mTc-MIBI and 123-Iodine images. ***Materials and Methods:*** Retrospective data on parathyroid scintigraphy in 26 patients were selected from the database and anonymized. MIBI and Iodine image pairs included 25 early and 22 delayed pinhole scintigrams and 24 early and 18 delayed planar images. RPC was performed with all 89 image pairs using inhouse software. Image scaling was automatic. The method resulted in two images demonstrating common and difference structures of each input pair. Subsequent rotation (analogy to image subtraction) was performed to emphasize unique structures specific exclusively for MIBI image on flat background (removing both oversubtracted and residual common image segments). Three rotation procedures were compared: (A) manual procedure under visual supervision (reference method), (B) semi-automatic procedure that required manual definition of background ROI, and (C) automatic procedure that defined background

ROI automatically. Parametric images visualizing entropy in the neighbourhood of each pixel were also calculated. ***Results:*** All 37 lesions found in 25 early pinhole image pairs were well reproduced by both semi-automatic and automatic procedures (100 %). While semi-automatic procedure reproduced 100 % of the lesions found in delayed pinhole reference images, automatic procedure failed in 8 % probably due to low counts in iodine scans. In early planar images, semi-automatic and automatic procedures found 96 % and 93 % of the lesions revealed by supervised manual procedure. There were only 10 lesions found in 18 delayed planar images that were reproduced in 100 %. In comparison with reference manual procedure, both semi-automatic and automatic RPC were faster and more comfortable. Parametric images supported interpretation of difference images by emphasizing positive lesions by locally lowest image entropy. ***Conclusion:*** In well registered images with sufficient counts, automatically rotated principal components perform as well as manual stepwise subtraction procedure under visual supervision. The advantage is the speed of the method, comfort of a user, and potential future inclusion in the procedures of machine learning. ***References:*** None

OP-969

A cross-scanner robustdeep learning method for the recovery of full-dose imaging quality from low-dose PET

S. Xue[1], R. Guo[2], K. P. Bohn[1], J. Matzke[3], M. Viscione[1], M. Viscione[1], B. Li[2], A. Rominger[1], K. Shi[1];
[1]University of Bern, Bern, SWITZERLAND, [2]Ruijin Hospital, Shanghai Jiaotong University, Shanghai, CHINA,
[3]Technical University of Munich, Munich, GERMANY.

Aim/Introduction: Despite the fact that radiation dose of modern PET imaging became much less than in early days, it still remains a major bottleneck for extensive application of this modality. Artificial intelligence has been recently developed to recover high-quality imaging from low-dose scans. However, it is not clear if the methods developed on one scanner can be applied to other scanners. ***Materials and Methods:*** Brain PET imaging of 245 patients scanned with scanner 1 was included for the development of the AI technology. Then the developed algorithm was tested on data of 8 patients with scanner 1, 27 patients scanned with scanner 2 and 9 patients scanned with scanner 3. All data was scanned in list mode for 15 min. In addition to the reconstruction of full dose imaging of 15 min, reduced frames of 7.5 min, 3.75 min, 1.5 min and 0.75 min were reconstructed to mimic a dose reduction fraction (DRF) of 2, 4, 10 and 20. A 2D generative adversarial network (GAN) was developed with a U-net generator and a convolutional neural network (CNN) based discriminator. For each DRF, a corresponding GAN was trained. The normalized root mean squared error (NRMSE), structural similarity index (SSIM) and peak signal-to-noise ratio (PSNR) were calculated to evaluate the results generated by AI. Analysis of variance (ANOVA) was performed to examine the robustness and generalization ability of our algorithm, where the level of significance α is set to 0.05. Two independent nuclear medicine physicians assessed the interpretation ability towards a diagnosis. ***Results:*** The developed AI method can achieve a good physical performance with an average SSIM of 0.99±0.004, PSNR of 39.4±3.7, and NRMSE of 0.66±0.32% for DRF=2. The performance decreased as DRF increased and for DRF=20 it achieved the average SSIM of 0.94±0.018, PSNR of 26.8±3.3 and NRMSE of 2.9±1.1%. The ANOVA test showed no significant difference of NRMSE, PSNR and SSIM between the AI predictions on the three scanners in most cases, exception occurred to NRMSE and PSNR when DRF=2, where variation between scanner brands is the major source of difference. Clinical reading was performed in a subset of patients and after correction no significant impairment could be observed for DRF up to 20. ***Conclusion:*** The developed deep learning method is robust in the application on scanners of different vendors and technology. This encourages the further investigation of this method with emphasis on clinical interpretation. ***References:*** None

OP-970

Zero-TE MRI-based Attenuation Correction for Chest FDG PET/MRI: A Feasibility Study of Deep Learning Approach Using Unpaired PET/CT Data

***M. Nogami[1]**, H. Matsuo[1], M. Nishio[1], F. Zeng[1], J. Inukai[1], F. Wiesinger[2], S. Kaushik[2], T. Kurimoto[3], K. Kubo[1], T. Murakami[1];*
[1]Kobe University Hospital, Kobe, Hyogo, JAPAN, [2]GE Healthcare, Munich, GERMANY, [3]GE Healthcare, Hino, Tokyo, JAPAN.

Aim/Introduction: Deep learning approaches using pseudo computed tomography (pCT) for attenuation correction (AC) of chest positron emission tomography-magnetic resonance images (PET/MRI) is challenging as differences in subject's respiratory phase, body position, and scanner bed shape can hamper pairing data of images for training. Moreover, conventional generative adversarial networks (GANs) using unpaired training data suffer from significant deformation of the generated pCT. Here we propose using unsupervised GANs with adaptive layer-instance normalization for image-to-image translation (U-GAT-IT) in combination with a modality independent neighborhood descriptor (MIND) to create pCT for AC in the chest. ***Materials and Methods:*** The data of 125 patients who underwent chest fluorodeoxyglucose (FDG) PET/MRI with zero echo time (ZTE) were retrospectively analyzed. All ZTE images were scanned with a large field of view and reconstructed in-phase by central frequency adjustment. Unpaired training image data included bias-corrected ZTE (n=100) and CT component of PET/CT (n=100), and

were utilized for training U-GAT-IT/MIND model of pCT generation. Human annotation was not performed for the construction of unpaired training image data. Twenty-five cases with paired ZTE PET/MRI and PET/CT were used to validate the model for standardized uptake values (SUV) after AC. Mean SUV (SUVmean) of bone and liver in the chest region were measured by segmentation of bone on pCT and placement of a fixed region of interest in the liver, respectively. An MRI-based AC map with bone ($MRAC_{ZTE}$) was created by merging the segmented bone map onto a conventional 2-point Dixon-based AC map ($MRAC_{Dixon}$), and was applied to PET reconstruction on the offline workstation. Bland-Altman plots and ANOVA were used to compare SUVmeans between $MRAC_{Dixon}$, $MRAC_{ZTE}$ and CT-based attenuation correction (CTAC). ***Results:*** Mean differences in bone SUVmeans by $MRAC_{ZTE}$ and CTAC (-0.0252; 95% confidence interval (CI), -0.1014 to 0.05104) were significantly smaller than by $MRAC_{Dixon}$ and CTAC (-0.0988; 95%CI, -0.1741 to 0.02353) ($p<0.05$). Bone and liver SUVmean (0.918 and 2.300, respectively) by $MRAC_{ZTE}$ were significantly larger than by $MRAC_{Dixon}$ (0.844 and 2.252, respectively) ($p<0.0001$). ***Conclusion:*** AC maps with bone components from pCT yield smaller differences in bone SUV with CT-based AC than do $MRAC_{Dixon}$, and larger SUVs in the bone and liver than $MRAC_{Dixon}$, supporting the feasibility of deep-learning approaches with unpaired data sets for pCT and AC map creation for chest PET/MRI. ***References:*** 1. Kim J, et al. arXiv:1907.10830. 2. Heinrich MP, et al. Med Image Anal. 2012 Oct;16(7):1423-35. 3. Leynes AP, et al. J Nucl Med. 2018 May;59(5):852-858.

OP-971

Deep learning based scatter correction for PET imaging

D. Visvikis[1], T. Merlin[2], A. Bousse[1], D. Benoit[1], B. Laurent[1];
[1]LaTIM, INSERM, UMR 1101, Brest, FRANCE, [2]LaTIM, INSERM, UMR 1101, CHRU Brest, Brest, FRANCE.

Aim/Introduction: Scatter correction in PET imaging is routinely performed using a single scatter simulation (SSS) approach, where multiple scatter and scatter from outside the field of view are not accurately modeled leading to reduced qualitative and quantitative PET image accuracy. In this work we explore the potential of deep learning for the development of an accurate PET scatter correction methodology accounting for all scatter coincidences. ***Materials and Methods:*** The network used is based on a U-Net architecture with 5 convolutionnal layers. The input corresponds to emission data and attenuation sinograms, while the output corresponds to scatter sinograms of the same size as the input. The network training was performed using Monte Carlo (MC) simulated PET datasets. Multiple anthropomorphic XCAT phantoms of two different regions (lung and pelvis) were created, considering three different body sizes and different levels of statistics (1-6 minutes acquisitions). A total of 216 simulations were performed. Each sinogram contains 553 slices, leading to a total of 120 000 simulated slices. This entire dataset was subsequently divided in 3 parts: 2/3 for the training data, 1/6 for validation and 1/6 for testing data. Moreover, to train the network and evaluate its precision and robustness among different levels of statistics, acquisitions were simulated with various dose levels and acquisition times. In addition, two patient images acquired on an mMR scanner at the level of the lung and the pelvis were used to assess the expected performance of the algorithm relative to a perfect scatter correction based on MC simulations and the standard SSS algorithm used in clinical practice. ***Results:*** The results of the training were independent of data statistics for the use of acquisition times of >2 minutes per bed position. The quantitative accuracy in the simulated reconstructed images corrected using the estimated scatter sinograms output from the proposed network was equivalent to that achieved by a full MC based scatter correction. The results were not dependent on the body location (lungs or pelvis). In the case of the clinical patient datasets the results in the pelvis clearly demonstrated a reduction in the artefacts related to the use of the SSS approach. ***Conclusion:*** In this work we developed a deep learning based approach for scatter correction in PET imaging. The results obtained demonstrate the interest of this approach relative to the standard SSS methodology used clinically, improving both qualitative and quantitative image accuracy. ***References:*** None

OP-972

Data-driven motion compensation of [18F]FDG-PET brain imaging using conditional Generative Adversial Networks (cGANs)

D. Iommi[1], L. Shiyam Sundar[1], O. Muzik[2], Z. Chalampalakis[3], E. M. Klebermass[4], M. Hienert[5], L. Rischka[5], R. Lanzenberger[5], A. Hahn[5], E. Pataraia[6], T. Traub-Weidinger[4], T. Beyer[1];
[1]QIMP Team, Center for Medical Physics and Biomedical Engineering, Medical University of Vienna, Vienna, AUSTRIA, [2]Department of Pediatrics, Children's Hospital of Michigan, The Detroit Medical Center, Wayne State University School of Medicine, Detroit, MI, UNITED STATES OF AMERICA, [3]Service Hospitalier Frédéric Joliot, CEA, Inserm, CNRS, Univ. Paris Sud, Université Paris Saclay, Orsay, FRANCE, [4]Division of Nuclear Medicine, Department of Biomedical Imaging and Image-guided Therapy, Medical University of Vienna, Vienna, AUSTRIA, [5]Department of Psychiatry and Psychotherapy, Medical University of Vienna, Vienna, AUSTRIA, [6]Department of Neurology, Medical University of Vienna, Vienna, AUSTRIA.

Aim/Introduction: The quality of PET images and the accuracy of absolute quantification are affected by involuntary subject motion. We present here a fully-automated, motion correction (MC) approach based on conditional-generative adversarial networks (cGAN) that might promote dynamic

PET acquisitions in clinical routine. ***Materials and Methods:*** Ten healthy volunteers (5M/5F, (27±7) years, (70±10) kg) underwent a test-retest [18F]FDG-PET/MRI brain examination (N=20). The imaging protocol consisted of a 60-min PET list-mode acquisition with parallel MR-acquisitions including MR navigators and 3D time-of-flight MR-angiography (TOF-MRA). Arterial input function (AIF) was collected as the reference standard. A separate low-dose CT scan was used for brain attenuation correction. Training of the cGAN was performed using 70% of the total data sets (N=14, randomly chosen), which was corrected for motion using the MR navigator sequences. The PET frame corresponding to 55-60 min p.i. was considered as the target frame and all other frames (0 to 55 min p.i.) were individually paired to the target frame. cGAN training was individually applied to the image pairs (early frames to late PET frames) and the resulting cGAN models were applied to the testing data set (remaining 30%, N=6), generating artificial high-count early PET frames with increased image-quality. These volumes were then used for MC during the extraction of an image-derived input function (IDIF). Performance of the cGAN-method to carry out an accurate MC was tested by comparing the area-under-the-curve (AUC) of the so derived IDIF against the gold standard of AIF. The clinical relevance of this methodology was assessed by direct comparison of average cerebral metabolic rates of glucose (CMRGlc) values in grey matter (GM) calculated using the AIF and the IDIF. ***Results:*** The artificially generated images displayed excellent image quality for frames >2 min P.I, whereas the quality was suboptimal for frames <2 min P.I. Quantitative assessment of motion vector accuracy in the test data set resulted in an absolute % difference between AUCs derived using the motion-corrected IDIF and the AIF of only 1.2±0.9%. Moreover, the GM CMRGlc values determined using these two input functions differed on average by less than 5% (2.4±1.7%). ***Conclusion:*** A fully-automated data-driven MC approach was established and validated for quantitative [18F]FDG-PET imaging of the brain. The developed cGAN based MC scheme might be pivotal in enabling the translation of non-invasive clinical absolute quantification from PET/MR to PET/CT. ***References:*** None

OP-973

Automatic Classification of Data-Driven Respiratory Waveforms Using AI

M. D. Walker[1], *K. Su*[2], *S. D. Wollenweber*[2], *R. Johnsen*[2], *D. R. McGowan*[1,3];
[1]*Oxford University Hospitals NHS FT, Oxford, UNITED KINGDOM,* [2]*GE Healthcare, Milwaukee, WI, UNITED STATES OF AMERICA,* [3]*University of Oxford, Oxford, UNITED KINGDOM.*

Aim/Introduction: Data-driven respiratory gating for PET has been implemented clinically[1]. The decision to apply gating can be made during the acquisition, modifying the protocol and affecting image quality. This is currently done using a threshold on the signal-to-noise ratio for respiratory frequencies in the respiratory waveform (R-value). We aimed to develop an AI algorithm to improve the accuracy of this decision, and compare its performance to the existing method. ***Materials and Methods:*** 155 ^{18}F-FDG PET scans were used to train the AI and evaluate performance. The respiratory waveform was extracted from each of 1134 bed positions. Waveforms were previously scored by two readers using a three-point scale (0, 1, or 2)[2]. The AI uses a pattern recognition network, designed and trained to predict the readers' scores using ten-fold cross-validation. This provided 10 separate AI predictors, each of which was trained on 90% of the data and predicted the scores for the remaining 10%. Predictions for the entire dataset were thus obtained, with each test waveform not included in the training waveforms for its corresponding AI predictor. Those waveforms with an average reader score ≥1.5 were classified as being clinically useful. This classification provided the standard for performance evaluation of the two methods. The classification accuracies, sensitivities and specificities were calculated. The optimum R-value threshold of 12, found to give maximum accuracy, was used for the comparison. ***Results:*** The AI outperformed the R-value method. It had higher accuracy (93% vs. 88%), sensitivity (87% vs. 78%) and specificity (96% vs. 92%). The maximum discrepancy between the AI-predicted score and the readers' mean score was small. In all cases the AI correctly classified those waveforms with reader scores of 2 or ≤0.5, corresponding to waveforms where clinical utility was unambiguous. The R-value method had greater variance, leading to some waveforms with mean reader scores of 0 or 2 being misclassified, with R≥12 or R<12 respectively. The ^{18}F-FDG-trained AI performed well in similar, initial evaluation for ^{68}Ga-dotatate (24 waveforms; 96% accuracy). ***Conclusion:*** An AI-classifier of data-driven respiratory waveforms was developed. In the ^{18}F-FDG data used for evaluation, the AI had greater concordance with the scores assigned by two medical physicists as compared to the existing technique. This AI approach may allow for improved automation of respiratory gating workflows in PET/CT, with improved decision making as to when motion correction techniques can be confidently applied. ***References:*** [1] Walker et.al. jnumed.120.242248.(2020) [2] Walker et.al. EJNMMI.Res 9,1(2019)

OP-974

The effect of data preparation of small datasets to predict biochemical recurrence in prostate patients from PET/MR imaging

D. Krajnc*, L. Papp, C. P. Spielvogel, M. Grahovac, M. Hartenbach, M. Hacker, T. Beyer;*
Medical University of Vienna, Vienna, AUSTRIA.

Aim/Introduction: Machine learning (ML) approaches have demonstrated potential to improve the diagnostic value of medical imaging and patient management. However, the majority of these studies does not embrace adequate data preparation to address challenges, such as imbalanced subgroups, insufficient sample count and outliers. We aim to demonstrate the importance of applying data pre-processing of small patient cohorts, in order to support ML training processes to predict biochemical recurrence from prostate PET/MRI studies. ***Materials and Methods:*** 36 multi-parametric prostate PET/MRI cases with ^{18}F-FMC, ^{18}F-FMC+^{68}Ga-PSMA$^{HBED-CC}$ (dual-tracer) PET furthermore, T2, ADC, iAUC, KEP, Ktrans and Ve MRI images were involved in our study. Each case had biochemical recurrence yes/no information as well as annotated full-mount histopathological slices. Two nuclear medicine experts delineated in consensus the most aggressive lesion on each PET/MR image using the Gleason-annotated histopathological slices. 56 radiomics features were extracted from each delineation. Ensemble learning approaches were applied to predict biochemical recurrence yes/no information in a 100-fold Monte Carlo cross-validation scheme. This step was performed twice: first, with training the predictive models on the original training datasets, and second with processing the training datasets. In training data pre-processing, we performed imbalance data correction, outlier detection as well as data oversamling and undersampling across MC folds. Predictive performance was estimated for both executions over the ML fold validation cases with confusion matrix calculations (sensitivity (SENS), specificity (SPEC) and overall accuracy (ACC)). ***Results:*** The validation performance including ML models built on the original training data was SENS 35%, SPEC 71% and ACC 53%. In contrast, the validation performance including ML models built on the pre-processed training data was SENS 84%, SPEC 66% and ACC 75%, where sensitivity and overall accuracy significantly increased by 49% and 22% respectively, while specificity slightly decreased (5%) due to model overfitting built on original imbalanced dataset. ***Conclusion:*** We have demonstrated the added value of performing adequate data preparation steps (ACC 75% vs 53%), suggesting that applying these techniques can support the establishment of ML models based on small patient cohort for prediction of biochemical recurrence in prostate PET/MRI cases. ***References:*** None

OP-975

Novel Software for Computer-aided Differential Diagnosis of Parkinsonism Using Positron Emission Tomography

E. Lindström[1,2], C. Widström[2], T. Danfors[2], M. Lubberink[1,2], M. Jonasson[1,2];
[1]Uppsala University, Uppsala, SWEDEN, [2]Uppsala University Hospital, Uppsala, SWEDEN.

Aim/Introduction: The PET tracer ^{11}C-PE2I is a selective dopamine transporter (DAT) compound that has been successfully introduced for differential diagnosis of Parkinsonism [1]. Using tracer kinetic analysis of a dynamic ^{11}C-PE2I-PET scan, DAT availability and relative cerebral blood flow (rCBF) can be measured at the voxel level. The aim was to develop an automated workflow from dynamic PET-data to statistical comparison of the patient's regional rCBF and DAT availability values to a normal control database, allowing for computer-aided differential diagnosis of Parkinsonism. ***Materials and Methods:*** The automated workflow was based on previously validated and published methodology [2,3]. In brief, the dynamic PET images were realigned to correct for inter-frame patient motion. A volume of interest template in MNI space was projected onto an early sum image. rCBF images were generated from 40-min dynamic PET-data using a basis function implementation of the simplified reference tissue model and SUVR-1 was estimated for the 30-40 min interval, with cerebellar gray matter as reference region. Regionally average voxel values were extracted in conjunction with z-scores from comparison to a normal database (n=30). Surface projection maps of rCBF and rCBF z-score were computed after translation to MNI space. The software was written in Qt and C++ and implemented within the Hermes environment. Results in 22 subjects were compared to a previous analysis using in-house written software in Matlab. ***Results:*** Quantitative results of the automated software agreed well with previous analysis. Spearman rank correlation r was 0.92 (CI 0.86-0.96) and 0.84 (CI 0.79-0.88) for SUVR-1 in putamen and rCBF in the limbic area, respectively. So far, the software has been used for differential diagnosis of about 300 patients at Uppsala University Hospital. Total processing time of approximately 5 min/patient. ***Conclusion:*** ^{11}C-PE2I enables a differential diagnosis of Parkinsonism based on both DAT availability and general brain function (rCBF) using a single scan, replacing a dual scan approach using DATscan-SPECT and FDG-PET. The software-aided approach improves logistics and may be helpful for experienced ^{11}C-PE2I-PET readers analyzing challenging cases. The single scan approach and software have been successfully introduced as a routine clinical application at Uppsala University Hospital and the software is freely available for other interested centers. ***References:*** 1. Appel L, et al. 2015, J Nucl Med, 56:234-242. 2. Jonasson, M, et al. 2013, NeuroImage, 74:172-78. 3. Jonasson, M, et al. 2017, Am J Nucl Med Mol Imaging, 7:263-74.

1707

Teaching Session 7: Molecular Imaging in Thyroid Nodules

Friday, October 30, 2020, 15:30 - 17:00 Channel 7

OP-976

[99mTc]TcO4- Scintigraphy in the Evaluation of Thyroid Nodules

T. Jukic; University Hospital Center Sestre milosrdnice, Department of Oncology and Nuclear medicine, Zagreb, CROATIA.

OP-977

The Importance of [99mTc]Tc-MIBI Scintigraphy in Thyroid Nodules Assessment

S. Schenke; Department of Radiology and Nuclear Medicine, University Hospital Magdeburg, Magdeburg, GERMANY.

OP-978

The Role of 2-[18F]FDG PET/CT Imaging in the Characterization of Thyroid Nodules

A. Piccardo; Galliera Hospital, Department of Nuclear Medicine, Genoa, ITALY.

1708

Clinical Oncology Track - TROP Session: [177Lu] Lu-PSMA Radioligand Therapy

Friday, October 30, 2020, 15:30 - 17:00 Channel 8

OP-979

Prognostic markers for overall survival and outcome to LuPSMA radionuclide treatment in patients with metastatic castration-resistant prostate cancer

A. Gafita[1], J. Calais[1], H. Wang[2], M. Weber[3], H. Rathke[4], C. Kratochwil[4], R. Esfandiari[5], W. R. Armstrong[1], S. Sandhu[6], R. Tauber[2], E. S. Delpassand[5], U. Haberkorn[4], W. A. Weber[2], K. Herrmann[3], J. Czernin[1], M. S. Hofman[6], W. P. Fendler[3], M. Eiber[2]; [1]UCLA, Los Angeles, CA, UNITED STATES OF AMERICA, [2]Technical University Munich, Munich, GERMANY, [3]University of Duisburg-Essen, Essen, GERMANY, [4]Heidelberg University, Heidelberg, GERMANY, [5]Excel Diagnostics and Nuclear Oncology Center, Houston, TX, UNITED STATES OF AMERICA, [6]Peter MacCallum Cancer Center, Melbourne, AUSTRALIA.

Aim/Introduction: The aim of this international multicenter retrospective analysis was to identify prognostic markers for the clinical outcome in late-stage mCRPC patients treated with ^{177}Lutetium-prostate-specific membrane antigen (LuPSMA) radionuclide treatment. ***Materials and Methods:*** Patients with progressive mCRPC treated with LuPSMA at six centers in Germany, USA and Australia were considered for inclusion. Eligible patients had 24 predefined pretherapeutic covariates (demographics, prior mCRPC treatments, and PSMA PET/CT derived parameters) and survival data available. Endpoints included overall survival (OS) and PSA progression-free survival(PSA-PFS). Covariates were tested using univariate and mulitvariate proportional hazards regression Cox models. ***Results:*** 267/414 (64%) patients met inclusion criteria and were analyzed. 113 patients participated in clinical trials, while 154 were enrolled in compassionate access programs. After a median follow-up of 22.5 months, median OS was 13.0 months (95%CI 11.6-14.4); 83% of the patients died. Median PSA-PFS was 4.0 months (95%CI 3.2-4.7). In the multivariate analysis, factors associated with shorter OS were: shorter time since diagnosis of prostate cancer (HR = 2.04; p= 0.002), lower number of prior systemic therapies (≤3; HR = 1.56; p= 0.006), prior exposure to chemotherapy (HR = 1.42; p= 0.05), lower hemoglobin levels (HR = 1.13; p= 0.002), higher number of lesions (≥20: HR = 1.53; p= 0.009), multiple sites of metastases (bone/LN only vs. bone + LN; HR = 1.39; p= 0.03) and visceral involvement (M1c) (HR = 1.45; p= 0.01). Factors associated with longer PSA-PFS were: longer time since diagnosis of prostate cancer (HR = 0.44; p< 0.001), higher hemoglobin levels (HR = 0.32; p= 0.03), presence of pelvic lymph nodes (LN) metastasis (N1) (HR = 0.68; p= 0.01), no distant lymph node metastases (M1a) (HR = 0.66; p= 0.01), no skeleton involvement (HR = 0.44; p= 0.01), no visceral metastases (M1c) (HR = 0.51; p< 0.001), higher PSMA-positive tumor volume (HR = 0.87; p= 0.04), and higher SUVmean (HR = 0.94; p= 0.002). ***Conclusion:*** This retrospective analysis identified prognostic factors for survival and treatment response to LuPSMA. Along with the conventional risk factors in mCRPC, PSMA PET/CT can be a useful tool for stratifying patients and guide patient's selection for LuPSMA radionuclide treatment. ***References:*** None

OP-980

Circulating androgen receptor gene amplification and resistance to 177Lu-PSMA-617 in patients with metastatic castration-resistant prostate cancer: results of a phase 2 trial

G. Paganelli[1], S. Severi[1], M. Sansovini[1], S. Nicolini[1], I. Grassi[1], F. von Eyben[2], V. Conteduca[1], M. Monti[1], F. Foca[1], G. Gurioli[1], M. Celli[1], F. Matteucci[1], U. De Giorgi[1];
[1]Istituto Scientifico Romagnolo per lo Studio e la Cura dei Tumori, IRST IRCCS, Meldola (FC), ITALY, [2]Center of Tobacco Control Research, Odense M, DENMARK.

Aim/Introduction: Plasma androgen receptor (AR) aberrations have been associated with resistance to hormonal therapy in prostate cancer, however their impact on the prognosis of radio ligand therapy with 177Lu PSMA is unknown. In a phase 2 clinical trial, we aimed to determine if plasma AR

gene status enable early assessment of 177Lu-PSMA-617 activity in metastatic castration-resistant prostate cancer (mCRPC) progressing after standard survival-prolonging treatments. ***Materials and Methods:*** In this open-label, single-arm, phase 2 study mCRPC patients with a positive PSMA PET/CT scan received 3.7-5.5 GBq of 177Lu-PSMA-617 repeated 4-6 times at interval of 8 weeks. We determined AR copy number by droplet digital polymerase chain reaction (ddPCR) on pretreatment plasma samples. Logistic regression was used to estimate the odds ratio (OR) and 95% confidence intervals (95% CI) in order to evaluate the independent relevance of AR status and patients without PSA response (PSA decline >50%) and those with early progressive disease defined as treatment interruption occurring within 4 months of the start of 177Lu-PSMA-617. ***Results:*** Forty-three patients were enrolled, 40 of whom were included in the analysis, 15 (32.5%) with AR gain and 25 (62.5%) with AR normal. A PSA response was reported in 15 (37.5%) of the 40 pts, 3 of 15 (20%) with AR gene gain, and 12 of 25 (48%) with no gain (P = 0.080). Early progressive disease was observed in 17 (42.5%) of the 40 pts, 12 of 15 (80%) with AR gene gain and 5 of 25 (20%) with no gain (P = 0.0002). The OR for patients without PSA response having AR gain was 3.69, 95% confidence interval (0.83-16.36), P = 0.085. The OR for patients with early PD having AR gain was 16.00, 95% confidence interval (3.23-79.27), P = 0.0007. ***Conclusion:*** Plasma AR status assessment using ddPCR identifies mCRPC resistant to 177Lu-PSMA-617. These data suggest potential better activity of 177Lu-PSMA-617 in earlier phases of prostate cancer. ***References:*** None

OP-981

Overall survival after177Lu-PSMA-617 molecular radiotherapy in patients with metastatic castrate-resistant prostate cancer: Post-hoc analysis of a prospective phase II trial

J. Calais[1], W. R. Armstrong[1], J. Gartmann[1], P. Thin[1], K. Nguyen[1], V. Lok[1], L. Gosa[1], R. Slavik[1], M. Dalhbom[1], K. Herrmann[2], M. Eiber[3], W. P. Fendler[4], J. Czernin[1];
[1]UCLA, Los Angeles, CA, UNITED STATES OF AMERICA, [2]University Hospital Essen, Essen, GERMANY, [3]Technical University Munich, Munich, GERMANY, [4]University Clinic Essen, Essen, GERMANY.

Aim/Introduction: This was an open-label randomized prospective bi-centric single-arm phase II clinical trial of 177Lu-PSMA-617 molecular radiotherapy in patients with progressive metastatic castrate-resistant prostate cancer (mCRPC) conducted at University of California Los Angeles (USA) and Excel Diagnostics & Nuclear Oncology Center (Houston, TX, USA) (NCT03042312). The study was investigator-initiated under an investigational new drug approval protocol (IND#133661) with authorization of charging for investigational drug (cost-recovery, Title 21 CFR 312.8). We report here the post-hoc analysis of overall survival (OS) in a single-study site cohort (UCLA). ***Materials and Methods:*** Patients with progressive mCRPC (biochemical, radiographic, or clinical) after ≥1 novel androgen axis drug (NAAD), either chemotherapy (CTX) naïve or post-CTX, with sufficient bone marrow reserve, normal kidney function, and sufficient PSMA-target expression by PET were eligible. Patients received up to 4 cycles of 177Lu-PSMA-617 every 8±1 weeks and were randomized into 2 treatment activities groups (6.0 or 7.4 GBq). Efficacy was defined as serum PSA decline of ≥50% from baseline and served as primary endpoint (hypothesis: ≥40% of responders after 2 cycles). ***Results:*** 43 patients were randomized to the 6.0 GBq (n= 14) and 7.4 GBq (n=29) treatment arms. 11/43 (26%) were CTX naïve while 10/43 (23%), 12/43 (28%), 5/43 (12%) and 5/43 (12%) had received 1, 2, 3 or 4 CTX regimens. Median baseline PSA was 29.2 ng/ml (mean 228.8, range 0.5-2082.6). 21/43 (49%) completed 4 cycles of 177Lu-PSMA-617 whereas 4/43 (9%), 13/43 (30%) and 5/43 (12%) underwent 1, 2 and 3 cycles. PSA decline of ≥50% was observed in 11/43 of patients (26%) after 2 cycles and in 16/43 (37%) at any time (best PSA response). 9/43 (21%) had a PSA decline of ≥90% and 23/43 (53%) had any PSA decline (>0%). After a median follow-up of 19.5 months the median OS was 14.8, 15.7 and 13.5 months in the whole cohort, the 6.0 GBq and 7.4 GBq treatment arms, respectively (p=0.68). Patients showing a PSA decline of ≥50% after 2 cycles and at any time had a longer OS: median 20.1 months vs. 13.6 (p=0.091) and 20.1 vs. 11.6 (p=0.002), respectively. ***Conclusion:*** In this post-hoc analysis of a single-site cohort of 43 patients included in a prospective phase II trial the median OS after 177Lu-PSMA-617 molecular radiotherapy in patients with progressive mCRPC was 14.8 months. There was no difference of efficacy between the 6.0 GBq and 7.4 GBq treatment arms. ***References:*** None

OP-982

[^{177}Lu]Lu-PSMA-617 in low-volume metastatic hormone sensitive prostate cancer: a prospective pilot study

B. Prive[1], *S. M. B. Peters[1], C. H. J. Muselaers[1], P. Zamecnik[1], M. J. R. Janssen[1], T. W. J. Scheenen[1], M. W. Konijnenberg[1], J. Verzijlbergen[1], W. R. Gerritsen[1], N. Mehra[1], D. M. Somford[2], J. A. Van Basten[2], I. M. Van Oort[1], J. Sedelaar[1], J. O. Barentsz[1], S. Heskamp[1], M. Gotthardt[1], J. Witjes[1], J. Nagarajah[1];*
[1]Radboudumc, Nijmegen, NETHERLANDS, [2]Canisius Wilhelmina Hospital, Nijmegen, NETHERLANDS.

Aim/Introduction: To date, [^{177}Lu]Lu-PSMA-617 (Lu-PSMA) is solely used in end-stage high-volume metastasized prostate cancer (PC) with promising efficacy. However, because of high PSMA expression in metastatic hormone-sensitive PCa (mHSPC), Lu-PSMA could also be effective in this patient cohort. Here we present the results of the first prospective study analyzing dosimetry, tolerability and treatment response of Lu-PSMA as a first-line systemic

treatment in oligometastatic mHSPC patients. ***Materials and Methods:*** In this prospective study (NCT03828838), 10 mHSPC patients with a maximum of 10 metastatic lesions on [^{68}Ga]Ga-PSMA PET (PSMA-PET) and serum-PSA doubling time <6 months received two cycles (3+6 GBq) of Lu-PSMA in an 8 week interval. Whole-body SPECT/CT and blood dosimetry was performed (1, 24, 48, 72, and 168 hours p.i.) to calculate the doses to tumor lesions and organs at risk (salivary glands, kidneys, liver and bone marrow). Adverse events (AE), toxicity (hematology, renal/liver functions and PSA) and quality of life were monitored weekly until 12 weeks after cycle two (end of treatment; EOT) and followed up until week 24 after cycle two. All patients underwent PSMA-PET at screening, 8 weeks after cycle one, EOT and 24 weeks after cycle two. ***Results:*** All 10 patients completed the study protocol till EOT. At baseline the median number of metastases was 3 (range 1-10) and PSA level was 1.75 µg/l (0.43-20). According to dosimetry, Lu-PSMA was safe with a mean total dose of 6.34 Gy (2.25-10.77), 7.92 Gy (5.65-10.46), 1.49 Gy (1.11-1.93), 0.16 Gy (0.12-0.21) to salivary glands, kidney, liver and bone marrow, respectively. No grade 3/4 AEs were observed during the study. None of the patients reported xerostomia at EOT. All patients had at least a stabilization of PSA. 5/10 patients had a drop of >50% in PSA. On baseline PSMA-PET, a total of 36 metastases were identified with SUVmax higher (mean 16.1 ±10.7) than liver SUVmean (mean 5.1 ±1.3). In 12 of these 36 metastases, the SUVmax dropped below liver SUVmean, with one patient having complete response. Furthermore, none of the patients showed new metastases on the EOT PSMA-PET. ***Conclusion:*** Lu-PSMA appears to be safe in mHSPC. Even with this relatively low dose of Lu-PSMA, all patients responded by at least stabilizing disease. 5/10 patients showed >50% PSA drop and one patient showed complete remission on PSMA-PET. Based on the results of this study, we initiated a prospective randomized multicenter phase II/III trial in oligometastatic mHSPC. ***References:*** None

OP-983

Extended radioligand therapy with Lu-177-PSMA-617 in patients with advanced metastatic castration-resistant prostate cancer

N. Mader[1], *J. Baumgarten*[1], *D. Gröner*[1], *C. Nguyen Ngoc*[1], *K. Davis*[1], *S. Banek*[2], *N. Tselis*[3], *C. Happel*[1], *F. Grünwald*[1], *A. Sabet*[1]; [1]*Department of Nuclear Medicine, University Hospital Frankfurt, Frankfurt am Main, GERMANY,* [2]*Department of Urology, University Hospital Frankfurt, Frankfurt am Main, GERMANY,* [3]*Department of Radiooncology, University Hospital Frankfurt, Frankfurt am Main, GERMANY.*

Aim/Introduction: Treatment regimens with predefined treatment cycles of Lu-177-PSMA-617 radioligand therapy (RLT) may be suboptimal in patients with more aggressive high tumor load metastatic castration-resistant prostate cancer (mCRPC). We assessed the outcome, toxicity and clinical response in patients receiving extended RLT with a mean cumulative activity of >45 GBq and no other promising treatment alternatives. ***Materials and Methods:*** Eighteen patients with high tumor burden (miTNM classification, PROMISE) and low PSA-doubling time of <2 months were treated with 6.7±1.2 GBq Lu-177-PSMA-617 at 9±8 weeks interval. Treatment was discontinued in case of 1) biochemical progression defined as a rise of >30% in PSA-Level from baseline (PCWG3), 2) progressive disease in routine Ga68-PSMA-11 PET/CT examinations done every 2-3 cycles using mPERSIST criteria, 3) new lesions in intra-therapeutic Lu-177-PSMA-617 scintigrams, 4) the onset of significant renal or hematological toxicity (grade 3/4) using maximal Common Terminology Criteria for Adverse Events (CTCAE v. 5.0), 5) xerostomia (grade 3/4, CTCAE v.5), 6) pain exacerbation, defined as >2 step increase in VAS, or 7) clinical deterioration (ECOG >2). Progression free survival analysis was performed with the Kaplan-Meier curve method. ***Results:*** Patients were treated with 10±2 cycles. Mean cumulative activity was 67.1±14.6 GBq, resulting in a median cumulative renal dose of 31.5±11.3 Gy. Mean eGFR declined from 90.4 ml/min/1.73 m^2 at baseline to 72.4 ml/min/1.73 m^2 after a mean follow-up period of 17±9 months (p=0.003). Moderate renal function reduction (grade 2) was observed in 4 patients (22 %) but no patient developed severe nephrotoxicity (grade 3/4). Significant pancytopenia of grade 3 occurred in 1 patient (6 %) leading to therapy cessation after 7 cycles. Eight patients (44 %) developed xerostomia (grade 1-2) after 5±2 cycles. The median progression free survival (PFS) was 31 months (CI 95 % 14-48). Five out of 7 patients with painful metastases (VAS >5) improved significantly (VAS-reduction >2 steps) throughout the treatment and no patient showed pain progression. Two of three patients starting the treatment with restricted performance status (ECOG 2) at baseline improved to grade 1. ***Conclusion:*** Long progression free survival times and the absence of serious adverse events in this patient group encourage further evaluation of extended radioligand therapy in patients with advanced disease. ***References:*** None

OP-984

Early prostate-specific antigen changes and clinical outcome following ^{177}Lu-PSMA radionuclide treatment in patients with metastatic castration-resistant prostate cancer

A. Gafita[1], *M. M. Heck*[2], *I. Rauscher*[1], *R. Tauber*[2], *C. Franz*[1], *L. Cala*[1], *C. D'Alessandria*[1], *M. Retz*[2], *M. Eiber*[1], *W. A. Weber*[1]; [1]*Department of Nuclear Medicine, Technical University Munich, Munich, GERMANY,* [2]*Department of Urology, Technical University Munich, Munich, GERMANY.*

Aim/Introduction: The availability of multiple new treatments for metastatic castration-resistant prostate cancer (mCRPC)

mandates early treatment switch decisions in the absence of a response. Prostate-specific antigen (PSA) is widely used to monitor treatment response, however, PSA measurements are considered only after 12 wk of treatment. We aimed to evaluate the prognostic value of early PSA changes following ^{177}Lu-labelled prostate specific membrane antigen (LuPSMA) radionuclide treatment in mCRPC patients. ***Materials and Methods:*** Men who were treated under a compassionate access program with LuPSMA at our institution and had available PSA values at baseline, and at 6 wk after treatment initiation were included in this retrospective analysis. Patients were assigned to three groups based on PSA changes: 1) response: ≥30% decline, 2) progression: ≥25% increase and 3) stable: <30% decline and <25% increase. The co-primary endpoints were overall survival and imaging-based progression-free survival. The secondary endpoints were PSA changes at 12 wk after LuPSMA initiation and PSA flare-up. ***Results:*** We identified 124 eligible patients with PSA values at 6 wk, with 115 patients had available PSA levels at both 6 wk and 12 wk time-points. A ≥30% decline in PSA at 6 wk was associated with longer overall survival (median 16.7 mo; 95%CI 14.4-19.0) compared with patients with stable PSA (median: 11.8 mo; 95%CI 8.6-15.1;) and progression (median: 6.5 mo; 95%CI 5.2-7.8; p<0.001). Patients with ≥30% decline in PSA at 6 wk also had a reduced risk of imaging-based progression compared with patients with stable PSA (HR: 0.60; 95%CI 0.38-0.94; p=0.02), while patients with PSA progression had a higher risk of imaging-based progression compared with those showing stable PSA (HR: 3.18; 95%CI 1.95-5.21; p<0.001). The percentage changes of PSA at 6 wk and 12 wk were highly associated (r=0.90; p<0.001). 29 of 31 (94%) patients who experienced early PSA progression at 6 wk achieved biochemical progression also at 12 wk. Overall, only 1 of 36 (3%) patients with PSA progression at 6 wk achieved any PSA decline at 12 wk (1% of the entire cohort). ***Conclusion:*** PSA changes at 6 wk after LuPSMA initiation are an early indicator of long-term clinical outcome. Patients progressing by PSA after 6 wk of treatment could benefit from a very early treatment switch decision. PSA flare-up during LuPSMA treatment is very uncommon. Prospective studies are now warranted to validate our findings and potentially inform clinicians earlier on the effectiveness of LuPSMA. ***References:*** None

OP-985

Risk and Concomitant Factors of Renal Insufficiency throughout Radioligand Treatment with ^{177}Lu-PSMA-617

C. Nguyen Ngoc[1], N. Mader[1], K. Davis[1], D. Groener[1], C. Happel[1], P. Mandel[2], N. Tselis[3], F. Gruenwald[1], A. Sabet[1];
[1]Department of Nuclear Medicine, University Hospital Frankfurt, Frankfurt am Main, GERMANY, [2]Department of Uology, University Hospital Frankfurt, Frankfurt am Main, GERMANY, [3]Department of Radiooncology, University Hospital Frankfurt, Frankfurt am Main, GERMANY.

Aim/Introduction: Kidneys are exposed to continuous low dose radiation during radioligand therapy with ^{177}Lu-PSMA-617 (Lu-RLT) due to excretion of the ligand and specific binding. This may result in glomerular damage and gradual renal function loss. This study is to define the extent and potential risk factors of renal impairment in patients with metastatic castration-resistant prostate cancer (mCRPC) undergoing Lu-RLT using serial eGFR measurements driven from serum creatinine levels. ***Materials and Methods:*** 105 patients received 4 ± 1 cycles of Lu-RLT with 6.5 ± 1.4 GBq ^{177}Lu per cycle, resulting in a mean cumulative activity of 27 ± 13 GBq and a total renal radiation dose of 13 ± 8 Gy. eGFR was measured for a median of 6 ± 4 times per patient. Yearly change in eGFR was calculated using linear curve fit. Common Terminology Criteria for Adverse Events (CTCAE) v5.0 was used to classify renal toxicity. Correlation of eGFR reduction and potential risk factors like renal impairment prior to Lu-RLT, diabetes mellitus, hypertension, previous chemotherapy and cumulated administered dose was assessed using nonparametric testing. ***Results:*** Alterations in eGFR differed widely among the patients during the follow-up period of 13 ± 9 months. 57 patients (54 %) experienced a mild (2-10 ml/min/m^2 per year) and 35 patients (33 %) a significant (> 10 ml/min/m^2 per year) decline of eGFR. In 18 patients, on the other hand, eGFR increased > 10 ml/min/m^2 per year. Mean eGFR of the cohort decreased 4.5 ± 26 ml/min/m^2 per year from 83 ± 19 ml/min/m^2 at baseline to 72 ± 21 ml/min/m^2. 58 patients showed renal impairment of grade I (n=30) or II (n=28) subsequent to the treatment. 3 patients developed postrenal (sub)acute kidney injury and significant renal function loss (grade 3) due to progressive bladder infiltration and subsequent ureteral stenosis. No radiation induced nephrotoxicity of grade 3/4 was observed. However, cumulated renal dose was significantly correlated with renal function decline per year (p < 0.01). No other parameter including previous chemotherapy affected renal function (p > 0.05). ***Conclusion:*** Slight reduction in renal function may be expected in patients undergoing radioligand therapy with ^{177}Lu-PSMA-617 and correlates with cumulative doses. Acute kidney injury was observed only in a small number of cases with subrenal obstruction. ***References:*** None

OP-986

Tracer kinetics in the dual time-point ^{177}Lu-PSMA post-therapy SPECT/CT scan predicts treatment outcome in prostate cancer patients

F. Fiz[1], H. Dittmann[2], M. Straub[3], C. la Fougère[2];
[1]Humanitas Clinical and Research Center - IRCCS, Milan, ITALY, [2]Nuclear Medicine Unit, Department of Radiology, University of Tübingen, Tübingen, GERMANY, [3]University of Tübingen, Tübingen, GERMANY.

Aim/Introduction: ^{177}Lu-PSMA is a promising, radionuclide therapy in metastasized castration-resistant prostate cancer (mCRPC), as it can induce a PSA and clinical response in most cases. However, some patients do not respond and progress quickly in course of the ^{177}Lu-PSMA cycles, independently from the pre-therapeutic PSMA uptake on PET/CT. Kinetics of tracer uptake/elimination might indeed influence the absorbed dose.In this study, we investigated whether tracer kinetic inside the metastatic lesions is associated with the therapy outcome. ***Materials and Methods:*** 91 mCRPC patients were retrospectively enrolled. Every patient underwent at least two 177Lu-PSMA cycles. Mean SUV on a representative lesion was calculated on the pre-therapy PSMA-PET/CT, using an isocontour method. Each patient then underwent two consecutive SPECT/CT scans the first and the second day after each 177Lu-PSMA administration. The target-to-background ratio (TBR) of the same representative lesion was calculated on each SPECT/CT. Patients presenting at least a 50% PSA-drop after two 177Lu-PSMA cycles were classified as responders. ***Results:*** Fifty-five patients (59%) were classified as responders. In these patients, mean TBR increased by 34±19% from the first to the second SPECT/CT. Conversely, non-responders showed a significantly smaller mean TBR increase (5±9%, p=0,016). Mean TBR increase showed a direct correlation with PSA decrease after two 177Lu-PSMA cycles (R=0,63; p<0,001).Mean SUV, mean starting PSA, and absolute TBR were not significantly different between responders and non-responders. ***Conclusion:*** Effectiveness of the 177Lu-PSMA seems to be related to the tracer residence time, rather than to the absolute uptake value. Increasing uptake values between the first and the second day after the 177Lu-PSMA administration could be compatible with a longer biological half-life of the radiopharmaceutical within the lesions, possibly purporting a higher dose to the tumour. ***References:*** None

OP-987

Efficacy and safety of ^{177}Lu-PSMA radionuclide treatment in patients with diffuse bone marrow involvement: a multicenter retrospective study

A. Gafita[1], *W. P. Fendler*[2], *H. Wang*[3], *S. Sandhu*[4], *M. Weber*[2], *R. Esfandiari*[5], *J. Calais*[1], *I. Rauscher*[3], *H. Rathke*[6], *R. Tauber*[3], *E. S. Delpassand*[5], *W. Weber*[3], *K. Herrmann*[2], *J. Czernin*[1], *M. Eiber*[3], *M. S. Hofman*[4], *LuPSMA;*

[1]UCLA, Los Angeles, CA, UNITED STATES OF AMERICA, [2]University of Duisburg-Essen, Essen, GERMANY, [3]Technical University Munich, Munich, GERMANY, [4]Peter MacCallum Cancer Center, Melbourne, AUSTRALIA, [5]Excel Diagnostics, Houston, TX, UNITED STATES OF AMERICA, [6]University of Heidelberg, Heidelberg, GERMANY.

Aim/Introduction: 177 Lu-labelled prostate-specific membrane antigen (LuPSMA) radionuclide therapy for metastatic castration-resistant prostate cancer is under investigation in a Phase III trial (VISION: NCT03511664). However, patients with diffuse bone involvement, diagnosed with a superscan by bone scintigraphy at baseline, were excluded due to lack of efficacy and safety data. We therefore aimed to investigate the feasibility of LuPSMA in patients with diffuse bone marrow involvement on baseline PSMA-targeted PET. ***Materials and Methods:*** The primary end points were PSA response (PCWG3), hematologic safety profile (CTCAE), and overall survival. Secondary end points of quality of life (assessed with Brief Pain Inventory-Short Form questionnaires), and radiological response (RECIST) were assessed. ***Results:*** Through retrospective screening of databases, we identified 43 eligible patients across four centers worldwide who received 154 cycles of LuPSMA under clinical trials or compassionate access programs. Median baseline PSA was 1000 (IQR 431-2151) ng/ml. PSA decline of at least 50% at 12 weeks was achieved in 22 (58%) patients, while median time to pain progression was 8.3 (95%CI 4.1-12.6) months. Median overall survival was 11.6 (95%CI 8.8-14.3) months. Objective response in nodal or visceral disease was reported in seven (39%) of 18 patients with RECIST measurable disease. Grade 3 anemia, thrombocytopenia and neutropenia occurred in nine (22%), seven (17%) and three (8%) patients, respectively. Grade 4 thrombocytopenia was noticed in three (8%) patients. ***Conclusion:*** Patients with diffuse bone marrow involvement demonstrated similar LuPSMA efficacy and safety compared to Phase II evidence. Acceptable safety outcomes do not support exclusion of patients with a superscan from future LuPSMA treatment protocols. ***References:*** None

OP-988

Intermittent radioligand therapy with Lu-177-PSMA-617 in metastatic castration-resistant prostate cancer patients with favorable characteristics and early response

N. Mader[1], *C. Nguyen Ngoc*[1], *J. Baumgarten*[1], *D. Gröner*[1], *K. Davis*[1], *J. Wichert*[1], *N. Tselis*[2], *P. Mandel*[3], *F. Grünwald*[1], *A. Sabet*[1];

[1]Department of Nuclear Medicine, University Hospital Frankfurt, Frankfurt am Main, GERMANY, [2]Department of Radiooncology, University Hospital Frankfurt, Frankfurt am Main, GERMANY, [3]Department of Urology, University Hospital Frankfurt, Frankfurt am Main, GERMANY.

Aim/Introduction: Various treatment regimens have been recommended for radioligand therapy (RLT) with Lu-177-PSMA-617 in metastatic castration-resistant prostate cancer (mCRPC). Extending the time to maximal renal absorbed dose is highly desirable in patients with more favorable tumor biology, and longer life expectancy. Therefore, we assessed the feasibility of intermittent RLT in patients with an early initial response achieving a low tumor burden during the first three treatment cycles. ***Materials and Methods:*** RLT was discontinued in 15 responding patients with a PSA doubling time ≥3 months, achieving low tumor load after

only 2±1 cycles RLT with 6.6±3.8 GBq Lu-177-PSMA-617 per cycle. Treatment was initiated upon progression, consisting of 2±1 more cycles with 6.6±3.8 GBq each. The mean cumulative activity was 29.4±18.4 GBq. Treatment response was evaluated using PSA sampling according to Prostate Cancer Working Group 3 criteria (PCWG3) and ^{68}Ga-PSMA-PET/CT imaging using mPERCIST criteria. Tumor load was identified as low based on miTNM classification, PROMISE. Complete blood count and estimated glomerular filtration rate (eGFR) were measured at baseline, during treatment course and follow-up period. Toxicity was classified using Common Terminology Criteria for Adverse Events (CTCAE v. 5.0). Kaplan-Meier curve method was used for survival analysis. ***Results:*** Re-initiation of RLT with Lu-177-PSMA-617 resulted in partial response in 5 patients (33 %), stable disease in 3 patients (20 %) and progressive disease in 7 (47 %). Median progression free survival (PFS) was 10±3 months after initial treatment and 7±2 after re-initiation. The cumulative renal absorbed dose during the treatment period of 18±7 months was 13.3±8.5 Gy. No patient developed significant renal function loss or bone marrow dysfunction (CTC grade III/IV). ***Conclusion:*** Intermittent radioligand therapy with Lu-177-PSMA-617 seems not to comprise the outcome of early responders with low PSA doubling time and tumor load. This treatment regime may be worth considering to prolong the time to maximal cumulative renal absorbed dose enabling further treatment cycles in patients with longer life expectancy. ***References:*** None

OP-989

Efficacy of Lu-177-PSMA-617 Therapy in Metastatic Castration-resistant Prostate Cancer Patients, A Single-Center Experience

T. Telli*, M. Tuncel, M. Caglar;*
Hacettepe University Faculty of Medicine, Ankara, TURKEY.

Aim/Introduction: Lu-177 labeled prostate-specific membrane antigen(PSMA) radioligand therapy is an emerging treatment in metastatic castration-resistant prostate cancer(mCRPC). The study aims to share our experience on clinical, biochemical, and PET response rates of the mCRPC patients treated with at least two cycles of Lu-177-PSMA-617 therapy. ***Materials and Methods:*** The study included 52 patients(median age: 70,5(range:56-86)) with mCRPC who received Lu-177-PSMA-617 treatment. Serum PSA levels were regularly monitored 2-weekly during the therapy and three months after completion of the therapy. Biochemical responses were evaluated according to the Prostate Cancer Clinical Trial Working Group3(PCWG3). For subjective responses, the patients were clinically followed for ECOG and Karnofsky performance scores(PS), the visual analog scale(VAS) for pain. The patients were evaluated with Ga-68-PSMA PET/CT 6-8 weeks after the second therapy and 8-12 weeks after completion of the therapy to four. PET responses were categorized according to EORTC Response Criteria. ***Results:*** The patients received 163 cycles of Lu-177-PSMA-617(median cumulative dose: 21,09 GBq, range 13,5-44,4 GBq, 24/52(46,2%) two cycles; 7/52(13,5%) three cycles; 15/52(28,8%) four cycles; 2/52(3,8%) five cycles; 4/52(7,7%) six cycles). Any PSA decline was seen in 44 patients (84,6%). Maximum PSA response rates were as follows: ≥%90 decrease in 11(21,2%), ≥%50 decrease in 31(59,7%), ≥%30 decrease in 37(71,1%) patients. Eight patients(15,4%) showed PSA progression despite the therapy. PSA response rates three months after completion of the therapy(PCWG3 criteria) were as follows: ≥%90 decrease in 7(13,7%), ≥%50 decrease in 25(49%), ≥%30 decrease in 26(51%) patients. Four patients (7,8%) had biochemical stable disease (SD), while 21 patients(41,2%) had progressive disease (PD). Eleven(21,2%) patients showed at least one score improvement in ECOG PS, and 15/52(28,8%) patients showed improvement at least 10 scores in Karnofsky PS after Lu-177-PSMA therapy. Among the patients with bone metastases and baseline pain score(VAS) ≥2, 19/36(52,7%) of the patients showed two points or more improvement(or ≥30%) in VAS. There was a significant difference between pre and post-therapy mean VASs(4,1±2,35 and 2,8±2,4, p: 0,03). 5/16 patients with a regular need for non-opioid-analgesics and 2/9 patients with a regular need for opioids before Lu-177-PSMA therapy, no longer needed any analgesic after Lu-177-PSMA therapy. During the follow-up (median:10,93 months), 24/52(46,2%) patients died. Estimated median overall survival was 17 months(95% CI:15,4-18,6) and median progression-free survival was 6,7 months(95% CI:3,65-9,8). ***Conclusion:*** Lu-177-PSMA therapy is a promising therapy option for mCRPC patients in terms of both objective responses and pain palliation. ***References:*** None

OP-990

The efficacy of Lu177-PSMA treatment at chemotherapy-naive metastatic prostate cancer

F. Beytur[1]*, S. Sager*[1]*, S. Bilgic*[1]*, A. Nazari*[1]*, L. Uslu-Besli*[1]*, S. Asa*[1]*, H. B. Sayman*[1]*, D. Tural*[2]*, C. Demirdağ*[3]*, K. Sonmezoglu*[1]*;*
[1]Cerrahpasa Faculty of Medicine, Nuclear Medicine Department, Istanbul, TURKEY, [2]Bakirköy Sadi Konuk Teaching Hospital, Medical Oncology Division, Istanbul, TURKEY, [3]Cerrahpasa Faculty of Medicine, Urology Department, Istanbul, TURKEY.

Aim/Introduction: Hematotoxicity is one of the most serious side effects and also a limiting factor of Lu177-PSMA treatment in prostate cancer patients and it is seen more often in the patients who were treated with taxane-based chemotherapy regimes previously. In this retrospective study, we aimed to evaluate the efficacy and hematotoxicity of Lu177-PSMA therapy in chemotherapy-naive patients with metastatic prostate cancer. ***Materials***

and Methods: Retrospectively, we recruited 12 patients with a diagnosis of metastatic prostate cancer who received Lu-177 PSMA-617 treatment without a previous taxane-based chemotherapy between December 2015 and September 2019. All patients had pretreatment serum PSA measurements and Ga-68 PSMA PET/CT or PET/MR imaging. Mean pretreatment age was 71.33±11.0 (ranged 59-86). Efficacy of the treatment was assessed with serum PSA levels, clinical performance, and Ga68-PSMA PET imaging as well. ***Results:*** Patients received a median of 3.5 cycles (ranged 1-8) of Lu177-PSMA with an average dose of 6.98 GBq per cycle and a mean total administered activity of 23.85 GBq (ranged 7.4-65). According to the PROMISE criteria[1], the patients were categorized according to their pretreatment Ga68-PSMA PET imaging findings and there were 3 patients (25%) as miN2, 1 patient (8.3%) as miM1a, 1 patient (8.3%) as miM1b(oligo), 2 patients (16.7%) as miM1b(diss), 1 patient (8.3%) as miM1b(dmi), and 4 patients (33.3%) as miM1c. In this study, we grouped miM1b(diss) and prior stages as early-stage and miM1b(dmi) and miM1c stages as advanced-stage. Early-stage group consists of 7 patients and advanced-stage group consists of 5 patients. The median overall survival was 35.0 (ranged 4.7-49.5) months at early-stage group and 2.8 months (ranged 1.2-14.5) at advanced-stage group after emerging of Lu177-PSMA treatment. Grade 3-4 nephrotoxicity developed only in 2 patients (16.7%) and grade 3-4 hematotoxicity was not observed in any patient. In 4 patients (33.3%), PSA levels decreased >50% from baseline, but elevated in 8 patients (67.7%). Post-treatment Ga-68 PET scans revealed a regression in 4 patients (33.3%), and progression in 8 patients (67.7%). Only 5 patients (41.7%) described a symptomatic relief due to the treatment. ***Conclusion:*** Our preliminary data suggests that Lu177-PSMA treatment is useful and could be an alternative to taxane-based chemotherapy in early-stage prostate cancer with less severe side effects. However, it has not got a considerable positive impact on survival in advanced-stage disease. ***References:*** 1. Eiber, M., et al. (2018). "Prostate Cancer Molecular Imaging Standardized Evaluation (PROMISE): Proposed miTNM Classification for the Interpretation of PSMA-Ligand PET/CT."

1709

TROP Session: Novel Molecular Brain Imaging Approaches

Friday, October 30, 2020, 15:30 - 17:00 Channel 9

OP-991

A Positron Emission Tomography (PET) Study to Examine the Brain Binding of[^{11}C]-PXT012253 in Healthy Subjects

P. Stenkrona[1], *R. Arakawa*[1], *H. Holst*[2], *S. Nag*[1], *M. Mahdi Moein*[1], *Z. Jia*[1], *C. Halldin*[1], *A. Varrone*[1];
[1]*Karolinska Institutet, Stockholm, SWEDEN,*
[2]*H. Lundbeck A/S, Valby, DENMARK.*

Aim/Introduction: The metabotropic glutamate receptor 4 (mGlu4) has been proposed as a target for Parkinson's disease (1). [^{11}C]PXT012253 is a PET radioligand for mGlu4 (3.4 nM), previously characterized in non-human primates (2). This study evaluated the quantification and replicability of [^{11}C]PXT012253 binding in healthy subjects. ***Materials and Methods:*** Two 93-min PET measurements with [^{11}C]PXT012253 on the same day using an HRRT system were planned for 6-10 subjects. Metabolite corrected input function was measured. Regions of interests delineated using the Anatomical Automatic Labeling template on co-registered MRI. The regions with the highest binding was identified using quantification by kinetic analysis using 1-tissue (1T) and two-tissue (2T) compartment modeling (CM), Logan graphical analysis (GA) and Multilinear analysis (MA1). The outcome measure was the total distribution volumes (VT). Test-retest metrics were absolute variability (AbsVar, %) and intraclass correlation coefficient (ICC). ***Results:*** Six subjects (4 females, age 23±3.5y, weight 66±14kg) completed the study (373±77MBq, 1090±416GBq/μmol, 0.11± 0.4 μg). [^{11}C]PXT012253 displayed high uptake (peak SUV whole brain 4.7±0.9 kg/ml) at about 5 min, and a rapid wash-out. There was 10-20% of unchanged [^{11}C]PXT012253 in plasma at 20 min. The parent fraction curve was extrapolated by 3-exp fitting from 45-60 min and onwards. VT in subcortical regions (2TC: pons: 6.1±1.0, thalamus: 5.5±0.9, putamen: 5.3±1.1) was higher than in cortical regions (frontal-cortex: 4.0±0.8, cerebellum: 3.6±0.6), consistent with the known distribution of mGlu4. 2TC provided better fits than 1TC (Akaike information criterion 16 vs 85, model selection criterion 4.6 vs 2.7). VT by Logan GA and MA1 analysis were highly correlated with VT (Logan GA:y=0.97x+0.36, R2=0.95; MA1:y=0.96x+0.36, R2=0.95). MA1 showed better identifiability as smaller standard error than Logan GA (1.2 vs 1.7). Test-retest metrics were good for all models and regions (AbsVar 2TC: pons: 3.3±2.6%, thalamus: 2.8±1.7%, putamen: 4.2±5.5%, frontal-cortex: 6.4±5.3%, cerebellum: 8.0±5.8%), (ICC 2TC: (95% CI): thalamus 0.98 (-0.87,1.0), putamen 0,93 (-0.56,0.99), frontal-cortex 0.95 (-0.67,0.99), cerebellum 0.83 (-0.27,0.97), pons 0.97 (-0.78,1.0)). Time stability analysis showed that VT values estimated using 63 minutes of imaging were within 10% of the values obtained with 93 minutes. ***Conclusion:*** [^{11}C]PXT012253 showed high brain uptake and rapid washout. VT was reliably estimated using 2TC, Logan GA and MA1. The test-retest metrics in pons, putamen and thalamus showed AbsVar lower than 7% and ICC higher than 0.93, indicating replicability. [^{11}C]PXT012253 is a suitable PET radioligand for mGlu4 in humans. ***References:*** 1. Charvin D. Mov Disord. 2018;33:1619-16312. Takano A. Mol Imaging

Biol. 2019;21:500-508

OP-992

First-in-human PET imaging and dosimetery of [^{11}C] NOP46, a novel visualization agent of protein kinase G (PKG) pathway activation

M. Doubrovin[1], J. Kim[1], S. Oya[1], J. Castrillon[1], S. Deng[1], P. Zanzonico[2], M. Soffing[1], A. Molotkov[1], P. Carberry[1], D. Landry[1], A. Mintz[1];
[1]Columbia University H. Irving Medical Center, New York, NY, UNITED STATES OF AMERICA, [2]Memorial Sloan-Kettering Cancer Center, New York, NY, UNITED STATES OF AMERICA.

Aim/Introduction: Protein kinase G-1α (PKG) activation controls long-term hyper-excitability (LTH) of the primary sensory neurons and has been shown to contribute to chronic pain. It is also associated with the pathogenesis of several malignancies, including in the breast, stomach and pancreas. The NOP46 protein kinase inhibitor was developed to have over 3-log higher specificity to PKG pathway compared to other PKs. We initiated a first in human clinical trial [^{11}C]NOP46 to visualize PKG related biological processes. Our objective is to establish human dosimetry to enable further clinical trial in subjects afflicted with diseases affected by the PKG pathway. ***Materials and Methods:*** The dosimetry and initial pharmacokinetic assessment was performed in four informed and consented healthy volunteers according to the IRB-approved protocol. The whole-body [^{11}C]NOP46 PET/CT was acquired in a dynamic mode over approximately 90 minutes following the radiotracer injection (6.2-9.8 mCi). The radiotracer uptake data analysis was performed on PMOD software generating residence times for individual organs and tissues. The dosimetry calculations were performed using OLINDA 1.1. Serum samples harvested from the patients were used to assess the [^{11}C]NOP46 stability. ***Results:*** The [^{11}C]NOP46 administration for PET was well tolerated and was estimated to deliver Effective Dose Equivalent (EDE) 2.8 +/-0.5 mSv or Effective Dose (ED) of 1.7+/-0.8 mSv, which represented EDE 12.3 +/- 2.4 microSv/MBq or ED 7.4 +/- 3.8 microSv/MBq. With predominantly hepatic clearance of the radiotracer, the critical organ was identified as a gall-bladder, which accumulating up to EDE 0.44+/-0.25 mSv. Appearance of [^{11}C]NOP46 degradation metabolites were identified around 30 minutes. ***Conclusion:*** Dosimetry evaluation of the first 4 human subjects with [^{11}C]NOP46 PET/CT demonstrated safety of the radiotracer for the human subjects. In future studies, we will assess [^{11}C] NOP46 PET/CT accumulation in chronic pain and tumors with activated PKG. ***References:*** Support: Study was sponsored by Medtech Innovation. The PET Center early drug development program is supported by the Columbia Dept. of Radiology and Irving Institute CTSA Translational Therapeutics Accelerator (UL1TR001873).

OP-993

Functional Dynamics of Dopamine Synthesis During Reward Processing

A. Hahn[1], M. B. Reed[1], V. Pichler[2], P. Michenthaler[1], L. Rischka[1], G. M. Godbersen[1], W. Wadsak[2,3], M. Hacker[2], R. Lanzenberger[1];
[1]Department of Psychiatry and Psychotherapy, Medical University of Vienna, Vienna, AUSTRIA, [2]Department of Biomedical Imaging and Image-guided Therapy, Division of Nuclear Medicine, Medical University of Vienna, Vienna, AUSTRIA, [3]Center for Biomarker Research in Medicine (CBmed), Graz, AUSTRIA.

Aim/Introduction: Although the competition model enables the assessment of dopamine release, cognitive paradigms only elicit 5-15% signal change and comparison with a control condition requires several PET measurements. We introduce a novel approach to assess rapid changes in dopamine neurotransmission during task performance in a single PET scan. The technique combines functional PET (fPET) [1] and 6-[^{18}F]FDOPA imaging by exploiting the dynamic regulation of dopamine synthesis. Specifically, dopamine synthesis is activated by neuronal firing to refill the synaptic vesicles [2,3] and is also increased by the dopamine releasing agent amphetamine [4]. ***Materials and Methods:*** Dopamine synthesis was obtained in 16 healthy participants (24.8±4.8 years, 7 female) using 6-[^{18}F]FDOPA fPET (injected dose=5.5 MBq/kg as bolus+infusion, 70x43 s frames). During the scan the monetary incentive delay (MID) task was carried out with separate evaluation of monetary gain and loss (4x5 min task blocks). Task effects were obtained by the general linear model [1] and dopamine synthesis was quantified with the Gjedde-Patlak plot. For comparison, BOLD fMRI was obtained in the same subjects (3T, TE/TR=30/2050 ms). ***Results:*** Compared to baseline, dopamine synthesis rates in the nucleus accumbens of men increased by 77.6±32.9% during monetary gain and 49.4±26.7% for loss (p&lt0.001). These task-specific effects were reversed in women with higher dopamine synthesis during loss (78.4±18.6%) than gain (51.2±16.5%, p&lt0.001), leading to a significant sex difference for gain vs. loss (p&lt0.01). Task changes in dopamine synthesis were further correlated with behavioral metrics of reward sensitivity in men (rho=-0.7, p<0.05) and punishment sensitivity in women (rho=0.89, p&lt0.01). Although robust activation of the nucleus accumbens for gain vs. loss was also obtained with fMRI (p&lt0.001), this was not different between men and women (p=0.4). ***Conclusion:*** Assessment of functional dynamics in dopamine neurotransmission with 6-[^{18}F]FDOPA fPET is highly sensitive and specific to task stimulation, enabling direct investigation of dopamine action during numerous cognitive and emotional processes. Our findings provide a biological rationale for well-known behavioral sex differences in reward and punishment processing, which is usually not observed in fMRI-based neuronal activation [5]. This may have important implications in several psychiatric

conditions with sex-specific prevalence rates, altered reward processing and dopamine signaling. ***References:*** [1] Rischka et al., NeuroImage 181: 323-330 (2018).[2] Morgenroth et al., PNAS 71: 4283-4287 (1974).[3] Neff et al., Prog Brain Res 106: 91-97 (1995).[4] Kehr et al., J Neural Transm 40: 129-147 (1977).[5] Oldham et al., Hum Brain Mapping 39: 3398-3418 (2018).

OP-994

Assessment ofα4(α6)β2* nicotinic acetylcholine receptor (nAChR) availability before and after rewarding food-cue stimulation in human obesity and normal-weight controls

S. Hesse[1,2], M. Rullmann[1,2], J. Luthardt[1], E. Schweickert-de Palma[2], T. Günnewig[2], G. A. Becker[1], F. Zientek[1,2], T. Jochimsen[1], A. Landsmann[2], S. Martin[2], P. M. Meyer[1], M. Patt[1], J. Neumann[2,3,4], P. Brust[5], M. Blüher[6,7], A. Hilbert[2,8], O. Sabri[1];
[1]University of Leipzig, Department of Nuclear Medicine, Leipzig, GERMANY, [2]University of Leipzig, Integrated Research and Treatment Center (IFB) AdiposityDiseases, Leipzig, GERMANY, [3]Ernst-Abbe-Hochschule, University of Applied Sciences, Department of Medical Engineering and Biotechnology, Jena, GERMANY, [4]Max Planck Institute for Human Cognitive and Brain Sciences, Department of Neurology, Leipzig, GERMANY, [5]Helmholtz-Zentrum Dresden-Rossendorf, Department of Neuroradiopharmaceuticals, Leipzig, GERMANY, [6]Helmholtz Zentrum München, Helmholtz Institute for Metabolic, Obesity and Vascular Research (HI-MAG), Leipzig, GERMANY, [7]University of Leipzig, Department of Internal Medicine, Leipzig, GERMANY, [8]University of Leipzig, Department of Psychosomatic Medicine and Psychotherapy, Leipzig, GERMANY.

Aim/Introduction: Cholinergic modulation of brain reward and attentional networks appears to play a crucial role in information processing about salience as a key biological mechanism in obesity (OB). Changes in acetylcholine (Ach) transmission, however, that are associated with abnormal eating behavior have not been demonstrated in vivo in human OB so far. We investigated the α4(α6)β2*-nAChRs availability by applying simultaneous PET-MRI and (-)-[^{18}F] flubatine in individuals with OB and normal-weight controls (NW) at rest and in response to salient food cues (stim). ***Materials and Methods:*** Thirty-one individuals with OB (n=15; 10♀ ; age 38±14 yrs; BMI 38±3 kg/m2) and NW (n=16; 13♀ ; 27±7 yrs; BMI 22±2 kg/m2) underwent simultaneous PET-MRI with (-)-[^{18}F]flubatine twice on separate days (rest and stim) using a bolus-infusion protocol (294±7 MBq) with list-mode acquisition 0-60 min and 120-165 min p.i. paralleled by anatomical MPRAGE and functional EPI sequences. Total distribution volumes VT (mL/cm3) were estimated as the ratio between mean (–)-[^{18}F]flubatine activity in tissue between 120 and 165 min and free parent (–)-[^{18}F]flubatine in plasma obtained from venous blood. Food pictures (stim) were shown 120-135 min p.i.. Disinhibited eating behaviour was assessed by using the German version of the Three-Factor Eating Questionnaire (TFEQ). High TFEQ score indicates high disinhibition (cut-off 7 according to Niemeyer et al., 2012). ***Results:*** VT_{stim} was significantly higher in OB compared with NW in the thalamus, in particular in those with high TFEQ disinhibition (left: 30.7±4.5 vs. 25.6±3.3, p=0.01; right: 29.5±4.4 vs. 25.4±3.3, p=0.03) while VT_{rest} in the ventral tegmental area and in the nucleus basalis Meynert tend lower in OB compared with NW (e.g. left: 16.4±2.2 vs. 17.5±2.3; p=0.1 and 11.7±2.0 vs. 10.3±1.8, p=0.08). VT_{stim} values compared with VT_{rest} appear only to increase in OB with high TFEQ disinhibition in the thalamus and the mesolimbic system (without reaching significance yet) but not in NW and in OB with low TFEQ disinhibition. ***Conclusion:*** Compared with NW and low-disinhibited eaters with OB, α4(α6)β2*-nAChR availability of high-disinhibited eaters with OB seems to be altered in the thalamus, the mesolimbic system and in the basal forebrain. Whether these changes are associated with an attentional bias towards incentive food cues in high-disinhibited eaters and changes in large-scale networks as markers for differences in eating traits is currently under investigation. ***References:*** Niemeier HM, Leahey T, Palm Reed K, et al. An acceptance-based behavioral intervention for weight loss: a pilot study. Behav Ther 2012; 43: 427-435.

OP-995

Brain metabolism and related connectivity after EMDR in PTSD of military veterans: a ^{18}F-FDG PET study sensitized by virtual reality exposure to war scenes

A. Verger[1], P. Rousseau[2], E. Malbos[3], M. Chawki[1], F. Nicolas[4], C. Lancon[3], S. Khalfa[2], E. Guedj[5];
[1]Department of Nuclear Medicine and Nancyclotep Imaging Platform, CHRU Nancy, Nancy, FRANCE, [2]Laboratoire de Neurosciences Sensorielles et Cognitives, Marseille, FRANCE, [3]Department of Psychiatry, La Conception University Hospital, Marseille, FRANCE, [4]Department of Psychiatry, Hôpital d'Instruction des Armées Sainte-Anne, Toulon, FRANCE, [5]Department of Nuclear Medicine, Assistance Publique Hôpitaux de Marseille, Timone University Hospital, Marseille, FRANCE.

Aim/Introduction: The prevalence of posttraumatic stress disorder (PTSD) is high among military veterans, and can lead to disastrous consequences such as suicide. Eye Movement Desensitization and Reprocessing (EMDR) is recommended in first-line psychotherapies for PTSD. The objective of this study is to identify, after EMDR therapy, the metabolic and related connectivity changes in military veterans suffering from PTSD. ***Materials and Methods:*** Fifteen military veterans with PTSD performed a brain ^{18}F-FDG-PET sensitized by virtual reality exposure to war scenes, before and after EMDR treatment. Statistical parametric mapping (SPM) was used to compare brain metabolism before and after treatment, to evaluate connectivity of previously

identified areas (through inter-regional correlation analysis), and to study correlations between metabolism and evolution scores on PTSD clinical scales (PTSD Checklist Scale, PCLS; Clinician Administered PTSD Scale, CAPS). ***Results:*** After EMDR therapy, the metabolic activity of the precuneus was increased, and a decrease of metabolic connectivity was observed between this area and two bilateral clusters of the cerebellum (bilateral Crus I and VI cerebellar lobules, p<0.005 for the voxel, k>180). Moreover, the metabolic values of precuneus were associated before and after therapy with respectively the PCLS scale (r=-0.667 and p=0.006) and the CAPS scale (r=-0.73 and p<0.001) after EMDR. Furthermore, higher cerebellar metabolism before treatment was associated with reduced clinical PTSD scores after EMDR (p=0.03). ***Conclusion:*** The precuneus metabolism and its related connectivity with the posterior cerebellum upon VR stress exposure are correlated and predictive of the clinical improvement after EMDR in military patients with PTSD. ***References:*** None

OP-996

Can ^{18}F-FDG PET be used as a surrogate marker in autoimmune encephalitis?

S. ArunRaj[1], *D. Khan*[1], *K. Ihtisham*[2], *M. Tripathi*[2], *A. Garg*[3], *A. Kumar*[1], *D. Yadav*[1], *M. Tripathi*[1], *C. Bal*[1];
[1]*Department of Nuclear Medicine, All India Institute of Medical Sciences, New Delhi, INDIA,* [2]*Department of Neurology, All India Institute of Medical Sciences, New Delhi, INDIA,* [3]*Department of Neuroradiology, All India Institute of Medical Sciences, New Delhi, INDIA.*

Aim/Introduction: Autoimmune encephalitis (AIE) is an immune-mediated, paraneoplastic or non-paraneoplastic process of the central nervous system. Initial diagnosis is based on the clinical presentation as well as antibody profiles and MRI findings. Timely diagnosis is essential for initiation of appropriate therapy, response to which is usually good in non-paraneoplastic AIE. Though the utility of ^{18}F-FDG PET has been suggested in limbic encephalitis when MRI findings are normal it has not been included in the diagnostic algorithm of AIE.[1] This study investigates the combined potential of ^{18}F-FDG-PET and MRI in AIE. ***Materials and Methods:*** This was a retrospective analysis in 60 patients diagnosed and treated for AIE, 40 were antibody negative and 20 antibody positive. Patient inclusion was based on the clinical diagnosis of AIE and whether both MRI and PET had been done. All patients had undergone a dedicated brain and whole body ^{18}F-FDG PET/CT in the department of Nuclear Medicine. MRI had been done in a separate setting on a dedicated MRI scanner. The PET and MRI dataset was independently reviewed by a nuclear medicine physician and neuroradiologist. ***Results:*** In the antibody negative group (40 patients) MRI was positive in 23 and FDG PET in 20. Both MRI and PET were positive in 12, MRI was positive but PET negative in 11 while MRI was negative and PET positive in 8. Thus when both PET and MRI were combined the detection rate for AIE was 77 % (31/40). In the antibody positive group (20 patients), MRI was positive in 7, PET was positive in 9. Both MRI and PET were positive in 4, MRI was positive and PET negative in 3 while MRI was negative and PET positive in 5. Thus the correct identification of AIE by both combined was 60% (12/20). Based on combined PET and MRI findings 43/60 (71 %) patients were found to show morphologic and functional changes indicative of AIE. ***Conclusion:*** MRI findings play an important role in the diagnostic criteria for AIE. Neverthless the inclusion of functional information from PET along with MRI findings has definite potential to improve the imaging diagnosis of AIE. ***References:*** 1. Graus F, Titulaer MJ, Balu R, Benseler S, Bien CG, Cellucci T, et al. Clinical approach to diagnosis of autoimmune encephalitis. Lancet Neurol. 2016Apr;15(4):391-404.

OP-997

Predictive value of metabolic and perfusion beyond the seizure onset zone as predictors of postoperative outcome in patients with refractory focal epilepsy

M. Haemels[1], *D. Van Weehaeghe*[1], *E. Cleeren*[2], *P. Dupont*[3], *J. Van Loon*[4], *T. Theys*[4], *K. Van Laere*[1], *W. Van Paesschen*[2], *K. Goffin*[1];
[1]*Department of Nuclear Medicine, University Hospitals Leuven, Leuven, BELGIUM,* [2]*Department of Neurology, University Hospitals Leuven, Leuven, BELGIUM,* [3]*Department of Neurosciences, Laboratory of cognitive neurology, KU Leuven, Leuven, BELGIUM,* [4]*Department of Neurosurgery, University Hospitals Leuven, Leuven, BELGIUM.*

Aim/Introduction: Interictal ^{18}F-fluorodeoxyglucose (FDG)-PET and ictal/interictal perfusion SPECT are established imaging tools to identify the seizure onset zone (SOZ) in patients with refractory focal epilepsy, who are eligible for epilepsy surgery. Functional changes beyond the SOZ may provide predictive information regarding surgical outcome. The aim of this retrospective study was to evaluate relative metabolic and perfusion changes beyond the SOZ as predictors of postoperative outcome in patients with refractory focal epilepsy. ***Materials and Methods:*** Eighty-six patients with refractory unifocal epilepsy underwent ^{18}F-FDG-PET prior to epilepsy surgery. Ictal and interictal perfusion SPECT was available in 65 patients (75%). Good postoperative outcome was defined as International League Against Epilepsy class 1&1a. Univariate statistical analysis quantified the predictive ability for outcome of metabolism/perfusion in composite volumes of interest (VOIs) by the area under the ROC-curve (AUC). The composite VOIs were based on the Hammers atlas (orbitofrontal, frontal, temporal, parietal, occipital and central VOIs). Results were cross-validated and a false discovery rate (FDR) correction was applied for multiple comparisons. A subgroup analysis was performed on patients with temporal lobe epilepsy

(TLE). ***Results:*** Increased ictal perfusion in the contralateral central region was significantly correlated with good surgical outcome both in the total population (AUC 0.79, p_{FDR}=0.009) and the TLE-subgroup (AUC 0.80, p_{FDR}=0.028). Higher ictal perfusion showed a trend to be correlated with good outcome in the ipsilateral central region (total population AUC 0.69, $p_{non\text{-}FDR}$=0.012; TLE-subgroup AUC 0.68, $p_{non\text{-}FDR}$=0.048) as well as in the ipsilateral orbitofrontal cortex (total population AUC 0.65, $p_{non\text{-}FDR}$=0.046). Also higher interictal perfusion in the contralateral central region tended to correlate with good outcome (total population AUC 0.69, $p_{non\text{-}FDR}$=0.01). Reduced ictal perfusion, on the other hand, tended to correlate with good outcome in the contralateral temporal lobe (total population AUC 0.70, $p_{non\text{-}FDR}$=0.007). No significant correlations or trends between metabolic changes and postoperative outcome were detected. ***Conclusion:*** Ictal perfusion in the contralateral central region significantly predicted outcome after epilepsy surgery in patients with refractory focal epilepsy, potentially reflecting a variable degree of ictal neuronal network recruitment. ***References:*** None

OP-998

Epileptogenic zone localization on SISCOS in drug refractory epilepsy

D. Khan*, S. T. Arun Raj, S. Sagar, M. Tripathi, M. Tripathi, R. Doddamani, A. Garg, P. Chandra, C. Sarkar, N. Damle, C. S. Bal; All India Institute of Medical Sciences, New Delhi, INDIA.*

Aim/Introduction: Drug refractory epilepsy (DRE) can be effectively treated by surgical resection of the epileptogenic zone (EZ) if it is correctly localized. The pre-surgical work-up of such patients includes interictal and ictal SPECT followed by SISCOS (subtraction ictal spect coregistered to SPECT). We have been routinely performing SISCOS for our DRE patients. In this retrospective analysis we determined the concordance of SISCOS for localization of the EZ in DRE patients who underwent surgery. ***Materials and Methods:*** This retrospective analysis was conducted in 148 patients of DRE who underwent presurgical workup followed by surgical resection at All India Institute of Medical Sciences, New Delhi. During workup vEEG, MRI, FDG PET/CT and SISCOS was done for all these patients. The concordance of these modalities for localization of the EZ was compared with the reference standard which was surgical resection/ biopsy and assessed along with post surgical outcomes (ILAE surgical outcome scales). ***Results:*** Age range of patients was 1.7 to 51 years, there were 96 male and 52 females. Seizure onset was during the first decade of life in 51 patients, with a mean duration of symptoms of 9.3+ 6 years. There were 71 cases of extratemporal epilepsy and 77 cases of temporal lobe epilepsy. FCD (n=30) was the most common histopathological diagnosis in the resected samples. Concordance for localization of the EZ on MRI, vEEG, FDG-PET, and SISCOS was 85.8%, 64%, 71.2% and 75.8% with the surgically resected EZ. Concordance of SISCOS with MRI, VEEG, and FDG PET for lesion detection was 42.9%, 45.6% and 35.5%. Thus SISCOS had highest concordance with MRI. Good surgical outcomes (ILAE scale; Grade 1) were seen in 58% of the patients with localization on SISCOS. Localization of the EZ for SISCOM (subtraction ictal spect coregistered to MRI) has been reported as 88.2% (1) while one study in literature has similar results for SISCOS 87%(2). ***Conclusion:*** Localization of the EZ by SISCOS was the second highest of all modalities used in pre-surgical evaluation of DRE after MRI. This is comparable to the localization of EZ by SISCOM and can therefore be effectively used for DRE patients. ***References:*** (1) O'Brien et al; Subtraction ictal SPECT co-registered to MRI improves clinical usefulness of SPECT in localizing the surgical seizure focus ;Neurology. 1998 Feb;50(2). (2) Lewis et al; Does performing image registration and subtraction in ictal brain SPECT help localize neocortical seizures; JNM. 2000 Oct;41(10).

OP-999

Reduced pulmonary function is associated with global brain function on ^{18}F-FDG brain PET in lung cancer patients

S. Son*, E. Kong; Yeungnam University Medical Center, Daegu, KOREA, REPUBLIC OF.*

Aim/Introduction: While a growing number of studies have demonstrated a relationship between pulmonary function and brain function, especially cognition, the relationship has been only studied with clinical or structural imaging technique, such as MRI. Imaging techniques using ^{18}F-FDG positron emission tomography (PET) provide measures of true functional activation of whole brain. This study was performed to determine the relationship of pulmonary function to brain metabolic parameter and to examine the mediating factors for any relationships. ***Materials and Methods:*** A random sub-sample of 102 patients who were diagnosed as lung cancer, underwent ^{18}F-FDG brain PET and pulmonary function test. Pulmonary function was analyzed according to the percentage predicted values (% pred) for forced vital capacity (FVC), forced expiratory volume in the first second (FEV1), and diffusing capacity for carbon monoxide (DLCO). The semiquantitative FDG uptake (standardized uptake values [SUVs]) was calculated in brain by using the PMOD Neuro tool (version 3.6). The quantifications mostly performed by cortical-to-cerebellum SUV ratio (SUVr). ***Results:*** Five of 102 patients, who had brain metastasis, were excluded, therefore, 97 patients were final subjects (mean age, 67.7±10.3). Mean FVC was 80.0±15.4%; mean FEV1 was 77.6±17.8%; mean DLCO was 71.0±20.9%. There was significant correlation between

FVC or FEV1 or DLCO and SUVr in all brain regions (frontal, parietal, occipital, temporal) (p<0.01). The result was also significant in cognition-related regions (posterior cingulate gyri, precuneus, and posterior temporal and parietal lobes). In multivariate regression, FVC, FEV1, and DLCO were significantly associated with SUVr in cognition-related regions (p<0.05), after adjusting the data for confounding factors (age, sex, lung cancer type [NSCLC or SCLC], smoking [pack-year]). In addition, lung cancer type (NSCLC) was also associated with SUVr in cognition-related regions (p<0.05). ***Conclusion:*** These findings suggest that reduced pulmonary function was significantly associated with decreased brain function, especially in cognition-related regions. ***References:*** None

OP-1000

Relation Between Amyloid Deposition and Microbleeds in CAA

Y. Chang, J. Liu, B. Xu;
Chinese PLA General Hospital, Beijing, CHINA.

Aim/Introduction: Our aim was to investigate the relationship between amyloid deposition and strictly lobar cerebral microbleeds (CMBs) in cerebral amyloid angiopathy (CAA), Alzheimer's disease (AD) and cognitively normal healthy controls (NC) by integrated PET/MR, and to assessed the diagnostic value of PIB PET/MR in probable CAA patients. ***Materials and Methods:*** 8 probable CAA patients (per modified Boston criteria, n=7; pathologically defined CAA, n=1), 15 probable AD patients and 15 NC subjects underwent static head PET/MR scan using ^{11}C-PIB at 40 min after injection. Cortical PIB deposition was assessed quantitatively (standardized uptake value ratio [SUVR]) and visually classified as positive or negative. SUVR were calculated using the cerebellum as reference region. Patients with CAA and AD and NC subjects were compared for region cortical and global cortical PIB SUVR values. Brain MRI were assessed for detecting the location of CMBs. ***Results:*** All CAA patients had evidence of lobar CMBs, Eight of 15AD patients(53.3%) presented with CMBs. Fourth of 15 NC subjects(26.7%) detected lobar CMBs. PIB deposition was detected at CMB sites were observed in CAA patients when compared with AD patients and NC subjects (1.72± 0.11vs 1.63± 0.08 vs 1.17±1.08; p<0.0001). PIB deposition was associated with lobar CMBs and was greatest in occipital and temporal regions in CAA patients. The global cortical PIB deposition was significantly higher in CAA than in NC subjects (1.71±0.61vs1.21±0.60; p<0.0001) and significantly less than in AD patients (1.86±0.17; p<0.0001). In contrast, the occipital-to-global PIB ratio was significantly increased in CAA (occipital/global cortex 1.07± 0.03) relative to AD patients (0.95 ± 0.02). ***Conclusion:*** Amyloid deposition associated with strictly CMBs, indicate CMBs occur preferentially in local regions of concentrated amyloid and suggest underlying CAA pathology. PIB-PET can detect cerebrovascular amyloid in patients with CAA and the distribution differ from that seen in AD patients. We recommend PET/MR may serve as a noninvasive method for diagnose CAA in appropriate clinical setting. ***References:*** None

OP-1001

Comparison between regional cerebral blood flow estimates using different MR arterial spin labelling approaches and early-phase amyloid PET on a simultaneous PET/MR

J. Anton Rodriguez[1,2], J. C. Matthews[3], L. Scott[3], M. Lohezic[4], K. Herholz[3], L. M. Parkes[3];
[1]The Christie NHS Foundation Trust, Manchester, UNITED KINGDOM, [2]Division of Informatics, Imaging and Data Sciences, MAHSC, University of Manchester, Manchester, UNITED KINGDOM, [3]Division of Neuroscience and Experimental Psychology, Faculty of Biology, Medicine and Health, University of Manchester, Manchester, UNITED KINGDOM, [4]Applications and Workflow, GE Healthcare, Manchester, UNITED KINGDOM.

Aim/Introduction: Amyloid-PET can be used as dual-phase biomarker enabling differential diagnosis between dementias by providing images of amyloid load (late-phase) and functional estimates of regional cerebral blood flow (rCBF) (early-phase) [1]. MRI arterial spin labelling (ASL) can quantify CBF and can provide similar patient classification information as [^{18}F]FDG PET [2]. Here, we compare rCBF obtained with ASL with the early-phase distribution of amyloid-PET using [^{18}F]flutemetamol (FLUT). ***Materials and Methods:*** Twenty participants, 70(60-80) years old, 14 cognitively normal/6 mild cognitive impairment, were scanned on a SIGNA PET/MR (GE-Healthcare). PET list-mode data were acquired for 30 minutes following the injection of ~185MBq of FLUT. PET images were reconstructed using GE Q.Clear (β=250) for two separate time frames corresponding to 20s-80s and 120s-300s post-arrival of tracer in the brain. Enhanced-ASL with pCASL labelling and 3D spiral FSE acquisition was acquired with 6 post-labelling delays to obtain voxel-wise arrival-time-corrected CBF maps [3] (scan duration: 9min). CBF maps were calculated using either global (CBF_{global}) or local (CBF_{local}) correction for equilibrium magnetisation and also using a single time point post-labelling of 2.2s ($CBF_{2.2}$) (scan duration: ~3min). FreeSurfer brain segmentation on each participant's T1w MPRAGE image (1mm isotropic resolution) was used to estimate median CBF values for 12 'meta-regions'. Linear regression was used to compare intensity normalised early phase PET and ASL. ***Results:*** For PET_{20-80} vs CBF_{global}, CBF_{local}, $CBF_{2.2}$ the ***r*** (median(range)) values across the 20 participants were 0.56(0.26-0.65), 0.67(0.33-0.82) and 0.59(0.27-0.82) respectively. Removing subcortical ROIs caudate and striatum (clear outliers on the scatter-plots) improved the

r values to 0.63(0.36-0.81), 0.82(0.48-0.96), 0.85(0.42-0.96). Lower r values for $PET_{120-300}$ were observed. ***Conclusion:*** For cortical regions, there is a good proportional relationship between ASL and PET measurements (improved using earlier PET (PET_{20-80}) to $PET_{120-300}$ proposed in [1]) with this proportion not holding for the subcortical ROIs with values underestimated for ASL. ASL CBF maps with local magnetisation correction have a closer association with PET suggesting that spatial inhomogeneity in coil sensitivities cause significant errors if uncorrected. Good association is maintained with single time point ASL suggesting that 2.2s is sufficient delay for complete transit of labelled blood; enabling faster ASL acquisition. These close associations suggest that simultaneous ASL with late-phase amyloid-PET and injection of FLUT off the bed could provide excellent classification of dementia patients in a single scan. ***References:*** [1]Asghar M. et al. EJNMMI 2019 [2]Ceccarini J. et al. EJNMMI 2020 [3]Parkes L.M. and Tofts P.S. MRM 2002

OP-1002

Association of Retention of [18F]-APN-1607, a Novel Tau PET Tracer, with Brain Glucose Metabolism and Cognition in Patients of Alzheimer's Disease

J. Lu[1], W. Bao[1], M. Li[1], L. Li[1], Z. Zhang[1], I. Alberts[2], M. Brendel[3], P. Cumming[2], C. Zuo[1], Y. Guan[1], Q. Zhao[4], K. Shi[2], A. Rominger[2];
[1]PET Center, Huashan Hospital, Fudan University, Shanghai, CHINA, [2]Department of Nuclear Medicine, University Hospital Bern, Bern, SWITZERLAND, [3]Department of Nuclear Medicine, University Hospital of Munich, Ludwig-Maximilian-University Munich, Munich, GERMANY, [4]Department of Neurology, Huashan Hospital, Fudan University, Shanghai, CHINA.

Aim/Introduction: Specific molecular imaging of tau pathologies in patients of Alzheimer's Disease (AD) with positron-emission-tomography (PET) is complicated by off-target binding properties of the first-generation of tau radioligands. We aimed to characterize the cerebral binding of [18F]-APN-1607 ([18F]-PM-PBB3), a newly developed tau tracer, in AD patients compared to normal control (NC) subjects. ***Materials and Methods:*** We obtained static late frame PET recordings with [18F]-APN-1607 and [18F]-FDG in patients with a clinical diagnosis of AD group (N=19), along with an age-matched NC group ([18F]-APN-1607 only, N=11). Group differences were tested by statistical parametric mapping (SPM) and volume of interest (VOI) analyses of the reference region normalized standard uptake value ratio (SUVR) maps. Relationships between both PET biomarkers as well as their associations with clinical cognition were assessed by Spearman correlation. ***Results:*** In the AD group, [18F]-APN-1607 binding was elevated in widespread cortical regions (P< 0.001 for VOI analysis, family wise error-corrected P< 0.01 for SPM analysis). The regional uptake in AD correlated significantly with global cognitive function (mini-mental state examination (MMSE); frontal lobe: R= -0.632, P= 0.004; temporal lobe: R= -0.593, P= 0.008; parietal lobe: R= -0.552, P= 0.014; insula: R= -0.650, P= 0.003; cingulum: R= -0.665, P= 0.002) and cognitive functions of specific domains including memory (Delay Recall of Rey-Osterrieth Complex Figure Test (CFT-delay); frontal lobe: R= -0.725, P <0.001; temporal lobe: R= -0.616, P= 0.005; occipital lobe: R= -0.611, P= 0.005; parietal lobe: R= -0.687, P= 0.001; insula: R= -0.669, P= 0.002; cingulum: R= -0.717, P= 0.001), visuospatial function (CFT-copy; frontal lobe: R= -0.502, P= 0.029; occipital lobe: R= -0.485, P= 0.035; parietal lobe: R= -0.510, P= 0.029; insula: R= -0.478, P= 0.038; cingulum: R= -0.526, P= 0.021), attention and working memory (Trail Making Test A (TMT-A); frontal lobe: R= 0.526, P= 0.021; occipital lobe: R= 0.536, P= 0.018; parietal lobe: R= 0.566, P= 0.012; insula: R= 0.521, P= 0.021; cingulum: R= 0.547, P= 0.015). The hypometabolism to [18F]-FDG PET in AD patients also showed negative correlations with regional [18F]-APN-1607 binding in some signature areas of AD (temporal lobe: R= -0.530, P= 0.020; parietal lobe: R= -0.637, P= 0.003; occipital lobe: R= -0.567, P= 0.011). ***Conclusion:*** Our results demonstrate that [18F]-APN-1607 retention differentiates patients of AD from normal subjects and the distribution of [18F]-APN-1607 matches the expected patterns of tau deposition in AD. Furthermore, [18F]-APN-1607 retention correlates with impaired cerebral glucose metabolism and cognitive function. ***References:*** None

1711

e-Poster Presentation Session 12: Onco Diagnostics - Mixed Bag

Friday, October 30, 2020, 15:30 - 16:50 Channel 11

EPS-183

Additional Diagnostic Value of Metabolic Parameters Measured by Pretreatment F-18 FDG PET/CT in patients with early stage endometrial carcinoma

J. Hwang;
Soonchunhyang University Hospital Bucheon, Bucheon, KOREA, REPUBLIC OF.

Aim/Introduction: The aim of this retrospective study was to determine whether delayed glucose metabolism assessed by pretreatment F-18 FDG PET-CT provides additional diagnostic information independent of established pathologic factors in patients with early stage endometrial carcinoma ***Materials and Methods:*** We reviewed retrospectively the medical records of 54 patients (mean age 52 ± 10 years) with pathologically proven endometrioid carcinoma of endometrium. They underwent F-18 FDG PET-CT and enhanced MRI as part of a pretreatment workup from Jan 2016 to Jan 2019. For the analysis, patients were classified by age, FIGO stage, SUVmax, MRI pattern [No demonstrable

(ND), SI change or thickness (ST), mass forming (MF)] and histopathology (size, lymphovascular invasion (LVI), invasion depth, LN metastasis). The relationship between FDG uptake, MRI pattern and diagnostic value was analyzed using the parametric and nonparametric tests and multiple regression methods. ***Results:*** Median SUVmax for all 54 study subjects was 15.9 (range: 3.5 - 35.4). The correlation of SUVmax and MRI pattern was found to be significantly related [median SUVmax of ND 8.7 ± 5.1, ST 14.6 ± 6.0, MF 20.8 ± 8.8 (p = 0.0008)] and revealed that the patients with a higher SUVmax showed mass forming MRI pattern (p = 0.045) than non-mass forming pattern. In univariate analysis, FIGO stage (p = 0.01), LN metastasis (p = 0.001), MRI pattern (p = 0.003) and LVI (p = 0.003) showed significant correlation with pretreatment SUVmax. Among the all patients, 6 patients showed recurrence (5 stage 3, 1 stage 2, 5 MF and 1 ST with LN metastais). The result revealed that higher SUVmax (p = 0.0001), MF pattern of MRI (p = 0.03), higher stage (p = 0.008), prescence of LN metastasis (p = 0.001) and LVI (p = 0.003) showed a recurrence in multiple regression analysis. ***Conclusion:*** SUVmax on pretreatment F-18 FDG PET-CT can provide additional diagnostic information with MRI pattern and predictive value in patients with early stage endometrial cancer. ***References:*** None

EPS-184

^{18}F-FDG PET/CT in the Preoperative Staging of Endometrial Cancer

A. Gutta[1,2], W. J. Pilloy[1], T. Mosehle[1,2], P. B. Nemutaduni[1,2]; [1]SMU Health Sciences University, Garankuwa, Pretoria, SOUTH AFRICA, [2]Dr George Mukhari Academic Hospital, Garankuwa, Pretoria, SOUTH AFRICA.

Aim/Introduction: The incidence of Endometrial cancer (EC) is lower in developing than developed countries. Patients in developing countries such as South Africa frequently present with advanced disease due to limited access to health care services and a lack of awareness of EC symptoms and treatment. EC prognosis and management is guided by accurate initial staging. Five-year-survival rates in early-stage EC are >95%, but drop to 20% in more advanced cases. Surgery is the mainstay of treatment, with extent of resection and the use of external beam radiotherapy and intracavitary brachytherapy directed by staging. Routine lymphadenectomy remains controversial. The aim of this study was to evaluate the diagnostic performance of ^{18}F-FDG PET/CT in the preoperative assessment of lymph node and distant metastases in patients with EC at a South African tertiary hospital. ***Materials and Methods:*** A retrospective analysis of 56 women with histologically proven EC was undertaken. All patients underwent a preoperative ^{18}F-FDG PET/CT scan (Philips Ingenuity TF) at 50-70 minutes p.i (8,12 ±1,192 mCi), followed by surgery. Scans were visually assessed by an experienced nuclear medicine physician and a radiologist. Findings were compared with histology, complementary imaging and/or follow up. Using appropriate statistical methods, the diagnostic accuracy of PET/CT was determined. ***Results:*** Complete records were available for 49 patients, with a mean age of 65 years (range 52-86). 69% (34/49) were endometroid adenocarcinomas. Primary tumours were all FDG avid (mean SUV_{max}:6,8 [range 3,22-32,1]). No correlation was determined between SUV_{max} and histologic subtype, but a statistical significance was observed between higher SUV_{max} values and histologic grading (p=0,002). Extra pelvic nodes were observed in 37% (18/49) of patients, with para-aortic adenopathy being the most common site. Distant metastases were present in 27% (13/49), predominantly in the lungs (54%[7/13]), followed by skeletal, liver, splenic and adrenal lesions respectively. The sensitivity, specificity, PPV and NPV of PET/CT for (1) nodal disease was 82,8%, 90%, 92,3% and 78,3% respectively; and for (2) distant metastases was 100%, 94,3%, 87,5% and 100% respectively. ***Conclusion:*** In this cohort, whole body ^{18}F-FDG PET/CT demonstrated high diagnostic accuracy for the detection of nodal and distant metastases in EC. The retrospective design (and probable selection bias) may account for a higher diagnostic accuracy than is quoted in the literature, but PET/CT may be valuable in the preoperative workup of EC in a setting where advanced disease at presentation is likely. A prospective study is planned to validate our results. ***References:*** None

EPS-185

The Relationship Between HER-2 Expression Levels and ^{18}F-FDG PET/CT Parameters in Gastric Cancer Patients

S. Ertürk*, Z. Hasbek, H. Özer, Ö. Ulaş Babacan; Sivas Cumhuriyet University, Sivas, TURKEY.*

Aim/Introduction: Gastric cancer is one of the most common cancers worldwide.HER-2 is a protooncogene encoded by ERBB2 on chromosome 17.The main role of HER-2 protein in these tissues is to support cell proliferation and prevent apoptosis. ^{18}F-FDG PET/CT examination is frequently used for the detection of distant metastasis in gastric cancer imaging.Our aim in this study is to investigate the relationship between the data obtained in the ^{18}F-FDG PET/CT examination and HER-2 expression status in gastric cancer patients. ***Materials and Methods:*** In our study,patients who underwent HER-2 examination with a diagnosis of gastric cancer and ^{18}F-FDG PET / CT examination for staging purposes between 2016 and 2020 are included.All patients were staged with ^{18}F-FDG PET / CT examination.HER-2 immunohistochemical examination was performed on all patients.SPSS 23.0 program was used for statistical analysis. ***Results:*** In our study, there were 115 patients, including 85 men (73.9 %) and 30 women (26.1 %).According to the HER-2 immunohistochemical examination, 71 patients (61.7%)

were negative and 44 patients (38.3%) were positive. The median SUVmax,SUVmean,MTV,TLG values of HER-2 positive patients were 9.95, 5, 30.44, 139.16, whereas HER-2 negative patients were 9.3, 5.4, 36.62 and 190.424 respectively (p> 0.05).The median CA 19-9 levels of HER-2 positive patients was 33.52, whereas those who were negative were 11.79 (p = 0.016).The mean age was 69.3 ± 9.35 in patients with distant metastases, while the mean age was 65.2 ± 10.9 in those without distant metastases (p = 0.042).Median SUVmax and SUVmean values in patients with distant metastases were 11.1 and 6.3, respectively, and 8.2 and 4.5 in those without distant metastases (p = 0.002, p = 0.001, respectively).The median CA 19-9 and CEA levels in patients with distant metastases were 31.34 and 9.20, respectively, whereas those without distant metastases were 11.55 and 2.26, respectively (p = 0.011 and p = 0.001, respectively). ***Conclusion:*** In our study, there was no statistically significant difference in terms of HER-2 status and SUVmax, SUVmean, MTV, TLG, presence of distant and lymph node metastasis, age, gender, tumor diameter, tumor grade, tumor localization, and CEA levels in gastric cancer patients.A statistically significant difference was found between HER-2 status and CA 19-9 levels.While there was a statistically significant relationship between distant metastases in the ^{18}F-FDG PET/CT examination and SUVmax, SUVmean, age, CEA levels; the relationship between distant metastasis , and MTV, TLG, tumor diameter, tumor localization, and tumor grade was not statistically significant. ***References:*** None

EPS-186

The comparative performances of ^{18}F-FDG PET/MRI and ^{18}F-FDG PET/CT for the detection of pancreatic neoplasms

H. Xing[1], *B. Hou*[2], *W. Zhu*[1], *H. Ding*[3], *X. Li*[4], *Y. Hu*[5], *H. Xue*[2], *F. Feng*[2], *K. Lv*[6], *X. Wu*[7], *F. Li*[1], *Z. Jin*[2], *D. Li*[5], *L. Huo*[1], *Y. Zhao*[5];
[1]*Department of Nuclear Medicine, Peking Union Medical College Hospital,Chinese Academy of Medical Science & Peking Union Medical College, Beijing Key Laboratory of Molecular Targeted Diagnosis and Therapy in Nuclear Medicine, Beijing, CHINA,* [2]*Department of Radiology, Peking Union Medical College Hospital, Chinese Academy of Medical Science & Peking Union Medical College, Beijing, CHINA,* [3]*Center for Biomedical Imaging Research, Department of Biomedical Engineering, School of Medicine, Tsinghua University, Beijing, CHINA,* [4]*Division of Nuclear Medicine, Department of Biomedical Imaging and Image-guided Therapy, Medical University of Vienna, Vienna, AUSTRIA,* [5]*Department of General Surgery, Peking Union Medical College Hospital, Chinese Academy of Medical Science & Peking Union Medical College, Beijing, CHINA,* [6]*Department of Doppler Ultrasonic, Peking Union Medical College Hospital, Chinese Academy of Medical Science & Peking Union Medical College, Beijing, CHINA,* [7]*Department of Gastroenterology, Peking Union Medical College Hospital, Chinese Academy of Medical Science & Peking Union Medical College, Beijing, CHINA.*

Aim/Introduction: Pancreatic cancer is one of the leading causes of cancer death with an increasing incidence. Noninvasive determination of malignancy is of major interest for patient therapeutic management. We aim to evaluate the diagnostic performance of ^{18}F-FDG PET/MRI and ^{18}F-FDG PET/CT in preoperative assessment of patients with pancreatic neoplasms. ***Materials and Methods:*** Forty-four Patients (18 male, 56.2 ± 11.1 yrs) with suspected pancreatic neoplasms were recruited prior to resection or biopsy. All underwent PET/CT (Biograph TruePoint 64, Siemens) and PET/MR (Signa 3T, GE) on the same day, using a single tracer ^{18}F-FDG injection. PET protocol in PET/CT included 5 bed positions (2 min/bed). PET/MR protocol included T_1-weighted, T_2-weighted and diffusion-weighted MR sequences and single bed position for PET scan. ^{18}F-FDG was injected with 3.7-7.4 MBq/kg averaged 95 min before PET/CT scan and 165 min before PET/MR scan. Tumor with high-grade dysplasia and invasive pattern were defined as malignance based on the histological examinations. Patients were grouped into malignant (n = 25) and benign (n=19) groups. Subjective diagnosis was made according to clinical routine process. Regions of interest (ROIs) were defined on the lesions on MRI for PET/MR. Regions of interest (ROIs) were defined as PET-positive lesions with anatomic CT correlate (if visible). The maximum standardized uptake value (SUVmax) of placed RIOs was assessed on PET. The uptake ratio (SUVR) was calculated by SUVmax of the lesion targeted to the mean of SUV on liver of 1 cm ROI (SUVmean). Diagnosis agreement between the two scans and the corresponding calculation of sensitivity, specificity, and accuracy to differentiate malignance and benign tumors were performed. Paired t tests and correlations were performed to compare the SUVmean of liver, the SUVmax of lesion and the SUVR measured on PET/CT and PET/MRI, respectively. ***Results:*** SUVR values in malignant group were significantly elevated than those in benign group (2.82 ± 1.97 vs. 0.71 ± 0.28 with P < 0.001) for PET/CT and (4.98 ± 2.98 vs. 0.99 ± 0.40 with P < 0.001) for PET/MR. All the SUV measurements differed (P < 0.001) but significantly correlated (P < 0.05) between PET/CT and PET/MRI. The diagnosis showed total sensitivity, specificity, and accuracy were 79.2%, 82.35% and 79.6% for PET/CT and 91.67%, 70.59% and 81.8% for PET/MR, respectively. The overall agreement between PET/CT and PET/MRI reached 77% (95% CI, 0.59-0.96). ***Conclusion:*** ^{18}F-FDG PET/MRI and ^{18}F-FDG PET/CT seem comparably accurate for the detection of malignant neoplasms. ***References:*** None

EPS-187

Does diffuse gastric FDG uptake infer Helicobactor pylori infection?

Z. Al Bimani[1,2], *S. Samman*[3], *W. Zeng*[1];
[1]*University of Ottawa, Ottawa, ON, CANADA,* [2]*Ministry Of Health, Muscat, OMAN,* [3]*University of*

Miami, Miami, FL, UNITED STATES OF AMERICA.

Aim/Introduction: Helicobacter pylori (H. pylori) is a common cause of peptic ulcers and may be present in more than half of the people in the world. Diffuse Fluoro-Deoxy-Glucose (FDG) uptake in the stomach is usually an incidental finding in patients referred for FDG Positron Emission Tomography (PET) scan for cancer staging. Several studies have shown good correlation between gastric FDG uptake and the presence of H. pylori infection in Asian patients. However, no studies have been done in the North American population. The aim of the study is to test if the presence of diffuse gastric FDG uptake on PET without a CT correlate is associated with H. pylori infection. ***Materials and Methods:*** All patients referred to our institution for FDG PET/CT for cancer staging from April 2017-Dec. 2019 were retrospective reviewed for the presence of diffuse gastric uptake if the gastric uptake is much higher than the liver. The patients with gastroesophageal cancer or abnormal gastric findings on CT were excluded. The presence of H. Pylori infection was identified by endoscopy, C-14 urea breath test and blood test. Continuous variables are presented as mean ± standard-deviation. P-values less than 0.05 were considered statistically significant. ***Results:*** There are 96 patients with diffuse gastric FDG uptake, with the activity much higher than the liver (stomach SUV_{max}:7.6±3.7, liver SUV_{max}: 3.4±0.8). 18 patients had follow-up results for H. pylori. There is no difference in FDG uptake in the stomach between the follow-up and non follow-up groups (SUV_{max} 7.1 ± 2.6 vs. 7.7±3.9, p=0.57). Of the patients who had follow-up results for H. pylori, 13 were negative and 5 were positive or intermediate probability for H. pylori infection, with no significant difference in gastric uptake (SUV_{max} 7.0±1.9 vs. 7.4±3.4, p=0.77). ***Conclusion:*** Incidental diffuse gastric uptake on FDG PET in cancer patients is not an uncommon finding. Different from the results from the studies with Asian patients, our study from North America showed no significant association between the diffuse gastric uptake and the presence of H. pylori infection. ***References:*** Kobayashi S, Ogura M, Suzawa N, Horiki N, Katsurahara M, Ogura T, et al. (18)F-FDG uptake in the stomach on screening PET/CT: value for predicting Helicobacter pylori infection and chronic atrophic gastritis. BMC med imaging 2016;16(1):58.

EPS-188

Impacts of malnutrition on ^{18}F-FDG PET/CT measurements on healthy organs in patients with esophageal cancer

E. Deshayes[1], *S. Thezenas*[2], *I. Berkane*[1], *N. Flori*[3], *P. Senesse*[3], *T. Galvez*[3];
[1]*Nuclear Medicine Department, Institut du Cancer de Montpellier, Montpellier Cedex 5, FRANCE,* [2]*Biometrics Unit, Institut du Cancer de Montpellier, Montpellier Cedex 5, FRANCE,* [3]*Clinical Nutrition and Gastroenterology Department, Institut du Cancer de Montpellier, Montpellier Cedex 5, FRANCE.*

Aim/Introduction: Malnutrition characterized by reduced food intake, involuntary weight loss and change in body composition is frequent in cancer patients, impairing quality of life and overall survival[1]. ^{18}F-FDG PET-CT is routinely performed as part of initial staging of numerous cancers owing to its ability to detect increased glycolytic activity of cancer cells. The aim of this study was to determine, in patients with esophageal cancer (with a high incidence rate of malnutrition), whether 18F-FDG uptake in healthy organs was influenced by malnutrition status (weight loss, fat and muscle wasting) and correlated to overall survival (OS). ***Materials and Methods:*** Patients over 18 years-old diagnosed with oesophageal cancer, who underwent an initial ^{18}F-FDG PET-CT between 2014 and June 2019, were included in this retrospective study. Patients whose brain scanning was not performed or who presented with diabetes were excluded. SUV (max, peak, mean) normalized to patient's weight (bw) or lean mass (lm) were obtained from brain, liver, spleen and bone marrow. Nutritional status and survival data were obtained from patient records. Patients were defined as sarcopenic according to cut-off values obtained from a reference healthy population[2] of skeletal muscle index (SMI). SMI is the Skeletal Muscle Area using CT imaging at the 3rd lumbar vertebra normalized by height squared. Group differences were tested using the Kruskal-Wallis test and correlation with overall survival (OS) was assessed using a Cox proportional hazards model. ***Results:*** Sixty patients (51 males), with median age of 65.5 years at diagnosis, were included. Twenty had a weight loss WL ≥ 10 %. Median OS was 25.8 months. Nineteen showed a SMI consistent with sarcopenia. SUV(bw and lm) in brain were significantly lower in patients with WL ≥ 10% compared to WL < 10% (p<1e-3). No difference between SUV in these 2 groups were observed for any other normal tissues. In sarcopenic patients, SUV_{bw} were consistently lower in every tissue tested but no difference was observed when using SUV_{lm}, except for brain with values still lower in sarcopenic patients (p = 0.003). Patients with lower brain SUV(bw and lm) had poorer OS (p<0.05). No association between SUV and OS in other organs was seen. ***Conclusion:*** SUV should be corrected for lean mass in malnourished patients. Brain ^{18}FDG uptake is significantly lower in malnourished patients and correlated to poor OS. FDG uptake in other studied organs was not associated with OS. ***References:*** 1. Arends, J.(2017). 2. Van der Werf, A. (2018)

EPS-189

Clinical Value of ^{18}F FDG Bio-distribution in Metabolic Characterization of Pancreatic Masses on PET/CT

S. Tatlidil[1], *E. Guler*[2], *B. Karasah*[1], *G. Hakverdi*[3], *Z. Ozcan*[1];
[1]*Department of Nuclear Medicine, Ege University Medical Faculty, Izmir, TURKEY,* [2]*Department of Radiology, Ege*

University Medical Faculty, Izmir, TURKEY, [3]Department of Statistics, Ege University Medical Faculty, Izmir, TURKEY.

Aim/Introduction: FDG PET/CT imaging for the initial evaluation of pancreatic tumors is challenging. In the current study, we aimed to assess the possible effects of metabolic/clinical factors and bio-distribution of FDG on pancreatic tumor detectability. ***Materials and Methods:*** he study group included 162 patients (pts) with a pancreatic mass referred for initial metabolic characterization between July 2012 and January 2019. PET/CT was performed using non-contrast low-dose CT. Clinical records, biochemical and radiologic findings were reviewed retrospectively including biochemical profile, personal variables, and SUV measurements of reference tissues. Patients were divided into groups as benign lesions, pancreatic adenocarcinoma (AC), and liver metastasis (LM) as a subgroup of AC. Only one primary lesion and/or metastatic lesion from each patient was included for quantitative analysis. In order to assess FDG bio-distribution, SUVmax were measured in the cerebrum, psoas muscle, and liver using standard ROIs. Data were analyzed using SPSS Statistics 22.0 Program and binary logistic regression analysis was used to test variables related to lesion detectability. CI was accepted as %95 for all tests. ***Results:*** There were 17 benign and 145 AC pts. LM was found in 47. The median SUVmax was 4.2 (1-10.7) and 9.6 (1.5-65) respectively in benign lesions and ACs (Mann Whitney U test, p<0,001). In the AC group, primary lesions >1cm did not show FDG uptake in 9 pts. In the LM group, 13 liver lesions could not be detected on PET/CT though they had a confirmed metastasis > 1cm. In Pts with false (-) FDG findings, high blood glucose level was noted (Mann-Whitney U test, p<0,001) which was also negatively correlated with low SUVmax cerebrum (r:-0,571; p<0,001). The sensitivity of PET/CT for the detection of the primary lesion was 94% (CI:%88-97) and 90% (CI: 82-96) respectively in the overall group and hyperglycemic pts. SUVmax cerebrum was found to be the most robust variable which predicted the undetectability of a primary or metastatic lesion (OR=0,3(0,2-0,6);p<0,001). ROC analysis showed cut-off value for SUVmax cerebrum was 8.2 (AUC=0,9(0,7-0,9),p<0,001) and 7.9 (AUC:0,8(0,7-0,9); p<0,01) for the overall and hyperglycemic pts (>120 mg/dl,n:71). ***Conclusion:*** FDG PET/CT appears to be useful in discriminating benign and malignant pancreatic lesions while SUVmax values may overlap. Detectability of pancreatic AC found to be inter-related both with high blood glucose and low cerebral FDG uptake. Therefore, in daily practice of PET/CT, reviewing cerebral uptake might improve diagnostic evaluation of pancreatic tumors in cases with high glucose levels ***References:*** None

EPS-190

FDG-PET/CT versus Conventional Imaging to Distinguish Between Benign and Malignant Pathology of the Gallbladder

A. Sabaté-Llobera[1], *G. Reynés-Llompart*[2], *J. Mestres-Martí*[1], *J. J. Robles-Barba*[1], *L. M. Gràcia-Sánchez*[1], *P. C. Notta*[1], *I. Sánchez-Rodríguez*[1], *M. Cortés-Romera*[1];
[1]*IDI - Hospital Universitari de Bellvitge - IDIBELL, L'Hospitalet de Llobregat, SPAIN,* [2]*ICO - Hospital Universitari de Bellvitge - IDIBELL, L'Hospitalet de Llobregat, SPAIN.*

Aim/Introduction: Gallbladder lesions are frequent findings in routine imaging tests. Though usually benign (adenomyomatosis or inflammation), malignant lesions are sometimes found incidentally. This study aimed to determine the ability of PET/CT to distinguish between benign and malignant conditions of the gallbladder compared with the conventional imaging approach (CT or MRI), and to find cut-off values for metabolic parameters that could help the diagnosis. ***Materials and Methods:*** Imaging studies of 50 patients (28 men, mean age 67.5) were retrospectively reviewed. Imaging findings were considered as benign, malignant or indeterminate. PET/CT images were analyzed visually and semiquantitatively (SUVmax of the gallbladder lesion and lesion-to-liver ratio (LLR)). Agreement between conventional imaging and PET/CT was calculated (weighted kappa). Using histology or evolution as gold-standard, ROC curves were obtained to calculate the optimal cut-off values for PET semiquantitative parameters. ***Results:*** Conventional imaging classified 22 studies as benign, 17 as malignant and 11 as indeterminate, while for PET/CT they were 25, 21 and 4, respectively. There were 16 discordant results between both imaging procedures, obtaining a fair agreement (k=0.36). Visually, PET/CT findings were dichotomized as FDG-avid (32 studies, 64%) and non-FDG-avid. Median SUVmax and LLR in FDG-avid cases were 6.15 and 2.19, respectively, while in non-FDG-avid studies they were 2.0 and 0.66, respectively.Overall, 37 patients (74%) were operated, while the remaining were considered for follow-up (all of them with suspected adenomyomatosis). Among operated patients, 28 (87.5%) were FDG-avid (proving 23 carcinomas and 5 chronic cholecystitis) and 9 were non-FDG-avid (5 cholecystitis, 2 cholelithiasis without additional pathology, 1 lymphoplasmacytic colangitis and 1 adenocarcinoma). PET/CT considered all these non-FDG-avid findings as benign, while conventional imaging considered 2 of them as malignant (the lymphoplasmacytic colangitis and the adenocarcinoma) and 3 as indeterminate.Regarding the final diagnosis (histology or clinical/radiological follow-up), PET/CT showed a diagnostic accuracy of 87% and conventional imaging of 92.3%, though indeterminate results were not considered in this analysis. Metabolic parameters showed significant differences between finally

benign and malignant lesions, with median SUVmax of 3.0 and 6.8, respectively ($p=6.4 \cdot 10^{-6}$), and median LLR of 0.86 and 2.3, respectively ($p=3.4 \cdot 10^{-6}$). Optimal cut-off values to distinguish between benign and malignant pathology were 3.7 for SUVmax and 1.16 for LLR. ***Conclusion:*** PET/CT shows a good performance in distinguishing benign and malignant gallbladder lesions, with less indeterminate results than conventional imaging techniques. In our study, significant differences between benign and malignant conditions were obtained for PET metabolic parameters, aiming the diagnosis. ***References:*** None

EPS-191

Potential Value of Quantified Metabolic Indices Obtained in^{68}Ga (DOTATOC) PET/CT to Distinguish Between G1 and G2 Low-Grade Neuroendocrine Tumors. A Pilot Experience in a Single Center of Spain

J. Rodríguez Gomez[1], M. Ollarves Carrero[1], M. Cabrera Martín[1], F. Ferrando-Castagnetto[2], C. Wakfie Corieh[1], M. Meneses Navas[1], P. Romero Fernández[1], J. Carreras Delgado[1];
[1]Servicio de Medicina Nuclear, Hospital Clínico San Carlos, Madrid, SPAIN, [2]Departamento de Cardiología-CCVU, Hospital de Clínicas, Facultad de Medicina, Universidad de la República., Montevideo, URUGUAY.

Aim/Introduction: The detection of neuroendocrine tumors (NET) is favored by over-expression of somatostatin receptors (STTR) in tumor cells. The precision of diagnosis obtained through PET/CT with ^{68}Ga (DOTATOC) and ^{18}F-FDG depends on the STTR membrane receptor subtype and histopathological grade. The following experience explored the potential usefulness of some clinical variables and quantified indices of molecular activity in ^{68}Ga (DOTATOC) PET/CT to differentiate G1 from G2 histopathological degrees in NET patients over-expressing SSTR. ***Materials and Methods:*** All diagnosed/highly suspicious NET patients who underwent ^{68}Ga (DOTATOC) PET/CT between April 2019 and march 2020 were included. Patients with high-grade NET (grade G3 histological tumor according to Ki67 criteria) were excluded. The clinical data, anatomy of the primary tumor, and the indices maximum and mean standardized uptake value (SUVmax, SUVmean) in primary/metastatic lesions, metabolic tumor volume (MTV), and total lesion glycolysis (TLG) were compared between histological grades G1 and G2. All indices were correlated using the Pearson coefficient (r). Data in subjects with G1 and G2 tumors were compared using Fisher's exact and nonparametric Mann-Whitney tests. A multiple linear regression model was applied to detect possible predictors of histological G1 (p-value = 0.05). ***Results:*** Thirty-two patients with ^{68}Ga (DOTATOC) PET/CT results were available, 50% women, aged 40-81 years, 44% were gastrointestinal-pancreatic primary tumors. Histopathological confirmation was obtained in 19 patients; 74% of them were classified as low-grade G1 and G2 (n=14). In aggregated low-grade NETs, the sensitivity of ^{68}Ga PET/CT (DOTATOC) was 91%, with a positive predictive value of 100%. There was an inverse strong correlation between VMT and TLG (r= -0.96) with a moderate/weak correlation among other indices. Patients in both subgroups were similar in age, anatomic site of the primary tumor, functional status, recurrence rate an treatment. Quantified parameters did not differ between patients with G1 and G2 tumors SUVmax +SEM: 67.78+21.58 vs. 30.21+10.94, p=0.13; SUVmean +SEM: 13.07+1.60 vs. 9.86+3.01, p=0.49; MTV +SEM: 42.38+14.64 vs.20.17+5.34, p=0.41; TLG +SEM: 607.9+297.2 vs. 226.4+82.12, p=0.34).The only variable associated with G1 tumors after multivariate analysis was male sex, with a non-significant trend to lower age (p=0.06) and bigger SUVmax (p=0.08) in G1 subjects. ***Conclusion:*** ^{68}Ga PET-CT (DOTATOC) demonstrates high sensitivity for diagnosing low-grade NETs. The quantified molecular indices measured in the primary tumor and/or metastatic lesions are similar in histological grades G1 and G2. These preliminary findings and the potential prognostic value of different parameters should be tested in larger multicenter case series. ***References:*** None

EPS-192

Impact of PET data driven respiratory motion correction of ^{68}Ga-DOTATATE PET/CT for differentiating neuroendocrine tumors (NET) and intrapancreatic accessory spleens (IPAS)

V. Liberini[1,2,3], F. Kotasidis[4], V. Treyer[2], M. Messerli[2], E. Orita[2], I. Engel-Bicik[2], A. Siebenhüner[5], M. Huellner[2];
[1]Department of Nuclear Medicine, A.O.U. Città della Salute e della Scienza di Torino, University of Turin, Turin, ITALY, [2]Department of Nuclear Medicine, University Hospital Zürich, University of Zürich, Zürich, SWITZERLAND, [3]ENETS CoE Training Fellowship Grant 2019, Berlin, GERMANY, [4]GE Healthcare, Waukesha, WI, UNITED STATES OF AMERICA, [5]Department of Hematology and Medical Oncology, University Hospital Zürich, University of Zürich, Zürich, SWITZERLAND.

Aim/Introduction: To evaluate whether quantitative PET parameters of motion-corrected ^{68}Ga-DOTATATE PET/CT may allow differentiating between intrapancreatic accessory spleens (IPAS) and pancreatic neuroendocrine tumor (pNET). ***Materials and Methods:*** A total of 498 patients underwent a clinically indicated ^{68}Ga-DOTATATE PET/CT for staging/restaging of NET. All subjects with accessory spleens (n = 43, thereof 7 IPAS) and pNET (n = 9) were included, resulting in a total of 45 scans. PET images were reconstructed using TOF PSF OSEM ($OSEM_{PSF}$) and TOF PSF BSREM with a beta value of 1000 ($BSREM_{1000}$). A data-driven gating (DDG) technique (MotionFree^{TM}, GE Healthcare) was applied to extract respiratory triggers and use them for PET motion correction within both reconstructions. An R-value threshold of > 10.0 defined respiratory motion. PET

parameters among different samples were compared using non-parametric tests. Receiver operating characteristics (ROC) analyzed the ability of PET parameters to differentiate IPAS and pNETs. ***Results:*** SUVmax and SUVmean were able to distinguish pNET from accessory spleens and IPAs in OSEM as well as in all $BSREM_{1000}$ reconstructions (all $p < 0.05$), except SUVmax of OSEM. This result was more reliable using DDG-based motion correction ($p < 0.003$) in both OSEM and $BSREM_{1000}$ reconstruction. For differentiating accessory spleens and pNETs, the ROC analysis yielded an AUC of 0.742 (sensitivity 56%, specificity 100%) / 0.765 (sensitivity 56%, specificity 100%) / 0.846 (sensitivity 62%, specificity 100%) / 0.840 (sensitivity 63%, specificity 100%) for SUVmax 36.7 / 41.9 / 36.9 / 41.7 in $OSEM_{PSF}$ / $BSREM_{1000}$ / $OSEM_{PSF}$ + DDG / $BSREM_{1000}$ + DDG, respectively. ***Conclusion:*** An SUVmax > 42 identifies a pNET with a specificity of 100%, regardless of the reconstruction technique used. A lesion with SUVmax < 42 may need more specific imaging examinations, such as ^{99m}Tc-HDRBC, if the suspicion of IPAS is still high, in order to avoid surgery. DDG-based motion correction increases the ability of PET/CT parameters (SUVmax and SUVmean) to discriminate IPAS/accessory spleens from pNET. $BSREM_{1000}$ leads to a significant increase of SUV parameters compared to OSEM, while data-driven gating (DDG) leads to a significant increase of SUV parameters and reduced PET volume compared to reconstructions without DDG. Hence, SUV cut-offs need to be adapted to different reconstruction settings. ***References:*** None

EPS-193

Image quality for two administration schedules for PET/CT-imaging of 68Ga-DOTATOC

C. Hindorf[1], A. Stenvall[1,2], L. Jönsson[1,2], B. Olsson[3], A. Svensson[3], U. Bitzén[3], F. Hedéer[3];
[1]Radiation physics, Skåne university hospital, Lund, SWEDEN, [2]Medical radiation physics, Lund university, Lund, SWEDEN, [3]Clinical physiology and nuclear medicine, Skåne university hospital, Lund, SWEDEN.

Aim/Introduction: For 68Ga-DOTATOC PET it is attempting to administer a low fixed activity per patient to facilitate a high patient throughput since the yield per batch is limited. Guidelines for 68Ga-DOTA-conjugated peptides recommend an injected activity of 100-200 MBq. However, each examination has to provide images with an acceptable quality. The aim was to compare image quality obtained by two different administration schedules: fixed injected activity and activity injected per body weight. ***Materials and Methods:*** Twelve patients referred for ^{68}Ga-DOTATOC PET were included (mean: 59years, 83kg, 6 females). The patients were divided into three groups based on body weight (3 patients <70kg, 6 patients 70-100kg, and 3 patients >100kg). Each patient received 2 MBq/kg body weight and an hour thereafter images were acquired in list mode (Discovery MI). Images were reconstructed with a block-sequential regularization expectation maximization reconstruction algorithm (Q.Clear, beta 900) both for our clinically used acquisition time of 3 minutes/bed position and for a shorter acquisition time/bed position to mimic an injected activity of 100 MBq. Images were assessed for image quality by one expert reader. Scores were given by a five-grade scale (1=unacceptable to 5=very high image quality). From regions-of-interest drawn in liver, muscle and fat max and mean activity concentration and standard deviation (std) were noted, and signal to noise ratios (SNR=mean/std) were calculated. Visually assessed image quality and SNR was compared for the two administration schedules and for the three patient groups. ***Results:*** The administration schedule of 2 MBq/kg gave a mean scored image quality of 3.7, 3.8 and 3.7 for patient groups <70kg, 70-100kg and >100kg, respectively. For a fixed activity of 100 MBq, the mean image quality decreased to 92%, 71% and 44%, respectively, of that for the 2MBq/kg-schedule for the patient groups. The SNR follows the results for the scored image quality. The administration schedule of 2 MBq/kg gave mean SNR of 19.3, 20.2 and 18.6 for patient groups <70kg, 70-100kg and >100kg, respectively. For a fixed injected activity of 100 MBq, the visually assessed image quality decreased to 94%, 92% and 65%, respectively, of that for the 2MBq/kg-schedule for the patient groups. Similar trends were seen for muscle and fat. ***Conclusion:*** Our study shows that an image quality independent of body weight is obtained for these patients if an administration schedule of 2 MBq/kg is applied, compared to if a schedule of 100 MBq fixed activity is applied. ***References:*** None

EPS-194

Integration of PET/MRI Hybrid Imaging into Radiotherapy Planning of Cervical Cancer Patients: First Results

S. Ahangari[1], N. Liv Hansen[1], A. Beck Olin[1], T. Jakobi Nøttrup[2], A. Kiil Berthelsen[1], J. Olof Löfgren[1], A. Loft Jakobsen[1], A. Kjær[1,3], F. Littrup Andersen[1], B. M. Fischer[1,4], A. Espe Hansen[1];
[1]Department of Clinical Physiology, Nuclear Medicine and PET, Rigshospitalet, University of Copenhagen, Copenhagen, DENMARK, [2]Department of Oncology, Section of Radiotherapy, Rigshospitalet, University of Copenhagen, Copenhagen, DENMARK, [3]Cluster for Molecular Imaging, University of Copenhagen, Copenhagen, DENMARK, [4]The PET Centre, School of Biomedical Engineering and Imaging Sciences, Kings College London, St Thomas' Hospital, London, UNITED KINGDOM.

Aim/Introduction: The integration of multiparametric PET/MRI imaging into the radiation treatment (RT) planning process and its potential to improve local disease control is promising but remains challenging. The objective of this study is to investigate how multiparametric PET/MRI can be integrated into RT planning of patients with cervical cancer. This includes attenuation correction (AC) of MRI hardware

and dedicated positioning equipment and evaluating MRI derived synthetic CT (sCT) of the pelvis region for PET AC and dose calculation to enable a PET/MRI-only setup. ***Materials and Methods:*** Nine patients underwent PET/MRI (Siemens Biograph mMR) scan in RT position. Each patient had a CT available and one patient was referred for RT. The PET/MRI scan protocol included multiparametric imaging with a total scan time of 35 minutes. The PET signal attenuation and CT-based attenuation correction of the dedicated RT setup including a flat table overlay, leg fixation device, flexible surface coil, and coil holders were evaluated using both phantom and clinical measurements.A deep convolutional neural network was trained to generate sCT from the corresponding Dixon MRI by including also data of sixteen patients from another ongoing study. For one patient the sCT was evaluated by measuring the mean absolute difference between the dose distributions calculated on sCT and CT. PET images reconstructed with sCT and co-registered CT were compared by the voxel-wise relative difference. ***Results:*** Phantom imaging with the RT flat table overlay revealed 2.3% reduction in total prompt. The PET photon attenuation for the phantom was up to 14.6% near to the table, which was reduced to 0.5%±3.2% using the generated hardware AC map. Comparable results were found in the patient study resulting in a 16% underestimation of SUV_{mean} without AC of the RT equipment.AI based sCT was inferred for each patient in less than 5 seconds. There was an excellent voxel-by-voxel correlation between CT and sCT ($P < 0.01$). The dosimetric analysis of the sCT-based dose planning showed a mean absolute error (MAE) of 0.12 Gy within the body contour and 0.18 Gy inside the planning target volume (PTV). PET image reconstructed with sCT compared to the one reconstructed with CT had relative differences of 6.2%±1.7% within the tumor. ***Conclusion:*** These preliminary results suggest that multiparametric PET/MRI-only can be successfully integrated in the radiotherapy workflow of patients with cervical cancer. Patient recruitment is ongoing for validation of the robustness of the setup. ***References:*** None

EPS-195

Utility of the Sentinel Lymph Node Biopsy in Breast Cancer after Neoadjuvant Chemotherapy with Negative Axillary Lymph Nodes or Node Involvement

N. Álvarez Mena*, F. Sebastián Palacid, P. Turbay Eljach, B. Pérez López, M. Alonso Rodríguez, C. Gamazo Laherrán, A. Sainz Esteban, M. Ruiz Gómez, M. González Soto, R. Ruano Pérez; Hospital Clínico Universitario de Valladolid, Valladolid, SPAIN.*

Aim/Introduction: To assess the usefulness of sentinel lymph node biopsy (SLNB) technique in patients with breast cancer after neoadjuvant chemotherapy (NAC). ***Materials and Methods:*** Retrospective series of 80 women with breast cancer who underwent a lymphoscintigraphy after the periareolar/peritumoral injection of 111MBq of 99mTc-nanocoloid for the detection of the sentinel lymph node post-NAC between June 2016 and April 2020. Variables such as age, carcinoma histology, molecular subtype, BRCA gene mutations, focality, axillary staging pre-NAC (clinical, US/MRI, FNA), tumor size, type of surgery, radiological response, lymphoscintigraphy result and intraoperative SLNB result (by using OSNA method) were analyzed. ***Results:*** Average age was 50 years (48% between 45-60 years). The main histological type was invasive ductal carcinoma (75), followed by infiltrating lobular carcinoma (4) and metaplastic (1). Regarding tumor characteristics we found that: 29 patients were triple-negative (36%), 19 luminal B-HER2, 13 HER2neu, 16 luminal B and 3 luminal A. BRCA1 gene mutations were detected in 3 patients. 1 tumor was multifocal and 7 multicenter. Axillary involvement pre-NAC was observed in 40 patients (50%): 4 clinically+ and US/MRI/FNA-, 7 US/MRI+ and FNA-, and 29 with axillary FNA+. 33 of them (83%) showed a tumor size <5cm (T1-T2) and the remaining 7 >5cm (T3-T4). Conservative surgery (lumpectomy/quadrantectomy) was performed in 54 patients (68%). 54% showed complete radiological response. Lymphoscintigraphy detected the SLN in 76 patients (95%). 4 were not detected despite reinjection, so an axillary lymph node dissection (ALND) was performed (3 without lymphatic invasion and 1 with 5/9 macrometastases). When evaluating SLNB result, it was observed to be: 1. Negative in 61 patients: -Axillary lymph-node preservation in 42 (69%): 1 metaplastic carcinoma. 17 triple-negative (1 of them synchronous bilateral carcinoma), 5 HER2neu (1 showed partial radiological response) and 8 luminal B-HER2. 1 multifocal and 4 multicenter. 8 patients with axillary affectation pre-NAC (1 clinically, 1 US/MRI+ and 6 FNA+) and 34 with negative axillary lymph nodes. 9 patients operated with a mastectomy. -ALND was performed in 19: they showed partial radiological response and/or suspicious lymph nodes intraoperatively (14 with lymphatic invasion pre-NAC). However, 73% without metastases. 2. Positive in 15 patients: -Axillary lymph-node preservation in 3 (20%) with micrometastases. -ALND in 12 with macrometastases: 9 showed axillary involvement pre-NAC. ***Conclusion:*** SLNB is a very useful technique in patients with NAC by avoiding a high number of unnecessary axillary lymphadenectomies, even in those with a worse prognosis, improving their quality of life. ***References:*** None

EPS-196

Impact Of Sentinel Lymph Node Biopsy In Breast Cancer Patients Treated With Neoadjuvant Chemotherapy

A. Roteta*, D. Nogueira Souto, E. Galindo Lalana, L. Tardin Cardoso, A. Andrés Gracia, P. Razola Alba, M. Delgado Castro, T. Escalera Temprado, E. Prats Rivera, M. Abós Olivares; Clinic Hospital "Lozano Blesa", Zaragoza, SPAIN.*

Aim/Introduction: To analyze how many of the patients undergoing neoadjuvant chemotherapy (NCT) may benefit from SLNB, as well as the impact on patient management, especially in those with early axillary involvement. ***Materials and Methods:*** We included patients with breast carcinoma candidates to NCT discussed at the Tumor Committee of our hospital (April/2017-August/2019). All of them were subjected to clinical assessment, ultrasound and, if appropriate, histological analysis, axillary pre and post-NCT. Sentinel lymph node detection was performed after periareolar injection of [99mTc]Tc-nanocoloid (74 MBq) the day before surgery. In some cases, blue dye was injected and/or a pre-NPC metal clip was placed in the affected node. ***Results:*** Sixty-two patients were included. NCT achieved a complete breast response in 12 patients, partial in 46 and non-response in 4. Initially, 31 patients were classified as N0 and 31 as N+ (28 N1 and 3 N2), achieving a complete axillary response in 58% of N+ (18). SLNB was performed in 49 patients (79%; 100% in N0 and 58% in N+ from baseline). The gamma detection rate of the sentinel lymph node was 91.8% (93.5% in N0 and 88.9% in N+). 28 lymphadenectomies were undergone (45.2%; 22.5% in N0 and 67.7% in N+), 11 due to positive SLNB (5 N0 and 6 N1), 13 owing to lack of axillary response and 4 caused by the non-localization of the sentinel lymph node. SLNB was performed in 58% of N+ patients, of which 44.4% were negative, avoiding lymphadenectomy. Metal clip and/or blue dye techniques were used in 31 cases (50%). ***Conclusion:*** SLNB is viable in a high percentage of patients with previous NCT, with a high detection rate, even in patients with early affected axilla, avoiding lymphadenectomy to patients who achieve a complete response of the axillary lymph node. ***References:*** None

EPS-197

Tumor Recurrence at 5 Years in Patients with Breast Cancer, Previous Surgery Treatment and Sentinel Lymph Node Biopsy

N. Álvarez Mena*, F. Sebastián Palacid, P. Turbay Eljach, B. Pérez López, C. Gamazo Laherrán, M. Alonso Rodríguez, A. Sainz Esteban, M. Ruiz Gómez, M. González Soto, R. Ruano Pérez; Hospital Clínico Universitario de Valladolid, Valladolid, SPAIN.*

Aim/Introduction: To assess the probability of tumor recurrence at 5 years in patients with personal history of breast cancer in whom sentinel lymph node biopsy (SLNB) was performed. ***Materials and Methods:*** Retrospective series of 123 patients with breast cancer who underwent lymphoscintigraphy to detect the SLN and subsequent intraoperative exeresis between January 2014 and December 2014. Variables such as age, sex, SLNB result, tumor recurrence at 5 years and exitus until January 2020 were analyzed. Data were also collected from patients with disease recurrence: age, sex, histology and tumor size, if triple-negative (negative estrogen and progesterone receptors and also negative HER2), percentage of nuclei with positive staining in tumor cells (Ki-67 score), SLNB result and location of recurrence. ***Results:*** 122 women and 1 man with average age of 55 years were studied. SLNB was negative in 76 patients (62%). Recurrence was detected in 6 patients, all of them women with mean age of 60 years. Regarding tumor characteristics in this group: histological types found were invasive ductal carcinoma (IDC) in 5 patients and carcinosarcoma in 1, and an average size of 20mm. 33% of them were triple-negative and showed Ki-67 percentage score of 70-80%. When evaluating SLNB result, it was observed to be: 1. Negative in 2 of the relapsed patients: 1 showed distant recurrence at 3 years in the liver, and 1 presented new lesion in the contralateral breast at 2 years (second SLNB also negative). 2. Positive in 4 patients, with axillary lymph node dissection (ALND) performed: 2 showed local recurrence (surgical site) and 2 presented distant disease (1 in the liver and 1 had a mass with superior vena cava thrombosis). Therefore, the recurrence of disease at 5 years is 5% in our sample (6/123): 33% (2/6) with previous negative sentinel lymph node biopsy; 66% (4/6) with positive SLNB and ALND. Until January 2020, 6 of the 123 patients deceased, but just 3 due to recurrence. ***Conclusion:*** The recurrence of the disease at 5 years is not relevant in patients undergoing sentinel lymph node biopsy. However, there is a higher incidence in those who showed positive SLNB and ALND was performed, probably due to some prognostic factors such as tumour size, histology, hormone receptors expression, or Ki-67 score. ***References:*** None

1801

Honorary Member Award, Marie Curie Award, Plenary 4: Highlights Lecture, Closing

Friday, October 30, 2020, 17:05 - 18:25 Channel 1

OP-1003

Honorary Member Award

OP-1005

Marie Curie Award

OP-1006

Plenary 4: Highlights Lecture

A. Chiti*; Humanitas University, Nuclear Medicine, Milan, ITALY.*

OP-1007

Plenary 4: Highlights Lecture

R. Hustinx*; Centre hospitalier Universitaire de Liège, Service de Médecine Nucléaire, Liege, BELGIUM.*

OP-1012

Closing

S. Fanti; EANM Congress Chair, Bologna, ITALY.

EP-01

All about the Prostate

e-Poster Area

EP-001

Decision impact study on the use of PET-PSMA for the initial staging of men with high-risk localized prostate cancer (PCa)

A. Viaouet[1], C. Verrier[2], S. Mengue[2], S. Leroux[2], G. Desrez[2], T. Haaser[1], R. Herve[2], O. Couturier[2], P. Gustin[2];
[1]University Hospital of Bordeaux, Bordeaux, FRANCE, [2]General Hospital of French Polynesia, Papeete, FRENCH POLYNESIA.

Aim/Introduction: The standard-of-care conventional imaging for men with high-risk localized PCa are the MRI and the 99mTc-Bone scan. We aimed to investigate to what extent the use of gallium-68 PSMA PET-CT (Prostate Specific Membrane Antigen), because of its better sensitivity, could induce a change in management during the multi-disciplinary genitourinary oncology teams. *Materials and Methods:* This monocentric retrospective study was conducted at the General Hospital of French Polynesia on 23 patients with high-risk localized PCa who underwent PET-PSMA in New-Zealand for their initial staging. The primary outcome was the frequency of staging modification. The secondary outcomes were the proportion of change in management intent (curative to palliative) or modality (prostatectomy or radiotherapy) (major change), and the proportion of change in modality delivery (minor change). *Results:* The median age was 64 years-old. The mean initial PSA was 44,26 ng/mL. 11 patients were T3a (48%), 2 were T3b (9%). The distribution between ISUP group 1, 2, 3, 4, 5 was respectively 4 (17%), 3 (13%), 8 (35%), 1 (4%) and 6 (26%). 18 were at high-risk according to D'Amico's risk classification (78%) and 5 were at intermediate risk (22%). A change in staging occurred for 13 patients (56%): 7 UP-staging (30%), including 4 on T, 2 on N, 2 on M. 6 DOWN-staging (26%), including 0 on T, 4 on N, 3 on M. 10 were stable (43%). A change in treatment intent occurred for 11 patients (48%) with 6 « major » changes and 5 « minor » changes. *Conclusion:* Despite their retrospective and their low power, these results are consistent with the recent available literature. Thus, the prospective study "proPSMA" confirmed to a lesser extent these results with a change in treatment intent occurring for 39 (27%) of the 146 patients who underwent PET-PSMA. *References:* None

EP-02

Bone and Soft Tissues

e-Poster Area

EP-002

^{18}F-NaF Uptake by Fibrous Dysplasia Lesions in the Skull is Signficantly Higher in Patients with Optic Neuropathy

G. Papadakis[1,2,3], G. Giannakakis[2], A. H. Karantanas[3], K. Marias[2], M. T. Collins[1], A. M. Boyce[1];
[1]National Institute of Dental and Craniofacial Research (NIDCR), Bethesda, MD, UNITED STATES OF AMERICA, [2]Computational Biomedicine Laboratory (CBML), Foundation for Research and Technology Hellas (FORTH), Heraklion, GREECE, [3]Department of Medical Imaging, Medical School, University of Crete, Heraklion, GREECE.

Aim/Introduction: Fibrous dysplasia (FD) of bone is a benign skeletal disorder characterized by the replacement of normal bone and normal bone marrow with abnormal fibro-osseous tissue leading to significant morbidity. Since the skull is a frequent site of FD lesions, aim of the current study was to explore potential association between FD-related ^{18}F-NaF uptake in the skull and the presence of optic neuropathy. *Materials and Methods:* Forty four FD patients (26 females, 18 males) underwent whole-body ^{18}F-NaF-PET/CT scans at the NIH Clinical Center. All study participants underwent neuro-ophthalmologic evaluation in order to determine the presence of optic neuropathy (36 patients without optic neuropathy, 8 patients with optic neuropathy). Mean age±std at the time of the scan was: 30.1±14.9 years. PET scans were obtained (mean ± SD) 61.8±5.1minutes after intravenous administration of an average±std of 2.69±0.73mCi of ^{18}F-NaF. Low dose, non-contrast, CT scans were acquired for coregistration and attenuation correction purposes. FD-related ^{18}F-NaF activity in the skull was assessed by using MIM vista (version 6.5.9). Firstly, a VOI encompassing the head was drawn, and afterwards a SUVmax threshold-based approach -customized per patient- was employed in order to include all FD-related craniofacial uptake. Separate VOIs encircling all areas above the SUVmax threshold, were automatically generated, while areas with non-FD related ^{18}F-NaF activity were manually removed. Subsequently, the following craniofacial FD-related ^{18}F-NaF uptake parameters were automatically obtained:Total Volume (TV) of all ^{18}F-NaF positive skull FD lesions and FD-related Total ^{18}F-NaF craniofacial Activity (TA) determined as the product of TV multiplied by SUVmean of all craniofacial FD lesions (TA = TV×SUVmean). Finally the aforementioned ^{18}F-NaF parameters were correlated with the presence of optic neuropathy. *Results:* T-test revealed that both TV and TA were significantly higher in FD patients with optic neuropathy in comparison to FD patients without

optic neuropathy. (TV: t=2.37, p=0.022<0.05) (TA: t=2.04, p=0.048<0.05). ***Conclusion:*** The significant association between craniofacial FD-related ^{18}F-NaF uptake and the presence of optic neuropathy, indicates the effectiveness of ^{18}F-NaF PET/CT in reflecting clinically relevant skeletal outcomes in patients with FD. ***References:*** None

EP-003

Prognostic value of ^{18}F-FDG PET/CT-based metabolic parameters in patients with bone sarcoma

L. García Belaústegui, C. Wakfie Corieh, R. Valhondo Rama, A. Blanes García, M. Cabrera Martin, J. Carreras Delgado; Clinico San Carlos Hospital, Madrid, SPAIN.

Aim/Introduction: The aim of the study was to assess the prognostic significance of maximum standardized uptake value (SUVmax), metabolic tumor volume (MTV), and total lesion glycolysis (TLG) from ^{18}F-FDG PET/CT scans performed in patients with bone sarcoma by correlating these metabolic parameters with clinicopathological features of the tumor. ***Materials and Methods:*** In total, 35 patients initially diagnosed with bone sarcoma and who underwent ^{18}F-FDG PET/CT with contrast enhacement at the time of initial diagnosis were retrospectively reviewed. The SUVmax, MTV (cm^3) and TLG of primary tumors were measured and correlated with tumor grade, histological subtype and presence of lymph node or distant metastasis. ***Results:*** Mean age was 42 years and 57.7% of the patients were women. Primary tumor was located in lower (53.85%) and upper limbs (23.07%) or pelvis (23.07%). The 7.7% of the patients presented lymph node metastasis at the time of diagnosis and the 30.8% had distant disease in lung, bone or peritoneum. Tumors histologically classified as high grade presented mean values of SUVmax 20.60, $VMT_{2,5}$ 319.67, $VMT_{40\%}$ 51.83 and TLG 1605.30; moderate grade tumors showed an average of SUVmax 8.24, $VMT_{2,5}$ 71.58, $VMT_{40\%}$ 46.80 and TLG 283.20 and mean values in low grade tumors were SUVmax 4.75, $VMT_{2,5}$ 8.32, $VMT_{40\%}$ 39.9 and TLG 25.09. Metabolic parameters were also measured according to the histological subtype of the tumor: 34.6% were osteosarcoma (SUVmax 12.80, $VMT_{2,5}$ 80.47, $VMT_{40\%}$ 27.09, TLG 463,98), 34.6% were chondrosarcoma (SUVmax 7.16, $VMT_{2,5}$ 59.07, $VMT_{40\%}$ 50.08, TLG 228.35) and 11.5% were Ewing sarcoma (SUVmax 12.02, $VMT_{2,5}$ 123.77, $VMT_{40\%}$ 59 and TLG 669.84). ***Conclusion:*** The pretreatment SUVmax, MTV and TLG from ^{18}F-FDG PET/CT were directly related with histologic tumor grade and aggressiveness of the tumor subtype and therefore could be useful for providing important prognostic information at initial diagnosis. However, these results need to be validated in standardized prospective studies. ***References:*** None

EP-004

Correlation between 18F-sodium fluoride uptake by PET and dual-energy X-ray absorptiometry in the second lumbar spine vertebra

R. Piri[1,2]*, P. Hermann*[3]*, H. Petersen*[1]*, O. Gerke*[1,2]*, A. B. Jespersen*[4,5]*, M. Ø. Andersen*[4,5]*, P. F. Høilund-Carlsen*[1,2]*;*
[1]Research Unit of Clinical Physiology and Nuclear Medicine, Department of Clinical Research, University of Southern Denmark, Odense C, DENMARK, [2]Department of Nuclear Medicine, Odense University Hospital, Odense, DENMARK, [3]Department of Endocrinology, Odense University Hospital, Odense C, DENMARK, [4]Center for Spine Surgery and Research, Lillebælt Hospital, Middelfart, DENMARK, [5]Institute of Regional Health Research, University of Southern Denmark, Odense, DENMARK.

Aim/Introduction: 18F-Sodium Fluoride (NaF) is a known positron emission tomography (PET) tracer used to track micro-calcification at the molecular level, i.e., "active calcification" in the body. In comparison, dual-energy X-ray absorptiometry (DXA) is common modality used to examine bone mineral density (BMD) and bone mineral content (BMC). Thus, these modalities are used to evaluate molecular and physical bone features, respectively. Focusing on the second lumbar spine vertebra (L2), we examined the potential association between results obtained by NaF-PET/CT and DXA scans. ***Materials and Methods:*** A total of 78 patients were included from the PARA-DESIS study, i.e., a randomized controlled trial aiming to elucidate the effect of parathyroid hormone (Teriparatide) given to patients, aged 60+ years, for three months following spondylolisthesis operation for disabling spinal stenosis. All patients underwent NaF-PET/CT and DXA scans 3 months after operation, and measured variables were obtained from L2, distant from the operation site in all patients. PET variables included volume of interest (VOI), and maximal, peak, mean and total standardized uptake values (SUVmax, SUVpeak, SUVmean, SUVtotal), including the latter two after partial volume correction (cSUVmean and cSUVtotal). Finally, the association between demographics and variables from the two modalities were examined. ***Results:*** The mean age of the patients was 70.49±6.14 years (62 females). Weight (r=0.31, p=0.007) and height (r=0.34, p=0.002) had weak positive correlations with BMC and with total VOI uptake (r=0.34, p=0.002) and (r=0.44, p<0.001), respectively. BMC correlated with VOI volume (r=0.51, p<0.001), SUVtotal (r=0.37, p<0.001) and cSUVtotal (r=0.34, p=0.002). Similarly, BMD correlated with SUVpeak (r=0.24, p=0.03), SUVtotal (r=0.24, p=0.04) and cSUVtotal (r=0.27, p=0.02). ***Conclusion:*** Positive correlations between relevant SUV measures and physical features of bone, including BMD and BMC, were observed indicating that the metabolic activity of bone increases with increasing bone density and mineral content. ***References:*** None

EP-005

Comparison of thoracic, abdominal and pelvic SPECT/CT with wholebody bone scan in bone metastases. Can we avoid planar wholebody bone scan?

A. Sainz Esteban, P. Turbay Eljach, N. Álvarez Mena, F. Sebastian Palacid, M. González Soto, M. Ruíz Gómez, C. Gamazo Laherrán, B. Pérez López, R. Ruano Pérez;
Hospital Clinico Universitario, Valladolid, SPAIN.

Aim/Introduction: To compare thoracic, abdominal and pelvic SPECT/CT (wSPECT/CT) with wholebody bone scan (WBS) in the assessment of bone metastases. ***Materials and Methods:*** A total of 32 patients with suspected or confirmed bone metastases underwent WBS and a wSPECT/CT (from the base of the cervical spine to the pelvis) after the intravenous injection of 99mTc-diphosphonates. Images were visually interpreted in two separate reading sessions. For anatomical analysis, the skeleton was divided in nine anatomical sections as skull and cervical spine, clavicle and sternum, ribs and scapula, thoracic spine, lumbar spine, sacrum, pelvis, humerus and femur. In patients with generalized bone metastases, only one dominant lesion in each anatomical section was selected for analysis. Lesions were interpreted as malignant or equivocal in WBS and malignant, benign or equivocal in wSPECT/CT. Lesions with unsuspicious morphological alterations located around the joints, degenerative changes (e.g. osteophytes), osteoporotic patterns and/or fractures detected in WBS were excluded from the study. ***Results:*** A total of 130 lesions were assessed, 10 were only positive on WBS (located in parts of the body not covered by wSPECT/TC) and 21 were only positive on the wSPECT/CT. WBS showed 31 equivocal lesions, 12 were benign on wSPECT/CT, 18 malignant and 1 equivocal. In a patient-based analysis, in 16 patients wSPECT/CT didn't supply additional information to the WBS: two patients showed a normal scan and 14 patients showed the same lesions presented in the WBS or more lesions but without impact on the final diagnosis. In 16 patients wSPECT/CT add crucial information to the diagnosis: in one patient wSPECT/CT showed metastatic disease not visible in WBS, in 13 patients improved equivocal lesion characterization and in two patients dismiss false positive findings on WBS. However, in all the patients the performance of a WBS and a SPECT/TC of one anatomical section would have been sufficient to provide the same data. In 8 patients showed lesions not covered in the wSPECT/CT but it didn't modify the final diagnosis. ***Conclusion:*** wSPECT/TC can replace the WBS in all the patients studied and add crucial information to the diagnosis in 50% of the patients. However, in all the patients the performance of a WBS and a SPECT/TC of one anatomical section would have been sufficient to provide the same data. ***References:*** None

EP-006

Necessity of Whole Body Bone Scintigraphy In Patients With Lung Or Breast Cancer Who Underwent Whole Body ^{18}F FDG-PET/CT For Initial Staging

F. Görtan[1], Z. Kaya Döner[2], Ö. Vural Topuz[3], E. Arslan[4], M. Halaç[5];
[1]Turkish Ministry of Heath, Ankara City Hospital, Department of Nuclear Medicine, Ankara, TURKEY, [2]Health Sciences University Bursa Higher Specialization Training And Research Hospital, Department of Nuclear Medicine, Bursa, TURKEY, [3]Istanbul Okmeydani Training and Research Hospital, Department of Nuclear Medicine, Istanbul, TURKEY, [4]Istanbul Training and Research Hospital,Department of Nuclear Medicine, Istanbul, TURKEY, [5]Neo Life Medical Center, Istanbul, TURKEY.

Aim/Introduction: The aim of our study is to analyze the necessity of performing whole body bone scintigraphy (WBS) for revealing potential metastatic bone lesions in patients with lung or breast cancer who underwent whole body fluorodeoxyglucose positron emission tomography/computerized tomography (^{18}F FDG-PET/CT) for initial staging. ***Materials and Methods:*** In the study, the patients diagnosed with histopathologically poven lung or breast cancer who underwent ^{18}F FDG-PET/CT scan at our department for initial staging were evaluated retrospectively. Among these patients, 82 of them were included in the study (41 female and 41 male; average age 57.7 (34-76); 48 lung cancer and 34 breast cancer) who had underwent also WBS within maximum 30 days (average 5,4± 6,4 days) in order to be evaluated for bone metastases before any treatment. ***Results:*** Either one of ^{18}F FDG-PET/CT or WBS revealed 292 bone lesions which were evaluated to possibly be bone metastasis in 36 (43.91 %) out of 82 patients. In 22 of those 36 patients, both methods revealed positive results. 7 out of remaining 14 patients had true positive results in ^{18}F FDG-PET/CT and false negative results in WBS. The remaining 7 patients revealed false positive results in WBS and true negative in ^{18}F FDG-PET/CT. According to the final diagnosis, all but 2metastatic bone lesions were demonstrated in ^{18}F FDG-PET/CT while only 122 of 292 lesions were demonstrated in WBS. In identifying bone metastasis, sensitivity, specificity, accuracy, positive and negative predictive values of ^{18}F FDG-PET/CT and WBS were 99.32%; 100%; 99.41%; 100%; 95.92% and 41.78%; 56.79%; 45.04%; 77.70%; %15.75, respectively. The relation between computerized tomography (CT) characteristics and ^{18}F FDG uptake concentration indicated that SUVmax values in lytic lesions tend to be higher. ***Conclusion:*** Our study revealed higher values of sensitivity, specificity, positive and negative predictive values in ^{18}F FDG-PET/CT than those in WBS for diagnosis of bone metastasis. ^{18}F FDG-PET/CT could reveal all but two bone metastasis. These two lesions were in the upper extremity and therefore out of imaging area. Besides, there wasn't any lesion where ^{18}F FDG-PET/CT predicted false negative results. On the other hand, WBS wasn't able to

detect all metastatic bone lesions. Furthermore, it predicted false positive lesions. Accordingly it might be concluded that it is not necessary to perform WBS for revealing other potential bone metastasis in patients who underwent ^{18}F FDG-PET/CT for initial staging. ***References:*** None

EP-007

Additional clinical impact of single photon emission computed tomography/computed tomography bone scintigraphy (SPECT/CT) 16 slices to planar whole body BS in evaluation of equivocal lesions

N. Kapsoritakis[1], *P. Simos*[2], *O. Bourogianni*[1], *M. Stathaki*[1], *A. Tsaroucha*[1], *E. Papadaki*[1], *S. Koukouraki*[3];
[1]*Nuclear Medicine Department, University Hospital, Heraklion-Crete, GREECE,* [2]*School of Medicine, University of Crete, Institute of Computer Science, Foundation for Research and Technology-Hellas, Heraklion-Crete, GREECE,* [3]*School of Medicine, University of Crete, Heraklion-Crete, GREECE.*

Aim/Introduction: In clinical practice, one of the most frequent diagnostic dilemmas is evaluating oncological patients in order to confirm or rule out bone metastatic disease. Despite more advanced imaging modalities, bone scintigraphy (BS) continues to play a major role. However, indeterminate lesions require further imaging with higher specificity. Nowadays, new hybrid imaging modalities SPECT/CT 16 or more slices is increasingly being used in clinical nuclear medicine practice. The aim of this study was to assess the additional value of targeted SPECTCT 16 slices acquisition to whole body planar BS (wbPBS) in characterizing equivocal bone lesions. ***Materials and Methods:*** Between January 2019 and January 2020, a total of 600 pts with different types of histopathologically proven cancer were prospectively recruited for staging and restaging purposes. Inclusion criteria were bone pain, elevated tumor markers and equivocal/suspicious CT results. All 600 oncological pts underwent wbPBS and all patients with equivocal/suspected for bone metastasis lesions on wbPBS (n=265), underwent additionally a targeted SPECT/CT. Image interpretation was based on lesion and patient based analysis. According to lesion based analysis, lesions were scored as benign (score 1), malignant (score 2) or equivocal (score 3). ***Results:*** 215/600 pts had a negative test result (35.9%) on wbPBS. In the remaining 385 patients a total of 803 lesions of abnormal uptake of the radiotracer were found: 62 (7.7%) lesions were evaluated as metastatic (score 2), 60 (7.7%) were evaluated as lesions of benign origin (non-metastatic) (score 1) and 681 (84.8%) as unclear lesions (score 3). A targeted SPECT/CT was performed immediately after the wbPBS in 265 pts. 668 lesions considered as unclear and were reevaluated with targeted SPECT/CT. Diagnostic findings on SPECT/CT were obtained for 592/668 (88.6%) lesions and 227/265 (85.7%) of patients, 317/668 lesions (47.5%) were classified as score 1, 275/668 (41.2%) as score 2. 76/668 lesions (11.4%) in 38 patients (14.3%) were classified as score 3. The percentage of indeterminate lesions on SPECT/CT vs PBS was 11.4% vs 84.8%.Moreover, the addition of SPECT/CT provided 36 more lesions vs wbPBS. The diagnostic yield was 83% (30/36 lesions), with 8/30 (26.7%) were evaluated as score 1 and 23/30 as score 2 (76.7%). 5/36 lesions (13.9%) were classified as score 3. ***Conclusion:*** The introduction of SPECT/CT has further enhanced the diagnostic accuracy of wbPBS offering a better characterization of equivocal findings distinguishing metastasis from benign lesions. SPECT/CT could be a promising tool for the accurate staging and restaging. ***References:*** None

EP-008

Bone scan indications in patients under 30 years of age

N. Manevska*, N. Bozinovska, T. Makazlieva, S. Stojanoski, V. Majstorov, D. Miladinova;*
Medical Faculty, Skopje, NORTH MACEDONIA.

Aim/Introduction: Bone scintigraphy can be a useful tool in evaluating bone disorders in young adults. Although it has a low specificity, combining planar dual phase bone scan (DPBS) and hybrid imaging (SPECT/CT), can help in detecting metabolic activity of bone lesions (BL) of various etiology. ***Materials and Methods:*** Bone scan indications in young patients under 30 years were retrospectively evaluated in a two-year period at our Nuclear Medicine Department. The DPBS and afterwards SPECT/CT procedure on the region of interest was performed 3 hours after i.v application of 99mTc-MDP in dose calculated by age. ***Results:*** We evaluated 65 patients (27 males, 38 females), average - 15.32±7.25y. The most frequent indication was metabolic activity of primary BL of non-malignant etiology (38/65, 58.46%), followed by primary malignant BL (12/65 patients, 18.46%). In 10 (15.38%) patients the indication was to detect bone mets due to non-bone malignancies (Malignant Melanoma, Neuroblastoma, Nephroblastoma, Medulloblastoma, Hodgkin Lymphoma, Histiocytosis). The non-malignant etiology was predominantly due to primary benign bone tumors (22/38, 57.89%) including Osteoid osteoma - 8, Fibroma Non-Ossificans - 4, Enchondroma - 1, Osteochondroma - 1, followed by Aneurysmal Bone Cyst-7, Exostosis-1. Other rare indications were trauma, sacroiliitis, rheumatologic diseases and fibrous dysplasia. In suspected malignant bone tumors histopathology revealed Osteosarcoma in 4 patients, Chondrosarcoma - 2, Ewing sarcoma - 1, Histiocytosis - 3, Malignant Lymphoma - 1, NET - 1. More than 2/3 of the patients complained of bone pain and in 23% the pain was associated with an injury. In 50/55 patients, BL presented in the appendicular skeleton, mainly in the inferior extremities. DPBS was performed in all except 9 patients (with malignancy of non-bone etiology), where indication was detecting distant

mets. From 56 patients, DPBS was positive in 36.92%, while negative in the pool phase and positive only on the late phase in 27.69%. Positive both planar and SPECT/CT were detected in more than half of the patients (52.31%), while 4 patients had negative planar and positive SPECT/CT (ABC-1, Ewing - 1, Sacroiliitis - 1, Nephroblastoma - 1). ***Conclusion:*** Bone scintigraphy is still a valuable nuclear method complementary to other diagnostic modalities. In young adults the main clinical indication is evaluation of primary BL of non-malignant etiology. Because of its high sensitivity, it can detect metabolic activity of BL and their turnover (osteoblastic reactions) of various etiologies (benign, malignant, traumatic, inflammatory, rheumatic) and assists in further management of the patient. ***References:*** None

EP-009

The role of bone scan in the diagnosis of bone metastases in Ewing's sarcoma

D. Travaglio Morales*, J. M. Cordero García, L. García, D. Monachello Araujo, E. López Llobet, S. Rodado Marina, M. Coronado Poggio, C. Lancha Hernandez, C. Escabias del Pozo, E. Ortiz, R. Sebastián, L. Dominguez Gadea;*
Hospital Universitario La Paz, Madrid, SPAIN.

Aim/Introduction: To review the experience of the conventional bone scan in the evaluation of Ewing's sarcomas metastases in a sarcomas expert center. ***Materials and Methods:*** A review of the bone scans performed in the last 6 years in our center was carried out, evaluating the presence of metastases in the initial assessment and follow up of Ewing's sarcoma (ES). The data concerning the age at initial diagnosis, histological type and anatomic origin of the primary tumor were collected, as well as the data of evolution of these patients. The presence of metastases in the initial diagnosis or during follow up was confirmed by CT, RM, PET-CT or biopsy. ***Results:*** A total of 42 patients (p) (average age: 16.8 years, 14 women and 28 men) were reviewed, in whom a total of 191 bone scan had been carried out. Eight out of 42 patients were diagnosed of soft tissue ES, and 34/42 with bone ES. The primary tumor was located in the lower extremities in 20 patients, followed by pelvis (9 patients), trunk (9), upper extremities (3) and head (1). The follow up ranged between 1 and 204 months, with a mean of 58 months. A total of 18/42 patients (43%) had metastases: 18/18 in the lungs and 5/18 (28%) in bone tissue. 15/18 patients had metastasis at initial diagnosis (16 pulmonary and 2 osseous) and 3/18 during the follow up (3 osseous and 2 pulmonary). The bone scan identified the presence of lesions in 4 of 5 patients with bone metastases. (S=83% and E=100%). The false negative case was due to diffuse bone marrow involvement. ***Conclusion:*** The bone scan constitutes nowadays an important diagnostic tool in the initial evaluation and follow up of Ewing's sarcomas, with a high sensitivity in the detection of bone metastases. Bone marrow involvement may not be identified in bone scans, leading to false negative results ***References:*** None

EP-010

Usefulness of ^{18}FDG PET/CT in Ewing sarcoma In Morocco

A. Sallak*, E. Iris, G. Amal;*
University Hassan II of medicine, Casablanca, MOROCCO.

Aim/Introduction: This is a retrospective descriptive study done at the nuclear medicine department of the Ibn Rochd University Hospital in Casablanca, from February 01, 2015 to December 31, 2017. We analysed the 18FDG TEP-TDM exams done as part of the initial extension assessment or follow-up of patients with Ewing's sarcoma (ES). The purpose of this work is to understand the usefulness of PET / CT in these patients. ***Materials and Methods:*** The 18FDG PET / CT examination done in fasted patients for at least 6 h, with a fasting capillary blood glucose lower than 7mmol / l. The injected activity is 3 MBq / Kg for children and 4 to 5.5 MBq / kg of 18FDG in adults. The acquisitions made 60 minutes after the injection. The exams analyse was done by two seniors. Positive lesions are those in which the max SUV is greater than the hepatic max SUV ***Results:*** Fourteen patients, and 15 scans, 6 scans for initial assessment of extension, 5 for suspected recurrence and 4 for evaluation of treatment. The average age was 23.5 years [5 to 55 years]. The sex ratio F/M was 1.67. The ES was skeletal in 88 % of the cases. For the extension assessment, PET / CT was strongly positive in the initial lesion in 5/6 patients, the mean maximum SUV was 8, the hepatic max SUV [1.14, 4.42]. The mean lesion metabolic volume was 641.7 cm^3. Two patients had satellite lymph node hypermetabolism, SUV max at 2.65. Three patients (50%) have osteo- medullary and pulmonary metastatic at diagnosis, the SUV max average value at 4.5. For suspected relapse, ^{18}FDG PET / CT was positive in 5/6 patients. The initial site was hyper metabolic in 5/6 patients, the maximum mean SUV was 8.5 associated in 50 % of cases with a satellite lymph node hypermetabolic and in 83 % of cases to a distant metastasis. Four patients underwent end-of-treatment ^{18}FDG PET / CT. The ^{18}TEP / CT was negative in 3 patients, the disease was stable in one. ***Conclusion:*** The level of FDG uptake faithfully reflects the grade and aggressiveness of the tumor and remains a guiding factor in the management of Ewing's sarcomas by offering one of its great advantages, whole-body imaging and exhaustive mapping of all the targets to be treated as well as possible risk lesions. ***References:*** None

EP-03
Brain tumours

e-Poster Area

EP-011
Differential diagnosis between progression and radionecrosis in brain metastases after stereotactic radiosurgery using hybrid FDG-PET and MRI coregistered images

H. Otman[1], J. Deverdin[2], N. Menjot de Chamfleur[2], F. Molino[2], M. Bilal Chawki[3], F. Cachin[1], C. Bouvet[1], B. Fayçal[2], L. Emmanuelle[2], D. Mariano Goulard[2];
[1]Centre Jean Perrin, Clermont Ferrand, FRANCE,
[2]University Hospital of Montpellier, Montpellier, FRANCE,
[3]University Hospital of Nancy, Nancy, FRANCE.

Aim/Introduction: Dual phase 18 FDG-PET has been proven helpful to assess FDG-avid cerebral tumors as tracer will build up in metastases or tumor recurrences while its retention remains stable within normal tissue or inflammatory process. This is useful when MRI can't discriminate brain tumor recurrence (TR) from radionecrosis (RN) after stereotaxic radiosurgery (SRS) for brain metastases (BM). Many studies have sought to improve diagnostic performance by associating FDG-PET and MRI with interesting results but many bias, mostly within image post-processing. Coregistered MRI and dual phase FDG-PET images could alleviate these biases and be used to extract prognostic biomarkers. ***Materials and Methods:*** We retrospectively evaluated patients treated with SRS for BM which developed a contrast-enhanced MRI lesion with non-conclusive diagnosis for TR or RN. All patients underwent MRI and FDG-PET at least 3 months after their last SRS session. Dual FDG-PET comprised a one hour "based image" (H1) followed by a 4 hours "delayed image" (H4). MRI included contrast enhanced T1 (T1), FLAIR, ASL (BAT, CBF), T1 Perfusion (ktrans, SER) and T2* Permeability (k2,rBF, rBV). PET and MRI data were all coregistered on the T1 images. Semi-automated Regions of Interest (ROI) of the tumor were drawn on the T1 MRI, H1 and H4 FDG-PET images; a reference contralateral white-matter ROI (WM) was drawn for standardization. Imaging metrics were then evaluated for their association with TR or RN based on histological, radiological and clinical criteria after at least 6 months follow-up. ***Results:*** Eleven patients matched the inclusion criteria; 7 with TR and 4 with RN; no additional treatment was introduced. On visual analysis, FDG-PET and MRI respectively obtained 100% and 83% Sensitivity and 100% and 80 % Specificity. The two MRI-false negative diagnoses were subsequently identified on follow-up (1 patient, RN) and histology (1 patient, TR). When standardized on WM, PET SUVmax values were significantly different across groups at H1 (p<0,044) and H4 (p<0,00285). Among MRI metrics, relCBF (p<0.02055), T1-perfusion AUC (p< 0.00425), SER (Signal Enhancement Ratio, p<0.0195) and Washout (p<0.0212) could significantly discriminate between TR or RN. ***Conclusion:*** Coregistered PET-MRI images accurately discriminates between TR and RN. With FDG being the most commonly used PET radiotracer, this protocol remains easily transposable and should be encouraged to obtain non-invasive prognostic and clinically relevant biomarkers. ***References:*** None

EP-012
[^{11}C]Methionine Uptake In Grade II-III Diffuse Gliomas Does Not Allow To Classify Tumors According To IDH1 Mutation Status

T. Skvortsova*, Z. Savintseva, D. Zakhs;*
N. P. Bechtereva Institute of the Human Brain of Russian Academy of Sciences, Saint-Petersburg, RUSSIAN FEDERATION.

Aim/Introduction: The aim of the study was to assess the relationships between [^{11}C]methionine (MET) positron emission and computed tomography (PET/CT) and histomolecular markers in patients with untreated grade II-III glioma. ***Materials and Methods:*** We included 109 patients with histologically proven grade II-III gliomas (47 males, 62 females, age 39±11 years) who had undergone PET/CT using [^{11}C]methionine (PET-MET) prior surgery/biopsy. The sample included diffuse gliomas grade II (57 astrocytomas (AST), 27 oligodendrogliomas (ODG), n = 84) and grade III (18 AST, 7 ODG, n = 25). All were tested for the presence of a mutation in the IDH1 gene (R132H IDH1). 1p/19q status was assessed in 42 cases. On PET-MET tumor-to brain uptake ratio (TBR) was calculated by dividing the MET uptake in the tumor (hot spot 10 mm in diameter) to radiotracer uptake in the contralateral unaffected cortex. Imaging-derived parameters were compared between gliomas stratified according to glioma type, WHO grade, IDH1 status using non-parametric tests. ***Results:*** Diffuse astrocytic and oligodendroglial tumors grade II-III were divided into three subgroups: astrocytic gliomas with a mutation in the IDH1 gene (n = 51), astrocytic gliomas without a mutation in the IDH1 gene (n = 24) and IDH1 mutated oligodendrogliomas (n = 34). In mutated gliomas (n = 85) TBR was 1,79 ± 0,7 (mean ± standard deviation), in IDH1-wild type glioma TBR was 1,8 ± 0,97 (p=0,59, Mann-Whitney test). The median TBR in grade II-III astrocytomas with and without the IDH1 mutation was 1,52 (range 0,8 - 3,8) and 1.47 (range 1,0 - 5,1), respectively (p=0,31). Oligodendrogliomas showed significantly higher MET uptake values (median TBR=1,9, range 1,0 - 4,36) compared with astrocytic gliomas (median TBR=1,5, range 0,8 - 3,8) (p=0,0008). Moreover, significant differences were revealed between IDH1 mutated astrocytoma and oligodendroglioma (p=0,0007). Significant differences in TBR were also found between grade II and

III gliomas (p=0,03). ***Conclusion:*** MET uptake in grade II-III gliomas seems not to be dependent on the IDH1 (R132H) status of the tumor and PET-MET does not allow to classify gliomas according to their IDH1 genotype. Differences in MET uptake metrics in lower grade gliomas are associated with their histological subtypes and the grade of malignancy. Acknowledgment: The reported study was funded by Russian Foundation of Basic Researches according to the research project № 18-29-01015. ***References:*** None

EP-013

Initial Experience With 18F-DOPA PET/CT For Differentiating Radionecrosis From Tumour Progression In Brain Metastasis And Malignant Primary Tumors Of The Central Nervous System

V. Lopez Prior*, R. Diaz Expósito, F. Manchón Adsuar;*
Valencian Oncologic Institution (IVO), Valencia, SPAIN.

Aim/Introduction: This study highlights our initial experience evaluating the efficacy of 18F- DOPA PET/CT for distinguishing changes post-radiation treatment (CPRT) from disease progression (DP) in patients with brain metastasis and malignant primary tumors of the central nervous system. ***Materials and Methods:*** In 16 patients (11 men (68.80%)-5 women (31.20%); 56.00 ±9.93 years) with a total of 30 previously irradiated brain lesions (metastasis 10 (62.50%) or primary tumors 6 (37.50%)) 18F-DOPA PET/CT was performed. PET studies were analyzed semiquantitatively (maximum lesion uptake value (SUVLmax), lesion-to-estriatum (SUVmaxL/Smax), and lesion-to-normal brain tissue (SUVLmax/SUV Bkgrmax) ratios).Diagnosis of DP was defined radiologically as an increment in lesion size on MR images or clinical follow-up.Relative cerebral blood volume (rCBV) derived from perfusion-MR was available in 10 lesions.A comparison was made between SUVmaxL/Smax, SUVLmax/SUV Bkgrmax ratios and rCBV values from our results, and the results obtained by Cicone et al (Eur J Nucl Med Mol Imaging (2015) 42:103-111). ***Results:*** Primary tumors were lung(7 patients), breast(1 patient), colon(1 patient), melanoma(1 patient), astrocytoma(1 patient), glioblastoma(5 patients).Median maximum diameter of the lesions was 25.00±11.58mm (range 10-50 mm).All patients had undergone radiation therapy before the PET scan: whole brain radiation(WBR) 4(26.70%), radiosurgery(RS) 4(26.70%), stereotactic radiotherapy(SRT) 7(46.70%).Median treatment doses were (Gy): WBR 47.50(range 30-60), RS 19.50(range18-24), SRT 27.35(range18-60).The median time interval from the completion of radiation treatment to PET was 10.25 mo (2.00-23.00mo).Of the 30 lesions, the diagnosis of DP was established in all of them as a definitive outcome by radiological and clinical criteria.The median of SUVLmax of the total of 30 lesions was 2.85±0.87; SUVmaxL/Smax 1.04±0.27; SUVLmax/SUV Bkgrmax 2.10±0.65. Using Cicone´s best differentiating SUVmaxL/Smax cut-off value (0,75) we have 83.33% (25/30 lesions) of accuracy in our study (Cicone:78.2%).Using Cicone´s best differentiating SUVLmax/SUV Bkgrmax cut-off value (1,59) we have 79.31% (23/29 lesions) of accuracy in our study (Cicone:91.3%). The rCBV was available in 10 lesions (6.04±4.23).Using Cicone´s best differentiating cut-off value (2,14) we have 90%(9/10lesions) of accuracy in our study (Cicone:75,6%). The mean time of follow-up after PET scan was 5.64±2.92 mo.The management strategies after PET scans include RS 3/14(21.43%); SRT 8/14(57.14%), surgery 1/14(7.14%); chemotherapy 1/14(7.14%); palliative treatment 1/14 (7.14%).One patient died and a new recurrence was observed in another patient. ***Conclusion:*** Semiquantitative indices from 18F-DOPA PET/CT images could be used for differentiating DP from CPRT.In this specific setting, these parameters could be predictors of progression-free survival but need to be confirmed with longitudinal studies on a larger population. ***References:*** None

EP-014

^{18}F-FET or ^{18}F-FLT PET/CT in diagnosis of low-grade gliomas? A pilot study

J. Vasina[1]*, M. Hodolič*[2]*, R. Jančálek*[3]*, Z. Mackerle*[3]*, M. Hendrych*[3]*, R. Hejnová*[1]*, T. Kazda*[1]*, Z. Řehák*[1]*;*
[1]Masaryk Memorial Cancer Institute, Brno, CZECH REPUBLIC, [2]University Hospital, Olomouc, CZECH REPUBLIC, [3]St. Anne´s University Hospital, Brno, CZECH REPUBLIC.

Aim/Introduction: The diagnosis of low-grade glioma (LGG) is challenging, as conventional imaging modalities can often give inconclusive results. PET, as functional imaging modality, can provide additional metabolic information. Given that thymidine is a nucleoside encountered in DNA, 3'-deoxy-3'-[^{18}F]-fluorothymidine (^{18}F-FLT) was proposed as a PET marker for cell proliferation rate. ^{18}F-FLT has a high detecting rate for high-grade gliomas (HGG) but is considered less valuable in diagnosis of LGG. O-(2-[^{18}F]-fluoroethyl)-L-thyrosine (^{18}F-FET) is a radiopharmaceutical approved for the characterization of glioma-suggestive lesions.The aim of this study was to determine the diagnostic accuracy of ^{18}F-FET and ^{18}F-FLT PET/CT in patients with primary LGG. ***Materials and Methods:*** Patients with MRI-suspected LGG planned for biopsy or resection surgery underwent preoperative ^{18}F-FET and ^{18}F-FLT PET/CT within one week. Surgery and histopathological diagnosis was performed by the next two weeks. The histopathological results were correlated to PET findings. ***Results:*** Six patients (22-43 years) with MRI suspected LGG underwent ^{18}F-FET and ^{18}F-FLT PET/CT followed by a surgery and tissue diagnostics. PET findings can be divided into three diagnostic groups according to ^{18}F-FET and ^{18}F-FLT PET positivity: the first group counting one patient (n=1/6) was characterized by positive ^{18}F-FET PET (SUVmax 5.52/T5, 6.05/T40) and negative ^{18}F-FLT PET had histopathological diagnosis of oligodendroglioma

(grade II).The second group was characterized by positive ^{18}F-FET PET but only slightly positive ^{18}F-FLT PET. This PET pattern ws presented in two patients (n=2/6) with lower SUVmax in the one suffering diffuse astrocytoma WHO grade II (^{18}F-FET PET SUVmax 3.13/T5, 3.48/T40; ^{18}F-FLT PET SUVmax 0.84/T15) compared to the patient with final diagnosis of anaplastic astrocytoma WHO grade III (^{18}F-FET PET SUVmax 5.6/T5, 5.9/T40; ^{18}F-FLT PET SUVmax 0.96/T15). The main feature of the third PET group was marked positivity on both PET procedures. Three patients (n=3/6) with ^{18}F-FET (SUVmax 6.69/T5, 4.74/T40; 8.85/T5, 6.85/T40; and 13.31/T5, 9.15/T40) and ^{18}F-FLT PET (SUVmax 2.69/T15; 3.91/T15; and 1.75/T15) avid lesion had a final diagnosis of diffuse midline glioma harbouring the H3 K27M mutation (grade IV), anaplastic astrocytoma (grade III), and anaplastic astrocytoma (grade III), respectively. ***Conclusion:*** Preliminary results on the small number of patients document the need for appropriate diagnostic tool in patients with LGG because of the low specificity of MRI. Opposed to the MRI findings, ^{18}F-FET and ^{18}F-FLT PET were sufficient for diagnosis of HGG. However, ^{18}F-FET was superior to ^{18}F-FLT in imaging of LGG. ***References:*** None

EP-015

Molecular imaging ^{99m}Tc-CXCR4-L SPECT in brain tumors

P. Vallejo Armenta[1], G. Ferro Flores[2], O. Pérez-García[1], J. Soto Andonaegui[3], B. Sandoval-Bonilla[3], B. Nettel-Rueda[3], C. Bautista-Wong[3];
[1]Instituto Nacional de Cancerología, Mexico City, MEXICO, [2]Instituto Nacional de Investigaciones Nucleares (ININ), Mexico City, MEXICO, [3]UMAE Hospital de Especialidades. Centro Médico Nacional Siglo XXI. IMSS., Mexico City, MEXICO.

Aim/Introduction: Overexpression of the chemokine-4 receptor (CXCR4) in brain tumors (BT) is associated with high cancer cell invasiveness. 99mTc-CXCR4-L is a new SPECT radioligand capable of specifically detecting the CXCR4 protein. The aim of the study was to assess the feasibility of 99mTc-CXCR4-L (CXCR4-SPECT) for imaging BT and correlate the radiotracer uptake by BT in patients with the histological grade of differentiation and the CXCR4 expression evaluated by immunohistochemistry. ***Materials and Methods:*** Twenty-seven patients (age, 44.6±15.8 years; 16 males, 11 females) with suspected brain tumor (20 indeterminate brain tumor [IBT] and 7 with suspected glioma recurrence detected by enhanced MRI were evaluated with preoperative brain SPECT scan 3 hours after intravenous injection of 750 MBq 99mTc-CXCR4-L. Both visual and semiquantitative analyses were performed. Maximum target-to-background ratio (TBRmax) was calculated using contralateral tissue uptake as background. The expression of PSMA was analyzed by immunohistochemistry in 11 patients. TBRmax was correlated with IHC findings and pathological grade (low-grade glioma [LGG], high-grade gliomas [HGG]). The gold standard was pathological diagnosis using specimens obtained by biopsy or surgical resection. ***Results:*** In vivo CXCR4 expression was seen in all patients with malignant BT and glioma recurrence (n=24). CXCR4-SPECT was positive in 3 LGG (astrocytoma), 14 HGG (1 anaplastic astrocytoma and 13 GBM) and 2 breast mets with TBRmax 1.8±0.6, 7.5±2.1 and 5.0±3.0, respectively; while for the rest, the result was negative with a histological report of gliosis. TBRmax significantly correlated with the pathological grade (Spearman rs=0.90, $p < 0.0001$). CXCR4 was highly expressed in the cancer cells of HGG and mets, while its expression in LGG was low and completely absent in gliosis. The sensitivity, specificity, PPV, NPV and accuracy with TBRmax evaluation with a cut-off value of 1.3 were 100%. ***Conclusion:*** The radiopharmaceutical uptake in malignant BT was significantly higher than the background brain uptake, which demonstrated the ability of the new 99mTc-CXCR4-L to detect tumours with CXCR4 expression. CXCR4-SPECT is a potentially useful imaging tool for assessing of glioma grading, to detect tumor recurrence (negative scan in treatment-related changes), planning treatment and biopsy guidance (the background uptake in normal brain parenchyma is absent, thus enhancing tumor detection). ***References:*** None

EP-016

^{99m}Tc-EDDA/HYNIC-iPSMA SPECT Imaging in differentiating radiation necrosis from tumor recurrence in gliomas

P. Vallejo Armenta[1], G. Flores Ferro[2], J. Soto Andonaegui[3], O. García Pérez[4], B. Sandoval Bonilla[3], B. Nettel Rueda[3], K. Contreras Contreras[3], C. Bautista Wong[3];
[1]Instituto Nacional de Cancerología., Mexico City, MEXICO, [2]Instituto Nacional de Investigaciones Nucleares (ININ)., Mexico City, MEXICO, [3]UMAE Hospital de Especialidades. Centro Médico Nacional Siglo XXI., Mexico City, MEXICO, [4]Instituto Nacional de Cancerología, Mexico City, MEXICO.

Aim/Introduction: Prostate-specific membrane antigen (PSMA) is upregulated on endothelial cells of solid tumors, including gliomas. Glioblastoma (GBM) is the most malignant glioma, the current standard therapy includes surgery followed by concurrent radiotherapy and chemotherapy with temozolomide. However, combination therapy can lead to radiation necrosis that often mimics recurrent brain tumor on MRI. PSMA-targeted imaging may potentially identify patients with disease recurrence and help direct changes in therapy. The aim of this study was to investigate the diagnostic value of ^{99m}Tc-EDDA/HYNIC-iPSMA (iPSMA-SPECT) in distinguishing tumor recurrence from radiation necrosis. ***Materials and Methods:*** Eighteen patients (age, 43.8±15.0 years; 9 males, 9 females) with suspected glioma recurrence (8 low-grade glioma [LGG] and 10 high-grade glioma [HGG]) detected by enhanced

MRI after surgery and radiation therapy (median interval was 11 months) were evaluated with iPSMA-SPECT. Both visual and semiquantitative analyses were performed. Maximum target-to-background ratio (TBR_{max}) was calculated using contralateral tissue uptake as background. The expression of PSMA was analyzed by immunohistochemistry in 6 patients. TBR_{max} was correlated with IHC findings and pathological grade. The gold standard for diagnosing radiation necrosis (RN) or glioma recurrence (GR) was pathological diagnosis using specimens obtained by biopsy or surgical resection. ***Results:*** In vivo PSMA expression was seen in all patients with GR (n=12). iPSMA-SPECT was positive in 4 LGG (astrocytoma) and 8 HGG (1 anaplastic oligodendroglioma and 7 GBM) with TBR_{max} 7.6±0.7 and 22.7±4.8, respectively; while for the rest, the result was negative with a histological report of RN. TBR_{max} significantly correlated with the pathological grade (Spearman rs=0.87, $p < 0.0001$). Immunohistochemical results corroborated that PSMA was highly expressed in the vascular endothelium of HGG, whereas its expression in LGG was low and absent in RN. Furthermore, a trend toward a positive correlation between the degree of iPSMA-SPECT uptake and PSMA expression levels in tumor specimens was observed. The sensitivity, specificity, PPV, NPV and accuracy of TBRmax evaluation with a cut-off value of 2.8 were 100%. ***Conclusion:*** The extremely low background uptake in normal brain tissue and consequently high TBR_{max} make iPSMA-SPECT highly promising for discrimination between recurrence and RN. PSMA expression in recurrent glioma opens a potential way for targeted peptide therapy as well as for prediction of treatment with antiangiogenic agents. Substantial advantages to iPSMA-SPECT were seen including low dosimetry, high availability and low cost. Further study with a larger population using external data is required for translation of the future clinical potential. ***References:*** None

EP-04

Cognitive Impairment

e-Poster Area

EP-017

The metabolic amyloid signature of ^{18}F-FDG PET/CT in Alzheimer's disease

S. Pacella[1], *V. Isella*[2,3], *E. Preza*[1], *V. Polonia*[4], *A. Franchini*[1], *C. Crivellaro*[5], *C. Landoni*[2,5], *L. Guerra*[2,5], *C. Ferrarese*[2,3], *A. Formenti*[4], *M. Musarra*[5];

[1]*Postgraduate School of Nuclear Medicine, University of Milano Bicocca, Milan, ITALY,* [2]*School of Medicine and Surgery, University of Milano Bicocca, Milan, ITALY,* [3]*Neurology Unit, ASST Monza San Gerardo Hospital, Monza, ITALY,* [4]*Postgraduate School of Neurology, University of Milano Bicocca, Milan, ITALY,* [5]*Department of Nuclear Medicine, ASST Monza San Gerardo Hospital, Monza, ITALY.*

Aim/Introduction: Alzheimer's disease (AD) represents the most common cause of dementia in elderly patients, accounting for about 60-70% of all cases. 18F-FDG-PET/CT is an important tool in the diagnostic workout of AD: the typical pattern of hypometabolism involved the posterior cingulate cortex (PC), precuneus (Pr) and temporoparietal areas (TP). The aim of our study is to determine if 18F-FDG-PET/CT may predict amyloid pathology at the individual level in patients with confirmed AD using three methods of analysis of PET/CT images and comparing the three approaches. ***Materials and Methods:*** Two Nuclear Medicine Physicians retrospectively reviewed 101 PET/CT scans of patients referred to the Neurology Unit of our Hospital for dementia or suspect dementia, who had undergone lumbar puncture or amyloid-PET as biomarker for amyloid status, or carried a genetic mutation for AD or non-AD dementia. They used three rating methods: the visual evaluation (also named visual rating, VR) of PET/CT transaxial re-elaborated images and two semiautomatic softwares that are Cortex ID, developed and marketed by GE Healthcare (Waukesha, WI, USA) and SPM INLAB, an automated software based on Statistical Parametric Mapping (SPM; http://www.fil.ion.ucl.ac.uk/spm), developed by the National Research Council (http://inlab.ibfm.cnr.it/inlab/SPM.php). Cohen's kappa (κ) was run to determine the degree of concordance between the three rating methods in defining the presence/absence of PC-Pr-TP hypometabolism. Total accuracy, sensitivity, specificity and positive and negative predictive values (PPV, NPV) were calculated for each of the three FDG-PET rating methods. ***Results:*** Cortex ID showed the best sensitivity (91%), specificity (75%) trade off and highest total accuracy (83%) of all three rating methods. For VR, inter-rater reliability was also calculated and indicated near-perfect agreement between the two Nuclear Medicine physicians in defining presence/absence of PC-Pr-TP hypometabolism (Cohen's $\kappa = 0.85$ [95% CI, 0.74 to 0.96], $p = 0.000$). Cohen's κ showed substantial agreement between the two automated ratings ($\kappa = 0.80$ [95% CI, 0.68 to 0.92], $p = 0.000$). There was substantial agreement also between SPM INLAB and VR ($\kappa = 0.73$ [95% CI, 0.59 to 0.86], $p = 0.000$). ***Conclusion:*** Our study confirmed the important role of 18F-FDG PET/CT in patients with confirmed AD. The high sensitivity of all three methods supports the idea that underlying amyloid pathology strongly correlates with a typical topography of hypometabolism. Semiautomatic softwares as Cortex ID could improve specificity in order to reduce the possibility of false positive results that could lead to overdiagnosis of amyloid-related dementia. ***References:*** None

EP-018

Alternatives to static F-18-FDG brain PET using early-phase F-18-FPN brain PET

H. Yoon[1], Y. Jeong[1,2], J. Jeong[1], H. Shin[2], D. Kang[1,2];
[1]Dong-A University Medical Center, Busan, KOREA, REPUBLIC OF, [2]Dong-A University, Busan, KOREA, REPUBLIC OF.

Aim/Introduction: Early-phase amyloid PET images represent perfusion and are known to be associated with the metabolism of F-18-FDG. F-18-Florapronal (FPN, Alzavue, FutureChem Pharma, Korea) is a newly developed radio-pharmaceutical for amyloid PET imaging that is being used clinically in Korea. The aim of this study is to find the optimal frame in early-phase F-18-FPN PET that can replace the F-18-FDG PET image, to generate perfusion images and use it for AD diagnosis. ***Materials and Methods:*** Seventeen AD patients (age: 69.0±9.3 yrs) and 15 age-matched normal subjects (age: 69.9±8.0 yrs) underwent F-18-FDG and F-18-FPN brain PET scans, within an interval of 4 weeks. Dynamic PET data were acquired 0-60 min after intravenous injection of F-18-FPN (370 MBq) and F-18-FDG (185 MBq). Early-phase F-18-FPN PET images were merged by frame within 15 minutes with 0-3 minutes as the start time, and voxel-wise and region-based correlation coefficients with F-18-FDG PET were calculated. Region-based correlation coefficients were calculated using the average SUVr values in 83 brain regions using Hammer's brain atlas of PMOD 3.6. Optimal frames were determined by considering the correlation coefficient, noise in the initial state, image quality, and personal similarities between early-phase F-18-FPN perfusion PET images and F-18-FDG delayed static PET images. ***Results:*** The voxel-wise correlation coefficient of early-phase F-18-FPN PET and static F-18-FDG brain PET images was 0.934 at 1.5-2 min, and the region-based correlation coefficient was 0.984 at 2.7-4.5 min. Considering the PET image quality, and voxel-wise and region-based correlation coefficients, the early-phase F-18-FPN image generated in 1.5-4 minutes was optimal to replace the static F-18-FDG brain PET image. Early-phase F-18-FPN images were generated for each patient for 1.5-4 minutes and compared to static F-18-FDG PET images. The two images were visually similar. Correlation coefficients of minimum value 0.873 or higher were observed. The regions for classifying AD and HC in early-phase F-18-FPN images were anterior orbital gyrus, lateral orbital gyrus, and amygdala, and SUVr thresholds were 0.900, 0.889, 0.763 using ROC. ***Conclusion:*** We found an early-phase F-18-FPN image with a high correlation coefficient to replace the static F-18-FDG brain PET image. In this study, the threshold value of SUVr, which can be classified as AD and HC, was proposed using a time-optimized early-phase F-18-FPN brain PET image. Now, quantitative diagnosis of amyloid negative AD patients will be possible. ***References:*** None

EP-019

Severe Obstructive Sleep Apnea and Increased Cortical Amyloid-beta Deposition

T. Laitinen[1], *S. Ylä-Herttuala[2], M. Hakulinen[1], P. Poutiainen[1], T. M. Laitinen[1], A. Koivisto[3], A. Remes[4], M. Hallikainen[3], J. Lehtola[3], T. Saari[2], M. Könönen[1], R. Vanninen[1], H. Mussalo[1], E. Mervaala[1];*
[1]Diagnostic Imaging Center, Kuopio University Hospital, Kuopio, FINLAND, [2]Institute of Clinical Medicine, University of Eastern Finland, Kuopio, FINLAND, [3]KUH Neurocenter, Kuopio University Hospital, Kuopio, FINLAND, [4]Research Unit of Clinical Neuroscience, University of Oulu, Oulu, FINLAND.

Aim/Introduction: Human studies have suggested that sleep deprivation may act as a risk factor of Alzheimer´s disease (AD) via brain amyloid-β (Aβ) burden. Patients with obstructive sleep apnea (OSA) have poor quality of sleep, insufficient sleep, and chronic partial sleep deprivation. The suggested association between severe OSA and risk of Alzheimer´s disease (AD) needs further study. So far only few reports exist on associations between brain Aβ burden and severe OSA. ***Materials and Methods:*** The study cohort was collected retrospectively from a routine diagnostic patient population from the years 2011-2018 that was evaluated in our hospital due to a clinical suspicion of OSA. Inclusion and exclusion criteria were 1) severe OSA (Apnea-Hypopnea Index > 30/h) in diagnostic polygraphy, 2) age 30-50 years, 3) no medical history of major neurological or psychiatric diseases, 4) diabetes, when present, had to be in good treatment balance, 5) no use of medication influencing on the central nervous system or any substance abuse, 6) no subjective or objective symptoms or signs of any cognitive difficulties. We performed detailed multimodal neuroimaging in 19 cognitive intact middle-aged patients with severe OSA. Brain Aβ uptake was studied with [^{11}C]-PiB -PET, glucose metabolism with [^{18}F]-FDG-PET, and structural imaging was performed with 3.0 T MRI. ***Results:*** Increased cortical grey matter [^{11}C]-PiB uptake (Z-score >2 in any of the regions of interest) was found in 6 out of the 19 patients (32 %). Two of these 6 patients showed Z-scores above 3. The increased Aβ uptake was seen individually in precuneus/posterior cingulum regions (5 patients), sensorimotor regions (2 patients), and prefrontal, temporal mesial, anterior cingulum, and occipital regions (1 patient in each, respectively). Cortical glucose hypometabolism in [^{18}F]-FDG-PET was seen in only two patients and localized to primary visual cortices in both of them. MRI did not show structural changes suggestive of AD-related pathology. ***Conclusion:*** OSA may predispose to cerebral Aβ burden, which reflects a future risk for AD, or a possible preclinical prevailing pathology. In OSA patients findings of increased [^{11}C]-PiB uptake were less pronounced and regional compared with more pronounced and widespread Aβ burden typically seen in AD. In OSA patients Aβ clearance may be compromised without simultaneous

evidence of metabolic or structural alterations. Our results emphasize the importance of early diagnostics and proper treatment of severe OSA in cognitively intact subjects, possibly diminishing the individual risk for later cognitive dysfunction. ***References:*** None

EP-020

^{18}F-FDG PET/CT study on the changes of brain FDG metabolism in patients with DLBCL after chemotherapy

H. Yang[1], Q. Zhao[2], J. Cao[1], J. Tian[1], J. Ren[1];
[1]Ningxia Medical University, Yinchuan, Ningxia, CHINA, [2]General Hospital of Ningxia Medical University, Yinchuan, Ningxia, CHINA.

Aim/Introduction: The aim of this study was to illustrate the glucose metabolism changing pattern of "chemo-brain" in patients with diffuse large b-cell lymphoma (DLBCL). The relationship between brain glucose metabolism and clinical staging and chemotherapy cycles were also explored. ***Materials and Methods:*** Fourty-five patients with DLBCL were retrospectively included. All patients received standard CHOP or R-CHOP chemotherapy. A baseline before chemotherapy and follow-up ^{18}F-FDG PET/CT whole-body imaging were performed in all subjects (9 after 4 cycles, 26 after 6 cycles, and 10 after 8 cycles). Clinical data, such as staging, was recorded. ^{18}F-FDG PET/CT cerebral images and raw data were analyzed using SPM8 and ScAnVP. A VOI based brain metabolism changing pattern image was obtained. An AAL template was used to perform the ROI based semi-quantitative analysis. SPSS17.0 was applied as the statistical software. Paired samples t-test and Pearson correlation analysis were conducted. ***Results:*** After chemotherapy, the glucose metabolism of bilateral temporal pole, bilateral hippocampus, bilateral parahippocampal gyrus, bilateral pons, , bilateral amygdala, left inferior frontal gyrus, right gyrus rectus, vermis, bilateral olfactory cortex, right thalamus and bilateral cerebellum were significantly decreased ($p< 0.05$). In contrast, bilateral inferior occipital gyrus, bilateral middle occipital gyrus, right middle frontal gyrus, right inferior frontal gyrus, bilateral precuneus, bilateral superior occipital gyrus, bilateral cuneus, right precentral gyrus, bilateral postcentral gyrus, bilateral supramarginal gyrus and bilateral angular gyrus showed an increase of FDG uptake after chemotherapy ($p< 0.05$). The changes of glucose metabolism in bilateral pons positively correlated with chemotherapy cycles ($p< 0.05$). No correlation was found between the changes of glucose metabolism and clinical staging ($p< 0.05$). ***Conclusion:*** Chemotherapy changed the brain glucose metabolism in DLBCL patients, especially in frontal lobe, temporal lobe, collapse and cerebellum. The change of glucose metabolism in bilateral pons was associated with chemotherapy cycles. ***References:*** None

EP-021

Brain amyloid load assessed by ^{11}C-PIB PET/CT for predicting long-term severity of cognitive impairment in patients with amnestic mild cognitive impairment. A comparison with ^{18}F-FDG PET/CT scan

J. Jiménez-Bonilla[1], R. Quirce[1], M. De Arcocha-Torres[1], I. Martínez-Rodríguez[1], S. López-García[2], C. Lage[2], M. García[2], A. Pozueta[2], E. Rodríguez-Rodríguez[2], P. Sánchez-Juan[2], A. Sánchez-Salmón[1], N. Martínez-Amador[1], S. Ruiz-Llama[1], G. Molina[1], O. Cuenca-Vera[1], J. Andrés[1], A. Gutiérrez-González[1], I. Banzo[1];
[1]Nuclear Medicine Service. Marqués de Valdecilla University Hospital. Molecular Imaging Research Group. University of Cantabria, Santander, SPAIN, [2]Neurology Service. Marqués de Valdecilla University Hospital, Santander, SPAIN.

Aim/Introduction: To study in patients with amnestic mild cognitive impairment (A-MCI) if brain amyloid load (BAL) is associated with the severity of cognitive impairment after 5-year follow-up and to compare it with the prognostic value of regional glucose metabolic findings. ***Materials and Methods:*** We prospectively studied 45 consecutive A-MCI patients (all Stage 3 on Global Deterioration Scale [GDS]) with 11C-PIB and 18F-FDG PET/CT at diagnosis. Five years later, 33 patients were clinically re-evaluated; re-evaluation was not possible in 12 patients (5 died, 7 lost to follow-up). Clinical status was evaluated using the GDS. PIB-PET was acquired 60-90 minutes after iv 555MBq 11C-PIB, and FDG-PET 30 minutes after iv 185 MBq 18F-FDG.In PIB-PETs, regional SUV indices were obtained in cerebellar, temporal, occipital, frontal, parietal, anterior cingulated and posterior cingulated cortex. Using the cerebellar cortex as reference region, regional SUV ratios (SUVr) were obtained. BAL was obtained as an average of these regional SUVr in each patient. FDG-PET was visually analyzed considering temporo-parietal hypometabolism as key finding to consider the scan as positive or negative for AD. ***Results:*** At diagnosis, 7/33 A-MCI patients were PIB+/FDG+ (Group A); 14/33 were PIB+/FDG- (Group B); 3/33 were PIB -/FDG + (Group C), and 9/33 were PIB-/FDG- (Group D). In the group A, the averaged BAL was 2.2034+0.441 (range: 1.664-2.7677), and in group B was 2.2191+0.3582 (range: 1.779-3.0175) (p= ns). Five years later, in the Group A 3/7 patients were GDS 6-7, 1/7 was GDS 5, and 3/7 were GDS 3-4; and in the Group B, 3/14 patients were GDS 6-7, 5/14 were GDS 5, and 6/14 were GDS 3-4 for AD. In the Group C and D, none of them developed Alzheimer's disease dementia (ADdm). When the proportion of patients who developed a severe-very severe ADdm (GDS 6-7) was compared between A and B groups, statistically significant differences were not found. However, when only BAL was considered, we found that the cut-off value to predict a deeper cognitive impairment was 1.96. Above 1.96, (n=11) 6/11 patients were GDS 6-7 and 5/11were GDS 4-5; and below 1.96, (n=10) 1/10 patient was GDS 6-7 and 9/10 were GDS 4-5 ($p< 0.05$). ***Conclusion:*** BAL in

A-MCI patients may be a better predictor of the long-term severity of cognitive impairment than FDG PET/CT findings. BAL may play a role in the progressive neurodegeneration beyond initial regional FDG abnormalities. It may deserve more studies focussed on anti-amyloid therapies. ***References:*** None

EP-022

Concordance between amyloid PET imaging and CSF biomarkers in clinical setting

G. Marotta*, L. Sacchi, G. G. Fumagalli, A. M. Pietroboni, A. Arighi, L. Ghezzi, A. Colombi, T. Carandini, M. Scarioni, F. Buffoni, M. Rognoni, D. Galimberti, E. Scarpini;*
Fondazione IRCCS Ca' Granda Ospedale Maggiore Policlinico, Milan, ITALY.

Aim/Introduction: Increased uptake of Aβ tracers in the brain on PET and decreased concentrations of amyloid β (Aβ) in the cerebrospinal fluid (CSF) are considered the most specific biomarkers of Alzheimer's disease (AD).Despite a high rate of concordance, results show discrepancies.Our aim was to investigate concordance between amyloid PET scans and CSF amyloid measurements. ***Materials and Methods:*** We included 76 subjects from a mixed cohort of demented and non-demented patients, who had undergone a lumbar puncture for CSF analysis and an amyloid PET with either florbetapir (N=49) or florbetaben (N=27) compounds. CSF specimens were assayed for Aβ, total Tau and phosphorylated Tau, using cut-offs for positivity of <600 pg/mL, >450 pg/mL and >61 pg/mL, respectively.Amyloid-PET scans were subdivided into positive and negative on the basis of quantitative measurement of global amyloid uptake in the brain. ***Results:*** 45 out of 76 (59%) subjects showed concordant results between amyloid PET scans and CSF Aβ levels. Of these, 38 (84%) were positive and 7 (16%) negative exams. Among discordant cases, the majority (23/31 or 74%) had a positive PET scan in spite of normal CSF-Aβ levels (F+/A-).Interestingly, mean CSF concentration of Aβ in the F+/Agroup was significantly different from F-/A- cases (683.3 vs 963.7 pg/mL). ***Conclusion:*** In our cohort, overall concordance was 59% (florbetapir 61%, florbetaben 56%).According to our results, PET and CSF-Aβ measurements cannot be used interchangeably and PET imaging is particularly helpful for settling uncertain cases near the CSF-Aβ threshold. ***References:*** None

EP-023

Differences of Perfusion Correlates between Apathy and Depression in Patients with Alzheimer's disease. A Brain SPECT Study with Brodmann Areas Mapping

V. Valotassiou*[1], N. Sifakis[2], C. Tzavara[1], E. Lykou[3], N. Tsinia[4], V. Kamtsadeli[3], D. Sali[5], G. Angelidis[1], D. Psimadas[1], I. Tsougos[1], A. Ziaka[1], E. Theodorou[1], C. Tzioumerka[1], C. Ziangas[1], S. Papageorgiou[6], P. Georgoulias[1], J. Papatriantafyllou[3,7];*
[1]Dpt of Nuclear Medicine, University Hospital of Larissa, Larissa, GREECE, [2]Dpt of Nuclear Medicine, "Alexandra" University Hospital, Athens, GREECE, [3]IASIS Third Age Center, Athens, GREECE, [4]1st University Psychiatric Department, Aeginition Hospital, Athens, GREECE, [5]Neurology Dpt, Evrokliniki, Athens, GREECE, [6]2nd University Neurological Dpt, Attikon Hospital, Athens, GREECE, [7]Memory Disorders Clinic, Medical Center, Athens, GREECE.

Aim/Introduction: Apathy and depression are among the most clinically important neuropsychiatric symptoms (NPSs) in Alzheimer's disease (AD). The prevalence of apathy and depression ranges from 19% to 88% and from 19% to 78%, respectively. Apathy is characterized by lack of initiative and interest and emotional blunting, while loss of interest is also a core feature of depression. Apathy and depression often co-occur, which results, in combination with the similarity of symptoms, in misdiagnosis. The aim of this study was to evaluate differences of perfusion correlates between apathy and depression in AD patients using SPECT with Brodmann areas (BAs) mapping and comparison with healthy controls, in order to reveal BAs associated specifically with these NPSs. ***Materials and Methods:*** We studied 65 consecutive patients (20 men, 45 women, age±SD 69.9±8.1 years, duration of disease±SD 3.4±2.4 years, education±SD 9.4±4.7 years) from an outpatient Memory Clinic. We used the established DSM-IV criteria for the diagnosis of dementia and the specific established criteria (NINCDS-ADRDA) for the diagnosis of AD. All the patients had a neuropsychological evaluation with a battery of tests including the mini-mental state examination (MMSE, mean±SD 19.6±5.5) and the Neuropsychiatric Inventory. All the patients underwent a brain SPECT scan 20 min after the intravenous administration of 740MBq of ^{99m}Tc-HMPAO. We applied the NeuroGam^{TM} software on the reconstructed data, for the comparison of brain perfusion in BAs in the right (R) and left (L) hemispheres with the software's normal data base consisted of healthy subjects of the same age. ***Results:*** Compared with normal subjects, we found a statistically significant correlation of apathy with hypoperfusion in right anterior prefrontal cortex (BA 10R), dorsolateral prefrontal cortices (BAs 8L, 9LR, 46R), ventral posterior cingulate cortices (BA 23LR), left dorsal anterior cingulate cortex (BA 32L), right entorhinal and perirhinal cortices (BAs 28R, 36R). Depression was correlated with hypoperfusion in primary motor, primary somatosensory and dorsolateral prefrontal cortices, on the left (BAs 1L, 2L, 3L, 4L, 8L), ***Conclusion:*** Apathy and depression in AD are mediated through different underlying neural mechanisms. Functional nuclear imaging may contribute significantly in the differential diagnosis between them and the improvement of patients' management. ***References:*** 1. Lanctôt KL, Amatniek J, Ancoli-Israel S, et al. Neuropsychiatric signs and symptoms of Alzheimer's disease: New treatment paradigms. Alzheimers Dement (N Y). 2017;3(3):440-449. 2. Rosenberg PB, Nowrangi MA, Lyketsos CG. Neuropsychiatric

symptoms in Alzheimer's disease: What might be associated brain circuits? Mol Aspects Med. 2015;43-44:25-37

EP-024

Brain Perfusion SPECT Imaging with Brodmann Areas Mapping in the Evaluation of Eating Disorders in Frontotemporal Dementia

V. Valotassiou[1], *N. Sifakis*[2], *C. Tzavara*[1], *V. Kamtsadeli*[3], *N. Tsinia*[4], *E. Lykou*[3], *D. Sali*[5], *G. Angelidis*[1], *I. Tsougos*[1], *D. Psimadas*[1], *E. Theodorou*[1], *A. Ziaka*[1], *C. Tzioumerka*[1], *C. Ziangas*[1], *S. Papageorgiou*[6], *P. Georgoulias*[1], *J. Papatriantafyllou*[3,7]; *[1]Dpt of Nuclear Medicine, University Hospital of Larissa, Larissa, GREECE, [2]Dpt of Nuclear Medicine, "Alexandra" University Hospital, Athens, GREECE, [3]IASIS Third Age Center, Athens, GREECE, [4]1st University Psychiatric Department, Aeginition Hospital, Athens, GREECE, [5]Neurology Dpt, Evrokliniki, Athens, GREECE, [6]2nd University Neurological Dpt, Attikon Hospital, Athens, GREECE, [7]Memory Disorders Clinic, Medical Center, Athens, GREECE.*

Aim/Introduction: Eating disorders (ED) represent a prominent feature in frontotemporal dementia (FTD), and especially in the behavioral variant of FTD (bvFTD), where the prevalence of ED ranges from 60% to 80%. In bvFTD, the spectrum of ED involves overeating, changes in food preference with a craving for sweets and inappropriate eating behaviors. In semantic dementia (SD), ED include stereotypical eating, alterations in food preference and hyperorality, characterized by oral exploration of inappropriate objects. The aim of this study was to reveal hypoperfused Brodmann areas (BAs) implicated specifically in the manifestation of ED in FTD. ***Materials and Methods:*** We studied 56 consecutive patients (18 men, 38 women, age±SD 65.5±9 years, mean duration of disease 3.6 years, education±SD 10.1±4.6 years) from an outpatient Memory Clinic. We used the established DSM-IV criteria for the diagnosis of dementia and the Neary criteria for the diagnosis of FTD. Twenty-seven patients received the diagnosis of bvFTD and 29 patients the diagnosis of SD. All the patients had a neuropsychological evaluation with a battery of tests including the mini-mental state examination (MMSE, mean 17.7±8.5) and the Neuropsychiatric Inventory (NPI, ED score 5.4). All the patients underwent a brain SPECT scan 20 min after the intravenous administration of 740MBq of ^{99m}Tc-HMPAO. We applied the NeuroGam™ software on the reconstructed data, for the comparison of brain perfusion in BAs in the right (R) and left (L) hemispheres with the software's normal data base consisted of healthy subjects of the same age. ***Results:*** Compared with normal subjects, we found statistically significant correlation of ED with hypoperfusion in bilateral anterior prefrontal and right dorsolateral prefrontal cortices (BAs 10LR, 46R), orbitofrontal cortices bilaterally (BAs 11LR), orbital part of inferior frontal gyrus (posterior lateral) on the right (BA 47R) and left parahippocampal gyrus (BA 36L). ***Conclusion:*** Our findings suggest that neurodegeneration of an integrated network which involves the orbitofrontal and prefrontal cortices, especially in the right hemisphere, and other connected areas in temporal cortices, is the underlying cause of ED and their sub-syndromes in FTD. These brain regions are implicated in the organization of feeding in response to internal and external behavioral signals and in cognitive control on appetite. ***References:*** 1. Ahmed RM, Irish M, Kam J, et al. Quantifying the eating abnormalities in frontotemporal dementia. JAMA Neurol. 2014;71(12):1540-1546. 2. Piguet O. Eating disturbance in behavioural-variant frontotemporal dementia. J Mol Neurosci. 2011;45(3):589-593.

EP-05

Endocrine/Parathyroid

e-Poster Area

EP-025

Optimization of ^{18}F-Fluorocholine PET/CT protocol in parathyroid imaging

I. Bossert[1], *M. Hodolic*[2,3], *S. Chytiris*[4], *D. D'Ambrosio*[5], *A. Marchetto*[1], *C. Vellani*[1], *A. J. Mallia*[6], *M. Boniardi*[7], *L. Chiovato*[4], *G. Trifirò*[1]; *[1]Nuclear Medicine Unit, Istituti Clinici Scientifici Maugeri SpA SB IRCCS, Pavia, ITALY, [2]Nuclear Medicine Department, Faculty of Medicine and Dentistry, Palacký University, Olomouc, CZECH REPUBLIC, [3]Nuclear Medicine Research Department, Iason, Graz, AUSTRIA, [4]Endocrinology Unit, Istituti Clinici Scientifici Maugeri SpA SB IRCCS, Pavia, ITALY, [5]Medical Physics Unit, Istituti Clinici Scientifici Maugeri SpA SB IRCCS, Pavia, ITALY, [6]Division of Nuclear Medicine, Department of Medical Imaging, Mater Dei Hospital, Msida, MALTA, [7]Department of Endocrine Surgery, Niguarda Hospital, Milan, ITALY.*

Aim/Introduction: Identification of pathological parathyroid glands in primary hyperparathyroidism, based on neck ultrasound (US) and/or 99mTc-SestaMIBI (MIBI) scintigraphy, is challenging. With respect to MIBI scan, ^{18}F-Fluorocholine (FCH) PET/CT improve detection rate of pathological parathyroid glands thanks to its better spatial resolution and lesion-to-noise ratio. Different authors proposed different protocols, with variations in administered activity, scanning time and bed time duration. Our aim was to propose a protocol for FCH PET/CT imaging, optimizing every variable and preserving the good quality of the exam. ***Materials and Methods:*** On the basis of published literature and the characteristics of our PET/CT scanner (Discovery 690 VCT, GE Healthcare) we decided to inject less than 2,5 MBq/kg of FCH, perform a dual-time point acquisition (15 and 60 min after FCH injection) with a duration of 3 minutes per bed (neck and upper mediastinum), and to skip dynamic acquisition. To test our method we plan to enroll 50 patients

with primary o tertiary hyperparathyroidism and negative or inconclusive MIBI scan. FCH PET results will be confirmed with cito-hystological examination whenever possible. ***Results:*** We prospectively enrolled 41 patients. The median injected FCH dose was 2,3±0,13 MBq/kg (range 1,79-2,55). The median injected FCH per patient was 172,9±45,5 MBq (range 108,9-283,6). FCH PET/CT was positive in 35 out of 41 patients. One patient had bilateral lesions (then sent for genetic evaluation) and 1 patient had a focal FCH uptake in the superior-anterior mediastinum. So far 15 patients had a cito-hystological confirmation of FCH PET result. We obtained a perfect correlation between PET and the gold standard evaluation results, even in case of a very small lesion or uncommon localization (i.e. para-esophageal). ***Conclusion:*** Although we have a relatively small number of patients, our method showed a good sensitivity allowing a reduction in patient's dose and exposure, bed time duration and avoiding dynamic acquisition, resulting in an easier patient's management. ***References:*** - PETC/CT with 18F-Choline localizes hyperfunctioning parathyroid adenomas equally well in normocalcemic hyperparathyroidism as in overt hyperparathyroidism. Bossert I, Chytiris S, Hodolic M, Croce L, Mansi L, Chiovato L, Mariani G, Trifirò G. J Endocrinol Invest. 2019 Apr;42(4):419-426. doi: 10.1007/s40618-018-0931-z. Epub 2018 Aug 9. - Diagnostic performance of choline PET for detection of hyperfunctioning parathyroid glands in hyperparathyroidism: a systematic review and meta-analysis. Treglia G, Piccardo A, Imperiale A, Strobel K, Kaufmann PA, Prior JO, Giovanella L. Eur J Nucl Med Mol Imaging. 2019 Mar;46(3):751-765. doi: 10.1007/s00259-018-4123-z. Epub 2018 Aug 9.

EP-06

Epilepsy

e-Poster Area

EP-026

Brain FDG PET/CT in Patients with Epilepsy : Single Center Experience

A. Arçay*, F. Aydın, E. Apaydın Doğan, M. Akyüz, U. Şenol, K. Karaali;*
Akdeniz University, Antalya, TURKEY.

Aim/Introduction: The aim of this study is to determine the consistency between visual and quantitative evaluation in brain FDG PET/CT which are performed to seek epileptic focus and assess surgical therapy options in epilepsy patients. We also aim to investigate the correlation between brain PET findings, brain MRI and clinical findings. ***Materials and Methods:*** 42 epilepsy patients who underwent brain FDG PET/CT in our hospital between April 2016 and January 2020 were included in the study. The 42 PET/CT scans were evaluated visually without quantitative results by the experienced nuclear medicine specialist. The correlation between the quantitative values which were obtained from the workstation by comparing to the data in normal individuals and the visual evaluation results were examined. In addition, the consistency of PET data with the clinical course of the patients and brain MRI findings was determined. ***Results:*** In 29 of 42 PET/CT scans, visual and quantitative evaluation were found compatible. Out of the remaining 13 incompatible scans, in 11 scans epileptic focus could be determined by visual evaluation while the quantitative evaluation was within normal limits. In 7 of these patients, visual evaluation was compatible with the clinical and MRI findings and contributed to treatment planning. Visual PET and MRI findings were compatible in 28 patients while they were incompatible in 14 patients. Out of these 14 patients,in 8 patients epileptic focus could be determined with PET but not with MRI. Total 13 patients underwent epilepsy surgery and 10 of these patients (8 patients with mesial temporal sclerosis, 1 patient with cortical dysplasia and 1 patient with diffuse astrocytoma) have been followed up without post-operative seizures. While visual and quantitative PET evaluation, MRI and clinical findings were compatible in 8 of these patients who were followed-up without seizures after successful surgery, 2 patients had quantitative values within normal limits, and epileptic focus was determined by visual PET evaluation and this guided the surgery option. While the compatibility rate between clinical (seizure semiology and EEG findings) and visual PET evaluation was 56%, this rate was determined as 54% with MRI and 50% with quantitative evaluation. ***Conclusion:*** Although the quantitative data contributes to the evaluation of brain FDG PET/CT , visual evaluation should be as effective as quantitative evaluation on PET/CT interpretation, as it appears that collective assessment of visual evaluation, MRI and clinical findings will provide additional benefits to the clinical course of epilepsy patients. ***References:*** None

EP-07

Imaging Clinical Studies -> Cardiovascular Imaging Clinical Study -> Heart Failure (including Sarcoidosis and Amyloidosis)

e-Poster Area

EP-027

Description of the typical patient with suspected cardiac amyloidosis due to transthyretin deposits and a positive result on the ^{99mTc}DPD scintigraphy in our health area

F. Sebastián Palacid*, N. Álvarez Mena, P. Turbay Eljach, B. Pérez López, C. Gamazo Laherrán, M. Alonso Rodriguez, A. Sáinz Esteban, M. Ruiz Gómez, M. González Soto, R. Ruano Pérez;*

Hospital Clínico Universitario Valladolid, Valladolid, SPAIN.

Aim/Introduction: Describe the clinical, epidemiological and scintigraphic characteristics of the typical patient with suspected cardiac amyloidosis due to transthyretin deposits (TTR) with a positive result on the ^{99m}Tc-DPD scintigraphy in the population of our health area. ***Materials and Methods:*** A retrospective study carried out between February 2017 and April 2020. We have evaluated 152 patients (95 men and 57 women) aged between 51 and 90 years, with suspected TTR cardiac amyloidosis by pathological echocardiography with diagnostic ^{99m}Tc-DPD scan (60 positive and 92 negative results).Variables such as the result of the scintigraphy, the degree of uptake intensity of the radio tracer in the myocardium, the distribution pattern, as well as demographic and clinical variables of each patient were analyzed. ***Results:*** The results obtained allow us to characterize the typical patient with a positive result on the ^{99m}Tc-DPD scintigraphy as a male patient (91.7% p =0.000), with a mean age of 81.5 years (p=0.000), with or without arrhythmias (p= not statistically significant (nss)), non-pacemaker carrier (76.7% p=nss), with no history of infarction (95% p=nss), and without alterations in the proteinogram (63.3% p=nss). Regarding the scintigraphic pattern of radiotracer uptake, 91.7% of patients with amyloidosis present a type 3 pattern and, in 88.3% of patients, a biventricular distribution patterns is evident. Finally, regarding the rest of the complementary diagnostic techniques, 10% of patients with a positive scintigraphic result have a histological study, 28.3% have a genetic study (100% with a negative result), 76.3% present signs of left ventricular hypertrophy in ecochardiography (p=0.000) and 26.7% present a late subendocardical enhancement pattern typical of TTR amyloidosis on cardiac magnetic resonance imaging (p=0.000). ***Conclusion:*** A positive ^{99m}Tc-DPD cardiac scintigraphy is more common in older men, with echochardiographic signs of left ventricular hypertrophy and a pattern of late subendocardical enhancement on cardiac MRI. We have not been able to demonstrate any other clinical or demographic variable that allows us to predict which scans will be positive before being performed. We find that in clinical practice, 99mTc-DPD scan obviates the need to perform a biopsy for the diagnosis of TTR amyloidosis. ***References:*** None

EP-028

^{99m}Tc PYP planar and SPECT bone scan in the diagnosis of transthyretin cardiac amyloidosis

M. Garcheva-Tsacheva[1], *M. Gospodinova*[2], *G. Kirova*[3], *A. Todorova*[4];
[1]*Acibadem City clinic, Sofia, BULGARIA,* [2]*Clinic of Cardiology, Medical Institute, Ministry of Interior, Sofia, BULGARIA,* [3]*Clinic of Medical Imaging, Acibadem City clinic Tokuda, Sofia, BULGARIA,* [4]*Department of Medical Chemistry, Biochemistry , Medical University Sofia, Genetical Medico-Diagnostics Laboratory, Genica, Sofia, BULGARIA.*

Aim/Introduction: Transthyretin cardiac amyloidosis (ATTR-CA) is a devastating disease, more common than previously thought. Early diagnosis is vital for timely treatment and better prognosis. Endomyocardial biopsy with histology for amyloid typing is an invasive procedure with potential risks. The aim of the study is to determine the value of combined planar and SPECT ^{99m}Tc PYP bone scan in the noninvasive diagnostic algorithm of the disease. ***Materials and Methods:*** Forty patients (29 males, 11 females, aged 39-88 y) with suspicion for cardiac amyloidosis from clinic, echocardiography, or cardiac magnetic resonance) were submitted to ^{99m}Tc-PYP bone scan for evaluation of eventual myocardial uptake. Two planar projections (anterior and left lateral) were registered at the 1st hour after injection of 10-15 mCi of ^{99m}Tc-PYP followed by SPECT/CT imaging. Beside visual assessment of planar cardiac uptake (according to Perugini score) and semiquantitative evaluation by the ratio heart to contralateral region (H/CL), a visual assessment of SPECT images was also done to prove myocardial deposition of radiotracer. Serum and urine electrophoresis with immunofixation and free light chain assays were performed to rule out light chain amyloidosis (AL) as well as genetic analyses for differentiation of hereditary from wild type ATTR-CA. ***Results:*** Eleven patients had score ≥2, in 10 of them in combination with H/CL≥1.5, suggesting ATTR-CA. Parallel test results suggested AL amyloidosis in 11 patients, only 3 of them with score≥2, two - with H/CL≥1.5, accepted to be false positive for ATTR-CA. The visual evaluation of SPECT images confirmed myocardial deposition in all, but one of patients with H/CL≥1.5, and did not show myocardial deposition in patients positive for AL and the rest of the patients (n=21), which were referred for further diagnostic assessment. Bone scan with additional SPECT images evaluation correctly identify 8 patients to have ATTR-CA, with only one false positive result. The further genetic analysis confirmed hereditary type in 6 of them, 2 were with wild type of the disease. ***Conclusion:*** Bone scan by 99mTc PYP is a reliable method for the diagnosis of the Transthyretin cardiac amyloidosis with low rate of false positive results. SPECT/CT helps the differentiation of myocardial deposition from blood pool persistence of radiopharmaceutical. This noninvasive examination reduces significantly the percentage of patients with unclear diagnosis, which need EMB. ***References:*** None

EP-029

Evaluation of technetium-99m DPD uptake in cardiac amyloidosis using myocardial perfusion imaging quantification software

M. O'Connell[1,2], *F. Delaney*[1], *M. Dore*[3], *M. Coyne*[2], *G. Giblin*[1], *D. O Sullivan*[1];
[1]*Mater Misericordiae University Hospital, Dublin, IRELAND,* [2]*University College Dublin, Dublin, IRELAND,* [3]*Mater Private Hospital, Dublin, IRELAND.*

Aim/Introduction: Multiple technetium 99m (Tc99m)-labelled bone avid radiotracers, such as 3,3-diphoshono-1,2-propanodicarboxylic acid (DPD), reliably identify myocardial amyloid deposition, facilitating the non-invasive diagnosis of cardiac transthyretin (ATTR) Amyloidosis. We aimed to map the distribution and extent of myocardial DPD uptake in ATTR amyloidosis using commercially available myocardial perfusion imaging (MPI) quantification software. The polar plot data which is produced may enhance understanding of the distribution of DPD uptake and help quantify severity over serial studies. MPI quantification software has not previously been validated in the assessment of myocardial DPD uptake. ***Materials and Methods:*** Tc99m-DPD radionuclide studies to evaluate for cardiac ATTR amyloidosis in 26 patients who demonstrated significant uptake (graded as Perugini Score 2 or 3) on planar thoracic imaging were included. Additional SPECT/CT imaging was performed in all cases. Images were analysed using AutoQUANT® software (Cedars Sinai, CA) and polar plot maps were produced based on the 20-segment model with relative uptake quantified in each segment from 0-100. Segments were grouped into five anatomical regions to evaluate relative uptake in the left ventricular myocardium. Data was compared to echocardiographic and MRI findings. ***Results:*** Quantification was successful in all patients. The average relative left ventricular myocardial uptake values across the 26 cases in each segment were: anterior = 56, inferior = 58, anteroseptal = 66, inferoseptal = 69, anterolateral = 56, inferolateral = 58, apical = 60. Follow-up imaging to date in one patient on Patisiran treatment showed an overall increase in DPD uptake with clear increase in 12 out of 20 individual segments. ***Conclusion:*** This study demonstrates the ability to re-purpose standard commercially available software to assess left ventricular myocardial uptake of Tc99m DPD in a deposition disease. While formal validation is required, there is the possibility to greatly improve the quantification of DPD uptake and map its distribution in cardiac ATTR Amyloidosis. This may allow assessment for disease progression on serial studies in patients undergoing novel treatments, such as Patisiran ATTR gene silencer. ***References:*** None

EP-030

Left ventricular ejection fraction improvement predicted by postoperative gated blood pool SPECT performed on CZT camera

V. Shipulin*, K. Zavadovsky, S. Andreev, A. Pryakhin, V. M. Shipulin; Cardiology Research Institute, Tomsk National Research Medical Centre, Russian Academy of Sciences, Tomsk, RUSSIAN FEDERATION.*

Aim/Introduction: To assess the value of gated blood pool SPECT (GBPS) carried out on CZT camera in early postoperative period in term of prediction of left ventricular (LV) ejection fraction (EF) improvement after 1 year follow-up period in patients with ischemic cardiomyopathy (ICM). ***Materials and Methods:*** Thirty six patients with ICM were enrolled. Before and within 2 weeks after surgery all patients underwent GBPS and 2D echocardiography. The values of LV and right ventricular (RV) volumes, global contractile function and LV mechanical dissynchrony were calculated. In the follow-up period (476 ± 36 days), patients were divided into two groups based on 2D echocardiography data. Group 1 (n=12) - patients with improving of LV ejection fraction (EF) ≥5% in comparison to early postoperative period study. Group 2 (n=24) - without improving of LV EF. ***Results:*** According to univariate U-test there were no statistically differences between two groups in clinical variables as well as GBPS indices before surgery. Early postoperative study showed significant differences between groups in terms of LV end diastolic volume index (EDVI) (109,6 (94,2; 129,5) vs. 146 (89,8;232,8), p<0,0001), end systolic volume index (ESVI)(69,7 (45,6; 94,4) vs. 107,7 (47,3; 200,6), p=0,001), LV EF (40 (35; 49) vs. 30 (26;39), p=0,02) as well as dissynchrony indices like LV Entropy (64 (60;70) vs. 74 (69; 77), p=0,003), RV SD (13 (8;17) vs. 69 (57; 102), p<0,0001), RV bandwidth (45 (36;60) vs. 69 (57; 102), p=0,0008), and interventricular dissynchrony (IVD) (8,5 (5;17) vs. 24 (8;40), p=0,01), respectively. It had been shown that long-term LV EF has a strong negative correlation (r=-0,7, p<0,05) with postoperative LV Entropy indices, middle negative correlation with RV SD indices (r=-0,66, p<0,05) and RW Bandwidth indices (r=-0,64, p<0,05). Multivariate logistic regression analysis showed that all of this variables were independent predictors of LV EF improvement.: LV EDVI (OR = 0,93; 95% CI 0,88; 0,98; p=0,0001), LV ESVI (OR = 0,95; 95% CI 0,92; 0,99; p=0.004), LV EF (OR = 1,06; 95% CI 1,02; 1,14; p<0,003), LV Entropy (OR = 0,85; 95% CI 0,76; 0,95; p<0,002), RV SD (OR = 0,7; 95% CI 0,56; 0,88; p<0,0001); RV bandwidth (OR = 0,7; 95% CI 0,56; 0,88; p<0,0001), IVD (OR = 0,92; 95% CI 0,87; 0,98; p<0,0001). ***Conclusion:*** The values of LV and RV indices, obtained from GBPS carried out in early postoperative period after surgical ICM correction, are associated with LV EF improving in 1 year follow-up period. ***References:*** None

EP-031

Diagnostic accuracy of bone scintigraphy in the assessment of cardiac amyloidosis: comparison among different methods of evaluation

C. Cottignoli, C. Romagnolo, F. Fringuelli, G. Biscontini, A. Palucci, L. Burroni;
Nuclear Medicine, Ancona, ITALY.

Aim/Introduction: Cardiac transthyretin-related amyloidosis (ATTR) is a severe and progressive cardiomyopathy. Bone scan with bone-seeking radiotracers is able to detect myocardial amyloid deposits, especially in ATTR patients. In all previous studies, several different tracers (Tc99m-DPD, -PYP, -HMDP, -MDP and -HDP) and different acquisition times are used for bone scan. The scintigraphic images were analyzed qualitatively (Grade 0-3) by means visual analysis and also semi-quantitatively in about 75% of studies. For the semi-quantitatively analysis different methods were also described in literature. Aim of our work is to compare these different methods of analysis to identify the most simple and accurate method for diagnostic use. ***Materials and Methods:*** Bone scintigraphy (Tc99m-HDP; 740 MBq) was performed in 28 patients (8 females and 20 males; mean age: 76 yrs) with 3 age-related groups of cardiomyopathy: cardiac TTR Amyloidosis (ATTR; n=10, qualitative grade 2), other Infiltrative Cardiac Disease (ICD; n=4) and Hypertensive Cardiomyopathy (HC; n=18). For the semi-quantitative analysis, we used the anterior image (ANT) and the geometric mean of anterior and posterior images (GM), drawing ROIs to obtain: hearth/contralateral lung count ratio (H/CL), hearth/skull count ratio (HS) and heart/iliac bone count ratio (H/IB). The values obtained were compared between groups with statistical evaluation tests for unpaired data. ***Results:*** The results obtained by comparison (p value) between the groups and the methods are shown in the table below. Non-significant p values were found in the comparison between ICD and HC with all the methods used. ***Conclusion:*** Our data confirm that bone scintigraphy represent a non-invasive tool for the assessment of cardiac ATTR with high sensitivity and specificity values. To differentiate infiltrative from hypertensive cardiomyopathies, any method has proven to be accurate, but if you want to distinguish ATTR from other infiltrative cardiomyopathies, it is better to perform the measurements with the calculation of the geometric mean between the anterior and posterior acquisition. The most reliable reference regions of interest were the iliac wing and the contralateral thoracic region. The skull region is the least reliable, probably because it is most affected by individual bone metabolic activity. ***References:*** None

EP-032

Volumetric Evaluation of ^{99m}Tc-pyrophosphate SPECT/CT in the Diagnosis of Transthyretin Cardiac Amyloidosis

S. Watanabe, K. Nakajima, H. Yoneyama, H. Wakabayashi, A. Inaki, T. Konishi, J. Komatsu, S. Yoshida, S. Kinuya;
Kanazawa University Hospital, Kanazawa, JAPAN.

Aim/Introduction: Quantitative evaluation of ^{99m}Technetium-pyrophosphate (PYP) uptake using standardized uptake value (SUV) has been reported in the diagnosis of transthyretin cardiac amyloidosis (ATTR-CA). However, SUV changes depending on volume of interest because blood pool PYP uptake is relatively high. The aim of this study was to evaluate a feasibility of a volumetric PYP parameter, which can be calculated more objectively, for differentiating ATTR-CA patients from control patients. ***Materials and Methods:*** We retrospectively evaluated all patients who underwent PYP SPECT/CT at our hospital between October 2018 and February 2020. Among them, 35 patients who underwent endomyocardial biopsies (29/35) and/or TTR gene tests (18/35) were included in this study. Seventeen patients were diagnosed as ATTR-CA (9 variant types and 8 wild types) and 18 patients were diagnosed as non-ATTR (control: 1 light chain cardiac amyloidosis, 1 cardiac sarcoidosis, and 16 other myocardial disorders). There was no significant difference in age between two groups. First, we evaluated blood pool PYP uptake by SUVmean in the ascending aorta at the level of the main pulmonary artery and defined as Amean. Then, we objectively evaluated the total volume of the region with PYP uptake above 1.5 times of Amean within the left and right ventricular myocardium and defined as a cardiac metabolic volume (CMV, i.e., a volume of voxels with abnormal PYP uptakes). SUVmean and CMV were calculated using xSPECT Quant. Accuracy of determining abnormal or normal volume was examined by receiver operating characteristic analysis and the area under the curve (AUC) was calculated. ***Results:*** The average CMV was 130.8 ± 118.2 cm^3 in the ATTR-CA group and 0.4 ± 0.5 cm^3 in the control group. CMV was significantly higher in the ATTR-CA group than the control group ($p = 0.0003$, AUC = 0.96). Using the cutoff value of 1.6 for diagnosing ATTR-CA, CMV showed sensitivity and specificity of 94% and 94%, respectively. There was no significant difference in CMV between patients with variant type ATTR-CM and patients with wild type ATTR-CM. ***Conclusion:*** A novel volumetric assessment of PYP SPECT/CT could accurately differentiate ATTR-CA patients from control patients, which should be studied in a larger prospective manner. ***References:*** 1) Ramsay SC et al. Eur J Hybrid Imaging. 2018; 2: 17-29. 2) Caobelli F et al. J Nucl Cardiol. 2019; online ahead of print. 3) Ramsay SC et al. J Nucl Cardiol. 2019; online ahead of print. 4)Ahmadian A et al. J Nucl Cardiol. 2017; 24, 413-424.

EP-033

Conduction disturbances in cardiac amyloidosis patients and 99mTc-HDP bone scintigraphy

A. Scarale[1], C. Dolci[1], A. Capozza[1], A. Franchini[1,2], I. Gotuzzo[1,2], E. Gay[1], G. Cabrini[1], M. Milella[1], C. Rossetti[1];
[1]ASST Grande Ospedale Metropolitano Niguarda, Milano, ITALY, [2]Nuclear Medicine School, University of Milan-Bicocca, Milan, ITALY.

Aim/Introduction: Cardiac amyloidosis is a disorder caused by extracellular protein fibril accumulation in the myocardium leading to restrictive heart failure. Both atrial and ventricular arrhythmias, along with conduction disease are common in cardiac amyloidosis. Planar imaging alone or with single-photon emission computed tomography (SPECT) using bone-seeking radiotracers (e.g. 99mTc-DPD, 99mTc-HDP) have been found to be more effective in detecting transthyretin (TTR) myocardial deposits. Aim of this study is to evaluate the prevalence of conduction disease in cardiac amyloid population in relation to 99mTc-HDP heart uptake. ***Materials and Methods:*** 99mTc-HDP scans performed, between 01/2015 and 04/2020, in patients with suspected or known cardiac amyloidosis were retrospectively reviewed. All underwent clinical evaluation, trans-thoracic echocardiography (TTE), electrocardiography (ECG), and total-body scintigraphy with 99mTc-HDP. Perugini visual score and semiquantitative analysis of cardiac uptake normalized to background activity (H/CL), defined as [total counts (myocardial ROI) / total counts (right hemithorax background ROI)] were performed. ROIs dimensions were identical in the same patient. TTE assessed LV volumes, function and mass. Final diagnosis was obtained by biopsy (28/77), or clinical follow-up. To compare differences between moderate/high and absent/low tracer's uptake, the unpaired t-test or Mann-Whitney was performed for normally or non-normally distributed variables, respectively for continuous variables and Pearson chi-squared for categorical ones. To evaluate the magnitude effect of the moderate/high and absent/low heart uptake and the presence of atrial fibrillation (AF) or other arrhythmias standardized mean differences (SMD) for each variable were computed. ***Results:*** Seventy-seven patients (63 males, 14 females) were enrolled. Population had median age of 77.0 (IQR: 70-83) years, 39/77 TTR cardiac amyloidosis patients and 38/77 AL-amyloidosis or other forms. The population was divided in two groups: patients with moderate/high or absent/low 99mTc-HDP heart uptake. Thirty-eight (49%) patients (35 males, 3 females) resulted with moderate/high heart uptake, significantly older (79.8±6.4 years; p-value<0.001) and with a significantly higher number of AF (n=28, 70%; p-value<0.001) respect to the absent/low heart uptake group (n=39, 51%). The sample was homogeneous for BMI and TTE and ECG measures. Among patients with AF higher SMDs were found for age (0.83) and FE% (0.65). ***Conclusion:*** These preliminary data on a small cohort suggest an higher prevalence of arrhythmias in cardiac amyloidosis patients with high heart 99mTc-HDP uptake than in low or absent one. ***References:*** None

EP-034

^{99m}Tc-DPD SPECT/CT Quantification In Cardiac Transthyretin Amyloidosis. A Pilot Descriptive Study

***C. Wakfie Corieh[1]**, J. Rodríguez Gómez[1], F. Ferrando-Castagnetto[2], M. Pérez Castejón[1], M. Pedrera Canal[1], I. Vilacosta[1], P. Romero Fernández[1], K. Bayardo[2], R. Ferrando[2], J. Carreras Delgado[1];*
[1]Hospital Clínico San Carlos, Madrid, SPAIN, [2]Hospital de Clínicas Dr. Manuel Quintela, Facultad de Medicina, Universidad de la República, Montevideo, URUGUAY.

Aim/Introduction: Scintigraphy with ^{99m}Tc-bisphosphonate derivatives (^{99m}Tc-DPD, ^{99m}Tc-HMDP and ^{99m}Tc-PYP) provides critical information on transthyretin cardiac amyloidosis (ATTR-CA). Unlike ^{99m}Tc-HDMP, a detailed quantification about myocardial distribution of amyloid transthyretin (ATTR) has not been evaluated so far with ^{99m}Tc-DPD. While it is suggested that can be used interchangeably, there is also no comparison between both tracers. This pilot experience quantified the myocardial distribution of ^{99m}Tc-DPD on of SPECT/CT in ATTR-CA patients. ***Materials and Methods:*** Eleven patients with Perugini score 2 and 3 diagnosed with ATTR-CA were consecutively selected between September 2019 and February 2020. All of them underwent planar and cardiac SPECT/CT images. ^{99m}Tc-DPD uptake through left ventricle (LV) was analyzed by obtaining the number of counts over each cardiac wall (anterior, septal, inferior, lateral and apex), both in non-corrected (NC) images and after applying iterative reconstruction with attenuation correction (IRAC). ***Results:*** Mean age was 83.8 years, 90.9% were men. Tracer distribution over LV walls tended to be more intense in septal-inferior walls and through basal segments, reflecting a lower amyloid accumulation in the apex. In NC images, ATTR deposit in LV walls was distributed, in decreasing order, as follows: septal, inferior, anterior, lateral and apex (23.3±4.4, 21.0±3.0, 19.8±3.6, 19.3±3.0 and 16.6±5.1%, respectively, p=0.002 for ANOVA and Bonferroni posthoc test for septal vs. apex). After IRAC, regional amyloid distribution tended to be higher in inferior than in septal walls, with a more prominent apex-to-base gradients. The decreasing uptake order obtained in IRAC images was: inferior, septal, lateral, anterior and apex (23.3±2.8, 23.1±4.4, 20.9±2.8, 19.0± 3.2 and 13.9±4.2%, respectively, p<0.05 for multiple comparisons: anterior vs. inferior, anterior vs. apex, septal vs. apex, inferior vs. apex and lateral vs. apex). ***Conclusion:*** In ATTR-CA subjects with high Perugini scores, ^{99m}Tc-DPD SPECT/CT allows to quantify the distribution and extension of regional amyloid burden. These results agree with recent findings provided by ^{99m}Tc-HDMP SPECT/CT. The image activity obtained after IRAC could be derived

from soft tissue attenuation (described in patients with CA) and from ribs and sternum uptake related with DPD bone avidity. Clinical diagnostic and prognostic impacts of different attenuation correction algorithms should be evaluated in larger series, head-to-head with other noninvasive diagnostic techniques. ***References:*** None

EP-08

Imaging Clinical Studies -> Cardiovascular Imaging Clinical Study -> Metabolism and Innervation

e-Poster Area

EP-035

^{123}I-Metaiodobenzylguanidine Cardiac Scintigraphy In Patients With Clinical Suspicion Of Parkinson´s Disease

L. García Zoghby, *S. Rizkallal Monzón, C. Lancha Hernández, D. Monachello Araujo, D. Travaglio Morales, E. López Llobet, S. Rodado Marina, C. Escabias del Pozo, J. Cordero García, M. Coronado Poggio, L. Domínguez Gadea;*
Hospital Universitario La Paz, Madrid, SPAIN.

Aim/Introduction: The aim of our study is to determine the heart / mediastinum ratio cutoff value for Parkinson´s disease (PD) diagnosis in our population, and also determine which image has more correlation with the final diagnosis (early vs delayed vs both). ***Materials and Methods:*** We retrospectively analyzed 51 patients (29 females, 22 males; mean age 66.6 years) with clinical suspicion of PD studied in our nuclear medicine department from January 2016 to October 2019. All of them underwent a ^{123}I-MIBG cardiac scintigraphy: anteroposterior and left oblique thorax planar images, 15 minutes and 4 hours after intravenous administration of the tracer (370 MBq). These images were quantitatively evaluated with the heart / mediastinum ratio. Patients were followed up for a mean of 20 months (range 3 to 48). We divided our sample (51 patients) into two groups according to final diagnosis: PD or non-PD. Final diagnosis was achieved with clinical findings, laboratory and imaging tests, treatment response and follow-up. The optimal e-H/M ratio cutoff and d-H/M ratio cutoff were determined by Receiver Operating Characteristic (ROC) curve analysis. We compared the delayed heart / mediastinum (d-H/M) ratio capability vs the early heart / mediastinum (e-H/M) ratio capability to separate PD patients from non-PD patients with non-parametric test (Mann-Whitney test). Statistical significance was defined as $p < 0.005$. ***Results:*** 18/51 patients with PD and 33/51 patients with non-PD (4/33 Lewy body dementia, 5/33 multiple system atrophy, 9/33 progressive supranuclear palsy, 2/33 corticobasal degeneration, 2/33 pharmacological parkinsonism, 2/33 vascular parkinsonism, 9/33 others). The optimal e-H/M ratio cutoff was 1.50 (73% sensitivity, 78% specificity, 0.785 area under the ROC curve) and the optimal d-H/M ratio cutoff was 1.49 (70% sensitivity, 83% specificity, 0.756 area under the ROC curve). We found statistical differences between patients with PD and non-PD in both e-H/M ($p=0.001$) and d-H/M ($p=0.003$). ***Conclusion:*** The e-H/M ratio cutoff was 1.50 and the d-H/M ratio cutoff was 1.49, both of them were able to differentiate PD from non-PD in our population. ***References:*** None

EP-09

Imaging Clinical Studies -> Cardiovascular Imaging Clinical Study -> Other Cardiovascular Imaging (including Plaque)

e-Poster Area

EP-036

Significance of epicardial and visceral adipose tissue measurement by 18F-FDG-PET / CT in type 2 diabetes mellitus

D. Dezso[1], *K. Zámbó*[1], *Z. Ritter*[1], *Z. Bán*[1], *Z. Szabó*[1], *E. Várady*[1], *B. Bódis*[2], *O. Nemes*[2], *K. Rucz*[2], *S. Szujó*[2], *E. Mezősi*[2], *L. Bajnok*[2], *E. Schmidt*[1];
[1]*University of Pécs, Medical School, Department of Diagnostic, Pécs, HUNGARY,* [2]*University of Pécs, Medical School, 1st Department of Medicine, Pécs, HUNGARY.*

Aim/Introduction: Type 2 diabetes (T2DM) is a leading risk factor of cardiovascular diseases. There is a strong correlation between coronary artery diseases and the volume of epicardial adipose tissue (EAT) deposits located between myocardium and visceral pericardium. This metabolically active ectopic adipose tissue is in strong relationship with visceral adipose tissue (VAT) developmentally and correlates with its amount. The aim of our study was to investigate the relationship between BMI, calcification of large arteries, VAT and EAT in the diabetic population studied with FDG-PET/CT. ***Materials and Methods:*** Examinations of 33 T2DM patients' and 62 non-diabetic patients were investigated during our retrospective study. The volume of EAT and VAT was determined with FDG-PET/CT scans using Slicer 4.10.0 software (free and open source software package). SUVmax (Standardized Uptake Value calculated with Interview Fusion software, Mediso), the volume of calcified arterial plaque (density above 130 Hounsfield Units), EAT and VAT were measured and the results were evaluated using SPSS software. The mean SUVmax of the mediastinal blood-pool was measured to correct the SUVmax value of the adipose tissue. ***Results:*** Results of our ongoing research showed significant correlation between EAT volume ($r=0.242$, $p<0.05$), mediastinal blood-pool corrected EAT SUVmax ($r=0.270$,$p<0.05$) and the calcification of the vascular system on the whole examined population. The amount of EAT

(p<0.001) and VAT (p<0.05), mediastinal blood-pool corrected SUVmax (p<0.001) and the degree of vascular calcification (p<0.001) in patients with T2DM were significantly higher than in the control group. The amount of EAT and VAT showed significant correlation (r=0.495,p<.00001) in both group. The mediastinal blood-pool corrected EAT SUVmax is significantly higher than VAT SUVmax in both groups (p<0.001), and showed significant correlation (r=0.442, p<0.001) with each other. There is a significant correlation between the volume of VAT and mediastinal blood-pool corrected VAT SUVmax (r=0.221,p=0.036), which correlation is significantly stronger in patients with T2DM (r=0.455,p=0.011). EAT (r= 0.072,p=0.491)and VAT SUVmax (r=0.084,p=0.427) is independent of pre-examination blood glucose. ***Conclusion:*** Based on our results, patients with T2DM have significantly higher levels of EAT and VAT, higher FDG uptake, and increased calcification of large arteries too. According to our results, the higher epicardial and visceral fat deposits may contribute to the higher cardiovascular risk in T2DM patients. Our results confirm that EAT is in strong relationship with VAT developmentally and correlates with its amount, and these metabolically active ectopic adipose tissues activity are independent of pre-examination blood glucose. ***References:*** Under the 20765-3/2018/FEKUTSTRAT research program.

EP-037

The use of gated blood-pool SPECT for evaluation of cardiac dyssynchrony in patients with ventricular tachycardia

V. Saushkin*, D. Lebedev, S. Popov, Y. Lishmanov;*
Tomsk National Research Medical Center of the Russian Academy of Sciences, Cardiology Research Institute, Tomsk, RUSSIAN FEDERATION.

Aim/Introduction: The aim of the study was to evaluate the impact of idiopathic ventricular tachycardia and premature ventricular beats on cardiac function and dyssynchrony. ***Materials and Methods:*** The study included 21 patients with ventricular arrhythmias (VA) (mean age of 43,5±11,7 years). The control group consisted of 15 patients (mean age of 56,3±8,3 years) without cardiac arrhythmias. Electrophysiological study (EPS) and radiofrequency ablation (RFA) procedure for patients with VA were performed according to indications. Phase images were used for calculating the first harmonic Fourier transform. The phase standard deviation (PSD), histogram bandwidth (HBW) and phase entropy (E) were used as an indicator of mechanical dyssynchrony for the both ventricles. ***Results:*** Patients with VA had local areas of asynchronous myocardial contraction (AMC). Patients with VA had significantly higher values of the end-diastolic and end-systolic volumes, and lower indices of contractility than patients of the control group. More negative changes observed in the right ventricle. The negative association found between the total number of AMC areas and cardiac contractility indices. Ectopic localization (based on EPS data) associated with topography of AMC areas (based on GBP SPECT). Radiofrequency ablation procedure significantly improved cardiac contractility indices and reduction of intraventricular dyssynchrony. The AMC areas completely disappeared or decreased in a number compared with the preoperative conditions. ***Conclusion:*** Patients with VA have AMC areas which mostly localized in the right ventricle. The presence of AMC zones is a scintigraphy symptom of arrhythmogenic focus. ***References:*** None

EP-038

Assessment of vulnerable atherosclerotic plaques in coronary arteries using somatostatin receptor scintigraphy (SRS) and head-to-head comparison with myocardial perfusion scintigraphy (MPI): A paradigm under construction

M. Assadi*, A. Amini, E. Jafari, M. Pourbehi, D. Iranpour, R. Nemati;*
Bushehr University of Medical Sciences (BUMS), Bushehr, IRAN, ISLAMIC REPUBLIC OF.

Aim/Introduction: Activated macrophages can lead to cardiac events by rupturing the vulnerable atherosclerotic plaques. It has been shown that activated macrophages express somatostatin receptor-2 (SSTR-2), therefore, we aimed first, to detect atherosclerotic plaques by somatostatin receptor scintigraphy (SRS) using 99mTc-Octreotide SPECT which bind to somatostatin receptor 2, and second, comparison of SRS with myocardial perfusion scintigraphy (MPI) using 99mTc-MIBI SPECT and angiography in detection of atherosclerotic plaques. ***Materials and Methods:*** 737 patients with suspicious coronary artery disease who referred to the Nuclear Medicine Department for MPI were participated in this prospective controlled trial, 52 of them representing the final study cohort, performed additional SRS . The SRS analysis was done according to severity of uptakes (mild, moderate , severe) into five cardiac regions (apex, anterior, inferior, septal, lateral) . The MPI defects were also reported according the above segments. According to the standard cardiovascular guideline, the angiography was performed during 1 month after SRS . The coronary arteries in all modalities divided into three main arteries inducing LAD, RCA, and LCX. Statistical analysis of all modalities was performed for three main coronary arteries separately and compared. ***Results:*** In 17 out of 52 patients who underwent coronary angiography, 11 female and 6 male aged from 28 to 84 (54.83±19.7) years old, had been shown remarkable uptake on cardiac SRS. The SRS and angiography in the LAD territory was concordant in 13/17 patients while only 7/17 cases were concordant between MPI and angiography. In RCA territory, the SRS and angiography were concordant in 14/17 cases while MPI and angiography were 11/17 cases.

In LCX territory, SRS and angiography were concordant in 13/17 cases while MPI and angiography were 6/17 cases. In all 35 remaining patients who had not been performed coronary angiography based upon cardiovascular profile, cardiac event was not showed over follow up period of 2-9 months (5.52±2.71) , and interestingly they didn't depicted remarkable uptake on SRS. An example of such cases is presented ***Conclusion:*** 99mTc-octreotide uptake was more concordant relative to 99mTc-MIBI SPECT findings with coronary plaques, suggesting a potential role for 99mTc-octreotide in the evaluation of atherosclerosis. In addition, coronary uptake may provide a molecular guide for the representation of coronary atherosclerotic lesions. Specific regional uptake is warranted to be ascertained by histology. ***References:*** None

EP-039

Prevalence of transthyretin cardiac amyloidosis (ATTR-CA) in a population of patients with hip and knee arthroplasty: could they be early signs?

A. Paccagnella[1], *R. Bonfiglioli*[1], *F. Mattana*[1], *R. Mei*[1], *G. Saturi*[2], *P. Massa*[2], *G. Caponetti*[2], *M. Sguazzotti*[2], *A. Ponziani*[2], *C. Gagliardi*[2], *S. Longhi*[2], *N. Galiè*[2], *S. Fanti*[1];
[1]*Department of Nuclear Medicine, Policlinico S.Orsola, University of Bologna, Bologna, ITALY,* [2]*Department of Cardiology, Policlinico S.Orsola, University of Bologna, Bologna, ITALY.*

Aim/Introduction: ATTR-CA is an under-diagnosed progressive disorder in which excessive extracellular cardiac deposition of mutant (ATTRm) or wild-type ATTR (ATTRwt) causes a restrictive cardiomyopathy.It's well known that ATTR preferentially deposits in ligaments, tendons, articular cartilage and soft tissues (ST), causing carpal tunnel syndrome and lumbar spinal stenosis. We hypothesized that patients with total hip (THA) and/or knee (TKA) arthroplasty would have a significative prevalence of ATTR-CA visualized at whole body scintigraphy (WBS); this may precede and be a red flag of ATTR-CA diagnosis. ***Materials and Methods:*** we collected all WBS scans performed from March 2010 to March 2020 using technetium-99m (99mTc)-diphosphonate (DPD). Out of all patients, we selected only those with presence of THA or TKA (group-1) and in this group we investigated the further presence of cardiac uptake with visual score (VS) as well as ST and lung uptake-LU- (group-2). Group-2 was analyzed at cardiologic department, using echocardiography, laboratory test, and/or magnetic resonance in order to define the significance of cardiac uptake. A binary linear regression was used to evaluate correlation between VS and cardiological diagnosis. ***Results:*** out of 14858 patients, group-1 was formed by 418 patients (2,8%); 37/418 patients (9%) were included in group-2, of which 8 were excluded for the absence of cardiological data with a remaining total of 29 (7%)(mean age at WBS: 79 years; male: 65%; female: 35%; THA: 59%; TKA: 41%; VS 1: 21%, VS 2: 65%, VS 3: 14%). Out of 29, 20 (69%, 4,8% of group-1) received ATTR-CA diagnosis (all ATTRwt) with a mean time of 15 months between scan and diagnosis. WBS detected also ST uptake in 55% and LU in 80%. Positive correlation was found between VS and cardiological diagnosis (OR 7,064, CI95% 1,173-42,526, p=0,033). Date of arthroplasty intervention was only available in 2 patients, in which it occurred on an average of 7,7 years before ATTR-CA diagnosis. 9 patients with no cardiological diagnosis (VS 1: 45%; VS 2: 55%) showed a low prevalence of ST uptake (22%). ***Conclusion:*** early recognition of ATTR-CA may be critical for emerging therapeutic options. In our study, all confirmed cardiological diagnosis were ATTRwt, this is consistent with the hypothesis that ATTRwt disease has a course over a period of decades such as articular degeneration.History of THA and TKA, like carpal tunnel syndrome and lumbar spinal stenosis, may be an important clinical historical marker indicating the presence or future development of ATTR-CA. ***References:*** None

EP-10

Imaging Clinical Studies -> Cardiovascular Imaging Clinical Study -> Perfusion

e-Poster Area

EP-040

Intra- and inter-observer repeatability of three myocardial perfusion scintigraphy software packages in quantification of perfusion abnormalities

C. Sachpekidis[1], *V. Sachpekidis*[2], *A. Kopp-Schneider*[3], *G. Arsos*[1], *E. Moralidis*[1];
[1]*Department of Nuclear Medicine, Aristotle University of Thessaloniki, Papageorgiou Hospital, Thessaloniki, GREECE,* [2]*Department of Cardiology, Papageorgiou Hospital, Thessaloniki, GREECE,* [3]*Department of Biostatistics, German Cancer Research Center (DKFZ), Heidelberg, GERMANY.*

Aim/Introduction: In the quantification of the extent of abnormalities in myocardial perfusion scintigraphy (MPS), the repeatability (agreement between different analyses of a single acquisition of MPS data) of commercially available software packages has not been evaluated, yet. The aim of the present study was to evaluate the intra- and inter-observer repeatability of commonly applied software packages for ischemia quantification. ***Materials and Methods:*** 182 consecutive patients referred for routine 1-day ^{99m}Tc-sestamibi MPS were prospectively enrolled. Half patients underwent a stress/rest protocol and 91 patients underwent a rest/stress protocol. Automated quantitative analysis was performed with the Cedars Quantitative Perfusion SPECT, Version 4.0, Cedars-Sinai Medical Center (QPS), the Emory Cardiac Toolbox, Version 3.0, Emory

University Medical Center (ECTb), and the 4D-MSPECT, Version 4.0, University of Michigan Medical Center (4DM). From stress images, the parameters summed stress score (SSS) and the total defect extent (TDE), expressed as % percentage of the LV, were automatically calculated with each software tool. Data were analyzed independently by an experienced nuclear cardiologist and a trainee. The Bland-Altman analysis (bias±95% limits of agreement) was used to assess repeatability. ***Results:*** Based on the Bland-Altman analysis, the intra-observer repeatability results of SSS assessment for the experienced physician and the trainee using the different software programs were 0.0%±4.3% and 0.2%±5.9% (4DM), 0.2%±7.8% and 0.0%±7.5% (ECTb), -0.6%±7.6% and -0.5%±5.4% (QPS), respectively. Further, the intra-observer repeatability results of TDE assessment for the experienced and the trainee were 0.1%±5.2% and 0.3%±6.6% (4DM), 0.1%±7.9% and -0.1%±6.4% (ECTb), 0.1%±2.8% and -0.1%±2.4% (QPS), respectively. Regarding inter-observer repeatability, the results of SSS assessment were 0.2%±5.4% (4DM), 0.1%±9.6% (ECTb), and 0.2%±8.1% (QPS), while the results of TDE assessment were 0.6%±6.4% (4DM), -0.2%±10.3% (ECTb) and -0.1±4.3 (QPS). ***Conclusion:*** Those data provide evidence for bothersome limitations in intra-observer repeatability when using commercially available software packages for the assessment of SSS in MPS. Similar were the findings in the assessment of TDE, with only QPS offering a satisfying degree of repeatability. No substantial differences were noted between the experienced and the trainee observer. Concerning inter-observer agreement, 4DM for SSS and QPS for TDE assessment provided the best, yet suboptimal, results, whereas considerable problems were noted with the ECTb package. ***References:*** None

EP-041

Coronary Flow Reserve (CFR) Obtained with SPECT Discovery NM 530c Camera - Comparison with Coronary Angiography

M. Blaszczyk[1], P. Cichocki[2], K. Cygulska[3], J. Kuśmierek[2], P. Lipiec[3], J. D. Kasprzak[3], K. Frynas – Jończyk[3], P. Wejner – Mik[3], A. Płachcińska[1];

[1]Department of Quality Control and Radiological Protection, Medical University of Lodz, Łódź, POLAND, [2]Department of Nuclear Medicine, Medical University of Lodz, Łódź, POLAND, [3]Chair and Department of Cardiology, Medical University of Lodz, Bieganski Hospital, Łódź, POLAND.

Aim/Introduction: CFR is an important parameter that complements a myocardial perfusion study (MPS), especially in case of a multivessel CAD, due to a frequent underestimation of the disease extent, sometimes resulting even in omission of abnormal perfusion, especially when all 3 vessels are stenosed. CZT cameras are an attractive alternative to PET CFR studies which are more expensive and less available.The aim of the study was to check whether CFR reflects hemodynamic effects of coronary artery stenoses. ***Materials and Methods:*** The study involved 34 patients (19 men) with known or suspected CAD, in whom standard MPS (2-day protocol-dipirydamol stress and rest) were preceded by dynamic radiopharmaceutical administration. After injection of 37 MBq of 99mTc-MIBI (for camera positioning), patients were administered a bolus of 550 MBq, simultaneously with start of dynamic image acquisition lasting 8 min. Scintigraphic list mode data was converted to 15 frames 6s, 4 frames 30s and 4 frames 60s and reconstructed to 3-dimensional SPECT images. Then the study was processed with a Corridor 4M software. Results assess CFR of the entire left ventricular myocardium (CFR_{TOT}) and individual coronary vessel areas (CFR_{LAD},CFR_{RCA}, CFR_{LCx}). Coronary angiography (CA) was the verification of results in all patients, where artery stenosis was presented as a percentage reduction in its diameter. ***Results:*** Mean CFR_{TOT} values in patients without critical (≥70%) coronary stenoses (n=16) and with stenoses (n=18) differed statistically significantly (p=0.018) and amounted to 2.21±0.55 and 1.70±0.65, respectively. In patients without critical stenosis of LAD (n=20), mean value of the CFR_{LAD} was 2.19±0.60 and was significantly higher (p=0.004) than in patients (n=14) with critical stenosis of this vessel :1.56±0.58. In patients with significant stenosis on RCA (n=9), this difference was close to statistical significance: 2.01±0.52 vs 1.56±0.82, p=0.07. After a division of patients with significant stenoses into 2 subgroups: without or with one stenosis (n=22) and with at least 2 stenoses (n=12), a significant (p=0.031) difference between mean values of the CFR_{TOT} (2.17±0.58 vs 1.52±0.58) was found. In addition, a statistically significant (p=0.00007) correlation (r=-0.63) between CFR_{LAD} and percentages of stenosis of this vessel in CA was demonstrated. ***Conclusion:*** CFR obtained with CZT camera reflects, in a non-invasive way, hemodynamic effects of coronary artery stenoses, especially on LAD. A significant reduction of the CFR_{TOT} in multivessel patients allows to expect a quantitative criterion for a reliable, non-invasive recognition of multivessel patients, that nees to be worked out on a larger material. ***References:*** None

EP-042

Optimize the calculation of the left ventricular ejection fraction with myocardial perfusion gated-SPECT in small hearts

C. Martínez[1,2], *C. Espinet*[1], *M. N. Pizzi*[1], *A. Cardoso*[1], *S. Aguadé-Bruix*[1];
[1]*Hospital Universitari Vall d'Hebron, Barcelona, SPAIN,*
[2]*Complejo Hospitalario Universitario de Vigo, Vigo, SPAIN.*

Aim/Introduction: The geometric methods used for calculate the left ventricular ejection fraction(LVEF) with gated-SPECT myocardial perfusion(MP) gives a clear overvaluation when ventricular volumes are small. There are several approaches that can be used to correct the problems related to the effect of partial volume on the LVEF calculation . This study is based on applying the reconstruction zoom correction of a study acquired with a 64x64 matrix, which allows to decrease the pixel size from 6.8mm to 2mm, so we can evaluate the changes obtained in the LVEF and the ventricular volumes applying the reconstruction zoom compared to the normal study. *Materials and Methods:* We analyze 205patients (139 women, mean age: 72 years±10) with low prevalence of coronary heart disease (up to 10% pretest probability), who have performed a study of myocardial stress perfusion, without clinical, electrical or scintigraphic abnormalities, and with a normal LVEF obtained after post-stress (we did not perform a rest study). LVEF, ventricular volumes, and cardiac output have been assessed with and without reconstruction zoom. *Results:* We obtained global results with the normal processing methods(b) and with reconstriction zoom(z). Also, ventricular function results were grouped according to the following EDV ranges:EDV<40: LVEF: 83,8±7,4(b); 72,2±8,6(z), EDV: 33,3±3,6(b), 56,2±7,1(z), ESV: 5,44±2,5(b), 15,7±5,6(z), Heartbeat volume(HV): 27,9±3,6(b), 40,5±6,9(z), Cardiac output(CO): 2,31±0,53(b), 3,35±0,8(z). EDV 40-54: LVEF: 75,6±9(b); 66,3±8,6(z), EDV: 47,2±4,3(b), 73,1±6,2(z), ESV: 11,5±4,7(b), 24,7±7,2(z), HV: 35,6±4,7(b), 48,4±6,8(z), CO: 2,74±0,54(b), 3,74±0,76(z). EDV 55-69: LVEF: 68,7±6,6(b); 60,5±6,8(z), EDV: 61,4±4,3(b), 89,1±5,2(z), ESV: 19,2±4,3(b), 35,1±6,4(z), HV: 42,1±4,7(b), 54±6,8(z), CO: 3,17±0,55(b), 4,07±0,77(z). EDV 70-84: LVEF: 63,5±7,7(b); 55,9±7,8(z), EDV: 75,7±4,7(b), 103,3±9,2(z), ESV: 27,5±6,6(b), 45,9±10,3(z), HV: 48,3±6,9(b), 57,4±7,7(z), CO: 3,54±0,7(b), 4,23±0,95(z). EDV>84: LVEF: 58,5±4,3(b); 49,8±3,6(z), EDV: 98,7±11,6(b), 126,9±9,2(z), ESV: 40,9±5,8(b), 63,8±10,3(z), HV: 57,8±8,5(b), 63,1±5,8,7(z), CO: 4,24±1,03(b), 4,62±0,97(z).The differences obtained by group respect to the EDV were: EDV<40: Mean EDV: 33,3; HV:12,6; CO:1,03. EDV 40-54: Mean EDV: 47,2: HV:12,8; CO: 1.EDV: 55-69, Mean EDV:61,4; HV:11,9; CO:0,9. EDV: 70-84; Mean EDV: 75,7; HV:9,2; CO: 0,69.EDV>84: Mean EDV: 98,7; HV:5,3; CO:0,38. All calculated LVEF, volumes, and CO show statistically significant differences (p<0.001), overall and by EDV segments. The evaluation of the differences shows a clear decrease between them in HV and CO from EDV bigger than 69 ml. *Conclusion:* The application of the reconstruction zoom in the calculation of the LVEF, volumes and cardiac output corrects the alterations due to the effect of the partial volume on the gated-SPECT. This reconstruction zoom achieves better performance at EDV values <70 ml. *References:* None

EP-043

Preliminary Comparison of Myocardial Perfusion Study Results on a Standard Dual-head Scintillation Camera and a CZT Semiconductor Camera

M. Blaszczyk[1], *P. Cichocki*[2], *J. Kuśmierek*[2], *A. Płachcińska*[1];
[1]*Department of Quality Control and Radiological Protection, Medical University of Lodz, Łódź, POLAND,* [2]*Department of Nuclear Medicine, Medical University of Lodz, Łódź, POLAND.*

Aim/Introduction: Scintillation cameras are reliable diagnostic tools allowing non-invasive assessment of myocardial perfusion. A semiconductor CZT camera is characterized by higher resolution and sensitivity, which should allow obtaining high-quality images in shorter time. Comparison of myocardial perfusion images obtained with scintillation and CZT cameras and assessment of the impact of differences on diagnosis and size of ischemia. *Materials and Methods:* 41 patients (24 men, aged 33 to 83, mean 67 years) were selected randomly from patients referred for myocardial perfusion study (MPS). 2-day protocol was used: rest and stress (exercise/pharmacological). 99mTc-MIBI was administered in activity of 10 MBq / kg. Acquisition, carried out twice, using Discovery NM 530c camera (5 min) and Optima 640 (15 min), was completed with a low-dose CT on Optima camera to correct images for attenuation. Images were assessed according to the semi-quantitative method (17-segment model), assigning each segment values from 0 (normal perfusion) to 4 (no perfusion). First, images reconstructed without attenuation correction (NC) and with correction (AC) were evaluated separately, and then both sets were combined, using a 3-point scale: normal-n, equivocal-e and abnorma-a. First, all images from Optima were assessed, and after a few days - from Discovery. *Results:* Correlation coefficient between SSS values for both cameras, without attenuation correction (NC), was 0.95, for SRS - 0.94. Assuming SSS value≥4 as a criterion for abnormal stress study, results were concordant (normal/abnormal) in 95% (39/41) of studies. SSS lesions detected with both cameras, after division into small (SSS = 4-8) and large (SSS≥9), were concordant in 55% (6/11). With AC, correlations between SSS and SRS obtained with both cameras improved to 0.98 and 0.96, respectively. Accepting SSS≥2 as a criterion for abnormal stress study with AC allowed to achieve agreement between results (normal/abnormal) of 90% (37/41). AC improved agreement of size of defects (small/large) to 100% (10/10). After combined assessment of NC and AC studies on Optima, 21n, 9e and

11a results were obtained, and on Discovery - 25, only 5 and 11, respectively. ***Conclusion:*** Satisfactory agreement was obtained between results of MPS on Discovery NM530c (3 times shorter acquisition) and Optima 640 camera. AC based on a CT scan performed on Optima applied to images obtained with both cameras fulfilled its role properly. The study needs to be continued on a larger group of patients. ***References:*** None

EP-044

Evaluation of the dyssynchrony difference between pharmacological stress and rest of gated myocardial perfusion single photon emission computed tomography in patients after acute myocardial infarction

M. Ota[1], T. Kato[1], S. Matsuo[2];
[1]Gifu prefectural general medical center, Gifu, JAPAN,
[2]Matsuo Medical Clinic, Hirakata, JAPAN.

Aim/Introduction: Quantification of left ventricular (LV) dyssynchrony has been developed by using gated myocardial perfusion single photon emission computed tomography (GMPS). Heart Function View (HFV) software activated on GMPS was introduced which can investigate clinical usefulness for LV phase analysis. Hence, we reported that the results of calculating phase analysis were changed by the accumulated counts of myocardium at baseline of GMPS[1)]. Presumably, the high-count GMPS data can provide better quantification of LV dyssynchrony. The aim of this study is evaluation of comparison post pharmacological stress dyssynchrony with rest dyssynchorny on the same revel accumulated counts of myocardium at baseline of using 2days protocol GMPS in acute myocardial infarction (AMI) patients after successful percutaneous coronary intervention (PCI). ***Materials and Methods:*** We retrospectively examined 53 consecutive AMI patients (39 men and 14 women; mean age 68.5±11.5 years old) who underwent successful PCI on admission were enrolled in this study. All patients were referred for routine rest and post pharmacological stress ^{99m}Tc-GMPS imaging on the two days protocol. Rest ^{99m}Tc-GMPS was performed within 12 days after the PCI of achieving successful coronary reflow. After within 9 days from rest imaging, post pharmacological stress GMPS imaging was performed. Rest ^{99m}Tc-MIBI GMPS images were obtained at 1 hour after the injection of ^{99m}Tc-MIBI at a dose of 740 MBq. Post stress ^{99m}Tc-MIBI GMPS images were obtained at 1 hour after adenosine stress (120μg/kg/min, infusion) and the injection of ^{99m}Tc-MIBI at a dose of 740 MBq. Phase standard deviation (SD) and Bandwidth was analyzed using HFV of ^{99m}Tc-GMPS stress and rest. Data from the perfusion defect score of each GMPS were used to divide patients into 3 groups: patients with SDS≥7 group, patients with SDS<7 and SSS≥9 group, patients with SDS<7 and SSS<9. (SSS: summed stress score, SRS: summed rest score, SDS: summed difference score) In 3 groups, Phase SD and Bandwidth were compered between pharmacological stress and rest of GMPS. ***Results:*** In the patients after successful PCI on AMI, the dyssynchrony was no significant difference between rest and post pharmacological stress GMPS on the same revel accumulated counts of myocardium. Hence, in stress-induced severe ischemia group (patients with SDS≥7 group, patients with SDS<7 and SSS≥9 group), it was significant difference between rest EF with post parmarogical stress EF. ***Conclusion:*** We suggested myocardial dyssynchrony is not chaneged between rest GMPS with post pharmacological GMPS in the patients after successful PCI on AMI. ***References:*** None

EP-045

Relevance Of Myocardial Perfusion Gated-SPECT(gMPS) As A Pre-Trasplant Screening Method To Detect Ischemia

B. Pérez López*, F. Sebastián Palacid, N. Álvarez Mena, P. J. Turbay Eljach, C. Gamazo Laherrán, M. Alonso Rodríguez, M. J. González Soto, A. Sainz Esteban, M. A. Ruiz Gómez, R. Ruano Pérez;*
Hospital Clínico Universitario de Valladolid, Valladolid, SPAIN.

Aim/Introduction: To assess the importance of myocardial perfusion gated-SPECT (gMPS) as a screening method to detect ischemia in patients with cardiovascular risk factors (CVRF) before kidney transplantation. ***Materials and Methods:*** We analysed all patients with cardiovascular risk factors (CVRF) considered eligible to be included in kidney transplantation list referred to our Nuclear Medicine Department from January-2017 to December-2019. Pharmacologic vasodilator stress test with dipyridamole and gMPS with ^{99m}Tc- MIBI (1 day protocol, stress-rest) was perfomed in all patients. Variables such as demographic data, CVRF, stress test result, gMPS result and clinical course were studied. ***Results:*** 62 patients were studied (42 males and 20 females) with average age of 63.3 years old (range 31-83). The 30.6% of patients had a personal history of ischemic cardiopathy, being stable angina pectoris the most frequent pathology (58.9%) followed by myocardial infarction (42.1%). Regarding pharmacologic vasodilator stress test, the majority of patients (74.2%) showed a negative result (both clinical and electrographic), the 3,2% showed a positive result (both clinical and electrographic) , the 12.9% clinically positive without EKG changes and the 9.7% showed EKG changes without symptoms due to ischemia. gMPS result was reported as normal in 38.8% of cases, ischemia in 53.2 % (mainly slight), transmural myocardial infarction in 3.2%, ischemia+ non-transmural myocardial infaction in 1.6% and ischemia+ transmural myocardial infarction in 3.2%. In the cases with pathological gMPS result, a subsequent cardiac catheterization was performed in the 52.7% of cases, being normal in the 7.9% of them, revealed non-significant lesions in coronary arteries in the 13.2% , and significant lesions with stent placement in the 31.6 % . Furthermore,

a bypass surgery (internal mammary artery to left anterior descending artery) was carried out in 1 patient. Finally, the 24.2% of patients were transplanted and the 22.6% are included in the waiting list for kidney trasplantation. The 8% are still pending of being reassessed and kidney transplantation was dismissed in the 45.2% ***Conclusion:*** The inclusion of gMPS in clinical practice as a screening method to detect ischemia in patients considered eligible to kidney transplantation with cardiovascular risk factors is justified given the high prevalence of ischemic cardiopathy that revealed. ***References:*** None

EP-046

Locating The Latest Site Of Left Ventricular Mechanical Contraction Through Gated-SPECT Phase Analysis In Subjects With Normal Perfusion And Functional Parameters

F. Ferrando-Castagnetto[1], *C. Real*[2], *M. Pedrera Canal*[3], *I. Vilacosta*[2], *M. Ollarves Carrero*[3], *L. García Belaustegui*[3], *P. Pascual*[3], *R. Ricca-Mallada*[1], *M. Pérez Castejón*[3], *J. Carreras Delgado*[3]; [1]*Departamento de Cardiología - CCVU, Hospital de Clínicas, FM, UdelaR, Montevideo, URUGUAY,* [2]*Instituto Cardiovascular, Hospital Clínico San Carlos, Madrid, SPAIN,* [3]*Servicio de Medicina Nuclear, Hospital Clínico San Carlos, Madrid, SPAIN.*

Aim/Introduction: Detecting the site of latest mechanical contraction in the left ventricle (LV) acquires special therapeutic relevance in patients with symptomatic systolic dysfunction and prolonged QRS complex. However, the normal location of this site has been characterized only by some non-invasive techniques. The objective of this experience was to locate the final site of mechanical LV contraction in subjects with normal myocardial perfusion, as reference values for next researches. ***Materials and Methods:*** Phase histograms at rest were obtained in 20 consecutive non-diabetic patients derived to 99mTc-MIBI gated-SPECT, without coronary artery disease, in sinus rhythm, with narrow QRS, no renal dysfunction, and normal perfusion images and quantified functional parameters. Phase standard deviation (PSD) and phase bandwidth (PBW) were obtained at rest applying SyncTool (Emory Cardiac Toolbox®), comparing them with a control sample already reported (1) using multiple "t" tests. The latest mechanical contraction region was obtained by freezing the digital video of ventricular contraction on the polar map during the last 10-40 degrees of phase. ***Results:*** PSD and PBW of the sample were higher than controls, both in men (PSD = 26.6 + 13.3 vs. 14.2 + 5.1, PBW = 72.3 + 35.6 vs. 38.7 + 11.8 degrees, $p < 0.05$ for all comparisons) as in women (PSD = 17.5 + 7.7 vs. 11.8 + 5.2, PBW = 48.2 + 21.5 vs. 30.6 ± 9.6 degrees, $p < 0.05$). The latest site of mechanical contraction was located predominantly at the anteroseptal (45%) and inferior (40%) regions. The mechanical contraction ended in two simultaneous regions (antero-septal and antero-lateral) in two patients. ***Conclusion:*** Subjects with normal myocardial perfusion derived to gated-SPECT exhibit some degree of LV mechanical dyssynchrony. The region of the latest mechanical contraction obtained by gated-SPECT phase analysis agrees with previous findings obtained through other imaging modalities. It is required to validate these results in a head-to-head design with other imaging techniques and to expand the series in candidates for resynchronization therapy. ***References:*** 1) Chen J, Garcia EV, Folks RD, et al. Onset of left ventricular mechanical contraction as determined by phase analysis of ECG-gated myocardial perfusion SPECT imaging: development of a diagnostic tool for assessment of cardiac mechanical dyssynchrony. J Nucl Cardiol 2005;12:687-695.

EP-047

The Effect Of Respiration Motion Correction On Myocardial Perfusion Quality

E. Popov*, A. Mochula;*
FSBSI «Tomsk National Research Medical Center, Russian Academy of Sciences», Cardiology Research Ins, Tomsk, RUSSIAN FEDERATION.

Aim/Introduction: Breathing is a source of motion artifacts during myocardial perfusion scintigraphy. Currently, there are methods for correcting of the motion of the heart [1] and heart motion during breathing [2], but they were originally developed for radiation therapy [4]. The use of these methods in cardiology imaging will also eliminate artifacts from heart motion during breathing and will improve the diagnostic value of the images. ***Materials and Methods:*** . 15 healthy male volunteers (age 28 ± 2 years) underwent two-day stress-rest myocardial perfusion scintigraphy with 99mTc-MIBI (370 MBq). All data was acquired in List-mode. There were used two methods for respiratory correction. The first technique was to acquire SPECT data on the background of a breath holding. Respiratory arrest was carried out for 15 seconds. The study time increased from five to ten minutes. The second method was to process the native SPECT data using software - Motion Detection and Correction for Alcyone. This software allows the exclusion of offset scintigrafic images from common scintigram pool. Correction was carried out along three perpendicular axes of heart movement. Subsequent analysis of the processed data was performed using 4DM SPECT software. ***Results:*** A comparative analysis of myocardial perfusion data showed that the SSS obtained with breath-holding test was significantly less than software method correction motion detection or standard technique processing MPS: 2 (1.5; 3); 3 (1.5; 4.5); 4.5 (3.5; 5), respectively ($p<0.05$). SRS and SDS were not significant different for three methods. ***Conclusion:*** Using the breath-holding test allows to identify the size of the perfusion defect with more accuracy. The correction of respiratory movements of the heart for SPECT is promising

and requires further study. ***References:*** 1. Zavadovsky K.V, Mishkina A.I., Mochula A.V., Lishmanov Yu.B. The method for correction of motion artefacts to improve myocardial perfusion imaging. REJR. 2017; No. 7 (2), pp. 56-64 (In Russ.)].2. Correction for respiration artefacts in myocardial perfusion SPECT is more effective when reconstructions supporting collimator detector response compensation are applied. Kovalski G, Keidar Z, Frenkel A, Israel O, Azhari H. J Nucl Cardiol. 2009 Nov-Dec;16(6):949-55.3. Impact of data-driven cardiac respiratory motion correction on the extent and severity of myocardial perfusion defects with free-breathing CZT SPECT. Daou D, Sabbah R, Coaguila C, Boulahdour H. J Nucl Cardiol. 2018 Aug;25(4):1299-1309

EP-048

Safety of Regadenoson MPI in STEMI Patients Treated with Ticagrelor

A. Jimenez-Heffernan*, C. Salgado-Garcia, A. Amr-Rey, T. Aroui-Luquin, J. Lopez-Martin, E. Sanchez de Mora;*
Hospital Juan Ramon Jimenez, Huelva, SPAIN.

Aim/Introduction: Ticagrelor, a direct-acting P2Y12-adenosine diphosphate receptor blocker, is associated with a significant increase in adenosine plasma concentration through inhibition of cellular reuptake. More frequent and severe side effects, especially bradycardia and dyspnea, may be anticipated in patients undergoing adenosine and dipyridamole stress testing. However, the interaction with regadenoson has not yet been studied. We aim to assess the safety profile of MPI with regadenoson combined with low-level exercise in STEMI patients receiving ticagrelor. ***Materials and Methods:*** We studied 12 STEMI patients (83.3% male, age 64.2±14.3 years) treated with ticagrelor who underwent MPI for ischemia guided PCI of nonculprit vessel. Stress was 4 minutes of low-level exercise with a 15-s bolus injection of regadenoson (0.4 mg) at 1.5 minutes, followed by a saline flush, ^{99m}Tc-tetrofosmin, and a new saline flush. Medical history, adverse events, changes in systolic blood pressure (SBP), heart rate (HR), and oxygen saturation ($SatO_2$) were registered. ***Results:*** Cardiovascular risk factors were dyslipidemia (66.7%), hypertension (41.7%), obesity/overweight (20.0% and 50.0%, respectively), smokers/exsmokers (41.7% and 50.0%, respectively), and diabetes mellitus (8.3%). Clinical symptoms were self-limiting and well tolerated: fatigue (75%), dyspnea (25%), gastrointestinal discomfort (25%), dizziness (16.7%), headache (16.7%), dry mouth (8.3%), feeling hot (8.3%), and chest pain (8.3%). We observed significant increases in SBP and HR from baseline (127 mmHg ± 20 vs 137 mmHg ± 19, and 74 bpm ± 14 vs 106 bpm± 13, respectively, $p<0.05$). No ECG or $SatO_2$ changes were observed following regadenoson administration (97.1% vs 97.5%, p=0.4). ***Conclusion:*** MPI with regadenoson in combination with low-level exercise is safe and well tolerated in STEMI patients treated with ticagrelor.

References: None

EP-050

Could music positively influence cardiac perfusion studies?

M. Guiote Moreno*[1], B. Luque Espejo[1], F. R. Maza Muret[1], J. F. Labraca[1], R. Zurera Pareja[2], J. A. Vallejo Casas[1];*
[1]Hospital Universitario Reina Sofía, Cordoba, SPAIN, [2]Instituto Maimonides de Investigación Biomédica, Cordoba, SPAIN.

Aim/Introduction: The aim of the study is to verify if during pharmacological stimulation for a ^{99m}Tc-Tetrofosmin SPECT / CT, music could be a factor that decreased the cardiac stimulation adverse effects and therefore contributed to the well-being of the patient. ***Materials and Methods:*** 63 patients were recruited, 2 of whom were excluded due to Alzheimer's disease and the other due to hearing loss. The mean age was 69.13 years (S = 10.15 years), 27 were men and 34 women. The study was requested for the diagnosis of inducible myocardial ischemia in 45 of the patients, and for the prognostic purpose of evaluating their known ischemic heart disease in 16 of them. 35 of these patients were stimulated with Atepodin, and 25 with Regadenoson for obesity or respiratory pathology. The patients were randomly selected to make two groups, one listen to "Clair de Lune" of Debussy during the administration of the medication, and another control without music. All of them subsequently underwent a survey with the following variables, tolerability, presence of palpitations, sweating / heat, nausea, headache, central thoracic pain, gastralgia, dyspnea, cough, tingling sensation. At the end of the survey we asked if the music had positively influenced in them. These variables were included, since most of them are possible adverse effects of both drugs. Blood pressure constants (BP) were taken before and after pharmacological stimulation, heart rate (HR), saturation of 02 (Sat02), as well as the electrocardiogram. ***Results:*** 29 patients were placed with music, of which 25 of them had a positive influence according to the survey. 85% of all the patients tolerated well. Dyspnea and sweating were the predominant adverse effects in 27 patients respectively. Of the patients that underwent music stimulation 14 presented dyspnea and only 9 presented sweating. Given the small sample, we did not obtain statistically significant differences between the adverse effects and the different drugs. We will later conduct the study with a larger group. ***Conclusion:*** Music could be a useful tool for patients to better tolerate the administration of Atepodin and Regadenoson during cardiac stimulation for subsequent acquisition of studies with ^{99m}Tc-tetrofosmin. ***References:*** None

EP-051

Spleen uptake of sestamibi as an unexpected witness of sympathetic response to exercise in myocardial perfusion imaging

S. Raffa[1], M. Pennone[2], M. Bauckneht[2], A. Borra[1], A. Miceli[1], I. Donegani[1], S. Marra[1], S. Morbelli[1], C. Marini[3], G. Sambuceti[1]; [1]Dept. of Health Sciences (DISSAL), University of Genoa, Genoa, ITALY, [2]IRCCS Ospedale Policlinico San Martino, Genoa, ITALY, [3]Istituto di Bioimmagini e Fisiologia Molecolare (IBFM), CNR, Milan, ITALY.

Aim/Introduction: Spleen volume decreases around 40% during vigorous exercise due to an increased drive of alpha-adrenergic fibers in the splenic nerves. Defining this autonomic response in humans might help verify the competence of the ortho-sympathetic nervous system in a variety of clinical conditions. In the present study, we aimed to verify whether myocardial perfusion imaging can provide information about spleen perfusion response to the sympathetic drive induced by exercise. ***Materials and Methods:*** We re-evaluated the images of 120 patients consecutively submitted to myocardial ^{99m}Tc-Sestamibi gated single-photon emission computed tomography (G-SPECT) because of known or suspected coronary artery disease (CAD) in the last three months. Images reconstruction was performed by filtered back projection using the Volumetrix software (Xeleris, GE). Regions of interest (ROI) were manually drawn to estimate average counts of spleen and liver as well maximal counting rate of left ventricular myocardium. Clinical and follow-up data of enrolled patients were also collected. ***Results:*** Stress was induced by physical exercise or by dipyridamole infusion (0.56 mg/Kg over 4 minutes) in 99 and 21 subjects, respectively. Exercise stress test significantly increased the spleen to liver radioactivity ratio (SLR) compared to dipyridamole (123±37% vs. 76±32%, respectively, p<0.05). This difference was not observed in the corresponding rest images (88±41% vs. 89±38%, p=ns, respectively). Similarly, spleen to myocardial radioactivity ratio (SMR) was remarkably similar in the two subgroups at rest G-SPECT (9±3% vs. 9±7%, respectively, p=ns). By contrast, SMR significantly increased during exercise (to 21±10%, p<0.001 vs. baseline), while it remained stable after dipyridamole infusion (10±8%, p=ns vs. baseline). Moreover, SMR was higher in the 53 patients performing a maximal exercise (maximal heart rate ≥85% of age-predicted maximum) than in the remaining 46 ones (15±3% vs. 11±2%, p<0.01, respectively). This difference was obviously reproduced when absence or presence of active betablocker treatment was considerd. By contrast, SMR was not virtually independent of reversible ischemia (SDS >3) or contractile dysfunction (rest LV ejection fraction ≤45%). ***Conclusion:*** Physical exercise increases splenic Setamibi uptake. This effect is not reproduced by dipyridamole and is not related to the occurrence of ischemia or left ventricular dysfunction. Accordingly, it seems to reflect the increased splenic perfusion caused by the alpha-mediated contraction of splenic smooth muscle cells. ***References:*** None

EP-052

Effect of Ischemia Percentage in MPS on Patient Management and Revascularization Decision in CAD with Solid-State Cardiac Gamma Camera

N. Talay[1,2], E. Özdemir[1,2], N. Coşkun[1,2]; [1]Nuclear medicine, Ankara, TURKEY, [2]Ankara şehir hastanesi, Ankara, TURKEY.

Aim/Introduction: Myocardial Perfusion Scintigraphy (MPS) is a highly sensitive noninvasive diagnostic method used in coronary artery disease (CAD). With this method, visual, quantitative / semi-quantitative evaluation is made. In this study, we aimed to evaluate the effect and results of the percent of ischemic area calculated on a semiquantitative basis on the revascularization decision in follow-up. ***Materials and Methods:*** : 611 patients who were sent to our clinic for MPS and taken with Cardiac Spect NM 530 GE device were scanned retrospectively. 93 patients (C: 36, M: 57, mean age: 60.11 ± 9.07) who underwent coronary angiography (CAG) were included in the study. Percentages of ischemic area were calculated by semictitative evaluation (average 6.16 ± 5.85%, median: 4%, minimum: 0%, maximum: 40%). In the follow-up of patients, the relationship between the choice of medical treatment or revascularization treatments (PTCA / Stent and CABG) and the percentage of ischemic area was evaluated statistically. ***Results:*** When the frequency of risk factors for CAD was examined, DM: 52% (n: 48), HT: 62% (n: 58), HPL: 17% (n: 16), smoking: 18% (n: 17) detected. 24 of the patients (25.8%) had known CAD. The number of patients with ischemia on MPS images was 85 (91%). In patients with ischemic area above 5%, stenosis detection rate in CAG was 85.4% (p: 0.002), and the rate of application of revascularization treatments (Stent, CABG) was found as 56.1% (p: 0.000).% Of ischemic area <% It was found to be statistically significantly higher than 5 patients. In patients with an ischemic area below 5%, the rate of patients who were decided to undergo medical treatment as a result of CAG was found to be 65.4% (p: 0.001). In addition, multivascular stenosis was detected in 68.3% of patients with ischemic area percentage of 5% and above, and the percentage of ischemic area was found to be significantly higher than patients below 5% (p: 0.000). In our study, the percentage of ischemic area above 5% was found to be 89% sensitivity and 69% specificity in determining patients to undergo revascularization, and it was found to be an important marker in clinical patient management. ***Conclusion:*** The percentage of ischemic area calculated by semi-quantitatively calculated MPS imaging with solid-state cardiac gamma cameras was observed to play an

important role in post-scintigraphic KAG planning and revascularization decision. ***References:*** None

EP-053

The results of myocardial perfusion SPECT and coronary angiography in Russian patients with different pretest CAD probability

A. Ansheles[1], *E. Denisenko-Kankiya*[2], *I. Sergienko*[1], *V. Sergienko*[1];
[1]*National Medical Research Center of Cardiology, Ministry of Healthcare, Moscow, RUSSIAN FEDERATION,*
[2]*Sity Hospital №4, Moscow, RUSSIAN FEDERATION.*

Aim/Introduction: To study the relationship between pretest probability (PTP) of coronary artery disease (CAD), calculated according to 2013/2019 European Society of Cardiology (ESC) guidelines, LV myocardial perfusion according to single-photon emission tomography (SPECT), and the results of invasive coronary angiography (CAG). ***Materials and Methods:*** The study included data from 220 patients with suspected CAD assigned to invasive CAG. All patients underwent rest-stress perfusion SPECT within 1 month before or after CAG with the assessment of standard quantitative parameters of left ventricle (LV) perfusion. Clinical data was retrospectively analyzed and CAD PTP was calculated according to 2013 and 2019 ESC guidelines. ***Results:*** Invasive CAG revealed obstructive lesion of one or more coronary arteries (CA) in 204 out of 220 patients (92.7%). In a retrospective analysis, taking into account gender, age and nature of symptoms, according to the 2013 ESC guidelines PTP was rated as low (<15%) in 13 patients (5.9%), as intermediate (15-85%) in 207 patients (94.1%). Based on the results of comprehensive examination, including SPECT and CAG, 8 patients with low PTP (61.5%) underwent CA revascularization. Among patients with intermediate PTP, significant (>10%) transient ischemia according to SPECT was revealed in 31 (15.0%), initial (5-10%) - in 107 patients (51.7%). According to CAG data, among 207 patients with intermediate PTP, obstructive CA lesion was detected in 192 (92.7%), of which 113 patients (58.8%) underwent CA revascularization. According to 2019 ESC guidelines, corrected PTP (clinical likelihood) was rated as low (<15%) in 117 patients (53.2%), including 98 (44.5%) with PTP 5-14%. After complete examination, 68 of them (58.1%) underwent CA revascularization. ***Conclusion:*** The principles of corrected CAD PTP evaluation proposed by 2019 ESC guidelines cannot be applied without significant amendments to the patients of Russian population with suspected CAD. 2013 ESC guidelines with higher CAD PTP values for all categories reflected Russian population better, while the 2019 guidelines mistakenly attributed patients with obstructive CAD and proved significant ischemia to a low clinical likehood in at least 58% of cases. We suggest that underestimation of the symptoms by the patients and physicians may play a role. These results are preliminary and will be expanded in subsequent studies in a larger group. ***References:*** None

EP-054

Rubidium Myocardial Perfusion PET/CT: Initial Experience In First 200 Patients

L. Price*, C. Copland, B. Ade-Ojo, M. Burnistion, M. Costa, S. Ferreira, R. Gregory, T. Hussain, B. Ribeiro, A. Simeonova, G. Testanera, L. Menezes;*
Barts Health NHS Trust, London, UNITED KINGDOM.

Aim/Introduction: Positron Emission Tomography/Computed Tomography (PET/CT) has many advantages over Single Photon Emission Computed Tomography in Myocardial Perfusion Scintigraphy (MPS) (1). However, UK availability, has been limited (2). We describe a new Rubidium (Rb) PET MPS service; the third in the National Health Service in England. ***Materials and Methods:*** Audit of the first 200 patients from November 2019 to February 2020. 131 men, 69 women, mean age 65 ±11, mean Body Mass Index 29.7±6.8. Imaging comprised CT for attenuation correction, CT for Agatston scoring (CAC) if no known Coronary Artery Disease (CAD) or prior intervention, and PET with and without adenosine vasodilation, in List mode. ***Results:*** The commonest indication was symptoms post-revascularization (29%). 29% had had previous percutaneous intervention, 16% had had previous coronary surgery. 21% had had prior cardiac CT. 96% received 140 mcg/kg/min adenosine, 4% received 210 mcg/kg/min. Two patients did not show adequate vasodilation. 1 scan was not of diagnostic quality. 47% had Agatston scoring. The mean total Agatston score was 564 ±1040. 14% had no coronary calcium, 24% had CAC <100, 31% had CAC<400, and 17% CAC >400. The normalcy rate for PET MPS was 63%. The prevalence of myocardial infarction was 19%. The mean global stress myocardial blood flow was 2.32 ±0.8 mL/g/min, and global Myocardial Flow Reserve was 2.36 ±0.9. The mean wait from request to scan was 32 days, and to report 33 days. ***Conclusion:*** Rb PET MPI is feasible and high quality in a new service. It provides detailed coronary assessment, with plaque burden, relative perfusion and absolute myocardial blood flow quantification (3). It will be an essential contributor to patient diagnosis, treatment response and risk stratification. ***References:*** (1) Chatal J-F, Rouzet F, Haddad F, et al. Story of Rubidium-82 and Advantages for Myocardial Perfusion PET Imaging. Front Med (Lausanne) 2015;2:65(2) Groves AM, Speechly-Dick M-E, Dickson JC, et al. Cardiac 82Rubidium PET/CT: initial European experience. Eur J Nucl Med Mol Imaging 2007;34:1965-72.(3) Taqueti VR, Hachamovitch R, Murthy VL, et al. Global coronary flow reserve is associated with adverse cardiovascular events independently of luminal angiographic severity and modifies the effect of early revascularization. Circulation 2015;131:19-27

EP-055

Myocardial Perfusion Imaging SPECT May Reveal Silent Myocardial Ischemia In Patients With Epilepsy

C. Sioka, A. Tsoumani, C. Votti, M. Beltsiou, L. Lakkas, K. Pappas, D. Kiortsis, A. Fotopoulos, A. Kyritsis, S. Markoula;
University Hospital of Ioannina, Ioannina, GREECE.

Aim/Introduction: The aim of the study was to assess whether asymptomatic myocardial ischemia can be diagnosed in patients with epilepsy employing myocardial perfusion imaging (MPI) with 99mTc tetrofosmin stress - rest single photon emission computer tomography (99mTc - SPECT). ***Materials and Methods:*** Twenty-nine adult epileptic patients were compared to 32 age and gender matched individuals, all with atypical cardiac symptoms and negative ECG and cardiologic examination. MPIs SPECT were performed and summed stress scores (SSS), summed rest scores (SRS) and summed difference scores (SDS) images were acquired. MPIs were designated as pathological with SSS ≥4. In addition, lower SDS score denoted more irreversible ischemia at rest. ***Results:*** In the patient group, 20 of 29 (69%) patients had abnormal MPI; in the control group, 14 of 32 (43.8%) had abnormal MPI (p=0.04). The difference was significant in males, since 18/23 (78.2%) male patients and 11/25 (44%) male controls had abnormal MPI (p=0.01). However, male patients demonstrated more reversible myocardial ischemic abnormalities in their MPI than the control group, assessed by SDS. In addition, differences in the reversibility at rest of their myocardial ischemia was also detected in patients treated with inducers and patients treated with VPA. ***Conclusion:*** Patients with epilepsy with atypical cardiac symptoms are at high risk for cardiovascular disease. MPI SPECT may represent a non-invasive tool to detect early myocardial ischemia, in order to treat and possibly reduce sudden cardiac death in patients with epilepsy. ***References:*** None

EP-056

Increased Hypotensive Response With Regadenoson In Elderly Patients

J. Villena-Salinas, J. Alors Ruiz, S. Ortega Lozano, E. Ramos Moreno;
Hospital Universitario Virgen de la Victoria, Malaga, SPAIN.

Aim/Introduction: Analyze the variability of arterial pressure (AP) and cardiac frecuency (CF) in a series of patients that were exposed to regadenoson stimuli according to the age of each. ***Materials and Methods:*** Demographic data (age, gender) and clinical data (basal and maximum CF, basal AP and AP after 3 minutes) were gathered for an observational, prospective study, from 170 patients to which Regadenoson 400mcg was administered before performing a Myocardial Perfusion SPECT with 99m-Tetrofosmin (25mCi). Side effects and their treatment were registered. All the variables showed a normal distribution, according to Kolmogorov-Smirnov test. A bivariate logistic regression was used, dividing the sample in age groups and establishing the cut off point at 71 years of age. The variability in the 10% AP decrease and the variability >20% of the CF were analyzed in both groups. ***Results:*** 170 patiens were analyzed: 79 male and 91 female, mean age being 72.4+/-9.1 years. The basal CF was 142.2+/-20mmHg and mean basal DAP was 76.3+/-11.7mmHg. SAP after 3 minutes was 90.8+/-8.3mmHg and DAP after 3 minutes 51+/-8.2mmHg. 78.82% of the patients showed >20% increase in basal CF. The variability was <10% in 64.71% of the patients, with >10% increase in 8.82%, and >10% decrease in 26.47%. In patients older than 71 years of age, a lower variability of the CF was obtained (OR:0.78, p>0.05), having the tendency to remain constant. In the group of patients older than 71 years of age, an OR of 2.68 (p<0.05) was obtained for a decrease in the SAP of >10%. ***Conclusion:*** The results fit our experience in administering Regadenoson, by obtaining a higher risk of decrease in SAP in patients older than 71 years of age, with more constant values of the CF in this group. ***References:*** None

EP-057

Repeatability of Coronary Flow Reserve Values Determined with SPECT Technique Using a CZT Semiconductor Camera

P. Cichocki[1], M. Błaszczyk[2], K. Cygulska[3], K. Filipczak[2], J. Kuśmierek[1], P. Lipiec[3], J. D. Kasprzak[3], A. Płachcińska[2];
[1]Department of Nuclear Medicine, Medical University of Lodz, Lodz, POLAND, [2]Department of Quality Control and Radiological Protection, Medical University of Lodz, Lodz, POLAND, [3]Chair and Department of Cardiology, Medical University of Lodz, Bieganski Hospital, Lodz, POLAND.

Aim/Introduction: Scintigraphic coronary flow reserve (CFR) examination is one of the most recent diagnostic methods in nuclear cardiology. It allows, in contrast to FFR determination in coronary angiography, to assess CFR of the whole myocardium of the left ventricle and of selected vascular territories. This expands the diagnostic potential of myocardial perfusion scintigraphy, especially in diagnosis of multivessel coronary artery disease, where standard study is characterized by lower sensitivity. CFR assessment with CZT semiconductor cameras is an alternative to analogous PET study using ^{82}Rb, ^{15}O or ^{13}N isotopes that is expensive and less available.The methodology of processing scintigraphic data obtained in this study (both in SPECT and PET techniques) is not free from subjective factors and must be performed with utmost care. Therefore, it is reasonable to evaluate reliability of this method, by assessing intra- and interobserver repeatability of values obtained by one and two independent operators. ***Materials and Methods:*** 33 patients were included in the study. CFR was assessed using CZT camera Discovery NM530c in a two-day protocol - at rest

and after stress test with dipyridamole. Each time patients were given 37MBq ^{99m}Tc-MIBI (for positioning on the camera) followed by 550MBq bolus injected simultaneously with the start of image acquisition lasting 8 minutes. Scintigraphic data in list-mode format was converted to 23 frames (15x6s, 4x30s, 4x60s) and reconstructed into SPECT images, that were processed using the Corridor 4DM program 3 times by one operator (twice on the same day and once after 2 weeks) and once by another independent operator. ***Results:*** Repeatability of CFR values was assessed in the myocardium of the whole left ventricle (Total) and in vascular territories of main coronary arteries (LAD, LCX and RCA). Pearson's correlation coefficients were as follows: 1) One operator, the same day: Total: 0,92; LAD: 0,91; LCX: 0,94; RCA: 0,92 2) One operator, 2 weeks apart: Total: 0,90; LAD: 0,89; LCX: 0,93; RCA: 0,86 3) Two independent operators: Total: 0,87; LAD: 0,91; LCX: 0,92; RCA: 0,73 ***Conclusion:*** CFR values obtained by the same and two independent operators displayed high repeatability in the whole myocardium and territories of LAD and LCX. In RCA territory, results obtained by different operators were less reproducible. This may be explained by the so-called "cardiac creep" phenomenon - motion of the heart, especially its inferior wall, probably caused by faster and deeper breathing in response to dipyridamole. ***References:*** None

EP-058

The evaluation of myocardial blood flow and coronary flow reserve in MINOCA patients: comparison with cardiac magnetic resonance

A. Mochula*, O. Mochula, A. Maltseva, D. Vorobyeva, V. Ryabov, K. Zavadovsky;*
Cardiology Research Institute, Tomsk NRMC, Tomsk, RUSSIAN FEDERATION.

Aim/Introduction: Aim. To assess the global and regional myocardial blood flow and coronary flow reserve impairment in MINOCA patients compared to CMR. ***Materials and Methods:*** The study group comprised 28 patients with acute coronary syndrome. Based on ICA results all patients were divided into two groups: 1) MINOCA (n=11); 2) patients with MI and obstructive CAD (MICAD) (n=17). Within 7-10 days after admission to the hospital all patients underwent SPECT MPS with the assessment of standard indices and quantitative parameters: stress /rest MBF and CFR (on CZT gamma-camera)[1]. Also, all patients underwent CMR with evaluation of infarct size (IF), microvascular obstruction (MVO), size of myocardial edema (ME) and transmural extent of myocardial infarction (TE)[2]. ***Results:*** According to the quantitative MPS data analysis, global sMBF and CFR values were significantly higher in MINOCA than in MICAD patients group: 1.2 (0.82;1.69) ml/min/g vs 0.62 (0.52;0.9) ml/min/g; 1.96 (1.23;2.42) vs 1.16 (0.98;1.64) , respectively.CMR indices such as IS, ME and TE were significantly lower in MINOCA compared to MICAD patients: 1.6 (0;7.8) vs 14.8 (6.3;22.6)%; 8(0;14) vs 18.5 (10;23)%; 0 (0;5) vs 18 (10;25), respectively. Seven(40%) MICAD group patients showed MVO, whereas there were no such patients in MINIOCA group.The regional analysis revealed that sMBF and CFR were significantly lower in LV regions characterized by myocardial injury compared to non-injured regions (based on CMR data): 0.78 (0.51;0.94) ml/min/g vs 1.11 (0.82;1.4) and 1.22 (0.91;1.74) vs 1.52 (1.14;2.42), respectively. Also, we found out significant correlation between regional quantitative SPECT indices and TE evaluated by CMR: r=-0.4 for sMBF; r=-0.35 for CFR ($p<0.05$). ***Conclusion:*** The analysis of quantitative MPS SPECT parameters showed that such approach allows identifying MBF and CFR disturbances both on global and regional level. These results showed that MINOCA patients characterized by mild reduction of MBF and perfusion assessed visually and quantitatively. It means that despite the absence of obstructive coronary artery lesion this group of patients has more pronounced risk of cardiac events and need more aggressive observation and treatment. The study was supported by a grant of President Russia (MK-1347.2020.7). ***References:*** 1. Zavadovsky K.V., Mochula A.V., Boshchenko A.A., et al. Absolute myocardial blood flows derived by dynamic czt scan vs invasive fractional flow reserve: correlation and accuracy // Journal of Nuclear Cardiology. 2019. doi:10.1007/s12350-019-01678-z2. Alexeeva Ya.V., Vyshlov E.V., Ryabov V.V., Mochula O.V., et al. Phenomenons of microvascular injury in primary myocardial infarction with ST-segment elevation // Kardiologicheskij Vestnik. 2019. 14(2):54-60.

EP-059

Association of electrocardiographic changes during adenosine stress with perfusion defect on myocardial perfusion SPECT

O. Ben Hamida*, W. El ajmi, A. Sellem, H. Hammami;*
Military hospital of instruction of tunis, Tunis, TUNISIA.

Aim/Introduction: Myocardial perfusion single-photon emission computed tomography (SPECT) is a valuable and noninvasive imaging modality in the evaluation of patients with coronary artery disease(CAD). Adenosine stress may occasionally be associated with electrocardiographic (ECG) changes, but significance of ECG changes is controversial. The aim of this study is to evaluate the strength of association between adenosine stress-related ECG changes and perfusion defects on scintigraphy. ***Materials and Methods:*** One hundred and fifty (mean age: 63,69 years; sex: men 67, women 83) patients with known/suspected CAD underwent adenosine stress myocardial perfusion SPECT. Patients with baseline ECG abnormalities, previous history of coronary artery bypass graft surgery or myocardial infarction (MI) were excluded. ECG was monitored continuously during adenosine stress for ST-

depression. On the basis of the summed difference score, reversible perfusion defects were categorized as follows: normal: less than 4, mild: 4-8, moderate: 9-13, and severe: more than 13. ***Results:*** ST-depression was observed in 43/150 (28.6%) and reversible perfusion defects were observed in 22/43 (51.16%) patients. 12/27, 6/27, and 4/27 patients had mild, moderate, and severe ischemia, respectively. 21/43 patients had normal perfusion. ECG changes and perfusion defects showed a moderate strength of association. The sensitivity, specificity, positive predictive value, and negative predictive value of ECG findings for prediction of ischemia were 27.8, 69.44, 51.16, and 42.72%, respectively. ***Conclusion:*** ECG changes during adenosine stress are not uncommon. It shows a moderate strength of association with reversible perfusion defects. Studies showed that patients with ischemic ECG response to adenosine administration and normal perfusion on SPECT are at low risk of cardiovascular events. Nevertheless, ECG changes during adenosine merit critical evaluation of myocardial perfusion SPECT findings. ***References:*** 1. Taywade SK, Ramaiah VL, Basavaraja H, Venkatasubramaniam PR, Selvakumar J. Prevalence of ECG changes during adenosine stress and its association with perfusion defect on myocardial perfusion scintigraphy. Nucl Med Commun. avr 2017;38(4):291 8. 2. Paladugu N, Shaqra H, Blum S, Bhalodkar NC. Positive Vasodilator Stress ECG With Normal Myocardial Perfusion Imaging and Its Correlation With Coronary Angiographic Findings in African Americans and Hispanics. Clin Cardiol. 2010;33(10):638 42. 3. Electrocardiographic profile of adenosine pharmacological stress testing [Internet]. [cité 30 avr 2020]. Disponible sur: https://www.spandidos-publications.com/10.3892/etm.2015.2279

EP-11

Imaging Clinical Studies -> Nephro-Urological Imaging Study -> Nephro-Urology

e-Poster Area

EP-060

Comparison of different simplified methods to determinate Glomerular Filtration Rate with 99mTc-DTPA

M. A Hernandez Fructuoso[1], *J. E. Romero Herrera*[2], *B. Santos Montero*[1], *C. G. Franco Monterroso*[2], *S. Ruiz Llama*[2], *J. Castell Conesa*[2];

[1]*Hospital Universitario Vall d'Hebron. Institut de Diagnòstic per la Imatge., Barcelona, SPAIN,* [2]*Hospital Universitario Vall d'Hebron., Barcelona, SPAIN.*

Aim/Introduction: Due to [51Cr]Cr-EDTA withdrawal in January 2019, centers had to adapt the technique to calculate glomerular filtration rate (GFR) using [99mTc]Tc-DTPA. The aim of this study was to validate different simplified method of determining GFR with [99mTc]Tc-DTPA by analyzing the radioactive concentration of three and two plasma samples, compared to the validated reference method with 10 extractions. ***Materials and Methods:*** GFR of 30 patients was analyzed after intravenous administration of 18.5MBq of [99mTc]Tc-DTPA. Blood samples were withdrawn from the contralateral arm post-injection at different times: t=5', t=10', t=20', t=30', t=60', t=90', t=120', t=150', t=180' and t=240'. Blood samples were centrifuged at 1500g for 5 min to isolate the plasma. 1 ml of plasma samples in duplicate and standards in triplicate were counted 10 minutes in a gamma-counter (Wallac 1470, Wizard), correcting the values obtained by decay at time zero (dose administration). The GFR of the reference method, (RM), calculated by two-compartment bi-exponential kinetic analysis using 10 samples, was compared against the values obtained from 4 simplified methods (SM), calculated by "slope-intercept", one compartment mono-exponential analysis:1)SM1: using 3 extractions at 120', 180' and 240' and Bröchner-Mortensen correction; 2)SM2: using 3 extractions at 120', 180' and 240 and Chandler's correction; 3)SM3`: using 2 extractions at 120 'and 240' and Bröchner-Mortensen correction; 4)SM4:using 2 extractions at 120 'and 240' and Chandler correction (SM4). The GFR was normalized with respect to the body surface and the absolute errors (EA, EA=reference GFR-simplified GFR) and relative errors (ER, ER=GFR reference/EA x100) of each method were determined. ***Results:*** The mean values of GFR obtained by the MS1, MS2, MS3 and MS4 was 90.16±29.35ml/min/1.73m2, 93.12±33.82ml/min/1.73m2, 90.10±29.32ml/min/1.73m2, 92.96±33.37 ml/min/1.73m2 respectively and that of the MR was 92.79±30.55ml/min/1.73m2. All the simplified evaluate method showed a significant correlation with respect to the reference method (MS1:r=0.994, MS2: r=0.992; MS3: r=0.993 and MS4: r = 0.995). The average AE for MS1, MS2,MS3 and MS4 were of 2.62±3.36 ml/min/1.73m2,-0.33±5.25ml/min/1.73m2, 2.69±3.17 ml/min/1.73m2; 0.17±4.96 ml/min/1.73m2 respectively and the mean ER were 2.75±3.15%, 1.21±6.17%, 2.84±2.95%, 1.41±6.07% respectively. ***Conclusion:*** All this methods simplify the GFR measurement test and all show good correlation with the reference methods. Small differences without clinical relevance were found. In our series, one compartment mono-exponential analysis with 2 samples and Chandler correction was the most accurate test (least relative and absolute errors). ***References:*** None

EP-061

Correlation between the findings in the first post-transplantation Renogram and the allograft renal function twelve months after surgery

G. Guzmán Prudencio*, S. Álvarez Ruiz, L. M. Del Barco Diez Canseco, M. Calderón Calvente, L. Nieto Morcillo, L. De la Cueva Barrao, M. Falgás Lacueva, M. Sangrós Sahún, P. Navarro Beltrán, D. Abós Olivares;*

Hospital Universitario Miguel Servet, Zaragoza, SPAIN.

Aim/Introduction: To study the correlation between findings in the first renogram post-trasplantation, and the evolution of the renal function of the graft twelve months after surgery. ***Materials and Methods:*** 20-minute duration renogram with [^{99m}Tc]Tc-MAG3, performed in the first 72 hours post-kidney transplantation, of patients attended at the Nuclear Medicine Service between January-December of 2018 are reviewed, extracting: a) the concentration angle (CA) that measures the inclination of the ascent section of the concentration phase with respect to the vertical axis (cutoff thershold <40° vs ≥40°); b) the time, in minutes (Tmax), at which the maximum concentration occurs (<10 vs ≥10min); and c) the percentage of cortical retention (CR) at the end of the study (<80% vs ≥80%). These 3 parameters are correlated with renal function at 12 months post-transplantation, through the need or not of dialysis. ***Results:*** A total of 62 renograms were obtained, excluding 7 due to death as a result of intercurrent diseases and 2 due to vascular complications and graft loss, before the first year after surgery. 53 patients, 15 female and 38 male, aged between 20-80 years, were included in the analysis. Functional failure (dialysis) of the graft one year after the transplantation ocurred in 15% (8/53). In patients with CA ≥40° the probability of failure was 28% (5/18) and in CA <40° 8.6% (3/35), with relative risk (RR) of 3.2. 7/34 (20,6%) patients incluided in the group with Tmax ≥10 min were on dialysis one-year after, unlike just 1/19 (5,3%) if Tmax<10min (RR 3,8). Among the 37 patients with CR ≥80%, 8/37 (22%) were dialyzed one year after, while none of the 16 in the group of patients with CR <80% (0% probability if CR <80%). The matching of parameteres CA ≥40°, Tmax ≥10 min and CR ≥80% together do not improve the prediction of dialysis one year after (27%, 5/18). ***Conclusion:*** 1. Renogram parameters 72 hours post-transplantation, such as concentration phase angle ≥40°, time at maximun concentration ≥10min and percentage of cortical retention ≥80%, allow recognize a group of patients with greater probability of needing dialysis in the first year after surgery, but they do not are capable of indentify in which specific patients it will occur. 2. The parameter that best predicts the viability of the graft is cortical retention <80%. ***References:*** None

EP-062

Usefulness of Additional Quantitative Parameters of Dynamic Renal Scintigraphy (DSN) in the Diagnosis of Obstructive Uro- and Nephropathy

P. Cichocki[1], *K. Filipczak*[2], *A. Płachcińska*[2], *J. Kuśmierek*[1];
[1]*Department of Nuclear Medicine, Medical University of Lodz, Lodz, POLAND,* [2]*Department of Quality Control and Radiological Protection, Medical University of Lodz, Lodz, POLAND.*

Aim/Introduction: One of the main indications for DSN is diagnosis of obstructive uro-/nephropathy. In standard practice, this study includes assessment of sequential scintigraphic images, renographic curves and such quantitative parameters as: T_{MAX}, $T_{1/2}$ and split function of each kidney (SF). Due to the relative nature of SF and limitations of diagnostic capabilities of T_{MAX} and $T_{1/2}$, DSN was expanded to include new quantitative parameters describing kidney function in absolute values. This study aims to evaluate usefulness of kidney efficiency index (KEi) - new, in-house developed parameter proportional to clearance function of the kidney, as well as mean and parenchymal transit times (MTT and PTT). ***Materials and Methods:*** Study included 226 people aged 18-84 (average 53). First group, from which normative values of new parameters were determined, consisted of 20 healthy volunteers. Second group consisted of 206 patients selected retrospectively, based on archived scintigraphic data. Values of KEi were determined twice, by two independent operators, to assess their repeatbility. In addition, "normalcy rate" (percentage of normal results among selected 62 patients with low likelihood of obstructive uro-/nephropathy) was used to evaluate reliability of all new parameters. Reliability of KEi and PTT was also assessed by their correlation with each kidney's eGFR calculated using CKD-EPI formula (in 92 patients who had current serum creatinine levels in archived medical records). A comparative differential analysis of obstructive uro-/nephropathy, based on standard and new DSN parameters, was performed on selected 74 patients (92 kidneys) with single functioning kidney or bilateral obstructive uropathy, where SF is unreliable. ***Results:*** Normative values: KEi≥8, MTT≤250s, PTT≤225s. Inter-observer reproducibility of KEi results: 0.987 Normalcy rate: 95% for KEi, 91% for PTT, 81% for MTT. KEi vs eGFR correlation was 0.84 ($p<0.0001$) and was significantly higher than SF vs eGFR (0.66) and PTT vs eGFR (-0.53). In comparison with standard DSN evaluation, application of KEi changed the diagnosis in 34% of assessed kidneys (from uropathy to nephropathy in 27/92 kidneys and vice versa in 4 kidneys). ***Conclusion:*** KEi enables repeatable, quantitative assessment of absolute kidney function without any modifications of the standard DSN protocol. Its values can be compared between independent studies (e.g. follow-up examinations). KEi corrected the diagnosis of obstructive uro-/nephropathy in 1/3 cases of single functioning kidney or bilateral obstructive uropathy. MTT and PTT displayed limited utility in diagnosis of obstructive uro-/nephropathy. *References:* None

EP-063

Who Can We Trust More? A Comparison of Three Methods for GFR Determination

I. Grierosu[1,2], M. Starcea[3,2], R. Tibu[1], A. Tarca[1], C. Gavrilovici[3,2], C. Stolniceanu[1,2], W. Jalloul[1,2], T. Ionescu[1,2], A. Statescu[1], R. Iacob[2], C. Stefanescu[1,2];
[1]Hospital Sf. Spiridon, Nuclear Medicine Laboratory, Iasi, ROMANIA, [2]University of Medicine and Pharmacy Grigore T. Popa, Iasi, ROMANIA, [3]Hospital Sf. Maria, Paediatric Nephrology Department, Iasi, ROMANIA.

Aim/Introduction: We would like to share our experience, in consequence of more than a decade of fruitful collaboration between the Paediatric Nephrology Clinic and the Nuclear Medicine Department. The glomerular filtration rate (GFR) remains a subject of multiple controversies, especially in children. We found studies in literature data, for instance Garcia-Covarrubias L. et al. who demonstrated the strong correlation between estimated GFR by cystatin C equations and measurement by 99mTc-DTPA nephrogram. ***Materials and Methods:*** From the total of 974 nephrograms in children we considered only 539 cases diagnosed with congenital hydronephrosis. Granting a maximum of 2 days interval between scintigraphy and mandatory creatinine dosage, we finally selected 485 pediatric cases, with an age range between 1 month and 17 years. 99mTc-DTPA images were acquired with a Siemens Diacam double headed gamma camera. ***Results:*** We compared the GFR by three methods: one scintigraphical and two creatinine based mathematical equations, Schwartz and bedside Schwartz. The patients were devised in four groups: group I = 87 cases (under 1 year), group II = 198 cases (between 1 and 6 years), group III =124 cases (6 - 12 years) and finally, group IV = 76 cases (12-17 years old). For each group we correlated the GFR using statistic Pearson correlation factor (R): A. Schwartz and scintigraphy, B = bedside Schwartz and scintigraphy, C = Schwartz and bedside Schwartz. We found: no correlation between scintigraphy and mathematical formulas in any group: RIA = 0.0157, RIB = 0.0408, RIIA = 0.2193, RIIB = 0.2256, RIIIA = 0.3298, RIIIB = 0.3321, RIVA = 0.4994, RIVB = 0.5445. Oppositely, the correlation between the two mathematical equations is very high: RIC = 0.9985, RIIC = 0.9959, RIIIC = 0.9998, RIVC = 0.8811. ***Conclusion:*** It is obvious that the smaller the age, the less does mathematical GFR correlate with scintigraphic GFR. Even if the 99mTc-DTPA scintigraphical GFR may not be perfect, we acknowledge its tremendous usefulness when other techniques such as serum cystatin C dosage or Gates' method with plasma sample measuring are not available. To conclude, we do not recommend the use of a mathematical formula for GFR alone, but in comparison with an alternative method to serum cystatin C dosage, such as scintigraphical GFR. ***References:*** Garcia-Covarrubias L et al. Correlation of the Glomerular Filtration Rate Measured With the Use of DTPA-Tc99m in Live Kidney Donors With Equations Based on Creatinine and Cystatin C. Transplant Proc. 2018; 50(2): 423-427.

EP-12

Imaging Clinical Studies -> Oncological Imaging Clinical Study -> Any Other Malignant (including Primary of Unknown Origin)

e-Poster Area

EP-064

The Diagnostic Contribution of 18F-FDG PET/CT SCAN in Cancer of BMUO

Y. Liu;
The First Affiliated Hospital of Zhengzhou University, Zhengzhou, CHINA.

Aim/Introduction: The purpose of this study was to investigate the value of 18F-FDG PET / CT in finding primary tumors in patients with bone metastasis of unknown primary origin (BMUO). ***Materials and Methods:*** A total of 223 patients were enrolled from November, 2017 to April, 2018 in the Department of Nuclear Medicine of the First Affiliated Hospital of Zhengzhou University to find the primary tumor for ^{18}F-FDG PET/CT examination due to the discovery of bone metastases. The patients who found bone metastasis by routine examination were performed ^{18}F-FDG PET/CT examination to find the primary tumor within 3 days after routine examination. All patients were finally diagnosed by histopathology. The diagnostic efficacy of ^{18}F-FDG PET/CT to find the primary lesion was calculated by comparing the histopathological results with the ^{18}F-FDG PET/CT imaging results. ***Results:*** A total of 223 patients were enrolled in this study, including 122 males and 101 females, with a median age of 62 years. Among 223 cases, the primary tumor was found in 205 cases, but 18 cases were not found. ^{18}F-FDG PET/CT imaging was positive in 203 cases, including 199 true positives and 4 false positives. ^{18}F-FDG PET/CT imaging was negative in 20 cases, including 14 true negatives and 6 false negatives. The sensitivity, specificity, accuracy, positive predictive value and negative predictive value of ^{18}F-FDG PET/CT in detecting primary tumors in patients with BUMO were 97.1% (199/205), 77.8% (14/18), 91.9% (205/223), 98.0% (199/203), and 17% (14/20) respectively. ^{18}F-FDG PET/CT detected all previously known metastases and found new metastases in 173 patients. ***Conclusion:*** ^{18}F-FDG PET/CT, as a non-invasive examination method, is of great value in finding primary tumors in patients with unknown primary tumor bone metastasis. It can be used as the first choice for finding primary lesions. ***References:*** [1] Anqin, Han,Jie, Xue,Man, Hu,Jinsong, Zheng,Xiaohui, Wang. Clinical value of 18F-FDG PET-CT in detecting primary

tumor for patients with carcinoma of unknown primary. [J].Cancer epidemiology,2012,36(5):470-5.[2] Park S B, Lee K H, Kim S J, et al. Value of 18F-FDG PET/CT in the evaluation of suspected bone metastasis with an unknown primary origin[J]. Journal of Nuclear Medicine, 2015, 56(supplement 3): 632-632.[3] Budak E, Yanarateş A. Role of 18F-FDG PET/CT in the detection of primary malignancy in patients with bone metastasis of unknown origin[J]. Revista Española de Medicina Nuclear e Imagen Molecular (English Edition), 2019.

EP-065

Role of ^{18}F-FDG PET/CT in assessment of treatment response in transitional cell carcinoma

P. Kaushik, S. Shamim, J. Hussain, G. Arora, S. Datta Gupta, R. Kumar, C. Bal;
All India Institute of Medical Sciences, New Delhi, INDIA.

Aim/Introduction: Role of ^{18}F-FDG PET/CT in transitional cell carcinoma (TCC) has been mostly limited to detection of metastatic disease. There are very few studies evaluating the application of this modality in response assessment. This retrospective study aims to determine utility of FDG PET/CT in assessing response to chemotherapy in TCC. ***Materials and Methods:*** Patients with newly diagnosed as well as recurrent metastatic TCC who underwent chemotherapy and were referred to our department for assessing response with FDG PET/CT were retrospectively included in the study. Whole body (vertex to mid thigh) PET/CT scans were acquired on dedicated PET/CT scanner (Biograph mCT, Siemens, Germany and 710 Discovery, GE, USA) 45- 60 minutes after injection of 10 mCi of FDG intravenously. A delayed abdomen spot image was acquired at 120 minutes post-injection of FDG. FDG PET/CT done at baseline and at 4-6 weeks after starting chemotherapy were analyzed by an experienced nuclear medicine physician. Response was assessed as per PERCIST criteria. Clinical follow-up was used as reference standard. ***Results:*** A total of 9 patients (7 male and 2 female) were retrospectively analyzed in this study. Mean age of the patients was 58.1±5.4 years. The site of primary disease was kidney in 7 and urinary bladder in two. Lymph node metastases were present in all 9 patients with additional extra-nodal disease in 4 patients including bone (n=2), lung (n=1) and peritoneum (n=2). On response assessment four patients had stable disease, 4 had disease progression, 3 patients had complete metabolic response and 2 patients had partial metabolic response on FDG scan. ***Conclusion:*** FDG PET/CT may be a useful modality to assess chemotherapy response in patients with TCC. With its increasing use in metastatic workup and detecting recurrence, it may be a 'one stop shop' modality for staging, response assessment and detecting recurrence in TCC. ***References:*** None

EP-066

Performance of digital PET/CT in the assessment of liver metastases

F. Fuentes-Ocampo, A. Flotats, D. López-Mora, M. Sizova, S. Abouzian, V. Camacho, A. Fernández, M. Estorch, J. Duch, A. Domènech, I. Carrió;
Hospital de la Santa Creu i Sant Pau, Barcelona, SPAIN.

Aim/Introduction: Recent studies have established a superior lesion detectability of digital PET/CT over analog PET/CT in cancer patients. In this study we evaluated the performance of digital PET/CT in the assessment of liver involvement in patients with known or suspected liver metastases. ***Materials and Methods:*** We prospectively included 83 oncological patients with various primary tumors (24 colorectal cancer, 16 lung cancer, 11 breast cancer, 3 sarcomas, 2 urothelial, 2 cancer of unknown primary origin and 9 others) from February 2018 to October 2019. All patients had previous history or liver metastases or were considered at risk of liver metastases because of type of primary, blood biomarkers and clinical presentation. All patients underwent a 18F-FDG PET/CT with a conventional digital scanner (Philips VEREOS). To compose a reference standard, the findings on digital PET/CT were compared with other imaging modalities (including magnetic resonance, contrast CT and echography), with biopsy when available, and with subsequent follow-up including PET/CT and other imaging modalities. Three nuclear medicine physicians evaluated the liver parenchyma to determine the presence or absence of liver metastases. Results on digital PET were compared with the composite reference standard. ***Results:*** Fourteen patients were excluded because confirmation of the results was not possible (death or follow up not appropriately performed). Finally, a total of 67 patients were considered evaluable, with a mean age of 69±12 years, 36 women and 31 men. A total of 54 patients had a true positive result and only 2 patients were considered false positive. Eleven patients were considered true negative, and none had a false negative result. This analysis based on our composite reference standard indicates a sensitivity of Digital PET/CT of 100%, with a specificity of 85% with a diagnostic accuracy of 97%. In addition, the false negative rate was 0 and the false positive rate was 0.15. Finally, the positive predictive value was 0.98 and the negative predictive value of 1. ***Conclusion:*** Digital PET/CT offers high sensitivity and diagnostic accuracy in the assessment of liver involvement in patients with known or suspected liver metastases, and may be considered the instrument of choice when available. ***References:*** None

EP-067

Diagnosis of Inmunotherapy Adverse Effects with 18Fdg Pet-Ct.Our Experience:

M. Agolti, L. Solari;
Centro de Medicina Nuclear Clinica Modelo, Parana, ARGENTINA.

Aim/Introduction: Immunotherapy is an increased usefull therapy in oncology . Adverse effects can be diagnose through 18 PET CT , and this is very important in life threatening effects to start treatments. We describe our incidence and findings during one year . ***Materials and Methods:*** We have made 46 18FDG PET CT since 31st March 2019 to 31st March 2020 to patients treated with Immunotherapy : the treatments were ordered for Lung Cancer in 15 patients , renal cancer in 11 patients , melanoma in 15 patients , pancreatic cancer in 3 patients , 2 head and neck cancer . ***Results:*** We found possible IrAE in 7 patients: 1 increased uptake in Hipophysitis, without clear symptoms ,3 patients with findings possibly related to Colitis ,however one of them was discharged for he was under oral treatment for Type II Diabetes , 2 Patients with increased uptake in Thyroid, without clear Hyperthyroid symptoms 2 findings compatible with pneumonitis ***Conclusion:*** The incidence of our findings was 15,21%. When reporting 18 FDG PET CT in immunotherapy evaluation , to look after IrAE is very important for findings , and every nuclear medicine physician should have a check list for some of these undesirable effects maybe life threatening and once diagnosed they can be correctly treated . ***References:*** None

EP-068

Dual time point PET/CT adds little to standard PET/CT in patients with renal cell carcinoma

L. Geertsen[1], *J. A. Simonsen*[2], *S. Hvidsten*[2], *P. Høilund-Carlsen*[2,3], *L. Lund*[1,3];
[1]*Department of Urology, Odense University Hospital, Odense, DENMARK,* [2]*Department of Nuclear Medicine, Odense University Hospital, Odense, DENMARK,* [3]*Department of Clinical Research, University of Southern Denmark, Odense, DENMARK.*

Aim/Introduction: FDG PET/CT is a well-established method of diagnosing and staging several types of cancer. In renal cell carcinoma (RCC) the use of FDG PET/CT is hampered by low tumour FDG uptake and high urine excretion. Dual time point (DTP) PET/CT has been proposed for better distinction between malignant and benign processes. The aim in this prospective pilot study was to investigate the potential advantages of DTP PET/CT in patients with RCC. ***Materials and Methods:*** Seven patients with primary or recurrent RCC had DTP FDG PET/CT (4 MBq ^{18}F-FDG per kg bodyweight) performed 1 and 3 hours p.i. Images were interpreted by visual assessment with supplementary measurements of standardized uptake values (SUVs). The tumour or metastases were delineated manually based on CT scans. Both early and delayed PET scans were aligned with the early, contrast-enhanced CT scan. SUVmax and SUVmean in volumes of interest were read automatically. ***Results:*** Five patients had primary RCC with no known metastases. Two patients had recurrent disease after nephrectomy; one had a lymph node metastasis in the renal hilus, the other multiple lung metastases. Judged by visual evaluation primary tumours showed varying FDG uptake, while the FDG uptake of all metastases was low. Quantitative results showed varying FDG uptake in tumours and metastases with SUVmax 1.60-17.70 g/mL and SUVmean 0.61-9.70 g/mL in scans performed at 1 h p.i. There was no significant or consequent change in SUVs from early (1h) to delayed (3h) images; some increased while others decreased. Average SUVmax was 7.4 g/mL vs. 6.9 g/mL, p=0.85, and average SUVmean was 3.7 g/mL vs. 3.2 g/mL, p=0.72, at the two time points. Delineation of tumours turned out to be quite difficult and prone to intra-observer variation, since tumours were not well-defined. SUVmean was influenced by a generally heterogeneous structure with varying degrees of central necrosis or cystic components. SUVmax was affected by the partial volume effect to different degrees in early and delayed PET images, since calices contained different amounts of urine at the two time points. Hence, delayed imaging did not facilitate delineation or quantification. ***Conclusion:*** Quantitative DTP FDG PET/CT appears to be of limited value in RCC, even when supplied by delayed imaging. ***References:*** None

EP-069

$^{64}CuCl_2$: New Radiopharmaceutical PET for Urological Cancers

M. Mascia[1], *C. Villano*[1], *V. De Francesco*[1], *M. Marchioni*[2], *L. Schips*[2], *L. Cindolo*[3];
[1]*SS.Spirito Hospital, Dept. of Nuclear Medicine, Pescara, ITALY,* [2]*G. D'annunzio University, Dept. of Urology, Chieti, ITALY,* [3]*CDC Villa Stuart, Dept. of Urology, Rome, ITALY.*

Aim/Introduction: This study was designed to evaluate safety and efficacy of ^{64}Copper(II)dichloride ($^{64}Cu(IICl_2)$ as a new positron emission tomography radiopharmaceutical PET for urological malignancies (UM). ***Materials and Methods:*** Patients diagnosed with UM were enrolled in a prospective single-center study. All Patients were staged with preoperative computed tomography (CT) and $^{64}Cu(II)Cl_2$PET/CT. Patient characteristics, anatomical and functional imaging, final histopathology were recorded. Surgical specimens for histopathological examination were collected after biopsy or surgery. To determine time-activity curves for $^{64}Cu(II)Cl_2$ uptake in UM and normal tissues, standardized uptake values (SUVs) were calculated in tumors and corresponding normal tissue in healthy subjects, in liver and gluteus muscle. The safety of $^{64}Cu(II)Cl_2$ was assessed and based on subjective symptoms and objective findings.

All the patients involved in this study have expressed their written informed consent including the use of their data for scientific purpose. The EudraCTnumber 2017-000940-17 has been issued for Sponsor's Protocol Code Number 64Cu in date 27/02/2017. The study was registered at ISRCTN as 11735211 on 21/11/2017 and it obtained the approval of the Ethical Committee of Chieti/Pescara on 12/03/2018 and the authorization of the OsSC-AIFA on 07/05/2018. ***Results:*** Twenty-three patients were included (mean age:69.6) and 82.6% were men. As dosimetry, an administered dose of 174.75 MegaBequerel for $^{64}Cu(II)Cl_2$ was equal to 9.80milliSievert of the effective dose. The median SUVmax were 5.7, 0.9, 1.8 and 9.8 for the prostate, bladder, penis and kidney, respectively. All patients had histopathological report: 26.1%(6/23) with prostate cancer, 21.7%(5/23) with renal cancer, 21.7%(5/23) with bladder cancer, 22.7%(5/23) with penile cancer; 8.7%(2/23) patients had no cancer at the final pathological report. Median SUVmax were higher in organs with a malignancy in comparison with healthy tissue [prostate (11.5vs5.3,p<0.001), bladder (6.2vs0.9,p=0.007) and penis (3.9vs1.3,p=0.027)], but not in the kidneys (5.0vs10.4,p=0.998). the highest area under curve (AUC) was reported for prostate cancer (AUC=0.978), the lowest for penile cancer (AUC=0.775). The detection rates based on the best suggested cut-off according to the SUVmax were 85.7%(6/7) for prostate and bladder, 83.3%(5/6) for penile cancer. Neither drug-related effects or physiologic responses occurred, not adverse reactions observed. ***Conclusion:*** $^{64}Cu(II)Cl_2$ is an effective and well tolerated tracer in patients with UM. Our results show higher SUVmax in cancer patients than in healthy subjects. Although large prospective trials are needed in order to extend the indication of this PET tracer, our findings suggest that $^{64}Cu(II)Cl_2$PET/CT is useful in patients affected by prostate, bladder and penis cancer. ***References:*** None

EP-070

The Role Of 18F-FDG PET/CT In The Management Of Merkel Cell Carcinoma: The Experience Of 51 Studies In Our Institution

V. Lopez Prior*, B. LLombart Cussac, R. Diaz Expósito, F. Manchón Adsuar;*
Valencian Oncologic Institution (IVO), Valencia, SPAIN.

Aim/Introduction: Merkel cell carcinoma (MCC) is a rare and aggressive neuroendocrine tumor with limited evidence on the role of 18F-FDG PET/CT. The aim of this study was to assess the impact of the 18F-FDG PET/CT in the management of MCC. ***Materials and Methods:*** Fifty-one studies of 18F-FDG PET/CT of 35 patients (19 men (54,30%); 72,17+-14,63 years) with histologic diagnosis of MCC were retrospectively evaluated. The change in tumor staging and the impact on the treatment were analysed. ***Results:*** There were 23 PET/CT positive studies (45,10%) and 28 (54,90%) negative. Thirty four (66,7%) studies were performed for assessment of stage at initial presentation and 17(33,3%) were performed during the follow up: 6(35,29%) for suspected recurrence; 7(41,18%) for restaging; 4(23,53%) as a part of ongoing surveillance. On the basis of PET/CT results, there was a change in disease stage (SC) in 20 studies (39,20%) and impact in the management (MI) in 28 (54,90%): 11 (32,40%) SC and 12 (35,30%) MI in the initial staging; 5(71,43%) SC and 7(100%) MI in the restaging; 3 (50,00%) SC and 6 (100%) MI in suspected recurrence; 1 (25,00%) SC and 3 (75,00%) MI in the surveillance. 18F-FDG PET/CT incidentally detected 1 additional histologically confirmed cancer. The presence of nodal involvement in the beginning (0,0098; HR 3,82; IC95% 1,38-10,6), chemotherapy treatment (6e-04; HR 7,06; IC95% 2,30-21,60), size of primary tumor >2 cm (6e-04; HR 7,06; IC95% 2,30-21,60) and positive resection margin (0,00069; HR 4,01; IC95% 1,46-11,00) were statistically significant prognostic factors for overall survival. There was a trend towards significance for worse overall survival with initial positive 18F-FDG PET/CT but the trend did not reach statistical significance. ***Conclusion:*** 18F-FDG PET/CT altered the stage in 2 out of 5 studies and changed the treatment in more than half of the studies performed. The study confirms the important impact of 18F-FDG PET/CT on the management of MCC patients. ***References:*** None

EP-071

Quantification of 18F-FDG accumulation in the intact testes of oncological patients

G. Arsos*, D. Katsampoukas, P. Exadaktylou, A. Kalaitzogloy, V. Mpalaris, S. Georga, E. Moralidis;*
3rd Dept. of Nuclear Medicine, Aristotle University of Thessaloniki School of Medicine, Papageorgiou Gen. Hospital, Thessaloniki, GREECE.

Aim/Introduction: From childhood to adulthood, testicular function first matures and then declines. Accordingly, testicular metabolic activity and 18F-FDG accumulation varies with age. Despite the existence of the blood-testis barrier, testis can be nevertheless affected by both neoplastic disease and antineoplastic agents, resulting in 18F-FDG uptake alterations. Considering symmetry, right and left testis have differing venous vasculature and also show subtle size and position differences. We aim to assess the levels of 18F-FDG uptake in the intact testes in relation to age and in comparison to other established reference sites, as well as their symmetry in the setting of the ordinary oncological 18F-FDG PET/CT scan. ***Materials and Methods:*** M A selected age-balanced sample of male patients admitted for oncological 18F-FDG-PET/CT scan from October 2018 to December 2019 was retrospectively analyzed. Patients with pediatric genitourinary operation, nephrourological malignancies or detectable testicular lesions were excluded. The 18F-FDG skull-base to mid-thigh

PET/CT scan was performed in all according to recognized guidelines. Properly sized spherical volumes of interest were drawn over each of both testes, mediastinum, right lobe of the liver and left thigh musculature, omitting any lesions and maximum standardized uptake value (SUVmax) was obtained. ***Results:*** Eighty-three patients with an age range 6-89 years (mean 46.3), were included. SUVmax (mean ± standard deviation) was: left testis (L) 3.4±0.9, right testis (R) 3.5±0.9, mediastinum (MD) 2.3±0.4, liver (LIV) 3.2±0.5, left thigh (TH) 0.9±0.1. There was no significant difference between either L and R or between their ratios to mediastinum (L/DM and R/MD), liver (L/LIV and R/LIV) and thigh (L/TH and R/TH). Both L and R were significantly higher than MD, LIV and TH ($p<0.001$ in every case). L and R were strongly linearly correlated each other (r 0.936, p less than 0.005). The correlation of R with age was positive until the age of 23 years (r 0.842, p less than 0.0001) and slightly negative (r -0.251, p 0.04) thereafter. Interestingly, in the younger group (18 patients), the ratios R/MD, R/LIV and R/TH were also significantly increased with age (r 0.610, 0.666 and 0.713 respectively, p less than 0.05 for all) up to 23 years. ***Conclusion:*** 18F-FDG uptake in the intact testis of oncological patients shows considerable inter-testes parity. The correlation of 18F-FDG uptake with age is biphasic with fast increase of the former from childhood to early adulthood; this must be kept in mind considering uptake normality at this period. ***References:*** None

EP-072

18-F-fluorodeoxyglucose positron emission tomography (18FDG PET) as an attractive oncology imaging modality in patients with brain metastasis of unknown origin - initial experience

P. Nikolova[1], V. Hadzhiyska[1], K. Mladenov[1], M. Ilcheva[1], V. Grudeva[2];
[1]University Hospital Alexandrovska, Sofia, BULGARIA,
[2]Department of Imaging Diagnostics, University Hospital „Sv.Ekaterina", Sofia, BULGARIA.

Aim/Introduction: The aim of the study is to evaluate the role of positron emission tomography/computed tomography (PET/CT) in detecting primary site in patients with brain metastasis of unknown primary as well as the extent of the disease. ***Materials and Methods:*** Thirty-nine patients (23 men; 16 women; aged from 26 to 85 years, mean: 62 years old) with a diagnosis of brain metastasis according to histopathology and/or MRI were included in this retrospective study. Almost half of them had solitary metastases (49%), followed by those with several (33%) and multiple (18%) metastatic foci. Twenty-eight out of 39 patients were proved to have metastases histopathologically and 11 patients had highly suspicious metastases by conventional imaging. The most common histology types were adenocarcinoma, poorly- and undifferentiated carcinoma and other rarer variants as melanoma, anaplastic blastoma, NHL and etc. Half of the patients had available baseline examinations and previous imaging studies prior to PET/CT, with only 9 of them (23%) having a whole-body CT. ***Results:*** 18FDG PET/CT suggested primary site in 31 cases (79%), 27 of which were subsequently proved to be correct either by direct histological verification or indirectly by the observation of lesion appearance or lesion growth on structural imaging as the standard of reference (true positive rate; 69%), mainly in the following locations: lung (21), testis (2), colorectal (1), prostate (1), uterus(1) and primary brain tumor(1). Findings for the other 4 cases were categorized as false positive since another primary location was confirmed by further investigations. Of 8 PET/CT-negative patients, no primary lesion was identified by other diagnostic procedures and formal clinical follow-up results in a false-negative rate of 0 and a true negative rate of 21%. Sensitivity, specificity, and accuracy were calculated as 100%, 67%, and 90%, respectively. PET/CT revealed additional metastasis in 77% (30/39) with most frequent sites being: lymph nodes(59%), lung(31%), bones(28%) and liver(18%). The calculated average survival rate, based on the date of PET/CT examination was around 9 months and in 8/39(21%) patients it was under 40 days, respectively. ***Conclusion:*** Our results demonstrate positive PET/CT findings in almost three-quarters of the patients with the lung being the most common primary location. Therefore, we believe that CUP patients may benefit from PET/CT assessment because of its highly sensitive and noninvasive nature - detection of possible primary site, determining the best location for biopsy as well as the extent of the metastatic disease. ***References:*** None

EP-073

Tonsils are the Most Frequent Primary Source of Cancer of Unknown Primary by FDG-PET/CT

G. Al-Obthani[1], J. Hatazawa[2];
[1]Hadramout University, Mukalla, YEMEN,
[2]Osaka University, Osaka, JAPAN.

Aim/Introduction: Cancer of unknown primary (CUP) refers to metastatic malignancy without an identified primary source. Carcinoembryonic antigen (CEA) is a glycoprotein, present at very low levels in the blood normally, but may elevate in many cancers. To check the detection rate (DR) for the primary lesions of CUP by FDG PET/CT and its correlation with the CEA level. ***Materials and Methods:*** 287 cases of CUP that were referred for FDG PET/CT during the period 2007-2017 at Osaka University Hospital, Japan. The cases had biopsy-proven malignancy whose primary origin remains unidentified. ***Results:*** DR of the primary lesions of CUP by FDG PET/CT was 18% (52/287). The primary sources in 40% (21/52) were located in the cervical area, and extra cervical in 60% (31/52). Neck lymph nodes metastases were

the initial presentation in 23% (67/287) of the CUP cases, while 77 % (220/287) with extra cervical metastases. DR for the primary lesion of the CUP cases that presented with neck LN metastases was 39% (26/67). The location of the primary tumor was also in the neck area in 80% (21/26) of the detected primary cancer with cervical metastases presentation. Tonsils were the most frequent primary lesion of CUP in the neck; 52% (11/21), followed the base of the tongue, and larynx, each of them 14% (3/21). While the primary source of 20% (5/26) of the detected primaries that presented with neck LN metastases, were located in extra cervical areas; 3 cases in the thoracic esophagus and one case in each of the stomach and sigmoid colon. 77% (220/287) of the CUP cases presented by extra cervical metastases, DR was 12% (26/220). The common primary sources were: lung 27% (7/26), the stomach 15% (4/26). 32 cases of the CUP cases had high carcinoembryonic antigen (CEA). Of them, the primary cancers were detected in 34% (11/32), While 66% (21/32), their primary cancers were not detected. ***Conclusion:*** DR was higher for the primary cancers of the CUP with cervical lymph nodes metastases than non-cervical.Tonsils should be checked carefully in cases with cervical metastases. The efficacy of FDG PET/CT in the detection of the CUP was not correlated with the level of CEA. ***References:*** None

EP-074

Utility ^{18}F-FDG PET/CT of the detection of unknown primary tumors (UPT)

A. Baena-Garcia*, M. Cruz-Montijano, S. Garcia-Martinez, M. De Bonilla-Candau, J. Rodriguez-Rubio Corona, Y. Santaella-Guardiola, M. Pajares-Vinardell;*
Hospital Universitario Puerta del Mar, Cadiz, SPAIN.

Aim/Introduction: The aim of this study is to evaluate the utility 18F-FDG PET/CT of the detection of unknown primary tumors (UPT). ***Materials and Methods:*** We analysed all the ^{18}F-FDG PET/CT studies with an indication of UPT addressed to our department from the start of PET/CT from March 2016 to December 2019.We defined as pathological all studies with positive metabolic malignancy findings. We differentiated studies with primary localized tumour (PLT), studies with positive metabolic without primary located tumour (P), and studies without pathological findings (WP). Final diagnosis criteria were histological confirmation by guided PET/CT or other techniques biopsy and/or clinical/radiological follow-up for at least six months. ***Results:*** Under the established criteria, 66 patients (43 males, 25 females) with an average age of 62 years old were identified. 59 of all the cases showed correctly tumor etiology.Positive metabolic lesions were identified in 57/66 patients, 96% of them were diagnosed as pathological (55/57. PLT+P). 4 patients were diagnosed as false positive by PET-CT.The primary tumor was identified in 36 patients, 41% of those were diagnosticated by guided PET-CT biopsy. The PET-CT was decisive in the final diagnosis of 37% (22/59) of the patients with UPT. ***Conclusion:*** The primary tumor was correctly diagnosticated by PET-CT in 41% of the patients where a malignant origin was found. PET-CT contributed to establish the final diagnosis in 37% of all cases. ***References:*** 1.Talavera-Rubio, M. D. P., García-Vicente, A. M. (2013). Utilidad de la tomografía por emisión de positrones con 18F-Fluorodesoxiglucosa-tomografía computarizada en la identificación del tumor primario en pacientes con cáncer de origen desconocido. Medicina Clinica, 140(1), 14-19. 2. Budak E, Yanarateş A. Papel de la PET/TC con 18F-FDG en la detección del tumor primario en pacientes con metástasis óseas de origen desconocido. Rev Esp Med Nucl Imagen Mol. 2020;39:14-19

EP-075

It Takes Two to Tango: Detection Efficiency of ^{18}F-FDG PET-CT and High Resolution Contrast Enhanced CT in the evaluation of Hidden Primary Malignancy

M. Siddique[1]*, A. Iqbal*[2]*, A. B. Rai*[3]*, M. K. Nawaz*[1]*;*
[1]*Pakistan Kidney and Liver Institute & Research Centre, Lahore, PAKISTAN,* [2]*LINCS Diagnostic & IR Services, Lahore, PAKISTAN,* [3]*Oxford University, Oxford, UNITED KINGDOM.*

Aim/Introduction: ^{18}F-FDG PET-CT is an astute detective in unraveling unknown primaries in cases presenting either with metastatic disease or constitutional symptoms that remains unspecified despite thorough diagnostic evaluation. We took a slingshot by adding anatomical probe high resolution contrast enhanced (HR CECT) in diagnostic regimen. ***Materials and Methods:*** Retrospectively, 92 patients [52 males, 40 females; age 8 - 73 y, mean: 49.8 y] with unknown parimaries or negative nodal or extra-nodal diseases who underwent multimodal imaging (combined ^{18}F-FDG PET-CT and HR CECT) from June 2019 till March 2020 were evaluated. We assessed combined work of both as compared with them working alone. Tissue diagnosis and follow up particularly in negative cases was considered reference standard. Statistical analysis included detection rate, sensitivity, specificity, positive predictive value (PPV), negative predictive value (NPV) and area under curve (AUC) for FDG PET alone and combined molecular-diagnostic imaging. Linear regression was calculated to interpret PET-CT outcome based on background corrected target nodal / extra-nodal SUVmax values. ***Results:*** Of 92 cases, pre-scan biopsy was suggestive of metastases in 29.5% (n=27), inconclusive in 14% (n=13) and rest of 56.5%(n=52) had only constitutional symptoms. Of 66 patients with hypermetabolic disease, 52.2%(n=48) turned out to be true positive for primary tumor on biopsy and false positive in rest of 19.6% (n=18) cases due to underlying granulomatous disease. Of 26(28%) FDG non-avid cases, three were false negative while rest of 23(25%) were true negative. The

primary tumor was detected in gastrointestinal (n=8), pancreaticobiliary (n=10), genitourinary (n=2) and respiratory (n=6) systems. Two cases had breast carcinoma, 17 lymphoproliferative origin, three of malignant melanoma and miscellaneous sites in 3 cases. Putting all the pieces of jigsaw puzzle revealed that combined molecular - high resolution anatomical imaging was more precise in picking the true positives. Receiver operating character curve (ROC) revealed that the working model of two was accurate in detecting unknown primary with statistically significant (P-value < 0.01) difference. ***Conclusion:*** High resolution CECT when added to ^{18}F-FDG PET-CT works much better providing higher detection quotients and reducing the number of false positives. In unison, both work as an effective tool for identifying occult primary pathology. ***References:*** None

EP-13

Imaging Clinical Studies -> Oncological Imaging Clinical Study -> Breast

e-Poster Area

EP-076

Diagnostic Yield of F-18 FDG PET-CT in Staging and Restaging of Breast Cancer: Where Do We Need the Addition of Metabolic over Conventional Radiological Imaging?

M. Siddique[1], A. Iqbal[2], M. K. Nawaz[1], A. B. Rai[3];
[1]Pakistan Kidney and Liver Institute & Research Centre, Lahore, PAKISTAN, [2]LINCS Diagnostic & IR Services, Lahore, PAKISTAN, [3]Oxford University, Oxford, UNITED KINGDOM.

Aim/Introduction: Over the years, addition of metabolic over anatomical imaging is being investigated in intermediate to high risk breast cancer. In current study, we will evaluate the potential role of FDG PET-CT in different clinical settings by comparing its precision with conventional radiological imaging. ***Materials and Methods:*** 43 female breast cancer patients (age range:21-79 years, mean:52.6 years) with histological diagnosis of invasive ductal carcinoma/IDCA between June 2019 and March 2020 were evaluated retrospectively. Patients were stratified into cases with preoperative staging, post chemo and/or radiotherapy (CRT) or recurrence? Initial staging was performed based on clinico-pathological results, according to the American Joint Committee on Cancer(AJCC) classification. Following PET-CT imaging, modification in the staging was executed in patients with metastatic findings. Pearson's correlation coefficient was implicated to evaluate the impact of various factors. ***Results:*** Of 43 cases, PET-CT was performed preoperatively in 26%(n=11), post-treatment in 48%(n=21) and 26%(n=11) patients with suspicion of recurrence. 61%(n=27) had IDCA grade II while 39% (n=17) had grade III histology. Immunohistochemistry revealed 7(16%) ER/PR+ HER/2+, 15(35%) ER/PR+ HER/2-, 10(23%) ER/PR+ HER/2 equivocal and 6(14%) ER/PR- HER/2- cases, missing data in 5(12%) cases. By AJCC staging system; stage I, 7(16%); stage II, 12(28%); stage III, 13(30%) and stage IV 11(26%). 13 cases underwent CRT following mastectomy and axillary nodal dissection, while 21 had neo-adjuvant chemotherapy alone. Of total, 9(21%) were upstaged, 11 (25.6%) down-staged, two (4.6%) cases were equivocal, required MR correlation. Of baseline(n=11) cases, apart from primary tumor(mean size: 2.8 cm), hypermetabolic nodal, visceral and osseous metastases were seen in five, three and one case respectively. Cases with suspicious recurrence(n=11), local recurrence was identified in three, axillary and distant nodal metastases in three and extra-nodal metastases in five. Of post treatment cases (n=21), 10 cases had progressive disease, four had partial response and seven were unremarkable. No statistically significant difference seen in maximum standardized uptake value (SUV_{max}) of primary tumor with grade II versus III. Addition of PET-CT showed statistically significant impact on modification of tumor staging in intermediate, IIB[T_2N_1/T_3N0] disease, or higher clinical stage, tumor size > 2 cm and axillary nodal metastases. ***Conclusion:*** F-18 FDG PET-CT has been shown to be of utmost importance in recognizing the site of relapse in breast cancer cases where traditional imaging features are equivocal or conflicting. For baseline staging, PET has imperative role in high grade tumors with suspicious axillary and/or non-axillary metastases. ***References:*** None

EP-077

^{18}F-FDG digital PET/CT performances for initial axillary lymph node status in breast cancer

C. Provost[1,2], A. Belly-Poinsignon[3], O. Madar[1], L. Champion[2];
[1]Radiopharmacology department, Institut Curie, Saint Cloud, FRANCE, [2]Nuclear Medicine department, Institut Curie, Saint Cloud, FRANCE, [3]Medical Physics department, Institut Curie, Saint Cloud, FRANCE.

Aim/Introduction: Breast cancer represents 11.6% of new tumors in 2018 in the world. Axillary lymph node status is one of the most important prognostic factors at diagnosis. PET/CT is an efficient imaging tool in oncology. Evolution of PET technology (Time-of-Flight TOF and then digital detectors) permits to improve small lesions detectability. In literature, sensitivity of analog and analog TOF PET/CT in the assessment of axillary lymph node status is between 24 and 85%. In this study, we analyzed ^{18}F-FDG digital PET/CT results for the detection of axillary lymph nodes in initial breast cancer staging. ***Materials and Methods:*** Eighty-eight women with breast cancer (mean age 51; range 24-79 years) underwent ^{18}F-FDG digital PET/CT before surgery, between September 2018 and February 2019. Mid-thigh

acquisition (1min/bed position) was performed 60 min after injection of the radiotracer (3MBq/Kg). Images were reconstructed to a target image voxel size of 2×2×2 mm. Digital PET performances were compared with surgical pathology and analog PET results. ***Results:*** Sixty-six patients with T2 or higher breast carcinoma and 22 patients with T1 carcinoma were included. Axillary lymph node metastases were histologically confirmed in 37 of 88 patients (42%). For axillary lymph node evaluation, ^{18}F-FDG digital PET/CT accuracy, sensitivity, specificity, positive and negative predictive values were 89, 86, 90, 86 and 90 %, respectively. Mean SUVmax value was 6.6 ± 3.8 (range 2.5-18.2) and mean size was 10.5 ± 3.6 (range 5-22 mm). In comparison with ^{18}F-FDG analog PET/CT sensitivity, digital PET/CT results are significantly better (p=0.002). In comparison with analog TOF PET/CT, there is no significant difference between the both PET technologies (p=0.7). Even if specificity seems better with digital PET than TOF PET (90% vs 78%), no significant difference was found (p=0.1). ***Conclusion:*** Accurate evaluation of axillary lymph nodes status is crucial for treatment choice and prognosis prediction. In this study, axillary lymph node detection by ^{18}F-FDG digital PET/CT is promising with high index performances. ***References:*** Cooper KL, et al. Positron emission tomography (PET) for assessment of axillary lymph node status in early breast cancer: a systematic review and meta-analysis. Eur J Surg Oncol 2011; 37:187-198 Yiyan Liu. Role of FDG PET-CT in evaluation of locoregional nodal disease for initial staging of breast cancer. World J Clin Oncol. Dec 10, 2014; 5(5): 982-9895. Mio Mori, et al. Diagnostic Performance of Time-Of-Flight PET/CT for Evaluating Nodal Metastasis of the Axilla in Breast Cancer. Nucl Med Commun. 2019 Sep;40(9):958-964.

EP-078

Metabolic activity by 18F-FDG-PET/CT is predictive of early response after ribociclib combination therapy in previously treated hormone positive advanced carcinoma breast : a hope of future

H. Rathore*, N. Thaker, I. Talwar, B. Smruti, R. Pai, M. Ansari, R. Jaiswar;*
Bombay Hospital and Medical Research Centre, Mumbai, INDIA.

Aim/Introduction: Therapy with Ribociclib and aromatase inhibitor (Letrozole) is a novel combination for hormone positive metastatic carcinoma breast. To assess the efficacy of Ribociclib combination therapy by clinical, radiological and metabolic responses, and toxicity. ***Materials and Methods:*** Ribociclib combination therapy was given to two patients(AandB) with HR+/HER2-CABreast and kept under observation for 8 months. 18F-FDG-PET/CT was performed prior to initiation and after 8 months of treatment and evaluated for radiological and metabolic response assessment by size of lesions and SULpeak by using RECISTv1.1 and PERSIST1.0 criteria respectively, metabolic tumour volume(MTV) and total lesion glycolysis(TLG) were also calculated. FISH study was negative for HER2. In addition, early response and toxicity of ribociclib was also evaluated by ECOGperformance scale and CBC, liver and renal function tests(LFTandRFT), serum electrolytes, LDH and alkaline phosphate(ALP) prior to therapy and followed by 4 weekly as per ECOG-CTCcriteria. ***Results:*** A complete to partial metabolic response as SULpeak to ribociclib combination therapy was observed in both patients which were further categorised to individual organs. All lesions detected by 18F-FDG-PET/CTscan exhibited significant reduction in metabolic activity(MA). First patient(A) showed a reduction in MA of 48.71% in lung nodules, 28.23% in mediastinal nodes, 22.89% in liver lesions, 30% in skeletal lesions with increased sclerosis, 100% in subcutaneous deposits and 68.04% in muscle deposits. Another patient(B) showed reduction in MA of 100% in mediastinal nodes, 52.63% in right axillary nodes, 6.09 % in liver lesions and 48.18 % in skeletal lesions suggestive of CMR and PMR according to PERSIST1.0, however increase in size of liver lesions seen in both patient as increase in extent of necrosis (24.48%and15.08 %) suggestive of PD and SD respectively according to RESIST1.1criteria. There are no new lesions seen in any of the patients with no significant haematological, lung, liver, kidney toxicity. ALP and LDH remains constant(gradeI) from the baseline values. ***Conclusion:*** Metabolic responses by 18F-FDGuptake (especiallyTLG) are closely associated with therapeutic response and survival at 8 month after Ribociclib and endocrine therapy. Even if morphological changes on CT-scans it is difficult to distinguish between responders and non-responders. Thus, the 18F-FDG-uptake on PET/CT appears to be a promising biomarker for predicting the therapeutic efficacy of ribociclib and should be implemented in clinical practice. ***References:*** Gabriel N. Hortobagyi et al. Ribociclib for the first-line treatment of advanced hormone receptor-positive breast cancer: a review of subgroup analyses from the MONALEESA-2 trial. Hortobagyi Breast Cancer Research (2018)20:123.doi.org/10.1186/s13058-018-1050-74.

EP-079

PET-CT And Breast Cancer: Indications And Interest

A. Hind*, H. Maha;*
Faculty of Medicine, Casablanca, MOROCCO.

Aim/Introduction: Positron emission tomography is an expensive examination with reduced availability in our country from where the interest to limit its indications and to approach them in a spirit of evaluation and rationalization of the requests. Our study aims to describe the place that PET currently occupies in our context in the staging of the disease, in the evaluation of the response to treatment as well as its role in the therapeutic decision-making in patients with breast cancer. ***Materials and Methods:*** This is

a retrospective observational study of patients with breast cancer treated in the Mohammed VI cancer center in Casablanca and having performed a PET-CT scan between January 2016 and December 2018. ***Results:*** 46 patients were included in the study. Their mean age at diagnosis was 47.91 (SD=10.61). The PET in the initial extension assessment allowed upstaging and downstaging at the lymph node stage in respectively 21.43% and 7.14% of the patients. It made it possible to classify 50% of patients as metastatic. In the recurrence assessment, PET allowed upstaging in 27.27% of cases and downstaging in 3.03% of Lymph node level 19.23% of patients underwent upstaging and 7.69% had downstaging. In the evaluation of the therapeutic response, PET showed a favorable response to treatment in 35% of the cases at the lymph node level and 30% of the cases at the metastatic level. It made it possible to detect a progression of the disease in 5% and 10% of the cases respectively at the lymph node and metastatic level. ***Conclusion:*** It remains essential to target its indications as well as possible to avoid duplication of examinations and to offer patients the best therapy, taking into account cost-effectiveness. ***References:*** 1. Berriolo-Riedinger A, Touzery C, Riedinger J-M, Toubeau M, Coudert B, Arnould L, et al. [18F] FDG-PET predicts complete pathological response of breast cancer to neoadjuvant chemotherapy. Eur J Nucl Med Mol Imaging. déc 2007;34(12):191524. 2. Caresia Aroztegui, A. P., García Vicente, A. M., Alvarez Ruiz, S., Delgado Bolton, R. C., Orcajo Rincon, J., Garcia Garzon, J. R., ¨ Garcia-Velloso, M. J. (2017). 18F-FDG PET/CT in breast cancer: Evidence-based recommendations in initial staging. Tumor Biology. https://doi.org/10.1177/1010428317728285 3. Riedl CC, Pinker K, Ulaner GA, Ong LT, Baltzer P, Jochelson MS, et al. Comparison of FDG-PET/CT and contrast-enhanced CT for monitoring therapy response in patients with metastatic breast cancer. Eur J Nucl Med Mol Imaging. août 2017;44(9):142837.

EP-080

Prospective comparison of early interim 18F-FDG PET/CT and 18F-FLT PET/CT for predicting treatment response and survival in metastatic breast cancer

S. Chan[1], *T. Su*[2], *P. Chang*[2];
[1]*Hualien Tzu Chi Hospital, Hualien, TAIWAN,* [2]*Keelung Chang Gung Memorial Hospital, Keelung, TAIWAN.*

Aim/Introduction: Our purpose was to compare the value of 3'-deoxy-3'-18F-fluorothymidine (18F-FLT) and 18F-fluorodeoxyglucose (18F-FDG) positron emission tomography/computed tomography (PET/CT) for early prediction of treatment response and survival in patients with metastatic breast cancer after salvage therapy. ***Materials and Methods:*** Twenty-five patients with metastatic breast cancer were prospectively enrolled and received PET/CT using 18F-FLT and 18F-FDG at baseline, after 1st cycle , and after 2nd cycle of systemic chemotherapy. The standard reference for treatment response was classified according to Response Evaluation Criteria in Solid Tumors (RECIST) 1.1 criteria for contrast-enhanced CT (CE-CT) after 3 months of systemic chemotherapy. The metabolic response on PET was assessed according to PET response criteria in solid tumors (PERCIST) criteria. The metabolic response on PET was correlated to the treatment response, progression-free survival (PFS), and overall survival (OS). ***Results:*** Complete response was observed in 4% (n=1), partial response in 44% (n = 11), stable disease in 24% (n = 6), and progressive disease in 28% (n = 7) of the study patients. The median follow-up time was 38 months. The responders had a significant greater reduction of maximal SUV of the tumor on 18F-FDG-PET after 2 cycles of chemotherapy than non-responders (P=0.03). Metabolic response on 18F-FDG-PET after 2 cycles of chemotherapy showed a higher area under the receiver operating characteristics curve (AUC) of 0.801 in predicting treatment response compared with AUCs of 18F-FLT PET after 1 cycle or 2 cycles (AUC=0.593 and 0.587, respectively; P = 0.09 and 0.08, respectively) and 18F-FDG uptake after 1 cycle (AUC=0.679; P = 0.17). Patients who were responders at 18F-FDG-PET after 2 cycles of chemotherapy had significantly longer PFS (53.8% vs. 16.7%, P = 0.014) and OS (100% vs. 47.6%, P = 0.046) than non-responders. Survival differences between responders and non-responders in 18F-FLT PET were not significant. ***Conclusion:*** Early-interim 18F-FDG-PET is more accurate than 18F-FLT PET in predicting treatment response and survivals in metastatic breast cancer patients. ***References:*** None

EP-081

Prediction of recurrence in locally advanced breast cancer using deep learning analysis

I. Jo[1], *J. Kim*[2], *S. Jeong*[1], *Y. Chae*[3], *S. Lee*[1];
[1]*Department of Nuclear Medicine, School of Medicine and Chilgok Hospital, Kyungpook National University, Daegu, KOREA, REPUBLIC OF,* [2]*School of Computer Science and Engineering, Kyungpook National University, Daegu, KOREA, REPUBLIC OF,* [3]*Department of Hematology/Oncology, Kyungpook National University Hospital, Kyungpook National University School of Medicine, Daegu, KOREA, REPUBLIC OF.*

Aim/Introduction: The purpose of this study was to identify whether convolutional neural network (CNN)-based features can predict recurrence in locally advanced breast cancer. ***Materials and Methods:*** This retrospective study included 265 breast cancer patients who diagnosed from Jun 2007 to Dec 2015. Pre-treatment PET/CT images, clinicopathologic data such as age, clinical T and N stages, histologic grade, estrogen and progesterone receptors, HER2 status were given for the prediction of the recurrence. Regions of interest (ROIs) were manually drawn to place primary tumors in the individual PET/CT images. Then, we

cropped ROIs using 3D cuboids with standard size (130 x 114 x 60) for all subjects. We implemented a 3D residual neural network following the architecture of ResNet-34 with 34 convolutional layers with skip connections. The individual clinicopathologic data were transformed into one-hot vectors and were concatenated with convolutional feature vectors through a fully-connected layer. The concatenated features were passed through two fully-connected layers followed by sigmoid activation function for the binary prediction of recurrence. The network was trained using binary cross-entropy loss. ***Results:*** Sixty-one patients had recurrence (23%). To validate the prediction accuracy, we performed 5-fold cross-validation. Without clinical variables, the model achieved a prediction accuracy of 0.804 (sensitivity 0.358 and specificity 0.946) on the validation sets. When clinicopathologic data were incorporated, the accuracy for the validation sets showed no significant change (accuracy 0.804, sensitivity 0.359, and specificity 0.939). We also observed large variations of sensitivity from 0.231 to 0.5 according to the validation sets, which are thought to include outliers. ***Conclusion:*** It was able to predict recurrence of breast cancer with a model from pre-treatment PET/CT images regardless of additional clinicopathologic data. We suggest that these data will be leveraged to improve patient management. ***References:*** None

EP-082

NaF-PET/CT has very limited clinical impact as a routine adjunct to FDG-PET/CT in breast cancer staging

S. Hess[1,2], *R. Horvat*[1], *E. H. Jakobsen*[3], *P. C. Holdgaard*[4];
[1]*Dept. of Radiology and Nuclear Medicine, Hospital South West Jutland, University Hospital of Southern Denmark, Esbjerg, DENMARK,* [2]*Department of Regional Health Research, University of Southern Denmark, Odense, DENMARK,* [3]*Dept. of Oncology, Lillebælt Hospital, University Hospital of Southern Denmark, Vejle, DENMARK,* [4]*Dept. of Nuclear Medicine, Lillebælt Hospital, University Hospital of Southern Denmark, Vejle, DENMARK.*

Aim/Introduction: Correct staging of breast cancer is essential. Previous strategies included CT and bone scintigraphy, but FDG-PET/CT has replaced CT. Sclerotic metastases may be less FDG-avid than lytic ones, but it remains controversial whether routine supplemental bone imaging is warranted. We retrospectively assessed the added clinical value of NaF as an adjunct to FDG in staging breast cancer patients. ***Materials and Methods:*** All breast cancer patients referred to Hospital South West Jutland for staging with both NaF and FDG within 2 weeks during a one-year period were retrospectively divided into group A (novel diagnosis with intended neoadjuvant treatment) and group B (confirmed local recurrence). Medical records were reviewed for results of PET/CT scans and clinical course on a per-patient basis. Scans were classified as FDG(+/-), CT(+/-) or NaF(+/-) with regards to bone metastases and concordance. Clinical impact was based on composite MDT decisions. ***Results:*** 66 consecutive patients were eligible for group A (n=45) or group B (n=21). In group A, most patients were without any metastases (n=17), or with loco-regional lymph node metastases on FDG and CT only (n=20). The remaining eight patients were NaF+, i.e. multiple bone metastases and concordant with FDG and CT (n=2), or solitary bone lesions with discordance, i.e. FDG-/CT+/NaF+ (n=3), FDG+/CT-/NaF+ (n=1), and FDG-/CT-/NaF+ (n=2). In the case with concordant PET scans (FDG+/CT-/NaF+), and the two NaF-only positive cases (FDG-/CT-/NaF+), PET results were considered false positive and treatment strategy remained unchanged. Of the three cases with discordant PET scans (FDG-/CT+/NaF+), two were considered false positive, and in one patient suspicion was maintained but treatment strategy remained unchanged. In group B, most patients were also without any metastases (n=9), or with soft tissue metastases only (n=4). The remaining seven patients were NaF+, i.e. multiple bone metastases concordant with FDG and CT (n=4), or solitary bone lesions with discordance, i.e. FDG-/CT+/NaF+ (n=1) and FDG-/CT-/NaF+ (n=1). Both cases with solitary NaF+ findings were considered false positive. One patient was considered true positive for bone metastases based in CT only and discordant with PET (FDG-/CT+/NaF-). ***Conclusion:*** The clinical impact of NaF-PET/CT as an adjunct to FDG-PET/CT is very limited; Of 66 patients, only seven displayed solitary NaF-positive findings discordant with FDG, and only one was considered suspicious, but with no consequence for treatment strategy. Thus, NaF-PET/CT does not seem warranted as a routine supplement to FDG-PET/CT for staging of breast cancer, but prospective confirmation is needed. ***References:*** None

EP-083

Bone Scan Index as Overall Survival predictor in Breast cancer patients with bone metastases at diagnosis

V. Frantellizzi*, A. Matto, M. Conte, G. Brunotti, L. Cosma, J. Lazri, M. S. De Feo, G. De Vincentis;*
Sapienza University of Rome, Rome, ITALY.

Aim/Introduction: Bone metastases represent a leading cause of death in patients with advanced breast cancer. It is not clear whether the bone metastatic load might have an impact on Overall Survival (OS) in patients with bone metastatic breast cancer at diagnosis. For this purpose we used Bone Scane Index (BSI) which is a reproducible and quantitative expression of the tumor load observed at bone scintigraphy. The aim of this analysis was to correlate BSI with OS in bone metastatic breast cancer patients. ***Materials and Methods:*** In this retrospective study breast cancer patients with bone metastases at the first bone scan and no visceral metastatic involvement (from the beginning of 2000 untill 2015) were enrolled. All patients underwent

scintigraphic bone scan for staging purposes in our centre, after administration of 740 (550-800) MBq of 99mTc labelled with HDP (hydrodiphosphonates); images were acquired approximately 2 hours after injection. The BSI was then calculated using the DASciS software and a statistical analysis of the obtained results was carried out. Other clinical variables relevant for OS analysis such as age, any treatments (radiotherapy, hormonal therapy, diphosphonate therapy and chemotherapy) and post- treatment response were taken into account. ***Results:*** 94 patients were studied and scintigraphic bone scans were analyzed to correlate the BSI with OS in breast cancer patients using DASciS program. On a total of 94 patients 30 (32%) died. In 90% of cases the histotype was ductal infiltrating carcinoma. The median OS from diagnosis was 72 months (CI 95%: 62-NA). The univariate analysis with COX regression showed that only hormone therapy is significantly correlated with OS (HR 0.417, CI 95%:0.174-0.997, p<0.049), resulting as protective factor. Regarding the BSI value, our statistical analysis showed that it does not represent a significant predictor of OS in breast cancer patients (HR 0.960, 95% CI: 0.416-2.216, p<0.924). The other variables included in the statistical analysis specifically age, radiotherapy, treatment with diphosphonates, chemotherapy and post-treatment response, resulted not significantly correlated with OS. ***Conclusion:*** Although the BSI showed to be useful as OS predictor in several tumours (such as prostate cancer), in this study we observed that the metastatic load of bone disease has no key role in prognostic stratification in this setting of patients. ***References:*** None

EP-084

Comparison of 1 day protocol and 2 day protocol of lymphoscintigraphy by subareolar injection in the detection of sentinel lymph nodes in breast cancer patients

J. Seok;
Chung-Ang University, Colleage of Medicine, Seoul, KOREA, REPUBLIC OF.

Aim/Introduction: Lymphoscintigraphy and sentinel node biopsy were used for the detection of axillary lymph node metastasis in breast cancer patients. We compared the results of subareolar injections on the day of surgery (1 day protocol) with injections the day before surgery (2 day protocol). ***Materials and Methods:*** This study included 1,266 breast cancer patients who underwent surgery between 2001 and 2020. For the 1 day protocol 0.8 ml of Tc-99m Tin-Colloid (37MBq) was injected in 887 patients in the subareolar region on the morning of the surgery. For the 2 day protocol 0.8 ml of Tc-99m Tin-Colloid (185MBq) was injected in 379 patients on the afternoon before surgery. Lymphoscintigraphy was performed in the supine position and sentinel node identification was performed by hand-held gamma probe during surgery. ***Results:*** Among 887 patients with the 1 day protocol, 855 cases (96.4%) were identified by sentinel node lymphoscintigraphy, and 860 cases (97.0%) were identified by gamma probe. Among the 379 patients, in the 2 day protocol, 356 cases (93.9%) had the sentinel node identified by lymphoscintigraphy, and 346 cases (91.3%) had the sentinel node identified by the gamma probe. There was no significant difference in the identification rate of the sentinel node between the 1 day and 2 day protocol by lymphoscintigraphy and the gamma probe. ***Conclusion:*** The results of the identification of the sentinel node according to 1 day or 2 day protocols showed no significant differences. Because the 2 day protocol allows for an adequate amount of time to perform the lymphoscintigraphy, it is a more useful protocol for the identification of sentinel nodes in patients with breast cancer. ***References:*** 1. Seok JW, Kim IJ, Heo YJ, Yang YJ, Choi YS, Kim BG, Park SJ. Comparison of subareolar injection lymphoscintigraphy with the 1-day and the 2-day protocols for the detection of sentinel lymph nodes in patients with breast cancer. Ann Nucl Med. 2009 Jul;23(5):465-9.

EP-085

Negative Predictive Value Of ^{18}F-FDG PET/CT In The Axillary Response to Neoadjuvant Chemotherapy In Patients Diagnosed Of Locally Advanced Breast Cancer

M. Lara Martínez[1], *M. López Acosta*[2], *A. Díaz Silván*[2], *O. Vilahomat Hernández*[2], *D. Cabello García*[2], *J. Uña Gorospe*[2], *A. Allende Riera*[2];
[1]*Hospital Universitario de Canarias, Santa Cruz de Tenerife, SPAIN,* [2]*Hospital Universitario Nuestra Señora de La Candelaria, Santa Cruz de Tenerife, SPAIN.*

Aim/Introduction: To determine the negative predictive value of ^{18}F-FDG PET/CT (PET/CT) in the detection of axillary metastatic disease response after neoadjuvant chemotherapy (NACT) in patients with complete structural response. ***Materials and Methods:*** Retrospective descriptive study of 45 patients diagnosed of locally advanced breast cancer who had undergone studies of conventional image (MRI, axillary ultrasound and mammography) with the result of axillary complete structural response after NACT. PET/CT was performed on this group of patients and those who presented complete metabolic response at the axillary level that underwent sentinel lymph node biopsy (SLNB). We have analyzed the pathological results of the sentinel nodes. ***Results:*** In the period from January 2019 to January 2020 a total of 45 patients with T1-T3 cN1 breast cancer received QTN with clinical and morphological response assessment using conventional imaging tests (MRI, ultrasound and mammography), who afterwards underwent a PET/CT. Twenty-six of them presented a complete axillary metabolic response result by PET/CT. The SLNB preformed to this group showed metastatic axillary lymph node in 10 patients, so the negative predictive value of PET/CT in

this type of patients is 61.5%, similar to the referenced in the literature found at values of 65%.The mean age of the patients attended was 53 years, of which 73% presented infiltrating breast tumor, being predominantly affected the right breast in 54% of the patients. ***Conclusion:*** PET/CT together with SLNB after NACT along with conventional morphological imaging that detects complete structural response are a complementary diagnosis tool to rule out disease and avoids lymphadenectomy to be done in this group of patients. ***References:*** None

EP-086

Positron Emission Mammography In The Evaluation Of Interim Response To Neoadjuvant Chemotherapy In Patients With Locally Advanced Breast Cancer

S. Medina-Ornelas[1], I. Soldevilla-Gallardo[1], F. García-Perez[1], C. Villarreal-Garza[1], E. Bargallo-Rocha[1], E. Estrada-Lobato[2];
[1]Instituto Nacional de Cancerologia, Mexico City, MEXICO, [2]IAEA, Vienna, AUSTRIA.

Aim/Introduction: Neoadjuvant chemotherapy (NAC) has an important role in patients with locally advanced cancers, treating distant micrometastases, downstaging tumors, improving operability, and sometimes allowing breast-conserving surgery to take place. We studied the association between two Positron Emission Mammography with ^{18}F-FDG (^{18}F-FDG-PEM) semi-quantitative parameters in 108 patients and correlated with pathologic response in each of the following breast cancer subtype: ***Triple negative breast cancer (TPN), HER2-positive, and ER-positive/HER2-negative cancers., our objective is*** Examine the association between two Positron Emission Mammography (PEM) semi-quantitative parameters: PUVmax (maximum uptake value) and LTB (lesion to background) baseline and the end of NAC with pathologic response in each breast cancer subtype. ***Materials and Methods:*** 108 patients, 71 with invasive ductal carcinoma and 37 with infiltrating lobular carcinoma were evaluate with ^{18}F-FDG-PEM scans baseline and after end of NAC. We assessed the impact of 2 PEM semi-quantitative parameters for molecular subtype correlated with pathologic response according Miller-Payne grade (MPG) ***Results:*** After NAC, an overall reduction of 2 PEM semi-quantitative parameters was found. Neither breast cancer subtypes nor Ki67 modified chemotherapy responses. Compared to PUVmax, an overall increase of LTB was found in baseline condition, independent of the expressed immunophenotype. Post-treatment values of PUVmax revealed a significant reduction compared to baseline values (4.8±0.26 vs. 1.9±0.18; p<0.001) and LTB exhibited a significant decay after the first course of NACT (15.8±1.36 vs. 5.5±0.49; p<0.001). Using the Kruskal-Wallis H test which showed no correlation between the different molecular subtypes and the MPG and PUVmax and LTB (p=0.52), but if a correlation was found between the response rate by MPG and both semiquantitative parameters (p=0.05). ***Conclusion:*** 2 PEM semi-quantitative parameters demonstrated a statically significant correlation and equivalence across the different breast cancer subtypes correlated with pathologic response according to MPG. PEM did not allow for prediction of NAC response in terms of breast cancer biomarkers, it is not discarded that this technology might be helpful for individual treatment stratification in breast cancer. ***References:*** None

EP-088

Is there a correlation between PET and histopathology findings of the invasive ductal carcinoma of breast with the histopathological features of coexisting DCIS?

I. Sarikaya[1], A. Sarikaya[2], A. N. Albatineh[1], E. Tastekin[2], Y. A. Sezer[2];
[1]Kuwait University Faculty of Medicine, Kuwait, KUWAIT, [2]Trakya University Faculty of Medicine, Edirne, TURKEY.

Aim/Introduction: Ductal carcinoma in-situ (DCIS) often coexists with invasive ductal carcinoma (IDC) of the breast. DCIS is recognized as non-obligate precursor of IDC when it coexists with IDC. ^{18}F-fluorodeoxyglucose (FDG) positron emission tomography/computed tomography (PET/CT) is commonly used in the staging and follow-up assessment of high risk and inflammatory breast cancers. In this study, we aimed to determine if there is any correlation in primary tumor's PET and histopathology findings with the histopathological features of the coexisting DCIS. In other words, we wanted to determine if PET findings can support the hypothesis of DCIS to be the precursor of IDC in cases with IDC-DCIS. ***Materials and Methods:*** FDG PET/CT images and histopathology results of the patients with newly diagnosed IDC-DCIS were selected for further analysis. Primary tumor's grade and the largest dimension, pathological staging, nuclear grade of DCIS, and architectural subtype of DCIS were noted from the post-operative histopathology results. Weight and lean body mass corrected maximum standardized uptake values (SUV_{max} and SUL_{max}) of the primary tumor were measured. Statistical analysis was conducted to determine if there is any correlation between between PET and histopathological findings of the primary tumor with the nuclear grade and architectural subtype of the coexisting DCIS. ***Results:*** Forty six (46) female patients with IDC-DCIS of the breast were included in this study. Grade of the primary tumor was significantly correlated and associated with the nuclear grade of the coexisting DCIS (r=0.616, Polychoric correlation and P-value=0.001). Size of the primary tumor was mildly correlated with the nuclear grade of the coexisting DCIS (0.285, Polyserial correlation). There was no significant difference in median primary tumor SUV in cases with nuclear grade-3, -2 and -1 DCIS (p >0.05). There was no significant difference in median primary tumor SUV in cases with comedo and non-comedo

DCIS (p >0.05). There was a weak correlation between the primary tumor's SUV with the nuclear grade and no correlation with the architectural subtype of the coexisting DCIS (r=0.185, Polyserial correlation, and r=-0.033, Point biserial correlation). ***Conclusion:*** Primary tumor's grade is significantly and positively correlated with the nuclear grade of the coexisting DCIS but the metabolic activity of the primary tumor does not seem to be correlated with the nuclear grade and architectural subtype of the coexisting DCIS. ***References:*** Sarikaya I, etal. Is there a difference in FDG PET findings of invasive ductal carcinoma of the breast with and without coexisting DCIS? AOJNMB 2020;8:27-35.

EP-089

The comparative study of the validation for Tc-99m Tin-colloid and Tc-99m Phytate in sentinel node detection in breast cancer patients

J. Seok;
Chung-Ang University, Colleage of Medicine, Seoul, KOREA, REPUBLIC OF.

Aim/Introduction: Lymphoscintigraphy and sentinel node biopsy has become a standard method for detection of axillary lymph node metastasis in breast cancer patients, but the standard radiopharmaceutical was not prepared. About detection of axillary lymph node metastasis by lymphoscintigraphy and sentinel node biopsy in breast cancer patient, we compared the results of Tc-99m Tin-colloid and Tc-99m Phytate by subareolar injection. ***Materials and Methods:*** This study included 1,266 breast cancer patients who were performed operation during 2001-2020. Four hundred twelve patients were injected 0.8 ml of Tc-99m Tin-colloid (37-185 MBq) by subareolar injection. Eight hundred thirty-eight patients were injected 0.8 ml of Tc-99m Phytate (37-185 MBq). Lymphoscintigraphy was performed in supine position and sentinel node localization was performed by hand-held gamma probe in operation. ***Results:*** Among 412 patients by Tc-99m Tin-colloid, 374 cases (90.8%) were localized the sentinel node by lymphoscintigraphy and 367 cases (89.1%) were localized by gamma probe. Among 838 patients by Tc-99m Phytate, 821 cases (98.0%) were localized by lymphoscintigraphy and 823 cases (98.2%) were localized by gamma probe. The detection rate by lymphoscintigraphy and gamma probe was superior for Tc-99m Phytate compared to that for Tc-99m Tin-colloid, with a statistically significant difference. ($p<0.05$, $p<0.05$) ***Conclusion:*** Tc-99m Phytate is a better choice for localization of sentinel node than Tc-99m Tin-colloid in breast cancer patients. ***References:*** 1. Seok JW, Choi YS, Chong S, Kwon GY, Chung YJ, Kim BG, Park SJ. Sentinel lymph node identification with radiopharmaceuticals in patients with breast cancer: a comparison of 99mTc-tin colloid and 99mTc-phytate efficiency. Breast Cancer Res Treat. 2010 Jul;122(2):453-7.

EP-090

Evaluation of low glucose uptake of lymph nodes in patients with advanced breast cancer

C. Romagnolo[1], *G. Biscontini*[1], *C. Cottignoli*[1], *D. Morichetti*[2], *A. Savini*[3], *F. Fringuelli*[1], *A. Palucci*[1], *L. Burroni*[1];
[1]*Nuclear Medicine, Ancona, ITALY,* [2]*Pathological Anatomy department, Ancona, ITALY,*
[3]*Oncology Department, Ancona, ITALY.*

Aim/Introduction: Breast cancer is frequently characterized by expression of the glucose transporter protein Glut-1 and elevated glucose consumption. ^{18}F-FDG PET / CT is the suitable examination to detect lesions with these characteristics and therefore particularly useful for staging and restaging of cancer. Unfortunately, recent studies have shown that distant metastases of breast cancer are capable of changing their immuno-phenotype compared to primary tumor because of reduced expression of the glucose transporter protein Glut-1. The aim of our study was to evaluate the reduced or absent glucose metabolic activity of the thoracic lymph nodes in breast cancer operated patients and to compare these findings with the morphological positive ones obtained by high resolution CT (HRCT). ***Materials and Methods:*** 14 patients (14 F; mean age 51.6 yrs) underwent a ^{18}F-FDG PET/CT scan and HRCT survey 3 months after breast cancer surgery. The patients presented infiltrating ductal carcinoma (6/14), lobular carcinoma (4/14) and mixed carcinoma (4/14).All of them had tumor grade G3 and pT2N3a disease stage. HRCT images were evaluated by two expert radiologists who described all positive or suspected lymph node lesions of the chest. The reconstructed PET/CT images were assessed separately by two nuclear medicine physicians who also provided for the semi-quantitative calculation of glucose uptake (SUV_{max}) of the lesions. Because of mismatched findings in the two methods used, all the patients underwent Fine Needle Aspiration Cytology (FNAC) and cytological evaluation of chest pathological lymph nodes. ***Results:*** The lymphadenopathies reported with contrast-enhanced HRCT were compared with ^{18}F-FDG PET/CT scan. All lymph nodes detected as positive at HRCT exams showed glucose metabolism and SUV_{max} values slightly modified compared to normal limits (SUV_{max}=2.1-3.1). Of the 14 patients studied with FNAC, three tested positive for lymph node metastasis (SUV_{max}=3.07) ***Conclusion:*** In patients with breast cancer (pT2N3a stage) with lymph node morphology suspected for contrast-enhanced HRCT disease and low glucose metabolism detected at PET ^{18}F-FDG, FNAC is recommended for the diagnosis of metastatic lesions. The lymph nodes with low-grade activity of ^{18}F-FDG are characterized by reduced expression of the glucose transporter protein Glut-1, normally expressed in the primary tumor. However, this reduced expression is probably present also in the primary tumor, especially

when increasing in size. ***References:*** None

EP-091

Usefulness of PET/CT scan in Brest Cancer Patient

A. Guensi*, I. Essongue, A. Sallak, H. Benider, S. S. Zouine; Hassan II University, Casablanca, MOROCCO.*

Aim/Introduction: Breast cancer is the leading cause of death from cancer in women, with an incidence of 6,650 new cases / year in 2014 in Morocco. The prognosis for breast cancer patients improved by the new treatments available in addition to radiotherapy, hormone therapy and chemotherapy. The objective of this work is to show the usefulness of 18-FDG PET / CT in the assessment of the initial staging, in the assessment of the reclassification of patients with breast cancer ***Materials and Methods:*** This is a retrospective work carried out in the nuclear medicine department of the Ibn Rochd University Hospital from January 2019 to December 2019. The study carried out based on data from the PET-CT files. The 18-FDG PET / CT was investigated in first assessment and also for restaging if recurrence is suspected ***Results:*** Among the 1412 scans carried out, 36 were for breast cancer patients. The average age was 52 years. Six scans carried out for the initial extension assessment and 30 scans for the relapse suspicion. On the 18 FDG PET/CT scan, the 9 scans done for initial extension assessment were positive and found in 5 cases a hypermetabolic breast mass associated with hypermetabolic axillary lymphadenopathy and in 1 case a hypermetabolic breast mass associated with a hypermetabolic lung mass. Of the 30 exams done for relapse suspicion, 9 were negative. The 21 positive PET / CT distributed as follows: contralateral breast recurrence associated with a bone extension (1 case). A local recurrence associated with axillary lymphadenopathy (4 cases). a local recurrence with lymph node and bone extensions (5 cases), local recurrence with bone extension (1 case), local recurrence with pulmonary extension (2 cases), lymph node and pulmonary extension (2 cases). Only mediastinal lymph node recurrence (3 cases), lymph node and bone extension (1 case), lymph nodes, bone and pulmonary extension (1 case), one only hepatic extension (1 case). ***Conclusion:*** The indication of 18 FDG PET-CT at during the initial assessment remains limited to triple negative patients and advanced tumors. In the event of suspected recurrence, the PET / CT scan at 18FDG is very useful for carrying out an extension assessment and allows precise reclassification which allows the continuation of treatment to be adapted to the actual stage of the disease. ***References:*** None

EP-092

Paraneoplastic Cerebellar Degeneration: Initial Presentation of Occult Breast Cancer

N. Filizoglu*, S. Kesim, C. O. Engur, T. Ones, S. Ozguven, T. Y. Erdil; Marmara University Pendik Training and Research Hospital, Istanbul, TURKEY.*

Aim/Introduction: Paraneoplastic cerebellar degeneration (PCD) is a rare type of paraneoplastic syndrome characterized by the progressive onset of cerebellar dysfunction as a result of immune-mediated response against neoplasm rather than metastasis. We present a case of occult breast cancer who had PCD at initial presentation with diffuse cerebellar uptake depicted on the FDG PET/CT scan. Six months after the treatment, a follow-up FDG PET/CT scan revealed complete resolution of the cerebellar hypermetabolism. ***Materials and Methods:*** FDG PET/CT was performed to A 64-year-old female patient presented with complaints of progressive dysarthria, ataxia, nystagmus, headache and gait disturbance. ***Results:*** FDG PET/CT showed diffuse and intensely increased uptake in both cerebellar hemispheres and vermis (A). FDG PET/CT images also depicted moderate hypermetabolic lymph node in the right axillary region; however, no hypermetabolic foci was detected in breast tissues (A). Histopathology of the right axillary lymph node revealed metastasis of breast cancer. Based on these findings, the diagnosis of paraneoplastic cerebellar degeneration associated with occult breast cancer was made and treatment with doxorubicin-docetaxel-trastuzumab-pertuzumab was initiated. After four cycles of chemotherapy, follow-up FDG PET/CT showed complete regression of cerebellar hypermetabolism (B). ***Conclusion:*** PCD is a rare central nervous system disorder that is triggered by an immune system response to a neoplasm. PCD affects 1-3 % of all cancer patients, and it occurs typically in patients with cancer of the ovary, uterus, breast cancer, small-cell carcinoma of the lung and Hodgkin lymphoma. Patients typically develop subacute cerebellar ataxia, dysarthria, diplopia, and vertigo, which often precede the detection of the primary tumor. PCD is characterized by extensive loss of Purkinje cells and the presence of highly specific antineuronal antibodies in the serum and cerebrospinal fluid. Proteins expressed by tumors induce the production of onconeural antibodies leading to a T-cell mediated destruction of Purkinje cells in the cerebellum. The treatment of the underlying malignancyis considered the optimal treatment for PCD. FDG PET/CT is crucial in the early detection of the unknown primary tumors. Most of the recently published studies emphasizing the potential of FDG PET/CT in the assessment of the functional neurologic consequences of the disease in the brain as well as changes that follow after therapeutic interventions. To the best of our knowledge, this is the first case in the literature that uses FDG PET / CT to assess the current state of occult

breast cancer with PCD and subsequently following up the disease. ***References:*** None

EP-14

Imaging Clinical Studies -> Oncological Imaging Clinical Study -> Colorectal

e-Poster Area

EP-093

Value of Volumetric and Textural Analysis in Predicting the Treatment Response in Patients with Locally Advanced Rectal Cancer

N. Karahan Sen*, A. Aksu, G. Capa Kaya;*
Dokuz Eylül University, Izmir, TURKEY.

Aim/Introduction: The aim of this study was to assess the value of 18F-FDG PET/CT in predicting the response to neoadjuvant chemo-radiotherapy (NCRT) in patients with locally advanced rectal cancer (LARC) via the volumetric and texture data obtained from 18F-FDG PET/CT images. ***Materials and Methods:*** Patients with staging FDG PET/CT and who had diagnosed LARC were evaluated retrospectively. In total, 110 patients who had undergone NCRT after PET/CT and followed by surgical resection were included in this study. Patients were divided into two groups randomly as train set (n:88) and test set (n:22). Pathological response using three-point tumor regression grade (TRG) and metastatic lymph nodes (increased size, changes in shape and high FDG uptake visually detectable from background were considered as metastatic) in PET/CT images were determined. TRG1 were accepted as responders and TRG2-3 as non-responders. Region of interest for the primary tumors was drawn and texture features were calculated. In train set, the relationship between these features and TRG was investigated with Mann Whitney U test. Receiver operating curve analysis was performed for features with p<0.05. Correlation between features were evaluated with Spearman correlation test, features with correlation coefficient <0,8 were evaluated with the logistic regression analysis for creating a model. The model obtained was tested with a test set that has not been used in modeling before. ***Results:*** In train set 32 (36.4%) patients were responders. The rate of visually detected metastatic lymph node at baseline PET/CT was higher in non-responders than responders (71.4% and 46.9% respectively=0.022). There was a statistically significant difference between TLG, MTV, SHAPE_compacity, NGLDMcoarseness, GLRLM_GLNU, GLRLM_RLNU, GLZLM_LZHGE and GLZLM_GLNU between responders and non-responders. (All of these parameters were at higher values in non-responders except NGLDMcoarseness). MTV and NGLDMcoarseness demonstrated the most significance (p=0.011). However, conventional SUV parameters did not demonstrate any significant difference (p>0.05). A multivariate logistic regression analysis that included MTV, coarseness, GLZLM_LZHGE and lymph node metastasis was performed. Multivariate analysis demonstrated MTV and lymph node metastasis were the most meaningful parameters. The model's AUC was calculated as 0.714 (p=0.001,0.606-0.822,95%CI). In test set, AUC was determined 0.838 (p=0.008,0.671-1.000,95%CI) in discriminating non-responders. ***Conclusion:*** In this study, it was thought higher MTV value and metastatic lymph nodes in PET/CT images could be a predictor of low treatment response in patients with LARC. The combine evaluation of MTV and lymph node metastasis in pre-treatment PET/CT images should be considered to predict pathologic response to NCRT. ***References:*** None

EP-094

^{18}F-FDG PET/CT Metabolic Tumor Burden in Primary Staging of Colorectal Cancers

E. Etchebehere*, J. S. Fonseca, A. O. Santos, M. C. L. Lima, M. S. Mendes, M. N. Silveira, B. J. Amorim, C. R. Martinez, L. P. Cunha, P. Fanti, J. B. Carvalheira;*
The University of Campinas, Campinas, BRAZIL.

Aim/Introduction: FDG PET/CT metabolic tumor burden (whole-body and primary tumor MTV (wbMTV; tuMTV) and TLG (wbTLG; tuTLG) parameters) has shown a direct correlation with prognosis in several solid tumors. However, the impact of these parameters in staging colorectal cancer (CRC) has not been studied. The purpose of this study was to determine if metabolic tumor burden plays a prognostic role in the primary staging of CRC. ***Materials and Methods:*** A retrospective analysis of 115 CRC patients submitted to a staging FDG PET/CT were studied. Semi-automatic calculation of metabolic tumor burden (hSUVmax, tuMTV, wbMTV, tuTLG, wbTLG) was performed. Cox proportional hazards regression was used to analyze predictors of survival. ***Results:*** The wbMTV (p< 0.0001; HR= 1.082), tumor histology (p= 0.0024; HR= 32.258) and clinical stage (IV vs I+II+III; p= 0.0116; HR= 7.407) were independent predictors of overall survival (OS). Only the presence of neural invasion was an independent predictor of progression-free survival (PFS) (p= 0.0479; HR= 4.902). ***Conclusion:*** wbMTV should be considered as a tool to make the fine adjustments in the treatment choice since it is a good predictor of survival. The evaluation of the primary tumor alone (tuMTV, tuTLG) are not able to predict OS and PFS. A higher number of patients and a longer period of observation should better demonstrate the reliability of these markers, cutoff values and the precise cases in which they are helpful. ***References:*** None

EP-095

The role of ^{18}F- FDG PET-CT in the decision making of radiotherapy treatment in patients with anal cancer

A. Palucci[1], M. di Benedetto[2], C. Cottignoli[1], L. Vicenzi[2], C. Romagnolo[1], F. Fringuelli[1], G. Biscontini[1], F. Fenu[2], S. Costantini[2], L. Burroni[1], G. Mantello[2];
[1]Nuclear Medicine, Ancona, ITALY, [2]Radiotherapy Department, Ancona, ITALY.

Aim/Introduction: Chemo-radiotherapy represents the standard treatment in patients with anal cancer. Intensity Modulated Radiotherapy (IMRT) leads to a precise treatment of the tumor, with dose escalation on Gross Tumor Volume (GTV), saving the surrounding healthy tissues. ^{18}F-FDG PET-CT and MRI of the pelvis are both used to for the definition of radiotherapy treatment plans. Our study assessed the impact of FDG PET-CT on the radiotherapy contouring process and its contribution to the assessment of the lymphatic spread allowing a personalization of Clinical Target Volume (CTV) and dose prescription. ***Materials and Methods:*** We carried out a retrospective study on 31 patients (25 females and 6 males) affected by anal cancer, treated with concomitant chemo-radiotherapy. Initial staging was based on MRI of the pelvis and ^{18}F-FDG PET-CT performed in radiation treatment position. The whole pelvis, plus bilateral inguinal lymph node stations were include in the Radiotherapy Target volume. A total dose of 54 Gy (up to 59 Gy) was delivered to the primary tumor and 45 Gy to the elective lymph node areas; a simultaneous integrated boost of 50-54Gy was planned on involved lymph nodes. ***Results:*** 25 out of 31 patients presented lymph nodes involvement, in one or more areas detected on PET-CT and/or MRI. In 9 patients, PET-CT showed positive lymph nodes not detected on MRI: the lymph node stations involved were pre-sacrum-coccygeal (in 2 patients), external iliac (in 3 patients) and inguinal (in 6 patients). In 8 patients, MRI reported lymph nodes involvement not described on PET-CT: the lymph node stations reported were mesorectal (in 6 patients), pre-sacral (in 1 patient) and obturator (in 3 patients). Radiotherapy Clinical Target Volume (CTV) was modified including common iliac region only in 1 patient. Both diagnostics (PET-CT and MRI) had reported the presence of disease. Simultaneous integrated boost was performed in the 25 patients with lymph nodes involvement. ***Conclusion:*** PET-CT and MRI are both useful to define the Clinical Target Volume (CTV). An accurate definition of lymph nodes involvement allows dose escalation and CTV personalization. In our experience, MRI seems to be more accurate in defining perivisceral lymph node involvement, like mesorectal stations. PET-CT may be more useful in defining lymph node disease spread in the remaining pelvic and inguinal stations. ***References:*** None

EP-096

Metabolic parameters of primary tumor in preoperative ^{18}F-FDG PET/CT do not accurately predict occult regional lymph node metastasis in patients with clinically N0 colorectal cancer

M. Zhou[1,2], X. Wang[1,2], Y. Wang[1,2];
[1]Department of Nuclear Medicine, the Third Affiliated Hospital of Soochow University, Changzhou, CHINA, [2]Changzhou Key Laboratory of Molecular Imaging, Changzhou, CHINA.

Aim/Introduction: To investigate whether metabolic parameters of primary tumor in preoperative ^{18}F-FDG PET/CT could predict occult regional lymph node metastasis in patients with clinically N0 colorectal cancer. ***Materials and Methods:*** The present study consecutively enrolled a total of 60 patients (male: female = 2:1, age 64.5 ± 10.5 years) from January 2012 to June 2019 with clinically N0 colorectal cancer based on preoperative 18F-FDG PET/CT and contrast-enhanced CT. The SUVmax, tumor metabolic volume (MTV) and total glycolysis (TLG) of the primary tumor were measured on the dedicated PET/CT workstation. Using a logistic regression model, the relationships between clinicopathologic characteristics including PET/CT parameters and regional lymph node metastasis were analyzed. ***Results:*** 15 out of 60 patients were pathologically confirmed to have regional lymph node metastasis. No significant difference was found in SUVmax of regional lymph nodes between LNM(+) and LNM(-) groups (1.6 ± 0.8 vs 1.4 ± 0.8, t = 0.730, P = 0.472). There were also no significant differences in SUVmax, MTV and TLG of the primary tumor between two groups [20.4 ± 9.6 vs 23.4 ± 11.2, t = 0.907, P = 0.368; 32.5 (20.4, 43.2) vs 24.2 (14.7, 40.0), u = 0.810, P = 0.417; 200.7 (117.2, 432.1) vs 174.3 (86.3, 376.0), u = 0.248, P = 0.804]. The ROC curve analysis showed the area under the curve of SUVmax, MTV and TLG for predicting occult regional lymph node metastasis was 0.430, 0.570 and 0.521, respectively (all P>0.05). Univaraite and multivariate analysis showed that PET/CT metabolic parameters, age, gender, preoperative serum CEA and clinical T stage were not risk factors associated with occult regional lymph node metastasis (all P>0.05). ***Conclusion:*** Metabolic parameters of primary tumor in preoperative 18F-FDG PET/CT have no ability to accurately predict occult regional lymph node metastasis in patients with clinically N0 colorectal cancer. ***References:*** None

EP-15

Imaging Clinical Studies -> Oncological Imaging Clinical Study -> Gastro-Intestinal (including Liver and Non-Endocrine Pancreas)

e-Poster Area

EP-097

Dual-Time Point Imaging (DTPI) in Gastrointestinal Stromal Tumors (GIST)

M. Aly[1,2], E. Kothekar[1], T. Seierstad[3], C. Rojulpote[1], Ø. Bruland[4], T. J. Werner[1], A. Alavi[1], M. E. Revheim[1,5,6];
[1]Department of Radiology, University of Pennsylvania, Philadelphia, PA, UNITED STATES OF AMERICA, [2]Department of Radiology, Asyut University Hospital, Asyut, EGYPT, [3]Department of Research and Development, Oslo University Hospital, Oslo, NORWAY, [4]Department of Oncology, Oslo University Hospital, Oslo, NORWAY, [5]Division of Radiology and Nuclear Medicine, Oslo University Hospital, Oslo, NORWAY, [6]Institute of Clinical Medicine, Faculty of Medicine, University of Oslo, Oslo, NORWAY.

Aim/Introduction: Increased activity between dual time point imaging (DTPI) was shown to be correlated with more malignant behavior in different cancers. With the introduction of tyrosin kinase inhibitors (TKI), the overall survival increased tremendously but some patients did not respond to first line treatment with imatinib or developed drug-resistant tumor clones. Approximately 20% of GISTs do not show sufficient FDG uptake or are too small to be detected by PET. We aim to evaluate the clinical value of DTPI of FDG-PET/CT in patients with metastatic GIST. ***Materials and Methods:*** 21 patients were included with metastatic GIST imaged after 60 and 90 minutes before treatment (timepoint 0 (Tp0)) and 2 weeks (Tp1) and 3 months after onset of TKI treatment (Tp2). 32 were responders according to RECIST and Choi criteria at Tp2. Examinations were using a Siemens Biograph 64PET/CT scanner. Scans were analyzed using an adaptive thresholding system (ROVER software; ABX GmbH, Radeberg/Germany). ROIs were placed over the active malignant lesions and the adaptive thresholding algorithm delineated the boundaries of active lesions. Quantitative PET parameters as SUVmean and SUVmax were automatically computed in addition to partial volume corrected (PVC). Volumetric measures of global disease burden included: metabolic tumor volume (MTV), total lesion glycolysis (TLG=SUVmean×MTV), and partial volume corrected TLG (pvcTLG=pvcSUVmean×MTV). Liver background was obtained by placing region of interest (ROI) of 3 cm in the right liver lobe. ***Results:*** 1)Strong correlations between pvcTLG at 60 and 90 minutes: 0.99 for Tp0 and Tp1, and 0.96 for Tp2 ($p<t0.05$). 2)Strong correlation between change based on 60 minutes and change based on 90 minutes between the three time-points. 3)No significant difference between liver background values at 60 minutes (median;2.2, range;1.2-3.2) and 90 minutes (median;1.9, range;1.1-2.9) ($p<0.05$) ***Conclusion:*** Total TLG and liver background activity provided the same result at 60 and 90 minutes after FDG injection in metastatic GIST patients during TKI treatment. Imaging after 90 minutes did not give any additional information. The low SUV results exhibited with GISTs compared with such values in aggressive tumors like lung cancer, indicate the relatively benign nature of these GISTs, and this also applies to the DTP imaging where SUV values may jump by even 30-40, after 30 minutes. And due to this benign-nature of GISTs (32 patients responded to TKI treatment), there was no significant elevation of metabolic activity as imaged between DTPI. ***References:*** None

EP-098

Comparison of ^{18}F-FDG PET-CT and ^{68}GA-PSMA PET-CT in Hepatocellular Carcinoma

S. Shamim*, G. Arora, J. Hussain, S. Gupta, Shalimar, S. Gamanagatti, C. Bal;*
AIIMS, New Delhi, INDIA.

Aim/Introduction: Hepatocellular carcinoma (HCC) is the sixth most common malignancy globally with a rising trend owing to increase in chronic liver disease. FDG PET is known to have low sensitivity in HCC due to variable FDG avidity and physiological uptake in liver. Few studies have demonstrated PSMA expression in HCC. Although, there is paucity in data available comparing FDG and PSMA avidity in HCC. Our objective was to assess the feasibility of HCC evaluation using ^{68}Ga-PSMA PET-CT in HCC and compare it with the established ^{18}F-FDG PET-CT. ***Materials and Methods:*** This prospective study recruited treatment naive radiological proven HCC patients from liver cancer clinic, in whom ^{18}F-FDG PET-CT and ^{68}Ga-PSMA PET-CT were performed within 2 weeks of one another. Institutional ethical clearance was sought and written informed consent was taken from each participant. ^{18}F-FDG PET/CT images were acquired at 45-60 minutes after intravenous administration of 8-10mCi of ^{18}F-FDG. ^{68}Ga-PSMA PET/CT images were acquired at 30-40 minutes after intravenous administration of 2-4mCi of ^{68}Ga-PSMA. Images were visually analysed by two expert nuclear physicians independently. Semi-quantitative image analysis was done by drawing region of interests and estimating standardized uptake values (SUVmax) of positive lesions, liver background & mediastinum; and calculating ratios between the same. ***Results:*** Five patients (4 male; 1 female) of HCC were prospectively recruited, who underwent FDG PET/CT and PSMA PET-CT. Mean age of patients was 67±8.7 years. Mean imaging interval between two scans was 5.2±3.3 days. On qualitative assessment PSMA showed better liver lesion to background contrast as compared to FDG in three cases (mean tumor to liver ratio: 3.28 vs 2.33)

and inferior to FDG in 2 cases (mean tumor to liver ratio: 5.62 vs 2.28). FDG detected more liver lesions than PSMA in one case and FDG missed additional liver lesions that were detected on PSMA in another case. Overall mean tumor to liver ratios in FDG PET/CT was 3.64 (range: 1.29 -9.87) and PSMA PET/CT was 2.87 (0.69 - 5.01), with no significant difference (p=0.893). Overall mean tumor to mediastinum ratios of FDG vs PSMA was 5.70 (1.84 -12.95) and 9.56 (6.42 - 15.86), also comparable (p=0.080). ***Conclusion:*** PSMA PET/CT may be a promising imaging modality for HCC, which can be complimentary to existing FDG PET/CT in staging and detection of multifocal liver disease. This opens up a theranostic avenue with PSMA targeted radionuclide therapy in patients of HCC. ***References:*** None

EP-099

Asphericity as a measure of spatial heterogeneity predicts therapy outcome in FDG-PET of patients with esophageal carcinoma

F. Hofheinz[1], *Y. Li*[2], *J. Maus*[1], *P. Nikulin*[1], *J. Rogasch*[3], *J. van den Hoff*[1], *S. Zschaeck*[4];
[1]*Helmholtz-Zentrum Dresden-Rossendorf, Institute of Radiopharmaceutical Cancer Research, Dresden, GERMANY,* [2]*Department of Radiation Oncology, Xiamen Cancer Hospital, The First Affiliated Hospital of Xiamen University, Xiamen, CHINA,* [3]*Department of Nuclear Medicine, Charite – Universitätsmedizin Berlin, Berlin, GERMANY,* [4]*Department of Radiation Oncology, Charite – Universitätsmedizin Berlin, Berlin, GERMANY.*

Aim/Introduction: It has been previously demonstrated that the quantifying the primary tumor asphericity (ASP) adds prognostic information to what is provided by standard parameters (SUV, MTV, TLG) in FDG-PET of patients with head and neck cancer. In the present study we address the question if ASP is also able to predict therapy outcome in patients with esophageal carcinoma. ***Materials and Methods:*** FDG-PET/CT was performed in 143 consecutive patients ((62+/-10)y, 112 males) with newly diagnosed esophageal squamous cell carcinoma prior to definitive radiochemotherapy. In the PET images, the metabolic active volume (MTV) of the primary tumor was delineated with an adaptive threshold method. For the resulting ROIs, SUVmax and ASP were computed. Kaplan-Meier analysis and univariate Cox regression were performed with respect to overall survival (OS) and event-free survival (EFS) for the PET parameters and clinically relevant parameters. Additionally, a multivariate Cox regression including clinical parameters as confounding factors was performed. ***Results:*** Survival analysis revealed MTV and ASP as prognostic factors for OS and EFS (p<0.001). SUVmax was not prognostic for any of the clinical endpoints (p>0.15). Among the clinical parameters, T-stage, N-stage, and UICC-stage were prognostic for OS and EFS (p=0.001-0.02). In multivariate analysis, MTV remained a significant factor indicating its independent prognostic value. ASP was independent of clinical parameters (p=0.024-0.049) but not independent of MTV (p=0.12-0.23). ***Conclusion:*** In the investigated group of patients with esophageal carcinoma, ASP of the pretherapeutic FDG uptake pattern in the primary tumor adds prognostic information to clinical parameters but not to MTV. ***References:*** None

EP-100

DNA synthesis PET imaging with 4DST: A radiomics approach for predicting prognosis in patients with esophageal cancer

M. Hotta*, R. Minamimoto, K. Yamada;*
National Center for Global Health and Medicine, Tokyo, JAPAN.

Aim/Introduction: 4′-[methyl-11C] thiothymidine (4DST) has been developed as a cell proliferation imaging positron emission tomography (PET) tracer that directly incorporates into DNA. The aim of this study was to investigate whether a radiomics approach using 4DST PET/computed tomography (CT) is helpful for predicting prognosis in patients with esophageal cancer compared to fluorodeoxyglucose (FDG) PET/CT. ***Materials and Methods:*** This prospective study was approved by the Institutional Ethics Review Board. Between August 2015 and October 2018, 74 patients with pathologically proven esophageal cancer underwent 4DST PET/CT. Among them, 49 patients (44 men and 5 women; mean age, 67.9 ± 10.0 years) who underwent pretreatment 4DST and FDG PET/CT were used for the analysis. To obtain the volume of interest of the primary tumor, a three-dimensional sphere was set to encompass the lesion; the area showing a threshold of 40% of the maximum standardized uptake value was contoured; and PET features including conventional features and global, local, and regional textural features were measured. The study endpoint was overall survival (OS). Important PET features for predicting cancer-related death were selected using a machine-learning method: the Boruta algorithm. The selected features were evaluated based on Kaplan-Meier analysis and Cox proportional hazards regression analysis after determining the optimal cut-off value based on receiver-operating characteristic curve analysis. ***Results:*** Twenty patients died during the follow-up period [median 19.4 (interquartile range: 10.1-30.7) months]. Among all 4DST PET features, kurtosis and skewness were selected as statistically significant prognostic factors, and kurtosis was the most important feature, whereas none of the FDG PET features showed statistical significance in the feature selection. Patients with high 4DST kurtosis (>3.37) showed significantly short OS (log-rank p-value = 0.008; hazard ratio = 1.61). 4DST kurtosis was an independent statistically significant prognostic factor in multivariate analysis of clinical features including clinical stage, treatment method, and histological type. ***Conclusion:*** Radiomics features of

4DST PET are helpful for predicting prognosis in patients with esophageal cancer. Higher 4DST kurtosis, which potentially represents intratumoral heterogeneity, can lead to poor prognosis. ***References:*** None

EP-101

Digital vs Analog PET/CT in the detection of liver metastases

F. Fuentes-Ocampo*, D. López-Mora, A. Flotats, M. Sizova, S. Abouzian, V. Camacho, A. Fernández, M. Estorch, J. Duch, A. Domènech, I. Carrió;*
Hospital de la Santa Creu i Sant Pau, Barcelona, SPAIN.

Aim/Introduction: To determine if digital PET/CT improves liver lesion detectability in patients with known or suspected liver metastases. ***Materials and Methods:*** Eighty-three oncological patients were prospectively included from February 2018 - October 2019 (42 women, mean age 69 ± 11 years) with one of the following criteria: previous history or liver metastases, risk of presenting liver metastases and/or presence of at least one liver lesion in the first scan performed (digital or analog). All patients underwent a dual imaging protocol (digital and analog PET/CT) during the same day. The order of acquisition was aleatory: the digital PET/CT was performed first in 43 patients (group 1) and the analog PET/CT first in 40 patients (group 2). Three nuclear medicine physicians assessed and counted liver lesions suspicious of malignancy. ***Results:*** The mean number of liver lesions detected per patient by the digital PET/CT was significantly higher than the analog PET/CT (digital: 3.25±4.03 vs. analog: 2.49±3.20; P<0.001). We found no statistically significant difference in the time delay between scans of groups 1 and 2. Sixty-seven patients were considered positive for liver lesions by any PET/CT. The digital PET/CT detected more liver lesions than the analog PET/CT in 30/67 patients (45%), of whom 11/30 patients (16%) only had lesions detected by the digital system. The analog PET/CT detected more liver lesions in only 2/67 patients (3%). Thirty-five patients had the same number of liver lesions detected by both systems and 16 patients were considered negative for liver lesions. A total of 32 patients had different number of liver lesions detected between both PET/CT. In 7/32 patients (22%) their oncological disease upstaged due to the increased detectability by the digital system. In the remaining 25/32 patients (78%) their disease staging was not modified. ***Conclusion:*** Digital PET/CT offers higher liver lesion detectability in patients with known or suspected liver metastases. ***References:*** None

EP-102

Usefulness of regionally different cut-off SUVmax of the lymph nodes for the N staging of esophageal cancer

K. Takahashi[1]*, K. Takanami*[2]*, K. Takase*[2]*, T. Kamei*[1]*;*
[1]*Department of surgery, Tohoku University, Sendai, JAPAN,* [2]*Department of Diagnostic Radiology, Tohoku University Hospital, Sendai, JAPAN.*

Aim/Introduction: Although F-18 Fluorodeoxy-glucose (FDG) PET/CT is useful for the diagnosis of lymph node (LN) metastasis of esophageal cancer, it is often difficult to differentiate the FDG avid LNs as a reaction to inflammation from metastatic LNs and the inflammation might be different at each region. The aim of this study was to determine the usefulness of regionally different cut-off SUVmax of the lymph nodes (LNs) for N staging of esophageal cancer. ***Materials and Methods:*** We retrospectively reviewed a clinical data in our institution. This study included the patients with thoracic esophageal cancer who had undergone F-18 FDG PET/CT and contrast-enhanced CT (CE-CT) before radical esophagectomy with two- or three-field node dissection. We measured a nodal short-axis diameter on CE-CT image and a SUVmax of the LNs on PET/CT image. The LN regions were divided to "upper thoracic", "middle to lower thoracic" and "abdominal" regions. The common cut-off SUVmax and the regionally different cut-off SUVmax at each region of the LNs for detecting LN metastases were determined using receiver operating characteristic (ROC) analysis. Diagnostic accuracy in the metastatic LNs using the common cut-off SUVmax was compared with that using the regionally different cut-off SUVmax. ***Results:*** In this study, we included 216 LNs in 75 patients and identified 42 metastatic LNs in 27 patients. The short axis diameter and SUVmax were 8.65±3.31 mm and 5.41±3.96 for the metastatic LNs and 5.53±1.71 mm and 1.94±1.44 for the non-metastatic ones, respectively. The numbers of the metastatic LNs and non-metastatic ones were 15 and 91 at the upper thoracic region, 7 and 40 at the middle to lower thoracic region and 20 and 43 at the abdominal region, respectively. The SUVmax did not differ significantly among the three groups (Kruskal-Wallis test). Based on the ROC analysis, the common cut-off SUVmax was 2.61, and the regional cut-off SUVmax at upper thoracic, middle to lower thoracic and lower thoracic region, were 4.33, 3.36 and 2.40, respectively. The overall accuracy for detecting LN metastases was improved from 0.80 to 0.87 by using the regionally different cut-off SUVmax. ***Conclusion:*** Regionally different cut-off SUVmax of the lymph nodes may be useful for the N staging of esophageal cancer. ***References:*** None

EP-103

The Relationship Between Microsattelite Instability and ^{18}F-FDG PET / CT Parameters in Colorectal Cancer Patients

Z. Hasbek[1], *N. Demir*[2], *M. Yılmaz*[1], *H. Özer*[1], *S. A. Ertürk*[1], *Ö. Ulaş Babacan*[1], *F. Arslan*[1];
[1]*Sivas Cumhuriyet University School of Medicine, Sivas, TURKEY,* [2]*Sivas Medicana Hospital, Sivas, TURKEY.*

Aim/Introduction: Microsatellite Instability (MSI) is due to incompatibilities in the DNA repair mechanism (mismatch repair) caused by DNA replication errors resulting from the accumulation of somatic changes in nucleotide repeat sequences which are called microsatellites and some of these changes occur in gene promoter regions.MSI is considered stable (MSS) when patients without unstable marker.The effectiveness of immunotherapy is lower in patients with MSS colorectal cancer.Our aim in this study was to evaluate the relationship between MSI status and ^{18}F-FDG PET / CT parameters in patients with colorectal cancer. ***Materials and Methods:*** There were 58 patients (39M / 19F, mean age: 63; range: 41-89) with colorectal adenocarcinoma in this study.In the immunohistochemical examination,nuclear staining was considered positive for all antibodies.Normal colon mucosa and lymphocytes in tissue were used as an internal positive control group.The absence of nuclear staining in tumor cells was considered "loss" in "Mismatch Repair Gen" proteins.MSI status of the patients was divided into 3 groups according to the number of MSI genes.The first group was determined as patients without MSI (MSS),the second group as MSI with only 1 gene (MSI-L), and the third group with MSI with 2 or more genes (MSI-H).The relationship between MSI status and both PET parameters and clinicopathological data were evaluated. ***Results:*** MSI was not observed in 46 (79.3%) of 58 patients in the study.The incidence of MSI was low (MSH-L) in 4 patients (6.9%) and high in 8 patients (13.8%) (MSH-H).There was a statistically significant relationship between MSI status and SUVmax value (p = 0.02).In patients with MSI-H, the median SUVmax value was higher than MSS and MSI-L patients (18, 14.75, 14, respectively).In addition, although not statistically significant, the rate of distant metastasis in PET / CT was higher in patients without MSI (p = 0.082) (Table 1).17.2% of our patients had a family history of colorectal cancer. There was no statistically significant relationship between family history and MSI (p = 0.141). ***Conclusion:*** In our study, although it was not statistically significant the rate of distant metastasis in PET / CT was found lower in patients with high MSI.In addition, SUVmax values were found to be higher in patients with high MSI.In our literature review,although a positive correlation was reported between MSI and SUVmax values in gastric cancers,we think that the results of our study are valuable since no studies evaluating MSI and PET / CT data in colorectal cancers were found. ***References:*** None

EP-16

Imaging Clinical Studies -> Oncological Imaging Clinical Study -> Gynaecological

e-Poster Area

EP-104

PET and cervical cancer: staging and therapeutic impact

A. Hind, *H. Hajar;*
Faculty of Medicine, Casablanca, MOROCCO.

Aim/Introduction: Cervical cancer is the second most common cancer in the world after breast cancer. The most disadvantaged countries are the most affected by this disease. The aim of our work is to study, in our context, the role of PET in staging the disease and its impact on therapeutic decision in patients with cervical cancer. ***Materials and Methods:*** We conducted a descriptive study including patients with cervical cancer referred for treatment to Mohammed VI cancer center at university hospital IBN ROCHD in Casablanca, between January 2017 and December 2018 and explored with PET-CT. ***Results:*** We included 39 women (among 284 referred during this period). The mean age was 52 years +/- 11.5 years. PET has shown its superiority by making a contribution to other explorations (CT and MRI) in the assessment of lymph node invasion. (77% vs 48% respectively) in the pelvic region, and (20% vs 14% respectively) in the lumbo-aortic region. A secondary localization was revealed by PET in 26% of cases (lymph nodes, bone and parietal), with a change in the stage of the disease (Up staging to IVB) and therefore an impact on the therapeutic management. Morever, PET revealed intercurrent pathologies in 20% of cases. ***Conclusion:*** If MRI remains essential in the assessment of local extension of cervical cancer, PET is very effective in the evaluation of pelvic and lombo-aortic lymph node involvement, as well as in the distant metastasis detection. ***References:*** 1. Liu B, Gao S, Li S. A Comprehensive Comparison of CT, MRI, Positron Emission Tomography or Positron Emission Tomography/CT, and Diffusion Weighted Imaging-MRI for Detecting the Lymph Nodes Metastases in Patients with Cervical Cancer: A Meta-Analysis Based on 67 Studies. Gynecol Obstet Invest. 2017;82(3):20922. 2. Stecco A, Buemi F, Cassarà A, Matheoud R, Sacchetti GM, Arnulfo A, et al. Comparison of retrospective PET and MRI-DWI (PET/MRI-DWI) image fusion with PET/CT and MRI-DWI in detection of cervical and endometrial cancer lymph node metastases. Radiol Med (Torino). juill 2016;121(7):53745. 3. Yang Z, Xu W, Ma Y, Liu K, Li Y, Wang D. (18)F-FDG PET/CT can correct the clinical stages and predict pathological parameters before operation in cervical cancer. Eur J Radiol. mai 2016;85(5):87784. 4. Morkel M, Ellmann A, Warwick J, Simonds H. Evaluating the Role of F-18 Fluorodeoxyglucose

Positron Emission Tomography/Computed Tomography Scanning in the Staging of Patients With Stage IIIB Cervical Carcinoma and the Impact on Treatment Decisions. J Int Gynecol Cancer Soc. 2018;28(2):37984.

EP-105

Role of earlyFDG PET/CT at 6 weeks for the prediction of response in cervical cancer treated with chemoradiotherapy

I. Zerizer[1], *A. Divoli*[1], *S. Chua*[1], *A. Parsai*[2];
[1]*Royal Marsden Hospital, London, UNITED KINGDOM,*
[2]*Barts Healthcare, London, UNITED KINGDOM.*

Aim/Introduction: We have evaluated the role of early FDG PET/CT performed at 6 weeks following chemotherapy and external beam radiotherapy in predicting final response in patients with advanced cervical cancer (CC) ***Materials and Methods:*** 43 female patients had a PET/CT(1) for staging, PET/CT(2) 6 weeks after platinum-based chemotherapy and external beam radiotherapy (prior to brachytherapy) and an end of treatment PET/CT(3) 3 months after completion of chemoradiotherapy. Maximal and peak standardized uptake values ($SUV_{max,}$ SUVp), size and volumes were measured on each PET/CT and percentage differences in ΔSUV_{max}, ΔSUVp, size and metabolic volumes between responders (R) and non-responders (NR) were calculated between the baseline PET/CT(1) and early PET/CT(2) as well as PET/CT(1) and end of treatment PET/CT(3). ***Results:*** Final treatment response as determined by the end of treatment response PET/CT(3) at 3 months revealed 32 patients as responders (R) having reached a complete metabolic response, 11 patients as non-responders (NR) with 10 having had a partial metabolic response and 1 progressing with new disease outside the pelvis. On the early PET/CT (2), the ΔSUV_{max}% and ΔSUVp % were significantly higher in the R (65-97%) compared with the NR (22-64%) and correlated with the ΔSUV_{max}% and ΔSUVp % on the end of treatment PET/CT(3) ($P<0.001$, $P<0.002$ respectively). Similarly the percentage difference in metabolic volume was highly predictive of an early response with a marked decrease in volume of the primary tumour on the early PET/CT(2) in R (56-100%) compared with NR (15-55%), which also correlated with the end of treatment response ($P<0.001$). However difference in tumour size did not correlate with a response on the early PET/CT(2) or end of treatment PET/CT (3). ***Conclusion:*** An early PET/CT performed at 6 weeks following induction chemotherapy and external beam radiotherapy for CC is predictive of a final response on the end of treatment PET/CT. This provides valuable information on early tumour response in CC and can identify NR early with the possibility of treatment intensification and escalation. ***References:*** None

EP-106

Correlation between tumor biological parameters at diagnosis and response to chemo-radiation therapy in cervical cancer patients

O. Kagna*, R. Abdah-Bortnyak, Z. Keidar;*
Rambam Health Care Campus, Haifa, ISRAEL.

Aim/Introduction: Cervical cancer is the fourth most common cancer among women both in incidence and in mortality. The treatment of choice in locally advanced cervical cancer is a combination of radiation with chemotherapy. However, 20-40% of patients do not achieve complete response. FDG PET/CT is a major diagnostic tool in the management of cervical cancer. The aim of this study was to assess the ability of quantitative pre-treatment FDG-PET/CT parameters to predict treatment response in newly diagnosed cervical carcinoma patients. ***Materials and Methods:*** 93 cervical carcinoma patients (29-85 years), were retrospectively enrolled in the study. All patients underwent FDG PET/CT scan at diagnosis and 3 months after treatment completion. For each patient demographical-biological parameters, treatment regimens (radiation and chemotherapy dosages) and metabolic-radiological parameters of the tumor at diagnosis and after completion of treatment (including tumor SUV max, SUVmean, primary tumor and metastatic lymph nodes size) were recorded. A complete response of the primary tumor was defined as no FDG uptake in the cervix on post treatment PET/CT. Based on this definition, the patients were divided into complete response (CR) and non-complete response (Non-CR) groups. ***Results:*** Primary tumor SUV max, SUV mean and tumor size measurements were found to be significantly lower in the CR group in comparison to the non-CR group. No statistically significant difference however was observed between these groups regarding the same parameters measured in metastatic lymph nodes. In addition, no satisfactory PET/CT derived parameters threshold in the primary tumor that enables distinguishing responders from non-responders could be established. Histologically, 73 patients had squamous cell carcinoma, 11 had adenocarcinoma and in 9 patients the tumor type record was not available. The complete response rate was 77% in patients with squamous cell carcinoma and 64% in those with adenocarcinoma. A sub-group of 14 (15%) patients had achieved complete response in the primary tumor but had metabolically active metastatic lymph nodes or distant metastases after completion of therapy. In this group patient age, lymph nodes SUVmax/mean, and size at diagnosis were significantly higher in comparison to the same parameters in those patients who achieved complete metastatic response. ***Conclusion:*** Primary tumor metabolic parameters at diagnosis were found to be associated to complete tumor response rate. Parameters related to lymph nodes involvement however, are not significantly associated to the primary tumor

treatment response. These finding might indicate that the primary tumor and its metastases may response differently. ***References:*** None

EP-107

FDG-PET/CT Leads A Better Target Volume Definition In Radiotherapy Of Locally Advanced Cervical Cancer

A. Palucci[1], *L. Vicenzi*[2], *C. Romagnolo*[1], *M. di Benedetto*[2], *G. Biscontini*[1], *F. Fringuelli*[1], *C. Cottignoli*[1], *F. Cucciarelli*[2], *G. Mantello*[2], *L. Burroni*[1];
[1]*Nuclear Medicine, Ancona, ITALY,* [2]*Radiotherapy Department, Ancona, ITALY.*

Aim/Introduction: Concurrent chemo-radiotherapy is the elective therapeutic strategy in locally advanced cervical cancer. CT and MRI are routinely performed at diagnosis to evaluate disease extension. In our study, we assessed the impact of ^{18}FDG-PET/CT acquired before radiotherapy in optimizing dose and volume prescription. ***Materials and Methods:*** 43 patients (pts) with locally advanced cervical carcinoma, treated between December 2015 and April 2020, were retrospectively analyzed. All patients underwent definitive Intensity Modulated Radiotherapy (IMRT) of pelvis +/- para-aortic region, followed by brachytherapy. All patients received Platinum based concomitant chemotherapy. CT was assessed in 35 patients and MRI in 41 patients. All the 43 patients underwent planning ^{18}FDG-PET/CT. The total delivered dose was 45-50.4 Gy, 1.8 Gy/fr on the pelvis +/- paraaortic region and 54 Gy (50-56 Gy , 2-2.16 Gy/fr) with simultaneous integrated boost (SIB) on ^{18}FDG-PET/CT positive nodes. ***Results:*** Local lymph nodal involvement was identified in 29 patients (67%). In 11 patients (26%), ^{18}FDG-PET/CT showed pelvic positive lymph nodes in one or more areas, not detected in the other imaging techniques (PET+, CT SCAN- , MRI-): common iliac lymph nodes (LN) were shown in 3 pts, internal iliac LN in 4 pts, obturator LN in 4 pts, external iliac LN in 3 pts and perirectal LN in 2 patients. Radiotherapy Clinical Target Volume (CTV) was modified including para-aortic region in 8 patients with metabolically active nodes not evidenced in CT and MRI reports. ***Conclusion:*** In our experience, ^{18}FDG-PET/CT leads to a better definition of the target volume, playing a crucial role in dose escalation and organ at risk sparing. ***References:*** None

EP-108

PET/CT in calcified metastatic ovarian serous papillary cystadenocarcinoma, mimicking a benign lesion on CT: two case reports

Z. Dancheva[1], *A. Konsulova*[2], *P. Bochev*[3], *B. Chaushev*[1], *M. Dyankova*[1], *T. Yordanova*[1], *A. Klisarova*[1];
[1]*St Marina University Hospital, Varna, BULGARIA,* [2]*Department of Oncology, Complex Oncological Centre, Burgas, BULGARIA,* [3]*Acibadem Cityclinik Oncology center Sofia, Sofia, BULGARIA.*

Aim/Introduction: Calcification is detected in 8% of all ovarian carcinomas and ~12% of serous ovarian tumours on computer tomography (CT) but is nonspecific as it may also be seen in benign serous tumours, following chemotherapy or in granulomatous diseases. The ability of PET/CT for metabolic activity assessment and the knowledge to expect a disease progression in calcified lesions could guide the biopsy, prompting initiation of treatment in patients with progressive ovarian carcinoma. ***Materials and Methods:*** We present two cases of patients with serous papillary ovarian carcinoma with calcified lesions. ***Results:*** During follow-up, both patients had progressive elevation of their tumor marker (Ca-125), and no other suggestion of progression, detected by clinical or conventional radiological imaging. CT findings included generalized lymphadenopathy, presented with small to medium size lymph nodes with calcifications and pleural masses with calcifications, initially falsely interpreted by CT as benign. Subsequently, patients were followed up by CT scans and no progression by RECIST criteria was registered. In view of the progressive CA 125 dynamics, a PET/CT was organized and it was helpful to identify disease progressionin both patients. PET/CT also identified a biopsy site for histological confirmationof the disease progression. In both cases we observed similar findings -calcified lymph nodes and pleural masses presented with increased metabolic activity up to SUVmax 10.4. In general, serous ovarian cancer metastases rarely present with calcifications in contrast to metastatic lymph nodes in osteosarcoma, tuberculosis, silicosis, treated lymphoma, medullary thyroid carcinoma or colorectal mucinous adenocarcinoma. Large calcified pleural masses could be seen in tuberculosis, osteosarcoma, chondrosarcoma, mucinous adenocarcinoma types, etc. Although in ovarian carcinoma with progressively rising tumor marker, calcified lymph nodes and soft tissue masses might be taken into account and further examined. ***Conclusion:*** Calcified metastatic ovarian carcinoma may becomeма pitfall in CT imaging and RECIST criteria are unreliable in follow up of this kind of metastatic tumors as they only rely on dynamics of size. PET/CT lead to diagnosis of disease progression and identified the site for biopsy, thus prompting subsequent treatment in patients with progressive disease.It is an important diagnostic modality in elevated tumor marker and negative CT studies in ovarian carcinoma. ***References:*** Burkill G, Allen S, A'hern R, Gore M, Significance of tumour calcification in ovarian carcinoma., Br J Radiol. 2009 Aug;82(980):640-4.Michail P, Amith I, George S, George MK., A case of calcified metastatic colorectal adenocarcinoma mimicking a benign lesion: pitfalls in diagnosis, Case Rep Oncol Med.2015

EP-17

Imaging Clinical Studies -> Oncological Imaging Clinical Study -> Head and Neck

e-Poster Area

EP-109

Detection of Second Primary Tumors in patients with head and neck cancers using FDG PET/CT as a screening imaging tool

T. Yordanova[1], A. Klisarova[1], B. Chaushev[1], T. Stoewa[1], Z. Dancheva[1], S. Chausheva[1], M. Dyankova[1], N. Sapundzhiev[2]; [1]Medical University Prof. dr P.Stoyanov, Department of nuclear medicine, Varna, BULGARIA, [2]Medical University Prof. dr P.Stoyanov, Department of neurosurgery and ENT diseases, Varna, BULGARIA.

Aim/Introduction: The purpuse of this study was to assess the efficacy of 18F fluorodeoxyglucose positron emission tomography and computed tomography (PET/CT) in detecting second primary tumors in patients with head and neck cancers (HNC). ***Materials and Methods:*** Retrospectively we analyzed 120 patients with initial HNC diagnosed between 2015-2017. The selected patients were with previous untreated HNC referred for FDG-PET/CT for staging and detection of unexpected second primary malignant neoplasms. The diagnoses of malignancy were confirmed with hystopathology and imaging. ***Results:*** Nine second primary malignancy were identified from 120 patients. FDG-PET/CT correctly identifed unexpected second primary cancers in 8 of these 9 patients, there was 1 false positive result. Most common localisation of the second primary malignancy were colorectal region 50%, thyroid gland 12.5%, lung 12.5%, head and neck 12.5% and renal 12.5%. FDG-PET/CT showed a sensitivity of 100%, a specificity of 99%, a positive predictive value 88.9%, a negative predictive value 100% and accuracy 99% identifying additional primary malignant neoplasms. ***Conclusion:*** The non-invasive whole body FDG-PET/CT is an useful as a screening imaging tool for detecting unexpected second primary malignancy in patients with Head and neck tumors. ***References:*** None

EP-110

Usefulness of MTV, TLG and SUVmax as predictive values of the response to definitive chemo-radiotherapy treatment in head and neck tumors

A. Santos Bueno[1,2], M. Guite Moreno[1,2], L. Rodriguez Perez[1], A. Herrero Muñoz[3], J. Gutierrez Jodas[1], M. Albala Gonzalez[1,2]; [1]Hospital Universitario Reina Sofía, Córdoba, SPAIN, [2]IMIBIC, Córdoba, SPAIN, [3]Facultad de Medicina. Universidad de Córdoba, Córdoba, SPAIN.

Aim/Introduction: To assess the usefulness of tumor metabolic volume (MTV), total lesion glycolysis (TLG) and SUV maximum (SUVmax) as predictors of the response to treatment in patients with head and neck tumors and the threshold value in which they present the highest diagnostic value. ***Materials and Methods:*** Retrospective study that includes 30 patients (27 males and 3 females) with a mean of age of 59.6 years old (range 42-72) who were diagnosed with head and neck cancer and underwent treatment with definitive chemo-radiotherapy. The response to the treatment was assessed in all cases by PET-CT 12 weeks after the end of treatment. Patients were labelled in two categories: whether they presented a complete response (responder group) or did not present it (non-responder group) (22 and 8 respectively). The SUVmax value and the MTV and TLG values, were measured in pre-treatment PET-CT by a VOI sphere with a threshold value of 40%, 45% and 50% of the SUVmax in the primary lesion. We performed hypothesis testing using the Mann-Whitney U test between each threshold value of MTV, TLG and SUVmax and the responder /non-responder groups, with a statistical significance value of $p < 0.05$. Receiver operating characteristic (ROC) curve analysis was accomplished to obtain optimal predictive cut-off values. ***Results:*** We found statistically significant differences ($p < 0.05$) of the MTV and TLG values in all the threshold values (40, 45 and 50%) between the responder group and the non-responder group, while the SUVmax value was not significant ($p = 0.056$). Analyzing the ROC curves of each of the threshold values of MTV and TLG, we found that all of them have an AUC (area under the curve) value greater than 0.79; being the highest one the MTV45 (AUC = 0.84; sensitivity 0.77, specificity 0.76, for a cut-off point value of 8.27). SUVmax AUC is 0.7 (sensitivity 0.66, specificity 0.8, for a cut-off point value of 18.85). ***Conclusion:*** Both MTV and TLG are good predictors of the response to treatment with definitive chemo-radiotherapy in patients with head and neck tumors, with the value of MTV45 showing the highest AUC value. ***References:*** None

EP-111

Comparison between the efficacy of physical examination/endoscopy with the efficacy of FDG-PET/CT for the identification of recurrence in head and neck squamous cell carcinoma after curative treatment

T. Yordanova[1], A. Klisarova[1], B. Chaushev[1], T. Stoewa[1], Z. Dancheva[1], S. Chausheva[1], M. Dyankova[1], N. Sapundzhiev[2]; [1]Medical University Prof. dr. P. Stoyanov, Deparment of nuclear medicine, Varna, BULGARIA, [2]Medical University Prof. dr P.Stoyanov, Department of neurosurgery and ENT diseases, Varna, BULGARIA.

Aim/Introduction: The aim of our study was to compare the efficacy of physical examination/endoscopy (PE/E) with the efficacy of fluorodeoxyglucose (FDG)-positron

emission tomography/computer tomography (PET)/CT) for the detection of recurrence in head and neck squamous cell carcinoma (HNSCC) after curative treatment. ***Materials and Methods:*** We retrospectively reviewed total 21 curatively treated patients with primary head and neck squamous cell carcinoma. They were referred to Medical University Department of nuclear medicine Varna Bulgaria in the period 2015- 2017. All patients underwent physical examination/endoscopy and FDG-PET/CT scan during their follow-up period. The final diagnosis of local recurrence were confirmed by hystopathology report. ***Results:*** PET/CT correctly identified local recurrence of the head and neck squamous cell carcinoma in 16 cases, 1 false positive and 4 true negative findings, there were no false negative results. Physical examination/endoscopy demonstrated 13 true-positive, 5 false positive, 3 false negative and 0 true-negative findings in a patient-basis. The sensitivity, specificity, accuracy, positive and negative predictive values for detecting local recurrence were 100%, 80%, 95%, 94% and 100%, respectively, for PET/CT versus 81%, 0%, 62%, 72%, and 0%, respectively, for PE/E. FDG- PET/CT scan identified sites suggestive local recurrence of HNSCC in 17 patients. The malignancy was located in the following localizations: larynx (n=6), nasopharynx (n=2), oropharynx (n=3) and oral cavity (n=6). ***Conclusion:*** FDG PET/CT has a high sensitivity and negative predictive value in the identification of the local recurrence in patients with head and neck squamous cell carcinoma and it is effective non-invasive method even if there is a diagnostic doubt after physical examination/endoscopy. ***References:*** None

EP-18

Imaging Clinical Studies -> Oncological Imaging Clinical Study -> Lung (including Mesothelioma)

e-Poster Area

EP-112

Study on the Relationship Between SUVmax in F-18-FDG PET/CT and Expression of Ki-67 in Patients with Non-small Cell Lung Cancer

R. Wang[1,2], X. Liao[1], M. Liu[1], Y. Cui[1], Y. Fan[1], J. Zhang[1], X. Zhang[1], L. Di[1], Q. Jiang[1];
[1]Peking University First Hospital, Beijing, CHINA, [2]Peking University International Hospital, Beijing, CHINA.

Aim/Introduction: To investigate the association between the preoperative maximum standardized uptake value (SUVmax) of primary lesions measured on 18F-fluorodeoxyglucose positron emission tomography/computed tomography (F-18-FDG PET/CT) and expression of Ki-67 labeling index (Ki-67) in patients with non-small cell lung cancer (NSCLC). ***Materials and Methods:*** One hundred and eleven patients with NSCLC received surgical treatment and the F-18-FDG PET/CT examination was performed preoperatively. The SUVmax values of F-18-FDG PET/CT were estimated, and the expression of Ki-67 in cancer tissue was detected with histoimmunochemistry SP method. The association between SUVmax and Ki-67 expression, and the association of dichotomized SUVmax (2.5), mean SUVmax and median SUVmax with Ki-67 was analyzed with multivariate Logistic regression, respectively. ***Results:*** Multiple linear regression showed regardless of pathological subtypes, TNM stage and maximum diameter of primary lesion, Ki-67 and SUVmax displayed a moderate correlation (r=0.66). In acinar predominant adenocarcinoma, N0 or N1-3, SUVmax was significantly correlated with Ki-67. Dichotomous SUVmax (cutoff point:2.5) was significantly associated with Ki-67 (P=0.01). ***Conclusion:*** A moderate relationship exists between the SUVmax values and Ki-67 expression. SUVmax ≥2.5 of primary lesion may suggest active tumor proliferation and poor prognosis of patients with NSCLC. ***References:*** None

EP-113

Evaluation of Different Registration Landmarks for Thoracic MR-PET/CT Fusion Using High-Frequency Non-Invasive Ventilation (HF-NIV) for Lung Nodule Assessment

M. Jreige*, M. Neury, M. Nicod Lalonde, N. Schaefer, E. Darçot, C. Beigelman, J. O. Prior;*
Lausanne University Hospital, Lausanne, SWITZERLAND.

Aim/Introduction: To evaluate the co-registration of thoracic MR and PET/CT images acquired under HF-NIV and assess the effect of this ventilation technique in providing reproducible lung volume that would optimize sequential image fusion and thus allow the feasibility of low-cost, virtual thoracic PET/MR imaging. ***Materials and Methods:*** Four patients known for a suspicious lung nodule underwent both PET/CT and MR under HF-NIV. On both HF-NIV axial MR and CT images, eleven thoracic anatomical landmarks were manually located, including the lesion center, using landmark co-registration application (AW workstation, GEMS). For each pair of landmarks, mean and maximum co-registration errors were calculated for fusion of HF-NIV-MR with either HF-NIV-CT or free-breathing-(FB)-CT of PET/CT. Co-registration of HF-NIV-CT and an undersampled-HF-NIV-MR reconstruction using only movement-free raw data were tested in cases of significant respiratory motion (n=3). ***Results:*** For the 11-thoracic landmarks, the mean and maximum co-registration errors were 20.6±7.3 and 32.8±13.9 mm in HF-NIV-MR/FB-CT; 8.0±2.9 and 15.6±7.1 mm in HF-NIV-MR/HF-NIV-CT; 6.4±3.1 and 12.3±7.8 mm in undersampled-HF-NIV-MR/HF-NIV-CT. Mean lesion co-registration error was 16.3±6.0 mm, 5.3±3.2

mm and 5.0±4.2 mm in HF-NIV-MR/FB-CT, HF-NIV-MR/HF-NIV/CT and resampled-HF-NIV-MR/HF-NIV-CT, respectively. HF-NIV allowed to reduce co-registration error by 61%, 52%, 68% for mean, maximum and pulmonary lesion errors, reaching 69%, 62% and 70% with HF-NIV-MR motion-free-sampling. ***Conclusion:*** We showed a notable error reduction of sequential thoracic PET/CT and MR co-registration using HF-NIV. This optimization of thoracic HF-NIV-PET/MRI fusion for assessing lung nodules has the advantage of creating a low-cost hybrid "PET/MR" from sequential, separate PET-MR acquisitions, which allows for easier accessibility and better hybrid fusion results. ***References:*** None

EP-114

Diagnostic effect of benign lung changes in initial cancer staging with F-18 FDG PET/CT. The Kwa-Zulu Natal experience

N. Nyakale[1,2], J. Kabunda[2], C. Kalinda[3,2], L. Harry1[2], P. Ramdass[2], T. Ebrahim[2];
[1]Sefako Makgatho Health Sciences University, Pretoria, SOUTH AFRICA, [2]University of Kwa-Zulu Natal, Durban, SOUTH AFRICA, [3]University of Namibia, Namibia, SOUTH AFRICA.

Aim/Introduction: The incidence of lung pathology in sub-Saharan Africa is high due to the high prevalence of pulmonary infections and inflammatory disorders including granulomatous diseases such as tuberculosis or sarcoidosis. This is known to compromise evaluation of metastatic lung involvement when staging patients with malignancy. The aim of this study was to determine the ability of a single phase PET to characterize lung disease involvement during the staging of treatment naïve cancer patients in our patient population in Kwa-Zulu Natal. ***Materials and Methods:*** A retrospective analysis of patients referred for initial staging of cancer with F-18 FDG PET/CT scan in the period between 2014 and 2017. The PET and CT lung findings, reported by an experienced Nuclear Physician and Radiologist respectively, were recorded and confirmatory findings were assessed based on pathological results and /or follow-up imaging. Lung findings were classified as benign, metastases or equivocal. Patients with lung cancer, no confirmed primary or no histological confirmation of malignancy were excluded. Data obtained was analysed by comparing the level of agreement between the PET and CT lung findings using the variance-ratio test and concordance correlation tests. ***Results:*** A total of 326 patients (180 females, 146 males) with a mean age (±SD) of 50.9±16.5 were included. The cancer types were variable with the most common being lymphoma, oesophagus and breast cancer. There was no FDG uptake noted in the lungs in 55% of patients, no CT changes were noted in 32%. The PET scan reported lung metastases in 28% (n=91), benign changes in 12% (n=40) and equivocal in 4.6% (n=15) of patients. The CT reported the lung metastases in 29% (n=96), benign changes in 23% (n=74) and equivocal in 15% (n=49) of patients. The mean SUVmax in metastases was 7.5±0.598 while reported benign disease was 3.88±0.615. Using the variance ratio test, statistical differences were observed in the PET and CT lung findings ($F_{325, 325}$=0.6672, P=0.003). There was no concordance achieved in the PET with the CT lung findings (rho-c=0.348, 95% CI: 0.266-0.430, p≤0.001) nor with the final diagnosis (rho-c =0.341, 95%CI: 0.245-0.437, p≤ 0.001). ***Conclusion:*** PET findings are not able to successfully characterize the changes in the lungs at initial staging of cancer patients due to the high prevalence of pulmonary infection and inflammation in the Kwa-Zulu Natal population and require anatomical description as well as histological confirmation to increase specificity. ***References:*** To be provided during the presentation

EP-115

Semi-quantitative analysis of ^{18}F-FDG PET/CT in single pulmonary lesion: the role of blood glucose level and body mass index normalization

A. Capozza[1], *C. Dolci[1], A. Scarale[1], A. Franchini[2], I. Gotuzzo[2], E. Gay[1], G. Cabrini[1], M. Milella[1], C. Rossetti[1];*
[1]Nuclear Medicine Unit, ASST Grande Ospedale Metropolitano Niguarda, Milan, ITALY, [2]Nuclear Medicine, University of Milano-Bicocca, Milan, ITALY.

Aim/Introduction: ^{18}F-FDG PET/CT is widely applied for metabolic characterization of pulmonary nodules. In clinical practice, FDG uptake is commonly evaluated with a standard parameter normalized by body weight, SUV_{MAX}. Nevertheless, this value is burdened by several factors that limit its reliability. Few correction factors have been proposed to overcome this limitation, such as blood glucose level (SUV_{BGL}) and body mass area (SUV_{BMI}). Aim of this study is to evaluate the accuracy of different normalization of FDG uptake, in detecting malignancy in single lung lesions, both in general population and in a sub-group of diabetic subjects. ***Materials and Methods:*** ^{18}F-FDG PET/CT scans performed, between 04/2014 and 02/2020, were retrospectively reviewed. Patients, referred to our Unit for metabolic characterization of single pulmonary lesions, were selected. Semi-quantitative analysis was performed to assess FDG uptake in pulmonary lesions; the uptake value, SUV_{MAX}, was then normalized by blood glucose level (BGL) and body mass index (BMI). Histological analysis reports, performed on bioptical or surgical samples on each patient, were collected. Student's t-test was performed to evaluate the association between malignancy of pulmonary single lesion and tracer uptake entity, normalized by body weight, BMI and glycemia. ***Results:*** Seventy-nine patients (55male/24female) were enrolled. Population had median age of 70 years (range 51-89) and mean BMI 26.2 (16.66-41.80); 11/79 (14%) patients were treated for diabetes and presented mean BGL= 131 ng/mL (90-155) pre-FDG

injection.The population was divided in two groups: benign abnormalities (n=22) vs malignant lesions (n=57), according to histopathological findings. FDG-PET/CT semi-quantitative analysis showed an overall mean SUV_{MAX}=7.76 (0.45-29.21); SUV_{MAX} 3.69 (0.45-24.97) and 9.59 (0.54-29.21) in benign and malignant group of patients, respectively. A statistically significant correlation was found between histopathological findings and all three uptake parameters evaluated, SUV_{BMI} showing a slightly less significant correlation: SUV_{MAX} p <0.01, SUV_{BGL} p <0.01 and SUV_{BMI} p= 0.03.Selecting diabetic patients, the sub-population presented mean BMI= 27.31 (28.13-29.14), with 55% (6/11) patients overweight and the remaining 5/11 in healthy BMI-range. In diabetic patients' subgroup, no significant correlation was seen between malignancy and SUV_{MAX}, nor with SUV_{BMI}: p value= 0.17 and 0.33 respectively. The only statistically significant correlation (p value= 0.01) was found between malignancy and SUV_{BGL}. ***Conclusion:*** Overall, SUV_{MAX} measured on FDG-PET shows good accuracy in differentiating benign alterations from malignancy, in pulmonary lesions. However, in diabetic population, normalizing the uptake value according to glycemia might be a more reliable method to properly identify lesions with higher malignant likelihood. ***References:*** None

EP-116

Value Of [^{18}F]FDG PET/CT In The Diagnosis Of Thoracic Lymph Node Metastasis In Non-Small Cell Lung Cancer

M. Calderón Calvente[1], *S. Álvarez Ruiz*[1], *M. Sangrós Sahún*[1], *L. Nieto Morcillo*[1], *G. Guzmán Prudencio*[1], *L. Del Barco Diez Canseco*[1], *P. Navarro Beltrán*[2], *M. Falgás Lacueva*[1], *L. De la Cueva Barrao*[1], *D. Abós Olivares*[1];
[1]*Hospital Universitario Miguel Servet, Zaragoza, SPAIN,*
[2]*hospital universitario miguel servet, Zaragoza, SPAIN.*

Aim/Introduction: To assess the diagnostic effectivity of [^{18}F] FDG PET/CT in thoracic nodal characterization of recently diagnosed patients with non-small cell lung cancer in our hospital, relating it to nodal histopathological results. ***Materials and Methods:*** Patients with non-small cell lung cancer who had PET/CT scan during initial staging (May to December 2019) were selected. Data was collected of nodal SUVmax, considering positive nodes those with SUVmax ≥2'5.When available, citohistopahological results from linfadenectomy were used as Gold Standard, using those of US guided bronchoscopy otherwise.To evaluate the results, contingency tables were constructed for each node station, assigning values for TP, TN, FP and FN. Secondly, an analysis "per station" was performed, in two groups, bronchopulmonary and mediastinal, calculating sensitivity (SE), Specificity (SP), Positive Predictive Value (PPV) Negative Predictive Value (NPV) and its 95% confidence intervals (95% CI).Finally an analysis "per patient" was performed with imaging findings that involve N2-N3 staging (any positive node in PET/CT in mediastinal or contralateral bronchopulmonary stations) according to the 8th edition of the TNM classification. ***Results:*** 43 patients were collected (mean age 68 years old, 88% men, 12% women) with non-small cell lung cancer (adenocarcinoma 53%, squamous 37%, big-cell 5%, undifferentiated 5%).When evaluating all lymph node stations, prevalence of metastasis in our sample is 25%, obtaining SE 0'81 (95%IC(0'64-0'93)), SP 0'84 (95%IC(0'77-0'92)), PPV 0'64 (95%IC(0'5-0'78)) and NPV 0'93 (95%IC(0'88-0'98)) in PET/CT's identification of nodal metastasis.When comparing bronchopulmonary and mediastinal territories, we find SE 0.75 (95%IC(0'35-0'97)), SP 0.81 (95%IC(0'64-0'93)), PPV 0.5 (95%IC(0'21-0'79)) and NPV 0.93 (95%IC(0'77-0'99)) for the former and SE 0.84 (95%IC(0'64-0'95)), SP 0.86 (95%IC(0'75-0'93)), PPV 0.7 (95%IC(0'51-0'85)) and NPV 0.93 (95%IC(0'83-0'98)) for the latter. The prevalence for positive nodes was 19'5% and 28% respectively.When analyzing "per patient", the results for the identification of patients with N2-N3 stage were SE 0'9 (95%IC(0'68-0'98)), SP 0'78(95%IC(0'56-0'92)), PPV 0'78 (95%IC(0'56-0'92)) and VPN 0'93 (95%IC(0'68-0'99)) (prevalence 46'5%). ***Conclusion:*** 1 SE and SP results of PET/CT for diagnosis of thoracic lymph node metastasis is in line with the published evidence. 2. In view of the low PPV, PET/CT positive results which establish N2-N3 staging must be citohistologicaly confirmed so as not to deprive FP patients of an appropriate curative treatment. However, we must bear in mind that some FP in our study may be due to EBUS low sensitivity. 3. Negative results allow to generally rule out node metastasis, as long as clinical suspicion (prevalence) is not high. ***References:*** None

EP-117

Lymphonodular anthracosis in patients undergoing FDG PET/CT for initial lung cancer diagnostics and/or staging is a mayor pitfall: a comparison to the histological gold standard

H. Hautzel[1], *T. Plönes*[2], *K. Darwiche*[3], *W. P. Fendler*[1], *C. Rischpler*[1], *D. Theegarten*[4], *C. Aigner*[2], *K. Herrmann*[1];
[1]*University Hospital Essen, Department of Nuclear Medicine, Essen, GERMANY,* [2]*University Medicine Essen - Ruhrlandklinik, Department of Thoracic Surgery and Thoracic Endoscopy, Essen, GERMANY,* [3]*University Medicine Essen - Ruhrlandklinik, Department of Pneumology, Division of Interventional Bronchology, Essen, GERMANY,* [4]*University Hospital Essen, Department of Pathology, Essen, GERMANY.*

Aim/Introduction: Coal miners demonstrate an increased incidence of various pneumoconioses, especially coal dust induced anthracosis. Case reports indicate that anthracosis might lead to false positive findings in FDG PET/CT for diagnosing or staging of lung cancer with regards to lymph node involvement. However, no larger series of patients with lung cancer and anthracosis undergoing FDG

PET/CT have been investigated so far. Nonetheless, the concurrent appearance of these diseases is of particular relevance in areas with coal mining industries. Aim of this study was to elucidate the diagnostic performance of FDG PET/CT in n-staging of patients synchronously suffering from lung cancer and anthracosis with respect to the histopathological gold standard. ***Materials and Methods:*** 23 patients were retrospectively identified in the period from 01/2018 to 03/2020 who were referred for FDG PET/CT imaging of previously untreated lung cancer or pleural mesothelioma, subsequently underwent either surgery (n=14), mediastinoscopy (n=4) or systematic ultrasound-guided bronchoscopic (EBUS-TBNA) lymph node sampling (n=5), and finally were diagnosed with lymph node anthracosis with or without lymph node metastasis. Per patient 12+/-6 lymph nodes were investigated. Sensitivity, specificity, accuracy, positive predictive value (PPV) and negative predictive value (NPV) of FDG PET/CT for thoracic n-staging were calculated taking the lymph node histology as gold standard. ***Results:*** In 15 of 23 patients the final diagnosis was lung cancer, in 2 of 23 pleural mesothelioma and 6 of 23 had a benign lesion. In the context of concurrent anthracosis FDG PET/CT identified lymph node malignancy with a sensitivity of 100% and NPV of 100% but with severely impaired specificity (23%), accuracy (32%) and PPV (6%). ***Conclusion:*** Due to an increased glucose consumption in thoracic lymph nodes with anthracotic changes FDG PET/CT yields a high rate of false positive results when used for n-staging of lung cancer or pleural mesothelioma. Therefore, its diagnostic accuracy is limited in patients with pulmonary malignancies and potentially coexisting anthracosis. In this specific setting only a negative FDG PET/CT is reliable in terms of an appropriate n-staging. ***References:*** None

EP-118

The relationship between the standard uptake value and the BMI in the patients with lung cancer:A study of PET-CT scans

Z. Zhao[1], S. Jia[1], J. Zhang[2], H. Yang[3];
[1]Shenzhen Yunshan Yinghe medical imaging diagnosis center, Shenzhen, CHINA, [2]Shenzhen shajing people's hospital, Shenzhen, CHINA, [3]Peking University Shenzhen Hospital, Shenzhen, CHINA.

Aim/Introduction: The standard uptake value (SUV)was widely used in the positron emission tomography (PET) examination in the patients with cancer. In general, the focal zone of the malignant tumor often has a higher SUV. As a measure of overweight ,BMI was also used to evaluate the patients' physical condition. For patients with cancer, physical condition was also important. While, the relationship between the SUV and BMI in the patients with lung cancer is not clear. In this study, we intended to explore this relationship using 18F-FDG PET. ***Materials and Methods:*** 31 patients with lung cancer were enrolled in this study. 15 of them had the BMI less than 22.4 (group 1) and 16 matched controls had the BMI more than 22.4 (group 2). All of these patients received the 18F-FDG PET/CT scanning. The SUVmax was used only in this study and it was get by the hand-painted measurement. The students t test was used to estimate the differences between groups. Nominal P values of less than 0.05 were considered to demonstrate statistically significant differences. ***Results:*** The media SUVmax was 10.57±6.86 in group 1 and 11.91±5.86 in group 2. The highest SUVmax was 25.4 in group 1 and 24.6 in group 2. The lowest SUVmax was 1.4 in group 1 and 4.9 in group 2. There was no significant difference between the two group (P = 0.565). ***Conclusion:*** This study demonstrated there was no significant difference of SUVmax between the high BMI patients and the low BMI patients with the lung cancer. As the diagnosis of these patients were same, the characteristic of PET/CT scanning were also same in spite of the difference of the BMI. That means for the patients with the same cancer, different BMI of the patients indicate the same characteristic of the cancer. This can give us more information about this disease and help us to know better about the lung cancer. ***References:*** None

EP-119

Comparison of the image quality and precision of fused lung images acquired by FDG PET/MRI with ZTE and PET/CT

J. Inukai[1], M. Nogami[1], F. Zeng[1], T. Kurimoto[2], T. Murakami[1];
[1]Department of Radiology, Kobe University Graduate School of Medicine, Kobe, JAPAN, [2]GE Healthcare, Hino, JAPAN.

Aim/Introduction: Although lung imaging by magnetic resonance imaging (MRI) remains challenging, advent of newer technologies such as pulse sequences, including zero echo-time imaging (ZTE), yields better image quality than conventional sequences. This study examined images acquired by positron emission tomography (PET)/MRI using ZTE and PET/computed tomography (CT). The image quality of normal lung structures and the precision for identifying lung lesions in fused images acquired by hybrid scanners were compared statistically. ***Materials and Methods:*** For image quality assessment, one hundred age-, sex-, and body-mass index- matched patients who underwent FDG PET/MRI (n=50) or PET/CT (n=50) were retrospectively evaluated. Normal lung structures were separately evaluated for subjective image quality in the upper and lower lung fields on two-point-Dixon T1-weighted (Dixon), ZTE, and CT images by two radiologists using a 5-point visual scoring system, followed by statistical comparison using Kruskal-Wallis test. Inter-reader agreement was tested by Cohen's kappa coefficient. To evaluate precision from the fused images, the FDG-avid lung nodules (diameter, ≦1 cm) of 118 matched patients were assessed on FDG PET/MRI (n=59) and PET/

CT (n=59) images for both lung fields. The distances of the lung lesions between PET and MRI (dist-PET/ZTE and dist-PET/Dixon) images and that between PET and CT (dist-PET/CT) images were semi-automatically calculated by measuring the distance between the coordinates of the centre of the regions of interest placed on respective lung lesions. The degree of misregistration of the lung lesions were statistically compared between dist-PET/ZTE, dist-PET/Dixon and dist-PET/CT images by Kruskal-Wallis test. ***Results:*** Image quality of normal lung structures by PET/MRI with ZTE was significantly superior to that by Dixon between both readers and in both lung fields ($p<0.000001$), but significantly inferior to CT ($p<0.000001$). A substantial agreement (weighted kappa=0.68) was firmed in the inter-rater assessments for image quality. The degrees of lung lesion misregistration with PET/Dixon (3.574±1.520 mm) and PET/ZTE (2.832±1.432 mm) were significantly smaller than that with PET/CT images (6.806±4.457 mm) ($p<0.0001$ and $p=0.0006$, respectively) in lower lung fields. The upper lung fields showed no significant differences in misregistration when compared between dist-PET/ZTE and dist-PET/Dixon with dist-PET/CT ($p=0.6346$ and $p=0.5774$, respectively). ***Conclusion:*** PET/MRI with ZTE provides superior image quality of the normal lung structures than conventional Dixon sequences, but inferior to the CT component of PET/CT. Fused images of lung lesions with PET/MRI provides significantly better precision than PET/CT images. Therefore, PET/MRI could be used to acquire spatially-matched, precise, hybrid images of lung lesions. ***References:*** None

EP-120

Establishment and Verification of an ^{18}F-fluorodeoxyglucose (FDG) PET/CT Based Prediction Model for Identifying Malignant from Benign Ground-Glass Nodules

R. Niu, *X. Shao, X. Shao, J. Wang, Y. Wang;*
The Third Affiliated Hospital of Soochow University, Changzhou, CHINA.

Aim/Introduction: In recent years, with the popularity of low-dose CT in lung cancer screening, the detection rate of ground-glass nodule (GGN) has gradually increased. GGN is common in early-stage lung adenocarcinoma but can also be a result of inflammation, interstitial fibrosis, or local bleeding. But,any single CT morphological feature or quantitative parameter is ideal for the differential diagnosis of GGN, and a multivariate prediction model is likely to improve the diagnostic performance for GGN. Currently, few prediction models are dedicated to GGN prediction. In this study, we aim to build a prediction model based on ^{18}F-FDG PET/CT imaging, and take both functional metabolism and CT image characteristics into account, in order to improve the efficacy of identifying malignant from benign GGNs. ***Materials and Methods:*** We retrospectively analyzed 170 patients with GGN (197 GGNs in total) who underwent PET/CT examination in our hospital from November 2011 to December 2019. The clinical and imaging data of all patients were collected, and the nodules were evenly and randomly divided into derivation set and validation set. For the derivation set, we used multivariate logistic regression to develop a prediction model for distinguishing benign and malignant GGNs. The receiver operating characteristic (ROC) curve was used to evaluate the diagnostic efficacy of the model, and the data in the validation set was used to verify the prediction model. ***Results:*** The 197 GGNs were classified into benign group (27) and adenocarcinoma group (170). A total of 5 parameters, including the patient's gender, nodule location, margin, pleural depression, and SUV index (the ratio of nodule SUVmax to liver SUVmean), were selected to develop a prediction model for distinguishing benign and malignant GGNs. The AUC of the model was 0.875 in the derivation set, with a sensitivity of 0.702 and specificity of 0.923. The positive likelihood ratio was 9.131, and the negative likelihood ratio was 0.322. In the validation set, the AUC of the model was 0.874, which was not significantly different from the derivation set ($P = 0.989$). ***Conclusion:*** The prediction model based on PET/CT imaging has good diagnostic efficacy and high specificity. It can be used to distinguish benign and malignant GGNs. ***References:*** None

EP-121

Value of total metabolic tumor burden as predictor of overall survival in NSCLC patients treated with pembrolizumab

D. Calabro'[1], *F. G. Dall'Olio*[2], *F. Formica*[2], *G. Argalia*[1], *S. Fanti*[1], *A. Ardizzoni*[2], *V. Ambrosini*[1];
[1]*Nuclear Medicine, S.Orsola-Malpighi Hospital, DIMES University of Bologna, Bologna, ITALY,* [2]*Sant'Orsola-Malpighi Teaching Hospital, University of Bologna, Medical Oncology Unit, Bologna, ITALY.*

Aim/Introduction: Pembrolizumab has improved the outcome of patients with advanced NSCLC and ≥ 50% PDL1 expression. Predictive factor of benefit from immunotherapy alone are lacking. Total metabolic tumour volume (TMTV)≥75cm3 has been shown to be a predictor of shorter overall survival (OS) in non-small cell lung cancer (NSCLC) patients (pts) treated with immunotherapy in advanced setting(DOI:10.1007/s00259-019-04615-x). Our aim is to confirm this finding in first line pembrolizumab. ***Materials and Methods:*** We retrospectively enrolled pts with advanced NSCLC (stage IV) and PD-L1 expression ≥50% (Ethical Committee approvation no. 2381/2019). Only those with a positive [18F]18F-FDG PET/CT performed at our center within 60days of treatment initiation were included in the study. MTV was calculated for each lesion by a

dedicated software (PET VCAR, GE Healthcare) on transaxial PET images, that semi-automatically delineates the tumour contours with a SUVmax threshold of 42% within the lesion. The results were checked by comparison with the fused CT images to determine if percentage threshold adjustment was needed and therefore was performed until a satisfactory outcome was achieved. TMTV was obtained summing each single lesion's MTV. Potential prognostic parameters for OS were analysed (TMTV, SUVmax, presence of bone/live metastasis, neutrophil/lymphocyte ratio≥4, ECOG Performance Status≥2, LDH>ULN). ***Results:*** Overall, 32 pts (squamous=5; non-squamous=27) were included (median follow up= 13.5 months, 95% CI [10.1 - 17.0]). Pts with a TMTV≥ 75cm3 (18/32 pts) showed a worse outcome (median OS= 4.7 mo, 95% CI [1 - 8.4] vs not reached). Parameters associated with worse outcome both in univariate and multivariate analysis were TMTV≥ 75cm3 (HR=11.3; 95% CI [2.3 - 55.2], p=0,01), neutrophils/lymphocyte ratio≥4 (HR=13.3; 95% CI [2.8- 64], p=0,002), ECOG PS ≥2 (HR=9.1; 95% CI [1.8-46.2], p=0,006). ***Conclusion:*** Our data showed that TMTV≥ 75cm3 can be used as predictor of outcome in pts candidated to first line pembrolizumab, suggesting that this parameter could be useful for the early identification of pts needing the association of chemo-immunotherapy. ***References:*** DOI:10.1007/s00259-019-04615-x

EP-122

Molecular imaging as a predictive biomarker response to Ceritinib in ALK-Rearranged Non-Small-Cell Lung Cancer

S. Medina-Ornelas*, F. García-Perez, O. Arrieta-Rodriguez, F. Barron-Barron;*
Instituto Nacional de Cancerologia, Mexico City, MEXICO.

Aim/Introduction: Demonstrate the usefulness of ^{18}F-FDG-PET/CT as a predictive tool for response to treatment of patients with non-small-cell lung cancer with ALK-rearrangement (NSCLC-ALKr) treated with ceritinib. ***Materials and Methods:*** We studied 20 patients with NSCLC-ALKr with 18F-FDG-PET/CT as a baseline study from two institutions between April 2017 to February 2020. All patients were treated with ceritinib at dose of 750mg/day. An evaluation was made by 18F-FDG-PET/CT after 1 month of treatment (28±7 days) and one month after 6-10 cycles (mean 6 cycles). Obtaining SUVmax, SUVmean, VTMA (metabolically active tumor volume) and TLG (total lesion glycolysis) values, RECIST 1.1 and PERCIST 1.0 criteria was performed. The best cut discriminative values for SUVmax, VTMA and TLG were identified by ROC curves. The analysis of semicuantitative values was made with Fisher's exact test and Cox regression. A significant value of p was considered when this was ≤0.05. ***Results:*** The mean values of the initial SUVmean was 8.2±3.9 SD, after the first cycle (interim) SUVmean was 6.3±3.8 SD in target lesions; and 3.7±4.1 SD after the last cycle. The mean values of the initial SUVmax were 13.4±7.6 SD, 6.2±5.8 SD interim; and 4.6±4.3 SD after the last cycle. The mean values of the initial VTMA were 34.9±65.8 SD, 23.0±49.8 SD interim, and 21.0±39.5 SD after the last cycle. The mean values of the initial TLG were 269.4±1028.1 SD, 231.8±667.2 SD interim, and of 208.0±395.9 SD after the last cycle. In the analysis after the first cycle, no patient presented disease progression assessed. In the analysis after the last cycle, 15 patients presented a partial metabolic response, of which 12 had a statistically significant decrease in TLG after the first cycle; while those with stable disease did not show a statistically significant decrease after the first cycle. At the end of the last cycle through the RECIST criteria, 5 patients had stable disease. The measurement of the TLG was the most significant parameter for the prediction of response to treatment in the univariate analyzes (p=0.001). In the multivariate analysis with the Cox regression method, a low TLG, and the clinical stage before therapy were significant prognostic factors to present good response to treatment (p=0.001). ***Conclusion:*** The TLG is an excellent response prediction parameter superior to values of SUVmax, SUVmean or VTMA. Low TLG values after firs cycle associated with a clinical stage IIIC or IVa can predict a good response to treatment. ***References:*** None

EP-123

Clinical role of F-18 FDG PET/CT in thymic epithelial tumors

K. Hayasaka*, T. Saitoh, H. Inoue, Y. Shiraishi, J. Atsumi, T. Tohgoh, M. Hiramatsu, K. Shimoda, H. Yoshimori, K. Ohta;*
Fukujuji Hospital, Anti-Tuberculosis Association, Tokyo, JAPAN.

Aim/Introduction: We aimed to determine whether 18-F FDG PET/CT is useful for the 8th UICC staging and WHO classification of thymic epithelial tumors. ***Materials and Methods:*** We retrospectively reviewed the medical records, PET and other findings of 36 patients (male, n = 16; mean age [SD], 64.8 [10.9] y) with thymic epithelial tumors who underwent 18-F FDG PET/CT. The maximum standardized uptake (SUVmax) of 18-F FDG within one hour was determined and the findings of thymic epithelial tumors, lymph nodes and distant metastases were reviewed. According to the WHO classification, thymic epithelial tumors were grouped as low risk (types A, AB, B1), high risk (types B2, B3) and carcinoma. All data were statistically analyzed using SPSS version 11.0 software (SPSS Inc., Chicago, IL, USA). Statistical significance was set at $p < 0.05$. ***Results:*** Thymic epithelial tumors were confirmed in 32 surgical and four surgical biopsy specimens. The histological classifications were thymoma (n = 23; A, n = 3; AB, n = 7; B1, n = 4; B2 and B3, n = 9), carcinoma (n = 13, squamous cell carcinoma (n = 10), adenocarcinoma (n = 1) and well-differentiated neuroendocrine carcinoma (n = 2). The thymomas were staged as I (n = 14), II, (n = 1), III (n = 5), and IV (n = 1). The mean (SD) tumor size (mm) and SUVmax

were respectively 57.1 (25.6) and 3.24 (1.04)I n low risk, 67.4 (21.6) and 6.57 (2.50) in high risk, 64.6 (30.0) and 9.53 (4.86) in carcinoma, 55.1 (23.0) and 3.81 (2.07) in stage I/II, and 72.8 (16.1) and 3.81 (2.07) in stage III/IV thymomas. Pearson correlation analysis revealed a statistically significant association between tumor size and SUVmax in stage III/IV thymomas (r = -0.855, p = 0.030). Analysis of variance showed that differences were statistically significant for low vs. high risk (p = 0.008), low risk vs. carcinoma (p = 0.001), and stage I/II vs. III/IV thymoma (p = 0.007). ***Conclusion:*** We found that 18-F FDG PET/CT was useful for differentiating histological types and staging the extent of thymic epithelial tumors. ***References:*** Park SYet al. Value of F18-FDG PET/CT for predicting the World Health Organization malignant grade of thymic epithelial tumors. Clin Nucl Med 2016;20: 15-20

EP-124

Prediction of overall and free progression survival by means of post-induction chemo/chemoradiotherapy ^{18}F-FDG PET/CT in non-small cell lung cancer patients

P. García-Talavera San Miguel, F. Gómez-Caminero, J. G. Villanueva, B. Lucas, C. Riola, A. C. Peñaherrera, J. C. Cañadas, E. Martín, P. Tamayo;
Nuclear Medicine. University Hospital of Salamanca, Salamanca, SPAIN.

Aim/Introduction: To demonstrate the value of post-induction ^{18}F-FDG PET-CT as a predictive factor of the progression free survival (PFS) and overall survival (OS), in locally advanced non-small cell lung cancer patients (LA-NSCLC), treated with neoadjuvant Chemotherapy (CH), or Chemoradiotheraphy (CH-RT) ***Materials and Methods:*** Thirty patients with LA-NSCLC were included (20 males; mean age: 62,3 ± 9,2 years old; histology: 13 adenocarcinomas and 17 squamous cell carcinomas; Staging (8th ed. AJCC): IIB (3), IIIA (13), IIIB (10), IIIC (4).Two ^{18}F-FDG PET-CT studies were acquired to all patients. One of staging (PET1), and the other post-neoadjuvant CH (28 patients) or CH-RT (2 patients) (PET2), acquired 3 weeks after the end of treatment.SUVmax, SUVmean, MTV (metabolic tumor volume) and TLG (total lesion glycolysis) were analyzed in PET2, as well as Δ TLG and Δ SUVmax.Patients were monitored by means of clinical and radiological follow up (CT or PET-CT). PFS and OS were collected from the moment of PET2 acquisition. PFS and OS Curves were performed, by means of Kaplan Meir analysis and Log Rank test, after calculation of cut off values of the variables, based on ROC curves.SPSS 22.0 version was used for the statistical analysis (statistical significance: p< 0.01) ***Results:*** Regarding to the ROC curves for PFS, only ΔSUVmax reached established statistical significance, getting 45.4% as the best cut off (p=0.004), with a sensitivity of 92% and specificity of 71%. In survival curves, a PFS of 25 months for a decrease > 45.4% vs 7.6 months for a decrease < 45.4% were obtained (p=0.003). For ROC curves of OS, SUVmean and SUVmax achieved statistical significance. We obtained as optimal cut off 7.9 (p=0.007) for SUVmean and 14.1 (p=0.01) for SUVmax. Sensitivity of 71% and 100% of specificity, for both parameters, were found. In Kaplan Meier curves, a OS of 15.8 months vs 34.6 months were obtained, for a SUVmax >14.1 and SUVmax <14.1 (p=0.000), respectively. With regard to SUVmed, 12.4 months vs 34.6 months, for a SUVmean >7.9 and <7.9 (p=0.000), respectively. ***Conclusion:*** Some parameters, SUVmean and SUVmax, from post-induction ^{18}F-FDG PET-CT, and ΔSUVmax (from PET1 and PET2), have demonstrated to be predictive factors for PFS and OS, in patients with LA-NSCLC, treated with neoadjuvant CH or CH-RT. ***References:*** None

EP-125

Evaluation of regional lymph node involvement in the staging of non-small cell lung cancer with 18F FDG PET/CT

M. Keskin;
Mersin City Training and Research Hospital, Mersin, TURKEY.

Aim/Introduction: To evaluate the diagnostic performance of mediastinal blood pool activity (MBP) threshold for lymph node staging of non-small cell lung cancer (NSCLC) in PET / CT and examining other variables that may improve the diagnostic performance of 18F FDG PET / CT in evaluating regional lymph node involvement by taking advantage of mediastinal blood pool activity. ***Materials and Methods:*** Patients diagnosed with NSCLC who underwent endobronchial ultrasound guided transbronchial needle aspiration (EBUS-TBNA) and 18F-FDG-PET / CT were included in the study. Analysis of lymph node station and lymph node staging, MBP threshold value and five other PET / CT parameters (lymph node SUVmax value, lymph node short diameter, lymph node / MBP SUVmax ratio, lymph node / tumor SUVmax ratio, and lymph node SUVmax / lymph node short diameter ratio) compared with histopathological results. Optimal threshold values were determined using receiver operating characteristic curve analysis to compare the diagnostic value of all parameters examined in PET / CT. ***Results:*** Eighty eight patients were included in the study and pathological samples were performed from 250 lymph node stations. The higher lymph node activity in PET / CT than MBP showed a sensitivity of 95.3%, a specificity of 36.1%, a positive prediction value of 33.1% and a negative prediction value of 96.2%. From the other five PET / CT parameters examined, lymph node SUV max value and lymph node / MBP SUVmax ratio were the most diagnostic parameters. The 3.8 threshold value for lymph node SUVmax showed a sensitivity of 90.2% and a specificity of 61.7%, and the 1.8 threshold for lymph node/MBP SUVmax ratio showed a sensitivity of 90.1% and a specificity of 60.5%. ***Conclusion:*** Compared to the MBP

threshold value in the nodal staging of the NSCLC, the use of higher lymph node / MBP SUVmax ratio threshold value and other PET / CT variables may increase the diagnostic value of PET / CT. ***References:*** None

EP-126

Role of 18F-FDG PET/CT in the evaluation of reponse to therapy in non-small-cell lung cancer (NSCLC) patientes treated with inmunotherapy (prelimary results)

M. Suarez-Piñera[1], A. Taus[2], D. Ramal[3], L. Pijuan[4], A. Mestre-Fusco[5], E. Arriola[2];
[1]Nuclear Medicine Department, Hospital del Mar, Barcelona, SPAIN, [2]Medical Oncology Department, Hospital del Mar, Barcelona, SPAIN, [3]Radiology Department, Hospital del Mar, Barcelona, SPAIN, [4]Pathology Department, Hospital del Mar, Barcelona, SPAIN, [5]Nuclear Medicine Department, Hospital del Mar, Barcelona, SPAIN.

Aim/Introduction: The main issue to evaluate response to inmunotherapy with FDG PET/TC in NSCLC patients, are the inflammatory infiltration secondary to this treatment that might also show FDG uptake, hamper reliability of PET signal. We aimed to analyze reponse to inmunotherapy (anti-PD-1/PD-L1) in a sample of NSCLC patients. ***Materials and Methods:*** Retrospective study of 14 NSCLC stages III-IV in immunotherapy treatment. All underwent a baseline 18F-FDG PET/CT (PET1), prior to the start of immunotherapy and another (PET2) during / at the end of it, due to clinical / radiological suspicion of progressionPET analysis was visual and quantitative: SUVmax, SUVlbmy ratio SUVmax / SUVfund. The results of PET1 and PET2 were compared. Patients were classified into local progression and non-local progression. PET findings will correlate with clinical, CT, and histology when available. ***Results:*** Time between the start of treatment and PET2 was 15.4 ± 8.8 months. PET identified 8 patients in local progression (7true positive/1false positive) in 6 patients PET was negative (6 true negative). A reduction in SUVmax of 75.5% ± 12 and a ratio in PET2 SUVmax / SUV background of 1.8 were established as quantitative response criteria. The PET showed a sensitivity 100%, specificity 83%, positive predictive value 87% and negative predictive value 100% in the assessment of the local response. ***Conclusion:*** FDG PET/TC let to evaluate response to inmunotherapy in NSCLC patients . Quantitative analyze might give support when visual analysis show doubts. Prospective long-series studies are needed that can assess the actual role of PET in these patients. ***References:*** None

EP-19

Imaging Clinical Studies -> Oncological Imaging Clinical Study -> Lymphoma

e-Poster Area

EP-127

Added Value of SPECT/CT in the Monitoring and Long-Term Follow-up of Malignant Lymphomas

L. Chavdarova, E. Piperkova;
University Specialized Hospital for Active Treatment in Oncology, Sofia, BULGARIA.

Aim/Introduction: Modern hybrid imaging assists monitoring and treatment individualization with PET/CT undoubtedly being the "gold imaging standard" in FDG-avid lymphomas. SPECT/CT evolved later but could offer a lot in oncology, using different tumor-seeking radiopharmaceuticals (TSRP). Compared to PET/CT, there is still much less evidence about the place of improved SPECT/CT imaging in lymphoma. Our aim was to study the added value of SPECT/CT with TSRP 99mTc-MIBI or TF in Hodgkin and Non-Hodgkin lymphomas: diagnostic and staging capacity, predictive role for multi-drug resistance, assessment of cardiotoxicity and as a probable alternative for 18F-FDG-PET/CT. ***Materials and Methods:*** We studied 42 adult (22-77y) patients with proven or suspected lymphoma (16 HL, 23 NHL, 3 undefined) with clinical indication for: primary diagnosis/staging (5 pts), restaging after first-line therapy (33 pts); relapse-restaging (3 pts). Using previous "non-hybrid" experience, we introduced a new one-day protocol including whole-body (WB: base of skull-upper thigh) SPECT/CT tumor-seeking scan followed by myocardial perfusion imaging MPI-Gated-SPECT/CT with only one application of the RP. Overall 71 scans were performed on a Symbia-T16-SPECT/(low-dose) CT in our Clinic of Nuclear medicine during 3 year-period: 45 for tumor imaging and 26 MPI. We checked all nodal and extranodal/organ regions for lymphoma engagement, assessed concordant and discordant SPECT vs CT findings and looked for multidrug resistance and myocardial toxicity. In 2 patients SPECT/CT was compared to a previously done PET/CT without intermittent therapy. ***Results:*** SPECT was concordant to CT in 36 pts. In 9 pts SPECT showed non-viable tumor residues after therapy. Comparing SPECT/CT and PET/CT, one patient was diagnosed with MDR and the other showed totally concordant PET and SPECT viable lymphoma lesions. 9/26 MPI showed pathologic myocardial perfusion and/or kinetics, 8 patients were diagnosed with post-therapeutic cardiotoxicity. ***Conclusion:*** Tumor-seeking SPECT/CT shows significant added value for primary diagnosis and staging in lymphoma patients with very high SPECT vs CT concordance. During restaging/follow up SPECT/CT could confirm clinical remission or relapse

and differentiate between viable tumor and post-therapy fibrosis with up to 100% accuracy. 99mTc-MIBI/TF-SPECT/CT allows non-invasive pre-therapeutic assessment of chemo-sensitivity and can predict multidrug resistance. The introduced protocol for subsequent tumor-seeking and myocardial perfusion hybrid imaging gives simultaneous multifunctional assessment and supports individualized treatment design. In the case of non-sufficient PET/CT equipment, the more readily available 99mTc-MIBI/TF-SPECT/CT might serve as an alternative in lymphoma monitoring at a lower cost and reduced radiation burden. Additional studies could give further evidence. ***References:*** None

EP-128

Inter reader agreement andvariabilityof FDG PET volumetric parameters in a cohort of patients with Diffuse Large B-Cell Lymphoma (DLBCL)

M. Simó[1], *A. Hernandez Martinez*[2], *M. Cortes Romera*[3], *M. Sarandeses Fernández*[4], *A. Rotger Regi*[5], *X. Setoain Perego*[6], *M. Coronado Poggio*[7];
[1]*Hospital Universitari Vall De Hebron, Barcelona, SPAIN,* [2]*Hospital Santa Lucia, Cartagena, Murcia, SPAIN,* [3]*Hospital Universitario de Bellvitge. Idibell, Barcelona, SPAIN,* [4]*Hospital Universitario 12 de octubre, Madrid, SPAIN,* [5]*Hospital Universitario Gregorio Marañon, Madrid, SPAIN,* [6]*Hospital Universitari Clinic, Barcelona, SPAIN,* [7]*Hospital Universitari La Paz. On Behalf on the imaging subcomitte of GELTAMO, Madrid, SPAIN.*

Aim/Introduction: Measurement of metabolic tumor volume (MTV) and tumor lesion glycolysis (TLG) in patients with advanced (DLBCL) is challenging due to large amount of nodal and extranodal lymphomatous involvement. The purpose of this study was to evaluate the inter reader agreement and variability of these two parameters in our group of patients. ***Materials and Methods:*** Fifty patients with unfavourable DLBCL and baseline staging FDG PET/CT scans from a clinical trial (NCT01848132) were included. Three observers in-dependently read the scans and segmented metabolic tumor volume and total lesion glycolysis using a custom semi-automated workflow in the MIM Encore™ software (MIM Software Inc., Cleveland, OH, USA). Lesions were identified by visual assessment with PET images scaled to a fixed SUV of 2.5 and by Positron Emission Tomography Response Criteria in Solid Tumors (PERCIST) value. Contours of all hypermetabolic lesions were automatically created by fixed threshold method at 41% of SUVmax. Bland-Altman plots were used to compare volume parameters between observers. Inter-observer reproducibility was assessed using an intraclass correlation test. Based on Landis and Koch scale, agreement between operators was considered excellent if the intraclass correlation coefficient (ICC) was superior to 0.8. ***Results:*** The average MTV and TLG values measured by SUV max: 2.5 and PERCIST in all patients were 1634cc and 1542cc respectively. No significant differences were documented between two methods. (t student 0.8). Using the SUV max:2.5 criteria, a greater dispersion of measures were found between the observers at a higher disease volume. This effect was not found when the PERCIST criteria was used. In 24 of 50 patients (48%) at least one VOI had to be manually modified, since it included some physiological uptake, as kidney or bladder. In this subgroup of patients there were also no differences between the observers, although there was also a greater dispersion at higher volumen. From a time consuming point of view, RECIST Criteria was better than fix SUV max method since fewer VOIS had to be removed. An excellent inter-observer reproducibility (higher than 0.90, $p < 0.05$) between the 3 observers were found considering TLG (SUVmax:2.5), MTV (SUVmax:2.5), $TLG_{41\%}$ (SUVmax:2.5), $MTV_{41\%}$ (SUVmax:2.5), MTV (percist), $MTV_{41\%}$ (percist), $TLG_{41\%}$ (percist) analysis ***Conclusion:*** There was good interreader agreement for measurement of metabolic tumor volume and total lesion glycolysis in our patients with DLBCL. A major dispersion had been observed at a greater volume of disease. ***References:*** None

EP-129

End of therapy ^{18}F-FDG PET/CT for assessment of persistent bone involvement in B-cell lymphoma

L. Michaud*, R. Nakajima, E. Joffe, P. Ghione, S. Ahsanuddin, A. Navitski, H. Schöder;*
MSKCC, New York, NY, UNITED STATES OF AMERICA.

Aim/Introduction: Bone involvement in B-cell lymphoma is often perceived by oncologists to indicate a more aggressive disease. Radiographic resolution of the lesions post-treatment is crucial for prognosis.^{18}F-FDG PET/CT has become the standard for response assessment in most lymphomas. However, there are many reasons for residual FDG uptake in bone, other than persistent disease. To assess this hypothesis, we evaluated and characterized PET response patterns in patients with B-cell lymphoma with initial bone involvement. ***Materials and Methods:*** Lymphoma patients with reported initial bone involvement and end of therapy ^{18}F-FDG PET/CT(=EoT-PET) evaluation between 2001 and 2018 were identified from our institutional data base(n=413). We selected all cases with FDG uptake in bone higher than reference liver in EoT-PET report (n=54). In addition, we randomly selected 55cases without EOT bone uptake. Thus,109 patients were evaluated(74DLBCL,19FL,16HL). Two independent nuclear medicine physicians, blinded to original PET report and patient clinical outcome, retrospectively reviewed baseline(n=101) and EoT-PETs(n=109). Response on EoT-PET was evaluated using Deauville/Lugano criteria to which three criteria for FDG bone uptake were added: M=diffuse reactive medullar uptake, S=uptake around surgery site,

F=uptake around a fracture site. In case of discordant results between the two readers, a third independent expert reader (HS) established the final classification. ***Results:*** Discordant results between the two readers occurred in 26patients(24%): Deauville≤3 versus ≥4(n=7); fracture or surgery overlooked by one reader(n=6); disagreement regarding M status:Deauville≤3 versus M(n=12); and classification as X vs 5(n=1). After consensus, 60patients were classified as D≤3 for bone involvement (including n=6 with extra-osseous status D≥4). The 49 other patients showed the following bone uptake: D≥4(n=21), S(n=11), F(n=5), M(n=8), X(n=2) and indeterminate(n=2). The latter two patients had a paravertebral/vertebral lesion impossible to characterize without biopsy and unchanged mild femoral uptake. Among these 49patients, only 8 had confirmed persistent/progressive disease in bone(n=5 with D≥4, n=1 with S and n=2 indeterminate). The EoT response was evaluated by the clinician (complete response=negative biopsy, follow up imaging with resolved uptake, or no treatment despite persistent stable uptake and unremarkable clinical course). Particularly, among the 21patients D≥4, 15(71%) had a complete response ***Conclusion:*** Non-tumoral residual FDG uptake in bone with intensity higher than reference liver background (e.g.,due to surgery, fractures, or diffuse reactive marrow), is common on EoT PET, whereas true residual bone disease is rare. Of note, 71% of patients with residual bone uptake on EoT PET achieve a complete response, particularly when there is no residual extra-osseous uptake. ***References:*** None

EP-130

PET/CT for Detecting Bone Marrow Involvement in Diffuse Large B-cell Lymphoma Compared with Bone Marrow Biopsy

C. Soldevila[1], *M. Cortés-Romera*[1], *A. Sabaté-Llobera*[1], *S. Mercadal-Vílchez*[2], *A. Palomar-Muñoz*[1], *F. Climent-Esteller*[3], *E. Llinares-Tello*[1], *M. Pudis*[1], *E. González-Barca*[2];
[1]*PET/CT Unit (IDI)- Department of Nuclear Medicine. Hospital Universitari de Bellvitge, L'Hospitalet de Llobregat (Barcelona), SPAIN,* [2]*Department of Hematology. ICO. Hospital Duran i Reynals-IDIBELL, L'Hospitalet de Llobregat (Barcelona), SPAIN,* [3]*Department of Pathology. Hospital U. de Bellvitge-IDIBELL, L'Hospitalet de Llobregat (Barcelona), SPAIN.*

Aim/Introduction: Diffuse large B-cell lymphoma (DLBCL) is the most commonly occurring lymphoma subtype. Detection of bone marrow involvement (BMI) is important in these patients because it may have prognostic and therapeutic implications. Focal bone or bone marrow FDG uptake in PET/CT is highly sensitive to detect bone marrow involvement (BMI) in Hodgkin lymphoma and in aggressive non-Hodgkin lymphoma (NHL). However, diffuse FDG uptake in PET/CT is more controversial in aggressive NHL. The aim of this study was to compare PET/CT with BMB for detecting BMI in patients with newly diagnosed DLBCL. ***Materials and Methods:*** One hundred fifty-two patients (73 women; mean age 57 years) newly diagnosed with DLBCL underwent a pretreatment FDG PET/CT and BMB. PET/CT was considered positive for BMI at the visual assessment when there was a focal, heterogeneous or diffuse bone marrow uptake (BMU) higher than liver uptake. Focal pattern was subclassified as unifocal, bifocal and multifocal. Morphological changes on CT were studied in patients with BMI and they were subclassified as diffuse increased bone density, lytic and/or sclerotic lesions. Concordance between PET/CT and BMB was analyzed. ***Results:*** BMI was detected in 25 patients (16%) by BMB and in 48 (31%) by PET/CT. Of all positive PET/CT, diffuse uptake was observed in 10 cases, heterogeneous in 8 and focal pattern in 30 (20 multifocal, 4 bifocal and 6 unifocal). Morphological changes on CT were observed in 24 patients (8 with diffuse increased bone density, 10 with lytic lesions and 6 with mixed sclerotic and lytic lesions). Concordant results between PET/CT and BMB were obtained in 119 cases (78%): 20 of them with positive PET/CT (6 diffuse, 3 heterogeneous and 11 focal pattern) and BMB results (16%), and 99 patients with negative PET/CT and BMB results (83%). Discordant results were obtained in 33 cases (22%): 28 of them with positive PET/CT (4 diffuse, 5 heterogeneous and 19 focal pattern) and negative BMB (85%), and 5 with negative PET/CT and positive BMB (15%). ***Conclusion:*** PET/CT detects more BMI compared with BMB in DLBCL, though there is a good concordance between both techniques. Around 60% of patients with a focal and/or heterogeneous pattern at the PET/CT had a negative BMB, so the omission of BMB in these cases should be considered. However, 60% of patients with a diffuse pattern had a positive BMB, so in these cases we recommend the BMB. ***References:*** None

EP-131

Disease Free Survival on Follow-up ^{18}FDG PET/CT in NHL Patients with Complete Metabolic Response on Interim scans

N. Fatima[1], *M.U. Zaman*[1], *A. Zaman*[2], *U. Zaman*[3], *S. Zaman*[4], *R. Tahseen*[1];
[1]*Aga Khan University, Karachi, PAKISTAN,* [2]*Department of Medicine, Dr Ruth Hospital, Karachi, PAKISTAN,* [3]*Dept of Medicine Suny Downstate, Hospital, New York, NY, UNITED STATES OF AMERICA,* [4]*Dow Medical College, Dow University of Health Sciences (DUHS), Karachi, PAKISTAN.*

Aim/Introduction: Aim of this retrospective study was to determine disease free survival (DFS) in patients with non-Hodgkin's lymphoma (NHL) on follow-up ^{18}FDG PET/CT who had complete metabolic response (CMR) on interim scan (iPET). ***Materials and Methods:*** This retrospective study was conducted at PET/CT Section of a JCIA accredited healthcare facility from December 2015 till February 2020.

NHL patients with CMR on iPET were selected and followed for a median period of 11 months (4-144 months). End point response on follow- PET/CT (either end of treatment or surveillance) was categorized as sustained CMR (sCMR) and disease recurrence using Deauville 5-point scoring. Kaplan Meier survival curve was used to measure DFS and receiver operating characteristics (ROC) was plotted for age, largest lesion size, highest standardized uptake value (SUVmax), disease stage and body mass index (BMI) on baseline scan to find their impact on disease recurrence on follow-up ^{18}FDG PET/CT ***Results:*** During study period, 185 NHL patients achieved CMR on iPET with a median age 55 years (19 - 88 yr.) with male predominance (63% male). On follow-up, 123 (66%) patients were found to have sCMR while recurrence was found in 34% ($p < 0.05$). No significant difference in demographics was found between two groups. Median DFS time was 34 months (22.8 - 45.1 months). On ROC analysis, baseline highest SUVmax was found to be a significant independent predictor of disease recurrence at a cut off >22.6 (highest area under curve: 0.595; SE 0.046; $p < 0.05$). ***Conclusion:*** We conclude that significant higher proportion of NHL patients with CMR had a DFS of median 34 months (range: 22.8 - 45.1 months) and highest baseline SUVmax (>22.6) was found to be an independent predictor of disease recurrence. ***Key words***: Interim PET/CT; Non-Hodgkin's Lymphoma; Responder; Disease free survival; predictor. ***References:*** None

EP-132

Can Metabolic Parameters Obtained From PET/CT Images Be Used As A Prognostic Factor For Hodgkin Lymphoma?

C. Sezgin*, G. Mutevelizade, E. Sayit, I. Aydogdu, G. Gumuser;*
Celal Bayar University, Manisa, TURKEY.

Aim/Introduction: F-18-fluorodeoxyglucose (F-18 FDG)PET/CT is currently used as the gold standard method in patients with Hodgkin lymphoma for staging, evaluation of response to therapy, detecting residual tumor tissue and recurrence. In this study, we investigated PET/CT metabolic parameters' value for predicting the treatment response. In addition, the relationship between Ann Arbor staging and international prognostic score 3 (IPS3) with metabolic parameters and treatment response was evaluated. ***Materials and Methods:*** Seventy-two patients with histopathologically proven Hodgkin lymphoma underwent F-18 FDG PET/CT (Philips, True Flight Select, USA) imaging for staging and response to therapy evaluation. 35 patients (20 men,15 women; mean age 38.3±16 years) with available laboratory, pathology and treatment data were evaluated retrospectively. Metabolic tumor parameters [(SUVmax, SUVmean, lesion/liver SUVmax ratio, metabolic tumor volume (MTV) and metabolic index max (MImax)] achieved from PET/CT images taken for initial staging. After 4 cycles of Adriamycin, Bleomycin, Vinblastin, Dakarbazin (ABVD) treatment patients underwent PET/CT for evaluation of response to therapy and Deauville response scale were identified. Metabolic tumor parameters and Deauville response scale were compared. Ann Arbor stages and IPS3 scores (age≥45, stageIV disease, Hgb<10.5; each were given 1 point) were determined. Deauville score 1-3 was considered as response to treatment, score 4-5 as treatment failure. The relationship between Ann Arbor stages and IPS3 scores with metabolic tumor parameters and Deauville response scores were examined. ***Results:*** Nineteen of 35 patients were nodular sclerosing, 7 were mixed cellular, 4 were in lymphocyte predominant subtype, whereas 5 patients subtypes could not be determined pathologically. There was a significant relationship between response to 4 cycles of ABVD treatment with SUVmax, SUVmean, lesion / liver SUV max ratio and MImax (p=0.016,p=0.020,p=0.033,p=0.013, respectively). There was no significant relationship between total tumor volume and treatment response. Patients' IPS3 scores and SUVmax; Ann Arbor stages and tumor volumes were found to be related (p=0.039,p=0.014, respectively); whereas there was no significant relationship between IPS3 scores and Ann Arbor stage with treatment response. There was a statistical relationship between MTV and MImax values with serum LDH levels (p=0.002,p=0.038, respectively). ***Conclusion:*** We conclude that SUVmax, SUVmean, lesion/liver SUV max ratio and MImax values achieved from PET/CT images taken for initial staging of patients with Hodgkin's lymphoma are promising in terms of creating a new prognostic scoring system and treatment guidance. ***References:*** Barrington SF. Time to prepare for risk adaptation in lymphoma by standardising measurement of metabolic tumour burden. J Nucl Med. 2019;jnumed.119. 227249. doi:10.2967/jnumed.119.227249

EP-133

Impact of Gender on Metabolic Response in Patients with Non-Hodgkin's Lymphoma using Interim ^{18}FDG PET/CT

N. Fatima[1]*, M. U. Zaman*[1]*, A. Zaman*[2]*, U. Zaman*[3]*, S. Zaman*[4]*, R. Tahseen*[1]*;*
[1]Aga Khan University, Karachi, PAKISTAN, [2]Department of Medicine, Dr Ruth Hospital, Karachi, PAKISTAN, [3]Dept of Medicine Suny Downstate, Hospital, New York, NY, UNITED STATES OF AMERICA, [4]Dow Medical College, Dow University of Health Sciences (DUHS), Karachi, PAKISTAN.

Aim/Introduction: The purpose of this study was to determine the impact of gender on response in patients with non-Hodgkin's lymphoma (NHL) based on interim ^{18}-fluorodeoxyglucose (FDG) positron-emission tomography/computed tomography (PET/CT). ***Materials and Methods:*** This retrospective study was conducted at PET/CT section of a JCI-accredited healthcare facility from January 2019 to February 2020. Patients with baseline and interim ^{18}FDG PET/CT scans were selected. Interim

scans were performed not earlier than 2nd or later than 4th chemotherapy. The study population was divided on the basis of gender and various demographic factors were compared among them. Furthermore, predictors for responders between two groups were analysed using receiver operating characteristics (ROC) and logistic regression analysis (LRA). ***Results:*** Total 330 patients with NHL were categorized on the basis of gender into male (211/330) and female (119/330) cohorts. Female group was significantly obese (Body Mass Index ≥30 kg/m^2). Rest of the demographic factors (age, fasting blood level, FDG dose, uptake time, mean liver uptake, baseline highest SUVmax and the largest lesion size) were statistically similar. Male group was found to have significantly higher Stage III disease while rest of disease burden was found to have similar distribution in both groups. Significantly higher proportion of female was found as responders (with Deauville Score: 1-3) than males (82% vs. 66%; p value <0.05). Among responders, obesity was found significantly higher in female responders (32% vs. 19%; p-value <0.05). Rest of the factors were found non-significant in both groups. Using ROC, baseline BMI (>26.8 Kg/m^2) was found to be an independent predictor of response in female responders. While stage IV disease, was found to be a predictor of non-responders in male. Using LRA, a negative correlation was found for baseline highest SUVmax for BMI >26.8 Kg/m^2 in female responders. ***Conclusion:*** We conclude that prevalence of NHL is higher in males but females are good responders and baseline BMI >26.8 Kg/m^2 is an independent predictor in female responders. Furthermore, baseline SUVmax has inverse correlation with baseline BMI in female responders. ***References:*** None

EP-20

Imaging Clinical Studies -> Oncological Imaging Clinical Study -> Melanoma

e-Poster Area

EP-134

Melanoma patients: is it really necessary a whole-body PET/CT scan?

D. Calabro'[1], *L. Vetrone*[1], *A. Farina*[1], *F. Serani*[1], *P. Castellucci*[2], *S. Fanti*[1];
[1]*Nuclear Medicine, DIMES University of Bologna, S.Orsola-Malpighi Hospital, Bologna, ITALY,* [2]*Nuclear Medicine, S.Orsola-Malpighi Hospital, Bologna, ITALY.*

Aim/Introduction: The aim of the study is to assess the utility of performing a whole body 18F-FDG PET/CT scan (head to toe) in patients (pts) with uveal, mucosal and cutaneous melanoma. ***Materials and Methods:*** Inclusion criteria were: i) pts with histologically proven diagnosis of uveal, mucosal and cutaneous melanoma of the head and neck, trunk and proximal extremities, ii) at least one whole body PET/CT scan (head to toe) performed for post-surgical restaging of melanoma. Exclusion criteria were: i) pts with melanoma unknown primary tumour ii) primary lesion in the upper/lower limbs. Each scan was reviewed by two experienced nuclear medicine physicians, in order to assess the presence of secondary lesions that would have been excluded by a shorter field of view (FOV) from the vertex to the thighs. PET findings were considered positive when the uptake was more than two times the surrounding tissues. Data analysis was performed both per patient and per examination. ***Results:*** Among 506 scans performed from January 2016 and March 2020, 148 scans in 82 pts matched the inclusion criteria. PET/CT was positive in 29/82 pts (35%) and negative in 53/82pts (65%). PET/CT was positive in 48/148 scans (32.4%) and negative in 100/148 scans (67.6%). Among the 48 positive PET scans, only in two cases (4.2 %; 2 pts) secondary lesions outside the shorter FOV were found: in the tibia in one patient and in the distal arm and distal femoral diaphysis in the other. It is important to note that these two patients had already a known widespread disease, for which they were under immunotherapy, so the detection of lesions outside the standard field of view had no clinical impact in these two patients. Main limitation of the study is that most PET positive findings (although reported by two experienced nuclear medicine physicians) were not validated by biopsies or other imaging. ***Conclusion:*** This analysis shows that it is not strictly necessary to routinely extend FOV to the toes, in pts with uveal, mucosal and cutaneous melanoma of the head and neck, trunk and proximal extremities, sparing dose to the patient and shortening the acquisition time. ***References:*** None

EP-135

Interim^{18}F-FDG PET/CT in survival prediction ofanti-PD-1 immunotherapy in metastatic melanoma

C. Sachpekidis[1], *J. C. Hassel*[2], *A. Dimitrakopoulou-Strauss*[1];
[1]*Clinical Cooperation Unit Nuclear Medicine, German Cancer Research Center (DKFZ), Heidelberg, GERMANY,* [2]*Department of Dermatology and National Center for Tumor Diseases, University Hospital Heidelberg, Heidelberg, GERMANY.*

Aim/Introduction: A growing amount of literature has highlighted the potential role of ^{18}F-FDG PET/CT in the prediction of treatment response to immunotherapeutic agents in metastatic melanoma. In quest of identifying reliable biomarkers for the prediction of long-term outcomes to immunotherapy, we aim in the present prospective study to assess the value of interim ^{18}F-FDG PET/CT performed after the first two cycles of anti-PD-1 treatment. ***Materials and Methods:*** 29 patients with metastatic melanoma underwent immunotherapy with pembrolizumab (n=9), nivolumab (n=4) or a combination

of nivolumab/ipilimumab (n=16). All patients were examined with dynamic PET/CT (dPET/CT) of the thorax and upper abdomen as well as static, whole body PET/CT with ^{18}F-FDG before the start (baseline) and after two cycles (interim) of treatment. PET-based patient response evaluation to treatment was based on the European Organization for Research and Treatment of Cancer (EORTC) criteria and the recently proposed PET Response Evaluation Criteria for Immunotherapy (PERCIMT). The evaluation of dPET/CT studies was based on semi-quantitative (SUV) and quantitative analysis, based on two-tissue compartment modeling and a fractal approach. Progression-free survival (PFS) from the beginning of treatment was calculated. ***Results:*** According to the EORTC criteria, interim PET/CT demonstrated progressive metabolic disease (PMD) in 14 patients, stable metabolic disease (SMD) in 7 patients, partial metabolic response (PMR) in 7 patients, and complete metabolic response (CMR) in 1 patient. According to the PERCIMT, interim PET/CT demonstrated PMD in 8 patients, SMD in 13 patients, PMR in 7 patients and CMR in 1 patient. The results of semi-quantitative and quantitative PET analysis as well as PFS analysis data will be presented. ***Conclusion:*** Interim ^{18}F-FDG PET/CT performed after the first two cycles of immunotherapy provides significant prognostic information in metastatic melanoma patients treated with PD-1 inhibitors, which, in turn, may affect therapeutic decisions. ***References:*** None

EP-136

The application of 18F-FDG PET/CT for the assessment of tumor response to immunotherapy with PD-1/PD-L1 blockage in patients with advanced melanoma

I. Kostadinova;
Clinic of nuclear medicine, University Hospital Acibadem City Clinic, Mladost, Sofia, BULGARIA.

Aim/Introduction: The advent of immune checkpoint inhibitors has revolutionized metastatic melanoma treatment, as they have led to longer progression free survival and overall survival rates. However their introduction in the clinics has raised the issue of appropriate treatment response evaluation since the tumor responses are typically longer than in conventional treatment and they are partially associated with immune related adverse events. The aim of the study was to evaluate the treatment response of patients with metastatic malignant melanoma to check point inhibitors, using 18F-FDG PET-CT. ***Materials and Methods:*** We have studied retrospectively 21 patients (12 women and 9 men), treated with pembrolizumab (18 patients) and with nivolumab (3 patients) for the period 2016-2019, performing 89 PET-CT investigations (on the average 4.2 per patients), before and after beginning of the immunotherapy (the first follow up scan was performed on 3 month in order to escape visualization of eventual early pseudoprogression).We have used metabolic criteria PERCIST and morphological criteria- RECIST 1.1 and irRC for treatment response evaluation. ***Results:*** Progression was registered in 7/21 patients with 43.5% metabolic increase of activity of the target lesions on average (including new lesions) and the treatment was discontinued; complete response in 5/21 patients (without active lesions); partial response in 5/21 patients with 40.8% metabolic decrease of activity of the target lesions on average and stable disease was registered in 4/21 patients. In 6 of the patients the therapeutic answer was visualized earlier on PET than on CT (in some lymph nodes, bone marrow, peritoneum and muscles). Three of the patients with negative PET findings and residual lesions on CT had no signs of the progression in the following 2 years. Five of the patients showed adverse effects of the treatment such as sarcoidosis, pneumonitis, hypophisitis, colitis, skin changes. From these, three were successfully early visualized with PET but not with CT and were treated later on. ***Conclusion:*** We consider PET-CT a promising tool for evaluating patients with metastatic melanoma under PD-1/PD-L1 blockage in order to optimize treatment. It could show earlier therapeutic answer and visualization of the adverse effects on the basis of the changed metabolism, compared to usage of CT only. ***References:*** None

EP-137

^{18}FDG PET/CT role in a case of Pembrolizumab associated sarcoidosis mimicking progression in metastatic melanoma patient

Z. Dancheva[1], A. Konsulova[2], B. Chaushev[1], P. Bochev[3], M. Dyankova[1], T. Yordanova[1], A. Klisarova[1];
[1]St Marina University Hospital, Varna, BULGARIA, [2]Department of Oncology, Complex Oncological Centre, Burgas, BULGARIA, [3]Acibadem Cityclinik Oncology center Sofia, Sofia, BULGARIA.

Aim/Introduction: Pembrolizumab is a widely used cancer immunotherapy humanized antibody. It is an IgG4 isotype antibody that blocks a protective mechanism of cancer cells and thereby, allows the immune system to destroy them. It is used in the treatment of metastatic melanoma, and recently for many other malignant diseases as lung cancer, head and neck cancer, urothelial cancer, lymphoma and many others. Most adverse effects of Pembrolizumab are immune-related and may affect any organ in the human body. Sarcoidosis is a rarely described in the literature adverse reaction. ***Materials and Methods:*** We report a case of a female patient with a diagnosis of metastatic skin melanoma of the left leg, treated with first line immunotherapy with pembrolizumab, who developed a granulomatous sarcoidosis-like reaction. ***Results:*** While on treatment, the patient had a PET/CT as a procedure for response assessment 3 and 5 months after initiation of pembrolizumab. She developed at first mediastinal lymph nodes (Stage 1 sarcoidosis), which were

interpreted as pseudoprogression and the treatment was continued as the condition of the patient was unchanged and very good. To exclude rapid disease progression, a second re-assessment by PET/CT 2 months later was organized and granulomatous sarcoidosis-like reaction in lungs (stage 2) was observed. It was misinterpreted as progressive disease by another institution and treatment with pembrolizumab was interrupted. ***Conclusion:*** This case enriches the literature, enlarging the knowledge of immune-related adverse events spectrum and mimicking condition. As PET/CT is largely used for treatment response assessment, it is important to remain vigilant and not to interpret the immunotherapy-associated imaging changes, e.g. sarcoidosis as disease progression. ***References:*** 1. Cheshire SC1, Board RE1, Lewis AR1, Gudur LD1, Dobson MJ1. Pembrolizumab-induced Sarcoid-like Reactions during Treatment of Metastatic Melanoma., Radiology. 2018 Nov;289(2):564-567. doi: 10.1148/radiol.2018180572. Epub 2018 Aug 14. 2. Abdel-Wahab N, Shah M, Suarez-Almazor ME. Adverse events associated with immune checkpoint blockade in patients with cancer: a systematic review of case reports. PLoS One 2016;11(7):e0160221. 3. Cotliar J, Querfeld C, Boswell WJ, Raja N, Raz D, Chen R. Pembrolizumab-associated sarcoidosis. JAAD Case Rep 2016;2(4):290-293. 4. Firwana B, Ravilla R, Raval M, Hutchins L, Mahmoud F. Sarcoidosis-like syndrome and lymphadenopathy due to checkpoint inhibitors. J Oncol Pharm Pract 2017;23(8):620-624.

EP-138

Significance of FDG PET/CT in the Evaluation of Melanoma Patients

J. Stojanovic*, I. Grozdic Milojevic;*
Centre for Nuclear medicine, Clinical Center of Serbia, Faculty of Medicine University of Belgrade, Belgrade, SERBIA.

Aim/Introduction: The aim of this study was to determine the usefulness of FDG PET / CT in the evaluation of patients with advanced malignant melanoma. ***Materials and Methods:*** The retrospective analysis of data from 102 patients with a confirmed pathohistological diagnosis of advanced malignant melanoma who underwent FDG PET/CT scanning was performed. The FDG acquisition was quantitatively analyzed in the form of maximum standardized value (SUVmax). PET/CT was interpreted as positive or negative depending on the SUVmax value, with values ≥ 2.5 considered pathological. The examination was done with PET/CT scan, 60 minutes after 18F-FDG injection in standard whole body mode including orbits. ***Results:*** Based on the results the disease was present in 71% patients on FDG PET/CT, average SUVmax value was 12.9 ± 11.06. The evaluation of distant areas identified the disease predominantly located in the in the retroperitoneal lymph nodes in 48% (SUVmax 10.12 ± 8.51) and in the liver in 39% patients (SUVmax 9.18 ± 6.24). The disease was present in lymph nodes of the neck in 28% (SUVmax 7.71 ± 7.49) , in the axillary lymph nodes in 15% (SUVmax 12.3 ± 19.43), in the mediastinal lymph nodes in 35% (SUVmax 10.65 ± 14.09), , in the lymph nodes of the pelvis in 35% (SUVmax 11.3 ± 8.07) and in the inguinal lymph nodes in 35% (SUVmax 6.96 ± 4.85), in the bones in 34% (SUVmax 10.65 ± 10.55) , in the lungs in 21% (SUVmax 7.4 ± 4.78) and in the brain in 4% (SUVmax 10.67 ± 5.85) patients. ***Conclusion:*** Due to its ability in detecting functional and anatomical changes, FDG PET/CT has become a powerful tool in identification of distant metastases, assessment of response to therapy, and selecting candidates for surgical treatment. ***References:*** None

EP-21

Imaging Clinical Studies -> Oncological Imaging Clinical Study -> Neuroendocrine (Pancreatic and Others)

e-Poster Area

EP-139

^{18}F-FDG PET/CT in Primary and Recurrent Adrenocortical Carcinoma

S. Shamim*, G. Arora, J. Hussain, S. Datta Gupta, R. Kumar, C. Bal;*
AIIMS, New Delhi, INDIA.

Aim/Introduction: Adrenocortical Carcinoma (ACC) that originates from the cortex of adrenal gland is a rare but aggressive tumor. The prognosis is generally poor with 5-year survival of <35%. Surgery is the only curative option, which makes early diagnosis of operable disease imperative. We assess the role of ^{18}F-FDG PET/CT in diagnosis of primary and recurrent ACC. ***Materials and Methods:*** FDG PET/CT scans of 15 patients (3 female; 12 male) with primary/recurrent ACC were retrospectively analyzed. Patients who were referred to our department for evaluation of ACC underwent whole body (vertex to mid thigh) FDG PET/CT scan on dedicated PET/CT scanners (Biograph mCT, Siemens and 710 Discovery, GE) 60 minutes post-injection of 10 mCi ^{18}F-FDG. First, low dose CT scan was acquired followed by PET scan with 1.5-2 min per bed position. Images were reconstructed with iterative reconstruction technique. Scans were visually evaluated by an experienced nuclear medicine physician. Semi-quantitative analysis was done by estimating SUVmax and tumor to background ratio (TBR) of primary lesion using normal liver as background. ***Results:*** Mean age of the patients was 41.2±13.7 year. Of the 15 patients, 4 underwent FDG scan for baseline disease evaluation for metastatic work up prior to surgery, while 11 were follow up (F/U) cases to assess recurrent or residual disease. Two of the 11 follow up cases, were inoperable and

hence were only treated with chemotherapy. In all the cases referred for baseline staging (n=4), FDG PET/CT detected primary lesion (mean SUVmax=11.2; mean TBR=4.99) as well as metastatic sites (lung =3; liver=2; nodes=3). In the 2 inoperable F/U cases, FDG PET/CT detected residual primary (mean SUVmax=4.95; mean TBR=3.22) as well as metastatic sites (lung =2; nodes=1; bone=1). Of the remaining 9 post-operative F/U cases, 5 patients had recurrent disease at primary site and metastasis was present in 8 patients (lung =7; bone=3; nodes=5). ***Conclusion:*** ^{18}F-FDG PET/CT appears to be of diagnostic utility in primary, metastatic as well as recurrent ACC and may assist in guiding its management. ***References:*** None

EP-140

Results of a sequential strategy ^{68}Ga (DOTATOC) - ^{18}F-FDG PET/CT in real-life diagnosis and staging of neuroendocrine tumors

M. Ollarves Carrero[1], J. Rodriguez Gomez[1], M. Cabrera Martin[1], F. Ferrando-Castagnetto[2], C. Wakfie Corieh[1], A. Blanes Garcia[1], R. Couto Caro[1], J. L. Carreras Delgado[1];
[1]Hospital Clinico San Carlos, Madrid, SPAIN, [2]Universidad de la República Montevideo, Montevideo, URUGUAY.

Aim/Introduction: Neuroendocrine tumors (NETs) are a rare family of malignancies characterized by overexpression of somatostatin receptors (STTRs) in tumor cells. This molecular hallmark has established the basis for pharmacological treatment with analogues and diagnostic imaging. Following investigation was aimed to characterize our clinical experience by applying a sequential diagnostic algorithm with ^{68}Ga PET/CT (DOTATOC) followed by ^{18}F-FDG PET/CT in selected patients with NET ***Materials and Methods:*** This is an observational, analytical, and retrospective real-life experience developed in a single reference center. All patients with confirmed/highly suspicious diagnosis of NET who underwent ^{68}Ga PET-CT (DOTATOC) between April 2019 and March 2020 were included. Patients with a negative result of ^{68}Ga PET/CT (DOTATOC) and/or high clinical suspicion of NET or with high-grade tumors (histological G3 according to the Ki67 criteria) were sequentially referred to ^{18}F-FDG PET/CT. Clinical and anatomical data, histological grade (G1-G2 or G3), diagnostic accuracy, and changes in therapy after PET results are reported ***Results:*** Thirty-two patients with ^{68}Ga PET/CT (DOTATOC) results were included, 50% women, aged 40-81 years, 48% with metastatic NET. Fourteen patients (44%) had gastrointestinal and pancreatic primary tumors. The technique aimed at control/staging (confirmed NET) in 23 patients, diagnosing NET (highly suspicious NET) in 5 patients and locating the primary tumor (NET with unknown primary) in 4 cases. SSTR overexpression was detected in 22/32 patients (69%). Histopathological confirmation was obtained in 19 patients exhibiting a high tracer affinity for the SSTR; 88% of available histological grading were classified as low-grade (G1-G2) and 12% as high-grade (G3). The sequential PET strategy yielded better sensitivity than isolated ^{68}Ga PET/CT (DOTATOC); 91% vs. 95% and optimal PPV; 100% vs. 100% in diagnostic indications. Based on PET results, oncology therapy was modified in 63% and continued as previously defined in 37% of patients ***Conclusion:*** ^{68}Ga PET/CT (DOTATOC) allows the diagnosis and staging of NETs in the real-life care of patients and provides clinically useful information to improve treatment individually. In our experience, a complementary sequential ^{68}Ga PET/CT (DOTATOC) strategy followed by ^{18}F -FDG PET/CT in selected patients is associated with better sensitivity over ^{68}Ga PET/CT (DOTATOC) alone ***References:*** None

EP-141

Evaluating Neuroblastoma - Role of 18F-DOPA PET/CT Compared with 131I-MIBG Scintigraphy

A. Hemrom, A. Tupalli, K. S. Reddy, S. Agarwala, R. Seth, S. Bakhshi, M. Prabhu, A. Kumar, N. A. Damle, C. Bal;
All India Institute Of Medical Sciences, New Delhi, INDIA.

Aim/Introduction: 131I-MIBG scintigraphy and 18F-DOPA PET/CT are established imaging modalities in evaluation of neuroblastoma. This study intends to compare 131I-MIBG scintigraphy and 18F-DOPA PET/CT in picking up the lesions and to evaluate extent of the disease in children with neuroblastoma using standardised scoring methods i.e SIOPEN and Curie Scoring systems. ***Materials and Methods:*** Biopsy proven consecutive neuroblastoma patients underwent 131I-MIBG (planar and SPECT/CT) scan and 18F-DOPA PET/CT scan (±1 month). 131I-MIBG scan (whole body Planar and SPECT/CT) and whole body 18F-DOPA PET/CT were acquired according to standard guidelines. Curie and SIOPEN system scoring of both the modalities were compared and correlation between the same were assessed. Number of lesions detected in planar 131I-MIBG vs MIP image of 18F-DOPA and SPECT/CT vs fused regional PET/CT images were correlated. ***Results:*** In total 42 patients were included, (27 males, 15 females). Age ranged from 3 months to 84 months (Mean age was 34.4 ± 23 months). Out of 42 patients, 27 patients were indicated for initial staging and 15 patients for restaging. They were staged according to INRGSS staging. In 17 patients urinary catecholamines were elevated. Bone marrow biopsy was performed in 28 patients (12 positive, 14 negative and 2 inadequate). 131I-MIBG was positive in 38 and negative in 4 patients and 18F-DOPA PET/CT scan was positive in 39 patients and negative in 3 patients. Curie score in 131I-MIBG scan ranged from 0-28 (Mean - 5.9±8.2) and in 18F-DOPA PET/CT ranged from 0-30 (Mean - 7.6±9.5) with statistically significant difference (p=0.0147). SIOPEN score in 131I-MIBG ranged from 0-44 (Mean - 7.3±13.8) and in 18F-DOPA PET/CT ranged from 0-51 (Mean - 9.0±15.3). Strong correlation in describing the disease extent was

noted between 131I-MIBG and 18F-DOPA in both Curie (Spearman correlation, ρ = 0.83) and SIOPEN scoring (ρ = 0.82). Total no. of lesions detected in planar 131I-MIBG v/s MIP 18F-DOPA were 205 v/s 305 (ρ = 0.84) and SPECT/CT 131I-MIBG v/s fused PET/CT 18F-DOPA were 194 v/s 329 (ρ = 0.8). Higher number of bone/bone marrow lesions were picked up on 18F-DOPA PET/CT. ***Conclusion:*** Total number of lesions picked up were more in 18F-DOPA MIP and corresponding PET/CT images in comparison to 131I-MIBG planar and SPECT/CT images, respectively. When curie scoring is considered in staging, F-DOPA PET/CT performs better compared to 131I-MIBG scan. ***References:*** None

EP-142

Are we enough for insulinoma?

P. Soeiro*, L. Fadiga, R. Silva, J. Saraiva, A. Moreira, G. Costa, J. Pedroso de Lima;*
Centro Hospitalar e Universitário de Coimbra, Coimbra, PORTUGAL.

Aim/Introduction: Neuroendocrine Neoplasms of the pancreas account for less than 2% of all pancreatic tumors, and insulinomas are the most frequent. Even though mostly benign, insulinomas cause significant morbidity due to hypoglycemia. The aim of this study was to assess the accuracy of all available nuclear medicine imaging techniques in a tertiary center, without GLP-1R molecular-based imaging, for the diagnosis and identification of insulinoma. ***Materials and Methods:*** Data from all insulinoma patients diagnosed at our center was thoroughly reviewed, including clinical information, imaging studies, and genetic profiling. ***Results:*** Between 1986 and 2020 twenty four patients were found to have histology proven insulinomas (54% women). Four of these tumors were malignant. The average age at diagnosis was 60±4.3 (25-89) years. In 87.5% of cases, the initial symptom was hypoglycemia; and in 1 case, secondary hepatic lesions. Three patients had previously been diagnosed with MEN1, and insulinoma was detected in follow-up.Out of 11 insulinoma patients who performed nuclear medicine techniques, including [^{68}Ga]Ga-DOTA-NOC, 2-[^{18} F]FDOPA and 2-[^{18}F]FDG PET/CT and Octreoscan, only 4 tumors were detected, and only 2 not detected by morphologic techniques. [^{68}Ga]Ga-DOTA-NOC PET/CT detected 1 in 5 patients scanned, 2-[^{18}F]FDG PET/CT 1/1 and octreoscan 2/4. 2-[^{18} F]FDOPA PET/CT was performed in only 1 patient, and was not able to detect the tumour. In contrast, CT was able to detect 13/24, echoendoscopy 9/13 and MRI 4/8. In the remaining 4 patients, tumor localization was achieved only by angiography with intra-arterial calcium stimulation. The average size of the tumors detected by nuclear medicine techniques was 2.0±1.5, in contrast to 1.8±0.5cm for the undetected tumors. One tumor was located in the head, 2 in the tail and 1 in the body of the pancreas. ***Conclusion:*** Nuclear medicine techniques, including [^{68}Ga]Ga-DOTA-NOC, 2-[^{18} F]FDOPA and 2-[^{18}F]FDG PET/CT and Octreoscan are not sensitive for insulinoma detection, and should play a minor role in these tumors. New nuclear medicine techniques, with improved accuracy, such as GLP-1R based imaging, are eagerly awaited. ***References:*** None

EP-143

Are post-therapeutic SPECT/CT acquisitions useful to predict response to PRRT in patients with gastroenteropancreatic neuroendocrine tumors ? Preliminary results

T. Godefroy*, C. Ansquer, Y. Touchefeu, M. Barbaud, T. Matysiak-Budnik, F. Kraeber-Bodéré, T. Carlier;*
CHU de Nantes, Nantes, FRANCE.

Aim/Introduction: PRRT is a well-established therapeutic option in advanced gastroenteropancreatic neuroendocrine tumors (GEP-NET). This study analyzed some parameters extracted from post-therapeutic SPECT-CT for the prediction of PET response at 12 months. ***Materials and Methods:*** Five patients (3 males, median age: 68 years), diagnosed with metastatic Grade 1 and 2 GEP-NETs were treated with a total of 4 cycles of 7.4 GBq of ^{177}Lu-DOTATATE every 2 months. Two of them had pancreatic NETs, two others midgut NETs and one a rectal NET. A thoracic-abdominal-pelvic SPECT/CT was performed 24h after ^{177}Lu-DOTATATE injections. Data were reconstructed with attenuation, scatter and point spread function correction using 64 MLEM-equivalent iterations (voxel size: 2.4x2.4x2.4 mm^3). Normalized peak count (NPC) of the focus with the highest uptake at cycle 1 was considered. Its variation between cycle 1 and 4 (DeltaNPC) was calculated. The same computation was derived between the most intense lesion of cycle 1 and cycle 4 (PERCIST-like). Each patient had a ^{68}Ga-DOTATOC PET/CT before and one year after PRRT1. DeltaNPC was compared with the PET-based SUVpeak variation of this same lesion (DeltaSUVpeak). Outcome defined with PERCIST criteria using the two ^{68}Ga-DOTATOC PET/CT was then compared with parameters derived from SPECT/CT (DeltaNPC, PERCIST-like) and DeltaSUVPeak from ^{68}Ga-DOTATOC PET/CT. ***Results:*** At one year, one patient (patient 1) had complete metabolic response (CMR), three patients (patients 2, 3 and 4) had partial metabolic response (PMR), and one patient (patient 5) had stable metabolic disease (SMD) according to PERCIST criteria. A decrease was observed in DeltaNPC (-73%), as well as in the DeltaSUVPeak (-57%) for the patient who had CMR after one year. Among patients who achieved PMR, two showed decreased DeltaNPC and DeltaSUVpeak (respectively -91% and -79% for patient 2 and -17% and -58% for patient 3). Patient 4 showed heterogeneous results with rising DeltaNPC (33%) but decreased DeltaSUVpeak (-52%). Finally, patient 5, who had SMD, showed stable DeltaNPC (-3%) and DeltaSUVpeak

(-7%). PERCIST-like using SPECT/CT exhibited the same trend as results obtained with DeltaNPC. ***Conclusion:*** These preliminary results obtained using parameters extracted from post-therapeutic SPECT/CT, seem to be predictive of the 12-month metabolic response after PRRT. These results need to be confirmed on a larger cohort of patients. ***References:*** None

EP-144

Post Lu-177 PRRT Scintigraphy; Value of SPECT-CT

M. Numair Younis*, I. U. Khan, M. Masood, A. Shahid;*
Institute of Nuclear Medicine and Oncology-INMOL, Lahore, PAKISTAN.

Aim/Introduction: Theranostic application for detection and treatment of gastroenteropancreatic neuroendocrine tumors (GEP-NETs) using Ga-68 Dotatate (Ga-tate) and Lutetium-177 Dotatate (Lu-tate) is being widely applied as clinical trials have shown survival benefit with Lu-tate based Peptide Receptor Radionuclide Therapy (PRRT). Guidelines suggest multiple doses of Lu-tate PRRT each of maximum 200 mCi to NET patient. Lu-tate PRRT is available and being applied in Pakistan for over 2 years (1). Post therapy imaging using gamma camera is routinely performed between day 1-7 post therapy. There is no consensus on routine use of SPECT-CT in these patients. We conducted study to determine if there is any additional value of performing SPECT-CT imaging post Lu-tate PRRT. ***Materials and Methods:*** 10 patients of biopsy proven NET with metastatic disease documented on Ga-tate PET scan underwent Lu-tate PRRT. In a previous institutional study performed earlier, 10 patients underwent whole body scans on days 1, 3 and 5 post therapy. It was established that there was no difference between day 3 and 5 scans as far imaging characteristics, tumor to background ratio and detection of disease sites is concerned. Day 1 scan showed higher soft tissue background, relatively lower tumor to background and less number of disease sites as compared to days 3 and 5 scans. So in this study SPECT-CT was performed on day 3 following whole body imaging. Scans were compared with immediate pre therapy Ga-tate PET scans. ***Results:*** In our study a total of 72 disease sites were detected on Ga-tate PET scans performed in 10 patients. Whole body Lu-tate scans showed 64 disease sites, with successfully showing 8 of 8 in neck, 14 of 16 in thorax, 32 of 38 in abdomino-pelvic region and 10 of 10 in bones or bone marrow when compared with Ga-tate PET scans. SPECT-CT imaging identified all 16 of 16 in thorax and 38 of 38 in abdomino-pelvis region showing 100% concordance with Ga-tate PET scans. ***Conclusion:*** Our study concludes that there is no statistically significant benefit of using SPECT-CT scans post Lu-tate PRRT as far lesion detection rate is concerned. We suggest that SPECT-CT in post PRRT setting may be used judiciously in selected patients only after reviewing whole body scans in combination with Ga-tate PET scans for detection of obscured lesions only, keeping radiation concerns in mind. ***References:*** 1. Bashir H, et al. Nuclear Medicine Theranostics: Perspective from Pakistan. Nucl Med Mol Imaging. 2019;53(1):38-41.

EP-145

18F-FDG PET/CT diagnosis of adrenal tumors

J. Liu*, X. Han, Henan Medical Key Laboratory of Molecular Imaging;*
Hospital, Zhengzhou, CHINA.

Aim/Introduction: To investigate the diagnostic criteria and differential diagnosis of 18F-FDG PET/CT in the diagnosis of adrenal tumors by summarizing the characteristics of adrenal tumors on 18F-FDG PET/CT imaging. ***Materials and Methods:*** A total of 134 patients with adrenal tumors underwent 18F-FDG PET/CT scans in our department were analyzed for tumor size, morphology, density, and tumor FDG uptake. Plotted ROC curves of tumor SUVmax for diagnosis of benign and malignant adrenal tumors, and compared different tumor sizes and tumor SUVmax difference. ***Results:*** Of the 134 patients, 6 cases of myelolipoma , 17 cases of adenoma, 4 cases of Adenocarcinoma , 3 cases of malignant pheochromocytoma, 9 cases of neuroblastoma, 34 cases of lymphoma and 61 cases of adrenal metastases. The threshold value of SUVmax for the diagnosis of benign and malignant adrenal tumors was 4.85. The sensitivity and specificity were 88.5% and 88.9%, respectively. There were differences between different adrenal tumor sizes and tumor SUVmax. ***Conclusion:*** Different types of adrenal tumors generally have certain characteristics in ^{18}F-FDG PET/CT. It was easy to make a diagnosis in combination with laboratory tests and clinical symptoms. ***References:*** None

EP-146

^{90}Y- or ^{177}Lu-DOTATOC therapy improves symptoms control and impacts on clinical management of metastatic insulinoma

M. Freitag*[1], M. Braun[2], E. Christ[1], B. Goichot[3], T. O'Dorisio[4], D. Bushnell[4], M. Walter[1], D. Wild[1], N. Guillaume[1];*
[1]University Hospital of Basel, Basel, SWITZERLAND, [2]Claraspital, Basel, SWITZERLAND, [3]Hôpitaux Universitaires de Strasbourg, Strasbourg, FRANCE, [4]University of Iowa, Iowa City, IA, UNITED STATES OF AMERICA.

Aim/Introduction: Metastatic insulinoma is an extremely rare neuroendocrine neoplasia with estimated incidence of 1-4/10'000'000. Uncontrolled hypoglycaemia is a major cause of acute morbidity and mortality in this disease. Here, we retrospectively evaluate the hitherto largest patient series on this topic assessing the value of radiolabelled somatostatin analogue (DOTATOC) for the clinical control of progressive, metastatic insulinoma. ***Materials***

and Methods: All Patients with diagnosis of malignant insulinoma were enrolled between 2001-2018. Patients were treated with repeated cycles of Yttrium-90-DOTATOC, with consecutive cycles of Yttrium-90-DOTATOC and Lutetium-177-DOTATOC, or with Lutetium-177-DOTATOC alone. Symptomatic response was assessed using a score of hypoglycaemia between 0 (no hypoglycaemic events), 1 (some hypoglycaemic events, treatment conservative with optimization of nutrition) and 2 (severe hypoglycaemic requiring medication, history of coma). Standard of reference of a successful therapy was defined as reduction of medication necessary to maintain stable blood glucose level during the observation time. ***Results:*** Within 18 years, 23 patients were included and observed for a median time of 205 days (102.1 - 526.7). 7 patients received Yttrium-90-DOTATOC only (2.7 ± 1.0 cycles, 165 - 200 mCi), 12 patients received Yttrium-90-DOTATOC and Lutetium-177-DOTATOC (4.2 ± 2.3 cycles, 150 - 220 mCi) and 4 patients received Lutetium-177-DOTATOC only (3.5 ± 0.6 cycles, 150 mCi - 200 mCi). 16 of 23 patients experienced grade 1/2 hematotoxicity (88%), no higher grade occurred. 17 patients of 23 patients (73.9%) demonstrated improvement of hypoglycemia during the observation period. In 10 of 17 responders, anti-hypoglycemic medication could be reduced after DOTATOC therapy. ***Conclusion:*** Yttrium-90/Lutetium-177 DOTATOC therapy is able to reduce anti-hypoglycaemic medication in a significant proportion of patients with progressive malignant insulinoma and therefore helps to control hypoglycaemic events. In conclusion, radiolabelled DOTATOC therapy is a promising therapeutic option in this rare disease. ***References:*** None

EP-147

Role of [68Ga]68Ga-DOTANOC PET/CT in presurgical staging of small intestine neuroendocrine tumour

D. Calabro'[1,2], S. Telo[1,2], G. Argalia[1,2], E. Fortunati[1,2], E. Tabacchi[1,2], L. Zanoni[1,2], C. Ricci[2,3], R. Casadei[2,3], D. Campana[2,3], S. Fanti[1,2], V. Ambrosini[1,2];
[1]Nuclear Medicine, S.Orsola-Malpighi Hospital, DIMES University of Bologna, Bologna, ITALY, [2]NET team Bologna, ENETS Center Of Excellence, Bologna, ITALY, [3]DIMEC University of Bologna, Bologna, ITALY.

Aim/Introduction: Although recommended by current guidelines, [68Ga]68Ga-DOTANOC PET/CT (SSA-PET) is not often performed in the pre-surgical staging of small intestine (si) neuroendocrine tumour (NET), due to the frequent presentation as intestinal obstruction needing urgent surgery. The aim of this study is to retrospectively evaluate the usefulness of pre-surgical PET staging in patients (pts) with not occlusive siNET, comparing it with conventional imaging (CI). ***Materials and Methods:*** Inclusion criteria were: i) si lesion detected on CI (entero-CT, CT, EUS, MRI); ii) SSA-PET performed before surgery, within 60 days from CI. SSA-PET/CT was performed and interpreted following standard EANM procedure. All images were reviewed by two experienced nuclear medicine physicians. CI and SSA-PET were compared by lesions' site and number. ***Results:*** Twenty-two pts were included in the final analysis. SSA-PET was positive in all cases. SSA-PET and CI were concordant in 10/22 pts (45.5%) while in the remaining 12/22 pts (54.5%) SSA-PET and CI were discordant. Among discordant cases, in 4/12 pts (33%) CI detected more lesions than SSA-PET: 2/4 a higher number of hepatic lesions, 1/4 peritoneal carcinosis, 1/4 a necrotic lympho-adenopathy. In the remaining 8/12 pts (67%), SSA-PET showed more lesions than CI: 4/8 (50%) multiple ileal localizations, 1/8 multiple hepatic lesions (missed by EUS but later confirmed by CT performed after SSA-PET), in 2/8 sub-centimetric nodal findings (in 1/2 PET also showed bilateral lesions in normal-sized ovaries, confirmed as additional NET secondary metastasis after surgery). ***Conclusion:*** Despite the small population: in more than half of the cases pre-surgical SSA-PET showed more lesions than CI and, in particular, for the detection of multiple sub-centimetric primary ileal lesions. Additionally, PET/CT proved to be useful to identify small pathologic nodes not reaching the dimensional criteria for CT positivity. ***References:*** None

EP-148

Early post-surgical 68Ga-DOTANOC PET/CT imaging in GEP NET patients

S. Telo[1,2], E. Fortunati[1,2], G. Argalia[1,2], D. Calabrò[1,2], E. Tabacchi[1], L. Zanoni[1], D. Campana[3], S. Fanti[1,2], V. Ambrosini[1,2];
[1]Nuclear Medicine, Policlinico S.Orsola-Malpighi, Bologna, ITALY, [2]DIMES University of Bologna, Bologna, ITALY, [3]DIMEC University of Bologna, Bologna, ITALY.

Aim/Introduction: To evaluate the value of early-post-surgery-68Ga-DOTANOC-PET/CT in patients (pts) with gastro-entero-pancreatic-neuroendocrine-tumours (GEP-NET). ***Materials and Methods:*** Inclusion criteria: 1) Pts with GEP-NET enrolled in a prospective electronic archive from September 2017 to April 2019 2) first 68Ga-DOTANOC-PET/CT performed within 3-months from surgery 3) not receiving any treatment prior to PET/CT-imaging 4) diagnostic CT performed before surgery. ***Results:*** 102/822 pts were included: in most cases (77/102) early-post-surgery-68Ga-DOTANOC-PET/CT was negative. In 25/102 pts detected the presence of active-disease confirmed at follow-up (grade 1: 11/25 pts; grade 2: 14/25 pts). Among grade-1 pts, 5/11 underwent radical-surgery and early-post-surgery-68Ga-DOTANOC-PET/CT showed additional lesions not detected by pre-surgical-CT. A subcentimetric mesenteric lymph-node (SUVmax=7), a second concordant primary ileal-lesion (SUVmax=13.9) and 2 liver metastases (SUVmax=10.8) were detected in 3 pts with ilieal-primary-NET. A mesenteric lymph-node (SUVmax=11) was detected

in 1 pt with jejunum-primary-NET. A pelvic lymph-node (SUVmax=17.5) was detected in 1 pt with rectum-primary-NET. Non-radical surgery was performed in 6/11 pts with ileum-primary-NET and known metastatic lesions reported at pre-surgery-CT. Early-post-surgery-68Ga-DOTANOC-PET/CT was concordant with pre-surgical CT in 4/6: liver metastases (SUVmax-range=6-27) were detected in 3 pts, peritoneal carcinomatosis (SUVmax=12.5) in 1 pt. Lung-metastases (SUVmax=23), undetected by pre-surgical-CT with a field of view not including the thorax, were observed at early-post-surgery-PET/CT in 1 pt. Finally, an additional subcentimetric primary-ileal-lesion (SUVmax=16.3) was detected by PET/CT in 1 pt in which both CT and PET/CT showed nodal spread. Among grade 2 pts, 5/14 underwent radical-surgery: early-post-surgery-68Ga-DOTANOC-PET/CT detected additional lesions not detected by pre-surgical-CT: a local sub-centimetric lymph-node (SUVmax=8.5) and a mesenteric lymph-node (SUVmax=18.2) in 2 pancreatic-primary-NET pts, an iliac lymph-node (SUVmax=9.6) in an ileum-primary-NET pt, and multiple unknown liver lesions (SUVmax=10.1;15.2) in 2 caecum-primary-NET pts. 9/14 underwent non-radical-surgery: early-post-surgery-68Ga-DOTANOC-PET/CT was concordant with pre-surgery-CT in all cases, confirming liver metastases in 3 pancreatic-primary pts and in 2 ileum-primary pts (SUVmax range=9.3-38.6); multiple (mesenteric and pelvic) lymph-nodes in 1 pancreatic, 1 caecum and 2 ileum-primary-NET pts (SUVmax range=6.6-29.4). Overall, early-post-surgery-68Ga-DOTANOC-PET/CT was positive in 25/102 pts. In particular, PET/CT showed lesions undetected by pre-surgical CT in 10/10 cases after radical surgery and in 2/15 cases after non radical surgery. ***Conclusion:*** Our data, though limited by the small sample, show that early-post-surgery-68Ga-DOTANOC-PET/CT is positive in approximately one fourth of cases. PET/CT detected additional lesions in half of the cases when performed after radical surgery. On the contrary, in the non-radical setting, PET/CT detected additional lesions in a small minority of cases. ***References:*** None

EP-149

G1/G2 discrimination of pNET with [68Ga]Ga-DOTANOC PET/CT quantitative parameters: is it feasible?

D. Calabro'[1,2], S. Malavasi[3], A. Bevilacqua[3], C. Ricci[4,2], S. Telo[1,2], G. Argalia[1,2], E. Fortunati[1,2], E. Tabacchi[1,2], L. Zanoni[1,2], R. Casadei[4,2], D. Campana[4,2], S. Fanti[1], V. Ambrosini[1,2];

[1]Nuclear Medicine, S.Orsola-Malpighi Hospital, DIMES University of Bologna, Bologna, ITALY, [2]NET team Bologna, ENETS Center Of Excellence, Bologna, ITALY, [3]Advanced Research Center for Electronic Systems (ARCES), University of Bologna, Bologna, ITALY, [4]DIMEC University of Bologna, Bologna, ITALY.

Aim/Introduction: To evaluate if [68Ga]Ga-DOTANOC PET/CT derived TLRE (tumour lesion receptor expression) and SUVmax/SUVmean ratio of the primary lesion, can be used to discriminate G1 from G2 pancreatic neuroendocrine tumours (pNET). ***Materials and Methods:*** Among the patients (pts) with pancreatic tumour eligible for primary tumour surgery and included in a prospective electronic archive, only those with a neuroendocrine primary and a positive 68Ga-DOTANOC PET/CT performed before surgery were included in the study. 68Ga-DOTANOC PET/CT was performed and interpreted following standard EANM procedure. TLRE, defined as the product of receptor tumour volume and the SUVmean of the lesion, was calculated by a dedicated software (PET VCAR, GE Healtcare) that semi-automatically delineates the tumour contours by using a threshold of 42% of the maximal SUV within the lesion. The results were checked by comparison with the fused CT images to determine if percentage threshold adjustment was needed and therefore was performed until a satisfactory outcome was achieved. The mean and maximum SUV of each primary lesion were assessed by expert nuclear medicine physicians. TLRE and SUVmax/mean ratio results were correlated with tumour grade G1/G2 as assessed on the primary tumour mass after surgical excision. ***Results:*** In the final analysis, 25 pts with pNET and a positive [68Ga]Ga-DOTANOC PET/CT were included (G1= 13 pts; G2=12pts). TLRE (G1: 132.7±187.0 [5.8-587.4]; G2=696.9±1098.9 [8.8-3988.5] showed a good correlation with pathological grade (p=0,0276; AUC= 0.76) and sensitivity, specificity, accuracy, positive predictive, negative predictive value were respectively 75%, 77%, 76% 75% and 77%. SUVmax/mean ratio (G1: 2.1±0.4 [1.5-2.7]; G2: 1.8±0.3, 1.2-2.4] showed a weaker correlation (p=0.0414, AUC= 0.74) with sensitivity, specificity, accuracy, positive predictive and negative predictive value of 92%, 54%, 72%, 65%, 88%. ***Conclusion:*** Considering the clinical implications derived from accurate evaluation of tumour heterogeneity, the definition of easily accessible and measurable PET-derived parameters is mandatory. Although preliminary, our data show potential utility of using the TLRE and the SUVmax/mean ratio to discriminate G1 from G2 tumours. If confirmed in larger population, these results may prove valuable especially in patients not amenable to biopsy of the primary lesion. ***References:*** None

EP-150

Role of [18F] FDG-PET/CT in assessment of effectiveness of paraganglioma embolization

J. Maczewska[1], K. Kulesza[2], M. Kobylecka[1], K. Fronczewska[1], L. Królicki[1];

[1]Nuclear Medicine Department Warsaw Medical University, Warsaw, POLAND, [2]Department of General, Endocrine and Vascular Surgery Warsaw Medical University, Warsaw, POLAND.

Aim/Introduction: Preoperative embolization of carotid paragangliomas is a common procedure in interventional

neuroradiology. It appears to decrease estimated blood loss and operative time when compared with that without preoperative embolization. However, the effect depends on the effectiveness of embolization Aim of the study was to assess the effectiveness of paraganglioma embolization using [^{18}F]FDG-PET / CT. ***Materials and Methods:*** 10 patients (5 women and 5 men) with neck paraganglioma were analyzed. One week before embolization CECT and [^{18}F]FDG-PET/CT were performed to assess morphology, size and location of tumors. All patients had paraganglioma embolization according to standard procedure. Angiography performed after procedure was used to assess early effectiveness of embolization. Follow-up [^{18}F]FDG was repeated minimum 3 months after embolization. ***Results:*** All patients had single neck tumor. Average size of the tumor was 32 ± 18,5mm (range 8 - 60mm), average SUVmax in initial examination was 12,2 ± 11,6 (range 3-34,1). Angiography after embolization confirmed good result of procedure. In the control PET study, lack of [^{18}F] FDG accumulation was found only in one patient, decrease of tumor diameter as well decrease of tracer accumulation was observed in 5 patients and no changes was described in 4 patients. ***Conclusion:*** [18F] FDG PET/CT can be useful method in assessment of effectiveness of paraganglioma embolization. In our study 40% of patients had stable image of tumor in [^{18}F] FDG-PET/CT examination, despite angiography showing successful embolization. ***References:*** None

EP-151

[68Ga]-DOTA-TOC PET-TC prospective comparison with [99mTc]-HYNIC-TOC SPECT-CT and [18F]-FDG PET-CT in patients with low grade gastroenteropancreatic neuroendocrine tumors (GEPNETs)

M. Simó[1], *A. Garcia*[2], *J. Hernando*[3], *D. Villasboas*[2], *F. Dellepiane*[2], *I. Navales*[2], *M. Barios*[2], *M. Boronat*[2], *J. Capdevila*[3], *J. Castell*[2]; [1]*Hospital Universitari Vall De Hebron, Barcelona, SPAIN,* [2]*Hospital Universitari Vall de Hebron, Barcelona, SPAIN,* [3]*Vhio, Barcelona, SPAIN.*

Aim/Introduction: Initial workup in GEPNETs is usually challenging due to their heterogeneity, and accurate staging is important for selecting the appropriate treatment. [^{68}Ga]-DOTATOC imaging is a promising approach and could help in selecting optimal therapeutic strategies, but it is not yet available in all centers. The aim of this study was to prospectively determine the impact of [^{68}Ga]-DOTATOC-PET/CT versus [^{99m}Tc]-HYNIC-TOC SPECT-CT , and the role of [^{18}F]-FDG PET-CT in low grade tumors. ***Materials and Methods:*** Patients underwent [^{68}Ga]-DOTATOC-PET/CT, [^{18}F]-FDG PET/CT and [^{99m}Tc]-EDDA/HYNIC-TOC whole body planar imaging and thoracic-abdominal SPECT/CT, with less than four-week interval. Primary objective was accuracy assessment in diagnosis of [^{68}Ga]-DOTATOC-PET/CT compared with [^{99m}Tc]-EDDA/HYNIC-TOC, determine the different binding patterns of [^{18}F]-FDG and [^{68}Ga]-DOTA peptides in this group of patients and assess the therapeutic impact on treatment decision. ***Results:*** 29 and 27 patients were positive for [^{68}Ga]-DOTATOC-PET/CT and for [^{99m}Tc]-EDDA/HYNIC-TOC, respectively. [^{68}Ga]-DOTATOC-PET/CT found the primary tumor in 14/16 non resected patients, whereas [^{99m}Tc]-EDDA/HYNIC-TOC fount it in 8/14 patients. Neither could detect the primary in two patients with primary unknown origin. In liver, [^{68}Ga]-DOTATOC-PET/CT was positive in 25 patients (all histological confirmation) and negative in 5. The only patient with false negative result had both lung carcinoid and pancreatic TNE. [^{99m}Tc]-EDDA/HYNIC-TOC could not detect liver metastases in two [^{68}Ga]-DOTATOC-PET/CT positive patients. In one patient, with potentially resectable hepatic disease by [^{99m}Tc]-EDDA/HYNIC-TOC, [^{68}Ga]-DOTATOC-PET/CT detected multiple unresectable liver disease. [^{68}Ga]-DOTATOC-PET/CT was superior to [^{99m}Tc]-EDDA/HYNIC-TOC in detecting the number and localization of liver metastases, bone metastasis and peritoneal carcinomatosis detection. Only [^{68}Ga]-DOTATOC-PET/CT could detect extrahepatic disease in 43% of patients, with a major impact on therapeutic management 3 out of 26 patients potentially candidates for peptide receptor radionuclide therapy using [^{68}Ga]-DOTATOC-PET/CT were not by [^{99m}Tc]-EDDA/HYNIC-TOC. [^{18}F]-FDG PET/CT added clinical information in only one of all cohort patients. ***Conclusion:*** [^{68}Ga]-DOTATOC-PET/CT provides important information for accurate workup of GEPNETs and selection of appropriate treatment decisions, compared to [^{99m}Tc]-EDDA/HYNIC-TOC. [^{18}F]-FDG PET/CT provides residual information in this group of G1/G2 patients and it is not recommended in daily routine. ***References:*** None

EP-152

Utility of suvmax values of PET / TC 68GA-DOTATOC in the diagnosis and monitoring of patients with pulmonary neuroendocrine tumors (NPT)

T. Moreno-Monsalve*, T. Rodríguez -Locarno, D. Cáceres- Silva, M. Castellón -Sánchez, J. Navarro- Fernández, L. Frutos- Esteban, L. Mohamed-Salem, J. Contreras- Gutiérrez, M. Claver Valderas; Hospital Universitario Virgen De La Arrixaca, Murcia, SPAIN.*

Aim/Introduction: TNPs express somatostatin receptors according to the degree of differentiation and the histological type. Our objective is to study the correlation between the SUVmax values of the 68Ga-DOTATOC PET / CT and the different histological subtypes of the TNP. ***Materials and Methods:*** We conducted a retrospective study in 32 patients with suspected or previous diagnosis of TNP between December 2018 and 2019, who had histological confirmation and PET / CT 68Ga-DOTATOC. Subjects were 13 women (40.6%) and 19 men (59.4%) with a mean age of 60.84. Diagnostics comprised 16 typical carcinoids

(CT) (50%), 6 atypical carcinoids (CA) (18.75%), 1 diffuse idiopathic neuroendocrine cell hyperplasia (3.12%), 1 large cell neuroendocrine carcinoma (CNCG) (3, 12%), 2 with undetermined pathological diagnosis, and finally 6 subjects with negative histology (18.75%). ***Results:*** We analyzed the SUVmax of 32 patients out of which 6 reported baseline PET / CT 68Ga-DOTATOC and PET / CT 18F-FDG. The CTs had a mean SUVmax for the 68Ga-DOTATOC PET / CT of 16.21, and 6.06 for the PET / CT 18F-FDG. In the CA, the SUVmax for the 68Ga-DOTATOC PET / CT was 3.19, and for the 18F-FDG PET / CT it was 5.2. In the CNCG the mean was 3.06 for the PET / TC 68Ga-DOTATOC, and 5.7 for PET / TC 18F-FDG. Regarding the 68Ga-DOTATOC PET / CT performed after treatment, of 12 CT, only 4 showed pathological uptake with a mean SUVmax of 33.38. And of 6 CA, 5 were pathological with an average SUVmax of 11.4. ***Conclusion:*** There is a correlation between the SUVmax values and the different histological subtypes of the TNP, where CT shows greater affinity for the PET / CT 68Ga-DOTATOC than the CA, and an inverse relationship with the PET / CT 18F-FDG. Prospective epidemiological studies are necessary to validate this association. ***References:*** None

EP-153

Characterization and surveillance of cardiac metastasis in well-differentiated gastroenteropancreatic neuroendocrine tumor using Ga68-DOTATATE PET/CT and PET/MR

J. Renfrew*, R. Shrestha, M. Yang, T. Halfdanarson, R. Arsanjani, M. Sonbol;*
Mayo Clinic - Arizona, Phoenix, AZ, UNITED STATES OF AMERICA.

Aim/Introduction: Gastroenteropancreatic (GEP) neuroendocrine tumor (NET) has gained growing recognition thanks to the clinical utilization of Ga68-labelled somatostatin analogue PET tracers, which target the somatostatin receptor subtype 2 (SSTR2) expressed on the tumor cell membrane. While hepatic and nodal metastases are commonplace at the time of NET diagnosis, cardiac metastases are found much less frequently. In this study, we aim to evaluate the prevalence, distribution pattern, and radiotracer uptake characteristics of cardiac metastasis on Ga68-DOTATATE PET/CT and PET/MR images. ***Materials and Methods:*** In this IRB approved retrospective study, the diagnostic criterion of cardiac metastasis is focal myocardial tracer uptake on PET with confirmative space-occupying lesion on chest CT or cardiac MR. The SUVmax of the cardiac metastasis and left ventricular chamber (blood pool), the Krenning score of the cardiac metastasis, and the presence of multisystem metastasis were documented and analyzed. ***Results:*** From Oct. 2017 to Mar. 2020, there were 1,426 Ga68-DOTATATE PET/CT and PET/MR scans performed at our institution. Twenty-one GEP NET patients (mean age of 64 ± 10.17 years old, male : female ratio of 11:10) were diagnosed with asymptomatic cardiac metastasis, always with coexistence of multisystem metastases on PET, including liver, lymph node, lung and bone marrow, as well as elevated chromogranin A. In this cohort of patients, there were 29 total lesions, including those at the left ventricular free wall (16), septum (8), and right ventricular free wall (5). The average maximal SUV of these lesions was 9.2 (range 2.6-24.1) with the Krenning score of 2 to 4. The average maximal SUV of blood pool was 1.2 (range 0.5-2.4). The average lesion to blood pool SUV ratio was 8.3 (range 2.6-18.2).Seven patients had multiple Ga68-DOTATATE PET/CT scans while on Octreotide therapy. Among them, two (29%) showed initial progression with subsequent lesion stabilization on imaging. ***Conclusion:*** The prevalence of cardiac metastasis is associated with high tumor burden. Ga68-DOTATATE PET/CT and PET/MR is an established imaging modality in detection and surveillance of this rare clinical entity, and provides further guidance of clinical management. The clinical significance of cardiac metastasis needs to be further investigated. ***References:*** 1.Bonsen LR, Aslbersberg EA, Tesselaar M, Stokkel MP. Cardiac neuroendocrine tumour metastases: case reports and review of the literature. Nucl Med Commun. 2016, 37(5):461-52.Kunz WG, Eschbach RS, Stahl R, et al. Identification and characterization of myocardial metastases in neuroendocrine tumor patients using 68Ga-DOTATATE PET-CT. Cancer Imaging. 2018, 20;18(1):34.

EP-154

Retrospective Analysis of the Indications to 18F-FDG-PET/CT in NET Patients

G. Argalia*[1], D. Calabrò[1], S. Telo[1], E. Fortunati[1], E. Tabacchi[2], L. Zanoni[2], D. Campana[3], S. Fanti[1], V. Ambrosini[1];*
[1]Nuclear Medicine, S.Orsola-Malpighi Hospital, DIMES University of Bologna, Bologna, ITALY, [2]Nuclear Medicine, S.Orsola-Malpighi Hospital, Bologna, ITALY, [3]DIMEC University of Bologna, Bologna, ITALY.

Aim/Introduction: To retrospectively analyze the indications to 18F-FDG-PET/CT (FDG) performed before or after biopsy and 68Ga-DOTANOC-PET/CT (SSA) in patients (pts) with Grade-1 (G1) and Grade-2 (G2) neuroendocrine tumours (NET). ***Materials and Methods:*** Among pts collected in a CE-approved electronic archive between September2017-June2019, those with confirmed G1-G2 NET and both SSA and FDG were included. ***Results:*** 33 pts were included: Group-A (FDG positive=21) and Group-B (FDG negative=12). Group-A: indication to FDG in 9/21 pts was conventional imaging (CI:CT/US/MRI) equivocal (not suggestive for NET) findings characterization before biopsy (performed on average 1month after FDG) and before SSA. In 2/9 pts biopsy revealed a G1-tumour (lung primary: 1pt, ileum primary: 1pt) but the subsequent SSA showed mismatch lesions in one

case and matched lesions in the other. In the remaining 7/9 pts, biopsy showed a G2-tumour (primary: lung 3pts, ileum 1pt, pancreas 1pt, gallbladder 1pt, 1pt with retroperitoneal paraganglioma with ki67>10%). In the remaining 12/21, FDG was performed after biopsy and SSA. In 4/12 pts FDG was performed to characterize equivocal CT findings: SSA was positive in 2pts (1 ileum primary-G1 with suspected peritoneal lesions; 1 paraganglioma with ki67:5.4% studied for suspected relapse) and negative in 2pts (primary: 1 G1-ileum, 1 G1-lung with lung nodules suspicious for non-NET lesions but later confirmed as NET). In 5/12 FDG was performed for disease progression in pts with an originally well-differentiated lesion (biopsy performed before FDG respectively at 68months in one G1-ileum, at 156months in a G2-ileum, at 15months in two G2-pancreas and at 48months in one G2-pancreas), in 1/12 pt for low uptake at SSA (G2-ileum with suspected lung secondary lesions), in 2/12 pts for pre-surgical staging (G2-pancreas and G2-ileum respectively). Group-B (12pts): in 7/12 pts FDG was performed to characterize equivocal CI findings not suggestive for NET (6 hepatic lesions; 1 abdominal mass) before biopsy and before SSA. Biopsy later revealed ileum primary in 6/7 (G1:4; G2:2) and UPC in 1/7 (G1:1). In 2/12 pts FDG was performed to characterize equivocal CT findings after a NET-positive biopsy and negative SSA: 1/2 hepatic lesions (G2-lung) and 1/2 abdominal nodes (G2-pancreas). Indication to FDG in 3/12 pts was suspected disease progression (1 G1-pancreas, 1 G2-pancreas, 1 MEN1): SSA was respectively positive in the first 2 pts and negative in the latter. ***Conclusion:*** Indications to FDG in NETG1-G2 pts were CI equivocal findings characterization, disease progression and negative/low-uptake SSA. ***References:*** None

EP-155

Corticomedullary mixed tumor of the adrenal gland with apparent 18F-FDG activity but no 68Ga-DOTATATE uptake on PET/CT

C. Engur[1], T. Apaydin[2], T. Ones[1], H. I. Gozu[2], T. Y. Erdil[1];
[1]Marmara University Pendik Training and Research Hospital, Istanbul, TURKEY, [2]Marmara University Pendik Training and Research Hospital, Endocrinology Department, Istanbul, TURKEY.

Aim/Introduction: Corticomedullary mixed tumor (CMT) is a single adrenal tumor mass composed histologically by an admixture of adrenal cortical and medullary cells. It is a rare condition with approximately 20 cases reported to date. To our knowledge, the PET imaging findings of this mostly benign tumor have not been reported in the literature. We present a case of CMT who was evaluated with both 18F-FDG and 68Ga-DOTATATE. ***Materials and Methods:*** A 63-year-old woman referred to endocrinology clinic for a 23x22 millimeter left adrenal adenoma, detected incidentally in abdominal CT which performed for abdominal pain in her left flank. In the laboratory examination; the 1 mg over night dexamethasone suppression test (DST) was 5.32 µg/dL (normal value(NV):<1.8 µg/dL) , 2-day low-dose DST was 3.26 µg/dL (NV: < 1.8 µg/dL). There was no obvious cushingoid features and the patient was diagnosed as subclinical Cushing's syndrome. The patient was evaluated with both 18F-FDG and 68Ga-DOTATATE. ***Results:*** The hypermetabolic tumor seen on 18F-FDG (SUVmax was 4.4, clearly higher than the background liver SUVmax 2.2, Figure 1A) which was localized on the medial crus of the left adrenal gland, showed no abnormal uptake on 68Ga-DOTATATE (Figure 1B). Laparascopic left adrenalectomy was performed. The tumor diameter was 2.4x2.3x2 centimeters and histopathologically demonstrated two different cell types composed of cortical and chromaffin cells. The Weiss score was 1, compatible with adefinitive pathologic diagnosis of a benign CMT. The patient was followed up at the endocrine outpatient clinic and 1 mg overnight DST was 0.26 µg/dL at postoperative third month. ***Conclusion:*** In the vast majority of patients with CMT, the symptoms were related to the tumor's hormone hypersecretion. Most of them are benign with a favourable prognosis but some malignant tumors with a poor prognosis have been reported. Due to the lack of specific clinical features, these tumors are discovered accidentally on histological examination. 18F-FDG is a useful imaging technique in characterizing adrenal masses. However false-positive interpretations may result from benign lesions. Our case is the first one to our knowledge to report a case of a benign CMT who was evaluated with PET imaging findings and it should be kept in mind that it may exhibit false-positive results for malignancy with 18F-FDG . Negative 68Ga-DOTATATE findings may be a clue for benignity in this patient group. It may be important to obtain further PET imaging results, especially in patients with pathologic diagnosis of malign CMT. ***References:*** None

EP-156

Influence of somatostatin analogue type for result of 68Ga-somatostatin analogue PET/CT and its effect on therapeutic decisions in patients with neuroendocrine neoplasm - which result to believe? - case study

***M. Opalinska[1]**, A. Sowa-Staszczak[2,1], K. Skórkiewicz[1], M. Buziak-Bereza[2,1], A. Stefańska[1], A. Hubalewska-Dydejczyk[2,1];*
[1]Nuclear Medicine Unit, Endocrinology Department, University Hospital, Krakow, POLAND, [2]Endocrinology Clinic of the Endocrinology Department , Faculty of Medicine, Jagiellonian University Medical College, Krakow, POLAND.

Aim/Introduction: Confirmation of the somatostatin receptors expression in neuroendocrine neoplasm is a basis for choice of diagnostic and therapeutic procedures. Lack of such expression limits treatment options. The somatostatin analogues used for diagnostics may have different affinity for the somatostatin receptors subtypes. The selection of ligand(NOC, DOTA, TATE) often is limited by its availability and

usually is not connected to the real profile of somatostatin receptors expression in the tumor tissues. ***Materials and Methods:*** Case report: In 03.2009 a 34-years old male was referred to Endocrinology Clinic with suspicion of pancreatic NET. MRI revealed presence of a 54x42mm tumor of the distal part of the pancreas and 2 metastatic changes in the liver. Liver biopsy confirmed neuroendocrine neoplasm. Resection of the pancreatic body and tail with splenectomy was performed on 04.2009(pathology: neuroendocrine cancer, Ki67 50%, metastases in 17/20 nodes). The tumor had good expression of somatostatin receptors (sstr) in the primary and metastatic lesions.Due to the high expression of sstr, patient received 1 dose of PRRT with the next Gemzar and Erlotinib therapy which was ended in 08.2011. From 2015, the PET/CT scan with 68GaDOTA-TATE show pathological (Krenning score 3 and 4) expression of sstr in the retropharyngeal node. The lesion had slowly progressed in various follow-up studies. In 09.2016, the conglomerate of neck nodes group II and V, the submandibular salivary gland and the node of the mandible angle were removed (metastases to lymph nodes were confirmed, Ki67 3%). The follow-up PET/CT studies with 68Ga DOTA-TATE started from 11.2016 showed the persistent pre-vertebral SSTR+ space infiltration extending from the base of the skull to level C1/C2 and involvement of cervical IIa nodes. A follow-up study with 68Ga DOTA-TOC showed only slightly elevated (Krenning score 1) expression of sstr in the pre-vertebral space (previously with high pathological expression of sstr seen on 68GaDOTA-TATE PET/CT). The next follow-up study with 68GaDOTA TATE again revealed high, pathological expression of sstr in the neck area. ***Results:*** Patient with pancreatic NETG3 was found to have incompatible imaging results using both 68Ga-TOC and -TATE ligands. ***Conclusion:*** The result of PET/CT 68Ga-somatostatin analogue imaging with different ligands may give different results in the same patient and in extreme cases may lead to the suboptimal choice of therapeutic procedures (disqualification from long-acting somatostatin analogue treatment and PRRT in case of dissemination of the disease). ***References:*** None

EP-157

Prognostic impact of phenotype heterogeneity of grade 1-2 metastatic gastroenteropancreatic neuroendocrine tumors documented by 18FDG PET-CT and 68Ga-DOTANOC PET-CT

M. Barbaud[1], *Y. Touchefeu*[2], *M. Le Bras*[3], *V. Fleury*[4], *T. Carlier*[1,5], *C. Bailly*[1,5], *E. Frampas*[6], *A. Rauscher*[7], *F. Kraeber-Bodere*[1,5], *C. Ansquer*[1]; [1]*Nuclear Medicine Unit, University Hospital, Nantes, FRANCE,* [2]*Digestive Oncology, Institut Des Maladies De l'Appareil Digestif, University Hospital, Nantes, FRANCE,* [3]*Department of Endocrinology, University Hospital, Nantes, FRANCE,* [4]*Nuclear Medicine Unit, Institut de Cancérologie de l'Ouest, Saint-Herblain, FRANCE,* [5]*CRCINA, INSERM, CNRS, Angers University, Nantes University, Nantes, FRANCE,* [6]*Department of Radiology, University Hospital, Nantes, FRANCE,* [7]*Pharmacy Unit, Institut de Cancérologie de l'Ouest, Saint-Herblain, FRANCE.*

Aim/Introduction: The identification of prognostic factors for survival in patients with metastatic gastroenteropancreatic neuroendocrine tumors (GEP-NET) represents a challenge for patient management. This retrospective study investigated the phenotype presentation of these tumors with 18FDG and 68Ga-DOTANOC-PET-CT and analyzed its prognostic impact on survival. ***Materials and Methods:*** Patients with metastatic histologically proven grade 1 (G1) or 2 (G2) GEP-NET (WHO 2019 classification), who underwent 18FDG-PET-CT and 68Ga-DOTANOC-PET-CT within 2 months between 2013 and 2017, were included. For 18FDG-PET-CT analysis, pathological foci which exceeded in intensity healthy liver were considered significant. Progression was assessed with clinical and radiological criteria. Progression free survival (PFS) and overall survival (OS) were evaluated. Kaplan-Meier method was used (curves being compared with log-rank test). Prognostic factors were evaluated with univariate and multivariate analysis (Cox proportional hazards model), with a p value of less than 0.05 considered significant. ***Results:*** A total of 39 patients (23 males, 16 females, median age: 59 years), 10 with G1 (26%) and 29 with G2 (74%) tumors were included, mainly pancreatic (n=20; 51%) or midgut (n=13; 33%) origin. Median Ki67 index was 7%, >10% in 11 patients (28%). 68Ga-DOTANOC-PET-CT was positive (at least one lesion) in 100% of patients and 18FDG-PET-CT in 72% of patients (n=28). At least one 18FDG+/68Ga-DOTANOC- lesion was found in 4 patients (10%). After a median follow-up of 39 months, 24 patients had progressive disease (64%) and 11 died (28%). PFS was significantly lower in 18FDG-PET-CT positive patients than in 18FDG-PET-CT negative patients (14vs55.9 months; p=0.0249). Furthermore, the number of 18FDG positive lesions and the presence of at least one 18FDG+/68Ga-DOTANOC- lesion were significantly correlated with PFS in univariate (respectively, p<0.0001 and p=0.007) and multivariate analysis (respectively p=0.0012 and p=0.020). Despite the low number of event, the presence of at least one 18FDG+/68Ga-DOTANOC- lesion was associated with poor OS (p=0.017). The number of previous treatment was associated with PFS in univariate analysis (p=0.0396) but not in multivariate analysis. None of the other clinical, biological (including WHO grade, Ki67 index) or 68Ga-DOTANOC-PET-CT data were significantly associated with PFS or OS. ***Conclusion:*** Our results showed the high prevalence of 18FDG positive lesions in G1 and G2 metastatic GEP-NET illustrating the heterogeneity of these tumors and confirmed the prognostic impact of 18FDG-PET-CT on PFS. In particular, the number of 18FDG positive lesions and the presence of at least one 18FDG+/68Ga-DOTANOC- lesion were associated with a poorer prognosis in our patients. ***References:*** None

EP-22

Imaging Clinical Studies -> Oncological Imaging Clinical Study -> Other Hemato-Oncology

e-Poster Area

EP-158

Prognostic value of ^{18}F-FDG PET / CT in patients with Multiple Myeloma treated with autologous haematopoietic stem-cell transplantation

L. Brero Sánchez, R. Álvarez Pérez, J. Cuenca Cuenca, E. Carrillo Cruz, J. Tirado Hospital, J. Jiménez-Hoyuela García; Virgen del Rocio University Hospital, Seville, SPAIN.

Aim/Introduction: To assess the prognostic value of ^{18}F-FDG PET / CT in patientes with Multiple Myeloma (MM) treated with autologous haematopoietic stem-cell transplantation (HSCT). ***Materials and Methods:*** Retrospective study of 17 patients (11 women and 6 men with a mean age of 57.18 years) diagnosed with MM between 2015 and 2019, with avaible clinical information about disease status before chemotherapy induction treatment, before HCST and a minimum clinical follow-up of 6 months after HCST. All of them underwent a ^{18}F-FDG PET / CT before HCST (PET0) and at least 3 months after it (PET1). We analized the number of lesions and the maximum standardized uptake values (SUVmax) of each study before and after HCST. After literature review, we considered as poor prognosis indicator a SUVmax &gt 4.2. ***Results:*** 3/17 patients had negative studies on both PET0 and PET1. 9/17 showed a decrease of SUVmax in PET1 compared to the previous one, with a SUVmax reduction over 25% in 5 of them, all of them had a progression-free survival (PFS) &gt 12 months. 5/17 patients showed SUVmax increase in PET1 compared to PET0, with PFS &lt 6 m. 3/5 patinetes presented a significant increase (25%) in SUVmax between PET0 and PET1 and they were exitus during the follow-up. 2/3 patients showed extramedullary disease and study SUVmax &gt 4.2 on PET0. We did not observe a correlation between the number of lesions in PET0 and PFS. ***Conclusion:*** Visual and semiquantitative analysis of 18F-FDG PET / CT pre and post-HCST in patients with MM, as well as the evaluation of SUVmax value, may predict patient response to HCST. ***References:*** Multiple myeloma: ESMO Clinical Practice Guidelines for diagnosis, treatment and follow-up. Annals of Oncology 28 (Supplement 4): iv52-iv61, 2017. Interest of Pet Imaging in Multiple Myeloma. Front Med April 9; 6:69. 2019.

EP-159

PET / CT Imaging in Smoldering Multiple Myeloma Patients F 18-Fluorodeoxyglucose and Ga68-Pentixafor: Preliminary results

U. Korkmaz, E. G. Umit, G. Durmus-Altun; Trakya University, Edirne, TURKEY.

Aim/Introduction: Smoldering multiple myeloma (SMM) is a subgroup of MM, limited to bone marrow, with no other organ involvement. Patients are face the risk of developing active MM over time. The risk increases with bone marrow involvement. Tumor burden is the most important factor for prognosis. FDG PET/CT has proven to be a sensitive technique for the detection of metabolically active MM and has recently been included in the diagnosis of MM by the International Myeloma Study Group (IMSG). Accurate evaluation of bone disease is important in MM, order to be managed clinically correctly. The aim of this study is to evaluate the contribution of Ga68-Pentixafor PET / CT by comparing it with F18-FDG data in the special patient group followed up without tumor after SMM or otolog bone marrow transplantation (OBMT). ***Materials and Methods:*** In this study, 155 patients (67 years, 46K) who were diagnosed and treated with MM in between 2016-2018 were included. All patients were evaluated with the FDG PET/CT after the initial and remission induction. In patients with suspected SMM, Ga 68-Pentixafor PET / CT was performed. The Ga-68 Pentixafor PET / CT and F-18 FDG PET / CT images taken in the same system with the proposed routine protocol were independently evaluated on the basis of patients and lesions by two experienced nuclear medicine specialists. Data of each patient were obtained from the hematology follow-up files. PET / CT findings were evaluated together with accompanying clinical follow-up data. ***Results:*** No metabolic active focus was detected in F-18 FDG PET / CT images in 30 of 155 patients at the time of diagnosis. Three patients were accepted as SMM and 3 patients were in complete remission after first line therapy and OBMT according to the IMSG criteria. None of them had evidence that could be associated with bone lesion. ***Conclusion:*** The findings of this study supported that FDG PET / CT is a sensitive technique for the detection of metabolically active MM. Limited but valuable data has been generated for 68Ga-Pentixafor in six MM patients. It has been possible to show metabolic changes with PET / CT in both SMM patients and MM patients in remission. As a disease that is still considered "incurable", Ga68-Pentixafor PET / CT promises the correct use of newer definitions such as "minimal residual disease" and "limited complete remission" in the clinical approach in MM. ***References:*** None

EP-160

^{11}C-Methionine and ^{18}F-FDG PET/CT in multiple myeloma: Comparative study

O. Cuenca-Vera[1], M. de Arcocha-Torres[1], I. Martínez-Rodríguez[1], R. Quirce[1], J. Jiménez-Bonilla[1], A. Sánchez-Salmón[1], N. Martínez-Amador[1], G. Molina-Mendoza[1], J. Andrés-Pacheco[1], Á. Gutiérrez-González[1], S. Ruiz Llama[1], A. Bermúdez[2], I. Banzo[1];
[1]Nuclear Medicine Service. Marqués de Valdecilla University Hospital. Molecular Imaging Group (IDIVAL). University of Cantabria, Santander, SPAIN, [2]Hematology Service. Marqués de Valdecilla University Hospital. University of Cantabria, Santander, SPAIN.

Aim/Introduction: Our objective was to evaluate and compare the diagnostic efficacy of ^{11}C-Methionine (MET) and ^{18}F-FDG (FDG) PET/CT in patients with a diagnosis of multiple myeloma. ***Materials and Methods:*** We performed a retrospective study involving 12 patients with multiple myeloma (9 men; mean age: 57.5±9.7 years). In all patients both MET and FDG PET/CT were acquired with an interval between examinations ranged from 11.8 to 12.9 days (november-17th to January-20th). In total, 13 sets of PET/CT were evaluated (one patient had two sets of examinations). PET/TC studies were performed prior to treatment in 4 cases (30.8%) and during follow-up in 9 (69.2%). MET and FDG were produced in an in-house cyclotron and using an automated synthesis system. Whole-body PET/CT scans were acquired 20 minutes after iv injection of 555-740 MBq of MET and 90 minutes after iv injection of 7 MBq/kg of FDG. MET and FDG images were blindly visually analysed. Any focal accumulation of the radiotracer higher than the background was considered as positive. The results obtained with MET and FDG were compared, considering both the number and extend of bone uptake foci. ***Results:*** MET and FDG findings matched in 10 out of 13 studies included (76.9%) and mismatched in 3 (23.1%). Of the 10 matched studies, 6 (46.1%) were MET and FDG positive: in 1 of them both examinations showed the same bone uptake foci, in 4 MET showed more foci than FDG and in 1 the FDG showed more foci than MET. In 3 studies (23.1%) MET and FDG were negative. Finally, in 1 study (7.7%) MET and FDG were inconclusive. Of the 3 mismatched studies, in 1 (7.7%) MET was positive and FDG negative, and in 2 (15.4%) FDG was positive and MET negative. MET detected multiple myeloma involvement in 7/13 studies (53.8%), in 4 of them with greater extent than FDG and in 1 with a negative FDG. FDG detected myeloma involvement in 8/13 studies (61.5%), in 1 of them with greater extent than MET and in 2 with a negative MET. ***Conclusion:*** MET and FDG PET/CT scans showed a complementary role in the evaluation of patients with multiple myeloma. When both studies, MET and FDG, were positive MET detected a more extensive involvement. These results should be confirmed by a larger population. ***References:*** None

EP-161

Can ^{18}F-NaF PET/CT Before Autologous Stem Cell Transplantation Predict Survival In Multiple Myeloma?

C. Sachpekidis[1], A. Kopp-Schneider[2], M. Merz[3], A. Jauch[4], M. Raab[3], H. Goldschmidt[3], A. Dimitrakopoulou-Strauss[1];
[1]Clinical Cooperation Unit Nuclear Medicine, German Cancer Research Center (DKFZ), Heidelberg, GERMANY, [2]Department of Biostatistics, German Cancer Research Center (DKFZ), Heidelberg, GERMANY, [3]Department of Internal Medicine V, University Hospital Heidelberg and National Center for Tumor Diseases (NCT), Heidelberg, GERMANY, [4]Institute for Human Genetics, University of Heidelberg, Heidelberg, GERMANY.

Aim/Introduction: There is an unmet need for positron emission tomography (PET) radiotracers that can image bone disease in multiple myeloma (MM) in a more sensitive and specific way than the widely used ^{18}F-fluorodeoxyglucose (^{18}F-FDG). Sodium fluoride (^{18}F-NaF) is a highly sensitive tracer of bone reconstruction, evolving as an important imaging agent for the assessment of malignant bone diseases. We attempted to investigate for the first time the prognostic significance of ^{18}F-NaF PET/CT in newly diagnosed, symptomatic MM patients planned for autologous stem cell transplantation (ASCT). ***Materials and Methods:*** Forty-seven patients underwent dynamic and static PET/CT with ^{18}F-NaF before treatment. After correlation with the respective findings on CT and ^{18}F-FDG PET/CT that served as reference, the ^{18}F-NaF PET findings were compared with established factors of high-risk disease, like cytogenetic abnormalities as well as bone marrow plasma cell infiltration rate. Furthermore, the impact of ^{18}F-NaF PET/CT on progression-free survival (PFS) was analyzed. ***Results:*** Correlation analysis revealed a moderate, significant correlation of the ^{18}F-NaF parameters $SUV_{average}$ and K_1 in reference tissue with bone marrow plasma cell infiltration rate. However, no other significant correlation was observed regarding all other ^{18}F-NaF PET parameters. Survival analysis revealed that patients with a pathologic ^{18}F-NaF PET/CT have a shorter PFS than those with a physiologic scan. Nevertheless, no quantitative ^{18}F-NaF parameter adversely affected PFS. ***Conclusion:*** The herein presented findings highlight the rather limited role of ^{18}F-NaF PET/CT as a single PET approach in MM. ***References:*** None

EP-162

The role of 18F-FDG PET/CT and beta-2-microglobulin in diagnostic assessment of patients with multiple myeloma

K. Mladenov[1], V. Hadzhiyska[1], D. Vasileva[2], P. Nikolova[1], M. Ilcheva[1];
[1]Clinic of Nuclear medicine, University Hospital "Alexandrovska", Sofia, BULGARIA, [2]Department of Nuclear Medicine, Specialized Hospital for Active Therapy of Haematological diseases, Sofia, BULGARIA, .

Aim/Introduction: Multiple myeloma (MM) is a malignant haematological disorder characterized by bone marrow infiltration with neoplastic plasma cells, paraproteinemia and osteolytic bone destruction. The detection of extramedullar tissue involvement is important for the treatment planning and prognosis of MM patients (pts). Standard diagnostic imaging methods, such as radiography and bone scan, have certain limitations for early evaluation of bone and bone marrow lesions. FDG-PET/CT has been shown to be able to detect extramedullar lesions and to improve bone lytic lesions detection for appropriate staging of the process. Serum beta-2-microglobulin (β_2M) levels have been used to evaluate tumour burden in MM pts. However data regarding correlations between PET findings with serum β_2M levels in MM pts are limited. The aim of the study was to investigate the clinical usefulness of 18F-FDG-PET/CT imaging and correlations with serum-beta-2-microglobulin in MM pts. ***Materials and Methods:*** Fifty eight MM patients were evaluated retrospectively (32 males and 26 females) a median age 58.3 years. 18F-FDG-PET/CT scans were performed according to the standard protocol. Serum β_2M levels were measured by radioimmunoassay. ***Results:*** In 3 pts without bone lesions, disease was detected in the bone marrow with PET/CT scintigraphy (diffuse uptake), before other visual methods. The PET marrow uptake correlated with the percentage of bone marrow plasma cells. The median serum β_2M levels were 4.8mg/l (normal range 1.2-2.4 mg/l). The scintigraphy data showed hypermetabolic bone lesions in 55 pts. The focal and multifocal patterns of FDG-PET/CT were detected in four and 51 pts, respectively. A total of 102 bone lesions were detected in the calvaria, spine, ribs, sternum, pelvis and long bones. The median SUV max was 8,5 mg/l. The extramedullary lesions in the soft tissues were detected in 12.1% (7/58) pts (thyroid gland, mammary gland, lungs, orbita, stomach). The median serum β_2M levels were 9.8 mg/l. 18F-FDG PET revealed 2 previously unknown additional lesions in two patients undetected by conventional visualization methods. The diagnosis was confirmed by bone and bone marrow biopsy. confirmed by bone and bone marrow biopsy. ***Conclusion:*** The results showed the effectiveness of the 18F-FDG-PET/CT in the detection of skeletal, bone marrow and extramedullar involvement in MM patients. The positive scintigraphy showed a good correlation with the data of serum beta-2-microglobulin in patients with MM. The potential of PET/CT to detect medullary and extramedullary lesions in a single examination is important advantage over other visualization methods. ***References:*** None

EP-163

^{18}F-Fluorocholinein the staging of Multiple Myeloma patients . First impressions

P. Garrastachu Zumaran[1], X. Boulvard[1], M. Albornoz[1], P. Hernández Pérez[2], F. Cañete Sanchez[1], L. Romero Robles[1], A. Cabrera Villegas[1], M. Hermosilla Fernández[2], R. Ramirez Lasanta[1]; [1]Fundacion Riojasalud. CIBIR, Logroño, Rioja, SPAIN, [2]Hospital San Pedro, Logroño, Rioja, SPAIN.

Aim/Introduction: It is well known the negative results obtained when staging some patients diagnosed with MM. The objective of this study is to evaluate the possible role of ^{18}Fluorocholine -PET/TAC(FCH-PET) in this scenario and compare it with the established imaging work up, the ^{18}Fluorodesoxiglucose-PET/TAC (FDG-PET). ***Materials and Methods:*** It is a prospective study that includes patients with diagnosis of MM and candidates for bone marrow autologous transplant (AT). Each patient undergoes PET-CT studies with two tracers: 18-FCH and18-FDG. For each tracer we evaluate the presence of bone marrow infiltration and its metabolic pattern as well as the presence of focal bone lesions and paramedular and extramedular disease according to the proposed IMPeTus criteria (Italian myeloma criteria for PET Use). We compare the findings obtained for both tracers per lesion and per patient. ***Results:*** We included 9 patients (the study is still opened). The median time between 18FDG-PET and 18FCH-PET scans was 4 days(1-28). 4 out of the 9 patients studied had diffuse bone marrow infiltration in FDG-PET. FCH showed a diffuse pattern in 8 of the 9 patients and a patchy distribution in 1 of them. The FDG-PET visualized 5 focal bone lesions in contrast to the 13 observed in the FCH-PET. 3 of the FDG-PET positive bone lesions were also positive in FCH-PET and 2 of them were negative: one corresponded to a costal fracture and the other to degenerative origin. The 10 bone lesions observed only in the FCH-PET were located in the axial skeleton. 1 patient presented a plasmocitoma, detected by both tracers, although the intensity of the uptake was higher in the FDG-PET. 2 extramedular foci were detected: one in vagina and the other in the cervical area, both of inflammatory-infectious origin. According to the patient based analysis 3 patients showed more axial foci in the FCH-PET than the FDG-PET. ***Conclusion:*** FCH-PET could be a useful tool for the staging of MM patients, although, it is still a challenge to determine what patients should benefit from this new tracer. ***References:*** Nanni C. et al. Image interpretation criteria for FDG PET/CT in multiple myeloma: a new proposal from an Italian expert panel. IMPeTUs (Italian Myeloma criteria for PET USe). Eur J Nucl Med Mol Imaging. 2016 Mar;43(3):414-21 Cassou-Mounat T. et al 18F-fluorocholine versus 18F-fluorodeoxyglucose for PET/CT imaging in patients with suspected relapsing or progressive multiple myeloma: a pilot study. Eur J Nucl Med Mol Imaging. 2016 Oct;43(11):1995-2004.

EP-164

18F-FDG PET / CT findings of Rosai Dorfman Disease with diffuse extranodal involvement

N. Filizoglu, S. Kesim, C. O. Engur, K. Oksuzoglu, S. Ozguven, T. Ones, H. T. Turoglu, T. Y. Erdil;
Marmara University Pendik Training and Research Hospital, Istanbul, TURKEY.

Aim/Introduction: Rosai Dorfman disease (RDD) is a rare benign disease characterized by permanent massive lymphadenopathy mimicking malignant tumors. Extranodal involvement, including the skin, upper respiratory tract, salivary gland, bone, central nervous system and rarely kidneys, may occur in approximately 43% of patients. Although RDD can usually recover spontaneously, it may persist in some patients and mimic lymphoproliferative disorders clinically and visually. We present the 18F-FDG PET / CT findings of the patient with RDD with diffuse extranodal involvement. ***Materials and Methods:*** An 18F-FDG PET / CT examination was performed to investigate malignancy in a 57-year-old male patient with multiple cervical lymph nodes. ***Results:*** 18F-FDG PET / CT demonstrated 2.5 cm sized intense hypermetabolic lymph nodes in the bilateral cervical chain. Intense hypermetabolic soft tissue density lesions were observed in the subcutaneous fatty plans of the T12 vertebra left posterolateral section and the right lower quadrant of the abdomen. 12 mm sized mild hypermetabolic soft tissue density nodular lesion was seen in the right adrenal gland medial crust and 3x2.5 cm sized mild hypermetabolic soft tissue density nodular lesion was found in the left adrenal gland corpus. In the skeletal system, intense hypermetabolic lytic lesions compatible with metastasis were observed in the left occipital condyle, the posterior elements of the T6 vertebra, the C1 vertebra transvers process, the posterior part of the right acetabulum and the posterior part of the right iliac bone. Excisional biopsy was performed on the lymph node in the submandibular area and the lesion observed in the subcutaneous fatty plan in the right lower quadrant of the abdomen and the histopathology was found compatible with Rosai Dorfman disease. ***Conclusion:*** RDD, first described by Rosai and Dorfman in 1969, is a rare benign lymphoproliferative disease. RDD is usually manifested by cervical lymphadenopathy and typically mimics lymphoma. Diseases such as lymphoma, tuberculosis, sarcoidosis, reactive hyperplasia and nasopharyngeal carcinoma can be considered in the differential diagnosis. Extranodal disease is observed in approximately 43% of cases, most commonly in the skin, nasal cavity, eyes and bone. Although Rosai-Dorfman disease is usually self-limited, patients with extranodal involvement may have a more fulminant course and need active treatment. Since lesions show increased FDG uptake, 18F-FDG PET-CT may be useful in determining the extent of the disease, including lymph node involvement. Therefore, the present case emphasized the importance of 18F-FDG PET-CT scan in the diagnosis, staging and treatment selection of the disease. ***References:*** None

EP-23

Imaging Clinical Studies -> Oncological Imaging Clinical Study -> Prostate BC Recurrence

e-Poster Area

EP-165

^{68}Ga-PSMA PET/CT in prostate cancer patients with biochemical recurrence after primary treatment: diagnostic accuracy and impact on management strategy

R. Wang, G. Shen, L. Pan, R. Tian;
Sichuan University West China Hospital, Chengdu, CHINA.

Aim/Introduction: ^{68}Gallium prostate-specific membrane antigen positron emission tomography/computed tomography (^{68}Ga PSMA PET/CT) is a promising imaging modality in assessing prostate cancer. The aims of our study is to evaluate the diagnostic performance of ^{68}Ga PSMA PET/CT for detecting relapse or metastasis in prostate cancer patients with biochemical recurrence (BCR) after primary treatment, and to assess the potential impact of ^{68}Ga PSMA PET/CT on the management strategy of prostate cancer patients with BCR. ***Materials and Methods:*** The PubMed, EMBASE and Cochrane Library databases were searched until April 20, 2019. Studies regarding the diagnostic performance of ^{68}Ga-PSMA PET/CT in detecting prostate cancer patients with BCR after definitive treatment and/or studies reporting proportion of management changes after ^{68}Ga PSMA PET/CT in patients with BCR were included. The quality of each study was assessed using the Quality Assessment of Diagnostic Accuracy Studies-2 (QUADAS-2) tool. The detection rate of ^{68}Ga PSMA PET/CT and the proportion of management changes were pooled using random-effects model. The quality of the studies was evaluated using the GRADE system. Subgroup analyses and meta-regression analyses were performed to explore heterogeneity. ***Results:*** A total of 45 studies were included, and 17 studies of them evaluated the impact of ^{68}Ga PSMA PET/CT on management of patients. For prostate cancer patients with BCR, the pooled detection rate of ^{68}Ga PSMA PET/CT was 77% (95%CI, 76-78). For PSA categories 0-0.19 ng/ml, 0.2-0.49 ng/ml, 0.5-2.0ng/ml, 2.0-1.9ng/ml and > 2ng/ml, the pooled detection rates were 26% (95%CI, 22-29), 48% (95%CI, 45-52), 59%(95%CI, 56-62), 81%(95%CI, 79-84) and 95%(95%CI, 94-96). For the impact of ^{68}Ga PSMA PET/CT on the management, the pooled proportion of management changes was 53%(95%CI, 51-55). Among

these management changes, the increasing proportion was seen in the treatments including radiotherapy (42%-49%), surveillance (29%-32%) and surgery (0.4%-3.5%), whereas the proportion of systemic treatment (56%-42%) decreased due to the ^{68}Ga PSMA PET/CT. ***Conclusion:*** For prostate cancer patients with BCR, the diagnostic accuracy of ^{68}Ga PSMA PET/CT was high, and the detection rate correlated positively with PSA levels. In addition, ^{68}Ga PSMA PET/CT had a significant impact on the management of patients. ***References:*** None

EP-166

Role of ^{68}Ga-PSMA PET/ CT in men with biochemical recurrence after definitive treatmentofadenocarcinoma prostate

R. Kumar[1], *A. Sharma*[1], *S. Kumar*[1], *C. Das*[1], *A. Seth*[1], *A. Pandey*[1], *C. Patel*[1], *E. Estrada-Lobato*[2], *J. Cerci*[3], *S. Fanti*[4];
[1]*AIIMS, New Delhi, INDIA,* [2]*Division of Human Health, IAEA, Vienna, AUSTRIA,* [3]*Diretor do Serviço de PET/CT Quanta - Diagnóstico e Terapia, Curitiba, BRAZIL,* [4]*University of Bologna, Bologna, ITALY.*

Aim/Introduction: Early localisation of disease recurrence after definitivetreatment of prostate cancer is vital to determine suitabilityfor salvage treatment. The aim of present study was toprospectively determine therelationship between prostate specific antigen (PSA) level anddetection of suspected cancer recurrence using ^{68}Ga-PSMAPET/CT in patients with biochemical recurrence after radicalprostatectomy (RP) or radiotherapy, particularly at low PSAlevels. ***Materials and Methods:*** Sixty patients with histopathologically proven prostate adenocarcinoma who had undergone primary treatment in the form of RP or radiotherapy with rising serum PSA were recruited in the study. Serum PSA levels on which biochemical relapse was diagnosed were assured to be less than or equal to 4 ng/ml. Each patient underwent a whole body PET/CT scan on BiographmCT 64 slice after 30 minutes of injecting2 - 5 mCi (74-185MBq)/kg of ^{68}Ga- PSMA intravenously. PET/CT scans were interpreted independently by two nuclear medicine experts who were blinded to patient information. Data was analysed to determine the relationship of pre-scan PSA level to the probability of a positive scan finding for recurrent prostate cancer. ***Results:*** Of 60 men, 46 had previous RP and 14had prior radiotherapy. Median PSA of RP groupwas 0.346ng/mL and inradiotherapy group was 0.555ng/mL. Inpost RP group, the overall detection rate of ^{68}Ga-PSMA PET/CT was 43.5% (n=20/46). The detection rate was 37.5% (n=6/16) for PSA 0.01 to <0.2 ng/mL, 8.3% (n=1/12) for PSA0.2 to <0.5 ng/mL, 60% (n=3/5) for PSA 0.5 to <1 ng/mL, 80% (n=4/5) forPSA 1 to <2 ng/mL and 75% (n=6/8) for PSA 2 to 4. Lymph nodemetastasis post RP was identified in 60%(n=12/20) and bone metastasis in 45% (n=9/20) of men withsuspected disease recurrence. In the post radiotherapy groupthe overall detection rate was 64.3% (n=9/14). The detection rate was 33% (n=2/6) for PSA 0.01 to <0.5 ng/mL,80% (n=4/5) for PSA 0.5 to <2ng/mL, and 100% (n=3/3) for PSA 2 to 4 ng/ml. Out of 9 PET/CT positive patients post radiotherapy, local recurrence was detected in 89% (n=8/9) of men, lymph node metastasisin 66.66% (n= 6/9)and bone metastasis in 44% (n=4/9) of men. ***Conclusion:*** ^{68}Ga-PSMA PET/CT has an important role in detection of suspectedrecurrence in prostate cancer post definitive treatment. Detection rate for suspected recurrence increases with increase in PSA levels. Detection of suspected recurrent disease outside thepelvis at low PSA levels will influence the decision for salvagetreatment options. ***References:*** None

EP-167

Diagnostic accurancy of ^{68}Ga-PSMA-11 PET/CT in patients with recurrent prostate cancer

V. Fech, *C. Sachpekidis, I. Alberts, C. Mingels, B. Vollnberg, A. Rominger, A. Afshar-Oromieh;*
Department of Nuclear Medicine, Bern, SWITZERLAND.

Aim/Introduction: The high sensitivity of ^{68}Ga-PSMA-11-PET/CT has been shown in numerous studies. Recently, many case reports have been published describing various benign and malignant entities exhibiting PSMA-ligand uptake. The present evaluation was performed in order to further analyze the positive predictive value of ^{68}Ga-PSMA-11 PET/CT. ***Materials and Methods:*** A retrospective analysis was performed for all patients who underwent ^{68}Ga-PSMA-11 PET/CT between January 2017 and March 2019 at our institute in order to detect recurrent PC (n=523). Hitherto, 80 patients were identified who had received radiation therapy, histology or surgical removal of PSMA-positive lesions, enabling a comparison with PSMA-avidity in the previous PET/CT. ***Results:*** So far, 87 PSMA-positive lesions in the 80 patients have undergone external radiation, were biopsied or surgically removed. 78 of them (89,7%) were true-positive PC lesions (proven by falling PSA following external radiation or by histology). Amongst the mentioned lesions were 42 local relapses, 11 lymph node metastases and 25 distant metastases. ***Conclusion:*** Our analysis demonstrates the high positive predictive value of ^{68}Ga-PSMA-11 PET/CT. To our conviction, PSMA-positive lesions with a CT-correlate in patients with recurrent PC can be classified as PC lesions with high confidence. Although uptake of PSMA-ligands in various non-prostatic tissues have been described, it must be assumed that their numbers represent only a fraction of the overwhelming numbers of PC lesions detected daily in clinical practice by ^{68}Ga-PSMA-11 -PET/CT worldwide. ***References:*** None

EP-168

^{68}Ga-PSMA-11 PET/CT detection rate in very low risk recurrent PCa patients: a single center experience

S. Telo, A. Farolfi, R. Mei, S. Mattoni, L. Calderoni, P. Castellucci, S. Fanti;
Nuclear Medicine, Policlinico S.Orsola-Malpighi, Bologna, ITALY.

Aim/Introduction: To evaluate ^{68}Ga-PSMA-11-PET/CT detection rate in a cohort of very low risk biochemically relapsed (BCR) Prostate Cancer (PCa) patients. ***Materials and Methods:*** We reviewed all ^{68}Ga-PSMA-11 PET/CTs of PCa patients who were referred to our Center, from December 2016 to December 2019. Inclusion criteria were 1) patients with BCR after radical therapy with or without subsequent salvage therapy; 2) ISUP group ≤3; 3) no ongoing androgen-deprivation-therapy (ADT) in the last 6 months; 4) Time to PSA recurrence ≥12 months; 5) PSA doubling time (DT) ≥ 10 months; 6) PSA at time of ^{68}Ga-PSMA-11 PET/CT ≤0.5 and ≥0.2 ng/ml. ^{68}Ga -PSMA PET/CT findings were categorized as positive and negative by two experienced Nuclear Medicine Physicians. Doubtful findings were re-evaluated and categorized by consensus. Positive findings were categorized as: local relapse in prostate bed, pelvic lymph-nodes, distant lymph-nodes, bone and visceral. Patients with a maximum of 3 lesions were categorized as oligometastatic. ***Results:*** Out of 1702 patients reviewed, 78 matched the inclusion criteria. ^{68}Ga-PSMA-11 PET/CT resulted positive in 9/78 cases (detection rate 11,5%). Characteristics of positive patients were: mean PSA at time of ^{68}Ga-PSMA-11 PET/CT= 0,30 ng/ml (range=0,2-0,46); mean PSA DT =14,8 months (range= 10,2-29,9); mean SUVmax of the positive lesions =3,9 (range=3-7,6). Characteristics of negative patients were: mean PSA= 0,31 ng/ml (range=0,2-0,50); mean PSA DT= 20,5 months (range=10-32,8). Single lesions were detected in 5 patients (prostate bed relapse in 2 patients, pelvic lymph-nodes in 2 patients, bone in 1 patient). Oligometastatic disease was detected in 2 patients (bone/pelvic lymph-node and prostate bed relapse in 1 patient; 2 pelvic lymph-nodes in 1 patient). Multimetastatic disease was detected in 2 patients (multiple bone lesions in 1 patient; multiple pelvic lymph-nodes in 1 patient). In our population of very low risk BCR patients ^{68}Ga-PSMA-11-PET/CT turned out positive in 11,5% of patients. In patients with low PSA values, long PSA doubling times, low ISUP, no ongoing ADT therapy and time to PSA recurrence longer than 1-year indication to ^{68}Ga-PSMA-11-PET/CT should be carefully considered. ***Conclusion:*** In our population of very low risk BCR patients ^{68}Ga-PSMA-11-PET/CT turned out positive in 11,5%. This result needs to be validated in further studies including larger populations. ***References:*** None

EP-169

Pharmacokinetic PET/CT studies with ^{68}Ga-PSMA-11 in patients with biochemical recurrence and progression of a prostatic cancer

D. Strauss[1], C. Sachpekidis[1], K. Kopka[2], A. Dimitrakopoulou-Strauss[1], L. Pan[1], U. Haberkorn[3];
[1]German Cancer Research Center CCU Nuclear Medicine, Heidelberg, GERMANY, [2]Institute of Radiopharmaceutical Cancer Research at Helmholtz-Zentrum Dresden-Rossendorf, Dresden, GERMANY, [3]Department of Nuclear Medicine, University of Heidelberg, Heidelberg, GERMANY.

Aim/Introduction: To investigate the biodistribution and pharmacokinetics of ^{68}Ga-PSMA-11 PET in patients with biochemical recurrence or progression of prostate cancer (PC) using multiparametic (dynamic and whole-body) PET/CT. ***Materials and Methods:*** In total 128 PET/CT scans of 112 patients with PC biochemical relapse or progression were extracted from our database. All patients underwent dynamic PET/CT (dPET/CT) scanning of the pelvis and lower abdomen for 60 minutes as well as whole-body PET/CT with ^{68}Ga-PSMA-11. Dynamic and whole-body PET/CT assessment was based on qualitative evaluation and SUV calculation. Moreover, dPET/CT data from the pelvis underwent quantitative analysis based on a two-tissue compartment model and a non-compartmental approach leading to the extraction of fractal dimension (FD). ***Results:*** Mean plasma PSA in all patients was 8.09 ng/mL (range <0.01-132 ng/mL), and mean Gleason-Score was 7.53 (range 5-10). 100/128 scans of 98/112 patients were PET-positive (detection rate: 87.5%). 11/98 ^{68}Ga-PSMA-11 positive patients had a PSA of < 0.5 ng/mL. 24 local recurrence lesions were detected in dPET/CT with following mean values (range): $SUV_{average}$: 14.2 (2.3-62.5), SUV_{max}: 24.7 (3.3-84.6); k1 = 0.16 (0.04 - 0.64), k3= 0.35 (range <0.01 - 0.99), FD = 1.25 (0.94-1.37). 191 lymph node metastases were detected in dPET/CT with the following mean values (range): $SUV_{average}$: 14.9 (range 0.3-171.3), SUV_{max}: 26.4 (range 0.6-250.8), k1 = 0.19 (<0.01-0.83), k3= 0.33 (<0.01 - 0.99), FD = 1.25 (0.85-1.92). Respectively, 49 bone metastases had the following values: $SUV_{average}$: 9.8 (range 1.9-80.5), SUV_{max}: 16.9 (2.8-117.5), k1 = 0.19 (0.02-0.96), k3= 0.25 (<0.01 - 0.99), FD = 1.21 (1.04-1.36). In most lesions time-activity curves revealed an increasing ^{68}Ga-PSMA-11 accumulation during dPET acquisition. No statistical significant difference was observed in the pharmacokinetics between metastases und recurrent tissue. ***Conclusion:*** ^{68}Ga-PSMA-11 shows satisfying results in the detection of PC recurrence with a detection rate of 87.5%. A non-negligible number of patients with very low PSA values could benefit from the detection of suspect lesions, though patients with higher PSA have a higher tracer accumulation. ***References:*** None

EP-170

PET/CT with ^{68}Ga-PSMA-11 for detection of rib involvement in a subgroup of prostate cancer patients

L. Calderoni, A. Farolfi, R. Mei, S. Telo, S. Fanti;
Nuclear Medicine, Sant'Orsola University Hospital, Bologna, ITALY.

Aim/Introduction: In the last years several studies have shown that recommended imaging techniques, including computed tomography (CT) or magnetic resonance imaging (MRI) and bone scintigraphy (BS), have shown a limited detection rate for the detection of lesions in patients with a history of prostate cancer (PCa) in staging, biochemical recurrence (BCR), with particular regard for the detection of costal lesions, which are often misdiagnosed. The objective of this study was to evaluate the performance of ^{68}Ga-PSMA-11 PET/CT for the detection of rib involvement with particular attention to oligometastatic patients (defined as having 5 or more lesions), who can benefit considerably from targeted therapy, such as external beam radiotherapy. ***Materials and Methods:*** In our retrospective, single-center study patients were included with the following criteria: histopathological diagnosis of PCa and ^{68}Ga-PSMA-11 PET/CT during staging or BCR. We reviewed all the reports of the patients who underwent a 68Ga-PSMA-11 PET/CT between March 2016 and February 2018 matching all the inclusion criteria. ***Results:*** Overall we included 808 ^{68}Ga-PSMA-11 PET/CT scans and we found 93/808 scans with reported rib findings at ^{68}Ga-PSMA PET/CT (occurrence 11.5%). Out of 93 positive scans, 18 scans (in 18 patients) were PSMA positive at a single rib (occurrence 2.2%); 7 scans (in 7 patients) showed increased ^{68}Ga-PSMA-11 uptake in a single rib and in another site (prostate bed 3/7, pelvic lymph nodes 5/7); 10 scans (9 patients) were PSMA positive but could be classified as oligometastatic patients (less than 5 bone lesions); 34 scans (in 30 patients) showed advanced disease (greater than 4 lesions). In 18 cases PET/CT scans showed suspect but inconclusive findings (low PSMA uptake); 6 scans (6 patients) were reported as rib fracture or small high density areas only seen at CT. ***Conclusion:*** In our study a significant number of PET scans (11.5%) showed one or more lesions with rib involvement, with a significant number of patients (2.2%) with only one rib lesion, who would have been misdiagnosed with standard imaging procedures. Based on PET/CT 68Ga-PSMA-11 4.2% of patients could be classified as oligometastatic and be a candidate for targeted therapy, avoiding any hormone therapy and its side effects. ***References:*** Sarkar S, Das S. A Review of Imaging Methods for Prostate Cancer Detection. Biomed Eng Comput Biol. 2 marzo 2016;7(Suppl 1):1-15.

EP-171

18F-Choline PET/CT in Biochemical Recurrence of Prostate Cancer

C. Riola-Parada, B. Lucas-Velázquez, F. Gómez-Caminero, J. Villanueva, P. García-Talavera, L. Díaz, A. Peñaherrera, J. Cañadas Salazar, M. Tamayo;
Nuclear Medicine Department. Hospital Clínico Universitario de Salamanca, Salamanca, SPAIN.

Aim/Introduction: The aim of this study was to prove the usefulness of 18F-choline PET/CT in the suspicion of prostate cancer recurrence in our patients and to relate 18F-choline PET/CT detection rate with analytical and pathological variables. ***Materials and Methods:*** We prospectively analyzed 116 consecutive patients with prostate cancer (mean age 68 years, range 47-87 years) who received local therapy as primary treatment and who underwent 18F-choline PET/CT due to suspicion of recurrence (persistently rising serum PSA level). The patients were recruited from the Nuclear Medicine Department of Hospital Clínico Universitario de Salamanca, Spain, from November 2015 to March 2019. 18F-choline PET/CT findings were validated by anatomopathological analysis, other imaging tests or by biochemical response to oncological treatment. ***Results:*** 18F-choline PET/CT detected disease in 81 of 116 patients (detection rate 69.8 %). 20 patients (17.2%) presented exclusively local recurrence, 32 (27.5%) lymph node metastases, 28 (24.1%) bone metastases and 1 (0,8%) esplenic metastases. Mean PSA (PSAmed) at study time was 5.55 ng/mL (median 3.8, range 0.017-38 ng/mL). PSAmed in patients with positive PET/CT was 6.33 ng/mL (median 4.03, range 0.7-38 ng/mL), higher than in patients with negative PET/CT: PSAmed 3.71 ng/mL (median 2.89, range 0.017-15.90 ng/mL) ($p<0.05$). The percent of positive scans was 25% for PSA less than 1 ng/ml, 66,7% for PSA 1-1,9 ng/ml, 60% for PSA 2-2,9 ng/ml and 77% for PSA ≥3 ng/ml. PSA level could not differentiate between patients with local recurrence, lymph node metastases or bone disease. Mean total Gleason score at diagnosis was 6.89 (range 4-10). Mean total Gleason score in patients with a positive study was 7.04 (range 4-10) higher than in patients with a negative study: mean total Gleason score 6.56 (range 4-9) ($p<0.05$). Gleason score could differentiate between patients with local recurrence, lymph node metastases or bone disease ($p<0.05$). ***Conclusion:*** 18F-choline PET/CT was able to detect disease in an important number of our patients (69.8%). PSA level could differentiate between positive and negative 18F-choline PET/CT. ***References:*** None

EP-172

Utility of 68Ga-PSMA PET / CT in occult biochemical recurrence of prostate carcinoma with negative 18F-Choline PET / TC. Our experience

P. Plaza López[1], E. Puertas[1], J. Aguiló[1], B. Domenech[1], S. Sanjosé[1], M. Suarez-Piñera[2], E. Rivera[3], J. Casals[1], J. Chicharo[4];
[1]Hospital Quironsalud Barcelona, Barcelona, SPAIN, [2]Hospital del Mar Barcelona, Barcelona, SPAIN, [3]Hospital Dexeus Barcelona, Barcelona, SPAIN, [4]Cimes. Fundación

General Universidad de Málaga., Málaga, SPAIN.

Aim/Introduction: To assess the utility of 68Ga-PSMA PET / CT studies in the clinical practice of patients with occult biochemical recurrence of prostate carcinoma, with negative or inconclusive radiological imaging and PET / CT 18F-Choline studies. ***Materials and Methods:*** Retrospective descriptive study. The first 10 patients with a history of prostate carcinoma, treated with curative intent and who had suspected biochemical recurrence with low PSA values (range: 0.04-2.35 ng / ml) were selected. Imaging, prostate ultrasound, CT, and / or pelvic MRI were negative, and all of them had negative or inconclusive 18F-Choline PET / CT. All patients were referred for a 68Ga-PSMA PET / CT. Protocol: Dose 2.2MBq / Kg. 20mg of furosemide at minute 15. Images from the skull to the proximal third to mid-thigh at 60 min . Late images at 3 hours if needed. ***Results:*** In 6 of the 10 patients (60%), the 68Ga-PSMA managed to locate the occult biochemical recurrence, and in all of them there were changes in the therapeutic attitude. In 3 of the patients (30%) 68Ga-PSMA was negative, and the vigilant attitude was continued with PSA controls and imaging studies according to the usual protocols. These patients had the lowest PSA values (less than 0.4). One of the 68Ga PSMA studies was inconclusive, reporting the presence of a dubious right iliac adenopathy. ***Conclusion:*** 68Ga-PSMA PET / CT allows early diagnosis, with low PSA values, of occult biochemical recurrence of prostate carcinoma, even in patients with negative 18F-choline PET / CT. The 68Ga-PSMA findings changed the therapeutic attitude in a significant proportion of patients. ***References:*** Comparison of PET imaging with a 68Ga-labelled PSMA ligand and 18F-choline-based PET/CT for the diagnosis of recurrent prostate cancerAli Afshar-Oromieh, Christian M. Zechmann, Anna Malcher, Matthias Eder, Michael Eisenhut, Heinz G. Linhart, Tim Holland-Letz, Boris A. Hadaschik, Frederik L. Giesel, Jürgen Debus & Uwe Haberkorn European Journal of Nuclear Medicine and Molecular Imaging volume 41, pages11-20(2014)68Ga-PSMA PET/CT for restaging recurrent prostate cancer: which factors are associated with PET/CT detection rate?Francesco Ceci, Christian Uprimny, Bernhard Nilica, Llanos Geraldo, Dorota Kendler, Alexander Kroiss, Jasmin Bektic, Wolfgang Horninger, Peter Lukas, Clemens Decristoforo, Paolo Castellucci, Stefano Fanti & Irene J. VirgoliniEuropean Journal of Nuclear Medicine and Molecular Imaging volume 42, pages1284-1294(2015)

EP-173

Predictors Of Positivity Of [^{18}F]F-Choline PET-CT In Prostate Cancer Recurrence. Preliminary Results

L. Nieto Morcillo*, M. Falgás Lacueva, L. de la Cueva Barrao, A. Borque Fernando, A. Méndez Villamón, I. Guerrero Fernández de Alba, M. Calderón Calvente, G. Guzmán Prudencio, L. del Barco Diez Canseco, D. Abós Olivares;*

Hospital Universitario Miguel Servet, Zaragoza, SPAIN.

Aim/Introduction: To analyze the validity of [^{18}F]F-Choline PET-CT results in prostate cancer recurrence in our daily practice, based on theoretical cut-off points of prostate-specific antigen (PSA), its kinetic, and PSA doubling time (PSADT), to identify predictors of positivity and modify the indication criteria. ***Materials and Methods:*** Prior to the validity analysis, a descriptive, prospective analysis of consecutive patients with prostate cancer treated with curative intent by radical prostatectomy (RP) or radiotherapy (RT), who underwent PET-CT scan with recurrence criteria: PSA ≥1 or PSA 0.4-1 with PSADT <6 months after RP; PSA> Nadir + 2 after RT, was performed. ***Results:*** From April to December 2019, 69 patients were included, 40 were treated with RP (58%) and 29 with RT (42%). In 45 patients (65%) PET-CT was able to identify recurrence of the disease (positive PET) and in 24 it was not (negative PET). Of patients treated with RP, 82,5% (33/40) had PSA>1, and of those, 61% were positive PET. 17,5% (7/40) had PSA<1 and PSADT< 6 months (28/69), with positive PET in 43% of patients. 76% of patients had a positive PET after RT. Positive PET results were obtained in 57% of patients with PSADT>6months (28/69), in 71% if PSADT<6months (41/69) and in 81% of patients if PSADT<3 months (16/69). After RP and RT, PET was positive in 50% and 62,5% of patients respectively if PSADT>6 months, in 61% and 92% if PSADT<6 months and in 77% and 100% if PSADT<3 months. ***Conclusion:*** Preliminarily and awaiting validation, it seems that PSA>1 after RP or Nadir +2 after RT is an indicator of PET-CT. There seems to be a tendency that shows that PSA<1 after RP is an indicator of PET-CT if PSADT<3 months. PSADT <3 or <6 months could be the best predictor of positivity of PET-CT with [^{18}F]F-Choline in recurrent prostate cancer. ***References:*** None

EP-174

Evaluation Of ^{18}F-Fluorocoline PET-CT Findings In Patients With Suspicion Of Prostate Cancer Tumor Recurrence And Gleason <7 Or PSA <2ng / mL Prior To PET

S. Garcia Martinez*, Á. Baena García, M. De Bonilla Candau, M. Cruz Montijano, J. Rodríguez-Rubio Corona;*
Puerta del Mar University Hospital, Cadiz, SPAIN.

Aim/Introduction: To analyze the PET CT findings visualized in studies with ^{18}F-FCH, with tumor recurrence suspicion in patients treated of prostate cancer with Gleason score less than 7 or with a PSA value less than 2ng / mL prior to PET. ***Materials and Methods:*** Retrospective study was made from March 2016 to October 2019, including 20 patients (22 explorations) treated of prostate cancer (mean age 73 years) with tumor recurrence suspicion and doubtful imaging tests, considering two independent samples: those with Gleason <7 (14 patients) and those with PSA <2ng / mL prior to PET (6 patients). The PET findings, the

subsequent therapeutic management and the evolution of the patients (mean follow-up period 9.06 months) were analyzed. ***Results:*** In the sample of 15 studies (14 patients) with Gleason score <7 (PSA 2.2-25ng / mL), local or locoregional ^{18}F-FCH uptake was seen in 11 studies (73%) and focal bone uptake was seen in 2/15 (13.3%). In 7 cases (46.6%) there were changes in therapeutic management with a clear decrease in PSA. 2/15 were negative studies (Gleason 5-6). There were no therapeutic changes if the PET findings were doubtful or unconfirmed. In the sample of 7 studies (6 patients) with PSA prior to PET <2ng / mL (Gleason 7-9), only 2/7 (28.5%) showed lymph node uptake: one received radiotherapy (PSA 1.34) and another did not modify further treatment (PSA 1.96). The rest of them were negative studies (3/7) or inconclusive (2/7). None showed progression at follow-up. ***Conclusion:*** PET-CT with ^{18}F-FCH allows a better therapeutic approach after suspicion of tumor recurrence due to prostate cancer despite Gleason score <7; providing lower therapeutic profitability in cases of PSA <2ng / mL. ***References:*** None

EP-24

Imaging Clinical Studies -> Oncological Imaging Clinical Study -> Prostate Other

e-Poster Area

EP-175

Comparison between 99mTc-MDP bone scintigraphy combined with SPECT/CT and 68Ga-PSMA PET/CT in evaluation of bone involvement in patients with prostate cancer. Preliminary results

G. Mateva*, M. Garcheva-Tsacheva;*
Acibadem CityClinic Mladost, Sofia, BULGARIA.

Aim/Introduction: The aim of the study was to compare the diagnostic value of whole body bone scintigraphy (WBS) combined with SPECT/CT and 68Ga-PSMA PET/CT in evaluation of bone involvement in patients with prostate cancer. ***Materials and Methods:*** 151 68Ga-PSMA PET/CT scans executed in 10 months were retrospectively reviewed. In 14 of the examined patients, a WBS (99mTc-MDP) was done in the previous 1- 6 months. The used protocols were: WBS combined with SPECT/CT after injection of 555 MBq 99mTc-MDP on GE Discovery NM/CT 670 Pro and head to mid thigh PET scan on GE Discovery IQ, 60 -70 min. after 1-2 mBq/kg 68Ga-PSMA -11. 68Ga-PSMA-11 was produced on site with labeling efficiency > 98%. Three groups were identified according to the indications. Group 1- patients with biochemical recurrence n= 4, all on androgen deprivation therapy (ADT), PSA levels from 1,74 ng/ml to 22 ng/ml with median doubling time of PSA 1-3 months. Group 2 - high risk patients for staging before the start of therapy n=5. Group 3 - patients with bone dissemination confirmed by WBS, n=5 treated with ADT, or radiotherapy, for which the levels of PSA did not correspond with the suspicion for progression. ***Results:*** All patients in gr. 1 (n=4) had negative WBS, and positive for skeletal involvement 68Ga-PSMA scans, 3 of which bone marrow lesions. Three had additionally local recurrences and/or lymph nodes lesions. In gr. 2 the WBS was positive in 1/5, while 68Ga-PSMA scans were positive in all 5 (2 bone marrow lesions, including lymph node dissemination in 3 of them). In 3 of patients from gr. 3, the WBS positive lesions did not demonstrate increased 68Ga-PSMA uptake, which corresponded to the PSA regression. In 2 other cases - 68Ga-PSMA scan revealed more bone lesions than WBS, including generalized involvement in 1 patient. The bone marrow lesions had higher 68Ga-PSMA SUVmax (mean 43,98) versus lesions with sclerotic substrate (mean value 14,5). ***Conclusion:*** According to this preliminary study 68Ga -PSMA PET/CT detects skeleton lesions in patients with prostate cancer compared to WBS and SPECT/CT. The interpretation of skeletal involvement was changed in 11/14 patients /78%/ in addition to detected local recurrences and/or lymph nodes involvement in 12/14 of the patients /85%/. That makes 68Ga -PSMA PET/CT indispensable not only in patients with biochemical recurrence, bit in primary staging of high risk patients and for evaluation of therapy response. ***References:*** None

EP-176

Detailed advantages of ^{18}F-DCFPyL over ^{18}F-FDG PET imaging in the diagnosis of metastatic and non-metastatic prostate cancers: a comparative study

J. Ning*, Y. Liu, C. Li, Y. Chang, G. Wang, P. Yu, J. Gao, B. Xu;*
Chinese PLA General Hospital, Beijing, CHINA.

Aim/Introduction: To explore the detailed advantages of ^{18}F-FDG over ^{18}F-PSMA PET targeting the precise assessment of metastatic and non-metastatic prostate cancers (PCa). ***Materials and Methods:*** We retrospectively analyzed the imaging data of ^{18}F-FDG and ^{18}F-PSMA PET/CT in 20 patients with metastatic and non-metastatic PCa in the Chinese PLA General Hospital, each of whom was confirmed by histopathology. Then a series of parmameters including SUV and size of each Volume of Interest (VOI) and lesion distribution were taken into account among the PCa foci and metastases. ***Results:*** Among the total of 20 patients with PCa, 10 cases were diagnosed as primary PCa without any metastases while multiple metastases were detected on ^{18}F-FDG or ^{18}F-PSMA PET in the other 10 cases. The overall analysis of metastases' number turned out that PSMA imaging did not show proper advantages (P = 0.034) while the subgroup analysis found that PSMA imaging, thanks to high sensitivity and specificity, showed significant advantages in the detection of metastatic lesions' number (P = 0.034), size (P = 0.019) and SUV (P =0.001), and the

primary lesion's size (P = 0.014) and SUV (P<0.001). As for the detection potential in lesion distribution, PSMA PET's ability to detect LNs' metastases in the groin region is slightly inferior to FDG PET. But in the metastases' detection of pelvic lymph nodes (LNs), upper abdominal LNs, bones metastases, mediastinal, hilar LNs and clavicle LNs, PSMA modality far overweighed FDG imaging, especially in detection of pelvic LN metastases. ***Conclusion:*** PSMA PET has more potential to facilitate the identification of PCa primary lesions and metastases, in particular, the LNs in the pelvic cavity and upper abdomen. ***References:*** None

EP-177

PET/CT with 11C-Choline, 68Ga-PSMA, 18F-FACBC in castration resistant prostate cancer patients: evaluation of MTV and TLA

E. Tabacchi[1], *G. Argalia*[1], *S. Vichi*[1], *C. Malizia*[1], *C. Fonti*[1], *F. Massari*[2], *V. Mollica*[2], *V. Di Nunno*[2], *E. Nobili*[2], *C. Nanni*[1], *S. Fanti*[1];
[1]*Nuclear Medicine, S.Orsola-Malpighi Hospital, DIMES University of Bologna, Bologna, ITALY,* [2]*Division of Oncology, S.Orsola-Malpighi Hospital, Bologna, ITALY.*

Aim/Introduction: to investigate, on preliminary data, which radiotracer among 11C-Choline, 68Ga-PSMA, 18F-FACBC provides features better representing the volume of active disease in metastatic castration resistant prostate cancer (mCRPC) patients. This could be useful, on a greater number of patients, to identify the most suitable radiotracer to assess therapy response ***Materials and Methods:*** in the contest of a wider prospective interventional monocentric explorative study (granted project RF-2016-02364809), we evaluated mCRPC pts enrolled from January 2019 to January 2020 that have been assigned randomly to receive 11C-Choline, 68Ga-PSMA or 18F-FACBC PET/CT respectively. Each patient underwent two PET/CT scans: one before therapy onset with abiraterone or enzalutamide and one two months later. No changes in therapy derived from PET/CT results. We evaluated the Metabolic Tumor Volume (MTV) calculated with a fixed threshold set at 40% of SUV max with a licensed software (GE VCAR) and Total Lesion Activity (TLA:MTVxSUVmean) on each scan. Correlation between PSA value and SUVmax, MTV and TLA for the three groups of radiotracers was calculated. For statistical analysis we used a non parametric test (SPEARMAN). ***Results:*** to date we enrolled 16 mCRPC pts randomized for of 11C-Choline (6pts), 68Ga-PSMA(5 pts)and 18F-FACBC (5 pts). For 11C-Choline group we found a strong significant correlation between PSA value and MTV (rho=0.8667, p-value =0,0027), PSA value and TLA (rho=0.9125, p-value=0,0005) and no significant correlation between PSA and SUVmax. For 68Ga-PSMA group we found a significant correlation (although weaker than 11C-Choline) between PSA value and MTV (rho=0.8167, p-value=0,0108), PSA value and TLA (rho=0.85, p-value=0,0061)and no significant correlation between PSA and SUVmax. No significant correlation has been found for 18F-FACBC group between PSA and SUVmax,MTV,TLA. ***Conclusion:*** limited to the small number of patients, 11C-Choline seems the tracer providing parameters that better correlate with PSA value, possibly indicating a more accurate representation of the volume of active disease. It is not clear yet whether this suggests a better performance of 11C-Choline for assessing therapy response. Similarly, no conclusion can be drawn about the correlation for 68Ga-PSMA between PSA value and MTV,TLA. A larger number of patients is needed as well as a longer follow up to draw conclusions. ***References:*** None

EP-178

Assessment of Bone Metastasis Using Deep Learning Software in Prostate Cancer Patients: Correlation with Evaluation by Experts

K. Nomura*, M. Nakayama, A. Okizaki;*
Asahikawa Medical University, Asahikawa, JAPAN.

Aim/Introduction: The purpose of this study was to assess the utilization of a deep learning-based software for bone metastases in patients with prostate carcinoma. ***Materials and Methods:*** 32 patients (52-90 years old) with prostate carcinoma, who had one or more bone metastases, were studied. A deep learning-based software (bone scan index automated calculation software by Tc-99m-HMDP: VSBONE BSI®) was used to evaluate whole body bone scintigraphy. Using the software, bone metastases and nonspecific uptakes were evaluated. A gold standard was determined by two experienced radiologists. When the results of interpretation were not matched, the consensus was used as the gold standard after their discussions. Spearman's rank correlation coefficient was used for evaluation of the correlation between the result with the deep learning-based software and radiologists. ***Results:*** 632 bone metastases in 32 patients were identified by radiologists. 502 of 632 lesions (79.4%) were also identified by the software. There was a statistically significant correlation (r=0.976; P<0.01). ***Conclusion:*** The deep learning-based software showed significant correlation with the diagnosis by experienced radiologists, and the software may be useful to assess the bone metastases in patients with prostate carcinoma. ***References:*** None

EP-179

Incidence of lung nodules positive at ^{68}Ga-PSMA-11 PET/CT- a single center experience

S. Telo*, A. Farolfi, R. Mei, S. Mattoni, L. Calderoni, P. Castellucci, S. Fanti;*
Nuclear Medicine, Policlinico S.Orsola-Malpighi, Bologna, ITALY.

Aim/Introduction: To evaluate incidence of lung nodules showing uptake at ^{68}Ga-PSMA-11-PET/CT in prostate-

cancer (PCa) patients. ***Materials and Methods:*** We consecutively reviewed ^{68}Ga-PSMA-11-PET/CTs of PCa patients referred to our Center from December-2016 to December-2019. Inclusion criteria: 1) positive ^{68}Ga-PSMA-11-PET/CT in one or more lung nodules 2) one of the following clinical settings: PSA-persistence after radical-therapy; biochemical-recurrence after radical-therapy; castration-resistant PCa-patients with PSA progression. ***Results:*** 36/1702 patients were included. Incidence of ^{68}Ga-PSMA-11-PET/CT-uptaking-lung-nudules in our cohort was 2,1%. Characteristics of included patients were: Mean PSA at time of ^{68}Ga-PSMA-11-PET/CT(PET-PSA):5,8 ng/ml (range:0,21-80); Mean lung-lesions-SUVmax (SUVmax):5,9 (range:faint uptake-43,5); 26 patients had single lung lesions, 10 had several lung lesions; Most of lung lesions studied were small sized (subcentimetric nodules in 28 patients; centimetric nodules in 8 patients with maximum diameters range:1-3,6 cm). Follow-up data were available in 21/36 cases:^{68}Ga-PSMA-11-PET/CT results were surgically validated in 11 patients (Group 1) and with subsequent imaging/follow-up in 10 (Group 2). Group 1: 7/11 turned out true-positives for PCa-lung-metastases (Mean SUVmax:9,1; range:faint uptake-43,5; Mean PET-PSA:2,3ng/ml; range:0,27-4,5); Localized lung disease was detected in 4 patients, multiple lymph-nodes and a single lung lesion in 1; spread (lung/bone/lymph-node) disease in 2. 4/11 cases turned out consistent with other neoplastic localizations: Small-Cell-Lung-Cancer (SUVmax:faint uptake;PET-PSA:0,30ng/ml) in 1 pt with localized lung-disease, colon adk metastasis (SUVmax:11,7;PET-PSA:4,13ng/ml), primary lung adk (SUVmax:3,3;PET-PSA:2,8ng/ml) and follicular-LNH (SUVmax:3,7;PET-PSA:6,7ng/ml) in 3 cases with concomitant multi-nodal disease. Group 2 (Mean SUVmax:3,9; range:faint uptake-6,6; Mean PET-PSA:3,9ng/ml; range: 0,46-5): 4 were compatible with true-positives, their consecutive ^{68}Ga-PSMA-11-PET/CT showed respectively: no pulmonary nodule uptake after stereotactic radiation-therapy in 1 patient, bone/lung/lymph-nodes disease progression with concomitant increasing of PSA levels in 2 patients, decreased PSA levels after androgen-deprivation-therapy (ADT) in 1 patient. Disease stability at follow-up ^{68}Ga-PSMA-11-PET/CT was detected in 3 patients (2 with multiple lymph-node and lung lesions/1 with a single lung lesion). Multiple bone/lung/lymph-node lesions were detected in 2 patients and, despite starting ADT, a patient deceased and the other had a PSA-increase. Finally, a single pulmonary lesion turned out to be inflammatory after normalization at HRCT follow-up. ***Conclusion:*** In our population of recurrent, persistent and castration resistant PCa patients ^{68}Ga-PSMA-11-PET/CT was positive in 1 or more lung nodules in about 2% of patients. This result needs to be validated in further studies including larger populations. ***References:*** None

EP-180

^{11}C-Choline PET/CT Performance in Prostate Cancer Surveillance. Ten Years Evaluation of Effectiveness

F. Gomez-De La Fuente*, I. Martínez-Rodríguez, M. de Arcocha-Torres, R. Quirce, J. Jiménez-Bonilla, A. Sánchez-Salmón, N. Martínez-Amador, G. Molina-Mendoza, O. Cuenca-Vera, J. Andrés-Pacheco, Á. Gutiérrez-González, S. Ruiz Llama, I. Banzo;*
Nuclear Medicine Service, Marqués de Valdecilla University Hospital, Molecular Imaging Group (IDIVAL), University of Cantabria, Santander, SPAIN.

Aim/Introduction: ^{11}C-Choline PET/CT has shown good results in prostate cancer (PCa) surveillance, especially in patients with serum levels of prostate specific antigen (PSA) above 1 ng/ml. Our aim was to analyse the performance of the test in our centre over 10 years and evaluate its effectiveness. ***Materials and Methods:*** Three hundred and twenty-nine ^{11}C-Choline PET/CT examinations from 191 patients with PCa (mean age: 69.2 ± 7.4 years) were retrospectively evaluated. They were randomly selected from a total of 804 tests performed in our centre (from 2009 to 2018) in patients with active surveillance or suspected relapse of PCa. Initial treatment was radical prostatectomy (RP) with or without adjuvant treatment in 81 patients, and other treatments (radiotherapy, chemotherapy, hormonotherapy) in 110 patients. PET/CT scans were acquired 20 minutes after intravenous administration of 555-740 MBq of ^{11}C-Choline. Minimum follow-up time was 12 months. ***Results:*** From the 329 examinations, 219 (66.6%) were ^{11}C-Choline PET/CT positive and 110 (33.4%) were negative. Of the 219 positive examinations, 130 (59.3%) showed local recurrence, 49 (22.4%) distant recurrence and 40 (18.3%) local plus distant recurrence. One hundred and forty-nine examinations (45.3%) were performed in patients treated initially with RP, with 65 (43.6%) of positive and 84 (56.4%) of negative results, while 180 (54.7%) examinations were performed in patients with other initial forms of treatment, with 154 (85.6%) of positive and 26 (14.4%) negative results. Mean serum PSA level at PET/CT study was 13 ng/ml (range: 0.02-1337.9 ng/ml) and mean Gleason index was 6. In the subgroup of 81 ^{11}C-Choline PET/CT examinations performed with serum PSA levels <1 ng/ml, 23 (28.4%) showed a positive result, and 9 (11.1%) of them prompted a change in the planned therapeutic management. ***Conclusion:*** ^{11}C-Choline PET/CT demonstrated its effectiveness in PCa surveillance, as two thirds of the examinations showed tumour activity. The diagnostic performance was different depending on the initial treatment. Finally, one third of the ^{11}C-Choline PET/CT examinations performed in patients with serum PSA levels <1 ng/ml showed tumour activity. ***References:*** None

EP-181

The Relationship Between Four Parameters: 68Ga PSMA PET/CT, Gleason Score, PSA Levels and Metastasis

C. Sezgin, G. Mutevelizade, Y. Parlak, G. Gumuser, E. Sayit; Celal Bayar University, Faculty of Medicine, Department of Nuclear Medicine, Manisa, TURKEY.

Aim/Introduction: 68Ga PSMA PET/CT imaging is a valuable method used for staging prostate cancer, evaluating treatment response, and detecting recurrent disease. We aimed to evaluate the relationship between PSA values and pathological data obtained from 68Ga PSMA PET/CT imaging, which were taken for staging in patients with prostate cancer, and the relationship between pathological data and presence of metastasis. ***Materials and Methods:*** The data of 55 patients with prostate cancer (mean age 69.8±8.7) underwent 68Ga PSMA PET/CT (Philips, True Flight Select) imaging for initial staging were analyzed retrospectively. None of them had a prostatectomy. We evaluated the relationship between primary tumor parameters [primary lesion PSMA tumor volume (PSMA-TV), SUVmax, SUVmean], serum PSA values and Gleason Score, and also the relationship of all these values with extraprostatic spread and metastases were investigated. ***Results:*** Fifty-five newly diagnosed patients were included in the study. The extraprostatic spread was not observed in 16 (29%) of them, whereas extraprostatic spread was observed in 39 (71%) patients. Lymph node metastasis was not observed in 23 (42%) of the patients, while 18 (33%) patients had regional and 14 (25%) patients had distant lymph node metastases. Bone metastasis was not observed in 35 (64%) of the patients, 2 (4%) had limited metastases to the pelvic bones, and 18 (33%) had distant bone metastases. Six of the patients (10%) had solid organ metastases. There was a statistically significant relationship between PSA values and primary lesion PSMA-TV ($p<0.05$), whereas no significant relationship was observed between SUVmax and SUVmean values. There was a statistically significant relationship between Gleason Score and primary lesion PSMA-TV, SUVmax and SUVmean values ($p<0.05$). There was a significant relationship between primary lesion PSMA-TV values and the presence of extraprostatic spread and lymph node metastasis no significant relationship was found between TV and bone metastasis. There was a significant relationship between primary tumor SUVmax value and the presence of extraprostatic spread and distant bone metastasis ($p<0.05$). ***Conclusion:*** Gleason Score and PSA values are the main parameters used in risk classification in patients with prostate cancer. The parameters we obtained from PSMA PET/CT images correlate with both Gleason Score and PSA values. We concluded that PSMA PET/CT parameters of the primary lesion might contribute to the risk classification in prostate cancer patients. Although there is no clear relationship between the presence of metastasis and PSMA PET/CT parameters, studies with higher patient numbers are promising in this regard. ***References:*** None

EP-182

Requirements and complexity: interprofessional cooperation within a prospective multicenter clinical trial using [^{68}Ga]Ga-PSMA-11 - The German Cancer Consortium (DKTK) experience

O. Neels[1,2], *C. Zippel*[3,2], *S. Biedenstein*[4], *F. L. Giesel*[4,5,6], *K. Kopka*[1,5,7]; [1]*Helmholtz-Zentrum Dresden-Rossendorf (HZDR), Institute of Radiopharmaceutical Cancer Research, Dresden, GERMANY,* [2]*Formerly: German Cancer Research Center (dkfz), Heidelberg, GERMANY,* [3]*Witten/Herdecke University, Faculty of Management and Economics, Witten, GERMANY,* [4]*University Hospital Heidelberg, Department of Nuclear Medicine, Heidelberg, GERMANY,* [5]*German Cancer Consortium (DKTK), Heidelberg, GERMANY,* [6]*German Cancer Research Center (dkfz), Clinical Cooperation Unit Nuclear Medicine, Heidelberg, GERMANY,* [7]*German Cancer Research Center (dkfz), Heidelberg, GERMANY.*

Aim/Introduction: Prospective clinical trials are initiated within the field of nuclear medicine to translate the most promising radioligands into clinical routine [1]. A close cooperation and communication between experts from different fields is necessary for the efficiency and efficacy of the clinical trial which can then have a positive impact on the timely start of recruitment and subsequent patient inclusions [2]. ***Materials and Methods:*** Given the exemplary phase 1/2 multi-center clinical trial „Ga-68-PSMA-11 in high-risk Prostate Cancer" (NCT03362359) [3], we demonstrate how professions from clinical research, drug manufactur-ing and administration can be involved in the planning, preparation and realisation of prospective clinical trials in nuclear medicine. Organisational measures are derived to support the interprofessional cooperation within diagnostic prospective multicenter clinical trials. ***Results:*** Besides nuclear medicine physicians, urologists and pathologists, other professions like technicians and technologists (nuclear medicine, biology, chemistry), study nurses, radiochemists/-pharmacists and nursing staff are involved in the clinical setting. In addition, radiation safety officers, quality manager, clinical monitors, lawyers, data protection officers, project managers and study coordinators are embedded in the setting of in total eleven study sites in Germany, Austria and Switzerland. ***Conclusion:*** Interprofessional cooperation is of great importance for high-quality work in health care and re-search in general, as well as the accomplishment of prospective clinical trials in nuclear medicine in particular. Readiness to put oneself in the position of other professions, cooperation under no professional constraints, ade-quate time for mutual exchange, the ability and skills for interprofessional project management and an integral view on the required expertise by strengthening overall communication skills are required

in particular on senior management level. ***References:*** 1. Zippel C, Ronski SC, Bohnet-Joschko S, Giesel FL, Kopka K. Current Status of PSMA-Radiotracers for Prostate Cancer: Data Analysis of Prospective Trials Listed on ClinicalTrials.gov. Pharmaceuticals (Basel, Switzerland). 2020;13. doi:10.3390/ph13010012. 2. Reeves S, Pelone F, Harrison R, Goldman J, Zwarenstein M. Interprofessional collaboration to improve professional practice and healthcare outcomes. The Cochrane database of systematic reviews. 2017;6:Cd000072. doi:10.1002/14651858.CD000072.pub3. 3. Neels O, Zippel C, Giesel F, Kopka K. Initiation Of A Prospective Clinical Multicentre Trial With Local Production Of A Short-Lived PSMA-PETRadiopharmaceutical In The D-A-CH-Region: Chances And Experiences. Annual Congress of the European Association of Nuclear Medicine October 12 - 16, 2019. 2019;46:S732. doi:10.1007/s00259-019-04486-2.

EP-183

Meningeal carcinomatosis in patients with a diagnosis of prostate carcinoma visualized in [18F]18F-PSMA, report of three cases

M. Acuña Hernandez[1], *Q. Pitalua Cortes*[2];
[1]*Universidad Autónoma de Bucaramanga, Bucaramanga, Santander, COLOMBIA,* [2]*Instituto Nacional de Cancerología (INCan), Ciudad de México, MEXICO.*

Aim/Introduction: Meningeal carcinomatosis is a uncommon pathology that can occur in solid or hematological malignancies present between 1 and 2 years after the initial diagnosis. When its presence is determined, between 60-70% of cases present associated systemic progression. In prostatic cancer, only have in the literature report o series cases. Its origin may be secondary to hematogenous infiltration, by contiguity to parenchymal or bone metastatic lesions or by neural and perivascular route. Patients may report neurological symptoms according to the location of the lesion. The diagnosis is based on cerebrospinal fluid studies, diagnostic images (preferably MRI) and signs and symptoms suggestive of meningeal involvement. ***Materials and Methods:*** A series cases of three patients with a diagnosis of castration-resistant prostate adenocarcinoma were staged with [18F]18F-PSMA and incidental meningeal involvement was observed. ***Results:*** Case 1 is a 61-year-old male patient diagnosed in 2013 with prostate adenocarcinoma Gleason 7 who received initial management with radiotherapy and hormone blockade. In 2017, presented bone progression, treatment with docetaxel was indicated. In 2019, presented an elevate PSA (40.7 ng/ml) and a moderate intensity headache, [18F]18F-PSMA was performed, evidence compromise in bone structures of the skull with extension in the metabolism over the right frontoparietal region towards the cerebral parenchyma. Subsequently, MRI was performed with contrast that reported pachymeingeal reinforcement of the right hemisphere and study of cerebrospinal fluid that reported pleocytosis. Case 2 is a 66-year-old male patient diagnosed with prostate adenocarcinoma Gleason unknown, indicating treatment surgical. At follow-up in 2019 elevated PSA (15.0 ng/ml) with no neurological symptoms, indicating [18F]18F-PSMA was performed, evidence compromise in bone structures of the right skull base with extension in the metabolism on the cerebral parenchyma. Subsequently, MRI was performed with contrast which reported meningeal reinforcement in this area. Case 3 is a 76-year-old male patient diagnosed in 2012 with prostate adenocarcinoma Gleason 7 indicating surgical treatment. At follow-up in 2019 elevated PSA (40.0 ng/ml) and a headache, [18F] 18F-PSMA was performed, evidence compromise in bone structures of the frontal and parietal right skull with extension in the tracer uptake on the cerebral parenchyma. ***Conclusion:*** Meningeal carcinomatosis is an infrequent event in patients diagnosed with prostate carcinoma, which should be taken into account, according to our cases, in patients with compromised cranial bone structures that may affected by contiguity. ***References:*** None

EP-25

Imaging Clinical Studies -> Oncological Imaging Clinical Study -> Prostate Staging

e-Poster Area

EP-184

Ga 68 PSMA PET/CT at the initial staging of high risk patients with prostate cancer

V. Prassopoulos*, T. Pipikos, D. Kechagias, V. Filippi, F. Vlachou, J. Andreou, K. Dalianis, R. Efthymiadou;*
PET/CT department, Hygeia Hospital, Athens, GREECE.

Aim/Introduction: Ga68 PSMA is a specific PET agent for the investigation of prostate cancer patients. Although it is not routinely used at initial staging, in selected cases it can be of great value. Aim of this study is to evaluate the results of Ga68 PSMA PET/CT study in high risk prostate cancer patients at initial staging ***Materials and Methods:*** The data of 38 patients who underwent a Ga68 PET/CT study between 1/2019 and 12/2019 were retro prospectively evaluated. They were categorized as high risk based on their Gleason score (8 or higher). The area from the base of the skull to the mid-thigh was covered in the scan. SUVmax values in the prostate gland as well as in possible other sites of abnormal uptake were calculated ***Results:*** Twenty-two patients (22/38-58%), had abnormal extra prostatic uptake, with twelve of them showing only lymph node lesions (12/22,54%), eight (8/22, 36%) mixed lymph node and bone foci , while two (2/22, 9%) patients had only bone lesions. Usual sites of abnormal lymph node uptake were the inner inguinal lymph nodes,

lymph nodes in the anatomic space by the prostatic bed, the outer inguinal lymph nodes, the pre-sacral area and less frequently the para-aortic lymph nodes. Mean SUVmax of the lymph nodes foci was 22,17 (4,6 to 42). In the majority of the cases the lymph nodes were not abnormal using CT criteria alone (16/20, 80%). Mean SUVmax of the bone lesions was 20,25 (5,7 to 31), with most usual sites of pathology the spine and the pelvis. Sixteen patients had only uptake in the prostatic gland lesions, with mean SUVmax of 14,6, while the mean SUVmax in the prostate lesions in the group of patients with also extra-prostatic abnormal uptake was 25,65. There was no significant statistical difference of the SUVmax between the two groups (p=0,36). On the contrary when comparing the mean PSA values, the extra-prostatic group showed significantly higher PSA values compared to the prostate limited only group (59,2 to 10,95 respectively, p=0,006). ***Conclusion:*** Ga68 PSMA PET/CT study can be of great value in the initial staging of patients with high risk prostate cancer. In the majority of patients extra prostate pathology can be identified , with a great impact in the therapy planning. ***References:*** Silver DA, Pellicer I, Fair WR, Heston WD, Cordon-Cardo C. Prostate-specific membrane antigen expression in normal and malignant human tissues. Clin Cancer Res. 1997;3:81-5

EP-185

Primary staging of untreated prostate cancer in two-phase Ga-68-PSMA-11 PET/CT: The clinical impact of semi-quantitative parameters

F. Weitzer[1], *B. Pernthaler*[2], *R. Riedl*[3], *R. M. Aigner*[2];
[1]*Medical University of Graz, Graz, AUSTRIA,* [2]*Medical University of Graz, Department of Radiology, Division of Nuclear Medicine, Graz, AUSTRIA,* [3]*Medical University of Graz, Institute for Medical Informatics, Statics and Documentation, Graz, AUSTRIA.*

Aim/Introduction: The value of Ga-68-PSMA-11 in diagnosing both nodal and bone metastases in recurrent prostate cancer is undoubted. The aim of this retrospective study was to evaluate the value of semi-quantitative PET parameters in a two-phase imaging protocol in patients with untreated prostate cancer (PC). ***Materials and Methods:*** We retrospectively evaluated 128 patients with newly diagnosed histopathologically confirmed untreated PC who underwent Ga-68-PSMA-11 PET/CT at our division from January 2017 to October 2019. 28 patients did not meet our inclusion criteria. Static Ga-68-PSMA-11 PET/CT scan of the pelvis was performed 6 min p.i. (early image) and a total-body PET/CT scan was performed 60 min p.i. (late image). Regions of interest for calculating SUVmax and SUVmean were drawn manually around the prostate gland, avoiding the bladder activity in both early and late images. Associations of SUVmax and SUVmean with Gleason score and PSA levels were investigated. ***Results:*** In 94 patients (94%) the primary tumor in the prostate gland could be detected in both early and late phase.In 29 (29%) patients metastases could be detected at a median PSA level of 32.2 (range 0.4 - 503.0) ng/ml vs 10.1 (range 0.6 - 102.9) ng/ml in patients without metastasis (p=< 0.001). PC associated lesions demonstrated in the early vs late images a median SUVmax value of 8.2 (range 3.1 - 45.3) vs. 12.2 (range 3.1 - 73.4) and a median SUVmean of 4.2 (range 1.6 - 4.1) vs 5.8 (range 1.6 - 39.9) statistically significantly increase over the time. (p=<0.001). Higher SUVmax and SUVmean were observed for higher Gleason grading (p=0.004 and p=0.003, respectively) and PSA levels positively correlate with SUVmax (Spearman's rank correlation coefficient: r=0.40, p<0.001) und SUVmean (r=0.35, p<0.001). ***Conclusion:*** Two-phase Ga-68-PSMA-11 PET/CT demonstrated a high overall detection rate of untreated PC of 94% and improves the diagnostic accuracy in primary staging as metastases could be detected in 29 (29%) patients. In primary PC SUVmax and SUVmean values are significantly increasing over the acquisition time points. Higher PSA levels and higher Gleason grading were associated with higher SUVmax and SUVmean levels in the primary lesion. ***References:*** Demirci E, Kabasakal L, Şahin OE, Akgün E, Gültekin MH, Doğanca T, et al. Can SUVmax values of Ga-68-PSMA PET/CT scan predict the clinically significant prostate cancer? Nucl Med Commun. 2019;40(1):86-91.

EP-186

The Role Of Fluciclovine 18F-FACBC-PET/CT In The Characterization Of High Risk Primary Prostate Cancer: Comparison With 11C-Choline-PET/CT And Histopathological Analysis

R. Mei[1,2], *L. Maltoni*[2], *L. Zanoni*[1], *C. Pultrone*[3], *F. Giunchi*[4], *C. Nanni*[1], *I. Bossert*[5], *A. Matti*[2], *R. Schiavina*[3], *M. Fiorentino*[4], *L. Bianchi*[3], *C. Fonti*[1], *F. Lodi*[1], *E. Brunocilla*[3], *S. Fanti*[1,2];
[1]*Nuclear Medicine Policlinico S.Orsola-Malpighi, Bologna, ITALY,* [2]*DIMES, University of Bologna, Bologna, ITALY,* [3]*Urology, AOU di Bologna Policlinico S.Orsola-Malpighi, Bologna, ITALY,* [4]*Pathology, AOU di Bologna Policlinico S.Orsola-Malpighi, Bologna, ITALY,* [5]*Nuclear Medicine, Istituti Clinici Scientifici Maugeri, Padua, ITALY.*

Aim/Introduction: To explore the potential role of ^{18}F-fluciclovine PET/CT in the differentiation of malignant from benign intraprostatic lesions in patients with high-risk primary prostate cancer (PCa) eligible for radical surgery, compared with ^{11}C-choline PET/CT and confirmed by prostatectomy histopathological examination. ***Materials and Methods:*** Among patients (n=94) who underwent additional ^{18}F-fluciclovine PET/CT for staging high-risk PCa as part of a prospective monocentric investigational study (139/2014/O/Sper), the following inclusion criteria were considered for this subgroup analysis: histologically confirmed high-risk Pca, staging PET/CT performed both with standard ^{11}C-choline and ^{18}F-fluciclovine (within max 1 month), radical surgery within 3 months, availability of

all pre-operative investigations in our hospital and of an accurate histopathological analysis of each intraprostatic malignant/benign lesion. A 6 sextants prostate template was created and used independently by PET readers and pathologists for data comparison and validation. PET visual and semiquantitative analyses (SUVmax; SUVmean; target-to-background ratios[TBR], using abdominal aorta, bone marrow, liver and healthy prostate as backgrounds) were performed on both ^{11}C-choline and ^{18}F-fluciclovine scans: at first patient-based, blinded to histopathology (imaging only) and subsequently lesion-based, unblinded, according to pathology reference template. All staging clinical data were collected. ***Results:*** Overall 19 out of 94 patients were included. Main clinical characteristics were mean age 63 (range 51-72) years, 89% high and 11% very-high-risk [D'Amico], mean PSA 9.15 (range 4.2-25ng/mL), whereas pathological ones were pT3a 53%, R1 47%, extracapsular/seminal vesicle/perineural involvement respectively 74%, 21% and 84%; pGS 4+3 42%, 4+5 37%. Overall, 45 malignant and 31 benign lesions were found.For both tracers, the location of the "blinded" prostate SUVmax matched with the lobe of the index lesion (highest pGS) in 17/19 cases (89%).A significant positive correlation was found between SUVmax and pGS with ^{18}F-fluciclovine (p=0.0082), but not with ^{11}C-choline (p=0.30).SUV max was not significantly higher in malignant than benign lesions (p=0.12 and p=0.10) but was significantly higher in malignant than healthy tissue (Mann Whitney, p=0.0012 and p=0.0004 for ^{18}F-fluciclovine and ^{11}C-choline, respectively). Overall TBRs differed significantly between malignant and benign groups. Diagnostic performance of SUVmax resulted significant with both tracer (AUC=0.662, p=0.004 for ^{18}F-fluciclovine; AUC=0.675, p=0.001 for ^{11}C-choline). ***Conclusion:*** In our setting, ^{18}F-fluciclovine SUVmax demonstrated a significant performance in identifying PCa lesions, not different from standard ^{11}C-choline, however still inadequate to accurately differentiate malignant from benign intraprostatic lesions. A significant correlation was found between SUVmax and pGS, with ^{18}F-fluciclovine only. TBRs should be further investigated as more promising parameters. ***References:*** None

EP-187

The Value of the Gleason Score and the Initial PSA (Prostate Specific Antigen) Level in Predicting the Results of Bone Scan in Patients with Newly Diagnosed Prostate Cancer

M. Habbache*, Q. Naili, M. Abdi, B. Said;*
Nuclear medicine Center or Blida, Algier, ALGERIA.

Aim/Introduction: The factors that can predict a higher risk of bone metastasis (BMets) from prostate cancer (PC) are still a subject of debate. The aim of this work is to assess the value of the GLEASON score, and the PSA level, in the prediction of BMets from newly diagnosed PC, and thus determine the indications for basic bone scan (BS) ***Materials and Methods:*** From 2017 to 2019, 256 patients have been enrolled in this retrospective study, with an average age of 71.45 (44 to 88 years). The following informations were collected for each patient: initial PSA level, GLEASON score, and the result of bone scan. We analyze the correlation of the results of the BS, with the PSA level, then with the Gleason score according to whether this score is ≤7, or> 7, and finally with the association of the PSA level and the GLEASON score. ***Results:*** The frequency of BMets increased as the PSA level increased (p <0.01). 5 groups were distinguished. Group 1 (PSA≤10ng/ml): 28 patients, all having a negative BS. Group 2 (PSA: 10-20ng/ml): 3/80 patients (3.7%), have BMets, two of which had a Gleason score>7, and one was classified T4N1. Group 3 (PSA: 20-50ng/ml): 10/58 patients are metastatic (17%). Group 4 (PSA: 50-100ng/ml): 25/52 patients, are metastatic (48%). Group 5 (PSA> 100ng/ml): 29/38 patients are metastatic (76%). The number of metastatic patients also increased according to the Gleason score, ranging from 19% (37/194 patients) for a Gleason≤7, to 48% (30/62 patients) if the Gleason score is>7 (p <0.01). In patients with a PSA level>20ng/ml, the number of metastatic patients increased from 35% (36/104) if the Gleason score is ≤7, to 63% (28/44) if the GLEASON score is>7 (p <0.01). The frequency of BMets in patients with PSA≤20, increased from 1% (1/90) if the Gleason score is ≤7, to 11% (2/18) if the GLEASON score is>7 (p <0.01). ***Conclusion:*** Bone scan is not indicated if the PSA level is ≤10ng/ml. It does't seem necessary if the PSA level is between 10-20ng/ml, unless the GLEASON score>7,There is a lymph node involvement, or a large tumor. The risk of the existence of BMets increases from a PSA level>20ng/ml, especially if the GLEASON score is>7.Thus it can be considered that a PSA level>20ng/ml, or a Gleason score>7, would be predictors of BMets in newly diagnosed prostate cancer, which may therefore indicate to perform an initial bone scan ***References:*** None

EP-188

The Relationship Between The SUVmax Value Obtained in Ga-68 PSMA PET / CT Examination and LDH and ALP in Prostate Cancer Patients

Z. Hasbek*, I. Salk, S. A. Erturk, B. Yücel, Ö. Ulaş Babacan, G. Gökçe, R. T. Bulut;*
Sivas Cumhuriyet University School of Medicine, Sivas, TURKEY.

Aim/Introduction: Lactate Dehydrogenase (LDH) and Alkaline Phosphatase (ALP) are known to have prognostic significance in patients with prostate cancer.Our aim in this study was to evaluate the relationship between the SUVmax values obtained with Ga-68 PSMA PET/CT and LDH and ALP. ***Materials and Methods:*** Patients with prostate adenocarcinoma who underwent Ga-68 PSMA PET/CT for

primary staging or restaging in our department in 2019-2020 and whose LDH and ALP levels were studied in the same month were included in the study. ***Results:*** There were 61 patients in this study and median age was 73(range: 57-89). Distribution of metastasis localization in the patients was as follows:Bone-lymph node 22(36.1%),only-bone 13(21.3%), only-lymph node 4(6.6%),bone-lung 3(4.9%),bone-lymph node-lung 3(4.9%),lymph node-lung 2(3.3%), only-lung 1(1.6%),bone-liver 1(1.6%),bone-liver-brain 1(1.6%),no distant metastasis 11(18%).There was a significant positive correlation between serum PSA and ALP and LDH levels (p=0.0001,r=0.43 and p=0.033,r=0.26,respectively).There was a significant but weak correlation between the prostate SUVmax value and ALP levels of the patients (p=0.019,r=0.271).There was no significant correlation between patients' prostate SUVmax value and LDH levels (p=0.345).Also, no significant correlation was found between the SUVmax of the metastatic lesion with the highest PSMA uptake and LDH and ALP levels in patients with distant metastasis (p=0.238 and 0.277, respectively). No statistically significant correlation was found between prostate SUVmax value and presence of distant metastasis (p=0.729).When the LDH cut-off value was taken as 240, no significant relationship was found between the rate of metastasis and LDH (p= 0.811).When ALP cut-off value was taken as 120, a significant relationship was found between the rate of metastasis and ALP (p=0.039).Considering the presence of bone metastases alone; in patients with ALP levels of 120 and above, there was no significant relationship between the rates of bone metastasis and ALP levels (p=0.052).However, in patients with ALP levels of 120 and above, there was a significant relationship between the presence of diffuse bone metastasis and ALP levels (p=0.052).However, there was no significant relationship between LDH levels and the presence of diffuse bone metastases (p=0.109). ***Conclusion:*** In our study, it was found that ALP was high in the presence of both bone and other organ metastases, and there was a significant relationship between ALP levels and the prostatic SUVmax values. However, according to the data of our study, there was no such relationship with LDH.It is thought that this may be due to a limited number of patient populations in our study. ***References:*** None

EP-189

Dual-phase 68Ga-PSMA-11 PET/CT may increase rate of detected Lesions in Low PSA Levels of Prostate Cancer

M. Assadi[1], *H. Dadgar*[2], *N. Norouzbeigi*[2], *F. Emami*[2], *H. Ahmadzadehfar*[3];

[1]*Bushehr University of Medical Sciences (BUMS), Bushehr, IRAN, ISLAMIC REPUBLIC OF,* [2]*Razavi Cancer Research Center, Razavi Hospital, Mashhad, IRAN, ISLAMIC REPUBLIC OF,* [3]*Klinikum Westfalen, Knappschaft Hospital, Dortmund, GERMANY.*

Aim/Introduction: Recently, 68Ga-PSMA-11 has been introduced as a promising tracer for evaluation of recurrences in prostate cancer (PC). While standard whole-body scans (one hour post injection (p.i.)) are performed routinely, because of high accumulation of radiotracer in the bladder interpretation of the results must be considered with caution. Regarding to this issue, early static imaging can show higher uptake in PC lesions earlier than tracer accumulation in the urinary bladder. Therefore, the aim of the current study was to compare the early static (3-6 min post-injection (p.i.)) and standard whole body (1h p.i.) 68Ga-PSMA-11 PET/CT imaging for detection of recurrences in PC patients. ***Materials and Methods:*** PC patients with prostate-specific antigen (PSA) less than 2.0 ng/ml choose for 68Ga-PSMA-11 PET with mean injected activity 170 MBq. Early static imaging contained the pelvis and the lower abdomen while whole body scan was performed as a routine site from the skull to the mid-thigh one hour after injection. Semi-quantitative analysis (SUVmax) was performed in suspicious lesions. ***Results:*** PSMA uptakes were observed at the small sites of primary tumor and lymph node metastases in patients. Comparing early and one-hour pelvic images in patients demonstrated that no significant differences were detected in the number of lesions. ***Conclusion:*** Early imaging (5 min p.i.) of 68Ga-PSMA-11 PET/CT in addition to whole-body scans (60 min p.i.) may increase the detection rate of local recurrence in PC patients with biochemical recurrence where the urinary bladder has a high uptake during the scan acquisition time. ***References:*** None

EP-26

Imaging Clinical Studies -> Other Imaging Clinical Studies -> Other Clinical Studies

e-Poster Area

EP-190

Measurement of blood flow of thoracic vertebral body using O-15 water PET

K. Matsunaga*, M. Yanagawa, E. Shimosegwa, J. Hatazawa; Osaka University, Suita city, JAPAN.*

Aim/Introduction: There were few reports about human bone blood flow (BBF)(1). The relationship between human BBF and blood cell counts has not been examined. Inhibition of vascular endothelial growth factor (VEGF) was reported to reduce BBF in mice (2), however the BBF change in human after anti-VEGF treatment has been rarely reported (3). The objectives of this study were to measure human BBF using ^{15}O-H_2O PET, to examine the relationship between BBF and age, sex, blood cell counts, and to examine the BBF change after the anti-VEGF treatment (bebacizumab:BEV). ***Materials and Methods:*** Twelve patients with advanced lung cancer

underwent 10 min dynamic ^{15}O-H_2O PET before/after the chemotherapy. Using nonlinear regression, time activity curve of thoracic vertebral body was fitted to the single-tissue compartment model using image derived input functions, which were determined using volumes of interest over ascending aorta. We also evaluated the relationship between BBF, age and blood cell counts. In patients treated BEV (n=6), we compared the difference before/after administration of BEV including chemotherapy. ***Results:*** The mean of BBF was 0.1 ml/min/cm^3 , which was consistent with reported values derived from other methods (1,3). There was no significant correlation between BBF and age or BBF and blood cell counts. Significant BBF changes 1-2 days after BEV including chemotherapy were not observed. ***Conclusion:*** Human BBF could be measured using ^{15}O-H_2O PET. The sex, age, blood cell counts would not be the main regulatory factors in BBF. Anti-VEGF treatment did not affect BBF in human. ***References:*** (1)Lahtinen, T et al. Eur J Nucl Med. 1979;4(6):435-439. (2)Lane NE, et al. Bone Reports. 2019;10:100210. (3)Van der Veldt AAM, et al. Cancer Cell. 2012;21(1):82-91.

EP-192

Paget's Disease on Bone Scintigraphy: the Role of Scintigraphic Patterns and Bone SPECT/CT in Diagnosis

H. Turoglu*, S. Kesim, C. O. Engur, N. Filizoglu, S. Ozguven, K. Oksuzoglu, S. Inanir, T. Ones, T. Y. Erdil;*
Marmara University Istanbul Pendik Training and Research Hospital, Istanbul, TURKEY.

Aim/Introduction: Paget's disease of Bone (PDB) is a chronic and benign bone disease with unknown etiology, which is more common in men and middle-aged or older adults. PDB is usually polyostotic and most of the bone lesions are asymptomatic. The scintigraphic and radiographic appearances of pagetoid bones depend on the disease stage. In this study, the frequency of PDB in bone scintigraphy, the role of SPECT/CT and scintigraphic patterns were investigated. ***Materials and Methods:*** Two hours after the intravenous injection of 20 mCi Tc99m-MDP, routine whole body skeletal survey and if necessary SPECT/CT images were acquired. For 14 patients who were clinically suspicious of PDB, immediate dynamic blood flow images and 2-5 minutes after injection, static blood pool images were also performed. ***Results:*** A total of 2665 patients, referred to the nuclear medicine clinic for bone scintigraphy, between years 2012 and 2019, were retrospectively investigated. Out of 2665 patients, 28 patients (17 males, 11 women) were identified as known/clinically suspicious or asymptomatic PDB. The age of patients ranged from 25 to 90 (mean 66.1±15.8). Five cases diagnosed by radiography, CT and bone scan were also confirmed by histopathology. In eight patients, malignancies and metastatic work-up were present. Although both were seen in elderly aged men, it was noteworthy that the number of patients who have coexisting metastatic prostate cancer and PDB was small. Hearing loss, fracture and deformity complications of PDB were present, in five patients, in one patient and in five patients, respectively. In our patient series, "Mickey Mouse sign" was found in one patient and hemi-pelvis involvement was seen in 13 patients. It was observed that increased total ALP levels and metabolic active PDB on scintigraphy correlate well (p=0.002). Monostotic and symptomatic lesions were more frequent in our patient series, than that reported in the literature; which can be considered as a result of selection of the patients in a tertiary hospital setting. ***Conclusion:*** Clinical indications are the diagnosis and evaluation of the extent of PDB, assessment of treatment response and detecting complications in the follow-up. It was revealed that with the recognition of scintigraphic patterns ("Mickey Mouse sign" in the vertebrae, "Lincoln" sign in the mandible, hemi-pelvis involvement), and the addition of SPECT/CT in metabolic active PDB cases; high diagnostic accuracy can be achieved with prevention of unnecessary biopsies in monostotic cases. ***References:*** None

EP-193

Audit Of Reporting Ventilation-Perfusion (V/Q) Lung Scans In Pregnancy Over A Decade Apart And Across Two Different Institutions

G. Shabo*;*
University Hospital Lewisham, London, UNITED KINGDOM.

Aim/Introduction: Pregnancy is associated with a five-fold increase in the prevalence of venous thromboembolism (VTE) and pulmonary embolism (PE). The diagnosis of PE is challenging as the physiologic changes during pregnancy can mimic pulmonary embolism. The ventilation-perfusion lung scintigraphy (V/Q scan) is a well-established investigation of suspected PE in pregnancy with low radiation burden. In pregnancy, up to 5% of scans are positive and 75% of scans are normal. This audit looks at the reports from earlier and recent years, using planar and tomographic imaging in two different hospital settings, to evaluate whether the findings are in line with those of the literature. ***Materials and Methods:*** Data were collected retrospectively (via PACS, CRIS and Patient Centre), covering two years from January 2006 to December 2007 and two years from January 2018 to December 2019. The scans from 2006, 2007 and 2018 were performed at East Kent hospitals (UK) whereas the scans from 2019 were performed in a South East London hospital. The scans in 2006 and 2007 were planar imaging whereas those in 2018 and 2019 were SPECT imaging. All scans were ventilation-perfusion studies. ***Results:*** Total of 182 scans were reviewed. 51 studies in 2006 and 2007, aged 17 to 44 (mean 27.65, median 26.5 in 2006; mean 27.65, median 27 in 2007), 62 studies in 2018, aged 19 to 45 (mean 28.5; median 28) and 69 studies in 2019, aged

17 to 47 (mean 31.36; median 32). In 2006 and 2007, 31 scans (60.8%) were reported "normal" and 20 scans (39.2%) were "low probability". No "positive" scans were reported during this period. In 2018, 51 scans (82.3%) were reported "normal", 3 scans (4.8%) were "negative for PE", 5 scans (8%) were "positive", 2 scans (3.2%) were "low probability" (performed as planar imaging) and 1 scan (1.6%) was reported "uncertain whether recent or old PE". In 2019, 56 scans (81.2%) were reported "normal", 5 scans (7.3%) were "negative for PE" and 8 scans (11.6 %) were "positive". Overall, 138/182 scans (75.8%) were "normal" and only 13/182 scans (7.1%) were reported "positive". ***Conclusion:*** The reports are largely in line with the literature findings in pregnancy. Reporting "low probability" in planar imaging can be subjective and these scans may be considered "normal" by other reporters. SPECT-V/Q scintigraphy is unquestionably superior to planar imaging. Positive scans can occur and the perception that V/Q scans in pregnancy are always normal is erroneous. ***References:*** None

EP-194

Incidental Findings on Single-Photon Emission Computerized Tomographic (SPECT) Studies

J. Koutsikos[1,2], *S. Episkopopoulou*[1], *S. Mpakalis*[1], *S. Vasileiou*[1], *K. Athanasiou*[1], *S. Giourgouli*[2], *A. Kokkini-Pashou*[1];
[1]*401 General Army Hospital, Athens, GREECE,* [2]*Henry Dunant Hospital Center, Athens, GREECE.*

Aim/Introduction: SPECT is a complementary and, in many cases, a necessary technique in the Nuclear Medicine studies. An important step in the interpretation of SPECT images is to study of the unprocessed imaging data, known as raw data. The raw imaging data contain the original information about captured physical quantities, which describe internal aspects of the body. This is followed by the application of the appropriate processing filters and algorithms to display the reconstructed final image. In some cases, an incidental finding is observed out of the region of investigation. The purpose of this study is to identify random findings on SPECT studies. ***Materials and Methods:*** A retrospective study was conducted. A total of 352 SPECT images were evaluated, including 233 myocardial perfusion scans, 14 bone scintigraphies, 5 inflammatory detection scans, 13 somatostatin receptors studies and 87 brain tomographies. Special attention was given in the evaluation of unprocessed data, in order to highlight possible random findings. ***Results:*** Nine unexpected findings were observed; thymoma, breast tumor, myelodysplastic syndrome, lung tumor, adenoma of the parathyroid gland, brain tumor and lymphoma. Seven of them were confirmed histologically or with other imaging techniques, such as MRI and PET. The other findings were an accessory spleen and sarcoidosis. Myocardial perfusion scintigraphic studies were the most common studies where an incidental finding was observed (6/9). ***Conclusion:*** In our study, the occurrence of incidental findings in SPECT scans that should lead to additional medical care is 2,5%. Even if this is a small percentage, we can't ignore the fact that any further information may be crucial for the patient. So nuclear medicine physicians should keep in mind to study carefully the unprocessed data, while evaluating the tomographic nuclear medicine studies, to avoid overlooking such findings. ***References:*** None

EP-195

Exploratory study of the utility of clinical images with half dose ^{18}F-FDG in a Biograph Vision PET/CT system

S. Tagawa*, A. Ohnishi, A. Ohhashi, K. Hayashi, M. Nobuhara, N. Sakamoto, T. Nakamura;*
Kakogawa Central City Hospital, Kakogawa, JAPAN.

Aim/Introduction: The Biograph Vision PET/CT device is equipped with a silicon photomultiplier (SiPM), which has higher photodetection efficiency and faster processing speed than a conventional photomultiplier (PMT). Effective sensitivity is greatly increased due to its high time-of-flight (TOF) timing resolution. In addition, the smaller crystal size in SiPM results in improved spatial resolution and higher quality clinical images compared with PMT. The recent focus on dose reduction to the patient in the clinical setting requires a reduction in ^{18}F-FDG dosage. Accordingly, we explored the clinical value of PET images obtained using Biograph Vision in half-dose ^{18}F-FDG. ***Materials and Methods:*** In two sessions 2 days apart, three healthy subjects (body mass index [BMI] 18.7, 22, and 27.2) were injected with ^{18}F-FDG of 3.7 MBq/kg (normal dose) or 1.85 MBq/kg (half dose) and underwent whole-body PET/CT starting at 60 minutes post-injection. Whole-body PET/CT images were acquired in step-and-shoot mode for 3 min/bed. One subject (BMI 22) underwent whole-body PET/CT in whole-body dynamic mode for 78 minutes (3 min/pass) after ^{18}F-FDG injection at normal and half doses. In each subject, PET images obtained with normal and half dose ^{18}F-FDG were compared and evaluated using liver signal-noise ratio (SNR; cut-off value, 10) and visual evaluation. In the whole-body dynamic scan images, summation images of passes 1-6 from 60 minutes post-injection were generated and evaluated. ***Results:*** In two of the subjects (BMI 18.7 and 22), liver SNR was slightly lower in the half-dose than normal-dose images, but above the cut-off value. In the other subject (BMI 27.2), liver SNR was 7.0 in the half-dose images, which is below the cut-off value. In all subjects, visual evaluation revealed almost no difference between the half-dose and normal-dose images. In whole body dynamic scanning, liver SNR was less than the cut-off value (6.0 and 9.1) in the summation images of the 6 passes from 60 minutes post-injection in both the half-dose and normal-dose images. However, in visual evaluation, even the summation images

of 3 passes from 60 minutes post-injection with half dose were relatively clear, and these images showed almost no difference from images with normal dose. ***Conclusion:*** These results indicate the quality of half-dose images is sufficient for clinical use. Clinically acceptable images can be obtained even in subjects with a large physique and with a short scan time. The use of Biograph Vision enables a reduction in dose and scan time in PET examinations. ***References:*** None

EP-196

Can we really trust bone scan for condylar hyperplasia?

D. Calabro'[1], *R. Mei*[1], *G. Argalia*[1], *L. Vetrone*[1], *N. Fraccascia*[1], *R. Bonfiglioli*[2], *E. Tabacchi*[2], *M. Levorato*[2], *S. Fanti*[1];
[1]*Nuclear Medicine, S.Orsola-Malpighi Hospital, DIMES University of Bologna, Bologna, ITALY,* [2]*Nuclear Medicine, S.Orsola-Malpighi Hospital, Bologna, ITALY.*

Aim/Introduction: Condylar hyperplasia (CH) is a pathology of the temporomandibular joint resulting in a progressive unilateral non-neoplastic growth. Single photon emission computed tomography (SPECT) with Tc-99m-3,3-diphosphono-1,2-propanodicarboxylic acid (Tc-99m-DPD) has a pivotal role in the diagnosis of CH since the decision to perform condylectomy is almost exclusively based on finding a % condylar uptake difference ≥ 10%. Aim of this study was to compare two different quantitative evaluation methods to interpret the 99TC-DPD SPECT/CT in patients (pts) with clinically suspected unilateral CH. ***Materials and Methods:*** Pts who performed a 99TC-DPD SPECT/CT for clinical suspicion of unilateral CH between January 2016 and March 2020 were included. % condylar uptake difference was evaluated with two different quantitative methods: 1) total counts of 5 fixed-size regions of interest (ROI) drawn on 5 consecutive transaxial images for each condyle 2) total counts calculated on a fixed-size volume of interest (VOI) on fused transaxial SPECT/CT images. All the exams were reviewed by two nuclear medicine experts. Reproducibility (inter-operator variability) was assessed for both methods using contingency tables and K-coefficient. ***Results:*** Overall, 26 pts were included in the final analysis. % condylar uptake difference values were significantly different between the two methods (p=0.08). A low grade of diagnostic agreement was obtained in both ROI method (K=0.07) and VOI method (K=0.03). Limitations of this analysis are: i) the small population, ii) the lack of clinical follow-up data supporting a real evaluation of sensitivity and specificity for both methods. ***Conclusion:*** 5 fixed-size ROI method is the most commonly used in nuclear medicine departments. Despite its more easily evaluation, VOI method provides data that significantly differ from the 5 ROI method. Both methods also showed a poor reproducibility in terms of inter-observer agreement, so it is mandatory to identify a standardized method of quantitative evaluation of this test that offers the best possible CH diagnostic precision and accuracy. ***References:*** None

EP-197

Whole-body PET/CT recognizes two distinct patterns of osteolytic lesions in adult Langerhans cell histiocytosis

R. Wang*, M. Su, R. Tian;*
Sichuan University West China Hospital, Chengdu, CHINA.

Aim/Introduction: Langerhans cell histiocytosis (LCH) is a histicocytosis disease which always accompanied multisystem lesions. Previous studies have assessed the role of FDG PET/CT in the management of adult multisystem LCH. The aim of our article is to explore the ability of ^{18}F-FDG PET/CT in distinguishing two distinct patterns of osteolytic lesions in LCH patients. ***Materials and Methods:*** Ten consecutive adult patients with histologically proven LCH was included in this respective study, ^{18}F-FDG PET/CT scan was performed for staging. The findings of other imaging features and treatment history were collected. The images of PET/CT were analyzed and compared between two different patterns of osteolytic lesions in LCH. The relationship between these clinical and PET/CT findings also analyzed. ***Results:*** Forty-two osteolytic bone lesions were detected on whole-body CT, mostly involving skull, ribs, spine and pelvis. These lesions separated two types of metabolic lesions containing of 16 high metabolisms and 26 low or no metabolisms on whole-body PET. According to the results of ^{18}F-FDG PET/CT, low or no metabolic osteolytic lesions presented low SUVmax and SUVmean values(2.03±0.62 and 1.84±0.51), whereas high metabolic osteolytic lesions showed the pattern of high FDG intake, characterized by higher SUVmax and SUVmean values(6.36±1.14 and 5.71±0.9). we also found that the metabolic features in PET/CT have no relationship with treatment history. ***Conclusion:*** Two different metabolic patterns of osteolytic lesions were detected by ^{18}F-FDG PET/CT in adult LCH. The lesions with high metabolism may be indicative for active or progressive disease, no metabolic lesions may present no-active or resolved disease. These two types of lesions were indicative for the diagnose of LCH, although only high metabolic lesions presented increased FDG uptake on ^{18}F-FDG PET/CT. ***References:*** None

EP-198

Small steps driving big changes - How we implemented a new Gastric Emptying Protocol

M. Botelho Cruz*, A. Pereira, A. Nunes, D. Bailey, C. Sibley-Allen, D. Dasgupta, F. Ul-Hassan, A. Eccles;*
Guy's and St. Thomas' Hospital, London, UNITED KINGDOM.

Aim/Introduction: Gastric emptying (GE) scintigraphy is commonly used as a diagnostic procedure for the assessment of gastric motility and function. A plethora of literature is available to evaluate different meals for this

procedure, nevertheless standardisation is still lacking. The latter has been well demonstrated by Notgi, A. et al (2018) in their national survey. To optimise the quality and consistency of gastric emptying reporting and patient compliance with our standard meal (porridge with milk), we made it our goal to identify areas requiring improvement. Our initial focus was turned to the adult patient cohort. ***Materials and Methods:*** Multiphase gradual approach based on Kaizen methodology was adopted. This methodology is a process where workers at all levels of the department are engaged in constantly identifying opportunities for change and improvement. A motivated and skilled taskforce worked together to address current GE hurdles. This involved members of different staff groups with varying levels of seniority and expertise within Nuclear Medicine. The entire team was made aware of the aim and progressive results via departmental meetings. Phase 1 consisted in literature review of multiple meal options and reference ranges. An audit on consistency of reports and variation from our standard meal was conducted. On Phase 2 the impact of GE procedure on different staff groups workflow was analysed. This was followed by weighing pros and cons to drive a protocol change. The Nottingham test meal (NTM) was agreed upon as the test solution. Phase 3 encompassed contacting the Nottingham team to obtain authorisation and establish collaboration. On Phase 4 we performed protocol and software validation with a gastric phantom, produced in-house. The results were satisfactory; hence the protocol was accepted for clinical trial. Local standard operating procedures were produced. ***Results:*** The new protocol was clinically approved and fourteen adult patients have already been successfully scanned. A staff training programme is being developed and further qualitative research to evaluate staff and patient experience is the next step of this taskforce. Moreover, evaluation of suitability for paediatric population will also be addressed. ***Conclusion:*** In conclusion, multidisciplinary and co-operation between staff groups and bridging with other departments' knowledge is crucial to improve practices and drive changes in the Nuclear Medicine community. The use of Kaizen method was shown to be very effective in this project. ***References:*** Notghi, A. and Hansrod, S., 2018. National survey of gastric emptying studies in the UK. Nuclear Medicine Communications

EP-199

Conceptions of quality of nuclear medicine care services: A prospective two-center study

E. Giannoula[1], I. Katsikavelas[2], N. Papadopoulos[3], C. Sachpekidis[4], A. Doumas[1], F. Spyroglou[1], V. Chatzipavlidou[5], I. Iakovou[1]; [1]Nuclear Medicine dpt of Aristotle University AHEPA Academic hsp, Thessaloniki, GREECE, [2]Faculty of Engineering, Aristotle University of Thessaloniki, Thessaloniki, GREECE, [3]G.Gennimatas hsp, Thessaloniki, GREECE, [4]Clinical Cooperation Unit Nuclear Medicine, German Cancer Research Center, Heidelberg, GERMANY, [5]Nuclear Medicine dpt of THEAGENEIO Anticancer hsp, Thessaloniki, GREECE.

Aim/Introduction: Nuclear Medicine has a unique characteristic: the use of radiopharmaceuticals and exposure to ionizing radiation. Hence, quality and safety assurance is considered a sine qua non. Although, several reports have been issued, on how qualitative and safe management of patients in nuclear medicine departments (NMD) should be done, limited data are available in terms of the level of the quality of service and patients' perceptions regarding them. In this context, the objective of the current study was the assessment of patient satisfaction level and all aspects of perceived quality for medical, nursing and organization in NM settings as well as the evaluation of patients' attitude to exposure to ionizing radiation for medical purposes. ***Materials and Methods:*** The survey was contacted by using two SERVQUAL type questionnaires. The inpatient and outpatient questionnaires, were transformed and validated to reach out to thyroid cancer patients, submitted to nuclear medicine departments. A total number of 551 patients (354 who received therapeutic doses of ^{131}I and 197 who underwent diagnostic ^{131}I-scintigraphy) enrolled in this study. ***Results:*** High level satisfaction was measured from the medical services (98.8% of the inpatient and 99.5% of the outpatient survey participants were satisfied or very satisfied) and the nursing facilities (81.6% and 67.7% respectively were very satisfied). Patient satisfaction was obviously lower in respect with organization (55.1%) and hotel facilities (42.7% and 45.9%). The score of the overall perceived quality of services was high (98.5% and 91.8%). Waiting had a great impact on the perception of service quality for 34.4% of the participants. There were statistically significant differences in patient satisfaction and perceived quality of services observed according to sex, age, rural or urban residency, nationality, marital status, education level and profession, as well as health status. Patients' attitude towards radiation treatment efficacy and safety matters was revealing of the poor awareness towards the effects of exposure to ionizing radiation for medical reasons, showing the necessity for further informative campaign. ***Conclusion:*** Most NMD provide the same type of services but not equally qualitative. Quality assurance procedures, compliance with regulations and clinical practice based on evidence-based medicine do not seem to be enough, since perceptions in terms of safety, quality and satisfaction from the provided services differ between patients. Patient-centered practice, communication and proper information play a decisive role in ensuring satisfied patients. ***References:*** None

EP-200

Relevance of investigation of deep lymphatic vessels in lower limbs lymphoscintigraphy: a single Center experience

C. Dolci[1], R. Dentici[2], A. F. Scarale[1], A. Capozza[1], A. Franchini[3], I. Gotuzzo[3], E. Gay[1], G. Cabrini[1], M. Milella[1], C. Rossetti[1]; [1]Nuclear Medicine Unit, ASST Grande Ospedale Metropolitano Niguarda, Milan, ITALY, [2]Nuclear Medicine Unit, ASST Rhodense, Caduti Bollatesi Hospital, Bollate, ITALY, [3]Nuclear Medicine, University Milano-Bicocca, Milan, ITALY.

Aim/Introduction: Lymphoscintigraphy (LSG) is a reliable tool for diagnosis of lymphedema but its execution protocol is not standardized and differs among diagnostic centers. Aim of this study was to evaluate the value of deep lymphatic circulation assessment together with superficial one in lower limbs (LL) LSG. ***Materials and Methods:*** One hundred and four patients (68 females, 36 males; mean age 40 years, range 11-78) with LL LSG performed at Caduti Bollatesi Hospital from 2016 to 2019 were retrospectively analyzed. Indications were suspect primary and secondary lymphedema in 87 and 17 patients respectively. Deep and superficial lymphatic circulation were investigated sequentially on the same day. One deep injection of 37 MBq technetium-99m labeled albumin nanocolloids was performed in the plantar arc of each foot and scintigraphic planar images were obtained at 5 and 25 minutes, after centripetal stimulation (walking). Superficial circulation was then examined with the same protocol after subcutaneous injections in first and fourth interdigital spaces and peroneal malleolus area (37 MBq overall for each foot). Pathologic findings were absent or reduced visualization of lymphatic vessels/nodes and dermal backflow. ***Results:*** Twenty-three out of 104 (22%) LSGs were negative, while 81/104 (78%) were positive for alterations of LL lymphatic system. Among positive LSGs, only 1/81 (1%) showed alterations of superficial lymphatic circulation alone; 42/81 (52%) showed alterations of both deep and superficial circulation and in 38/81 (47%) pathologic findings concerned only deep lymphatic system. In 33/38 (87%) LSGs with deep lymphatic system impairment, superficial compensation was observed as early visualization of superficial lymphatic channels/nodes after radiotracer deep injection. In 47/81 patients (58%) clinical presentation of limb swelling (left, right, bilateral) was concordant with lymphoscintigraphic abnormalities; among the 34/81 "nonmatch" patients (42%) 28 had bilateral lymphoscintigraphic abnormalities but unilateral clinical swelling, while in only 6 cases there was a discrepancy between clinical manifestation and scintigraphic findings. ***Conclusion:*** In this series most patients presented alterations of deep lymphatic vessels, with or without alterations of superficial one, so in these cases investigation of superficial circulation alone could cause lack of clinical information: in LL LSG it is useful to study both deep and superficial circulation because alterations of deep circulation can be offset by a superficial one that functionally corrects a deficiency of primary or secondary nature. LSG can show bilateral lymphatic abnormalities in patients with unilateral lymphedema, thus detecting subclinical changes to lymphatic pathways before clinical evidence of disease. ***References:*** None

EP-201

FDG-PET/CT in neurofibromatosis type 1: the experience of a reference center

D. Peres e Leiro Gonçalves Ferraz*, I. Patrocínio Carvalho, P. Ratão, J. Passos, M. Rio Carvalho, M. Silvestre, D. Fraga, I. Vitorino, F. Norton Brandão, R. Sousa, T. Cruz Ferreira, L. Salgado; Instituto Português de Oncologia de Lisboa Francisco Gentil, Lisbon, PORTUGAL.*

Aim/Introduction: Neurofibromatosis type 1 (NF-1) is an autosomal dominant neurocutaneous pathology, which results in the loss of function of the oncossupressant gene NF and predisposes affected individuals to develop tumors. This pathology has an incidence at birth of 1-2500 to 1-3000 and also carries a risk of malignization in the range of 8-12% during the patient's expected life span. The objective of the present study is to assess the degree of metabolic activity of neurofibromatous lesions and the correlation with malignant transformation. The preliminary results of the study are presented. ***Materials and Methods:*** A single-center retrospective study was carried out, with 85 patients (pts) with NF-1 undergoing FDG-PET/CT between February 2014 and January 2020, to assess possible malignant transformation of neurofibromatous lesions in the context of: pain, increase in size, change in consistency, associated neurological deficits. Seven pts were excluded: four, for having previously undergone systemic / surgical therapy and three, for not being followed at our institution. We included 78 pts (median age 23 years 6-69 years, 40 females and 38 males), corresponding to a total of 78 exams, with 149 lesions identified. [^{18}F]FDG was administered at a dose of 37Mbq / 10 kg weight and the average time between injection and image acquisition was 72 minutes [45-120 min]. The lesions were divided into three groups according to the maximum SUV: Group A: <2.5 (not suspect), Group B: 2.5-3.5 (doubtful), Group C:> 3.5 (suspect). Etiological confirmation was obtained by histological characterization or by a follow-up of more than 24 months (27 lesions). Lesions with a follow-up of less than 24 months and without histological evaluation to date, were classified as indeterminate and excluded from the present analysis. ***Results:*** Group A- 6 lesions: two benign (histological characterization) and four benign (follow-up). Group B- 5 lesions: three benign (histological characterization) and two benign (follow-up). Group C- 16 lesions: 11 benign (histological characterization), two malignant

(histological characterization) and 3 atypical (histological characterization). ***Conclusion:*** In this preliminary study, maximum SUV value of 3.5 appears to be a good cut-off to indicate benignity. Benignity was confirmed in all lesions with maximum SUV bellow 3.5. However, the reduced sample, as a consequence of the short follow-up time and the absence of histological characterization of all lesions, does not allow us to determine at this time the nature of the lesions through their metabolism. ***References:*** None

EP-27

Imaging Clinical Studies -> Other Oncological Clinical Study -> Radioguided Surgery and Radiation Therapy Planning

e-Poster Area

EP-202

Radioguided Occult Lesion Localization of Pulmonary Nodules in Video-Assisted Thoracic Surgery: Initial Experience

A. Cánoves-Llombart[1], *H. Rodríguez-Parra*[1], *I. Casáns-Tormo*[1], *M. Redal-Peña*[1], *V. Carrero-Vásquez*[1], *J. Sabater-Sancho*[1], *P. Cárcamo-Ibarra*[1], *M. Rengel-Ruiz*[2], *S. Figueroa-Almanzar*[3], *R. Wins-Birabén*[3], *G. Galán-Gil*[3];
[1]*Nuclear Medicine, Valencia, SPAIN,* [2]*Radiology, Valencia, SPAIN,* [3]*Thoracic Surgery, Valencia, SPAIN.*

Aim/Introduction: To evaluate the results obtained in our initial experience in the radioguided occult lesion localization (ROLL) of small and solitary pulmonary nodules in video-assisted thoracic surgery (VATS). ***Materials and Methods:*** We analyzed 6 patients, age 24 - 78 y/o (mean 56), with single, small and peripherally located pulmonary nodules by computed tomography (CT). In all cases radiotracer administration and surgery were performed on the same day. We administered 1mCi of ^{99}mTc-macroaggregated albumin in a volume of 0.2ml through CT-guided injection. Before the surgery, the radiotracer localization was verified by lung SPECT and SPECT-CT fusion. During the surgery, a gamma probe and portable gamma camera were used to locate and verify the nodule and to check the removed piece. After the surgery, it was obtained the pathological confirmation. ***Results:*** In 3 patients, the suspected diagnosis was primary lung neoplasia, and lung metastases in the other 3. Two nodules were localized in the right lower lobe, one in the right upper lobe and three in the left upper lobe. The distance to the pleural surface was 0.38-2.3cm (mean 1.3cm). The size of the nodules ranged from 3 to 12.8mm (mean 7.8mm).The intraoperative detection and excision rate were 100%. In all cases, the presence of radiotracer in the resected piece was confirmed. The pathological study confirmed the localization of the nodule in the removed piece, with the results of one cancer, two metastases, one atypical adenomatous hyperplasia and two benign tumors. Patients' tolerance of the procedure was good. Regarding the technique, there was an extravasation of the radiotracer to the pleural space in one case, but the incident did not suppose any difficulty in radioguided localization of the nodule. After surgery, one patient had late postoperative complications, not related with ROLL technique. ***Conclusion:*** Radioguided occult lesion localization of pulmonary nodules allows a safe removal of no-detectable lesions by video-assisted thoracic surgery, without the need of thoracotomy. It reduces morbidity, allowing a minimally invasive surgery, with preservation of large volume of health pulmonary parenchyma and improves the patient recovery. ***References:*** None

EP-203

Role Of Double-Phase Parathyroid Scintigraphy With SPECT-TC, Probe And Portable Gamma Camera In The Detection And Extraction Of Parathyroid Adenomas

P. Turbay Eljach*, M. González Soto, B. Pérez López, A. Sainz Esteban, N. Álvarez Mena, F. Sebastián Palacid, M. Alonso Rodríguez, C. Gamazo Laherrán, M. Ruíz Gómez, R. Ruano Pérez; Hospital Clínico Universitario de Valladolid, Valladolid, SPAIN.*

Aim/Introduction: To assess the diagnostic capacity of parathyroid scintigraphy with planar 99mTc-MIBI and SPECT-CT (GP) and the portable gammacamera in radioguided parathyroid surgery. ***Materials and Methods:*** Nineteen patients referred for suspicion of parathyroid pathology have been studied. A double-phase parathyroid scan was performed with 99mTc-MIBI and early cervicothoracic SPECT-CT. On the day of surgery, a 370 MBq dose of 99mTc-MIBI was administered one hour before surgery. During surgery, a probe and a portable gammacamera were used. Demographic data, scintigraphy detection capacity, SPECT-CT detection capacity and location, portable gammacamera and probe detection capacity, other imaging tests, pathological results and clinical evolution were evaluated. ***Results:*** All the cases were studied with ultrasound /CT before surgery, being negative for parathyroid disease in ten patients. The GP detected 19 unique adenomas (upper right 3, lower right 10, upper left 2 and lower left 3), one of them ectopic. All of them were extracted during surgery with the help of the probe and portable gammacamera. In 10 patients, the portable gammacamera was of great help in removing doubtful pathological glands. The pathological results confirmed the existence of 16 adenomas and 3 hyperplastic glands. During the surgical act, other parathyroid glands were removed (5), of which none had uptake with the portable gammacamera with pathological result of clear cell hyperplasia (1) and without pathological changes (4). Scintigraphic localization was confirmed during surgical excision in all cases. A significant decrease in

PTHi values was confirmed after excision and normalization of calcium levels. ***Conclusion:*** GP is useful in the detection and presurgical location of parathyroid pathology. The probe and portable gammacamera have proven to be very useful during the excision, successfully solving doubtful cases. ***References:*** None

EP-204

γ-probe guided minimally invasive parathyroidectomy in selected cases of solitary parathyroid adenomas

I. Iakovou[1], *T. Papavramidis*[2], *E. Giannoula*[1], *F. Spyroglou*[1], *G. Gerasimou*[1], *E. Papanastasiou*[3], *A. Doumas*[1];
[1]*Nuclear Medicine dpt of Aristotle University AHEPA Academic hsp, Thessaloniki, GREECE,* [2]*1st Propedeutic Surgery dpt of Aristotle University AHEPA Academic hsp, Thessaloniki, GREECE,* [3]*Laboratory of Medical Physics dpt of Aristotle University AHEPA Academic hsp, Thessaloniki, GREECE.*

Aim/Introduction: Our objective was to assess the efficacy of γ-probe guided minimally invasive parathyroidectomy (γP-MInP) inselected cases of solitary parathyroid adenomas without intra-operative quick parathyroid hormone (qiPTH) measurement. ***Materials and Methods:*** Our cohort comprised 24 patients (21 female), 53±12yrs old, with primary hyperparathyroidism (HPT) without history of familial HPT nor MEN syndrome, no ultrasound thyroid nodule presence and ^{99m}Tc-MIBI scan and ultrasound concordant localisation of a solitary parathyroid adenoma. They were all operated by a high volume, parathyroid dedicated surgeon of the endocrine surgery department of our hospital from March 2017 to January 2019. All patients were operated within 1-3 weeks after the detection of a solitary parathyroid adenoma by ultrasound and confirmation by dual phase ^{99m}Tc-MIBI scintigraphy. γP-MInP was performed under local anesthesia, without qiPTH measurement, 1.5-2 hours after the i.v injection of 740 MBq ^{99m}Tc-MIBI. γ-probe Navigator GPS (RMD-Instruments) was used. A follow-up of at least one year was performed. ***Results:*** All patients discharged from the hospital after one day of hospitalization. A significant (higher than 50%) reduction of the 1st postoperative day serum PTH in respect to the preoperative PTH levels was noticed in all cases while an easily-treated transient hypocalcemia was detected in just one patient. Operation duration time was 31.1±6 min significantly shorter than the 1,5 hours duration of typical approach with the use of qiPTH measurement, under general anesthesia. There was no hyperparathyroidism relapse during the one year of follow-up period. ***Conclusion:*** γP-MinP is a really trustful operative technique in selected patients with hyperparathyroidism due to solitary parathyroid adenomas as defined by preoperative concordant ^{99m}Tc-MIBI and ultrasound findings. In such cases the use of qiPTH measurement is of little value. ***References:*** None

EP-205

18F-FDG PET/CT in staging and delineation of tumoral volume in radiotherapy planning

F. Manchon Adsuar*, V. Lopez Prior, R. Diaz Exposito;*
Fundacion Instituto Valenciano De Oncologia, Valencia, SPAIN.

Aim/Introduction: The aim is to investigate the use of 18F-FDG (fluorine-18 fluorodeoxyglucose) PET/CT in cancer staging and its effect on the therapeutic strategy and radiotherapy (RT) planning. ***Materials and Methods:*** Twenty four patients were included.12 man and 12 women. Primary tumor sites: 10 lung, 4 head and neck, 5 gastrointestinal, 3 gynecological and 2 others (1 renal and 1 prostate). The mean age was 63.4 years. All of them had a CT and / or MRI. A contrast-enhanced CT and a 18F-FDG PET/CT acquired under radiotherapy position were performed. Both exams were compared to analyze patients staging reclassification. Changes in therapeutic strategy were analyzed. ***Results:*** 18F-FDG PET-CT changed the treatment management in 13 patients (54.16%); in 6 it modified the treatment (4 canceled the radiotherapy and treatment intention changed to palliative, chemotherapy was added in one patient and another a synchronous tumor of the rectum was operated). In 3 patients GTV (Gross Tumor Volume) decreased (PET ruled out malignancy in one of two pulmonary nodules, local recurrence in the cancer renal and differentiated pulmonary atelectasis vs tumor), in 4 patients the treatment volume increased (in unsuspected lymph node territories and nodular pulmonary lesions) .Also two synchronous rectum tumors, were detected. It did not mean a longer PET exploration time, in addition to the saving of the previous planning CT. ***Conclusion:*** 18F-FDG PET-CT changed the treatment management in 13 patients (54.16%); in 6 it modified the treatment (4 canceled the radiotherapy and treatment intention changed to palliative, chemotherapy was added in one patient and another a synchronous tumor of the rectum was operated). In 3 patients GTV (Gross Tumor Volume) decreased (PET ruled out malignancy in one of two pulmonary nodules, local recurrence in the cancer renal and differentiated pulmonary atelectasis vs tumor), in 4 patients the treatment volume increased (in unsuspected lymph node territories and nodular pulmonary lesions) .Also two synchronous rectum tumors, were detected. It did not mean a longer PET exploration time, in addition to the saving of the previous planning CT. ***References:*** None

EP-28

Imaging Clinical Studies -> Other Oncological Clinical Study -> Sentinel Node

e-Poster Area

EP-206

Women with cN0 Breast Cancer and Negative Hormonal Receptors: Is It Time to Reconsider the Use of Sentinel Lymph Node Biopsy After Neoadjuvant Chemotherapy?

J. Alors-Ruiz[1], B. D. Patrût[1], S. Sanz-Viedma[1], A. Montellano-Fenoy[1], F. Fernández-García[2], F. Sendra-Portero[3];
[1]UGC Medicina Nuclear. Hospital Clínico Universitario Virgen de la Victoria, Málaga, SPAIN, [2]UGC Cirugía General y Digestiva. Unidad de Patología Mamaria. Hospital Clínico Universitario Virgen de la Victoria, Málaga, SPAIN, [3]Departamento de Radiología. Universidad de Málaga, Málaga, SPAIN.

Aim/Introduction: High rates of negative sentinel lymph node (SLN) biopsies in women with cN0 breast cancer with triple negative (TNBC) or ERBB2 gene overexpression (ERBB2-positive) subtypes, with complete clinical and radiologic response (CCRR) after neoadjuvant chemotherapy (NACT), have been described. Our purpose is to evaluate the association between clinical and molecular variables and presence of SLN metastasis. ***Materials and Methods:*** 152 women was included prospectively in this study. The inclusion criteria was patients with breast cancer cN0 who underwent NACT before the breast surgery and SLN biopsy. Complete axillary dissection was performed if no drainage of the radiotracer or in case of SLN metástasis in intraoperative biopsy. We analyzed the relation between the SLN result with the ERBB2-positive, TNBC, positive hormonal receptors with negative ERBB2 (HR+/ERBB2-) and the NACT response. ***Results:*** From the 152 patients included (51±11.2 years old), 23.7% had SLN metastasis. The HR-negative subtypes (TNBC and HR-/ERBB2+) had lower rates of SLN metastasis (9.8% and 10.7%), compared to HR-positive subtypes (HR+/ERBB2+ and HR+/ERBB2-): 30.4% and 51.9% each. From the 74 women ERBB2+, 41.9% reached CCRR, and only one presented SLN metastasis (3.2%; IC-95%: 0.4%-19.1%; p=0.0005). In TNBC group who reached CCRR (27/51; 52.9%) there was no case of SLN metastasis. The residual breast disease was 92.3% in HR+/ERBB2- group, and the SLN metastasis rate in this group was 58.3%, notably higher than in ERBB2+ and TNBC groups with residual breast disease (33.3% and 24% each, p=0.0025). The multivariable regression analysis has proven that initial tumor size >30mm (OR=3.42; IC-95%:1.45-8.06; p=0.005) and HR+ (OR=5.53; IC-95%: 2.27-13.49; p=0.0002) are related to SLN metastasis (p<0.0001). ***Conclusion:*** In our series, the initial tumor size >30 mm and HR+ relate significantly to SLN metastasis. Patients with HR-/ERBB2+ and TNBC have higher rates of complete clinical and radiological response, with very low rates of SLN metastasis, which suggests the need to individually evaluate the axillary surgery indication after NACT in these patients. ***References:*** None

EP-207

Sentinel lymph node biopsy in oral squamous cell carcinoma: SPECT-CT over planar lymphoscintigraphy

B. Luna[1], C. Sampol[1,2], V. Lasa[1], M. Pastor[1], A. Repetto[1], N. Orta[1,2], C. Peña[1,2];
[1]Hospital Universitari Son Espases, Palma, SPAIN, [2]IdISBa, Palma, SPAIN.

Aim/Introduction: Analyze the value of ^{99m}Tc-labelled nanocolloid SPECT-CT over planar lymphoscintigraphy for sentinel lymph nodes(SLN) detection in Oral squamous cell carcinoma(OSCC). Evaluate the lymphatic drainage by surgical levels of the neck with SPECT-CT and assess the value and the reliability of sentinel lymph node biopsy(SLNB) over lymphadenectomy. ***Materials and Methods:*** Retrospective study(2011-2019) of 38 patients(7 women/31 men;median age:71,5 years) referred for SLNB of OSCC T1-2 cN0.Dynamic images were acquired immediately after peritumoral/submucosal injections of 148MBq ^{99m}Tc-labelled nanocolloid.Static images and SPECT-CT were acquired at 30 minutes-1h p.i in all patients.The acquisitions were obtained using a dual-head camera(NM/CT D670,GE).The number and anatomical localization of SLN by surgical levels of the neck were compared.A gamma probe(Navigator GPS) was used for intraoperative localization of SLN at a maximum of 24 hours p.i.,and then it was referred for intraoperative anatomopathological analysis.Long-term follow-up(mean: 26.7 months) and recurrence analysis were performed. ***Results:*** The tumor localization were lower lip(14), upper lip(1), tongue(12), palate(1), floor of the mouth(9) and retromolar trigone(1). SLN identification rate was 100%. 132SLN were obtained in planar study(mean 3,47 SLN/patient) vs 155SLN in SPECT-CT(mean 4,08 SLN/patient). 152SLN were excised from the total necks(mean 4 SLN/patient); 12SLN were malignant (7,89%).All of the 23SLN extra provided by the SPECT-CT were negative.Only 2 of 17 lymphadenectomies showed other affected nodes (3/325 nodes).After surgery 31/38patients were T1,beeing the most frequent levels of lymphatic drainage Ib, IIa and III. Unsuspected contralateral lymphatic drainage was obtained in 13 patients: lower lip(4), tongue(4), palate(1) and floor of the mouth(4). One of them had a micrometastasis (8%) with a tumour on the tip of right tongue and unilateral drainage to the left side. The ipsilateral lymphadenectomy in this patient was negative.In addition, aberrant drainage was obtained in 2 patients:1SLN in parapharyngeal space(palate tumour) and 1SLN localized between bellies of the digastric muscle(tongue tumour), both negative in the anatomopathological analysis. During

follow-up, just one patient had bilateral cervical lymph node recurrence with bone metastasis at 13 months after surgery(tumour localized on the right side of the tongue and bilateral drainage with SLN negatives). ***Conclusion:*** ^{99m}Tc-labelled nanocolloid SPECT-CT detects a higher number of SLN and in more surgical levels of the neck than planar imaging. Furthermore, it can detect atypical and unexpected lymphatic drainages, positive in a 8% of cases. The most frequent lymphatic drainage was in levels Ib, IIa y III.SLNB has proved to be a useful and reliable technique in OSCC over lymphadenectomy. ***References:*** None

EP-208

The Diagnostic Value Of Hybrid SPECT/CT For Sentinel Lymph Node Mapping In Patients With Malignant Melanoma. Comparison To Dynamic Planar Radioisotopic Lymphoscintigraphy

M. Stathaki[1], N. Kapsoritakis[1], D. Michelakis[2], O. Bourogianni[1], E. Papadaki[1], A. Tsaroucha[1], E. De Bree[2], S. Koukouraki[1]; [1]Nuclear Medicine Department, University Hospital, Heraklion-Crete, GREECE, [2]Department of Surgical Oncology, University Hospital, Heraklion-Crete, GREECE.

Aim/Introduction: Sentinel lymph node (SLN) biopsy and preoperative imaging constitute an important component in surgical treatment of oncologic patients. This study aims to evaluate the added diagnostic value of hybrid SPECT / CT with 16 slice CT in the detection and localization of SLN in patients with melanoma compared to dynamic planar radioisotopic lymphoscintigraphy (dLS). ***Materials and Methods:*** Between January 2019 - February 2020, 56 patients with malignant melanomas (head-neck:8, trunk: 28, limbs: 10 upper and 10 lower) underwent dLS as well as SPECT/CT imaging. Dynamic images were acquired first after intradermal administration of 2-4 injections of ^{99m}Tc-nanocolloidal albumin, around the lesion. Qualitative analysis was based on evaluating the exact number and anatomical localization of SLNs detected on each imaging method. Sensitivity, specificity, PPV and NPV were calculated. ***Results:*** SPECT/CT demonstrated 40 (33,3%) additional SLNs vs dLS in 24 pts (2 patients with head-neck, 16 with truncal, 4 with upper limb, 2 with lower limb melanoma). In 2 cases of truncal melanoma, dLS failed to detect one SLN found on SPECT/CT (false negative). In 4 patients with head-neck melanomas, no SLNs were identified with any of the above-mentioned imaging techniques. Moreover in 2 cases of truncal melanoma, the foci of increase activity interpreted on planar scintigraphy were found to be non-nodal site of uptake on SPECT/CT (false positive). Analysis of dLS imaging revealed sensitivity, specificity, PPV and NPV of 96%, 66,6%, 96%, and 66,6% respectively. For SPECT/CT imaging all the above-mentioned parameters were excellent, reaching 100%. ***Conclusion:*** SPECT/CT is an important complementary imaging modality to dLS imaging improving detection and anatomical localization of SLN in patients with melanoma. Moreover, it helps to reduce false positive and false negative results, especially in cases of head-neck and truncal melanoma, aiding in more accurate patients' staging, treatment planning and prognosis. ***References:*** 1. Perissinotti A, Rietbergen DD, Vidal-Sicart S, et al. Melanoma & nuclear medicine: new insights & advances. Melanoma Manag.2018; 28:5: MMT06. 2. Chapman BC, Gleisner A, Kwak JJ, et al. SPECT/CT improves detection of metastatic sentinel lymph nodes in patients with head and neck melanoma. Ann. Surg Oncol. 2016; 23:2652-7. 3. Jimenez-Heffernan A, Ellmann A, Sado H, et al. Results of a Prospective Multicenter International Atomic Energy Agency Sentinel Node Trial on the Value of SPECT/CT Over Planar Imaging in Various Malignancies. J Nucl Med. 2015; 56:1338-44.

EP-209

Survival Analysis in Patients with cN0 Breast Cancer who underwent Selective Lymph Node Biopsy after Neoadjuvant Chemotherapy

J. Alors-Ruiz[1], S. Sanz-Viedma[1], A. Montellano-Fenoy[1], B. D. Patrût[1], R. Gómez-Pérez[2], F. Sendra-Portero[3]; [1]UGC Medicina Nuclear. Hospital Clínico Universitario Virgen de la Victoria, Málaga, SPAIN, [2]UGC Cirugía General y Digestiva. Unidad de Patología Mamaria. Hospital Clínico Universitario Virgen de la Victoria, Málaga, SPAIN, [3]Departamento de Radiología. Universidad de Málaga, Málaga, SPAIN.

Aim/Introduction: There is a need for more survival analysis in women with cN0 breast cancer who have received neoadjuvant chemotherapy (NACT). Our objective is to contribute by collecting survival data and locoregional recurrence rates which associate results from the sentinel lymph node (SLN) biopsy with the response to NACT and the different molecular subtypes. ***Materials and Methods:*** It is a prospective study with 123 female patients with cN0 breast cancer, who received NACT before the axillary SLN surgery. Previous lymphoscintigraphy with periareolar injection of ^{99m}Tc-nanocoloid and radioguided surgery with a surgical gamma probe was performed. Complete axillary dissection was performed in case there was no radiotracer drainage or if the intraoperative examination of the SLN was positive for metastasis. The complete pathological response (CPR) was defined according to the criteria from the Residual Cancer Burden system (RCB). Survival rates was calculated from the date of diagnosis until death, recurrence or last follow-up. A Kaplan-Meyer analysis was performed in order to evaluate the association between overall and disease-free survival rates, molecular subtype, NACT response and SLN biopsy result. ***Results:*** The median follow-up was 53.8 months (98.9-8.6). There was no axillary relapse in the 95 female patients (77.2%) who had negative SLN. Overall and disease-free survival rate from our series

was 92.7% and 85.4%, respectively. These rates was 88.5% and 76.9%, respectively, for the non-CPR group. The patients with negative SLN showed a higher disease-free survival rate compared to the patients with SLN metastasis (91.6% vs 64.3%, Log-Rank p=0.0003), reaching 98% if they presented also overexpression of the ERBB2 gene. There were no recurrence cases in women with CPR after NACT. ***Conclusion:*** In our series, the highest global, disease-free survival rates were shown by women with negative SLN, who did not present axillary relapse. The follow-up showed that certain groups of patients had excellent survival rates related to the NACT response and overexpression of ERBB2 gene. The results suggest a personalized strategy when it comes to recommend axillary surgery after NACT. ***References:*** None

EP-210

Sentinel lymph node detection in breast cancer patients depending on the tracer application site

M. Rodrigues*, F. Schmidt, R. Moncayo, I. Virgolini;*
Department of Nuclear Medicine, Innsbruck Medical University, Innsbruck, AUSTRIA.

Aim/Introduction: Breast cancer is the most often diagnosed malignant tumour in women worldwide. The assessment of the regional lymph nodes is an essential factor to notice a potential tumour spread into the lymphatic system and furthermore to plan the following therapeutical approach. Sentinel lymph node (SLN) scintigraphy aims to mark the first few lymph nodes into which the tumour drains before these SLN become excised and histopathologically examined. We aimed to compare the efficacy of periareolar and peritumoral injections for SLN detection in breast cancer patients. ***Materials and Methods:*** Anonymised data of 231 female patients investigated with SLN scintigraphy for breast cancer were retrospectively evaluated. All patients underwent planar (anteriror) and SPECT/CT (360°, low dose CT) imaging of thorax 1h after injection of 30 MBq Tc-99m human serum albumin nanocolloids (injection volume: 0,2-1,0 ml). Tracer application was periareolar in 117 patients and peritumoral (ultrasound-guided) in 114 patients. Tracer application was performed 18-24h before breast surgery and SLN biopsy. ***Results:*** SLN detection rate was 95,73 % in the periareolar group and 86,84 % in the peritumoral group. Histopathologic confirmed false negative rate in the periareolar group A was 0 % while in the peritumoral group B it was 12,12 %. ***Conclusion:*** The periareolar injection showed to be more sensitive for SLN mapping and for avoiding false negative results as compared with the peritumoral application. For routine investigation the periareolar injection should be applied in as much as the method is easier to carry out than the peritumoral procedure. ***References:*** None

EP-211

Sentinel Lymph Node Detection In Patients With Breast Cancer And Positive Axillary Lymph Node After Neoadjuvant Chemotherapy

P. Cárcamo-Ibarra[1]*, H. Rodríguez-Parra*[1]*, M. Redal-Peña*[1]*, I. Casáns-Tormo*[1]*, V. Carrero-Vásquez*[1]*, A. Cánoves-Llombart*[1]*, J. Sabater-Sancho*[1]*, U. López-González*[2]*, M. Soria-Merino*[1]*;*
[1]Nuclear Medicine. Universitary Clinic Hospital, Valencia, SPAIN, [2]Preventive Medicine. Universitary Dr Peset Hospital, Valencia, SPAIN.

Aim/Introduction: To assess the results of sentinel lymph node biopsy (SLNB) after neoadjuvant chemotherapy (NACT) in patients with breast cancer and initial axillary affectation, evaluating the coincidence with the axillary radiological marker (ARM) and comparing the anatomopathological analysis (APA) of the sentinel lymph node (SN) with the rest of lymph nodes of the axillary lymph node dissection (ALND). ***Materials and Methods:*** Cross-Sectional study (September 2016 to November 2019) in patients with infiltrating breast cancer and axillary lymph nodes with positive metastatic affectation by FNA/CNB and with ARM. After NACT, SLNB and ALND were performed, analyzing in 42 women (36-76 years old, mean 53) with scintigraphic detection of SN, the coincidence of SN with ARM, anatomopathological response of SN and the other axillary lymph nodes. ***Results:*** In 33/42 patients (78.6%) the histological type was ductal and 21/42(50%) Luminal B. SN coincided with ARM in 39/42(92.9%). The APA of the ALND showed complete remission of the axillary lymph nodes in 14/42(33.3%), partially in 18(42.8%) and no response in 10(23.8%), one of the latter group showed no coincidence between the SN and ARM. Among the 28 patients with partial or no response, SN was the only affected node in 10/28(35.7%), while in the other 18 patients there was 1-11 additional lymph nodes affected in ALND. Among the 14 patients with complete response, none of them had affectation of SN nor in other lymph nodes in ALND. The analysis of validity of SLNB in the 39 cases of coincidence SN-ARM with relation to APA of the ALND, shows sensitivity 94%, false negative rate 6%, negative predictive value (NPV) 95%, and OR of 19 between TN and FN (CI 95% 2,1-171,2, p:0.004). ***Conclusion:*** In our group of patients with breast cancer and initial positive axillary lymph node, SNLB after NACT showed a high percentage of concordance with the radiological marker and high NPV. Thus, it is possible to consider that SLNB could provide valuable and reliable information of the state of the axillary nodes, and allows to avoid unnecessary ALND when the SN is negative. ***References:*** None

EP-212

Alydra Index, a Tool for Quantifing the Drainage in the Preoperative Lymphoscintigraphy for Breast Cancer

J. Alors-Ruiz[1], F. Sendra-Portero[2], B. D. Patrût[1], A. Montellano-Fenoy[1], F. Fernández-García[3], S. Sanz-Viedma[1];
[1]UGC Medicina Nuclear. Hospital Clínico Universitario Virgen de la Victoria, Málaga, SPAIN, [2]Departamento de Radiología. Universidad de Málaga, Málaga, SPAIN, [3]UGC Cirugía General y Digestiva. Unidad de Patología Mamaria. Hospital Clínico Universitario Virgen de la Victoria, Málaga, SPAIN.

Aim/Introduction: The purpose of this study was to improve the results of the lymphoscintigraphy by developing a semiquantification tool which is able to evaluate the axillary drainage of the radiotracer, in order to investigate the variables that affect the lymphatic pathophysiology of breast cancer. ***Materials and Methods:*** It is a prospective study of 108 women with clinically node-negative breast cancer (cN0) who received neoadjuvant chemotherapy (NCT). Lymphoscintigraphy with periareolar injection of ^{99m}Tc-nanocolloid was performed before the sentinel lymph node (SLN) biopsy. The Alydra (Axillary Lymph Drainage) Index was calculated by estimating the quantity of radiotracer migrated from the injection site, using the proportion of injected activity that is present in the axillary area. The logistical regression analysis determined the correlation between the Alydra Index with the lymph nodes number in the images and the SLN results. ***Results:*** The Alydra Index value was significantly higher as more lymph nodes were visualized in the lymphoscintigraphy (p<0,0001). 7.27±2.51 vs 20.47±7.11 between 0 and 1 lymph nodes (p=0.035); 20.47±7.11 vs 42.9±10.68 between 1 and 2 lymph nodes (p<0.0001) and 42.9±10.68 vs 75.47±23.68 between 2 and 3 or more lymph nodes (p=0.004). The patients with negative SLN had significantly higher values of the Alydra index compared to the patients with SLN metastasis (Median differences=21.76; IC 95%: 5.13-38.39; p=0.0035). The multivariant logarithmic regression showed that the number of lymph nodes in lymphoscintigraphy (OR=1; IC 95%; 0.51-1.95; p=0.999) didn´t show differences regarding the SLN results; however, lower values of the Alydra Index (OR=4.56; IC-95% 1.58-13.2 p=0.005) were related to SLN metastasis. ***Conclusion:*** Alydra, as a new semiquantitative index measured in lymphoscintigraphy, was able to evaluate the quantity of lymph drainage in women with cN0 breast cancer and NCT candidates, with better discrimination than using the number of sentinel lymph nodes visualized. The results suggested potential value in clinical research, with the objective of comparing subpopulations and variables related to lymphatic physiopathology of breast cáncer, as the presence of SLN metastasis. ***References:*** None

EP-213

Our experience in Sentinel lymph node biopsy after neoadjuvant chemotherapy treatment

A. Utrera*, M. Agudelo, J. Bernal, J. Cañon, P. Olivan, A. Yepes, P. Bello, V. Vera;*
Hospital la Fe, Valencia, SPAIN.

Aim/Introduction: The aim of the study is to follow patients with locally advanced breast cancer after neoadjuvant chemotherapy and being clinically negative on axillary, following Sentinel lymph node biopsy (SLNB). ***Materials and Methods:*** 47 patients with locally advanced breast cancer and SLNB were studied after chemotherapy during 5 years (December 2014 to January 2019). whose ages range from 25 to 70.The histological classification showed the following results: Invasive Ductal (91%), Lobular (4%) , others (4%);. The 55% were triple negative. The response to chemotherapy according to Miller & Fisher scale was 51 % G5 and 12% G4., SLNB with OSNA technique (One Step Nucleic Acid Amplification) was performed and , if the node had 250 or more > copies, was considered positive node and is required to complete lymphadenectomy . After surgery, patients went through with annual checks. Breast cancer was controlled in 85% while 15% had progressesion, and one even died. ***Results:*** The detection rate of sentinel node was 80% (38/47), with an average of 1.27 lymph nodes removed. The tracer did not reach the lymph nodes in 9 out of 47 patients (20%), Six of them presented cancer spread to axillary lymph nodes SLN was detected in 38 patients., 7 were positive nodes followed complete lymphadenectomy. Only 2 out of 7 presented metastasis during their annual checks, and one eventually died. During the study of 31 negative sentinel nodes; 87% of them were BIRADS 2 ;and 13 % had metastatic progression. Two of the patients presented cerebral metastasis; other patient had local affection BIRADS 5; and only one had lymph node affection. ***Conclusion:*** The SNLB results in patients with breast cancer after neoadjuvant treatment, has demonstrated to be of help reducing the number of unnecessary lymphadenectomies ***References:*** None

EP-214

Sentinel lymph node biopsy in oral cavity squamous cell carcinoma: our experience

D. Monachello Araujo*, C. Escabias del Pozo, L. García Zoghby, D. Travaglio Morales, E. López Llobet, J. Cebrian Carretero, P. Losa Muñoz, A. Guzmán Cruz, L. Domínguez Gadea;*
Hospital Universitario La Paz, Madrid, SPAIN.

Aim/Introduction: To asses our experience in the implementation of sentinel lymph node biopsy (SLNB) in oral cavity squamous cell carcinoma (OCSCC). ***Materials and Methods:*** Retrospective study of 11 patients (p), 6 women, mean age 63 years (51-79), with the diagnosis of OCSCC,

all of them localized in mobile tongue, cT1-T2/N0 by head and neck CT, referred to our nuclear medicine unit for SLNB between December 2017 and August 2019. All patients underwent the procedure according to standard protocol: four submucosal injections of the radiotracer (74 MBq of 99mTc Albumin Nanocoloid), immediate acquisition of dynamic images, early and late acquisition of planar images and SPECT-CT of the neck. Elective neck dissection (END) was performed in 4p after SLNB as initial validation. The average follow-up was 11 months (1-24). ***Results:*** The sentinel node (SN) was detected by lymphoscintigraphy in all patients, 9p (82%) had 2-3 SN. The most frequent locations were levels II-IV (15 SN), followed by level I (5 SN), supraclavicular fossa (2 SN) and level V (1 SN). 4p had bilateral drainage in unilateral lesions. SNs were found during surgery in all cases and were concordant with the locations provided by SPECT-CT. Pathologic evaluation of SN was negative in 10/11p. END of patient with SN metastasis was negative for other node metastasis (0/29). Pathologic evaluation of the other 4p who underwent END was concordant with the SN (negative).During follow-up, only 1p with negative SN showed non-lymph node locoregional relapse (soft tissue) 10 months after. ***Conclusion:*** In our series, SN detection was possible in all cases, being a useful technique in patients with clinically localized OSCC. Lymphoscintigraphy identified unsuspected contralateral drainage, being the SPECT-CT the one that allowed a precise localization of the SN, facilitating its identification during surgery. ***References:*** None

EP-215

Role of selective sentinel node biopsy in T2-3 breast carcinomas converted to T0-1 after receiving neoadjuvant chemotherapy

P. Turbay Eljach*, A. Sainz Esteban, B. Pérez López, M. González Soto, N. Álvarez Mena, F. Sebastián Palacid, M. Alonso Rodríguez, C. Gamazo Laherrán, M. Ruíz Gómez, R. Ruano Pérez;*
Hospital Clínico Universitario de Valladolid, Valladolid, SPAIN.

Aim/Introduction: To assess the usefulness of selective sentinel node biopsy (BSGC) in patients with T2 (greater and less than 3 cm) and T3 breast carcinoma, converted to T0 and T1 (a, b or c), after receiving treatment with neoadjuvant chemotherapy. ***Materials and Methods:*** We included all the patients referred to our service (from 2017 to 2019) for the performance of BSGC, with biopsy-confirmed infiltrating breast carcinoma and previously treated with neoadjuvant chemotherapy.All of them underwent lymphoscintigraphy after injection of 185 MBq of 99mTc-nanocoloids (if the breast lesion has disappeared or was not palpable after the action of neoadjuvance, the injections were administered periareolar). Static planar images were performed 60 min post-injection for the analysis of the lymphatic drainage. ***Results:*** Forty seven patients, all women with a mean age of 54.1 years (range 26-74 years), were studied. The CG was visualized in the lymphoscintigraphy in 95.7% (45/47). The BSGC technique was performed in all patients, locating the sentinel node intraoperatively in 95.7%. The sentinel node was negative in 29 patients; positive in 18 patients, of whom 3 presented micrometastases and 11 macrometastases (> 10,000 cp), with axillary lymphadenectomy being performed in all cases of macrometastases. In the 2 cases of absence of intraoperative localization of the sentinel node, lymphadenectomy was performed directly (1 negative case and one positive case for metastasis). ***Conclusion:*** The BSGC in breast cancer with conversion to T0-1 post-neoadjuvant presents good results, with a low false negative rate. ***References:*** None

EP-216

In the sites of blinding lights: the role of lymphoscintigraphy in melanoma

A. Farina*[1], R. Bonfiglioli[1], M. Levorato[1], M. Maccagnani[1], F. Giorgini[2], R. Cipriani[2], S. Fanti[1];*
[1]Nuclear Medicine Department, Sant'Orsola-Malpighi Hospital, University of Bologna, Bologna, ITALY, [2]Plastic and Reconstructive Surgery Department, Sant'Orsola-Malpighi Hospital, University of Bologna, Bologna, ITALY.

Aim/Introduction: The sentinel node (SL) lymphoscintigraphy may shows multiple sites of drainage and hypercaptant lymph-nodes in patients with histologically proven melanoma skin cancer localized in the trunk. In this cases the nuclear physician indicates the projection of multiple lymphatic sites (MLS). The aim of this retrospective single centre study is to analyze the concordance between the histological exam of SL removed and compared to those marked by lymphoscintigraphy in a group of patients with different sites described by the procedure. ***Materials and Methods:*** From March2018 to February2020, overall 80 consecutive patients (21F, 33M, age21-93, mean59) showing histologically proven melanoma skin cancer at the first excision of atypical nevus. All patients had lesions localized in trunk and underwent lymphoscintigraphy for the SL localization performing an early anterior dynamic acquisition followed by anterior, lateral and oblique static acquisitions. The procedure starts with a subcutaneously injection of 99Tc-NanoAlbumon (range1-2mCi, depending by the timing gap to the surgery, according to EANM guidelines) around the melanoma removal scar, immediately followed by first dynamic acquisition. For this examination we used GE-Discovery NM/CT 670 ES. The same day or the next day all patients underwent enlargement with removal of the SL. All of the specimens tissues were analyzed by our pathological anatomy department. ***Results:*** Out of80, 57lymphoscintigraphy indicated only one site for SL (53unilateral axillary cable, 3unilateral groin, 1 deep supraclavicular); in23/80lymphoscintigraphy we

indicated2different sites of SL (16bilateral axillary cable, 1bilateral groin, 3unilateral axillary cable and simultaneous unilateral groin; 3unilateral axillary cable and peri-scapular or back-nape side). In 21/23cases the surgeon has removed all the lymph-nodes marked. Pathological analysis demonstrated: in 11/21patients all lymph-nodes were reactive, 10/21had at least one metastatic lymph-node (in 3/10all limph-nodes removed were metastatic). In case of the pathological analysis demonstrated micro or macro-metastasis, we have seen in 60% of cases (6/10) that the closest site to the injection one was only interested by reactive lymph-nodes, instead of the more unusual and farthest site of drainage was site of metastatic lymph-nodes. ***Conclusion:*** As previously described, lymphoscintigraphy of SL is an important diagnostic tool for the surgeons to identify and remove all lymph-nodes with micro or macro-metastasis, especially in case of different uptake in multiple sites indicating unusual and distance site of drainage. The possible detection of metastatic MLS in unusual sites of drainage could guide the surgeons to modify the surgery approach from a localized to an extended surgical exeresis. ***References:*** None

EP-217

Application Of The Sentinel Lymph Node Biopsy In Patients With Axillary Lymph Node Metastasis (cN1) Of Breast Carcinoma After Neoadjuvant Chemotherapy. Triple Marking Protocol

C. Sampol[1,2], P. Camarasa[3], O. Cordoba[4], L. Carrillo[4], A. Lopez[5], G. Matheu[6], A. Pozo[3], A. Perello[7], A. Repetto[1], C. Peña[1,8];
[1]Nuclear Medicine. Hospital universitario Son Espases, Palma De Mallorca, SPAIN, [2]IDISBA, Palma de Mallorca, SPAIN, [3]Radiology. Hospital universitario Son Espases, Palma De Mallorca, SPAIN, [4]Gynecology department. Hospital universitario Son Espases, Palma De Mallorca, SPAIN, [5]Plastic Surgery. Hospital universitario Son Espases, Palma De Mallorca, SPAIN, [6]Anamopathology department. Hospital universitario Son Espases, Palma De Mallorca, SPAIN, [7]Oncology. Hospital universitario Son Espases, Palma De Mallorca, SPAIN, [8]IDISBA, Palma De Mallorca, SPAIN.

Aim/Introduction: Application of a triple axillary marking protocol in cN1 patients with a complete axillary pathological response after NAQT and analysis the coincidence of the clipped positive lymph node with the SLNB obtained from the combination technique of ^{99m}Tc-Albumin nanocolloid and Blue-dye. ***Materials and Methods:*** After confirming cN1 previously to NACT, the positive node was marked.After completing therapy, the axillary response is assessed by ultrasound.If response, triple axillary marking protocol is applied.In contrary, lymphadenectomy is performed.Planar lymphoscintigraphy and SPECT/CT were performed after the injection of ^{99m}Tc-Albumin nancolloid for SLNB and methylene blue dye was injected in the surgery room.During surgery,by ultrasound-guide the clipped node is removed and sentinel lymph node by gammaprobe scanning.The technique is considered optimal if the clipped node and at least one other SLN(radioactive and/or blue) are removed. If the clipped node is not located, will be optimal if at least 3SLNs are identified.We avoided lymphadenectomy when technique is optimal and the anatomopathogical result is negative. ***Results:*** Included 35p(mean age 56 years[40-78]),with a diagnosis of locally advanced Breast Cancer(cN1, 2 with intramammary nodes).Axillary marker placed in 33p before treatment.In re-staging ultrasound:9p no/partial response(positive lymphadenectomy only in 5)and 26p complete response whose underwent triple axillary marking protocol,with a mean SLN/p:3.19(marker and/or radioactive and/or blue);of which 3p was not possible to identify the marker on the ultrasound,but we could identify a minimum of 3 SLNs in all cases.Of the remaining 23p where the marker is identified,19 were detected intraoperatively (82.6%),in 100%we detected radioactive nodes and in 78% we found at least one blue node.Of the 19p wich marker is located in the surgical piece,13 are concordant with Technetium.Blue and technetium do coincide in all,excepting 1which coincide marker and blue dye.Discordance between clipped node and Technetium is 31.5% and 53.8% with blue.From this group, 3 lymphadenectomies were performed and just in 1p more affected nodes apart from the SLNs were found.The marker itself detected 11 positive, technetium 12 and blue dye 7.A total of 22/35 lymphadenectomies were performed(10 after non-response and 12 for positive SLN after triple tagging). Finally we could avoid 13 lymphadenectomies (37.1%). ***Conclusion:*** In our sample the triple tagging protocol has allowed us to avoid 37% of lymphadenectomies in cN1 patients after NACT with complete pathological response. Despite of 31% of disagreement between the marked positive node and the SLN,the triple marking protocol was optimal in 95% of patients thanks of the detection of a minimum of 3SLNs in most cases. ***References:*** None

EP-218

Relevance of Lymphoscintigraphy for Detection of the Sentinel Lymph Node in Males with Breast Cancer

N. Álvarez Mena*, F. Sebastián Palacid, P. Turbay Eljach, B. Pérez López, M. Alonso Rodríguez, C. Gamazo Laherrán, A. Sainz Esteban, M. Ruiz Gómez, M. González Soto, R. Ruano Pérez;*
Hospital Clínico Universitario de Valladolid, Valladolid, SPAIN.

Aim/Introduction: To assess the usefulness of lymphoscintigraphy for detecting the sentinel lymph node (SLN) in men with breast cancer. ***Materials and Methods:*** Retrospective series of 14 male patients with breast cancer who underwent lymphoscintigraphy for the detection of the sentinel lymph node (SLN), between October 2010 and December 2019. 111MBq of 99mTc-albumin nanocoloid were injected the day before surgery, into the affected

breast and a lymphoscintigraphy was subsequently performed until the SLN was visualized. Variables such as age, carcinoma histology, size and location of the lesion, the expression of hormonal receptors and HER2, lymphoscintigraphy result, intraoperative SLN biopsy result and the existence of recurrence until April 2020 were analyzed. ***Results:*** Average age of our patients was 67 years. The main histological type was infiltrating ductal carcinoma (13 patients) followed by 1 intracystic papillary (1 patient). Regarding tumor characteristics we found that: the mean size of the lesions was 17 mm (range 10-26 mm), being retroareolar the most frequent location (58% of cases). All of them showed positive hormonal receptors and 2 expressed the HER2/neu proto-oncogene. Lymphoscintigraphy detected the SLN after the first injection in 12 patients (86%). 2 patients needed reinjection, being unable to detect SLN in 1 of them so lymphadenectomy was performed directly (2/9 nodes with macrometastases). Intraoperatively, the SLN removed from the 13 patients with sentinel node visualization on the lymphoscintigraphy were analyzed by using OSNA method (One Step Nucleic Acid Amplification): - 8 patients showed positive SNL biopsy (including 1 with intramammary sentinel lymph node and drainage in the internal mammary chain) so axillary lymph node dissection (ALND) was performed. - 5 patients showed negative SNL biopsy so axillary lymph node preservation was decided. Until April 2020, no tumor recurrence was observed in any of the patients studied, with special attention in the 5 patients in whose ALND was not performed. ***Conclusion:*** Lymphoscintigraphy for the detection of sentinel lymph node is an acceptable and feasible technique in men with breast cancer, avoiding unnecessary lymphadenectomies without increasing the incidence of tumor recurrence. ***References:*** None

EP-29

Imaging Clinical Studies -> Paediatric Imaging Study -> Paediatric Study

e-Poster Area

EP-219

Re-staging post therapy with radioactive iodine and follow-up in pediatric patients with thyroid cancer

T. Tairo-Cerron[1,2], R. Morales-Guzman-Barron[1], R. Ledesma-Vasquez[1], P. Saavedra-Sobrados[1], L. Araujo-Cachay[1], D. Valdivia-Alvarado[1];
[1]Department of Nuclear Medicine, National Institute of Neoplastic Diseases, Lima, PERU, [2]Universidad Peruana Cayetano Heredia, Lima, PERU.

Aim/Introduction: To provide an overview of the management with I-131 in our institution, to evaluate pre and post radioactive iodine (RAI) staging, follow-up one year and long term after the first therapy./ The evaluation of the response to treatment with images (cervical ultrasound and/or thyroid tissue scan) and biochemical markers (TSH, Tg, AbTg) have been described. Differentiated thyroid cancer (DTC) in patients under 18 years old is relatively rare, accounting for 1.4% of pediatric malignancies, with a standardized incidence rate in Peru of 0.4 per 100,000, predominantly female (GLOBOCAN 2018). They usually debut with and distant metastases (25% to the lungs). Fortunately, papillary thyroid cancer (PTC) shows an avid absorption of RAI. An excellent prognosis is achieved when proper treatment is administered. To date there are no clear prospective studies on the management of this disease. The American Thyroid Association (ATA) addresses a series of guidelines; however, many open questions remain. ***Materials and Methods:*** A retrospective observational study was performed, twelve patients under the age og 18 years old submitted to total thyroidectomy with diagnosis of DCT were identified from 2012 to 2018. ***Results:*** This study included 10 women and 2 men (5:1), with a mean age of 10.25 years old (range between 4-17 years old). All the patients were diagnosis with papillary cancer. A mediam dose of 30-100 mCi (1110-3700 MBq) was administered in the first session. The examination was performed between the 5th and 7th day after the RAI, where 5 patients were re-staged as EC-II for lung metastases. During the one-year follow-up, 5 patients (41.7%) had an excellent response with Thyroglobulin (Tg) <1ng/ml and remained free of recurrence after 3 years of follow up, 5 patients (41.7%) remained with lung metastases (micronodular pattern) with decreased Tg in a follow-up of 3 to 7 years (with a cumulative dose of 130 to 370 mCi), and 2 (16.7%) presented lymphatic disease progression with stationary pulmonary metastasis ***Conclusion:*** This study shows the value of post-therapy scan, not only as a diagnostic tool, but also as re-staging. Furthermore, the Tg measured at one year of follow-up is the most reliable for evaluating the response to RAI. These results cannot be extrapolated to the pediatric population, but show the importance of the appropriate use of dynamic stratification of recurrence risk and individualized monitoring of patients with DTC, since approximately 30% have recurrence in the first 5 years of follow-up ***References:*** None

EP-220

The effect of manual and automatic motion correction on the result of radiorenography in infants

T. Czékus[1], S. Urbán[1], D. Hirling[2], J. Csirik[2], L. Pávics[1];
[1]Department of Nuclear Medicine, University of Szeged, Szeged, HUNGARY, [2]Department of Computer Algorithms and Artificial Intelligence, Szeged, HUNGARY.

Aim/Introduction: Technetium-99m

diethylenetriaminepentaacetic acid (^{99m}TcDTPA) renography is widely available diagnostic method, for the evaluation of separate renal function and urodynamic. The selection of appropriate background and kidney ROI-s (region of interest) are essential for the correct interpretation of the investigations. Patient movement effect significantly the results. The aim of our study was to investigate the efficacy of manual and automatic motion correction algorithms on the radiography parameters. ***Materials and Methods:*** From 360 dynamic renography we re-evaluated the studies of 14 infants (age: 5 months -7 years; male: 8, female: 6). In all these cases with conventional technique it was impossible to get appropriate time activity curves because of the restlessness of the children. We used an in-house developed method for motion corrections and to generate renogram curves, which based on pairwise registration of the image frames. During the course of manual correction the frames were moved only horizontally and vertically to get the kidneys on the series of images in the same position. The automatic correction beside horizontal and vertical movements rotated the frames as required. The differences of the renography curve parameters were compared and significance were calculated by Wilcoxon-test. ***Results:*** The manual movement correction took 15 minutes time while the automatic version less than a minute. With both correction methods we received appropriate time activity curves ready for evaluation. The T-max (mean ± SD) were 8.48 ± 6.65 min, the T1/2: 9.75 ± 6.72 min with manual correction, vs. 8.6±6.87 min. and 10.02±6.94 min by the automatic correction. The differences were insignificant (p=0.90 and 0.82). The counted left and right kidneys' relative functions were 50.1±5.01%; 49.9±50.1% with manual correction and 50.46±4.55%; 49.54±4.55% with automatic method. The differences were insignificant (p=0.71 and 1.0). Both method helped the visual interpretations of the images as well. ***Conclusion:*** Both manual and automatic correction method used by us is helpful in the evaluation of radiorenography of restless infants, but the automatic program is more faster, than the manual one. ***References:*** None

EP-221

Added value of SPECT/CT for diagnosing biliary atresia

T. Andersen*, R. Aleksyniene, L. J. Pedersen;*
Department of Nuclear Medicine, Aalborg, DENMARK.

Aim/Introduction: Hepatobiliary scintigraphy (HBS) is an important tool in diagnosing biliary atresia in infants. There is limited evidence on the use of SPECT/CT as additional imaging method to the dynamic and static images. We evaluated the value of SPECT/CT in unclear cases of planar HBS. ***Materials and Methods:*** Consecutive patients with suspected biliary atresia who underwent guideline-compliant HBS from January 2010 until March 2020 were reviewed, and cases with SPECT/CT were identified. Each step within the imaging procedure (dynamic, static [early and late], and SPECT/CT) were blindly re-read in consensus by two observers and categorized on a 5-point scale; 0, definitely no bowel excretion (i.e., atresia confirmed); 1, probably positive; 2, equivocal; 3, probably negative, and 4, definite negative (i.e., atresia not confirmed). In this analysis, categories were dichotomized as negative for biliary atresia (score 3-4) or positive (scores 0-2, including equivocal scans). Available follow up information constituted the standard of truth (SoT). ***Results:*** Twenty-three infants had a HBS among which ten (4 boys and 6 girls; mean age 36 days; range 8-108) had a SPECT/CT. SPECT/CT was performed as early examination (<8 h) in 3 subjects, late (8 to 24 h) in 7 infants. The re-read SPECT/CT was categorized as positive for atresia in three infants, negative in seven. The SoT showed biliary atresia in one of ten patients. SPECT/CT was true positive in one case, false positive in two, true negative in seven; there was no false negative cases. The diagnostic performance of SPECT/CT showed sensitivity 100%, specificity 78%, positive predictive value (PPV) 33%, negative predictive value (NPV) 100%, and accuracy 90%. For comparison, the diagnostic performance of planar HBS showed sensitivity 100%, specificity 67%, PPV 25%, NPV 100%, and accuracy 70%. In summary, the addition of SPECT/CT to planar HBS improved specificity and PPV, and marginally improved PPV. SPECT/CT provided more confidence in the final conclusion; the category score changed in 8/10 patients; seven changed one category (e.g., 3 to 4), and one showed a 3-point change (1 to 4, a true negative case). In 7 of 8 patients, the SPECT/CT improved confidence by changing categories in the middle to the more confident categories, e.g. 1 to 0 or 3 to 4. ***Conclusion:*** The diagnostic performance without SPECT/CT was very good. SPECT/CT improved reader confidence. These preliminary data indicted predominantly improved specificity of add-on SPECT to planar HBS. ***References:*** None

EP-222

Early Diagnosis of Focal Congenital Hyperinsulinism: a Fluorine-18-labeled Ldihydroxyphenylalanine(^{18}F-DOPA) PET/CT study

L. Burroni[1]*, F. Fringuelli*[1]*, G. Biscontini*[1]*, A. Palucci*[1]*, C. Romagnolo*[1]*, C. Cottignoli*[1]*, A. Iannilli*[2]*, M. Marino*[2]*, V. Cherubini*[2]*;*
[1]*Nuclear Medicine, Ancona, ITALY,* [2]*Pediatric Endocrinology and Diabetology, Ancona, ITALY.*

Aim/Introduction: Congenital hyperinsulinism (CHI) is a rare but complex disorder caused by unregulated secretion from the beta-cells of the pancreas. Maintenance of euglycemia is necessary to minimize neurologic damages like cerebral palsy, epilepsy, neurodevelopemental deficits and even death. CHI occurs due to mutations in key genes and now is classified into three groups: diffuse, focal and atypical forms. The diffuse form is medically unresponsive and will

require a near total (>95%) pancreatectomy; the focal form, requires a limited pancreatectomy. Thus, the pre-operative differentiation of these two subgroups is necessary. Because US, CT and/or MRI are unable in distinguishing the diffuse and focal forms of CHI, the imaging modality of choice to diagnose CHI is ^{18}FDOPA PET/CT scan. ***Materials and Methods:*** An infant boy, body weight 4,446 g, length 52 cm, head circumference 35 cm, showed normal APGAR scores. Due to the early detection of hypoglycemia the infant was transferred to the neonatal intensive care unit, was on full enteral feeding, and received intravenous glucose treatment at 1.2 gr/kg/day dose to maintain normal blood glucose values. Therefore, genetic analysis and ^{18}F-DOPA PET/CT scan were organized. The patient received 4 MBq/kg of ^{18}F-DOPA intravenously. After 60 min, a whole-body scan was obtained in 3 bed positions. Iterative reconstruction was performed and the images were evaluated in a 3D display using axial, coronal, and sagittal views to define pancreas. ***Results:*** Laboratory tests showed persistent high insulin levels (over 30 mcg/ml), negative ketonemia, low free fatty acid (213 mcmol/l), normal IGF-1, cortisol, and ammonia levels in the setting of hypoglycemia, suggesting diagnosis of CHI. Diazoxide treatment produced limited response while subcutaneous octreotide allowed a significant decrease of intravenous glucose infusion. The diazoxide unresponsiveness suggested a potassium channel gene mutation. Next generation sequencing method allowed the identification of a mutation variant in ABCC (p.Leu 40 Arg). ^{18}F-DOPA PET/CT images showed intense ^{18}F-FDOPA uptake in the head of the pancreas, confirmed by a semi-quantitative evaluation (SUVmax = 6.67). ***Conclusion:*** We confirm that ^{18}F-DOPA-PET/CT is a safe, non-invasive and the investigation of choice in distinguishing between the focal and diffuse forms of CHI; the prompt and accurate localization permits the correct enucleation of the focal lesion preventing the risk of developing iatrogenic diabetes mellitus and pancreatic insufficiency. We confirm that advances in molecular genetics, imaging methods (^{18}F-DOPA PET-CT), medical therapy and surgical approach have completely changed the management and improved the outcome of these children. ***References:*** None

EP-223

The role of split function quantification of kidney segments using DMSA scan in the choice of appropriate treatment in children with ren duplex or duplicated collecting system - a retrospective study

D. Chroustova[1], L. Cerna[1], J. Trnka[2], J. Langer[3], R. Kocvara[4], D. Zogala[1], L. Lambert[5];
[1]Institute of Nuclear Medicine, Charles University - 1st Faculty of Medicine and General University Hospital, Prague, CZECH REPUBLIC, [2]Department of Medical Physics, General University Hospital, Prague, CZECH REPUBLIC, [3]Clinic of Paediatrics and Adolescent Medicine, Charles University - 1st Faculty of Medicine and General University Hospital, Prague, CZECH REPUBLIC, [4]Clinic of Urology, Charles University - 1st Faculty of Medicine and General University Hospital, Prague, CZECH REPUBLIC, [5]Radiodiagnostic clinic, Charles University - 1st Faculty of Medicine and General University Hospital, Prague, CZECH REPUBLIC.

Aim/Introduction: Ren duplex or renal duplicated collecting system (DCS) is one of the most common congenital renal tract abnormalities. They can be associated with a variety of other abnormalities such as obstruction, ureterocele or vesicoureteral reflux (VUR). Early diagnosis followed by an appropriate therapeutic procedure in children at an early age is essential for the prevention of persistent renal impairment. In our retrospective study, we focused on the functional assessment of renal segments using ^{99m}Tc-DMSA scintigraphy and its influence on the choice of therapy including surgical solution. ***Materials and Methods:*** A total of 138 patients (48 boys and 90 girls aged from 3 months to 10 years) with ren duplex or DCS were retrospectively evaluated. Static renal scintigraphy was performed 2 hours after i.v. administration of the ^{99m}Tc-DMSA (18-70 MBq) on gamma camera MB 9200 (Mediso) or a dual-head gamma camera Infinia (GE). The total kidney counts and total counts per renal segment were determined using the geometric mean of anterior and posterior projections to compensate for kidney depth. The split total renal and segmental functions were calculated according to the established formulas. ***Results:*** The method detected DCS on left (51), right (60), and bilateral (27) sides. Most patients (118) had asymmetrical distribution of renal function, from whom 36 had decreased function in right upper segment (US), 23 in left US, 11 in right lower segment (LS), and 21 in left LS. Bilateral DCS was detected in 27 children. Based on scintigraphy combined with ultrasonography and micturating cystourethrogram, 34 of 118 children with asymmetrical segmental results required no intervention, the rest underwent surgery: heminephrectomy with or without ureteropyeloanastomosis was performed in patients with ureterocele or obstructive megaureter of the US; surgical solution of VUR in patients with VUR into LS. ***Conclusion:*** The assessment of the parenchymal function of the separate parts of the kidney with a duplex system by ^{99m}Tc-DMSA scintigraphy has value for subsequent management of the patients. ***References:*** None

EP-224

Simplify scoring System vs SIOPEN in prognosis risk assessment in Neuroblastoma

C. Olianti[1], M. Allocca[2], A. Martini[2], A. Tondo[3], H. Gauthier[4];
[1]University Hospital of Florence, Florence, ITALY, [2]University of Florence, Florence, ITALY, [3]University Hospital Meyer, Florence, ITALY, [4]Oscar Lamberet Center, Lille, FRANCE.

Aim/Introduction: SIOPEN scoring is commonly used to semi-quantify metastatic tumor load in HR-NB to stratify patients with good/poor response to therapy (1). A cut-off score of ≤3 is the most useful predictor to define good responders after induction-chemotherapy (I-CH). Perhaps a simplified method is likely able to stratify risk. The study compares the SIOPEN scoring and three proposed Simplified Scoring System (SSS) and assess the prognostic value of scoring in terms of progression free survivor (PFS) and relapse. ***Materials and Methods:*** The study included 16F and 27M, mean age 3.5±3.2 years at the first scintigraphy, 18HR-NB-1 (VI stage) and 25 intermediate (III stage) or low risk (II stage)—NB referred for I-123 MIBG scintigraphy (January 2009-December 2019) were investigated by 123I-MIBG scans for staging (ST) and I-CH for a total of 86 whole-body+SPECT scans. SIOPEN scoring (for 12 anatomical body segments with a 0-6 scale and 72 as maximal score) was compared with tree proposed Simplified Scoring System (SSS), and the cut-off SCORE-value at ST and I-CH was evaluated respect PFS and relapse in whole cohort. Log-rank Cox analysis was used for cut-off assessment and Kaplan-Maier Curves were build for each cut-off at ST and I-CH, for each simplified method. SSS1 analyzes three great sector: neural, body and arms, with the same SIOPEN 0-6 scale, SSS2 analyzes the same sectors with a simplified 0-4 scale, SSS3 analysis 12 body segments as SIOPEN scoring, with a simplified 0-2 scale. ***Results:*** At staging no significant predictive SCORE value was found for PFR and Relapse. After-I-CH log-rank Mantel-COK showed a cut-off value >3 as expected (*1) able to divide the population into a group with a of 6Y PFS versus a group with 3Y PFS. The mean Score into 3 sectors were significant different for neural and body sectors mean 0.88+/-2,5 and 0.75+/-2.2 respectively vs 3.07+/-7.3 of arms sector ($p<0.001$ HSD Turkey ANOVA). ***Conclusion:*** SSS1 and SSS3 don't bring a real advantage respect SIOPEN scoring cause the first has the same grading in lesions-extension characterization, and the second has the same numbers of segments : they result superimposable. All 3 methods seems to gain the same prognostic value with a cut-off Score >3 at post-induction chemotherapy scan in stratify PFS. This prognostic value should be tested on larger population of HR-NB. ***References:*** Eur J Nucl Med Mol Imaging. 2018 February; 45: 292-305, Eur J Nucl Med Mol Imaging DOI 10.1007/s00259-017-3829-7)

EP-225

Experience in our center of pediatric thyroid scintigraphy: a useful tool for the etiologic diagnosis of congenital hypothyroidism

G. Castillo Simón, V. Rodriguez Morales, C. Martínez Ramos, B. Núñez Arana, I. Dominguez-Prado, J. Muñoz Iglesias, F. Loira Bamio;
Hospital Meixoeiro, Vigo, SPAIN.

Aim/Introduction: Demonstrate the efficacy of thyroid scintigraphy as a non-invasive method with a great sensitivity for the etiologic diagnosis of congenital hypothyroidism. ***Materials and Methods:*** Retrospective study from 2010 to 2019 of 41 pediatric patients (7 days to 8 years old) who underwent thyroid scintigraphy after suspected congenital hypothyroidism. Review of the newborn blood spot screening, thyroid function at diagnosis, treatment and its duration, ultrasound and X-ray, genetic test, concomitant pathologies and scintigraphy findings. Thyroid scintigraphies were performed following regular protocol: static image acquisition of the anterior cervical region, with Pin-hole and/or planar collimator, in different projections, 20 minutes after the intravenous administration of [99mTc] NaTcO4 (activity calculated according to weigh: 11,1-199,8 MBq, average: 72,52 Mbq). Our studies were performed after 3-weeks hormonal-treatment suppression, excluding neonates. ***Results:*** Among the 41 patients, 27 (65,85%) were female. 14 had a scintigraphy performed during the first month of life, 22 between 2 and 4 years old and 5 patients were older than 5 years old. The scintigraphic findings showed 22 (53,65%) thyroid dysgenesis (15 ectopic glands, 4 hypoplastic glands, 2 agenesis and 1 hemiagenesis) and 19 (46,34%) eutopic glands (6 of those patients had a positive genetic test for mutations related with dyshormonogenesis and 5 patients were eventually diagnosed with a transient hypothyroidism). 7 patients showed a discrepancy between the ultrasound and scintigraphy results, being the scintigraphy more accurate regarding the final clinical diagnosis, particularly among those patients with a diagnosis of ectopic gland (5 of the 7 patients showing this discrepancy). Continuation of the levothyroxine treatment in neonates did not interfere in the scintigraphy results. ***Conclusion:*** Thyroid scintigraphy is a non-invasive test with great sensitivity for the etiologic diagnosis of congenital hypothyroidism, even during the neonatal period, showing superior performance than ultrasound, with no need of levothyroxine treatment delay. ***References:*** None

EP-30

Inflammation & Infection

e-Poster Area

EP-226

The role of three-phase bone scintigraphy in indentifying complications after hip replacement in liquidators of accident at the Chernobyl Nuclear Power Plant with septic and aseptic osteoarthrosis

P. Korol[1], *M. Tkachenko*[2], *N. Ponomarenko*[1];
[1]*Kiev Clinic City Hospital # 12, Kiev, UKRAINE,* [2]*A.A. Bohomolets National Medical University, Kiev, UKRAINE.*

Aim/Introduction: To evaluate the prognostic role of kinetic parameters of three-phase bone scintigraphy in identifying complications after hip replacement of liquidators of accident at the Chernobyl Nuclear Power Plant (ChNPP) with septic and aseptic osteoarthrosis (OA). ***Materials and Methods:*** 241 patients (185 men and 56 women) aged 31 to 85 years were imaged by three-phase bone scintigraphy: I stage - angiographic phase, II stage - early static phase, III stage - delayed static phase. Intestinal uptake was observed visually 3 hours after the intravenous administration of 740 MBq ^{99m}Tc MDP. ***Results:*** According to the results of microbiological analysis of diagnostic puncture of the hip joints, the patients were divided into two cohorts. The first cohort included 152 patients with aseptic OA of the hip joint, the second - 89 patients with septic OA. Significant increase of the parameters of arterial inflow ($t = 2.27$; $p < 0.05$) and integral perfusion ($t = 2.52$; $p < 0.05$) in the angiographic phase of patients with septic OA, due to the intensification of osteoblastic activity and angiogenesis, in comparison with indicators of aseptic OA. The kinetic of ^{99m}Tc MDP in lesions of septic OA is characterized by significant predominance of retention ($t = 3.04$; $p < 0.05$) and specific accumulation of the drug in the early static phase ($t = 2.17$; $p < 0.05$) and delayed static phase of scintigraphy ($t = 2.11$; $p < 0.05$), compared with indicators for aseptic OA. According to the results of kinetic analysis, aseptic OA results in rapid elimination of ^{99m}Tc MDP from the lesion, due to the active leaching of the radiopharmaceutical, due to the decrease in blood supply to the tissues of the area - a retentive "failure". In septic OA there was a gradual increase in the percentage of accumulation of the radiological indicator in the lesion, which is due to the intensification of integral perfusion, increased permeability of blood vessels due to the action of infectious agents, activation of resorption factors and synthesis of mineral components. ***Conclusion:*** The use of three-phase bone scintigraphy contributes to the early detection of paraendoprosthetic complications in the postoperative period, the reduction of the number of revision endoprosthetics and the shortening of the rehabilitation measures after the hip replacement in the liquidators of accident ChNPP. ***References:*** None

EP-227

Usefulness of ^{99m}Tc-Besilesomab in infection after fracture osteosynthesis: our experience

P. Guardia Jimena*, M. Martínez del Valle Torres, M. Bermúdez Morales, R. Arenas Aguaza, M. Sánchez Torrente, A. Castro López, E. Moratalla Aranda, A. Villena García, R. Nieto Serrano, D. Becerra García;*
Hospital Universitario Clínico San Cecilio, Granada, SPAIN.

Aim/Introduction: To contribute our experience in the diagnosis of post-fracture osteosynthesis material infections in the peripheral skeleton with ^{99m}Tc- Besilesomab. ***Materials and Methods:*** We included 31 patients with age ranges from 26 to 75 years with suspicion of osteomyelitis due to the presence of osteosynthesis material after fracture in the lower extremities (femur, tibia, fibula and tarsus). Three phase bone scan (^{99m}Tc-oxidronate) was previously performed on all patients with positive result in all cases. The infection study was performed after injection of 555 MBq ^{99m}Tc-Besilesomab with static imaging 4 and 24 hours post injection, once the absence of human anti-murine antibodies (HAMA) was confirmed. The evaluation of the study was made qualitatively and after semiquantitative analysis, making regions of interest (ROIs) on the suspicious areas of infection both in early and late images, using a total counts intensity scale with the same intensity threshold. The studies whose quantification was superior in the 24 hour images in comparison with 4 hour images were considered as positive, considering the decay of the radiopharmaceutical. SPECT-CT studies were performed to locate the anatomical areas of infection in the bone or outside the bone (soft-tissue infection). The definitive diagnosis was established after the clinical monitoring of all patients, either following the result of the microbiological culture, after response to the medical and/or surgical treatment, as well as the result of other imaging studies. ***Results:*** 18 negative results (18 TN and 0 FN) and 13 positive results (12 TP y 1 FP) were obtained. According to these results, 100 % sensitivity and 94 % specificity were obtained. A positive predictive value of 92 % and a negative predictive value of 100 %. The FP result corresponded to a patient with a large inflammatory component in tarsus. ***Conclusion:*** The scintigraphy with ^{99m}Tc -Besilesomab shows a high diagnostic precision for infections due to post-fracture osteosynthesis material in the peripheral skeleton in our patient sample. ***References:*** None

EP-228

Hybrid imaging in muscular sarcoidosis

I. Grozdic Milojevic[1]*, D. Sobic-Saranovic*[2]*, V. Artiko*[2]*;*
[1]*Clinical Center of Serbia, Belgrade, SERBIA,*
[2]*Clinical center of Serbia, Belgrade, SERBIA.*

Aim/Introduction: To determine the prevalence of muscle sarcoidosis (MUS) and evaluate the role of hybrid molecular imaging in MUS. ***Materials and Methods:*** Between 2010 and 2011, 90 patients with chronic sarcoidosis and presence of prolonged symptoms of active disease were referred to FDG PET/CT. Active disease was found in 74 patients, and they were all screened for the presence of MUS. All the patients underwent MDCT and the assessment of the serum ACE level. Follow-up FDG PET/CT examination was done 12.0±5.2 months after the baseline ***Results:*** MUS was present in 7.6%. Patients usually had thoracic disease (57%), nonspecific symptoms and high ACE levels.Most of the patients had more than one symptom of the disease and

muscle pain was present in 29%. The disease was usually present in lower limbs (4/7 patients), with nodular FDG avid lesion. Less frequent localisation were: skeletal striated muscles and heart muscle. ACE levels were not in correlation with the SUVmax level (p>0.05). Follow-up PET/CT revealed complete remission in one patient and partial remission in two. ***Conclusion:*** FDG PET/CT can be useful in the detection of MUS and in the evaluation of the therapy response. It can resolve which muscular pattern of the disease is present in patient, which can affect the therapy and prognosis of the disease. ***References:*** None

EP-229

The diabetes impact on the course of community-acquired pneumonia according to ventilation scintigraphy

V. Udodov*, A. Zaitseva, V. Zavadovskaia, E. Bukreeva, I. Degtyarev, M. Zamyshevskaya, M. Zorkaltsev, T. Saprina;*
SSMU, Tomsk, RUSSIAN FEDERATION.

Aim/Introduction: To evaluate ventilation scintigraphy results of diabetic patients with community-acquired pneumonia as more severe disease with frequent complications and high mortality rates in this category of patients. ***Materials and Methods:*** 10 patients (6 males and 4 females) with diabetes mellitus and community-acquired pneumonia both and 13 patients with community-acquired pneumonia without diabetes (8 males and 5 females) were studied. Mean age of patients was 55.8 ±5.4 years. All patients underwent ventilation scintigraphy with 99mTc MAA (370 Mbq in aerosol, SPECT Philips Brightview). ***Results:*** By using ventilation scintigraphy the measurement of radioactive impulses number was calculated in the area of pneumonia in comparison with the symmetric intact region (count difference) in two groups of patients. At the first group consisted of diabetic patients with community-acquired pneumonia count difference was 2.99 [1.54-5.41]. Patients with community-acquired pneumonia without diabetes were in the second group which was characterized count difference 1.47 [1.13-2.05]. It was shown a statistically significant (p <0.05) count difference increase in patients with diabetes mellitus and community-acquired pneumonia. The value of the count difference reflects in this situation the degree of bronchial patency, the higher the score difference, the lower the bronchial patency, therefore, the more severe the course of community-acquired pneumonia. When assessing $T_{1/2}$ in both groups, this indicator was reduced: in the first group 45.5min [31.0-60.3] and in the second group 47.0 min [38.0-53.5], with no statistically significant differences. ***Conclusion:*** The count difference as result of ventilation scintigraphy confirm a more pronounced abnormality of bronchial patency in patients with diabetes mellitus, which may to indicate a more severe course of community-acquired pneumonia in these patients. ***References:*** None

EP-230

Metabolic Features of Patients with COVID-19 Lung Infection: Contribution of ^{18}FDG-PET / CT

J. Ardila Mantilla*, A. Rotger Regí, M. Baquero Oliveros, A. Marí Hualde, J. Orcajo Rincón, I. Gómez Fernández, C. Durán Barquero, D. Zamudio Rodríguez, Y. Henao Celada, J. Atance García de la Santa, J. C. Alonso Farto;*
Hospital General Univeristario Gregorio Marañón, Madrid, SPAIN.

Aim/Introduction: One of the most frequent complications that increases the morbidity of patients infected with COVID-19 is lung infection. The radiological patterns and their evolution are already being studied and described. However ^{18}FDG-PET / CT metabolic image may also offer valuable information about the inflammatory / infectious process. Since the declaration of the state of alarm in Spain, our service has only performed urgent PET / CT scans. Our aim is to study the metabolic characteristics of lung disease in patients with COVID-19. ***Materials and Methods:*** From March 14 to April 24, 2020, we performed 240 urgent ^{18}FDG-PET / CT most of them with an oncological indication. All of them underwent PET / CT using the usual protocol, performing a questionnaire for screening for covid-19 infection before the examination. They were considered asymptomatic when they did not present any of the following clinical manifestations: myalgia, cough, headache, fever, dyspnea or others, and oligosymptomatic those presenting with only one of them. Imaging was considered positive for infection in the presence of hypermetabolic lung infiltrates unjustified by other causes. ***Results:*** 19 patients were diagnosed with COVID-19 infection. 6 of the patients were clinically diagnosed and the other 13 with a positive result of reverse transcriptase polymerase chain reaction (PCR) for covid-19. Image characteristics were as follows: unilateral pneumonia 2/19 (1 right, with pleural and hiliomediastinal involvement resulting in exitus, and 1 left); bilateral 2/19; multifocal 12/19 one of them with pleural involvement (63.2%); without pulmonary alterations 3/19. The predominant location was in the lower lobes 10/16 (62.5%); 5/16 in the upper lobes and 1/16 in the middle lobe. There was agreement between PET and CT findings in lung parenchyma in all patients except one that showed abnormalities in CT without increased uptake in PET, this patient was oligosymptomatic with negative PCR. There was more discordance in hilio-mediastinal lymph node involvement; 12 had pathologic FDG uptake compared to 4 who had increased lymph node size on CT (all positive in PET). The median SUVmax of lung lesions was 4.05. ***Conclusion:*** The typical pattern of presentation of Covid-19 lung disease is multifocal involvement, predominantly in the lower lobes. Lung lesion detection is highly concordant in PET and CT, however lymph node detection seems to be

higher in PET imaging. ***References:*** None

EP-231

Clinical Manifestations of Patients with Pulmonary Abnormalities in ^{18} FDG-PET with COVID-19 Infection

J. Ardila Mantilla*, A. Rotger Regí, M. Baquero Oliveros, A. Marí Hualde, J. Orcajo Rincón, I. Gómez Fernández, C. Durán Barquero, D. Zamudio Rodríguez, Y. Henao Celada, J. Atance García de la Santa, J. C. Alonso Farto;*
Hospital General Univeristario Gregorio Marañón, Madrid, SPAIN.

Aim/Introduction: With more than 200,000 infections and 20,000 deaths from covid-19, Spain is one of the countries most affected by this virus. During the declaration of alarm status, all non-urgent PET / CT scans were suspended. Our aim is to describe the relationship between patients´ symptomatology and PET / CT findings. ***Materials and Methods:*** From March 14th to April 24th, 2020, we performed 240 urgent ^{18}FDG-PET / CT scans. All of them underwent PET / CT using the usual protocol, performing a questionnaire for screening for covid-19 infection before the examination. They were considered asymptomatic when they did not present any of the following clinical manifestations: myalgia, cough, headache, fever, dyspnea or others, and oligosymptomatic those presenting with only one of them. Imaging was considered positive for infection in the presence of hypermetabolic lung infiltrates unjustified by other causes. ***Results:*** 19 patients were diagnosed with Covid-19 infection, 16 with oncological disease and 3 with infectious indication. 6 of the patients were clinically diagnosed and the other 13 with a positive result of reverse transcriptase polymerase chain reaction (PCR) for covid-19. In 9 of the patients Covid-19 diagnosis was suspected on the findings of the PET CT. Regarding clinical manifestations 4 were asymptomatic, 6 oligosymptomatic and 9 symptomatic. 15 patients presented with positive imaging of which 8 were asymptomatic or oligosymptomatic and only 7 were symptomatic. Only in one oligosymptomatic patient with negative PCR, CT abnormalities were found without increased FDG uptake. No statistically significant differences were found between clinical manifestations and the presence of hypermetabolic infiltrates on PET ($p = 0.65$ Yates correction; Fisher 0.66). ***Conclusion:*** Despite being a small and very defined sample, we found no statistically significant differences between clinical manifestations and the presence of hypermetabolic abnormalities in lungs of patients diagnosed with Covid-19. ***References:*** None

EP-232

18F-FDG and 18F-Fluorocholine PET/CT findings in symptomatic and asymptomatic patients with COVID-19, a French case series

S. Mekhail*, J. Chalaye, B. Emsen, L. Lerman, E. Evangelista, M. Abulizi, J. M. Israel, S. Bonnot-Lours, M. Marie, M. Borel, M. Gueremy, S. Hamel, C. Juin, S. Larrous, N. Latouche, N. Marin, P. Blanc-Durand, E. Itti;*
Nuclear Medicine Department, Henri Mondor Hospital APHP, UPEC, Créteil, FRANCE.

Aim/Introduction: With more than 3 millions confirmed cases and more than 200 000 deaths worldwide, the COVID-19 outbreak became quickly a public health emergency of international concern. Diagnosis relies - among others - on RT-PCR and chest CT showing typically multiple and bilateral patchy ground glass opacities and bilateral pulmonary consolidations (1). Some studies (2,3) have reported the glycolytic activity of these pulmonary abnormalities on 18F-FDG PET/CT in small cases series and, to our knowledge, no case wase reported to date with 18F-Fluorocholine (FCH) PET/CT. The aim of our study was to illustrate FDG and FCH PET/CT findings in patients affected by COVID-19. ***Materials and Methods:*** We retrospectively reviewed the PET/CT results from 11 consecutive patients diagnosed with COVID-19 on the basis of clinical, radiological and laboratory data, between March 24 and April 30, 2020. Studies were performed for routine oncologic indications (n=8) and infectious/inflammatory disease (n=3). Symptoms, RT-PCR results and biological data were retrospectively collected if available. ***Results:*** Ten of the 11 patients had CT imaging features of COVID-19 pneumonia with variable FDG-uptake (SUVmax range, 1.2 to 5.8) and a strong uptake of FCH in one patient (SUVmax = 6,3). The patient without pulmonary abnormalities was on day-13 of the infection when PET/CT was performed. We reported mediastinal lymph node involvement in 8 of the 11 patients with mild to high FDG uptake (SUVmax range, 3.4 to 8.6) and high FCH uptake (SUVmax = 5,5). Two others patients demonstrated FDG uptake in mediastinal lymph nodes that could be reported either to neoplastic involvement or to COVID-19. Four of the 11 patients were asymptomatic. RT-PCR was positive in 4/6 patients. Diagnosis was first suspected based on the PET/CT findings in 5 patients. ***Conclusion:*** Although PET/CT is not recommended in routine practice to evaluate COVID-19 pneumonia, knowing the pattern of FDG and FCH uptake within the lungs and mediastinal nodes can help to identify infected patients, even when asymptomatic. ***References:*** 1. Huang C. et al. Clinical features of patients infected with 2019 novel coronavirus in Wuhan, China. The Lancet 395, 497-506 (2020).2. Qin C. et al. X. 18F-FDG PET/CT findings of COVID-19: a series of four highly suspected cases. Eur J Nucl Med Mol Imaging 1-6 (2020).3. Albano D. et al. Incidental Findings Suggestive of COVID-19 in Asymptomatic Patients Undergoing Nuclear Medicine Procedures in a High-Prevalence Region. J Nucl Med 61, 632-636 (2020).

EP-233

3D Volume Rendering Model and Pixelated Quantitative CT for Accurate Assessment of the Extent and Severity of Patients with COVID-19

M. Masoomi, L. Alkhandari, I. Alshammeri, H. ELrahman, H. Ramsy, S. Almutairi;
ADAN Hospital- MOH, Kuwait, KUWAIT.

Aim/Introduction: Coronavirus disease 2019 (COVID-19), caused by severe acute respiratory syndrome coronavirus 2 (SARS-CoV-2), has become an increasingly prevalent worldwide, declared a pandemic on March 11, 2020 by WHO. Early diagnosis of novel COVID-19 is crucial to detect the disease at the early stage for disease treatment and control which has medical and economic impact regardless of how well you are prepared. In this multi-center study, we are aiming to develop a combination of 3D-360 visual rendering model of lung COVID-19 disease and the quantitative CT data to better categorize the CT findings with regard to the extent and severity of COVID-19 lung and to provide an objective approach to rapidly and accurately identify patients in need of hospital admission. ***Materials and Methods:*** We use a multistep Materialize Mimics Care Suite-3D to produce unrestricted 360 orientations of the patient lung disease, where one can see through the lungs, the pattern of disease distributions in a virtual reality concept. In addition, we use DICOM file and a Matrix Laboratory (MATLAB) to generate a unique colour pixelated visual map and semi quantitative analysis of the CT of disease regions to create a data base for quantitative scoring based on HU value for 50 proved COVID-19 patients initially and therefore to set an optimal threshold value for assessing and categorizing negative, mild, moderate and sever cases. ***Results:*** We are anticipating that combination of 3D-360 rendering model of lung disease (COVID-19) and the quantitative of the COVID-19 CT data provide a more accurate assessment of extent and severity of COVID lung disease for better categorizing patients as typical appearance, indeterminate appearance, atypical appearance or negative and therefor plan a better program to handle the flux of COID-19 patients at locality with regard to health/safety and financial burden in mind. The initial results are promising. ***Conclusion:*** Combining 3D Modelling and quantitative CT of COVIS-19 Lung has a potential for significant impact within the Healthcare, with its ability to create personalized healthcare and cost effective solutions. ***References:*** None

EP-234

Prevalence of incidental pneumonia consistent with COVID19 infection an 18F-Fcholine (FCH) PET/CT in patients referred for prostate cancer

L. Turpin[1], Q. Pouliot[1], J. Zhang[1], B. Sgard[1], M. Glikman[2], F. Denise[1], J. Talbot[1], F. Montravers[1];
[1]Hôpital Tenon, Paris, FRANCE, [2]Medical office, Pantin, FRANCE.

Aim/Introduction: COVID-19-induced lung lesions are already known to frequently take-up FDG, but such a finding has not yet been described with FCH, first line radiopharmaceutical in France for prostate cancer, that may be taken-up by inflammatory lesions.Our aim was to evaluate the prevalence of incidental interstitial pneumonia consistent with COVID19 infection on CT and the FCH uptake of the lesions in patients referred to FCH PET/CT for prostate cancer. ***Materials and Methods:*** We retrospectively reviewed all the PET/CTs of patients referred to FCH PET/CT between 22nd February and 30th April 2020 for prostate cancer imaging. They had no respiratory symptoms at the time of PET/CT. We selected the cases showing lung lesions evocative of COVID-19 interstitial pneumonia on CT (ground-glass opacities, multifocal patchy consolidation, and interstitial changes with a peripheral distribution predominating in lower and posterior regions) and we determined the radiotracer uptake by these lesions. ***Results:*** 96 FCH PET/CT were performed during this period of time. We noticed lung lesions on CT consistent with COVID 19 infection in 4 of the 96 patients. Median age of these patients was 72.5 years (range 68 to 76).All 4 patients were asymptomatic at the time of FCH PET/CT, but 2 of them reported a history of symptomatic pneumopathy compatible with COVID infectious syndrome, 4 weeks and .6.5 weeks before FCH PET/CT, respectively. One of them had been sampled for RT-PCR when he was symptomatic and the diagnosis of Covid-19 infection was settled.The lung lesions took-up FCH in all 4 patients with a mean SUVmax of 4.2 (range: 2.8 to 6.6). Ground-glass opacities were more hypermetabolic (SUVmax 6.6 and 3.9 respectively) and more diffuse (over more than 30% of pulmonary surface) in the 2 patients who had presented with symptomatic pneumonia. ***Conclusion:*** During the COVID 19 outbreak in France, we incidentally observed hypermetabolic lung lesions consistent with COVID-19 infection in 4.1% of patients referred to FCH PET/CT for prostate cancer. Patients with recurrent prostate cancer belong to a population at high risk of aggressive Covid-19 infection (male patients aged over 60) and the incidental discovery of pneumopathy evocative of COVID-19 on CT could be expected. However, FCH uptake by the lung lesions was not expected in asymptomatic patients several weeks after the contamination. Its prognostic significance (delayed recurrence? parenchymal fibrosis?) needs to be determined by patients' follow-up. ***References:*** None

EP-235

Deployment of a Dedicated "Covid-19" CT in Nuclear Medicine : Strategic Issues in the Context of an Epidemic Emergency

E. Itti, T. Pillon, D. Giacometti, E. Brimboeuf, T. Barbosa, N. Ambiehl,

D. Bazas, S. Mekhail, J. Chalaye, M. Milliner, A. Quilichini, C. Lhermite, A. Maraval, H. Kobeiter, A. Luciani, P. Blanc-Durand; CHU Henri Mondor, AP-HP, U-PEC, Creteil, FRANCE.

Aim/Introduction: With rapid spread of the new SARS-CoV-2 Coronavirus (Covid-19) and high prevalence of pulmonary involvements leading to respiratory failure, clinical needs for thorax CTs have dramatically increased in our hospital. The Nuclear Medicine department is equipped with a hybrid SPECT/CT camera ideally located at an extremity of the department, close to the Emergency Room (ER). ***Materials and Methods:*** In this context, and owing to the close collaborations between all imaging departments already set up, we decided to deploy a "Covid-19" CT in Nuclear Medicine, dedicated to ER out-patient workflow, another "Covid-19" CT in the Neuroradiology department being deployed for in-patient workflow, the remaining CTs in the Radiology department being reserved for non-Covid patients. This deployment required to take into account several strategic issues. First, creating 3 distinct pathways would help reducing internal spread of the infection. Regulation of these pathways was ensured by a senior radiologist with a dedicated phone number. Then, we thought preferable for ER patients to be scanned as close as possible from the ER department, without using the elevator to reach the Neuroradiology CT. Nuclear Medicine technologists were rapidly formed to the disinfection procedures and were paired with Radiology technologists. ***Results:*** This organization was set up in only 24 hours thanks to the collaboration between technologists, physicians, physicist, radiation protection specialist, biomedical engineer and staff : a contrast media injector was connected to the SPECT/CT, all necessary CT protocols were programmed and validated on a phantom to ensure dose level conformity and DACS integration, and written declaration of this activity was performed to the Nuclear Security Agency (ASN) as the CT from the SPECT/CT does not have an authorization for diagnostic examinations, but a temporary derogation could be obtained if technical performances and medical organization were clearly stated. During 10 weekdays (08:00-18:00) of deployment at the pandemic peak, 111 CT scans were performed on the SPECT/CT, including 50% thorax CT angiographies and 50% thorax CT without contrast. A typical Covid-19 lung pattern was found in 63% of patients and pulmonary embolism was diagnosed in 11% of patients who underwent thorax CT angiography. ***Conclusion:*** In the context of an epidemic emergency, multidisciplinary cooperation between imaging professionals allowed us to arm a dedicated "Covid-19" CT in Nuclear Medicine within 24 hours and to optimize patient pathways. This reactive organization is a pledge for increased collaborations especially when healthcare pathways are essential for population safety. ***References:*** https://ebulletin.radiologie.fr/covid19

EP-236

The Novel Coronavirus: Our Experience in Facing an Invisible Enemy

L. Cunha[1], *P. Ratão*[1,2], *A. Roda*[1,3], *M. Capoulas*[1,4], *F. Ferreira*[1], *M. Sousa*[5], *H. Vasconcelos*[6], *A. S. Moreira*[1], *L. F. Metello*[1,7]; [1]*IsoPor-Azores, Angra do Heroismo, PORTUGAL,* [2]*Nuclear Medicine Department, IPOFG, Lisbon, PORTUGAL,* [3]*Medical Physics Department, IPOFG, Coimbra, PORTUGAL,* [4]*Pharmacy Department, HBA, Loures, PORTUGAL,* [5]*Interdisciplinary Studies Research Center, ISEP.IPP, Porto, PORTUGAL,* [6]*Sc. Techn. Fac., Univ. Azores, Ponta Delgada, PORTUGAL,* [7]*ESS-IPP, Porto, PORTUGAL.*

Aim/Introduction: Early this year, Chinese authorities identified a new type of coronavirus that was causing a disease named COVID-19. It disseminated quickly, and immediate action was needed to control the further spread of the infection. Many Governments imposed severe restrictions on people's and on companies' actions. After almost two months of lockdown, we had to prepare our Nuclear Medicine Department for a new reality. This paper aims to share the implemented measures and policies. ***Materials and Methods:*** We defined our action in three axes: 1)people; 2)spaces/infrastructures; 3)practices; and three moments: A.before; B.during and C.after the procedure (diagnostic or therapeutic). Each of these axes has branches: 1.1)social distancing; 1.2)epidemiological and health questionnaire; 1.3)communication and welfare; 2.1) definition of entrances and routes; 2.2)signs and posters regarding handwashing, respiratory etiquette and COVID-19 alert symptoms; 3.1)assessment of the procedure urgency level; 3.2)patient appointment order; 3.3)procedures' time slot; 3.4)infection prevention and control; 3.5)remote meetings and reporting. ***Results:*** Due to the universal application of the three basic rules of radioprotection: time, distance, and shielding, we believe that somehow the adoption of the above-mentioned special measures in Nuclear Medicine Departments might have been easier. Regarding people axis, social distancing among patients and staff was implemented as a rule of thumb, as well as the use of personal protective equipment (for staff: head cap, goggles, and disposable gown, face mask, and gloves, the latter two were indicated for outpatients not tested for COVID-19). Waiting rooms were rearranged to increase distances between people and members of staff avoided having meals together. Patients were contacted by phone before the procedures, to ascertain the presence of any symptoms, and to be informed about dedicated entrances and routes. Confirmed or suspected COVID-19 patients were managed according to institutional and national rules. The urgency level of the procedure was carefully assessed by both the referring physician, the patient himself, and the Nuclear Medicine physician, with non-urgent tests postponed. Inpatients who tested negative for COVID-19 were the first in the daily agenda, followed

by non-suspected outpatients, with positive inpatients for last. Suspected outpatients were advised to seek first for being tested for coronavirus. The time slot per patient was increased to allow cleaning and disinfection procedures after each patient. ***Conclusion:*** The preparedness for the current coronavirus outbreak required the review of procedures as well as the adoption of special measures to assure health professionals and public safety, to prevent infection transmission and spread. ***References:*** None

EP-237

The importance of being retrospective": medical directivities in COVID-19 time

A. Farolfi*, R. Bonfiglioli, A. Paccagnella, F. Mattana, S. Fanti;*
Nuclear Medicine Unit, S. Orsola Hospital,
University of Bologna, Bologna, ITALY.

Aim/Introduction: More than 2 million people worldwide had tested positive for COVID-19, and more than 200,000 deaths are attributed to this virus. In order to minimize the diffusion of the infection through hospital operators, that are people with highest risk, we analyzed the efficient impact of medical directivities in our hospital unit. ***Materials and Methods:*** 66 operators have worked at our high volume PET center located in a red zone from February 2020 until today: 55 in the nuclear medicine unit, 11 in the radiopharmaceutical unit at cyclotron site. In this setting, in order to limit patients and especially operators' exposure, adoption of preventive measures was needed. Our directives were: everyday change of individual protection devices, use of alcohol solution for disinfection (hand and equipment), repeated sanification of ambients during the day, respect of social distancing and limitation of operators contact with patients to the minimum necessary. In addiction, we set up a new entrance triage protocol in order to try to reduce the risk of contact with possible infective patients: nurses measured patients' temperature at their arrival, the head chief checked if the exam requests were appropriate, excluding suspected infective patients in which nuclear imaging tools were not necessary. All the operators underwent serology lab rapid tests on peripheral blood to check the presence of SARS-CoV-2019 IgG and IgM. ***Results:*** we reduced the number of PET performed every day from 70 before COVID time to around 40. Out of 66, 62 (94%) of our operators had negative tests not only for IgM but also for IgG. Only 4 operators resulted to have IgG positivity; of these, one had positive COVID nasopharyngeal swab (one before and one after blood test) while 2/4 were negative. ***Conclusion:*** Changing our daily clinical practise we have created a new filter in addition to the face mask, resulting in a free COVID-zone in our department until now. At this point the readers may be thinking that the limit of this study is its retrospective design. But this is the rhythm of the science (oh science, oh yeah): retrospective view is indeed the real power of this study. We hope that a prospective design, to confirm these data, will not be possible thanks to the advent of a new definitive treatment and if you are now here, reading this study, maybe the dream has become truth. ***References:*** None

EP-238

Nuclear Medicine in the times of COVID-19 - expected and possible (unexpected) risks and new safety standards-single institution experience

M. Vlajkovic*, M. Rajic, M. Stevic, M. Kojic, N. Topic, F. Velickovic, L. Kojic, L. Vranic, N. Todorovic, J. Vidojevic, G. Ignjatovic, S. Cvetic, P. Stoiljkovic;*
Center of Nuclear Medicine, Clinical Center Nis, Nis, SERBIA.

Aim/Introduction: The first cases of coronavirus disease (COVID-19) were seen in Wuhan, China, in late December 2019 before spreading globally.The current outbreak was officially recognized as a pandemic on 11 March 2020. The aim of this paper is to demonstrate the changed mode of operation, safety measures and procedures at the Center of Nuclear Medicine, Clinical Center Niš (CNM), the only nuclear medicine center in Serbia that had no work lockdown during the epidemic, and to propose a system of protective measures to be taken in the face of potential new pandemic waves. ***Materials and Methods:*** At the beginning of March, CNM had already scheduled all diagnostic and therapeutic procedures for March and April. Out of an average of 250 scintigraphies, 238 were scheduled for March and 88 for April. Twenty-six out of 34 treatment procedures were scheduled for the therapy unit. An epidemiological survey was conducted on all patients. More serious protective measures were introduced at the height of the coronavirus epidemic in the Republic of Serbia. PPE II was used when receiving the scan or treatment according to WHO guidelines. In addition to the standard epidemiologic survey conducted by telephone 1-2 days prior to admission to the hospital, blood samples were obtained from patients in order to test blood counts, CRP and LDH. ***Results:*** In March, 123/238 diagnostic procedures were performed (51%), while in April 35/88 (40%) diagnostic procedures were performed, exclusively bone scintigraphy. Twenty one out of 26 therapy procedures were performed in the therapy unit, mainly iodine treatment of differentiated thyroid carcinomas, whereas 4 patients were canceled due to the inability to import ^{177}Lu-DOTA-TATE, and one was canceled due to suspended traffic and inability to reach the hospital. The number of radioimmunology and complementary analyses had also dropped from an average of 5,000 a month to 910 in March and 93 in April. None of the staff involved in performing diagnostic or therapeutic procedures tested positive for Covid-19 disease. ***Conclusion:*** The emerging situation at the time of the pandemic requires additional protection of personnel working in nuclear medicine to

be undertaken and, in addition to radiation protective equipment, epidemiological protective equipment must be used until an effective and safe SARS-CoV-2 virus drug and vaccine is found. In the coming months, only patients with a negative test for the presence of the virus no older than 24 hours should be admitted for hospital treatment. ***References:*** None

EP-239

Casual cases of nuclear medicine examinations in Patients with concurrent/subsequent diagnosis of COVID-19

C. Olianti[1], *D. Malandrino*[2], *T. Tagliente*[2], *M. Allocca*[2];
[1]*University Hospital of Florence, Florence, ITALY,*
[2]*University of Florence, Florence, ITALY.*

Aim/Introduction: The study is a retrospective cross-referencing clinical data on a cohort of Patients admitted to University Hospital of Florence in 8 COVID-19 departments from 6.03.20 to 20.04.20, to find patients underwent to nuclear medicine scans than diagnosed for SARSCoV-2 infection. ***Materials and Methods:*** We crossed diagnostic and clinical data of 172 patients (40-97y; 108 M, 64 F) hospitalized in COVID-19 dedicated/reconverted department with different intensity of care, 3 internal medicine (60pz), 1 cardio-anesthesia and cardio-resuscitation (8pz), 1 trauma intensive care and severe organs failure (14pz), 1 infectious and tropical diseases (17pz), high intensity internal medicine (12pz) , 1 Thoracic-pulmonary physio pathology and pneumology (8pz). Each Patent underwent to different imaging diagnostic examinations with a wide variability on the basis of care intensity and the different clinical presentation of disease. We evaluated how many nuclear medicine examinations were performed in the whole cohort. ***Results:*** Only 4 Patients with SARSCoV-2 positivity underwent nuclear medicine exams, 2 of them some days before the confirmed infection: 1) a 84 Male hospitalized on 8.03.20 for bowel subocclusion in laryngeal/esophageal neoplasm and suspected intestinal primary cancer who underwent an FDG-Pet/CT scan for lung thickening showing a very complex oncologic situation. He underwent also 8 RX-thorax, 3 abdominal echo-sonography and 2 abdomen CT, before dying on 23.3.20. 2) a 85 Male hospitalized 28.3.20 for recurrence of congestive heart and respiratory failure, not sustained ventricular tachycardia in presence of normally functioning ICD cardioverter defibrillator. He underwent to a pulmonary perfusion scan for D-dimer very high levels with abnormal not-segmental bilateral perfusion defects, incongruent with pulmonary embolism (PE), 3 RX-thorax and 2 thorax-CT before dying on 31.3.20. 3) a 84 Male guest of an assisted elderly residence and hospitalized on 9.4.20 for dispnea, respiratory failure, bilateral pleural effusion and bibasal pneumonia and initially negative COVID-19 buffer. Perfusion lung scintigraphy demonstrated a homogeneous MAA distribution. 4) a 86 Male hospitalized 11.4.20 for bilateral pneumonia and recurrence of renal and heart failure in recent PTCA and high-frequency atrial fibrillation. He underwent a myocardial SPECT positive for viable perinecrotic tissue. He died on 13.4.20. ***Conclusion:*** Our results demonstrates that only 4/172 (2,3 %) hospitalized patient underwent nuclear medicine examinations, 2 during SARSCoV-2 infection, 2 just-before COVID-19, indicating a very good clinical selection of dispnoic patients referred for suspect PE. Interestingly the lung scans of Pz2) not-typical for PE and that of Pz3) without perfusion abnormalities. ***References:*** None

EP-31

Movement Disorders

e-Poster Area

EP-241

Longitudinal change in dopamine transporter availability in idiopathic REM sleep behavior disorder

Y. Kim[1], *J. Shin*[1], *J. Lee*[1], *S. Shin*[1], *H. Nam*[1], *H. Kim*[1], *B. Jeon*[2];
[1]*Seoul National University Boramae Medical Center, Seoul, KOREA, REPUBLIC OF,* [2]*Seoul National University Hospital, Seoul, KOREA, REPUBLIC OF.*

Aim/Introduction: To elucidate the longitudinal change in the nigrostriatal dopamine transporter (DAT) availability in idiopathic rapid-eye-movement sleep behavior disorder (iRBD) patients predicted by the baseline motor and non-motor biomarkers through prospective analysis over 4 years. ***Materials and Methods:*** This study cohort consisted of 40 polysomnography-confirmed iRBD patients, 31 drug-naïve Parkinson's disease (PD) patients and 19 healthy controls. All participants were evaluated for olfactory function test, neuropsychological tests and the Movement disorders society-Unified PD Rating Scale, and underwent 18F-FP-CIT PET scan. Participants were re- evaluated every 2 years, prospectively. We calculated DAT-pattern with principal component analysis from tracer uptakes in 6 striatal regions at each time point. ***Results:*** Baseline DAT-pattern in PD and healthy controls formed distinct clusters whereas that in iRBD group were distributed over the two clusters. DAT-patterns in iRBD patients with hyposmia, constipation, urinary dysfunction or mild parkinsonian sign were significantly biased toward PD pattern at baseline. Hyposmia was the only biomarker significantly associated with progression of DAT-pattern toward PD pattern during the follow-up. During the follow-up, 10 iRBD patients developed neurodegenerative diseases and they were all hyposmic at the baseline, except for 1 MSA converter. Baseline DAT-pattern predicted 70% of disease converters, and annual DAT-pattern change greater than 2.0 predicted

another 20% of disease converters those who had healthy control pattern at baseline. ***Conclusion:*** Hyposmia is the most efficient predictor of impending DAT decline in iRBD. DAT-pattern can identify individuals at risk reliably with longitudinal PET scan data, even those with normal DAT uptakes at baseline. ***References:*** 1. Postuma RB, Berg D. Prodromal Parkinson's Disease: The Decade Past, the Decade to Come. Mov Disord. 2019. 2. Iranzo A, Stefani A, Serradell M, et al. Characterization of patients with longstanding idiopathic REM sleep behavior disorder. Neurology. 2017. 3. Postuma RB, Iranzo A, Hu M, et al. Risk and predictors of dementia and parkinsonism in idiopathic REM sleep behaviour disorder: a multicentre study. Brain. 2019. 4. Lee JY, Yoon EJ, Kim YK, et al. Nonmotor and Dopamine Transporter Change in REM Sleep Behavior Disorder by Olfactory Impairment. J Mov Disord. 2019.

EP-242

Role of Functional Neuroimaging in early onset Parkinson's disease, 123I-MIBG - DaTscan, a multicenter study

J. Lazri[1], *A. Di Rocco*[1], *S. Nuvoli*[2], *M. L. Stazza*[2], *M. Rondini*[2], *M. S. De Feo*[1], *L. Cosma*[1], *V. Frantellizzi*[1], *A. Farcomeni*[3], *G. De Vincentis*[1], *A. Spanu*[2];

[1]*Sapienza University of Rome, Rome, ITALY,* [2]*University of Sassari, Sassari, ITALY,* [3]*University of Rome Tor Vergata, Rome, ITALY.*

Aim/Introduction: Neuroimaging markers for Parkinson's disease (PD) or other neurodegenerative parkinsonian syndromes (non-PD) include123I-ioflupane SPECT (DaTscan) to detect presynaptic dopamine neuronal dysfunction, and myocardial 123I-metaiodobenzyl guanidine (MIBG) scintigraphy to evaluate the cardiac sympathetic nerve fibers. The aim of this multicenter study is to assess if the use of both of these molecular imaging techniques can predict PD with higher sensitivity in early onset disease patients which diagnosis was confirmed after 3 years of clinical follow-up. ***Materials and Methods:*** This was a retrospective study of two centers. In a two years period patients with suspected diagnoses of PD or non-PD syndromes were enrolled. Also, patients had to have undergone both DaTscan and MIBG imaging. The caudate nuclei (C/O) and putamina (P/O) to the non-specific occipital region ratios in both the basal ganglia were analysed. Early and Late Heart to Mediastinum ratio (eH/M and lH/M) were calculated for MIBG examination. ***Results:*** 260 subjects were analysed. Patients baseline characteristics were: mean age 66± 9,8 years, symtomps appeared for less than one year, male 147 (56.5%). The patients' neurologic diagnoses after 3 years of clinical follow-up were PD in 143 and non-PD (including essential tremor, Multiple system atrophy and other parkinsonisms) in 117. Diagnostic odds ratio (OR) with 95% confidence interval (CI) was calculated for both the exams. As regards the MIBG scan OR was 0.22 (95% CI 0.19-0.26) for eH/M and 0.29 (95% CI 0.25-0.32) for lH/M (p=0.001) while the DaTscan OR was 0.98 (95% CI 0.93-1.03) for Right C/O (p=0.55); 0.98 (95% CI 0.93-1.03) for Right P/O (p=0.46); 0.97 (95% CI 0.91-1.02) for Left C/O (p=0.28) and 0.97 (95% CI 0.91-1.02) for Left P/O (p=0.25). The ROC showed an AUC 0.954 for both eH/M and lH/M. ***Conclusion:*** MIBG examination has a higher diagnostic accuracy in early onset PD patients than DaTscan. Given the superiority of the heart study, the combined use of the DaTscan in association with the MIBG in this phase of disease does not appear to be mandatory. ***References:*** None

EP-243

Impact of dopamine depletion on gait initiation in Parkinson's disease

G. Marotta[1], *C. Palmisano*[2], *G. Brandt*[2], *M. Vissani*[3], *N. G. Pozzi*[2], *A. Canessa*[4], *J. Brumberg*[2], *J. Volkmann*[2], *A. Mazzoni*[3], *C. A. Frigo*[5], *I. U. Isaias*[2];

[1]*Fondazione IRCCS Ca' Granda Ospedale Maggiore Policlinico, Milan, ITALY,* [2]*University Hospital Würzburg and Julius-Maximilian-University, Department of Neurology, Würzburg, GERMANY,* [3]*Scuola Superiore Sant'Anna, The Biorobotics Institute, Translational Neural Engineering Area, Pontedera, ITALY,* [4]*Department of Informatics, Bioengineering, Robotics and System Engineering, Università di Genova, Genova, ITALY,* [5]*Politecnico di Milano, Department of Electronics, Information and Bioengineering, MBMC Lab, Milan, ITALY.*

Aim/Introduction: The contribution of the basal ganglia and dopamine on postural control is still largely unknown, but indirect evidence points towards their possible involvement in the production of anticipatory postural adjustments. In addition, the influence of initial stance condition on gait initiation in Parkinson's disease (PD) has never been consistently assessed. The aim of this work was to define which biomechanical resultants at gait initiation are PD-related and dopamine (putamen)-dependent, accounting for the influence of anthropometric measures and the base of support. ***Materials and Methods:*** The biomechanical resultants of anticipatory postural adjustments contributing to gait initiation (imbalance, unloading and stepping phase) were studied in 26 unmedicated subjects with idiopathic PD (18 males, mean age 61.0 years) and in 27 healthy subjects (17 males, mean age 61.2 years). A subset of 13 patients (8 males) was analysed under standardized medication conditions and the striatal dopaminergic innervation was studied in 22 patients using FP-CIT SPECT. The imaging data were processed with the Basal Ganglia Matching Tool. We investigated the correlation between the biomechanical values and the DAT density of the putamen, as the main motor structure in the striatum, contralateral to the swing foot ($putamen_{SWING}$) and contralateral to the stance foot ($putamen_{STANCE}$). ***Results:*** PD patients showed a significant reduction in center of

pressure displacement and velocity during the imbalance phase, reduced first step length and velocity, and decreased velocity and acceleration of the center of mass at toe off of the stance foot. All these measurements correlated with the dopaminergic innervation of the putamen ($p<0.01$) and substantially improved with levodopa. These results were not influenced by anthropometric parameters or by the initial stance condition. In contrast, most of the measurements of the unloading phase were influenced by the foot placement and did not correlate with putaminal dopaminergic innervation. ***Conclusion:*** Our results suggest a significant role of dopamine and the putamen particularly in the elaboration of the imbalance phase of anticipatory postural adjustments and in the execution of the first step. The basal ganglia circuitry may contribute to defining the optimal referent body configuration for a proper initiation of gait and possibly gait adaptation to the environment. ***References:*** None

EP-244

Brain metabolic alterations herald falls in patients with Parkinson's disease

G. Marotta[1], *J. Brumberg*[2], *N. Pozzi*[2], *J. Volkmann*[2], *G. Pezzoli*[3], *I. U. Isaias*[2];
[1]*Fondazione IRCCS Ca' Granda Ospedale Maggiore Policlinico, Milan, ITALY,* [2]*University Hospital Würzburg and Julius-Maximilian-University, Department of Neurology, Würzburg, GERMANY,* [3]*ASST G.Pini-CTO, Centro Parkinson, Milan, ITALY.*

Aim/Introduction: The specific factors that are critical to fall prediction and prevention in Parkinson's disease (PD) remain elusive and the best single variable to predict falls is two or more falls in the previous year. Pathophysiological understanding of gait and balance disorders in Parkinson's disease is insufficient; late recognition of fall-risk patients limits efficacious follow-up to prevent/delay falls. The aim of this study was to identify specific metabolic patterns with brain FDG PET associated with motor and cognitive symptoms. ***Materials and Methods:*** We retrospectively evaluated the clinical records and molecular imaging findings of over 200 patients with a diagnosis of idiopathic Parkinson's disease (PD) who underwent FDG PET at our center between 2012 and 2017. We identified one group of 11 right-handed patients (8 males; disease duration: 7 ± 4 years; age at onset: 57 ± 11 years; UPDRS-III: 35 ± 14) who experienced their very first fall episode between 6 and 8 months after the execution of the FDG PET. We then collected the clinical and imaging data of a second group of 19 right-handed patients (13 males; disease duration: 8 ± 4 years; age at onset: 54 ± 8 years; UPDRS-III: 32 ± 13) and a group of 12 healthy controls (HC) matched for demographic and clinical data. Brain metabolic differences between fallers, non-fallers and HC were tested by Statistical Parametric Mapping (SPM) with age and disease duration as covariates, and a post hoc volume-of-interest (VOI) analysis. ***Results:*** Clinical and demographic data did not differ significantly between groups.PD fallers showed distinctive hypometabolism in the left parietal cortex (inferior and superior parietal lobules) and increased bilateral cerebellar glucose consumption. ***Conclusion:*** We demonstrate a distinctive reduction of glucose metabolism in the left posterior parietal cortex, with increased metabolic activity in the cerebellum, in parkinsonian patients 6-8 months before their first fall. Falls in PD might arise from altered cortical processing of body spatial orientation, possibly predicted by abnormal cortical metabolism. ***References:*** None

EP-32

Non-Oncological Treatments

e-Poster Area

EP-245

Response Assessment At One Year After 131I Treatment In Patients With Grave's Disease And Multinodular Goiter

V. Carrero-Vásquez*, H. Rodríguez-Parra, M. Redal-Peña, I. Casáns-Tormo, A. Cánoves-Llombart, P. Cárcamo-Ibarra, J. Sabater-Sancho, R. Maestre-Cutillas, M. Soria-Merino;*
Nuclear Medicine, University Clinical Hospital, Valencia, SPAIN.

Aim/Introduction: The administration of 131I is an effective therapeutic option for the control of hyperthyroidism. We assessed the response at one year after treatment, analyzing the influence of age, sex, thyroid function (clinical-CH and subclinical hyperthyroidism-SH), anti-TSH receptor antibodies (AB), thyroid volume (TV) through echography, glandular characteristics in thyroid scan, and administered 131I activity (A) in patients with Graves' disease (GD) and multinodular goiter (MNG). ***Materials and Methods:*** From 100 consecutive patients(p) (2017-2018) treated with 131I, 70 (38 MNG-32 GD) were selected who received a first 131I treatment and had clinical follow-up for one year, evaluating euthyroidism-hypothyroidism as a therapeutic response (R) and persistent hyperthyroidism as the absence of it (noR). In 38 MNG (28 women, 30-87 years y/o (mean 65), there were 23/38 with SH. In 32 GD (24 women, 31-75 y/o (mean 52), there were 19/32 with SH. AB determination was available in 37/70p, TV could be calculated in 51/70p, establishing 3 subgroups: <20ml, 21-50ml and >50ml. Overall A was 8-18mCi (mean 12mCi), that was calculated according to patient age and weight, TV, and scintigraphic characteristics. ***Results:*** Patients with MNG: there was R in 34/38 (89.4%), with A: 8.5-16.6mCi (mean 12.5), TV: 20-50ml, SH in 31/34, AB: 0.3-4.29 (mean 1.8 UI/L), available in 6/34, and noR in 4/38 (10.5%), A: 12-18 mCi (mean 14.6), with TV: 52.9-149.4ml, SH in 1/4, AB not available. Patients with GD: there was R in 28/32 (87.5%) with A: 8-15mCi (mean

10.7), TV: <20-80.9ml, SH in 17/28, AB: 0-6.87 (mean 2.58 UI/L) available in 20/28, and noR in 4/32 (12.5%), with A: 10-17mCi (mean 12.8), TV: 21.8-46.3ml, SH in 2/4, AB 2.68-28.53 (mean 11.63UI/L) available in 3/4. No significant differences between R and noR in terms of age, sex, A, CH or SH. ***Conclusion:*** After one year of follow-up, in our group of patients there was a good therapeutic response and without significant differences between MNG (89.4%) and GD (87.5%). Persistent hyperthyroidism was associated with a higher thyroid volume in MNG and in the group of GD with a tendency for higher AB levels, but without relation with the other assessed factors. ***References:*** None

EP-246

10-Years Results After 90-Yttrium and 166-Holmium Radiosynoviorthesis In Chronic Knee Synovitis Of Different Origin /820 patients/

M. Szentesi, Z. Nagy, G. Csőre;
Hospital of the Hospitaller Brothers of St. John of Budapest, Budapest, HUNGARY.

Aim/Introduction: In the case of chronic synovitis, the synovial membrane proliferates, producing fluid, then creeps onto the cartilage, causing first pannus formation, then serious destruction to both cartilage and bone. Our aim is to stop this process. ***Study objectives***: Examination of anti-inflammatory effect of 90-Yttrium and 166-Holmium injections. ***Materials and Methods:*** Out of these 820 patients 460 suffered from rheumatoid arthritis, 68 ankylosing spondylitis, 52 other seronegative spondylarthritis, 188 suffered from inflamed osteoarthritis , 4 hydrops articulorum intermitterns, 4 synovitis villonodularis, 44 from chronic traumatic synovitis . Evaulation was based on the criteria as described by Müller, Rau and Scütte the score system was developed by the authors. ***Results:*** In the first 10 years excellent and good results were recorded in 71%. They achieved excellent as well as good results at 83% of patients with rheumatoid arthritis, at 50% of patients with ankylosing spondylitis and at 55% of patients with osteoarthritis. 10 years after radiosynoviorthesis 72% of patients did not need another punction. ***Conclusion:*** Radiosynoviorthesis is as effectiv method of treating chronic synovitis as surgical synovectomy. Even after a 10 years period 71% the findings were rated as excellent or good. 72% of the patients do not need another punction even after a 10 years period. The effectiveness is worsened significantly by the stadium of the disorder and the local x ray phase and diagnosis. P 0.00001. The treatment must be done in rheumatoid arthritis Steinbrocker stadium I-II, local stadium I-II. ***References:*** no Szentesi M[1], Papp I[1], Farbaky Zs[2], Nagy Z[3], Berkes I.4, Nagy Gy[1]: Treatment of Chronic Knee Synovitis with Radiosynoviorthesis After Failure of Surgical Interventions. EC Orthopaedics 11.2 (2020): 01-14.Margit Szentesi1), Zoltán Nagy1), Pal Géher1), István Papp1), Willm Uwe Kampen2): A prospective observational study on long-term results of 90Yttrium Citrate radiosynoviorthesis of synovitis in osteoarthritis of the knee joint. Eur. J. Nucl. Med. Mol. I. 46: 8pp. 1633-1641. 9p. (2019)Szentesi M.,1 Takács S.,1 Farbaky Zs.,1 Nagy E.,1 Környei J.,2 Antalffy M.,2 Törkő J.,2 Géher P. 1,:166Holmium-phytate-radiosynoviorthesis in rheumatoid arthritis. One year clinical results Phase III prospectiv studyAnn. Rheum. Dis. 2006. 65. Suppl. 2. 346.

EP-247

Knee radiosynovectomy with Sm-153 hydroxyapatite compared to Y-90 hydroxyapatite: initial results of a prospective trial

E. Etchebehere[1], M. Lima[1], L. Pereira[1], R. Pagnano[1], E. Bortoletti[2], J. Mengatti[2], S. Q. Brunetto[1], M. Takahashi[1], E. Brunetto[1], M. Ozelo[1], A. Santos[1];
[1]The University of Campinas, Campinas, BRAZIL, [2]Institute of Research and Nuclear Energy (IPEN), Sao Paulo, BRAZIL.

Aim/Introduction: ***Introduction***: The most common clinical presentation in hemophilia patients consists of hemarthrosis. Various treatment strategies aim to control hemarthrosis to prevent secondary arthropathy, among them, radiosynovectomy with Y-90 hydroxyapatite (^{90}Y-HA). A few studies have shown a lower efficiency of knee radiosynovectomy with Sm-153 hydroxyapatite (^{153}Sm-HA) compared to ^{90}Y-HA. ***Purpose:*** The purpose of this investigation was to assess the efficacy and safety of knee radiosynovectomy with ^{153}Sm-HA compared to ^{90}Y-HA. ***Materials and Methods:*** Forty patients were prospectively assigned to undergo knee radiosynovectomy with ^{153}Sm-HA (19 patients) or with ^{90}Y-HA (21 patients). The frequency of hemarthrosis episodes before and after treatment was compared. ***Results:*** The response to knee radiosynovectomy stratifying according to radiotracer showed that after 6 months the median response rate with ^{153}Sm-HA was not significantly different from ^{90}Y-HA (87.5% vs 80.9%; $p = 0.576$). However, after 12 months the median response rate of knee radiosynovectomy with ^{153}Sm-HA was significantly better than with ^{90}Y-HA (87.5% vs 50%; $p = 0.037$), respectively. The reduction of joint bleeding by at least 50%, after 12 months, was greater in the group of patients treated with ^{153}Sm-HA compared to ^{90}Y-HA (74% vs 52%), respectively. ***Conclusion:*** Knee radiosynovectomy with high doses of ^{153}Sm-HA is safe, with an efficiency rate similar that is described in the literature by the ^{90}Y-HA. ***References:*** None

EP-33
Other Neurological Imaging

e-Poster Area

EP-248
Disentangling conscious visual processing by a multimodal approach in disorders of consciousness

G. Marotta[1], D. Sattin[2], D. Rossi Sebastiano[2], L. D'Incerti[2], D. Guido[2], E. Orunesu[1], R. Benti[1], S. Tirelli[2], F. G. Magnani[2], A. Bersano[2], D. Duran[2], S. Ferrero[2], L. Minati[2], A. Nigri[2], C. Rosazza[2], S. B. Marzoli[3], M. Leonardi[2];
[1]Fondazione IRCCS Ca' Granda Ospedale Maggiore Policlinico, Milan, ITALY, [2]Fondazione IRCCS Neurologico Carlo Besta, Milan, ITALY, [3]Istituto Auxologico Italiano, Milan, ITALY.

Aim/Introduction: Differentiating between Vegetative (VS) and Minimally Conscious State (MCS) is a challenge for scientists. Recent studies have highlighted that the visual responses to tailored stimuli might be one of the first evidence of a transition from VS to MCS. Furthermore, the visual fixation, visual pursuit, and reproducible movement to command responses were observed in more than 50% of patients in MCS. We aimed at exploring the functional and structural integrity of neural structures of the visual system of VS and MCS, namely who shows visual blink and who shows visual pursuit, with a multimodal approach by collecting several measures deriving from both behavioral, neurophysiological, and neuroimaging tools. ***Materials and Methods:*** The difference between groups in instrumental data (flash Visual Evoked Potentials, structural MRI and FDG-PET) was explored in 54 patients with disorders of consciousness, all diagnosed with VS according to the Coma Recovery Scale-revised (CRS-r) without considering its visual sub-scale score. The Wilcoxon test was used to assess hemispheric differences in MRI within subjects. For FDG-PET imaging, a voxel-by-voxel two-sample t test between patients with the visual blink response only and patients with visual pursuit was performed using SPM12, applying a threshold of FDR corrected $p<0.001$ for cluster containing at least 100 voxels. ***Results:*** Forty-two (77.7%) patients out of 54 showed only visual blink reflex in the CRS-r visual function subscale, and twelve (22.2%) showed visual pursuit. Among non-traumatic aetiologies, sixteen (29.62%) patients had a hemorrhagic etiology, two (3.7%) ischemic, and nineteen (35.18%) had post-anoxic damage. Flash Visual Evoked Potentials were absent in 88.9% and in 11.1% for the visual blink and visual pursuit groups respectively. For MRI, a significant statistical differences between the two groups (p-values<0.01) were found for the right V1 area and the right optic radiation scores. For FDG-PET, a significant difference ($p<0.001$ FDR-corrected) was also found between the two groups: the visual blink group showed a significant decrease metabolism in right calcarine and lingual gyrus cortex then visual pursuit group. ***Conclusion:*** We showed that patients manifesting visual blink have different patterns, as detected by instrumental tools, compared with patients manifesting visual pursuit especially in occipital areas. These results set the rationale to identify those markers associated with consciousness that could be of help in the next future to better understand if a certain visual behavior is determined by conscious or non-conscious processing. ***References:*** None

EP-249
A multimodal assessment of residual language processing in disorders of consciousness patients

G. Marotta[1], S. Ferraro[2], A. Nigri[2], L. D'Incerti[2], C. Rosazza[2], D. Sattin[2], D. Rossi Sebastiano[2], E. Visani[2], D. Duran[2], G. Demichelis[2], E. Catricala[3], S. Kotz[4], L. Verga[4], M. Leonardi[2], S. Cappa[3], M. Schiavini[1], M. F. Bardo[1], M. G. Bruzzone[2];
[1]Fondazione IRCCS Ca' Granda Ospedale Maggiore Policlinico, Milan, ITALY, [2]Fondazione IRCCS Neurologico Carlo Besta, Milan, ITALY, [3]Scuola Universitaria Superiore, Pavia, ITALY, [4]Maastrict University, Maastricht, NETHERLANDS.

Aim/Introduction: The impact of language impairment on the clinical assessment of patients sufferering from disorders of consciousness (DOC) is unknown or underestimated, and may mask the presence of conscious behavior.The aim of the study was to investigate the main neural functional and structural underpinnings of linguistic processing, and their relationship with the behavioral measures of the auditory function, using the Coma Recovery Scale-Revised (CRS-R) and to assess the integrity of the brainstem auditory pathways of the left superior temporal gyrus and arcuate fasciculus, the neural activity elicited by passive listening of an auditory language task and the mean hemispheric glucose metabolism. ***Materials and Methods:*** We included 11 patients with DOC included 4 with vegetative state (VS) and 7 with minimally conscious state (MCS): 5 MCS- and 2 MCS+ (4 males; median age: 57 years, range: 19-69 years; etiology: 4 traumatic brain injury, 5 hemorrhagic brain injury, 2 anoxic brain injury; median time post-injury: 27 months).The clinical assessment of the patients was performed with the CRS-R1.The multimodal evaluation comprised BAEPs, sMRI, DTI, fMRI during the administration of a passive hierarchical auditory language paradigm, and FDG-PET. ***Results:*** One VS and 3 MCS- patients, showed the auditory startle at the CRS-R auditory function subscale: in VS patient the lack of fMRI related activity was possibly supported by a very low-level metabolism; in MCS- patients the lack of fMRI-related activity was possibly sustained by severe anatomical damage of the leftsided investigated structures or by a very severe impairment of the brainstem auditory pathways. Three VS and 2 MCS- patients presented the localization to sound at the CRS-R auditory function

subscale: these patients presented a relative integrity of BAEPs and a certain degree of fMRI-related activity with metabolism was quite variable. Two MCS+ presented or integrity of the core structures of language processing or a complete preservation of bilateral BAEPs and both patients presented high-level left-lateralized fMRI activity. ***Conclusion:*** The results support the hypothesis that MCS- patients presenting the auditory startle might be aphasic in the receptive domain, independently from the level of cerebral metabolism and, therefore, from the level of consciousness. Moreover, our results support the hypothesis that MCS- patients exhibiting the localization to sound, might present a lower level of consciousness in comparison to MCS+ patients. ***References:*** Nigri A et al. The neural correlates of lexical processing in disorders of consciousness. Brain imaging and behavior 2017;11(5):1526-1537

EP-250

Sex difference in Cerebral blood flow and Cerebral glucose metabolism: An activation likelihood estimation Meta-analysis

K. Pak[1], *S. Kim*[2], *S. Lee*[3];
[1]*Pusan National University Hospital, Busan, KOREA, REPUBLIC OF,* [2]*Pusan National University Yangsan Hospital, Yangsan, KOREA, REPUBLIC OF,* [3]*Kyungpook National University Hospital, Daegu, KOREA, REPUBLIC OF.*

Aim/Introduction: We investigated the sex difference in cerebral blood flow and cerebral glucose metabolism using positron emission tomography and single photon emission computed tomography ***Materials and Methods:*** We performed a systematic search of MEDLINE and EMBASE for English-language publications using the keywords of "positron emission tomography", "single-photon emission computed tomography", and "sex". The inclusion criteria were original research articles that reported the difference between males and females in cerebral blood flow or cerebral glucose metabolism. For each experiment, the modeled activation map is calculated by finding the maximum across each focus's Gaussian. On the basis of empiric estimates of between-subject variability from the number of subjects in each study, the width of the Gaussian probability distribution is determined individually for each experiment. A threshold of uncorrected p<0.001 (minimum volume of 200mm3) was applied to the resulting ALE map. ***Results:*** 7 studies were eligible for inclusion in the study. Four studies of CBF with 15O-H2, 99mTc-ECD, and 99mTc-HMPAO, and 3 studies of CMRglu were included. A. Cerebral blood flow- In females, significant increases in CBF were identified in 6 clusters including right precuneus, left superior temporal gyrus, left inferior temporal gyrus, left inferior frontal gyrus, right cerebellar tonsil, and right middle temporal gyrus. In males, a significant increase in CBF was observed in 1 cluster of left anterior cingulate. B. Cerebral metabolic rate of glucose- In females, significant increases in CMRglu were identified in 7 clusters including left thalamus, left cingulate gyrus, right inferior parietal lobule, left medial frontal gyrus, right middle frontal gyrus, right midbrain, and left inferior parietal lobule. In males, no significant increase in CMRglu was observed. ***Conclusion:*** With the help of neuroimaging of PET and SPECT, significant sex difference of cerebral blood flow and cerebral metabolic rate of glucose was identified. ***References:*** Journal of Neuroscience Research 95:189-199 (2017)

EP-251

Determination of embolic brain distribution caused by right to left shunt in people with patent foramen ovale

M. Assadi*, R. Nemati, M. Jalali, H. Salimipour, A. Amini, E. Jafari;*
Bushehr University of Medical Sciences (BUMS), Bushehr, IRAN, ISLAMIC REPUBLIC OF.

Aim/Introduction: One of the etiologies for stroke, especially in younger patients, is patent foramen ovale (PFO). It is found in about 25% of healthy people and it is asymptomatic most of the time but during a valsalva maneuver, a transient right to left shunt can occur and if there would be emboli in it, it can bypass the lungs and enter the aorta and if it migrates to the brain, it can cause stroke. Some recent studies have been shown that these strokes mostly occur in posterior circulation, although a few says no. The overall epidemiology of posterior circulation strokes is about 20% of all strokes which seems to be much higher in PFO patients. There are not sufficient data about it. This study is about determination of distribution of emboli in brain in patients with PFO. ***Materials and Methods:*** We studied 51 patients with PFO. We injected 99mTc-macroaggragated Albumin, then we asked them to accomplish valsalva maneuver, then they underwent brain SPECTs in right lateral and left lateral views. ***Results:*** Te most flow of MAA was respectively in cerebellar, occipital, frontal and temporoparietal regions. ***Conclusion:*** We showed that posterior circulation is dominant in PFO people, in contrary to non-PFO people. It may because of valsalva maneuver that makes the posterior blood flow more dominant. Further studies about cerebral blood flow with and without valsalva maneuver is highly recommended. ***References:*** None

EP-252

Association of dizziness and brain perfusion SPECT : voxel-based analysis of a pilot sample

M. Assadi[1], *R. Nemati*[1], *M. Nayeri*[1], *N. Chabi*[1], *E. Jafari*[1], *H. Dadgar*[2];
[1]*Bushehr University of Medical Sciences (BUMS), Bushehr, IRAN, ISLAMIC REPUBLIC OF,* [2]*Razavi Cancer Research Center, Razavi Hospital, Mashhad, IRAN, ISLAMIC REPUBLIC OF.*

Aim/Introduction: The presence of perfusion and structural abnormalities on brain imaging in people with dizziness

has not been widely studied. The purpose of this study was to investigate the brain perfusion in patients with dizziness using single photon emission computed tomography (SPECT). ***Materials and Methods:*** We studied 34 people with self-reported dizziness who had experienced intermittent or constant dizziness within the past month or more. The study was carried out between January 2014 and November 2015. Dizziness-related impairment was assessed with the dizziness handicap inventory (DHI) and short physical performance battery (SPPB). Carotid intima-media thickness (CIM) also measured by ultrasonography. Brain perfusion data were analyzed either qualitatively in all cases or semi-quantitatively in 11 cases using statistical parametric mapping (SPM) software. ***Results:*** Overall, 34 patients (mean age 72.01 years, SD = 8.28 years) with a history of dizziness precipitated in the study. Dizziness severity of 34 patients was classified as 20(58.8%) cases were in mild group,9(26.5%) cases in moderate group and 5(14.7%) cases in severe group. Finding of brain perfusion scan revealed that 4 (11.2) patients had a normal scan and 30(88.2%) patients had an abnormal scan. In SPM analysis of the brain perfusion imaging, patients showed a significantly decreased brain perfusion in right precuneus, cuneus, superior and inferior occipital lobe, inferior frontal, middle frontal, temporal, inferior parietal and left superior parietal, precuneus, cerebellar, insula, and putamen. In qualitative assessment of brain SPECT, significant association was seen between perfusion defect severity with SPPB test (p=0.019), gait speed test 4 meter (p=0.003) and balance test(p=0.021) parameter, but not with chair stand (p=0.11). ***Conclusion:*** Our results showed that multiple regions of the brain involvement in patients with dizziness that supported dizziness may be manifestation of an abnormal integration of multisensory modality. We found that parietal hypoperfusion associated with impairment of balance and gait. In addition, frontal lobe involvement predominately affects gait speed. Key words: brain SPECT, dizziness, statistical parametric mapping (SPM), 99mTc-ECD. ***References:*** None

EP-253

DWI and SPECT findings in patients with acute ischemic stroke

M. Assadi*, A. Moradi, M. Emami, K. Mirzaei;*
Bushehr University of Medical Sciences (BUMS), Bushehr, IRAN, ISLAMIC REPUBLIC OF.

Aim/Introduction: Stroke or stroke is a common disease characterized by a rapid development of neurodegenerative defects that can lead to illness and death. Considering the increasing incidence of this disease, we look at the events that occur during MRI imaging in the form of weight distribution (DW MRI) and SPECT. ***Materials and Methods:*** 30 patients with acute ischemic stroke referred to a neurologist clinic confirmed their diagnosis by a neurologist. Then, two types of DWI and SPECT imaging were performed for these patients to investigate the events occurring during acute stroke. ***Results:*** In this study, 40 patients with stroke were enrolled in the study. Among them, 30 patients had SPECT and DWI scans, of which 16 were female and 14 were male. Of these, 14 were left hemiparesis And 14 patients with right hemiparesis and 4 patients with dysarteria, of which 4 had 2 simultaneous hemiparesis (a patient with dysarteria and right hemiparesis and one patient with dysarteria and left hemiparesis). DW MRI is also found in 40% of the patients with acute left frontal infarction, 33. 3% of the acute infarction in the right frontal, 20% in the right parietal, 13. 3% of the patients with acute left parietal infarction, 10% in the brain stem and right cerebellum. SPECT and DWI findings with patient complaints and the side of the conflict in the hemiparesis. Significant differences were found in the SPECT and DWI findings in patients with hemiparesis. ***Conclusion:*** This study showed that high percentage of patients with ischemic stroke had lesion in the left temporal and parietal lobes and right frontal and frontal lobes in DWI. It was also found that SpPECT in showing areas of reduction an impression that indicates ischemia is more sensitive than DWI. Also, the findings of the SPECT and DWI have also been correlated with complaints from patients and the side of the hemorrhagic conflict. DWI and SPECT compounds in showing ischemic lesions and the brain infarction was very sensitive. The DWI is useful for detecting TIA from stroke, and SPECT is more beneficial for differentiation due to the higher sensitivity, and when combined, there is a very high sensitivity to the differentiation of TIA from stroke. ***References:*** None

EP-34

Preclinical Studies -> Preclinical Studies -> In Vitro Studies

e-Poster Area

EP-254

Biological Characterization of the ^{47}Sc Labelled PSMA Ligand

D. Pawlak, W. Wojdowska, M. Żółtowska, M. Wyczółkowska, U. Karczmarczyk, P. Garnuszek, J. L. Parus, R. Mikołajczak; National Institute for Nuclear Research Radioisotope Centre POLATOM, Otwock, POLAND.

Aim/Introduction: In recent years, ^{47}Sc has attracted attention due to its favorable decay characteristic (T1/2 =3.35d, Eβmax = 600 keV; Eγ, 159 keV) and chemical properties similar to lutetium or yttrium, since it can be useful for therapy and allows imaging using SPECT. Herein we present the preclinical assessment of chemical and biological properties of our new PSMA analogue (PSMA-D4) when labelled with ^{47}Sc. ***Materials and Methods:*** ^{47}Sc was produced by irradiation of ^{46}Ca enriched targets in ^{46}Ca(n,γ)^{47}Ca→^{47}Sc nuclear reaction, either at target at ILL (Grenoble) or NCBJ (Otwock). ^{47}Sc was separated from the irradiated target by extraction chromatography on DGA resin [1]. Radiochemical purity of [^{47}Sc]Sc-PSMA-D4 was assessed by iTLC and HPLC. The affinity to the PSMA antigen was assessed using cell membranes isolated from LNCaP (PSMA+) and PC3 (PSMA-) cells by saturation binding assays to evaluate the specific binding, dissociation equilibrium constant (Kd), and maximal receptor concentration on cell surface (Bmax). For comparison, the same testing procedures applied to [^{90}Y]Y-PSMA-D4. Biodistribution of both [^{47}Sc]Sc-PSMA-D4 and [^{90}Y]Y-PSMA-D4 was studied in Balb/c nude mice bearing LNCaP xenografts. ***Results:*** Irradiation of 50 mg of ^{46}Ca resulted in approximately 350 MBq of ^{47}Sc. ^{47}Sc was separated from excess of Ca on DGA resin with about 90% yield. Radiolabeling of [^{47}Sc]Sc-PSMA-D4 resulted in over 90% radiochemical yield and the specific activity up to 5,5 MBq/nmol. Both [^{47}Sc]Sc-PSMA-D4 and [^{90}Y]Y-PSMA-D4 revealed high specific affinity to PSMA antigen in vitro with over 99% of the total binding. The Kd and Bmax values for [^{47}Sc]Sc-PSMA-D4 were 5,0±1,9 nM and 7,8±3,1 nmol/mg, while for [^{90}Y]Y-PSMA-D4 they were 5,6±1,5 nM and 20,4±6,3 nmol/mg, respectively. In vivo radioactivity uptake of [^{47}Sc]Sc-PSMA-D4 in the tumor reached maximum value of 9,24 ±2.21 %ID/g at 4hp.i.v. in Balb/c nude mice bearing LNCaP xenografts. Retention of radioactivity in the blood and in non-targeted organs and tissues decreased rapidly over time, reaching background levels after 6 h. ***Conclusion:*** We demonstrated that ^{47}Sc can be obtained via ^{46}Ca(n,γ)^{47}Ca→^{47}Sc nuclear reaction and successfully used for preparation of radiopharmaceuticals. Our newly developed PSMA-D4 ligand labelled with ^{47}Sc shows potential for targeted radionuclide therapy of prostate cancer metastasis. ***References:*** [1] D. W. Pawlak, et al. Comparison of separation methods for ^{47}Ca/^{47}Sc radionuclide generator. ApplRadiatIsot. 2019;151: 140-144 Acknowledgement:CERAD project is financed under Smart Growth Operational Programme 2014-2020, Priority IV, Measure 4.2.

EP-255

Molecular Imaging as a Quantitative Tool to Assess the in Skin Malaria Parasite Deposition: Mosquito Bites vs. Needle Injection

C. de Korne, B. M. F. Winkel, M. N. van Oosterom, S. C. Chevalley-Maurel, J. C. Sijtsma, E. Baalbergen, B. M. D. Franke-Fayard, F. W. B. van Leeuwen, M. Roestenberg; LUMC, Leiden, NETHERLANDS.

Aim/Introduction: An effective malaria vaccine could potentially prevent >200 million malaria cases each year. Vaccines comprising live attenuated malaria parasites (sporozoites; spz) are currently considered most promising. However their feasibility and efficacy critically depends on the means of administration; spz are much more efficacious in inducing protection when deposited by mosquito bite as opposed to needle injection[1,2]. This difference in efficacy is thought to be explained in part by the enhanced migratory capacity of mosquito-delivered spz. To understand what causes the difference in efficacy of the administration routes we used fluorescence imaging and custom image analysis software to study the injection site appearance and spz migration after injection. ***Materials and Methods:*** Plasmodium berghei spz expressing mCherry and luciferase were administered to mice by 30 mosquito bites (MB) or by intradermal needle injection of 3k spz in 10 µl (NI). The parasite burden in the liver of mice, assessed by bioluminescence imaging 44h post injection, was determined for the different administration routes. The intradermal injection sites were visualized using a spinning disk confocal microscope. Movies were obtained of migrating spz (NI: n=1251, MB: n=566) and quantitatively analyzed with our in-house written analysis tool $SMOOT_{mouse}$. Comparison of spz motility after delivery by MB vs. NI was performed based on key motility parameters: movement pattern, track tortuosity and velocity. ***Results:*** The number of spz able to migrate from the skin to the liver after NI was 3-fold lower compared to MB. Mapping the injection sites revealed that NI resulted in a spz hotspot (nearest neighbor distance (NND): 23 µm, IQR: 13-43) and increased interstitial space, while MB resulted in a higher spz spread (NND: 55 µm, IQR: 18-132) and small hemorrhages. $SMOOT_{mouse}$ analysis revealed that 88% of the spz tracked in mouse skin were motile. Following delivery by NI, the spz velocity

decreased (mean: 1.84 µm/s, SD: 0.24) and they travelled with a more random turn angle (angular dispersion: 0.57, SD: 0.14) compared to spz delivered by MB (mean velocity: 2.41 µm/s, SD: 0.31; angular dispersion: 0.73, SD: 0.10). ***Conclusion:*** Comparing routes of spz administration using molecular imaging combined with quantitative image analysis revealed differences in spz distribution and motility, which might explain the low efficacy of spz administration by intradermal needle injection. This indicated that alternative intradermal administration routes (e.g. microneedles) should be explored to better mimic the spz distribution and motility seen after delivery by mosquito bite. ***References:*** 1.doi.org/10.1086/339409; 2.doi.org/10.1126/science.1211548

EP-35

Preclinical Studies -> Preclinical Studies -> Other Medical Preclinical

e-Poster Area

EP-256

Targeted pharmacological inhibition and kinetic modeling to improve the performance of [^{99m}Tc] mebrofenin as probe to study MRP2 activity at the liver-bile interface

S. Marie[1], I. Hernández-Lozano[2], L. Breuil[1], W. Saba[1], M. Goislard[1], A. Novell[1], J. Gennisson[1], O. Langer[2], C. Truillet[1], N. Tournier[1];
[1]Laboratoire d'Imagerie Biomédicale Multimodale (BIOMAPS), Université Paris-Saclay, CEA, CNRS UMR9011, Inserm UMR1281, Service Hospitalier Frédéric Joliot, Orsay, FRANCE, [2]Department of Clinical Pharmacology, Medical University of Vienna, Vienna, AUSTRIA.

Aim/Introduction: Multidrug resistance-associated protein 2 (MRP2, ABCC2) mediates the biliary excretion of drugs from hepatocytes. Deficiency of this efflux transport may result in drug-induced liver injury. Quantitative imaging techniques are needed to explore the MRP2 transport in vivo. The interplay of other hepatic transporters and the liver metabolism of most probes complicate the interpretation of imaging data. [^{99m}Tc]mebrofenin (MEB) is a metabolically stable probe for hepatic imaging, predominantly transported by MRP2 at the canalicular (liver-bile) interface. However, its liver kinetics also depends on sinusoidal transporter-mediated uptake (blood-liver) by organic anion-transporting polypeptides (OATP, SLCO) [1]. A safe protocol for targeted inhibition of hepatic MRP2 is needed to study the intrinsic transport capacity of this transporter apart from other transporter systems, as would be achieved using MRP2-deficient animals versus wild-type animals. ***Materials and Methods:*** MEB was injected (39±4MBq iv, n=5-6 per condition) in control rats (CTRL) or after pretreatment with rifampicin (RIF 40mg/kg iv, OATP/MRP2 inhibitor) or ciclosporin (CsA, 0.01, 0.1, 0.5, 1 or 5mg/kg iv). Planar dynamic acquisitions were acquired during 40 minutes. Regions of interest were drawn over the heart blood-pool, liver and intestine to generate time-activity curves. Pharmacokinetic modeling was performed to describe the transfer rate constants between compartments [2]. The liver perfusion was measured before and after injection of the maximal dose of each inhibitor using Doppler ultrasound. Outcome parameters were compared using one-way ANOVA for imaging data and a paired t-test for ultrasound results. ***Results:*** A significant and comparable decrease in k_3 (rate constant for transfer from hepatocytes to excreted bile) was observed for all tested conditions (from $CsA_{0.01}$=0.03±0.00min^{-1} to RIF40=0.05±0.02min^{-1}) suggesting effective MRP2 inhibition compared to CTRL (k_3=0.15±0.08min^{-1}). RIF and the highest doses of CsA significantly decreased k_1 (rate constant for blood-to-liver transfer, RIF_{40}=0.88±0.09min^{-1}, CsA_5=2.82±0.87min^{-1}) compared to CTRL (k_1=7.37±1.62min^{-1}). The effect on k_1 was dose-dependent with no impact of the lowest dose of CsA ($CsA_{0.01}$=8.69±1.90min^{-1}). Highest dose of CsA did not affect the liver perfusion. ***Conclusion:*** Low dose CsA is a potent inhibitor in vivo of the MRP2-mediated canalicular efflux of MEB with impact on neither the OATP-mediated sinusoidal influx nor liver perfusion. MEB±CsA provides a safe, available and clinically feasible protocol to selectively unveil the MRP2 transport activity at the liver-bile interface in vivo. ***References:*** [1]S. Neyt et al., J. Nucl. Med., vol. 54, no 4, p. 624630, 2013. [2]I. Hernández Lozano et al., AAPS J., vol. 21, no 4, 2019.

EP-257

PET and MR imaging for in ovo evaluation of nanoparticle biodistribution

J. Loeffler[1,2], N. Eberhardt[2], R. Fiedler[3], M. Lau[3], M. Raabe[4], M. N. Alam[4], A. B. Koch[2], E. Scheidhauer[2], A. Abaei[1], H. Herrmann[2], C. Solbach[2], T. Weil[5], M. Lindén[3], F. Jelezko[6], A. J. Beer[2], V. Rasche[7,1], G. Winter[2];
[1]Ulm University, Core Facility Small Animal Imaging, Ulm, GERMANY, [2]Ulm University Medical Center, Department of Nuclear Medicine, Ulm, GERMANY, [3]Ulm University, Department of Inorganic Chemistry II, Ulm, GERMANY, [4]Max Planck Institute for Polymer Research, Synthesis of Macromolecules Department, Mainz, GERMANY, [5]Max Planck Institute for Polymer Research, Synthesis of Macromolecules Department, Ulm, GERMANY, [6]Ulm University, Institute for Quantum Optics, Ulm, GERMANY, [7]Ulm University Medical Center, Department of InternalMedicine II, Experimental Cardiovascular Imaging, Ulm, GERMANY.

Aim/Introduction: Surface-modified nanoparticles (NP) including nanodiamonds (ND), mesoporous silica (MSN) and superparamagnetic iron oxide nanoparticles (SPION) are of growing interest for medical applications. The different NP-

structures facilitate the potential use for high-resolution/high-sensitivity in vivo imaging (ND), for drug delivery (MSN) and as contrast agent (SPION). The assessment of biodistribution and accumulation in organs and target regions of those particles is crucial for their evaluation as medical compound. Using the HET-CAM (Hen's Egg Test - Chorioallantoic Membrane) model allows the reduction of usually necessary animal experiments in accordance with the 3Rs principles (reduction, refinement, replacement). Combined PET and MRI was used for evaluation of NPs in the HET-CAM model. ***Materials and Methods:*** NDs (microdiamond, IOM Leipzig) coated with PEGylated HSA and p-SCN-Bn-deferoxamine (DFO, Macrocyclics), SPION modified using polyethylenimine and MSN surface-modified with a fragment of CD47 and DFO were used. All particles were radiolabelled with ^{89}Zr. Labelling stability was monitored by thin-layer chromatography in sodium chloride (0.9%), cell culture medium and human serum over a 5 days period. Tumour xenografts of cell lines LNCaP C4-2, PC-3, HeLa, TZM-bl and AR42J were established. After intravenous injection of NPs, MRI data was acquired with an 11.7T small animal system (BioSpec117/16, Bruker) followed by PET measurements (Focus120, Siemens Medical Solutions, Inc.). Studies were performed between embryo development day 12 and 16. For quantification of radioactivity accumulation in xenografts, tumours were analysed in a gamma counter (Cobra II, Perkin Elmer). ***Results:*** An ^{89}Zr-labelling efficiency of at least 76% was obtained for all particles. Labelling stability was validated in human serum over a period of 5d, ranging from 77% (SPION) to 93% (MSN). However, SPIONs indicated instability in human serum at day 2 (35%). MSN and ND biodistribution was measured in eggs using PET and MRI. By superimposing the images, particle accumulation was assigned to the heart and liver area. Similar results were obtained for SPIONs in T1 weighted images. Signal intensity ratios (SIR, muscle/liver) of 2.7±0.2 before and 10.2±1.2 (0h) to 9.6±3.7 (4h) after injection, indicate a particle accumulation in the liver region. ***Conclusion:*** The HET-CAM model was successfully used to assess the biodistribution of different radiolabelled NPs by high-resolution MRI and highly sensitive PET imaging in ovo. Analysed NPs predominantly accumulated in organs of the reticuloendothelial system. Information on the biodistribution of nanoparticles can be obtained in ovo at early stages of drug development, thus reducing the number of animal experiments required. ***References:*** None

EP-258

The 5-HT2A receptor antagonist altanserin affects motor activity and hippocampal D2 receptor binding in the rat

S. Nikolaus[1], H. Wittsack[1], M. Beu[1], C. Antke[1], H. Hautzel[2], Y. Mori[1], E. Mamlins[1], G. Antoch[1], H. Müller[1];
[1]University Hospital Düsseldorf, Düsseldorf, GERMANY,
[2]University Hospital Essen, Essen, GERMANY.

Aim/Introduction: 5-HTergic projections run from the raphe nucleus to dopamin(DA)ergic cells in substantia nigra/ventral tegmental area and to their terminal fields in nucleus accumbens, caudateputamen and prefrontal cortex. Altanserin (ALT) acts a a 5-HT2A receptor (R) antagonist. In the present study, we assessed the effect of ALT on motor and exploratory behavior and on cerebral D2R binding in the same rats with the method of small animal SPECT. ***Materials and Methods:*** In 21 male Wistar rats, D2R binding was measured after injection of ALT (10 mg/kg ip) as well as vehicle (VEH; dimethylsulfoxide, 0.5 ml/kg ip). After injection of ALT, motor/exploratory behavior was registered for 45 min in an open field using EthoVisionXT. In 20 further rats, D2R binding and behavior were assessed after pre-treatment with VEH. Iodine-123-IBZM (29±3MBq iv) was injected 45 min post-challenge. Imaging data were acquired at 90 min post-challenge with the TierSPECT. Furthermore, rats were scanned with a dedicated small animal MRI (MRS3000 Pre-clinical MRI, 3.0 T, MR Solutions, Guildford, UK). Based on the Paxinos rat brain atlas, regions of interest were defined on SPECT-MRI overlays. Binding potentials (BPs) were computed for ALT and VEH in various regions (nucleus accumbens, caudateputamen, substantia nigra, thalamus, frontal, motor and parietal cortex, anterior and posterior hippocampus), for which the presence of D_2Rs has been confirmed (1). ***Results:*** After ALT, the BP in the posterior hippocampus was increased relative to VEH (p=.03). No other regional differences were observed between treatments. However, ALT reduced ambulation (min 1-35), rearing (min 6-40), head-shoulder-motility (min 6-45) and grooming (min 6-45) relative to VEH ($.0001 \leq p \leq .050$). ***Conclusion:*** The 5-HT2AR antagonist ALT reduced motor/exploratory behavior, whereas nigrostriatal and neocortical D2R binding was unaltered relative to VEH. However, an increase of D2R binding was observed in the posterior hippocampus, which may reflect a reduction of DA availability in this region. ***References:*** (1) Bouthenet et al., Neuroscience. 1987;20:117-55.

EP-259

Different effects of the 5-HT2A receptor agonist DOI and the 5-HT2A receptor antagonist altanserin on D2 receptor binding in the rat brain

S. Nikolaus[1], *H. Wittsack*[1], *M. Beu*[1], *C. Antke*[1], *H. Hautzel*[2], *Y. Mori*[1], *E. Mamlins*[1], *G. Antoch*[1], *H. Müller*[1];
[1]*University Hospital Düsseldorf, Düsseldorf, GERMANY,*
[2]*University Hospital Essen, Essen, GERMANY.*

Aim/Introduction: The serotonin 5-HT2A receptor (R) is known to modulate the relase of dopamine (DA) in the mammalian brain (1). 2,5-Dimethoxy-4-iodoamphetamine (DOI) and altanserin (ALT) act as 5-HT2AR agonist and antagonist, respectively. In the present study, we assessed the effects of DOI and ALT on D2R binding in the rat brain with the method of small animal SPECT. ***Materials and Methods:*** In 19 male Wistar rats, D2R binding was measured after injection of DOI (0.5 mg/kg ip) as well as vehicle (VEH; 0.9% NaCl, 0.5 ml/kg ip). In 21 further rats, D2R binding was measured after treatment with ALT (10 mg/kg ip) and the respective VEH dimethylsulfoxide (0.5 ml/kg ip). Iodine-123-IBZM (30±3MBq iv) was administered 30 min after injection of DOI and 45 min after injection of ALT. Imaging data were acquired with the TierSPECT starting at 74 and 90 min post-challenge, respectively. Additionally, all rats were scanned with a dedicated small animal MRI (MRS3000 Pre-clinical MRI, 3.0 T, MR Solutions, Guildford, UK). Based on the Paxinos rat brain atlas, regions of interest were defined on SPECT-MRI overlays. Binding potentials (BPs) were computed for each treatment in various regions (nucleus accumbens, caudateputamen, substantia nigra, thalamus, frontal, motor and parietal cortex, anterior and posterior hippocampus), for which the presence of D_2Rs has been confirmed. ***Results:*** DOI increased BPs in caudateputamen (p=.018), frontal cortex (p≤.001), motor cortex (p≤.001) and posterior hippocampus (p=.020) relative to VEH, while ALT increased the BP in the posterior hippocampus relative to VEH (p=.03). ***Conclusion:*** The 5-HT2AR agonist DOI increased D2R binding in caudateputamen, frontal cortex, motor cortex and posterior hippocampus. The 5-HT2A antagonist ALT merely increased D2R binding in the posterior hippocampus. The observed elevations of D2R binding may be conceived to reflect reductions of synaptic DA in these regions. Previous microdialysis studies have reported that both 5-HT2AR agonists and antagonists imcrease DA efflux (1). It may be hypothesized that the regional reductions of DA in the present study were due to D2 autoreceptor activation in response to initially increased DA levels, incurring compensatory decreases of DA efflux in the caudateputamen and in the cortical and limbic target regions of DAergic projections. ***References:*** (1) Di Matteo et al. Prog Brain Res 2008; 172:7-44

EP-260

[^{89}Zr]-labeled mesenchymal stem cells biodistribution in rats with local radiation injuries

O. Klementyeva, *K. Luneva, A. Larenkov, V. Bubenschikov, T. Astrelina, V. Brunchukov;*
Federal Medical Biological Agency, Federal State Budget Institution, State Research Center "Burnasyan", Moscow, RUSSIAN FEDERATION.

Aim/Introduction: The aim of this work: study of biodistribution of mesenchymal stem cells (MSC) labeled [^{89}Zr]Zr-oxine in animals at different times after the local irradiation. The local radiation injuries are one of the serious complications of external beam radiation therapy. There is no possible to integrate cellular technologies in the radiation burns treatment without information about the stem cells migration pathways in the body. PET imaging with [^{89}Zr]-labeled stem cells is the most informative method for preclinical studies and clinical applications. ***Materials and Methods:*** [^{89}Zr]Zr-oxine complex had been synthesized from [^{89}Zr]Zr-oxalate (Cyclotron Co., Ltd, Obninsk, Russia). Radiochemical purity (RCP) was tested using ITLC. [^{89}Zr]^{89}Zr-oxine with RCP not less 95% was used for labeling MSC. All animal experiments were performed based on the Russian Animal Protection laws and guidelines for scientific animal trials. Local irradiation of Wistar rats (male) was carried out using X-ray with dose of 110 Gy (dose rate of 21.4 Gy/min). This led to acute radiation skin damage (RSD). The biodistribution of[^{89}Zr]^{89}Zr-oxine-labeled MSC was studied in latent and acute phase of RSD (1 and 14 days after irradiation). [^{89}Zr]^{89}Zr-oxine-labeled MSC ($0.4 \cdot 10^6$ cells, 37.2-52.8 kBq) were transferred to rats by intradermal injection in irradiation area. Rats (5 ones per time point) were killed in 3h, 24h and 48h after injection. Each sample (blood, lungs, liver, spleen, kidneys, femur, RSD site, intact skin) was counted with a γ-counter to obtain percentage of the injected dose (% ID/g) and differential uptake ratio (DUR) in locus of RSD to intact skin. ***Results:*** The MSC labeling efficiency was about 60%. In the latent phase [^{89}Zr]Zr-oxine-MSC uptake at the RSD site decreased from 82% ID (3h p.i.) to 52% ID (48h p.i.). DUR values was ranged from 66 (3h p.i.) to 151 (48h p.i.). In the acute phase [^{89}Zr] Zr-oxine-MSCs were linked firmly at the RSD site. Uptake levels up to 48 hours after injection were 70-90% ID. There were DUR values: 333.4 (3h p.i.), 768.5 (24h p.i.) and 344.8 (48h p.i.). It's fact suggests about inflammatory response development in the RSD site promotes retention of MSCs. MSCs migration to the liver was observed (up to 2.8% ID 48h p.i.). There was minimal ^{89}Zr uptake in the bone tissue for 48 hours after injection (less 0.4% ID/g). ***Conclusion:*** Local injection of [^{89}Zr]Zr-oxine labeled MSCs will allow using PET imaging of the radiation lesion focus at the earliest possible time after irradiation. ***References:*** None

EP-261

Time after synthesis does not affect 4FMFES biodistribution and PET imaging

M. Paquette, S. Phoenix, B. Guérin, É. E. Turcotte;
Université de Sherbrooke, Sherbrooke, QC, CANADA.

Aim/Introduction: The Estrogen Receptor (ER)-targeting molecule 4-fluoro-11β-methoxy-16α-[18F]fluoroestradiol (4FMFES) is currently under investigation in combination with FDG-PET for the diagnosis of breast and uterine cancer patients in 2 separate phase 2 clinical trials. Its post-synthesis shelf-life was previously set to 2 hours, which limits the number of patients imaged per production and hinders its distribution to peripheral sites. In order to extend its shelf-life, we sought to demonstrate that 4FMFES does not lose its imaging properties and does not change its biodistribution even after many half-lives have passed. ***Materials and Methods:*** Athymic female nude mice were implanted with the human ER+ breast cancer cell line MCF7, and tumors were grown up to 3-4 mm diameter. Cohorts of mice (n = 4 each) were injected with 4FMFES at 1 hour (100 kBq and 10 MBq), 3 hours (100 kBq), 6 hours (100kBq) and 20 hours (10 kBq) post-synthesis, then dissected to assess biodistribution. Other groups (n = 4 each) were injected with 1.2 ± 0.3 MBq 4FMFES at 1-, 3- and 6- hours post-synthesis, then imaged for 15 minutes at 60 minutes post-injection in a small animal PET scanner. ROIs were drawn on the tumor, the pituitary, muscle and liver, and %ID/g were extrapolated. In parallel, product stability was tested by radio HPLC at the same post-synthesis time points. ***Results:*** Tumor uptake did not vary according to the time post-synthesis or the injected dose, as assessed by both biodistribution and PET. Other specific ER+ organs (uterus and ovary by dissection, pituitary by PET) had slight uptake fluctuations through the post-synthesis time points but were non-significant. Non-specific tissues, such as blood pool, muscle and liver yielded consistent uptake regardless of the time after synthesis, and as such tumor-to-muscle ratio was also unaffected. PET image looked of equal quality irrespective of the post-synthesis time. Radio-HPLC analysis of the compound at different time did not reveal any sign of degradation. The injection of 10 kBq at 20 hours post-synthesis yielded a normal biodistribution and tumor uptake, despite the large excess of decayed by-products which are likely to have low or nonexistent affinity for ER. ***Conclusion:*** 4FMFES can generate optimal PET images up to at least 6 hours after radiosynthesis. This breakthrough will increase the clinical throughput per synthesis, decrease the cost per scan and allow loco-regional distribution of the tracer. ***References:*** None

EP-262

Isotonic saline and dimethylsulfoxide differentially affect motor behavior and nigrostriatal and mesolimbic D2 receptor binding in the rat

S. Nikolaus[1], *H. Wittsack*[1], *M. Beu*[1], *C. Antke*[1], *H. Hautzel*[2], *Y. Mori*[1], *E. Mamlins*[1], *G. Antoch*[1], *H. Müller*[1];
[1]*University Hospital Düsseldorf, Düsseldorf, GERMANY,*
[2]*University Hospital Essen, Essen, GERMANY.*

Aim/Introduction: In scientific investigations, including behavioral and in vivo imaging studies on small laboratory animals, treatment effects are generally related to a "baseline", which is either the state before or after the pharmacological intervention, or the state induced by the administration of the "vehicle". In the present study, D2 receptor (R) binding was determined with small animal SPECT with no precedent treatment (BAS) and after challenge with isotonic saline (SAL) and dimethylsulfoxide (DMSO). ***Materials and Methods:*** In 51 male Wistar rats, D2R binding was measured either in BAS or after injection of SAL (0.9%, 1 ml/kg i.p.) or DMSO (100%, 0.5 mg/kg ip). Motor activity (travelled distance) was analyzed for 30 min after SAL and DMSO with EthoVisionXT. Subsequent to behavioral tests, rats were injected Iodine-123-IBZM (30±5MBq iv). Imaging data were acquired with the TierSPECT starting at 74 min post-challenge. Additionally, all rats were scanned with a dedicated small animal MRI (MRS3000 Pre-clinical MRI, 3.0 T, MR Solutions, Guildford, UK). Based on the Paxinos rat brain atlas, regions of interest were defined on SPECT-MRI overlays. Binding potentials (BPs) were computed for each condition in various regions (nucleus accumbens, caudateputamen, substantia nigra, thalamus, frontal, motor and parietal cortex, anterior and posterior hippocampus), for which the presence of D_2Rs has been confirmed. ***Results:*** After SAL, BPs were decreased in nucleus accumbens (p=0.011), caudateputamen (p=0.005) and thalamus (p=0.031) relative to BAS and decreased in nucleus accumbens (p=0.028) and caudateputamen (p=0.028) relative to DMSO. After DMSO, the BP was diminished relative to BAS in the posterior hippocampus (p=0.016). The distance travelled in the open-field was increased after SAL releative to DMSO (p≤0.0001). ***Conclusion:*** Findings show that vehicles may differentially affect motor activity and D2R binding in relevant regions of the nigrostriatal and mesolimbic system. This must be considered after treatment with substances dissolved in SAL as well as when comparing substances dissolved in different vehicles. ***References:*** None

EP-36

Preclinical Studies -> Preclinical Studies -> Preclinical Cardiology and Neurology

e-Poster Area

EP-263

Microglial activation in the right amygdala-entorhinal-hippocampal complex is associated with improved spatial learning in App^{NL-G-F} mice

G. Biechele[1], K. Wind[1], T. Blume[2], C. Sacher[1], L. Beyer[1], F. Eckenweber[1], S. Lindner[1], F. Gildehaus[1], B. von Ungern-Sternberg[1], S. Tahirovic[2], M. Willem[3], C. Haass[2], P. Bartenstein[1], P. Cumming[4], A. Rominger[4], J. Herms[1], M. Brendel[1];
[1]University Hospital of Munich, Munich, GERMANY, [2]DZNE Munich, Munich, GERMANY, [3]Biomedical Center LMU Munich, Munich, GERMANY, [4]Inselspital Bern, Bern, SWITZERLAND.

Aim/Introduction: Asymmetries of neuropathology, including β-amyloid burden and microglial activation, in patients of Alzheimer`s disease (AD) are a well-known phenomenon. Recently we described a high frequency of asymmetric plaque burden and microglial activation in amyloid mouse models of AD as assessed by positron-emission-tomography (PET). Though yet, it has not been investigated, if there is a correlation between asymmetry of neuropathology and spatial learning performance in β-amyloid mouse models. ***Materials and Methods:*** Cross-sectional 18 kDa translocator protein (TSPO-PET, ^{18}F-GE-180) and β-amyloid-PET (^{18}F-florbetaben) scans of 30 App^{NL-G-F} mice (15 female, 15 male) were acquired at 10.3±0.6 months of age. Spatial learning was assessed by Morris water maze within two weeks before or after PET scanning. PET and spatial learning results were correlated by voxel-wise and bilateral region-based (frontal cortex, entorhinal/piriform cortex, amygdala and hippocampus) analyses. Control data was obtained from 18 age- and sex-matched C57Bl/6 wild-type mice. Spatial learning results were compared between App^{NL-G-F} mice with left and right lateralization of PET quantification. ***Results:*** App^{NL-G-F} mice revealed association clusters of improved spatial learning performance with higher TSPO-PET signals in the amygdala, entorhinal and piriform cortices, the hippocampus and the hypothalamus. Region based quantification indicated significant correlations between TSPO expression and spatial learning in the right entorhinal/piriform cortex (escape latency: R = -0.441, p = 0.017; frequency: R = 0.529, p = 0.003) and the right amygdala (frequency: R = 0.377, p = 0.044), whereas associations in the left hemisphere did not reach significance. β-amyloid-PET showed no relevant associations with spatial learning. App^{NL-G-F} mice with right lateralized TSPO expression in the amygdala showed improved performance in Morris water maze when compared to mice with left lateralization, independently of absolute bilateral TSPO expression and amyloidosis (escape latency: 9.1 [0.6 - 17.6] vs. 22.4 [17.2 - 27.5] seconds, $F_{(1,25)}$ = 7.470, p = 0.011; platform frequency: 4.4 [3.3 - 5.5] vs. 2.8 [2.2 - 3.5] seconds, $F_{(1,25)}$ = 6.503, p = 0.017). ***Conclusion:*** Microglial activation in the right amygdala-entorhinal-hippocampal complex of App^{NL-G-F} mice is associated with improved spatial learning. Our findings provide new insights into the lateralized nature of hemispheric predominance of neuropathology and its consequences for cognitive function. ***References:*** None

EP-264

The heterogeneous effect of chronic hyperglycaemia on brain 18F-FDG uptake: an experimental study

A. Miceli[1], M. Donegani[1], S. Raffa[1], S. Marra[1], V. Cossu[1], L. Emionite[1], S. Morbelli[1], C. Marini[2], G. Sambuceti[1], M. Bauckneht[3];
[1]DISSAL, Genoa, ITALY, [2]CNR Institute of Molecular Bioimaging and Physiology (IBFM), Milan, ITALY, [3]IRCCS Ospedale Policlinico San Martino, Genoa, ITALY.

Aim/Introduction: Hyperglycaemia severely influences the quality of 18F-FDG PET images due to a competitive mechanism lowering brain metabolic signal. It's debated if this reduction is regional rather than uniform and if it can reduce the accuracy of reporting when evaluating neurodegenerative diseases. Indeed, previous studies showed that hyperglycaemia lowers 18F-FDG uptake preferentially in the posterior cortical areas, thus mimicking an Alzheimer-like (AD) pattern. However, other authors suggested that the regional hyperglycemia effect is negligible and mostly dependent on the images normalization method. The present experimental study aims to evaluate if chronic hyperglycaemia can produce different metabolic effects according to the brain region. ***Materials and Methods:*** 40 mice were enrolled (23 with streptozotocin-induced type-I diabetes -STZ- and 17 healthy controls) and submitted to a dynamic 18F-FDG PET scan lasting 50 minutes. Induced diabetes was tested using the OGTT curve in STZ mice. The serum glycaemic level was tested few minutes before the scan in each animal. Image analysis was performed employing PMOD application. Three different volumes of interest (VOI) were manually placed, named whole brain (WB), anterior cortex (ANT), and posterior cortex (POST), respectively. SUV_{avg} and $mrGLU_{avg}$ data were extracted. The ratio between anterior cortex to the whole brain (A/WB), posterior cortex to the whole brain (P/WB), and posterior to the anterior cortex (P/A) were also calculated to normalize obtained results. ***Results:*** While OGTT curve confirmed diabetes in all STZ mice, the serum glycaemic level at the time of imaging was 105±37 and 88.7±27.2 mg/dl in STZ and controls, respectively (p=ns). WB-$mrGLU_{avg}$ was significantly reduced in the STZ group compared to controls (p<0.01). Moreover,

when compared to healthy mice, the A/WB $mrGLU_{avg}$ was higher in the STZ group ($p<0.01$), while P/WB and the P/A ratio were considerably lower ($p<0.001$). Similarly, while WB-SUV_{avg} was only slightly lower in STZ ($p=ns$ vs. controls), A/WB-SUV_{avg} was significantly higher in this subgroup ($p<0.01$ vs. controls). In contrast, P/WB and P/A SUV_{avg} were significantly lower ($p<0.01$ vs. controls). ***Conclusion:*** Chronic hyperglycaemia, rather than pre-injection episodic hyperglycaemia, heterogeneously affects brain regional FDG uptake. In particular, it selectively lowers the posterior cortical metabolic activity. The difference in the local brain cytoarchitecture may cause an impact on the expression of glucose transporters and hexokinase activity, thus determining a regional variation in the lumped constant. This phenomenon may, ultimately, affect the accuracy of reporting when 18F-FDG PET is performed in humans for suspected neurodegenerative diseases. ***References:*** None

EP-265

Metabolic changes in an animal model of Amyotrophic Lateral Sclerosis by [^{18}F]-Fluorodeoxyglucose

B. Giacobbo, T. Mediavilla, J. Axelsson, M. Ericsson, D. Marcellino, F. Sultan;
Umeå University, Umeå, SWEDEN.

Aim/Introduction: Amyotrophic Lateral Sclerosis (ALS) is a fatal neurodegenerative disorder that affects motor neurons, leading to muscle atrophy, paralysis, and eventually respiratory failure. As with many other neurodegenerative disorders, neuronal apoptosis is often associated with a loss of neuronal function and metabolic changes. [^{18}F]-FDG is a well-validated biomarker to observe metabolic changes in several brain disorders in humans, but its use in preclinical ALS research is not yet widespread. We aim to compare [^{18}F]-FDG uptake in SOD1^{G93A} and wild-type before the development of terminal ALS symptoms. ***Materials and Methods:*** animals (6 SOD1^{WT}, 7 SOD1^{G93A}) were previously genotyped for mutant SOD1 using qPCR. When SOD1^{G93A} animals started to develop ALS-like symptoms, animals were fasted for 4 hours and then injected intravenously with [^{18}F]-FDG (injected dose of 10.8±2 MBq). One hour after injection, animals were placed in a microPET-CT scanner (Mediso nanoPET-CT) and scanned (5 minutes for CT, 10 minutes for PET). CT data was used for attenuation correction. After reconstruction, data were coregistered to an MRI template and brain VOIs were created for several regions and divided between left and right hemispheres using the Allen mouse brain atlas as a VOI template and the uptake of each ROI was calculated to the whole-brain (SUVR) with T-test. $P<0.05$ was used for statistical significance. ***Results:*** Our SUVR data suggest a significant metabolic deregulation in SOD1^{G93A} animals when analyzing [^{18}F]-FDG in the brain. There was significant hypometabolism in anterior cingulate cortex (9% decrease in SOD1^{G93A} vs. SOD1^{WT} for both left and right hemispheres), in left entorhinal cortex (14% decrease), left hippocampus (12% decrease), right nose-associated primary somatosensory cortex (6% decrease), left supplementary somatosensory cortex (8% decrease), thalamus (11% and 8% for left and right, respectively), and right vermal region of the cerebellum (9% decrease). Hypermetabolism was, on the other hand, found in pallidum (12% increase in SOD1^{G93A} vs. SOD1^{WT}), lateral amygdala (41% and 64% increase in left and right, respectively), and cortical amygdala (98% increase for both left and right). ***Conclusion:*** These preliminary findings suggest a significant metabolic deregulation in animals with mutant SOD1 that develop ALS disease. Since animals were scanned after developing ALS symptoms, further studies aimed to study brain metabolism with [^{18}F]-FDG in prodromal stages of disease are warranted. This would provide us better insight into the usefulness of metabolic radiotracers for the detection of disease onset and progression, as well as the efficacy of therapeutic treatment strategies. ***References:*** None

EP-266

Quercetin as a potential psychotherapeutic agent in a mouse model with acute exposure to cocaine: a preclinical PET study

F. Ribeiro[1], *C. Nicolucci*[2], *M. Lapo Pais*[3,4,5], *A. C. Santos*[4,5,6], *P. M. C. C. Encarnação*[1], *A. L. M. Silva*[1,7], *I. F. Castro*[7], *P. M. M. Correia*[1,7], *V. I. Assunção*[1], *J. F. C. A. Veloso*[1], *D. G. Priolli*[2];
[1]*Institute for Nanostructures, Nanomedelling and Nanofabrication (i3N), University of Aveiro, Aveiro, PORTUGAL,* [2]*Multidisciplinary Research Laboratory, São Francisco University, Bragança Paulista, BRAZIL,* [3]*Faculty of Sciences and Technology, University of Coimbra, Coimbra, PORTUGAL,* [4]*Institute for Clinical and Biomedical Research (iCBR), Center for Innovative Biomedicine and Biotechnology (CIBB), Coimbra, PORTUGAL,* [5]*Institute of Biophysics, University of Coimbra, Coimbra, PORTUGAL,* [6]*Faculty of Medicine, University of Coimbra, Coimbra, PORTUGAL,* [7]*Radiation Imaging Technologies Lda (RI-TE), Ílhavo, PORTUGAL.*

Aim/Introduction: The use of cocaine is increasing worldwide and currently represents one of the most frequent indications for drug treatment. Although cocaine chronic addiction shows neurovascular complications associated with high morbidity and mortality rates, its recreational use, leading to addicted consumption, is often neglected. In the absence of a specific treatment for addiction, there is an urgent need to develop therapeutic alternatives, having also a brain-protective effect from injuries caused by cocaine abuse. Flavonoids are pharmacological bases of drugs used to treat drug addiction, having antioxidant, neuroprotective, neurovascular, GABAergic and benzodiazepine properties. Quercetin, a flavonoid found in fruits and vegetables, has unique biological properties that can improve mental/physical performance and reduce infection risk, also acting

as an important antioxidant, a blocker of neuronal toxicity and neurovascular changes[1]. This work aims to assess the functional activity of quercetin as a protective psychotropic drug, in animals exposed to a single and low dose of cocaine. ***Materials and Methods:*** A total of 48 male Balb/c (6 weeks) mice were randomly divided into 4 groups according to the administration of Saline (0.9%), Cocaine (0.5mg/kg), Quercetin (50mg/kg) or Cocaine followed by Quercetin (referred dosages). Behaviour tests (Open Field Maze) were performed for functional analysis. Mice underwent ^{18}F-FDG PET imaging using the easyPET.3D scanner (RI-TE Lda, Portugal[2]) to assess brain glucose metabolic activity according to the stimuli. Anatomopathological studies were performed to ascertain morphological brain changes. ***Results:*** Mice receiving quercetin or cocaine revealed similar global behaviour, while the ones receiving quercetin after exposure to cocaine showed similar behaviour to controls, in tests which identify the level of anxiety or avoidance. The easyPET.3D images revealed a higher ^{18}F-FDG uptake mainly in the striatum for the quercetin or cocaine groups, while the cocaine group associated with quercetin was similar to controls. The hippocampus region and prefrontal cortex of animals exposed to cocaine presented morphological changes, which were minimized when quercetin was administered immediately after cocaine. For the first time, it has been demonstrated that cocaine, even in single and low doses, has the potential to induce structural neurological damage[3,4]. ***Conclusion:*** In vivo ^{18}F-FDG PET imaging proved to be a crucial tool to measure the brain metabolic activity resulting from the stimuli to which mice were exposed. Quercetin proved to be a neuropsychoprotective agent against this exposure. Cocaine changes, both in behaviour and brain structure, must be considered regardless of the used dosage. ***References:*** 1.doi:10.2174/1871527317666171221110139 2.WO2016147130(PCT/IB2016/051487), www.ri-te.pt 3.doi:10.1038/npp.2017.109 4.doi:10.3389/fpsyt.2017.00218

EP-267

Preliminary Evaluation of (S)-7-[^{18}F]Fluorotryptophan as a Tracer for the Imaging of Serotonin Synthesis in Pig Brain

V. Shalgunov[1,2], *N. R. Raval*[3], *L. L. Donovan*[3], *A. Nasser*[3], *B. D. Zlatopolskiy*[4], *B. Neumaier*[4], *G. M. Knudsen*[3], *M. M. Herth*[1,2]; *[1]Department of Drug Design and Pharmacology, Faculty of Health and Medical Sciences, University of Copenhagen, Copenhagen, DENMARK, [2]Department of Clinical Physiology, Nuclear Medicine & PET, Copenhagen University Hospital, Rigshospitalet, Copenhagen, DENMARK, [3]Neurobiology Research Unit and CIMBI, Rigshospitalet and University of Copenhagen, Copenhagen, DENMARK, [4]Institute of Neuroscience and Medicine, Forschungszentrum Jülich, Jülich, GERMANY.*

Aim/Introduction: Tryptophan is an essential amino acid of key importance for brain function. It is a precursor of the neurotransmitter serotonin. ^{11}C-labeled tryptophan analogs (e.g. [^{11}C]AMT and [^{11}C]HTP) have been used to measure serotonin synthesis by positron emission tomography (PET) both clinically and preclinically [1].However, complicated synthesis procedures and short half-life of carbon-11 limit the potential scale of application for these tracers. Recently, (S)-7-[^{18}F]-fluorotryptophan (7-[^{18}F]FTrp), a tracer labeled with a longer-lived fluorine-18 and prepared via a simple ^{18}F-fluorination-deprotection scheme, was reported. In rats, 7-[^{18}F]FTrp showed good brain penetration and accumulated in the raphe nuclei - known area of serotonin production [2]. We assessed the brain uptake of 7-[^{18}F]FTrp in pigs and investigated if fenfluramine, a drug that depletes neurons of serotonin, could increase 7-[^{18}F]FTrp binding in the raphe nuclei. Serotonin transporter tracer [^{11}C]DASB was used to locate the raphe nuclei, which have high densities of the serotonin transporter. ***Materials and Methods:*** 7-[^{18}F]FTrp was prepared as described in [2] with slight modifications. [^{11}C]DASB was prepared as described in [3]. Anesthetised pigs (~20 kg body weight) received bolus injections of either [^{11}C]DASB (478 MBq, 1.06 nmol, N=1) or 7-[^{18}F]FTrp (194-486 MBq, 1.17-2.7 nmol, N=2). The pigs were subsequently PET-scanned for either 120 min ([^{11}C]DASB) or 180 min (7-[^{18}F]FTrp). Uptake of 7-[^{18}F]FTrp in the brain was investigated at baseline and after a within-scan challenge with fenfluramine (0.5 mg/kg, given intravenously 60 min after tracer injection). Arterial blood samples were analyzed for radioactivity and radiometabolites to obtain an input curve. ***Results:*** Preparation of 7-[^{18}F]Trp lasted 100-110 min, producing 7-[^{18}F]FTrp in RCY of 30-40% from dried [^{18}F] fluoride with molar activity of 70-425 GBq/µmol at end of synthesis. In the porcine brain, 7-[^{18}F]FTrp accumulated in the raphe nuclei (to SUV 0.8-0.9). Fenfluramine injection did not influence 7-[^{18}F]FTrp uptake in the raphe nuclei. ***Conclusion:*** 7-[^{18}F]FTrp penetrates the porcine blood-brain barrier and accumulates in the raphe nuclei where serotonin synthesis is known to take place. However, treatment with fenfluramine had no discernible effect on 7-[^{18}F]FTrp uptake in that region. In order to conclusively demonstrate that 7-[^{18}F]FTrp uptake in the raphe nuclei reflects serotonin synthesis rate, other methods to manipulate serotonin synthesis are being tested. ***Acknowledgements:*** This work was supported in part by DFG (grant: ZL 65/3-1). ***References:*** 1. Visser AKD et al. Eur J Nucl Med Mol Imaging. 2011;38:576-91. 2. Zlatopolskiy BD et al. J Med Chem. 2018;61:189-206. 3. Houle S et al. Eur J Nucl Med 2000;27:1719-22.

EP-268

Social stress-dependent changes on behavior and inflammatory parameters in animals with HPA-axis disruption

B. Giacobbo[1], *R. Moraga-Amaro*[2], *L. Reali Nazario*[2], *A. Schildt*[2], *R. A. J. O. Dierckx*[2], *J. Doorduin*[2], *E. F. J. de Vries*[2]; *[1]Umeå University, Umeå, SWEDEN, [2]University Medical*

Center Groningen, Groningen, NETHERLANDS.

Aim/Introduction: Chronic stress is associated with a deregulation of the hypothalamus-pituitary adrenal (HPA) axis and can result in behavioral abnormalities, such as depressive behavior. Adrenalectomy (ADX) inhibits the production and release of corticosterone, impairing the response towards stressors, and thus may prevent stress-induced depressive behavior. We aim to determine behavioral and neuroinflammatory effects of HPA-axis disruption via bilateral adrenalectomy (ADX) in animals submitted to repeated social defeat (RSD). ***Materials and Methods:*** 8-weeks old male Wistar rats were divided into four groups: ADX+RSD; ADX+Control; Sham+RSD; Sham+Control. Seven days after ADX surgery, animals were submitted to a 5 days RSD or Control protocols. One- and two days after the last RSD trial, animals went through an open field and social interaction test, respectively. 14 days after RSD, animals went through a 30 minutes [^{11}C]-PBR28 scan for microglia activation. Multifactorial ANOVA was performed for statistical assessment. ***Results:*** There was a significant effect of RSD (p=0.038) and ADX (p=0.049) on the social interaction of the animals, as well as an interaction between surgery and RSD (p=0.042). Post-hoc analysis showed a significantly lower social interaction of Sham+RSD when compared with the other groups (vs. Control+ADX, p=0.032; Control+Sham, p=0.023; ADX+RSD, p=0.035). Open field analysis showed no anxiety-like behavior nor locomotion effect of RSD or ADX (p>0.05). Microglial activation assessed through [^{11}C]-PBR28 also showed no effect of RSD or ADX (p>0.05). ***Conclusion:*** HPA-axis signaling disruption is able to counterbalance the impairment on the social behavior of these animals. In contrast, no effects of ADX or RSD were observed in other behavioral paradigms. Neuroinflammation was also not observed two weeks after the RSD, suggesting that the inflammatory response of microglial cells is too mild to be detected by PET or that neuroinflammation was only transient and already resolved at the time of measurement. ***References:*** None

EP-269

A Single Day of Accelerated rTMS Causes No Cerebral Glucose Metabolism Change Assessed by FDG-PET in Beagle Dogs

Y. Xu[1], *R. Dockx*[1], *B. J. G. Broeckx*[2], *A. Dobbeleir*[3], *K. Peremans*[3], *J. H. Saunders*[3], *C. Baeken*[1];
[1]*Department of Psychiatry and Medical Psychology, Faculty of medicine and health sciences, Ghent University, Ghent, BELGIUM,* [2]*Department of Nutrition, Genetics and Ethology, Faculty of veterinary medicine, Ghent University, Merelbeke, BELGIUM,* [3]*Department of Veterinary Medical Imaging and Small Animal Orthopedics, Faculty of veterinary medicine, Ghent University, Merelbeke, BELGIUM.*

Aim/Introduction: Repetitive transcranial magnetic stimulation (rTMS) is an FDA-approved technique for major depressive disorders (MDD), but the underlying neurobiological mechanisms of action are not yet unraveled, and the stimulation parameters need to be optimized. According to our previous research, rTMS applied to the left frontal cortex alters regional cerebral perfusion in dogs using HMPAO-SPECT; more, the serotonin transporter (SERT) binding indices alterations in different brain regions were reported with [^{11}C]DASB-PET. Similar changes have been observed in humans. This strengthens the idea that further functional imaging techniques in dogs could be used to investigate the neurobiological mechanism and refine the rTMS treatment parameters and efficacy. This study aims to investigate the effect of one-day rTMS on cerebral glucose metabolism by FDG-PET in healthy beagle dogs. ***Materials and Methods:*** Twelve beagle dogs were randomly divided into two unequal groups: five active high frequency (HF) rTMS (20Hz) sessions (n=8) and five sham sessions (n=4). The protocol for each dog is: an anatomical magnetic resonance imaging (MRI) scan and neuronavigation were conducted to locate the left frontal cortex; FDG-PET scan was applied before and 24-hour, 1-month and 3-month after the rTMS treatment; A linear mixed model and a likelihood ratio test were used to evaluate significance of the interaction. ***Results:*** No significant differences in glucose metabolism between active and sham accelerated HF rTMS were noted for just after the stimulations (24h), nor for the stimulated area, the left frontal cortex, or other brain regions compared to the baseline. And no long-term metabolic change was noticed in both active and sham group. ***Conclusion:*** Though the single day of accelerated HF rTMS study did not show a significant cerebral glucose metabolism change in beagle dogs, probably due to the limited rTMS sessions and the relatively small sample size, additional accelerated HF rTMS days should be added to evaluate the effects of accelerated HF-rTMS treatment in beagles. ***References:*** None

EP-37

Preclinical Studies -> Preclinical Studies -> Preclinical Oncology

e-Poster Area

EP-270

Feasibility of PET-guided surgery with ^{64}Cu-labeled-cetuximab for intraoperative resection of residual tumors in an orthotopic pancreatic tumor mouse model

Y. Yoshii[1], *C. Igarashi*[1], *H. Tashima*[1], *Y. Iwao*[1], *E. Yoshida*[1], *H. Wakizaka*[1], *G. Akamatsu*[1], *T. Yamaya*[1], *H. Matsumoto*[2], *M. Yoshimoto*[3], *F. Hihara*[1], *T. Tachibana*[1], *M. Zhang*[1], *K. Nagatsu*[1], *A. Sugyo*[1], *A. B. Tsuji*[1], *T. Higashi*[1];
[1]*National Institutes for Quantum and Radiological Science and*

Technology, Chiba, JAPAN, [2]Nihon Medi-Physics Co., Ltd., Tokyo, JAPAN, [3]National Cancer Center Hospital East, Kashiwa, JAPAN.

Aim/Introduction: Pancreatic cancer (PC) has one of the poorest prognoses among all types of cancer. Surgery is the standard treatment for patients with resectable PC. However, positive resection margins were often found after surgery, which is associated with increased local recurrence and decreased survival in PC patients. Therefore, development of methods to observe spread of PC lesion within the pancreas under surgery is quite significant. We have developed a novel open-typed positron emission tomography (PET) system (called "OpenPET"), which enables high-resolution PET-guided surgery in real time. Our previous study has also demonstrated that the OpenPET-guided surgery with ip-administered ^{64}Cu-labeled anti-epidermal growth factor receptor (EGFR) antibody cetuximab was useful to detect and resect PC in a small (less than 1 cm) resectable PC orthotopic xenograft mouse model (Yoshii et al. Scientific Reports 2020). In the present study, we further investigated usefulness of the OpenPET-guided surgery for intraoperative detection and resection of residual tumors using a locally advanced PC (over 1 cm) orthotopic xenograft mouse model. ***Materials and Methods:*** To make the model, the cell suspension of human PC xPA cells stably expressing red fluorescent protein (xPA-RFP) (5×10^6) with an extracellular matrix were injected into the mouse pancreas at 1 week before the experiments. ^{64}Cu-labeled-cetuximab (7.4 MBq / mouse) was intraperitoneally administered and the OpenPET-guided surgery was performed 24 h later (n=7). One-pass list-mode DRAMA (dynamic row-action maximum-likelihood algorithm) on graphics processing unit was used for high-speed reconstruction, which enables updating cycle of image less than one second while accumulating list-mode data. ***Results:*** The OpenPET-guided surgery was able to detect and resect not only primary tumors but also small residual tumors during the surgery. In this experiment, 10 residual tumor specimens were isolated in total with OpenPET guidance; 3 tumors were 10-5 mm and 7 tumors were 5-3 mm in size. The all isolated tumor specimens by the OpenPET-guided surgery were detected tumor RFP signals. In contrast, the naked eyes could not clearly identify location of these tumors within the pancreas in this model. ***Conclusion:*** We demonstrated the feasibility of OpenPET-guided surgery with ^{64}Cu-labeled-cetuximab for intraoperative resection of residual tumors in the orthotopic PC mouse model. This technology would be useful to avoid the occurrence of positive resection margins in PC during surgery. ***References:*** Yoshii et al. Immuno-OpenPET: a novel approach for early diagnosis and image-guided surgery for small resectable pancreatic cancer. Scientific Reports 2020. in print.

EP-271

In vivo imaging of mast cell infiltration to lung cancer lesion by sodium iodide symporter gene

Y. Jeon[1], *J. Lee*[1], *S. Kim*[1], *S. Lee*[2];
[1]Laboratory Animal Center, Daegu-Gyeongbuk Medical Innovation Foundation, Daegu, KOREA, REPUBLIC OF, [2]Kyungpook National University, Daegu, KOREA, REPUBLIC OF.

Aim/Introduction: Herein, we demonstrated the mast cell infiltration into lung cancer lesion in living mice using sodium iodide symporter gene (NIS) and I-124 Positron emission tomography-computed tomography (PET/CT). ***Materials and Methods:*** Murine mast cell line MC-9 cells was transduced with lentivirus co-expressing NIS and enhanced green fluorescent protein (EGFP), which called as MC-9/NG cells. Iodide uptake was determined in MC-9/NG cells with inhibition study of $KClO_4$. Cell proliferation of luciferase expressing Lewis Lung Cancer (LLC/Luc) cells was evaluated in the presence of serum free media (SFM) or conditioned media (CM) of MC-9/NG cells using a bioluminescence imaging (BLI). The migration ability of MC-9/NG cells was evaluated in the presence of SFM or CM of LLC cells. LLC-tumor bearing mice received MC-9/NF cells via retro-orbital injection and its migration to tumor lesion was determined with I-124 PET/CT, which was accompanied by bio-distribution analysis. ***Results:*** Iodide uptake was higher in MC-9/NG cells than in MC-9 cells and increased iodide uptake in MC-9/NIS cells was inhibited by $KClO_4$ treatment. In vitro BLI showed higher proliferation of LLC/Luc cells in CM of MC-9 cells than SFM. Trans-well migration assay revealed enhanced mast cell migration in CM of LLC cells than SFM as a negative control. In vivo I-124 PET/CT imaging demonstrated the infiltrated MC-9/NIS cells to lung tumor lesion at 24h post-transfer, which was consistent with the finding of bio-distribution analysis. ***Conclusion:*** These finding suggest that sodium iodide symporter is feasible nuclear medicine reporter gene to visualize the biological behavior of mast cells in living mice with lung tumor. The mast cell imaging with nuclear medicine reporter gene enables us to better understand their biological role in tumor microenvironment. ***References:*** None

EP-273

Relevance of molecular tracer based on Fludarabine for detection and monitoring of primary brain lymphomas evolution

V. Tran[1], *S. Antoine*[2,3], *M. Mekhfi*[1], *G. Torquet*[1], *F. Assayag*[2,3], *F. Pouzoulet*[3], *F. Caillé*[1], *B. Kuhnast*[1], *A. Kas*[4], *V. Lebon*[1], *C. Soussain*[2], *C. Truillet*[1];
[1]Université Paris-Saclay, CEA, CNRS, Inserm, BioMaps, Orsay, FRANCE, [2]Institut Curie, Site de Saint-Cloud, Saint-Cloud, FRANCE, [3]Institut Curie, PSL Research University, Translational Research Department, Experimental Radiotherapy Platform, Orsay, FRANCE, [4]AP-HP Sorbonne

Université, Pitié-Salpêtrière hospital, Department of Nuclear Medecine, and LIB, Inserm U1146 F-75013, Paris, FRANCE.

Aim/Introduction: [^{18}F]Fludarabine ([^{18}F]Fluda) appears to be a promising PET tracer for detecting specifically different types of B-cell non-Hodgkin lymphoma. It also showed less susceptibility to inflammation-induced false-positive and much lower basal signal in normal brain tissue compared to [^{18}F]FDG.[1,2] In this study, we investigated the potential of this tracer to evaluate over time the progression of primary central nervous system lymphoma (PCNSL) in an orthotopic xenograft mouse model. Detailed whole body pharmacokinetic characterization was performed. We have also investigated the ability to monitor the pharmacological change on PCNSL under the effect of a Bruton Tyrosine Kinase inhibitor (Ibrutinib) using [^{18}F]Fluda. ***Materials and Methods:*** TMD8 human lymphoma cells were injected into the right striatum of the NMRI nude mice. A three-week longitudinal study (n = 8) was conducted in tumor-bearing mice by i.v. injecting [^{18}F]Fluda (364.3 ± 12.9 kBq/g) using dynamic PET acquisitions. Tumor evolution was determined by SUVmax. The results were compared with [^{18}F]FDG PET scan. Tumor volume was determined by applying a threshold equal to SUV_{mean} + 2SD of $VOI_{cerebellum}$. Pixel-wise kinetic modeling was applied to calculate volume of distribution (V_T) images. Immunofluorescence (IF) was performed on frozen sections of mice brains using antibody against human CD20 overexpressed in malignant B-cells. Finally, the efficacy of daily oral dose of ibrutinib (60 mg/kg) was evaluated by [^{18}F]Fluda and [^{18}F]FDG imaging compared to placebo solution (n = 8 for each group). Survival rate in each group were monitored until humane endpoints were reached. ***Results:*** [^{18}F]Fluda provided higher tumor-to-background ratios than [^{18}F]FDG (1.7 ± 0.1 versus 1.2 ± 0.1). Tumor delineation on [^{18}F]Fluda PET images were confirmed by CD20 immunofluorescent images. Longitudinal [^{18}F]Fluda PET images showed a clear evolution of tumor volume and uptake of [^{18}F]Fluda from week 1 (V = 31.0 ± 12.8 mm^3, SUVmax = 0.37 ± 0.13) to week 3 (V = 152.0 ± 64.3 mm^3, SUV_{max} = 0.56 ± 0.18) post inoculation. V_T images confirm the specific binding of [^{18}F]Fluda to tumor. In ibrutinib treated group, the uptake of [^{18}F]Fluda is significantly lower than in placebo group, which correlated with the survival curves. ***Conclusion:*** Our results confirmed the potential of [^{18}F]Fluda for early diagnosis of B-cell lymphatic malignancies especially PCNSL as well as for evaluating therapeutic efficacy of new treatments for PCNSL such as Ibrutinib. ***References:*** 1. Hovhannisyan, N. et al. EJNMMI Res. 5, (2015). 2. Hovhannisyan, N., et al. Mol. Pharm. 13, 2136-2139 (2016).

EP-274

Comparative preclinical biodistribution, dosimetry and endoradiotherapy in mCRPC of ^{177}Lu-rhPSMA-7.3 and ^{177}Lu-PSMA I&T

N. Yusufi[1], *S. Nekolla*[1], *A. Wurzer*[2], *M. Herz*[1], *C. D'Alessandria*[1], *W. Weber*[1], *H. J. Wester*[2], *M. Eiber*[1];
[1]*Technical University Munich, Klinikum rechts der Isar, Department of Nuclear Medicine, Munich, GERMANY,*
[2]*Technical University Munich, Chair of Pharmaceutical Radiopharmacy, Garching, GERMANY.*

Aim/Introduction: Radiohybrid prostate-specific membrane antigen (rhPSMA)-ligands are currently under evaluation as prostate cancer theranostics. Based on preliminary experiments the single isomer rhPSMA-7.3 is regarded as a promising candidate for potential endoradiotherapy. The aim of this preclinical evaluation was to assess biodistribution, dosimetry and therapeutic efficacy of ^{177}Lu-rhPSMA-7.3 in comparison to with established therapeutic agent, ^{177}Lu-PSMA-I&T. ***Materials and Methods:*** Biodistribution of ^{177}Lu-rhPSMA-7.3 and ^{177}Lu-PSMA-I&T was performed in LNCap tumour bearing SCID-mice after sacrifice at defined time points up to 7 days (n=5). Organs and tumours were dissected, injected dose per gram (%ID/g) was determined and dosimetry calculations were performed using OLINDA/EXM1.0. The therapeutic efficacy of a single dose of 30 MBq ^{177}Lu-rhPSMA-7.3 (222.6 ± 49.7 mm^3; n=7) was compared with ^{177}Lu-PSMA-I&T (457.9 ± 286.1 mm^3; n=7) and control groups (n=6-7) using C4-2 tumour bearing SCID-mice by evaluating tumour growth, tumour uptake and survival over 7 weeks post treatment. ***Results:*** The biodistribution of ^{177}Lu-rhPSMA-7.3 revealed fast blood clearance (0.67 %ID/g at 1 h p.i.) and highest activity uptake in the spleen and kidneys, particularly in the first hours (35.63 %ID/g and 223.6 %ID/g, respectively at 1 h p.i.) indicating a renal excretion pathway. A similar longitudinal biodistribution pattern was shown for ^{177}Lu-PSMA-I&T with a higher initial blood level (3.05 %ID/g), but lower kidney uptake (165.5 %ID/g). Compared with ^{177}Lu-PSMA-I&T, ^{177}Lu-rhPSMA-7.3 exhibited an initially (1 h) 2.6-fold higher tumour uptake in LNCap xenografts and a longer retention (4.5 %ID/g vs. 0.9 %ID/g at 168 h). The tumour dose of ^{177}Lu-rhPSMA-7.3 was substantially higher (1.96E+03 mGy/MBq vs. 7.47E+02 mGy/MBq at a volume of 200 mm^3) compared with ^{177}Lu-PSMA-I&T, with similar effective doses for both ligands (6.93E-03 mSv/MBq vs. 7.81E-03 mSv/MBq). A single dose of ^{177}Lu-rhPSMA-7.3 showed a significantly higher tumour size reduction compared with ^{177}Lu-PSMA-I&T (abs. volumes: 170.3 ± 122.1 mm^3 vs. 712.2 ± 206.8 mm ^{3}, respectively; or relative change to initial volumes: 1.2 ± 0.8- vs. 6.2 ± 4.7-fold increase, respectively; p=0.0167). At the pre-defined termination of the experiment (43 days), 7/7 and 3/7 mice were still alive in the ^{177}Lu-rhPSMA-7.3 and ^{177}Lu-PSMA-I&T groups, compared with a median survival of 10.5 and 14 days for the control

groups. ***Conclusion:*** ^{177}Lu-rhPSMA-7.3 can be considered as suitable candidate for clinical translation due to the similar clearance kinetics and radiation dose, and the superior tumour uptake and retention compared with ^{177}Lu-PSMA-I&T. Preliminary treatment experiments showed favourable anti-tumour response. ***References:*** None

EP-275

Preclinical assessment of octreotate-IRDye800CW for tumor targeting in intracranial meningioma for molecular fluorescence guided surgery

B. Dijkstra[1], F. A. E. Kruyt[2], F. Andreae[3], S. E. Dulfer[1], M. C. Stroet[4], J. Nonnekens[4,5], W. F. A. den Dunnen[6], M. de Jong[4], R. J. M. Groen[1];
[1]Department of Neurosurgery, University Medical Center Groningen, University of Groningen, Groningen, NETHERLANDS, [2]Department of Medical Oncology, University Medical Center Groningen, University of Groningen, Groningen, NETHERLANDS, [3]piCHEM Forschungs und EntwicklungsGmbH, Raaba-Grambach, AUSTRIA, [4]Department of Radiology and Nuclear Medicine, Erasmus MC, Rotterdam, NETHERLANDS, [5]Department of Molecular Genetics, Erasmus MC, Rotterdam, NETHERLANDS, [6]Department of Pathology and Medical Biology, University Medical Center Groningen, University of Groningen, Groningen, NETHERLANDS.

Aim/Introduction: Meningiomas are the most frequently occurring primary intracranial tumors in adults. Although these tumors are most often benign, symptoms arise due to compression of brain tissue, leading to for example focal neurological deficits or mental status changes. Treatment is only curative with complete surgical resection, which is not possible in all cases. To facilitate safe and complete resection, intraoperative guidance should be optimized, e.g. by applying molecular fluorescence guided surgery (MFGS). This technique utilizes the targeting of a biomarker, which is overexpressed on meningiomas, with a fluorescent tracer. Somatostatin receptor type 2 (SST_2) is overexpressed on all meningiomas, regardless of WHO grade or subtype. In this study, SST_2 was targeted with tyr^3-octreotate-IRDye800CW. In order to investigate whether this compound can be applied in MFGS in intracranial meningiomas, we have determined binding affinity of this tracer in vitro, and tumor targeting and binding specificity in a mouse model. ***Materials and Methods:*** Binding affinity of octreotate-IRDye800CW was evaluated using displacement assays with H69 xenograft slides. ^{177}Lu-DOTATATE was displaced with various concentrations of DOTATATE or octreotate-IRDye800CW. For determining tumor targeting, 3µg octreotate-IRDye800CW was injected in (SST_2-positive) human H69 xenograft bearing mice. To evaluate binding specificity, H69 xenograft bearing mice were injected with 3mg DOTATATE and 3µg octreotate-IRDye800CW. As a control, (SST_2-negative) CH157MN xenograft bearing mice were injected with 3µg octreotate-IRDye800CW. In vivo imaging was performed using the FMT2500 at 1, 2, and 4 hours post injection. Mice were terminated after the last scan and tissues and organs were imaged ex vivo using two fluorescence imagers: the PEARL and OdysseyCLx. Lastly, SST_2-expression was determined using immunohistochemistry. ***Results:*** Octreotate-IRDye800CW showed an affinity of 72 nM, sufficient to support further in vivo testing. Fluorescence was blocked for 61.5±5.8% after the additional administration of 3mg DOTATATE. In the (SST_2-negative) CH157MN model, fluorescence was 81.5±8.7% lower compared with the (SST_2-positive) H69 model. Furthermore, in and ex vivo, fluorescence was mainly located in the tumor, kidneys, urine and liver, whereas the brain, skull, muscle, blood and skin showed low fluorescence intensity. The tumor-to-brain-ratio (TBR) was high: 24.4 (95%CI: 19.7-29.1). Lastly, fluorescence uptake was compared to SST_2 expression levels based on immunohistochemistry. ***Conclusion:*** Considering the binding affinity, SST_2-mediated tumor uptake, biodistribution and high TBR, octreotate-IRDye800CW seems very promising for clinical application in the future. It could potentially aid in safer and completer resection of meningioma tissue, especially in the high grade meningiomas or in complex anatomical localizations. ***References:*** None

EP-276

PET Imaging of Lung Cancer with $^{64}CuCl_2$: A Pilot Study

L. Jiang;
Shanghai Pulmonary Hospital, Shanghai, CHINA.

Aim/Introduction: Recently, human copper transporter 1 (CTR1) has been proven to be overexpressed in many types of cancer cells, and copper (II)-64 chloride ($^{64}CuCl_2$) has been used as an effective tracer for positron emission tomography (PET) imaging in tumor-bearing animal models. Thus, this study aimed to investigate the potential application of $^{64}CuCl_2$ in PET imaging of lung cancer through targeting CTR1. ***Materials and Methods:*** The expression of CTR1 in a series of lung cancer cell lines was measured by quantitative real-time polymerase chain reaction (Q-PCR), western blot, enzyme-linked immunosorbnent assay (ELISA), and immunofluorescent staining. Then in vitro cell uptake assay of $^{64}CuCl_2$ was investigated in lung cancer cell lines with different levels of CTR1 expression. And small animal PET imaging and quantitative analysis were performed in lung cancer tumor-bearing mice after intravenous injection of $^{64}CuCl_2$, respectively. ***Results:*** The CTR1 expression in multiple lung cancer cells was identified and confirmed, and lung cancer cell lines H1299 with high CTR1 expression, H460 with moderate CTR1, and H1703 with low CTR1 were selected for further experiments. In vitro cellular uptake assay displayed that the $^{64}CuCl_2$ uptake by these three kinds of cells was positive correlated with their CTR1 expressed levels. And the blocking experiments testified

the specificity of $^{64}CuCl_2$ to target CTR1. Moreover, small animal PET imaging and quantitative results showed that $^{64}CuCl_2$ accumulation in H1299, H460, and H1703 tumor-bearing mice was consistent with CTR1 levels and cell uptake experiments. ***Conclusion:*** The expression of CTR1 in lung cancer could be successfully visualized by $^{64}CuCl_2$ PET examination. With the expected growth of PET/CT examination to be an essential strategy in clinical lung cancer management, $^{64}CuCl_2$ has the great potential to be a promising PET imaging agent of lung cancer. ***References:*** None

EP-277

Influence of macrocyclic bifunctional chelators on Self-assembling supramolecular dendrimer nanosystem biodistribution and in pancreatic adenocarcinoma patient derived cells L-IPC

B. Louis[1], *L. Ding*[2], *Z. LYU*[2], *A. Moyon*[3], *A. Bouhlel*[1], *L. Balasse*[1], *S. Fernandez*[1], *J. Yifan*[2], *S. Simoncini*[4], *G. Hache*[3], *F. Dignat-George*[5], *L. Peng*[2], *P. Garrigue*[3], *B. Guillet*[3];
[1]*C2VN INSERM 1263 INRA 1260 CERIMED Aix-Marseille Université, Marseille, FRANCE,* [2]*CINaM CNRS, UMR 7325 Aix-Marseille Université, Marseille, FRANCE,* [3]*C2VN INSERM 1263 INRA 1260 CERIMED, APHM, Aix-Marseille Université, Marseille, FRANCE,* [4]*C2VN INSERM 1263 INRA 1260 Aix-Marseille Université, Marseille, FRANCE,* [5]*C2VN INSERM 1263 INRA 1260, APHM, Aix-Marseille Université, Marseille, FRANCE.*

Aim/Introduction: Because of EPR effect, dendrimers can preferentially accumulate in tumor tissues, this kind of nanotechnology constitute a tool in diagnostic probe development and in the future, in a possible nanotheranonostic strategy [1-6] Based on our previous nanotechnology developments for PET [7], this study aimed at developing [^{111}In]In-nanotechnology-based bioimaging and at optimizing dendrimers biodistribution in a human primary pancreatic adenocarcinoma tumor mice model, and therefore compared the influence of two macrocyclic bifunctional chelators (DOTA and NODAGA) enabling the modification of global nanoparticle surface charge. ***Materials and Methods:*** Both dendrimers were produced and radiolabeled with [^{111}In]$InCl_3$ in ammonium acetate buffer 1M, with a supplemental 15-minute 57°C heating for [^{111}In]In-DOTA-dendrimer. Radiochemical purities were assessed in 37°C human serum up to 48h after synthesis by radiochromatography on iTLC-SG paper and 0.1M sodium citrate buffer (pH=5). µSPECT/CT acquisitions were performed 2h, 24h and 48h p.i under isoflurane anesthesia in six-week-old L-IPC tumor-bearing mice (n=3) on a NanoSPECT/CT camera (Mediso). SPECT signal quantifications were performed on Vivoquant software (Invicro). Data were analyzed with 2way-ANOVA statistical test after being checked for normality. ***Results:*** Satisfying radiochemical purities over 93% were obtained up to 48 h after radiosynthesis. [^{111}In]In-NODAGA enabled a significant reduction of µSPECT signal quantification in the liver compared to that of [^{111}In]In-DOTA-dendrimer as soon as 2h post-injection (3.78 %ID/g ± 0.27 vs 6.02 %ID/g ± 0.32 ; ****P < 0.0001), maintained 24 h (3.14 %ID/g ± 0.19 vs 6.37 %ID/g ± 0.33; ****P < 0.0001) and 48 h post-injection (2.70 %ID/g ± 0.1 vs 5.74 %ID/g ± 0.85; ****P < 0.0001). Tumor-to-muscle ratio was significantly higher for [^{111}In]In-NODAGA-dendrimer at 48 h p.i. compared to [^{111}In]In-DOTA-dendrimer respectively 324.57 ± 35.3 and 212.47 ± 38.13 (**P =0.0052). Contrariwise, Tumor-to- liver ratio was significantly higher for [^{111}In]In-NODAGA-dendrimer 24 h p.i. (30.11 ± 3.37 vs 16.66 ± 0.61 ; ***P < 0.0007), 48 h p.i. (27.06 ± 4.09 vs 17.89 ± 1.56;**P = 0.0075). ***Conclusion:*** In line with previous results focusing on radiolabeled peptides or proteins, this SPECT study highlights the importance of chelator's influence for the biodistribution of radiolabeled nanoparticles [8-10]. These findings provide perspectives of importance in the field of nanotheranostics for reducing nanoparticle trapping in the liver. ***References:*** (1) https://doi.org/10.1002/smll.201600635.(2) https://doi.org/10.1021/am5036225.(3) https://doi.org/10.1259/bjr.20150207.(4) https://doi.org/10.1016/j.addr.2012.06.006.(5) https://doi.org/10.1016/j.biopha.2016.09.035.(6) https://doi.org/10.1038/natrevmats.2017.24.(7) https://doi.org/10.1073/pnas.1812938115.(8) https://doi.org/10.1039/c3cs60304k.(9) https://doi.org/10.1371/journal.pone.0070028.(10) https://doi.org/10.1039/C9CC07750B.

EP-278

The significance of intraperitoneal administration of 18F-FDG in a preclinical mouse model

Z. Ritter[1], *K. Zámbó*[1], *P. Balogh*[2], *D. Szöllősi*[3], *J. Xinkai*[2], *D. Dezső*[1], *H. Alizadeh*[4], *I. Horváth*[3], *N. Hegedűs*[3], *D. Máthé*[3], *E. Schmidt*[1];
[1]*University of Pécs, Department of Diagnostic, Division of Nuclear Medicine, Pécs, HUNGARY,* [2]*University of Pécs, Department of Immunology and Biotechnology, Pécs, HUNGARY,* [3]*Semmelweis University Faculty of Medicine, Department of Biophysics and Radiation Biology, Budapest, HUNGARY,* [4]*University of Pécs, 1st Department of Internal Medicine, Pécs, HUNGARY.*

Aim/Introduction: Bc-DLFL.1 is a novel spontaneous, reproduciable, well-characterized high-grade lymphoma isolated from BALB/c mice. After intraperitoneal inoculation this lymphoma attaches to the omentum and mesentery and shows dissemination towards the mesenteric lymph nodes. We aimed to compare detection methods for spreading of Bc-DLFL.1 lymphoma using in vivo FDG PET or ex vivo autoradiography of FDG. The results of these imaging techniques were compared with results of immunohistochemistry. ***Materials and Methods:*** BALB/c mice were used as lymphoma recipients aged between 8-12 weeks. One million lymphoma cells were injected intraperitoneally per animal. Twenty-four hours after

injection, FDG was administered either intravenously or intraperitoneally. In both groups we investigated nine animals. For the immunhistochemistry detection, ex vivo carboxyfluorescein (CFSE) labeled lymphoma cells were injected to each animal. This allowed immunohistochemical diagnosis of lymphoma presence using anti-FITC antibodies. In order to monitor the expansion of the tumor in a later stage, next we examined whether PET would allow lymphoma detection. To assess whole-body spread of the disease, one day and 6 days after lymphoma inoculation in 3-3 animals, FDG was administered intravenously and PET examination was performed. ***Results:*** We could not detect specific tracer accumulation with PET in the early stage (1 day post-inoculation) either by intraperitoneal or intravenous tracer administration. Autoradiography results were also negative after intravenous FDG injection, circumscribed accumulation of FDG could not be detected in the mesentery or omentum, whereas clearly marked selective foci were observed after intraperitoneal FDG treatment.To confirm these results with IHC, we have observed focal anti-FITC signals which were exactly corresponding to the distribution of FDG accumulating foci. While specific tracer accumulation could not be detected with these imaging methods in the early stage (1 day after lymphoma inoculation), we found that tracer accumulation could be clearly detected at a later stage of tumor growth (beyond day 6 post-injection) by intravenous administration of FDG. FDG accumulating lymphoma foci were observed in the enlarged mesenteric lymph nodes. ***Conclusion:*** Based on our results, it can be hypothesized that even with early adhesion of tumor cells in the abdomen, the delivery of FDG (glucose) into the cells intravenously is partially restricted. This highlights the importance of local use of FDG in diagnostic procedures for the diagnosis of early peritoneal manifestations or metastases of certain diseases (colon, stomach, ovary) and raises the importance of local therapy in addition to systemic treatments. ***References:*** None

EP-279

The Feasibility of ^{68}Ga Replacing ^{89}Zr for CAR T Cell PET Monitoring

X. Wang*, Y. Wang, D. Pan, Q. Wu, J. Liu, M. Yang;*
Jiangsu Institute of Nuclear Medicine, Wuxi, CHINA.

Aim/Introduction: Chimeric Antigen Receptor (CAR) T-cells are important players in immunotherapy for oncology. In vivo characterizations of the spatio-temporal distribution and homing dynamics of CAR-T-cells would facilitate the customization of treatment regimens. In vivo PET imaging of CAR-T-cells have been reported with radionuclides ^{89}Zr and ^{64}Cu, which have long half-life. Although long-term tracking of CAR-T-cells would offer more information about homing and distribution dynamics, the overdose of irradiation made it almost impossible in clinical translation. Thus, replacement of radionuclides with shorter half-life may overcome this challenge. Here, we use ^{68}Ga-oxine for CAR-T-cells labeling and track it in vivo for the first time. ***Materials and Methods:*** ^{68}Ga solution was obtained from ITG ^{68}Ge/^{68}Ga generator. After pH adjustment by 1 N NaAc, the ^{68}Ga solution was mixed with oxine solution to form ^{68}Ga-oxine. CAR-T-cells were then incubated with ^{68}Ga-oxine solution for radiolabeling. In vivo distribution was assessed by PET imaging in NSG mice. ^{89}Zr-oxine labeled CAR-T-cells were used as control. ***Results:*** ^{68}Ga-oxine labeled CAR-T-cells have good stability in FBS within several hours with cell viability >90%. The ^{68}Ga-oxine labeled CAR-T-cells mainly distributed in lung, liver and spleen, which was similar with that of ^{89}Zr-labeled CAR-T-cells. For ^{68}Ga-oxine labeled CART cells, the lung uptake (%ID/g) was decreased from 76.68±7.07 at 10 min to 35.72±4.27 at 4 h post intravenous injected (pi) with 1*10^6 cells per animal, the liver and spleen uptake (%ID/g) were up to 27.49±6.89 and 17.03±6.52 at 4 h pi. While for ^{89}Zr-labeled CAR-T-cells, lung uptake (%ID/g) was decreased from 85.57±26.28 at 10 min to 26.67±7.22 at 4 h pi, liver and spleen uptake (%ID/g) were 23.85±3.56 and 14.44±4.90 at 4 h pi, respectively. With time increased, the liver and spleen uptakes of ^{89}Zr-labeled CAR-T-cells kept high and stable until 48 h pi, still were 34.44±10.20 and 21.24±12.01, respectively. Significant correlation appeared between PET imaging with ^{68}Ga and ^{89}Zr-labeled CAR-T-cells, the Pearson correlation coefficient in lung, liver and spleen uptake were 0.780, 0.872 and 0.959, respectively. Early phase of CAR-T-cells distribution and migration monitoring with ^{68}Ga was similar with ^{89}Zr-labeled CAR-T-cells. Effective dose of total body irradiation for ^{68}Ga-labeled CAR-T-cells is 5.30E-02 mSv/MBq, which is 24-fold lower than that of ^{89}Zr-labeled CAR-T-cells. ***Conclusion:*** We successfully proposed ^{68}Ga-labeling for CAR-T-cells in vivo tracking by PET imaging. It can offer spatio-temporal distribution and homing dynamics information just like ^{89}Zr, but reduce the effective dose of total body irradiation substantially. ***References:*** None

EP-280

Multi-modal PET and MRI biodistribution studies of ^{89}Zr-labelled nanodiamonds in mice

N. Eberhardt[1]*, J. Löffler*[1,2]*, M. Raabe*[3]*, M. N. A. Alam*[3]*, H. Li*[2]*, A. Abaei*[2]*, H. Herrmann*[1]*, C. Solbach*[1]*, F. Jelezko*[4]*, T. Weil*[3]*, A. J. Beer*[1]*, V. Rasche*[5,2]*, G. Winter*[1]*;*
[1]Ulm University Medical Center, Department of Nuclear Medicine, Ulm, GERMANY, [2]Ulm University, Core Facility Small Animal Imaging, Ulm, GERMANY, [3]Max Planck Institute for Polymer Research, Synthesis of Macromolecules Department, Mainz, GERMANY, [4]Ulm University, Institute for Quantum Optics, Ulm, GERMANY, [5]Ulm University Medical Center, Department of Internal Medicine II, Experimental Cardiovascular Imaging, Ulm, GERMANY.

Aim/Introduction: Due to their biocompatibility,

nanodiamonds (ND) are of great interest for medical applications. They are chemically inert and can harbour nitrogen vacancies (NV-centres) that potentially facilitate highly sensitive MRI measurements after hyperpolarization. Protein-coating is used to provide coupling sites for ligands/therapeutics and to improve the biodistribution by appropriate masking. To evaluate and optimize these surface modifications, in vivo biodistribution studies of radiolabelled NDs were performed. Combined PET and MR imaging with image fusion allowed a quantitative localization of NDs in organs and tumour over time. ***Materials and Methods:*** PEGylated human serum albumin surface-coated fluorescent NDs (Ø100nm, Microdiamant, IOM Leipzig) were coupled with the chelator p-SCN-Bn-deferoxamine (Macrocyclics) and radiolabelled using zirconium-89 or gallium-68. Tumour xenografts of prostate carcinoma cell lines LNCaP C4-2 and PC-3 (each $1x10^6$ cells) were established in the subscapular region of a CB17/Icr-Prkdc-scid/Crl (Charles River) mouse model. (42.4±4.4)µg of radiolabelled NDs were applied intravenously. Dynamic 60-min PET scans (Focus120, Siemens Medical Solutions, Inc.) were performed 1h and 3h (^{68}Ga-labelled), or 3h, 24h, 3d and 7d (^{89}Zr-labelled) p.i.. Anatomic MR imaging was performed at 11.7T (BioSpec117/16,Bruker Biospin) in a subgroup. Activity accumulation at each time point (n=4) was measured in excised organs using a gamma counter (Cobra II, Perkin Elmer). PET/MR image superposition and data analysis were performed with 3DSlicer and AsiPro. ***Results:*** ^{89}Zr-Labelling was stable in sodium chloride (0.9%), cell culture medium and serum during a 4d observation period. In the first 60min of observation, activity accumulated in liver and spleen, while simultaneously decreased in the heart region. The activity in the blood, responsible for the heart signal, decreased over time. A slight increase of activity was detected in LNCaP C4-2 tumours starting at (0.4±0.3)%ID up to (1.5±0.6)%ID after 3d followed by a decrease to (0.9±0.6)%ID after 7d. For PC-3 a short peak of (0.6±0.4)%ID followed by a constant level of (0.2±0.1)%ID were detected. Fast increase (40.4±17.7)%ID to (66.9±3.4)%ID after 3h and decrease over time to (49.5±8.6)%ID after 7d were observed for the liver. In the spleen an increase was detected from (2.1±0.5)%ID to (6.0±1.4)%ID at 24h followed by a decrease at 7d (3.4±0.9)%ID. ***Conclusion:*** Successful ^{89}Zr-radiolabelling and initial in vivo studies regarding biodistribution and accumulation of specifically coated NDs were performed. Main organs of accumulation were part of the reticuloendothelial system. Crucial data for the further optimization of the surface modifications with regard to pharmacokinetic and pharmacodynamic properties of the protein-coated NDs were obtained. ***References:*** None

EP-281

The feasibility of ^{64}Cu-PSMA I&T for specific PSMA PET imagings

I. Lim, S. Woo, C. Lee, K. Song, S. Lim;
Korea Cancer Center Hospital, Seoul, KOREA, REPUBLIC OF.

Aim/Introduction: To investigate the feasibility of ^{64}Cu labeling with PSMA I&T for PSMA PET imaging and biodistribution evaluation. ***Materials and Methods:*** PSMA I&T was labeled with ^{64}Cu and stability in human and mouse serum was evaluated. Prostate cancer cell lines were used for specific uptake assay (22RV1 for PSMA positive, PC-3 for PSMA negative). Both PC-3 and 22RV1 cells were transplanted left and right thigh in a mouse for PET/CT imaging. Biodistribution was performed using 22RV1 tumor models. ***Results:*** ^{64}Cu-PSMA I&T was successfully labeled (more than 95%) compared to free ^{64}Cu peak. Serum stability of ^{64}Cu-PSMA I&T was maintained more 90% until the 60 h. The specific binding of 22RV1 cells to ^{64}Cu-PSMA I&T was 7.5-fold higher than that of PC-3 cells ($p < 0.001$). From PET/CT imaging, more specific ^{64}Cu-PSMA I&T uptake was observed in 22RV1 tumor than PC-3 tumor. In PSMA blocking study using 2-PMPA, ^{64}Cu-PSMA I&T signal was significantly decreased in 22RV1 tumor region. In biodistribution study, kidney uptake at 2 h after the intravenous injection was the highest (52.6 ± 20.8%ID/g) but sharply decreased, and liver uptake was similar from 2 h to 48 h (ranges from 10 to 12%ID/g). On the other hand, ^{64}Cu-PSMA I&T uptake in the tumors increased as time went by and peaked at 48 h (5.6 ± 0.1%ID/g). ***Conclusion:*** ^{64}Cu-PSMA I&T can be labeled and demonstrated specific binding to PSMA in vitro and in vivo. Furthermore, ^{64}Cu-PSMA I&T might be used for evaluating the distribution of PSMA I&T labeled with metals. ***References:*** Weineisen M, Schottelius M, Simecek J, et al. ^{68}Ga- and ^{177}Lu-labeled PSMA I&T: optimization of a PSMA-targeted theranostic concept and first proof-of concept human studies. J Nucl Med. 2015;56:1169-1176. Mesters JR, Barinka C, Li W, Tsukamoto T, Majer P, Slusher BS, Konvalinka J, Hilgenfeld R: Structure of glutamate carboxypeptidase II, a drug target in neuronal damage and prostate cancer. EMBO J 2006, 25:1375-1384.

EP-282

Preliminary Evaluation of (S)-7-[^{18}F]Fluorotryptophan as a Tracer for the Imaging of Tryptophan Metabolism Alterations in Tumor Xenografts

L. Hvass[1], V. Shalgunov[2], J. T. Jørgensen[1], B. D. Zlatopolskiy[3], B. Neumaier[3], A. Kjær[1], M. M. Herth[2];
[1]Department of Clinical Physiology, Nuclear Medicine & PET, Copenhagen University Hospital, Rigshospitalet, Copenhagen, DENMARK, [2]Department of Drug Design and Pharmacology, Faculty of Health and Medical Sciences, University of Copenhagen, Copenhagen, DENMARK, [3]Institute of Neuroscience and Medicine,

Forschungszentrum Jülich, D-52425 Jülich, GERMANY.

Aim/Introduction: Tryptophan is an essential amino acid in mammals including humans. Tryptophan metabolism is altered in cancer, and the imaging of these alterations with positron emission tomography (PET) has been successfully used for tumor detection and staging. Such imaging can be done with ^{11}C-Labeled tryptophan analogs, e.g. [^{11}C] AMT and [^{11}C]HTP [1]. However, complicated synthesis procedures and short half-life of carbon-11 limit the potential scale of application for these tracers. Recently, (S)-7-[18F]-fluorotryptophan (7-[^{18}F]FTrp), a tryptophan analogue labeled with a longer-lived isotope fluorine-18 and prepared via a simple ^{18}F-fluorination-deprotection scheme, was shown to accumulate in tumor xenografts grown in chick embryos [2]. We aimed to assess the ability of 7-[^{18}F]FTrp to detect tumors in a mouse xenograft model, which is more advanced in a translational sense. ***Materials and Methods:*** 7-[^{18}F]FTrp was prepared as described in [2] with slight modifications. Nude Balb/c mice, 7-8 weeks of age, with LS 174T human colon adenocarcinoma xenografts (170-240 mm^3 volume), received injections of 3.7-4.7 MBq of 7-[^{18}F]FTrp into the lateral tail vein. At 10 and 90 min post-injection, the mice were placed into the PET camera and scanned for 20 min. CT scanning was performed to obtain anatomical information. Radioactivity concentration was measured in the tumor, in the leg muscle and in the heart (as a surrogate for blood uptake). ***Results:*** Average tumor uptake of 7-[^{18}F]FTrp was 5.9±1.1 %ID/g in the first scan (20 min post-injection) and 4.8±1.1 %ID/g in the second scan (100 min post-injection). Tumor-to-muscle ratios measured in the first and the second scans were 1.6±0.3 and 1.5±0.6, respectively. Corresponding tumor-to-heart ratios were 1.0±0.2 and 1.2±0.2 ***Conclusion:*** Despite decent absolute uptake in LS 174T xenografts, the contrast between tumor and healthy tissue for 7-[^{18}F]FTrp was poor in the chosen model. Evaluation of 7-[^{18}F]FTrp in tumors with greater known elevation of tryptophan metabolism (e.g. neuroendocrine tumors) is pending. ***Acknowledgements:*** This work was supported in part by DFG (grant: ZL 65/3-1) ***References:*** 1. Sun A et al. Front Chem 2018;5. 2. Zlatopolskiy BD et al. J Med Chem. 2018;61:189-206.

EP-283

Preclinical tumor imaging with ^{89}Zr-labeled monoclonal antibody ramucirumab

Z. Novy[1], *J. Janousek*[2], *P. Barta*[2], *M. Petrik*[1], *M. Hajduch*[1], *F. Trejtnar*[2]; [1]*Faculty of Medicine and Dentistry, Olomouc, CZECH REPUBLIC,* [2]*Charles University in Prague, Hradec Kralove, CZECH REPUBLIC.*

Aim/Introduction: The angiogenesis suppression has become one of the key anti-tumor strategies. This also includes blocking of VEGFR2 binding site by the monoclonal antibody ramucirumab (RAM). The aim of this study was to prepare RAM radiolabeled with positron emission tomography (PET) imaging radionuclide zirconium-89 and subsequently determine in vitro and in vivo biological properties of ^{89}Zr-labelled ramucirumab. ***Materials and Methods:*** The conjugation of RAM with the bifunctional chelator p-SCN-Bn-deferoxamine (DFO) was carried out at pH 9.0 in sodium bicarbonate. DFO-RAM was radiolabeled with (^{89}Zr)Zr-oxalate at pH 5.5 in sodium acetate solution. The binding affinity of prepared 89Zr-DFO-RAM to VEGFR2 was tested in vitro on prostate adenocarcinoma (PC-3) and ovary adenocarcinoma (SK-OV-3) cell lines. The PET/CT imaging and ex vivo biodistribution studies were performed in mice engrafted with PC-3 and SK-OV-3 tumors. ***Results:*** The in vitro experiments showed preserved binding ability of ^{89}Zr-DFO-RAM to VEGFR2 with the KD values 38.93±2.04 and 36.59±8.36 nM for PC-3 and SK-OV-3 cells respectively. The obtained ex vivo biodistribution data revealed the activity uptake in PC-3 and SK-OV-3 tumors at about 8.7±0.2 and 12.1±1.6 %ID/g respectively. The tumor-to-blood ratio for 1, 3 and 6 days p.i. was 0.4, 0.6 and 0.8 for PC-3 and 0.5, 1.0 and 1.3 for SK-OV-3 tumors respectively. The PET/CT images showed high radioactivity accumulation in the tumors starting already at first day p.i. ***Conclusion:*** The labeling of DFO-RAM with Zr-89 provided anti-VEGFR2 radiopharmaceutical with promising binding to the target receptors both in vitro and in vivo. The results of in vivo experiments proved the potency of ^{89}Zr-DFO-RAM to target and image VEGFR2-positive tumors. However, several non-target organs like e.g. heart, spleen and liver showed also increased accumulation of the radioactivity. ***References:*** None

EP-284

Quantification using 2D scintigraphic versus 3D SPECT imaging in pre-clinical oncology studies: A Comparative Analysis

M. Rouchota[1], *P. Tsialios*[2], *S. Sarpaki*[1], *M. Georgiou*[1], *L. Fysikopoulos*[1], *I. Pilatis*[3], *P. Papadimitroulas*[1], *G. Loudos*[1]; [1]*BIOEMTECH, Athens, GREECE,* [2]*Medical School, National and Kapodistrian University of Athens, Athens, GREECE,* [3]*University of West Attica, Athens, GREECE.*

Aim/Introduction: Preclinical studies hold the most prominent tool in oncology research. The gold standard in any oncology experiment is still ex vivo biodistributions, an invasive method that requires a large number of animals. Studies have shown that both planar (2D) and tomographic (3D) imaging provide high correlation to ex vivo studies and can be trusted as an alternative to bio kinetics [1]. Usually, tumours are subcutaneous thus do not overlap with other organs. In this study, a set of oncology imaging studies, performed both on 2D and 3D commercial systems and are compared against biodistribution data, to evaluate the correlation between the two methods. ***Materials***

and Methods: We have studied 6 oncology experiments, with more than 30 mice and 3 different isotopes, in 2D and 3D SPECT and ex vivo bio-distributions. Real-time, dynamic screening was performed on a commercial high resolution, 2D scintigraphic system, while quantification on its embedded analysis software. Tomographic SPECT/CT imaging was performed with a commercial microSPECT/CT scanner and post-processing on commercial processing software. ROIs or VOIs respectively, are drawn on major organs and the counts are translated to %ID/organ. For the biodistributions studies, organs were measured in a gamma counter and results calculated as %ID/organ. The agreement between the two methods was assessed using pairwise comparisons with repeated-measures ANOVA and the Bland - Altman plot. ***Results:*** The difference in uptake values between 2D and 3D imaging was (4.9 ± 3.2)%. The correlation between imaging and ex vivo bio-distribution values differs on average by (8.1 ± 2.6)%. Both imaging techniques present a very similar trend in comparison to ex vivo biodistributions. However, 2D imaging offers a number of additional advantages, such as speed, simplicity, real time imaging, and ability to provide very short time frames and extraction of time activity curves by the end of the experiment. ***Conclusion:*** This study demonstrates that for applications were organs are well separated, 2D scintigraphy provides similar results to 3D SPECT. In addition, it allows the reproduction of time activity curves with the same accuracy as ex vivo biodistribtuions, while significantly reducing in the number of animals required and increasing overall statistical accuracy. ***References:*** [1]. Dan Yang et al. Exogenous Gene Expression in Tumors: Noninvasive Quantification with Functional and Anatomic Imaging in a Mouse Model. Radiology, 235, 3 (2005).

EP-285

Preliminary study on the value of ^{18}F-FDG, ^{18}F-PSMA and ^{68}Ga-FAPI PET in the evaluation of hormone dependence in prostate cancer

J. Ning[1], *C. Yang*[1,2], *X. Zhang*[1], *J. Zhang*[1], *J. Liu*[1], *Y. Yin*[1], *B. Xu*[1]; [1]*Chinese PLA General Hospital, Beijing, CHINA,* [2]*Institute of Systems Biomedicine, Department of Pathology, School of Basic Medical Sciences, Beijing Key Laboratory of Tumor Systems Biology, Peking-Tsinghua Center for Life Sciences, Peking University Health Science Center, Beijing, CHINA.*

Aim/Introduction: To visualize the different biological behaviors of androgen-dependent and androgen-independent prostate cancer (PCa), drug-resistant and non-resistant PCa via multimodal PET imaging (^{18}F-FDG , ^{18}F-DCFPyL, ^{68}Ga-FAPI-04) . ***Materials and Methods:*** We planned to establish subcutaneous and orthotopic mouse models of androgen-dependent PCa (LNCaP: 12 subcutaneous masses in 6 mice) and androgen-independent PCa (PC-3: 12 subcutaneous masses in 6 mice), and docetaxel-resistant PCa (22RV1-DR: 12 subcutaneous masses in 6 mice and 12 orthotopic masses in 6 mice) and non-resistant PCa (22RV1: 12 subcutaneous masses in 6 mice and 12 orthotopic masses in 6 mice). Among these PCa cell lines, 22RV1-DR and 22RV1 were genetically modified to cell lines with fluorescent protein (mCherry) overexpression so as to differentiate tracer concentration in the prostate foci from tracer accumulation in the bladder of orthotopic mouse models. Then, perform ultrasound imaging, fluorescence imaging, and PET imaging of ^{18}F-FDG, ^{18}F-DCFPyL, ^{68}Ga -FAPI-04, and analyze and compare the imaging characteristics of different types of mouse models from different perspectives. After euthanizing the mice, every mass was extracted for immunohistochemistry analysis, whose indicators include PSAP, CD31, CD56, CgA, CK7, Ki-67, NKX3.1, NSE, P504S, CK20, PSMA and Syn. ***Results:*** For some reason, the construction of orthotopic mouse model all failed. So, the following results came from subcutaneous mouse models. On PSMA PET, LNCaP PCa was shown positive while PC-3 was none concentrated. As for PC-3 mice, PSMA PET indicated no tracer concentration while the FDG and FAPI imaging came out positive. 22RV1 and 22RV1-DR PCa were both shown negative on FAPI PET and positive on FDG and PSMA PET. And on FDG and PSMA PET, SUVmax of 22RV1-DR PCa were both higher than that of 22RV1 PCa (P_{FDG}=0.012, P_{PASM}=0.007). Among all the tested IHC indicators, some difference of CD56, CgA, CK7, Ki-67, NKX3.1, P504S and PSMA were observed between 22RV1-DR and 22RV1 PCa neoplasms. ***Conclusion:*** Multimodal molecular imaging has certain potential in the evaluation of androgen dependence in prostate cancer. Further studies are required to clarify the mechanism of PCa drug-resistance with the added value of molecular imaging to basic science. ***References:*** None

EP-38

Preclinical Studies -> Preclinical Studies -> Preclinical Therapy

e-Poster Area

EP-286

FAP radioligand therapy in a pancreatic adenocarcinoma patient-derived xenograft

C. Mona*, K. Lückerath, R. Riahi, F. Hikmat, K. M. Current, R. Slavik, T. R. Donahue, C. G. Radu, D. W. Dawson, J. Czernin; UCLA, Los Angeles, CA, UNITED STATES OF AMERICA.*

Aim/Introduction: There are no effective treatments for pancreatic ductal adenocarcinoma (PDAC), accounting for the abysmal statistic of fewer than 9% of patients surviving 5 years post diagnosis. Fibroblast Activation Protein (FAP) is almost exclusively expressed on cancer associated fibroblasts

that reside in the stroma of cancers. FAP is a key effector that promotes tumorigenesis and immunosuppression. Preclinical studies suggested that depletion or pharmacological inhibition of FAP-positive cells lead to decreased tumor growth and invasion. Thus, FAP-targeted radioligand therapy (RLT) may represent a promising modality to achieve tumor control. Aim: evaluating FAP-RLT FAPi-46 radiolabeled with alpha or beta particle as new therapeutic agent to treat PDAC. ***Materials and Methods:*** To study the relevance of 177Lu-FAPi-46 and 225Ac-FAPi-46 in PDAC, we used a PDAC patient-derived xenograft (PDX; AM1283) model. We performed both biodistribution and activity escalation study. In vivo FAP stromal expression was confirmed by 68Ga-FAPi-46 positron emission tomography, immunohistochemistry (IHC), FACS and immunoblot. In the biodistribution study, mice bearing AM1283 were sacrificed 1, 2, 4, 6, and 24 h post treatment with 225Ac-FAPi-46 (n=5 mice/group). At the indicated timepoints, multiple organs and tumor were resected, weighed and subjected to ex vivo gamma-counting. In the activity escalation study, NCG mice (n=8/group) were intravenously injected with 20, 40, or 60 MBq ^{177}Lu-FAPi-46, or 10, 20, or 40 kBq ^{225}Ac-FAPi-46. Acute toxicity and efficacy were evaluated by body weight measurements and tumor volumes determined by micro-CT. Two days post-RLT, tumors were resected in a subset of mice (n=3) to quantify FAP expression and DNA double-strand breaks. ***Results:*** Biodistribution analysis revealed an increased uptake of 225Ac-FAPi-46 in the tumors versus pancreas. However, we noted an important uptake in the kidneys and liver. All groups treated with FAP RLT exhibited a delayed tumor growth onset with respect to the vehicle-treated mice for both isotopes. We observed an activity-dependent inhibition of tumor growth with both isotopes. A more drastic effect was observed using 225-Actinium radiolabeled FAPi-46 at an activity of 40kBq without any toxicity. ***Conclusion:*** We report PDAC-PDX tumor growth inhibition in mice treated with single injection of 177Lu- or 225Ac-FAPi-46 in a subcutaneous tumor model. We observed a tendency toward an increased inhibition of tumor growth when using 225Ac rather than 177Lu. This study shows that FAP-RLT and more specifically alpha therapy targeting FAP appears to be a novel promising avenue for the FAP-positive PDAC and paves the way for new combination treatment strategy. ***References:*** None

EP-287

^{225}Ac-Pertuzumab Enhances Efficacy Against a Trastuzumab/Pertuzumab Resistant HER2-Positive Breast Cancer Xenograft Model

B. Khan[1], *F. Sanaulla*[1], *M. Khan*[1], *S. Karkare*[1], *P. Causey*[2], *R. Perron*[2], *D. Gendron*[2], *H. Fonge*[1];
[1]*University Of Saskatchewan, Saskatoon, SK, CANADA,*
[2]*Canadian Nulear Laboratories, Chalk River, ON, CANADA.*

Aim/Introduction: Background: Cell signaling through the epidermal growth factor family of receptors (EGFR, HER2, and HER3) promotes tumour cell proliferation and survival in a variety of epithelial malignancies notably in metastatic breast cancer (MBC). 25-30% of MBC overexpress HER2 and this is associated with aggressive disease and poor prognosis. A combination of trastuzumab and pertuzumab is approved for the treatment of HER2 positive MBC. However, very few patients qualify for this treatment and 20 - 50% of patients initially selected for therapy do not respond to treatment, while up to 70% of initial responders subsequently acquire resistance. In this study we hypothesize that targeting HER2 using ^{225}Ac-pertuzumab can enhance the therapeutic efficiency of pertuzumab. ***Materials and Methods:*** Pertuzumab was conjugated with an eighteen-membered macrocyclic chelator p-SCN-Bz-macropa and radiolabeled with ^{225}Ac for alpha particle therapy. The radiochemical yield of ^{225}Ac-pertxumab was >95%. The (radio)immunoconjugate was characterized by flow cytometry, radioligand binding assays, HPLC and internalization rate (live-cell imaging). In vitro cytotoxicity was studied in HER2 positive JIMT-1 cells, a pertuzumab/trastuzumab resistant model with medium to low HER2 expression. In vivo radioimmunotherapy using ^{225}Ac-pertuzumab was studied using JIMT-1 xenograft following treatment with three doses of 350 nCi/dose administered 10 days apart. In vivo study endpoint was tumor volume >= 1500 mm^3. Control treatment groups included PBS, pertuzumab and ^{225}Ac-labeled isotype control IgG. ***Results:*** Flow cytometry showed > 90% binding to the cells. In vitro studies in JIMT-1 showed enhanced cytotoxicity (IC_{50}) of ^{225}Ac-pertxumab (5.7 ±1.2 nM) which was 41 folds less than pertuzumab (215 ± 1.01 nM). ^{225}Ac-pertuzumab was effective at inhibiting the growth of JIMT-1 tumors. 9/8 mice treated injected with ^{225}Ac-Pertuzumab had tumor decreased to <50mm^3. Median survival after > 90 days since start of treatment are: ^{225}Ac-Pertuzumab (not yet reached); PBS-treated (51 days). ***Conclusion:*** ^{225}Ac-labeled Pertuzumab displayed promising therapeutic efficiency towards HER2 positive BC. Efficiency of this radioimmunoconjugate in 3D spheroids and other Her2 positive xenografts is ongoing ***References:*** None

EP-288

Radionuclide Therapy Using ^{177}Lu-labeled ABD-fused ADAPT6 Scaffold Protein

J. Garousi[1], *E. Von Witting*[2], *M. Oroujeni*[1], *J. Borin*[2], *A. Vorobyeva*[1,3], *M. Altai*[1], *O. Vorontsova*[1], *M. W Konijnenberg*[4], *A. Orlova*[3,5,6], *S. Hober*[2], *V. Tolmachev*[1,3];
[1]*Uppsala University, Rudbeck laboratory, Uppsala, SWEDEN,* [2]*Department of Protein Technology, KTH - Royal Institute of Technology, Stockholm, SWEDEN,* [3]*Research Centrum for Oncotheranostics, Research School of Chemistry and Applied Biomedical Sciences, Research Tomsk Polytechnic*

University, Tomsk, RUSSIAN FEDERATION, [4]Department of Radiology and Nuclear Medicine, Erasmus MC, Rotterdam, NETHERLANDS, [5]Science for Life Laboratory, Uppsala University, Uppsala, SWEDEN, [6]Department of Medicinal Chemistry, Uppsala University, Uppsala, SWEDEN.

Aim/Introduction: ADAPT6 is a small (5 kDa) scaffold protein, which binds to HER2 with high affinity. Radiolabeled ADAPT6 provides a high-contrast imaging of HER2-expressing tumors in clinics, but a high renal reabsorption prevents its use for radionuclide therapy. We tested a hypothesis that a fusion with an albumin-binding domain (ABD) from protein G would result in a binding of radiolabeled ADAPT6 to albumin in blood. Such binding would prevent glomerular filtration and reabsorption. In this way, an absorbed dose to kidneys will be reduced, which would enable radionuclide therapy. ***Materials and Methods:*** ABD_{035}-ADAPT6 (N-terminal position of ABD) and DOTA-ADAPT6-ABD_{035} (C-terminal position of ABD) were produced recombinantly and maleimido-derivative of DOTA was coupled site-specifically to C-terminal cysteines of constructs. The conjugates were labeled with ^{177}Lu and characterized in vitro using HER2-expressing SKOV-3 and BT474 cells. To select the best variant, their biodistribution 48 h p.i was measured in mice bearing SKOV-3 xenografts. Biodistribution of ^{177}Lu-DOTA-ADAPT6-ABD_{035} was measured at 4, 24, 48, 72, 168 and 236 h p.i. and absorbed doses were calculated. In experimental therapy, one group of mice was treated with a single injection of 18 MBq (6 μg) ^{177}Lu-DOTA-ADAPT6-ABD_{035} and another with two such injections, three weeks apart. Control groups were treated with PBS, 6 μg of non-labeled DOTA-ADAPT6-ABD_{035} and 18 MBq (6 μg) control protein ^{177}Lu-DOTA-$ADAPT_{Neg}$-ABD_{035}, which binds to albumin but not to HER2. ***Results:*** Both ^{177}Lu-DOTA-ADAPT6-ABD_{035} and ^{177}Lu-DOTA-ABD_{035}-ADAPT6 bound to HER2-expressing cell lines specifically and with high affinity (485 ± 88 and 432 ± 158 for ^{177}Lu-DOTA-ADAPT6-ABD_{035} and ^{177}Lu-DOTA-ABD_{035}-ADAPT6, respectively). ^{177}Lu-DOTA-ADAPT6-ABD_{035} provided higher tumor uptake and lower renal uptake than ^{177}Lu-DOTA-ABD_{035}-ADAPT6 at 48 h p.i. Uptake of ^{177}Lu-DOTA-ADAPT6-ABD_{035} in HER2-positive SKOV-3 xenografts (35±12 %ID/g) was significantly ($p < 0.005$) higher than in HER2-negative Ramos xenografts (2±12 %ID/g) at 48 h p.i. Absorbed doses were 94, 1060 and 3479 mGy/MBq for bone marrow, kidneys and tumor, respectively. Median survival in the control groups was 25, 25, and 31 d for treatment with PBS, unlabeled DOTA-ADAPT6-ABD_{035}, and ^{177}Lu-DOTA-$ADAPT_{Neg}$-ABD_{035}, respectively. A single injection of 18 MBq of ^{177}Lu-DOTA-ADAPT6-ABD_{035} resulted in a significant ($p<0.0001$) extension of a median survival to 70 d. In the mice treated with 20 injections ^{177}Lu-DOTA-ADAPT6-ABD_{035}, only 1 mouse died at the time of experiment termination. ***Conclusion:*** In the preclinical setting, ^{177}Lu-DOTA-ADAPT6-ABD_{035} has a strong effect on HER2-expressing xenografts and has no long-term toxicity. This variant should be considered for clinical translation. ***References:*** None

EP-289

Preclinical evaluation of targeted alpha therapy using ^{225}Ac-DOTA-E[c(RGDfK)]$_2$ for pancreatic cancer

M. Yoshimoto[1], *K. Washiyama*[2], *Y. Yoshii*[3], *K. Ohnuki*[1], *H. Fujii*[1]; *[1]Division of Functional Imaging, EPOC, National. Cancer Center, Kashiwa, JAPAN, [2]Advanced Clinical Research Center, Fukushima Medical University, Fukushima, JAPAN, [3]National Institute of Radiological Sciences, National Institutes for Quantum and Radiological Science and Technology, Chiba, JAPAN.*

Aim/Introduction: There is no curable therapeutic strategy for advanced pancreatic cancer up to now. This has led to its low survival rate. Many studies have revealed that targeted alpha therapy, radionuclide therapy using alpha particles such as ^{225}Ac and ^{211}At, would be a new attractive cancer treatment strategy. We have reported that SPECT imaging using ^{111}In-DOTA-c(RGDfK) as an $\alpha_v\beta_3$ imaging agent could successfully detect small tumors in a pancreatic carcinogenesis model, indicating that RGD containing peptides would be possible candidates as a radionuclide carrier for pancreatic cancer. In this study, we investigated tumor uptake of ^{111}In-DOTA-E[c(RGDfK)]$_2$ in human pancreatic cancer xenograft mice. Besides, the therapeutic efficacy and side effects of ^{225}Ac-DOTA-E[c(RGDfK)]$_2$ were estimated in human pancreatic cancer BxPC-3 xenograft mice. ***Materials and Methods:*** In this study, AsPC-1, BxPC-3, Capan-1, PANC-1, and PSN-1 as human pancreatic cancer cell lines, were used. Biodistribution of ^{111}In-DOTA-E[c(RGDfK)]$_2$ was determined at 1, 4, and 24 h after the injection. In the therapeutic experiment, ^{225}Ac-DOTA-E[c(RGDfK)]$_2$ (20, 40, and 65 kBq/mouse) was injected. Body weight and tumor size were measured. Hematological, hepatic, and renal toxicity was also examined. ***Results:*** The biodistribution study indicated the high uptake of ^{111}In-DOTA-E[c(RGDfK)]$_2$ in BxPC-3 and PANC-1 (7.04 and 5.76 %ID/g at 1 h). AsPC-1 was the lowest uptake (3.41 %ID/g at 1 h). More than 50 % of the tumor uptake was retained up to 24 h. In the therapeutic experiment using BxPC-3 xenograft mice, ^{225}Ac-DOTA-E[c(RGDfK)]$_2$ successfully suppressed the tumor growth. The 65 kBq of ^{225}Ac-DOTA-E[c(RGDfK)]$_2$ significantly inhibited the tumor growth, while the decrease in the body weight was observed from 40 days after the administration. In the blood toxicity, ^{225}Ac-DOTA-E[c(RGDfK)]$_2$ decreased in white blood cells and platelets. The liver toxicity dose-dependently appeared, though the kidney toxicity was not obvious. ***Conclusion:*** These results suggested that ^{225}Ac-DOTA-E[c(RGDfK)]$_2$ has great potential to treat intractable pancreatic cancers. However, we need to further investigate administration protocols to reduce the radiotoxicity. ***References:*** None

EP-290

Size-controlled ^{224}Ra-labelled calcium carbonate microparticles against peritoneal carcinomatosis

R. Li[1,2,3], T. B. Bønsdorff[3], I. S. Jorstad[3], K. Lindland[3], S. K. Tonstad[3], Ø. S. Bruland[1,4], S. Westrøm[3], R. H. Larsen[3];
[1]Institute of Clinical Medicine, University of Oslo, Oslo, NORWAY, [2]Department of Radiation Biology, Institute of Cancer Research, the Norwegian Radium Hospital, Oslo University Hospital, Oslo, NORWAY, [3]Oncoinvent AS, Oslo, NORWAY, [4]Department of Oncology, the Norwegian Radium Hospital, Oslo University Hospital, Oslo, NORWAY.

Aim/Introduction: Calcium carbonate microparticles functioning as carriers of ^{224}Ra provide intraperitoneal retention of the alpha emitter to deliver its radiation dose to micrometastases originating from cancers with peritoneal seeding. Addition of excipient is done with the purpose of stabilizing the size of ^{224}Ra-labelled microparticles in suspension. Further, the method of radiolabelling can be varied as ^{224}Ra may be either surface labelled or inclusion labelled into the calcium carbonate microparticles. We have evaluated whether these steps of optimization influence the therapeutic efficacy in two different models of peritoneal carcinomatosis: one xenograft ovarian cancer model and one syngeneic colorectal cancer model. ***Materials and Methods:*** Calcium carbonate microparticles for surface labelling of ^{224}Ra were produced by spontaneous precipitation, where after ^{224}Ra was adsorbed on the microparticles. Inclusion labelling was performed by simultaneous incorporation of ^{224}Ra into the bulk of the microparticles during $CaCO_3$ precipitation. Labelled microparticles were suspended in 0.9% NaCl, with or without the presence of size controlling excipients, followed by terminal sterilization in an autoclave. Models for peritoneal carcinomatosis were established by intraperitoneal inoculation of either human ovarian cancer cells (ES-2) in athymic nude mice, or murine colorectal cancer cells (CT26.WT) in immunocompetent BALB/c mice. Antitumour efficacy was evaluated by a single injection of 14-26 kBq of each variant of the ^{224}Ra-labelled microparticle suspension. ***Results:*** Addition of size controlling excipients to the radiolabelled microparticle suspension stabilized the median particle diameter at 5-9 µm for up to 8 days, while the diameter increased more than 2-fold when no excipient was present. Suspensions containing excipients were easier to handle because of longer microparticle sedimentation times. The ^{224}Ra-labelled $CaCO_3$ microparticles extended the survival compared to control in both tumour models, and there was no difference among groups receiving the different variants of the labelled suspension, neither with respect to addition of excipient nor the method of labelling. ***Conclusion:*** Radium-224-labelled $CaCO_3$ microparticles represent a promising therapy against peritoneal carcinomatosis. The tested excipients yield control of microparticle size and a product which remained well suspended, while maintaining the therapeutic effect in preclinical tumour models. ***References:*** None

EP-291

Feasibility of MR-guided intratumoral treatment with Holmium-166 microspheres in a brain tumor model

N. Klaassen[1], *N. Morsink[2], M. de Vries[3], J. van den Dobbelsteen[3], M. Boswinkel[1], S. van Nimwegen[2], J. Nijsen[1,4];*
[1]Radboud university medical center, Radboud Institute for Molecular Life Sciences, Department of Radiology, Nuclear Medicine and Anatomy, Nijmegen, NETHERLANDS, [2]Utrecht University, Department of Clinical Sciences of Companion Animals, Faculty of Veterinary Medicine, Utrecht, NETHERLANDS, [3]Delft University of Technology, Department of BioMechanical Engineering, Delft, NETHERLANDS, [4]Quirem Medical B.V., Zutphen, NETHERLANDS.

Aim/Introduction: Brain cancer is one of the most aggressive and difficult-to-treat malignancies. Standard of care includes neurosurgery, radiotherapy, and chemotherapy. However, treatment is rarely curative. A minimally invasive intratumoral treatment, in which radioactive particles are injected directly into the tumor, might improve the overall outcome. Intratumoral needle-injection of holmium-166 (^{166}Ho) microspheres (MS) has potential to be a successful therapy. ^{166}Ho (half-life 26.8h) emits high-energy beta rays (mean 0.67 MeV, max 1.85 MeV) with a limited penetration depth (mean 2.2 mm, max 8.7 mm) enabling high local tumor ablative radiation dose with minimal side effects. Visualization of holmium can be performed by SPECT, MRI and CT, due to emission of gamma rays (6.7%, 81 keV), paramagnetic properties, and high mass attenuation coefficient, respectively. These multimodal imaging options offer the possibility to visualize and quantify distribution of ^{166}Ho-MS directly after injection and during follow-up. Initial results of this 'microbrachytherapy' approach are promising. However, due to the relatively shallow penetration, a proper distribution of microspheres in tumor tissue is crucial for lethal dose-coverage of the entire tumor. This can be achieved by using image-guided injection of ^{166}Ho-MS and realtime quantitative imaging-dosimetry to guide additional injections during the treatment procedure (dose-painting). The purpose of this study was to evaluate feasibility of intratumoral dose-painting with ^{165}Ho-MS in a brain tumor mimicking phantom with dedicated delivery device. ***Materials and Methods:*** A tissue phantom, resembling a brain with embedded tumor, was developed mimicking the specific imaging and mechanical responses of both brain and tumor tissues. Among others, the phantom was composed of polyvinyl alcohol and phytagel. Predefined volumes of ^{165}Ho-MS suspended in an injection fluid, were injected in a controlled manner at different positions in the phantom tumor using a dedicated delivery device. The procedures were performed under full MR-guidance. To

evaluate the dose distribution, simulated dosimetry was performed using Q-suite. ***Results:*** The phantom resulted in a model with MR imaging properties comparable to normal brain and tumor tissue. Administration of ^{165}Ho-MS resulted in a controlled near-real-time MR-guided injection with the dedicated delivery device. MR guided administration resulted in the possibility to observe the ^{165}Ho-MS distribution within the phantom during and after injection. The direct quantitative distribution feedback enabled the spatial deposition of ^{165}Ho-MS in the target area, resulting in a dose distribution covering the artificial tumor volume. ***Conclusion:*** We demonstrated the feasibility of controlled MR-guided tumor dose-painting using ^{165}Ho-MS in a tissue phantom. ***References:*** None

EP-292

Conjugation of GRPR-targeting antagonist RM26 to albumin-binding domain extends antagonist's blood circulation and residence in tumours

A. Abouzayed[1], S. S. Rinne[1], F. Wadeea[1], H. Tano[2], Á. Nagy[2], A. E. Karlström[2], V. Tolmachev[1], A. Orlova[1];
[1]Uppsala University, Uppsala, SWEDEN, [2]KTH Royal Institute of Technology, Stockholm, SWEDEN.

Aim/Introduction: imaging of gastrin-releasing peptide receptors (GRPR) can be used for diagnostic of prostate cancer. Recently it was proposed for targeting radiotherapy. However, due to rapid blood clearance, multiple frequent injections of radioagent would be required. The aim of this study was to extend blood circulation of GRPR antagonist RM26 (D-Phe-Gln-Trp-Ala-Val-Gly-His-Sta-Leu-NH_2) by its conjugation to an albumin-binding domain (ABD) and to evaluate utility of new conjugate for therapy. ***Materials and Methods:*** DOTA-ABD-RM26 conjugate was produced by peptide synthesis and labelled with ^{111}In. The [^{111}In]In-DOTA-ABD-RM26 was evaluated in vitro for binding specificity, stability, competitive inhibition (IC_{50}), and cellular retention (with or without the addition of human serum albumin (HSA)) using PC-3 cells. The in vivo specificity and biodistribution of [^{111}In]In-DOTA-ABD-RM26 up to 144 h pi were studied on PC-3 tumour bearing mice. For comparison, the biodistribution of [^{111}In]In-DOTA-RM26 was evaluated 1 h pi. ***Results:*** DOTA-ABD-RM26 was labelled with ^{111}In with moderate radiochemical yields. After purification on size-exclusion column, the radiochemical purity was >99.5%. Labelled conjugate was stable in PBS (0.9±0.2% release within 24 h). However, there was considerable release of ^{111}In in the presence of EDTA (2.6±1.8% within 1 h incubation and 15.2±1.2% within 24 h). It bound specifically to GRPR-expressing cells in presence of HSA and to PC-3 xenografts in vivo. Affinity of DOTA-ABD-RM26 to GRPR was worse than for DOTA-RM26 (30.1±2.7 nM vs 4.5±0.7 nM), and was additionally compromised when measured in presence of HSA (48.7±5.4 nM). Slow internalization of new conjugate corroborate with antagonistic function of RM26. Residence time in blood was significantly extended for ABD-fused RM26 (1 h pi 32±4 %ID/g vs 0.27±0.03 %ID/g). In vivo, tumour activity uptake of [^{111}In]In-DOTA-ABD-RM26 reached 11±2 %ID/g and did not decrease up to 144 h pi. However, this was accompanied by high uptake over time in various organs such as liver, spleen, and bone. Activity uptake in kidneys was higher than in tumours. ***Conclusion:*** this proof-of-principle study demonstrated that conjugation of short GRPR-binding peptide RM26 with ABD resulted in a high and retained agent's tumour uptake. Conjugate can be used for GRPR-targeted delivery of cytotoxic drugs. However, the elevated uptake in kidneys and other organs due to label instability and compromised affinity to both GRPR and albumin abolish its use for radionuclide therapy. Further changes in the molecular design of the conjugate might improve its biodistribution profile. ***References:*** None

EP-293

Integration of diagnosis and treatmentof lymph node metastasis with radioactive upconversion luminescent nanoprobes

S. Xiumin[1,2], Z. Chuan[1,2], Q. Shanshan[1,2], Z. Jianfeng[1,2], Z. Ruijuan[1,2], C. Yanni[1,2], F. Longfei[1,2], L. Yamin[1,2], Z. Lulu[3], W. Feng[3], Z. Ran*[1,2];
[1]Radiation Medicine and Protection, Soochow University, Suzhou, CHINA, [2]State Key Laboratory of Radiation Medicine and Protection, Soochow University, Suzhou, CHINA, [3]Department of Nuclear Medicine,Nanjing First Hospital,Nanjing Medical University, Nanjing, CHINA.

Aim/Introduction: The detection and treatment of lymph node metastasis is of great importance for therapy planning and prognosis of cancers, but remains challenging in the clinic. In the current study, we report a tumor-specific imaging probe constructed with NaGdF4:Yb,Tm,Ca@NaLuF4 core@shellupconversion nanoparticles showing distinctive near infrared emission.The feasibility of binding of nuclide labeledthe upconversion nanoparticles NaGdF4:Yb,Tm,Ca@NaLuF4coupled with anti-epidermal growth factor receptor 2 (HER2) as a theranostic platform was investigated. ***Materials and Methods:*** The up-conversion nanoparticles NaGdF4:Yb,Tm,Ca@NaLuF4 with distinctive nearinfrared emissionwere prepared by thermal decomposition. Asymmetric polyethylene glycol (PEG) bearing a maleimide group at one end was used to replace the oleate ligand. And then the Herceptin antibody was conjugated to upconversion nanoparticles through a "click" reaction. Using a 177Lu-labeled nanoparticle. For in vitro experiments, SKBR3 (HER2 high expression) and MCF7(low expression) cells were incubated with 177Lu-NP-mAb. For in vivo experiments, SKBR3 and MCF7 tumor-bearing lymph node metastasismice were intravenously injected with 177Lu-NP-mAb and imaged before and 24 h,48h,72h,7d,14d,30d post-injection. ***Results:*** The synthesized probe has good

biocompatibility and is stable in vivo and in vitro. For vitro experiments, The NP-mAb demonstrated high affinity toward HER2, the distribution of NP-mAb probe in SKBR3 cells was 14 times higher than that in MCF7 cells. In the vivo experiments, up-conversion luminescence imaging and SPECT imaging showed a high degree of agreement, SKBR3 tumor-bearing lymph node metastasismice treated with 177Lu-NP-mAb exhibited significant tumor load reduction than MCF7tumor-bearing lymph node metastasismice ($P<0.05$). ***Conclusion:*** SPECT imaging and up-conversion imaging complement each other, forming their advantages. By monitoring drug metabolism and distribution, up-conversion imaging provides imaging diagnosis and treatment basis, while SPECT imaging provides longer term monitoring. The resulting 177Lu-NP-mAb nanoprobes presented excellent targeting ability and remarkable binding specificity to HER2-overexpressing cells in vitro, which enabled successful detection and treatment of metastatic lymph nodes through upconversion luminescence. Most importantly, the SPECT imaging suggest that antibody conjugation can prolong the blood half-life of UCNPs by evading the MPS uptake, which explains the outstanding performance of the resulting nanoprobes in diagnosing lymph node metastasis and therefore177Lu-NP-mAb can be used as a potential means to identify patients well-suited for treatment with theranostics nanoparticlesand provides a new basic research of diagnosis and treatment strategy for tumor lymph node metastasis. ***References:*** None

EP-294

A rat preliminary study on medication-related osteonecrosis of the jaw

F. Ribeiro[1], *M. Laranjo*[2,3], *P. M. C. C. Encarnação*[1], *C. M. Marto*[3,4], *R. Santos*[5,3,2], *A. Paula*[3,4], *A. C. Santos*[3,2,4], *A. L. M. Silva*[1,6], *R. Oliveira*[7], *N. Lima*[3], *I. F. Castro*[6], *N. Pereira*[5], *P. M. M. Correia*[1,6], *M. Piñeiro*[5], *G. F. S. Figueiredo*[1], *E. Carrilho*[3,4], *T. Pinho e Melo*[5], *M. F. Botelho*[2,3], *M. Marques-Ferreira*[3,8], *J. F. C. A. Veloso*[1];

[1]*Institute for Nanostructures, Nanomodelling and Nanofabrication (i3N), University of Aveiro, Aveiro, PORTUGAL,* [2]*Institute of Biophysics, Faculty of Medicine, University of Coimbra, Coimbra, PORTUGAL,* [3]*Institute for Clinical and Biomedical Research (iCBR) Area of Environment Genetics and Oncobiology (CIMAGO), Center for Innovative Biomedicine and Biotechnology (CIBB), Coimbra, PORTUGAL,* [4]*Institute of Integrated Clinical Practice, Faculty of Medicine, University of Coimbra, Coimbra, PORTUGAL,* [5]*Faculty of Sciences and Technology, University of Coimbra, Coimbra, PORTUGAL,* [6]*RI-TE, Radiation Imaging Technologies Lda, Ílhavo, PORTUGAL,* [7]*Pathology Service, Centro Hospitalar e Universitário de Coimbra (CHUC), Coimbra, PORTUGAL,* [8]*Institute of Endodontics, Faculty of Medicine, University of Coimbra, Coimbra, PORTUGAL.*

Aim/Introduction: Medication-related osteonecrosis of the jaw (MRONJ) is characterized by progressive bone destruction in the maxillofacial region, associated with severe drug side-effect and having a major impact on patients' quality of life. With no effective treatment or optimal therapy strategy, new approaches are highly expected. To our knowledge, few studies have applied PET to the diagnosis of MRONJ in animal models. This work aims to detect metabolic changes in soft tissue and bone using a novel microPET system in an animal model of MRONJ under photodynamic therapy, based in our recently developed photosensitizers (PS)[1,2]. ***Materials and Methods:*** A previously validated MRONJ animal model was used[3]. Wistar female rats (10 weeks) were administered with Zoledronate (Zol) (0.1 mg/kg) for 8 weeks, to induce ONJ. At week 4, the first upper right molar was extracted and, 72 hours before this procedure, rats were medicated with PS. Since photodynamic therapy (PDT) activates PS, the animals were randomly divided into two groups to ascertain the action of PS over ONJ: group 1, animals not submitted to PDT; group 2, animals submitted to PDT. Immediately after tooth extraction, irradiation of the surgical area was performed with LASER (635 nm, 1 min, 24 J). Two weeks post-surgery, rats underwent ^{18}F-FDG PET imaging, using the easyPET.3D scanner (RI-TE Lda, Portugal[4]). Animals were occised and samples collected for histologic and histomorphometric evaluation. ***Results:*** The easyPET.3D images, for group 1 (without PDT), showed a similar ^{18}F-FDG uptake compared to control, proving that PS remained inactive; while for group 2 (with PDT) presented a higher tracer uptake, which was focal and unilateral, matching the site of tooth extraction, therefore indicating the PS activation by the PDT. PS effect over ONJ was reflected by the higher metabolic activity of soft tissues. This study has not yet been completed, hence results regarding the histological evaluation of the collected samples are not yet available. ***Conclusion:*** This pilot results, obtained with ^{18}F-FDG PET imaging in the selected rat model, by revealing the activation of PS with PDT, suggest that PS is a potential treatment for MRONJ. Further PET studies will be performed with ^{18}F-NaF to assess the effect of PS directly over the bone. ***References:*** 1. Pereira N. et al., Eur J Med Chem. 2015, 103:374. 2. Nascimento B. et al., ACS Omega 2019, 4:17244. 3. Paulo S. et al., Materials 2020, 13:1955. 4. WO2016147130 (PCT/IB2016/051487), www.ri-te.pt

EP-39

Technical Studies -> Data Analysis -> Image Reconstruction

e-Poster Area

EP-295

Yttrium-90 PET imaging with digital photon counting for radioembollization absorbed dose monitoring

J. Labour, P. Boissard, F. Khayi, P. Veyrat Durebex, D. Kryza, S. Parisse-Dimartino, T. Mognetti, D. Sarrut, J. N. Badel;
CREATIS; Centre Léon Bérard; CNRS UMR 5220; INSERM U1044; Université de Lyon; INSA Lyon; Université Lyon 1, Lyon, FRANCE.

Aim/Introduction: We investigated the accuracy of image-based ^{90}Y PET dosimetry quantification with a SiPM-based PET/CT for radioembolization dose monitoring purposes. Different image reconstruction protocols from published studies [1,2] were used to compare with the clinical protocol in our centre. ***Materials and Methods:*** Three ^{90}Y phantoms were imaged: (1) a NEMA NU 2-1994 PET phantom with an insert filled with an uniform activity concentration (AC) = 1.71 MBq/mL, (2) a cylindrical phantom with AC = 0.29 MBq/mL, and (3) a NEMA body phantom containing six spheres of varying diameters (10-37 mm), with AC = 2.18 MBq/mL in all spheres and a sphere-to-background ratio of 9:1. Listmode PET data were acquired with a Philips Vereos digital photon counting (DPC)-PET/CT for 15 minutes in a single-bed position. Images were reconstructed using OSEM iterative algorithm with 3 iterations, 5 subsets, time-of-flight (ToF) and point-spread function (PSF). 2mm full-width at half-maximum (FWHM) Gaussian post-reconstruction filter was applied to all reconstructions. Phantoms (1) and (2), less influenced by partial-volume effects, were used for absolute quantification measurements. Phantom (3) was used to determine the AC recovery coefficients (RCs) of the hot spheres and background, based on CT-defined VOIs. We compared the results with those obtained from reconstruction parameters proposed by [1] (1 iteration, 21 subsets, ToF, PSF, 4.5mm FWHM filter) and [2] (3 iterations, 12 subsets, ToF, PSF, 5.2mm FWHM filter). Reconstructions were also performed with only the first 11 minutes of the acquisitions. ***Results:*** The relative differences between the reference and measured ACs in phantoms (1) and (2) were less than 1.5% and 2.5%, respectively. RCs for the hot spheres in phantom (3) for all reconstruction sets were between 0.74-0.78, 0.71-0.78 and 0.3-0.4 for the 37, 22 and 13mm spheres, respectively. RCs for the background using our parameters and the ones from [1] and [2] were 0.96, 0.86 and 0.94, respectively. RCs obtained with 11-minutes reconstructions were within 5% of the 15-minutes ones. ACs standard deviations were below 0.8 MBq/mL for the hot spheres. ***Conclusion:*** Reconstructions using 3 iterations provided overall better RCs than 1 iteration. Acquisition duration could be reduced by 30% (15 to 11 minutes) without accuracy degradation, thus improving patient comfort. ***References:*** [1]Pasciak et al. "A comparison of techniques for 90Y PET/CT image-based dosimetry following radioembolization with resin microspheres." Frontiers in Oncology 4(2014): 121
[2]Siman et al. "Dose volume histogram-based optimization of image reconstruction parameters for quantitative 90Y-PET imaging." Medical Physics 46.1(2019): p.229-237

EP-40

Technical Studies -> Dosimetry and Radiobiology -> Clinical Dosimetry

e-Poster Area

EP-296

Analysis of results of effective dose estimation obtained from RADAR 2017 dose assessment model for nuclear medicine procedures

L. Del Barco, M. Calderón Calvente, L. de la Cueva Barrao, A. Gandia Martinez, S. Moñux Salvador, G. Guzmán Prudencio, L. Nieto Morcillo, M. Falgás Lacueva, P. Navarro Beltrán, S. Álvarez Ruíz, M. Sangrós Sahún, D. Abós Olivares;
Hospital Universitario Miguel Servet, Zaragoza, SPAIN.

Aim/Introduction: To analyze the results of effective dose (E) estimation of the most frequent procedures using photon emitters in Nuclear Medicine, obtained from RADAR 2017 dose assessment model. To compare these results with those obtained from ICRP 128 (2015) recommendations, and to assess how using each dose assessment model can change E results. ***Materials and Methods:*** E estimation data was collected from photon emitter procedures performed during the last year in our department, obtained from RADAR 2017 dose estimation model for age groups: ≤ 1 year old; >1-5 years old ; >5- 10 years old, >10- 15 years old and adults. Injected activity was the one recommended by international guidelines and EANM Pediatric and Dosimetry Committees. Hybrid exams (SPECT / CT) and procedures for which there is no RADAR 2017 dosimetry estimation were excluded. Results for (E) were compared with those obtained by using ICRP 128 (2015) recommendations. ***Results:*** With RADAR 2017 dose evaluation model we obtained a lower mean value of E on most of the procedures that were analyzed, being significantly lower for Renogram, Renal scintigraphy on >10-15 years old, Thyroid scintigraphy, Meckel's scan and Bone Scan (0.12 to 1.16 mSv, 25% to 67%). Brain perfusion and Renal scintigraphy on ages under 10 obtained a significantly greater difference for E (0.33 to 2.85 mSv, 26% to 29%). ***Conclusion:*** These results are an updated collection of estimated E values for photon-

emitting radiopharmaceuticals commonly used in Nuclear Medicine, considering RADAR 2017 dose assessment model compared to ICRP 128) recommendations. Methodological changes on estimation lead to lower E for most of diagnostic procedures using photon emitters, this is of special interest for patients undergoing repeated ionizing radiation (dosimetry history). ***References:*** None

EP-297

Patient Radiation Doses from hybrid NM/CT Scans: Manitoba, Canada Vs. Europe

S. Eustace[1,2], Y. Kady[3], M. Al-Abedi[1,2], I. Elbakri[1,2];
[1]CancerCare Manitoba, Winnipeg, MB, CANADA, [2]Department of Radiology, University of Manitoba, Winnipeg, MB, CANADA, [3]Physics Department, Beirut Arab University, Beirut, LEBANON.

Aim/Introduction: This study documented patient radiation doses from common clinical hybrid nuclear medicine / computed tomography (NM/CT) procedures in the Canadian province of Manitoba (population 1.34 million). Results were compared to European values and used to establish diagnostic reference levels (DRLs). ***Materials and Methods:*** All hybrid NM/CT facilities in Manitoba participated, comprising of eight SPECT/CT systems and one PET/CT system. Data were collected for six clinical SPECT/CT procedures and three PET/CT procedures: Bone (Torso only), Myocardial Perfusion, Lung V/Q, Parathyroid, Octreotide, Sentinel Lymph Node / Melanoma Mapping, then PET/CT brain, Near Whole Body(NWB), and Head/Neck (H/N) + NWB. DLP (mGy·cm) and administered activity (MBq) data were collected for 10-20 patients weighing 70+/- 20kg. Paediatric and pregnant patients were excluded. Comparison was drawn to relevant values presented in recent European publications. ***Results:*** Provincial CT DRLs have been established for the following procedures; Bone (190 mGy.cm), Cardiac MPS (55 mGy.cm), Lung V/Q (140 mGy.cm), Parathyroid (115 mGy.cm), and In-111 Octreotide (155 mGy.cm) SPECT/CT procedures. Site DRLs were established for the following PET/CT procedures; Near Whole Body (NWB 335 mGy.cm), H/N + NWB (525 mGy.cm), and Brain (645 mGy.cm). Provincial NM DRLs were calculated for Bone (815 MBq), Cardiac MPS (1490 MBq), Lung V/Q (40/210 MBq), Parathyroid (785 MBq MIBI), and In-111 Octreotide (135 MBq) SPECT/CT procedures. Site DRLs were calculated for all F-18 FDG PET/CT procedures; NWB or H/N +NWB (435 MBq), and Brain (270 MBq). The Sentinel Lymph Node/Melanoma procedures were too varied to establish DRL values. These values are comparable to values published in the literature. CT DRL ranges observed were Bone (150-200mGy.cm), Cardiac MPS (36-70mGy.cm), Lung V/Q (100mGy.cm, perfusion only), Parathyroid (160-170mGy.cm), In-111 Octreotide (240mGy.cm) and PET/CT NWB (400-750mGy.cm). For the radionuclide administration, the observed activity ranges were as follows; Bone (600-800 MBq), Cardiac MPS (950-1600 MBq), Lung V/Q (40/120-200 MBq), Parathyroid (700-900 MBq MIBI), In-111 Octreotide (220 MBq) F-18 FDG Near Whole Body PET (350-400 MBq), and F-18 FDG PET Brain (250 MBq). ***Conclusion:*** Several dose optimization opportunities were identified and are being pursued. For example, one system had average DLPs equal to or higher than the provincial DRL for all but cardiac studies, almost 1.5 times larger for parathyroid imaging, and double the DRL for octreotide imaging. Ongoing optimization work focuses on standardizing CT protocols. Results of the survey, comparison to European values and initial optimization efforts will be presented. ***References:*** None

EP-298

Quantification of myocardial dosimetry and glucose metabolism using a 17 segment model of the left ventricle in esophageal cancer patients receiving radiotherapy

X. Sha[1], G. Gong[1], C. Han[2], Y. Yin[1];
[1]Shandong Cancer Hospital and Institute, Shandong First Medical University and Shandong, Jinan, CHINA, [2]Turku PET Centre, Turku University Hospital, Turku, FINLAND.

Aim/Introduction: Previous studies have shown that increased cardiac uptake of 18F-fluorodeoxyglucose (FDG) from positron emission tomography (PET) may be an indicator of myocardial injury after radiotherapy. The primary objective of this study was to quantify cardiac subvolume dosimetry and 18F- FDG uptake in oncologic PET using a17-segment model of the left ventricle (LV) and to identify dose limits related to changes in cardiac FDG uptake after radiotherapy (RT). ***Materials and Methods:*** Twenty-four esophageal cancer (EC) patients who underwent consecutive oncologic 18F-FDG PET/CT scans at baseline and post-RT were enrolled in this study. The radiation dose and the 18F-FDG uptake were quantitatively analyzed based on a 17-segment model. The 18F-FDG uptake and doses to the basal, mid and apical regions, and the changes in the 18F-FDG uptake for different dose ranges were analyzed. ***Results:*** A heterogeneous dose distribution was observed, and the basal region received a higher median mean dose (18.36 Gy) than the middle and apical received the highest doses, all of which were greater than 10 Gy. Three patterns were observed for the myocardial 18F-FDG uptake related to the radiation dose before and after RT: an increase (5 patients), a decrease (13 patients) and no change (6 patients). In the pairing analysis, the 18F-FDG uptake after RT decreased by 28.93% and 12.12% in the low-dose segments (0-10 Gy and 10-20 Gy,respectively) and increased by 7.24% in the high-dose segments (20-30 Gy). ***Conclusion:*** The RT dose varies substantially within LV segments in patients receiving thoracic EC RT. Increased 18F-FDG uptake in the myocardium after RT was observed

for doses above 20 Gy. ***References:*** None

EP-299

^{177}Lu-DOTATATE Quantification for Patient Personalised Dosimetry in Therapy of Neuroendocrine Tumours

C. Rodrigues[1,2], *P. Ferreira*[1], *F. P. M. Oliveira*[1], *Â. Silva*[1], *L. Peralta*[2,3], *D. C. Costa*[1];
[1]*Champalimaud Foundation, Champalimaud Centre for the Unknown, Lisbon, PORTUGAL,* [2]*Faculdade de Ciências da Universidade de Lisboa, Lisbon, PORTUGAL,* [3]*Laboratório de Instrumentação e Física Experimental de Partículas, Lisbon, PORTUGAL.*

Aim/Introduction: Peptide Radionuclide Radiotherapy (PRRT) with ^{177}Lu-DOTATATE is a nuclear medicine therapeutic option with increasing interest over the last few years due to its efficacy in the treatment of metastatic and/or inoperable neuroendocrine tumors overexpressing somatostatin receptors. Toxicity may represent a limitation of this therapy. The evaluation of absorbed dose, besides being required by law, is an essential tool for the improvement of treatment plans. The present study investigates the average dose absorbed by the liver, kidneys, spleen and bone marrow, for further customization of future treatments. ***Materials and Methods:*** From August 2017 to March 2019, 4 patients, treated with 7.4±0.3 GBq of ^{177}Lu-DOTATATE per treatment cycle (four cycles/patient), accepted to undertake whole-body planar images, single photon emission computed tomography (SPECT) and X-ray computerized tomography (CT) images of the abdomen, at specific time points (1h, 4h, 24h and 120h), after radiopharmaceutical administration. Patient data were retrospectively selected from our institution's database. After processing, structural images were used to perform manual segmentation of the volume for all organs of interest. For each organ, the radiopharmaceutical kinetic distribution was analysed, the voxel-wise absorbed dose distribution was determined based on SPECT activity images, and the organ toxicity was assessed. ***Results:*** After completion of the four treatment cycles, the mean absorbed dose, for the 4 patients investigated, was as follows: liver 22±22 Gy; right kidney 20.3±8.6 Gy; left kidney 18±12 Gy; spleen 21.7±6.5 Gy and bone marrow 4.7±5.7 Gy. Additionally, we observed that approximately half of the mean absorbed dose on each cycle has occurred within the first five days after the radiopharmaceutical's administration. ***Conclusion:*** The mean absorbed doses in the kidneys, after all four therapy cycles, are below the established limits. On the other hand, the average value of the mean absorbed dose by the bone marrow is higher than expected[1,2]. This indicates that, in an overall analysis, the administered activity could have been altered, not in an attempt to optimize treatment effectiveness, but rather to improve bone marrow toxicity. Despite the reduced number of patients investigated, so far, our results are in agreement with the values presented by others. Ongoing work is designed to measure the absorbed dose by tumour lesions, and to optimize a protocol to implement personalized therapeutic medicine in patients with metastatic neuroendocrine tumours. ***References:*** [1] Sandstrom, M., et al. (2013), [2] Sonbol, M., et al. (2020).

EP-300

An Analysis of Post-Therapy Lu177 Uptake Progression for Individual Volumes of Interest Across a Full Treatment Cycle

S. McGurk*, D. R. McGowan, D. Morgan;*
Oxford University Hospitals NHS Foundation Trust, Oxford, UNITED KINGDOM.

Aim/Introduction: Lutetium-177 dotatate has been shown to significantly improve progression-free survival rates in patients with mid-gut NETs , however response to the treatment can vary between patients and between tumours in a given patient. The aim of this project is to use quantitative analysis of SPECT-CT images to monitor changes in Lutetium-177 uptake on a tumour by tumour basis throughout a 4 treatment cycle. ***Materials and Methods:*** Volumetric structures outlining regions of interest were generated using Hermes Hybrid Viewer on SPECT-CT studies acquired on a GE Discovery 670 24 hours after administration of the first treatment in the cycle. For each patient the liver, kidneys and spleen were outlined in addition to distinct foci of activity within or outside of these organs. The same structure sets were then applied to subsequent registered imaging studies following second, third and fourth treatments. To date in 3 patients 11 total organ volume structures were generated for liver, kidneys and spleen. In addition 17 regions of high uptake (10 within patient livers, 3 in chest and 4 in abdomen) with volumes ranging from 2.5cm^3 to 206cm^3 were identified and delineated. Count data from these volumes were converted to activities using a Lu177 sensitivity factor derived from phantom scanning. This data was used to calculate changes in uptake activity for each individual VOI relative to first treatment of the cycle at each post treatment scan. ***Results:*** To date the mean difference in measured counts across all regions was found to be -12.5% (range: -92.1% to +97.3%, n=28) from T1 to T2; +22.8% from T2 to T3 (range: -55.7% to 204.1%, n=29); -4.5% from T3 to T4 (range: -76.4% to 151.5%, n=15). The resulting total change from T1 to T4 was -4.1% (n=15), range: -95% to +148%. The rapid growth of small volume tumours can result in large proportional increases in uptake. Of the 17 tumour regions identified 5 were <10cm^3. ***Conclusion:*** This work demonstrates variability within cycles and the need for personalised dosimetry in order to understand patient response to treatments. ***References:*** None

EP-301

Effect of attenuation and scatter correction of Tc99m MAA SPECT images on dose evaluations in patients treated with Y90 resin microspheres

C. Pettinato, C. Mosconi, A. Cappelli, E. Tabacchi, E. Lodi Rizzini, S. Civollani, E. Terzi, L. Strigari, R. Golfieri;
AOU S. Orsola Malpighi - Bologna, Bologna, ITALY.

Aim/Introduction: The aim of this work was to evaluate the effect of attenuation and scatter correction on Tc99m-MAA SPECT images to calculate tumor and whole liver doses. ***Materials and Methods:*** 20 patients, treated with Y90 resin microspheres, were randomly retrospectively selected for this study. Each SPECT/CT scan data was reconstructed without any correction (IRNC), with CT based attenuation correction (IRAC) and with attenuation correction + scatter correction based on the two windows method (IRACSC). Tumor and liver doses were calculated using partition model, assuming a uniform distribution of the activity inside each compartment. The same ROI sets were applied on the three image data to calculate activities based on MAA distribution and Y90 doses.IRNC, IRAC and IRACSC results were compared in terms of tumor and liver doses by evaluating the statistical differences using a two sample t-test and calculating the relative percentage difference among values. ***Results:*** When tumor dose values were compared we found no statistically significant differences between the three data sets of images (IRNC - IRAC - IRASC). The average relative percentage differences, respectively for IRNC vs IRAC, IRNC vs IRACSC and IRAC vs IRACSC, were 2.2, 6 and 3.8% and always less than 10%. The highest tumor dose values belonged to IRACSC images while the lowest to IRNC images.On the contrary whole normal liver doses showed a statistically significant difference for all the three groups of analyses with p values less than 0.001. The average relative percentage differences, respectively for IRNC vs IRAC, IRNC vs IRACSC and IRAC vs IRACSC, were 6.7, 22.7 and 16.8%. Despite tumor doses, whole normal liver doses where higher for IRNC images and lower for IRACSC images. ***Conclusion:*** When partition model is used and uniform distribution is assumed in the different compartments, attenuation and scatter correction don't significantly affect the tumor dose calculations. On the other hand they can affect the whole liver dose evaluation. From the safety point of view if the SPECT/CT scanner is not available, that means that attenuation and scatter corrections can't be applied, the IRNC images give an overestimation of liver dose that is safe for the patient. ***References:*** None

EP-41

Technical Studies -> Dosimetry and Radiobiology -> Preclinical Dosimetry and Radiobiology

e-Poster Area

EP-302

Use of tumour control probability model for determination of treatment efficiency of head-and-neck cancer

E. Sukhikh[1,2], *Y. Sutygina*[1,3], *L. Sukhikh*[3];
[1]*Tomsk Regional Oncology Center, Tomsk, RUSSIAN FEDERATION,* [2]*National Research Tomsk Polytechnic University, Toms, RUSSIAN FEDERATION,* [3]*National Research Tomsk Polytechnic University, Tomsk, RUSSIAN FEDERATION.*

Aim/Introduction: External beam radiotherapy based on volumetric modulated arc radiotherapy technic delivery is widely used for the treatment of the locally advanced head-and-neck cancer (LAHNC). There are some approaches of irradiation of LAHNC, for example, simultaneous integrated boost (SIB) and sequential boost (SEQ). Analysis of the developed treatment plans based on tumour control probability (TCP) models (Niemierko's TCP model) could help to estimate expected efficiency of the developed plans and to find optimal treatment schemes with respect to total dose value, fractional dose and overall treatment time (OTT). In this study, the simultaneous integrated boost VMAT (SIB-VMAT) plans and sequential boost VMAT (SEQ-VMAT) plans were developed and obtained TCPs based on the anatomical data of 11 patients. ***Materials and Methods:*** The anatomical data of 11 patients with LAHNC (larynx, oropharynx and oral cavity) were used. For each patient two treatment plans were developed, SIB-VMAT (70 Gy to tumour, 50 Gy to lymph nodes, 25 fractions) and SEQ-VMAT (70 Gy to tumour, 50 Gy to lymph nodes, 35 fractions). The developed plans were analyzed using the Niemierko's TCP model with Maciejewski's parameters (TCD50=70.26 Gy) taking into account dose-volume histograms and OTT. ***Results:*** The developed SIB-VMAT and SEQ-VMAT plans had the physical coverage of the CTV tumours more than 97% of prescribed dose delivered to more than 97% of the volume, except one. The average TCP value of SIB-VMAT was equal to 99.9% due to short OTT. The average value of TCP for SEQ-VMAT was equal to 61.0%. For one patient, the both SIB-VMAT and SEQ-VMAT plans showed zero expected efficiency due to CTV coverage 95%-95%. ***Conclusion:*** According to the Niemierko TCP model using Maciejewski's parameters (Maciejewski B et al., 1989), the 50% efficiency of the treatment could be reached at EUD equal to EUD = 70.26 Gy, when the prescription dose values higher than 71-72 Gy or 70 Gy delivered in less than 35 fractions. The

analysis of selected clinical trials showed that the reported results of treatment efficiency rather well correspond to the model predictions. However, the results of DVHs calculated for real patients' anatomical data showed that even small volumes of the tumour that were irradiated to doses less than 70 Gy in 35 fractions could significantly decrease the expected TCP value. The results of simulation and analysis of clinical practice show that the DVH of each patient should be analyzed on the expected TCP. ***References:*** None

EP-42

Technical Studies -> Instrumentation -> SPECT and SPECT/CT

e-Poster Area

EP-303

Scatter correction in ^{99m}Tc SPECT by energy window narrowing and Monte Carlo simulation

S. Arvola, M. Seppänen, T. Noponen;
Turku University Hospital, Turku, FINLAND.

Aim/Introduction: Two novel methods, energy window narrowing in digital SPECT/CT scanner and Monte Carlo simulation -based method, were evaluated for ^{99m}Tc SPECT scatter correction. ***Materials and Methods:*** A Jaszczak phantom was filled with 442 MBq of ^{99m}Tc-pertechnetate and scanned using Discovery NM/CT 670 CZT camera (GE Healthcare, Tirat Hacarmel, Israel) as follows: wide-energy high resolution collimators, 120 projections over 360° with 39-s acquisition time per view, 128 × 128 matrix, and 15% energy window centered at 140 keV. A low-dose CT scan was performed for attenuation map. The SPECT acquisition was performed in list mode, which allowed generation of additional sinograms with narrower energy windows. The energy window was narrowed from 15 to 6% in one percentage point intervals producing ten separate sinograms. The data of each sinogram were reconstructed with and without Monte Carlo simulation -based scatter correction using HybridRecon-Oncology (version 3.0, Hermes Medical Solutions AB, Stockholm, Sweden) and ordered-subset expectation-maximization algorithm with six iterations and 15 subsets. Attenuation and collimator response corrections were always used, and the images were post-filtered using a Gaussian filter with 7-mm full width at half maximum. From the reconstructed images, a 15 x 15 -pixel uniform region was segmented as background, and the five largest cold spheres were segmented using spherical volumes of interest with the actual diameters (9.5 - 31.8 mm) of the spheres. Total counts, background noise, and cold sphere contrasts were measured from all 20 SPECT images. ***Results:*** Energy window narrowing from 15 to 6% reduced the number of total counts by up to 35% and increased background noise from 6 to 16%. Depending on the energy window width (EWW), Monte Carlo -simulation further reduced total counts by 12 (EWW = 6%) to 19 % (EWW = 15%) and increased background noise by 0 to 2 percentage units. Average contrast of the five largest cold spheres was not affected by EWW until it was set narrower than 9%. Then the average contrast started to decrease from 44% (EWW = 9%) to 38% (EWW = 6%). Depending on the EWW, Monte Carlo -simulation increased the average contrast by 7 (EWW = 6%) to 15 % (EWW = 15%) compared to the images without Monte Carlo -simulation. ***Conclusion:*** Monte Carlo -simulation based scatter correction increases the contrast of cold spheres in ^{99m}Tc SPECT scan when energy window narrowing preserves the contrast. ***References:*** None

EP-43

Technical Studies -> Radiation Protection -> Radiation Exposure and Protection

e-Poster Area

EP-304

Internal Audits: an Ally in the Promotion of a Radiation Protection Culture

L. Cunha[1], A. R. Roda[2,1], P. Ratão[3,1], M. Capoulas[4,1], F. Ferreira[1], M. Sousa[5], H. Vasconcelos[6,7], A. S. Moreira[1], L. F. Metello[1,8];
[1]IsoPor-Azores, Angra do Heroismo, PORTUGAL, [2]Medical Physics Department, IPOFG, Coimbra, PORTUGAL, [3]Nuclear Medicine Department, IPOFG, Lisbon, PORTUGAL, [4]Pharmacy Department, HBA, Loures, PORTUGAL, [5]Interdisciplinary Studies Research Center, ISEP.IPP, Porto, PORTUGAL, [6]Sc. Techn. Fac., Univ. Azores, Ponta Delgada, PORTUGAL, [7]CEFITEC, Physics Dept, Universidade Nova de Lisboa, Lisbon, PORTUGAL, [8]ESS-IPP, Porto, PORTUGAL.

Aim/Introduction: Internal audits are between the most important tools supporting the management board of any organization. Regardless if they are conducted by an internal or an external auditor, the goals are to assist the organization in defining areas of improvement, while providing precise information needed to accomplish the established goals. We aim to contribute to improving the community awareness of the value of conducting regular audits and its impact on promoting a culture of radiation protection. ***Materials and Methods:*** In our department, the first audit started informally, essentially consisting of a checklist of legal requisites to become licensed. Further, the implementation of a quality management system created the need for undergoing regular internal audits on a process-centered analysis. Key staff members received formal training on defining goals and conducting internal audits. The main goals for internal audits are: continuously monitoring and analyzing the risks (either new or previously identified), the implemented mitigation

measures to address those risks; verifying the compliance regarding the legal framework; identifying opportunities for improvement, and any non-conformities; making recommendations to the board. ***Results:*** Currently, the outcomes and the level of compliance of several processes are systematically checked. Examples of audited processes are patients' and referring physicians' satisfaction, work practices regarding radiation protection issues, nosocomial infection prevention and control, and written records and record keeping. During auditing, items of a checklist are scored according to the level of conformance. When no or partial conformance is detected, a recommendation is released. In the next auditing, particular attention is given to the previously identified items to check whether the level of conformance has improved and the specific issue has been completely solved. If not, a new recommendation is released. The regular auditing process had a significant impact on the overall quality of services. It also led to changes in work practices such as the implementation of stricter rules regarding record keeping, equipment quality control, survey areas for radioactive contamination, cleaning procedures, waste management, and the correct use of shielding devices. ***Conclusion:*** The auditor's role in challenging the implemented practices in a pedagogic, non-penalizing way, as well as the involvement of the management board and the entire staff, demonstrated to be THE key to a successful outcome. By challenging the implemented practices and looking at them from a different angle, we created a safer, more effective, and efficient working environment, solidifying a stronger culture on radiation protection. ***References:*** None

EP-305

Attitude and commitment of Nuclear Medicine staff towards Safety Culture working in Nuclear Medicine department

N. Marwat;
Nuclear Medicine Oncology and Radiotherapy Institute, Islamabad, PAKISTAN.

Aim/Introduction: This study aimed to measure and access the knowledge, attitude and commitment that Nuclear Medicine staff had toward safety culture in Nuclear Medicine department ***Materials and Methods:*** The study is survey based upon a questionnaire designed to access attitude towards Safety Culture.This questionnaire consisted of 10 safety culture aspects: job satisfaction, knowledge, feedback and communication about errors, teamwork, communication openness, management support, frequency of error reported, non punitive response to errors and working conditions. Nuclear Medicine staff grouped into 4 as physicians, technologists, Pharmacists and Physicists. 28 questionnaires forms have been distributed with a response rate of 100%. ***Results:*** Analysis provided an insight into attitude and commitment towards safety culture. Analysis of 10 of the broad domains of safety culture resulted: 4 of them showed strength, 4 of them has potential improvement and 2 has come up as weakness towards safety culture. Team work resulted as greatest strength while in contrary communication openness identified as weakest link towards safety culture. The survey result indicates that technologists working in Nuclear Medicine department consider the support from department and management inadequate, they report fewer incidents among the 4 professions. Punitive response analysis signifies that significant number restrain from reporting errors and events, and highlights that disciplinary response to events are major barrier to reporting. Staff have positive attitude towards safety culture, technologist have insufficient knowledge about safety culture. Positive attitude towards communicating errors is seen in maximum number of staff. Technologists do not have the required knowledge regarding safety culture as participant respondents shows the absence of training courses and unavailability of any protocols directing the staff behavior toward safety measures ***Conclusion:*** Safety Culture is vital component of safety in Nuclear Medicine. The survey suggested presence of management committed towards patient safety and encourages to report errors and near misses, who aim to improve communication and to eliminate the blame culture will serve to improve safety culture. Number of events reported can be increased by creating openness to communication. Importance of near misses is to be understood because these are powerful in identifying work process problems that can lead to an incident. Nuclear Medicine is technologically demanding field which is dependent on well trained and highly skilled staff, better safety culture demands continuous training of staff ***References:*** 1. Pfeiffer Y. Manser T. Development of the German version of the Hospital Survey on Patient safety Culture Saf Sci.2010;48:1452-1462

EP-306

Estimation of Conversion Cactors for Quality Reference mAs for Child to Adult Reference Patient in Child SPECT-CT Protocols

S. Hansen[1], *N. Bebbington*[2];
[1]*Rigshospitalet, Copenhagen, DENMARK,*
[2]*Siemens Healthineers, Aarhus, DENMARK.*

Aim/Introduction: CT image quality and radiation dose are influenced by tube voltage (kV), tube current (mAs) and patient size and shape. CARE Dose 4D modulates mAs according to patient size and shape, performing topogram (scout scan) and angular based modulation, whilst maintaining a user-defined reference image quality. On the Symbia SPECT-CT systems, the reference patient for child scans was a 20kg child prior to software version

VB10 and is a 75kg adult thereafter. The aim was to estimate conversion factors for translating quality reference mAs between child protocols using child and adult reference patients for topogram-based patient-size-related dose level adaptations, following software upgrade or procurement of a new system. ***Materials and Methods:*** The thorax, abdomen and pelvis of a Kyoto Kagaku Pediatric Whole Body Phantom PBU70, representing a 20kg child, were first scanned on the T16 with child reference (software version VA60D) at 110kV and 80kV, with 100mAs quality reference, and the actual delivered effective mAs recorded. The scans were repeated on the Intevo Bold with adult reference (VB20B), with the phantom scanned at a range of quality reference mAs settings. The delivered average mAs values were plotted against the quality reference mAs settings for both scanners. The required quality reference mAs on the Intevo Bold (adult reference) that was necessary to achieve the same delivered mAs on the T16 (child reference) was then interpolated. The factor of difference between the quality reference mAs settings for both scanners giving the same delivered mAs was then calculated. ***Results:*** To give comparable delivered mAs to the child phantom across both systems, the CT quality reference mAs for the child protocols using the child reference (T16 VA60D) should be divided by the following factors, to provide the necessary quality reference mAs setting using the adult reference (Intevo Bold VB20B): Arms up at 110kV: 3.9 (thorax), 4.3 (abdomen), 5.1 (pelvis); arms up at 80kV: 4.1 (thorax), 4.0 (abdomen), 4.7 (pelvis); arms down at 110kV: 3.5 (thorax), 3.6 (abdomen), 4.5 (pelvis); arms down at 80kV: 3.2 (thorax), 3.3 (abdomen), 4.0 (pelvis). ***Conclusion:*** Conversion factors are provided for translating quality reference mAs from child to adult reference patients in child protocols in which topogram-based patient-size-related dose level adaptations are applied, to achieve the same delivered mAs to a child phantom. The conversion factors vary slightly according to tube voltage, body region and whether the arms are up or Down. ***References:*** None

EP-307

Dose Rate from Patients after Bone and Myocardial Perfusion Scintigraphies

B. Martins*, C. Varela Pinto, D. Calado, R. Jorge, M. Correia, A. Duarte, N. Alves, M. Rézio, C. Loewenthal;*
Hospital da Luz, Lisboa, PORTUGAL.

Aim/Introduction: Our Nuclear Medicine (NM) department follows good practice recommendations, in particular regarding administered activities to patients. The aim of this study is to ascertain whether after administering recommended activities of Technetium-99m agents, the dose rate from patients leaving the unit is below the limit suggested in the literature (50μSv/h at 1 meter). The dose rate values were obtained from patients that underwent Bone Scintigraphy (BS) with ^{99m}Tc-HMDP and Myocardial Perfusion Scintigraphy (MPS) 1 day protocol with ^{99m}Tc-Sestamibi, since these two are the most commonly performed conventional studies. The study was abruptly suspended by the COVID-19 pandemia, in which only absolutely necessary tasks were performed. For this reason the number of patients included is less than initially planned. Nonetheless, the study will soon resume, as the unit gradually returns to its normal workflow. ***Materials and Methods:*** The dose rate (μSv/h) was measured in 68 patients (BS:31; MPS:37) just before leaving the department. Measurements were made with a geiger-muller detector at 1 meter from the patient anteriorly at the level of the urinary bladder, always after micturition. The administered activity, time of administration, dose rate values adjusted to the background and time of measurement were registered. Renal function was verified, whenever available, to better understand higher than expected values. ***Results:*** As expected, dose rate values were was lower with longer intervals between injection and dose rate measurement. After Bone Scintigraphy, the majority of patients left the unit more than 3h after radiopharmaceutical injection and the mean dose rate was measured at 5.6μSv/h. Following Myocardial Perfusion Scintigraphy, the majority of patients left 1-2h after the second injection of ^{99m}Tc-Sestamibi with an average dose rate of 14.2μSv/h. ***Conclusion:*** Keeping in mind the most recent concerns regarding administered activities to patients, as well as reducing the environmental impact factor of NM clinical practice, the data obtained demonstrates that the patients evaluated were well below the established dose-rate limits. Our aim is to continue to verify the dose rate from patients leaving the department for these procedures and extend it to the rest of the procedures that we normally perform, as a standard of good clinical practice. ***References:*** 1 - Florida Administrative Code - 64e-5.622 Release of Patients or Human Research Subjects Treated with Radiopharmaceuticals, Implants or Remote Afterloader Units

EP-308

Barriers and challenges in incident reporting faced by healthcare staff of Nuclear Medicine department in Rawalpindi Islamabad region

N. Marwat*;*
Nuclear Medicine Oncology and Radiotherapy Institute, Islamabad, PAKISTAN.

Aim/Introduction: The aim of the study was to explore the under reporting of incident by health care staff ***Materials and Methods:*** The study was qualitatively designed in a form of interviews with all the health care staff working in Nuclear Medicine department individually. It was a voluntary study, Nuclear Medicine working group in twin city were approached and the one who agreed were

interviewed. Interview were design With a technique of conversation, health professionals were invited to discuss their experiences, perceptions and behavior about the practice and process of incidents reporting. what challenges they come across while reporting an Incident, factors that refrain them from reporting an Incident. ***Results:*** Response rate of the study was 64 % from the overall group of health care staff , where the maximum of the response rate was 68% from the technologists working in Nuclear Medicine and minimum was from Physicians which was 58 %. The reason for not being part of the study by26 % was unclear as they remain non respondent. The analysis of this study showed that healthcare professionals, particularly doctors, are reluctant to report adverse events to a superior because of the fear of bad and irresponsible image they might develop. The biggest barrier faced by the technologists that refrain from reporting was the blame culture. Coordination between the healthcare staff and superior is second major barrier in reporting. Lack of appreciation or no appreciation to staff who come forward and report. Competency can be judged on the bases of number of incident reported by a person or a department another factor to limit incidents being non reported. No follow up of incidents being reported, lack of interest by seniors and supervisors in reported incident and stakeholders not taking responsibility for reported incident. ***Conclusion:*** Incident reporting can be a powerful tool for developing and maintaining an awareness of risks in healthcare practice in Nuclear Medicine departments. Reporting of near misses over adverse events offers numerous benefits, for that frequency of these events has to be increased. This can only be possible by increasing the trust between management and staff. Blame culture needs to be discouraged strongly. Small incentives can be given to staff who reports incidents. Balance shall be maintained between blame and feeling responsible. Safety Culture shall be promoted, openness to communication and more trust shall be developed between all the healthcare staff. ***References:*** 1. https://www.researchgate.net/publication/234703108_Can_incident_reporting_improve_safety_Healthcare_practitioners%27_views_of_the_effectiveness_of_incident_reporting 2. https://www.researchgate.net/publication/265213107_What_to_do_With_Healthcare_Incident_Reporting_Systems

EP-309

Investigation into the excretion rates and contact restrictions of Lu^{177} Dotatate patients

L. Hutton[1], *D. Morgan*[1], *D. McGowan*[1,2], *A. Hallam*[1];
[1]*Oxford University Hospitals NHS Foundation Trust, Oxford, UNITED KINGDOM,* [2]*University of Oxford, Oxford, UNITED KINGDOM.*

Aim/Introduction: ^{177}Lu Dotatate is a radiopharmaceutical which gained approval in August 2018 from the National Institute for Health and Care Excellence (NICE) and therefore there is a need for more data to be collected to investigate the radiation protection issues associated with patients undergoing this treatment. The aim of this project is to obtain detailed data to better quantify excretion rates of ^{177}Lu Dotatate from patients. ***Materials and Methods:*** Dose rate data was obtained from seven patients (1st treatment - 3, 2nd treatment - 4) to date who were given radiation monitors, calibrated against a secondary standard by Public Health England. They took dose rate/count rate readings at regular time intervals after administration of the radiopharmaceutical. Two patients were given dose rate monitors which automatically recorded their dose rate at regular intervals. The other seven patients were issued with Geiger Muller tube detectors and recorded readings in counts per second. These seven patients were encouraged to record data as often as possible with a minimum of twice per day. Two patients were issued with both types of monitors. ***Results:*** It was found that the clearance of ^{177}Lu follows a biphasic model with average effective half-life of the fast phase 25.9 hours (range: 8.4 - 73.9 hours; 3rd quartile: 27.6 hours) and the slow phase average effective half-life was 100.1 hours (range: 75.6 - 145.1 hours; 3rd quartile: 104.64 hours). This differs in comparison to values published by Levart et al. of 4.7 ± 1.4 hours for the fast clearance phase and 87.2 ± 14.7 hours for the slow phase clearance[1]. The fast clearance effective half-life is significantly longer than that quoted by Levart et al. The implications of this on patient contact restrictions is that there is an increase in their length due to family & friends and members of the public being exposed for longer and therefore to higher external dose rates. ***Conclusion:*** Although there is no published data regarding contamination from these patients, we found that significant amounts of excretion happen after patients left the hospital, potentially resulting in contamination on household items. This is due to the longer clearance times and needs to be taken into consideration when calculating contact restrictions. ***References:*** [1] D. Levart, E. Kalogianni, B. Corcoran, N, Mulholland and G. Vivian. Radiation precautions for inpatient and outpatient ^{177}Lu-Dotatate peptide receptor radionuclide therapy of neuroendocrine tumours. EJNMMI Physics. 2019;6(1):7 doi: 10.1186/s40658-019-0243-1.

EP-310

Optimisation of Lu-177 therapy administration

R. Fernandez[1], *S. Rai*[1], *A. Perry*[2], *J. Johnson*[1], *P. Croasdale*[1], *N. Eftychiou*[1];
[1]*Guy's and St Thomas' Hospital, London, UNITED KINGDOM,* [2]*King's College London, London, UNITED KINGDOM.*

Aim/Introduction: With the rapid increase in utilisation of Lutetium-177 (^{177}Lu) for molecular radiotherapy (e.g. labelling with dotatate, or more recently, PSMA or monoclonal antibodies), safe administration is crucial - both for patients

and staff involved. Various methods for ^{177}Lu treatment delivery exist. This study, based on a large UK single-centre experience, considers various scientific aspects of our established method which ensure effective ^{177}Lu therapy administration. ***Materials and Methods:*** Approximately 200 ^{177}Lu-dotatate administrations are performed annually at our centre. For a prescribed treatment activity of 7400MBq, pre-labelled ^{177}Lu-dotatate is dispensed into a plastic syringe (under sterile conditions) and infused via a 3-way tap/PVC extension tubing set and shielded syringe driver. Recent hospital-wide adoption of a different syringe driver model prompted re-evaluation of the ^{177}Lu-dotatate administration protocol, to ensure that correct activity was administered without causing significant increase in staff radiation dose. In addition to routinely worn whole-body and extremity dosimeters, all staff involved in the procedure (Radiopharmacists, Physicists, Clinicians) wore automatic real-time fingertip electronic personal dosimeters (EPDs), to determine the specific tasks contributing to their extremity exposure. ***Results:*** The administration method adopted is flexible, if required, and generates minimal solid radioactive waste (both in terms of volume and activity). Using the new syringe driver resulted in slight, but statistically significant, increase in median residual ^{177}Lu solid waste activity - 180MBq from 130MBq. Dead space of tubing/syringe was approximately 1ml. This delivery method is sufficiently sensitive to venous line patency/occlusion issues mid-therapy administration - to date only one extravasation incident has occurred using this system. Radiation dose rate at the surface of the unshielded 50ml plastic administration syringe was 75.6mSv/hour which was reduced by >99% through the use of a bespoke 12mm thick lead 'barrel shield'. All staff extremity doses as measured by EPD were reassuringly low. The level of involvement during assay/administration/dismantling/disposal meant that of all craft groups, Physicists recorded the largest extremity dose per procedure of 28.1[16.6]µSv (Mean[SD]). Although this is a non-trivial extremity dose, it is deemed acceptable. The greatest proportion of Physicist extremity dose arose from connection of the therapeutic syringe to the tubing. ***Conclusion:*** A multidisciplinary approach, together with appropriate shielding and radiation monitoring equipment, ensure that ^{177}Lu therapy can be safely and effectively administered with minimal staff radiation exposure. ***References:*** None

EP-311

Approach "Lean Thinking" to improving performance and efficiency in a Nuclear Medicine Department: a tool for radioprotection

L. Burroni[1], *F. M. Fringuelli*[1], *G. Biscontini*[1], *A. Palucci*[1], *C. Romagnolo*[1], *C. Cottignoli*[1], *C. Bianciardi*[2], *J. Guercini*[3]; [1]*Nuclear Medicine, Ancona, ITALY,* [2]*Health gestional department, Alessandria, ITALY,* [3]*Healthcare Hospital Department, Pisa, ITALY.*

Aim/Introduction: Recently Lean thinking has been introduced in healthcare for the benefit of patients, employees and hospital organisation. Applying a Lean approach in diagnostic departments, such as Nuclear Medicine, there are many opportunities for, reduce clinical and technical errors and mistakes, reduce patients and report waiting times, improve patients outcomes, increase staff productivity, decrease costs and improve employee and customer satisfaction. Aim of our work is to demonstrate that the Lean approach may be applied to a Nuclear Medicine Department improving performance and efficiency. ***Materials and Methods:*** The "spaghetti diagram" is a tool to help you establish the optimum layout for a department or ward based on observations of the distances travelled by patients, staff or radionuclides. By analysing the lines, you can identify any areas with unnecessary movements. This helps staff decide whether to bring two points closer together and how optimise the flow. The construction of the spaghetti diagram on the layout allows us to consider the pathways of health care workers and patients. In terms of radioprotection, the paths should be separated as much as possible between the radioactive patients and health professionals. In this regard, it is also necessary to calculate transit times and rest of the patients in the various areas of the department. ***Results:*** Patients wait times in hospital are long. One of the key ideas in Lean is to increase velocity by examining the revenue generating sequence of activities called VSM. When waste such as delays, errors, transportation, motion, and so forth are eliminated from these operations what remains is the ability to provide the same value in less time. Flow is the right key to increasing velocity, reducing radiations burden to the staff and population. A workcell is a work unit larger than an individual machine or workstation but smaller than the usual department. Once processing begins, they move directly from process to process. The result is very fast throughput. Communication is easy since every operator is close to the others. This improves quality and coordination. ***Conclusion:*** Lean is an innovative management approach that has proven successful in health care organizations. Lean principles hold the promise of reducing or eliminating wasted time, money and energy in health care, creating a system efficient, effective, and truly responsive to the needs of patients. The goal of Lean is to improve value for the patient and organization, also in term of radioprotection. ***References:*** None

EP-312

Improving the reliability of the assessment of the skin exposure of the hands of workers handling selected radiopharmaceuticals based on the correction of finger dosimeter readings

J. Hudzietzova[1], *M. Fulop*[2], *J. Sabol*[3], *P. Povinec*[4], *A. Vondrák*[5], *D. Baček*[4], *P. Vlk*[4], *P. Nemček*[5], *L. Foltínová*[6];

[1]Czech Technical University in Prague, Kladno, CZECH REPUBLIC, [2]ABRS, s.r.o., Samorin, SLOVAKIA, [3]Faculty of Security Management PACR in Prague, Prague, CZECH REPUBLIC, [4]PET center BIONT, a.s., Bratislava, SLOVAKIA, [5]IZOTOPCENTRUM, s.r.o., Nitra, SLOVAKIA, [6]University of Economics in Bratislava, Bratislava, SLOVAKIA.

Aim/Introduction: Recently, some new devices for the preparation or application of radiopharmaceuticals have been put into operation in order to reduce the exposure of hands. Although many workplaces are equipped with modern technology, there are still situations where workers, due to the contamination or performance of non-standard operations, may receive the elevated exposure. The aim of the paper is to overview the skin exposure related to the use of some new technologies developed over the last 10 years. At the same time, the evaluation of the local skin exposure and the correction factor associated with the manipulation involving ^{68}Ga-labelled positron radiopharmaceuticals is analysed and compared with the situation involving the use of ^{18}F-labelled radiopharmaceuticals. ***Materials and Methods:*** Two nuclear medicine departments using ^{18}F and ^{68}Ga labelled radiopharmaceuticals participated in this pilot study. Thermoluminescent dosimeters placed at 10 different locations on the palm or back of the hand were used to assess personal dose equivalent $H_p(0.07)$. The measured maximum exposure of each worker was related to the activity being manipulated. Subsequently, the average values (related to the position at the tip of the index finger) of selected groups of workers engaged in radiopharmaceutical labelling, filling into syringes and applications have been applied to establish relevant correction factors for each monitored workplace. ***Results:*** The paper presents a summary of the comparison of results from finger dosimeters in selected occupational groups in the period of 2009 - 2019 and highlights new findings regarding the correction factor for selected radiopharmaceuticals over the last decade. In addition, the pilot experiments with ^{68}Ga are discussed in terms of the average exposure of the skin of the hand in the position at the tip of the index finger of the workers. The paper also illustrates the cases of manipulation with ^{68}Ga-labelled radiopharmaceuticals, which resulted in the significantly higher exposure of the skin. ***Conclusion:*** A more detailed monitoring of the radiation exposure of the skin on more locations on the workers' hand can reveal cases of abnormal working operations or elevated local exposure, which is often found on the fingertips. Consequently, the appropriate measures should be taken to eliminate non-standard working operations in a timely manner and thus minimize this exposure. If adequate correction factors are used, the exposure at the tip of the finger can be straightforwardly estimated from the results of the routinely used finger dosimeters. ***Acknowledgments:*** Paper was partially supported by project SGS18/00/OHK4/1T/17. ***References:*** None

EP-313

Dosimetric evaluation to medical workers operating in a PET/CT department after the use of dynamic techniques

K. Dalianis[1], G. Kollias[1], K. Gogos[1], T. Pipikos[2], F. Vlachou[2], J. Andreou[2], R. Eftymiadou[2], V. Prassopoulos[2];
[1]Medical Physics Deparment, Hygeia Hospital, Athens, Marousi, GREECE, [2]PET/CT Department, Hygeia Hospital, Athens, Marousi, GREECE.

Aim/Introduction: Due to the high-energy tracers emitting 511 KeV used in PET/CT departments and considering the risks associated to ionizing radiation that have been derived from previous studies, special attention is needed when dealing with radiation protection aspects in a PET/CT modality . New radiopharmaceuticals such us [18F]-fluorothymidine and 18F fluoromethylcholine are used, new imaging dynamic techniques are performed new measurements concerning the doses to staff are needed. Aim of this study was to measure the effective wholebody dose of the personnel in comparison with measurements that have been made in the past. ***Materials and Methods:*** The estimation of equivalent dose from external dosimetry for all members of the staff was monitored with the use of TLDs badges and electronic dosimeters. In our department 18F-FDG, 18F-FCT, 18F-FCH is available in multi dose vials. ***Results:*** We compared the first six months of 2019 a period in which no FLT or FCH procedures were performed, with the second semester in which 97 FLT and 74 FCH examinations were performed. The average number of FDG patients was the same for every day. The measurements for the nurses show increased wholebody dose of about 7-12% and that is due to the longer time spent near the patient. Concerning the technologist doses, an increase of about 15-21% was measured because they are near to patient at the time of the injection. ***Conclusion:*** From our results we can observe that although there is an increase of the doses for technologists and nurses the numbers are significantly lower than the recommended annual dose limit. ***References:*** Dalianis K, Malamitsi J, Gogou L, Pagou M, Efthimiadou R, Andreou J, Louizï A, Georgiou E Dosimetric evaluation of the staff working in a PET/CT department, Nuclear Instruments and Methods in Physics Research A 569, 548 - 550.

EP-314

Validation of an alternative measurement method to verify [131I]-NaI capsules activity by dose rate determination

C. Franco Monterroso[1], A. Hernández Fructuoso[2], B. Santos Montero[2], J. Romero Herrera[1], J. Castell Conesa[1];
[1]Hospital Universitari Vall d'Hebron, Barcelona, SPAIN, [2]Hospital Universitari Vall d'Hebron. Institut de Diagnòstic per la Imatge, Barcelona, SPAIN.

Aim/Introduction: Handling of [^{131}I]-NaI capsules to check

the reference activity leads to a radiation exposition increase, especially in hands. The aim of this study was to validate an alternative method to verify each capsule activity by dose rate determination, with the purpose of reducing this exposition. ***Materials and Methods:*** Two study groups (A and B) were established according to capsule lead container thickness (mm). 17 capsules of 555MBq and 13 of 1110 MBq contained in 18.7mm lead shields were included in Group A (n=75) and 10 capsules of 3700 MBq and 9 of 5550 MBq in leads containers of 28, 5mm thick in Group B (n=40). Each capsule dose rate was determined keeping itself in the original container with a commercially dose rate meter (E0111280 series MiniTrace Gamma). 3 measurements were taken for each capsule, turning it around its axis. All capsules were placing on a template to 30cm from a dose rate detector to warrant the reproducibility of the measurements. The exact activity of the [^{131}I]-NaI capsules was subsequently measured using a dose calibrator (Capintec CRC-55tR). Calibrating curves were created by linear correlation between the obtained results for each group (MBq vs μSv/h). ***Results:*** The average activities and dose rates obtained for 555 and 1110 MBq capsules (group A) were 601.5±8.23 MBq, 1200.17±31.06 MBq and 11.28±0.37 μSv/h, 22.06±1 μSv/h respectively. For 3700 and 5550 MBq capsules (group B) the average measurements were 4012.87±37.08 MBq, 5979.20±97.69 MBq and 21.9±0.98 μSv/h, 33.05±0.71 μSv/h respectively. Regression analysis showed a high correlation (r = 0.992 for group A and r = 0.987 for group B). The measurement uncertainty of the method was under 5%. ***Conclusion:*** This alternative method allows an accurate measurement activity before dispensing [^{131}I] -NaI, keeping itself in the shielded lead container and reducing personnel dosimetry. ***References:*** None

EP-315

Radiation Exposure of the Fingers during Preparation and Administration of ^{90}Y-Ibritumomab-Tiuxetan for Radioimmunotherapy of Non Hodgkin Lymphoma (NHL)

C. Happel*, W. T. Kranert, B. Bockisch, D. Gröner, A. Sabet, F. Grünwald;*
University Medical Center Frankfurt, Department of Nuclear Medicine, Frankfurt, GERMANY.

Aim/Introduction: Radioimmunotherapy of NHL with ^{90}Y-Ibritumomab-Tiuxetan has been increasingly implemented during the last decade. Handling of pure beta-emitters can cause significant radiation exposure due to external irradiation by Bremsstrahlung and contamination during preparation and administration. Influence of different locations of ring dosimeters on the obtained dose should be determined. ***Materials and Methods:*** For radioimmunotherapy of NHL ^{90}Y-labelled monoclonal CD20 antibodies were used. Preparation was carried out by the technical staff in a lead shielded workbench according to the manufactures instructions and averaged 67min (50-90min). The substance was injected intravenously by a physician and lasted around 10min in each case. In both cases extra dense gloves were worn to avoid contamination. Syringes and vials were shielded with acrylic glass belonging to the preparation kit. Radiation exposure during preparation and administration was determined using thermoluminescence ring dosimeters (GSF-TL-TD Typ X). The detection limits are 7.6keV to 3MeV for photons and >50keV for beta-. Physicians and technical staff wore 5 TLDs on each hand in each case (fingertip and first phalanx of index and middle finger and on the thumb). ***Results:*** All the following results are given in mSv/GBq administered ^{90}Y-Ibritumomab-Tiuxetan. Mean finger exposure during preparation was for the right hand: 3.72 for the index fingertip, 2.57 for the phalanx of the index finger, 1.37 (fingertip) and 1.54 (phalanx) of middle finger (right hand); for the left hand: 5.15 (fingertip) and 12.3 (phalanx) of index finger and 7.20 (fingertip) and 6.05 (phalanx) for the middle finger. The thumbs showed a mean exposure of 1.72 (right) and 4.33 (left). The mean finger exposure during administration was for the right hand: 2.91 (index fingertip), 1.32 (index phalanx); 0.58 (middle fingertip) and 0.49 (middle finger phalanx); and for the left hand: 121.1 (index fingertip), 28.7 (index phalanx); 108.5 (middle fingertip) and 19.6 (middle finger phalanx). The thumbs showed a mean exposure of 1.77 (right) and 2.23 (left). All physicians and technical employees were right handed. ***Conclusion:*** In both cases the highest exposures were detected at the index finger of the left hand. Therefore the index finger of the left hand is the best location to wear a ring dosimeter for handling, labelling and administration of ^{90}Y-Ibritumomab-Tiuxetan. ***References:*** None

EP-316

Effective dose of for medical workers operating in a PET/CT department

K. Dalianis[1]*, G. Kollias*[1]*, K. Gogos*[1]*, T. Pipikos*[2]*, M. Vogiatzis*[2]*, F. Vlachou*[2]*, V. Prassopoulos*[2]*;*
[1]*Medical Physics Deparment, Hygeia Hospital, Athens, Marousi, GREECE,* [2]*PET/CT Department, Hygeia Hospital, Athens, Marousi, GREECE.*

Aim/Introduction: The PET/CT applications have been continuously increasing for diagnostic procedures. Although such an increase is a positive trend for the benefit of patients, the associated risk of radiation exposure of staff needs to be properly evaluated. The aim of this study was to measure the radiation exposure of the staff and evaluate the doses in the first PET/CT department in Greece at Hygeia S.A. ***Materials and Methods:*** To estimate the effective dose from external exposure all 6 members of the staff (2 nurses, 2 medical physicists, 2 technologists, had TLD badges worn at the upper pocket of their overall, TLD

rings on the second finger of each hand constning of disk measuring diameter by 0,9 mm thickness. The basics stages for the PET/CT procedures involve 4 steps: segmentation of the dose, injection of the radiopharmaceutical, nursing care during uptake and positioning of the patient. ***Results:*** The results of our study for the average cumulative whole body dose for 100 patients (μSv±SD) at different stages were: segmentation of the dose 189±7,23, injection of the radiopharmaceutical 245±6,67, nursing care during uptake 70±5,63, positioning of the patient 146±12,3. The statistical analysis showed small differences between stages 1, 2 and 4 (p>0,05) but a great statistical difference was observed between stages 2,3 p=0,023. The results for the finger doses (μSv±SD) regarding the same stages were: segmentation of the dose 284±77.4, injection of the radiopharmaceutical 225±62.3, positioning of the patient 26,79±5.87. ***Conclusion:*** N} The personnel dose results are significantly lower than the recommended annual dose by International Commission for Radiological Protection. However a greater effort should be made to reduce the doses further in line with the ALARA principle ***References:*** Dalianis K, Malamitsi J, Gogou L, Pagou M, Efthimiadou R, Andreou J, Louizï A, Georgiou E Dosimetric evaluation of the staff working in a PET/CT department, Nuclear Instruments and Methods in Physics Research A 569, 548 - 550.

EP-317

CT radiation dose in whole-body PET/CT in relation to arm position in patients with different Body Mass index

G. Marotta*, M. F. Bardo, M. Schiavini, F. Buffoni, R. Leo, M. Rognoni, D. Capolongo, R. Pino, N. Basilico, E. Orunesu, E. Galli, R. Casati, I. Martina, C. Fabbri, L. D'Antonio, D. Marchelli, F. Voltini, C. Canzi;*
Fondazione IRCCS Ca' Granda Ospedale Maggiore Policlinico, Milano, ITALY.

Aim/Introduction: In whole-body PET/CT examinations a large contribution to patient radiation exposure is due to CT scan. Automatic Exposure Control (AEC) software initially determines tube current modulation using scout images and then modifies it during CT acquisition. Aim of the study was to evaluate the role of arm position on CT exposure reduction in patients with different body mass index (BMI). ***Materials and Methods:*** In whole-body PET/CT, radiation exposure doses with AEC routinely used with postero-anterior view (PA) scout images with arms up and down was investigated, using a 4-ring PET/CT scanner and with a AEC proprietary software. Ninety adult patients, who underwent whole-body PET/CT twice, once with their arms up and once with their arms down, were divided into 3 groups according to the Body Mass index: 10 underweight, 42 with normal weight and 38 overweight or obese. Changes of mAs affecting CTDIvol between arms up and down were determined. ***Results:*** Normalised tube current was significantly higher with the arms up than down in the head and neck and significantly lower in the shoulder, abdomen, pelvis, and proximal thigh . Analysis of variance showed that the effective dose was reduced significantly with arms up than arms down in all groups (p<0.01). The means of mAs and CTDIvol (in mGy) were respectively in underweight patients 53 and 3.58 with arms down and 43 and 2.95 (-22%) with arms up, in patients with normal weight 62 and 4.24 with arms down and 52 and 3.54 (-20%) with arms up, and in overweight or obese patients 78 and 5.41 with arms down and 66 and 4.58 (-19%) with arms up. ***Conclusion:*** Raising the arms increased radiation dose in the head and neck and decreased it in the chest and abdomen, resulting in overall reduction of effective dose, of greater relevance in underweight patients. These characteristics of AEC behaviour should be considered to determine an optimal imaging protocol for whole-body PET/CT. ***References:*** None

EP-318

Dose Optimization Of Brain Tomographic Studies Through Quantitative Analysis Of The ASIR Reconstruction Technique

J. Bustos*, A. Ruiz;*
Nuclear and Molecular Medicine Center Foundation Entre Rios, Entre Rios, ARGENTINA.

Aim/Introduction: ASIR is a hybrid Reconstruction Method that combines the Filtered Back Projection Analytical Method (FBP) and the Statistical Iterative Method that models noise. This algorithm is implemented in discrete quantities by adjusting the percentage from 10 to 100% and is used in conjunction with dose reduction.Therefore, studies were carried out whose purposes are to determine the Relationship of Compromise Between Image Quality and Radiation Dose by applying dose reduction and the ASIR reconstruction algorithm in brain tomography studies. ***Materials and Methods:*** The experimental development was carried out at the CEMENER facilities, in the nuclear medicine service. Discovery PET / CT 710 equipment was found with 64-slice CT. Tests were performed on phantoms of QA provided by General Electric and Capthan 500. In the first instance, the protocol for brain tomographic studies was particularly addressed. A quantitative and qualitative analysis of image quality was performed. The aspects evaluated quantitatively were noise, the signal-to-noise ratio, the high and low contrast ratio and the Hounsfield Units. Regarding the qualitative analysis, the CEMENER medical imaging specialist carried out a subjective evaluation taking into account noise, artifacts, sharpness and diagnostic acceptability. ***Results:*** The Results show that it is possible to remarkably improve the image quality and decrease the radiation dose to the patient by applying a dose reduction of 40% and 60% of ASIR. Therefore, it is

concluded that the application of ASIR has a positive impact with respect to the radiation received by the patient, and the impact on the useful life of the tube in relation to the milliamperage used. It was applied to the brain protocol used in the CEMENER, resulting in less radiation to the patient, going from 320mA to 190mA, with a CTDIvol of 59 mGy to 35 mGy with medical endorsement in image quality in terms of noise, sharpness and diagnostic acceptability. ***Conclusion:*** As a corollary, the use of the ASIR reconstruction algorithm was found to allow for a significant 40% dose reduction in brain CT studies and to use 60% ASIR or higher, without compromising image quality. ***References:*** None

EP-44

Technical Studies -> Radiopharmacy/ Radiochemistry -> New Biological Targets and Ligands

e-Poster Area

EP-319

Evaluation of Iodine-131 Labelled Lawsone (2-Hydroxy-1,4-Naphthoquinone) Compound's Transdermal and Intravenous Biodistribution

V. Tekin[1], U. Korkmaz[2], I. Ince[1], I. Kutlubay[2], G. Durmus Altun[2], F. Biber Muftuler[1];
[1]Ege University, Izmir, TURKEY, [2]Trakya University, Edirne, TURKEY.

Aim/Introduction: One of the popular therapeutic herbs is Lawsonia inermis, which has many local names such as Mhendi, Shudi, Madurang, and Goranti, known as 'Henna'. Lawsone (2-hydroxy-1,4-naphthoquinone) (LW) is one of the main compounds of the henna plant and colors with its own orange-red colorants. Many studies have reported that the LW compound has anticoagulant, anticancer, antioxidant, antibacterial and antifungal effects. The systemic distribution of LW is unknown, because of direct use to the skin surface as traditionally method. In presented study, systemic biodistribution of I-131 labeled LW, after intravenous injection and transdermal use was evaluated with the aim of highlight the potential of the clinical use of LW. ***Materials and Methods:*** Lawsone (LW) compound was radiolabeled with 131I. Radiolabelling yield was calculated as 92.70±4.312% by Thin Layer Chromatography (TLRC). Six female adult SD rats (mean weight 214±14g) were used in the study. Study groups were planned as 3 rats for the use of transdermal gel (TDJ LW) and 3 rats for the intravenous (IV LW) injection. I-131 labeled LW Carbomer Gel (5 mCi, 100 mg/ml) was prepared for the TDJ use and 0.5 mCi I-131 LW was injected intravenously for the systemic biodistribution study. For both study groups of TDJ and IV, 1 hour dynamic imaging and 2,4,12 and 24h static imaging were performed after use and injection. The biodistribution of LW was quantitatively evaluated by using whole body images for all time periods. After imaging study, tissue weights were measured and the distribution of homogenized tissues was determined using a gamma counter. 1 hour dynamic imaging was performed with HE collimators (64x64 matrix) and static imaging was performed with 512x512 matrix by recording anteriorly and posteriorly. ***Results:*** It was observed that I-131 labeled LW compound showed high uptake in liver, kidney, stomach, muscle and blood compared to other organs after TDJ and IV. ***Conclusion:*** Although henna is a bioactive which is directly used to skin surface, the main component of the henna (LW) is able to use for systemic circulation. The blood level is high even after 24 hours after intravenous injection. ***References:*** None

EP-45

Technical Studies -> Radiopharmacy/ Radiochemistry -> New Radiopharmaceuticals - PET

e-Poster Area

EP-320

Influence of the glutamate concentration on [^{18}F] PEB binding to metabotropic receptor subtype 5 : a translational study

A. Dupont[1,2], S. Serrière[2], L. Barantin[2], J. Vercouillie[2,3], V. Gissot[3], S. Bodard[2], G. Chicheri[2], S. Chalon[2], F. Bonnet-Brihault[2,4], M. Santiago Ribeiro[5,2,3], N. Arlicot[1,2,3];
[1]Radiopharmacie, CHRU Tours, Tours, FRANCE, [2]UMR1253, iBrain, Inserm, Tours, FRANCE, [3]CIC 1415, Inserm, CHRU Tours, Tours, FRANCE, [4]Centre universitaire de Pédopsychiatrie, CHRU Tours, Tours, FRANCE, [5]Service de Médecine nucléaire, CHRU Tours, Tours, FRANCE.

Aim/Introduction: Glutamate is the most abundant excitatory neurotransmitter in the human brain and altered glutamate signaling is thought to be involved in a myriad of neurological disorders. Positron emission tomography (PET) imaging with [^{18}F]PEB allows assessing dynamic changes in metabotropic glutamate receptor 5 (mGluR5) availability underlying neuropathological conditions. However the influence of endogenous glutamate levels on the receptor binding has not been well established yet. The purpose of this study was to explore the [^{18}F]PEB binding regarding to physiological fluctuations or acute changes of glutamate synaptic concentrations by a translational approach; i.e. a PET/MRS imaging study in healthy human volunteers combined to a PET imaging after an N-acetylcysteine (NAc) pharmacological challenge in rodents. ***Materials and Methods:*** Glutamate (Glu) and glutamine (Gln) levels from 12 healthy adult males were assessed from MRS data collected from the anterior-cingulate cortex (ACC) with

PRESS, and mGluR5 binding (BP_{ND}) was assessed from PET data collected with [^{18}F]PEB. We correlated the [^{18}F]PEB (ACC BP_{ND}/Cerebellum BP_{ND}) with Glu/Cr, Gln/Cr ratios in the ACC. MicroPET [^{18}F]PEB dynamic acquisitions were conducted in 9 rats after an i.v. injection of either water (test/retest) or NAc 50mg/kg (challenge), a promoter of the cystine-glutamate antiporter that increases extra synaptic glutamate release. The microPET images for the regions of interest (ROI) of caudate putamen, amygdala, thalamus, cingulate and cerebellum were analyzed. Time-activity curves were obtained from ROI defined on the rat MRI T2 template and all SUV ratios were calculated using the cerebellum as the reference region. ***Results:*** In healthy humans, no statistically significant correlation was evidenced between the physiological concentrations of Glu and Gln and [^{18}F] PEB binding. ACC BP_{ND}/Cerebellum BP_{ND} vs Glu/Cr: r=0.303, p=0.315; Gln/Cr: r=-0.299, p=0.320.In rats, no changes in SUVr measurements were observed in the test and retest conditions nor in the NAc condition in any ROIs analyzed (p>0.17). ***Conclusion:*** In humans, [^{18}F]PEB binding did not show sensitivity to glutamate concentrations in physiological conditions as an independent outcome. In rodents, a pharmacological challenge with NAc did not affect the [^{18}F]PEB binding in rodents. These data suggest that the in vivo affinity of [^{18}F]PEB to an allosteric site of mGluR5 is not sensitive to changes in glutamate levels. [^{18}F] PEB seems therefore as a reliable radioligand to quantify the mGluR5 availability despite potential heterogeneity of glutamate concentrations. ***References:*** None

EP-321

Synthesis and Pre-clinical Evaluation of Novel Piperazine Amide-modified ^{18}F-Rhodamines as Myocardial Perfusion Imaging Agents

J. Inkster[1,2], J. L. J. Dearling[1,2], E. Snay[1], A. B. Packard[1,2];
[1]Boston Children's Hospital, Boston, MA, UNITED STATES OF AMERICA, [2]Harvard Medical School, Boston, MA, UNITED STATES OF AMERICA.

Aim/Introduction: Rhodamine dyes are fluorescent lipophilic cations that exhibit affinity for cells with high mitochondrial activity, such as cardiomyocytes. Rhodamine esters bearing ^{18}F-fluorinated aliphatic chains have been identified as a new class of myocardial perfusion imaging agents.[1] Our goal is to develop "next generation" ^{18}F-rhodamines that exhibit enhanced in vivo stability. Thus, we are targeting derivatives in which the ^{18}F pendant group is a) aromatic and b) attached to the rhodamine via an amide (vs. ester) bond. In addition, the amide linkage should decrease radiotracer lipophilicity and potentially improve heart uptake while decreasing uptake in the liver. Secondary rhodamine amides have the potential to cyclize to form neutral lactams. Thus the 1-(4-[^{18}F]fluorobenzoyl)piperazine group was chosen for investigation, as piperazine amides are tertiary and cannot cyclize. ***Materials and Methods:*** The precursors (RhoB-pip and Rho6G-pip) of 1-(4-[^{18}F]fluorobenzoyl) piperazine-modified rhodamine B ([^{18}F]FRhoB-pip-Ar) and rhodamine 6G ([^{18}F]FRho6G-pip-Ar) were prepared by coupling N-Boc-piperazine with rhodamine B base or rhodamine 6G inner salt, respectively, in the presence of amidation reagent HBTU and triethylamine (TEA), followed by TFA-mediated Boc-deprotection. A second HBTU/TEA amidation reaction with 4-fluorobenzoic acid (FBA) yielded the ^{19}F standards. [^{18}F]FBA was synthesized in two steps from ethyl 4-(trimethylammonium triflate)benzoate under standard ^{18}F-fluorination conditions ($K_{2.2.2}$/K_2CO_3/Δ), then conjugated to RhoB-pip or Rho6G-pip (HBTU/TEA, DMSO, RT, 15 min). HPLC-purified [^{18}F]FRhoB-pip-Ar (3.4 MBq) or [^{18}F]FRho6G-pip-Ar (9.5 MBq) was injected into the lateral tail vein of a Sprague-Dawley rat. PET/CT data was collected over 60 minutes. ***Results:*** [^{18}F]FRhoB-pip-Ar and [^{18}F]FRho6G-pip-Ar were prepared in 4-21% DC-RCYs. PET images reconstructed over 5-min intervals show modest heart uptake that remains essentially unchanged over 60 min (SUVs: 0.23→0.19 and 0.14→0.15 %ID/mL, respectively). The ratio of activity concentration in heart vs. liver was <1 and increased marginally over time (0.06→0.14 and 0.08 →0.20, respectively). In contrast, the heart/liver ratios of ^{18}F-diethyleneglycol-bearing rhodamine 6G ester [^{18}F] FRho6G-DEG[1a] increased from 0.38→2.0 over the same interval. ***Conclusion:*** PET imaging of [^{18}F]FRhoB-pip-Ar and [^{18}F]FRho6G-pip-Ar in rats suggest that both radiotracers exhibit higher in vivo stability than the established tracer [^{18}F]FRho6G-DEG, but lower overall heart uptake. The 1-(4-[^{18}F]fluorobenzoyl)piperazine moiety is likely responsible for both of these phenomena. Thus, our next efforts will include the preparation of ^{18}F-rhodamines in which the stabilizing piperazine group is retained, but the radioisotope is attached via a hydrophilic oligo(ethylene glycol) chain rather than a lipophilic benzyl moiety. ***References:*** [1]a) M.D. Bartholoma et al., Nucl. Med. Biol. 2015, 42, 796;b)M.D. Bartholoma et al., J. Med. Chem. 2012, 55, 11004.

EP-322

Head to head comparison of [^{15}O]H_2O and [^{11}C]MMP in non-human primates; tracers for measuring regional cerebral blood flow

J. Toyohara[1], T. Kakiuchi[2], H. Ohba[2], M. Kanazawa[2], T. Tago[1], M. Sakata[1], N. Harada[2];
[1]Tokyo Metropolitan Institute of Gerontology, Tokyo, JAPAN, [2]Hamamatsu Photonics, Hamamatsu, JAPAN.

Aim/Introduction: Increases in fasting plasma glucose (PG) levels lead to a decrease in [^{18}F]FDG uptake, especially in the precuneus, resulting in an Alzheimer's disease (AD)-like pattern. Therefore, patients with higher PG levels, such as those with diabetes, can be erroneously diagnosed with AD when PET imaging is done using [^{18}F]FDG, due

to reduced uptake of [^{18}F]FDG in the precuneus. To help avoid an erroneous diagnosis of AD due to differences in glucose metabolism, evaluating cerebral blood flow (CBF) in the brain is useful. However, current techniques such as SPECT and ^{15}O-water PET have limitations in early diagnosis of AD because the images of they produce are of low resolution. Recently, we developed N-isopropyl-p-[^{11}C] methylamphetamine ([^{11}C]MMP) as a carbon-11-labeled alternative of the standard CBF SPECT tracer N-isopropyl-p-[^{123}I]iodoamphetamine. In this study, we evaluated the brain kinetics of [^{11}C]MMP in the non-human primate. Head-to-head comparison with [^{15}O]H_2O was also evaluated. ***Materials and Methods:*** Two successive PET measurements with [^{15}O]H_2O and [^{11}C]MMP under vehicle and acetazolamide (AZM: 10 mg/kg or 20 mg/kg) loading conditions were performed in 3 conscious state male monkeys (Macaca mulatta) with arterial blood sampling. Metabolite-corrected plasma and whole-blood time-activity curves were used as an input function for pharmacokinetic modeling of [^{11}C]MMP. The preferred model was chosen according to the Akaike Information Criterion (AIC) and were used to calculate the influx constant (K_1). Moreover, standardized uptake values (SUV) were estimated using different time intervals. ***Results:*** The preliminary kinetic analysis of the comparison of AIC (paired t test, $P < 0.05$) in all regions investigated showed that 1-tisue-compartment model provided significantly better AIC scores than the 2-tissue-compartment model ($n = 3$). The regional K_1 values of [^{11}C]MMP in vehicle treated monkey were well correlated with that in rCBF (Pearson $r = 0.9230$, $p < 0.0001$). Furthermore, short duration scan (0-10 min) of SUV showed good correlation with rCBF ($r = 0.9042$, $p < 0.0001$), too. The data suggest that [^{11}C]MMP probably detect changes of rCBF in the low to normal range of flows. However, this correlation was decreased at higher flow range under AZM-loading (10 mg/kg: $r = 0.6581$, $p = 0.0041$; 20 mg/kg: $r = 0.7510$, $p = 0.0005$), due to the underestimation of rCBF at higher flows. ***Conclusion:*** The K_1 and early phase SUV (0-10 min) of [^{11}C]MMP well reflect rCBF in vehicle treated non-human primate, but that in higher flow region after AZM-loading did not. ***References:*** None

EP-323

Development and Preclinical Evaluation of New Theranostic ^{64}Cu-Folates for Folate Receptor-Positive Tumor

I. Aljammaz[1], *B. Alotaibi*[1], *Y. Almalki*[1], *N. Alhokbani*[2], *S. Okarvi*[1];
[1]*King Faisal Specialist Hospital and Research centre, Riyadh, SAUDI ARABIA,* [2]*King Saudi University, Riyadh, SAUDI ARABIA.*

Aim/Introduction: Membrane-folic acid receptor is a glycosylphosphatidylinositol protein that overexpressed in approximately 100% of ovarian adenocarcinomas and various epithelial cancers. Meanwhile, this receptor is highly restricted in most normal tissues which make these tumors as excellent candidates for molecular targeting through the folate receptor system. Folic acid has been conjugated with various chelates via its carboxylate of the glutamic acid fragment. These conjugates have shown considerable success for delivering various radionuclides to folate-receptor-positive KB cell tumor xenografts in athymic mouse models. Among these radionuclides gallium-67/68, indium-111, technetium-99m and fluorine-18 appeared to be feasible in targeting folate receptor expressing tumors in-vivo. Recently, radiolabeled $^{67/68}$Ga-DOTA and NOTA based folate conjugates were synthesized and their characteristics were similar to ^{111}In-DTPA-folate, which has been used in clinical trials. Due to the known high stability of Cu^{II}-NOTA complex and in an attempt to develop new folate radiotracers with favorable properties for detecting folate receptor-positive cancers, we here report the synthesis and preclinical evaluation of new ^{64}Cu-NOTA- and NATOAM-folate conjugates using 1,4,7-triazacyclononane-1,4,7-triacetic acid (NOTA) and 1,4,7-triazacyclononane-1,4,7-triamine (NOTAM) as chelating groups. ***Materials and Methods:*** The synthetic approaches for the preparation of ^{64}Cu-NOTA- and ^{64}Cu-NOTAM-folate conjugates were straightforward. Solutions of $^{64}CuCl_2$ (37-300 MBq) were reacted with NOTA- and NOTAM-folate conjugates in acetate buffer (pH ~4.5) at 80°C and different time range. Work up of these conjugates gave ^{64}Cu-NOTA- and ^{64}Cu-NOTAM-folate conjugates in quantitative radiochemical yields and purities as assessed by TLC and HPLC in less than 20 min. ***Results:*** The stability of these radioconjugates were determined in human plasma and revealed that radioconjugates remained stable during incubation at 37°C for at least 4 h. In vitro receptor binding studies performed using folate receptor-positive KB cell-line, showed that significant amount of these radioconjugate were associated with cell-fractions and the in vivo biological characterizations were carried out in normal Balb/c mice revealed rapid blood clearance of radioconjugates with excretion predominantly by the urinary system. Biodistribution studies in nude mice bearing human KB cell-line xenografts, demonstrated substantial tumor uptake (~20%, ID/g). This uptake was blocked by excess co-injection of folic acid suggesting a receptor-mediated process. ***Conclusion:*** These results demonstrate that ^{64}Cu-NOTA- and ^{64}Cu-NOTAM-folate conjugates may be useful as molecular theranostic probe for detecting and staging of folate receptor-positive cancers and possibly treatment. ***References:*** None

EP-324

Novel radiofluorinated silicon rhodamines for bimodal PET and NIR-optical imaging

T. Kanagasundaram[1,2], *M. Laube*[1], *S. Stadlbauer*[1], *C. Kramer*[3], *J. Pietzsch*[1], *K. Kopka*[1];
[1]*Helmholtz Zentrum Dresden Rossendorf, Institute of Radiopharmaceutical Cancer Research, Dresden,*

GERMANY, [2]Heidelberg University, Faculty of Chemistry and Earth Sciences, Heidelberg, GERMANY, [3]German Cancer Research Center, Heidelberg, GERMANY.

Aim/Introduction: Radiolabelled fluorophores are decisive for bimodal imaging and currently in demand for PET- and optical imaging. Fluorescent dyes show unique optical properties such as high quantum yields and extinction coefficients. FDA approved fluorophores (e.g. 5-ALA or ICG) are well-known for their use in fluorescence-guided intraoperative surgery. The goal of this work was the development of near-infrared (NIR) light-emitting silicon-rhodamines for PET- and optical imaging. The synthesized first-in-class dyes were prepared for their subsequent conjugation to the PET-compatible radioisotope fluorine-18 with the aim to elucidate their potential as imaging agent for the detection of tumors and their metastases. Moreover, the Si-rhodamines were bioconjugated to the PSMA-binding motif as a generic prominent tumor targeting binding vector for an enrichment in prostate tumors (1). For this reason the introduced dyes are intended to be used for non-invasive PET imaging (prestaging) followed by fluorescence/(radio)-guided R0-tumor-resection. ***Materials and Methods:*** The combination of PET- and optical imaging leads to new approaches in tumor imaging and resection. This powerful method enables the accurate differentiation of healthy and affected tumor tissues. We have designed fluorophores of the silicon (Si)-rhodamine family with absorption and emission properties in the near-infrared region of about 650 nm (2). The Si-rhodamines were radiolabelled by using the alcohol-enhanced and copper-mediated approach for radiofluorination (3). Finally, the dyes were characterized using NMR-, UV/VIS/NIR-spectroscopy and mass spectrometry and their radiolabelling properties were analyzed. ***Results:*** The classical synthesis pathway of novel Si-rhodamines through xanthone building blocks provided boronic acid functionalized Si-rhodamines with overall yields of 43%. The acid functionalized Si-rhodamines were conjugated to the PSMA-inhibitor binding motif to receive an increased selective enrichment in tumors (1). The dyes show large extinction coefficients up to 72.000 $M^{-1}cm^{-1}$, quantum yields of 0.33 and high photostabilities making them potentially useful for NIR-optical imaging. As shown by human serum stabilities the radiofluorinated Si-rhodamines show valuable and promising performance for in-vitro and in-vivo experiments. ***Conclusion:*** Novel NIR-fluorescent dyes based on the Si-rhodamine lead structure were synthesized and chemically characterized and their efficiency under radiolabelling conditions were determined. Profitable optical- and radiolabelling properties show promising performance for biological performance. For this reason, our first-in-class radiolabelled and bioconjugated Si-rhodamine dyes are subject of current and future biological evaluation. ***References:*** (1) K. Kopka et al., J. Nucl. Med. 2015, 56, 914-920. (2) T. Nagano et al., J. Am. Chem. Soc. 2012, 134, 5029-5031. (3) B. Neumaier et al., Chem. Eur. J. 2017, 23, 3251-3556.

EP-325

Radiosynthesis and initial evaluation of [^{18}F]FBAT forin vivoPET imaging of inducible nitric oxide synthase

H. Yeh[1], *W. Huang*[2], *C. Chiu*[3], *C. Chen*[4], *K. Ma*[5], *H. Tian*[6], *T. Yu*[7], *P. Wang*[7], *Y. Kuo*[2], *C. Chang*[2];
[1]National Yang-Ming University, Taipei, TAIWAN, [2]Department of Nuclear Medicine, Taipei Veterans General Hospital, Taipei, TAIWAN, [3]Department of Nuclear Medicine, Tri-Service General Hospital, Taipei, TAIWAN, [4]Department of Biomedical Imaging and Radiological Sciences, National Yang Ming University, Taipei, TAIWAN, [5]Departments of Nuclear Medicine and Biology and Anatomy, National Defense Medical Center, Taipei, TAIWAN, [6]Departments of Biomedical Engineering and Radiology, Case Western Reserve University, Taipei, OH, UNITED STATES OF AMERICA, [7]Brain Research Center, National Yang Ming University, Taipei, TAIWAN.

Aim/Introduction: The role of inducible nitric oxide synthase (iNOS), a nitric oxide synthase, in neuroinflammation—specifically the function of microglia in inflammatory processes—has been widely investigated; iNOS may be an important biomarker of the risk of neuroinflammation. Development of radiopharmaceuticals based on selective iNOS inhibitors has enabled positron emission tomography (PET) imaging of iNOS protein levels. However, the low brain levels of iNOS (even under neurodegenerative conditions), expression of iNOS by cells other than microglia (astrocytes, peripheral macrophages during blood brain barrier breakdown), genetic polymorphisms that affect the binding affinity of most iNOS PET radiopharmaceuticals, and similar levels of iNOS expression in activated microglia regardless of polarization (pro- or anti-inflammatory state) limit the potential of iNOS as a PET biomarker. ***Materials and Methods:*** We carefully defined a strategic plan to develop iNOS-targeted molecular PET imaging using (4′-amino-5′,8′-difluoro-1′H-spiro[piperidine-4,2′-quinazolin]-1-yl)(4-fluorophenyl)methanone ([^{18}F]FBAT) as a tracer to detect iNOS in a mouse model of lipopolysaccharide (LPS)-induced brain inflammation. ***Results:*** [^{18}F]FBAT yield ranged from 2.2-3.1% (EOS), radiochemical purity was higher than 99% and specific radioactivity at the end of synthesis was typically 125 to 137 GBq/μmol. Compared to the control group, the 3 h ratios of [^{18}F]FBAT accumulation at 30 min post-i.v. injection of the radiotracer reached 1.64 ± 0.57 in the whole brain, 1.53 ± 0.52 in the cortex and 1.34 ± 0.29 in the cerebellum. Quantitative immunostaining confirmed preferential accumulation of iNOS in the cortex and cerebellum in lipopolysaccharide (LPS)-induced mice. ***Conclusion:*** This study indicates [^{18}F]FBAT has potential prognostic utility to indicate the progression of neuroinflammation-

mediated brain disease. ***References:*** 1.Beaton H, Hamley P, Nicholls DJ, Tinker AC, Wallace AV. 3,4 Dihydro-1-isoquinolinamines: a novel class of nitric oxide synthase inhibitors with a range of isoform selectivity and potency. Bioorg Med Chem Lett. 2001;11(8):1023-1026.2.Haibin Tian ZL. Radiosynthesis of 8-Fluoro-3-(4 [18F]Fluorophenyl)-3,4-Dihydro-1-Isoquinolinamine ([18F]FFDI), a Potential PET Radiotracer for the Inducible Nitric Oxide Synthase. Current Radiopharmaceuticals. 2008;1:49-53.3. Zhou D, Lee H, Rothfuss JM, et al. Design and synthesis of 2-amino-4-methylpyridine analogues as inhibitors for inducible nitric oxide synthase and in vivo evaluation of [18F]6-(2-fluoropropyl)-4-methyl-pyridin-2-amine as a potential PET tracer for inducible nitric oxide synthase. J Med Chem. 2009;52(8):2443-2453.

EP-326

Site-directed conjugation chemistry of the hexahistidine tag

T. Tshibangu[1], M. Sillen[2], F. Cleeren[1], N. Geukens[2], P. Declerck[2], G. Bormans[1];
[1]Laboratory for Radiopharmaceutical Research, KULeuven, Leuven, BELGIUM, [2]Laboratory for Therapeutic and Diagnostic Antibodies, KULeuven, Leuven, BELGIUM.

Aim/Introduction: Despite its potential for site-specific bioconjugation (1,2), the functionalization of histag is barely explored by radiopharmaceutical scientists (3). To fill this gap, we report the controlled ligation of an histagged scFv targeting plasminogen activator inhibitor-1, by a bifunctional PEG-monosulfone. Owing to its high potential, the bioconjugation on histag could become a standard methodology for the radiolabeling of recombinant proteins. ***Materials and Methods:*** Based on literature procedures (1,2), hexahistidine peptide was used to explore the bioconjugation strategy. Parameters including the peptide-monosulfone ratio, temperature, pH, and duration of the reaction were monitored using LC-HRMS. The azido-monosulfone was reacted with sulfo-Cy5-DBCO to obtain a probe identifiable by a UV-vis detector. Stability of sulfo-Cy5-hexahistidine was assessed by LC-HRMS, after storage at 4°C for 5 months in PBS at pH5 to 7 as well as at room temperature for 10 days in PBS pH 6.6. A scFv served as model for complex proteins, the bioconjugation was monitored by LC-HRMS and size-exclusion chromatography (SEC). ***Results:*** LC-HRMS monitoring of the reaction showed a fast bioconjugation of hexahistidine peptide, both at 4°C, room temperature and 40°C (70% conversion after 30 minutes at room temperature). The efficiency of the bioconjugation was highest at pH 6.5-7. Independently of the pH of the reaction, the entire monosulfone reagent was conjugated after 17 hours. A molar ratio 2:1 of peptide: monosulfone reagent results in exclusively mono alkylated hexahistidine. LC-HRMS analysis did not detect any release of the sulfo-Cy5 derivative after storage at 4 ° C for 5 months or at room temperature for 10 days proving the stability of the bioconjugate. The reaction condition optimized with hexahistidine peptide served as a launching pad for the site-specific bioconjugation of recombinant proteins, LC-HRMS and SEC analyzes confirmed the successful functionalization of scFv. ***Conclusion:*** Site-specific bioconjugation with PEG-monosulfone leads to better control of the degree of conjugation, achieving homogenous functionalization. The simplicity of the conjugation reaction makes this method suitable for the development of radio-biopharmaceuticals. The biological evaluation of site-specific radiolabeled scFv is underway. ***References:*** 1) Peciak, Karolina, et al. Chemical science 10.2 (2019): 427-439. 2) Jivan, Faraz, and Daniel L. Alge. Advanced Therapeutics 3.1 (2020): 1900148. 3) Waibel, Robert, et al. Nature biotechnology 17.9 (1999): 897.

EP-327

Copper-64 based Radiopharmaceuticals as Potential Theranostic Agents

I. Khan[1], R. Zahoor[1], M. Numair[1], A. Shahid[1], A. J. Abrunhosa[2];
[1]Institute of Nuclear Medicine and Oncology (INMOL), Lahore, PAKISTAN, [2]Institute of Nuclear Sciences Applied to Health (ICNAS), University of Coimbra, Coimbra, PORTUGAL.

Aim/Introduction: Copper radionuclides offer a varying range of half-lives and positron energies. The well-established coordination chemistry of copper allows for its reaction with a wide variety of chelator systems that can be linked to antibodies, proteins, or peptides,. This paper will focus on ^{64}Cu radiopharmaceuticals for positron emission tomography (PET) imaging applications. Cu-64 can be safely used in imaging glioma and Alzheimer disease. ***Materials and Methods:*** We optimized the radiolabeling of ^{64}Cu with NODAGA-NOC and NODAGA-RGD at various labeling conditions, tested the stability of radioligands at room temperature and in human serum, evaluated the protein binding, lipophilicity, and tested binding affinity of radioligands on 143B and PANC-1 cells. Then the potential of these novel radioligands was tested in animal models bearing tumor xenografts. Finally, the potential of $^{64}CuCl_2$ as a theranostic agent was tested in metastatic prostate cancer and brain glioma patients. ***Results:*** These scientific investigations produced very encouraging results, e.g., the radiolabeling of both NODAGA compounds with Cu-64 was done with high radiochemical purities without further purification. Both radioligands were found stable till 24h. Two peaks for ^{64}Cu-NODAGA-NOC were found using HPLC and it seem to be explained due to the formation of isomers. This is in contrast with ^{64}Cu-NODAGA-RGD, where only one peak was found. Serum stability studies showed that both radioconjugates remained more than 75% intact till 24h. Displacement assays showed that the ^{64}Cu-NODAGA-RGD precursor had higher retention(%) in 143B cells as compared

to ^{64}Cu-NODAGA-NOC precursor. Finally, the $^{64}CuCl_2$ tracer showed very intense uptake in metastatic prostate cancer patient which retained until 24h while no remarkable uptake could be detected in patient suffering from brain glioblastoma because he had already undergone surgery followed by several cycles of radiotherapy. ***Conclusion:*** Keeping in view the potential merits of Cu-64 labeled ligands and uptake of $^{64}CuCl_2$ in human patients, copper-64 based PET radiotracers seem interesting candidates which deserve to be investigated further so that they could also be clinically evaluated. ***References:*** 1. Papotti M, Kumar U, Volante M, et al. Immunohistochemical detection of somatostatin receptor types 1-5 in medullary carcinoma of the thyroid. Clin Endocrinol (Oxf). 2001; 54:641-649. [PubMed: 11380495] 2. Weiner RE, Thakur ML. Radiolabeled peptides in oncology: role in diagnosis and treatment. BioDrugs. 2005; 19:145-163. [PubMed: 15984900] 3. Kulaksiz H, Eissele R, Rossler D, et al. Identification of somatostatin receptor subtypes 1, 2a, 3, and 5 in neuroendocrine tumors with subtype specific antibodies. Gut. 2002; 50:52-60. [PubMed: 11772967]

EP-328

New radiopharmaceuticals for PET from inhibitors of mechanistic target of rapamycin

U. Jauregui-Haza[1], *A. Ferino-Perez*[2], *F. Vélayoudom-Céphise*[3], *L. Belia*[4], *S. Gaspard*[3];
[1]*Instituto Tecnológico de Santo Domingo (INTEC), Santo Domingo, DOMINICAN REPUBLIC,* [2]*1Instituto Superior de Tecnologías y Ciencias Aplicadas (InSTEC), Universidad de La Habana, Havana, CUBA,* [3]*Université des Antilles, Pointe-à-Pitre, GUADELOUPE,* [4]*University Hospital of Pointe-à-Pitre, Pointe-à-Pitre, GUADELOUPE.*

Aim/Introduction: Communications 16.00 Normal 0 21 false false false PT-BR JA X-NONE /* Style Definitions */ table. MsoNormalTable {mso-style-name:"Tableau Normal"; mso-tstyle-rowband-size:0; mso-tstyle-colband-size:0; mso-style-noshow:yes; mso-style-priority:99; mso-style-parent:""; mso-padding-alt:0cm 5.4pt 0cm 5.4pt; mso-para-margin:0cm; mso-para-margin-bottom:.0001pt; mso-pagination:none; mso-hyphenate:none; text-autospace:ideograph-other; font-size:12.0pt; font-family:"Times New Roman",serif; mso-bidi-font-family:Mangal; mso-font-kerning:1.5pt; mso-ansi-language:PT-BR; mso-fareast-language:ZH-CN; mso-bidi-language:HI;} Rapamycin is a macrolide that in the past few decades have shown to be useful as an immunosuppressant and in other therapeutic applications. It is the natural inhibitor of the mechanistic target of rapamycin (mTOR), a kinase protein that plays a key role as a sensor of nutritional status at the cellular and organismal levels. Therefore, mTOR is a central node in the regulation of cell growth, proliferation, and metabolism. Several tumors are predicted to be potentially sensitive to its inhibitors, the reason why it could be an interesting target for radiopharmaceuticals oriented to the diagnosis of several diseases. The aim of this work is to evaluate the utility of several compounds obtained from rapamicyn and its semi-synthetic analogs everolimus and temsirolimus as possible radiopharmaceuticals. ***Materials and Methods:*** DFT calculations of these molecules were performed and further analysis of the dual descriptor, charges population and of the electrostatic potential surfaces were made. Molecular docking simulations were employed for evaluating the interactions of the protein with the studied candidates. ***Results:*** DFT studies allowed the proposal of two strategies of synthesis of novel compounds based on electrophilic reactions. Molecular docking results give us the opportunity to eliminate those molecules that do not interact correctly with the target. Finally, it was obtained that compounds synthesized through the electrophilic addition reaction that employed ^{18}F-selectfluor, as a fluorinating agent, the interactions with the target proteins are conserved. ***Conclusion:*** We propose three candidates to PET-radiopharmaceuticals targeting mTORC1. Two labeling strategies were analyzed, a direct one using ^{18}F-selectfluor as an electrophilic fluorinating agent and an indirect one in two steps through the "click chemistry" approach. Thanks to docking simulations, we conclude that directly labeled derivatives of rapalogues should maintain the biological activity of original compounds and therefore are suitable as possible PET-radiopharmaceuticals targeting the mTORC1 system. However, the compounds synthesized through the "click chemistry" approach are not suitable for this application because they are not able to correctly interact with the binding site due to the size of the prosthetic group introduced that does not allow the correct formation of the ternary complex ligand/FKBP12/FRB. ***References:*** None

EP-329

Novel [^{18}F] FBPA synthesis method from pinacol boran precursor and [^{18}F] fluoride ion using automatic synthesizer

Y. Kanai[1,2], *Y. Ohta*[3,4], *T. Watanabe*[5], *Y. Hottori*[3], *H. Takenaka*[4], *K. Uehara*[4], *S. Naka*[6], *T. Sakai*[7], *J. Hatazawa*[6], *M. Kirihata*[3];
[1]*Osaka University of Pharmaceutical Science, Takatsuki, JAPAN,* [2]*Kansai BNCT Medical Center, Osaka Medical College, Takatsuki, JAPAN,* [3]*Research Center of Boron Neutron Capture Therapy, Osaka Prefecture University, Sakai, JAPAN,* [4]*STELLA PHARMA CORPORATION, Sakai, JAPAN,* [5]*Sumitomo Heavy Industry, LTD., Tokyo, JAPAN,* [6]*Osaka University, Suita, JAPAN,* [7]*Hanwa Intelligent Medical Center, Sakai, JAPAN.*

Aim/Introduction: 2-[^{18}F] Fluoro-4-borono-phenylalanine (FBPA) is an important PET tracer for determination of Boron Neutron Capture Therapy (BNCT). Because it is used for BNCT applicability. [^{18}F] FBPA is mostly produced from [^{18}F] F_2 gas. Final product of [^{18}F] FBPA radioactivity is small

in amount. Recently [^{18}F] fluorination of aromatic ring with pinacol boran derivatives and copper reagent was reported. We previously reported [^{18}F] FBPA synthesis from [^{18}F] F^- which is produced by ^{18}O (p, n) ^{18}F nuclear reaction. In this study, we tried to adopt this method for automatic synthesizer. ***Materials and Methods:*** We used modified type of MPS-200 Aβ (Sumitomo Heavy Industry, Tokyo) as automatic synthesizer. Pinacol boran precursor and copper reagent was used for [^{18}F] fluorination step. After the fluorination reaction, reaction mixture was passed through silica gel cartridge column to remove copper reagent. In the borylation step, we used bis(pinacolato)diboron, bis(dibenzylideneacetone)-palladium(0), tricyclohexylphosphine and potassium acetate. Then, hydroiodic acid was added to reaction mixture for hydrolysis. Crude mixture was purified by HPLC. Finally, [^{18}F] FBPA fraction was collected. ***Results:*** Radiochemical yield of [^{18}F] FBPA from [^{18}F] HF was about 5~10 % (non-decay collected). Total synthesis time from End of bombardment was about 90 min. Radiochemical purity of [^{18}F] FBPA was more than 98 % and specific activity was about 1,000 GBq/μmol. About 9 GBq of [^{18}F] FBPA was produced by our method with 60 min and 40 microA irradiation using 12 MeV cyclotron (HM-12S, Sumitomo Heavy Industry, Tokyo, Japan). ***Conclusion:*** We succeeded to synthesis [^{18}F] FBPA from [^{18}F] HF using automatic synthesizer. ***References:*** None

EP-330

Synthesis and In Vivo Behavior Study of Target-directed Zr-89 Labeled Nanorods

G. Kim*, J. Chae, G. Kang, C. Lee, S. Kim;*
Dongguk Univ., Gyeongju, KOREA, REPUBLIC OF.

Aim/Introduction: The purpose of this study is to selectively treat colorectal cancer by synthesizing target-oriented silica nanorods and roading anti-cancer drugs inside the rods, and to study the behavior of nanocarrier by labeling Zr-89 on nanorods. The behavior of the body varies according to the shape of the nanoparticles, and the uptake of cancer cells is also different. In the case of the hollow rod shape, the drug can be carried inside the particle, thereby making it highly useful. In addition, CT-26, a folate receptor overexpressing cancer cell line, is targeted by binding folic acid to the nanoparticle surface. ***Materials and Methods:*** In this study, silica nanorods were synthesized using a stober reaction using a silicon source (TEOS, tetraethoxy silane) on the AAO (Anodic Aluminum Oxide) template, chemically bound folic acid to the synthesized silica rod surface, and doxorubicin was supported inside the particles. And Zr-89 was introduced to the particle surface for the study of the In vivo behavior. ***Results:*** The shape and size of the silica nanorods were confirmed by SEM and TEM, and it was found through spectroscopic analysis (FT-IR and NMR) whether folic acid and doxorubicin were introduced. The Zr-89 labeling experiment showed high radiochemical purity of > 95%, and PET studies showed typical RES uptake. ***Conclusion:*** Rod-shaped nanoparticles were successfully synthesized uniformly, and Zr-89 could be stably introduced to the particle surface by a method without using a chelator. As a result of PET study, the distribution of silica nanorods in vivo could be confirmed, but it was not effectively accumulated in cancer site. It is thought that the target-oriented effect of folic acid was not shown by RES accumulation. ***References:*** None

EP-331

Scale-down production of [68Ga]Ga-NODAGA-Exendin-4 PET tracer

S. Migliari*[1,2], A. Sammartano[1,2], M. Scarlattei[1,2], G. Baldari[1,2], B. Janota[3], R. Bonadonna[4,5], L. Ruffini[1,2];*
[1]AZ. Osp. Universitaria di Parma, Parma, ITALY, [2]Nuclear Medicine Department, University Hospital of Parma, Parma, ITALY, [3]National Centre for Nuclear Research Radioisotope Centre POLATOM, Otwoch, POLAND, [4]AZ. Osp. Universitaria di Parma, PARMA, ITALY, [5]Division of Endocrinology and Metabolic Diseases, Parma, ITALY.

Aim/Introduction: Glucagon-like peptide 1 receptor (GLP-1R) is preferentially expressed in pancreatic islets, especially in β-cells, but it's highly expressed in human insulinomas and gastrinomas. In recent years several GLP-1 receptor-avid radioligands have been developed to image insulin-secreting tumors or to provide a tentative quantitative in vivo biomarker of pancreatic β-cell mass. Exendin-4 is a 39-amino acid high affinity ligand of the GLP1-R with full agonist activity. It was labeled with PET isotope for imaging purposes. Here, we report results of a semi manual procedure to label [Lys40,Nle14(Ahx-NODAGA) NH2]exendin-4, as a kit, with Ga-68 ([68Ga]Ga-NODAGA-Exendin-4). To develop and validate a labeling procedure to obtain [68Ga]Ga-NODAGA-Exendin-4 in order to make it available for a clinical community. ***Materials and Methods:*** A 68Ge/68Ga Generator (GalliaPharma®,Eckert and Ziegler) was eluted with 0.1M HCl to obtain the PET tracer Ga-68. The eluate $^{68}GaCl_3$ was purified using a cationic-exchange cartridge (SCX) on an automated synthesis module (Scintomics GRP®). The peptide contained in the kit vial (prepared by the Institute of Atomic Energy, Radioisotope Center POLATOM) in different amounts (10 - 20 - 30 ug) was reconstituted with 3.2 mL of HEPES solution and then 1.5 mL $^{68}GaCl_3$ (300-1850 MBq) was added to the dissolved peptide, followed by 15 min incubation at 100°C in a thermoblock. The reaction solution was purified through an HLB cartridge and the resulted product was diluted with PBS buffer and passed through a 0.22 μm sterile filter into a sterile 25 mL capped glass for the final formulation. A sample of the radiopharmaceutical product was tested for quality controls (e.g. radionuclidic purity, radiochemical and chemical purity, pH, endotoxins and sterility). ***Results:*** The

synthesis of [68Ga]Ga-NODAGA-Exendin-4 starting from 10 ug of peptide gets the best radiochemical yield of reaction (6.47±2.4 %), specific radioactivity (5.04 MBq/µg) and radiochemical purity (91.69 %), also representing the ideal amount for clinical application. All different quality control parameters tested were in accordance with the European Pharmacopoeia. ***Conclusion:*** The NODAGA-Exendin-4 was successfully labeled with Ga-68 with a semi manual procedure, fitting all the required QCs. ***References:*** None

EP-55

Technical Studies -> Radiopharmacy/ Radiochemistry -> New Radiopharmaceuticals - SPECT

e-Poster Area

EP-332

Evaluation of Bivalent Fibroblast Activated Protein Inhibitor [^{99m}Tc-DTPA-(8-OH-quinoline)$_2$] for SPECT imaging of tumor

A. Wadhwa[1,2], *S. Chaturvedi*[3,2], *A. K. Mishra*[3], *F. Hussain*[4];
[1]*Institute of Nuclear Medicine and Allied Science, DRDO, Delhi, INDIA,* [2]*INMAS,DRDO, Delhi, INDIA,* [3]*Defence Research Development Organization, Delhi, INDIA,* [4]*Department of chemistry, University of Delhi, Delhi, INDIA.*

Aim/Introduction: Aim: Despite the progress in diagnostic and therapeutic techniques, cancer remains one of the leading causes of death. It is speculated that the tumor stromal micro-environment may present specific and sensitive targets that can aid in early diagnostics. Fibroblast activated protein (FAP) are being explored as promising targets for tumor delineation and diagnostic confirmation. FAP are expressed in more than 90 % of the epithelial carcinomas including pancreatic, colon and breast cancer. FAP, being involved in tumor migration, growth and progression presents an ideal target for diagnosis and therapy, especially in scenarios with limited FDG applicability. Imaging of FAP has better tumor demarcation, shorter scan time and is patient friendly with no dietary regulation before scan. Here, we report synthesis and preclinical evaluation of quinoline based FAP inhibitor, ^{99m}Tc-labelled-FAPI (^{99m}Tc(8-OHquinoline)$_2$DTPA) as SPECT tracer. ***Materials and Methods:*** Synthesis of bis-quinoline based FAPI inhibitor was done through conjugation of carboxylate group of DTPA with amine group of amino hydroxy quinoline. ADME properties and docking studies (PDB:1Z68) were assessed using Schrodinger software to analyze binding affinity and the fate of compound in vivo. The molecule was radiolabeled with ^{99m}Tc and the complex was characterized after purification using HPLC. Physicochemical characterization included evaluation of stability constants and non-specific binding through fluorescence quenching of bovine serum albumin (BSA). Biocompatibility was evaluated using cellular and haemato-toxicity. Biodistribution at predefined time was done to assess the tissue distribution. ***Results:*** The DTPA-(8-OH-quinoline)$_2$ analogue was synthesized in more than 80% yield and characterized using spectroscopic methods. Docking with FAP gave GSscore of -9.67. Fluorescence quenching with bovine serum albumin revealed no to minimum non-specific binding. Non-toxicity of the tracer was established by less than 85% HEK-cell kill when incubated with 1 µM for 48 h and hemolysis data. The ^{99m}Tc-radiolabeled yield was more than 98±1% and the tracer was stable when challenged with serum for more than 24 h with 95±1% activity being retained. Biodistribution data indicate tumor specific accumulation ***Conclusion:*** Bis-quinoline based FAPI radiotracer was synthesized and characterized by NMR and ESI-MS spectroscopic techniques and evaluated as SPECT tracer. Radiolabeling was achieved more than 98%. In vitro studies revealed specific binding to HEK cell and less toxicity of synthesized radiopharmaceuticals. Future work will concentrate on SPECT imaging of tumor bearing mice. ***References:*** Thomas Lindner, Anastasia Loktev, Annette Altmann, Frederik Giesel, Clemens Kratochwil, Jürgen Debus, Dirk Jäger, Walter Mier, Uwe Haberkorn Journal of Nuclear Medicine, 2018; 59(9): 1415-1422

EP-333

Radiolabelling, stability and in vivo biodistribution studies of albumin nanoparticles with gallium-67 and technetium-99m

M. De Arcocha Torres[1], *G. Quincoces*[2], *A. L. Martínez-López*[3], *A. Erhard*[2], *M. Collantes*[4], *I. Martínez-Rodríguez*[1], *I. Luis-De Redin*[3], *M. Ecay*[4], *I. Banzo*[1], *J. M. Irache*[3], *I. Peñuelas*[2];
[1]*Nuclear Medicine Service. Marqués de Valdecilla University Hospital. Molecular Imaging Group (IDIVAL). University of Cantabria, Santander, SPAIN,* [2]*Radiopharmacy Unit, Nuclear Medicine Service, University Clinic of Navarra, IdiSNA, Pamplona, SPAIN,* [3]*Department of Pharmacy and Pharmaceutical Technology, University of Navarra, Pamplona, SPAIN,* [4]*Micropet Unit. Nuclear Medicine Service, University Clinic of Navarra, IdiSNA, Pamplona, SPAIN.*

Aim/Introduction: To optimize the radiolabelling of Gantrez-mannosamine polymer-coated (GPM2) albumin nanoparticles (NPs) with technetium-99m and gallium-67 in order to evaluate their in vivo biodistribution by SPECT/CT after intravenous administration. ***Materials and Methods:*** All NPs were prepared by solvent displacement They were radiolabeled at different temperatures (22ºC, 40ºC, 60ºC) with 74±3.1 MBq of tin-reduced [^{99m}Tc]$NaTcO_4^-$. For gallium-67 radiolabeling, albumin was modified with NOTA before marking. Labelling of NOTA-modified NPs was carried out with [^{67}Ga]Cl_3 obtained from ^{67}Ga-citrate. A mixture of 2 mg NPs, 0.2M sodium acetate and 37 MBq

[^{67}Ga]Cl_3 was incubated at different temperatures (22ºC, 30ºC, 60ºC) and times (10, 30 minutes). Radiolabelled NPs were purified using microconcentrators. Radiochemical purity was evaluated by radio-TLC (Whatman-1, NaCl 0.9 % for technetium-99m and Whatman-1, HCl 0.05M for gallium-67). The particle size and zeta potential were determined by photon correlation spectroscopy and laser Doppler anemometry, respectively. Stability of radiolabeled NPs was evaluated in saline and human plasma (37ºC). All experiments were repeated thrice. Biodistribution studies were carried out in Wistar rats after intravenous administration (n=12, 3 per group: [^{99m}Tc]-GPM2, [^{67}Ga]-NOTA-GPM2, [^{99m}Tc]Tc-GPM2)[^{67}Ga]Ga-NOTA-GPM2[^{99m}Tc] $NaTcO_4^-$ and [^{67}Ga]Cl_3). After SPECT/CT imaging, animals were humanly killed and activity in organs measured in a gamma counter. ***Results:*** Highest yield (97.59 ± 0.52%) for technetium-99m radiolabeling of NP was obtained at 22 ºC for 10 minutes, while for gallium-67 the highest yield was roughly 70 % (69.2 ± 2.6%) and obtained at 30º C, 30 min. In both cases RCP was >97% after purification. [^{67}Ga]-NOTA-GPM2 NPs[^{67}Ga]Ga-NOTA-GPM2 showed >90% stability in saline and >80% in plasma, while it was >75% and >70% for [^{99m}Tc]-GPM2 NPs.^{99m}Tc]Tc-GPM2 (The size of NPs was slightly increased after radiolabeling: 257±1.35 vs 244±3.40 for [^{99m}Tc]-GPM2 and 251.3±2.25 vs 243.5±6.62 for [^{67}Ga]-NOTA-GPM2. The potential Z increased slightly in both cases but remained within adequate values. In vivo SPECT/CT biodistribution studies showed in both cases a high accumulation of activity in the liver at 2 and 24 hours after administration (as measured by semi-quantitative analysis of VOIs derived from the corresponding CT images), with a very different biodistribution between treated and control animals. These results were coincident with those obtained ex vivo in the gamma counter. ***Conclusion:*** Albumin nanoparticles coated with the GPM2 polymer can be easily labeled with technetium-99m and gallium-67, obtaining high radiolabelling yield and adequate in vitro stability. In vivo SPECT/CT studies show a similar biodistribution for both isotopes, remaining stable for long periods. ***References:*** None

EP-334

Evaluation of mercaptoacetyl-based amino acid containing chelators for labeling of GRPR antagonist PEG2- RM26 with ^{99m}Tc

H. Sabahnoo[1], A. Abouzayed[1], S. Rinne[1], V. Tolmachev[2], A. Orlova[1]; [1]Department of Medicinal Chemistry, Uppsala University, Uppsala, SWEDEN, [2]Department of Immunology, Genetics and Pathology, Uppsala University, Uppsala, SWEDEN.

Aim/Introduction: Bombesin (BN) analogs bind with high affinity to gastrin-releasing peptide receptor (GRPR/BB2) that is up regulated in prostate cancer. This receptor can be used as a potential molecular target to visualize and treat this tumor. The specific aim of this study was to investigate the influence of ^{99m}Tc-amino acids-based chelator complex on the targeting properties of the bombesin-based GRPR antagonist PEG_2-D-Phe-Gln-Trp-Ala-Val-Gly-His-StaLeu-NH2 (PEG2-RM26). ^{99m}Tc-peptide based-chelator complexes can be improved by substituting glycyl residues in the chelating sequence with more hydrophilic seryl and provided the best labeling stability by negatively charge glutamic acid residues. ***Materials and Methods:*** Synthetically produced analogs N-terminally conjugated with the chelator sequences mercaptoacetyl-Ser-Ser-Ser (maSSS-PEG2-RM26) and mercaptoacetyl-Ser-Glu-Ser (maSES-PEG2-RM26) were radiolabeled with ^{99m}Tc via ligand exchange using glucoheptonate. Radiochemical yield, stability in PBS, and analysis of radiocatabolites in urine and and gastrointestinal tract were determined by radio-RP-HPLC. In vitro binding specificity, kinetic properties, and cellular processing tests were performed using GRPR-expressing cells PC-3. The pharmacokinetics and in vivo binding specificity of the compound were studied in NMRI mice. ***Results:*** Radiolabeling of the peptides with ^{99m}Tc was efficient and stable, >98% radiochemical yield within 60 min at 90°C. Binding of ^{99m}Tc-maSXS-PEG2-RM26 was specific both in vitro and in vivo with binding affinity (K_D) of 61 pM for ^{99m}Tc-maSSS-PEG2-RM26 and 846 pM for ^{99m}Tc-maSES-PEG2-RM26. The cellular processing of all compounds indicated slow internalization. Labeled conjugates were rapidly eliminated with high degree of hepatobiliary excretion, 3 h pi most activities remained in GI tract. Analyses of activity showed that ^{99m}Tc-maSSS-PEG2-RM26 remained intact in GI content (~70%) and in urine (~30%), while for ^{99m}Tc-maSES-PEG2-RM26 only less hydrophobic catabolites were detected. ***Conclusion:*** The use of amino acid-based chelator could be used for stable labeling of GRPR antagonist with ^{99m}Tc. ***References:*** None

EP-335

A Novel Tc-99m-labeled and MAG_3-chelated Arginine-Arginine-Leucine containing Peptide for Tumor Imaging in Hepatoma Xenografts Model

R. Wang[1,2], Y. Du[1], Z. Chen[1], P. Yan[1], Q. Jiang[1], X. Duan[1]; [1]Peking University First Hospital, Beijing, CHINA, [2]Peking University International Hospital, Beijing, CHINA.

Aim/Introduction: In this study, arginine-arginine-leucine (RRL) a tumor targeting peptide is designed to link the bifunctional chelator mercaptoacetyltriglycine (MAG_3), aiming to explore the labeling conditions of Tc-99m and to evaluate the imaging of this probe in vivo. ***Materials and Methods:*** Tc-99m was labeled through the $SnCl_2$ reduction method, and the main factors affecting the labeling were investigated respectively to obtain the suitable labeling conditions. The paper chromatography was used to determine the labeling rate and radiochemical

purity. Cysteine replacement experiment and incubation experiment of normal saline/bovine serum albumin was utilized to evaluate the stability of Tc-99m-MAG_3-RRL in vitro. HepG2 tumor-bearing models were established and after tail vein injection, gamma camera imaging and biodistribution study were respectively performed periodically. ***Results:*** The purity of MAG_3-RRL was 98.94%. Under the suitable labeling conditions, the labeling rate was 93.67% ± 1.10%, and the radiochemical purity was 94.32% ± 0.19% (n=3). Tc-99m-MAG_3-RRL was placed in normal saline at room temperature and 50% BSA at 37°C, the radiochemical purity of Tc-99m-MAG_3-RRL was more than 90% (n=3) within 6 hours. The highest replacement rate of Tc-99m-MAG_3-RRL was 0.57% ± 0.21% in cysteine solution, and 0.41% ± 0.04% in normal saline control (n=3, P>0.05). The distribution coefficient lgP of Tc-99m-MAG_3-RRL was -0.15 ± 0.01 (n=3). Gamma camera imaging revealed substantial uptake of Tc-99m-MAG_3-RRL in tumors. The specific uptake of Tc-99m-MAG_3-RRL in tumor was significantly higher than that of control test after injection (P<0.05). In planar gamma imaging study, the tumors were imaged clearly at 2-4h after injection of Tc-99m-MAG_3-RRL, with the highest tumor-to-muscle ratio 5.63 ± 0.40 in 30min. Biodistribution data showed that Tc-99m-MAG_3-RRL was rapidly accumulated in tumor within 30min with the highest tumor-to-muscle ratio 5.50 ± 0.74. And then it was rapidly cleared from the blood and predominantly accumulated in the kidneys. ***Conclusion:*** The results show that MAG_3 could successfully be connected to RRL polypeptide and further improve the labeling rate, and the preparation method of Tc-99m-MAG_3-RRL is simple and fast. Tc-99m-MAG_3-RRL probe has good stability in vitro. Animal study shows that Tc-99m-MAG_3-RRL can be used as a potential candidate for visualization of malignant carcinomas. ***References:*** None

EP-336

Influence Of Different Factors On Labelling Yield And Image Quality Of Leukocytes Labelled With ^{99m}Tc-HMPAO

V. Mendi Barcina*, E. Martínez Montalbán, E. Dobra, L. Arias Buendía, M. García Ruiz, S. Rizckallal Monzón, B. Martínez de Miguel;*
Hospital Universitario La Paz, Madrid, SPAIN.

Aim/Introduction: Study the possible variables that may affect the labelling efficiency of white blood cells with ^{99m}Tc-HMPAO and the image quality. ***Materials and Methods:*** Retrospective study in which 123 patients in who we carried out leukocyte labelling with ^{99m}Tc-HMPAO were analysed, according to the protocol of the Radiopharmacy Unit, during 2018 and 2019. The variables to be evaluated are: age, white blood cells count present in the initial analysis and isolated white blood cells, leukocyte labelling yield and image quality. Data analysis is performed through the SPSS statistical program, using the Mann-Whitney statistical test. ***Results:*** A low correlation is obtained between the number of pre-labelled leukocytes (2.95 * 10^3 - 12.6 * 10^3 leukocyte /µL) and the labelling yield (50 - 83%) (p = 0.034). About post-labelling leukocytes (17.08 * 10^3 - 101 * 10^3 leukocyte / µL) and the labelling yield there is a low correlation (p = 0.020). A proportional association is observed between pre-labelling leukocytes and post-labelling leukocytes (p = 0.000). In 100% of the cases, isolated leukocytes are above the ones in the initial analysis, obtained a ratio of 6.27 ± 1.15 isolated white blood cells for each initial white blood cell. A low correlation is obtained between the variation obtained in the count of both leukocytes and the yield (p = 0.019). No statistically significant association can be determined between white blood cell count and image (p = 0.440) and (p = 0.587), in the same way as between age (12-90 years) and yield (p = 0.838). ***Conclusion:*** The results obtained in our case show that there isn't relationship between the different variables analysed and the labelling yield and the diagnostic imaging. Thus, the number of pre-labelling and post-labelling leukocytes does not influence the labelling efficiency, which was over 50% in all cases. ***References:*** None

EP-56

Technical Studies -> Radiopharmacy/ Radiochemistry -> New Radiopharmaceuticals - Therapy

e-Poster Area

EP-337

Re-188 N-DEDC lipiodol for trans-arterial therapy in HCC: labeling efficiency and bio-distribution

S. Datta Gupta[1]*, P. Gupta*[1]*, S. A. Shamim*[1]*, J. Hussain*[1]*, Shalimar*[1]*, S. Gamanagatti*[1]*, M. B. Mallia*[2]*, V. Chirayil*[2]*, A. K. Dash*[2]*, C. S. Bal*[1]*;*
[1]*All India Institute of Medical Sciences, New Delhi, INDIA,*
[2]*Bhabha Atomic Research Centre, Mumbai, INDIA.*

Aim/Introduction: Lipiodol labeled trans-arterial radionuclide therapy (TART) is a promising treatment in patients with hepatocellular carcinoma (HCC). Various agents are available for Re-188 lipiodol labeling. However, due to low labeling yields (50-60%), variable tumor retention and high cost, the search for an ideal agent is on-going. Novel bis-(diethyldithiocarbamato) nitrido (N-DEDC) compound is an attempt at achieving high labeling yield and tumor retention at an affordable cost. We aimed at studying the labeling efficiency and bio-distribution of Re-188 N-DEDC lipiodol in HCC. ***Materials and Methods:*** Sodium perrhenate was eluted from W-188/Re-188 generator for labeling. Eluted perrhenate was added to kit-1 of N-DEDC and heated at 65°, followed by addition of eluted kit-2 contents. Thereafter, lipiodol was added and the complex mixed well

in vortex and centrifuged. Activity in separated lipiodol phase was measured and injected trans-arterially. Whole-body images at 24 and 48 hours and abdomen SPECT images at 24 hours post therapy were acquired for patients to assess bio-distribution. Region of interests were drawn over the tumor lesions, normal liver parenchyma, lungs and thigh (background) in planar images for semi-quantitative analysis. ***Results:*** Seven patients with radiological diagnosis of HCC were recruited prospectively and underwent Re-188 N-DEDC lipiodol TART. Mean dose synthesized and injected was 72.7±7.7mCi (2.6±0.3GBq). Mean labeling efficiency was found to be 80.75±9.84%, with short time to synthesis of 82.5±5.8minutes. It was observed during measurement, that iodinated lipiodol led to attenuation of activity in lipiodol phase by 24.18±9.76%. Whole-body imaging revealed distribution of radiopharmaceutical in target lesions, surrounding liver parenchyma and bladder. Mean tumor to liver ratio at 24 hours was 1.21±0.12 and at 48 hours 1.24±0.16 (p=0.176). Mean tumor to background ratio increased from 4.33±1.20 at 24 hours to 5.36±1.69 at 48 hours (p=0.116). Mean tumor to lung ratio at 24 hours and 48 hours was 1.98±0.41 and 1.99±0.48, respectively (p=0.310). ***Conclusion:*** N-DEDC appears to be a promising novel agent for Re-188 lipiodol TART in HCC having similar bio-distribution with the advantage of higher labeling yield, shorter time to synthesis and lower cost. Further, clinical studies are underway to assess its efficacy in HCC. ***References:*** None

EP-338

In vitro characterizations of ^{177}Lu-anti-CEA antibody and HSP90 inhibition for potentiated radioimmunotherapy of gastrointestinal cancer

T. Mohajer Shojai[1], *P. Jha*[1], *A. Boström*[2], *F. Y Frejd*[1], *P. J Yazaki*[3], *M. Nestor*[1];
[1]*Uppsala University, Uppsala, SWEDEN,* [2]*Ridgeview Instruments AB, Uppsala, SWEDEN,* [3]*Beckman Research Institute, Duarte, CA, UNITED STATES OF AMERICA.*

Aim/Introduction: Carcinoembryonic antigen (CEA) is an antigen overexpressed in colorectal cancers, and widely used as a tumor marker. Radiolabeled anti-CEA monoclonal antibodies (mAbs) have previously been used in clinical trials with ^{90}Y as a therapeutic radionuclide, demonstrating promising results. However, ^{177}Lu may be an even more favorable therapeutic radionuclide compared to other widely clinical used radionuclides. This is owing to its unique chemical characteristics, well suited physical and biological half-life and desired energy in order to minimize off-target effects for therapy. The heat shock protein 90 (HSP90) has been shown to be overexpressed in colorectal cancer, where the HSP90 inhibitor Onalespib has previously demonstrated radiotherapy potentiation effects in combination with external radiotherapy. Consequently, in the present study, we aimed to create and evaluate a ^{177}Lu radiolabeled anti-CEA hT84.66-M5A (M5A) mAb, and investigate the potential therapeutic effects of ^{177}Lu-M5A mAb and Onalepib, as monotherapies or in combination, in multicellular colorectal cancer spheroid models. ***Materials and Methods:*** ^{177}Lu-radiolabeling of DOTA conjugated M5A mAb was first optimized. Labeling yield and stability were analyzed using instant thin-layer chromatography, high-performance liquid chromatography, serum stability and EDTA challenge assays. Binding specificity and affinity was evaluated in three colorectal cancer cell lines (HT29, LS174T and HT55) and one gastric (MKN45) cancer cell line by blocking assays and LigandTracer real-time measurements. The effect on spheroid growth and cell viability from radioimmunotherapy with ^{177}Lu-M5A mAb and HSP90 inhibition was assessed alone and in combination in two different 3D multicellular tumor spheroid models. ***Results:*** Stable and reproducible radiolabeling was obtained, with labeling yields above 92%, serum stability above 92%, and EDTA stability above 87% at 48 hours after radiolabeling. Antigen-specific binding of the radiolabeled conjugate was demonstrated on all CEA-positive cell lines. Dose-dependent and antigen-specific therapeutic effects of ^{177}Lu-M5A mAb and Onalespib was demonstrated for the monotherapies in the spheroid models. Moreover, therapeutic effects could be further potentiated by combining ^{177}Lu-M5A mAb and Onalespib. ***Conclusion:*** Administration of either ^{177}Lu-M5A mAb or Onalespib as single compounds may be a promising treatment for colorectal cancer. Combinatorial therapy using both compounds could further potentiate therapeutic effects, however further in vitro and in vivo studies would be required to confirm current study findings. ***References:*** None

EP-339

DOTA-conjugation and ^{177}Lu-DOTA-radiolabeling optimizations of IgG4 antibodies

P. Jha*, H. Berglund, T. M. Shojai, A. C. L. Mortensen, M. Nestor; Immunology, Genetics and Pathology, Uppsala University, Uppsala, SWEDEN.*

Aim/Introduction: The high-specific tumor-affinity of IgG4 has made it one of the emerging therapeutic monoclonal antibody (Ab) subclasses employed for cancer immunotherapy. In addition to the inherent structural properties, the therapeutic efficacy of IgG4-Ab's is also affected by the post-radiolabeling specific activity or crude radiolabeling yield of the Ab-radiometal conjugates, and type of macrocyclic chelator used for radiometal incorporation. In this work, we optimized the physicochemical parameters for ^{177}Lu-labeling of various IgG4-Ab's. ***Materials and Methods:*** Conjugation with NHS- and p-SCN-Bn derivatives of DOTA was first tested with a commercially available IgG1 antibody followed by ^{177}Lu-labeling. Various IgG4-Abs to a cancer-

associated antigen were conjugated with p-SCN-Bn-DOTA using the1:10 molar ratio. The temperature-effect on DOTA-conjugation was assessed at 4°C, room temperature (RT), and 37°C. Purification of DOTA-Ab conjugates was tested using NAP-5 and Amicon Ultra 0.5 spin columns. Sodium and ammonium acetate buffers of different molarity and pH were then evaluated, as well as the incubation time for ^{177}Lu-labeling (42°C). Labeling yield was assessed using Instant Thin Layer Chromatography developed in 0.2 M citric acid and purity was determined using size exclusion (SE)-HPLC progressed in isocratic 0.1 M, pH 6.8 phosphate buffer. Binding specificity of the top candidates was assessed in vitro using LigandTracer and in vivo in mice xenografted with tumors of varying antigen density. ***Results:*** p-SCN-Bn-DOTA chelator produced enhanced conjugation and ^{177}Lu-labeling yields for all IgG4-Abs. RT and 4°C DOTA-Ab conjugated samples demonstrated varied ^{177}Lu-labeling yields (30-97%) for IgG4-Ab variants, whereas consistent ^{177}Lu-labeling yields (95-100 %) were obtained for the DOTA-IgG4-Ab samples conjugated at 37°C. Highest specific activity (285-300 MBq/mg for 50µg of Ab) was obtained with 15 MBq of ^{177}Lu following a 2 h incubation for most of the IgG4-Abs. Optimum ^{177}Lu-labeling yields were noted for ammonium buffer (pH 5.4) rather than sodium buffer (pH 5.5) when used in 0.1-0.2 M range. The SE-HPLC of DOTA-Ab and ^{177}Lu-DOTA-Ab conjugates of the IgG4-variants, post-DOTA-conjugation (37°C) and post-^{177}Lu-labeling (42°C) revealed little or no aggregation when stored at -20°C compared to 4°C. In vitro and in vivo studies demonstrated antigen-specific binding of the assessed radioconjugates. ***Conclusion:*** The first comprehensive physicochemical studies of DOTA-conjugation and ^{177}Lu-labeling of IgG4-Ab's provide reproducible results with improved labeling yields with high specific activity and no or minimal aggregate formation and retained antigen binding. This approach could lead to improved in vitro and in vivo outcomes of ^{177}Lu-loaded-IgG4-Ab's for cancer immunotherapy. ***References:*** None

EP-340

Radiolabeling with Tb-161 and Lu-177: defining the impact of metal impurities

M. Ooms[1], A. R. Burgoyne[1], B. Ponsard[1], D. Elema[1], T. Cardinaels[1,2], M. Van de Voorde[1];
[1]SCK CEN, Mol, BELGIUM, [2]KU Leuven, Department of Chemistry, Leuven, BELGIUM.

Aim/Introduction: ^{161}Tb and ^{177}Lu prove to be highly valuable in the fight against cancer as they can be deployed in targeted radionuclide therapy. ^{177}Lu-based radiopharmaceuticals are currently being widely explored, whereas interest in ^{161}Tb as therapeutic radioisotope is growing rapidly because of its very comparable decay properties. Moreover, ^{161}Tb is expected to have an improved therapeutic effect because of its simultaneous emission of conversion and Auger electron emission. SCK CEN recently developed in-house production methods for ^{161}Tb [1] and ^{177}Lu with high radionuclidic purity. However, also metal impurities are of major concern since they have the potential to compete with the radionuclide during radiolabeling. In this study we aimed to identify and quantify the effect of metal impurities on the radiolabeling of ^{161}Tb and ^{177}Lu. ***Materials and Methods:*** The effect of metals on the radiolabeling of p-SCN-Bn-DOTA and p-SCN-Bn-DTPA with ^{161}Tb and ^{177}Lu was investigated. Radiolabeling yields in the presence of increasing amounts of common metal ion impurities (Al, Ca, Cu, Fe, Mg and Zn) were evaluated using radio-TLC. Also the effect of target matrix remnants on the radiolabeling yield of ^{161}Tb and ^{177}Lu was studied by addition of Gd and Yb impurities, respectively. Metal ion impurities were added in 250 to 10^4 molar excess. A 10^6 molar excess of the respective metal ion impurities was added to the radiolabeled complexes to evaluate their stability against transchelation. ***Results:*** The presence of low amounts of multivalent transition metal impurities showed dramatic decrease in radiolabeling yield. Target material remnants and high amounts of Ca also had a significant impact on radiolabeling. Partial transchelation of the radionuclide from the complex was observed in the presence of Al, Fe and Cu. ***Conclusion:*** In conclusion, this study confirms that metals can have a high impact on the radiolabeling efficiency of a radionuclide solution. This makes it possible to identify the metals that need to be closely monitored during the production process of ^{161}Tb and ^{177}Lu. Also after radiolabeling, an high impact of certain metal ions on the stability of radiolabeled compounds was found ***References:*** [1] A. Burgoyne et al., J. Labelled Comp. & Radiopharm., 62 (2019) S303

EP-57

Technical Studies -> Radiopharmacy/ Radiochemistry -> Radionuclide Production

e-Poster Area

EP-341

New Y Solid Target Concept for ^{89}Zr Cyclotron-based Production

S. Cisternino[1], *H. Skliarova[1], E. Cazzola[2], G. Gorgoni[2], A. Baldini[3], U. Anselmi-Tamburini[3,4], J. Esposito[1];*
[1]Istituto Nazionale di Fisica Nucleare - Laboratori Nazionali di Legnaro, Legnaro (PD), ITALY, [2]IRCCS Sacro Cuore Don Calabria Hospital, Negrar (VR), ITALY, [3]Department of Chemistry, University of Pavia, Pavia (PV), ITALY, [4]Istituto Nazionale di Fisica Nucleare, Sezione di Pavia, Pavia (PV), ITALY.

Aim/Introduction: One of the most promising radioisotope candidate to perform immuno-PET imaging investigations

is ^{89}Zr, thanks to its main features [1]: 3.27 d physical halflife, relatively low energy positrons (maximum β+ energy 0.897 MeV, β+ =22.7%) providing high resolution PET images. At last the production is straightforward by means of medium-to-small medical cyclotrons. The ^{89}Y(p,n)^{89}Zr nuclear reaction route on 100% natural Y target isotope, commercially easily available, is the main one aimed at ^{89}Zr yielding. Demand for ^{89}Zr batches for research purposes is indeed growing up in the last years and different research groups have been working on it to improve radioisotope's production steps: target design and manufacturing, radiochemical purification, recovery and labelling studies. In the framework of the LARAMED research program at INFN-LNL [2], a new cyclotron solid target concept, based on Y foil bonded to Nb backing by means of Spark Plasma Sintering technique, has been investigated for the first time. ***Materials and Methods:*** Y targets were realized through a specific bonding manufacturing process of Y foils (i.e. 150 μm thickness, 12 mm dimeter) to Nb backing plate (Ø 23.5 mm x 1 mm) performed out by both a commercial SPS machine (in a private company) and by a prototype machine in-house developed at the University of Pavia and INFN-Pv department. Irradiation runs (energy 13 MeV, current 50 μA), automatic purification and recovery steps were carried out in collaboration with Radiopharmacy of Sacro Cuore Don Calabria Hospital. The production yield and the recovery efficiency were measured and compared with the ^{89}Zr produced by irradiating simple Y foils. ***Results:*** Any visible damage on targets surfaces has been seen after the irradiation runs (mean heat power areal density of around 650 W/cm^2), thus confirming the robustness of the SPS Y targets manufacturing process adopted. An integral yield of 0.4 mCi/μAh of ^{89}Zr was thus determined with high ^{89}Zr recovery efficiency (95%). A set of labelling procedures were performed with the ^{89}Zr produced by SPS Y target. ***Conclusion:*** The success and the advantage of the SPS Y targets could be the solution for a consistent ^{89}Zr radionuclide supply using small medical cyclotron. Moreover, the advantages of the SPS technique can be exploited for the manufacturing of other cyclotron targets for the production of different interesting radioisotopes. ***References:*** 1. Jalilian, A.R. et al., Journal of Radioanalytical and Nuclear Chemistry 2017, 314, 7-21.2. Esposito, J. et al., Molecules 2019 24, 20.

EP-342

Cyclotron-Production of $^{51/52}$Mn Isotopes: an Update on the METRICS Project

P. Martini[1,2], *A. Boschi*[2], *E. Cazzola*[3], *S. Cisternino*[1], *A. Duatti*[2], *G. Gorgoni*[3], *L. Marvelli*[2], *M. Pasquali*[1,2], *L. Mou*[1], *G. Pupillo*[1], *C. Rossi Alvarez*[1], *H. Skliarova*[1], *G. Sciacca*[1], *J. Amico*[3], *L. Uccelli*[2], *J. Esposito*[1];

[1]*Legnaro National Laboratories of the National Institute of Nuclear Physic (INFN-LNL), Legnaro (PD), ITALY,* [2]*University of Ferrara, Ferrara, ITALY,* [3]*Sacro Cuore Don Calabria Hospital, Negrar (VR), ITALY.*

Aim/Introduction: The aim of the ongoing METRICS project (acronym for Multimodal pET/mRI imaging with Cyclotron-produced $^{51/52}$Mn iSotopes), is to develop all the technology needed to get a cyclotron-driven $^{52/51}$Mn radionuclide production aimed at the so-called Multi Modal Imaging (MMI). Final goal is to achieve a perfect molecular matching between PET and MRI diagnostic techniques, by using both paramagnetic and radioactive properties shown by some manganese isotopes, which might allow for an unprecedented PET/MRI hybrid imaging modality. Such activities are funded by INFN in the framework of LARAMED (LAboratory of RAdioisotopes for MEDicine) research program [1], running at Legnaro National Laboratories (LNL) on the development of cyclotron-based production strategies, either of emerging or conventional radionuclides for nuclear medicine applications. ***Materials and Methods:*** ^{nat}Cr metal pellets have been produced and attached to Cu/Au or Nb baking materials by means of the SPS (Spark Plasma Sintering) manufacturing technique. Both the backing selection and the design step process has been taken into account in order to achieve an, as high as possible, improvement in the backing thermal conductivity, while ensuring surface inertness required to the next chemical process (e.g. acid dissolution). To meet such a demand, we also realized a solid target dissolution system by making some technical modifications to an automatic module available on the market, which moreover allows performing the on-line dissolution process with a cassette-based system. Anion exchange chromatography has been used for the Mn/Cr separation. The efficiency of the process has been evaluated by gamma-spectrometry analysis. In addition, a series of paramagnetic Mn(II) complexes were prepared and characterized by HPLC chromatography, IR-spectroscopy, elemental analysis, and mass spectrometry. ***Results:*** So far, irradiation runs with TR19 cyclotron were performed to evaluate target thermomechanical resistance under a proton beam up to 50μA (~1.2kW/cm^2) and to perform a preliminary production test to optimize dissolution and purification process. Moreover, a series of Mn(II) complexes were prepared, in aqueous conditions, with different bidentate ligands with the goal to identify the most robust ligand arrangement, capable of stabilizing the Mn^{2+} ion in a biological environment. Along with stability, the pharmacokinetic properties of these complexes are currently under analysis. ***Conclusion:*** The preliminary results of the METRICS project are here presented, in terms of technology improvement, such as target, dissolution system, etc., to obtain cyclotron-produced $^{52/51}$Mn and development of a new bimodal probe for manganese-based PET-MRI imaging. ***References:*** [1] J. Esposito, et al. Molecules 2019, 24, 20; DOI:10.3390/molecules24010020.

EP-58

Technical Studies -> Radiopharmacy/ Radiochemistry -> Radiopharmaceutical Preparation and Quality Control

e-Poster Area

EP-343

Multifunctional crown-5-calix[4]arene based phase-transfer catalysts for aromatic ^{18}F-fluorination

W. Lee[1,2], S. Kang[3], D. Kim[3], B. Lee[2,4], W. Lee[2], S. Kim[1,2,4];
[1]Department of Transdisciplinary Studies, Graduate School of Convergence Science and Technology, Seoul National University, Suwon, KOREA, REPUBLIC OF, [2]Department of Nuclear Medicine, Seoul National University Bundang Hospital, Seongnam, KOREA, REPUBLIC OF, [3]Department of Chemistry, Inha university, Incheon, KOREA, REPUBLIC OF, [4]Center for nanomolecular imaging and innovative drug development, Advanced Institutes of Convergence Technology, Suwon, KOREA, REPUBLIC OF.

Aim/Introduction: Fluorine-18 has been used predominantly as a useful positron emitting isotope to prepare the radiotracer in the application of positron emission tomography (PET). In particular, incorporation of fluorine-18 into arenes is more required to avoid the metabolic defluorination of radiotracer by the reason of a high in vivo stability of a C_{Ar}-F bond. Herein, we intend to achieve an effective nucleophilic aromatic ^{18}F-fluorination in various arenes by using multifunctional BTC5A-based phase-transfer catalysts (PTC). ***Materials and Methods:*** We prepared six different leaving groups substituted biphenyl precursors for aromatic fluorination. After evaluating the reactivity of precursors in the presence of BTC5A-based PTCs, we have chosen diaryliodonium tosylate as the desirable precursor and optimized the condition of nucleophilic aromatic fluorination by changing various solvents, PTCs and temperature. To monitor the stability of the precursor, it was reacted with PTCs and base ($K_{2.2.2}$ or BTC5A-based PTCs/K_2CO_3) in various solvents except the fluoride sources. Aromatic [^{18}F]fluorination was conducted with various diaryliodonium tosylate substrates in different amount of PTCs ($K_{2.2.2}$, BTC5A-based PTCs), solvents, and radical scavenger (TEMPO). Radiochemical yield (RCY) was measured by the radio-TLC. ***Results:*** Various diaryliodonium tosylate precursors were synthesized as following the reported method. In the stability test of precursors, the BTC5A-based PTCs treated group showed approximately 30% higher stability than the $K_{2.2.2}$ treated group. When using TEMPO as radical scavenger, we found that precursor was more stable in basic condition. The optimized aromatic fluorination by using BTC5A-based PTCs showed the highest yields up to 80%, which is 10 times higher than that using $K_{2.2.2}$. In ^{18}F-labeling experiments, RCY in the presence of BTC5A-based PTCs is 3 times higher (82%) than that of $K_{2.2.2}$. When applying this ^{18}F-labeling protocol in various substrates, RCYs were showed in maximum 3 times higher compared with the conventional method employing $K_{2.2.2}$. Especially, the well-known aromatic ^{18}F-labeled radiopharmaceuticals, [^{18}F]Flumazenil, was prepared in 95% RCY which is 2 times higher than that of followed the reported method. ***Conclusion:*** In this study, we have successfully optimized the condition for aromatic fluorination by using a new type of multifunctional PTC, BTC5A-based PTCs, which is far better than general PTC ($K_{2.2.2}$). With these promising results of ^{18}F-labeling experiments, we are expecting that multifunctional BTC5A-based PTCs could serve as a facile and efficient tool for the development of radiopharmaceuticals. ***References:*** D. W. Kim, et al. Chem. Eur. J. 2016, 22, 4515-20; B. C. Lee, et al. Org. Biomol. Chem. 2011, 9, 8346-55

EP-344

Evaluation of DOTA-TATE kit formulation for multi isotope labelling

M. Maurin, P. Garnuszek, M. Radzik, W. Wojdowska, D. Pawlak, R. Mikołajczak;
National Centre for Nuclear Research, Radioizotope Centre POLATOM, Otwock, POLAND.

Aim/Introduction: Peptide receptor radionuclide therapy (PRRT) using radiolabelled somatostatin analogues like DOTA-TATE peptide is a treatment option for patients with disseminated neuroendocrine tumours (NET). Depending on the type of the lesions a one isotope treatment or combination treatment using the high-energy ^{90}Y beta emitter for larger lesions and a lower energy ^{177}Lu for smaller lesions has been postulated in the literature. Additionally, recently the role of the theragnostic isotopes such as Sc-44 (4h half-life PET tracer) and Sc-47 (β^- therapeutic isotope) is increasing showing the potential for use in the diagnostic and therapeutic procedures. The aim of the study was evaluation of POLATOM designed sterile DOTA-TATE kit (MultiSom) as a kit for multi isotope labelling. ***Materials and Methods:*** MultiSom kit containing 100µg of DOTA-TATE as an active substance and excipients like ascorbic acid and sodium hydroxide was tested for labelling with ^{90}Y (ItraPol), ^{177}Lu ca (LutaPol) and nca, ^{44}Sc and ^{47}Sc. The radiolabelling was performed according to the standard aseptic procedures. The kit was evaluated on basis of radiolabelling yield, resulting radiochemical purity and pH of final mixture. Radiochemical purity and radiolabelling yields were determined by RP-HPLC method (Phenomenex Kinetex 150x4.6mm column, flow of 80% 0.1%TFA in water and 20% of 0.1%TFA in acetonitrile, 1mL/min) and TLC method for unbound radionuclide determination (ITLC SG; mobile phase: 1M sodium acetate/methanol (50:50). ***Results:*** It has been proved that the specific content of

ascorbic acid in the kit successfully buffers 0.5mL of 0.04M HCl (medium for LutaPol/ItraPol). The MultiSom kit was efficiently (RCP> 98%) labelled with 4.4 GBq of c.a. ^{177}Lu (LutaPol of spec. act. ca. 700GBq/mg) and up to 8GBq with nca ^{90}Y (ItraPol). In case of Sc theragnostic pair it has been confirmed that the kit can be labelled to high RCP (>98%) with ^{44}Sc of radioactivity ca. 1.8 GBq and 0.95 GBq/kit for ^{47}Sc of low specific radioactivity. The resulting radiolabelled DOTA-TATE preparations are sterile and endotoxin and are ready for human use. ***Conclusion:*** The study showed that MultiSom kit developed by Polatom can be effectively labelled with ^{177}Lu, ^{90}Y, ^{44}Sc and ^{47}Sc. When radioisotope is sterile, endotoxin free and of GMP grade, the radiolabelled DOTA-TATE radiopharmaceuticals can be prepared directly in the hospital radiopharmacies just before application to patients. ***References:*** This work was partly financed by grant No. POIR/01.02.00-00-0041/15 „Multivariate formulations of DOTATATE peptide as precursor for preparation of radiopharmaceuticals (MultiSom)" from the National Centre for Research and Development.

EP-345

Automated production of a quinoline-based FAP-inhibitor^{68}Ga-FAPI-46 for clinical use

F. Lodi[1], *C. Malizia*[1], *V. Cabitza*[1], *S. Telo*[2], *C. Nanni*[2], *C. Drake*[3], *F. Valla*[3], *S. Fanti*[2];
[1]*PET Radiopharmacy, Nuclear Medicine Dept. S.Orsola-Malpighi University Hospital, Bologna, ITALY,* [2]*Nuclear Medicine Dept. S.Orsola-Malpighi University Hospital, Bologna, ITALY,* [3]*SOFIE Co., Totowa, NJ, UNITED STATES OF AMERICA.*

Aim/Introduction: Cancer-associated fibroblasts (CAFs) can contribute up to 90% of the gross tumor mass. CAFs have common properties distinct from normal fibroblasts like the expression of FAP (fibroblast activation protein), a type II transmembrane serine protease which plays multiple biologic roles in cancer and it is associated with a poor prognosis in a variety of tumors. FAP is considered a promising target for the development of diagnostic and therapeutic radiotracers. The quinoline-based FAP-inhibitor ^{68}Ga-FAPI-46 is a promising radiotracer for imaging of CAFs. Aim of this work was to perform the synthesis of this tracer for clinical use by using a fully automated synthesizer. ***Materials and Methods:*** ^{68}Ga-FAPI-46 synthesis was performed in a synthesis module equipped with single-use sterile cassettes (Modular-Lab PharmTracer) using the eluate of a GalliaPharm generator (1850 MBq). The eluate was purified with a cation exchange column and the labeling reaction with the precursor FAPI-46 was carried out at 95°C in acetate buffer. The crude product was then purified on C18 column, eluted with ethanol, diluted with saline and sterilized by 0.22 µm filter. Different labeling conditions were investigated by varying cation post processing purification methods, reaction times, precursor amounts and the type of scavenger added to prevent radiolysis. ***Results:*** Labelling rate increased by time using both post processing purification methods and different precursor amounts. The use of ascorbic acid as scavenger provided better radiochemical purity than ethanol. The latter provided also an incomplete product trapping during purification step, even after dilution of the reaction mixture with saline. Better synthesis yield achieved was 82±1% corrected for the decay (n = 5) with 34 nmol of precursor in 35 minutes, including generator elution. Radiochemical purity was >97% (RP-HPLC) and colloids <3% (TLC), pH 5.5, ethanol and residual ^{68}Ge content complied with European Pharmacopoeia limits. The product was sterile and apyrogenic. ***Conclusion:*** ^{68}Ga-FAPI-46 synthesis and quality control were performed for studying oncological patients in a FAPI-based clinical trial. The labeling conditions found with Modular-Lab PharmTracer synthesizer allowed to obtain ^{68}Ga-FAPI-46 in good yield enough for multiple patients administration and in a good radiopharmaceutical quality with high radiochemical and radionuclidic purity. Further stability study of ^{68}Ga-FAPI-46 in higher radioactive concentrations, by using the eluate of 2 generators, is under evaluation in order to increase the number of patients studied for each synthesis. ***References:*** None

EP-346

Impact of Synthesis Procedure, Patient and Procedure-related Parameters on Image Quality of ^{68}Ga-PSMA-11 PET/CT

L. Calderoni[1], *A. Farolfi*[1], *F. Lodi*[2], *S. Telo*[1], *G. Ricci*[1], *D. Pianori*[3], *E. Maietti*[3], *V. Cabitza*[2], *M. Fantini*[3], *P. Castellucci*[1], *S. Fanti*[1];
[1]*Nuclear Medicine, Sant'Orsola University Hospital, Bologna, ITALY,* [2]*PET Radiopharmacy Unit, Sant'Orsola Universital Hospital, Bologna, ITALY,* [3]*Department of Biomedical and Neuromotor Sciences, Unit of Hygiene, Public Health and Biostatistics, Alma Mater Studiorum, University of Bologna, Bologna, ITALY.*

Aim/Introduction: ^{68}Ga-labeled urea-based inhibitors of the prostate-specific membrane antigen (PSMA), such as ^{68}Ga-PSMA-11, are promising small molecules for targeting prostate cancer (Pca). Production of this radiopharmaceutical is generally performed by using an automated synthesis module, nevertheless recently a sterile cold kit for ^{68}Ga-PSMA-11 production was introduced and commercially available. Aim of our study was to evaluate the human imaging characteristics of^{68}Ga-PSMA-11 PET/CT prepared with two different synthesis procedures: synthesis module and ANMI sterile cold kit using the eluate of a GalliaPharm generator (Eckert & Ziegler) in PCa patients population. Secondary aim was to assess among patients characteristics and technical features which ones most influence image quality. ***Materials and Methods:*** Two different groups of 100 consecutive PCa patients who underwent ^{68}Ga-PSMA-11 PET/CT and images were reviewed independently by two

experienced nuclear medicine physicians with at least two years of PSMA imaging practice and unaware of clinical history. The two reviewers rated quality of each ^{68}Ga-PSMA-11 PET/CT using a 3-point likert-type scale (excellent, good and moderate). The performance was evaluated on the basis of the expected biodistribution, lesion detection, physiologic background uptake and presence of artifacts. The first group of patients was studied with ^{68}Ga-PSMA-11 obtained with synthesis module while the second group underwent imaging with ANMI sterile cold kit synthesis based radiopharmaceutical. ***Results:*** Overall 97/200 (48.5%) ^{68}Ga-PSMA-11 PET/CT resulted positive. Patient indications were 7/200 (3.5%) primary staging, 168/200 (84.0%) biochemical recurrence and 25/200 (12.5%) castration-resistant PCa. No significant differences in image quality between cold kit and synthesis module were found (p=0.176) but a higher amount of excellent images was observed among kit examinations (35% vs. 26%).According to multivariable regression analysis patient age (OR=1.49; CI 95%=1.09-2.02; p<0.05), patient weight (OR=1.68; CI 95%=1.38-2.05; p<0.05) and ^{68}Ga-PSMA-11 uptake time (OR=1.38; CI 95%=1.11-1.71; p<0.05) were significantly associated with an excellent image quality. ***Conclusion:*** No significant differences were found on image quality between two groups of patients studied respectively with ^{68}Ga-PSMA-11 synthetized with cold kit or synthesis module. Patient age, patient weight and ^{68}Ga-PSMA-11 uptake time were significantly associated with image quality. ***References:*** Perera M, Papa N, Christidis D, et al. Sensitivity, Specificity, and Predictors of Positive 68Ga-Prostate-specific Membrane Antigen Positron Emission Tomography in Advanced Prostate Cancer: A Systematic Review and Meta-analysis. Eur Urol. 2016;70:926-937.

EP-347

Automated radiosynthesis of [^{18}F]LBT999 on two different platforms

J. Vercouillie[1], *C. Vala*[2], *C. Mothes*[3], *G. Chicheri*[1], *P. Magadur*[3], *G. Viot*[3], *J. Deloye*[2], *S. Maia*[4], *Y. Bouvet*[2], *N. Arlicot*[4], *D. Guilloteau*[4], *P. Emond*[1];
[1]*INSERM 1253, CERRP, Tours Hospital, Tours, FRANCE,* [2]*Zionexa, Paris, FRANCE,* [3]*Cyclopharma, Tours, FRANCE,* [4]*Tours Hospital, Tours, FRANCE.*

Aim/Introduction: Fluorine labelled 8-((E)-4-fluoro-but-2-enyl)-3β-p-tolyl-8-aza-bicyclo[3.2.1]octane-2β-carboxylic acid methyl ester ([^{18}F]LBT999) is a selective radioligand for in vivo neuroimaging and quantification of the dopamine transporter by Positron Emission Tomography (PET). (1-3) In regards with potent interest of this radiopharmaceutical in routine application, we report herein fully automated methodologies on two commercial modules, TRACERlab FX_{FN} (FXFN) and AllinOne (AIO) in accordance with criteria for human use. ***Materials and Methods:*** Automated production of [^{18}F]LBT999 was first developed on FXFN module and then transferred on AIO synthesizer to comply with GMP. These automations were based on a previously reported radiosynthesis of [^{18}F]LBT999 in a one-step reaction strategy from a chlorinated precursor, with slight modifications.(1, 4) On AIO module, an optimization of various parameters was performed to get high reproducibility, repeatability as well as to shorten radiosynthesis process ***Results:*** Automation of [^{18}F]LBT999 radiosynthesis on FXFN was carried out in 35% yield (decay-corrected) in 65 min (n=16), with a radiochemical purity higher than 99 % and a molar activity of 158 GBq/µmol at the end of synthesis. The transfer on the AIO platform followed by optimizations allowed the production of [^{18}F]LBT999 in 32.7% yield (decay-corrected) within 48 min (n=5), with a radiochemical purity better than 98% and a molar activity in average higher to 154 GBq/µmol at the end of synthesis. Quality controls of both methods met the specification for clinical application. ***Conclusion:*** Both modules allow efficient and reproducible radiosynthesis of [^{18}F]LBT999 with good radiochemical yields and a reasonable synthesis time. The developments made on AIO as its ability to meet pharmaceutical criteria and to more easily comply with GMP requirements make this approach as the best for a potent industrial production of the [^{18}F]LBT999 and a future wider use ***References:*** (1) Serriere S et al. Nucl Med Biol. 2014;41(1):106-13; (2) Varrone A, et al. JNM 2011;52(8):1313-21.(3) Arlicot N et al.Q J Nucl Med Mol Imaging. 2019. under press. (4) Dollé F, et al. WO/2008/059349. 2008

EP-348

Full quality control of ^{11}C- and ^{18}F-radiobalelled compounds using compact and automated Quality Control device

B. Kuhnast[1], *O. Carvalho*[1], *J. Witczak*[2], *R. Grugel*[2], *X. Franci*[2];
[1]*CEA, BioMaps, Orsay, FRANCE,* [2]*TRASIS, Ans, BELGIUM.*

Aim/Introduction: Quality control (QC) is a crucial step in the development of original radiotracers and in the pharmaceutical quality assurance of radiopharmaceuticals injected to Humans. In the clinical practice, QC meets requirements, which are laid down by the pharmaceutical authorities. Specifications in terms of organoleptic characteristics, purity, identity, concentration, molar activity and biological burden must be observed. QC1 is a compact and automated quality control device in development that allows for checking these quality parameters of a large array of radiotracers and radiopharmaceuticals, according to the European Pharmacopeia (EP) recommendations, as well as internal specifications depending on the tracer. ***Materials and Methods:*** Samples of [^{11}C]PIB, [^{18}F]DPA-714 and [^{18}F]AV1451 have been submitted to radiophysico-chemical quality control using QC1 device. Chemical and radiochemical purity and identity have been evaluated by

analytical radioHPLC (according to "Liquid chromatography" monograph, 01/2019 :20229). Radionuclide purity and identity have been measured by gamma spectrometry (according to "Radiopharmaceutical preparations" monograph, 07/2016:0125). Residual solvent content has been determined by head-space gas chromatography (according to "Identification and control of residual solvents" monograph, 01/2017:20424). Kryptofix has been identified using spot-test and pH using pH paper-strip (according to "Approximative pH of solutions" monograph, 01/2016 :20204), both based on camera image analyses. Molar activity and radioactive concentration of the radiotracers have as well been calculated. This set of controls has been performed starting from a unique 200 µL sample of the radiotracer. ***Results:*** The entire QC process lasted between 20 and 25 min including three successive HPLC injections (in-house practice) from a unique sample of [^{11}C]PIB, [^{18}F] DPA-714 or [^{18}F]AV1451. On the same production-batch of these radiotracers, standard analyses using regular apparatus were conducted in parallel to the exception of the gas chromatography that is not adapted for radioactive samples in our laboratory. All measured parameters were in accordance with the EP or in-house specifications for each radiotracer e.g. radiochemical purity > 95%; half-life for fluorine-18 between 105 and 115 min and > 99% 511 keV photons…. A final report was automatically generated summarizing the nature of the tests, the specifications and the compliance of the measures. Graphs of the chromatographies and spectrometries were also included. Analyses (type and number) were fully customizable. ***Conclusion:*** The compact and automated device QC1 is fully adapted for the QC of radiotracers and radiopharmaceuticals in a time compatible with the half-life of the radioisotopes. The implementation of the QC of other radiopharmaceuticals is ongoing. ***References:*** None

EP-349

Fast, reliable and universal spot test for the detection of TBA$^+$ in radiopharmaceutical preparations

F. Morelle, A. Vas;
Trasis, Liège, BELGIUM.

Aim/Introduction: Spot testing is a cheap method to determine the presence or absence of compounds in radio-pharmaceutical preparations. However, no separation of the analyte from other substances is performed in such tests. Therefore, the possibility of false positive or false negative results due to the presence of interfering substances in the product hampers the implementation of such test and can redirect to more time-consuming chromatography methods. The tetrabutylammonium cation (TBA$^+$) is used as a phase-transfer catalyst for the labelling of ^{18}F-radiopharamceuticals and its presence in the final product is limited to 2.6 mg per dose according to the European Pharmacopeia (EP). Its presence can be detected by a spot test on thin layer chromatography (TLC) silica plate using iodine or iodoplatinate as revealing agent. In the presence of sodium ascorbate (NaAsc), which is widely used as antioxidant for injectable solutions, iodine and iodoplatinate become ineffective at revealing the presence of TBA. This study aims at the development of a fast and reliable spot test method for TBA that remains valid for formulations containing NaAsc. ***Materials and Methods:*** The new method is based on the radial elution on a few mm scale of the initial spot. This is sufficient to separate the TBA from the interfering NaAsc. The detection limit was estimated and the specificity of the test was verified for several ^{18}F-compounds matrices. ***Results:*** The detection limit of TBA with the new method was shown to be close to 0.1 µmol/ml. This value was not affected by the presence of NaAsc in the sample matrix. Considering a dose volume of 20 ml, this is 5 times below the accepted limit for TBA. The equipment required for the test is limited to a silica TLC plate, a reference solution of TBA, water for injection, iodoplatinate spray reagent and pipetting equipment. The method has been validated for manual and automated processes on systems such as QC1. ***Conclusion:*** The new spot test can be used for the quality control of radiochemical preparations using TBA in their preparation process regardless of the presence of sodium ascorbate in the final formulation. ***References:*** European Pharmacopeia 8.2 01/2015:1325

EP-350

Automation and High yield production of [^{18}F] MK-6240, a promising PET Tracer for quantification of Human Neurofibrillary tangles in Alzheimer disease

C. Vriamont, C. Warnier, M. Otabashi;
Trasis, Ans, BELGIUM.

Aim/Introduction: Tau PET tracers are well known radioactive probes designed for imaging of the accumulation and regional spread of brain neurofibrillary tangles and characteristic of neurodegenerative disorders known as taupathies. Second generation Tau tracers, such as [^{18}F]-MK-6240, show an improvement in their binding properties and lower the off-target binding. First in human studies with [^{18}F]-MK-6240 underlined it as a promising PET radioligand for in vivo imaging of neurofibrillary Tau aggregates in Alzheimer disease. Automation of the [^{18}F]-MK-6240 radiotracer to ensure high and reproducible synthesis yields and to allow starting with multi-curies on a platform with disposable cassettes and reagent kits is therefore needed to allow production centers to produce and dispense this PET tracer. ***Materials and Methods:*** The production of [^{18}F]-MK-6240 is performed along the synthesis method described hereafter and performed with an AllinOne-18 with HPLC. The resulting solution is clear, isotonic and can be used for quality control. The [^{18}F]$^-$ produced in the

cyclotron is separated from the aqueous solvent by trapping on an anion-exchange cartridge followed by elution with a solution of tetrabutylammonium hydrogen carbonate and evaporation to dryness. MK-6240 precursor is then added. The fluoride anion displaces the Nitro leaving group in a S_NAr reaction. Heating the reaction to 160°C in DMF allows a thermal deprotection of the Boc groups to afford the crude [^{18}F] MK-6240 radiotracer in one single step. The [^{18}F]-MK-6240 is purified by a semi-preparative HPLC, followed by collection and trapping on an SPE cartridge. The [^{18}F]-MK-6240 is eluted with ethanol and saline. The product is ready for QC and dispensing. ***Results:*** [^{18}F]-MK-6240 was produced on the AllinOne unit- in 65 minutes- with an average yield of 30 +- 5 % non-decay-corrected (NDC)- with a final volume of 20+- 1 ml The HPLC purification was performed on the embedded HPLC unit and allows to selectively collect the [^{18}F]-MK-6240 peak, free from any radiochemical or chemical impurities. Stability studies were conducted during 8 hours with a product vial containing 750 mCi (28 GBq) at the end of synthesis time and showed a radiochemical purity higher than 98%. [^{18}F]-MK-6240 Synthesis have been performed on different AllinOne units and at different facilities and showed consistent results, highlighting the reliability of the process. ***Conclusion:*** The automation of the [^{18}F]-MK-6240 PET tracer synthesis on the AllinOne platform afford reliable cassette-based synthesis, providing high yields (30+-5% NDC) and stable product over time. ***References:*** None

EP-351

A Generic GC Protocol for the Residual Solvent Analysis of PET Radiopharmaceuticals

C. Marcolan*, M. Glaser, F. Twyman, K. Sander, R. Awais, E. Årstad; University College London, London, UNITED KINGDOM.*

Aim/Introduction: Testing for residual organic solvents is a regulatory requirement for quality control (QC) of PET radiopharmaceuticals prepared under Good Manufacturing Practice (GMP) for use in humans[1]. As it is impractical and time consuming to use distinct GC methods for residual solvent analysis for each individual PET tracer produced in a GMP facility, we sought to develop a generic assay that allows robust identification and quantification of all solvents and volatile organic commonly used for PET tracer productions. ***Materials and Methods:*** A stock solution was prepared containing the following analytes; dimethylamine, dimethylaminoethanol, methanol, ethanol, acetonitrile, isopropanol, dichloromethane, acetic acid, dimethylformamide and dimethylsulfoxide. Selected diluents were then used to dilute the stock solution to concentrations ranging from 10-120% of the target value. Several GC columns and temperature gradients were evaluated and assessed for accuracy, repeatability, linearity, as well as resolution, peak tailing and sensitivity. ***Results:*** Of the GC columns investigated, the CP-Volamine capillary column (PN: CP 7447, 30 m x 0.32 mm diameter) proved best suited for analysis of complex solvent mixtures. Dimethylacetamide gave optimal results when used as a diluent. 1-propanol was chosen as the internal standard as it readily could be resolved from the analytes investigated. The optimised GC system demonstrated satisfactory results for all analytes investigated. The accuracy ranged from 93-107%, with excellent linearity ($R^2 > 0.99$) and injection repeatability (RSD% in the range of 0.2-1.2). Resolution, peak tailing and sensitivity met ICH guidelines. The validated protocol was implemented for routine residual solvent analysis of a range of PET tracers, including ^{18}F-FDOPA, ^{18}F-D_4-FCholine, and ^{18}F-DPA-714. ***Conclusion:*** We have developed a generic GC assay that allows analysis of all solvents and volatile organic commonly used for PET tracer productions. The method overcomes the need for dedicated residual solvent analysis methods for individual PET tracers and can substantially simplify QC testing of residual solvents in PET GMP facilities. ***References:*** [1] ICH Harmonised Guideline, Impurities: Guideline for residual solvents Q3C(R6). (2016).

EP-352

Investigations on formulation of freeze dried kit for preparation of ^{99m}Tc-PSMA-peptid (Mepromostat)

S. Keresztes*[1], T. Mándoki[1], Z. Kiss-Gombos[1], E. Szemenyei[1], M. Antalffy[1], J. Környei[1], G. Trencsényi[2], L. Pávics[3]; [1]Institute Of Isotopes Co., Ltd., Budapest, HUNGARY, [2]Department of Nuclear Medicine, University of Debrecen, Debrecen, HUNGARY, [3]Department of Nuclear Medicine, University of Szeged, Szeged, HUNGARY.*

Aim/Introduction: To formulate freeze dried cold kits for preparation of ^{99m}Tc-PSMA-peptid (Mepromostat) which is suitable for routine use in nuclear medicine laboratories for diagnostic imaging of prostata cancer. ***Materials and Methods:*** Systematic investigations were carried out on the impact of different excipient concentrations for the API content and on the radiolabeling efficiency of freeze dried cold kit. Three different compositions were tested in formulation by five batch preparation. Quality control tests were carried out to establish compliance of specifications: pH, tin(II) content, loss on drying, API assay and radiochemical purity of injection. In addition solubility studies were conducted in order to identify which buffer provides the highest solubility of API thus minimizing the API filtering loss. A Quality Control kit has been developed with a simple, end-user method for 'on-the-spot' testing of radiolabeling. Two radolabeling methods were compared in every batch. Finally, all formulas were tested regarding biodistribution in male Wistar rats. ***Results:*** All formulas were compliant to the predefined quality specifications and were successfully labeled with ^{99m}Tc. One specified phosphate buffer is proved to be a good candidate for ensuring high

solubility of API and robust manufacturing process. The different compositions showed similar biodistribution in male Wistar rats and two of them were successfully utilized for detection of prostata cancer in patients. Initial clinical trials demonstrated the high utility of ^{99m}Tc-PSMA (^{99m}Tc-mas3-y-nal-k(Sub-KuE)) in diagnostic imaging of prostate cancer. ***Conclusion:*** The formulated kits provide consistently high radiolabeling yields with ^{99m}Tc and appropriate API content. Quality tests are repeated in every six months to ensure compliance of cold kit specifications. ***References:*** None

EP-353

Time-dependent sterility testing to determine the viability of microorganisms and autosterilisation in radiopharmaceutical therapeutics

A. Gummesson[1], S. Protze[2], S. Knolle[2], M. Joksch[3], S. M. Schwarzenboeck[1], M. Heuschkel[1], B. J. Krause[1], C. Bergner[1]; [1]Department of Nuclear Medicine, Rostock University Medical Center, Rostock, GERMANY, [2]CUP – CUP Laboratorien Dr. Freitag GmbH, Radeberg, GERMANY, [3]Core Facility Multimodal Small Animal Imaging, Rostock University Medical Center, Rostock, GERMANY.

Aim/Introduction: Sterility testing is used to assess the presence or absence of microorganisms in products made for human use. Most products can usually be tested directly after production, radiopharmaceuticals mostly with a significant time delay. Only few laboratories are equally authorized to handle radioactivity, and are also equipped to carry out sterility tests. According to the Radiation Protection Regulations, samples can only be sent from the manufacturing laboratory to a test laboratory without an authorization to handle radioactive materials after reaching the legal limit for unrestricted release of a particular nuclide. This value for the nuclide Lu-177 is 100 Bq/g. For the usual range of Lu-177-activities applied in the synthesis of radiopharmaceuticals as Lu-177-PSMA or Lu-177-DOTATOC this would correspond to a decay time of 20 to 22 weeks before a sample can be submitted for sterility testing. The aim of this project is to develop a concept for monitoring the sterility over the mentioned period of sample storage under varying storage conditions. ***Materials and Methods:*** Different sample compositions starting from the pure sample matrix to the manufactured Lu-177-DOTATOC sample are used. After the validation of methods for sterility testing and bioburden measurement, the recovery of microorganisms depending on the monitored sample volume, storage time and amount of inoculated microorganism have to be evaluated. According to USP and EP regulations, the inoculation of 7 different types of microorganisms in 3 different amounts varying from 10 to 100 CFU is used. Sterility tests are carried out for samples with varying activity concentrations between 0.26 GBq/mL and 1.33 GBq/mL. Individual batches are stored at -20 °C, 4 °C and at room temperature, respectively, and tested at least 3 points in time. ***Results:*** A work flow has been developed to examine the impact of long term storage parameters on the detection of microbiological species, which could potentially contaminate the radiopharmaceutical during its manufacturing process. ***Conclusion:*** The proposed method of time-dependent sterility testing can be used to determine the impact of autosterilisation during long term storage of Lu-177-containing radiopharmaceuticals. It is transferable to other nuclides and radiopharmaceutical preparations. ***References:*** [1] StrSchV, 29.11.2018, p. 111. [2] EP, Chapter 2.6.1, Sterility, 8th edn, 2014. [3] USP, Chapter <71>, Sterility, US Pharmacopeial Convention, Rockville, MD, 2014.

EP-354

Study of Separation and Formulation Using Solid-Phase Extraction Method to Produce [^{11}C]DPA713 and [^{18}F] DPA714 as a Translocator Protein Ligands

***S. Naka[1,2]**, K. Kurimoto[1], K. Matsunaga[1], T. Watabe[1], M. Tatsumi[2], E. Shimosegawa[1], H. Kato[1], J. Hatazawa[1]; [1]Osaka University Graduate School of Medicine, Suita, Osaka, JAPAN, [2]Osaka University Hospital, Suita, Osaka, JAPAN.*

Aim/Introduction: [^{11}C]DPA713 and [^{18}F]DPA-714 have been developed to evaluate the relevance of expressed translocator protein (TSPO) and the activation of microglia in various neurodegenerative diseases. For the synthesis of both tracers, after labeling, HPLC separation and formulation with evaporation system were performed, however the cleaning validation of these device is required. We tried to establish a single-use system with solid-phase extraction (SPE) method. ***Materials and Methods:*** In the synthesis of [^{11}C] DPA713, [^{11}C]CH_3OTf as a labeling agent was adopted, and its production was performed by gas-phase method. On the other hand, for the [^{18}F]DPA714 synthesis, the precursor was used tosyl group and hydroxy group (same with [^{11}C]DPA713 precursor). The radiolabeling with tosyl group precursor was performed according to previous report (Michelle L. James, J Nucl Med 2008) and hydroxy group was labeled by [^{18}F]fluoroethyl bromide. After radiolabeling, reaction mixture was processed in SPE columns (reverse phase) and any concentration ethanol. ***Results:*** In the [^{11}C]DPA713 synthesis, 10-fold dilution solution of reaction mixture was passed through the tC2 column and then the column was washed with 20 mL of 25 % ethanol. [^{11}C]DPA713 eluted with 1mL ethanol from tC2 column was obtained the high radioactivity (> 1.5 GBq) radiochemical purity (> 99%). [^{18}F] DPA714 synthesis with tosyl group could not be separated any chemical impurities using SPE column, however, good separation of radiochemical and chemical impurities were obtained by hydroxy group precursor and [^{18}F]fluoroethyl bromide. ***Conclusion:*** We could establish a single-use system

with SPE method for the synthesis of [^{11}C]DPA713 and [^{18}F] DPA714 using same precursor. ***References:*** None

EP-355

Production of [^{18}F]PSMA-1007 using different starting activities of 18F-fluoride: yield and stability of the radioligand

C. Maisto*, A. Morisco, E. Squame, L. D'Ambrosio, M. Aurilio, P. Gaballo, S. Lastoria;*
Istituto Nazionale Tumori IRCCS Fondazione G. Pascale, Naples, ITALY.

Aim/Introduction: Prostate-Specific Membrane Antigen (PSMA), overexpressed in prostate cancer (PC), is considered a good target for staging of this disease. Different ^{68}Ga-radiolabeled-PSMA ligands have been investigated as PET probes, showing excellent imaging properties. Unfortunately, they can be produced in small amounts because of the limited quantity of ^{68}Ga obtained from the generator with a limited number of studied patients. Recently, [^{18}F]PSMA-1007 has been introduced, matching the possibility of a large-scale production. Our aim was to evaluate the influence of different starting amounts of 18F-fluoride on radiochemical yield (RCY), radiochemical purity (RCP) and stability of the final product. ***Materials and Methods:*** [^{18}F]PSMA-1007 was produced under GMP-compliant conditions on a TRASIS AllinOne platform according to the manufacturing process. Briefly, [^{18}F]-fluoride is trapped on QMA and then eluted with 75mM TBA; the PSMA-precursor in DMSO (1,6mg/2,2ml) is heated at 105°C for 10 min. The product was purified by C18ec cartridge and washed with 5.7% ethanol, then it was eluted with 30% ethanol on PS-H$^+$ cartridge and buffered in PBS. The product was tested for RCP and stability by radio-HPLC using a Jupiter® 5 µm C18 300 Å, 250 x 4.6 mm column and a gradient method with solvent A (acetonitrile 0,1% TFA) and solvent B (water 0,1% TFA), flow 1ml/min. Starting [18F]-fluoride activities were: 58.2±5 GBq (A) and 88.4±3.9 GBq (B). ***Results:*** RCYs were determined as no decay corrected yields at end of synthesis (EOS). Four syntheses were performed with starting activity A with a final RCY of 49.2±3.8%; eight syntheses were performed with starting activity B with a final RCY of 51.9±3.6%. The [18F]PSMA-1007 radiotracer was stable up to 8 h post synthesis with lack of degradation products due to radiolysis. ***Conclusion:*** The described method is very reliable and provides excellent RCYs in 35 min. The different activities did not affect the final RCY and the stability over a period of 8 hours, enabling to study up to 18 patients with PC by a single synthesis. ***References:*** None

EP-59

Technical Studies -> Radiopharmacy/ Radiochemistry -> Radiopharmacokinetics and Drug Development

e-Poster Area

EP-356

CYP3A4 inhibitors affect the pharmacokinetics of the TSPO radioligand [^{18}F]DPA-714 in PET imaging studies in humans

M. Peyronneau*[1], B. Jego[1], C. Letaillandier[2], C. Leroy[1], S. Lavisse[3], F. Caillé[1], B. Kuhnast[1], M. Bottlaender[4];*
[1]CEA, BioMaps, Orsay, FRANCE, [2]APHP, Hôpital Saint-Antoine, Paris, FRANCE, [3]CEA, MIRCen, Fontenay-aux-Roses, FRANCE, [4]CEA , Neurospin, UNIAC, Gif-sur-Yvette, FRANCE.

Aim/Introduction: [^{18}F]DPA-714, a known TSPO radioligand, has been recently evaluated by PET imaging in humans for investigating the role of neuroinflammation in the development and progression of neurodegenerative diseases like Alzheimer, Parkinson and multiple sclerosis [1,2]. During this study, we aimed to assess the effect of co-medications on the metabolism and pharmacokinetics of [^{18}F]DPA-714, in a large cohort of 192 subjects (genotyped for TSPO polymorphism) and consequently on the human brain input function that may be required for PET data analyses. ***Materials and Methods:*** Venous blood samples were collected from all subjects during PET (129 patients and 63 controls). Among them, arterial blood samples were also collected from 16 healthy controls free of any medication (HC). [^{18}F]DPA-714 and metabolites fractions were determined by a solid phase extraction method and used for the correction of individual input functions. The mean percentages of parent tracer in plasma at 70-90min ([^{18}F]DPA-714$_{70\text{-}90}$) and corresponding concentrations of [^{18}F] DPA-714 ($AUC_{0\text{-}90}$) in co-medicated patients were compared to HC. For statistical analyses, impact of endogenous factors such as age, gender, TSPO polymorphism was verified. ***Results:*** The metabolism of [^{18}F]DPA-714 was significantly lower in patients than HC ([^{18}F]DPA-714$_{70\text{-}90}$; 61.35±11.02 % vs 51.50±6.83 %, $p<0.05$). In order to investigate the potential source of variability, 38 subjects exhibiting a huge decrease of metabolites formation (parent radiotracer fraction higher than 70%) were analysed separately. Among the most common co-medications given, amlodipine, atorvastatine, metformin, nicardipine, sartans, verapamil were identified. All these drugs are known inhibitiors of CYP3A4, the isoform mainly responsible for the metabolism of DPA-714 [3]. Considerable modifications of the plasma pharmacokinetics were observed, leading to an increase of the parent plasma concentration with $AUC_{0\text{-}90}$ values from 20.03±7.93 to 73.13±44.82 SUV·min in co-treated individuals

vs 15.57±5.24 SUV.min in HC. Finally, while [18F]DPA-714 is administrated at tracer dose, the toxicity of the radiotracer should be highly reduced as compared to pharmacological dose, co-medications may affect individual input functions. ***Conclusion:*** Thus any co-medication that inhibits CYP3A4 should be taken into account since it may lead to a decrease of [18F]DPA-714 metabolism that will likely produce an increase of the parent tracer in plasma and a potential increase of the brain uptake. Individual input functions should be preferred for the analysis of imaging patients data, instead of averaged input function derived from HC. ***References:*** [1]Hamelin et al. Brain. 2018;141(6):1855-1870. [2] Bodini et al., J Nucl Med. 2020 Jan 31. [3]Peyronneau et al., Drug Metab Dispos. 2013;41(1):122-31.

EP-357

A Physiologically Based Pharmacokinetic Model of 68Ga-DOTATATE to Describe Organ Distribution

H. Siebinga[1,2], B. J. de Wit-van der Veen[2], J. H. Beijnen[1], M. P. M. Stokkel[2], T. P. C. Dorlo[1], A. D. R. Huitema[1,3], J. J. M. A. Hendrikx[1,2]; [1]Department of Pharmacy & Pharmacology, The Netherlands Cancer Institute, Amsterdam, NETHERLANDS, [2]Department of Nuclear Medicine, The Netherlands Cancer Institute, Amsterdam, NETHERLANDS, [3]Department of Clinical Pharmacy, University Medical Center Utrecht, Utrecht, NETHERLANDS.

Aim/Introduction: Physiologically based pharmacokinetic (PBPK) models combine drug specific information with prior knowledge on the physiology and biology at the organism level (system specific information). Whole-body PBPK models contain an explicit representation of the organs and tissue and can be used as a tool to predict pharmacokinetic behavior of drugs. The aim of this study was to develop a PBPK model to describe organ distribution of 68Ga-DOTATATE based on clinical PET/CT data. ***Materials and Methods:*** Clinical 68Ga-DOTATATE PET/CT data from 41 patients without any visible somatostatin receptor (SSTR) overexpressing tumors were included. Scans were performed at 45 minutes (range 30-60 min) after intravenous bolus injection of approximately 100 MBq 68Ga-DOTATATE (~10 µg peptide). Organ (spleen, liver, thyroid) and blood activity levels were derived from PET-scans and corresponding peptide concentrations were calculated. A whole-body PBPK model was developed using a standardized protein model in PK-Sim and MoBi (Open System Pharmacology, version 8.0). Organs were linked by blood compartments and each organ was further characterized by a specific blood-flow, volume, tissue-partition coefficient and permeability. The internalization reaction, enzymatic reaction for intracellular degradation and renal clearance were included in the model and SSTR2 expression was added to several organs (1). Input parameters were fixed or fitted using a built-in Monte Carlo algorithm for parameter identification. ***Results:*** 68Ga-DOTATATE was administered with a median peptide amount of 12.5 µg (range 8.0-16.9 µg) labeled with 92.7 MBq (range 43.4-129.9 MBq). SSTR2 expression for spleen, liver and thyroid were fitted at 24.3, 4.86 and 1.09 nmol/L, respectively. Variability in observed organ concentrations was described by variability in SSTR2 expression and differences in administered peptide amounts. Using this variability, the model predicted 78.0%, 90.2% and 94.1% of observed data for spleen, liver and thyroid, respectively. Fraction unbound in plasma was fitted at 0.28 and 13% of the peptide was excreted unchanged in the urine within 4 hours. ***Conclusion:*** To conclude, biodistribution of 68Ga-DOTATATE can be described with a whole-body PBPK model, where tissue distribution is mainly determined by variability in SSTR2 organ expression. Besides, variability in observed concentrations was described by differences in administered peptide amounts. This PBPK model showed the feasibility to model concentration-time profiles for specific organs and, hereafter, can be used to predict distribution throughout other tissues. ***References:*** 1. Sandström M, et al. Comparative biodistribution and radiation dosimetry of 68Ga- DOTATOC and 68Ga-DOTATATE in patients with neuroendocrine tumors. J Nucl Med. 2013;54(10):1755-9.

EP-358

Investigation of structure-affinity relationship of novel 18F-labeled norepinephrine analogue tracers

S. Mühlig[1,2], X. Chen[1,2,3], Y. Ohshima[1,2,4], Y. Yagi[5], H. Kimura[5], K. Koshino[6], N. Nose[7], C. Lapa[3], A. Buck[1], T. Higuchi[1,2,7]; [1]Department of Nuclear Medicine, University Hospital of Würzburg, Würzburg, GERMANY, [2]Comprehensive Heart Failure Center, University Hospital of Würzburg, Würzburg, GERMANY, [3]Department of Nuclear Medicine, University Hospital of Augsburg, Augsburg, GERMANY, [4]Department of Radiation-Applied Biology Research, Quantum Beam Science Research Directorate, National Institutes for Quantum and Radiological Science and Technology, Gunma, JAPAN, [5]Department of Analytical and Bioinorganic Chemistry, Kyoto Pharmaceutical University, Kyoto, JAPAN, [6]Department of Systems and Informatics, Hokkaido Information University, Ebetsu, Hokkaido, JAPAN, [7]Graduate School of Medicine, Dentistry and Pharmaceutical Sciences, Okayama University, Okayama, JAPAN.

Aim/Introduction: The norepinephrine transporter (NET) is one of the major targets for radionuclide imaging of the cardiac sympathetic nerve condition and neuroendocrine tumors. Most radiotracers, which target NET-function, consist of derivatives of norepinephrine (NE). In this study two newly designed NE analogue 18F-labeled PET compounds, which have identical structure rather than meta-fluoride (compound ***a***) or meta-iodide (compound ***b***), were evaluated to understand the relationship with NET affinity. ***Materials and Methods:*** In vitro study with competitive uptake assay was performed with 3H-NE and human neuroblastoma SK-N-SH cell line to characterize

uptake via NET. Cells were treated with ^{3}H-NE (12 kBq/ml) in 0.1% BSA/DMEM containing non-radioactive compounds ***a*** or ***b*** in concentrations from 10^{-10} - 10^{-3} M. In the presence of 20 µM pyrogallol (catechol-O-methyl-transferase inhibitor) and 100 µM pargyline (monoamine oxidase inhibitor), cells were incubated for 60 min then washed with PBS, lysed in 0.1 M NaOH, followed by measurement of radioactivity. Cold hydroxyephedrine (HED), metaiodobenzylguanidine (MIBG) and NE were used as references for the target compounds. In vivo biodistribution study was performed on healthy male Wistar rats, whereby ^{18}F-labeled compound ***a*** or ***b*** were administered via tail vein. After 10 min tracer injection, heart, liver and blood were obtained for tissue counting study. ***Results:*** The in vitro study demonstrated that cold compound ***a*** had an IC_{50} value (3.4 µM) in a comparable range as the cold references NE (5.4 µM) and HED (2.1 µM). To be noted, these IC_{50} values are about 5 hold higher than clinical tracer MIBG (15.4 µM). In contrast, compound ***b*** greatly lost its NET affinity (IC_{50} value 98.1 µM). Animal study of both ^{18}F-labeled compound ***a*** and ***b*** showed homogeneous cardiac uptake, while higher cardiac uptake (heart-to-blood ratio) was seen with compound ***a*** than ***b***: 12.0 and 13.1(n=2) vs 5.8± 0.3 (n=4). ***Conclusion:*** In cell uptake studies, two ^{18}F-labeled compounds with an identical structure rather than meta-fluoride or -iodide greatly differ in NET affinity. The former has similar affinity as NE or HED and even better affinity than MIBG, whereas the latter showed a much lower affinity. In contrast, in vivo rat experiments revealed high cardiac uptake in both ^{18}F tracers. Considering the existence of an extra-neuronal cardiac uptake mechanism in rats, the uptake may be mediated by other transporters, such as organic cation transporters, which is currently under investigation. ***References:*** None

EP-60

Therapy Clinical Study -> Oncological Therapy Clinical Study -> Local Radionuclide Therapy (including Spheres)

e-Poster Area

EP-359

Can SPECT/CT lung shunt quantification improves dose optimisation with ^{99m}Tc-MAA study for ^{90}Ymicrosphere workup

A. Poon[1,2], J. Dal Santo[1], S. T. Lee[1,3,4], B. M. Chappell[1], K. Pathmaraj[1], A. M. Scott[1];
[1]Austin Hospital, Heidelberg, AUSTRALIA, [2]University of Melbourne, Parkville, AUSTRALIA, [3]Olivia Newton-John Cancer Research Institute, Heidelberg, AUSTRALIA, [4]La Trobe University, Heidelberg, AUSTRALIA.

Aim/Introduction: ^{90}Y microspheres radioembolisation is a recognised treatment of inoperable liver cancer. Radioembolisation involves intrahepatic-arterial injection of ^{90}Y microspheres into tumour via the hepatic artery performed under angiogram guidance. To optimise risk/benefit for patients receiving ^{90}Y microspheres, a pretreatment ^{99m}Tc-MAA shunt study is required to assess lung shunting in order to minimise potential radiation pneumonitis. Current practice calculate percentage of lung shunt from planar imaging, however, implementation of software to quantify shunting from SPECT/CT may allow for more accurate assessment of lung shunt and therapeutic dose optimisation. To quantify and compare the percentage of ^{99m}Tc-MAA lung shunting calculated from planar and SPECT/CT imaging in patients being worked up for ^{90}Y microspheres radioembolisation and calculation of expected radiation dose to the lungs. ***Materials and Methods:*** A pilot study of patients with hepatic malignancies undergoing imaging workup for ^{90}Y microspheres radioembolisation was conducted. Planar and SPECT/CT imaging of chest and abdomen were acquired on a GE Discovery-670 system. ^{99m}Tc-MAA injected dose and patient demographics were collected. Percentage lung shunt was calculated using regions of interest drawn over the whole lungs and whole liver. The lung shunt is calculated by equation (lung shunt%=geometric mean lung counts/[geometric mean liver counts+geometric mean lung counts]x100) and GE Q.Volumetrix software for planar and SPECT/CT imaging respectively. Lung radiation dose(Gy) was calculated by 49670xActivity(lung)(GBq)/Mass(lung)(g)- as per SIR-Spheres® product insert. Statistical analysis was performed. ***Results:*** Twenty patients were reviewed. Using planar analysis, the percentage lung shunt ranged from 2.5-38% (mean ±SD=11.61% ± 7.22%). Using SPECT/CT analysis, the percentage lung shunt ranged from 1.41-13.3% (mean ±SD=3.54% ± 2.64%); indicating a lower calculated lung shunt using SPECT/CT analysis. Two patients did not receive ^{90}Y microspheres therapy, one of which was due to lung shunt >20% on planar calculation but was only 13.3% on SPECT. Assuming a lung mass of 1000g, the estimated radiation dose to the lungs from the treated ^{90}Y microspheres dose ranged from 2.24-16.58Gy (mean ±SD= 7.78 ±4.06 Gy) from planar and 0.73-5.99Gy (mean ±SD= 2.39 ±1.55 Gy) from SPECT calculations. ***Conclusion:*** Quantification of lung shunting and hence radiation dose to the lungs calculated from SPECT/CT was lower when compared with planar imaging for patients undergoing workup for ^{90}Y microspheres radioembolisation, which may allow for better dose optimization in cases where lung shunting was the primary limiting factor. However, given the pilot study's small size, further investigation is needed to validate this technique for clinical practice. ***References:*** None

EP-61

Therapy Clinical Study -> Oncological Therapy Clinical Study -> Neuroendocrine Therapy

e-Poster Area

EP-360

Neuroendocrine Tumours (NET) Quantitative SUV-SPECT/CT Change during ^{177}Lu-DOTATATE MRT

T. Alkahtani[1,2], L. Livieratos[1,2], V. Lewington[1,2];
[1]King's College London, London, UNITED KINGDOM,
[2]Guy's & St Thomas' Hospitals NHS Foundation Trust, London, UNITED KINGDOM.

Aim/Introduction: Post-treatment imaging is routinely used to, verify radiopharmaceutical distribution in patients undergoing molecular radiotherapy (MRT). Beyond its role as a visual assessment tool, image quantification may have a role in monitoring changes induced by MRT. This project examines the role of quantitative SUV-SPECT during ^{177}Lu-DOTATATE MRT to determine whether Standardised Uptake Values (SUV) change in patients undergoing repeated radionuclide treatments. ***Materials and Methods:*** We retrospectively analysed serial SPECT/CT data for three patients undergoing ^{177}Lu-DOTATATE MRT for metastatic neuroendocrine tumours. 3D quantitative SUV-SPECT/CT data were reconstructed and analysed using Hybrid3D 3.01 software (HERMES Medical Solutions, Sweden). The SUV of normal and abnormal tissues was calculated following the first and fourth cycle of 177Lu- DOTATATE. Seventeen lesions and healthy organs (liver, kidneys, and spleen) were assessed after both cycles to derive SUVmax, SUVmean, SUVpeak, and SUVratio. Wilcoxon Signed-Rank test using SPSS (IBM SPSS Statistics 2019 v26.0; Armonk, NY) was applied testing of SUV changes. Paired sample t-test was used to evaluate differences for non-target organs. ***Results:*** SUV values changed significantly between the first and fourth PRRT cycles ($p < 0.05$). The mean overall SUV decrease in index tumour lesions was 70%. The mean total lesion: spleen SUV ratio decreased from 4:1 to 0.9:1 between PRRT cycles 1 and 4. The SUV of non-target organs such as liver, spleen and kidneys was stable between treatment cycles in all patients. ***Conclusion:*** Quantitative SPECT/CT appears feasible to evaluate changes in tumour and normal tissue uptake following MRT. SUV change has potential as a clinical marker to evaluate response between MRT cycles and might improve the optimisation and individualisation of MRT. ***References:*** None

EP-361

Peptide Receptor Radionuclide Therapy With [^{177}Lu-DOTA^{0},Tyr^{3}]octreotate. Experience At Our Center

M. Lara Martínez[1], M. De Sequera Rahola[2], A. Díaz Silván[2], O. Vilahomat Hernández[2], E. Martínez[2], D. Cabello García[2], M. López Acosta[2], A. Allende Riera[2];
[1]Hospital Universitario de Canarias, Santa Cruz de Tenerife, SPAIN, [2]Hospital Universitario Nuestra Señora de La Candelaria, Santa Cruz de Tenerife, SPAIN.

Aim/Introduction: There are limited therapeutic options for patients with advanced Neuroendocrine Tumors (NETs) progressing on first-line somatostatin analog therapy. Peptide receptor radionuclide therapy (PPRT) is an innovative technique that delivers cytotoxic radiation to tumor cells using a β- emitting radionuclide such as [^{177}Lu-DOTA^{0},Tyr^{3}]octreotate (^{177}Lu-DOTATATE) that is chelated to a somatostatin analog allowing targeted action on NETs which usually overexpress somatostatin receptors. PRRT is thus a new therapeutic option for NETs patients. Indicated for the treatment of unresectable or metastatic, progressive, well differentiated (G1 and G2), somatostatin receptor positive gastroenteropancreatic (GEP) and bronchial neuroendocrine tumours (NETs) in adults. ***Materials and Methods:*** Descriptive retrospective study of patients with GEP and bronchial NETs who were treated with ^{177}Lu-DOTATATE from 2018 to 2019. In this period, 15 patients were treated. In addition to demographic parameters, we analyzed NET type, stage, side effects and progression-free survival. ***Results:*** We analyzed 15 canarian patients treated with 177Lu-DOTATATE who had previously progressed to somatostatin analogues and chemotherapy (11 men and 4 women), with a mean age of 58 years, with diagnoses of pancreatic NET (7 patients), ileal NET (6 patients), and pulmonar NET (2 patients), all of them in stage IV, 12 patients being G2 and 3 patients were G1. Three patients received 2 doses due to liver progression, both of them kept experiencing disease progression and only one patient received 3 doses due to severe thrombocytopenia, however this last one remains in stable disease until now with a mean progression-free survival of 12 months. The median progression-free survival after treatment of the 11 patientes who completed all the 4 doses was 18 months, lower compared to the 28,5 months reported in the Netter study, probably because of the small sample and the scarce 2-year follow up since the first treatment was administered at our center. Of whom 7 remain in stable disease and 4 showed disease progression. Hematological toxicity was seen on 3 patients due to thrombocytopenia. ***Conclusion:*** PPRT with ^{177}Lu-DOTATATE is a favorable therapeutic option in patients with metastatic bronchial and GEP NETs that express somatostatin receptors that have progressed to other lines of treatment with few side-effects. ***References:*** None

EP-362

Tandem High-Dose 131I-MIBG Therapy For Paediatric Patients With Relapsed-Refractory High Risk Neuroblastoma: A Dosimetry Based Treatment

C. Altini[1], M. Villani[1], B. Cassano[2], M. Pizzoferro[1], A. Serra[3], A. Castellano[3], V. Cannatà[2], M. Garganese[1];
[1]IRCCS Bambino Gesù Children's Hospital, Nuclear Medicine Unit, Imaging Department, Rome, ITALY, [2]IRCCS Bambino Gesù Children's Hospital, Medical Physics Unit, Rome, ITALY, [3]IRCCS Bambino Gesù Children's Hospital, Paediatric Haematology/Oncology Department, Rome, ITALY.

Aim/Introduction: ^{131}I-meta-iodobenzylguanidine (^{131}I-MIBG) combined with myeloablative chemotherapy represents an useful modality of treatment in children affected by relapsed/refractory neuroblastoma (NB) for increasing palliation and progression-free survival. Aim of our study is to evaluate the feasibility, safety and response of tandem high-dose therapy based on two administrations of ^{131}I-meta-iodobenzylguanidine (^{131}I-MIBG) followed by Melphalan. ***Materials and Methods:*** 13 patients (age range: 3-17 years) affected by relapsed/refractory NB, (all previously subjected to several lines of treatment) were included. Each treatment included two administrations of ^{131}I-MIBG (with a dosimetric approach); the WB absorbed dose resulting from the first administration was used to determine the second activity to be administered to reach a total WB absorbed dose of 4 Gy. 96 hours after second ^{131}I-MIBG administration, a single dose of Melphalan (110 mg/m2) with peripheral blood stem cell (PBSC) rescue was given. In all patients, a ^{123}I-MIBG scintigraphy was performed before treatment and SIOPEN score was determined. ***Results:*** after first treatment no one experienced grade 4 of neutropenia; three patients needed an RBC transfusion. After second treatment twelve patients experienced grade 4 neutropenia and one grade 3, three patients presented fever and all needed a RBC and PTL transfusions; six patients showed mucositis. Cumulative WB absorbed doses ranged from 1.6 to 4.8 Gy (median: 3.6 Gy). Regarding treatment response, five patients showed progressive disease (they died after 6, 6, 10, 10 and 16 months respectively); four patients showed stable disease (FUP ranging from 14 to 24 months); two patient showed partial response (FUP: 12 and 14 months respectively) and 2 patients showed complete response (FUP of 9 and 30 months). ***Conclusion:*** in our experience, high-dose ^{131}I-MIBG therapy combined with chemotherapy is a feasible and safe modality of treatment in heavily pre-treated patients affected by relapsed/refractory NB in order to achieve an effective myeloablation; dosimetric approach allows to prescribe a tailored treatment, administering activities as high as possible. Moreover it can be considered an effective therapy too, even though further studies with more patients and a longer FUP are mandatory. ***References:*** None

EP-363

Quantitative assessment of SUVs obtained in ^{68}Ga-labeled somatostatin analogue PET/CT for estimation of long term response to PRRT in patients with neuroendocrine tumors

A. Sowa-Staszczak[1], M. Opalińska[2], A. Kania-Kuc[2], I. Al Maraih[2], M. Buziak-Bereza[1], A. Hubalewska-Dydejczyk[1];
[1]Chair and Department of Endocrinology, Jagiellonian University CM, Krakow, POLAND, [2]Nuclear Medicine Unit, Endocrinology Department, University Hospital in Krakow, Krakow, POLAND.

Aim/Introduction: PRRT is an effective treatment for disseminated NETs, especially for control of disease progression. Currently there is not known any effective predictors of the final response to PRRT. Aim: Quantification of SUVs obtain in ^{68}Ga-somatostatin analogue PET/CT in prediction of the long-term response to PRRT. ***Materials and Methods:*** Out of 20 people treated with PRRT using ^{177}Lu and ^{177}Lu/^{90}Y DOTA-TATE in 2017-2019 due to dissemination of G1 and G2 neuroendocrine neoplasm, 13 patients were eligible for study. In this group ^{68}Ga-DOTA-TATE PET/CT was performed in average 4.5 months before and 3.6 months after PRRT. A total of 83 metastatic lesions were evaluated and they were located in the liver, bones, lungs and lymph nodes of the neck, chest, abdominal and pelvic cavity. For every lesion in both PET/CTs (before and after PRRT) SUVmax, mean value of SUV, and ROI volume were measured. SUVmax in target lesion was compared to the mean value of SUV in the lesion volume to assess the homogeneity of the lesions. Further for all lesion corrected SUVmax was counted, taking into account individual for each patients SUV max of reference organs (normal liver and spleen). Finally corrected SUVmax change(before and after PRRT) was counted. Obtained results were assigned to three groups of variations: 1. SUV increase 2. SUV decrease 3. Insignificant variation. Those results were correlated with the progression, stabilization (SD) or regression of the disease seen in other imaging studies after mean 9 months of observation. ***Results:*** The mean follow-up was 8.9 months, during which progression was found in 3 patients, regression in 4 and disease stabilization in 6 patients. Among patients with regression, a decrease in the mean value of corrected SUVmax in comparison to the baseline study of 281% was observed. Among patients with SD, a mean of corrected SUVmax in comparison to the baseline study decreased by 190%. Stable values were observed among progressive patients, where change of corrected SUVmax was in average -1%. ***Conclusion:*** A decrease in the value of corrected SUVmax in metastatic lesions obtained from routine PET/CT tests with ^{68}Ga-DOTA-TATE may indicate a lower risk of neuroendocrine tumor progression within a 9 months from the end of PRRT and may constitute an additional independent parameter helping to estimate the risk of progression in this group of patients. ***References:*** None

EP-364

Complications During The Treatment Administration Of 177Lu-Oxodotreotide And Adverse Effect In The Patients

***S. Rodríguez Gadea**, E. Cobreros Peña, A. Cuadra Plaza, M. Bravo Perez, D. Gimeno Gállego, M. Marín Ferrer, Á. Galiana Morón, M. Gonzalez Martín;*
Hospital Universitario 12 Octubre, Madrid, SPAIN.

Aim/Introduction: The present study aims to describe the complications and adverse effects observed during the administration of 177Lu-oxodotreotide in the treatment of neuroendocrine tumours (NET), according to the technical specifications sheet of the radiopharmaceutical. ***Materials and Methods:*** Nineteen patients (average age 60.4± 12.65) including 9 women were treated with 177Lu-oxodotreotide (4 doses/7400MBq every 8 weeks) between March 2016 and November 2019. Fourteen patients had a primary lesion in the digestive system and 5 in the lungs. A total of 67 doses were administered, 13 patients completed the treatment, in 4 patients the treatment was discontinued because progression disease or toxicity and 2 patients were pending completion of the treatment. The procedure was carried out by a nurse of our department, supervised by Nuclear Medicine physician or a third-year internal resident. During each patient procedure we collected the following data: percentage of radiopharmaceutical injected, injection instruments malfunctions, changes in pump injection pressure or flow rate to the patient, radioactive contaminations, problems with urine incontinence requiring bladder catheterization and stopping the treatment. And finally any adverse symptoms referred by the patient during the procedure or the following days. ***Results:*** According to our data, the average dose injected to the patients was 98.40%±2.23 of the total amount in the vial. The problems observed during the procedures were: instrument malfunctions 8 (11.94%); changes in pressure/flow rate of perfusion pump 13 (19.24%); radioactive contaminations: floor 2 (2.98%), bed and sheets 2 (2.98%), staff skin 3 (4.17%); 3 patients (4.47%) required bladder catheter due to urinary incontinence (4.47%). Adverse reactions: nausea 13 patients (G1- 42.1%, G2 21.1%, G3 5.2%); vomits 6 patients (G1 26.3%, G2 5.2%), diarrhoea 3 patients (G1 10.5%, G2 5.2%), abdominal pain 4 patients (G1 10.5), headache 2 patients (10.52%). ***Conclusion:*** The perfusion technique employed in our department allows for a 98.4% administration of the total dose prescribed. All the problems occurred during the procedure were successfully resolved. The adverse effects observed are few and similar to the published data. ***References:*** Nuclear Medicine Service, Hospital12 de Octubre

EP-365

^{131}I-MIBG treatment in patients with metastatic paraganglioma and pheochromocytoma

***J. Bernal**, S. Prado, M. Agudelo, A. Utrera, J. Cañón, P. Bello;*
Hospital Universitario y Politécnico La Fe, Valencia, SPAIN.

Aim/Introduction: To describe our experience with ^{131}I-MIBG in patients with metastatic paraganglioma and pheochromocytoma during the last decade. ***Materials and Methods:*** Descriptive, retrospective study of 7 patients (4 men, one of them child), with an age range between 5-77 years (mean: 45.14), diagnosed with metastatic paraganglioma/pheochromocytoma and treated with ^{131}I-MIBG from 01-01-2010 until 01-17-2020. All of them were previously studied with ^{123}I-MIBG scintigraphy, somatostatin receptor scintigraphy and/or PET-CT (^{18}F-FDG or ^{68}Ga-DOTATOC). ***Results:*** 4/7 pheochromocytomas and 3/7 paragangliomas were treated. 2/7 patients presented SDHB mutation. In 2/7 cases a second cycle of ^{131}I-MIBG was administered and one cycle in the remaining patients. The average activity administered was 165.37mCi (83-222.5mCi). The treatment was clinically well tolerated by all patients. The most frequent adverse event was hypertensive crisis (2/7 patients) despite premedication, with improvement after adjusting the supportive treatment. The mean follow-up after treatment was 23.42 months. During the first year: 1/7 patient had a partial response, 3/7 stable disease, 2/7 progression of disease, and 1/7 died due to advanced disease. Clinical improvement was reported in 5/7 cases and laboratory parameters normalization in 3/7. In the long-term follow-up 2/3 patients are with stable disease, and do not have any clinical change and 1/3 patients have progressed in 22 months. The pediatric patient is into partial response and remains asymptomatic after 62 months follow-up. ***Conclusion:*** Treatment with ^{131}I-MIBG has shown excellent tolerance and improves the life quality in most of the patients, with bearable short-term adverse events. Although larger series are necessary, about half of the patients remain free of disease progression, and it could be advisable to assess the use of this treatment in earlier stages of the disease. ***References:*** None

EP-366

Assessment of early cardiotoxicity following the use of radiotheranostics agents177Lu-PSMA for prostate cancer and177Lu-DOTATATE for neuroendocrine tumors

***M. Assadi**[1], A. Amini[1], E. Jafari[1], H. Ahmadzadehfar[2], D. Bagheri[3];*
[1]Bushehr University of Medical Sciences (BUMS), Bushehr, IRAN, ISLAMIC REPUBLIC OF, [2]Klinikum Westfalen, Knappschaft Hospital, Dortmund, GERMANY, [3]Persian Gulf University, Bushehr, IRAN, ISLAMIC REPUBLIC OF.

Aim/Introduction: Cardiovascular diseases and cancer are the most common causes of morbidity and mortality around the world. Nowadays, with progression in technology

and patient care procedures, the survival rate of cancer patients is improved significantly. Nevertheless, all of the therapy procedures lead to short and late-term adverse side effects which can decrease the clinical efficacy such as cardiovascular toxicity (CVT). Therefore, evaluation of novel cancer treatment procedures associated CVT is necessary for its efficiency. Aim of this study was evaluation of early cardiotoxicity following radionuclide therapy (RNT) including peptide receptor radionuclide therapy (PRRT) with 177Lu-DOTATATE for treatment of patients with neuroendocrine tumors (NETs) and radioligand therapy (RLT) with 177Lu-PSMA by measurement of serum troponin as a cardiac injury indicator. ***Materials and Methods:*** From December 2018 to October 2019, patients with prostate cancer and NET referred for PRRT and RLT, respectively, were enrolled to this study. To measure troponin, blood samples were taken immediately before treatment and 48 hours after treatment for each patient and the serums were separated and frozen. ***Results:*** 42 RNT cycles were evaluated in 26 patients with mean age of 60.08±17.55 years from 27 - 99) including 13 NET patients (23 cycles) and 13 prostate cancer patients (19 cycles) underwent PRRT and RLT, respectively. The NET patients included five females and eight male. The median administered dose was 6.6 with range of 3.7 to 7.4 GBq. The serum values of troponin before and after treatment were 0.61±0.49 and 0.47±0.54 ng/ml, respectively (p=0.12). In prostate cancer patients, the serum values or troponin before and after treatment were 0.59±.42 and 0.53±0.38 ng/ml, respectively (p=0.4). In NET patients, the serum values or troponin before and after treatment were 0.62±0.47 and 0.42±0.51 ng/ml, respectively (p=0.39). ***Conclusion:*** In this study, it has been shown that PRRT and RLT as novel cancer treatment have no significant effect of the early values of serum troponin as a cardiac injury indicator, therefore, these procedures have no significant cardiotoxicity. ***References:*** None

EP-62

Therapy Clinical Study -> Oncological Therapy Clinical Study -> Other Oncological Treatments

e-Poster Area

EP-367

Peptide receptor radionuclide therapy for glioma tumors: An extended report on a pilot study

M. Assadi[1], R. Nemati[1], A. Amini[1], H. Ahmadzadehfar[2], H. Shooli[1], S. Rekabpour[1], E. Jafari[1];
[1]Bushehr University of Medical Sciences (BUMS), Bushehr, IRAN, ISLAMIC REPUBLIC OF, [2]Klinikum Westfalen, Knappschaft Hospital, Dortmund, GERMANY.

Aim/Introduction: The prognosis for high-grade glioma is impoverished yet despite application of optimal available treatment (surgery, radiation, and chemotherapy). We aim to report our ongoing pilot study in which we assess the therapeutic effectiveness of intravenous (iv) ^{177}Lu-DOTATATE in glioma tumors. ***Materials and Methods:*** Between January 2017 and April 2020, eighteen patients with glioma tumors were included. Inclusion criteria are defined as tissue-based confirmation of glioma tumors, blood brain barrier (BBB) interruption, and sufficient expression of somatostatin receptors (SSTRs) by the tumor tissue. In all patients, ^{99m}Tc-octreotide SPECT or ^{68}Ga-DOTATATE PET-CT scan was acquired as a screening evaluation for confirming high level of SSTR expression. Our interdisciplinary group, consist of oncologist, neurologist, neurosurgeon, nuclear medicine specialist, and cardiologist, visited each patient and discussed him/her individually. Accordingly, if no other alternative therapeutic option was available (failed state-of-the-art treatment, inoperable tumors, or patient refusal to available treatment), every patient was individually treated on a compassionate basis. We planned to treat all cases with 1 to 4 cycles of iv ^{177}Lu-DOTATATE (50-200 mCi for each cycle). After each cycle, ^{177}Lu-DOTATATE brain and whole-body scan (24-hr, 48-hr, and if needed 72-hr after treatment) were obtained to evaluate drug delivery and SSTR-binding capacity. Tumor response was assessed using response assessment in neuro-oncology (RANO) criteria. Eastern Cooperative Oncology Group (ECOG) (score: 0-5) and Karnofsky Performance Score (KPS) (score: 0-100) were used to assess Patients' quality of life (QOL) before and after treatment. ***Results:*** Sixteen adults (m/f=9/7) and two children (2 girls) with a mean age of 54.75 and 6.5 years, respectively, were included in our study. The mean ECOG and KPS score (pre-/post-treatment) were respectively (2.3/2.1) and (57.5/60.6) for adults and (2/2) and (65/65) For children. Of note, the pattern of radionuclide uptake on post-therapy imaging (^{177}Lu-DOTATATE scans) was spatially corresponded to enhancing-areas on MRI. ^{177}Lu-DOTATATE effectively bound to SSTR receptor-positive regions and it was also able to identify new brain masses. The participants' response to the treatment were observed as complete remission (n=1), partial remission (n=6), stable disease (n=3), progressive disease (n=8). Nonetheless of the promising radiologic response, QOL was not significantly improved (p<0.05). These clinical and radiological inconsistency can be attributed to the well-established injury to the critical structures in the brain. ***Conclusion:*** PRRT approach using ^{177}Lu-DOTATATE seems promising option in treating brain tumors and warrant further well-designed trials to solidify current evidence. ***References:*** None

EP-368

Initial practice with Gallium-68 DOTATATE PET/CT and peptide receptor radionuclide therapy for pediatric patients with relapsed or refractory metastatic neuroblastoma: A promising point-of-care after failure 131I- MIBG therapy

M. Assadi[1], G. Fathpour[1], E. Jafari[1], H. Dadgar[2];
[1]Bushehr University of Medical Sciences (BUMS), Bushehr, IRAN, ISLAMIC REPUBLIC OF, [2]Cancer Research Center, Razavi Hospital, Mashhad, IRAN, ISLAMIC REPUBLIC OF.

Aim/Introduction: There are limited therapeutic methods for pediatric patients with refractory neuroblastoma. Since somatostatin receptors (SSTRs) expression had been shown in neuroblastoma lesions, we aimed to evaluate STTR expression in these patients for imaging and therapeutic purpose with 68Ga-DOTATATE PET/CT and peptide receptor radionuclide therapy (PRRT) with 177Lu-DOTATATE, respectively. ***Materials and Methods:*** 13 pediatric patients with refractory neuroblastoma were enrolled in this study with mean age of 5.18±.188 from 2-8 years old including 6 (46.2%) males and 7 (53.8%) females. Among them 4 patients were underwent PRRT. Treatment response, survival and therapy related toxicity were assessed in these patients. ***Results:*** Of 13 patients underwent 68Ga-DOTATATE PET/CT, 9 (69.2%) patients were referred for restaging and 4 (30.8%) were referred for staging. 68Ga-DOTATATE was positive in 9 (69.2%) of patients and median number of detected lesions was 2 (1-13) in patients with positive 68Ga-DOTATATE. Of 4 patients who were refractory or relapsed after 131I-MIBG therapy and showed significant 68Ga-DOTATATE uptake underwent PRRT, 1 showed partial response following 7 PRRT cycles (24.8 GBq) and has 19 months overall survival. One of the patients with complete response following 4 cycles PRRT (13.69 Gbq) has no sign of disease and overall survival of 16 months. Another patient with complete response following 4 PRRT cycles (19.95 GBq) has overall survival of 18 months. One patient showed progressive disease following 2 PRRT cycles (7.4 GBq) and died 2 months after PRRT begins. No significant PRRT associated toxicity was observed. ***Conclusion:*** 68Ga-DOTATATE was positive in a high proportion of neuroblastoma patients, therefore, it can be used as imaging modality for management of primary or relapsed neuroblastoma patients and identifying suitable candidates for PRRT with 177Lu-DOTATATE. In addition, safety and feasibility of PRRT for refractory neuroblastoma pediatric patients were proved. ***References:*** None

EP-369

Technical and procedural aspects of high dose-personalized brachytherapy using a not sealed ^{188}Rhenium-resin in patients with non-melanoma skin cancer

A. Farina[1], F. Savoia[2], G. Lima[1], A. Patrizi[3], F. Zagni[4], S. Vichi[4], G. Argalia[1], E. Dika[3], L. Strigari[4], A. Morganti[5], S. Fanti[1], P. Castellucci[1]; [1]Nuclear Medicine Department, Sant'Orsola-Malpighi Hospital, University of Bologna, Bologna, ITALY, [2]Dermatology Department, Sant'Orsola-Malpighi Hospital, University of Bologna, Bologna, ITALY, [3]Dermatology Medicine Department, Sant'Orsola-Malpighi Hospital, University of Bologna, Bologna, ITALY, [4]Medical Physics Department, Sant'Orsola-Malpighi Hospital, University of Bologna, Bologna, ITALY, [5]Radiation Oncology Department, Sant'Orsola-Malpighi Hospital, University of Bologna, Bologna, ITALY.

Aim/Introduction: High dose-personalized brachytherapy with a non-sealed ^{188}Rhenium-resin (OncoBeta®GmbH for Rhenium-SCT®) is a new option for the treatment of non-melanoma skin cancer (NMSC) especially in patients were surgical approach would be sub-optimal as concerns the features of the lesion or the aesthetic outcome after surgery. The aim of this study is to describe the technical and procedural aspects and the times required for the treatment of NMSC with ^{188}Rhenium-resin. ***Materials and Methods:*** From September2017 to February2020, we performed 57 treatments in 48patients (15F,33M, age56-97, mean81) showing 57 histologically proven NMSC (40BCC;14SCC;2Spino-CC;1BCC&SCC). Lesions were located on face, ears, nose or scalp (45/57), extremities (8/57), trunk (4/57). Mean surface areas 6,4cm^2 (range1-36cm^2); mean thickness invasion 1,1mm (range0.2-2.5mm). The procedure consists in three consecutive steps: Preparation, Treatment, Discharge. ***Results:*** Preparation: 1) lesion curettage; delineation of tumor margins and application of plastic foil over the lesion avoiding any direct contact of the resin with the skin; 2) loading of ^{188}Re-carpoule in the applicator. This phase takes approximately 15-20minutes and it is the most critical since the application of the protective foil in not-planar surfaces may result difficult to perform. Treatment: 1) measure the initial ^{188}Re-activity; 2) apply the ^{188}Re-resin over the foil following the lesions margins; 3) measure the remaining ^{188}Re-activity in the applicator; 4) calculate the treatment time using the simutation software (WARSKIN5.2). This phase usually does not present significant problems and it takes usually less than 10minutes, however the effective treatment time vary a lot depending on lesion size, lesion thickness and the required effective dose delivered to the lesion. In our population the mean dose delivered to the lesions was 62Gy (range 18-126Gy), the mean treatment time was 78minutes (range21-285minutes). In this phase, we have never observed any discomfort or pain during or soon after the treatment. Discharge: 1) removing the foil from the lesion 2) performing contamination control 3) clean the lesion and 4) provide the information to the patient for home care and follow up checkpoint. This phase takes about 10minutes. We have never observed any contamination after removing the protective foil. In conclusion, the whole procedure takes approximately 35-40minutes to be added to effective treatment time. ***Conclusion:*** In pur experience

high dose brachytherapy with a not-sealed 188Rhenium-resin in NMSC is easy to perform, quick and patient friendly. It may offers many advantages over surgery, in particular no pain and simple patient care during and after treatment. ***References:*** None

EP-370

Initial experience with 177Lu-PSMA therapy for patients with advanced liver cancer

M. Assadi[1], *S. Rekabpour*[1], *E. Jafari*[1], *N. Shakibazad*[1], *H. Ahmadzadehfar*[2], *Z. Alipour*[1], *A. Amini*[1];
[1]*Bushehr University of Medical Sciences (BUMS), Bushehr, IRAN, ISLAMIC REPUBLIC OF,* [2]*Klinikum Westfalen, Knappschaft Hospital, Dortmund, GERMANY.*

Aim/Introduction: Patients with advanced liver cancer typically have poor survival outcomes. Until recently, few agents especially sorafenib were the systemic therapy options available .The aim of this study was evaluation of clinical efficacy of radioligand therapy (RLT) with 177Lu-PSMA on liver cancer patients. ***Materials and Methods:*** We enrolled 3 liver cancer patients showed intensive PSMA uptake on pre-therapy diagnostic scan with 68Ga-PSMA PET/CT and/or 99mTc-PSMA scintigraphy in this study. The patients underwent RLT and for evaluation of response to therapy, follow up conventional imaging had been performed. In addition, for evaluation of therapy associated toxicity, laboratory tests were obtained. The interval time between RLT cycles was 4 weeks. ***Results:*** In this study 3 males patients included 2 hepatocellular carcinoma (HCC) patients (61 and 56 years old) and one 12 years old child with hepatoblastoma were underwent RLT. HCC cases had local involvement but hepatoblastoma case in addition to local involvements, had multiple pulmonary involvements. Of two HCC patients , one who had portal vein thrombosis (PVT) and cirrhosis received 2 cycles of RLT (8 GBq) and another one took 4 cycles (14 GBq) till now. The hepatoblastoma case underwent 3 cycles of RLT (7 GBq) till now. Stable disease was observed in all patients according to the imaging analysis. The patient with HCC , PVT and cirrhosis showed stable lesions with some evidence in thrombosis resolution. One HCC patient died after 3 months from RLT beginning due to complications of cirrhosis. The two other patients are alive since from starting of RLT in 4 months ago. No significant therapy associated toxicity was observed in all patients. ***Conclusion:*** The therapy of advanced liver cancer remains challenging and complex. RLT with 177Lu-PSMA might take in consideration in therapy of liver cancer patients with progression despite multimodality treatment. These data support ongoing clinical trials in such challenging patients. ***References:*** None

EP-371

Molecular Imaging in the selection and evaluation of response in patients treated with Radium-223 in six different solid tumors: A single center experience

S. Medina-Ornelas*, F. García-Perez, M. Alvarez-Avitia, N. Sobrevilla-Moreno, D. Garcia-Ortega, F. Barron-Barron, M. Jimenez-Rios, O. Arrieta-Rodriguez;*
Instituto Nacional de Cancerologia, Mexico City, MEXICO.

Aim/Introduction: Evaluate impact after ^{223}Ra therapy and ^{18}F-NaF (sodium fluoride) PET/CT in the selection and evaluation of response in patients treated with ^{223}Ra in six different solid tumors. ***Materials and Methods:*** Twenty patients with metastatic castration-resistant prostate cancer (mCRPC), seven metastatic castration-sensitive prostate cancer (mCSPC), three osteosarcoma, two breast cancer, two non-small cell lung cancer (NSCLC), one chondrosarcoma, one chordoma and one patient lung neuroendocrine carcinoma. Three groups of study were defined according total skeletal tumor-burden obtained by ^{18}F-NaF PET/CT, group 1 <1000cm^3, group 2 1001-2999cm^3 and group 3 >3000cm^3 VOI´s. A semi-quantitative comparison was performed measuring the SUVmax values of VOIs values in all bone metastases in each patient previous to receive the first cycle of ^{223}Ra, after 3 and 6 cycles. ***Results:*** 30 patients non-progress disease was documented after 24±4 weeks. 8 patients progress disease was presented after three cycles of ^{223}Ra, two patients with osteosarcoma, four patients with mCRPC, one patient with chondrosarcoma and one patient with NSCLC. Group 1 patients showed better response rates compared to group 3 ($p<0.05$). Group 2 patients who showed improvement clinical and radiological, had prostate malignancies compared to those in the same group, but non-prostatic malignancies ($p<0.05$). No significant difference in group 2 patients compared to group 3 ($p<0.67$). Symptomatic skeletal-related event was observed in 7 patients. ***Conclusion:*** ^{18}F-NaF PET/CT allows to identify patients who show osteoblastic bone activity and discard or confirm progression in the interval PET/CT image, allowing change of treatment, reducing costs. High tumor-burden strongly suggests a poor response to treatment. ***References:*** None

EP-372

Complex treatment of bone metastases of tumors of different origin

O. Solodyannikova[1]*, Solodyannikova OI, Danilenko VV, Stolyarova OY, V. Danilenko*[2];
[1]*Institute of Oncology AMS of Ukraine, Kiev, UKRAINE,* [2]*National Institute of Cancer, Kiev, UKRAINE.*

Aim/Introduction: Radionuclide therapy is quite widely used in developed countries in the treatment of multiple bone metastases, as "last-line" therapy. The aim is to perform

a comparative analysis of radionuclide, radiation and accompanying treatment of bone metastases of malignant tumors ***Materials and Methods:*** Radionuclide therapy was performed in accordance with standardized treatment protocols by radiopharmaceutical (European Nuclear Medicine Guide, 2018). Among the treated patients, 58 were with breast cancer, 30 - prostate cancer, 6 - lung cancer, 4 - kidney cancer, 1 - cervical cancer and 1 - rectal sigmoid angle of the colon. Of these, 64 are women and 36 are men. The age of those treated is 32 to 78 years. Mean age (55.0 ± 11.6) years. In 94 patients (90%) the presence of bone metastases was determined by osteoscintigraphy with ^{99m}Tc-MDP. In 6 patients, the diagnosis of bone lesion was verified by other methods of radiodiagnosis.Radiation therapy was performed for 30 patients, 20 of them with prostate cancer and 10 with breast cancer. During treatment, patients received a total dose of 30 Gy, 3 Gy for 10 fractions.All patients were treated with bisphosphonate as an accompaniment therapy. ***Results:*** It was found that the intensity of pain before and after treatment with different radiopharmaceutical varied as follows: ^{32}P - before treatment 7.1 ± 1.5, after treatment - 5.0 ± 3.1 * (p <0.05); ^{89}Sr - before treatment 8.0 ± 2.2, after treatment - 4.8 ± 1.5 * (p <0.05); ^{153}Sm - before treatment 8,4 ± 1,3, after treatment - 3,5 ± 1,8 * (p <0,05). Thus, under the influence of radionuclide therapy, pain levels were reduced to 3-5 points, averaging 47%.The effectiveness of the analgesic influence of radiation therapy averaged 52.2% ± 4.1%, i,e, before treatment on the LACOMED scale the level of pain syndrome fluctuated within 7.2 ± 3.6 points, and after treatment 3.7 ± 4.4, respectively (p <0.05). ***Conclusion:*** 1. Complex treatment of metastatic damage of the bone system in malignant tumors of different localization is as effective as possible when using both radionuclide therapy and remote radiation.2. The most effective compared to ^{32}P and ^{89}Sr in the treatment of bone metastases for analgesic influence and tolerability is ^{153}Sm oxabiphor (p <0.05).3. The effectiveness of the analgesic action of radiation therapy is significantly higher in the treatment of single but larger metastatic bone lesions, it achieves high reliability. ***References:*** None

EP-63

Therapy Clinical Study -> Oncological Therapy Clinical Study -> Prostate Cancer Therapy

e-Poster Area

EP-373

Prognostic implications of dual tracer PET/CT: additional FDg PET/CT in patients undergoing [^{177}Lu]PSMA radioligand therapy

K. Michalski[1], *J. Ruf*[1], *P. Meyer*[1], *A. Buck*[2], *C. Lapa*[3], *P. Hartrampf*[2];
[1]*University hospital Freiburg, Freiburg, GERMANY,*
[2]*University hospital Würzburg, Würzburg, GERMANY,*
[3]*University hospital Augsburg, Augsburg, GERMANY.*

Aim/Introduction: A recent study has shown poor survival of patients with metastatic castration-resistant prostate cancer (mCRPC) scheduled for [^{177}Lu]PSMA radioligand therapy (RLT) who presented with lesions positive on FDG PET/CT but without relevant concordant uptake on PSMA PET/CT [1]. These patients were subsequently not treated with RLT, and the overall survival (OS) in this group was 3.9 months [1]. In contrast, patients without any discordant FDG-positive lesions underwent RLT with a distinct higher OS of 12.0 months [2]. The aim of the following analysis was to investigate the prognostic value of the combination of PSMA PET/CT with FDG PET/CT for outcome prediction in patients undergoing RLT. ***Materials and Methods:*** This bicentric, preliminary analysis included 54 patients with mCRPC who underwent both FDG and PSMA PET/CT prior to RLT. In all patients, the pattern of PSMA-ligand and FDG uptake was visually assessed. Patients with lesions positive on FDG PET but without relevant concordant uptake on PSMA PET were compared to patients without any discordant FDG-positive lesions. A log-rank analysis was used to assess the difference in OS between groups. ***Results:*** A significant lower OS was found for patients with lesions positive on FDG PET but without relevant concordant uptake on PSMA PET (n=17) with a median OS of 6.0 ± 0.8 months (95% CI 4.4 - 7.6) vs. the patients without any discordant FDG-avid disease (n=37) with a median OS of 13.0 ± 0.9 months (95% CI 11.3 - 14.7; p = 0.000). ***Conclusion:*** This preliminary analysis demonstrates a significantly poorer response to treatment with RLT in patients with mCRPC and discordant FDG-positive lesions. In how far this patient population still (partially) benefits from RLT remains to be elucidated. ***References:*** [1] Thang, SP et al. Poor outcomes for patients with metastatic castration-resistant prostate cancer with low prostate-specific membrane antigen (PSMA) expression deemed ineligible for 177Lu-labelled PSMA radioligand therapy. European urology oncology 2.6 (2019): 670-676. [2] Sandhu SK et al. Lutetium-177 PSMA617 theranostics in metastatic castrate-resistant prostate cancer (mCRPC): interim results of a phase II trial. J Clin Oncol 2018;36 (15 Suppl):5040.

EP-374

Myelotoxicity after Treatment with ^{177}Lu-PSMA-617 in Patients with Metastatic Prostate Cancer

D. Gröner[1], *J. Baumgarten*[1], *K. Davis*[1], *C. Happel*[1], *N. Mader*[1], *C. Nguyen Ngoc*[1], *J. Wichert*[1], *P. Mandel*[2], *N. Tselis*[3], *F. Grünwald*[1], *A. Sabet*[1];
[1]*Nuclear Medicine, University Hospital Frankfurt, Frankfurt, GERMANY,* [2]*Urology, University Hospital Frankfurt, Frankfurt, GERMANY,* [3]*Radiation Oncology, University Hospital Frankfurt, Frankfurt, GERMANY.*

Aim/Introduction: Repeated cycles of radioligand therapy (RLT)

may be associated with an increased risk of myelosuppression. This study aims to investigate the incidence, severity and reversibility of hematotoxicity in a large patient cohort with progressive metastatic prostate cancer undergoing RLT with ^{177}Lu-PSMA-617. The impact of pre-existing risk factors and the cumulative administered activity were of particular interest. ***Materials and Methods:*** RLT was performed in 156 patients. Previous treatments included second-generation antiandrogenes (enzalutamide, abiraterone) in 116, at least one line of chemotherapy in 79, and ^{223}Ra-dichloride in 66 patients. A mean activity of 6.7± 1.3 GBq ^{177}Lu-PSMA-617 per cycle was administered in a median of 4 treatment cycles (IQR 2 to 5) at intervals of 6 to 8 weeks. Median cumulative activity was 19.3 GBq (IQR 11.5 to 35.6). Hematological parameters were measured at baseline, prior to each treatment course, 2 to 4 weeks thereafter and throughout follow-up. Toxicity was classified using Common Terminology Criteria for Adverse Events v5.0. ***Results:*** Significant treatment-induced hematotoxicity (grade 3 or 4) occurred in 18 patients (12 %), with anemia in 9% leukopenia in 4 % and thrombocytopenia in 5%. Bone marrow impairment was reversible throughout a median follow-up of 8 months (IQR 9 months) in all but two patients who died from disease progression within less than 3 months after RLT. Severe myelosuppression was significantly more frequent in patients with pre-existing grade 2 cytopenias (p=0.04) or high bone tumor burden (disseminated pattern based on PROMISE miTNM criteria, p<0.001). A history of chemotherapy, treatment with ^{223}Ra-dichloride and cumulative RLT treatment activity were not associated with an increased incidence or higher degree of hematotoxicity (p=0.20, 0.15, 0.11) . ***Conclusion:*** Hematotoxicity after RLT is frequently reversible and has an acceptable overall incidence. High bone tumor burden and pre-existing moderate cytopenia (grade 2) were identified as risk factors for developing relevant hematotoxicity (grade 3 to 4). Previous chemotherapy, ^{223}Ra-dichloride treatment or cumulative RLT activity have no impact on the incidence of significant hematoxicity. ***References:*** None

EP-375

Whole-Body Dosimetry in Therapy of Metastatic Prostate Cancer with ^{177}Lu-PSMA-617

C. Happel, L. Völler, W. T. Kranert, D. Gröner, B. Bockisch, N. Mader, F. Grünwald, A. Sabet;
University Medical Center Frankfurt, Department of Nuclear Medicine, Frankfurt, GERMANY.

Aim/Introduction: Molecular radiotherapy with ^{177}Lu-labelled prostate specific membrane antigen (PSMA) is being increasingly implemented as therapeutic option for patients with metastatic prostate cancer. However, accumulation in metastases as well as physiologic uptake in several organs necessitate dosimetric considerations. Aim of this study was therefore to calculate the mean whole body dose of patients undergoing ^{177}Lu-PSMA-617 treatment. ***Materials and Methods:*** In this study the course of 672 ^{177}Lu-PSMA-617 therapy cycles in 198 consecutive patients was analyzed retrospectively. The median age of the patient cohort was 72.9 years (41 - 89.6 years) at administration of ^{177}Lu-PSMA-617. Median administered activity per cycle was 6.96 GBq (1.08 - 11.2 GBq) depending on tumor burden, physiological condition, blood parameters and kidney function. Whole body dosimetry was performed by measuring the geometric mean of the remaining activity in the whole body at three timepoints per day over the complete in-patient stay of 72h with an individually calibrated collimated gamma probe with attached multi-channel analyzer (2"x2" NaI(Tl)-detector scintiSPECT; SCINTRONIX). The individual calibration resulted from an initial measurement of the remaining activity directly after administration of the ^{177}Lu-PSMA-617 prior to micturition. Mean whole-body doses were calculated with Microsoft Excel 2010 using a bi-exponential fit to the measurements as time activity curve. ***Results:*** The effective doses to the whole-body ranged from 27.7 to 1,794 mGy per cycle (median: 226 mGy). Related to the administered ^{177}Lu-PSMA-617 activity the whole body dose ranged from 9.62 to 251 mGy/GBq (median: 33.1 mGy/GBq). The primary exponential rapid declining phase of ^{177}Lu in the whole-body which is mainly caused by renal elimination, varied from 1.43 to 97.8 h (median: 7.32 h). In contrast, the effective half-life during the secondary exponential slow phase which is mainly influenced by metastatic burden and physiological accumulation ranged from 4.75 - 160h (median: 51.5 h). ***Conclusion:*** The course of ^{177}Lu-PSMA-617 in the whole body can be subdivided into a first rapid phase which is mainly influenced by renal elimination and a second slow phase mainly influenced by metastatic tumor burden. Individual doses vary for a huge range and may reflect tumor accumulation and changes of it during fractionated treatment of one patient. The calculated median whole-body dose of 226 mGy is comparable to the whole body doses known from radioiodine-131 therapy. Due to multiple influences to the time course it gives only limited information to organ doses and tolerability to further applications. *References:* None

EP-376

Brazilian Profile of Ra-223 Therapy - a Multicenter Study

E. Etchebehere[1], *F. P. P. Lopes*[2], *S. A. L. Matedi*[2], *R. Fockink*[3], *D. A. Anjos*[3], *G. V. Gomes*[4], *L. R. Silva*[4], *A. O. Santos*[5], *T. Minekawa*[1], *V. M. Araújo*[6], *A. B. M. J. Teixeira*[6], *R. Martins*[7], *G. E. Bier*[7], *A. Sanches*[8], *N. Hanaoka*[9], *R. M. Tavares*[2], *F. Mourato*[10], *M. C. L. Lima*[1], *P. Almeida*[10], *A. E. T. Brito*[10];
[1]*The University of Campinas, Campinas, BRAZIL,* [2]*Clinica de Medicina Nuclear Villela Pedras, Rio de Janeiro, BRAZIL,* [3]*Hospital Santa Paula, São Paulo, BRAZIL,* [4]*Núcleos, Brasília, BRAZIL,* [5]*Medicina Nuclear de Campinas, Campinas, BRAZIL,* [6]*Centro de Diagnósticos por Imagem de Goiânia, Goiás, BRAZIL,* [7]*Centro*

de Tomografia e Medicina Nuclear (CETAC), Curitiba, BRAZIL, [8]Santa Casa de Misericórdia da Bahia, Salvador, BRAZIL, [9]Dimen, Campinas, BRAZIL, [10]Real Hospital Português, Recife, BRAZIL.

Aim/Introduction: Although Ra-223 therapy has been available since 2013 for metastatic castrate-resistant prostate cancer (mCRPC), only in 2017 was Ra-223 approved by the National Health Surveillance Agency in Brazil. Purpose: To perform a multicenter analysis of the profile of mCPRC submitted to Ra-223 in the Brazilian Nuclear Medicine institutions and to describe their clinical outcomes. ***Materials and Methods:*** A retrospective analytical study of mCRPC patients who underwent Ra-223 treatment was undertaken. All clinical and laboratory data (age, previous treatments, previous imaging and laboratory tests, pain scale and performance status, number of Ra-223 cycles, reasons for discontinuation, possible adverse effects) as well as follow-up data (time to death, progression or bone event) was evaluated. ***Results:*** A total of 303 submitted to 1,402 Ra-223 cycles between August/2017 and March/2020 from 9 centers were studied. The mean age of the patients was 74 years (43 - 100 years). 229 patients underwent previous treatments (mean 3.4 months) prior to Ra-223 as follows: chemotherapy (44%), radiation therapy (42%), hormone therapy (70%). Ra-223 was used as first line treatment in 3%, 25% as second line, 35% as third line and 37% fourth or more. The mean number of Ra-223 cycles was 4.6, 51% of patients completed all six cycles and 15% interrupted Ra-223 due progression. Association of Ra-223 with other treatments occurred in 34% of patients, 62% due to secondary hormone therapy. Major hematologic toxicity causing interruption of Ra-223 occurred in 6%. After the 1st Ra-223 cycle 33.6% patients progressed (median 3.4 months) and 13.5% had bone events. The most common bone event was intractable bone pain (20.3%). The median overall survival was 8 months. ***Conclusion:*** The survival benefit of Ra-223 was not satisfactory most likely because >70% of the patients were submitted to Ra-223 as third or more-line therapy. This data is an important and clear demonstration of the necessity to educate the referring physician as to the proper timing for Ra-223 in order to have maximum benefit. ***References:*** None

EP-377

Bone scintigraphy to evaluate response to therapy with Radium-223 for castration-resistant prostate cancer patients with bone metastases: a single-center experience

E. Martínez Albero*, A. Gómez Grande, A. Saviatto Nardi, Á. Galiana Morón, D. Vega Pérez, V. Godigna Guilloteau, J. Pilkington Woll, S. Ruiz Solís, P. Sarandeses Fernández, M. Tabuenca Mateo, J. Estenoz Alfaro;*
Hospital Universitario 12 de octubre, Madrid, SPAIN.

Aim/Introduction: We aimed to assess treatment-related changes on conventional bone scans (BS) in metastatic castration-resistant prostate cancer (mCRPC) patients treated with Radium-223 (^{223}Ra). ***Materials and Methods:*** We included 62p (median age 77y; range: 56-93 years) with mCRPC and bone metastases treated with ^{223}Ra from March 2013 to December 2019. Radium-223 therapy was given intravenously every 4 weeks, at a dose of 50 kBq/kg body weight for up to six cycles. Fifty-six patients had undergone conventional bone scintigraphy (^{99m}Tc-HDP) before the start of treatment and 4 weeks from last cycle. Pre and post-treatment bone scans were evaluated visually. Patients were classified according to extent of bone disease (EOD) in four groups: EOD1 (<6 metastatic lesions), EOD2 (6-20), EOD3 (>20) and EOD4 (superscan). Changes with each scan pair were assessed as one of three response patterns: Partial Response (PR), defined as decrease and/or disappearance of HDP uptake in metastatic foci; Stable Disease (SD) and Progression Disease (PD), if at least two new foci of HDP uptake are seen. We also evaluated the correlation between the response pattern observed in the bone scan and the number of cycles administered, Gleason score, the levels of prostatic-specific antigen [PSA] and alkaline phosphatase [ALP]. Changes in PSA and ALP, were defined as an increase or a decrease of ≥ 30% from baseline. ***Results:*** Thirty-six patients (64,3%) had high risk prostate cancer (Gleason score >7; range 8-10). Most of them, 35/56p (62,5%) were treated with ^{223}Ra post-docetaxel. The mean of bone lesions observed in baseline bone scintigraphy was 15,5 (range 1-68): 22p (EOD1),13p (EOD2), 15p (EOD3) and 6p (EOD4). Among the patients who received 6 and 5 cycles, 71% showed PR or SD in bone images. Significant differences between Gleason score and response (PR+SD) were not found: Gleason 7 (10p), Gleason 8 (10p), Gleason 9 (11p). Increase in PSA level was similar in patients who presented PR+SD (71%) and those who presented PD (76%), while ALP levels decrease in 55% of patients included in the PD/SD groups. No correlation was observed between the extent of metastatic bone disease and the response patterns shown on BS. ***Conclusion:*** BS is useful to evaluate the response of metastatic bone disease in the follow-up of patients with mCRPC treated with ^{223}Ra. No progression of bone disease was observed in most of the patients during treatment. PSA levels showed no correlation with the response pattern on BS. ***References:*** None

EP-378

Initial experience with somatostatin receptor (SSTR) imaging and peptide receptor radionuclide therapy for patients with neuroendocrine differentiation (NED) of prostate cancer

M. Assadi[1]*, S. Rekabpour*[1]*, H. Ahmadzadehfar*[2]*, E. Jafari*[1]*, A. Amini*[1]*;*
[1]Bushehr University of Medical Sciences (BUMS), Bushehr, IRAN, ISLAMIC REPUBLIC OF, [2]Klinikum Westfalen, Knappschaft Hospital, Dortmund, GERMANY.

Aim/Introduction: Nowadays, neuroendocrine differentiation

(NED) of prostate cancer has increasing attention duo to its limited and challenge for treatment modalities. The aims of this study were, first, evaluation of somatostatin receptor (SSTR) expression in castrate resistant prostate cancer (CRPC) patients who is refractory or progressive to radioligand therapy (RLT) with 177Lu-PSMA. As second aim, we evaluated the clinical efficacy of peptide receptor radionuclide therapy with 177Lu-DOTATATE for CRPC patients with NED. ***Materials and Methods:*** In this study, the patients who are refractory to multiple cycles of RLT were asked to perform 68Ga-DOTATATE PET/CT or 99mTc-octerotide for evaluation of SSTR expression and NED. The patients who showed positive SSTR, underwent PRRT. For evaluation of treatment response, in addition to post therapy imaging, chromogranin A (Cg-A) had been measured before and 2 months after PRRT. For evaluation likely toxicity, periodically laboratory tests were taken after therapy. ***Results:*** In this study, we evaluated 5 CRPC patients with mean age of 67.6±10.73 ranged from 55-80 years old. For evaluation of SSTR expression, 4 patients underwent 99mTc-octerotide and one of them underwent 68Ga-PET/CT. One of them, despite had widespread metastases on 99mTc-MDP bone can showed no abnormal uptake on 99mTc-PSMA scintigraphy suspected for NED but interestingly octreotide scan was normal as well. 4 other patients, showed progressive or stable response to several cycles of 177Lu-PSMA, therefore they underwent evaluation of SSTR expression. 2 of them showed negative SSTR expression and 2 showed significant uptake of radiotracer. Pre-PRRT Cg-A in both patients was several times more than normal value. Therefore, these two patients underwent 2 cycles of PRRT with 177Lu-DOTATATE (3.7 GBq per cycles with time interval of 6-8 weeks). Interestingly, in addition to reduction in number and size of metastases and improvement in quality of life in both patients, the value of Cg-A significantly decreased after 2 cycles of PRRT (in one patient, the Cg-A reached to normal value). There was no significant toxicity observed after PRRT. ***Conclusion:*** Our results suggested that in CRPC patients showed refractory or progressive disease following several cycles of RLT, the SSTR expression has been checked for NED. In CRPC patients with positive SSTR expression, PRRT can be considered as a valuable therapeutic option. ***References:*** None

EP-379

Fractionated ^{177}Lu-PSMA-617 therapy with 101 GBq in a patient with metastatic prostate cancer

C. Happel*, J. Wichert, W. T. Kranert, L. Völler, B. Bockisch, D. Gröner, F. Grünwald, A. Sabet;*
University Medical Center Frankfurt, Department of Nuclear Medicine, Frankfurt, GERMANY.

Aim/Introduction: 177Lu-labelled prostate-specific membrane antigen (^{177}Lu-PSMA-617) has evolved as promising therapeutic target for patients with castration resistant prostate cancer (CRPC). The German consensus-protocol is based on therapeutic cycles with standard activities of 6 GBq up to a recommended cumulated maximum activity of 18 GBq and a kidney dose of 23 Gy. ***Materials and Methods:*** A 73-years-old patient with CRPC and osseous metastases (Gleason 8) was treated over a period of 2.6 years with all in all 14 cycles of ^{177}Lu-PSMA-617. Previous therapy included ADT, local radiation, chemotherapy and ^{223}RaCl2. During each in-patient-stay dosimetric monitoring was performed including measurements with an individually calibrated gamma-probe (SCINTRONIX), whole-body scintigraphy and SPECT (Mediso AnyScan). Therapeutic monitoring was ensured by frequent ^{68}Ga-PSMA-11-PET/CT and functional scintigraphy of the kidneys. Mean whole-body dose (MWBD) was calculated from integrating the bi-exponential activity course. Kidney dosimetry was performed using a combination of planar scintigraphy, SPECT and gamma-probe. ***Results:*** Mean administered activity was 7.5GBq per cycle (5.6-9.2GBq) taking into account the tumor burden, PSA and kidney function. In total, 101 GBq ^{177}Lu-PSMA-617 were administered. Treatment was continued after exceeding the cut-off of 18 GBq even after the 8th and 12th therapy due to scintigraphic detection of tumor tissue and biochemical response in accordance with the recommendation of an interdisciplinary tumor-board to avoid further metastatic progression and disease specific complications. The cumulative MWBD was 5.1Gy. Median MWBD was 354 mGy per treatment cycle (48mGy/GBq) decreasing dependent on the time after initial treatment. Mean calculated kidney dose was 1.4 Gy per treatment corresponding to a median activity-related dose of 0.19Gy/GBq. The cumulative kidney dose was 19Gy. Therefore, the cut-off value for the kidneys was not exceeded. Blood parameters (leucocytes and thrombocytes) did not change significantly over the treatment. Hemoglobin stayed stable up to the 12th cycle and showed a slight drop afterwards. Kidney function parameters (GFR, creatinine) stayed stable throughout the therapy. After the 14th cycle, the patient showed an overall improvement of symptoms compared to the 1st cycle with good general condition. PSA continuously decreased during ^{177}Lu-PSMA-617-therapy from 50 to less than 1 ng/ml. ***Conclusion:*** A cumulative activity beyond 100 GBq ^{177}Lu-PSMA-617 during a treatment course of 2.6 years was well tolerated without relevant complications. Depending on kidney and MWBD, considering the good therapeutic response and state of health, an escalation of the cumulative activity to up to 100 GBq seems to be feasible and effective in selected cases. ***References:*** None

EP-64
Thyroid

e-Poster Area

EP-380
Gallium-68 DOTATATE PET/CT and peptide receptor radionuclide therapy for patients with refractory/ recurrence metastatic medullary carcinoma of thyroid

M. Assadi[1], H. Dadgar[2], S. Rekabpour[1], E. Jafari[1], H. Ahmadzadehfar[3], A. Amini[1];
[1]Bushehr University of Medical Sciences (BUMS), Bushehr, IRAN, ISLAMIC REPUBLIC OF, [2]Razavi Cancer Research Center, Razavi Hospital, Mashhad, IRAN, ISLAMIC REPUBLIC OF, [3]Klinikum Westfalen, Knappschaft Hospital, Dortmund, GERMANY.

Aim/Introduction: Medullary thyroid carcinoma (MTC) is a kind of thyroid malignancies originated from the parafollicular cells (C cells) which are responsible for the hormone calcitonin production. Accurate detection of MTC has great impact on management of MTC patients. Since it has been proved that MTC tumors express somatostatin receptors (SSTR), the aim of this study was the clinical efficacy of 68Ga-DOTATATE PET/CT on detection of MTC. As a secondary aim we evaluated the treatment efficacy of 177Lu-DOTATATE for MTC patients. ***Materials and Methods:*** We retrospectively evaluated 15 MTC patients referred for evaluation of staging, workup for metastasis, recurrence disease and response evaluation. 68Ga-DOTATATE PET/CT was performed following injection of 70-180 MBq radiotracer. Images were interpreted with two blind nuclear medicine specialists. Patients who showed intensive 68Ga-DOTATATE uptake according to our clinical team consideration underwent peptide receptor radionuclide therapy (PRRT) with 177Lu-DOTATATE. ***Results:*** We evaluated 15 MTC patients with mean age of 52.2±13.44 (27-71) years old included 8 (53.3%) males and 7 (46.7%) females. Of 15 patients, 5, 7, 2, 1 were referred for evaluation of staging, recurrence, workup of metastasis and response evaluation, respectively. Thyroidectomy was performed for 12 (80%) of patients. 68Ga-DOTATATE was positive on 13 (86.7%) of patients. Of 13 positive scans, 3, 5, 5 scans showed locoregional, distant and locoregional/distant involvement, respectively. The total number of detected lesions in patients with positive scan were 46 in all patients with median of 2 (range: 1-16). Of these patients, 5 patients underwent PRRT included 3 females and 2 males with mean age of 50.2±13.36 (34-70) years old. Patients totally underwent 13 cycles of PRRT with median of 2 cycles (1-4) and median of injected dose of radiotracer was 14 GBq (6-29 GBq). All patients showed partial response with improvement in quality of life. Overall survival was 12.2±7.79 months (4-21). Of 5 patients, only one of them died duo to GI bleeding after 11 months from the beginning of PRRT. ***Conclusion:*** Our results reveal that SSTR agents are clinically suitable for management of MTC patients as a diagnostic procedure using 68Ga-DOTATATE PET/CT or therapeutic option as PRRT with 177Lu-DOTATATE.
References: None

EP-65
Thyroid Cancer

e-Poster Area

EP-381
^{131}I-SPECT/CT after radioiodine therapy in patients with differentiated thyroid carcinoma (DTC)

S. Nuvoli, A. Marongiu, I. Gelo, L. Mele, M. Rondini, M. L. Stazza, G. Madeddu, A. Spanu;
University of Sassari, Sassari, ITALY.

Aim/Introduction: We further investigated ^{131}I-SPECT/CT usefulness after radioiodine therapy in DTC patients to achieve the best strategy in the affected patient management during follow-up. ***Materials and Methods:*** We retrospectively enrolled 89 DTC patients, 81 with papillary carcinoma, 3 with follicular and 5 with Hürthle cell carcinomas. In 36 patients, papillary carcinoma was multifocal; in 17 cases extra-thyroid tumor extension was present and in 10 neck cervical lymph node (LN) metastases were ascertained. Moreover, 16 patients were at high risk (H), 55 at low risk (L) and 18 at very low risk (VL). All patients underwent ^{131}I-whole body scan (WBS) followed by SPECT/CT 5-7 days after 1.85-5.66 GBq radioiodine therapeutic dose using a hybrid dual head gamma camera with high energy, parallel hole collimators. ***Results:*** SPECT/CT detected 206 radioiodine-avid foci in the 89 patients, while WBS identified 194 foci, all positive at SPECT/CT. Both procedures concordantly classified 153 foci (139 residues, 8 lung metastases, 5 soft tissue metastases, 1 cutaneous contamination). SPECT/CT also characterized 39 foci unclear at WBS (24 residues, 8 neck LN metastases and 5 LN outside neck, 1bone metastasis and 1 physiologic uptake). Moreover, SPECT/CT identified 12 foci occult at WBS (9 residues, 2 neck LN metastases and 1 LN metastasis outside neck). SPECT/CT also changed WBS classification of 2 foci in neck LN metastasis and muscle metastasis in the thorax, wrongly classified as residue and lung metastasis, respectively. Globally, SPECT/CT correctly classified 32 malignant foci in 12/89 patients (6H, 4L, 2VL). WBS evidenced 29/32 foci; however, it classified as unclear 14/29 foci, wrongly classified 2 foci and missed 3 further foci. At surgery, 6 of the12 metastatic patients had carcinomas with extra-thyroid extension and 5/6 also with loco-regional LN metastases and one with multifocal disease, too; of the remaining 6/12 patients, 2 had multifocal papillary carcinoma and 4 unifocal intracapsular carcinomas. Thyroglobulin was >10 ng/dl in 8/12 patients, between 2.5 to 5 ng/dl in 1 patient, < 2.5 ng/dl

in 1 patient and undetectable in the remaining 2 patients (1L, 1VL). SPECT/CT had an incremental value over WBS in 23.6% of patients and changed the classification and therapeutic management in 12.3 % of cases. ***Conclusion:*** ^{131}I-SPECT/CT with therapeutic dose improved loco-regional and distant metastasis identification and characterization than WBS with more correct disease staging and more appropriate patient management in DTC follow-up. Thus, SPECT/CT complementary use of WBS is routinely suggested after radioiodine therapy. ***References:*** None

EP-382

FDG PET/CT versus Somatostatin Receptor PET/CT in TENIS Syndrome:a systematic review and meta-analysis

E. Etchebehere[1], F. Mourato[2], A. Maria[2], A. Brito[2], A. Leal[3], P. Almeida Filho[2];
[1]The University of Campinas, Campinas, BRAZIL, [2]Real Hospital Português de Beneficência em Pernambuco, Recife, BRAZIL, [3]Real Hospital Português de Beneficência em Pernambuco, Re, BRAZIL.

Aim/Introduction: In patients with de-diffferentiated thyroid cancer (or TENIS Syndrome - ***T***hyroglobulin-***E***levated ***N***egative ***I***odine ***S***cintigraphy), radiotracers that are specific for PET/CT imaging may be used to identify metastases, such as FDG PET/CT and somatostatin analogs (SSTR PET/CT). Objective: This study aims to compare capability and current diagnostic performance of identifying metastatic lesions in patients with TENIS syndrome using FDG PET/CT and SSTR PET/CT through a systematic review of the literature and meta-analysis. ***Materials and Methods:*** A literature search was performed in electronic databases (Medline / Pubmed, Scopus, Web of Science, Scielo, and LILACS) until February 2020 to identify relevant studies on ^{18}F-FDG and ^{68}Ga-somatostatin analogs tracers in patients with TENIS Syndrome. The search terms used were: "Thyroid cancer", "somatostatin analog", "Positron emission tomography" and "FDG". ***Results:*** A total of 3551 abstracts were obtained from electronic databases and bibliographic references. The initial review of these articles identified 13 candidates for full-text analysis. Of these, six articles were included in qualitative and quantitative analyses and a total of 179 patients that were submitted to both SSTR PET/CT and FDG PET/CT to evaluate performance of these radiotracers were analyzed. FDG PET/CT images identified significantly ($p = 0.006$) more patients with metastases when compared to SSTR PET/CT (143 vs 103, respectively). Even though FDG PET/CT outperformed SSTR PET/CT, in FDG PET/CT- negative cases, SSTR PET/CT was able to detect metastases in approximately 17% of them. ***Conclusion:*** FDG PET/CT has a higher capability to detect metastases than SSTR PET/CT in patients with TENIS Syndrome. However, when an FDG PET/CT study is negative, SSTR PET/CT can still help by detecting metastases in approximately 1 out of every 5 patients. ***References:*** None

EP-383

Comparison between [^{11}C]-acetate and [^{18}F]-FDG positron emission tomography (PET) in radioactive-iodine-refractory (RAIR) differentiated thyroid cancer (DTC)

S. Li*, E. Kretschmer-Chott, M. Wibbe, E. Rainer, S. Rasul, R. Dudczak, M. Hacker;*
Medical University of Vienna, Vienna, AUSTRIA.

Aim/Introduction: The purpose of this study is to evaluate the diagnostic value of [^{11}C]-acetate PET in patients with radioactive-iodine-refractory differentiated thyroid cancer (RAIR-DTC) as compared with [^{18}F]-FDG PET. ***Materials and Methods:*** The study population comprised 7 patients with RAI-DTC who underwent both [^{18}F]-FDG PET and [^{11}C]-acetate PET. The presence of recurrent cancer was evaluated on a patient-related and lesion-related basis. Histology, elevated thyroglobulin and prior as well as follow-up examinations (such as CT, sonography) served as the standard of reference. ***Results:*** Recurrent or metastatic tumour lesions were confirmed in all 7 patients. [^{18}F]-FDG PET correctly identified the tumour lesions in 6 of 7 (86 %) patients. In 3 patients tumour lesions were missed by [^{11}C]-acetate PET (57%). In the lesion-related analysis, overall lesion detection rates were 33/44 (68 %) and 15/44 (34 %) for [^{18}F]-FDG PET and [^{11}C]-acetate PET, respectively. [^{18}F]-FDG PET was significantly ($p < 0.05$) superior to [^{11}C]-acetate PET in the overall lesion evaluation. Whereas, no significant difference was found in the detection of pulmonary metastases between [^{18}F]-FDG PET and [^{11}C]-acetate PET. ***Conclusion:*** This study demonstrated that [^{18}F]-FDG PET has significantly higher lesion-related sensitivity as compared with [^{11}C]-acetate PET in the detection of overall DTC lesions. No significant difference between these two tracers was found in the detection of pulmonary lesions. Therefore, [^{11}C]-acetate cannot replace [^{18}F]-FDG PET for evaluation of patients with RAIR-DTC. ***References:*** None

EP-384

The diagnostic value of stimulated serum thyroglobulin in the follow-up of low and intermediate-risk patients with differentiated thyroid cancer

I. Mihaljevic*[1,2,3], V. Wagenhofer[1,2], T. Kralj[1,2], D. Vrdoljak[1], T. Kizivat[1,2], D. Mudri[1,2], M. Franceschi[4,2,3], T. Jukic[4,2];*
[1]Clinical Institute of Nuclear Medicine and Radiation Protection, University Hospital Osijek, Osijek, CROATIA, [2]Faculty of Medicine Osijek, Josip Juraj Strossmayer University of Osijek, Osijek, CROATIA, [3]Academy of Medical Sciences of Croatia, Zagreb, CROATIA, [4]Department of Oncology and Nuclear Medicine, Sestre milosrdnice University Hospital Centre, Zagreb, CROATIA.

Aim/Introduction: The aim of this study was to evaluate the diagnostic value of stimulated serum thyroglobulin (sTg) in the follow-up of patients with differentiated thyroid cancer (DTC) with respect to new classification criteria for risk groups

(American Thyroid Association, ATA 2015) and to determine whether repeated measurement of sTg had an additional clinical benefit for detecting structural recurrent or persistent disease if the first sTg was negative. ***Materials and Methods:*** The negative predictive value (NPV) of the first sTg for detecting structural persistent or recurrent disease obtained 12 months after the initial therapy has been compared with NPV of sTg performed during 3 consecutive examinations in the follow-up of patients with DTC. The retrospective study included 388 consecutive patients with DTC treated and followed-up between 2004 and 2018 in the Clinical Institute of Nuclear Medicine and Radiation Protection, Osijek University Hospital. Patients were categorised based on risk group according to the classification criteria for risk groups of the American Thyroid Association (ATA, 2015). ***Results:*** NPV of the first sTg, measured 12 months after initial treatment, amounted to 99.5 % in the group of low-risk patients and 96.1 % in the group of intermediate-risk patients. In both groups (low- and intermediate-risk) there were no differences between NPV of the first sTg and NPV of sTg performed in 3 consecutive tests during a minimum of a 3 year monitoring period. ***Conclusion:*** Repeating the measurement of the stimulated serum thyroglobulin after negative result of the first stimulated thyroglobulin had a limited clinical value for detecting structural recurrent or persistent disease, and is not recommended for routine use in the group of low- and intermediate-risk patients with DTC. ***References:*** Prpic M, Franceschi M, Romic M, Jukic T, Kusic Z. Thyroglobulin as a tumor marker in differentiated thyroid cancer - clinical considerations. Acta Clin Croat 2018;57(3):518-27. Haugen BR, Alexander EK, Bible KC, Doherty GM, Mandel SJ, Nikiforov YE et al. 2015 American Thyroid Association management guidelines for adult patients with thyroid nodules and differentiated thyroid cancer: the American Thyroid Association guidelines task force on thyroid nodules and differentiated thyroid cancer. Thyroid. 2016;26(1):1-133. Kowalska A, Walczyk A, Pałyga I, Gąsior-Perczak D, Gadawska-Juszczyk K, Szymonek M et al. The delayed risk stratification system in the risk of differentiated thyroid cancer recurrence. PloS One 2016;11(4):e0153242.

EP-385

Standardised uptake value (SUV) of iodine-131 at post-treatment SPECT/CT in patients with differentiated thyroid cancer

A. Trukhin*, P. Rumyantsev, A. Bubnov, E. Kolpakova, K. Slaschuck, Y. Sirota, M. Degtyarev, S. Serzhenko;*
Endocrinology Research Cener, Moscow, RUSSIAN FEDERATION.

Aim/Introduction: Standardized uptake value of 131-I accumulation in tumor foci at whole body scintigraphy of patients after radioiodine therapy of differentiated thyroid cancer (DTC) is strongly required by clinical practice. ***Materials and Methods:*** Study included 148 patients (f-105, m-43) with DTC treated with 131-iodine. Administered treatment activities of ^{131}I calculated according to clinical features including tumor recurrence risk group. Patients were divided into three groups using ATA 2018 recommendations. Absolute risk groups: low risk (L), medium risk (M), high risk (H). Administered 131-I activity [MBq]: $<A_L>$ = 3223±729, $<A_M>$ = 3696±456, $<A_H>$ = 4589±1078; Tg [ng/ml]: $<Tg_L>$ = 7,4±1.7 ng/ml, $<Tg_M>$= 14,8 ±5,9, $<Tg_H>$ = 68,3 ±18,5; TgAb [IU/ml]: $<TgAb_L>$ = 124,3 ± 81.7, $<TgAb_M>$ = 29,2 ±15,9, $<TgAb_H>$ = 85,7 ±28,9. All null hypothesis was checked using paired Mann-Whitney U-test. Calibration of system SPECT/CT and evaluation SUVs completed according to protocols designed using Jaszczak phantom Deluxe. Model development based on logistic regression with ROC-analysis, regularization and cross-validation. ***Results:*** Reference intervals of SUVpeak and SUVmax calculated for all groups of risk. SUVpeak: low risk >155, medium risk 105-155, high risk 0-105 pL-M=0.069 pL-H=0.0037 pM-H=0.7514; SUVmax: low risk >38, medium risk 29-38, high risk 0-29 pL-M=0.052 pL-H=0.0033 pM-H=0.949. Logit model based on SUVpeak without regularization has: AUC = 0.67 (95%CI 0.33-1.00); Accuracy = 0.82; SE = 0.89; SP = 0.4; PPV = 0.41; NPV = 0.89, cross-validated AUC =0.67 (0.4-0.88), regression coefficients: B_0=0.037, B_1=0.001. Regularization (SUVpeak<100) lead to AUC = 0.75, (95%CI 0.44-1.00); accuracy = 0.89; SE = 0.98; SP = 0.4; PPV = 0.76; NPV = 0.87, cross-validated AUC = 0.513 (0.36-0.71) regression coefficients: B_0=0.473, B_1=0.003. ***Conclusion:*** Study shows that SUV has wide range of values and can be matched with existed model of risk assessment of DTC. Algorithm of image segmentation and evaluation of SUVpeak and SUVmax for SPECT/CT systems was developed. According to the ROC analysis, developed predictive model shows an acceptable performance for further clinical investigation and advancement focused on refining model parameters and introducing additional predictors. ***References:*** None

EP-386

Rare sites of metastasis in differentiated thyroid carcinoma:case series study

N. Bashank*[1], H. Farghally[2], S. Hassanein[3], M. Abdeltawab[3], M. Wahman[4];*
[1]Assuit university,AUH, clinical oncology and nuclear medicine department, Assuit, EGYPT, [2]Assuit university, clinical oncology and nuclear medicine department, Assuit, EGYPT, [3]Assuit University Hospitals, Diagnostic Radiology department, Assuit, EGYPT, [4]South Vally University,Clinical Oncology and Nuclear Medicine Department, Qena, EGYPT.

Aim/Introduction: The most common sites of metastasis in differentiated thyroid cancer are the neck lymph nodes with distant metastasis to lungs and bone. The liver, brain, adrenal gland, kidney, pancrease, eye, muscle and skin can be sites for rare metastasis .Rare metastases can be missed resulting in diagnostic pitfalls and inappropriate treatment

.Identification of such cases has a great impact on patients management . There is lack of knowledge about dealing with such patients and what treatment they should receive and response of therapy due to rarity of such cases. More studies are needed to establish a therapeutic algorithm with an accurate and definitive treatment for these patients.Our study aims to study and report these rare cases of distant metastasis in patients with differentiated thyroid cancer (DTC) increasing the awareness about these cases and their methods of treatment and response to therapy. ***Materials and Methods:*** A retrospective review of 1,200 cases of thyroid cancer cases was performed. A total of 9 cases of DTC that had a rare distant metastasis were recognized . ***Results:*** 9 patients were included in this study (7 females ,2 males) with median age 57 years (range:32-79). 6 patients had follicular carcinoma , 2 patients had papillary carcinoma & 1 patient had insular carcinoma.4 cases(44.4%) had multi-organs distant metastasis. the metastases were as following:, kidney and pancrease metastases (1), sella-turcica metastasis(1) muscle metastasis(1) paragharyngeal metastasis(1) , solitary brain metastasis (1),solitary bone metastasis(1)papillary carcinoma with bone metastasis(1)liver metastasis (1)and Malignant jugular vein thrombus (1).All patients received the initial therapy (total thyroidectomy with lymph node dissection & radioactive iodine therapy) in addition to external beam radiotherapy in 4 cases & tumour excision with vertebral fixation in one patient.5 patients showed disease regression while progression in 3 patients with disease stability in one patient. ***Conclusion:*** Rare metastases Identification has a significant impact on patients management . However, distant metastasis in DTC patients carries a bad prognosis, disease remission can occur especially if they are iodine avid or surgically resectable. More studies are needed to establish a therapeutic algorithm promoting an accurate and definitive treatment for such rare cases ***References:*** 1. Kunadharaju, R., et al., New Treatment Options for Metastatic Thyroid Cancer. Federal Practitioner, 2015. 32(Suppl 7): p. 21S.2. Farina, E., et al., Unusual thyroid carcinoma metastases: a case series and literature review. Endocrine pathology, 2016. 27(1): p. 55-64.

EP-387

18F-FDG PET-CT: impact in the diagnosis and management of a population of thyroid cancer patients

C. Varela Pinto*, B. Martins, D. Calado, D. Macedo, A. Martins, F. Sobral do Rosário, C. Loewenthal;*
Hospital da Luz Lisboa, Lisbon, PORTUGAL.

Aim/Introduction: To evaluate the impact of 18F-FDG PET-CT results on the therapeutic management of patients with thyroid cancer. ***Materials and Methods:*** Retrospective analysis of clinical electronic records of 44 patients (mean age 52 years, range 30-86) who underwent 18F-FDG PET-CT at the time of diagnosis or follow-up of thyroid cancer between January 2008 and April 2020. Biochemical, clinical, imaging and pathological findings were reviewed. We compared results of all other imaging modalities combined, with PET-CT results, and evaluated clinical impact of PET-CT on management. ***Results:*** Forty-four patients (25 women, 19 men) underwent 18F-FDG PET-CT, 11 for initial staging and 33 for re-staging of thyroid cancer. The most common histological subtypes was papillary (28), followed by medullary (8), follicular (4) and anaplastic (4). On PET-CT, 3 patients had disease confined to the thyroid gland, 10 had locoregional disease, 17 had metastatic disease (10 lung lesions, 5 bone lesions, 1 liver lesion and 1 bone plus liver lesions) and 14 patients had no detectable lesions. PET-CT and other imaging modalities results were similar in the diagnosis and management of the disease in 38 patients (86%). In the remaining 6 patients (14%), PET-CT results detected unknown disease and determined a change in strategy. PET-CT detected hypermetabolic lesions in cervical lymph nodes in 2 patients, lung lesions in another 2 and bone lesions in 2. In 4/6 patients, PET-CT results were confirmed pathologically. In the other 2/6 patients, PET-CT results were confirmed during follow-up, with reduction of serum thyroglobulin after radioactive iodine therapy in one patient and stereotactic body radiation therapy on the other. ***Conclusion:*** PET-CT with 18F-FDG appears to bring added value in the diagnosis and management of patients with thyroid cancer. A percentage of patients seem to benefit from the additional information provided, altering the therapeutic management at least in 14% of the patients, all of them in the follow-up of papillary thyroid cancer. ***References:*** None

EP-388

A critical review of the contact restrictions following radioiodine (I-131) therapy in the UK

E. Stamou*, D. Morgan, A. Hallam;*
Oxford University Hospitals NHS Trust, Oxford, UNITED KINGDOM.

Aim/Introduction: Radioiodine therapy is particularly effective in managing differentiated thyroid cancers. Upon therapy completion, patients are given restrictions to minimize doses to the public, family and friends. IRR17[1] established the 1 mSv/year limit for keeping doses ALARP, whereas IRMER[2] yields for differentiated doses for the latter if justified as "comforters and carers", where employers establish constraints, those being 5mSv in 5yrs in our hospital. Following MDGN[3] guidelines, the UK release criterion is the retained activity, with 800MBq threshold. Given restrictions are currently calculated based on radioiodine's biological half-life. This study assessed this model against a proposed one and investigated their effectiveness in complying with legislation. ***Materials and Methods:*** Data from 32 patients (16 Female, 16 Male) (69% papillary carcinoma, 31% follicular carcinoma) with age range 25-77yrs, over a period of 2yrs (2018 to 2020) were analysed. 77% of patients underwent a single treatment ($Activity_{average}$=3.7GBq) while 22% (13% within a year, 9% within 4 years) received a second treatment

($Activity_{average}$=5.6 GBq). Restrictions were generated using the proposed bi-phasic model based on the physiological kinetics, utilising a slow and fast clearance component. ***Results:*** For 41% of the patients (68% males, 32% females) the current dose to bedsharing adults exceeded the 1mSv/yr limit by 31% (D_{mean}=1305μSv; D_{max}=9353 μSv), while for children <5yrs it was D_{mean}=620 μSv; D_{max}=2913 μSv. According to the proposed model, doses to bedsharing adults could be brought to 1mSv with 2 additional days and significantly optimised with 4 extra days (we currently instruct for 2 days on average, following the 3-day hospital isolation). With up to 30% recurrence probability [1], a second treatment with 3.7GBq could result in high doses to close contact adults, with 20% of cases approaching the 5mSv in 5 yrs limit. Interestingly, positive correlations were found between the doses to adults and children, and the % of tumour uptake ($r_{Pearson's\_children<5yrs}$ =0.77; $r_{Pearson's\_Adults(bedshare)}$ =0.82) while no correlation was shown between whole-body counts and doses to adults and children, respectively ($p_{adults(bedshare)}$=0.04; $p_{children<5yrs}$=0.01). ***Conclusion:*** Notwithstanding minimising children's exposure to radioiodine patients due to greater radiosensitivity, we highlight that prolonged close contact to patients, occurring mainly with adults, could result in higher total dose potentially exceeding the dose constraints, especially with repeat treatment. It is, therefore, vital to carefully consider the outcomes of the study and review the current guidelines to avoid underestimating the restrictions given to patients. ***References:*** [1]Legislation.gov.uk.Available from:http://www.legislation.gov.uk/uksi/2017/1075/pdfs/uksi_20171075_en.pdf [2]Ionising_Radiation_(Medical_Exposure)_Regulations_(IR(ME)R)_Available from:https://www.cqc.org.uk/guidance-providers/ionising-radiation/ionising-radiation-medical-exposure-regulations-irmer [3][Internet].Available from: http://files.site fusion.co.uk/webfusion117640/file/medicalguidancenotes_1.pdf [4]Shaha_A.Recurrent_differentiated_thyroid_cancer. Endocrine_Practice.2012_Jul_1.18(4):600-3.

EP-389

The Diagnostic Contribution and Clinical Impact of ^{131}I SPECT/CT in the Evaluation of Extrathyroidal Uptake in Patients with Differentiated Thyroid Carcinoma after Radioiodine Therapy

T. Bahceci, *E. Özdemir;*
Ankara City Hospital, Ankara, TURKEY.

Aim/Introduction: The purpose of this study was to determine the diagnostic contribution and clinical impact of adding SPECT/CT to posttherapy ^{131}I whole body scan (WBS) in the evaluation of equivocal extrathyroidal ^{131}I uptake in patients with differentiated thyroid cancer (DTC). ***Materials and Methods:*** We retrospectively reviewed ^{131}I-WBS imaging findings in 280 patients (March 2019-January 2020) who were operated for DTC and treated with RAI. A total of 116 patients (93F, 23M; mean age:48.34±13.41) who had extrathyroidal uptake on WBS and who underwent SPECT/CT imaging were included in the study. We assigned an incremental value to SPECT/CT when it provided better interpretation and identification of the foci of radioiodine, more correct anatomic localization and characterization, and precise differentiation between malignant lesions and physiologic uptake. The contribution of SPECT/CT imaging was evaluated in both lesion-based analysis and on patient-based analysis. Changes in staging and patient management were investigated after SPECT/CT evaluation. Serum thyroglobulin level, histopathology, other imaging modalites and clinical follow-up served as the gold standard. ***Results:*** The contribution of SPECT/CT to distinguish various causes of false-positive uptake images showed that the most common I-131 uptake site, except the thyroid bed, was observed in the thyroglossal duct (n:64(55%)) and thyroglossal duct uptake was correctly localized by SPECT/CT in all cases. The physiological uptake was most frequently observed in the salivary glands (n: 10 (9%)) and most commonly detected benign nonthyroidal pathology was the dental pathology (n: 25 (21%)). In 60 patients (51.7%) with doubtful findings in planar imaging, SPECT/CT was excluded pathological uptake. Overall, SPECT/CT changed therapy management for 17 patients (14.6%), by upstaging nodal staging (n: 12) and distant metastasis staging (lung metastasis n: 5, bone metastasis n: 1). ***Conclusion:*** SPECT/CT imaging after RAI therapy in patients with DTC improves diagnostic accuracy of WBS imaging by identification of physiological uptake and the differentiation of benign pathologies from malignancy and accurate localization and diagnosis of lymph node/distant metastases; It contributes significantly to the clinical impact and patient management. ***References:*** None

EP-390

Six-Year Experience With The ROLL Technique In The Detection And Treatment Of Loco-Regional Recurrence In Thyroid Cancer

J. Villena Salinas, *E. Ramos Moreno, J. Alors Ruiz, A. Montellano Fenoy, T. Amrani Raissouni, S. Ortega Lozano;*
Hospital Universitario Virgen de la Victoria, Malaga, SPAIN.

Aim/Introduction: Describing the experience gained in radioguided surgery with ROLL technique (Radioguided Occult Lesion Localization), in order to detect and excise loco-regional reccurences in patients diagnosed with thyroid cancer. ***Materials and Methods:*** It is a prospective study with 39 patients: 19 men and 20 women, with suspected tumoral recurrence, previously treated with surgery. The differentiated carcinomas received complementary therapy with 131I. 0,4-0,6mCi of MAA-99mTc was administered in 0,07ml of saline solution by ultrasound-guided intralesional injection. The Navigator2.0 (Dilon technologies Inc®) radiation detector probe was used to localize on skin the highest radioactivity

point, in order to guide the surgeon towards the suspicious lesion. After its excision, lack of activity in the surgical field and its presence in the ex-vivo piece were proven and the piece was sent to conventional histopathological study. ***Results:*** The patient´s average age was 56,6+/- 13,1 years old. The histological types of the primary tumor were: papillary (30/39, 76,92%), medular (4/39, 10,26%), follicular (1/39, 2.56%) and Hurtle (1/39, 2.56%). The performed surgical treatment was total thyroidectomy with radical lymphadenectomy (23/39, 85.97%) and total thyroidectomy without lymphadenectomy (16/39, 41.03%). From all the patients, 33/39 (84.62%) received complementary therapy with 131I, average dose of 115+/-24mCi. The average preoperative values of thyroglobulin were 12.02+/-18.62 ng/ml and 58.28+/-150 ng/ml of antithyroglobulin antibodies. The average size of the recurrences was of 2.6+/-1.6cm, with 21 of them (53.85%) being tumor recurrence, and 18 (46.15%) lymph nodes recurrence. The lesion was localized in 100% of the cases, and in 33 cases (82.62%) it was positive in the histopathological analysis, and negative in 6 cases (15.38%). ***Conclusion:*** Radioguided surgery with ROLL technique in thyroid cancer can be established as a reliable procedure which has allowed, since the beginning of its use in 2013, the localization of the suspected recurrence. ***References:*** None

EP-391

The influences of TSH stimulation level, stimulated Tg level and Tg/TSH ratio on the prognosis of ^{131}I treatment in DTC patients

W. Zheng*, Z. Rui, X. Wang, N. Li, Z. Meng, J. Tan, Q. Jia;*
Department of Nuclear Medicine, Tianjin Medical University General Hospital, Tianjin, CHINA.

Aim/Introduction: To study the influences of preablation TSH stimulation level, sTg and sTg/TSH ratio on the prognosis of ^{131}I treatment in DTC patients. ***Materials and Methods:*** According to the TSH levels (mU/l), all the 479 patients were divided into two groups: TSH < 30 and TSH ≥ 30. And then, the TSH ≥ 30 group was divided into three subgroups: 30 ≤ TSH < 60, 60 ≤ TSH < 90 and TSH ≥ 90. The clinical features and the prognosis were analyzed. The cutoffs of sTg and sTg/TSH were calculated to predict the prognosis of DTC. ***Results:*** The TSH ≥ 90 subgroup was younger and less possible with LNM. The postoperative L-T4 dose in the 30 ≤ TSH < 60 subgroup was higher than 60 ≤ TSH < 90 subgroup. In the TSH < 30 group, the postoperative L-T4 dose was higher and THW (d) was longer. The response rate six months after the first ^{131}I treatment among the three subgroups and between the two groups were no statistical significances. The distribution of different TSH stimulation levels among each response group was similar. The cutoffs for good prognosis in sTg and sTg/TSH were < 9.51 ng/ml and < 0.11, respectively. Both univariate and multivariate logistic regressions showed that LNM, distant metastasis and higher sTg, sTg/TSH predicted poor prognosis. ***Conclusion:*** There was no significant effect of TSH stimulation level before the first ^{131}I treatment on the prognosis of DTC. Both preablation sTg and sTg/TSH can be considered as predictors of ^{131}I treatment outcome. ***References:*** None

EP-392

Outcome related to changes of stimulated and suppressed thyroglobulin

C. Hong*, S. Lee, J. Lee, S. Jeong, B. Ahn;*
Kyungpook National University Hospital, Daegu, KOREA, REPUBLIC OF.

Aim/Introduction: Stimulated thyroglobulin (off-Tg) and suppressed thyroglobulin (on-Tg) are widely used for risk assessment of thyroid cancer patients. However, there is only few studies about outcome related to changes of off-Tg and on-Tg. ***Materials and Methods:*** We retrospectively reviewed DTC patients who underwent total thyroidectomy and radioactive iodine (RAI) ablation between Jan-2000 and Feb-2002. Response to therapy risk (RTT) assessment using both off-Tg and on-Tg were performed 6-15 months after high-dose RAI therapy. All the patients were under TSH suppression. Median follow-up period after RAI ablation was 15.6 ± 5.4 years. ***Results:*** Finally, 411 patients were included in this study. 80 patients were low risk, 165 were intermediate and 166 were high-risk according to ATA risk stratification. At initial RTT (off-Tg/on-Tg), 176/156 patients were excellent response (ER), 130/159 were indeterminate response (IR), 62/53 were biochemical incomplete response (BIR), and 43/43 were structural incomplete response (SIR) and. Progression rates of DRS using off-Tg/on-Tg were 1.7%/5.8% in ER, 15.4%/12.6% in IR, 43.5%/39.6% in BI, 69.8%/69.8% in SI. During the follow-up, 41 patients were down-staged to ER (from IR/BI) or IR (from BI) using off-Tg without any kind of procedures, and only 1 patient (2.4%) showed progression. And 30 patients were down-staged using on-Tg during follow-up and only 1 patient (3.3%) showed progression. ***Conclusion:*** Off-Tg shows better prognostic value than on-Tg on DRS. The patients who down-staged without any procedure showed excellent prognosis. ***References:*** None

EP-393

^{131}I Effective Half-life in Children and Adolescents with Thyroid Cancer Patients

X. Zhang*, B. Liu;*
Department of Nuclear Medicine, West China Hospital, Sichuan University, Chengdu, CHINA.

Aim/Introduction: The kinetics of ^{131}I in therapy of children and adolescents with thyroid cancer is poorly studied. The goal was to investigate the effective half-life of ^{131}I in children and adolescents with thyroid cancer treated in our center in relation to clinical parameters. ***Materials and Methods:*** Fifty-

two thyroid cancer patients <20 years of age at diagnosis were included. Probe measurement of whole-body dose rate was serially performed after ingestion of ^{131}I. ***Results:*** The median age was 16 years, and the majority were female (73.1%). All patients underwent total thyroidectomy and received ^{131}I therapy after thyroid hormone withdrawal. The mean effective half-life was 10.9 hours, ranging from 6.4 to 26.0 hours. Significant correlation coefficient was only found between effective half-life and body surface area (r=0.349; p=0.11). ***Conclusion:*** Effective ^{131}I half-life in children and adolescents with thyroid cancer is shorter than that in adult populations reported previously, suggesting that age may be an affecting factor. Body surface area should be included in specific recommendations regarding ^{131}I activity retention during ^{131}I therapy in children and adolescents with thyroid cancer. ***References:*** None

EP-66

Thyroid Therapy

e-Poster Area

EP-395

Impact of 18F-FDG PET/CT on the management of well differentiated thyroid cancer (DTC) persistence/recurrence in the suspect of radio-iodine refractory disease (RAI-R-DTC)

E. Lodi Rizzini[1], *L. Zanoni*[1], *E. Tabacchi*[1], *A. Repaci*[2], *A. G. Morganti*[3], *S. Fanti*[1], *F. Monari*[3];
[1]*Nuclear Medicine Unit, S.Orsola-Malpighi Hospital, Bologna, ITALY,* [2]*Endocrinology Unit, S.Orsola-Malpighi Hospital, Bologna, ITALY,* [3]*Radiation Oncology Center, S.Orsola-Malpighi Hospital, Bologna, ITALY.*

Aim/Introduction: Prognostic role of 18FDG-PET/CT imaging in advanced DTC has already been reported in literature. However, there is still lack of data about the real impact of 18FDG-PET/CT on treatment management in the case of advanced and aggressive disease, so the first aim of our study was to retrospectively assess the impact of 18F-FDG PET/CT and secondly to confirm the prognostic role of clinical and semi-quantitative metabolic 18F-FDG PET/CT parameters in comparison with scientific literature. ***Materials and Methods:*** A monocentric retrospective/observational study was performed from a database of 208 pts treated, from January 2011 to July 2019, for local/metastatic DTC with several RAI courses in our Radiation Oncology Center. 53 pts who started to perform 18FDG-PET/CT scan after the second RAI course because of strong suspect of RAI-R-DTC (negative Rx-WBS scan and/or high thyroglobulin levels) were included. Clinical, laboratory and imaging data were collected. Metabolic response was defined according to PERCIST criteria. SUVmax, SUVmean,MTV,TLG were calculated. Kruskal-Wallis,Chi-Square-Pearson tests and Cox regression were used to compare metabolic/clinical parameters and PFS. ***Results:*** In our sample (mean age: 52±19.9 years; 31F-22M) 20/53(38%) pts had a negative RxWBS and a positive PET/CT scan, 7/53(13%) pts had positive RxWBS and PET/CT scans, 24/53 (45%) pts had negative RxWBS and PET/CT scan and 2/53(4%) pts had a positive RxWBS and a negative PET/CT scan. Therapeutic approaches addressed after PET/CT positivity were external-beam-radiation therapy in 4/27(15%) pts, surgery in 4/27(15%), further RAI course in 2/27(7.4%), surgery+EBRT in 1/27(4%) and observation in 16/27(59%) pts. PERCIST response was evaluated in 14/27 FDG/PET positive scans. Median FU and median PFS were 5.8±3.9 years and 38±21.8 months respectively. At the last FU, 13/53(24.5%) pts had persistence of structural disease, 25/53(47%) persistence of biochemical disease and 15/53(28%) excellent response. Significant associations were found between clinical response assessment and therapeutic approach(p=0.01) and between PFS and metabolic response (p=0.02). Linear correlation between MTV and TLG and suppressed-Tg was found. At Cox-Regression multivariate analysis only MTV (p=0.034 HR 1.100 CI95% 1.007-1.202) and PERCIST response (p=0.004 HR 2.434 CI95% 1.322-4.481) were independently associated to persistent disease. ***Conclusion:*** In our analysis 18F-FDG-PET/CT turned out to be a guide for clinical management of RAI-R-DTC, particularly to avoid further ineffective/toxic RAI administrations. Randomized trials are needed to confirm our results and the real impact of 18F-FDG-PET/CT on therapy choice. ***References:*** Prognostic value of 18F-FDG PET/CT metabolic parameters in metastatic differentiated thyroid cancers. Masson-Deshayes et al. ClinNuclMed 2015; 40(6): 469-475.

EP-396

To compare high turnover and normal turnover Graves' disease outcomes after ^{131}I-Radioiodine therapy and determine prognostic factors

S. Arora*, D. Chakraborty, K. S. Reddy, M. Prabhu, A. Behera, A. Tupalli, A. Passah, B. S. Mangu, A. Hemrom, C. Bal;*
All India Institute of Medical Sciences, New Delhi, INDIA.

Aim/Introduction: To compare the outcomes after 131I-Radioiodine therapy in high turnover and normal turnover Graves' disease patients. ***Materials and Methods:*** High turnover (HTO), was defined as 2h RAIU/24h RAIU ratio ≥1 and normal turnover (NTO) as 2h RAIU/24h RAIU ratio <1 (1,2). These two cohorts of Graves' disease (GD) patients were selected for a retrospective cohort design study (1:2 ratio, n=104: n=208) and then matched using propensity score matching (PSM) (1:1, 77:77). ^{131}I cure rate (euthyroid plus hypothyroid) at 12 months was compared. Univariate and multivariate analysis were done to determine prognostic factors. The binary logistic regression model was used to predict the factors responsible for the failure of RIT. ***Results:***

There was a significant difference in cure rates, 28% vs 66% (unadjusted) and 31% vs 61% (adjusted for covariates using PSM) in HTO and NTO groups, respectively noted (P 0.001). The median number of RIT (2 vs 1) and median cumulative activity (15 vs 7 mCi) was required to achieve cure in two groups respectively. The variables associated with the failure after 131 RIT (at 12 months) were; age >44years (odds ratio-2.6, p 0.001), grade 2 goitre (odds ratio-2.8, p 0.029), high turnover group (odds ratio-2.6, P 0.007) and 2h RAIU >37% (odds ratio 2.7, p-value 0.005). ***Conclusion:*** High turnover Graves' disease patients differ significantly from normal turnover in outcome (failing after routine lower activities of ^{131}I). Factors predicting high failure rate are higher age (>44 years), higher grade of goiter, high turnover of the gland and higher 2h RAIU (>37%). ***References:*** 1. Aktay R, Rezai K, Seabold JE, Bar RS, Kirchner PT. Four- to twenty-four-hour uptake ratio: an index of rapid iodine-131 turnover in hyperthyroidism. J Nucl Med. 1996; 37(11):1815-9. 2. Van Isselt JW, de Klerk JMH, Koppeschaar HPF, Koppeschaar HP, Van Rijk PP. Iodine-131 uptake and turnover rate vary over short intervals in Graves' disease. Nucl Med Commun2000; 21(7): 609-616.

EP-397

Dynamic risk stratification to evaluate prognostic factors (PrFs) for differentiated thyroid cancer (DTC): A retrospective cohort study

E. Giannoula[1], N. Papadopoulos[2], C. Sachpekidis[3], A. Doumas[1], G. Gerasimou[1], F. Spyroglou[1], V. Chatzipavlidou[4], I. Iakovou[1]; [1]Nuclear Medicine dpt of Aristotle University AHEPA Academic hsp, Thessaloniki, GREECE, [2]G.Gennimatas hsp, Thessaloniki, GREECE, [3]Clinical Cooperation Unit Nuclear Medicine, German Cancer Research Center, Heidelberg, GERMANY, [4]Nuclear Medicine dpt of THEAGENEIO Anticancer hsp, Thessaloniki, GREECE.

Aim/Introduction: Despite excellent prognosis, small cohorts of DTC-patients experience a more aggressive form of disease often associated with certain poor PrFs. Identifying these patients at an early stage and dynamically evaluating them is imperative for guiding treatment decisions. Risk stratification should be a dynamic process to predict the appropriateness for minimalistic initial therapy, disease-specific-mortality, risk of recurrence, and the most likely response to initial therapy. In this respect, the objective of our study is to investigate the factors (demographic,clinical,pathologic,treatment administrated characteristics) influencing treatment response. ***Materials and Methods:*** Our cohort comprised all 551 patients_(47,2±14yrs) with DTC,who underwent a first radioiodine ablation procedure or follow-up-WBS at our institutions from June_2016 to June_2018. All demographic and pathologic characteristics were recorded. TSH,Tg,TgAb and AntiTPO levels were measured after TSH stimulation. Thyroid remnant in post-therapy and follow-up 131I_WBScan was retrospectively given classification scores based on visual assessment of the number of foci of thyroid bed uptake and their overall intensity on 131I_WBScan. Response to therapy was assessed according to the ATA2015-guidelines response to therapy re-classification. ***Results:*** Cohort overwhelmingly comprised patients with papillary type_(76.8%). Despite favorable histotypes, a large proportion of patients had characteristics suggested higher risk or uncertainty regarding risk, or both: Almost, half of the cohort_(46.25%) was diagnosed with primary tumors ≥2cm. Multifocality was detected in_53.95% patients. Invasiveness was documented for_40.5% of the patients.Lymph node metastases were detected in_39.4% and distant metastases in less than_5% of the patients. Virtually, all patients had evidence of postsurgical thyroidremnant (thyroid-bed uptake was absent in only_7.75% of cases). Response to treatment evaluation showed 37.7%_Excellent_Response-ER, 14.7%_Biochemical_Incomplete_Response-BIR, 21.7%_Structural_Incomplete_Response-SIR and 26%_Indeterminate_Response-IR which were significantly correlated with histological type(p=0.001), stage(p=0.039) preablation_Tg(p=0.001) and remnant scoring(p<0.001). ***Conclusion:*** Several PrFs (clinical, pathologic, treatment administrated characteristics) for DTC have emerged and should be addressed. However, their role has yet to be determined not only for achieving an adequate therapeutic approach, but also for avoiding overtreatment of low-risk patients. Dynamic-risk-assessment should be used to guide all aspects of DTC management, beginning before a definitive diagnosis is made and continuing through the final follow-up visit. ***References:*** -Frangos_S,Iakovou_IP,Marlowe_RJ et al.Difficulties in deciding whether to ablate patients with putatively "low-intermediate-risk" DTC: do guidelines mainly apply in the centres that produce them? Results of a retrospective, two-centre quality assurance study.Eur_J_Nucl_Med_Mol_Imaging_2015;42(13)-Frangos_S,Iakovou_IP,Marlowe_RJ et al.Acknowledging gray areas: 2015 vs. 2009 American Thyroid Association DTC guidelines on ablating putatively low-intermediate-risk patients.Eur_J_Nucl_Med_Mol_Imaging.2017;44(2)-Giannoula_E,Iakovou_I,Chatzipavlidou_V.Risk factors and the progression of thyroid malignancies.Hell_J_Nucl_Med_2015,18(3)

EANM'21

WORLD LEADING MEETING

34th Annual Congress of the European Association of Nuclear Medicine

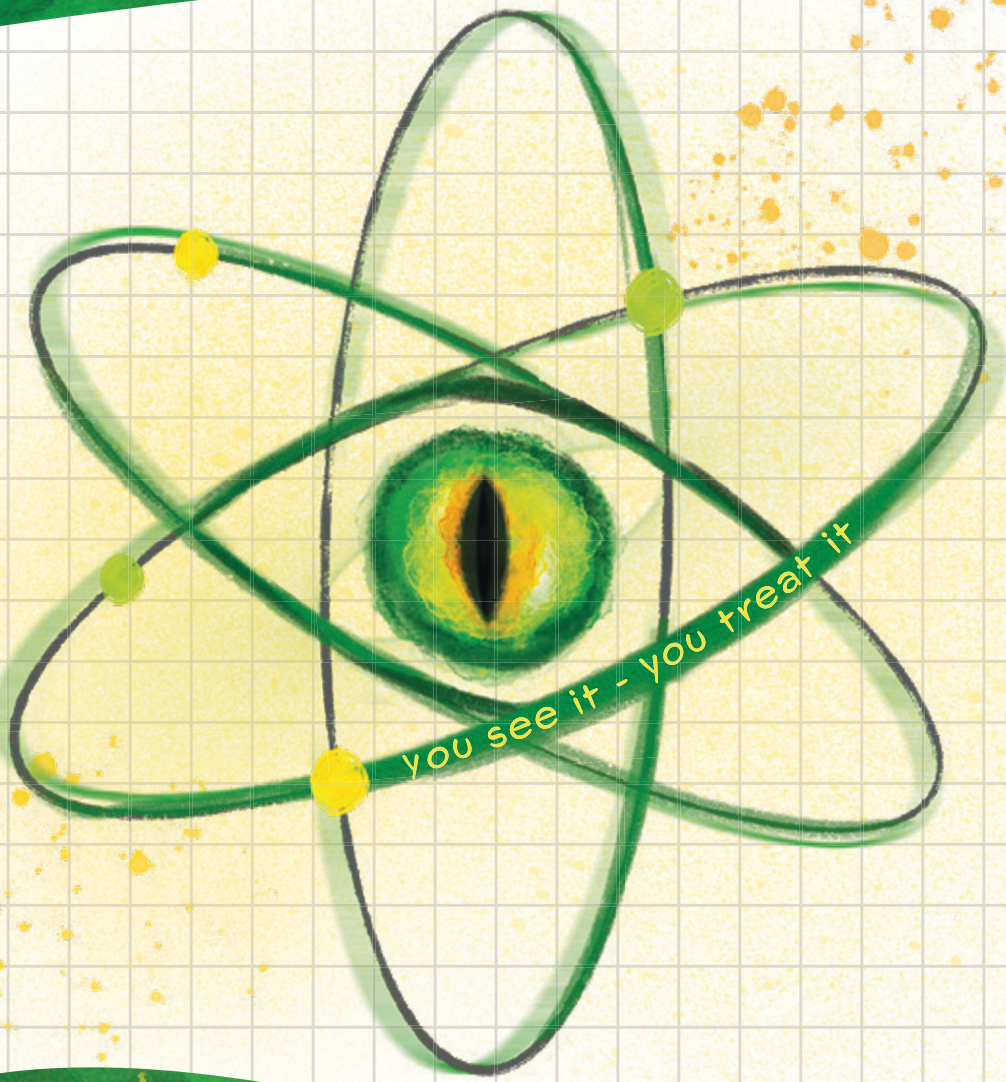

HAMBURG

Oct 23 - 27, 2021

eanm21.eanm.org

ESMIT

European School of Multimodality Imaging and Therapy

ESMIT Live Webinar series - to be continued!

Place: EANM'20 WORLD LEADING MEETING VIRTUAL

Nuclear Imaging Technology: Where we came from, where we are and where we are heading

PHYSICS

Speakers:
Ian Armstrong, John Dickson, Stephan Nekolla, Dimitris Visvikis

Moderator:
Michel Koole

Place: EANM'20 WORLD LEADING MEETING VIRTUAL

PET MPI: Tracers, Equipment, Protocols, Flow Quantification, Viability

CARDIOLOGY

Speakers:
Mark Lubberink, Roberto Sciagra

Moderator:
Christoph Rischpler

For more information visit the ESMIT Booth of EANM'20

Stay tuned for more ESMIT Live Webinars coming up in 2021!

ESMIT

European School of Multimodality Imaging and Therapy

Course Programme 2021

Dosimetry	**Practical Implementation of Clinical Dosimetry in NM Therapy**	**Feb 2021**
Oncology I	**Therapy Assessment**	**Mar 2021**
Physics	**Advanced Features of Quantification**	**Apr 2021**
Neurology	**Quantification in Neurology**	**Apr 2021**
Bone & Joint	**Post-Operative Skeleton**	**Jun 2021**
Oncology II	**Prostate Cancer (advanced)**	**Sep 2021**
Thyroid	**Management of Thyroid Cancer (advanced)**	**Nov 2021**
Tba	**Theranostics**	**Dec 2021**

Please note that the information given above is subject to change.
For regular updates, please visit the EANM website or
subscribe to the ESMIT vNewsletter.

eanm.org/esmit

Acknowledgement

The ESMIT leadership likes to thank all contributors of this initiative. Special thanks to the EANM Committees and the ESMIT Project Groups for their continuing support.

HERMES MEDICAL SOLUTIONS

FOCUSMEETING.EANM.ORG

POSTPONED DUE TO COVID-19

SEVILLE, SPAIN

NEW DATES: FEBRUARY 3-5, 2022

EANM 4 FOCUS

MOLECULAR IMAGING AND THERAPY IN HAEMATOLOGICAL TUMOURS

EUROPEAN ASSOCIATION OF NUCLEAR MEDICINE

EARL RELEASED

^{18}F STANDARD 2 ACCREDITATION,

Allowing sites to benefit from state-of-the-art PET/CT technology while still ensuring harmonized scanners performance,

UNIQUE ^{89}Zr PET/CT ACCREDITATION

Based on and derived from the procedures performed for the ^{18}F-FDG PET/CT accreditation which is a prerequisite for ^{89}Zr accreditation

EANM RESEARCH LTD (EARL)

EARL is a 100% subsidiary of the EANM, which aims to enhance the quality of nuclear medicine practice for the benefit of public health.

RESEARCH 4 LIFE©

an EANM initiative